NAT'L INST. OF STAND & TECH R.I.C.
A11104 938263

Precision Measurement and Calibration

Heat and Mechanics

Handbook 77 — Volume II

United States Department of Commerce
National Bureau of Standards

UNITED STATES DEPARTMENT OF COMMERCE • Frederick H. Mueller, *Secretary*
NATIONAL BUREAU OF STANDARDS • A. V. Astin, *Director*

Precision Measurement and Calibration

Selected Papers on Heat and Mechanics

A compilation by Sherman F. Booth of previously published technical papers by the staff of the National Bureau of Standards.

Issued in three volumes*

I. Electricity and Electronics.
II. Heat and Mechanics.
III. Optics, Metrology, and Radiation.

National Bureau of Standards Handbook 77 — Volume II

Issued February 1, 1961

For sale by the Superintendent of Documents, U.S. Government Printing Office, Washington 25, D.C.
*Prices: Volume I $6.00, Volume II $6.75, Volume III $7.00. The three volumes at $19.75 a set.

National Bureau of Standards
1931
104,747 Ref.

Abstract

This Handbook is a three-volume compilation of approximately 150 selected papers previously published by the staff of the National Bureau of Standards on precision measurement, calibration, and related subjects. It was prepared to meet the urgent need of newly established standards laboratories for a "textbook" and reference source in these fields. Volume I contains papers in electricity and electronics; Volume II, heat and mechanics; and Volume III, optics, metrology, and radiation. Each volume contains a complete index of the entire Handbook by author, subject, and title.

Foreword

The National Bureau of Standards is charged with the responsibility of establishing and maintaining the national standards of physical measurement, and of providing means for their effective utilization. This responsibility carries with it the mission of providing the central basis for a complete, consistent system of physical measurement, adequate for national growth in research and technology.

The recent tremendous increase in industrial activity, particularly in the missile and satellite fields, has led to an unprecedented demand for precision measurement, which, in turn, is bringing about the establishment of hundreds of new standards laboratories. Many of these new laboratories must cover the entire field of measurement, and must do so with a staff not previously trained in work on standards of precision measurement.

To aid these laboratories in transmitting the accuracies of the national standards to the shops of industry, the Bureau has prepared this three-volume Handbook. It is a compilation of publications by the Bureau staff that have been found of value to those who are establishing and operating new standards laboratories. Omitted are some extended works, as well as a few shorter papers that are otherwise readily available.

It is hoped that this compilation will serve both as a "textbook" and a reference source for the many scientists and engineers who must be trained in the shortest possible time to fill responsible positions in this critical area.

A. V. Astin, *Director.*

Preface

Because of the urgent need for this Handbook, it has been reproduced by a photoduplication process. As a result, the individual publications that make up the compilation will be found to vary in such details as style, size of type, and method of pagination.

Each paper reproduced for the compilation is essentially complete as originally published and retains its original page numbering. All pages have also been numbered in regular sequence throughout the three volumes. Thus, the volume page number and the original page number are combined, for example 100/10.

Because of the short time available, a complete review of each paper included was not possible. However, some efforts were made to bring the older papers up to date, and only those papers have been included that are of current value. Nevertheless, users should be cautioned that the state of the art may have advanced beyond that represented in some of the older papers.

These three volumes, extensive as they are, include only a fraction of the published work of the National Bureau of Standards relating to standards. However, many of the reprinted papers contain extensive bibliographies that will enable the user who is confronted with a special problem to locate additional information.

The papers that appear or are cited in this three-volume Handbook were originally published over a period of several years as circulars, research papers, chapters of books, and as articles in scientific and technical periodicals. Thus individual copies of many papers are no longer readily available. More recent Bureau publications, and in some cases the older papers for which prices are given, may still be obtainable by purchase from the Superintendent of Documents, U.S. Government Printing Office, Washington 25, D.C. Other papers may often be obtained directly from the authors or from the publishers of the Journals in which the papers appeared. The papers referred to in the various lists, if not generally available as stated above, are usually available for reference in technical, university, Government depository, and public libraries.

Contents

Heat

Mechanics

Selected Papers on

Heat

(Contents on page V)

U. S. Department of Commerce
National Bureau of Standards

Research Paper RP1962
Volume 42, March 1949

Part of the Journal of Research of the National Bureau of Standards

The International Temperature Scale of 1948

By H. F. Stimson

The International Temperature Scale is based upon six fixed and reproducible equilibrium temperatures to which numerical values have been assigned and upon specified interpolation formulas relating temperature to the indications of specified measuring instruments. This is the first revision of the scale adopted in 1927. It is designed to conform as nearly as practicable to the thermodynamic centigrade scale as now known, while incorporating certain refinements based on experience to make the scale more uniform and reproducible than its predecessor. A new value for the temperature of the silver point and the use of Planck's law with a new value for the radiation constant, c_2, are the only changes which produce significant effects on numerical values assigned to temperatures.

The first International Temperature Scale was adopted by the Seventh General Conference on Weights and Measures in 1927, and is now known as the International Temperature Scale of 1927.[1] The General Conference on Weights and Measures is the diplomatic body, representing 33 participating nations, which has power to adopt recommendations concerning standards of weights and measures for international use. The recommendations are made by the International Committee on Weights and Measures which nominally consists of 18 scientists (not more than one from any nation) elected by the General Conference. The General Conference is scheduled to meet at intervals of 6 years and the International Committee at intervals of 2 years.

The Seventh General Conference recommended that international thermometric conferences be called by the International Committee to revise the temperature scale as occasion required. The Eighth General Conference, in 1933, made official provision for these conferences. In June 1937 the International Committee approved the creation of an Advisory Committee on Thermometry, subject to the sanction of the Ninth General Conference.

A meeting of the Advisory Committee was first called in July 1939. It approved a revision of the text of the scale of 1927 for proposal to the International Committee, but no action was taken because World War II began before the date originally scheduled for the Ninth General Conference. At the call of the International Committee, the Advisory Committee met again in May 1948. At this meeting three resolutions and a new text for the International Temperature Scale were approved.

Both the International Committee and the Ninth General Conference met in October 1948. On the recommendation of the International Committee, the General Conference sanctioned the creation of this Advisory Committee, which is to be known as the "Advisory Committee on Thermometry and Calorimetry". The General Conference then examined and adopted the resolutions which had been proposed by the Advisory Committee and had been transmitted by the International Committee with minor modifications.

The first of these resolutions concerns the International Temperature Scale directly and is as follows:

> "1. With the present-day technique, the triple point of water is susceptible of being a more precise thermometric reference point than the 'melting point of ice'.
>
> "The Advisory Committee considers, there-

[1] Comptes Rendus des Séances de la Septième Conférence Générale des Poids et Mesures, p. 94 (1927); also in Travaux et Mémoires du Bureau international des Poids et Mesures 18 (1930); also George K. Burgess, BS J. Research 1, 635 (1928) RP22.

fore, that the zero of the thermodynamic centigrade scale should be defined as being the temperature 0.0100 degree below that of the triple point of pure water."

The Conference also adopted the International Temperature Scale of 1948 as proposed by the Advisory Committee on Thermometry and Calorimetry; and, on this occasion, decided to give to the degree of temperature the designation of degree Celsius in place of degree centigrade or centesimal. Before the end of 1948 the official text of the scale was approved for publication in the Procès-Verbaux des Séances du Comité international des Poids et Mesures, t. XXI, 1948.

The National Bureau of Standards, therefore, in common with other national laboratories, began using the definitions of the International Temperature Scale of 1948 on January 1, 1949, both in its own scientific work and for calibrating instruments for other scientific and industrial purposes. It is recommended that scientists and industrial workers elsewhere conform to the definitions of the revised scale as set forth in the text.

A translation of the official text follows.

Text of The International Temperature Scale of 1948

Part I. Introduction

The Kelvin scale, on which temperatures are designated as ° K and denoted by the symbol T, is recognized as the fundamental thermodynamic scale to which all temperature measurements should ultimately be referable. On this scale the interval from the ice point, T_0, to the steam point, T_{100}, is 100 degrees. The Kelvin scale and the thermodynamic centigrade[2] scale, on which the temperature is $T-T_0$, are hereby adopted, in principle, by the Ninth General Conference on Weights and Measures. Any temperature interval expressed on one of these scales will have the same numerical value as when expressed on the other.

The experimental difficulties inherent in the measurement of temperature on the thermodynamic scale led to the adoption in 1927, by the Seventh General Conference on Weights and Measures, of a practical scale which was designated as the International Temperature Scale. This scale was intended to be as nearly identical with the thermodynamic centigrade scale as was possible with the knowledge then available. It was designed to be conveniently and accurately reproducible and to provide means for specifying any temperature on the International Scale within much narrower limits than was possible on the thermodynamic scale.

The scale herein defined represents the first revision of the scale adopted in 1927 and is designed to conform as nearly as practicable to the thermodynamic centigrade scale as now known, while incorporating certain refinements, based on experience, to make the scale more uniform and reproducible than its predecessor.

The experimental procedures by which the scale is to be realized are substantially unchanged. Only two of the revisions in the definition of the scale result in appreciable changes in the numerical values assigned to measured temperatures. The change in the value for the silver point from 960.5° to 960.8° C changes temperatures measured with the standard thermocouple. The adoption of a different value for the radiation constant, c_2, changes all temperatures above the gold point, while the use of the Planck radiation formula instead of the Wien formula affects the very high temperatures. The Planck formula is consistent with the thermodynamic scale and consequently removes the upper limit which was imposed by Wien's law in the 1927 scale.

Other important modifications, which cause little or no change in the numerical values of temperatures, but serve to make the scale more definite and reproducible are (a) the termination of one part of the scale at the oxygen point instead of at −190° C, (b) the division of the scale at the freezing point of antimony (about 630° C) instead of at 660° C, (c) the requirements for higher purity of the platinum of the standard resistance thermometer and standard thermocouple, and for smaller permissible limits for the electromotive force of the standard thermocouple at the gold point.

The scale defined by the resistance thermometer remains substantially identical with the 1927 scale. In the range between 630° and 1063° C, numerical values of temperature on the 1948 scale are higher than on the 1927 scale, the maximum difference being about 0.4 degree near 800° C.

[2] The General Conference, held in October 1948, decided to discontinue the use of the words "centesimal" and "centigrade" and to replace them by "Celsius".

Temperatures on the International Temperature Scale of 1927 were designated as ° C or ° C (Int.). Inasmuch as the designation "C" is retained in this revision, it should be applied in the future to temperatures on the last scale adopted previous to the time at which the designation is used. Where any doubt might arise, the designation should be specified as ° C (Int. 1927) or ° C (Int. 1948).

Part II. Definition of The International Temperature Scale of 1948

1. Temperatures on the International Temperature Scale of 1948 will be designated as "° C" or "° C (Int. 1948)" and denoted by the symbol, t.

2. The scale is based upon a number of fixed and reproducible equilibrium temperatures (fixed points) to which numerical values are assigned, and upon specified formulas for the relations between temperature and the indications of the instruments calibrated at these fixed points.

3. The fixed points and the numerical values assigned to them are given in Table I. These values, in each case, define the equilibrium temperature corresponding to a pressure of 1 standard atmosphere, defined as 1,013,250 dynes/cm². The last decimal place given for each of the values of the primary fixed points only represents the degree of reproducibility of that fixed point.

TABLE I.—*Fundamental and primary fixed points under the standard pressure of 1,013,250 dynes/cm²*

	Temperature ° C
(a) Temperature of equilibrium between liquid oxygen and its vapor (oxygen point)	−182. 970
(b) Temperature of equilibrium between ice and air saturated water (ice point) (*Fundamental fixed point*)	0
(c) Temperature of equilibrium between liquid water and its vapor (steam point) (*Fundamental fixed point*)	100
(d) Temperature of equilibrium between liquid sulfur and its vapor (sulfur point)	444. 600
(e) Temperature of equilibrium between solid and liquid silver (silver point)	960. 8
(f) Temperature of equilibrium between solid and liquid gold (gold point)	1063. 0

4. The means available for interpolation lead to a division of the scale into four parts.

(a) From 0° C to the freezing point of antimony the temperature, t, is defined by the formula

$$R_t = R_0(1 + At + Bt^2),$$

where R_t is the resistance, at temperature, t, of the platinum resistor between the branch points formed by the junctions of the current and potential leads of a standard resistance thermometer. The constant, R_0, is the resistance at 0° C, and the constants, A and B, are to be determined from measured values of R_t at the steam and sulfur points. The platinum in a standard resistance thermometer shall be annealed, and of such purity that R_{100}/R_0 is greater than 1.3910.

(b) From the oxygen point to 0° C, the temperature, t, is defined by the formula

$$R_t = R_0[1 + At + Bt^2 + C(t-100)t^3],$$

where R_t, R_0, A, and B are determined in the same manner as in (a) above, and the constant, C, is calculated from the measured value of R_t at the oxygen point.

(c) From the freezing point of antimony to the gold point, the temperature, t, is defined by the formula

$$E = a + bt + ct^2,$$

where E is the electromotive force of a standard thermocouple of platinum and platinum-rhodium alloy when one junction is at 0° C and the other is at the temperature, t. The constants, a, b, and c, are to be calculated from measured values of E at the freezing point of antimony and at the silver and gold points. The antimony used in determining these constants shall be such that its freezing temperature, determined with a standard resistance thermometer, is not lower than 630.3° C. Alternatively the thermocouple may be calibrated by direct comparison with a standard resistance thermometer in a bath at any uniform temperature between 630.3° and 630.7° C.

The platinum wire of the standard thermocouple shall be annealed and of such purity that the ratio R_{100}/R_0 is greater than 1.3910. The alloy wire shall consist nominally of 90 percent platinum and 10 percent rhodium by weight. When one junction is at 0° C, and the other at the freezing point of antimony (630.5° C), silver, or gold, the completed thermocouple shall have electromotive forces, in microvolts, such that

$$E_{Au} = 10{,}300 \pm 50\ \mu v$$

$$E_{Au} - E_{Ag} = 1185 + 0.158(E_{Au} - 10{,}310) \pm 3\ \mu v$$

$$E_{Au} - E_{Sb} = 4776 + 0.631(E_{Au} - 10{,}310) \pm 5\ \mu v$$

(d) Above the gold point the temperature, t, is defined by the formula

$$\frac{J_t}{J_{Au}} = \frac{e^{\frac{c_2}{\lambda(t_{Au}+T_0)}}-1}{e^{\frac{c_2}{\lambda(t+T_0)}}-1},$$

in which

J_t and J_{Au} are the radiant energies per unit wavelength interval at wavelength, λ, emitted per unit time by unit area of a black body at the temperature, t, and at the gold point, t_{Au}, respectively.

c_2 is 1.438 cm degrees.

T_0 is the temperature of the ice point in ° K.

λ is a wavelength of the visible spectrum.

e is the base of Naperian logarithms.

Part III. Recommendations

The recommendations in the following sections are advisory rather than mandatory. The apparatus, methods, and procedures recommended represent good practice at this time, but there is no intention of retarding the development and use of improvements and refinements. Experience has shown these recommendations to be in the interest of uniformity and reproducibility in the realization of the temperature scale defined in part II.

1. Standard Resistance Thermometer

A standard resistance thermometer should be so designed and constructed that the wire of the platinum resistor is as nearly strain-free as practicable and will remain so during continued use. The most suitable platinum wire is that drawn from a fused ingot, not from forged sponge.

Satisfactory thermometers have been made with wire as small as 0.05 mm and as large as 0.5 mm in diameter, a short portion of each lead adjacent to the resistor being made of platinum and continuing with gold wire through the region of temperature gradient. The completed resistor of the thermometer should be annealed in air at a temperature not lower than about 450° C, or if it is to be used at temperatures above 450° C, at a temperature higher than the highest temperature at which it is to be used. It is recommended that the tube protecting the completed resistor be filled with gas containing some oxygen.

A useful criterion, which serves as a safeguard against inferior construction of the completed thermometer and against errors in the calibrations at the fixed points, is that $(R_s-R_0)/(R_{100}-R_0)$ (where R_s is the resistance at the sulfur point) should be between 4.2165 and 4.2180. Similarly, if the thermometer is calibrated for use in the range below 0° C, the ratio, $(R_s-R_{O_2})/(R_{100}-R_0)$ (where R_{O_2} is the resistance at the oxygen point) should be between 6.143 and 6.144. The constancy of resistance at a reference point, such as the triple point of water (or the ice point), before and after use at other temperatures, is also a valuable criterion of the adequacy of the annealing and the reliability of the thermometer in service.

2. Standard Thermocouple

Satisfactory standard thermocouples have been made of wires not less than 0.35 mm and not more than 0.65 mm in diameter. Before calibration, the wires of the couple should be annealed in air for an hour at about 1100° C. The wire of the thermocouple should be mounted so as to avoid all mechanical constraints in the region where steep temperature gradients are likely to occur.

3. Pressure

Each of the fixed points is given as a temperature of equilibrium at a pressure of 1,013,250 dynes/cm^2. This pressure corresponds to the pressure exerted by a column of mercury 760 mm high, having a density of 13.5951 g/cm^3 and subject to a gravitational attraction of 980.665 dynes/g. Except for work of the highest precision, pure ordinary (commercial) mercury may be taken as having a mean density of 13.5951 g/cm^3 at 0° C in such a mercury column.

In the following sections concerning fixed points, the formulas giving the relation between the pressure, p_t, at the midpoint of the platinum resistor and the corresponding equilibrium temperature, t_p, are given in two forms. The poly nomial is a convenient form when the pressure is near 1 standard atmosphere, whereas the logarithmic form is applicable, as is well known, over a much larger range. Both of these forms are given as functions of the ratio of p to p_0 (standard atmospheric pressure) and, consequently, are equally applicable whether p and p_0 are expressed in dynes/cm^2 or in mm of mercury at 0° C and under a gravitational attraction of 980.665 dynes/g.

4. Zero Point of the Scale

The temperature 0° C may be realized experimentally well enough for nearly all purposes by the use of a mixture of finely divided ice and water saturated with air at 0° C in a well-insulated container such as a Dewar flask. It is recommended, however, that for work of the highest precision the zero point be realized by means of the triple point of water, a point to which the temperature +0.0100° C has been assigned.

This value agrees with all existing experimental determinations up to the present time within about 0.0002 degree.

(a) Triple Point of Water

The temperature of equilibrium between ice, liquid water, and water vapor has been realized in glass cells from 4 to 7 cm in diameter, which have an axial reentrant well for thermometers and contain only water of high purity. The amount of water should be such as to permit adequate immersion of the thermometer and to ensure the existence of the three phases during measurements. Such cells, when properly prepared for use and kept entirely immersed in an ordinary ice bath, have been found to be capable of maintaining a temperature constant to 0.0001 degree for several days.

Cells have been prepared for use by cooling the entire contents until small crystals are present throughout the liquid. A preferred method is to freeze a thick mantle of ice around the well by rapid cooling from within. With this method, the water ahead of the forming ice contains most of the impurities initially in the water frozen. This will result in an appreciable lowering of the temperature at the outside of the mantle unless the initial purity of the water is sufficiently high. If a thin layer of the pure ice next to the well is then melted, a very pure water-ice interface immediately surrounding the well is obtained, and this fixes a temperature that is constant and reproducible to better than 0.0001 degree, provided the initial outside temperature is not more than 0.001 degree lower than the temperature produced on the interior after melting the thin layer of ice.

The equilibrium temperature, t, corresponding to the depth, H (in mm), below the vapor-liquid surface, may be calculated from the formula

$$t=0.0100-0.7\times10^{-6}H.$$

(b) Ice Point

By observing precautions in regard to purity of ice and water, the saturation of the water at 0° C with uncontaminated air, and the effect of pressure, a temperature reproducible within a few ten-thousandths of a degree may be realized.

The effect of pressure may be calculated from the formula[3]

$$t=0.0099\left(1-\frac{p}{p_0}\right)-0.7\times10^{-6}H,$$

where t is the equilibrium temperature, p is the prevailing atmospheric pressure at which the water is saturated with air, and H is the depth (in mm) below the surface of the mixture of water and ice.

5. Oxygen Point

The temperature of equilibrium between liquid oxygen and its vapor is usually realized experimentally by the static method. The platinum resistor of the standard thermometer and the free surface of the liquid oxygen in its container are brought to the same temperature in a suitable cryostat, such as a metal block in a well-stirred bath of liquid oxygen. The tube which connects the space containing the pure liquid oxygen to the manometer used for the measurement of the vapor pressure should be protected against temperatures lower than the temperature of the pure liquid oxygen at the location of the resistor of the standard resistance thermometer.

The equilibrium temperature, t_p, corresponding to a pressure, p, may be found to an accuracy of a few thousandths of a degree over the range from $p=660$ to $p=860$ mm, by means of the formula

$$t_p=-182.970+9.530\left(\frac{p}{p_0}-1\right)-3.72\left(\frac{p}{p_0}-1\right)^2+2.2\left(\frac{p}{p_0}-1\right)^3,$$

or to the same accuracy but over a wider range by the formula

$$t_p=-182.970+\frac{21.94\log_{10}\frac{p}{p_0}}{1-0.261\log_{10}\frac{p}{p_0}}.$$

[3] Author's note. In this formula the value, 0.0099, which appears in the official text, should be 0.010. Ordinarily the incorrect value will not lead to a significant error.

6. Steam Point

The temperature of equilibrium between liquid water and its vapor has been realized by the dynamic method with the thermometer in the saturated vapor, using apparatus of various designs, some closed and others open to the atmosphere. Closed systems, in which a steam-point apparatus and manometer are connected to a manostat of large volume filled with helium are preferable for precise calibrations at the steam point.

The design of the steam-point apparatus should be such as to avoid any superheating of the water vapor around the thermometer, contamination with air or other impurities, and radiation effects. A criterion that the equilibrium temperature has been attained is that the observed temperature corrected to a constant pressure is independent of elapsed time, of variations in the heat supply to the liquid, of variations in the heat loss from the walls, and of the depth of immersion of the thermometer.

The equilibrium temperature, t_p, corresponding to the pressure, p, may be found to an accuracy within 0.001 degree over the range from $p=660$ to $p=860$ mm by means of the formula

$$t_p=100+28.012\left(\frac{p}{p_0}-1\right)-11.64\left(\frac{p}{p_0}-1\right)^2 +7.1\left(\frac{p}{p_0}-1\right)^3,$$

or to the same accuracy over a wider range by the formula

$$t_p=100+\frac{64.500\ \log_{10}\frac{p}{p_0}}{1-0.1979\ \log_{10}\frac{p}{p_0}}.$$

7. Sulfur Point

The sulfur used in a sulfur boiling-point apparatus should not contain more than 0.005 percent of impurities. Selenium and arsenic are the impurities that have been found most likely to be present in quantities sufficient to affect the temperature of equilibrium to a significant extent.

In the conventional type of sulfur boiling-point apparatus which has proved satisfactory for an accuracy of 0.01 to 0.02 degree, the sulfur is contained in a tube of glass, fused silica, or similar material with an internal diameter of 4 to 5 cm. The length of the tube is determined by the consideration that the vapor column must be long enough to accommodate a radiation shield and to permit the necessary depth of immersion of the resistance thermometer. Electric heating is preferable. Above the source of heat the tube is surrounded by heat-insulating material.

In a recent work in which an accuracy of about 0.001 degree was desired, the thermometer was not immersed directly in the sulfur vapor, but in an aluminum thermometer well, thus adapting the apparatus for use with a closed system. The thermometer well was provided with one or more radiation shields so designed that the interior of the shield approximated a black body, but with ample openings for circulation of sulfur vapor throughout the interior. An electric heater was provided to control the heat loss from the walls.

A criterion that equilibrium temperatures have been attained is that the observed temperatures corrected to a constant pressure should be independent of elapsed time, of variations in the heat supply to the liquid, of variations in the heat loss from the walls, and of the depth of immersion of the thermometer.

The equilibrium temperature, t_p, corresponding to a pressure, p, may be found to an accuracy of about 0.001 degree over the range from $p=660$ to $p=800$ mm by means of the formula

$$t_p=444.6+69.010\left(\frac{p}{p_0}-1\right)-27.48\left(\frac{p}{p_0}-1\right)^2+ 19.14\left(\frac{p}{p_0}-1\right)^3,$$

or, over a wider range, by the formula

$$t_p=444.6+\frac{158.92\ \log_{10}\frac{p}{p_0}}{1-0.234\ \log_{10}\frac{p}{p_0}}.$$

8. Silver and Gold Points

Data on the effect of the impurities most likely to be present in carefully purified silver or gold indicate that the addition of 0.01 percent by weight of metallic impurities to pure silver, or of 0.005 percent to pure gold will probably not change the freezing point in either case by more than 0.1 degree.

For calibrating a thermocouple, the metal is contained in a crucible of pure graphite or other

refractory material which will not contaminate the metal. Crucibles of artifical graphite about 3 cm inside diameter and 15 cm deep with a wall about 1 cm thick have been found very satisfactory. The amount of metal required in such a crucible is about 1600 g of gold or about 900g of silver. Silver must be protected from oxygen while hot.

The crucible and metal are placed in a furnace capable of heating the contents to a uniform temperature. The metal is melted and brought to a uniform temperature a few degrees above its melting point, then allowed to cool slowly. The thermocouple, mounted in a porcelain tube with porcelain insulators separating the two wires, is immersed in the molten metal through a hole in the center of the crucible cover. The depth of immersion should be such that the observed electromotive force of the thermocouple is not changed by more than 1 microvolt when the immersion is increased or decreased by 1 cm. During freezing, the electromotive force should remain constant within 1 microvolt for a period of at least 5 minutes.

9. Freezing Point of Antimony

The procedure in using the freezing point of antimony as a calibration temperature is substantially the same as outlined above for the silver and gold points. Antimony has a marked tendency to undercool before freezing. The undercooling will not be excessive if the metal is heated only a few degrees above its melting point and if the liquid metal is stirred. During freezing, the electromotive force should remain constant within 1 microvolt for a period of at least 5 minutes.

10. Temperature of the Ice Point on the Kelvin Scale

For the sake of uniformity, it is recommended that the temperature of the ice point on the Kelvin scale be taken as 273.15° K.[4] [5]

Part IV. Supplementary Information

1. Resistance-Temperature Formulas

The interpolation formula, for the range 0° C to the freezing point of antimony, as given in the definition of the scale,

$$R_t = R_0(1 + At + Bt^2),$$

may be written in the Callendar form

$$t = \frac{1}{\alpha}\left(\frac{R_t}{R_0} - 1\right) + \delta\left(\frac{t}{100} - 1\right)\left(\frac{t}{100}\right),$$

where

$$\alpha = \frac{1}{100}\left(\frac{R_{100}}{R_0} - 1\right).$$

The relations between the coefficients are

$$A = \alpha\left(1 + \frac{\delta}{100}\right), \qquad \alpha = A + 100B,$$

$$B = -\frac{\alpha\delta}{100^2}, \qquad \delta = -\frac{100^2 B}{A + 100B}.$$

The condition that R_{100}/R_0 shall be greater than 1.3910 is equivalent to requiring that α shall be greater than 0.003910. The condition that $(R_S - R_0)/(R_{100} - R_0)$ shall be between 4.2165 and 4.2180 is equivalent to requiring that δ shall be between 1.488 and 1.498.

Similarly, the interpolation formula, for the range 0° C to the oxygen point, as given in the definition of the scale.

$$R_t = R_0[1 + At + Bt^2 + C(t - 100)t^3],$$

may be written in the Callendar-Van Dusen form

$$t = \frac{1}{\alpha}\left(\frac{R_t}{R_0} - 1\right) + \delta\left(\frac{t}{100} - 1\right)\frac{t}{100} + \beta\left(\frac{t}{100} - 1\right)\left(\frac{t}{100}\right)^3.$$

---

[4] This value 273.15° K was not ratified by either the International Committee or the General Conference. The choice of the last decimal figure was postponed.

[5] *Author's note.* The value 273.15° K±.02 for the temperature of the ice point was originally proposed by the Advisory Committee on Thermometry in 1939; and, in 1948, the Committee did not consider that enough new knowledge had been gained to change this value. That some uncertainty was felt about this action is indicated by a clause in Resolution 2, which already had been approved by the Advisory Committee, and was later adopted by the General Conference. This resolution resulted from a proposal the committee had received to define an absolute thermodynamic temperature scale by assigning a value to the temperature of a single fixed point.

"Resolution 2. The Advisory Committee recognizes the principle of an absolute thermodynamic scale requiring only one fundamental fixed point, which would now be the triple point of pure water, for which the absolute temperature will be chosen later.

"The introduction of this new scale in no way affects the International Scale which continues to be the recommended practical scale."

This resolution defers the establishment of a precise value for the temperature of the ice point. Inasmuch as it is definitely stated at the beginning of Part III of this text that "The recommendations in the following sections are advisory rather than mandatory", many scientists will not consider it mandatory to accept this recommended value for the ice point. In the United States of America the value, 273.16° K, for the temperature of the ice point has been so generally accepted that its use now prevails in scientific publications, and this value will probably continue to be used until a more accurate one has been agreed upon.

The relations between A, B and α, δ are as given above and the other relations are

$$C=-\frac{\alpha\beta}{100^4}, \text{ and } \beta=-\frac{100^4 C}{A+100B}.$$

The condition that $(R_S-R_{O_2})/(R_{100}-R_0)$ shall be between 6.143 and 6.144 is equivalent to requiring that $0.5852\delta-\beta$ shall be between 0.7656 and 0.7598.

2. Secondary Fixed Points

In addition to the six fundamental and primary fixed points, certain other fixed points are available and may be useful for various purposes. Some of the more constant and reproducible of these fixed points and their temperatures on the International Temperature Scale of 1948 are given in Table II. The temperatures given are those corresponding to a pressure of 1 standard atmosphere, except for the triple points of water and of benzoic acid. The formulas for the variation of temperature with pressure are intended for use over the range from $p=680$ to $p=780$ mm of mercury.

TABLE II. *Secondary Fixed Points under the pressure of 1 standard atmosphere (except for the triple points)*

	Temperature °C (Int. 1948)
Temperature of equilibrium between solid carbon dioxide and its vapor	−78. 5

$$t_p=-78.5+12.12\left(\frac{p}{p_0}-1\right)-6.4\left(\frac{p}{p_0}-1\right)^2$$

Temperature of freezing mercury	−38. 87
Temperature of equilibrium between ice, water and its vapor (Triple Point)	+0. 0100
Temperature of transition of sodium sulphate decahydrate	32. 38
Temperature of triple point of benzoic acid	122. 36
Temperature of equilibrium between naphthalene and its vapor	218. 0

$$t_p=218.0+44.4\left(\frac{p}{p_0}-1\right)-19\left(\frac{p}{p_0}-1\right)^2$$

Temperature of freezing tin	231. 9
Temperature of equilibrium between benzophenone and its vapor	305. 9

$$t_p=305.9+48.8\left(\frac{p}{p_0}-1\right)-21\left(\frac{p}{p_0}-1\right)^2$$

Temperature of freezing cadmium	320. 9

TABLE II. *Secondary Fixed Points under the pressure of 1 standard atmosphere*—Continued

	Temperature °C (Int. 1948)
Temperature of freezing lead	327. 3
Temperature of equilibrium between mercury and its vapor	356. 58

$$t_p=356.58+55.552\left(\frac{p}{p_0}-1\right)-23.03\left(\frac{p}{p_0}-1\right)^2+14.0\left(\frac{p}{p_0}-1\right)^3$$

Temperature of freezing zinc	419. 5
Temperature of freezing antimony	630. 5
Temperature of freezing aluminum	660. 1
Temperature of freezing copper in a reducing atmosphere	1083
Temperature of freezing nickel	1453
Temperature of freezing cobalt	1492
Temperature of freezing palladium	1552
Temperature of freezing platinum	1769
Temperature of freezing rhodium	1960
Temperature of freezing iridium	2443
Temperature of melting tungsten	3380

3. Relation Between the International Temperature Scale of 1948 and the Thermodynamic Centigrade Scale

At the time of the adoption of the International Temperature Scale of 1927, the evidence available was insufficient to establish definite differences between that scale and the thermodynamic centigrade scale. The earlier investigations, such as those published in 1911 by the Physikalisch-Technische Reichsanstalt, indicated no differences exceeding 0.05 degree in the range 0° C to the sulfur point.

Recent investigations at the Massachusetts Institute of Technology indicate larger differences between 200° C and the sulfur point. Intercomparisons of two nitrogen gas thermometers with platinum resistance thermometers were made at 0°, 25°, 50°, 75°, 100°, 150°, 200°, 250°, 300°, 350° C, the mercury boiling point, 400° C and the sulfur point. The differences found between t(thermodynamic scale) and t(International Scale) have been formulated as follows:

$$t\ (\text{therm})-t\ (\text{Int})=\frac{t}{100}\left(\frac{t}{100}-1\right)(0.04217-7.481\times10^{-5}t).$$

The sulfur point on the thermodynamic scale was found to be 444.74° C, the results obtained with the two gas thermometers differing by about 0.05 degree.

In the range from 0° C to the oxygen point, intercomparisons published by the Physikalisch-Technische Reichsanstalt in 1932 and by the Leiden Laboratory in 1935 indicate that the differences between the International and thermodynamic scales are less than 0.05 degree. Agreement is lacking as to the sign of some of the reported differences, which are of the order of magnitude of the possible uncertainties in the gas thermometer measurements.

In the range extending below the oxygen point, there is evidence that temperatures on the International Temperature Scale of 1927 are progressively higher than those on the thermodynamic scale, amounting to several hundredths of a degree at −190° C. For this reason, and also because it is advantageous to terminate the various parts of the scale at calibration points, the International Temperature Scale of 1948 extends only to the oxygen point.

In the range from the freezing point of antimony to the gold point, there is little evidence relative to the sign or magnitude of departures of the International from the thermodynamic scale. The value 1063.0° C for the gold point has been accepted as a conventional definition and will doubtless remain so until the appearance of new and more accurate basic data. The change from 960.5° to 960.8° C is well within the uncertainty of the location of the silver point on the thermodynamic scale. This change makes the thermocouple scale join more smoothly, not only with the resistance thermometer scale at the freezing point of antimony, but also with the optical pyrometer scale at the gold point when $c_2=1.438$ cm degrees.

It is of interest to note that, granting the validity of Planck's formula, temperatures above the gold point on the International Temperature Scale of 1948 will differ from those on the thermodynamic centigrade scale only to the extent caused by errors in the constants, c_2, t_{Au}, and T_0, used in the formula.

WASHINGTON, January 14, 1949.

574278 O - 61 - 2

Reprinted from THE JOURNAL OF CHEMICAL PHYSICS, Vol. 27, No. 2, 378–389, August, 1957
Printed in U. S. A.

Absolute Temperatures below 1°K: Chromic Methylammonium Alum as a Thermometric Substance

E. AMBLER AND R. P. HUDSON
National Bureau of Standards, Washington, D. C.
(Received February 19, 1957)

The method of gamma-ray calorimetry has been employed to determine the entropy-temperature relation for a single-crystal of chromic methylammonium alum in the range 0.015°–1°K. A critical discussion of possible sources of error is given; the accuracy in T is estimated to be approximately 5% throughout the region investigated. There is close agreement between the Hebb-Purcell theoretical $S-T$ relation and the present data down to 0.07°K. The fact that the susceptibility-entropy relation varies considerably for different specimens at temperatures below 0.06°K suggests that $S-T$ measurements are of limited value in that region, especially from a thermometric point of view.

I. INTRODUCTION

THE choice of a paramagnetic salt as the working substance in the magnetic cooling process is governed primarily by (a) how low a temperature range may be reached, (b) the heat capacity, which governs the length of time that such temperatures can be maintained, (c) the susceptibility, or rather the temperature variation of the susceptibility, which is generally used as the thermometric indicator. These properties vary considerably with crystallographic and chemical constitution, so that for any particular experiment it is often necessary to make a careful choice of working substance. In the widening field of research on paramagnetism at low temperatures many new salts have been investigated, some showing unusual properties which have enabled novel experiments to be done in the range of temperature below 1°K. For many applications, however, a good "all-round" material is needed. For such a role the alums have long held sway, and in particular one has been led to select chromic methylammonium alum (CMA), $Cr_2(SO_4)_3\cdot(CH_3NH_3)_2SO_4\cdot 24H_2O$, as ideal.[1] Since one would expect that this substance would be widely used, it is important that the above-mentioned properties should be accurately determined and checked for reproducibility.

A number of investigations have been made on CMA in the region below 1°K in recent years[2–6] but only one of these[3] involved a major effort to determine thermodynamic temperatures. In order to complete the low temperature studies made on CMA in this Laboratory, similar measurements were carried out by the authors in 1954. These were in generally good agreement with the findings of Gardner and Kurti[3] but were of unsatisfactory accuracy (see the following). The measurements were resumed recently and the outcome forms the subject of this report. Although the difficulties and causes of inaccuracy in this type of measurement have been recognized for some time, no attempt seems to have been made to estimate errors quantitatively. (They are usually depressingly large.) The questions of precision for a specific series of measurements, and of the value of the latter when used for the subject substance generally, will be examined closely in this paper.

II. APPARATUS

The demagnetization and susceptibility-measurement apparatus has been described earlier by Hudson and McLane.[4] For introducing heat uniformly into the salt (see Procedure) a 250-mc Co^{60} gamma-ray source was employed, comprising sixteen cobalt wires, each 2 in. long, sealed in aluminum tubes. These were held in cylindrical array (four inches in diameter) coaxial with the cryostat by a rigid assembly of thin-walled brass tubes. The source-assembly could be raised from a massive lead pig some four feet below the cryostat into the heating position in roughly two seconds. The heating produced in the salt amounted to 1300 ergs/mole/sec. The background heating was reduced to about 4% of this figure by using an extremely fragile (95 mm long and over the central 40 mm portion about 1.2 mm o.d., 0.2 mm wall thickness) glass supporting tube to the crystal. In the first series of experiments (Series A) a one-inch sphere ground from a single crystal[7] was employed, but with this arrangement the crystal extended too far along the axis of the gamma-ray source so that the absorption was not uniform. Conditions were considerably improved in Series B by there using a smaller specimen, S.C. IIIb, 19 mm in diameter (0.012 mole).

III PROCEDURE

The magnetic thermometer was calibrated in the 1°–2.2°K region, using the T_{55E} helium vapor-pressure

[1] For more detailed discussion, see, for example, the review articles by D. de Klerk and M. J. Steenland, *Progress in Low Temperature Physics* (Interscience Publishers, Inc., New York, 1955), Chap. XIV; E. Ambler and R. P. Hudson, Repts. Progr. Phys. 18, 251 (1955).
[2] D. de Klerk and R. P. Hudson, Phys. Rev. 91, 278 (1953).
[3] W. E. Gardner and N. Kurti, Proc. Roy. Soc. (London) A223, 542 (1954).
[4] R. P. Hudson and C. K. McLane, Phys. Rev. 95, 932 (1954).
[5] E. Ambler and R. P. Hudson, Phys. Rev. 96, 907 (1954).
[6] Beun, Steenland, de Klerk, and Gorter, Physica 21, 767 (1955).
[7] This was the specimen designated S.C. II in references 4 and 5.

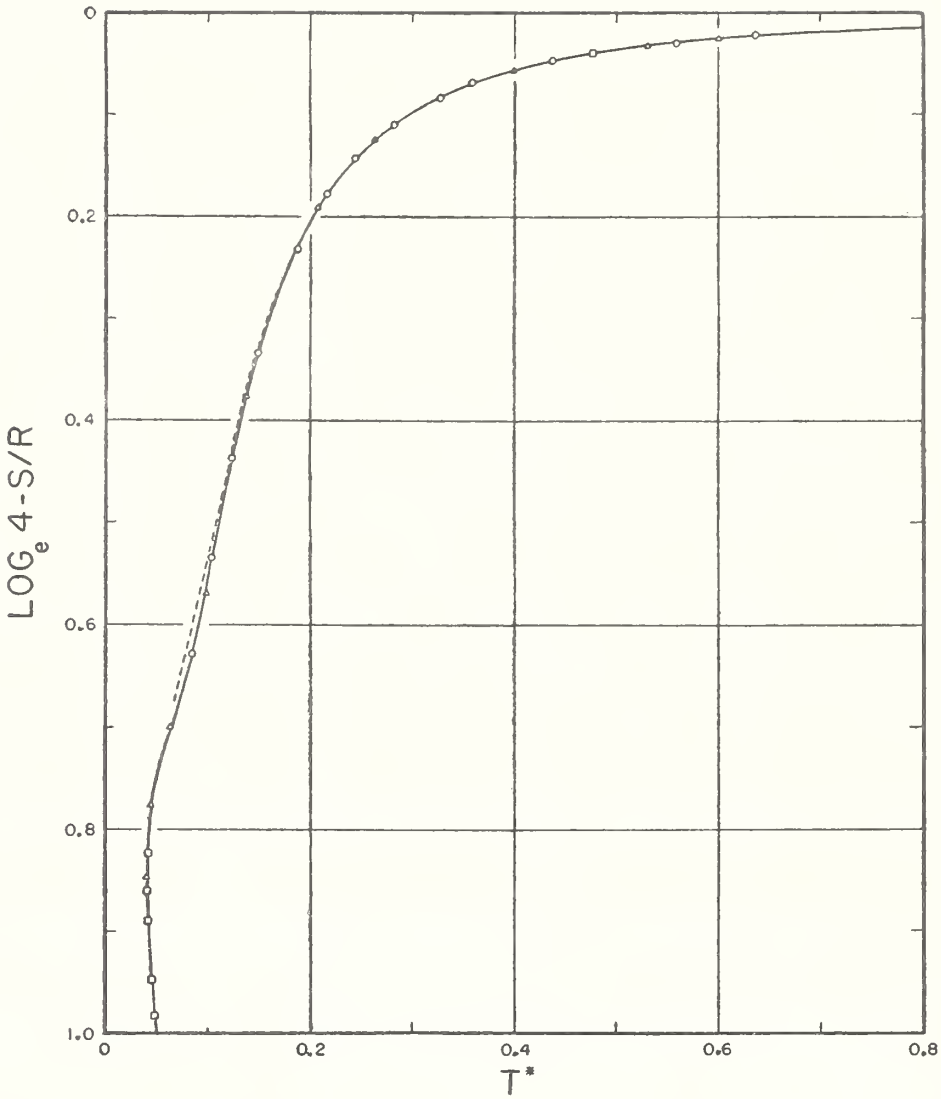

FIG. 1. Entropy *vs* magnetic temperature for spherical crystal specimen S.C. IIIb. The broken line is calculated according to Hebb and Purcell's theory with $\delta/k = 0.267°K$.

scale of temperature[8]; the scatter of individual points from a Curie law plot was less than one millidegree. Major procedural details have also been given earlier.[2,4] Susceptibility determinations were made continuously during the heating periods as well as during "drift" intervals, there being only a small correction to the ac-bridge readings because of the proximity to the measuring coils of the metal in the source-assembly. A 267-cps measuring field was employed, of magnitude 0.3 oersted for the high temperature region and 0.1 oersted at the lowest temperatures.

In the experiments with S.C. II, the strong initial magnetizing field and the small ac measuring field were each applied along cubic axes of the crystal. S.C. IIIb was arbitrarily oriented, but this has only a very small effect on the entropy[9] and no effect on the zero-field susceptibility measurements, even below the Néel point.[6]

The method of deriving absolute temperatures from calorimetric and magnetic measurements, and of heating by means of gamma irradiation, was developed some twenty years ago by Kurti and Simon.[10] One measures both Q and S as functions of a suitably sensitive thermometric parameter, e.g., the susceptibility, χ, (in "zero" field) whence, making use of the fundamental relation $T = dQ/dS$,

$$T = (dQ/d\chi)(dS/d\chi)^{-1}. \tag{1}$$

More frequently, the magnetic temperature, $T^*(=c/\chi$, where c is the Curie constant) is employed since T^* remains a fair approximation to T in the tenths-of-a-degree region and dQ/dT^* is then a pseudo specific heat, denoted by C^*. (The susceptibility, χ, as used here is, of course, an apparent susceptibility as measured on a spherical specimen.)

[8] See Clement, Logan, and Gaffney, Phys. Rev. **100**, 743 (1955), note added in proof.

[9] J. M. Daniels and N. Kurti, Proc. Roy. Soc. (London) **A221**, 243 (1954). These authors derived a general formula (arbitrary orientation of H) valid for the condition $g\beta H \gg \delta$. For the case $g\beta H \approx \delta$ we have made the further check of deriving exact expressions for S/R for several specific orientations of H. The computation was very kindly carried out by Dr. W. G. Nef.

[10] N. Kurti and F. Simon, Proc. Roy. Soc. (London) **A149**, 161 (1935), footnote; *ibid.* **A152**, 21 (1935); see also W. H. Keesom, J. Phys. radium **5**, 373 (1934).

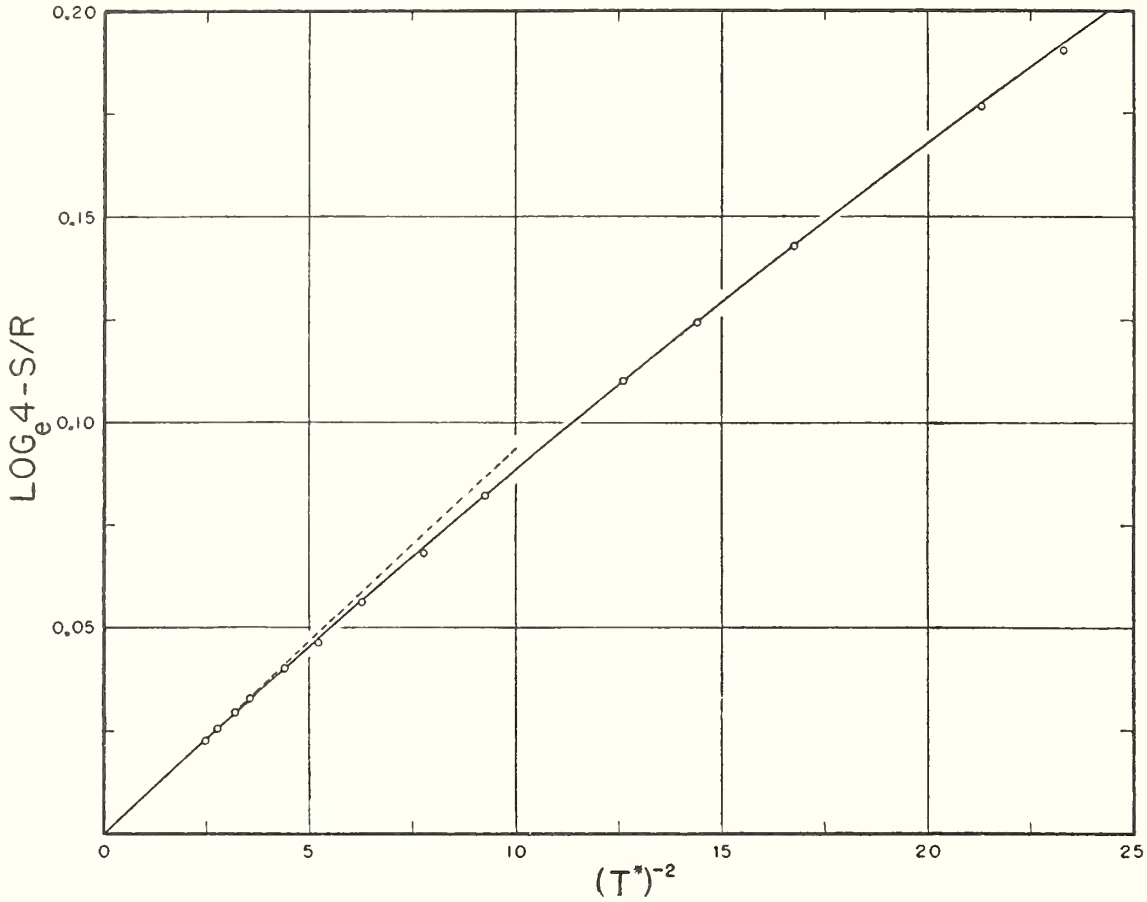

FIG. 2. Entropy *vs* inverse square of magnetic temperature. The solid line is calculated for $\delta/k = 0.267°K$ and the broken line is the tangent to this at the origin.

The coefficient of absorption of the γ rays is assumed to be temperature independent (see Discussion). The heat supply, dQ/dt, is therefore constant for all demagnetizations and

$$C^* = dQ/dT^* = (dQ/dt)(dT^*/dt)^{-1}, \quad (2a)$$

$$= \text{const}(dT^*/dt)^{-1}. \quad (2b)$$

Each C^* point was determined by the normal calorimetric procedure, i.e., observing heating and "drift" periods successively. In the high temperature region, i.e., above 0.1°K, for each demagnetization some four or five points were obtained, care being taken that the last (highest temperature) point of a set lay within the region spanned by the points of the set from the preceding demagnetization (to a higher temperature). This provided a means of checking whether points obtained at the end of a set, i.e., after rather prolonged heating, were accurate or whether because of the poor thermal diffusivity surface (drift) heating and nonuniformity of the gamma-ray heating had caused major temperature inhomogeneities within the specimen. The object in view was, of course, to obtain as many points per demagnetization as was consistent with a high accuracy, since magnetic cooling is a time-consuming procedure.

IV. RESULTS

(1) The $S - T^*$ Relation

For each demagnetization the entropy, S, was calculated in the usual way from the known starting conditions of magnetizing field and temperature, with $g = 1.976$,[11] applying a small correction for the effect of the crystalline field.[9,12] The results for Series B, i.e., with S.C. IIIb, are shown in Fig. 1 where the experimental $S - T^*$ points are compared with a curve derived on the basis of the theory of Hebb and Purcell[13] using a value of 0.267°K for δ/k, the crystalline field splitting of the ground-state spin-quadruplet in the Cr^{+++} ion. The above value for δ/k was also found for S.C. II, in Series A and on prior occasions,[4,5] although marked differences in the curves appear at the lowest temperatures (see below). These are most probably due to varying internal strains or structures arising from different rates of precooling[4] through the region of 160°K where a structural change occurs. This is indicated by anomalous dielectric behavior and the onset of ferroelectricity,[14,15] and below this point the electric field

[11] J. M. Baker, Proc. Phys. Soc. (London) **B69**, 633 (1956).
[12] R. P. Hudson, Phys. Rev. **88**, 570 (1952).
[13] M. H. Hebb and E. M. Purcell, J. Chem. Phys. **5**, 338 (1937).
[14] Pepinsky, Jona, and Shirane, Phys. Rev. **102**, 1181 (1956).
[15] E. Ambler and R. P. Hudson (to be published).

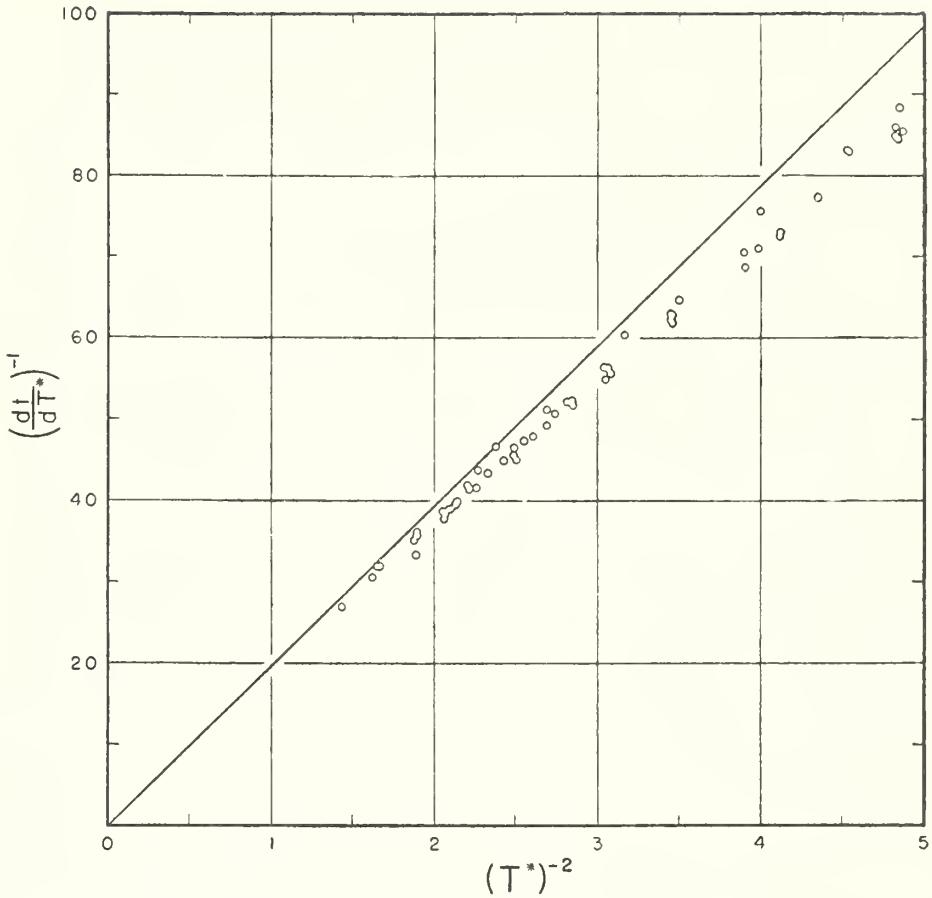

FIG. 3. Reciprocal of rate of change of T^* under gamma-ray heating (after "drift" correction) *vs* $(T^*)^{-2}$. The solid line is tangent at the origin to the best curve through the experimental points (not shown) the necessary extrapolation being carried out as explained in the text.

acting on the magnetic ions develops a small component of tetragonal symmetry.[11]

At "high" temperatures ($T \approx 1$°K) both the entropy and specific heat vary as T^{-2} to a good approximation[13]:

$$\ln 4 - S/R = b/T^2 = \tfrac{1}{8}(\delta/kT)^2 + 1.2(\tau/T)^2, \quad (3a)$$

$$C/R = 2b/T^2, \quad (3b)$$

where $\tau = 3c = 0.0189$°K. Thus one may use the $S - T^*$ data to derive b and hence C^* (for this temperature region where $T^* \approx T$), and so finally the value of the gamma-ray heater calibration constant in Eq. (2b).

An approximate value for b may be obtained by plotting $\ln 4 - S/R$ as a function of $(T^*)^{-2}$ and drawing a straight line through the points nearest the origin.[3] To obtain b more precisely, however, it is preferable to find the value of δ by fitting a Hebb-Purcell curve to the data, and then to calculate b from Eq. (3a).

In Fig. 2 we have plotted $\ln 4 - S/R$ as a function of $(T^*)^{-2}$ and drawn in both the theoretical curve for $\delta/k = 0.267$°K and the tangent at the origin. It will be observed that the slope of the latter is significantly greater than that of a straight line passing through the origin and, say, the first five points. The figures are 9.335×10^{-3} and 9.185×10^{-3}, respectively.

(2) The "Specific Heat" C^*

With the value of b determined, one may similarly plot the (dt/dT^*) data against $(T^*)^{-2}$ and equate the initial slope to $2b(\dot{Q}/R)^{-1}$. The graph is shown in Fig. 3. The same objections apply here, however, as were raised in the preceding section. One needs a smoothing function which will fit the data closely and permit a calculation of the slope at the origin. Unfortunately the scatter in the calorimetric data (about two percent) permitted a variety of analytical curves to be fitted and it was not possible to arrive thus at an unambiguous value for the slope.

The solution to the problem was found in the use of a "normalizing" function, namely the theoretical $C^* - T^*$ relation. The quantity $(dt/dT^*)(C_{\text{th}}^*/R)^{-1} = (\dot{Q}/R)^{-1}$ should be essentially independent of temperature and it should be possible to plot its values as a function of $1/T^*$ and make an accurate extrapolation to zero. These expectations were realized and the extrapolated value was 1055 ± 20 min deg^{-1}, the error being largely determined by the scatter in the calorimetric data. Hence $\dot{Q}/R = 9.48 \pm 0.18 \times 10^{-4}$ deg min^{-1}, or $\dot{Q} = 7.88 \times 10^4$ ergs mole^{-1} min^{-1}. A preliminary computation, by fitting a straight line by the method of least squares to the points in Fig. 3 for $(T^*)^{-2} < 3$, gave $\dot{Q}/R = 10.06 \times 10^{-4}$, a value some 6% greater than that previously quoted.

The entire C^* curve is shown in Fig. 4. Here are plotted the data from Series B together with the smoothed results of Gardner and Kurti. Below $T^* = 0.05°$ the curve rises rapidly toward infinity as the maximum in susceptibility is approached (compare Fig. 1). The differences between the current results and

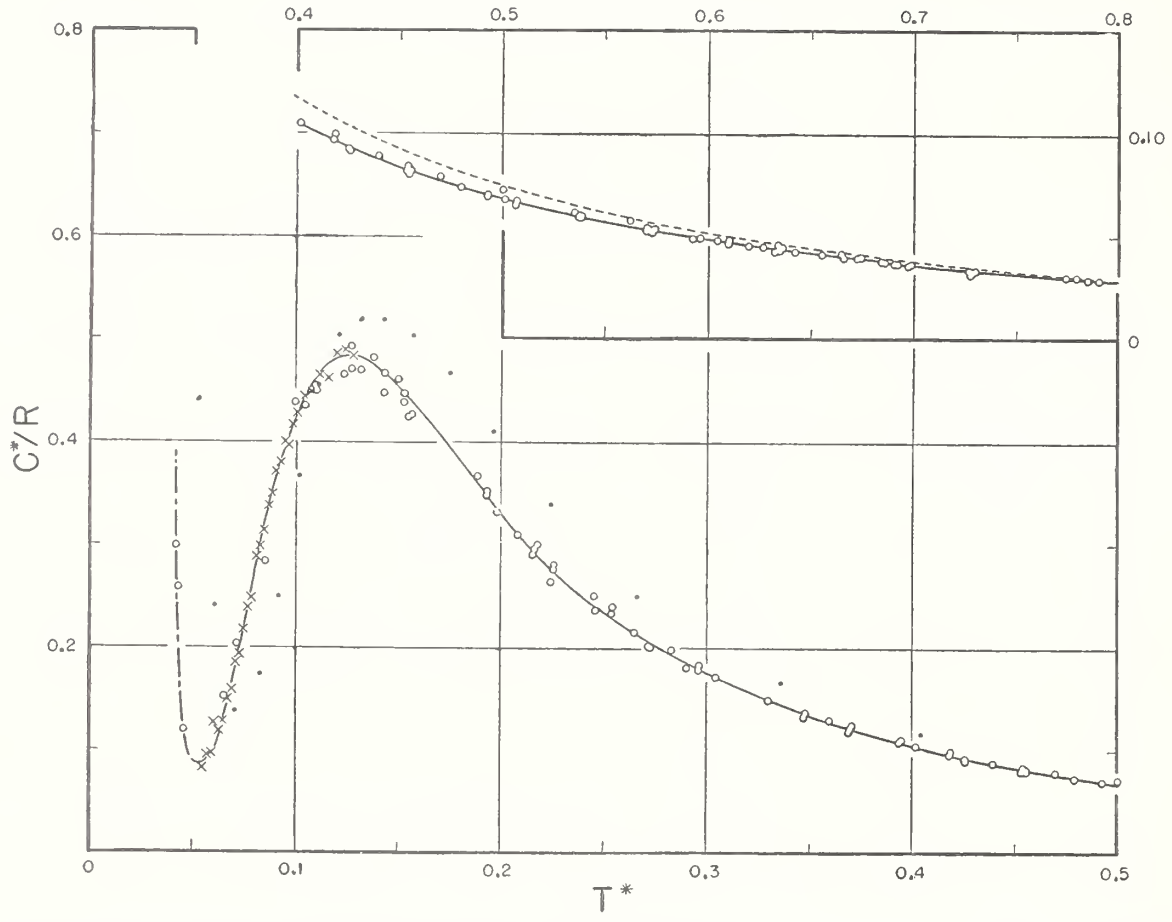

FIG. 4. Pseudo specific heat, C^*, *vs* magnetic temperature. ○ = direct measurements, × = points obtained from differentiation of "master-Q curve" (see text), ● = data of Gardner and Kurti. Inset is the high temperature region drawn to a larger scale, with the broken line corresponding to the solid line of Fig. 3.

the Gardner-Kurti data are quite large below $T^*=0.3°$ and must be due in part, at least, to the different procedures for calibrating the heater, as described above; the points for Series A (not shown) lie in between. As we discuss in more detail in the following, the latter results are suspect in the low-temperature region on the grounds of nonuniform heating, but the separation from Series B above $T^*=0.1°$ was nowhere greater than 8% (this at 0.22°) which is within the estimated precision of measurement, *viz.* ±5% (see Discussion) and part of which at least could represent genuine differences between the specimens.

(3) Susceptibility in the Region of the Maximum

Although the nonreproducible behavior of the alums shows up to a certain extent in the different values of δ which may be obtained for different specimens, and also in different laboratories,[1,4] the greatest variations in T^* are manifested in the region of the Néel point, or susceptibility maximum.[4] This fact is illustrated in Fig. 5 where we compare the data for S.C. IIIb, for S.C. II on two different occasions, and those for the Gardner-Kurti specimen. The fact that the latter was a compressed-powder ellipsoid rather than a single-crystal sphere might be invoked to account for its egregious behavior, but an explanation[3] in terms of the ballistic method of measurement contrasting with ac determinations is unlikely to be valid. Where both types of measurement have been employed on the same specimen (crystal) the difference in susceptibility is relatively small.[4,6] The ballistic susceptibility, furthermore, is larger (for small measuring fields) than the ac susceptibility in the neighborhood of the maximum. Finally, a *loosely-packed* powder specimen also showed essentially "single-crystal behavior."[2]

It is obvious from these and earlier results that any one $T-T^*$ correlation has no general value at the lowest entropies. Thus the highest value of χ_{max} observed, $55\times10^{-8}R$ (Fig. 5), and the lowest,[3] $44\times10^{-8}R$ (Fig. 5) correspond to a range in T^*—for the *same* entropy, and supposedly same T—of 0.41° to 0.51°.

(4) The $Q-S$ Relation

Determination of absolute temperatures by the calorimetric method requires a knowledge of the relation between the heat content, Q (= the internal energy, U, in zero field), and the entropy, S. The $Q-T^*$ relation may be obtained by integration of the C^*-T^* curve, then combining with the $S-T^*$ relation gives Q *vs* S which may be differentiated to yield T. Alternatively,

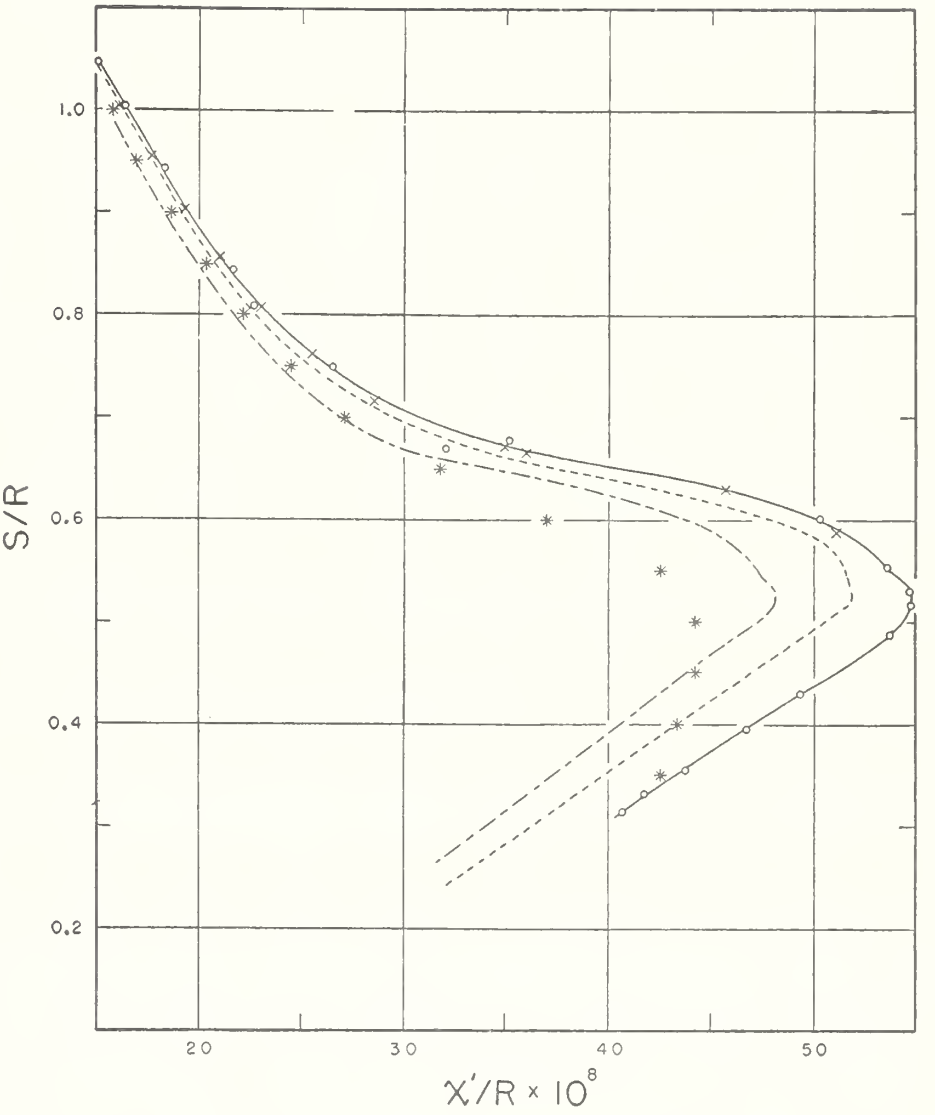

FIG. 5. Entropy *vs* ac susceptibility, showing nonreproducible behavior in different specimens. ———, ○, ×, S. C. IIIb June and July, 1956; – – – –, S. C. II September, 1953; — — — —, S. C. II November, 1954; * data of Gardner and Kurti (compressed-powder ellipsoid). (The entropy values here are all slightly low as a result of using a g value of 2 in the early computations.)

one may differentiate $S-T^*$ and combine with C^* (since $T=C^*\,(dS/dT^*)^{-1}$)—a procedural difference only.

The measurement of C^* by the method described in III, however, cannot be continued down to very low temperatures. First, C^* rises rapidly towards infinity in the neighborhood of the susceptibility maximum. Second, below about $T^*=0.06°$ for the case of a single crystal, and probably below 0.1° for a compress of powder, the thermal diffusivity of the salt becomes very small and it is impossible to make a valid correction for the "drift" heating. The latter warms the surface preferentially and the (apparent) susceptibility becomes an arbitrary function of the entropy. The situation is made worse by any inhomogeneity in the gamma-irradiation.

In such a region one resorts to the "total Q method," namely, upon demagnetization one heats the salt rapidly back into the "high temperature" region, noting the time taken to arrive at some suitably chosen reference T^*. The value of S corresponding to the latter being known, and setting Q arbitrarily equal to zero at this point, one may thus obtain a series of $Q-S$ points, construct the curve and extend it into the high temperature region by combining it with that portion already obtained from the integration of C^*.[16] The essential condition is that an adequately high value of T^* be selected for the reference point. (If the heating-rate be large compared with the drift, a fairly large error in the estimated value of the latter will give rise to a much smaller error in the Q values.)

With the salt being heated continuously, susceptibility determinations were made at intervals determined by the rate of change of bridge balance (ranging from a few seconds to one minute) until the salt had warmed to $T^*\approx 0.1°$ (actually, to a bridge dial-setting of 25.000 for Series B). This reference temperature was chosen since the work of Daniels and Kurti on a com-

[16] This technique forms part of the lore of gamma-ray calorimetry below 1°K, as developed at the Clarendon Laboratory, Oxford. To the writers' knowledge, the first published account of its use, however, is by J. M. Daniels and F. N. H. Robinson, Phil. Mag. 44, 630 (1953). It is only reliable to the extent that the background-heating is negligible compared with the irradiation-heating, or that the former is the same at all temperatures and for each demagnetization.

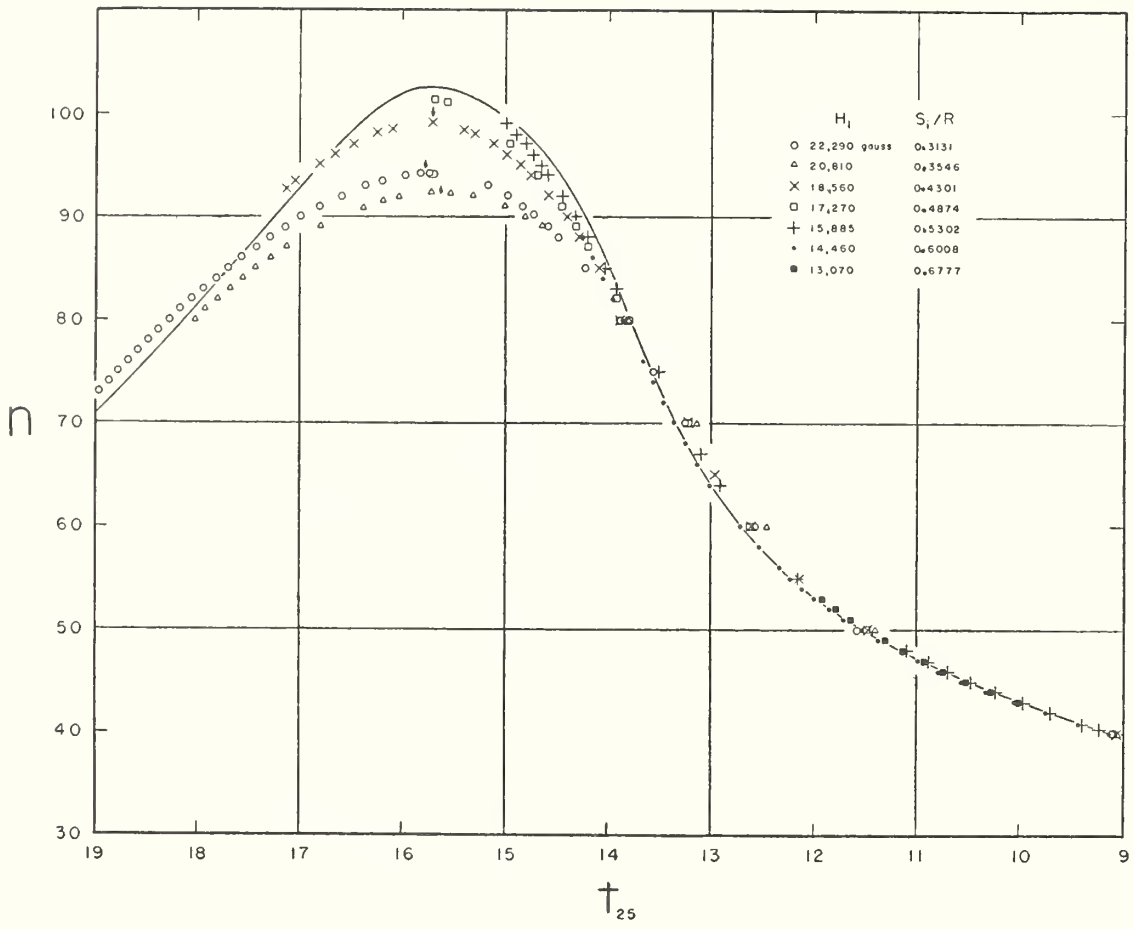

FIG. 6. Warmup curves under continuous gamma-irradiation for various initial entropies. The bridge balance, n, is plotted as a function of (negative) time, all curves being adjusted to a common time-zero, namely the instant when the bridge balanced at 25.000. The solid line is the ideal curve (homogeneity of temperature) calculated back from the final results.

pressed-powder specimen of potassium chromic alum[17] had indicated that the thermal diffusivity was adequate above $T^*=0.07°$. With the superior conductivity of a single crystal, the even higher temperature of 0.1° could confidently be expected to suffice.

In the event, it was found that the heating curves (bridge turns, n, *vs* time) for all demagnetizations could be superimposed for $n<40$ i.e., for $T^*>0.08°$. (Numerical details are given in Table I, wherein times are

TABLE I. Continuous-heating curves for different entropies. Data are times (in seconds) prior to zero chosen as the instant when $n=25$.

	Bridge turns and approximate T^*				
H_i/T_i	80 0.050	60 0.062	40 0.081	35 0.088	30 0.095
9930				423½	245
10 500			548	421½	244
10 955			545	420½	244½
12 155	831½	763	545½	420	243½
13 375	827	757½	543	419	243
13 635	827	756½	545	420	243
14 195	828½	758	544½	420	243½
15 410	833	756½	543	···	···
16 210	829½	752½	544	419½	244
17 260	828	748	542½	418½	243
17 900	831½	751	544	···	243½
18 445	833	753½	543½	419	243

[17] J. M. Daniels and N. Kurti, Proc. Roy. Soc. (London) **A221**, 243 (1954).

negative with zero at $n=25$.) This is also evidence that the drift rate must have been the same for all demagnetizations, to a good approximation. The drift rates determined in the "high temperature" region varied from about 3% of the gamma-ray heating at $T^*=0.1°$ to about 5% at $T^*=0.7°$ with a local scatter of about ½%. In order to apply a correction to the total $-Q$ data, a fixed allocation of 4% drift was made.

In Fig. 6 are plotted curves of bridge reading *versus* (negative) time for a representative series of demagnetizations in Series B, all curves being adjusted to $t=0$ when the bridge reading passed through the value 25. The abscissae are therefore equivalent to Q, with $Q=0$ at $n=25$. Beyond $n=40$ (off the graph) all points lie, within experimental accuracy, on a single curve. It will be observed that the separation of the curves increases as the temperature is lowered beyond that corresponding to $n=40$ and the value of $n_{\max}$ diminishes with decreasing initial entropy. This is due to the inhomogeneous gamma-heating and, to a lesser extent, to the drift heating on the surface. The longer that heat is supplied under conditions of poor thermal diffusivity the greater, of course, will be the nonuniformity and the higher will be the temperature to which the temperature gradients persist. For perfectly uniform heating and zero drift there would be, of course, a unique $n-t$ curve (solid line in Fig. 6) and the higher the initial entropy the more nearly will the experimental

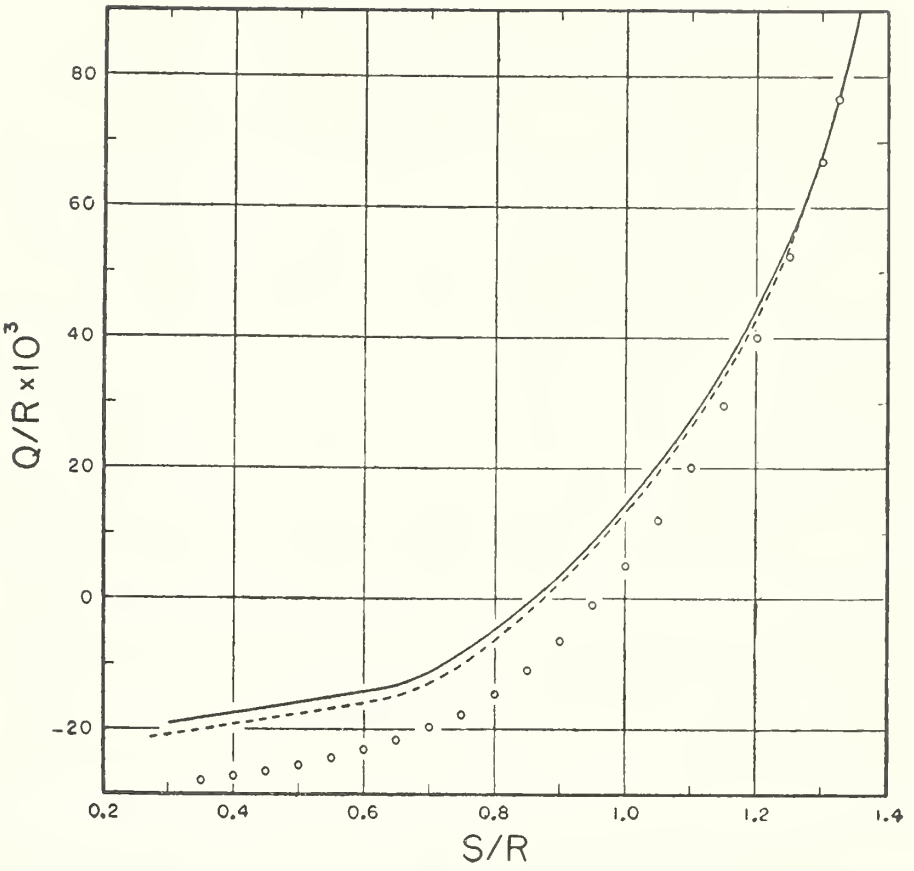

FIG. 7. Heat content, Q/R, *vs* entropy, S/R (smoothed). ———, results of Series *B*, June, 1956, S.C. IIIb; – – – –, results of Series *A*, November, 1954, S. C. II; ○, results of Gardner and Kurti.

curve reproduce this ideal curve.[18] With this in mind, observing the trend within the group of curves at the right in Fig. 6, one may hope to draw in a close approximation to the ideal curve between $n=80$ and $n=40$ as a limit towards which the group is tending. By such a procedure it was possible to obtain a continuous ("master") $Q-T^*$ curve between $n=80$ ($T^*=0.05°$) and $n=25$, which should be viewed with reserve only at the very lowest points. (Referring again to Table I, it may be seen that the curves superimpose to within 2% down to $n=80$, the maximum spread occurring in the region of $n=70$.)

The $Q-S$ curve is shown in Fig. 7 and the low temperature portion of this on a larger scale in Fig. 8. Referring to the latter it will be seen that the master Q curve is evidently valid over its whole extent since the $Q-S$ points derived from it are in excellent agreement with the individual total Q points obtained by demagnetizing into the region over which the master Q curve extends rather than demagnetizing to much lower temperatures and returning by prolonged gamma-heating. (For Series A, our reference temperature of $T^*=0.1°$ proved subsequently to be too low for use to be made of this method of interpolation.) In Fig. 4 we have included points derived from the master Q curve to demonstrate their consistency with the straightforward C^* determinations; the C^* curve evidently becomes inaccurate below $S/R=0.66$ (see Fig. 8) so that the C^* points cannot be trusted below this entropy, which corresponds to $T^*=0.056°$ or the minimum in C^*.

Figures 7 and 8 also show the data obtained in Series A and the final smoothed curve of Gardner and Kurti. To obtain these graphs we have arbitrarily lowered the latter [an absolute value for Q could only be given if the measurements could be extended down to absolute zero] to coincide with our curve at the highest entropy listed in the relevant table published by Gardner and Kurti. The latter authors only carried out total Q measurements for $S/R<0.4$ and made use of integrated C^* data down to $S/R=0.6$ (see Fig. 4, reference 3). Our experience with a single crystal suggests that straightforward C^* determinations should not be trusted below $T^*=0.1°$ ($S/R=0.8$) for a compressed-powder specimen unless the heating is exceptionally uniform. In addition, the results of Series A and those of Gardner and Kurti deviate from Series B in the same direction, and there is good reason to believe that Series A was invalidated by nonuniform gamma-

[18] Very roughly, one may describe the effect of nonuniform heating by considering the crystal as being made up of a large number of segments which are receiving energy at different rates. Each will have a $n-t$ curve similar to the ideal curve of Fig. 6 but scaled down vertically proportional to volume and appropriately stretched or contracted along the t axis but all with a common t_0 where the enhanced thermal diffusivity eliminates temperature gradients and results in a uniform, average heating rate. The fact that the several curves in Fig. 6 have their maxima (indicated by arrows) at very much the same value of t (i.e., Q) suggests that there is a dominant component in this segmentation analysis i.e., that the heating is essentially uniform over a large fraction of the crystal.

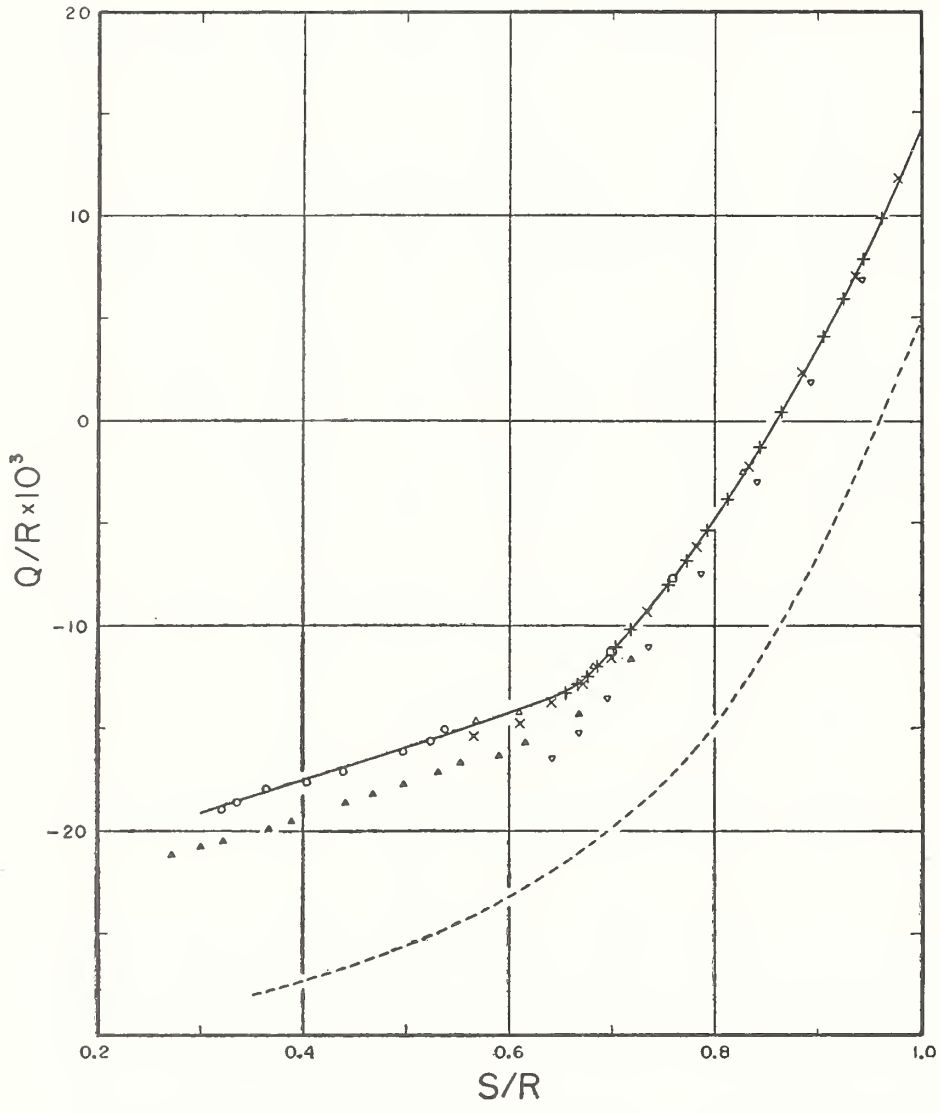

FIG. 8. Q–S curve for low-temperature region (see Fig. 7). ———, series Series B: ○, △, □, total-Q points; × from integration of C^* curve; + from master-Q (see text); ▲, ▽, Series A, total Q and integrated C^*, respectively. – – – – –, Gardner and Kurti.

ray heating.[19] The maximum separation, $\Delta Q/R$, between our two sets of data was 2.2×10^{-3} in the region of $S/R=0.8$, or 2% of the total $\Delta Q/R$ between this point and the upper limit of measurement.

(5) Absolute Temperatures; the $S-T$ Relation

The slope of the $Q-S$ curve gives the value of T at that particular point, and the final $S-T$ curve for the results of Series B is shown in Fig. 9, together with the smoothed data of Gardner and Kurti. The theoretical Hebb-Purcell curve has also been drawn in. The steep drops in entropy associated with the Stark-splitting and magnetic interaction (specific heat anomalies) are well separated for the current measurements. The slope becomes extremely steep for the Néel-point anomaly, T remaining essentially constant over a large entropy interval ($0.35<S/R<0.55$). Similar behavior was observed by Daniels and Kurti in the case of potassium chromic alum.[17]

The Néel point is usually defined as the temperature below which hysteresis and remanence may be observed. The entropy at such a point has been found to be variously, $S/R=0.50$,[3] 0.53,[4] and 0.54.[6] For $S/R=0.50$ Gardner and Kurti find $T_c=0.020$°K. For $S/R=0.53$, we find $T_c=0.016$°K. In Table II we list corresponding values of T^*, C^*/R, Q/R, T, and T_{theor} (the last-mentioned computed from the entropy and the Hebb-Purcell $S-T$ relation*) at selected intervals of S/R for Series B, together with the absolute temperatures derived by Gardner and Kurti for the purpose of comparison. H_i/T_i values are not given since S/R is not a unique function of this quantity, there being a significant entropy correction due to the effect of the crystalline field even at $T_i\approx1.1$°K. (Table I in ref-

[19] Nonuniformity effects showed up as pronounced curvature in the initial part of the drift curves. These could be exaggerated by deliberately displacing the gamma-ray assembly small distances in a vertical direction.

* *Note added in proof.*—We are indebted to Dr. Horst Meyer for drawing our attention to an error in the formula for the "omega function" quoted in reference 13. The correction when carried through, however, merely alters the very lowest values of T_{theor} in Table II, and even these to a negligible extent—about 0.001°.

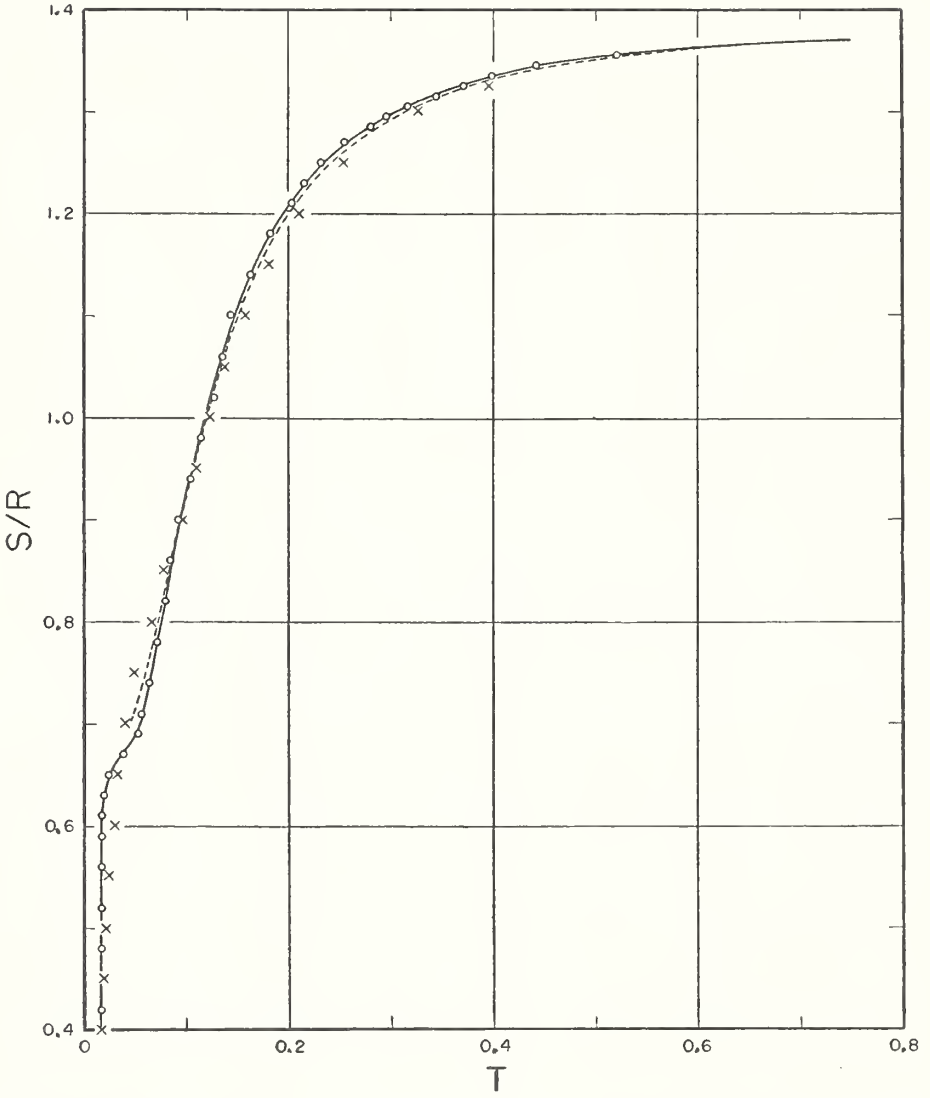

FIG. 9. Entropy *vs* absolute temperature. The points are derived from differentiating Q–S (Fig. 7), taking increments at small intervals, and the solid line is a smooth curve through them. The broken line is the Hebb-Purcell curve for $\delta/k=0.267$°K and the crosses are the results of Gardner and Kurti.

erence (4) provides this information for the condition $T_i=1.15$°K.)

V. DISCUSSION

The experimental data in Fig. 9 lie very close to the theoretical (Hebb-Purcell) $S-T$ curve for all values of T above 0.08°K. In this region the maximum deviation is 4% (at 0.26°K) and since this falls within the estimated experimental error (see the following) it would be quite permissible to accept that curve as an analytical representation of the data. We have, however, drawn in the best curve through the experimental points and used this to supply the data of Table II.†

† *Note added in proof.*—It will be noticed that, for all temperatures above 0.04°K, T differs from T^* by about 0.018°, which immediately brings to mind the possibility of Curie-Weiss behavior, $x=c(T-\Delta)^{-1}$ with $\Delta=0.018$°. It would then be necessary, however, to derive a new calibration formula consistent with this (which *can* be done) and as a result a quite different value for x is derived for a given bridge reading. Thus, the constant value of T^*-T evident in Table II is seen to be accidental, and not truly evidence of Curie-Weiss behavior. One would expect T^*-T to approach zero as T^* increases above 0.1°; although our data do not show this, our estimated error in T of 5% could readily account for this defect.

The existence of curvature in a plot of susceptibility *versus* time at the beginning of a drift period has been cited above as an indication of inhomogeneous heating and poor thermal diffusivity. Such effects were observed up to as high as $T^*=0.13$°, but they were not serious enough, evidently, to significantly affect the results beyond $T^*\approx 0.06$°, as has been discussed already in Sec. IV (4).

Assuming that the quantum-mechanical calculation of the entropy is valid,[20] errors will only enter through uncertainties in the values of H_i and T_i. Random errors

[20] Direct experimental evidence for this comes from measurements of magnetic moment as a function of H and T (W. E. Henry, Phys. Rev. 88, 559 (1952)). The small correction due to the crystalline-field splitting can be adequately estimated and the resultant value of b, the $1/T^2$ term in the zero-field $S-T$ curve, has been verified by "relaxation" measurements [A. H. Cooke (private communication)]. At 1°K the contribution to the entropy from the lattice is negligible [D. G. Kapadnis, Physica 22, 159 (1956)]. The true value of δ/k is probably 0.255°K rather than 0.267°K,[11] demanding the postulation of another small interaction besides dipole-dipole coupling—but this does not affect the argument here. Finally, the values of the $1/T^2$ term obtained by different workers agree within 3%, though T_i varies from 0.9° to 1.2°K.

TABLE II. Corresponding values of entropy, heat content, pseudo-specific heat, magnetic temperature and absolute temperature (smoothed values). The T_{GK} values (Gardner and Kurti data) and T_{theor} (after Hebb and Purcell) are those corresponding to the given *entropies* only.

S/R	$10^3 \times Q/R$	C^*/R	T^*	T	T_{GK}	T_{theor}	S/R	$10^3 \times Q/R$	C^*/R	T^*	T	T_{GK}	T_{theor}
1.35	86.75	0.068	0.501	0.480		0.496	0.80	−4.80	0.384	0.0935	0.0752	0.065	0.0720
1.325	76.40	0.113	0.383	0.365	0.396	0.377	0.75	−8.30	0.301	0.0832	0.0656	0.048	0.0600
1.30	68.10	0.157	0.320	0.305	0.326	0.314	0.70	−11.30	0.177	0.0705	0.0540	0.039	
1.25	54.90	0.232	0.251	0.234	0.254	0.242	0.675	−12.55	0.104	0.0613	0.0415		
1.20	44.20	0.303	0.211	0.194	0.210	0.200	0.65	−13.35		0.0525	0.0240	0.032	
1.15	35.20	0.371	0.184	0.167	0.180	0.172	0.625	−13.85			0.0180		
1.10	27.45	0.420	0.164	0.147	0.157	0.150	0.60	−14.30			0.0172	0.028	
1.05	20.60	0.456	0.148	0.131	0.137	0.132	0.55	−15.15			0.0164	0.023	
1.00	14.30	0.478	0.135	0.118	0.122	0.119	0.50	−16.00			0.0162	0.020	
0.95	8.55	0.482	0.123	0.106	0.109	0.106	0.45	−16.80			0.0160	0.018	
0.90	3.65	0.470	0.113	0.0950	0.096	0.0940	0.40	−17.60			0.0160	0.016	
0.85	−0.80	0.437	0.103	0.0850	0.077	0.0825	0.35	−18.35			0.0156	0.013	

will show up as scatter in the $S-T^*$ curve, and the assignment of a figure of 1%, as evidenced in Fig. 2, should be safely conservative. Systematic errors in H_i and T_i (possibly 0.5% in H_i/T_i) could contribute an uncertainty of the same order of magnitude in the "high" temperature region, where the entropy is a function of $(H_i/T_i)^2$. The mean scatter in the dt/dT^* data is ±2%. In calibrating the gamma-ray heater, however, where we have to consider the joint effect of an error in b (used to derive the theoretical C^*) and the scatter in the dt/dT^* data, we may effectively discount the effect on the value derived for b of random errors in the entropy since the Hebb-Purcell curve is assuredly a valid smoothing function in this "high" temperature region. Hence, the probable error in $\dot{Q}$ is $\pm 1 \pm 2 = \pm 3\%$, and that in C^* is therefore ±5%. The probable error in $T = dQ/dS$, from combining Q and S, will be somewhat less than the sum of the respective errors in the latter quantities since systematic errors in H_i and T_i affect both S (directly) and Q (via b and $\dot{Q}$). This contribution is therefore zero at the highest temperatures and tends towards its above-estimated value of 1% at the lowest temperature, where the effect on S of an error in H_i/T_i is much smaller.

The total estimated error in deriving T from the entropy and specific heat data therefore amounts to ±5% for the high temperature region, increasing towards 6% for lower temperatures, if it be assumed that the errors incurred in differentiating $S-T^*$ (or integrating C^*-T^*) are rendered negligible by the process of smoothing. The latter assumption was strengthened by processing the data both ways and also reversing the individual procedures to back-check.

For the lowest temperatures, where the total $-Q$ method was employed, the total probable error in T is about the same as that estimated for the C^* region (above). The probable error in Q/R is made up of 1% for incorrect drift estimation and 3% for the heater calibration, yielding a resultant ±4%. The error in S/R being 2%, the derived values of T should be valid to ±6%.

In the region of $S/R = 0.67$, where the curvature of $Q-S$ has a maximum, it is possible that the accuracy for T diminishes due to errors in deriving dQ/dS. These would have to arise mostly through errors in the $S-T^*$ curve, since the $Q-T^*$ curve can be made continuous through the device of the master-Q determination, the validity of which is confirmed by its exact agreement with individual C^* determinations. Even so, the physical restriction on the manner in which one may drawn a curve through the experimental points $-d^2Q/dS^2$ always positive—assists one in making a valid smoothing of the experimental irregularities.

The most notable differences between the present results and those of Gardner and Kurti occur in the range below 0.09°K, our T values being the higher for $0.67 < S/R < 0.90$ and the lower elsewhere. In the upper portion of this region Gardner and Kurti relied exclusively on the C^* method which is open to serious objection, and in consequence their precision was undoubtedly diminished. At the very lowest temperatures, where we have used only the total Q method and Gardner and Kurti the same but supplemented by some measurements of $dQ/d\Sigma$, where Σ is the remanence, the agreement is quite satisfactory. It is significant that the divergence is greatest (see Fig. 9) in the region of link-up between the two calorimetric procedures.

It is, of course, unremarkable that two different $Q-S$ curves should agree fairly well (Fig. 7) and yet their slopes at a particular value of S be quite widely different. The necessary condition is that the divergence be non-systematic. Hence it is possible, by making accurate measurements at the ends of the curve and inaccurate ones in the middle, to arrive at a large error in slope in the transition region. It may be seen from Fig. 8 that our $Q-S$ curve would not be altered by ignoring all points save those involving a measurement of total Q. A reliable estimate for the slope-error should hence be obtainable from the sum of the errors in Q and S. We submit that the errors in the work of Gardner and Kurti are probably considerably greater in the intermediate region due to the change-over there in the method of measurement with no region of overlap for a check.

A comment is in order on the fundamental reliability of measurements employing gamma-irradiation for

heating. The method has been criticized in the past, on the grounds of a possibility of a delay in communication of the energy to the spin-system, so that the effective heating-rate would not be temperature-independent.[21] This has been examined in some detail by Platzmann[22] and a defense of the method given in reply by Kurti and Simon.[23] Our conclusions are in agreement with the latter. In all our measurements we employed a 250 millicurie Co^{60} source; Gardner and Kurti used a 60-Mc radioactive silver source for total Q and 500 mC of radium for C^*. Despite the wide variation in gamma-ray energies and in specific absorption, the results agree quite well—especially the overall $Q-S$ relation, if not the more exacting dQ/dS. As stated earlier, above $T^*=0.08°$ [0.063°K] the Q value at any point was not dependent upon the amount of prior heating required to reach that particular entropy. It does not seem necessary, furthermore, to go beyond poor thermal diffusivity and imperfect geometry to explain time-lag effects at the very lowest temperatures.

We believe that Fig. 9 represents the entropy-temperature relation of a slowly precooled single crystal of CMA to the estimated accuracy of 6% down to 0.06°K. The same degree of confidence may be placed in the $T-T^*$ correlation of Table II. Below this temperature, where the susceptibility begins to increase rapidly with decreasing entropy, the significance of the present results may be notably less, from a general thermometric point of view. The variation in value of χ_{max} for such crystals (about 15%) suggests that in this, the most sensitive, region the $S-T$ relation may well vary considerably from sample to sample so that a "thermometer" could only be calibrated by the laborious calorimetric procedure. The data of Table I and Fig. 6 show, moreover, that below 0.06°K the diminished thermal diffusivity of the salt would limit its value as a thermometer, even if the surface were in excellent thermal contact with the particular substance under investigation.

[21] De Klerk, Steenland, and Gorter, Nature (London) **161**, 678 (1948). The thesis was evolved to account for wide divergence between results obtained in Oxford and, by a different method of heating, in Leiden. New measurements by Beun, Miedema, and Steenland [Physica **23**, 1 (1957)] indicate, however, that the early Leiden measurements were in error and that the above criticism need be supported no longer.

[22] R. L. Platzmann, Phil. Mag. (7) **44**, 497 (1953).

[23] N. Kurti and F. E. Simon, Phil. Mag. (7) **44**, 501 (1953).

Journal of Research of the National Bureau of Standards Vol. 53, No. 3, September 1954 Research Paper 2530

Installation for Adiabatic Demagnetization Experiments at the National Bureau of Standards

D. de Klerk[1] and R. P. Hudson

A description is given of the National Bureau of Standards equipment for the production and measurement of very low temperatures by the method of adiabatic demagnetization. The construction of the cryostat and that of the mutual-inductance bridge are described in detail and the relative advantages of iron-cored electromagnets and iron-free solenoids are discussed.

1. Introduction

In recent years, with the rapid increase in the number of low-temperature laboratories throughout the world, there has been a coincident growth in the number of installations for the production and measurement of very low temperatures by the magnetic method. In the period from July 1951 to July 1952, an adiabatic demagnetization apparatus was set up at the National Bureau of Standards. A detailed description of this installation is given. It was built with the special purpose of making accurate determinations of absolute temperatures in the region between 1° and 0.001° K, but the construction is such that other investigations in the region below 1° K can also be performed with it.

2. General Description

The principle of cooling by adiabatic demagnetization was enunciated in 1926 [1] [2] and first applied successfully 7 years later [2]. A detailed description of the physical principles involved would not be appropriate here; for this the reader is referred to the literature [3]. Briefly, however, use is made of the fact that certain salts retain their paramagnetic properties down to temperatures in the region of 10^{-2}° K and possess, at liquid-helium temperatures, a large entropy by virtue of their almost free electronic magnetic moments. This entropy may be removed for the greater part by isothermal magnetization at about 1° K in readily obtainable fields. A subsequent adiabatic removal of the field will result in a fall in the temperature of the salt, until the small internal interaction forces in the crystal bring about the same degree of order as does the strong magnetic field at 1° K. It is self-evident that the final temperature is the lower, the stronger is the magnetic field and the lower the starting temperature. In fact, for most of the salts used in the adiabatic demagnetization process the entropy removed in the isothermal magnetization is a function of H/T.

Thus one needs a suitable paramagnetic salt in a cryostat with liquid helium of as low a temperature as possible, and mounted in such a way that it can be magnetized in heat contact with the liquid (isothermally) and demagnetized under thermal insulation (adiabatically).

The cryostat is located between the poles of an electromagnet or along the axis of a high-power solenoid. With an iron magnet one can obtain fields of the order of 20,000 oersteds, making use of the high B value of the iron. If much higher fields are required (up to 100,000 oersteds), the contribution of iron is relatively small and high-power iron-free solenoids are used. The energy consumption in the case of an iron magnet is of the order of 25 kw; the above-mentioned solenoids require about 1,000 kw.

In order to obtain a low starting temperature for the demagnetization process, the liquid helium is evaporated under reduced pressure. This is accomplished by means of a large-capacity mechanical vacuum pump operating through a large-diameter pumping line. A suitable diffusion pump inserted in the system may bring about a further reduction in the vapor pressure. (As mentioned above, the entropy removal in the isothermal magnetization is a function of H/T, and it is a more economical process to achieve a very low T rather than an enormously high H).

The heat contact between the salt and the liquid-helium bath is made and broken with the help of exchange gas: The sample is mounted in a vacuum space, and during the isothermal magnetization the space is filled with helium gas at a pressure of 10^{-3} to 10^{-2} mm Hg. Thereafter the gas is pumped off with a diffusion pump and then the field is removed. As the specimen is now thermally isolated from the surrounding liquid, the demagnetization is isentropic and the temperature of the salt falls.

The final temperature, which is well below 1° K, cannot be measured by conventional high-temperature methods, but indirect processes must be applied, often rather laborious ones [4], in which use is made of the magnetic properties of the salt, such as the static susceptibility χ, the real and imaginary parts of the dynamic susceptibility, χ' and χ'', or, in the case that hysteresis effects occur, the residual magnetic moment Σ. These quantities, the so-called "thermometric parameters", are usually determined by an induction bridge method. Both self- and mutual-inductance bridges are in use, and the measurement can be performed ballistically as well as with alternating current. An a-c method has the advantage that many measurements can be taken in

[1] Present address: University of Leiden, Netherlands.
[2] Figures in brackets indicate the literature references at the end of this paper.

a short time and with high precision, but ballistic methods become particularly useful at the very lowest temperatures where relaxation and hysteresis effects appear, since here an alternating magnetic field may cause an appreciable heat supply to the salt.

If an iron-cored magnet is employed, provision must be made for the separation of the cryostat and electromagnet immediately after the demagnetization because the iron may have a considerable influence on the setting of the induction bridge for the temperature determination. If the magnet is relatively small, it is possible to have a cryostat in a fixed position and to mount the magnet on wheels or an elevating mechanism, but for a very heavy magnet this is impossible, and the cryostat with its pumping lines must be movable. If a solenoid magnet is used, its influence on the induction coils is much smaller, but even in this case the coupling between the measuring coils and the coaxial windings of the large solenoid produces undesirable effects unless special precautions are adopted in the construction of the measuring coils [5].

It is often desirable to study the magnetic properties of the salt as a function of a magnetic field, and if relatively low fields (up to about 500 oersteds) are sufficient, it is advantageous, for the above-mentioned reasons, not to use the big electromagnet or solenoid itself but to construct a separate small iron-free coil magnet. The influence of the coupling of this magnet with the measuring coils can be decreased drastically by mounting them mutually perpendicular.

In some cases even the earth's magnetic field has a noticeable influence on the magnetic properties of the salt, and then special earth-field compensation coils must be installed.

The components of the new NBS demagnetization equipment are described separately in the following sections.

3. Electromagnet

The electromagnet is a rotatable, adjustable-height model [6]. The pole gap, which must be as small as possible, was determined by the amount of space necessary to accommodate a salt specimen of about 1-in. diameter surrounded by a vacuum chamber and two glass Dewar vessels, the inner one of which contains liquid helium and the outer liquid nitrogen. The gap is 2¼ in. and the pole face 5¾ in. Designed to be operated up to a level of 125 kw, the magnet is being used at present at 25 kw, the rating of the available d-c generator. The loss in magnetic field is not great, however, owing to the rapid saturation that sets in at about 20 kw. At 25 kw the field is 23,000 oersteds; at 125 kw it is 26,000 oersteds. The magnet was calibrated, using a Rawson "gaussmeter", checked in turn in fields stabilized by proton resonance, through the kind cooperation of Dr. Hipple. The accuracy of this instrument is about one-half percent, and within this limit the field was found to be uniform out to within 1½i in. of the edge of the pole face.

The magnet is energized by a four-unit a-c–d-c synchronous motor-generator set mounted in the basement of the Bureau's Cryogenics Laboratory. This method has the advantage that the complete control of the magnet current, and the action of the protection devices (against, for instance, failure of cooling supply, overload, surge on current-break, etc.) can take place through the exciter field. The generator is started with a motor-control panel, and the current is adjusted at a separate exciter-control panel. Both panels are placed in the magnet room. The current is measured accurately by means of a millivoltmeter and a series of 50-mv shunts.

Several automatic control circuits have been developed for the elimination of slow drifts in the magnet current [7], but in the present case manual adjustment proved to be satisfactory. A more serious source of trouble may be the ripple in the magnet current, which has the commutator frequency. If the ripple in the field is large, it will cause relaxation heating in the paramagnetic salt during the evacuation of the exchange gas, such that, by the time that the field is removed, the starting temperature of the demagnetization is much higher than that of the liquid-helium bath. For any frequency above a few hundred cycles per second the solid mass of iron in the electromagnet becomes ineffective, and the only choking effect is due to the self-inductance of the coils, which is generally quite small. But, on the other hand, in the contribution of the ripple current to the magnetic field the iron is ineffective as well, and this is one reason why in most iron magnets the influence of the ripple voltage of the generator on the field is negligible. Another is, of course, that the windings are generally quite far removed from the pole gap and the direct effect of the current is small.

The ripple voltage, with a load current of 100 amp d-c, was 2 v at a frequency of 2,400 c/s (commutator ripple). From the values of the self-inductance at $\nu=2{,}400$ and $\nu=0$ and from the initial slope of the calibration curve of the magnet, it was estimated that this ripple voltage might cause a ripple in the field of not over 0.04 oersted. No ripple in the field could be detected by means of a search coil connected to a cathode-ray oscilloscope. It should have been possible in this way to detect 0.1 oersted at this frequency. (With respect to the ripple, an iron-cored magnet has an advantage over an iron-free high-power solenoid. In the latter the ripple voltage is higher because a higher energy is used, and moreover the contribution of the ripple voltage to the field is larger because the windings are much closer to the field space than in the case of a Weiss-type magnet. Usually, special precautions must be taken to filter out the ripple current of a solenoid magnet.)

The magnet is cooled by circulating a low viscosity silicone oil through the coils and through a heat exchanger, the heat being carried off by means of tap water. The heat exchanger and the circulation pump are mounted in the basement just below the magnet, but the circulation can be started and stopped from the magnet room.

4. Movable Cryostat and Vacuum Installations

The cryostat, consisting essentially of two coaxial Pyrex Dewar vessels, is mounted on the far end of a rotating wooden framework that pivots, by means of steel collars, on a vertical steel pillar. This framework carries the entire high-vacuum system and a 3-in. copper pumping line, which enters the side of a brass cryostat cap. The whole installation is shown in figure 1, and a vertical cross section of the cryostat is given in figure 2.

The inner Dewar vessel (liquid helium) is fitted with its upper end in a brass ring held in place by sealing wax. The ring fits smoothly into the cryostat cap on the wooden arm and thus alines the Dewar vertically. A wired-on rubber sleeve provides vacuum tightness and helps support the weight of the cryostat. The outer vessel (liquid nitrogen) fits around the liquid-helium Dewar; it also is provided with a brass ring, which fits into a brass cap waxed to the outer wall of the helium Dewar. This ring is also a close fit in its cap, and with a rubber sleeve over this joint, too, the weight may be supported; for extra safety, however, a simple harness of string is provided.

The helium Dewar becomes single-walled about 20 cm from its upper end and about 10 cm below the nitrogen cap. If the nitrogen Dewar is kept well-

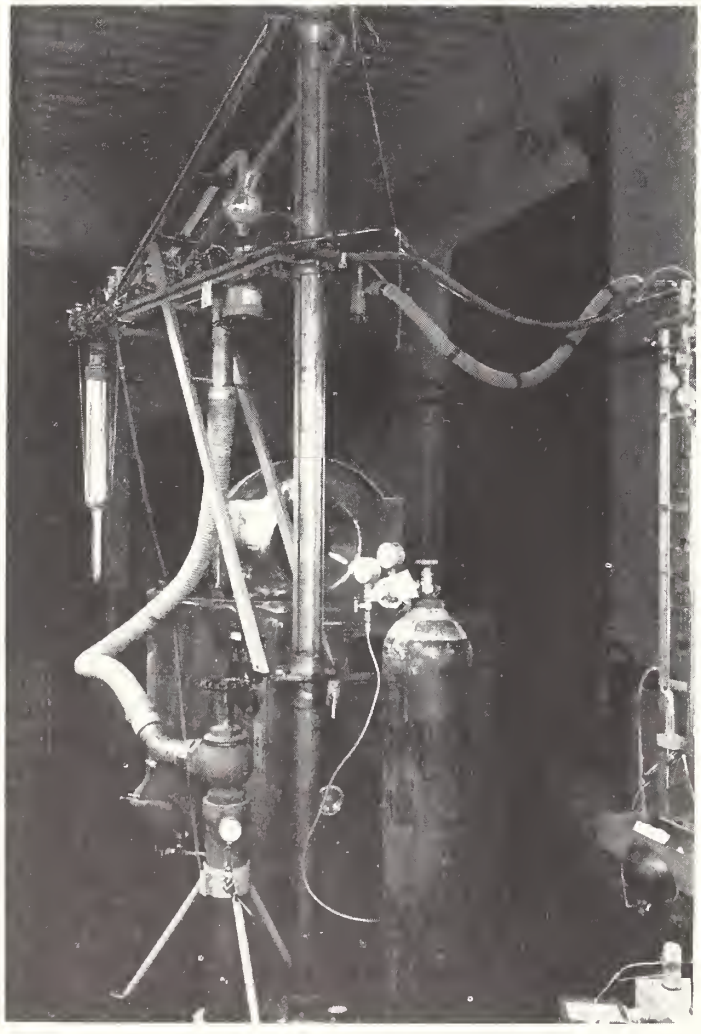

FIGURE 1. *General view of the adiabatic demagnetization installation.*

The Dewar-vessel assembly is suspended from the far end of the rotating arm, which carries the high-vacuum equipment. The electromagnet is in the background.

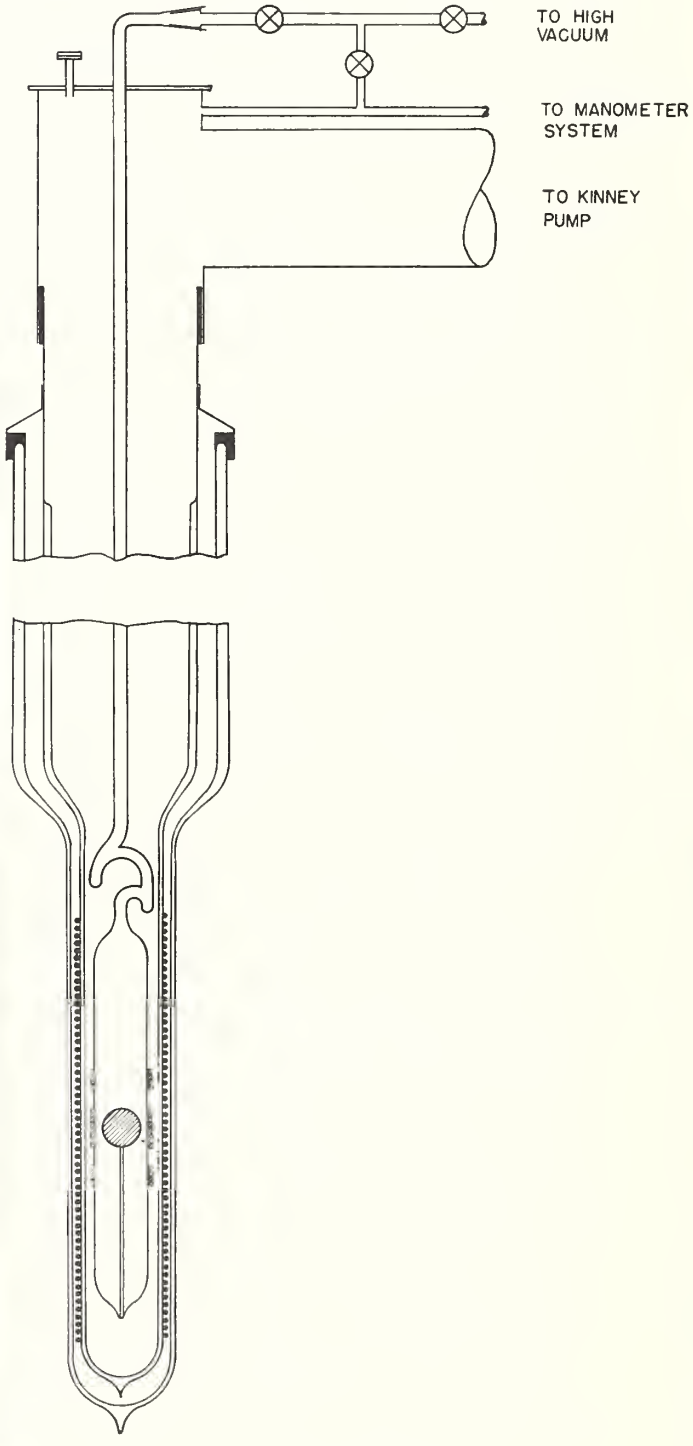

FIGURE 2. *Cryostat.*

The paramagnetic specimen is mounted within the vacuum case, on which is wound the secondary of the pickup mutual inductance. The primary of the latter is shown on the outside of the tail of the inner (liquid helium) Dewar vessel.

filled, the rim of the helium vessel is at liquid-nitrogen temperature, and the heat leak to the liquid helium is smaller than if the rim were at room temperature. Hence the evaporation is less and experiments can be carried out for a longer time.

The two Dewar vessels are made with a narrow lower portion (the "tail") so that, although containing a large quantity of refrigerant, they may fit into a relatively small pole gap in the magnet. The tail of the liquid-helium Dewar is 33 cm long and 3.2-cm inside diameter; it then widens to 7-cm inside diameter for 43 cm up to the ring seal; the single-walled section (20 cm long) is 8-cm inside diameter. The tail of the nitrogen vessel is 5.45-cm outside diameter, the tolerance between a pole face and the glass being only 0.5 mm. The wide part is 58 cm long; the outside diameter is 11.5 cm.

The nitrogen Dewar cap is provided with monel tubes for the admission of liquid nitrogen and escape of vapor. Five monel tubes pass through the helium Dewar cap. One accommodates the transfer syphon and may be sealed off after transfer by a plug and a rubber sleeve; glass tubes pass through each of two others (sealed in by black wax) for connection between the experimental apparatus and the high-vacuum system; the remaining two, which are much narrower, provide the connection to the manometer system and an inlet for the leads to the coils of the mutual-induction bridge.

The rough-vacuum pump (capacity 50 liters/sec) is located in the basement beneath the cryomagnetic laboratory. It is mounted on vibration eliminators, because even the energy of small vibrations of the cryostat is sufficient to develop an appreciable amount of heat in a demagnetized sample [8]. A vertical 5-in. copper line passes from a short length of flexible steel tubing at the inlet to the pump to the room above and is surmounted by a 3-in. globe valve; the latter connects through an S-shaped 3-in. inside diameter reinforced flexible rubber hose to the 3-in. copper line, which is mounted on the moving arm. The arm is then free to rotate about its supporting pillar without interruption of pumping the bath, and the vibrations of the pump are not transmitted to the cryostat. As a final step in the suppression of vibrations, a large sandbox was built around the 5-in. line and valve in the upper room. The cryostat can be conveniently swung out of the magnet and into the framework supporting the earth's field compensation coils, which may then be raised into position (see section 6).

The temperature of the liqiud helium in the cryostat is derived in the conventional way from its vapor pressure. A system of three manometers was constructed: First, a mercury manometer; a millimeter scale engraved on a glass mirror was mounted directly behind the tubes of the manometer and permitted readings of pressures in the region between 1 atm and 5 cm with sufficient precision without the use of a cathetometer. For the region between 5 and 0.5 cm of mercury, a similar oil manometer was constructed. Lower pressures are read with the help of a small McLeod gage with a wide capillary. It is sensitive in the region between 1 and 0.01 mm of mercury. The whole manometer assembly is shown in figure 3.

The high-vacuum system as a whole is mounted on the rotating arm and follows the movements of the cryostat. It consists of an oil-diffusion pump (capacity 20 liters/sec), a spherical Pyrex liquid-air trap, and a valve system. A side tube permits the admission of exchange gas to the experimental chamber directly from the cryostat (see fig. 2). Pressures in the region between 1 and 10^{-3} mm of Hg are measured by means of a Pirani-gage, and lower pressures (down to 10^{-5} mm) are read with an ion gage.

When the cryostat is between the electromagnet poles or in the earth's field compensator, it is rigidly held in position by means of locking clamps on the beam, which are provided with a screw for accurate adjustment (fig. 4).

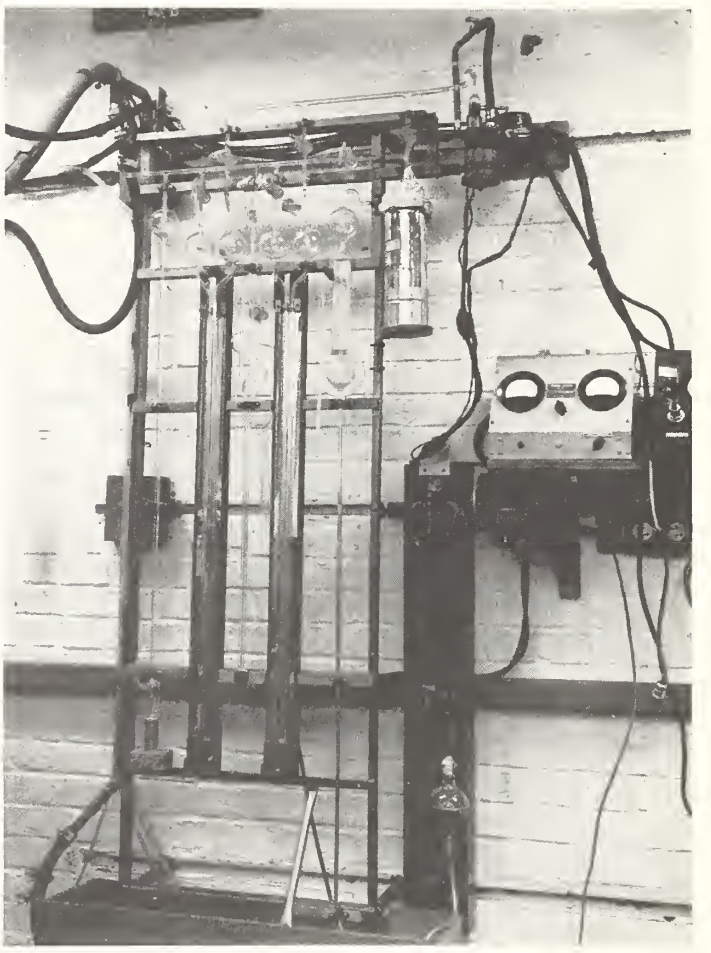

FIGURE 3. *Manometer system.*

Mounted on the framework, from left to right, are (1) over-pressure release "bubbler," (2) mercury manometer, (3) differential oil manometer, (4) oil manometer, and (5) McLeod gage.

574278 O - 61 - 3

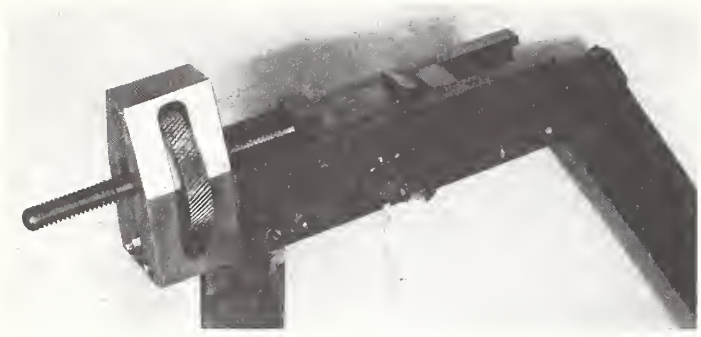

FIGURE 4. *Clamping deviee for locking in position the rotating arm.*

Two are used, one above the electromagnet and one above the earth's-field compensation coils.

5. Experimental Chamber

For adiabatic demagnetization experiments, in which only the temperature and magnetic properties of the salt itself are investigated, the apparatus is extremely simple. It comprises a paramagnetic salt specimen mounted within a vacuum case and thermally isolated from the walls as efficiently as possible. This may be achieved by suspending the specimen from fine nylon fibers or mounting it in an "egg-cup" fixed to the lower end of the vacuum case by a thermally insulating pedestal. The vacuum case may be made either of metal or of glass. Glass apparatus is always preferable to metal because the latter can cause undesirable electromagnetic effects in the measuring equipment through the agency of eddy currents and, on occasion, ferromagnetic impurity. A metal apparatus is more convenient, however, for repeated assembly and dismantling. In this case the tubing should be very thin-walled, and of high electric resistivity nonmagnetic material. Finally, the "cleanup" of exchange gas on pumping is markedly more rapid when glass is used rather than metal.

In this apparatus the vacuum case is made of glass. Soft glass is used to avoid the possibility of heating (and so seriously damaging) the salt during assembly. (Some paramagnetic salts lose their water of crystallization even at 25° C.) The Pyrex of the high-vacuum system is joined to the soft-glass tubing emerging from the cryostat cap by means of a tapered joint (see fig. 2). If the egg-cup type of specimen support is used, the pedestal may be of thin-walled glass tubing with an extra-thin midsection.

The pumping tube emerging from the vacuum case is bent as shown in figure 2 to provide radiation traps. With the sample mounted inside the vacuum case the whole apparatus is silvered externally to a point above the traps, and a protecting coating of suitable varnish is applied. The radiation-screening precautions are of paramount importance in minimizing the heat influx into the specimen after demagnetization. The glass tube above the silvering is coated with aquadag over its whole length so that only a very small cone of room-temperature radiation can penetrate into the first trap. The secondary coil of the mutual inductance (see below) is wound on to the tube around the specimen and covered with a wrapping of very thin paper. Care must be taken to avoid electrical leaks from the lead wires to the aquadag layer.

The paramagnetic salt may be in the form of powder or a single crystal. In order to be able to calculate the internal field of the specimen, it should be spherical or ellipsoidal. Not only is heating dangerous for the salt, but also pumping may cause loss of water of crystallization, expecially if the sample is in powdered form. The experimental chamber must never be evacuated at room temperature; evacuation is safe, however, at temperatures well below 0° C. A single-crystal specimen may be protected by a coating of varnish, collodion, etc.

6. Earth's Field Compensation and Auxiliary Field Coils

The necessary apparatus, which is strictly free of iron or other magnetic material, was built into one unit and is mounted in a brass-tubing framework. By means of counterweights and supporting cables over pulleys, the unit, weighing some 180-lb, can be conveniently raised and lowered to permit movement of the cryostat (see above) into and out of the field.

The earth's field compensation is effected by means of three pairs of mutually perpendicular square coils, the units of each pair being separated a distance of 0.55 times the side of the square, which is a "pseudo-Helmholtz" condition for maximum uniformity of field at the center of the unit. The windings are set in peripheral slots cut in wooden frames, and the current in each of the three pairs of coils (which are fed from a common accumulator source) is controlled through a rheostat and read on a small d-c milliammeter. The wooden frames are secured together at their points of contact by small brass right-angle brackets and wood screws. A flip-coil and ballistic galvanometer circuit is used as a detector of magnetic field, and the currents are adjusted to reduce to zero each of the three components of the field at the center.

The 500-oersted coils are wound on cylindrical wooden cores between end-plates of Bakelite. They are made in two sizes, the smaller pair just far enough apart to accommodate the tail of the cryostat and the larger pair approaching close to the walls of the cryostat where it widens. The end-plates of the larger pair are square and ¾-in. threaded brass rods pass through holes at the corners. These rods are fitted with pulleys at each end, and these guide the assembly along the vertical members of the supporting framework. The smaller coils are bolted to the large ones, and the end-plates of each coil are held by bolts passing through the cores. These bolts must be sufficiently strong to withstand the large strains set up during the winding. In

each pair the coils are separated by a distance equal to the mean radius of the windings to obtain a reasonably uniform field at the center. The assembly is shown in figure 5.

The constructional details are as follows: Large coils: Each winding is 1,080 turns of No. 14½ gage Formex wire, resistance 10.8 ohms; calculated fields for the two coils in parallel, 23.15 oersteds/amp; calculated initial rate of rise of temperature, 4.2 deg/min at 6 amp. Small coils: Each winding is 588 turns of No. 16 gage Formex wire, resistance 4.7 ohms; calculated field for the two coils in parallel, 24.75 oersted/amp; calculated initial rate of rise of temperature 8.4 deg/min at 6 amp.

The coils are connected in a symmetrical series-parallel manner and fed from a battery d-c supply, giving 52.5 oersteds/amp. In general, two sources of 10 v and 100 v, respectively, are used, which may be selected by means of a double-pole double-throw switch. For fast measurements it is convenient to be able to vary the field in predetermined steps, and for this a panel was constructed to carry a network of ohmite resistors. A rotary selector switch mounted on the front of the panel permits the cutting in or out of the resistors in succession, and a second rotary selector switch permits one to select the appropriate current range on one or other of two 3-range d-c ammeters.

To reduce contact-sparking a small thyratron is connected across the coils as shown in figure 6, so that when the main circuit breaker is opened the energy stored in the coils may be dissipated in the circuit now closed by the thyratron instead of in a spark across the switch contacts.

The control panel is shown in figure 7.

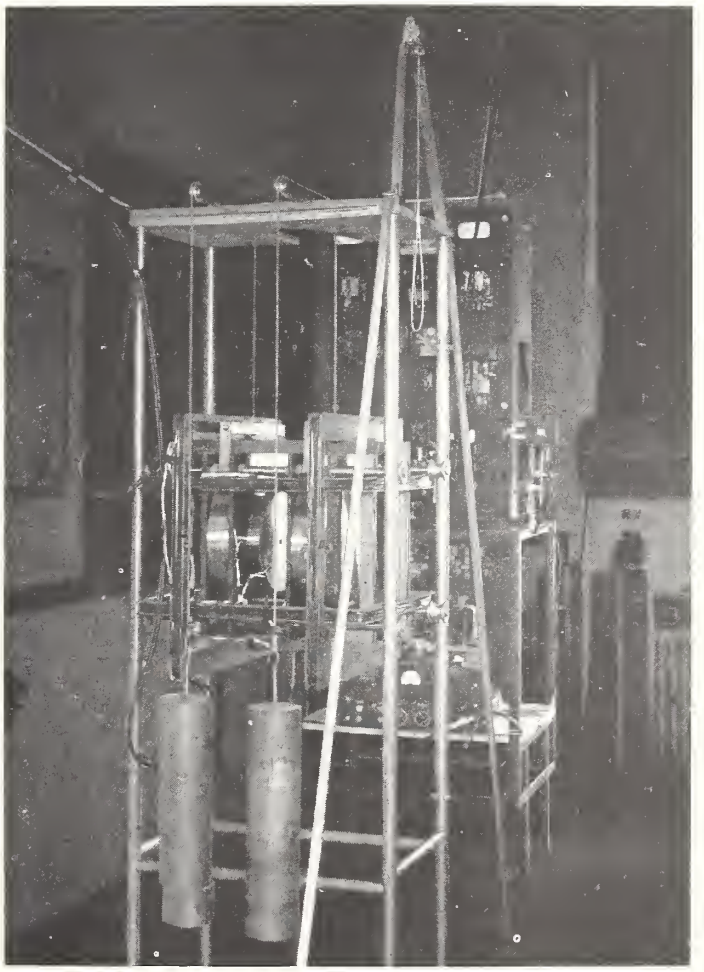

FIGURE 5. *Earth's-field compensation coils and 500-oersted Helmholtz-coils unit.*

The control panel for the synchronous motor of the 25-kw motor-generator set is in the background.

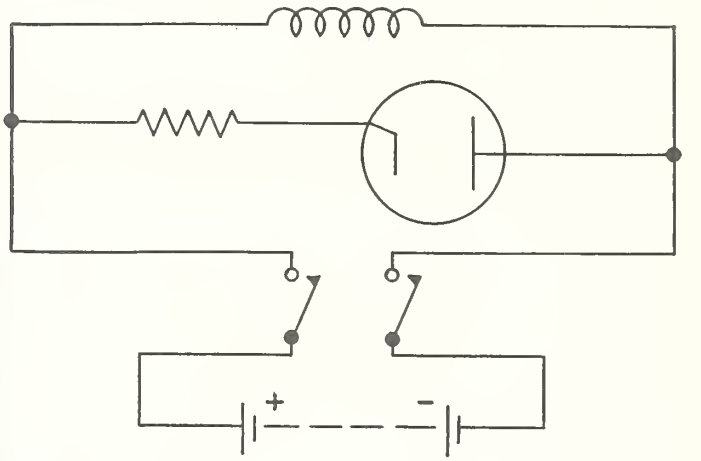

FIGURE 6. *Thyratron circuit for reducing arcing at switch contacts on deenergizing 500-oersted coils.*

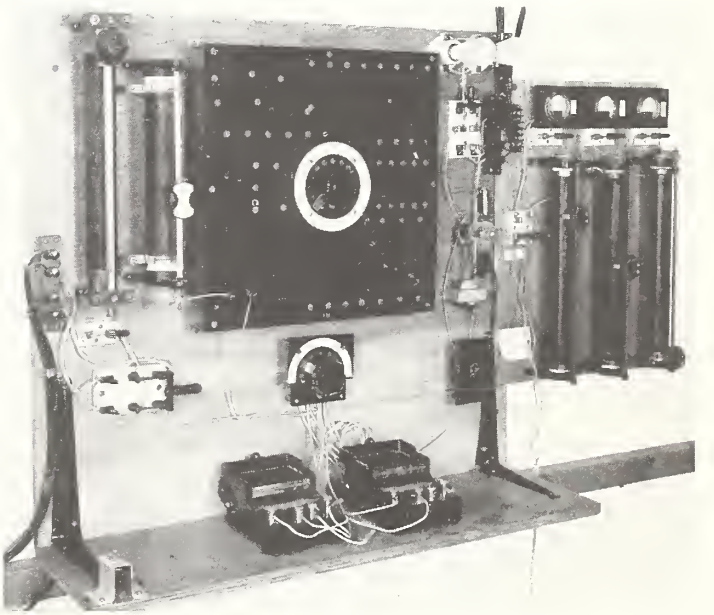

FIGURE 7. *Auxiliary-field control unit.*

The main panel contains the control circuit for the 500-oersted coils and the three rheostats for adjusting the current in each of the earth's-field compensation coil-pairs may be seen at the right.

7. Mutual-Inductance Bridge

The bridge is of the Hartshorn type [9] and is a close copy of the one used for the demagnetization work in the Kamerlingh Onnes Laboratory [10]. It can be used both for ballistic and a-c measurements. As was already mentioned, the a-c method is the more convenient one: A higher precision can be obtained by it and more measurements can be taken per unit time; moreover, at the lowest temperatures, where hysteresis and relaxation phenomena occur, the bridge gives valuable information on the heat absorption by the salt from the alternating magnetic field. On the other hand, this heat may give rise to a fast warming up of the sample, and hence, when measurements are required at constant temperature, the ballistic method must be preferred in this region. With the latter, moreover, data can be obtained on the remanent magnetic moment and the shape of the hysteresis loop.

Schematic diagrams for both the a-c and the ballistic bridges are given in figure 8, a and b. S represents the paramagnetic salt surrounded by the primary and secondary windings of a mutual inductance, M_1. This is connected in series with a variable mutual inductance, M_2, provided by the bridge circuit. In the case of the a-c bridge the primary circuit is fed from a low-frequency (about 200 c/s) signal generator, SG, the detecting device being a vibration galvanometer, VG, preceded by an amplifier, A. The mutual inductance, M_2, is continuously variable so that exact compensation of M_1 is possible, VG being used as a null detector. If a-c losses occur in S, these will give rise to a phase shift in the secondary voltage of M_1. Now this voltage can be resolved into two components, of which only one can be compensated by M_2. The other component, which is in quadrature with the voltage of M_2 (and hence in phase, or 180° out of phase, with the primary current) can be compensated by taking off a small voltage from a potentiometer, R, in the primary circuit. Zero deflection of VG can only be obtained if both M_2 and R are set to the correct value.[2]

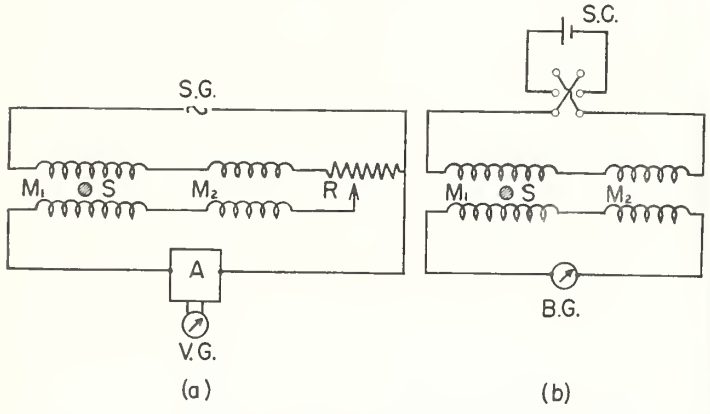

FIGURE 8. *Schematic drawing of alternating. current and ballistic measuring circuits.*

(a) a-c measuring circuit: SG, signal generator; S, paramagnetic salt; M_1, eryostat mutual inductance; M_2, variable mutual induetance, opposing M_1; T, phase-shift potentiometer; A, amplifier; and VG, vibration glavanometer.
(b) ballistie measuring eireuit. SC, storage cell; BG, ballistie galvanometer.

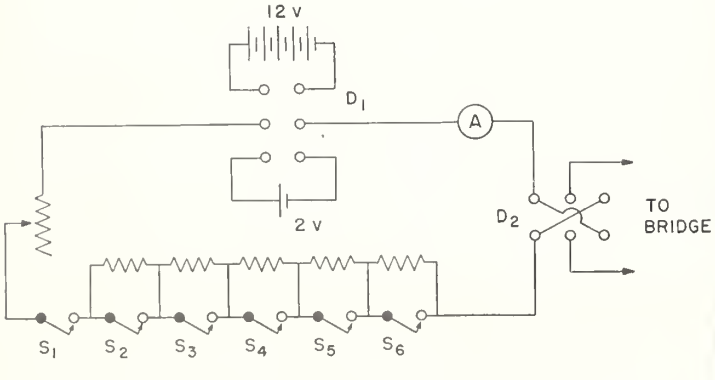

FIGURE 9. *Direct-current power-supply circuit.*

D_1, 2- to 12-v selector switeh; A, ammeter; S_1 to S_6, switches for step-variation of current; D_2, reversing switch.

For ballistic measurements the primary circuit is fed from a storage cell, SC, with a combination of switches and adjustable resistors. In this case only larger dials of M_2 are used, and M_1 is only approximately compensated by M_2. The susceptibility (or the magnetic moment) of S is now calculated from M_2 and the residual deflection of a ballistic galvanometer, BG. In this case the resistance, R, is not needed in the circuit.

The a-c and ballistic bridges are built into one network. The transition from one to the other can be made in a few seconds by setting some switches. SG is then replaced by the storage cell, VG, and A by BG, and R is switched out of the circuit.

The following are short descriptions of the separate components of the bridge network.

The a-c power supply consists of a commercial audiofrequency signal generator. The frequency can be varied between 20 and 20,000 c/s, but generally frequencies of a few hundred cycles per second are used. In the present work the standard frequency is 210 c/s, just between two of the mains harmonics, so that disturbing influences from the mains are as small as possible. At the rated power output of 5 w the distortion of the signal is less than 1 percent. The current is read on a precision milliammeter, with a set of internal shunts for different ranges.

The d-c power supply is shown diagrammatically in figure 9. With the dp-dt switch, D_1, either of two storage batteries (2 and 12 v) may be selected. Ballistic susceptibility measurements are performed by reversing the primary current through M_1 and M_2 by means of D_2. Measurements of hysteresis loops can be made by switching the current on or off in six approximately equal steps with the help of

[2] If a-c losses of the above-mentioned kind oeeur, the magnetic behavior of the salt can be described by means of a complex suseeptibility: $\chi=\chi'-i\chi''$, where χ', the "induetive component," gives rise to the part of the magnetie moment that can be eompensated by M_2, and χ'', the "resistive component," ean be compensated by R. Sinee the heat absorption per second from an alternating magnetic field is equal to $\frac{1}{2}h_0^2\omega\chi''$ [4] (where h_0 is the amplitude of the field), this heat can be derived at once from the value of R. For the caleulation of the magnetic moment (in magnitude and in phase) both M_2 and R are needed.
It should be noted that spurious a-c losses in the bridge also gave rise to a contribution to R.

S_1 . . . S_6. If only the remanent magnetic moment is of interest, the current is made and broken by S_1. This can be done in both directions by reversing D_2, when S_1 is open. The current is read on the precision milliammeter, A, with a set of internal shunts for different ranges.

The primary coil in the mutual inductance, M_1, consists of one layer of No. 30 double-silk covered enameled copper wire wound onto the tail of the liquid-helium Dewar and hence immersed in the liquid nitrogen (see fig. 2). The secondary coil is wound, in three sections, on the outside of the vacuum case. The center section surrounds the salt specimen and consists of several hundred turns of No. 42 Formvar-enameled copper wire (Formex) the number being the greater, the weaker is the paramagnetism of the salt and the smaller the size of the sample. The remaining two sections are wound above and below this in the opposite direction at a separation of about 1 cm, each containing half the number of turns in the center winding. With this arrangement of coils the mutual inductance of the whole set will be zero until the salt is placed within the center winding. Thus at high temperatures where χ' is very small, the bridge may be balanced at a low value of M_2. As both the primary and secondary coils are at a low temperature, their resistance is low, and this is advantageous for the stability of the bridge.

The mutual inductance, M_2, is mounted on the measuring table, of which an over-all view is given in figure 10. Different equipment is used for a-c and ballistic measurements.

The a-c part of M_2 consists of three units. The main unit is variable up to 3 mh in steps of about 3 μh, the variation being made by switching the turns of the secondary coil in and out of the circuit by means of a three-decade dial system. The second unit, the so-called "tenths of turns unit", consists of one decade, each setting being equivalent to one-tenth of the smallest unit of the main mutual inductance. The third unit, the "variometer" is continuously variable and is a fine adjustment on the foregoing one.

The primary coil of the main mutual inductance comprises two parallel solenoids wound in opposite directions and connected in series. They consist of one layer of No. 20 Formex wire, wound on cylindrical ceramic formers, 40 cm long and 4-cm outside diameter. In order to reduce the capacity between subsequent turns, a nylon thread of 0.3-mm thickness was wound between the turns of the copper wire. In order to prevent the accumulation of moisture between the windings, the solenoids were vacuum-impregnated with microcrystalline wax and covered with oil tape before the wax had hardened.

Bakelite bobbins fitting closely over the primary solenoids carry the secondary coil. The latter is wound from 10-strand cable made up from No. 30 double-silk covered enameled copper wire as described below. Three coils are wound on a bobbin, one having 100 turns of this cable, one having 10 turns, and one consisting of a single loop. The location of the turns is shown in figure 11; they are wound in such a way that all the coils have the same average diameter. The secondary coils are impregnated in the same way as the primary solenoids.

The 10-strand cable is made with the help of a simple device, as follows: Wires from 10 supply spools spaced around the perimeter of a large plywood disk are led radially toward the center of the disk and then through right-angled glass tubes parallel to the axle. The latter projects from the opposite face and is mounted in a lathe. As the disk is rotated the 10 wires are pulled continuously outward and the cable forms; in winding it on to a storage spool the latter must be given an occasional turn to reduce the possibility of kinking. Doubtless, an automatic device could be devised to carry out this process somewhat more conveniently and rapidly,

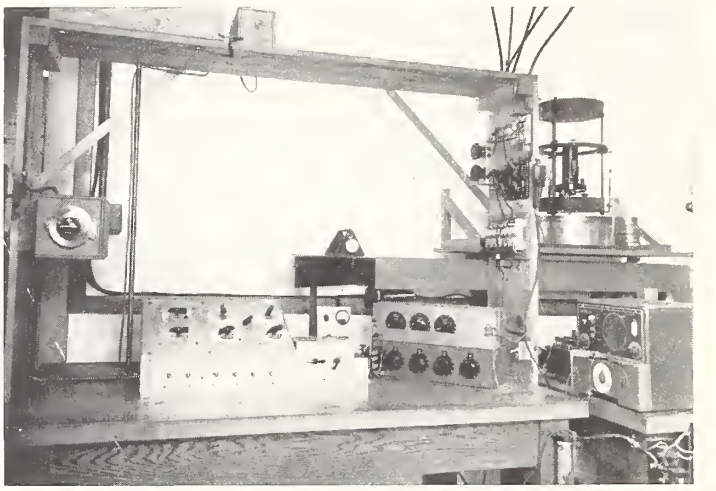

FIGURE 10. *General view of bridge table.*

From left to right, variometer, mutual-inductance dial box, sensitivity control and galvanometer selector, and resistance boxes for P_{eff} network (see fig. 15 and text). The main mutual inductances and the "one-tenths" unit are enclosed in the two boxes at top left, and the ballistic galvanometer may be seen at top right.

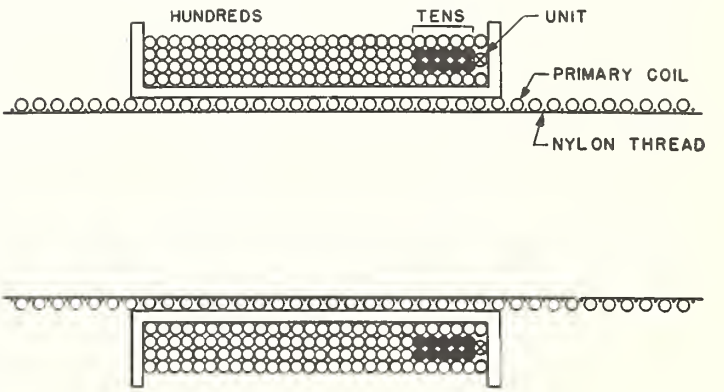

FIGURE 11. *Mutual-inductance unit (detail) showing location of secondary windings which are made from 10-strand cable.*

○, Hundreds of turns; ●, tens of turns; ⊗, unit turns.

but it has been found that two persons (one pulling steadily and one storing the cable) can manufacture the cable at a rate of 5 to 10 m/min with no difficulty.

The advantage of the use of this tenfold stranded wire in the bridge is obvious. It is the easiest way to obtain 10 coils that are identical to a high degree of precision (a few parts in 10^4). The disadvantage, however, is that the capacitive coupling between the 10 coils is not very small, so that the bridge can only be used for investigations at relatively low frequencies. In practice, the upper limit is of the order of 500 cycles.

As mentioned above, two parallel primary solenoids wound in opposite directions and connected in series are used. They are set in a wooden box on a board 3 ft above the table (fig. 10). Each solenoid is surrounded by a secondary bobbin, as described above, and the turns of these bobbins are also connected in series. This arrangement has the advantage of both a negligible stray field from the primaries on the measuring table and a negligible pickup in the secondary coils from spurious alternating magnetic fields. The resultant 1,110 turns (in fact, pairs of turns on the two bobbins) are led to three selector switches providing decades of hundreds, tens, and units of turns. Due to the fact that all the windings have the same average diameter, the relations 10×10 turns$=1\times100$ turns and 10×1 turn$=1\times10$ turns hold with a high degree of precision. Their validity can be improved further by shifting the secondary bobbins along the primary coils, making use of the fact that the field of a solenoid of finite length is not exactly homogeneous. After some adjustment we obtained: 10×10 turns-1×100 turns$=0.003$ turn, and 10×1 turn-1×10 turns$=0.013$ turn. In this position the units of turns correspond to a mutual inductance of 3.061 μh each. For very precise investigations this correction may be applied, but for ordinary demagnetization work it can be neglected. The rotary selector switches (commercial low-thermal-emf type, with 11 contacts) are mounted in an aluminum switchbox placed on the bridge table. The cables are led from the bobbins to the switchbox through a copper tube to minimize electrical pickup (see fig. 10).

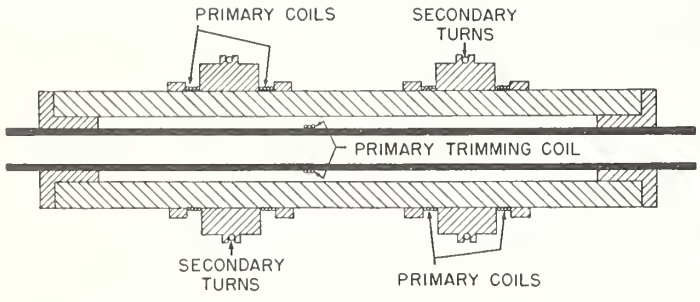

FIGURE 12. *"One-tenths" mutual inductance (see text).*

The secondary winding for each half of the unit comprises a single turn of 10-strand cable and is located at a position of minimum primary field to ensure that each strand encompasses the same magnetic flux.

The "tenths of turns unit" is constructed in a similar manner to the above-described unit and is depicted diagrammatically in figure 12. This unit also consists of two symmetrical parts wound in opposite directions in order to minimize stray fields and pickup effects. The primary of each part is wound in the shape of a Helmholtz coil, with three turns on each half. The secondary consists of one turn of tenfold stranded cable of such a diameter that the wires pass through a region of minimum primary field, so that the flux linkage is little affected by irregularity of winding. It is connected to a fourth rotary selector switch in the switch box on the table. A small trimming coil wound on a glass tube inside the unit and connected in series with the primary winding may be moved along the axis of symmetry in order to adjust the total mutual inductance exactly to that of one turn of the main mutual inductance.

The variometer is shown in figure 13. Again, this unit is double to minimize stray fields and pickup. The Bakelite former (11-cm diameter) holds a peripheral primary winding of 5 turns of No. 20 Formex. The secondary winding is actually a single, incomplete, loop of brass fixed to one face of the Bakelite former, with one lead soldered in the rear to the midpoint of the loop and the other connected to the sliding contact, which moves over the brass ring. The mutual inductance is positive or negative according to whether the contact is moved clockwise or counterclockwise away from the midpoint. The position of the sliding contact is indicated by a dial; the point for which the mutual inductance is equal to one-tenth of a turn of the main unit is found by experiment and marked. The space between this point and the midpoint is then graduated linearly with 100 divisions, and this is repeated for the opposite rotation.

The ballistic part of M_2 is very similar to the main unit of the a-c part. Actually, the same primary solenoids are used in both cases. Another pair of

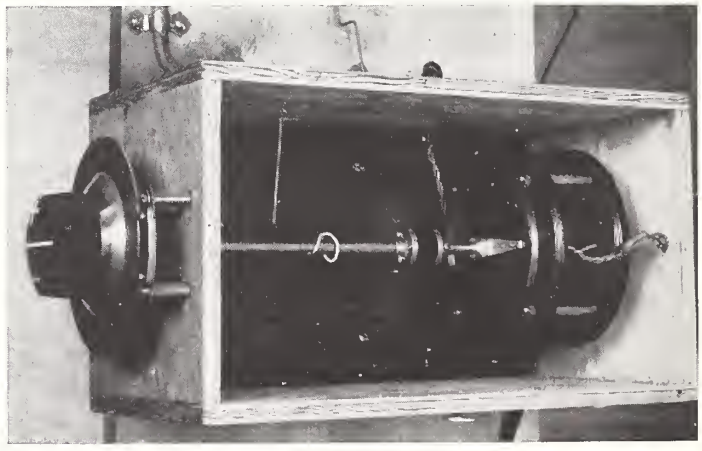

FIGURE 13. *Variometer.*

The two halves of the primary winding and one of the secondaries—a single (split) ring of brass—may be seen at the right. The dial (left) is graduated ±100, one scale division corresponding to approximately 0.003 microhenry.

bobbins was mounted on the primaries, and secondary coils of tenfold stranded cable were wound on them, but only the hundreds and tens of turns, since the ballistic measurements require only partial compensation of M_1 by M_2 (see the beginning of section 7). The coils were connected to double (22 point) rotary selector switches and 20 noninductive spools of copper wire were wound, each trimmed to the resistance of a particular mutual-inductance winding. The connections were then made in such a way that as inductance turns are switched out (for instance) the appropriate noninductive resistance is switched in. By this means the total resistance of the secondary circuit remains constant, and hence the ballistic sensitivity of the galvanometer is constant. The reason that these coils are not also used for the a-c measurements is that the compensator resistances give a noticeable increase of the spurious a-c losses in the bridge circuit. An inside view of the switchbox showing the wiring to the switches and the ballistic compensator resistances is given in figure 14.

The phase-shift potentiometer may be constructed as R in figure 8,a, but a practical difficulty is that resistances of the order of 10^{-4} and 10^{-5} ohm must be measured with some precision. For this reason the circuit shown in figure 15 was built, in which r_1 is a 0.1-ohm fixed resistance, R is a three-decade resistance-box variable between 100 and 10^5 ohms, and r_2 is a four-decade box variable from 0.1 to 1,000 ohms. The voltage taken off in the secondary circuit per unit current of the primary is $(r_1r_2)/(r_1+r_2+R)$. This quantity is called the "effective resistance of the circuit," R_{eff}. If R is set at a constant value well above r_1 and r_2 (for instance, 10^4 ohms), R_{eff} is practically linear in r_2, the proportionality factor being r_1/R. The complete layout of the bridge is given in figures 16 (schematic) and 17.

The grounding of the bridge is a point of importance. The system of figure 16 has the advantage that both the signal generator and the preamplifier of the vibration galvanometer are grounded. A reversing switch must be included in the circuit, however, so that phase shifts in both directions may be compensated with the R_{eff} network. This problem was solved by connecting the reversing switch between P and Q.

The a-c detecting device consists of a vibration galvanometer preceded by an amplifier. The design of the amplifier is very simple. It consists of three stages, a 6AK5, a 6AS6, and a 6AQ5 resistance-capacitance coupled to each other, and the last stage is coupled to the galvanometer with a transformer. No frequency-sensitive element has been inserted, and the maximum amplification is about a factor 10^4. Under these circumstances, special attention must be given during the construction that no oscillations will take place. Signals down to 10^{-7}v must be detected, and the reason that no difficulties occur with the noise level from the first stage is that the frequency width of the galvanometer is very narrow, only a few cycles per second.

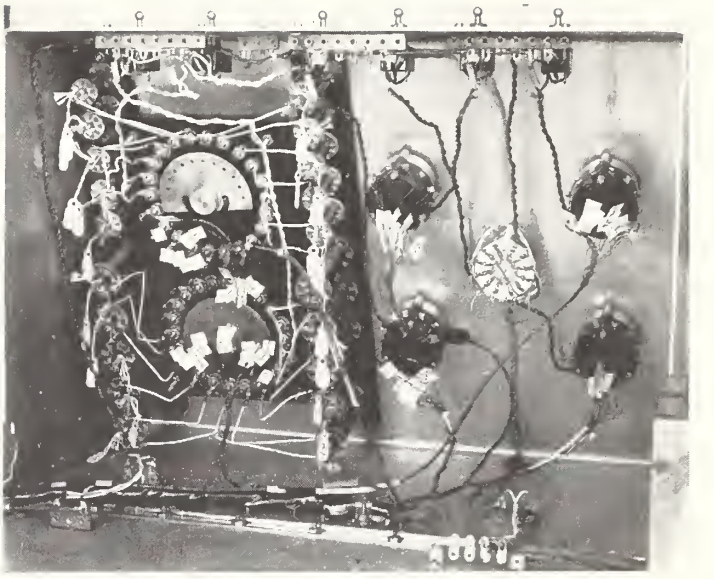

FIGURE 14. *Interior of mutual-inductance dial box.*

The two ballistic turns selectors (100-10) and 20 noninductive resistance-compensation coils are at the left; the four a-c turns selectors (100–10–1–0.1) and the a-c–ballistic selector are at the right.

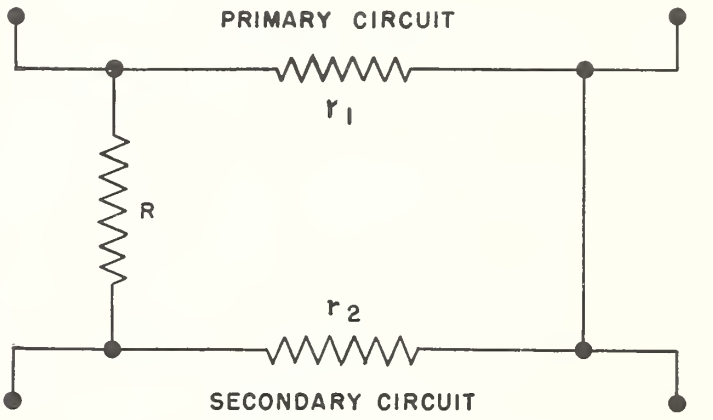

FIGURE 15. *Phase-shift potentiometer.*

$R_{eff}=e_s/i_p=r_1r_2(R+r_1+r_2)^{-1}$

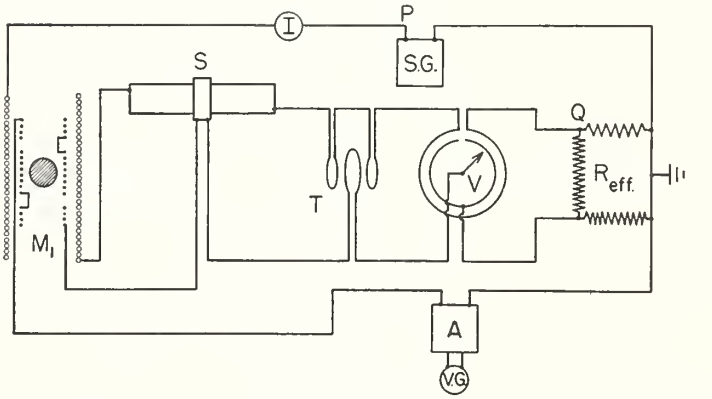

FIGURE 16. *Mutual-inductance bridge circuit (schematic).*

SG, signal generator; I, ammeter; M_1, cryostat mutual inductance; S, main variable mutual-inductance unit; T, "one-tenths" unit; V, variometer; R_{eff}, phase-shift potentiometer; A, amplifier; VG, vibration galvanometer. For PQ, refer to text.

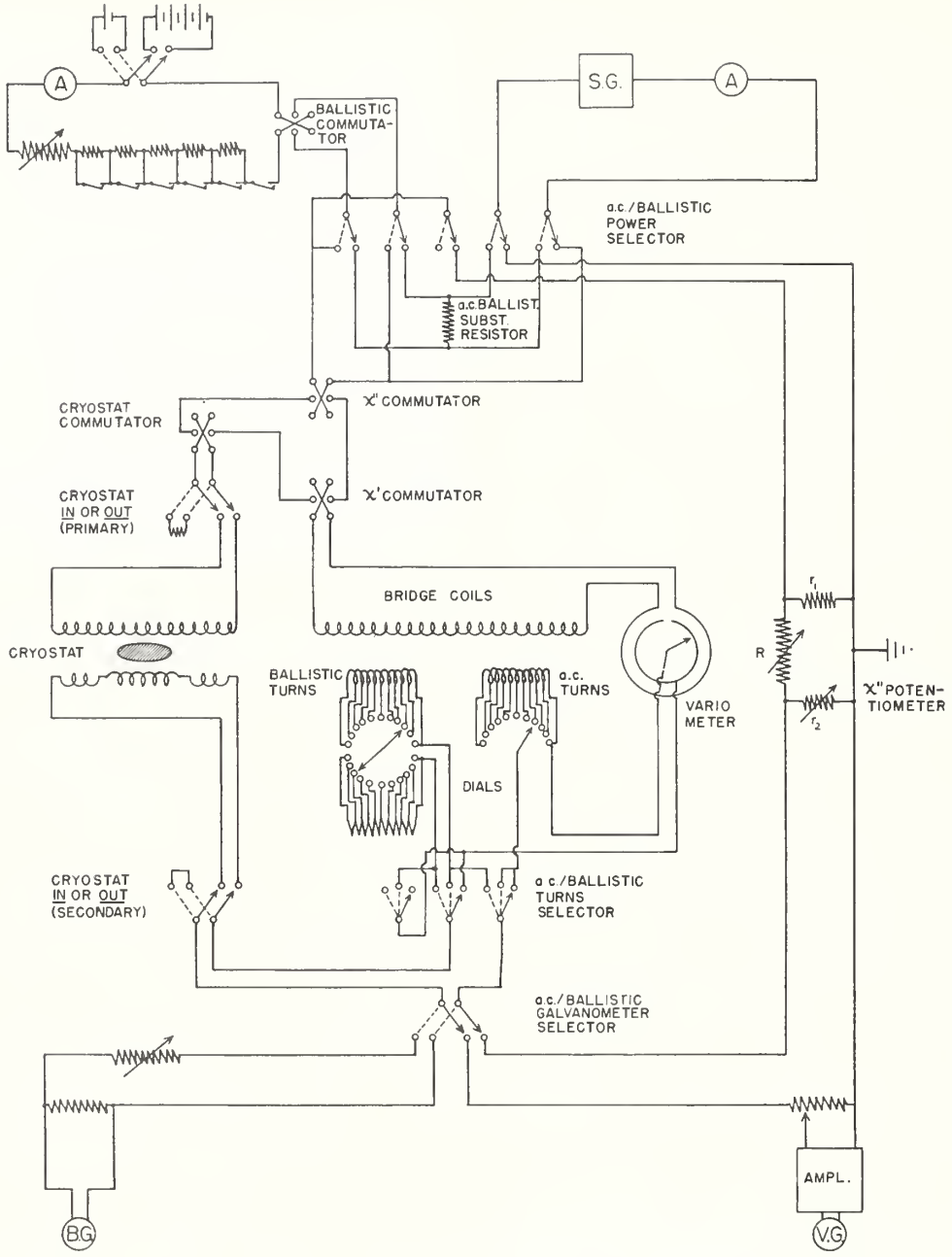

FIGURE 17. *Circuit diagram of alternating-current/ballistic mutual-inductance bridge*

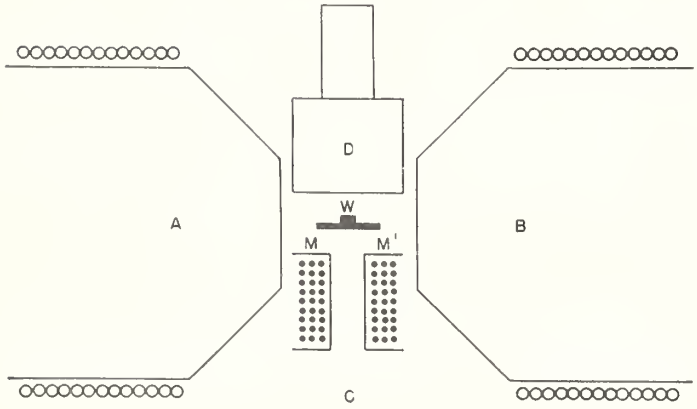

FIGURE 18. *Casimir-type vibration galvanometer (horizontal cross section).*

AB, electromagnet; MM′, magnetic-alloy mirror; W, phosphorbronze suspension; C, deflecting coils; D, copper damping block.

The vibration galvanometer was originally designed by Casimir and constructed in the Kamerlingh Onnes Laboratory. A cross section is shown in figure 18. The vibrating system consists of a small piece of highly magnetic alloy, MM′, 2 mm square and 0.2 mm thick attached to a flat strip of phosphorbronze, W. MM′ is magnetized perpendicular to the strip, and one side is ground to a mirror. The a-c coil, C, is mounted in front. The resonance of MM′ with the a-c frequency is adjusted by applying a constant d-c magnetic field, the current through electromagnet AB being adjusted to such a value that the deflection of MM′ is maximum for a given a-c current through C. In this way the galvanometer can be tuned to any frequency between 100 and 500 c/s. D is a movable copper block, which is used for damping the vibrating system. If D is far away from the mirror, the damping is very small; it takes a long time for MM′ to reach its final amplitude for a given current through C, and the frequency band width is so narrow that the resonance adjustment can hardly be found. If D is placed very close to MM′, the mirror changes from one amplitude to another in a fraction of a second, the band width is still a few cycles per second, and the sensitivity of the galvanometer is quite satisfactory. If the galvanometer is in resonance and well-damped, the sensitivity is about 1mv in the neighborhood of 200 c/s; hence, in combination with the amplifier, signals of the order of 10^{-7} v can be detected.

The ballistic detector device is a voltage-sensitive galvanometer with a sensitivity of 10 mm/μv and a period of 5.1 sec. It is aperiodically damped with a shunt resistance, and the deflections are read by means of a telescope and a lighted scale. The commercial "ballistic galvanometers" with periods of half a minute or more are not suitable for these investigations as their ballistic sensitivity is smaller by about a factor 10, and the long period prevents one from taking more than one reading a minute. Measurements with a fast galvanometer require some experience, but if the deflections are kept under 10 cm (by proper adjustment of M_2) tenths of millimeters can be estimated easily. With the above arrangement, it is possible to take at least six readings a minute.

The possibility was considered of using a still faster galvanometer and registering the deflections photographically. This system has been applied successfully in Leiden, using galvanometers with periods of 1.3 and 0.2 sec. The method works quite satisfactorily, but in some cases difficulties occur in the interpretation of the results when the relaxation time of the salt becomes of the same order of magnitude as the swinging time of the galvanometer.

The first author, who was at the National Bureau of Standards for 1 year as a consultant, expresses his gratitude to members of the staff of the Bureau for the ready cooperation and assistance he received during his stay, for the many valuable discussions, and for the high priority that was often awarded to his work.

8. References

[1] P. Debye, Ann. Phys. **81,** 1154 (1926); W. F. Giauque, J. Am. Chem. Soc. **49,** 1864 (1926).
[2] W. F. Giauque and D. P. McDougall, Phys. Rev. **43,** 768 (1933); W. J. de Haas, E. C. Wiersma, and H. A. Kramers, Physica **1,** 1 (1933).
[3] N. Kurti and F. E. Simon, Proc. Roy. Soc. **149,** 152 (1935); M. H. Hebb and E. M. Purcell, J. Chem. Phys. **5,** 338 (1937); H. B. G. Casimir, Magnetism and very low temperatures, Cambridge Physical Tracts (1940).
[4] D. de Klerk, Science **116,** 335 (1952); D. de Klerk, Phys. Today **6,** ii, p. 4–9 (February 1953).
[5] H. B. G. Casimir, D. Bijl, and F. K. du Pré, Physica **8,** 449 (1941); D. Bijl, thesis, Leiden, p. 97 (1950); W. F. Giauque, J. J. Fritz, and D. N. Lyon, J. Am. Chem. Soc. **71,** 1657 (1949).
[6] F. Bitter and F. E. Reed, Rev. Sci. Instr. **22,** 171 (1951).
[7] M. E. Packard, Rev. Sci. Instr. **19,** 435 (1948); H. S. Sommers, P. R. Weiss, and W. Halpern, Rev. Sci. Instr. **20,** 244 (1949) and **22,** 612 (1951).
[8] R. A. Hull, K. R. Wilkinson, and J. Wilks, Proc. Phys. Soc. [A] **64,** 379 (1951).
[9] L. Hartshorn, J. Sci. Instr. **2,** 145 (1925).
[10] H. B. G. Casimir, W. J. de Haas, and D. de Klerk, Physica **6,** 241 (1939); W. J. de Haas and F. K. du Pré, Physica **6,** 705 (1939); D. de Klerk, thesis, Leiden, p. 36–43 (1948); D. de Klerk, M. J. Steenland, and C. J. Gorter, Physica **15,** 649 (1949); M. J. Steenland, thesis, Leiden, p. 12–23 (1952).

Washington, April 19, 1954.

ournal of Research of the National Bureau of Standards Vol. 56, No. 2, February 1956 Research Paper 2654

An Examination of the Helium Vapor-Pressure Scale of Temperature Using a Magnetic Thermometer[1]

E. Ambler and R. P. Hudson

The variation of the mutual inductance of two coils surrounding a paramagnetic crystal has been measured as a function of the saturation vapor pressure of helium in the range 1.3° to 4.2° K. The fact that this quantity should vary inversely as the absolute temperature has been made use of to investigate the consistency of two recently proposed vapor-pressure temperature scales. The results suggest errors above 2° K in the empirical equation proposed by Clement, Logan, and Gaffney (in contrast to the experiences of Erickson and Roberts with a magnetic thermometer) and are in closer accord with the thermodynamic calculation of Van Dijk and Durieux.

1. Introduction

All practical thermometry in the "liquid-helium region" (that is, between 1° and 5.2° K) is dependent, directly or indirectly, upon a knowledge of the relation between the saturation vapor pressure of helium and the absolute temperature. Many investigators measure directly the pressure over the liquid-helium cryostat and derive T from p-T tables; others use the same procedure to calibrate a resistance thermometer or magnetic thermometer, etc. In this type of vapor-pressure measurement the accepted practice is to apply a depth correction ("hydrostatic head") to the measured value of p; this correction is, however, of somewhat doubtful validity and can be avoided by measuring the pressure in a vapor-pressure bulb that is in thermal equilibrium with the material under investigation (effectively zero immersion).

The p-T tables in general use at the present time comprise the "1948 scale" [1][2] and are based on the work of Schmidt and Keesom [2], Bleaney and Simon [3], and Kamerlingh Onnes and Weber [4]. Possible errors in the 1948 scale were admitted at the time of its preparation, notably in the 1.3° to 2.2° K region from consideration of the helium isotherm measurements of Kistemaker [5], and between the normal boiling point and the critical point due to the sparseness of the experimental data upon which the scale was based in the latter region. The investigations of Erickson and Roberts [6] with a magnetic thermometer for the region 1° to 4.2° K and those of Berman and Swenson [7] above 4.2° K with a gas thermometer provided a strong basis for a revision of the 1948 scale, and an empirical formula was developed by Clement and coworkers [8] from which a p-T table could be conveniently calculated to any desired precision, and which fitted the new data to within 0.002 deg throughout the entire range. A summary of the situation obtaining in October 1954, prior to the development of the Clement formula and the publication of the supporting evidence obtained by Corak et al. [9] from calorimetric work and by Keller [10] from He^4 and He^3 isotherm data, has been given by Hudson [11]. The latter report made reference to some preliminary magnetic thermometer investigations by Hudson and de Klerk (unpublished) that were in qualitative agreement with the findings of Erickson and Roberts [6] but suggested somewhat larger errors in the 1948 scale in the region of 3.5° K. These measurements have now been extended, using improved apparatus, and the results provide the subject of the present report. While this work was in progress, Keesom and Pearlman [12] reported that some anomalies in their calorimetric data could be removed upon reevaluating their data in terms of the Clement equation.

In summary, the evidence available in mid-1955 strongly supported the validity of the Clement equation. A revision of the 1948 scale, long overdue, therefore seemed feasible and the time opportune with the approach of the Fourth International Conference on Low Temperature Physics in Paris in September 1955. During this conference, however, the results of a new thermodynamic calculation of the p-T relation, which differs by several millidegrees from the Clement equation below 1.5° K and above 2.2° K, were announced by Van Dijk and Durieux.[3]

The first part of section 4 of this paper deals with an analysis of our data in terms of the Clement equation. In section 4.2 the same data are reanalyzed in terms of the Van Dijk-Durieux table.

2. Apparatus

To reduce uncertainties in the measurement of p, the saturation vapor pressure, occasioned by measurement of the bath-pressure and application of the hydrostatic-head correction, a vapor-pressure bulb was employed. A series of measurements was performed with the apparatus shown in figure 1, a.

The magnetic thermometer comprised a paramagnetic salt specimen, A (a 1-in. sphere ground from a large crystal of chromic methylammonium alum)[4]

[1] A brief account of this work was presented at the Fourth International Conference on Low Temperature Physics, Paris, August 30 to September 8, 1955.

[2] Figures in brackets indicate the literature references at the end of this paper.

[3] H. van Dijk and M. Durieux, paper presented at the Fourth International Conference on Low Temperature Physics, Paris Aug. 30 to Sept. 8, 1955. We are indebted to Dr. van Dijk for kindly providing us with advance information on this calculation.

[4] The choice of salt was based upon the requirements: Reproducible behavior, small crystal field splitting and dipole-dipole interaction, absence of direct exchange interaction, and ease of growth of large crystals.

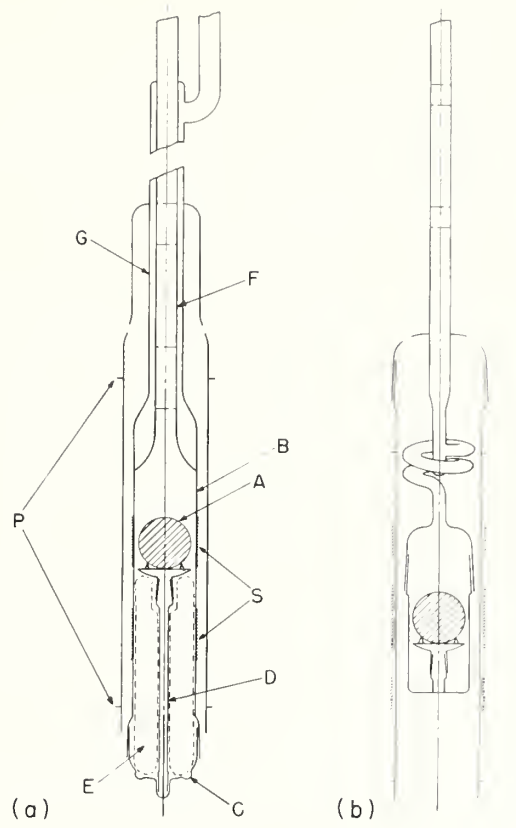

FIGURE 1. *Vapor-pressure bulb and magnetic thermometer.*

a, First apparatus, used in June 1955 measurements; b, modification as used in August 1955 measurements. For explanation of symbols, see text.

located within a mutual inductance, P-S, which was wound, in a rigid assembly, on concentric glass tubes. The latter was connected to an a-c mutual-inductance bridge [13]. For convenience of removal and inspection of the crystal, the bulb, B, was extended to project beyond the coil windings, and closed at the bottom by a ground-joint plug, C. A pedestal, D, supported the crystal, and the volume of the bulb was reduced by means of a hollow glass "filler", E. The tube, F, connected the bulb to the manometer system and was protected by a vacuum jacket, G. Sealed-in glass disks, each perforated by one small hole (about 2 mm in diameter), provided radiation shielding, and F and B were silvered internally.

The purpose of the jacket, G, was to avoid a "cold spot" on F: Due to the hydrostatic head effect, the liquid helium in the surrounding bath is coldest at the surface and, if the vapor in F comes to thermal equilibrium with the bath liquid at this point, the pressure indicated on the manometers will be that corresponding to the temperature at the liquid surface and not at the paramagnetic salt (but see below).

As the temperature of A changed with changing bath pressure, the variation in susceptibility was detected as a change in the bridge setting, n. Since the approximate calibration formula of the thermometer was $T=34/n$ and the precision of bridge setting was $\Delta n=0.001$, temperature changes could be observed as follows: At 4° K, 5×10^{-4} deg; at 3° K, 2.5×10^{-4} deg; at 2° K, 1.2×10^{-4} deg; at 1.3° K, 5×10^{-5} deg. This precision was not realized in practice because of small fluctuations at the lowest pressures and to the necessity for applying small corrections for the nonlinearity of the bridge, but the probable error due to such effects was less than 1 millidegree thoughout the range of measurement (1.3° to 4.2° K).

Subsequently the apparatus was redesigned, for reasons given below, and the second version is shown in figure 1, b In this modification there was no vacuum jacket shielding the tube, F, the vapor-pressure bulb was shortened considerably, and access to the latter was made possible by winding the coils of the mutual inductance on demountable formers. This assembly proved thoroughly satisfactory from the point of view of rigidity.

3. Experimental Procedure

With liquid helium in the cryostat, liquid helium was introduced into the vapor-pressure bulb by condensation of gas under a small overpressure. Prior to the silvering and final assembly, a test filling was carried out to determine the exact quantity of helium required to submerse the crystal, A, and to observe the change of liquid level within the bulb during continuous cooling of the bath. This level will tend to rise because of condensation of the helium gas in the manometer system and fall because of increased density of the liquid as the lambda point is approached. In the present apparatus, the former effect tended to outweigh the latter, and there resulted about a 3-mm submersion at the lambda point. As the precise depth varied with bath level (a large part of the dead-space gas is contained in the section of F that is immersed), the possible correction of 0.03 mm of Hg was not applied to the measured value of p. [The corresponding error in T is 3×10^{-4} deg at the lambda point and becomes progressively smaller as T increases; below the lambda point there is, of course, no depth correction.]

In an experimental determination of helium vapor pressure the most probable sources of error, i. e., extraneous heat influxes to the bulb, will lead to an overestimate of p. Apart from the more familiar radiation and conduction effects, there is one peculiar to low-temperature apparatus; viz., a heat influx due to oscillations in the gas column in a tube such as F. As a result of these heat leaks, the surface temperature of the bulb liquid will be raised, and temperature inhomogeneity will persist because of the low thermal conductivity of the liquid. A thermometer below the surface will therefore be at a lower temperature than that corresponding to the measured value of p. The paramagnetic salt is a much better heat conductor than liquid helium, but, even so, a very small heat influx (if all passes through the salt) will suffice to set up a differential of several millidegrees across a 1-in. sphere. (A rough calculation gives: at 4.2° K, 5×10^{-4} watt per millidegree; at 2.2° K, 10^{-4} watt per millidegree.) The employment of a vacuum jacket in order to

avoid a cold spot on tube F (fig. 1), was found to do more harm than good; heat flow along F from above is prevented from entering the bath-liquid, and the conduction heat leak into the vapor-pressure bulb is greatly intensified. A strong manifestation of this effect was observed in the first apparatus, and it was found necessary to admit "exchange gas" into the erstwhile vacuum space, G, in order to minimize this heat leak. [In fact, the "cold-spot hypothesis" appears, upon closer examination, to be invalid for liquid-helium vapor-pressure thermometry in a glass apparatus. This was not appreciated, however, at the time of designing the first apparatus. The hypothesis supposes that a pressure drop exists along the tube corresponding to the full hydrostatic head, which is, for example, 1 mm of Hg for a 10-cm depth. (This is equivalent to 1.5 millidegrees at 4° K, 3.7 millidegrees at 3° K.) Under such a Δp, there would be a very large flow of vapor up the tube, which, for the maintenance of the supposed conditions, must cool to the cold-spot temperature and then return downward by convection or condense and flow back as liquid. A rough calculation shows at once that in a tube of the size used (1-cm i. d.) the required heat transfer could not possibly take place through the wall and the process must be self-stifling.]

The presence of gas oscillations in the tube, F, was sought for by connecting a small oil manometer of 2-mm bore between F and the bath.[5] None could be detected with the arm connected to the bath closed off. (With this arm open, the oil meniscus oscillated with a period of some 15 sec and an amplitude of about 1 mm.) The same manometer could be used as a direct check on the hydrostatic-head effect. In the first apparatus, the hydrostatic head as measured in this way was always considerably higher than that computed from the level of the liquid in the bath. With the second apparatus, the two values always checked much more closely, which suggests that a heat leak was present in the first apparatus.

The second apparatus was accordingly built without the vacuum shield, G (fig. 1, a) and with smaller holes in the radiation shields (which were also increased in number and more closely spaced). Enough liquid was condensed to reach, initially, the equator of the sphere, A, to make better use of the thermal conductivity of the salt as opposed to that of liquid helium.

The manometers were of sufficiently large bore to obviate the necessity for meniscus-height corrections. Thermomolecular pressure effects, and the reflux of helium due to film flow in the He II region, were negligible for the 1-cm-diameter tube used. Pressures were measured to 0.01 mm by means of a Wild cathetometer and the readings corrected to standard gravity and 20° C. Pressures were stabilized through simultaneous adjustment of a fine-control pumping valve and the current through a small heating coil in the bottom of the cryostat.

[5] We are indebted to J. R. Clement for suggesting this procedure.

The bridge reading, n, is a linear function of the susceptibility of the paramagnetic salt specimen, χ, which varies as the inverse of the absolute temperature (Curie law). Departures from the Curie law due to the crystalline field splitting of the ground state spin-quadruplet are negligible down to 1.3° K, the lower limit of measurement [14]. The calibration formula actually has the form

$$n-B=A/T, \tag{1}$$

where A is proportional to the Curie constant of the material, and B is a second constant, equivalent to the bridge balance value at infinite temperature. In order to examine the over-all consistency of a given p-T relation the two constants A and B may be determined by plotting n as a function of $1/T$ and fitting a straight line to the data. Inserting these values into eq (1), magnetic temperatures, T_m, are then computed for each measured value of n, and the differences $\Delta T=T-T_m$ provide a measure of the "over-all validity" of the given p-T relation. [As the latter may be a priori in error in any part of the temperature range investigated, the correct values of A and B are, within limits, infinitely variable and the final choice correspondingly arbitrary. The two constants may be fixed by considering the scale to be correct at any two chosen points, preferably at opposite ends of the temperature interval (cf. Erickson and Roberts [6]).] Values of $\Delta T/T_m$ are then plotted against T_m for a more sensitive check of the quality of the above fit: for let us suppose that the derived ΔT's are entirely due to incorrect choices of the values for A and B. Then

$$\Delta T=T-T_m=\frac{\partial T_m}{\partial A}\Delta A+\frac{\partial T_m}{\partial B}\Delta B$$

$$=\frac{\Delta A}{A}T_m+\frac{\Delta B}{A}T_m^2, \tag{2}$$

and

$$\frac{\Delta T}{T_m}=\frac{\Delta A}{A}+\frac{\Delta B}{A}T_m. \tag{2a}$$

Bearing in mind that this type of plot will tend to exaggerate deviations at the lowest temperatures, the best straight line may now be drawn and the originally chosen values of A and B modified accordingly (see footnote 5). By such a procedure it was found possible to assign final values to A and B with confidence that any alternative choices that could be readily permitted would only affect the values of ΔT in a minor way and would not invalidate the general conclusions as to the over-all correctness of the scale. [This procedure becomes the more acceptable, the better is the p-T relation under examination. In the case of the 1948 Scale, for example, the errors are so large that the choice of B would have to be supported by an independent determination of this quantity from measurements at high temperatures; this was not possible in the present apparatus where the measuring coils were immersed in liquid helium.]

TABLE 1. *Corresponding values of pressure in millimeters of mercury, p (corrected to 20° C and standard gravity), and bridge dial-setting, n (corrected for nonlinearity in decade scale)*

June 7, 1955		June 8, 1955		June 16, 1955		June 17, 1955		August 17, 1955	
p	n	p	n	p	n	p	p	p	n
768.00	11.223_1	748.67	11.164	758.94	11.202_0	769.97	11.227_3	726.55	17.012_3
751.77	11.178_3	413.42	9.876_5	758.12	11.200_0	750.63	11.173_5	726.22	17.013_2
627.49	10.803_0	41.060	3.805_8	680.15	10.977_8	550.49	10.520_8	603.46	17.280_8
508.12	10.334_1	37.894	3.577_8	603.56	10.723_2	547.46	10.510_3	495.96	17.573_7
341.13	9.443$_7$	23.473	2.182_7	501.32	10.3174	315.84	9.258_6	320.30	18.263_1
254.04	8.736_5	16.987	1.240_4	402.33	9.829_6	45.486	4.110_3	181.73	19.224_2
153.91	7.473_0	13.827	0.6384	173.72	7.794_0	36.834	3.492_2	96.08	20.385_0
71.02	5.378_0	13.581	.585_0	88.05	5.992_2	21.691	1.959_5	24.595	23.100_0
70.71	5.376_1	8.526	$-.795_0$	87.81	5.984_1	8.576	-0.775_2	17.795	23.755_2
26.03	2.478_5	8.556	$-.788_5$	14.676	0.814_7	3.502	-3.515_7	13.126	24.371_7
25.80	2.451_5	6.415	-1.650_8	14.774	.836_7	---------	---------	9.367	25.070_4
---------	---------	3.907	-3.173_0	---------	---------	---------	---------	6.141	25.951_0
---------	---------	2.229	-4.927_0	---------	---------	---------	---------	3.770	27.003_0
---------	---------	1.263	-6.765_7	---------	---------	---------	---------	2.358	28.010_9

4. Results

The experimental data, i. e., corresponding values of pressure in millimeters of mercury (corrected to 20° C and standard gravity) and bridge reading (corrected for nonlinearity), are given in table 1.

4.1. Comparison With the Clement Equation

Four runs on different days were made with the first apparatus and the results could be harmonized, using slightly different values for the constants A and B, with a quite small scatter. This is shown in fig. 2,a.[6]

The signal feature of these results is a large positive deviation hump ($\Delta T \sim 5$ millidegrees) in the middle of the He I region. The deviations are very small in the He II region (less than 1 millidegree) and achieve significant negative values above 4°K. From what has been said in the preceding section, the good fit in the He II region could be fortuitous, and one might, for example, reassess the thermometer calibration to give a zero deviation in the region of the boiling point and again somewhere in the middle, say, of the He II region. This has been done in figure 2, b. The main effect is to exaggerate the 3°K "hump" while only slightly affecting the points below the lambda point.

On either assessment, however, the suggestion remains that the "Clement temperature" (T_{Cl}) is too high by several millidegrees in the neighborhood of 3°K. Equally well, of course, the measured vapor pressures could be too high here due to errors of measurement, such as would be occasioned by extraneous heat influx to the bulb. All the data of figure 2 were obtained with exchange gas introduced into the jacket, G (fig. 1, a). Without exchange gas the 3°K hump became several times larger, and this finds a ready explanation in terms of heat conducted down tube F (fig. 1, a), as discussed in section 3. By the same token, the hump of figure 2 might be due to an ineradicable heating effect, and that it is partly so is supported by the data obtained with the second apparatus, shown in figure 3.

[6] The results as presented in figs. 2a and 3 were actually obtained using the same A, B values as finally chosen for the corresponding Van Dijk-Durieux evaluation (figs. 4 and 5, respectively). It so happens that these values provide as good a general fit as any others.

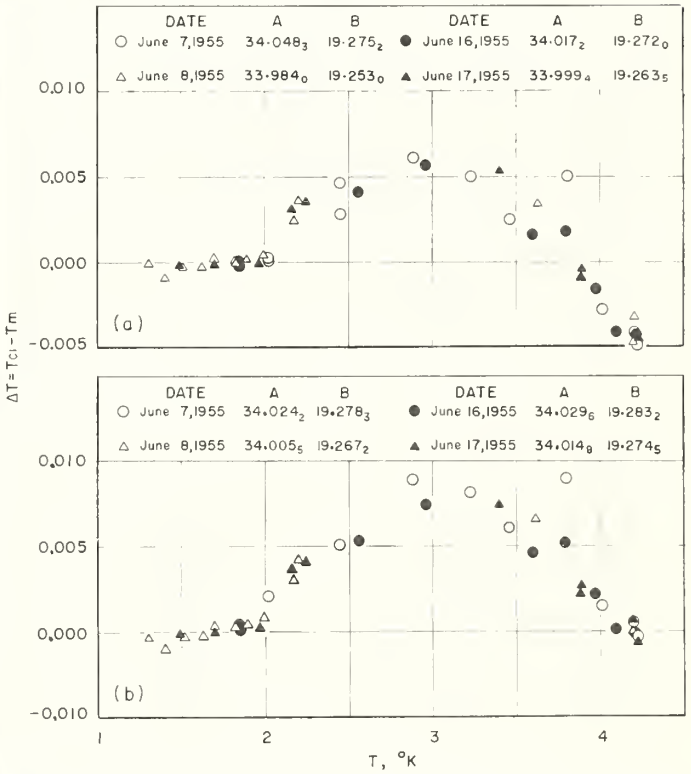

FIGURE 2. *Deviation of temperature as indicated by vapor pressure and Clement p-T relation (T_{Cl}) from magnetic temperature (T_m) as a function of T.*

a, Results of June 1955; b, data reanalyzed with different values of constants A and B, equation (1), to give $\Delta T=0$ at normal boiling point.

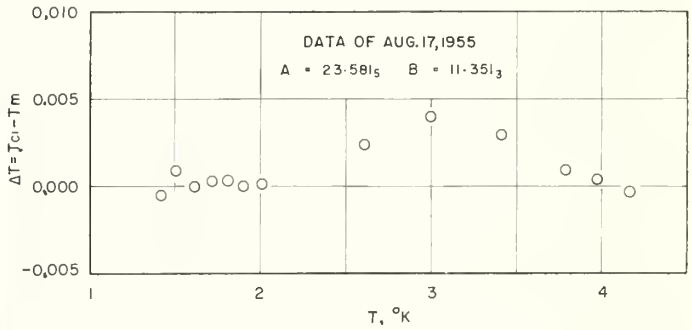

FIGURE 3. *Results of August 1955 analyzed in terms of Clement temperatures, corresponding to June data of figures 2a and 2b.*

Only one experiment was carried out with this apparatus, and the data are accordingly somewhat sparse. The thermometer calibration was quite different from the previous case, i. e., one was then operating upon a different section of the bridge windings, which is an advantage in checking the internal consistency of the bridge. The results are very similar to those of figure 2, b, but the hump in the He I region is much less pronounced (see footnote 6).

4.2. Comparison With the Van Dijk-Durieux Table

Recently Van Dijk and Durieux (see footnote 3) have recalculated the p-T relation for helium, making a reassessment of the best available thermodynamic data. Their results are not in exact accord with the Clement equation and, in fact, deviate from it in the He I region after the manner of the points in figure 3, with a ΔT_{max} of 3.6 millidegrees at 2.9°K. In the He II region, $\Delta T(=T_{C1}-T_{VDD})$ increases steadily from −0.001 deg at 1.9°K to +0.0016 deg at 1.0°K.

In consequence, the magnetic thermometer data of this report can be fitted somewhat more closely to the Van Dijk-Durieux table than to the Clement equation. Figure 3 has been obtained in a rather subjective manner, with an eye to the general features of a plot of $T_{C1}-T_{VDD}$ versus T.

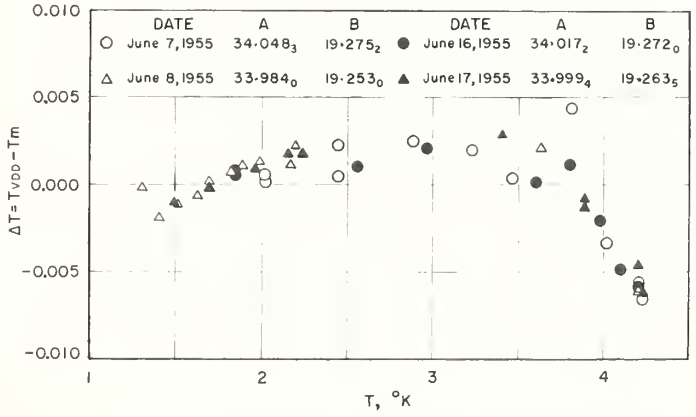

FIGURE 4. *Deviation of temperature as indicated by vapor pressure and Van Dijk-Durieux p-T relation (T_{VDD}) from magnetic temperature, T_m, as a function of T.*

Results of June 1955.

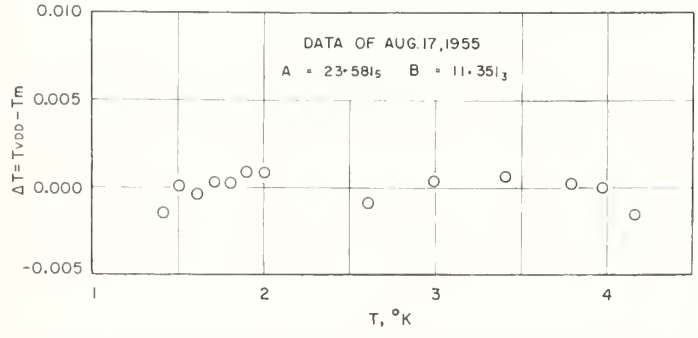

FIGURE 5. *Results of August 1955 analyzed in terms of "Van Dijk-Durieux temperatures," corresponding to June data of figure 4.*

(Compare fig. 3.)

The latter [not shown] shows zero deviation at 1.7°K and a minimum deviation at about 3.8°K; these features have been used as a guide in obtaining the calibration curves from which figure 4 is derived. It can be seen that a two-point tie-down is forced on one here, as it is impossible to choose values of A and B (eq (1)) that will give effectively zero ΔT over a significantly large temperature interval without causing unduly large deviations elsewhere. Thus one may keep the magnitude of $\Delta T(=T_{VDD}-T_m$ small throughout the entire range of measurement but then one also obtains a systematic deviation in the He II region.

The August data are plotted in figure 5, which is to be compared with figure 3. Figure 5 was obtained as the best fit throughout the entire range of measurement, and it, too, has the feature of practically zero deviation at 1.7° and 3.8° K. The magnitude of ΔT now lies within $\pm$1.5 millidegrees throughout the range of measurement.

5. Discussion

The two sets of data, viz., the June results with the first apparatus and the August results with the second, do not agree quantitatively but do show qualitatively the same behavior. It is felt that the August data are the more valid (smaller heat leaks into vapor-pressure bulb), and these agree very closely with the Van Dijk-Durieux calculated p-T table. Both Van Dijk and Clement have recently made significant modifications to their respective p-T tabulations. In a subsequent report the present authors will reevaluate the above data together with the results of a new series of measurements.

None of the present measurements can be brought into very close accord with the Clement equation, in contrast to the results of Erickson and Roberts [6]. The greater part of the latter data was obtained from bath-pressures plus hydrostatic-head correction, which might account for the discrepancy, since the conditions necessary for the exact validity of applying such a correction are impossible to achieve in practice.

The significant differences among the data of Erickson and Roberts and the first and second series reported here point up a major problem in vapor-pressure thermometry in the liquid-helium region, viz., the difficulty of reproducing results from one apparatus to another and of checking any p-T relation to the desirable accuracy of 1 millidegree. From the practical point of view, one desires to obtain accurate values of absolute temperature from simply performed measurements of vapor pressure, the latter being an essentially minor part of any given investigation. It is not entirely unreasonable to seek a solution in the direction of making rigid stipulations concerning the technique of vapor-pressure measurement and to evolve a "practical p-T relation" that is different from that calculated on a thermodynamic basis.

On the other hand, it is true that the differences between the Clement equation and the Van Dijk-

Durieux table are never greater than a few millidegrees. Allowing a 2-millidegree precision for the latter table (as its authors claim), a "Clement temperature" should have a maximum deviation from the thermodynamic temperature of 5.6 millidegrees at 2.9° K, a probable error that is tolerable for many of the common research problems in this region. Experiments demanding a knowledge of dT/dp (e. g., specific-heat determinations) are, of course, most sensitive to deficiencies in the temperature scale.

The authors are greatly indebted to J. R. Clement of the U. S. Naval Research Laboratory for many stimulating discussions and helpful suggestions. It is a pleasure to acknowledge the further benefit derived from general discussions of the problem with R. A. Erickson (Ohio State University), M. P. Garfunkel (Westinghouse), P. H. Keesom (Purdue University), W. E. Keller (Los Alamos), L. D. Roberts (Oak Ridge), C. A. Swenson (Iowa State College); and with H. van Dijk, D. de Klerk, and M. P. Durieux (Kamerlingh Onnes Laboratory).

6. References

[1] H. van Dijk and D. Shoenberg, Nature **164,** 151 (1949).
[2] G. Schmidt and W. H. Keesom, Physica **4,** 963, 971 (1937).
[3] B. Bleaney and F. Simon, Trans. Faraday Soc. **35,** 1205 (1939).
[4] H. Kamerlingh Onnes and S. Weber, Leiden Commun. 147b (1915).
[5] J. Kistemaker, Physica **12,** 272 (1946).
[6] R. A. Erickson and L. D. Roberts, Phys. Rev. **93,** 957 (1954).
[7] R. Berman and C. A. Swenson, Phys. Rev. **95,** 311 (1954).
[8] J. R. Clement, J. K. Logan, and J. Gaffney, Phys. Rev. **100,** 743 (1955).
[9] W. S. Corak, M. P. Garfunkel, C. B. Satterthwaite, and A. Wexler, Phys. Rev. **98,** 1699 (1955).
[10] W. E. Keller, Phys. Rev. **97,** 1 (1955); **98,** 1571 (1955).
[11] R. P. Hudson, "Temperature, its measurement and control in science and industry," vol. II, p. 185 (Rheinhold Publishing Corp., New York, N. Y., 1935).
[12] P. H. Keesom and N. Pearlman, Phys. Rev. **98,** 548 (1955).
[13] D. de Klerk and R. P. Hudson, J. Research NBS **53,** 173 (1954) RP 2530.
[14] R. P. Hudson, Phys. Rev. **88,** 570 (1952).

Washington, November 22, 1955.

"Temperature, its Measurement and Control in Science and Industry, Vol. 2, American Institute of Physics Symposium, 1939, New York City, Rheinhold Pub. Co.

9. PRECISION RESISTANCE THERMOMETRY AND FIXED POINTS

H. F. Stimson

National Bureau of Standards

Introduction

The definition of the International Temperature Scale[1] gives the interpolation formulas relating temperature to the resistance of a standard resistance thermometer. The standard resistance thermometer and formula together provide the means for determining an unknown temperature relative to the ice point temperature from a determination of the ratio of two resistances of the thermometer, one at the unknown temperature and the other at the ice point. Precision resistance thermometry with a standard resistance thermometer, therefore, depends upon the precision and accuracy with which these ratios can be determined.

The standard resistance thermometer is calibrated at the ice, steam, and sulfur points for determinations of temperatures from the ice point to 630°C, and further calibrated at the oxygen point for determinations of temperatures between the oxygen and ice points. The accuracy of resistance thermometry depends fundamentally upon the accuracy with which the fixed-point temperatures can be realized. Precision resistance thermometry therefore requires not only precision measurements of resistances but also accurate realizations of the fixed points when the standard resistance thermometers are being calibrated.

The paper, "Precision Resistance Thermometry," at the temperature symposium held in New York in 1939, was contributed by E. F. Mueller.[2] He mentioned the beginning of precision resistance thermometry in 1887, when Callendar's paper on resistance thermometry was published. He then described the procedures of precision resistance thermometry that were the best practice a half century later. The present paper describes some of the techniques which have been developed in the 15 years since Mueller's paper was written.

At the time of the earlier symposium there had been some studies at the Massachusetts Institute of Technology[3, 11] on the reproducibility of the

steam, sulfur and ice points which are the fixed points for the first resistance-thermometry part of the International Temperature Scale. Recognizing the importance of this work, the National Bureau of Standards began in 1942 to develop apparatus and techniques to improve the accuracy of the realization of all four fixed points which are the basis of both of the resistance-thermometry parts of the scale. The aim was to make the accuracy of realization of these fixed points comparable with the precision of measurement.

Recent Developments in Technique for Precision Determinations of Thermometer Resistances

Measurements of the resistances of platinum resistance thermometers are made with a small electric current flowing in the coils of the thermometers. This small current heats the platinum and raises its temperature above that of the surroundings. The amount which the temperature of the platinum is raised depends upon the construction of the platinum thermometer and often on the environment of the thermometer. For thermometry of the highest precision the effects of this heating must be taken into account.

When the surface of the protecting envelope of the thermometer is in direct contact with a substance which absorbs the heat of the measuring current, the platinum is heated only the amount of the temperature drop to the outside of the envelope itself. This condition might exist when the thermometer is directly in an ice bath or a stirred liquid bath. See Fig. 1. There are times, however, when this heat flows beyond the outside surface of the protecting envelope before it is absorbed. At these times there is a further temperature drop outside the envelope. This condition exists, for example, when the thermometer is being calibrated in a triple point cell (described later). See Fig. 2. In this instance there is a temperature drop from the envelope to the inside wall of the triple-point-cell well through the fluid in the well, usually water. There is a further drop in temperature through the glass of the well to the outside of the well and then another small drop through the film of water outside the well before the heat reaches the water-ice surface where the fixed point temperature is maintained by the liquid-solid equilibrium.

Sometimes the temperature drop from the outside of the thermometer envelope to the temperature of interest may be made smaller by the use of liquids or solids which improve the thermal contact. In the triple point cell, for example, it is convenient to use water in the well of the cell. Water is a much better thermal conductor than air but a free fitting metal bushing occupying most of the space in the water outside the thermometer coil helps a good deal more. In the triple point cell, when 2 milliamperes are

574278 O - 61 - 4

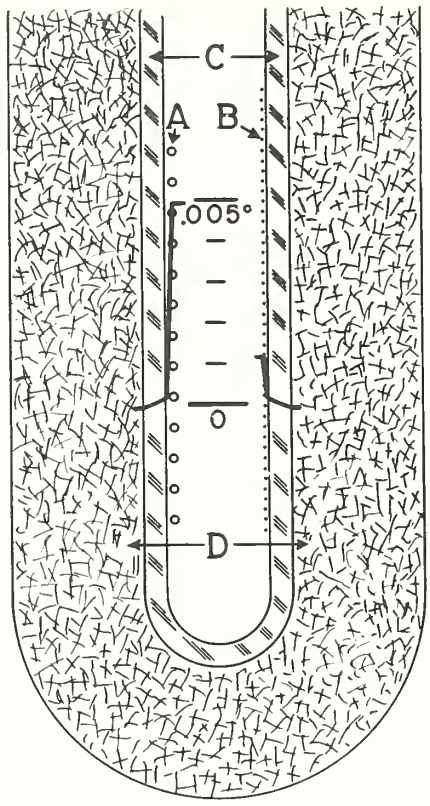

FIG. 1. Thermometers in ice bath. Temperature distribution from axis of thermometer with 2 milliamperes current. A. Platinum coils of coiled filament thermometer; only alternate coils are indicated. B. Platinum of single layer helix thermometer; alternate turns indicated. C. Pyrex thermometer envelope. D. Ice bath.

flowing in the thermometer coils, an aluminum bushing has reduced the temperature drop outside the thermometer envelope from about 0.0008°C to about 0.0002°C. In the benzoic acid cell[4] at about 122.36°C one can not use water, so bushings are of great help. See Fig. 3. In the benzoic acid cells especially, it is wise not to use a bushing much longer than the coils because the upper parts of the cells cool much sooner than the lower parts. Glycerine or oil has been used in the wells of benzoic acid cells to improve the thermal contact, but care must be taken lest these conducting fluids undergo a chemical reaction when they are at these temperatures and thus produce an independent source of energy to cause an erroneous determination of temperature. Obviously a thicker film of a given conducting medium will maintain a greater temperature difference across it.

Inasmuch as the platinum is heated by the measuring current it is necessary to wait till a sufficiently steady state of heat flow is established so that the resistance of the thermometer is constant enough for precision measure-

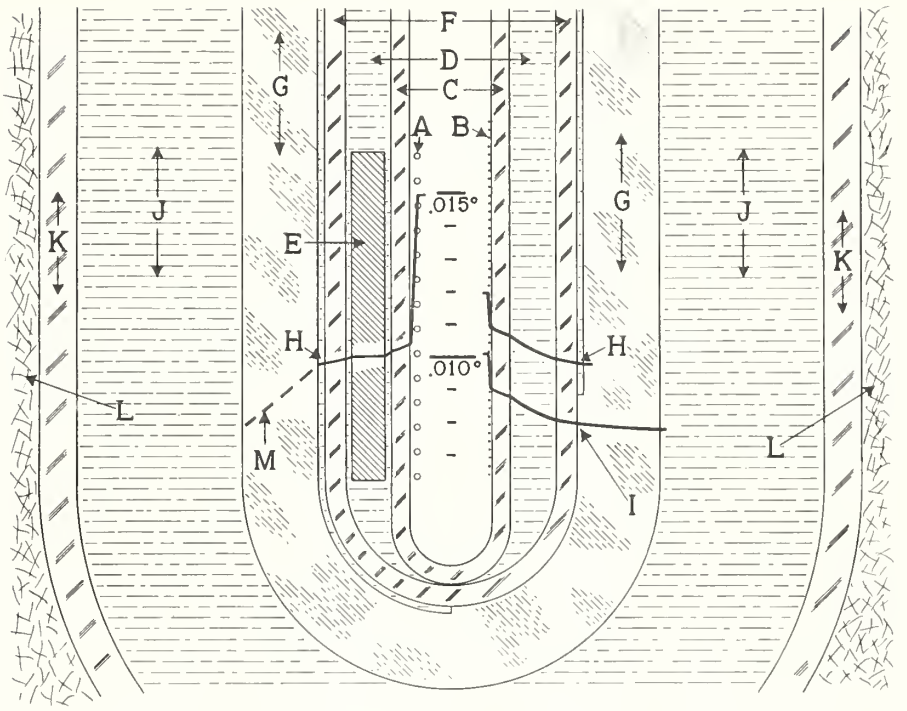

FIG. 2. Thermometers in triple point cell. Temperature distribution from axis of thermometer with 2 milliamperes current. A. Coiled filament. B. Single layer. C. Pyrex thermometer envelope. D. Water. E. Metal bushing. F. Pyrex thermometer well. G. Ice mantle. H. Inner melting. I. No inner melting. J. Water in cell. K. Cell wall. L. Outside ice bath. M. Temperature gradient through mantle.

ments. The time that it is necessary to wait depends upon the temperature rise of the platinum and the various heat capacities and thermal conductivities of the parts of the thermometer and the surroundings that intervene between the platinum and the substance whose temperature is being measured. The approach of the thermometer resistance to the steady state value, therefore, is not a simple exponential function of time. For precision measurements it is necessary to have a continuous current flowing in the thermometer coil and to wait till the resistance of the coil has reached its final value within the desired precision of measurement. Under different conditions this time has been found to range from a half to five minutes.

When the thermometer is to be used for precision measurements of temperature in places where the temperature is maintained beyond the outside boundary of the protecting envelope, the reliable way to make the resistance determinations is to measure the resistances at two different currents and extrapolate to the resistance which it would have if no current were flowing through the thermometer coil. In instances where the highest precision is not demanded the temperature drop outside the thermometer

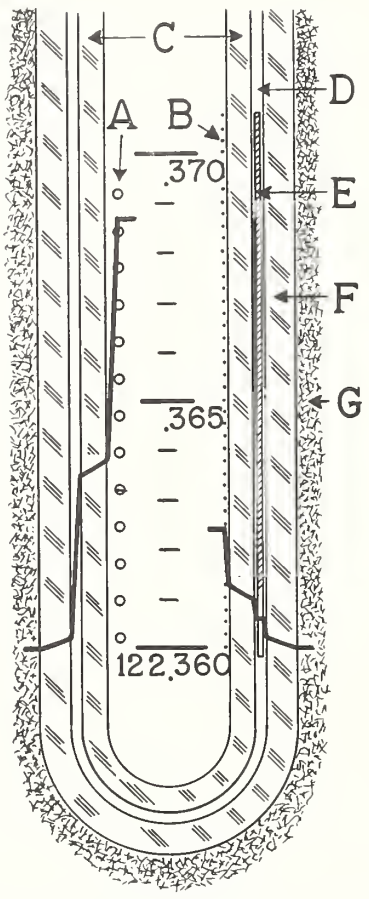

FIG. 3. Thermometers in benzoic-acid cell. Temperature distribution from axis of thermometer with 2 milliamperes current. A. Coiled filament. B. Single layer. C. Pyrex thermometer envelope. D. Air space. E. Metal bushing. F. Well. G. Solid and liquid benzoic acid.

envelope may be small enough to be neglected. For these, the thermometer coefficients obtained with 2 milliamperes in the coils may be used. In the Callendar formula the alpha coefficient for the 2 milliampere current, however, will probably differ from the calibration at zero milliamperes by several units in the sixth significant figure. The delta coefficients will not differ significantly. During the past few years, certificates from the National Bureau of Standards have stated: "The following values were found for the constants in the formula,

$$t = \frac{R_t - R_0}{\alpha R_0} + \delta\left(\frac{t}{100} - 1\right)\frac{t}{100},$$

in which t is the temperature at the outside surface of the tube protecting

the platinum resistor—and R_t and R_0 are the resistances of the platinum resistor at $t°$ and 0°C respectively, measured with a continuous current of 2.0 milliamperes." In some instances, where the user needed to make measurements with higher precision, the alpha coefficients have been determined for the current extrapolated to zero. It is possible, however, as we shall see presently, to compute the difference in the alpha coefficient to a satisfactory approximation from a determination which one can make of the heating effect in an ice bath.

The alpha coefficient is defined by the equation $\alpha = (R_{100} - R_0)/100\ R_0$. When a measuring current (for example 2 ma) is flowing in the thermometer coil the resistances, R_0 and R_{100}, will be increased to $R_0 + \Delta R_0$ and $R_{100} + \Delta R_{100}$. If we now call α_Δ the apparent alpha coefficient, at this measuring current, then

$$\alpha_\Delta = \frac{(R_{100} + \Delta R_{100}) - (R_0 + \Delta R_0)}{100(R_0 + \Delta R_0)}$$

Performing the division indicated by the fraction we can write the equation in the form

$$\alpha_\Delta = \frac{R_{100} - R_0}{100R_0} + \frac{\Delta R_{100} - (R_{100}/R_0)\Delta R_0}{100(R_0 + \Delta R_0)} = \alpha + \frac{\Delta R_{100} - (R_{100}/R_0)\Delta R_0}{100(R_0 + \Delta R_0)}$$

With any given measuring current, the power dissipated in a coil is proportional to its resistance, so at 100° the power dissipated is greater than the power dissipated at 0° by the ratio R_{100}/R_0. At 100°, however, the thermal conductivity of air is 30 % greater than at 0° and the thermal conductivity of Pyrex glass is 13.5 % greater. In thermometers of widely different construction the part of the temperature drop through glass from the platinum to the outside of the protecting envelope tube may range from 5 % to 15 % of the total drop. Although radiation from the platinum is a few times greater at 100° than at 0° it probably accounts for less than 1 % of the heat transfer. The temperature drop from the platinum to the thermometer envelope tube, therefore, is predominantly through air so if we select the value, 1.29, for the ratio of the average coefficient of heat transfer at 100° to that at 0° our computations probably will not be in error by more than one or two percent. We can, therefore, take $\Delta R_{100} = \Delta R_0(R_{100}/R_0)/1.29$. Since the value R_{100}/R_0 is about 1.392 we can write

$$\alpha_\Delta = \alpha + \frac{1.392\Delta R_0(1/1.29 - 1)}{100(R_0 + \Delta R_0)} = \alpha - \frac{0.313\Delta R_0}{100R_0} \text{ approximately.}$$

For two milliamperes current the values of ΔR_0 for two widely different thermometers were found to be 460 microhms and 125 microhms respectively. The corresponding values for $\alpha - \alpha_\Delta$ are 53×10^{-9} and 15×10^{-9}

respectively. We can get the significance of these values when we consider that 39×10^{-9} for $\alpha - \alpha_\Delta$ is equivalent to 0.001° in 100°, hence for these thermometers the values for $\alpha - \alpha_\Delta$ are equivalent to about 0.0014° and 0.0004° in 100° respectively. For one milliampere these values would be reduced by a factor of four.

In striving for a precision of a few microhms in the determination of the resistance extrapolated to zero current it is necessary to control carefully the ratio of the currents used for the measurements and to consider the variance of the measurements at each of these currents. Thermometers having larger heating of the platinum at a given current require greater precision in the determination of the ratio of the two currents. Ordinary milliammeters are not sufficient for the highest precision and an auxiliary potentiometer for setting the current is desirable. When using these measurements for extrapolation to zero-current determinations it will be shown that precision in the resistance measurements at the lower current is more important than precision in the measurements at the higher current. Statistical theory shows that

$$s_Y^2 = \left(\frac{x_2}{x_2 - x_1}\right)^2 s_{\bar{y}_1}^2 + \left(\frac{x_1}{x_2 - x_1}\right)^2 s_{\bar{y}_2}^2$$

where s_Y^2 is the estimate of the variance of the zero-current resistance, $s_{\bar{y}_1}^2$ and $s_{\bar{y}_2}^2$ are the estimates of the variance of the means of the lower and the higher-current resistances respectively, and x_1 and x_2 are proportional to the power (current squared) put into the thermometer coils at the lower and higher currents respectively. The values of $s_{\bar{y}_1}^2$ and $s_{\bar{y}_2}^2$ can be determined by experiment.

It sometimes happens that $s_{\bar{y}_1}^2$ is greater than the $s_{\bar{y}_2}^2$ because the lower current is so small that the deflections of the balancing instruments are more difficult to detect. At different periods in the past we have used currents ranging from 1 and 1.41 ma to 2 and 7.5 ma but with the instrumentation used at the National Bureau of Standards it was found that the optimum value of $s_{\bar{y}_1}^2$ was for currents of about 2 ma. With higher currents the amount of the extrapolation to the zero-current resistance is greater and the determination of the ratio of the high to the low current is more important. A potentiometer of moderate precision should be sufficient, but the higher the current the more attention has to be given to the control of the current.

Let us assume that n observations are to be made to determine the resistance at zero current and of these n_1 are at the lower current and n_2 are at the higher. Having determined the estimates $s_{\bar{y}_1}^2$ and $s_{\bar{y}_2}^2$ by experiment we can choose the proportion of the observations that should be made at the two currents in order to get the smallest value for s_Y^2. Again using sta-

tistical theory, we find

$$\frac{n_1}{n_2} = \frac{x_2 s_{\bar{y}_1}}{x_1 s_{\bar{y}_2}}$$

approximately. As an example let us assume that the currents are 2 ma and 5 ma. Then if we take, for simplicity, $s_{\bar{y}_1} = s_{\bar{y}_2}$ we have $n_1/n_2 = {}^{25}\!/\!_4$ which is the ratio of the number of observations which must be made at x_1 to those at x_2 in order to get the best results. As another example let us assume with these same currents that $s_{\bar{y}_1} = 3s_{\bar{y}_2}/2$. We then have $n_1/n_2 = {}^{25}\!/\!_4 \times {}^{3}\!/\!_2 = {}^{75}\!/\!_8$. In both of these examples it is evident that many more observations should be made at the lower current than at the higher in order to obtain the best precision with a given time spent in observing.

Thermometer Developments

In his symposium paper in 1939, Mueller mentioned the coiled filament thermometer construction described by C. H. Meyers.[5] The purpose of this construction was to confine the resistor of the thermometer to a shorter length and a smaller diameter than had been thought practical for standard thermometers before. About 25.5 ohms at 0°C of 0.087 mm wire are wound in a helix about 0.4 mm in diameter. This helix, in turn, is bifilar wound in a larger helix about 20 mm long which is supported on a mica cross within a Pyrex protecting tube ranging from 7 to 7.5 mm outside diameter. Gold leads extend up the protecting tube about 43 cm to a head where the leads pass through a hermetic seal to copper leads.

In 1943 there came to the author's attention some other small thermometers which were made in Russia. These thermometers were intended for measurements of temperature in a range extending up to temperatures which are too high for mica to be used for supporting the coils. The resistor has a resistance of about 10 ohms at 0°C and is wound in a helix of about 0.6 mm in diameter. This helix is supported bifilarly on opposite sides of a twisted silica ribbon and the coils extend about 40 mm. The coils are enclosed in a fused silica protecting envelope of about 6 mm outside diameter. Platinum leads extend up to a head corresponding to that of the Meyers-type thermometers.

A platinum thermometer of small dimensions was described by C. R. Barber[6] of the National Physical Laboratory in 1950. Some of these thermometers had a resistance of about 28 ohms at 0°C. They were made of 0.05-mm wire wound, while hard drawn, on a 1-mm mandrel and supported inside a fine Pyrex tube of 1.5-mm inside diameter and 0.2-mm wall thickness. The fine tube is bent into the form of a U, the helix is held in place by fusing at the bottom of the U and 0.2-mm platinum extensions of the helix are sealed into the top of the U. The coils are in a space over 30 mm

long. At the top of the U the platinum leads are fused to 0.5-mm gold leads which extend up to a head as in the other small thermometers. A 6-mm outside diameter Pyrex protecting envelope encloses the leads and the U with the enclosed coils.

These three small thermometers which were developed within the last 25 years have proved their superiority for measuring temperatures in smaller diameter spaces than was heretofore possible. This superiority over the older type, however, has been somewhat offset in some of these small thermometers by the disadvantage that the platinum temperature is not as near the temperature of the outside of the protecting envelope. To be sure, the resistance at any temperature can be extrapolated to that at zero current, as we have seen; but the precision of this extrapolation does depend upon the amount to be extrapolated. In using these small coils some of the parts of the helices are several diameters of the wire away from the wall of the protecting envelopes, and furthermore the area through which heat flows to the protecting envelope is smaller in this type than it was in the older types. Meyers recognized this disadvantage in his coiled filament type of thermometer and developed another type to correct it. About 1943 he began making thermometers of this new design using 0.077-mm wire wound in a single-layer bifilar helix 22 mm long with the wire only 0.03 or 0.04 mm away from the inside wall of the protecting envelope. The helix is supported on a mica cross in U-shaped notches spaced about 0.25 mm on centers. The notches are about 1.5 diameters of the wire deep and just wide enough to allow freedom for the wire to adjust itself with a minimum of constraint. Gold leads 0.2 mm in diameter extend up the envelope to the head. In this type of construction the thermal contact of the wire with the envelope is so good that, when a current of 2 ma is in the coils, the temperature rise of the wire above the outside of the protecting envelope is less than 0.002°. In the other types of small thermometers, described above, the temperature rise ranges from 2 to 4 times as great.

One effect which must be guarded against in precision thermometry is the effect on the resistance of the thermometer coil caused by heat conduction along the leads. This effect is easily determined by experiment. One procedure is to pack the thermometer in a slush of ice and water till the ice is just above the coil of the thermometer. The resistance of the coil is then measured. Packing more ice up around the stem of the thermometer to increase the depth of immersion will change the resistance of the coil. This process is continued till further packing does not change the resistance by a significant amount. A plot of these data on semi-log paper shows the immersion necessary for the precision desired.

Thermometers with heavy gold leads in poor thermal contact with the envelope obviously will require greater immersion than those with light

platinum leads near the envelope wall. The immersion necessary to reduce the effect to within the equivalent of 0.0001° on some of the small thermometers described above ranged from 11 cm to 26 cm from the ends of the protecting envelopes. Usually there is provision for sufficient immersion so that the lead conduction will produce no significant error in the determination of temperature, but this effect must be kept in mind for precision temperature determinations. Some special thermometers have been constructed where special attention was paid to thermal contact of the leads with the envelope wall in order to make the necessary immersion very small. Ordinarily this precaution is not demanded.

Thermometers for calorimetry at temperatures below the oxygen point are made of the coiled filament type and enclosed in platinum capsules, 5.5 mm in diameter and 48 mm long. When in use, these thermometers are usually soldered into the calorimeters with low melting solder so heat conduction outside the protecting envelopes is seldom a problem. Platinum leads are sealed through glass which covers the end of the platinum capsule. At the sulfur point, however, the glass seals become conducting and increase the difficulty and uncertainty of the calibrations at that temperature. The electrical conduction in the glass insulation of these resistance thermometers has been discussed by H. J. Hoge.[7] In order to have thermal contact of the platinum wire with the envelopes of these thermometers at temperatures ranging down to near 10°K these capsules are filled with hydrogen-free helium containing some oxygen.

In Mueller's paper in 1939[2] there was a speculation about the changes in the coefficients of a thermometer accompanying progressive changes in ice-point resistances. He stated "The changes of resistance which occur in the resistor of the thermometer are likely to be additive. Changes which affect the resistance of the thermometer at all temperatures in the same proportion are less likely to occur." This is to say $R_{100} - R_0$ was expected to be more constant than R_{100}/R_0. Since that time we have some evidence, with thermometers made of high purity platinum, that the ratio R_{100}/R_0 remains constant within our precision of measurement even when the resistance of the thermometer at 0°C does increase by significant amounts. There is also some confirming evidence of this from other national laboratories. It appears, therefore, that changes affect the resistance of thermometers proportionally at all temperatures when the thermometers are of high purity platinum and well annealed.

R. J. Corruccini,[8] on the other hand, has shown that rapid chilling of platinum does cause changes which are more nearly additive. He attributes these changes to strains set up by the chilling because reannealing restores the platinum to the old condition. In general, however, it seems unlikely that standard resistance thermometers in protecting envelopes could be

subjected to such drastic chillings as he was able to give to his platinum. We conclude, therefore, that additive changes are not likely in standard thermometers.

Bridge Developments

Since Mueller's paper[2] in 1939 two new bridges have been designed and constructed, and are being used for precision resistance thermometry. One is an improved Smith Bridge that is in use at the National Physical Laboratory. Since this bridge is described elsewhere[9] it will not be discussed here. The other is a bridge which Mueller, using his many years of experience, designed after his retirement from the National Bureau of Standards. Prototypes of this design were delivered to the Bureau in 1949. Since an extensive description of this bridge is not in prospect in the near future a brief description will be given here.

The intention of the design of this bridge was to make measurements possible within an uncertainty not exceeding two or three microhms. This bridge has a seventh decade which makes one step in the last decade the equivalent of ten microhms. One uncertainty which was recognized was that of the contact resistance in the dial switches of the decades. Experience shows that with care this uncertainty can be kept down to the order of 0.0001 ohm. Switches made with well-planed copper links bridging well-planed copper posts and making contact with an excess of mercury, have uncertainties of contact resistance of considerably less than one microhm.

Iu Mueller's design the ends of the equal-resistance ratio arms are at the dial-switch contacts on the one ohm and the tenth ohm decades. He has made the resistances of the ratio arms 3000 ohms so that the uncertainty of contact resistance, 0.0001 ohm, produces an uncertainty of only one part in 30,000,000. With 30 ohms, for example, in each of the other arms of the bridge, these two ratio-arm contacts should produce an uncertainty of resistance measurement of 1.41 microhms. The next largest uncertainty would appear to be in the hundredth ohm decade which has the largest steps of four Waidner-Wolff elements. In the zero position of this decade the 0.0001-ohm uncertainty in contact resistance is part of a shunt of over 20 ohms and produces an uncertainty of 0.4 microhm.

The 10-ohm decade has mercury contacts and the commutator switch has large mercury contacts. One new feature in the commutator switch is the addition of an extra pair of mercury-contact links which serve to reverse the ratio coils simultaneously with the thermometer leads. This feature was suggested by Hoge, who was then at the National Bureau of Standards. This feature automatically makes the combined error of the normal and reverse readings only one in a million, for example, when the ratio arms are unequal by as much as a part in a thousand, and thus prac-

tically eliminates an error from lack of balance in the ratio-arms. It does not eliminate any systematic error in the contact resistance at the end of the ratio arms on the decades, however, because the mercury reversing switch has to be in the arms.

The commutators on these bridges are made so as to open the battery circuit before breaking contacts in the resistance leads to the thermometer. This makes it possible to lift the commutator, rotate it, and set it down in the reversed position in less than a second and thus not disturb the galvanometer or the steady heating of the resistor by a very significant amount. In balancing the bridge, snap switches are used to reverse the current so the heating is interrupted only a small fraction of a second. This practice of reversing the current has proven very valuable. It not only keeps the current flowing almost continuously in the resistor but also gives double the signal of the bridge unbalances.

In striving for greater precision in resistance thermometry we may ask what our limit is. One limit which we cannot exceed is that imposed by the Johnson noise which exists in all resistors. The random voltage in resistors at 300°K is given by the formula $\delta V = 1.12 \times 10^{-10}\sqrt{R/\tau}$ where R is the resistance in ohms and τ is the time in seconds over which the voltage is averaged. The quantity, τ, could, for example, be the time constant of the galvanometer. From this formula it would appear that the magnitude of the Johnson noise in a circuit including an instrument having a one-second period would be of the same order of magnitude as an unbalance of 1 microhm in the measuring arm of a bridge when one milliampere was flowing in a 25-ohm thermometer. In practice there seems to be a discrepancy between this limit and what we realize. We have found that for a net time of over a minute of observing, for observations at 1.5 and 2.5 ma to extrapolate to zero current, the determinations of the resistance of thermometers in triple point cells have a standard deviation of a single determination of about 8 microhms. We have not yet been able to attribute this discrepancy either to the bridge, the thermometer, the galvanometer, the triple point cell, or the observer and it remains one of the unsolved problems of precision resistance thermometry.

Fixed Points

For the calibration of platinum resistance thermometers on the International Temperature Scale four equilibrium fixed points are defined, one of which is a freezing point and the others are boiling points. To realize these fixed points it is assumed that it is better to strive for realizations of the definitions rather than to follow recommended procedures which were set up as standard practice in the past. At the National Bureau of Standards the triple point of water sealed in cells is used exclusively to derive the ice

point. The boiling points of sulfur and water are realized by active ebullition in boilers connected to a pressure-controlled reservoir of helium. The pressure of the helium is controlled manually by means of a precision manometer to give one atmosphere pressure at the level of the thermometer coils. The boiling point of oxygen is realized in an apparatus which contains saturated liquid oxygen and its vapor at one atmosphere pressure. The oxygen is separated from the helium of the reservoir by a thin metal diaphragm which indicates the balance between the oxygen and helium pressures.

Triple Point of Water

At the General Conference on Weights and Measures in 1948 the following resolution was adopted:

"With the present-day technique, the triple point of water is susceptible of being a more precise thermometric reference point than the 'melting point of ice'.

"The Advisory Committee considers, therefore, that the zero of the thermodynamic centigrade scale should be defined as being the temperature 0.0100 degree below that of the triple point of pure water."

The triple point of water has been realized for the past several years in glass cells of about 5 cm in diameter with reentrant coaxial walls for the thermometers about 39 cm long and 1.3 cm in inside diameter. Figure 4 shows a sectioned drawing of a triple point cell in an ice bath. Extending up from the cell is a tube which is sealed off above the cell after filling with gas-free distilled water. Below the sealing-off point is a side tube, extending horizontally which serves as a handle for lifting and turning the cell and also for supporting the cell when it is packed in a bath of flaked ice and water.

After the cells are blown and annealed they are cleaned with acid and distilled water and then steamed for several days until the condensed steam on the walls runs down in a continuous film over the entire inner surface. They are then connected to a still which removes 99.9 per cent of dissolved gases from distilled water. They are evacuated and filled with water to within about 2 cm of the top and sealed off.

To prepare the cell for measurements it is first immersed into an ordinary ice bath for several minutes to cool the cell and its contents. A mantle of ice from 3 to 10 mm thick is then frozen onto the outside of the well. One procedure for freezing the ice mantle is to dry the well and keep it filled with crushed dry ice (solid CO_2) until the ice mantle is thick enough. This procedure takes about thirty minutes. When the cooling with dry ice is first started it may take a minute or more to initiate freezing. Crystals first appear as fine needles along the outside of the well. As cooling is continued these initial needle crystals disappear and a clear glass-like mantle builds

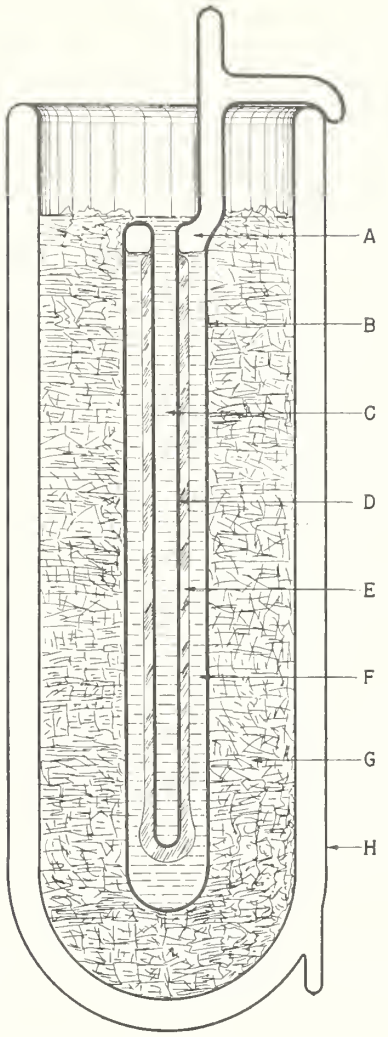

FIG. 4. Triple point cell. A. Water vapor. B. Pyrex cell. C. Water from ice bath. D. Thermometer well. E. Ice mantle. F. Air-free water. G. Flaked ice and water. H. Insulated container.

up. When sufficient ice has been frozen on the well, the dry ice is withdrawn from the well and the cell immersed below the water level in the ice bath so that ice-cold water fills the well in order to improve the thermal contact of the thermometer with the water-ice interface.

The process of freezing purifies the water and concentrates the impurities in the water ahead of the ice as it forms on the outside surface of the ice mantle. These concentrated impurities lower the temperature on the outside mantle surface by a significant amount unless the water was very pure before freezing. If, now, a warm tube is immersed into the well for a few

seconds, enough of the pure ice next to the well will be melted to free the mantle and provide a new water-ice interface. It is easy to see when the ice mantle is free by giving the cell a quick rotation about the axis of the well and noting whether or not the mantle rotates with the cell. This new water-ice surface provides the temperature for calibrating thermometers. See Fig. 2.

This procedure of inner melting is believed to be very valuable for obtaining reproducibility of temperature. We have seen that freezing purifies the sample from the well outward and that the inner melting produces liquid from ice which is much purer than the water outside the mantle. This means that less effort has to be expended in preparing and filling the cells than would be necessary if other procedures for freezing were used. Experience shows that the *inner* melting procedure, in the cells at the National Bureau of Standards, provides temperatures which are as identical to each other and as reproducible as we are now able to differentiate temperatures, namely, within about 0.00008°C.

Temperatures at the *outside* of thick mantles in some cells about two years old, on the other hand, were found to be about 0.002° low, when first determined within a half hour of freezing, but were rising for several hours thereafter. These low temperatures are believed to be caused by impurities (including dissolved glass) and the rising temperatures by diffusion of the concentrated impurities away from the outside surface of the mantle into the water. The lower temperature at the outside of the mantle causes no error when the inner melting technique is used. Small transfers of heat caused by radial temperature gradients merely cause freezing or melting at the water-ice interfaces and do not change the temperature by significant amounts.

Previous investigators have frozen the water in their triple point cells by supercooling until spontaneous freezing fills the cells with mush ice. When the water in these same NBS cells was spontaneously frozen, the temperatures were a few ten-thousandths of a degree low, presumably due to impurities. This result again emphasizes the value of the simple inner-melting technique for obtaining reproducible temperatures.

Precision Manometer

The precision manometer at the National Bureau of Standards was designed for precision gas-thermometer measurements. The apparatus consists of two large cells for mercury surfaces connected by an articulate tube and supported on a base by long and short columns of end standards. The aim in the design was to make this manometer capable of determining pressure to an accuracy of one part in a million but this accuracy is not demanded by present-day precision thermometry. Fig. 5 shows a scale di-

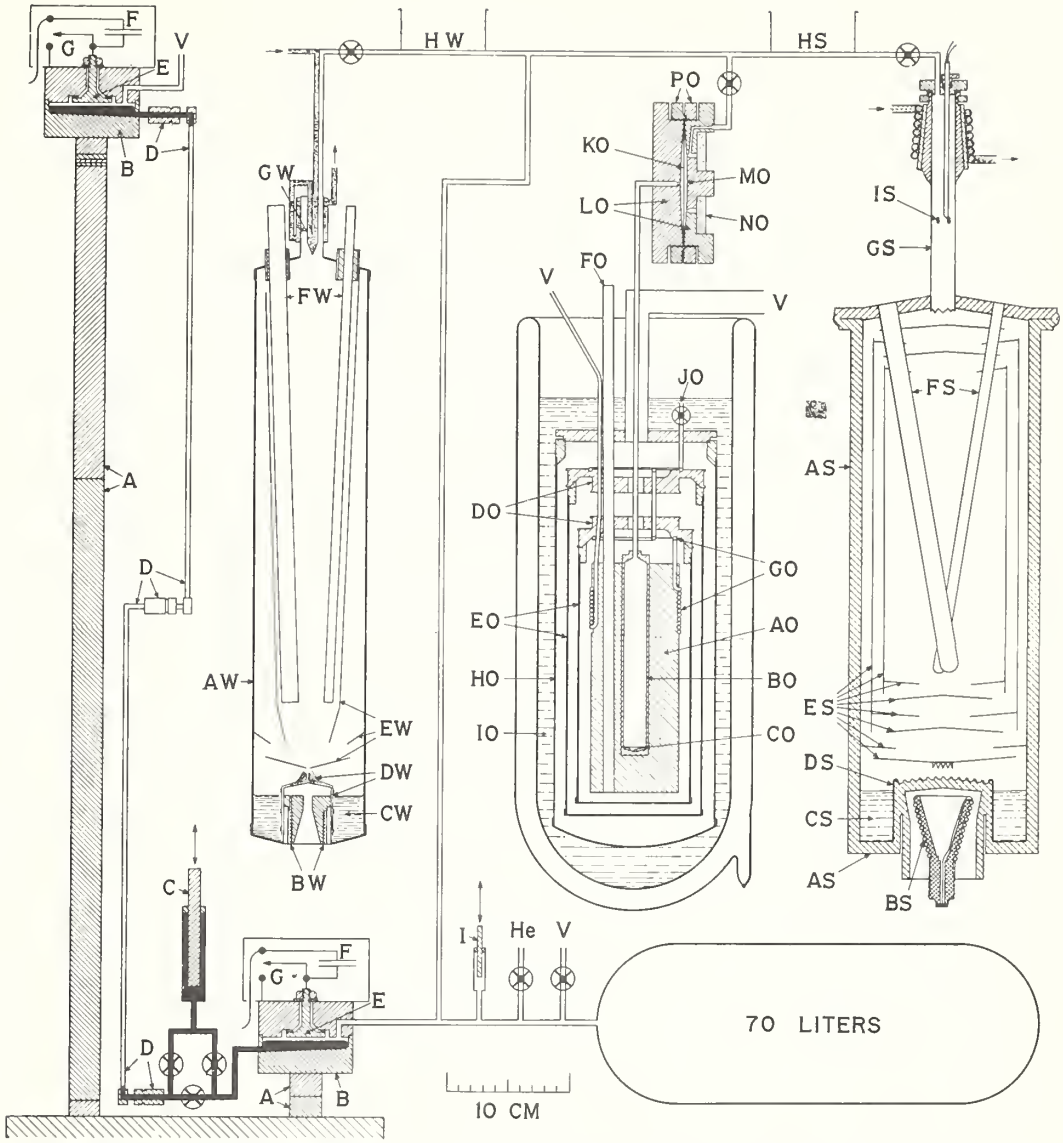

FIG. 5. Manometer: A. Hoke blocks. B. Mercury cell. C. Mercury pump. D. Articulate tube. E. Insulated capacitor plate. F. Reference capacitor. G. Pneumatic switch. H. Helium supply. I. Helium pump. V. Vacuum line.

Steam point boiler: AW. Boiler wall, tinned copper. BW. Heater. CW. Liquid water. DW. Layer of silver wires. EW. Radiation shields. FW. Thermometer wells. GW. Water vapor condenser. HW. Dry ice trap.

Oxygen point apparatus. AO. Copper block. BO. Oxygen bulb. CO. Liquid oxygen. DO. Heat interceptors. EO. Radiation shields. FO. Thermometer well. GO. Cooling tubes. HO. Envelope. IO. Liquid nitrogen. JO. Liquid nitrogen inlet for cooling. KO. Metal diaphragm. LO. Diaphragm cell wall. MO. Insulated island. NO. Glass insulator. PO. Clamp for diaphragm. V. Vacuum lines.

Sulfur point boiler. AS. Boiler wall, aluminum. BS. Radiant heater. CS. Liquid sulfur. DS. Layer of aluminum wires. ES. Radiation shields. FS. Thermometer wells. GS. Sulfur vapor condenser. HS. Dry ice trap. IS. Feeler thermocouple.

agram of the manometer at the left connected to the steam point boiler, the oxygen point apparatus, and the sulfur point boiler.

The pressure which is measured with this manometer is balanced by a column of mercury. Pressure is the product of the height of the column multiplied by the density of the mercury and by the gravitational acceleration. It is believed that the height of the column can be determined with this apparatus to the accuracy of calibration of the end standards, which heretofore has been about two parts in a million. The value of the density of mercury at 0°C, according to recent reports, may be uncertain to one or two parts in 100,000 but it is the opinion at the National Bureau of Standards that differences of more than about four parts in a million are not to be expected between different samples of virgin mercury, gathered anywhere on the earth. The value for the gravitational acceleration may be uncertain by nearly one part in 100,000 but values relative to the value determined at Potsdam are known with high precision. For these reasons it is believed that the reproducibility of the steam point in different laboratories could be in the order of 0.0001°C, inasmuch as this corresponds to about four parts per million in pressure.

The principal features of this manometer, which make such precision possible, are the large cells for the mercury surfaces to eliminate the uncertainties of capillary depression, an electrostatic capacitance scheme for determining the height of the mercury surface, and the use of end-standards 2.4 cm square for supporting these cells.

The mercury cells are about 7.3 cm in inside diameter. They are made of steel with the tops and bottoms about 2 cm thick, which is thick enough to prevent a significant flexure by a change of pressure of one atmosphere. A steel tube about 3 mm inside diameter permits mercury to flow from one cell to the other. To permit raising the upper cell to the desired height, this tube has three joints with horizontal axes, referred to as the "shoulder," "elbow," and "wrist" joints.

Both cells are supported on a cast iron base by Hoke gage blocks which are end-standards as precise as the better-known Johansson blocks, but, being square, are more suitable as columns for supporting the cells. The ends of these blocks are accurately parallel. The columns of blocks are 18 cm apart at the base. One block is fastened securely to the bottom of each cell and another block is fastened securely to the base at the bottom of each column. The two blocks under the lower cell are seldom moved but the intermediate blocks in the column supporting the upper cell are changed every time the length of the column is changed. The top surface of the supporting block for the upper cell was carefully leveled. The set has enough blocks to permit a column of blocks to be selected having a nominal height of any desired ten-thousandth of an inch. Blocks of this type can be wrung

together with a separation of less than a hundredth of a micron. In 14 years the blocks have been calibrated a few times at the National Bureau of Standards and none has changed for more than four parts in a million.

Above the mercury there is an electrically insulated steel plate 3.5 cm in diameter for determining the height of the mercury in the cells. The electrostatic capacitance between the plate and the mercury is part of the capacitance in one of the two circuits of a beat frequency oscillator. In a shielded chamber above the cell is a reference capacitor which is adjusted so that its capacitance is equal to the capacitance between the plate and the mercury for the desired height of the mercury. A pneumatic mercury switch permits the interchange of these two capacitors in a few seconds. It has been found convenient to have the spacing of the mercury from the plate about 0.15 mm. At that height, a change of pressure of one micron changes the capacitance by 0.2 $\mu\mu$f which changes the beat frequency by 60 cycles; hence the manometer is sensitive to much less than 0.1 micron of mercury pressure.

Ripples are always present on the surface of the mercury in a cell of this diameter (7.3 cm) at any place within the National Bureau of Standards. Their wavelength is small in comparison with the radius of the plate and the effect of the crests of ripples compensates for that of the troughs. No effect of these ripples on the capacitance is noticeable until the mercury approaches to within 0.1 mm of the plate.

It is obvious that temperature control is important not only for the length of the steel blocks but especially for the density of mercury. The combined effect is such that a change in pressure of one part in a million is produced by a change in temperature of about 0.006°C. To provide for temperature control the manometer is mounted on a low pier in a cellar below the basement floor where temperature fluctuations are minimized. The cellar is about 4.5 meters deep, 4.3 meters long and 2.1 meters wide. The manometer is operated by remote control. The air is circulated in the cellar and the relative humidity reduced below 50 per cent by passing it over refrigerated coils and reheating it.

At the base of the manometer a platinum resistance thermometer is placed in a copper block. On the surface of this block are placed reference junctions of three sets of multiple-junction thermocouples for determining the mean temperature of three different parts of the mercury column. There are twelve measuring junctions in series on the manometer arm from the shoulder to the wrist joint, six junctions on the tube from the lower cell down to the shoulder joint, and three junctions from the wrist joint up to the upper cell. These provisions make it possible to determine the mean temperature of the mercury itself and, should the temperature not be the same on the tubes to the upper and lower cells, the difference in density can be accounted for. The temperature of the manometer ordinarily drifts only a

574278 O - 61 - 5

few hundredths of a degree per day. This rate is so small that occasional measurements taken during the day are sufficient for corrections. The temperature of the blocks is assumed the same as the mean temperature of the mercury.

The procedure for obtaining the desired pressure by means of the height of mercury column is, first, to determine the "zero level," and then to increase the height of the upper cell by the height of the desired column. For the zero level, the proper blocks can be found and the reference capacitance made equal to the mercury capacitance on each cell when both cells are evacuated. When this equality of capacitances is again realized, with pressure in the lower cell and with the upper cell still evacuated, the height of the mercury column is the same as the extra height of blocks added to the upper cell column.

Since the two columns of gage blocks are spaced 18 cm apart it is important to know whether they maintain their relative heights. For this reason the zero level of the manometer has been followed for several days before and after the time when the manometer is used at one atmosphere. Experience shows that the drift in zero level is less than one micron. The effect of the change of level caused by the extra weight of 30 inches of gage blocks (about 3.4 kg) was determined experimentally and found to be about 0.2 micron. The compression of the 30 inches of gage blocks by half the weight of these blocks and by the weight of the cell with its mercury contents was found to be about 0.3 micron. These effects are small but are accounted for.

To control the pressure of the helium there are needle valves for admitting or removing helium from the lines. Small changes in the helium pressure are controlled by a piston about 0.75 cm^2 cross section area which can be moved in or out of a small chamber in the helium line at the control bench, 4.5 meters above the manometer. The piston is moved by a screw of such pitch that one turn changes the volume connected to the helium line by about one part in a million. The helium pressure may be affected by small drifts in the temperature of the 70-liter reservoir or by larger and more rapid changes in the temperature of the tubes above the floor. The pressure changes are indicated by the beat frequency oscillator and usually are so small they can be compensated for by a fraction of a turn of the piston screw. Such sensitive control of pressure enables the operator to keep the pressure controlled to within a part in a million for as long a time as is needed for thermometer calibrations.

Steam Point Boiler

The steam point apparatus is a closed system with helium gas transmitting the water vapor pressure to the precision manometer. See Fig. 5.

The boiler is made of copper heavily tinned on the inside to prevent contamination of the water. It is made of a tube 8.7 cm in diameter and 46 cm long, closed at the ends. There are six reentrant thermometer wells 35 cm long extending from the top cap down into the vapor space. These wells are of various diameters of thin-wall copper-nickel tubing which is also tinned on the surface exposed to the water. These wells are separated where they extend through the top but at the bottom they are as close together as is convenient without touching. Surrounding the wells is a conical radiation shield of tinned copper which is sufficiently open at the top and bottom for free passage of vapor around the wells.

At the bottom of the boiler there is a reentrant copper-nickel heater dome with a shallow conical cap at the top. Inside this dome is a heater, wound on mica on a copper spool which is enlarged at the top for a short length for soldering into the reentrant dome. By this construction most of the heating power is supplied in a zone just below the surface of the water in the annular space at the bottom of the boiler surrounding the heater dome. On the outside of the heater dome is a single layer of closely spaced vertical silver wires about 0.4 mm in diameter. These wires are bound to the surface with three horizontal hoops of silver wire. The vertical silver wires extend from the bottom of the dome to about 2 cm above the top of the dome and there the ends are brought together in a bundle around the axis. This construction was adopted for the purpose of holding a small residual of vapor in the cusp-shaped spaces between the dome and the wires, to avoid explosive vaporization. It has proven most effective.

Below the radiation shield around the thermometer wells are two shallow conical shields which serve to prevent direct radiation from the walls to the outside walls of the boiler and also serve to drain condensed water from the boiler wall to the axis where it drips onto the bundle of silver wires at the top of the dome. By this construction it is believed that these wires are kept wet continually during operation and there are no exposed surfaces at temperatures above the saturation temperature.

Since the temperature of the boiler is about 75° above that of the room, considerable heat flows out through the boiler wall. This heat is supplied on the inside of the boiler by condensation of the water vapor to liquid which flows down the wall in a film computed to be 0.05 mm thick. Assuming the liquid-vapor surface to be at the saturation temperature there is a temperature gradient through the liquid film so that the inside wall of the boiler is probably less than 0.1 degree below the saturation temperature. Since the boiler is a little below the saturation temperature, the radiation shield radiates a small amount of energy to the boiler most of which it receives by condensation of vapor on both its inner and outer wall surfaces. The radiation shield, therefore, is nearer to the saturation tempera-

ture than the wall of the boiler is by a factor of several hundred. The wells, in turn, radiate heat to the radiation shield; but, since the temperature of the radiation shield itself is very near the saturation temperature, the wells certainly should be at the saturation temperature within our precision of temperature measurements. Indeed, computations indicate that there might have been sufficient attenuation by the wells alone but the radiation shields provide enough more attenuation so there can be little chance that the wells containing the thermometers are at a temperature that is significantly low.

From the top of the boiler the excess vapor flows up through a short tube, about 1.8 cm inside diameter, to a condenser which starts above the boiler. The condenser is cooled by ice-cold water first flowing in a core on the axis and then in a water jacket on the outside of the 1.8-cm tube. The inner and outer water-cooled surfaces are about 3.7 cm long. This construction provides an annular space with a radial separation of about 0.4 cm for the vapor to flow through on its way to the cold walls where it is condensed to liquid. In this space the water vapor meets helium from above. The level of this water-vapor to helium interface depends on the amount of excess water vapor that must be condensed. The area over which condensation is taking place is determined by the temperature of the metal, the thickness and thermal conductivity of the liquid film, and the power flowing through this film. The liquid-vapor surface may be assumed to be at the saturation temperature.

Above the condenser, the helium extends up in a tube which is soldered to the incoming cold water tube. At this place there is a shut-off valve. From the valve the helium line extends in a 0.5-cm horizontal tube that is soldered to a copper tray for dry ice (solid CO_2) and then down to the manometer and a 70-liter helium reservoir on the pier in the cellar.

The radiation shields and wells in the boiler provide such effective protection against a temperature that is too low, that the question arose whether or not the wells might be superheated by the measuring current in the thermometers and the temperature be above the saturation temperature. To test this, two strips of silver gauze were placed so that one drains the liquid from the axial condenser surface to the surface of one well and the other drains the liquid from the outer condenser surface to another well. Thermometers interchanged from these wells to wells without draining have, so far, failed to indicate any difference in temperature depending on the wells. This indicates not only that the liquid film running down the wells has approached the saturation temperature but also that no superheating exists on the other wells.

On the outside the boiler is insulated by two coaxial radiation shields made of aluminum-coated paper and these are enclosed in a metal cover.

This construction furnishes enough thermal insulation so that only about 70 watts of power are necessary to maintain the boiler at 100°C. The power in excess of 70 watts goes to maintaining a flow of vapor into the condenser where it meets the helium. It is common practice to use 125 watts in the boiler at the steam point.

Since the steam point is defined as the temperature of equilibrium between liquid and its vapor at 1 atmosphere pressure it is necessary to determine this pressure at the height of the center of the thermometer coils when they are in the wells. The accounting for pressure considers the fluid heads of columns of water vapor, helium, and liquid mercury at their respective temperatures and the saturation pressure of mercury vapor at the upper cell temperature.

Increasing the power input to the boiler increases the flow of water vapor into the condenser and raises the helium because more surface is required for condensation of the water vapor. This increases the pressure a little because the head of water vapor is greater than that of helium. The more noticeable change, however, is the volume of helium which must be withdrawn from the system to maintain the pressure constant.

Some flow into the condenser is necessary to oppose diffusion of helium down to the level of the thermometer coils. Helium near the thermometer wells would decrease the water-vapor partial pressure and hence the temperature. It is for this reason that the tube to the condenser is not large. The fact that helium is lighter than water vapor is favorable for avoiding convective instability. Too great an excess of power can be undesirable, however, because it increases both the length and the velocity of the stream of vapor ascending into the condenser. This increases the head loss due to viscous or turbulent flow. Experience shows, however, that the excess power can be increased by 100 watts without producing any significant error in the determination of temperature near 100°C. It is not until low pressure measurements in the neighborhood of 30°C are being made with this boiler that these effects become significant.

Sulfur Point Boiler

In the text of the 1927 International Temperature Scale[10] the recommended experimental procedure for the sulfur point was specified in considerable detail. At that time the precision of temperature realization at the sulfur point was considered good when it was in the order of 0.01°. Since that time it has been demonstrated that a greater precision is attainable when the sulfur boiler is connected to a closed system. This led in 1948 to the definition of the sulfur point temperature as 444.600°C,[1] where the last figure only represents the degree of reproducibility of that fixed point. A temperature change of 0.001° at the sulfur point corresponds to a change of pressure of about 10 microns of mercury.

In 1951 a closed-system sulfur boiler was completed at the National Bureau of Standards and connected to the precision manometer. In the design of this boiler the same principles were used that proved successful in the steam boiler. In this new boiler the liquid and vapor sulfur are exposed only to 2S aluminum (which is the purest commercial grade). The boiler was constructed from sheet nearly 1 cm thick. It is 45 cm tall and 13 cm in inside diameter. The entire apparatus was welded together by means of an inert-gas arc using welding rods of the same 2S aluminum.

At the bottom is a heater dome which is analogous to that in the steam boiler. This dome is surrounded by a single layer of closely spaced vertical aluminum wires, 1.5 mm in diameter, analogous to the silver wires in the steam boiler. These also are effective for avoiding explosive vaporization. Heat for boiling is supplied by a radiant heater which has a nominal rating of 660 watts but only about 420 watts are normally used. On the boiler itself is wound an additional heater with a capacity of about 1000 watts which aids in raising the temperature of the boiler and contents from room temperature to near the sulfur temperature in about an hour. As the sulfur temperature is approached the power in this heater is reduced until the whole load can be taken on the radiant heater. The heat conducted away from the boiler itself is about 380 watts when the steady state has been established.

Ten thermometer wells of various sizes extend down from the top into the vapor space. The axes of these wells approach each other as they extend down into the vapor space so they are closest together at the level of the centers of the thermometer coils. Stainless steel liners 0.25 mm thick were drawn with the aluminum tubing for the thermometer wells. These liners serve not only to stiffen the wells but also to prevent the aluminum from rubbing off onto the protecting tubes of the thermometers when they are hot.

Between these wells and the walls of the boiler are two cylindrical radiation shields; at the top there are four, and at the bottom six conical radiation shields alternately diverting the fluid flow to and away from the axis yet preventing direct radiation away from the wells. These shields are spaced not less than 9 mm apart which should be ample to avoid any significant drop in pressure of the vapor as it enters these spaces. As it was found for the steam boiler, computations indicate that one less shield might have been sufficient, so, with the present number of radiation shields, there is little chance that the wells containing the thermometers are at a temperature significantly lower than the saturation temperature.

On the axis above the top of the boiler is a stack, 1.9 cm inside diameter, for condensing the excess of sulfur vapor. In all, the stack extends up with this diameter nearly 18 cm above the body of the boiler. For about 9 cm above the top of the boiler the stack has a wall thickness of only about 1

mm. Above this thin section is welded a thick section on which is turned a cone about 5.3 cm long with a taper of 1 in 10 from the axis. On this cone there rests a sleeve of brass to which are soldered several turns of copper tubing for cooling water. Above the cooling section is a cap, sealed with a Teflon gasket, from which a tube leads away to the manometer. Down through this cap there also extends an aluminum tube, about 4 mm in diameter, carrying a pair of thermoelement wires to a ring of aluminum within the thin section of the stack. This is a feeler thermoelement which serves to indicate the height at which the helium meets the hot sulfur vapor during the operation of the boiler. Its height is adjustable but it is usually kept about 3 cm below the thick section of the stack.

It may seem paradoxical that water cooling is used for sulfur which freezes at about 119°C. The hot saturated sulfur vapor at 1 atmosphere pressure, however, does not reach the thick section of the stack which is water cooled but stops at the level where the heat of vaporization has all been given up to the thin wall of the stack at temperatures well above the freezing point. At this level the stack temperature differs most from that of the saturated vapor so the rate of heat flow to the stack is a maximum as is also the temperature gradient in the stack. Above this level there is little condensation and the gradient decreases slightly owing to the loss of heat from the side of the stack.

Experiments were made changing the power input into the boiler to change the height of the hot saturated vapor in the stack. Temperature gradients along the stack were determined by means of ten thermocouples spaced uniformily. From these experiments it was concluded that the height of the top of the hot vapor was about at the level of the feeler thermocouple in the stack where the thermocouple electromotive force increases most rapidly with an increase in vapor height. From these experiments it also was concluded that viscous flow of vapor in the stack caused an insignificant loss of head, as it was found for the steam boiler.

It is important to know the height of the saturated vapor at one atmosphere, because, according to the values used at the Massachusetts Institute of Technology,[11] its density is such that 4.0 cm of vapor head corresponds to a change of saturation temperature of 0.001°. Having determined the height of the hot saturated vapor with the feeler thermocouple, a better accounting can be made of the pressure of the vapor at the height of the thermometer coils. In the helium above the top of the hot vapor the stack temperature is so much lower than the sulfur point that the cooler saturated sulfur vapor at these temperatures contributes very little partial pressure head.

The stability of this sulfur boiler has brought to light a phenomenon which heretofore had escaped attention. When the sulfur is started to boil,

after a period of rest, the temperature is observed to fall for a period of about a day. The temperature then approaches constancy at about a hundredth of a degree below the initial temperature and has been found to remain there for periods lasting over a week. On account of this phenomenon the practice is to delay calibrations in the sulfur boiler until at least a day after the boiling is begun.

An analysis was made of the purity of the sulfur which had been used for sulfur boilers. It was found to contain less than a part in a million each of selenium, arsenic, and tellurium. Mueller[12] reported that one part in a thousand of selenium and arsenic added to the sulfur gave a combined raising in boiling temperature of less than 0.1°. After having been boiled the sulfur did, however, contain about 140 parts per million of carbon, 76 parts per million of nonvolatile matter, and about 8 parts per million of iron. Sulfur was purified by T. J. Murphy in the NBS Chemistry Division and the resulting sulfur was found to contain 2 parts per million of carbon, 3 parts per million of nonvolatile matter, and less than 1 part per million of iron. When this purified sulfur was used in the sulfur boiler no changes were found either in the final boiling temperature or the phenomenon of falling temperature. The practice in the use of the sulfur boiler has been to boil a new batch of sulfur for several hours to drive off gases and then to cool the sulfur in order to evacuate these gases before starting the boiling for calibration work. During use a small amount of helium is in the boiler stack for transmitting the pressure out to the manometer. Between runs this helium is left in the boiler. Our present conclusion is that the phenomenon of falling temperature is not a result of impurities in the sulfur, but is another unsolved problem concerning precision thermometry.

Oxygen Point Apparatus

A new oxygen boiling point apparatus is now in operation. It also is connected to the precision manometer. This apparatus uses the stable equilibrium between liquid oxygen and its vapor rather than active boiling as in the steam and sulfur boilers. The essential part of this apparatus is a copper block which contains an oxygen vapor-pressure bulb and eight wells for resistance thermometers. In operation the oxygen bulb contains a few drops of liquid oxygen in equilibrium with vapor near the position of the resistors of the thermometers being calibrated. Superheated oxygen vapor extends from the saturated oxygen in the bulb out to a diaphragm cell which is at about room temperature. The diaphragm transmits the pressure from the oxygen to the helium of the precision manometer.

The copper block is a cylinder about 7 cm in diameter and 18 cm tall. The eight wells of the thermometers extending up from the copper block are of thin copper-nickel tubing which has a low thermal conductivity.

These wells lead up through liquid nitrogen to the outside of the apparatus near room temperature. Above the copper block are two heat interceptors soldered to the wells. In thermal contact with these heat interceptors are copper shields which surround the entire copper block.

Outside the shields is a brass envelope placed in a bath of liquid nitrogen which boils at about 13° below the oxygen point. The brass envelope is evacuated in order to eliminate heat transfer by gaseous conduction from the copper block and the surrounding shields. The heat interceptors are heated electrically and controlled to temperatures close to that of the copper block. These interceptors serve to isolate the block so completely that temperature variations do not exceed 0.001° in the block near the thermometer resistors. For the initial cooling of the block and interceptors, tubes are soldered to them so that liquid nitrogen from the bath can be admitted through a valve above the envelope. The vaporization and heating of the nitrogen remove energy at a rate which makes it possible to cool the apparatus to a temperature below the oxygen point in about 2 hours.

In the helium line from the precision manometer to the steam and sulfur bath it is a simple matter to prevent either the steam or sulfur vapor from reaching the manometer by the use of dry ice to cool a horizontal portion of the transmitting line. For the oxygen point apparatus, however, it is not so simple. The method chosen is to use a plane metal diaphragm about 60 microns thick which separates the oxygen from the helium yet is so sensitive and so reproducible that it will permit the determination of the oxygen pressure within the equivalent of 0.0001° in its saturation temperature. The diaphragm is held in a cell with walls so close that the diaphragm is supported after it has been displaced a small amount by pressure, and thus the support prevents the diaphragm from being strained beyond its elastic limit.

The diaphragm cell is made of stainless steel and has an over-all diameter of about 13 cm. This diameter is for flanges, which extend out from each of two central supporting walls which are about 10.2 cm in diameter. The diaphragm is held between these supports on plane areas about 6 mm wide near the 5-cm radius. Inside this supporting surface the wall is ground, lapped, and polished to a spherical concave surface having a radius of curvature of about 15 meters. On the helium side of the diaphragm the cell wall has a central electrically insulated island about 4.5 cm in diameter which is used for determining the null position of the diaphragm. This island is spaced about 0.15 mm from the main wall. The insulation is an annular sheet of Pyrex glass about 8 mm thick which is clamped both to the island and to the body of the cell. The insulator was used to hold the island in place when the cell body wall was being made spherical. Subsequently the island was removed for cleaning and replaced so the spherical

surface of the island was continuous with that of the body wall within a fringe of light. Between the flanges there is a recessed space for a pair of clamping rings, each about 13 cm in diameter and 1 cm thick, which clamp the diaphragm at a diameter of about 11 cm. When the diaphragm is clamped in its rings, it is laid on the island side of the cell and drawn axially toward the flange by means of screws. This stretches the diaphragm to a plane in a manner analogous to the tuning of a kettle drum.

The center of the diaphragm is about 70 microns from the island surface when the diaphragm is in equilibrium. The difference in electrostatic capacitance between that of a reference capacitor and that of the island to the diaphragm indicates the displacement of the diaphragm away from its equilibrium position. A beat frequency oscillator is used for this indication in a manner analogous to that for the precision manometer.

An excess of pressure on one side forces the diaphragm against the wall on the other side of the cell and further excess pressure makes little change. When the excess pressure is removed the diaphragm returns nearly to its original position. In order to be effective for a precision of 0.0001°, the diaphragm must return to its original position within the equivalent of 10 microns of mercury pressure. This has been done to within the equivalent of a few microns pressure so the reproducibility appears adequate. The diaphragm cell, however, has been found to be somewhat sensitive to temperature changes so it is enclosed inside a pair of thick-walled aluminum boxes with the outside box thermostatted at 28°C.

The diameters of the protecting envelopes of the thermometers which must be calibrated in this apparatus differ so much that various diameters of wells are provided, ranging from 7.5 to 13 mm in diameter. The length of the wells is a compromise at about 41 cm long. This provides sufficient immersion for most thermometers but may be too long for a few special thermometers with short stems. Since the boiling point of oxygen is below that of some of the gases in air, such as carbon dioxide and water vapor which are present in small quantities, it is desirable to avoid these gases in the wells. Provision is made, therefore, for sealing the thermometers in the wells by means of rubber sleeves at the top, evacuating the air, and introducing dry helium in the wells. The use of helium in the wells has the added advantage that helium has a greater thermal conductivity than air and hence improves the thermal contact of the well with the thermometer envelope.

Conclusion

In conclusion we may ask how far we have come in precision resistance thermometry and how much farther we may expect to go with the experimental possibilities that are known to us now. The precision of resistance

thermometry has been increased by the attention to some details in the technique of measurement and by improved designs of instruments. It has been seen that the present triple point cells and the boilers for realizing the steam, sulfur, and oxygen points make it possible to attain an accuracy that is comparable to that indicated in the text of the International Temperature Scale. These accomplishments, however, yield results which fall short of the precision in resistance thermometry which appears to be possible before it is limited by Johnson noise.

References

1. Stimson, H. F., "The International Temperature Scale of 1948," *J. Research NBS*, **42**, 209 (1949).
2. Mueller, E. F., "Precision Resistance Thermometry," in "Temperature, Its Measurement and Control in Science and Industry," Reinhold Publishing Corp., 1941.
3. Beattie, J. A., and Blaisdell, B. E., "The Reproducibility of the Steam Point. The Effect of Pressure on the Steam Point," *Proc. Am. Acad. Arts Sci.*, **71**, 361 (1937).

   Beattie, J. A., Tzu-Ching Huang, and Benedict, M., "The Reproducibility of the Ice Point and the Triple-Point of Water. The Temperature of the Triple-Point of Water," *Proc. Am. Acad. Arts Sci.*, **72**, 137 (1938).
4. Schwab, F. W., and Wiehers, E., "Freezing Temperature of Benzoic Acid as a Fixed Point in Thermometry," *J. Research NBS*, **34**, 333 (1945).
5. Meyers, C. H., "Coiled Filament Resistance Thermometers," *BS J. Research*, **9**, 807 (1932).
6. Barber, C. R., "Platinum Resistance Thermometers of Small Dimensions," *J. Sci. Instruments*, **27**, 47 (1950).
7. Hoge, H. J., "Electrical Conduction of Glass Insulation of Resistance Thermometers," *J. Research NBS*, **28**, 489 (1942).
8. Corruccini, R. J., "Annealing of Platinum Thermometers," *J. Research NBS*, **47**, 94 (1951).
9. Barber, C. R., Gridley, A., and Hall, J. A., "An improved construction of the Smith bridge, type 3," *J. Sci. Instruments*, **32**, 213 (1955).
10. Burgess, G. K., "The International Temperature Scale," *BS J. Research*, **1**, 635 (1928).
11. Beattie, J. A., Benedict, M., and Blaisdell, B. E. "The Reproducibility of the Sulfur Point. The Effects of Pressure on the Sulfur Point," *Proc. Am. Acad. Arts Sci.*, **71**, 327 (1937).
12. Mueller, E. F., and Burgess, H. A., "The Standardization of the Sulfur Boiling Point," *J. Am. Chem. Soc.*, **41**, 745 (1919).

Reprinted from Journal of Applied Physics, Vol. 11, No. 6, 388–407, June, 1940

Thermoelectric Thermometry*

By Wm. F. Roeser

National Bureau of Standards, Washington, D. C.

The fundamental laws and theories of thermoelectric phenomena and their historical development as well as the application of these phenomena to the measurement of temperature are discussed in this paper in considerable detail. Thermoelectric thermometry, with particular regard to types of thermocouples, protection of thermocouples, fundamental considerations in temperature measurements, etc. are treated primarily from the practical standpoint.

I. Introduction

STUDY in the field of thermoelectricity began in 1821 with the discovery of Seebeck[1] that an electric current flows continuously in a closed circuit of two dissimilar metals when the junctions of the metals are maintained at different temperatures. In the early investigations of thermoelectric effects the results were expressed more qualitatively (in terms of the direction of the current flowing in a closed circuit) than quantitatively, because the relations between the measurable quantities in an electric circuit were not well known at the time.†

II. Fundamental Laws

As a result of a large number of investigations of thermoelectric circuits in which accurate measurements were made of the electromotive force, current, and resistance, several "established facts" or "laws" have been formulated. These facts or laws, variously stated in different ways and combinations and sometimes consolidated into a general statement of the phenomenon discovered by Seebeck, can be reduced to three fundamentals:

(1) The law of the homogeneous circuit
(2) The law of intermediate metals
(3) The law of successive or intermediate temperatures.

The latter two may be arrived at by applying the laws of thermodynamics to the thermoelectric circuit, but the fundamental experimental fact regarding a homogeneous circuit, which enters into all measurements of temperature by thermoelectric methods, cannot be derived from such considerations. The law of the homogeneous circuit is incorporated into most statements of the law of intermediate metals. In any case all of these facts or laws, as stated below and used in the measurement of temperatures, have been established experimentally beyond a reasonable doubt and in order that temperatures may be measured by this method the laws must be accepted in spite of any lack of rigor that may appear in any of the thermodynamic derivations given here or elsewhere.

The discussion will be simplified by defining a few terms at this point. It will be considered that all the metals comprising a thermoelectric circuit are solids unless otherwise stated.

A pair of electrical conductors so joined as to produce a thermal e.m.f. when the junctions are at different temperatures is known as a thermocouple. The resultant e.m.f. developed by the thermocouples generally used for measuring temperatures ranges from 1 to 7 millivolts when the temperature difference between the junctions is 100°C.

If in a simple thermoelectric circuit, Fig. 1, the current flows from metal A to metal B at the colder junction, A is generally referred to as thermoelectrically positive to B. In determining or expressing the e.m.f. of a thermocouple as a

* Presented at the American Institute of Physics Symposium on Temperature, Its Measurement and Control in Science and Industry, November 4, 1939.

† The relation between the current and potential difference in an electric circuit was first clearly stated by G. S. Ohm in 1826. Schweigger's J. 46, 137 (1826).

function of the temperature, one junction is maintained at some constant reference temperature, such as 0°C, and the other is at the temperature corresponding to the e.m.f. In the present paper, the order in which the metals are named and the sign of the numerical value of the e.m.f. will be used to indicate which of the metals is

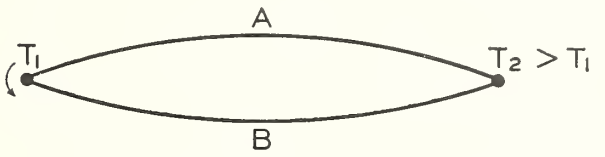

Fig. 1. Simple thermoelectric circuit.

positive to the other at the junction which is at the reference temperature. For example, if, in Fig. 1, T_1 is the reference temperature and the current flows in the direction indicated, the e.m.f. of thermocouple AB will be positive, and the e.m.f. of thermocouple BA will be negative.

1. The Law of the Homogeneous Circuit

An electric current cannot be sustained in a circuit of a single homogeneous metal, however varying in section, by the application of heat alone. As far as we know this principle has not been derived theoretically. It has been claimed from certain types of experiments that a nonsymmetrical temperature gradient in a homogeneous wire gives rise to a galvanometrically measurable thermoelectric e.m.f. However, the overwhelming weight of evidence indicates that any e.m.f. observed in such a circuit is to be attributed to the effects of local inhomogeneities. As a matter of fact, at the present time any current detected in such a circuit when the wire is heated in any way whatever, is taken as evidence that the wire is inhomogeneous. The more important of a large number of investigations of this subject are adequately discussed by Foote and Harrison.[2]

In the present paper, we accept, as an experimental fact, the general statement that the algebraic sum of the electromotive forces in a circuit of a single homogeneous metal however varying in section and temperature is zero. As a consequence of this fact, if one junction of two dissimilar homogeneous metals is maintained at a temperature T_1 and the other junction at a temperature T_2, the thermal e.m.f. developed is independent of the temperature gradient and distribution along the wires.

2. Law of Intermediate Metals

This law is stated in one of several ways, and although the statements may appear quite different, they are really equivalent with the exception that the law of the homogeneous circuit is included in some of the statements. One statement of this law is: *The algebraic sum of the thermoelectromotive forces in a circuit composed of any number of dissimilar metals is zero, if all of the circuit is at a uniform temperature.* This law follows as a direct consequence of the second law of thermodynamics, because if the sum of the thermoelectromotive forces in such a circuit were not zero, a current would flow in the circuit. If a current should flow in the circuit, some parts of it would be heated and other parts cooled, which would mean that heat was being transferred from a lower to a higher temperature without the application of external work. Such a process is a contradiction of the second law of thermodynamics and therefore we conclude that the algebraic sum of the thermoelectromotive forces is zero in such a circuit.

Combining this law with that for a homogeneous circuit, it is seen that in any circuit, if the individual metals between junctions are homogeneous, the sum of the thermal electromotive forces will be zero provided only that the junctions of the metals are all at the same temperature.

Another way of stating the law of intermediate metals is:

If in any circuit of solid conductors the temperature is uniform from any point P through all the conducting matter to a point Q, the algebraic sum of the thermoelectromotive forces in the entire circuit is totally independent of this intermediate matter and is the same as if P and Q were put in contact. Thus it is seen that a device for measuring the thermoelectromotive force may be introduced into a circuit at any point without altering the resultant e.m.f. provided that the junctions which are added to the circuit by introducing the device are all at the same temperature. It is also obvious that the e.m.f. in a thermoelectric circuit is independent of the method employed in

forming the junction as long as all of the junction is at a uniform temperature, and the two wires make good electrical contact at the junction, such as is obtained by welding or soldering.

A third way of stating the law of intermediate metals is:

The thermal e.m.f. generated by any thermocouple AB with its junctions at any two temperatures T_1 and T_2, is the algebraic sum of the e.m.f. of a thermocouple composed of A and any metal C and that of one composed of C and B, both with their junctions at T_1 and T_2 or $E_{AB}=E_{AC}+E_{CB}$.

From this statement of the law it is seen that if the thermal e.m.f. of each of the metals A, B, C, D, etc. against some reference metal is known, then the e.m.f. of any combination of these metals can be obtained by taking the algebraic differences of the e.m.f.'s of each of the metals against the reference metal. Investigators tabulating thermoelectric data have employed various reference metals such as mercury, lead, copper, and platinum. At present it is customary to use platinum because of its high melting point, stability, reproducibility, and freedom from transformation points.

3. Law of Successive or Intermediate Temperatures

The thermal e.m.f. developed by any thermocouple of homogeneous metals with its junctions at any two temperatures T_1 and T_3 is the algebraic sum of the e.m.f. of the thermocouple with one junction at T_1 and the other at any other temperature T_2 and the e.m.f. of the same thermocouple with its junctions at T_2 and T_3. Considering the thermocouple as a reversible heat engine and applying the laws of thermodynamics to the circuit, it will be shown in the next section that

$$E=\int_{T_1}^{T_3}\phi dT,$$

from which it follows that

$$E=\int_{T_1}^{T_2}\phi dT+\int_{T_2}^{T_3}\phi dT.$$

This law is frequently invoked in the calibration of thermocouples and in the use of thermocouples for measuring temperatures. It will be discussed in detail in Section IV.

The above are all the fundamental laws required in the measurement of temperatures with thermocouples. They may be and frequently are combined and stated as follows: The algebraic sum of the thermoelectromotive forces generated in any given circuit containing any number of dissimilar homogeneous metals is a function only of the temperatures of the junctions. It is seen then that if all but one of the junctions of such a given circuit are maintained at some constant reference temperature, the e.m.f. developed in the circuit is a function of the temperature of that junction only. Therefore, by the proper calibration of such a device, it may be used to measure temperatures.

It should be pointed out here that none of the fundamental laws of thermoelectric circuits which make it possible to utilize thermocouples in the measurement of temperatures, depends upon any assumption whatever regarding the mechanism of interconversion of heat and electrical energy, the location of the e.m.f.'s in the circuit, or the manner in which the e.m.f. varies with temperature.

III. Historical Investigation and Theory

Although a knowledge of the location of the electromotive forces in a thermoelectric circuit and the mechanism by which heat is converted into electrical energy, is not required in order to measure temperatures with thermocouples, any information available on these subjects may be used advantageously in studying the characteristics of thermocouples and their behavior during use. Various theoretical and experimental investigations of thermoelectric circuits give us the location of the electromotive forces in such a circuit, and the relation between these electromotive forces, but they have not yielded a satisfactory explanation of the mechanism by which heat is converted into electrical energy or of the manner in which the electromotive force varies with temperature, except empirical relations.

In 1834 Peltier[3] found that when a current is passed across the junction of two dissimilar metals in one direction heat is absorbed and the junction cooled, and that when the current is

passed in the opposite direction the junction is heated. Peltier and others observed that for a given current the rate of absorption or liberation of heat at the junction of two dissimilar metals depends upon the thermoelectric power (dE/dt) of the two metals and is independent of the form and dimensions of the metals at the junction. In 1853 Quintus Icilius[4] showed that the rate at which heat is absorbed or generated at a junction of two dissimilar metals is proportional to the current. This heating or cooling effect discovered by Peltier should not be confused with the Joule heating effect which, being proportional to the electrical resistance and to the square of the current, depends upon the dimensions of the conductor and does not change sign when the current is reversed.

Inasmuch as heat is absorbed when a current flows up a potential gradient and heat generated when the current flows down a potential gradient, the heating or cooling effect at a junction of two dissimilar metals (being proportional to the current) is evidence that the junction is the seat of an electromotive force. If we let P be the rate at which heat (in joules per second or in watts) is generated or absorbed when a current of one ampere flows across a junction, then P is the Peltier coefficient of the junction (in watts per ampere) or more simply the Peltier e.m.f. (in volts). The direction and magnitude of this e.m.f. depend upon the metals which form the junctions and upon the temperature.

In 1851, W. Thomson[5] (later Lord Kelvin) concluded from thermodynamic reasoning and the then known characteristics of thermocouples, that the reversible absorption of heat at the junctions of dissimilar metals was not the only reversible heat effect in a thermoelectric circuit. In brief he reasoned as follows:

(1) Assuming that the Peltier e.m.f.'s represent the only reversible effects in a simple thermoelectric circuit, the resultant e.m.f. E in the circuit is given by

$$E=P_2-P_1, \tag{1}$$

where P_1 is the Peltier e.m.f. of the junction which is at temperature T_1 and P_2 is the Peltier e.m.f. of the junction which is at temperature T_2.

(2) Neglecting the effect of thermal conduction (an irreversible process) and considering the thermocouple as a reversible heat engine with a source at the temperature T_2 in degrees Kelvin and a sink at the temperature T_1, we have as a consequence of the second law of thermodynamics

$$P_2/T_2-P_1/T_1=0 \tag{2}$$

or

$$(P_2-P_1)/P_1=(T_2-T_1)/T_1, \tag{3}$$

which combined with (1) gives

$$E=P_1(T_2-T_1)/T_1. \tag{4}$$

It would follow therefore that if one junction were maintained at a constant temperature T_1, P_1 would be constant, and the e.m.f. E would be proportional to (T_2-T_1). It had been definitely shown by a number of investigators that E was not proportional to (T_2-T_1). Thomson therefore concluded that the Peltier effects were not the only reversible heat effects in such a circuit and that there must be a reversible absorption of heat due to the flow of current through that part of the conductors in which there is a temperature gradient.

In 1854 Thomson[6] succeeded in showing experimentally that in certain homogeneous metals, heat is absorbed when an electric current flows from colder to hotter parts of the metal and heat is generated when the current flows from the hotter to colder parts. In certain other metals the opposite of this effect occurs, that is, heat is absorbed when an electric current flows from the hotter to colder parts, and in still other metals, the effect is too small to be detected by the methods used. This heating or cooling effect, called the Thomson effect, being reversible and occurring only where there is a temperature gradient in a metal, is entirely distinct from the irreversible Joule heating.

The reversible absorption of heat in a homogeneous conductor has the same effect as if an electromotive force existed in the temperature gradient. The direction and magnitude of this e.m.f. between any two points depend upon the metal, the temperature, and the temperature difference between the two points. If in any metal we let σ equal the rate at which heat is absorbed or generated per unit difference of temperature when a current of one ampere flows, then the total e.m.f. between any two points at

temperatures T_1 and T_2 is given by

$$\int_{T_1}^{T_2} \sigma dT.$$

In a simple thermoelectric circuit of two metals A and B, Fig. 2, there exist then four separate and distinct electromotive forces, the Peltier e.m.f.'s at the two junctions and the Thomson e.m.f.'s along that part of each wire which lies in the temperature gradient. The only e.m.f. that can be measured as such in this circuit is the resultant e.m.f. The identity of the individual e.m.f.'s can only be established by observations

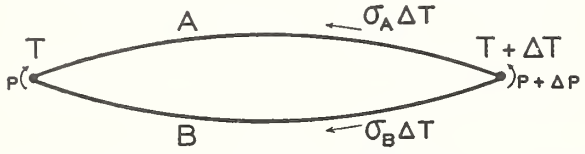

FIG. 2. The location of the electromotive forces in a thermoelectric circuit.

of the reversible heat effects. The Thomson e.m.f. will be considered positive if heat is generated when the current flows from the hotter to colder parts of the conductor and negative if the reverse occurs.

Thomson took into consideration the reversible heat effects in the temperature gradient of the conductors, (Thomson effects), as well as those at the junctions, (Peltier effects), and applied the laws of thermodynamics to the thermoelectric circuit. A complete discussion of this application together with the hypothesis involved is given in the original paper by Thomson.[7]

Consider a simple thermoelectric circuit of two metals A and B, Fig. 2 and let P and $P+\Delta P$ be the Peltier e.m.f.'s of the junctions at temperature T and $T+\Delta T$ in degrees Kelvin, respectively, and let σ_A and σ_B be the Thomson e.m.f.'s per degree along conductors A and B, respectively. Let the metals and temperatures be such that the e.m.f.'s are in the directions indicated by the arrows. The resultant e.m.f. ΔE in the circuit is given by

$$\Delta E = P + \Delta P - P + \sigma_A \Delta T - \sigma_B \Delta T, \qquad (5)$$

$$\Delta E = \Delta P + (\sigma_A - \sigma_B)\Delta T, \qquad (6)$$

or in the limit

$$dE/dT = dP/dT + (\sigma_A - \sigma_B). \qquad (7)$$

By virtue of the second law of thermodynamics $\Sigma Q/T = 0$, for a reversible process. If then we regard the thermocouple as a reversible heat engine and pass a unit charge of electricity q around the circuit, we obtain by considering only the reversible effects*

$$\frac{q(P+\Delta P)}{T+\Delta T} - \frac{qP}{T} + \frac{q\sigma_A \Delta T}{T+\frac{\Delta T}{2}} - \frac{q\sigma_B \Delta T}{T+\frac{\Delta T}{2}} = 0, \qquad (8)$$

* The following quotations are from the paper by W. Thomson.

"···The following proposition is therefore assumed as a fundamental hypothesis in the Theory at present laid before the Royal Society.

"The electro-motive forces produced by inequalities of temperature in a circuit of different metals, and the thermal effects of electric currents circulating in it, are subject to the laws which would follow from the general principles of the dynamical theory of heat if there were no conduction of heat from one part of the circuit to another.

"In adopting this hypothesis, it must be distinctly understood that it is only a hypothesis, and that, however probable it may appear, experimental evidence in the special phenomena of thermo-electricity is quite necessary to prove it. Not only are the conditions prescribed in the second Law of the Dynamical Theory not completely fulfilled, but the part of the agency which does fulfill them is in all known circumstances of thermo-electric currents excessively small in proportion to the agency inseparably accompanying it and essentially violating those conditions. Thus, if the current be of the full strength which the thermal electromotor alone can sustain against the resistance in the circuit, the whole mechanical energy of the thermo-electric action is at once spent in generating heat in the conductor;—an essentially irreversible process. The whole thermal agency immediately concerned in the current, even in this case when the current is at the strongest, is (from all we know of the magnitude of the thermo-electric force and absorptions and evolutions of heat) probably very small in comparison with the transference of heat from hot to cold by ordinary conduction through the metal of the circuit. . . . It is true, we may, as has been shown above, diminish without limit the waste of energy by frictional generation of heat in the circuit, by using an engine to do work and react against the thermal electromotive force; but as we have also seen, this can only be done by keeping the strength of the current very small compared with what it would be if allowed to waste all the energy of the electromotive force on the frictional generation of heat; and it therefore requires a very slow use of the thermo-electric action. At the same time, it does not in any degree restrain the dissipation of energy by conduction, which is always going on, and which will therefore bear an even much greater proportion to the thermal agency electrically spent than in the case in which the latter was supposed to be unrestrained by the operation of the engine. By far the greater part of the heat taken in at all, then, in any thermo-electric arrangement, is essentially dissipated, and there would be no violation of the great natural law expressed in Carnot's principle, if the small part of the whole action, which is reversible, gave different, even an enormously different, and either a greater or a less, proportion of heat converted into work to heat taken in, than that law requires in all completely reversible processes. . . ."

which may be written

$$\Delta\left(\frac{P}{T}\right)+\frac{(\sigma_A-\sigma_B)\Delta T}{T+\frac{\Delta T}{2}}=0, \tag{9}$$

or in the limit

$$\frac{d}{dT}\left(\frac{P}{T}\right)+\frac{1}{T}(\sigma_A-\sigma_B)=0 \tag{10}$$

or

$$\sigma_A-\sigma_B=P/T-dP/dT. \tag{11}$$

Eliminating $(\sigma_A-\sigma_B)$ between (7) and (11) we have

$$P=TdE/dT. \tag{12}$$

Substituting (12) in (10) we have

$$-(\sigma_A-\sigma_B)=Td^2E/dT^2. \tag{13}$$

From (12) it is seen that

$$E=\int_{T'}^{T}\frac{P}{T}dT=\int_{T'}^{T}\phi dT, \tag{14}$$

which is the expression referred to earlier.

The Peltier e.m.f. at the junction of any two dissimilar metals at any temperature can be calculated from Eq. (12) and measurements of the variation of the thermal e.m.f. with temperature. The magnitude of the e.m.f. existing at the junction of two dissimilar metals ranges from 0 to about 0.1 volt for the metals generally used in temperature measurements.

Although the thermoelectric theory as developed above does not enable us to determine directly the magnitude of the Thomson coefficient in any individual metal, the difference between the Thomson coefficients in two metals can be calculated from Eq. (13) and measurements of the variation in thermal e.m.f. with temperature. Various types of experiments indicate that the Thomson effect in lead is extremely small, if not zero, at ordinary atmospheric temperatures. Consequently some information regarding the magnitude of the Thomson coefficients in other metals at these temperatures can be determined if it is assumed that this coefficient is zero for lead. On this basis it is found that the Thomson coefficient at 0°C in microvolts per °C is −9 for platinum, −8 for iron, +2 for copper, −23 for constantan,† −8 for Alumel,† −2 for 90 platinum −10 rhodium,† and +9 for Chromel-P.†

In order to justify the assumption involved in the application of the second law of thermodynamics, it is necessary and sufficient to verify experimentally the relation

$$P=TdE/dT \tag{12}$$

or

$$-(\sigma_A-\sigma_B)=Td^2E/dT^2. \tag{13}$$

Inasmuch as the individual e.m.f.'s cannot be measured as such, we must depend upon calorimetric measurements of the heating and cooling effects. In order to measure these small reversible effects, it is necessary to separate them from the much larger irreversible Joule heating and the thermal conduction which take place in any experiment of this nature. Practically all of the experimental work on this subject has been on the relation given by Eq. (12) because the reversible heating effects involved in it are in general much larger and more localized than those in Eq. (13).

The most carefully conducted experiments particularly those of Edlund,[8] Jahn,[9] Caswell,[10] and Borelius[11] indicate that the above relations hold within the accuracy of the measurements, about 5 to 10 percent. As far as we know, there is no evidence available which would indicate that the above relations are not exact.

We cannot integrate Eq. (12) or (13) and obtain a general relation between E and T, without some information on the manner in which P or σ varies with T. Experiments indicate that P and σ both depend upon T but the manner in which they vary with T has not been established either theoretically or experimentally with any degree of accuracy.

A number of hypotheses have been made as to the manner in which σ varies with the temperature and Eq. (13) then integrated, but in each case it has been found that the type of equation so obtained represents the experimentally determined values of E and T only over limited temperature ranges. Consequently the relation between E and T for any pair of metals must be determined experimentally and corresponding

† Alloys used in the measurement of temperatures.

574278 O - 61 - 6

values given by tables or empirical relations for limited temperature ranges.

Later theories of thermoelectricity may be divided into two general classes: (1) those in which attempts are made to avoid the hypothesis made by Thomson, and (2) those in which the

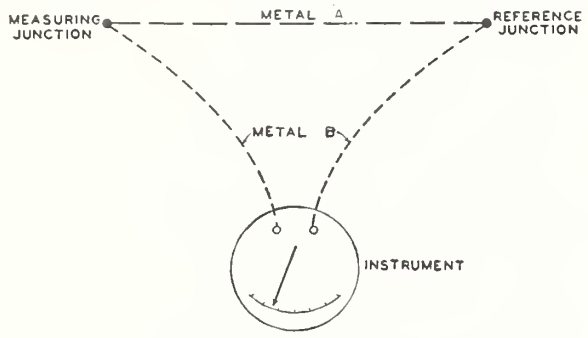

FIG. 3. Simple thermoelectric thermometer.

theory as developed by Thomson is accepted as far as it goes, and attempts are made to derive a reversible mechanism or process for converting heat into electrical energy by the application of the electron theories of metals. The theories in the first general class have added little, if anything, to our knowledge of thermoelectricity. The assumptions involved in most of these appear more objectionable than the one made by Thomson. The relations derived between the quantities involved are either equivalent to or less useful than those derived by Thomson.

The existence of the Peltier and Thomson e.m.f.'s in a thermoelectric circuit may be deduced, qualitatively at least, from the electron theories of metals, but the uncertainties in the quantities involved are so large that we cannot determine whether the theories are in agreement with experimental data or not. The most that can be claimed for the more complete of these theories at the present time, is that they give the order of magnitude of the various effects for certain metals.

IV. Thermoelectric Thermometers

A thermoelectric thermometer is a device for measuring temperatures by utilizing the thermoelectric effects. In its simplest form, it consists of a thermocouple of two dissimilar metals which develop an e.m.f. when the junctions are at different temperatures and an instrument for measuring the e.m.f. developed by the thermocouple, connected together as shown in Fig. 3.

As long as the instrument is at essentially a uniform temperature, all the junctions in the instrument including the terminals, will be at the same temperature, and the resultant thermal e.m.f. developed in the circuit is not modified by including the instrument. If the reference junction is maintained at some reference temperature, such as 0°C, the e.m.f. developed by the thermocouple can be determined as a function of the temperature of the measuring junction. The device can then be used for measuring temperatures. It is not necessary to maintain the reference junction at the same temperature during use as during calibration. However, the temperature of the reference junction in each case must be known. For example, let the curve in Fig. 4 be the relation between the e.m.f. E and temperature t for a particular thermocouple with the reference junction at 0°C. Suppose the device is used to measure some temperature and an e.m.f. E_x is observed when the reference junction is at 30°C. We may add the observed e.m.f. E_x to E_{30} (the e.m.f. given by the thermocouple when one junction is at 0 and the other at 30°C) and obtain from the curve the true temperature t_A of the measuring junction. Certain types of instruments which are used with thermocouples in the manner shown in Fig. 3 are such that they can be adjusted manually for changes in the reference

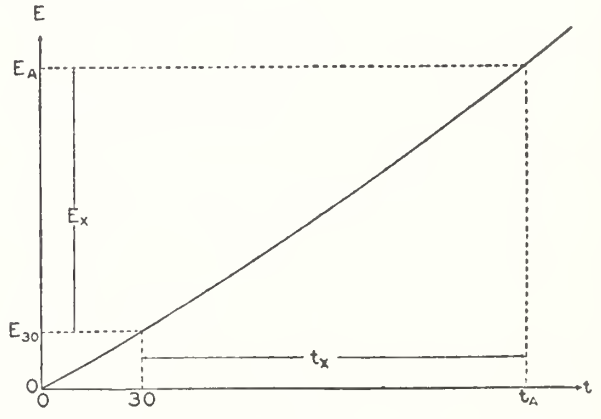

FIG. 4. Illustrating how corrections may be applied for variations in the temperature of the reference junction.

junction temperature and the e.m.f. E_A read directly on the instrument.

Inasmuch as the curves giving the relation between e.m.f. and temperature are not, in

general, straight lines, equal increments of temperature do not correspond to equal increments of e.m.f.

In many cases the thermocouple is connected to the instrument by means of copper leads as shown in Fig. 5.

If the junctions C and C' are maintained at the same temperature, which is usually the case, the circuit shown in Fig. 5 is equivalent to that shown in Fig. 3. If the junctions C and C' are not maintained at the same temperature the resultant thermal e.m.f. in the circuit will depend not only upon the thermocouple materials and the temperature of the measuring junction but also upon the temperatures of these junctions and the thermoelectric properties of copper against each of the individual wires. Such a condition should be and usually is avoided.

Circuits such as shown in Figs. 3 and 5 are used extensively in laboratory work where it is usually convenient to maintain the reference junctions either at 0°C by placing them in a thermos bottle filled with cracked or shaved ice and distilled water or at some other conveniently controlled temperature.

In most commercial installations where it is not convenient to maintain the reference junctions at some constant temperature, each thermocouple wire is connected to the instrument with a lead of essentially the same chemical composition and thermoelectric characteristics as the thermocouple wire, in the manner shown in Fig. 6. This is equivalent to using a thermocouple with the reference junctions at the instrument terminals. Leads which have the same thermoelectric characteristics as the thermocouple wires are

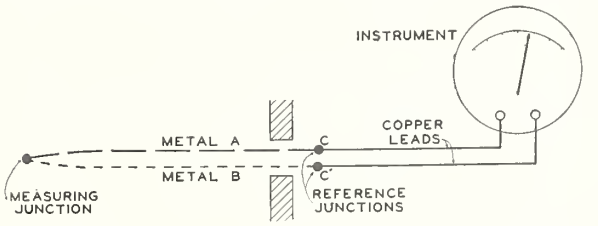

FIG. 5. Diagram for thermoelectric thermometer with copper leads for connecting thermocouple to instrument.

called extension leads. In most installations of this nature the instrument is equipped with an automatic reference junction compensator which automatically changes the indication of the

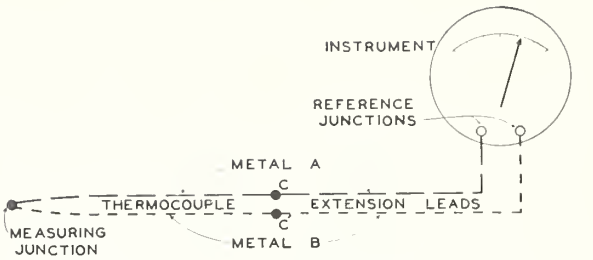

FIG. 6. Thermoelectric thermometer with extension leads.

instrument to compensate for changes in the temperature of the reference junctions, thus eliminating the necessity of measuring or controlling the reference junction temperature. Such automatic devices are usually part of the instrument and in such cases the reference junctions should be located in or at the instrument or at some point which is at the same temperature as the instrument.

In some cases where expensive thermocouple wires are used, extension lead wires of less expensive materials are available which give practically the same temperature-e.m.f. relation as the thermocouple over a limited temperature range, usually 0 to 100°C. Although the combined leads give practically the same temperature-e.m.f. relation as the thermocouple wires, the individual lead wires are not identical thermoelectrically with the thermocouple wires to which they are attached and therefore the two junctions where the leads are attached to the thermocouples (C and C' in Fig. 6) should be kept at the same temperature. This is not necessary in the case of thermocouples where each lead and thermocouple wire to which it is attached are of the same material.

V. Types of Thermocouples

Although a thermal e.m.f. is developed when the junctions of any two dissimilar metals are maintained at different temperatures, only certain combinations of metals have been found suitable for use as thermocouples in the measurement of temperatures. Obviously these thermocouples must be such that:

(1) The thermal e.m.f. increases continuously with increasing temperature over the temperature range in which the thermocouple is to be used.

(2) The thermal e.m.f. is great enough to be measured with a reasonable accuracy.

(3) Their thermoelectric characteristics are not appreciably altered during calibration and use either by internal changes such as recrystallization or by contamination from action of surrounding materials.

(4) They are resistant to any action such as oxidation, corrosion, etc. which destroys the wire.

(5) The melting points of the metals used must be above any temperature at which the thermocouple is to be used.

(6) The metals are reproducible and readily obtainable in uniform quality.

The combinations of metals and alloys extensively used as thermocouples for the measurement of temperatures in this country, are listed in Table I, together with the temperature ranges in which they are generally used and the maximum temperature at which they can be used for short periods. The period of usefulness of a thermocouple depends upon such factors as the temperature, diameter of wires, accuracy required, conditions under which it is used, etc.

There are two types* of platinum to platinum-rhodium thermocouples used in this country, the platinum to 90 platinum-10 rhodium and the platinum to 87 platinum-13 rhodium. These thermocouples develop, at high temperatures, 10 to 14 microvolts per °C as compared to 40 to 55 for the other thermocouples listed in Table I. The platinum to platinum-rhodium thermocouples at temperatures from about 400 to 1600°C being more stable than any other combination of metals, are used (1) for defining the International Temperature Scale from 660°C to the freezing point of gold, 1063°C (only the platinum to 90 platinum-10 rhodium thermocouple is used for this purpose), (2) for very accurate temperature measurements from 400 to 1500°C, and (3) for temperature measurements where the lower melting point materials cannot be used. They are not suitable for temperature measurements below 0°C because the thermoelectric power (dE/dT) is only about 5 microvolts per °C at 0°C and decreases to zero at about −138°C.

The nominal composition of the Chromel-P alloy is 90 percent nickel and 10 percent chromium. Alumel contains approximately 95 percent nickel, with aluminum, silicon, and manganese making up the other 5 percent. Chromel-P-Alumel thermocouples, being more resistant to oxidation than the other base metal thermocouples listed in Table I, are generally more satisfactory than the other base metal thermocouples for temperature measurements from about 650 to 1200°C (1200 to 2200°F). The life of a No. 8 gage (0.128″) Chromel-P-Alumel thermocouple is about 1000 hours in air at about 1150°C (2100°F).

Constantan was originally the name applied to copper-nickel alloys with a very small temperature coefficient of resistance but it now has become a general name which covers a group of alloys containing 60 to 45 percent of copper and 40 to 55 percent of nickel (with or without small percentages of manganese, iron, and carbon) because all the alloys in this range of composition have a more or less negligible temperature coefficient of resistance. Constantan thus includes the alloys made in this country under such trade names as Advance (Ideal), Copel, Copnic, Cupron, etc., most of which contain approximately 55 percent of copper and 45 percent of nickel.

Iron-constantan thermocouples give a slightly higher e.m.f. than the other base metal thermocouples in Table I. They are extensively used at temperatures below about 760°C (1400°F). The life of a No. 8 gage iron-constantan thermocouple is about 1000 hours in air at about 760°C (1400°F).

* Neither one of these thermocouples has any distinct advantage over the other. For several years prior to 1922, there were two classes of supposedly platinum to 90 platinum-10 rhodium thermocouples available which differed in thermoelectric properties by about 10 percent. It was found that one of these contained a large percentage of impurities and that the removal of these impurities eliminated one class of platinum to 90 platinum-10 rhodium thermocouples. However, the scales of a large number of instruments had been graduated to read temperatures directly with these impure thermocouples and in order to provide thermocouples which would give approximately correct readings with these instruments the manufacturers supplied platinum to 87 platinum-13 rhodium thermocouples, which were found to give roughly the same temperature-e.m.f. relation as the "impure 10 percent rhodium thermocouple." New instruments were graduated to read temperatures directly with these new thermocouples and consequently more thermocouples were required. This has gone on and now this type of thermocouple is considered unavoidable.

Copper-constantan thermocouples are generally used for accurate temperature measurements below about 350°C (660°F). They are not suitable for much higher temperatures in air because of the oxidation of the copper.

Combinations of metals other than those listed in Table I are sometimes used for special purposes. As examples, at temperatures above −200°C (−300°F) Chromel-P-constantan gives a thermal e.m.f. per degree somewhat greater than that of any of the thermocouples listed in Table I and is sometimes used when the greater e.m.f. is required. Graphite to silicon carbide has been recommended[12] for temperatures up to 1800°C (3300°F) and for certain applications in steel plants.

VI. Reproducibility of Thermocouples

One of the first requirements of thermoelectric pyrometers for general industrial use is that the scales of the instruments shall be graduated to read temperature directly. Although the indications of the measuring instruments used with thermocouples depend upon the resultant e.m.f. developed in the circuit, the scale of the instrument can be graduated in degrees of temperature by incorporating a definite temperature-e.m.f. relation into the graduation of the scale. The temperature can then be read directly if the temperature-e.m.f. relation of the thermocouple is identical with that incorporated in the scale of the instrument.

All the thermocouples which have the same nominal composition do not give identical relations between e.m.f. and temperature. As a matter of fact, in most cases, two samples of metal which are identical as far as can be determined by chemical methods, are not identical thermoelectrically. This is due in part, to the fact that the thermoelectric properties of a metal depend to some extent upon the physical condition of the metal.

It is not practicable to calibrate the scale of an instrument in accordance with the temperature-e.m.f. relation of a particular thermocouple and to change the scale each time the thermocouple is replaced. Consequently the scales of such instruments are calibrated in accordance with a particular temperature-e.m.f. relation which is considered representative of the type of thermocouple, and new thermocouples are purchased or selected to approximate the particular temperature-e.m.f. relation.

If the temperature-e.m.f. relations of various thermocouples of the same type are not very nearly the same, corrections must be applied to the readings of the indicator, and the corrections will be different for each thermocouple. When several thermocouples are operated with one indicator, and when thermocouples are frequently renewed, the application of these corrections becomes very troublesome. For extreme accuracy it is always necessary to apply such corrections, but for most industrial processes, thermocouples can be manufactured or selected with temperature-e.m.f. relations which are so nearly the same that the corrections become negligibly small.

The accuracy with which the various types of thermocouple materials can be selected and matched to give a particular temperature-e.m.f. relation, depends upon the materials and the degree to which the temperature-e.m.f. relation is characteristic of the materials available. The differences in the temperature-e.m.f. relations of the new platinum to platinum-rhodium thermocouples available in this country rarely exceed 4 to 5°C at temperatures up to 1200°C. Consequently, there is no difficulty in selecting a relation between e.m.f. and temperature which is adequately characteristic of these thermocouples. The temperature-e.m.f. relations used in this

TABLE I. *Types of thermocouples and temperature ranges in which they are used.*

Type of Thermocouple	Usual Temperature Range		Maximum Temperatures	
	°C	°F	°C	°F
Platinum to platinum rhodium	0 to 1450	0 to 2650	1700	3100
Chromel-P to Alumel	−200 to 1200	−300 to 2200	1350	2450
Iron to constantan	−200 to 750	−300 to 1400	1000	1800
Copper to constantan	−200 to 350	−300 to 650	600	1100

country for platinum to platinum-rhodium thermocouples are such that new thermocouples which yield these relations within 2 or 3°C up to 1200°C are readily available.

The differences in the temperature-e.m.f. relations of base metal thermocouples of any one type are so large that the selection of a temperature-e.m.f. relation which might be considered characteristic of the type of thermocouple is difficult and more or less arbitrary. The relations generally used for some of these thermocouples by some manufacturers have been changed from time to time because of differences introduced in the thermoelectric properties of the materials by variations in raw materials and methods of manufacture. However, the relations in use at the present time are such that materials can generally be selected and matched to yield the adopted relations with an accuracy of about ±3°C up to 400°C and to ±¾ percent at higher temperatures. In special cases, materials may be selected to yield the adopted relations within 2 or 3°C for limited temperature ranges.

VII. Temperature-E.M.F. Relations

Corresponding values of temperature and e.m.f. which are considered characteristic of the various types of thermocouples are given in Table II. More detailed tables will be found in the references given in the table. As far as we know the corresponding values given for platinum to 90 platinum-10 rhodium, platinum to 87 platinum-13 rhodium, and Chromel-P-Alumel thermocouples are more or less standard and are the only ones used in this country for these types of thermocouples. The temperature-e.m.f. relation of Chromel-P-Alumel thermocouples has been fairly well controlled because these materials are manufactured primarily with controlled thermoelectric properties for thermocouples by only one company.

The values for iron-constantan headed *A* were determined at the National Bureau of Standards a few years ago as being characteristic of the iron and constantan generally available at that time. The values for iron-constantan headed *B* have been used by certain pyrometer manufacturers for a number of years and presumably are characteristic of the materials available at the time the corresponding values were determined. Owing to the differences in the thermoelectric properties of different lots of iron and constantan, materials must be selected and properly matched in order to obtain a thermocouple which will approximate a selected temperature-e.m.f. relation for this type of thermocouple.

Until recent years copper-constantan thermocouples were used primarily for accurate measurements at temperatures below about 350°C, and in such cases it is customary to calibrate each thermocouple or lot of wire and use an instrument calibrated in millivolts. However, in recent years, there has been an increasing demand for direct reading instruments for use with copper-constantan thermocouples. There are large differences in the temperature-e.m.f. relations of copper-constantan thermocouples and consequently the materials must be selected in order to obtain thermocouples which will yield any specified temperature-e.m.f. relation. No difficulty has been encountered in obtaining thermocouples which will give very closely the temperature-e.m.f. relation in Table II.

VIII. Instruments

Instruments used to measure the e.m.f. developed by thermocouples or to indicate the

TABLE II. *Corresponding values of temperature and e.m.f. for various types of thermocouples.*

Temp. °C	90 Pt-10 Rh to Platinum[1] mv	87 Pt-13 Rh to Platinum[1] mv	Chromel-P to Alumel[2] mv	Iron to Constantan		Copper to Constantan[5] mv
				A[3] mv	*B*[4] mv	
−200			−5.75	−8.27		−5.539
−100			−3.49	−4.82		−3.349
0	0.000	0.000	0.00	0.00	0.00	0.000
+100	0.643	0.646	+4.10	+5.40	+5.28	+4.276
200	1.436	1.464	8.13	10.99	10.78	9.285
300	2.315	2.394	12.21	16.56	16.30	14.859
400	3.250	3.398	16.39	22.07	21.82	20.865
500	4.219	4.454	20.64	27.58	27.39	
600	5.222	5.561	24.90	33.27	33.16	
700	6.260	6.720	29.14	39.30	39.19	
800	7.330	7.927	33.31	45.72	45.48	
900	8.434	9.177	37.36	52.29	51.82	
1000	9.569	10.470	41.31	58.22	58.16	
1100	10.736	11.811	45.14		64.50	
1200	11.924	13.181	48.85			
1300	13.120	14.562	52.41			
1400	14.312	15.940	55.81			
1500	15.498	17.316				
1600	16.674	18.679				
1700	17.841	20.032				

[1] Nat. Bur. Stand. J. Research **10**, 275 (1933), R.P. 530.
[2] Nat. Bur. Stand. J. Research **14**, 239 (1935), R.P. 767.
[3] Nat. Bur. Stand J. Research **20**, 337 (1938), R.P. 1080.
[4] Catalogs, Leeds & Northrup Co. and Brown Instrument Co.
[5] *Pyrometry*, (Symposium published by Am. Inst. Mining Met. Engrs. 1920), p. 165. Int. Crit. Tab. 1, 58 (1926). Nat. Bur. Stand. J. Research 20, 337 (1938), R.P. 1080.

temperature of the measuring junction of a thermocouple may be divided into two general classes: (1) Those operating upon the galvanometric principle such as ordinary millivoltmeters; and (2) those operating upon the potentiometric principle. At one time there was considerable interest in a class of instruments which operate upon a combination of the galvanometric and potentiometric principles but at the present time there appears to be no place or demand for such instruments.

Millivoltmeters

A millivoltmeter consists of a coil of wire suspended between the poles of a permanent magnet so that the coil is free to move. A pointer is attached to the coil and moves over a scale graduated in millivolts or in degrees. Leads from the thermocouple are connected to the terminals of the coil usually through a series resistance, and the e.m.f. generated in the thermocouple circuit sends a current through the coil, causing it to deflect in the magnetic field. The magnitude of the deflection depends upon the current through the coil which in turn depends on the e.m.f. generated by the thermocouple and the resistance of the circuit.

The current I in the circuit is given by

$$I=E/(R_g+R_x),$$

where E is the resultant e.m.f. in the circuit, R_g the resistance of the millivoltmeter, and R_x the resistance of the thermocouple and leads. The potential difference, E_g, across the terminals of the instrument is given by

$$E_g=\frac{R_g}{R_g+R_x}E.$$

Millivoltmeters are ordinarily calibrated to indicate E correctly when connected to a thermocouple and leads of combined resistance R_x. Any change then in either R_g or R_x causes a change in the indications of the instrument. Inasmuch as instruments are frequently used with more than one thermocouple and inasmuch as R_x varies with the temperature and the amount of the wire heated, it is desirable to make R_g large compared to R_x or at least to variations in R_x. However, this cannot be accomplished in most instances because the design of a millivoltmeter for any particular service is a compromise between sensitivity and ruggedness, which to a large extent determines the resistance. Millivoltmeters

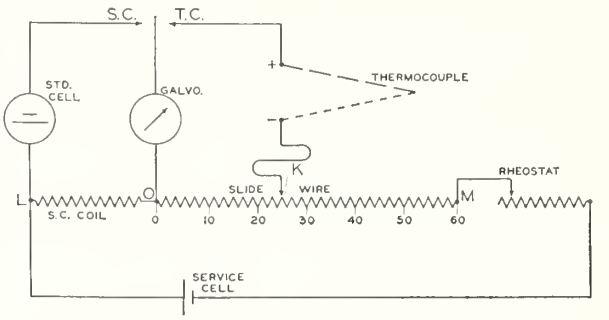

Fig. 7. Diagram of a potentiometer circuit.

with a resistance of much over 600 ohms become extremely delicate and cannot be used in many locations. In order to obtain the ruggedness required it is necessary in some instances to make R_g as low as 12 or 15 ohms. This means that variations in the resistance of the circuit have an appreciable effect upon the indications of the instrument. Owing to these inherent sources of error, millivoltmeters are not very extensively used at the present time.

Potentiometers

The fundamental principle of the potentiometer may be seen by referring to Fig. 7. The current from a service cell which may be a dry cell or a storage cell, passes through the main circuit composed of a series of fixed resistors and can be adjusted by a variable rheostat. The relative values of the fixed resistors and the magnitude of the current determine the range of the instrument. By means of a switch either the standard cell or the thermocouple can be connected to the main circuit and its voltage balanced, through a galvanometer, against an equal voltage drop developed in a portion of the main circuit. The potential drop across the various fixed resistors is made to correspond to definite and reproducible values of voltage by adjusting the current to some standard value.

To standardize the battery current, the switch $S.C.$ is closed and the current adjusted until the potential drop across the resistor LO is equal to the e.m.f. of the standard cell. The e.m.f. of the

thermocouple can then be determined by closing the *T.C.* switch and moving the contact *K* until the potential drop in the resistors in the main circuit from *O* to *K* is equal to the e.m.f. of the thermocouple. The potential drop from *O* to *K* is read on some suitable scale. The resistors included between *O* and *M* may be made up of fixed coils, a slidewire, or a combination of the two.

The galvanometer has no measuring function but serves solely to indicate zero current in its branch of the circuit. As there is no current through the galvanometer and thermocouple when a balance is obtained, the reading of the potentiometer is independent of the resistance of the thermocouple circuit. However, large changes in this resistance affect the precision of balancing because as the resistance is increased the sensitivity of response of the galvanometer is decreased and the greater is the change in e.m.f. required to produce a perceptible deflection of the galvanometer. It is therefore advisable to keep the resistance of the thermocouple and leads within reasonable limits as determined by the characteristics of the galvanometer.

There are several important advantages in the potentiometer method. The scale is easily made very open, thus permitting precise readings if a suitable galvanometer is used. The accuracy of the potentiometer is in no way dependent upon the constancy of magnets, springs, or jewel bearings, nor upon the level of the instrument. Insofar as temperature measurements with thermocouples are concerned, the greatest advantages are the accuracy and the complete elimination of any error due to ordinary changes in the resistance of the thermocouple and leads. The objections to the potentiometer are its higher initial cost and the fact that, except for automatic instruments, a manual adjustment must be made to obtain a reading. In the recording and controlling potentiometer equipment, however, all the various manipulations may be performed automatically even to the standardizing of the battery current.

Potentiometers are used for practically all laboratory work where the highest accuracy is required. At the present time the large part of the instruments in industrial use operate upon the potentiometric principle.

The scales of millivoltmeters or potentiometers may be calibrated either in millivolts or in degrees of temperature for a particular type of thermocouple. Either type of instrument can be made automatically recording and can be equipped with devices for automatically controlling the temperature of a process or furnace.

Inasmuch as the e.m.f. developed by a thermocouple depends upon the temperature of the reference junctions as well as upon the temperature of the measuring junction, corrections must be made for changes in the reference junction temperature unless they are automatically taken care of by the instrument. If properly calibrated, an ordinary millivoltmeter will indicate the temperature of the measuring junction, when the pointer of the indicator is set to read the reference junction temperature on open circuit. If the reference junction temperature is well controlled, this adjustment may be made conveniently by hand. However, if this junction is subject to frequent temperature changes it is advisable to locate the reference junctions at the instrument and use an instrument which automatically changes the indication to compensate for changes in the reference junction temperature. In the case of millivoltmeters this is accomplished automatically by attaching a properly adjusted bimetallic spring to the control spring of the moving coil. If an instrument is equipped with an automatic reference junction compensator for one type of thermocouple, it should not be used with other types of thermocouples nor should it be used in any case unless the reference junctions are located at the instrument.

Potentiometers for industrial use are usually provided with either a hand-operated or an automatic reference junction compensator. A hand-operated compensator is an adjustable resistor, having a scale graduated in millivolts, which the operator sets to correspond with the observed reference-junction temperature. This operation is equivalent to moving the fixed end of the thermocouple circuit (point 0 Fig. 7) to a point corresponding with reference-junction temperature. For use with any one type of thermocouple the compensator may include a nickel coil which varies in resistance as the temperature changes and thus compensates automatically for

changes in the reference-junction temperature. An instrument so equipped is usually calibrated directly in degrees of temperature. Although it is usually at the instrument, an automatic compensator can be located wherever desired. Lead wires from thermocouple to the compensator location in any case must have the same thermoelectric characteristics as the thermocouple wires.

Instruments calibrated in millivolts are generally used:

(1) When very accurate temperature measurements are to be made with individually calibrated thermocouples.
(2) When used with various types of thermocouples.

Instruments are generally calibrated in degrees of temperature:

(1) When used in industrial plants with only one type of thermocouple.
(2) When the inconvenience of converting millivolt values to temperature is considered more important than the errors introduced by the lack of reproducibility of thermocouples of any one type.

Instruments are ordinarily equipped with manually operated reference junction compensators:

(1) When used with various types of thermocouples.
(2) When the reference junctions are not located at the instrument.

Instruments are ordinarily equipped with automatic reference junction compensators:

(1) When the reference junctions are located at the instrument and subject to considerable variations in temperature.
(2) When the inconvenience of making manual adjustments or arithmetical corrections is considered more important than the errors introduced by using automatic compensators.

IX. Protection Tubes

One of the reasons why the materials listed in Table I have come into common use for thermocouples is that they are reasonably stable thermoelectrically when heated in a clean oxidizing atmosphere. The standards of performance which are generally accepted for the various combinations of thermocouple materials are based upon their performance in air. Although it has not been shown that a reducing atmosphere, in itself, necessarily contaminates or alters the thermoelectric properties of thermocouple materials, it is nevertheless generally observed that exposure of thermocouples to such atmospheres is accompanied by contamination or changes in the chemical composition which seriously alter the thermoelectric properties. In order to obtain the best performance of thermocouples, it appears necessary to maintain them in an atmosphere having essentially the same composition as air. Consequently the selection of a proper protection tube, which will protect the thermocouple from vapors, fumes, or furnace gases, is sometimes as important as the selection of the thermocouple materials.

Changes in thermoelectric characteristics result from causes such as the following.

(1) Metals (solid, liquid, or vapor) coming into contact with the thermocouple materials and altering their chemical composition.

(2) Furnace gases and fumes coming into contact with the thermocouple materials. Sulphur and sulphur compounds are particularly deleterious.

(3) Materials normally stable in an oxidizing atmosphere coming into contact with the thermocouples in a reducing atmosphere. One common cause of contamination, which is serious in the case of rare metal thermocouples, is the reduction of silica (usually present in insulating and ceramic protection tubes) to silicon which readily combines with the thermocouple materials.

(4) Preferential oxidation and reduction of base metal alloys exposed alternately to oxidizing and reducing atmospheres. This results in a gradual change in chemical composition, because all the elements which comprise an alloy are not oxidized and reduced at the same rates under all conditions.

Many types of protection tubes are required in order to meet all needs. In many cases, the conditions under which thermocouples are used are such that two tubes are required to provide the desired protection. For instance, a primary

tube of porcelain or fused silica may be placed inside a secondary tube of metal, silicon carbide, or fire clay. The primary tube of low volatility is intended to provide imperviousness to gases at high temperatures, and the secondary tube to provide resistance to thermal and mechanical shock and to corrosion.

In thus providing protection for the thermocouple, however, one should not lose sight of the fact that a thermocouple can perform its function only when the conditions of heat transfer are such that the measuring junction attains or at least approaches the temperature to be measured. When a tube of large cross section or more than one tube is used, particularly if the tubes have a high thermal conductance, it should be carefully considered whether the depth of immersion is sufficient to insure that the temperature of the thermocouple junction is reasonably close to the temperature to be measured. Short thick-walled tubes may cool the junction so much that the indications are comparatively worthless.

Platinum to platinum-rhodium thermocouples are particularly susceptible to contamination and should be protected by ceramic tubes which are impervious to gases and vapors at all operating temperatures. Metal protection tubes usually provide sufficient protection for base metal thermocouples. The oxide coatings on the thermocouple wires are fairly effective in protecting the wires from contamination by metallic vapors. Metal tubes which provide sufficient protection in an oxidizing atmosphere may be entirely unsatisfactory if large amounts of furnace gases are present. In some installations it has been found advisable to ventilate the interior of the protection tube with a slow stream of air in order to minimize the deleterious effects of furnace gases.

The primary ceramic tubes which meet most requirements of stability and imperviousness to gases are: highly refractory porcelain, sometimes called "Sillimanite" or "Mullite" for temperatures up to about 1550°C (2800°F), fused silica for temperatures up to about 1050°C (1900°F) in an oxidizing atmosphere, and Pyrex glass for temperatures up to about 600°C (1100°F).

The secondary or metal tube most suitable for a particular application depends to a large extent upon the type of corrosion encountered. Nickel-chromium-iron tubes are particularly useful in oxidizing atmospheres, chromium-iron tubes in atmospheres containing sulphur, and nickel or iron tubes in hot caustic and molten metal baths. The temperature limits given in Table III for the various types of tubes are those which will, in general, result in a reasonably long life. The tubes may be used at higher temperatures than those given but higher operating temperatures will result in a shorter life.

Fire clay, silicon-carbide, and graphite meet certain requirements of secondary tubes at temperatures above the useful limits of metal tubes. Numerous other types of tubes have been developed for specific purposes. Recommendations regarding tubes for any particular purpose may be obtained from pyrometer manufacturers.

X. Calibration of Thermocouples

Various methods used for calibrating thermocouples and of testing thermocouple materials and the precautions which must be observed in order to attain various degrees of accuracy are given in a separate paper, which is essentially the same text as the paper entitled "Methods of testing thermocouples and thermocouple materials" published originally in the *Journal of Research of the National Bureau of Standards*.[13] The numerical values in the original text have been brought into agreement with later published data.

XI. Measurement of Temperatures

The measurement of the temperature of any particular object or space is in many cases a problem in itself, even after a suitable thermocouple has been selected and calibrated. The methods employed in many instances are described elsewhere in this symposium. However, there are certain fundamentals that must be observed in any case.

The temperature indicated by a thermocouple is that of its measuring junction, but usually this is of no interest in itself. The accuracy obtained in measuring the temperature of any object or space usually depends upon how closely the junction of the thermocouple can be brought to the same temperature as that of the object or space, or to some temperature which is definitely related to that of the object or space.

Table III. *Recommended maximum operating temperature of metal protection tubes.*

Type of Tube	Recommended Maximum Temperature	
	°C	°F
Seamless steel	550	1000
Wrought iron	700	1300
Cast iron	700	1300
Calorized wrought iron	800	1500
14 percent chromium iron	800	1500
28 percent chromium iron	1100	2000
18 (Cr)-8 (Ni)-stainless steel	850	1600
32 Ni-20 Cr-48 Fe	1100	2000
62 Ni-13 Cr-25 Fe	1150	2100
Nickel	1100	2000

If under steady conditions there is a net exchange of heat between the thermocouple junction and an object, then there is a difference in temperature between the two. The magnitude of this difference in temperature depends upon the rate of heat transfer and the thermal resistance between the junction and the object. The idea then is to bring the thermocouple junction into as good thermal contact as possible with the object and to insulate the junction as well as possible against the transfer of heat to or from other objects or spaces. Greater precautions are obviously necessary in accurate measurements than in rough ones.

As an illustration, suppose we desire to measure the temperature of a metal plate which is heated from within by some means. The bare thermocouple junction is brought into contact with the metal plate. The junction will receive some heat from the plate by thermal conduction and probably a smaller amount, by radiation and convection. The junction will lose heat by conduction along the thermocouple wires, and by convection, conduction, and radiation to the surroundings. Obviously the junction will be at a lower temperature than the plate. However, this difference in temperature can be reduced by the following.

(A) By improving the thermal contact. (1) By flattening the junction to obtain a larger area of contact or better still (2) by soldering, brazing, or welding the junction to the plate.

(B) By reducing the heat loss from the junction. (1) By keeping the wires close to the plate for some distance so as to reduce the temperature gradient in the wires near the junction, and/or (2) by raising the temperature of the space immediately surrounding the junction (a) by insulating the junction from that space or (b) by utilizing an auxiliary source of heat as is done in the compensated contact thermometer.[14,15]

The thermocouple junction may be at either a higher or lower temperature than the object depending upon the direction of the net heat transfer. The use of thermocouple protection tubes usually makes it more difficult to bring the thermocouple junction to nearly the same temperature as that of an object, because of the additional thermal resistance introduced between the junction and object and the additional transfer of heat along the protection tubes. For example, the junction of a thermocouple may be brought within a few hundredths of a degree of the temperature of a liquid by immersing the bare wires in the liquid for a distance of 5 to 10 diameters of the wire, whereas if a protection tube is used with the thermocouple it will be necessary to immerse the junction 5 to 10 diameters of the protection tube to obtain the same degree of accuracy. In most applications, the best that can be done is to bring the thermocouple junction and object as close together as possible and immerse the thermocouple as far as practicable in the heated medium.

In the measurement of certain temperatures, particularly those of small objects and materials of low thermal conductivity, consideration must be given to the possibility that the temperature to be measured may be altered by the introduction of the temperature measuring device.

In the measurement of temperatures varying with time, heat capacity of thermocouples and protecting tubes as well as thermal contacts are involved. If the temperature is rising, the temperature of the junction itself will at any instant be lower than that of the surroundings. The reverse will be true if the temperature is falling. This is referred to as thermal lag. By appropriate auxiliary measurements, however, it is usually possible to determine the lag[16] under the particular conditions of use, and apply corrections to the thermocouple readings.

XII. Installations

The cost of pyrometer equipment is great enough to warrant installing it, not only so that the desired temperature can be measured with

the required accuracy but also in such a manner as to protect the equipment, as far as practicable, from changes and deterioration. The installation of simple pyrometer equipment for more or less temporary service in an air-conditioned laboratory, far removed from the vibrations set up by heavy equipment such as trip hammers, rolling mills, etc., is a comparatively simple matter. However, in the large installations required in many industrial plants, every precaution should be taken to protect the thermocouple, wiring, and instruments from the various deleterious conditions which may seriously affect their accuracy and life.

1. General Precautions

The installation of extensive thermocouple equipment requires the services of competent electricians. Just as much attention, if not more, should be given to the wiring, switches, switchboards, etc., as is given in the case of ordinary power installations. Proper fixtures should be used to mount the thermocouples in the furnaces. Lead wires should have a weatherproof covering and should be run in a metal conduit except possibly for a short length of flexible cable at the ends of the conduit. The conduit should be grounded to prevent leakage from power installations or lighting circuits. All joints in the lead wires should be soldered and taped. When indicators or recorders of low resistance are employed, it is of the greatest importance to have a well-constructed electrical installation to insure a constant line resistance. Since instruments of low resistance are usually calibrated for a low line resistance of definite value, special attention must be given to contact resistances at switches. Frequently switches rated at 100 amperes are required, although the actual thermoelectric current is only a few milliamperes. If the indicator is of high resistance, or operates upon the potentiometric principle, the factor of very low line resistance is not of great importance, but the wiring should be well installed, to avoid large changes in the resistance. Stationary indicating and recording instruments usually should be mounted upon switchboards, with suitable selective or commutating switches when several thermocouples are to be used with one indicator. When the junction between the thermocouple

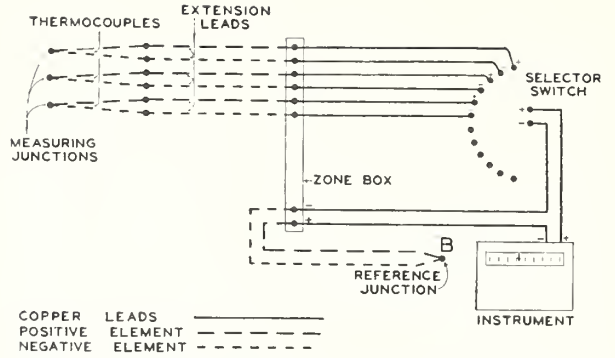

Fig. 8. Connections between several thermocouples and a distant instrument.

and leads is exposed to severe conditions, rain, etc., as in outside kilns, a weatherproof terminal head should be used. This consists of an outside casing which fits over both binding posts. The cover may be tapped for conduit wiring or provided with a packing gland or stuffing box if a length of flexible cable is used between the thermocouple and the conduit.

The indicator or recorder should be conveniently located. If the instrument is desired especially for the use of the operator of a furnace, it should be placed where it is readily visible. It should be mounted where vibration and excessive dirt and dust will not injure delicate parts of the mechanism. In almost all industrial installations an outside protecting case is required to prevent dust from filtering through the case of the indicator. Special devices are employed to damp out vibration when this is serious, as in the neighborhood of a trip hammer or rolling mill. Frequently the instruments are suspended on "vibration-proof mountings."

2. Location of Thermocouples

The proper location of the thermocouple in a furnace depends upon the particular process and the use to which the furnace is put. The primary consideration is to locate the measuring junction so that it acquires the temperature which it is desired to measure. This requires taking into consideration the thermal lag and heat transfer to and from the thermocouple junction. Both of these factors are materially affected by protection tubes. A secondary consideration, however, is to locate the thermocouple where the lead wires may be conveniently located. The space between

the protecting tube and the furnace wall should be plugged with refractory cement, so that hot air cannot strike through the hole onto the terminals of the thermocouple, nor cold air be drawn in, thus cooling the measuring junction of the thermocouple.

3. Common Return

The use of a common return wire for a multiple installation is in general unsatisfactory. When grounds or short circuits occur at any point between the measuring junctions and the instrument—for example, between the common return and the other lead wire of one thermocouple—all the thermocouples on the common return have, in addition to their own e.m.f., an impressed potential drop due to the current flowing in the shorted thermocouple. This may cause a large error in the reading of every thermocouple in the system. With the common return, leakage from a power installation affects the readings of every thermocouple connected to the return and a leakage through a high resistance may alter the readings of every thermocouple by the same amount so that the presence of such leaks is not always readily detected. It is also possible by leakage from different thermocouples to the ground to obtain very erratic and erroneous readings when the common return is employed. The insulation resistance of materials becomes very low at high temperatures making it difficult to insulate the various thermocouple wires from one another and from the furnace parts, even when individual returns are used. Base-metal thermocouples are frequently constructed with the measuring junction welded to the end of the metal protecting tube in order to reduce thermal lag. Even when the thermocouple is not welded at this point, the measuring junction usually touches the protecting tube and is in good electrical contact with it. If a common return is used when the thermocouples are mounted in this way, any electrical connection or leakage between the metal protecting tubes (through the furnace structure, etc.) will produce serious errors. However, if individual returns are used, the metal protecting tubes need not be insulated from one another. The troubles ordinarily encountered with common return installations are sufficient to warrant the extra cost of the wire required to install individual thermocouple circuits.

4. Use of a Zone Box

Extension lead wires are rather costly and should not be employed extravagantly. Also the use of long lengths of extension leads increases the line resistance, since the resistivity of the lead materials is much higher than that of copper.

For an installation in which several thermocouples are connected through a selector switch to an instrument located at some distance from a furnace, a wiring scheme similar to that shown in Fig. 8 may be very useful in saving extension lead wire and consequently in reducing the cost and resistance of the line. The common reference junction "*B*" for each thermocouple can be located at any conveniently controlled point or at the instrument if the latter is equipped with an automatic reference junction compensator by running only one pair of extension leads from the zone box to the controlled point or the instrument. A zone box is a box or zone of uniform temperature which need not be measured or maintained constant. It should be pointed out that although a common reference junction is used for all the thermocouples, the system is not subject to any of the objections which have been raised against the use of a common return.

5. Thermocouples Purposely Insufficiently Immersed

In many processes a furnace is operated at such a high temperature that a thermocouple or protecting tube cannot withstand the severe conditions inside the furnace. In this case the thermocouple may be advantageously inserted only part way through the furnace wall, or flush with the inner wall of the furnace. The temperatures indicated by thermocouples installed in this manner are always lower than those of the furnace interior, but they may bear a fairly definite relationship to the temperature of the furnace, and hence the method may be satisfactory for temperature control and reproduction of furnace conditions from day to day.

6. Measurement of Average Temperature

It is frequently desirable to measure "the average temperature" of an object or a heated

space by using thermocouples. No discussion of what is meant by the average temperature of an object or space or why anyone would be interested in measuring any such average will be given here. The average temperature that can be measured with thermocouples is only a mean of the temperatures of the measuring junctions of a number of thermocouples. This average may or may not be a close approximation to the average temperature which one desires to measure, depending upon such factors as the temperature distribution, the number and location of the thermocouples, etc.

If the measuring junctions of a number of thermocouples are placed in thermal contact with an object or located in a heated space, the average temperature of the junctions may be obtained by any one of three methods: (1) by reading the thermocouples individually and averaging the readings; (2) by connecting them in series and reading the total e.m.f.; or (3) by making all the thermocouples of equal resistance and connecting them in parallel so that the average e.m.f. is read directly. Although each of these methods has certain practical advantages over the others, they are all equivalent in that one is no more accurate than the others and that the same average temperature (that of the junctions) is measured in each case. In the following discussion, it will be assumed that the temperature-e.m.f. relations of all the thermocouples used in any one case are identical and that any correction or compensation required for the reference junctions is properly cared for.

The important advantages of taking readings of the individual thermocouples are that (1) one obtains not only the average temperature but also some idea of the temperature distribution, (2) the thermocouple junctions may be placed in contact with or welded to metal objects, thus insuring good thermal contact, and (3) the failure of any individual thermocouple is immediately detected. The disadvantage is that several observations must be taken, requiring several instruments if the observations are to be taken simultaneously or considerable time during which the temperatures may change if the observations are to be taken with one instrument.

One may average the values of the e.m.f. of the individual thermocouples and obtain the average temperature from the average e.m.f. or one may average the temperature values obtained for each thermocouple. The average values obtained in these two different ways will not necessarily agree exactly owing to the fact that the e.m.f. of a thermocouple is not a linear function of the temperature. If the temperature gradients in the object or heated space are not very large (less than about 50°C) the difference in the averages obtained in the two different ways is usually insignificant. If the temperature gradients in the object or heated space are so large (several hundreds of degrees) that there is an appreciable difference in the average temperature obtained in the two different ways, the average temperature obtained by using thermocouples located at several selected points probably has no exact significance.

Because values of temperature may be obtained with the individual thermocouples and averaged with this method, it is not necessary to use thermocouples with approximately the same temperature-e.m.f. relation.

The important advantage of connecting the thermocouples in series or in parallel is that only one observation is required to obtain the average e.m.f. of a number of thermocouples. However, such a single observation yields no information regarding the temperature distribution in the object or space. Connecting the thermocouples in series requires that the thermocouple wires and measuring junctions be electrically insulated from one another. This makes it difficult under certain conditions to bring the junctions in good thermal contact with an electrically conducting medium.

The objections to connecting a number of thermocouples in series are: (1) The e.m.f. developed by the thermocouples in series may be too great to be measured with the instruments available; (2) A short circuit which might materially reduce the e.m.f. of one of the thermocouples would not be detected by a single observation of the total e.m.f.

It can be shown by applying Kirchhoff's laws, that the potential difference across the terminals of a number of thermocouples of equal resistance connected in parallel is the average of the e.m.f.'s of the individual thermocouples. Inasmuch as the

average e.m.f. is measured directly when the thermocouples are connected in parallel, the e.m.f. can be measured with any instrument that is used for measuring the e.m.f. of a single thermocouple.

It should be pointed out that the temperature indicated when the two individual thermocouple wires are attached to a metal object at two points which may be designated P and Q (so that the electric circuit is completed through the metal), depends upon the thermoelectric power of the metal with respect to the thermocouple wires and is not necessarily the temperature of the metal at any point between P and Q and consequently is not the average temperature of the metal between P and Q except in very special cases. If the metal to which the thermocouple wires are attached is thermoelectrically positive to one element of the thermocouple and negative to the other, the temperature measured will be somewhere between those of P and Q. The thermocouple will indicate a temperature approximately midway between those of P and Q only if the metal is approximately midway between the two thermocouple wires thermoelectrically.

It is readily seen that if the wires of an iron-constantan thermocouple are attached to a piece of iron, the temperature measured will be that where the constantan wire is attached and if they are attached to a piece of constantan the temperature measured will be that where the iron wire is attached.

If the metal to which the thermocouple wires are attached is thermoelectrically positive or negative to both wires of the thermocouple, the value of the temperature indicated will not be between those of P and Q. For example, suppose that the wires of a platinum to 90 platinum-10 rhodium thermocouple are attached to a piece of constantan, and that the temperature of the point where the platinum wire is attached is 700°C and that where the platinum-rhodium is attached is 750°C. Let the reference junctions of the thermocouple be at 0°C. The circuit is equivalent to a 90 platinum-10 rhodium to constantan thermocouple with its junctions at 750° and 0°C in series with a constantan to platinum thermocouple with its junctions at 700° and 0°C. The resultant e.m.f. developed in the circuit will be approximately 9.14 mv which corresponds to 962°C for the platinum to 90 platinum-10 rhodium thermocouple.

XIII. Conclusion

In conclusion the author would like to emphasize that the success attained in the measurement of temperatures with thermocouples depends primarily upon the ability of the observer to bring the junctions of the thermocouples to the desired temperatures and upon the stability of the thermocouple materials. The reader's attention is directed to a number of papers in this symposium which deal with (1) the measurement of temperatures in particular cases, (2) the stability of thermocouples, and (3) the instruments available for use with thermocouples in the measuring, recording, and controlling of temperatures.

XIV. Bibliography

1. T. J. Seebeck, Gilb. Ann. **73**, 115, 430 (1823); Pogg. Ann. **6** 1, 133, and 253 (1826).
2. P. D. Foote and T. R. Harrison, J. Wash. Acad. Sci. **8**, 545 (1918).
3. J. C. A. Peltier, Ann. chim. Phys. 2nd ser. **56**, 371 (1834).
4. Quintus Icilius, Ann. d. Phys. und Chem. Pogg. **89**, 377 (1853).
5. W. Thomson, Proc. Roy. Soc. Edin. December 15, 1851.
6. W. Thomson, Proc. Roy. Soc. Lon. VII, May, 1854. Phil. Mag. July, 1854.
7. W. Thomson, Trans. Roy. Soc. Edin. **21**, 123 (1857); Read May 1, 1854.
8. E. Edlund, Pogg, Ann. **140**, 435 (1870); Pogg. Ann. **143**, 404, 534 (1871).
9. H. Jahn, Wied. Ann. **270**, 755 (1888).
10. A. E. Caswell, Phys. Rev. **33**, 379 (1911).
11. G. Borelius, Ann. d. Physik. (4) **52**, 398 (1917); **56**, 388 (1918).
12. G. R. Fitterer, A. I. M. E., Iron & Steel Div. **105**, 290 (1933); A. I. M. E. **20**, 189 (1936).
13. W. F. Roeser and H. T. Wensel, J. Research Nat. Bur. Stand. **14**, 247 (1935), R.P. 768.
14. M. W. Boyer and J. Buss, Ind. & Eng. Chem. **18**, 728 (1926).
15. W. F. Roeser and E. F. Mueller, Bur. Stand. J. Research **5**, 793 (1930), R.P. 231.
16. D. R. Harper, 3rd, Bul. Bur. Stand. **8**, 659 (1912), S185.

UNITED STATES DEPARTMENT OF COMMERCE • Sinclair Weeks, *Secretary*
NATIONAL BUREAU OF STANDARDS • A. V. Astin, *Director*

Methods of Testing Thermocouples and Thermocouple Materials

Wm. F. Roeser and S. T. Lonberger

National Bureau of Standards Circular 590

Issued February 6, 1958
(Superesedes Research Paper 768)

Contents

574278 O - 61 - 7

Methods of Testing Thermocouples and Thermocouple Materials

Wm. F. Roeser and S. T. Lonberger [1]

Various methods used for testing thermocouples and thermocouple materials and the precautions that must be observed in order to attain various degrees of accuracy are described. In particular, the methods that have been developed and used at the National Bureau of Standards are outlined in detail, and some guidance is given to the reader in the selection of the method best adapted to a given set of conditions.

Consideration is given primarily to the calibration of platinum versus platinum-rhodium, copper-constantan, Chromel-Alumel, and iron-constantan thermocouples.

1. Introduction

Methods of testing thermocouples and thermocouple materials have been developed to supply the need of those industries to which the measurement and control of temperature are essential. The recognition by the various industries in this country that the measurement and control of temperature are essential to a uniformly high quality of product has led, in recent years, to a tremendous increase in the use of temperature-measuring equipment. Where the higher temperatures are involved, by far the greater portion of such measurements is made with thermocouples, and therefore these devices must be regarded as one of the important tools of modern industry.

The users of thermoelectric pyrometers have been demanding ever-increasing accuracy in these instruments. Thermocouple materials are being bought on closer specifications, and the pyrometer manufacturers have been setting up smaller tolerances in the inspection and calibration of their product, with the result that practically all pyrometric equipment now being sold is of very high quality. Reliable methods of testing thermocouples and thermocouple materials are required to realize the degree of accuracy now demanded. The purpose of this Circular is to describe the more important of these methods and to point out certain precautions that must be observed to secure reliable results. The essential features of many of these methods and much of the apparatus described here have been devised and described in whole or in part by various writers, but references to their papers will be made only when it is felt that a more detailed description than is given here will be helpful to the reader.

Combinations of metals and alloys extensively used in thermocouples for the measurement of temperatures in this country are listed in table 1, together with the temperature ranges in which they are generally used and the maximum temperatures at which they can be used for short periods. The period of usefulness at high temperatures depends largely upon the temperature and the diameter of the wires. The methods described in this Circular were devised primarily for calibrating thermocouples in the usual temperature ranges, but unless otherwise indicated they may be used up to the maximum temperatures at which the various types of thermocouples can be used.

TABLE 1. *Types of thermocouples and temperature ranges in which they are used*

Type of thermocouple	Usual temperature ranges		Maximum temperatures	
	°C	°F	°C	°F
Platinum versus platinum-rhodium	0 to 1,450	32 to 2,650	1,700	3,100
Chromel-Alumel	−190 to +1,100	−310 to +2,000	1,350	2,450
Iron-constantan	−190 to +760	−310 to +1,400	1,000	1,800
Copper-constantan	−190 to +300	−310 to +570	600	1,100

2. General Considerations

2.1. Temperature Scale

The object in the calibration of any thermocouple is to determine an emf-temperature relationship in which the temperature is expressed on a definite and reproducible scale. The International Temperature Scale, adopted in 1927 [1] [2] by 31 nations and revised in 1948 [2], is now in practically universal use. The methods of realizing this scale are described in detail in the references

[1] Now with American Machine & Foundry Co., Alexandria, Va.

[2] Figures in brackets indicate the literature references at the end of this Circular.

TABLE 2. *Instruments, calibration points, and interpolation equations of the International Temperature Scale of 1948*

Temperature ranges		Instruments	Calibration points (values for pressure of 1 standard atmosphere)			Interpolation equations [a]
° C	° F		*Fixed point*	° C	° F	
−182.970 to 0	−297.346 to 32	Platinum resistance thermometer.	Boiling point of oxygen.	−182.970	−297.346	$R_t=R_0[1+At+Bt^2+C(t-100)t^3]$.
			Ice point [b]	0	32	
			Boiling point of water	100	212	
			Boiling point of sulfur	444.600	832.280	
0 to 630.5	32 to 1,166.9	Platinum resistance thermometer.	Ice point [b]	0	32	$R_t=R_0(1+At+Bt^2)$.
			Boiling point of water	100	212	
			Boiling point of sulfur	444.600	832.280	
630.5 to 1,063.0	1,166.9 to 1,945.4	Platinum versus platinum-10-percent-rhodium thermocouple.	Freezing point of antimony.	[c] 630.5	[c] 1,166.9	$E=a+bt+ct^2$.
			Freezing point of silver.	960.8	1,761.4	
			Freezing point of gold.	1,063.0	1,945.4	
1,063.0 and above	1,945.4 and above	Optical pyrometer	Freezing point of gold.	1,063.0	1,945.4	$\frac{J_t}{J_{Au}}=\frac{e^{\frac{c_2}{\lambda(t_{Au}+T_0)}}-1}{e^{\frac{c_2}{\lambda(t+T_0)}}-1}$.

[a] R_t is the resistance at t°C, R_0, the resistance at 0°C; A and B are constants determined by calibration at the boiling points of water and sulfur, and C is an additional constant determined by calibration at the boiling point of oxygen. E is the emf at t°C, and a, b, and c are constants. J_t and J_{Au} are the radiant energies per unit wavelength interval at wavelength, λ, emitted per unit time by unit area of a black body at the temperature, t, and at the gold point, t_{Au}, respectively, c_2 is 1.438 cm degrees, T_0 is the temperature of the ice point in degrees K. λ, is a wavelength of the visible spectrum, and e is the base of Naperian logarithms.

[b] It is recommended that for work of the highest precision, the zero point be realized by means of the triple point of water, a point to which the temperature +0.0100° C has been assigned.

[c] The freezing temperature of the antimony used in determining these constants shall be determined with a standard resistance thermometer, and shall be not lower than 630.3° C. Alternatively, the thermocouple may be calibrated by direct comparison with a standard resistance thermometer in a bath at any uniform temperature between 630.3° and 630.7° C.

cited. The instruments, calibration points, and interpolation equations to be used in the various ranges of the scale are summarized in table 2.

Methods of improving the International Temperature Scale are subjects of continuous study in many laboratories. Although such studies may result in minor changes in the values assigned to fixed points or in the substitution of one fixed point for another, they will not alter, in general, the methods of calibrating thermocouples.

2.2. General Methods

In order to calibrate thermocouples to yield temperatures on the International Temperature Scale, it is apparent from the definition that they must be so calibrated that their indications agree with those of the standard platinum-resistance thermometer in the range −182.970° to 630.5° C, the standard platinum versus platinum-10-percent-rhodium thermocouple in the range 630.5° to 1,063.0° C, and the optical pyrometer above 1,063.0° C. The most direct procedure would therefore be to compare the thermocouples directly with these primary instruments in the appropriate temperature ranges. However, to follow such a procedure in the calibration of every thermocouple requires more time and apparatus than is justifiable or necessary because, in most cases, other methods are available which yield results sufficiently accurate. For example, a thermocouple may be compared indirectly with any of the primary instruments by determining its emf at a number of fixed points, either those which are used in defining the scale or others, the values for which have been determined with the primary instruments. If a few laboratories maintain the apparatus necessary to calibrate thermocouples as working standards to yield temperatures on the International Temperature Scale, these standards may be used subsequently to calibrate other thermocouples. This procedure is used far more than any other because the comparison of the indications of two thermocouples is usually simpler than the comparison of two different types of instruments.

The temperature-emf relationship of a homogeneous [3] thermocouple is a definite physical property and, therefore, does not depend upon the details of the apparatus or method employed in determining this relation. Consequently, there are innumerable methods of calibrating thermocouples, the choice of which depends upon the type of thermocouple, temperature range, accuracy required, size of wires, apparatus available, and personal preference.

Thermocouple calibrations are required with various degrees of accuracy, ranging from 0.1° to 5° or 10° C. For an accuracy of 0.1° C, agreement with the International Temperature Scale and methods of interpolating between the calibration points become problems of prime importance, but for an accuracy of about 10° C, comparatively simple methods of calibration will usually suffice. The most accurate calibrations in the range −190° to 300° C are made by comparing the thermocouples directly with a standard platinum resistance thermometer in a stirred liquid bath. In the range 300° to 630.5° C (and below if a platinum resistance thermometer or stirred liquid bath is not available) thermocouples are most accurately calibrated at the freezing or boiling points of pure substances. Between 630.5° and 1,063.0° C, the platinum versus

[3] A homogeneous thermocouple is one in which each element is homogeneous, in both chemical composition and physical condition, throughout its length.

platinum-10-percent-rhodium thermocouple calibrated at the freezing points of gold, silver, and antimony serves to define the International Temperature Scale, and other types of thermocouples are most accurately calibrated in this range by direct comparison with the standard thermocouple calibrated as specified. Other platinum, versus platinum-rhodium thermocouples may be calibrated just as accurately at the fixed points as the platinum versus platinum-10-percent-rhodium thermocouple, but interpolated values at intermediate points may depart slightly from the International Temperature Scale. Above 1,063.0° C, the most basic calibrations are made by observing the emf when one junction of the thermocouple is in a black-body furnace, the temperature of which is measured with an optical pyrometer. However, the difficulties encountered in bringing a black-body furnace to a uniform temperature make the direct comparison of these two types of instruments by no means a simple matter. Other methods of calibrating a thermocouple above 1,063.0° C are given under melting points and under methods of interpolation.

Although the platinum versus platinum-10-percent-rhodium thermocouple serves to define the scale only in the range 630.5° to 1,063.0° C, this type of thermocouple calibrated at fixed points is used extensively both above and below this range as a working standard in the calibration of other thermocouples. For most industrial purposes, a calibration accurate to 2° or 3° C in the range room temperature to 1,200° C is sufficient. Other thermocouples can be calibrated by comparison with such working standards almost as accurately as the calibration of the standard is known. However, it might be pointed out that outside the range 630.5° to 1,063.0° C any type of thermocouple suitable for the purpose, and calibrated to agree with the resistance thermometer or optical pyrometer in their respective ranges, has as much claim to yielding temperatures on the International Temperature Scale as the platinum versus platinum-10-percent-rhodium thermocouple. In fact, at the lower temperatures, certain types of base-metal thermocouples are definitely better adapted for precise measurements.

The calibration of thermocouples then may be divided into two general classes, depending upon the method of determining the temperature of the measuring junction, (1) calibration at fixed points and (2) calibration by comparison with standard instruments, such as thermocouples, resistance thermometers, etc.

In order to obtain the high accuracies referred to above and usually associated with calibrations at fixed points, it is necessary to follow certain prescribed methods and to take the special precautions described in detail in the following sections, but for an accuracy of about 5° C the more elaborate apparatus to be described need not be employed.

2.3. Homogeneity

The magnitude of the emf developed by a thermocouple depends upon the temperatures of the measuring and reference junctions and the composition of the wires in the region of temperature gradients. The emf developed by an inhomogeneous thermocouple is characteristic of the temperature of the measuring junction only when the region of inhomogeneity is not in a region of temperature gradients. Therefore, in order to obtain a high degree of accuracy with a thermocouple, the homogeneity of the wires must be established.

Thermocouple wire now being produced by the manufacturers in this country is sufficiently homogeneous in chemical composition for most purposes. Occasionally, inhomogeneity in a thermocouple may be traced to the manufacturer, but such cases are rare. More often it is introduced in the wires during tests or use. It usually is not necessary, therefore, to examine new thermocouples for inhomogeneity, but thermocouples that have been used for some time should be so examined before an accurate calibration is attempted.

Although rather simple methods are available for detecting thermoelectric inhomogeneity, no satisfactory method has been devised for quantitatively determining it or the resulting errors in the measurement of temperatures. Tests for inhomogeneity must be so designed that the method of testing does not of itself introduce inhomogeneities into the wire being tested. Abrupt changes in the thermoelectric power may be detected by connecting the two ends of the wire to a sensitive galvanometer and slowly moving a sharp temperature gradient, such as that produced by a piece of solid carbon dioxide, a Bunsen burner, or small electric furnace, along the wire. This method is not satisfactory for detecting gradual changes in the thermoelectric power along the length of the wire. Inhomogeneity of this nature may be detected by doubling the wire and inserting it to various depths in a uniformly heated furnace, the two ends of the wire being connected to a galvanometer as before. If, for example, the doubled end of the wire is immersed 25 cm in a furnace with a sharp temperature gradient so that two points on the wire 50 cm apart are in the temperature gradient, the emf determined with the galvanometer is a measure of the difference in the thermoelectric properties of the wire at these two points.

After reasonable homogeneity of one sample of wire has been established, it may be used in testing the homogeneity of similar wires by welding the two together and inserting the junction into a heated furnace. The resulting emf at various depths of immersion may be measured by any convenient method. Other similar methods have been described for detecting inhomogeneity [3].

Tests such as those described above will indicate the uncertainty in temperature measurements

due to inhomogeneity in the wires. For example, if a difference in emf of 10 microvolts (abbreviated hereafter μv) is detected along either element of a platinum versus platinum-rhodium thermocouple by heating various parts of the wire to 600° C, measurements made with it are subject to an uncertainty of the order of 1° at 600° C or of 2° at 1,200° C. Similarly, if an emf of 10 μv is detected along an element of a base-metal thermocouple with a source of heat at 100° C, measurements made with it are subject to an uncertainty of the order of 0.2° C at this temperature. The effects of inhomogeneity in both wires may be either additive or subtractive, and, as the emf developed along an inhomogeneous wire depends upon the temperature distribution, it is evident that corrections for inhomogeneity are impracticable if not impossible.

2.4. Annealing

Practically all base-metal thermocouple wire produced in this country is annealed or given a "stabilizing heat treatment" by the manufacturer. Such treatment is generally considered sufficient, and seldom is it found advisable to further anneal the wire before testing.

Although the new platinum and platinum-rhodium thermocouple wires as sold by some manufacturers are already annealed, it has become regular practice in many laboratories to anneal or "stabilize" all platinum versus platinum-rhodium thermocouples, whether new or previously used, before attempting an accurate calibration. This is usually accomplished by heating the wire electrically in air. The entire length of wire is supported between two binding posts, which should be close together so that the tension in the wires and stretching while hot are kept at a minimum. The temperature of the wire is most conveniently determined with an optical pyrometer.[4] It is necessary, however, to add a correction to the observed apparent temperature to obtain the true temperature, which is always the higher. The correction (based on an emissivity of 0.33) amounts to 130° and 145° C, respectively, for apparent temperatures of 1,270° and 1,355° C.

There is some question as to the optimum temperature or length of time at which such thermocouples should be annealed to produce the most constant characteristics in later use [4]. As a matter of fact, there is some question as to whether annealing for more than a few minutes is harmful or beneficial. Most of the mechanical strains are relieved during the first few minutes of heating at 1,400° to 1,500° C, but it has been claimed that the changes in the thermal emf of a thermocouple in later use will be smaller if the wires are heated for several hours before calibration and use. The principal objection to annealing thermocouples for a long time at high temperatures, aside from the changes in emf taking place, is that the wires are weakened mechanically as a result of crystal growth. For a number of years prior to 1935, the practice at the National Bureau of Standards was to anneal all platinum versus platinum-rhodium thermocouples electrically in air for 6 hr at 1,500° C before calibration. The emf of a number of new thermocouples was determined both after annealing for 5 min and for 6 hr at 1,500° C, and in no case did the change in emf correspond to as much as 2° C at 1,200° C. After 6 hr of heating, the wires, particularly the platinum element, become much softer. It has been found, however, that annealing at temperatures much above 1,500° C produces rapid changes in the emf and leaves the wire very weak mechanically. The National Bureau of Standards, on January 2, 1935, adopted the procedure of annealing all platinum versus platinum-rhodium thermocouples for 1 hr at 1,450° C.

It has not been demonstrated conclusively that platinum versus platinum-rhodium thermocouples after contamination can be materially improved in homogeneity by prolonged heating in air, although it is logical to suppose that certain impurities can be driven off or, through oxidation, rendered less detrimental.

2.5. Instruments

One of the factors in the accuracy of the calibration of a thermocouple is the accuracy of the instrument used to measure the emf. Fortunately, in most instances, an instrument is available whose performance is such that the accuracy of the calibration need not be limited by the accuracy of the emf measurements. For work of the highest accuracy, it is advisable to use a potentiometer of the type designed by Diesselhorst [5], White [6], Wenner [7], or Bonn,[5] in which there are no slide wires and in which all the settings are made by means of dial switches. However, for most work, in which an accuracy of a few microvolts will suffice, slide-wire potentiometers of the laboratory type are sufficiently accurate. Portable potentiometers accurate within about 50 μv and capable of being read to about 5 μv are also available. Aside from the greater sensitivity obtained, an important advantage of using a potentiometer is the fact that the reading obtained is independent of the resistance of the thermocouple.

Indicators of the galvanometric type are seldom used in making calibrations. Galvanometer indicators should be graduated for a specified external resistance of thermocouple and extension wires, and the resistance of the indicator itself should be high in order to reduce the effects of changes in the resistance of the thermocouple and leads. A discussion of these factors is given in NBS Technologic Paper T170 (1921).

[4] The ordinary portable type of optical pyrometer is very satisfactory for this purpose. As commonly used, the magnification is too low for sighting upon an object as small as the wires of rare-metal thermocouples, but this is easily remedied by inserting an additional piece of telescoping tubing so that the objective lens of the pyrometer is about twice as far from the pyrometer lamp as it is when sighting upon distant objects, or by using an objective lens of higher magnification.

[5] Designed by N. E. Bonn, of the Rubicon Co.

3. Calibration at Fixed Points

One of the important applications of the method of calibrating thermocouples at fixed points is found in the calibration of platinum versus platinum-10-percent-rhodium thermocouples, to realize the International Temperature Scale in the range 630.5° to 1063.0° C. From such a calibration, together with methods of extrapolation described later, the temperature-emf relationship of this type of thermocouple may be determined with an accuracy of about 2° C at 1,450° C. Calibration at a few other selected points below 630.5° C will yield a working standard that is accurate to a few tenths of a degree in the range 0° to 1,100° C.

Fixed points are also conveniently used with various degrees of accuracy ranging from 0.1° to 5° C in the calibration and checking of various types of thermocouples in the range −190° C to the melting point of platinum (1,769° C). The fixed points for which values have been assigned or determined accurately and at which it has been found convenient to calibrate thermocouples are given in table 3. The values in the table apply for a pressure of 1 standard atmosphere (760 mm of Hg) and the variations of the boiling temperatures with pressure are given in the last column.

TABLE 3. *Fixed points available for calibrating thermocouples*

Thermometric fixed point	Values on the International Temperature Scale of 1948				Temperature of equilibrim (t_p) in degrees C as a function of tbe pressure (p) between 680 and 780 mm of mercury. p_0 is standard atmospheric pressure.
	Assigned (primary points)		Determined (secondary points)		
	°C	°F	°C	°F	
Boiling point of oxygen	−182.970	−297.346			$t_p=-182.970+9.530\left(\frac{p}{p_0}-1\right)-3.72\left(\frac{p}{p_0}-1\right)^2+2.2\left(\frac{p}{p_0}-1\right)^3$
Sublimation point of carbon dioxide.			−78.5	−109.3	$t_p=-78.5+12.12\left(\frac{p}{p_0}-1\right)-6.4\left(\frac{p}{p_0}-1\right)^2$
Freezing point of mercury			−38.87	−37.97	
Ice point	0	32			
Triple point of water			+0.0100	32.0180	
Boiling point of water	100	212			$t_p=100+28.012\left(\frac{p}{p_0}-1\right)-11.64\left(\frac{p}{p_0}-1\right)^2+7.1\left(\frac{p}{p_0}-1\right)^3$
Triple point of benzoic acid			122.36	252.25	
Boiling point of naphthalene			218.0	424.4	$t_p=218.0+44.4\left(\frac{p}{p_0}-1\right)-19\left(\frac{p}{p_0}-1\right)^2$
Freezing point of tin[a]			231.9	449.4	
Boiling point of benzopbenone			305.9	582.6	$t_p=305.9+48.8\left(\frac{p}{p_0}-1\right)-21\left(\frac{p}{p_0}-1\right)^2$
Freezing point of cadmium			320.9	609.6	
Freezing point of lead[a]			327.3	621.1	
Freezing point of zinc[a]			419.5	787.1	
Boiling point of sulfur	444.600	832.280			$t_p=444.600+69.010\left(\frac{p}{p_0}-1\right)-27.48\left(\frac{p}{p_0}-1\right)^2+19.14\left(\frac{p}{p_0}-1\right)^3$
Freezing point of antimony			630.5	1166.9	
Freezing point of aluminum[a]			660.1	1220.2	
Freezing point of silver	960.8	1761.4			
Freezing point of gold	1063.0	1945.4			
Freezing point of copper[a]			1083	1981	
Freezing point of palladium			1552	2826	
Freezing point of platinum			1769	3216	

[a] The values given in this table for tbese materials are the values stated in the International Temperature Scale of 1948. Standard Samples of tbese materials are procurable from the National Bureau of Standards with certificates giving the freezing point of the particular lot of metal.

In selecting the points at which to calibrate a thermocouple, one sometimes has a choice between a boiling or a freezing point [6] as, for example, between the boiling point of sulfur (444.600° C) and the freezing point of zinc (419.5° C); between the boiling point of naphthalene (218.0° C) and the freezing point of tin (231.9° C); or between the boiling point of benzophenone (305.9° C) and the freezing point of cadmium (320.9° C) or lead (327.3° C). In determining the emf of a thermocouple at a freezing point, the time in which observations may be taken is limited to the period of freezing, after which the material must be melted again before taking further observations. In the case of boiling points, there is no such limit in time since the material can be boiled continuously. In addition, there is sometimes a question as to the beginning and end of the interval of constant-temperature characteristic of freezing. On the other hand, it is not necessary to observe the pressure during freezing and, in general, simpler apparatus and less skill are required to obtain a given accuracy with freezing points.

[6] In this Circular, "boiling point" is used for tbe temperature of equilibrium between the liquid and vapor phases, although the point is usually realized experimentally by immersing the thermocouple in the condensing vapor. "Freezing point" is used for the temperature of equilibrium between the solid and liquid phases when the point is realized experimentally by immersing the thermocouple in the freezing material, and "melting point" is used for the same point when it is realized experimentally by determining the emf of a thermocouple while the material is melting. When conditions permit a choice, freezing points are preferable to melting points of metals because the molten metal can be brought to a uniform temperature just prior to freezing by stirring more easily than the solid can he brought to a uniform temperature just prior to melting, a condition that must be met to obtain accurate results.

3.1. Freezing Points

The emf developed by a homogeneous thermocouple at the freezing point of a metal is constant and reproducible if all of the following conditions are fulfilled: (1) The thermocouple is protected from contamination, (2) the thermocouple is immersed in the freezing-point sample sufficiently far to eliminate heating or cooling of the junction by heat flow along the wires and protection tube, (3) the reference junctions are maintained at a constant and reproducible temperature, (4) the freezing-point sample is pure, and (5) the metal is maintained at essentially a uniform temperature during freezing. The methods of obtaining these conditions are subject to a choice. However, the essential features of the methods employed at the National Bureau of Standards are described here.

a. Protection Tubes

Closed-end porcelain or Pyrex-glass tubes are generally used to protect thermocouples from contamination, which usually results from the thermocouple wires coming in contact with other metals or metallic vapors or from the action of reducing gases at high temperatures. In the latter case, the silica of the insulating or protecting tube is reduced to silicon, which alloys with the thermocouple wires [8]. For temperatures above 500° C, the wires should be insulated by porcelain tubing and protected from contamination by a glazed porcelain tube. It is advisable to heat these tubes before use, to about 1,200° C in an oxidizing atmosphere to burn out any carbonaceous material that may have collected in them during storage and shipping. Protection tubes 5-mm inside diameter, 7-mm outside diameter, and 50 cm long are convenient for platinum versus platinum-rhodium thermocouples insulated by two-hole insulating tubes 50 cm long and 4 mm in diameter with 1-mm holes. For temperatures below 500° C, Pyrex tubes are very satisfactory for both protecting and insulating the wires.

b. Depth of Immersion

The depth of the immersion necessary to avoid heating or cooling of the junction by heat flow along the thermocouple wires and protection tube depends upon the material and size of the wires, the dimensions of the insulating and protecting tubes, and the difference between the temperature of the freezing-point sample and that of the furnace and atmosphere immediately above it. The safest method of determining whether the depth of immersion is sufficient is by trial. It should be such that during the period of freezing the thermocouple can be lowered or raised at least 1 cm from its normal position without altering the indicated emf by as much as the allowable uncertainty in the calibration. For platinum versus platinum-rhodium thermocouples in the protection tube described above, a depth of 10 cm, which is greater than necessary, is used at the National Bureau of Standards.

c. Reference-Junction Temperature Control

The temperature of the reference junctions is most easily controlled at a known temperature by placing them in an ice bath. A wide-mouthed Dewar flask filled with shaved ice saturated with water is very satisfactory. Electrical connection between a thermocouple wire and a copper lead wire is easily made by inserting them into a small glass tube containing a few drops of mercury. The glass tubes are then inserted into the ice bath to a depth of about 10 cm. The extension wires must be insulated from the thermocouple wires, except where they make contact through the mercury. It is preferable that the insulation on the wires extends below the level of the mercury. The glass tubes should be kept clean and dry inside. Moisture is likely to condense in the tube from the atmosphere but should not be allowed to accumulate. A little moisture and dirt at the bottom of the tube will form a galvanic cell, which may vitiate the readings. A later section deals with reference-junction temperatures in general.

d. Purity of Freezing-Point Samples

The temperature at which a metal freezes depends upon the amount and kind of impurities present. The values in table 3 apply for metals, the purity of which is of the order of 99.99 percent. The freezing temperature of silver, gold, or copper may be lowered by as much as 0.1° C and that of antimony, aluminum, zinc, lead, cadmium, tin, or mercury by as much as 0.05° C by 0.01 percent of impurities. The purity of the Standard-Sample freezing-point materials issued by the National Bureau of Standards is not of great importance, as a certificate is issued with each sample giving the freezing temperature determined on that particular lot of metal. However, the purest metals available are selected for these Standard Samples because a high degree of purity is necessary in order that the metal may give a flat freezing curve.

e. Crucibles

Of the crucible materials ordinarily used, highly purified graphite has the greatest utility and is used almost exclusively at NBS for this work. It can be machined into any desired shape, and can be used in contact with any of the freezing-point materials in table 3 except palladium and platinum without detectable contamination of the metals. At high temperatures, the gases formed from its oxidation provide the reducing atmosphere usually necessary for the protection of the freezing-point metal. Copper and copper oxide form a eutectic which melts about 20° C lower than pure copper, and it is possible for molten silver to absorb enough oxygen from the air to lower its freezing point as much as 10° C [9]. Therefore, copper and silver must be protected from oxygen, and it is advisable also to protect aluminum and antimony from oxygen. This is

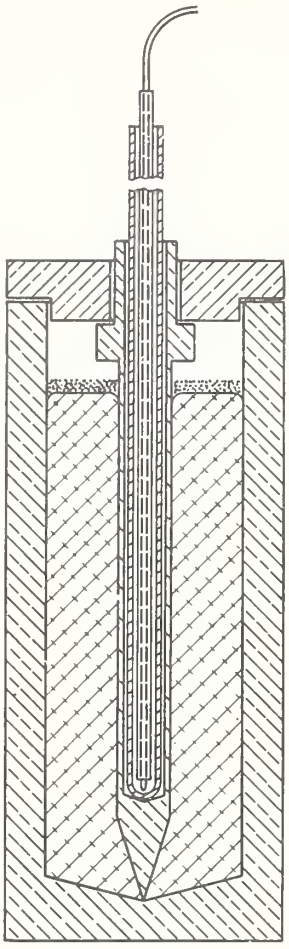

FIGURE 1. *Arrangement for protecting a thermocouple in molten aluminum.*

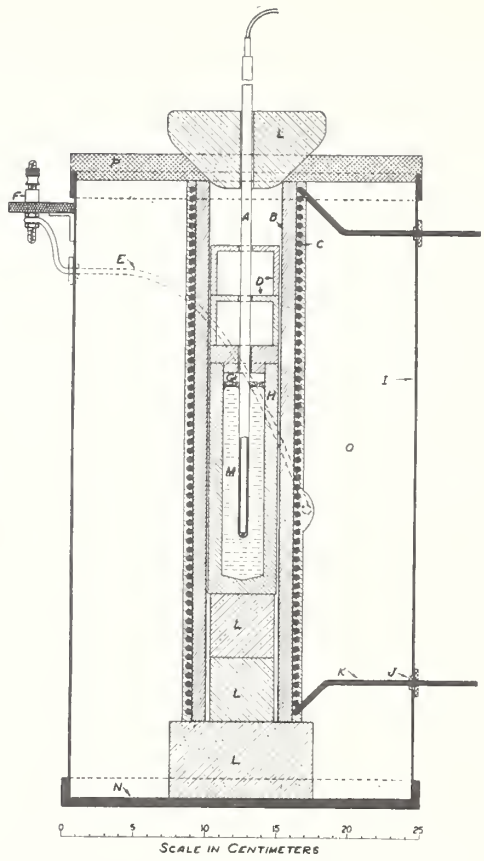

FIGURE 2. *Furnace used in calibrating thermocouples at freezing points of metals.*

A, Porcelain protecting tube; B, refractory furnace tube; C, heating element (80 nickel, 20 chromium); D, graphite diaphragms; E, control thermocouple (Chromel-Alumel); G, graphite powder; H, graphite crucible; I, sheet steel; L, insulating blocks; M, freezing-point metal; N, cast-iron base; O, powdered diatomaceous earth insulation.

done by using graphite crucibles with covers of the same material, and as an added precaution these freezing-point metals are covered with powdered graphite or charcoal.

Porcelain tubes or crucibles, or any material containing silica, cannot be used in contact with aluminum, as the silica is readily attacked. Aluminum is melted in a graphite crucible and the porcelain protecting tube separated from the aluminum by a very thin sheath of graphite. Figure 1 illustrates one convenient manner in which the sheath may be mounted in the crucible. The sheath is held down in the metal by the weight of the cover and is allowed to remain in the crucible after the aluminum is frozen. The thermocouple protecting tube fits snugly inside the sheath. At the National Bureau of Standards the graphite crucibles used for gold, silver, antimony, and zinc are 3-cm inside diameter and 15 cm deep. The crucibles used for copper, aluminum, lead, and tin are 5-cm inside diameter and 15 cm deep. Porcelain, silica, clay, clay graphite, and Pyrex glass are also used as crucible materials. Pyrex glass is very suitable for mercury.

f. Furnaces

Figure 2 shows the type of furnace used in the freezing-point determinations. The heating element is No. 6 or 8 gage nickel(80)-chromium(20) wire wound on a refractory tube and imbedded in refractory cement. The space between the heating element and the outside wall is filled with powdered diatomaceous earth. Graphite diaphragms are placed above the crucible in order to reduce the oxidation of the crucibles and to promote temperature uniformity in the metal.

g. Procedure

In the calibration of a thermocouple at freezing points, the thermocouple, properly protected, is slowly immersed in the molten metal. The metal is brought to essentially a uniform temperature at the beginning of freezing by holding its temperature constant at about 10° C above the freezing point for several minutes and then cooling slowly, or by agitating the metal with the thermocouple protection tube just before freezing begins. The emf of the thermocouple is observed at regular intervals of time. These values are plotted, and

the emf corresponding to the flat portion of the cooling curve is the emf at the freezing point of the metal.

Antimony and tin have a marked tendency to undercool before freezing, but the undercooling will not be excessive if the liquid metal is stirred.

3.2. Melting Points

The emf of a thermocouple at the melting point of a metal may be obtained in the same manner and with the same apparatus as that just described for freezing points, but the latter are found to be more satisfactory. However, melting points are used to advantage when only a limited amount of material is available. One method of obtaining the emf of a thermocouple at a melting point with a small amount of material is the wire method [10]. In this method, the thermocouple wires are placed in a two-hole insulating tube and a short length of the melting-point sample, in the form of wire about the same diameter as the thermocouple elements, is welded between the measuring junction ends of the two wires. The dimensions of the melting-point sample are not critical, but there should be at least 1 mm of wire between the two welds. In order that the melting-point sample shall not break before the melting point is reached, the weld should be made and the thermocouple placed in the furnace so that there is a minimum of strain on the melting-point sample. The measuring junction end of the thermocouple with the melting-point sample, is placed in a uniformly heated section of a furnace and the temperature increased very slowly as the melting point is approached. When the sample reaches its melting point, its temperature and consequently the emf of the thermocouple remain constant for a fraction of a minute (varying with the rate of temperature rise). After melting is complete, the temperature of the wire and the emf may rise somewhat before the circuit is broken by the separation of the molten metal. The value of the emf corresponding to the melting point is, therefore, the value at the halt in the emf rise and is obtained by continuous observation of the emf as melting is approached or by plotting time versus emf.

The metal most often used in the calibration of thermocouples by the wire method is gold, and it has been demonstrated that results can be obtained which are in agreement with those obtained with a crucible of freezing gold to a few tenths of a degree. The same method has been used with palladium, but with much less satisfactory results because of electric leakage through the refractory insulation at high temperatures and the oxidation of the palladium. This method is not well adapted to metals that oxidize rapidly, and if used with materials whose melting temperature is altered by the oxide, the metal should be melted in a neutral atmosphere.

If very accurate observations of the emf are not required, the emf at the instant the circuit is broken may be taken, but if this is done the thermocouple should be withdrawn from the furnace immediately and the sample examined to see whether the circuit was broken by the sample melting or by strain on it before melting occurred.

It is not necessary to weld the wire between the thermocouple elements, as fairly good results may be obtained by wrapping a small amount of the wire around the junction. This practice is often applied to base-metal thermocouples by wrapping wires of tin, lead, zinc, or aluminum around the measuring junction and heating it until a halt is observed in the heating curve.

One method of checking platinum versus platinum-rhodium thermocouples at the highest possible point is by heating the junction of the thermocouple until the platinum wire melts. To avoid electric leakage, the insulating tube is withdrawn to the colder parts of the heating device leaving only the wires and junction in the hotter parts.

3.3. Boiling Points

Boiling points play an important part in the definition of the International Temperature Scale, because 3 of the 4 points upon which the scale between −182.970° and +630.5° C is based are the boiling points of oxygen, water, and sulfur. However, boiling points, with the exception of that of water, are seldom used in the calibration of thermocouples, and consequently the methods of realizing these various points will be mentioned only briefly here. References are given to complete discussions for those interested, as boiling points might profitably be employed to a greater extent, when a platinum-resistance thermometer or a stirred liquid bath is not available.

a. Water (Steam Point)

The temperature of condensing water vapor is realized experimentally by the use of a hypsometer so constructed as to avoid superheat of the vapor around the thermocouple and contamination with air and other impurities. Simple types of hypsometers are shown in various trade catalogs. Mueller and Sligh [11] give a detailed description of a hypsometer used in precision measurements. If the proper conditions are attained, the observed emf of the thermocouple will be independent of the rate of heat supply to the boiler, the length of time the hypsometer has been in operation, and the depth of immersion of the thermocouple. The thermocouple for some distance from the junction must be shielded from radiation from hotter and colder surfaces. The relationship between the temperature (t_p) (in degrees C) and the pressure (p) given in table 3 holds for the range 660 to 860 mm of Hg. The steam point as realized by utilizing the condensing vapor in a hypsometer is certainly accurate to 0.01° C. An accuracy of about 1° C can be obtained by merely immersing a thermocouple in boiling water.

b. Sulfur, Benzophenone, and Naphthalene

The boiling points of the three materials above are near the freezing points of available pure metals and are very seldom used in the calibration of thermocouples. The specifications to be followed in realizing the sulfur point are given in the International Temperature Scale [12]. Detailed description of the apparatus and precautions to be observed for the sulfur boiling point are given by Mueller and Burgess [13]. The relationship between temperature and pressure for sulfur in table 3 holds for the range 660 to 800 mm of Hg. The procedure and apparatus for realizing the boiling points of naphthalene and benzophenone are the same as those for the boiling point of sulfur. Detailed information regarding these points is given by Waidner and Burgess [14] and by Finck and Wilhelm [15].

c. Oxygen

The temperature of equilibrium between liquid and gaseous oxygen is best realized experimentally by the static method, the oxygen vapor-pressure thermometer being compared with the thermocouple to be calibrated in a suitable low-temperature bath. An oxygen vapor-pressure thermometer is nothing more than a glass tube containing very pure oxygen at a pressure of several atmospheres at room temperature, and connected to a mercury-filled manometer for measuring the pressure in the tube [16]. When the thermometer tube is immersed in the bath, part of the oxygen liquefies. The relationship between the temperature (t_p) (in degrees C) of the bath and the pressure (p) in the thermometer given in table 3 holds for the range 660 to 860 mm of Hg. This requires that the temperature of the bath be kept within the limits −184.3° to −181.8° C. This is most conveniently done by stirring liquid oxygen in a Dewar flask.

d. Carbon-Dioxide Point

Although the sublimation point of carbon dioxide is not a boiling point, the highest accuracy is obtained in utilizing this point, by employing the same method as that for the boiling point of oxygen. An instrument of this type suitable for use as a carbon-dioxide vapor-pressure thermometer is container type 3, described by Meyers and Van Dusen [17]. The sublimation point of carbon dioxide may also be utilized by immersing the thermocouple in a slush made by mixing carbon-dioxide snow with a liquid such as acetone. The slush should be stirred and the air excluded from the vapor above the surface of the slush. Whereas the accuracy obtained with a vapor-pressure thermometer is of the order of a few hundredths of a degree, an accuracy of 1° C is all that can be claimed for the temperature of the slush.

4. Calibration by Comparison Methods

The calibration of a thermocouple, by comparison with a working standard is sufficiently accurate for most purposes and can be done conveniently in most industrial and technical laboratories. The success of this method usually depends upon the ability of the observer to bring the junction of the thermocouple to the same temperature as the actuating element of the standard, such as the measuring junction of a standard thermocouple or the bulb of a resistance or liquid-in-glass thermometer. The accuracy obtained is further limited by the accuracy of the standard. Of course, the reference-junction temperature must be known, but this can usually be controlled by using an ice bath as described earlier or measured with a liquid-in-glass thermometer. The method of bringing the junction of the thermocouple to the same temperature as that of the actuating element of the standard depends upon the type of thermocouple, type of standard, and the method of heating.

4.1. Platinum Versus Platinum-Rhodium Thermocouples

Platinum versus platinum-rhodium thermocouples, either the 10- or 13-percent rhodium, are seldom used for accurate measurements below 300° C (572° F) and are practically never used below 0° C, because the thermal emf per degree of these thermocouples decreases rapidly at low temperatures, becoming zero at about −138° C (−216° F). These thermocouples are usually calibrated above 300° C by comparison with standard thermocouples in electrically heated furnaces. The standard thermocouple may be either a platinum versus platinum 10- or 13-percent-rhodium thermocouple that has been calibrated at fixed points or by comparison with other thermocouples so calibrated.

The method employed at the National Bureau of Standards for the comparison of two such thermocouples permits simultaneous reading of the emf of each thermocouple without waiting for the furnace to come to a constant temperature. In order to insure equality of temperature between the measuring junctions of the thermocouples, they are welded together. A separate potentiometer is used to measure each emf, one connected to each thermocouple, and each potentiometer is provided with a reflecting galvanometer. The two spots of light are reflected onto a single scale, the galvanometers being set in such a position that the spots coincide at the zero point on the scale when the circuits are open and, therefore, also when the potentiometers are set to balance the emf of each thermocouple. Simultaneous readings are obtained by setting one potentiometer to a desired value and adjusting the other so that

both spots of light pass across the zero of the scale together as the temperature of the furnace is raised or lowered.

By making observations, first with a rising and then with a falling temperature, the rates of rise and fall being approximately equal, and taking the means of the results found, several minor errors, such as those due to differences in the periods of the galvanometers, etc., are eliminated or greatly reduced. The differences between the values observed with rising and falling temperatures are usually less than a few microvolts with platinum versus platinum-rhodium thermocouples, if the periods of the galvanometers are approximately the same.

This method is particularly adapted to the calibration of thermocouples at any number of selected points. For example, if it is desired to determine the temperature of a thermocouple corresponding to 10.0 mv, this emf is set up on the potentiometer connected to this thermocouple, the emf of the standard thermocouple observed as described above, and the temperature obtained from the emf of the standard. If it is desired to determine the emf of a thermocouple corresponding to 1,000° C, the emf of the standard corresponding to this temperature is set up on the potentiometer connected to the standard and the emf of the thermocouple being tested is observed directly.

In order to calibrate a thermocouple in the least possible time by this method, it is necessary to use a furnace that is so constructed that it will cool rapidly. The heating element of the furnace used at NBS for the routine testing of thermocouples consists of a nickel(80)-chromium(20) tube clamped between two water-cooled terminals. The tube, which is 13/16-in. inside diameter, 1$\frac{5}{16}$-in. outside diameter, and 24 in. long, is heated electrically, the tube itself serving as the heating element or resistor. The large current necessary to heat the tube is obtained from a transformer. A large cylindrical shield of sheet metal is mounted around the heating tube to reduce the radiation loss. To reduce lag no thermal insulation is used between the heating tube and the radiation shield. The middle part of this furnace, for about 18 in., is at practically a uniform temperature, and the water-cooled terminals produce a very sharp temperature gradient at each end. This furnace can be heated to 1,200° C in about 10 min with 12 kw and, if all the power is shut off, will cool from this temperature to 300° C in about the same time. This type of furnace can be used up to 1,250° C (2,282° F).

The thermocouples are insulated and protected by porcelain tubes. It is essential that the two potentiometers and thermocouple circuits be separate except at the point where the junctions are welded together. The reference junctions are maintained at 0° C.

The above method and apparatus were devised primarily for the rapid testing of thermocouples, but it is not necessary to follow this method literally or to procure identical apparatus to obtain good results. If it is not convenient to weld the junctions of the thermocouples together, they may be brought into fairly good contact by wrapping with platinum wire or foil. The only advantage of the furnace described above, over any other type of furnace in which several inches of the thermcocouples may be heated to a uniform temperature, is the flexibility of control. Electric tube furnances suitable for such comparison tests can be obtained, designed to operate on either 110 or 220 v, and may be obtained equipped with an adjustable power supply for regulating the current. For temperatures up to 1,150° C (2,102° F), a furnace with a heating element of nickel (80)-chromium (20) will suffice. Furnaces with heating elements of platinum or platinum-rhodium are available for higher temperatures. A convenient size of heating tube is 1 in. in diameter and 18 in. long. Even though the furnace tube is kept fairly clean, it is advisable to protect platinum versus platinum-rhodium thermocouples by a porcelain tube. If two potentiometers are not available for taking simultaneous readings, the furnace may be brought to essentially a constant temperature and the emf of each thermocouple read alternately on one instrument.

When the thermocouples are calibrated by welding or wrapping the junctions together, the difference between the temperatures of the junctions should not be great even when the temperature of the furnace is changing. If it is necessary or advisable to calibrate the thermocouples without removing them from the protection tubes, then the junctions of the thermocouple being tested and that of the standard should be brought as close together as possible in a uniformly heated portion of the furnace. In this case, it is necessary that the furnace be brought to approximately a constant temperature before taking observations. It is usually not possible to maintain the reference junctions at 0° C when the thermocouples are completely enclosed in protection tubes. However, extension leads may be used with the thermocouple or the temperature of the reference junctions may be measured with a thermometer.

There are a number of other methods of heating and of bringing the junctions to approximately the same temperature, for example, inserting the thermocouples properly protected into a bath of molten metal or into holes drilled in a large metal block. The block of metal may be heated in a muffle furnace or, if made of a good thermal conductor such as copper, may be heated electrically. Tin, which has a low melting point, 232° C (450° F), and low volatility, makes a satisfactory bath material. The thermocouples should be immersed to the same depth with the junctions close together. Porcelain tubes are sufficient protection, but to avoid breakage by thermal shock when immersed in molten metal it is preferable to place them inside of secondary tubes of iron, nickel-

chromium, graphite, or similar material. In all of these methods, particularly in those cases in which the junctions of the thermocouples are not brought into direct contact, it is important that the depth of immersion be sufficient to eliminate cooling or heating of the junctions by heat flow along the thermocouple and the insulating and protecting tubes. This can be determined by observing the change in the emf of the thermocouple as the depth of immersion is changed slightly. If proper precautions are taken, the accuracy yielded by any method of heating or bringing the junctions to the same temperature may be as great as that obtained by any other method.

4.2. Base-Metal Thermocouples in Laboratory Furnaces

The methods of testing base-metal thermocouples above room temperature are generally the same as those just described for testing rare-metal thermocouples with the exception, in some cases, of the methods of bringing the junctions of the standard and the thermocouple being tested to the same temperature and the methods of protecting platinum versus platinum-rhodium standards from contamination. One arrangement of bringing the junction of a platinum versus platinum-rhodium standard to the same temperature as that of a large base-metal thermocouple for accurate calibration is to insert the junction of the standard into a small hole (about 1.5 mm in diameter) drilled in the measuring junction of the base-metal thermocouple as shown in figure 3. The platinum versus platinum-rhodium standard is protected by porcelain tubes to within a few millimeters of the measuring junction; and the end of the porcelain tube is sealed to the thermocouple by Pyrex glass or by a small amount of kaolin and water-glass cement. This prevents contamination of the standard thermocouple, with the exception of the small length of 2 or 3 mm, which is necessarily in contact with the base-metal thermocouple. If the furnace is uniformly heated in this region (and it is of little value to make such a test unless it is) contamination at this point will not cause any error. If the wire becomes brittle at the junction, this part of the wire may be cut off and enough wire drawn through the seal to form a new junction. The seal should be examined after each test and remade if it does not appear to be good. More than one base-metal thermocouple may be welded together and the hole drilled in the composite junction. The thermocouples should be clamped in place so that the junctions remain in contact. If two potentiometers are used for taking simultaneous readings, the temperature of the furnace may be changing as much as a few degrees per minute during an observation, but if a single instrument is used for measuring the emf, the furnace temperature should be maintained practically constant during observations.

In testing one or more small base-metal thermocouples, they may be welded to the junction of the standard. If a base-metal standard is used, the best method is to weld all the junctions together. If a large number of base-metal thermocouples are to be tested at the same temperature, the method of immersing the thermocouples in a molten-metal bath or into holes drilled in a large copper block is very advantageous. If a tin bath is used, iron or nickel-chromium tubes are sufficient protection for base-metal thermocouples. When wires, insulators, and protection tubes of base-metal thermocouples are large, tests should be made to insure that the depth of immersion is sufficient to eliminate heating or cooling of the junction by heat flow along these materials.

4.3. Thermocouples in Fixed Installations

After thermocouples have been used for some time at high temperatures, it is difficult if not impossible to determine how much the calibrations are in error by removing them from an installation and testing in a laboratory furnace. The thermocouples are usually inhomogeneous after such use and in such a condition the emf developed by the thermocouples depends upon the temperature distribution along the wires [18]. If possible, such thermocouples should be tested under the same conditions and in the same installation in which they are used. Although it is not usually possible to obtain as high a precision by testing the thermocouples in place as is obtained in laboratory tests, the results are far more accurate in the sense of being representative of the behavior of the thermocouples.

The exact method of procedure depends upon the type of installation. A standard thermocouple is usually employed with extension leads and preferably a portable potentiometer, although a portable high-resistance millivoltmeter may be used. In this case, as in the calibration of any thermocouple by comparison methods, the main objective is to bring the measuring junction of the standard thermocouple to the same temper-

FIGURE 3. *Arrangement to assure good thermal contact between the junction of a base-metal thermocouple and that of a protected platinum versus platinum-rhodium thermocouple.*

ature as that of the thermocouple being tested. One method is to drill a hole in the furnace at the side of each thermocouple permanently installed, large enough to permit insertion of the checking thermocouple. The hole is kept plugged, except when tests are being made. The standard thermocouple is immersed in the furnace through this hole to the same depth as the thermocouple being tested, with the measuring junctions ends of the protection tubes as close together as possible.

In many installations, the base-metal thermocouple and protecting tube are mounted inside another protecting tube of iron, fire clay, silicon carbide, or some other refractory which is permanently cemented or fastened into the furnace wall. Frequently there is room to insert a small test thermocouple in this outer tube alongside of the fixed thermocouple. A third method, much less satisfactory, is to wait until the furnace has reached a constant temperature and make observations with the thermocouple being tested, then remove this thermocouple from the furnace, and insert the standard thermocouple to the same depth.

If desired, comparisons can be made preferably by either of the first or second methods at several temperatures, and a curve obtained for each permanently installed thermocouple showing the necessary corrections to be applied to its readings. Although testing a thermocouple at one temperature yields some information, it is not safe to assume that the changes in the emf of the thermocouple are proportional to the temperature or to the emf. For example, it has been observed that a thermocouple which had changed in use by the equivalent of 9° C at 315° C had changed only the equivalent of 6° C at 1,100° C.

It may be thought that this method of checking thermocouples is unsatisfactory because, in most furnaces used in industrial processes, large temperature gradients exist and there is no certainty that the standard thermocouple is at the same temperature as the thermocouple being tested. This objection, however, is not serious, because if temperature gradients do exist of such a magnitude as to cause much difference in temperature between two similarly mounted thermocouples located close together, the reading of the standard thermocouple represents the temperature of the fixed thermocouple as closely as the temperature of the latter represents that of the furnace.

The principal advantage of this method is that the thermocouple, leads, and indicator are tested as a unit and under the conditions of use.

4.4. Thermocouples in Stirred Liquid Baths

Thermocouples and resistance thermometers are not usually directly compared above 300° C because of the difficulty encountered in bringing the thermocouple junction and the thermometer bulb to the same temperature, but these two types of instruments may be very accurately compared below 300° C, where a stirred liquid bath can be conveniently used. A type of bath suitable for use above 0° C is shown in figure 5 of a paper by N. S. Osborne [19]. The container, which is insulated on the outside, consists of two cylindrical vertical tubes connected at the bottom and near the top by rectangular ports. A frame carrying the heating element, cooling coils if desired, and stirring propeller are inserted in one of the vertical tubes. The instruments being compared are placed in the other vertical tube and held in place by any convenient means. The chief advantage of this arrangement is that local irregularities, due to direct conduction from the vicinity of the heating or cooling elements, are eliminated. A stirred liquid bath for use below 0° C has been described by Scott and Brickwedde [20].

The liquids used in the baths should be capable of being stirred readily at any temperature at which they are used and they should not be highly flammable. At NBS oil is used between 100° and 300° C; water in the range 0° to 100° C; mixtures of carbon tetrachloride and chloroform in the range 0° to −75° C; a five-component mixture containing 14.5 percent of chloroform, 25.3 percent of methylene chloride, 33.4 percent of ethyl bromide, 10.4 percent of *trans*dichloroethylene, and 16.4 percent of trichloroethylene in the range −75° to −140° C; and commercial propane below −140° C. Propane is highly flammable, and every precaution must be taken to prevent it from mixing with liquid air or oxygen. A complete series of nonflammable liquids for cryostats is given by C. W. Kanolt [21] for temperatures down to −150° C.

A number of thermocouples can be calibrated at one time in a stirred liquid bath. Platinum-resistance or liquid-in-glass thermometers or thermocouples may be used as standards.

5. Methods of Interpolating Between Calibration Points

5.1. Platinum Versus Platinum-Rhodium Thermocouples

After a thermocouple has been calibrated at a number of points, the next requirement is a convenient means of obtaining corresponding values of emf and temperature at other points. A curve may be drawn or a table giving corresponding temperature and emf values may be prepared. The values in such a table may be obtained by computing an empirical equation or series of equations through the calibration points, by direct interpolation between points, or by drawing a difference curve from an arbitrary reference table which closely approximates the temperature-emf relationship of the thermocouple. The method to be selected for a particular calibration depends upon such factors as the type

of thermocouple, number of calibration points, temperature range, accuracy required, and personal preference.

For the highest accuracy in the range 630.5° to 1063.0° C with platinum versus platinum-10-percent rhodium thermocouples, the method is that prescribed in the International Temperature Scale. An equation of the form $e=a+bt+ct^2$, where a, b, and c are constants determined by calibration at the freezing points of gold, silver, and antimony, is used. By calibrating the thermocouple also at the freezing point of zinc and using an equation of the form

$$e=a'+b't+c't^2+d't^3,$$

the temperature range can be extended down to 400° C without introducing an uncertainty [22] of more than 0.1° C in the range 630.5° to 1063.0° C. By calibrating the thermocouple at the freezing points of gold, antimony, and zinc and using an equation of the form $E=a''+b''t+c''t^2$, a calibration is obtained for the range 400° to 1,100° C, which agrees [22] with the International Temperature Scale to 0.5° C. The freezing point of copper may be used instead of the gold point, and the aluminum point used instead of the antimony point without introducing an additional uncertainty [22] of more than 0.1° C.

For temperatures outside the range 630.5° to 1063.0° C, the method of drawing a smooth curve through the temperature and emf values has just as much claim to accuracy as the method of passing empirical equations through the calibration points, because an empirical equation performs the same function as a curved ruler. For the temperature range 0° to 1,450° C, a curve for interpolation to 1° or 2° C requires calibration points not more than 200° C apart and a careful plot on a large sheet of paper, which is tedious to read. A reduction in the number of calibration points increases the uncertainty proportionately. If, however, we plot as ordinates the differences between the observed emf and that calculated from the first degree equation $e=10t$, and emf as abscissas, the difference at intermediate points may be taken from the curve and added to the quantity $10t$ to obtain values of emf corresponding to the appropriate temperature in which the uncertainty in the interpolated values is much less than in the case in which the emf is plotted directly against the temperature. If we go one step further and plot differences from an arbitrary reference table, the values of which closely represent the form of the temperature-emf relationship for the type of thermocouple in question, the maximum differences to be plotted will be only a few degrees. In this way, interpolated values are obtained in which the uncertainty in the interpolated values is not appreciably greater than that at the calibration points. The more accurately the values in the arbitrary reference table conform to the emf-temperature relationship of actual thermocouples, the fewer the number of calibration points required for a given accuracy.

Reference tables [23] for platinum versus platinum-rhodium thermocouples which are based on the temperature-emf relationships of a considerable number of representative thermocouples from various sources have recently been published. These tables represent the shape of the relations for both the 10- and 13-percent-rhodium thermocouples in the entire range 0° to 1,700° C. The difference curve for any thermocouple from the appropriate table is a smooth curve.

In the calibration of platinum versus platinum-10-percent-rhodium thermocouples to be used as working standards, the emf is observed at the freezing points of gold, silver, antimony, and zinc. The constants in the equation $E=a+bt+ct^2$ are computed from the observations at the gold, silver, and antimony points. The observed value at 419.5° C and the values calculated from the equation for the range 630.5° to 1063.0° C are used to construct a difference curve from the reference table mentioned previously. This difference curve is then extended graphically above 1063.0° C. When the highest accuracy is required at the lower temperatures, additional observations are taken at the freezing points of lead and tin and at the boiling point of water. Values taken from this difference curve when added algebraically to the values in the reference table yield the corresponding temperature-emf values at any temperature. A numerical example follows.

The observed values of emf at the calibration points are given in table 4, together with the values at 50° C intervals from 650° to 1,050° C computed from the equation,

$$E=-270.73+8.15786t+0.00169396t^2.$$

Corresponding values of E and Δe are plotted in figure 4.

TABLE 4. *Data for construction of difference curve*

Temperature, t	Reference table emf NBS Circular 561, E_r	Observed emf standard thermocouple, E	Difference, $\Delta e=E_r-E$
° C	μv	μv	μv
0.0	0.0	0.0	0.0
419.5	3437.6	3443.6	−6.0
630.5	5536.8	5546.2	−9.4
650.0	5738.0	5747.6	−9.6
700.0	6259.7	6269.8	−10.1
750.0	6790.0	6800.5	−10.5
800.0	7328.9	7339.7	−10.8
850.0	7876.4	7887.3	−10.9
900.0	8432.4	8443.4	−11.0
950.0	8996.9	9008.0	−11.1
960.8	9120.0	9131.1	−11.1
1000.0	9570.1	9581.1	−11.0
1050.0	10151.8	10162.6	−10.8
1063.0	10304.4	10315.2	−10.8

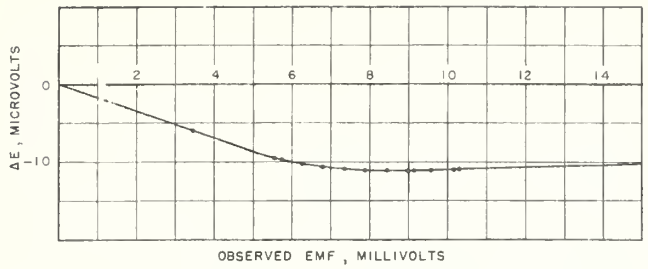

FIGURE 4. *Difference curve for a platinum versus platinum-10 percent-rhodium thermocouple, using the reference table in NBS Circular 561.*

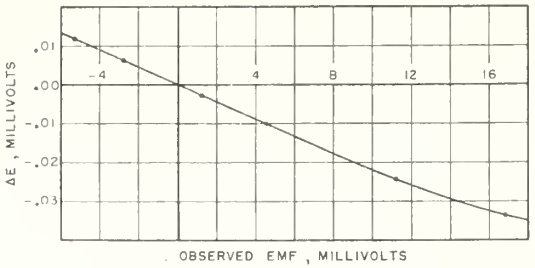

Figure 5. *Difference curve for a copper-constantan thermocouple, using the reference table in NBS Circular 561.*

For accurate extrapolation above the gold point, it is essential that the shape of the emf-temperature relationship given in the reference table conform closely to that of actual thermocouples so that the difference curves will be linear both above and below this point. If the difference curve has a large curvature or if there is an abrupt change in slope near the gold point, the extrapolation of the difference curve may involve considerable uncertainty. The difference curves of actual thermocouples both 10- and 13-percent-rhodium alloys from the reference tables given in NBS Circular 561 are in most cases smooth curves in the entire range 0° to 1,700° C and the difference curves can therefore be extrapolated with but little uncertainty. The extrapolated values for a number of thermocouples have been checked by means of actual comparison with an optical pyrometer, and in no case was the difference as great as 3° C at 1,500° C and in most cases it was not over 1° C. These differences are not much greater than the accidental errors in the comparisons.

Difference curves can be drawn from observations obtained in comparison calibrations as well as from observations at fixed points. Two points (accurate to ±0.3° C at about 600° and 1,100° C) are usually sufficient to determine the difference curve from the tables in NBS Circular 561 for either a 10- or a 13-percent-rhodium thermocouple, such that the resulting calibration is accurate to ±1° C at any point in the range 0° to 1,100° C and to ±3° C up to 1,450° C. (The reference junction temperature at which the emf difference is zero constitutes a third point.)

5.2. Copper-Constantan Thermocouples

The relationship between the temperature and emf of copper-constantan thermocouples has been very well established in the range −190° to +300° C. The temperature of the measuring junction of such a thermocouple can be very accurately determined in this range with a platinum-resistance thermometer in a stirred liquid bath. Consequently, the accuracy obtained with this type of thermocouple is, in general, limited by the stability of the wires above 200° C, and by the accuracy of the emf measurements and the homogeneity of the wire below 200° C. The stability of the larger sizes of wire is greater than that of the smaller wires under the same conditions.

Figure 5 shows a difference curve from the values in NBS Circular 561 for a typical copper-constantan thermocouple. Two points above and two below 0° C suitably spaced are usually sufficient to give an accuracy of 0.3° C.

Equations are used to good advantage with copper-constantan thermocouples for interpolating between calibration points, but it has not been demonstrated that the accuracy obtained with equations is any greater than that obtained by drawing difference curves from reference tables except when the differences are large. One convenient method of obtaining a calibration accurate to ±0.2° C in the range 0° to 100° C is to use an equation of the form $e=at+0.04t^2$ where a is a constant determined by calibration at 100° C, e the emf in microvolts, and t the temperature in degrees C. An equation of the form $e=at+bt^2+ct^3$, where a, b, and c are constants determined by calibration at three points (about 100°, 200°, and 300° C), will give interpolated values as accurately as the thermocouple can be relied upon to retain its calibration (about 0.2° C). The same type of equation with the constants determined at three points about equally spaced in the range 0° to −190° C, may be used in this range to give interpolated values almost as accurately as the emf can ordinarily be measured (about 2 μv). An equation of the form $e=at+bt^2$ will yield interpolated values in the range 0° to 100° C almost as accurately as the emf is determined at the calibration points, if the constants are determined by calibration at about 50° and 100° C. The same is true of this equation in the range 0° to −100° C if the constants are determined at −50° and −100° C.

5.3. Chromel-Alumel Thermocouples

Figure 6 shows a difference curve for a typical Chromel-Alumel thermocouple from the standard tables published in NBS Circular 561. The difference curve from these tables can be determined in the range 0° to 1,300° C (2,372° F) with an uncertainty not more than 1° C greater than at the calibration points by calibration at 500°, 800°, and 1,100° C (or at 1,000°, 1,600°, and

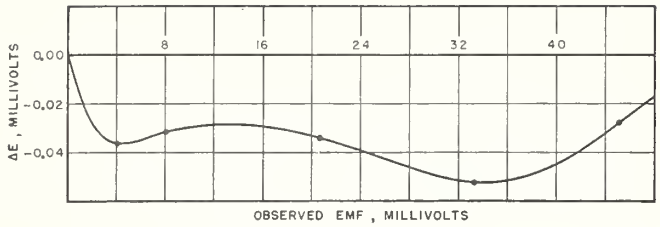

FIGURE 6. *Difference curve for a Chromel-Alumel thermocouple, using the reference table in NBS Circular 561.*

2,000° F). These tables represent the average temperature-emf relationship of Chromel-Alumel thermocouples now being manufactured.

Little success has been met in fitting equations to the calibration of Chromel-Alumel thermocouples in the range 0° to 300° C. An equation of the form $e=at+bt^2+ct^3$ may be in error by 1°C at 50° C if the constants are determined by calibration at about 100°, 200°, and 300° C. However, it will be accurate to about 0.5° C at 150° C and to about 0.2° C between 200° and 300° C. In the range 0° to −190° C, an equation through three points about equally spaced will give interpolated values in which the uncertainty is not more than 2 μv greater than at the calibration points.

5.4. Iron-Constantan Thermocouples

Until recently, several iron-constantan reference tables had been used by the suppliers of this material. One such table still being used by some Government agencies was published in a paper on "Reference Tables for Iron-Constantan and Copper-Constantan Thermocouples" [24].

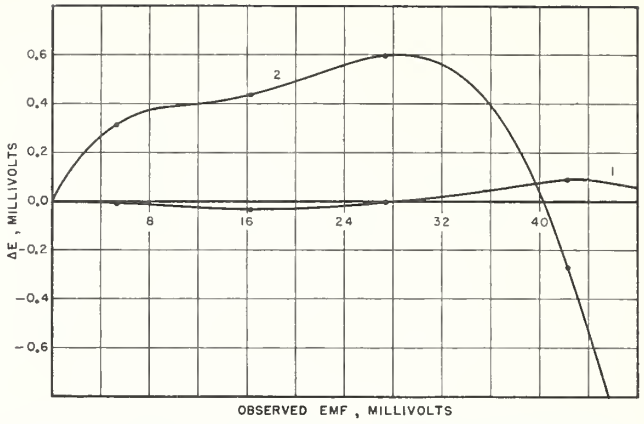

FIGURE 7. *Difference curves for an iron-constantan thermocouple, using (1) the reference table in NBS Circular 561 and (2) a straight line, $e=56t$.*

More recently, a reference table that closely represents the temperature-emf relationship of the iron-constantan thermocouples now being supplied by most producers of this type of thermocouple was developed. This table is not very different from that which had been in use by some producers since 1913 and consequently has been referred to as the "Modified 1913 Reference Tables for Iron-Constantan Thermocouples" [25].

Figure 7 shows a difference curve from the modified 1913 tables and from a straight line, $e=56t$ (where e is in microvolts and t is in degrees C) for a typical thermocouple. This latter method of drawing difference curves from a straight line may be used if the thermocouple does not match existing reference tables.

We have no data as to how closely the temperature-emf relationships of iron-constantan thermocouples may be fitted by equations.

6. Reference-Junction Corrections

It is not always possible to maintain the reference junctions (commonly called cold junctions) at a desired temperature during the calibration of a thermocouple, but if the temperature of the reference junctions is measured, it is possible to apply corrections to the observed emf, which will yield a calibration with the desired reference-junction temperature. If the emf of the thermocouple is measured with the reference junctions at temperature t, and a calibration is desired with these junctions at temperature t_0, the measured emf may be corrected for a reference-junction temperature of t_0 by adding to the observed value the emf which the thermocouple would give if the reference junctions were at t_0 and the measuring junction at t. For example, suppose the observed emf of a platinum versus platinum-10-percent-rhodium thermocouple with the measuring junction at 1,000° C and the reference junction at 25° C is 9.427 mv and the emf of the thermocouple with the measuring junction at 1,000° C and the reference junctions at 0° C is required. Since emf of the thermocouple when the reference junctions are at 0° C and the measuring junction at 25° C is 0.143 mv, the sum of these emf (9.427 and 0.143) gives the desired value.

The sign must be considered when applying reference-junction corrections. For example, suppose the observed emf of the thermocouple with the measuring junction at 1,000° C and the reference junctions at 0° C is 9.570 mv and the emf of the thermocouple with the measuring junction at 1,000° C and the reference junctions at 25° C is required. The emf of the thermocouple when the reference junctions are at 25° C and the

measuring junction at 0° C is −0.143 mv, and when this is added to the observed emf the desired value 9.427 mv is obtained. Whether the reference-junction correction is positive or negative should not cause any confusion if it is remembered that the emf of the thermocouple is lowered by bringing the junction temperatures closer together and increased by making the difference greater.

In the calibration of thermocouples, the temperature-emf relationship is not always accurately determined in the range of reference-junction temperatures, in which case the average temperature-emf relationship of the type of thermocouple may be used. The average relations for the various types of thermocouples are given in table 5. The errors caused by using these average relations, instead of the actual relation, for a particular thermocouple are, in general, less than 1° C.

If the thermocouple is very short, so that the reference junctions are near the furnace and subject to considerable variations or uncertainty in temperature, it is usually more convenient to use extension leads to transfer the reference junctions to a region of more constant temperature than to measure the temperature of the reference junctions near the furnace. The extension leads of base-metal thermocouples are usually made of the same materials as the thermocouple wires, but in the case of platinum versus platinum-rhodium thermocouples, a copper lead is connected to the platinum-rhodium wire and a copper-nickel lead to the platinum wire. Leads for any of the thermocouples discussed here are available at all the pyrometer instrument manufacturers. Although the temperature-emf relationship of the copper versus copper-nickel lead wire is practically the same as that of platinum versus platinum-rhodium thermocouples, the individual lead wires are not identical thermoelectrically with the thermocouple wires to which they are attached and, therefore, the two junctions where the leads are attached to the thermocouple should be kept at nearly the same temperature. This is not as necessary in the case of base-metal thermocouples when each lead and the thermocouple wire to which it is attached are the same material.

TABLE 5. *Average temperature-emf relations for thermocouples for applying reference-junction corrections*

Temperature		Electromotive force			
		Platinum versus platinum-rhodium [a]	Chromel-Alumel	Iron-constantan	Copper-constantan
°C	°F	mv	mv	mv	mv
−20	−4	−0.103	−0.77	−1.00	−0.75
−15	+5	−.079	−.58	−0.75	−.57
−10	14	−.054	−.39	−.50	−.38
−5	23	−.027	−.19	−.25	−.19
0	32	.000	.00	.00	.00
+5	41	+.028	+.20	+.25	+.19
10	50	.056	.40	.50	.39
15	59	.084	.60	.76	.59
20	68	.113	.80	1.02	.79
25	77	.143	1.00	1.28	.99
30	86	.173	1.20	1.54	1.19
35	95	.204	1.40	1.80	1.40
40	104	.235	1.61	2.06	1.61
45	113	.266	1.81	2.32	1.82
50	122	.299	2.02	2.58	2.03

[a] The values in this column apply for either the 10- or 13-percent rhodium thermocouples. The difference between the average temperature-emf relationships in this range does not exceed 2 μv.

7. Testing of Thermocouple Materials

Thermocouples are ordinarily made up to yield a specified emf at one or more temperatures, and in order to select and match materials to do this, a convenient method of testing each element is required. One method of accomplishing this is to determine the thermal emf of the various materials against some stable and reproducible material. At low temperatures copper is sometimes used for this purpose, but platinum appears to be the most satisfactory because it can be used at any temperature up to its melting point, can be freed from all traces of impurities, and can be readily annealed in air. Two samples of platinum, both of which are spectrochemically pure, may differ slightly in thermal emf, but the same is true of any other metal. To avoid the ambiguity that might arise from this fact, the thermal emf of thermocouple materials tested at the National Bureau of Standards (since 1922) is referred to an arbitrary piece of platinum designated as standard Pt 27. This standard is spectrochemically pure, has been thoroughly annealed, and although it may not be the purest platinum that has been prepared, serves as a satisfactory standard to which the thermal emf of other materials may be referred. However, there is nothing to prevent any other laboratory from setting up a laboratory standard for their own use, but in order that the various laboratories and manufacturers may specify and express values of thermal emf on a common basis, a common and ultimate standard is necessary.

Platinum is used as a working standard for testing thermocouple materials in some laboratories, but it is generally more convenient to use a working standard of the same material as that being tested. In any case, the thermal emf of a material against the standard Pt 27 is the algebraic sum of the emf of the material against the working standard, and the emf of the working standard against the standard Pt 27 (the law of intermediate metals). When platinum is used as a working standard in testing some other material, the thermal emf measured is great. To obtain the thermal emf of the material against the standard Pt 27, the relatively small emf of the platinum working standard against the standard Pt 27 is

574278 O - 61 - 8

added to the large measured emf. When the working standard is of the same kind of material as that being tested, the thermal emf measured is small. To obtain the thermal emf of the material against the standard Pt 27 in this case, the relatively large emf of the working standard against the standard Pt 27 is added to the small measured emf.

Except in the case of constantan, two samples of a similar material which will develop more than 0.5 μv/°C against one another are exceptional. In most cases, the value is less than 0.2 μv/°C. Even in the case of constantan, the thermal emf between 2 extreme samples does not exceed 3 μv/°C. Therefore, in determining the difference in thermal emf between two samples of a similar material, it is not necessary to measure the temperature accurately.

The average thermal emf per degree C of platinum against other thermocouple materials is given in table 6. It is seen that in measuring the thermal emf of these materials directly against platinum working standards, it is necessary to measure an emf which changes by a large amount for a small change in temperature. An accurate measurement of the emf corresponding to a given temperature, therefore, requires an accurate measurement of the temperature of the junctions. The necessity for this accurate measurement of temperature, however, is avoided when the measurements are made by using a working standard of material similar to that being tested, since in this case the emf developed is small and changes very little even for large changes in temperature. In the latter method, the accurate measurement of temperature is not entirely avoided but merely shifted to the laboratory that determines the thermal emf of the working standards against the standard Pt 27.

The small thermal emf of a platinum working standard against the standard Pt 27 at any temperature can be determined as accurately as the emf can be measured. These standards are subject to change during use but, if properly used and occasionally checked, can be relied upon to about 2 μv at 1,000° C. The thermal emf of working standards of other materials is determined and certified at the National Bureau of Standards to the equivalent of ± 1° C at high temperatures.

In any event the testing of a thermocouple material is essentially the determination of the emf of a thermocouple in which the material being tested is one element and a working standard the other. Some of the precautions that must be observed to obtain accurate results are given in the following sections.

TABLE 6. *Average thermal [a] emf per degree C of platinum against other thermocouple materials.*

Material	Temperature	Average change in thermal emf with temperature
	°C	μv/°C
Platinum-10-percent rhodium	1,000	11.6
Platinum-13-percent rhodium	1,000	13.2
Chromel	900	31.5
Alumel	900	8.7
Iron	600	11.6
Constantan	600	46.8
Constantan	100	37.4
Copper	100	9.4

[a] Complete tables giving the average thermal emf of platinum-10-percent rhodium, and platinum-13-percent rhodium against platinum are given in NBS Circular 561. The average thermal emf of Chromel and of Alumel against platinum are given in Research Paper 767; of copper and constantan against platinum in RP1080; of iron and constantan against platinum in RP2415.

7.1. Platinum

The thermal emf of the thermocouple platinum against the standard Pt 27 is usually less than 20 μv at 1,200° C and in testing one sample of platinum against another it is not necessary to measure the temperature of the hot junction to closer than 50° C to obtain a comparison accurate to 1 μv. The reference-junction temperature need not be accurately controlled. The platinum standard (i. e., the wire previously compared with the standard Pt 27) is welded to the wire being tested to form a thermocouple and the emf measured at one or more temperatures by any of the methods described for calibrating platinum versus platinum-rhodium thermocouples. The wires should be carefully insulated and protected. Measurements at two temperatures, about 600° and 1,200° C, are sufficient to give the emf at any temperature as the emf is small and practically proportional to the temperature.

In many laboratories the platinum standard and the platinum element of the thermocouple used to measure the temperature are one and the same. The sample or wire being tested is then welded to the junction of the thermocouple and the emf of the thermocouple and that between the two platinum wires are measured simultaneously with two potentiometers or alternately with one instrument. Simultaneous readings of these electromotive forces should not be made with a millivoltmeter or with a current flowing in either circuit because one wire is common to both circuits and in this case the potential difference measured by one instrument is influenced by the current flowing in the other circuit. However, this objection is not encountered in the method described above in which the platinum standard is not the same wire as the platinum of the thermocouple.

7.2. Platinum-Rhodium Alloy

The testing of platinum-rhodium thermocouple wire directly against platinum is exactly the same as the calibration of platinum versus platinum-rhodium thermocouples. Platinum against platinum-10-percent rhodium gives 11.6 μv/°C and platinum against platinum-13-percent rhodium

gives 13.2 μv/°C at 1,000° C. Therefore, in order to determine the thermal emf of a sample of platinum-rhodium against platinum to ±20 μv, it is necessary to measure the temperature to ±1.5° C. Such an accuracy in temperature measurements is obtained only with a very homogeneous and accurately calibrated thermocouple in a uniformly heated furnace, but if the emf of one sample of wire is known with this accuracy, it may be used to determine the emf of other samples without the necessity of accurately measuring the temperature. For example, the thermal emf per degree of any sample of platinum-10-percent rhodium against any other sample rarely exceeds 0.05 μv/°C (50 μv at 1,000° C). Therefore, if the thermal emf of one sample against platinum is known to ±20 μv at 1,000° C, the emf of other samples against the same platinum can be determined to about the same accuracy by comparing the samples of platinum-rhodium and measuring the temperature of the hot junction to 10° or 20° C. The same applies for platinum-13-percent rhodium.

The working standard used to determine the thermal emf of the platinum-rhodium may be a sample of platinum, of platinum-rhodium, or either element of the thermocouple used in measuring the temperature. Platinum-10-percent rhodium against platinum-13-percent rhodium gives about 1.6 μv/°C at 1,000° C so that if the thermal emf of one of these materials against platinum is known to ±20 μv at 1,000° C, the thermal emf of the other against the same platinum can be determined to ±30 μv by comparing the two and measuring the temperature to ±6° C.

A number of wires can be welded together and tested by any of these methods.

7.3. Base-Metal Thermocouple Materials

a. At High Temperatures

In testing base-metal thermocouple materials (Alumel, Chromel, constantan, copper, and iron) the procedure is very much the same as in calibrating base-metal thermocouples. Although such thermal-emf measurements are ultimately referred to platinum, it is not necessary to measure each sample directly against platinum. When the measurements are made against platinum (and this must frequently be done), the platinum wire should be sealed through the end of a glazed porcelain protection tube with Pyrex glass, leaving about 1 cm of the wire exposed for welding to the base-metal wire or wires. The largest uncertainty in the measurements arises from the uncertainty in the determination of the temperature of the hot junction. The junction of a standard platinum versus platinum-rhodium thermocouple may be inserted into a hole drilled in the junction formed by welding the material to platinum. This brings the junctions to the same temperature.

In the use of platinum or platinum-rhodium for testing thermocouple materials, the wires are used a large number of times before checking or scrapping. Base-metal thermocouple wires used for testing similar materials should not be used more than once if the highest accuracy is required, because there is a slight change in these materials when heated to a high temperature and if they are used repeatedly, the wires become inhomogeneous. The procedure then is to select a coil of wire and test it for homogeneity by taking several samples from different parts of the coil, welding them all together, and measuring the emf between the various samples. If the coil is sufficiently homogeneous as found from such tests, one or more samples may be taken from it and the thermal emf determined as accurately as necessary by comparison with a standard, the emf of which against the standard Pt 27 is known. The average value for the thermal emf of the few selected samples from the coil against the standard Pt 27 will apply for the remainder of the coil with sufficient accuracy for most purposes. Any sample from this coil may then be used as a working standard for testing similar materials. The accuracy with which the temperature must be measured depends upon the difference between the standard and the material being tested. In case of some materials that have been well standardized, the differences are small enough that an accuracy of 50° C is sufficient. Seldom, if ever, should it be necessary to measure the temperature closer than 10° C.

b. At Low Temperatures

Annealed electrolytic copper is very uniform in its thermoelectric properties and is often used as a standard for thermoelectric testing at temperatures below 300° C. The thermal emf of other materials against either copper or platinum may be determined very accurately by using a stirred liquid bath or fixed points. The steam point is an excellent one for this purpose.

Table 7 gives the thermal emf of annealed electrolytic copper against NBS standard Pt 27 and may be used to convert values of the thermal emf of any material against one of these standard materials to values of emf of the same material against the other standard material.

TABLE 7. *Thermal emf of annealed electrolytic copper against NBS platinum standard Pt 27*

Temperature	Electromotive force	Temperature	Electromotive force
°C	μv	°C	μv
−200	−194	100	766
−150	−354	150	1,265
−100	−367	200	1,831
−50	−242	250	2,459
0	0	300	3,145
+50	+340	350	3,885

7.4. Reference-Junction Corrections

It is not convenient for everyone to obtain the same reference-junction temperature in determining the emf of the various thermocouple materials against platinum and, therefore, corrections must be applied to arrive at values for a common reference-junction temperature. The method of applying these corrections is the same as that discussed under the testing of thermocouples. The average temperature-emf relationships for the various thermocouple materials against platinum are given in table 8 and may be used for making reference-junction corrections.

In comparing two samples of a similar thermocouple material at high temperatures, it is not necessary to measure or control accurately the temperature of the reference junctions. The emf developed by two samples of platinum-rhodium, even the 10- against the 13- percent-rhodium alloy, is practically independent of the temperature of the reference junctions between −20° and +50° C. In all other cases, with the possible exception of iron, the emf may be taken as proportional to the difference between the temperatures of the two junctions, and when the emf is small, the corrections for the temperature changes of the reference junctions are negligible. In comparing two samples of iron, the emf developed is changed more by changing the temperature of the reference junctions than by changing that of the hot junction by the same amount, for example it was observed (in one case) that the emf (320 μv) developed by two samples of iron when one junction was at 600° C and the other at 25° C changed by 0.1 μv for each degree change in the temperature of the hot junction and 1.4 μv for each degree change in the temperature of the reference junctions.

TABLE 8. *Average temperature-emf relationships of various thermocouple materials against platinum for applying reference-junction corrections*

Temperature		Electromotive force					
		Platinum versus platinum-rhodium [a]	Chromel versus platinum	Alumel versus platinum	Constantan versus platinum	Iron versus platinum	Copper versus platinum
°C	°F	mv	mv	mv	mv	mv	mv
−20	−4	−0.103	−0.50	0.27	0.64	−0.36	−0.109
−15	+5	−.079	−.38	.20	.48	−.27	−.084
−10	14	−.054	−.25	.14	.32	−.18	−.057
−5	23	−.027	−.13	.07	.16	−.09	−.029
0	32	.000	.00	.00	.00	.00	.000
+5	41	+.028	+.13	−.07	−.16	+.09	+.030
10	50	.056	.26	−.14	−.33	.18	.060
15	59	.084	.40	−.20	−.49	.27	.091
20	68	.113	.52	−.28	−.66	.36	.124
25	77	.143	.66	−.34	−.83	.45	.158
30	86	.173	.79	−.41	−1.00	.54	.193
35	95	.204	.93	−.47	−1.17	.63	.229
40	104	.235	1.07	−.54	−1.34	.72	.265
45	113	.266	1.21	−.60	−1.51	.81	.302
50	122	.299	1.35	−.67	−1.69	.90	.340

[a] These values apply for either 10- or 13-percent rhodium.

8. Accuracies Obtainable

The accuracies obtained in calibrating the various types of thermocouples by different methods and the uncertainty in the interpolated values by various methods are given in table 9.

These accuracies may be obtained with homogeneous thermocouples when reasonable care is exercised in the work. More or less accurate results can be obtained by the same methods. In the case of Chromel-Alumel and iron-constantan thermocouples at low temperatures, the accuracy given in table 9 is limited by the uncertainty in interpolated values. However, this uncertainty can be greatly reduced by observing the emf of the thermocouples at more points. The accuracy obtained with copper-constantan thermocouples at low temperatures is usually limited by the emf measurements and in such cases the accuracy may be improved by employing a number of thermocouples in series (multiple-junction couples). When it is desired to test a thermocouple and leads or thermocouple, leads, and indicator as a unit by any of the methods described in the preceding sections, no additional difficulties are encountered.

The following services are provided by the National Bureau of Standards for fees covering the cost.

(1) Thermocouples are calibrated and certified as accurately as the conditions of use and the homogeneity and stability of the wires justify. The accuracies given in table 9 have been found to meet most needs.

(2) Indicators used with thermocouples are calibrated separately or in combination with a particular thermocouple.

(3) The thermal electromotive forces of thermocouple materials against the standard Pt 27 are determined and the results certified to the limits justified by the material.

(4) Standard Samples of metals are distributed, each with a certificate giving the value of the freezing point. The freezing-point metals being distributed at present are tin, lead, zinc, aluminum, and copper.

TABLE 9. *Summary of methods and accuracies obtainable in calibrating thermocouples*

Type of thermocouple	Methods of calibration	Temperature range	Calibration points	Accuracy at observed points	Method of interpolating	Uncertainty in interpolated values
		°C		°C		°C
Platinum versus platinum-10-percent-rhodium.	International Temperature Scale (fixed points).	630.5 to 1,063.0	Freezing point of Sb, Ag, and Au.	0.2	Equation: $E=a+bt+ct^2$	0.3
Platinum versus platinum-rhodium.[a]	Fixed points	0 to 1,450	Freezing point of Zn Sb, Ag, and Au.	.2	Difference curve from reference table	0.5 to 1,100 and 2 at 1,450.
	NBS Standard Samples, fixed points.	0 to 1,450	Freezing point of Sn, Zn, Al, and Cu.	.2	do	.5 to 1,100 and 2 at 1,450.
	Comparison with standard thermocouple.	0 to 1,450	About every 100° C	.3	do	.5 to 1,100 and 2 at 1,450.
	do	0 to 1,450	About 600° and 1,100° C (or more points).	.3	do	1 to 1,100 and 3 at 1,450.
Chromel-Alumel	Comparison with standard thermocouple.[a]	0 to 1,100	About every 100° C	.5	Linear	1
	do	0 to 1,100	About 500°, 800°, and 1,100° C (or more points).	.5	Difference curve from reference table	2
	Comparison with standard resistance thermometer [b] or at fixed points.	0 to 350	About every 100° C	.1	do	0.5
	Comparison with standard resistance thermometer.[b]	0 to −190	About every 50° C	.1	do	.5
Iron-constantan	Comparison with standard thermocouple.[a]	0 to 760	About every 100° C	.5	Linear	1
	do	0 to 760	About 100°, 300°, 500°, and 750° C	.5	Difference curve from reference table	1
	Comparison with standard resistance thermometer [b] or at fixed points.	0 to 350	About every 100° C	.1	do	0.5
	Comparison with standard resistance thermometer.[b]	0 to −190	About every 60° C	.1	do	.5
Copper-constantan	Comparison with standard resistance thermometer [b] or at fixed points.	0 to 300	About every 100° C	.1	Equation: $e=at+bt^2+ct^3$ or difference curve from reference table.	.2
	Comparison with standard resistance thermometer.[b]	0 to 100	About 50° and 100° C	.05	Equation: $e=at+bt^2$ or difference curve from reference table.	.1
	Fixed points	0 to 100	Boiling point of water	.05	Equation: $e=at+0.04t^2$	.2
	Comparison with standard resistance thermometer.[b]	0 to −190	About every 60° C	.1	Equation: $e=at+bt^2+ct^3$ or difference curve from reference table.	.2
	Fixed points	0 to −190	Sublimation point of CO_2 and boiling point of O_2.	.1	Difference curve from reference table	.3

[a] Either 10- or 13-percent rhodium. [b] In stirred liquid bath.

9. References

[1] George K. Burgess, BS J. Research **1,** 635 (1928) RP22.

[2] H. F. Stimson, J. Research NBS **42,** 209 (1949) RP1962; R. J. Corruccini, J. Research NBS **43,** 133 (1949) RP2014.

[3] W. P. White, Phys. Rev. **23,** 449 (1906); **31,** 135 (1910); J. Am. Chem. Soc. **36,** 2292 (1914); P. D. Foote, C. O. Fairchild, and T. R. Harrison, Tech. Pap. BS **14** (1920–21) T170.

[4] R. J. Corruccini, J. Research NBS **47,** 94 (1951) RP2232.

[5] H. Diesselhorst, Z. Instrumentenk. **28,** 1 (1908).

[6] W. P. White, Z. Instrumentenk. **27,** 210 (1907).

[7] L. Behr, The Wenner potentiometer, Rev. Sci. Instr. **3,** 109 (1932).

[8] A symposium on the contamination of platinum thermocouples, J. Iron Steel Inst. (London) **155,** 213 (1947).

[9] Wm. F. Roeser and A. I. Dahl, BS J. Research **10,** 661 (1933) RP557.

[10] Von Fr. Hoffmann and W. Meissner, Ann. phys. **60,** 201 (1919); Von Fr. Hoffmann, Z. Physik, **27,** 285 (1924); C. O. Fairchild, W. H. Hoover, and M. F. Peters, BS J. Research **2,** 931 (1929) RP65.

[11] E. F. Mueller and T. S. Sligh, J. Opt. Soc. Amer. and Rev. Sci. Instr. **6,** 958 (1922).

[12] George K. Burgess, BS J. Research **1,** 635 (1928) RP22; H. F. Stimson, J. Research NBS **42,** 209 (1949) RP1962.

[13] E. F. Mueller and H. A. Burgess, BS Sci. Pap. **15,** 163 (1919–20) S339.

[14] C. W. Waidner and G. K. Burgess, Bul. BS **7,** 1 (1911) S143.

[15] J. L. Finck and R. M. Wilhelm, J. Am. Chem. Soc. **47,** 1577 (1925).

[16] R. B. Scott, Temperature, its measurement and control in science and industry, p. 206 (Reinhold Publishing Corp., New York, N. Y., 1941).

[17] C. H. Meyers and M. S. Van Dusen, BS J. Research **10,** 381 (1933) RP538; R. B. Scott, Temperature, its measurement and control in science and industry, p. 212 (Reinhold Publishing Corp., New York, N. Y., 1941).

[18] A. I. Dahl, J. Research NBS **24,** 205 (1940) RP1278.

[19] N. S. Osborne, Bul. BS **14,** 133 (1918–19) S301.

[20] R. B. Scott and F. G. Brickwedde, BS J. Research **6,** 401 (1931) RP284.

[21] C. W. Kanolt, BS Sci. Pap. **20,** 619 (1924–26) S520.

[22] Wm. F. Roeser, BS J. Research **3,** 343 (1929) RP99.

[23] Henry Shenker, John I. Lauritzen, Jr., Robert J. Corruccini and S. T. Lonberger, NBS Circ. 561 (1955).

[24] Wm. F. Roeser and A. I. Dahl, J. Research NBS **20,** 337 (1938) RP1080.

[25] R. J. Corruccini and H. Shenker, J. Research NBS **50,** 229 (1953) RP2415; NBS Circ. 561, Reference tables for thermocouples (April 1955).

WASHINGTON, June 10, 1957.

U. S. Department of Commerce National Bureau of Standards

RESEARCH PAPER RP1278

Part of Journal of Research of the National Bureau of Standards, Volume 24, February 1940

STABILITY OF BASE-METAL THERMOCOUPLES IN AIR FROM 800° TO 2,200° F

By Andrew I. Dahl

ABSTRACT

A study has been made of the changes in the emf of Chromel-Alumel and iron-constantan thermocouples heated in an oxidizing atmosphere at various temperatures and for various periods of time. The thermocouples were held at definite temperatures, ranging from 800° to 2,200° F, in steps of 200° F. Calibrations were made of the thermocouples in their original condition, and again after heating them at each temperature for total times of 10, 50, 100, 200, 400, 600, 800, and 1,000 hours, or as long as the thermocouples remained serviceable. The thermal emf of each element against platinum was measured in order to determine the relative stability of the individual elements. A few tests were made to determine the effect of wire size on the stability. The effects of changing the depth of immersion of thermocouples after they had been used under controlled conditions were also studied.

Since all tests were made in an atmosphere of clean air, the results give no information on stability except under oxidizing conditions.

CONTENTS

I. INTRODUCTION

With the widespread use of base-metal thermocouples for temperature measurement and control in industrial processes, there are numerous instances where high accuracy is of vital importance. Some processes require that a given temperature be maintained within narrow limits for an extended period of time, if efficiency in operation and uniformity in production are to be maintained. In order to meet these requirements, a more complete knowledge of the thermoelectric stability of base-metal thermocouple materials is necessary.

Practically all base-metal thermocouple wire produced in this country is annealed or given a stabilizing heat treatment by the manufacturer. For most purposes this treatment renders the product sufficiently stable, so that further changes which may occur while the thermocouple is in service may be neglected. However, when high accuracy is required throughout the useful life of the thermocouple,

these changes must be taken into account. In many industrial processes, thermocouples, when placed in service, are left undisturbed until there is evidence of either mechanical failure or of serious error in the temperatures indicated. However, long before this occurs, the thermocouple may have changed to such an extent as to make it unreliable for accurate temperature measurement. The changes in the thermoelectric characteristics of thermocouple materials due to ordinary service conditions are usually gradual and cumulative. They depend upon such factors as the temperatures encountered, the length of time in service, and the atmosphere surrounding the thermocouple. The various types of thermocouple materials are affected in various ways and to various degrees.

When the reference-junction temperature is maintained constant, the emf developed by a homogeneous thermocouple depends only on the temperature of the measuring junction. The emf developed by an inhomogeneous thermocouple depends not only on the temperature of the measuring junction but also on the temperature distribution throughout the inhomogeneous portions of the wires. All base-metal thermocouples become inhomogeneous with use at high temperatures. However, if all the inhomogeneous portions of the thermocouple wires are in a region of uniform temperature, the inhomogeneous portions have no effect upon the indications of the thermocouple. Therefore, an increase in the depth of immersion of a used couple has the effect of bringing previously unheated portions of the wires into the region of temperature gradient, and thus the indications of the thermocouple will correspond to the original emf-temperature relation, provided the increase in immersion is sufficient to bring all of the previously heated part of the wires within the zone of uniform temperature. If the immersion is decreased, the more inhomogeneous portions of the wires will be brought into the region of temperature gradient, thus giving rise to a change in the indicated emf. Furthermore, a change in the temperature distribution along inhomogeneous portions of the wire nearly always occurs when a couple is removed from one installation and placed in another, even though the measured immersion and the temperature of the measuring junction are the same in both cases. Thus the indicated emf is changed.

Although it is recognized that there are differences in composition and thermoelectric properties between various lots of thermocouple materials of the same general type, it is believed that the changes in the thermoelectric properties of a few selected lots of material will give a general idea of the changes which would occur in other lots of the same general type, provided that all the lots have received the same initial heat treatment.

II. MATERIALS INVESTIGATED

The thermocouple materials studied were Chromel *P*, Alumel, iron, and constantan. Chromel *P* and Alumel wire of No. 18 gage and iron and constantan of No. 14 gage were used for the tests at 800° and 1,000° F. For the tests at 1,200° F and above, No. 8 gage wires were used. To determine the relation of wire size to the thermoelectric stability, additional tests were made on No. 18 and No. 22 gage Chromel and Alumel at 1,200° and 1,600° F, and on No. 18 gage iron and constantan at 1,200° and 1,400° F.

Samples of the various materials were secured from several sources. Each of the materials used in the investigation had the temperature-emf relation characteristic of the large percentage of the material of its particular type now being manufactured. All of the wires had been heat treated by the manufacturers in the manner considered standard for the particular type of wire.

III. TEST METHODS

Since Chromel *P* is generally used in combination with Alumel, and iron with constantan, the materials were paired in this manner. In addition to determining the temperature-emf relation for each pair, the thermal emf of the individual elements of each pair against the platinum standard [1] Pt 27 was determined. In this way the thermoelectric changes of each thermocouple material were determined independently. The difference of the thermal emfs of the individual elements of a thermocouple against a third material is equal to the emf of the thermocouple. As all three were measured in this work, any two served as a check upon the third.

The temperatures were measured with a standard platinum to platinum—10 percent rhodium thermocouple calibrated in accordance with the specifications for the International Temperature Scale.[2] The platinum working standard used was checked periodically against Pt 27.

The pair or pairs of wire under test were insulated by two-hole porcelain insulators. The platinum reference wire was protected by a glazed porcelain tube and was sealed through the end of the protection tube with a Pyrex glass, leaving about 1 cm of the end of the wire protruding beyond the seal. The platinum-rhodium thermocouple, insulated with a two-hole porcelain tube inside a glazed porcelain protection tube, was likewise sealed through the end of its protection tube with a Pyrex glass, leaving the welded junction protruding about 1 cm beyond the seal. The ends of the base-metal wires, the platinum reference wire, and the standard thermocouple were then welded together to form a single composite junction.

The furnace used in this work was of the resistance type wound with platinum-rhodium wire. The furnace tube of Alundum was 60 cm long and 3-cm inside diameter. The wires under test, together with the platinum reference wire and the platinum-rhodium thermocouple, were placed in the furnace with the composite junction at about the midpoint. The wires were then securely clamped with respect to the furnace. Although the ends of the furnace tube were closed with asbestos wool to promote temperature uniformity, no attempt was made to exclude air from the heated chamber, so that the atmosphere prevailing within the tube was oxidizing. The reference junctions were maintained at 32° F during all the measurements. The temperature of the furnace was maintained practically constant during any observation at a given point by means of a hand-operated voltage regulator in the power circuit.

To obtain data on the effect of long-time exposure to high temperatures upon the thermoelectric properties of the materials, the following procedure was adopted. The initial measurements were made on the sample as received from the manufacturer. Measurements of the

[1] The thermoelectric reference standard maintained at the National Bureau of Standards.
[2] G. K. Burgess, BS J. Research 1, 635 (1928) RP22.

thermal emfs of the various combinations were made at intervals of 200° F up to and including in each case the temperature at which the effect of heating was to be determined. The furnace was then allowed to cool to room temperature, and the measurements were repeated. The differences between the two sets of measurements were ascribed to the initial heating and will be referred to as the "initial changes." Similar measurements were then made after the materials had been held at the test temperature for total elapsed times of 10, 50, 100, 200, 400, 600, 800, and 1,000 hours, or as long as the materials remained serviceable. The test temperatures included every temperature from 800° F to and including 2,000 °F, in steps of 200° F. Chromel *P* and Alumel were also tested at 2,200° F. A fresh sample was used for the test at each temperature. During heating periods, the temperature of the furnace was maintained constant within ±5° F by means of an automatic temperature controller.

The procedure followed in studying the effect of decreasing the depth of immersion was as follows:

The materials were heated in the electric furnace for a period of 20 hours at a constant temperature. Following this heat treatment, the thermal emf of the samples was determined, the position of the samples being maintained the same as that during the 20-hour heating period. The furnace was then allowed to cool to room temperature, and the immersion was decreased 3 inches and the thermal emf determined in this new position. The difference between the observations for a given sample is due only to the change in immersion, since no heating took place between the two sets of measurements. This type of test was carried out on No. 8 gage iron and constantan at temperatures from 600° to 1,800° F, in 200° F steps, and on No. 8 gage Chromel *P* and Alumel from 600° to 2,200° F.

IV. RESULTS

1. TEMPERATURE EXPOSURE TESTS

(a) CHROMEL P AND ALUMEL

Figures 1 and 2 show the results obtained on No. 18 gage Chromel *P* and Alumel heated at 800° and 1,000° F, respectively. The changes in the completed Chromel-Alumel thermocouples are also shown. The changes in the individual elements are in the same direction, so that each becomes thermoelectrically positive to the material in its original condition. The convention followed in regard to sign is as follows:

If in a simple thermoelectric circuit the current flows from metal *A* to metal *B* at the colder junction, *A* is thermoelectrically positive to *B*. On the basis of this convention, Chromel *P* is positive to Alumel. Therefore, a positive change in Chromel *P* will increase the emf of a Chromel-Alumel thermocouple, while a positive change in Alumel will decrease the emf of the thermocouple. The changes observed in the tests at 800° and 1,000° F are small, in all cases less than the equivalent of 1° F for a Chromel-Alumel thermocouple.

Figures 3 to 8, inclusive, show the results obtained with No. 8 gage Chromel *P* and Alumel at temperatures from 1,200° to 2,200° F, inclusive. The changes in the emf of Chromel *P* are in the positive direction throughout all tests, with the exception of the test at 2,200° F, where a negative change was observed at temperatures above 1,600°

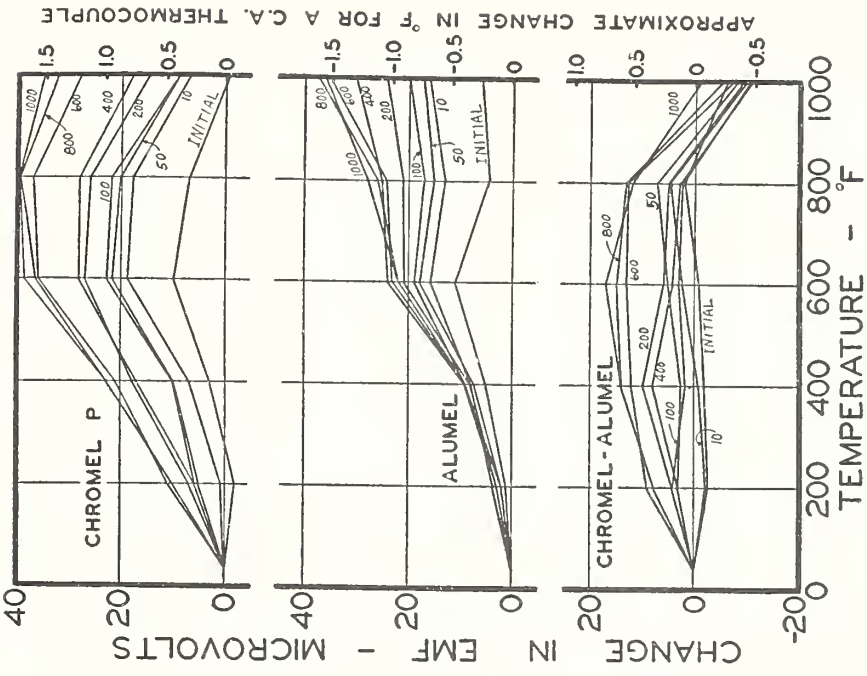

FIGURE 2.—*Changes in No. 18 gage Chromel P and Alumel due to heating at 1,000° F for the total times indicated on the graphs.*

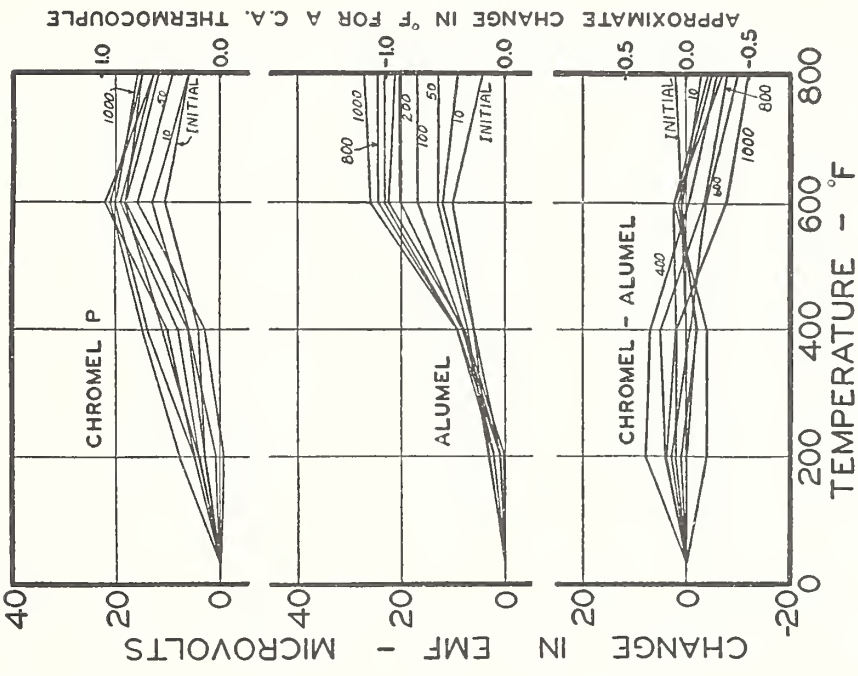

FIGURE 1.—*Changes in No. 18 gage Chromel P and Alumel due to heating at 800° F for the total times indicated on the graphs.*

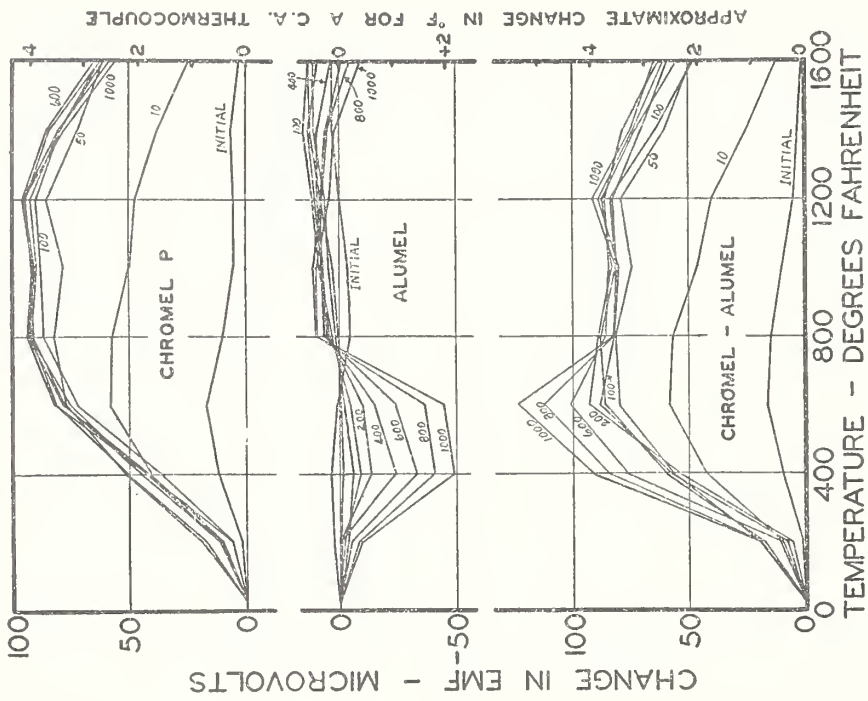

FIGURE 4.—*Changes in No. 8 gage Chromel P and Alumel due to heating at 1,400° F for the total times indicated on the graphs.*

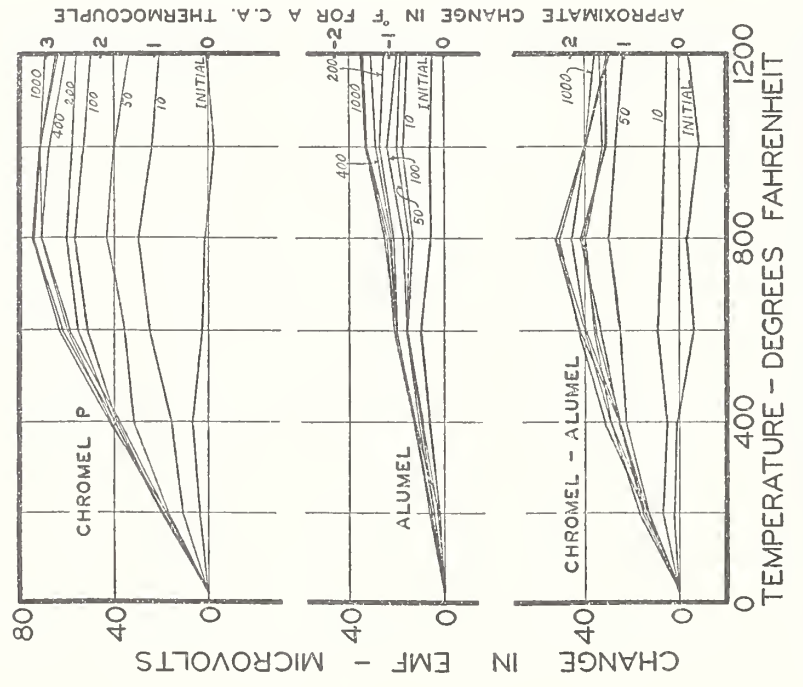

FIGURE 3.—*Changes in No. 8 gage Chromel P and Alumel due to heating at 1,200° F for the total times indicated on the graphs.*

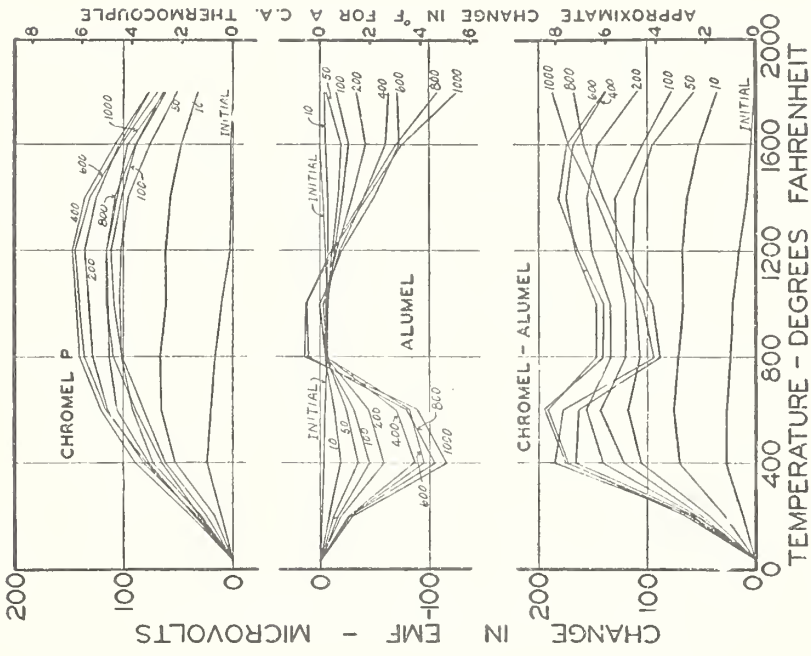

FIGURE 6.—*Changes in No. 8 gage Chromel P and Alumel due to heating at 1,800° F for the total times indicated on the graphs.*

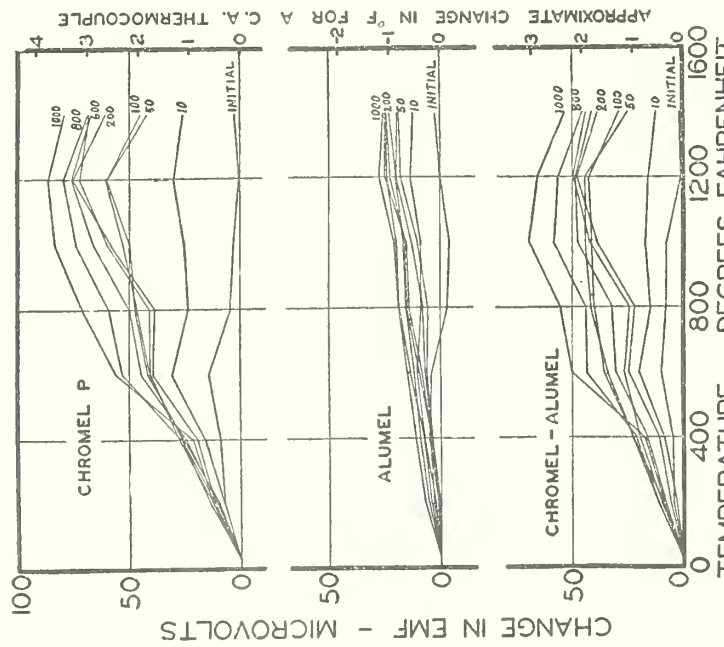

FIGURE 5.—*Changes in No. 8 gage Chromel P and Alumel due to heating at 1,600° F for the total times indicated on the graphs.*

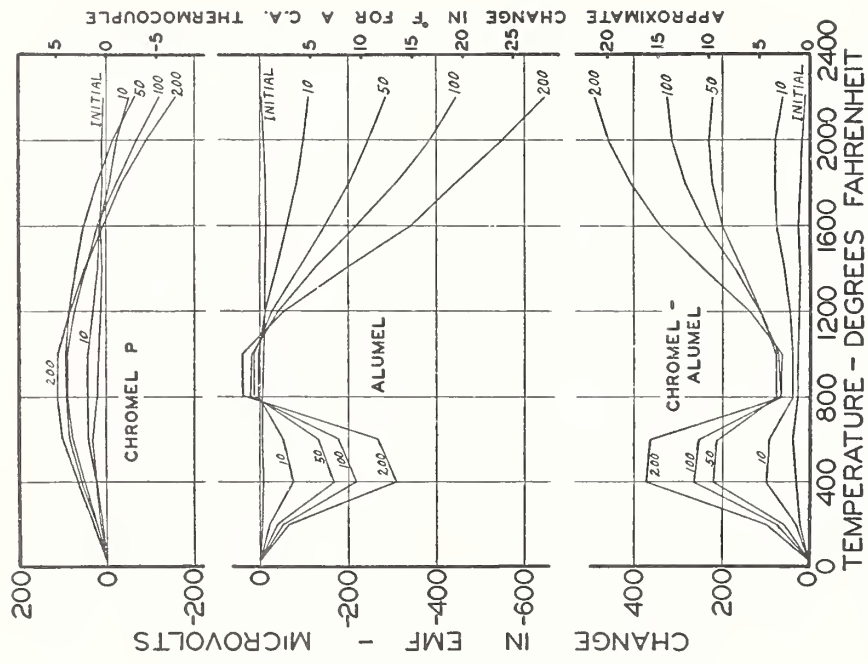

FIGURE 8.—*Changes in No. 8 gage Chromel P and Alumel due to heating at 2,200° F for the total times indicated on the graphs.*

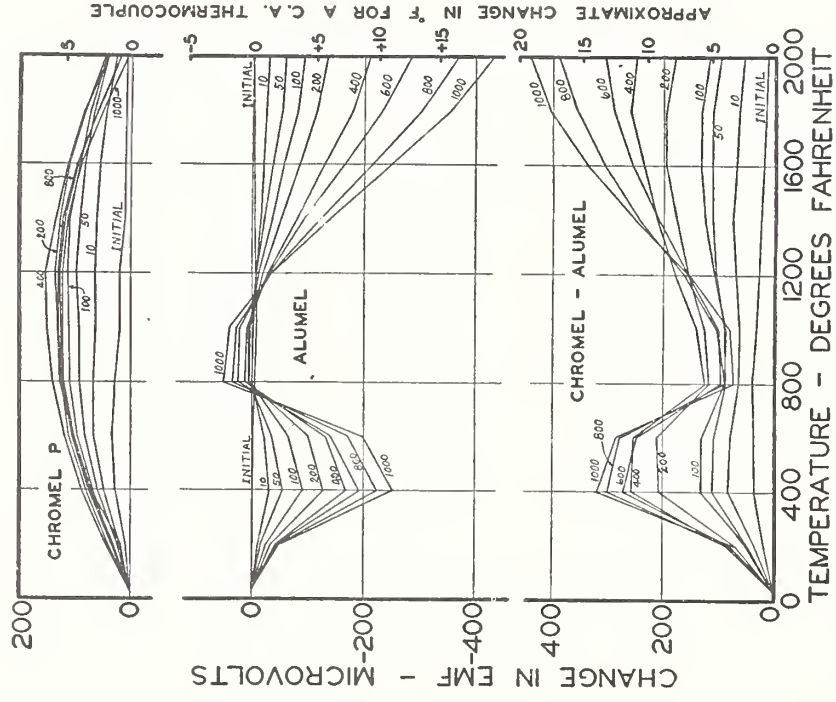

FIGURE 7.—*Changes in No. 8 gage Chromel P and Alumel due to heating at 2,000° F for the total times indicated on the graphs.*

F. The magnitude of the changes is, in nearly all cases, in the order of the duration of the heating periods, the maximum change occurring at about 1,200° F. The changes in the Alumel are in the positive direction throughout the tests at 1,200° and 1,400° F. In the tests at 1,600° F and above, the changes in the emf of the Alumel between about 800° and 1,100° F are extremely small. Above 1,100° F the changes are negative and of appreciable magnitude. This is most clearly shown in figure 7. The materials used in the test at 2,200° F failed after about 300 hours of heating.

Tests of No. 8, No. 18, and No. 22 gage Chromel-Alumel thermocouples heated at 1,200° F for a total of 1,000 hours indicated that

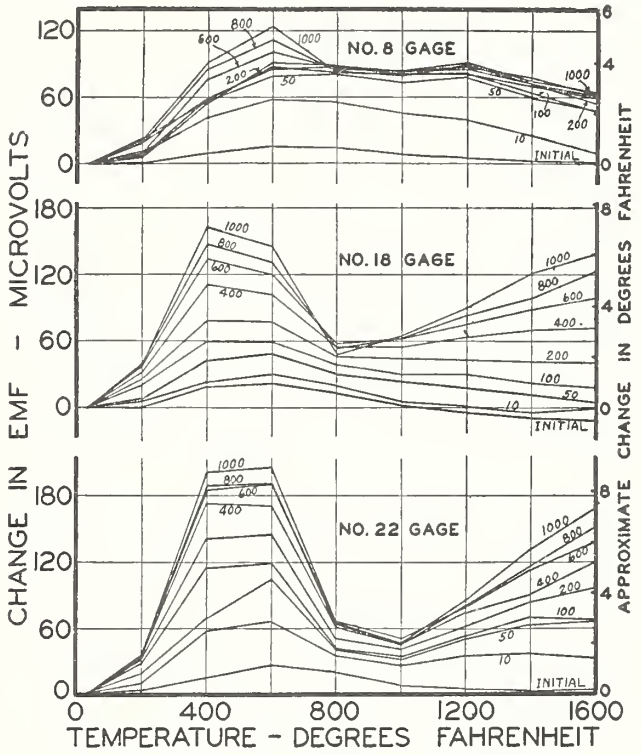

FIGURE 9.—*Changes in No. 8, No. 18, and No. 22 gage Chromel-Alumel thermocouples due to heating at 1,600° F for the total times indicated on the graphs.*

the changes in the thermocouples of the various sizes were nearly the same, and in all cases less than the equivalent of 2.5° F. Figure 9 shows the effects on the same sizes of Chromel-Alumel thermocouples when heated at 1,600° F. The change in calibration at 400° F is largest in the smallest size, but the reverse is true for the change at 1,000° F.

The changes in the emf of the Chromel-Alumel thermocouples produced by the total heating time in each of the tests are shown in figure 10 (reproduced from fig. 1 to 8, inclusive). In the test at 2,200° F the change after only 200 hours is shown, this being the elapsed time when the last measurements preceding failure were made. The peculiar change in the Alumel previously mentioned is reflected in change of the thermocouples.

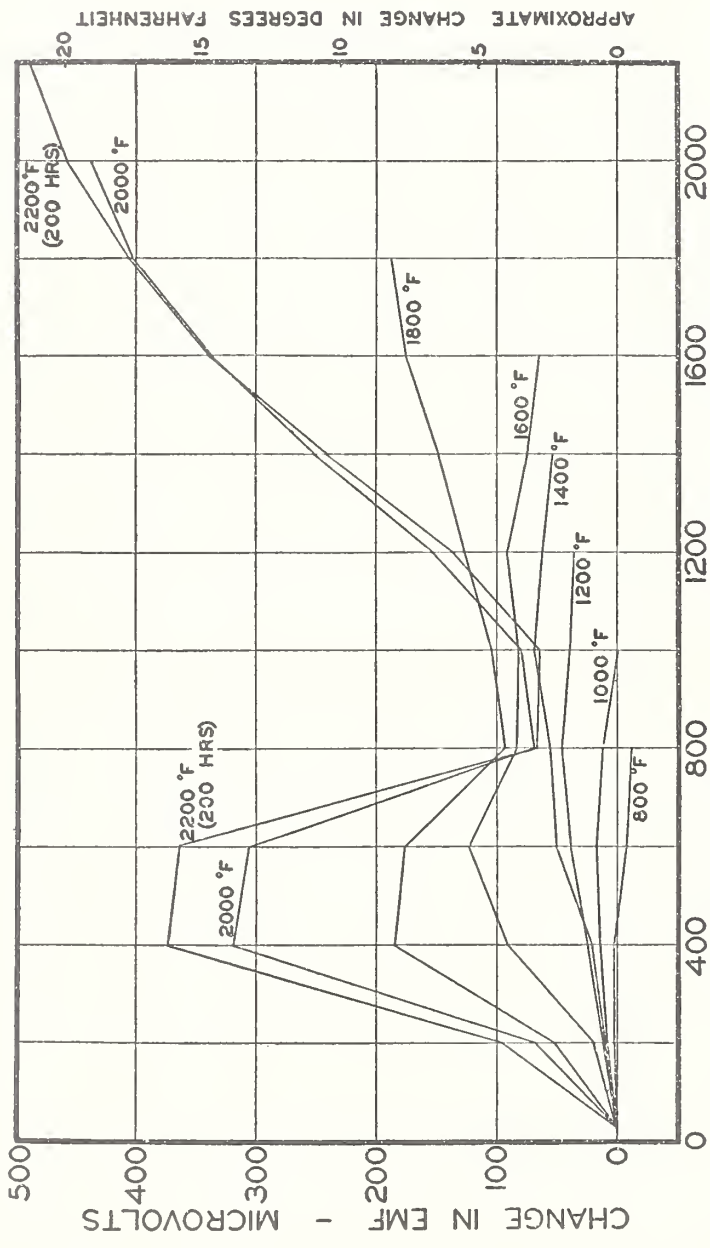

FIGURE 10.—*Changes in Chromel-Alumel thermocouples due to 1,000 hours of heating at temperatures indicated on the graphs.*

(b) IRON AND CONSTANTAN

Figures 11 and 12 show the results obtained on No. 14 gage iron and constantan tested at 800° and 1,000° F, respectively. The changes in all cases are small, being less than the equivalent of 1° F.

The results on No. 8 gage iron and constantan tested at 1,200° to 2,000° F, inclusive, are shown in figures 13 to 17. The time intervals between calibrations were shortened for the tests at 1,800° and 2,000° F, since at these temperatures the materials change at a rapid rate. The tests were continued until the materials failed.

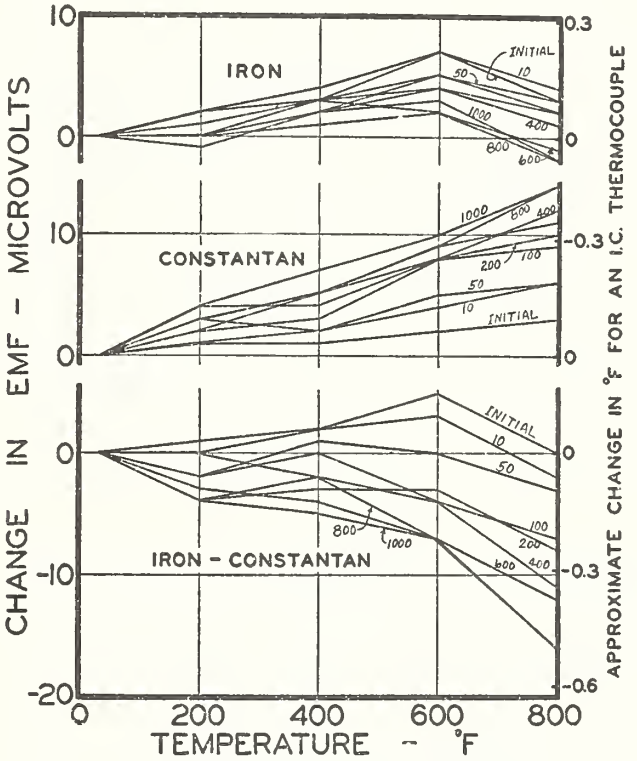

FIGURE 11.—*Changes in No. 14 gage iron and constantan due to heating at 800° F for the total times indicated on the graphs.*

The relative thermoelectric stability of No. 8 and No. 18 gage iron-constantan thermocouples heated at 1,400° F is shown in figure 18. As might be expected, the emf changes in the smaller wire proceed more rapidly. The No. 18 gage thermocouple failed after about 400 hours of heating, while the No. 8 gage remained serviceable throughout the 1,000 hours of the test. However, the measurements made on the thermocouple at the end of the 1,000-hour period indicated that failure was near. A test on these same sizes at 1,200° F showed no appreciable difference in their thermoelectric stability at this test temperature, the maximum change after 1,000 hours of heating being about the equivalent of 4° F.

The change in the emf of constantan was gradual and cumulative throughout each test. In the case of iron the change in emf was relatively small until failure of the wire was approached. When this stage was reached, the change was rapid and relatively large. This

574278 O - 61 - 9

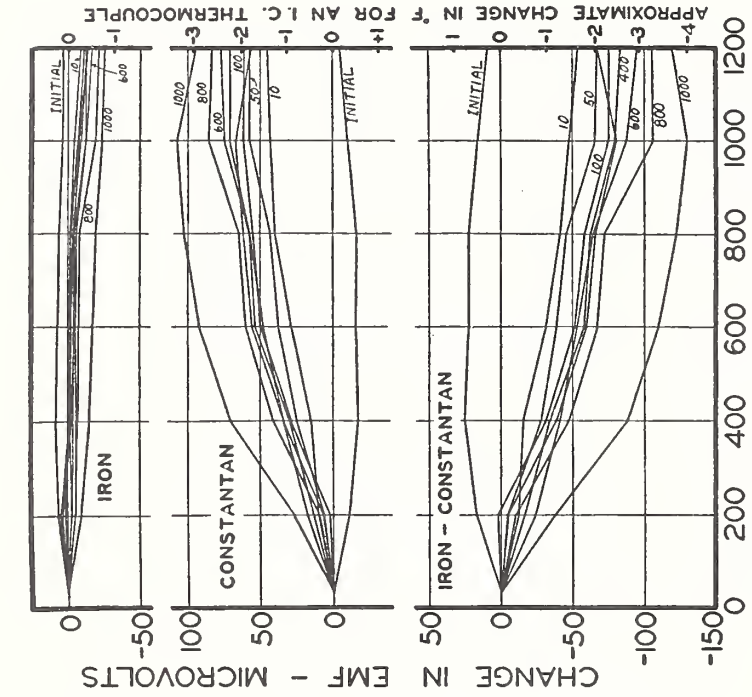

FIGURE 13.—*Changes in No. 8 gage iron and constantan due to heating at 1,200° F for the total times indicated on the graphs.*

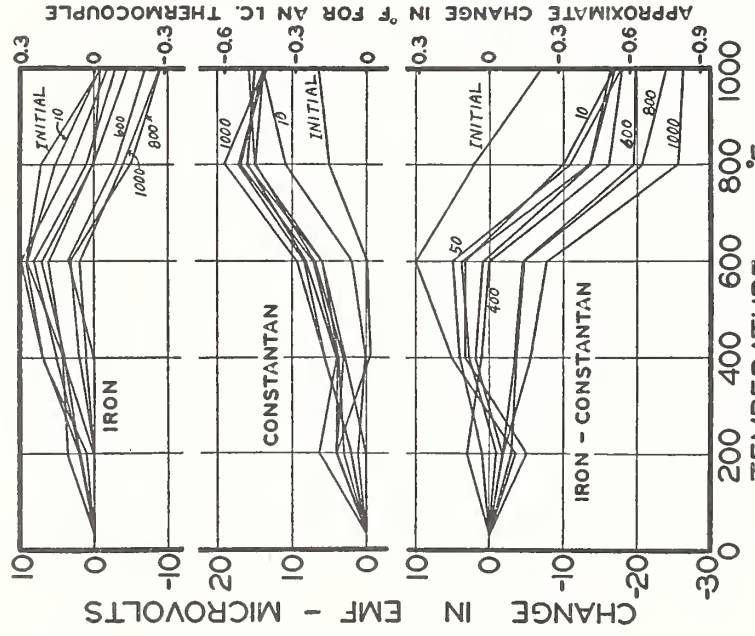

FIGURE 12.—*Changes in No. 14 gage iron and constantan due to heating at 1,000° F for the total times indicated on the graphs.*

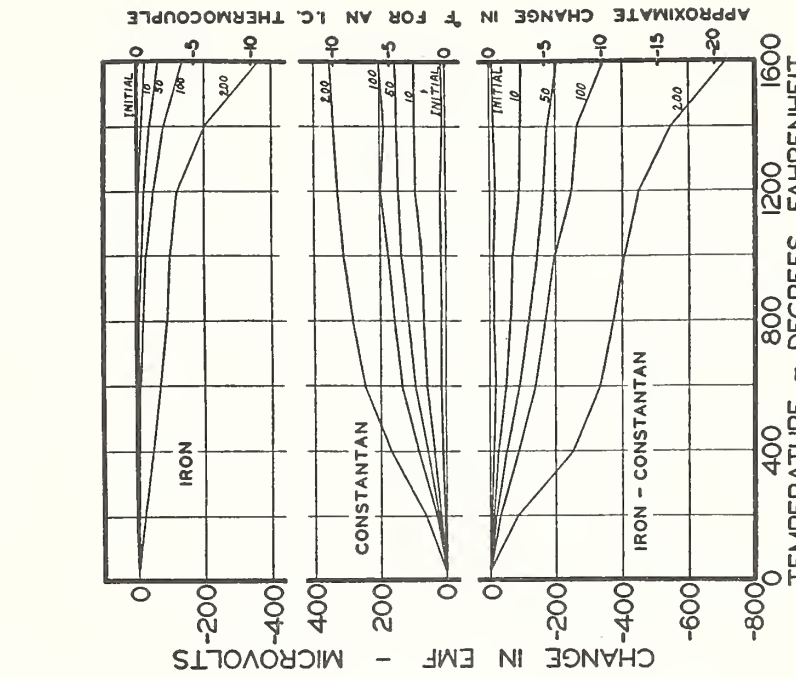

FIGURE 15.—*Changes in No. 8 gage iron and constantan due to heating at 1,600° F for the total times indicated on the graphs.*

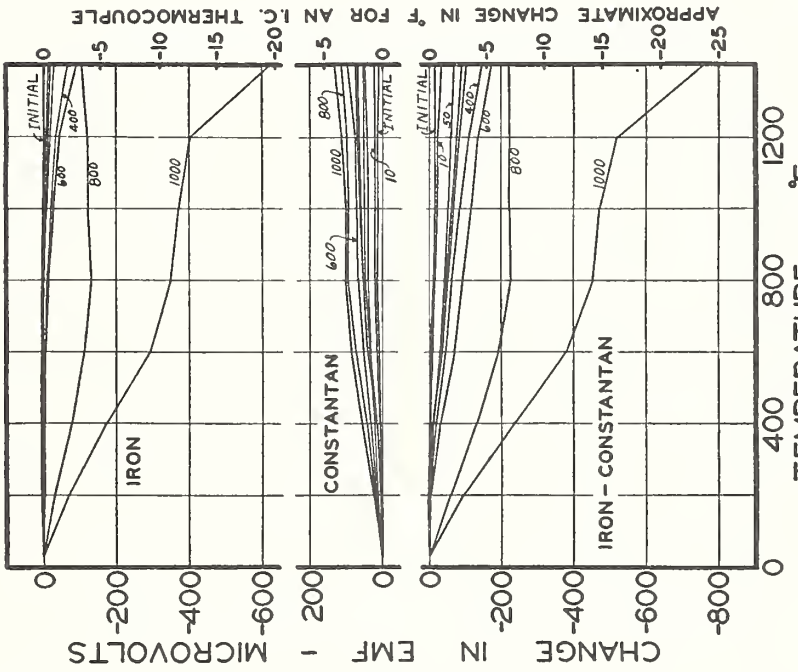

FIGURE 14.—*Changes in No. 8 gage iron and constantan due to heating at 1,400° F for the total times indicated on the graphs.*

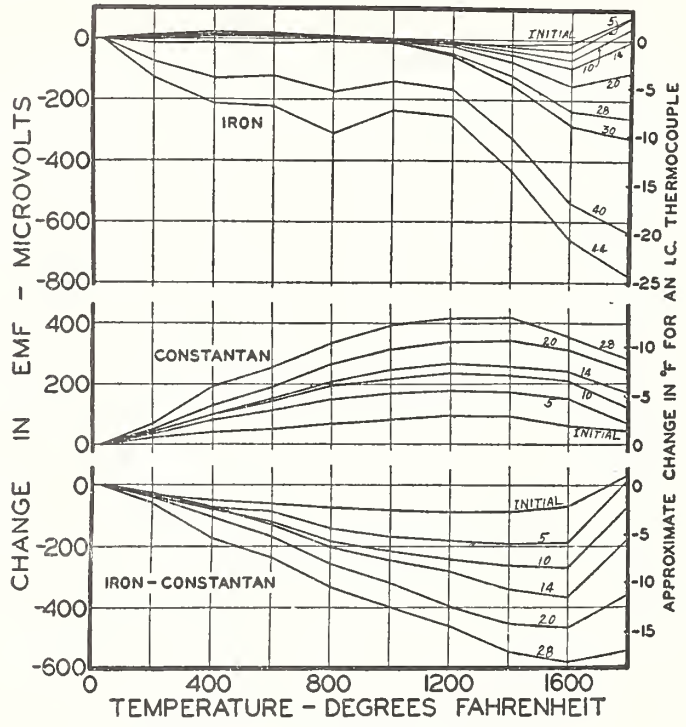

FIGURE 16.—*Changes in No. 8 gage iron and constantan due to heating at 1,800° F for the total times indicated on the graphs.*

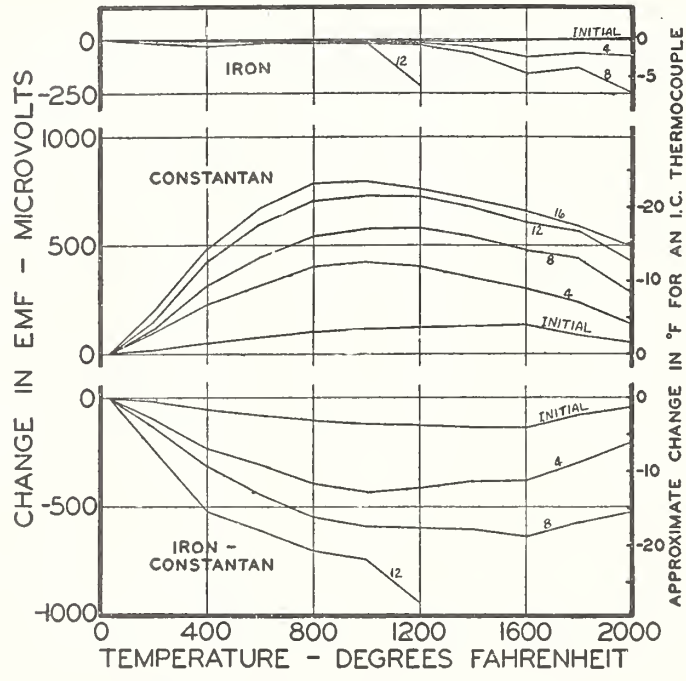

FIGURE 17.—*Changes in No. 8 gage iron and constantan due to heating at 2,000° F for the total times indicated on the graphs.*

was true for all tests in which iron was heated until failure occurred. The life of the iron element was found to be approximately the same as that of the constantan.

2. IMMERSION TESTS

Table 1 gives the observed changes in the thermal emf of No. 8 gage iron and constantan produced by a 3-inch decrease in immersion following the 20-hour heating period. The changes in both of the elements are gradual and regular throughout, the magnitude of the emf changes in constantan being everywhere considerably greater than in the case of iron. Figure 19 shows the change in the emf of the iron-constantan thermocouple under the various conditions of heating (test at 1,800° F not shown in graph). A greatly increased, though regular, change is clearly shown for the test at 1,600° F. At 1,800° F the change is about four times as great as that observed at 1,600° F.

TABLE 1.—*Changes (in thermal emf) at various temperatures caused by decreasing the depth of immersion 3 inches, after heating the wires in air at the temperatures indicated for 20 hours*

IRON

Calibration temperature	Heating temperature						
	600 °F	800 °F	1,000 °F	1,200 °F	1,400 °F	1,600 °F	1,800 °F
°F	μv	μv	μv	μv	μv	μv	μv
200	1	5	3	1	−2	−1	−2
400	0	7	4	3	−2	−4	−9
600	1	8	3	4	−2	−7	−18
800		7	2	4	−3	−12	−29
1,000			3	4	−6	−19	−43
1,200				1	−9	−30	−58
1,400					−13	−43	−72
1,600						−57	−80
1,800							−100

CONSTANTAN

200	4	10	13	14	14	25	83
400	7	18	20	30	28	62	224
600	9	27	26	43	41	93	374
800		35	37	52	53	127	504
1,000			49	60	54	156	615
1,200				65	65	182	735
1,400					68	208	837
1,600						223	935
1,800							1,078

IRON-CONSTANTAN

200	−3	−5	−10	−13	−16	−26	−85
400	−7	−11	−16	−27	−30	−66	−233
600	−8	−19	−23	−39	−43	−100	−392
800		−28	−35	−48	−56	−139	−533
1,000			−46	−56	−60	−175	−658
1,200				−64	−74	−212	−793
1,400					−81	−251	−909
1,600						−280	−1,015
1,800							−1,178

Table 2 gives the observed effects for No. 8 gage Chromel *P* and Alumel of changes in immersion, as outlined above. In the tests up to and including 1,600 °F the effect is gradual and approximately regular. At 1,800 °F and above, the Alumel element exhibited an irregular effect, somewhat similar to that observed in the exposure tests, which became more pronounced as the heating temperature was increased. Figure 20 illustrates the results for the Chromel-Alumel thermocouples.

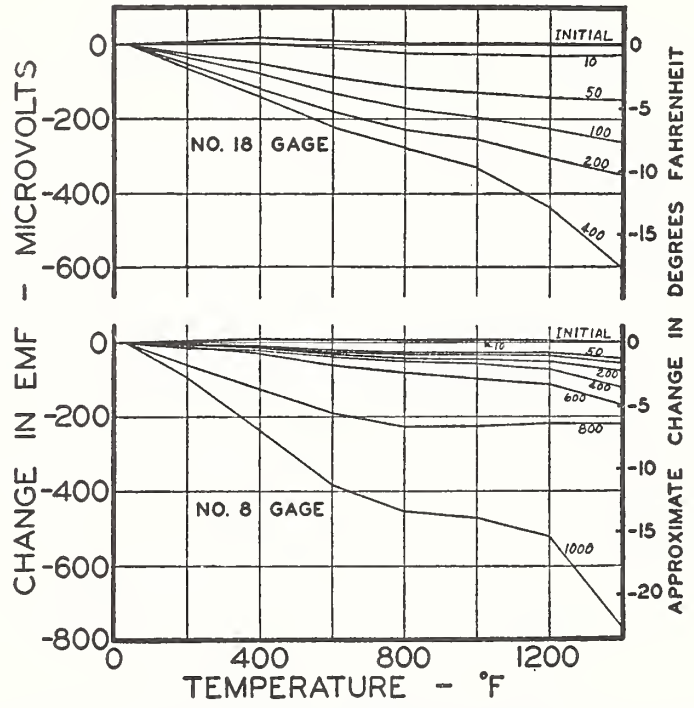

FIGURE 18.—*Changes in No. 8 and No. 18 gage iron-constantan thermocouples due to heating at 1,400° F for the total times indicated on the graphs.*

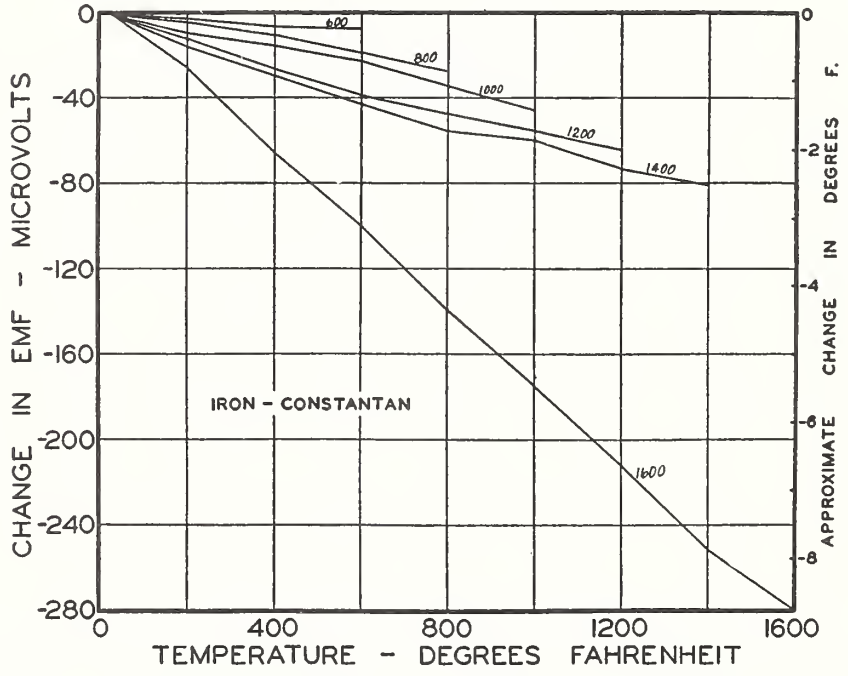

FIGURE 19.—*Changes in the indications of No. 8 gage iron-constantan thermocouples due to a 3-inch decrease in immersion after the couples had been heated for 20 hours at the temperatures indicated on the graphs.*

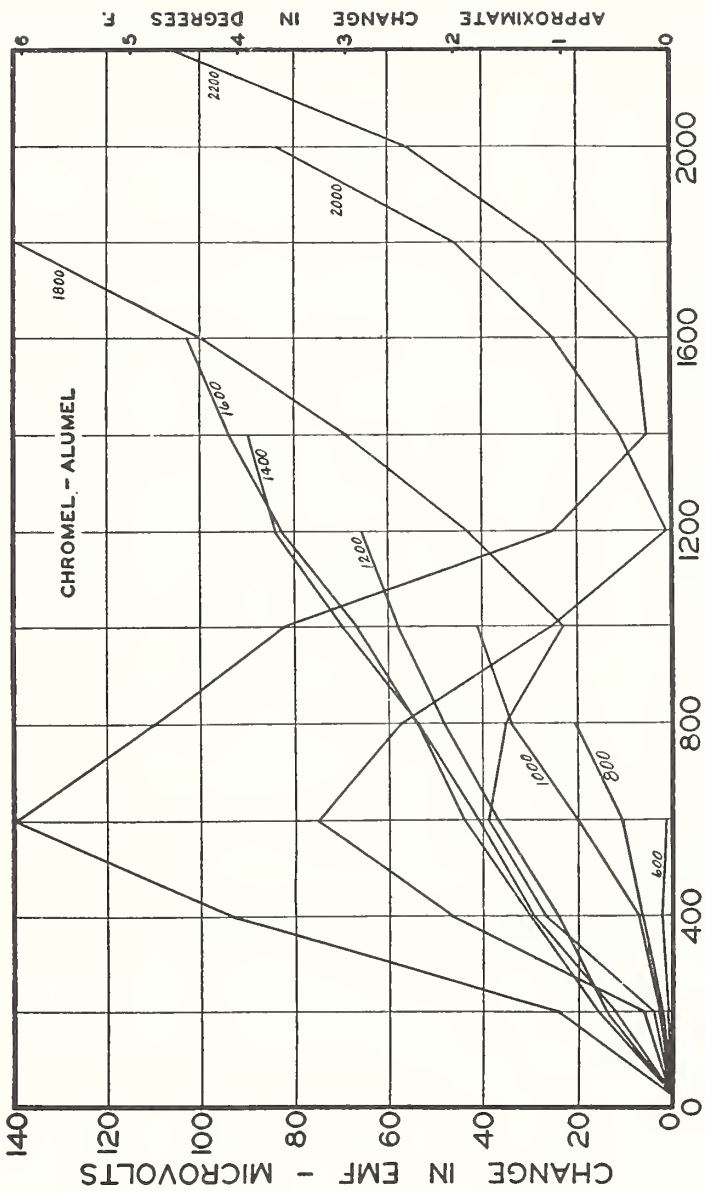

FIGURE 20.—*Changes in the indications of No. 8 gage Chromel-Alumel thermocouples due to a 3-inch decrease in immersion after the couples had been heated for 20 hours at the temperatures indicated on the graphs.*

TABLE 2.—*Changes (in thermal emf) at various temperatures caused by decreasing the depth of immersion 3 inches after heating the wires in air at the temperatures indicated for 20 hours*

CHROMEL *P*

Calibration temperature	Heating temperature								
	600° F	800° F	1,000° F	1,200° F	1,400° F	1,600° F	1,800° F	2,000° F	2,200° F
°F									
200	2	4	5	12	10	13	−1	−7	−7
400	5	9	8	21	25	24	+1	−12	−35
600	10	18	19	31	35	36	4	−14	−50
800		31	30	36	45	45	10	−16	−49
1,000			40	41	54	57	13	−21	−52
1,200				49	59	71	31	−32	−53
1,400					65	79	48	−28	−81
1,600						86	68	−29	−103
1,800							95	−28	−130
2,000								−18	−158
2,200									−176

ALUMEL

200	1	1	2	−2	−2	−3	−5	−13	−31
400	3	2	1	−3	−4	−6	−26	−59	−128
600	9	7	−1	−6	−6	−8	−35	−89	−193
800		10	−4	−12	−11	−9	−25	−73	−159
1,000			+1	−17	−17	−10	−10	−46	−134
1,200				−17	−25	−12	−13	−33	−78
1,400					−25	−15	−21	−39	−86
1,600						−17	−32	−54	−110
1,800							−45	−74	−157
2,000								−102	−214
2,200									−281

CHROMEL-ALUMEL

200	1	3	3	14	12	16	4	6	24
400	2	7	7	24	29	30	27	47	93
600	1	11	20	37	41	44	39	75	140
800		21	34	48	55	54	35	57	110
1,000			41	58	71	67	23	25	82
1,200				66	84	83	43	1	25
1,400					90	94	69	11	5
1,600						103	100	25	7
1,800							140	46	27
2,000								84	56
2,200									105

V. DISCUSSION OF RESULTS

As has been previously pointed out, the materials were heated in an oxidizing atmosphere. Furthermore, the depth of immersion of the materials in the furnace was constant throughout each exposure test. Direct application of the results obtained must be limited to cases where these conditions prevail.

From the observations reported, it is seen that long-time exposure of a Chromel-Alumel thermocouple to high temperatures causes the emf corresponding to a given temperature to increase or the temperature corresponding to a given emf to decrease. The effect on an iron-constantan thermocouple is just the reverse.

Failure of a Chromel-Alumel thermocouple (No. 8 gage) occurred within the 1,000-hour heating period only in the test at 2,200° F. In this case an open circuit was indicated after 300 hours, and examination of the sample showed that the metal forming the welded junction and the individual wires for some distance from the welded junction were oxidized nearly through.

The 1,000-hour heating periods at 2,000° and 1,800° F for No. 8 gage Chromel *P* and Alumel also produced appreciable oxidation of the materials. In the test at 2,000° F the diameter of the wires, after the oxide was removed, was 2.3 mm for the Alumel and 2.6 mm for the Chromel *P*, as compared with 3.3 mm for the original diameters. For the test at 1,800° F the diameter, after removing the oxide, was 2.6 mm for the Alumel and 3.1 mm for the Chromel *P*. In the tests at 1,600° F and below, the oxidation had not materially decreased the diameter of the wires.

The exposure tests on No. 8 gage iron-constantan thermocouples showed failure of the materials within the 1,000-hour heating time for the tests at 1,600° F and above. Failure occurred after 12 hours at 2,000° F, after 28 hours at 1,800° F, and after 300 hours at 1,600° F. The No. 18 gage iron-constantan thermocouple failed after about 500 hours at 1,400° F, while the No. 8 gage thermocouple remained serviceable throughout the 1,000-hour test at 1,400° F. However, at the conclusion of the test the diameters of the No. 8 gage materials had been reduced to about one-tenth of their original value.

A summary of the changes observed for Chromel-Alumel, iron-constantan, and Chromel-constantan thermocouples produced by long-time exposure to various temperatures is given in table 3. The values for Chromel-constantan were obtained indirectly by combining the changes in the individual elements. Though the changes in both Chromel *P* and constantan are considerably larger than those of the completed thermocouple, the directions are such that the changes counteract each other, so that the change in a Chromel-constantan thermocouple is small. The life of this thermocouple is limited by that of the constantan element.

TABLE 3.—*Changes in the calibration of base-metal thermocouples heated in air in an electric furnace*

Exposure temperature	Chromel-Alumel		Iron-constantan		Chromel-constantan	
	Hours of exposure	Maximum change	Hours of exposure	Maximum change	Hours of exposure	Maximum change
°F		°F		°F		°F
800	1,000	<1	1,000	<1	1,000	<1
1,000	1,000	<1	1,000	<1	1,000	<1
1,200	1,000	+2	1,000	−4	1,000	−1
1,400	1,000	3	800	−7	1,000	−2
1,600	1,000	5	100	−10	100	−4
1,800	1,000	8	28	−18	----	----
2,000	1,000	19	8	−19	----	----
2,200	200	21	----	----	----	----

The relatively large changes in calibration observed for Chromel-Alumel thermocouples at 400° and 600° F, after the couples have been exposed to temperatures of 1,600° F and above, are not as serious as may at first appear. When a thermocouple is used for accurate measurement of temperatures of 1,600° F or above, it is seldom required that this same couple be used for accurate measurements at temperatures as low as 400° or 600° F. Therefore, the relatively large changes at these lower temperatures are of no great importance. A thermocouple which is to be used for accurate measurements below 1,000° F should not be exposed to the higher temperatures. If this

procedure is followed, the relatively large changes at 400° and 600° F will be avoided.

The results on the immersion tests emphasize the importance of never decreasing the depth of immersion of a thermocouple after it has once been placed in service. The practice of using a single base-metal thermocouple for high-temperature measurements in a number of different installations should be avoided. It is even difficult to obtain consistent and accurate results by using a thermocouple in a single installation if the couple is withdrawn and replaced between periods of service. The results obtained by removing a used base-metal couple from an installation to determine the corrections to the original calibration by testing it in a laboratory furnace are unreliable. The temperature gradients in the two furnaces usually differ widely, and hence the results will not be applicable to the actual service conditions. If it is practicable by any means to remove the inhomogeneous portions of the thermocouple from the temperature gradient, then the original calibration of the couple is applicable.

WASHINGTON, December 14, 1939.

Note:

The reader should bear in mind that the data appearing in this research paper is representative of the types of base metal thermocouple wire that were manufactured during or prior to 1940. The base metal thermocouple wire that is manufactured today, due to modern manufacturing techniques, is, in most instances, superior to the above mentioned wire.

[Reprinted from The Journal of The American Ceramic Society, Vol. 39, No. 2. February, 1956.]

Calibration of Pyrometric Cones

by H. P. BEERMAN

National Bureau of Standards, Washington, D. C.

Pyrometric cones produced by the Standard Pyrometric Cone Company (now known as The Edward Orton, Jr., Ceramic Foundation) were calibrated at the National Bureau of Standards in 1926. Cones available from the 1926 calibration were recalibrated, and new working standards were obtained by calibrating specimens of present production from the Orton Foundation. Heating rates of 150° and 60°C. per hour were used in determining the end points of a series of large cones, whereas a rate of 300°C. per hour was employed for the small cones through cone 12. The pyrometric cone equivalent (P.C.E.) series was calibrated and extended down to cone 12.

I. Introduction

PYROMETRIC cones are slender trihedral pyramids made of mixtures of various mineral oxides. They are used to determine when the desired heat-treatment of all types of kiln-fired ceramic products has been attained, to measure uniformity of heat-treatment throughout a kiln, and to gauge the relative refractoriness of ceramic materials and products.[1] These cones range from cone No. 022 (expressed as cone 022) to cone 01, and from cone 1 to cone 42. Their end points cover a temperature range from approximately 600° to 2000°C. The cones are set in a plaque so that one side of the cone makes an angle of 82° with the base and so that a fixed length of the cone protrudes above the plaque. When a cone is heated to a sufficiently high temperature, it bends over and at some temperature the tip of the cone just touches the upper surface of the plaque. The temperature at the time of contact is known as the end point. The cone, however, must have been subjected to a known rate of temperature increase if the end point is to have any significance in terms of temperature. Appropriate cones are set alongside the ware in the kiln and, because the heating rate of the ware and of the cones is the same, the end points of the cones are an indication of the thermal treatment the ware has undergone.

End points of a series of large pyrometric cones (through cone 20) manufactured by the Standard Pyrometric Cone Company, now known as The Edward Orton, Jr., Ceramic Foundation, were determined in 1926 at the National Bureau of Standards for heating rates of 20° and 150°C. per hour in various atmospheres. Small calcined cones 23 through 38 were heated at 100°C. per hour, and cones 34 through 42

Received May 19, 1955.

The author is senior engineer, Tube Laboratory, Philco Corporation, Lansdale, Pa. At the time this work was done, he was research associate at the National Bureau of Standards for The Edward Orton, Jr., Ceramic Foundation.

[1] Properties and Uses of Pyrometric Cones, p. 9. Edward Orton, Jr., Ceramic Foundation, Columbus, Ohio, 1949. 55 pp.

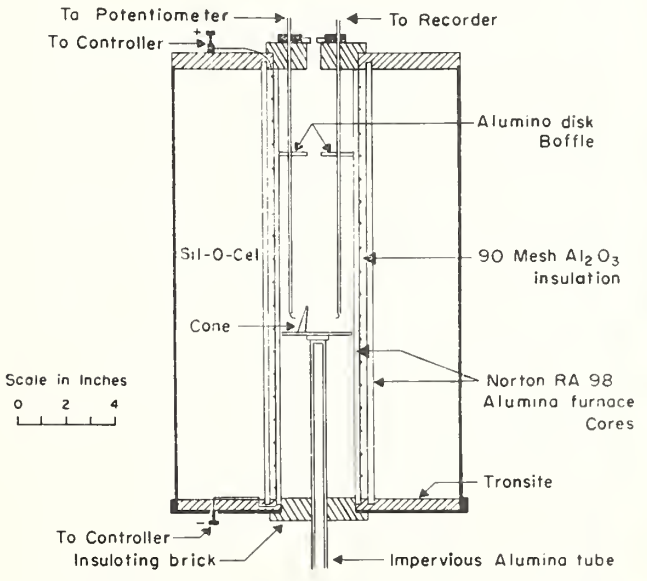

Fig. 1. Furnace with Pt-Rh resistance used for calibration of cones 022 through 20.

Fig. 2. Photograph of Pt-Rh resistance furnace and control equipment.

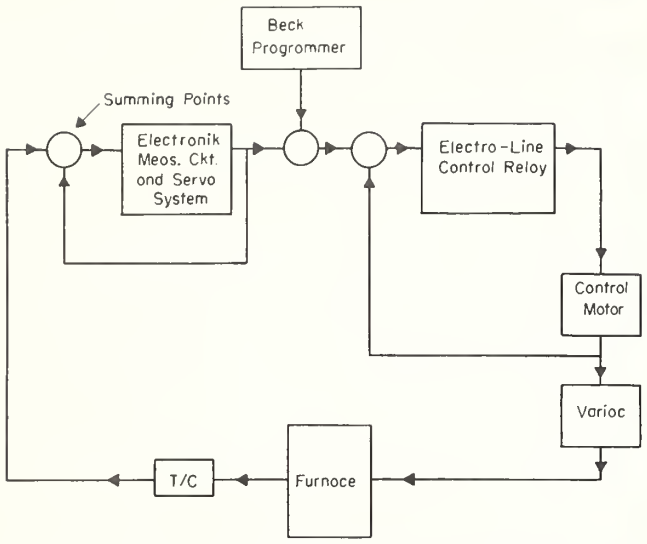

Fig. 3. Diagram of temperature cantrol system for Pt-Rh resistance furnace.

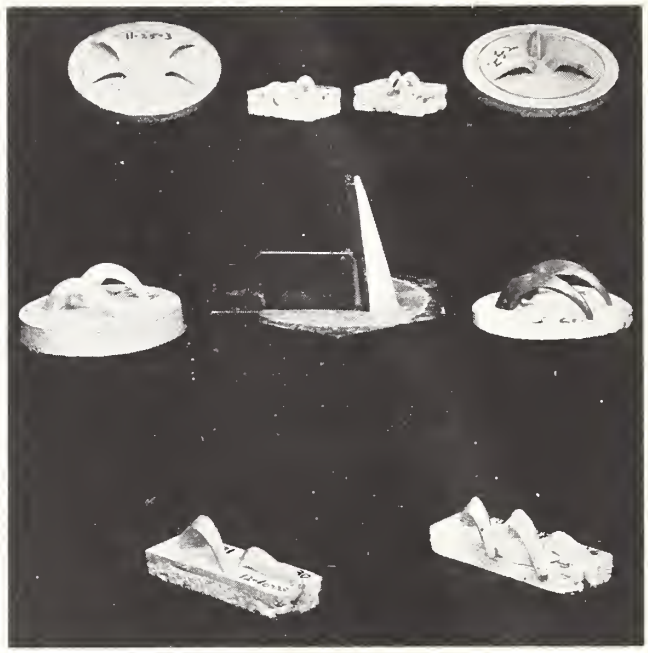

Fig. 4. Photograph of cone plaque with gauge (center) for mounting cones at 82° and of cone plaques after calibration tests. The round plaques were used in the Pt-Rh resistance furnace; the rectangular plaques were used in the rhodium resistance furnace.

were heated at a rate of 600°C. per hour.[2] Since that time the original stiff-mud method of fabricating cones has been improved by the adoption of the dry-press technique. Also, a new cone (No. $32^1/_2$) was added to the series about 20 years ago. In addition, a series of P.C.E., or small calcined cones from cone 12 through cone 20, is now being supplied for tests according to the A.S.T.M. method.[3] Thus it was felt that a determination of the end points of cones as now supplied would be desirable to determine if there had been any significant changes in their properties. Still another cone, No. $31^1/_2$, was introduced when the need became apparent in the course of this investigation.

Two heating rates, 60°C. per hour and 150°C. per hour, were used for the end-point determinations of the large cones and the P.C.E. cones. To meet the demands of many ceramic hobbyists, whose small kilns are heated rapidly, two special series of small uncalcined cones, 021 through 015 and 010 through 12, were calibrated at a heating rate of 300°C. per hour.

II. Equipment and Procedure

(1) Platinum-Rhodium Resistance Furnace

An electrically heated furnace (Figs. 1 and 2) was constructed in which the resistance was platinum-20% rhodium wire. This was used for all determinations of end points for cones 022 through 20. An electrically heated furnace was chosen instead of a gas-fired furnace because the former permits more exact control of the rate of temperature rise, avoids disturbing turbulences inside the furnace and the resulting thermal gradients, and insures an oxidizing atmosphere.

The Brown Division of the Minneapolis-Honeywell Regulator Company assembled the control equipment (Fig. 3) which provided proportional control depending on the unbalance between the temperature required by the programmer and the temperature indicated by a Pt-10% Rh thermocouple.

A circular test plaque (Fig. 4) that almost completely filled the cross-sectional area of the furnace was used. This plaque and a refractory ring cemented in place near the top of the furnace served as baffles and thus reduced convection currents and radiation losses. In the furnace the plaque rested on a thin alumina disk supported by a pedestal that could be raised and lowered with an elevating mechanism. This disk was checked frequently to be sure it was level when it was in position in the furnace.

In every test, three thermocouples (Pt to Pt-10% Rh), previously calibrated at the National Bureau of Standards on the 1948 International Temperature Scale,[4] were inserted in the furnace. One thermocouple supplied a signal to the controller and thus maintained the proper heating rate and the other two were used in making measurements of end points of the cones. The latter two thermocouples were inserted so that the junctions came halfway up the height and alongside a cone. All thermocouples were checked periodically against calibrated thermocouple wire.

Axial temperature gradients were measured in the platinum-rhodium resistance furnace for the three heating rates, 60°, 150°, and 300°C. per hour. For this purpose, thermocouples were used, of which one (*B*, Fig. 5) was located at the base of the cone, one halfway up the cone (*M*), and one (*T*) at the top of the cone. Using thermocouple *M* as the reference, temperature differences were observed between the top and middle, and the bottom and middle, thermocouple.

In the platinum-rhodium resistance furnace, which required vertical sighting, usually only cones of the same cone number were tested at the same time. As soon as it appeared that an end point had been reached, the plaque bearing the cones was lowered from the furnace to determine whether or

[2] C. O. Fairchild and M. F. Peters, "Characteristics of Pyrometric Cones," *J. Am. Ceram. Soc.*, 9 [11] 701–743 (1926).

[3] "Standard Method of Test for Pyrometric Cone Equivalent (P.C.E.) of Refractory Materials," A.S.T.M. Designation C 24–46. Manual of A.S.T.M. Standards on Refractory Materials, February 1952, pp. 74–77; 1952 Book of A.S.T.M. Standards, Part 3, pp. 628–31. American Society for Testing Materials, Philadelphia, Pa.

[4] H. F. Stimson, "International Temperature Scale of 1948," *J. Research Natl. Bur. Standards*, 42 [3] 209–18 (1949); RP 1962; *Ceram. Abstr.*, 1949, August, p. 193*d*.

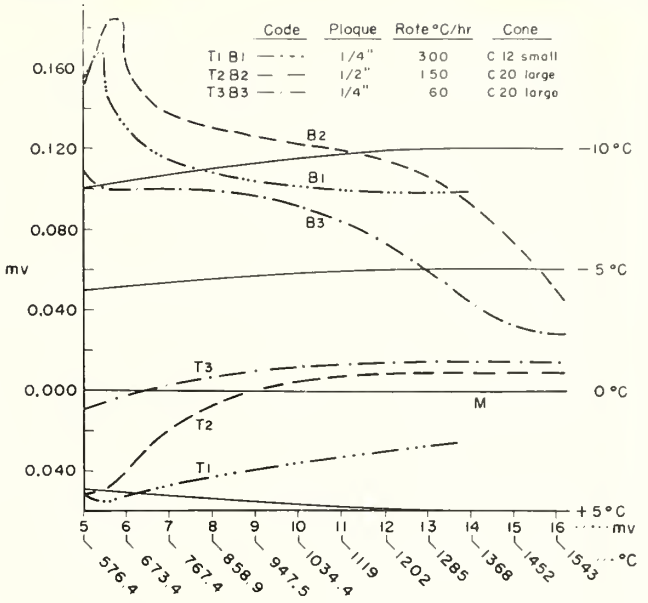

Fig. 5. Curves showing variation in temperature between thermacouple *B* at base of cone and thermocauple *T* at tip of cane, wlth reference ta thermocouple *M* at middle af cane. Temperatures carresponding ta millivolts alang the abscissa are based an the calibration of the thermocouple wire used in the tests.

not the position of the tip of the cone actually corresponded to that of an end point. If the end point had not been reached, the plaque was not reinserted into the furnace, and the test was repeated with a new set of cones.

(2) Rhodium Resistance Furnace

This furnace was used to calibrate cones 23 through 37. Because an oxidizing atmosphere had to be maintained around the cones at temperatures as high as 1800°C., a furnace was built in which the heating element was 62 feet of rhodium wire 0.030 in. in diameter wound on a helically grooved 99% Al_2O_3 tube, 3 in. in diameter (Figs. 6 and 7). The melting point of rhodium, 1960°C. in the pure state,[5] and the ability of alumina to withstand temperatures of 1900°C. and above, provided assurance that the desired temperature could be achieved. The metal furnace shell was water-cooled and two insulating materials were used. The inner layer of the insulation was, as shown in Fig. 7, bubble alumina, and the outer layer was diatomaceous earth.

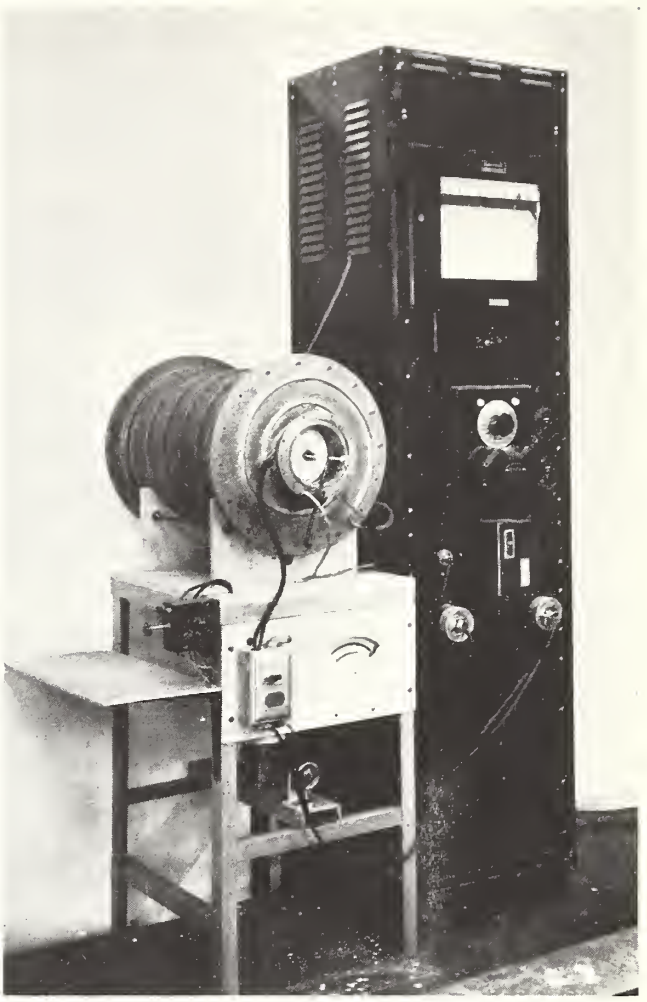

Fig. 6. Photograph af rhadium resistance furnace and cantral equipment.

This furnace was controlled automatically only to about 1475°C. (the insulating tube that held the controlling thermocouple in a horizontal position in the furnace started to bend at that temperature) and manually above that temperature. Readings were taken continuously with an optical pyrometer, calibrated at the National Bureau of Standards, to maintain the proper heating rate in the higher range.

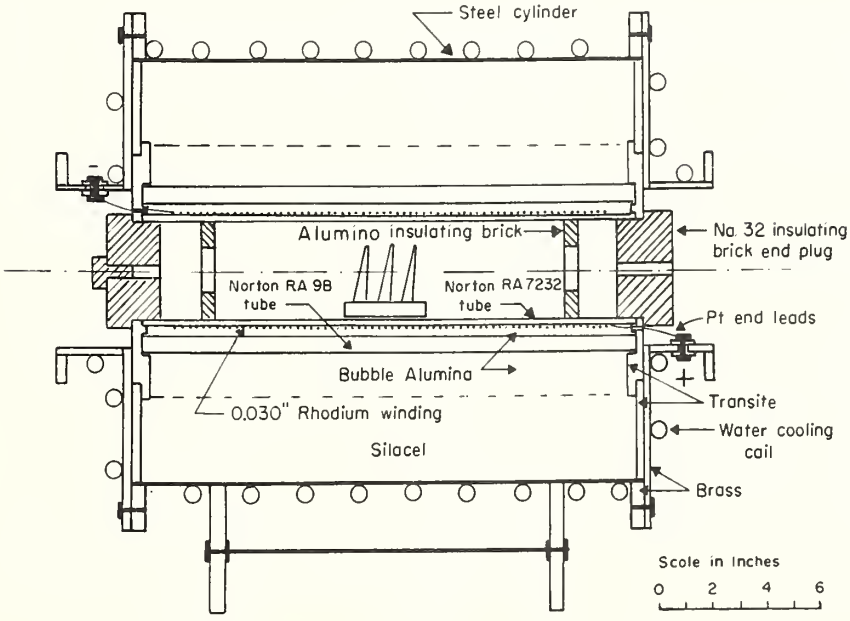

Fig. 7. Rhodium resistonce furnace used for colibrotion of cones 23 through 37.

[5] Converted to the 1948 temperature scale; W. F. Roeser and H. T. Wensel "Freezing Point of Rhodium," *Bur. Standards J. Research*, 12 [5] 519–26 (1934); RP 676.

The rhodium resistance furnace was operated successfully to 1830°C. at a rate of 150°C. per hour and possibly could have been heated slightly higher. Some of the rhodium seems to have volatilized. It was noted during the last tests that the required voltage for a given power input had increased approximately 25% over that of the initial test to 1800°C.

The cone plaques used in the rhodium resistance furnace were in the shape of bars 1/2 in. thick, 1 in. wide, and either 1 1/2 in. or 3 in. long (Fig. 4) and were adjusted to be level inside the furnace by sighting along a horizontal wire on the outside of the furnace.

(3) Cones

For every cone number to be tested, The Edward Orton, Jr., Ceramic Foundation selected at random 10 boxes of 50 cones each from their current stock. Five cones from each of the 10 boxes of like cone number were placed together in one box and forwarded to the National Bureau of Standards where cones were removed at random for testing. Care was taken, through the use of gauges, that the cones made the prescribed angle of 82° with the cone plaque and that they protruded the correct height above the surface of the plaque.

The small uncalcined cones 021 through 015 and 010 through 12 were inserted into plaques 1/4 in. thick so that 1 in. protruded above the base and were subsequently heated at a rate of 300°C. per hour. The large cones 022 through 20, calibrated at a heating rate of 150°C. per hour, projected 2 in. above a plaque 1/2 in. thick. For the 60°C. per hour heating rate on large cones 022 through 20, the cones extended 2 1/4 in. above a plaque 1/4 in. thick and 2 in. above a 1/2-in. plaque. As no significant difference was observed for the different lengths, all the results for any one cone number were averaged together in the data and, in tests above cone 20, measurements for the heating rate of 60°C. per hour were continued only for cones protruding 2 in. above a 1/2-in. plaque. In the case of the large cones heated at 150° and 60°C. per hour, it was found that these rates need be maintained carefully only during the last 3 or 4 hours of a test. The testing time could be shortened without influencing the end point by using a faster rate of heating at the beginning so long as the organic binder in the cone was not driven off so fast that bubbles were formed.

Table I. End-Point Values Reported in 1926 Compared with Values Obtained in Present Study on Cones Left Over from 1926 Investigation*

Cone No.	1926 calibration (°C.)†	1952–1953 recalibration (°C.)‡	
022	603–608	602	
021	615–620	622	
018	718–719	715	
017	770–775	771	(772 774)
07	987–989	(988 990)	
04	1062–1063	(1064 1066)	
01	1144–1147	1144§	
2	1165	(1163 1165)	
5	1205	1202§	
8	1260	(1265 1266)	
11	1325	(1319 1320)	
12	1335	1331§	
13	1350	(1346 1347)	
17	1475	(1484 1485)	(1483 1485)

* Heating rate in both calibrations was 150°C. per hour.

† See footnote 2. The spread of end-point values obtained in 1926 is given for cones 022 through 01. Only the average values obtained in 1926, rounded off to the nearest 5°C., are given for cones 2 through 17.

‡ Each value for a given cone number in this column represents one determination, except as noted. Values in parentheses for any one cone number are from one test.

§ Obtained for two cones in one test.

The small (P.C.E.) cones had been calcined by the Orton Foundation as follows:

Cone 12 through cone 15: Calcined to the end point of large cone 4 by heating at a rate of 60°C. per hour.
Cone 16 through cone 19: Calcined to the end point of large cone 8 by heating at a rate of 60°C. per hour.
Cone 20 through cone 37: Calcined to the end point of large cone 12 by heating at a rate of 60°C. per hour.

The P.C.E. cones were mounted in the plaque to protrude 15/16 in. above the base. Cones 12 through 20 were heated to 1200°C. at the rate of 1200°C. per hour by manual control, and then a rate of 150°C. per hour was maintained by automatic control to the end point. P.C.E. cones 23 through 37 were heated to 1400°C. at a rate of 1200°C. per hour, and above 1400° at 150°C. per hour. Whereas all P.C.E. cones through cone 34 were mounted so that 15/16 in. protruded above the plaque surface, this height had to be shortened to 7/8 in. for P.C.E. cones 35, 36, and 37 because these more refractory cones are somewhat shorter due to having been calcined at a higher temperature by the manufacturer.

Initially, small holes were drilled near the base of the cone to assure black-body conditions when sighting with the optical pyrometer. Drilling of holes in cones for sighting was discontinued after finding that measured temperatures of the holes and surfaces were the same in the region above 1500°C.

(4) Cone Plaques

The compositions of the plaques were as follows:

Cone size	Range (cone)	Composition
Small	021–12	75% Kentucky ball clay, 25% 40–100 mesh grog
Large	022–01	80% ball clay, 20% grog
Large	1–10	80% ball clay, 10% 40-mesh grog, 10% 90-mesh Al_2O_3
Large	11–13	40% ball clay, 40% Georgia kaolin, 20% 40-mesh grog
Large	14–20	1/3 ball clay, 1/3 kaolin, 1/3 90-mesh Al_2O_3
P.C.E.	12–20	50% kaolin, 50% Al_2O_3

P.C.E. and large cones above 20: 25% ball clay, 25% kaolin, 50% Al_2O_3

III. Results

A number of cones remaining from the 1926 investigation were tested in order to compare the over-all effect of determining end points by the present technique with the procedure used by Fairchild and Peters.[2] The results are presented in Table I. For comparison with the 1926 values it is necessary to consider the relation of the temperatures reported for the 1926 determinations to the 1948 International Temperature Scale used in this study. From an examination of the original data of Fairchild and Peters it is evident that they used the same temperature scale as adopted in 1927 for the International standard. Therefore, the corrections to the 1926 end-point values are less than 1°C. up to cone 5 and 2°C. or less to cone 17 (Table I). The amounts to be subtracted for the entire temperature scale involved are indicated as follows[4]:

International 1948 Scale (°C.)	International 1927 Scale (°C.)
1200	1200.6
1300	1301.1
1400	1401.7
1500	1502.3
1600	1603.0
1700	1703.3
1800	1804.6
1900	1905.5

In considering differences between the present values and those determined originally, one must take into account not only the changes introduced in the temperature scale in 1948 but also the fact that in 1926 all measurements above 1100°C. were made with the optical pyrometer. In the present investigation, noble-metal thermocouples were used to deter-

mine temperatures up to 1550°C.; an optical pyrometer was used only for higher temperatures.

The accuracy of the thermocouples is ±1/2° from 0° to 1100°C., decreasing to ±2° at 1450°C. and an estimated ±3° at 1550°C. The optical pyrometer has an accuracy of ±3° at 1063°C., decreasing to ±8°C. at 2800°C., or approximately ±5° at 1800°C. The precision with which the operator of the optical pyrometer can make a match is estimated at one-half the value given for the accuracy of the instrument. It is believed that the precision with which the end points of the cones were determined was within ±2°C. through cone 20 and ±3°C. above cone 20.

Variations of −7° and +8° from the prescribed angle of 82° in a large cone 10 sample fired at a rate of 150°C. per hour made a significant difference in the end point. The cone inserted at an angle of 75° came down at a temperature 15°C. lower than that for one set at the proper angle of 82°, whereas the cone inserted at an angle of 90° had not given any indication of bending over by the time the end point was reached for the cone that had been set at 82°.

The spread in end-point values for any one cone number rarely exceeded 6°C. and averaged about 3°C.

The temperature gradients from cone base to tip, within the furnace with platinum-rhodium resistance wire, are typified by the curves in Fig. 5. Generally, the gradient was negligible along the upper half of the cone (between thermocouples *M* and *T*) but was significant along the lower half (between thermocouples *M* and *B*) owing to the mass of the plaque. However, with increasing temperature, this gradient was greatly reduced because radiation played a greater, and conduction a relatively smaller, role in heat transfer.

Results of tests at a heating rate of 300°C. per hour for the small, uncalcined cones made especially for use in small kilns, such as used by hobbyists, are given in Table II. Comparison with the values in Table III will show that the end points as determined for the small cones range from 16° to 41° higher than for the comparable large cones heated at 150°C. per hour. A further comparison may be made of the values in Table III with the values in Tables IV and V. Here the only variable is the heating rate. The end points for large cones heated at 150° per hour range from 4° to 28° higher than comparable cones heated at 60° per hour, with two exceptions. The exceptions, cones 013 and 14, have end points 17° and 22° lower, respectively, when heated at 150°C. per hour.

Certain air-setting mortars, ladle lining brick, and chimney tile are appreciably less refractory than the brick and shapes for which the A.S.T.M. pyrometric cone equivalent test[3] was originally designed. Their increasing use made it desirable to broaden the application of the A.S.T.M. test to cones of lower number. For this purpose, the small P.C.E. cones have been produced also in Nos. 12 through 20 and their calibration is given in Table VI for a heating rate of 150°C. per hour. When compared with the large cones of the same numbers heated at 150°C. per hour (Table III) it is seen that their end-point differences range from 1° lower (cone 15) to 32° higher (cone 14).

The end points for large cones 23 through 36, heated at 150° per hour and at 60°C. per hour, are given in Tables VII and VIII, respectively. For the cones heated at 150°C. per hour the comparable end points range from 2° lower (cone 36) to 21° higher (cone 29) than the end points of cones heated at the slower rate.

P.C.E. cones 23 through 37 were calibrated for a heating rate of 150°C. per hour (Table IX). For cones 23 through 30 the end points range from 11° to 16° higher than the end points for the same series of large cones heated at the same rate (Table VII). Comparable differences for cones 31 through 35 are 4°, or less, except cone 32 1/2, for which the end point of the small (P.C.E.) cone is 6° lower than that of large cone 32 1/2.

In comparing the data published by Fairchild and Peters[2] in 1926 on large cones fired at the 150°C. per hour rate with the new data, it is observed that the deviations in the results

Table II. End Points of Small Uncalcined Cones 021 through 015, and 010 Through 12, Heated at 300°C. per Hour in Pt-Rh Resistance Furnace*

Cone No.	End points (°C.)			Average
021	(642 642)	(642 642)	(643 645 645)	643
020	(666 668 668)	(666 666 666)	(665 665 665 665)	666
019	(723 723)	(722 724)	(723 723 723)	723
018	(750 750)	(753 754)	(754 754 752 752)	752
017	(783 783)	(784)	(784 784 784 784)	784
016	(822 822)	(825 826)	(826 826 826 826)	825
015	(841 841)	(843 843 845)	(843 843 843)	843
010	(918 918)	(917 922)	(919 921 921 921)	919
09	(952 952)	(956 958)	(956 956 956)	955
08	(982 982)	(983 983 983 983)	(983 983 984)	983
07	(1005 1007)	(1010 1010)	(1007 1007 1007 1007)	1008
06	(1022 1022 1023)	(1021 1021 1022)	(1023 1025 1025)	1023
05	(1059 1059)	(1063 1064)	(1063 1063 1063)	1062
04	(1095 1095)	(1099 1100)	(1100 1100 1100)	1098
03	(1130 1130)	(1130 1130 1131 1131)	(1132 1133 1133)	1131
02	(1147 1148)	(1148 1147)	(1149 1149 1149 1150)	1148
01	(1181 1181)	[1175] [1179]	(1177 1178 1178)	1178
1	(1179 1181)	[1177] [1179]	(1179 1179 1180 1180)	1179
2	(1180 1179)	(1176 1178) [1179]	(1179 1181 1181 1182)	1179
3	(1192 1194)	(1197 1197 1197 1197)	(1196 1196 1196 1196)	1196
4	(1212 1210)	(1209 1207)	(1209 1209 1209 1209)	1209
5	(1223 1221)	(1221)	(1221 1221 1221 1221)	1221
6	(1256 1254)	(1256 1257)	(1255 1255 1255 1255)	1255
7	(1260 1263)	(1266 1266)	(1263 1263 1264 1264)	1264
8	(1302 1302)	(1298 1298 1299)	(1299 1299 1300 1300)	1300
9	(1318 1318)	(1318 1316)	(1315 1315 1315 1316)	1317
10	(1330 1330)	(1329 1329)	(1332 1332 1332 1332)	1330
11	(1336 1336)	(1336) (1335 1335 1335)	(1338 1338)	1336
12	(1353 1353)	(1356) (1356 1356)	(1354 1354 1354) (1356 1356)	1355

* Values in parentheses, or in brackets, are for individual cones on a plaque from one test.

Table III. End Points of Large Cones 022 Through 20 Heated at 150°C. per Hour in Pt-Rh Resistance Furnace*

Cone No.	End points (°C.)	Average	Cone No	End points (°C.)	Average
022	(600 600) (600 600)	600	01	(1137 1137) (1137 1137)	1137
021	(613 613) (615 615)	614	1	(1155 1155) (1153 1153)	1154
020	(635) (635 635)	635	2	(1162 1162) (1162 1162)	1162
019	(683 683) (683 683)	683	3	(1169 1169) (1168 1168)	1168
018	(715 715) (719 719)	717	4	(1186 1186) (1186 1186)	1186
017	(747 747) (748 746)	747	5	(1195 1195) (1197 1197)	1196
016	(792 792) (792 792)	792	6	(1221 1221) (1222 1225)	1222
015	(804 804) (804 804)	804	7	(1239 1239) (1239 1242)	1240
014	(836 836) (841 838)	838	8	(1263 1264) (1263 1264)	1263
013	(851 851) (852 853)	852	9	(1281 1281) (1279 1279)	1280
012	(884 884) (884 884)	884	10	(1305 1305) (1305 1305)	1305
011	(893 893) (894 895)	894	11	(1315 1315) (1315 1315)	1315
010	(894 894) (896 894)	894	12	(1327 1327) (1325 1326)	1326
09	(924 924) (923 923)	923	13	(1347 1347) (1346 1346) (1346 1346)	1346
08	(955 955) (955 955)	955	14	(1368 1368) (1366 1366) (1365 1365)	1366
07	(983 983) (985 985)	984	15	(1430 1430) (1433 1433)	1431
06	(999 999) (999 999)	999	16	(1473 1473) (1473 1473)	1473
05	(1046 1046) (1047 1045)	1046	17	(1485 1485) (1485 1485)	1485
04	(1061 1061) (1059 1060) (1061)	1060	18	(1507 1507) (1505 1507)	1506
03	(1100 1100) (1102 1102)	1101	19	(1529 1529) (1528 1528) (1528)†	1528
02	(1120 1120) (1121 1121)	1120	20	(1548) (1551 1551) (1548 1548) (1549)†	1549

* Values in parentheses are for individual cones on a plaque from one test.
† Obtained in Rh resistance furnace.

Table IV. End Points of Large Cones 022 Through 01 Heated at 60°C. per Hour in Pt–Rh Resistance Furnace*

Cone No.	End points (°C.) Group A†	Group B‡	Average
022	(586 587)	(585 586) (585 585) (584 584)	585
021	(602 602)	(601 601) (602 602) (602 602)	602
020	(624 624)	(624 624) (624 624) (628 628)	625
019	(668 668)	(667 667) (668 668) (667 669)	668
018	(699 699)	(693 694) (697 697) (695 695)	696
017	(725 725)	(731 731) (728 728) (725 725)	727
016	(767 767)	(763 763) (761 762) (764 764)	764
015	(789 789)	(791 791) (790 790) (789 789)	790
014	(838 838)	(833 833) (833 833) (831 831)	834
013	(869 869) (869)	(872 873) (868 868) (867 867) (871)	869
012	(869 869)	(866 866) (864 866) (866)	866
011	(886 886)	(886 886) (884 884) (885 885)	886
010	(888 888)	(887 887) (887 887)	887
09	(915 916)	(914 914) (915 916)	915
08	(944 946)	(946 946) (945 945)	945
07	(973 973)	(972 973) (973 973)	973
06	(993 995)	(987 988) (990 990)	991
05	(1034 1034)	(1029 1030) (1030 1030)	1031
04	(1053 1053) (1053)	(1047 1048) (1047 1047)	1050
03	(1087 1087)	(1084 1084) (1086 1087)	1086
02	(1102 1102)	(1099 1101) (1100 1100)	1101
01	(1118 1119)	(1117 1117) (1116 1116)	1117

* Values in parentheses are for individual cones on a plaque from one test.
† Group A: Cones protruded 2 in. above a $^1/_2$-in.-thick plaque.
‡ Group B: Cones protruded $2^1/_4$ in. above a $^1/_4$-in.-thick plaque.

for cones 022 through 011 are not in any direction. From cone 010 through cone 15 the general trend has been toward lower end points for the new cones, whereas the reverse holds true for cone 16 through cone 20. Comparing the data on P.C.E. cones with the 1926 results (Table X) it is seen that the end points for cones 23 through 30, and for cone 32, are appreciably higher than the formerly given values. The agreement of the old and new data for P.C.E. cone 31, and cones 33 through 37, is 7° or less.

IV. Summary and Conclusions

The end points of three series of pyrometric cones have been determined under reproducible conditions. A series of large cones was calibrated at heating rates of 150° and 60°C. per hour; small uncalcined cones 021 through 015, and 010 through 12, were calibrated at a heating rate of 300°C. per hour for the benefit of the hobbyist; the range of P.C.E. cones was extended downward to cone 12; and a new cone ($31^1/_2$) was produced to fill an important gap.

Certain observations can be made from the data. The small uncalcined cones 01, 1, and 2 heated at 300°C. per hour have practically the same end point. The end points of the large cones 01, 1, and 2, however, are in proper sequence when used at heating rates of both 150° and 60°C. per hour and, because all cones of the same cone number have the same composition regardless of size, it is believed inadvisable to change the composition of the small uncalcined cones 01, 1, and 2. Large cones fired at a rate of 150°C. per hour generally have a higher end point than those fired at 60°C. per hour, the ex-

Table V. End Points of Large Cones 1 Through 20 Heated at 60°C. per Hour in Pt-Rh Resistance Furnace*

Cone No.	End points (°C.)		Average
	Group A†	Group B‡	
1	(1134 1134)	(1136 1136) (1136 1137)	1136
2	(1144 1144)	(1141 1141) (1141 1141)	1142
3	(1150 1152)	(1153 1153) (1152 1152)	1152
4	(1170 1170)	(1167 1167) (1167 1168)	1168
5	(1175 1176)	(1177 1177) (1177 1177)	1177
6	(1199 1199)	(1202 1202) (1201 1201)	1201
7	(1214 1214)	(1215 1215) (1215 1216)	1215
8	(1235 1236)	(1235 1236) (1235 1237)	1236
9	(1261 1262)	(1260 1259) (1258 1258)	1260
10	(1286 1288) (1286 1286)	(1284 1285) (1285 1285)	1285
11	(1295 1295)	(1294 1294) (1293 1293)	1294
12	(1308 1308)	(1306 1305) (1306 1306)	1306
13	(1324 1326) (1324 1324)	(1319 1319) (1318 1318)	1321
14	(1390 1391) (1389 1389)	(1385 1386) (1385 1385) (1386 1386)	1388
15	(1425 1425)	(1424 1424) (1422 1422)	1424
16	(1456 1456)	(1456 1456) (1455 1455)	1455
17	(1478 1478) (1479 1479)	(1477 1477) (1476 1476)	1477
18	(1500 1500)	(1500 1500) (1499 1501)	1500
19	(1521 1521)	(1520 1520) (1520 1520)	1520
20	(1544)§ (1543 1543) (1542 1542)	(1540 1540) (1540 1540)	1542

* Values in parentheses are for individual cones on a plaque from one test.
† Group A: Cones protruded 2 in. above a $^1/_2$-in.-thick plaque.
‡ Group B: Cones protruded $2^1/_4$ in. above a $^1/_4$-in.-thick plaque.
§ Obtained in Rh resistance furnace.

Table VI. End Points of P.C.E. Cones 12 Through 20 Heated in Pt-Rh Resistance Furnace to 1200°C. at 1200°C. per Hour and Above 1200°C. at 150°C. per Hour*

Cone No.	End points (°C.)	Average
12	(1336) (1338 1338) (1337 1337 1339)	1337
13	(1346 1346) (1350 1350 1351 1351) (1348 1348 1348)	1349
14	(1397 1398 1398 1399) (1397 1397 1397 1397) (1397 1399 1399)	1398
15	(1429 1429 1431) (1430 1430) (1430 1430 1430 1430)	1430
16	(1490 1490 1493) (1491 1491 1491 1491) (1490 1490 1490 1490)	1491
17	(1510 1510 1513) (1511 1511 1514 1514) (1514 1512 1512 1513) (1510)†	1512
18	(1524 1524) (1520 1520 1522 1522) (1522 1522 1522 1522) (1521)†	1522
19	(1538 1541 1540 1543) (1541 1541 1541 1544) (1541 1541 1541 1544) (1541)†	1541
20	(1562 1562 1563 1564) (1563 1565 1566) (1564 1565 1565 1565) (1565)†	1564

* Values in parentheses are for individual cones on a plaque from one test.
† Obtained in Rh resistance furnace.

Table VII. End Points of Large Cones 23 Through 36 Heated at 150°C. per Hour in Rh Resistance Furnace*

Cone No.	End points (°C.)	Average
23	1589 1590 1590	1590
26	1605 1605 1605	1605
27	1630 1625 1625	1627
28	1634 1635 1630	1633
29	1647 1643 1646	1645
30	1658 1652 1653	1654
31	1681 1678 1678	1679
32	1719 1714 1719	1717
$32^1/_2$	1730 1727 1731 1731	1730
33	1742 1742 1738	1741
34	1759 1758 1761	1759
35	1785 1785 1782	1784
36	1798 1795	1796

* Each value represents an end point of an individual cone that was one of several consecutively numbered cones in a plaque.

Table VIII. End Points of Large Cones 23 Through 36 Heated at 60°C. per Hour in Rh Resistance Furnace*

Cone No.	End points (°C.)	Average
23	1588 1587 1584	1586
26	1590 1590 1586	1589
27	1617 1615 1610	1614
28	1616 1612 1613	1614
29	1626 1623 1622	1624
30	1636 1635 1636	1636
31	1663 1660 1660	1661
32	1707 1705 1706	1706
$32^1/_2$	1715 1720 1720	1718
33	1734 1731 1732	1732
34	1758 1758 1754	1757
35	1787 1783 1784	1784
36	1800 1796	1798

* Each value represents an end point of an individual cone that was one of several consecutively numbered cones in a plaque.

ceptions being cone 013 and cone 14. The end points of cones 011 and 010 in the large series, and for the same heating rate, are identical and therefore one of the cone numbers appears to be superfluous. Large cones 27 and 28 give the same end point for the 60°C. per hour heating rate but appear in proper sequence at the 150°C. per hour rate. For the large cones 34, 35, and 36, any difference due to different heating rates is insignificant.

The end-point values for cones 23 through 32 tested in this study are appreciably higher than the values published in

574278 O - 61 - 10

Table IX. End Points of P.C.E. Cones 23 Through 37 Heated to 1400°C. at 1200°C. per Hour and Above 1400°C. at 150°C. per Hour in Rh Resistance Furnace*

Cone No.	End points (°C.)								Average
23	1605	1604	1602	1605	1608	1604	1608		1605
26	1618	1623	1620	1620	1617	1625	1621		1621
27	1639	1641	1640	1639	1642				1640
28	1645	1647	1647	1644	1648	1646			1646
29	1660	1658	1658	1656	1661	1660			1659
30	1665	1666	1664	1663	1662	1665	1667		1665
31	1682	1683	1683	1684	1681	1683	1682	1683	1683
31½	1700	1698	1702	1700	1697				1699
32	1717	1717	1717	1716	1718	1716	1717		1717
32½	1724	1722	1726	1722	1724	1725			1724
33	1743	1741	1742	1746	1743				1743
34	1765	1760	1760	1764	1766				1763
35	1786	1782	1785	1785	1785				1785
36	1805	1803	1804	1803	1806				1804
37	1819	1820	1820	1820					1820

* Each value represents an end point of an individual cone that was one of several consecutively numbered cones in a plaque.

Table X. Comparison of End-Point Values for P.C.E. Cones Reported in 1926 with 1952–1953 Calibration*

Cone No.	1926 values (°C.)		1952–1953 values (°C.)
	As reported†	Corrected to 1948 scale‡	
23	1580	1577	1605
26	1595	1592	1621
27	1605	1602	1640
28	1615	1612	1646
29	1640	1637	1659
30	1650	1647	1665
31	1680	1676	1683
32	1700	1696	1717
33	1745	1741	1743
34	1760	1756	1763
35	1785	1781	1785
36	1810	1805	1804
37	1820	1815	1820

* Heating rate, 150°C. per hour.
† See footnote 2.
‡ Correction to nearest 1°.

1926. This would cause rejections in acceptance tests on refractory materials when following specifications for P.C.E. based on the 1926 values.

Acknowledgment

The author expresses his sincere appreciation to R. E. Wilson, formerly chief of the Temperature Measurements Section; A. M. Bass, assistant chief of the Temperature Measurements Section; R. J. Corruccini, formerly physicist, Temperature Measurements Section; W. J. Youden, Statistical Engineering Section; R. A. Heindl, chief of the Refractories Section; and S. T. Lonberger, physicist, Temperature Measurements Section (all of the National Bureau of Standards) for their constructive criticism of the project, and to The Edward Orton, Jr., Ceramic Foundation for sponsoring the project. Special credit is due R. F. Geller, chief of the Porcelain and Pottery Section, for his aid in revising the manuscript.

Reprinted from JOURNAL OF THE OPTICAL SOCIETY OF AMERICA, Vol. 46, No. 4, 246–254, April, 1956
Printed in U. S. A.

Spectral Absorption Method for Determining Population "Temperatures" in Hot Gases*†

HENRY J. KOSTKOWSKI AND HERBERT P. BROIDA
National Bureau of Standards, Washington, D. C.

(Received September 26, 1955)

A spectroscopic method, useful for strongly absorbed lines, has been investigated for measuring temperatures of hot gases. The minimum transmission of discrete spectral lines in gases at equilibrium has a simple dependence upon the absolute temperature and this relation is used to measure temperature from a straight line plot. An experimental study has been made of the absorption due to the rotational lines of OH ($^2\Sigma \leftarrow {}^2\Pi$) between 3067 and 3090 A in an oxygen-acetylene flame. It is shown that temperatures measured by this method are less affected than the conventional one by lack of sufficient resolving power, flame thickness, and various light sources (either continuous or line).

I. INTRODUCTION

INTEREST in nonequilibrium phenomena, combustion kinetics and control in the development of jet engines has provided a stimulus for investigating new methods of measuring high gas temperatures. Temperatures in flames and hot gases often are determined from spectra by measuring the distribution of intensities among the lines or bands.‡ These spectral measurements usually have been made in emission. However, if the self-absorption is great, the measured "temperature" may be considerably larger than the actual temperature. Furthermore, if the temperature of the system is low, the radiation emitted generally is small, making measurements very difficult. In such cases it would be desirable to make the measurements in absorption. Unfortunately, the conventional method for determining population "temperatures" in absorption requires that the peak absorption of the lines be small, thus limiting the applicability and accuracy of such measurements. In addition very high resolving power is needed to measure a weak absorption line. Because of these experimental difficulties, little use has been made of line absorption for "temperature" determinations. We have investigated a method by which "temperatures" may be determined in absorption when the peak absorption is as great as 98%. This paper reports on the method and compares it with the conventional one under a variety of conditions. Recently Huldt and Knall[1a] reported one such comparison.

II. THEORY

A. Conventional Method

The integrated absorption, $\mathfrak{A}$, of a spectral line as measured by a spectrometer is given by the expression

$$\mathfrak{A}=\int_{\text{line}} A(\nu)d\nu=\int_{\text{line}} \times\left\{\frac{\int_{\nu-\Delta x}^{\nu+\Delta x} I_0(x)\sigma(\nu,x)(1-e^{-K(x)u})dx}{\int_{\nu-\Delta x}^{\nu+\Delta x} I_0(x)\sigma(\nu,x)dx}\right\}d\nu \quad (1)$$

where $A(\nu)$ is the fractional absorption measured with the spectrometer when it is set on frequency ν and Δx is the spectral slit width of the spectrometer whose slit function is $\sigma(\nu,x)$. $I_0(x)$ is the intensity of radiation at the frequency x incident on the absorber, $K(x)$ the absorption coefficient and u the optical path length of the absorber.§ Equation (1) usually[1b] can be reduced to

$$\mathfrak{A}=\int_{\text{line}}(1-e^{-K(\nu)u})d\nu. \quad (2)$$

If the maximum value of $K(\nu)$ is sufficiently small

$$\frac{\mathfrak{A}}{u}=\int_{\text{line}} K(\nu)d\nu. \quad (3)$$

Equation (3) is correct to within two percent if the peak absorption is 5% or less.

Quantum electrodynamics[2] shows that for gases in thermal equilibrium

$$\int_{\text{line}} K(\nu)d\nu=\frac{8\pi^3}{3hc}\nu_0\frac{(1-e^{-h\nu_0/kT})|R|^2e^{-E''/kT}}{Q}=S \quad (4)$$

where S is the intensity per molecule per unit volume of the absorption line, ν_0 is the frequency of the line, k is the Boltzmann constant, T is the absolute temperature of the absorber, $|R|^2$ is the sum of the squares of

* This research was supported by the United States Air Force through the Office of Scientific Research of the Air Research and Development Command.

† This paper was presented in part at the April, 1955 meeting of the Optical Society of America.

‡ Since such temperatures are determined from the relative populations of energy levels, they are called population "temperatures." Quotation marks are used unless thermal equilibrium is clearly indicated.

[1](a) L. Huldt and E. Knall, Naturwiss. 41, 421 (1954); (b) E. Bright Wilson, Jr., and A. J. Wells, J. Chem. Phys. 14, 578 (1946).

§ The optical path length is defined here as the product of the geometrical path length and the number of molecules per unit volume of the gas. Frequently, other quantities are used, e.g., the product of the geometrical path length and pressure of the gas in atmospheres at 0°C.

[2] B. L. Crawford, Jr., and H. L. Dinsmore, J. Chem. Phys. 18, 983 (1950); 18, 1682 (1950).

the matrix elements of all the transitions producing the line, E'' is the energy of the lower level of the transition, Q is the state sum or partition function, h is Planck's constant, and c the velocity of light. In many circumstances, $h\nu_0$ is very large compared to kT and $1-e^{-h\nu_0/kT}$ may be set equal to one. For example, if $T\leqslant 3000°\text{K}$ and $\nu_0\geqslant 9700\ \text{cm}^{-1}$ ($\lambda\leqslant 10309$ A), $e^{-h\nu_0/kT}$ is less than 0.01. Thus from Eqs. (3) and (4) and for $h\nu_0\gg kT$

$$\mathfrak{A}=C_1\nu_0|R|^2e^{-E''/kT} \tag{5}$$

where the quantity $C_1=8\pi^3u/3Qhc$ is constant for our purposes. The conventional equation with which population "temperatures" in absorption have been determined is obtained directly from Eq. (5). It is

$$\log\frac{\mathfrak{A}}{\nu_0|R|^2}=\log C_1-\frac{\log e}{kT}E''. \tag{6}$$

The significant assumption used in deriving Eq. (6) is that the maximum value of Ku (or if one prefers, the peak absorption of the line) is sufficiently small so that in the expansion of the exponential in Eq. (2), no terms beyond the linear one need be retained. An equation similar to Eq. (6) can be obtained using the peak rather than the integrated absorption.[3] Though such a relation depends on the functional form of the absorption coefficient,‖ differences obtained using a Doppler and a Lorentz shaped line usually are negligible for "temperature" determinations.

B. Method Using Minimum Transmission

From the defining equation for the absorption coefficient, the minimum transmission of a spectral line, $\tau_{\min}$, in terms of the maximum value of the absorption coefficient, $K_{\max}$, is given by

$$\tau_{\min}=e^{-K_{\max}u}. \tag{7}$$

If the line has a Doppler shape

$$K_{\max}=\frac{Sc}{\nu_0}\left(\frac{m}{2\pi kT}\right)^{\frac{1}{2}} \tag{8}$$

and if the line has a Lorentz (pressure-broadened) shape

$$K_{\max}=\frac{S}{\pi\alpha} \tag{9}$$

where m is the mass of the absorbing molecule and α is the half-width of the absorption coefficient at half its maximum value. α is usually called the line half-width. Using Eqs. (4) and (7) in conjunction with (8) and (9) one may obtain, again assuming that $h\nu_0\gg kT$, for a line with a Doppler shape

$$\log\left(\frac{\ln 1/\tau_{\min}}{|R|^2}\right)=C_2-\frac{\log e}{kT}E'' \tag{10}$$

and for a Lorentz shape

$$\log\left(\frac{\ln 1/\tau_{\min}}{|R|^2\nu_0}\right)=C_3-\log\alpha-\frac{\log e}{kT}E'' \tag{11}$$

where all the constants have been incorporated into

$$C_2=\log\left[\frac{u}{3hQ}\left(\frac{32\pi^5m}{kT}\right)^{\frac{1}{2}}\right]$$

and

$$C_3=\log\frac{8\pi^2u}{3hcQ}.$$

Equations (10) and (11) represent the extended method by which population "temperatures" in absorption may be obtained. Usually ν_0, the frequency of each line in Eq. (11), varies only slightly over the band and can be considered as constant. Thus if, in addition, α, the line half-width does not vary from line to line, Eqs. (10) and (11) become identical for temperature measurements. For the present paper this will be assumed and Eq. (10) used even though the spectral lines have a combination of Doppler and pressure-broadened shape.

The method of Eq. (10) is not restricted to the case of only small absorption and, therefore, can be used in many more situations. However, it does require measuring the minimum transmission of the absorption lines which usually requires far better resolution than is available. This is probably the reason why the method has not been applied extensively. If a suitable discrete line source rather than a continuous source is used, however, the minimum transmission of an absorption line may be determined even with poor resolution.

Such a discrete line source exists for measuring OH lines in a flame at atmospheric pressure. Therefore the method was tried by measuring the minimum transmission of the rotational lines of the 0,0 band in the $^2\Sigma\leftarrow{}^2\Pi$ electronic transition of OH in an oxygen-acetylene flame. The results were so encouraging that a detailed study of the method under a variety of experimental conditions was made. Effects of resolution, amount of absorption and types of sources were compared with the results obtained from the conventional method [Eq. (6)].

III. EXPERIMENTAL

A. Instrumentation

Figure 1 is a schematic diagram of the experimental setup. "Temperature" measurements were made of a premixed oxygen-acetylene flame burning in air on a

[3] S. S. Penner, J. Chem. Phys. **20**, 507 (1952).
‖ This is usually called the line shape.

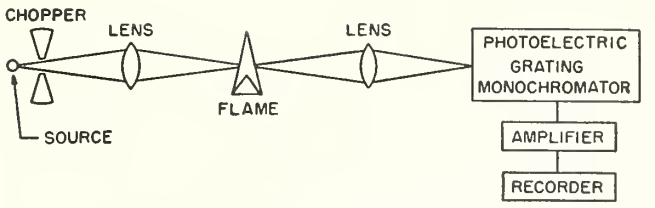

FIG. 1. Schematic diagram of arrangement of apparatus.

0.075 mm×50 mm water-cooled slot burner (Fig. 2). The flow rates, determined to within 5% by float type flowmeters, were 49 cc/sec for acetylene and 122.5 cc/sec for oxygen. Observations were made well into the hot gases above the reaction zone about 25 mm above the top of the burner.

Two discrete line sources and one continuum source were used in the experiments. One of the discrete line sources was an electrodeless discharge through water vapor. Figure 3 is a sketch of this apparatus, which is a simplification of a discharge system used previously.[4] It consists of a section of quartz tubing connected through ball and sphere joints to a glass system containing a supply of distilled water, a pressure gauge and a mechanical pump and trap. The discharge is excited by a 2450 megacycle signal from a continuous wave 125 watt magnetron source which is coupled to the quartz tubing through the modified wave-guide resonator shown in Fig. 3. This method of coupling produces an intense and stable discharge. The OH emission from this discharge is greater than that from the usual oxygen-acetylene welding torch. A stability of the order of 1% was possible for several hours. The water flow rate was adjusted to give maximum brightness of the OH emission by regulating the stopcock above the water supply. The pressure in the discharge was about 0.6 mm Hg. The "temperature" of the discharge was approximately 650°K[5] or, as will be seen, about $\frac{1}{4}$ that observed for the oxygen-acetylene flame.

Oldenberg and Rieke[6] have observed that the half-widths of OH lines are about 0.29 cm^{-1} at atmospheric pressure and 1473°K; pressure broadening contributes 0.19 cm^{-1} to this width. From this information, in a flame at one atmosphere and 2550°K, the half-width is computed to be 0.28 cm^{-1}. In a low-pressure discharge at 650°K, the half-width is computed to be 0.07 cm^{-1}. Therefore the half-widths of OH lines in the flame are four times those in the discharge. Thus the electrodeless discharge through water vapor is a bright, stable discrete line source of OH lines which are considerably narrower than those in the flame.

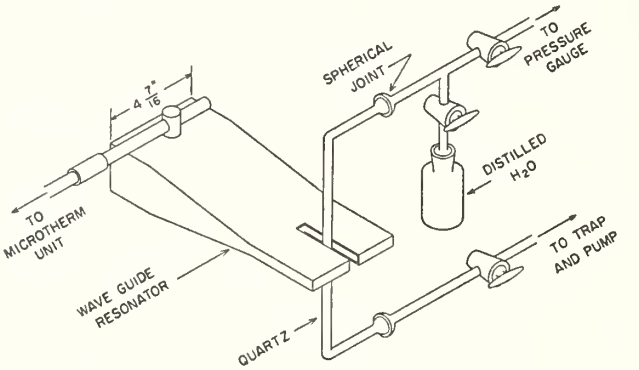

FIG. 3. Sketch of the discharge line source.

The other discrete line source was a premixed oxygen-acetylene flame at atmospheric pressure on a small burner whose bore diameter was 0.575 mm. The gas flow rates were 12.5 cc/sec of acetylene and 20 cc/sec of oxygen. The width of the OH lines in this source should be approximately the same as those in the slot burner.

The continuum source was a 1000 watt high pressure xenon lamp similar to those described by Baum and Dunkleman[7] operating with a direct current of 30 amperes.

The spectroscopic measurements were made with a scanning, grating monochromator¶ with photomultiplier detection.[8] The grating was a 75 mm×75 mm replica with 90 000 lines blazed for the first order at 6000 A.

FIG. 2. Photograph of flame on slot burner. The reaction zone is the small bright line just above the burner. The remainder of the luminous zone is due to the hot gases in which there is little chemical reaction.

[4] Broida, Morowitz, and Selgin, J. Research Natl. Bur. Standard 52, 293 (1954).

[5] A. M. Bass and H. P. Broida, "A spectrophotometric atlas of the $^2\Sigma^+ - ^2\Pi$ transition of OH", National Bureau of Standards Circular 541 (1953).

[6] O. Oldenberg and F. F. Rieke, J. Chem. Phys. 6, 439 (1938); R. J. Dwyer and O. Oldenberg, J. Chem. Phys. 12, 351 (1944).

[7] W. A. Baum and L. Dunkelman, J. Opt. Soc. Am. 40, 782 (1950).

¶ This instrument was constructed by the Research Department of Leeds and Northrup Company and loaned to the Heat and Power Division at the National Bureau of Standards on a field trial basis.

[8] William G. Fastie, J. Opt. Soc. Am. 42, 641 (1952).

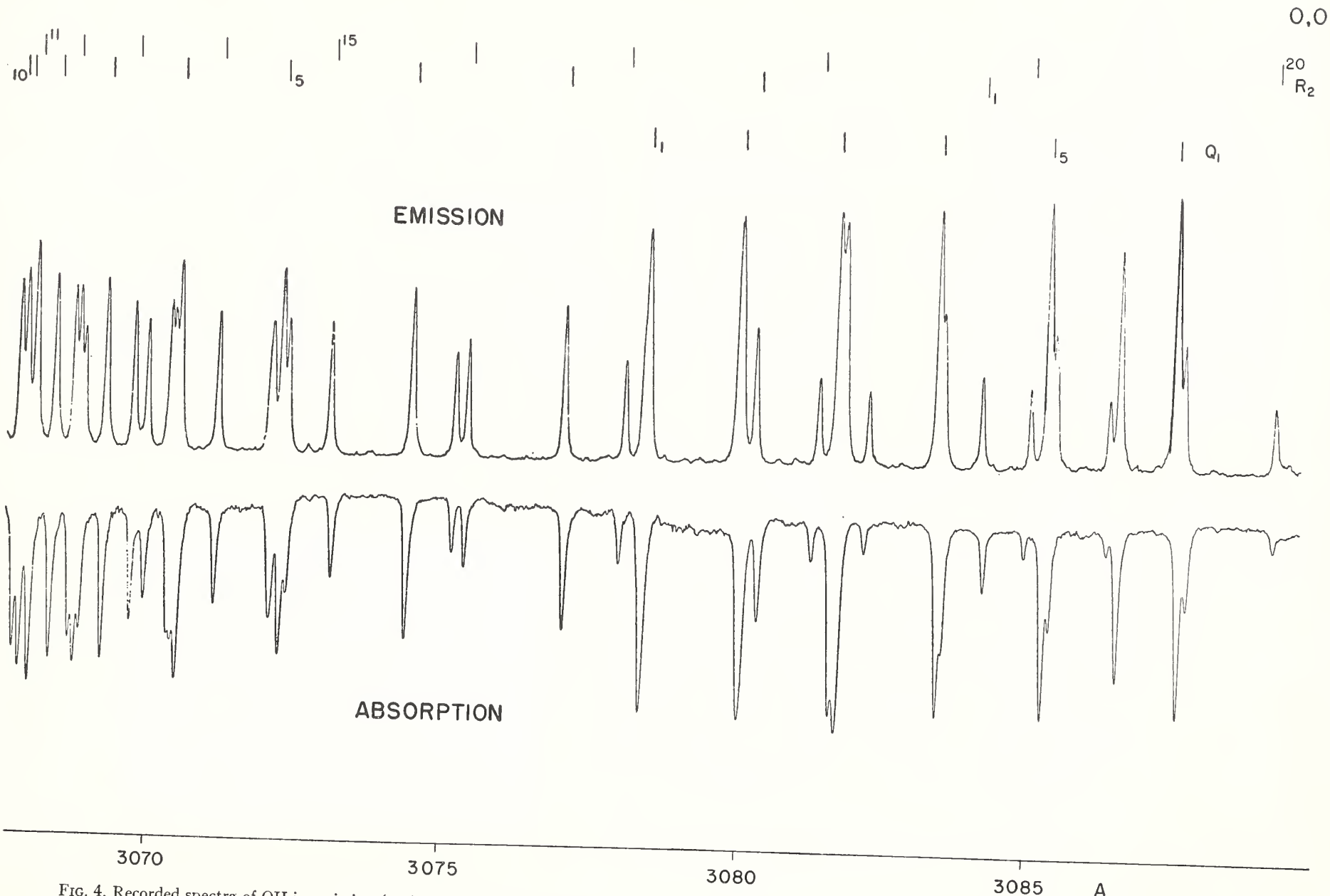

FIG. 4. Recorded spectra of OH in emission (top) and absorption (bottom) of an oxygen-acetylene flame. A high pressure xenon lamp was the continuum source.

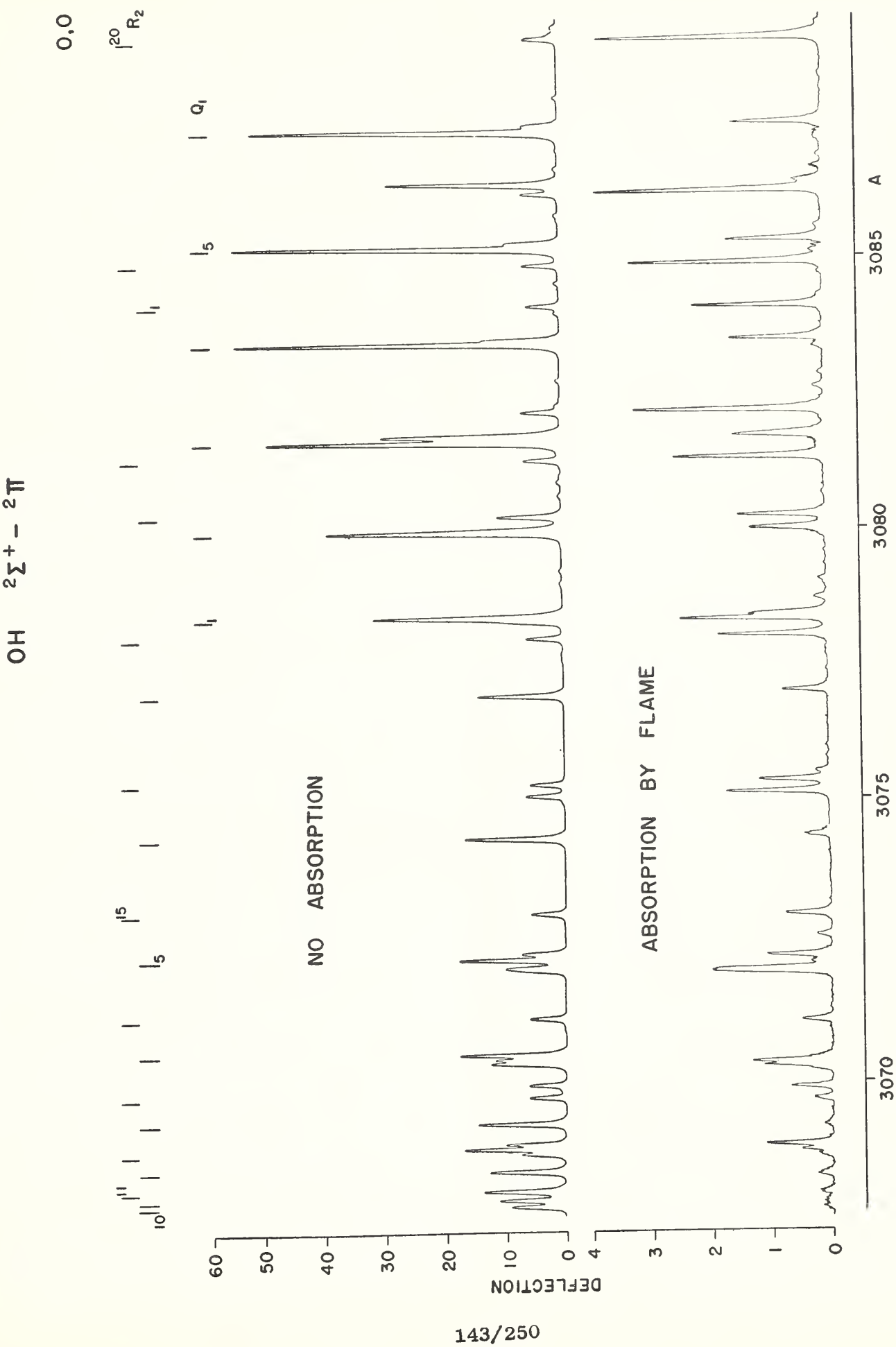

FIG. 5. Recorded spectra of OH from an electrodeless discharge through water vapor as seen with no absorption (top) and through a strongly absorbing oxygen-acetylene flame (bottom).

Two sets of entrance and exit slit widths of 6 (approximately) and 50 microns were used to determine the effect of resolving power on the measured absorption "temperature." These widths are equivalent to 0.03 A and 0.25 A in the second order. With a slit height of 0.5 mm, lines of OH in the second order near 3100 A whose centers were separated by 0.07 A and 0.45 A could be clearly resolved in the two cases. The detector was a 1P28 RCA photomultiplier. Radiation from the source was modulated at a frequency of 60 cycles per second by a metal chopper placed between the source and the flame. Thus, since the detected signal was amplified by a narrow band synchronous ac amplifier, radiation from the source alone is "seen" regardless of the relative intensities of the emission lines in the source and absorber. The spectra were recorded on a pen recorder.

B. Spectra

Absorption spectra of the R_2 branch of the 0,0 band in the $^2\Sigma \leftarrow ^2\Pi$ electronic transition of OH between 3067 A and 3090 A were obtained (see Figs. 4 and 5) with high and low resolution using the three sources mentioned previously. This branch, as pointed out by Dieke and Crosswhite,[9] is particularly suitable for temperature measurements because the first 20 lines occur in a wavelength region of 20 A and the branch is relatively free of overlapping lines. For each source, successive spectra were obtained for the source alone, the source and absorber, source alone, source and absorber and a final check on the source stability by recording the first few lines. In general the recorder deflections for the lines of the repeated spectra agreed with one another to within a few percent.

Figures 4 and 5 are examples of the spectra obtained under high resolution. Height above the base lines is proportional to the radiation intensity. Satellite lines, lines of the R_1 and P_1 branches and Rowland "ghosts" are not identified in the figures. The upper spectrum of Fig. 4 is an emission spectrum for the oxygen-acetylene flame on the slot burner. The lower spectrum is the absorption of this flame using the continuum source.

Figure 5 shows the spectrum of the discharge through water vapor with and without absorption by the flame. Since the OH discharge lines are considerably narrower than those in the flame, the ratio of the observed deflections of the absorbed to the nonabsorbed lines in Fig. 5 should be nearly equal to the minimum transmission of the respective lines. Thus a close look at Fig. 5 shows that the Q_1 lines have a transmission of only a fraction of one percent, i.e., they are almost completely absorbed. This large absorption produces an interesting effect on the weak lines. For example, the satellites close to the strong Q_1 lines can be seen only as shoulders on the $Q_1(1)$ to $Q_1(6)$ lines in the nonabsorbed spectrum. However in the lower spectrum of Fig. 5, the strong lines are almost completely absorbed leaving the six satellites of the Q_1 lines clearly visible. In addition satellites of the weaker R_1 lines also are observable. This, incidentally, illustrates a way in which the wavelengths of weak lines near very strong lines could be obtained more accurately.

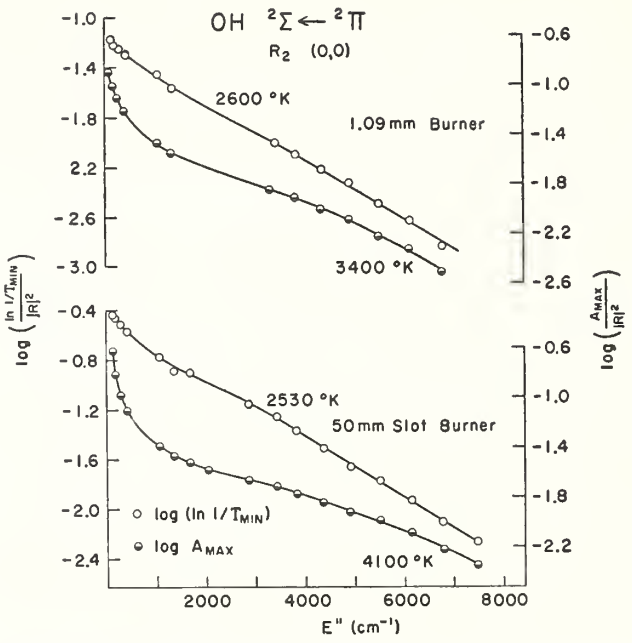

FIG. 6. Log and log ln plots of OH absorption in two thicknesses of an oxygen-acetylene flame. "Temperatures" are measured from the slopes of the curves between 4000 and 7500 cm^{-1}.

Minimum transmission (i.e., at the peak of the observed line) for all useable lines in the R_2 branch for each of the various runs were measured and averaged. Other quantities required in order to use Eq. (10) were obtained from the compilation of Dieke and Crosswhite.[9]

IV. RESULTS

"Temperature" plots were constructed for all the spectra obtained using both Eqs. (6)** and (10). Figure 6 compares the two methods for the case of high resolution and a discharge source.†† In order to observe the effect of changing the amount of absorption, a small welding torch with a port diameter of 1.09 mm was used as well as the slot burner.

Peak absorption in each flame for the R_2 lines is given in Table I. Except for slight dips in the vicinity of the stronger lines of the branch, the log ln plots give fairly straight lines in both flames. The slopes of these lines and therefore the respective "temperatures" are nearly equal. The temperature of the flame on the slot burner is expected to be somewhat lower than that

[9] G. H. Dieke and H. M. Crosswhite, Bumblebee Series Report No. 87 (November, 1948) (unclassified).

** For the sake of convenience, the peak absorption rather than the integrated absorption was measured.

†† We shall call the conventional method a log method or plot and the method using minimum transmission, log ln; this nomenclature follows from Eqs. (6) and (10).

TABLE I. Peak absorption of the R_2 branch of OH in an oxygen-acetylene flame as measured using a narrow discrete line source

K''	Peak absorption 1.09 mm burner	50 mm slot burner
1	0.34	0.62
2	0.54	0.85
3	0.69	0.93
4	0.78	0.97
5		
6		
7	0.86	0.98
8	0.84	0.98
9		0.98
10		0.97
11		0.95
12		
13	0.68	0.93
14	0.63	0.90
15	0.55	0.83
16	0.49	0.74
17	0.38	0.67
18	0.32	0.56
19	0.32	0.44
20	0.22	0.35

on the small burner because in the former case measurements were made a greater distance above the inner cone. Moreover, the experimental error estimated from the scatter of slopes is about 3% (75°K at 2500°K). While greater accuracy and closer comparison might be obtained, there would be no additional advantage since large differences and trends were the primary interest of this study.

The log plots in Fig. 6 deviate considerably from straight lines. In order that quantitative comparisons might be made, however, the straight line best fitting the higher energy transitions was used for obtaining a "temperature." These "temperatures", as seen in Fig. 6, are not only very high but differ greatly for the two flames. Thus the usual log method is greatly dependent upon the amount of absorption in the flame while the log ln method using a discrete, narrow line source is not.

The slight dip at the most intense lines in the log ln plot was unexpected and the cause of this is not definitely known. A greater half-width for the more highly populated transitions as is obtained in resonance type pressure broadening[10] would produce such an effect [see Eq. (11)]. However, the partial pressure of OH was only of the order of 16 mm Hg‡‡; this was calculated using our data on the integrated absorption of the $R_2(1)$ line corrected for lack of sufficient resolution, Oldenburg and Rieke's[6] absolute intensity for this line and Eqs. (3) and (4). This is probably too small for resonance broadening to have an effect. Another possible cause of the dip could be the amplifier passing a small signal from the slot burner itself, i.e., some of the unchopped radiation. A careful test definitely showed this not to be the case.

[10] H. M. Foley, Phys. Rev. **69**, 616 (1946); P. W. Anderson, Phys. Rev. **76**, 647 (1949).

‡‡ 14.5 mm Hg is the calculated equilibrium pressure of OH in the combustion products at this temperature.

A slight dip probably is due to the finite width of the OH lines in the discharge and the lack of sufficient resolving power. Even though the discharge lines are $\frac{1}{4}$ as wide as those in the flame, a small amount of absorption due to the wings is present in the measured peak absorption. This is so small, however, that its effect is only observed in the strongly absorbed lines. For example, if the peak fractional absorption for a line is 0.99 but due to a small wing contribution we obtain 0.98 at the peak of an observed discharge line, the reciprocal of the transmission should be 100 but is measured as 50. However, when the peak absorption is 0.50, even if the measured value were 0.40, the reciprocal of the transmission would change only from 2 to 1.7. This tentative explanation is consistent with the explanation given below of the effects of resolving power and source line width on the measured "temperature." The dip, whatever its cause, does not appear to affect seriously the "temperatures" obtained.

Figure 7 presents log ln plots for the slot burner under the various experimental conditions. For the low resolution case, fewer lines in the R_2 branch were free of overlapping from neighboring lines, resulting in fewer points. "Temperatures" obtained from these plots together with those from log plots and isointensity plots (Fig. 8) are listed in Table II.

Another method of using spectral data for determining temperature has been called the isointensity method.[9] It is most useful for branches of molecular bands which form a band head and is particularly well

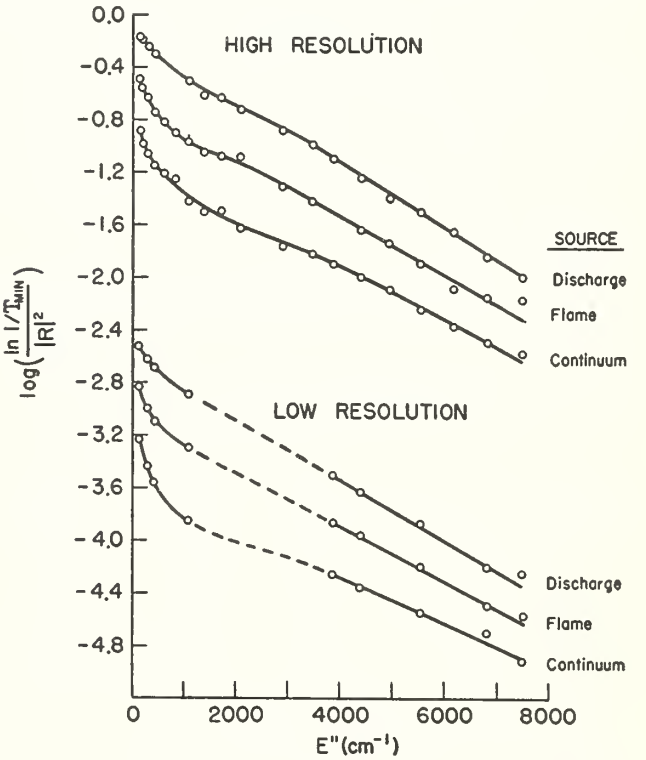

FIG. 7. Effect of resolving power on log ln plots of OH absorption with different light sources.

suited for the R_2 branch of OH[11,12] Heretofore this method has not been used for absorption. The isointensity method is based on the intensities of two lines being equal. For example, setting expressions for respective intensities of two lines equal to each other, e.g., in absorption Eq. (4), and assuming that their frequencies are the same, the temperature is found to depend only upon the difference in the energy levels and the ratio of the transition probabilities, $|R|^2$, of the two lines. Figure 8 compares isointensity plots of the same spectrum for the slot burner using the logarithm of the reciprocal transmission and the maximum absorption. Although the curve of the maximum absorption *versus* the rotational quantum number is considerably flatter than the corresponding transmission curve, both curves give the same isointensity "temperatures" for the first three lines. The lower curve is so flat that the precision for other pairs of lines is very low. These "temperatures" also agree with those obtained in the infrared in OH emission[13] for the same electronic and vibrational state. The isointensity method in absorption thus gives reasonable "temperatures" even when the absorption is large. However, one disadvantage of the method is that it provides no simple way of detecting nonequilibrium, i.e., the nonexistence of a temperature. When this possibility exists it is more desirable to use the log or log ln plot where a straight line indicates equilibrium.

The isointensity "temperatures" in Table II are approximately the same and with greater care would be closer. It is quite possible that the low "temperature" measured with the flame source at the higher resolving power is caused by a slight difference in the position of the slot burner flame. From the infrared and these present measurements, it appears that the rotational energy in the (0,0) band of the ground electronic state of the OH about 25 mm above the inner cone of an acetylene-oxygen flame with a mixture ratio of 2 to 5 is distributed as though the average "temperature" were 2550°±100°K.

Table II emphasizes two points in comparing the log and log ln methods of measuring "temperature." The first is that the log ln method with the discharge source

TABLE II. Measured OH rotational "temperatures."

Resolution	Source	Method of determination: log (ln $1/\tau$)	Log A_{max}	Isointens.
0.03 A	Discharge	2530°K	4100°K	2570°K
	Flame	2800	3750	2400
	Continuum	3000	3200	2520
0.25 A	Discharge	2650	4300	2480
	Flame	3000	4100	2490
	Continuum	3600	3600	2700

[11] K. E. Shuler, J. Chem. Phys. **18**, 1466 (1950).
[12] H. P. Broida, J. Chem. Phys. **21**, 1165 (1953).
[13] Benedict, Plyler, and Humphreys, J. Chem. Phys. **21**, 398 (1953).

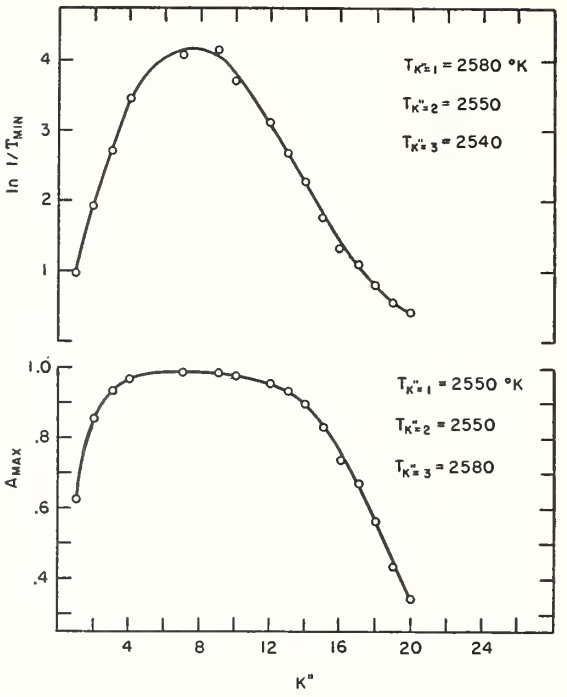

FIG. 8. The logarithm of the reciprocal transmission and the maximum fractional absorption plotted against the rotational quantum number, K'', of the initial state. Measured isointensity "temperatures" from the first three pairs of lines are listed.

gives correct "temperatures" independent of the resolution whereas the "temperatures" obtained from the log method are as much as 70% high. Second, regardless of the source or the resolution, the log ln "temperatures" are not in error by as much as the log "temperatures."

The trends exhibited by the different methods of "temperature" measurement and the different experimental conditions as shown in Table II can be explained in a rather simple manner. Consider first the group of "temperatures" obtained using the log ln method under high resolution. The "temperature" of 2530°K using the discharge source was shown to be correct. When a flame source is used the "temperature" is increased about 10%. Since the straight line portion of the plots from $K''=14$ to $K''=20$ ($E''=4000$ to 7500 cm^{-1}) were used in the nonlinear cases to obtain a "temperature," the relative changes in the reciprocal of the minimum transmission (or maximum absorption for log plots) for lines near $E''=4000$ cm^{-1} as compared to those at $E''=7500$ cm^{-1} will show how the slope of the plot or the "temperature" will vary. Lines near $E''=4000$ cm^{-1} have a peak fractional absorption of approximately 0.9 while those at $E''=7500$ cm^{-1} are about 0.4 (from discharge source). These values will decrease using a flame source since now source radiation is present not only at the center but also in the wings of the OH lines where absorption is less. The source lines are thus absorbed less in the wings than in the center and since the spectrometer "sees" more than just the center of the line when set on this wavelength (i.e., $\Delta x_{\text{spectrometer}} \sim \alpha_{\text{flame}}$), the observed absorption is less.

The decrease is probably somewhat less for the strongly absorbed lines since these transmitted lines (not the absorption coefficient) are broader. Even so, if the peak absorption changed from 0.9 to 0.8 and from 0.4 to 0.2, respectively, the corresponding change in reciprocal transmission would be from 10 to 5 and 1.66 to 1.25. This would cause the point at $E''=4000\ \text{cm}^{-1}$ to drop more than that at 7500 cm^{-1} resulting in a reduced slope and a greater "temperature." In going to a continuous source the same effect is present but since the source radiation in the wings of the OH lines is now the same as that at the peak, the transmitted energy in the wings is greater resulting in even less observed absorption and a still higher "temperature." The somewhat higher "temperatures" obtained when using the log ln method under poorer resolution is expected since the spectrometer now passes more of the wing transmission when set on the peak of the line (i.e., much broader slit function).

The very high "temperature" measured using the log method with the discharge source is to be expected since Eq. (6) is valid only for small absorption. For the spectral lines near $E''=7500\ \text{cm}^{-1}$ where the peak absorption is about 0.4, the intensity of the absorbed line is still roughly (15% error) proportional to the peak absorption. However, when the fractional peak absorption is 0.9, the absorption has increased far less than the intensity simply because the intensity is in the exponent. Thus the plotted points near $E''=4000\ \text{cm}^{-1}$ are much lower than they should be, producing a very high "temperature" measurement. This effect, which might be called saturation, is analogous to self-absorption in the case of emission measurements.

It is interesting to note that the "temperatures" obtained using the log method decrease in changing from a discharge to a continuous source—the opposite of that for the log ln method. This is simply due to the fact that we are plotting a function of absorption rather than reciprocal transmission. Since the relative absorption decreases more, as mentioned before, when it is weak, i.e., near $E''=7500\ \text{cm}^{-1}$, these points are lowered when using the flame and continuum source more than those at $E''=4000\ \text{cm}^{-1}$. This increases the slope of the log plot and therefore reduces the measured "temperatures."

Thus it is seen that the various trends in "temperature" can be explained by a combination of effects: plotting a function of absorption rather than reciprocal transmission, measurement of absorption in the wings as well as at the peak, and finally the spectral slit width of the spectrometer.

V. CONCLUSION

The log ln method based on Eq. (10) provides a more accurate means of measuring population "temperatures" in absorption in flames and hot gases. If a line source of radiation is available whose line widths are less than one-fourth those in the absorber, accurate "temperatures" may be determined, even when the peak line absorption is as great as 98%. Even with broader line sources or with a continuum, the "temperatures" will be more accurate than those obtained using the conventional method based on Eq. (6).

Reprinted from JOURNAL OF THE OPTICAL SOCIETY OF AMERICA, Vol. 46, No. 12, 1060–1064, December, 1956
Printed in U. S. A.

Slit Function Effects in the Direct Measurement of Absorption Line Half-Widths and Intensities*†

HENRY J. KOSTKOWSKI AND ARNOLD M. BASS
National Bureau of Standards, Washington 25, D. C.

(Received February 15, 1956)

The distortion of spectral lines by the finite band pass of spectrometers is an effect which must be considered in measuring line shape parameters. The differences between actual line half-widths and line intensities and those which would be obtained directly from measurements by spectrometers with Gauss and Cauchy shaped slit functions have been calculated for Lorentz and Doppler lines of varying widths and intensities. A method of utilizing these results to correct actual measurements is developed.

INTRODUCTION

THERE has been for some time considerable interest in the determination of half-widths and intensities of lines in the absorption spectra of gases. Line half-widths may be used to obtain information concerning the forces between molecules, while intensities give information on the forces within molecules. Moreover, both of these parameters can be used for determining the temperature of a hot gas and are important in considering energy transfer within the gas.

When a spectral line is observed with a spectrometer, its shape is distorted by the instrument, the distortion being greater the poorer the resolving power of the spectrometer. This effect is well known and various methods have been used to attempt to correct for such distortion.[1,2] In general, in the infrared region of the spectrum the available resolving power has been inadequate to obtain a spectral line with negligible distortion so that its true width and intensity could be measured directly. These parameters have been determined[3] usually by indirect means involving considerable effort and yielding only fair accuracy. However, recent instrumental advances[4,5] in the infrared have increased the available resolving power so that the possibility of direct measurements of line half-width and intensity in this region have increased considerably. In order to determine the resolving power necessary for this task, or the error committed with the resolving power available, calculations have been made of the intensity and half-width of an absorption line as a function of the resolving power, the line shape, the peak absorption, and the overlap of neighboring lines.

* Presented in part before the Optical Society of America, October, 1955.

† This research was supported in part by the U. S. Air Force through the Office of Scientific Research of the Air Research and Development Command under Contract CSO 680-56-30.

[1] A. C. Hardy and F. M. Young, J. Opt. Soc. Am. **39**, 265 (1949).
[2] A. Adel and E. F. Barker, Revs. Modern Phys. **16**, 236 (1944).
[3] W. S. Benedict and S. Silverman, Phys. Rev. **95**, 752(A) (1954).
[4] Jaffe, Rank, and Wiggins, J. Opt. Soc. Am. **45**, 636 (1955).
[5] W. G. Fastie and H. M. Crosswhite, J. Opt. Soc. Am. **45**, 900(A) (1955).

CALCULATIONS

The transmittance of a gas as obtained with a spectrometer set on frequency ν may be expressed as

$$T_{\text{obs}}(\nu)=\exp(-k_{\text{obs}}(\nu)pl)$$
$$=\frac{\int_{\sigma}\sigma(\nu,x)\exp(-k(x)pl)dx}{\int_{\sigma}\sigma(\nu,x)dx}, \quad (1)$$

where $\sigma(\nu,x)$ is the slit function at frequency ν and represents the intensity of radiation as a function of frequency transmitted by the spectrometer when the latter is on ν, $k(x)$ is the absorption coefficient of the gas (the variation of $k(x)$ with frequency when only one line is present is called the line shape), p is the partial pressure of the absorber in atmospheres, l is the path length through the gas, and k_{obs} and T_{obs} are the observed absorption coefficient and transmittance, respectively. The half-width, α, of an absorption line is defined as half the width of the absorption coefficient for that line alone at half its peak value and the intensity of the line,‡ S, is equal to the integral of the absorption coefficient over the line. In addition, we shall be concerned with the peak value of the absorption coefficient, k^{peak}, a quantity which relates both the intensity and width of a line through its shape.

When the absorption coefficient, $k(x)$, varies negligibly over the frequency range of the slit function, the exponential in Eq. (1) can be removed from the integral and $k_{\text{obs}}=k$. It is then a trivial matter to determine α, S, and k^{peak}. The questions of current interest are: how narrow must the slit function be in order to do this, and, if the slit function is not sufficiently narrow, what are the errors that result? In particular we wish to know how these errors depend on the following variables:

1. ratio of spectral slit width§ to line half-width, $\Delta\nu/\alpha$,
2. shape of the line, $k(x)$,
3. shape of slit function, $\sigma(\nu,x)$,
4. overlap of neighboring lines, $\beta=2\pi\alpha/d$,‖
5. peak absorption, A^{peak}.

The integral in Eq. (1) has been evaluated on a high-speed electronic digital computer as a function of the variables listed above for intervals of ν of one-tenth the width of the lines or less. The line shapes chosen were the Lorentz (Cauchy function) and Doppler (Gauss function) i.e.,

$$k_L(x)=\frac{S\alpha/\pi}{(x-x_0)^2+\alpha^2}, \quad (2)$$

$$k_D(x)=\frac{S}{\alpha}\left(\frac{\ln 2}{\pi}\right)^{\frac{1}{2}}\exp[-(\ln 2)(x-x_0)^2/\alpha^2]. \quad (3)$$

To a first approximation, at least, absorption lines are expected to have either of these shapes or some combination of the two.

Similar functional relationships were assumed for the slit function, with $\Delta\nu=2\alpha$, and the peak value of σ normalized to unity. The validity of the Gauss assumption was checked by determining experimentally the slit function of our two spectrometers. One was an $f/6$ double pass spectrometer utilizing a 2-in. grating

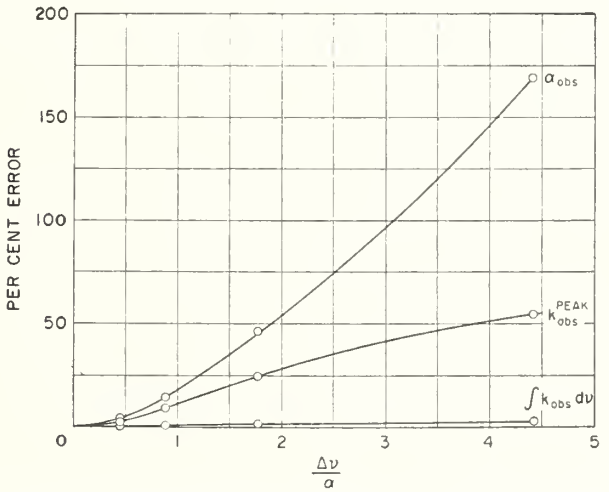

FIG. 1. Error made in direct measurement of line width, peak absorption coefficient, and line intensity as function of ratio of spectral slit width to line half-width for a single Lorentz line with 30% peak absorption and a Gauss slit function.

‡ The absorption coefficient is here defined so that intensity has the dimensions cm^{-2} atmos^{-1}.

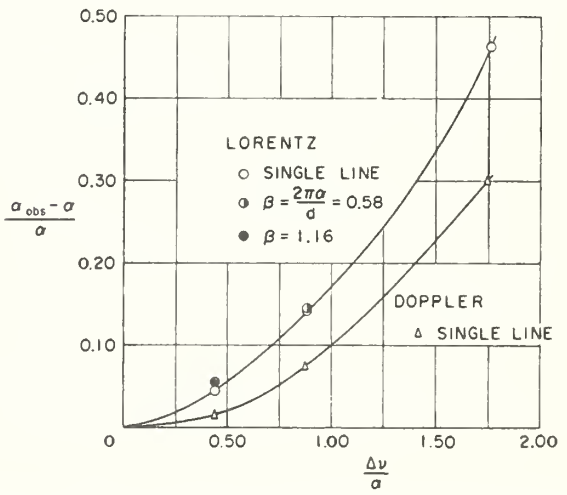

FIG. 2. Error made in direct measurement of line half-width as function of ratio of spectral slit width to line half-width, for Lorentz and Doppler lines with 30% peak absorption.

§ The spectral slit width, $\Delta\nu$, is the width of the slit function at half its peak value. It is approximately the frequency interval just resolved by a spectrometer and is a function of the mechanical slit width, the theoretical resolving power, the optical performance, etc.

‖ β is a parameter whose value is a measure of the amount of overlap. d is the distance between the lines.

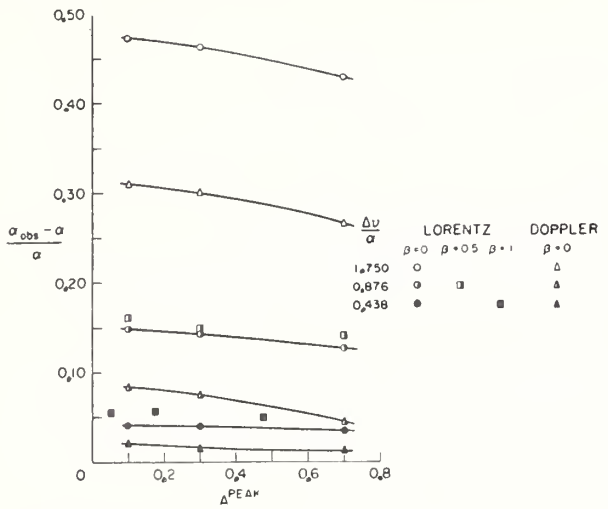

FIG. 3. Error made in direct measurement of line half-width as function of peak absorption for Lorentz and Doppler lines.

and an off-axis parabola. The other was an $f/10$ single pass Ebert System with a 3-in. grating. The entrance and exit slit widths, $s_1=s_2=s$, were such that the ratio of slit width to diffraction width, $sD/2\lambda F$, varied from 1 to 2 (D is the aperture, F the focal length, and λ the wavelength). The check was performed at 2.05 μ using a sharp emission line from a low pressure electrodeless discharge in helium.¶ Within the experimental error of about $\frac{1}{2}\%$, the result was a Gauss function.** The Cauchy function was also used as a slit function to observe the effect of a slit function with large wings. Conveniently, a Cauchy function follows a Gauss function of the same width fairly well in the central region making it possible to compare the effects of two slit functions which differ principally in the wings.

To see the effect of measuring α, S, and k^{peak} of lines with different amounts of absorption, calculations

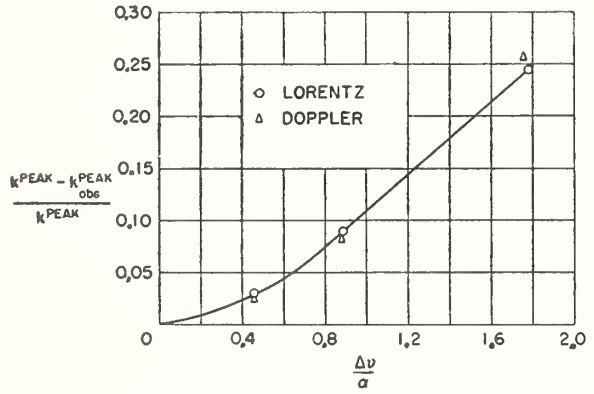

FIG. 4. Error made in direct measurement of peak absorption coefficient as function of ratio of spectral slit width to line half-width, for Lorentz and Doppler lines with 30% peak absorption.

¶ By replacing $\exp(-kpl)$ in Eq. (1) with the intensity of radiation from a narrow ($\alpha \ll \Delta\nu$) emission line which approximates a delta function, it is clear that the result of scanning over such a line is proportional to the slit function.

** When $sD/2\lambda F \ll 1$, one would expect the slit function to have secondary maxima and resemble a single slit diffraction pattern. This has been confirmed experimentally by Rank, Shearer, and Bennett, J. Opt. Soc. Am. 35, 762 (1955).

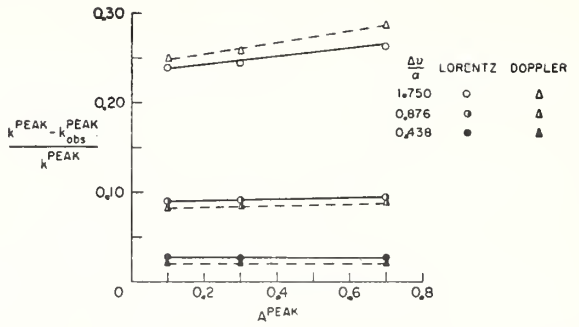

FIG. 5. Error made in direct measurement of peak absorption coefficient as function of peak absorption for Lorentz and Doppler lines.

were made assuming peak absorptions of approximately 10%, 30%, and 70%.

Finally, the effect of neighboring lines overlapping the line of interest was considered. An absorption line is not always sufficiently distant from all other lines so that the contributions to the absorption from the wings of the adjacent lines may be neglected. This effect was considered only for the simple case of a set of three absorption lines of slightly different intensity and separation. However, it is a rather good approximation to the lines in an absorption band of a linear molecule. Calculations were performed for two values of the parameter β corresponding to a trough absorption of approximately 10% and 25% of the absorption at the center of the line.

RESULTS

Figure 1 shows the percent difference between the "observed"†† and actual line half-widths, line intensities, and peak values of the absorption coefficient as a function of the ratio of the spectral slit width to line half-width. The greatest difference appears in measuring the line half-width because this measurement is affected by distortion in both the width and peak of the line. Though it was expected that the observed intensity be

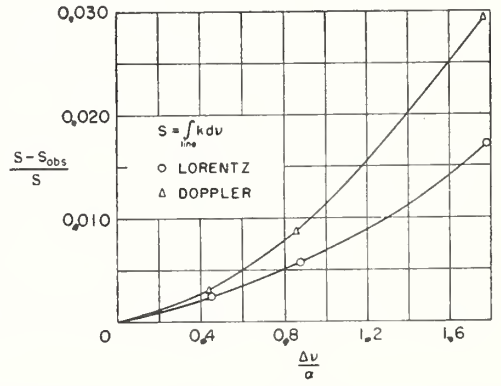

FIG. 6. Error made in direct measurement of line intensity as function of ratio of spectral slit width to line half-width for Lorentz and Doppler lines with 30% peak absorption.

†† "Observed" refers to the value calculated from Eq. (1). This would be the value measured if an experiment were performed under the conditions stated herein.

least affected, it is surprising that even at 30% peak absorption the error is only 2.5% when the spectral slit width is more than four times as large as the line half-width. The broadening of the absorption coefficient largely compensates for the depression of the peak, thus keeping the area nearly constant.

Figures 2 and 3 illustrate the error in direct measurements of line half-width as a function of line shape, resolving power, and peak absorption. Results are not given for $\Delta\nu/\alpha>2$ because in this region the difference exceeds 50%. To make accurate corrections of this magnitude, the slit function and line shape must be so accurately known as to make direct measurements impractical.

The effect of overlapping lines was determined for $\beta=0.58$ and 1.16. In order to measure the half-width of an absorption line, it is first necessary to determine the peak value of the absorption coefficient for that line alone. This can be done by calculating the absorption coefficient contributed to the peak of the line from neighboring lines in terms of a fraction of the total

TABLE I. Comparison of Cauchy and Gauss slit function effects on line shape parameters.

$\frac{\Delta\nu}{\alpha}$	$\frac{\alpha_{obs}-\alpha}{\alpha}$		$\frac{k_{peak}-k_{obs\,peak}}{k_{peak}}$		$\frac{S-S_{obs}}{S}$	
	Lorentz line, 30% peak absorption					
	Cauchy	Gauss	Cauchy	Gauss	Cauchy	Gauss
0.438	0.21	0.04	0.16	0.03	0.01	0.00
0.876	0.44	0.14	0.30	0.09	0.03	0.01
1.750	0.88	0.46	0.47	0.24	0.05	0.02
	Doppler line, 30% peak absorption					
0.876	0.25	0.08	0.30	0.09	0.04	0.01

absorption coefficient of an adjacent trough. In order to determine this fraction one must know the width, relative intensity, shape, and position for each line. Fortunately, the fraction is very insensitive to each of these parameters except the distances between the lines, which are known or can be measured independently. In this case, where a series of only three lines is considered, the ratio is approximately 0.25. Figure 2 illustrates that for $\beta=0.58$ and 1.16 the overlap, when handled in this way, has little effect on the accuracy with which the line width may be measured.

It is often useful to know the peak value of the absorption coefficient of a line. Figures 4 and 5 show that the error made in obtaining the peak value of k as a function of $\Delta\nu/\alpha$ in the range from 0 to 2.0 is very nearly the same for both Lorentz and Doppler lines. Actually, this is expected because both shapes are very similar around the center of the line. If one is interested in the total absorption coefficient at the center of the line, these graphs are applicable. If the peak value of the absorption coefficient for the single line alone is desired, the amount of overlap must be subtracted.

Line intensities may be determined by the extrapolation method which Wilson and Wells[6] used for band intensities. However, the method is time consuming and at times the present, more rapid method would be preferable. Figure 6 demonstrates the accuracy possible when measuring directly the line intensity of a 30% peak absorbed line. Graphs of this type for peak absorptions of greater or less than 30% can be prepared from Figs. 7 and 8.

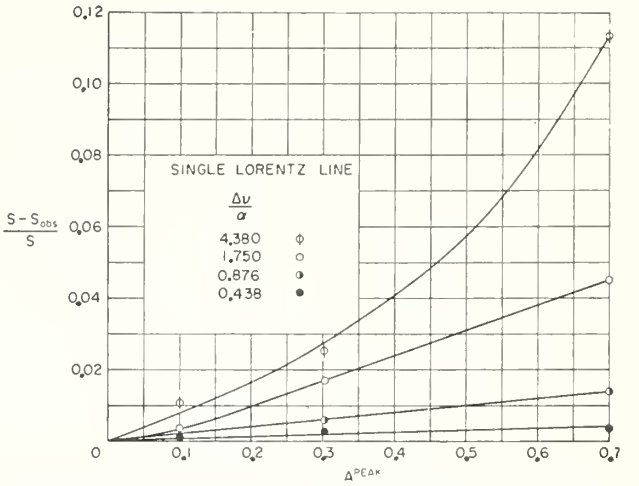

FIG. 7. Error made in direct measurement of line intensity as function of peak absorption for a Lorentz line.

In order to determine the effect produced by a slit function which has large wings, the line half-width, peak absorption coefficient, and intensity were calculated using a Cauchy slit function, i.e.,

$$\sigma(\nu,x)=\frac{(\Delta\nu/2)^2}{(x-\nu)^2+(\Delta\nu/2)^2}.$$

The comparison between the effects of a Gauss slit function and a Cauchy slit function is given in Table I, and the results show that even if $\Delta\nu/\alpha$ is small, the error

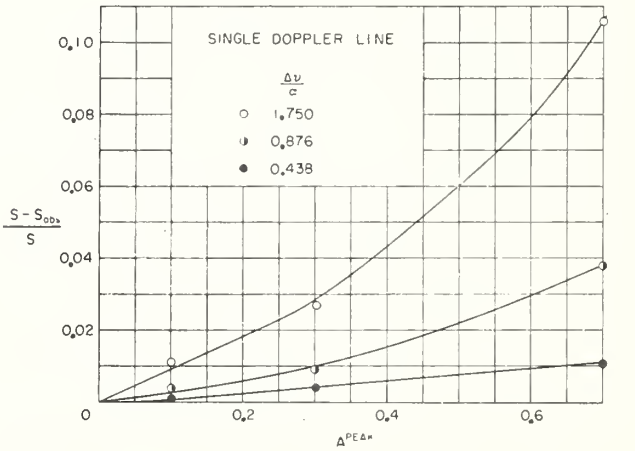

FIG. 8. Error made in direct measurement of line intensity as function of peak absorption for a Doppler line.

[6] E. B. Wilson, Jr., and A. J. Wells, J. Chem. Phys. 14, 578 (1946).

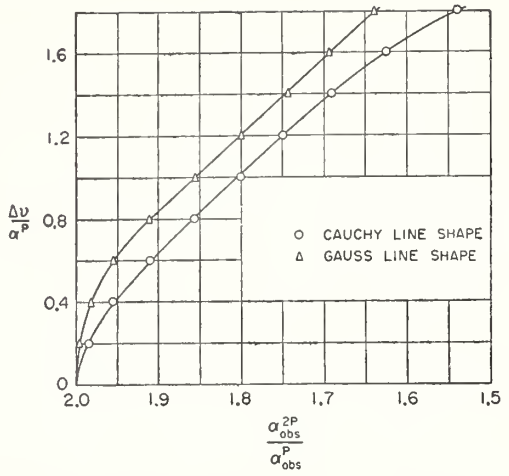

FIG. 9. Curves for determining ratio of spectral slit width to line half-width from direct measurement of line half-widths at pressures of P and $2P$. The curves are drawn for Cauchy and Gauss shaped lines of which the width varies linearly with pressure.

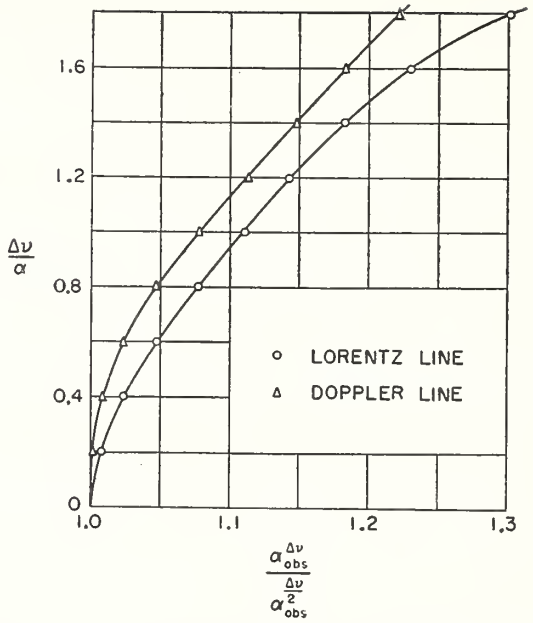

FIG. 10. Curves for determining ratio of spectral slit width to line half-width from direct measurement of line half-widths at spectral slit widths of $\Delta\nu$ and $\Delta\nu/2$.

can be large if the slit function has strong wings. The effects indicated in Table I are for an extreme case since it appears from our observations that a high resolution spectrometer will tend to have a slit function somewhere between a Gauss function and a single slit diffraction function. Nevertheless, this does emphasize the importance of determining in some way the particular slit function which is used in an experiment.

APPLICATION OF RESULTS

In order to use the various graphs, presented in this paper, to correct the directly measured quantities, it is necessary to know the ratio of the spectral slit width to line half-width, $\Delta\nu/\alpha$, and the actual peak absorption of the line, A^{peak}. In Fig. 9, $\Delta\nu/\alpha$ has been plotted against the ratio of two observed half-widths where actual half-widths differ by a factor of two.‡‡ Though the curves have been prepared for a peak absorption of 30%, $\alpha_{\text{obs}}-\alpha/\alpha$ does not vary greatly with the peak absorption (see Fig. 3) and, therefore, these curves can be used for other absorptions. Whenever it is possible to vary the pressure in an absorption experiment (and if α varies linearly with pressure) it is a simple matter to obtain spectra for the same spectral slit width but for the two values of α. The desired $\Delta\nu/\alpha$ can then be obtained from Fig. 9.

When experimental conditions are such that the pressure cannot be changed easily or α does not vary with pressure in a known way, the slit width can be changed and $\Delta\nu$ determined for each using a sharp emission line. Then a graph such as Fig. 10†† can be used to obtain $\Delta\nu/\alpha$.

It should be emphasized again that the graphs in this study have been prepared for a Gaussian slit function and the shape of the slit function ought to be checked experimentally by using some narrow emission line as described earlier. This emission line, however, need not be in exactly the region in which measurements are desired, for the shape of the slit function is expected to change little as a function of frequency compared with the change in its width.

SUMMARY

Direct measurements of absorption line half-widths and peak absorption coefficients can be made with an error of only 5.0% with a ratio of spectral slit width to line half-width of about 0.50. Under similar conditions direct determination of line intensity can be made with an error of 0.5% when the peak absorption is 30%.

The ratio of spectral slit width to line half-width can be determined experimentally by making observations at two known pressures or at two mechanical slit widths. If the shape of the slit function is approximately Gaussian, which also can be confirmed experimentally, this value of $\Delta\nu/\alpha$ and the graphs given can be used to correct direct measurements of line half-width and intensity for the slit function distortion.

The electronic computer calculations were performed by Mr. John Cooper of the National Bureau of Standards' Computation Laboratory; we gratefully acknowledge his cooperation and assistance.

‡‡ Curves of this type can be prepared from Fig. 2 for α or $\Delta\nu$ changing by a factor other than 2.

UNITED STATES DEPARTMENT OF COMMERCE • Lewis L. Strauss, *Secretary*
NATIONAL BUREAU OF STANDARDS • A. V. Astin, *Director*

Calibration of Liquid-in-Glass Thermometers

James F. Swindells

National Bureau of Standards Circular 600
Issued January 8, 1959

[Supersedes Circular 8]

For sale by the Superintendent of Documents, U. S. Government Printing Office, Washington 25, D. C.
Price 20 cents

574278 O - 61 - 11

Preface

The liquid-in-glass thermometer is probably the most widely used temperature measuring device in both science and industry. In spite of its fragile nature, its relative simplicity makes this type of thermometer singularly attractive where reliable temperature measurements are required but the highest attainable accuracy is not necessary.

The liquid-in-glass thermometer is not an entirely foolproof instrument, however. If the user is to realize the accuracy of which his thermometer is capable, and to recognize its inherent limitations as well, he must have, in addition to its calibration, some knowledge of the behavior to be expected of such a thermometer. It is the purpose of this Circular to emphasize the important features of good practice in the design and use of liquid-in-glass thermometers, and to describe the techniques used by the National Bureau of Standards in their calibration. This information is intended to be of value not only to those who wish to submit thermometers to the Bureau for calibration, but also to manufacturers, to other standards laboratories, and to those who wish to calibrate their own instruments.

A. V. Astin, *Director.*

Contents

Calibration of Liquid-in-Glass Thermometers

James F. Swindells

This Circular contains information of general interest to both manufacturers and users of liquid-in-glass thermometers, as well as those who wish to calibrate thermometers or submit them to the National Bureau of Standards for calibration. Important elements of thermometer design are discussed, and eligibility requirements for certificates or reports of tests are given. Factors affecting the use of common types of liquid-in-glass thermometers are included together with tables of tolerances and reasonably attainable accuracies. The calculation of corrections for the temperature of the emergent stem is given in detail for various types of thermometers and conditions of use. The Circular also describes the techniques and equipment used in the calibration procedures and provides instructions for applicants requesting thermometer calibration services.

1. Introduction

It is the responsibility of the National Bureau of Standards to establish, maintain, and assume custody of the Nation's standards of physical measurement. One important activity under this responsibility is the accurate reproduction of the International Temperature Scale as a basis for the uniform measurement of temperature throughout the scientific and industrial activities of the United States. To this end the Bureau accepts for calibration with reference to this scale selected types of temperature-measuring instruments [1][1] for use as reference or working standards where precise-temperature measurements are required. Less precise types of instruments are not accepted, nor are the more routine calibrations performed in cases where such work can be done in qualified commercial testing laboratories or elsewhere. It is the purpose of this Circular to describe the practices employed at the Bureau in the calibration of acceptable types of liquid-in-glass thermometers. The information is intended for those who wish to submit thermometers for calibration or who have occasion to use thermometers calibrated at the Bureau. Important features of good practice in the use of liquid-in-glass thermometers are emphasized to assure the realization of the accuracy of which the thermometers are capable, as well as to point out their inherent limitations.

In this Circular, which supersedes the fourth edition of Circular 8, much of the material formerly deleted in the third and fourth editions of Circular 8 has been retained. It appears that much of this information is of continuing interest to both manufacturers and users and is most useful when collected in one publication. Consistent with the purpose of this Circular, however, only material relating to liquid-in-glass thermometry is included.

2. Temperature Scales and Standards

The calibration of a thermometer consists of comparing its indications with known temperatures on an accepted scale of temperature. The Kelvin Scale is recognized as the absolute thermodynamic scale to which all temperatures should be ultimately referable. In 1954 the Tenth General Conference on Weights and Measures defined this scale by means of a single fixed point, the triple point of water, to which was assigned the temperature 273.16° K, exactly. Because of the difficulties encountered in the realization of the Kelvin Scale, however, a practical working scale, the International Temperature Scale, was first adopted in 1927 and later revised in 1948. This Scale was intended to have close correspondence with the Kelvin Scale and to provide scientific and industrial laboratories throughout the world with a common basis for stating temperatures. Calibrations of thermometers at the Bureau are therefore made with reference to temperatures on the International Temperature Scale.

In the range of temperatures covered by liquid-in-glass thermometry, the International Temperature Scale is defined by four fixed points, the normal boiling points of oxygen at −182.970° C, water at 100° C, sulfur at 444.600° C, and the normal freezing point of water (ice point) at 0° C. It is recommended that the ice point be taken as the temperature exactly 0.01° C below the temperature of the triple point of water. This makes 0° C correspond to 273.15° K. Temperatures in the range 0° to 630.5° C, other than the fixed points, are defined on the International Temperature Scale in terms of a standard platinum resistance thermometer calibrated at the ice (or triple point), steam, and sulfur points.[2] The oxygen point is added as a fourth calibration point when the standard resistance thermometer is used below 0° C. For international uniformity the name of the scale was changed in 1948 from "centigrade" to "Celsius." In the range from −182.97° to 630.5° C no significant change in the values of temperature was effected as compared with the 1927 scale.

Thermometers graduated on the Fahrenheit scale are calibrated with reference to the Inter-

[1] Figures in brackets indicate the literature references at the end of this Circular.

[2] Because of the uncertain nature of the sulfur point, it is probable that action by the International Conference on Weights and Measures in 1960 will result in the use of the freezing point of zinc, with an assigned temperature close to 419.505° C, as a defined fixed point on the ITS.

national Temperature Scale using the conversion formula,

$$t_{°F}=\frac{9}{5}t_{°C}+32°\text{ F.}$$

When the highest accuracy is required in a calibration, the thermometer indications are compared directly with temperatures obtained with a standard resistance thermometer. If lesser accuracy is adequate, one of a series of mercury-in-glass standards is used, except below 0°C, where the calibration is always made directly with a resistance thermometer regardless of the accuracy required. The series of mercury-in-glass thermometers which serve as standards for total-immersion comparisons is shown below.

Range	Smallest graduation	Auxiliary scale
°C	°C	°C
0 to 50	0. 1	------
0 to 100	0. 2	------
50 to 100	0. 1	at 0
100 to 200	0. 2	at 0
200 to 300	0. 5	at 0
300 to 500	1. 0	at 0

These standards are calibrated with reference to the International Temperature Scale through comparisons with a standard resistance thermometer.

Partial-immersion standards, known as "like standards," are maintained for the calibration of accepted designs of partial-immersion thermometers. These standards are calibrated for stem-temperature conditions expected to prevail during the calibration of similar thermometers. This use of like standards eliminates the need for many of the precautions necessary when dissimilar thermometers are compared. The procedure permits the direct comparison of the indications of similar thermometers, as long as the bulbs are at the same temperature and the stem temperatures are essentially the same for all of the thermometers under comparison.

For the use of those who may want to set up reproducible fixed points in their own laboratories, the Bureau issues triple-point-of-benzoic-acid cells and freezing-point standards of tin, lead, zinc, aluminum, and copper together with their appropriate measured temperatures. Detailed information on these samples and their procurement is given in NBS Circular 552.

3. Kinds of Thermometers Accepted for Test

Liquid-in-glass thermometers include a wide variety of types, not all of which are accepted for test. In general, considerations of design, intended use, and probable stability of the thermometer indications are the principal factors governing acceptability for test. Thermometers belonging to the large and varied group which may be classed as laboratory or "chemical" thermometers are regularly accepted. These may be of the etched-stem or enclosed-scale (Einschluss) type. Other acceptable types include such special-purpose thermometers as Beckmanns, calorimetrics, and clinicals. Thermometers of the so-called industrial or mechanical types, with special mountings for their various intended uses, can be accepted for test only when their construction permits testing with the equipment available. Ordinary household or meteorological thermometers will not, in general, be accepted unless the scale is graduated on the glass stem itself and the thermometer can be readily detached from its mounting for insertion in a testing bath.

Every thermometer submitted must pass a preliminary examination for details of construction before being finally accepted for test. The examination is made with optical aid (about 10 to 15 ×) for fineness and uniformity of graduation, cleanness of the mercury and capillary bore, and freedom from moisture, gas bubbles, and cracks in the glass. Among other possible defects are omission of gas filling where needed, insufficient annealing, misnumbered graduations, and numerous others. A complete listing of all possible defects is not practicable. When serious defects are found the thermometer is returned untested.

4. Certificates and Reports

A certificate of test issued by the Bureau for a liquid-in-glass thermometer, in addition to giving the results of the test, may be taken as an indication that the thermometer is free from serious defects of design, material, or workmanship, and that it has been tested at a sufficient number of points to provide reasonable assurance that the indications throughout the scale are as nearly correct as can be expected with good manufacturing practice.

The test requirements and tolerances outlined in sections 5, 6, and 7 indicate the standard to which a thermometer should conform in order to be eligible for certification.

If a thermometer that is accepted for test is not eligible for certification, a report giving the

results of the test will be issued. This report also contains a statement of the reasons for not issuing a certificate. The issuing of a report means that the thermometer is usable, but in most cases it also means that the manufacturer has failed to meet requirements such as those listed at the end of this section which he could reasonably be expected to meet. There may be some other cases where a thermometer is carefully manufactured, but is designed to meet a particular government or commercial specification which, while adequate for its intended purpose, is in some particular in conflict with the NBS requirements for certification. A report of test will usually serve to enable the user to secure satisfactory and reliable temperature measurements with the thermometer if it is properly used and the reported corrections are applied.

In addition to the results of test, a certificate or report will show the following information: the manufacturer's identification markings and numbers; the agency or firm for which the test was made; the NBS test number and date of test; and such explanatory notes as will define the conditions under which the results of test are applicable and which will enable the user to apply the results of the test to advantage. The authenticity of a certificate is evidenced by an impressed seal of the Bureau. When necessary, the certificate will be accompanied by a sheet showing how to calculate the correction for emergent stem. If the thermometer is of the metastatic (Beckmann) type, the certificate will be accompanied by a table of setting factors to enable the user to apply the results of test when the thermometer is used with a setting other than that for which the corrections are given.

Figure 1 shows the face of a certificate and figure 2 the back of the same certificate.

Some of the reasons why a thermometer may not be certified are given in detail in the following three sections and are briefly summarized below:

(a) Defects of design or workmanship, in general.

(b) Omission, where required, of ice point or other reference point.

(c) Part of graduated scale not usable.

(d) Defects in graduation or numbering, or graduation in unsuitable intervals.

(e) Omission of required marking on partial-immersion thermometers.

(f) Unsuitable glass in bulb.

(g) Inadequate annealing.

(h) Inadequate gas filling.

(i) Scale error in excess of tolerance.

(j) Not tested over entire range of scale.

5. Thermometer Design Requirements

The first requirements for certification are that the thermometer shall be of good design, material, and workmanship and shall be permanently marked with a serial number which will serve to uniquely identify the thermometer with its certificate of calibration. No attempt is made to list specifically all possible defects of design and workmanship, since some latitude for judgment must be reserved to deal with individual cases as they arise. Certain important requirements of general applicability can be singled out, however, and these are described below.

5.1. Materials of Construction

While the cleanliness of the thermometer bulb, bore, and liquid filling have a pronounced effect upon the performance of a finished thermometer, of equal importance is the proper choice of the glass from which the thermometer is manufactured. Particularly, the thermometer bulb must be made of a glass suitable for use in the temperature range for which the thermometer is graduated. In addition, the thermometer must be adequately annealed so that continued use will not greatly change its indications. This is especially important for a thermometer graduated above 300° C or 600° F. The quality of the thermometer glass and the adequacy of the annealing process may be judged in part by the stability of reference-point readings (such as ice points). To be eligible for certification, reference-point readings taken before and after test must not differ by more than the accuracy bounds stated for the particular type of thermometer in the applicable table in section 6.

All high-temperature thermometers should be filled with a dry inert gas under sufficient pressure to prevent separation of the mercury at any temperature for which the scale is graduated. Total-immersion thermometers graduated above 150° C or 300° F must be gas filled to minimize the distillation of mercury from the top of the column. Gas filling for lower temperatures is optional, but is strongly recommended.

5.2. Scale Design and Workmanship

Thermometers of the plain-stem type shall have the graduation marks etched directly on the stem and so located as to be opposite the enamel back. In thermometers of the enclosed-scale (Einschluss) type, the graduated scale must be securely fastened to prevent relative displacement between scale and capillary—for example, by fusing the scale to the enclosing tube—or if this is not done, a mark should be placed on the outer tube to locate the scale and indicate at any time whether the scale is in its original position. The graduation marks shall be clear cut, straight, of uniform width, and in a plane perpendicular to the axis of the thermometer. The spacing of the gradua-

NBS186C
(Rev. 11-1-56)

UNITED STATES DEPARTMENT OF COMMERCE
NATIONAL BUREAU OF STANDARDS
WASHINGTON 25, D. C.

National Bureau of Standards

Certificate

Liquid-in-Glass Thermometer

Tested for
National Bureau of Standards
Division 3, Section 1

Marked
Surety 1495

Range
-5° to +105°C in 0.2°

Thermometer Reading	Correction
- 0.02°C	+0.02°C
20.00	+ .02
40.00	- .02
60.00	+ .02
80.00	+ .04
100.00	+ .06

If the correction is + the true temperature is higher than the indicated temperature; if the correction is — the true temperature is lower than the indicated temperature. To use the corrections properly, reference should be made to the notes marked by asterisks on the reverse side of this sheet.

For the Director

Geneva Williams

Geneva Williams, Physicist
Thermometry Laboratory
Heat Division

Test No. G-25060
Completed: April 9, 1958
JST:dh

FIGURE 1. *Facsimile of face of a thermometer certificate.*

NOTES

✳ NOTE A.—The tabulated corrections apply for the condition of total immersion of the bulb and liquid column. If the thermometer is used at partial immersion, apply an emergent stem correction as explained in the accompanying stem correction sheet.

NOTE B.—The tabulated corrections apply for the condition of total immersion of the bulb and liquid column. Although this thermometer is not ordinarily used in this way, no significant errors should be introduced by neglecting the corrections for emergent stem.

NOTE C.—The thermometer was tested in a large, closed-top, electrically heated, liquid bath at an immersion of . The temperature of the room was about 25° C (77° F). If the thermometer is used under conditions which would cause the average temperature of the emergent liquid column to differ markedly from that prevailing in the test, appreciable differences in the indications of the thermometer would result.

NOTE D.—The tabulated corrections apply provided the ice-point reading is . If the ice-point reading is found to be higher (or lower) than stated, all other readings will be higher (or lower) by the same amount.

✳ NOTE E.—The tabulated corrections apply provided the ice-point reading, taken after exposure for not less than 3 days to a temperature of about 25° C (77° F) is −0.02°C . If the ice-point reading is found to be higher (or lower) than stated, all other readings will be higher (or lower) by the same amount. If the thermometer is used at a given temperature shortly after being heated to a higher temperature, an error of 0.01° or less, for each 10° difference between the two temperatures, may be introduced. The tabulated corrections apply if the thermometer is used in its upright position; if used in a horizontal position, the indications may be a few hundredths of a degree higher.

NOTE F.—The tabulated corrections apply provided the reading when the thermometer is immersed in steam at 100° C (212° F) is If the reading is found to be higher (or lower) than stated, all other readings will be higher (or lower) by the same amount. The temperature of steam is 100° C (212° F) only if the pressure is 760 mm (29.921 inches). If the pressure differs from 760 mm (29.921 inches) allowance must be made for this. If the pressure is higher (or lower) than 760 mm (29.921 inches) the temperature will be higher (or lower) than 100° C (212° F) by approximately 0.037° C per mm difference (1.68° F per inch difference).

NOTE G.—The thermometer, before testing, was heated to the temperature of the highest test point. The application of the tabular corrections to the readings of the thermometer will give true temperature differences provided the thermometer is used in its upright position and is heated previously (within an hour before using) to the highest temperature to be measured.

NOTE H.—The thermometer was tested for use in differential measurements, such as the measurement of temperature differences in a flow calorimeter. The two thermometers used in a flow calorimeter should be compared occasionally in stirred water at some convenient temperature and if their indications, after application of the tabular corrections, are found to differ, an additional correction equal to the difference, should be applied to the indications of one of them.

NOTE I.—The tabulated corrections apply for a "setting" of 20° C. Setting factors for use with other settings are given on the accompanying sheet.

NOTE J.—The tabulated corrections apply for the condition of immersion indicated provided the ice-point reading, taken after heating to for not less than 3 minutes, is If the ice-point reading, which should be taken within 5 minutes after removal of the thermometer from the heated bath, is found to be higher (or lower) than stated all other readings will be higher (or lower) by the same amount.

FIGURE 2. *Facsimile of back of a thermometer certificate.*

tions shall be free from significant irregularities which would produce uncertainties in the indications by amounts exceeding the limits otherwise set for the type of thermometer.

The scale shall be graduated either in 1.0-, 0.5-, 0.2-, or 0.1-degree intervals, or in decimal multiples or submultiples of such intervals. Thermometers with scales graduated in 0.25-degree intervals, or in 0.25-degree intervals further subdivided, have occasionally been submitted for test. Such thermometers are sometimes difficult to read and their elimination is desirable. The divisions shall be numbered in such a way that the identification of any graduation is not unnecessarily difficult. Thermometers graduated in 0.1- or 0.2-degree intervals, or decimal multiples or submultiples of these, should have every fifth mark longer than the intermediate ones and should be numbered at every tenth mark. Thermometers graduated in 0.5-degree intervals, or in decimal multiples or submultiples of 0.5 degree, require three lengths of graduation marks consisting of alternating short and intermediate marks, with every tenth mark distinctly longer than the others, and numbering at every 10th or 20th mark.

The range of scale must not be extended to temperatures for which the particular thermometer glass is unsuited. An example would be that of a thermometer of borosilicate glass graduated to 1,000° F; an attempt to use the instrument at that temperature would ruin it in a short time.

5.3. Dimensional Requirements of Scale

Excessively coarse graduation marks do not represent good design. The optimum line width, however, will depend in some measure upon the use for which a particular thermometer is intended. If the thermometer indications are to be observed precisely, for example to 0.1 division, the width of the graduation marks in the extreme case should not be more than 0.2 of the interval between center lines of the graduations. In cases where the thermometer must be read quickly or in poor light, and less precision is expected, somewhat wider lines may be acceptable.

In addition, the graduation marks must not be too closely spaced. The closest permissible spacing will depend upon the fineness and clearness of the marks. In no case, however, shall the distance between center lines of adjacent graduation marks on an etched-stem thermometer be less than 0.4 mm. The minimum permissible interval between graduation marks for an enclosed-scale thermometer is 0.3 mm if the lines are ruled on a milk-glass scale; for other scales the minimum is 0.4 mm. The minimum in no case represents good design, and well-designed thermometers will have graduation intervals considerably larger than the specified minimum.

In order that a thermometer scale be usable over its entire range, graduation marks must not be placed too close to any enlargement in the capillary. Insufficient immersion of the mercury in the main bulb or a capillary enlargement, graduation marks placed over parts of the capillary that have been changed by manufacturing operations, or graduations so close to the top of the thermometer that excessive gas pressure results when the mercury is raised to this level, may lead to appreciable errors. The following distances between graduations and the bulb and between graduations and enlargements in the bore are considered as minimum limits for thermometers acceptable for certification:

(a) A 13-mm length of unchanged capillary between the bulb and the lowest graduation, if the graduation is not above 100° C (212° F); a 30-mm length if the graduation is above 100° C (212° F).

(b) A 5-mm length of unchanged capillary between an enlargement and the graduation next below, except at the top of the thermometer.

(c) A 10-mm length of unchanged capillary between an enlargement, other than the bulb, and the graduation next above, if the graduation is not above 100° C (212° F); a 30-mm length if the graduation is above 100° C (212° F).

(d) A 10-mm length of unchanged capillary above the highest graduation, if there is an expansion chamber at the top of the thermometer; a 30-mm length if there is no expansion chamber. For the purposes of this requirement, "an expansion chamber" is interpreted as an enlargement at the top end of the capillary bore which shall have a capacity equivalent to not less than 20 mm of unchanged capillary.

5.4. Reference Point on Scale

To be acceptable for certification, thermometers graduated above 150° C or 300° F, or precision thermometers to be certified to an accuracy better than 0.1° C or 0.2° F, when calibrated for the measurement of actual temperatures rather than temperature differences, must have a reference point at which the thermometer can be conveniently retested from time to time. From these reference-point tests, the effects of changes in bulb volume on the thermometer indications may be followed throughout the life of the thermometer, and the proper corrections applied at any time. If no suitable reference point such as the ice or steam point is included in the range of the main scale, a short auxiliary scale including a fixed point shall be provided. To avoid making the thermometer unduly long, an enlargement in the capillary may be introduced between the auxiliary scale and the main scale. The graduations on an auxiliary scale must extend for a short interval both above and below the reference point. Similarly, when the main scale ends near a temperature to be used as a reference point, the graduations must be continued for a short interval above or below the reference point as the case may be.

Any auxiliary scale must have graduations identical to those of the main scale, both dimensionally and in terms of temperature.

Reference points are not required on thermometers certified for differential measurements (calorimetric, gas calorimetric, etc.), nor on thermometers not graduated above 150° C or 300° F, if these are not to be certified to an accuracy better than 0.1° C or 0.2° F.

5.5. Marking of Partial-Immersion Thermometers

Partial-immersion thermometers will not be certified unless plainly marked "partial immersion", or its equivalent (for example, "76-mm immersion"), and unless a conspicuous line is engraved on the stem to indicate the depth to which the thermometer is to be immersed. This mark must not in any case be less than 13 mm above the top of the bulb. Special partial-immersion thermometers adapted to instruments which fix definitely the manner of use (for example, viscometers and flash-point testers in which the thermometer is held in a ferrule or other mounting fitting the instrument) need not be marked, although even in these cases it is desirable that the thermometers be marked "partial immersion".

6. Common Types of Thermometers and Factors Affecting Their Use

In this section the more common types of high-grade thermometers are mentioned briefly with a discussion of some of the factors affecting their use.

Tolerances allowed by the Bureau in issuing certificates are given in the tables for individual types of thermometers. The values of these tolerances are the same as those given in the fourth edition of Circular 8 (1926). The accuracy bounds shown in the tables may seem broad in some instances, but the definite limitations of liquid-in-glass thermometry become apparent when all factors are considered. For example, if one keeps expanding the scale for more precise reading by reducing the capillary-bore diameter, a practical limit is reached beyond which capillary forces will prevent a smooth advance or retreat of the mercury column. Particularly with a slowly falling temperature, the movement of the mercury meniscus may be found to occur erratically in steps appreciably large in comparison to the graduation interval. If the mercury and glass are clean, no significant sticking of the mercury column should occur if the diameter of the bore of circular cross section is at least 0.1 mm. Excessively elliptical or flattened bores are not recommended. It is evident from the above that increasing the length of a degree on the scale, for practical bulb sizes, improves thermometric performance to a certain point only, beyond which the precision of reading may readily be mistaken for accuracy in temperature measurement.

In addition, other factors such as ice-point changes, unless exactly accounted for, and differences in external pressure may account for inaccuracies much greater than the imprecision with which a scale having 0.1- or 0.2-degree graduations may be read.

6.1. Total-Immersion Thermometers

Thermometers pointed and graduated by the manufacturer to read correct, or nearly correct, temperatures when the bulb and entire liquid index in the stem are exposed to the temperature to be measured are known as "total-immersion" thermometers. While these thermometers are designed for complete immersion of all the mercury, it is not necessary, and in some cases not desirable, that the portion of the stem above the meniscus be immersed. The heating of this portion to high temperatures might cause excessive gas pressures resulting in erroneous readings if not permanent damage to the bulb.

In practice a short length of the mercury column often must be left emergent from the bath (or region) so that the meniscus will be visible when the temperature is being measured. If a large enough temperature difference exists between the bath and its surroundings, an appreciable temperature gradient may be found in the thermometer stem near the surface of the bath for which a correction to the thermometer reading may be required. The condition becomes more serious when a thermometer designed and calibrated for total immersion is intentionally used at partial immersion, that is with a significant portion of the liquid column at a temperature different from that of the bath. The reading will be too low or too high depending upon whether the surrounding temperature is lower or higher than that of the bath. For a total-immersion thermometer so used, an emergent stem correction must be determined and applied in addition to the calibration corrections. The correction may be as large as 20 Celsius degrees (36 Fahrenheit degrees) if the length of emergent liquid column and the difference in temperature between the bath and the space above it are large.

A method for determining this correction is given in section 10.2.

The scale tolerances allowed in awarding certificates to total-immersion thermometers are given in tables 1 and 2. These tolerances are based on the fact that in the manufacture of thermometers certain small errors in pointing and graduation are inevitable, and also that the indications of thermometers are subject to variations due to the inherent properties of the glass. The tolerances must be sufficiently rigid to insure to the user a satisfactory high-grade thermometer and at the same time must not be so rigid as to cause undue manufacturing difficulties.

TABLE 1. *Tolerances for Celsius total-immersion mercury thermometers*

Temperature range in degrees	Graduation interval in degrees	Tolerance in degrees	Accuracy in degrees	Corrections stated to
Thermometers not graduated above 150° C				
°C				
0 up to 150	1.0 or 0.5	0.5	0.1 to 0.2	0.1
0 up to 150	.2	.4	.02 to .05	.02
0 up to 100	.1	.3	.01 to .03	.01
Thermometers not graduated above 300° C				
0 up to 100	1.0 or 0.5	0.5	0.1 to 0.2	0.1
Above 100 up to 300		1.0	.2 to .3	.1
0 up to 100	.2	0.4	.02 to .05	.02
Above 100 up to 200		.5	.05 to .1	.02
Thermometers graduated above 300° C				
0 up to 300	2.0	2.0	0.2 to 0.5	0.2
Above 300 up to 500		4.0	.5 to 1.	.2
0 up to 300	1.0 or 0.5	2.0	.1 to 0.5	.1
Above 300 up to 500		4.0	.2 to .5	.1

TABLE 2. *Tolerances for Fahrenheit total immersion mercury thermometers*

Temperature range in degrees	Graduation interval in degrees	Tolerance in degrees	Accuracy in degrees	Corrections stated to
Thermometers not graduated above 300° F				
32 up to 300	2 0	1.0	0.2 to 0.5	0.2
32 up to 300	1.0 or 0.5	1.0	.1 to .2	.1
32 up to 212	.2 or .1	0.5	.02 to .05	.02
Thermometers not graduated above 600° F				
32 up to 212	2 or 1	1.0	0.2 to 0.5	0.2
Above 212 up to 600		2.0	.5	.2
Thermometers graduated above 600° F				
32 up to 600	5	4.0	0.5 to 1.0	0.5
Above 600 up to 950		7.0	1. to 2.0	.5
32 up to 600	2 or 1	3.0	0.2 to 1.0	.2
Above 600 up to 950		6.0	.5 to 1.0	.2

In addition to the requirements shown in the tables, the error in any temperature interval must not exceed 5 percent of the nominal value of the interval. The intent of this requirement is to eliminate thermometers having large corrections of alternating signs.

Tables 1 and 2 also give suitable values for the subdivisions, the accuracy which may be expected, and the decimal figure to which the calibration corrections are stated for thermometers that have the ranges shown. The word "accuracy" used in these tables refers to the best values attainable in the use of the thermometer when all corrections are applied. The final columns state the magnitudes to which the corrections are given for thermometers calibrated by the Bureau. They are stated to somewhat higher accuracy than can be attained with certainty in calibrating the thermometers. This is done because it is preferable to give the corrections as found, since the results actually obtained are the best that can be deduced for the tests, and any rounding off might introduce an additional uncertainty.

6.2. Partial-Immersion Thermometers

In many instances it is required to measure temperatures under conditions where it is inconvenient or impossible to use a liquid-in-glass thermometer at total immersion. For such uses partial-immersion thermometers are designed with scales graduated to indicate true temperatures when the thermometers are immersed to specified depths. No stem temperature correction is necessary, therefore, when these thermometers are used with the same depth of immersion and emergent-stem temperature for which they are calibrated. Unless otherwise stated, each certificate of calibration issued by the Bureau gives corrections that apply for the temperatures prevailing above the comparison baths. When such a thermometer is to be used with a different stem temperature, the necessary emergent stem correction may be calculated as shown in section 10.3.

The accuracy attained with this type of thermometer will usually be significantly less than that possible with total-immersion thermometers. This is particularly the case when partial-immersion thermometers are used with stem temperatures greatly different than the temperature being measured. An unsteady or irreproducible environment surrounding the emergent stem, together with the inherent difficulty of estimating or measuring the emergent-stem temperature with sufficient accuracy, can contribute markedly to the uncertainty of a given thermometer indication. For this reason tables 3 and 4 show that accuracies expected of partial-immersion thermometers are not so high as those for total-immersion thermometers nor are the calibration corrections stated so closely.

TABLE 3. *Tolerances for Celsius partial-immersion mercury thermometers*

Temperature range in degrees	Graduation interval in degrees	Tolerance in degrees	Accuracy[a] in degrees	Corrections stated to
Thermometers not graduated above 150° C				
0 up to 150	1.0 or 0.5	1.0	0.1 to 0.5	0.1
Thermometers not graduated above 300° C				
0 up to 100	1.0	1.0	0.1 to 0.3	0.1
Above 100 up to 300	1.0	1.5	.5 to 1.0	.2
Thermometers graduated above 300° C				
0 up to 300	2.0 or 1.0	2.5	0.5 to 1.0	0.5
Above 300 up to 500		5.0	1.0 to 2.0	.5

[a] The accuracies shown are attainable only if emergent stem temperatures are closely known and accounted for.

TABLE 4. *Tolerances for Fahrenheit partial-immersion mercury thermometers*

Temperature range in degrees	Graduation interval in degrees	Tolerance in degrees	Accuracy in degrees	Corrections stated to
Thermometers not graduated above 300° F				
32 up to 300	2.0 or 1.0	2.0	0.2 to 1.0	0.2
Thermometers not graduated above 600° F				
32 up to 212	2.0 or 1.0	2.0	0.2 to 0.5	0.2
Above 212 up to 600	2.0 or 1.0	3.0	1.0 to 2.0	.5
Thermometers graduated above 600° F				
32 up to 600	5.0 or 2.0	5.0	1.0 to 2.0	1.0
Above 600 up to 950	5.0 or 2.0	10.0	2.0 to 3.0	1.0

6.3. Low-Temperature Thermometers

The lowest temperature to which a mercury-filled thermometer can be used is limited by the freezing point of mercury at about −38.9° C (−38.0° F). This limit may be extended to considerably lower temperatures, however, by alloying thallium with the mercury. The eutectic alloy of 8.5 percent of thallium by weight has a freezing point of −59° C and is used successfully in thermometers for temperatures down to about −56° C. The freezing temperature of the alloy is critically affected in the neighborhood of the eutectic by the amount of thallium present. Small differences in composition, resulting in either too much or too little thallium, have the effect of markedly raising the freezing point of the alloy. It is therefore somewhat difficult to achieve the lowest freezing temperature in practice. In addition, some thermometers with this filling have been found to behave erratically in the range of about two degrees above the freezing point. For these reasons thermometers of this type probably should not be used below −56° C (−68.8° F).

Other low-temperature thermometers are commonly filled with organic liquids. While not considered to be as reliable as mercury-thallium-filled thermometers, they serve to extend the range below −56° C. Some of these liquids are used as low as −200° C (−328° F).

Alcohol, toluene, and pentane have all been used as fluids for low-temperature thermometers. All of these fluids, however, have limitations of one kind or another, but their performance can be improved for some uses by admixing other liquids. Other organic liquids, alone or in mixtures, have been found by some manufacturers to show better characteristics for particular applications.

All of these organic liquids have the disadvantage of wetting the bore of the thermometer tubing which may lead to significant error in the indications of such thermometers if sufficient precautions are not taken. Any liquid that wets the tube will leave a film on the wall as the meniscus falls, the thickness of the film being dependent among other things on the viscosity of the liquid, the interfacial action between the liquid and glass, and the rate at which the thermometer is cooled. Where possible the rate of cooling should be slow with the bulb cooled first. In this way the viscosity of the part of the filling fluid in the thermometer bore is kept as low as possible until the final temperature is reached, thus minimizing the amount of liquid left behind on the wall. Even so, sufficient time should be allowed for drainage from the wall to be essentially completed. Under adverse conditions it may take a very long time, an hour or more, before the effect of drainage is no longer noticeable.

In addition to having good drainage characteristics, a satisfactory low-temperature fluid should be free of water, dirt, or other foreign material which will crystallize or otherwise separate out at temperatures for which the thermometer is graduated. Furthermore, low-temperature thermometers are frequently designed for use up to room temperature or above. In these cases the vapor

TABLE 5. *Tolerances for low-temperature total-immersion thermometers*

Temperature range in degrees	Type of thermometer	Graduation interval in degrees	Tolerance in degrees	Accuracy in degrees	Corrections stated to
Celsius thermometers					
−35 to 0	Mercury	1 or 0.5	0.5	0.1 to 0.2	0.1
−35 to 0	do	.2	.4	.02 to .05	.02
−56 to 0	Mercury-thallium.	.5	.5	.1 to .2	.1
−56 to 0	do	.2	.4	.02 to .05	.02
−200 to 0	Organic liquid.	1.0	.2	.2 to .5	.1
Fahrenheit thermometers					
−35 to 32	Mercury	1 or 0.5	1.0	0.1 to 0.2	0.1
−35 to 32	do	.2	0.5	.05	.02
−69 to 32	Mercury-thallium.	1 or .5	1.0	.1 to .2	.1
−69 to 32	do	.2	0.5	.05	.02
−328 to 32	Organic liquid.	2 or 1.0	3.0	.3 to .5	.2

TABLE 6. *Tolerances for low-temperature partial-immersion thermometers*

Temperature range in degrees	Type of thermometer	Graduation interval in degrees	Tolerance in degrees	Accuracy in degrees	Corrections stated to
Celsius thermometers					
−35 to 0	Mercury	1.0 or 0.5	0.5	0.2 to 0.3	0.1
−56 to 0	Mercury-thallium.	1.0 or .5	.5	.2 to .3	.1
−90 to 0	Organic liquid.	1.0	3.0	.4 to 1.0	.2
Fahrenheit thermometers					
−35 to 32	Mercury	1.0 or 0.5	1	0.3 to 0.5	0.1
−69 to 32	Mercury-thallium.	1.0 or .5	1	.3 to .5	.1
−130 to 32	Organic liquid.	2 or 1	5	.8 to 2.0	.5

pressure of the filling liquid becomes important. A low vapor pressure is necessary to prevent distillation of the liquid at the higher temperatures. Any dye added to improve the visibility of the thermometer liquid should be chosen for good color fastness with respect to light exposure or chemical action with the thermometer liquid.

Tolerances applicable to low-temperature thermometers are given in tables 5 and 6.

6.4. Beckmann Thermometers

A metastatic or Beckmann thermometer is usually of the enclosed-scale type, so constructed that portions of the mercury may be removed from, or added to, the bulb permitting the same thermometer to be used for differential measurements in various different temperature ranges. The scales are kept short, usually 0 degree to 5 or 6 degrees C, although some so-called micro types have a scale of only about 3 degrees C. The "setting" of such a thermometer refers to the temperature of the bulb when the reading is 0° on the scale. When the setting is changed to allow for use at a higher or lower temperature, the quantity of mercury affected by a temperature change is different. It follows that two equal changes in temperature at different settings cause different indications on the scale. Therefore a "setting factor" must always be used to convert reading differences into true temperature differences whenever the thermometer is used at any setting different from the one at which its scale was calibrated. These setting factors combine corrections for the different changes in volume of different quantities of mercury during equal temperature changes, and the difference between the mercury-in-glass scale and the International Temperature Scale.

Table 7 lists setting factors calculated for thermometers of Jena 16^{III} glass, or its American equivalent, Corning normal. The scale calibrations for Beckmann thermometers as reported by the Bureau are applicable to a setting of 20° C, and the factor is consequently 1.0000 at this temperature. For a setting of any other temperature the observed temperature difference must be multiplied by the appropriate factor from the table. An illustrative example is given below the table.

In a common design of the Beckmann thermometer the large bulb is joined to the fine capillary, backed by the milk-glass scale, by a capillary of much larger diameter. When such an instrument is used at partial immersion this large capillary is a source of some uncertainty, since the temperature of this relatively large quantity of mercury, enclosed in the glass case, cannot be actually measured. When an estimate can be made of the temperature of the emergent stem, however, a correction may be calculated as described in section 10.5.

Tolerance requirements for the certification of Beckmann thermometers are given in table 8.

Table 7. *Setting factors for Beckmann thermometers*

Setting	Factor	Setting	Factor
°C.		°C.	
0	0.9934	55	1.0096
5	.9952	60	1.0107
10	.9969	65	1.0118
15	.9985	70	1.0129
20	1.0000	75	1.0139
25	1.0015	80	1.0148
30	1.0030	85	1.0157
35	1.0044	90	1.0165
40	1.0058	95	1.0172
45	1.0071	100	1.0179
50	1.0084		

As an illustration, suppose the following observations were made:

Setting = 25° C. Lower reading = 2.058°
Stem temperature = 24° Upper reading = 5.127°

	Lower	*Upper*
Observed reading =	2.058	5.127
Correction from certificate =	+0.005	−0.008
Corrected upper reading =		5.119
Corrected lower reading =		2.063
Difference =		3.056
Difference multiplied by setting factor (1.0015) =		3.061
Emergent stem correction (see accompanying stem correction sheet) =		+.004
Corrected difference =		3.065

Under the heading "Accuracy of interval in degrees" is given the estimated accuracy attainable in the measurement of any interval within the limits of the scale.

No tolerances for scale error are given although it is desirable that the scale error be small.

Table 8. *Tolerances for Beckmann and calorimeter thermometers*

Type of thermometer	Graduation interval in degrees	Allowable change in correction in degrees	Accuracy of interval in degrees	Corrections stated to
Beckmann	0.01° C	0.02 over a 1° interval for setting of 20° C.	0.002 to 0.005	0.001
Bomb calorimeter.	.01° C	0.03 over a 2° interval.	.005 to .01	.002
Do	.02° C	0.03 over a 2° interval.	.005 to .01	.002
Do	.05° F	0.08 over a 5° interval.	.01 to .02	.005
Gas calorimeter.	.1° F	0.15 over a 5° interval.	.02 to .05	.02

6.5. Calorimeter Thermometers

Calorimeter thermometers include a specialized group of etched-stem mercury-in-glass thermometers which are used for accurate differential measurements. Since, in the use of these thermometers, the accuracy at any one temperature is of less importance than the accuracy of the temperature intervals, no reference point is required for certification.

Table 8 gives the scale tolerances required of some typical calorimeter thermometers. No tolerances for scale error are given although it is desirable that the scale corrections be small.

6.6. Clinical Thermometers

Clinical, or medical, thermometers are small maximum-reading thermometers used in measuring body temperatures. In this country they are usually graduated in degrees Fahrenheit, and the range covers about 10 to 16 degrees Fahrenheit, from at least 96° to 106° F. When graduations are in degrees Celsius, the range usually covers 6 to 9 degrees Celsius, from at least 35° to 41° C. The bulb, made of a suitable grade of thermometer glass, has the least volume, that is, the least heat capacity consistent with a reasonably steady motion of the mercury along the very fine capillary of the lens front tubing. A constriction above the bulb formed by collapsing a bubble blown in the capillary permits the expanding mercury to pass when the bulb is being warmed, but is "tight" enough to prevent the retreat of the mercury after the warming ceases. At the same time, the constriction must be "loose" enough so that the mercury can be shaken down by hand or by whirling in a suitable centrifuge.

In order to accurately indicate the temperature of the body, the thermometer must be left in place for a time sufficiently long for all the mercury to reach the body temperature. For most thermometers this requires 3 min or more.

Clinical thermometers submitted to the Bureau are usually tested for compliance with Commercial Standard CS1–52. Thermometers meeting the requirements of this specification are marked NBS followed by a two-digit number indicating the year in which the test was made. A note explaining the certification is issued with each thermometer certified.

7. Number and Choice of Test Points

In calibrating a thermometer, corrections to its indications must be determined at a number of test points sufficient to give reasonable assurance that the corrections between test points can be reliably obtained by interpolation. In general, if the readings of a thermometer are to to be trusted to one- or two-tenths of the smallest scale division, the interval between test points should not exceed 100 divisions and usually need not be less than 40. If, for example, a thermometer is graduated in 0.1° intervals, and the correction at 20° is +0.07° and at 25° it is +0.12°, the correction at 22° may be taken as +0.09° with considerable confidence as to its correctness. If interpolation between test points from 40 to 100 divisions apart on any particular thermometer are considered untrustworthy, it is better to discard the thermometer and obtain one which is worthy of confidence.

Occasionally requests are received for tests of thermometers graduated in 1- or 2-degree intervals at a series of points only 1 or 2 degrees apart. In general such requests are declined, since the extra work involved would not improve the accuracy of the calibration. In another case, a request may call for test at only two points on a long scale. If the thermometer is to be used only at or near these points, such a test may serve the purpose satisfactorily, but a report instead of a certificate will be issued if the number of test points is insufficient to justify the use of the entire scale of the thermometer. In no case will a thermometer be tested at less than two points on the main scale nor will test of at least one reference point be omitted when such a point (or points) is included in the scale.

In general, when a thermometer is to be tested without reference to any special use, the choice of test points may well be left to the testing laboratory. If the thermometer is to be used for a special purpose, a knowledge of the use for which it is intended will be useful to the laboratory in choosing test points. The Bureau does not, however, undertake to make tests at more points than in its judgment are necessary, although due consideration will be given special requests. In some cases the proper number and distribution of test points can be decided only after a careful inspection of the thermometer, and occasionally only after the test has been partly completed.

For some special types of thermometers, set procedures have been established with regard to choice of test points. For example, Beckmann thermometers with scales 3 to 6° C long are calibrated every degree and calorimetric thermometers are calibrated every 2° C or 2.5° F.

8. General Calibration Procedures

At the Bureau all liquid-in-glass thermometers are calibrated in terms of the International Temperature Scale as defined by the indications of the standard platinum resistance thermometer. Indications of the thermometer under test may be compared directly with a resistance thermometer, or indirectly through the use of a mercury-in-glass standard, as the situation dictates. Through considerations of accuracy, direct comparisons are made with Beckmann thermometers, calorimeter thermometers, and thermometers graduated in tenths of a degree Fahrenheit. Below 0° C, all calibrations are made directly both for convenience and accuracy. Above 316° C (600° F), the platinum thermometer is used because of its greater stability. All other calibrations are generally made against mercury-in-glass standards (listed in section 2) which have been calibrated directly with a standard resistance thermometer.

When comparing thermometers with liquid-in-glass standards two standards are always used. In this way reading errors are more readily

detected and cross checks of the standards are maintained. The comparison procedures are described in simplified form in the following hypothetical test of four thermometers (T1 through T4) which are assumed to have been found free of gross defects such as are discussed in section 5.

Table 9 shows the observations taken in obtaining the corrections applicable to the thermometers at 20°. To simplify the illustration, all of the entries in the table assume perfect thermometer performance and no observer error.

TABLE 9. *Comparison of test thermometers with liquid-in-glass standards*

	S1	T1	T2	T3	T4	S2
Ice-point readings of test thermometers						
Observer A	-----	+0.02	−0.02	+0.02	0.00	------
Observer B	-----	+.02	−.02	+.02	0.00	------
Mean ice points	-----	+.02	−.02	+.02	.00	------
Thermometer comparisons						
Observer A reading left to right	19.87	19.98	19.96	20.02	20.03	19.89
Observer A reading right to left	19.88	19.99	19.97	20.03	20.04	19.89
Observer B reading left to right	19.88	19.99	19.97	20.04	20.05	19.90
Observer B reading right to left	19.89	20.00	19.98	20.04	20.05	19.90
Means	19.88	19.99	19.97	20.03	20.04	19.89_5
Ice-point readings of standards						
Observer A	−0.01	-----	-----	-----	-----	−0.08
Observer B	−.01	-----	-----	-----	-----	−.08
Mean ice points	−.01	-----	-----	-----	-----	−.08
Calculations of corrections						
Correction to standards	+0.12	-----	-----	-----	-----	+0.04
Mean temperature, each standard	20.01	-----	-----	-----	-----	20.01_5
Mean temperature of all readings	-----	-----	20.01	-----	-----	-----
Corrections to test thermometers	-----	+0.02	+0.04	−0.02	−0.03	-----

The first observations are the ice points of the thermometers under test. These are entered in the upper part of the table. The thermometers are then mounted in the comparison bath between the two standards, and the power to the bath is so adjusted that its temperature is slowly increasing at a steady rate. The data shown in the table are for a temperature rise of 0.001° between each observation. Two observers (A and B) are used, first with one observer reading and the other recording, and next with the observers interchanged. Observer A reads in the order left to right as the thermometers appear in the table and then repeats the observations in the order right to left. Observer B then immediately reads in the same manner. The observations are spaced uniformly in time so that with the bath temperature increasing steadily with time, the mean of the observations with any one thermometer will correspond to the mean temperature of the comparison bath during the observations of all of the thermometers. Immediately after the comparison observations ice points are taken of the two standards. Using these ice-point data together with the known scale corrections for the standards, the temperatures indicated by the standards are calculated and an over-all mean temperature for the observations is obtained. This over-all mean temperature is compared with the mean of the observations with a particular thermometer to obtain a correction to the scale of the thermometer at this point. The thermometer comparisons are then repeated at the next higher test point and so on until corrections are obtained at a sufficient number of points to calibrate the complete scale, as specified in section 7.

Ice-point readings are not usually taken with each test point on the scale. For thermometers not graduated above 300° C or 600° F ice points taken before the first test point on the scale and after the last point will usually suffice. With high-temperature thermometers, however, it is the practice to take an ice point and then test immediately at the highest test point on the scale. After a rest period of 3 days at room temperature a second ice point is taken. If a change in ice point is found that is greater than the expected accuracy of the thermometer, the thermometer is deemed unsuitable for certification and further tests are unnecessary.

The corrections obtained in this manner apply as long as the ice point remains the same as that observed during calibration. Subsequent changes in the ice point will be a result of small changes in the glass which affect the volume of the thermometer bulb. The volume of the capillary stem also changes, but the volume of mercury contained in the stem is so small in comparison to that in the bulb that changes in the stem volume can usually be ignored. As a result, changes in the ice-point reading will be duplicated by similar changes in readings at each point along the scale. Thus, when during use the correction at the ice point is found to be higher (or lower) than that observed at the time of calibration, the other reported corrections to the scale can confidently be taken to be higher (or lower) by the same amount.

9. Testing Equipment

9.1. Ice Bath

Through the use of an ice bath, the ice point may be realized conveniently to better than 0.01° C. A thermos bottle or Dewar flask serves as a container for the ice, the melting of the ice being retarded by the insulating properties of such a vessel. Ice shaved from clear cakes and distilled water are mixed to form a slush. Enough water is used to afford good contact with the thermometers, but not so much as to float the ice. From time to time excess water is syphoned from the

bath. Precautions are taken to prevent contamination of the ice and water. A small reading telescope with a magnification of about 10 diameters aids in reading the thermometer indication and reduces errors due to parallax. Gently tapping the thermometer just before reading may prevent the sticking of a falling meniscus. On the other hand too vigorous a tap will occasionally cause the mercury to rebound to an erroneously high reading.

9.2. Steam Bath

The steam point may be realized in a steam-point apparatus or hypsometer either by comparing the thermometers with standards or by the determination of the temperature of the steam from a measurement of the prevailing atmospheric pressure.

The steam bath shown in figure 3, consists of a double-walled steam jacket in which steam from a boiler circulates. The thermometers are suspended in such a manner as to insure free circulation of steam around them. Provision is made for either relieving any excess pressure in the space surrounding the thermometers, or for determining the excess by means of a small differential manometer.

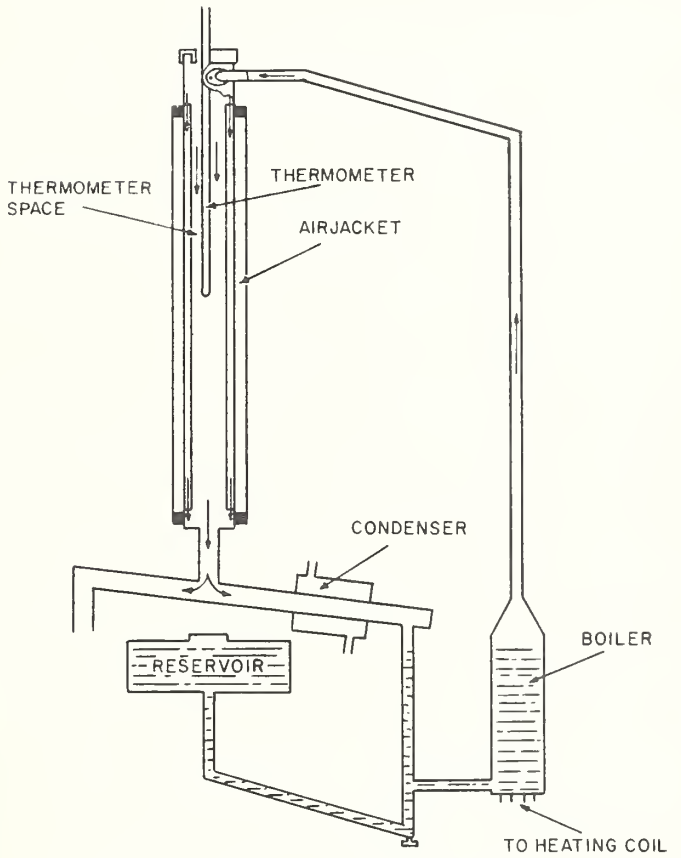

FIGURE 3. *Schematic drawing of steam bath.*

When the steam bath is used as a fixed-point apparatus a barometer is a necessary accessory since the true temperature of the steam is dependent upon the prevailing pressure. The usual corrections are applied to the barometer reading including any corrections necessary for the value of local acceleration of gravity, for the difference in height of the steam bath and the barometer, and for any excess pressure in the hypsometer. The steam temperature may then be found from the pressure-temperature values given in table 10, reproduced from a paper by Osborne and Meyers [2]. With a good barometer, accurate to 0.1 mm Hg, this procedure is capable of an accuracy of 0.002 to 0.003 degree C. The Fortin type barometer will usually serve for all but the most exacting measurements.

The steam bath is also used as comparison bath, in which case the temperature of the steam is determined at the time of test by means of a previously standardized thermometer. This method is simpler than determining the steam temperature from a barometer reading, and may be preferable, particularly when a resistance thermometer can be used as the standard.

9.3. Comparison Baths

Stirred liquid baths of two designs are used at the Bureau as comparators in which thermometers are calibrated in the range −40 to +500 degrees C. This equipment is of design appropriate to accommodate the thermometers to be tested, to permit stirring adequate for uniform temperature distribution, and to provide for controlled heat input for temperature regulation.

A type suitable for use with media which do not solidify at room temperature is shown in figure 4. This bath [3] is constructed with two tubes of different diameters having connecting passages at the top and bottom. The heating coil, cooling coil for circulating cold water for comparisons below room temperature, and stirrer are located in the smaller tube, the larger tube being left clear for immersion of the thermometers.

The type shown in figure 5 is designed for use at high temperatures with molten tin as the bath liquid. The bath is made with two coaxial tubes of which the inner tube is open at both ends. The stirring propeller is mounted near the bottom of the inner tube leaving the space above the propeller free to receive thermometers which are inserted in reentrant tubes. Heat is supplied by heater coils wound on the outside tube. As is also the case with the bath shown in figure 4, the thermometers are shielded from direct radiation from the hotter parts of the bath.

In both types of baths a 2- or 3-in. thickness of insulation reduces heat loss and thus aids in maintaining a uniform temperature distribution throughout the bath liquid. Each bath is provided with an insulated cover carrying a thermometer holder which can be rotated to bring

TABLE 10. *(Thermometric) condensation temperature of steam* [2]

[Star (*) indicates change in integer]

P	Pressure in mm mercury (standard)									
	0	1	2	3	4	5	6	7	8	9
	Temperature in degrees of International Scale									
500	88.678	0.730	0.782	0.834	0.886	0.938	0.990	*0.042	*0.093	*0.144
510	89.196	.247	.298	.350	.401	.452	.502	.553	.604	.655
520	0.705	.756	.806	.856	.907	.957	*.007	*.057	*.107	*.157
530	90.206	.256	.306	.355	.405	.454	.503	.553	.602	.651
540	0.700	.749	.798	.846	.895	.944	.992	*.041	*.089	*.138
550	91.186	.234	.282	.330	.378	.426	.474	.521	.569	.617
560	0.664	.712	.759	.806	.854	.901	.948	.995	*.042	*.089
570	92.136	.182	.229	.276	.322	.369	.415	.462	.508	.554
580	0.600	.646	.692	.738	.784	.830	.876	.922	.967	*.013
590	93.058	.104	.149	.195	.240	.285	.330	.375	.420	.465
600	0.5100	.5548	.5996	.6443	.6889	.7335	.7780	.8224	.8668	.9112
610	.9554	.9996	*.0438	*.0879	*.1319	*.1759	*.2198	*.2636	*.3074	*.3511
620	94.3948	.4384	.4820	.5255	.5689	.6123	.6556	.6989	.7421	.7852
630	0.8283	.8713	.9143	.9572	*.0001	*.0429	*.0857	*.1284	*.1710	*.2136
640	95.2562	.2987	.3411	.3834	.4257	.4680	.5102	.5523	.5944	.6365
650	95.6785	.7204	.7623	.8041	.8459	.8876	.9293	.9709	*.0125	*.0539
660	96.0954	.1368	.1782	.2195	.2607	.3019	.3431	.3842	.4252	.4662
670	0.5072	.5480	.5889	.6297	.6704	.7111	.7517	.7923	.8329	.8734
680	.9138	.9542	.9946	*.0349	*.0751	*.1153	*.1555	*.1956	*.2356	*.2756
690	97.3156	.3555	.3954	.4352	.4749	.5146	.5543	.5939	.6335	.6730
700	0.7125	.7519	.7913	.8307	.8700	.9092	.9484	.9876	*.0267	*.0657
710	98.1048	.1437	.1827	.2216	.2604	.2992	.3379	.3766	.4153	.4539
720	0.4925	.5310	.5695	.6079	.6463	.6846	.7229	.7612	.7994	.8376
730	.8757	.9138	.9519	.9899	*.0278	*.0657	*.1036	*.1414	*.1792	*.2170
740	99.2547	.2924	.3300	.3675	.4051	.4426	.4800	.5174	.5548	.5921
750	0.6294	.6667	.7039	.7410	.7781	.8152	.8523	.8893	.9262	.9631
760	100.0000	.0368	.0736	.1104	.1471	.1838	.2204	.2570	.2936	.3301
770	0.3666	.4030	.4394	.4758	.5121	.5484	.5846	.6208	.6570	.6932
780	.7293	.7653	.8013	.8373	.8733	.9092	.9450	.9808	*.0166	*.0524
790	101.0881	.1238	.1594	.1950	.2306	.2661	.3016	.3371	.3725	.4079

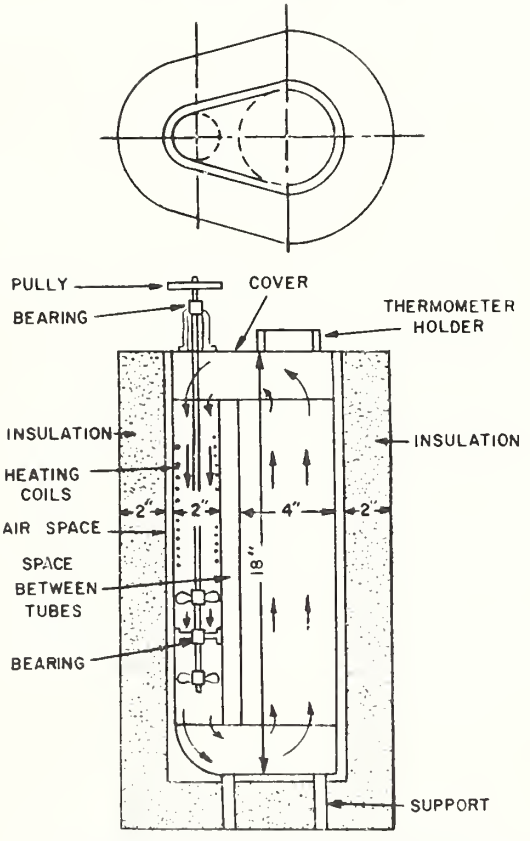

FIGURE 4. *Stirred bath for use with liquids which do not solidify at room temperature.*

successive thermometers into the field of a vertically adjustable reading telescope.

For calibrations in the range 5 to 99 degrees C, or 40 to 210 degrees F, water is used as the bath liquid. One grade of petroleum oil is used between 99° and 200° C and a second between 200° and 315° C. The oils are chosen with properties such that they are not too viscous for adequate stirring at the lower temperature and at the same time have flash points which are not exceeded at the higher temperatures. The tin bath is used from 315° C up to about 540° C.

Calibrations from 0° to −110° C are made in a cryostat similar in essentials to that described by Scott and Brickwedde [4]. The cryostat, shown in figure 6, consists of an inner Dewar flask, D, which contains the bath, surrounded by liquid nitrogen in the outer Dewar flask, C. The rate of heat transfer between the bath liquid and the liquid nitrogen is controlled by varying the gas pressure between the walls of the inner Dewar flask, which is connected to a vacuum system through the side tube, M. Vigorous stirring of the bath liquid is maintained by the propeller, I, which circulates liquid upwards through the inside of the stirrer tube, P, and down the outside. Excess refrigeration is compensated by thermostatically controlled heat supplied by the heater coil, J, wound outside the stirrer tube.

For temperatures down to −75° C, the bath liquid used is the eutectic mixture of carbon tetrachloride and chloroform (49.4 percent, by

weight, of CCl_4 and 50.6 percent of $CHCl_3$), which freezes at about −81° C. For temperatures between −75° and −110° C a five-component mixture is used containing 14.5 percent of chloroform, 25.3 percent of methyl chloride, 33.4 percent of ethyl bromide, 10.4 percent of transdichloroethylene, and 16.4 percent of trichloroethylene. This mixture freezes at about −150° C, but absorbs moisture readily and becomes cloudy at somewhat higher temperatures.

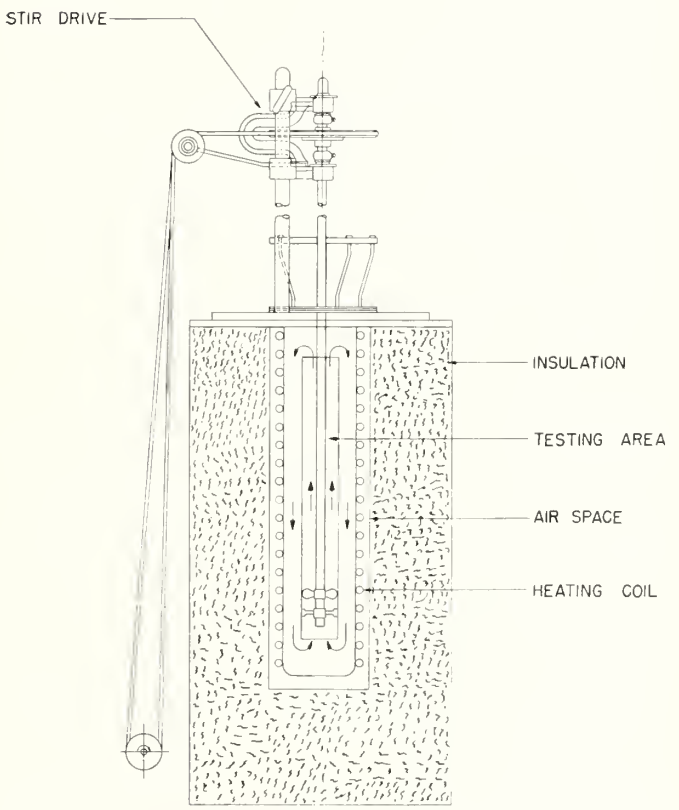

FIGURE 5. *Stirred bath suitable for use with liquids which do solidfy at room temperature.*

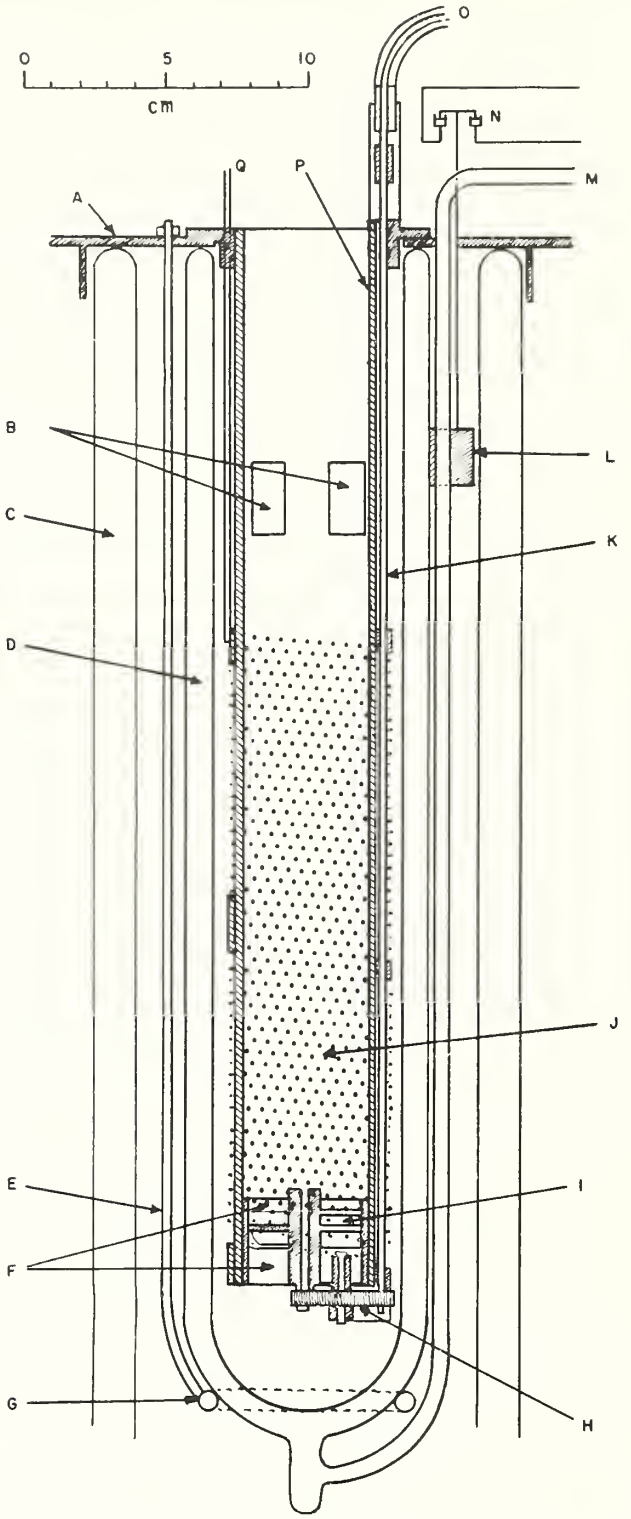

FIGURE 6. *Vertical section of cryostat.*

10. Corrections for Emergent Stem

The proper application of scale corrections as reported in NBS Certificates and Reports presents no difficulties in cases where thermometers are calibrated and used under conditions of total immersion. In such cases the temperature of the thermometer, including the stem up at least to the top of the mercury thread, is definitely specified and may be readily reproduced in use. Instances may occur in use, however, where some part of the mercury column is emergent from the region whose temperature is being measured. In these cases the emergent part of

574278 O - 61 - 12

the stem may be in an environment not only in which the temperature is markedly different from that of the thermometer bulb, but in which pronounced temperature gradients may be present. If such a situation exists in the use of a thermometer which has been calibrated at total immersion, a correction may be calculated to account for the difference in temperature between the bulb and the emergent stem. The calculation of this correction requires a reliable estimate of the mean temperature of the emergent stem, which, for the best work, will be made from measurements. But if the stem temperature measurements are not repeated each time the thermometer is used, the accuracy of the correction will depend upon the constancy of the stem temperature over periods of time. For example, if the emergent stem is exposed to the air above a liquid bath, variations in ambient temperature and air circulation will sometimes cause significant variations in the temperature of the emergent stem.

The same situation can occur in the case of partial-immersion thermometers. For this type of thermometer, the reported scale corrections apply only for the indicated depth of immersion and a particular stem temperature. If the thermometer is then used under conditions where the mean stem temperature is different, the reported scale corrections are not applicable, and a stem temperature correction is required.

In the following paragraphs methods for determining stem temperatures and formulas for calculating the corrections are given. For a given known or assumed condition, the use of these formulas will serve to indicate the importance of the stem correction in relation to a desired accuracy, and the corrections can then be applied as necessary.

10.1. Measurement of Emergent-Stem Temperature

The mean temperature of the emergent stem may be measured approximately by means of one or more small auxiliary thermometers suspended near the emergent stem, or more accurately by exposing an exactly similar stem and capillary mercury thread beside the emergent stem and thus measuring its mean temperature [5]. This is conveniently carried out with a faden thermometer ("thread thermometer") in which the expansion of the mercury in a capillary tube (bulb) is measured in a still finer capillary stem.

The methods used at NBS in calibration work are based upon the use of faden thermometers whenever possible. These thermometers have very long bulbs (5 to 20 cm) with wall thicknesses and bore sizes nearly the same as the stem of an ordinary thermometer. They are calibrated to read approximately true temperatures when immersed to the top of the bulb. If a faden thermometer is immersed beside a thermometer to be observed, to such a depth that the top of the faden thermometer bulb is at the same level as the top of the mercury column in the thermometer, the faden thermometer reading will give approximately the mean temperature of the adjacent portion of the thermometer stem and mercury thread. For example, a faden thermometer with a 10-cm bulb will give the mean temperature of the adjacent 10 cm of the thermometer stem. This method of using the faden thermometer is convenient for correcting the readings of a total-immersion thermometer when being used at partial immersion. If the stem temperature of a partial-immersion thermometer is to be measured, one or more faden thermometers are mounted so as to indicate the mean stem temperature between the immersion mark and the top of the mercury column.

In calculating the correction for the emergent stem, it is convenient to express the length of thermometer stem adjacent to the faden bulb in terms of degrees on the thermometer scale. Thus, for a 10-cm faden thermometer, the number of degrees corresponding to 10 cm must be found by measurement of a portion of the thermometer scale. This measurement should be made over the portion of the graduated scale which was adjacent to the faden bulb. This is particularly important with high-temperature thermometers where the length of a degree is generally not the same at all parts of the scale.

10.2. Formula for Total-Immersion Thermometers

When a thermometer, which has been graduated and calibrated for use at total immersion is actually used at partial immersion, the correction for the emergent stem may be calculated by the general formula,

$$\text{stem correction} = Kn(T-t),$$

where

K = differential expansion coefficient of mercury (or other thermometric liquid) in the particular kind of glass of which the thermometer is made,

n = number of thermometer scale degrees adjacent to the faden thermometer,

t = average temperature of n degrees of the thermometer stem (faden thermometer reading),

T = temperature of the thermometer bulb.

The coefficient K is different for different kinds of glass, and even for the same glass, it differs for different temperature intervals, i. e., different values of $(T-t)$. Since, however, most of the change results from the varying coefficient of the

mercury, the change in K with temperature for one glass may with some certainty be inferred from the change for another glass.

10.3. Formula for Partial-Immersion Thermometers

The scale corrections for partial-immersion thermometers calibrated at the Bureau are reported for the conditions of immersion to the depth of the immersion mark on the thermometer and unless otherwise requested, for the unspecified stem temperatures resulting from the particular environments prevailing over the comparison baths in the course of the calibration. Frequently, however, thermometers are submitted for calibration with a request for scale corrections which are applicable to a specified mean temperature of the emergent stem. In such cases the emergent stem temperatures are measured during the process of calibration. The calibration observations are then corrected as necessary to account for any differences found between the stem temperatures observed during test and the specified stem temperature for which the scale corrections are to apply. In this case, the magnitude of the stem correction is proportional to the difference between the specified and observed stem temperatures and may be calculated for Celsius mercurial thermometers by means of the relation,

$$\text{stem correction} = 0.00016n(t_{sp} - t_{obs}),$$

where

t_{sp} = specified mean temperature of emergent stem (for which reported scale corrections apply),

t_{obs} = observed mean temperature of emergent stem,

n = number of scale degrees equivalent to the length of emergent stem.

The above relation, of course, may also be used to correct the indications of a partial-immersion thermometer when used under stem-temperature conditions other than specified ones for which the scale corrections apply. In using the formula it should be noted that n applies to the whole length of emergent stem, i. e., from the immersion mark to the top of the mercury column. The ungraduated length between the immersion mark and the first graduation on the scale must therefore be evaluated in terms of scale degrees and included in the value of n.

For purposes of computing the emergent-stem correction, the value of K may be considered as depending on the average of T and t, that is $(T+t)/2$. Values of K as a function of $(T+t)/2$ for two widely used thermometer glasses are given in table 11. If the kind of glass is not known, K may be taken as 0.00016 for Celsius mercury thermometers and 0.00009 for Fahrenheit thermometers.

The calculation of the stem correction may be illustrated by the following example:

TABLE 11. *Values of K for mercury-in-glass thermometers*

Mean temp. $\frac{T°+t°}{2}$	K for "normal" glass	K for "borosilicate" glass
For Celsius thermometers		
0°	0.000158	0.000164
100	.000158	.000164
150	.000158	.000165
200	.000159	.000167
250	.000161	.000170
300	.000164	.000174
350	----------	.000178
400	----------	.000183
450	----------	.000188
For Fahrenheit thermometers		
0°	0.000088	0.000091
200	.000088	.000091
300	.000088	.000092
400	.000089	.000093
500	.000090	.000095
600	.000092	.000097
700	----------	.000100
800	----------	.000103

Suppose a total-immersion thermometer reads 90° C in a bath when immersed to the 80° C graduation mark on the scale, and a 10-cm faden thermometer placed alongside the thermometer is adjacent to the scale between 60° and 90° C. For this case $n=90-60=30$. If the faden thermometer indicates 80° C, then the stem correction $=0.00016\times30(90-80)=+0.048$, or $+0.05$° C. Note that when the temperature of the emergent stem is lower than the bath temperature, the sign of the correction is +.

If a faden thermometer were not available in the above example, the emergent-stem temperature could be estimated by suspending a small auxiliary thermometer above the bath adjacent to the main thermometer and with its bulb centered at about the level of the 85° graduation. The reading of the auxiliary thermometer will then approximate the mean temperature of the 10 degrees C (80° to 90° C) emergent from the bath. For this condition $n=10$. If the auxiliary thermometer reads 60° C, the stem correction $=0.00016\times10(90-60)=+0.048$ or $+0.05$° C. This method, however, will usually not be as reliable as the method using a faden thermometer.

10.4. Formula for Calorimeter Thermometers

The stem correction is often important when thermometers are used for differential temperature measurements, as in calorimetry. In this case, provided the mean temperature of the stem remains constant, the correction may be computed from the following formula, involving the difference of the initial and final readings:

$$\text{stem correction} = Kd(T_1 + T_2 - S - t),$$

where

K=factor for relative expansion of glass and mercury,
T_1 and T_2=the initial and final readings, respectively,
$d=T_2-T_1$,
S=scale reading to which the thermometer is immersed, and
t=mean temperature of the emergent stem.

This correction must be applied (added if +, subtracted if −) to the difference of the readings to give the true difference of temperature.

Example: Suppose the thermometer was immersed to its 20° mark; its initial reading, T_1, was 25° C; its final reading, T_2, was 30° C; and the stem temperature was 20° C. Then the correction is $0.00016\times5(25+30-20-20)=+0.012°$ C. The difference between T_1 and T_2 is 5°. The true difference between the initial and final temperatures was T_2-T_1+correction$=5.012°$ C.

10.5. Formula for Beckmann Thermometers

For a Beckmann thermometer the correction may be readily computed from the following formula, differing only slightly from that for calorimeter thermometers, provided the thermometer is immersed to near the zero on its scale and that the temperature of the stem remains constant:

$$\text{stem correction}=Kd(S+T_1+T_2-t),$$

where

S=setting of the thermometer (section 6.4), and the other symbols have the same meanings as for calorimeter thermometers.

A Beckmann thermometer of the ordinary type should not be used with any part of the lower portion of the stem exposed, as this part may contain 5 to 10 times as much mercury per centimeter as the graduated portion and, if exposed, introduces a large and uncertain error. If it is unavoidable, however, to use such a thermometer with some of the lower portion of the stem emergent from the bath, the necessary correction may be computed from the above formula, provided S in the formula is replaced by $S+m$, where m is the number of degrees the temperature of the thermometer must be lowered to bring the meniscus from the zero mark on its scale to the point of immersion.

If the thermometer is immersed to some point other than its zero mark, as would ordinarily be the case with thermometers having the zero graduation at the top of the scale, the differential stem correction may be calculated from the above formula if S is replaced by $S+m$. The formula is applicable whether the point of immersion is on the scale or below it, provided the points at which readings are made are above the point to which the thermometer is immersed.

11. Lag of Thermometers

Practically all theoretical treatment of the question of thermometer lag is based on the assumption that Newton's law of cooling (i. e., that the rate of change in the reading of the thermometer is proportional to the difference between thermometer temperature and bath temperature) holds for the thermometer. It is an immediate consequence of this law that when a thermometer is immersed in any medium it does not take up the temperature immediately, but approaches it asymptotically. A certain time must elapse before the thermometer reading agrees with the temperature of the medium, to 0.1 degree, still longer to 0.01 degree, the temperature remaining constant. If the temperature is varying, the thermometer always indicates, not the true temperature, but what the temperature of the medium was at some previous time. The thermometer readings are thus said to "lag" behind the temperature by an amount which may or may not be negligible, depending upon the rapidity of temperature variation and the construction of the thermometer. A more complete treatment of this subject has been given by Harper [6].

For a thermometer immersed in a bath, the temperature of which is changing uniformly, the lag may be defined as the interval in seconds between the time when the bath reaches a given temperature and the time when the thermometer indicates that temperature. This lag, λ, is dependent upon the dimensions and material of the thermometer bulb, the medium in which it is immersed, and the rate at which this medium is stirred. For instance, the lag when in the air of the room would be perhaps 50 times that of the same thermometer when immersed in a well-stirred water bath.

Since the value of λ for mercurial thermometers is not large, being from 2 to 10 sec in a well-stirred water bath, it is not generally necessary to correct for it. For example, if two thermometers, one having a lag of 3 and another of 8 sec, are read simultaneously in a bath whose temperature is rising at the rate of 0.001 degree in 5 sec, the former will read 0.001 degree higher than the latter, due to the lag. In the intercomparison of thermometers the rate of temperature rise may nearly always be kept so small that this lag correction is negligible.

If a thermometer at a given initial temperature is plunged into a bath at a different temperature,

the lag, λ, is the time required for the original difference in temperature between thermometer and bath to be reduced to $1/e$ (that is 1/2.8) of itself. In a length of time 4λ the difference will have become about 1.5 percent and in a length of time 7λ about 0.1 percent of the original difference.

This shows that it is necessary to wait 10 to 45 sec after placing a thermometer in stirred water in order to get a reading correct to within 1 percent of the original difference between bath and thermometer.

When a thermometer is used to measure changes of temperature, as in calorimetry, it has been shown by White [7] that the lag enters into the observations in such a way as to be eliminated from the results in applying the usual radiation corrections. Therefore the lag need not be considered, provided only that the initial and final readings are made when the temperature is varying uniformly. This is not strictly true, however, in the case of some Beckmann thermometers that have no true value of λ, as has been explained in the paper referred to above.

An idea of the magnitude of the lag, λ, of thermometers of various types, when immersed in a well-stirred water bath, may be obtained from table 12.

TABLE 12. *Lag of thermometers*

Type of thermometer	Lag, λ
	sec
Laboratory thermometer, small bulb	2
Calorimeter thermometer, large bulb	5
Beckmann thermometer, large bulb	9
Inclosed capillary portion of Beckmann thermometer	50+

12. Notes on Thermometry

The following brief notes on the characteristic behavior of mercury-in-glass thermometers are added to aid the user in understandmg the behavior of such thermometers and in a better utilization of the information that is contained in the certificates or reports of tests.

12.1. Gradual Changes in Glass

There is a gradual change in the volume of a glass thermometer bulb which will continue for years. This change manifests itself by a slow rise in the thermometer indications at all points. With better grades of thermometer glasses the change will not exceed 0.1° C in many years, provided the thermometer has not been heated to temperatures above about 150° C. In addition permanent changes in bulb volumes have sometimes been observed with thermometers which have been repeatedly cycled at low temperatures, for example between −30° and +25° C. Allowance for these changes can readily be made by determining the ice-point reading from time to time, since if the reading at this point is found to be higher (or lower) than at the time of test all readings will be higher (or lower) to the same extent.

12.2. Temporary Changes in Bulb Volume

When a thermometer which has been at room temperature for a long time is heated to a higher temperature, the glass quickly expands to its final equilibrium condition corresponding to the higher temperature. When cooled to the original temperature, the glass does not completely return to its original volume for a long time (months or even years), although if the bulb is made of suitable glass and has not been heated above 100° C. the original volume will be recovered within the equivalent of 0.01 or 0.02 degrees C in about 3 days. Obviously, this phenomenon has an important bearing on the precision attainable with mercury thermometers and must be taken into consideration in precision thermometry, especially in the interval 0 to 100 degrees C. Thus, if a thermometer is used to measure a given temperature, it will read lower than it otherwise would if it has a short time previously been exposed to a higher temperature. With the better grades of thermometric glasses the error resulting from this hysteresis will not exceed (in the interval 0 to 100 degrees) 0.01 of a degree for each 10-degree difference between the temperature being measured and the higher temperature to which the thermometer has recently been exposed and with the best glasses only a few thousandths of a degree for each 10-degree difference. The errors due to this hysteresis become somewhat erratic at temperatures much above 100° C. For the reasons briefly set forth above it is customary, in precision thermometry, to determine the ice point immediately after each temperature measurement.

12.3. Changes in Bulb Volume Due to Annealing

Another change to which the indications of thermometers are subject is the annealing change at high temperatures. If the glass has not been properly annealed, it will slowly and progressively contract when exposed to high temperatures (above 300° C), thus causing the indications of the thermometer to rise progressively. These annealing changes may amount to 30 or 40 degrees C, and hence thorough annealing of a high-temperature thermometer is very important. No amount of annealing will make the ice-point reading of a thermometer constant if the thermometer is exposed for a long period to high temperatures

(450° C or thereabouts). For well-annealed thermometers such changes will be small and can be readily allowed for by occasional determinations of the fixed-point reading and application of the necessary additional corrections. In the use of high-temperature thermometers care must be taken not to overheat them. When the glass becomes "soft", the high internal gas pressure enlarges the bulb and thus causes a lowering in the indications of the thermometer.

13. Separated Columns

Many inquiries are received concerning separated mercury columns, particularly after shipment. Since no means of avoiding such occurrences has yet been found, the recourse of stating some directions for joining the mercury is adopted. The mercury may separate somewhat more readily in thermometers which are not pressure-filled, but it can be more easily joined since there is little gas to separate the liquid. The process of joining broken columns consists of one or a series of manipulations which may be effective, and these are briefly described here.

1. The bulb of the thermometer may be cooled in a solution of common salt, ice, and water (or other cooling agent) to bring the mercury down into the bulb. Moderate tapping of the bulb on a paper pad or equally firm object or the application of centrifugal force usually serves to unite the mercury in the bulb. If the salt solution does not provide sufficient cooling, carbon dioxide snow (dry ice) may be used. Since the temperature of dry ice is about −78° C and mercury freezes at about −40° C, it will cause the mercury to solidify. Care must be taken to warm the top of the bulb first so that pressures in the bulb due to the expanding mercury may be relieved. Care should also be taken in handling dry ice as it may cause severe "burns".

2. If there is a contraction chamber above the bulb or an expansion chamber at the top of the thermometer the mercury can sometimes be united by warming the bulb until the column reaches the separated portions in either enlargement. Great care is necessary to avoid filling the expansion chamber completely with mercury, which might produce pressures large enough to burst the bulb. Joining the mercury is more readily accomplished if the quantity in either cavity has first been shattered into droplets by tapping the thermometer laterally against the hand.

3. As a last resort, especially for thermometers having no expansion chambers, small separated portions of the column can sometimes be dispersed by warming, into droplets tiny enough to leave space for the gas to by-pass, and these droplets can then be collected by a rising mercury column.

The procedure for thermometers in which organic liquids are used is similar. Liquids in the stem can more readily be vaporized and may then be drained down the bore. The latter process is aided by cooling the bulb. All of these manipulations require patience, and experience is helpful, but they will yield results if care is used. A convenient method of ascertaining that all the liquid has been joined is a check of the ice point, or some other point on the scale.

14. General Instructions to Applicants for Tests

Tests in accord with the policies of the National Bureau of Standards, and of the types indicated in the fee schedules as published in the "Federal Register", will be undertaken. If need arises for a special test, not listed in the fee schedule but of a similar nature, the Bureau should be consulted. If the required measurements appear feasible, and, in the opinion of the Bureau, sufficiently important to justify the work, such tests will be undertaken for a special fee determined by the nature of the work. In all requests the following procedures and information are pertinent.

14.1. Initial Arrangements

A letter or purchase order, stating the tests desired and referring to the appropriate sections and subsections of the fee schedule, should be sent to the Bureau prior to any shipment. The purpose of this requirement is to determine whether or not the Bureau will undertake the test and to insure correct procedure in reporting, shipping, and billing. In the case of routine or periodic tests, of a type made in the past for the requester, this letter may be sent at the time shipment is made. In general, the purpose of the test and the manner in which the results are to be used should be stated. If the thermometer submitted has been previously calibrated by the Bureau, reference should be made to the former test number. A test number will be assigned by the Bureau to each project, and this test number must be referred to in all subsequent communications.

14.2. Shipping and Packing

Shipping charges, both to and from the Bureau, must be assumed by the applicant. Return shipments are made by the Bureau in accordance with its judgment of the best method of shipping unless specific instructions are received. Such instructions should be supplied at the time that arrangements are being made for the test. If a test number has been assigned prior to the shipment, this number should appear on the shipping container. If a test number has not been assigned at this

time, an invoice, purchase order, or letter should be enclosed in the shipment for identification purposes.

All possible care will be taken in handling thermometers at the Bureau, but the risk of damage either in shipment or in testing must be assumed by the applicant. The applicant should consider the nature of the equipment he is shipping and pack it accordingly, with appropriate labeling. Attention is called to the availability of security express in shipping thermometers.

Appreciation is expressed for the use of the following material: (a) Figure 3, which first appeared in the Journal of the Optical Society of America; (b) figure 4, which first appeared in the Proceedings of the American Society for Testing Materials; and (c) section 13, Separated Columns, is from the paper by Johanna Busse, Liquid-in-glass thermometers, which appeared in the book, Temperature, its Measurement and Control in Science and Industry (Reinhold Publishing Corp., New York, N. Y.).

15. References

[1] Federal Register, Title 15, Chapter 11, Part 203 (copies available from NBS on request).
[2] N. S. Osborne and C. H. Myers, A formula and tables for the pressure of saturated water vapor in the range 0 to 374 C, J. Research NBS **13**, 1 (1934) RP691.
[3] E. F. Mueller and R. M. Wilhelm, Methods of testing thermometers, Proc. ASTM **38**, Part I, 493 (1938).
[4] R. B. Scott and F. G. Brickwedde, A precision cryostat with automatic temperature regulation, BS J. Research **6**, 401 (1931) RP284.
[5] E. Buckingham, The correction for emergent stem of the mercurial thermometer, Bul. BS **8**, 239 (1911) S170.
[6] D. R. Harper 3d, Thermometric lag, Bul. BS **8**, 659 (1912) S185.
[7] W. P. White, Lag effects and other errors in calorimetry, Phys. Rev. **31**, 562 (1910).

Washington, April 24, 1958.

The Library of Congress has cataloged this publication as follows:

Swindells, James F

Calibration of liquid-in-glass thermometers. Washington, U. S. Dept. of Commerce, National Bureau of Standards, 1958.

21 p. illus. 26 cm. (U. S. National Bureau of Standards. Circular 600)

1. Thermometers and thermometry. I. Title.

QC100.U555 no. 600 — Copy 2. 536.51 QC272.S9 58–62396 ‡

Library of Congress

U. S. Department of Commerce National Bureau of Standards

RESEARCH PAPER RP1676

Part of Journal of Research of the National Bureau of Standards, Volume 35, November 1945

DETERMINATION OF THE PURITY OF HYDROCARBONS BY MEASUREMENT OF FREEZING POINTS[1]

By Augustus R. Glasgow, Jr., Anton J. Streiff,[2] and Frederick D. Rossini

ABSTRACT

An improved and simplified procedure is described for determining the freezing points of hydrocarbons from time-temperature freezing and melting curves, and for calculating the purity when the freezing point for zero impurity is (a) known and (b) not previously known. A procedure for determining the cryoscopic constant is also described.

CONTENTS

I. INTRODUCTION

In connection with the work of this laboratory on the analysis, purification, and properties of hydrocarbons, the freezing point, determined from time-temperature freezing and melting curves, has been used to evaluate the purity of given samples of hydrocarbons. Since the previous reports on this subject [1, 2, 3],* improvements have been made in the apparatus and the procedure has been clarified and simplified. This report describes the present apparatus and procedure for determining the freezing point from time-temperature freezing and melting curves and for calculating the purity when

[1] This investigation was performed at the National Bureau of Standards as part of the work of the American Petroleum Institute Research Project 6 on the "Analysis, Purification, and Properties of Hydrocarbons."

[2] Research Associate on the American Petroleum Institute Research Project 6 at the National Bureau of Standards.

* Figures in brackets indicate the literature references at the end of this paper.

the freezing point for zero impurity is known and also when the freezing point for zero impurity is not previously known. A procedure for determining the cryoscopic constant is also described.

II. PRINCIPLES INVOLVED

The definitions, abbreviations, and symbols used in this paper are the same as those given in the preceding report [2], to which the reader is referred for details not covered here.

For the equilibrium between a crystalline phase consisting of the major component alone and a liquid phase consisting of the major component and one or more other components, the thermodynamic relation between the temperature of equilibrium and the composition of the liquid phase, for an ideal or sufficiently dilute solution, is

$$-\ln N_1 = -\ln (1-N_2) = A(t_{f_0}-t)[1+B(t_{f_0}-t)+ \ . \ . \ .], \qquad (1)$$

where

N_1 = the mole fraction of the major component in the liquid phase;

$N_2 = (1-N_1)$ = the sum of the mole fractions of all other components in the liquid phase;

t_{f_0} = the temperature, in degrees centigrade, of the freezing point of the major component when pure (that is, when $N_2=0$);

t = the given temperature of equilibrium, in degrees centigrade;

$A = \Delta H_{f_0}/RT_{f_0}^2$;

$B = 1/T_{f_0} - \Delta C_{p_0}/2\Delta H_{f_0}$;

R = the gas constant, per mole;

$T_{f_0} = t_{f_0} + 273.16$

ΔH_{f_0} = the heat of fusion; per mole, of the major component in the pure state at the temperature T_{f_0};

ΔC_{p_0} = the heat capacity, per mole, of the pure liquid less that of the pure solid, for the major component in the pure state at the temperature T_{f_0}.

It is seen that the three constants (t_{f_0}, A, and B) in eq 1 are properties only of the major component, so that the relation between the temperature of equilibrium and the mole fraction of solute is the same for all solutes, of which there may be more than one in the same solution, provided they remain in the liquid phase and form with the major component an ideal solution.

If r is the fraction crystallized of the total number of moles of all components in the system, then, as previously shown [2],

$$t = t_{f_0} - a/[\{1-(b/a)\}-r], \qquad (2)$$

where a and b are constants for the given sample. Equation 2 gives

the relation between the temperature of equilibrium and the fraction of material crystallized.

When the experiment is one performed according to the procedure described in the present report, the rate of crystallization or melting of the major component is substantially constant with time, and, as previously shown [2],

$$r=k(z-z_f), \tag{3}$$

where k is a constant characteristic of the given experiment, z is any given time, and z_f is the time at which freezing begins or melting is complete. Furthermore,

$$t=t_{f_0}-a'/[1-k'(z-z_f)], \tag{4}$$

where a' and k' are constants [2]. Equation 4 gives the relation between the temperature of equilibrium and the time during the part of the experiment in which equilibrium between the liquid and solid phases of the major component exists.

III. APPARATUS AND MATERIALS

The freezing-point apparatus in its present form is shown in figures 1, 2, and 3, which give, respectively, the assembly, the details of the freezing tube,[3] and the details of the stirring assembly. With the stirrer shown in figure 3, the vertical stroke is usually made 1½ inches over-all, and the rate about 120 strokes per minute.

The thermometric system consists of a 25-ohm platinum resistance thermometer, a resistance bridge (Müeller-type)[4] in which the main coils are thermostated, and a highly sensitive galvanometer, adjusted so that 1 mm on the scale is equivalent to from 0.0001 to 0.0005 degree centigrade.

The apparatus also includes a vacuum system and a stop watch or clock.

The cooling and warming baths used are listed in table 1.

TABLE 1.—*Cooling and warming baths used*

Type of experiment	Range of freezing points	Cooling or warming bath
	°C	
Freezing	+30 to −50	Slush of solid carbon dioxide in a 50–50 mixture of carbon tetrachloride and chloroform.
Do	−50 to −170	Liquid air, or preferably, liquid nitrogen.
Melting	+30 to −10	Water maintained constant (±1 degree centigrade) at 10 to 25 degrees centigrade above the freezing point of the sample.
Do	−10 to −90	Ice and water.[a]
Do	−90 to −170	Slush or solid carbon dioxide in a 50–50 mixture of carbon tetrachloride and chloroform.[a]

[a] See the discussion at the end of section V.

[3] Acknowledgment is gratefully made of the assistance of F. W. Rose, Jr. (formerly Research Associate on the API Research Project 6, and since October 1940, with the Houdry Process Corporation, Marcus Hook, Pa.), in fixing the details of the first design of the freezing tube shown in figure 2.

[4] Leeds & Northrup No. 8069, type G-2.

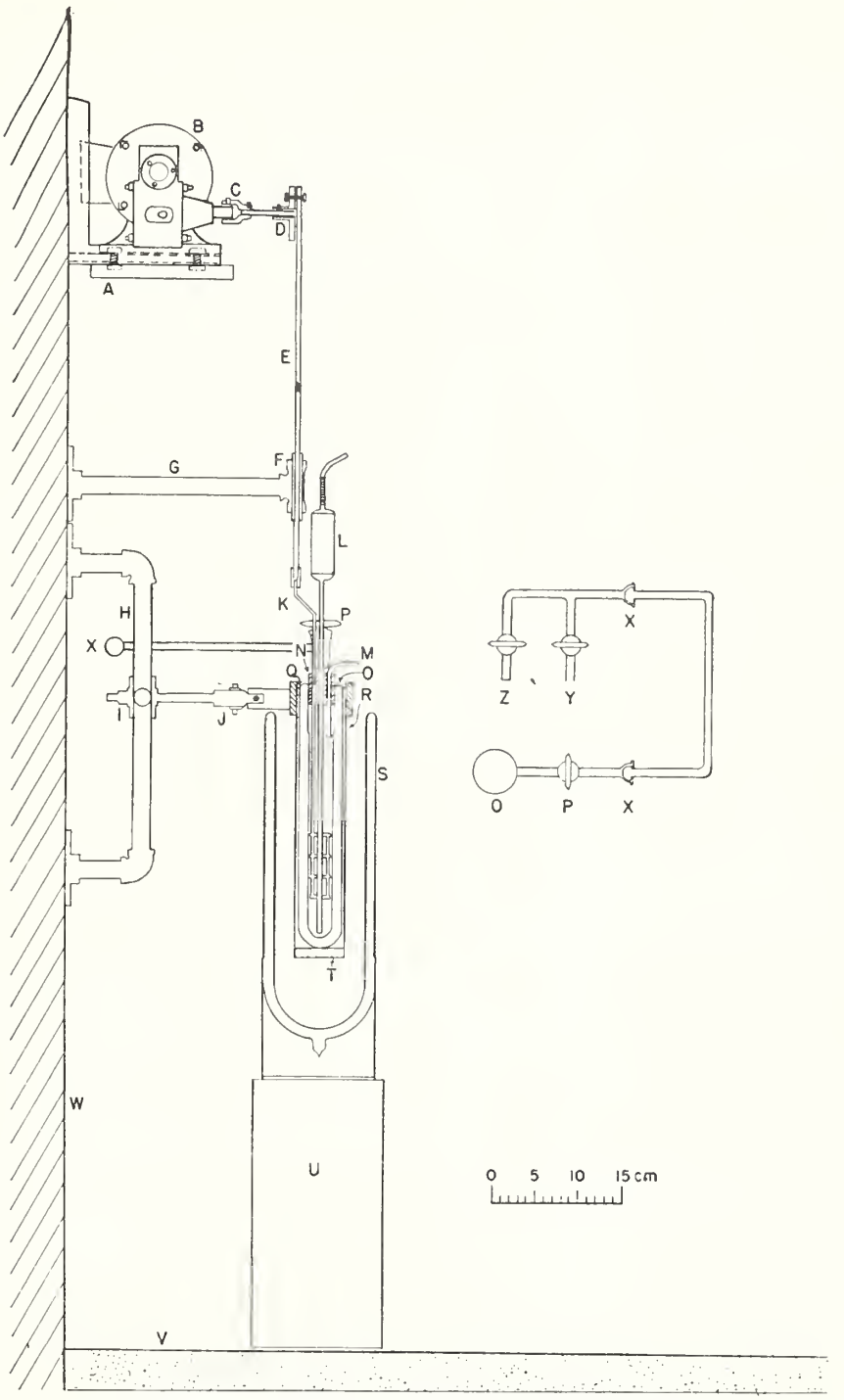

FIGURE 1.—*Assembly of the freezing-point apparatus.*

A, Braeket for motor, with rubber pad; *B*, motor, with reduction gears, to give 120 rpm; *C*, eoupling; *D*, wheel; *E*, steel rod; *F*, bearing; *G*, support for bearing; *H*, support for freezing tube; *I*, adjustable clamp holder; *J*, clamp for freezing tube; *K*, stirrer; *L*, thermometer; *M*, tube for inlet of dry air; *N*, cork stopper, with boles as shown, plus a small hole for the "seed" wire; *O*, freezing tube, with silvered jacket; *P*, stopcock on freezing tube; *Q*, asbestos collar; *R*, brass eylinder, 12½ inehes long and 2⅛ inches inside diameter, with Bakelite eollar; *S*, Dewar flask, for cooling or warming bath; *T*, asbestos pad at bottom of eylinder *R*; *U*, wood-block support; *V*, table top; *W*, wall; *X*, spherical joint, 18/7; *Y*, connection to vacuum; *Z*, eonneetion to air, through drying tube.

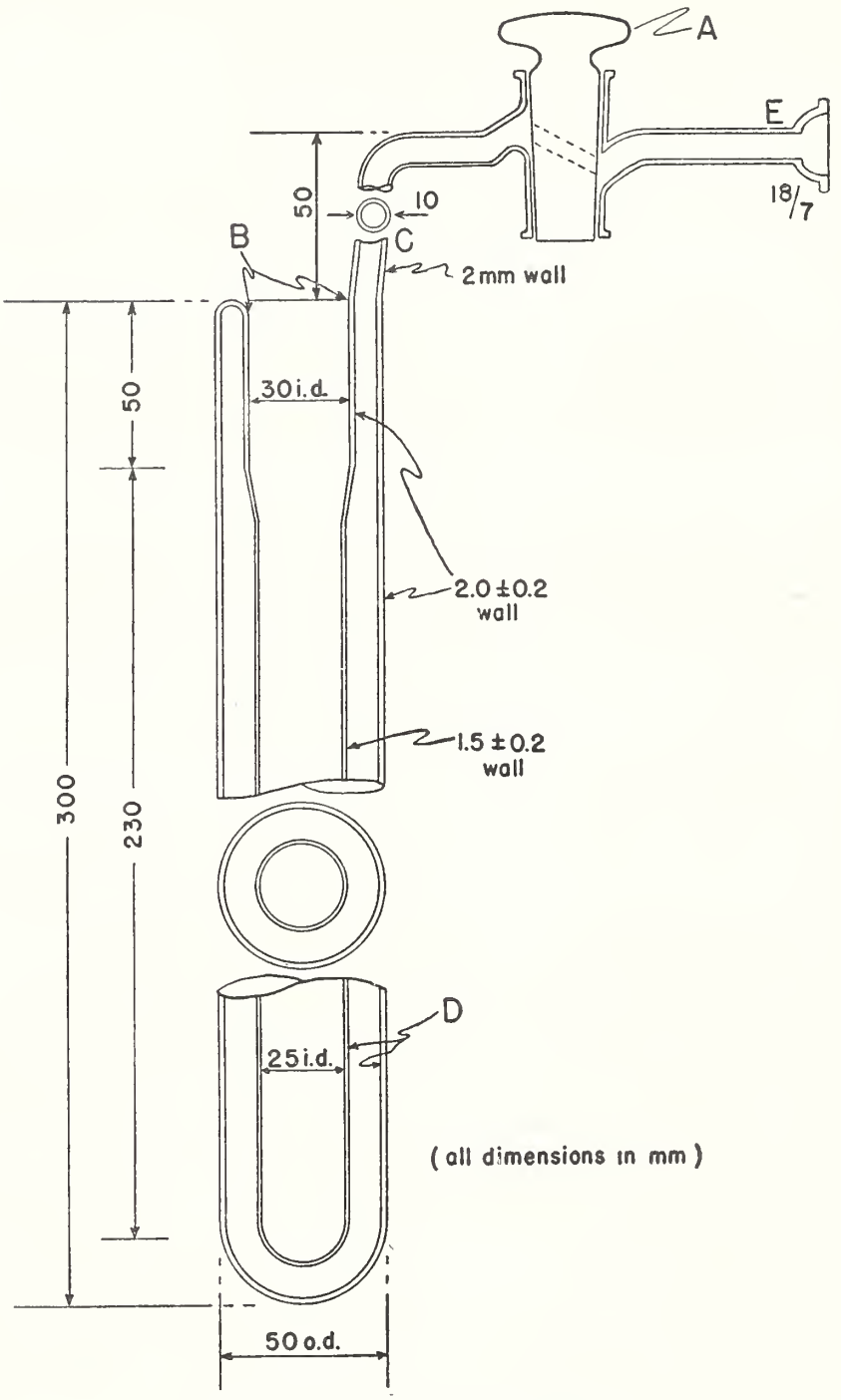

FIGURE 2.—*Details of the freezing tube.*

A, High-vacuum stopcock, hollow plug, oblique 3½-mm bore; *B*, inside opening of freezing tube, which must have no bulge at this point; *C*, slanted connection to jacket of freezing tube; *D*, internal walls of jacket of freezing tube, silvered; *E*, spherical joint, 18/7.

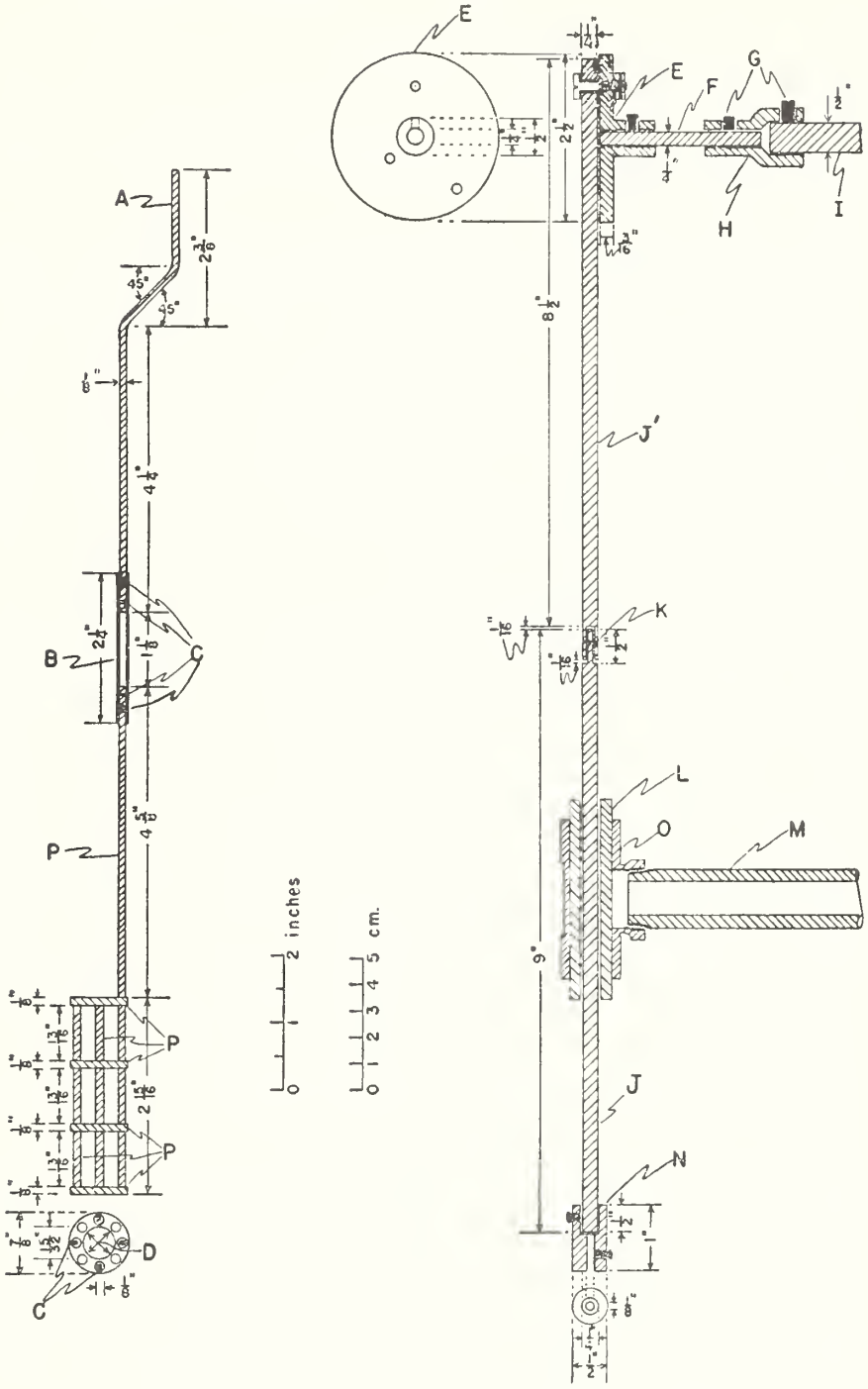

FIGURE 3.—*Details of the stirring assembly and supports.*

A, Stainless steel rod, round; *B*, German-silver tube; *C*, pins; *D*, holes, ⅛-inch in diameter; *E*, brass wheel, with three holes, tapped for machine screws, spaced ½, ¾, and 1 inch from center; *F*, steel rod; *G*, set screws; *H*, brass coupling; *I*, steel shaft; *J*, steel rod, round; *J'*, steel rod, square; *K*, connecting pin; *L*, brass-sleeve bearing; *M*, steel pipe, ½-inch nominal size; *N*, brass coupling; *O*, brass tee; *P*, aluminum.

IV. EXPERIMENTAL PROCEDURE FOR A FREEZING EXPERIMENT

The procedure for performing a freezing experiment is as follows: The apparatus is assembled, with no refrigerant and no sample of hydrocarbon yet in place, but with a stream (10 to 20 ml a minute) of dry air flowing. The jacket of the freezing tube is filled with air freed of carbon dioxide and water.

As required, the operator must be prepared to induce crystallization in the hydrocarbon sample as soon as possible after the temperature has passed below the freezing point of the sample. In some cases, crystallization may be induced by introducing, into the hydrocarbon sample at the appropriate time, a small metal rod, which has been kept at liquid air temperatures. In other cases, crystallization may be induced by introducing, into the hydrocarbon sample at the appropriate time, crystals of the hydrocarbon on the coiled end of a small metal rod. These crystals are made by placing several milliliters of the hydrocarbon in a small test tube (incased in a thin metal tube) immersed in a refrigerant whose temperature is below the freezing point of the hydrocarbon.

The Dewar flask surrounding the freezing tube is filled with the appropriate refrigerant. The thermometer and stopper are temporarily removed and the hydrocarbon sample (50 ml of liquid) is introduced. When the hydrocarbon is volatile or normally gaseous at room temperature, the freezing tube is cooled before introducing the sample in order to minimize loss by evaporation. The flow of dry air into the freezing tube is continued in order to keep out water vapor. The stirrer is started and the sample is allowed to cool down to within about 15 degrees centigrade of the freezing point, when evacuation of the jacket of the freezing tube is begun.

The time and the resistance of the thermometer are observed at even intervals of 0.1 ohm (about 1 degree centigrade) to determine the rate of cooling. When a cooling rate is obtained that will give a change of 1 degree in about 2 to 3 minutes, in the range of about 5 to 10 degrees above the freezing point, the stopcock controlling the jacket of the freezing tube is closed. (The optimum rate of cooling will vary with the hydrocarbon being examined.)

When the temperature reaches a point about 5 degrees above the expected freezing point, the time is recorded to 1 second (or 0.01 minute), at which the resistance of the termometer equals certain preselected values (every 0.1 or 0.05 ohm). At the appropriate time (see above), crystallization is induced. The beginning of crystallization will be accompanied by a halt in the cooling of the liquid. After recovery from under cooling is substantially complete, the resistances, including the reading of the scale of the galvanometer at full sensitivity as well as the scale reading with no current through the galvanometer, are recorded at intervals of about 1 minute. These observations, together with the sensitivity of the galvanometer system in terms of ohms per millimeter of scale reading, yield a sensitivity near 0.0001 degree centigrade in the measurement of temperature. These observations are continued until the stirrer begins laboring.

Then the stirrer is stopped and comparison of "N" and "R" readings

is made through the commutator. These latter readings are made at fixed intervals of about 1 minute, alternately for "N" and "R," and the difference between the two at any given instant of time is determined from a plot of the several values against time.

V. EXPERIMENTAL PROCEDURE FOR A MELTING EXPERIMENT

The procedure for performing a melting experiment is exactly the same as for a freezing experiment, up to the point where the stirrer begins laboring. When the stirrer shows signs of laboring, a comparison of "N" and "R" readings is made through the commutator, as in the previous section, except that the stirrer is still operating. When the laboring of the stirrer becomes quite pronounced, the cooling bath is replaced by the appropriate warming bath, and, simultaneously, further evacuation of the freezing tube is begun, with the stirrer still operating. After evacuation for an appropriate length of time (3 to 10 minutes), the stopcock on the freezing tube is closed, and observations of time and resistance are continued along the equilibrium portion of the melting curve as along the equilibrium portion of the freezing curve. When melting is substantially complete, as evidenced by a marked change in the rate of change of resistance, the time is recorded when the resistance reaches certain preselected values at even intervals of 0.05 ohm (0.5 degree centigrade). The experiment is concluded when the temperature has reached a point 5 to 10 degrees above the freezing point.

For substances having freezing points in the range $-135°$ to $-170°$ C, the melting experiment may be performed by letting the cooling bath of liquid air remain in position and evacuating the jacket of the freezing tube as much as possible. This will make the thermal conductivity across the jacket so small that the energy introduced by the stirrer may be used to provide the energy of melting. A similar procedure may be used for melting experiments with substances having freezing points in the range from about -50 to $-80°$ C, utilizing the bath of solid carbon dioxide in a 50-50 mixture of carbon tetrachloride and chloroform.

VI. EVALUATION OF THE FREEZING POINT FROM A FREEZING CURVE

To locate zero time (the time at which crystallization would have begun in the absence of undercooling), a preliminary plot is made of the time-resistance observations covering the liquid cooling line and the equilibrium portion of the freezing curve. For this plot, as shown in figure 4, the time scale is taken so that 1 cm is equivalent to 1 minute and the resistance scale (for a 25-ohm thermometer) so that 1 cm is equivalent to 0.02 ohm (0.2 degree centigrade). Usually the extent of undercooling is small enough that no correction for zero time need be made, in which case zero time can usually be determined by a visual extrapolation, on this plot, of the equilibrium portion of the freezing curve back to its intersection with the liquid-cooling line. However, if undercooling is appreciable, correction for its effect on the time may be required (see part II–2 of reference [1]).

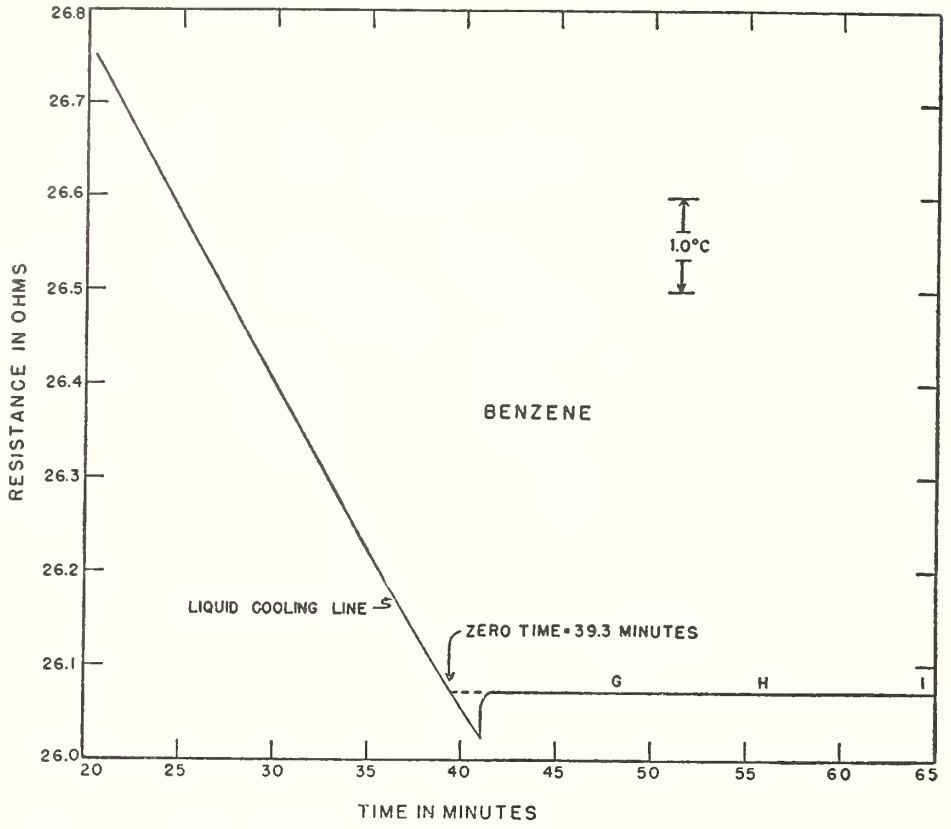

FIGURE 4.—*Time-temperature cooling curve for determining "zero" time in an experiment on a sample of benzene.*

The scale of ordinates gives the resistance in ohms of the platinum resistance thermometer, and the scale of abscissas gives the time in minutes. GHI represents the equilibrium portion of the freezing curve. Zero time is given by the intersection of the liquid cooling line with GHI extended. The same data are plotted in figure 5 with a magnified scale of temperature.

In order to locate accurately the resistance corresponding to the freezing point, the time-resistance observations are plotted as shown in figure 5, with the same time scale as before but with the scale of temperature magnified 10 to 200 times. The equilibrium portion of the curve, GHI, is extended back to its intersection at F with the liquid line by the simple geometrical construction shown in figure 6 (taken from reference [2]), selecting, for this purpose, three points (near the ends and the middle) of the equilibrium portion of the curve. The point F gives the resistance corresponding to the freezing point. (For details regarding the identification of the equilibrium portion of the curve, and the geometrical construction for determining the freezing point, see reference [2].)

If there is any doubt about the location of the equilibrium portion of the time-temperature curve, the criterion described on pages 210 and 211 of reference [2] may be applied. This procedure [2] involves plotting values of $(z-z_m)/(R-R_m)$ versus $(z-z_m)$, where (R_m, z_m) is an arbitrary fixed point near the middle of the equilibrium portion and (R, z) is any other point on the curve. This plot yields a straight line for that portion of the time-termperature curve representing the

equilibrium portion, and which has been obtained according to the experimental method described in this report.[5]

The observed resistance at the point F, corrected by one-half the difference between the "N" and "R" readings, and by appropriate calibration corrections to the coils of the bridge, if necessary, is converted to temperature in degrees centigrade. A convenient procedure to follow for this purpose is to put the calibration constants of the platinum resistance thermometer in the equation

$$R=R_0\{1+ct[(1+0.01\delta)-10^{-4}\delta t-10^{-8}\beta(t-100)t^2]\}, \qquad (5)$$

where t is the temperature in degrees centigrade and R_0, δ, β, and c,$=(R_{100}-R_0)/100R_0$, are the calibration constants provided by the National Bureau of Standards Thermometer Laboratory for the given

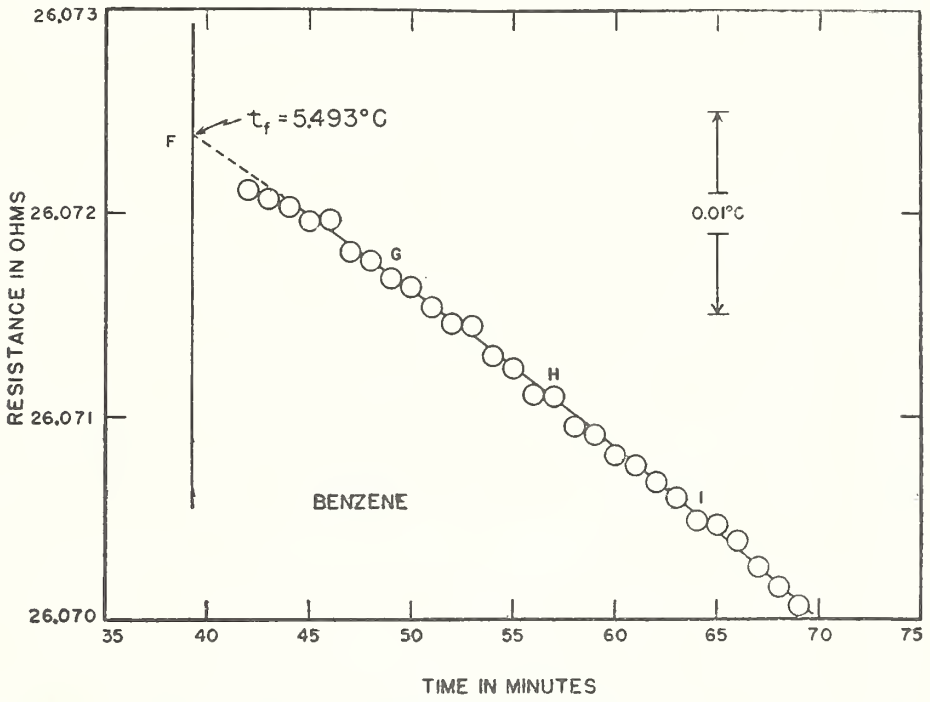

FIGURE 5.—*Time-temperature cooling curve for determining the freezing point of a sample of benzene.*

The scale of ordinates gives the resistance in ohms of the platinum resistance thermometer, and the scale of abscissas gives the time in minutes. GHI represents the equilibrium portion of the freezing curve. The freezing point F is determined as described in the text (see [2]). These data are the same as those plotted in figure 4.

thermometer. The foregoing equation with four constants is used for the range −190° to 0° C. For the range above 0° C, β is taken as zero, and the equation is simplified to

$$R=R_0\{1+ct[(1+0.01\delta)-10^{-4}\delta t]\}. \qquad (6)$$

With this equation, values of R are calculated to 0.00001 ohm, for unit degrees in the range of interest. (If determinations are to be

[5] This plot of $(z-z_m)/(R-R_m)$ versus $(z-z_m)$ may also be used to evaluate t_f and t_{t_0}, as described on pages 210 and 211 of reference [2].

574278 O - 61 - 13

made on many different hydrocarbons, time will be saved by making up at the start a table of such values of R for unit degrees in the entire range). Linear interpolation between unit degrees may be used without significant error to obtain the temperature corresponding to the given resistance. A table of this kind covering the range —190° to 50° C can be put on a sheet 14 by 17½ inches in size.

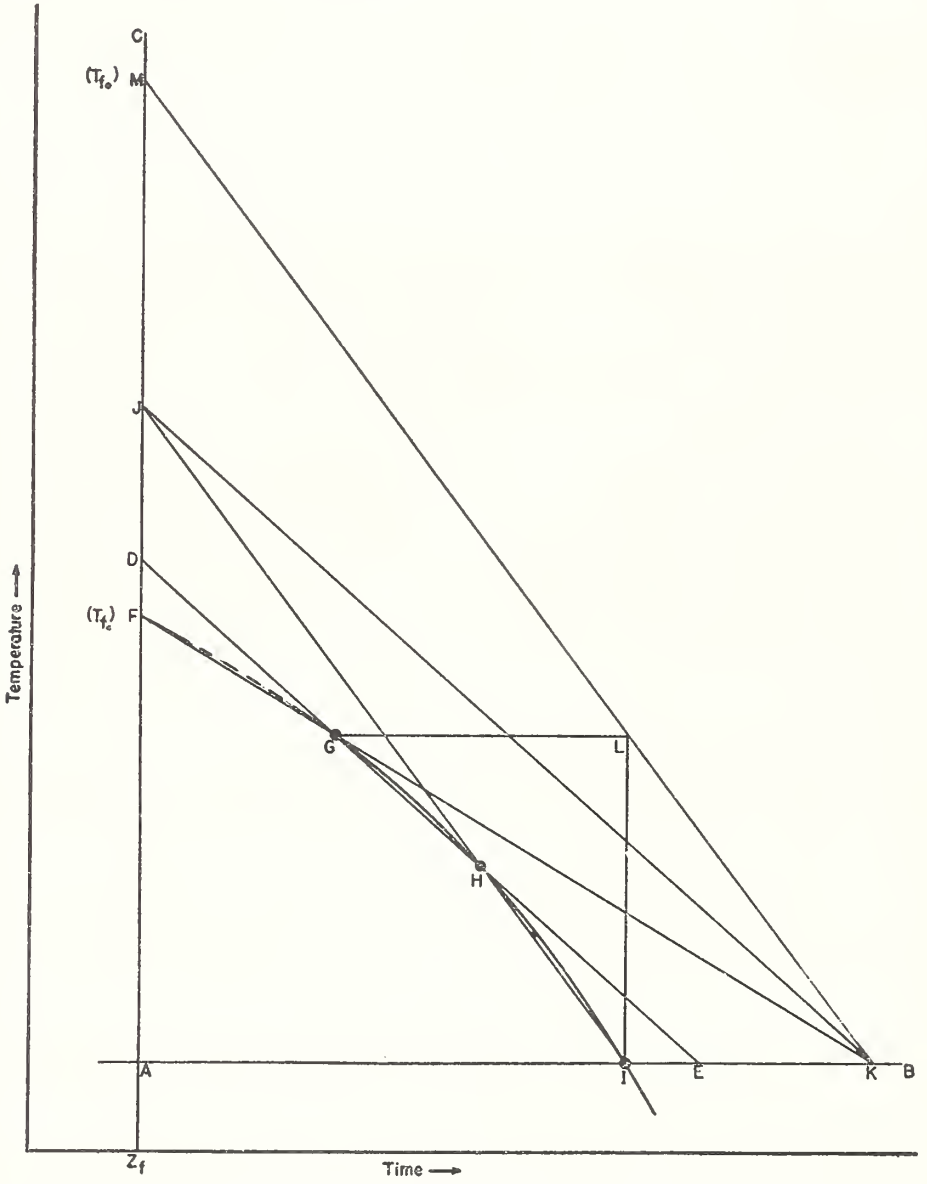

FIGURE 6.—*Geometrical construction for determining the freezing point.*

Given G, H, and I as any three points on the equilibrium portion of the freezing curve, preferably spaced approximately as shown. Construction to determine t_f: Draw AC parallel to the temperature axis at "zero" time (the time at which crystallization would have begun in the absence of undercooling). Draw AB through I parallel to the time axis. Draw a line through G and H intersecting AB at E and AC at D. Draw a line through H and I intersecting AC at J. Draw a line through J parallel to DE, intersecting AB at K. Draw a line through K and G, intersecting AC at F. F is the desired point, representing the freezing point of the given sample. Construction to determine t_{f_0}: Draw a line through G parallel to AB and a line through I parallel to AC, the two lines intersecting at L. Draw a line through points K and L, intersecting AC at M. M is the desired point, representing the freezing point for zero inpurity, t_{f_0}.

VII. EVALUATION OF THE FREEZING POINT FROM A MELTING CURVE

Zero time is determined from a preliminary plot (as for the freezing curve) of the time-resistance observations covering the equilibrium portion of the melting curve and the liquid warming line, as shown in figure 7. Zero time can usually be determined by visual extrapolation, on this plot, of the equilibrium portion of the melting curve to its intersection with the liquid warming line extended down in tem-

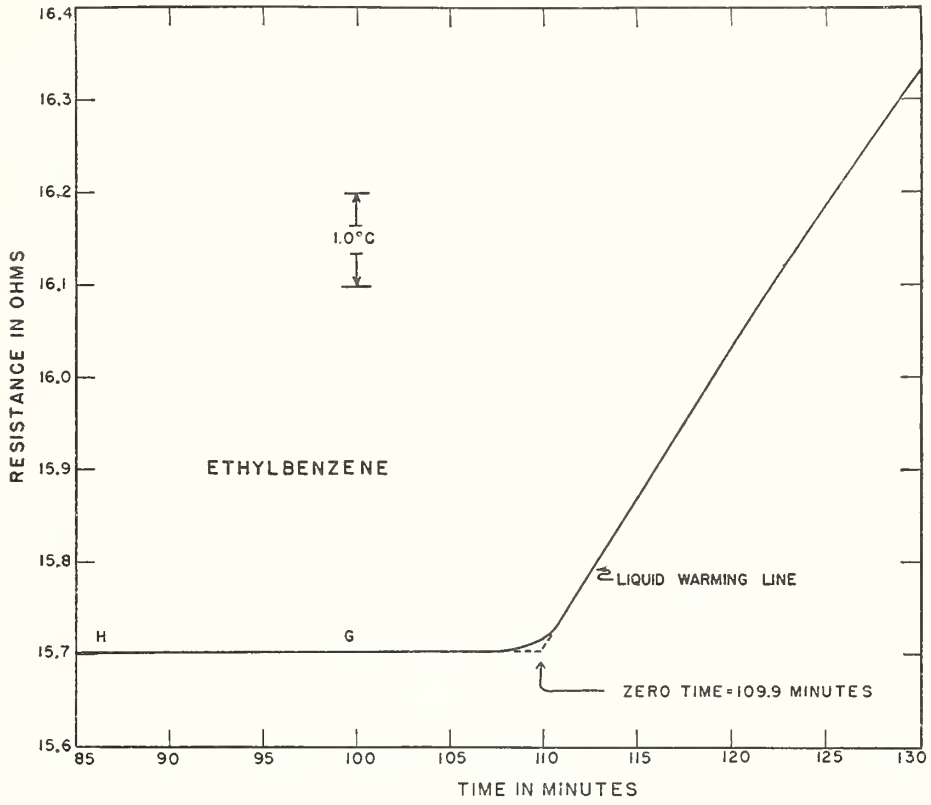

FIGURE 7.—*Time-temperature warming curve for determining "zero" time in an experiment on a sample of ethylbenzene.*

The scale of ordinates gives the resistance in ohms of the platinum resistance thermometer, and the scale of abscissas gives the time in minutes. HG represents part of the equilibrium portion of the melting curve. Zero time is given by the intersection of HG extended to its intersection with the backward extension of the liquid warming line. The same data are plotted in figure 8 with a magnified scale of temperature.

perature to its intersection with the extension of the equilibrium portion of the curve.

The location of the freezing point at F is done exactly as in the case of the freezing experiment, except that the geometrical construction is made to the right, as in figure 8. See figure 6 and reference [2] for details.

The conversion of resistance to temperature is made as previously described.

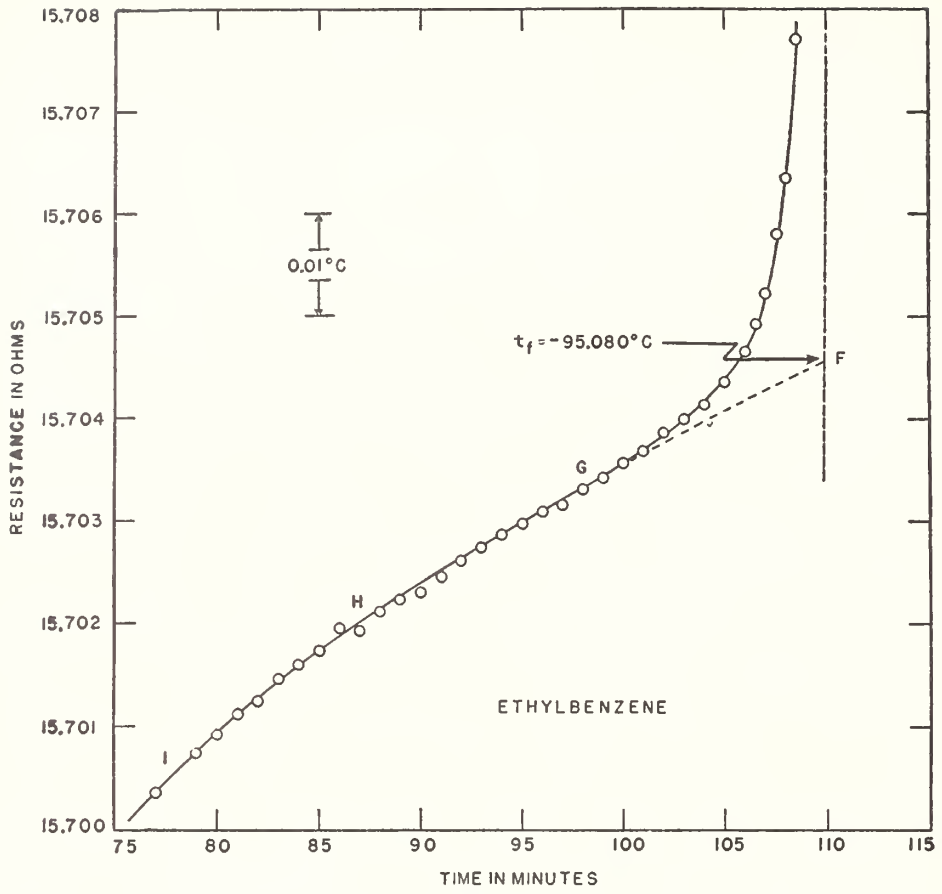

FIGURE 8.—*Time-temperature warming curve for determining the freezing point of a sample of ethylbenzene.*

The scale of ordinates gives the resistance in ohms of the platinum resistance thermometer, and the scale of abscissas gives the time in minutes. IHG represents the equilibrium portion of the melting curve. The freezing point F is determined as described in the text (see [2]). These data are the same as those plotted in figure 7.

VIII. CALCULATION OF THE PURITY WHEN THE FREEZING POINT FOR ZERO IMPURITY IS KNOWN

When the values of the freezing point for zero impurity and the cryoscopic constants are known, the measured value of the freezing point may be used to calculate the purity of the given sample by means of the equation

$$\log_{10}p = 2.00000 - (A/2.30259)(t_{f_0} - t_f)[1 + B(t_{f_0} - t_f)]. \qquad (7)$$

In eq 7, p is the purity in mole percent, t_f is the freezing point, t_{f_0} is the freezing point for zero impurity, and A and B are the cryoscopic constants [6] defined in section II.

For many hydrocarbons of low molecular weight, the value of the constant A lies in the range 0.005 to 0.06 deg^{-1} and that of the constant

[6] Selected "best" values of the cryoscopic constants of the more important hydrocarbons of the various classes are being compiled for publication in a joint investigation of the Thermochemical Laboratory and the American Petroleum Institute Research Project 44 at the National Bureau of Standards.

B in the range 0.000 to 0.005 deg^{-1}. In many cases, therefore, the constant B may be neglected, and eq 3 reduces to

$$\log_{10}p=2.00000-(A/2.30259)(t_{f_0}-t_f). \tag{8}$$

For small values of $t_{f_0}-t_f$, eq 8 reduces further to

$$p=100[1-A(t_{f_0}-t_f)]. \tag{9}$$

In terms of mole fraction of the major component, N_1, the equations corresponding to 7 and 9 are

$$\log_{10}N_1=-(A/2.30259)(t_{f_0}-t_f)[1+B(t_{f_0}-t_f)] \tag{10}$$

$$N_1=1-A(t_{f_0}-t_f). \tag{11}$$

In terms of mole fraction of the impurity, N_2, which is $1-N_1$, the limiting equation corresponding to eq 11 is

$$N_2=A(t_{f_0}-t_f). \tag{12}$$

The foregoing equations relating purity and temperature involve the two assumptions that all of the impurity in the given sample (a) remains in the liquid phase during crystallization, and (b) forms with the major component a substantially ideal solution. With regard to assumption (b), it is apparent that when a given hydrocarbon has been put through a logical system of purification there will remain as impurity only those hydrocarbons (usually close-boiling isomers) that are very similar to the major component. These latter hydrocarbons are, however, precisely those that are most likely to form with the major component a substantially ideal solution. With regard to assumption (a), involving the absence of solid solutions, the following points should be noted: The possible existence of solid solutions need be considered only for the case of the major component and its most probable impurities (usually close-boiling isomers); among hydrocarbons of low molecular weight, close-boiling isomeric impurities fortunately seldom possess the required shape and size of the molecule to favor the formation of solid solutions.

However, when there are known cases where a given hydrocarbon and its most probable impurity (for the given process of purification) form solid solutions, or otherwise do not conform to the requirements for the ideal relations, and if it is desired to translate into purity the freezing points of such systems, observations should be made on known mixtures of such hydrocarbons for the purpose of evaluating the actual relation between freezing point and purity. In general, in those cases where the identity of the impurity is known, the actual relation between purity and freezing point may be determined experimentally from known mixtures. In such cases, the observed relation, rather than the theoretically calculated relation for the ideal solution, should be used if the former is found to differ significantly from the latter.

IX. CALCULATION OF THE PURITY WHEN THE FREEZING POINT FOR ZERO IMPURITY IS NOT PREVIOUSLY KNOWN

When for the given compound under examination, the freezing point for zero impurity is not previously known, its value may be determined by application of the procedures previously described [1, 2].

The first of these procedures may be performed simply as follows: The time of crystallization is determined as described in part II–3 of reference [1]. If this experiment is not identical with the one from which the freezing point has been determined, the time of crystallization for the latter is related to that for the former (with the same quantity of sample in both experiments) as follows:

$$(z_{xln})_1/(z_{xln})_2=(\Delta t/\Delta z)_2/(\Delta t/\Delta z)_1, \tag{13}$$

where z_{xln} is the time of crystallization in minutes, $\Delta t/\Delta z$ is the cooling rate (or the negative of the warming rate) of the liquid phase at the freezing point in degrees per minute or ohms per minute, and the subscripts 1 and 2 identify the two experiments.[7]

Taking the rate of crystallization to be substantially constant [1], the fraction, r, crystallized at any time z_r is

$$r=(z_r-z_f)/z_{xln} \tag{14}$$

where z_f is "zero" time or the time at which crystallization begins (with no significant amount of undercooling). In the proper application of eq 9 and 10, it is necessary that the rate of introduction of energy by stirring be small in comparison with the total rate of heat flow to or from the sample.[8] If the stirring energy is significantly large, appropriate correction for it must be made in evaluating the time of crystallization, as described in part II–3 of reference [1]. The time z_r is selected as far as possible down the equilibrium portion of the curve (see GHI in fig. 5 and 8). Then the freezing point for zero impurity is

$$t_{f_0}=t_f+\left(\frac{1-r}{r}\right)(t_f-t_r), \tag{15}$$

where t_r is the equilibrium temperature at the time z_r. It is desirable to make the determination of t_{f_0} from several experiments on the same or different samples of the highest purity.

When the value of the freezing point for zero impurity is thus determined, and a value of the cryoscopic constant (or constants) is known, the calculation of the purity is made by means of the appropriate equations given in the preceding section.

Whenever the value of the cryoscopic constant A is not known, a value for it may be determined as described in the following section.

The second procedure for determining t_{f_0} is described on pages 205–207 of reference [2]. This procedure, which requires no additional experimental data, is applicable only to those experiments in which the time-temperature observations extend over a sufficiently large fraction (of the order of ¼ to ½) of material crystallized. The geometrical construction for determining t_{f_0} by this procedure is illustrated in figure 6. If the point M lies off the available plotting space,

[7] If the resistance-time curve at the freezing point, for either a melting or a freezing experiment, is not sufficiently linear to permit reasonably accurate evaluation of the slope directly from the resistance-time plot, the slope at the freezing point may be readily evaluated, from the data of either the freezing or the melting experiment, by plotting, as a function of time, values of the slope of successive chords of the resistance-time curve taken as the difference in successive readings of resistance divided by the time interval in minutes, and extrapolating these slopes to the "zero" time, z_f, at the freezing point.

[8] The energy of stirring may be readily determined by having the substance and container at the temperature of the jacket (0°, —80°, or —185° C), taking observations of resistance, with stirring, for a period of 10 minutes, stopping the stirrer for a period of 5 minutes, again taking observations of resistance, with stirring, for another period of 10 minutes, etc. The cessation of stirring in a given period produces, between the two periods adjacent to it, an offset (decrease) of the resistance (temperature) curve with respect to time. The actual displacement of the resistance-time line between the two stirring periods, measured at the middle of the period of no stirring, divided by 5, the number of minutes in which the stirrer was halted, gives the value of the stirring energy in terms of the change of resistance (temperature) per minute, of the given system.

its value may be determined analytically as follows [2]: Given the three points G, H, and I on the equilibrium curve, having values of time equal to z_G, z_H, and z_I (with point H having been selected midway between G and I in point of time, so that $z_G - z_H = z_H - z_I$) and values of temperature (resistance) equal to t_G, t_H, and t_I, respectively. Then (see footnote 5)

$$t_{f_0} = t_G + (t_G - t_I)/(u-1), \tag{16}$$

where

$$u = (t_H - t_I)/(t_G - t_H). \tag{17}$$

In general, it is desirable to utilize both of the foregoing procedures where possible. The two procedures should give the same result within the respective limits of uncertainty. (See fig. 5 in reference [2].)

X. DETERMINATION OF THE CRYOSCOPIC CONSTANT

When enough of the given compound is available, the cryoscopic constant may be determined directly by measuring the lowering of the freezing point caused by the addition to it of a measured amount of an appropriate solute. The amount of the given compound required is about 40 ml, and its purity should be about 97 or more mole percent. The solute required to be added is one that will form with the given compound a substantially ideal solution (with no solid solutions), its purity should be about 97 or more mole percent, and the amount required is about 2 ml. Preferably, the solute added should be isomeric with the given compound and the impurity in the solute should not include any significant amount of the given compound. Furthermore, the solute added must be one that does not form a eutectic mixture with the given compound at the resulting concentration in the solution formed. In general, eutectic mixtures of this low concentration will be likely to occur only for solutes that have freezing points much higher than the given substance.[9]

Let H be the given hydrocarbon compound under examination. Measurement is made of the freezing point, t_f^p, of a sample of "pure" H, according to the procedure described in the preceding sections of this report. To a weighed amount of 40 ml of pure H is added 2 ml of the given solute, with the weight of the solute being determined from the increase in weight. The solution thus formed is one in which the concentration of the hydrocarbon H is about 5 mole percent less than in the pure H. Measurement is made of the freezing point, t_f^s, of the solution. Let

m^p = the mass of the pure H used in making the solution of H.
m^q = the mass of the solute, Q.
M^p = the molecular weight of pure H, taken to be that given by the molecular formula of H;
M^q = the molecular weight of the solute, Q, taken to be that given by the molecular weight of Q;
N^p = the mole fraction of H in pure H;
N^s = the mole fraction of H in the solution formed from H and Q, calculated from the masses and molecular weights. If H and Q are isomeric, the mole fraction is identical with the weight fraction.

[9] For example, *p*-xylene (fp=13.26° C) forms with ethylbenzene (fp=−94.95° C) a eutectic mixture in which there is about 3½ mole percent of *p*-xylene.

Then the following relations hold

$$-\ln N^p = A(t_{f_0} - t_f^p) \tag{18}$$

$$-\ln N^s = A(t_{f_0} - t_f^s) \tag{19}$$

$$-\ln (N^s/N^p) = A(t_f^p - t_f^s) \tag{20}$$

$$A = -2.3026 \, [\log_{10} (N^s/N^p)]/(t_f^p - t_f^s). \tag{21}$$

For many compounds, the value of $t_f^p - t_f^s$ in the foregoing experiments will be, for the amounts indicated, about 1° to 2° C, and the uncertainty in the resulting value of the cryoscopic constant should be not more than several percent. (See reference [3]).

In case 40 ml of the given compound in a purity of about 97 percent is not available for making up a solution as described above, the cryoscopic constant, A, may be determined, without contaminating the sample, from a value of the heat of fusion estimated by a comparison with observations on a substance whose heat of fusion is known [1]. The procedure is as follows: Select a similar compound F whose heat of fusion is known and whose freezing point is within about 15° C of that of the compound G whose heat of fusion is to be estimated. Perform a complete time-temperature freezing experiment on the substance F, and likewise on the substance G, using substantially the same number of moles in each case and the same jacket temperature. For each of the experiments, the corrected time of crystallization is determined. Then, approximately,

$$(\Delta Hm)_G = (\Delta Hm)_F \frac{(\Delta t/\Delta z)_G (z_{x\,ln})_G}{(\Delta t/\Delta z)_F (z_{x\,ln})_F}. \tag{22}$$

The foregoing relation will yield a value for the heat of fusion, and hence the cryoscopic constant, which will in most cases be uncertain by not more than about 20 percent of itself. The accuracy of this procedure can be improved by using two reference substances, one of freezing point above and the other below that of the given substance, and appropriately interpolating.

Where possible, the method of determining the cryoscopic constant by direct measurement of the lowering of the freezing point is to be preferred over the approximate method described in the preceding paragraph. For use in the ideal systems discussed in this report, the most accurate values of the cryoscopic constants are usually derived from heats of fusion measured calorimetrically.

XI. DISCUSSION

Duplicate determinations of the freezing point of a given sample made by a given operator with the apparatus and procedure described in sections III to VII will usually differ by not more than 0.002 to 0.005 degree centigrade, except for very impure samples and for compounds having rather small values of the cryoscopic constant A. It follows that duplicate determinations would yield values of purity (in mole percent) differing usually by not more than 0.2 to 0.5 times the cryoscopic constant A (in deg^{-1}).

Determinations of the freezing point of a given sample made in different laboratories with the apparatus and procedure described in sections III to VII should normally differ by not more than about 0.01 to 0.02 degree centigrade, if the resistance bridges and the plati-

num resistance thermometers have been properly calibrated, as with constants certified by the National Bureau of Standards, and measurements of the ice point are made at appropriate intervals.

Assuming that the impurity remains entirely in the liquid phase during crystallization and forms with the major component a substantially ideal solution, the uncertainty in the value of the purity of a given sample determined with the present apparatus and procedure will include (a) an uncertainty in the value of the freezing point t_f, which uncertainty has been discussed above, and (b) an uncertainty in the given value of t_{f_0}. For substances having a large value of the cryoscopic constant A, the uncertainty in t_{f_0} will usually be near 0.01 to 0.03 degree centigrade, if the sample available for measurement has a purity of about 99.8 or more mole percent. For substances having a small value of the cryoscopic constant A, the uncertainty in t_{f_0} may be near 0.05 to 0.10 degree centigrade, when the determination is made on a sample having a purity of about 99.8 or more mole percent. The uncertainty in the value of t_{f_0} will, of course, decrease with increase in the purity of the sample. As discussed in section VIII, calculations relating to systems of known components should be based, when possible, upon actual experimental observations on known mixtures of such compounds.

For those compounds that have one or more metastable forms whose freezing points can be determined, it becomes necessary to ascertain for which crystalline form the determined freezing point has been obtained. For those cases where the freezing point (for zero impurity) of metastable form II is more than a few degrees below that of the stable form I, there is little difficulty in identifying the forms, as it would usually require a rather impure sample of form I to have a freezing point below that of a pure sample of form II. When the difference in the freezing points (for zero impurity) of the two forms is less than several degrees, and especially when the difference is less than one degree, the problem of identifying the forms is somewhat more involved. However, except in the most complicated case, it is possible to determine the value of t_{f_0} yielded by the given experiment (as outlined in section IX) and to identify the crystalline form from the value of t_{f_0}.

Measurements of freezing points of actual "best" samples, with evaluation of freezing points for zero impurity, together with determinations of cryoscopic constants as required, have been made, according to the method and procedures described in this report, on approximately 80 different purified hydrocarbons of the paraffin, alkylcyclopentane, alkylcyclohexane, alkylbenzene, monoolefin, diolefin, and cyclomonoolefin series in connection with the work at this Bureau of the American Petroleum Institute Research Project 6 on the purification and properties of hydrocarbons. Determinations of the purity of the NBS Standard Samples of hydrocarbons are also being made by the procedures described in this report. Complete details of this experimental work will appear in other reports from the National Bureau of Standards [7].

XII. REFERENCES

[1] B. J. Mair, A. R. Glasgow, Jr., and F. D. Rossini, J. Research NBS **26,** 591 (1941) RP1397.
[2] W. J. Taylor and F. D. Rossini, J. Research NBS **32,** 197 (1944) RP1585.
[3] A. J. Streiff and F. D. Rossini, J. Research NBS **32,** 185 (1944) RP1584.
[4] G. K. Burgess, J. Research NBS **1,** 635 (1928) RP22.
[5] E. W. Washburn, J. Am. Chem. Soc. **32,** 653 (1910).
[6] G. N. Lewis and M. Randall, Thermodynamics and the free energy of chemical substances (McGraw-Hill Book Co., Inc., New York, N. Y., 1923).
[7] American Petroleum Institute Research Project 6 and Hydrocarbon Standard Samples Laboratory; National Bureau of Standards. Unpublished data.

WASHINGTON, May 20, 1945.

Reprinted from ANALYTICAL CHEMISTRY, Volume 20, Page 321, April 1948

Double Freezing-Point Method for Determination of Styrene Purity

JOSEPH F. MASI AND RUTH K. CHENEY

National Bureau of Standards, Washington, D. C.

A method is described for determining the purity of recycle and blended styrene monomer, in which the purity is from 87 to 98% and the principal impurities are ethylbenzene, 4-vinylcyclohexene, and 1,3-butadiene. The data required are the freezing points of the original sample and of a portion from which the volatile impurities have been removed. The separation of low-boiling hydrocarbons is accomplished by complete evaporation of a portion of the sample under low pressure and condensation of the styrene and heavy impurities as solid in a trap at −65° C. The probable error of the method is estimated at ±0.15 weight % of styrene in samples of lower purity.

THE measurement of the freezing-point depression is one of the most convenient ways of determining the purity of hydrocarbons in general. The method presented here demonstrates what may be accomplished by the use of liquid-in-glass thermometers for routine work in industrial laboratories where the time, personnel, and equipment may not be available for the more accurate technique using platinum resistance thermometers. The method also includes a simple and effective procedure for separating very volatile impurities when they are present in amounts up to a few per cent.

The method was developed for determination of the purity of recycle and blended styrene in the synthetic rubber plants under the control of the Office of Rubber Reserve of the Reconstruction Finance Corporation.

THEORETICAL

If a solution which is predominantly styrene is ideal with respect to all the constituents, and if the impurities remain in the liquid phase while the styrene is being frozen, we may write (*4, 5*):

$$-\ln N_1 = A\,\Delta t(1 + B\,\Delta t \ldots) \qquad (1)$$

where N_1 is the mole fraction of styrene, $\Delta t = t_0 - t_f$, the difference between the freezing points of pure styrene and solution,

$$A = \frac{\Delta H_0}{RT_0^2} \qquad (2)$$

and

$$B = \frac{1}{T_0} - \frac{\Delta C_{p_0}}{2\,\Delta H_0} \qquad (3)$$

T_0, ΔH_0, and ΔC_{p_0} represent, respectively, the freezing point (degrees Kelvin), molar heat of fusion, and change of molar heat capacity on fusion, of pure styrene. Terms of higher order than those indicated in the parentheses in Equation 1 may be neglected.

Since in plant practice it is required that the purity of the sample be given in weight per cent, it is necessary to have an evaluation of the number, nature, and relative amounts of the impurities, in addition to the conditions imposed in Equation 1. The principal impurities in recycle styrene are ethylbenzene, 4-vinylcyclohexene, and 1,3-butadiene (*1, 2*); it has been assumed that others are present in negligible amounts. If it is further assumed that the ratio of ethylbenzene to 4-vinylcyclohexene is approximately constant, only two independent measurements are needed to fix the weight per cent of styrene. The last assumption is justified because the molecular weights of the two C_8 impurities are so close together that for a given number of total moles of ethylbenzene and 4-vinylcyclohexene, even large variations in their molecular ratio will cause only small differences in their total weight per cent actually present in the sample and also calculated from freezing-point depression if, again, the solution is ideal.

The two independent measurements chosen are the freezing points of the sample before and after separation of the light hydrocarbons from it. It is obviously of practical advantage to have a single procedure for both measurements.

By applying Equation 1 to both freezing points, equations were developed for the weight per cent of C_8 impurity in the C_8-free sample, the weight per cent

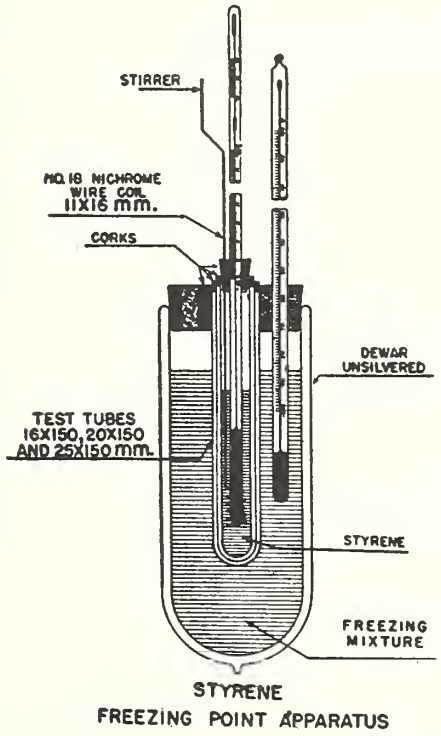

Figure 1. Styrene Freezing Point Apparatus

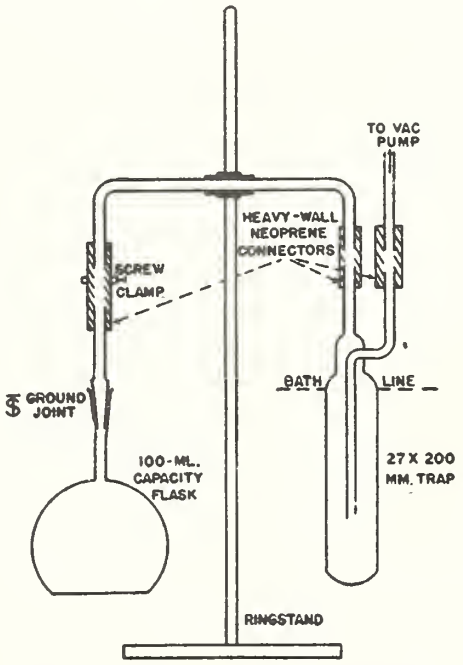

Figure 2. Apparatus for Separation of Low-Boiling Impurities

of butadiene, and the weight per cent of styrene. The assumption of ideality, on which these equations were based, is invalid, however, for solutions of ethylbenzene and butadiene in styrene. Since it was found that an error of as much as 0.7%, in 90% styrene solutions, can be introduced by the use of the theoretical equations, they were discarded in favor of empirical relations obtained from experimental data, as described below.

APPARATUS AND MATERIALS

The freezing-point apparatus (Figure 1) consists of a 665-ml. unsilvered Dewar vacuum flask of Pyrex, a nest of three test tubes, and a stirrer operated by a reciprocating vacuum-type stirrer motor. (This apparatus is substantially the same as that designed by Irving Madorsky, Rubber Section, National Bureau of Standards, for freezing-point purity of fresh styrene.) The temperature of the styrene is measured with a mercury-thallium–filled thermometer, designed in this laboratory especially for freezing points of recycle styrene. This thermometer is graduated from −42° to −29° C. in 0.05° with an auxiliary scale from −0.5° to +0.5° C., and has a total length of 470 to 480 mm., a bulb length of 50 to 60 mm., and a diameter of 6 to 7 mm.

The apparatus for separation of low-boiling impurities (Figure 2) consists of an evaporating flask and a cold trap, connected as shown by glass tubing (8 to 10 mm. in outside diameter) and heavy-walled neoprene connectors. The bath surrounding the cold trap is contained in a Dewar flask, preferably silvered. The vacuum pump used with this apparatus is capable of reducing the pressure to less than 0.5 mm. of mercury and has a capacity sufficient to maintain the pressure below 10 mm. of mercury when pumping on the impure styrene solution.

The materials necessary for an analysis are dry ice and a freezing mixture made of equal parts by volume of chloroform and carbon tetrachloride.

The following materials were used in making up the solutions for investigation of the method:

Styrene. Two lots of styrene monomer were specially purified by the Dow Chemical Company. The purities of the two lots, by freezing point, were 99.80 and 99.90 weight %.

Ethylbenzene. A sample purified by the Petroleum Laboratory of the Pennsylvania State College, at least 99.5% pure by melting point, was used.

4-Vinylcyclohexene. The sample used was purified by fractional distillation by the Koppers Company. From refractive index and specific gravity measurements, its purity was judged to be better than 95%.

1,3-Butadiene. Phillips Petroleum Company's Pure Grade butadiene, 99% pure by freezing point, was used without further purification.

PROCEDURE

The following procedure, although describing operations on plant samples, is also applicable to the synthetic mixtures discussed later. The first step in an analysis is to determine the freezing point, t_1, of a portion of the original sample. The next step is to remove the light hydrocarbon impurities from another portion of the sample and determine its freezing point, t_2. From t_2 is computed the weight per cent of heavy impurity, p_i, in this sample from which the light hydrocarbons have been removed. Finally the weight per cent of light impurity, p_2, in the original material is computed from the difference in the two freezing points, $t_2 - t_1$.

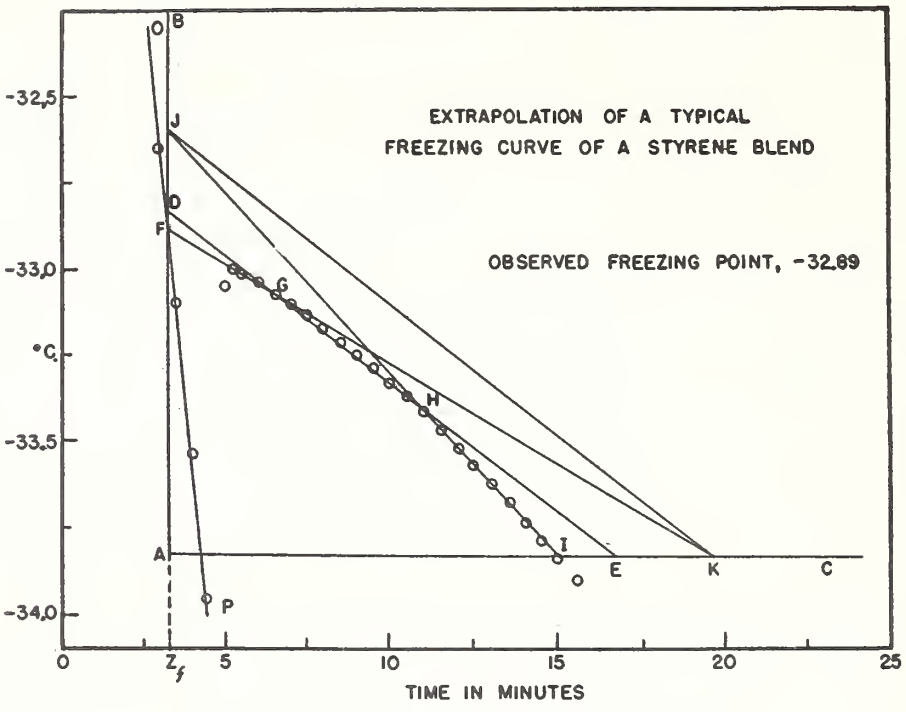

Figure 3. Freezing Curve of Styrene Blend

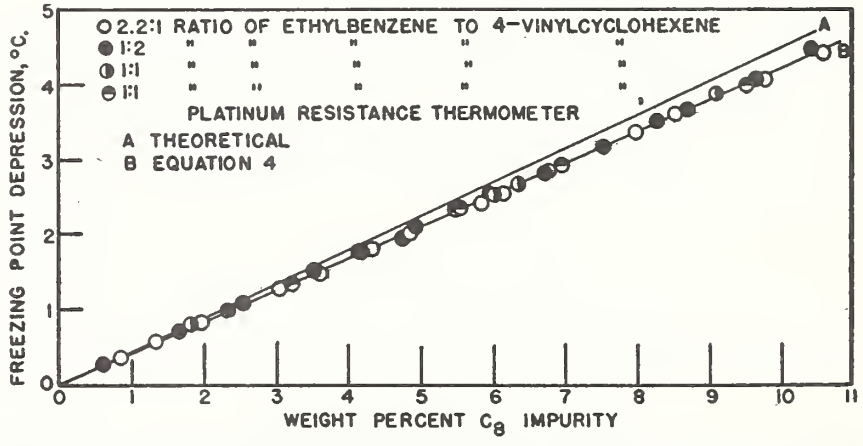

Figure 4. Experimental Freezing Point Depression of Styrene by Ethylbenzene and 4-Vinylcyclohexene

Samples of recycle and blend styrene to be analyzed are obtained in clean screw-cap bottles of about 1-pint capacity. These samples are chilled to 40° F. (4.4° C.) before analysis in order to minimize the loss of light hydrocarbons by evaporation.

Determination of Freezing Points. The freezing mixture in the Dewar flask is cooled with dry ice to −43° C. Approximately 10 ml. of the sample are placed in the innermost test tube and the apparatus is assembled as in Figure 1. The thermometer is immersed at least 2 cm. above the bulb and the bath level is about 2 cm. above the sample. Throughout the determination the sample is stirred at the rate of about 150 strokes per minute, and the bath is maintained (by addition of small pieces of dry ice) within 0.5° of a temperature selected so that the rate of cooling of the sample, while freezing, is near 0.1° C. per minute. This rate of freezing is produced by temperatures from −42° to −44° C. with the apparatus shown in Figure 1.

The temperature of the sample is read to 0.01° C. at 30-second intervals; at least three readings are taken before freezing begins and from 20 to 25 after freezing begins. The time-temperature readings are plotted on a graph which is scaled so that 1° (on the ordinate) is equal to 10 cm. and 10 minutes are equal to 10 cm.

The uncorrected freezing points are determined by extrapolat-

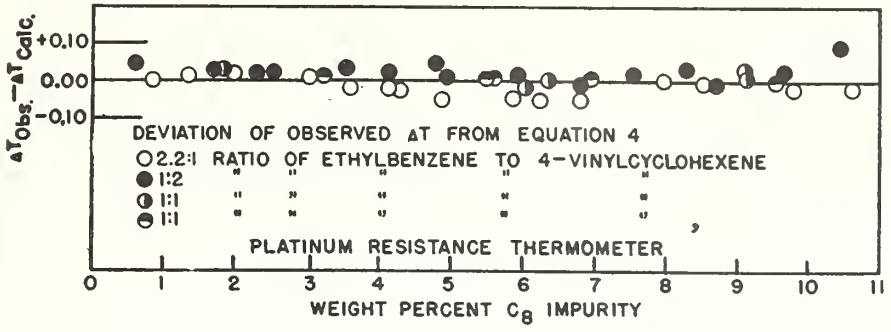

Figure 5. Deviation of Experimental Freezing Points from Empirical Equation 4 for Mixtures with No Butadiene

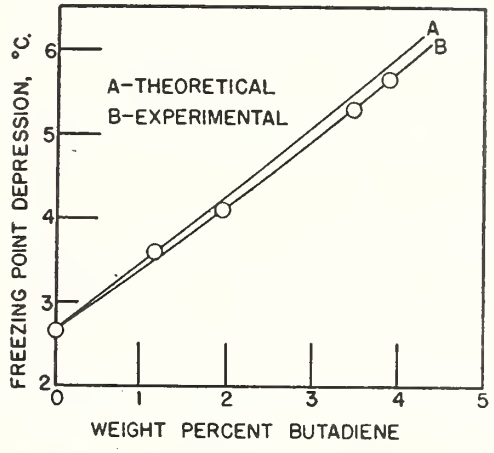

Figure 6. Freezing Point Depression by 1,3-Butadiene of Styrene Containing 6.37 Weight % C_8 Impurity

ing the time-temperature curves by a graphical method described by Taylor and Rossini (*4*). This method is illustrated in Figure 3.

After the liquid cooling curve, *OP*, and a vertical line, *AB*, are drawn at the estimated time, Z_f, that freezing would have begun in the absence of undercooling, three experimental points *G*, *H*, and *I* are chosen about equally spaced and as far apart as possible; *G* is sufficiently far from the beginning of freezing so that essential equilibrium has been established. A horizontal line is drawn through *I*, *DE* is drawn through *H* and *G*, *JI* is drawn through *H* and *I*, and *JK* is drawn parallel to *DE*. The extrapolated freezing point, *F*, is obtained by drawing a line from *K* through *G* to intersection with *AB*.

The corrected freezing points are obtained by adding algebraically to the uncorrected values, the calibration correction, the change in ice-point correction since the original calibration, and the correction for emergent stem, for the thermometer used. The corrected freezing point of the original sample is called t_1, and the corrected freezing point of the sample after removing butadiene is called t_2. The respective freezing-point lowerings, Δt_1 and Δt_2, are obtained by subtraction from −30.63° C., the freezing point of pure styrene (*3*). The per cent styrene is calculated from Equations 4, 5, and 6, or from a nomogram prepared from them.

In order to realize the greatest possible accuracy with liquid-in-glass thermometers it is necessary to check their calibration and the freezing-point procedure being followed. These thermometers are prone to change in bulb volume and rise in ice point, particularly during the first few months after manufacture. It is not unusual for this change to be as great as 0.1° C.

The thermometers are calibrated before use by the National Bureau of Standards.

Calibration corrections are obtained under total immersion conditions at −40°, −35°, −30°, and 0° C., are stated to 0.01° C., and are good to 0.02° C. If the bulb volume changes, the calibration at all points on the scale will be changed by a constant amount; this correction is obtained by taking ice points weekly during the first six months of the life of the thermometer, or until it appears that only small changes are taking place. Ice points are checked every month or two after that. Good ice points are obtained by crushing clean, clear ice, washing it, and making a thick slush with distilled water. The thermometer is immersed to the 0° mark in this slush, in a vessel protected from radiation.

A further control measure is freezing of a standard material of known freezing point. A stable reference substance, having a freezing point close to that of styrene, is bromobenzene. A sampleof this substance, with a freezing point certified by the National Bureau of Standards, is frozen in the same way as a sample of styrene, except that freezing is continued until the stirrer begins to labor or until the sample has been freezing about 20 minutes. The points are plotted with a temperature scale about 5 times as sensitive as that for styrene. In following the extrapolation procedure given above, it is important to disregard the initial flat portion of the freezing curve, by choosing points *G*, *H*, and *I* (Figure 3) so that *G* is on the downward-sloping portion of the curve. Errors of several hundredths of a degree were discovered after failure to observe this precaution on two occasions.

By making use of these checks, an accuracy of ±0.02° C. can be obtained.

Separation of Low-Boiling Impurities. Since the low-boiling impurities (principally butadiene) differ so greatly in volatility from the remainder of the impure styrene mixture, they may be effectively removed by the following simple procedure.

About 15 ml. of the original sample are poured into the flask of the evaporating apparatus (Figure 2), and the apparatus is assembled as shown and connected to the pump and a small manometer. Before the clamp above the flask is opened, the system is pumped out to less than 0.5 mm. and the cold trap is cooled with a carbon tetrachloride–chloroform mixture maintained at −65° C. with dry ice. While the flask is shaken gently, the clamp is opened slowly enough so that the pressure does not rise above 10 mm. After the clamp is open, a beaker of warm water placed around the flask aids evaporation. The styrene, ethylbenzene, and 4-vinylcyclohexene are condensed as solid on the walls of the trap, while the light hydrocarbons pass through as vapor. When the sample has completely evaporated, the cold trap is detached, the contents are allowed to melt, and the freezing point of the condensate is determined.

DATA ON SYNTHETIC MIXTURES

In order to investigate the method and develop the required empirical relationships between freezing point and composition, a series of experiments was made on 68 synthetic mixtures ranging from 87 to 98% styrene. The mixtures were made up with known composition and their freezing points determined by the procedure described above. The first thirty of these styrene solutions contained the solutes ethylbenzene and 4-vinylcyclohexene in ratios of 2.2 to 1 and 1 to 2. At a much later time, freezing points of eight solutions containing ethylbenzene and 4-vinylcyclohexene in various ratios were obtained. Some freezing points were also obtained with a platinum resistance thermometer on solutions containing ethylbenzene and 4-vinylcyclohexene in 1 to 1 ratio. The freezing-point lowering is plotted against weight per cent, for all these solutions containing no light hydrocarbons, in Figure 4. Various equations were fitted to these points by the method of least squares. Separate equations through the points representing different ratios of the impurities could be obtained, but at 90% styrene, the difference in per cent styrene found by using 2.2 to 1 ratio of ethylbenzene to 4-vinylcyclohexene instead of 1 to 2 was only 0.16%. Since there does not exist at this time a good independent method for determining

the ratio of these two impurities, and there is some evidence that the ratio is usually in the neighborhood of 1 to 1 (*2*), a least square fit was obtained using a quadratic function of Δt_2 for all the points together. This equation is

$$p_1 = 2.389\,\Delta t_2 + 0.003\,\Delta t_2^2 \qquad (4)$$

and is shown by curve *B* in Figure 4. Curve *A* is obtained from the laws of ideal solutions. The deviations of observed freezing-point depressions from those calculated by Equation 4 are shown in Figure 5. As expected, most of the points representing 2.2 to 1 ratio of ethylbenzene to 4-vinylcyclohexene give negative deviations, while those of the inverse ratio are positive.

By low-temperature condensation in vacuum, butadiene in various amounts was added to various mixtures of styrene and the 1 to 1 mixture of ethylbenzene and 4-vinylcyclohexene. The nonideality of the butadiene-styrene solutions is shown by the points of one series of solutions in Figure 6. The solutions in this series were made by adding butadiene to styrene containing 6.37 weight % of ethylbenzene and 4-vinylcyclohexene (1 to 1). Other series containing different amounts of heavy impurities gave similar curves. After the freezing-point determinations, the added butadiene was removed (from fresh portions of the solutions) by the vacuum evaporation procedure given above, and freezing points (t_2) were determined. It was found that the weight per cent of butadiene could be represented within the experimental error by the equation

$$p_2 = 1.366(t_2 - t_1) - 0.025(t_2 - t_1)^2 \qquad (5)$$

The deviations of the experimental values of $t_2 - t_1$ from those calculated by Equation 5 are plotted against weight per cent of butadiene in Figure 7. No correlation with content of heavy impurities is observed.

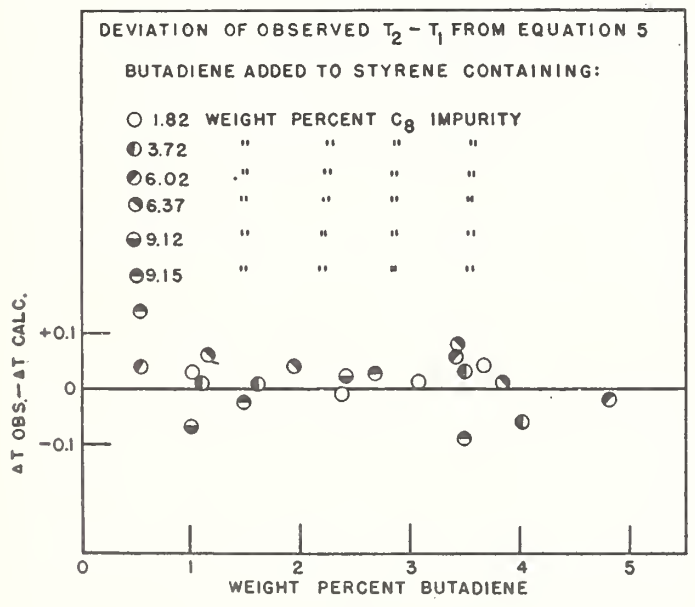

Figure 7. Deviation of Experimental Freezing Point Lowering by Butadiene from Empirical Equation 5

The weight per cent of styrene in the original sample was obtained from the equation

$$p_3 = \frac{(100 - p_1)(100 - p_2)}{100} \qquad (6)$$

The average of the deviation of all the solutions from the calculated value of p_1 obtained by Equation 4 was ±0.06 weight %. The average deviation of p_2, in the synthetic mixtures containing butadiene, from the value calculated by Equation 5, was ±0.05.

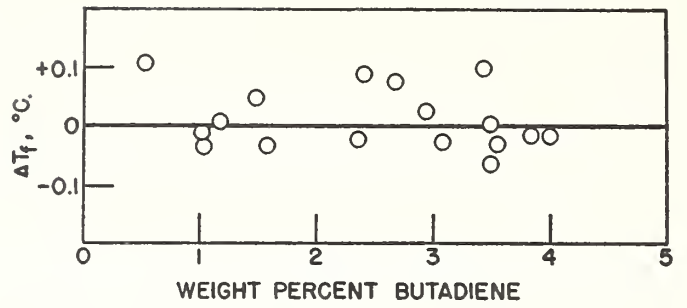

Figure 8. Change in Freezing Point of Impure Styrene Solutions Caused by Adding and Removing 1,3-Butadiene, Plotted against Weight Per Cent of 1,3-Butadiene

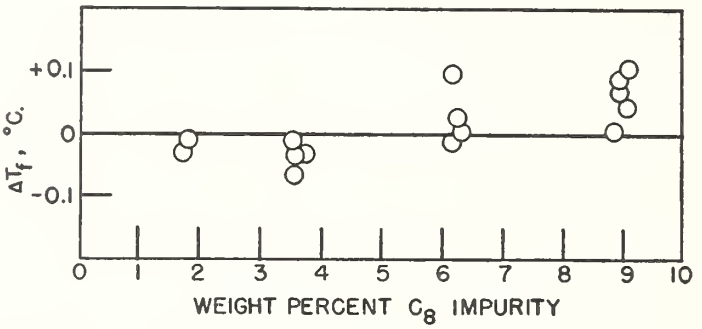

Figure 9. Change in Freezing Point of Impure Styrene Solutions Caused by Adding and Removing 1,3-Butadiene, Plotted against Weight Per Cent of C_8 Impurity

The weight per cent of styrene in all solutions was calculated by use of Equations 4, 5, and 6, and compared with the actual values; the average deviation in p_3 was ±0.06.

The efficiency of the separation of low-boiling impurities is shown by the results obtained on seventeen synthetic mixtures, which are plotted in Figures 8 and 9. The difference in freezing point of the sample before adding butadiene and after removing it by vacuum evaporation is plotted against per cent butadiene in Figure 8. No correlation is observed. In Figure 9 the change in freezing point of the same samples, due to the addition and removal of butadiene, is plotted against per cent heavy impurity in the sample. The positive side of the Δt_f axis is the direction of increase of purity upon separation. From these two graphs, it is evident that the greater the percentage of ethylbenzene and 4-vinylcyclohexene, the more of these substances are removed in the separation, regardless of the amount of butadiene. This observation seems to indicate that the error is caused by distillation of the heavier fraction rather than by the sweeping of solid particles through the trap. The latter effect would be the first error suspected in the arrangement of this apparatus, but such effects are partly dependent upon the amount of gas passing through.

ACCURACY

The error in the freezing-point determinations which is caused by the use of a liquid-in-glass thermometer should not exceed 0.03° C. Reproducibility of freezing points in this laboratory, using different thermometers and different operators, has been of the order of 0.02° C.

There is no evidence that there is any error in the first freezing point (t_1) caused by evaporation of light hydrocarbons from the sample in the freezing tube, at least for samples containing less than 3% butadiene, provided the sample is thoroughly chilled before testing. If the first freezing point is correct, any error in the second freezing point (t_2) such as indicated by Figures 8 and 9, will result in a portion of the heavy impurity's being calculated as butadiene, or the reverse. Thus the error in per cent styrene is

essentially the difference between the error in p_1 and in p_2, or approximately the value of the error in t_2.

The error which can be made by assuming that the ratio of ethylbenzene to 4-vinylcyclohexene is 1 to 1 may be as large as 0.5% if the impurity is entirely one or the other. However, those recycle styrenes which have been investigated have contained these impurities in ratios from 1:2 to 2:1.

An appreciable error in the method is introduced by the assumption that the only impurities are ethylbenzene, 4-vinylcyclohexene, and 1,3-butadiene. The presence of C_4 hydrocarbons other than butadiene is not important, but there is recent evidence that recycle styrene contains C_9 hydrocarbons, particularly isopropylbenzene, in amounts which may be as large as 1.5% (*2*). An error of as much as 0.2 in the weight per cent of styrene may thus be made.

After consideration of all the above sources of error, the probable error in weight per cent of styrene as determined by the double freezing point method is set at ±0.15, for samples of 90% purity.

ACKNOWLEDGMENT

The authors wish to express their appreciation to Daniel R. Stull and the Dow Chemical Company for the specially purified lots of styrene which they furnished for this investigation.

LITERATURE CITED

(1) Frieden, E., Freeman, L., and Ebrey, G. O., Technical Report to Reconstruction Finance Corp., Office of Rubber Reserve, OPS-24, Aug. 20, 1945.
(2) National Bureau of Standards, Thermochemistry Section, unpublished data contained in analytical reports to Reconstruction Finance Corp., Office of Rubber Reserve.
(3) Rands, R. D., and Brickwedde, F. G., recent unpublished work at National Bureau of Standards.
(4) Taylor, W. J., and Rossini, F. D., *J. Research Natl. Bur. Standards*, **32**, 197–214 (1944).
(5) Washburn, E. W., *J. Am. Chem. Soc.*, **32**, 666 (1910).

RECEIVED August 16, 1947. Presented before the Division of Analytical and Micro Chemistry at the 111th Meeting of the AMERICAN CHEMICAL SOCIETY, Atlantic City, N. J.

Revised
1960

U. S. DEPARTMENT OF COMMERCE

NATIONAL BUREAU OF STANDARDS

List of
Publications
LP 32

TEMPERATURE MEASUREMENTS

Publications by Members of the Staff of the

National Bureau of Standards

Liquid-in-Glass Thermometry

C. W. Waidner and L. A. Fischer, The testing of clinical thermometers, Bul. BS 1, 275 (1904-05), S13.

H. C. Dickinson, Heat treatment of high-temperature mercurial thermometers, Bul. BS 2, 189 (1906), S32.

E. Buckingham, The correction for "emergent stem" of the thermometer, Bul. BS 8, 239 (1912), S170.

Testing of thermometers. (Contains general information of interest to those who desire to submit thermometers to the NBS for test.) Circ. BS, C8 4th ed, (1926).

Clinical thermometers, Commercial Standard CS1-52. 4th ed., CS1-52 (1951), (Commodity Standards Division, Office of Technical Services, U. S. Department of Commerce, Washington 25, D. C.)

E. F. Mueller and R. M. Wilhelm, Methods of testing thermometers, Proc. A. S. T. M. (260 s. Broad Street, Philadelphia, Pa.), 38, 1 (1938).

J. Busse, Liquid-in-glass thermometers. Temperature, Its Measurement and Control in Science and Industry, p. 228 (Reinhold Publishing Corp., New York, N. Y., 1941).

J. Busse, Thermometry. Medical Physics, p. 1555 (The Year Chicago, Ill., 1944).

A. Q. Tool and J. B. Saunders, Expansion effects of annealing borosilicate thermometer glasses, J. Research NBS 42, 171 (1949), RP1960.

Resistance Thermometry

C. W. Waidner and G. K. Burgess, Platinum resistance thermometry at high temperatures, Bul. BS 6, 149 (1909-10), S124.

E. F. Mueller, Wheatstone bridges and some accessory apparatus for resistance thermometry, Bul. BS 13, 547 (1916-17), S288.

T. S. Sligh, Jr., Recent modifications in the construction of platinum resistance thermometers, Sci. Pap. BS17, 49 (1922), S407.

M. S. Van Dusen, Note on platinum resistance thermometry at low temperatures, J. Am. Chem. Soc. (1155 16th St., N. W., Washington 6, D. C.), 47, 326 (1925).

E. F. Mueller, Precision resistance thermometry, Temperature, Its Measurement and Control in Science and Industry, P. 162 (Reinhold Publishing Corp., New York, N. Y., 1941).

574278 O - 61 - 14

C. H. Meyers, Coiled-filament resistance thermometers, BS J. Research 9, 807 (1932), RP508.

H. J. Hoge and F. G. Brickwedde, Establishment of a temperature scale for the calibration of thermometers between 14° and 83° K, J. Research NBS 22, 351 (1939), RP1188.

H. J. Hoge and F. G. Brickwedde, Intercomparison of platinum resistance thermometers between -190° and 445° C, J. Research NBS 28, 217 (1942), RP1454.

H. J. Hoge, Electrical conduction in the glass insulation of resistance thermometers, J. Research NBS 28, 489 (1942), RP1466.

J. L. Thomas, Precision resistors and their measurement, NBS Circ. 470, (1948) 20 cents.

Thermoelectric Thermometry

W. F. Roeser, The passage of gas through the walls of pyrometer protection tubes at high temperatures, BS J. Research 7, 485 (1931), RP354.

H. B. Brooks and A. W. Spinks, A multi-range potentiometer and its application to the measurement of small temperature differences, BS J. Research 9, 781 (1932), RP506.

W. F. Roeser and H. T. Wensel, Reference tables for platinum to platinum-rhodium thermocouples, BS J. Research 10, 275 (1933), RP530.

W. F. Roeser, F. H. Schofield, and H. A. Moser, An International comparison of temperature scales between 660° and 1,063°C, BS J. Research 11, 1 (1933), RP573.

W. F. Roeser, A. I. Dahl and G. J. Gowens, Standard tables for chromel-alumel thermocouples, J. Research NBS 14, 239 (1935), RP767.

W. F. Roeser and H. T. Wensel, Methods of testing thermocouples and thermocouple materials, J. Research NBS 14, 247 (1935). Also in Temperature, Its Measurement and Control in Science and Industry, p. 284 (Reinhold Publishing Corp., New York, N. Y., 1941). RP768.

W. F. Roeser and A. I. Dahl, Reference tables for iron-constantan and copper-constantan thermocouples, J. Research NBS 20, 337 (1938), RP1080.

A. I. Dahl, Stability of base-metal thermocouples in air from 800° to 2200°F, J. Research NBS 24, 205 (1940), RP1278. Also in Temperature, Its Measurement and Control in Science and Industry, p. 1238 (Reinhold Publishing Corp., New York, N. Y., 1941).

R. B. Scott, Calibration of thermocouples at low temperatures, J. Research NBS 25, 459 (1940), RP1339. Also in Temperature, Its Measurement and Control in Science and Industry, p. 206 (Reinhold Publishing Corp., New York, N. Y., 1941).

W. F. Roeser, Thermoelectric thermometry, J. Applied Phys. 11, 388 (1940). Also in Temperature, Its Measurement and Control in Science and Industry, p. 180 (Reinhold Publishing Corp., New York, N. Y., 1941).

E. F. Fiock and A. I. Dahl, The use of thermocouples in high-velocity gas streams, J. Am. Soc. Naval Engrs. 60, 139 (1948).

A. I. Dahl and E. F. Fiock, Shielded thermocouples for gas turbines, Trans. A. S. M. E. 71, 153 (1949).

E. F. Fiock, L. O. Olsen, and P. D. Freeze, The use of thermocouples in streaming exhaust gas, published in collected papers of the Third Symposium on Combustion, Flame and Explosion Phenomena (Waverley Press, Williams and Wilkins Co., Baltimore, Md., Copyright 1949).

R. J. Corruccini and H. Shenker, Modified 1913 reference tables for iron-constantan thermocouples, J. Research NBS 50, 229 (1953), RP2415.

H. Shenker, J. I. Lauritzen, Jr., R. J. Corruccini, and S. T. Lonberger, Reference tables for thermocouples, NBS Circ. 561 (1955). Supersedes NBS C508.

Optical and Radiation Pyrometry

G. K. Burgess and P. D. Foote, The emissivity of metals and oxides, I. Nickel oxide (NiO) in the range 600° to 1,300° C, Bul. BS 11, 41 (1915), S224.

G. K. Burgess and R. G. Waltenberg, The emissivity of metals and oxides. II. Measurements with the micropyrometer, Bul. BS 11, 591 (1915), S242.

P. D. Foote, The emissivity of metals and oxides. III. The total emissivity of platinum and the relation between total emissivity and resistivity, Bul. BS 11, 607 (1915), S243.

G. K. Burgess and P. D. Foote, The emissivity of metals and oxides. IV. Iron oxide, Bul. BS 12, 83 (1915-16), S249.

G. K. Burgess and P. D. Foote, Characteristics of radiation pyrometers, Bul. BS 12, 91 (1915-16), S250.

P. D. Foote, "Center of gravity" and "effective wave length" of transmission of pyrometer color screens, and the extrapolation of the high temperature scale, Bul. BS 12, 483 (1915-16), S260.

P. D. Foote, F. L. Mohler, and C. O. Fairchild, The proper type of an absorption glass for an optical pyrometer, J. Wash. Acad. Sci. (450 Ahnaip St., Menasha, Wis.), 7, 545 (1917).

C. O. Fairchild and W. H. Hoover, Disappearance of the filament and diffraction effects in improved forms of an optical pyrometer, J. Opt. Soc. Am. and Rev. Sci. Insts. (Cornell Univ., Ithaca, N. Y.), 7, 543 (1923).

H. T. Wensel and W. F. Roeser, Temperature measurements of molten cast iron, Trans. Am. Foundrymen's Assn. (222 W. Adams St., Chicago, Ill.), 36, 191 (1928).

W. F. Roeser, Spectral emissivity (at 0.65 u) of some alloys for electrical heating elements, Proc. A.S.T.M. (260 S. Broad Street, Philadelphia, Pa.) 39, 780 (1939).

Miscellaneous

E. Buckingham, On the establishment of the thermodynamic scale of temperature by means of the constant-pressure gas thermometer, Bul. BS 3, 237 (1907), S57.

R. D. Harper, 3rd., Thermometric lag, Bul. BS 8, 659 (1912), S185.

F. Wenner and E. Weibel, The testing of potentiometers, Bul. BS 11, 1 (1915), S223.

P. D. Foote, C. O. Fairchild, and T. R. Harrison, Pyrometric practice, Tech. Pap. BS, T170 (1921), T170.

E. F. Mueller and T. S. Sligh, Jr., A laboratory hypsometer, J. Opt. Soc. Am. and Rev. Sci. Insts. (Cornell Univ., Ithaca, N. Y.) 6, (1922).

C. W. Kanolt, Nonflammable liquids for cryostats, Sci. Pap. BS 20, 619 (1924-26), S520.

W. F. Roeser and C. O. Fairchild, Pyrometry of molten brass, Trans. Am. Foundrymen's Assn. (222 W. Adams St., Chicago, Ill.), 34, 675 (1926).

C. O. Fairchild and M. F. Peters, Characteristics of pyrometric cones, J. Am. Ceram. Soc. (2525 N. High St., Columbus, Ohio), 9, 701 (1926).

R. F. Geller and E. E. Pressler, A comparison of the softening points of some foreign and American pyrometric cones, J. Am. Ceram. Soc. (2525 N. High St., Columbus, Ohio), 9, 744 (1926).

G. K. Burges, The International Temperature Scale, BS J. Research 1, 635 (1928), RP22.

H. B. Henrickson, Thermometric lag of aircraft thermometers, thermographs, and barographs, BS J. Research 5, 695 (1930), RP222.

W. F. Roeser and E. F. Mueller, Measurement of surface temperatures, BS J. Research 5, 793 (1930), RP231.

R. B. Scott and F. G. Brickwedde, A precision cryostat with automatic temperature regulation, BS J. Research 6, 401 (1931), RP284.

W. H. Swanger and F. R. Caldwell, Special refractories for use at high temperatures, BS J. Research 6, 1131 (1931), RP327.

R. B. Kennard, An optical method for measuring temperature distribution and convective heat transfer, BS J. Research 8, 787 (1932), RP452.

J. L. Thomas, Reproducibility of the ice point, BS J. Research 12, 323 (1934), RP658.

H. T. Wensel, D. B. Judd, and W. F. Roeser, Establishment of a scale of color temperature, BS J. Research 12, 527 (1934), RP677.

D. N. Craig, Electrolytic resistors for direct-current applications in measuring temperatures, J. Research NBS 21, 225 (1938), RP1126.

H. T. Wensel, International Temperature Scale and some related physical constants, J. Research NBS 22, (1939), RP1189.

H. T. Wensel, Temperature, J. Applied Phys. 11, 373 (1940). Also in Temperature, Its Measurement and Control in Science and Industry, p. 3 (Reinhold Publishing Corp., New York, N. Y., 1941).

F. W. Schwab and E. Wichers, Precise Measurement of the freezing range as a means of determining the purity of a substance, Temperature, Its Measurement and Control in Science and Industry, p. 256 (Reinhold Publishing Corp., New York, N. Y., 1941).

C. P. Saylor, Control and measurement of temperature under the microscope, Temperature, Its Measurement and Control in Science and Industry, p. 673 (Reinhold Publishing Corp., New York, N. Y., 1941).

A. R. Glasgow, Jr., A. J. Streiff, and F. D. Rossini, Determination of the purity of hydrocarbons by measurement of freezing points, J. Research NBS 35, 355 (1945), RP1676.

Temperature interconversion tables (^{o}C-^{o}F) and melting points of the chemical elements, NBS Misc. Pub. (1947), M183.

A. I. Dahl and P. D. Freeze, Laboratory evaluation of a method proposed by Gnam for measuring the temperature of rotating parts, J. Research NBS 41, 601 (1948), RP1942.

H. F. Stimson, The International Temperature Scale of 1948, J. Research NBS 42, 209 (1949), RP1962.

R. J. Corruccini, Differences between the international Temperature Scales of 1948 and 1927, J. Research NBS 43, 133 (1949), RP2014.

J. B. Peterson and S. H. J. Womack, Electrical thermometers for aircraft, N.A.C.A. Report No. 606.

Tentative method of test for determination of purity by measurement of freezing points, ASTM Designation: D940-47T, (1916 Race St., Philadelphia, Pa.).

D. B. Judd, The 1949 scale of color temperature, J. Research NBS 44, 1 (1950), RP2053.

A. I. Dahl and E. F. Fiock, Response characteristics of temperature-sensing elements for use in the control of jet engines, J. Research NBS 45, 292 (1950), RP2136.

R. W. Murdock and E. F. Fiock, Measurement of temperatures in high-velocity steam, Trans A.S.M.E. 71, 1155 (1950).

A. I. Dahl, Measurement of high temperatures in gas streams, Bul. Agri. and Mech. College of Texas, Petroleum Refiner 29, 115 (1950).

R. J. Corruccini, Annealing of platinum for thermometry, J. Research NBS 47, 94 (1951), RP2232.

G. T. Lalos, A sonic-flow pyrometer for measuring gas temperatures, J. Research NBS 47, 179 (1951), RP2242.

P. D. Freeze, Bibliography of the measurement of gas temperatures, NBS Circ. 513 (1951).

F. Ordway, Techniques for growing and mounting small single crystals of refractory compounds, J. Research NBS 48, 152 (1952), RP2299.

H. F. Stimson, The present status of temperature scales, Science 116, 339 (1952).

E. F. Fiock and A. I. Dahl, The measurement of gas temperatures by immersion-type instruments, J. Am. Rocket Soc. 23, 155 (1953).

Standard samples and reference standards issued by the National Bureau of Standards, August 31, 1954, C552.

Thermometric Fixed Points

R. M. Wilhelm, Freezing point of mercury, Bul. BS 13, 655 (1916-17), S294.

E. F. Mueller and H. A. Burgess, Standardization of the sulphur boiling point, Sci. Pap. BS 15, 163 (1919-20), S339.

R. M. Wilhelm and J. L. Finkelstein, A standardized method for the determination of solidification points, especially of naphthalene and parafin, Sci. Pap. BS 15, 185 (1919-20), S340.

C. O. Fairchild, W. H. Hoover, and M. F. Peters, A new determination of the melting point of palladium, BS J. Research 2, 931 (1929), RP65.

H. T. Wensel and W. F. Roeser, The freezing point of nickel as a fixed point of the International Temperature Scale, BS J. Research 5, 1309 (1930), RP258.

W. F. Roeser, F. R. Caldwell, and H. T. Wensel, The freezing point of platinum, BS J. Research 6, 1119 (1931), RP326.

W. F. Roeser and A. I. Dahl, Conditions affecting the freezing temperature of silver, BS J. Research 10, 661 (1933), RP557.

F. Henning and H. T. Wensel, The freezing point of iridium, BS J. Research 10, 809 (1933), RP568.

W. F. Roeser and H. T. Wensel, The freezing point of rhodium, BS J. Research 12, 519 (1934), RP676.

W. F. Roeser and H. T. Wensel, Freezing temperatures of high-purity iron and some steels, J. Research NBS 26, 273 (1941), RP1375.

H. J. Hoge, A practical temperature scale below the oxygen point and a survey of fixed points in this range, Temperature, Its Measurement and Control in Science and Industry, p. 141 (Reinhold Publishing Corp., New York, N. Y., 1941).

F. W. Schwab and E. Wichers, Freezing temperature of benzoic acid as a fixed point in thermometry, J. Research NBS 34, 333 (1945), RP1647.

H. F. Stimson, The measurement of some thermal properties of water, J. Wash. Acad. Sci. (450 Ahnaip St., Menasha, Wis.), 35, 201 (1945). (triple point of water)

M. S. Van Dusen and A. I. Dahl, Freezing points of cobalt and nickel, J. Research NBS 39, 291 (1947). See also, Freezing points of cobalt and nickel and a new determination of Planck's constant c_2, Science 106, 428 (1947), RP1828.

A. I. Dahl and H. E. Cleaves, The freezing point of uranium, J. Research NBS 43, 513 (1949), RP2042.

"The Extension of the International Temperature Scale below the Oxygen Point", by H. Van Dijk, Maintenance of Standards Symposium 51-8, London: Her Majesty's Stationery Office, 1952.

"Present Status of Temperature Scales", by H. F. Stimson, Science, Vol. 116, pp. 339-41, 1952.

"Temperature - Its Measurement and Control in Science and Industry", by R. B. Scott (H. C. Wolfe, ed.), Vol. II, pp. 179-184, Reinhold, New York; Chapman & Hall, London. Low Temperature Scales from 90° to 5°K.

"A Low Temperature Scale from 4 to 300°K in Terms of a Gold-Cobalt Versus Copper Thermocouple", Jour. Phys. Chem., Vol. 61, pp. 644-646, 1957.

"Calibration of Thermocouples at Low Temperatures", by M. D. Bunch and R. L. Powell, CEL NBS, Proc. Cry. Eng. Conf. 1957, p. 269, 1958.

"The Use of Thermocouples for Measuring Temperatures below 70°K to ±0.5°K", by T. M. Dauphinee, D.K.C. MacDonald and W. B. Pearson, Jour. Sci. Instr., Vol. 30, pp. 399-400, 1953.

"Measurements on Thermo-electric Forces of Some Alloys at Temperatures from 2.5° to 17.5°K", by W. H. Keesom and C. J. Matthijs, Physica, Vol. 2, p. 623, 1935.

"Precision Nuclear Resonance Thermometer", by G. B. Benedek, and T. Kushida, Rev. Sci. Instr., Vol. 28, p. 92, 1957.

"Indium Resistance Thermometer; 4° - 300°K", by G. K. White and S. B. Woods, Rev. Sci. Instr., Vol. 28, p. 638, 1957.

"Germanium Resistance Thermometers Suitable for Low-Temperature Calorimetry", by J. E. Kunzler, T. H. Geballe, and G. W. Hull, Rev. Sci. Instr., Vol. 28, p. 96, 1957.

"Calorimetry of a Fluid", by Nathan S. Osborne, NBS Jour. Res., Vol. 4, p. 609, 1930.

"Measurements of Heat Capacity and Heat of Vaporization of Water in the Range 0° - 100°C", by N. S. Osborne, H. F. Stimson, and D. C. Ginnings, NBS Jour. Res., Vol. 23, p. 197, 1939.

"The Low Temperature Characteristics of Carbon-Composition Thermometers", by J. R. Clement and E. H. Quinell, Naval Research Lab. Rev. Sci. Instr., Vol. 23, pp. 213-216, 1952.

"Carbon-Resistor Thermometry below 1°K", by A. H. Markham, R. G. Netzel, and J. R. Dillinger, Note Rev. Sci. Instr., Vol. 28, p. 382, 1957.

"Carbon Resistor Thermometry between 0.3 and 2°K", by D. C. Pearce, A. H. Markham, and J. R. Dillinger, Rev. Sci. Instr., Vol. 27, p. 240, 1956.

"Universal Calibration Curves for Carbon Resistance Thermometers", by Clement, Logan and Gaffney, Phys. Rev., Vol. 100, p. 743, 1955.

"Resistance-Temperature 'Scaling' of Carbon-Composition Thermometers", by J. R. Clement, R. L. Dolecek, and J. K. Logan, Proc. of the 1956 Cryogenic Eng. Conf., p. 104, 1957.

"The Accuracy and Precision of Measuring Temperatures above 1000°K", by H. J. Kostkowski, Proc. International Symposium on High Temperature Technology, Asilomar, Calif., Oct. 6-9, 1959, sponsored by Stanford Research Institute.

"Rapport Sur L'Etalonnage De Deux Lampes Etalons Secondaires A Ruban de Tungstène par Quatre Laboratoires Nationaux", by D. R. Lovejoy, H. J. Kostkowski, H. Kunz, and H. Wagenbreth, Procés-Verbaux des Séances du Comité International des Poids et Measures, 26-A, 1959.

"Bibliography on the Measurement of Gas Temperature", by Paul D. Freeze, NBS Circular 513, August 20, 1951.

"Constant Temperature Liquid Helium Bath and Reproducibility of Resistance Thermometers", by H. H. Plumb and M. H. Edlow, Rev. Sci. Instr., Vol. 30, No. 5, pp. 376-377, May 1959.

"Design and Construction of a Blackbody and its Use in the Calibration of a Grating Spectroradiometer", by G. T. Lalos, R. J. Corruccini, and H. P. Broida, Rev. Sci. Instr., Vol. 29, No. 6, pp. 505-509, June 1958.

"Incomplete Equilibrium and Temperature Measurement", by C. M. Herzfeld, Jour. Wash. Acad. Sci., Vol. 46, No. 9, September 1956.

"Apparatus for Measuring Freezing Points 'in Vacuum' at Saturation Pressure", Glasgow, Krouscop, and Rossini, Anal. Chem., Vol. 22, p. 1521, 1950.

"An Improved Apparatus for the Determination of Liquidus Temperatures and Rates of Crystal Growth in Glasses", by O. H. Grauer and E. H. Hamilton, NBS Jour. Res. RP2096, Vol. 44, pp. 495-502, 1950.

"Accuracy of the Cutler-Hammer Recording Gas Calorimeter when Used with Gases of High Heating Value", by J. H. Eiseman and E. A. Potter, NBS Jour. Res. RP2754, Vol. 58, No. 4, pp. 213-226, April 1957.

"An Apparatus for Measurement of Thermal Conductivity of Solids at Low Temperatures", by R. L. Powell, W. M. Rogers, and D. O. Coffin, NBS Jour. Res. RP2805, Vol. 59, p. 349, November 1957.

"Design and Performance of a Block-type Osmometer", by D. M. McIntyre, G. C. Doderer, and J. H. O'Mara, NBS Jour. Res. RP2931, Vol. 62, p. 63, February 1959.

"Reference Tables for Thermocouples", by H. Shenker, J. I. Lauritzen, Jr., R. J. Corruccini, and S. T. Lonberger, NBS Circular 561, April 27, 1955.

"Comparison of Cryoscopic Determinations of Purity of Benzene by Thermometric and Calorimetric Procedures", by A. R. Glasgow, Jr., G. S. Ross, A. T. Horton, D. Enagonio, H. D. Dixon, C. P. Saylor, G. T. Furukawa, M. L. Reilly, and J. M. Henning, Analytica Chimica Acta, Vol. 17, No. 1, pp. 54-79, July 1957.

"Measurements of Heat of Vaporization and Heat Capacity of a Number of Hydrocarbons", by N. S. Osborne and D. C. Ginnings, NBS Jour. Res. RP1841, Vol. 39, pp. 453-477, November 1947.

"Vapor Pressures and Boiling Points of Some Paraffin, Alkylcyclopentane, Alkylcyclohexane, and Alkylbenzene Hydrocarbons", by C. B. Willingham, W. J. Taylor, J. M. Pignocco, and F. D. Rossini, NBS Jour. Res. RP1670, Vol. 35, pp. 219-244, September 1945

"Theoretical Analysis of Certain Time-Temperature Freezing and Melting Curves as Applied to Hydrocarbons", by W. J. Taylor and F. D. Rossini, NBS Jour. Res. RP1585, Vol. 32, pp. 197-213, May 1944

"A Cryoscopic Study of the Solubility of Uranium in Liquid Sodium at 97.8°C", by T. B. Douglas, NBS Jour. Res. RP2493, Vol. 52, No. 5, pp. 223-226, May 1954

"Calorimetric Determination of the Half-Life of Polonium", by D. C. Ginnings, Anne F. Ball, and D. T. Vier, NBS Jour. Res. RP2392, Vol. 50, No. 2, pp. 75-79, February 1953

"Annealing of Platinum for Thermometry", by R. J. Corruccini, NBS Jour. Res. RP2232, Vol. 47, No. 2, pp. 94-103, August 1951

"Reference Tables for Thermocouples", by H. Shenker, J. I. Lauritzen, Jr., R.J. Corruccini, and S. T. Lonberger, NBS Circular 561, April 27, 1955 -

"Calculation of Cryoscopic Data", by C. P. Saylor, Analytica Chimica Acta, Vol. 17, No. I, pp. 36-42, July 1957.

"Gas Calorimeter Tables", by R. S. Jessup and E. R. Weaver, NBS Circular 464, March 25, 1948.

"Freezing Temperature of Benzoic Acid as a Fixed Point in Thermometry", by F. W. Schwab and E. Wichers, NBS Jour. Res. RP1647, Vol. 34, pp. 333-372, April 1945.

"Heat of Combustion of the Two Butadienes", by E. J. Prosen, F. W. Maron and F. D. Rossini, NBS Jour. Res. RP1968, Vol. 42, p. 269, 1949.

"Heats of Isomerization of the Five Hexanes", by E. J. Prosen and F. D. Rossini, NBS Jour. Res. RP1420, Vol. 27, p. 289, 1941.

"Some Experimental Data on the Heats of Combustion of Benzoic Acid and Carbon (Graphite)", by E. J. Prosen and F. D. Rossini, NBS Jour. Res. RP1619, Vol. 33, p. 439, 1944.

"Heats of Combustion in a Bomb of Compounds Containing Carbon, Hydrogen, Oxygen, and Nitrogen", by E. J. Prosen, Chapter 6 of "Experimental Thermochemistry", edited by F. D. Rossini, Interscience Publishers, Inc., New York, 1956.

"Heats of Combustion of Benzoic Acid, with Special Reference to the Standardization of Bomb Calorimeters", by R. S. Jessup, NBS Jour. Res. RP1499, Vol. 29, p. 247, 1942.

"Viscosities of Sucrose Solutions at Various Temperatures: Tables of Recalculated Values", by J. F. Swindells, C. F. Snyder, et al., Supplement to NBS Circular 440, July 31, 1958.

"Thermal Expansion of Solids", by P. Hidnert and W. Souder, NBS Circular 486, March 15, 1950

"Adiabatic Demagnetization of Chromium Methylamine Alum", by D. DeKlerk and R. P. Hudson, Phys. Rev., Vol. 91, No. 2, pp. 278-281, July 15, 1953.

"Determination of the Purity of Hydrocarbons by Measurement of Freezing Points", by A. R. Glasgow, Jr., A. J. Streiff, and F. D. Rossini, NBS Jour. Res. RP1676, Vol. 35, p. 355 (1945).

"Theoretical Analysis of Certain Time-Temperature Freezing and Melting Curves as Applied to Hydrocarbons", by W. J. Taylor and F. D. Rossini, NBS Jour. Res. RP1585, Vol. 32, p. 197 (1944).

"Instructions and Precautions on the Use of Benzoic Acid Thermometric Standard Cells", NBS mimeographed sheet.

Reprinted from Journal of Applied Physics, Vol. 13, No. 2, 128–137, February, 1942

Note on Temperature Correction Methods in Calorimetry

R. S. Jessup
National Bureau of Standards, Washington, D. C.
(Received November 17, 1941)

The problem of correcting calorimetric data for thermal leakage has been discussed by King and Grover in a recent paper in this Journal. From their analysis of the problem these authors have concluded that large errors are involved in the usual methods of correcting the data of bomb-calorimetric measurements, and of experiments by the method of mixtures. In the present note it is shown, in agreement with W. P. White's treatment of calorimetric lag, that in the case of bomb-calorimetric measurements the errors in question are practically completely eliminated by calibrating the calorimeter experimentally. Since experimental calibration of the calorimeter is the usual practice in modern bomb-calorimetric measurements, the results of such measurements are not affected by the errors discussed by King and Grover. In the case of measurements by the method of mixtures these errors can be avoided by so conducting the experiment that the final temperature of the calorimeter will be very near the convergence temperature.

IN a recent paper in this Journal, King and Grover[1] have presented a mathematical treatment of the problem of correcting calorimetric data for thermal leakage. They conclude from their analysis of the problem that large errors are introduced into the results of bomb-calorimetric measurements, and of measurements by the method of mixtures, by the usual methods of calculating the correction for thermal leakage. For a particular hypothetical experiment they report that the usual methods of calculation lead to errors of the order of 0.2 percent. As the precision of modern bomb-calorimetric measurements is 0.01 or 0.02 percent, an error of 0.2 percent in the results of such measurements would be very serious. In the present note it will be shown that in the case of bomb-calorimetric measurements, the errors discussed by King and Grover are practically completely eliminated if the calorimeter is calibrated by supplying a measured quantity of energy and observing the resulting temperature rise, and if the usual methods of correcting for thermal leakage are used for both the calibration experiments and the measurements of heats of combustion. It will be shown also that in the case of experiments by the method of mixtures, errors resulting from the usual methods of correcting for thermal leakage can be avoided by a suitable experimental procedure.

The problem discussed by King and Grover is that of a calorimeter in which is immersed a charge, such as a bomb. It is assumed that at a time $t_0=0$ the charge is at a uniform temperature Θ_0, and the calorimeter is at a lower uniform temperature $\theta_0=0$. It is further assumed that the temperatures Θ and θ of charge and calorimeter, respectively, vary with time in a manner which is described by the differential equations

$$d\Theta/dt=-a(\Theta-\theta) \qquad (33)^2$$

[1] Allen King and Horace Grover, "Temperature correction methods in calorimetry," J. App. Phys. **12**, 557 (1941).

[2] Equations taken from reference 1 are given the same numbers (expressed in Arabic numerals) as in that paper. The numbers of other equations given in this paper are expressed in roman numerals.

and

$$d\theta/dt = b(\Theta - \theta) - c(\theta - \theta_k), \qquad (34)$$

where a, b, and c are constants of the apparatus, and θ_k is the convergence temperature of the calorimetric system, that is, the temperature which the system would attain in an infinite time if the rate of stirring and all external conditions remained constant.

Elimination of Θ from Eqs. (33) and (34) yields the second-order differential equation

$$d^2\theta/dt^2 + 2pd\theta/dt + q\theta = q\theta_k, \qquad (35)$$

where $2p = (a+b+c)$ and $q = ac$. The second-order differential equation in Θ is of the same form as (35). The solutions of these differential equations may be written in the form

$$\theta = \theta_k + Ae^{-\epsilon t} + Be^{-(2p-\epsilon)t} \qquad (36)$$

and

$$\Theta = \theta_k + Ce^{-\epsilon t} + De^{-(2p-\epsilon)t}, \qquad (I)$$

where $\epsilon = p - (p^2 - q)^{\frac{1}{2}}$, and A, B, C, and D are constants of integration. Insertion of the numerical data given by King and Grover into Eq. (36) leads to the following expression for the time-temperature relation for the hypothetical experiment

$$\theta = 1.7082 + 1.010029e^{-0.005t} - 2.718229e^{-0.5t}. \qquad (II)$$

It can be shown that the temperature rise of the calorimeter corrected for thermal leakage is given by

$$\theta_\infty{}^* - \theta_0 = \frac{-\epsilon A - (2p-\epsilon)B + c(\theta_0 - \theta_k)}{a+b}. \qquad (III)$$

The value of $(\theta_\infty{}^* - \theta_0)$ calculated from Eq. (III), using the values of the constants given by King and Grover is 2.69302°.[3]

It should be noted that although the mathematical treatment of the problem under consideration by King and Grover leads to the correct value of the temperature $\theta_\infty{}^*$ which the calorimeter would attain if there were no thermal leakage, this temperature can be calculated by means of Eq. (III), or the equivalent equation given by King and Grover, only when the time-temperature relation is of the form given by Eq. (36). Experimental time-temperature curves usually cannot be represented by equations of this form. After the ignition of a sample of combustible material in a bomb, or after a heated charge is dropped into a calorimeter, there is usually a short interval of time during which the rate of temperature rise is much smaller than the rate which would be calculated by means of an equation of the form of (36). This is the result of various kinds of lag, especially stirring lag. The form of experimental time-temperature curves after the temperature has begun to rise rapidly indicates also that the rate of transfer of heat between calorimeter and charge is not a linear function of $(\Theta - \theta)$ as was assumed in the derivation of Eq. (36). It will be shown later that the value of the corrected temperature rise for some types of calorimetric experiments would differ from that calculated from Eq. (III) even if the time-temperature curve were of the form represented by Eq. (36).

The calculation of the thermal leakage correction for a bomb-calorimetric experiment will now be considered. The time-temperature relation for such an experiment may be represented qualitatively by the curve $ABDFG$ of Fig. 1. The parts AB and FG of this curve represent data obtained in the "rating periods" for use in calculating the thermal leakage. Even though the rates of change of Θ and θ may not be in accord with Eqs. (33) and (34) when $(\Theta - \theta)$ is large, it will be assumed that these equations are valid during the rating periods when $(\Theta - \theta)$ is small.

During the rating periods Eqs. (36) and (I) reduce to

$$\theta = \theta_k + Ae^{-\epsilon t} \qquad (IV)$$

and

$$\Theta = \theta_k + Ce^{-\epsilon t}. \qquad (V)$$

Imposing the conditions (see Fig. 1) that $\theta = \theta_B (= \theta_0)$ when $t = t_B$, and $\theta = \theta_F$ when $t = t_F$, Eq. (IV) leads to the following equations for the initial and final rating curves

$$\theta = \theta_k + (\theta_B - \theta_k)e^{\epsilon(t_B - t)}, \qquad (VI)$$

$$\theta = \theta_k + (\theta_F - \theta_k)e^{\epsilon(t_F - t)}. \qquad (VII)$$

It is easily shown that the temperature of the

[3] King and Grover give the value 2.6931° for $(\theta_\infty{}^* - \theta_0)$. The difference may be due to the use of rounded values of some of the constants in the present paper. The value given in the text is consistent with Eq. (II) and the values of $(a+b)$ and c given in reference 1.

bomb will be represented by

$$\Theta=\theta_k+\frac{a}{a-\epsilon}(\theta_B-\theta_k)e^{\epsilon(t_B-t)} \qquad \text{(VIII)}$$

during the initial rating period, and by

$$\Theta=\theta_k+\frac{a}{a-\epsilon}(\theta_F-\theta_k)e^{\epsilon(t_F-t)} \qquad \text{(IX)}$$

during the final rating period.

The observed temperature rise of the calorimeter will be taken as $(\theta_F-\theta_B)$ It follows from Eqs. (VI), (VII), (VIII), and (IX) that if θ' and Θ' are the temperatures of calorimeter and bomb, respectively, at any time t' in the initial rating period, and θ'' and Θ'' are the corresponding temperatures at any time t'' in the final rating period, then

$$\Theta''-\Theta'=\frac{a}{a-\epsilon}(\theta''-\theta'). \qquad \text{(X)}$$

In particular, the temperature rise of the bomb corresponding to the observed temperature rise, $(\theta_F-\theta_B)$, of the calorimeter will be given by

$$\Theta_F-\Theta_B=\frac{a}{a-\epsilon}(\theta_F-\theta_B). \qquad \text{(XI)}$$

If the heat capacities of calorimeter alone and bomb alone are K_1 and K_2, respectively, the quantity of heat corresponding to the temperature rise $(\theta_F-\theta_B)$ of the calorimeter, and the temperature rise $(\Theta_F-\Theta_B)$ of the bomb will be given by

$$Q_{BF}=K_1(\theta_F-\theta_B)+K_2(\Theta_F-\Theta_B)$$

$$=\left(K_1+\frac{a}{a-\epsilon}K_2\right)(\theta_F-\theta_B). \qquad \text{(XII)}$$

The heat gained by the calorimeter by thermal leakage between the times t_B and t_F will be given by

$$\Delta Q=-cK_1\int_{t_B}^{t_F}(\theta-\theta_k)dt.$$

This quantity may be taken as equivalent to an increase $\Delta\theta$ in the temperature of the calorimeter, and an increase $\Delta\Theta=\Delta\theta a/(a-\epsilon)$ in the temperature of the bomb, where

$$\Delta\theta=-\frac{cK_1}{K_1+K_2a/(a-\epsilon)}\int_{t_B}^{t_F}(\theta-\theta_k)dt. \qquad \text{(XIII)}$$

The constant preceding the integral sign in (XIII) evidently may be considered as a cooling coefficient which could be used to calculate the increase in temperature $\Delta\theta$ of the calorimeter due to thermal leakage on the basis that the corrected temperature rise, $(\theta_F-\theta_B-\Delta\theta)$, of the calorimeter corresponds to a temperature rise of the bomb equal to

$$\frac{a}{a-\epsilon}(\theta_F-\theta_B-\Delta\theta).$$

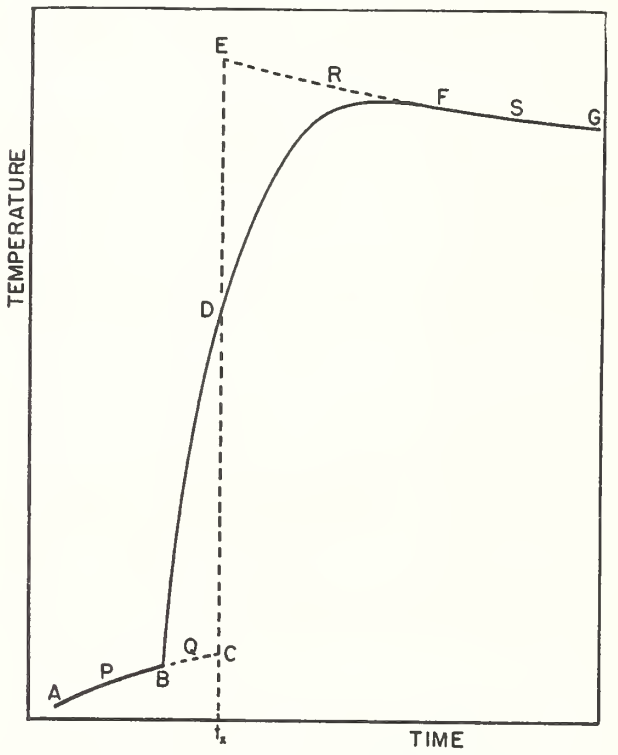

FIG. 1. Diagram to illustrate Dickinson's method of calculating the corrected temperature rise.

This cooling coefficient can be shown to be equal to the constant ϵ. From Eqs. VI and VII it follows that during the rating periods the rate of change of the temperature of the calorimeter is given by

$$d\theta/dt=-\epsilon(\theta-\theta_k). \qquad \text{(XIV)}$$

In other words the constant ϵ is the cooling coefficient for the calorimeter which would be

calculated from the data of the rating periods on the basis of Newton's law of cooling as expressed by Eq. (XIV). Therefore the use of these data for calculating the correction to the observed temperature rise would lead to a corrected temperature rise, $(\theta_F-\theta_B-\Delta\theta)$, for the calorimeter which would correspond to a temperature rise of the bomb equal to

$$\frac{a}{a-\epsilon}(\theta_F-\theta_B-\Delta\theta).$$

The fact that the corrected temperature rise of the calorimeter calculated from the rating period data is not equal to the corresponding temperature rise of the bomb is of no consequence in bomb-calorimetric measurements for the following reasons. In order to obtain accurate results by means of a bomb calorimeter the energy equivalent, or effective heat capacity of the calorimetric system, must be determined experimentally by supplying a measured quantity of energy to the system, either electrically or by burning a standard material of known heating value, and observing the resulting temperature rise. If the corrected temperature rise in the calibration experiments is calculated from the data of the rating periods on the basis of Eq. (XIV), then the value obtained for the energy equivalent will be that corresponding to a temperature rise of the bomb equal to $a/(a-\epsilon)$ times that of the calorimeter. The experimental value of the energy equivalent is therefore not the true heat capacity of the calorimetric system. It is evident, however, that it is the value appropriate for use in calculating the results of measurements of heat of combustion when the thermal leakage correction for such measurements is computed as described above.

The fact that the effect of lag of parts of a calorimeter is completely eliminated by an experimental calibration has been pointed out by White.[4] The preceding discussion in the present paper is a somewhat more detailed demonstration of this fact for the special case in which the lagging part of the calorimeter is a bomb.

[4] W. P. White, *The Modern Calorimeter* (Reinhold Publishing Corporation, New York, 1928), p. 88.

It has been shown by Dickinson[5] that the correction for heat of stirring in a bomb-calorimetric experiment is included in the correction for thermal leakage, when this correction is calculated from the data of the rating periods in the manner described above. The effect of the production of heat at a constant rate by stirring is merely to raise the convergence temperature slightly above the temperature at which the rate of heat transfer between calorimeter and surroundings would be zero. The heat of stirring is also taken care of in the calculation of $(\theta_x^*-\theta_0)$ by means of Eq. (III) if the value of θ_k used in this equation is the convergence temperature of the stirred calorimeter. The temperature θ_∞^* is then the temperature which the system would attain if the rate of loss of heat were at all times equal to the rate of production of heat by stirring.

As an example of the correction of bomb-calorimetric data for thermal leakage, Dickinson's method[5] of calculating the corrected temperature rise will now be applied to a hypothetical bomb-calorimetric experiment for which the time-temperature relation is that represented by Eq. (II). The time-temperature relation during the initial rating period for such an experiment would be given by

$$\theta=1.7082(1-e^{-0.005t}). \qquad \text{(XV)}$$

This equation was obtained by substituting the numerical values of θ_B, θ_k, and ϵ given by King and Grover into Eq. (VI). The corresponding relation for the final rating period is represented by Eq. (II) with the last term omitted.

Dickinson's method of finding the corrected temperature rise consists in extrapolating the rating curves AB and FG (Fig. 1) to a time t_x such that the areas BCD and DEF are equal. The difference between the temperatures θ_E and θ_C obtained in this way is the corrected temperature rise. The value of t_x for the experiment under consideration was calculated from the relation

$$\int_0^{t_x}(A+\theta_k)e^{-\epsilon t}dt+\int_0^{\infty}Be^{-(2p-\epsilon)t}dt=0 \qquad \text{(XVI)}$$

and found to be 2.01 minutes. The values of θ_C and θ_E calculated by inserting $t=t_x=2.01$ into

[5] H. C. Dickinson, Bull. Bur. Stand. 11, 189 (1914).

the equations for the rating curves are, respectively, 0.01708° and 2.70813°. The difference between these temperatures is 2.69105°, which is lower by 0.073 percent than the value 2.69302° calculated from Eq. (III) for $(\theta_\infty{}^* - \theta_0)$.

The reason for the discrepancy is that the two values of temperature rise of the calorimeter correspond to different values for the temperature rise of the bomb. Thus the temperature rise $(\theta_\infty{}^* - \theta_0)$ for the calorimeter corresponds to a temperature rise of $(\theta_\infty{}^* - \Theta_B)$ for the bomb, where Θ_B, in accordance with Eq. (VIII), is given by

$$\Theta_B = (a\theta_B - \epsilon\theta_k)/(a - \epsilon).$$

Hence the temperature rise for the bomb in this case is

$$\theta_\infty{}^* - \Theta_B = \theta_\infty{}^* - \frac{a\theta_B - \epsilon\theta_k}{a - \epsilon}. \qquad \text{(XVII)}$$

On the other hand the temperature difference $(\theta_E - \theta_C)$ for the calorimeter, in accordance with Eq. (X), corresponds to a temperature difference of

$$\Theta_E - \Theta_C = \frac{a}{a - \epsilon}(\theta_E - \theta_C) \qquad \text{(XVIII)}$$

for the bomb.

It is easily shown by actually performing the calculation that the quantity of heat required to produce the temperature rise $(\theta_\infty{}^* - \theta_0) = 2.69302°$ in the calorimeter, and the corresponding temperature rise $(\theta_\infty{}^* - \Theta_B) = 2.71376°$ in the bomb is exactly the same as the quantity of heat required to produce the temperature increases $(\theta_E - \theta_C) = 2.69105°$ and $(\Theta_E - \Theta_C) = 2.72373°$ in calorimeter and bomb, respectively. Hence either $(\theta_\infty{}^* - \theta_0)$ or $(\theta_E - \theta_C)$ may be considered as the corrected temperature rise for the bomb-calorimetric experiment under consideration if used with the proper value for the energy equivalent of the system. From Eq. (XVIII) and the discussion given in the text following Eq. (XIV) it will be seen that the value of the energy equivalent appropriate for use with the temperature rise $(\theta_E - \theta_C)$ is the value which would be obtained as the result of an experimental calibration of the calorimeter in which the thermal leakage correction was calculated on the basis of Newton's law of cooling in the form (XIV).

TABLE I. Values of temperature and corresponding time in a hypothetical bomb-calorimetric experiment.

Time minutes	Temperature degrees	Differences degrees	Time minutes	Temperature degrees	Differences degrees
−10	−0.08758		12	2.6527	
		0.00895			
− 9	− .07863	.00892	14	2.64747	
		.00886			−0.00372
− 8	− .06971	.00883	15	2.64375	
		.00878			− .00409
− 7	− .06085	.00873	16	2.63966	− .00429
− 6	− .05202	.00869	17	2.63537	− .00441
− 5	− .04324	.00864	18	2.63096	− .00447
− 4	− .03451	.00862	19	2.62649	− .00450
− 3	− .02582	.00856	20	2.62199	− .00451
− 2	− .01718		21	2.61748	− .00451
− 1	− .00856		22	2.61297	− .00449
0	.00000		23	2.60848	− .00448
0.5	.5987		24	2.60400	− .00446
1	1.0645		25	2.59954	− .00445
2	1.7082		26	2.59509	− .00442
4	2.3304		27	2.59067	− .00439
6	2.5591		28	2.58628	− .00438
8	2.6288		29	2.58190	− .00436
10	2.6507		30	2.57754	

The value of the energy equivalent of a bomb calorimeter appropriate for use with the temperature rise $(\theta^*{}_\infty - \theta_0)$ depends to a slight extent upon the magnitude of this temperature rise, apart from any dependence of heat capacity upon temperature. In general it cannot be as conveniently determined experimentally as the energy equivalent corresponding to the temperature rise $(\theta_E - \theta_C)$. In the case of an experiment by the method of mixtures, the value of the energy equivalent which is equal to the effective heat capacity of the calorimeter alone, multiplied by $(\theta_\infty{}^* - \theta_0)$ will yield the heat given up by the charge in cooling from its initial temperature to $\theta_\infty{}^*$. This energy equivalent can be determined experimentally either by electrical heating of the calorimeter alone, or by the use of a charge of known heat capacity. However, in general it will not be possible to use Eq. (III) to evaluate $(\theta_\infty{}^* - \theta_0)$ either for bomb-calorimetric experiments or for experiments by the method of mixtures, because of the fact that experimental time-temperature relations are not of the form assumed in the derivation of Eq. (III). The calculation of the thermal leakage correction for an experiment by the method of mixtures will be considered later in this paper.

In practice the time-temperature relation for a calorimetric experiment is not given in terms of equations, but in terms of temperatures measured at definite times. Ordinarily, therefore, the method used above of calculating the

TABLE II. Calculation of corrected temperature rise for a hypothetical bomb-calorimetric experiment.

Initial period	Final period
$\theta_A = -0.08758°$	$\theta_F = 2.62199°$
$\theta_B = 0.00000$	$\theta_G = 2.57754$
$\Delta\theta = 0.08758$	$\Delta\theta = -0.04445$
$\left(\frac{\Delta\theta}{\Delta t}\right)_P = 0.008758$ deg. min.$^{-1}$	$\left(\frac{\Delta\theta}{\Delta t}\right)_S = -0.004445$ deg. min.$^{-1}$
$\theta_P = -0.04324°$	$\theta_S = 2.59954°$

$$\Delta\left(\frac{\Delta\theta}{\Delta t}\right) = -0.013203 \text{ deg. min.}^{-1}$$

$$\Delta\theta = 2.64278°$$

$$\Delta\left(\frac{\Delta\theta}{\Delta t}\right)/\Delta\theta = -0.0049959 \text{ min.}^{-1}$$

$t_Q - t_B = \frac{2.01}{2} = 1.005$ min.	$t_F - t_R = \frac{17.99}{2} = 8.995$ min.
$1.005 \times 0.008758 = 0.00880°$	$-8.995 \times -0.004445 = 0.03998°$
$\theta_B = 0.00000$	$\theta_F = 2.62199$
$\theta_Q = 0.00880$	$\theta_R = 2.66197$
$\theta_P = -0.04324$	$\theta_S = 2.59954$
$\Delta\theta = 0.05204$	$\Delta\theta = -0.06243$
$0.05204 \times -0.0049959$	$+0.06243 \times -0.0049959$
$= -0.000260$ deg.	$= -0.000312$ deg. min.$^{-1}$
$\left(\frac{\Delta\theta}{\Delta t}\right)_P = 0.008758$ min.$^{-1}$	$\left(\frac{\Delta\theta}{\Delta t}\right)_S = -0.004445$
$\left(\frac{\Delta\theta}{\Delta t}\right)_Q = 0.008498$ deg. min.$^{-1}$	$\left(\frac{\Delta\theta}{\Delta t}\right)_R = -0.004757$ deg. min.$^{-1}$
$0.008498 \times 2.01 = 0.01708°$	$-0.004757 \times -17.99 = 0.08558°$
$\theta_B = 0.00000$	$\theta_F = 2.62199°$
$\theta_C = 0.01708°$	$\theta_E = 2.70757°$

Corrected temperature rise $= 2.70757 - 0.01708 = 2.69049°$

temperatures θ_C and θ_E from equations for the rating curves would not be applied. It will be of interest to consider the calculation of the corrected temperature rise for a bomb-calorimetric experiment, using numerical data rather than equations. In Table I are given values of temperature calculated by means of Eqs. (II) and (XV). It will be assumed that these temperatures were obtained from observations in a bomb-calorimetric experiment, and they will be used to calculate the corrected temperature rise of the calorimeter by Dickinson's method. The period from $t = -10$ to $t = 0$ will be taken as the initial rating period. Since the equation for the final rating period is assumed not to be known, it would be necessary for the experimenter to judge from the data when the final rate of temperature change has been attained. If temperatures were read each minute to 0.0001° it would be evident to the experimenter that the final rate had not been attained before $t = 18$, and he might be expected to take the period from $t = 20$ to $t = 30$ as the final rating period.

Ordinarily the value of t_x would be obtained from numerical data by plotting such data on large-size coordinate paper and determining areas by some such method as counting squares. In the present case, however, we are interested in comparing the results of extrapolating the rating curves to t_x by means of the equations for these curves, with the results of extrapolating the curves by the use of numerical data, without introducing the effect of possible errors in the determination of t_x. Therefore the value $t_x = 2.01$ which was calculated by means of Eq. (XVI) will be used here.

Since the present writer, using Dickinson's method, has obtained a distinctly different value for the corrected temperature rise from that reported by King and Grover as having been obtained by the same method, the details of the present calculation are given in Table II. The following description of the method of calculation will be understood by reference to Table II and Fig. 1.

The average rate of change of temperature, $\Delta\theta/\Delta t$, in each of the rating periods is taken as corresponding to the "observed" temperature at the mid-time of that period. From the values of the two rates and the corresponding temperatures the average change in rate per degree change in temperature, $\Delta(\Delta\theta/\Delta t)/\Delta\theta(=-\epsilon)$, is calculated. The approximate temperature, θ_Q, which would have been attained at the time t_Q (Fig. 1) midway between t_B and t_x if the rating period had continued to the time t_Q, is then calculated by linear extrapolation of the curve AB. From the value of $\Delta\theta/\Delta t)_P$, the difference between the temperatures θ_Q and θ_P (Fig. 1), and the value of $\Delta(\Delta\theta/\Delta t)/\Delta\theta$, the value of the rate $(\Delta\theta/\Delta t)_Q$ corresponding to the temperature θ_Q is calculated, and this rate is multiplied by $(t_x - t_B)$ to obtain $(\theta_C - \theta_B)$. Similarly, the rate corresponding to the temperature θ_R (Fig. 1) is calculated and multiplied by $(t_F - t_x)$ to obtain $(\theta_E - \theta_F)$. These data, together with the values of θ_B and θ_F, give the corrected temperature rise $(\theta_E - \theta_C)$.

The value of the corrected temperature rise obtained in the manner just described is 2.69049°, which is lower by 0.021 percent than the corresponding value 2.69105° calculated by means of the equations for the rating curves. Three factors contribute to this discrepancy: (1) Although the experimenter would probably think

that the final rate had been attained at time $t=20$, the calculated value of the last term of Eq. (II) for $t=20$ is 0.00012°, so that the observed value of the temperature for $t=20$ is lower by this amount than the temperature corresponding to the final rating curve. (2) The linear extrapolation of the final rating curve gives too low a value for θ_R. (3) Although $d\theta/dt$ in the rating periods varies linearly with temperature, $\Delta\theta/\Delta t$ does not vary linearly with the temperature at the midtimes of the intervals for which the values of $\Delta\theta/\Delta t$ are calculated.[6] All three of these factors enter into the calculations in such a manner as to lower the resulting value of θ_E. The corresponding error in θ_C arising from factors (2) and (3) is negligible because the extrapolation of the initial rating curve is over such a short interval.

The errors arising from the factors (2) and (3) mentioned above result from the fact that the method of extrapolating the final rating curve by the use of the numerical data does not take full account of the curvature of this curve. The small error from this source could be avoided by so conducting the experiment that the final temperature of the calorimeter is very nearly equal to the convergence temperature. The final rate would then be very small, and the change in rate between the temperatures θ_R and θ_S (Fig. 1) would be negligible.

The hypothetical experiment under consideration differs in several important respects from an actual bomb-calorimetric experiment with apparatus suitable for measurements of high precision. The differences are such as to make the errors in the calculation of the thermal leakage correction from rating period data larger for the hypothetical experiment than for an actual experiment. The curves of Fig. 2 represent the time-temperature relation for the hypothetical experiment, and a time-temperature relation obtained by multiplying the observed temperatures in a routine bomb-calorimetric experiment by the ratio of the corrected temperature rise, 2.69105°, for the hypothetical experiment to the corrected temperature rise, 2.9519°, calculated from the data of the actual experiment. The "observed" curve of Fig. 2 may therefore be considered as representing the data of an actual bomb-calorimetric experiment for which the corrected temperature rise is the same as for the hypothetical experiment. The final rate in the actual experiment was about 0.0001° per minute, so that the change in rate corresponding to the temperature difference $(\theta_R-\theta_S)$ (Fig. 1) is negligible.

It will be seen that the observed curve (Fig. 2) approaches a steady final rate much more rapidly than the hypothetical curve. Even though the observed curve rises more slowly at the start, its later rise is so rapid that the final rate is reached at $t=10$, while for the hypothetical curve the final rate is not reached until about $t=20$. This more rapid approach of the actual curve to the final rate, and the consequent smaller interval over which the observed final rating curve must be extrapolated to obtain θ_E, result in a smaller error in this temperature arising from the factor (1) mentioned above, even if the error in θ_F is the same as in the hypothetical experiment. The value of ϵ for the actual experiment is less than half that assumed for the hypothetical experiment. The thermal leakage correction for the actual experiment is less than for the hypothetical experiment because of the smaller value of ϵ, because of the shorter time of the actual experiment, and because $|(\theta-\theta_k)|$ is smaller during a relatively large part of the actual experiment. This correction amounts to less that 0.3 percent for the actual experiment, while for the hypothetical experiment it is over 2 percent.

Although the above discussion has been restricted to Dickinson's method of calculating the thermal leakage correction, it is evident that the proper use of any method based on Newton's law of cooling can lead to only one result.

The significance of the constants c and ϵ occurring in Eqs. (34) and (36), respectively, and the relation between them will now be discussed briefly. It is evident from Eq. (34) that the constant c is the cooling coefficient of the calorimeter alone, that is, not including a bomb or other charge. From (VI) and (VII) it is evident that the cooling coefficient of a calorimetric system which includes a bomb or other charge is not c but ϵ. From the definition of ϵ it follows that if

[6] Except in the special case that the intervals are all equal. The three intervals involved in the calculation of θ_E are $t_B-t_A=t_G-t_F=10$, and $t_F-t_x=17.99$.

$(\epsilon^2-\epsilon c)$ is negligible in comparison with ac, then $\epsilon=ca/(a+b)$. In other words, the ratio ϵ/c is approximately equal to the ratio of the heat capacity of the calorimeter alone to the heat capacity of calorimeter plus bomb. Thus, from the values of a, b, and c given by King and Grover the value of $ca/(a+b)$ is calculated to be 0.00501 as compared with their value 0.00500 for ϵ. The fact that ϵ is not exactly equal to $ca/(a+b)$ is due to the lag of the temperature of the charge or bomb behind that of the calorimeter.

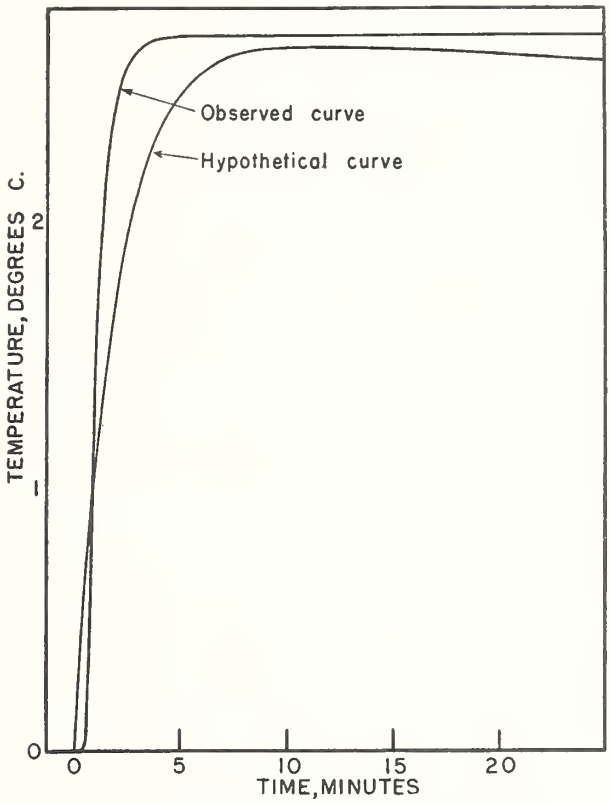

FIG. 2. Comparison of the hypothetical time-temperature curve represented by Eq. (II) with a time-temperature curve observed in a routine bomb-calorimetric experiment.

The discussion of the thermal leakage correction for the case of a bomb-calorimetric experiment may be summarized as follows. The data of the rating periods, which correspond to the cooling coefficient ϵ rather than to c, are the appropriate data to use in calculating the thermal leakage correction on the basis of Newton's law of cooling. The results of such calculations will be affected by the lag of the temperature of the bomb behind that of the calorimeter, but errors due to this lag will be completely eliminated by the use of an experimentally determined value of the energy equivalent of the calorimetric system. Errors in the calculation of the thermal leakage correction can be made negligible by suitable experimental procedure, especially by so conducting the experiments that the final temperature of the calorimeter will be approximately equal to the convergence temperature of the system.

The above conclusions were reached on the basis of certain assumptions regarding the conditions existing during a bomb-calorimetric experiment, which were introduced in order to simplify the mathematical treatment. The conclusions have been shown to be valid, therefore, only for the type of ideal experiment defined by the assumptions. King and Grover, in their discussion, have introduced essentially the same simplifying assumptions, and therefore their conclusions are necessarily subject to the same restrictions. The treatment given in this paper is not a complete justification of the usual methods of correcting for thermal leakage, but it does show the fallacy of the conclusion of King and Grover that the usual methods are not applicable to the type of ideal bomb-calorimetric experiment which has been discussed.

A rigorous mathematical treatment of the problem of correcting the data of actual bomb-calorimetric experiments for thermal leakage will not be attempted here. However, it appears from the following discussion that the errors involved in the usual methods of correcting such data are probably negligible. It follows from the mathematical analysis given in this paper that, in the case of the ideal type of experiment considered, the effect of the difference between the temperatures of bomb and calorimeter during the rating periods is fully taken into account by an experimental calibration of the calorimeter. It is evident that this would be true also for actual calorimetric experiments provided the time-temperature curves of calibration experiments and combustion experiments are identical. This condition is practically satisfied when the calibration is by means of a standard substance of known heat of combustion, but is not satisfied when the calibration is by electrical heating. It is conceivable, therefore,

that when a bomb calorimeter is calibrated by electrical heating the difference in temperature between bomb and calorimeter during the rating periods might not be taken into account completely, although it is evident that this difference would be at least approximately taken into account. For the calorimeter used in obtaining the data represented by the observed time-temperature curve of Fig. 2 it has been calculated that the difference between the temperatures of bomb and calorimeter affects the observed temperature rise by about 0.03 percent. It seems highly probable that the error resulting from the difference in form of the time-temperature curves of electrical calibration experiments and combustion experiments is a small fraction of this amount.

This conclusion is supported by results obtained by Dickinson[5] in two sets of electrical calibration experiments one set with a heater which was not in contact with the bomb and the other with a heater which was in good thermal contact with the bomb. The time-temperature curves for the first set of experiments were nearly linear during the heating period, while those for the second set were somewhat similar in form to the time-temperature curve for a combustion experiment. The results of the two sets of experiments were in practically perfect agreement. This indicates that the difference in form of the time-temperature curves had no measurable effect on the corrected temperature rise calculated by the usual methods.

The method described above for calculating the thermal leakage correction for a bomb calorimetric experiment is not applicable to an experiment by the method of mixtures, because in this case the data of the initial and final rating periods correspond to different heat capacities of the calorimetric system, and because of the fact that the effect of the lag of the charge in such an experiment is not eliminated by an experimental calibration of the calorimeter. A method of calculation appropriate for experiments by the method of mixtures will now be described.

It is assumed that the charge is dropped into the calorimeter at time t_B (when $\theta=\theta_B$), and that the mass and initial temperature of the charge are such that the final temperature of the calorimeter will be so nearly equal to θ_k that the lag of the charge will not cause its temperature to differ by a significant amount from that of the calorimeter during the final rating period. The final rating period is assumed to begin at a time $t=t_F$.

The cooling coefficient of the calorimeter alone will be represented by c. The rate of increase in temperature of the calorimeter alone due to thermal leakage will then be represented by

$$d\theta/dt=-c(\theta-\theta_k). \qquad \text{(XIX)}$$

If K_1 represents the heat capacity of the calorimeter alone, the expression

$$dQ/dt=-cK_1(\theta-\theta_k) \qquad \text{(XX)}$$

will represent the rate at which heat is added to the calorimeter by thermal leakage. This rate is assumed not to depend on whether the charge is or is not in the calorimeter.

From Eq. (XX) it follows that the heat added to the calorimeter by thermal leakage between the times t_B and t_F is given by

$$\Delta Q=-cK_1\int_{t_B}^{t_F}(\theta-\theta_k)dt. \qquad \text{(XXI)}$$

That part of the temperature rise $(\theta_F-\theta_B)$ which is due to thermal leakage is therefore given by

$$\Delta\theta=\frac{\Delta Q}{K_1+K_2}=-\alpha\int_{t_B}^{t_F}(\theta-\theta_k)dt, \qquad \text{(XXII)}$$

where K_2 represents the heat capacity of the charge and

$$\alpha=c\frac{K_1}{K_1+K_2}$$

is the (approximate) cooling coefficient of calorimeter plus charge.

The constant α may be calculated from the data of the rating periods. Thus if $(\Delta\theta/\Delta t)_{P'}$ and $(\Delta\theta/\Delta t)_S$ are the average rates of change of temperature during the initial and final rating periods, respectively, we may write

$$\left(\frac{\Delta\theta}{\Delta t}\right)_{P'}=-c(\theta_{P'}-\theta_k)$$

$$\left(\frac{\Delta\theta}{\Delta t}\right)_{S}=-c\frac{K_1}{K_1+K_2}(\theta_S-\theta_k),$$

whence

$$-c\frac{K_1}{K_1+K_2}=-\alpha$$

$$=\frac{\frac{K_1}{K_1+K_2}\left(\frac{\Delta\theta}{\Delta t}\right)_{P'}-\left(\frac{\Delta\theta}{\Delta t}\right)_{S}}{\theta_{P'}-\theta_S} \quad \text{(XXIII)}$$

The constant $-\alpha$ is thus equal to the value of $\Delta(\Delta\theta/\Delta t)/\Delta\theta$ for a calorimeter having a heat capacity of (K_1+K_2), and thermal leakage represented by Eq. (XIX).

The thermal leakage correction to the observed temperature rise can be calculated by inserting the value of α into Eq. (XXII), and evaluating the integral by any convenient method. As the object of an experiment by the method of mixtures is usually the determination of K_2, it will be necessary to use an approximate value of this constant in calculating α, and more than one approximation may be required to obtain the desired accuracy. An alternative, and perhaps better procedure, would be to calculate the quantity of heat represented by $Q=K_1(\theta_F-\theta_B)$ and to calculate the thermal leakage correction to this quantity by means of Eq. (XXI), using the value of c calculated by means of Eq. (XXIII). An error in the value used for K_2 would then be multiplied by $(\Delta\theta/\Delta t)_S$, which is small, rather than by $(\Delta\theta/\Delta t)_{P'}$, which is large, and the error would therefore have a much smaller effect on the final result.

It should be emphasized that the above procedures for correcting the data of an experiment by the method of mixtures are based on the assumption that the final rate is so small that the lag of the charge does not affect the final temperature by a significant amount. The effect of the lag in such experiments is not eliminated by an experimental calibration of the calorimeter. These procedures are also subject to the restriction that the rate of production of heat by stirring does not change when the charge is dropped into the calorimeter.

It appears from the discussion in this paper that the important contribution of King and Grover consists in pointing out that the lag of the bomb in a determination of heat of combustion, or of a solid body introduced into a calorimeter in an experiment by the method of mixtures, affects the observed temperature rise of the calorimeter, and the corrected temperature rise calculated by the usual methods. It is possible that failure to appreciate this fact has been a source of error in bomb-calorimetric measurements in cases where the energy equivalent of the system was calculated from the masses and specific heats of the various component parts of the calorimeter, and in measurements by the method of mixtures made under conditions such that the rate of temperature change in the final period was large.

The effect of the lag of the bomb in a bomb-calorimetric experiment is practically completely eliminated by an experimental calibration of the calorimeter. In this case, any method of calculation based on Newton's law of cooling, if properly applied, should yield the correct result. Small errors in the calculation of the thermal leakage correction can be reduced by arranging the experiment so that the final temperature is very near the convergence temperature, and the final rate, therefore, very small. If the effects of evaporation are to be considered, it is preferable that this final temperature be below the convergence temperature rather than above it, so that any heat transfer by evaporation will be always in the same direction. Since experimental calibration of the calorimeter has been the usual practice in precise measurements for twenty-five years or more, the results of modern bomb-calorimetric experiments are not affected[7] by the errors discussed by King and Grover.

In the method of mixtures, in which a solid body is introduced into the calorimeter at the end of the initial rating period, the effect of the lag of the body can be practically eliminated by so arranging the experiment that the final temperature is at or very slightly below the convergence temperature. In this case also the usual methods of calculation based on Newton's law of cooling should yield the correct result.

[7] See F. D. Rossini, Chem. Rev. 18, 243–244 (1936).

Journal of Research of the National Bureau of Standards Vol. 55, No. 6, December 1955 Research Paper 2636

A New Bunsen-Type Calorimeter

Ralph S. Jessup

A new Bunsen-type calorimeter, using diphenyl ether as the calorimetric substance, is described. Tests of this calorimeter show that it can be used to measure quantities of heat of the order of 38 calories with a precision of about 0.05 percent.

1. Introduction

A new Bunsen-type [1][1] calorimeter for use in measurements of small quantities of heat, such as heats of mixing of polymers and solvents is described. The calorimeter uses diphenyl ether (phenyl ether, phenoxybenzene) as the calorimetric substance instead of water. The data reported in the literature indicate that Bunsen calorimeters using organic compounds as calorimetric substances have considerably higher sensitivity than that reported for the ice calorimeter [2, 3]. The organic compounds that have been used for this purpose include acetic acid [4], anethole [5], diphenylmethane [6, 8, 9] naphthalene [10,11], phenol [7, 12], benzalacetone [13], and diphenyl ether [14, 15, 16, 21]. The last-named substance has the important advantages that it is quite stable, it can be easily prepared in a state of high purity, and its melting point (26.87° C) is conveniently near room temperature.

2. Description of Calorimeter

The calorimeter is shown schematically in figure 1. It is similar in design to the ice calorimeter described by Ginnings, Douglas, and Ball [3], but has a larger central well to accommodate a "reaction vessel" for use in measurements of heats of reaction or heats of mixing.

The central well of the calorimeter was made from a piece of 1¾ in. stainless-steel pipe that was turned down to a wall thickness of 0.02 in. at the upper end to reduce thermal leakage, and is hard soldered to a copper insert in the jacket cover, K, and to the brass piece, I, which constitutes the top of the calorimeter proper. The brass bottom of the well is hard-soldered to the stainless-steel pipe. The copper fins, F, which are soldered to the outer wall of the well are partly to improve thermal contact between the well and the diphenyl ether, and partly for supporting the solid diphenyl ether, which is denser than the liquid. The copper spacers, C, between the fins at the lower end of the well are to promote uniformity in the vertical distribution of heat transferred between the well and the diphenyl ether outside of it. The outer shell, E, of the calorimeter is of stainless steel 1/16 in. in thickness and is soft-soldered to the brass piece, I. The diphenyl ether occupies the space enclosed by the shell, E, the top, I, and central well of the calorimeter, with the exception of the space occupied by the pool, H, of mercury in the bottom of E.

An electric heater having a resistance of about 30 ohms is wound on the outside of the cylindrical part of shell E of the calorimeter, and a heater of about 10 ohms is wound on the hemispherical part of the bottom. Both heaters are cemented to the shell with glyptal lacquer, and are covered with aluminum foil to reduce radiation. They can be used separately or in series. The use of these heaters is described in section 4.

When the calorimeter is in use the outer surface of the central well is covered by a mantle of solid diphenyl ether. Heat transferred between the central well and the diphenyl ether causes partial melting or freezing, with a consequent change in volume of the diphenyl ether and a flow of mercury into or out of the calorimeter through the platinum tube, W, and the stainless steel tube, J, so as to keep the total volume of liquid plus solid in E constant.[2] The quantity of heat is measured by the volume or weight of mercury so transferred. If this is small, it can be determined from the displacement of the mercury meniscus in the 40-cm graduated glass capillary, G, the steel valve, V, being kept closed. If the volume of mercury is large it can be determined from the combination of the change in weight of the contents of the beaker, B, and the change in position of the meniscus in the capillary.

The capillary, G, is horizontal so that the changes in the position of the mercury meniscus in it do not affect the pressure on the diphenyl ether in the calorimeter. Changes in barometric pressure might be large enough to affect the position of the meniscus significantly. To reduce any such effect the open end of capillary G is connected to a 1-liter flask immersed in oil in a Dewar flask. The pressure in this system is adjusted to atmospheric at the beginning of an experiment and has been shown by measurements with a closed-end mercury manometer to remain practically constant during the time of an experiment.

The T-joint in the stainless-steel tube near the valve, V, and the connections to the valve and the glass capillary, G, are made with Apiezon wax.

The interchange of heat between the calorimeter and its environment is reduced to a minimum by

[1] Figures in brackets indicate the literature references at the end of this pape .

[2] The calorimeter was originally constructed with the stainless-steel tube J, extending nearly to the bottom of the pool of mercury. Difficulties were encountered due to creeping of the diphenyl ether past the mercury seal between diphenyl ether and the stainless-steel tube. This was overcome by replacing the lower end of the stainless-steel tube with the platinum tube, W [17]. The nickel sleeve connecting tubes J and W is sealed to them with a low-melting-point glass made of equal parts by weight of soda glass, borax, and zinc oxide.

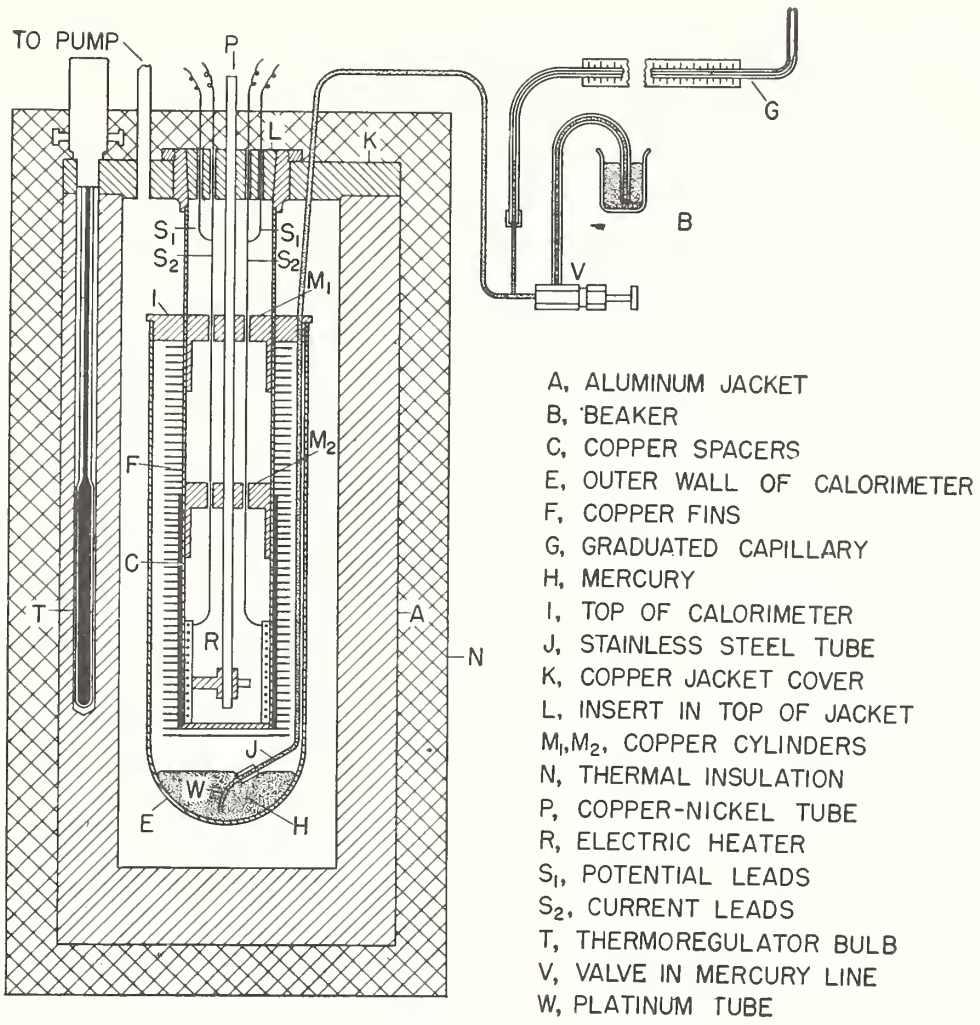

FIGURE 1. *Schematic drawing of calorimeter.*

surrounding the calorimeter with the aluminum jacket, A, with its copper cover K. The jacket is maintained at the temperature of the calorimeter within ± 0.001 deg C by means of thermoregulator T. The temperature difference between the top of the calorimeter, I, and the copper jacket cover, K, is measured by means of a 10-junction copper-constantin thermocouple (not shown in fig. 1) and a Diesselhorst potentiometer. The coefficient of thermal leakage between calorimeter and jacket is reduced by radiation shields (not shown in fig. 1) of aluminum foil and by evacuating the space between calorimeter and jacket to a pressure of about 1μ.

The 100-ohm electric heater, R, the $\frac{3}{16}$-in. copper-nickel tube, P, the cylindrical copper pieces, M_1 and M_2, and the conical copper piece, L, form a unit, the lower part of which fits closely inside the central well. This unit, which is used only for calibrating the calorimeter, can be removed and replaced by a similar unit having a reaction vessel instead of the heater, R, together with suitable tubes for introducing reactants. The purpose of copper pieces M_1 and M_2 is to provide zones of good thermal contact with the wall of the well, and thereby trap heat that would otherwise escape by conduction along the leads, or by radiation and convection. The conical piece, L, fits into a conical hole in the jacket cover and forms a part of the jacket cover, and M_1 forms part of the top of the calorimeter proper.

The heater leads are brought out in such a manner that they are in intimate thermal contact with jacket L and calorimeter M_1. The potential leads are connected to the current leads midway between L and M_1. As the total resistance of the current leads between L and M_1 is approximately 0.01 ohm, or 0.01 percent of the heater resistance, the uncertainty in the heat developed between calorimeter and jacket is negligible.

The current through the heater was turned on and off by a double-pole double-throw switch similar to one described by Osborne, Stimson, and Fiock [20]. It is operated by a spring and a release that is actuated by second signals from a standard clock.

3. Filling the Calorimeter With Diphenyl Ether

3.1. Diphenyl Ether

The diphenyl ether used was purified under the direction of F. L. Howard by fractional freezing and distillation in the Engine Fuels Section of the Bureau. The purity was determined by R. E. McCoskey and G. T. Furukawa from measurement of the equilibrium temperature of a solid-liquid mixture for various known values of the mass ratio of solid to liquid. The value reported for the purity is 99.9985 mole percent and that for the triple-point temperature is 300.03° K. It was later found [18] that the purity of this sample of diphenyl ether after heating to about 360° K in a tin-lined calorimeter had decreased to 99.9926 mole percent.

3.2. Cleaning the Calorimeter

Before shell E (fig. 1) was soldered to brass piece I, it was washed internally, and the central well and attached vanes were washed externally with organic solvents to remove traces of oil or grease. After shell E was soldered in place, the interior surfaces were washed repeatedly with boiling distilled water until tests showed only a slight change in the resistivity of the water after such washings. The system was then heated internally and externally to a temperature somewhat lower than the melting point of the soft solder, and was evacuated for about a week at a pressure less than 10^{-4} mm of mercury to remove water and other adsorbed materials.

3.3. Introducing Diphenyl Ether and Mercury into the Calorimeter

The method of introducing diphenyl ether and mercury into the calorimeter can best be explained by reference to figure 2. The liquid diphenyl ether was first put into a 1-liter spherical flask, F, and slowly frozen under vacuum. This process was repeated several times until most of the dissolved gas was removed. Then with the diphenyl ether frozen the flask was disconnected from the vacuum system and sealed to the 2-in. glass tube, T (fig. 2), and connecting tubing, and connected to a vacuum pump and to the calorimeter as indicated. The system was then evacuated to a pressure less than 10^{-4} mm of mercury.

During this procedure the end of glass capillary G (fig. 1) was sealed, and beaker B (fig. 1) was replaced by a short glass test tube containing mercury and closed at the top by a rubber stopper with a hole of the proper size to fit the glass capillary leading to valve V. This tube was evacuated through a side tube above the mercury surface. Valve V was then opened so that the pressure in it and the glass capillary above it was reduced to that in the calorimeter

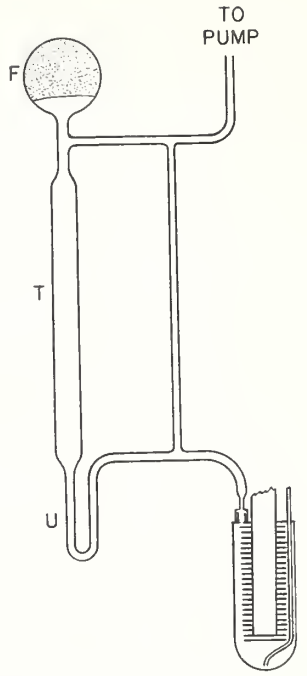

FIGURE 2. *Schematic diagram to illustrate method of introducing diphenyl ether into calorimeter.*

(less than 10^{-4} mm). Valve V was then closed, and air admitted to the glass tube, which replaced beaker B, thus filling the valve and connecting glass capillary completely with mercury. The beaker, B, containing a weighed amount of mercury, was then replaced in its normal position, as shown in figure 1.

An attempt was made to remove any residual gas in the diphenyl ether before introducing it into the calorimeter, as follows:

With the vacuum pump operating, a small amount of diphenyl ether in flask F (fig. 2) was melted and allowed to run down into tube T, where it was refrozen by surrounding the tube with ice. The diphenyl ether in T was then remelted and allowed to run down into the U-tube at the lower end of T. After this the U-tube was kept in an ice bath to prevent any premature flow of diphenyl ether into the calorimeter. The procedure of melting a small amount of the diphenyl ether in F, freezing it in T, and finally remelting it and allowing it to flow to the bottom of T, was followed repeatedly until the entire amount had been transferred from F into T.

Valve V (fig. 1) was then opened, and the desired amount of mercury was introduced into the calorimeter. After this, the temperature of the room was raised above the melting point of diphenyl ether, the entire amount of diphenyl ether in tube T (fig. 2) and in the U-tube at the bottom was melted, and the liquid allowed to flow into the calorimeter. When the flow stopped, a small amount of liquid remained in the tube connecting to the calorimeter. Air was then admitted to the system through the line to the vacuum pump, raising the pressure to atmospheric. The connection to the calorimeter was then removed and the small opening

into the calorimeter was closed by a conical stainless-steel pin forced into the opening by means of a screw-cap. Holes in ths screwcap permitted washing out any diphenyl ether remaining outside the calorimeter proper in the space around the conical pin.

It is believed that by the above procedure the diphenyl ether introduced into the calorimeter was substantially free from dissolved gases. Unfortunately, however, a small amount of air was later introduced into the system due to failure of the room thermostat during a weekend, resulting in an excessively low room temperature and consequent freezing of enough diphenyl ether to draw all the mercury from beaker B (fig. 1), together with a small amount of air, into the calorimeter. The part of the air that was trapped in valve V and tube J was easily removed, but that which actually got into the calorimeter could not be removed without a major operation, which it seemed desirable to avoid. The air is normally dissolved in the liquid diphenyl ether and apparently does not seriously reduce the accuracy of measurements with the calorimeter, but it does cause considerable inconvenience in the use of the instrument.

4. Forming a Mantle of Solid Diphenyl Ether

The inconvenience in the use of the calorimeter resulting from dissolved air in the diphenyl ether has been greatest in attempts to form a satisfactory mantle of solid around the central wall. Because it is not possible to see into the calorimeter, some parts of the following discussion were inferred from the observed behavior of the calorimeter.

Because diphenyl ether may undercool several degrees, it is necessary to cool some part of the material in the calorimeter several degrees below its melting point to start freezing. This is done most conveniently by pressing a piece of ice against the wall of the central well. If any considerable amount of diphenyl ether is frozen in this way, air in the gas phase accumulates in the calorimeter, as shown by the fact that the change with pressure in the position of the mercury meniscus in the capillary, G, increases by a factor of as much as five in some cases. The excess sensitivity to pressure disappears due to solution of air in the remaining liquid, but mantles formed entirely by cooling with ice have never given satisfactorily consistent results in calibration experiments. It is inferred that this is due to air entrapped inside the solid in such a manner that it did not contribute appreciably to the apparent compressibility of the diphenyl ether, but that it dissolved in the liquid when the adjacent solid is melted in a calibration experiment, thus causing the observed increase in volume of the system to be low.

In some cases the freezing of the diphenyl ether was started with ice, and the central well was then filled with water and freezing continued slowly by bubbling air through the water. This procedure did not always lead to satisfactory precision in the calorimetric experiments. In some cases it appeared that in this procedure the mantle did not spread uniformly over the central well, but tended to grow over only a small area, and finally to bridge over the space between the central well and shell E (fig. 1) of the calorimeter.

The most satisfactory results were obtained with the following procedure: (1) A small amount of diphenyl ether was frozen by cooling with ice, and the calorimeter was left overnight to permit any gaseous air to redissolve. (2) The central well was filled with water, which was stirred by bubbling air through it; heat was supplied by means of the heaters wound on the outer shell E (fig. 1) of the calorimeter, and small pieces of ice were added periodically to the water in the central well. By proper adjustment of the heating current and the rate of addition of ice, the rate of freezing of diphenyl ether could be made as low as desired, and the temperature of the water could be maintained from 0.5 to 2 deg below the freezing point. Under these conditions it was expected that the mantle would spread over the central well so as to form a more or less uniform layer.

After the above procedure had been followed for about 1.5 hr, the addition of ice to the central well was stopped, and the current through the heaters was reduced gradually to zero as the temperature of the water in the well rose to the melting point of the diphenyl ether. Slow freezing of the diphenyl ether was then continued over a period of 2 or 3 days by bubbling air through the water in the central well, at first with the well filled with water up to the top of the calorimeter proper, and finally with about half of this amount in order to make the mantle thicker in the lower part where heat was to be added to it. During this slow freezing a small current was passed through the electric heaters on the outside of shall E.

Even with a mantle formed in the manner indicated, it was necessary to melt part of it by means of the heater, R, before consistent results could be obtained. It seems probable that the part of the solid diphenyl ether which was frozen with ice contained entrapped gaseous air, and this part must be melted and the air dissolved in order to obtain satisfactory results.

It is believed that the difficulties encountered in forming a satisfactory mantle are due to the air in the system, and that if no air were present, a mantle could be formed much more quickly and easily.

5. Thermal Leakage

The results of typical experiments to determine the thermal-leakage coefficient of the calorimeter are plotted in figure 3. The slope of the straight line corresponds to a thermal leakage of 0.0042 j (0.0010 cal) per minute for a temperature difference of 0.001 deg C between calorimeter and jacket. That part of the thermal leakage due to conduction along metallic connections between calorimeter and jacket has been calculated to be approximately half of the observed total, so that the other half may be assumed to be due to radiation.

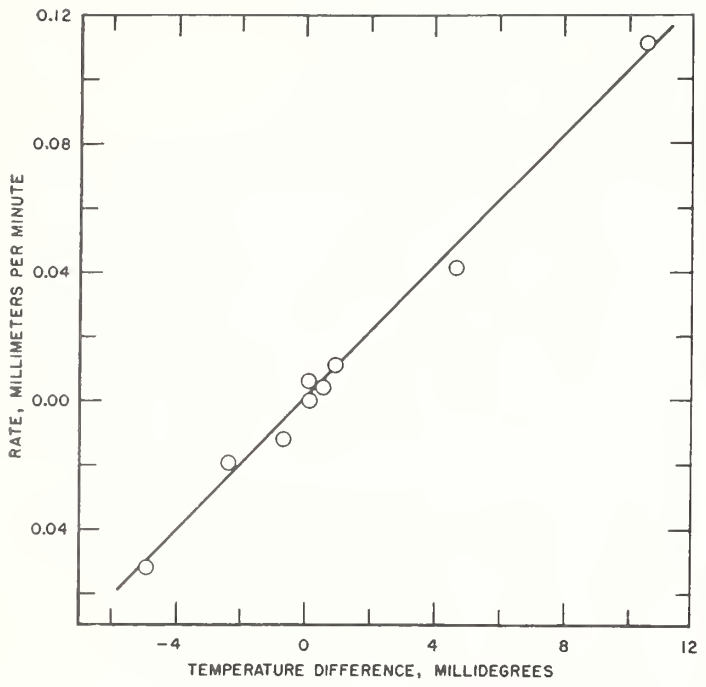

FIGURE 3. *Thermal leakage between calorimeter and jacket.*

Ordinate represents the rate change of position of the mercury meniscus in the graduated capillary tube. (1 mm is approximately equivalent to 0.1 cal) Abscissa represents temperature differenee between ealorimeter and jaeket.

The observed thermal-leakage coefficient is a little larger than is desirable for measurements to a precision of one or two hundredths of a calorie. The "reaction period" for an electrical calibration experiment is about 30 min, and the temperature of the jacket varies in an irregular manner over a range of a few ten thousandths of a degree up to 0.001 deg. It is found, however, that the observed rate of heat transfer remains more nearly constant over periods of 1 or 2 hr than would be expected on the basis of the curve in figure 3 and the observed variation in jacket temperature. This is undoubtedly due to damping of the effect of fluctuations in jacket temperature by the radiation shields between calorimeter and jacket, the relatively heavy calorimeter wall, and the layer of liquid between the calorimeter wall and the mantle of solid diphenyl ether. Although this damping of the effect of fluctuations in jacket temperature probably reduces the uncertainty in the thermal leakage, this uncertainty nevertheless is very probably one of the major sources of error in the calorimeter, particularly in experiments extending over long periods of time.

6. Calibration of the Calorimeter

The graduated capillary, G (fig. 1), was calibrated by observing at various points along the capillary the lengths of 2- and 8-cm mercury threads with reference to the scale etched on the capillary, and by weighing the mercury removed from the capillary when the reading of the meniscus changed from 40 cm to zero. Corrections found for nonuniformity of the capillary bore did not exceed 0.2 mm (0.02 cal), and the mass of mercury required to fill the capillary was found to be $0.05239_8 \pm 0.000004_3$ (sdm) g/cm. This corresponds to an average capillary diameter of 0.71 mm.

TABLE 1. *Electrical calibration experiments*

Series	Experiment	Calibration faetor	Deviation from mean for series	Deviation from mean of all experiments
		j/cm	*j/cm*	*j/cm*
1	1	4.1435	−0.0021	−0.0012
	2	4.1452	−.0004	+.0005
	3	4.1458	+.0002	+.0011
	4	4.1473	+.0017	+.0026
	5	4.1433	−.0023	−.0014
	6	4.1485	+.0029	+.0038
Mean		4.1456		
Standard deviation of mean			$\pm 0.0008_4$	
2	1	4.1461	+0.0021	+0.0014
	2	4.1438	−.0002	−.0009
	3	4.1418	−.0022	−.0029
	4	4.1421	−.0019	−.0026
	5	4.1444	+.0004	−.0003
	6	4.1450	+.0010	+.0003
	7	4.1443	+.0003	−.0004
	8	4.1449	+.0009	+.0001
Mean		4.1440		
Standard deviation of mean			$\pm 0.0005_2$	
3	1	4.1470	+0.00025	+0.0023
	2	4.1448	+.00003	+.0001
	3	4.1436	−.00009	−.0011
	4	4.1448	+.00003	+.0001
	5	4.1425	−.00020	−.0022
Mean		4.1445		
Standard deviation of mean			$\pm 0.0007_5$	
Mean of all results		4.1447		
Standard deviation of mean				$\pm 0.0004_0$

The calorimeter was calibrated electrically, using the 100-ohm heater, R, shown in figure 1, a Wolff-Diesselhorst potentiometer, a Wolff 0.1-ohm standard resistor, a 20000/20-ohm volt box, and a saturated cadmium standard cell maintained at a constant temperature of about 32.8° C by means of a temperature-control box [19]. The potentiometer, volt box, standard resistor, and standard cell were calibrated in the Electricity and Electronics Division of the Bureau immediately following the calibration experiments reported.

The results of three series of calibration experiments are given in table 1, expressed in absolute joules per centimeter displacement of the mercury meniscus in the graduated capillary, G. The results of each series were obtained on a separate mantle formed in the manner described in section 5. The amount of heat supplied to the calorimeter in each experiment was approximately 159 j (38 cal).

Table 1 shows that the results of each series of experiments are in satisfactory agreement among themselves, the maximum deviation from the mean in any one series being about 0.07 percent, which corresponds to about 0.11 j (0.02_7 cal) in the 159 j supplied to the calorimeter. However, the mean of

the results of the first series differs from the means for the other two series by somewhat more than would be expected in view of the precision attained in the separate series. This suggests that perhaps the method of forming a mantle of solid does not entirely prevent the entrapment of air in the solid, and that the amount entrapped in different mantles may be significantly different, but that in any one mantle it is small enough and distributed uniformly enough through the solid to permit a relatively high precision in measurements with that mantle. It is to be expected, therefore, that to obtain a precision of the order of 0.1 j in the measurement of a small quantity of heat with the calorimeter it will be necessary to make a new calibration of the calorimeter for each new mantle.

If the individual results of all three series are averaged, the maximum deviation from the mean result so obtained of the mean for any one series is about 0.02 percent, corresponding to 0.03_5 j (0.01cal), but the maximum deviation of individual results from this mean is now 0.09_5 percent (0.15 j, or 0.04 cal).

Combination of the calibration factor 4.1447 j/cm with the value 0.05239_8 g/cm for the mercury required to fill the capillary yields the calibration factor 79.10 ± 0.010 (sdm) j/g of mercury. This may be compared with the value 270.46 j/g of mercury reported by Ginnings, Douglas, and Ball [3] for the calibration factor of the ice calorimeter. The sensitivity of the diphenyl ether calorimeter is thus about 3.4 times that of the ice calorimeter.

Combination of the value 79.10 j/g of mercury for the calibration factor with the value 300.06° K for the freezing point of diphenyl ether under the pressure (114 cm of mercury) in the calorimeter yields the value $-\Delta H/T\Delta V = 35.6_6$ bars per deg C. This value is subject to some uncertainty because of the fact that the observed value of $\Delta H/\Delta V$ may be affected by gaseous air in the solid diphenyl ether.

It is of interest to compare the calibration factor obtained in the present work with those reported by other investigators—who have reported their results in terms of weight (or volume) of mercury expelled per calorie. The results on this basis are as follows:

Author	Calibration factor
	g Hg/*cal*
Sachse [14]	0.0364
Holmberg [15]	.0488
Klemm, Tilk, and Jacobi [16]	.0528
Giguère, Morissette, and Olmos [21]	.05260
Present work	$.05289_5$

7. References

[1] R. Bunsen, Pogg. Ann. **141,** 1 (1870).
[2] D. C. Ginnings and R. J. Corruccini, J. Research NBS **38,** 583 (1947) RP1796.
[3] D. C. Ginnings, T. B. Douglas, and A. F. Ball, J. Research NBS **45,** 23 (1950) RP2110.
[4] L. E. O. de Visser, Z. physik. Chem. **9,** 767 (1892).
[5] V. Grassi, Soc. Linc. (5) **221,** 494 (1913).
[6] A. N. Shchukarev, I. P. Krivobalko, and L. A. Shchukareva, Physik. Z. Sowjetunion **5,** 722 (1934).
[7] A. N. Shchukarev, T. V. Ass, and N. I. Putilin, Méd. exptl. (Ukraine), **1936,** No. 6, 114.
[8] K. S. Evstrop'ev, J. Phys. Chem. (USSR) **8,** 130 (1936).
[9] M. M. Gordon, Zentralblatt **1938,** II 561.
[10] C. C. Coffin, J. C. Devine, J. R. Dingle, J. H. Greenblatt, T. R. Ingraham, and S. Schrage, Can. J. Research [B] **28,** 579 (1950).
[11] A. Thomas, Faraday Soc. Trans. **47,** 569 (1951).
[12] S. J. Gregg, J. Chem. Soc. **1927,** 1494.
[13] E. J. Caule and C. C. Coffin, Can. J. Research [B] **28,** 639 (1950).
[14] H. Sachse, Z. physik. Chem. [A] **143,** 94 (1929).
[15] Toivo Holmberg, Soc. Sci. Fennica, Commentationes Phys.-Math. **9,** No. 17 (1938).
[16] W. Klemm, W. Tilk, and H. Jacobi, Z. anorg. allgem. Chem. **207,** 187 (1932).
[17] R. S. Jessup, J. App. Phys. **23,** 543 (1952).
[18] G. T. Furukawa, D. C. Ginnings, R. E. McCoskey, and R. A. Nelson, J. Research NBS **46,** 195 (1951) RP2191.
[19] E. F. Mueller and H. F. Stimson, J. Research NBS **13,** 699 (1934) RP739.
[20] N. S. Osborne, H. F. Stimson, and E. F. Fiock, BS J. Research **5,** 429 (1930) RP209.
[21] P. A. Giguère, B. G. Morissette, and A. W. Olmos, Can. J. Chem. **33,** 657 (1955).

Washington, August 16, 1955.

Journal of Research of the National Bureau of Standards Vol. 60, No. 4, April 1958 Research Paper 2848

An Adiabatic Calorimeter for the Range 30° to 500°C [1, 2]

E. D. West and D. C. Ginnings

An adiabatic calorimeter accurate to 0.1 percent and suitable for heat capacity measurements of solids and liquids over the the temperature range 30° to 500° C is described. Factors affecting the design and accuracy are discussed. Automatic controls permit one-man operation of the apparatus. Measurements of the heat capacity of Al_2O_3 agree to 0.1 percent with earlier measurements made with other calorimeters at the National Bureau of Standards.

1. Introduction

An ideal adiabatic calorimeter may be defined as one which has no heat transfer to its environment. As commonly used for the measurement of heat capacities, an adiabatic calorimeter is one which is heated over a small temperature interval, keeping the temperature of the environment as near as possible to the temperature of the calorimeter. This type of calorimeter has been used extensively at moderate and low temperatures. However, at high temperatures, the large coefficient for heat transfer by radiation increases the difficulty of avoiding heat transfer between the calorimeter and its environment. Only a few adiabatic calorimeters have been used above 500° C and even at this temperature, an accuracy as high as 1 percent is unusual [1, 2, 3, 4].[3] Consequently, at the high temperatures, the "drop" method has been more commonly used for the determination of heat capacities [5]. Although the drop method can reduce uncertainties due to increased heat transfer by radiation, it has one basic limitation which prevents its universal application. This limitation is that the method can be used only for materials which reach a thermodynamically reproducible state at the temperature of the calorimeter. With certain materials having slow transitions, this reproducible state may not be reached. The element sulfur is such a material, because it has slow transitions which make accurate measurements impossible by the drop method. The calorimeter described in this report was developed for the temperature range 30° to 500° C with the intention that it would be used first to measure the heat capacity of sulfur.

2. Principles of Design

This adiabatic calorimeter was designed primarily to be accurate to 0.1 percent in measuring heat capacity up to 500° C. In order to attain this accuracy, a number of factors were considered. The evaluation of electric energy input to 0.01 percent is relatively easy with modern techniques. The use of a platinum resistance thermometer for measurement of the temperature change in the calorimeter makes possible an accuracy comparable with that of the electric energy. The largest uncertainty in measuring heat capacity with adiabatic calorimeters in this temperature range is believed to be the uncertainty in "heat leak" (heat transfer between the calorimeter and its environment) which results from experimental departures from the ideal adiabatic condition. Two steps are taken to approach the ideal condition. First, the heat transfer coefficient between the calorimeter and its environment is made small. Second, the temperature of the environment is kept as close as possible to the temperature of the calorimeter. This second step is much more difficult because the surfaces of the calorimeter and its environment are not isothermal, especially during a heating period. Consequently, in many calorimeters thermocouple junctions are distributed over the surfaces to "integrate" the temperature gradients and obtain mean surface temperatures. This procedure introduces difficulties because the mechanism for heat transfer may be different over the various parts of the surface. For example, a part of the calorimeter having a metallic connection to the environment may lose heat mostly by metallic conduction. Another part may loose heat primarily by radiation or conduction through gas. The amount and proportion of heat transferred by various means change with temperature or other circumstances, so that the ideal distribution of thermocouples for proper integration is difficult to achieve.

In adiabatic calorimetry, one of the best procedures is to make two types of heat capacity experiments, one with an empty calorimeter (or with a small amount of sample) and one with the calorimeter filled with the sample. The purpose of the experiments with the empty calorimeter is twofold. The first purpose is to account for the heat capacity of the empty calorimeter by taking the difference in the results of the two experiments. A second purpose, which is sometimes overlooked, is to eliminate heat leak errors and certain other errors which have the same absolute value in the two types of experiments. This procedure can be extremely useful in the elimination of the effect of some unknown heat leaks. However, the procedure does not eliminate heat leak errors which are different in the two types of experiments. Unfortunately, the very existence of the sample in the calorimeter during the heating interval makes the temperature distribution in the full calorimeter different from that in the empty calorimeter. It is therefore vital, for high accuracy, to design a calorimeter having essentially the same temperature dis-

[1] This work was supported in part by the Allied Chemical and Dye Corporation and American Petroleum Institute Project 48A on the "Production, Isolation, and Purification of Sulfur Compounds and Measurement of Their Properties."

[2] This paper includes material from a thesis submitted by E. D. West to the University of Maryland in partial fulfillment of the requirements for the degree of Master of Science.

[3] Figures in brackets indicate the literature references at the end of this paper.

tribution over its outer surface in the two types of experiments. This has been accomplished in the present calorimeter by using a series of thin silver shields as described later.

In addition to high accuracy, the calorimeter was designed to require only one person for its operation. Adiabatic calorimeters capable of 0.1 percent accuracy over a moderate temperature range usually have required at least two operators. One of these operators has had to devote most of his time to controlling and recording the various temperatures pertinent to heat leak evaluation. The present calorimeter has been designed to use automatic equipment to make it possible for one person to operate the calorimeter without difficulty. The calorimeter was also designed to incorporate a sample container which could be removed from the calorimeter with a minimum of disturbance to the electrical system. To accomplish this, the calorimeter was designed in two parts, a sample container and a shield system surrounding and attached to the sample container.

3. Calorimetric Apparatus

Figure 1 is a schematic diagram of a vertical section of the apparatus. The calorimeter, defined as that part of the apparatus where energy changes are measured, is made in two main parts: (1) a sample container C surrounded by (2) a shield system consisting of the silver ring R_1 to which are attached two sets of silver shields S_1 and L_1. Surrounding the calorimeter is the adiabatic jacket which consists of the silver ring R_2 to which silver shields S_2 and L_2 are attached. Between the jacket ring R_2 and the calorimeter ring R_1 are two ten-junction thermopiles T_1 which indicate the vital temperature difference between the calorimeter and its jacket. Figure 2 is a photograph of the top of the calorimeter and jacket with lids L_1 and L_2 removed.

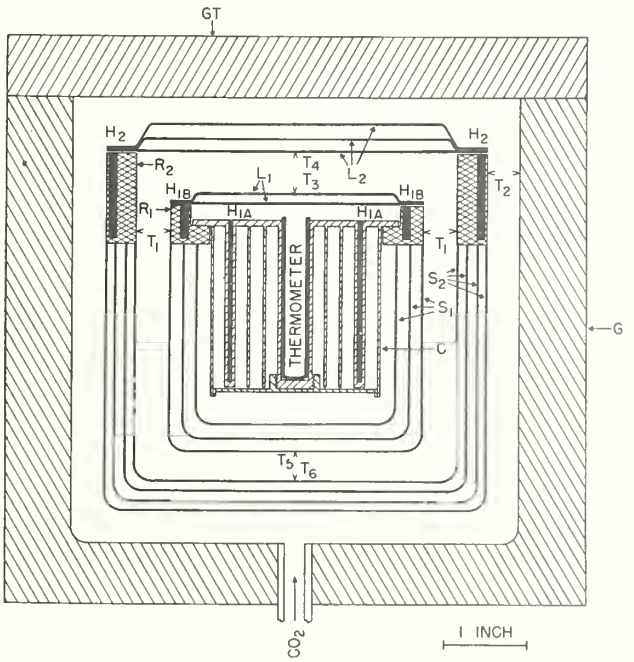

FIGURE 1. *Vertical cross section of the apparatus.*

C, sample container; G, GT, aluminum; H_2, jacket heater; H_{1A}, H_{1B}, calorimeter heater; L_1, L_2, silver lids; R_1, R_2, silver rings; S_1, S_2, silver shields; T_1, thermopile; T_{2-6}, thermocouples.

Surrounding the jacket is a "guard" G whose temperature is controlled a few tenths of a degree below that of the jacket to reduce the power required in the jacket and the consequent temperature gradients. It also guards the jacket from effects of changes in ambient conditions and in the temperature gradients in the glass fiber which is used for thermal insulation of the apparatus.

3.1. The Calorimeter

An essential requirement underlying the design of the calorimeter is that the temperature distribution on its outer silver surface must be independent of the amount of material in the sample container so that the empty calorimeter experiments will properly account for the exchange of small amounts of heat with the jacket. As a practical matter, it is important that the container be easily removed for filling. Consequently, the additional requirement must then be imposed on the design that the temperature distribution on the outer surface also be independent of variations in thermal contact due to differences in the way the sample container is installed. It is apparent that success in meeting these requirements will depend to a great extent on minimizing changes in temperature gradients on the container itself and between the container and ring R_1. It is desirable that these gradients be small so that their changes will be small.. For control purposes, the design must meet the further requirement that the calorimeter must reach thermal equilibrium quickly.

The sample container C, figure 1, is a cylinder 2 in. high and 2 in. in diameter made from aluminum alloy 1100 (99+ percent pure) with a stainless steel cover screwed on the bottom. Aluminum was used here so that the container could later be adapted to the measurements on sulfur. In order to distribute heat quickly to the sample and keep gradients small, the

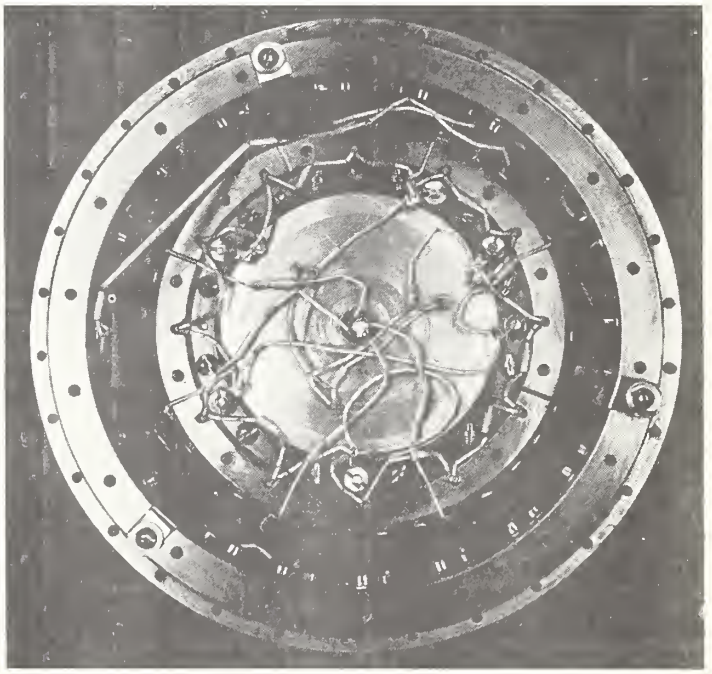

FIGURE 2. *Top view of the calorimeter and jacket.*

container is made from a solid cylinder of aluminum by boring many holes 2 to 5 mm in diameter and leaving a web of metal between holes so that no part of the sample is more than 2.5 mm from a good thermal conductor. The container has an internal volume of 70 cm^3 and a mass of about 112 g. In a central well in the container is a platinum resistance thermometer enclosed (but not sealed) in a Vycor tube which is ground cylindrical to permit a good fit in the well. Also inserted in the top of the sample container are three coils (H_{1A}, fig. 1) of the calorimeter heater. This placement of the heaters permits observation of the calorimeter temperature within a few hundredths of a degree while heating.

The sample container is held against the silver ring by a thin stainless steel ring and twelve stainless steel screws. To avoid contact of aluminum with silver, another thin stainless ring is silver-soldered to the ring where it is in contact with the sample container. This second stainless ring also provides a strong material for attaching the screws.

The ring R_1 is made of pure silver 0.8 cm^2 in cross section to reduce temperature gradients due to circumferential heat flow. It provides space for 12 short heater coils and 20 junctions of the thermopiles which measure the effective temperature difference between the calorimeter and its jacket. Silver-soldered to the ring are three silver shields each 0.25 mm thick. The function of the shields is to provide an external surface on which the effect of the gradients on the sample container and between the sample container and the ring is greatly attenuated. It is calculated that the attenuation by one shield is a factor of about 8, so that the attenuation by three shields should be about 500. The temperature differences on the surface of the sample container are significant only during the heating interval. They are calculated to be not greater than 0.02° C when empty and 0.04° C when full. The temperature difference between the sample container and the ring is made small by distributing the calorimeter heater between them approximately in proportion to their heat capacities. By various combinations of the heating coils allowance is made for the full or empty sample container. During heating, the temperature difference between the sample container and the ring is calculated to be about 0.05° C, which is less than 10 percent of what it would be if the heater were all in the ring. Assuming the uncertainty in the reproducibility of this gradient is as much as the calculated gradient, the variation in the average temperature of the outer surface of the calorimeter due to variations on the sample container is estimated to be only about 0.0001° C.

More critical than the thermal contact between the container and the ring is the contact between the lid L_1 and the ring R_1, because variations in this contact are not attenuated and directly affect the temperature over almost one-sixth of the outer surface of the calorimeter. This contact is made between the soft silver lid screwed down against a stainless steel ring. Although the heat capacity of the lid is small, all the heat required to raise its temperature during the heating interval must come from the heaters in the ring through this mechanical contact. In disassembling the calorimeter, this contact is usually found to be so good that the lid and ring must be forced apart, indicating that some heat is transferred by direct metal-to-metal conduction. However, to arrive at an estimate of how large the temperature difference between the ring and the lid may be, it is assumed that heat transfer is only by gaseous conduction through an effective spacing of 0.0002 in. With these assumptions, the temperature difference between lid and ring is calculated to be 0.001° C. The single-junction thermocouple T_3 is not sensitive enough to determine variations in this thermal contact, but it does set an upper limit of a few thousandths of a degree.

The calorimeter heater was designed to have large electrical resistance and small heat capacity. The coils for this heater (and also for the jacket heater) are made by winding helices of oxidized 38 Nichrome V wire to fit inside porcelain tubes 1 mm i. d. The lead from the lower end of each coil is brought up through a smaller porcelain tube inside the helix. To reduce the heat developed in the leads between coils, the helices are arc welded in helium to larger nickel leads. The total resistance of all calorimeter heaters in series would be 640 ohms, but the sections are connected in two series-parallel combinations to give 77 ohms for the empty calorimeter and 60 ohms for the full calorimeter. The heat capacity of the heater is about 1 j deg^{-1} C, which is less than 0.3 percent of the heat capacity of the full calorimeter.

3.2. The Adiabatic Jacket

The main purpose of the adiabatic jacket is to minimize heat transfer from the calorimeter. To accomplish this purpose, both the heat transfer coefficient and the temperature difference between the jacket and the calorimeter are made small. The jacket is adiabatic if its effective temperature is equal to that of the calorimeter. At equilibrium, this equality can be checked by following the calorimeter temperature. However, during the heating interval, no such check on the heat transfer is available. In place of effective temperature equality, the more feasible requirement has been substituted that temperature inequalities and the corresponding small heat losses be the same in the two experiments—one with the calorimeter full and one with it empty. If this substitute requirement is satisfied, then, when the empty heat capacity is subtracted from the full heat capacity, allowance is automatically made for those small heat losses which are the same in the two types of experiments. The uncertainty in the equality of these small heat losses is frequently the chief limitation on the accuracy of the heat capacity measurements.

In order that heat losses compensate, any errors in measuring the temperature difference between the calorimeter and its jacket must be the same in the two types of experiments. These errors are greatest during the heating interval. To make them the same in the empty and full experiments, the thermopile junctions must have the same thermal lags and the gradients on the outer surface of the calorimeter

and the inner surface of the jacket must be the same. The temperature difference between the jacket ring and the calorimeter ring is measured by means of two ten-junction Chromel-Alumel thermopiles (T_1, fig. 1) connected so that their emf's are additive. These two thermopiles are compared frequently by opposing their emf's to detect circumferential gradients on the silver rings. The junctions are made at "thermal tiedowns" which consist of small gold tabs sandwiched between mica washers for electric insulation and squeezed against the silver rings by stainless steel nuts. These thermal tiedowns are similar to, but larger than, those used previously in this laboratory [6]. At the usual heating rate of 0.5° C min^{-1}, tests indicate the junctions of the thermopile lag about 0.02° C below the rings. The lag in junctions on the calorimeter is compensated for by the lag in those on the jacket, so that the error in the observed temperature difference will be considerably less than 0.02° C. However, it is necessary to have this temperature difference reproducible to better than 0.001° C between the full and empty measurements. To insure maximum reproducibility, the thermopile junctions are not disturbed when the sample container is removed for filling. To prevent cooling of the thermopile junctions by conduction along the leads an extra thermal tiedown was installed in each of the four leads to bring them to the jacket temperature.

In addition to making the thermal lags the same, the gradients on the inner shield of the jacket must be reproducible, just as the gradients on the outer surface of the calorimeter must be reproducible. However, the variations to be attenuated by the jacket are due to disturbances on the outside and are considerably larger. The attenuation at 400° C has been determined by altering the guard temperature 0.75° C and observing the effect on the calorimeter. The change in the rate of heat transfer corresponds to an offset of the jacket temperature of 0.0056° C, an attenuation of 130. The attenuation is much greater at lower temperatures. The uncertainty in the guard temperature, estimated from observations of time and circumferential variations of thermocouples is less than 0.3° C. From this estimate the uncertainty in reproducing the temperature distribution inside the jacket is calculated to be about 0.002° to 400° C.

During the heating period, there are gradients on the shields S_1 and S_2 due to heat flowing from the rings R_1 and R_2 to raise the temperature of the shields. When the calorimeter is being heated at 0.5° C min^{-1}, the temperature difference between the ring and the center of the bottom of the corresponding shield is about 0.1° C. The maximum temperature difference between the outer shield of the calorimeter and the inner shield of the jacket occurs between the centers of the shield bottoms and is about 0.05° C. The gradients in these two shields and therefore the effective temperature difference between them are very nearly proportional to the rate of heating. Consequently, the rate at which heat is lost from the calorimeter by transfer between these shields is directly proportional to the rate of heating. On first thought, it may appear that the rate of heating in the empty experiment would have to be made the same as in the full experiment. That this is not the case may be seen from the following considerations: In any given experiment, the heating rate is virtually constant, so that energy lost from the calorimeter is directly proportional to the product of the heating rate and the time of heating. Since this product is equal to the change in the calorimeter temperature, the energy lost is the same in the empty and full experiments if they have the same initial and final temperatures. The rate of heating in both full and empty experiments was adjusted to 0.5° C min^{-1} within 3 percent, but, to establish the validity of the above conclusion, two experiments in which the heating rate was one-half the usual rate were carried out at 660.05 and 669.75° K. The data for these two experiments are given in table 1 (see note b). At these temperatures the large heat transfer coefficient would result in the largest effect on the heat capacity values, but no such effect is apparent.

In addition to reproducing the errors in measuring the temperature difference, it is necessary to avoid changes in the heat transfer coefficient between the empty and full experiments. During the heating interval, the gradient on the inner jacket shield is different from that on the outer calorimeter shield, resulting in a net temperature difference even when the ring temperatures are matched. If the heat transfer coefficient were to change between the empty and full measurements, there would be a systematic error equal to the product of this change and the average temperature difference between the shields, which is calculated to be about 0.026° C at the normal heating rate.

To avoid large absolute changes in the heat transfer coefficient, it has been made small by using silver for the outer surfaces of the calorimeter and the inner surfaces of the jacket. The silver surfaces were clean, but not polished. Silver loses its polish when heated, but the heat transfer by radiation is not changed much because the orientations of the new crystallite faces are at small angles with the average plane of the surface. The coefficient for heat transfer by radiation is calculated to be 0.10 w deg^{-1} C at 400° C. The coefficient for heat transfer by CO_2 gas conduction across the 1-cm space is calculated to be 0.07 w deg^{-1} C at 400° C. Although the heat transfer coefficient could be reduced by the amount of the gas conduction if the system were evacuated, the gain would be more than offset by the adverse effects where good thermal contact is desired, i. e., at the lids, heaters, thermocouple junctions and the thermometer.

Heat conduction along leads and supports is minimized by using small wires and poor conductors whenever possible. The thermopile is made of No. 36 AWG Chromel P and Alumel wires. The seven heater and thermometer leads are No. 32 AWG gold between the calorimeter and the jacket. The three supports for the calorimeter are Nichrome V, 6 mm wide and 0.1 mm thick. The total metallic conductance is about 0.006 w deg^{-1} C. The leads

TABLE 1. *Heat capacity of aluminum oxide* [a]

Temperature	Empty Calorimeter		Calorimeter+Al_2O_3		C_p° of Al_2O_3 This work	Standard deviation	C_p° of Al_2O_3 Ref. 5	Difference This work—Ref. 5
	Date	Heat capacity	Date	Heat capacity				
°K(*Int. 1948*)		*abs j deg*$^{-1}$		*abs j deg*$^{-1}$	*abs j deg*$^{-1}$ *mole*$^{-1}$	*abs j deg*$^{-1}$ *mole*$^{-1}$	*abs j deg*$^{-1}$	%
311.92	9–9–55	221.64	10–27–55	318.82	81.91	±0.019	81.90	+0.01
	9–13–55	221.59	10–28–55	318.79				
			11–3–55	318.79				
321.65	9–9–55	222.83	10–27–55	322.23	83.80	.019	83.82	−.02
	9–13–55	222.78	10–28–55	322.23				
			11–3–55	322.25				
331.35	9–6–55	224.17	10–27–55	325.81	85.66	.017	85.64	+.02
	9–9–55	224.17	10–28–55	325.79				
	9–13–55	224.15	11–3–55	325.82				
341.05	9–6–55	225.35	10–28–55	329.04	87.38	.019	87.36	+.02
	9–9–55	225.38	11–3–55	329.05				
	9–13–55	225.31						
350.65	9–6–55	226.47	10–28–55	332.06	89.01	.019	88.99	+.01
	9–9–55	226.48	11–3–55	332.09				
	9–13–55							
360.35	9–6–55	227.54	10–28–55	335.05	90.58	.019	90.58	.00
	9–9–55	227.57	11–3–55	335.06				
	9–13–55	227.57						
515.15	9–15–55	241.94	11–16–55	369.35	107.36	.022	107.19	+.16
	9–16–55	241.90	11–17–55	369.34				
	1–27–56	241.92	1–11–56	369.34				
524.95	9–15–55	242.66	11–16–55	370.92	108.05	.020	107.89	+.15
	9–16–55	242.66	11–17–55	370.91				
	1–27–56	242.69	1–11–56	370.90				
	2–7–56	242.67						
534.55	9–15–55	243.49	11–16–55	372.52	108.72	.020	108.57	+.14
	9–16–55	243.47	11–17–55	372.52				
	1–27–56	243.52	1–11–56	372.55				
	2–7–56	243.46						
544.15	9–15–55	244.28	11–16–55	374.05	109.34	.020	109.20	+.13
	9–16–55	244.25	11–17–55	374.04				
	1–27–56	244.30	1–11–56	374.04				
	2–7–56	244.21						
553.85	9–15–55	245.08	11–16–55	375.55	109.96	.020	109.83	+.12
	9–16–55	245.02	11–17–55	375.53				
	1–27–56	245.10	1–11–56	375.55				
	2–7–56	244.98						
563.55	9–15–55	245.82	11–16–55	377.04	110.56	.022	110.42	+.13
	9–16–55	245.80	11–17–55	377.02				
	1–27–56	245.80	1–11–56	377.03				
660.05	1–30–56	253.75	12–30–55	390.56	115.29	.053	115.39	−.09
	1–31–56	253.79	1–4–56	390.59				
	2–2–56	253.73	1–6–56	390.66				
	2–3–56	[b] 253.76						
669.75	1–30–56	254.62	12–30–55	391.90	115.68	.053	115.81	−.11
	1–31–56	254.55	1–4–56	391.80				
	2–2–56	254.58	1–6–56	391.97				
	2–3–56	[b] 254.58						
679.35	1–31–56	255.31	1–4–56	393.11	116.09	.065	116.20	−.09
	2–2–56	255.41	1–6–56	393.21				
689.05	1–30–56	256.27	12–30–55	394.58	116.52	.053	116.59	−.06
	1–31–56	256.19	1–4–56	394.48				
	2–2–56	256.32	1–6–56	394.65				

[a] Molecular weight 101.96. [b] Values obtained at one-half normal heating rate not included in heat capacity calculations.

are brought to the temperature of the rings by the same tiedown technique used for the thermopile junctions. The leads and supports are not disturbed when the container is removed. Calculations indicate that heat transfer by convection is wholly negligible, so that the over-all heat transfer coefficient for flow from the calorimeter is calculated to be about 0.18 w deg^{-1} C at 400° C.

By controlling the jacket temperature about 0.01° C hot or cold, the change in heat flow from the calorimeter leads to an experimental evaluation of the heat transfer coefficient. At 400° C, the mean value of this coefficient is 0.23 w deg^{-1} C, with a standard deviation of ±0.02 which is in reasonable agreement with the calculated value above. Estimating the average uncertainty in the temperature difference from all causes to be 0.001° C at 400 and considering a typical 40-min experiment, the heat loss due to this uncertainty is equivalent to 0.08 percent of the heat capacity of the Al_2O_3. This 0.08-percent uncertainty is comparable to the scatter of the heat capacity results around 670° K (table 1). This considerable heat effect from such a small temperature difference is indicative of the difficulties of adiabatic calorimetry at elevated temperatures.

3.3. Guard System

The guard G is made from aluminum 2 cm thick. The heaters are in three sections distributed over the surface. The guard temperature is automatically controlled about 0.3° C below the jacket temperature using a single junction Chromel-Alumel thermocouple between the jacket ring and the cylindrical section of the guard. This temperature difference permits

sufficient cooling to maintain automatic control of the jacket. The temperature of the top and bottom sections are controlled to the temperature of the cylindrical section by means of differential thermocouples. After temperature gradients in the guard were found to cause appreciable gradients in the jacket ring R_2, a series of thermocouples was installed to measure circumferential gradients in the guard. These gradients amounted to several degrees and were highly dependent on the variations in packing the glass fiber insulation around the guard. To reduce these gradients, which caused significant circumferential gradients on the jacket ring R_2, a heated aluminum cylinder was placed around the guard.

At the bottom of the guard is a connection to the CO_2 supply. Carbon dioxide is kept flowing into the calorimeter at all times at a rate of about 1 $cm^3\ sec^{-1}$. A fraction diffuses through small holes in the various silver shields and lids to insure a uniform atmosphere throughout. Changing the CO_2 flow by tenfold does not affect the heat transfer from the calorimeter.

4. Energy and Temperature Measurements

The power to the calorimeter is obtained from large capacity storage batteries. It is evaluated in the conventional way by determining the current through the calorimeter heater and the potential drop across it. The current is determined by the potential drop across a 1-ohm series resistor (certified to 0.005%). The potential drop across the calorimeter heater is divided by a 20,000-ohm volt box which has a 100:1 ratio certified to 0.01 percent. The current through the volt box is accounted for in evaluating the true calorimeter current. The potential across the 1-ohm resistor and across 1 percent of the volt box is determined by means of a Wenner potentiometer certified to 0.01 percent and standardized against a saturated standard cell which is accurate to 0.002 percent.

To allow for the small amount of heat generated in the current leads between the calorimeter and its jacket, one potential lead is brought from a terminal on the calorimeter, the other from a terminal on the jacket. If the current leads are alike, this procedure accounts for that part of the heat generated in them which flows to the calorimeter. All leads are brought to the temperature of the jacket and the calorimeter by means of thermal tiedowns like those used for the thermopile. The resistance of the leads is approximately 0.03 ohm, so that only about 0.02 percent of the heat to the calorimeter is generated in the leads. A very small correction is applied for heat generated in the resistance thermometer.

The heating interval (about 1,200 sec) is measured to about 0.02 sec with an electric timer synchronized with an accurate crystal oscillator. The interval is held to integral seconds by synchronizing the heater switch with a relay which closes once each second. The coincidence of these second signals is checked daily against standard time signals from WWV.

The 25-ohm platinum resistance thermometer was calibrated at the Bureau. The resistance at the ice point is checked each time the sample container is removed. A thermometer current of 2 ma was used. The resistance is measured with a Mueller bridge calibrated in this laboratory. Temperatures are reported in degrees Celsius as obtained by use of the International Temperature Scale (1948). Temperatures on the Kelvin scale were obtained by adding 273.15°.

5. Jacket Control System

Precise control of the temperature difference between the jacket and the calorimeter is essential for accurate measurements. The apparatus has been designed with low thermal lags in the thermopiles and heaters to facilitate precise control. A commercially available servo system, used in conjunction with the thermopiles, controls the jacket temperature more precisely and for longer periods than is possible for a human operator. The servo system consists of an amplifier, a recorder and a control unit. A few refinements have been added to permit closer control at the beginning and end of the heating period. The details of the control system are described elsewhere [7].

The control system holds the temperature difference within $\pm 0.001°$ C on the average. This control is much better than that obtained by manual operation, which was attempted in some preliminary experiments. Deviations from ideal control are integrated electronically over the time of an experiment and a small correction is applied. Frequent checks of the amplifier and recorder indicate that the indicated zero is stable to $\pm 0.2\ \mu v$, which corresponds to 0.0002° C. Random variations of the control zero will appear in the data; long-term changes will be taken into account by the operating procedure.

6. Experimental Procedure

In a normal day's work one operator can obtain the data for six to nine experiments, depending on how much time is required to adjust the apparatus to the desired initial conditions. So that the apparatus will not be too far from these conditions, its temperature is held overnight about 10 deg below the desired initial temperature by automatic control of the guard heaters. Prior to starting a series of experiments, the temperatures of the jacket and guard are brought under automatic control. The calorimeter is then heated to the initial temperature, adjusting the number of cells in the storage battery and a resistance in series with the calorimeter heater to give a heating rate of $0.5°\ min^{-1}$. This series resistance is kept about equal to the resistance of the calorimeter heater so that the change in heater resistance with temperature will produce only a very small change in the power level [8]. Whenever current is not desired in the calorimeter heater, it is switched to a "dummy" resistor which has about the same resistance as the calorimeter heater. This procedure keeps the external circuit at operating temperature and avoids most of the change in

574278 O - 61 - 16

external resistance which would otherwise occur when the current is turned on. From 7 to 10 minutes after the power is shut off, the temperature of the calorimeter (with the Al_2O_3 sample) can be determined. The temperature is obtained from four readings on a Mueller bridge taken at 30-sec intervals. After another 10-min period, the temperature is again observed to determine the initial temperature "drift", i. e., the rate of change of the calorimeter temperature with time. At 300° K this drift is only 0.005° hr^{-1}, but at 700° K it amounts to 0.03° hr^{-1}.

About 30 sec after the last temperature reading, the current from the storage batteries is switched from the dummy resistor to the calorimeter heater on an integral second. The emf's corresponding to the heater current and voltage are each read on the potentiometer at 3-minute intervals. The operator also has time during the heating period to check the operation of the automatic control equipment and read the various auxiliary thermocouples. About a minute before the end of the heating period, the resistance thermometer current is turned on and the temperature is observed continuously until it is a few hundredths of a degree below the desired final temperature. The power is then switched back to the dummy resistor on the nearest integral second.

The temperature is observed after the calorimeter reaches equilibrium and again after a 10-min interval to obtain the final temperature and its drift. Based on the final and initial drift experiments a correction for drift during an experiment is applied to the apparent heat capacity. This correction makes an allowance for a number of factors which change from one experiment to the next, such as changes in the control point of the jacket control system or changes in spurious emf's of the thermopile. In the time between heating periods, the apparent heat capacity is calculated, so that comparison with previous results can be made before the next experiment is begun.

To obtain the small correction for deviations of the jacket temperature from that of the calorimeter, the electronic integrator is read each time the calorimeter temperature is observed. Each day, the factor for converting the integrator readings to energy correction is evaluated by changing the jacket control point 0.01° C for 10 min and observing the corresponding integrator readings and temperature changes on the calorimeter.

After completion of a series of experiments with the empty container it is removed, filled with a sample, and replaced. When it is not necessary to seal the sample container (as with Al_2O_3) the time required for this operation is about 2 days. After filling the calorimeter, a second series of measurements is made.

7. Heat Capacity of Aluminum Oxide

The heat capacity of the Calorimetry Conference sample of Al_2O_3 [5] has been measured in this calorimeter from 305° to 365°, from 510° to 570°, and from 655° to 695° K, using a 120-g sample. The data are summarized in table 1. The data shown for the empty and full calorimeter have been corrected to the average temperature shown in the first column. The heat capacities calculated from these data have been corrected for the curvature of the heat capacity-temperature function, for buoyancy in weighing, and for the heat capacity of CO_2 displaced by the Al_2O_3. The experiments were carried out at a constant pressure of 1 atm so that C_p is determined directly. Included for comparison are smoothed data taken from earlier work in this laboratory with two different calorimeters [5]. In the last column are shown the percentage differences between the new data and the earlier work. The estimated uncertainty in the earlier data obtained in an adiabatic calorimeter is ±0.1 percent from 90 to 373° K; the uncertainty in the data obtained by the drop method increases from ±0.2 percent at 373 to ±0.4 percent at 1073° K. The agreement with the earlier data is well within these estimated uncertainties.

8. Analysis of Errors

The random errors associated with the results in table 1 have been estimated by ordinary statistical methods, using all the data in each temperature range to estimate the standard deviation of individual measurements in that range. This "pooled estimate" of the standard deviation is then used to compute the standard deviations of the heat capacity of Al_2O_3 at each temperature. These standard deviations are given in table 1. Confidence limits (99% level) for the heat capacity of Al_2O_3 are ±0.05 percent for the two lower ranges and ±0.14 percent for the highest range. These limits would include the average of an infinite number of observations 99 percent of the time, but they do not include an estimate of systematic errors.

It is believed that the variations in the data in table 1 are mainly due to heat transfer from the calorimeter which is not accounted for by the correction for the calorimeter drift experiments. This correction averages 0.05 j deg^{-1} in the lowest range, 0.12 j deg^{-1} in the middle range, and 0.50 j deg^{-1} in the highest range. The magnitude of the drift decreased with time after the heating interval in a manner which is nearly exponential with a time constant of 2 or 3 hr and probably results from thermal lags in the glass fiber insulation. The magnitude of the correction will accordingly depend on when the drift is determined. In general, the drift has been determined as described in section 6. The validity of corrections based on these drift experiments can be judged by the sets of data taken in the middle temperature range on November 16 and 17, 1955, and January 11, 1956 (table 1). These sets of data had very different drift corrections averaging respectively −0.15, +0.13 and +0.09 j deg^{-1}, yet the apparent heat capacities in the three sets agree on the average to 0.01 j deg^{-1}. By contrast, the sets of data taken in the highest range on December 30, 1955, January 4, 1956, and January 6, 1956, had corrections averaging respectively 0.55, 0.39 and 0.49 j deg^{-1}, and the average difference between the heat capacity data of January 4 and those of

January 6 is 0.14 j deg^{-1}. It is obvious that not only are the drift corrections larger at high temperatures, but they are also relatively more uncertain.

The variations in drift seem to be random in nature, not differing significantly between the empty and full calorimeter experiments. Therefore no allowance for errors in drift corrections has been made other than that for the random errors which appear as scatter in the data.

The systematic errors discussed below are estimated to be on about the same probability basis as the confidence limits given above for random variations.

An estimate of the over-all systematic error from the measuring instruments of ± 0.02 percent is obtained by taking the square root of the sum of the squares of the individual estimates in section 4. There is also a possibility of systematic errors in accounting for heat lost from the calorimeter. These errors might arise either from changes between empty and full experiments in the heat transfer coefficient or in the temperature distribution on the outer surface of the calorimeter or the inner surface of the jacket.

An estimate can be made of the systematic error which may be due to a change in the heat transfer coefficient. The error is possible because, during the heating interval, the gradient on the inner jacket shield is different from that on the outer calorimeter shield, resulting in a net temperatue difference even though the thermopiles indicate zero. If the heat transfer coefficient changes between the full and empty measurements, the empty measurement will not make the proper allowance for the small heat loss. It is therefore necessary to consider possible changes in the heat transfer coefficient.

The reproducibility of heat transfer by gas conduction depends only on the composition of the gas. The CO_2 is kept flowing through the system at all times so that a significant change in composition due to diffusion of air is unlikely. It has already been pointed out that conduction along leads and supports is the same in the full and empty experiments. It is therefore unlikely that the heat transfer coefficient might change because of changes in metallic or gas conduction.

There remains the possibility of a change in heat transfer by radiation due to a change in the emittance of the silver surfaces. This change might come about, for example, by the formation of a sulfide layer, although no such corrosion was discernible on the several occasions when the calorimeter was opened. The uncertainty in the observed heat transfer coefficient is too large to permit a significant statement about any systematic change between empty and full experiments. However, in the middle temperature range, empty experiments were made both before and after the full experiments. If there is a significant change in the heat transfer coefficient between the two series of empty measurements, it should result in a constant difference between the averages of the heat capacity values. It is apparent from table 1 that there is no evidence of such a difference.

Apart from the variation in the heat transfer coefficient, systematic error can be introduced if there is a change (between empty and full experiments) in the temperature distribution on either the outer surface of the calorimeter or the inner surface of the jacket. In section 3.1, the effect on the outer shield of the calorimeter due to loading the sample container and changing the gradient between the container and the ring is estimated to be about 0.0001° C. Taking the heat transfer coefficient at 400° C to be about 0.23 w deg^{-1}, the error in a 20-min heating period on a sample of 130 j deg^{-1} heat capacity is 0.002 percent. Also in section 3.1, the temperature drop from the ring R_1 to the lid L_1 is estimated to be 0.001° C. If the irreproducibility in squeezing the silver against the stainless steel is 50 percent, the systematic error may be 0.005 percent. A similar estimate applies to the jacket lid L_2. Both lids were removed several times during the measurements to allow work on the electrical system so that the error due to the lids appears to a considerable extent as a random error in the data.

One further possibility of error is in the reproducibility of a circumferential gradient in the silver rings which might arise from a large change in contact between the sample container and the ring, or from a change in the technique of packing the insulation around the guard. If this gradient is properly averaged around the ring by evenly spacing the thermopile junctions, no error results even if it is not reproducible; however, the thermopiles are distributed around only three-fourths of the circumference, so that one-fourth of the circumference is not included in the average. At equilibrium the thermopiles indicate a difference of less than 1 μv, and there is no apparent variation between the full and empty experiments. If a possible change in this gradient between the full and empty measurements is no greater than the limit of sensitivity of the temperature difference measurement, the resulting error is about 0.005 percent of the heat capacity of the Al_2O_3.

Taking into consideration the random and systematic errors, the error in the heat capacity of Al_2O_3 is estimated to be less than 0.1 percent in the lower ranges and less than 0.2 percent in the upper range.

The interest and cooperation of Professor William J. Svirbely is gratefully acknowledged.

9. References

[1] L. D. Armstrong, Can. J. Research [A] **28,** 44 (1950).
[2] J. H. Awberry and E. Griffiths, Proc. Roy. Soc. (London) [A] **174,** 1 (1940).
[3] H. Moser, Physik. Z. **37,** 737 (1936).
[4] J. M. North, Atomic Energy Research Establ. (G. Brit.) M/R 1016 (1952).
[5] G. T. Furukawa, T. B. Douglas, R. E. McCoskey, and D. C. Ginnings, J. Research NBS **57,** 67 (1956) RP 2694.
[6] N. S. Osborne, H. F. Stimson, and D. C. Ginnings, J. Research NBS **18,** 400 (1937) RP 983.
[7] E. D. West and D. C. Ginnings, Rev. Sci. Inst. **28,** 1070 (1957).
[8] H. J. Hoge, Rev. Sci. Instr. **20,** 59 (1949).

Washington, May 16, 1957.

Reprinted from THE REVIEW OF SCIENTIFIC INSTRUMENTS, Vol. 28, No. 12, 1070–1074, December, 1957
Printed in U. S. A.

Automatic Temperature Regulation and Recording in Precision Adiabatic Calorimetry

E. D. WEST AND D. C. GINNINGS
National Bureau of Standards, Washington, D. C.
(Received July 8, 1957)

In connection with a precision adiabatic calorimeter used for heat-capacity measurements up to 500°C, there is described apparatus for automatically controlling and recording the temperature difference between the calorimeter and its surroundings and for evaluation of the heat leak by electronic integration of the time-temperature difference function.

I. INTRODUCTION

AN ideal adiabatic calorimeter is an instrument in which quantities of heat are measured with no exchange of energy between the calorimeter and its surroundings (the adiabatic jacket). To eliminate energy exchange the ideal apparatus could have either the heat transfer coefficient or the temperature difference between the calorimeter and its jacket zero; in an actual apparatus, both are made as small as practicable and a correction is applied for known deviations from ideal temperature matching.

In a typical experiment, the jacket temperature is controlled as near as possible to the calorimeter temperature while the temperature of the calorimeter is measured at thermal equilibrium, energy is added, and the temperature is again measured after allowing a suitable time for equilibrium. This experimental procedure increases the complexity of the control problem because: (1) With the calorimeter at equilibrium, the jacket requires only sufficient power to balance that lost to its surroundings. (2) When energy is added to the calorimeter, the jacket requires additional power to raise its temperature at a matching rate. This additional power may be many times the equilibrium power, yet, to be effective, the adjustment must be made in a very short time. As the experimental temperature is increased, the demand for accurate control of the temperature difference increases because of the rapid increase in heat transfer by radiation. For precise work, the observation and control of the temperature difference between the jacket and the calorimeter usually require most of the attention of one person, so that two or more observers are required to operate the apparatus. To permit operation of the calorimeter by only one person, it is necessary to record and control automatically this temperature difference and to integrate it with respect to time.

Although versatile automatic control equipment is available for adaptation to temperature control problems in calorimetry, it is essential for best results to design the thermal system so as to facilitate the control problem. Large heat capacities and poor thermal contacts must be avoided in heaters and temperature-sensing devices.

In recent years, a number of experimenters have reported automatic control of adiabatic jackets,[1–4] but the present work is believed to offer the closest control when the calorimeter is intermittently heated. It was the purpose of the work described below to apply electronic instrumentation to the control and evaluation of heat exchange to permit one operator to measure heat capacities from 30 to 500°C with an accuracy of 0.1%. A detailed description of the calorimeter, together with measurements on the heat capacity of aluminum oxide, will be reported elsewhere.[5]

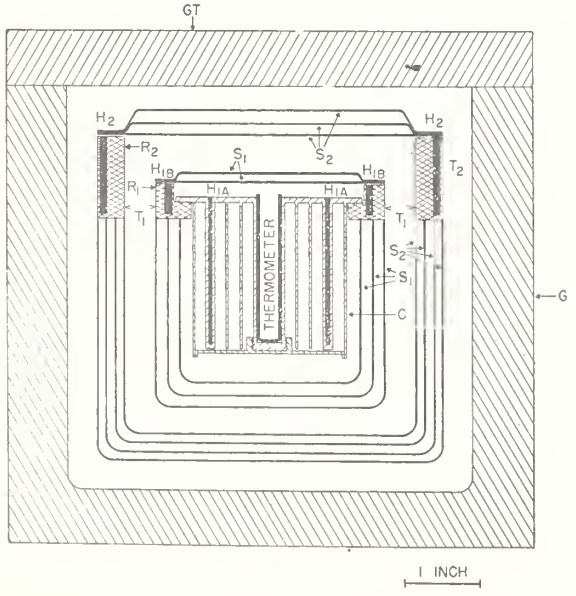

FIG. 1. Schematic diagram showing vertical section of the calorimeter.

II. ADIABATIC CALORIMETER

Figure 1 shows schematically the essential parts of the calorimetric apparatus. The calorimeter (defined as that part of the apparatus in which heat is accurately accounted for) consists of two parts, the sample container C and its silver shield system made up of thin silver shields S_1 attached to a silver ring R_1. In the center of the sample container is a platinum resistance thermometer. The calorimeter is surrounded

[1] T. M. Dauphinee and S. B. Woods, Rev. Sci. Instr. 26, 693 (1955).
[2] Worthington, Marx, and Dole, Rev. Sci. Instr. 26, 698 (1955).
[3] Dole, Hettinger, Larson, Wethington, and Worthington, Rev. Sci. Instr. 22, 818 (1951).
[4] M. G. Zabetakis, Dissertation Abstr. 16, 1077 (1956).
[5] E. D. West, and D. C. Ginnings, J. Research Natl. Bur. Standards (to be published).

by the adiabatic jacket which consists of a heavy silver ring R_2 to which are attached the thin silver shields S_2. The temperature difference between the jacket and the calorimeter is indicated by the 20-junction thermopile T_1. The jacket is enclosed by the "guard" G which is thermally insulated with two inches of glass fiber. The temperature difference between the guard and the jacket is indicated by the thermocouple T_2.

In designing this apparatus, much attention has been given to reducing heat capacities and obtaining good thermal contact in order to avoid excessive thermal lags. For example, it is necessary that temperature gradients in the container and on the guard have a negligible effect on the two important surfaces—the outer surface of the calorimeter and the inner surface of the jacket. Such gradients might be attenuated by a thick metal shield around the container and another for the jacket, but, to avoid the large heat capacity of such an arrangement, the more complex construction utilizing several thin shields has been used. To reduce lags in the calorimeter, the heater is placed partly in the container (H_{1A}) and partly in the ring R_1 (H_{1B}). Both the calorimeter heater and jacket heater (H_2) consist of a number of Nichrome V helices in porcelain tubing ($\frac{1}{16}$ in. o.d.) to combine a small heat capacity with a relatively large area of thermal contact. To obtain good thermal contact and low lags the junctions of the thermopile T_1 are made on gold tabs sandwiched between mica washers for electrical insulation and screwed down against the silver rings.[6]

III. THE JACKET CONTROL SYSTEM

In order to control the temperature of the jacket as closely as possible to the temperature of the calorimeter at all times, several different modes of temperature control are used. First, *proportional* control is used to change the power supplied to the jacket by an amount which is proportional to its temperature difference from the calorimeter. Second, *automatic reset* control is used to reduce gradually the average of this temperature difference to zero. Third, *rate* control is used to keep the time response of the controller as short as possible without causing sustained temperature oscillations known as hunting. The controller equation using these three modes of control may be written as follows[7]:

$$\dot{Q}=\dot{Q}_0-P\theta-RP\int\theta dt-DPd\theta/dt, \qquad (1)$$

where $\dot{Q}$ is the power supplied to the jacket heater, $\dot{Q}_0$ is the steady or uncontrolled part of this power,[8] θ is the temperature difference between the jacket and the calorimeter, and P, R, and D are control factors corresponding to the above three modes of control. These factors are set by the operator in the external control system in order to provide best temperature control consistent with short time response. The factor P is the *proportional control* setting which determines the amount of change in the power per degree of deviation from the control temperature (that of the calorimeter). If the average of the power $\dot{Q}$ differs from $\dot{Q}_0$, there will be an average temperature difference which is not zero. The heat-capacity measurements would have to be corrected for the corresponding energy exchange. However, *automatic reset*, represented in Eq. (1) by the term $RP\int\theta dt$, acts over a period of time to reduce this average temperature difference to zero. The term $DPd\theta/dt$ in Eq. (1) results from *rate* control which alters the power to the jacket by an amount proportional to the rate of change of the temperature difference θ. The three factors P, R, and D are all mutually dependent for optimum performance.

If the lags in the controller and thermopile are negligible compared to the thermal lags in the jacket and its heaters, one can, for illustrative purposes, derive an equation for the temperature control of the jacket by straightforward methods.[9,10] In the apparatus used, the jacket-heater lags are about ten times as large as the controller-thermopile lags. Defining the additional symbols,

T = control temperature (calorimeter temperature),
T_j = temperature of the adiabatic jacket ($\theta=T_j-T$),
C_j = heat capacity of the jacket,
C_h = heat capacity of the jacket heaters,
h_j = heat transfer coefficient between heaters and jacket,
h_s = heat transfer coefficient between jacket and surroundings,
T_h = temperature of heaters, and
T_s = temperature of surroundings,

the following equations, based on the first law of thermodynamics, can be written

$$h_s(T_j-T_s)=h_j(T_h-T_j)-C_jdT_j/dt, \qquad (2)$$

$$h_j(T_h-T_j)=\dot{Q}-C_hdT_h/dt. \qquad (3)$$

Combining Eqs. (1)–(3), imposing the experimental conditions that T_s-T is virtually constant and that T is either constant or increasing at a constant rate,

[6] Osborne, Stimson, and Fiock, Trans. Am. Soc. Mech. Eng. 52, 198 (1930).
[7] E. T. Davis, Instruments 24, 642 (1951).
[8] In the present apparatus, the current in the jacket heater is the controlled variable, so that Eq. (1) is rigorous only if the currents i and i_0 are substituted for $\dot{Q}$ and $\dot{Q}_0$. Therefore, in combining Eq. (1) with Eqs. (2) and (3), it has been tacitly assumed that $d\dot{Q}/dt$ is directly proportional to di/dt, which is an approximation of the true relationship $d\dot{Q}/dt=(i_0+i)di/dt$.
[9] C. E. Mason, Trans. Am. Soc. Mech. Engrs. 60, 327 (1938).
[10] C. E. Mason, and G. A. Philbrick, Trans. Am. Soc. Mech. Engrs. 62, 295 (1940).

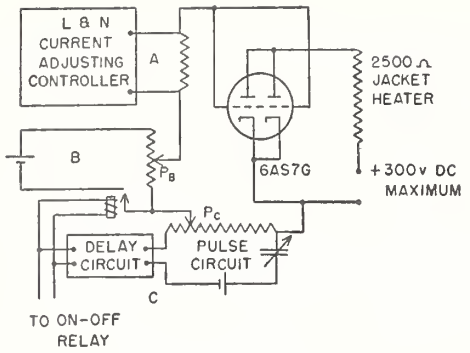

FIG. 2. Arrangement of the jacket heater control circuits.

one obtains

$$\frac{d^3\theta}{dt^3}+\frac{C_h(h_j+h_s)+h_j(C_j+PD)}{C_hC_j}\frac{d^2\theta}{dt^2}$$

$$+(h_s+P)\frac{h_j}{C_hC_j}\frac{d\theta}{dt}+\frac{RPh_j}{C_hC_j}\theta=0. \quad (4)$$

Equation 4 may be written

$$\theta'''+A_2\theta''+A_1\theta'+A_0\theta=0. \quad (5)$$

Defining the ratio of coefficients in Eq. (5) $\rho=A_1A_2/A_0$, the criteria for the performance of the controller are[11]; $\rho<1$, hunting with increasing amplitude of oscillations: $3>\rho>1$, damped oscillations, acceptable in most control problems; $\rho>3$, overdamped with slow response. From Eq. (4)

$$\rho=\left[\frac{h_s+h_j}{C_j}+\frac{h_j}{C_h}+\frac{PDh_j}{C_hC_j}\right]\frac{h_s+P}{PR}. \quad (6)$$

In designing equipment, this equation is useful in predicting qualitatively the performance of the temperature controller with an apparatus whose thermal constants are known. It can be seen from this equation that the effects of the proportional factor P and the rate factor D depend on the thermal constants of the apparatus. An indiscriminate increase of the reset factor R will result in increased hunting and loss of control. In the present apparatus, at the beginning and end of the heating period, the jacket power requirements may change by fifteen-fold. With this condition, the maximum reset action (maximum value of R) which could be used without causing hunting did not reduce the temperature difference to zero in a reasonable time. Consequently, the auxiliary circuit B, Fig. 2, described in the following, was incorporated to reduce the amount of reset action needed and improve response. Increasing the rate action D to damp oscillations should permit some increase in the reset action, but experience indicated that, in the first version of the control system, an electric positioning motor in the output provided more than sufficient damping. When the control motor was replaced with an all-electronic device, which has negligible lag, some damping was added by means of the rate control D. The effect of the proportional factor P depends on its value relative to the heat transfer coefficient h_s. P is about equal to h_s in these experiments so that increasing P may make ρ less than 1 and cause increasing hunting.

The effects of the other factors in Eq. (6) have been taken into account in the design of the calorimeter (Sec. II). If care is taken to keep the thermal lags in the jacket small, damping may be added in the control system. If thermal lags are too large, the controller cannot be made to give a rapid response.

The arrangement of the jacket control circuits is shown in Fig. 2. The controller system at A consists of three Leeds & Northrup components: a 9835-B breaker-type dc amplifier, a Type G Speedomax recorder which will respond to a full-scale deflection in one second, and a Series 60 CAT control unit. This controller system takes the emf (800 μv/deg C) from the thermopile (T_1, Fig. 1), amplifies and records it and adjusts the bias on the 6AS7G electron tube according to the controller equation. In the first version of the controller system, the grid bias imposed by circuit A was obtained from a ten-turn servo-type potentiometer positioned by a constant-speed motor operated by the controller. In the present version the controller adjusts the current through a fixed resistor at A. The tube supplies up to 50 ma to the 2500-ohm jacket heater. The advantages of using a tube are that the time lag in its operation is negligible and that the small power required in the grid circuit makes feasible the addition of the two simple auxiliary control circuits (B and C, Fig. 2).

The controller factors are selected so that a signal change from −5 to +5 μv (−0.006 to +0.006°C) changes the jacket power from 2.5 to 3.5 w during the heating period. The automatic reset action is adjusted to change the power in response to a given error signal at a rate which would duplicate in 6 sec the power added instantaneously by proportional action ($R=10$ min^{-1}). The rate factor D is set at 0.09 min; this means that the power added by rate action for a temperature change of 1° min^{-1} is equivalent to the power added by proportional action for a 0.09° error. In the first controller which had a lag due to the motor, R was set at 2 min^{-1} and D at zero.

The two auxiliary control circuits, B and C (Fig. 2), are used to improve control at the beginning and end of the heating period and operate simultaneously with the calorimeter heater switch. Circuit B automatically changes the bias on the grid of the tube by the voltage set on the potentiometer P_B. This potentiometer is adjusted so that the increase in power level to the jacket heater is approximately that needed to raise the jacket temperature at the desired rate. When the calorimeter power is turned off, the effect is reversed. By anticipating the need for large amounts of reset

[11] E. S. Smith, *Automatic Control Engineering* (McGraw-Hill Book Company, Inc., New York, 1940), p. 239–240.

action, this circuit permits close control with reasonable values of the reset constant.

Circuit (C) is used to anticipate a temperature surge at the beginning and end of the calorimeter heating period. This surge is due to the difference in thermal lags between the calorimeter and jacket systems. This circuit produces a voltage pulse on the grid of the tube. The delivery of this pulse may be delayed up to 10 seconds after the calorimeter power switch is thrown by a variable unbalancing resistor and capacitor in one side of the Eccles-Jordan trigger circuit. When this delay circuit triggers, it closes a relay in the pulse circuit allowing a direct current to charge a capacitor through potentiometer P_C in the grid circuit of the tube. By varying the voltage and capacitance, one controls the magnitude and duration of this pulse. Figure 3 illustrates the improvement in control due to the pulse circuit. Using optimum settings of all controls the lower trace was made without the pulse circuit; the upper traces were taken from the beginning and end of an actual 30-min experiment using the pulse circuit.

In Fig. 3, the record of the experiment with all controls shows that the maximum deviations in the recorded thermopile emf correspond to a few thousandths of a degree. However, these two deviations at the beginning and end of a heating period are reduced to less than 0.001°C within one minute after the power is turned on or off, so that the average temperature difference over an experiment of thirty minutes is still less than 0.001°C.

IV. INTEGRATOR

Near room temperature with an average temperature difference of about 0.001°C between the calorimeter and its jacket, the heat leak from the calorimeter is only about 0.01% of the total energy added in an average ten-degree experiment. At temperatures near 500°C, increased heat transfer by radiation makes this 0.001°C difference more significant. It is therefore desirable to integrate this temperature difference with respect to time. This integral, when used with the experimental heat transfer coefficient, determines a correction to the total energy supplied to the calorimeter. While it is possible to perform a mechanical integration using the paper record, as shown in Fig. 3, it is tedious and time-consuming. It is preferable to have an integrator which is observed only at the end of each experiment. For these experiments, a simple electronic analog integrator was developed to give the integral with an accuracy of about 10%, which is adequate for making the small correction. More accurate integrators can be assembled from commercially available sub-assemblies.[12]

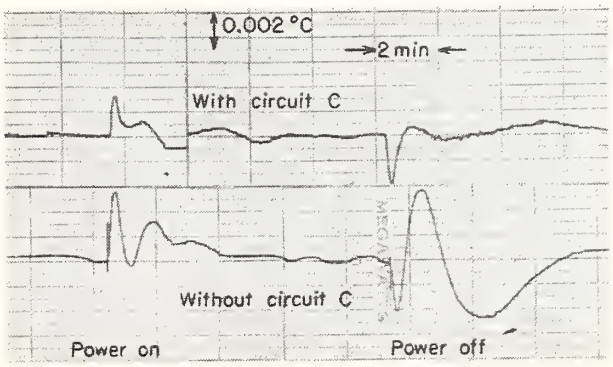

FIG. 3. Chart record showing effect of circuit C on temperature control.

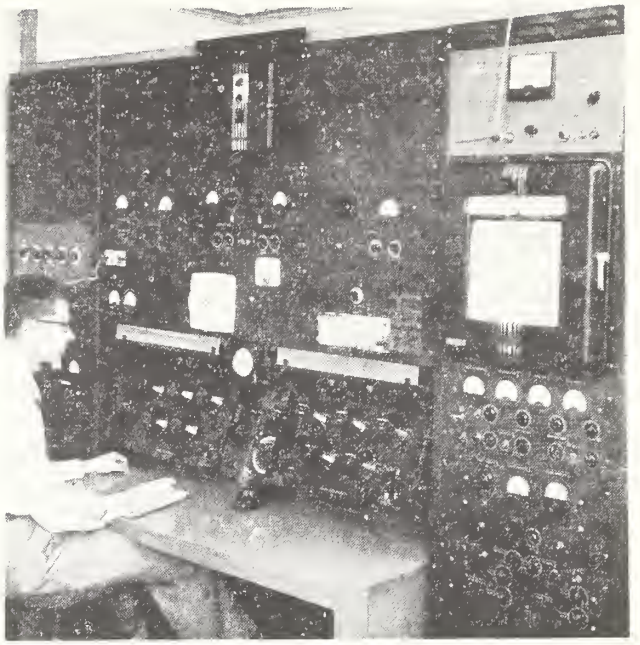

FIG. 4. Arrangement of control and observation apparatus.

The input signal to the integrator is taken from a 50 000-ohm ten-turn potentiometer geared to the drive mechanism of the recorder so that it delivers a voltage across the input resistor proportional to the deviation of the recorder from its zero. The zero signal to the integrator is adjusted by means of a ten-turn resistor. Power for the input circuit is obtained from a 45-v dry battery.

The over-all reliability of the integrator is about 0.001 deg-min over a forty-minute experiment. This corresponds to an uncertainty of about 0.001% in the heat capacity of the calorimeter.

V. GUARD CONTROL SYSTEM

The "guard" G which surrounds the jacket as shown in Fig. 1 supplies most of the heat which is lost to the outside, thereby reducing the power and the temperature gradients on the jacket. The four silver shields on the jacket are designed to eliminate errors resulting from a one-degree temperature difference on the surrounding guard. It is necessary therefore, to keep temperature differences in the guard to less than one degree. To accomplish this, the guard was made of

[12] G. A. Korn, and T. M. Korn, *Electronic Analog Computers*, (McGraw-Hill Book Company, Inc., New York, 1952).

aluminum 0.75 in. thick with separate heaters for the top, bottom, and cylindrical section, each with a separate control. The temperature of the cylindrical part was automatically controlled a few tenths of a degree below that of the jacket, using a thermocouple (T_2, Fig. 1) to indicate the temperature difference. The guard bottom and guard top were controlled to the same temperature as the main guard, also using differential thermocouples. To avoid ac pickup, dc power was supplied to the three guard heaters. This power was controlled by three simple proportional controllers.

With these controls, it was possible to control the guard temperatures to a tolerance of about 0.1°C corresponding to a few microvolts on the thermocouple, which was adequate for the guard control.

VI. GENERAL ARRANGEMENT OF CONTROL APPARATUS

A photograph of the observing and control station is shown in Fig. 4. Standard rack construction is used as much as possible to facilitate assembly, substitution, and rearrangement of the various components. The operator is shown in the position used most of the time during the experiments.

With the automatic jacket control, one observer can easily operate the calorimeter. The automatic controller maintains more precise and convenient control of the temperature difference than manual control which was used in some early experiments. The effectiveness of the controlling apparatus has contributed to the high over-all accuracy of the calorimeter.

Physical Properties of High-Temperature Materials

Part I. New Apparatus for the Precise Measurement of Heat Content and Heat Capacity from 0° to 1,500°C *

Thomas B. Douglas and William H. Payne

There is described in detail new apparatus for the accurate measurement of the heat content and heat capacity of solids and liquids over the temperature range 0° to approximately 1500°C (32° to 2750°F). For use of the "drop" method, a new Bunsen ice calorimeter and resistance-heated furnace were designed, and have been partly constructed. The ice calorimeter is similar to that developed earlier at the National Bureau of Standards, but embodies several minor modifications. To achieve regions of known and uniform temperature, the furnace was designed to have three concentric cores wound with 17 independently controlled wire-heater sections. Temperatures will be measured by several platinum-rhodium thermocouples, which are arranged to permit their periodic recalibration in place. After the performance of the apparatus has been tested, the first measurements undertaken are to be on standard-sample synthetic sapphire (aluminum oxide). These data will augment the Bureau's earlier measurements on this material from 0° to 900°C (32° to 1650°F), and permit its use as a heat-capacity standard up to approximately 1500°C (2750°F).

* Originally published as WADC Technical Report 57-374, Part I; ASTIA Document No. AD142119 (Wright Air Development Center, Wright-Patterson AFB, Ohio, June 1957).

I. GENERAL CONSIDERATIONS

The importance to science and engineering of haveing reliable heat capacities at high temperatures may be illustrated by two major applications. First may be mentioned the importance as a direct factor in heat transfer and the development of thermal stresses such as are likely to be encountered in high-speed flight. Secondly, physical and chemical changes in materials usually proceed so rapidly at high temperatures that from a practical standpoint these are largely governed by equilibrium relations (unless the rate of temperature rise is very great); in these cases the necessary heat capacities are the only data needed to extend the thermodynamic properties of the materials from room temperature, where they are often well known, to the high temperatures where they are needed.

The initial goal of the work described in this report was the development and use of new apparatus to extend accurate values on a high-temperature heat-capacity standard up to a temperature of about 1500°C. As in the Bureau's earlier work from 0° to 900°C, the "drop" method was adopted because of its simplicity of procedure and because the rapidity of dropping a sample from a furnace into a calorimeter minimizes the otherwise serious losses of heat by radiation. In fact, the latter advantage usually more than compensates for the large magnitudes of heat involved in always returning the sample to a low temperature.

Though stirred-liquid and metal-block calorimeters have often been used elsewhere in the "drop" method, and with proper precautions are capable of high accuracy, a Bunsen ice calorimeter was adoped in the present design. This type of calorimeter had been developed at the National Bureau of Standards into a precise instrument for the measurement of quantities of heat that are not too small [1] [1], and has been operated successfully for many years. The ice calorimeter must be capable of measuring extremely small percentage changes in volume accurately, but this requirement is not difficult to attain, principally by constructing the system from rigid parts and ensuring that it is free of gases and fluid leaks. Unlike calorimeters whose temperatures change, the ice calorimeter requires no temperature measurements, and only an occasional reading to determine the small heat leak.

In an attempt to explain why so many published heat capacities at high temperatures determined by the "drop" method show serious

---

[1] Numbers in brackets refer to literature references at the end of this report.

disagreement, the authors have reached the conviction that inaccurate determination of the average temperature of the sample in the furnace is the most common single source of error. After all, to enable this determination to be made accurately is the principal role of the furnace, aside from supplying to the sample the heat necessary for it to reach the elevated temperature. For this reason, in designing a suitable furnace for the present purpose, special attention was paid to verifying by calculation that the region of the furnace where the sample is to be held would be close to isothermal. In the first place, the use of a thick layer of solid silver around the core to minimize temperature gradients, earlier suggested for lower-temperature furnaces by Ginnings and Corruccini and used in a 900°C furnace subsequently described [2, 3] , is impossible in a furnace such as that described here, designed to operate above the melting point of silver. In the second place, the total radiation from a hot body to room temperature is about five times as great at 1500° as at 900°C. These facts necessitated some radical departures from the earlier furnace. It may be added that the furnace need not be the greatest limitation on the precision of the heat measurements. In a recent paper [3] it was pointed out that variations in duplicate measurements using the Bureau's older "drop-method" apparatus were approximately independent of temperature, a fact suggesting that the small variations in duplicate values must be attributed mostly to the calorimeter.

The next major problem in striving for accuracy is to measure the temperatures of the furnace and the sample by some reliable means. The International Temperature Scale [4] specifies what are generally believed to be the best practical means of reproducing the same temperature readings in different laboratories and at the same time following the true, or Thermodynamic Temperature Scale almost as closely as present information permits. According to this scale the gold-point (freezing point of pure gold) is taken to be 1063.0°C, and in addition all higher temperatures are based ultimately on the readings of the optical pyrometer and the use of Planck's radiation law.

In the case of the present apparatus the authors decided to measure temperatures entirely with platinum-rhodium thermocouples, even up to 1500°C. Good-quality thermocouples of this type are said not to change their calibrations at a rapid rate even at 1500°C. While their accuracy in terms of conformity to the International Temperature Scale depends on the thoroughness and frequency of calibration, as well as on various other factors, Roeser and Wensel [5] have stated that with favorable calibration the uncertainty in interpolated values of temperature should be as small as 0.3 degree near 1100°C and 2 degrees near 1500°C. The fact that such thermocouples can be read with considerable precision (to better than 0.1 degree) offers two possible advantages in the present type of work. In the first place, a thermocouple exhibiting about the same error at two neighboring high temperatures - say, 100 degrees apart - should lead to a more accurate heat capacity over the interval than if the two temperatures were each subject to independent uncertainties. In the second place, there is the possibility of basing the thermocouple calibration partly on one or more reproducible fixed

point above the gold point, such as the palladium point; in this event later, more accurate revisions by anyone of the temperatures corresponding to such fixed point would enable a corresponding revision of good thermal data without the need of their remeasurement. Just such revisions have occurred numerous times as the techniques of temperature evaluation have advanced.

II. DESIGN OF THE CALORIMETER

Structure Details

A diagram of the ice calorimeter designed for the present purpose is shown in Fig. 1, with the calorimeter itself drawn to scale. A detailed discussion of the two precision ice calorimeters originally designed and built in this laboratory is to be found in earlier references [1, 2, 3] , and needs no repetition here. Certain features of the older calorimeters were examined critically to see whether changes were needed or desirable because of the higher temperatures of samples that will enter the new calorimeter. In addition, as is normally the case in similar circumstances, long experience with the older calorimeters had suggested the wisdom of certain minor modifications. These topics will now be discussed.

Because of the expansion of water when it freezes, the transparency afforded by envelopes of glass seems an advantage too great to be sacrificed. Yet the glass-to-metal seal is probably the most vulnerable part of the calorimeter. A number of persons building ice calorimeters similar to the earlier ones mentioned have used seals of different types, e.g. O-rings or Kovar joints, apparently with success. The use of Kovar joints was considered, but not adopted after advice was received that soldering close to the glass-metal joint appeared hazardous. Except for occasional breakage, a thin film of hard Apiezon W wax between the glass and metal has worked well in the older calorimeters, and was adoped for the new.

The metal caps (I, J, Fig. 1) of the older calorimeters were constructed of brass, which has a linear coefficient of expansion of about 19×10^{-6} per deg. C. Because the coefficient of Pyrex glass is only 3×10^{-6}, the wax gap had to be sufficiently thick to avoid its undue compression as the calorimeter cooled by as much as 100 deg. C. In the new calorimeter the metal caps were constructed of a low-expansion alloy obtained from the Driver-Harris Co., of Harrison, N. J., under the trade name "Therlo" (29.0% Ni, 17.0% Co, 0.3% Mn, balance Fe). This has a coefficient of expansion of about 5×10^{-6}. The glass envelopes were cylindrically ground to allow for a wax gap of about 0.005" radially, which is considerably smaller than in the older ice calorimeters. This should make it more likely that when the calorimeter is allowed to warm to room temperature, the additional softness of the wax will not allow the hydrostatic pressure inside the calorimeter (about 35 cm Hg) to force the glass and metal apart within a reasonable time.

In the older calorimeters all metal surfaces inside the calorimeter exposed to the water, which must remain free of solutes, were covered with tin by the soldering technique. In the new calorimeter tin was replaced by silver-plating (after first making a "strike" of copper or nickel onto the Therlo alloy). The electroplaters estimated that the average thickness of silver is 0.005" and that since no anode of special shape was used, the thickness of plate would probably vary from 0.001" to 0.010". The copper "conduction" fins of the calorimeter had been assembled by soldering with pure tin, and special attention was given to avoiding crevices which might be bridged across by the silver plate and so lead to pockets of variable volume, a fatal disadvantage in a good ice calorimeter. In addition, earlier experience with one of the older calorimeters had sometimes shown a lack of precision in heat measurement that was interpreted as being caused by a variable degree of filling small crevices by the calorimeter fluids.

The mercury "tempering coil" (H, Fig. 1) should ideally hold as much mercury as will ever enter the calorimeter in one run, lest some of the mercury entering the calorimeter not be at the ice temperature and consequently contribute heat of its own to the measurements. The coil of the older calorimeter holds only about 80 gm of mercury; the coil of the new calorimeter retains approximately the same ID (0.113"), but is long enough to contain about 160 gms of mercury. This extra capacity is a minor disadvantage when the necessary amount of mercury is first introduced into the calorimeter, if this is accomplished by successively freezing part of the water and, on melting the ice, allowing mercury to enter in place of the displaced water. Any ultimate gain in mercury arises only from expansion in excess of the coil capacity, the latter being similar to a mechanical "back lash". In addition, any mercury entering the calorimeter from the room in a heat measurement has an excellent opportunity to be cooled thoroughly if ice (in the bath) has been packed carefully around the coil. In a few measurements using the older calorimeter, as much as 100 gm of mercury entered in a single run, yet the heats measured showed no evidence of being appreciably too great.

The whole transit tube for mercury must, of course, be constructed of some inelastic material which is highly insoluble in mercury. Inconel tubing was used. It was considered desirable that the tubing conducting mercury from the coil to the bottom of the calorimeter be of smaller bore than that of the coil. In addition, a simple calculation shows that the mercury outside the ice bath must have a quite small volume so that a small change in room temperature will not change the volume of the mercury enough to introduce appreciable error in the heat measurements. This dictates a small bore outside the calorimeter. Yet one wants to avoid so small a bore that the viscous flow of mercury during a run is highly restricted. Such a result would greatly lower the pressure inside the calorimeter and so might lead to troublesome volume hysteresis.

In the older ice calorimeter the three bores of mercury transit tubing were achieved by joining three pieces of tubing by wax seals, which occasionally broke under mechanical stress. (No solder can be used because of its high solubility in mercury.) In the new calorimeter such wax seals were avoided by constructing the transit tube of one piece, drawing down the ends of the 1/8" tubing to ID's of 0.04" outside the calorimeter and 0.065" inside. These are comparable to the corresponding bores in the older calorimeter.

The "mercury" valve (X in Fig. 1) must also be entirely insoluble in mercury. The valves used in the older calorimeter were of steel, with a rotating needle effecting closure on a seat of softer steel. This has been troublesome at times. Closure is apt to be imperfect, and the volume inside the valve accessible to mercury is unnecessarily large and, one may suspect, slightly variable.

Several years ago a new valve was designed by H. F. Stimson, of the National Bureau of Standards, to avoid these objections. This valve is drawn to scale in Fig. 2, and was adopted for the new calorimeter. The seat is of platinum, which seals against a small crater rim. The stem is not only rotationless, but effects seating with the reproducible force of a spring. It was advised that Teflon flows too readily under pressure to be useful as a long-time packing, but that Kel-F containing a small proportion of Teflon would be more suitable. A stronger spring (made from piano wire of diameter 0.049") had to be substituted, and the stem was then squeezed lightly in a vise, to achieve approximate vacuum tightness in later closings. A sharper cone or a softer seat material would probably have helped in obtaining good close with less force.

The Drop of the Sample

The gate to the well of the new calorimeter (not shown in any drawing in this report) followed almost precisely the design of Ginnings and Corruccini [1] . During the time the calorimeter is measuring heat, the gate is open for only a very short time (about 2 sec.) to allow the falling sample to pass, and calculation shows that even with the calorimeter at 1500°C the solid angle from furnace to calorimeter is so small that only a few hundreths of a calorie is radiated into the calorimeter. This error approximately cancels anyhow, because it occurs in the empty-container measurements too. The closed gate receives radiation at a somewhat greater rate (up to about 0.1 calorie per sec), but with a good ice bath the temperature of the gate remains so near the ice point that the heat delivered to the calorimeter from this source is but a small fraction of the total heat leak.

For a suitable container material for samples heated to 1500°C, it seems that most investigators have used platinum or a platinum-rhodium alloy, and one of these two materials appears to be the best general choice in the present case. Pt-Rh would remain much stronger than Pt mechanically, and thus seems to be much the better of the two. If oxygen were present, somewhere below 1000°C the rhodium would

form a dark coating of oxide which would decompose at highter temperatures and so, through large variations in the total emissivity, would lead to serious variations in the considerable heat lost during the drop into the calorimeter. But the flow of pure helium through the furnace core will greatly reduce any such oxidation. At the high temperatures these noble metals alloy appreciably with samples of most metals and metalloids, but inert refractory liners or spaces can be interposed, or in some cases one may use containers of other metals such as tantalum.

The heat lost as the sample drops with nearly free fall through the space between the furnace and the calorimeter may be estimated. Let us assume that there is 27 cm^2 of container surface at 1500°C. Assume furthermore that its total hemispherical emissivity is 0.2. Then, if the container is in the room-temperature region in the interval from 26 to 69 cm below the position from which it started falling, about 11 calories would be radiated during the 0.15 sec of time involved. Loss by convection, which is more difficult to estimate, might raise the total to something like 40 calories, much too large a heat to neglect in accurate work. However, using a container surface of constant emissivity and a fall of fixed time, the variation of this heat loss from one measurement to another may be kept small; e.g., a 3-percent variation would affect the reproducibility by only 3 percent of 40 calories, or about 1 calorie. Moreover, the procedure of always measuring the empty container in the same way as one measures the container plus sample leads to almost the same heat loss (largely a surface effect in the small time), and so causes a cancellation of most of this heat loss when the difference is taken in order to arrive at the heat due to sample alone. As in many calorimetric procedures, it is the variation that leads to error. And since the percentage variation tends to be constant, the larger the total effect the larger the resulting error is likely to be. The older "drop" apparatus in this laboratory has the same sources of error, but at 900°C the convective loss is perhaps only half as great and the radiation to room temperature is only one-fifth as great as at 1500°C, other factors being equal.

Some investigators have simply dropped the sample into the calorimeter. The procedure in this laboratory has always kept the sample connected to a suspension wire. This avoids mechanical impact of the sample against the bottom of the calorimeter well, and at the same time provides a very convenient way of returning the sample to the furnace for later "drop" measurements. If the suspension wire is of some fairly hard refractory metal such as molybdenum or tungsten, it would undoubtedly be strong enough at 1500°C but would probably act as a "getter" for traces of oxygen in the furnace atmosphere. Platinum metals offer less strength, but freedom from accummulative oxidation.

The present plan is to use Pt -20% Rh suspension wire, and to minimize the strain due to stopping the fall before the sample reaches the bottom of the calorimeter. The ideal way to minimize this strain would apparently be to impose a constant breaking force on the last 12 cm of fall, when the sample is inside the calorimeter. Since the sample

has by then already fallen about 69 cm, the uniform deceleration must be 5.75 g (g being the gravitational acceleration), which would produce a force of 2000 psi on a No. 26 suspension wire, assuming the mass of sample plus container to be 30 gm.

The tensile strength of Pt - 20% Rh at 1500°C was not found, but from extrapolation of Pt - 10% Rh to this temperature [6] a rough estimate of 6000 psi was arrived at. The tensile strengths of annealed Pt - 10% Rh and Pt - 20% Rh at room temperature have been reported [7] as 45,000 and 70,000 psi, respectively. The solidus temperatures of both alloys have been reported [8] to be in the neighborhood of 1850°C. A pertinent fact may be that in the case of gold the yield strength is about half the tensile strength at room temperature [6]. No. 26 Pt - 20% Rh may thus be strong enough at 1500°C if approximately constant deceleration is achieved.

Calculations of the braking action of air cushions or that resulting from the mechanical additions of increasing amounts of inertia led to unsatisfactory results; in the latter case, e.g., the added mass which itself must later be decelerated increases too rapidly. But a spring of small mass appears to provide a simple braking mechanism, and such an arrangement is shown in Fig. 1. It is planned to use a "plunger" (metal cylinder) falling in a vertical tube above the furnace and connected to the sample container by the suspension wire. Assuming that the total mass to be decelerated is 130 gm, calculation shows that such a spring will produce the desired deceleration if its modulus of elasticity is such that a mass of 715 gm (B in Fig. 1) will produce an initial stretch of 24 cm between the stops. The force of the spring is imparted suddenly to the taut spring attached to the falling system, and according to Hooke's law increases 50 percent during an additional 12 cm of stretch. Some device is necessary, of course, to keep the spring from oscillating appreciably at the end of the motion.

Heat Transfer from Sample to Calorimeter

Once the container and sample have come to rest near the bottom of the calorimeter well, how much heat is likely to be lost out of the calorimeter by conduction, convection, and radiation up the well in the most unfavorable case - viz., when the sample is at 1500°C.

As a "worst case" among those likely to be encountered, it was assumed that the sample remained at 1500°C while it evolved 2000 cal. as a heat of solidification or transition, then cooled to 0°C with a heat capacity of 4 cal./degree C, the total heat to be delivered to the calorimeter thus being 8000 cal. Where the margin of safety proved to be great, the environment of the sample could be assumed to remain at a constant temperature, a great simplification of the actually very complicated pattern of heat transfer. It should be noted that these sources of error are not eliminated by measurements on the empty container, for the latter remains at high temperatures in the calorimeter for a much shorter time than when a sample is present.

Conduction was found entirely negligible. The walls of the upper part of the calorimeter well are, except for a very thin coating of silver plate, entirely of poorly conducting monel. A rough computation indicated 0.002 cal. per min. as the conductive loss, and this would persist for only a few min. before diminishing greatly.

Heat loss by convection is undoubtedly more serious than by conduction, and very difficult to estimate reliably. The loss would be intolerable if any considerable fraction of the rising gas reached the region of the gate without being cooled by the walls of the calorimeter well. In designing an ice calorimeter of very similar dimensions, Ginnings and Corruccini [9] performed special experiments to test for such heat losses. Above a heater at about 900°C, which simulated a hot sample container, were spaced three polished silver disks each of 0.3 mm thickness and 1" apart. Thermocouples on the shields showed the excess temperature (compared with the ambient) to be smaller than the temperature of the shield just below by a factor of about 5, the temperature of the third shield being only about 3 degrees C above the ambient temperature. Ginnings and Corruccini [10] describe also special experiments in which the effect on the heat content showed that one shield was definitely needed but probably adequate when the sample was at 725°C. On the basis of those tests three thin platinum shields were adopted in the present case (C', Fig. 1).

The radiative loss outside the calorimeter can easily be shown to be negligible. The solid angle from the top shield to the part of the well outside the calorimeter is very small, and besides, the top shield itself will be at a much reduced temperature as discussed above. Each shield owing to its heat capacity, contributes a small part to the total heat measured, but its premature reduction in temperature below that of the sample container will tend to be independent of whether or not a sample is present, and the resulting error will thus largely cancel when the heat found for the empty container is subtracted.

In designing the present calorimeter for use with samples that may initially be at 1500°C, a final question was posed: Is the transfer of heat to the calorimeter likely to be so great that water in the calorimeter will be temperarily raised to its boiling point? Preliminary calculations indicated that without special precautions this might occur, and steps were taken to avoid it. In the first place, a "safety stop" (N, Fig. 1) was designed to be placed in the bottom of the calorimeter well. This consists of a tube of Pt - 10% Rh 1 cm long and of 1 mm wall thickness. If the suspension wire should stretch or break, this would prevent the hot sample container from coming in direct contact with the bottom of the well, where thermal contact would be too good. In the second place, the lowest 12 cm length of the well was surrounded by a cylindrical shell of copper 3 mm thick (L, Fig. 1). This will aid somewhat in distributing the heat over a larger height of ice, thus increasing the amount of an ice mantle which can be melted in heat measurements before a hole develops in the ice, when some hot water would escape and deliver part of its heat to the jacket. However, calculation showed that this advantage is not great, for it appears that only about 15 percent

574278 O - 61 - 17

of the heat from the sample will enter the calorimeter at levels above the top of the sample. The horizontal paths for heat conduction are still much shorter and of much greater cross-section than the vertical path up the copper shell.

The main purpose of the copper shell is to provide a temporary reservoir for heat, which will subsequently be delivered to the surrounding water from a far lower temperature than that of the hot sample container.

The time-temperature pattern of the sample and calorimeter parts was then solved by numerical integration over periods of time as short as 0.1 sec. As before, a sample was assumed to deliver 2000 cal. while at 1500°C, and then 6000 cal. more in cooling to 0°C. The surface of the sample container was assumed to have an emissivity of 0.17, that of the well surface to be unity, all conduction to occur through helium and the 1-cm-long Pt - Rh tube at the bottom, and ice to be directly in contact with the copper surfaces in the calorimeter when heat began to flow.

This calculation indicated that the sample would lose its 2000 cal of latent heat in about 12 sec. At the end of this time 65 percent of this heat would have melted ice, 25 percent would be stored in the copper shell, and the remaining 10 percent would be stored in the water formed from ice that had melted. The calculation indicated that 99.99 percent of the heat from the sample would have entered the calorimeter in 10 minutes after the sample was dropped. This result is a lower limit of the time actually required, largely because the thermal conductivity of the sample was assumed to be infinite, but the calculation did indicate that all parts of the water will remain well below the boiling point.

III. DESIGN OF THE FURNACE

Structure Details

A detailed diagram of the furnace designed for the present apparatus is drawn to scale in Fig. 3. There are three coaxial ceramic cores, which in the order of increasing diameter will be designated as Nos. 1, 2, and 3 respectively. On the outside of these are wound the various platinum-rhodium wire heaters as shown. Three "main" heaters, supplying most of the power, are on core 2. Three "auxiliary" heaters, altogether divided into 13 parts capable of independent control, are on core 1 and are designed to supply small additional quantities of power needed to make the center of the furnace where the sample will be suspended nearly isothermal. On core 3 is wound a single ("insulation") heater, which is designed to aid in heating the insulation and so shorten the time required to reach steady-state temperatures throughout the furnace. An approximately steady state throughout the insulation is highly desirable so that the environment of the sample can be kept at a constant temperature without having to make frequent reductions in the power supplied to the inner heaters while the

lags in the insulation are being overcome.

All parts of the furnace inside the main heaters (except near the top and bottom ends of the furnace) are designed to withstand temperatures up to 1500°C. Cores 1 and 2 are of a porous grade of alumina stated by their suppliers, the McDanel Refractory Porcelain Co., of Beaver Falls, Pennasylvania to be 99.5 percent Al_2O_3 and to be more stable at high temperatures than vitreous alumina. Fitting inside core 1 over the length of the furnace is a platinum liner of 0.012" wall thickness. This is tight to most gases, reduces radiation because of its low emissivity, and electrically shields the most important thermocouples. Fitting snugly inside this platinum liner and around the sample for a height of 4" is another platinum tube of 0.040" wall thickness. Inside these platinum tubes a stream of pure helium will flow when the furnace is in operation. An air gap separates cores 1 and 2, and between cores 2 and 3 is packed fine purified alumina powder having a bulk density of approximately 30 lb/ft^3. Calculations of radical heat conduction indicated that with the furnace interior at 1500°C, core 3 will not exceed a temperature of about 1100°C. This core is constructed of vitreous refractory Mullite, and the insulation material between it and the aluminum cylinder surrounding the furnace is so-called Thermoflex loose fiber packed to a density of about 10 lb/ft^3. (According to the supplier, the Johns-Manville Corporation, the effective thermal conductivity of this material is less the greater the density to which it is packed. The material is said to stand continuous exposure up to 1100°C.) The top and bottom cover plates of the furnace are of "18-8" stainless steel. The top plate really consists of three separate plates in a cascaded arrangement; by removing them separately, it is possible to remove an inner furnace core for changes or repairs without dislocating the cores outside it. Thermocouples of Pt -- Pt - 10% Rh measure the temperatures inside the cores at the levels where the various heaters are located. Tubing of pure alumina, with an OD of 1/8" and an ID of 1/16", conduct the thermocouple and heater leads out through the top and bottom furnace cover plates.

The adopted furnace design outlined above was based on numerous calculations of heat transfer in the furnace. With the aim of justifying the conclusions reached, the more important of these calculations will now be discussed.

Radiation in the Furnace

It is necessary to provide adequate clearance below the sample hanging in the furnace so that it may fall into the calorimeter without obstruction. The intensity of radiation inside the innermost core at the highest temperatures led to the question of how small the axial temperature gradients must be to prevent serious error in the mean temperature of the sample and container through radiation from the bottom of the container to the colder parts of the core. If the temperature of the 10-cm-long platinum cylinder surrounding the sample and container averages 1500°C and is sufficiently uniform, the tempera-

ture of the rest of the core could be 30 degs C different but the consequent mean temperature of the sample and container would not be in appreciable error. Assuming the region of the core above the sample to be isolated with respect to radiation by proper shielding, only about one-tenth the solid angle subtended by the container bottom and practically none of the angle to the container walls would be included in the region below the platinum cylinder. If e.g. this region of the core were at only 1470°C, a steady state would be reached with the sample at a temperature of about 1499.5°C. (The core will of course be far below 1470°C near its ends, but the solid angles between the sample container and these distant regions are very small and so allow little transfer of heat by radiation.) This simple calculation enables a good first estimate of how large the axial temperature gradients can be allowed to be inside the innermost core in regions fairly close to the sample.

The core will, as mentioned, be far colder near its ends, and one may question whether the greatly increased temperature factor for radiation from the sample overbalances the effect of the very small solid-angle factors. The following calculation was made, and it may be worthwhile to describe the results in some detail, in view of the general importance of this type of problem in the use of furnace cores at high temperatures.

Consider the total net power radiated (W) from all parts of the inside wall of an opaque cylinder to a band of the wall of width dx and absolute temperature T_o. Assuming all azimuthal temperature gradients to be negligible, let the absolute temperature of the wall be T at a distance along the axis of rL from the band in question, where r is the radius of the cylinder. The following equation was derived,

$$W = k\,E\,r\left\{\int_{-\infty}^{\infty} T^4\left[1 - L(L^2+6)/(L^2+4)^{3/2}\right]dL - 2\,T_o^4\right\}dx,$$

where k is the Stefan-Boltzmann radiation constant and E is the proper emissivity factor. The bracketed expression in the integrand may be replaced to an accuracy within a few percent by $e^{-|L|}$, but integration depends of course on a knowledge of the function T(L), which will be intricate if several heaters of variable power gradients are assumed.

The above equation was applied to a cylinder of 1" ID. The results obtained are exaggerated for the present case, since emissivities of unity were assumed, but the platinum liner need have an emissivity no greater than 0.2 or so. An exact solution was considered not worthwhile because of the necessary approximations to the actual conditions. The cylinder was taken to be 30 cm long and to correspond to the part of furnace core 1 which is below the bottom of the sample container. The upper half of the core was assumed, as before, to be blocked to radiation by proper shielding. The 30-cm core was divided into ten

bands 3 cm wide (along the axis); the power entering band i from adjacent heaters is W_i watts and the temperature of the band is assumed constant and equal to T_i °K, where the subscript i varies from 1 at the end of the cylinder corresponding to the center of the furnace core to 10 at the other end of the cylinder, which corresponds to the bottom of the core.

Setting up heat balances to arrive at a steady state, each of the tem temperatures (in terms of a defined quantity F_i) was solved for as a function of the ten heater powers (P_i)

$$F_i \equiv (T_i/100)^4 = \sum_i a_i P_i$$

The coefficients a_i thus found are given in the following table.

Equation giving \ Coefficient	a_1	a_2	a_3	a_4	a_5	a_6	a_7	a_8	a_9	a_{10}
F_1	3748	2741	2550	2219	1911	1600	1289	979	666	365
F_2	3322	2815	2538	2221	1911	1600	1290	979	667	365
F_3	2967	2447	2599	2209	1912	1599	1288	978	666	364
F_4	2602	2157	2223	2274	1901	1601	1288	978	666	364
F_5	2238	1853	1921	1899	1965	1590	1290	978	666	364
F_6	1874	1552	1607	1599	1590	1654	1279	980	665	364
F_7	1510	1251	1295	1287	1290	1279	1343	969	667	364
F_8	1146	949	983	977	978	980	969	1033	656	366
F_9	780	646	669	665	666	665	667	656	719	353
F_{10}	427	353	366	364	364	364	364	366	353	427

Radiation is reflected repeatedly throughout the length of the cylinder, so that, as the table shows, the temperature where the sample will be placed (given by F_1) is affected appreciably by the power input to any part of the cylinder. However, it will be noted from the table that the first coefficients in any one column are almost constant. In fact, closer examination of this constancy shows that varying the power input to any given band or section of the cylinder by several watts causes a change in the temperature of every section nearer the center of the furnace (smaller value of i) by substantially the same amount. It was

thus concluded that if close temperature control is needed in only the central 10 axial cm of the furnace core, no more than one heater is needed on any core above or below this region. Owing to an increasing axial temperature gradient, such an "end" heater (a "Bottom" heater in Fig. 3) will deliver decreasing amounts of power (per axial cm) to the inside of its core as one approaches an end of the core. But it appears from the table that this fact will contribute little to creating an axial temperature gradient near the center of the furnace.

A related problem which was considered is the magnitude of the direct transfer of heat by radiation between the inside of core 2 and the outside of core 1 at different levels, since this space is filled with air and is thus transparent. Aside from the unknown emissivities, which may here be taken as unity, such a computative problem is chiefly concerned with an adequate estimation of the solid angle involved. An equation was derived for the solid angle S from a point on the outermost surface (with an assumed radius of 2 cm) to a band, 1 cm wide and x cm displaced axially, on the innermost surface (with an assumed radius of 1.6 cm). After weighting with the cosine of the angle to the normal and then normalizing, for values of x not less than 1 cm the solid angle is given to a good approximation by

$$S = (0.507/x^4)\,(1 - e^{-0.8x}).$$

For a difference in temperature of 1 deg C at about 1500°C, it was found that the total radiation between two bands (on opposite walls) each 1 cm wide and displaced axially from each other by an average of x cm is as follows: For $x = 0$, 1 watt; for $x = 1$, 0.2 watt; for $x = 2$, 0.01 watt; and for $x = 3$, 0.002 watt. Because the two tubes are so close together, the radiation thus falls off so rapidly with increasing displacement parallel to the furnace axis that to a good approximation the transfer of heat between the two tubes is essentially horizontal for radiation (as well as for conduction), at all temperatures up to 1500°C.

Main Heaters

Taking into account both conduction and radiation but only in a somewhat approximate manner, the following results were calculated on the basis of three untapped "main" heaters only and a furnace temperature of 1500°C.

Extent of Section Along Furnace Axis (cm above center)	Which Main Heater	Heater Power for Steady State (watts per axial cm)	Extremes of Temperature of Core 1 (°C)
+30 to +22.5	none	0	room temp. - 1429°
+22.5 to +13.5	top	25	?
+13.5 to -13.5	center	16	1500.0° - 1500.5°
-13.5 to -22.5	bottom	25	1515° - 1429°
-22.5 to -30	none	0	1429° - room temp.

Since the heat losses from the furnace are difficult to estimate accurately, allowance was made for considerable error in the calculation of the heater powers required. All heater wire is of platinum-10% rhodium except that of the two end main heaters ("top" and "bottom"), which must carry the greatest currents. The end main heaters are of Pt -20% Rh because of its superior mechanical strength and slightly higher melting point. The use of windings of pure rhodium (melting point 1955°C) was considered, but rejected because, on the basis of advice that it would be more difficult to wind the rhodium in a properly annealed condition, it was feared that the advantage of its higher melting point might be more than offset by a larger spacing between the wire and the furnace core. One calculation of the probable maximum temperature of the platinum-rhodium heaters gave a value above 1800°C when the furnace is at 1500°C. While this is probably an exaggerated result, it is understood from others that platinum-rhodium furnace windings often have a short life at furnace temperatures above 1500°C. For this reason, because of the desire for a margin of safety, and because of the increasing rates of change of the calibration of platinum-rhodium thermocouples as the temperature increases, it was decided to limit the maximum furnace temperature to 1500°C. It will probably be possible to get a more reliable estimate of the actual maximum excess temperature of these windings from their electrical resistances while they are delivering power to the hot furnace.

It seems likely that enough heat may be conducted from the furnace to the calorimeter to justify water-cooling the tube leading from the bottom of the furnace. This would be simple to accomplish after the performance of the furnace has been tested.

Auxiliary Heaters

At 1500°C the thermal conductivity of core 1 (alumina and platinum, together) is computed to be such as to allow a longitudinal heat flow of 1.7 watt for a temperature gradient of 1 deg. C per cm, or an azimuthal heat flow of 0.2 watt per axial cm for an azimuthal temperature gradient of 1 deg C per cm. In each of these two cases the platinum contributes about two-thirds of the total. Even this much conductivity is an aid in creating an isothermal environment for the sample, but is far less than provided by the 1/2" thickness of silver in the older "900°C" furnace in this laboratory.

The possibility of using the platinum liner as a resistance element for "auxiliary" (fine-control) heaters was examined, but rejected because of the high heating currents that would be needed for such small electrical resistances.

The center auxiliary heater is wound on core 1 over the 10 cm of length whose temperature must be critically controlled, as discussed earlier. A simple calculation shows that if enough azimuthal asymmetry should exist in this region (different spacings of heaters, insulation, cores, etc.) to allow a difference of power input of, say, 1 watt per axial cm to exist at some azimuth, the temperature would probably vary by several degrees around the core. It would require several thermocouples azimuthally spaced to average these core-wall temperatures accurately, and the heat transfer to the sample would still need to be uniform to make this average applicable.

While the estimates of the extent of such asymmetry may prove to be exaggerated, it was decised to reduce its effect by dividing the central auxiliary heater into three parts which could compensate by supplying different powers to three equal azimuthal sectors of the core. Placing such azimuthal heaters farther from the axis (e.g., in the insulation) would give them large lags, making quick adjustments of the temperatures of core 1 impossible. The most obvious way to install a wire heater giving preference to one such azimuthal sector would be to wind the heater on that sector only, but this would pose the problem of anchoring the heater at its frequent sharp turns without creating unequal spacings on the core.

The design of center auxiliary heater adopted is shown schematically in Fig. 4, with the corresponding wiring diagram in Fig. 5. In Fig. 4 the pitch of winding and the distance between adjacent turns are greatly exaggerated, while the number of turns shown is much smaller than planned, in order to make clear how the winding is distributed on three separate groves of the alumina core. The whole outside tube surface is shown spread out flat, so that the continuity of wire in each groove can be followed. The whole heater is a continuous length of No. 26 (B&S) Pt - 10% Rh wire wound up one groove, down a second groove, and finally up the third groove. Butt welds (one of which might happen to be faulty) are thus avoided except

at the two ends, and anchorage of the wire is required at four places only. The heater is tapped at eight places, and ten leads being of No. 20 Pt - 10% Rh. The heater is thus divided into nine separate sections, each of which is fed from a step-down isolation transformer and a potentiometer as shown in Fig. 5. The heater sections are joined only to simplify the anchorage of their ends, although this makes it possible to impose common voltages on groups of them if this should prove desirable later.

The nine heater sections obviously make it possible to impose separate power on each "level", or distance of 3-1/3 cm along the axis. In addition, differential heating in the three azimuths of any one level is accomplished as follows. In each groove an additional Pt - 10% Rh wire (No. 22) is laid beside the No. 26 wire for each 2/3 of a turn; by platinum-soldering the short length of No. 22 wire at its ends to the No. 26 wire, the two wires are electrically in parallel. Each wire is thus equivalent to No. 26 wire for a third of a turn and to No. 20 wire, with about one-fourth the resistance per unit length, for the other two-thirds of a turn.

As shown in Fig. 4, the finer wire, in which is generated the greater power by the same current, covers a different azimuth in each of the three grooves. Each azimuth will be heated not only by the higher-resistance winding in one groove but also by the lower-resistance windings in the other two grooves. However, a change in current in any one heater section will affect more the azimuth in which its higher-resistance wire lies than the azimuths in which the lower-resistance wire lies. This can be illustrated by a simple example for the three heater sections at a given level.

Case (a). Assume the same voltage applied to each heater section, and of such magnitude as to give the following power contributions in each azimuth, as determined by the sum of the contributions from the three grooves (always tabulated below in the same order):

Azimuth 1: 1/2 + 1/2 + 2 = 3 watts
Azimuth 2: 1/2 + 2 + 1/2 = 3 watts
Azimuth 3: 2 + 1/2 + 1/2 = 3 watts

Case (b). Same as case (a) except the voltage on the heater section in groove 1 is multiplied by [2.25,] while that in each of grooves 2 and 3 is multipled by [0.75,] giving:

Azimuth 1: 9/8 + 3/8 + 3/2 = 3 watts
Azimuth 2: 9/8 + 3/2 + 3/8 = 3 watts
Azimuth 3: 9/2 + 3/8 + 3/8 = 5-1/4 watts

It is obvious that to be able to increase the power on one azimuth by a given amount without affecting that in the other two azimuths, sufficient current must have already been passing through the two heater sections whose currents must be reduced in the readjustment.

As shown in Fig. 5, the current in each heater section may be read on a common ammeter, with the DPDT switches provided with a spring return to prevent the inadvertent connection of the ammeter to more than one heater section at the same time. With a little practice, the simultaneous adjustment of these currents can doubtlessly be made manually and easily. It would be possible to gear the three potentiometers for each level to each other, but this is hardly worth the trouble. Besides, the ideal efficiency of power control illustrated above can never actually be reached. Since the thermal contact of the heater with its surroundings is never perfect, part of the extra heat generated in the fine wire will flow through it into the coarser wire, thereby tending somewhat to equalize the power available in each azimuth.

An exact calculation was made to determine the above-mentioned effect of heat flowing through the heater wire of non-uniform diameter. Assuming a steady state, the environment was assumed to be uniformly at 1600°C and, neglecting conduction from the wire to its surroundings, the heat transmitted was all assumed to be by radiation. For convenience the results were integrated over three equal lengths of one complete turn of the winding: (a) the one-third turn composed of No. 26 wire, (b) the middle one-third turn of No. 20 wire, and (c) the intervening two one-sixths of a turn of No. 20 wire. With t = the mean temperature of the wire section in degs. C and $\bar{I}$ = the amperes of current flowing through the wire, the results were as follows.

Part of Wire (see above)	Size of Wire (B. & S.)	Mean (t-1600) (degs. C)	Power Generated (watts)	Power Radiated (watts)
a	26	$11.4\ I^2$	$0.132\ I^2$	$0.112\ I^2$
b	20	$1.7\ I^2$	$0.033\ I^2$	$0.034\ I^2$
c	20	$2.6\ I^2$	$0.033\ I^2$	$0.051\ I^2$
		Total:	$0.198\ I^2$	$0.198\ I^2$

Below 1600°C radiation is of course less effective in removing heat from the wire. It was estimated, however, that at all temperatures conductive from the wire would be about as efficient as radiation is at 1600°C if the average spacing of the wire from its surroundings is 0.2 mm over half its perimeter but far greater over the other half. To ensure a comparably small spacing, it may be desirable to cement the bottom of the wire into its groove.

The ten leads of the center auxiliary heater are of No. 20 Pt - 10% Rh wire instead of smaller wire in order to reduce the heating produced by the leads themselves. Because of the rather small number of

turns in each of the nine heater sections, the power from the leads is relatively appreciable, but is made symmetrical by running the leads close to the azimuth most sensitive to the corresponding heater section. It will be noted that the eight leads which are taps are each common to two adjacent heater sections, an expedient that reduces the number of leads and the space occupied. A simple calculation seemed to indicate that this use of common leads of appreciable resistance will not cause an undue dependence of the current in one heater section on the voltage applied across another. Exemplifying the actual case at 1500°C by taking two heater sections, each of 1.2 ohms, in series and connected to two sources of voltage by three leads of 0.3 ohm each, the current in each heater section proved to be six times as sensitive to the voltage directly across it as to the voltage across the other heater section.

Additional temperature control is provided by top and bottom auxiliary heaters wound on core 1 as shown in Fig. 3. Their use seems necessary to ensure a sufficiently small temperature gradient longitudinally in the center of this core, and also to provide protection against the considerable lags which may be encountered at certain temperatures in the transfer of heat from the end main heaters to the innermost core. Each of these auxiliary heaters covers a length of 15 cm along the furnace axis, and is tapped once 5 cm from the inner end to provide additional variation in power gradient. Since this core has three grooves over its whole length, the "inner" section of each end auxiliary heater runs in all three grooves before joining onto the "outer" section. The latter in turn runs up and down in the same three grooves but over a different axial range.

In place of supplying power from separate potentiometers and variable transformers to the various sections of the auxiliary heaters, the alternative of using variable shunts outside the furnace was first considered, but rejected. The shunts would need to carry considerable current, and would presumably need variable contacts of dependably low resistance. The current through a heater section would be reasonably independent of the shunts across the other heater sections, particularly if all the heaters were in series with a large shunt outside the furnace. The method appears to be practical; but the resulting network circuit would be rather complicated, especially since platinum-rhodium heater windings have widely different resistances at widely different temperatures.

Heater Lags: Summary of Heater Specifications.

Most of the foregoing calculations have been for steady-state conditions. It is of practical importance to know the approximate magnitude of the temperature lags, particularly those in the transfer of heat from the main and auxiliary heaters to the innermost core. Approximate calculations for the auxiliary heaters led to the belief that the relaxation time in this case will be of the order of 1 minute.

The relaxation time of the lag of the main heaters was estimated roughly to vary from about 10 minutes near room temperature to a minute or less at 1500°C, being reduced greatly by radiation through the air gap at the higher temperature. So much current passes through the main heaters that a small percentage variation in this current would quickly vary the temperature of the platinum walls if the lag at high temperatures were so small. For this reason a thin platinum radiation shield was inserted midway between cores 1 and 2 for a length of 12 cm along the axis, making the lag at 1500°C more nearly the same as that at room temperature.

A Leeds and Northrup Speedomax control-recorder is available for automatic control of one temperature degree-of-freedom in the furnace. It is planned to place this control on the power generated in the center main heater. The potential of a thermocouple whose hot junction is attached to the inside surface of core 2, at the same level as the sample, will be opposed by an adjustable fixed potential, and the resulting amplified signal will be fed into a saturable-core reactor. The reactance of the secondary of the latter will control the current in the center main heater. It is expected in this way to avoid serious change in the largest power source near the sample, a change that might otherwise vary the temperature of the environment of the sample too rapidly for adequate correction by the center auxiliary heater when the sample is almost ready to be dropped into the calorimeter.

The following table summarizes the estimated dimensions and extreme electrical characteristics of each heater. In the case of each heater which is tapped to form more than one section, the figures in a given column apply to one section only. (The power uniformity of the "insulation" heater is not critical, so core 3 was obtained ungrooved at a considerable reduction in cost.) The estimates of maximum heater powers are based on a steady state.

Approximate Specifications of Furnace Heaters

Heater group	Insulation	Main	Main	Aux., Center	Aux., Top or Bottom	Aux., Top or Bottom
Individual heater or section	-	Center	Top or Bottom	Any 1 of the 9	Inner	Outer
Axial length (cm)	30	24	8	3-1/3	5	10
Diam. of 1 turn (in.)	5-1/8	2-3/4	2-3/4	1-1/2	1-1/2	1-1/2
Pitch of winding (in.)	1.3	1/12	1/12	1/4	1/4	1/4
Pt -X% Rh; X =	10	10	20	10	10	10
Size of wire (B. &S.)	26	20	20	26&20	26	26
Length of wire, heater only (ft)	80	82	27	2.1	6.2	12.4
Length of wire, leads only (ft)	1	1	1	1	1	1
Ohms of heater at 100°C	40(70°)	10.5	3.6	0.5	3	6
Ohms of heater at 1500°C	90(1100°)	28	9.3	1.4	8.5	17
Ohms of leads at 1000°C	1	0.3	0.2	0.3	1	1
Max. watts per axial cm, 100°C	-	2.3	4	0.3	0.5	0.7
Max. watts per axial cm, 1500°C	17	<35	<60	4	7.5	10
Max. watts, heater only, 100°C	-	56	32	1	2	7
Max. watts, heater only, 1500°C	500(1100°)	850	500	13	75	200
Min. watts, heater only, 100°C	0	56	32	0	0	0
Min. watts, heater only, 1500°C	0	850	500	0	0	0
Max. volts, heater+ leads, 1500°C	200	150	70	5	30	60
Min. volts, heater+ leads, 100°C	0	25	11	0	0	0
Max. amperes, 1500°C	2.4(1100°)	5.5	7.2	3	3	3.4
Min. amperes, 100°C	0	2.4	3	0	0	0

Temperature Measurement

The decision to use platinum-rhodium thermocouples to measure the temperatures of the furnace, and thereby the sample, was discussed in Section I.

At high temperatures the conventional Pt vs Pt - 10% Rh thermocouple has certain practical disadvantages which have led some to advocate the substitution of platinum "legs" with higher percentages of rhodium (e.g., Pt - 6% Rh vs. Pt - 30% Rh [11] and Pt - 20% Rh vs. Pt - 40% Rh [12] . Such thermocouples have been found to maintain their calibrations for comparable periods of time at temperatures some 300 deg. C higher than the Pt vs. Pt - 10% Rh couples. But without having further information it was feared that there might be disadvantages in striving for the highest accuracy up to 1500°C that would be unimportant in some applications. A number of persons in various parts of the country who were known to have had considerable critical experience with high-temperature thermocouples were consulted in this regard.

The following additional facts constitute a summary of the pertinent information brought out by this inquiry.

1. The pure-platinum wires of a thermocouple are ordinarily weakened by grain growth at temperatures around 1500°C much more than wires of the alloys containing rhodium. In the present case, however, provision is made to recalibrate the couples in place without their being removed, so the reduced strength may be only a minor handicap.

2. The Pt vs. Pt - 10% Rh thermocouple constructed of wire of high standards has been found not to change its calibration excessively - only by something like 1/4 deg. C during 6 hr. at 1450°C.

3. More rhodium distils out of Pt - 30% Rh than Pt - 10% Rh (probably through preferential oxidation of the rhodium) in the range 400° to 800°C. While both types of couple may have highly homogeneous leads to start with, the opinion was expressed that due to this fact serious inhomogeneities in the regions of large, poorly reproduced temperature gradients would develop faster in the couples of higher rhodium content.

4. One person stated that there is evidence that Pt - 30% Rh is difficult to obtain completely homogeneous.

5. It was thought that the couples containing more rhodium have particular advantage against rapid changes in calibration when the wires must be small, but that wires of diameter 0.025" (as adopted in the present case) would be more stable, for a given rhodium content.

6. Compared with the Pt vs. Pt - 10% Rh, the Pt - 6% Rh vs. Pt - 30% Rh thermocouple has a considerably smaller temperature

coefficient of EMF below about 500°C. This is advantageous when one is permitted to have the standard junction at room temperature (for less accurate work), but is not advantageous when, as here, a good ice bath is used. In fact, the smaller temperature coefficient may actually impair the precision slightly at the lower furnace temperatures. The Pt - 20% Rh vs. Pt - 40% Rh thermocouple is much less temperature-sensitive at all temperatures, especially near room temperature.

7. A great deal of experience with the Pt vs. Pt - 10% Rh couple has been accrued by many investigators and for many years, not only as to stability but also through numerous comparisons with other temperature standards. In fact, the International Temperature Scale specifies that this thermocouple be the standard means of interpolation of temperature from 630.5° to 1063.0°C [4, 13] . In contrast, there is not yet a standard method of interpolation for the other Pt-Rh thermocouples. One person stated that one currently used interpolation table for one of the less conventional Pt-Rh thermocouples is 2 deg C in error at 1200°C.

In view of the above facts it was recommended to the authors that the Pt - 6% Rh vs. Pt - 30% Rh thermocouple would seem preferable if only temperatures above 1300°C were to be measured, but that for temperatures below 1300°C or for one installation measuring temperatures from 0° to 1500°C (as in the present case) the Pt vs. Pt - 10% Rh thermocouple seems preferable. The latter type of thermocouple was adopted. Wire of the highest attainable specifications as to purity, homogeneity, and thermoelectric properties was obtained from the Sigmund Cohn Corporation, of Mount Vernon, New York, who had annealed the pure Pt at 500°C and the Pt - 10% Rh at 1450°C. While it has been found [14] that further annealing of the pure Pt up to 1450°C produces a small additional change in its thermoelectric calibration, it was advised that this step be omitted for working thermocouples to be used continuously, because of the mechanical weakening produced.

It is planned to keep one or two "standard" Pt vs. Pt - 10% Rh thermocouples for calibration purposes only. These may be calibrated at the gold point (1063°C) when necessary, and will have brief exposure to high temperatures, such as 1500°C, only during occasional comparison with each of the experience in this laboratory and the advice of others, it is believed that a Pt vs. Pt - 10% Rh thermocouple will tend to change its calibration more or less in proportion to temperature, so that the change found at the gold point alone will be an index of whether appreciable change has probably occurred at other temperatures.

A calculation was made of the efficiency of tempering the thermocouple leads, to see whether enough heat might be removed from the hot junction to make its temperature appreciably in error. The calculation was made specifically for a junction in a gold bath, but is indirectly applicable to the temperature measurements of the funace

near the sample. Leads of 0.6 mm (0.025") diameter were assumed to have an average spacing (air-filled) of 0.2 mm from the inside walls of ceramic insulating tubes, heat transfer was assumed to be by conduction only (predominant over radiation at 1063°C with the small spacing involved), the insulated leads were assumed to run down the axis of the furnace, and the center part of the furnace was assumed to have an axial temperature gradient of 1 deg per cm. At 1063°C it was calculated that the hot thermocouple junction would be colder than its environment depending on the immersion as follows: almost no immersion, 1 deg C; 1 cm immersion, 0.04 deg C; 2 cm immersion, 0.003 deg C; 3 cm immersion, 0.0002 deg C. Under these conditions an immersion of 2 or 3 cm is thus adequate. With a different spacing, the distance of immersion required to achieve a given closeness of temperature is proportional to the square root of the linear gap separating the wire from the object whose temperature is being measured.

As stated before, there is one thermocouple measuring junction in the center of each of the 17 heaters or heater sections indicated in Figs. 3 and 4. Many of these thermocouples could have been of the differential type, with the advantage that the less stable Pt - 10% Rh need not run through the large temperature gradients in order to reach ice junctions outside the furnace. However, it was considered an advantage that all the thermocouples be of the absolute type, each having its own ice junction, so that they would to some extent serve as checks on one another in measuring the mean temperature of the samples. The trouble of reading a number of thermocouples with differences in calibration values is avoided by introducing potentiometrically a small known potential, or "bias", in series with each thermocouple, as shown in Fig. 6. Each of these bias potentials can be connected separately across the potentiometer, and, according to the calibration value of that thermocouple at the furnace temperature in question, can be so adjusted that all the thermocouples on cores 1 and 2 give the same reading at the same temperature. Rapid operation of the selector switches then permits successive readings of all the most important thermocouples against a given potentiometer setting, from the galvanometer deflections alone.

The thermocouple junctions adjacent to the main and "insulation" heaters are "tied down" thermally by being welded to thin bands of Pt - 10% Rh fitting snugly inside the respective ceramic cores. On the other hand, the thermocouples for the auxiliary heaters (those inside core 1) run the length of the furnace, one lead passing out the top and the other out the bottom, with the use of a single alumina tube of 1/16" ID. According to the previously discussed calculation on tempering, the small axial temperature gradient in the center region of the furnace should obviate appreciable error in the readings of the thermocouples whose junctions are located there. The platinum liner could have been used as the platinum return lead for all thermocouples inside it, but this procedure has the disadvantage that the platinum-rhodium leads of two or more thermocouples could become shorted to one another without giving different readings that would reveal the consequent error.

An electrical "insulator" such as the alumina constituting the cores and insulating tubes of the new furnace can cause error in thermocouple readings through its increasing electrical conduction at higher temperatures. One common source of error of this type in high-temperature furnaces arises when the electric heaters, in which large potential drops exist, cause leakage to a thermocouple lead either through the presence of a D.C. component in the heating current or through a preferential rectifying action of the insulating material. However, in the new furnace a platinum liner runs the length of the furnace and shields against such an error by shorting out, and hence greatly reducing, any potential which would otherwise be imposed by the heaters acting through the alumina on the thermocouple leads.

Another potential source of error through electrical conductivity of alumina would not be prevented by the platinum liner; this is the shorting to each other of the leads of a thermocouple in regions at temperatures different from that of the junction but sufficiently high to give appreciable electrical conductivity. The effect would be the same as if an infinite number of thermocouples with junctions at various temperatures were connected in parallel, the leads all having high resistance except two.

A calculation was made to find the order of magnitude of this error in case the two (insulated) leads of the thermocouple ran side by side and the junction, in the center of the furnace, were at 1500°C. It was found that the thermocouple would indicate too low a temperature by 0.01 R deg C, where $\underline{R}$ is the ratio of the width of the alumina perpendicular to the plane through the two wires to the width in the plane of the wires. For the two insulating tubes side by side, $\underline{R}$ would presumably be of the order of unity, and for separated leads $\underline{R}$ would be less than unity, so that the error would seem to be negligible.

However, the results of such a calculation depend strongly on the specific electrical resistivity of the insulating material, and this in turn will vary from one sample of material to another, depending on its purity and other factors. The above calculation was based on a specific resistivity of the alumina of 10^4 ohm-cm at 1500°C, a figure found by extrapolation from the linear relation.

$$\log_{10} R_0 = (12,000/T) - 2.8,$$

which was plotted for the range 870° to 1060°C only [15] . ($\underline{T}$ is deg K.). At 500°C this equation gives log R_0 = 12.7. However, more recent investigators have found values of 6.5 to 10.5 for various aluminas and 11 for sapphire [16] ; according to these results in the error might well be many times as great as the calculation in the preceding paragraph indicates, if the two leads are side by side.

The decision to run the two leads out opposite ends of the furnace and to space the thermocouples as far apart azimuthally as possible may provide an additional margin of safety. At least it is hoped that

any such error will be sufficiently constant that it will effectively cancel out when each thermocouple located in a fixed position is calibrated by the juxtaposition of a standard thermocouple. The insulators of the leads of the latter do not need to touch the metal walls.

IV. PROGRESS OF CONSTRUCTION, AND FUTURE PLANS

At the time of this writing, the greater part of the apparatus described in the preceding sections has been constructed. The ice calorimeter and connecting accessories were completed. A typical ice mantle was then frozen, and the heat-leak of the calorimeter which was observed at intervals over a period of two days was found to correspond to a net absorption of between 1 and 2 calories per hour, a rate small enough to be followed accurately by only an occasional reading. The rate appeared to be quite constant, a requisite of accurate interpolation during a run when a sample is evolving heat to the calorimeter so that the heat leak cannot be followed.

After several days the calorimeter developed a leak where the inner glass vessel was sealed by wax to the metal cap (J, Fig. 1). Disassembly of the glass parts indicated that the leak had probably developed because friction had scraped most of the wax off one side of the ground glass. The glass surface was ground down so as to increase the average gap between glass and metal from 0.002" to 0.006", in an effort to prevent a recurrence of an imperfect wax gap. The calorimeter was then reassembled, evacuated, and filled with distilled, air-free water and triply distilled mercury in the usual way. This second assembly seems satisfactory.

All the wiring external to the furnace has been completed except further needed refinement of the control circuit so as to give sufficient sensitivity in controlling the temperature near the center main heater. The metal boundaries of the furnace have been constructed. All other parts of the furnace are on hand, but have been only partly assembled. Winding the platinum-rhodium heater wires on the cores is almost done.

It is unfortunate that by the time of this writing, the development of the apparatus has not progressed to the stage where it could have been given a complete test of operation. To be sure the new apparatus has certain features in common with other calorimeters and furnaces, and careful design can provide considerable confidence in what its general performance will be. Yet invariably in developing new apparatus there are elusive factors which can be evaluated fully only in operation. Undoubtedly many features described on previous pages of this report will prove satisfactory, while others will need modification as indicated by experience in operation. The authors hope these modifications will be minor and can be easily made.

Regardless of the future program employing the new apparatus, the first measurements of heat content will be on standard-sample

"synthetic sapphire" (pure polycrystalline alpha aluminum oxide). At furnace temperatures below 900°C, these measurements will be directly comparable with the same measurements on the same material made earlier in this laboratory with two other "drop-method" apparatuses [3, 10] . This will provide an overall check on the operation of the apparatus in the lower temperature range. In subsequent measurements on aluminum oxide above 900°C the aim is to extend values on this material as a heat capacity standard from 900° to 1500°C.

V. BIBLIOGRAPHY

[1] D. C. Ginnings and R. J. Corruccini, An Improved Ice Calorimeter - The Determination of Its Calibration Factor and the Density of Ice at 0°C, J. Research NBS 38, 583 (1947) RP 1796.

[2] D. C. Ginnings, T. B. Douglas, and A. F. Ball, Heat Capacity of Sodium Between 0° and 900°C, The Triple Point and Heat of Fusion, J. Research NBS 45, 23 (1950) RP 2110.

[3] G. T. Furukawa, T. B. Douglas, R. E. McCoskey, and D. C. Ginnings, Thermal Properties of Aluminum Oxide from 0° to 1,200°K, J. Research NBS 57, 67 (1956) RP 2694.

[4] H. F. Stimson, The International Temperature Scale of 1948, J. Research NBS 42, 209 (1949) RP 1962.

[5] Temperature, Its Measurement and Control in Science and Industry (a symposium), Reinhold Publishing Corp., New York, p. 311 (1941).

[6] J. L. Everhart, W. E. Lindlief, J. Kanegis, P. G. Weissler, and F. Siegel, Mechanical Properties of Metals and Alloys, NBS Circ. 447 (1943)., U. S. Government Printing Office, Washington D. C.

[7] Metals Handbook, The American Society for Metals, Cleveland, Ohio, (1948).

[8] M. Hansen, Der Aufbau der Zweistofflegierungen, Julius Springer, Berlin (1936).

[9] D. C. Ginnings, Private communication.

[10] D. C. Ginnings and R. J. Corruccini, Enthalpy, Specific Heat, and Entropy of Alluminum Oxide from 0° to 900°C, J. Research NBS 38, 593 (1947) RP 1797.

[11] H. R. Wisely, Thermocouples for Measurement of High Temperatures, Ceramic Age, Newark, N. J.(1955).

[12] R. C. Jewell, E. G. Knowles, and T. Land, High-Temperature Thermocouple, Metal Ind. 87, 217 (1955).

[13] H. F. Stimson, Heat Units and Temperature Scales for Calorimetry, Am. J. Phys. 23, 614 (1955).

[14] R. J. Corruccini, Annealing of Platinum for Thermometry, J. Research NBS 47, 94 (1951) RP 2232.

[15] H. Rogener, Uber den Gleichstromwiderstand Keramischer Wekstoffe, Z. Elektrochem. 46, 25 (1940).

[16] B. Schwartz and W. E. Hauth, Jr. (International Resistance Co., Philadelphia, Pa.), Resistivity of Ceramic Materials, Fall Meeting, Basic Science Division, American Ceramic Society, Clemson, S. C., November 1-2, 1956.

SUPPLEMENTARY DISCUSSION

The operational experience acquired by the authors with the furnace during the two or three years since this report was written has led to several alterations in design which materially faciliate the main purpose of the furnace, namely, the control and accurate measurement of the sample temperature.

The platinum cylinder of 0.04 in. wall thickness directly surrounding the sample was replaced by one three times as thick. The gain in temperature uniformity achieved thereby (or by a still thicker wall if space had permitted) is well worth the additional cost of a high-precision design of this type. In addition, the moderate precaution exercised in striving for azimuthal symmetry around the furnace axis (mainly through uniformity of core thickness and of heater-wire closeness of contact with the wall) proved to have made the use of azimuthally biased heaters entirely unnecessary. (The design of azimuthal heaters described in the report, believed to be novel, should be of value in less favorable or more exacting installations.) As a result of these advantages, the number of independently controlled heaters on the important innermost furnace core was reduced from 13 to 3, with a corresponding reduction in the number of thermocouples to minitor them. The resulting reduction of human labor in controlling and measuring numerous temperatures proved to be indispensable. This was especially true when it was discovered that, owing to large power input and output at higher temperatures and to lower thermal inertia than expected (lack of massive core parts), any one temperature often began drifting rapidly without due warning. These facts indicate the desirability of using a separate automatic temperature control for each heater. Present plans call for use of a three-mode control on the heater closest to the sample, and simple inexpensive proportional-type controls on the other heaters.

Operational experience with the furnace has shown also that two precautions discussed in the report deserve being emphasized, especially since it has become apparent that many other designers of calorimetric apparatus tend to forget them and "hope for the best". First is the need for close, dependable thermal contact between every major thermocouple junction and the object whose temperature is to be measured. Second is the practical advantage of a design which permits as many parts of the apparatus as possible to be disassembled for repair or changes without disturbing other parts.

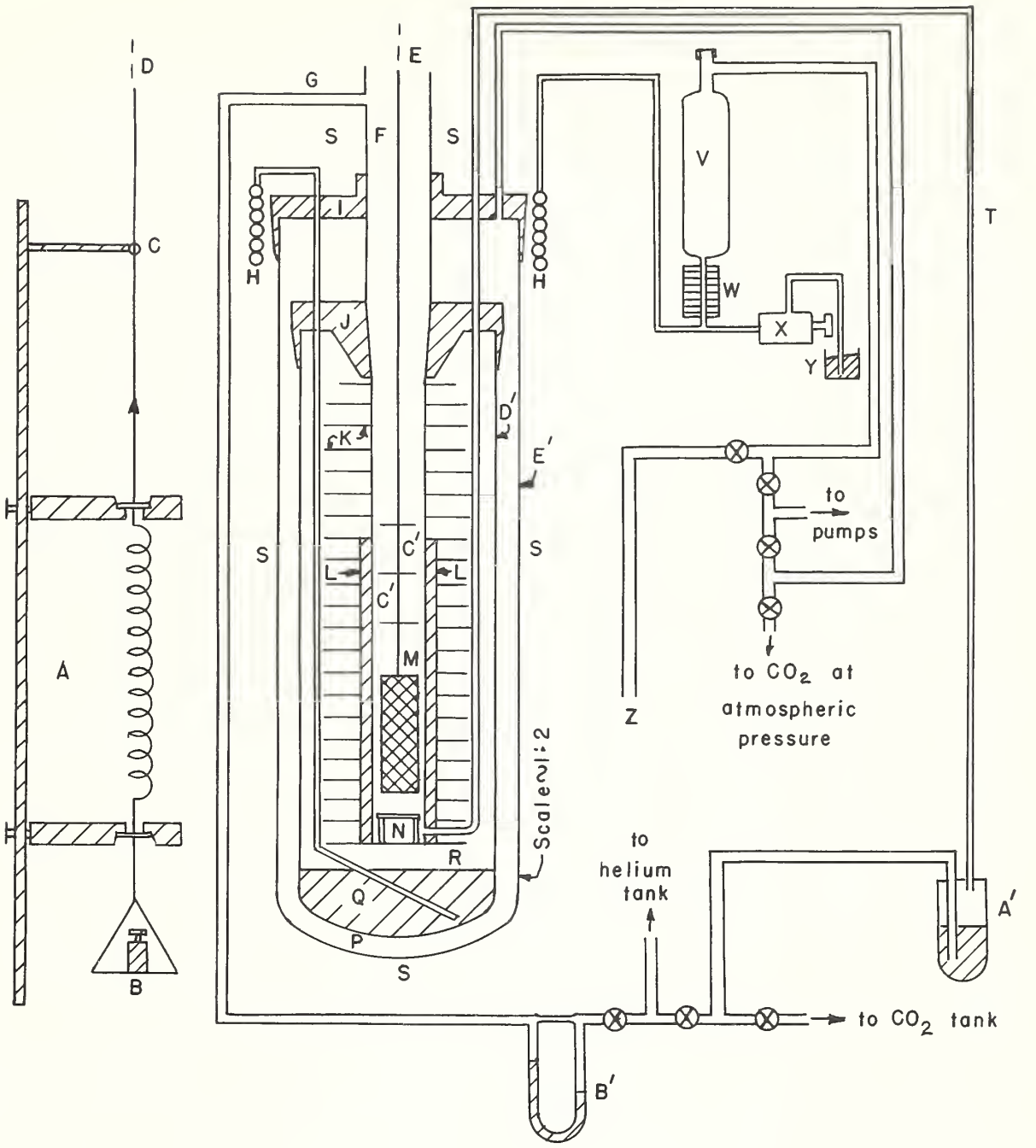

Figure 1 -- Ice Calorimeter,
Connecting Accessories, and
Braking Mechanism

A, braking mechanism; B, weight for calibrating spring; C, eye for damping oscillations; D, E, sample suspension wire and attached wire; F, calorimeter well; G, helium inlet to furnace; H, mercury tempering coil; I, J, metal covers; K, calorimeter fins; L, copper shell; M, sample container; N, safety stop; P, jacket space; Q, mercury; R, air-free water; S. location of surrounding ice bath; T, gas inlet to calorimeter; U, tube for evacuating jacket space; V, mercury reservoir; W, glass capillary, scale; X, "mercury" valve; Y, beaker of mercury; X, opening for varying pressure on mercury meniscus; A', gas bubbler; B', flowmeter; C', platinum shields; D', E', glass envelopes

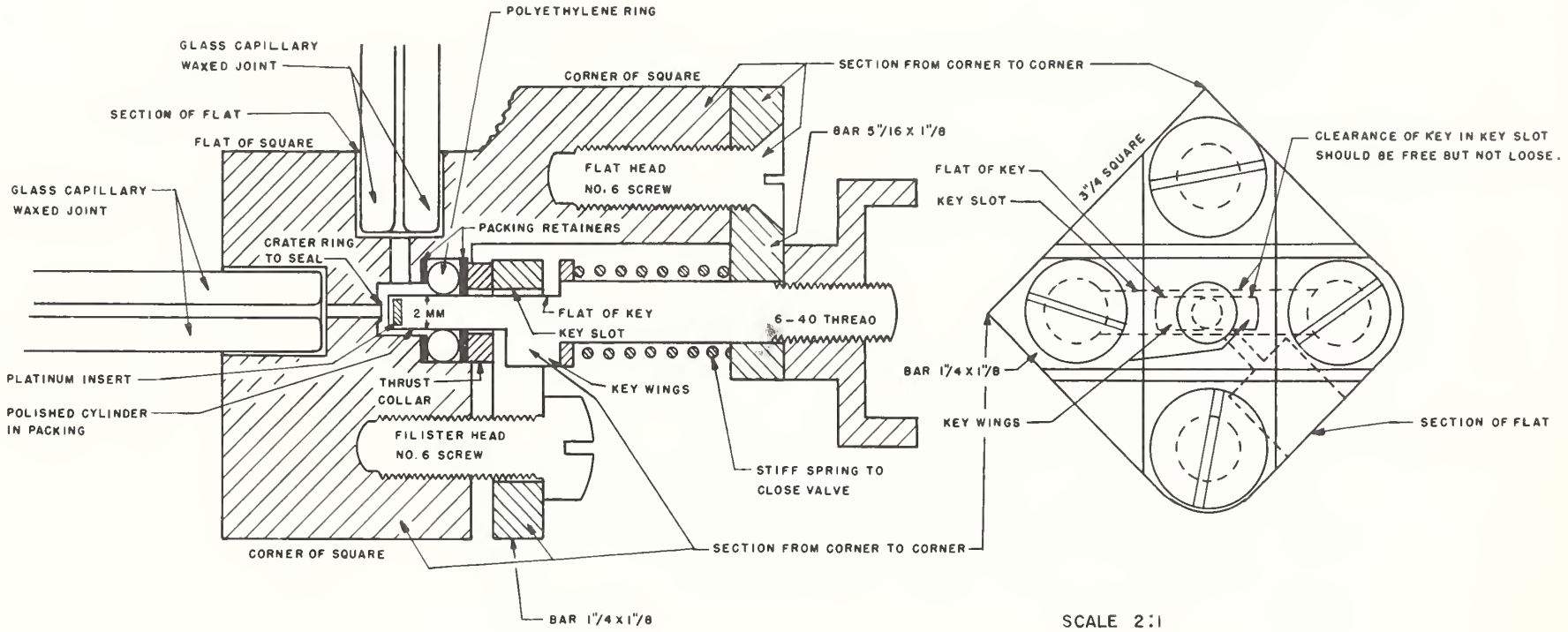

Figure 2 -- "Mercury" Valve of Ice Calorimeter

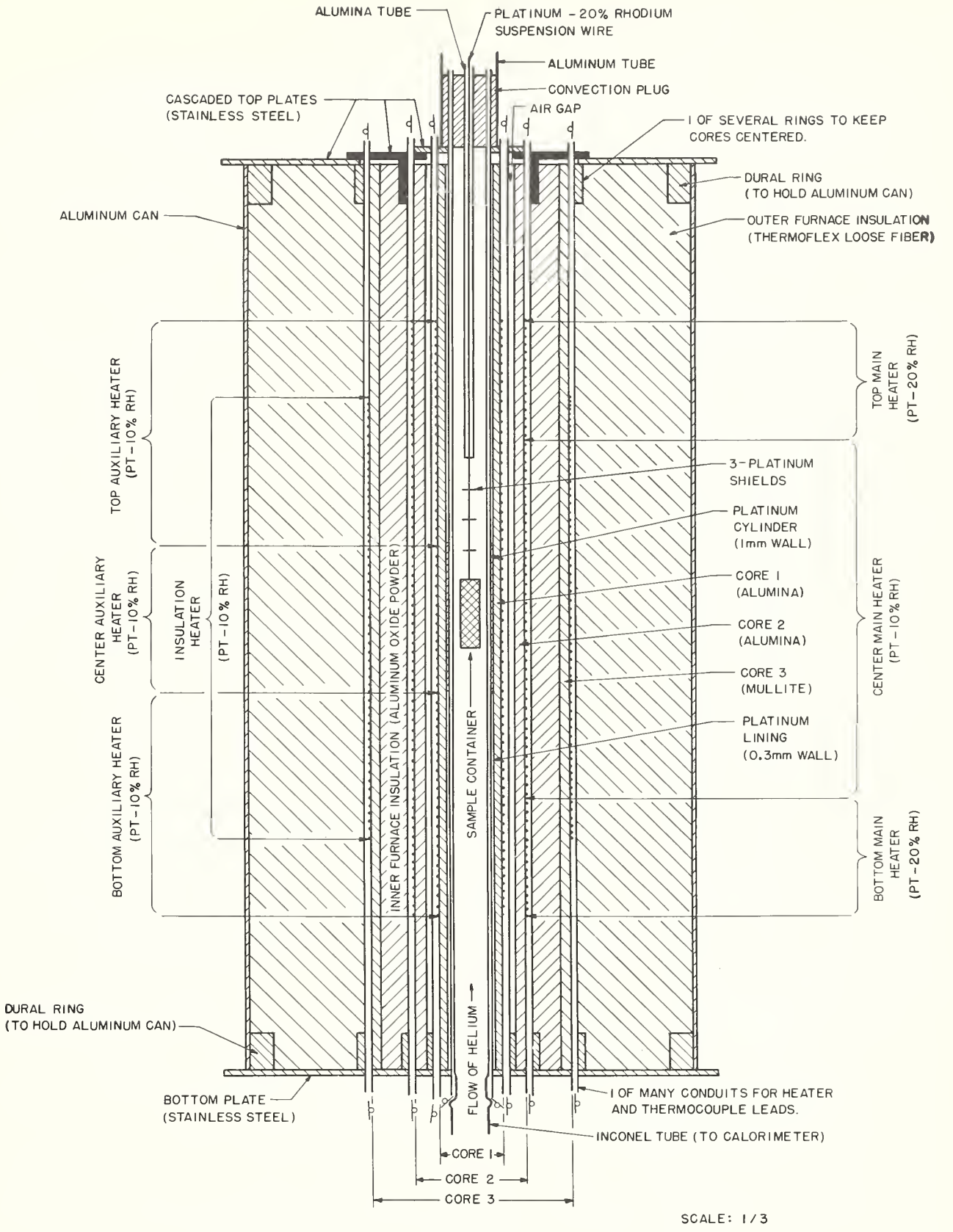

Figure 3 -- Furnace

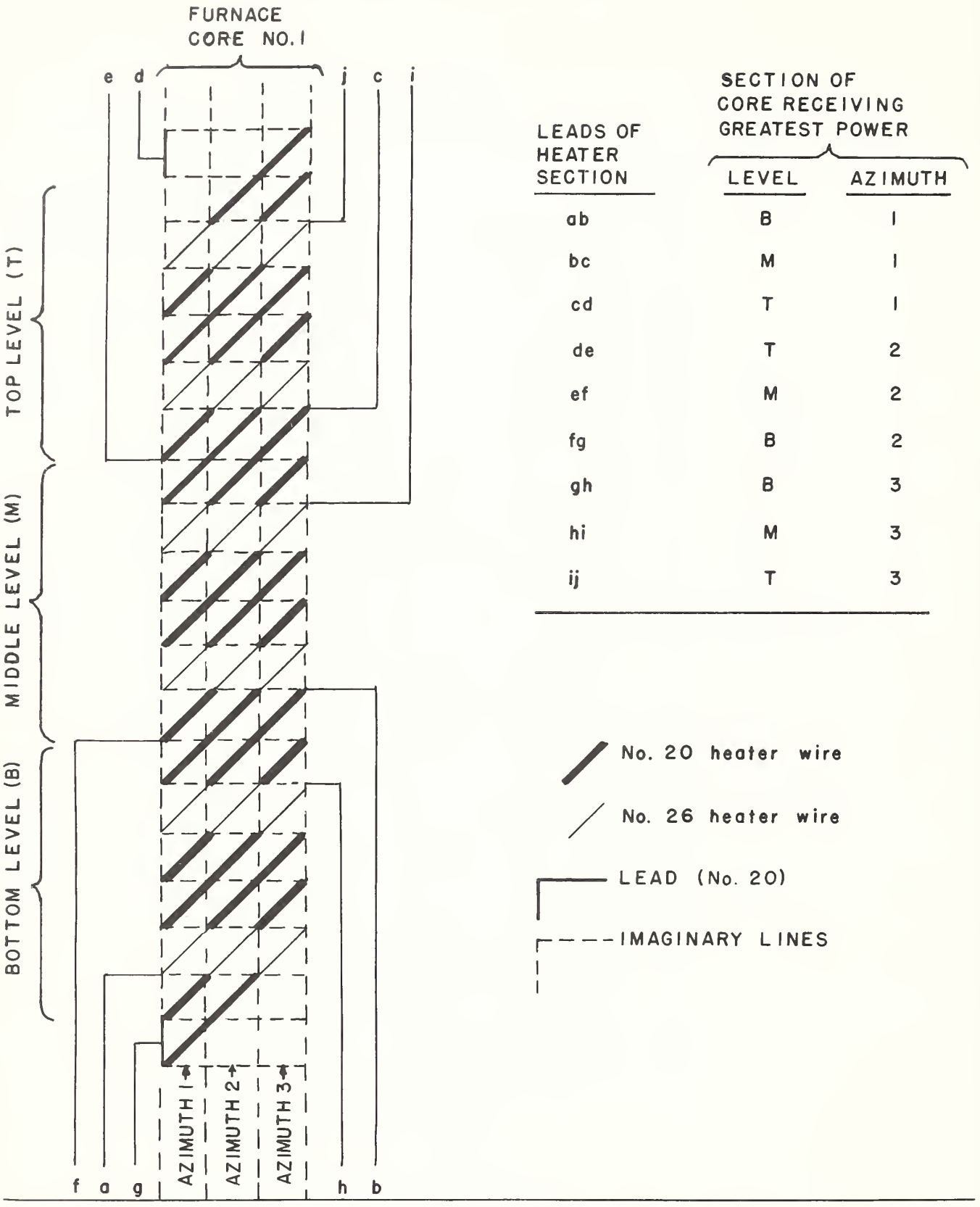

LEADS OF HEATER SECTION	SECTION OF CORE RECEIVING GREATEST POWER	
	LEVEL	AZIMUTH
ab	B	1
bc	M	1
cd	T	1
de	T	2
ef	M	2
fg	B	2
gh	B	3
hi	M	3
ij	T	3

No. 20 heater wire

No. 26 heater wire

LEAD (No. 20)

IMAGINARY LINES

Figure 4 -- Center Auxiliary Heater (schematic)

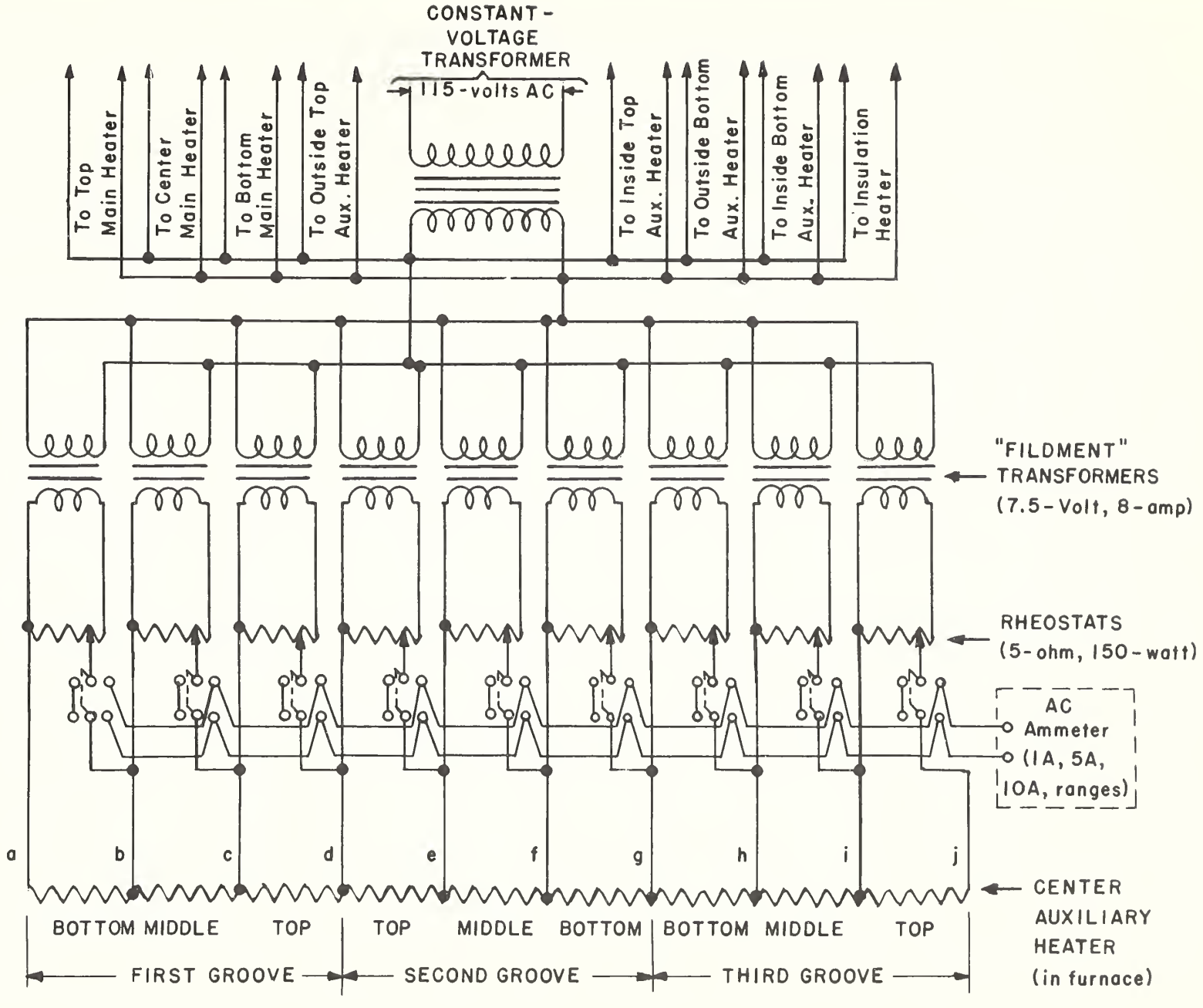

Figure 5 -- Center Auxiliary Heater (wiring diagram)

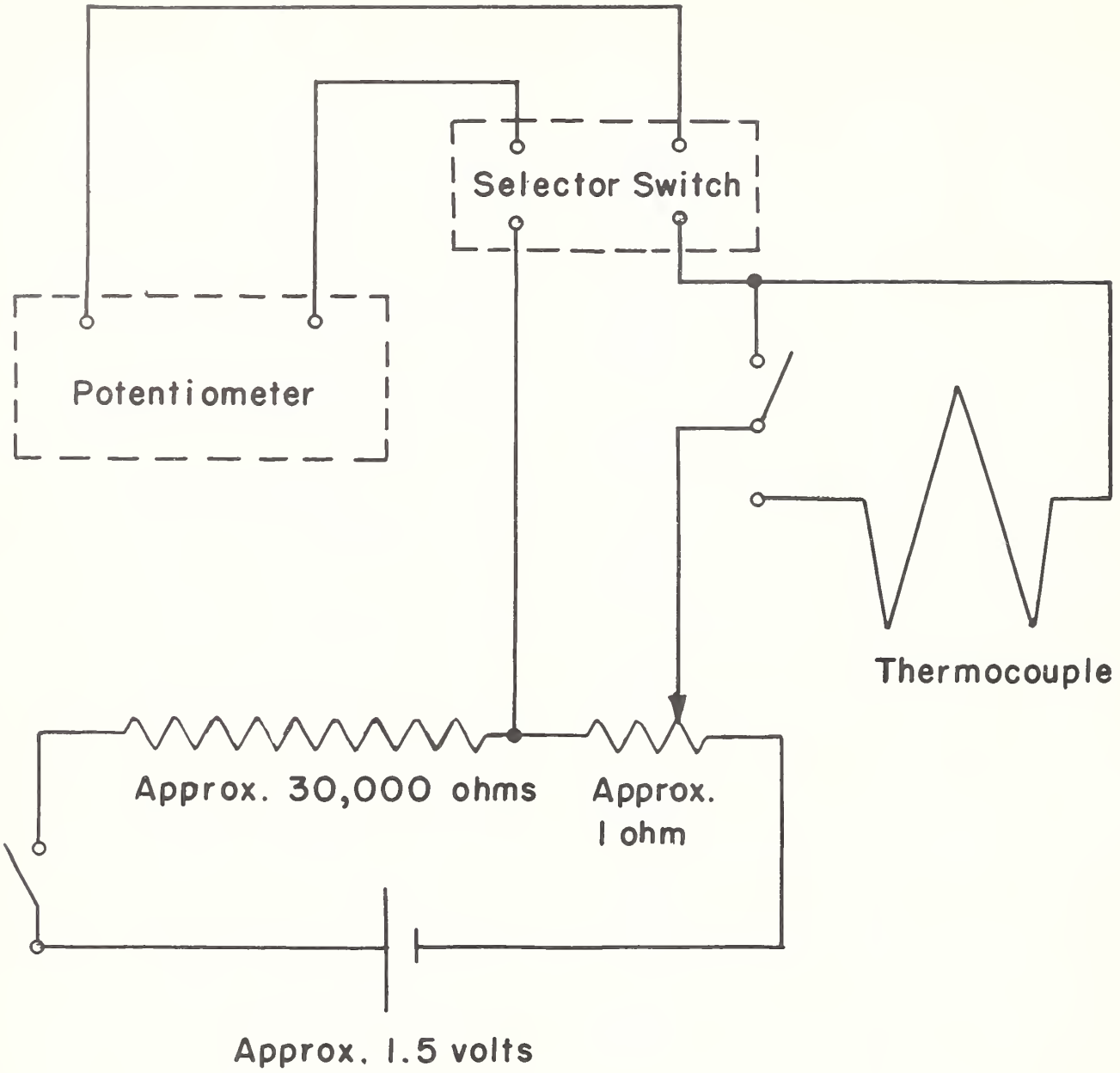

Figure 6 -- A thermocouple and Its Bias (wiring diagram)

U. S. Department of Commerce National Bureau of Standards

RESEARCH PAPER RP1228

Part of Journal of Research of the National Bureau of Standards, Volume 23, August 1939

MEASUREMENTS OF HEAT CAPACITY AND HEAT OF VAPORIZATION OF WATER IN THE RANGE 0° TO 100° C

By Nathan S. Osborne, Harold F. Stimson, and Defoe C. Ginnings

ABSTRACT

The present series of measurements of heat capacity and heat of vaporization of water in the range 0° to 100° C have been made to provide greater certainty in the values of the specific heat of water for calorimetric purposes and also to provide greater reliability in the values of enthalpy and the other derived properties for use in steam tables.

To insure the desired accuracy in the specific-heat determinations, complete new calorimetric equipment was designed and built. The same fundamental principles of fluid calorimetry by the electric-heating method were used as in previous measurements extending from 0° to 374° C. In the present case, the limited range of temperature and pressure allowed greater freedom of design to provide for higher accuracy in measurements. Heat leak was accounted for by observation, although it was kept practically nil by insulation and by thermal control of the envelope.

Temperature uniformity in the calorimeter was secured by an efficient circulation pump. Temperature uniformity in the envelope was secured by a controllable saturated-steam bath. Temperatures were measured by platinum resistance thermometers supplemented with numerous thermoelements. Heat added was measured electrically. The process of evaporation was closely controlled by manipulation of a sensitive throttle valve.

From 256 heat-capacity experiments and 152 vaporization experiments, as finally reduced and formulated, there was obtained a group of properties of water comprising specific heat, enthalpy of both liquid and vapor, heat of vaporization, and specific volume of saturated vapor in the range 0° to 100° C.

The values of specific heat have been compared with values from several important researches by both the mechanical and the electrical method. This comparison shows a more satisfactory accord of the present results with the results of Rowland, of Laby and Hercus, and of Jaeger and von Steinwehr, than with those of Callendar and Barnes.

CONTENTS

PART 1. A CALORIMETER FOR MEASURING THE HEAT CAPACITY AND HEAT OF VAPORIZATION OF WATER IN THE RANGE 0° TO 100° C

PART 2. HEAT CAPACITY OF WATER IN THE RANGE 0° TO 100° C

PART 3. HEAT OF VAPORIZATION OF WATER IN THE RANGE 0° TO 100° C

Part 1. A Calorimeter for Measuring the Heat Capacity and Heat of Vaporization of Water in the Range 0° to 100° C

I. INTRODUCTION

The principal purpose of the calorimeter described here was to provide for a systematic determination of the heat capacity of water from 0° to 100° C. A secondary purpose was to provide for a determination of the heat of vaporization over the same range. It was desired to obtain new experimental data on these properties to remove, if possible, some of the existing uncertainty. Of the earlier determinations of the specific heat of water, some are limited in range and the degree of accord is unsatisfactory. The measurements which have been completed, and which are described in part 2 of this report, were in part repetitions of previous measurements made in this laboratory. These previous determinations of the heat capacity of water were made for the purpose of obtaining data on the properties of saturated steam, using a calorimeter designed to operate at pressures up to 1,200 lb/in^2. While the values obtained for enthalpy of liquid water were of adequate precision for use in compiling steam tables for engineering purposes, the derived values of specific heat in the range below 100° C were not sufficiently accurate for use as calorimetric standards.

In providing apparatus for a resurvey of the heat capacity, the moderate range of pressure between 0° and 100° C allowed more freedom of design to avoid sources of experimental error. The design also provided for the determination of the heat of vaporization from 0° to 100° C. The results of these measurements are given in part 3.

II. GENERAL DESCRIPTION OF METHOD AND APPARATUS

The principles of the method used in the measurements have been described in previous publications [1],[1] and therefore are not repeated in detail in this report. This method was applied previously [2, 3] to measurements on saturated water and saturated steam from 0° to 374° C. The description given here includes mention of both the heat-capacity and the vaporization measurements.

The apparatus consists essentially of a calorimeter in which a sample of water may be so isolated from other bodies as to enable its amount, state, and energy to be accounted for. The sample may be made to pass through a chosen definite change in state while the accompanying gain or loss of energy is being determined.

A quantity of water, part liquid and part vapor, is enclosed in a metal calorimeter shell. An electric heater immersed in the water provides a means of adding measured energy to the calorimeter and its contents. Outlets with valves provide for filling and emptying the calorimeter and for withdrawing vapor. Detachable receivers suitable for weighing are connected to the outlets to hold the samples of water transferred.

For confining the energy, the calorimeter is well insulated from the influence of external sources of heat. In operation, the temperature of an enveloping shell is kept very close to that of the calorimeter shell. The small amount of heat which passes by leakage to or from the calorimeter is taken into account.

Two general types of experiments were made with this calorimetric apparatus. In the first type (heat-capacity measurements) the calorimeter with a sample of water was heated over a measured temperature range. By making some experiments with the calorimeter nearly full of liquid water and others with it nearly empty of liquid, it is possible to account for the tare heat capacity of the calorimeter, and to obtain the change of a quantity called alpha, α, which is a property of the water alone. It previously has been shown in the theory [1] that this quantity, α, differs from the enthalpy, or heat content, H, of saturated liquid water by another quantity beta, β. In other words,

$$\alpha = H - \beta.$$

The quantity β has been shown to be

$$\beta = L\frac{u}{u'-u} = Tu\frac{dP}{dT},$$

where L is the heat of vaporization, u is the specific volume of saturated liquid, u' is the specific volume of saturated vapor, T the absolute temperature, and dP/dT is the vapor-pressure derivative. In the previous experiments the quantity β was measured calorimetrically at higher temperatures, but between 0° and 100° C it is so small that its value can be calculated from liquid-volume and vapor-pressure data with greater accuracy than can be obtained by calorimetric measurements.

[1] Figures in brackets indicate the literature references at the end of this paper.

The second type of experiment (vaporization) made with this calorimeter is virtually an isothermal process. Heat is supplied to evaporate a sample of water which is withdrawn from the calorimeter at a controlled rate, collected, and weighed. From this experiment, there is obtained a value of a quantity gamma, γ, which differs from the latent heat of vaporization, L, by the same quantity, β, mentioned above. In other words,

$$\gamma = L + \beta.$$

III. APPARATUS

The essential features of this calorimeter may be explained by reference to a schematic diagram, figure 1, which shows the metal calorimeter shell, C, containing a water sample; an electric heater, H;

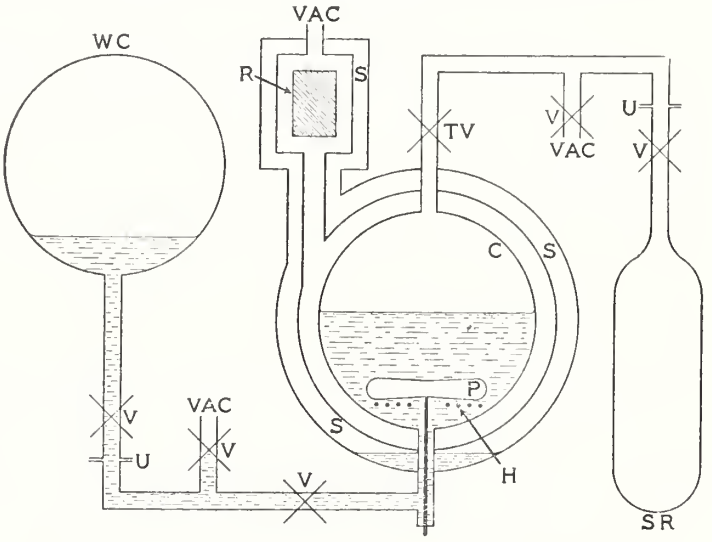

FIGURE 1.—*Schematic diagram of calorimetric apparatus.*

C, calorimeter shell; *H*, electric heater; *P*, water circulating pump; *R*, reference block; *S*, saturated steam bath; *SR*, steam receiver; *TV*, throttle valve; *U*, union; *V*, valve; *VAC*, vacuum line; *WC*, water container.

and a water-circulating pump, P. This shell is supported within an evacuated space which is surrounded by a controlled bath, S, of saturated water vapor, hereafter called the steam bath, which shields it against heat exchange with the surroundings. Provision is made for the introduction of a water sample from the water container, WC, into the calorimeter, or the withdrawal of saturated vapor through the throttle valve, TV, into the glass receiver, SR. The calorimeter and flow lines may be evacuated through lines VAC. The reference block, R, provides a temperature datum determined by a platinum resistance thermometer. Auxiliary thermoelements are used for measuring temperatures on the calorimeter shell and its surroundings, relative to this datum. The reference block is located in an inclosure surrounded by an extension of the steam bath. The calorimeter and the essential parts are shown in detail in the scale drawings, figures 2 and 3. Figure 2 shows more of the calorimeter detail, whereas figure 3 shows more of the accessory parts.

1. CALORIMETER SHELL AND INCLUDED PARTS

The purpose of the calorimeter shell shown at *C* is to hold the sample of water whose thermal properties are being determined. The shell was made nearly spherical in shape for compactness and calorimetric efficiency. It was spun from pure copper and has a thickness of about 0.55 mm. The two hemispherical ends were joined by solder,

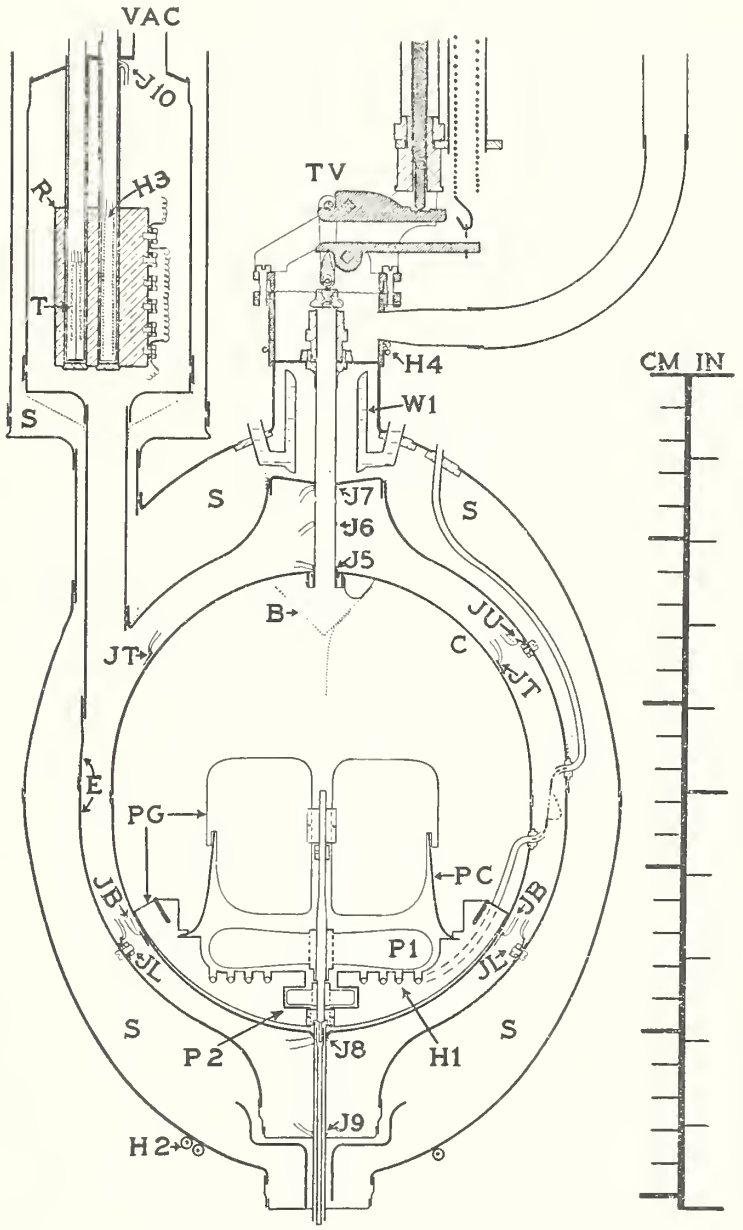

FIGURE 2.—*Scale drawing of calorimeter.*

B, gauze baffle; *C*, calorimeter shell; *E*, envelope shell; *H1*, calorimeter heater; *H2*, steam bath heater *H3*, reference block heater; *H4*, throttle valve heater; *JT*, *J5*, etc., thermoelement principal junctions; *P1*, *P2*, pump propellers; *PC*, pump casing; *PG*, pump guides; *R*, reference block; *S*, saturated steam bath; *T*, resistance thermometer; *TV*, throttle valve; *VAC*, vacuum line; *W1*, condenser.

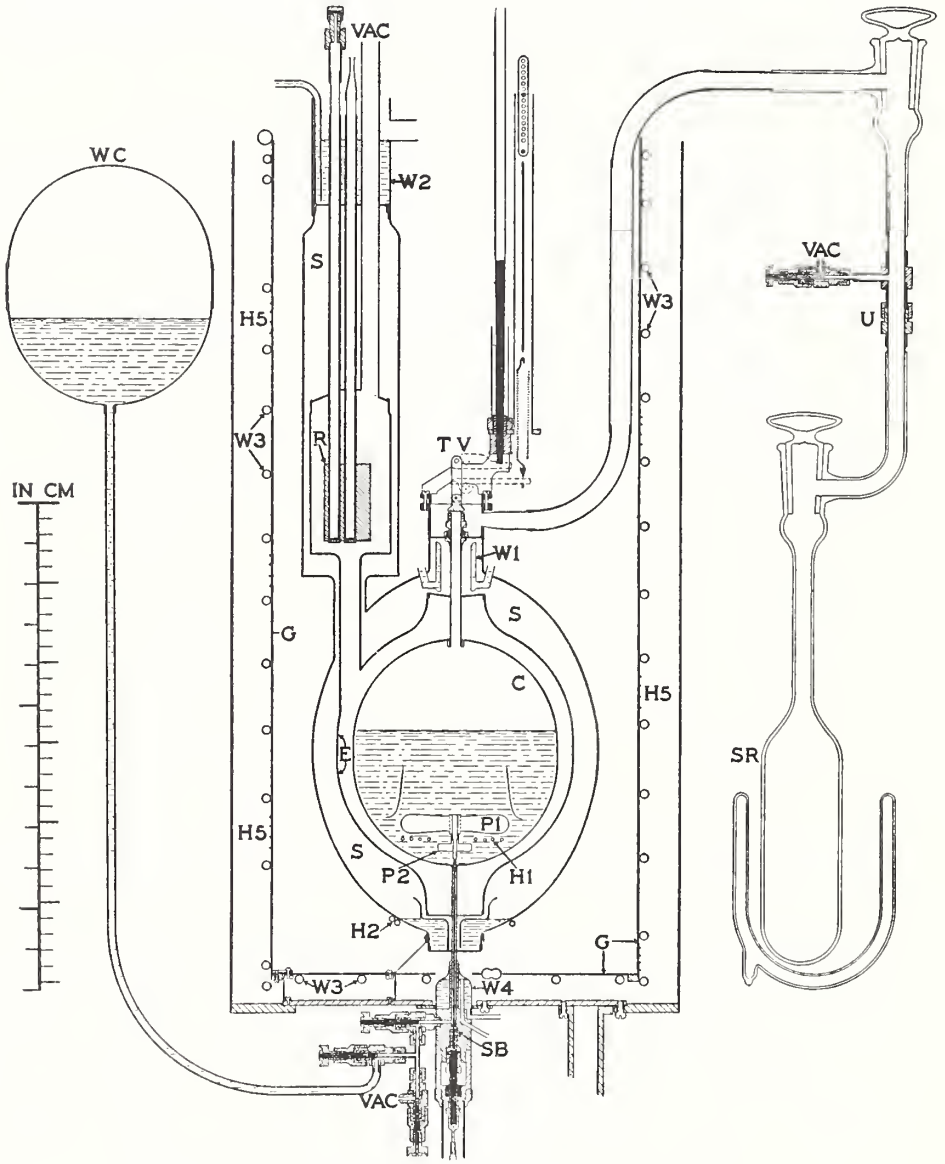

FIGURE 3.—*Scale drawing of calorimetric apparatus.*

C, calorimeter shell; *E*, envelope shell; *G*, guard; *H1*, calorimeter heater; *H2*, steam bath heater; *H5*, guard heater; *P1*, *P2*, pump propellers; *R*, reference block; *S*, saturated steam bath; *SB*, stuffing box; *SR*, steam receiver; *TV*, throttle valve; *U*, union; *VAC*, vacuum line; *W1*, condenser; *W2*, condenser; *W3*, cooling water tubes; *W4*, cooling water chamber; *WC*, water container.

with a narrow cylindrical copper band at the equatorial zone. As assembled with the various parts in place, the shell has a capacity of 1,190 cm^3.

Two tubes connected axially at the top and bottom of the calorimeter shell are designated as the "upper tube" and "lower tube", respectively. These tubes serve for the transfer of fluid to and from the calorimeter and to hold the calorimeter shell in place.

All surfaces of the calorimeter shell and the parts inside were gold-plated. The outer surface of the shell was polished to reduce heat transfer by radiation. Eight thermoelement junctions, *J*, distributed over the outer calorimeter surface were used in the evaluation of calorimeter temperature, as described later in the section "Thermometric installation."

The circulating pump consists of two screw propellers, shown at *P1* and *P2*, and a system of guides to direct flow. The larger propeller, *P1*, performed most of the work in circulating water, while the smaller propeller, *P2*, was used to avoid stagnation in the extreme bottom of the calorimeter. The specially designed blades of the larger propeller were formed from sheet copper and soldered to a hub of brass, all plated with gold and polished. The two propellers were fastened to a phosphor-bronze pump shaft, which was squared at its lower end so that it could be engaged from below by a shaft extension.

In addition to the propellers, there is a system of guides designed to direct flow and increase the pumping efficiency. The liquid water flows downward next to the inner surface of the calorimeter shell and is directed by radial guides at the bottom so that the water flows without swirl past the heater into the propellers. The water from the propeller is guided upward by a casing, *PC*, and by guide vanes *PG*, curved to remove the swirl imparted to the water by the propeller.

The pump guides form a rigid framework which supports the two pump bearings and the electric heater, *H1*. The downward thrust on the pump shaft is taken on a copper-nickel washer located just below the small propeller, *P2*. This whole pump framework is held down against the calorimeter shell by a threaded connection to a short piece of the lower outlet tube which extends into the calorimeter.

The electric heater shown at *H1* is an insulated resistor encased in a coiled metal tube sealed hermetically through the shell. It consists of about 107 ohms of a chromium-nickel-alloy wire, 0.2 mm in diameter with 0.4-mm copper leads. This resistor was wound in helical form, 0.6-mm outside diameter, and embedded in magnesia for insulation. The resistor with leads was sheathed in a copper tube drawn down tightly on the magnesia to an outside diameter of about 2 mm. This sheathed resistor was then bent to form a flat spiral of five turns, the largest being 6 cm in diameter. This coil was fastened in slots in the metal guides just below the large circulating pump propeller, *P1*. The resistor is so located as to concentrate the heating in the region just below the large propeller. The leads extending out from the envelope shell, both for current and potential connections, were made like the leads of the sheathed resistor.

For measuring the potential drop in the calorimeter heater, two potential leads were joined to the current leads where they cross the vacuum space between the calorimeter shell and the envelope. These junctions were located to include in the measured electric-energy input that part of the heat developed in the leads, which went to the calorim-

eter. Choice of suitable proportions of the leads in this boundary region of the calorimeter was a compromise between thermal conductance, electrical resistance, and convenient battery voltage. As made, the two current leads contributed but little to the total heat-leak transfer, and their combined electrical resistance was only 1/3000 of the calorimeter heater resistance of 107 ohms. Therefore, only 1/3000 of the energy input was developed in the current leads between the calorimeter and envelope shells, and so a small inequality in the eventual distribution of this extraneous heat was negligible.

To minimize the uncertainty of the accounting for the heat developed in this small resistance, the current leads, their insulation, and their sheaths were all made as much alike as possible on both sides of the vacuum space. The sheaths were soldered into the shells similarly, and the leads extended about 3 mm beyond their sheaths. In this way, the two electric connecting links had equal thermal connection with the calorimeter and the envelope shells. The current links were made of 0.3-mm gold wire about 4 cm long. One potential lead was connected to the calorimeter end of one link. The other potential lead was connected to the envelope end of the other link. In this way, the electric power developed in one link was apportioned to the calorimeter, and the power developed in the other link was apportioned to the envelope. Thus it was not necessary to connect potential leads within the vacuum space to the midpoints of the links, where the temperature of the wire rose above the calorimeter temperature during the heating period. These potential leads were made small and long to keep their thermal conductance negligible.

In order to prevent passage of liquid drops during the vapor withdrawal experiments, a baffle, *B*, shown in figure 2, made of conical-shaped wire gauze, was installed near the vapor outlet tube.

2. THERMAL-PROTECTING ENCLOSURE

In an ideal calorimeter no unmeasured heat would be gained or lost. This ideal may be approached by three means: First, the calorimeter may be thermally insulated from its surroundings. Second, the surroundings may be kept approximately at the temperature of the calorimeter. Third, the heat transferred may be accounted for by observation. In the present calorimeter, all three means were provided by use of a protecting enclosure for the calorimeter. This thermal-protecting enclosure will next be described.

The enclosure which surrounds the calorimeter is used to control heat leak to or from the calorimeter and to provide for determining the correction for the small unavoidable heat leak. The inner wall of the enclosure is a shell called the envelope, shown at *E*. It is a closed copper shell made in the same manner as the calorimeter shell, but larger. At the bottom of the envelope, the seal to the lower tube was made with a thin copper disk to accommodate differential expansion. The copper envelope shell is 0.55 mm thick, gold-plated and the inside surface polished to reduce heat transfer by radiation to the calorimeter. The space between the calorimeter shell and the envelope was evacuated for improving the insulation, leaving radiation between the polished gold surfaces as the chief path for heat leak. In the preliminary cooling of the calorimeter, this space was filled with helium to promote heat removal. Eight thermoelements on the inner surface of the envelope are used in the control and evaluation of

heat leak, as described later. To provide a space for the reference block, *R*, described later, an extension to the envelope is located as shown.

Control of the envelope temperature is an important factor in the operation of the calorimetric equipment. Upon this control depends not only the magnitude of the heat leak, but also its correct evaluation. In the calorimetric measurement, it is important that the envelope temperature be kept uniform and close to the average temperature of the calorimeter, not only when at the initial and final steady states, but also during the heating period. Another function of the envelope is the cooling of the calorimeter as a preliminary to a series of measurements. In consideration of the several functions of the envelope, a saturated-steam bath was chosen to control its temperature. An electric heater for vaporizing water and water-cooled condensers furnished the means for controlling the steam bath. The saturated steam furnished the medium for distribution of heat or refrigeration to the parts of the envelope, and thus automatically provided the desired uniformity of temperature distribution and the desired responsiveness in temperature regulation.

The saturated-steam bath, *S*, occupies the space between the envelope and a third shell of brass. This shell, or steam jacket, as it is called, is entirely closed except for small tubes for introducing or removing liquid water and vapor. A flexible copper disk was used to join the brass shell to the axial lower tube. The volume of this steam space between the steam jacket and the envelope was about 2,000 cm^3. The sheathed heater, *H2*, soldered to the outside of the steam jacket just below the level of the pool of water inside, furnished the controlled source of heat input. The vapor spaces were sufficiently open so that only negligible pressure differences could exist, even when there was flow of vapor to the remote parts.

The action of this vapor bath depends upon the latent heat of the water vapor and upon the principle that the temperature of a wet surface is determined by the vapor pressure. It therefore follows that the temperature of the entire envelope responds to any increase in saturation temperature of the vapor. In other words, the saturated steam acts as an automatic thermodynamic distributor of heat and equalizer of temperature for the space which it occupies. In heating, the saturation temperature of the vapor is raised above that of the metal, and condensation takes place, using up the latent heat of the vapor to add heat. The heat flows to the shells through whatever condensed liquid is on the metal. Gravity tends to make the condensed water run down to the pool at the bottom, where it receives heat and goes through the cycle again. Since the entire mass of fluid in this space is small and the metals of the envelope and jacket are thin, the temperature of the envelope is quickly responsive to changes in power imparted to the heater.

For the purpose of initial cooling preliminary to a day's experiments, or for a steady heat drain to be compensated by heat for regulation, two condensers are provided in the steam bath, as shown at *W1* and *W2*. Cooling was supplied to these condensers by water, regulated in flow and temperature. The water condensed within the steam bath was directed by wire-gauze leaders to parts which needed to be kept wet. The surplus returned by gravity to the pool at the bottom.

It is possible that the surfaces are not always completely wetted,

but even so, large temperature gradients could not be produced in the well-conducting envelope shell. The steam-bath enclosure was found to have a very small air leak, which made it necessary to purge it of air occasionally to secure the best operation. This was done by drawing off a small amount of steam from the region of the condenser, *W2*.

In order to protect the steam bath from the influence of the outside temperature, it was surrounded except at the top by a controlled metal casing called the "guard", shown at *G* in figure 3. This guard was a sheet-copper cylinder with a plane bottom. It could be cooled by means of a system of cooling-water tubes, *W3*, distributed over its surface. Heat could be supplied by an electric heater, *H5*, distributed over the surface. By thus controlling the temperature of the guard, the operation of the steam bath was improved.

Outside the guard there is another shell made of aluminum, for a cover. For the purpose of insulation, the blank spaces inside the cover and the guard were filled with insulating material consisting of wool and kapok.

3. CONNECTIONS TO THE CALORIMETER

The calorimeter shell is held in place by two tubes of copper-nickel alloy. In addition to furnishing a firm support for the shell without too great heat conduction, these tubes serve also for the transfer of fluid to or from the calorimeter. The "upper tube," which has an outside diameter of 6.35 mm and a wall thickness of 0.25 mm, connects to the vapor throttle valve, *TV*, which permits control of the rate of flow of outgoing steam in the evaporation type of experiments. The diameter of this upper tube was large enough to allow for adequate rates of withdrawal of steam at the lower temperatures. Near 0° C, where the specific volume of saturated steam is over 200,000 cm^3/g, it was possible to withdraw about 0.63 g/min.

During the heat-capacity experiments, which preceded the vaporization measurements, the upper tube was sealed at both the bottom and top by disks across the ends. This was to exclude water which might distill from end to end and thereby transfer unmeasured heat. These disks were removed prior to the vaporization experiments.

The "lower tube", which has an outside diameter of 3.0 mm and wall thickness of 0.35 mm, encloses the propeller drive shaft of the circulating pump. It also connects to the valve through which the calorimeter is filled or emptied.

The container, *WC*, for storing and transferring water samples was a copper shell similar to but slightly larger than the calorimeter shell, tinned on the inside to avoid contamination of the water sample, and with a tubular stem ending in a valve. It was connected to the calorimeter by a union. The long stem was to give head for running the water in or out when the vapor pressure was low.

4. STUFFING BOX AND PUMP DRIVE

The calorimeter circulating pump is driven from a 1/75-hp synchronous motor, using controlled-frequency alternating current to provide a constant speed. The drive is transmitted through a speed-reducing gear train to a vertical shaft running in a stuffing box below the calorimeter. From this shaft, a tubular extension with squared

ends transmits the rotation to the bottom of the calorimeter pump shaft.

The stuffing box, shown at *SB* in figure 3, was taken from an older calorimeter and has been more fully described in a previous publication [2]. The shaft through this stuffing box is of hardened tool steel 1 mm in diameter where it runs in the packing. A packing material of soft kid leather impregnated with a mixture of paraffin and vaseline was found to be satisfactory. This packing is kept compressed to the proper tightness around the shaft by a spring acting between the retaining ring and the threaded cap. Clearances were made small to avoid exuding the packing. The agreement of the amounts of water put in and taken out of the calorimeter was a check on the satisfactory tightness of the stuffing box.

The stuffing box was cooled with water circulating in a chamber, *W4*, around the shaft tube at the top of the stuffing box. In experiments at temperatures near 0° C, this cooling was found necessary to prevent transfer of unmeasured heat to the calorimeter by boiling in the lower tube, whereas in experiments at higher temperatures, it was necessary to keep the packing cool to prevent leaking.

5. VAPOR LINE AND THROTTLE VALVE

The vapor throttle valve used in the vaporization experiments is an extremely vital part. On it depends the precision with which the experimental process of evaporation can be controlled. The valve opening must necessarily be large enough to allow sufficient flow of vapor when the specific volume is large at temperatures near 0° C. It should also be capable of closing tightly in order to permit accurate accounting for mass and energy. It should also allow steady, continuous adjustment, so that the evaporation temperatures can be controlled by regulating the flow.

The vapor throttle valve is shown at *TV*. It is made as a cylindrical cell joined to the top of the steam jacket, capped by a flexible corrugated-copper diaphragm, clamped tightly to the upper rim of the cell. This diaphragm seals against the atmosphere and carries a short valve stem at the center. The stem projects above and below the diaphragm, to which it is sealed by hard solder. The flexibility of the diaphragm permits about 1-mm linear motion of the stem to open or close the flow aperture. The outflow tube ends in a brass plug, which forms the seat. The actual seat (6.1-mm diameter) is merely a 45° sloped ridge rising about 0.15 mm above the plane end of the brass plug. The part of the stem which bears on the seat has a flat face and is fastened to the diaphragm with a threaded stud. The stem face was covered with a thin film of soft rubber, applied by dipping in latex and vulcanizing. The performance of this soft-rubber coating exceeded all expectations. It enabled the valve to be closed tightly with no perceptible leak and permitted fine regulation of throttling. One application of rubber served for the entire series of evaporation experiments.

The valve stem is operated by two levers acting axially on the stem outside the diaphragm. One lever thrusts a strut against the stem to close the valve, and the other lifts it by a stirrup to open the valve. These levers act on knife-edges to avoid any irregularity in their motion. The closing lever is actuated by a spring which not only removes any backlash but keeps a steady moderate force against the

seat of the valve when closed. The opening lever with a mechanical reduction of motion of 4 to 1 is operated by a screw with a pitch of 32 threads per inch. The shaft of this screw extends up to a grooved pulley above the calorimeter and is driven by remote control with a wire belt from a small pulley over the observing bench. A shaft from this pulley extends down to a handwheel and lever easily accessible to the operator. Using an additional lever 20 cm long, which could be clamped to the handwheel, there was a total reduction of motion of over 30,000 to 1 from the end of this lever to the valve stem. In spite of this large reduction, there was no detectable backlash in the operation of the valve. The nicety of the mechanical operation of the throttle, and the consequent excellent control of evaporation conditions amply repaid for the effort expended on the refinement of this throttle valve.

A sheathed heater, shown at *H4* in figure 2, was soldered to the body of the throttle valve to maintain both the valve and the upper tube warmer than the calorimeter. This was to prevent water from condensing in the upper tube during the evaporation experiments.

The outlet tube from the throttle was made larger than the inlet to accommodate the larger specific volume of vapor after throttling. The vapor line from the throttle to the receiver is nowhere less than 1 cm in diameter. The vapor line extends up and out of the guard space, through copper and copper-nickel tubes to a glass stopcock. Beyond the stopcock, a union, *U*, provides for the attachment of either of two Pyrex-glass containers for collecting the samples of vapor by condensation in liquid air. A side tube with valve permits evacuation of the vapor line. The glass containers, of about 225-cm^3 capacity, are provided with unions and stopcocks so that they can be detached and weighed for determining the amounts of samples.

6. THERMOMETRIC INSTALLATION

Platinum resistance thermometers and thermoelements were used in the control and measurement of temperature in this apparatus. A resistance thermometer, *T*, placed in the copper reference block, *R*, determines a reference datum on the International Temperature Scale, from which small temperature differences to the calorimeter or other points are measured by means of thermoelements. Thermoelements were also used differentially for the survey of temperature distribution and for regulation of the calorimetric processes.

The reference block, *R*, is located in a space somewhat apart from the calorimeter to avoid direct interchange of heat but is connected to it through a tube for evacuation and for installing differential thermoelement wires. The surrounding steam jacket maintains the temperature of the enclosure approximately at the temperature of the calorimeter. The reference block was designed to give adequate thermal connection between the resistance thermometer and the reference junctions of the thermoelements. It is of copper in the form of a right hexagonal prism, 5 cm tall, with three broad vertical faces on which the reference junctions of the thermoelements and attachments for the leads are located. These attachments are for intercepting heat conducted along the leads and will be referred to as "thermal tie downs."

Four vertical round holes in the reference block are the sockets into which fit the several tubes containing resistance thermometers

and the tube containing an electric heater, *H3*. The heater socket is at the axis and the thermometer sockets are located symmetrically. Tubes of thermally resistant Cu–Ni alloy extend up from these four sockets successively through the envelope, the steam space, the outer wall of the steam jacket, and the water in the condenser, *W2* in figure 3, to the outside. A length of 4.5 cm was allowed in the vacuum space to give thermal separation from the envelope and a length of 12 cm in the steam space permitted a resistance thermometer coil to be placed there for automatic regulation of the steam-bath temperature.

The platinum resistance thermometer used as a working standard for the temperature measurement was of the four-lead potential-terminal type described by C. H. Meyers [4]. The windings were of pure platinum wound on a mica cross, and the initial strains were relieved by annealing the completed thermometer at 660° C. The thermometer was then sealed in an atmosphere of helium in a tubular sheath of copper-nickel, 6.3-mm in diameter and 46 cm long. The calibration was made according to the specifications for the International Temperature Scale [5], using the fixed points of ice, steam, and boiling sulphur as 0°, 100°, and 444.6° C, respectively. The thermometer fulfilled the requirements of the specifications for the International Temperature Scale and was recalibrated several times during the calorimetric experiments.

There are, in all, 22 thermoelements within the vacuum space, all having their reference junctions on the reference block. Some of the thermoelement principal measuring junctions are shown at points labeled *J* in figure 2. Eight of these thermoelements have their principal junctions uniformly spaced on the outer surface of the calorimeter so as to evaluate the average temperature. Four of these on the bottom hemisphere are connected in series and designated as *JB*. The other four on the top hemisphere, which have separate leads to allow for examining temperature uniformity in azimuth, are also connected in series and designated as *JT*. All eight in series may be used to refer the average temperature of the calorimeter to the reference block, i. e., to the standard thermometer. Similarly, eight principal junctions on the inside surface of the envelope evaluate its average surface temperature; four of these on the lower part are designated as *JL*, and four on the upper part as *JU*. All eight on the envelope may be opposed to the eight on the calorimeter for heat-leak control and measurement.

In addition to the 16 thermoelement junctions located on the surfaces of the calorimeter and envelope shells, there are five more located on the connecting tubes between the shells. These thermoelements are used in the control and measurement of heat leak by metallic conduction along the tubes. The three principal junctions on the "upper tube" are shown at *J5*, *J6*, and *J7*. Junction *J6*, located midway between *J5* and *J7*, was used for determining the temperature of the steam withdrawn in the evaporation experiments. The two junctions on the "lower tube" are shown at *J8* and *J9*.

One thermoelement, shown at *J10*, is placed near where the tubes from the reference block pass through its envelope. This thermoelement is useful as a detector or purge indicator, since it quickly shows local temperature differences when enough air eventually leaks into the steam jacket to interfere with the free transfer of heat by the steam. For the purpose of regulating the temperature of the guard

shell, one thermoelement was placed near the top of the guard. During the evaporation experiments, a thermoelement was used on the outside of the throttle valve for regulating the heat applied.

The thermoelements used in this apparatus were made of No. 32 (0.20-mm) Chromel *P* wire containing about 90 percent of Ni and 10 percent of Cr, and No. 34 (0.16-mm) constantan wire containing about 60 percent of Cu and 40 percent of Ni. These wires, which gave about 60 μv°C for single elements, were insulated with silk and covered with Glyptal lacquer. The junctions of these elements were made in three different ways, depending on the way the thermal contact had to be made to acquire the temperature of the surface where they were placed.

The usual type of junction was on a copper terminal made in the form of a narrow washer with a radial tag to which the wires were soldered with the least bit of solder. These terminals were clamped with a screw stud and nut between thin mica washers to the metal whose temperature they were to acquire. They were somewhat larger but made according to the same principles as those described in previous reports [2, 3]. These terminals were used on the reference block for the "reference junctions" and for the first "tie-downs," and for the eight principal junctions on the envelope shell.

A second type of junction, used on the outside of the calorimeter shell, was made by soldering the two wires to larger plates of copper. These plates were insulated with thin sheets of mica and lacquer and held down with two narrow thin bands of copper extending around the shell in great circles.

The third type of attachment was used on the tubes between the calorimeter and envelope shells. In this type, the two wires were soldered together end to end, reinsulated with silk, and bound and lacquered to the tube for several turns away from the junction to insure that the junction was at the temperature of the tube.

Each thermoelement had two reference junctions on the reference block, although in cases where the elements were connected in series, some of the reference junctions were common to several elements. Eighteen copper leads from reference junctions sufficed for all of the temperature exploration it was desired to make. Their leads were carried in coils from the reference junction terminals near the bottom of the reference block to "thermal tie-downs" with similar terminals near the top of the block. From these tie-down terminals, the wires led up through a flat copper-nickel sheath which extended through the steam jacket to above the liquid in the condenser. These silk-insulated wires were in a single layer and sealed into the flat copper-nickel sheath with Glyptal for electric insulation and thermal contact. The length in thermal contact with steam sufficed to bring the temperature of the wire at the envelope boundary very close to the steam temperature. The tie-downs on the upper part of the reference block still further eliminated any temperature gradients on the lead wires toward the reference junctions.

Various combinations of the thermoelements for the several functions mentioned above were provided for by connections to specially built all-copper distributing switches. By manipulation of these switches, the observer could quickly shift from one to another combination, with little more delay than for galvanometer response.

The electromotive forces of the thermoelements were measured on a Wolff potentiometer designed by F. Wenner. The potentiometer

measurements were referred to a standard cell, described in part 2 under "Accounting for energy." The electromotive forces measured were so small that the potentiometer calibration errors were negligible.

The eight thermoelements used to measure the temperature of the calorimeter and contents were calibrated in place against the resistance thermometer in the reference block. This calibration procedure was first to observe the resistance thermometer and thermoelements, when the reference-block temperature was very close to that of the calorimeter. The reference block was then heated for a few seconds, keeping the calorimeter temperature constant, and the thermometer and thermoelements observed again. The change in the electromotive force of the thermoelements was then given directly in terms of the change in temperature by the resistance thermometer. No evidence was found that the calibration of any of the other thermoelements differed at all from this one and furthermore, even moderate differences could have had no significant effect on the results.

The resistance of the thermometer was measured with a Mueller bridge [6] built by O. Wolff and calibrated several times during the experiments. The addition of a commutator with normal (N) and reverse (R) positions adapts the bridge for measuring the resistance between the branch points of a four-terminal resistance thermometer. A bridge current of 5 ma was used, half of which passed through the resistance thermometer. The bridge current could be quickly reversed by a double-pole tapping switch. This automatically compensates for a drifting bridge zero and doubles the bridge sensitivity. To further increase the sensitivity, a special galvanometer arrangement was used. A stationary mirror inside the galvanometer case was so placed that the beam of light from the movable galvanometer mirror was reflected back to the movable mirror before emerging to the scale. This arrangement doubles the deflection with less loss in light intensity than doubling the scale distance. With these arrangements, a sensitivity of 0.0001° C was attained.

For the purpose of automatic regulation of the envelope temperature, one resistance thermometer was inserted only to the region between the reference block envelope and condenser so that its temperature was quickly affected by the steam bath. This resistance thermometer was connected in a simple Wheatstone bridge and was used with a galvanometer, photelelectric cell, and amplifier to automatically maintain constant temperature of the steam bath.

7. AUXILIARY COOLING APPARATUS

Cold water was used for cooling the apparatus in the experiments below room temperature. About 30 liters of water circulating in a storage reservoir was cooled by an electric refrigerating unit and the temperature was controlled by a kerosene-filled thermostat. The cooled water from the reservoir was led by gravity through several different flow lines on the apparatus and emptied into a small centrifugal pump which returned it to the reservoir. The reservoir and flow lines were insulated with wool to avoid dew and excessive loss in refrigeration.

In all experiments starting near 0° C, the cooling water was maintained at a constant temperature by circulating over a layer of ice frozen to the refrigerator unit. In order to have the cooling water

temperature somewhat below 0° C to compensate for heating in the flow lines, enough ethyl alcohol was mixed with the water to lower the freezing point in the reservoir by the required amount. A special device was used for maintaining a covering of ice on the cooling unit. This device consisted of a straight tube with a small open end which rested against the unit. Thus tube was filled with water from the reservoir and the end sealed shut with ice as soon as ice began to form on the unit. Further freezing displaced the water in the tube and actuated the thermostat in the usual manner.

8. MEASURING INSTRUMENTS AND CALIBRATIONS

The water samples were weighed by the method of substitution, using a balance having a capacity of 2 kg. Below the balance pans there was a closed cabinet in which the water containers, tare containers, and counterpoises were suspended. The platinum-plated brass weights used were calibrated at this Bureau. Corrections were made for buoyancy of the air on the brass weights. Since the water sample is in a closed container, no correction for the air buoyancy on the sample is necessary. Correction for air buoyancy on the container was avoided by using counterpoises having approximately the same displacement as containers.

A Wolff-Diesselhorst potentiometer was used for measurements of current and potential drop in the calorimeter heater. A 0.1-ohm four-terminal resistor in series with the heater was used for the current determination and a 1,000 to 1 ratio volt box for the potential drop. Correction was made for the fraction of the main current shunted through the volt box, whose resistance was about 20,000 ohms. The potential drop in the calorimeter heater was measured by means of the two potential leads which join the current leads at points which had been chosen to account properly for the heat developed in the current leads between the calorimeter shell and envelope.

All electrical-measuring instruments were carefully calibrated several times during this series of experiments. The standard resistors and the volt boxes used were calibrated before, during, and after the series of measurements and showed no significant changes. The potentiometric measurements of power input were referred to a group of three cadmium standard cells. These cells were of the saturated type and were maintained at a constant temperature in a special temperature-controlled box described by Mueller and Stimson [7]. Frequent calibration of the standard cells proved their reliability to about a microvolt.

The Wolff-Diesselhorst potentiometer which was available for this work was not ideally adapted to these measurements. The calibration of the potentiometer showed a seasonal variation of nearly 1 part in 10,000 and a smaller daily variation. A scheme was devised using two permanent standard resistors to calibrate the potentiometer in place. By making this calibration two or three times a day, errors due to changes in the potentiometer were avoided.

The potentiometer was intended for use with standard cells having voltages between 1.01800 and 1.01930. The saturated standard cells at the temperature used in these experiments, however, gave about 1.01762 v. It was necessary, therefore, to set the potentiometer arbitrarily for some voltage in its range of adjustment and to correct for the true standard-cell voltage. In practice, the potentiometer

was set for a standard-cell electromotive force of 0.0005 v higher than that of the standard cells used, thereby giving a correction to each potentiometer reading of about 1 part in 2,036. This correction appears in the sample computation sheet as "correction for potentiometer ratio."

The description of the temperature-measuring instruments and their calibrations is given in the preceding section, "Thermometric installation."

Part 2. Heat Capacity of Water in the Range 0° to 100° C

I. INTRODUCTION

The heat capacity [2] of water has been the subject of various experimental determinations extending back to the time of Regnault. Some of them have been inspired by the usefulness of water as a calorimetric medium and definitive standard for determining heat capacities, while others have had for their objective the evaluation of the "mechanical equivalent of heat." The study of these past measurements for appraisal and correlation of results has been the subject of many reviews and reveals diligent effort to overcome inherent obstacles to accuracy in heat measurements by developing refinements of laboratory technique. During this development, the art of calorimetry has been far advanced by the evolution of standards and technique in electrical measurements of temperature and energy.

Notwithstanding all the advances in the laboratory arts, the appraisal of past experimental results has been unsatisfactory because so many uncertain factors have been involved regarding former units, standards, and calorimetric technique. Consequently, any interpretation of past results is subject to some arbitrary choice, and the various reviews have failed to bring the results into the accord to be expected from the accounts of the experimenters.

In 1921 the Cambridge, Mass. [8], conference on the properties of steam, as their first recommendation, made the proposal "the specific heat of water should be determined with the greatest possible accuracy up to the boiling point of water at atmospheric pressure for the more accurate determination of the mechanical equivalent of the mean heat unit."

Measurements made at the National Bureau of Standards and published in 1930 included data on the heat capacity of saturated water between 0° and 100° C., from which the specific heat at one atmosphere pressure could be derived. Since the experiments were not made especially for establishing accurate specific heats, the derived values were of only moderate precision. They have nevertheless been used in preference to earlier data as a basis for measurements of the enthalpy of superheated steam by several of the laboratories cooperating in the international steam research project. Recognizing that the accord of steam data was limited by the uncertainty in the values of the specific heat of water, the Third International Conference on Steam Tables [9], held in America in 1934, adopted a recommendation "that new measurements of the enthalpy or total heat of water between 0° and 100° C be undertaken by the National

[2] The expression "heat capacity" is used in this paper in the general sense of the energy required to produce a change of temperature, without necessarily restricting its application to unit mass, to unit temperature change, or to derivatives only.

Bureau of Standards to provide greater accuracy in these values for use in other calorimetric measurements." The present series of measurements was undertaken in response to this request and in extension of the program of steam research already completed.

In planning the work, it was the aim to provide for refinement of the technique of heat-balance accounting comparable with the accuracy of the temperature and power measurements, and if possible, to avoid an error of more than 1 part in 5,000 in the final results. To do this, it was necessary to design the new calorimetric equipment described in part 1 of this report.

II. METHOD AND APPARATUS

The method and apparatus have been described in detail in part 1 of this report, and therefore will be given only very brief mention here. The apparatus consisted essentially of a metal calorimeter shell containing a quantity of water, part liquid and part vapor. Immersed in the water are an electric heater and a circulating pump. Valves provide for filling and emptying the calorimeter. The calorimeter is well insulated from its surroundings, which are controlled to its temperature. Resistance thermometers and thermoelements are used in measuring temperatures.

In the measurement of heat capacity, the calorimeter with a sample of water was heated over a measured temperature range. By making some experiments with the calorimeter nearly full of liquid water, and others with it nearly empty, the tare heat capacity of the calorimeter was accounted for and there was obtained the change of a quantity called alpha, α, which is a property of the water alone. This quantity alpha differs from the enthalpy, or heat content, H, of saturated liquid water by another quantity beta, β. In other words,

$$\alpha = H - \beta$$

The quantity beta, β, had been measured calorimetrically in previous experiments at higher temperatures. However, between 0° and 100° C, it is so small that its value can be calculated from other data with greater accuracy than can be obtained by calorimetric measurements.

In addition to the enthalpy, H, of saturated liquid, values of specific heat, etc., may be derived.

III. EXPERIMENTAL PROCEDURE

In the heat-capacity measurements it was necessary to measure the amount of water subjected to the process, the amount of energy exchanged, and the change in state produced. It was the aim to account accurately for all three of these main factors. The following description of the experimental procedure indicates how these essential accountings were made.

1. ACCOUNTING FOR MASS OF WATER

The mass of water subjected to a change of state enters as a direct factor in the reduction of the data. The results, therefore, would be no more reliable than the determinations of the masses. Special care was therefore taken that the weighings were accurate and free from systematic errors. An account was kept of the amount in the calorim-

eter at any time and a check made by completely exhausting and weighing each charge before refilling with a new one.

The water used in these experiments was purified by preliminary distillation and then redistilled in a specially designed still under a pressure of about 0.1 atmosphere for the purpose of removing dissolved gases. These gases were removed by continuously withdrawing a part of the mixture of gas and water vapor from the condenser of the still. This kept the partial pressure of the gas at the condensing surface less than 0.001 atmosphere. The fraction of gas dissolving in the condensing water at this low pressure was too small to have any significant effect on any of the measurements.

The purified sample of water was then transferred from the still to an evacuated container, which was then weighed. When filling the calorimeter, this container was connected to the evacuated calorimeter, as shown in figure 3, and the connecting line evacuated. The water was transferred by gravity from the container to the calorimeter, leaving only a few grams in the container and line. The water in the line was collected and weighed by pumping through a detachable liquid-air trap in the vacuum line. The container with the water remaining in it was then reweighed. From the weights of the container before and after filling the calorimeter, and the weight of the water from the line, the amount of the water in the calorimeter was obtained by differences. When emptying the calorimeter, a similar procedure was followed, except that the water container was placed below the calorimeter, so that the water would flow from the calorimeter down to the container. The water remaining in the line and calorimeter was accounted for by condensing in liquid air and weighing as before.

The same charge of water was usually left in the calorimeter for several days' experiments. Comparison of the amount put in with the amount taken out was a check on the accuracy of accounting for the mass. Such a sum check was carefully kept in this work, and when the accounts did not agree, the results were discarded. Usually the check was to about 0.020 g, which amounts to about 1 part in 50,000 in a 1-kg water sample.

2. ACCOUNTING FOR ENERGY

Measured energy was supplied electrically to the calorimeter and contents by means of the calorimeter heating coil installed within the calorimeter shell and immersed in the water sample. Power was supplied by a separate storage battery of large current capacity. Potentiometer readings of current and potential drop across the calorimeter heater were made periodically for obtaining the energy added electrically, as described later. Reduction of these readings took account of the timing of the readings and of the slight gradual change in power which sometimes occurred.

In order to avoid too rapid an initial change when the current was switched to the calorimeter heater at the start of an experiment, a substitute resistor was used to steady the battery output. Between heating periods, the battery current was adjusted to a selected value to make the final temperature of the calorimeter come close to the desired even temperature after the power had been on an integral number of minutes. It was usually possible to adjust the current,

so that the final temperature would be within 0.01° C of the desired temperature.

The resistance of the calorimeter heater increased, during the first few seconds after the power was switched on, until the resistor temperature had reached a steady value. Since this change was practically completed before the first current reading was made (½ min after the start), the correction for it was determined by separate experiments. The correction for the current change was found by leaving the galvanometer connected when the current was shifted to the calorimeter and observing the deflections periodically for 15 sec. The integral of the galvanometer deflections over this time was used to compute the starting correction to the current. The starting correction for the potential drop, which is of the opposite sign, was obtained in a similar manner. These corrections were then combined to get the energy correction. This amounted to only 1 part in 10,000 of the whole energy input, even in the extreme case.

The shift in current from the substitute resistor to the calorimeter heater, was made automatically by means of double-pole double-throw switch, which was actuated by a tensed spring and released by the electric seconds-signals furnished by the standard clock. Since the heating periods were integral numbers of minutes, no significant errors have been attributed to the mechanism for transmitting the electric signals from the clock. Some experiments made to determine the time error due to the switch showed it to be 0.002 sec. or less and therefore insignificant.

The auxiliary electrical-measuring apparatus used in the measurement of the power and its calibration have been described in part 1, The routine of current and potential-drop observations for evaluating the power input are described later in the description of heat-capacity measurements.

The small amount of energy transmitted to the calorimeter by the pump and appearing as heat added was included in the accounting for total energy added in any experiment. The pump speed was kept constant at approximately 70 rpm, by a geared drive from a synchronous motor. Determinations of the pump power thus dissipated as heat were a part of the regular routine of the entire experimental program. These determinations were made calorimetrically by observing the rise in temperature produced in the calorimeter by running the pump alone with no electric-power input, keeping control and account of heat leak just as in a heat-capacity measurement. These pump-power experiments usually lasted for half an hour and the energy per minute was derived for each.

About 70 pump-power determination were made during the series of heat-capacity experiments. Pump-power determinations were made with both large and small masses of water in the calorimeter and, at one time or another, at most of the even temperatures where stops were made in the experiments. These determinations gave values of pump power about 0.2 to 0.3 j/min. After a study of the resulting values of pump power, simple formations were derived for use in calculating pump energies in the heat-capacity experiments.

The accidental variation of the observed pump power from the general mean was larger than could be accounted for by the uncertainty of the temperature measurement, but this was usually not more than would correspond to about 1 part in 20,000 in the value of alpha.

The characteristics of the pump, i. e., speed, power input, and corresponding heat-distributing effect, had been investigated by preliminary measurements before installing the pump in the calorimeter shell and served as a guide in choice of speed for the most advantageous operation in the final measurements.

The control and evaluation of heat leak is a vital part of any calorimetry when high precision is sought. The means provided for this purpose have been described in part 1. In operation, there were usually slight deviations from the ideal control which would nullify heat leak. The small corrections for this remaining heat leak were evaluated with the aid of the differential thermoelements, which indicated temperature differences between the calorimeter and its envelope by the number of microvolts. These differences were observed every minute and added algebraically to give sums in microvolt-minutes, called "heat-leak factors." These factors, when multiplied by "heat-leak coefficients," give the heat-leak corrections for the individual experiments. As previously stated in another way, the calorimeter was designed to make the coefficient small by construction and by evacuation of the insulating space, and means were provided to make the factor small by manipulation of the envelope temperature.

The total heat leak as determined experimentally consists of several parts, designated as "envelope," "upper-tube," and "lower-tube" heat leaks. The envelope heat leak is the chief part and results mainly from radiation between the surface of the calorimeter and of the envelope. The two tube heat leaks account for the heat transfer by metallic conduction along the tubes between the calorimeter and envelope. These tube heat leaks were nearly proportional to the envelope heat leak but not always exactly so for all experimental conditions, and therefore they were corrected for separately. Their coefficients were computed with sufficient accuracy from the knowledge of their dimensions and the thermal conductivity of their material.

The envelope heat-leak coefficient (in joules per microvolt-minute) was determined experimentally during the early part of the program and were checked occasionally later. This was done by exaggerating the temperature difference between the envelope and the calorimeter for a suitable time, observing this temperature difference and the two tube-temperature gradients every minute by means of the thermoelements, and summing these thermoelement indications (in microvolt-minutes) for the whole period to give the heat-leak factor. The total energy change in the calorimeter was computed from the measurements of the calorimeter temperature before and after this exaggerated heat leak. This energy, when corrected for the pump energy and the upper- and lower-tube heat leaks, was divided by the heat-leak factor, to give the envelope heat-leak coefficient, in joules per microvolt-minute, at the mean temperature of the experiment. This coefficient included, beside the radiation, any conduction (except by the two tubes) which was proportional to the temperature difference between the shells. This accounted for conduction through the heater and thermoelement wires. The gaseous conduction between these shells was probably negligible with the evacuation (less than 0.000,001-atmosphere pressure) maintained during all the experiments.

The factors of the three heat leaks were determined from observations made every minute during the experiments and were summed

algebraically for the whole periods. The experimental manipulation was usually such as to make the envelope heat-leak factor very small. During the heat-capacity experiments, the entire heat-leak correction would seldom affect the individual results by as much as 1 part in 50,000. It might be thought that corrections as small as these could have been disregarded, but had they not been regularly observed there would be no assurance that they were always insignificant.

The lower tube was always full of liquid, and precautions were taken to keep this tube always cool enough to prevent boiling, which might have caused transfer of heat to the calorimeter.

In addition to the various heat leaks mentioned, there is the possibility of a residual heat leak which could have been overlooked in the accounting for energy. This residual heat leak would be one which still occurred when everything else was eliminated and could be observed during periods when the pump was stopped and all other heat-leak factors kept as near zero as possible. A few such experiments were made but gave little more than a detectable coefficient. These experiments were discontinued, because whatever this residual heat leak was, it was included always in determinations of the pump power and therefore not neglected.

In the heat-capacity experiments, the usual procedure was to start observing the calorimeter temperature at 3 min after the end of the heating period. Investigation showed that thermal equilibrium was not complete in that time and that a small correction should be made if that temperature were used. This correction was found to be a function of the amount of water in the calorimeter and the temperature of the experiment. Although it was very small, it was applied to all heat-capacity experiments.

3. ACCOUNTING FOR CHANGE IN STATE

The temperature of the calorimeter and contents was measured by a platinum resistance thermometer used in conjunction with thermoelements, as previously described. The temperature change of the calorimeter and contained water sample was thus accurately observed in all experiments. All observed temperatures are expressed on the International Temperature Scale.

For determining either the initial or final temperature, each temperature reading consisted in simultaneous observations of resistance thermometer and thermoelements. The eight thermoelements on the calorimeter were connected in series to indicate the mean temperature of the calorimeter with respect to the reference block. Four successive temperature readings were made at half-minute intervals. This method of making several successive temperature readings is desirable for several reasons. The four-lead potential-terminal resistance thermometer requires at least two observations to eliminate the lead resistance from the measurement. Increasing the number of readings decreases the accidental error of observation. A regular schedule of readings takes account of slight drift in temperature.

A change in the proportion of liquid and vapor in the calorimeter occurs in the experiments. This change is analyzed in the theory of the method and is accounted for by use of the supplementary quantity, which is designated as β.

Special details of the experimental procedure that apply to the carrying out of the calorimetric measurements will next be described.

4. DESCRIPTION OF HEAT-CAPACITY MEASUREMENTS

It will be recalled that these experiments yield values of the change with temperature of the quantity α. Combined algebraically with corresponding changes of the quantity β, obtained from calculations, the data suffice to determine the change in enthalpy, H, of the saturated liquid.

The procedure in these heat-capacity experiments consisted essentially in heating a sample of water, part liquid and part vapor, over an accurately measured temperature range and in accounting for the energy added in the process. Two such heat-capacity determinations, a gross and a tare, are required for an evaluation of the change in α. These two determinations over the same temperature interval are made with different amounts of water, always maintaining the saturation condition. One determination, made with a large charge, yields a gross value of energy added. The other, made with a small charge, yields a tare value. The difference, or net value, of energy added, divided by the net mass, gives the value of the change in α for that temperature interval. This method of differences avoids the necessity of determining the heat capacity of the empty calorimeter.

In an experiment starting, for example at 0° C, the calorimeter is first cooled by the following procedure. The cold water from the cooling tank, where the temperature is a few tenths of a degree below 0° C, flows through the condenser (*W1* in fig. 3) located at the top of the main steam jacket, the condenser, *W2*, located at the top of the reference block steam jacket, the guard cooling coil, *W3*, and the stuffing-box cooling cell, *W4*. The space between the envelope and calorimeter is filled with helium to increase heat transfer between the two. Heat from the calorimeter and contents is transferred to the colder surroundings until the temperature of the calorimeter and contents is about 0° C. This process took many hours when the calorimeter contained a large charge and was usually done overnight. In a few of the experiments starting near zero the temperature of the calorimeter and contents was reduced to a few hundredths of a degree below zero. At no time was there any evidence of freezing in the calorimeter.

The envelope and the reference block are then brought to the temperature of the calorimeter. The helium is then pumped out of the envelope space to reduce heat transfer. The circulating pump is started at the desired speed, and the apparatus is ready for the beginning of an experiment.

The equilibrium temperature of the calorimeter and its contents is observed as described in section 3. The storage battery is connected to the calorimeter heater by the switch actuated by the time signals. At about the same time, the power is supplied to the envelope heater and reference-block heater. The currents in these heaters are adjusted so that the temperatures of the envelope and reference block stay very close to the temperature of the calorimeter. The differential thermoelement indications for determining the heat leak are observed almost continuously and recorded once each minute. One or more complete surveys with all thermoelement combinations are usually recorded in each individual experiment. The current and potential drop in the calorimeter heater are observed on alternate minutes starting with the first half-minute of the interval. The calorimeter heating

is continued for an integral number of minutes and stopped when the desired temperature interval has been completed.

The rate of heating was chosen as 0.5° C/min, and the calorimeter heater current was adjusted before the beginning of each experiment, so that after the integral number of minutes, the calorimeter temperature ended very close to the desired even temperature. The envelope and reference-block heater currents were adjustable to keep the temperatures of the envelope and reference block very near that of the calorimeter at all times. After several minutes, to allow the calorimeter and contents to come to temperature equlibrium, the final temperature was observed. This completed the heat-capacity experiment.

Two groups of such experiments were made, one with large charges of water in the calorimeter and the other with small charges. The experiments with small charges may be regarded as determinations of the tare-heat capacity of the calorimeter. Choice of the extent of the temperature intervals was governed by the rate of change of heat capacity with temperature. It was found that 10° intervals were suitable to determine the trend over most of the temperature range. Toward 0° C, where the change was increasingly rapid, the shorter intervals of 5°, 2.5°, and finally 1° C, gave more convincing evidence about this rate of change, even at the cost of some loss in the percentage of accuracy of the intervals.

During the heat-capacity experiments, the upper tube was closed at both its upper and lower ends by metal disks. In this way, possible error from condensation of water in the upper tube was avoided.

IV. RESULTS OF HEAT-CAPACITY EXPERIMENTS

The observations made during the experiments were recorded on separate laboratory-data sheets as soon as they were made. The computations from these sheets were often begun before all of the day's data sheets had been completed, and it was the rule to have preliminary results of the data for one day before the experiments of the next day were under way. This made it possible to arrange the day's observations with the full knowledge of what was most needed and what special precautions, if any, needed to be taken in observing. As more data were collected, it was possible to get and use more complete knowledge of contributory results, such as pump power, heat-leak coefficients, etc., that enter into the final reductions. Lastly, corrections were made for all known factors. The energies thus determined for the actual temperature intervals were then interpolated to even temperature intervals. These were reduced to determinations of the change of α over separate temperature intervals. These data were then formulated for use in the computation of tables and for computations involving the heat capacity of water.

In table 1, a typical data sheet is shown for a "large-mass" experiment made with 1,093.647 g of water in the calorimeter. The observations recorded under "Power" consist of the potentiometer readings of potential drop and current in the calorimeter heater after applying the decimal factors for standard resistor and volt box to reduce the readings to volts and amperes. Under "Thermometer" are given both "normal" (N) and "reverse" (R) bridge readings of the resistance of the thermometer in the reference block. The remaining observations are thermoelement readings, in microvolts. The column "Calorimeter minus reference block" shows the thermoelement readings of the eight

thermoelements ($JT+JB$) used in the measurement of the average temperature of the calorimeter. Under "Envelope minus calorimeter" are recorded the readings of the eight thermoelements on the envelope ($JU+JL$) opposed to the eight on the calorimeter ($JT+JB$). The column "Lower tube" shows the indications of the thermoelements ($J9-J8$), while the column "Upper tube" shows ($J7-J5$). In the last column, a survey of thermoelement indications is shown, starting just after the routine observations at 11:57. At least one such survey, taking less than a minute, was made in each experiment.

TABLE 1.—*Sample data sheet*

[Temperature interval 25° to 30° C ---------- October 27, 1937]

Time	Power		Thermometer, Bridge readings	Thermoelement readings				
	Potential drop	Current		Calorimeter minus reference block	Envelope minus calorimeter	Lower tube	Upper tube	Survey of other thermoelements
	v	*amp*	*Ohms*	*μv*	*μv*	*μv*	*μv*	*μv*
11:53			30.41524 N	−0.4	1	−1	0	
53.5			30.41517 R	−.5				
54			30.41516 R	−.5	2			
54.5			30.41524 N	−.6				
55	On				1	−1	0	
55.5		0.60268						
					2	−3	5	
56.5	65.965							
				0	0	−3	5	
57.5		.60269						JU 1
					0	−3	5	JL 1
58.5	65.965							JT 0
					−1			JB −1
59.5		.60274						J1 0
					−1	−4	5	J5 −12
12:00.5	65.964							J8 −2
					0			J10 −3
01.5		.60278						
					0	−3	5	
02.5	65.963							
					−1			
03.5		.60283						
					−1	−3	5	
04.5	65.963							
05	Off				−1			
06					−2			
07					0			
08			30.96171 N	−0.3	2			
08.5			30.96162 R	−.3				
09			30.96165 R	−.4	0	−1	0	
09.5			30.96171 N	−.5				

Table 2 shows a computation sheet, using the data given in table 1. The first step is the calculation of the temperature of the calorimeter. The average of the first four bridge readings is taken as the resistance of the thermometer at the mean time. Using the thermometer and bridge calibrations, the temperature of the reference block corresponding to this resistance value is obtained. Likewise, the average of the first four readings of the thermoelements ($JT+JB$) is found and from this and the calibrations, the difference in temperature called "temp. cal. minus temp. ref. block" is obtained at the same mean time. Combination of these temperature measurements gives the initial temperature of the calorimeter at that time, considered as the beginning of the experiment. The same method is used in the computation of the final temperature.

TABLE 2.—*Sample computation sheet, using data shown in table 1*

[Temperature interval 25° to 30° C ---------- October 27, 1937]

Steps in computations	Temperature	
	Initial	Final
Average of bridge readings (ohms)	30.41520	30.96167
Temperature of reference block (°C)	25.0034	30.0036
Average thermoelement reading (μv)	−0.50	−0.38
Temp. cal. minus temp. ref. block (°C)	− 0.0010	−0.0008
Temperature of calorimeter (°C)	25.0024	30.0028

	Energy	
	Potential drop	Current
	v	*amp*
Average of potentiometer readings	65.9640	0.602744
Correction for timing of readings	0.0001	.000009
Potentiometer calibration correction	.0090	.000090
Correction for potentiometer ratio	−.0324	−.000296
Volt-box current		−.003298
Correction for volt-box factor	.0011	
Correction for standard resistance factor		−.000086
	65.9418	0.599163
	int. j	
Electric energy for 600 sec	23,705.9	
Pump energy for 15 min	3.7	
Envelope heat leak (for −2 μv min)	0.0	
Lower tube heat leak (for −36 μv min)	−.1	
Upper tube heat leak (for 50 μv min)	0.3	
Starting correction	2.3	
Equilibrium correction	−0.2	
Energy added to calorimeter and contents	23,711.9	
Energy to correct initial temp. to 25° C	11.4	
Energy to correct final temp. to 30° C	−13.3	
Energy for even temp. interval, 25° to 30° C	23,710.0	

The next step is the computation of the electric-energy input to the calorimeter during the heating period, 11:55 to 12:05. The potential drop across the calorimeter heater is calculated from the average of the five potentiometer readings of potential drop. Since these potentiometer readings are not distributed symmetrically about the middle of the heating period, a small correction is made to account for the drift during the experiment. This is recorded as "correction for timing of readings." The "potentiometer calibration correction" is computed, taking into account the calibrations made during the day of the experiment. The "correction for potentiometer ratio" has been explained in part 1 of this report under "measuring instruments and calibrations." The correction for the volt-box calibration factor is also recorded. Applying all of these corrections to the average of the potentiometer readings, the average calorimeter potential drop, expressed in international volts, is computed.

Likewise, the average calorimeter heater current (international amperes) is computed. In this case, corrections must be made for the current through the volt box and for the standard 0.1-ohm calibration factor. By multiplying together the current, the potential drop, and the time of electric heating (600 sec), the total electric energy (international joules) is computed.

The next step is the computation of the total energy added to the calorimeter and contents during the experiment. This is obtained by adding to the total electric energy the following small energy corrections. The pump energy is calculated from the value of power formulated from pump-power experiments. This pump power was multiplied by the time of the experiment (15 min) to give the pump energy. The three heat leaks (envelope, upper tube, and lower tube) were computed by summing the thermoelement readings from table 1 to give heat-leak factors in microvolt-minutes. These factors were multiplied by their respective heat-leak coefficients to give the heat-leak corrections. The "starting correction" and "equilibrium correction," which have been described in the previous section, were calculated from the results of the special experiments. The sum of the electric energy and all the energy corrections gives the entire energy added to heat the calorimeter and its contents from the initial temperature, 25.0024° C, to the final temperature, 30.0028° C.

In the reduction of the results, it was convenient to use the even temperature interval 25° to 30° C. Therefore, corrections were made for the small deviations of the measured temperatures from the intended even temperatures. Only approximate values of the heat capacity of the calorimeter and contents were necessary to make these corrections. The resulting energy is recorded as "energy for even temperature interval," and will be referred to as ΔQ.

The sample computation just described is one of the 256 assembled in table 3. This table contains the substance of the principal data and preliminary reductions of the heat-capacity experiments made with a large mass of water in the calorimeter. Table 4 contains a similar assembly of the principal data of the 137 experiments made with a small mass of water. These two tables comprise an abstract of the record of all the experimental data which were accepted as trustworthy. Only those experiments in which the technique was faulty or the record incomplete were excluded. Further reductions of these data are included in these tables, as next described.

Each experiment for the temperature interval Δt gives a value of ΔQ which, according to the theory [1], should satisfy the equation

$$\frac{\Delta Q}{\Delta t}=\frac{\Delta Z}{\Delta t}+\frac{M\Delta\alpha}{\Delta t},$$

where M is the mass of water in the calorimeter, $\Delta Z/\Delta t$ is a property of the calorimeter independent of the amount of water in it, and $\Delta\alpha/\Delta t$ is a specific property of the water. By taking all the equations for one temperature interval for both the large- and small-mass experiments, it is possible to solve for the $\Delta\alpha/\Delta t$ and $\Delta Z/\Delta t$ for that interval by the method of least squares, as was done in previous publications. Actually, however, since approximate values of $\Delta\alpha/\Delta t$ were available from previous researches, it was found expedient to solve for preliminary values of $\Delta Z/\Delta t$ as the experimental work progressed, using these tentative values of $\Delta\alpha/\Delta t$ together with the data from experiments with small mass. These values of $\Delta Z/\Delta t$ were smoothed by formulating dZ/dt and were then used with the large-mass data to compute corresponding values of $\Delta\alpha/\Delta t$. Successive substitutions of these tentative values of $\Delta Z/\Delta t$ and $\Delta\alpha/\Delta t$ gave rapid approach to the limiting mean values, since the ratio of the large to the small masses was usually about 8.6. This method of reduction facilitated

the preliminary survey of results as the experimental data accumulated and served as a guide in the choice of temperature intervals best suited to determine the trend of the heat-capacity curve.

As finally reduced and recorded in table 4, the result of each experiment with small mass constitutes a separate determination of $\Delta Z/\Delta t$, and the entire series of these results is a calibration of the calorimeter. Similarly, the result of each experiment with large mass, as reduced by use of the calibration results and recorded in table 3, constitutes a separate determination of $\Delta\alpha/\Delta t$, and the entire series is a determination of the heat capacity of water in the range 0° to 100° C.

A comparison of the individual results with the average values indicates the degree of consistency of the measurements, and comparison of the averages with the formulated values indicates the degree of consistency of the trend with temperature. The manner of formulation of these results will next be described.

Since all experiments are necessarily made over finite temperature intervals, the results, in terms of increments $\Delta\alpha/\Delta t$ and $\Delta Z/\Delta t$, differ slightly from the corresponding derivatives, $d\alpha/dt$ and dZ/dt. These differences were computed by use of preliminary approximate equations and were used to get the corresponding values of $d\alpha/dt$ and dZ/dt[6] at the mid temperatures to be fitted by formulas.

The empirical formula chosen for dZ/dt has the following form:

$$dZ/dt=A+Bt+C(t+60)^{5.14}.$$

The final coefficients determined from the average values of $\Delta Z/\Delta t$ listed in table 4 are $A=168.69$, $B=0.089$, and $C=68.85214\times10^{-10}$, where t is in degrees centigrade and dZ/dt is in international joules per degree centigrade. Values of $\Delta Z/\Delta t$ calculated from this formula are given in table 4 as formulated values of $\Delta Z/\Delta t$. It appears that a further adjustment of the dZ/dt formulation by another approximation would have changed the final value of $d\alpha/dt$ by about 1 part in 80,000 at 0° C and by successively smaller amounts up to 100° C. This change was considered as sufficiently insignificant to be neglected.

The formulation for $d\alpha/dt$ was based on the values of $\Delta\alpha/\Delta t$ given in table 3. The average values of $\Delta\alpha/\Delta t$ were computed for each of the 20 temperature intervals and then corrected for deviations from the derivatives to get corresponding mean values of $d\alpha/dt$. It is obvious that some of these experimental means should have more weight than others. For example, the 19 experiments over the 10° interval from 40° to 50° C should have more weight than the 4 experiments over the 1° interval from 0° to 1° C. The means were therefore weighted approximately proportionally to the number of experiments times the number of degrees in the interval. A least-squares solution was then made for the constants in the following empirical equation:

$$d\alpha/dt=A+Bt+C(10)^{-0.036t}.$$

The constants were found to be $A=4.1699$, $B=0.000\,015\,27$, and $C=0.0467$, where t is in degrees centigrade, and $d\alpha/dt$ is in international joules per gram-degree centigrade. Using this equation, the values of $\Delta\alpha/\Delta t$ for each of the intervals have been computed and are recorded in table 3 for each interval. The deviations from these formulated values are tabulated in the last column of table 3.

It may be seen from table 3 that in the later experiments there is a trend to lower values of $\Delta\alpha/\Delta t$. The experiments above 5° C made after October 28, 1937, show values of $\Delta\alpha/\Delta t$ which average about 1 part in 10,000 less than those before that date. No explanation is offered for this change, and the fact is taken merely as evidence of the limitation of accuracy due to unknown systematic causes.

Since the specific heat at ordinary atmospheric pressure is the property of water most commonly utilized for calorimetric purposes, this property was determined by further reduction of the experimental average values of $\Delta\alpha/\Delta t$ given in table 3. This computation will next be described.

The reduction may be considered in three steps, which are indicated in table 5, starting with the average of the measured values of $\Delta\alpha/\Delta t$. At saturation pressure, the mean enthalpy change, $\Delta H/\Delta t$, exceeds $\Delta\alpha/\Delta t$ by the quantity $\Delta\beta/\Delta t$, as shown in the theory. The values of this reduction term, as given in column 3, were calculated by the relation $\beta=TudP/dT$, as explained in part 1 of this report. Values of the specific volume, u, were obtained from the density data of Chappuis [10] up to 50° C and of Thiesen [11] up to 100° C, and the compressibility data of Smith and Keyes [12]. Values of dP/dT were obtained from an unpublished formulation of the vapor-pressure data of the Reichsanstalt as reformulated by Harold T. Gerry and used for the saturation pressure table by the International Steam Conference of 1934 [9, 36].

Next, values of the term for reduction to mean enthalpy change at 1-atmosphere pressure, $(\Delta H/\Delta t)_{p=1}-(\Delta H/\Delta t)_{sat.}$, as given in column 4, were calculated by the relation

$$\left(\frac{dH}{dP}\right)_T = V - T\left(\frac{dV}{dT}\right)_p,$$

using the same data as above. There is still the difference between the mean value of the change of enthalpy per degree at 1 atmosphere and the derivative, $C_{p=1}$, the desired specific-heat value at the mid-temperature of the interval. This reduction term, $C_{p=1}-(\Delta H/\Delta t)_{p=1}$, given in column 5, was computed by using a preliminary approximate equation for C_p.

The 20 experimental values of C_p in column 6, which were obtained by applying the three reduction terms just described, were then formulated, using the same weighting factors previously used in the formulation of $d\alpha/dt$. After tests of types of functions to represent the experimental data, the empirical equation finally chosen was

$$C_p = A + B(t+100)^{5.26} + C(10)^{-0.036t}.$$

The coefficients were determined by least squares to be $A=4.169\,036$, $B=0.000\,3639(10)^{-10}$, and $C=0.0467$, when t is expressed in degrees centigrade, and C_p in international joules per gram-degree centigrade at 1-atmosphere pressure. Both the formulated and the experimental values of C_p are given in table 5, together with the deviations. The midtemperatures of the temperature intervals are given also.

Figure 4 shows graphically the comparison of the experimental values with the formulated values of C_p. In this figure the areas of the circles representing the observed means are made proportional to the weights assigned in the formulation. In other words, the larger

circles indicate that more experiments or larger temperature intervals are represented. The degree of accord of the formulation with the experimental results shows that this fairly simple empirical equation is adequate to represent the results over the entire 100° C range. However, this agreement must not be taken as an estimate of the accuracy of the results, since it takes no account of unknown systematic errors, which may well be larger than the accidental errors.

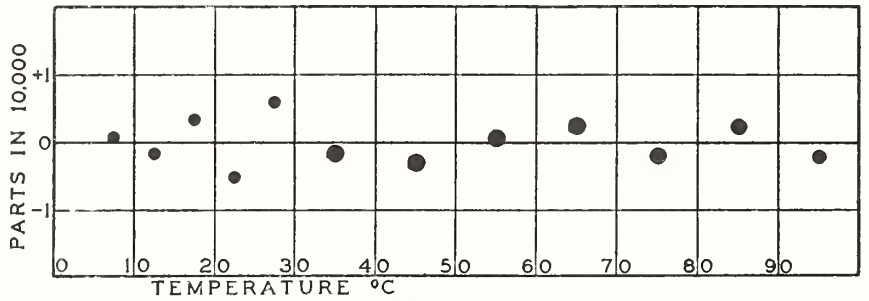

FIGURE 4.—*Deviations of mean measured C_p from formulation. Areas of circles are proportional to the weights assigned to the mean values.*

Figure 5 shows a comparison of the heat capacities. It should be noted from the figure that the scale of the heat capacities is very much exaggerated and that the extreme range of the values of C_{p1} between 0° and 100° C is only about 1 percent. The $d\alpha/dt$ line gives essentially the measured values of heat capacity. The departure of the $(dH/dt)_{sat}$ line from the $d\alpha/dt$ line represents the magnitude of the $d\beta/dt$ reduction. The difference between the C_p line and the

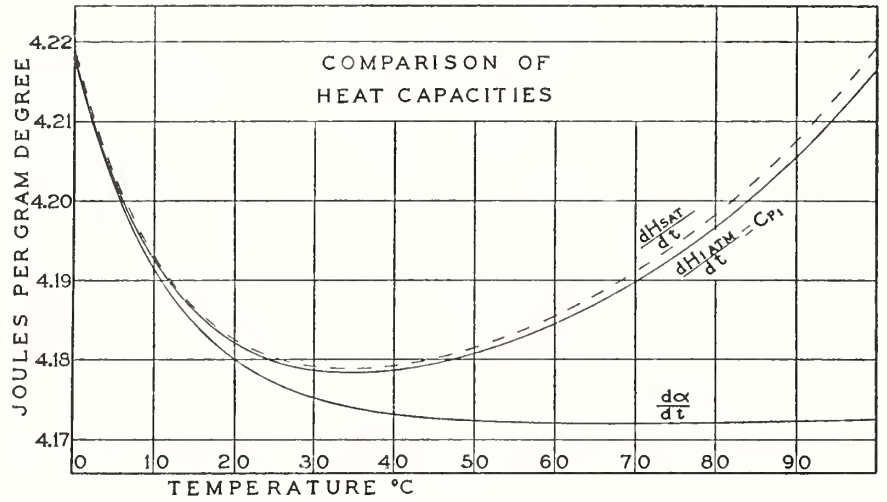

FIGURE 5.—*Comparison of heat capacities.*

$(dH/dt)_{sat}$ line shows the magnitude of the reduction to 1-atmosphere pressure. The experimental values have not been plotted on this figure, because only one or two values would fall outside the width of the line in spite of the exaggerated scale.

Water is often used as a calorimetric medium and also as a standard of heat capacity, as, for example, in a condensing calorimeter for measuring the enthalpy of superheated steam or for measuring

specific heats by the method of mixtures. For such purposes, it is useful to know the integral of the specific heat (C_p) function, since these calorimetric measurements must necessarily apply to finite temperature intervals. A table of values of the integral, giving the heat content, or enthalpy, from 0 to each temperature at intervals of 1° from 0° to 100° C has been prepared for this use. This table has been compiled in terms of absolute joules per gram and international steam-table calories per gram instead of any of the numerous heat units which have been used in the past, and defined variously in terms of the heat capacity of water.

Since the absolute practical electrical units are expected to replace the present international units on January 1, 1940, it seems desirable to use the absolute joule rather than the international joule which has been used in the measurements, but which is likely so soon to be obsolete. Also since the international steam-table calorie (IT Cal), defined as 1/860 int. whr, has now become the basis of heat units used in steam tables, values are included in this unit.

The conversion factor from international joules to absolute joules, being based on measurement, can not be exactly known, but the uncertainty has been greatly reduced by the more recent measurements of the absolute ohm and absolute ampere in terms of the electrical standards maintained in National laboratories. Since a final official figure for this factor has not yet been announced, the value 1 int. j=1.00019 abs. j used here was an estimate of the probable value of the absolute joule in international joules as derived from electrical standards maintained in this laboratory and was based on recent measurements, partly unpublished. It is believed that this value expresses the equivalent of the units actually used within 1 or 2 units in the last place.

The equation for C_p in international joules per gram-degree centigrade has been converted to absolute joules per gram-degree by multiplying the coefficients by the factor 1.00019, giving the new equation

$$C_p=4.169828+0.000364(t+100)^{5.26}\times10^{-10}+0.046709(10)^{-0.036t},$$

where t is in degrees centigrade and C_p is in absolute joules per gram-degree centigrade at 1-atmosphere pressure. By integration of $C_p dt$, the equation for enthalpy, H_p, at 1-atmosphere pressure in absolute joules per gram is obtained. Taking the value of $H_{sat.}$ as 0 at 0° C, the equation is

$$H_p=0.102559+4.16928t+[5.8142(t+100)^{6.26}\times10^{-15}-0.563485(10)^{-0.036t}]^{t}_{0},$$

where t is in degrees centigrade, and H_p in absolute joules per gram at 1-atmosphere pressure.

Values of both C_p and H_p are given in table 6. The values of H_p, in IT Cal, have been computed from the values in absolute joules per gram by use of the conversion factor 1 abs. j=0.238846 IT Cal.

This gives values of H_p which are larger by 1 part in 100,000 than correspond to the present definition of the IT Cal but are in agreement with a redefinition of the IT Cal as 0.001163 abs. whr, which has been suggested for adoption when the change in electrical units takes place. This small discrepancy is less than the amount which is important in steam tables, and likewise less than the uncertainty of the present measurements.

The enthalpy of saturated liquid water is one of the important items in the compilation of steam tables. Values of this property were computed by use of the formula for $d\alpha/dt$ and values of β.

The formula for $d\alpha/dt$ in international joules per gram-degree centigrade is

$$d\alpha/dt=4.1699+15.27\ \ t\times10^{-6}+0.0467(10)^{-0.036t}.$$

By integration, the following equation for the increment of α is obtained:

$$\alpha^t{}_0=[4.1699t+7.635t^2\times10^{-6}-0.56376\times10^{-0.036t}]^t{}_0.$$

Values of $\alpha^t{}_0$ computed by this equation, at every 5° point from 0° to 100° C, are given in table 7. Values of β, computed as previously described, are also given. Values of enthalpy are found by adding the increment of β to $\alpha^t{}_0$, and are given in the table in international joules per gram and also converted to absolute joules per gram and to International Steam Table Calories per gram, using the conversion factors stated above.

TABLE 3.—*Principal data from large-mass heat-capacity experiments*

Date	Mass of water, M	Initial temperature	Final temperature	Heat leak	Pump energy	Energy for even temperature interval	$\Delta\alpha/\Delta t$	Deviation from formulation
	g	°C	°C	*Int. j*	*Int. j*	*Int. j*	*Int. j/g-°C*	*Int. j/g-°C*
12-7-37	1093.989	0.0104	0.9974	0.0	1.7	4,778.4	4.21286	−0.00187
12-9-37	603.781	.0565	.9522	.0	6.1	2,714.9	4.21563	.00090
12-10-37	603.781	.3232	1.0068	.1	15.6	2,713.9	4.21398	−.00075
12-14-37	603.781	.0324	.9938	.0	2.9	2,713.9	4.21398	−.00075
Average							4.21411	
Even temperature interval 0.0° to 1.0° C. $\Delta Z/\Delta t$=169.577 int. j/°C. Formulated value of $\Delta\alpha/\Delta t$=4.21473 int. j/g-°C								
9-23-37	1091.161	0.1772	2.4587	0.6	2.7	11,918.6	4.21363	0.00153
10-6-37	1092.517	.4886	2.4624	−.1	2.4	11,932.5	4.21349	.00139
10-8-37	1092.517	.2433	2.4981	−.4	2.7	11,931.7	4.21320	.00110
10-14-37	1092.517	.1884	2.4990	−.2	2.4	11,932.1	4.21334	.00124
10-21-37	1093.647	−.0385	2.5184	−.1	2.4	11,939.6	4.21173	−.00037
10-26-37	1093.647	−.0376	2.4947	−.1	2.4	11,941.4	4.21239	.00029
10-27-37	1093.647	.0120	2.4972	.2	2.4	11,941.1	4.21228	.00018
10-28-37	1093.647	.0070	2.4992	.1	2.4	11,941.1	4.21228	.00018
11-16-37	1096.489	−.0174	2.4588	.0	2.4	11,970.4	4.21205	−.00005
11-18-37	1096.489	−.0037	2.4867	−.1	2.4	11,971.1	4.21231	.00021
12-2-37	1093.989	−.0586	2.5191	.4	2.9	11,945.7	4.21265	.00055
Average							4.21267	
Even temperature interval 0.0° to 2.5° C. $\Delta Z/\Delta t$=169.688 int. j/°C. Formulated value of $\Delta\alpha/\Delta t$=4.21210 int. j/g-°C								
9-14-37	1091.161	0.1830	4.9763	1.3	5.6	23,809.2	4.20833	0.00016
9-21-37	1091.161	.1920	5.1873	.5	4.1	23,806.8	4.20789	−.00028
Average							4.20811	
Even temperature interval 0.0° to 5.0° C. $\Delta Z/\Delta t$=169.879 int. j/°C. Formulated value of $\Delta\alpha/\Delta t$=4.20817 int. j/g-°C								
12-7-37	1093.989	1.0078	2.0054	−0.1	1.7	4,776.7	4.21118	0.00000
12-9-37	603.781	.9518	1.9649	.0	6.1	2,712.3	4.21109	−.00009
12-10-37	603.781	1.0041	2.0051	.0	15.6	2,712.2	4.21093	−.00025
12-14-37	603.781	.9964	1.9944	.0	2.9	2,711.8	4.21027	.00009
Average							4.21087	
Even temperature interval of 1.0° to 2.0° C. $\Delta Z/\Delta t$=169.725 int. j/°C. Formulated value of $\Delta\alpha/\Delta t$=4.21118 int. j/g-°C								

TABLE 3.—*Principal data from large-mass heat-capacity experiments*—Continued

Date	Mass of water, M	Initial temperature	Final temperature	Heat leak	Pump energy	Energy for even temperature interval	$\Delta\alpha/\Delta t$	Deviation from formulation
	g	°C	°C	*Int. j*	*Int. j*	*Int. j*	*Int. j/g-°C*	*Int. j/g-°C*
12-7-37	1093.989	2.0054	3.0051	−.01	1.7	4,772.5	4.20719	−0.00072
12-9-37	603.781	1.9649	2.9776	−.1	2.5	2,710.7	4.20818	.00027
12-10-37	603.781	2.0051	2.9997	−.1	6.4	2,710.6	4.20802	.00011
12-14-37	603.781	1.9944	2.9979	.0	1.2	2,710.1	4.20719	−.00072
Average							4.20765	

Even temperature interval 2.0° to 3.0° C. $\Delta Z/\Delta t$=169.876 int. j/°C. Formulated value of $\Delta\alpha/\Delta t$=4.20791 int. j/g-°C

9-23-37	1091.161	2.4587	4.9962	0.0	2.4	11,890.7	4.20306	−0.00118
10-6-37	1092.517	2.4624	4.9935	−.3	2.4	11,905.5	4.20326	−.00098
10-8-37	1092.517	2.4981	4.9767	−.1	2.4	11,908.4	4.20432	.00008
10-14-37	1092.517	2.4990	4.9990	−.1	2.4	11,907.9	4.20414	−.00010
10-19-37	1093.647	2.5092	5.0043	−.2	2.4	11,918.8	4.20378	−.00046
10-21-37	1093.647	2.5184	5.0021	−.1	2.4	11,922.0	4.20495	.00071
10-26-37	1093.647	2.4947	5.0025	.0	2.4	11,919.6	4.20409	−.00015
10-27-37	1093.647	2.4963	5.0439	.4	2.4	11,918.4	4.20363	−.00061
10-28-37	1093.647	2.4983	4.9961	.4	2.4	11,919.6	4.20409	−.00015
11-16-37	1096.489	2.4585	5.0015	−.1	2.4	11,948.0	4.20354	−.00070
11-18-37	1096.489	2.4886	4.9970	.0	2.4	11,949.2	4.20397	−.00027
12-3-37	1093.989	2.4637	4.9717	.0	2.4	11,921.4	4.20342	−.00082
Average							4.20385	

Even temperature interval 2.5° to 5.0° C. $\Delta Z/\Delta t$=170.071 int. j/°C. Formulated value of $\Delta\alpha/\Delta t$=4.20424 int. j/g-°C

12-7-37	1093.989	3.0051	4.0045	0.0	1.7	4,770.4	4.20513	0.00023
12-9-37	603.781	2.9776	3.9911	−.1	2.5	2,708.8	4.20479	−.00011
12-10-37	603.781	2.9997	4.0005	−.1	6.4	2,709.1	4.20528	.00038
12-14-37	603.781	2.9979	3.9993	.0	1.2	2,709.6	4.20611	.00121
Average							4.20533	

Even temperature interval 3.0° to 4.0° C. $\Delta Z/\Delta t$=170.030 int. j/°C. Formulated value of $\Delta\alpha/\Delta t$=4.20490 int. j/g-°C

12-7-37	1093.989	4.0045	5.0036	0.0	1.7	4,766.4	4.20133	−0.00081
12-9-37	603.781	3.9911	5.0052	.0	2.5	2,707.6	4.20253	.00039
12-10-37	603.781	4.0005	5.0015	.0	6.4	2,707.8	4.20286	.00072
12-14-37	603.781	4.9993	4.9990	−.1	1.2	2,707.3	4.20204	−.00010
Average							4.20219	

Even temperature interval 4.0° to 5.0° C. $\Delta Z/\Delta t$=170.188 int. j/°C. Formulated value of $\Delta\alpha/\Delta t$=4.20214 int. i/g-°C

9-14-37	1091.161	4.9763	10.0026	1.3	4.4	23,741.4	4.19515	−0.00012
9-16-37	1091.161	5.0018	9.9480	.1	4.6	23,742.5	4.19536	.00009
9-21-37	1091.161	5.1873	9.9846	1.0	3.9	23,739.9	4.19488	−.00039
9-23-37	1091.161	4.9962	9.9910	−.4	3.7	23,743.6	4.19556	.00029
10-6-37	1092.517	4.9935	10.0029	−.6	3.7	23,771.7	4.19550	.00023
10-8-37	1092.517	4.9767	10.0084	−.2	3.7	23,772.9	4.19571	.00044
10-14-37	1092.517	4.9990	10.0050	−.1	3.7	23,772.5	4.19564	.00037
10-19-37	1093.647	5.0043	10.0104	−.2	3.7	23,795.6	4.19553	.00026
10-21-37	1093.647	5.0021	9.9988	.3	3.7	23,799.0	4.19615	.00088
10-26-37	1093.647	5.0025	10.0018	.0	3.7	23,797.3	4.19584	.00057
10-27-37	1093.647	5.0432	10.0077	.2	3.7	23,796.5	4.19570	.00043
10-28-37	1093.647	4.9954	9.9905	.3	3.7	23,795.9	4.19559	.00032
11-16-37	1096.489	5.0011	10.0036	−.2	3.7	23,853.3	4.19518	−.00009
11-18-37	1096.489	4.9965	10.0005	.0	3.7	23,853.9	4.19529	.00002
12-3-37	1093.989	4.9701	9.9808	.0	3.7	23,799.4	4.19491	−.00036
12-7-37	1093.989	5.0036	10.0067	−.3	3.7	23,798.3	4.19471	−.00056
12-9-37	603.781	5.0052	10.0755	.0	5.4	13,516.1	4.19445	−.00082
12-10-37	603.781	5.0015	10.0029	−.1	13.8	13,517.3	4.19485	−.00042
12-14-37	603.781	4.9990	9.9994	−.3	2.6	13,516.9	4.19472	−.00055
Average							4.19530	

Even temperature interval 5° to 10° C. $\Delta Z/\Delta t$=170.687 int. j/° C. Formulated value of $\Delta\alpha/\Delta t$=4.19527 int. j/g-°C

TABLE 3.—*Principal data from large-mass heat-capacity experiments*—Continued

Date	Mass of water, M	Initial temperature	Final temperature	Heat leak	Pump energy	Energy for even temperature interval	$\Delta\alpha/\Delta t$	Deviation from formulation
	g	*°C*	*°C*	*Int. j*	*Int. j*	*Int. j*	*Int. j/g-°C*	*Int. j/g-°C*
9-14-37	1091.161	10.0026	15.0032	0.9	3.9	23,697.0	4.18619	−0.00059
9-16-37	1091.161	9.9480	14.9471	−.1	3.7	23,699.1	4.18658	−.00020
9-21-37	1091.161	9.9846	15.0031	1.3	4.1	23,699.9	4.18672	−.00006
9-23-37	1091.161	9.9910	14.9987	−.5	3.7	23,701.9	4.18709	.00031
10-6-37	1092.517	10.0029	15.0069	.1	3.7	23,728.9	4.18684	.00006
10-8-37	1092.517	10.0084	15.0045	−.3	3.7	23,730.5	4.18713	.00035
10-13-37	1092.517	10.0020	15.0123	−.2	3.7	23,724.7	4.18607	−.00071
10-14-37	1092.517	10.0050	15.0064	.0	3.7	23,729.6	4.18696	.00018
10-19-37	1093.647	10.0104	15.0098	−.1	3.7	23,752.1	4.18675	−.00003
10-21-37	1093.647	9.9988	14.9970	.3	3.7	23,753.9	4.18708	.00030
10-26-37	1093.647	10.0018	15.0000	.0	3.7	23,754.5	4.18719	.00041
10-27-37	1093.647	10.0077	15.0024	.0	3.7	23,755.2	4.18732	.00054
10-28-37	1093.647	9.9905	14.9997	.0	3.7	23,755.1	4.18730	.00052
11-16-37	1096.489	10.0036	14.9993	.0	3.7	23,808.8	4.18624	−.00054
11-18-37	1096.489	9.9999	15.0004	.0	3.7	23,810.4	4.18654	−.00024
12-3-37	1093.989	9.9808	14.9891	−.1	3.7	23,757.9	4.18650	−.00028
12-7-37	1093.989	10.0067	15.0097	.0	3.7	23,754.8	4.18594	−.00084
12-9-37	603.781	10.0755	15.1357	−.3	8.9	13,496.4	4.18644	−.00034
12-10-37	603.781	10.0004	15.0065	−.3	23.0	13,494.7	4.18587	−.00091
12-14-37	603.781	9.9996	15.0019	−.2	4.3	13,497.7	4.18687	.00009
Average							4.18668	

Even temperature interval 10° to 15° C. $\Delta Z/\Delta t$=171.588 int. j/° C. Formulated value of $\Delta\alpha/\Delta t$=4.18678 int. j/g-°C

9-16-37	1091.161	14.9471	19.8801	0.0	3.7	23,675.9	4.18140	0.00021
9-21-37	1091.161	15.0031	20.0047	−.2	3.7	23,673.5	4.18096	−.00023
9-23-37	1091.161	14.9987	19.9959	−.4	3.7	23,675.9	4.18140	.00021
10-6-37	1092.517	15.0069	20.0025	.0	3.7	23,704.0	4.18135	.00016
10-8-37	1092.517	15.0045	20.0133	−.2	3.7	23,705.6	4.18165	.00046
10-13-37	1092.517	15.0123	19.9903	.0	3.7	23,705.3	4.18159	.00040
10-14-37	1092.517	15.0064	20.0082	−.1	3.7	23,704.5	4.18145	.00026
10-19-37	1093.647	15.0098	20.0137	.2	3.7	23,728.5	4.18151	.00032
10-21-37	1093.647	14.9970	19.9951	.0	3.7	23,729.6	4.18171	.00052
10-26-37	1093.647	15.0000	20.0426	.0	4.4	23,725.3	4.18093	−.00026
10-27-37	1093.647	15.0024	19.9990	.1	3.7	23,730.5	4.18188	.00069
10-28-37	1093.647	14.9997	20.0012	.1	3.7	23,730.9	4.18195	.00076
11-16-37	1096.489	14.9993	20.0001	−.1	3.7	23,784.3	4.18085	−.00034
11-18-37	1096.489	15.0004	20.0018	.0	3.7	23,785.8	4.18113	−.00006
12-3-37	1093.989	14.9891	19.9982	−.2	3.7	23,732.0	4.18085	−.00034
12-7-37	1093.989	15.0097	20.0096	.0	3.7	23,732.2	4.18088	−.00031
12-9-37	603.781	15.1357	19.9751	−.2	5.4	13,485.8	4.18125	.00006
12-10-37	603.781	15.0065	20.0009	.4	13.8	13,485.5	4.18115	−.00004
12-14-37	603.781	15.0025	20.4957	.2	2.7	13,484.5	4.18082	−.00037
Average							4.18130	

Even temperature interval 15° to 20° C. $\Delta Z/\Delta t$=172.600 int. j/°C. Formulated value of $\Delta\alpha/\Delta t$=4.18119 int. j/g-°C

9-16-37	1091.161	19.8801	24.9932	−0.2	3.7	23,657.6	4.17700	−0.00053
9-21-37	1091.161	20.0047	25.0045	−.7	3.7	23,658.5	4.17716	−.00037
9-23-37	1091.161	19.9959	24.9938	−.3	3.7	23,659.5	4.17735	−.00018
10-6-37	1092.517	20.0025	25.0089	0	3.7	23,686.6	4.17712	−.00041
10-8-37	1092.517	20.0133	25.0031	−.1	3.7	23,689.1	4.17758	.00005
10-13-37	1092.517	19.9903	24.9999	0	3.7	23,687.0	4.17720	−.00033
10-14-37	1092.517	20.0082	25.0133	0	3.7	23,687.8	4.17734	−.00019
10-19-37	1093.647	20.0137	24.9982	.2	3.7	23,713.5	4.17773	.00020
10-21-37	1093.647	19.9951	24.9970	−.1	3.7	23,710.6	4.17720	−.00033
10-26-37	1093.647	20.0426	25.0031	0	3.7	23,713.9	4,17780	.00027
10-27-37	1093.647	19.9990	25.0024	.1	3.7	23,713.6	4.17775	.00022
10-28-37	1093.647	20.0012	25.0023	.2	3.7	23,714.9	4.17798	.00045
11-16-37	1096.489	20.0001	25.0008	−.1	3.7	23,768.8	4.17699	−.00054
11-18-37	1096.489	20.0018	25.0001	0	3.7	23,770.8	4.17735	−.00018
12-3-37	1093.989	19.9982	25.0048	−.1	3.7	23,716.6	4.17699	−.00054
12-7-37	1093.989	20.0096	25.0079	0	3.7	23,716.1	4.17690	−.00063
12-9-37	603.781	19.9751	25.0376	−.3	5.4	13,478.4	4.17691	−.00062
12-10-37	603.781	20.0009	25.0050	0	13.8	13,477.9	4.17675	−.00078
Average							4.17728	

Even temperature interval 20° to 25° C. $\Delta Z/\Delta t$=173.739 int. j/°C. Formulated value of $\Delta\alpha/\Delta t$=4.17753 int. j/g-°C

TABLE 3.—*Principal data from large-mass heat-capacity experiments*—Continued

Date	Mass of water, M	Initial temperature	Final temperature	Heat leak	Pump energy	Energy for even temperature interval	$\Delta\alpha/\Delta t$	Deviation from formulation
	g	°C	°C	*Int. j*	*Int. j*	*Int. j*	*Int. j/g-°C*	*Int. j/g-°C*
9-16-37	1091.161	24.9932	29.9906	−0.1	3.7	23,655.1	4.17537	0.00024
9-21-37	1091.161	25.0045	29.9953	−.9	3.7	23,655.3	4.17540	.00027
9-23-37	1091.161	24.9938	29.9913	−.1	3.7	23,656.1	4.17554	.00041
10-6-37	1092.517	25.0089	29.9926	−.1	3.7	23,683.9	4.17546	.00033
10-8-37	1092.517	25.0031	30.0106	−.1	3.7	23,685.8	4.17581	.00068
10-13-37	1092.517	24.9999	30.0000	0	3.7	23,684.0	4.17548	.00035
10-14-37	1092.517	25.0133	30.0068	.1	3.7	23,683.4	4.17537	.00024
10-19-37	1093.647	24.9982	30.0054	0	3.7	23,706.9	4.17535	.00022
10-21-37	1093.647	24.9970	29.9945	.3	3.7	23,709.6	4.17584	.00071
10-26-37	1093.647	25.0031	29.9981	0	3.7	23,709.0	4.17573	.00060
10-27-37	1093.647	25.0024	30.0028	.2	3.7	23,710.0	4.17592	.00079
10-28-37	1093.647	25.0023	30.0017	−.1	3.7	23,709.4	4.17581	.00068
11-16-37	1096.489	25.0008	30.0012	−.1	3.7	23,764.4	4.17502	−.00011
11-18-37	1096.489	25.0001	30.0015	0	3.7	23,765.4	4.17519	.00006
11-19-37	1096.489	24.9997	30.0644	−.1	3.1	23,764.6	4.17505	−.00008
12-3-37	1093.989	25.0048	30.0131	0	3.7	23,712.6	4.17509	−.00004
12-7-37	1093.989	25.0079	30.0051	−.1	3.7	23,711.0	4.17480	−.00033
12-9-37	603.781	25.0376	29.9672	−.1	5.4	13,479.1	4.17502	−.00011
12-10-37	603.781	25.0050	30.0028	.1	13.8	13,479.7	4.17522	.00009
12-14-37	603.781	25.0430	30.0016	−.2	4.3	13,479.2	4.17506	−.00007
Average							4.17538	

Even temperature interval 25° to 30° C. $\Delta Z/\Delta t$=175.025 int. j/°C. Formulated value of $\Delta\alpha/\Delta t$=4.17513 int. j/g-°C

9-16-37	1091.161	29.9906	39.9768	−0.5	6.1	47,308.5	4.17313	0.00006
9-21-37	1091.161	29.9953	39.9841	−1.9	6.1	47,314.3	4.17366	.00059
9-23-37	1091.161	29.9913	39.9938	−0.2	6.1	47,309.7	4.17324	.00017
10-6-37	1092.517	29.9926	39.9994	.0	6.1	47,365.0	4.17312	.00005
10-8-37	1092.517	30.0106	40.0110	−.1	6.3	47,368.8	4.17347	.00040
10-13-37	1092.517	30.0000	39.9973	.1	6.1	47,366.4	4.17325	.00018
10-14-37	1092.517	30.0068	39.9938	.0	6.1	47,364.7	4.17310	.00003
10-19-37	1093.647	30.0054	40.0252	.4	6.1	47,413.2	4.17322	.00015
10-21-37	1093.647	29.9945	40.4984	.7	6.3	47,411.3	4.17305	−.00002
10-28-37	1093.647	30.0017	40.0038	.3	6.1	47,412.4	4.17315	.00008
11-16-37	1096.489	30.0012	40.0003	.0	6.1	47,525.0	4.17260	−.00047
11-18-37	1096.489	30.0015	40.0054	.1	6.1	47,529.0	4.17296	−.00011
11-19-37	1096.489	30.0659	40.0052	.5	6.1	47,526.2	4.17271	−.00036
12-3-37	1093.989	30.0131	40.0228	.0	6.1	47,422.7	4.17278	−.00029
12-7-37	1093.989	30.0051	40.0159	−.2	6.1	47,420.5	4.17258	−.00049
12-9-37	603.781	29.9672	40.0050	.1	8.9	26,967.2	4.17275	−.00032
12-10-37	603.781	30.0028	40.0067	.1	23.0	26,967.4	4.17279	−.00028
12-14-37	603.781	30.0016	40.0000	.0	4.3	26,967.6	4.17282	−.00025
Average							4.17302	

Even temperature interval 30° to 40° C. $\Delta Z/\Delta t$=177.291 int. j/°C. Formulated value of $\Delta\alpha/\Delta t$=4.17307 int. j/g-° C

9-16-37	1091.161	39.9768	49.9916	−0.3	6.1	47,330.3	4.17174	0.00000
9-21-37	1091.161	39.9841	49.9863	−2.4	6.1	47,325.2	4.17127	−.00047
9-23-37	1091.161	39.9938	49.9831	−0.4	6.3	47,331.9	4.17189	.00015
10-6-37	1092.517	39.9994	50.0157	−.2	6.1	47,387.6	4.17181	.00007
10-8-37	1092.517	40.0110	50.0230	−.1	6.1	47,390.1	4.17204	.00030
10-13-37	1092.517	39.9973	50.0000	.0	6.1	47,386.8	4.17173	−.00001
10-14-37	1092.517	39.9938	50.0149	−.1	6.1	47,387.0	4.17175	.00001
10-19-37	1093.647	40.0252	49.9521	.3	6.1	47,433.4	4.17168	−.00006
10-21-37	1093.647	40.4984	49.9933	.5	5.9	47,435.8	4.17190	.00016
10-28-37	1093.647	40.0038	50.0085	.4	6.1	47,439.7	4.17226	.00052
11-16-37	1096.489	40.0003	50.0032	.0	6.1	47,548.0	4.17132	−.00042
11-18-37	1096.489	40.0054	49.9958	.0	6.1	47,551.4	4.17163	−.00011
11-19-37	1096.489	40.0052	50.0046	.3	6.1	47,549.8	4.17149	−.00025
11-20-37	1096.489	40.0003	50.0006	.4	6.1	47,549.7	4.17148	−.00026
12-3-37	1093.989	40.0228	50.0059	−.2	6.1	47,444.5	4.17139	−.00035
12-7-37	1093.989	40.0108	50.0111	.1	6.1	47,444.9	4.17143	−.00031
12-9-37	603.781	40.0050	49.9467	.1	8.9	26,997.3	1.17161	−.00013
12-10-37	603.781	40.0067	50.0083	−.1	23.0	26,996.2	4.17143	−.00031
12-14-37	603.781	40.0026	50.0011	−.2	7.0	26,997.2	4.17160	−.00014
Average							4.17165	

Even temperature interval 40° to 50° C. $\Delta Z/\Delta t$=180.989 int. j/°C. Formulated value of $\Delta\alpha/\Delta t$=4,17174 int. j/g-°C

TABLE 3.—*Principal data from large-mass heat-capacity experiments*—Continued

Date	Mass of water, M	Initial temperature	Final temperature	Heat leak	Pump energy	Energy for even temperature interval	$\Delta\alpha/\Delta t$	Deviation from formulation
	q	°C	°C	*Int. j*	*Int. j*	*Int. j*	*Int. j/q-°C*	*Int. j/q-°C*
9-16-37	1091.161	49.9916	59.9913	−0.1	6.1	47,375.0	4.17156	0.00032
9-21-37	1091.161	49.9863	59.9896	−1.9	6.1	47,374.8	4.17154	.00030
9-23-37	1091.161	49.9831	59.9923	−0.1	6.1	47,377.2	4.17176	.00052
10-6-37	1092.517	50.0157	60.0047	.0	6.1	47,432.1	4.17161	.00037
10-8-37	1092.517	50.0230	60.0065	−.2	6.1	47,434.1	4.17179	.00055
10-14-37	1092.517	50.0149	59.9958	.0	6.1	47,430.2	4.17143	.00019
10-19-37	1093.647	49.9521	59.9329	.3	6.1	47,477.8	4.17147	.00023
10-21-37	1093.647	49.9933	59.9976	.7	6.1	47,477.7	4.17146	.00022
10-28-37	1093.647	50.0085	60.0019	.4	6.1	47,482.4	4.17189	.00065
11-16-37	1096.489	50.0032	60.0024	.0	6.1	47,590.1	4.17090	−.00034
11-18-37	1096.489	49.9958	60.0050	−.1	6.1	47,594.8	4.17133	.00009
11-19-37	1096.489	50.0046	60.0081	.2	6.1	47,592.3	4.17110	−.00014
11-20-37	1096.489	50.0006	60.0114	.4	6.1	47,590.7	4.17096	−.00028
12-4-37	1093.989	50.0006	60.0322	.1	6.1	47,485.3	4.17086	−.00038
12-7-37	1093.989	50.0143	60.0080	−.1	6.1	47,487.5	4.17106	−.00018
12-9-37	603.781	49.9513	59.9329	−.2	8.9	27,040.3	4.17100	−.00024
12-10-37	603.781	50.0083	59.9993	.2	23.0	27,038.1	4.17063	−.00061
12-14-37	603.781	50.0009	59.9980	−.5	5.0	27,042.4	4.17135	.00011
Average							4.17132	

Even temperature interval 50° to 60° C. $\Delta Z/\Delta t$=185.663 int. j/°C. Formulated value of $\Delta\alpha/\Delta t$=4.17124 int. j/g-°C

9-16-37	1091.161	59.9913	69.9814	0.2	6.1	47,429.1	4.17114	0.00003
9-21-37	1091.161	59.9896	70.9984	−2.1	6.8	47,431.6	4.17137	.00026
9-23-37	1091.161	59.9923	69.9831	0.1	6.1	47,432.4	4.17145	.00034
10-6-37	1092.517	60.0047	70.0140	−.2	6.1	47,488.7	4.17142	.00031
10-8-37	1092.517	60.0065	70.0097	.0	6.1	47,491.3	4.17166	.00055
10-19-37	1093.647	59.9329	70.0336	.0	6.1	47,533.0	4.17116	.00005
10-21-37	1093.647	59.9976	69.9959	.3	6.1	47,535.5	4.17139	.00028
10-28-37	1093.647	60.0019	70.0089	−.1	6.1	47,538.1	4.17163	.00052
11-16-37	1096.489	60.0024	70.0021	.0	6.1	47,648.1	4.17085	−.00026
11-18-37	1096.489	60.0050	70.0038	−.2	6.1	47,654.0	4.17139	.00028
11-19-37	1096.489	60.0081	70.0056	.0	6.1	47,656.3	4.17160	.00049
11-20-37	1096.489	60.0114	70.0042	.4	6.1	47,649.5	4.17098	−.00013
12-3-37	1093.989	60.0104	70.0119	.0	6.1	47,547.4	4.17118	.00007
12-4-37	1093.989	60.0320	70.0076	.0	6.1	47,544.7	4.17093	−.00018
12-7-37	1093.989	60.0079	70.0183	.1	6.1	47,551.1	4.17151	.00040
12-9-37	603.781	59.9329	69.9511	−.3	8.9	27,098.0	4.17085	−.00026
12-10-37	603.781	59.9993	69.9990	.3	23.0	27,095.9	4.17050	−.00061
Average							4.17124	

Even temperature interval 60° to 70° C. $\Delta Z/\Delta t$=191.520 int. j/°C. Formulated value of $\Delta\alpha/\Delta t$=4.17111 int. j/g-°C

9-16-37	1091.161	69.9814	79.9916	0.0	6.1	47,504.6	4.17140	0.00026
9-21-37	1091.161	71.0327	80.0364	−.4	6.1	47,493.5	4.17038	−.00076
9-23-37	1091.161	69.9831	80.0028	.1	6.6	47,500.3	4.17101	−.00013
10-8-37	1092.517	70.0097	80.0089	.1	6.1	47,564.2	4.17168	.00054
10-19-37	1093.647	70.0336	80.0126	.2	6.1	47,607.4	4.17132	.00018
10-21-37	1093.647	69.9959	80.0016	.2	6.1	47,607.1	4.17129	.00015
11-16-37	1096.489	70.0021	80.0031	.0	6.1	47,721.0	4.17087	−.00027
11-18-37	1096.489	70.0038	80.0038	−.1	6.1	47,726.5	4.17137	.00023
11-19-37	1096.489	70.0056	80.0038	.0	6.1	47,721.2	4.17086	−.00028
11-20-37	1096.489	70.0042	79.9993	.2	6.1	47,722.4	4.17099	−.00015
12-3-37	1093.989	70.0119	80.0090	−.2	6.1	47,621.7	4.17132	.00018
12-4-37	1093.989	70.0076	80.0145	.0	6.1	47,615.5	4.17075	−.00039
12-7-37	1093.989	70.0183	80.0040	−.1	6.1	47,616.1	4.17081	−.00033
12-9-37	603.781	69.9511	79.9741	−.4	8.9	27,172.5	4.17114	.00000
12-10-37	603.781	69.9990	80.0085	.3	23.0	27,168.9	4.17054	−.00060
Average							4.17105	

Even temperature interval 70° to 80° C. $\Delta Z/\Delta t$=198.795 int. j/°C. Formulated value of $\Delta\alpha/\Delta t$=4.17114 int. j/g-°C

TABLE 3.—*Principal data from large-mass heat-capacity experiments*—Continued

Date	Mass of water, M	Initial temperature	Final temperature	Heat leak	Pump energy	Energy for even temperature interval	$\Delta\alpha/\Delta t$	Deviation from formulation
	g	°C	°C	*Int. j*	*Int. j*	*Int. j*	*Int. j/g-°C*	*Int. j/g-°C*
9–16–37	1091.161	79.9916	89.9950	0.0	6.1	47,597.1	4.17167	0.00043
9–21–37	1091.161	80.0364	89.9882	−.5	6.1	47,592.5	4.17125	.00001
9–23–37	1091.161	80.0028	89.9957	−.4	6.3	47,592.2	4.17123	−.00001
10–19–37	1093.647	80.0126	90.0150	.2	6.1	47,696.4	4.17127	.00003
10–21–37	1093.647	80.0016	89.9994	.0	6.1	47,698.2	4.17144	.00020
10–28–37	1093.647	79.9989	89.9751	.4	6.1	47,703.6	4.17193	.00069
11–16–37	1096.489	80.0031	90.0029	.0	6.1	47,809.8	4.17080	−.00044
11–18–37	1096.489	80.0038	90.0003	−.3	6.1	47,815.6	4.17133	.00009
11–19–37	1096.489	80.0041	90.0068	−.1	6.1	47,811.9	4.17099	−.00025
11–20–37	1096.489	79.9993	90.0060	.0	6.1	47,812.9	4.17109	−.00015
12–3–37	1093.989	80.0090	90.0074	.1	6.1	47,710.4	4.17125	.00001
12–4–37	1093.989	80.0145	90.0123	.1	6.1	47,708.6	4.17108	−.00016
12–7–37	1093.989	80.0040	90.0032	.1	6.1	47,711.2	4.17132	.00008
12–9–37	603.781	79.9741	90.0319	−.4	8.9	27,263.1	4.17133	.00009
12–10–37	603.781	80.0085	90.0092	−.1	23.0	27,263.7	4.17143	.00019
Average							4.17129	

Even temperature interval 80° to 90° C. $\Delta Z/\Delta t$=207.738 Int. j/°C. Formulated value of $\Delta\alpha/\Delta t$=4.17124 int. j/g-°C

9–16–37	1091.161	89.9950	99.9843	−0.4	6.1	47,704.3	4.17152	0.00015
9–21–37	1091.161	89.9882	99.9992	.2	6.3	47,693.1	4.17049	−.00088
9–23–37	1091.161	89.9957	99.9887	−.4	6.1	47,696.9	4.17084	−.00053
10–19–37	1093.647	90.0150	100.0086	−.4	6.2	47,806.1	4.17135	−.00002
10–21–37	1093.647	89.9994	100.0027	.1	6.1	47,807.6	4.17148	.00011
11–16–37	1096.489	90.0029	100.0024	−.2	6.1	47,920.8	4.17099	−.00038
11–18–37	1096.489	90.0003	100.0037	−.3	6.1	47,927.2	4.17158	.00021
11–19–37	1096.489	90.0068	99.9942	.0	6.1	47,925.5	4.17142	.00005
11–20–37	1096.489	90.0060	100.0045	−.3	6.1	47,921.9	4.17110	−.00027
12–3–37	1093.989	90.0074	100.0098	−.3	6.1	47,820.7	4.17138	.00001
12–4–37	1093.989	90.0123	100.0076	−.2	6.1	47,828.1	4.17205	.00068
12–9–37	603.781	90.0319	100.0076	−.3	8.9	27,371.6	4.17126	−.00011
12–10–37	603.781	90.0248	100.0075	.1	23.0	27,369.9	4.17098	−.00039
Average							4.17126	

Even temperature interval 90° to 100° C. $\Delta Z/\Delta t$=218.626 int. j/°C. Formulated value of $\Delta\alpha/\Delta t$=4.17137 int. j/g-°C

TABLE 4.—*Principal data from small-mass heat-capacity experiments*

Date	Mass of water, M	Initial temperature	Final temperature	Heat leak	Pump energy	Energy for even temperature interval	$\Delta Z/\Delta t$
	g	°C	°C	*Int. j*	*Int. j*	*Int. j*	*Int. j/°C*
11–5–37	126.708	−0.0646	2.5102	−0.1	2.3	1,758.0	169.49
11–6–37	126.708	−.0401	2.5830	−.3	1.9	1,758.4	169.65
11–11–37	126.713	.0309	2.5359	−.1	1.9	1,758.5	169.67
11–12–37	126.713	.0045	2.5027	−.2	1.9	1,758.3	169.59
11–23–37	126.842	.0321	2.6038	.5	3.7	1,760.5	169.93
11–24–37	126.842	−.0182	2.5545	.8	5.4	1,759.8	169.65
11–30–37	126.842	.0069	2.5444	.2	3.5	1,758.8	169.25
11–30–37	126.842	.0896	2.3173	.6	2.5	1,760.3	169.85
Average							169.64

Even temperature interval 0.0° to 2.5° C. $\Delta\alpha/\Delta t$=4.21210 int. j/g-°C
Formulated value of $\Delta Z/\Delta t$=169.69 int. j/° C

11–5–37	126.708	2.5111	5.0085	0.0	1.9	1,756.2	169.77
11–6–37	126.708	2.5430	5.0009	−.2	1.9	1,757.3	170.21
11–11–37	126.713	2.5368	4.9962	−.2	1.9	1,757.1	170.11
11–12–37	126.713	2.5030	4.9980	−.2	1.9	1,756.8	169.99
11–23–37	126.842	2.6240	4.9988	.6	3.7	1,758.7	170.21
11–24–37	126.842	2.5754	5.0040	.5	2.5	1,757.4	169.69
11–30–37	126.842	2.3173	5.0053	−.2	2.5	1,758.3	170.05
Average							170.00

Even temperature interval 2.5° to 5.0° C. $\Delta\alpha/\Delta t$=4.20424 int. j/g-°C
Formulated value of $\Delta Z/\Delta t$=170.07 int. j/°C

574278 O - 61 - 21

TABLE 4.—*Principal data from small-mass heat-capacity experiments*—Continued

Date	Mass of water, M	Initial temperature	Final temperature	Heat leak	Pump energy	Energy for even temperature interval	$\Delta Z/\Delta t$
	g	°C	°C	*Int. j*	*Int. j*	*Int. j*	*Int. j*/°C
9-27-37	127.140	5.0941	9.5974	−0.3	5.0	3,519.3	170.47
9-28-37	127.140	5.0468	10.0059	.1	4.2	3,520.3	170.67
9-29-37	127.140	5.0469	10.0019	−.2	4.2	3,520.6	170.73
9-30-37	127.140	4.9889	10.0055	.0	4.2	3,520.0	170.61
10-1-37	127.140	5.0698	9.9952	−.2	4.2	3,519.3	170.47
11-5-37	126.708	5.0086	10.0132	−.2	2.9	3,510.6	170.55
11-6-37	126.708	5.0013	9.9995	−.3	2.9	3,511.9	170.81
11-11-37	126.713	4.9966	10.0060	−.5	2.9	3,511.4	170.68
11-12-37	126.713	4.9985	10.0012	−.4	2.9	3,511.3	170.66
11-24-37	126.842	5.0065	10.0022	.4	3.8	3,513.0	170.46
11-30-37	126.842	5.0053	10.0091	−.2	3.8	3,514.1	170.68
Average							170.61

Even temperature interval 5° to 10° C. $\Delta\alpha/\Delta t$=4.19527 int. j/g-°C
Formulated value of $\Delta Z/\Delta t$=170.69 int. j/°C

9-27-37	127.140	9.5974	15.0994	−0.3	4.5	3,520.3	171.75
9-28-37	127.140	10.0059	15.0066	−.3	4.2	3,519.0	171.49
9-29-37	127.140	10,0019	15.0031	−.1	4.2	3,519.1	171.51
9-30-37	127.140	10.0055	15.0155	−.4	4.2	3,518.9	171.47
10-1-37	127.140	9.9952	15.1422	.1	4.2	3,518.4	171.37
11-5-37	126.708	10.0132	15.0025	−.2	2.9	3,510.0	171.50
11-6-37	126.708	9.9995	15.0001	−.3	2.9	3,511.1	171.72
11-11-37	126.713	10.0131	14.9993	−.4	2.9	3,510.9	171.66
11-12-37	126.713	10.0012	15.0015	−.2	2.9	3,510.5	171.58
11-24-37	126.842	10.0022	15.0063	−.3	3.9	3,512.1	171.36
11-30-37	126.842	10.0091	15.0004	−.2	3.8	3,513.1	171.56
Average							171.54

Even temperature interval 10° to 15° C. $\Delta\alpha/\Delta t$=4.18678 int. j/g-°C
Formulated value of $\Delta Z/\Delta t$=171.59 int. j/°C

9-27-37	127.140	15.0994	20.0230	−0.4	4.3	3,521.2	172.64
9-28-37	127.140	15.0066	19.9974	−.3	4.3	3,520.6	172.52
9-29-37	127.140	15.0031	20.0028	−.2	4.3	3,521.0	172.60
9-30-37	127.140	15.0155	19.9961	−.3	4.3	3,520.7	172.54
10-1-37	127.140	15.1422	20.0015	−.1	4.2	3,519.3	172.26
11-5-37	126.708	15.0025	20.0054	−.3	3.0	3,512.0	172.61
11-6-37	126.708	15.0001	20.0011	−.3	3.0	3,512.7	172.75
11-11-37	126.713	14.9993	20.0015	−.4	3.0	3,512.7	172.73
11-12-37	126.713	15.0015	20.0013	−.2	3.0	3,512.4	172.67
11-24-37	126.842	15.0063	20.0075	−.1	3.8	3,514.1	172.47
11-30-37	126.842	15.0004	19.9991	−.3	3.8	3,514.4	172.53
Average							172.57

Even temperature interval 15° to 20° C. $\Delta\alpha/\Delta t$=4.18119 int. j/g-°C
Formulated value of $\Delta Z/\Delta t$=172.60 int. j/° C

9-27-37	127.140	20.0230	24.9939	−0.2	4.6	3,524.2	173.71
9-28-37	127.140	19.9974	24.9946	−.3	4.3	3,523.7	173.61
9-29-37	127.140	20.0028	24.9979	−.4	4.3	3,524.3	173.73
9-30-37	127.140	19.9961	24.9962	−.2	4.3	3,524.0	173.67
10-1-37	127.140	20.0015	25.0055	−.4	4.3	3,522.8	173.43
11-5-37	126.708	20.0054	25.0067	−.3	3.0	3,514.9	173.65
11-6-37	126.708	20.0011	24.9988	−.3	3.0	3,515.6	173.79
11-11-37	126.713	20.0015	24.9971	−.3	3.0	3,515.8	173.81
11-12-37	126.713	20.0013	24.9966	−.2	3.0	3,515.4	173.73
11-24-37	126.842	20.0075	25.0031	−.2	3.9	3,517.2	173.55
11-30-37	126.842	19.9991	24.9978	−.4	3.9	3,517.4	173.59
Average							173.66

Even temperature interval 20° to 25° C. $\Delta\alpha/\Delta t$=4.17753 int. j/g-°C
Formulated value of $\Delta Z/\Delta t$=173.74 int. j/°C

TABLE 4.—*Principal data from small-mass heat-capacity experiments*—Continued

Date	Mass of water, M	Initial temperature	Final temperature	Heat leak	Pump energy	Energy for even temperature interval	$\Delta Z/\Delta t$
	g	*°C*	*°C*	*Int. j*	*Int. j*	*Int. j*	*Int. j/°C*
9-27-37	127.140	24.9939	29.9932	−0.2	4.3	3,530.2	175.21
9-28-37	127.140	24.9946	29.9991	−.1	4.3	3,529.3	175.03
9-29-37	127.140	24.9979	29.9949	−.3	4.3	3,529.2	175.01
9-30-37	127.140	24.9962	29.9948	−.2	4.3	3,529.8	175.13
10-1-37	127.140	25.0058	30.0080	−.4	4.3	3,528.9	174.95
11-5-37	126.708	25.0067	30.0113	−.2	3.0	3,520.1	175.00
11-6-37	126.708	24.9988	29.9981	−.2	3.0	3,520.5	175.08
11-11-37	126.713	24.9971	29.9968	−.2	3.0	3,521.0	175.16
11-12-37	126.713	24.9966	29.9974	−.2	3.0	3,520.4	175.04
11-24-37	126.842	25.0031	30.0057	−.2	3.9	3,522.4	174.90
11-29-37	126.842	25.0033	29.9767	−.3	4.2	3,523.0	175.02
Average							175.05

Even temperature interval 25° to 30° C. $\Delta\alpha/\Delta t$=4.17513 int. j/g-°C
Formulated value of $\Delta Z/\Delta t$=175.02 int. j/°C

9-27-37	127.140	29.9932	39.9929	−0.5	7.3	7,078.8	177.32
9-28-37	127.140	29.9991	39.9917	−.1	7.3	7,078.1	177.25
9-29-37	127.140	29.9949	39.9848	−.4	7.3	7,079.1	177.35
9-30-37	127.140	29.9948	39.9923	−.6	7.3	7,078.4	177.27
10-1-37	127.140	30.0080	39.9991	−.9	7.3	7,078.1	177.25
11-5-37	126.708	30.0117	40.0274	−.2	5.2	7,059.9	177.23
11-8-37	126.708	29.9930	39.9952	−.1	5.2	7,059.2	177.16
11-11-37	126.713	29.9968	39.9884	−.5	5.2	7,061.5	177.37
11-12-37	126.713	29.9974	39.9950	−.3	5.2	7,059.7	177.19
11-24-37	126.842	30.0057	40.0131	−.3	6.6	7,064.5	177.13
11-29-37	126.842	29.9797	40.0490	−.7	6.6	7,065.1	177.19
Average							177.25

Even temperature interval 30° to 40° C. $\Delta\alpha/\Delta t$=4.17307 int. j/g-°C
Formulated value of $\Delta Z/\Delta t$=177.29 int. j/°C

9-27-37	127.140	39.9929	49.9881	−0.6	7.5	7,115.4	181.14
9-28-37	127.140	39.9917	50.0028	−.5	7.5	7,113.2	180.92
9-29-37	127.140	39.9848	50.0068	−.5	7.5	7,114.9	181.09
9-30-37	127.140	39.9923	50.0015	−.6	7.5	7,113.3	180.93
10-1-37	127.140	39.9991	50.0037	−.7	7.5	7,114.2	181.02
11-5-37	126.708	40.0274	50.0222	−.3	5.3	7,095.7	180.98
11-8-37	126.708	39.9952	49.9983	−.2	5.3	7,095.1	180.92
11-11-37	126.713	39.9967	49.9975	−.3	5.3	7,095.5	180.94
11-12-37	126.713	40.0046	50.0032	−.4	5.3	7,094.4	180.83
11-24-37	126.842	40.0231	50.0078	−.3	6.7	7,099.9	180.84
11-29-37	126.842	40.0490	50.0050	−.4	6.7	7,100.5	180.90
Average							180.96

Even temperature interval 40° to 50° C. $\Delta\alpha/\Delta t$=4.17171 int. j/g-°C
Formulated value of $\Delta Z/\Delta t$=180.99 int. j/°C

9-27-37	127.140	49.9881	59.9833	−0.7	7.6	7,160.4	185.71
9-28-37	127.140	50.0028	59.9990	−.8	7.6	7,159.4	185.61
9-29-37	127.140	50.0068	59.9980	−.3	7.6	7,159.9	185.66
9-30-37	127.140	50.0015	60.0036	.1	7.6	7,159.9	185.66
10-1-37	127.140	50.0037	60.0053	−.7	7.6	7,160.1	185.68
11-5-37	126.708	50.0222	60.0165	−.2	5.4	7,142.6	185.73
11-8-37	126.708	49.9983	59.9981	−.5	5.4	7,141.6	185.63
11-11-37	126.713	49.9975	59.9969	−.6	5.4	7,142.2	185.67
11-12-37	126.713	50.0032	59.9945	−.1	5.4	7,141.1	185.56
11-24-37	126.842	50.0225	60.0085	−.2	6.9	7,145.8	185.49
11-29-37	126.842	50.0050	60.0022	−.3	6.8	7,146.1	185.52
Average							185.63

Even temperature interval 50° to 60° C. $\Delta\alpha/\Delta t$=4.17124 int. j/g-°C
Formulated value of $\Delta Z/\Delta t$=185.66 int. j/°C

TABLE 4.—*Principal data for small-mass heat-capacity experiments*—Continued

Date	Mass of water, M	Initial temperature	Final temperature	Heat leak	Pump energy	Energy for even temperature interval	$\Delta Z/\Delta t$
	g	°C	°C	*Int. j*	*Int. j*	*Int. j*	*Int. j*/°C
9-27-37	127.140	59.9833	69.9959	−1.1	7.7	7,219.3	191.61
9-28-37	127.140	59.9990	69.9834	−1.0	7.7	7,218.1	191.49
9-29-37	127.140	59.9980	69.9870	−0.2	7.7	7,217.9	191.47
9-30-37	127.140	60.0036	70.0132	−0.2	8.0	7,217.0	191.38
10-1-37	127.140	60.0053	69.9886	−1.1	7.7	7,218.7	191.55
11-5-37	126.708	60.0165	70.0135	−0.3	5.6	7,200.8	191.57
11-8-37	126.708	59.9973	70.0845	−.3	5.6	7,199.2	191.41
11-12-37	126.713	59.9945	69.9967	−.4	5.6	7,200.0	191.47
11-24-37	126.842	60.0085	69.9908	−.4	7.0	7,204.5	191.38
11-29-37	126.842	60.0022	69.9523	−.4	7.0	7,204.8	191.41
Average							191.47
Even temperature interval 60° to 70° C. $\Delta\alpha/\Delta t$=4.17111 int. j/g-°C Formulated value at $\Delta Z/\Delta t$=191.52 int. j/°C							
9-27-37	127.140	69.9959	79.9973	−1.2	7.8	7,292.0	198.88
9-28-37	127.140	69.9834	80.0011	−.5	7.8	7,291.1	198.79
9-29-37	127.140	69.9870	80.0073	−.3	7.8	7,290.8	198.76
9-30-37	127.140	70.0132	80.0058	−.2	8.8	7,289.9	198.67
10-1-37	127.140	69.9886	80.0043	−.6	7.8	7,291.5	198.83
11-5-37	126.708	70.0135	80.0056	−.1	5.7	7,273.6	198.84
11-8-37	126.708	70.0845	79.9952	−.4	5.7	7,272.8	198.76
11-29-37	126.842	69.9523	79.9922	−.3	7.1	7,277.7	198.69
Average							198.78
Even temperature interval 70° to 80° C. $\Delta\alpha/\Delta t$=4.17114 int. j/g-°C Formulated value of $\Delta Z/\Delta t$=198.79 int. j/° C							
9-27-37	127.140	79.9973	89.9929	−0.5	8.0	7,381.9	207.86
9-28-37	127.140	80.0011	90.0146	−.2	8.6	7,379.7	207.64
9-29-37	127.140	80.0073	90.0104	−.5	8.0	7,381.1	207.78
9-30-37	127.140	80.0058	90.0117	−.8	8.3	7,379.7	207.64
10-1-37	127.140	80.0043	89.9998	−.6	8.0	7,381.5	207.82
11-5-37	126.708	80.0056	89.9972	−.3	5.8	7,363.4	207.81
11-8-37	126.708	79.9952	90.0004	−.7	5.8	7,363.2	207.79
11-29-37	126.842	79.9922	90.0033	−.3	7.2	7,367.7	207.68
Average							207.75
Even temperature interval 80° to 90° C. $\Delta\alpha/\Delta t$=4.17124 int. j/g-°C Formulated value of $\Delta Z/\Delta t$=207.74 int. j/° C							
9-27-37	127.140	89.9929	99.9985	−0.7	8.1	7,489.8	218.63
9-28-37	127.140	90.0146	100.0007	.2	8.7	7,488.9	218.54
9-29-37	127.140	90.0104	99.9982	−.1	8.7	7,489.5	218.60
9-30-37	127.140	90.0117	99.9885	−.4	8.4	7,488.2	218.47
10-1-37	127.140	89.9998	99.9970	−.6	8.1	7,489.9	218.64
11-5-37	126.708	89.9972	99.9959	−.6	5.9	7,471.8	218.63
11-8-37	126.708	90.0004	100.0010	−.9	6.7	7,472.6	218.71
11-29-37	126.842	90.0170	100.0005	−.4	7.3	7,476.0	218.50
Average							218.59
Even temperature interval 90° to 100° C. $\Delta\alpha/\Delta t$=4.17137 int. j/g-°C Formulated value of $\Delta Z/\Delta t$=218.61 int. j/°C							

TABLE 5.—*Calculation of specific heat at 1-atmosphere pressure*

Temperature interval	$\Delta\alpha/\Delta t$, measured	Reductions to give C_p at 1 atmosphere			C_p, experimental	C_p, formulated	Deviation exp.—form.	Mid-temperature of interval
		$\frac{\Delta H}{\Delta t}-\frac{\Delta \alpha}{\Delta t}$	$\left(\frac{\Delta H}{\Delta t}\right)_{p=1}-\left(\frac{\Delta H}{\Delta t}\right)_{sat}$	$C_{p=1}-\left(\frac{\Delta H}{\Delta t}\right)_{p=1}$				
1	2	3	4	5	6	7	8	9
°C	*Int. j/g-°C*	*Int. j/g-°C*	*Int. j/g-°C*	*Int. j/g-°C*	*Int. j/g-°C*	*Int. j/g-°C*	*Int. j/g-°C*	°C
0 to 1	4.21411	0.00085	−0.00054	−0.00001	4.21441	4.21508	−0.00067	0.5
0 to 2.5	4.21267	.00089	−.00052	−.00008	4.21296	4.21242	.00054	1.25
1 to 2	4.21087	.00090	−.00051	−.00001	4.21125	4.21158	−.00033	1.5
0 to 5	4.20811	.00096	−.00051	−.00027	4.20829	4.20837	−.00008	2.5
2 to 3	4.20764	.00096	−.00051	−.00001	4.20808	4.20837	−.00029	2.5
3 to 4	4.20533	.00101	−.00050	−.00001	4.20583	4.20542	.00041	3.5
2.5 to 5.0	4.20385	.00103	−.00050	−.00006	4.20432	4.20472	−.00040	3.75
4 to 5	4.20219	.00107	−.00050	−.00001	4.20275	4.20272	.00003	4.5
5 to 10	4.19530	.00127	−.00047	−.00018	4.19592	4.19588	.00004	7.5
10 to 15	4.18668	.00167	−.00045	−.00012	4.18778	4.18784	−.00006	12.5
15 to 20	4.18130	.00217	−.00045	−.00008	4.18294	4.18280	.00014	17.5
20 to 25	4.17728	.00279	−.00045	−.00006	4.17956	4.17977	−.00021	22.5
25 to 30	4.17538	.00354	−.00047	−.00004	4.17840	4.17814	.00026	27.5
30 to 40	4.17302	.00500	−.00053	−.00010	4.17739	4.17744	−.00005	35
40 to 50	4.17165	.00761	−.00065	−.00007	4.17854	4.17866	−.00012	45
50 to 60	4.17132	.01122	−.00084	−.00006	4.18164	4.18161	.00003	55
60 to 70	4.17124	.01606	−.00110	−.00006	4.18614	4.18604	.00010	65
70 to 80	4.17105	.02239	−.00144	−.00007	4.19193	4.19200	−.00007	75
80 to 90	4.17129	.03049	−.00188	−.00008	4.19982	4.19972	.00010	85
90 to 100	4.17126	.04063	−.00241	−.00010	4.20939	4.20947	−.00008	95

TABLE 6.—*Heat capacity of air-free water at 1 atmosphere pressure*

Temperature	C_p	Enthalpy, H_p		Temperature	C_p	Enthalpy, H_p	
°C	Abs. j/g-°C	Abs. j/g	IT Cal/g	°C	Abs. j/g-°C	Abs. j/g	IT Cal/g
0	4. 2177	0. 1026	0. 0245	50	4. 1807	209. 3729	50. 0079
1	4. 2141	4. 3184	1. 0314	51	4. 1810	213. 5538	51. 0065
2	4. 2107	8. 5308	2. 0376	52	4. 1814	217. 7350	52. 0051
3	4. 2077	12. 7400	3. 0429	53	4. 1817	221. 9166	53. 0039
4	4. 2048	16. 9462	4. 0475	54	4. 1820	226. 0984	54. 0027
5	4. 2022	21. 1498	5. 0515	55	4. 1824	230. 2806	55. 0016
6	4. 1999	25. 3508	6. 0549	56	4. 1828	234. 4632	56. 0006
7	4. 1977	29. 5496	7. 0578	57	4. 1832	238. 6462	56. 9997
8	4. 1957	33. 7463	8. 0602	58	4. 1836	242. 8296	57. 9989
9	4. 1939	37. 9410	9. 0621	59	4. 1840	247. 0134	58. 9982
10	4. 1922	42. 1341	10. 0636	60	4. 1844	251. 1976	59. 9975
11	4. 1907	46. 3255	11. 0647	61	4. 1849	255. 3822	60. 9970
12	4. 1893	50. 5155	12. 0654	62	4. 1853	259. 5673	61. 9966
13	4. 1880	54. 7041	13. 0659	63	4. 1858	263. 7529	62. 9963
14	4. 1869	58. 8916	14. 0660	64	4. 1863	267. 9390	63. 9962
15	4. 1858	63. 0779	15. 0659	65	4. 1868	272. 1256	64. 9961
16	4. 1849	67. 2632	16. 0655	66	4. 1874	276. 3127	65. 9962
17	4. 1840	71. 4476	17. 0650	67	4. 1879	280. 5003	66. 9964
18	4. 1832	75. 6312	18. 0642	68	4. 1885	284. 6885	67. 9967
19	4. 1825	79. 8141	19. 0633	69	4. 1890	288. 8772	68. 9972
20	4. 1819	83. 9963	20. 0622	70	4. 1896	293. 0665	69. 9977
21	4. 1813	88. 1778	21. 0609	71	4. 1902	297. 2564	70. 9985
22	4. 1808	92. 3589	22. 0596	72	4. 1908	301. 4469	71. 9994
23	4. 1804	96. 5395	23. 0581	73	4. 1915	305. 6381	73. 0004
24	4. 1800	100. 7196	24. 0565	74	4. 1921	309. 8299	74. 0016
25	4. 1796	104. 8994	25. 0548	75	4. 1928	314. 0224	75. 0030
26	4. 1793	109. 0788	26. 0530	76	4. 1935	318. 2155	76. 0045
27	4. 1790	113. 2580	27. 0512	77	4. 1942	322. 4094	77. 0062
28	4. 1788	117. 4369	28. 0493	78	4. 1949	326. 6039	78. 0080
29	4. 1786	121. 6157	29. 0474	79	4. 1957	330. 7992	79. 0101
30	4. 1785	125. 7943	30. 0455	80	4. 1964	334. 9952	80. 0123
31	4. 1784	129. 9727	31. 0435	81	4. 1972	339. 1920	81. 0147
32	4. 1783	134. 1510	32. 0414	82	4. 1980	343. 3897	82. 0172
33	4. 1783	138. 3293	33. 0394	83	4. 1988	347. 5881	83. 0200
34	4. 1782	142. 5076	34. 0374	84	4. 1997	351. 7873	84. 0230
35	4. 1782	146. 6858	35. 0353	85	4. 2005	355. 9874	85. 0262
36	4. 1783	150. 8641	36. 0333	86	4. 2014	360. 1883	86. 0295
37	4. 1783	155. 0423	37. 0312	87	4. 2023	364. 3902	87. 0331
38	4. 1784	159. 2207	38. 0292	88	4. 2032	368. 5929	88. 0369
39	4. 1785	163. 3991	39. 0272	89	4. 2042	372. 7966	89. 0410
40	4. 1786	167. 5777	40. 0253	90	4. 2051	377. 0012	90. 0452
41	4. 1787	171. 7563	41. 0233	91	4. 2061	381. 2068	91. 0497
42	4. 1789	175. 9351	42. 0214	92	4. 2071	385. 4135	92. 0545
43	4. 1791	180. 1141	43. 0195	93	4. 2081	389. 6211	93. 0594
44	4. 1792	184. 2933	44. 0177	94	4. 2092	393. 8297	94. 0647
45	4. 1795	188. 4726	45. 0159	95	4. 2103	398. 0395	95. 0701
46	4. 1797	192. 6522	46. 0142	96	4. 2114	402. 2503	96. 0759
47	4. 1799	196. 8320	47. 0125	97	4. 2125	406. 4622	97. 0819
48	4. 1802	201. 0120	48. 0109	98	4. 2136	410. 6753	98. 0882
49	4. 1804	205. 1923	49. 0094	99	4. 2148	414. 8895	99. 0947
				100	4. 2160	419. 1049	100. 1015

TABLE 7.—*Enthalpy of saturated liquid water*

Temperature	$\alpha]_0^t$	β	Enthalpy		
°C	*Int. j/g*	*Int. j/g*	*Int. j/g*	*Abs. j/g*	*IT Cal/g*
0	0. 0000	0. 0121	0. 0000	0. 0000	0. 0000
5	21. 0408	. 0169	21. 0456	21. 0496	5. 0276
10	42. 0172	. 0233	42. 0283	42. 0363	10. 0402
15	62. 9511	. 0316	62. 9706	62. 9826	15. 0431
20	83. 8571	. 0425	83. 8875	83. 9034	20. 0400
25	104. 7447	. 0564	104. 7890	104. 8089	25. 0332
30	125. 6204	. 0741	125. 6824	125. 7063	30. 0244
35	146. 4883	. 0963	146. 5725	146. 6003	35. 0149
40	167. 3511	. 1241	167. 4631	167. 4949	40. 0055
45	188. 2108	. 1583	188. 3570	188. 3928	44. 9968
50	209. 0685	. 2002	209. 2566	209. 2964	49. 9896
55	229. 9251	. 2510	230. 1640	230. 2077	54. 9842
60	250. 7810	. 3123	251. 0812	251. 1289	59. 9811
65	271. 6366	. 3858	272. 0102	272. 0619	64. 9808
70	292. 4921	. 4730	292. 9530	293. 0087	69. 9839
75	313. 3477	. 5760	313. 9116	313. 9712	74. 9907
80	334. 2035	. 6970	334. 8883	334. 9519	80. 0019
85	355. 0596	. 8381	355. 8856	355. 9532	85. 0180
90	375. 9159	1. 0019	376. 9057	376. 9773	90. 0395
95	396. 7726	1. 1909	397. 9514	398. 0270	95. 0671
100	417. 6296	1. 4082	419. 0257	419. 1053	100. 1016

V. REVIEW OF EARLIER WORK AND COMPARISONS

It is of interest to present a résumé of comparisons between the present results and the earlier results, but unfortunately, it seems impossible to make all such comparisons on the basis of definite evaluation. As mentioned above, so many uncertain factors regarding units, standards, and experimental technique have been involved in some of the earlier work that the results of much of the pioneer research is difficult to interpret and appraise in terms of present standards. In spite of the care with which these various determinations were made, the diversity of results indicates that in some of the work, the uncertainties were greater than supposed.

Since the present determinations have been made by use of the present standards of electromotive force and electric resistance, they yield values for the heat capacity of water in international electric-energy units. They are comparable, in kind, to two types of previous measurements, those in which the variation of specific heat with temperature has been observed, and those in which the heat capacity of water has been measured, either in mechanical or electrical units of energy.

Comparisons of the determinations of the variation of specific heat may be made, independently of the absolute value of the energy units. These comparisons may easily be made by arbitrarily choosing a temperature at which the observed specific heat is taken as unity. Differences in temperature scales used and such calorimetric errors as heat leaks, however, would affect the accord.

For the evaluation of the heat capacity or specific heat of water in the fundamental or absolute units of energy, the choice of values for

the relations between units and standards of different periods is involved, particularly for measurements made by the method of electric heating. The data available for this purpose are not adequate to yield satisfactory appraisals of all the experimental data. The opinions of some who have studied this matter are interesting.

For example, in the discussion of T. H. Laby's [13] critical review paper on the mechanical equivalent of heat, several physicists have given their views. F. E. Smith said that he "had little faith in the values of physical constants obtained by applying corrections long after the date of the observations." G. M. Clark said "I doubt whether much is gained by discussing the results of other observers by making known corrections that arise through the light of later knowledge * * * the halo of nebulosity surrounding any physical determination is probably greater than the original experimenter cared to acknowledge to himself. I am also of the opinion that the only person who can revise any old determination is the person who made it." Ezer Griffiths said "I view with misgivings attempts to correct old work unless made by the investigators themselves, as they alone are acquainted with all the facts concerning the apparatus." E. H. Griffiths said "I confess that it appears to me that it is the final and not the earlier conclusions of an author which should be quoted." In this very frank discussion, several authors gave reappraisals of their earlier numerical values, which are most helpful to reviewers.

In comparing various appraisals made in the past, much can be found to support these views. It seems, however, that part of the discord which has baffled reviewers may be removed by use of more complete correction data, without too ruthless rejection of early experimental work.

In accord with the above warnings of caution, the present authors propose to accept at their face values the experimenters' own reappraisals, where available. In view of the impossibility of precise interpretation and reduction to present standards of much of the earlier work, and since this service has been already so thoroughly performed by previous reviewers, a complete review will not be undertaken here. Instead, only a few of the determinations which have been cited in the past as important or authoritative have been selected for examination and correlation to indicate the extent of corroboration. In order to coordinate them for intercomparison, some reductions have been made by using equivalents or ratios which are based on more complete experimental evidence than those used in former reviews. These data will be examined in two respects, the first by considering the experimental data yielding values for the mechanical equivalent of heat, each in terms of some definite heat unit, and second, by considering data on the change of specific heat with temperature.

James Prescott Joule

Joule [14] appears to have been the first to undertake systematic measurements of the mechanical equivalent. In 1850, from experiments by a number of methods, he chose a value of 772 foot-pounds per heat unit. Later, in 1878, by water friction in a calorimeter, he obtained the value 772.6 foot-pounds per 62° F heat unit. Because these experiments belong to an early period in the development of standards of physical measurements, it is impossible to evaluate the results in terms of present standards, but their pioneer nature and

classical refinement set them apart as exempt from any purely numerical appraisal of their relative accuracy. Tribute to Joule's work is perpetuated by the use of his name to designate the unit of work.

Henry A. Rowland

Rowland [15] followed Joule by making a series of elaborate experiments similar in principle to Joule's, but with greater care and refinements in some respects. Although the thermometry of that time was less precise than later, Rowland's measurements were made and recorded so carefully that they could be revised later when the thermometers that he used had been compared with better-known standards. William S. Day [16], with Rowland's permission and advice, compared Rowland's thermometers with the Paris Standard (international hydrogen scale) and made a revision of the results 20 years after the original work.

At the conclusion of his paper, Rowland says "Between the limits of 15° and 25° C, I feel almost certain that no subsequent experiments will change my values of the equivalent so much as 2 parts in 1,000, and even outside those limits, say between 10° and 30°, I doubt whether the figures will ever be changed much more than that amount." This concluding estimate seems to have been conservative.

Table 8 gives the values reported by Rowland and the values corrected by Day at five temperatures from 10° to 30° C. It also gives the NBS values reduced to the same temperature intervals and rounded to the same number of figures. The last two columns give the deviations of Rowland's original and Day's revision from the NBS. Rowland's smoothed results differ most from the NBS at the ends of the range from 10° to 30° C, and there, by less than his estimated 2 parts in 1,000.

TABLE 8.—*Comparison of specific heat values of Rowland with NBS values*

Temperature	Rowland, 1879	Day's revision, 1898	NBS 1939	Rowland minus NBS	Day's revision minus NBS
°C	*j/g-°C*	*j/g-°C*	*j/g-°C*	*j/g-°C*	*j/g-°C*
10	4.200	4.196	4.192	0.008	0.004
15	4.189	4.188	4.186	.003	.002
20	4.179	4.181	4.182	−.003	−.001
25	4.173	4.176	4.180	−.007	−.004
30	4.171	4.174	4.179	−.008	−.005
Average				−0.0016	−0.0010

Rowland's values are greater than the NBS values in the lower part of this range and less in the upper part. It seems probable that these departures can be explained by the correction he applied for heat leak, or "radiation," as he called it. This correction amounted to over 2 percent of the energy input when the temperature of the calorimeter differed from that of the jacket by 10° C. He determined the "coefficients of radiation" by measurement, but in discussing them he says "the circumstances in the experiments are not the same as when the radiation was obtained." These circumstances, he states, "tend to give *too small* [italics Rowland's] coefficients of radiation, and this is confirmed by looking over the final tables." He, however, did not feel at liberty to make corrections on this

basis. Had these coefficients been greater by nearly 4 percent, it would have accounted for the difference in slope of Rowland's curve from that of the NBS, as will be seen by referring to table 8. At 20° C, which is the midtemperature of the range in which Rowland estimated his greatest precision, Rowland's revised value is less than the NBS value by about 1 part in 4,000. At 15° C, which was about the average jacket temperature, and where the heat leak would have been zero, Rowland's revised value is greater than the NBS value by 1 part in 2,000.

It is possible that his remarkable accord with recent determinations is accidental, but it appears more likely to be due to the thoroughness with which he is known to have worked.

Reynolds and Moorby

These workers [17] determined the mechanical equivalent of heat by means of a hydraulic brake driven by a steam engine. The measurements were carried out on an engineering scale, the power input being in some experiments as large as 65 hp. This feature has sometimes been considered an advantage as compared with lesser proportions. The heat developed was used to raise the temperature of water over a range of nearly 100° C. These distinctions give these measurements an importance for purposes of comparison.

It must be recognized that in some other respects, the apparatus and technique were less refined than in the case of some of the other determinations. Although the work is described at great length, it is difficult to ascertain all details which would aid in correlating the numerical result with others. This is the case with the record of the initial and final temperatures and pressures of the water which absorbed the energy input as sensible heat. It seems that for the final value of 4.1832 abs. j/g-°C, the approximate range of state was from a temperature of 1.3° C and a pressure of 1.53 atmospheres, to a final temperature of 100° C and a pressure of 1.43 atmospheres. The change in enthalpy for this change of state may be computed from the NBS data as follows:

Enthalpy at 1.3° C, pressure 1 atm	5. 583 abs. j/g.
Change for 0.53 atm	0. 054 abs. j/g.
Enthalpy at 1.3° C, pressure 1.53 atm	5. 637 abs. j/g.
Enthalpy at 100° C, pressure 1 atm	419. 105 abs. j/g.
Correction for 0.43 atm	0. 033 abs. j/g.
Enthalpy at 100° C, pressure 1.43 atm	419. 138 abs. j/g.
Change in enthalpy 1.3° C, 1.53 atm, to 100° C and 1.43 atm	413. 501 abs. j/g.
Change per degree by NBS value	4. 1895 abs. j/g-°C.
Reynolds and Moorby's value	4. 1832 abs. j/g-°C.
R. and M.–NBS	0. 0063 abs. j/g-°C (or 1 part in 660)

The accord of this result with the NBS result is inferior to the accord of Rowland's result after Day's revision for temperature scale. Inasmuch as the means of protection from heat leak in Reynolds and Moorby's work were less complete and the range of temperature considerably greater, it is very probable that this may account in part for the greater discrepancy. Although this extensive research suffers by comparison with modern technique, the approximate confirmation of smaller scale laboratory measurements has served for many years as a classical contribution to engineering data.

Laby and Hercus

They [18] determined the mechanical equivalent of heat by direct mechanical measurements using an induction dynamometer and the method of continuous-flow calorimetry. The ingenuity of design and refinements of technique justify their aim at "the highest precision attainable with the present developments of physical technique."

There have been two serious criticisms of Laby and Hercus' work. Birge [19] has proposed a reevaluation of their result by disregarding the experiments near 20° C on account of their large residual. In a later paper, Laby and Hercus [20] have noted this criticism and have accepted the proposal. Jessel [21] has reported finding differences in the specific heat of air-free water and air-saturated water and has questioned Laby and Hercus' result on the score that air-free water was not used. In replying to this criticism, Laby and Hercus [20] deny the validity of Jessel's conclusions in their own case and show by computation that the effect is negligible. As a reappraisal in 1935 of the final result of their measurements, Laby and Hercus give for the mechanical equivalent for both deaerated and aerated water, the value of 4.1852×10^7 ergs/15° cal, which may be taken as their appraisal of their results for purposes of comparison. The present NBS measurements give the value of 4.1858 j (abs.)/g-°C for C_p at 15° C and 1 atmosphere, which agrees within 1 part in 7,000 with Laby and Hercus' value.

Callendar and Barnes

Their work [22] on the measurement of the heat capacity of water between 5° and 95° C by the continuous electric-calorimetric method is without doubt more pretentious and comprehensive than any of the other researches on this property of water. The results which were obtained from measurements made by Barnes in 1899 and 1900 in terms of the electrical standards of that period have since been the subject of numerous reviews [13, 22, 23, 24, 25], mostly with the object of deriving better appraisals of the value of the mechanical equivalent of heat by applying corrections to bring them into accord with known standards. The diversity of these reappraisals emphasizes the difficulty and uncertainty involved. Even Callendar, who cooperated in the design and preparation of the apparatus, and Barnes, who carried out the experimental part of the program, differed in their opinions of the validity of the accounting for heat leak. It seems that for the purpose of comparisons, the best course is to take the authors' own latest estimates. These along with others are given in table 9.

In 1909 Barnes [22] revised his original figures of 1902 by applying corrections for the value of the standard cells. Callendar [26] reviewed previous experiments on the variation of specific heat of water, described experiments by a new method, and derived a formula for specific heat. It is somewhat difficult to differentiate Callendar's interpretations of these several elements, and, for purposes of comparison, it seems best to take his tabulated figures, referred to the value at 20° C as unity. Callendar later, in 1925 [13], in a discussion of T. H. Laby's paper on the Mechanical Equivalent of Heat, has given a reappraisal of the value at 20° C from the Callendar and Barnes' experiments as 4.178 abs. j/g-°C. This value is practically the same as the value 4.1785 given by Barnes in 1909. Laby's

appraisal of Callendar and Barnes' value made at the same time is 4.1795 at 20° C. The NBS value for 20° C at present is 4.1819, which is about 1 part in 1,200 greater than Barnes' figure. Barnes' estimated values of the specific heats at other temperatures deviate from the NBS values by as much as 1 in 500, while Callendar's estimate is for the most part within 1 part in 1,000 of the NBS value. Barnes' mean value between 5° and 95° C of 4.1835 is about 1 part in 1,000 less than the corresponding mean value of 4.1877 from the NBS measurements.

TABLE 9.—*Comparison of specific heat value of Callendar and Barnes with NBS value*

Temperature	Barnes original 1902	Barnes revised 1909	Callendar revised 1925	Laby's revision of Callendar and Barnes 1925	Callendar 1912	Barnes 1909	NBS 1939
°C	*Abs.j/g-°C*	*Abs.j/g-°C*	*Abs.j/g-°C*	*Abs.j/g-°C*	*cal₂₀/g-°C*	*cal₂₀/g-°C*	*cal₂₀/g-°C*
0							1.00857
5	4.2105	4.2052			1.00596	1.00639	1.00487
10	4.1979	4.1926			1.00310	1.00337	1.00247
15	4.1895	4.1842			1.00122	1.00136	1.00094
20	4.1838	4.1785	4.178	4.1795	1.00000	1.00000	1.00000
25	4.1801	4.1748			0.99922	0.99911	0.99946
30	4.1780	4.1727			.99877	.99861	.99919
35	4.1773	4.1720			.99856	.99844	.99913
40	4.1773	4.1720			.99856	.99844	.99921
45	4.1782	4.1729			.99871	.99866	.99942
50	4.1798	4.1745			.99901	.99904	.99973
55	4.1819	4.1766			.99942	.99955	1.00013
60	4.1845	4.1792			.99994	1.00017	1.00061
65	4.1870	4.1817			1.00055	1.00077	1.00119
70	4.1898	4.1845			1.00125	1.00144	1.00185
75	4.1925	4.1872			1.00201	1.00208	1.00261
80	4.1954	4.1901			1.00288	1.00278	1.00348
85	4.1982	4.1929			1.00380	1.00345	1.00446
90	4.2010	4.1957			1.00479	1.00412	1.00556
95	4.2038	4.1985			1.00583	1.00479	1.00679
Mean		4.1835					
100							1.00817

Although it is difficult to explain this degree of discord, it seems possible that inaccurate accounting for heat leak may have been responsible for much of the difference. It is difficult to believe that Barnes' estimate in 1909 that the error of the measurements in any part of the range did not exceed 1 part in 10,000, or Callendar's estimate of 1 part in 4,000 for the absolute value of the mechanical equivalent, took into account all the possibilities for deviations from the true values.

Jaeger and von Steinwehr

Their measurements [27] were made at the Physikalisch-Technische Reichsanstalt in 1921, by the electric-heating method, and extending over the range from 5° to 50° C, are free from some of the uncertainties of units and standards which affect much of the earlier work. There is very little doubt that the temperature scale and the electrical standards used were substantially the same as those now in use as international standards. The numerical values as given originally may therefore be taken to represent the experimental data between 5° and 50° C smoothed by an empirical formula of the second degree.

These values are given in table 10 with corresponding NBS values for comparison.

Henning and Jaeger [28] quote the value of 4.1842 int. j/g °C for the heat capacity of water at 15° C., estimating the accuracy as about 2 parts in 10,000. The PTR formula accords with the NBS value at this temperature to this estimated accuracy but, elsewhere, the deviations are larger.

It is of interest to examine the individual experimental results to see to what extent this peculiarity may be the result of the type of formula used. It is a well-known fact that formulas of the power series type often show a pronounced tendency to deviate near the ends of an experimental range, even though fitted to the data by least-squares adjustment.

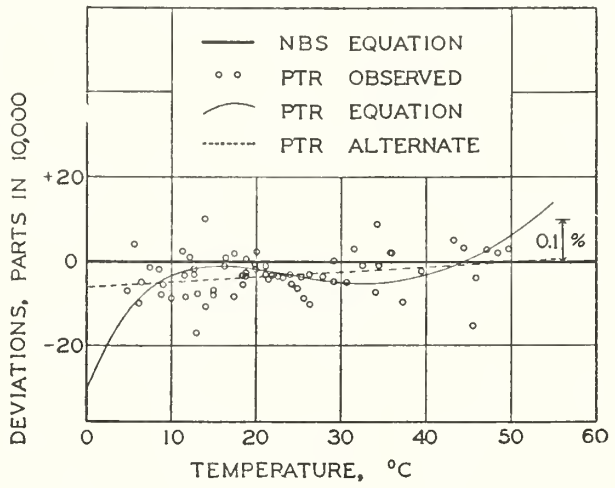

FIGURE 6.—*Deviations of PTR from NBS values of C_p.*

In figure 6 the deviation of the PTR formula from the NBS formula is shown by the smooth curved line. The deviations of the PTR (observed-minus-calculated) values as given by Jaeger and von Steinwehr in their table 11 are shown by the points designated as "PTR obs." The dotted line designated as "PTR Alternate" represents a re-formulation of the PTR data in the light of the present work. This was found by fitting a linear equation to the deviations of the PTR data from the NBS equation, and therefore this alternate interpretation of the PTR results differs from the NBS formulation of C_p only by addition of a correction equal to $[-0.00256+0.0000486t]$. This alternate formulation accords with the observed values slightly better than the PTR equation does, and is of a type which is consistent with experimental data outside their range of temperature. The greater spread of the PTR data is to be expected from the smaller temperature intervals used which were only about 1.4° C, and the general accord may be considered as satisfactory.

TABLE 10.—*Comparison of specific heat values of Jaeger and von Steinwehr with NBS value*

Temperature	Jaeger and von Steinwehr	Jaeger and von Steinwehr alternate	NBS 1939	Temperature	Jaeger and von Steinwehr	Jaeger and von Steinwehr alternate	NBS 1939
°C	*Int. j/g-°C*	*Int. j/g-°C*	*Int. j/g-°C*	*°C*	*Int. j/g-°C*	*Int. j/g-°C*	*Int. j/g-°C*
5	4.1966	4.1991	4.2014	30	4.1755	4.1766	4.1777
10	4.1897	4.1893	4.1914	35	4.1753	4.1765	4.1774
15	4.1842	4.1832	4.1850	40	4.1764	4.1772	4.1778
20	4.1800	4.1795	4.1811	45	4.1788	4.1783	4.1787
25	4.1771	4.1775	4.1788	50	4.1825	4.1798	4.1799

National Bureau of Standards

The earlier measurements of the enthalpy of saturated water made in this laboratory and published in 1930 [2] furnish data from which values of specific heat of water at 1 atmosphere in the range 0° to 100° C may be derived. These measurements were not intended primarily for determining the specific heat, having been made to furnish data for enthalpy of water and steam for compiling steam tables, and values of the specific heat were not published. Beside other limitations on the accuracy of the NBS 1930 data, the larger temperature intervals then used gave less convincing evidence of the trend of specific heat in the lower range of temperature where the change is most rapid.

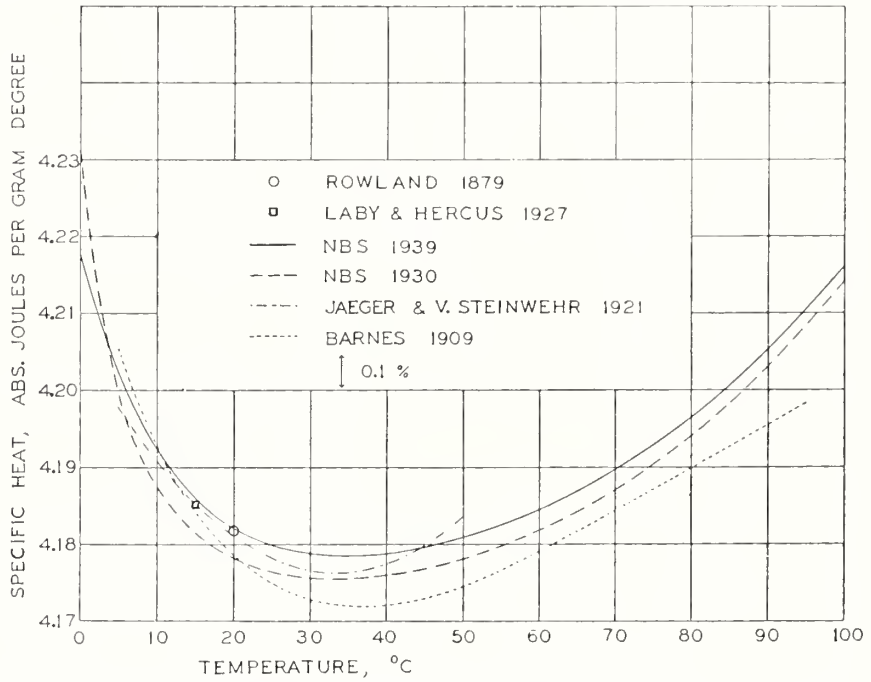

FIGURE 7.—*Comparison of values of C_p.*

Nevertheless, these results have been taken as a basis for values of heat capacity of water used in measurements of enthalpy of superheated steam by several of the laboratories cooperating in the international steam research project. It is therefore of interest to note the difference between the old and the new results, expressed as specific heat. For the purpose of intercomparison, the values of C_p at 1-atmosphere pressure have now been computed from the formulated results of the 1930 report as represented by the following formula given for alpha in the range 0° to 170° C:

$$\alpha = 1.240777 \log_{10}\left(\frac{t+7}{7}\right) + 415.2412\left(\frac{t}{100}\right) + 0.6912\left(\frac{t}{100}\right)^2 - 0.044874\left(\frac{t}{100}\right)^4$$

This computation of C_p was made in a manner similar to those for the present new results as previously described in this report, using the same value for β and $[H_t]^{1\ \text{atm}}_{\text{sat.}}$ The values of C_p thus derived are given in table 11 and are designated as $C_{p\ (\text{NBS 1930})}$, together with the 1939 NBS values.

Comparative values of specific heat in absolute joules from the determinations just reviewed are shown graphically in figure 7.

TABLE 11.—*Comparison of specific-heat values of NBS 1930 with NBS 1939 values*

Temperature	C_p NBS 1930	C_p NBS 1939	Temperature	C_p NBS 1930	C_p NBS 1939
°C	*Int. j/g-°C*	*Int. j/g-°C*	°C	*Int. j/g-°C*	*Int. j/g-°C*
0	4.2297	4.2169	50	4.1771	4.1799
5	4.1986	4.2014	55	4.1787	4.1816
10	4.1865	4.1914	60	4.1808	4.1836
15	4.1804	4.1850	65	4.1833	4.1860
20	4.1771	4.1811	70	4.1861	4.1888
25	4.1753	4.1788	75	4.1894	4.1920
30	4.1746	4.1777	80	4.1932	4.1956
35	4.1745	4.1774	85	4.1974	4.1997
40	4.1749	4.1778	90	4.2022	4.2043
45	4.1758	4.1787	95	4.2075	4.2095
			100	4.2134	4.2152

As a summary of the review and comparisons just made, it is found that the results of Rowland, Laby and Hercus, and Jaeger and von Steinwehr for the mechanical or electrical equivalent of the heat capacity of water in the range 15° to 20° C, are corroborated by the results of the present investigation, and are in accord with a value of 1.00019 for the ratio of the international volt-ampere to the absolute, or mechanical watt. It is further found that the results of Jaeger and von Steinwehr throughout their experimental range, 5° to 50° C, are in satisfactory accord with the present NBS results. It has not been found possible to reconcile the discord between the results of Callendar and Barnes and the present NBS results. The likelihood that uncertainty in heat-leak accounting may have been the cause of unsuspected error is suggested. The close control of this factor in the present work may be considered in a choice of definitive values without detracting from esteem of the earlier work.

The values of specific heat derived from the earlier (1930) determinations of the NBS are less trustworthy than the new results and are not considered by the authors as entitled to inclusion in any new appraisal of values of specific heat in the range 0° to 100° C.

Part 3. Heat of Vaporization of Water in the Range 0° to 100° C

I. INTRODUCTION

The heat of vaporization of water is not only a large part of the enthalpy, or heat content, of steam, but it is also one of the terms in the Clapeyron equation by which saturation specific volumes are correlated with saturation vapor pressure. Hence, independent values of this property are important data in the compilation of tables of the properties of steam.

The existing data from direct measurements in the range 0° to 100° C by different experimenters lacked the accord desired in standard steam tables. In the range 0° to 50° C, the deviations of these values from the international skeleton table were as much as 0.2 percent. Since the skeleton table was based on appraisal of the whole ensemble of available data, which in this region were relatively scanty, it was desired to obtain a more positive verification by a systematic redetermination of the heat of vaporization.

This was undertaken in connection with the redetermination of the heat capacity of liquid water from 0° to 100° C, and in the construc-

tion of the calorimeter, as described in part 1, provision was made for measurements of heat of vaporization. Without sacrifice of the aim of high precision in the heat-capacity measurements, it was possible to include features adapting the apparatus to accurate vaporization measurements over the range 0° to 100° C.

II. METHOD AND APPARATUS

Since the method and apparatus have been described in part 1, only a brief resumé is given here of the general scheme of measurement before describing the experimental procedure in detail.

The calorimeter, consisting of a metal shell, protected from unmeasured heat leak by a controlled insulating envelope, contained a sample of air-free water, both liquid and vapor. The liquid was vigorously circulated through an electric heater by an immersed pump.

In the vaporization experiments the measured heat was supplied electrically to evaporate liquid, while vapor was withdrawn at a rate which was controlled manually to keep a constant temperature of evaporation. The energy added per unit mass removed as vapor, designated as gamma, γ, exceeds the latent heat of vaporization, L, by the quantity beta, β. That is, according to the theory [1]

$$\gamma = L + \beta$$

where

$$\beta = T\, u \frac{dP}{dT}.$$

The values of β used in deriving values of L from the observed values of γ were calculated from known values of the vapor-pressure derivative, dP/dT, and of u, the specific volume of the liquid. This reduction term is very small at low pressures, and at 100° C amounts to only 1/1600 of γ.

III. EXPERIMENTAL PROCEDURE

1. ACCOUNTING FOR MASS, ENERGY, AND CHANGE IN STATE OF THE WATER SAMPLE

The accounting for the mass, energy, and change in state of the water sample in the vaporization experiments was for the most part the same as in the heat-capacity experiments. The few differences will be pointed out briefly here.

The amount of water evaporated and collected by condensation in an average experiment was about 20 g. To make the weighings with suitable precision, the glass containers holding the condensed water samples were subjected to a standard conditioning treatment before weighing them. The glass container, after a sample of water had been collected as ice by condensation in liquid air, was warmed carefully to melt the ice and bring it slightly above the temperature of the room. The container was then wiped dry and placed in the balance case. Air in the balance case was circulated by a fan for at least 5 min to bring the container to the balance case temperature as well as to insure a standard surface condition. Weighings were then made by substitution, estimating to one-tenth of a milligram. A substitute or tare glass container, which displaced the same amount

of air as the weighing container, was kept in the case and was weighed either just before or after the collecting container. This eliminated errors of weighing due to variation in length of the balance arm or change of weight of the counterpoise.

In the vaporization process, larger temperature gradients were induced in the calorimeter than in the heat-capacity experiments. In order to diminish these gradients, the pump speed was increased to 106 rpm at the expense of a larger pump power. Since the pump power was also less constant than before, determinations of it were made oftener. Several pump-power determinations were made on each day, the experiments being arranged so that pump-power determinations were made usually just before and just after one or two evaporation experiments. By interpolating between pump-power determinations, account was taken of changes in pump power, including that due to changes in liquid level. In all, 131 determinations of pump power were made during the 152 evaporation experiments.

Owing to the greater disturbance of temperature by the evaporation process, the heat-leak accounting was slightly less exact than in the heat-capacity measurements. A small supercorrection, depending on the location of the liquid level, was applied, sometimes amounting to as much as 1 part in 50,000.

During the withdrawal of steam from the calorimeter, the upper tube was tempered by the outgoing steam, so for this period there was no correction for heat leak in the upper tube.

The initial and final temperatures of the water in the calorimeter were observed in the same manner as in the heat-capacity experiments. The temperature of the steam leaving the calorimeter was indicated by the group of four thermoelements, *JT*, representing the average temperature of the upper part of the calorimeter, and the single thermoelements, *J7*, *J6*, and *J5*, representing the temperatures along the upper tube.

A study of the thermoelement indications and their correlation with the observed values of heat of vaporization indicated that the temperature of the upper part of the calorimeter (measured by *JT*) is the best representation of the temperature of the steam withdrawn from the calorimeter and likewise of the temperature of evaporation.

Special details of the experimental procedure will next be described.

2. DESCRIPTION OF VAPORIZATION EXPERIMENTS

In preparation for an experiment, the calorimeter was charged with about 800 g of air-free water in the manner described in part 2. Trials with different charges showed that amounts between about 800 and 500 g gave the most satisfactory operating conditions. The calorimeter temperature was adjusted to the chosen temperature of the experiment by either electric heating, or cooling by the process of withdrawing vapor. During this adjustment of the calorimeter temperature, the throttle valve was heated by its electric heater to maintain it warmer than the calorimeter. The envelope temperature also was maintained above the calorimeter temperature. These precautions opposed condensation of water in the upper tube, which later, by removal, might give erroneous accounting for mass and energy. Consistency of the results with varying rates of withdrawal showed that this danger had been removed.

574278 O - 61 - 22

The temperatures of the envelope and reference block were next brought very slightly above the calorimeter temperature. During this period of adjustment, the circulating pump was started and the space between the calorimeter and envelope was evacuated for the purpose of insulation. A weighed evacuated glass container, *SR*, was connected to the vapor line, as shown in figure 3 in part 1. After evacuation of the line, the glass container was opened to the vapor throttle valve. The apparatus was then ready for the beginning of an experiment.

The equilibrium temperature of the calorimeter and contents was observed. At the start of the heating period, the current from the storage battery was shifted from the substitute resistor to the calorimeter heater by the automatic switch actuated by the time signals. Using the indications of the four thermoelements, *JT*, as guides, the throttle valve was opened and steadily adjusted so as to keep the value of *JT* practically zero. The reference block was kept at a constant temperature, as shown by the resistance thermometer indications. In this way, the temperature of the upper part of the calorimeter, which closely followed the evaporation temperature, was maintained constant at the initial reference block temperature by withdrawing enough steam to balance the energy put into the calorimeter. During this time, the bottom part of the calorimeter, which was in contact with the circulating liquid, became warmer than the top part by the amount of superheating necessary to conduct the heat to the surface for evaporation.

In order to evaluate heat-leak factors and the temperature of the withdrawn steam, the thermoelements on the upper tube, lower tube, calorimeter, and envelope were observed at 1-min. intervals. The readings of the resistance thermometer were recorded every minute so that the thermoelement observations could be referred to the International Temperature Scale. Occasional surveys of all thermoelements were made to guide proper control of the experiments. The current and potential drop in the calorimeter heater were observed on alternate minutes starting ½ minute after the power was switched on. At the end of the chosen number of minutes, the calorimeter heating was stopped and enough more vapor withdrawn before closing the valve to bring the calorimeter and contents to final equilibrium temperature near the initial temperature. The final temperature was then observed.

In all, 152 satisfactory vaporization experiments were made between 0° and 100° C. For most of these experiments, the time of evaporation was about 20 min., and the total time of the experiment about 30 min. Of these, 64 experiments were made at an evaporation rate of about 1 g/min. In tests to detect any significant change of the result with the rate of withdrawal, a number of the other experiments were made at various rates ranging from 0.25 to 2.22 g/min. The purpose of these tests was to ascertain whether there was any appreciable amount of liquid in the steam withdrawn. Examination of the results revealed no definite evidence of such an effect.

IV. RESULTS OF VAPORIZATION EXPERIMENTS

The data and computations for the vaporization experiments were so similar to those described in part 2 for the heat-capacity experiments that sample sheets need not be given. The principal data from the

vaporization experiments, as reduced to give values of gamma, γ, are given in table 12. In addition to the data taken in the heat-capacity experiments, both thermometer readings and the thermoelement, JT, readings were observed every minute during the evaporation period. The combination of the readings permitted the calculation throughout the experiment of the temperature of the top part of the calorimeter, which was found to represent closely the temperature of evaporation.

The computations of temperature and electric energy were made in the same manner as in the heat-capacity computations. In computing the total energy, the corrections were made as shown previously, except that in the case of the upper tube the heat leak was considered as zero during the outflow of steam. A correction was always necessary to account for the energy involved in the difference of the final temperature of the calorimeter and contents from the initial temperature. This correction was usually for temperature changes of less than 0.01°C, and was calculated, using the data from the heat-capacity experiments. Values are given in table 12 as "corrections for change of temperature."

Dividing the total energy thus obtained by the mass of water withdrawn gives a value of gamma, γ, at the effective evaporation temperature. This temperature was usually within 0.03° C of the even temperature, making the correction applied to the energy for the difference usually less than 1 part in 30,000.

The mean values of γ at the even temperatures were then found, weighting the separate determinations in proportion to the rates of evaporation. These weighted means and the deviations of the measured values from them are given in table 12. Study of the deviations justifies this mode of weighting for the rates used. The results were then ready for final formulation for use in computing heat of vaporization.

TABLE 12.—*Principal data from vaporization experiments*

Date	Evaporation temperature	Approximate rate	Mass of vapor removed	Heat leak	Pump energy	Correction for change in temperature	Entire energy added	γ at even temperature	Deviation from weighted mean
	°C	g/min	g	Int. j	Int. j	Int. j	Int. j	Int. j/g	Int. j/g
5-5-38	0.13	0.63	12.6135	−1.9	33.3	−12.7	31,539.0	2500.73	0.01
5-5-38	.15	.63	12.6135	−2.3	31.8	−7.0	31,542.1	2501.01	.29
5-5-38	.15	.63	12.6076	−1.9	32.4	−33.0	31,522.9	2500.67	−.06
5-5-38	.16	.63	12.6365	−3.9	32.9	44.5	31,592.6	2500.49	−.23
5-5-38	.14	.63	12.6160	−2.0	33.5	−5.2	31,544.6	2500.69	−.03
Even temperature 0.0° C. Weighted mean value of $\gamma_{0.0}$=2500.72 int. j/g.									
3-14-38	1.12	0.28	5.5299	−1.9	20.6	19.7	13,810.9	2497.78	−0.14
3-14-38	1.12	.65	12.9825	−3.6	21.3	1.4	32,419.9	2497.48	−.44
3-15-38	1.09	.70	14.0974	−2.3	32.2	−2.4	35,212.4	2498.00	.08
3-15-38	1.11	.70	14.0984	−3.5	23.6	4.7	35,209.4	2497.66	−.26
3-30-38	1.03	.70	14.0606	−2.0	27.0	17.9	35,118.8	2497.74	−.18
3-30-38	1.02	.70	14.0586	−2.2	26.1	22.6	35,115.0	2497.81	−.11
3-30-38	1.03	.25	4.9895	−.2	25.5	−18.5	12,464.2	2498.15	.23
3-30-38	1.03	.25	5.0009	−.2	24.4	−2.5	12,488.1	2497.24	−.68
3-30-38	1.02	.25	5.0032	−.2	25.3	7.2	12,495.7	2497.59	−.33
3-30-38	1.03	.25	4.9988	−.5	25.7	−2.7	12,484.0	2497.47	−.45
5-4-38	0.99	.70	14.0962	−1.4	25.5	9.2	35,215.8	2498.23	.31
5-4-38	1.00	.71	14.1013	−1.5	26.1	9.9	35,228.3	2498.23	.31
5-4-38	1.00	.70	14.0920	−1.4	28.3	−12.8	35,205.0	2498.23	.31
5-4-38	1.00	.71	14.1014	−1.4	27.1	1.2	35,227.7	2498.18	.26
5-4-38	1.00	.71	14.1054	−1.3	27.6	6.8	35,236.7	2498.10	.18
Even temperature 1.0° C. Weighted mean value of $\gamma_{1.0}$=2497.92 int. j/g.									

TABLE 12.—*Principal data from vaporization experiments*—Continued

Date	Evaporation temperature	Approximate rate	Mass of vapor removed	Heat leak	Pump energy	Correction for change in temperature	Entire energy added	γ at even temperature	Deviation from weighted mean
	°C	g/min	g	Int. j	Int. j	Int. j	Int. j	Int. j/g	Int. j/g
3-31-38	5.00	0.91	18.1421	−2.6	28.7	26.7	45,142.0	2488.24	−0.10
3-31-38	5.00	.91	18.1191	−3.9	29.2	−11.8	45,089.1	2488.48	.14
3-31-38	5.01	.25	5.0913	−.8	29.6	−3.4	12,669.4	2488.46	.12
3-31-38	5.02	.25	5.0952	−.9	29.5	−13.3	12,677.7	2488.22	−.12
3-31-38	5.02	.25	5.0972	−1.1	29.3	−5.8	12,683.7	2488.32	−.02
5-3-38	5.00	.92	18.3058	−8.7	24.4	−12.4	45,553.6	2488.48	.14
5-3-38	5.00	.92	18.3167	−5.5	23.0	−15.1	45,579.2	2488.39	.05
5-3-38	5.00	.92	18.3298	−4.5	23.1	3.2	45,609.4	2488.27	−.07
5-3-38	5.00	.92	18.3372	−4.0	23.1	4.7	45,627.5	2488.25	−.09
5-3-38	5.01	.92	18.3425	−2.7	23.2	−1.9	45,639.9	2488.22	−.12
5-3-38	5.01	.92	18.3463	−2.2	23.3	2.3	45,651.5	2488.35	.01
Even temperature 5° C. Weighted mean value of γ_5=2488.34 int. j/g.									
3-22-38	10.04	0.56	11.2389	−5.6	27.3	−7.0	27,836.6	2476.90	0.17
3-22-38	10.05	.26	5.1646	−2.4	28.4	−8.8	12,788.6	2476.32	−.41
3-22-38	10.07	1.05	20.9428	−9.8	30.4	−12.1	51,862.3	2476.54	−.19
4-1-38	9.97	1.03	10.3408	−2.9	19.4	−9.9	25,609.1	2476.44	−.29
4-1-38	9.99	0.26	5.1040	−0.9	30.0	−2.6	12,640.0	2476.47	−.26
4-1-38	9.99	.26	5.1106	−.8	31.0	−0.7	12,659.3	2477.05	.32
4-1-38	10.01	.26	5.1326	−.9	31.5	7.4	12,711.9	2476.74	.01
4-1-38	10.01	.26	5.1070	−.8	31.5	−13.8	12,647.6	2476.54	−.19
4-1-38	10.01	.26	5.1057	−.9	31.5	−16.6	12,643.2	2476.31	−.42
4-25-38	10.00	1.03	20.5761	−6.7	24.5	27.5	50,971.4	2477.21	.48
4-25-38	10.01	1.03	20.5738	−6.3	21.9	−25.6	50,953.8	2476.65	−.08
4-25-38	10.02	0.57	11.3193	−2.4	26.0	−1.0	28,019.9	2477.14	.41
4-25-38	10.02	.57	11.3326	−2.1	27.3	8.4	28,037.4	2477.00	.27
4-25-38	10.03	.57	18.5282	−4.0	28.2	8.4	28,065.2	2476.55	−.18
Even temperature 10° C. Weighted mean value of γ_{10}=2476.73 int. j/g.									
3-28-38	15.04	1.04	20.8145	−13.2	27.4	5.6	51,306.7	2465.04	0.23
3-28-38	15.04	1.04	20.7958	−10.4	27.3	−7.4	51,255.2	2464.78	−.03
3-28-38	15.06	0.26	5.1292	−2.3	27.9	−3.9	12,642.1	2464.87	.06
3-28-38	15.06	.26	5.1420	−2.5	30.4	5.9	12,674.7	2465.08	.27
3-28-38	15.06	.26	5.1417	−2.6	28.9	−0.2	12,671.8	2464.66	−.15
3-28-38	15.06	.26	5.1421	−2.6	29.3	−3.7	12,669.3	2463.98	−.83
Even temperature 15° C. Weighted mean value of γ_{15}=2464.81 int. j/g.									
3-21-38	20.05	0.57	11.3473	−6.9	28.7	−12.4	27,841.8	2453.73	0.37
3-21-38	20.06	.57	11.3539	−6.4	28.3	2.3	27,860.8	2453.99	.63
3-21-38	20.08	.26	5.2151	−2.6	27.7	−10.8	12,797.3	2454.08	.72
3-21-38	20.10	1.06	16.9431	−9.8	23.0	1.9	41,561.4	2453.24	−.12
4-26-38	19.98	1.03	20.6986	−6.5	25.2	−20.2	50,779.4	2453.22	−.14
4-26-38	19.99	1.03	20.6905	−6.8	27.5	−20.1	50,758.2	2453.19	−.17
4-26-38	20.01	0.57	11.3518	−3.0	26.1	−4.8	27,849.1	2453.30	−.06
4-26-38	20.02	.57	11.3453	−3.1	26.3	−22.2	27,835.7	2453.55	.19
4-26-38	20.02	.57	11.3570	−3.2	26.5	1.4	27,856.5	2452.85	−.51
4-26-38	20.03	.57	11.3506	−3.3	27.7	2.0	27,845.5	2453.15	−.21
Even temperature 20° C. Weighted mean value of γ_{20}=2453.36 int. j/g.									
3-25-38	25.01	1.06	21.1489	−8.8	26.3	1.3	51,627.7	2441.17	−0.14
3-25-38	25.01	1.06	21.1399	−7.8	26.2	−.5	51,610.4	2441.39	.08
3-25-38	25.01	.26	5.2053	−1.6	26.1	−11.9	12,706.7	2441.13	−.18
3-25-38	25.03	.26	5.2216	−2.0	26.8	5.2	12,744.0	2440.70	−.61
3-25-38	25.03	.26	5.2151	−1.9	25.5	−11.4	12,726.1	2440.31	−1.00
4-4-38	24.99	.29	5.7987	−1.3	23.7	−44.6	14,160.0	2441.91	.60
4-4-38	24.99	.57	11.4234	−3.9	24.7	−18.9	27,893.9	2441.80	.49
4-4-38	25.00	1.05	21.1590	−5.2	28.0	−19.9	51,652.3	2441.21	−.10
4-4-38	25.01	1.05	20.9658	−4.6	15.6	28.6	51,188.2	2441.53	.22
4-8-38	24.98	1.05	21.2868	−13.6	24.5	23.2	51,952.5	2440.55	−.76
4-8-38	24.98	2.08	41.5416	−21.0	26.6	−40.3	101,426.3	2441.51	.20
4-8-38	25.01	.29	5.7624	−2.3	25.7	−12.0	14,071.6	2441.99	.68
4-8-38	25.01	.57	11.3594	−6.3	23.5	.3	27,735.8	2441.68	.37
Even temperature 25° C. Weighted mean value of γ_{25}=2441.31 int. j/g.									

TABLE 12.—*Principal data from vaporization experiments*—Continued

Date	Evaporation temperature	Approximate rate	Mass of vapor removed	Heat leak	Pump energy	Correction for change in temperature	Entire energy added	γ at even temperature	Deviation from weighted mean
	°C	g/min	g	Int. j	Int. j	Int. j	Int. j	Int. j/g	Int. j/g
3-19-38	30.02	0.57	11.4735	−6.4	25.1	−17.8	27,880.5	2430.04	0.61
3-19-38	30.03	.57	11.4791	−6.6	25.8	−7.4	27,893.3	2429.99	.56
4-12-38	30.03	2.15	42.9434	−11.9	25.9	−11.5	104,302.5	2428.91	−.52
4-12-38	30.04	2.15	42.9255	−12.0	23.9	−31.3	104,266.4	2429.12	−.31
4-13-38	30.00	.29	5.8389	−2.4	26.9	−5.0	14,185.1	2429.41	−.02
4-13-38	30.01	.29	5.8419	−2.5	26.9	5.2	14,194.9	2429.86	.43
4-13-38	30.01	.58	11.5218	−5.7	26.9	1.1	27,990.2	2429.34	−.09
4-13-38	30.01	.58	11.5076	−5.1	27.0	−11.2	27,959.8	2429.70	.27
4-13-38	30.01	1.07	21.4137	−10.7	27.7	−1.3	52,032.2	2429.88	.45
4-13-38	30.01	1.07	21.4173	−10.4	29.3	.2	52,037.6	2429.72	.29
4-13-38	30.01	1.07	21.4198	−10.1	30.7	3.6	52,041.0	2429.57	.14
Even temperature 30° C. Weighted mean value of γ_{30}=2429.43 int. j/g.									
3-18-38	40.03	0.58	11.6219	−6.2	24.3	9.3	27,962.7	2406.10	0.23
3-18-38	40.04	.58	11.6027	−5.9	25.5	−5.7	27,918.9	2406.34	.47
3-18-38	40.05	1.08	21.6436	−13.9	26.1	25.7	52,067.5	2405.82	−.05
3-18-38	40.05	.27	10.6672	−5.9	44.1	−2.5	25,664.4	2406.04	.17
4-18-38	40.02	.29	5.8071	−3.6	24.7	−3.7	13,971.8	2406.04	.17
4-18-38	40.02	.29	5.8067	−3.4	29.1	−9.8	13,968.9	2405.70	−.17
4-18-38	40.02	.58	11.5896	−7.6	25.1	8.5	27,883.7	2405.97	.10
4-18-38	40.02	1.10	22.0565	−14.6	25.5	1.3	53,065.9	2405.96	.09
4-18-38	40.03	2.10	42.0339	−26.8	26.8	5.8	101,117.2	2405.68	−.19
4-18-38	40.03	2.10	42.0039	−24.3	29.1	−9.2	101,049.1	2405.78	−.09
Even temperature 40° C. Weighted mean value of γ_{40}=2405.87 int. j/g.									
3-17-38	50.03	0.58	11.7417	−9.1	21.2	−4.2	27,971.7	2382.32	0.48
3-17-38	50.04	.58	11.7431	−8.7	23.4	0.3	27,975.5	2382.39	.55
3-17-38	50.05	.30	5.9655	−2.9	25.0	−26.5	14,211.8	2382.45	.61
4-15-38	50.03	2.13	42.6496	−16.8	18.9	−25.6	101,565.8	2381.47	−.37
4-15-38	50.04	0.30	6.0205	−2.0	18.6	8.6	14,336.3	2381.35	−.49
4-15-38	50.04	.30	6.0117	−2.3	20.0	−16.8	14,318.2	2381.82	−.02
4-15-38	50.04	.58	11.7121	−4.8	20.9	−1.9	27,894.8	2381.81	−.03
4-15-38	50.04	.58	11.7095	−4.8	21.4	−7.5	27,885.6	2381.55	−.29
4-15-38	50.05	1.09	21.8394	−7.4	22.8	−31.8	52,017.0	2381.92	.08
5-25-38	49.99	1.08	21.5345	−4.4	27.3	17.8	51,292.4	2381.85	.01
5-25-38	49.99	1.08	21.5660	−5.4	28.8	17.4	51,372.4	2382.08	.24
Even temperature 50° C. Weighted mean value of γ_{50}=2381.84 int. j/g.									
5-13-38	59.99	1.12	22.4288	−22.0	25.5	−10.7	52,891.7	2358.18	0.53
5-13-38	59.99	1.12	22.4230	−19.5	24.7	−21.0	52,870.3	2357.84	.19
5-13-38	60.01	2.20	44.0762	−29.6	29.9	−9.7	103,905.8	2357.43	−.22
5-13-38	60.00	2.20	44.0688	−24.2	27.3	14.0	103,889.5	2357.44	−.21
5-13-38	60.01	1.12	22.4740	−10.7	32.4	−7.7	52,983.3	2357.56	−.09
5-13-38	60.02	1.12	17.9796	−8.4	25.7	−2.1	42,392.7	2357.87	.22
5-25-38	60.01	1.09	21.7726	−8.9	26.5	−10.6	51,333.5	2357.73	.08
5-25-38	60.01	1.09	21.7708	−8.4	26.7	75.7	51,325.9	2357.58	−.07
Even temperature 60° C. Weighted mean value of γ_{60}=2357.65 int. j/g.									
5-9-38	70.01	2.18	21.7659	−14.3	16.7	−46.9	50,787.9	2333.39	0.14
5-9-38	70.02	1.12	22.4433	−19.1	25.7	34.5	52,366.3	2333.32	.07
5-9-38	70.02	1.12	22.4376	−18.0	22.5	−8.5	52,352.2	2333.29	.04
5-9-38	70.01	1.12	22.4550	−17.7	22.5	21.7	52,386.9	2332.99	−.26
5-9-38	70.02	1.12	22.4530	−14.7	23.3	1.9	52,381.7	2333.00	−.25
5-9-38	70.02	1.12	22.4598	−13.3	25.2	23.7	52,406.1	2333.38	.13
Even temperature 70° C. Weighted mean value of γ_{70}=2333.25 int. j/g.									
5-24-38	80.06	1.10	11.0280	−4.3	19.8	−28.7	25,456.1	2308.47	−0.04
5-24-38	80.08	1.10	22.0315	−15.3	25.5	−17.6	50,856.3	2308.54	.03
5-24-38	80.08	1.11	22.2351	−15.6	29.9	−0.1	51,329.2	2308.68	.17
5-24-38	80.09	1.11	22.2461	−12.3	28.8	9.9	51,349.2	2308.45	−.06
5-24-38	80.08	1.11	23.4033	−11.2	28.9	69.8	54,019.6	2308.40	−.11
5-26-38	80.00	1.10	22.0608	−12.3	38.3	−4.0	50,932.6	2308.74	.23
5-26-38	80.00	1.10	22.0742	−12.2	39.1	20.6	50,959.5	2308.55	.04
5-26-38	80.01	0.63	12.5791	−5.8	39.1	8.2	29,040.1	2308.62	.11
5-26-38	80.01	.63	12.5686	−6.2	38.7	−10.1	29,014.5	2308.51	.00
5-26-38	80.03	.63	12.5666	−6.5	38.2	2.4	29,007.1	2308.34	−.17
5-26-38	80.03	.63	12.5659	−6.5	38.0	5.0	29,002.5	2308.10	−.41
Even temperature 80° C. Weighted mean value of γ_{80}=2308.51 int. j/g.									

TABLE 12.—*Principal data from vaporization experiments*—Continued

Date	Evaporation temperature	Approximate rate	Mass of vapor removed	Heat leak	Pump energy	Correction for change in temperature	Entire energy added	γ at even temperature	Deviation from weighted mean
	°C	*g/min*	*g*	*Int. j*	*Int. j*	*Int. j*	*Int. j*	*Int. j/g*	*Int. j/g*
5-10-38	90.01	2.22	22.1958	−9.4	18.4	−2.8	50,683.1	2283.48	0.07
5-10-38	90.01	2.22	44.3722	−22.9	31.8	8.7	101,321.2	2283.47	.06
5-10-38	90.01	1.16	23.2875	−13.9	36.1	−8.9	53,171.6	2283.30	−.11
5-10-38	90.01	1.17	23.3241	−12.0	38.9	3.9	53,255.2	2283.30	−.11
Even temperature 90° C. Weighted mean value of γ_{90}=2283.41 int. j/g.									
5-11-38	99.99	1.18	23.5914	−13.7	33.9	4.3	53,261.8	2257.65	0.33
5-11-38	100.00	1.18	23.5977	−13.7	31.8	3.4	53,272.1	2257.51	.19
5-11-38	100.01	0.63	12.5763	−7.8	31.8	−7.0	28,392.8	2257.66	.34
5-11-38	100.01	.63	12.5796	−8.0	30.9	−4.2	28,396.0	2257.33	.01
5-11-38	100.01	.63	12.5795	−8.1	31.1	−6.7	28,393.3	2257.13	−.19
6-1-38	99.99	1.13	22.5785	−25.6	24.9	53.0	50,964.4	2257.18	−.14
6-1-38	99.99	1.13	22.5522	−24.8	21.5	−6.5	50,900.1	2256.96	−.36
6-1-38	99.99	1.13	22.5650	−18.4	21.4	17.4	50,932.4	2257.11	−.21
6-1-38	99.99	1.13	22.5745	−14.3	18.9	19.3	50,946.0	2256.76	−.56
6-2-38	100.00	1.12	22.4874	−14.3	28.0	−12.2	50,766.3	2257.54	.22
6-2-38	100.01	1.12	22.4909	−13.8	24.6	3.2	50,778.9	2257.78	.46
6-2-38	100.01	1.12	22.4899	−12.6	24.1	−2.6	50,764.6	2257.25	−.07
6-2-38	100.01	1.12	22.4959	−11.7	23.6	3.3	50,776.8	2257.19	−.13
6-3-38	100.01	1.13	22.5822	−11.2	29.2	29.0	50,977.9	2257.47	.15
6-3-38	100.01	1.13	22.5659	−10.9	29.9	1.2	50,939.2	2257.38	.06
6-3-38	100.02	1.13	22.5644	−10.2	30.2	3.1	50,931.4	2257.21	−.11
6-3-38	100.02	1.13	22.5616	−10.8	30.3	9.4	50,927.8	2257.33	.01
Even temperature 100° C. Weighted mean value of γ_{100}=2257.32 int. j/g.									

In addition to the measurements described here, there was a series of results of similar measurements made in this laboratory (1930–32) [2, 29] with an earlier stirred calorimeter and extending from 50° to 270° C; also another series (1937) [3] extending from 100° to 374° C, made with a later unstirred calorimeter.

Although these older measurements lacked some of the refinements of the present series, the fact that they were obtained with two calorimeters of different design from the present calorimeter and covered a much greater range of temperature, entitles them to inclusion in the scheme of formulation. In the range where they overlap or duplicate present measurements, the degree of accord furnishes a measure of the corroboration, while the greater range of the older data contributes greater directive control to a formulation than would result from the more accurate present results. A formulation was sought which comprised a smoothed appraisal of the experimental evidence over considerable range, and an empirical equation for γ was derived which satisfactorily does this over the range 0° to 200° C. After appraising the reliability of the various measurements, it was decided to weight them according to the number of observations and to give the observations of 1930–32 and those of 1937, respectively, one-fourth and one-half the weight of the observations of the present series.

The empirical equation for γ, as finally adjusted to these weighted data by the least-squares method, is written

$$\gamma=2500.5-2.3233t-10^{z},$$

where $z+5.1463-1{,}540/T$, t is in degrees centigrade, T is in degrees Kelvin ($t+273.16$), and γ is in international joules per gram. This equation represents not only the present values of γ between 0° and

100° C but also the earlier values between 50° and 200° C from previous reports. The degree of accord between the observed and calculated values is shown graphically in figure 8.

Between 170° and 200° C the equation gives values which are practically identical with the formulation of 1937, and therefore these values merge smoothly in this region. From 0° to 200° the new formulation supersedes the previous one, and together they complete the determination of γ over the entire range from the ice point to the critical region.

Values of the latent heat of vaporization, L, are calculated from γ by applying the corresponding values of β, which are computed as described in part 2 of this report. Table 13 includes the experimental mean values of γ which were used in the formulation, corresponding values of β, and calculated values of γ and L.

Values of the specific volume of the saturated vapor, u', were calculated from γ by the relation

$$\gamma = u' TdP/dT.$$

The values of the Clapeyron factor, TdP/dT, were calculated from vapor-pressure derivatives, as described in part 2.

TABLE 13.—*Formulation of data on heat of vaporization*

Temperature	γ, Observed				γ, calculated	β	Heat of vaporization, L	Clapeyron factor $T\frac{dP}{dT}$	Specific volume of vapor u'
	1930. 1932.	1937	1939	Weighted mean					
°C	*Int. j/g*	*Int. j/g*	*Int. j/g*	*Int. j/g*	*Int. j/g*	*Int. j/g*	*Int. j/g*	*Int. j/dm³*	*cm³/g*
0			2500. 72	2500. 72	2500. 18	0. 012	2500. 17	12. 1198	206288
1			2497. 92	2497. 92	2497. 84				
5			2488. 34	2488. 34	2488. 48	. 017	2488. 46	16. 9112	147150
10			2476. 73	2476. 73	2476. 76	. 023	2476. 74	23. 2730	106422
15			2464. 81	2464. 81	2465. 02	. 032	2464. 99	31. 6138	77973
20			2453. 36	2453. 36	2453. 25	. 042	2453. 21	42. 4173	57836
25			2441. 31	2441. 31	2441. 46	. 056	2441. 40	56. 2535	43401
30			2429. 43	2429. 43	2429. 64	. 074	2429. 57	73. 7846	32929
35					2417. 78	. 096	2417. 68	95. 7734	25245
40			2405. 87	2405. 87	2405. 88	. 124	2405. 76	123. 089	19546
45					2393. 93	. 158	2393. 77	156. 714	15275
50	2382. 0		2381. 84	2381. 85	2381. 93	. 200	2381. 73	197. 752	12045
55					2369. 88	. 251	2369. 63	247. 430	9578. 0
60			2357. 65	2357. 65	2357. 76	. 312	2357. 45	307. 097	7677. 6
65					2345. 58	. 386	2345. 19	378. 234	6201. 4
70	2333. 9		2333. 25	2333. 40	2333. 31	. 473	2332. 84	462. 470	5045. 3
75					2320. 97	. 576	2320. 39	561. 544	4133. 2
80			2308. 51	2308. 51	2308. 53	. 697	2307. 83	677. 319	3408. 3
85					2296. 00	. 838	2295. 16	811. 815	2828. 2
90	2283. 7		2283. 41	2283. 45	2283. 35	1. 001	2282. 35	967. 152	2360. 9
95					2270. 60	1. 191	2269. 41	1145. 57	1982. 1
100	2258. 71	2257. 79	2257. 32	2257. 73	2257. 71	1. 408	2256. 30	1349. 52	1673. 0
130	2177. 15			2177. 15	2177. 26				
150	2119. 64	2119. 50		2119. 57	2119. 87				
170	2058. 78			2058. 78	2058. 63				
200	1957. 96	1957. 11		1957. 44	1957. 93				

V. COMPARISONS WITH EARLIER WORK

A review of determinations of heats of vaporization of water previous to 1930 has already been made by Fiock [24]. No further attempt will be made here to review critically those determinations. However, since some of the results of earlier experiments are expressed in terms of the heat capacity of water, it is necessary to use heat-capacity data to convert those results to electric-energy units. In the review by Fiock these conversion data were obtained from the 1930 measurements at the NBS. The measurements given in part 2 of this report supply more accurate conversion data which will be used, where necessary, to interpret early results. The determinations of heats of vaporization will be briefly mentioned.

Dieterici

Dieterici [30] used a Bunsen ice calorimeter to measure the heat of vaporization at 0° C. In interpreting his results, uncertainty in units is avoided by using his own calibration of his ice calorimeter in terms of the mean calorie. By using the NBS value of the mean calorie along the saturated path (4.1903 int. j/g-°C) Dieterici's value of the heat of vaporization at 0° C becomes 2492.2 int. j/g.

Griffiths

Griffiths [31] measured the heats of vaporization at 30° and 40° C. The greatest uncertainty in the reduction of his data is in the evaluation of his electrical units. On the assumption that the electromotive force of his Clark cell was 1.4328 int. v instead of the 1.4342 that he used, his values are

$L_{30°}$=2425.2 int. j/g $\qquad$ $L_{40°}$=2400.0 int. j/g

Henning

Henning [32] made measurements in 1906 on the heat of vaporization between 30° and 100° C. His summary in 1919 gives values of his formulated results below 100° C, as follows:

$L_{30°}$=2426.0 int. j/g.	$L_{70°}$=2333.1 int. j/g.
$L_{40°}$=2403.8 int. j/g.	$L_{80°}$=2308.0 int. j/g.
$L_{50°}$=2380.8 int. j/g.	$L_{90°}$=2282.5 int. j/g.
$L_{60°}$=2357.4 int. j/g.	$L_{100°}$=2255.7 int. j/g.

A. W. Smith

Smith [33] made determinations between 14° and 100° C by evaporating water into a stream of air. Correction is made to the 1907 data for the revised Clark cell voltage. The values from Smith's experiments are as follows:

$L_{14°}$=2463.5 int. j/g.	$L_{40°}$=2401.4 int. j/g.
$L_{21°}$=2447.6 int. j/g.	$L_{100°}$=2261.6 int. j/g.
$L_{28°}$=2431.1 int. j/g.	

Richards and Mathews

Richards and Mathews, and Mathews [34] measured the heat of vaporization at 100° C by a condensation method. After correction of the 1911 series, as later suggested by Mathews, the 1911 and 1917

series yield essentially the same result. Using the 1939 NBS heat-capacity data, their average value for the heat of vaporization at 100° C is 2257.3 int. j/g.

Carlton-Sutton

Carlton-Sutton [35] used a modification of Joly's classical apparatus to measure the heat of condensation of water directly in terms of the mean calorie without any reference to electrical standards. His final value of 538.88 mean cal, when interpreted by the NBS–39 value for

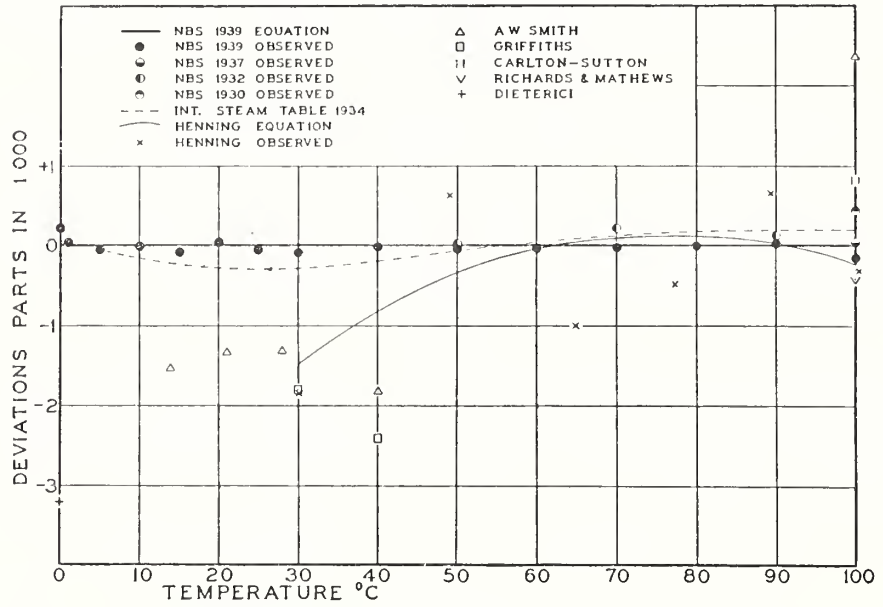

FIGURE 8.—*Comparison of values of heat of vaporization.*

the mean calorie along the saturated path, yields the value 2258.0 int. j/g for the heat of vaporization at 100° C.

National Bureau of Standards

Measurements at the National Bureau of Standards in 1930 [2] and 1932 [29] were made with an earlier calorimeter of different design from that of the present calorimeter. The observed values of heat of vaporization, L, in the range 50° to 100° C were:

$L_{50}° = 2381.8$ int. j/g. $\quad L_{90}° = 2282.7$ int. j/g.
$L_{70}° = 2333.6$ int. j/g. $\quad L_{100}° = 2257.3$ int. j/g.

Measurements above 100° C were made at the National Bureau of Standards in 1937 [3] with another calorimeter. The value observed in 1937 of heat of vaporization, L, at 100° C, was 2256.38 int. j/g.

It is believed that the measurements made with these two earlier calorimeters are inferior in precision to the present results using an improved calorimeter, but since these earlier results were obtained in calorimeters of different design from that of the present, they were included in the formulation in the present report.

In figure 8, a comparison is given of the various measurements of the heats of vaporization between 0° and 100° C. The base line in this figure is taken from the NBS–39 formulation.

The formulations of heat capacity and heat of vaporization, which have been given in this report, are considered more reliable than those given in previous reports from this laboratory in the range 0° to 100° C. Inasmuch as the values of some of the properties of saturated water and steam above 100° C depend partly on the values below 100° C a reappraisal has been made of all the measurements made at the National Bureau of Standards and the results compiled into a single table of smoothed values in the entire range 0° to 374.15° C. This compilation appears elsewhere in this journal [36].

REFERENCES FOR PARTS 1, 2, AND 3

[1] Nathan S. Osborne, *Calorimetry of a fluid.* BS J. Research **4,** 609 (1930) RP168.

[2] N. S. Osborne, H. F. Stimson, and E. F. Fiock, *A calorimetric determination of thermal properties of saturated water and steam from 0° to 270° C,* BS J. Research **5,** 411 (1930) RP209.

[3] N. S. Osborne, H. F. Stimson, and D. C. Ginnings, *Calorimetric determination of the thermodynamic properties of saturated water in both the liquid and gaseous states from 100° to 374° C.* J. Research NBS **18,** 389 (1937) RP983.

[4] Cyril H. Meyers, *Coiled-filament resistance thermometers.* BS J. Research **9,** 807 (1932) RP508.

[5] George K. Burgess, *The International Temperature Scale.* BS J. Research **1,** 635 (1928) RP22.

[6] E. F. Mueller, *Wheatstone bridges and some accessory apparatus for resistance thermometry.* Bul. BS **13,** 547 (1916) S288.

[7] E. F. Mueller and H. F. Stimson, *A temperature-control box for saturated standard cells.* J. Research NBS **13,** 699 (1934) RP739.

[8] *Conference on present state of knowledge of properties of steam.* Mech. Eng. **43,** 553 (1921).

[9] *The Third International Conference on Steam Tables.* Mech. Eng. **57,** 710 (1935).

[10] M. P. Chappuis, *Dilatation de l'eau.* Travaux et Mémoires du Bureau International des Poids et Mesures **13** (1907).

[11] M. Thiesen, *Bestimmung der Ausdehnung des Wassers für Temperaturen zwischen 50° und 100°.* Wiss. Abhandl. physik.-tech. Reichsanstalt **4,** 1 (1904).

[12] Leighton B. Smith and Frederick G. Keyes, *The volumes of unit mass of liquid water and their correlation as a function of pressure and temperature.* Proc. Am. Acad. Arts. Sci. **69,** 285 (1934).

[13] T. H. Laby, *Critical discussion of the determinations of the mechanical equivalent of heat.* Proc. Phys. Soc. (London) **38,** 169 (1926).

[14] James Prescott Joule, *On the mechanical equivalent of heat.* Phil. Trans. **40,** 61 (1850).
Joule's Scientific Papers Phys. Soc. (London) **1** and **2** (1884–87).

[15] Henry A. Rowland. *On the mechanical equivalent of heat, with subsidiary researches on the variation of the mercurial from the air thermometer, and on the variation of the specific heat of water.* Proc. Am. Acad. Arts Sci. **15,** 75 (1879).

[16] William S. Day, *A comparison of Rowland's thermometers with the Paris Standard, and a reduction of his value of the mechanical equivalent of heat to the hydrogen scale.* Phil. Mag., [5] **46,** 1 (1898).

[17] Osborne Reynolds, and W. H. Moorby. *On the mechanical equivalent of heat.* Phil. Trans. Roy. Soc. (London) [A] **190,** 301 (1897).

[18] T. H. Laby, and E. O. Hereus, *The mechanical equivalent of heat.* Phil. Trans. Roy. Soc. (London) [A] **227,** 63 (1927).

[19] Raymond T. Birge, *Probable values of the general physical constants (as of Jan. 1, 1929).* Rev. Modern Phys. **1,** 30 (1929).

[20] T. H. Laby and E. O. Hercus, *The effect of the aeration of the water used in the determination of the mechanical equivalent of heat.* Proc. Phys. Soc. (London) **47,** 1003 (1935).
[21] R. Jessel, *The effect of dissolved air on the specific heat of water.* Proc. Phys. Soc. (London) **46,** 747 (1934).
[22] Hugh L. Callendar, *Continuous electrical calorimetry.* Phil. Trans. Roy. Soc. (London) [A] **199,** 55 (1902).
Howard Turner Barnes, *On the capacity for heat of water between the freezing and boiling-points, together with a determination of the mechanical equivalent of heat in terms of the international electric units.* Phil. Trans. Roy. Soc. (London) [A] 199, 149 (1902).
Howard T. Barnes. *The mechanical equivalent of heat measured by electric means.* Trans. Int. Elec. Cong. **1,** 53 (1904).
Howard T. Barnes, *The absolute value of the mechanical equivalent of heat in terms of the international electric units.* Proc. Roy. Soc. (London) [A] **82,** 390 (1909).
[23] J. S. Ames, *L'équivalent mécanique de la chaleur.* Rapports Cong. Int. Phys. **1,** 178 (1900).
[24] Ernest F. Fiock, *A review of calorimetric measurements on thermal properties of saturated water and steam.* BS J. Research **5,** 481 (1930) RP210.
[25] W. A. Roth, *Die spezifischen Wärmen des Wassers (H_2O) zwischen 0° und 100° C.* Z. physik. Chem. [A] **183,** 38 (1938).
[26] H. L. Callendar, *On the variation of the specific heat of water, with experiments by a new method.* Phil. Trans. Roy. Soc. (London) [A] **212,** 1 (1912).
[27] W. Jaeger und H. von Steinwehr, *Die Wärmekapazitat des Wassers zwischen 5° und 50° in internationalen Wattsekunden.* Ann. Physik. **369,** 305 (1921).
[28] W. Jaeger, *Erzeugung von Wärme aus anderen Energieformen.* Handbuch der Physik **9,** 475, 439 (1926).
[29] E. F. Fiock and D. C. Ginnings, *Heat of vaporization of water at 50°, 70°, and 90° C.* BS J. Research **8,** (1932) RP416.
[30] C. Dieterici, *Die Verdampfungswärme des Wassers bei 0°.* Ann. Physik. **273,** 494 (1889).
[31] E. H. Griffiths. *The latent heat of evaporation of water.* Phil. Trans. Roy. Soc. (London) [A] **186,** pt. 1, 261 (1895).
[32] F. Henning, *Die Verdampfung des Wassers zwischen 30 und 100° C.* Ann. Physik. **326,** 849 (1906).
F. Henning. *Zur Verdampfungswärme des Wassers.* Ann. Physik. **363,** 759 (1919).
[33] Arthur Whitmore Smith, *Heat of evaporation of water.* Phys. Rev. **25,** 145 (1907).
Arthur Whitmore Smith, *Heat of evaporation of water.* Phys. Rev. **33,** 173 (1911).
[34] Theodore W. Richards and J. Howard Mathews, *A method for determining heat of evaporation as applied to water.* J. Am. Chem. Soc. **33,** 863 (1911).
J. Howard Mathews, *A redetermination of the heat of vaporization of water.* J. Phys. Chem. **21,** 536 (1917).
[35] T. Carlton-Sutton, *A determination of the heat of vaporization of water at 100° C and one-atmosphere pressure in terms of the mean calorie.* Proc. Roy. Soc. (London) [A] **93,** 155 (1916–17).
[36] Nathan S. Osborne, Harold F. Stimson, and DeFoe C. Ginnings, *Thermal properties of saturated water and steam.* J. Research NBS **23,** 261 (1939) RP1229.

Washington, May 28, 1939.

U. S. Department of Commerce
National Bureau of Standards

Research Paper RP2110
Volume 45, July 1950

Part of the Journal of Research of the National Bureau of Standards

Heat Capacity of Sodium Between 0° and 900° C, the Triple Point and Heat of Fusion

By Defoe C. Ginnings, Thomas B. Douglas, and Anne F. Ball

Using an improved ice calorimeter and furnace, the enthalpy changes of two samples of pure sodium have been accurately measured by a drop method at a number of temperatures between 0° and 900° C. Equations are derived to fit the data, and values of enthalpy and entropy, based on zero values at 0° C, as well as the heat capacity are tabulated for both the solid and liquid. Sources of significant experimental error are examined critically, and some theoretical implications of the results are discussed qualitatively.

I. Introduction

The advantages of liquid sodium for heat transfer at high temperatures have been known for some time. Not only have experimental values of the heat capacity of sodium been limited to the temperature range below 300° C, but these values have been widely discordant at 200° to 300°. It was the purpose of this investigation to measure the heat capacity of pure liquid sodium with higher accuracy and at higher temperatures than had been done previously.

II. Samples

The measurements were made on two samples of sodium enclosed in stainless steel containers of the type shown in figure 1. The stainless steel used was chosen for its resistance to attack by sodium at high temperatures. The sodium had been distilled once in glass in vacuum at or below 300° C. The weights of the samples were 5.3404 and 6.0297 g, respectively, and each was admitted in vacuum to a stainless steel cylinder weighing 16.840 g and having a capacity of 9.7 cm^3. After admitting helium to a pressure of one-thirtieth atm, each cylinder was sealed by welding and subsequently tested for leakage by noting whether exposure to 850° C for 15 min in an evacuated vessel caused any change in weight. The welding process utilized pulsed inductive heating [1].[1] With this welding technique, it was possible to seal the container without changing its weight by more than a milligram.

[1] Figures in brackets indicate the literature references at the end of this paper.

The sodium sample used for most of the measurements was analyzed spectrochemically at this Bureau after the heat-capacity experiments. Of the 47 elements tested for, including all the common metals, only three were detected. Calcium and lithium were found in amounts estimated at between 0.0001 and 0.001 weight percent, whereas potassium was estimated to be between 0.001 and 0.01 percent. The sample was completely soluble in water.

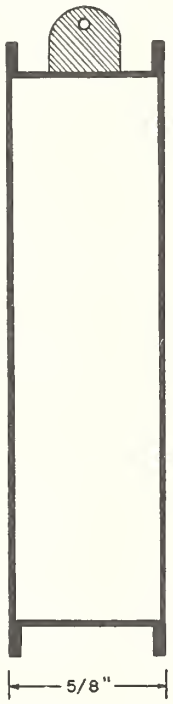

FIGURE 1. *Scale diagram of sample container.*

The spectrochemical analysis did not include a

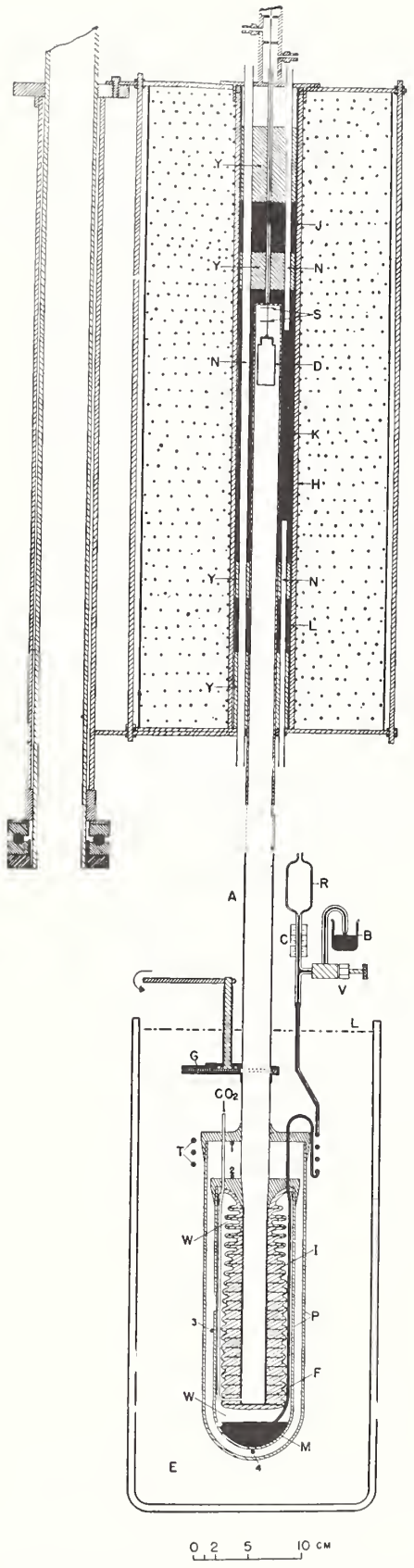

FIGURE 2. *Schematic diagram of furnace and ice calorimeter.*

A, Calorimeter well; *B*, beaker of mercury; *C*, glass capillary; *D*, sample container; *E*, ice bath; *F*, copper vanes: *G*, gate; *H*, platinum heater; *I*, ice mantel; *J*, *K*, *L*, silver cylinders; *M*, mercury; *N*, Inconel tubes; *P*, Pyrex containers; *R*, mercury reservoir; *S*, platinum shields; *T*, mercury "tempering" coil; *V*, needle valve; *W*, water; *Y*, porcelain spacers; 1, 2, 3, 4, thermocouple junctions.

search for the common nonmetals. However, other samples from the same original source and distilled by the same procedure were reported to contain as much as 0.01 percent by weight of oxygen (as Na_2O). The typical content of hydrogen before distillation amounted to 0.006 percent by weight. A melting curve observed by the authors on the principal sample is described in this paper. This indicated that the impurity in solution in the liquid but not in the solid amounted to about 0.0016 mole percent at the triple point.

III. Method and Apparatus

The method as applied to an earlier apparatus has already been described [2, 3, 4]. In brief, the method is as follows. The sample, sealed in its container, is suspended in a furnace until it comes to constant temperature. It is then dropped into a Bunsen ice calorimeter, which measures the heat evolved by the sample plus container in cooling to 0° C. A similar experiment is made with the empty container at the same temperature. The difference of the two values of heat is a measure of the change in enthalpy of the sample between 0° C and the temperature in the furnace. From enthalpy values of the sample so determined for a series of temperatures, the heat capacity can be derived.

1. The Ice Calorimeter

The construction, calibration, and use of an earlier Bunsen ice calorimeter in this Bureau have been described [2]. The present model, shown together with the furnace in figure 2, incorporates several improvements. In the first place, the mercury-water interface is now located in the bottom of the inner glass calorimeter vessel. This has two advantages. First, the area of the interface is much larger than before, so that for a given influx of heat, the level of mercury in the calorimeter changes very little. The calorimeter and its contents are slightly compressible, so that a change in pressure in the calorimeter results in a change in volume that must be distinguished from the change in volume due to heat input. With the earlier calorimeter, the change in volume produced by the change in head of mercury affected the calibration factor by about 0.01 percent, but with the present

calorimeter, the effect of the change in head is only about 0.004 percent. The electrical calibration experiments automatically compensate for this effect in heat measurements. However, reduction of the magnitude of the effect permits determination of the calibration factor of an "ideal" ice calorimeter (one that operates at constant head) with greater accuracy. A second reason for locating the mercury-water interface in the bottom of the calorimeter is to avoid danger of breaking the inner glass vessel. The inlet tube, now being filled with mercury rather than water, is not subject to blocking by freezing, an event that would burst the glass vessel. The present inlet tube includes a coil (T), for bringing the mercury to the temperature of 0° C before it enters the calorimeter.

The present calorimeter has been equipped with a tin-plated system of copper vanes, as pictured in figure 2. This results in more rapid distribution of heat from the well to the ice, so that the lag in reaching thermal equilibrium is now caused almost wholly by the thermal resistance between the heat source (sample in container) and the inner wall of the well. The latter lag has been considerably reduced by using a slow stream of dry helium gas up the well instead of carbon dioxide gas (as shown in fig. 1).

Unlike the earlier calorimeter, the new one has no built-in heater for electrical calibration. Calibrations were made with a removable heater provided with two zones of thermal contact with the calorimeter well for trapping the heat that would otherwise escape through the leads. This heater has a resistance of about 100 ohms instead of the 10 ohms in the earlier calorimeter. This reduces the uncertainty of accounting for the heat developed in the leads between the calorimeter and the jacket to a few thousandths of a percent of the total heat input to the calorimeter.

About one hundred electrical calibration experiments were made with the new calorimeter, with energies varying from 12,000 to 25,000 j. These experiments gave a calibration factor of 270.46 ± 0.03 abs j/g of mercury, which agrees with the value of 270.41 ± 0.06 obtained for the earlier calorimeter within the uncertainty assigned to the latter figure. About a hundred additional calibration experiments were made with low energies (about 100 j) in a search for small absolute errors that might not be detectable in high-energy experiments. These experiments indicated that the calorimeter failed to register about 0.4 j, an amount of heat that is negligible in most measurements.

2. The Furnace

The furnace is shown in position over the ice calorimeter in figure 2. It was mounted on a ball bearing so that it could be swung aside for access to the calorimeter. This furnace incorporated certain improvements that reduced temperature gradients in its central region and permitted more accurate temperature measurements over most of its temperature range.

In order to minimize end effects, the furnace was made 24 in. high, instead of 18 in. as with the earlier one [3]. The furnace was electrically heated by means of No. 26 platinum wire (H) wound on a grooved alundum tube having an inside diameter of 2 in. This heater was made in three separate sections corresponding in elevation to the three silver cylinders, which were located inside the alundum at J, K, and L. Silver was used because of its high thermal conductivity. By maintaining the silver cylinders J and L at the same temperature as the cylinder K, the temperature gradient in K could be made negligible. The silver cylinders were supported by porcelain spacers (Y). The silver and porcelain cylinders were lined with an Inconel tube (14% Cr, 80% Ni, 6% Fe) having an inside diameter of 1 in. in the central and lower parts of the furnace but with a diameter of one-eighth in. in the upper part. This tube served to enclose the sample container and its suspension wire (No. 32 Nichrome V), so that an inert atmosphere could be maintained at high temperatures where the stainless steel container would oxidize in air. Helium was used for the atmosphere in order to minimize the time necessary to hold the capsule in the furnace.

Figure 2 shows some of the vertical holes drilled through the silver and porcelain. These were placed 90 deg apart azimuthally. Three of them (one-fourth-in. in diameter) extended through the length of the furnace while two (three-sixteenth-in. in diameter) extended only to the top and bottom respectively of the center silver cylinder as shown in figure 2. These holes were fitted with thin-walled Inconel tubes, one of which served to hold the platinum-rhodium thermocouple sometimes used for temperature measurement of the central

silver section (K). In the two $\frac{3}{16}$-in tubes were placed differential thermocouples used to keep the end silver sections (J, L) at the same temperature as the central section. All thermocouples were insulated in four-hole porcelain tubes, which fit snugly in the Inconel tubes. A platinum resistance thermometer was encased in a platinum-rhodium tube, which also fit snugly in one of the one-fourth-in. Inconel tubes.

In another one-fourth-in. tube were placed three small auxiliary heaters, located at the elevations of the three silver cylinders. It was possible with these heaters to add heat at a low rate to any silver cylinder for fine-temperature regulation. It was possible to maintain the central silver cylinder constant to 0.01 deg and the end silver cylinders within a few tenths of a degree of the central silver. These auxiliary heaters were very useful in fine-temperature regulation since their heat was mostly delivered to the silver in 30 sec, thus avoiding the larger and troublesome lag that would have been encountered had the fine regulation been dependent on adjusting the currents in the main heaters.

In addition to the thermocouple mentioned, several more were installed just outside the main heaters (H). These thermocouples served to measure the temperature of this region and were used in a safety device to turn off automatically all current in the furnace if its temperature approached 961° C (the melting point of silver).

The suspension of the container in the furnace and its drop into the calorimeter is similar to that described earlier [3]. The braking started after the container entered the calorimeter. The weight of the falling system was kept constant in all experiments. Two platinum shields were used above the container in the same manner as formerly except that the diameters of the shields were increased from five-eighths in. to three-fourths in. since the diameter of the calorimeter well was increased from three-fourths in. to seven-eighths in.

3. Measurement of the Temperature of the Capsule in the Furnace

Up to 600° C, a strain-free platinum resistance thermometer was used to measure the temperature of the central silver cylinder that surrounded the capsule. This thermometer was calibrated at this Bureau on the International Temperature Scale [5] at the ice, steam, and sulfur points, and its resistance was always checked at the ice point after experiments at 600° C. Between 600° and 900°, the resistance thermometer was removed from the furnace, and the platinum-rhodium thermocouple was used. This thermocouple also was calibrated at this Bureau and was checked against a standard thermocouple before and after the measurements. A comparison of the resistance thermometer with the thermocouple showed agreement within 0.2 deg C in the temperature range up to 600° C. Both the resistance thermometer and thermocouple were made to have good thermal contact with the silver, so that their indications would not be affected by heat conduction along their leads. Experimental verification of this was found in tests with varying depths of immersion. The resistance thermometer winding and the principal junction of the thermocouple were both located at approximately the height of the sample container in the furnace.

It has been assumed that the sample container attains the temperature of the central silver, which surrounds it except at the bottom. Although calculations showed this assumption to be justified, experiments were made to test this. These experiments consisted of first making regular drop experiments at 700° C with the end silver pieces (J and L) regulated in the normal manner within a few tenths of a degree of the central silver (K). Then another series of drops was made, regulating both end silver pieces about 50 deg colder than the center. In other words, the temperature difference between the ends and the central silver was exaggerated by a factor of over one hundred. Even under these extreme conditions, the experiments gave a result only 0.1 percent lower. This indicated two main facts. First, with the exaggerated temperature difference, either the temperature gradient in the central silver was small, or the thermocouple was so placed that it represented the temperature of the sample container in spite of the gradient. Actually calculations show that the gradient is negligible in normal use. Second, this also indicated that any lowering of the temperature of the sample container below that of the main silver cylinder K due to radiation loss from the sample container out the bottom of the furnace is negligible. Calculations considering the solid angle had already shown that this should be true.

Since the temperature of the sample container was not directly measured, it was necessary to allow sufficient time for the container to reach the temperature of the silver. Special tests have been made to determine this time, similar to those described in detail in an earlier publication [3]. In the present experiments using helium in the furnace, the container with sodium acquired the temperature of the furnace (within 0.01 deg) within 15 min, whereas the empty container took less time in proportion to its heat capacity. In the experiments with sodium just above its melting point, extra time was taken to allow for absorption of the heat of fusion.

It was also necessary to consider the possibility of azimuthal temperature gradients in the silver due to the periodic addition of small amounts of heat by means of the auxiliary heaters that are located in one of the vertical holes in the silver. Calculations showed that no significant temperature gradients resulted with the relatively small amounts of heat supplied in this way.

4. Errors Due to Cooling of the Sample Container During Its Drop into the Calorimeter

Some users of the "drop" method in the past have simply subtracted the calculated enthalpy of the sample container from the measured enthalpy of the container plus sample. Of course, this procedure does not make allowance for heat lost during the drop. By making drop experiments with the empty container, most of this heat lost is accounted for, since it is approximately the same in both types of experiments. However, for the most accurate measurements, it is desirable to test the validity of this assumption that the heat loss is essentially the same for both empty and filled containers. The heat loss during the drop is dependent on the temperature difference between the container surface and its surroundings. This temperature difference will be slightly greater for the filled container, since its total heat capacity is higher than that of the empty container. This difference between the amounts of heat lost by the empty and the filled containers has been estimated by the authors for a sample assumed to have infinite thermal conductivity and perfect contact with the container. This gives the maximum possible difference. The radiation loss was estimated on the basis of a container with an area of 35 cm^2 with an emissivity of approximately unity. The heat lost by radiation from a container at 900° C dropping through a region near room temperature for one-quarter sec is about 80 j. The convective heat loss is much more difficult to estimate. Using the formula given in the International Critical Tables [6] for horizontal cylinders as being somewhat analogous, the convective loss in helium was calculated as about 80 j. Using these figures with the known heat capacities of the empty and filled containers, it is estimated that there would be a maximum error of about 4 j in the value for the enthalpy of the sample at 900° C. This is equivalent to about 0.06 percent on enthalpy, and a somewhat greater error on heat capacity.

Due to the approximate nature of the calculations of this error, some experiments were made to test if the heat losses calculated in this way were reasonable. Eight experiments were made at 300° C, dropping another container having about the same emissivity. In these experiments, the time of fall of the container was varied by factors of two and four greater than the normal time of fall (almost free fall). Assuming that the heat loss is directly proportional to the time of fall, it was estimated that the total heat lost in a normal fall at 300° C was about 6 j. This figure is considerably less than the value of about 16 j calculated in the manner described above (12 j by convection and 4 j by radiation). This would indicate that the heat loss is less than the calculations indicate and that at 900° C, the error due to this loss may be 0.02 to 0.03 percent. Since this error is small and is not known accurately, no attempt was made to apply a correction.

IV. Results of Enthalpy Measurements

A total of 129 measurements of enthalpy was made, 67 with the two empty containers and 62 with the two containers containing sodium. The average deviation from the mean was ± 0.02 percent with a given sample, and the difference between the values of enthalpy for the two samples did not exceed 0.3 j/g or 0.03 percent, whichever is larger. The detailed results of individual runs are given in table 1. Measurements were often repeated at lower temperatures after experiments at higher temperatures without disclosing any evidence that significant permanent changes had occurred in the samples meanwhile.

574278 O - 61 - 23

TABLE 1. *Corrected enthalpy values of individual experiments*

Temperature, t [a]	Measured heat		$(H_t-H_{0°C})$		
	Blank experiments	Experiments with sample	Observed	Calculated	Observed—Calculated
°C	*Abs j*	*Abs j*	*Abs j g*$^{-1}$	*Abs j g*$^{-1}$	
30.60	244.1	441.2	37.08	37.10	−0.02
	242.6	441.0			
	242.7	441.0			
	243.6	442.0			
59.00	474.1	862.4	72.64	72.61	+.03
	474.4	862.1			
	474.6	862.6			
	474.3	-------			
77.00	622.7	1,135.4	95.86	95.87	−.01
	623.3	1,135.2			
	623.7	1,134.9			
94.00	764.5	1,398.1	118.52	118.52	.00
	765.9	1,399.0			
	765.3	1,399.0			
	-------	[d] 1,479.2			
	-------	[d] 1,479.8			
	-------	[d] 1,479.1			
100.00	815.3	2,096.1	239.90	239.90	.00
	815.1	2,096.3			
	815.2	2,095.5			
	814.1	2,095.2			
	814.8	2,097.5			
	815.3	[d] 2,260.9			
	813.7	[d] 2,260.6			
	814.3	[d] 2,260.9			
	815.2	-------			
	[b] 814.0	-------			
	[b] 814.8	-------			
	[b] 814.6	-------			
150.00	1,241.2	2,889.0	308.48	308.47	+.01
	1,241.2	2,889.1			
	[c] 1,242.2	2,888.3			
200.00	1,676.8	3,682.2	375.84	375.95	−.11
	1,676.7	3,686.1			
	1,677.0	3,684.3			
	-------	3,683.1			
300.00	2,570.7	5,284.6	508.41	508.03	+.38
	2,570.2	5,285.5			
	2,571.7	5,285.2			
	-------	[d] 5,639.6			
	-------	[d] 5,636.7			
	-------	[d] 5,635.7			
	-------	[d] 5,636.3			
400.00	3,498.7	6,904.1	636.87	637.09	−.22
	3,496.1	6,897.2			
	[b] 3,496.9	6,901.3			
	[b] 3,507.4	6,900.0			
	[b] 3,499.0	-------			
	[b] 3,499.0	-------			
500.00	4,449.1	8,529.3	764.02	764.05	−.03
	4,449.1	8,529.2			
	4,448.3	8,528.4			
600.00	5,422.3	10,175.7	889.97	889.82	+.15
	5,423.3	10,173.3			
	5,422.2	[d] 10,791 6			
	-------	[d] 10,788.3			
	-------	[d] 10,788.8			
699.5	6,421	11,840	1,014.5	1,014.7	−.2
	6,418	11,836			
	6,420	11,837			
	-------	11,836			

See footnotes at end of table.

TABLE 1. *Corrected enthalpy values of individual experiments*—Continued

Temperature, t [a]	Measured heat		$(H_t-H_{0°C})$		
	Blank experiments	Experiments with sample	Observed	Calculated	Observed—Calculated
°C	*Abs j*	*Abs j*	*Abs j g*$^{-1}$	*Abs j g*$^{-1}$	
796.8	7,417	13,496	1,137.2	1,137.5	−.3
	7,420	13,492			
	7,417	13,491			
	[b] 7,423	-------			
	[b] 7,420	-------			
	[b] 7,422	-------			
	[b] 7,420	-------			
896.6	8,455	15,211	1,265.2	1,264.9	+.3
	8,458	15,211			
	8,454	15,210			
	[b] 8,458	[d] 16,083			
	[b] 8,453	[d] 16,080			
	[b] 8,453	-------			
	[b] 8,448	-------			
	[b] 8,449	-------			
	[b] 8,449	-------			
	[b] 8,452	-------			

[a] International Temperature Scale of 1948 [5].
[b] On alternate container of same mass.
[c] Weighted less because of unsteady heat leak.
[d] On alternate container, containing 6.0297 g of sodium. The other container had the same mass but contained 5.3404 g of sodium.

No corrections for impurities were made, since these were believed to be much smaller than the accidental error. All weights were reduced to an in-vacuum basis. Small corrections were made to bring the results to a common basis at the listed temperatures. The values of enthalpy (H_t-H_0) given in table 1 are at the vapor pressure (saturation pressure). Small corrections were made for the thin oxide coatings that the containers acquired in the furnace, using published heat capacities of Fe and Fe_3O_4 [7]. In addition, in order to evaluate the heat capacity of the liquid alone, it was necessary to make small corrections at the highest temperatures for the heat given up in condensing the sodium vapor. These corrections, based on published vapor pressure data and the volumes of the vapor, amounted to about 0.03 percent of the enthalpy at the highest temperature. The total corrections of all kinds did not amount to more than 0.1 percent of the enthalpy.

The experimental values found for the enthalpy of sodium (at saturation pressure) in absolute joules per gram, are represented by the following empirical equations. H_0 is the enthalpy of the solid at 0°C, and t represents degrees C.

$$H_t \text{ (solid)} - H_0 \text{ (solid)} = 1.19926t + (3.247)\ (10^{-4})t^2 + (3.510)(10^{-6})t^3 \qquad (0° \text{ to } 97.80° \text{ C})$$

$$H_t \text{ (liquid)} - H_0 \text{ (solid)} = 98.973 + 1.436744t - 2.90244)\ (10^{-4})t^2 + (1.54097)\ (10^{-7})t^3 + 24000e^{-\frac{13600}{t+273}} \qquad (97.80° \text{ to } 900° \text{ C})$$

The last term of the latter equation (liquid) accounts for the difference between $H_t - H_0$ and the net heat measured. As shown by Osborne [10], this difference is equal to PV/m, where P is the vapor pressure of the sodium, V is the volume of the container, and m is the mass of sodium. In the temperature range investigated, this term reaches a maximum value of 0.02 percent at 900° C and is entirely negligible for the solid. These equations give 113.2 abs j/g as the heat of fusion at the triple point, 97.80° C.

After dropping the last term in the equation for the enthalpy of the liquid, the two preceding equations then give the measured heat differences along the saturation curve. Therefore their direct differentiation gives the heat capacities (C_s) under saturation temperature and pressure, as follows:

$$C_s \text{ (solid)} = 1.19926 + (6.494)\ (10^{-4})t + (1.0531)\ (10^{-5})t^2 \qquad (0° \text{ to } 97.80° \text{ C})$$

$$C_s \text{ (liquid)} = 1.43674 - (5.8049)\ (10^{-4})t + (4.6229)\ (10^{-7})t^2 \qquad (97.80° \text{ to } 900° \text{ C})$$

From these equations directly result the following equations for the entropy (also at saturation pressure), absolute joules g^{-1} deg K^{-1}, in excess of that at 0° C. T represents degrees Kelvin (taking 0° C=273.16° K).

$$S_T \text{ (solid)} - S_{273.16°K} \text{ (solid)} = 4.16241 \log_{10} T - (5.1036)\ (10^{-3})\ T + (5.2656)\ (10^{-6})\ T^2 - 9.14016 \qquad (0° \text{ to } 97.80° \text{ C})$$

$$S_T \text{ (liquid)} - S_{273.16°K} \text{ (solid)} = 3.75276 \log_{10} T - (8.3303)\ (10^{-4})\ T + (2.3112)\ (10^{-7})\ T^2 - 8.67398 \qquad (97.80° \text{ to } 900° \text{ C})$$

Values of enthalpy, heat capacity, and entropy calculated from these equations for rounded temperatures are listed in table 2.

TABLE 2. *Enthalpy, specific heat, and entropy of sodium*

Temperature, t	$H_t - H_{0°C}$	C_s	$S_T - S_{273.16°K}$
°C	abs j g^{-1}	abs j g^{-1} deg^{-1}	abs j g^{-1} deg^{-1}
0	0	1.1991	0
25	30.25	1.2221	.10590
50	61.21	1.2555	.20569
75	93.26	1.3071	.30116
97.80 (solid)	123.68	1.3636	.38581
[Melting	113.2	------	*.30510*]
97.80 (liquid)	236.86	1.3845	.69090
100	239.90	1.3832	.69906
200	375.95	1.3393	1.0222
300	508.03	1.3042	1.2757
400	637.09	1.2786	1.4832
500	764.05	1.2619	1.6590
600	889.82	1.2548	1.8121
700	1,015.3	1.2569	1.9481
800	1,141.6	1.2682	2.0715
900	1,269.4	1.2887	2.1853

V. Determination of the Triple Point and the Temperature Change During Melting

In order to measure the triple point and the amount of impurities (liquid-soluble, solid-insoluble) in the sodium, a resistance thermometer (60 ohms of No. 40 enameled copper wire) was wound directly around the lower half of the sample container used in most of the enthalpy measurements. This container was raised into the furnace, and the copper resistance thermometer was then calibrated at 94° and 100° C against the platinum resistance thermometer located in the silver cylinder (K). Starting with this container and the furnace at equilibrium at 94° C, the container was heated adiabatically using the copper resistance thermometer as an electric heater and raising the temperature of the furnace at about the same rate. After an appropriate time interval the electric power was turned off, and

the container was allowed to come to a constant temperature, which was observed by the copper resistance thermometer. This cycle was repeated about 20 times, using electric power of one-fourth watt over a total heating period of 90 min. It was therefore possible to observe the relation between the temperature of the sodium and the fraction that had melted.

The temperature and fraction of the sample melted were consistent with Raoult's law within the precision of the measurements, and indicated the triple point of the sample to be 97.792° C and that of pure sodium to be 97.80°. This triple-point lowering corresponds to a liquid-soluble, solid-insoluble impurity of 0.000016 mole/gram-atom of sodium. The freezing point of pure sodium at 1-atm pressure is calculated to be 97.81° C.

VI. Effect of Mechanical State of the Solid

E. Griffiths [9] claimed that he found reproducible changes in the heat capacity of crystalline sodium amounting to as much as 1.5 percent, depending on whether in its previous heat treatment, the sample had been "quenched" or "annealed". Similar tests were made by the authors on the two sodium samples reported here, and with conditions of quenching and annealing somewhat more extreme than employed by Griffiths. The furnace temperatures used were chosen to cover the temperature range where he found the greatest difference. The results are summarized in chronological order in table 3.

The first set of experiments (Set 1) was made after freezing slowly over an interval of 1 hr and then cooling at the rate of about 5 deg/hr. Preceding the experiments in Set 2 and on the same day, the molten sample was quenched by putting its container into a tube immersed in ice. The treatments before Sets 3 and 4 were respectively similar, except that the annealing carried out on the day preceding Set 3 involved freezing the sample over a period of 3 hr and then cooling the solid to room temperature at a rate varying from 3 to 5 deg/hr. Before observing Set 5, the sample was remelted and requenched by immersing its container directly into a dry ice-acetone bath (−78° C). It was then kept at this temperature overnight until just before the experiments.

TABLE 3. *Experiments to determine the reproducibility of the mechanical state of solid sodium*

Set No.	Temperature t	Mass of Na in sample	Prior heat treatment	Measured heat (Na and container)	
				Individual experiment	Mean of set
	°C	g		abs j	abs j
1	59.00	5.3404	Annealed	860.7 861.7 863.4 862.2	862.0
2	59.00	5.3404	Quenched	864.5 862.7 863.2	863.5
3	39.90	6.0297	Annealed	619.2 615.8 616.0 616.7 617.9	617.1
4	39.90	6.0297	Quenched	616.3 616.8 616.0	616.4
5	39.90	6.0297	Requenched rapidly by dry ice	614.4 616.2 615.2 616.5	615.6

The results tabulated in table 3 indicate that the quenching and annealing treatments did not change the heat capacity of the sodium by more than 0.2 percent and that these changes seem to be accidental and within the precision of the measurements.

VII. Reliability

An index to the reproducibility, or "precision", of the enthalpy measurements is afforded by the deviations from the mean, as shown by the results of the individual measurements shown in table 1. Another index is provided by the deviations (also listed in table 1) from the smoothed values given by the empirical equations adopted. All the results for liquid sodium lead to a probable error of the mean of from 0.01 to 0.03 percent on enthalpy (depending on the temperature), and as much as 0.3 percent on the derived heat capacity values, with a somewhat increased uncertainty below 200° and above 800° C because of the difficulty of determining the derivative of an empirical function accurately near its ends. For solid sodium, the relative uncertainties become considerably greater at the low temperatures, owing to the inability to determine heats by the ice calorimeter with a precision of better than 0.4 j.

In addition, all factors suspected of contributing appreciable systematic errors were analyzed to determine their likely contributions. Direct comparisons between the platinum resistance thermometer and the platinum-rhodium thermocouple up to 600° indicated differences in temperature of from 0.0 to 0.2 deg. Calculations indicated that errors due to the very small temperature gradients inside the silver cylinder in the furnace were entirely negligible. As far as uncertainties in measuring the temperatures on the International Temperature Scale are involved, the resulting probable error [2] in the enthalpy is thought to be only about 0.02 percent between 100° and 600°, and perhaps three times this much at 900°, where it was necessary to resort to measurement using a thermocouple. As a consequence, the probable error in the heat capacity due to uncertainty in temperature measurement may be considered to lie within 0.03 percent from 100° to 600°, but may reach 0.2 percent at 900° C.

In case the sample contained 0.01 percent by weight of oxygen as sodium oxide, as discussed earlier in this report, the error in enthalpy or heat capacity due to its gradual deposition from solution as the temperature fell might be as much as 0.05 percent. A similar error would be present if the liquid sodium dissolved appreciable amounts of the steel container; but recent measurements on the solubility of iron in liquid sodium by L. F. Epstein [8], of the Knolls Atomic Power Laboratory, indicate a solubility at 900° C of 22 parts per million, which would lead to negligible error in the present measurements. The analysis of the difference between the heat lost, during the drop into the calorimeter, by the sample container and by the empty container, showed that this effect, greatest at the highest temperatures, might lead to errors of 0.03 percent on enthalpy and 0.1 percent on heat capacity at 900°. Taking due consideration of the sources of error mentioned and other less significant ones, the authors believe that the probable error of the enthalpy values of sodium reported here may be considered to be between 0.1 and 0.2 percent (except below 100°, as mentioned above), whereas the probable error of the heat capacity was similarly estimated to be between 0.3 and 0.4 percent.

One experimental check on the over-all accuracy of the apparatus in measuring enthalpy was made by measuring the heat delivered to the ice calorimeter by a Monel capsule containing water and dropping from 250° C. By thus determining in several measurements the difference in heats for two amounts of water differing by about 6 g, a value of 1042.05 abs j/g for $\alpha]_{0}^{250^\circ}$ of water, defined elsewhere [10], was obtained. This figure differs by only 0.02 percent from the value of 1041.85 published in the latest report [11] on the thermal properties of water as accurately measured earlier in this laboratory with an adiabatic calorimeter.

The value found for the triple point is considered to have a probable error of 0.03 deg, dependent mostly on the uncertainty in the calibration of the copper resistance thermometer used for the measurements. A probable error of 0.3 percent is assigned to the heat of fusion. This figure is based on the estimated reliability of the enthalpy values in the neighborhood of the triple point. If all the impurity indicated by the measured melting curve were actually in liquid solution at 94°, then 0.25 percent of the sample was liquid at this temperature. In that case, the value of the enthalpy of the solid given in table 1 would be 0.2 j/g too high due to this effect, making the calculated heat of fusion 0.3 j/g too low.

VIII. Comparison with Results of Other Investigations

A number of other investigators [9, 12, 13, 14, 15, 16, 17] have made measurements of the heat capacity of solid and liquid sodium above 0° C, and most of these are shown for comparison in figure 3, where the full-line curves represent the values of the present investigation as given by the equations presented earlier in this paper. Each experimental point (NBS) given for the liquid in figure 3 was calculated from two adjacent observed enthalpies given in table 1. Rengade's [12] measurements, which made use of an ice calorimeter, extended from 15° to 100°, and although he stated that his sample was not very pure, his precision amounted to about 0.2 percent. Griffiths [9] employed a dynamic method and covered the range 0° to 140°, claiming a

[2] "Probable error" as used in the remainder of this paper includes the authors' estimate of certain systematic errors. To each factor subject to error, there was assigned a figure such that it was believed that the actual error was as likely greater as smaller than this figure. These figures were then combined statistically to yield an over-all probable error in the given experimental quantity.

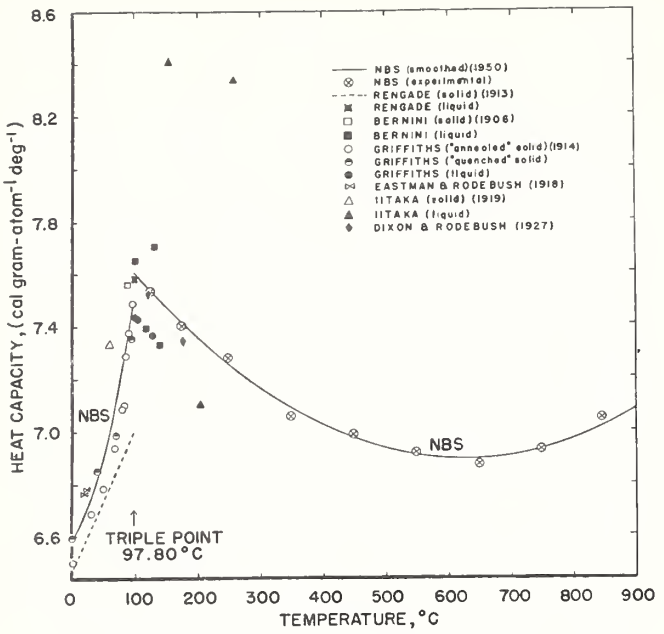

FIGURE 3. *Comparison of heat-capacity values.*

reproducibility of better than 0.1 percent, except for the variation of about 1.5 percent on the solid caused by varying the heat treatment, as mentioned above. Eastman and Rodebush's [13] measurements were mostly at low temperatures, but afford a comparison at 20° C. Iitaka [14] made determinations of the heat capacity of the liquid between 125° and 290°, the latter being the highest temperature attained prior to the present investigation. He dropped his samples from a furnace into his calorimeter and took due precaution to avoid certain systematic errors, but his precision was not better than several percent, and it will be noted from the graph that his values for heat capacity are considerably higher than those of the other investigators. Dixon and Rodebush [15] made measurements with a precision of about 1 percent, from 121° to 178°. Their method consisted in measuring the adiabatic temperature-pressure coefficient, and seems to have been subject to experimental difficulties due to the high thermal conductivity of the sodium.

TABLE 4. *Values for the melting point and heat of fusion of sodium*

Source	Melting point	Heat of fusion
	°C	*abs j g*$^{-1}$
This investigation	97.81±0.03	113.2
Ladenburg and Thiele [18]	97.8 ±0.1	----------
Edmondson and Egerton [19]	97.7	----------
Tammann [18]	97.8	----------
Griffiths [9]	97.61	115.35 (113.4, less accurate)
Bridgman [20]	97.63	125.5
Rengade [12]	97.90	----------
Bernini [11]	97.63	74.5
Iitaka [14]	----------	108.8
Joannis [16]	----------	132.6

The values reported for the melting point and heat of fusion of sodium are given in table 4. These melting point values in themselves are not, of course, a reliable criterion of the relative purity of the various samples used.

IX. Discussion of Results

The values of the heat capacity of sodium reported herein have practical importance, inasmuch as they cover the temperature range between 0° and 300° C with greater accuracy and precision than has been the case heretofore, and in addition extend the measurements to much higher temperatures, where experimental values for sodium have been entirely lacking until now. At the same time these values should be of considerable theoretical interest, since the extensive interest in the structure and properties of the liquid state in recent years has led to the theoretical calculation of the heat capacity of certain liquids, including sodium, whereas accurate experimental measurements on liquid metals have been relatively very meager.

The accuracy of the results given in this report is sufficient to show clearly the trends of the heat capacity curves of sodium with temperature, both below and above the triple point. The fall of the liquid curve to a minimum, a phenomenon in contrast to the steady rise with temperature for the great majority of liquids, is by no means unique in the case of metals, being paralleled by the heat capacity of mercury [21]. The entropy of fusion of sodium, 7.03 j deg^{-1} gram-atom^{-1}, is one of the lowest values for metals. According to current theories, the metal does not acquire complete randomness on melting, and the increased heat capacity of the liquid over what it displays at much higher temperatures is to be attributed to a further absorption of "communal" entropy above the melting point. Taking the values of the present investigation and extrapolating linearly to the melting point that part of the curve (fig. 3) above 700°, it was calculated

that the excess heat capacity between the triple point and 600° is equivalent to an entropy increase of 1.3 j deg^{-1} gram-$atom^{-1}$, a figure of the right order of magnitude to be explained in this way.

It has been pointed out further that the increase of heat capacity of the solid alkali metals with increasing temperature is enhanced in the regions of temperature just below the respective melting points, and this has been attributed to an acquisition of a part of the randomness, most of which occurs in fusion. The equation which Rengade [12] gave for the heat capacity of solid sodium from 15° to the melting point, being linear with temperature, does not of course show this feature. The equation found for the solid in this investigation, however, does have the sign of curvature just referred to, and so in this respect is at variance with an unmodified Debye function above the characteristic temperature.

Aside from any theoretical explanation of its approximate values, the heat capacity of liquid sodium is, as is well known, one of the determinants of the curvature of the vapor-pressure curve. Ladenburg and Thiele [18], in a critical evaluation of numerous vapor-pressure data of sodium, were forced to assume an average heat capacity of the liquid. Although their calculations are based on an approximate partition function for the vapor which is not accurate at these temperatures, the effect of this on the vapor pressures is probably relatively small, and they were able to show that for the range 100° to 500° C an average heat capacity of liquid sodium of 1.326 j g^{-1}, deg^{-1}, based on the measurements of Dixon and Rodebush [15], have better agreement with the vapor-pressure data and theoretically calculated "chemical constant" than a value of 1.452, the latter being Iitaka's [14] mean value. The results of the present investigation lead to an average heat capacity of 1.310 in this temperature interval.

X. Summary

The enthalpy of sodium has been measured in the range 0° to 900° C and with an accuracy of 0.1 to 0.2 percent over most of the range. Values of heat capacity are derived from the enthalpy values with an accuracy of 0.3 to 0.4 percent over most of the range. The triple point of sodium was shown to be 97.80°±0.03° C, whereas the heat of fusion is 113.2±0.4 abs j/g.

This investigation was made possible by the splendid cooperation of the Knolls Atomic Power Laboratory, Schenectady, N. Y., in preparing the samples and developing techniques of handling and sealing the samples without changing the mass of the containers. For this assistance, the authors are particularly indebted to Clifford Mannal and William D. Davis, who planned and supervised the work; and to William A. Ruggles, who was responsible for filling, sealing, and testing the sample containers.

XI. References

[1] R. J. Bondley, G. E. Research Laboratory Report No. RL–269.

[2] D. C. Ginnings and R. J. Corruccini, J. Research NBS **38,** 583 (1947) RP 1796.

[3] D. C. Ginnings and R. J. Corruccini, J. Research NBS **38,** 593 (1947) RP 1797.

[4] D. C. Ginnings and R. J. Corruccini, J. Research NBS **39,** 309 (1947) RP 1831.

[5] H. F. Stimson, J. Research NBS **42,** 209 (1949) RP 1962.

[6] International Critical Tables **5,** 234 (McGraw-Hill Book Co., New York, N. Y., 1929).

[7] K. K. Kelley, Contributions to the data on theoretical metallurgy. II. High-temperature specific-heat equations for inorganic substances. Bureau of Mines Bulletin 371. (U. S. Government Printing Office, Washington 25, D. C., 1934).

[8] Private communication.

[9] Ezer Griffiths, Proc. Roy. Soc. (London) **A89,** 561 (1914).

[10] N. S. Osborne, BS J. Research **4,** 609 (1930) RP168.

[11] N. S. Osborne, H. F. Stimson, and D. C. Ginnings, J. Research NBS **23,** 261 (1939) RP 1229.

[12] E. Rengade, Compt. Rend. **156,** 1897 (1913).

[13] E. D. Eastman and W. H. Rodebush, J. Am. Chem. Soc. **40,** 489 (1918).

[14] I. Iitaka, Sci. Reports Tohoku Imp. Univ. (Sendai) **8,** 99 (1919).

[15] A. L. Dixon and W. H. Rodebush, J. Am. Chem. Soc. **49,** 1162 (1927).

[16] A. Joannis, Ann. Chim. Phys. [7] **12,** 358 (1887).

[17] A. Bernini, Physik. Z. **7,** 168 (1906).

[18] R. Ladenburg and E. Thiele, Z. physik. Chem. **B7,** 161 (1930).

[19] W. Edmondson and A. Egerton, Proc. Roy. Soc. (London) **A113,** 521, 533 (1927).

[20] P W Bridgman, Phys. Rev. **3,** 153 (1914).

[21] T. B. Douglas, Anne F. Ball, and D. C. Ginnings, J. Research NBS (publication pending).

Washington, July 8. 1949.

For sale by the Superintendent of Documents, U. S. Government Printing Office
Washington 25, D. C. - Price 10 cents

Heat Capacity of Gaseous Carbon Dioxide[1]

Joseph F. Masi and Benjamin Petkof

The heat capacity (C_p) of gaseous carbon dioxide has been measured at −30°, 0°, +50°, and +90° C and at 0.5-, 1.0-, and 1.5-atmosphere pressure, with an accuracy of 0.1 percent. The flow calorimeter used was a modification of the one previously described by Scott and Mellors [1] [2] and Wacker, Cheney, and Scott [2]. In order to test the accuracy of the calorimeter, the heat capacity of oxygen was measured at 1 atmosphere at −30°, 0°, and +50°C. The measured values of C_p for oxygen were combined with an equation of state to give C_p°; these differed from the statistically calculated values by +0.03, −0.06 and −0.01 percent at the three temperatures.

The experimental values of C_p for carbon dioxide have been used to calculate new values of C_p° and values of the pressure coefficient of heat capacity at the four temperatures of measurement. The theoretical values of C_p° calculated in 1949 [8] were found to be too low by 0.2 to 0.3 percent; the results of a new calculation are in substantial agreement with the experiments. The pressure coefficients are in agreement with those obtained from the recent pressure-volume-temperature work of MacCormack and Schneider [7].

1. Introduction

The large number of experimental values of the specific heat of carbon dioxide reported in the literature are in serious disagreement with each other. Leduc, for the International Critical Tables [3], attempted to evaluate and correlate all of the work, both experimental and theoretical, up to 1929. It is now thought that these ICT values are in considerable error. There have been two calorimetric measurements of the heat capacity since that time [4, 5]. There have also been at least two good sets of pressure-volume-temperature measurements [6, 7] and two calculations of the ideal gas heat capacity from spectroscopic data [8, 9]. There have been several compilations, based almost entirely on the combination of equations of state with spectroscopic values of C_p° [10 to 13]. Values from several sources of the heat capacity in dimensionless units, C_p/R, at 1 atmosphere and 0° C, are given here.

Partington and Schilling, 1924 [14]	4. 40
Leduc, ICT 1929 [3]	4. 37
Eucken and v. Lude, 1929 [4]	4. 348
Sweigert, Weber and Allen, 1946 [10]	4. 487
NBS–NACA Table 13.24, 1949 [12]	4. 396
MacCormack and Schneider, 1950 [13]	4. 363

The present investigation was undertaken because of the impossibility of deciding which values to choose and because of the reluctance, on the part of some users of thermodynamic tables, to accept statistically calculated values without supporting experimental evidence.

Oxygen was chosen as a substance to test the accuracy of the apparatus, because its heat capacity is well known and because a pure sample is rather easily prepared.

2. Materials

The oxygen was prepared by heating potassium permanganate as described by Scott [15] and by Hoge [16]. This is a method that has been shown to produce very pure oxygen. The vapor pressure of the sample at the temperature of boiling nitrogen was found to agree with the value calculated from Hoge's data [16]. During the course of the last series of measurements (those at −30° C), a small air leak in the apparatus was suspected. As soon as the measurements were completed, a portion of the sample was dissolved in alkaline pyrogallol to determine the purity; the amount of residual gas was 0.2 percent, and it was assumed to be nitrogen from air that had leaked in.

Carbon dioxide was purified from commercial gas that had been made from limestone. A large cylinder containing 20 lb of carbon dioxide was opened and the gas allowed to escape until less than half of the contents remained. Several hundred grams were then transferred to a small evacuated cylinder, which was then attached to a purification train. The sample was slowly sublimed from the cylinder and condensed in a glass trap at liquid N_2 temperature, while a high vacuum was maintained by pumping on the trap. Transfer to the final receiver was also accomplished by sublimation and condensation. About 600 g were prepared in this way. The sample was tested several times for permanent gases by dissolving portions in concentrated potassium hydroxide and observing the volumes of residual gas. These were always less than 0.01 percent of the volume of the sample. A test performed by E. R. Weaver showed less than 0.001 percent of moisture.

3. Apparatus

The adiabatic flow calorimeter used in this work was a modification of one that was shown by Wacker, Cheney, and Scott [2] to give heat capacities reliable to better than 0.1 percent. The principal modifi-

[1] This work was financed in part by the National Advisory Committee for Aeronautics.

[2] Figures in brackets indicate the literature references at the end of this paper.

cation was the substitution of two resistance thermometers of nickel wire for the thermocouple previously used for measuring the rise in temperature of the heated gas. The main advantage of this substitution was that the thermometers could be calibrated in place at any time. A further advantage was that it could be demonstrated by the readings of the lower thermometer that the gas entering the calorimeter always reached the temperature of the bath, and that there was negligible heat leak "upstream" from the hot calorimeter to the incoming cold gas.

The flow calorimeter, as it was used, is shown in figure 1. Most of the essential features are as described by Scott, et al. [1, 2], but so many changes have been introduced that a brief description of the entire apparatus appears desirable.

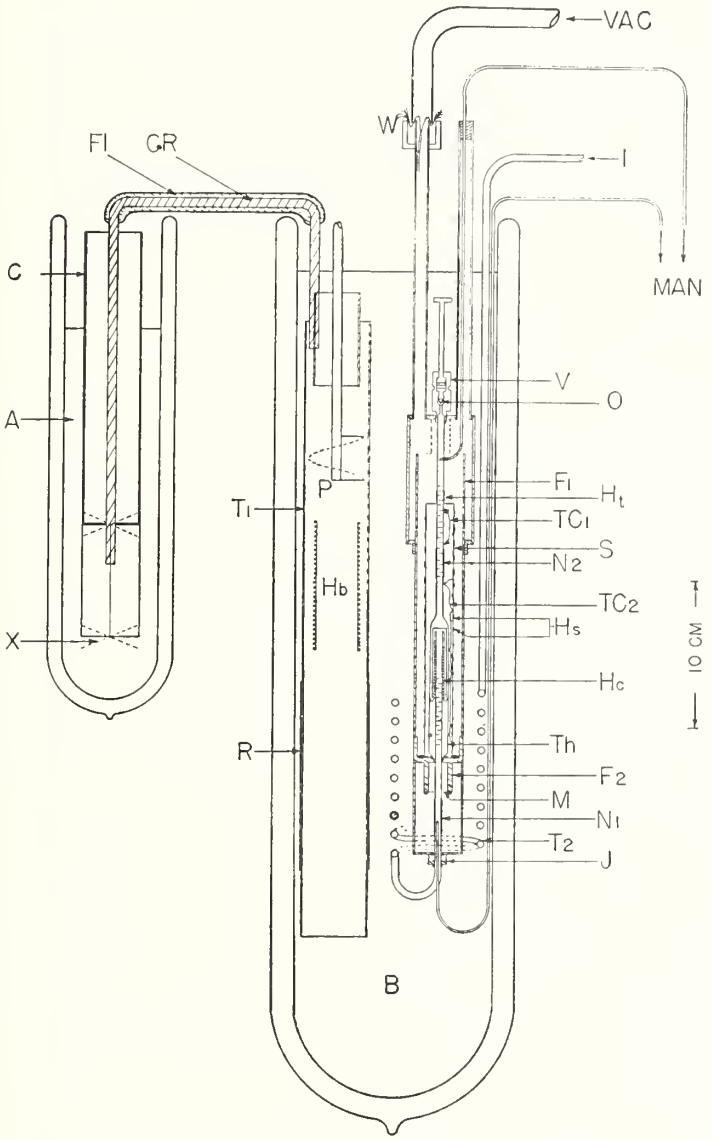

FIGURE 1. *Scale drawing of flow calorimeter.*

A, Liquid nitrogen; B, constant-temperature bath; C, protecting cylinder; CR, copper rod; F_1 and F_2, flanges; Fl, felt insulation; H_b, bath heater; H_c, calorimeter heater; H_s, shield heater; H_t, tube heater; I, inlet; J, bellows seal; M, mica spacer; MAN, manometer tubes; N_1 and N_2, nickel thermometers; O, outlet; P, propeller; R, bath-control thermometer; S, radiation shield; T_1, stirrer tube; T_2, helical tube; TC_1, tube thermel; TC_2, shield thermel; Th, metal thimble; V, throttle valve; VAC, vacuum line; W, wax seal; X, vanes.

3.1. Constant-Temperature Bath

The calorimeter is immersed in the bath, *B*, the temperature of which was controlled by supplying electric power to the heater, H_b. The stirring propeller, *P*, forced liquid down the brass tube, T_1, and over the copper resistance thermometer, *R*, which consisted of about 140 ohms of No. 37 AWG wire and which formed one arm of a Wheatstone bridge. An unbalance in the bridge circuit of 1 μv corresponded approximately to 0.001 deg K. The circuit was ordinarily attached to the galvanometer in a Rubicon phototube amplifier, the output of which was fed to a proportionating heat-control amplifier developed by the Electronic Instrumentation Section of the Bureau. This arrangement gave automatic control of the bath temperature within 0.002 deg, provided there were no large disturbances. The copper thermometer bridge could be switched from the controlling galvanometer to a sensitive wall galvanometer for manual control, or the two galvanometers could be placed in series for momentary observation of the efficiency of control.

When controlling the bath below room temperature, refrigeration was required, and this was provided by the apparatus shown at the left of figure 1. A solid copper rod, *CR*, with copper vanes, *X*, at one end and a copper cylinder at the other was immersed in liquid nitrogen, *A*. The metal tube, *C*, closed at the bottom end made the rate of heat transfer almost independent of the depth of the nitrogen in the dewar.

The bath liquid was a special light machine oil for temperatures above that of the room and an equivolume mixture of chloroform and carbon tetrachloride for temperatures below that of the room.

3.2 Flow Control

The source of gas flowing into the calorimeter is not shown in figure 1. For oxygen, this was a cylindrical brass boiler with heavy-copper vanes, wound with a heater and immersed in a cold dewar. The rate of flow was controlled by the power supplied to the heater on the boiler for evaporating the liquid oxygen. For carbon dioxide the boiler was replaced by a high-pressure system in which the carbon dioxide was contained in a steel cylinder immersed in melting ice. The pressure (34.38 atm) remained sufficiently constant for good flow control. The gas was admitted to the calorimeter, and its flow rate was controlled, by a very sensitive diaphragm valve. This valve was previously used by Osborne, Stimson, and Ginnings [17] for control of flow of high-pressure water. A silver seat moving down against a stainless steel crater-rim cone with a very small opening provided the closing action.

Both the rate of flow and the mean pressure during an experiment were adjusted, controlled, and measured by following the readings of a three-column manometer, two columns of which were connected to the calorimeter as shown in figure 1, whereas the third was open to the atmosphere.

3.3 Calorimeter and Shield

The gas being investigated entered at I and passed through the helical tube, T_2, where it was brought to the temperature of the bath. This tube passes into the vacuum jacket through the bellows joint, J, which was intended to prevent stresses caused by differential expansion.

The calorimeter, considered as the vertical tube between points J and O through which the gas flowed, was constructed of thin-walled seamless Monel tubing. The various pieces were soldered together as nearly coaxially as possible, and the whole length was supported only at the two ends, and at M by a mica spacer. The copper thimble, Th, was used to provide a surface of higher temperature to protect the incoming cold gas from radiation; it was thermally a part of the calorimeter. The latter, with the exception of the necessary lead wires, was completely isolated from contact with surroundings from points M to O. The thimble was gold-plated and polished; the Monel tubing was covered with thin aluminum foil, except for a short length that was highly polished The copper radiation shield, S, was gold-plated and polished on the inside, and covered with aluminum foil on the outside. It was supported and centered by string spacers.

The temperature of the gas entering the calorimeter was measured by the nickel resistance thermometer, N_1; the gas passed over a system of baffles and went twice past the glass-silicone-insulated No. 36 AWG constantan heater, H_c. The direction of flow was again reversed, and another system of baffles was encountered in the region where the exit temperature was measured with the nickel resistance thermometer, N_2. Heat leak to the upper tube was opposed by supplying heat to a tube heater, H_t, so that zero temperature gradient was maintained as indicated by a null reading of the copper-constantan thermocouple, TC_1. Radiation to or from the outer surface of the calorimeter was reduced almost to zero by heating the shield with the heaters, H_s, which were so arranged that any desired proportion of the heat could be supplied to the top half of the shield. The three junctions of the chromel-constantan thermocouple, TC_2, could be read in summation or individually, and the attempt was made to keep all of the readings near zero. Heat transfer from the bath by gas conduction was eliminated by evacuating the brass jacket.

Leads were brought in through the wax seal, W, and were tempered nearly to bath temperature on the brass cylinder, F_1. Leads from the thermometer, N_1, were taken directly to the brass ring, F_2, and further tempered; all other leads were wound twice around the shield. All leads were of AWG No. 34 copper wire, silk-and-enamel insulated. All wires, whether heaters, thermometers, thermal junctions, or leads, were cemented to the metal surfaces with glyptal lacquer and afterward baked.

Each nickel thermometer consists of about 55 ohms of AWG No. 40 enameled nickel wire with four copper leads. The thermometers were calibrated by comparing with one or more platinum resistance thermometers suspended in the bath when helium was in the calorimeter jacket. It was found that the resistance of the nickel thermometers in use fluctuated slowly over a range corresponding to 3 or 4 mdeg during a period of 3 months. Consequently, spot checks of the calibration were made each day of heat-capacity measurements.

After leaving the calorimeter through the throttle valve, V, the gas went to one or the other of two receivers through a snap-throw valve, capable of changing the flow from one receiver to the other in less than 0.1 second. This valve in one of the two positions closed the clutch circuit of an interval timer that was driven by a special constant-frequency 60-cycle current, accurate to 0.02 second. This valve was the same one described by Wacker, Cheney, and Scott [2]. The receivers were kept at the temperature of liquid nitrogen.

A Leeds & Northrup G–2 Mueller bridge was used to measure resistances. The potential and current in the calorimeter heater were measured with a precision potentiometer, in conjunction with a calibrated standard resistor and a calibrated volt box. The circuits were essentially the same as those described by Scott, Meyers, Rands, Brickwedde, and Bekkedahl [18].

4. Method

The selection of the temperatures and pressures at which to measure the heat capacity of carbon dioxide was made to cover the working range of the calorimeter and obtain as many points as necessary. The usual assumption was made, that the error in an apparent heat capacity caused by heat leak would be inversely proportional to the flow rate. Consequently, at each temperature and pressure, a number of determinations were made over as wide a range of flow rates as was consistent with a reasonable time for measurement, with the size of sample, or with the capacity of the calorimeter.

The determinations of the heat capacity included the measurements necessary to obtain the three fundamental quantities: the mass rate of flow, F, of the gas through the calorimeter; the electric power, W, to the calorimeter heater; and the rise in temperature of the gas, ΔT.

A heat-capacity experiment was begun by adjusting both the valve, V, and the flow of gas to the calorimeter until the selected values for the mean pressure and pressure drop were obtained. Meanwhile, power was supplied to the heater and adjusted. Neither valve V nor the power supply were changed after the initial adjustment, all control being at the source of gas. Heat was also supplied to the shields. After a length of time that was inversely proportional to the rate of flow, a steady state was reached in which the heated portion of the calorimeter and the shield were at a constant temperature that was approximately 10 deg higher than the constant bath temperature. At this time the gas was directed by means of the snap-throw valve to the other (weighed) receiver, thus starting the measurement. Contin-

uous measurements of the exit temperature (N_2) of the gas were made, and slight adjustments of the flow were made to keep that temperature constant within 0.03 deg. In addition to the measurements of the resistance of the thermometer, N_2, readings of current and potential of the heater, resistance of N_1 and the bath thermometer, and heights of the three mercury columns were recorded as often as possible in connection with each run. When about the desired weight of sample had been collected and the temperature was nearly constant and the same as that at the start of the run, the experiment was terminated and the gas was redirected to the other container. The barometric pressure was also recorded, as well as the reading of the interval timer. The receiver was weighed on a large analytical balance, and the weight of sample was corrected for buoyancy.

"Blank" experiments were required in which the temperature drop, δT, in the calorimeter was measured when no heat was applied. This temperature drop is chiefly due to Joule-Thomson cooling, but heat leaks and responsiveness of the nickel thermometers to the gas temperature usually contribute. The blank experiments were made with the bath temperature approximately at the mean temperature of the corresponding heat-capacity measurements, and they were made at the same mean pressures and over the same range of pressure drops as the heat-capacity experiments. The values of $\delta T/\Delta p$ were plotted as a function of Δp for each pressure and temperature for each gas. These graphs were used to obtain the quantity δT for each heat-capacity experiment. The value of δT varied from 0.005° to 0.4° in the extreme cases.

The apparent specific heat of the gas, C, at the mean temperature and pressure of the experiment was computed by the relation

$$C=\frac{WF^{-1}}{(\Delta T+\delta T)}. \quad (1)$$

The mean temperature, T_m, of the experiment was calculated as the bath temperature plus $\Delta T/2$. The average pressure, p_m, in the region of the calorimeter between the thermometers N_1 and N_2 was calculated, from the corrected manometer and barometer readings, as equal to the pressure at the entrance to the calorimeter minus three-eighths of the measured pressure drop, Δp. A consideration of the geometry of the calorimeter had led the authors to the opinion that the factor three-eighths is near the truth and that any uncertainty in this factor will not affect the result by a significant amount.

5. Results

5.1 Tests with Oxygen

All the heat-capacity data on oxygen from this investigation are given in table 1. The experiments

TABLE 1. *Data on oxygen*

Reciprocal of rate, F^{-1}	Mass of sample, m	Power, W	Pressure drop, Δp	Temperature rise, ΔT	Blank correction, δT	Heat capacity, C[a]	Correction for T_m and p_m, δC	Heat capacity, C_p (observed)
			−30.00° C=243.16° K: 1.00 atm					
sec. g^{-1}	*g*	*Watt*	*mm* Hg	°*K*	°*K*	*jg*$^{-1}$ *deg*$^{-1}$	*jg*$^{-1}$ *deg*$^{-1}$	*jg*$^{-1}$ *deg*$^{-1}$
11.9673	70.7703	0.762865	270.7	9.8817	0.0965	0.91489	−0.00012	0.91477
20.1028	49.0120	.457512	97.5	10.0141	.0382	.91487	−.00006	.91481
24.2569	41.3857	.381375	67.4	10.0837	.0271	.91488	−.00004	.91484
37.9589	26.9976	.240804	27.8	9.9815	.0141	.91435	−.00002	.91433
44.7503	26.0441	.203395	20.2	9.9454	.0096	.91419	−.00004	.91415
Extrapolated value								0.91519
			0.00° C=273.16° K: 1.00 atm					
11.1876	50.7721	0.796101	357.4	9.5978	0.1222	0.91624	−0.00008	0.91616
11.5440	99.1040	.781965	334.4	9.7381	.1157	.91606	−.00009	.91597
11.8257	79.9193	.796649	320.9	10.1718	.1117	.91608	−.00011	.91597
11.8486	62.8581	.796698	320.0	10.1910	.1115	.91632	−.00010	.91622
19.1670	27.8317	.420780	125.0	8.7491	.0501	.91646	−.00013	.91633
19.7966	68.4814	.418768	114.2	9.0000	.0462	.91639	−.00004	.91635
24.9887	33.1234	.344989	73.2	9.3736	.0311	.91655	+.00002	.91657
35.0715	26.4032	.232535	36.5	8.8815	.0177	.91629	.00000	.91629
37.2491	28.4235	.232170	33.2	9.4208	.0173	.91619	+.00002	.91621
46.1153	30.2936	.192647	22.2	9.6852	.0155	.91571	+.00001	.91572
Extrapolated value								0.91625
			50.00° C=323.16° K: 1.00 atm					
11.9923	111.6318	0.867217	297.8	11.1740	0.0887	0.92337	−0.00020	0.92317
12.1609	46.5598	.866257	284.7	11.3270	.0848	.92305	−.00023	.92282
23.6091	24.1352	.442883	78.1	11.3069	.0233	.92272	−.00018	.92254
31.9922	23.4676	.279146	43.3	9.6740	.0129	.92191	−.00002	.92189
41.8940	23.4888	.226012	26.0	10.2656	.0077	.92152	−.00007	.92145
Extrapolated value								0.92366

[a] The values of C are corrected for 0.0035 g of oxygen left in the delivery tubes because of the vapor pressure of oxygen at the temperature of boiling nitrogen.

are listed in the order of decreasing flow rate at each temperature. The values of C, given in column 7, are calculated by means of eq 1. These are adjusted by the amounts given in column 8, to correct for the difference between T_m and the nominal temperature and between p_m and 1-atm pressure, and there are obtained the values of C_p (observed) in column 9. The values of C_p (observed) are plotted as a function of F^{-1}. The straight line drawn through the points was determined by the method of least squares, and the value of C_p is obtained as the intercept. One of these plots is shown in figure 2, to illustrate the precision obtained. The values of C_p obtained by this process are labeled "Extrapolated value" in column 9 of table 1. These values, converted to dimensionless form, C_p/R, are listed again in table 3 (a). There are also given the corrections to ideality calculated by the Beattie-Bridgeman equation [19], and the resulting values of C_p°/R. These values are then compared with the values calculated by Woolley [20, 21] from the spectroscopic and molecular data.

5.2 Heat Capacity of Carbon Dioxide

All of the heat-capacity data on carbon dioxide in this research are given in table 2. In addition, plots of all the experimental results at $-30°$ and $+50°$ C are furnished in figures 3 and 4 to show the typical appearance of these plots and to indicate the precision. The value of C_p (observed) for each point (col. 9), after adjusting for the differences between T_m and p_m and the nominal temperature and pressure (col. 8), is plotted against the reciprocal of flow rate (col. 1). The slopes and intercepts of the lines were first obtained by the method of least squares. As the heat leak, of which the slopes of these lines is a measure, would be expected to be independent of pressure, the three lines at each of the temperatures except 90° C were adjusted slightly to a constant average slope. A small but regular change of slope with pressure was noted at 90° C, and these lines were therefore unchanged from the least-square values. The intercepts of these lines are the desired values of C_p and are listed in column 9 of table 2 as the "Extrapolated value." In order to furnish an estimate of the precision of these values of C_p, they are followed in table 2 by values of σ, where σ is defined as $\sqrt{\sum d^2/(n-1)}$, and d is the deviation from the extrapolated value of C_p, of each C_p (observed), after correcting for heat leak by use of the slope of the straight line previously found.

The values of C_p have been converted to dimensionless form and are given as C_p/R in table 3 (b). Although there are a number of experimental measurements at atmospheric pressure recorded in the literature, there is no interest other than historical in making comparisons with the very old work. Partington and Shilling [14], Leduc [3], and Quinn and Jones [22] have made studies that may be referred to. The most recent thermal measurements are those made by Kistiakowsky and Rice [5] by the isentropic expansion method. The values

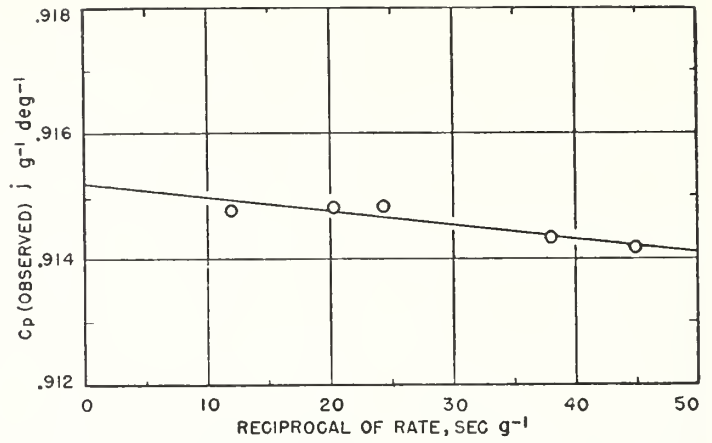

FIGURE 2. *Heat capacity of oxygen at −30° C and 1 atmosphere.*

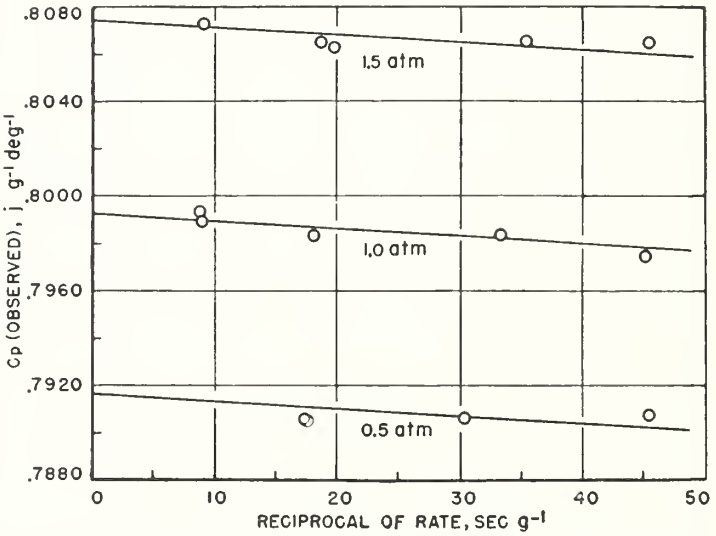

FIGURE 3. *Heat capacity of carbon dioxide at −30° C and three pressures.*

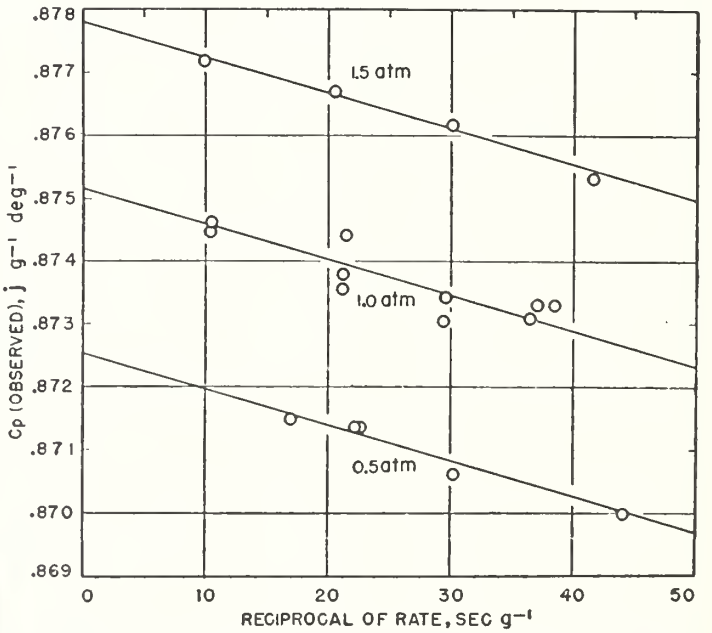

FIGURE 4. *Heat capacity of carbon dioxide at 50° C and three pressures.*

TABLE 2. *Data on carbon dioxide*

Reciprocal of rate, F^{-1}	Mass of sample, m	Power, W	Pressure drop, Δp	Temperature rise, ΔT	Blank correction, δT	Heat capacity, C	Correction for T_m and p_m, δC	Heat capacity, C_p (observed)
				−30.00°C=243.16°K; 1.50 atm				
sec g^{-1}	g	*Watt*	*mm* Hg	° K	° K	$jg^{-1}\ deg^{-1}$	$jg^{-1}\ deg^{-1}$	$jg^{-1}\ deg^{-1}$
8.8629	41.3700	0.883700	232.0	9.4287	0.2680	0.80772	−0.00044	0.80728
18.5247	28.5792	.483207	54.0	11.0151	.0740	.80721	−.00068	.80653
19.5828	40.5411	.470045	48.5	11.3377	.0674	.80708	−.00080	.80628
35,2678	27.3805	.238232	15.2	10.3897	.0230	.80689	−.00036	.80653
45.6761	37.3852	.171032	9.0	9.6685	.0181	.80648	−.00006	.80642
							Extrapolated value	0.80743
							σ	±0.00040
				1.00 atm				
8.7392	90.5234	0.884995	360.7	9.2665	0.4018	0.79995	−0.00056	0.79939
8.9149	66.0436	.873842	343.2	9.3580	.3843	.79963	−.00067	.79896
17.9871	34.4809	.472673	85.3	10.5263	.1148	.79898	−.00064	.79834
33.1864	30.2534	.237875	25.9	9.8478	.0393	.79844	−.00007	.79837
44.9014	27.7185	.179918	14.1	10.0914	.0353	.79775	−.00025	.79750
							Extrapolated value	0.79925
							σ	±0.00032
				0.50 atm				
17.2954	32.0664	0.471766	191.2	10.0748	0.2390	0.79111	−0.00044	0.79067
17.4880	33.8616	.468653	186.4	10.1265	.2340	.79107	−.00049	.79058
30.0616	13.5575	.268526	63.9	10.1155	.0928	.79076	−.00014	.79062
45.2457	26.3510	.169161	28.9	9.6347	.0469	.79055	+.00019	.79074
							Extrapolated value	0.79162
							σ	±0.00049
				0.00° C=273.16° K; 1.50 atm				
9.3013	57.1123	0.866418	201.4	9.5445	0.1454	0.83167	−0.00016	0.83151
9.3372	55.0724	.881983	233.6	9.6941	.2032	.83207	−.00040	.83167
9.3629	62.0585	.881506	233.4	9.7189	.2030	.83184	−.00035	.83149
9.5304	53.5353	.866533	191.6	9.7887	.1383	.83191	−.00035	.83156
18.0472	31.1528	.461388	54.1	9.9729	.0455	.83115	−.00022	.83093
18.4196	31.9291	.470372	60.9	10.3594	.0610	.83145	−.00049	.83096
18.5104	70.0752	.461507	51.5	10.2334	.0435	.83125	−.00036	.83089
18.5114	39.8565	.470610	60.6	10.4168	.0607	.83155	−.00041	.83114
19.0150	52.8550	.460423	49.4	10.4888	.0420	.83137	−.00032	.83105
27.9321	48.1789	.279317	23.0	9.3786	.0223	.83009	+.00005	.83004
33.2801	35.3785	.231057	19.3	9.2371	.0207	.83060	+.00014	.83074
33.2990	28.2507	.231259	19.4	9.2458	.0208	.83101	+.00013	.83114
36.3004	20.1507	.197887	13.9	8.6471	.0160	.28919	+.00048	.82967
36.9328	26.7567	.197941	13.6	8.7985	.0157	.82940	+.00047	.82987
44.0597	23.7691	.170483	11.0	9.0283	.0120	.83088	+.00011	.83099
52.5659	29.4592	.142725	7.0	9.0379	.0096	.82923	+.00043	.82966
							Extrapolated value	0.83178
							σ	±0.00042
				1.00 atm				
9.7661	76.8902	0.864573	288.1	10.0045	0.2132	0.82636	−0.00016	0.82620
19.1194	30.6709	.438435	72.7	10.0863	.0640	.82585	−.00031	.82554
19.4948	29.6885	.439721	69.7	10.3133	.0637	.82608	−.00026	.82582
19.6730	31.9056	.440429	68.2	10.4224	.0594	.82663	−.00057	.82606
26.8229	40.7983	.279254	37.6	9.0375	.0398	.82518	+.00039	.82557
27.3293	21.1385	.280370	35.7	9.2462	.0392	.82520	+.00027	.82547
28.7456	33.6643	.278591	32.2	9.6719	.0339	.82510	−.00017	.82493
29.5021	23.1136	.279038	31.0	9.9395	.0334	.82546	−.00002	.82544
38.6285	21.0078	.220050	18.3	10.2730	.0256	.82537	−.00040	.82497
49.6069	29.4923	.154452	11.0	9.2763	.0187	.82430	+.00030	.82460
							Extrapolated value	0.82657
							σ	±0.00029
				0.50 atm				
16.0773	55.3158	0.524271	226.5	10.0779	0.1857	0.82124	−0.00019	0.82105
20.7110	39.0001	.410999	129.2	10.2405	.1163	.82189	−.00037	.82152
20.8485	27.4840	.408322	128.3	10.2415	.1155	.82195	−.00033	.82162
26.7300	36.5463	.279879	77.6	9.0390	.0776	.82061	+.00030	.82091
27.0941	19.9896	.321382	73.8	10.5239	.0738	.82165	−.00059	.82106
38.8621	26.1406	.218921	36.3	10.3228	.0389	.82107	−.00047	.82060
39.4649	24.1511	.219418	35.3	10.5001	.0378	.82173	−.00054	.82119
51.4968	27.4060	.142761	21.2	8.9446	.0233	.81978	+.00028	.82006
							Extrapolated value	0.82198
							σ	±0.00029

TABLE 2. *Data on carbon dioxide*—Continued

Reciprocal of rate, F^{-1}	Mass of sample, m	Power, W	Pressure drop, Δp	Temperature rise, ΔT	Blank correction, δT	Heat capacity, C	Correction for T_m and p_m, δC	Heat capacity, C_p (observed)
50.00° C=323.16° K; 1.50 atm								
sec g^{-1}	g	*Watt*	*mm* Hg	° K	° K	jg^{-1} deg^{-1}	jg^{-1} deg^{-1}	jg^{-1} deg^{-1}
9.9533	62.1153	0.865713	201.7	9.7182	0.1035	0.87731	−0.00012	0.87719
20.5446	32.9410	.440265	49.0	10.2884	.0260	.87694	−.00024	.87670
30.0909	25.6955	.279579	23.4	9.5905	.0124	.87607	+.00010	.87617
41.6754	22.0562	.198506	12.5	9.4465	.0067	.87513	+.00018	.87531
							Extrapolated value	0.87779
							σ	±0.00010
1.00 atm								
10.4374	88.9567	0.866111	281.8	10.1896	0.1437	0.87484	−0.00037	0.87447
10.4894	73.2889	.866896	285.0	10.2484	.1453	.87488	−.00026	.87462
21.0786	40.0728	.447243	69.2	10.7445	.0377	.87434	−.00056	.87378
21.0995	25.2669	.445427	69.4	10.7141	.0379	.87410	−.00054	.87356
21.4479	37.7110	.406496	67.0	9.9321	.0366	.87459	−.00018	.87441
29.2761	21.0018	.280525	36.6	9.3880	.0202	.87293	+.00012	.87305
29.4729	22.2099	.280078	36.0	9.4321	.0199	.87333	+.00010	.87343
36.3511	25.2598	.226390	24.0	9.4134	.0133	.87300	+.00008	.87308
37.0996	28.1755	.234775	23.0	9.9595	.0123	.87347	−.00016	.87331
38.3836	27.9002	.219624	21.7	9.6411	.0120	.87329	+.00001	.87330
							Extrapolated value	0.87515
							σ	±0.00030
0.50 atm								
16.9244	33.9652	0.523830	232.6	10.0336	0.1375	0.87164	−0.00014	0.87150
22.0871	27.3684	.402422	131.4	10.1132	.0846	.87159	−.00023	.87136
22.6081	34.2599	.440823	125.3	11.3464	.0801	.87220	−.00083	.87137
30.2390	34.4856	.279988	69.9	9.6780	.0465	.87064	−.00001	.87063
44.1108	23.2882	.216601	33.7	10.9518	.0230	.87058	−.00060	.86998
							Extrapolated value	0.87251
							σ	±0.00012
90.00° C=363.16° K; 1.50 atm								
10.6379	53.2143	0.865605	199.9	10.0164	0.0780	0.91221	−0.00006	0.91215
10.6711	64.2950	.866260	197.7	10.0538	.0771	.91245	−.00010	.91235
21.8113	31.5644	.392277	48.9	9.3726	.0191	.91102	+.00028	.91130
22.1309	23.8029	.396665	47.9	9.6176	.0187	.91099	+.00018	.91117
31.8221	24.2740	.282280	23.6	9.8573	.0092	.91043	+.00009	.91052
43.3567	22.2464	.205021	13.5	9.7692	.0053	.90941	+.00012	.90953
							Extrapolated value	0.91310
							σ	±0.00008
1.00 atm								
11.1544	60.3069	0.866978	277.7	10.4979	0.1222	0.91060	−0.00029	0.91031
22.3219	26.4180	.396304	69.8	9.6914	.0307	.90991	−.00022	.90969
22.8647	23.1588	.396651	66.7	9.9364	.0294	.91004	−.00035	.90969
30.5500	25.0064	.280344	37.8	9.4027	.0166	.90930	−.00007	.90923
31.6170	26.8963	.279376	35.5	9.6989	.0156	.90926	−.00020	.90906
38.3123	25.9995	.220204	24.3	9.2771	.0107	.90837	+.00030	.90867
38.3154	24.6919	.220067	24.5	9.2728	.0108	.90826	+.00030	.90856
40.0074	29.5816	.219191	22.4	9.6382	.0099	.90891	−.00017	.90874
							Extrapolated value	0.91102
							σ	±0.00009
0.50 atm								
17.6983	33.4157	0.523971	232.3	10.0869	0.1171	0.90880	−0.00006	0.90874
17.8550	72.7266	.524275	227.0	10.1915	.1144	.90831	−.00012	.90819
23.6482	24.4505	.401379	125.3	10.3876	.0631	.90825	−.00022	.90803
31.5103	20.4568	.279808	71.4	9.6812	.0360	.90734	+.00011	.90745
44.7281	19.6214	.219747	36.3	10.8154	.0183	.90725	−.00037	.90688
44.8320	29.8347	.219444	36.1	10.8265	.0182	.90718	−.00037	.90681
							Extrapolated value	0.90948
							σ	±0.00019

TABLE 3. *Summary of results*

	Temperature, °C			
	−30.00	0.00	+50.00	+90.00
	(a) Oxygen			
C_p/R, 1.00 atm	3.5223	3.5264	3.5549	------
$(C_p=1-C_p^\circ)/R$	0.0100	0.0079	0.0055	------
C_p°/R, observed	3.5123	3.5185	3.5494	------
C_p°/R, spectroscopic	[a] 3.5112	3.5207	3.5499	------
Percentage difference, observed-spectroscopic	+0.03	−0.06	−0.01	------
	(b) Carbon dioxide			
C_p/R, 1.50 atm	4.2739	4.4028	4.6463	4.8332
1.00 atm	4.2306	4.3752	4.6324	4.8222
0.50 atm	4.1902	4.3509	4.6184	4.8141
C_p°/R, observed	4.148	4.324	4.604	4.804
C_p°/R, spectroscopic:				
Benedict [24]	4.148	4.325	4.600	4.800
Wagman [25]	----------	----------	4.600	4.799
Percentage difference, observed-spectroscopic	0.00	−0.02	+0.09	+0.08
$\Delta(C_p/R)/\Delta p$, atm^{-1}	.0837	.0519	.0279	.0192

[a] Corrected for presence of 0.2% of nitrogen.

of C_p/R at 1 atm obtained by those authors were 0.13, 0.04, and 0.08 percent higher than values obtained by interpolation in the present experimental results, at the three temperatures of their experiments: 26.9°, 58.7°, and 94.56° C.

The results at each temperature were extrapolated linearly to zero pressure to obtain the values of (C_p°/R, observed) listed in table 3 (b). These values were first compared with the most recently published theoretical ones [8, 23] and found to be 0.2 to 0.3 percent higher. Recalculation of the theoretical values was made by W. S. Benedict and independentally checked by H. W. Woolley [24]. The results are shown in table 2 on the line labeled "Benedict". Two values interpolated in the National Bureau of Standards tables of "Selected values of chemical thermodynamic properties" [25], which were recalculated by Wagman from the older calculations of Kassel [9], are also given.

A consideration of the possible errors of the various measurements involved in these heat-capacity determinations, as well as the precision of the results, and the agreement of the observed and calculated heat capacities of oxygen, leads to the conclusion that the error in the final values of C_p/R at each pressure should not exceed 0.1 percent. The extrapolated values of C_p°/R should therefore be reliable to 0.15 percent.

5.3. Equation of State of Carbon Dioxide

It is assumed here that in the low-pressure region covered by these experiments the equation of state of carbon dioxide is of the form

$$pV=RT+Bp, \tag{2}$$

where B is a function of the temperature. The thermodynamic relation

$$\left(\frac{\partial \frac{C_p}{R}}{\partial p}\right)_T=-\frac{T}{R}\left(\frac{\partial^2 V}{\partial T^2}\right)_p=-\frac{T}{R}\left(\frac{\partial^2 B}{\partial T^2}\right)_p \tag{3}$$

must be satisfied by the second derivative of the second virial coefficient, B. The values of the change in heat capacity with pressure, obtained in this research, are given in the last line of table 3 and plotted as circles in figure 5. Also in figure 5 are shown curves representing the right-hand side of eq 3 obtained from (1) the recent pVT isotherms of MacCormack and Schneider [13]; (2) the Berthelot equation, using the critical constants of Meyers and Van Dusen [26]; and (3) the Lennard-Jones potential function [27, 28]. The dashed curve affords a comparison with other experimental work through the equation

$$\left(\frac{\partial \frac{C_p}{R}}{\partial p}\right)_T=-\mu\left(\frac{\partial \frac{C_p}{R}}{\partial T}\right)_p-\frac{C_p}{R}\left(\frac{\partial \mu}{\partial T}\right)_p, \tag{4}$$

where the values of the Joule-Thomson coefficient μ, and its derivative were obtained by interpolation in the tables of Roebuck, Murrell, and Miller [29].

A simple calculation shows that the quantity given by eq 3 is approximately 1 percent of the heat capacity and also 1 percent of the values of the second virial coefficient, in the region covered by this investigation. Therefore, if second virial coefficients could be determined to the same percentage accuracy as the heat capacities, the values of $\partial(C_p/R)/\partial p$ calculated from the right-hand side of eq 3 would be about half as accurate (because of two differentiations) as those obtained from direct heat-capacity

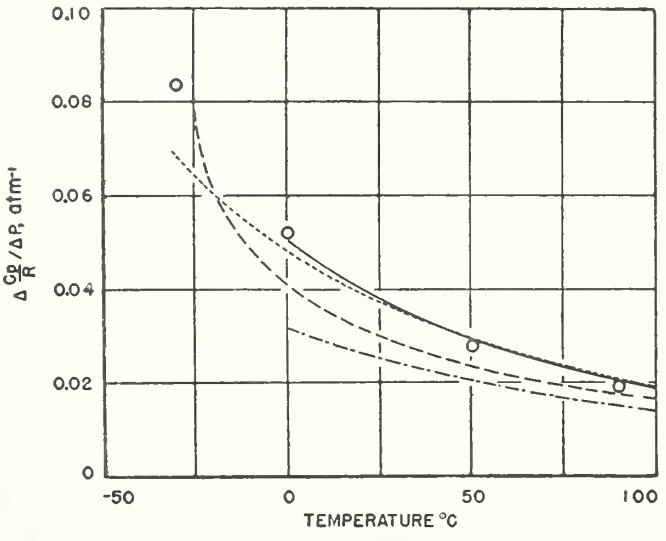

FIGURE 5. *Change of heat capacity of carbon dioxide with pressure as a function of temperature.*

○, This research; ——, MacCormack and Schneider [13]; — — —, Joule-Thomson-Roebuck, Murrell and Miller [18]; - - - - - -, Berthelot; ·—·—·, Lennard-Jones 6–12 potential function.

measurements. However, the limit of error generally to be expected from good pVT measurements, and that given by MacCormack and Schneider for their work [7], is about 0.5 percent of the value of B in this region. As the heat-capacity measurements are thought to be good to 0.1 percent, the values of $\partial(C_p/R)/\partial p$ obtained in this research are about an order of magnitude more accurate than those calculated from second virial coefficients.

The comparisons made in figure 5 show that the Lennard-Jones function cannot be used successfully to calculate the equation of state of carbon dioxide. An attempt was made to fit new Lennard-Jones constants to the results of this research, but unreasonable values ($b_0=25$ cm^3 mole^{-1} and $\epsilon/k=550$°K) were obtained. The difficulties presented by ellipsoidal molecules such as carbon dioxide have been mentioned by others [28].

The data of state of MacCormack and Schneider are evidently adequate to give good second derivatives of the second virial, as shown by figure 5. Other empirical equations, such as van der Waals' and the Beattie-Bridgeman equation, give curves similar to the Berthelot equation.

The authors are grateful for the valuable help and encouragement freely given by Russell B. Scott. For assisting at various times with the experimental work, we wish to thank William L. Cross, Jr., Dino Zei, and Richard J. Sherman.

6. References

[1] R. B. Scott and Jane W. Mellors, J. Research NBS **34,** 243 (1945) RP1640.
[2] P. F. Wacker, Ruth K. Cheney, and R. B. Scott, J. Research NBS **38,** 651 (1947) RP1804.
[3] A. Leduc, Int. crit. tables **V,** 83 (McGraw-Hill Book Co., Inc., New York, N. Y., 1929).
[4] A. Eucken and K. v. Lude, Z. physik. Chem. [B] **5,** 413 (1929).
[5] G. B. Kistiakowsky and W. W. Rice, J. Chem. Phys. **7,** 281 (1939).
[6] A. Michels and C. Michels, Proc. Roy. Soc. London [A] **153,** 201 (1935).
[7] K. E. MacCormack and W. G. Schneider, J. Chem. Phys. **18,** 1269 (1950).
[8] Serge Gratch, Trans. Am. Soc. Mech. Engrs. **71,** 897 (1949).
[9] L. S. Kassel, J. Am. Chem. Soc. **56,** 1838 (1934).
[10] R. L. Swigert, P. Weber, and R. L. Allen, Ind. Eng. Chem. **38,** 185 (1946).
[11] A. Michels and S. De Groot, Applied Scientific Research AI, 94 and 103 (1948).
[12] NBS-NACA tables of thermal properties of gases. Table 13.24, Carbon dioxide, specific heat (1949).
[13] K. E. MacCormack and W. G. Schneider, J. Chem. Phys. **18,** 1273 (1950).
[14] J. R. Partington and W. G. Shilling, The specific heats of gases, p. 204 (Ernest Benn, London, 1924).
[15] R. B. Scott, J. Research NBS **25,** 459 (1940) RP1339.
[16] H. J. Hoge, J. Research NBS **44,** 321 (1950) RP2081.
[17] N. S. Osborne, H. F. Stimson, and D. C. Ginnings, J. Research NBS **18,** 389 (1937) RP983.
[18] R. B. Scott, C. H. Meyers, R. D. Rands, Jr., F. G. Brickwedde, and N. Bekkedahl, J. Research NBS **35,** 39 (1945) RP1661.
[19] J. A. Beattie and O. C. Bridgeman, J. Am. Chem. Soc. **50,** 3133 (1928).
[20] H. W. Woolley, J. Research NBS **40,** 163 (1948) RP1864.
[21] NBS-NACA tables of thermal properties of gases. Table 1.10—Molecular oxygen (ideal gas state), specific heat, enthalpy, entropy.
[22] E. L. Quinn and C. L. Jones, Carbon dioxide (Reinhold Pub. Co., Inc., New York, N. Y., 1936).
[23] NBS-NACA tables of thermal properties of gases. Table 13.10—Carbon dioxide (ideal gas state), specific heat, enthalpy, entropy.
[24] W. S. Benedict and H. W. Woolley, Private communications.
[25] Selected values of chemical thermodynamic properties, NBS Circular 500 (in press).
[26] C. H. Meyers and M. S. Van Dusen, BS J. Research **10,** 381 (1933) RP538.
[27] NBS-NACA tables of thermal properties of gases. Tables of corrections of thermodynamic properties for gas imperfection, using the Lennard-Jones 6–12 potential (1950).
[28] R. B. Bird, Ellen L. Spotz, and J. O. Hirschfelder, J. Chem. Phys. **18,** 1395 (1950).
[29] T. R. Roebuck, T. A. Murrell, and E. E. Miller, J. Am. Chem. Soc. **64,** 400 (1942).

Washington, October 15, 1951.

UNITED STATES DEPARTMENT OF COMMERCE · Frederick H. Mueller, *Secretary*
NATIONAL BUREAU OF STANDARDS · A. V. Astin, *Director*

Precise Measurement of Heat of Combustion With a Bomb Calorimeter

R. S. Jessup

National Bureau of Standards Monograph 7

Issued February 26, 1960

For sale by the Superintendent of Documents, U.S. Government Printing Office, Washington 25, D.C. - Price 25 cents

574278 O - 61 - 24

361/II

Contents

Precise Measurement of Heat of Combustion With a Bomb Calorimeter [1]

R. S. Jessup

This Monograph gives detailed descriptions of apparatus and methods which are used at the National Bureau of Standards for precise determinations of heats of combustion of liquid hydrocarbon fuels. Numerical examples are given of methods of calculating results of measurements from observed data. The technique of making and filling glass bulbs to contain samples of volatile liquid fuels is described.

The accuracy of the methods described is about 0.1 percent. This is intermediate between the accuracy of 0.01 or 0.02 percent attained in certain measurements on pure compounds, and the accuracy of several tenths of one percent obtainable with published standard procedures for measurements on fuels.

1. Introduction

Standard methods of moderate precision for bomb-calorimetric measurement of heats of combustion of solid and liquid fuels are published by the American Society for Testing Materials [1,2].[2] These methods can be used to measure heat of combustion with an accuracy of several tenths of one percent. Apparatus and methods for measurements of heat of combustion with an accuracy of 0.01 or 0.02 percent have been described in the literature [3]. The attainment of such accuracy involves the use of rather laborious and time-consuming procedures. In some applications of fuels the heat of combustion is required with an accuracy of approximately 0.1 percent, which is probably not attainable with the standard methods referred to [1, 2], but can be attained with less expenditure of time and effort than is required in the most precise measurements.

This Monograph describes methods and apparatus used at the National Bureau of Standards in connection with several series of investigations of heats of combustion of aircraft fuels [4, 5, 6, 7]. The restrictions of the treatment to a particular set of apparatus, and a particular experimental procedure involves some loss of generality, but this is not believed to be serious. Most precise measurements of heats of combustion of materials containing essentially only the elements carbon, hydrogen, nitrogen, and oxygen have been made in apparatus of similar design, to which the same procedures are applicable. Descriptions of other equally satisfactory apparatus for this purpose will be found in reference [3] and the references there cited. There will also be found in some of these references descriptions of apparatus and procedures suitable for measurements on materials containing considerable amounts of such elements as sulfur and halogens. The apparatus and methods described in this Monograph are not suitable for measurements on such materials.

Although the apparatus described in this Monograph is suitable for measurement of heat of combustion with an accuracy of 0.01 or 0.02 percent, the procedure in measurements on fuels is such that a considerable saving in time was achieved at the cost of a somewhat lower precision. This lower precision resulted from several factors as follows:

(1) As a rule only two experiments were made on each fuel, as compared with six or more experiments where the highest possible accuracy is desired; (2) an approximate method was used to obtain the corrected temperature rise of the calorimeter, i.e., the temperature rise corrected for heat of stirring and heat transfer between calorimeter and surroundings; (3) because some liquid fuels are quite volatile there may be an appreciable loss of lighter components in handling. In spite of these effects the results of measurements even on the most volatile fuels (gasolines) are, in general, precise to about 0.05 percent. The results contain a nearly constant systematic error of approximately 0.03 percent (for hydrocarbon fuels) due to neglect of the Washburn correction [18] which takes account of the difference between heats of combustion in oxygen under a pressure of about 30 atm and at a pressure of 1 atm.

(If desired, this error can be approximately corrected, in the case of hydrocarbon fuels only, by reducing the observed heat of combustion by 0.03 percent.)

In other respects the methods described are applicable in measurements of the highest precision, and may serve as a useful guide to persons interested in such measurements.

1.1. Definitions of Terms

a. Heat Units

The heat units used in connection with measurements of heats of combustion of fuels are the IT calorie [3] and the Btu. These units are here defined as follows:

[1] The preparation of this Monograph was supported in part by the Air Force Ballistic Missiles Division, Air Research and Development Command, U.S. Air Force.

[2] Figures in brackets indicate the literature references on page 16.

[3] IT calorie is an abbreviation for International Steam Tables calorie. This calorie was adopted by the International Steam Table Conference held in London in July 1929 [12], and is in fairly general use in engineering practice both in this country and abroad.

1 IT calorie=4.1868 absolute joules
1 Btu=1055.07 absolute joules.

The definition of the Btu was obtained from that of the IT calorie by means of the relations

1 pound (avoirdupois)=453.5924 grams
1 IT calorie per gram=1.8 Btu per pound.

b. Heats of Combustion

The quantity directly measured in a bomb-calorimetric experiment is generally referred to as the "total (or gross) heat of combustion at constant volume"; this quantity is represented by the symbol Q_v (gross) in this Monograph. A precise definition of this term requires a specification of the initial states of the reactants (oxygen and fuel) and of the final states of the products of combustion. For most purposes the following definition is sufficient: *The total (or gross) heat of combustion at constant volume of a liquid or solid fuel containing only the elements carbon, hydrogen, oxygen, nitrogen and sulfur is the quantity of heat liberated when unit weight of the fuel is burned in oxygen in an enclosure of constant volume, the products of combustion being gaseous* CO_2, N_2, *and* SO_2 *and liquid* H_2O, *with the initial temperature of fuel and oxygen and the final temperature of the products of combustion at 25° C.*

Although the total heat of combustion is the quantity directly measured in a bomb-calorimetric experiment, the quantity required in many practical applications is the "net heat of combustion at constant pressure." This quantity is designated by the symbol Q_p (net), and may be defined as follows: *The net heat of combustion at constant pressure of a liquid or solid fuel containing only the elements carbon, hydrogen, oxygen, nitrogen, and sulfur is the quantity of heat liberated when unit weight of the fuel is burned in oxygen (or air) at a constant pressure of one atmosphere, the products of combustion being* CO_2, N_2, SO_2, *and* H_2O, *all in the gaseous state, with the initial temperature of fuel and oxygen and the final temperature of products of combustion at 25° C.*

For the most fuels to which these definitions apply the elements oxygen, nitrogen, and sulfur will be minor constituents if present at all. The methods described in this Monograph are not suitable for accurate measurements on materials containing more than about 2 percent sulfur.

2. General Discussion of Bomb-Calorimetric Measurements

A bomb calorimeter consists essentially of a calorimeter vessel containing a measured amount of water, in which are immersed (1) a thermometer for measuring the temperature of the water, (2) a stirring device for maintaining the water at a uniform, and therefore definitely measurable temperature, and (3) a "bomb" of constant volume in which combustible materials can be burned in oxygen under pressure. In order to control heat transfer between the calorimeter and its environment ("thermal leakage") the calorimeter vessel is enclosed by a "jacket" which is separated from the vessel by an air space about 1 cm thick, and which for a majority of precise calorimeters, is kept at constant temperature by means of a thermostat.

A schematic diagram of a bomb calorimeter and its jacket is shown in figure 1. The calorimeter vessel is made in the form shown in order to facilitate stirring of the calorimetric liquid. The effectiveness of a screw propeller stirrer is greatly increased by enclosing it in a tube which extends from near the top to near the bottom of the calorimeter vessel. Putting the tube outside of the main part of the calorimeter vessel, as shown in figure 1(b), reduces the total volume of the calorimeter necessary for a bomb of given size.

In principle, a measurement of the heat of combustion of a given material consists in comparing the corrected temperature rise of the calorimeter in an experiment in which a known quantity of energy is supplied to it, with that produced in another experiment by combustion

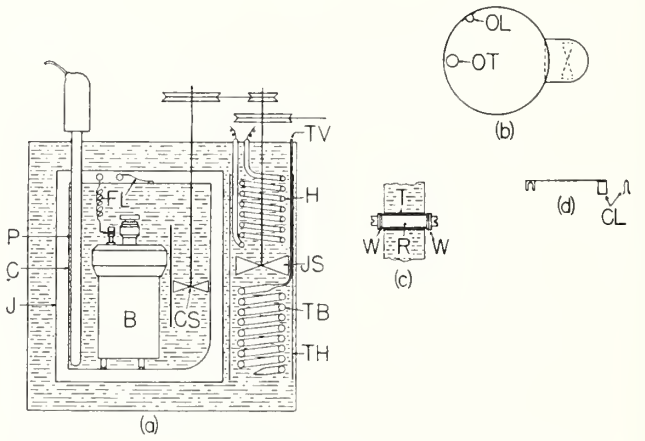

FIGURE 1. *Schematic diagram of a bomb calorimeter.*

(a) Assembled calorimeter with jacket: B, bomb; C, calorimeter vessel; J, jacket wall; P, resistance thermometer; FL, firing leads; CS, calorimeter stirrer; JS, jacket stirrer; TV, tube to thermostat valve; H, jacket heater; TB, thermostat bulb; and TH, tubular housing. (b) Top view of calorimeter vessel OL, opening for firing lead; and OT, opening for thermometer. (c) Firing lead through jacket T, tube; R, rod; and W, washers. (d) Firing lead to calorimeter vessel CL, clip.

in the bomb of a weighed sample of the given material. The temperature rise in both experiments should be as nearly as possible over the same temperature range from a standard initial temperature to a standard final temperature. This method of using the corrected temperature rise of the calorimeter to compare an unknown with a known quantity of energy eliminates some of the systematic errors of calorimetric measurements, in particular those associated with uncertainty as to the exact location of the boundary of the

calorimeter, and those associated with various kinds of lag, by virtue of which different parts of the calorimeter are at different temperatures when the temperature is changing.

Experiments to determine the corrected temperature rise of the calorimeter when a known quantity of energy is supplied to it are generally called calibration experiments, and the mean result of a series of such experiments expressed as energy supplied per unit of corrected temperature rise is called the "energy equivalent" of the calorimeter. The product of the energy equivalent and the corrected temperature rise of the calorimeter in an experiment in which a material of unknown heat of combustion is burned in the bomb gives the energy liberated in the combustion reaction plus any side reactions which may occur.

Calibration experiments are conveniently carried out by burning in the bomb weighed samples of a standard material, such as benzoic acid (NBS Standard Sample 39), the heat of combustion of which is accurately known. If the calorimeter is to be used for measurements of heats of combustion of volatile liquids, such as gasolines, it is desirable to supplement the calibration experiments with benzoic acid by making a series of measurements on NBS Standard Sample 217 of 2,2,4-trimethylpentane, which is a volatile liquid with a certified value for its heat of combustion. The difference between the measured and certified values of heat of combustion will give an overall check on the accuracy of the measurements, and in particular, on the effectiveness of precautions taken to eliminate effects of volatility.

Since a measurement of heat of combustion involves the comparison of two nearly equal changes in temperature covering the range from a standard initial temperature to a standard final temperature, the temperature scale used in the measurement is not important. Thus temperatures can be expressed in terms of the resistance in ohms of a given platinum resistance thermometer with the energy equivalent of the calorimeter in calories per ohm, or in Celsius degrees with the energy equivalent in calories per degree.

3. Factors Affecting Accuracy in Bomb-Calorimetric Measurements

The overall error in the result of a bomb-calorimetric measurement is the algebraic sum of individual errors contributed by various factors. Some of the individual errors may be positive and others negative, so that to some extent they may be expected to cancel. However, the extent to which cancellation may take place is uncertain, and may vary from one experiment to another, so that the percentage contribution of each individual error should be kept well below the permissible overall error of the determination. In the present Monograph the permissible difference between duplicate determinations is taken as 0.05 percent. In order to attain this precision, the error contributed by each of the various independent factors should be kept below 0.01 percent so far as possible.

The factors which may affect the accuracy of a bomb-calorimetric determination may be divided roughly into two classes, (1) side reactions which may take place in the bomb, the effect of which cannot be readily evaluated, and (2) the experimental techniques used in making the various individual measurements. These two classes of factors are discussed in sections 3.1 and 3.2, respectively.

3.1. Undesirable Side Reactions

These include (a) formation of carbon monoxide, carbon, or other products of incomplete combustion of the samples; (b) oxidation of the crucible in which combustion of the fuel sample takes place, or oxidation of other parts of bomb or fittings; (c) reaction of acids formed in combustion with the material of the bomb; (d) oxidation of combustible impurities such as hydrogen or hydrocarbon gases in the oxygen used.

a. Incomplete Combustion

In tests of volatile liquid fuels which must be enclosed in glass bulbs to prevent loss by evaporation, incomplete combustion sometimes occurs as a result of breakage of the bulb before ignition of the sample. In such cases large amounts of carbon will usually be formed, and the results of such tests should be discarded. Normally a bulb containing a volatile liquid sample does not break before ignition of the sample, and in such cases there is generally little or no evidence of incomplete combustion. It occasionally happens that globules of glass remaining in the crucible after combustion are gray or black in color. This may be due to metal oxides formed in combustion of the fuse wire, or to inclusion of a small amount of carbon in the glass while it is molten. Determinations of carbon dioxide in the products of combustion of pure liquid hydrocarbons which were enclosed in soft glass bulbs indicate that the amount of carbon in such glass globules does not exceed 0.01 percent of the carbon in the sample.

Incomplete combustion of solid materials, such as benzoic acid, is very likely to occur if these materials are placed in the crucible in powdered form. For this reason, such materials should be compressed into pellets. For samples of non-volatile liquid fuels which are not enclosed in glass bulbs, and for pelleted samples of benzoic acid, incomplete combustion almost never occurs in apparatus such as that described in the appendix.

b. Oxidation of Crucible and Fittings

Oxidation of the crucible and its support and other fittings exposed to the direct action of the flame can be avoided by using platinum crucibles and fittings (see appendix).

c. Reaction of Acids with Bomb Material

Reaction of acids formed in combustion with the material of the bomb can be made negligible by the use of suitable corrosion-resistant material for the bomb. The bomb described in the appendix has been found satisfactory in this respect. Bombs provided with gold or platinum linings have also been found to be satisfactory.

d. Combustible Impurities in Oxygen

Combustible impurities in the oxygen used may introduce very serious errors into the results of bomb-calorimetric measurements. Oxygen prepared by electrolysis of water may contain enough hydrogen to cause errors of 1 percent or more. The possibility of error from this source is eliminated by passing the oxygen over copper oxide at 500° C before admitting it to the bomb (see appendix).

3.2. Experimental Techniques of Individual Measurements

The most important of the individual measurements which go to make up a bomb calorimetric determination include measurements of (a) the weight of the sample of combustible; (b) the weight of the calorimeter plus water; and (c) the temperature rise of the calorimeter, including correction for thermal leakage and heat of stirring. A given percentage error in any one of these measurements introduces an equal percentage error into the final result of the experiment. Other individual measurements which determine relatively small correction terms and which can be easily made with the necessary precision include measurements of (d) the quantity of energy used to fire the charge of combustible; (e) the amounts of oxygen and other materials in the bomb; and (f) the amounts of nitric and sulfuric acid formed in the combustion reaction.

a. Weight of Sample of Combustible

The sample of combustible (0.8 to 1.5 g) is weighed with a precision of about 0.02 mg using an undamped semimicro balance with a keyboard arrangement for adding and removing the smaller weights (see appendix). Calibrated high grade (class M) weights are used, and the corrections to the weights given on the calibration certificate are applied in determining the weight of the sample. If weighings are made in the ordinary manner with weights and object weighed on opposite pans of the balance, the balance should be tested to determine whether the balance arms are of equal length. If the arms are found to differ in length by a significant amount a correction for this difference will be necessary.

The necessity for such a correction can be eliminated by using the method of weighing by substitution. This consists in placing on the left-hand pan a fixed weight or "tare," somewhat greater in weight than the heaviest object to be weighed, then placing the object to be weighed on the right-hand pan together with sufficient weights, including rider adjustment, to balance against the tare. The object being weighed is then removed and weights and rider again adjusted to obtain balance. The difference in the weights required in the two cases is the desired weight of the object. In addition to eliminating the effect of any difference in length of the balance arms, this method also eliminates any change in sensitivity with load, since the load is constant. The following description of the procedure is for this method of weighing by substitution.

Each half of the balance beam from the center knife edge to the outer knife edge is graduated in 100 equal divisions, so that if a 1 mg rider were used a change in position of the rider by one division on the scale would correspond to a change in weight of 0.01 mg. However, it may be inconvenient to use such a small rider because of the likelihood of its being deformed or lost. Instead, a 10 mg rider may be used so that one division on the scale corresponds to 0.1 mg in weight, and hundredths of a milligram obtained from the deflection of the pointer, as described below.

Weighings are normally made with the weights to the nearest milligram on the right-hand pan of the balance, and the 10 mg rider so placed (between 0 and +10 divisions on the beam scale) that the tare weight on the left-hand pan is balanced to the nearest 0.1 mg. The equilibrium position of the pointer with reference to the zero of the index scale is then determined by observing the turning points of the pointer in an odd number of swings (3 or 5).

The procedure in using the balance will be illustrated by an example of the weighing of a sample of benzoic acid. All weighings are made after time has been allowed for temperature equilibrium to be established, and for air currents set up when the balance case was open to die out. To determine when equilibrium has been established, the apparent weight is observed from time to time until no change has been observed during a period of about 10 min.

The following observations were made in determining the weight of a pellet of benzoic acid, the first set of observations were made with the empty crucible, and the second with the crucible containing the pellet:

Crucible empty:		
Weights	12. 493 g	Turning points of swings:
Rider	0. 0002	−2. 6 2. 0
Pointer deflection $\times 2, -0.55 \times 0.07 \times 10^{-3}$	− . 00004	−2. 5
Total weights	12. 49316	−2. 55 2. 0
		2×pointer deflection = −0.55
Crucible plus pellet:		
Weights	10. 971	Turning points of swings:
Rider	0. 0003	−2. 3 2. 6
Pointer deflection $\times 2, 0.45 \times 0.07 \times 10^{-3}$	. 00003	−2. 0
Total weights	10. 97133	−2. 15 2. 6
		2×pointer deflection = +0.45
Observed weight of pellet	1. 52183	
Weight correction [a]	+ . 00005	
Corrected weight of pellet	1. 52188	

[a] The weight correction is the algebraic sum of the certificate corrections to the individual weights used with the empty crucible minus the algebraic sum of the corrections to the weights used with crucible plus pellet.

In the above example the weight corresponding to the pointer deflection from the zero of the index scale was obtained by multiplying twice the average deflection (in divisions on the scale) by one-half of the sensitivity reciprocal of the balance, in this case $0.07 = 1/2 \times 0.14$ mg per scale division. (The same result would be obtained, of course, if the average deflection were multiplied by the sensitivity reciprocal, e.g., for the first weighing of the above example the average pointer deflection $= -0.28$ and $-0.28 \times 0.14 = -0.04$ mg).

The same procedure is followed, for example, in weighing a sample of a volatile liquid which must be enclosed in a glass bulb to prevent loss by evaporation, except in this case it is not necessary to include the crucible in either weighing. The empty bulb is first weighed against the tare, and then the filled bulb together with glass removed in sealing is weighed against the tare. It should be emphasized that the balancing weight against the tare with only the weights on the right-hand pan should be determined in weighing both the empty bulb and the filled bulb. The use of a fixed value for the balancing weight against the tare with only the weights on the right-hand pan would introduce errors if the rest point of the balance changes between the times of weighing the empty and filled bulbs. This is likely to occur if a considerable length of time elapses between the weighings with the bulb empty and filled. The use of a fixed value for the balancing weight with the empty crucible on the right-hand pan is ruled out by the fact that the crucible is subject to changes in weight in use.

b. Weight of Calorimeter Plus Water

The calorimeter plus water (3,700 g total weight)[4] is weighed on a magnetically damped balance having a capacity of 5 kg and a sensitivity of 0.5 mg (see appendix). The procedure in this weighing is as follows: The calorimeter is filled with approximately the desired quantity of water, the temperature of which is adjusted to a value such that after assembly of the calorimeter its temperature will be a few tenths of a degree below the desired initial temperature in the experiment. The choice of the temperature to which the water is to be brought before weighing will depend upon a number of factors, including room temperature, the desired initial temperature in the calorimetric experiment, and the relative heat capacities of calorimeter vessel, water, and bomb. No definite rule can be given for this choice, but the operator will learn by experience how to select the proper temperature under the conditions of his particular laboratory and apparatus.

After adjustment of the temperature the calorimeter is placed on one pan of the balance with the desired weights (see footnote 4) on the other. The amount of water in the calorimeter is adjusted so that the total weight of calorimeter plus water exceeds slightly that of the weights on the opposite balance pan, and the balance case is closed. Because of evaporation of water the weight of calorimeter plus water decreases slowly, and the pointer on the balance gradually moves toward the zero of the index scale. When the pointer reaches the scale zero the balance beam is arrested, the case is opened, and the calorimeter is removed from the balance and placed in position in its jacket preparatory to making a calorimetric experiment.

It is not feasible in weighing the calorimeter to wait for it to come to temperature equilibrium with the air, partly because this would require a very long time and partly because the desired initial temperature in the calorimetric experiment will usually differ from room temperature. Any difference in temperature between calorimeter and the air in the balance case will cause convection currents which will affect the observed weight. The effect of this will partially cancel if the difference between the temperature of calorimeter and the air in the balance case when the calorimeter is weighed is the same in all experiments, including both calibration experiments and measurements of heat of combustion.

The change in weight of the water in the calorimeter due to evaporation after weighing will affect the energy equivalent of the calorimeter, but the effect of this is small and will cancel if the

[4] The weight should correspond to an amount of water in the calorimeter such that when the bomb is immersed in the water the calorimeter cover can be put in place with its lower side in contact with the water.

procedure in placing the calorimeter in its jacket and completing the assembly of the system is carried out in the same manner and in the same length of time in the calibration experiments as in measurements of heat of combustion.

In addition to the water in the calorimeter vessel, 1 cm^3 of water is placed in the previously dried bomb before each experiment to insure that the space in the bomb is saturated with water vapor at the beginning of the experiment as well as at the end, when water formed in combustion will be present in any case. This water is introduced into the bomb by means of a buret or pipet accurate to about 0.01 cm^3, immediately before introducing the sample of combustible.

c. Temperature Measurements

The temperature rise of the calorimeter in a combustion experiment is approximately 3° C, and must be measured with an accuracy of 0.0003° if the error in temperature measurement is to contribute not more than 0.01 percent to the result of the calorimetric experiment. Measurements of temperature differences with this precision can be made conveniently with a suitable 25 ohm platinum resistance thermometer, and a Mueller bridge of the type commonly designated as G–2.

In precise measurements of temperature with a resistance thermometer it is customary to eliminate the resistance of the thermometer leads completely by making two resistance readings, with the commutator set first in the N position and then in the R position. In bomb calorimetric measurements where only a small temperature difference is to be measured and where time for making the temperature measurements is limited, it is permissible to omit changing the commutator setting. However, if this procedure is followed it is very important that all measurements in all experiments be made with the same commutator setting, since the change in observed resistance per degree change in temperature may be different for the N and R positions of the commutator. The possibility of error due to change in the commutator setting may be eliminated by permanently disconnecting one of the current leads (c or t) of the thermometer from the bridge. The thermometer is then effectively a 3-lead thermometer and the bridge can be operated with only one setting of the commutator.

It is also important that the thermometer be immersed to the same depth in all experiments, so that its contribution to the energy equivalent of the calorimeter will be the same in all experiments, and so that the temperature distribution along the leads will be the same.

The observations of the temperature of the calorimeter in a bomb-calorimetric experiment must be made in such a manner as to provide data from which can be derived a value for the temperature rise corrected for thermal leakage and heat of stirring. The following procedure is for a calorimeter with the jacket maintained constant at a standard temperature.[5]

Temperatures of the calorimeter are measured at definite times during three periods: (1) An initial period of 6 to 10 min during which the temperature change results solely from thermal leakage and heat of stirring; (2) a middle period of about 12 min, at the beginning of which the charge in the bomb is fired, and during which the temperature change is due partly to thermal leakage and heat of stirring but mostly to the heat liberated by the combustion reaction in the bomb—this period continues until the rate of change of temperature has become constant; and (3) a final period of 10 min or more, during which the temperature change is again due solely to thermal leakage and heat of stirring. It is desirable to choose the initial temperature of the calorimeter so that its final temperature will be slightly below that of the jacket. This reduces the total thermal leakage during the middle period and eliminates heat transfer by evaporation of water from the calorimeter and condensation on the jacket wall which would occur if the temperature of the calorimeter exceeded that of the jacket.

During the initial and final periods the resistance of the thermometer should be measured with the highest possible accuracy, since the overall accuracy of the determination depends directly upon the accuracy of these temperature measurements. During the middle period, because of the very rapid rate of temperature rise, it is not possible to make readings as accurately as during the initial and final periods, but this is not important because the readings of the middle period are used only for calculating the relatively small correction for thermal leakage and heat of stirring.

With a G–2 bridge and a thermometer having a resistance of approximately 25.5 ohms at 0°C, one step in the last dial of the bridge (0.0001 ohm) corresponds to approximately 0.001°C in temperature. Readings of the bridge are made to the nearest 0.00001 ohm (0.0001°) by interpolating between two adjacent settings of the last dial of the bridge. This interpolation is accomplished by observing the deflection of the galvanometer as follows: The galvanometer is located about 2 meters from a ground glass scale graduated in millimeters, which is so placed as to be conveniently observable by the operator of the bridge. In front of the galvanometer mirror is placed a lens of such focal length that the reflected image of the vertical filament of a light source is focused on the ground-glass scale.[6] The bridge current is adjusted so that with constant thermometer resistance a change of 0.001 ohm in the bridge

[5] The NBS calorimeter is located in an air-conditioned laboratory, the temperature of which is maintained at about 25° C. The jacket temperature is always maintained constant at 28° C and the calorimetric experiments cover the range from 25° to 28° C. If room temperature is not controlled the standard temperature of the jacket should be taken high enough so that it will be above room temperature at all seasons. A jacket temperature below that of the room is undesirable as it may result in the condensation of water on the calorimeter, the initial temperature of which is 3° C below that of the jacket.

[6] Lamp and scale devices for indicating galvanometer deflection are available commercially, and are as satisfactory as the device described here.

setting causes a galvanometer deflection corresponding to a 2.5 cm displacement[7] of the filament image on the scale. This is equivalent to a displacement of 2.5 mm per step in the last dial of the bridge, i.e., to 2.5 mm per millidegree. This sensitivity is doubled by reversing the current through the bridge and observing the resulting change in position of the filament image. The sensitivity is such that when the bridge current is reversed a displacement of the filament image by 0.5 mm corresponds to 0.00001 ohm (0.0001°). Reading the bridge by observing the deflection of the galvanometer when the bridge current is reversed not only increases the sensitivity but also reduces the effect of changes in the galvanometer zero. The reversal of the bridge current is conveniently made by means of a double-pole double-throw toggle switch connected in the battery circuit.

The above discussion of the deflection of the galvanometer when the bridge current is reversed tacitly assumes that the resistance of the thermometer remains constant during this operation. In an actual calorimetric experiment the resistance of the thermometer is usually changing with time; in the initial period for example the resistance of the thermometer is increasing at a rate of approximately 0.0007 ohm/min. (0.007° C/min). During this period readings are made once per minute in such a manner as to give the resistance of the thermometer to the nearest 0.00001 ohm at intervals of exactly 1 min. These readings are made as follows: The switch for reversing the bridge current is thrown in the direction such that as the temperature of the calorimeter rises the image of the filament of the galvanometer light source moves toward the observer's right. The bridge dials are adjusted occasionally so as to keep the filament image slightly to the left of its zero position. The time is observed by means of a stop watch, or preferably by means of a combination of stop watch and audible second signals from a standard clock. The position of the filament image is observed to the nearest 0.5 mm at a time 4 sec before the even minute and the reversing switch is thrown immediately. The position of the image is observed again at 4 sec after the even minute[8] and the switch is then thrown back to its original position in preparation for later readings. If the second position of the filament image is exactly the same as the first, then the galvanometer deflection on the even minute was zero, and the reading of the bridge is correct with zero in the next place after the reading of the last dial. If the second position of the filament image is x mm to the left (or right) of the original reading, then the reading of the bridge should be increased (or decreased) by $0.00002x$ ohm to obtain the reading corresponding to the even minute. For example, if the reading of the bridge is 27.3956 ohms and the upper and lower arrows in figure 2(a) represent the initial and final positions, respectively, of the filament image, then the corrected reading of the bridge at the even minute would be 27.39563 ohms. On the other hand the situation represented in figure 2(b) for the same setting of the bridge dials would correspond to a corrected bridge reading of 27.39556 ohms.

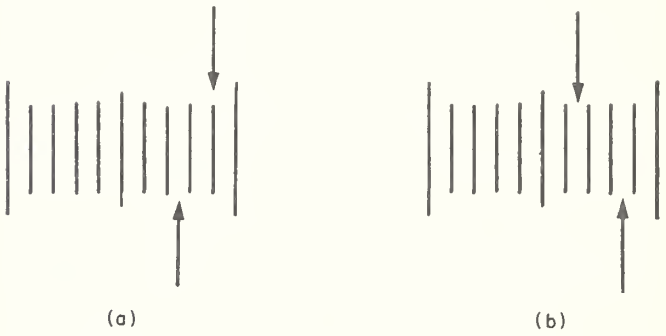

FIGURE 2. *Diagram to illustrate use of galvanometer deflections in reading bridge*

With a little practice an observer can learn to anticipate each bridge reading fairly closely after the first one or two of a series, and to preset the bridge dials for each subsequent reading so that the change in galvanometer deflection upon reversal of the current will not exceed 2.5 mm (0.00005 ohm or 0.0005° C).

As a result of the preliminary adjustment of the temperature of the water in the calorimeter before weighing it as described in section 3.2.b., it is to be expected that after assembling the calorimeter the temperature will be a few tenths of a degree below the desired initial temperature. The temperature should then be raised to about 0.05° (0.005 ohm) below the temperature at which the initial period is to start, and allowed to drift up to this temperature as a result of thermal leakage and heat of stirring. The observations of the initial period are then made as described above.

The heating of the calorimeter to 0.05° below the starting temperature is most conveniently done by means of an electric heater which is a permanent part of the calorimeter system. Another method which is frequently used is to place a heated brass rod (½ in. × 2 in.) on top of the calorimeter cover. The rod is inserted through a hole in the jacket cover which is normally closed by a brass plug. Care is taken to avoid having the heated rod come in contact with the jacket and thereby upset the control of its temperature.

[7] With the particular combination of bridge, thermometer, galvanometer, and galvanometer to scale distance used, the bridge current of 6.8 ma (thermometer current of 3.4 ma) gives the sensitivity indicated. Much higher bridge current is undesirable because of the increased heating of the thermometer and the consequent increased variation of thermometer resistance with slight variations in bridge current. A 6-volt low-discharge storage battery is a convenient source of bridge current.

[8] The time which should elapse between the two observations of the galvanometer deflection depends upon the free period of the galvanometer. The reading time of an underdamped galvanometer with a relative damping constant of 0.8 or 0.9 is roughly equal to the free period [19].

The above instructions may be illustrated by an example. The calorimeter temperature before weighing was adjusted to a value such that after assembly of the calorimeter the thermometer reading was 20.5+7.420 ohms.[9] By means of the heated rod referred to above, the temperature was raised until the reading of the bridge was 20.5+7.465 ohms. The rod was then removed, the plug replaced in the hole in the jacket, and the calorimeter temperature allowed to drift upward until the bridge reading was 20.5+7.4701 ohms when the readings of the initial period were begun. These are made once per minute as indicated previously.

Immediately after the observations of the initial period are completed the charge of combustible in the bomb is ignited by means of an electric fuse, the sensitivity of the galvanometer is reduced by reducing the bridge current to about one-third of its original value, and the observations of the middle period are begun. These must be made so rapidly that there is no time for reversing the bridge current for each observation. The observations are made by setting the bridge dials successively at certain predetermined readings and observing the times at which the galvanometer deflection becomes zero. After about 3 min the rate of temperature rise has decreased to such an extent that the bridge current can be increased to its original value and the precise readings of resistance each minute are resumed. These precise readings are continued until the rate of temperature change has been constant for at least 10 min. The observations made after the rate of temperature change has become constant constitute those of the final period.

TABLE 1. *Observations of time and thermometer resistance during a bomb-calorimetric experiment*

Time minutes	Resistance minus 27.5 ohms	Difference × 10^5	Time minutes	Resistance minus 27.5 ohms	Difference × 10^5
0	0.47015	63	7.614	0.7000	
1	.47078	64	7.747	.7100	
2	.47142	64	7.922	.7200	
3	.47206	128 (64)	9	.75050	870
4		(64)	10	.75920	350
5	.47334	63	11	.76270	140
6	.47397		12	.76410	60
6.528	.4900		13	.76470	29
6.621	.5100		14	.76499	16
6.682	.5300		15	.76515	10
6.754	.5500		16	.76525	9
6.820	.5700		17	.76534	6
6.894	.5900		18	.76540	6
6.970	.6100		19	.76546	7
7.066	.6300		20	.76553	7
7.170	.6500		21	.76560	6
7.320	.6700		22	.76566	20 (7)
7.399	.6800		23		(6)
7.496	.6900		24		(7)
			25	.76586	6
			26	.76592	7
			27	.76599	7
			28	.76606	

[9] The bridge has a 20.5-ohm coil in addition to the 10-, 20-, 30-ohm coils, etc., in the 10x10-ohm decade (see appendix).

Bridge readings made during the course of a typical bomb calorimetric experiment are given in table 1, and are shown graphically in figure 3. The values given for resistance represent the observed resistance of the thermometer minus 27.5 ohms. The initial period extends from $t=0$ to $t=6$ min, the middle period from $t=6$ to $t=18$ min, and the final period from $t=18$ to $t=28$ min. The constancy of the differences between consecutive readings in the initial and final periods is an indication that the system has attained a steady state. This is a necessary condition for the applicability of the method given in section 5 for calculating the corrected temperature rise.

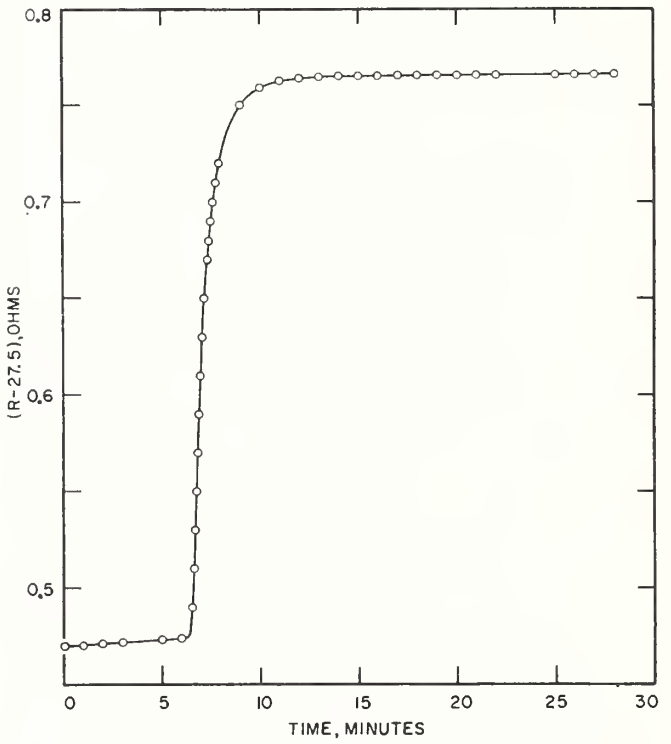

FIGURE 3. *Bridge readings versus time in a bomb calorimetric experiment.*

In the particular experiment illustrated in table 1 and figure 3 the time readings during that part of the middle period from $t=6$ to $t=9$ min were made by means of an electric timer which prints the time at which the operator presses a button when he observes the galvanometer deflection to pass through zero. This instrument is a convenience and would be an important part of the equipment in measurements of extremely high precision. It is not a necessary part of the apparatus for measurements of the precision aimed at in the procedures described in this Monograph. For such precision it is also not necessary to obtain as many readings in the middle period. It is sufficient to make three or four measurements in the range from 55 to 70 percent of the total temperature rise, and to read the time to the nearest second (or the nearest 0.01 min) by means of a stopwatch.

The corrected temperature rise for the experiment illustrated in table 1 and figure 3 is calculated in section 5.

d. Firing Energy

The quantity of energy used to fire the charge is the sum of the electric energy used to ignite the fuse plus the heat of combustion of the amount of fuse wire burned. The current for igniting the fuse is obtained from a small transformer with a secondary voltage of about 10. The total firing energy can be determined in a series of blank experiments in which only the fuse wire is burned. In such experiments the temperature rise of the calorimeter is very small, and the initial temperature of the calorimeter should be very near that of the jacket. The rate of change of temperature in the initial and final periods will then be small, and the correction for thermal leakage will also be small.

When a 2-cm length of fuse wire is used in the manner described in the appendix it has been found that if the wire is burned completely [10] the firing energy is constant and equal to 5.2 cal. No appreciable error will result from using this value in any case where the same type of fuse is used, i.e., a 2-cm length of Parr fuse wire wound into a helix and attached to platinum leads. The firing energy in this case is only 0.05 percent of the energy normally produced in a combustion experiment, and any error in the value 5.2 cal will largely cancel if this same value is used for both calibration experiments and measurements of heats of combustion, and if the temperature rise is about the same in the two kinds of experiment.

The most serious error likely to be encountered in accounting for the firing energy is that which may result from a short-circuit between the firing electrode and the bomb, either because of failure of the insulation around the electrode or because of moisture getting into the mica insulation inside of the bomb. This mica normally is wet by the acid solution formed in combustion and by the water introduced in washing the interior of the bomb after each experiment. It should be dried thoroughly before each experiment, and the insulation should be tested before attaching the fuse to its platinum leads. An insulation resistance of less than 10^6 ohms usually indicates either moisture in the insulation or some other failure of the insulating material which needs to be corrected. A "megger" or volt-ohmeter or other similar instrument may be used for testing the insulation resistance.

[10] Combustion of the fuse wire may not be complete in all blank experiments to determine the firing energy, although it is practically always complete when a sample of fuel is burned in the bomb. Blank experiments in which combustion of the fuse wire is incomplete should be rejected, or else a correction for the unburned wire should be applied.

e. Materials in Bomb

A calibration of the calorimeter yields a value for the energy equivalent E of the system as actually used, consisting of calorimeter vessel, stirrer, water, thermometer, bomb, and contents of the bomb at the beginning of the experiment. The calorimeter vessel, stirrer, mass of water, thermometer, and bomb will ordinarily be unchanged from one experiment to another, and the crucible and amount of water placed in the bomb will also be constant. However, the mass of the platinum leads to the fuse, the mass of oxygen, and the mass and kind of combustible material may change from one experiment to another. The heat capacity of the largest amount of platinum wire in the bomb amounts to only 0.001 percent of the total energy equivalent of the system, so that variations in the amount of platinum wire are entirely negligible. The mass of oxygen in the bomb is inversely proportional to absolute temperature and directly proportional to absolute pressure. The temperature is measured to about 0.5° C at the time the oxygen is admitted to the bomb, by means of a mercurial thermometer with its bulb near the bomb. The pressure of the oxygen (about 30 atm=450 psi) is measured to the nearest 0.1 atm (1.5 psi) by means of a calibrated Bourdon gage.

The values of the energy equivalent E obtained in calibration experiments are reduced to the energy equivalent E_s of a standard calorimeter system consisting of the calorimeter vessel with cover, the standard mass of water, stirrer, thermometer, and bomb containing 1 ml of water, the crucible, and oxygen under an absolute pressure of 30.0 atm at 28.0° C but no combustible material. In a measurement of heat of combustion the energy equivalent E_s of the standard calorimeter system is corrected for any excess of the oxygen pressure at 28° C over 30 atm and for the heat capacity of the charge of combustible.

The reduction of the observed E to the corresponding value of E_s, and vice versa, is discussed in section 5 on calculation of results.

f. Acids Formed in Combustion

Nitric acid is normally formed in the combustion reaction from nitrogen either in the fuel sample itself or present as an impurity in the oxygen. If sulfur is present in the fuel, oxides of sulfur will be formed. These are entirely converted to sulfuric acid if nitric acid is also formed. For this reason, if the fuel is known or suspected to contain a significant amount of sulfur, the air initially present in the bomb should not be flushed out with oxygen at the time oxygen is admitted to the bomb. The sulfur will then be all converted to aqueous sulfuric acid, and therefore to a determinate final state.

The total acid formed in combustion is deter-

mined by washing the inner surface of the bomb with distilled water and titrating the washings against 0.1 N sodium hydroxide, using methyl orange as the indicator.

If both nitric and sulfuric acids are formed the total acid is determined by titration as before, and the sulfur is determined by analyzing the bomb washings after titration, using the procedure described in ASTM Designation D129–58 [14]. The correction for nitric acid is 14.0 kcal/mole of acid formed. If sulfur is present in the fuel the total acid is corrected for as if it were all nitric acid, and an additional correction of 1,400 cal/g of sulfur is applied.

4. Summarized Directions for a Bomb-Calorimetric Experiment

Summarized directions will now be given for carrying out a bomb-calorimetric experiment with benzoic acid to determine the energy equivalent of the calorimeter. Following these directions there will be a brief discussion of the differences in procedure in an experiment to determine the heat of combustion of a fuel.

4.1. Preliminary Adjustment of Apparatus

Observe the temperature of the oxygen purifier and if necessary bring its temperature to 500° C. (Caution: The temperature and oxygen pressure should never be allowed to exceed values consistent with safety with respect to the possibility of explosive failure of the purifier. The manufacturer's recommendations regarding safety precautions should be adhered to rigidly.) Add water, if necessary, to fill the calorimeter jacket bath, bring its temperature to the desired standard value and put the thermostat into operation (see sec. 3.2.c.).

4.2. Preparation and Weighing of Sample of Benzoic Acid

Weigh out approximately an amount of benzoic acid somewhat in excess of 1.52 g [11] and compress it into a pellet. Weigh the pellet on a balance sensitive to about 0.01 g and adjust the weight, if necessary, to 1.52 ± 0.01 g (see footnote 11) by scraping the pellet. Carefully remove any powdered benzoic acid from the pellet by brushing. Weigh the crucible on the semimicro balance, first empty and then after placing the pellet of benzoic acid into it, following the procedure described in section 3.2.a.

4.3. Preparation of Bomb

Test insulation resistance. If less than 10^6 ohms, dry mica or replace cone insulator.

Attach fuse wire to platinum leads as described in the appendix.[12] Measure 1.00 cm^3 of distilled water into the bomb by means of a buret or pipet. Attach the crucible to its support in such a manner that the fuse is nearly touching the pellet of benzoic acid and assemble the bomb. Connect the bomb to the oxygen cylinder through the purifier and admit oxygen to a pressure of approximately 30 atm. The oxygen should be admitted slowly so as not to cool the copper oxide in the oxygen purifier below the temperature at which it will oxidize combustible impurities in the oxygen. Close the valve in the oxygen line and open the needle valve on the bomb, allowing the oxygen to escape until the pressure is reduced to atmospheric. This procedure removes about 97 percent of the nitrogen in the air initially in the bomb. Refill the bomb to the pressure of approximately 30 atm, read and record the temperature and pressure, and disconnect the bomb from the oxygen tank. Attach the binding post (fig. 6(b)) with the lead wire to the terminal nut on the bomb.

4.4. Weighing of Calorimeter Plus Water

Fill the calorimeter with water, adjust temperature of water, and weigh calorimeter plus water as described in section 3.2.b.

4.5. Assembly of Calorimeter

Immediately after the calorimeter is weighed carry it to the jacket and place it in its proper position in the jacket space. Place the bomb in the calorimeter,[13] put the calorimeter cover in place and press it down until its lower surface is in contact with the water. These operations should be performed rapidly and as nearly as possible in the same manner and in the same length of time in all experiments. Complete the firing circuit by connecting the lead to the bomb electrode to the binding post provided for this purpose (fig. 1.(c)) and connect the other lead (already attached to the other binding post) to the calorimeter vessel by means of the clip shown in figure 1.(d) (see appendix). Close the jacket cover and connect the calorimeter stirrer to its driving shaft. Measure the jacket temperature to 0.001° C (0.0001 ohm) by means of the bridge and resistance thermometer, then remove the thermometer from the jacket bath, dry it, and put it in place in the calorimeter.

[11] The standard mass of benzoic acid should be such as to give a temperature rise of approximately 3° C. The mass used should be within 0.01 g of the standard mass.

[12] It may be convenient to do this while waiting for the attainment of temperature equilibrium in the balance case in connection with weighing the sample of combustible.

[13] The bomb should be lowered into the calorimeter without touching the water with the fingers. This can be done by using some sort of hook on which the bomb can be hung and which can be removed after the bomb is in place. A hook made of a piece of brass or nichrome rod about $\frac{1}{16}$ in. in diameter and bent into the form shown in fig. 6(f) has been found satisfactory for this purpose with the Parr bomb. The hooked ends of the rod are inserted into holes on opposite sides of the screw cap of the bomb, and are easily removed after the bomb is in place. The amount of water which adheres to the hook when it is withdrawn from the calorimeter is negligible.

4.6. Adjustment of Initial Temperature of Calorimeter

Adjust the calorimeter temperature to 0.05° (0.005 ohm) below the starting temperature of the initial period, and allow it to drift up to the starting temperature as described in section 3.2.c. The starting temperature (in calibration experiments) always has the same value, which is so chosen that the final temperature of the calorimeter after combustion will be at, or preferably a few hundredths of a degree below, the temperature of the jacket.

4.7. Observation of Temperature and Ignition of Sample

After the temperature of the calorimeter has been allowed to drift up to the starting temperature, make and record the readings of time and temperature of the initial period each minute as described in section 3.2.c. Immediately after the last reading of the initial period fire the charge by closing the circuit through the fuse in the bomb. Observe the ammeter in this circuit when the charge is fired. The reading of the ammeter should rise abruptly to about 5 amp and then drop almost instantly to zero. Failure of the current to drop immediately indicates a short circuit, and the charge will probably not be ignited, or if it is ignited the result of the experiment will be in error by an unknown amount because of the excess electrical energy. If the ignition takes place normally, make and record the observations of the middle and final periods as described in section 3.2.c. After the end of the final period remove the thermometer from the calorimeter, insert it in the jacket bath and measure the temperature of this bath to 0.001° If the temperature control equipment has been operating properly the jacket temperature should remain constant to 0.005° or better during an experiment.

4.8. Analysis of Contents of Bomb

Remove the bomb from the calorimeter, dry it, open the needle valve and allow the gas to escape at a rate such as to reduce the pressure to atmospheric in not less than 1 min. Then open the bomb and examine the interior for unburned carbon, which would indicate incomplete combustion. If more than a slight trace of unburned carbon is found the experiment should be rejected. If no appreciable amount of unburned carbon is found wash all interior surfaces of the bomb with distilled water and collect the washings quantitatively in a beaker. The quantity of the washings should preferably not exceed 150 ml. Titrate the washings against a 0.1 N solution of NaOH using methyl orange as the indicator. Calculate the correction for nitric acid as described in section 5 on calculation of results.

The procedure in a measurement of heat of combustion follows the same steps outlined in paragraphs 4.1 to 4.8, with certain differences in individual steps as indicated below.

4.2.a. Preparation and Weighing of Sample of Fuel

If the material whose heat of combustion is to be determined is a sufficiently nonvolatile liquid, weigh the empty crucible by the method of substitution as described previously, decrease the weights on the pan with the crucible by the desired weight of sample,[14] and add the liquid drop-wise from a pipet until the weights plus sample plus crucible balance the tare weight on the opposite pan. Ordinarily this procedure will add more than the desired weight of sample, and the excess may be removed, for example, by dipping the end of a fine glass capillary into the liquid. Great care should be taken during the introduction of the sample into the crucible and making the final adjustment of the weight to avoid getting any of the sample on the outside of the crucible. The final weighing of crucible plus sample is carried out as described in section 3.2.a.

If the material whose heat of combustion is to be determined is a volatile liquid, the enclosure of the sample in a glass bulb (as described in the appendix) and the determination of its weight (as described in sec. 3.2.a.) will ordinarily have been done prior to the beginning of the calorimetric measurements. It is then only necessary to place the bulb in the crucible before starting the procedure described in section 4.3. and 4.3.a.

4.3.a. Preparation of Bomb

The procedure here is the same as that described in section 4.3 except that if the sample contains sulfur the air initially in the bomb is not flushed out before filling the bomb with oxygen. If the sample does not contain sulfur the air should be flushed out as described in section 4.3 by filling the bomb with oxygen to 30 atm, allowing the gas to escape until the pressure is reduced to atmospheric, and then refilling the bomb to 30 atm. Where the sample is enclosed in a glass bulb, premature breakage of the bulb when the pressure is first raised to 30 atm can sometimes be detected by the odor of the fuel in the escaping gas when the pressure is released.

4.6.a. Adjustment of Initial Temperature of Calorimeter

In the case of a nonvolatile liquid where the weight of sample is such as to give a temperature rise equal to that in a calibration experiment the adjustment of the initial calorimeter temperature is carried out in the same manner as described in section 4.6.

[14] The weight of sample should be such as to give approximately the same temperature rise of the calorimeter as in the calibration experiments.

In the case of volatile samples it is difficult to make the glass sample-bulbs sufficiently uniform in capacity to give the same temperature rise of the calorimeter in all experiments. Select the initial temperature for each experiment so that the mean of the initial and final temperatures of the calorimeter will be the same as in the calibration experiments.

4.8.a. Analysis of Contents of Bomb

If the sample contains no sulfur follow procedure described in section 4.8. If the sample contains sulfur titrate the bomb washings to determine total acid is described in section 4.8. After this titration analyze the bomb washings for sulfur using the procedure described in ASTM Designation D129–58 [14].

5. Calculation of Results

5.1. Calibration Experiment

Calculate a value for the energy equivalent E from the data of each calibration experiment, using the following formula:

$$E=\frac{Q_c\times m_s+c_1+c_2}{\Delta t}$$

where Q_c=heat of combustion of benzoic acid in IT calories per gram under the conditions of the experiment.
m_s=weight in air, in grams, of sample of benzoic acid burned.
c_1=correction for firing energy, in calories.
c_2=correction for nitric acid, in calories.
Δt=corrected temperature rise of calorimeter, in degrees Celsius (or ohms).

The value of E will be in calories per unit of the temperature scale used, e.g., in calories per deg C, or calories per ohm.

a. Heat of Combustion of Benzoic Acid

The certified value for the heat of combustion of the present standard sample (39h) of benzoic acid under the standard conditions of the bomb process is 6318.3 IT cal/g weight in air.[15] The standard conditions are:

A. The combustion reaction is referred to 25° C.

B. The sample is burned in a bomb of constant volume in pure oxygen at an initial pressure of 30 atm at 25° C.

C. The number of grams of sample burned is equal to three times the internal volume of the bomb in liters.

D. The number of grams of water placed in the bomb before combustion is equal to three times the internal volume of the bomb in liters.

If the conditions in the experiment differ from the standard conditions A, B, C, and D above, the value of Q_c for the heat of combustion of benzoic acid under the actual conditions of the experiment will be obtained from the following approximate equation, which was derived in accordance with the procedure recommended by Washburn [18]:

$$Q_c=6318.3\left\{1+10^{-6}\left[20\left(P-30\right)+42\left(\frac{m_s}{V}-3\right)+30\left(\frac{m_w}{V}-3\right)-45\left(t-25\right)\right]\right\}$$

where P=initial absolute pressure of oxygen, in atmospheres, at the temperature t,
m_s=weight of sample, in grams,
m_w=weight in grams, of water placed in bomb before combustion,
V=internal volume of bomb in liters,
t=temperature to which the combustion reaction is referred, in degrees C.

The temperature to which the reaction is referred is here taken as the final temperature of the calorimeter. The value of the energy equivalent E obtained from eq (1) is then that of the initial calorimetric system at the mean temperature of the calorimeter. By the initial calorimetric system is meant the system before combustion of the benzoic acid, i.e., it includes the benzoic acid, water, and oxygen in the bomb before combustion takes place.

For example let the following data be given:

Volume of bomb, V =0.380 liter
Weight of benzoic acid, m_s =1.522g; m_s/V=4.01g/liter
Weight of water in bomb, m_w =1.00g; m_w/V=2.63g/liter
Initial oxygen pressure =30.8 atm gage at 25.5° C
=31.8 atm abs at 298.7° K
Final temperature of calorimeter, t=28.00° C=301.2° K
Oxygen pressure

at 28.00° C, $P=31.8\times\frac{301.2}{298.7}$

=32.1 atm absolute

Substituting in eq (2) we obtain

$$Q_c=6318.3\{1+10^{-6}[20(32.1-30)+42(4.01-3)+30(2.63-3)-45(28.00-25.00)]\}$$

=6317.9 cal/g in air.

[15] The value for the heat of combustion of benzoic acid is given here in IT calories per gram weight in air against brass weights, the densities of air, brass, and benzoic acid being taken as 0.00116, 8.4, and 1.320 g/cm³, respectively.

b. Correction Terms c_1 and c_2

The correction c_1 for firing energy is preferably determined in a series of blank experiments as described in section 3.2.d. The use of the value $c_1=5.2$ cal will not lead to a significant error if the fuse is a 2-cm length of Parr fuse wire wound into a helix and attached to platinum leads. In some cases a greater length (5 cm or more) of fuse wire is attached to electrodes which are located a short distance away from the crucible. In such cases the fuse may not all burn, and the firing energy will be different in different experiments depending upon the length of wire burned. If this procedure is followed, the length of wire burned in each experiment must be determined and the correction c_1 may be taken as $2.6\times L$ calories, where L is the length of wire burned, in centimeters.

The correction c_2 for nitric acid is 14.0 kcal/mole of nitric acid formed, or 14.0 N cal/cm^3 of sodium hydroxide solution of normality N required to neutralize the acid. Thus if 2.4 cm^3 of 0.0987 N sodium hydroxide is required to neutralize the nitric acid formed, $c_2=2.4\times14.0\times0.0987=3.3$ cal.

c. Corrected Temperature Rise

The calculation of the corrected change in resistance of the thermometer in a bomb calorimetric experiment will be illustrated by carrying out the calculations for the experiment in which the data given in table 1 were obtained. As stated in section 3.2.c. the initial, middle, and final periods in this experiment extend from $t=0$ to $t=6$, $t=6$ to $t=18$, and $t=18$ to $t=28$ min, respectively. The observed change in resistance of the thermometer is taken as the difference between the bridge readings at $t=6$ and $t=18$ min, namely, $0.76540-0.47397=0.29143$ ohm. This difference is to be corrected for thermal leakage and heat of stirring. Correct methods for calculating this correction will be found in reference [3] and in a number of the references there cited. For the accuracy aimed at in this manual it is sufficient to use the following procedure which has been found empirically to give correct results within about 0.01 percent of the total resistance change. We first calculate the average rates of change of resistance r_1 and r_2 in the initial and final periods, respectively. These are seen to be

$$r_1=\frac{0.47397-0.47015}{6}=\frac{0.00382}{6}=0.000637 \text{ ohm min}$$

$$r_2=\frac{0.76606-0.76540}{10}=\frac{0.00066}{10}=0.000066 \text{ ohm min.}$$

Next we calculate from the data of the middle period the time t_m at which 63 percent of the observed resistance change has taken place. The resistance at t_m is given by that at the final reading of the initial period (at $t=6$), 0.47397, plus 63 percent of the observed resistance change. In other words

$$R_m=0.47397+0.63\times0.29143=0.65757 \text{ ohm.}$$

Referring to table 1 it is seen that this resistance is reached at a time intermediate between 7.17 and 7.32 min, and by interpolation we obtain $t_m=7.227$ min. The corrected initial and final resistances, R_i (corr.) and R_f (corr.), are then obtained by applying corrections to the observed resistance at $t=6$ and $t=18$ min as follows:[16]

$$R_i \text{ (corr.)}=R_6 \text{ (obs)}+r_1(t_m-6)$$
$$=0.47397+0.000637\times1.227=0.474752 \text{ ohm,}$$

$$R_f \text{ (corr.)}=R_{18} \text{ (obs)}-r_2(18-t_m)$$
$$=0.76540-0.000066\times10.773=0.764689 \text{ ohm.}$$

The change in resistance corrected for thermal leakage and heat of stirring is then

$$R_f \text{ (corr.)}-R_i \text{ (corr.)}=0.764689-0.474752=0.289937 \text{ ohm.}$$

Practically the same result would have been obtained if only three readings had been taken during the period of very rapid temperature rise, say at $R=0.6300$, 0.6600, and 0.6900 ohm.

This result must be corrected for errors in the bridge coils by applying a correction equal to the algebraic sum of the certificate corrections to the coils used in obtaining R_{18} (obs) less the algebraic sum of the corrections to the coils used in obtaining R_6 (obs.). It is evident that it is not necessary in this calculation of the change in resistance to include corrections to coils which enter into both R_6 (obs) and R_{18} (obs). In this case such coils include one of 20.5 ohms and one of 7 ohms. The bridge correction in the experiment under consideration was +0.000029 ohm, making the corrected resistance change $\Delta R=0.289966$ ohm.

Resistance of the thermometer can be converted to temperature with the aid of the formula or tables accompanying the NBS certificate for the thermometer. It is somewhat more convenient, however, to compute a table of factors $\Delta t/\Delta R$ which when multiplied by the corrected change in resistance ΔR will give the desired change in temperature Δt. Such a table may be calculated as follows. First the temperatures corresponding to certain given resistances, say $R=27.5000$, 27.6000, . . . – 28.5000. . . , are calculated, using the data in the certificate for the thermometer. These temperatures are then substituted into the formula

$$\frac{\Delta t}{\Delta R}=\frac{1}{R_0\alpha\left[1+\frac{\delta}{100}-\frac{2\delta t}{10000}\right]} \qquad (3)^{17}$$

[16] Resistances are read to 1 in the fifth decimal. The calculations are carried one place farther to avoid errors from rounding off.

[17] Strictly speaking, eq (3) gives the derivative dt/dR. This is exactly equal to $\Delta t/\Delta R$ for a finite interval ΔR, provided it is calculated for the *mean temperature* of the interval. If, as is customary, the value of dt/dR corresponds to the *mean resistance* of a finite interval, then dt/dR is not exactly equal to $\Delta t/\Delta R$, but the error is entirely negligible.

where R_0, α, and δ are constants given in the calibration certificate for the particular thermometer. The values of R and corresponding values of $\Delta t/\Delta R$ calculated from the above formula are tabulated. The value of $\Delta t/\Delta R$ to use in calculating the corrected temperature rise in a given experiment is that corresponding to the mean of the corrected initial and final values of R for the experiment. This value of $\Delta t/\Delta R$ is obtained from the table, by interpolation if necessary. For example, in the example given above the value of $\Delta t/\Delta R$ used should be that corresponding to the mean of $27.5+R_i$ (corr.) and $27.5+R_f$ (corr.) or

$$27.5+(0.47475+0.76469)/2=27.5+0.6197$$
$$=28.1197 \text{ ohms.}^{18}$$

It is found that $\Delta t/\Delta R$ increases by about 0.03 percent for an increase in temperature of 1 deg C (0.1 ohm).

It is not necessary, however, to convert resistance to temperature. If desired, the resistance change can be taken as the measure of the temperature change, with the energy equivalent E expressed in caloreis per ohm. The corrected resistance change ΔR (ohms) in a measurement of heat of combustion would then be multiplied by E (calories per ohm) to give the energy (calories) produced in the combustion reaction. One disadvantage of this procedure is that E in calories per ohm changes more for a given change in the mean temperature of the experiment than does E in calories per degree. For a typical bomb calorimeter it has been calculated that the change in the value of E for an increase of one degree (0.1 ohm) in the mean temperature of the experiment is about +0.03 percent if E is expressed in calories per ohm, but is less than 0.01 percent if E is expressed in calories per degree. Hence if temperatures are expressed in ohms, then for a precision of 0.01 percent, the mean temperature of the calorimeter should be kept within about 0.2 degree (0.02 ohm) of some fixed value, or else the value of E_s in each calibration experiment should be corrected to some standard temperature, and the mean value of E_s for this standard temperature should be corrected to the actual mean temperature of each measurement of heat of combustion. The greater change with temperature of E_s expressed in calories per ohm is due to the fact that the resistance of the thermometer is not a linear, function of temperature, i.e., the fact that $\Delta t/\Delta R$ is not constant.

A convenient check on the behavior of the calorimeter and the correctness of the temperature measurements may be obtained by calculating the "cooling constant," k, of the calorimeter. This is defined by

$$k=-\frac{r_2-r_1}{R_2-R_1}$$

where r_1 and r_2 are the average rates of change of resistance in the initial and final periods, respectively, and R_1 and R_2 are the observed resistances at the mid-points of these periods. Thus, using the data of table 1 at the beginning of this section (5.1c):

$$k=\frac{0.000637-0.000066}{0.76573-0.47206}=0.001944.$$

This quantity is a constant of the calorimeter and should remain constant to better than one percent in different experiments.

d. Example Illustrating the Calculations of E and E_s

The calculation of E may be illustrated by an example, using the following data taken from preceding sections as indicated.

Weight benzoic acid, $m_s=1.52188$ g (sec. 3.2 a)
Heat of combustion of benzoic acid, $Q_c=6317.9$ cal/g (sec. 5.1.a)
Firing energy (2 cm fuse wire), $c_1=5.2$ cal (sec. 5.1.b)
Correction for nitric acid, $c_2=3.3$ cal (sec. 5.1.b)
Corrected resistance change, $\Delta R=0.289966$ ohm (sec. 5.1.c)
Corrected temperature change, $\Delta t=2.87462$ deg C ($\Delta t/\Delta R=9.91364$)
Oxygen pressure at 28.0°, $P=32.1$ atm abs (sec. 5.1.a)

Substituting the above values in eq (1), the value of E is found to be

$$E=\frac{1.52188\times6317.9+5.2+3.3}{0.289966}=33188.7 \text{ cal/ohm}$$

$$=\frac{1.52188\times6317.9+5.2+3.3}{2.87462}=3347.78 \text{ cal/deg.}$$

To reduce the above values of E to the corresponding values of E_s, the energy equivalent of the standard calorimeter system, it is only necessary to subtract the heat capacity of the sample of benzoic acid, and of the amount of oxygen in excess of that required to fill the bomb to 30 atm absolute at 28° C, as follows:

	cal/° C	cal/ohm
Observed value of E	3,347.78	33,188.7
Heat capacity of excess oxygen=(32.1-30.0)×0.077	0.16	1.6
Heat capacity of benzoic acid=1.522×0.29=	0.44	4.4
Value of E_s	3,347.18	33,182.7

The factor 0.077 used in calculating the correction for excess oxygen is the increase in heat capacity (in calories per degree) per atmosphere

[18] Strictly speaking, the corrections to all the coils used should be applied in calculating the mean value of the resistance. In many cases, however, these corrections are too small to be significant in this calculation and may be neglected.

increase in pressure in the bomb used, which has an internal volume of 0.380 liter. For a bomb of volume V the corresponding factor is $0.077\ V/0.380$. The factor 0.29 used in correcting for the benzoic acid is the specific heat of benzoic acid in calories per gram degree Celsius. Both factors are greater by a factor of 10 if E is in calories per ohm (for a thermometer having a resistance of 25.5 ohms at 0° C).

5.2. Calculation of Heat of Combustion

Calculate a value of total (or gross) heat of combustion at constant volume from the data of each measurement, using the following formula.

$$Q_v \text{ (gross)} = \frac{E \times \Delta t - c_1 - c_2 - c_3}{m_s}, \qquad (4)$$

where:

Q_v (gross) = total heat of combustion at constant volume at the final temperature of the experiment, in IT calories per gram.

E = energy equivalent of the calorimeter as used, in IT cal/deg (or IT cal/ohm)

Δt = corrected temperature rise of calorimeter in degrees (or ohms)

m_s = mass of sample, in grams

c_1 = firing energy, in calories

c_2 = correction for energy of formation of nitric acid, in calories

c_3 = correction for energy of formation of sulfuric acid, in calories.

a. Energy Equivalent of Calorimeter as Used

The calorimeter as used differs from the standard calorimeter because it contains the sample of fuel and because, in general, the absolute pressure of the oxygen at 28° differs from 30.0 atm. The energy equivalent E of the calorimeter as used is obtained by adding to the energy equivalent E_s of the standard calorimeter the heat capacity of the charge of combustible and the heat capacity of the oxygen in excess of that required to fill the bomb to 30.0 atm absolute at 28° C. The calculation is illustrated as follows, taking the sample of combustible as 0.92231 g of gasoline, and the oxygen pressure at 28.0° as 29.0 atm absolute:

	cal/°C	cal/ohm
Energy equivalent of standard calorimeter, E_s =	3,347.18	33,182.7
Heat capacity of excess oxygen, (29.0–30.0)×0.077 =	−.08	−0.8
Heat capacity of sample, 0.922×0.51 =	+.47	+4.7
Energy equivalent of calorimeter as used, E =	3,347.57	33,186.6

The factor 0.51 used in calculating the heat capacity of the sample is the specific heat of gasoline [19] at 26.5°C in cal/g°C. The factor 0.077 used in calculating the heat capacity of the excess oxygen is defined in section 5.1.d. Both factors are greater by a factor of 10 if E_s is in calories per ohm (for a thermometer having a resistance of 25.5 ohms at 0°C). The heat capacity of the glass bulb (less than 0.1 g) used to enclose the sample of gasoline may be neglected.

b. Corrected Temperature Rise

Directions for calculating the corrected temperature rise are given in section 5.1.c. The value to be used in the example to be given later may be taken as 0.309617 ohm or 3.06943°C.

c. Corrections c_1, c_2, c_3

The correction c_1 for firing energy with a 2-cm length of fuse wire may be taken as 5.2 cal. The corrections c_2 and c_3 are calculated as follows: The correction c_2 is calculated as if all the acid found by titration were nitric acid, as described in section 5.1.b. Thus if it required 14.2 ml of 0.0987 N sodium hydroxide to neutralize the total acid the correction c_2 would be given by $c_2 = 14.2 \times 14.0 \times 0.0987 = 19.6$ cal. If the test for sulfur showed 0.0042 g sulfur present in the bomb washings the correction for sulfuric acid, as given in section 3.2.f., would be $c_3 = 1400 \times 0.0042 = 5.9$ cal.

d. Calculation of Q_v (gross)

Substituting the values of E in calories per degree (or calories per ohm), Δt (or ΔR), c_1, c_2, c_3, and m_s given in sections 5.2.a., b., and c. into formula (4) yields:

$$Q_v \text{ (gross)} = \frac{3347.57 \times 3.06943 - 5.2 - 19.6 - 5.9}{0.92231}$$

or

$$Q_v \text{ (gross)} = \frac{33186.6 \times 0.309617 - 5.2 - 19.6 - 5.9}{0.92231}.$$

Both of these expressions yield the value 11107.4 cal/g weight in air for the total (or gross) heat of combustion of the liquid gasoline at constant volume. The corresponding value in terms of engineering units is

$$Q_v \text{ (gross)} = 11107.4 \times 1.8 = 19993 \text{ Btu/lb.}$$

The method of calculation is such that the value obtained for Q_v (gross) is referred to the final temperature of the calorimeter, in this case 28.1° C. The observed value may be reduced to the standard temperature of 25° by means of the following formula:

[19] Taken from NBS Miscellaneous Publication M97 [15] for a gasoline having an API gravity of 70. Values of heat capacity of petroleum products given in this publication for a temperature of 80° F range from 0.42 to 0.52 for API gravities ranging from 10 to 80.

574278 O - 61 - 25

$$Q_v \text{ (gross, 25° C)} = Q_v \text{ (gross, } t\text{° C)} + A(t-25) \quad (5)$$

Where the value of the factor A is given in the following table.[20]

Q_v (gross)	A	Q_v (gross)	A
Btu/lb	*Btu/lb° C*	*Btu/lb*	*Btu/lb° C*
18,500	0.68	19,600	1.14
18,600	.72	19,700	1.18
18,700	.76	19,800	1.22
18,800	.80	19,900	1.26
18,900	.85	20,000	1.30
19,000	.89	20,100	1.35
19,100	.93	20,200	1.39
19,200	.97	20,300	1.43
19,300	1.01	20,400	1.47
19,400	1.05	20,500	1.51
19,500	1.09	20,600	1.55

Substituting the value of Q_v (gross, 28.1° C)= 19993 Btu/lb and the corresponding value $A=1.30$ from the above table in eq (5) we obtain

$$Q_v \text{ (gross, 25° C)} = 19993 + 1.30 \times 3.1 = 19997 \text{ Btu/lb.}$$

[20] The values of A were calculated using the specific heats of liquid petroleum fuels, of gaseous oxygen and carbon dioxide, and of liquid water. The masses of oxygen consumed and of carbon dioxide and water formed in combustion of unit mass of fuel were obtained from an empirical relation between Q_v (gross) and hydrogen content. See reference [5]. In general, the change in Q_v gross (Btu/lb) with temperature for any fuel may be calculated from the relation dQ_v (gross)$/dt = K_v$ (reactants) $- K_v$ (products).

Here K_v (reactants) denotes the heat capacity at constant volume of 1 lb of fuel plus the oxygen consumed in its combustion, and K_v (products) denotes the heat capacity of the products of combustion of one pound of fuel, including gaseous carbon dioxide and liquid water. In calculating K_v the heat capacities of solids and liquids may be taken as heat capacities at constant pressure.

e. Calculation of Q_p (net)

If the hydrogen content of the fuel is known the value of the net heat of combustion, Q_p (net, 25°), can be calculated from that for Q_v (gross) by means of the following formula [4]:

$$Q_p \text{ (net, 25° C)} = Q_v \text{ (gross, 25° C)} - 91.23 \text{ (\%H)} \quad (6)$$

Thus if Q_v (gross, 25° C)=19997 Btu/lb and (%H)=13.9, we obtain

$$Q_p \text{ (net, 25° C)} = 19997 - 91.23 \times 13.9 = 18729 \text{ Btu/lb.}$$

If the hydrogen content of the fuel is not known, an approximate value for Q_p (net, 25° C) can be calculated from the following empirical relation:

$$Q_p \text{ (net, 25° C)} = 4310 + 0.7195\ Q_v \text{ (gross, 25° C).} \quad (7)$$

Substituting the value Q_v (gross, 25° C)=19997 Btu/lb in this equation we obtain

$$Q_p \text{ (net, 25° C)} = 4310 + 0.7195 \times 19997 = 18698 \text{ Btu/lb (approximate)}$$

Equation (6) is preferable to eq (7) for calculating net from gross heat of combustion, since the latter equation is purely empirical. A fairly accurate value of (%H) is required in eq (6), since an error of 0.1 in this quantity introduces an error of about 0.05 percent in Q_p (net).

6. References

[1] ASTM Method D 240–57T. ASTM Standards **7,** 143, (1958).

[2] ASTM Method D 271–58, ASTM Standards, **8,** 999 (1958).

[3] F. D. Rossini, Experimental thermochemistry (Interscience Publishers, New York, N.Y., 1956), and the references there cited.

[4] R. S. Jessup and C. S. Cragoe, Nat. Advisory Comm. Aeronaut. Tech. Note No. 996 (1945) (copies not available).

[5] S. Rothberg and R. S. Jessup, Ind. Eng. Chem. **43,** 981 (1951).

[6] R. S. Jessup and J. A. Cogliano, ASTM Bull. No. 201 (Oct. 1954).

[7] G. T. Armstrong, R. S. Jessup, and T. W. Mears, Chem. Eng. Data Ser. **3,** 20 (1958).

[8] H. C. Dickinson, Bul. BS **11,** 189 (1914) S230.

[9] N. S. Osborne, H. F. Stimson, and T. S. Sligh, Bul. BS **20,** 119 (1925) S503.

[10] C. H. Meyers, J. Am. Chem. Soc. **45,** 2135 (1923).

[11] T. W. Richards and F. Barry, J. Am. Chem. Soc. **37,** 993 (1915).

[12] H. N. Davis, Mech. Eng. **51,** 791 (1929).

[13] See for example:
(a) N. Irving Sax, Handbook of dangerous materials (Reinhold Publishing Corp., New York, N.Y., 1951).
(b) Manufacturing Chemists Association, General Safety Committee, Guide for safety in the chemical laboratory (D. Van Nostrand and Co., New York, N.Y., 1954).
(c) National Safety Council, Accident prevention manual for industrial operations (Chicago, Ill., 1951).
(d) National Board of Fire Underwriters, National electrical code (Chicago, Ill., 1940).

[14] ASTM Method D 129–58, ASTM Standards **8,** 81 (1955).

[15] C. S. Cragoe, Thermal Properties of Petroleum Products, NBS Misc. Publ. M97 (this paper is out of print but may be found in many public libraries).

[16] E. J. Prosen and F. D. Rossini, J. Research NBS **27,** 289 (1941) RP1420.

[17] J. Coops, D. Mulder, J. W. Dienske, and J. Smittenberg, Rec. trav. chim. **66,** 153 (1947).

[18] E. W. Washburn, J. Research NBS **10,** 525 (1933) RP546; see also chapters 5 and 6 of reference [3].

[19] F. K. Harris, Electrical measurements, p. 57 (John Wiley & Sons, Inc., New York, N.Y., 1951).

[20] E. J. Prosen, W. H. Johnson, and Florence Y. Pergiel, J. Research NBS **62,** 43 (1959) RP2927.

7. Appendix

7.1. Apparatus

The major items of apparatus used in bomb-calorimetric measurements on fuels at the National Bureau of Standards are listed in table 2. On the basis of prices listed in manufacturers' catalogs at the present time (1959), the estimated total cost of replacement of the equipment listed is in the neighborhood of $15,000.

TABLE 2. *Major items of equipment used in measurement of heats of combustion of liquid fuels at the National Bureau of Standards*

Mueller bridge.	Set of weights for above.
Resistance thermometer.	Oxygen purifier.
Galvanometer.	Temperature controller for oxygen purifier.
Calorimeter, jacket, and thermostat.	Laboratory table for bridge.
Combustion bomb.	Laboratory bench.
Platinum crucibles and fittings.	Pellet press.
Balance.	Reducing valve.
Set of class M weights for above.	Julius suspension.
Heavy duty balance	

The approximate arrangement of the calorimeter and accessory apparatus is shown in figure 4. The reading station *R* provides support for the lamp *L* and ground glass scale *S*, as well as for some electrical equipment for measurements not covered in this Monograph. It also contains a convenient "desk" for use in recording the data of bomb calorimetric experiments. The arrangement of the equipment for purifying oxygen and admitting it to the bomb is shown schematically in figure 5.

The arrangements shown in figures 4 and 5 are not necessarily the best under all circumstances. For example, the bench *BE* (fig. 4) is considerably larger than necessary for the calorimeter alone, as part of this table is used for other purposes.

The essential features of the various items of apparatus are described below. Items not obtainable commercially, and modifications of commercial items are described in considerable detail.

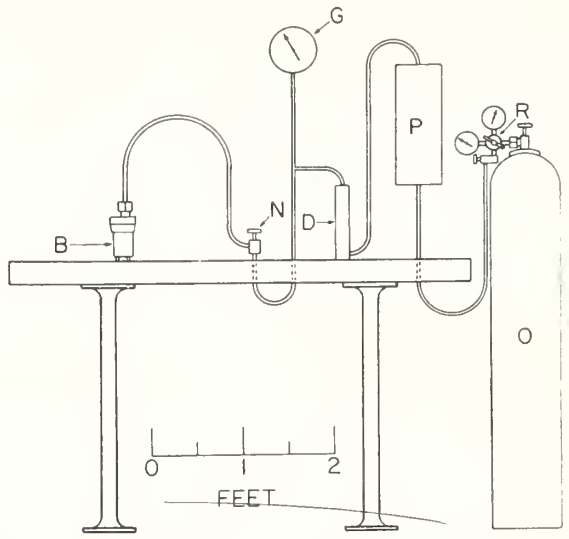

FIGURE 5. *Arrangement of apparatus for admitting oxygen to bomb.*

B, bomb; D, dryer; G, pressure gage; N, needle valve; O, oxygen cylinder; P, oxygen purifier; and R, reducing valve.

a. Bridge

The bridge used is a special Mueller bridge designed especially for bomb-calorimetric measurements. It is substantially equivalent to the commercially available bridge designated as *G*–2. In addition to the usual 10-, 20-, 30-ohm coils of the 10×10-ohm decade this bridge has a 20.5-ohm coil. Such a coil is useful in bomb-calorimetric measurements, where the change in resistance of the thermometer in an experiment is of the order of 0.3 ohm, since it makes it possible to avoid a change in setting of the dial of the 10×1-ohm decade which would otherwise be necessary in certain circumstances. Thus if the initial and final resistances of the thermometer are 27.8721

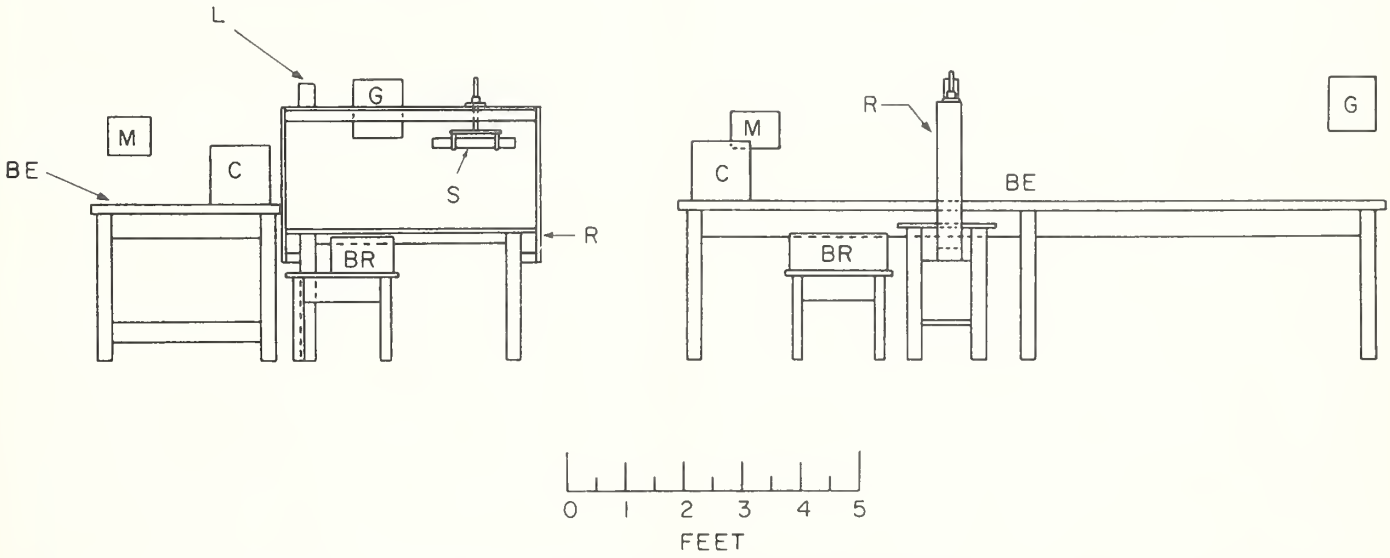

FIGURE 4. *Arrangement of calorimetric apparatus.*

BE, bench; C, calorimeter; BR, bridge; G, galvanometer; L, light source; M, stirring motor; R, reading station; and S, ground glass scale.

and 28.1806, the corresponding dial settings with the 20.5-ohm coil would be 20.5+7.3721 and 20.5+7.6806 and the change in dial setting would involve only the 10×0.1-ohm and lower decades. If no 20.5-ohm coil were available, it would be necessary to change the dial setting of the 10×1-ohm decade from 7 to 8 at a time when the temperature of the calorimeter was rising very rapidly. This would greatly increase the difficulty of following the temperature of the calorimeter during the period of rapid temperature rise, and might also involve a larger correction to the observed change in resistance of the thermometer.

b. Thermometer

The platinum resistance thermometer has a resistance of approximately 25.5 ohms at 0° C. It is of the strain-free type with coil windings very close to the wall of the enclosing glass tube. It was purchased under a specified requirement that the temperature of the coil with a current of 1 ma flowing through it should not exceed that of the bath in which the thermometer is immersed by more than 0.0003° C. Calorimetric resistance thermometers enclosed in metal sheaths are available commercially. These are less subject to breakage than glass-enclosed thermometers, but are subject to damage from bending the metal sheath. Such damage might not be obvious on casual examination, but could be detected by periodic determination of the ice point of the thermometer.

c. Galvanometer

The galvanometer has a sensitivity of about 0.2 μv/mm at 1 m, an external critical damping resistance of 40 ohms and a period of about 5 sec. The damping resistance used is so chosen that the galvanometer is slightly underdamped. The galvanometer is protected from air currents and abrupt changes in temperature by an enclosure made of cork pipe covering (for 6 in. pipe) about 10 in. in outside diameter. The galvanometer is supported by a Julius suspension, which is very effective in reducing the effect of vibrations.

d. Bomb

The combustion bomb [21] is made of a corrosion-resistant alloy (Illium). It is provided with a check valve for admitting oxygen and also with a needle valve for releasing the gases contained in it. It is sealed by a self-sealing neoprene gasket. The original bomb has been modified by replacing the three supporting feet furnished with it by new ones of monel metal about 12 mm in height. This permits freer circulation of water under the bomb.

The base-metal electrode inside of the bomb, and the crucible-support rod were cut off leaving lengths of about 3 cm from the point at which they enter the lock nuts. To the shortened electrode was hard soldered a 1/16 in. platinum rod about 3 cm in length. To the shortened crucible-support rod was hard soldered a 5-cm length of 1/8 in. o.d. platinum tube having a 0.01 in. wall. The arrangement of electrode, crucible support, crucible, electric fuse and 0.3 mm platinum leads thereto is shown in figure 6(a) (valves not shown). An enlarged view of the platinum crucible is shown at (c) figure 6. The crucible is put in place by sliding the split tube (5/32 in. o.d.) shown at the right of figure 6(c) over the end of the 1/8 in. platinum crucible-support tube referred to above until the fuse is nearly in contact with the sample of combustible. The split tube may be deformed slightly with the fingers to make it fit the 1/8 in. tube tightly enough to be held in place by friction. The length of the crucible-support, and the position of the crucible on this support should be such that the crucible cannot come in contact with the water in the bottom of the bomb when the bomb is assembled. If the crucible should come in contact with the water, combustion will be incomplete.

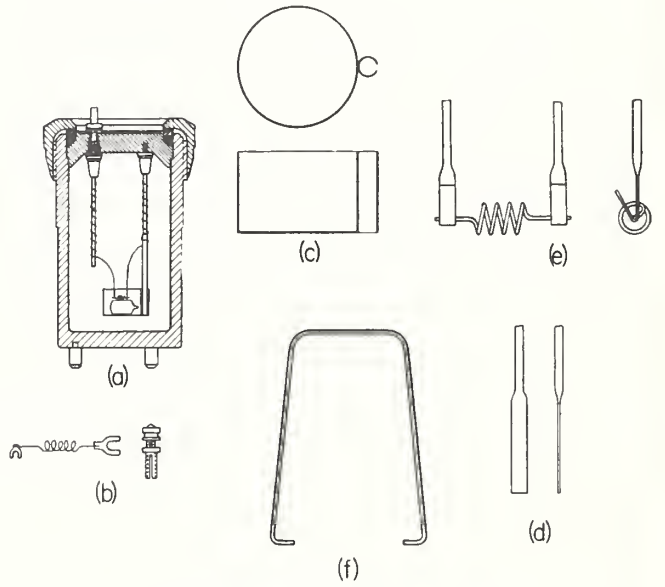

FIGURE 6. *Bomb and accessories.*

(a) Bomb, showing arrangement of crucible, crucible support, electrode, etc. (Valves not shown, see fig. 1); (b) Binding post and lead wire; (c) Enlarged view of crucible; (d) Platinum lead flattened at end; (e) Fuse wire attached to platinum leads; and (f) Hook for handling bomb.

A supply of platinum lead wire is wound around the electrode and crucible support rods as shown, and a sufficient amount of this to reach down to the crucible is unwound for each experiment. The electric fuse is a 2-cm length of Parr fuse wire (No. 34 AWG chromel C) which is formed into a small helix by winding it around a rod about 0.04 in. in diameter. The method of attaching the fuse to the platinum leads is illustrated at (d) and (e), figure 6. The ends of the lead wires are first flattened by hammering as shown at (d). The flattened ends are then bent and the fuse inserted as shown at (e), after which the turned-up ends

[21] Parr Instrument Company Catalog No. 1101.

of the lead wires are hammered down with a small hammer or squeezed together with pliers to clamp the ends of the fuse wires.

The terminal nut attached to the electrode outside of the bomb was replaced by one of the form shown at (a), figure 6. The binding post shown at (b), figure 6, has a split tube at its lower end which can be slipped over the upper part of the terminal nut, where it fits tightly so as to make good electrical contact. The lead wire shown at (b), figure 6, connects this binding post to one on the calorimeter jacket which is connected in the firing circuit. This wire is soldered to spade-type terminals at each end, the larger of which normally is permanently attached to the binding post shown at (b). This wire should be so insulated as to avoid any electrical contact with the calorimeter vessel. With alternating current the contact of the lead wire and bomb electrode with the water in the calorimeter does not result in any appreciable electrical leakage, provided actual metallic contact with the calorimeter vessel is avoided.

e. Calorimeter and Jacket

The calorimeter now used for fuel testing is of the type described by Dickinson [8]. The calorimeter vessel is of the form shown at (a) and (b), figure 1. The calorimeter cover is in the form of a flat circular disk with vertical wall about 1 cm in height at the edge. The holes OT and OL (fig. 1(b)) are surrounded by metal collars about 1 cm high. The cover fits tightly enough inside of the calorimeter vessel so that it is held in place by friction. Its lower surface is in contact with the water of the calorimeter. The calorimeter vessel is supported inside of the jacket by pins of stainless steel, in the manner described by Dickinson [8].

The Dickinson type calorimeter was constructed in the NBS shops. There is a commercially available "submarine" calorimeter, [22] based on a design developed at the National Bureau of Standards [20], which has been found to be substantially equivalent in performance to the Dickinson calorimeter. The submarine calorimeter is supplied without a thermostat for the jacket bath, so that a thermostat for controlling the bath temperature to a few thousandths of a degree must be purchased or constructed.

The thermostat [23] used with the particular Dickinson type calorimeter used for fuel testing is similar to one previously described by Osborne, Stimson, and Sligh [9]. It consists of a "bulb" filled with toluene and connected to a glass capillary U-tube (1.5 mm i.d.) containing mercury. Expansion of the toluene as a result of rising temperature causes the mercury to make contact with a needle closing an electrical circuit through an electronic relay [24] which shuts off the current in the electric heater in the jacket bath. The "bulb" *TB* (fig. 1) consists of about 3 m of $\frac{3}{16}$ in. copper tubing with 0.01 in. wall thickness wound into a helix and so located in the same tubular housing as the jacket bath stirrer that the water flows over the bulb immediately after leaving the stirrer. The glass U-tube and attached valve for admitting or removing toluene are shown in figure 7. The valve has tubular openings at the top and bottom for attaching the reservoir *B* and the capillary U-tube as described below.

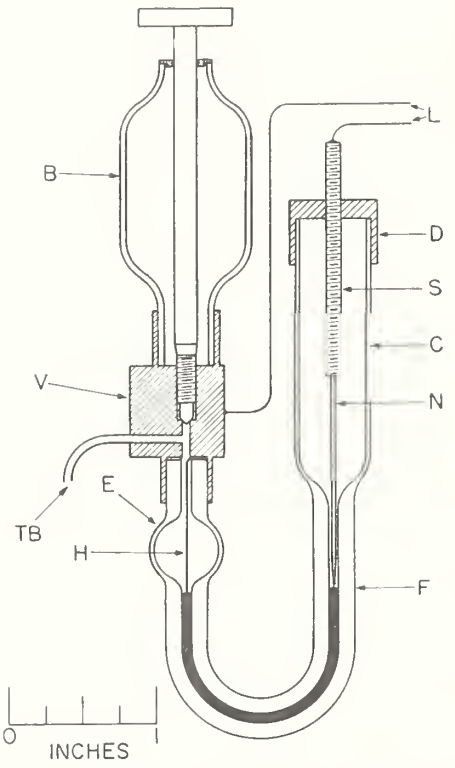

FIGURE 7. *Valve and glass parts of thermostat.*

V, valve; TB, tube to thermostat bulb; B, toluene reservoir; F, capillary U-tube; E, enlargement in capillary; H, platiuum wire; L, leads to relay; C, Pyrex tube; D, brass cap; S, screw; and N, steel needle.

The Pyrex reservoir *B* contains a supply of toluene which is separated from that in the "bulb" *TB* (fig. 1) by the valve *V* when it is closed. This valve is opened when the calorimeter is shut down thus permitting toluene to flow from the reservoir into the bulb as the bath cools. Failure to open the valve when the bath cools usually results in air being drawn into the system through the capillary *F* (fig. 7). The Pyrex bulb *C* (fig. 7) also contains toluene which protects the mercury surface in the capillary from oxidation. The enlargement *E* in the capillary is larger in volume than the mercury in the capillary so that no mercury will be drawn into the metal parts of the system if the valve *V* is inadvertently left closed when the calorimeter is shut down.

[22] Catalog No. 63090, Precision Scientific Co., Chicago, Ill. This calorimeter embodies an improved method of supporting the calorimeter vessel inside of the jacket [20].

[23] Temperature-control units for which a control accuracy of 0.001° C. is claimed are available commercially. Numerous other temperature-control devices are described in the literature. See for example the papers cited in reference [3]. For any temperature-control unit it is important that the relative locations of heater, stirrer, and temperature-sensing element should be as shown in figure 1, that is, the bath liquid should flow from the heater, through the stirring propeller, and over the temperature-sensitive element by the shortest path possible.

[24] American Instrument Company Catalog No. 4-5301.

Electrical connection between the Valve V and the mercury in the capillary U-tube is provided by a platinum wire H, long enough to reach from the top of the capillary to near the bottom of the U. The upper end of the wire is flattened and bent at a right angle to the rest of the wire so as to insure electrical contact with the valve.

The glass reservoir B and the capillary glass U-tube are soldered into the tubular openings in the brass valve V with pure tin following the procedure described by Meyers [10].

To fill the thermostat with toluene the tube C (with cap D removed) is connected to a large bulb G above C (at least 250 cm^3, not shown in fig. 7) by means of a short piece of Tygon tubing. Somewhat more than enough toluene to fill the thermostat is placed in the bulb G, and some is also placed in the reservoir B. Air can be removed from the thermostat system by heating the "bulb" (TB, fig. 1) to about 100° C and repeatedly evacuating the bulb G above the toluene and then admitting air. To test for air in the system, air is admitted above the toluene in G, the valve V is opened, the toluene meniscus is brought into the capillary at F, and the valve is closed. If the system is free of air, moderate air pressure applied by mouth above the toluene will not cause a movement of the meniscus in the capillary of more than 0.2 or 0.3 mm. The removal of air from the system should be done before introducing mercury into the capillary. If air is inadvertently admitted to the system after mercury has been introduced into the capillary, the mercury should be removed before attempting to remove the air.

In preparing for a calorimetric experiment the jacket is first heated to the desired temperature, the heating current is reduced to slightly more than enough to maintain the temperature constant, and the valve V is closed. Final adjustment of the temperature can be made by moving the needle N up or down by rotating the cap D relative to the screw S (fig. 7). The heating current should be adjusted so that the on and off periods are about equal in length.

The method of bringing the firing leads through the jacket is illustrated in figure 1(c).[25] Two metal rods, one of which is shown at R, are cemented with wax into tubes T which pass through the jacket, so that the rods are insulated from the jacket. Each rod is drilled and tapped at each end for a 4–40 brass screw, which is used to clamp the terminal of the lead wire between the two washers, W, thus forming a binding post at each end of the rod. The terminal at the left end of the lead wire shown in figure 1(d) is attached permanently to one of the inner binding posts and the clip at the other end of the wire (d) is slipped over the edge of the calorimeter vessel when it is assembled preparatory to making an experiment. The other lead wire, from the binding post on the bomb (see fig. 6(b)), is attached to the other inner binding post after the bomb has been put in the calorimeter and the calorimeter cover has been put in place. The two outer binding posts are connected through an ammeter and a switch to a small transformer having a secondary voltage of 8 or 10. The switch should be of the momentary contact push-button type normally open except when held closed by the operator.

[25] This method is not applicable to some types of calorimeters, for example, submarine calorimeters. The important feature of the method is that the leads are in good thermal contact with the jacket, but are electrically insulated from it.

f. Balance for Weighing Samples

The balance used for weighing samples of combustibles is an undamped semimicro balance (capacity 100 g) having a sensitivity reciprocal of 0.14 mg per division on the index scale. The balance is provided with a keyboard arrangement for adding and removing weights from 1 to 100 mg. Temperature gradients parallel to the balance beam are reduced by covering the walls of the balance case inside and out with aluminum foil, and by locating the balance where temperature gradients in the room are small. It has been found, however, that best results are obtained with the balance when there is a vertical temperature gradient such that the top of the balance case is warmer by 0.03 to 0.1° C than the bottom.

The weights used with the balance are high-grade one-piece (class M) weights and were calibrated in the Mass and Scale Section of the National Bureau of Standards.

For most purposes a good analytical balance would be satisfactory if provided with high grade calibrated weights, and properly used.

g. Balance for Weighing Calorimeter

This is a magnetically damped heavy duty balance having a capacity of 5 kg and a sensitivity of about 0.5 mg. The tantalum-plated weights used with this balance are of good quality but are not calibrated. Calibration was considered unnecessary since the purpose of weighing the calorimeter is not to determine its absolute weight, but to reproduce the same weight of calorimeter plus water for each experiment. For this purpose it is important that the weights remain constant in value, and that the same weights be used at all times, but the actual masses of the weights used need not be known accurately.

h. Oxygen Purifier

Combustible impurities in the oxygen are removed by passing it through a cylinder containing cupric oxide maintained at a temperature of 500° C (932° F). The purifier[26] consists essentially of a heavy-walled alloy-steel cylinder having inside dimensions of approximately 1 in. diameter by 10 in. length, and capable of withstanding a pressure of at least 2500 psi at 500° C. The cylinder is provided with an electric heater. It

[26] American Instrument Company 1942 Catalog No. 406-31.

has inlet and outlet at opposite ends, and a well for inserting a thermocouple for measurement of temperature. The cylinder is filled with wire-form cupric oxide. The temperature and oxygen pressure in the purifier should not be allowed to rise above values consistent with safety. The manufacturers recommendations regarding safety precautions should be adhered to rigidly. The strength of materials decreases rapidly with increasing temperature.

The temperature of the purifier can be controlled by means of a "Fail safe" controller. Such controllers are available commercially.[27] The pressure is easily controlled by a reducing valve attached to the oxygen cylinder.

i. Laboratory Table for Bridge

This table should be large enough to accommodate the bridge comfortably, and of a height which will afford convenience in the manipulation of the bridge dials. A table 22 in. square by 18 in. high is convenient for use with a G–2 bridge as it allows space for batteries, etc

j. Pressure Gage

The Bourdon pressure gage used has a 6 in. dial and is graduated from 0 to 800 psi in steps of 10 psi, so that it can be read to about 1 or 2 psi. The gage was calibrated in the Mechanical Instruments Section of the NBS and was set so as to read correctly at 450 psi.

7.2. Glass Sample Bulbs

For measurements of heat of combustion of kerosenes, gasolines, or other volatile liquids it is necessary, in order to permit accurate weighing of the sample and to insure that it is all in the liquid state until it is ignited in the bomb, to enclose the sample in a thin-walled glass bulb, so constructed and filled that it will not break under the pressure of the oxygen. The type of bulb[28] used in testing of volatile fuels at the National Bureau of Standards, and the method of making such bulbs are illustrated in figure 8. Attempts to obtain bulbs of this type from manufacturers of glass laboratory apparatus have been unsuccessful to date, and such bulbs are therefore made in our own laboratory. A brief description of the method of making the bulbs will be given below. It should be recognized, however, that it is virtually impossible to describe the method in such detail as to enable an inexperienced worker to make bulbs successfully on his first attempt. The best that can be done is to outline the method, and to depend upon the individual worker to develop the necessary techniques by trial. It is to be expected that in the early attempts failures will far outweigh successes, and that a reasonable degree of skill can be acquired only by long and patient practice.

[27] For example American Instrument Company Catalog No. 49–9570. Arthur S. Lapine and Company Catalog No. 357–70.

[28] Bulbs of this type were first described by Richards and Barry [11].

The starting material for making bulbs is soft glass tubing 4 to 6 mm in outside diameter.[29] Approximately 2 cm of such a tube is heated in a moderately hot air-gas flame of an ordinary laboratory blast burner. When the glass becomes soft it is removed from the flame and drawn down to a fine capillary having a minimum outside diameter of about 1 mm. This procedure is then repeated in such a manner as to leave a short section of the same diameter as that of the original tube, as shown at figure 8(a). The two capillaries are then broken at about their midpoints, leaving a piece such as that shown at figure 8(b). The remaining glass-working operations are carried out with an air-gas micro blast burner capable of producing relatively small flames. Using such a micro burner the piece illustrated at (b), figure 8, is rotated and heated by a small hot flame at the point indicated by the arrows, and is then drawn down to 1 mm outside diameter. This procedure is repeated on the other side of the enlargement in the tube, the final product being as illustrated at (c), figure 8. This piece is then rotated and heated by a small sharp flame at the center of the enlargement as indicated by the arrow at (c), and the two halves of the piece are pulled apart as shown at (d), figure 8, where the enlarged end of the piece at the left has been reduced in size by removal of surplus glass. This removal of surplus glass is accomplished by heating the end of the enlargement until it softens, and then pulling off small filaments of glass until an enlargement of the proper size remains. After such removal of surplus glass from both of the pieces shown at (d) a spherical bulb, not greater than 14 mm in diameter, is blown on each piece (fig. 8(e)). The spherical bulb is then flattened on one side by holding the bulb above a small soft flame (no primary air) about ¼ in. in diameter by ¼ in. high, and gradually lowering it until the glass on the under side of the bulb softens and flattens. This procedure is then repeated so as to flatten the opposite side of the bulb. The final form of the bulb is shown at figure 8(f). The operations of bringing the bulb down on to the flame and removing it after flattening is complete should be done gradually, since too rapid heating or cooling of the bulb may cause it to break.

The most difficult part of the procedure just described is that of blowing a bulb of the proper size. Success in this operation depends in part upon having the proper amount of glass on the end of the tube (fig. 8 (d)) and in part upon the type of flame used, as well as upon the procedure followed in blowing the bulb. A flame which has been found to be satisfactory is one about ¼ in. in diameter by ⅝ in. in height with just enough primary air so that there is a small yellow tip in the flame. The end of the tube (fig. 8(d)) on which the bulb is to be blown is heated in the

[29] Pyrex glass has been found unsatisfactory for this purpose, as unburned carbon is usually found on such glass after a combustion. This may be related to the fact that the Pyrex glass does not melt completely when the sample is burned, as does soft glass, and therefore partially retains its original form, thus inhibiting access of oxygen to the fuel.

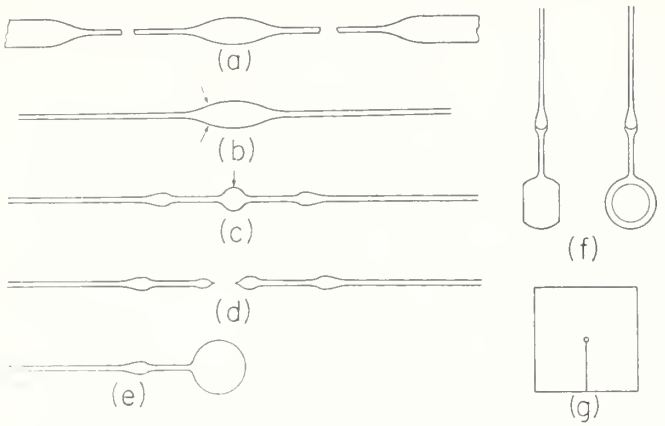

FIGURE 8. *Steps in making sample bulbs.*

flame until sufficiently hot, and is then removed from the flame and the bulb blown immediately. In order to prevent sagging of the end of the tube when heated, the tube is held at an angle of about 30° to the vertical and is rotated about its axis continuously. Usually the first few attempts to blow a bulb will be unsuccessful because the initial size of the bulb is so small that a relatively high pressure will be required to overcome surface tension and the viscous resistance to flow of the glass. If the pressure is not high enough the bulb will expand so slowly at first that the glass will harden before the desired size is reached. If the pressure is high enough to expand the bulb at a sufficiently high initial rate, the bulb may suddenly expand to too large a size before the glass hardens. The ideal procedure would be to blow very hard at first and then less so as the bulb becomes larger. This is very difficult to do because the whole operation must be carried out in a very short time before the glass hardens. It is therefore usually more successful to repeat several times the procedure of blowing the bulb to a diameter of 4 or 5 mm and then shrinking it by heating, before attempting to blow the bulb to the required size. This procedure also serves to provide a somewhat more uniform distribution of glass in the final bulb.

Too large an amount of glass in the bulb and too hot a flame are both conducive to too large size of the bulb. Too small an amount of glass and too low a flame temperature have the opposite effect. Success in blowing a suitable bulb of the proper size depends upon the proper combination of flame temperature, amount of glass and technique of blowing.

The spherical bulb should be not more than 14 mm in diameter, and the completed bulb should not contain more than about 1.3 cm^3 nor less than 0.7 cm^3 of liquid. The flat sides of the bulb should be thin enough to deflect visibly, but not so thin as to break, under moderate air pressure applied by mouth. The weight of the glass in the bulb after sealing off the stem near the bulb should be between 0.05 and 0.10 g. The outside diameter of the capillary adjacent to the bulb should be between 1.0 and 1.3 mm. The inside diameter should be at least 0.5 mm and preferably a little larger in order to permit easy insertion of a No. 27 hypodermic needle (0.4 mm diam.) in filling the bulb. The appearance of the flat sides of a completed bulb will give some indication as to whether it will be satisfactory. Usually the flat sides present a scalloped appearance, although if the amount of glass in the bulb is greater than normal they may be nearly plane. If the scallops are very fine, say 1 mm or less apart, the bulb is probably too thin and fragile to be satisfactory.

Samples of liquid fuel can be conveniently introduced into the previously weighed glass bulbs by means of a hypodermic syringe fitted with a No. 27 needle. The liquid should be introduced into the bulb slowly in order to permit escape of the air initially present without undue increase in pressure. The bulb should be filled completely so that the liquid extends up into the enlargement in the stem as indicated at figure 8(f). Usually a small bubble will be trapped in the bulb at the point where it joins on to the stem, but such a bubble can usually be removed without too much difficulty with the aid of the hypodermic needle or a piece of wire. In filling the bulbs the usual safety precautions for the handling of volatile organic solvents should be taken, particularly if the fuel contains tetraethyl lead [13].

In filling bulbs with very volatile liquid fuels such as gasolines, great care should be taken to avoid loss of material by evaporation, as this causes fractionation of the material with a consequent change in heat of combustion. The container should be kept tightly closed at all times except when withdrawing a sample with the hypodermic syringe. The sample can be withdrawn more quickly if the needle is detached from the syringe. In replacing the needle after withdrawal of the sample care should be taken to avoid contact of gasoline with the hands, particularly if it contains tetraethyl lead.

After the bulb is filled, the capillary is sealed off so as to leave a stem about 3 or 4 mm long attached to the bulb. In order to do this the bulb must be cooled so as to draw the liquid out of the capillary, and the bulb must be protected from the flame during the sealing operation. To protect the bulb from the flame a small piece of asbestos paper with a hole in the center and with a cut between the hole and the edge (fig. 8(g)) is slipped over the capillary via the cut so that the capillary goes through the hole, and the piece of asbestos paper is in contact with the bulb. The bulb is then cooled by placing it on a mass of shaved ice in a beaker, or on a copper plate in contact with ice, and when the meniscus in the capillary disappears below the asbestos paper, the capillary is sealed off with a small hot air-gas flame and removed from the bulb. The bulb should then be removed promptly from the ice to avoid possible breakage due to

excessive contraction of the liquid. The filled bulb is conveniently handled by the short projecting capillary by means of forceps of the type ordinarily used for handling balance weights. Particles of asbestos which may adhere to the bulb should be removed by means of a camel's hair brush. Any liquid remaining in the capillary detached from the bulb in sealing it should be removed before weighing the filled bulb together with this detached capillary. If the liquid is sufficiently volatile it can be removed by flaming the capillary several times with the micro-burner flame. The flame should be applied first to the closed end of the capillary, and moved gradually to the open end in such a manner as to avoid softening the glass. If the liquid is of low volatility, it should be washed out with a volatile solvent, such as benzene or petroleum ether, introduced into the capillary by means of a hypodermic syringe before flaming as described above.

When first sealed, the bulb may contain a small bubble of air. This will dissolve in the liquid after a time leaving the bulb completely filled with liquid. Bulbs prepared in the manner described should withstand changes in room temperature of 10° C or more, and pressures of at least 30 atm (450 psi) without breaking.

Glass sample bulbs of different types have been described by a number of workers [16, 17].

Washington, April 14, 1959.

U. S. Department of Commerce National Bureau of Standards

RESEARCH PAPER RP1499

Part of Journal of Research of the National Bureau of Standards, Volume 29,

October 1942

HEAT OF COMBUSTION OF BENZOIC ACID, WITH SPECIAL REFERENCE TO THE STANDARDIZATION OF BOMB CALORIMETERS

By Ralph S. Jessup

ABSTRACT

New measurements yielded the value 26428.4±2.6 International joules per gram mass for the heat of combustion, Q_B, of benzoic acid at 25° C under the conditions of the standard bomb process. The difference, 0.036 percent, between the above value and that reported in 1934 is due to five factors: (1) An error in the previous value, resulting from the effect of dissolved carbon dioxide on the determination of the nitric acid formed in the bomb, (2) a change in the value used for the energy of formation of nitric acid in the bomb, (3) taking account in the present work (in the calculation of the value of Q_B at 25° from the observed value at 30°) of the temperature dependence of the Washburn reduction, (4) a change in the value used for the temperature coefficient of the heat of combustion, arising from the use of a new value for the specific heat of benzoic acid, and (5) a small difference in the results of the calorimetric measurements. The 1934 results, when corrected for the first four of the above effects, are in agreement within 0.01 percent with the results of the present measurements. The procedure for correcting the results of calibration experiments originally calculated on the basis of the 1934 value of Q_B is described.

With one exception, values of Q_B at 25° C calculated from the results of previous measurements are in satisfactory agreement with the value given above.

When the amount of benzoic acid burned in each experiment was calculated from the mass of carbon dioxide formed, the present measurements yield the value 3226.39±0.32 International kilojoules per mole for $-\Delta H^\circ_{298.16}$, the decrease in heat content for the combustion reaction at 25° C when each of the gases involved in the reaction is in the thermodynamic state of the unit fugacity and the water formed in combustion is in the liquid state.

CONTENTS

I. INTRODUCTION

Benzoic acid has been used many years as a standard substance for calibrating bomb calorimeters, and has been selected as the primary standard substance for this purpose by the Standing Committee for Thermochemistry of the International Union of Chemistry [1].[1] Such use of benzoic acid requires an accurate value, in terms of some generally acceptable energy unit, for its heat of combustion under the conditions of the bomb process.

The results of heat of combustion measurements made at this Bureau on various lots of benzoic acid used as Standard Sample material have been reported previously [2, 3]. Because impurities might affect the heat of combustion of different lots of benzoic acid by significantly different amounts, it has been the practice at this Bureau to determine the heat of combustion of each lot of Standard Sample material.

The present paper gives the results of measurements of the heat of combustion of two lots of benzoic acid, designated as Standard Samples 39e and 39f, and of two samples of benzoic acid of a very high degree of purity that were prepared by Schwab and Wichers [4] of this Bureau.

These measurements were made primarily for the purpose of providing data for use in connection with the standardization of bomb calorimeters. For this purpose the quantity of interest is the heat of combustion per gram of sample under the conditions of the bomb process. However, since material of exceptionally high purity was available for this work, it seemed worth while to obtain also data on the heat of combustion per mole of benzoic acid. The values reported for the heat of combustion per mole apply for conditions other than those of the bomb process, and these values are not suitable for use in connection with the standardization of bomb calorimeters.

II. APPARATUS AND METHOD

The essential features of the apparatus and methods used in the present work have been described in detail [2, 3] previously, and only a brief description of them will be given here. The calorimeter system consists of a nickel-plated copper vessel, of about 3.5 liters capacity, containing a weighed amount of water, provided with a closely-fitting cover and an arrangement for stirring the water; an electric heater; a bomb of 377 ml capacity, made of a corrosion-resistant alloy (illium); and a platinum resistance thermometer. The calorimeter is completely inclosed by a jacket which can be maintained at a constant temperature by means of a thermostat, and which is separated from the calorimeter by a 1-cm air space.

The method consists in making two types of experiments with the calorimeter. In one of these a measured quantity of energy is supplied to the system electrically, and the resulting temperature rise of the calorimeter is observed. In the other type of experiment a weighed sample of a combustible material is burned in the bomb, and the resulting temperature rise is observed. The first type of experiment yields the energy equivalent (effective heat capacity) of the calorimeter system, and when the energy equivalent is known the

[1] Numbers in brackets indicate the literature references at the end of this paper.

temperature rise of the calorimeter in the second type of experiment is a measure of the heat produced by the combustion. In both types of experiments the bomb contained 1 ml of water, and oxygen under a pressure of approximately 30 atmospheres. The procedure in both types of experiments was such that the final temperature of the calorimeter was very nearly the same as the constant temperature of the jacket.

The apparatus and methods used in the present work differ from those described in the report of measurements made at this bureau in 1934 [3] principally in the following respects:

1. The power measurements in the determination of the energy equivalent of the calorimetric system were referred to a saturated cadmium standard cell, which was maintained at a constant temperature by means of a temperature-control box [5]. The cell was calibrated before each series of energy-equivalent determinations, and its electromotive force remained constant to 2 microvolts over a period of 6 months. Unsaturated standard cells of the type used in the 1934 measurements have a very low temperature coefficient, but have been found to exhibit hysteresis effects [6] when exposed to varying temperature. Errors from this source could be avoided by keeping the cells at a constant temperature, but with the temperature kept constant the saturated cells have been found to be more satisfactory.
2. The Wolff-Diesselhorst potentiometer used for the measurements of power was calibrated in place. The potentiometer ratio (ratio of reading to electromotive force) was measured before each energy-equivalent determination, using two recently calibrated standard resistors [7].
3. The platinum resistance thermometer used to measure the temperature change of the calorimeter was of the same type as that used in the 1934 measurements [3], but it did not exhibit the erratic behavior of the latter.
4. The Wheatstone bridge used in connection with the platinum resistance thermometer was designed especially for bomb-calorimetric measurements [8].
5. The "constant range" method [9, 31] was used, that is, all calibration and combustion experiments were made over very nearly the same range of temperature. This procedure largely eliminates the effect of constant errors in calibration of the Wheatstone bridge and of peculiarities in the temperature scale defined by the thermometer.
6. In some of the measurements the amount of carbon dioxide formed in combustion was determined in the manner described in 1938 [10].

III. CALIBRATION OF THE CALORIMETER

The energy equivalent of the calorimeter was measured in the manner described in the 1934 report [3], except for the changes in apparatus and procedure mentioned in section II of this paper. The values obtained for the energy equivalent of the calorimetric system were all reduced to correspond to an absolute pressure of 30 atmospheres at 30° C. All the calibration experiments were made over very nearly the same temperature range, the temperature rise being about 3 degrees and the final temperature 30° C in all cases.

The results of the first series of calibration experiments are given

in table 1. This series consisted of two groups of experiments, one made with 31 volts across the heater in the calorimeter and a time of heating of 7 minutes, the other with 47.5 volts and a time of heating of 3 minutes.

TABLE 1.—*Results of first series of electrical calibration experiments*

Experiment number	Date 1940	Approximate electromotive force across heater	Energy equivalent	Deviation from mean
		Volts	*Int. j/°C*	*Int j/°C*
1	July 24	31	13733.9	+0.6
2	24	31	35.5	+2.2
3	Aug. 2	31	30.4	−2.9
4	2	31	32.7	−0.6
5	2	31	33.1	−.2
6	3	31	32.3	−1.0
7	5	31	31.3	−2.0
8	5	31	34.2	+0.9
9	5	31	33.2	−0.1
10	5	31	34.0	+0.7
11	6	31	35.6	+2.3
12	6	31	32.8	−0.5
Mean for group			13733.3	[a] ±0.4$_6$
13	Aug. 7	47.5	13732.8	−0.9
14	7	47.5	33.5	−0.2
15	7	47.5	34.1	+0.4
16	7	47.5	34.3	+0.6
17	8	47.5	33.2	−0.5
18	8	47.5	34.9	+1.2
19	8	47.5	34.0	+0.3
20	8	47.5	33.2	−0.5
Mean for group			13733.7	[a] ±0.2$_6$
Weighted mean			13733.6	[a] ±0.2

[a] The standard deviation of the mean.

Table 1 shows that the mean values of energy equivalent from the two groups of calibration experiments are in agreement within about 0.003 percent. The results of measurements on Standard Samples 39e and 39f given in table 4 were calculated on the basis of the weighted mean value given in table 1 for the energy equivalent of the calorimeter.

The results of a second series of calibration experiments, made after some necessary repairs to the calorimeter, are given in table 2. All experiments in this group were made with an electromotive force of about 31 volts across the heater in the calorimeter, and with a heating period of 7 minutes. The results of measurements on Standard Samples 39e and 39f given in table 5, and the results of measurements on purified benzoic acid given in table 8 were calculated on the basis of the mean value given in table 2 for the energy equivalent of the calorimeter.

TABLE 2.—*Results of second series of electrical calibration experiments*

Experiment number	Date 1941	Energy equivalent	Deviation from mean	Experiment number	Date 1941	Energy equivalent	Deviation from mean
		Int. j/° C	*Int. j°/ C*			*Int. j/° C*	*Int. j/° C*
1	Feb 18	13732.0	−0.2	9	24	32.1	−.1
2	18	33.5	+1.3	10	24	31.7	−.5
3	19	32.6	+0.4	11	25	32.1	−.1
4	21	31.2	−1.0	12	25	31.3	−.9
5	21	30.8	−1.4	13	25	32.8	+.6
6	21	33.6	+1.4				
7	21	32.3	+0.1	Mean		13732.2	[a]±0.2[6]
8	24	32.7	+.5				

[a] The standard deviation of the mean.

IV. COMBUSTION EXPERIMENTS

1. MATERIAL

From the freezing behavior of Standard Samples 39e and 39f, Schwab and Wichers [4] have estimated the purity of these lots of benzoic acid to be 99.983 and 99.977 mole percent, respectively. From specific-heat measurements on the solid at temperatures near the melting point, the purity of Sample 39e was estimated to be 99.990 mole percent [4, 12].

The two samples of purified benzoic acid were prepared by Schwab and Wichers from Standard Sample 39e, one by eight fractional crystallizations from aqueous solution, the other by eight fractional crystallizations from benzene solution. The purity of the first of the purified samples was estimated from freezing behavior to be 99.995 mole percent, whereas that of the second sample was estimated from both freezing behavior and specific-heat measurements to be 99.999 mole percent [4, 12].

As noted by Schwab and Wichers [4], the estimates of purity from specific-heat measurements were made on samples that had been dried by passing dry air through liquid benzoic acid at a temperature a few degrees above the melting point. It was later found that this treatment results in the very slow formation of benzoic anhydride. It is possible, therefore, that these samples may have contained slightly larger amounts of impurity than the corresponding samples for which the estimates of purity were made on the basis of freezing behavior. On the other hand, the drying treatment may have removed some excess water from Standard Sample 39e, so that for this Sample the net effect of the drying treatment may have been either an increase or a decrease in purity. In view of the facts that the rate of formation of benzoic anhydride under the conditions of the drying treatment is extremely small, and that only a very small amount of water was found in the Standard Sample material in the special tests described later in this paper, it is not believed that the formation of anhydride or the removal of water caused any significant change in purity of the Samples.

It should be emphasized that both of the tests of purity mentioned above are sensitive only to impurities that are soluble in the liquid and insoluble in the solid benzoic acid. The Standard Sample material is known to contain some insoluble material, but the amount of this is so small as to be practically negligible.

Combustible impurities were removed from the oxygen used by

passing the gas through a tube filled with copper oxide maintained at a temperature of about 750°C.

2. IGNITION ENERGY

The samples of benzoic acid were ignited by passing electric current from a small transformer through a helix made from a 2-cm length of No. 36 AWG iron wire (about 0.13 mm in diameter). The procedure was the same as in the measurements reported in 1934 [3], except that the secondary voltage of the transformer in the present measurements was 9 instead of 14 as in the previous work. The energy, q_i, used to ignite the charge (q_i=electric energy plus heat of combustion of iron wire) was determined calorimetrically in a number of blank experiments in which only the iron wire was burned. The results of these measurements are given in table 3. The standard deviation of the mean of the results and the maximum deviation from the mean correspond to 0.001 and 0.005 percent, respectively, of the heat of combustion of a 1.5-g sample of benzoic acid.

TABLE 3.—*Energy used to ignite the charge*

Experiment number	q_i	Deviation from mean
	Int. j	*Int. j*
1	17.1	−1.5
2	20.6	+2.0
3	19.3	+0.7
4	19.0	+0.4
5	17.3	−1.3
6	18.2	−0.4
7	19.7	+1.1
8	17.5	−1.1
Mean	18.6	[a]±0.4$_8$

[a] Standard deviation of the mean.

In another method of ignition, which has been described by Huffman and Ellis [13], an electrically heated platinum wire ignites a small piece of filter paper, which in turn ignites the charge. In some preliminary experiments of the present work the method of Huffman and Ellis was compared with the iron-wire method of ignition by using the two methods alternately in a series of calorimetric experiments in which Standard Sample benzoic acid was burned in the bomb. These experiments yielded the following values for the energy equivalent of the calorimeter, which differed in some respects from the calorimeter used in the other experiments described in this paper:

Method of ignition	Number of experiments	Mean value of energy equivalent	Standard deviation of the mean
		Int. j/°C	*Int. j/°C*
Iron wire	6	13733.6	±0.6$_8$
Platinum wire and filter paper	6	13732.4	±0.7$_8$

These results indicate that the precision of the two methods is about the same. The difference between the two mean values of energy equivalent is no larger than might be expected if the procedure in the

two sets of measurements had been identical in all respects, and is in the direction opposite to that of the difference which might be expected to result from action of nitric acid on the products of combustion of the iron wire. The iron-wire technique is somewhat more convenient than the platinum-wire–filter-paper technique, and has the further advantage that it does not complicate the determination of the amount of carbon dioxide formed in the combustion of the charge.

3. CORRECTION FOR HEAT OF FORMATION OF NITRIC ACID

The amount of nitric acid formed in the bomb in each combustion experiment was determined by titrating the bomb washings against an 0.1 N solution of potassium hydroxide, using phenolphthalein [2] as an indicator. The correction, q_{HNO_3}, for the energy of formation of nitric acid in the bomb was calculated, using for the energy decrease, $-\Delta U_{HNO_3}$, for the reaction 1/2 N_2 (g)+5/4 O_2 (g)+1/2 H_2O (liq)=HNO_3 (aq) at 30° C the rounded value 60 kj/mole of nitric acid. This value is very near the mean of the value derived from the results of Becker and Roth [14], and that derived from data given by Bichowsky and Rossini [15]. The correction for the heat of formation of nitric acid rarely exceeded 0.02 percent of the heat produced in the bomb, and was usually less than this.

4. CALCULATION OF RESULTS

The corrected temperature rise, Δt, of the calorimeter for each calibration experiment and each combustion experiment was computed on the basis of Newton's law of cooling from data obtained in two "rating periods", using Dickinson's method [2] of calculation. It has been shown that the effect of the lag of the bomb and other parts of the calorimetric system is almost completely eliminated by this procedure [16, 17, 25].

The quantity of heat produced in each combustion experiment was computed by multiplying the corrected temperature rise, Δt, by the energy equivalent of the system, represented by $C=C_0+1.21\ m_s+0.32\ (P-30)$, where C_0 is the energy equivalent, determined by the calibration experiments, of the calorimetric system, including the bomb containing 1 g of water, and oxygen under an absolute pressure of 30 atm; m_s is the mass of the sample of benzoic acid; P is the initial oxygen pressure, in atmospheres, at 30° C. The factor 1.21 is the value recently obtained at this Bureau [12] for the specific heat of benzoic acid at 28.5° C (at constant pressure); and the factor 0.32 was calculated from the specific heat of oxygen at constant volume [18], the volume of the bomb, and the density of oxygen.

The value for the heat of combustion per gram of sample under the conditions of the actual bomb process was calculated for each experiment by means of the relation

$$q_B=\frac{C\Delta t-q_1-q_{HNO_3}}{m_s},$$

[2] Phenolphthalein is sensitive to dissolved carbon dioxide, and its use resulted in high values for nitric acid unless precautions were taken to remove dissolved carbon dioxide from the bomb washings before titrating. It is shown later in this paper that under the conditions of the present measurements the effect of dissolved carbon dioxide amounted to about 0.017 percent of the heat of combustion. The use of an indicator that is practically insensitive to carbon dioxide, such as methyl orange, would have been better.

The corresponding value for the heat of combustion per mole of benzoic acid was calculated from

$$-\Delta U_B = \frac{C\Delta t - q_i - q_{HNO_3}}{N/7},$$

where N is the number of moles of carbon dioxide formed in the combustion, the molecular weight of carbon dioxide being taken as 44.010. Since the value of C used in the above equations is the energy equivalent of the calorimetric system, including the oxygen and charge of benzoic acid rather than the products of combustion, the values of q_B and $-\Delta U_B$ are referred to the final temperature of the calorimeter, which was 30° C in all experiments.

With the aid of an equation similar to Washburn's [19] eq 81 (which applies at 20° C), but calculated by the writer for 30° C, there was computed from each value of q_B the corresponding value of Q_B, which is the heat of combustion (at 30° C) per gram of sample for the standard bomb process defined by the following initial conditions

$$m_S/V = 3.0 \text{ g/liter}$$
$$m_W/V = 3.0 \text{ g/liter}$$
$$P = 30 \text{ atm at } 30° \text{ C},$$

where V is the volume of the bomb, and m_W is the mass of water placed in the bomb before the experiment. The other symbols have been defined previously.

The values of $-\Delta U_B$ per mole of benzoic acid were reduced, with the aid of the modified Washburn equation, to the corresponding values of $-\Delta U_R$, which is the energy decrease for the reaction

$$C_6H_5COOH(c) + 7\tfrac{1}{2}O_2(g) = 7CO_2(g) + 3H_2O(liq.) \text{-----}, \quad (1)$$

where each of the reactants and products is under a pressure of 1 atm. at 30° C.[3]

5. RESULTS

In table 4 are given the results of the first series of measurements on Standard Samples 39e and 39f. The mean values of Q_B at 30° C given in this table are in good agreement with the corresponding mean values, 26415.3 and 26413.1 International joules per gram (mass), which were obtained for Samples 39d and 39e, respectively, in 1934[3]. In table 5 are given the results of the second series of measurements on Samples 39e and 39f. The measurements of the first and second series were made under the same conditions, except that in the second series the mass of carbon dioxide [4] formed in each experiment was determined by absorption in Ascarite in the manner described in 1938[10].

It will be seen from tables 4 and 5 that the values of Q_B at 30° C from the second series of measurements on both Samples are systematically higher by about 0.03 percent than those from the first series. It will also be seen that the correction for the heat of formation of nitric acid is systematically lower in the second series than in

---

[3] Washburn's eq 81 gives the value of $100\frac{\Delta U_B - \Delta U_R}{-\Delta U_B}$, that is, the percentage difference between $-\Delta U_B$ and $-\Delta U_R$. The percentage difference between the quantities q_B and Q_B is the difference between the values of $100\frac{\Delta U_B - \Delta U_R}{-\Delta U_B}$ for the actual and standard bomb processes.

[4] The results of the measurements of the mass of carbon dioxide formed in experiments 17 to 25, inclusive, were discarded because of a leak in the apparatus which was discovered after experiment 25.

574278 O - 61 - 26

TABLE 4.—*Results of first series of measurements on Samples 39e and 39f*

Experiment number	Date 1940	Mass of sample (weight in vacuum)	Initial oxygen pressure at 30° C	Total heat produced	Correction for heat of formation of HNO_3	Correction for ignition energy	Heat produced by combustion of benzoic acid	Observed heat of combustion, q_B	Reduction to standard bomb process	Q_B (30°C)	Deviation from mean
MEASUREMENTS ON SAMPLE 39e											
		g	*atm*	*Int. j*	*Int. j*	*Int. j*	*Int. j*	*Int. j/g*	*Int. j/g*	*Int. j/g*	*Int. j/g*
1	June 13	1.51865	31.7	40145.3	−11.9	−18.6	40114.8	26414.8	−1.7	26413.1	−2.0
2	13	1.52115	31.6	40215.6	−11.9	−18.6	40185.1	26417.6	−1.6	16.0	+0.9
3	13	1.52080	31.7	40211.5	−13.1	−18.6	40179.8	26420.2	−1.7	18.5	+3.4
4	14	1.51746	31.7	40116.3	−12.5	−18.6	40085.2	26416.0	−1.7	14.3	−0.8
13	21	1.53468	31.9	40578.9	−13.1	−18.6	40547.2	26420.6	−1.8	18.8	+3.7
14	24	1.52120	31.9	40214.5	−13.1	−18.6	40182.8	26415.2	−1.8	13.4	−1.7
15	24	1.52044	31.8	40195.7	−11.9	−18.6	40165.2	26416.8	−1.7	15.1	0.0
16	24	1.52153	31.8	40220.2	−12.5	−18.6	40189.1	26413.6	−1.7	11.9	−3.2
Mean										26415.1	*±1.0
MEASUREMENTS ON SAMPLE 39f											
5	June 14	1.51922	31.6	40164.5	−12.5	−18.6	40133.4	26417.1	−1.6	26415.5	+0.8
6	14	1.51711	31.8	40117.6	−10.1	−18.6	40088.9	26424.5	−1.7	22.8	+8.1
7	20	1.52153	31.9	40225.8	−10.7	−18.6	40196.5	26418.5	−1.8	16.7	+2.0
8	20	1.51974	31.9	40162.3	−11.3	−18.6	40132.4	26407.4	−1.8	05.6	−9.1
9	20	1.52141	31.8	40214.0	−11.9	−18.6	40183.5	26412.0	−1.7	10.3	−4.4
10	21	1.52050	32.0	40203.2	−12.5	−18.6	40172.1	26420.3	−1.9	18.4	+3.7
11	21	1.52111	32.0	40203.6	−11.3	−18.6	40173.7	26410.8	−1.9	08.9	−5.8
12	21	1.52075	32.0	40210.8	−12.5	−18.6	40179.7	26421.0	−1.9	19.1	+4.4
Mean										26414.7	*±2.1

* The standard deviation of the mean, calculated from the data of both calibration and combustion experiments.

TABLE 5.—*Results of second series of measurements on Samples 39e and 39f*

Experiment number	Date	Mass of sample (weight in vacuum)	Initial oxygen pressure at 30°C	Total heat produced	Correction for heat of formation of HNO_3	Correction for ignition energy	Heat produced by combustion of benzoic acid	Observed heat of combustion, q_B	Reduction to standard bomb process	Q_B (30°C)	Deviation from mean	CO_2 formed in combustion	Observed heat of combustion, $-\Delta U_B$	Washburn reduction, $\Delta U_B - \Delta U_R$	$-\Delta U_R$ (30°C)	Deviation from mean
MEASUREMENTS ON SAMPLE 39f																
	1940	*g*	*atm*	*Int. j*	*Int. j*	*Int. j*	*Int. j*	*Int. j/g*	*Int. j/g*	*Int. j/g*	*Int. j/g*	*Moles×7*	*Int. kj/mole*	*Int. kj/mole*	*Int. kj/mole*	*Int. kj/mole*
17	Nov. 29	1.52275	32.4	40267.7	−6.0	−18.6	40243.1	26427.9	−2.1	26425.8	+2.6					
18	Dec. 3	1.52111	32.6	40219.2	−6.0	−18.6	40194.6	26424.5	−2.2	22.3	−0.9					
19	27	1.52120	32.4	40223.5	−6.0	−18.6	40198.9	26425.8	−2.1	23.7	+0.5					
20	31	1.52077	32.3	40209.7	−6.0	−18.6	40185.1	26424.2	−2.1	22.1	−1.1					
	1941															
21	Jan. 2	1.52075	32.3	40205.0	−2.4	−18.6	40184.0	26423.8	−2.1	21.7	−1.5					
22	22	1.52182	32.3	40236.0	−5.4	−18.6	40212.0	26423.6	−2.1	21.5	−1.7					
23	27	1.52051	32.5	40200.1	−4.8	−18.6	40176.7	26423.2	−2.2	21.0	−2.2					
24	28	1.52144	32.4	40228.2	−2.4	−18.6	40207.2	26427.1	−2.1	25.0	+1.8					
25	30	1.52172	32.4	40235.3	−4.2	−18.6	40212.5	26425.7	−2.1	23.6	+0.4					
26	Feb. 6	1.52058	32.3	40212.6	−5.4	−18.6	40188.6	26429.8	−2.1	27.7	+4.5	0.0124527	3227.30	−2.53	3224.77	+0.16
27	7	1.52115	32.1	40214.9	−3.0	−18.6	41193.3	26423.0	−2.0	21.0	−2.2	.0124554	3226.98	−2.52	4.46	−0.15
Mean										26423.2	[a] ±0.8				3224.61	[a] ±0.17
MEASUREMENTS ON SAMPLE 39e																
28	Mar. 20	1.52141	32.2	40225.0	−6.6	−18.6	40199.8	26422.7	−2.0	26420.7	−1.8	0.0124582	3226.77	−2.53	3224.24	−0.04
29	25	1.51952	32.2	40185.2	−9.0	−18.6	40157.6	26427.8	−2.0	25.8	+3.3	.0124438	3227.12	−2.53	4.59	+0.31
30	26	1.52033	32.2	40201.3	−9.0	−18.6	40173.7	26424.3	−2.0	22.3	−0.2	.0124510	3226.54	−2.53	4.01	−0.27
31	27	1.52157	32.1	40228.4	−9.0	−18.6	40200.8	26420.6	−2.0	18.6	−3.9	.0124577	3226.97	−2.52	4.45	+0.17
32	Apr. 25	1.52175	32.2	40233.5	−5.4	−18.6	40209.5	26423.2	−2.0	21.2	−1.3	.0124623	3226.49	−2.53	3.96	−0.32
33	28	1.51853	32.2	40158.6	−7.8	−18.6	40132.2	26428.3	−2.0	26.3	+3.8	.0124365	3226.97	−2.53	4.44	+0.16
Mean										26422.5	[a] ±1.3				3224.28	[a] ±0.12

[a] Standard deviation of the mean, calculated from the data of both calibration and combustion experiments.

the first. The fact that the carbon dioxide was completely removed from the bomb before the nitric acid determinations in the second series of measurements, but not in the first, suggests that the nitric acid determinations of the first series may have been in error because of the sensitivity of the indicator, phenolphthalein, to carbon dioxide dissolved in the washings from the bomb.

In table 6 are given the values of the correction for nitric acid per gram of benzoic acid in the first and second series of measurements on Sample 39f.[5] The difference in the mean values of the correction for the two series is 4.5 j/g of benzoic acid (standard deviation ±0.4 j/g). If it is assumed that the difference is the result of dissolved carbon dioxide in the washings from the bomb in the first series of measurements, and the results of this series are corrected accordingly, the mean values of Q_B for the two series are brought into satisfactory agreement. The final values of Q_B at 30° C obtained in this way for the Standard Samples are given in table 7.

TABLE 6.—*Correction for nitric acid per gram of benzoic acid in the two series of measurements on Standard Sample 39f*

First series			Second series		
Experiment number	Correction	Deviation from mean	Experiment number	Correction	Deviation from mean
	Int. j.	*Int. j.*		*Int. j.*	*Int. j.*
5	8.2	+0.6	17	3.9	+0.8
6	6.7	−.9	18	3.9	+.8
7	7.0	−.6	19	3.9	+.8
8	7.4	−.2	20	4.0	+.9
9	7.8	+.2	21	1.6	−1.5
10	8.2	+.6	22	3.6	+0.5
11	7.4	−.2	23	3.2	+.1
12	8.2	+.6	24	1.6	−1.5
			25	2.8	−0.3
Mean	7.6	[a] ±0.2	26	3.6	+.5
			27	2.0	−1.1
			Mean	3.1	[a] ±0.3

[a] The standard deviation of the mean.

TABLE 7.—*Final values of Q_B at 30° C for the Standard Samples*

Series	Mean value of Q_B for Standard Sample 39e	Standard deviation of mean	Mean value of Q_B for Standard Sample 39f	Standard deviation of mean
	Int. j/g	*Int. j/g*	*Int. j/g*	*Int. j/g*
First	26419.6	[a] ±1.0$_5$	26419.2	[a] ±2.1$_5$
Second	26422.5	±1.3	26423.2	±0.8
Mean	26420.7	±0.8	26422.7	±0.7

[a] The results of the first series have been corrected for the effect of dissolved carbon dioxide in the washings from the bomb. The standard deviations for the results of the first series of measurements include the standard deviation (±0.4 j/g) of the correction for dissolved carbon dioxide.

The improved concordance of the results brought about by the application of the above correction is consistent with the hypothesis regarding the cause of the original differences, but it is not conclusive proof of this hypothesis. It was desirable, therefore, to make inde-

[5] The same oxygen tank was used in both series of measurements on Sample 39f, but different tanks were used in the two series of measurements on Sample 39e. The nitric acid determinations for the two series of experiments on Sample 39e are therefore not comparable.

pendent tests to ascertain the effect of dissolved carbon dioxide on the determination of nitric acid formed in the bomb. To this end, a measured volume of a dilute solution of nitric acid was placed in the bomb, which was then filled to a pressure of 30 atm with a mixture of oxygen and carbon dioxide. The mass and concentration of the nitric acid solution placed in the bomb and the composition of the O_2–CO_2 mixture were such as to duplicate approximately the conditions in the bomb after combustion of a 1.5-g sample of benzoic acid. After an hour or more had been allowed for the establishment of equilibrium, the pressure was released, the bomb opened and immediately washed out, and the washings were titrated, the procedure being as nearly as possible the same as in the first series of measurements on the Standard Samples. In other experiments the procedure was the same, except that after opening the bomb, it was flushed out with air and allowed to stand for a measured length of time before washing it out and titrating the washings.

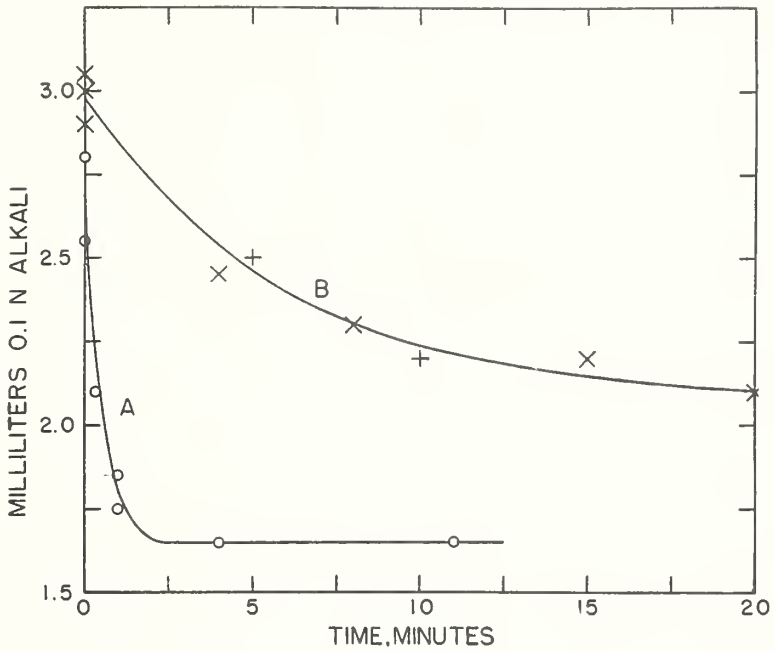

FIGURE 1. *Results of the tests to ascertain the effect of dissolved carbon dioxide on the determination of nitric acid.*

The results of these experiments are given by curve *A*, figure 1, where the amount of 0.1 *N* alkali solution required to neutralize the washings from the bomb is plotted as ordinate, and the time after opening and flushing out the bomb is plotted as abscissa. Curve *B* shows the results of two similar series of experiments, in which the carbon dioxide and nitric acid were formed by combustion of a 1.5-g sample of benzoic acid. Both curves are consistent, within the uncertainty of the measurements, with the conclusions drawn from the data of table 6 as to the magnitude of the effect of dissolved carbon dioxide. It is believed that this fact justifies the correction of the results of the first series of measurements on the basis of the data of table 6.

A surprising feature of figure 1 is the difference in form of the curves A and B, which indicates that the carbon dioxide was removed from solution much more slowly in the experiments represented by curve B than in those represented by curve A. It would be expected that the difference would be in the opposite direction, since in the experiments represented by curve A all the nitric acid solution was in the bottom of the bomb, whereas in those represented by curve B the solution was distributed over the entire inner surface of the bomb and therefore had a much larger free surface. No satisfactory explanation of this phenomenon has been found. A series of experiments similar to those represented by curve B, but in which naphthalene was burned instead of benzoic acid, gave results which were represented by a curve more nearly resembling curve A than curve B.

In addition to the values of Q_B per gram of sample, there are given in table 5 values of $-\Delta U_R$ (at 30° C) per mole of benzoic acid for the Standard Sample material. The results for the two Samples are in agreement within the uncertainty of the measurements.

In table 8 are given the results of measurements on the purified samples of benzoic acid. These samples were received in sealed glass containers, and in opening one of them some particles of glass were introduced into the sample. This made impossible an accurate determination of the mass of the sample burned in each experiment, and consequently only the values per mole of benzoic acid are given for this sample. In opening the other container great care was taken to avoid getting glass into the benzoic acid, and values of both Q_B per gram of sample and $-\Delta U_R$ per mole of benzoic acid are given for this sample.

The mean value of Q_B at 30° C given in table 8 for the benzoic acid purified by crystallization from benzene is in satisfactory agreement with the values given in table 7 for the Standard Samples. The values given in table 8 for $-\Delta U_R$ at 30° C for the purified samples of benzoic acid, and the corresponding values given in table 5 for the Standard-Sample materials are also in satisfactory agreement.

In view of the agreement of the results for the purified and Standard Sample materials, it may be concluded that the impurities in the Standard Sample materials are of such a nature that they have no appreciable effect on the heat of combustion. The weighted mean values of all results on both Standard-Sample and purified materials may therefore be taken as the results of the present measurements for pure benzoic acid or for the Standard Sample materials.

The weighted mean value of Q_B was obtained by taking the mean of all results on Standard Samples 39e and 39f that were obtained on the basis of the first calibration of the calorimeter, and the mean of all results on the Standard Samples and the purified materials that were obtained on the basis of the second calibration of the calorimeter, and weighting these two mean values inversely as the squares of their standard deviations. The final value of $-\Delta U_R$ is the mean of all results on both Standard Sample and purified materials.

The values obtained in the manner just described are Q_B (30° C)= 26422.4 Int. j/g (mass) and $-\Delta U_R$ (30° C)=3224.70 Int. kj/mole. The standard deviations of these mean values are, respectively, $\pm 0.6_5$ j/g and ± 0.12 kj/mole. Multiplication of these values of the standard deviation by appropriate factors will yield values of other measures of precision, such as "probable error" (factor=

TABLE 8.—*Results of measurements on samples of purified benzoic acid*

Experiment number	Date	Mass of sample (weight in vacuum)	Initial oxygen pressure at 30° C	Total heat produced	Correction for heat of formation of HNO_3	Correction for ignition energy	Heat produced by combustion of benzoic acid	Observed heat of combustion, q_B	Reduction to standard bomb process	Q_B (30° C)	Deviation from mean	CO_2 formed in combustion	Observed heat of combustion, $(-\Delta U_B)$	Washburn reduction, $(\Delta U_B - \Delta U_R)$	$-\Delta U_B$ (30°C)	Deviation from mean
SAMPLE 39e PURIFIED BY EIGHT CRYSTALLIZATIONS FROM WATER																
	1941	*g*	*atm*	*Int. j*	*Int. j*	*Int. j*	*Int. j*	*Int. j/g*	*Int. j/g*	*Int. j/g*	*Int. j/g*	*Moles* $\times 7$	*Int. kj/mole*	*Int. kj/mole*	*Int. kj/mole*	*Int. kj/mole*
34	Apr. 30		32.1	40199.4	−8.7	−18.6	40172.1					0.0124504	3226.57	−2.52	3224.05	−0.76
35	May 12		32.4	40216.2	−4.6	−18.6	40193.0					.0124568	6.59	−2.54	4.05	−.76
36	13		32.3	40241.8	−5.8	−18.6	40217.4					.0124629	6.97	−2.53	4.44	−.37
37	26		32.0	402.9.5	−3.5	−18.6	40197.4					.0124553$_5$	7.32	−2.52	4.80	−.01
38	28		32.2	40207.5	−2.9	−18.6	40186.0					.0124512	7.48	−2.53	4.95	+.14
39	29		31.5	40213.1	−4.1	−18.6	40190.4					.0124513	7.81	−2.48	5.33	+.52
40	June 12		32.1	40176.6	−4.6	−18.6	40153.4					.0124400	7.77	−2.52	5.25	+.44
41	18		32.4	40203.8	−1.2	−18.6	40184.0					.0124484	8.05	−2.54	5.51	+.70
42	19		32.0	40138.1	−2.3	−18.6	40117.2					.0124305	7.32	−2.52	4.80	−.01
43	20		31.9	40214.5	−3.5	−18.6	40192.4					.0124514	7.94	−2.51	5.43	+.62
44	23		31.5	40116.0	−3.5	−18.6	40093.9					.0124253	6.80	−2.48	4.32	−.49
Mean															3224.81	[a] ±0.18
SAMPLE 39e PURIFIED BY EIGHT CRYSTALLIZATIONS FROM BENZENE																
45	June 25	1.52107	31.7	40205.4	−2.9	−18.6	40183.9	26418.2	−1.7	26416.5	−6.8	0.0124543	3226.51	−2.49	3224.02	−0.87
46	26	1.52061	31.7	40209.7	−7.5	−18.6	40183.6	26426.0	−1.7	24.3	+1.0	.0124510	7.34	−2.49	4.85	−.04
47	27	1.52123	31.8	40228.4	−4.1	−18.6	40205.7	26429.7	−1.8	27.9	+4.6	.0124564$_5$	7.70	−2.50	5.20	+.31
48	30	1.52096	31.5	40220.1	−4.1	−18.6	40197.4	26429.0	−1.6	27.4	+4.1	.0124535	7.80	−2.48	5.32	+.43
49	July 21	1.52069	31.7	40199.0	−3.5	−18.6	40176.9	26420.2	−1.7	18.5	−4.8	.0124525	6.41	−2.49	3.92	−.97
50	22	1.52122	31.9	40217.8	−1.7	−18.6	40197.5	26424.5	−1.8	22.7	−0.6	.0124556$_6$	7.26	−2.51	4.75	−.14
51	23	1.52137	32.0	40226.3	−1.2	−18.6	40206.5	26427.8	−1.9	25.9	+2.6	.0124567$_8$	7.69	−2.51	5.18	+.29
52	24	1.52159	31.7	40227.3	−1.2	−18.6	40207.5	26424.7	−1.7	23.0	−0.3	.0124545	8.35	−2.49	5.86	+.97
Mean										26423.3	[a] ±1.5				3224.89	[a] ±0.24

[a] Standard deviation of the mean, calculated from the data of both calibration and combustion experiments.

0.6745), and the "uncertainty" (factor=2.0) proposed by Rossini and Deming [11] for the final results of thermochemical measurements. An estimated uncertainty of ±0.010 percent (±2.6 j/g, or ±0.32 kj/mole) is here assigned to the final results of the present measurements. In arriving at this figure, consideration was given to the precision of the data, the probable magnitudes of systematic errors, and the agreement of the results with those of previous measurements.

In order to obtain the value of Q_B at 25° C corresponding to the value given above for 30° C, it is necessary to take account of the temperature coefficient of $-\Delta U_R$, and of the change in the Washburn reduction with temperature. The temperature coefficient of $-\Delta U_R$ was calculated from the specific heats of benzoic acid [12], water [7], oxygen and carbon dioxide [18] to be −118.5 j/mole-degree (−0.97 j/g° C). The Washburn reduction, $(\Delta U_B - \Delta U_R)$, at 30° and 25°C is −2.30 and −2.44 kj/mole (−18.8 and −20.0 j/g), respectively. With these data it is calculated that for the standard bomb process

$$Q_B \text{ (25° C)} = 26428.4 \pm 2.6 \text{ Int. j/g (mass)}.^{6}$$

The value of $-\Delta H$ for the reaction (1) at 30° C, corresponding to the value of $-\Delta U_R$ (30° C) given above is 3226.03 ±0.32 Int. kj/mole. Using the value 115.5 j/mole-degree for the temperature coefficient of ΔH, and correcting for the departures of the gases, oxygen, and carbon dioxide, from the standard state of unit fugacity (1 atm), there is obtained for reaction (1) $-\Delta H°298.16 = 3226.39 \pm 0.32$ Int. kj/mole.[7]

It should be emphasized that the quantity of interest in connection with the standardization of bomb calorimeters is Q_B, the heat of combustion per gram under the conditions of the standard bomb process. The values of heat of combustion per mole are not suitable for this purpose, since they apply for conditions other than those of the bomb process and are based on the mass of carbon dioxide formed in combustion rather than on the mass of sample burned.

V. CORRECTION OF 1934 RESULTS

The procedure in the combustion experiments reported in 1934 [3] was the same as that in the first series of combustion experiments of the present work, and the same indicator, phenolphthalein, was used in the nitric acid determinations. It is inferred, therefore, that the 1934 results are low because of dissolved carbon dioxide in the bomb washings, and they have been corrected accordingly. The correction is somewhat uncertain because of the fact that the data of table 6 apply when a 1.52-g sample of benzoic acid is burned under an initial oxygen pressure of about 32 atm, whereas in the 1934 measurements the mass of sample was varied from 0.7 to 2.0 g and the oxygen pressure from 20 to 32 atm. In calculating the correction to be applied

[6] The heat of combustion under conditions differing by small amounts from those of the standard bomb process at 25° C is obtained by multiplying the value given for Q_B (25° C) by the factor

$$1+10^{-6}\,[20\,(P-30)+42\,(m_s/V-3)+30\,(m_w/V-3)-45\,(t-25).]$$

[7] As noted previously, this value was derived by calculating the number of moles of benzoic acid burned in each experiment from the mass of carbon dioxide formed in combustion. The value of $-\Delta H°298.16$ obtained by calculating the number of moles of benzoic acid burned from the mass of sample, using 122.118 for the molecular weight of benzoic acid, is 3226.04 ±0.32 Int. kj/ mole. Inert impurity in the sample would affect the value of heat of combustion per mole based on the weight of sample but not the value based on the weight of carbon dioxide formed. The effect of an error in the atomic weight of carbon would be 2.5 times as great in the value based on the weight of sample as in the value based on the weight of carbon dioxide.

to the 1934 results, it was assumed that the effect of dissolved carbon dioxide in any experiment is proportional to the mole fraction of carbon dioxide in the gas phase and to the total mass of water in the bomb at the end of the experiment.

The 1934 results have also been corrected for the change from 63 to 60 kj/mole in the value used for the energy of formation of nitric acid in the bomb, for the change in the value used for the temperature coefficient of $-\Delta U_R$, and for the dependence on temperature of the Washburn reduction. The last-named effect was neglected in 1934 in calculating the value of Q_B at 25° C from the observed value at 30° C.[8]

The values of Q_B at 25° calculated from the data of the 1934 measurements in the manner outlined above are given in table 9, together with the corresponding values resulting from the present measurements on Standard Samples 39e, 39f, and the sample of 39e that was purified by fractional crystallization from benzene.

TABLE 9.—*Values of Q_B at 25°C for Standard Samples, and for the sample purified by crystallization from benzene*

Date	Sample	Values for individual samples	Standard deviation of the mean	Mean of values for all samples	Standard deviation of the mean
		Int. j/g	*Int. j/g*	*Int. j/g*	*Int. j/g*
1934 [1]	39d	26427.7	±1.1	26426.6	±0.85
	39e	26425.6	±1.0		
1942	39e	26426.7	±0.7		
	39f	26428.8	±0.7	26428.4	±0.65
	Purified [2]	26429.3	±1.5		

[1] The results reported in 1934 have been corrected as described in the test.
[2] Sample 39e purified by crystallization from benzene.

It will be seen from table 9 that the corrected results of the 1934 measurements are in satisfactory agreement with those of the present work. The mean values of Q_B from the two investigations differ by only 0.007 percent, and the total range of values for the different lots of benzoic acid is 0.014 percent.

VI. PROCEDURE FOR CORRECTING RESULTS REPORTED ON THE BASIS OF THE 1934 VALUE OF Q_B

The mean value reported in 1934 for Q_B at 25° C, 26,419 International joules per gram mass, is lower by 9.4 j/g (0.036 percent) than the value obtained in the present measurements. The elements which enter into this difference may be summarized as follows:

1. Effect of dissolved CO_2	5.5 j/g
2. Temperature dependence of Washburn reduction	1.2 j/g
3. Change in temperature coefficient of $-\Delta U_R$	0.1 j/g
4. Change in nitric acid correction	0.8 j/g
5. Difference in calorimetric measurements	1.8 j/g
Total	9.4 j/g

The results of calibration experiments by means of benzoic acid which were calculated on the basis of the 1934 value of Q_B can be re-

[8] In other words, the temperature coefficient of $-\Delta U_R/M$, calculated from data on C_D at atmospheric pressure, was used in 1934 in deriving the value of Q_B at 25° C from the observed value at 30° C. The temperature coefficient of Q_B involves the temperature coefficients of both $-\Delta U_R/M$ and the Washburn reduction.

duced to the basis of the new value with the aid of the above data. The reduction will not in all cases involve all of the above elements of the difference between the two values of Q_B, and in deciding which of the elements are involved in any particular case, consideration will have to be given to the conditions under which the calibration experiments were performed. For example, consider the case of a bomb calorimeter calibrated with benzoic acid under the same (average) conditions as in the 1934 combustion experiments with respect to temperature, oxygen pressure, mass of sample, mass of water placed in the bomb, amount of nitric acid formed, procedure followed in the nitric acid determinations, and value used for the heat of formation of nitric acid. Under these circumstances the conversion of the value obtained for the energy equivalent of the calorimeter to the basis of the new value of Q_B would involve only that part of the difference between the old and new values which resulted from the difference in the calorimetric measurements (1.8 j/g=0.007 percent).

In the case where the calibration experiments were made under the same conditions as in the above example, except that the procedure was such that dissolved carbon dioxide did not affect the nitric acid determinations, the conversion to the basis of the new value of Q_B would involve both the difference in the calorimetric measurements (1.8 j/g) and the effect of dissolved carbon dioxide (5.5 j/g) on the nitric acid corrections in the 1934 experiments. If the calibration experiments were referred to some temperature other than 30° C, account would have to be taken of the change in the temperature coefficient of Q_B.

The following data on the average conditions in the 1934 measurements will be of use in reducing results originally calculated on the basis of the 1934 report to the basis of the present report:

Temperature to which experiments were referred	30° C
Mass of sample of benzoic acid	1.35 g
Nitric acid correction per gram of benzoic acid	17.4 j
Mole fraction of CO_2 in final gas phase in bomb	0.206
Water in bomb at end of experiment	0.089 mole
Effect of dissolved CO_2 per gram of benzoic acid	5.5 j

The value given above for the nitric acid correction was calculated, using the 1934 value, 63 kj/mole, for the heat of formation of nitric acid in the bomb.

The conversion of the results of calibration experiments by means of benzoic acid, originally calculated, using the 1934 value of Q_B, to the basis of the new value will be illustrated by a specific example. It is assumed that the calibration experiments were performed under the following conditions:

Volume of bomb	0.4 liter
Mass of sample burned	1.50 g
Mass of water placed in bomb	1.00 g
Nitric acid correction per gram of benzoic acid burned	6.8 j
Temperature to which experiments were referred	28.0° C
Initial oxygen pressure at 28° C	33.0 atm

The value for the heat of combustion of benzoic acid under these conditions would be 26418.6 Int. j/g, according to the 1934 report, and 26426.8 Int. j/g, according to the present report. The difference, 8.2 j/g, between these two values is less than the difference, 9.4 j/g, between the values of Q_B at 25° C reported in 1934 and in the present

paper. The discrepancy is due (1) partly to the fact that the coefficients of $(P-30)$, $(m_s/V-3)$, and $(m_w/V-3)$ in the formula given in footnote 6, page 161 differ slightly from the coefficients in the corresponding formula in the 1934 report, (2) partly to the fact that the change in the value used for the heat of formation of nitric acid does not enter into the calculations, and (3) partly to the fact that in the calculation of the heat of combustion at 28° C, according to data given in the 1934 report, the effect of the error in the temperature coefficient is reduced to 40 percent of its effect in the calculation of Q_B at 25° C from the observed value at 30° C.

The changes mentioned above in the coefficients of $(P-30)$, $(m_s/V-3)$, and $(m_w/V-3)$ are taken account of by applying a correction of -0.4_5j/g to the value of the heat of combustion of benzoic acid calculated on the basis of the 1934 report.

The other corrections that should be applied to the above value for the heat of combustion of benzoic acid calculated according to the 1934 report are related to the elements of the difference between the old and new values of Q_B at 25° C, and will be discussed in the order that these elements are listed on page 262.

1. The correction for the effect of dissolved carbon dioxide will depend upon how the nitric acid determinations were made in the calibration experiments under consideration. If the procedure in these experiments was the same as in the 1934 measurements, and in the first series of combustion experiments of the present measurements, then the effect of dissolved carbon dioxide in the calibration experiments here considered will partially cancel the effect in the 1934 value of Q_B. In this case the correction for dissolved carbon dioxide may be calculated as follows: Under the conditions of the calibration experiments under consideration the mole fraction of carbon dioxide in the bomb after combustion of the sample of benzoic acid is calculated to be 0.157, and the amount of water in the bomb after combustion is 0.092 mole. On the assumption that the total effect of dissolved carbon dioxide is proportional to the mass of water and the mole fraction of carbon dioxide, the above data, together with the data given previously regarding the average conditions in the 1934 combustion experiments, lead to 3.9_1 j/g of benzoic acid burned for the effect of dissolved carbon dioxide. This partially cancels the effect, 5.5 j/g of benzoic acid, in the 1934 value of Q_B, leaving a net correction of $+1.5_9$ j/g to be applied to the value of the heat of combustion calculated on the basis of the 1934 report.

On the other hand, if the procedure in the nitric acid determinations in the calibration experiments under consideration was such that these determinations were not affected by dissolved carbon dioxide, then a correction equal to the total effect of dissolved carbon dioxide in the 1934 value of Q_B, +5.5 j/g, will be necessary.

2 and 3. As noted previously, the effect (1.3 j/g) on Q_B at 25° C of the error in the value used in 1934 for the temperature coefficient of Q_B is partially eliminated in the calculation, on the basis of the 1934 report, of the heat of combustion of benzoic acid under the conditions of the calibration experiments here considered. There remains, however, 40 percent of the effect, or $+0.5_2$ j/g, which should be applied as a correction to the value of the heat of combustion calculated on the basis of the 1934 report.

4. The 1934 value of Q_B was too low by 0.8 j/g because of the

error in the nitric acid correction. This error in Q_B is partially cancelled in the original calculation of the results of the calibration experiments under consideration by the use of the value given in the 1934 report for the heat of formation of nitric acid in the bomb. A correction is necessary, however, for the error in the difference in the nitric acid corrections in the 1934 experiments and in the calibration experiments. This correction amounts to $+0.5_0$ j/g of benzoic acid burned.

5. A correction of +1.8 j/g is necessary to take account of the difference in the results of the calorimetric measurements of 1934 and the present work.

Taking account of the various factors discussed above, the value for the heat of combustion of benzoic acid which should be used in calculating the corrected value for the energy equivalent of the calorimeter from the data of the calibration experiments under consideration is obtained as follows:

(a) If the procedure in the nitric acid determinations was the same as in the 1934 experiments and in the first series of combustion experiments described in this paper:

Heat of combustion calculated on basis of 1934 report	26418.6 Int. j/g
Correction for:	
Changes in coefficients of $(P-30)$, etc	$-.4_5$ Int. j/g
Dissolved CO_2	$+1.5_9$ Int. j/g
Change in temperature coefficient of Q_B	$+0.5_2$ Int. j/g
Error in nitric acid correction	$+0.5_0$ Int. j/g
Difference in calorimetric measurements	+1.8 Int. j/g
Corrected value of heat of combustion	26422.6 Int. j/g

The correction to be applied to the original value of the energy equivalent of the calorimeter in this case is +0.015 percent.

(b) If the procedure in the nitric acid determinations was such that these determinations were not affected by dissolved carbon dioxide, the calculation of the corrected value for the heat of combustion of benzoic acid would differ from the above calculation only in that the correction for dissolved carbon dioxide in this case would be equal to the total effect, 5.5 j/g, in the 1934 experiments. The corrected value for the heat of combustion of benzoic acid in this case would be 26426.5 Int. j/g, and the correction to be applied to the original value of the energy equivalent of the calorimeter would be +0.030 percent.

The difference between the corrected value for the heat of combustion of benzoic acid given under (b) and the value 26426.8 Int. j/g calculated on the basis of the present measurements arises from the fact that a part of the change in the nitric acid correction does not appear in the above calculations but is taken care of in the original calculation of the energy equivalent of the calorimeter on the basis of the 1934 report.

VII. PREVIOUS WORK

Results of measurements of the heat of combustion of benzoic acid by various observers [2, 3, 20, 21, 22, 23, 32] are given in table 10. The correction of the 1934 results of Jessup and Green is discussed in section V of this paper.

The value of Q_B at 25° C attributed to Roth, Doepke, and Banse [22] in the 1934 report [3] was calculated from their published results, on

TABLE 10.—*Results of the measurements of the heat of combustion of benzoic acid by various observers*

Observer	Date	Material	Original value	Q_B at 25° C	Standard deviation of the mean	Deviation from result of present measurements
			Int. j/g (mass)	*Int. j/g* (mass)	*Int. j/g*	*Percent*
Fischer and Wrede	1909		26,475 at 17.5° C	26,436	±4.5	+0.029
Wrede	1910		26,466 at 17.5° C	26,427	±6.5	−.005
Dickinson	1914		26,441 at 25° C	26,434	[b] ±1.0	+.021
Roth, Doepke, and Banse	1928	Kahlbaum-Verkade [a]	26,433 at 20° C	26,405	±6.0	−.088
Jaeger and von Steinwehr	1928	Kahlbaum-Verkade [a] and National Bureau of Standards.	26,437 at 19.3° C—{NBS 26,426 / K−V [a] 26,411 ±}	26,418	{±9.0 / ±9.0} ±7.5	{−0.009 / −0.066} −.039
Jessup and Green	1934	Standard Samples 39d and 39e	26,419 at 25° C	[c] 26,426.6	±0.8 [b]	−.007
Prosen and Rossini	1939–41	Standard Sample 39e		26,428.9	±1.1	+.002
Present work	1942	Standard Samples 39e, 39f, and a specially purified sample.		26,428.4	±0.6 [b]	

[a] Obtained from Kahlbaum and compared with National Bureau of Standards material by P. Verkade [24], according to whom the two materials had the same heat of combustion. The National Bureau of Standards material was probably Standard Sample 39d.
[b] Dickinson did not give the necessary data for calculating the standard deviation. The value given was estimated by the present writer.
[c] Corrected as described in the text.

the assumption that they had placed 1 g of water in the bomb before each experiment. Professor Roth has since informed the writer that actually 10 g of water was placed in the bomb, and that the effect of the difference between 10 g and 1 g of water was found by experiment in his laboratory to be 0.064 percent. The difference between 0.064 percent and the value 0.10 percent calculated from the Washburn [19] equation was attributed to the lack of equilibrium between the gaseous carbon dioxide and the aqueous solution. On the basis of the information supplied by Roth, a correction of −0.064 percent has been applied to the value attributed to Roth, Doepke, and Banse in the 1934 report.

An additional correction of about 1 j/g has been applied to the values of Q_B at 25° C attributed in the 1934 report to Fischer and Wrede [20], Wrede [21], Roth, Doepke, and Banse [22], and Jaeger and von Steinwehr [23] to take account of the temperature dependence of the Washburn reduction, an effect which was partially neglected in the 1934 report.

The value attributed to Prosen and Rossini [32] in table 10 is the result of unpublished measurements made at this Bureau entirely independently of the measurements described in the present paper, and with different apparatus [34].

Because of uncertainty as to experimental procedure in the various investigations, and as to precautions taken to avoid the effect of dissolved carbon dioxide on the determinations of nitric acid, no correction for this effect has been applied to any previous results except those of the 1934 measurements at this Bureau. The results of Dickinson and those of Roth, Doepke, and Banse are probably not in error from this cause because the indicators they used, methyl orange and Congo red, respectively, are insensitive to carbon dioxide. The results of Prosen and Rossini are not in error from this cause, since they flushed out their bomb sufficiently to remove dissolved carbon dioxide. Fischer and Wrede, and Wrede do not state what indicators they used. Jaeger and von Steinwehr used phenolphthalein, and therefore their nitric acid determinations may have been in error because of dissolved carbon dioxide.

All of the final values given in table 10, with the exception of that due to Roth, Doepke, and Banse, are in as good agreement with the result of the present measurements as could be expected on the basis of the precision of the various measurements. The fact that the values obtained for the Kahlbaum-Verkade material by Jaeger and von Steinwehr and by Roth, Doepke, and Banse are in good agreement with each other and are lower than the other values in the table suggests that a difference in material may be responsible for the low values for the Kahlbaum-Verkade material. However, Verkade [24] has compared the Kahlbaum-Verkade and National Bureau of Standards materials and found no difference in their heats of combustion. It may be noted also that the values obtained for the two materials by Jaeger and von Steinwehr are in as good agreement with each other and with the value obtained in the present work for National Bureau of Standards material as could be expected from the precision of the measurements. Except for the low values for the Kahlbaum-Verkade material, there is nothing in the data of table 10 to indicate any differences in the materials used in the various investigations.

As noted in the 1934 report, the results of all measurements previous to that time may be too high because of combustible impurities in the oxygen. The estimate of 0.02 percent made in the 1934 report as the probable effect of combustible impurities on Dickinson's results is practically equal to the difference between Dickinson's value and that resulting from the present measurements.

VIII. SUITABILITY OF BENZOIC ACID AS A STANDARD SUBSTANCE FOR BOMB CALORIMETRY

The requirements that a standard substance for bomb calorimetry should satisfy have been summarized [28] as follows:

1. It should be easily obtainable in a pure state.
2. It should be stable.
3. It should not be hygroscopic.
4. It should not be too volatile.
5. It should be easily compressible into pellets.
6. It should burn completely in the bomb.

The tests of purity of Standard Samples 39e and 39f of benzoic acid [4], and the agreement of the results of measurements of heat of combustion of different samples given in table 10 indicate that benzoic acid satisfies the first of the above requirements. The low values given in table 10 for the heat of combustion of the Kahlbaum-Verkade material cast some doubt on this conclusion. However, as noted previously, the low values for this material are not in accord with results obtained by Verkade [24].

While it has been reported [29] that benzoic acid decomposes at temperatures above about 150° C, it appears to be quite stable under conditions to which it is likely to be subjected when used as a Standard Sample material. Thus no significant change in heat of combustion of Standard Sample 39e was observed during the period between the 1934 measurements and those of the present work.

In order to determine whether benzoic acid is appreciably hygroscopic, Schwab and Wichers [33] made measurements of the water content of Standard Sample 39f in its original condition and after exposure for 6 weeks at a relative humidity of 90 percent at about 23° C. Ten-gram samples of benzoic acid were fused in a glass apparatus, which was then evacuated through a trap immersed in liquid air. The trap was then closed off from the rest of the apparatus, and the liquid air was removed, allowing the trap to warm up to room temperature. The amount of water removed from the benzoic acid was estimated from the pressure, measured by means of a mercury manometer, and the temperature and volume of the closed system. The results indicated a water content of the untreated benzoic acid of 0.0015 to 0.0018 percent, and of the benzoic acid, after exposure to the high humidity, of 0.0014 to 0.0019 percent.

A less precise test of the hygroscopicity of benzoic acid was made by the writer by calibrating a calorimeter with (a) Standard Sample 39e from a recently opened bottle, (b) some of the same material which had been kept for about a year in an open bottle under conditions such that no appreciable amount of dust could get into the bottle, (c) some of the same material which had been kept for about a year in an open bottle in a desiccator vessel containing a saturated solution of ammonium chloride, which maintains a relative humidity of about

79 percent [27]. The values of the energy equivalent of the calorimeter obtained in these measurements are as follows:

Number of experiments	Treatment of benzoic acid sample	Energy equivalent of calorimeter	Standard deviation of the mean
		Int. j/°C	*Int. j/°C*
6	(a)	13730.6	0.6
2	(b)	13731.6	.7
4	(c)	13730.8	1.2
Mean		13731.0	0.4

Both of the above sets of data indicate that benzoic acid is not appreciably hygroscopic. However, data obtained by Weaver [29] indicated a moisture content of about 0.08 percent by weight in a sample of benzoic acid that had been kept in a glass-stoppered bottle for about a year. By a very sensitive test, Weaver also found small amounts of moisture in several other samples. In all cases the moisture could be removed by fusing the sample.

A number of years ago the writer found that a sample of benzoic acid obtained from another laboratory had a heat of combustion per gram that was lower by 0.2 percent than that of National Bureau of Standards material. The discrepancy disappeared after fusing the sample.

It appears, therefore, that some samples of benzoic acid may contain appreciable amounts of moisture. The source of such moisture is not known, but it is possible that samples crystallized from aqueous solution may contain trapped water unless special precautions are taken to dry them. Whatever the source of the water in the samples referred to, it appears that it is relatively easy to prepare benzoic acid which is substantially free from water, and that it will not absorb moisture from the atmosphere. It may be concluded, therefore, that benzoic acid is entirely satisfactory as a standard substance so far as hygroscopicity is concerned.

To determine the volatility of benzoic acid a pellet of 1.5 g was placed in a platinum crucible and weighed at intervals over a period of about 3 weeks. During this time the temperature of the room during the daytime varied from 29° to 32° C. The benzoic acid lost weight at the rate of about 0.15 mg, or 0.01 percent, per day. Evaporation at this rate is not serious, since not more than half an hour need elapse from the time a sample is weighed until it is ignited in the bomb.

Experience at this Bureau indicates that benzoic acid satisfies requirements 5 and 6, page 268. Some observers have reported negligible amounts of soot left in the crucible after burning a sample of benzoic acid, but no soot or other evidence of incomplete combustion was observed in any of the 1934 experiments at this Bureau or in those of the present work. In these experiments the samples were burned in a cylindrical platinum crucible ¾ in. in diameter and ⅝ in. high, weighing a little less than 8 g.

IX. SUMMARY

The present measurements yield the value 26428.4 International joules per gram mass for the heat of combustion, Q_B, of benzoic acid under the conditions of the standard bomb process.

When the amount of the reaction is determined from the mass of carbon dioxide formed in combustion, the present measurements yield for the combustion of benzoic acid $-\Delta H°_{298.16}=3226.39$ International kilojoules per mole when each of the gases involved in the reaction is in the thermodynamic state of unit fugacity. The estimated uncertainty of the final values of Q_B and $-\Delta H°_{298.16}$ is ± 0.010 percent (± 2.6 j/g, or ± 0.32 kj/mole).

X. REFERENCES

[1] Premier Rapport de la Commission Permanente de Thermochimie, Union Internationale de chimie, Paris (1934).
[2] H. C. Dickinson, Bul. BS **11,** 189 (1914) S230.
[3] R. S. Jessup and C. B. Green, J. Research NBS **13,** 496 (1934) RP721.
[4] F. W. Schwab and E. Wichers, J. Research NBS **25,** 747 (1940) RP1351.
[5] E. F. Mueller and H. F. Stimson, J. Research NBS **13,** 699 (1934) RP739.
[6] J. H. Park, BS J. Research **10,** 89 (1933) RP518.
[7] N. S. Osborne, H. F. Stimson, and D. C. Ginnings, J. Research NBS **23,** 197 (1939) RP1228.
[8] E. F. Mueller, Bul. BS **13,** 547 (1916) S288.
[9] L. J. P. Keffler and F. C. Guthrie, J. Phys. Chem. **31,** 58 (1927).
[10] R. S. Jessup, J. Research NBS **21,** 475 (1938) RP1140.
[11] F. D. Rossini and W. E. Deming, J. Wash. Acad. Sci. **29,** 416 (1939).
[12] R. S. Jessup. Unpublished data obtained at the National Bureau of Standards.
[13] H. M. Huffman and E. L. Ellis, J. Am. Chem. Soc. **57,** 41 (1935).
[14] G. Becker and W. A. Roth, Z. Elektrochem. **40,** 836 (1934).
[15] F. R. Bichowsky and F. D. Rossini, Thermochemistry of the Chemical Substances (Reinhold Publishing Corporation, New York, 1936).
[16] W. P. White, The Modern Calorimeter, p. 88 (Reinhold Publishing Corporation, New York, N. Y., 1928).
[17] R. S. Jessup, J. Applied Phys. **13,** 128 (1942).
[18] Int. Critical Tables **5,** 80, 82, 83 (1929).
[19] E. W. Washburn, BS J. Research **10,** 525 (1933) RP546.
[20] E. Fischer and F. Wrede, Z. physik. Chem. **69,** 218 (1909).
[21] F. Wrede, Z. physik. Chem. [A] **75,** 81 (1910).
[22] W. A. Roth, O Doepke, and H. Banse, Z. physik. Chem. **133,** 431 (1928).
[23] W. Jaeger and H. von Steinwehr, Z. physik. Chem. **135,** 305 (1928).
[24] P. Verkade, quoted by Roth, Doepke, and Banse [22] and by Jaeger and von Steinwehr [23].
[25] W. Jaeger and H. von Steinwehr, Ann. Physik **21,** 23 (1906).
[26] W. A. Roth, Thermochemie (Sammlung Goschen, Berlin, 1932).
[27] Int. Critical Tables **1,** 68 (1926).
[28] M. Beckers, Bul. soc. chim. Belg. **40,** 518 (1931).
[29] E. R. Weaver, J. Am. Chem. Soc. **35,** 1309 (1913).
[30] F. D. Rossini, J. Research NBS **22,** 407 (1939) RP1192.
[31] F. D. Rossini. BS J. Research **6,** 1 (1931) RP259.
[32] E. J. R. Prosen and F. D. Rossini. Unpublished data obtained at the National Bureau of Standards.
[33] F. W. Schwab and E. Wichers. Unpublished data obtained at the National Bureau of Standards.
[34] E. J. R. Prosen and F. D. Rossini, J. Research NBS **27,** 289 (1941) RP1420.

WASHINGTON, August 26, 1942.

574278 O - 61 - 27

U. S. Department of Commerce National Bureau of Standards

RESEARCH PAPER RP1711

Part of Journal of Research of the National Bureau of Standards, Volume 36, April 1946

NOTE ON THE DENSITY AND HEAT OF COMBUSTION OF BENZOIC ACID

By R. S. Jessup

ABSTRACT

The results of various determinations of the density of benzoic acid are summarized. The three most recent values are in reasonably good agreement with each other, but are higher by about 4.5 percent than the value most commonly referred to in the literature. The difference of 4.5 percent in density affects the reduction of weight in air to mass by an amount corresponding to 0.004 percent in mass, and in heat of combustion per gram mass.

The value 26428.4 ±2.6 international joules per gram mass reported [1] [1] in 1942 for the heat of combustion of Bureau Standard Sample 39f of benzoic acid under the specified standard conditions of the bomb process was obtained from the experimental values of heat of combustion per gram weight in air, using the value 1.260 g/cm ^{3} for the density of benzoic acid at 25° C in making the reduction to mass. This value was derived from the value 1.266 g/cm ^{3} for the density at 15° C given in International Critical Tables [2], and the value 0.00053 per degree centigrade reported by E. R. Smith [3] for the coefficient of cubical expansion of benzoic acid in the range 15° to 30° C. The value of density given in ICT is apparently that reported by Lumsden [4] in 1905.

It has recently been noted that two other values have been obtained for the density of benzoic acid, namely, the value 1.322 g/cm^3 at 20° C reported by Steinmetz [5] in 1913, and the value 1.3211 ± 0.0001 g/cm^3 at 23.3° C reported by Hendricks and Jefferson [6] in 1933. Steinmetz gave no information regarding his method of measurement or the accuracy of his result. Hendricks and Jefferson made measurements on single crystals grown from melts, by suspending the crystals in an aqueous salt solution, varying the concentration until the crystals just floated when the system was subjected to a centrifugal force of about 400 times gravity, and determining the density of the solution by means of a picnometer. The results were corrected for the effect of compressibility of solution and crystals. The individual results were not reported, but the probable error of the mean value was given as ±0.0001 g/cm^3.

[1] Numbers in brackets indicate the literature references at the end of this paper.

From the care with which the measurements of Hendricks and Jefferson were made, and from the agreement of their value with that of Steinmetz, it would seem that the older value of Lumsden is seriously in error. However, as no information was available regarding the reliability of the value reported by Steinmetz, and as it was not absolutely certain that the difference between the values of Lumsden and of Hendricks and Jefferson could be attributed entirely to error in Lumsden's data, an independent determination of the density of benzoic acid seemed desirable. Since an accuracy of 1 in the third decimal place is ample for the purpose of reducing weight in air to mass, it did not appear worth while to attempt to obtain higher accuracy than this.

To obtain samples of benzoic acid on which density determinations could be made, an attempt was made to grow single crystals from melts in the manner described by Hendricks and Jefferson. The product obtained was examined microscopically by C. P. Saylor, of the Chemistry Division of this Bureau, who reported that the samples were not single crystals, but were sufficiently compact and free from voids so that resasonably satisfactory density determinations could be made on them.

The density determinations were made by Mildred W. Jones, of the Weights and Measures Division of this Bureau, by the method of hydrostatic weighing in a saturated aqueous solution of benzoic acid. The density of this solution was determined by Mrs. Jones by means of a picnometer. Measurements on two samples of crystals prepared in separate experiments yielded the same value, namely, 1.316 g/cm^3 at 28° C.

The results of the various determinations of the density of benzoic acid are given in table 1. The reduction to 25° C was made by using for the coefficient of cubical expansion, γ, both the value 0.00040 reported by Schwab and Wichers [7][2] and the value 0.00067 that was obtained by recalculating the data of Smith [2] using the value 1.319 g/cm^3 at 25° for the density of benzoic acid rather than the value 1.266 g/cm^3 at 15° C originally used by Smith. It will be seen from table 1 that although the two values of the coefficient of expansion differ considerably, the difference has only a relatively small effect on the values obtained for the density at 25° C. It will also be seen from table 1 that the three most recent determinations are in reasonably satisfactory agreement with each other, whereas the value of Lumsden is lower by about 4.5 percent than the other three. It seems safe to conclude that the value reported by Lumsden is seriously in error. Any of the other values would be satisfactory for use in reducing weight in air to mass, as the value obtained for mass by using 1.3176 g/cm^3 for the density would differ by less than 2 parts in a million from that obtained with 1.3202 g/cm^3. In view of the fact that voids in the samples of benzoic acid would result in low values of density, and because of the care with which the measurements of Hendricks and

[2] Schwab and Wichers calculated the density of solid benzoic acid at its melting point (by means of the Clausius-Clapeyron equation) from (1) their observed value of the pressure coefficient of the freezing temperature, (2) a value derived from data reported by Timmermans and Burriel [8] for the density of the liquid at the freezing temperature, and (3) the value given in International Critical Tables for the heat of fusion. The value 1.27 g/cm^3 obtained in this way, and the value of density at 23.3° C reported by Hendricks and Jefferson, were then used to calculate the mean coefficient of cubical expansion in the range from 23° to 122° C.

Jefferson were made and the high precision of their results, their value is probably the most reliable one. It is therefore recommended that the value 1.320 g/cm³ be used for the density of benzoic acid at 25° C for the purpose of reducing weight in air to mass.

TABLE 1.—*Values for the density of benzoic acid*

Observer	Density reported	Density at 25° C	
		$\gamma=0.00040$	$\gamma=0.00067$
	g/cm³	*g/cm³*	*g/cm³*
Lumsden (1905)	1.266 (15° C)	1.2610	1.2577
Steinmetz (1913)	1.322 (20° C)	1.3194	1.3176
Hendricks and Jefferson (1933)	1.3211 ±0.0001 (23.3° C)	1.3202	1.3196
Jones (this paper, 1945)	1.316 (28° C)	1.3176	1.3186

With 1.320 g/cm³ as the value for the density, the value for the heat of combustion of Standard Sample 39f of benzoic acid becomes 26429.4 ±2.6 international joules per gram mass when the sample is burned under the standard conditions [1] of the bomb process. It should perhaps be emphasized that when this standard sample of benzoic acid is used to calibrate a bomb calorimeter, no appreciable error would result from using the value originally reported [1] for the heat of combustion per gram mass of the sample, provided the value 1,260 g/cm³ is used for the density of benzoic acid at 25° C in reducing weight in air to mass.

[1] R. S. Jessup, J. Research NBS **29,** 247 (1942) RP1499.
[2] Int. Critical Tables **1,** 208 (1926).
[3] E. R. Smith, BS J. Research **7,** 903 (1931) RP382.
[4] J. S. Lumsden, J. Chem. Soc. **87,** 90 (1905).
[5] H. Steinmetz, Z. Krystallographie **53,** 463 (1913).
[6] S. B. Hendricks and M. E. Jefferson, J. Opt. Soc. Am. **23,** 299 (1933).
[7] F. W. Schwab and E. Wichers, J. Research NBS **34,** 333 (1945) RP1647.
[8] J. Timmermans and F. Burriel, Chimie & industrie, Special No. pp. 196–7 (March 1931).

WASHINGTON, December 17, 1945.

U. S. Department of Commerce National Bureau of Standards

RESEARCH PAPER RP1661

Part of Journal of Research of the National Bureau of Standards, Volume 35, July 1945

THERMODYNAMIC PROPERTIES OF 1,3-BUTADIENE IN THE SOLID, LIQUID, AND VAPOR STATES

By Russell B. Scott, Cyril H. Meyers, Robert D. Rands, Jr., Ferdinand G. Brickwedde, and Norman Bekkedahl

This paper presents a detailed description of apparatus used and the results obtained in the following measurements relating to the thermodynamic properties of 1,3-butadiene in the solid, liquid, and vapor states: (1) Specific heats from −258° to +30° C, (2) heat of fusion, (3) heats of vaporization from −26° to +23° C, (4) vapor pressures from −78° to +110° C, (5) liquid densities from −78° to +95° C, (6) vapor densities from 30° to 150° C, and (7) the critical pressure, volume, and temperature of 1,3-butadiene. Tables embodying the results of these measurements are included for specific heats, enthalpy, and entropy of the solid, liquid, and vapor.

CONTENTS

I. INTRODUCTION

The measurements of the thermodynamic properties of 1,3-butadiene described in this paper were undertaken in response to requests for data needed in the Government's synthetic-rubber program. Most of the experimental data were made available previously to the synthetic-rubber industry in the form of reports [1, 2] [1] submitted to the Office of the Rubber Director and in a National Bureau of Standards Letter Circular [3]. As these reports were rather brief, more detailed descriptions of the apparatus, methods, and results are given here.

Empirical equations were constructed to represent the experimental results and used to calculate a thermodynamically consistent set of tables of various derived properties, including enthalpy and entropy of 1,3-butadiene in the solid, liquid, and vapor state. In these calculations use was made of measurements of the specific heat of 1,3-butadiene vapor previously published [4] and an equation of state for the vapor that represents measurements over a wide range of temperature and pressure.

II. PREPARATION OF SAMPLES

The butadiene from which the samples were prepared was furnished by the Dow Chemical Co. It was shipped in a steel cylinder refrigerated with solid carbon dioxide (−78° C). After it was received it was kept at or near −78° C, except while being transferred from one container to another. The butadiene was removed from the cylinder by evaporating it into one-half-liter Pyrex flasks at −78° C. These were provided with seals that could later be broken with magnetic plungers so that all the handling of the material could be carried out in the absence of air. The supply of butadiene, somewhat less than 2 liters, was stored in four such flasks.

It appeared that a small amount of carbon dioxide had leaked into the cylinder during transit while it was in a CO_2 atmosphere at such a low temperature that the pressure inside the cylinder was less than atmospheric. The carbon dioxide impurity was noticed during the transfer as it caused blocking by not condensing with the butadiene. It did condense readily in a liquid-air trap, which fact led to the belief that it was carbon dioxide and not air. The blocking occurred three times during the filling of the first half-liter flask. When it occurred, the flask and cylinder were connected through a stopcock to a vacuum system and pumped for a few seconds. In this way most of the carbon dioxide was removed, together with some butadiene. No difficulty was experienced during the filling of the three other half-liter flasks. These flasks are designated by the numbers 1, 2, 3, and 4 in the order of their filling.

[1] Figures in brackets indicate the literature references at the end of this paper.

During the course of the experiments four *samples* were prepared. Sample 1 was prepared by evaporating the 450-ml contents of flask 3 at about −30° C, separating a middle fraction of about 110 ml. This fraction was frozen with liquid air with the intention of pumping off any air that may have been present. However, a pressure measurement, made with a McLeod gage, showed this pumping to be unnecessary. The butadiene seemed to be free of any impurity that had an appreciable vapor pressure at the temperature of liquid air. After melting the butadiene, another evaporation was carried out, and the middle 95 ml was collected. This constituted sample 1. The unused material from both evaporations was returned to the half-liter flask.

The material from which sample 2 was prepared consisted of about 100 ml of butadiene also taken from flask 3. The distillate was separated into five fractions. Fraction 1, about 10 ml of liquid, was discarded. Fraction 2 was a very small amount, about 0.2 ml of liquid. Fraction 3 was the main body of the material, about 80 ml of liquid, which constituted sample 2. Fraction 4 was another small sample about the same size as fraction 2. Fraction 5, about 10 ml of liquid, was discarded.

The vapor pressures of fractions 2 and 4 were compared at a pressure of about 1 atm by means of a differential vapor-pressure apparatus similar to that described by Shepherd [5]. No difference in vapor pressures was detected, although a difference of 0.05 mm Hg could have been noticed. This equality of vapor pressures indicated that further distillation of fraction 3 would have little effect.

Sample 2 was prepared by fractional distillation by the use of a still with a rectifying column. This apparatus is shown in figure 1. The boiling reservoir, *A*, is surmounted by a rectifying column, *B*, consisting of a monel tube with a deep helical groove. The Pyrex container surrounding the rectifying column fits so closely that, during operation, the liquid sealed the space between the glass and the metal, causing all the vapor and most of the refluxing liquid to traverse the helical groove, a path of about 6 m. The evacuated space between the two walls of the Pyrex container insulated the boiler and rectifying column. The heat required for the boiling is supplied by the heater, *C*, consisting of 34 ohms of fiber-glass-insulated constantan wire wound on the stem of the copper piece, *D*. The inverted mushroom of copper conducts the heat from the constantan heater to the bottom of the boiling reservoir. The walls of the condenser, *E*, are in contact with the stirred alcohol bath in which the still is immersed. The bath is refrigerated by means of a copper coil into which high-pressure carbon dioxide expands. An electric heater is provided so that excess refrigeration can be compensated and a constant bath temperature maintained. During the operation of the still the temperature of the bath was kept at about −25° C and manually controlled so as not to vary more than 0.05 degree. The butadiene vapor was withdrawn at *F*. The withdrawal rate and the boiling rate were adjusted so that the reflux ratio was about 15.

Sample 3 was prepared by fractional crystallization of material from flask 2. The apparatus used is shown in figure 2. The butadiene in flask *A* was partially frozen by cooling produced by the liquid air surrounding tube *C*. The air space separating flask *A* and tube *C* provided enough insulation to prevent too rapid freezing. About 20 minutes were required to freeze 150 ml of butadiene. While the

freezing proceeded, the magnetic stirrer, *D*, kept the liquid agitated so that there would not be a concentration of impurity at the surface of the solid as it formed. Two fractional crystallizations were performed. After the first, about 50 ml remained liquid and was poured into flask *B*. The remaining solid was melted and again fractionally crystallized, this time discarding into flask *B* about 75 ml of unfrozen

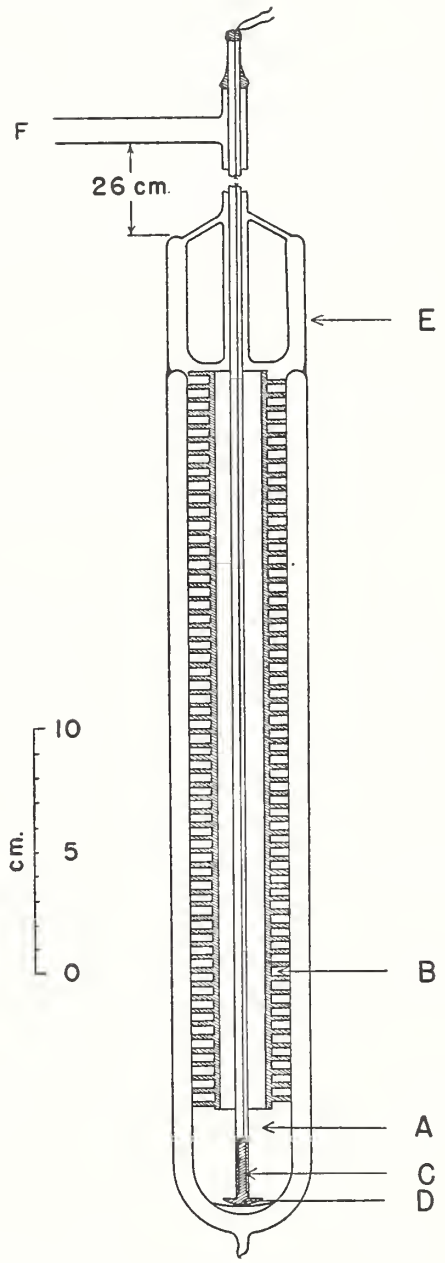

FIGURE 1.—*Still with rectifying column used to purify butadiene.*

A, boiling reservoir; *B*, rectifying column; *C*, heater; *D*, copper conductor; *E*, condenser; *F*, withdrawal line.

material. Flask *B* was then sealed off, and the 125 ml of butadiene remaining in flask *A* constituted sample 3.

Sample 4 was prepared by passing the butadiene, from flask 4, as a vapor over freshly outgassed silica gel. After condensing, the buta-

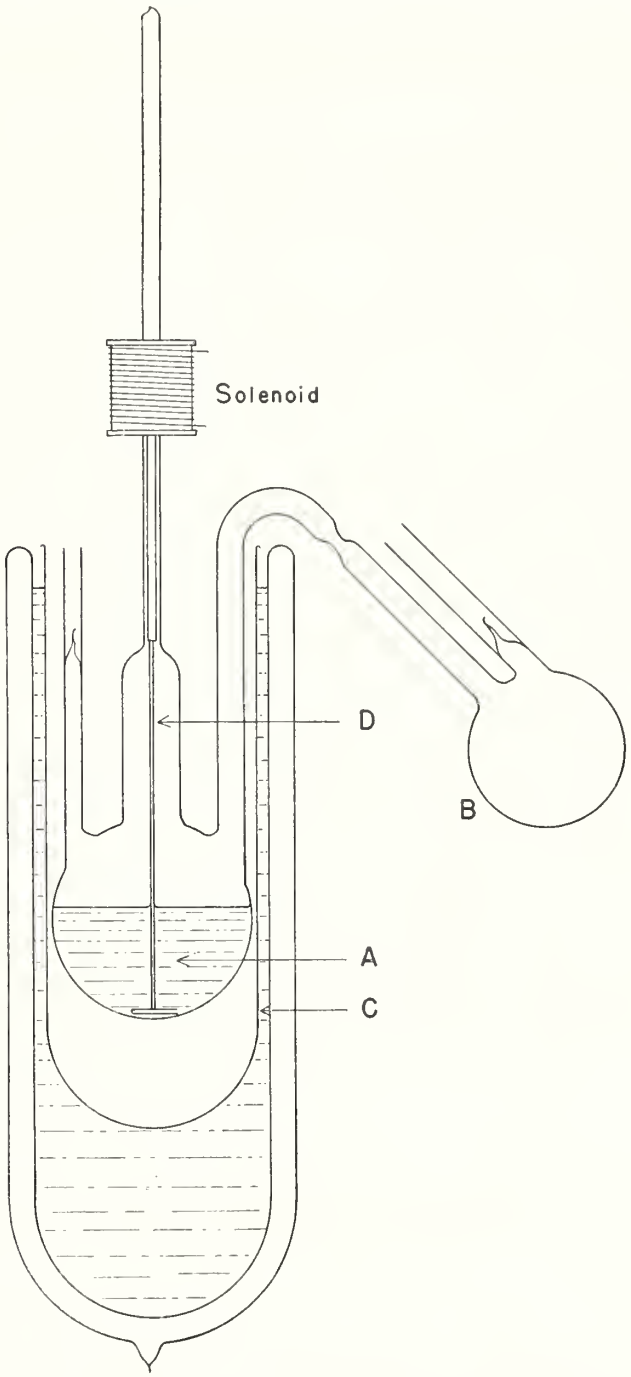

FIGURE 2.—*Fractional cystallization apparatus used to purify butadiene.*

A, butadiene in freezing flask; *B*, waste flask; *C*, tube providing air space around freezing flask; *D*, stirrer.

diene was fractionally crystallized three times, and finally the recrystallized material was distilled twice. In this process only about 60 ml of butadiene was obtained from an initial supply of 400 ml.

Estimates of purity of the various samples, based on melting data and vapor-pressure measurements, are given in section V.

III. CALORIMETRIC MEASUREMENTS

1. APPARATUS

(a) CALORIMETER

The calorimeter was of the adiabatic vacuum type, similar to one described by Southard and Brickwedde [6] for the measurement of the specific heats of nonvolatile solids. It was designed for the measurement of the specific heat and latent heats of a material that can be introduced into the calorimeter as a vapor and there condensed. Although the principal features are the same as those described by Southard and Brickwedde, several changes were necessary to adapt the design to the present use. Some changes were also made in the electric controls, by means of which adiabatic conditions are maintained. Because of these modifications and other differences in constructional detail, a description of the apparatus will be given here.

The term "calorimeter" may be properly applied to the complete apparatus with which thermal measurements are made, but for convenience in the following and later discussions in this paper, the word "calorimeter" will be used to designate that part of the apparatus containing the material being investigated, including all parts in intimate thermal contact with the material. The calorimeter is shown in vertical section at C, figure 3, and in horizontal section at C'. It consists of a cylindrical container of copper 1 mm in wall thickness, with domed ends of the same thickness, and contains two sets of vanes, V_1 and V_2, 0.2 mm thick, for the distribution of heat. The heater, H_1, by means of which measured amounts of electric energy were added, consists of two lengths of No. 34 AWG constantan wire with fiber-glass insulation. The wire was inserted into copper tubing, and then the tubing was drawn down snugly on the wire. The outside diameter of the tubing was about 1 mm after drawing. The tubing was wound in a single layer on the outside of vanes V_1. The heater is in two parts, the section nearer the bottom of the calorimeter having a resistance of about 28 ohms and the upper part having a resistance of about 37 ohms. The four ends of the copper tubes, with the projecting ends of the constantan wire, were brought out through the bottom of the calorimeter. Vanes V_2 are W-shaped pieces of copper formed to fit closely between the heater tubing and the wall of the calorimeter. The cone, B, just above the vanes, is a baffle intended to prevent droplets of liquid from being carried out of the calorimeter during vaporization experiments. The vanes, heater tubes, and inside surfaces of the calorimeter shell were tinned before assembling and the completed assembly heated to solder the parts together. About 2 mm of each end of the cylindrical wall was spun over the edge of the end cap to increase the strength of the calorimeter. The thermometer, T, used to determine the temperature of the calorimeter is a four-lead, strain-free, platinum resistance thermometer in a platinum

tube. This type of thermometer has been described by Southard and Milner [7]. The calibration of the thermometer used in this investigation has been described by Hoge and Brickwedde [8]. The thermometer contains helium and is sealed at the bottom by a soft glass cap, through which the platinum leads pass. Intimate thermal contact

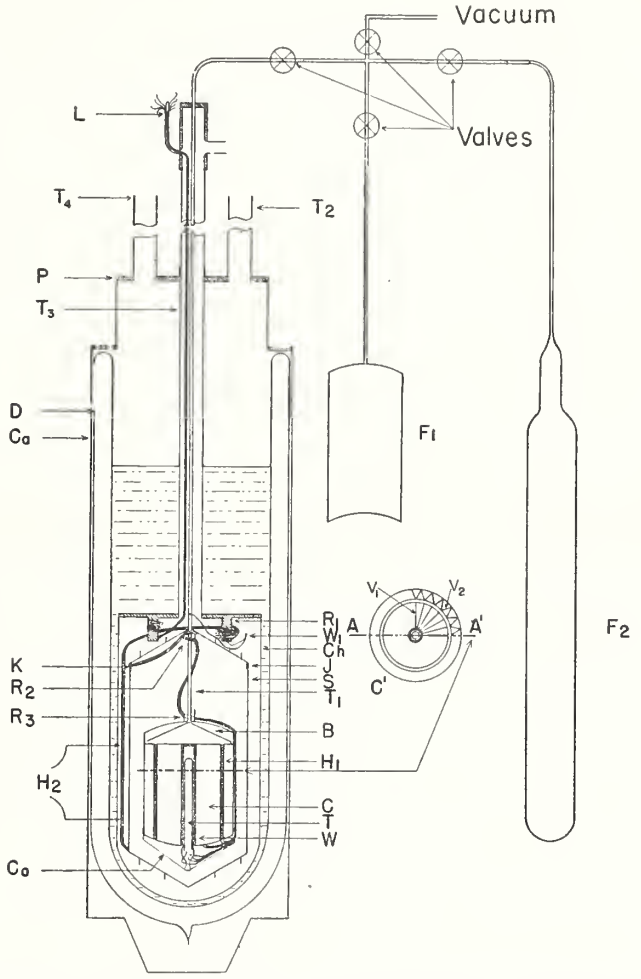

FIGURE 3.—*Sectional view of calorimeter and auxiliary apparatus.*

L, electrical leads; *P*, top plate of hydrogen container; T_3 monel tube for evacuation; *D*, Dewar flask; *Ca*, brass case; *K*, point at which leads pass through shield; R_2 and R_3, copper rings; H_2, cable heater; *Co*, aluminum cone; T_2, monel tube for exhausting over bath; R_1, brass ring; W_1, wire for thermal shunt; *Ch*, vacuum chamber; *J* sliding joint between top and side of shield; *S*, shield; T_1, filling tube; *B*, baffle; H_1, heater; *C*, calorimeter; *T*, resistance thermometer; *W*, thermometer well; F_1, weighing flask; F_2 reservoir; V_1 and V_2, copper vanes.

between the thermometer and the well, *W*, was attained by filling the excess space around the thermometer with low-melting (90° C) solder. The cone, *Co*, is a piece of aluminum foil 0.001 in. thick to trap heat radiated from the exposed ends of the heaters. The calorimeter is supported by the monel tube, T_1, through which the calorimeter was filled and emptied.

The radiation shield, *S*, is made of sheet copper 0.4 mm thick. It is cylindrical with conical ends. The bottom is soldered to the

cylindrical side, and the joint, J, at the top is a close sliding fit between the side and a flange on the top. Electric heaters on the shield and differential thermocouples between the calorimeter and shield were provided so that all parts of the shield could be kept at the temperature of the calorimeter. The heater on the side of the shield consists of a single layer of No. 30 AWG double silk-covered constantan wire entirely covering the side. Two wires were wound side by side and connected in parallel so as to obtain the desired resistance. The heaters on the top and bottom cones of the shield were wound on the projecting cylindrical copper rings shown in the figure. Although these heaters do not achieve as uniform distribution of heat as does the side winding, a calculation showed that errors arising from the nonuniformity of temperature would be negligible. Glyptal lacquer applied to the heater wires as they were wound served to cement them in place and to improve their thermal contact with the shield. After the heaters were wound, the shield was covered with aluminum foil to reduce radiation. The heater and thermocouple circuits and the distribution of the thermocouple junctions will be described later.

The radiation shield is supported by the tube, T_1, and the assembly thus far described hangs in the evacuated chamber, *Ch*. There is an opening in the shield through which the electric leads pass so that the space between the calorimeter and the shield is also evacuated. However, aluminum foil was placed over this opening so that there would be no direct path for radiation to leave the space inside the shield.

The temperature of tube T_1 was controlled by means of a heater of constantan wire wound in a single layer from a point about 2 cm above the top of the shield to a point level with the top of the Dewar flask, D. At the lower end of this heater was soldered a copper wire, W_1, No. 18 AWG, which provides a thermal path to the cold ring, R_1. The wire is in two parts, which were soldered together after assembling the shield system, the total length of wire from the tube to the ring being about 7 cm. A thermocouple junction on the tube just below the copper wire indicated the difference in temperature between this point and the shield. By means of this thermocouple and the tube heater the tube was kept about 0.01 degree warmer than the calorimeter to prevent condensation of butadiene in the tube.

The Dewar flask, D, contains a bath that supplies the refrigeration. Solid hydrogen was used for the lowest temperatures, which were obtained by closing the filler tube, T_4, and reducing the pressure over a bath of liquid hydrogen by pumping out the vapor through the tube, T_2, by means of a large vacuum pump. For successively higher temperatures the refrigerating materials were liquid hydrogen, liquid air, solid carbon dioxide, ice, and water. When liquid or solid hydrogen was used as the refrigerant, the brass case, *Ca*, surrounding the Dewar flask was immersed in liquid air, in a larger flask, to a level above the top plate, P.

The electric leads enter the vacuum space through the wax seal at L and pass down through the tube, T_3. They are brought to the temperature of the bath by being wound twice around the brass ring, R_1, and are cemented to it with Glyptal lacquer. Leaving the ring, the leads pass down outside the shield and are brought to the temperature of the shield by means of the heater, H_2, wound on the leads. This preheating of the leads before they come into contact

with the shield is done to avoid a cold spot on the shield. The leads are then wound in a single layer as a helix passing up the side of the shield under the shield heater and making four turns around the shield. At point K some of the leads are separated from the bundle and are connected to the heaters and thermocouples. The remaining leads enter the shield and make a turn around ring R_2, which is soldered to the top of the shield. They then pass to the calorimeter, making a turn around ring R_3, which is soldered to the top of the calorimeter. The leads are cemented to the rings with Glyptal lacquer and are bound down tightly with thread. Leaving ring R_3 the leads pass down the side of the calorimeter and are connected to the thermometer and heater. All the leads are No. 34 AWG copper wire insulated with enamel and silk.

The filling tube, T_1, communicates through the valves with the flasks, F_1 and F_2, or with the vacuum system. The amount of butadiene involved in an experiment was determined by transferring the butadiene from the calorimeter to the brass container, F_1, and weighing F_1 before and after the transfer. A union not shown permitted the removal of F_1 so that it could be weighed on an analytical balance. In the Pyrex flask, F_2, the approximate volume of the butadiene was visually estimated before transferring it to the calorimeter. This flask was also used as an auxiliary reservoir in experiments on the heat of vaporization.

(b) ELECTRIC CONTROL CIRCUITS

The thermocouple circuits and the locations of the junctions on the apparatus are shown in figure 4. The numbered arrows on the diagram of the calorimeter and shield show the locations of the junctions and refer also to the corresponding junctions shown in the circuit diagrams, A and B. Multiple-junction thermocouples were used between the shield and the calorimeter, as it is here that the most accurate control is necessary. The three-junction couple between the calorimeter and the side and bottom of the shield was wired so that the galvanometer, G_2, could be connected through the plug contacts, P, to any adjacent pair of leads from junctions 1, 2, 3, and 4. This allowed the operator to explore the temperature distribution over the shield so that the ratio of the heat supplied to the side and bottom could be adjusted to minimize the temperature differences. While measurements were being made the contacts, P, were connected to leads 1 and 4, thus using the total emf generated by the three-junction thermocouple. The six-junction thermocouple, between the top of the shield, 8, and the top of the calorimeter, 9, permits the detection of very small temperature differences between these two points. Very accurate control was desirable here to prevent heat conduction between the shield and the calorimeter along the leads and the filler tube. The elements of the multiple-junction thermocouples were constantan and Chromel-P. The combination of these alloys has a greater thermoelectric power than constantan-copper, and Chromel-P possesses the additional advantage that its thermal conductivity is much less than that of copper. Copper-constantan junctions at 11 and 12 with the reference junction at 10 were used in maintaining temperature equality between these points. Single junctions were used at 11 and 12 as high accuracy is not necessary in controlling the temperature

of these points. The constantan and Chromel-P thermocouple wires were No. 32 AWG, double silk insulated. All the junctions except 11 and 12 were enclosed in flat sheaths about 3 mm wide and 8 mm long, made of sheet copper 0.2 mm thick. Strips of mica were used to insulate the wires from the copper sheaths. A cross section of this arrangement is shown at *C*, figure 4. After inserting the junctions and the mica insulating strips into the copper sheath, the copper was crimped tightly on the mica by pressing in a vise. Junction 11 was insulated with silk floss and inserted into the bundle of leads, which were then bound together with thread and impregnated with Glyptal lacquer. Junction 12 was insulated with silk floss and bound to the

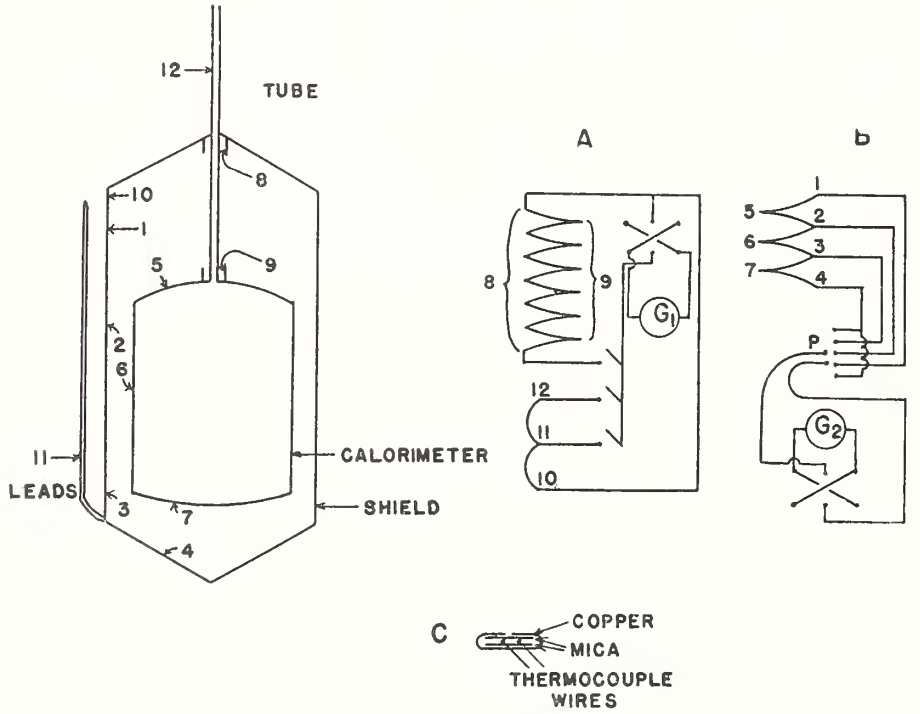

FIGURE 4.—*Diagram of thermocouple circuits showing locations of junctions.*

A, circuits for top, cable, and tube; *B*, circuits for side and bottom; *C*, enlarged diagram of thermojunction.

tube with thread, Glyptal lacquer again being used as a cement for improving thermal contact. The sheathed junctions were held in place on the surfaces of the calorimeter and shield by wedging them under small bridges of copper which were soldered to the surfaces. The junctions of the six-junction thermocouple were held against the inner surfaces of the rings, R_2 and R_3, by short pieces of watch spring coiled inside the rings. The sensitivity of the thermocouple circuits at 90° K were as follows: Top (six junction) 1.6 mm per millidegree; side (three junction) 0.8 mm per millidegree; ring and tube (single junction) 0.2 mm per millidegree.

The control circuit for the shield system is shown in figure 5. The resistances marked side, bottom, top, ring, and tube represent the electric heaters on the respective parts of the adiabatic shield system.

A_1, A_2, A_3, and A_4 are milliameters for measuring the current in each circuit. The currents supplied to the heaters are controlled by the 1-amp Variac transformers, V_1 and V_2, and the 500-ohm 50-w potential-divider rheostats, R_1, R_2, R_3, and R_4. When measurements are being made, the Variacs and rheostats are first adjusted so that the thermocouples on the shield system indicate approximately constant adiabatic conditions and then minor variations are compensated by the use of keys K_1 and K_2 in each circuit. K_1 shorts out a resistor of 100 ohms, thus momentarily increasing the current in the circuit, and K_2 opens the circuit momentarily. This operation is more convenient than changing the rheostat settings to compensate small variations in temperature. The 3,200-ohm potential divider is used

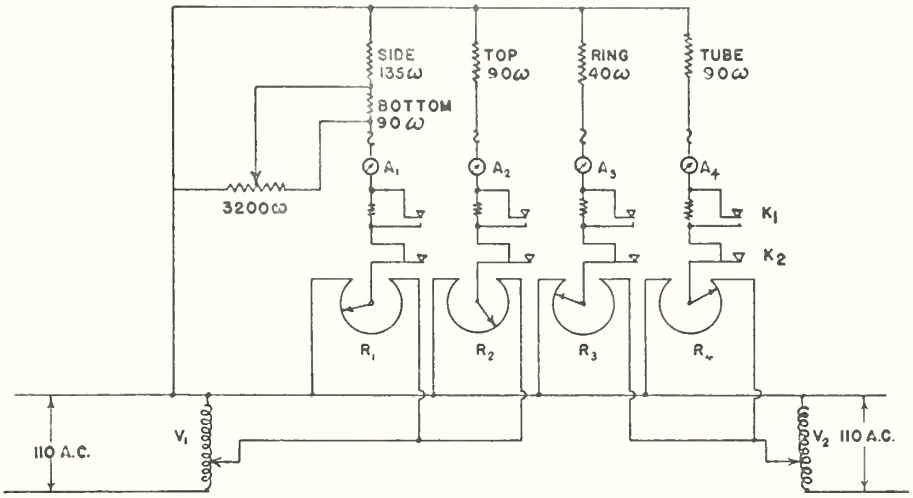

FIGURE 5.—*Diagram of electrical control circuits.*

A_1, A_2, A_3, and A_4, ammeters; K_1 and K_2, contact keys; R_1, R_2, R_3, and R_4, rheostats; V_1 and V_2, Variac transformers.

to adjust the ratio of the heat supplied to the side and bottom parts of the shield. After once adjusting this ratio, it was not found necessary to change it.

(c) MEASURING CIRCUITS

The circuits for measuring the electric energy supplied to the calorimeter and for measuring its temperature before and after heating are shown in figure 6. The current through the heater is determined by measuring the potential drop across a 1-ohm standard in series with the heater. The potential across the heater is determined by measuring a part of this potential by means of the volt box, which has a nominal ratio of 1 to 150. The leads from the volt box to the heater are actually part of the total volt-box resistance, so it is necessary to include their resistance when calculating the potential across the heater. Also part of the current that flows through the 1-ohm standard flows through the volt box; so this correction must be also made in calculating the current through the heater. One of the potential leads is connected to a current lead at its point of thermal

contact with the shield just before crossing the space between the calorimeter and shield. The other potential lead is connected to the other current lead at its first point of thermal contact with the calorimeter. Thus the measured electric energy is the energy developed in the heater plus the energy developed in that part of one current lead which traverses the space between the shield and the calorimeter. As the two sections of the current leads crossing from the shield to the calorimeter are equivalent, the same amount of heat will be developed in each. If it is assumed that this heat divides equally between the calorimeter and shield, then the heat supplied to the calorimeter will be that which is measured by this arrangement of the potential leads.

The time of heating was controlled and measured by making use of time signals supplied by the Riefler clock in the Time Section of this

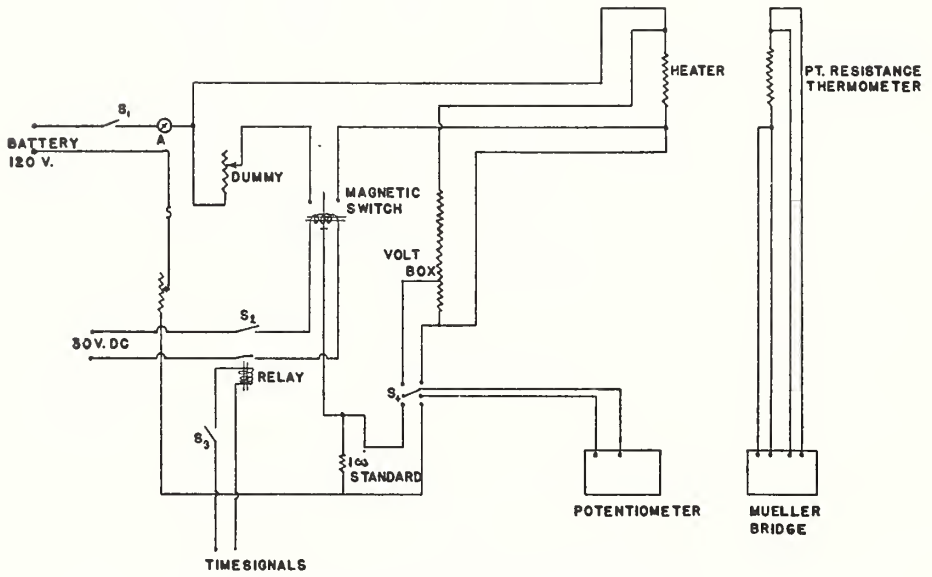

FIGURE 6.—*Diagram of measuring circuits.*

Bureau. The signals consist of electric impulses at 1-second intervals, except for a 2-second interval at the end of each minute. With switch S_3 closed, the operator notes the impulses actuating the relay. When the 2-second interval appears, the switch S_2 is closed, and the next impulse will close the 30-v circuit that actuates the magnetic switch. This switch is so constructed that it may be preset to snap either from left to right or from right to left when it receives the 30-v impulse. Thus the time of heating is an integral number of minutes. When the current is not flowing through the calorimeter heater, it flows through a dummy of equal resistance so that the battery current is constant.

Some tests were made in which the magnetic switch was used to operate the clutch of a synchronous interval timer driven by an accurately controlled 60-cycle supply. The reading of the interval timer were found to be within 0.01 second of the interval indicated by the clock-controlled circuit.

The temperature of the calorimeter was determined by measuring the resistance of the four-lead platinum resistance thermometer by means of the Mueller resistance bridge. The temperature rise during a heat was determined with an accuracy of about 0.001 degree except at temperatures below 20° K, where the sensitivity was of the order of 0.01 degree.

2. SPECIFIC HEAT

(a) METHOD OF MEASUREMENT

The specific heat of butadiene was obtained from measurements of the heat capacity of the calorimeter and contents. Two sets of heat-capacity measurements were required, one with a large amount of material in the calorimeter and one with a small amount. This procedure, which entails measurements with a small amount of material in the calorimeter rather than with the calorimeter empty, has been described by Osborne [9]. It not only takes into account the tare heat capacity of the calorimeter but makes possible an accurate correction for the effect of the vapor in the space above the solid or liquid in the calorimeter and connecting tube. In making the correction it is not necessary to know the volume of the vapor space nor the temperature of the filler tube, provided the temperature is the same during both sets of measurements.

The data from which heat capacities were calculated consisted of values of the temperature of the calorimeter and contents before and after a measured amount of electric energy had been added. The temperature rise during a heating period was usually about 10 degrees, although it was sometimes as small as 4 degrees or as large as 30 degrees. The rate of temperature rise was varied from about 0.5 degree per minute to 7 degrees per minute. The rate of 7 degrees per minute was taken between 20° and 30° K, where the heat capacity was small. This high rate could not safely be reached at temperatures above 100° K because the electric leads were too small for the required current. About 3 degrees per minute was the highest rate attained at temperatures above 100° K. One to two degrees per minute was the normal rate of rise. No consistent differences were observed between the data obtained from long heating intervals and those from short intervals, or between the data obtained from rapid heating and those from slow heating.

(b) METHOD OF CALCULATION

If a quantity of energy, ΔQ, is required to raise the temperature of the calorimeter and contents an amount, ΔT, the average heat capacity over this temperature interval is $\Delta Q/\Delta T$. The true heat capacity, dQ/dT, is the limit of this fraction as ΔT approaches zero. This limit, $dQ/dT=[G]_{Ta}$, may be calculated from the finite measured quantities by means of a relation given by Osborne, Stimson, Sligh, and Cragoe [10].

$$[G]_{T_a}=\left[\frac{dQ}{dT}\right]_{T_a}=\frac{\Delta Q}{\Delta T}-\left[\frac{\partial^2 G}{\partial T^2}\right]_{T_a}\frac{(\Delta T)^2}{24}-\left[\frac{\partial^4 G}{\partial T^4}\right]_{T_a}\frac{(\Delta T)^4}{1920}, \qquad (1)$$

where ΔQ is the heat added, ΔT is the temperature rise, and T_a is the average temperature of the heating. In making the calculations, the

574278 O - 61 - 28

derivatives of G with respect to T were replaced by derivatives of $\Delta Q/\Delta T$ with respect to T. This is permissible because $\Delta Q/\Delta T$ is approximately equal to G. Values of the derivatives were determined from graphs of $\Delta Q/\Delta T$ versus T. The last term involving the fourth derivative of G was found to be negligible for all the data for which this method was used. In fact, the term in which the second derivative of G appears was usually less than 0.1 percent of G.

The heat-capacity data were correlated and values obtained at intervals of 5 degrees by finding approximate analytical representations and plotting the deviations of the observed values from these formulas. At low temperatures the heat capacity was represented approximately by a modified Debye function $D[\Theta/(T+B)]$ suggested by Harold J. Hoge. The Debye function was evaluated from the tables prepared by Beattie [11]. By determining appropriate values of Θ and B, this function could be made to fit the heat-capacity data of the full calorimeter from 15° to 100° K. When the calorimeter contained only a small amount of butadiene it was possible to use this function from 15° to 150° K, the maximum deviation being about 2.5 percent of the heat capacity at 100° K. The conventional Debye function $D(\Theta/T)$ could not be used over such large ranges of temperature. At temperatures above 100° K for the full calorimeter and above 150° for the almost empty calorimeter, the heat-capacity data were represented approximately by equations of the form $G=a+bT+cT^2$. Tables were constructed giving G_b, the gross heat capacity when the calorimeter contained a large amount of butadiene, and G_a, the gross heat capacity when it contained a small amount.

The specific heat along the saturation line, $C_{sat.}$, was calculated by means of the equation

$$C_{sat.}=\frac{G_b-G_a}{M_b-M_a}+T\frac{d}{dT}\left(v\frac{dP}{dT}\right), \tag{2}$$

where v is the specific volume of the condensed phase and P is the vapor pressure. This equation was derived from relations given by Osborne [9]. The term $T\frac{d}{dT}\left(v\frac{dP}{dT}\right)$ allows for the fact that the gross heat capacity G includes some heat of vaporization. That is, sufficient butadiene evaporates to maintain saturation pressure in the space above the condensed phase in the calorimeter. The last term of equation 2 is negligible for solid butadiene because the vapor pressure of the solid is low.

Values of $v(dP/dT)$ for the liquid were obtained from vapor-pressure equation 4 (section IV–1, c) and values of v from table 13.

(c) RESULTS

The results of the specific-heat determinations are shown in figure 7 and in tables 1 and 2. The symbol $C_{sat.}$ is used to denote the specific heat at saturation. The graph at the bottom of figure 7 shows the differences between the specific-heat values obtained for the different

samples in the temperature range 60° to 215° K. In the liquid range there is excellent agreement, the differences usually being less than 0.1 percent. However, in the solid state the differences between the specific heats of the different samples is considerably larger. At 70° K the specific heat of sample 1 is about 1.8 percent larger than that of sample 4. It is unlikely that this difference can be accounted for by experimental error as different measurements on the same sample agreed within about 0.1 percent, and in the liquid state the agreement between the measurements on different samples was equally good. It was thought at first that the discrepancies might

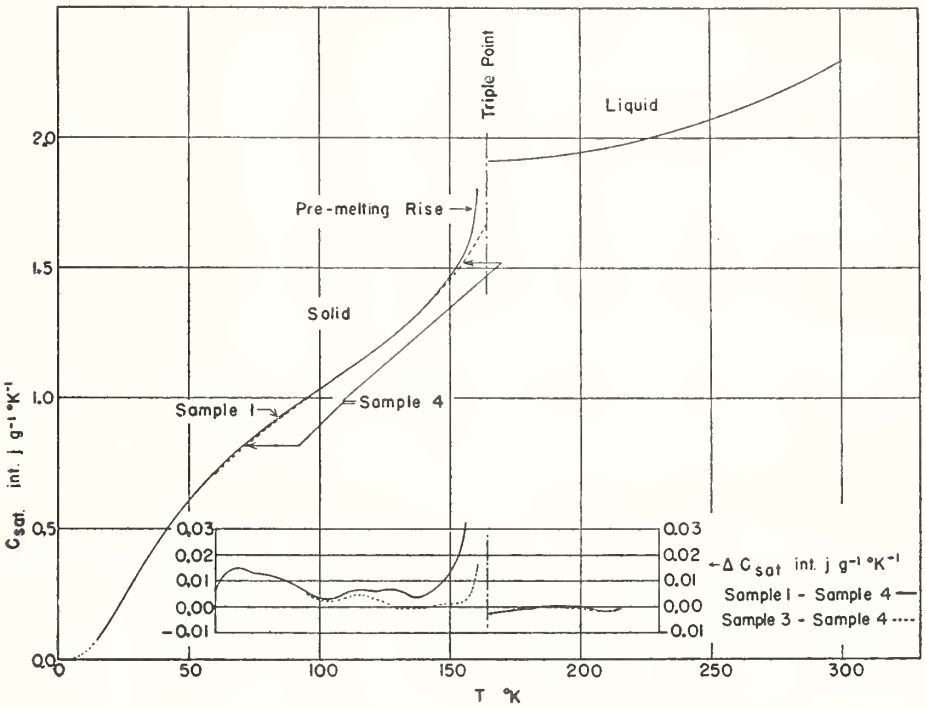

FIGURE 7.—*Specific heat along the saturation line for 1,3-butadiene as a function of temperature*

have resulted from different rates of cooling of the different samples, but a test made to detect such an effect gave a negative result. The most reasonable conclusion is that the differences were caused by different amounts of impurity in the different samples. This explanation requires that the impurity affect the specific heat to a much greater extent than would be expected from the additive law of specific heats. The large differences just below the triple point are caused by the premelting of samples 1 and 3. Sample 4, the specific heat of which is used as the reference in the deviation graph, contained so little impurity that there was no apparent premelting until the temperature was within 0.2 degree of the triple point.

TABLE 1.—*Specific heat of solid 1,3-butadiene*

T	$C_{sat.}$		
	Sample 1	Sample 3	Sample 4
° K	*Int. j* $g^{-1}°K^{-1}$	*Int. j* $g^{-1}°K^{-1}$	*Int. j* $g^{-1}°K^{-1}$
15	0.0747	----------	----------
20	.1492	----------	----------
25	.2341	----------	----------
30	.3193	----------	----------
35	.4012	----------	----------
40	.4762	----------	----------
45	.5447	----------	----------
50	.6081	----------	----------
55	.6654	----------	----------
60	.7186	----------	0.7136
65	.7670	----------	.7532
70	.8112	----------	.7964
75	.8522	----------	.8393
80	.8923	----------	.8800
85	.9307	----------	.9202
90	.9674	----------	.9585
95	1.0006	0.9999	.9954
100	1.0333	1.0328	1.0302
105	1.0668	1.0656	1.0636
110	1.1017	1.1000	1.0963
115	1.1376	1.1358	1.1312
120	1.1745	1.1718	1.1685
125	1.2136	1.2089	1.2071
130	1.2524	1.2474	1.2481
135	1.2963	1.2920	1.2926
140	1.3454	1.3408	1.3412
145	1.4019	1.3951	1.3942
150	1.4651	1.4533	1.4521
155	1.5450	1.5200	1.5186
160	1.7356	1.6097	1.5968

TABLE 2.—*Specific heat of liquid 1,3-butadiene*

T	$(G_b-G_a)/(M_b-M_a)$			$\frac{d}{dt}\left(v\frac{dp}{dt}\right)$	$C_{sat.}$
	Sample 1	Sample 3	Sample 4		Mean
° K	*Int. j* $g^{-1}°K^{-1}$	*Int. j* $g^{-1}°K^{-1}$	*Int. j* $g^{-1}°K^{-1}$	*Int. j* $g^{-1}°K^{-1}$	*Int. j* $g^{-1}°K^{-1}$
165	1.9104	1.9099	1.9130	0.000	1.911
170	1.9116	1.9116	1.9136	.000	1.912
175	1.9139	1.9141	1.9151	.001	1.915
180	1.9172	1.9172	1.9177	.001	1.918
185	1.9214	1.9211	1.9213	.001	1.922
190	1.9262	1.9257	1.9258	.002	1.928
195	1.9319	1.9311	1.9317	.002	1.934
200	1.9387	1.9379	1.9387	.003	1.941
205	1.9459	1.9454	1.9467	.004	1.950
210	1.9542	1.9539	1.9557	.006	1.961
215	1.9650	1.9657	1.9657	.008	1.973
220	1.9735	1.9744	----------	.009	1.983
225	1.9837	1.9854	----------	.012	1.997
230	1.9943	1.9964	----------	.015	2.010
235	2.0055	2.0078	----------	.018	2.025
240	2.0168	2.0192	----------	.021	2.039
245	2.0284	2.0308	----------	.025	2.055
250	2.0414	2.0440	----------	.030	2.073
255	2.0529	2.0551	----------	.035	2.089
260	2.0661	----------	----------	.041	2.107
265	2.0794	----------	----------	.047	2.126
270	2.0934	----------	----------	.054	2.147
275	2.1079	----------	----------	.062	2.170
280	2.1227	----------	----------	.070	2.193
285	2.1377	----------	----------	.080	2.218
290	2.1530	----------	----------	.090	2.243
295	2.1684	----------	----------	.101	2.269
300	2.1840	----------	----------	.112	2.296

In table 1 values of specific heat at 5-degree intervals at saturation are given for the different samples of butadiene in the solid state. Table 2 gives values at 5-degree intervals of $(G_b-G_a)/(M_b-M_a)$ for the three samples in the liquid state together with values of $T\frac{d}{dT}\left(v\frac{dP}{dT}\right)$. The values of $C_{sat.}$ in table 2 were obtained by averaging the values of $(G_b-G_a)/(M_b-M_a)$ at each temperature and adding the value of $T\frac{d}{dT}\left(v\frac{dP}{dT}\right)$.

3. HEAT OF FUSION

(a) METHOD OF MEASUREMENT

The heat of fusion of butadiene was determined by measuring the energy required to heat the calorimeter and contents from a temperature somewhat below the triple point to a temperature above the triple point. The initial temperature was chosen so as to be below the premelting region. The heat of fusion was obtained by subtracting from the total energy (1) the energy required to heat the calorimeter plus its solid contents from the initial temperature to the melting temperature, and (2) the energy required to heat the calorimeter plus its liquid contents from the melting temperature to the final temperature. In computing quantity (1), the specific heat of pure butadiene was used in obtaining the heat capacity of the calorimeter and contents so as to avoid errors that may be caused by the premelting of impure samples. In this way the heat of premelting is included in the value obtained for the heat of fusion. The heat of fusion was from 60 to 90 percent of the total energy added in the measurements on the different samples.

(b) RESULTS

The results of the determinations of the heats of fusion are as follows: Sample 1, 147.53; sample 3, 147.59; sample 4, 147.65 int. j g^{-1}. The mean of these values is 147.59 int. j g^{-1}. It may be noted that there is little difference in the heats of fusion of the samples, although they contain different amounts of impurity. The scattering of the results is no more than would be expected from ordinary errors of observation. Assigning a reasonable probable error, the heat of fusion of butadiene may be given as $147.6+0.1$ int. j g^{-1}, or 1908.4 ± 1.3 cal $mole^{-1}$.

4. HEAT OF VAPORIZATION

(a) METHOD OF MEASUREMENT

The measurement of the heat of vaporization consisted of determining the amount of electric energy required to vaporize a measured quantity of butadiene. This was accomplished in the following manner:

Referring to figure 3, the reservoirs, F_1 and F_2, were cooled by surrounding them with solid CO_2. The calorimeter was brought to the desired temperature and the shields adjusted to adiabatic conditions. Then the switch was closed, sending current through the calorimeter heater. The valve leading to F_2 was opened, and the valve leading to the calorimeter was used as a throttle and adjusted until the temperature of the calorimeter was almost constant. A final adjustment of the current through the calorimeter was necessary to obtain a steady temperature. After equilibrium had been established, the

valve leading to F_2 was closed and the valve to F_1 was opened without disturbing the adjustment of the throttling valve. After a measured interval of time, the valve to F_1 was closed and the calorimeter heater turned off. The amount of butadiene vapor removed from the calorimeter during the measured time was determined by weighing F_1 before and after each run. The temperature of the calorimeter was kept constant during a run by making small adjustments of the heating current at measured times, so that the total energy input could be measured by measuring the current and potential drop through the heater during each interval of time between these adjustments. The adjustments of heating current were of the order of 1 percent, and usually several minutes would elapse between adjustments. The platinum resistance thermometer was assumed to be at the temperature of the vaporizing liquid. This may not be strictly true, but if errors arise from this source they should be dependent on the power input, and no such dependence was observed. As the time of withdrawal of the measured sample is determined by manual operation of the valves, the error in timing may be as large as one-half second. The time of withdrawal ranged from 15 to 40 minutes.

(b) RESULTS

If Q is the energy input during the withdrawal of M grams of vapor, the heat of vaporization L_v is

$$L_v=\frac{Q}{M}\left(1-\frac{v}{V}\right), \tag{3}$$

where v is the specific volume of the liquid, and V is the specific volume of the vapor. Q/M is not the true heat of vaporization as part of the material vaporized does not leave the calorimeter but fills the space vacated by the vaporized liquid.

Table 3 gives the data and results on the heats of vaporization. The energy input, Q, and the mass withdrawn, M, are given for each individual vaporization at a given temperature, and the quantity Q/M is computed. In order to obtain the mean value of Q/M for each temperature the sum of the energy input was divided by the total amount withdrawn. This is shown in the bottom line of each group of measurements. This mean value is equivalent to that which would have been obtained by weighting the individual observations in proportion to the amount of butadiene vaporized. In calculating the latent heat, $L_v=\frac{Q}{M}\left(1-\frac{v}{V}\right)$, values of v and V were taken from table 13. The average deviations of the observations from the mean value of Q/M are given in the next to last column of table 3. These range from 0.04 to 0.06 percent, and the maximum deviation of a single observation is 0.20 percent.

TABLE 3.—*Data and results of heat-of-vaporization experiments*

T	Q	M	Q/M	Power input	$1-\frac{v}{V}$	$L_v=Q/M\left(1-\frac{v}{V}\right)$	Average deviation of observations	L, calculated from table 13
° K	*Int. j*	*g*	*Int. j* g^{-1}	*w*		*Int. j* g^{-1}	*Int. j* g^{-1}	*Int. j* g^{-1}
247.07	2043.3	4.6846	436.17	1.17				
	1282.2	2.9307	437.50	1.19				
	884.9	2.0267	436.62	0.74				
	915.1	2.0970	436.39	0.76				
	1708.4	3.9128	436.62	1.78				
	2324.6	5.3246	436.58	2.58				
Total	9158.5	20.9764	436.61		0.99843	435.92	0.27	435.21
268.60	1552.2	3.7147	417.85	0.86				
	3616.3	8.6651	417.34	2.08				
	2405.2	5.7582	417.70	0.93				
	1801.8	4.3165	417.42	2.00				
	1878.8	4.4975	417.74	1.01				
Total	11254.3	26.9520	417.57		0.99610	415.99	0.19	415.47
295.67	2594.4	6.6222	391.77	1.05				
	2286.0	5.8263	392.36	2.54				
	1128.4	2.8801	391.79	0.99				
	2324.2	5.9312	391.86	2.15				
	2709.6	6.9174	391.71	2.66				
Total	11042.6	28.1772	391.90		0.99012	388.03	0.20	388.17

The formulated values of L (see section VI–2) at temperatures of even degree centigrade (table 13) lead through interpolation to the values given in the last column of table 3. The agreement at 295.67° K is excellent, the calculated value being slightly higher than the observed. The calculated values at 268.60° and 247.07° K are only 0.13 and 0.16 percent lower than the respective observed values.

5. ACCURACY OF CALORIMETRIC MEASUREMENTS

Some tests were made with the calorimeter to determine the accuracy with which measurements could be made. Water was chosen as the test material as very reliable data [12] are available. The specific heat of water was measured in the calorimeter between 1° and 22° C. Three heats were made in this range of temperatures, and the maximum difference between the values obtained and those given by Osborne, Stimson, and Ginnings was 0.03 percent. Three determinations of the heat of vaporization of water at 20° C yielded a maximum difference of 0.17 percent, although the mean of the three measurements agreed with Osborne's values to 0.03 percent. The measurements on the specific heat of water are probably somewhat more reliable than those obtained on substances having lower specific heats, as the heat capacity of the water sample is a larger fraction of the total heat capacity of the calorimeter plus contents than it is for other substances. The measurements of the heat of vaporization of water, however, are probably comparable with the measurements on butadiene. The heating rates and total energy input during heats were about the same for the two substances.

Taking into consideration these tests, and the scattering of the observations previously mentioned, the estimates of the probable errors of the calorimetric measurements described in this paper are as follows: Specific heat, 0.1 percent between 40° and 300° K, becoming possibly as large as 1 percent below 20° K; heat of fusion, 0.07 percent; heat of vaporization, 0.15 percent.

IV. PRESSURE-VOLUME-TEMPERATURE MEASUREMENTS

1. VAPOR PRESSURE

The vapor-pressure measurements comprised two groups of observations made with two independent sets of apparatus. The first group of observations covered a temperature range from 195° to 288° K or a corresponding pressure range up to about 2 atm. The second group covered the temperature range 0° C to the critical temperature. Above 110° C, however, the accuracy was reduced considerably by rapid polymerization of the sample. The method used in both series of measurements was that in which static equilibrium was approached between the liquid and the vapor portions of the sample. At the higher temperatures the approach was always by condensation of some of the sample rather than by evaporation, as the former procedure had been found to be more rapid with other substances.

(a) MEASUREMENTS FROM 195° TO 288° K

The apparatus used for these observations consisted of a mercury manometer of 10-mm bore, which was read by means of a mirror-

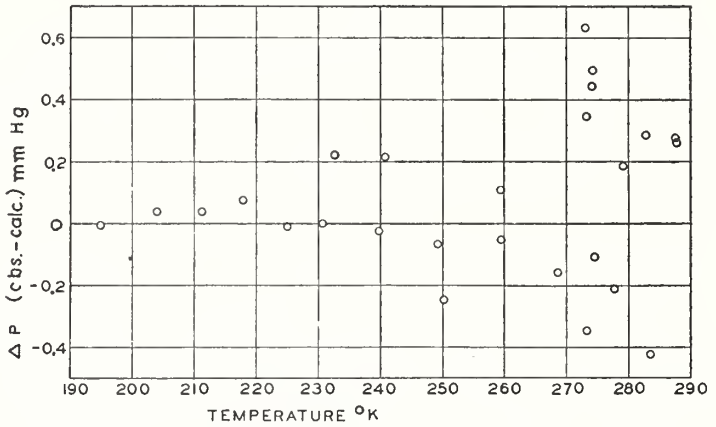

FIGURE 8.—*Comparison of vapor pressures observed in the first group of measurements with calculated values.*

backed glass scale graduated in millimeters and supported against the manometer tubes. One arm of the manometer was connected to the filler tube of the calorimeter, in which there was a quantity of butadiene from sample 4. When making measurements of vapor pressures below 1 atm the other arm of the manometer was evacuated. For measurements above 1 atm this arm was open to the atmosphere. In the latter case, one measurement of the atmospheric pressure was made with a precision barometer for each set of three readings of the manometer at a given temperature.

Figure 8 shows the deviations of the observations from the values calculated from equation 4. It was thought that the pressure measurements were reproducible to about ± 0.2 mm Hg. The deviations below 270° K confirm this. However, above this temperature there is considerably greater scattering, which has been attributed to the presence of some impurity, causing the vapor pressure to depend on the amount condensed, as described in the section on purity.

(b) MEASUREMENTS FROM 0° TO 152° C

The apparatus used in these measurements was entirely independent of that used in the group (a) measurements made in connection with the calorimetric experiments.

It is shown diagrammatically in figure 9. The vapor pressure of the butadiene in the closed end of one manometer is transmitted through the mercury and oil to either an open-ended auxiliary mercury manometer for the low-pressure measurements or to a dead-weight piston gage for the high-pressure measurements [14].

As static vapor-pressure measurements are susceptible to errors due to more volatile impurities, provision was made to vary the butadiene vapor space so that the vapor-pressure measurements could be extrapolated to large vapor volumes. The vapor space was varied

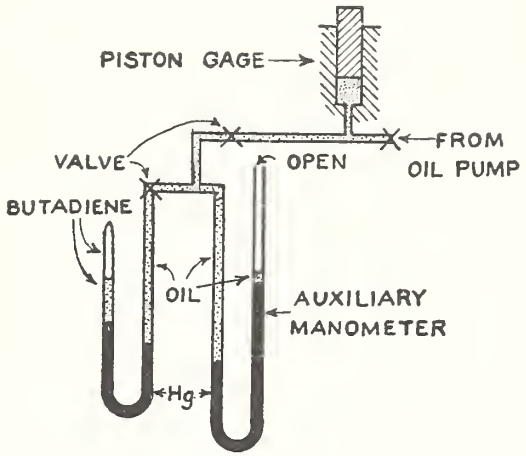

FIGURE 9.—*Connecting lines for vapor pressure measurements.*

by changing the amount of oil between the mercury manometers by means of the piston-gage oil pump.

Two types of manometers containing the butadiene were used and are shown in figure 10. Each consisted of a U-shaped glass tube with a metal valve soldered [13] to one arm. In the manometer shown in figure 10, *A*, the butadiene was distilled into a space above the mercury meniscus and sealed at *C*. In figure 10, *B*, the butadiene was distilled through a small third arm and sealed at *D*. By closing the main portion of the manometer with a mercury seal before sealing the glass, any gases freed during the sealing off and not removed by the vacuum pump were trapped at *D*. In the sealing of both types of manometers the butadiene was cooled with liquid air. The manometer shown in figure 10, *B*, was made with calibrated volumes as shown, and could also be used later in the measurement of vapor density.

The small size of the samples used in this group of observations necessitated great care in regard to the cleanliness of the apparatus. The glass manometers were washed with nitric acid, soaked several hours with freshly prepared chromic acid, and rinsed several times with

distilled water. The last rinse water, which remained in the manometers several hours, had substantially the same electric conductivity as the distilled water used. The manometers were outgassed by heating with a torch during evacuation, and the mercury was introduced by distillation. A small quantity of butadiene was admitted and then pumped out before condensing a sample into a manometer.

For the measurement at 0° C, the butadiene was completely im-

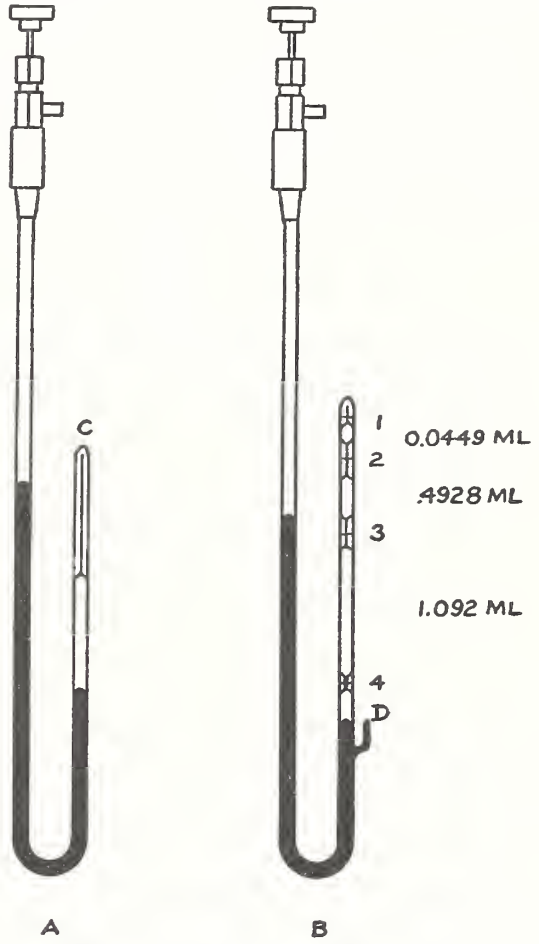

FIGURE 10.—*Manometers used in measurements of vapor pressure and of density of vapor.*

mersed in an ice bath. At higher temperatures, a stirred thermoregulated oil bath was used. Temperatures were measured with a four-lead, potential-terminal, platinum resistance thermometer of the coiled-filament type, calibrated according to specifications of the International Temperature Scale [15]. The elevations of the mercury surfaces were referred to steel scales graduated in millimeters and suspended between the arms of the manometers.

Seven samples were at various times distilled into manometers for these vapor-pressure measurements. The first five were subsamples taken from sample 3, already described in the section on preparation of samples, and were numbered 3a, 3b, 3c, 3d, and 3e, respectively. The other two (4a and 4b) were taken from sample 4.

The results of the measurements on samples 3b, 3e, and 4b are presented in figures 11, 12, and 13, respectively, in which the abscissas represent the volume occupied per gram of sample, whereas the ordinates represent pressures in centimeters of mercury corrected to 0° C and to standard gravity. In order to represent several isotherms with the same coordinates, a constant of appropriate amount for each isotherm is subtracted from the pressures. Observed values are represented in the three figures by various symbols, the same symbol being used uniformly for any one isotherm, calculated values are represented by black squares, the vapor pressure being calculated from vapor-pressure equation 4, and the corresponding volume being calculated from the equation of state 6. At 0° C the specific volume of the vapor (336 ml/g) is considerably off the scale.

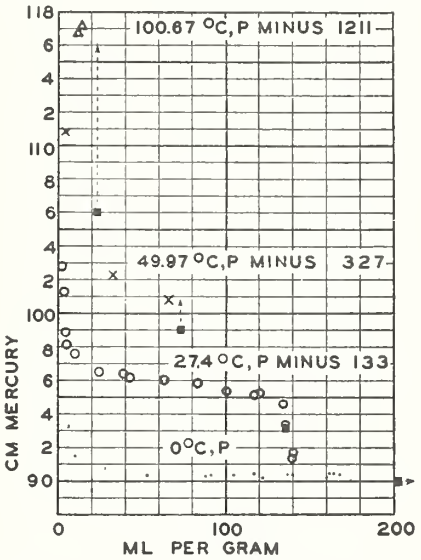

FIGURE 11.—*Vapor-pressure data for sample 3b.*

■=Values of pressure calculated from vapor pressure equation 11 and values of specific volume of saturated vapor calculated from equation of state 13. Specific volume at 0° C=335 ml/g. Dotted line and arrow indicate temperature to which ■ symbol belongs. Other symbols represent observed values.

The data at 0° C consist of numerous observations made initially on each sample, followed by observations at higher temperatures, with occasional repeated observations at 0° C. Such repeated observations after 62° C for samples 3e and 4b and after 112° C for sample 3e are represented in figures 12 and 13 by the same symbols as earlier measurements at 0° C. As their positions in the figures do not distinguish them from earlier measurements, it is believed that polymerization was thus far negligible. The agreement between the vapor pressures of the purer samples also indicates that at temperatures up to and including 112° C polymerization caused no appreciable effect.

Of the first four samples, which were not as pure as the others, only the data on sample 3b are presented. Besides comprising most of the data above 100° C, they are of special interest, as this sample was the only one in a manometer of sufficient capacity to permit the complete evaporation of the sample at room temperature, thus furnishing a better illustration of the variation of pressure with volume. The observed values for the vapor pressure of this sample (fig. 11) are

noticeably higher than the calculated. These differences are attributed to volatile impurities. On the other hand, the observed vapor pressure, 31,945 mm, at 152° C (not shown in fig. 11) is low by 484 mm, at least partially due to the extremely rapid rate of polymerization at this temperature.

Two observed values of vapor pressure at 62.05° C for sample 3e (see fig. 12) are notable for being considerably below the calculated pressure, even though the volume of sample was in one case slightly less than that calculated for saturated vapor. This is probably due to an impurity less volatile than butadiene, which appears to be absent in sample 4b (see fig. 13).

In addition to these data the vapor pressure of sample 4a was measured at 0°, 99.88° C, and at the critical temperature (discussed

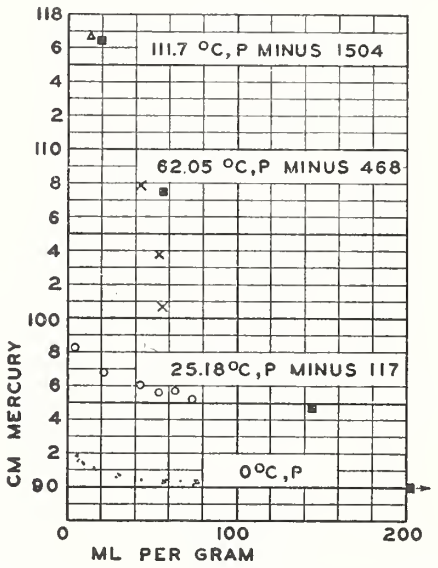

FIGURE 12.—*Vapor-pressure data for sample 3e.*

■=Values of pressure calculated from vapor-pressure equation 11 and values of specific volume of saturated vapor calculated from equation of state 13. Specific volume at 0°=335 ml/g. Other symbols represent observed values.

later). The observed values corresponding to the first two temperatures, 902.0 mm and 12,973 mm, are in very good agreement with the respective values calculated from the vapor-pressure equation, namely 899.7 and 12,971 mm, especially when one considers that observations with this sample at 0° C were possible only with a small portion evaporated on account of the relatively large mass of sample.

The results of these measurements show that the observed vapor pressures depended somewhat on the relative amounts of the sample that were in the liquid and vapor phases. This indicates the presence of an impurity. The data show that the first four samples, 3a, 3b, 3c, and 3d, contained approximately equal percentages of impurity, that sample 3e contained somewhat less impurity (probably due to the improved method of sealing the sample), and that samples 4a and 4b contained still less impurity (in consequence of a purer sup-

ply). The accuracy of reading at 0° C would lead one to expect results reproducible to within 0.5 mm, but the variation obtained was about three or four times that amount, as may be seen in figure 14, in which the observed pressures for samples 3e and 4b are represented at 0° C with a more open scale than in figures 12 and 13. It would

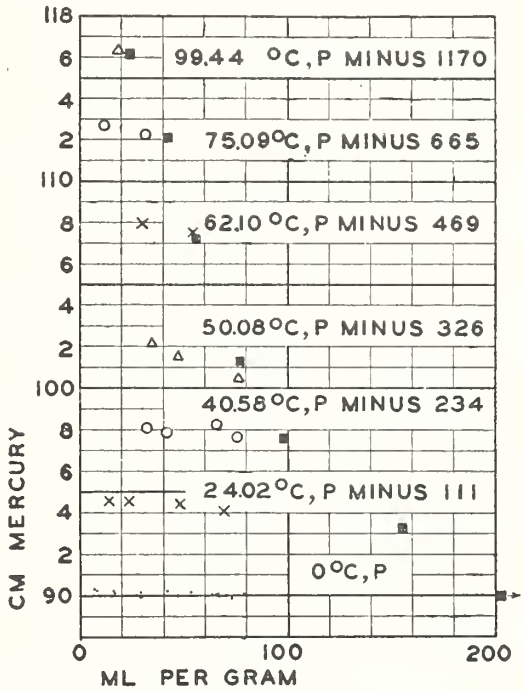

FIGURE 13.—*Vapor pressure data for sample 4b.*

Symbols are same as in figure 12.

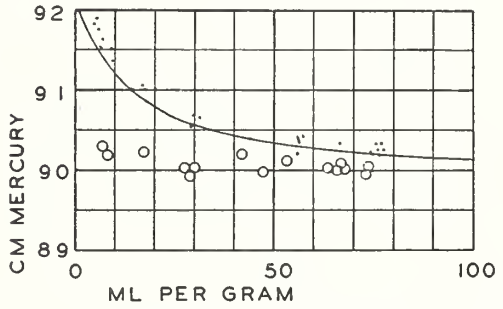

FIGURE 14.—*Vapor pressure of samples 3e and 4b at 0° C.*

appear that the excessive variation was due to a rather large lag in approaching equilibrium. The time required to remove the heat of condensation may have been supplemented by the time required for diffusion of an impurity between the butadiene liquid surface and the remainder of the liquid, especially in the earlier and less pure samples.

(c) VAPOR-PRESSURE EQUATION

The vapor pressure of 1,3-butadiene is represented over the temperature range from the triple point to the critical temperature by the empirical equation [2]

$$\log p = A - \frac{1}{T}[B + CX(10^{DX^2} - 1)] - E(T - 243.16)^6, \qquad (4)$$

where

$A = 7.2363$ for p in mm Hg
$B = 1165.21$
$C = 1.5875 \times 10^{-4}$
$D = 0.766 \times 10^{-10}$
$X = 125{,}000 - T^2$
$E = 2 \times 10^{-14}$ (not to be used above $-30°$ C)
$T = t + 273.16$ = temperature in degrees Kelvin.

The last term, which is not used above $-30°$ C, was added in order to produce a set of tables consistent with specific-heat data in the low-temperature region. This addition makes no change in the values of vapor pressure as great as 0.01 mm.

The equation represents the vapor-pressure measurements in the range from the triple point ($-108.92°$ C) to room temperature, as illustrated in figure 8 and in the range 0° C to the critical temperature, as shown in figures 11, 12, and 13. The representation is within the precision of the experimental data.

Differentiation of the vapor-pressure equation gives

$$\frac{d \ln p}{dT} = \frac{1}{T^2}[B + CX(10^{DX^2} - 1)] + 2C[10^{DX^2}(4.6052DX^2 + 1) - 1] - 6E(T - 243.16)^5. \qquad (5)$$

(d) COMPARISON WITH DATA OF OTHER OBSERVERS

The values for vapor pressure calculated from equation 4 are compared in table 4 with those obtained by previous observers. Some preliminary measurements made by R. S. Jessup of this Bureau are included in this table. These measurements were made with a Bourdon gage and samples of butadiene that were not as pure as those used to obtain the data presented in figures 8, 11, 12, and 13. The results of Vaughan [16] differ considerably from the present results both in pressure and in the rate of change of pressure with temperature. Heisig's [17] results are in much better agreement, although they are consistently higher than those obtained in this investigation. There appears to be a slight difference between Heisig's observations obtained with the platinum resistance thermometer below the freezing temperature of mercury and the observations with a mercury thermometer at higher temperatures. The data obtained

[2] A vapor-pressure equation of the form

$$\text{Log } p = A - \frac{1}{T}[B + CX(10^{DX^2} - 1)]$$

was first used to represent the observed vapor pressures of CO_2 within about 3 parts in 10,000. See BS J. Research 10, 381 (1933) RP538. It has also been used to represent the vapor pressures for several other substances. The value of X is usually approximately 0.7 $T_c^2 - T^2$, except for those substances having a low critical temperature, in which case the coefficient of T_c^2 is smaller. The value of C for substances previously tried has been between 1.1×10^{-4} and 1.22×10^{-4}. The exceptionally high value obtained for C for butadiene may be a consequence of the lack of accurate vapor-pressure data above 112° C.

by Moore and Kanep [18] deviate in an irregular manner, which suggests lack of equilibrium when their observations were made. The normal boiling temperature observed by Lamb and Roper [19] is only slightly lower than that calculated from equation 4 and agrees with that obtained for some of the less pure samples of the present investigation.

TABLE 4.—*Comparison of data of other observers with vapor pressures calculated from equation 4*

Temperature	$p_{obs.}$	$p_{obs.}-p_{calc.}$	Temperature	$p_{obs.}$	$p_{obs.}-p_{calc.}$	Temperature	$p_{obs.}$	$p_{obs.}-p_{calc.}$
R. S. Jessup. Sample 1			G. B. Heisig			Wm. E. Vaughan		
°C	mm	mm	°C	mm	mm	°C	mm	mm
0	917	17	−75.5	14.6	0.2	−81.9	9.2	0.8
25	2,142	37	−63.4	35.4	.1	−79.1	11.0	.3
50	4,340	76	−51.6	77.1	1.0	−38.5	156.9	−3.8
65	6,250	77	−39.4	153.4	0.2	−24.0	327.5	−3.2
			−38.6	161.7	1.8	−17.0	442.7	−10.0
			−32.7	219.0	1.9	−3.1	772.4	−27.2
			−26.1	301.4	1.8	+0.5	862.6	−54.1
			−19.9	400.5	1.6			
			−15.5	484.2	1.2			
R. S. Jessup. Sample 2			−10.4	599.9	1.6	G. Moore and E. K. Kanep		
			−5.6	729.7	4.2			
			−1.5	854.0	3.8			
0	904	4				−4.5	763	6
25	2,124	19	A. B. Lamb and E. E. Roper			3.0	957	−49
50	4,290	26				10	1,266	−24
65	6,210	37				16	1,627	47
			−4.51	760	2.9	22	1,926	9

2. DENSITY OF SUPERHEATED VAPOR

(a) METHOD AND APPARATUS

The density of the superheated vapor was measured for three samples of butadiene 3d, 3e, and 4b, the first of these being in the manometer illustrated in figure 10 *A*, and the other two in the manometer illustrated in figure 10 *B*. The volumes of these manometers were determined by weighing the mercury which filled the right-hand arms to various depths when in an inverted position.

A measured length of capillary in figure 10 *A*, and the space between marks 1 and 2 in figure 10 *B*, were used to measure the sample when nearly all condensed. A small vapor space was retained above the liquid to prevent sticking of the liquid in the top of the manometer. It had been previously observed that, after the sample was entirely condensed, the liquid broke away from the top of the manometer only after the pressure had been reduced considerably below the vapor pressure, and the violence of the separation was sufficient to scatter mercury droplets into undesirable places. In addition to this method of measuring the volume of the liquid and estimating the mass of sample from the known density, volume (about 120 ml), pressure, and temperature of the vapor were observed before the sample was condensed into the manometer. A correction was applied for the deviation from the ideal-gas law. This correction amounted to 1.5 parts in 1,000 for sample 3d, and 2.4 parts in 1,000 for samples 3e and 4b, which were filled with a charge at higher pressures than was sample 3d.

The measurements of vapor density may be divided into two classes. In the first class are a few measurements in which the vapor occupied the space down to either mark 3 or 4 (see fig. 10 and accompanying discussion in the text). In the second class are a larger number of measurements in which the vapor extends to unmarked parts of the manometers. This latter class of measurements is less accurate than the first. For sample 3d the position of only the dome of the meniscus was observed, whereas for samples 3e and 4b, both the dome and the edge of the meniscus were located with consequent improvement in accuracy.

(b) RESULTS OF MEASUREMENTS AND THEIR FORMULATION

The results of the measurements on samples 3d, 3e, and 4b are presented in tables 5, 6, and 7, respectively, together with a comparison of the observed values of pV/RT with those calculated from the empirical equation of state [3]

$$\frac{pV}{RT}=1-\frac{68.4\left[1-10^{-.045(T_c/T)^2}\right]-1.48}{V}+\frac{6\left(\frac{T_c}{T}\right)^4+3.5}{V^2}, \tag{6}$$

where v is in milliliters per gram, and the other variables are in consistent units. When p is in millimeters of mercury, and T is in degrees Kelvin ($T=273.16+°C$), the value of R is 1152.95 mm Hg (ml)/g mole° C. Only a few of the differences in tables 5, 6, and 7 exceed an amount appropriate to the accuracy of reading the position of the mercury-butadiene interface (see fig. 10, A and B). The consistent difference between data for samples 3d and 3e does not exceed the uncertainty in determining the mass of sample.

TABLE 5.—*Measurements of vapor density for sample 3d*

Mass of sample by measurement of vapor	0.01591
Mass of sample by measurement of liquid	.01591
Weigbted mean value	0.01591 gram

Date	Class of observation	Temperature	Pressure	Specific volume	pv/RT observed	pv/RT calculated	$10^4\frac{\text{col. 6}-\text{col. 7}}{\text{col. 7}}$
1943		°C	*mm* Hg	*ml/g*			
Mar. 2	2	30.78	2206.0	147.39	0.9279	0.9260	21
	2	30.80	2271.9	142.86	.9261	.9237	26
	2	30.81	2337.8	138.34	.9228	.9213	16
	2	30.80	2470.8	130.04	.9169	.9165	4
	2	36.41	2674.8	122.31	.9166	.9145	23
	2	36.41	2742.7	119.11	.9153	.9121	35
	2	36.41	2844.6	114.20	.9101	.9086	17
	2	36.41	2945.2	109.43	.9030	.9050	−22
Mar. 3	2	49.90	2680.2	129.04	.9286	.9256	33
	2	49.90	3365.6	100.64	.9094	.9049	50
	2	49.90	4062.5	81.14	.8850	.8831	22
	2	100.04	5,509	71.28	.9127	.9041	95
	2	99.99	9,110	39.09	.8277	.8268	10
	2	99.95	12,739	24.89	.7372	.7352	27
Average deviation							29

[3] Equation 6 expresses p at a given T as a cubic equation in V, necessitating the use of successive approximations for calculating the specific volume of the saturated vapor. For the first approximation it was convenient to obtain values of v [27] from the simpler equation

$$\left(1-\frac{pV}{RT}\right)_g=\frac{(p/2.718\ p_c)^{0.702}}{\left(1-\frac{pV}{RT}\right)_l},$$

where the subscripts g and l refer to gas and liquid, respectively, and p_c is the critical pressure.

TABLE 6.—*Measurement of vapor density for sample 3e*

Mass of sample by measurement of vapor 0.02749
Mass of sample by measurement of liquid ..... .02741

Weighted mean value ..... 0.02746 gram.

Date	Class of observation	Temperature	Pressure	Specific volume	pv/RT observed	pv/RT calculated	$10^4\frac{\text{col. 6}-\text{col. 7}}{\text{col. 7}}$
1943		° *C*	*mm* Hg	*ml/g*			
April 1	2	59.64	4283.7	79.24	0.8847	0.8881	−39
	2	59.65	4561.6	73.78	.8771	.8800	−33
	2	59.66	5117.6	64.79	.8641	.8635	+7
	2	62.03	4287.1	80.12	.8888	.8908	−22
	2	62.03	4562.7	74.58	.8806	.8830	−27
	2	62.03	4840.9	69.77	.8740	.8750	−12
	2	62.03	5120.1	65.44	.8670	.8669	+1
	1	62.03	5544.9	59.47	.8533	.8541	−9
April 3	2	111.71	5588.3	72.25	.9099	.9106	−8
	1	111.71	6665.5	59.43	.8928	.8917	+12
	2	111.70	9143.2	40.93	.8434	.8455	−25
	2	111.71	12,755	26.91	.7735	.7693	+55
	1	111.71	15,649	19.70	.6948	.6937	+16

Average deviation class 1 10
Average deviation class 2 23

TABLE 7.—*Measurement of vapor density for sample 4b*

Mass of sample by measurement of vapor 0.02757
Mass of sample by measurement of liquid ..... .02746

Weighted mean value ..... 0.02750 gram

Date	Class of observation	Temperature	Pressure	Specific volume	pv/RT observed	pv/RT calculated	$10^4\frac{\text{col. 6}-\text{col. 7}}{\text{col. 7}}$
1943		° *C*	*mm* Hg	*ml/g*			
May 5	2	50.08	4,060	80.87	0.8811	0.8831	−23
	2	50.08	4,264	76.15	.8713	.8765	−60
	2	62.10	4,288	80.43	.8922	.8910	+13
	1	62.10	5,557	59.37	.8536	.8540	+5
May 7	2	75.09	4,350	83.23	.9017	.9029	−13
	1	75.08	5,854	59.37	.8657	.8647	+12
	2	75.08	6,983	48.43	.8423	.8341	+98
	2	99.44	4,717	83.27	.9144	.9163	−21
	1	99.44	6,406	59.37	.8854	.8833	+24
	2	99.44	9,111	39.27	.8329	.8257	−34
	2	99.44	12,724	25.09	.7432	.7344	+120
	2	149.00	5,589	81.16	.9315	.9359	−47
	1	149.00	7,479	59.38	.9125	.9128	−3
	2	149.00	12,745	32.40	.8484	.8437	+56
	1	149.00	18,621	19.67	.7526	.7539	−17
	2	148.98	22,189	15.09	.6880	.6887	−10
	2	148.98	23,637	13.78	.6693	.6587	+160
	2	148.98	25,092	11.96	.6166	.6247	−133
	2	148.98	25,820	11.38	.6037	.6068	−52
	2	148.98	26,548	10.80	.5891	.5872	+33
	2	148.98	27,278	10.15	.5689	.5657	+39
	2	148.98	28,008	9.53	.5484	.5416	+125
	2	148.98	28,736	8.69	.5131	.5124	+14
	2	148.98	29,464	7.78	.4710	.4783	−155

Average deviation class 1 12
Average deviation class 2 63

574278 O - 61 - 29

3. DENSITY OF SATURATED LIQUID

(a) METHOD AND APPARATUS

The density of liquid butadiene was measured in the pyrex glass picnometer illustrated in figure 15. The picnometer was calibrated by weighing the amounts of mercury or water that filled the various parts of the picnometer. The results of these calibrations are given

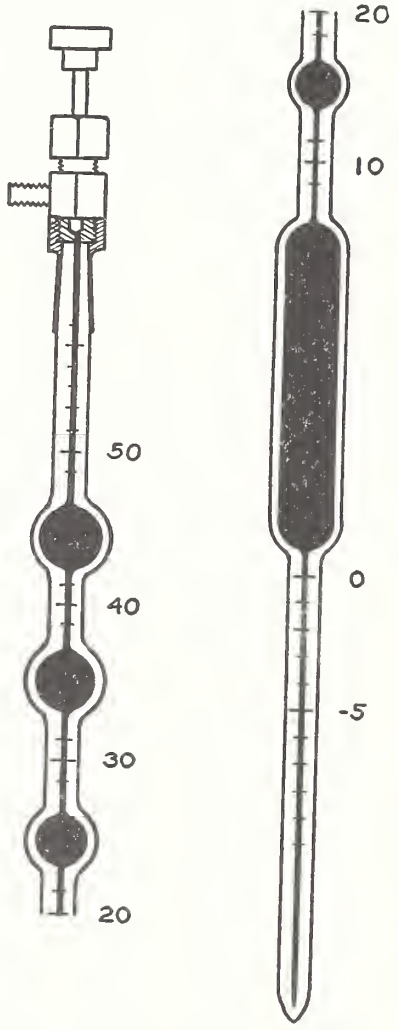

FIGURE 15.—*Semisectional view of picnometer.*

in table 8. The worst discrepancy between the two calibrations is at mark 40, which amounts to about 1 part in 7,000. The mean value, which is less than 1 part in 10,000 from either calibration, was used in calculating the results. The cross section of the capillary used in the picnometer was measured as an aid in correcting for readings not directly at a mark. The cross section of the capillary portions between the valve and the large bulb is 1.00 mm^2, that for the capillary below the large bulb is 1.38 mm^2. Both capillaries were calibrated by weighing mercury threads of measured length.

TABLE 8.—*Data from calibration of picnometer*

Space included	Capacity at 0°C			
	Water calibration (Sept. 15–16, 1943)	Mercury calibration (Oct. 1–12, 1943)	Mean	Total volume
	ml	*ml*	*ml*	*ml*
Valve to mark 50	0.0731		0.0731	15.6955
Mark 50 to mark 40	1.8348	1.8365	1.8356	15.6224
Mark 40 to mark 30	1.3442	1.3423	1.3433	13.7868
Mark 30 to mark 20	.8922	.8921	.8922	12.4435
Mark 20 to mark 10	.5667	.5665	.5666	11.5513
Mark 10 to mark 0	10.8448	10.8446	10.8447	10.9847
Mark 0 to bottom	.1400		.1400	.1400

The coefficient of volumetric expansion of the picnometer was assumed to be 1.00×10^{-5} per degree centigrade. The stretch of the picnometer with pressure, calculated from the dimensions of the large picnometer bulb (18-mm outside diameter and 1.8-mm wall thickness) and the elastic properties of Pyrex, was 1.61×10^{-5}/atm.

The measurement of the density of liquid butadiene was subject to error from polymerization, especially at the higher temperatures. On this account, the densities at low temperatures were observed first and a correction applied to the measurements at higher tempertures. This correction was determined by repeating the measurement at 0° C and noting the change in volume at 0° C resulting from polymerization at the higher temperature. Two subsamples, 4c and 4d, were taken from the larger sample 4 for the measurements of liquid density. Except at −78.72° C and at 0° C, the temperature was measured with the same platinum resistance thermometer used for measuring temperatures during the vapor-pressure investigation (IV–1 b).

Several different baths were used for measuring the density of these samples at various temperatures. At −78.72° C the picnometer was packed in finely divided dry ice up to the level of the meniscus. Precautions were taken to purge air from the space above the solid, and to pack the dry ice thoroughly enough to avoid radiation from the surroundings between the particles of solid CO_2. At 95.67° C the picnometer was totally immersed in a steam bath operated at a pressure below atmospheric. The data indicated that the temperature of this bath changed too rapidly with time, and in consequence of prolonged efforts to attain equilibrium, the correction for polymerization was unduly large, so that the corrected result is not as reliable as at the other temperatures. At 0° C an ice bath of shaved ice packed with enough water to fill the crevices but not to float the ice was used. In order to maintain the butadiene meniscus also at 0° C during the observations, a glass sight tube was placed between the picnometer and the bath container and ice was piled over the tube. At the remaining temperatures thermally controlled stirred liquid baths were used.

(b) RESULTS OF MEASUREMENTS AND THEIR FORMULATION

The data obtained are presented in tables 9 and 10. In these tables the "volumes occupied" include corrections to the volume of the picnometer at 0° C and 1 atm. It is to be noted that the density

of the vapor given in these tables is not necessarily that of the saturated vapor but that of the vapor existing in the picnometer. The "apparent liquid density" is the quotient obtained by dividing the mass of liquid by the volume occupied. The corrected density was obtained by adding to the apparent density (columns 8 of the tables 9 and 10) the correction for polymerization already discussed.

TABLE 9.—*Measurements of liquid density for sample 4c*

Mass of sample by weighing in..... 8.0392
Mass of sample by weighing out..... 8.0390

Mean value..... 8.0391 grams.

Date (1943)	Temperature t	Volume		Vapor density	Vapor mass	Liquid mass by difference	Liquid density		Col. 5+col. 9 +0.0010674t
		Liquid	Vapor				Apparent	Corrected [a]	
	°C	ml	ml	g/ml	g	g	g/ml	g/ml	g/ml
Oct. 15	−78.72	10.9808	4.711	0.00005	0.0002	8.0389	0.73209	0.73209	0.64811
Oct. 15	−44.92	11.5486	4.144	.00043	.0018	8.0373	.69595	.69595	.64844
Oct. 15	0	12.4463	3.252	.00277	.0089	8.0303	.64519	.64519	.64816
Oct. 20	+53.04	[b] 13.7909	1.833	.01456	.0267	[b] 7.9656	.5776	.5776	.6482
Oct. 21	+53.23	[c] 13.8016	1.824	.01423	.0260	[c] 7.9677	.5773	.5772	.6482
Oct. 27	95.67	15.704	.010	.036	.0004	8.0387	.5119	.5089	.6484

[a] Corrected for compressibility of liquid and for polymerization.
[b] Not including 0.0475 gram of liquid in top capillary next to valve.
[c] Not including 0.0454 gram of liquid in top capillary next to valve.

TABLE 10.—*Measurements of liquid density for sample 4d*

Mass of sample by weighing in..... 7.4635
Mass of sample by weighing out..... 7.4642

Mean value..... 7.4638 grams.

Date (1943)	Temperature t	Volume		Vapor density	Vapor mass	Liquid mass by difference	Liquid density		Col. 5+col. 9 +0.0010674t
		Liquid	Vapor				Apparent	Corrected [a]	
	°C	ml	ml	g/ml	g	g	g/ml	g/ml	g/ml
Nov. 3	−29.79	10.9814	4.71	0.00081	0.0038	7.4600	0.67933	0.67933	0.64844
Nov. 2	0	11.5494	4.146	.00277	.0115	7.4523	.64525	.64525	.64822
Nov. 8	+38.73	12.4487	3.253	.00961	.0313	7.4325	.59705	.59702	.64806
Nov. 9	79.62	13.794	1.914	.02613	.0500	7.4138	.53746	.53709	.64848

[a] Corrected for compressibility of liquid and for polymerization.

The rule of the rectilinear diameter by Cailletet and Mathias states that the sum of the densities of the liquid and the vapor is a linear function of temperature. A graph plotted for numerous substances shows that this rule gives a very close approximation if the rate of change with temperature of the sum of the densities is less than −1, when both variables are expressed in reduced units. The constants given for butadiene by Cragoe [20] lead to the equation

$$\rho_l+\rho_g=0.64817-0.0010674t, \tag{7}$$

where ρ_l and ρ_g are the densities of saturated liquid and vapor, respectively, in grams per milliliter and t is the temperature in degrees centigrade.

It will be seen that the sum of ρ_l, ρ_g, and $0.0010674t$ should be very nearly constant. Such sums are given in column 10 of tables 9 and 10 and are shown graphically as ordinate with temperature as abscissas in figure 16. The densities of the vapor used for this purpose are calculated from equations 4 and 6 in the same manner as the values in table 15 (discussed in section VII).

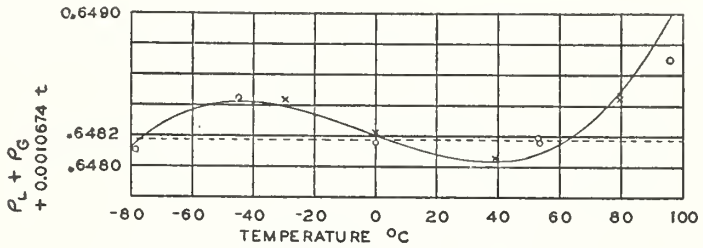

FIGURE 16.—*Comparison of observed with calculated densities of liquid 1,3-butadiene.*

⊙=ρ_l from sample 4c.
×=ρ_l from sample 4d.
----, ρ_l from equation 7.
——, ρ_l from equation 8.

The values calculated from equation 7 are represented by the dotted line in figure 16. The differences between the observed values and these calculated values are somewhat greater than the precision of the observed data, which are better represented by the continuous curve. This curve is calculated from the equation

$$\rho_l+\rho_g=0.64820-0.0010748t+1.6t^2 10^{-8}+1.5t^3 10^{-9}, \qquad (8)$$

in which the notation is the same as in equation 7. The constant 0.64820 in this cubic equation corresponds to a liquid density of 0.64523 g/ml at 0° C. This is nearly the mean of the observations on the two samples at 0° C, and is believed to be correct within a few units in the fifth decimal place. As may be seen from figure 16, equation 8 is in agreement with the observed values within five units in the fifth decimal place in the temperature range −80° to +40° C. Below −60° C the uncertainty in the expansion of the picnometer is relatively large, and above +50° C the observations are less accurate, in consequence of which the data in that temperature range are not considered accurate beyond the fourth decimal place, and above 100° C beyond the third decimal place. Values calculated from equation 8 are given in table 6 (discussed in section VI).

(c) COMPARISON WITH OTHER DATA

The densities measured by other observers are compared with the values calculated from the present formulation in figure 17. Prevost's [21] value for the density near the boiling point is notably low. The low normal boiling point (−4.75° C) for his sample suggests the presence of lighter hydrocarbons as impurities, which would explain the low density. The data given in Landolt-Bornstein [22] appear to be smoothed and have been represented by a dotted curve. The present data are intermediate between those from Pennsylvania State College [23] and those by Dean and Legatski [24]. The latter observers heated the surface of their sample above the average tem-

pcrature of the sample. In consequence, the liquid was subjected to a pressure exceeding the saturation pressure, and at the higher temperatures, where the liquid is more comprcssible, the observed densities may be appreciably too high.

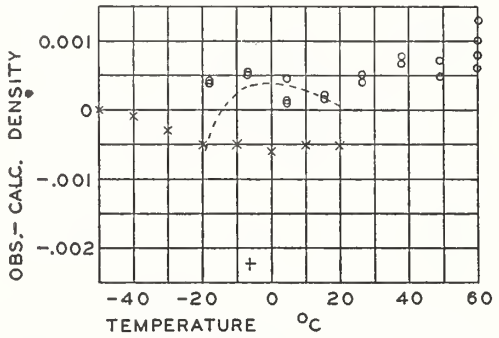

FIGURE 17.—*Comparison of values calculated from equation 16 with data of other observers.*

+=C. Prevost [19]
– – –=I. G. Farbenindustrie [20]
×=Pennsylvania State College [21]
O=M. R. Dean and T. W. Legatski [22]

4. RATE OF POLYMERIZATION

The observations taken during the measuremcnt of liquid density at 79.6° C, together with the assumption that the volumes of 1,3-butadiene and its dimer are additive upon mixing, lead to a rate of dimerization for pure butadiene of 0.12 percent/hr at 79.6° C. This is in very good agrecment with the value 0.11 percent at 82° C found by Robey, Wiese, and Morrell [25], who have made a thorough investigation of the rates of polymerization for pure butadiene and butadiene containing peroxides. It should be noted that in the present work the lower end of the column of butadiene was in contact with mcrcury, which has been reported to be a catalyst for polymerization [26].

5. CRITICAL CONSTANTS

Due to the rapid polymerization of the butadiene samples near the critical statc, accurate direct measurement of critical constants was not possible. The procedure near the critical temperature was to start with the sample in the vapor phase and to compress it by steps, observing thc pressure after each step and watching for the butadiene meniscus to appear. When sample 3b was thus treated at 152.0° C the meniscus suddenly appeared in the middle of the sample. At first it was very faint but soon became much more noticeable. Sudden expansion of the sample was accompanied by a transient opalescence, and as the sample was thus evaporated the meniscus took on the appearance of being considerably below the critical temperature. This cffcct is believed to be due to polymerization. The initial appearance only should be considered, on which basis 152° C is very near the critical temperature.

Sample 4b was observed at 149.0° C. The meniscus, very faint at first, appeared near the mercury at a volume considerably greater

than expected. Although "rain" and "fog" appeared during expansion (a phenomenon characteristic of the region near the critical), the volume at which the meniscus appeared indicated that the specific volume of the saturated vapor was considerably greater than the critical volume, and it was concluded that 149° C is below the critical temperature.

Sample 4a was observed at 157.36° C. The mass of the sample was unknown, hence only relative volumes were observed, but the pressure measurements are probably the best obtained near the critical state. These data are illustrated in figure 18, in which the upper portion

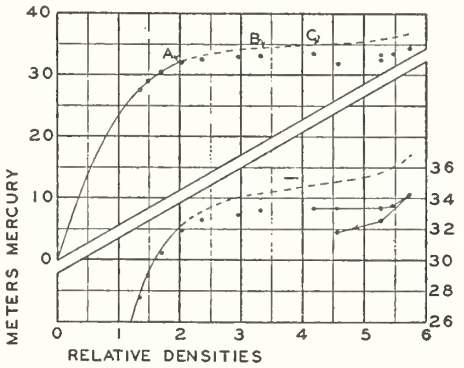

FIGURE 18.—*Isotherm at 157.36° C for sample No. 4a.*

Upper part—General view of whole isotherm.
Lower part—Magnified pressure scale near critical region.
Continuous curve represents calculated values from equation 13, with the assumption that the lowest observed point is unaffected by polymerization. Connected straight lines with arrows indicate chronological order of experiments.
A meniscus appears near mercury.
B meniscus disappears near middle of sample leaving opalescent band 1 or 2 mm wide.
C opalescent band disappears.

illustrates the whole isotherm and the lower portion illustrates the field covered by the observations with an enlarged pressure scale. After being compressed step by step until the highest density observed was reached, the sample was expanded. To avoid ambiguity, part of the points in figure 18 are connected with straight lines and the chronological order is indicated with arrows. The decrease in pressure indicated by the last two observations is obviously the result of polymerization. The continuous curve represents values calculated from the equation of state 6, which is believed to be valid up to about half the critical density, the relative volume scale being adjusted to fit the observed pressure at the lowest density. Assuming the value 0.245g ml^{-1} given in table 13 for the critical density, this adjustment places the critical density on the relative scale at approximately 3.7. The dotted curve was then drawn in to illustrate the path that would be expected had there been no polymerization. The course that this dotted curve should follow is uncertain for two reasons: (1) the rate of polymerization varies with the density, and (2) the data do not furnish an estimate of the effect on pressure of this rate except where pressures were observed with the densities varied in both directions. The short horizontal line in figure 18 represents a calculated pressure obtained from equations 4 and 5, together with the assumption that at the critical density, $(dp/dt)_V$ has a constant value above the critical temperature (152° C), an assumption

made by inference from the behavior of CO_2 and other substances with well-known properties.

The point A (fig. 18) represents the relative volume at which a liquid butadiene meniscus appeared near the mercury. At B this meniscus had approached the middle of the sample and vanished, leaving an opalescent band 1 or 2 mm wide. At C even this band had vanished without reaching the top of the sample. It may be inferred that the polymer at first condensed to form a solution relatively rich in polymers, the solution becoming diluted with more and more of the monomer until the critical temperature of the solution fell below 157° C, and the meniscus, and even the opalescent band, vanished. Thus the phenomenon just discussed, as well as the slope of the isotherm in figure 18, indicates that 157° C is above the critical temperature of pure butadiene. The discrepancy of about 1 atm between the isotherm as drawn and the pressure calculated from the vapor-pressure equation can be attributed to one or more of several causes, namely: (1) polymerization existing already at the first observation, (2) an underestimation of the rate of polymerization during experiments, and (3) a failure of the vapor-pressure equation to represent the facts.

The vapor pressure calculated from equation 4 for the critical temperature (152° C) is 32.42 meters of mercury. This value has been adopted for the critical pressure in producing a consistent set of tables, although the data in figure 18 suggest that the true critical pressure may be slightly lower.

The critical density is best determined from the mean of the data on the density of the liquid and the vapor. Two equations for the mean of these data are given. The linear equation 7 leads to 0.243 g/ml, whereas the cubic equation 8 leads to 0.245 g/ml. As the cubic equation represents the observed values of liquid densities better than the linear equation in the range −80° to +100° C. the larger value 0.245 g/ml is preferred.

The values P_c=32.42 meters of mercury, T_c=152+273.16° Kelvin, and P_c=0.245 g/ml give

$$\frac{p_c V_c}{RT_c}=0.270 \text{ or } \frac{RT_c}{P_c V_c}=3.70.$$

V. PURITY OF SAMPLES AND MELTING POINT OF PURE BUTADIENE

The melting curve of a material provides a sensitive method of determining the amount of impurity that is soluble in the liquid phase and insoluble in the solid phase. Such a curve is shown in figure 19 and was obtained as follows:

Starting with the calorimeter containing the sample (in the solid state) at the temperature A, measured amounts of electric energy were added and the temperature of the calorimeter observed after thermal equilibrium had been established following each heating. The resultant curve, A, E, B, C, gives the temperature of the calorimeter and contents as a function of the energy added. In order to obtain the more useful relation, fraction melted versus temperature,

the line AD is drawn. This is an extrapolation of the part of the curve representing the energy-temperature relation when the material is all solid. The horizontal distance EF from any observed point to the line AD represents the energy that has been used to melt part of the sample, as F represents the temperature energy condition which would have existed if no material had melted. Accordingly the distance DB represents the total heat of melting. Therefore, if the

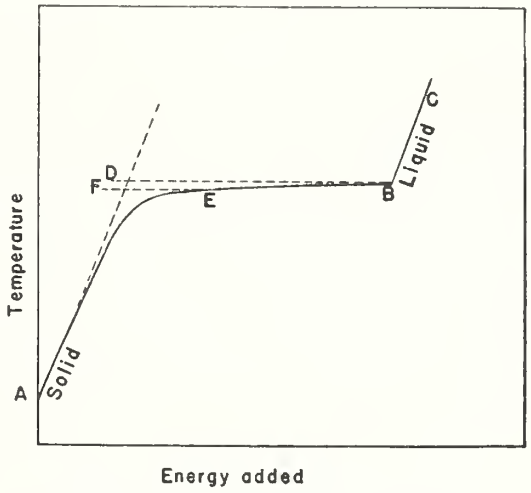

FIGURE 19.—*Illustrative melting curve.*

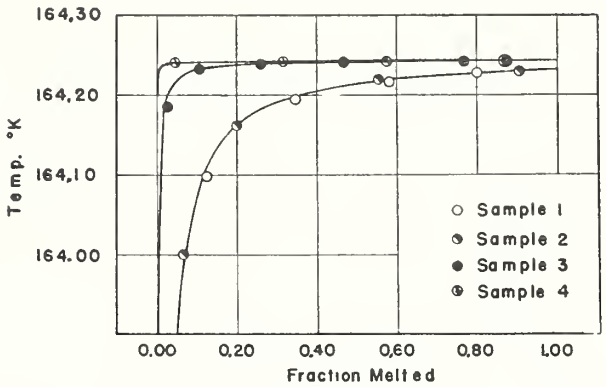

FIGURE 20.—*Melting curves for the four samples of 1,3-butadiene.*

heat of fusion is assumed to be constant, the fraction melted at point E is (EF/DB).

Figure 20 shows the melting curves of the four samples, giving the temperature as a function of the fraction melted. The data represented in these curves were used to obtain values for the purity of the samples and for the melting temperature of pure butadiene. If it is assumed that the impurity is soluble in the liquid and insoluble in the solid, then the curves shown in figure 20 will have approximately the form

$$T_m - T = (a/F), \tag{9}$$

where

T=temperature at a point on the curve
T_m=melting temperature of pure butadiene
F=fraction melted
a=constant=$T_m - T$ (when $F=1$).

This equation is derived from the formula relating the depression of the freezing point of a material with the mole fraction of impurity

$$x=\frac{L_f(T_m-T_f)}{RT_m^2}, \tag{10}$$

where

x=the mole fraction of impurity
L_f=the heat of fusion
T_m=the freezing (melting) temperature of the pure substance
T_f=the temperature at which the liquid containing x mole fraction of impurity starts freezing.

The constants in equation 9 were determined for the melting curve of sample 3, figure 20, by selecting a value of T_m that gave the most constant values for a. The results are shown in table 11. The data on this sample were best represented by equation 9 when 164.244° K was chosen as the value of T_m.

TABLE 11.— *Data from the melt of sample 3*

T_m-T	F	$a=F(T_m-T)$
° K		
0.059	0.027	0.00159
.011	.107	.00118
.005	.260	.00130
.0021	.466	.00098
.0017	.768	.00131
.0013	.872	.00113
	a (mean)	0.00125

The amount of liquid soluble, solid insoluble impurity may now be computed from equation 10. It is seen that the constant a in equation 9 is the same as T_m-T_f in equation 10. Using T_m=164.244° K, $T_m-T_f=a$=0.00125° K, L_f=7980 int. j mole^{-1}, the mole fraction impurity, x, in sample 3 is 0.000045, or 45 moles per million. Calculations of the amounts of impurity in samples 1 and 2 gave 552 moles per million and 516 moles per million, respectively. The treatment of the melting data of samples 1 and 2 yielded a value for T_m 0.006 degrees Kelvin higher than that obtained from the melt of sample 1. These two samples were so nearly alike that the melting data on both samples were well represented by a single curve.

The curve for sample 4, figure 20, shows that this was the purest sample obtained. In fact, the melting curve is so flat that only the point at 4.7 percent melted exhibited any measurable depression of the melting point, and even here it amounted to only 0.001 degree Kelvin. The temperature obtained for the other points on the melting curve was 164.242° K. The liquid soluble, solid insoluble impurity in sample 4 was calculated to be 2 moles per million.

The difference between the values of the melting point of pure butadiene, 164.244 degree Kelvin, obtained from the data on sample 3, and 164.242 degree Kelvin from the data on sample 4, may have been caused by small errors in the calibrations of the resistance bridges used. Two different Mueller bridges were used for these measurements. This difference of 0.002 degree Kelvin is considerably smaller than the absolute accuracy of temperature measurements, as platinum resistance thermometers, calibrated in the same way, can deviate from each other by as much as 0.01 degree centigrade at −110° C. The most probable value of the melting point of pure butadiene, as determined from the data on samples 3 and 4, is 164.243°±0.010° K or −108.917°±0.010° C.

The vapor-pressure measurements at the ice point and above indicated the presence of an impurity that did not appear to affect the melting curves. The vapor pressures of samples 1, 2, and 3 were found to depend somewhat on the fraction condensed, being higher when 95 to 98 percent was condensed than when 75 percent or less was condensed. This indicated the presence of an impurity that was more volatile than butadiene. With sample 3, which was relatively pure according to the melting curve test, the increase in vapor pressure upon condensing most of the sample amounted to about 6 mm at 0° C. The impurity of 45 parts per million, indicated by tne melting curve, was not great enough to have caused this increase in vapor pressure. The more elaborate procedure in preparing sample 4 was carried out primarily for the purpose of improving the vapor-pressure data. When 96 percent of this sample was condensed at 0° C the pressure was only 0.3 mm Hg higher than when 40 percent was condensed.

In figure 14 the continuous curve represents values calculated for a hypothetical liquid having a vapor pressure of 899 mm with 0.001 mole fraction of an ideal-gas impurity that is soluble in the hypothetical liquid to the extent of 5.5×10^{-7} moles/cm^3 of liquid for a partial pressure of 1 mm. These assumptions, together with the mass of the sample (0.0275 g), lead to the equation

$$P=899+\frac{1{,}000}{3.04v+45.4}, \tag{11}$$

where P is the total pressure in millimeters of mercury and v is the volume occupied per gram of sample. Although the curve represents the data for sample 3e very well, the spread in the data permits some variation in the assumed values; moreover, the impurity may not form an ideal solution as assumed.

No specific estimate of the impurity in sample 4b can be made because the spread of the data permits a considerable variation in the value assumed for the solubility of the impurity with a corresponding variation in the estimated amount present. It is evident, however, that the amount of more volatile impurity in sample 4b was considerably less than that in sample 3e.

VI. DERIVED PROPERTIES AND FORMULATED TABLES OF THE THERMODYNAMIC PROPERTIES OF 1,3-BUTADIENE

1. ENTROPY AND ENTHALPY OF SOLID AND LIQUID 1,3-BUTADIENE FROM 15° TO 300° K

The tables of specific heat, together with the value of the heat of fusion, were used to calculate the entropy and enthalpy of solid and liquid butadiene. It was first necessary to obtain values of $C_{sat.}$ between 0° and 15° K, the latter temperature being the lower limit of the observed data. This was accomplished by using the equation

$$C_{sat.}=0.7188D\left(\frac{134}{T}\right), \tag{12}$$

where $C_{sat.}$ is the specific heat in int. j $g^{-1}°K^{-1}$ and $D(\ )$ is the Debye function [11]. This function was selected to represent the data from 15° to 30° K, inclusive. The agreement between the observed values of $C_{sat.}$ and those calculated from equation 12 was not entirely satisfactory, but the function was considered adequate for the purpose of extrapolating the specific heat function to 0° K. The increases in entropy and enthalpy between 0° and 15° K are small compared with the total changes of these quantities between 15° and 300° K, so an error in the function used between 0° and 15° K would have little effect on the values obtained at 300° K.

The calculated values of entropy and enthalpy of the solid and liquid are given at 5-degree intervals in table 12. As different sets of measurements of $C_{sat.}$ were available it was necessary to make a selection in order to use the most reliable values for the calculation of entropy and enthalpy. From 15° to 55° K, inclusive, the data on sample 1 were used, as no other data were available in this temperature range. From 60° K to the triple point (164.24° K) the data of sample 4 were used because this was the purest sample measured. Above the triple point there was no choice between the data obtained for the different samples so the values of $C_{sat.}$ were simply averaged. Column 2 of table 12 gives these values of $C_{sat.}$

TABLE 12.—*Entropy and enthalpy of solid and liquid 1, 3–butadiene*

T	$C_{sat.}$	$S_{sat.}$	$\int_0^T C_{sat.}dT$	$\int_0^T V_{sat.}\frac{dP}{dT}dT$	$H_{sat.}-E_0^g$
			SOLID		
°K	*Int. j g⁻¹°K⁻¹*	*Int. j g⁻¹°K⁻¹*	*Int. j g⁻¹*	*Int. j g⁻¹*	*Int. j g⁻¹*
0	0	0	0	[a]0	0
5	.00291	.0010	.0036	----------	.0036
10	.02322	.0078	.0581	----------	.0581
15	.0747	.0257	.289	----------	.289
20	.1492	.0568	.844	----------	.844
25	.2341	.0991	1.798	----------	1.798
30	.3193	.1493	3.183	----------	3.183
35	.4012	.2047	4.985	----------	4.985
40	.4762	.2633	7.182	----------	7.182
45	.5447	.3234	9.737	----------	9.737
50	.6081	.3841	12.621	----------	12.621
55	.6654	.4448	15.807	----------	15.807
60	.7136	.5050	19.258	----------	19.258
65	.7532	.5637	22.929	----------	22.929
70	.7964	.6210	26.803	----------	26.803
75	.8393	.6775	30.892	----------	30.892
80	.8800	.7329	35.191	----------	35.191
85	.9202	.7875	39.692	----------	39.692
90	.9585	.8412	44.389	----------	44.389
95	.9954	.8940	49.274	----------	49.274
100	1.0302	.9460	54.339	----------	54.339
105	1.0636	.9970	59.574	----------	59.574
110	1.0963	1.0473	64.973	----------	64.973
115	1.1312	1.0968	70.541	----------	70.541
120	1.1685	1.1457	76.289	----------	76.289
125	1.2071	1.1942	82.228	----------	82.228
130	1.2481	1.2423	88.364	----------	88.364
135	1.2926	1.2902	94.715	----------	94.715
140	1.3412	1.3381	101.297	----------	101.297
145	1.3942	1.3861	108.134	----------	108.134
150	1.4521	1.4343	115.246	----------	115.246
155	1.5186	1.4830	122.669	----------	122.669
160	1.5968	1.5324	130.453	----------	130.453
164.24	1.6742	1.5752	137.384	----------	137.384
			LIQUID		
164.24	1.9110	2.4739	284.98	[a]0	284.98
165	1.911	2.4827	286.44	----------	286.44
170	1.912	2.5398	295.99	----------	295.99
175	1.915	2.5952	305.56	----------	305.56
180	1.918	2.6492	315.14	----------	315.14
185	1.922	2.7018	324.74	----------	324.74
190	1.928	2.7531	334.37	----------	334.37
195	1.934	2.8033	344.02	----------	344.02
200	1.941	2.8524	353.71	----------	353.71
205	1.950	2.9004	363.43	.00	363.43
210	1.961	2.9475	373.21	.01	373.22
215	1.973	2.9938	383.05	.01	383.06
220	1.983	3.0393	392.93	.01	392.94
225	1.997	3.0840	402.88	.02	402.90
230	2.010	3.1280	412.90	.02	412.92
235	2.025	3.1714	422.99	.03	423.02
240	2.039	3.2142	433.15	.04	433.19
245	2.055	3.2564	443.38	.05	443.43
250	2.073	3.2981	453.70	.07	453.77
255	2.089	3.3393	464.11	.08	464.19
260	2.107	3.3800	474.60	.10	474.70
265	2.126	3.4203	485.18	.13	485.31
270	2.147	3.4603	495.86	.16	496.02
275	2.170	3.4999	506.65	.19	506.84
280	2.193	3.5392	517.56	.23	517.79
285	2.218	3.5782	528.58	.28	528.86
290	2.242	3.6170	539.74	.33	540.07
295	2.269	3.6556	551.02	.39	551.41
298.16	*2.286*	*3.6799*	*558.22*	*.44*	*558.66*
300	2.296	3.6940	562.44	.46	562.90

[a] Column 5, zero from 0°K to 205°K.

The entropy, S, was calculated by integrating $(C_{sat.}/T)\,dT$ by means of Simpson's rule, and the results were checked by a graphical integration. The increase in enthalpy referred to the solid at absolute zero, $H-E_0^s$, is

$$H-E_0^s=\int_0^T C_{sat.}dT+\int_0^T v\frac{dp}{dT}dT, \tag{13}$$

where v is the specific volume of the liquid and p is the vapor pressure. The integrals were evaluated by Simpson's rule. Values of dp/dT were obtained from equation 5 and values of v from table 13. The calculated values of H were checked by performing the integration $\int_0^T SdT$ and comparing the values so obtained with the quantity $(TS-\mathrm{H}+E_0^s)$, which should equal $\int_0^T SdT$. This provides a check on the internal consistency of the calculations.

TABLE 13.— *Thermodynamic properties of 1,3-butadiene saturated vapor and liquid*

Temperature	log p_{mm}	Pressure	Liquid			Vapor		
			Volume	Density	pv/RT	Volume	Density	pv/RT
°C		mm Hg	ml/g	g/ml		ml/g	g/liter	
−108.92	$\bar{1}$.7157	0.520	1.3092	0.7638	0	364,200	0.00275	0.9999
−100	0.1638	1.46	1.3253	.7545	0	136,890	.0073	.9998
−90	.6064	4.04	1.3440	.7440	0	52,230	.0191	.9995
−80	.9960	9.91	1.3633	.7335	0	22,450	.0445	.9989
−70	1.3410	21.93	1.3833	.7229	.0001	10,660	.0938	.9978
−60	1.6482	44.49	1.4041	.7122	.0003	5,503	.1817	.9961
−50	1.92334	83.8	1.4257	.70140	.0005	3,050	.3279	.9935
−40	2.17098	148.2	1,4483	.69048	.0008	1,795	.5572	.9897
−30	2.39492	248.3	1.4718	.67945	.0013	1,112	.8993	.9847
−20	2.59836	396.6	1,4964	.66826	.0020	719.8	1.3892	.9781
−10	2.78399	608.1	1.5224	.65685	.0030	483.8	2.0668	.9698
0	2.95410	899.7	1.5499	.64522	.0044	335.9	2.977	.9595
10	3.11060	1,290	1.5790	.63331	.0062	239.8	4.171	.9473
20	3.25510	1,799	1.6102	.62106	.0086	175.3	5.706	.9330
25	3.32332	2,105	1.6265	.61480	.0100	151.0	6.621	.9250
30	3.38906	2,449	1.6436	.60842	.0115	130.8	7.647	.9164
40	3.51363	3,263	1.6797	.59533	.0152	99.3	10.069	.8976
50	3.62984	4,264	1.7191	.58169	.0197	76.6	13.060	.8763
60	3.73862	5,478	1.7624	.5674	.0251	59.8	16.73	.8526
70	3.84074	6,930	1.8104	.5524	.0317	47.2	21.20	.8260
80	3.93692	8,648	1.8643	.5364	.0396	37.5	26.66	.7967
90	4.02780	10,661	1.9259	.5192	.0490	30.0	33.33	.7640
100	4.11397	13,001	1.9975	.5006	.0604	24.1	41.54	.7274
110	4.19604	15,705	2.0833	.480	.0741	19.3	51.82	.686
120	4.27459	18,820	2.1909	.456	.0910	15.4	65.08	.638
130	4.35029	22,400	2.3351	.428	.113	12.0	83.17	.579
140	4.42389	26,540	2.5652	.390	.143	9.0	111.41	.500
150	4.49639	31,360						
152	4.51087	32,420	4.08	0.245	0.270	4.08	245	0.270

TABLE 13.—*Thermodynamic properties of 1, 3-butadiene saturated vapor and liquid*—Continued

Temperature	Enthalpy			Entropy			$C_{sat.}$	
	$H-E_0^*$ liquid	Evaporation	$H-E_0^*$ vapor	Liquid	Evaporation	Vapor	Liquid	Vapor
°C	*Int. j/g*	*Int. j/g*	*Int. j/g*	*Int. j/g° C*	*Int. j/g° C*	*Int. j/g° C*	*Int. j/g° C*	*Int. j/g° C*
−108.92	(284.98)	509.7	794.87	(2.4739)	3.1035	5.5782	(1.911)	−2.18
−100	(302.05)	501.2	803.30	(2.5749)	2.8944	5.4695	(1.914)	−1.934
−90	321.22	491.8	813.06	2.6826	2.6853	5.3679	1.922	−1.689
−80	340.50	482.7	823.18	2.7850	2.4989	5.2839	1.933	−1.471
−70	359.90	473.7	833.63	2.8829	2.3318	5.2147	1.947	−1.271
−60	379.45	464.9	844.38	2.9769	2.1811	5.1580	1.965	−1.090
−50	399.24	456.2	855.45	3.0675	2.0443	5.1118	1.990	−.926
−40	419.29	447.5	866.78	3.1555	1.9192	5.0748	2.019	−.776
−30	439.63	438.7	878.33	3.2408	1.8041	5.0449	2.048	−.641
−20	460.33	429.7	890.08	3.3241	1.6975	5.0216	2.083	−.518
−10	481.40	420.6	901.98	3.4055	1.5982	5.0037	2.122	−.407
0	502.88	411.1	913.99	3.4854	1.5050	4.9904	2.163	−.308
10	524.80	401.2	926.04	3.5640	1.4170	4.9810	2.207	−.220
20	547.24	390.9	938.11	3.6414	1.3333	4.9747	2.258	−.141
25	558.66	385.5	944.12	3.6798	1.2928	4.9726	2.286	−.108
30	570.23	379.9	950.11	3.7180	1.2531	4.9711	2.313	−.073
40	593.82	368.2	962.01	3.7940	1.1757	4.9697	2.367	−.014
50	618.01	355.7	973.72	3.8694	1.1007	4.9701	2.427	+.033
60	642.87	342.3	985.17	3.9442	1.0274	4.9716	2.489	+.070
70	668.41	327.8	996.25	4.0187	.9554	4.9741	2.551	+.093
80	694.67	312.2	1006.84	4.0930	.8839	4.9769	2.617	+.099
90	721.71	295.1	1016.77	4.1671	.8125	4.9796	2.688	+.084
100	749.59	276.2	1025.79	4.2411	.7402	4.9813	2.769	.038
110	778.5	255	1033.5	4.316	.665	4.981	2.87	−.06
120	808.9	230	1039.2	4.392	.586	4.978	3.02	−.24
130	841.4	200	1041.6	4.471	.496	4.967	3.34	−.63
140	878.8	158	1036.9	4.558	.383	4.941	----------	----------
150	----------	----------	----------	----------	----------	----------	----------	----------
152	(978)	0	(978)	(4.79)	0	(4.79)	----------	----------

2. THERMODYNAMIC PROPERTIES OF LIQUID AND VAPOR 1,3-BUTADIENE FROM −109° TO +150° C

The experimental data previously described, together with data on the specific heat of the vapor [4], have been used as a basis for the formulation of a consistent set of values for the thermodynamic properties given in tables 13 and 14. The values given in these tables were calculated from the following empirical equations: vapor pressure (eq 4), vapor density (eq 6), liquid density (eq 8), and

$$C_p^\circ = 1.3660 + 0.00445t - 1.88 \times 10^{-8}(t-30)^3, \qquad (14)$$

where C_p° is the specific heat of the vapor at zero pressure in international joules per gram degree centigrade, and t is in degrees centigrade.

TABLE 14.—*Thermodynamic properties of 1.3-butadiene superheated vapor*

Temperature	C_p°	$C_{p\ sat.}-C_p^\circ$	$H^\circ-E_0^\circ$	$H^\circ-H_{sat.}$	S°	$S^\circ-S_{sat.}$	$H^\circ-H_{1\ atm}$	$S^\circ-S_{1\ atm}$	$(pV/RT)_{1\ atm}$	$(1/V)_{1\ atm}$
°C	*Int. j/g °C*	*Int. j/g °C*	*Int. j/g °C*	*Int. j/g °C*	*Int. j/g °C*	*Int. j/g °C*	*Int. j/g*	*Int. j/g °C*		*g/liter*
−108.92	0.932	0.0000	794.9	0.00	4.4580	−1.1201	----------	--------	----------	--------
−100	.962	.0001	803.31	.01	4.5081	−0.9614	----------	--------	----------	--------
−90	.998	.0003	813.10	.04	4.5632	−.8047	----------	--------	----------	--------
−80	1.035	.0006	823.27	.09	4.6172	−.6667	----------	--------	----------	--------
−70	1.073	.0011	833.81	.18	4.6704	−.5443	----------	--------	----------	--------
−60	1.113	.0023	844.74	.36	4.7229	−.4351	----------	--------	----------	--------
−50	1.153	.0040	856.07	.62	4.7748	−.3370	----------	--------	----------	--------
−40	1.194	.0067	867.81	1.03	4.8263	−.2483	----------	--------	----------	-------
−30	1.237	.0106	879.96	1.63	4.8773	−.1676	----------	--------	----------	--------
−20	1.279	.0153	892.54	2.46	4.9280	−.0936	----------	--------	----------	--------
−10	1.323	.0229	905.55	3.57	4.9784	−.0253	----------	--------	----------	--------
0	1.366	.032	919.00	5.01	5.0286	+.0382	4.21	0.0102	0.9660	2.496
10	1.410	.044	932.88	6.84	5.0785	.0975	3.95	.0093	.9696	2.400
20	1.455	.059	947.21	9.10	5.1282	.1535	3.72	.0085	.9726	2.311
25	1.477	.068	954.54	10.42	5.1530	+.1804	3.60	.0081	.9740	2.268
30	1.499	.078	961.98	11.87	5.1777	+.2066	3.48	.0078	.9753	2.228
40	1.544	.101	977.20	15.19	5.2271	.2574	3.30	.0071	.9777	2.152
50	1.588	.130	992.86	19.14	5.2764	.3063	3.11	.0066	.9798	2.081
60	1.632	.167	1008.97	23.80	5.3254	+.3538	2.94	.0060	.9817	2.014
70	1.676	.214	1025.51	29.26	5.3744	.4003	2.78	.0056	.9833	1.952
80	1.720	.275	1042.49	35.65	5.4231	.4462	2.64	.0051	.9848	1.894
90	1.762	.356	1059.90	43.13	5.4718	.4922	2.50	.0048	.9861	1.840
100	1.805	.470	1077.74	51.95	5.5202	.5389	2.38	.0044	.9873	1.789
110	1.846	.641	1095.99	62.51	5.5684	+.5874	2.26	.0041	.9884	1.740
120	1.886	.925	1114.65	75.42	5.6166	.6391	2.15	.0038	.9893	1.694
130	1.926	1.508	1133.71	92.10	5.6644	.6973	2.04	.0036	.9902	1.651
140	1.964	----------	1153.16	116.29	5.7121	.7706	1.95	.0033	.9910	1.610
150	2.001	----------	1172.99	--------	5.7594	--------	1.85	.0031	.9917	1.571
200	----------	----------	----------	--------	--------	--------	[a]1.5	[a].002	[a].994	[a]1.400
300	----------	----------	----------	--------	--------	--------	[a]1.0	[a].001	[a].997	[a]1.152
400	----------	----------	----------	--------	--------	--------	[a]0.7	[a].001	[a].999	[a]0.980
500	----------	----------	----------	--------	--------	--------	[a].5	[a].000	[a].999	[a].852
600	----------	----------	----------	--------	--------	--------	[a].3	[a].000	[a]1.000	[a].755

[a] These values are obtained by extrapolation of the equation of state beyond the temperature range in which there are experimental data.

Equation 14 is in reasonable agreement with results recently reported [28, 29] and represents the results reported by Scott and Mellors [4] as follows:

Temperature	Specific heat, C_p° int. j/g °C	
	Reported	Calculated, eq 14
°C		
−35	1.217	1.215
0	1.366	1.366
40	1.549	1.544
80	1.721	1.720

Values of the tabulated quantities $H^\circ - E_0^s$ and S° for the vapor were calculated from equations obtained by substituting the definitions $dH = C_p dT$ and $dS = (C_p/T)dT$ in equation 14 and performing the integration. These equations are

$$H^\circ - E_0^s = 919.00 + 1.3660t + 0.002225t^2 - 0.47 \times 10^{-8} (t-30)^4 \tag{15}$$

and

$$S^\circ = 0.93615 + 1.55252 \log T - 0.0007335T + 8.549(10)^{-6}T^2 - 6.2667(10)^{-9}T^3, \tag{16}$$

where E_0^s is the internal energy of the solid at absolute zero, H° in international joules per gram, and S° in international joules per gram degree centigrade represent the ideal gas state at 1-atm pressure, t is in degrees centigrade, and $T = t + 273.16$. The constants of integration were chosen to make the calculated values for the liquid agree as closely as possible with the values in table 12.

The tabulated values for the specific heat of the liquid were calculated from the specific heat of the vapor with the aid of the following exact thermodynamic relations:

$$(C_s)_g = (C_s)_l + T\frac{d(L/T)}{dT} \tag{17}$$

$$(C_p)_{sat.} = (C_s)_g + T\left(\frac{\partial V}{\partial T}\right)_p \left(\frac{dp}{dT}\right)_{sat.} \tag{18}$$

$$C_v = C_p - T\left[\left(\frac{\partial V}{\partial T}\right)_p \left(\frac{\partial p}{\partial T}\right)_V\right] \tag{19}$$

$$C_v^\circ = C_v - \int_\infty^V T\left(\frac{\partial^2 p}{\partial T^2}\right)_V dV \tag{20}$$

$$C_p^\circ = C_v^\circ + R, \tag{21}$$

where $(C_s)_g$ and $(C_s)_l$ are the specific heats of saturated vapor and liquid, respectively, C_p and C_v are the specific heats of the vapor at constant pressure and volume, respectively, and C_p° and C_v° are the corresponding values at zero pressure. The procedure just described may appear to be reversed from the normal, as the experimental values of specific heat of the liquid are the more accurate and had already been tabulated in table 12. These values did not extend above

574278 O - 61 - 30

20° C, however, and at least a tentative formulation for the vapor would have been necessary to obtain values for the liquid above that temperature. Moreover, formulation for the liquid is necessarily limited to temperatures below the critical, whereas the limitations for the procedure used depend only upon the accuracy with which the chosen formula can be extrapolated.

The tabulated valus of L and L/T were calculated from the Clapeyron equation written in the dimensionless form

$$\frac{L}{RT}=\left[\left(\frac{pV}{RT}\right)_g-\left(\frac{pV}{RT}\right)\right]_l\left(T\frac{d\ ln\ p}{dT}\right), \tag{22}$$

values of pV/RT from table 13 being used. The quantity $T(d\ ln\ p)/dT$ was calculated from equation 5. Values of the quantity $d(L/T)/dT$ were calculated from the values of L/T by the Rutledge method. The various other derivatives were obtained through differentiation of equation 8.

The tabulated values of enthalpy and entropy were calculated from the equations

$$\frac{H^0-H}{RT}=\frac{14.1747(T_c/T)^2 10^{-0.045(Tc/T)^2}+68.4(1-10^{-0.045(Tc/T)^2})-148}{V}-\frac{36(T_c/T)^4+7}{2V^2} \tag{23}$$

$$\frac{S^0-S}{R}=\ln\frac{1.5171T}{V}+\frac{14.1747(T_c/T)^2 10^{-0.045(Tc/T)^2}-68.4(1-10^{-0.045(Tc/T)^2})+1.48}{V}-\frac{18(T_c/T)^4-3.5}{2V^2}, \tag{24}$$

where V is in milliliters per gram, $H°$ and $S°$ are given by equations 14 and 15, and R is 0.15369 int. j/g°C. Equations 23 and 24 were derived from equation 8. The values in table 13 are in excellent agreement with values interpolated from table 12. Except for the values shown in parentheses in table 13, which were obtained from table 12, the largest differences are 0.05 int. j/g in the enthalpy at −70° C, 0.0002 int. j/g°C in the entropy at several temperatures, and 0.002 int. j/g°C in the specific heat of the saturated liquid.

In order to retain accuracy on differences, most of the items in table 13 and some in table 14 are given to more places than the accuracy of the individual values would warrant. Although in some cases the values in the tables may be in error by a somewhat greater amount, the following are considered reasonable tolerances:

1. Vapor pressures: 0.1 mm or slightly better at low temperatures, 0.05 to 0.1 percent for −20° to +110° C, and about 1 percent at the critical temperature.
2. Liquid densities: 0.00005 g/ml near zero,
   0.0001 between −30 and +30° C,
   0.001 below 100° C.
3. Vapor densities: 0.1 or 0.2 percent,
   1 or 2 percent near the critical temperature.

4. Enthalpy of evaporation: Same as vapor densities.
5. Specific heats: Liquid below 20° C about 0.1 percent, the uncertainty increasing at higher temperatures, becoming very large near the critical temperature: vapor between −35° and +80° C about 0.5 percent, the uncertainty increasing greatly as the critical temperature is approached.
6. Enthalpy and entropy differences: Same as for specific heats.

The assistance of L. A. Matheson, of the Research Laboratory, Dow Chemical Co., in providing pure 1,3-butadiene for this investigation is gratefully acknowledged. The authors express their thanks to Patricia Husbands, who performed a large part of the calculations involved in determining the constants of the equations in this formulation and in preparing tables 13 and 14.

VII. REFERENCES

[1] R. B. Scott, R. D. Rands, Jr., F. G. Brickwedde, Report to the Office of the Rubber Director (July 23, 1943).
[2] C. H. Meyers, R. B. Scott, F. G. Brickwedde, R. D. Rands, Jr., Report to the Office of the Rubber Director (June 30, 1943).
[3] L. A. Wood and C. F. Higgins, NBS Letter Circular LC710 (1942).
[4] Russell B. Scott and Jane W. Mellors, J. Research NBS **34,** 243 (1945) RP1640.
[5] Martin Shepherd, BS J. Research **12,** 185 (1934) RP643.
[6] J. C. Southard and F. G. Brickwedde, J. Am. Chem. Soc. **55,** 4378 (1933).
[7] J. C. Southard and R. T. Milner, J. Am. Chem. Soc. **55,** 4384 (1933).
[8] Harold J. Hoge and F. G. Brickwedde, J. Research NBS **22,** 351 (1939) RP1188; **22,** 217 (1942) RP1454.
[9] N. S. Osborne, BS J. Research **4,** 609 (1930) RP168.
[10] N. S. Osborne, H. F. Stimson, T. S. Sligh, and C. S. Cragoe, BS Sci. Pap. **20,** 65 (1925) S501.
[11] J. A. Beattie, J. Math. Phys. **6,** 1 (1926).
[12] N. S. Osborne, H. F. Stimson, and D. C. Ginnings, NBS J. Research **23,** 197 (1939) RP1228.
[13] C. H. Meyers, J. Am. Chem. Soc. **45,** 2135 (1923).
[14] C. H. Meyers and R. S. Jessup, BS J. Research **6,** 1061 (1931) RP324.
[15] G. K. Burgess, BS J. Research **1,** 635 (1928) RP22.
[16] Wm. E. Vaughan, J. Am. Chem. Soc. **54,** 3863 (1932).
[17] G. B. Heisig, J. Am. Chem. Soc. **55,** 2304 (1933).
[18] G. Moor and E. K. Kanep, Trans. Experimental Research Lab., Chemgas [III] Leningrad (1936).
[19] A. B. Lamb and E. E. Roper, J. Am. Chem. Soc. **62,** 806 (1940).
[20] C. S. Cragoe, NBS Letter Circular LC 736 (1943).
[21] C. Prevost, Comp. rend. **186,** 1209 (1928).
[22] I. G. Farbenindustrie Ludwigshafen (1929) Landolt-Bornstein Physical Chemical Tables, 5th edition, 2d supplement, part I, page 207.
[23] Some physical constants of seven four-carbon-atom hydrocarbons and neopentane, Petroleum Refining Laboratory, Pennsylvania State College, Thesis (1941).
[24] M. R. Dean and T. W. Legatski, Ind. Eng. Chem. **36,** 7 (1944).
[25] R. F. Robey, H. K. Wiese, and C. E. Morrell, Ind. Eng. Chem. **36,** 3 (1944).
[26] The storage of 1,3-butadiene, Research Bul. 7.381–B, Mellon Inst. Ind. Research.
[27] C. H. Meyers, BS J. Research **11,** 691 (1933) RP616.
[28] J. G. Aston, G. W. Moessen, H. C. Hardy, and G. J. Szasz, J. Chem. Phys. **12,** 458 (1944).
[29] D. H. Templeton, D. D. Davies, and W. A. Felsing, J. Am. Chem. Soc. **66,** 2033 (1944).

Washington, April 30, 1945.

DEPARTMENT OF COMMERCE
BUREAU OF STANDARDS
George K. Burgess, Director

SCIENTIFIC PAPERS OF THE BUREAU OF STANDARDS, No. 501
[Part of Vol. 20]

SPECIFIC HEAT OF SUPERHEATED AMMONIA VAPOR

BY

N. S. OSBORNE, Physicist
H. F. STIMSON, Physicist
T. S. SLIGH, JR., Physicist
C. S. CRAGOE, Physicist

Bureau of Standards

March 2, 1925

WASHINGTON
GOVERNMENT PRINTING OFFICE
1925

460/64

SPECIFIC HEAT OF SUPERHEATED AMMONIA VAPOR

N. S. Osborne, H. F. Stimson, T. S. Sligh, Jr., and C. S. Cragoe

ABSTRACT

Measurements of the specific heat at constant pressure of superheated ammonia vapor were made within the range of temperature and pressure ordinarily used in refrigeration, namely, in the temperature interval −15 to +150° C. and at various pressures ranging from 0.5 to 20 atmospheres. Incidentally a few measurements of the Joule-Thomson effect were made in order to evaluate certain small correction terms.

The method employed is a familiar one in calorimetry, that of continuous flow combined with electric heating of the vapor. The principle of this method is to observe the rise in temperature produced by a measured electric power added as heat to a steady stream of vapor flowing through the instrument at a measured rate.

A flow calorimeter, which was developed for the particular purpose of making these measurements on ammonia, is briefly described. Refinements were incorporated into the calorimetric apparatus to limit size and thermal capacity, to secure sensitivity, to avoid thermal leakage, and to control experimental conditions which affect steadiness.

CONTENTS

I. INTRODUCTION

This series of measurements of the specific heat of superheated ammonia vapor is one of a group of experimental investigations of this fluid. The purpose of the whole experimental project has been to provide adequate data for tables of thermodynamic properties of ammonia (already published[1]) suitable for use in refrigeration engineering.

The results of the calorimetric measurements on superheated ammonia vapor have been expressed as values of the specific heat at constant pressure as a convenient intermediate step between the experiments and the final formulation of the properties of the vapor.

The aim has been to obtain calorimetric data for the superheated vapor comparable in accuracy with the results of the other experimental measurements of the group, so that consistent tables might be formulated which would agree throughout with the experimental data.

II. GENERAL DESCRIPTION OF METHOD AND APPARATUS

1. METHOD

The method employed in these measurements of the specific heat[2] is that known as the continuous-flow electric method. This method was used by Callendar and Barnes[3] for measurements of the specific heat of liquids. It has also been used successfully for the measurement of the specific heat of gases by a number of experimenters, notably Swann,[4] Scheel and Heuse,[5] Holborn and Jakob,[6] and Knoblauch and his associates.[7]

Measurements of the specific heat of gases are, in general, more difficult than of solids and liquids because larger volumes of gas must be subjected to the experimental process in order to have heat quantities large enough for accurate measurement. The flow method is particularly suited to calorimetry of superheated vapor because this method allows a large quantity of the vapor to be subjected to experiment in a given time in a relatively small apparatus. The heat capacity of the calorimeter does not enter as a direct element of the measurement, but does affect the time required to reach a steady state.

The principle of the electric-flow method is simple. The procedure is to observe the rise in temperature produced by a measured electric

---

[1] B. S. Circular No. 142, 1st edition; 1923.

[2] The term specific heat as used in this paper will refer to the specific heat at constant pressure; that is, the heat required per unit mass per degree to change the temperature of the vapor when kept at constant pressure.

[3] Brit. Assoc. Report, p. 552; 1897. Phil. Trans., 199 A, p. 55; 1902.

[4] Roy. Soc. Phil. Trans., 210, p. 199; 1910.

[5] Ann. d. Phys., 37, p. 79, 1912; 40, p. 473, 1913; 59, p. 86, 1919.

[6] Zs. des. Verein. Deutsch. Ing., 58, p. 1429, 1914; 61. p. 146, 1917; Phy. Zs., 6, p. 801, 1905.

[7] Zs. des. Verein Deutsch. Ing., 51, p. 81, 1907; 55, p. 665, 1911; 59, p. 376, 1915; 66, p. 418, 1922.

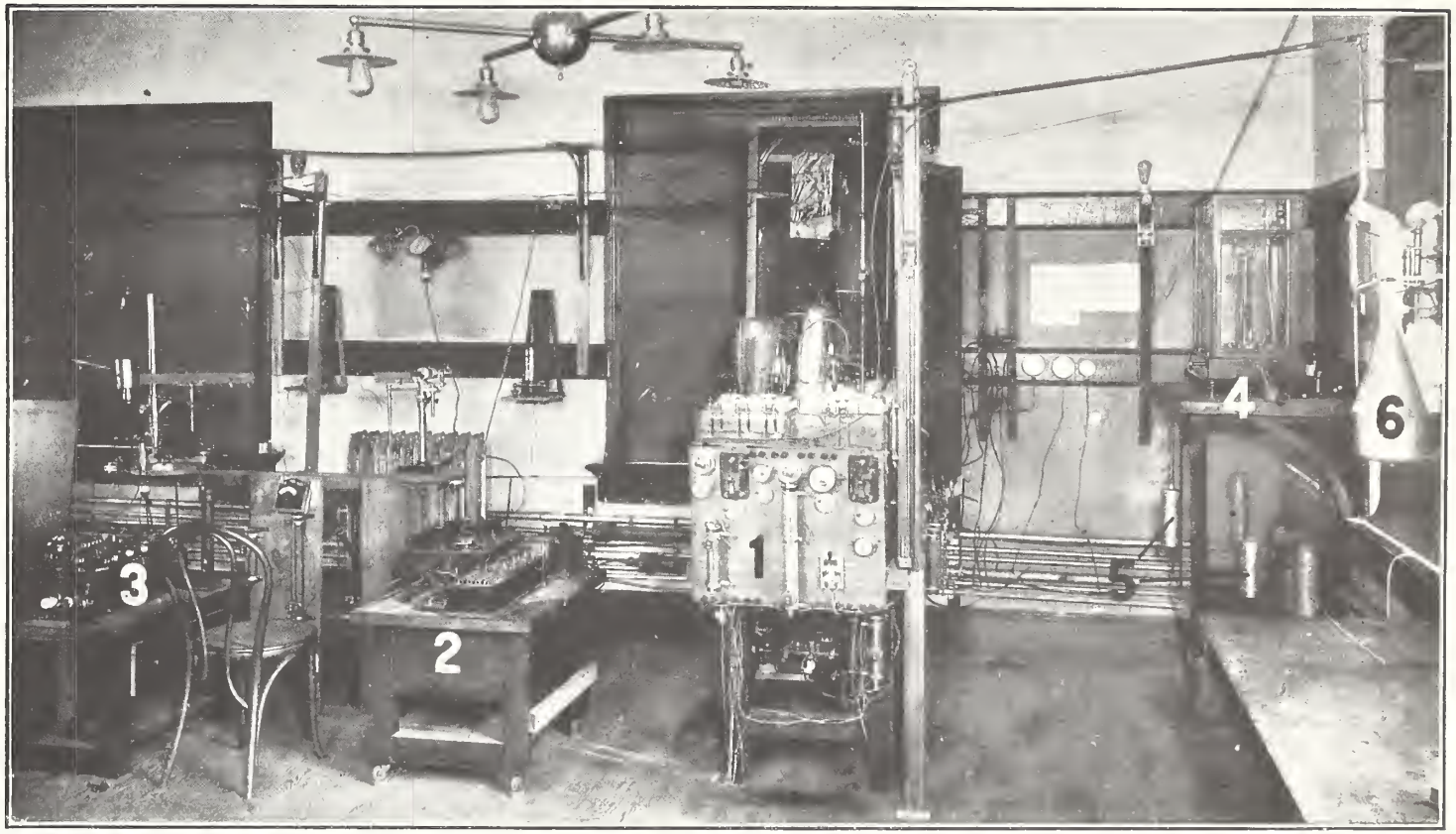

FIG. 1.—*General view of experimental set-up*

1, Assembled calorimeter with operating accessories; 2, potentiometer for observing thermocouples; 3, bridge for observing resistance thermometers; 4, balance and weighing chamber; 5, ammonia containers; 6, vacuum pump

power added as heat to a stream of fluid flowing through the calorimeter at a steady measured rate. In the apparatus described here, the rate of flow, when steady, is measured by condensing and weighing the ammonia vapor discharged from the calorimeter in a known interval of time. The electric power input is obtained from measurements of the potential drop across and the current flowing through the heater. The rise in temperature of the vapor is measured by two platinum resistance thermometers in the vapor stream, one before and one after the electric heater. The accuracy of the specific heat determinations depends to a large extent upon the constancy of these observed quantities during an experiment, and the accuracy with which they are measured. One of the important advantages of this method is that effects which could lead to constant or systematic errors may be eliminated by varying these three principal observed quantities through a series of experiments, and noting the effect on the results. Another important advantage is that the steady state required by the method favors accuracy of the observations because they may be made deliberately.

Other quantities which enter into the determinations of the specific heat as small corrections are heat leakage and the effect of pressure drop. The evaluation of these quantities is discussed in later sections of this paper.

2. ARRANGEMENT OF APPARATUS

A general view of the apparatus as actually used is shown in Figure 1. A diagram of the arrangement of the important parts is shown in Figure 2. The three large heavily dotted squares, *A*, *B*, and *C*, represent stirred, thermally controlled liquid baths. The parts within any one of these squares are supposed to be at or near that particular bath temperature. The first or "boiler bath," *A*, furnishes heat to evaporate the ammonia in the reservoirs, *D*, which are immersed in the liquid. From these reservoirs the vapor passes through three needle valves, *E*, *F*, and *K*, in series, where the pressure is reduced and regulated. Thus far the path of the vapor has been in a region controlled to a uniform temperature. From here the path of the vapor next leads into the second or calorimeter bath, *B*, which is a region of uniform temperature surrounding the calorimeter. Here the vapor first passes through a length of tube to bring it to the bath temperature, and is then led into the calorimeter itself. Within the calorimeter the vapor continues successively through thermometer cell, T_1, heater cell, *H*, and thermometer cell, T_2. From the calorimeter the path of the vapor leads through the throttle valve, *J*, through one or more control orifices, *L*, in parallel, and there leaves the calorimeter bath and enters the third or condenser bath, *C*. Here the ammonia is led into one of the reservoirs, *N*, which are cooled by the bath in order to condense and collect the ammonia.

The cell, H, contains the electric heater, by means of which measured electric power is added to the stream of vapor. Each of the cells, T_1 and T_2, contains a resistance thermometer to measure the temperature of the vapor, one before and one after the addition of the heat. Each of these thermometer cells has a connection to the pressure-measuring apparatus which enables the pressure to be observed simultaneously with the temperature. Two gauges are

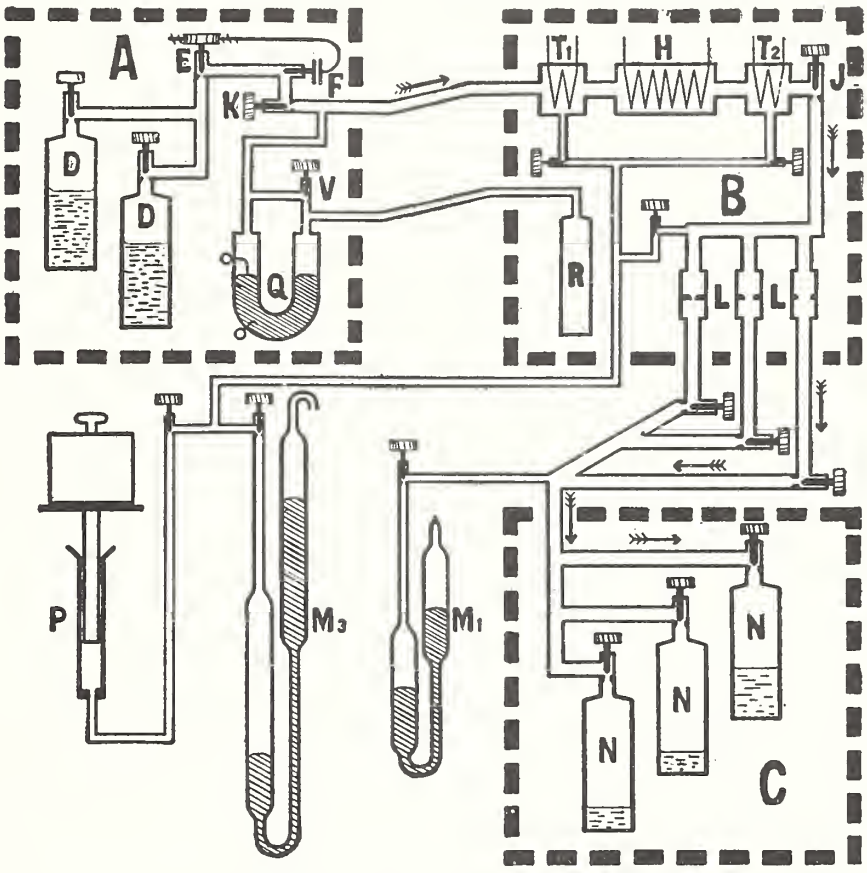

FIG. 2.—*Diagram of general arrangement*

A, boiler bath. *B*, calorimeter bath. *C*, condenser bath. *D*, reservoirs used as evaporators. *E*, *F*, and *K*, valves for regulating rate of flow. *H*, heater cell. T_1 and T_2, thermometer cells. *J*, reducing valve. *L*, flow control orifices. *N*, reservoirs used as condensers. M_1, one-atmosphere mercury manometer. M_3, three-atmosphere mercury manometer. *P*, piston gauge. *Q*, manometer for actuating pressure regulator. *V*, by-pass valve. *R*, reservoir for reference pressure.

provided, one a mercury gauge, M_3, for pressures up to 3 atmospheres, and the other a piston gauge, P, for higher pressures up to 100 atmospheres. The pressure just before the orifices, L, may also be observed by these gauges. The condenser line is provided with a mercury manometer, M_1, for pressures under 1 atmosphere.

The mercury manometer, Q, the reference pressure reservoir, R, and the valves, V, E, and F, are used in the automatic regulation of

pressure before the calorimeter. This pressure regulation combined with the action of the orifice control, L, regulates the flow. Constancy of the flow is a vital requirement of the continuous-flow method of calorimetry.

3. DESCRIPTION OF CALORIMETER

Although the term "calorimeter" might be applied to the entire group of apparatus used to measure the heat in an experimental process, this term will, for convenience, be used here to denote that portion of the apparatus where the experimental process occurs, the place where this process is isolated from external influences so that it may be accurately controlled and observed. The calorimeter and the more important parts of the equipment for its operation will be described in greater detail elsewhere.[8]

The calorimeter was designed and constructed primarily for measuring the specific heat of ammonia vapor at temperatures up to 150° C. and at pressures up to 20 atmospheres. To meet the requirements of the ammonia research it was desirable to combine into one instrument a number of features which are of obvious advantage, but which are not usually all found in a flow calorimeter. Among these features are: Utility over a wide range of temperature and pressure; small size and heat capacity; small thermal leakage; and means for accurately observing temperatures and heat added.

The function of this calorimeter is to provide a system within which we may account for the amount of vapor passing through, the state of the vapor, and the amount of energy added. The predominating influence in the design has been the development of means for conserving the heat added to the system. Our inability to avoid unmeasured leakage of heat limits the accuracy of determining the net amount of heat added, which is a direct factor of the result.

In this "calorimeter system," which is that part of the calorimeter in good thermal contact with the vapor stream between and including the two thermometer cells, the principal ways for loss or gain of heat other than through the electric heater are by (1) conduction, either along the tubes carrying the ammonia, the supports of the system, or the electric lead wires; (2) gaseous conduction and convection; (3) radiation. The second of these was the simplest to control, for it was found that the exhaustion of the space surrounding the calorimeter system to a pressure of 0.001 mm of mercury or less would reduce this element of the thermal leakage to a negligible amount. Heat conduction along the solid connections was controlled by first making the thermal resistance of these connections large and, second, by leading them away from the system to points outside kept at the same temperatures. Transfer of heat by radia-

[8] B. S. Sci. Paper on A Flow Calorimeter for Specific Heats of Gases.

tion was controlled by surrounding the system with metal guards maintained at temperatures nearly identical with the temperatures of the exposed parts of the system within. To make this possible a configuration of the system was devised which would keep practially all the exposed surface approximately at either the initial or the final temperature of the vapor. Only two protecting guards were then necessary, one at each temperature. One of these was kept at the initial temperature by the incoming gas stream and the other was controlled by an auxiliary electric heater and regulated by the observer to maintain that guard surface close to the temperature of the system within. The manner of accomplishing this result will appear as we describe the construction.

An idea of the actual figure of the calorimeter may be obtained from Figure 3. The important elements shown diagramatically in Figure 2 may be recognized here, namely, first thermometer cell, T_1, heater cell, H, and second thermometer cell, T_2. The figure of the channel in which the vapor is led along to the regions where its state is altered and observed is important. To get a clear idea of the thermal shielding we may again follow the path of the vapor through this vital portion of the instrument.

Before entering the calorimeter the vapor passes through a coil of tubing immersed in the bath to bring it to a definite temperature. It is important that on entering the calorimeter the vapor and the parts of the calorimeter in contact with it shall be near equilibrium with the temperature of the bath. To this end the vapor next passes through the coil, B, which is soldered to the calorimeter casing or envelope, and is bathed by the liquid. Thence the vapor tube passes through the envelope and across the vacuum space to the copper guard, G_1. The tube is soldered to this guard, winding spirally upward and then back to the lower end, where it passes inside the guard, G_1, to the entrance of thermometer cell, T_1. It is intended that the guard, G_1, should thus be kept automatically as nearly as possible at the temperature of the vapor as it enters the thermometer cell so that the initial temperature of the vapor may be correctly indicated. The connection, P_1, is for determining the initial pressure of the vapor. In passing from the thermometer cell to the heater cell the vapor is led through a coil of German silver tube bearing the copper shield, S_1, and thence on through the straight inlet tube into the heater cell. This is the place where the vapor enters the region where it is heated. Here the system is narrowed or necked down to the bare essentials to transmit the vapor across, and the shields are brought as close to the vapor tube and to each other as mechanical technique will permit, so that little area may be left exposed to radiation at an intermediate and uncontrolled temperature. The function of this "neck" is to confine, within clearly defined limits, the flow not

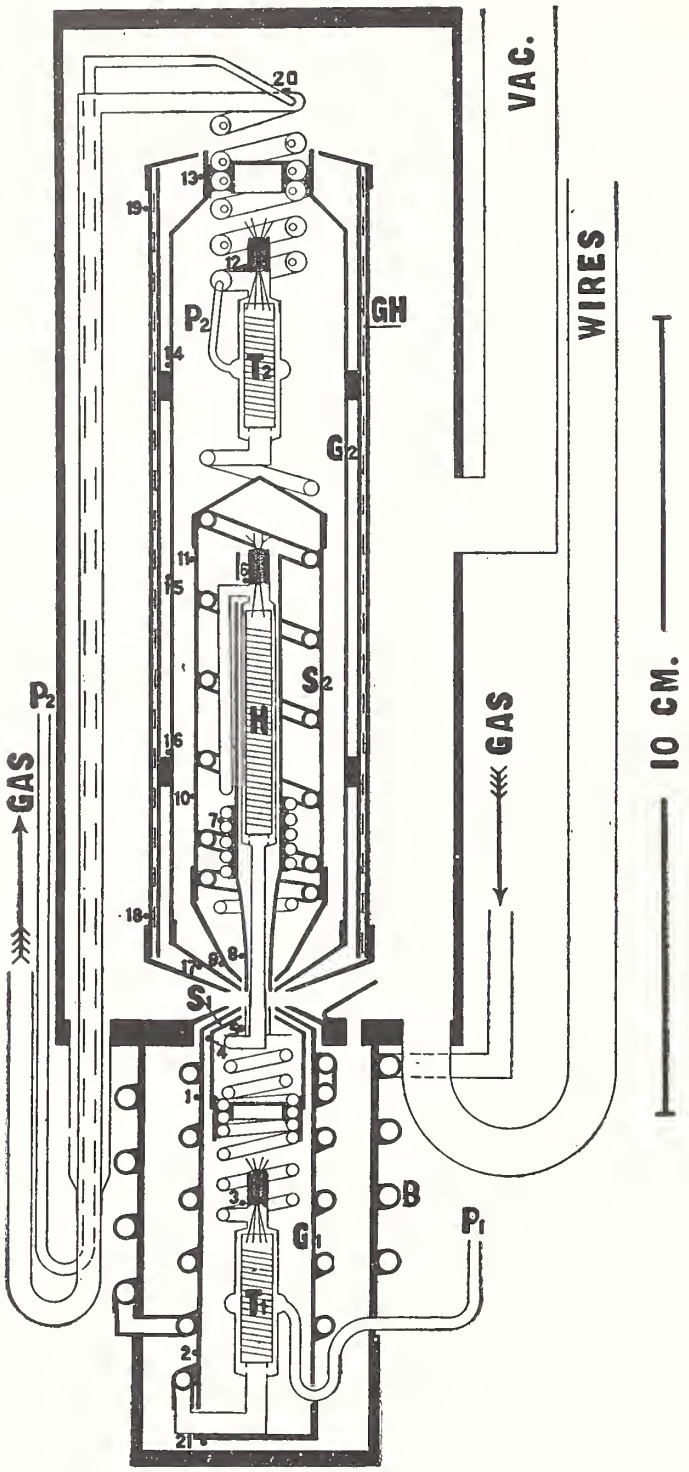

FIG. 3.—*Sectional drawing of calorimeter system (full scale)*

Copper in heavy lines; german silver in light lines; location of thermojunctions indicated by numbered dots. *B*, helix soldered to envelope. *H*, heater cell. T_1 and T_2, thermometers. S_1 and S_2, isothermal shields for conserving heat in calorimeter system. G_1 and G_2, isothermal guards for protecting calorimeter system from thermal leakage. P_1 and P_2, pressure connections to thermometer cells. *GH*, heater for guard G_2. *VAC*, connection to vacuum pump

only of the ammonia vapor, but also of the quantities of heat with which we are dealing.

The vapor enters the heater cell, H, and receives the energy which is added through the electric heater. The parts through which the vapor next flows tend to annul the differences in temperature between the vapor and its flow channel, and to provide temperature control of shielding surfaces to protect the inclosed parts against gain or loss of heat. At the upper end of the heater cell the channel turns abruptly to the side and again downward and then winds spirally for five turns about the cylindrical copper shell which incloses the heater cell itself. The vapor is then led through the coiled tube soldered to the cylindrical copper shield, S_2, so that the shield and vapor tend to approach the same temperature; that is, the final temperature of the vapor. A single spiral turn of german-silver tubing carries this isothermal stream of vapor to the second thermometer cell, T_2.

The vapor then passes on through the six turns of german-silver tubing to the straight channel which, turning abruptly, then leads down and out through the wall of the casing into the bath again. The pressure tube, P_2, is led out from the thermometer cell, T_2, through the flow tube for thermal reasons.

The guard, G_2, incloses virtually all the exposed portion of the calorimeter system which is at the higher or final temperature of the ammonia vapor. This guard is maintained at this same temperature by an electric heater. This heater is located in the annular cylindrical space between two concentric copper shells and is called the guard heater, *GH*. Thermocouples on the guard, on the shield, and on the thermometer cell permit the relative temperatures of these parts to be observed, and these indications are used for gauging the regulation of temperature of the guard so as to annul the thermal leakage to or from the calorimeter system.

Each thermometer coil contained about 54 cm of platinum wire 0.05 mm in diameter wound on a notched mica strip, about seven turns to the mm. The potential terminal arrangement of leads was used and the four platinum leads from each thermometer were brought out of the upper end of the thermometer cell through a glass seal. The heater coil, H, contained about 100 ohms of bare calido wire wound on a mica strip very much like the thermometers. The thermometers had fundamental intervals of 10.8 and 10.7 ohms, so that a sensitivity of the temperature measuring apparatus to 0.001° C. was not difficult to secure. As to the type of lead connections to the thermometers and the manner of their use, it might be inferred that the use of a pair of differentially connected Callendar type thermometers would have been appropriate, as such an arrangement would have required only a single reading of resistance to evaluate

the temperature rise instead of the four readings necessary with the arrangement used. Nevertheless, the choice of the potential terminal type of thermometer was made deliberately for the purpose of obtaining increased accuracy, as other considerations outweighed the one mentioned above.

The size or scale upon which the apparatus has been built has affected both its utility and its construction. In order to avoid useless bulk and thermal capacity which would require either preparation of unnecessarily large amounts of purified ammonia, or else sacrifice either time or accuracy in operation, some effort was made to keep the proportions small.

It had been found by experiment that the metals used in the construction of the calorimeter were not attacked by pure anhydrous ammonia.

4. THERMOREGULATED BATHS

Considerable attention was devoted to the design and construction of temperature control baths, to simplify construction, economize space, and promote reliability of operation. Three baths were used which were similar in general construction, each having modifications to adapt it to the performance of a particular service. Their shape favored the assembling of the calorimetric equipment upon a table in a compact group, the important elements of which were easily accessible, either for manipulation or observation.

Each bath was provided with a control unit which included a screw propeller, a refrigerating coil using carbon dioxide, an electric heating coil, and a thermoregulator, actuated by expansion of a confined liquid. These parts were assembled in a tubular housing which stood vertically in one corner and the rest of the space in the bath was available for installing such parts of the apparatus as required temperature control. The method of control was to overcool somewhat by a proper setting of the carbon dioxide throttle valve, and compensate the overcooling by electric heating, so controlled by an automatic regulating device as to keep the fluctuations of temperature within the desired limits. Extremely fine regulation was necessary only in the calorimeter bath, and it was found possible to control this bath so that no change of more than 0.001° C. could be observed over a period of 30 minutes or longer. The reliability of operation of this thermal control and the relief of the operator from this care was a factor contributing to the character of the final results.

5. REGULATION OF RATE OF FLOW

The rate of flow of the vapor is regulated by controlling the pressure in the line before and after the calorimeter. Use is made of the principle that gaseous flow through an orifice is practically inde-

pendent of the low side or back pressure, provided this pressure is less than a certain fraction of the high side or fore pressure. In applying this principle the ammonia lines are so arranged that the vapor after leaving the calorimeter is discharged into the condenser line through one or more orifices in parallel and the pressure thus reduced to a sufficiently low value. In the experiments with ammonia it was found that when the back pressure in the condenser line was kept less than 0.35 of the fore pressure on the orifices the flow was sensibly dependent only on the pressure in the calorimeter. In consequence, only a rough control on the condenser line pressure is needed, and having this the close regulation of flow results from control of the pressure in the calorimeter. Since constant flow is one of the essentials to accuracy, the device for regulating the calorimeter pressure is a vital part of the apparatus.

The pressure regulator is automatic and operates in a manner similar to the action of a familiar type of temperature regulator. One arm of the manometer, Q (fig. 2), is connected to the flow line ahead of the calorimeter and the other to a reservoir, R, which is immersed in the calorimeter bath for constancy of temperature. The pressure in this reservoir may be adjusted to any chosen reference value by transmitting ammonia through the by-pass valve, V. For automatic control the by-pass valve is closed, and then the pressure in the calorimeter line is balanced against the reference pressure. Departures of the line pressure from this reference value cause the mercury in the manometer to make or break electric contact with the platinum wires sealed through the glass. Making or breaking this contact controls through a relay the direction of rotation of an electric motor, which in turn through a mechanism controls the settings of valves, E and F.

The operation of the regulating device resulted in a periodic fluctuation of the line pressure, the amplitude and period of which were subject to the control of the operator. It was usually found possible to adjust the cycle of operation to a period of from 5 to 10 seconds and a fluctuation of not more than 1 mm of mercury. The device was so sensitive to fortuitous influences that it could not be left unattended for long without danger of spoiling an experiment, but with due vigilance it could be kept functioning indefinitely.

A detailed description, together with photographs of this regulating device, is given elsewhere.[9]

6. MEANS FOR INSURING DRYNESS OF VAPOR

Besides the provision made for observing the quantities from which the specific heat may be derived, there is another factor no less vital to accurate results than any of the refinements in equipment or operation. This factor is the quality of the vapor. Of course, if

[9] See footnote 8, p. 69.

the vapor is truly superheated and the state is truly indicated by the observed temperatures and pressures, no question of quality would be encountered except at the saturation limit. But if on the contrary a liquid spray or fog were to be formed at any place in the stream before it entered the calorimeter, and if these mechanically entrained droplets should be swept on into the calorimeter, the resulting value of the specific heat would evidently be in error on account of the heat required to evaporate this spray in the calorimeter.

The measures taken to avoid this occurrence are for the most part automatic in operation. The evaporation took place at a pressure from three to eight atmospheres higher than the working pressure in the calorimeter. The stream of vapor coming from the reservoirs in the boiler bath, *A* (fig. 2), passed to the needle valve, *E*, in the regulating train. It was then throttled successively in each of the three valves, *E*, *F*, and *K*. Each of these three valve bodies was in very good thermal connection with the boiler bath through a copper bracket soldered to the copper wall of the tank. This connection would tend to supply heat to the stream of ammonia at each valve to compensate for any cooling caused by the throttling. Besides this first approximation to isothermal throttling, further opportunity was given the ammonia stream to reheat between valves, *F* and *K*, and again after valve, *K*, by soldering a length of the flow tube directly to the wall of the tank. In operation the total reduction in pressure in this regulating train of valves was usually from three to eight atmospheres. This process of isothermal throttling in three stages would tend to eliminate any traces of liquid which might otherwise have been swept through.

Besides these precautionary measures to guard against wetness or nonuniformity in the ammonia stream entering the calorimeter, there was an effective means of test which would disclose any sensible effect produced on the result by wetness. This test was the repetition of experiments with different rates of flow. The principle of this test was that if spray or fog were entrained in the process of evaporation, the degree of wetness would depend upon the rapidity of the evaporation, and the elimination of entrained liquid would be the more perfect the slower the flow. Agreement of the resulting values of specific heat for different rates of flow assures us of the proper dryness of the vapor.

7. ACCESSORY APPARATUS

Accessory apparatus, such as vacuum pumps, McLeod gauges, pressure gauges, potentiometers, thermometer bridge, and balance, although essential parts of the experimental set-up, are so familiar and well described elsewhere that they need only be mentioned briefly here. Two vacuum pumps and McLeod gauges were used.

One set was used to evacuate the calorimeter envelope, and the other to evacuate the flow line for the connections to the condenser, as desired. The vacuum pumps are of the mercury-vapor type as designed and described by Stimson.[10]

Two pressure gauges were installed for measuring the pressure of the ammonia vapor during determinations. For pressures up to three atmospheres an ordinary open-end mercury-in-glass manometer was used, supplemented by a barometer. For higher pressures an oil-sealed, dead-weight, rotating piston gauge was used.

A Leeds & Northrup type K slide wire potentiometer was used for the power measurements, and a Wolff-Disselhorst potentiometer for the thermocouple readings. For the resistance thermometer readings a Mueller type Wheatstone bridge[11] with shunt decades was used.

The steel containers with ammonia were weighed on a Rueprecht balance rated at 2 kg capacity. The balance was mounted on a shelf and was provided with suspensions which extended from the scale pans down into an inclosed weighing chamber. (See fig. 1.)

The time signals used to measure the duration of flow in the determinations of the rate of flow were controlled by a Riefler clock with electric contacts.

About 40 valves were used on the closed ammonia system, which must needs be tight for trustworthy experimental work. Considerable study was devoted to the improvement of a type of small needle valve which had already been developed at this bureau for nice experimental work with fluids. Improvement in workmanship was found to be the most important element in attaining reliability. The thread, the stainless-steel conical tip, and the stuffing-box bearing of the stem were all ground or lapped and polished to reduce friction and avoid wear. A paraffin filled fine-grained leather stuffing held between two accurately fitted brass retainers was kept under a steady pressure by a stiff spring. Most of the valves were provided with extended stems of german-silver tubing so that the stuffing boxes could be at room temperature, and the seats at the temperature of the bath. The performance of all the valves was found to be entirely satisfactory, and their dependability both for vacuum and pressure contributed much to the reliability of the experimental results.

III. THEORY OF METHOD

In the preceding section the method of procedure in the experiments and the arrangement of the apparatus have been outlined. Consideration will now be given to the method of computation of the specific heat at constant pressure from the observed data. For this

[10] Jour. Wash. Acad. of Sci. 7, p. 477; 1917.
[11] B. S. Bulletin 13, p. 547; 1916 (Sci. Paper No. 288).

574278 O - 61 - 31

purpose we shall assume that the following quantities have been measured after the calorimeter has reached a steady state:

1. Current in electric heating coil.
2. Potential drop across heating coil.
3. Rate of flow of vapor through calorimeter.
4. Initial and final temperatures of vapor.
5. Initial and final pressures of vapor.
6. Temperature difference between heater shield and guard.

Given these data and some additional data for evaluating the corrections for thermal leakage and Joule-Thompson effect, our problem is to obtain an expression for the specific heat at constant pressure for a definite temperature and pressure.

1. NOTATION AND DEFINITIONS OF QUANTITIES

1, 2 = designations for initial and final states, respectively.
I = heating current, in amperes.
E = potential differences, in volts, across heating coil.
q = general symbol for heat added per unit mass.
Δq = heat added per unit mass for the change from state 1 to state 2.
F = rate of flow of vapor, in grams per second.
v = specific volume of vapor.
p = pressure.
θ = temperature.
$\Delta p = p_2 - p_1$ = pressure change from state 1 to state 2. (Since there is a drop in pressure, Δp is always negative.)
$\Delta\theta = \theta_2 - \theta_1$ = temperature change from state 1 to state 2. (In C_p experiments $\Delta\theta$ is positive, in Joule-Thomson experiments $\Delta\theta$ is negative.)

$p_m = \frac{p_1 + p_2}{2}$ = mean pressure.

$\theta_m = \frac{\theta_1 + \theta_2}{2}$ = mean temperature.

ϵ = internal energy per unit mass.
$H = \epsilon + pv$ = heat content per unit mass.

$\mu = \left(\frac{\partial\theta}{\partial p}\right)_H$ = Joule-Thomson coefficient.

C_p = specific heat at constant pressure.

X = heat added per second by thermal leakage in any experiment.
N = indicated excess of temperature of guard over that of heater shield, expressed in microvolts.
x = coefficient of thermal leakage, in watts per microvolt.

2. DETERMINATION OF C_p

Let us consider a fluid, in this case ammonia vapor, flowing steadily along a channel T_1HT_2 (fig. 4), in which T_1 and T_2 represent thermometer cells and H represents a heater cell. Let S_1 and S_2 be two sections of the channel, the entrance and exit sections. Let $p_1v_1\theta_1\epsilon_1$ be, respectively, the pressure, specific volume, temperature, and internal energy of the vapor as it passes the entrance section and let $p_2v_2\theta_2\epsilon_2$ be the corresponding quantities at the exit section. In these experiments the change of potential energy due to change of level and the change of kinetic energy due to change of speed are, taken together, always less than 0.01 per cent of the work equivalent of the heat added; and since this amount is negligible we may apply the first law of thermodynamics as if the fluid were at rest.

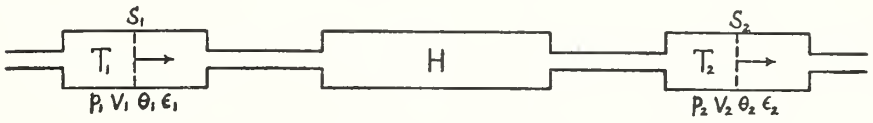

FIG. 4.—*Diagram of calorimeter system*

Since the vapor enters S_1 at the pressure p_1 and issues from S_2 at the pressure p_2 the net external work done by each gram in passing through the apparatus from the state 1 to the state 2 is $(p_2v_2-p_1v_1)$. The sum of this quantity of work and the simultaneous increase of internal energy $(\epsilon_2-\epsilon_1)$ is equal, by the first law, to the quantity of heat added so that we have

$$\Delta q=p_2\,v_2-p_1\,v_1+\epsilon_2-\epsilon_1 \tag{1}$$

all quantities of heat, work, and internal energy being expressed in the same units. But since $H=\epsilon+p\,v$ we have by substitution

$$\Delta q=H_2-H_1 \tag{2}$$

This equation shows that for the flow process under consideration the quantity of heat supplied is equal to the change in heat content. A similar reasoning applied to a constant pressure process also shows that the quantity of heat supplied is equal to the change in heat content so that

$$C_p=\left(\frac{\partial H}{\partial\theta}\right)_p$$

Inasmuch as the change of heat content H_2-H_1, depends only on the initial and final states, it would have been the same if the fall in pressure and the rise in temperature had occurred in two separate steps instead of simultaneously. Let us consider such a process in which the first step consists of an isothermal expansion of the vapor from p_1 to p_2 at the initial temperature θ_1 and the second

consists of a heating from θ_1 to θ_2 at the pressure p_2. The changes in heat content for these two steps are

$$\int_{p_1}^{p_2}\left(\frac{\partial H}{\partial p}\right)_{\theta_1} dp \text{ and } \int_{\theta_1}^{\theta_2}\left(\frac{\partial H}{\partial \theta}\right)_{p_2} d\theta$$

respectively, and the total change in heat content in passing from state 1 to state 2 is

$$H_2 - H_1 = \int_{p_1}^{p_2}\left(\frac{\partial H}{\partial p}\right)_{\theta_1} dp + \int_{\theta_1}^{\theta_2}\left(\frac{\partial H}{\partial \theta}\right)_{p_2} d\theta \tag{3}$$

Making use of the general relation

$$\left(\frac{\partial H}{\partial p}\right)_{\theta} = -\left(\frac{\partial H}{\partial \theta}\right)_{p}\left(\frac{\partial \theta}{\partial p}\right)_{H}$$

and substituting μ for $\left(\frac{\partial \theta}{\partial p}\right)_H$, C_p for $\left(\frac{\partial H}{\partial \theta}\right)_p$, and Δq for $H_2 - H_1$,

equation (3) may be written in the form

$$\int_{\theta_1}^{\theta_2}[C_p]_{p_2}\, d\theta = \Delta q + \int_{p_1}^{p_2}[\mu C_p]_{\theta_1}\, dp \tag{4}$$

The last term in this equation represents the correction for pressure drop. Since the pressure drop in these experiments is small and since the magnitude of this correction is small in comparison with the heat added, Δq, it is sufficiently accurate for our purpose to assume that $[\mu C_p]_{\theta_1}$ varies linearly with pressure, and write

$$\int_{\theta_1}^{\theta_2}[C_p]_{p_2}\, d\theta = \Delta q + [\mu C_p]_{\theta_1 p_m}\, \Delta p \tag{5}$$

The terms on the right of equation (5) may be evaluated by experimental observation, thus giving a value for the heat added in an ideal constant pressure process. But in order to evaluate C_p at definite temperatures and pressures it is necessary to take into account the manner in which C_p changes with temperature, especially near the saturation limit. Assuming that $[C_p]_{p_2}$ is a function of temperature we may apply Taylor's theorem and expand in powers of $(\theta - \theta_m)$ thus

$$[C_p]_{p_2} = [C_p]_{p_2\theta_m} + \left(\frac{\partial C_p}{\partial \theta}\right)_{p_2\theta_m}(\theta - \theta_m) + \left(\frac{\partial^2 C_p}{\partial \theta^2}\right)_{p_2\theta_m}(\theta - \theta_m)^2 + \text{etc.} \tag{6}$$

Integrating both sides of this equation between the limits θ_1 and θ_2, we have

$$\int_{\theta_1}^{\theta_2}[C_p]_{p_2}\, d\theta = [C_p]_{p_2\theta_m}\, \Delta\theta + \left(\frac{\partial^2 C_p}{\partial \theta^2}\right)_{p_2\theta_m}\frac{\Delta\theta^3}{24} + \left(\frac{\partial^4 C_p}{\partial \theta^4}\right)_{p_2\theta_m}\frac{\Delta\theta^5}{1924} + \text{etc.} \tag{7}$$

Combining equations (5) and (7) we have finally

$$[C_p]_{p_2\theta_m}=\frac{\Delta q}{\Delta\theta}+[\mu C_p]_{\theta_1 p_m}\frac{\Delta p}{\Delta\theta}-\left(\frac{\partial^2 C_p}{\partial\theta^2}\right)_{p_2\theta_m}\frac{\Delta\theta^2}{24}-\left(\frac{\partial^4 C_p}{\partial\theta^4}\right)_{p_2\theta_m}\frac{\Delta\theta^4}{1924}-\text{etc.} \quad (8)$$

We now have the desired result, namely, a means for computing the value of C_p at a definite temperature and pressure from the observed quantities and can discuss the physical meaning of the terms. The term $\frac{\Delta q}{\Delta\theta}$ represents the quantity of heat added per degree per gram of vapor. It would equal the specific heat at the mean temperature if the experiment were performed under the ideal condition of constant pressure and in case C_p were constant or a linear function of temperature. The remaining terms in the right member of the equation represent corrections for the departure of the actual experiment from the ideal conditions. The term involving μC_p represents a correction for the pressure drop. For the evaluation of this correction, the Joule-Thomson coefficient μ, must be known with moderate accuracy. The coefficient may be obtained with the same apparatus by means of auxiliary experiments in which the heat added electrically is zero. The remaining terms represent a correction for the variation in C_p with temperature within the temperature interval of the experiment. The magnitude of these terms can be determined only after the approximate values of C_p have been found.

The heat supplied to the vapor per unit time after the system has reached a steady state consists of two parts, namely, the heat developed by the heating coil, EI, and the correction for thermal leakage, X. Denoting by F the mass of vapor flowing per unit time, the heat added to each gram of vapor is

$$\Delta q=\frac{EI+X}{F} \quad (9)$$

A detailed account of the manner of evaluating the correction for thermal leakage is given in a later section of the paper.

3. DETERMINATION OF JOULE-THOMSON COEFFICIENT

As pointed out in the foregoing section, the Joule-Thomson coefficient, μ, can be determined with sufficient accuracy for the evaluation of the correction for pressure drop by performing supplementary experiments in which no heat is supplied electrically. A convenient expression for evaluating μ from the quantities observed in such experiments may be obtained by introducing certain approximations in equation (8). Neglecting second and higher powers of $\Delta\theta$, assuming $[C_p]_{p_2\theta_m}=[C_p]_{p_m\theta_1}=[C_p]_{p_m\theta_m}$, and solving for μ, equation (8) gives

$$\mu=\frac{\Delta\theta}{\Delta p}-\frac{\Delta q}{[C_p]_{p_m\theta_m}\Delta p} \quad (10)$$

These simplifications are very close approximations, since in any Joule-Thomson experiment performed in this calorimeter both $\Delta\theta$ and Δp are small. Since no heat is supplied electrically in these experiments, $EI=O$ and, from equation (9) $\Delta q=\frac{X}{F}$. The above equation then reduces to

$$\mu=\frac{\Delta\theta}{\Delta p}-\frac{X}{[C_p]_{p_m\theta_m}F\Delta p} \tag{11}$$

in which the last term represents a correction for heat leakage.

IV. MATERIAL

The ammonia used in these experiments was prepared by C. S. Taylor of the chemical division of this bureau. The method of preparation has already been described in detail elsewhere [12] and only a brief description of the process of purification is given here.

Commercial anhydrous ammonia, manufactured by the synthetic method, was used as a source of material. A previous analysis of this commercial ammonia indicated that it was very free from impurities with the exception of a small quantity of water. A sample was transferred by distillation from the original container into a small steel container. The first portion was discarded by blowing off the gas phase and about nine-tenths of the remainder was distilled into a similar vessel containing metallic sodium in the form of a fine wire to remove any remaining traces of water. Following this dehydration, about eight consecutive fractional distillations were made, rejecting the first and last tenths in each distillation. The first fractions were removed by blowing off the gas phase during active boiling of the liquid in order to extract the noncondensing gases present. The rejected last fractions, which remained in the container, mainly in the liquid phase, retained most of the soluble impurities.

Tests made upon several samples which were purified by the above process indicated the presence of less than 0.01 per cent by weight of water and less than 0.01 per cent by volume of noncondensing gases in the vapor phase.

A sample of about 500 g was used during the course of the specific heat experiments. As a matter of convenience this sample was distributed among several steel reservoirs which were used alternately as boilers and condensers, thus utilizing the ammonia repeatedly. On two occasions during the interval of time covered by the experiments the vapor pressure of the ammonia was observed in order to test the possibility of its contamination with gaseous impurities either by decomposition of the ammonia or by air leakage through

[12] Composition, Purification and Certain Constants of Ammonia. B. S. Sci. Papers, 18, p. 655; 1923 (Sci. Paper No. 465); also Refrigerating Engineering, 9, p. 213; 1923.

the packings of the valves into the condenser line, which was usually below atmospheric pressure. In both cases the observed pressure was in agreement with the pressure corresponding to the bath temperature as calculated from the results of an independent investigation on the vapor pressure of ammonia [13] within 0.3 mm of mercury which was within the limit of precision of the pressure observation.

V. EXPERIMENTAL DETAILS

1. CALIBRATION OF APPARATUS

THERMOMETERS.—The two platinum resistance thermometers, designated as thermometers 1 and 2, which were used in measuring the initial and final temperatures of the ammonia vapor, were especially designed and constructed for use in the flow calorimeter. These thermometers were placed directly in the vapor stream in order to obtain the best possible indication of the temperature of the vapor. This, of course, required that they be permanently installed in the calorimeter and that means be devised for their calibration in place. They were calibrated after the calorimeter was assembled by comparison with a third standard resistance thermometer. This reference standard thermometer was immersed, throughout the comparisons and experiments, in the stirred liquid bath used to control the temperature of the calorimeter. This thermometer was used not only to calibrate thermometers 1 and 2, but also to observe the temperature of the calorimeter bath in actual experiments for the purpose of checking the nicety of the temperature regulation.

In order to bring thermometers 1 and 2 to the temperature of the reference standard for the purpose of intercomparisons, a stream of hydrogen gas at about atmospheric pressure was passed through the calorimeter. Hydrogen was used as a medium for promoting thermal equilibrium on account of its high thermal conductivity and low Joule-Thomson effect. During the comparisons, hydrogen was also admitted into the envelope space, ordinarily evacuated, to favor still further the attainment of thermal equilibrium throughout the system. For the rates of flow used, the drop in pressure of the hydrogen was not enough to cause any appreciable rise in temperature due to the Joule-Thomson effect.

Comparisons were made previous to and during the course of the experiments as follows:

Date	Temperatures of comparisons
May, 1921	40°, 0°, 50°
February 21, 1922	25°, 50°.
February 23, 1922	50°, 75°, 100°, 125°.
March 8, 1922	50°, 75°, 100°, 125°, 150°.
March 13, 1922	−40°, −20°, 0°.
March 14, 1922	−40°, 0°.
March 15, 1922	−40°.

[13] B. S. Sci. Papers, 16, p. 1; 1920 (Sci. Paper No. 369); also Jour. Amer. Chem. Soc., 42, p. 206; 1920; and Jour. Amer. Soc. Refrg. Eng., 6, p. 307; 1920.

The platinum resistance thermometer, used as a reference standard in these comparisons and designated as Pt_7, had been in use as a working standard in the thermometer laboratory of this bureau for several years. Its history during this time indicated constancy and reliability. The complete calibration as a primary standard at 0, 100, and 444.6° (sulphur boiling point) had been recently verified. In addition, ice point observations were frequently made during the progress of the experiments as a check on its constancy.

The constants in the Callendar equation for Pt_7 and the constants for 1 and 2 determined from the above comparisons are:

Thermometer	R_0	$R_{100}-R_0$	δ
Pt_7	25.6093	9.9870	1.490
1	27.7266	10.8122	1.485
2	27.5069	10.7243	1.470

The calibration indicated that the readings of thermometers 1 and 2 were reliable to about 0.003° C., with a maximum error of possibly 0.005° C. at the higher temperatures. The sensitivity of the temperature measuring apparatus was such that readings were always possible to 0.001° C.

Pressure Gauges.—Observations of pressure were made for two purposes. The absolute value of the pressure was one of the specifications of the state of the ammonia vapor subject to the calorimetric measurement. For this purpose high accuracy in the pressure measurement was not necessary, since the specific heat does not change rapidly with changing pressure. The other purpose of the pressure observation was to evaluate the correction term for the drop in pressure which the vapor experienced in passing through the calorimeter, and for this purpose high sensitivity could be utilized.

The three-atmosphere gauge permitted direct observations of the pressure by reading the height of the mercury column upon a steel tape graduated in millimeters. The piston gauge, which was used for measuring pressures above three atmospheres, had been calibrated previously for use in another investigation by direct comparison with an open-end mercury manometer. In actual use the pressure of the ammonia vapor was transmitted to the piston gauge, first through a short mercury manometer and thence through oil to the piston. This small manometer served to indicate when the piston was in equilibrium and with a given load on the piston served to measure small pressure differences. The reading of each of these gauges could be estimated to a fraction of a millimeter of mercury.

Auxiliary Apparatus.—The auxiliary measuring apparatus consisting of the Wheatstone bridge used for the resistance thermometer observations, the two potentiometers and the electrical standards used with them, and the standard weights used in the measurements of rates of flow, had all been recently calibrated at this bureau.

2. EXPERIMENTAL PROCEDURE IN DETERMINATIONS OF C_p

Preparatory to a series of determinations, one or more reservoirs, each closed by a valve and each containing about 200 g of the purified ammonia, were placed in the boiler bath and connected to the vapor supply line leading to the calorimeter. Two or more similar reservoirs, each containing only a small amount of ammonia, were weighed, placed in the condenser bath, and connected to the discharge line from the calorimeter. The entire line from the boilers to the condensers was then evacuated, filled with ammonia vapor at about atmospheric pressure, and reevacuated to remove impurities.

At the beginning of an experiment the envelope of the calorimeter was evacuated to a pressure of 0.001 mm of mercury or less and the evacuation was continued throughout the course of an experiment. Frequent observations of this pressure were made to help control and evaluate the thermal leakage. Even at 150° C. no great difficulty was experienced in maintaining a pressure within the envelope of 0.001 mm of mercury after this pressure had been once attained; but it may be remarked that this was accomplished at the expense of considerable toil and patience in the discovery and repair of leaks.

Each of the three baths was brought to the desired temperature, which was thenceforth controlled. Close adjustment of the temperatures of the boiler and condenser baths was not required. After a little experience it was not difficult to choose a temperature of the boiler bath which was favorable to good regulation of the rate of flow. In the experiments at pressures less than about five atmospheres the temperature of this bath was usually maintained constant. In experiments at higher pressures, and also in those with the larger flows, better flow regulation was found possible when the bath temperature was made to rise slowly. The only requirement of the condenser bath temperature was that it be kept low enough to prevent the back pressure of the vapor from affecting the rate of discharge through the orifices. Experiments showed that this condition was realized when the indicated pressure on the condenser line was less than 35 per cent of the fore pressure on the orifices.

In most of the experiments a condenser bath temperature of −45° C. was found sufficiently low. In a few experiments at about one-half atmosphere pressure, and some with high rates of flow, lower condenser temperatures were maintained with the use of liquid air. The calorimeter bath temperature required extremely close regulation. This temperature was maintained constant to about 0.001° C. by means of the thermoregulator.

When all was ready, the flow was started. The final pressure, p_2, in the calorimeter was adjusted to the desired value and thereafter maintained constant by means of the pressure regulator. The calorimeter heating current from a storage battery was then turned on and

adjusted to produce the desired rise in temperature of the vapor. Heating current was also supplied to the guard heater in order to maintain the surface of the guard at the same temperature as the surface of the calorimeter system which it surrounds, and thus help control thermal leakage.

After the rate of flow and the calorimeter heating current had been maintained constant for a period of about one-half hour, observations were made periodically of the initial and final temperatures of the vapor. The constancy of these observations served to indicate that the calorimeter had reached a steady state. The initial and final pressures were then observed alternately, using the same pressure gauge, and a determination of the rate of flow was started by diverting the flow into a weighed reservoir.

During the flow determination several potentiometer readings were made of the current and potential drop in the calorimeter heating coil; the initial and final temperatures of the vapor were observed frequently, and the current in the guard heater was manually controlled to maintain a constant indication of the regulating thermocouples. After a chosen interval of time, usually 20 minutes, the flow was again diverted to another reservoir. This procedure provided the data for a single determination of specific heat, and could be repeated as often as desired.

The flow determinations were started and stopped on minute signals as indicated by a telegraph sounder which was operated by the standard clock of the bureau. The following procedure was adopted in order to avoid error in evaluating the duration of the flow determination. The minute signal from the clock gave the time for starting to close the valve to the condensing reservoir. When this was closed the valve to a weighed reservoir was opened. During the fraction of a second when both valves were closed the pressure in the condenser line did not rise to a value which would affect the rate of flow through the orifices and calorimeter. The same procedure was followed at the end of the time interval, first closing the valve to the weighed reservoir and then opening the valve to another reservoir.

Special handles were attached to these valve stems to facilitate rapid operation. With practice the time required to open or close a valve was less than one second and slight variations in the procedure at the beginning and end of the flow determinations introduced an error of only a small fraction of a second in the time interval, which was usually 1,200 seconds.

The weighed reservoirs, after a charge, were removed from the condenser bath, washed with water under the tap to bring them to room temperature, wiped with a towel, and placed for several minutes in a blast from an electric fan to bring them to room temperature and reference surface conditions before weighing.

All mass determinations were made to 1 mg by comparing the differences of the mass of the weighed reservoir with that of a dummy, substituted just before or just after the weighing. The dummy was one of the set of reservoirs and in form and surface was essentially identical with the rest of the set. The differences in weight were measured with platinum-plated brass weights placed on the same arm of the balance with the weighed reservoirs.

In carrying out the experiments it was found desirable and convenient to utilize the services of four persons in making the numerous manipulations, adjustments, and readings. The duties of this staff were apportioned somewhat as follows: First, regulation of boiler bath and rate of flow, manipulation and adjustment of pressure-regulating mechanism, orifices and appropriate valves, observations of the initial and final pressures in the calorimeter; second, operation of vacuum pumps and condenser bath, observations of jacket pressure, weighings and manipulations in the determinations of the rate of flow; third, regulation of calorimeter bath, and electric heating, adjustment of current in guard heater, observations of the power, thermometers and thermocouples; fourth, recording of all observations and computation of results.

3. EXPERIMENTAL PROCEDURE IN DETERMINATIONS OF μ

The procedure in the determinations of the Joule-Thomson coefficient, μ, was similar to that followed in the specific heat experiments, except that no electric heating was employed and the rate of flow was not measured during the course of those determinations. Frequently when working with the larger rates of flow such an experiment was made at the beginning of the day's observations because the calorimeter could be brought into approximate temperature equilibrium with comparative ease at that time. These experiments were not made previous to each specific heat experiment because of the length of time required to bring the calorimeter into temperature equilibrium after a portion of it had been heated several degrees in a preceding experiment and also because the correction for the effect of pressure drop in any experiment could be determined better from the data obtained with large flows.

4. THERMAL LEAKAGE

It has already been pointed out in Section II that the conservation of the measured heat intentionally added to the vapor and the avoidance of unmeasured heat leakage to or from the vapor are vital to the accuracy of the experimental results since the specific heat can be determined no more accurately than can the net amount of heat which the vapor gains in passing from the initial to the final state. The means adopted to meet these ideal conditions are: (1) Construction and operation of the calorimeter so as to make the

thermal leakage small, and (2) determination of the small amount of thermal leakage as a correction to the directly measured heat added. The constructive means have already been described and in operation they were found effective to the extent that only rarely did the correction for thermal leakage exceed 0.2 per cent of the entire heat supplied in any experiment. We shall next proceed to describe how this correction was evaluated.

The configuration of the apparatus is too complex to permit an analysis of the thermal leakage by the numerous possible paths and the alternative course was followed of evaluating the entire correction empirically. The fact that only a small quantity of heat remains to be evaluated after the means for reducing the thermal leakage had been effected, makes the selection of an empirical relation less critical than would otherwise be the case. What is more vital here is the method of testing as to the correctness of the evaluation of the leakage. This method is discussed later.

The empirical relation adopted to correct all the experiments for thermal leakage is

$$X = (N - 0.2\Delta\theta)x \tag{12}$$

in which N is the number of microvolts indicated by the regulating thermocouples on the guard and heater shield, $\Delta\theta$ is the observed temperature rise of the vapor expressed in degrees centigrade and x is the coefficient of thermal leakage; that is, the ratio between the total thermal leakage X and the mean effective temperature difference between the calorimeter system and its immediate surroundings. Experiments showed that this mean effective temperature difference could be obtained by applying a correction of 0.2 $\Delta\theta$ to the indicated temperature difference between the guard and the heater shield. The fact that the regulating thermocouples did not always indicate this exact mean effective temperature difference may have been the result either of imperfections of the individual couples or of the inherent difficulty of determining the average temperature of a complicated surface by means of a limited number of couples.

N and $\Delta\theta$ were observed in each determination of the specific heat, but the coefficient, x, required supplementary experiments to determine its value for various temperatures of the calorimeter and various degrees of evacuation of the envelope space. The coefficient of thermal leakage, x, was determined for any single combination of experimental conditions by making two successive, but separate experiments, in which the only conditions varied sensibly were the indicated temperature difference between the calorimeter shield and guard, N, and the resulting change in the temperature rise of the vapor, $\Delta\theta$.

These two coordinate changes were observed, the first by means of the regulating thermocouples on the shield and guard, and the second by means of the resistance thermometers in the vapor stream,

precisely as in a determination of the specific heat. In order to express numerically the results obtained by this procedure, equations (9) and (12) may be substituted in equation (8) and the result written as

$$[C_p]_{p_2\theta_m}=\frac{EI+(N-0.2\Delta\theta)x}{F\Delta\theta}+[\mu C_p]_{p_m\theta_1}\frac{\Delta p}{\Delta\theta}-\left(\frac{\delta^2 C_p}{\delta\theta^2}\right)_{p_2\theta_m}\frac{\Delta\theta^2}{24}-\text{etc.} \quad (13)$$

The two experiments yield two equations of this form in which the values of C_p at the respective mean temperatures are practically identical. Since determinations of x to a very moderate degree of accuracy are sufficient to evaluate the small amount of thermal leakage we may neglect the small differences of the correction terms and write

$$\frac{EI+(N_a-0.2\Delta\theta_a)x}{\Delta\theta_a}=\frac{EI+(N_b-0.2\Delta\theta_b)x}{\Delta\theta_b} \quad (14)$$

in which the subscripts refer to experiments a and b. Solving this equation for x, we obtain

$$x=\frac{EI(\Delta\theta_b-\Delta\theta_a)}{N_a\Delta\theta_b-N_b\Delta\theta_a} \quad (15)$$

The units in which the leakage coefficient, x, is expressed are watts per microvolt. It may be recalled that x is by definition the thermal leakage per unit temperature difference between the calorimeter system and its surroundings. Since the leakage takes place chiefly by radiation, and metallic and gaseous conduction, we may expect x, in general, to vary with the temperature of the calorimeter and the pressure of the gas within the envelope.

TABLE 1.—*Determinations of thermal leakage coefficient x*

Date	EI	$\Delta\theta_a$	$\Delta\theta_b$	$\Delta\theta_a-\Delta\theta_b$	N_a	N_b	Envelope		x
							Pressure	Temperature	
	Watts	°C	°C	°C	*μv*	*μv*	*mm Hg*	°C	*Watts/μv*
Nov. 8, 1921	0.3160	10.998	11.073	−0.075	+0.7	+7.0	----------	41	0.00034
Do	.3160	11.073	10.800	+.273	+7.0	−16.0	----------	41	.00034
Nov. 11, 1921	.1864	9.383	9.183	+.200	+0.1	−12.1	----------	40	.00033
Nov. 22, 1921	.1087	10.733	11.040	−.307	0.0	+10.0	----------	21	.00031
Nov. 26, 1921	.1109	8.899	9.085	−.186	+0.1	+10.0	----------	−11	.00023
Nov. 28, 1921	.0592	5.804	6.161	−.357	0.0	+10.0	----------	59	.00036
Feb. 1, 1922	.2153	9.310	8.652	+.658	0.0	−9.9	10.3	39	.00154
Do	.2151	9.344	8.952	+.392	0.0	−10.2	.12	39	.00088
Do	.2156	9.347	9.221	+.126	+0.1	−10.0	.0007	40	.00029
Feb. 2, 1922	.2135	9.249	9.038	+.211	0.0	−10.0	.0110	39	.00049
Do	.2131	9.236	9.045	+.191	0.0	−10.0	.0080	39	.00044
Do	.2128	9.221	9.104	+.117	0.0	−10.0	.0005	39	.00027
Feb. 3, 1922	.2294	9.875	9.768	+.107	+3.0	−7.0	.0001	40	.00025
Feb. 7, 1922	.3878	9.654	9.591	+.063	+3.0	−7.0	.0001	40	.00026
Feb. 9, 1922	.3526	9.800	9.725	+.075	+3.0	−6.9	.0003	60	.00027
Feb. 15, 1922	.2331	10.258	10.125	+.133	+3.0	−7.1	.0004	80	.00030
Feb. 28, 1922	.1824	9.968	9.632	+.336	+3.0	−7.0	.0090	155	.00062
Mar. 3, 1922	.3298	9.937	9.811	+.126	+1.5	−8.5	.0005	155	.00042
Mar. 9, 1922	.3365	9.754	9.660	+.094	+3.0	−7.0	.0002	120	.00033
Mar. 11, 1922	.6118	48.784	48,482	+.302	+8.0	−2.0	.0001	137	.00038
Mar. 17, 1922	.2504	10.017	9.950	+.067	+3.0	−7.0	.0001	5	.00017
Mar. 21, 1922	.1348	5.936	5.892	+.044	0.0	−7.0	.0001	−12	.00014

The results of several determinations of x at various calorimeter temperatures and envelope pressures are given in Table 1. The results are also shown in Figures 5 and 6. These results indicate, as shown in Figure 5, that at constant temperature x is a linear function of the envelope pressure for pressures below 0.01 mm mercury. The increase in the leakage with the envelope pressure may be interpreted as an increase in the gaseous conduction, since the leakage by other means is but slightly affected by the gas pressure. The linear relation shown in Figure 5 is in accord with kinetic theory, which states that gaseous conduction is directly proportional to the pressure of the gas at low pressures where the mean free path of the molecules is large compared with the distance between the boundaries of the conducting space. Thus, at zero pressure the gaseous conduction may be considered zero and the intercepts of the lines in Figure 5 with the axis of zero pressure are indications of the leakage by radiation and metallic conduction. It may be noted that the leakage by

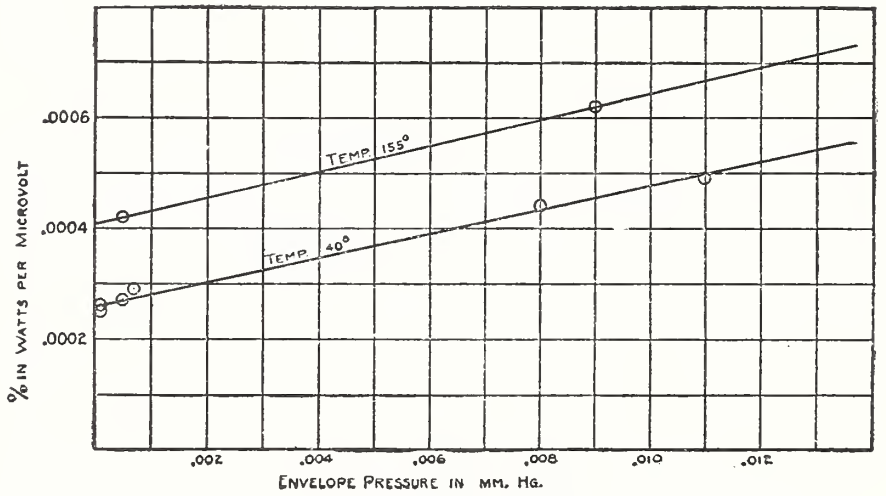

FIG. 5.—*Variation of thermal leakage coefficient, x, with evacuation*

these paths is large compared with the leakage by gaseous conduction in those experiments in which the envelope pressures are below 0.001 mm of mercury.

The determinations of x, which were made in 1922 with the envelope pressure below 0.001 mm of mercury, are shown in Figure 6, and indicate that x is approximately a linear function of the calorimeter temperature. The determinations made in 1921, without observing the envelope pressure throughout the experiments, are also shown in Figure 6 and indicate that the gaseous conduction was greater in these experiments. It is estimated by means of Figure 5 and by readings taken with the McLeod gauge previous to these experiments that the envelopes pressures were probably less than 0.005 mm of mercury. A discussion of the 1921 experiments and the reasons for not observing the envelope pressure are given in the next section.

Consideration has been given thus far to the evaluation of the correction for thermal leakage. We shall now consider the method of testing the correctness of this evaluation. The method chosen is based upon the assumption that the thermal leakage is independent of the power input and rate of flow as long as the temperature rise is sensibly constant. In other words, it is assumed that the temperature distribution within the calorimeter is independent of the power input and rate of flow under these conditions. There is experimental evidence in support of this assumption, for the indications of the thermocouples were found to be but slightly changed by doubling the rate of flow and keeping the temperature rise constant.

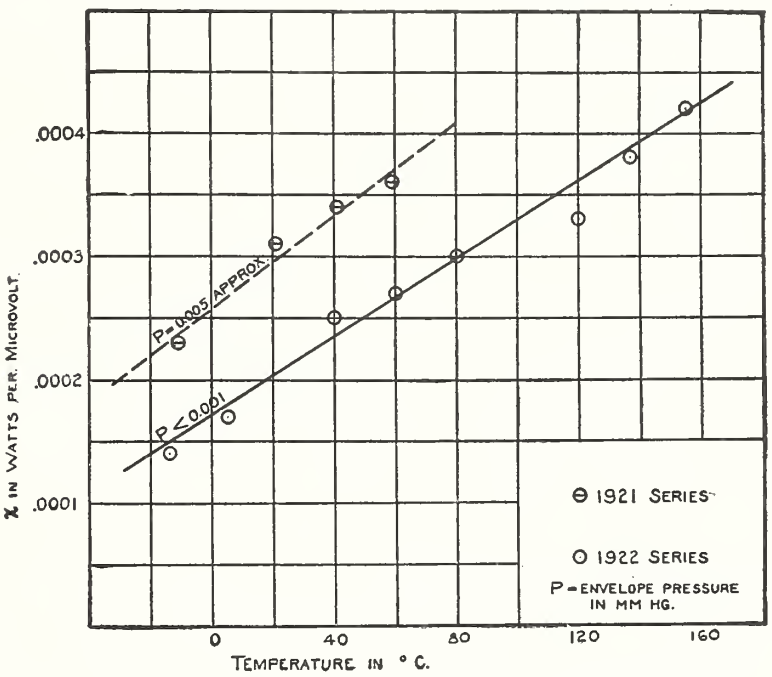

FIG. 6.—*Variation of thermal leakage coefficient, x, with temperature*

The principle of the method was to perform two or more specific heat experiments at the same temperature and pressure with approximately the same temperature rise, but different power inputs and different rates of flow.

The test of the proper correction for thermal leakage is that the values of C_p obtained from these experiments shall be independent of the rate of flow. Any appreciable outstanding leakage, which is not accounted for, will produce a different percentage error in the values computed for the heat added and consequently the resulting values of C_p will vary with the rate of flow. With very large flows the leakage will become negligible in comparison with the power input. Thus, by plotting the values of C_p against the reciprocal of

the rate of flow and extrapolating to infinite flow, the correct value of C_p may be obtained. This method of procedure is often called the method of extrapolation to infinite flow. This method was used in the selection of the empirical relation of equation (12) , but the ultimate test of the validity of the correction for thermal leakage was the constancy of the final result, C_p, with various rates of flow.

Experiments were performed with various rates of flow at each of the seven temperatures chosen for experimentation. That the above test was satisfied within the limits of accidental error is shown by the results given in Tables 3 and 4. It may be remarked incidentally that the constancy of the values of C_p obtained from experiments with different rates of flow is a crucial test not only of the correction for thermal leakage, but also of the Joule-Thomson correction for pressure drop.

TABLE 2.—*Determinations of C_p at 35° C. and 1.5 m of mercury*

Date	Regulating couples N	Power EI	Flow F	Temp. rise $\Delta\theta$	Pressure drop Δp	J-T correction $\mu C_p \frac{\Delta p}{\Delta\theta}$	Envelope pressure	C_p		Reciprocal of flow $\frac{1}{F}$
								Obs.	Cor.	
						Joules		*Joules*	*Joules*	
1922	μv	*Watts*	*g/sec.*	*° C.*	*m Hg*	*g deg*	*mm Hg*	*g deg.*	*g deg.*	*sec./g*
Jan. 26	0.0	0.48168	0.023159	9.242	−0.028	−0.0232	0.0004	2.2273	2.2251	43.18
Jan. 27	.0	.84251	.038773	9.531	−.067	−.0538	.0008	2.2261	2.2248	25.79
Feb. 1	.0	.21559	.010314	9.350	−.008	−.0065	.0007	2.2291	2.2241	96.96
Feb. 2	.0	.21280	.010315	9.224	−.008	−.0066	.0005	2.2300	2.2250	96.95
Feb. 3	3.0	.73374	.033218	9.742	−.053	−.0425	.0002	2.2249	2.2255	30.10
Do	3.0	.22917	.010423	9.864	−.008	−.0064	.0002	2.2231	2.2257	95.90

As an example of the information furnished by experiments with different rates of flow, the results of several such experiments are given in Table 2. These experiments were performed at a mean temperature of 35° and a pressure of 1.5 m of mercury with approximately 10° temperature rises. The apparent or observed values of C_p are plotted in Figure 7 against the reciprocal of the flow. In the first series of experiments the indication of the regulating thermocouples was made zero ($N=0$). The results indicated that a small quantity of heat was lost from the system, amounting to about 0.2 per cent of the heat supplied electrically at the lowest rate of flow. Two experiments were then performed with a regulating thermocouple indication of 3 mv ($N=3$) in order to compensate for this heat loss. As shown graphically in Figure 7, these experiments indicated a slight overcompensation. Correcting all of the experiments to $N=2$ gave values of C_p, which were constant within a few hundredths of a per cent. These experiments, together with others in which the temperature rises were approximately 5 and 50°, led to the selection of the empirical relation given by equation (12).

5. PRELIMINARY EXPERIMENTS ON C_p

In the series of experiments on specific heat performed in 1921 the importance of systematic control and observation of the residual envelope pressure was not recognized. Attempts to evaluate the thermal leakage correction in these experiments led to the installation of an additional vacuum pump and McLeod gauge in January, 1922, in order to obtain continuous service in the control and measurement of the envelope pressure.

During the progress of the final experimental series in 1922 (see Table 3) it was conclusively demonstrated that in order to evaluate the thermal leakage correction accurately it was necessary not only

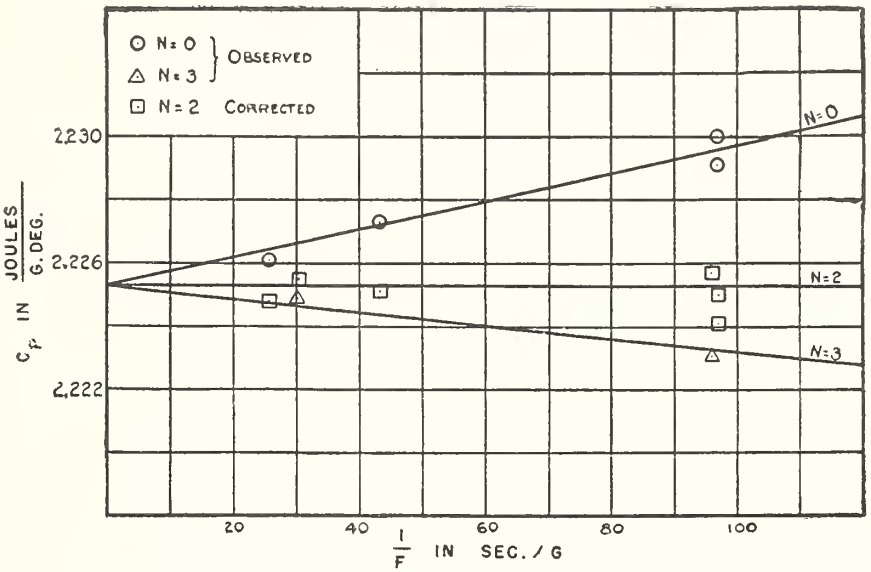

FIG. 7.—*Variation of apparent specific heat with rate of flow, F, and thermocouple indication, N*

to employ a certain degree of evacuation in the envelope space, but also to determine and control the constancy of the pressure therein.

Most of the 1921 experiments were made with small rates of flow in order to study the behavior of the various instruments more easily and also to acquire experience in manipulation. On account of the small rates of flow and the relatively high and indefinite pressure in the envelope space, the correction for thermal leakage was comparatively large and also uncertain. The results are, therefore, not as reliable as those obtained in the later series of experiments. The results are given as a matter of record in Table 5, but they have been excluded from the list of accredited determinations and no weight given to them in the final results.

574278 O - 61 - 32

6. EXPERIMENTS NEAR SATURATION

On account of the rapid increase in the value of C_p in the neighborhood of the saturation limit, several experiments were made in which the aim was to approach this boundary as closely as could be done safely. The danger in these experiments, of course, is the possibility of liquefaction taking place in the calorimeter and the uncertainty as to the result of such an occurrence.

In order to investigate what would happen in close proximity to saturation, an experiment was made on November 16, 1921, in which the calorimeter bath temperature was $-5°$ *C.*, and the pressure corresponded to 2° of superheat. No peculiarity in behavior was observed in any respect, and two complete determinations of C_p were obtained. After completing these determinations the pressure in the calorimeter was increased gradually, noting meanwhile the indications of the thermometers. When the pressure reached a value corresponding to 0.8° superheat, thermometer T_1 began to show slight fluctuations in temperature. These fluctuations increased as the pressure was raised until they became so large as to preclude reliable observations. The trend of this fluctuating temperature was upward as the pressure was raised. Upon stopping the flow the temperature promptly dropped several degrees, just as it would if liquid ammonia were present in that thermometer cell.

On the following day it was found that the calorimeter heater had developed a short circuit to its case. A plausible explanation was that a small particle of conducting material, such as a metal chip, had lodged between the coil windings and the case. This mishap did not preclude the use of the instrument, as the resistance of the heating coil still remained constant, but it was necessary to avoid grounding any other part of the heating circuit. Later on the fault disappeared. On November 18, 1921, two additional experiments with 2° of superheat were successfully made.

The foregoing experiments demonstrated that too close approach to the saturation limit caused pronounced manifestations of unsteadiness, and it was inferred that the appearance of unsteadiness marked the danger point in approach to saturation. The observations taken with 2° of superheat were believed to be far enough removed from this danger point to be reliable.

On February 13, 1922, two experiments were made with about 20 atmospheres pressure and approximately 3° of superheat. The temperature rise in these experiments was about 5°, and the agreement in the results was remarkably good. The time interval covered in these experiments was about two hours, and the measuring instruments indicated very steady conditions.

On March 28, 1922, an experiment was made with 0.9° superheat. In this experiment fluctuations of about 0.01° were observed in thermometer T_1. After completing the various measurements, an attempt was made to reduce the rate of flow and obtain a check

TABLE 3.—*Calorimeter data on C_p*

Date	Mean temperature θ_m	Temperature rise $\Delta\theta$	Final pressure p_2	Pressure drop $-\Delta p$	Rate of flow F	Power EI	Thermal leakage $(N-0.2\Delta\theta)x$	Number of determinations
1922	° C.	° C.	m Hg	m Hg	g/sec.	Watts	Watts	
Jan. 24	34.99	9.376	1.495	0.0080	0.010242	0.21462	−0.00046	1
Jan. 26	35.03	9.386	1.500	.0078	.010226	.21450	−.00050	2
Do	34.92	9.242	1.501	.0280	.023158	.48161	−.00043	2
Jan. 27	35.00	9.532	1.498	.0670	.038773	.84253	−.00049	1
Feb. 1	34.97	9.350	1.500	.0075	.010314	.21559	−.00052	2
Feb. 2	34.93	9.225	1.498	.0080	.010315	.21280	−.00050	1
Feb. 3	35.08	9.742	1.501	.0528	.033218	.73374	+.00026	1
Do	35.23	9.869	1.498	.0078	.010428	.22929	+.00026	2
Feb. 6	35.21	9.876	2.308	.0385	.035915	.82538	+.00026	1
Do	35.32	10.002	2.306	.0100	.016162	.37228	+.00026	1
Feb. 7	35.12	9.654	4.054	.0049	.016214	.38780	+.00026	1
Do	35.08	9.564	4.053	.0049	.016303	.38608	+.00026	1
Feb. 8	35.17	9.931	7.110	.0035	.015906	.45312	+.00026	1
Do	35.11	9.813	7.115	.0035	.016082	.45294	+.00026	1
Feb. 9	55.08	10.009	2.290	.0395	.034386	.79000	+.00028	1
Do	55.02	9.800	2.288	.0105	.015822	.35275	+.00028	1
Do	55.01	9.772	2.291	.0105	.015851	.35238	+.00028	1
Feb. 10	55.06	9.906	3.969	.0045	.015805	.37338	+.00028	2
Do	55.10	9.981	7.063	.0020	.015976	.41826	+.00028	2
Feb. 11	55.04	9.729	10.391	.0022	.015118	.43471	+.00028	1
Do	55.06	9.763	10.392	.0022	.015078	.43444	+.00028	1
Feb. 13	54.94	4.714	15.106	.0018	.016368	.27822	+.00015	1
Do	54.97	4.773	15.105	.0018	.016175	.27816	+.00015	1
Feb. 14	54.93	4.694	1.503	.0290	.022252	.23613	+.00013	1
Do	54.96	4.707	1.505	.0080	.010505	.11034	+.00015	2
Feb. 15	75.31	10.332	1.498	.0287	.021529	.50044	+.00031	2
Do	75.31	10.257	1.498	.0083	.010159	.23310	+.00029	2
Feb. 16	74.97	9.926	7.094	.0105	.027897	.69682	+.00030	2
Do	74.91	9.757	7.098	.0030	.015206	.37297	+.00032	1
Feb. 17	75.03	5.029	15.073	.0134	.061750	.96117	+.00015	2
Feb. 18	75.18	10.258	15.066	.0013	.014450	.45553	+.00029	2
Do	75.08	9.999	10.419	.0020	.015370	.41710	+.00030	2
Feb. 20	115.29	10.234	1.498	.0098	.009605	.22446	+.00046	2
Do	115.26	10.213	7.101	.0091	.026055	.64886	+.00036	2
Feb. 24	114.92	9.583	10.408	.0075	.028772	.70052	+.00048	1
Feb. 25	115.06	9.166	7.103	.0064	.017632	.39397	+.00043	1
Feb. 27	114.91	9.699	15.069	.0033	.026437	.69227	+.00038	3
Do	114.70	9.258	10.400	.0037	.017906	.42065	+.00042	2
Feb. 28	149.99	9.894	2.300	.0260	.021983	.51240	+.00080	2
Do	150.06	9.963	2.300	.0053	.007815	.18232	+.00068	3
Mar. 2	150.03	9.899	2.299	.0048	.007808	.18144	+.00048	2
Do	150.01	9.876	2.302	.0261	.022018	.51281	+.00042	2
Mar. 3	150.05	9.941	4.030	.0063	.013890	.32960	−.00021	3
Do	150.07	9.981	7.105	.0027	.011492	.28023	−.00020	2
Do	149.97	9.915	10.408	.0040	.016862	.41913	−.00021	2
Mar. 4	150.00	9.894	15.056	.0040	.024902	.64250	−.00021	2
Do	150.07	8.062	15.051	.0185	.053977	1.13722	−.00026	1
Mar. 6	150.06	9.742	1.502	.0101	.009240	.21122	−.00019	2
Do	150.05	9.752	10.386	.0040	.018431	.45076	−.00019	2
Mar. 7	150.00	9.862	0.376	.0273	.007727	.17757	−.00020	2
Do	150.01	8.025	15.049	.0185	.054030	1.13194	−.00025	1
Mar. 9	115.02	9.715	0.380	.0277	.008281	.18222	+.00036	2
Do	114.97	9.714	4.054	.0387	.041328	.94935	+.00036	2
Do	115.03	9.750	4.049	.0065	.014666	.33644	+.00036	2
Mar. 10	75.02	9.884	0.377	.0270	.008789	.19157	+.00030	2
Do	75.07	9.969	4.037	.0057	.015635	.36721	+.00030	2
Mar. 11	93.19	10.071	15.050	.0056	.028890	.82798	+.00032	2
Do	112.90	48.743	1.498	.0096	.010022	1.11540	−.00067	2
Do	113.02	48.787	1.501	.0043	.005484	.61238	−.00067	2
Mar. 17	−0.03	9.917	2.300	.0225	.028313	.70683	+.00018	2
Do	+0.06	10.015	2.301	.0036	.010044	.25036	+.00021	2
Mar. 20	0.01	9.804	0.380	.0235	.010075	.21166	−.00034	2
Do	0.12	10.037	1.501	.0148	.018215	.42602	−.00035	2
Mar. 21	−15.13	5.937	0.382	.0230	.010435	.13484	−.00017	2

TABLE 4.—*Calculation of* C_p

Date	θ_m	p_2	$\frac{\Delta q}{\Delta \theta}$	$\left[\mu C_p\right]_{p_m \theta_1} \frac{\Delta p}{\Delta \theta}$	$\left[\frac{d^2 C_p}{d\theta^2}\right]_{p_2 \theta_m} \frac{\Delta \theta^2}{24}$	$[C_p]_{p_2 \theta_m}$	C_p Empirical equation	Deviation obs.-calc.
1922	° C.	m Hg	Joules / g deg.	Joules / g deg.	Joules / g deg.	Joules / g deg.	Joules / g deg.	Per cent
Jan. 24	34.99	1.495	2.2302	−0.0066	0.0002	2.2234	2.2233	+0.00
Jan. 26	35.03	1.500	2.2296	−.0064	.0002	2.2230	2.2237	−.03
Do	34.92	1.501	2.2482	−.0234	.0002	2.2246	2.2239	+.03
Jan. 27	35.00	1.498	2.2783	−.0541	.0002	2.2240	2.2235	+.02
Feb. 1	34.97	1.500	2.2302	−.0062	.0002	2.2238	2.2237	+.00
Feb. 2	34.93	1.498	2.2311	−.0067	.0002	2.2242	2.2236	+.03
Feb. 3	35.08	1.501	2.2681	−.0418	.0002	2.2261	2.2237	+.11
Do	35.23	1.498	2.2305	−.0061	.0002	2.2242	2.2234	+.04
Feb. 6	35.21	2.308	2.3277	−.0311	.0005	2.2961	2.2953	+.03
Do	35.32	2.306	2.3046	−.0080	.0005	2.2961	2.2949	+.05
Feb. 7	35.12	4.054	2.4791	−.0043	.0010	2.4738	2.4741	−.01
Do	35.08	4.053	2.4778	−.0043	.0010	2.4725	2.4742	−.07
Feb 8	35.17	7.110	2.8702	−.0034	.0026	2.8642	2.8659	−.06
Do	35.11	7.115	2.8718	−.0035	.0026	2.8657	2.8676	−.07
Feb. 9	55.08	2.290	2.2962	−.0247	.0002	2.2713	2.2704	+.04
Do	55.02	2.288	2.2768	−.0067	.0002	2.2699	2.2703	−.02
Do	55.01	2.291	2.2768	−.0067	.0002	2.2699	2.2705	−.03
Feb. 10	55.06	3.969	2.3866	−.0030	.0005	2.3831	2.3820	+.05
Do	55.10	7.063	2.6248	−.0014	.0012	2.6222	2.6246	−.09
Feb. 11	55.04	10.391	2.9574	−.0018	.0024	2.9532	2.9489	+.15
Do	55.06	10.392	2.9512	−.0018	.0024	2.9470	2.9487	−.06
Feb. 13	54.94	15.106	3.6078	−.0035	.0014	3.6029	3.6085	−.16
Do	54.97	15.105	3.6049	−.0035	.0014	3.6000	3.6071	−.20
Feb. 14	54.93	1.503	2.2619	−.0370	.0000	2.2249	2.2229	+.09
Do	54.96	1.505	2.2345	−.0102	.0000	2.2243	2.2230	+.06
Feb. 15	75.31	1.498	2.2512	−.0140	.0001	2.2371	2.2364	+.03
Do	75.31	1.498	2.2398	−.0041	.0001	2.2357	2.2364	−.03
Feb. 16	74.97	7.094	2.5175	−.0059	.0006	2.5110	2.5134	−.10
Do	74.91	7.098	2.5160	−.0017	.0006	2.5137	2.5142	−.02
Feb. 17	75.03	15.073	3.0956	−.0177	.0007	3.0772	3.0767	+.02
Feb. 18	75.18	15.066	3.0751	−.0008	.0028	3.0715	3.0734	−.06
Do	75.08	10.419	2.7160	−.0012	.0011	2.7137	2.7153	−.06
Feb. 20	115.29	1.498	2.2882	−.0035	.0000	2.2847	2.2847	+.00
Do	115.26	7.101	2.4398	−.0034	.0002	2.4362	2.4381	−.08
Feb. 24	114.92	10.408	2.5424	−.0031	.0003	2.5390	2.5388	+.01
Feb. 25	115.06	7.103	2.4404	−.0026	.0002	2.4376	2.4382	−.02
Feb. 27	114.91	15.069	2.7013	−.0013	.0006	2.6994	2.6962	+.12
Do	114.70	10.400	2.5400	−.0015	.0003	2.5382	2.5390	−.03
Feb. 28	149.99	2.300	2.3595	−.0075	.0000	2.3520	2.3542	−.09
Do	150.06	2.300	2.3503	−.0015	.0000	2.3488	2.3543	−.23
Mar. 2	150.03	2.299	2.3537	−.0014	.0000	2.3523	2.3542	−.08
Do	150.01	2.302	2.3602	−.0075	.0000	2.3527	2.3543	−.07
Mar. 3	150.05	4.030	2.3855	−.0018	.0000	2.3837	2.3853	−.07
Do	150.07	7.105	2.4414	−.0008	.0001	2.4405	2.4421	−.07
Do	149.97	10.408	2.5057	−.0012	.0001	2.5044	2.5057	−.05
Mar. 4	150.00	15.056	2.6069	−.0012	.0002	2.6055	2.5999	+.21
Do	150.07	15.051	2.6127	−.0069	.0002	2.6056	2.5997	+.23
Mar. 6	150.06	1.502	2.3444	−.0030	.0000	2.3414	2.3402	+.05
Do	150.05	10.386	2.5068	−.0012	.0001	2.5055	2.5052	+.01
Mar 7	150.00	0.376	2.3276	−.0079	.0000	2.3197	2.3205	−.03
Do	150.01	15.049	2.6100	−.0069	.0002	2.6029	2.5997	+.12
Mar. 9	115.02	0.380	2.2695	−.0103	.0000	2.2592	2.2565	+.12
Do	114.97	4.054	2.3656	−.0147	.0001	2.3508	2.3521	−.06
Do	115.03	4.049	2.3547	−.0025	.0001	2.3521	2.3520	+.00
Mar. 10	75.02	0.377	2.2087	−.0135	.0000	2.1952	2.1896	+.26
Do	75.07	4.037	2.3579	−.0030	.0003	2.3546	2.3523	+.10
Mar. 11	93.19	15.050	2.8473	−.0029	.0013	2.8431	2.8408	+.08
Do	112.90	1.498	2.2819	−.0009	.0010	2.2800	2.2816	−.07
Do	113.02	1.501	2.2864	−.0004	.0010	2.2850	2.2819	+.14
Mar. 17	−0.03	2.300	2.5180	−.0314	.0020	2.4846	2.4861	−.06
Do	+0.06	2.301	2.4910	−.0050	.0021	2.4839	2.4854	−.06
Mar. 20	0.01	0.380	2.1394	−.0272	.0002	2.1120	2.1115	+.02
Do	0.12	1.501	2.3283	−.0187	.0011	2.3085	2.3097	−.05
Mar. 21	−15.13	0.382	2.1738	−.0550	.0002	2.1186	2.1191	−.02

determination with a smaller flow. Upon this occasion good additional evidence was obtained of the presence of liquid within the calorimeter. The result obtained in the preceeding experiment was, therefore, open to considerable doubt, and as a consequence it has been excluded from the list of accredited determinations.

It is of interest to consider how we may explain the apparently anomalous phenomenon of liquefaction when the indicated temperature and pressure corresponded to superheated vapor. On account of the precautions to prevent entrained wetness in the vapor supply delivered to the calorimeter it seems certain that whatever liquid appeared in the calorimeter was formed during the approach of the ammonia to thermometer cell T_1.

In the passage from the calorimeter bath to thermometer cell, T_1, the vapor experiences a moderate pressure drop, but has little opportunity to absorb heat. It is plausible that the cooling effect of this pressure drop accentuated by regenerative back conduction of heat may have cooled part of the ammonia stream down to the temperature of liquefaction, and that the entrained liquid was carried on mechanically for some distance within the calorimeter before equilibrium could again be established.

This speculation is supported by the fact that indications of the presence of liquid were fairly abrupt upon close approach to the saturation limit, and tends to strengthen the belief that for the experiments where no irregularities were observed, the ammonia entering the calorimeter system was homogeneous superheated vapor.

Apart from casting doubt on this critical experiment of March 28, the effect of crowding the conditions too far was disastrous for it was found on the following day that the calorimeter heating coil was short circuited between windings producing a variable resistance in that coil. In an attempt to remove the cause of this short circuit by excessive heating of the coil, a leak developed in one of the soldered joints rendering the calorimeter unsuitable for further experimentation. Enough experimental data had already been obtained to establish a formula for the specific heat of the superheated vapor in the region of greatest importance, and so this unexpected termination of the series was accepted with resignation.

VI. RESULTS OF MEASUREMENTS

1. CALORIMETRIC DATA

The data obtained from the calorimetric measurements of the specific heat are given in Table 3. The values given in each column represent, in most cases, average values obtained from several readings which were made during a determination of the rate of flow. When successive or duplicate experiments were made, only the averages of the various readings are given. The various observations taken during a single flow measurement constituted a complete determination.

The results of all the accredited experiments are included in Table 3. Except for one experiment very close to the saturation limit, Table 3 contains the results of all the complete experiments performed in 1922. The data obtained in the experiments of 1921, all of which were discredited on account of the uncertainty of the thermal leakage correction, are given in Table 5. This table also contains the computations of the specific heat from those data. In the last experiment performed in 1922, the results of which are also given in Table 5, the initial pressure and temperature were so close to the saturation limit that the results are considered doubtful.

The results of all the measurements on the Joule-Thomson coefficient, μ, are given in Table 6. The values given for Δp, $\Delta\theta$, and N are the averages of several readings. The rate of flow was not measured in these experiments at the time the other readings were made. It was held sensibly constant and measured, in several instances, during the specific heat experiment which followed. The values designated "Flow not measured" were estimated from the observed fore pressure and the calibration of the particular orifice or orifices used.

The scale of temperature used in the measurements given in this paper is the scale defined by the resistance thermometer of pure platinum, standardized at the temperatures of melting ice (0°C.), condensing steam (100°C.), and condensing sulphur vapor (444.6°C.), all at standard atmospheric pressure (760 mm of mercury at 0°C. and standard gravity). Using the Callendar equation

$$\theta=\frac{R_\theta-R_o}{R_{100}-R_o}\,100+\delta\left(\frac{\theta}{100}-1\right)\frac{\theta}{100}$$

as an interpolation equation, the scale so defined represents the thermodynamic scale in the interval −40 to +450°C. to the accuracy with which that scale is at present known. Temperatures on the absolute thermodynamic scale are obtained by adding 273.1° to the measured temperature.

All of the pressure measurements have been reduced to meters of mercury at 0°C. and at standard gravity ($g=980.665$).[14] The value of g in this laboratory is 980.091, based upon a determination made by the United States Coast and Geodetic Survey in 1910.[15]

The fundamental heat unit used in these measurements is the international joule, defined by the relation $\frac{Q}{t}=\frac{E^2}{R}$ where Q is the number of joules transformed into heat in a given electric circuit in t seconds, E is the number of volts potential drop, and R is the number

[14] This value was adopted by the International Committee on Weights and Measures in 1901. (Travaux et Mémoires du Bur. Int., third general conference, p 66; 1902).

[15] B. S. Bulletin, 8, p. 363; 1912 (Sci. Paper No. 171).

of ohms resistance; taking 1 volt $=\frac{1}{1.01830}\times$ emf of mean Weston normal cell at 20°, and 1 ohm = resistance at 0° C. of 106.300 cm mercury column of constant cross-sectional area and 14.4521 in mass. The difference between the international joule, realized thus, and the absolute joule is about 1 part in 3,000, according to Bureau of Standards Circular No. 60, 2d edition (1920). The ampere is used only as an intermediary unit, being determined by the relation $I=\frac{E}{R}$. As a secondary heat unit the 20° calorie, defined as 4.183 international joules, has been used in the table given in the appendix.

TABLE 5.—*Discredited experiments*

Date	Mean temperature $-\theta_m$	Temperature rise $\Delta\theta$	Final pressure p_2	Pressure drop $-\Delta p$	Rate of flow F	Power EI	Thermal leakage $(N-0.2\Delta\theta)x$	Number of determinations
1921	°C.	°C.	m Hg	m Hg	g/sec.	Watts	Watts	
Nov. 8	35.75	10.997	1.736	0.0090	0.012775	0.31596	−0.00062	1
Do	35.40	10.359	1.744	.0320	.026875	.63181	−.00081	1
Nov. 11	35.14	9.382	2.135	.0045	.008681	.18636	−.00062	2
Nov. 14	34.91	9.467	2.076	.0210	.023695	.51414	−.00061	1
Do	32.58	4.865	2.076	.0210	.023695	.26651	−.00036	1
Nov. 16	+0.02	9.762	2.450	.0080	.017215	.42637	−.00054	1
Do	+0.02	9.739	2.454	.0070	.017265	.42641	−.00054	1
Nov. 18	−0.33	9.069	2.453	.0100	.018813	.43398	−.00049	1
Do	+0.28	10.255	2.452	.0110	.018818	.48950	−.00047	1
Nov. 21	15.10	9.802	1.474	.0030	.006168	.13690	−.00065	1
Nov. 22	15.55	10.724	1.101	.0015	.004567	.10872	−.00065	2
Nov. 23	17.18	14.050	1.476	.0025	.006183	.19597	−.00087	1
Do	15.08	9.815	2.538	.0050	.010812	.25570	−.00060	2
Nov. 25	55.80	11.120	1.209	.0040	.004672	.11535	−.00072	1
Do	55.89	11.329	2.491	.0040	.009815	.25446	−.00081	1
Nov. 26	−15.37	8.899	1.198	.0025	.005308	.11093	−.00044	1
Do	−15.06	9.455	1.198	.0025	.005315	.11774	−.00044	1
Nov. 28	55.50	5.804	1.196	.0035	.004578	.05920	−.00042	1
Do	55.80	6.381	1.196	.0035	.004600	.06529	−.00046	1
Nov. 29	0.36	10.014	1.188	.0020	.005117	.11564	−.00054	1
Nov. 30	0.30	9.966	1.190	.0030	.005108	.11520	−.00060	1
Do	0.31	10.025	1.889	.0030	.008241	.19795	−.00054	1
Do	0.19	9.798	1.889	.0030	.008240	.19354	−.00050	1
Dec. 1	34.90	9.453	1.098	.0025	.004392	.09177	−.00060	2
Do	34.76	9.164	2.492	.0035	.010218	.21758	−.00058	2
Dec. 2	34.07	7.905	1.457	.0400	.028142	.50280	−.00052	1
Do	34.15	7.923	1.474	.0030	.005924	.10511	−.00052	1
Dec. 3	34.17	7.946	1.465	.0030	.005909	.10539	−.00052	1
Do	34.15	7.918	1.465	.0070	.009788	.17337	−.00052	1
1922								
Mar. 28	−15.00	6.012	1.484	.0140	.017395	.25957	−.00000	2

TABLE 5.—*Discredited experiments*—Continued

Date	θ_m	p_2	$\frac{\Delta q}{\Delta\theta}$	$\left[\mu C_p\right]_{p_m\theta_1}^{\frac{\Delta p}{\Delta\theta}}$	$\left[\frac{d^2C_p}{d\theta^2}\right]_{p_2\theta_m}\frac{\frac{\Delta\theta^2}{24}}{}$	$[C_p]_{p_2\theta_m}$	C_p Empirical equation	Deviation obs.-calc
1921	° C.	m Hg	Joules / g deg.	Joules / g deg.	Joules / g deg.	Joules / g deg.	Joules / g deg.	Percent
Nov. 8	35.75	1.736	2.2446	−0.0064	0.0004	2.2378	2.2434	−0.25
Do	35.40	1.744	2.2665	−.0240	.0004	2.2421	2.2444	−.10
Nov. 11	35.14	2.135	2.2806	−.0038	.0004	2.2764	2.2793	−.13
Nov. 14	34.91	2.076	2.2893	−.0175	.0004	2.2714	2.2746	−.14
Do	32.58	2.076	2.3088	−.0340	.0001	2.2747	2.2700	+.21
Nov. 16	+0.02	2.450	2.5339	−.0115	.0021	2.5203	2.5216	−.05
Do	+0.02	2.454	2.5328	−.0101	.0021	2.5206	2.5226	−.08
Nov. 18	−0.33	2.453	2.5407	−.0155	.0019	2.5233	2.5263	−.12
Do	+0.28	2.452	2.5341	−.0151	.0024	2.5166	2.5188	−.09
Nov. 21	15.10	1.474	2.2536	−.0031	.0006	2.2499	2.2479	+.09
Nov. 22	15.55	1.101	2.2066	−.0014	.0006	2.2046	2.2012	+.15
Nov. 23	17.18	1.476	2.2459	−.0018	.0013	2.2428	2.2442	−.06
Do	15.08	2.538	2.4039	−.0055	.0014	2.3970	2.4017	−.20
Nov. 25	55.80	1.209	2.2064	−.0022	.0001	2.2041	2.2065	−.11
Do	55.89	2.491	2.2811	−.0022	.0003	2.2786	2.2826	−.18
Nov. 26	−15.37	1.198	2.3391	−.0047	.0013	2.3331	2.3391	−.26
Do	−15.06	1.198	2.3342	−.0044	.0015	2.3283	2.3368	−.36
Nov. 28	55.50	1.196	2.2122	−.0036	.0000	2.2086	2.2055	+.14
Do	55.80	1.196	2.2087	−.0033	.0000	2.2054	2.2057	−.01
Nov. 29	0.36	1.188	2.2462	−.0025	.0008	2.2429	2.2478	−.22
Nov. 30	0.30	1.190	2.2512	−.0037	.0008	2.2467	2.2484	−.08
Do	0.31	1.889	2.3895	−.0040	.0015	2.3840	2.3885	−.19
Do	0.19	1.889	2.3910	−.0041	.0014	2.3855	2.3876	−.09
Dec. 1	34.90	1.098	2.1959	−.0020	.0002	2.1937	2.1900	+.17
Do	34.76	2.492	2.3174	−.0031	.0005	2.3138	2.3138	±.00
Dec. 2	34.07	1.457	2.2578	−.0388	.0002	2.2188	2.2209	−.09
Do	34.15	1.474	2.2284	−.0029	.0002	2.2253	2.2223	+.14
Dec. 3	34.17	1.465	2.2335	−.0029	.0002	2.2304	2.2215	+.40
Do	34.15	1.465	2.2303	−.0068	.0002	2.2233	2.2215	+.08
1922								
Mar. 28	−15.00	1.484	2.4821	−.0389	.0008	2.4424	2.4256	+.69

TABLE 6.—*Joule-Thomson data*

Date	Mean temperature θ_m	Mean pressure p_m	Specific heat C_p	Rate of flow F	Regulating couple N	Temperature drop $-\Delta\theta$	Pressure drop $-\Delta p$	$\frac{\Delta\theta}{\Delta p}$	Leakage correction $\frac{X}{C_pF\Delta p}$	μ	μC_p	Equation μC_p	Deviation obs.-calc.	Deviation expressed in—
			Joules					Deg.	Deg.	Deg.	Joules	Joules	Per	
1921	° C.	m Hg	g deg.	g/sec.	μv	° C.	m Hg	m Hg	m Hg	m Hg	m Hg	m Hg	cent	° C.
Nov. 9	30.16	1.760	2.252	[1] 0.027	−0.1	0.103	0.0300	3.43	−0.01	3.42	7.70	7.78	−1.0	−0.001
10	30.11	1.815	2.257	[1] .035	+0.5	.154	.0453	3.40	+.05	3.45	7.79	7.80	−0.1	−.000
11	30.15	2.308	2.308	[1] .052	+0.5	.244	.0723	3.37	+.02	3.39	7.82	7.96	−1.8	−.004
15	−5.35	2.307	2.553	[1] .058	−1.0	.460	.0826	5.57	−.03	5.54	14.14	14.03	+0.8	+.004
15	−4.98	2.478	2.594	.01593	+0.5	.038	.0075	5.07	+.40	5.47	14.19	14.12	+0.5	.000
28	+52.49	1.303	2.208	[1] .024	0.0	.099	.0366	2.70	.00	2.70	5.96	5.95	+0.2	.000
1922														
Jan. 27	30.09	1.532	2.230	.03877	0.0	.236	.0680	3.47	.00	3.47	7.74	7.70	+0.5	+.001
Feb. 3	30.10	1.527	2.230	.03322	−2.0	.185	.0525	3.52	−.13	3.39	7.56	7.70	−1.8	−.003
6	30.17	2.326	2.314	.03591	−0.1	.133	.0370	3.59	−.01	3.58	8.28	7.97	+3.9	+.005
7	30.23	4.060	2.511	.01621	+0.1	.023	.0065	3.54	+.10	3.64	9.14	8.55	+8.1	+.002
8	30.15	7.110	2.964	.01600	−0.1	.012	.0032	3.75	−.17	3.58	10.61	9.70	+9.4	+.001
9	49.98	2.308	2.275	.03439	0.0	.108	.0388	2.78	.00	2.78	6.32	6.26	+1.0	+.001
14	52.52	1.518	2.223	.02225	+0.2	.079	.0284	2.78	+.04	2.82	6.27	6.00	+4.5	+.004
15	70.05	1.513	2.232	.02153	0.0	.069	.0286	2.41	.00	2.41	5.38	5.05	+6.5	+.004
20	110.04	1.512	2.278	[1] .021	0.0	.052	.0304	1.71	.00	1.71	3.90	3.63	+7.4	+.004
24	110.06	10.411	2.550	[1] .030	−0.2	.021	.0118	1.78	−.08	1.70	4.33	3.87	+11.9	+.002
28	144.94	2.323	2.347	[1] .032	0.0	.053	.0428	1.24	.00	1.24	2.91	2.85	+2.1	+.001
Mar. 7	144.95	0.752	2.317	[1] .015	0.0	.056	.0448	1.25	.00	1.25	2.90	2.84	+2.1	+.001
20	−5.02	0.392	2.117	.01007	+0.9	.118	.0231	5.11	+.28	5.39	11.41	11.38	+0.3	.000
21	−18.22	0.394	2.141	.01043	+1.2	.146	.0227	6.44	+.37	6.81	14.58	14.22	+2.5	+.004
22	−12.92	1.475	2.449	[1] .035	−0.9	.299	.0481	6.22	−.03	6.19	15.16	15.02	+0.9	+.003

[1] Flow not measured.

2. COMPUTATION OF RESULTS

The computations of the specific heat, C_p, are given in Tables 4 and 5. These computations are made according to the equation (13),

$$[C_p]_{p_2\theta_m}=\frac{EI+(N-0.2\Delta\theta)\,x}{F\Delta\theta}+[\mu C_p]_{p_m\theta_1}\frac{\Delta p}{\Delta\theta}-\left(\frac{\partial^2 C_p}{\partial\theta^2}\right)_{p_2\theta_m}\frac{\Delta\theta^2}{24} \qquad (13)$$

The value of the correction term $\left(\frac{\partial^2 C_p}{\partial\theta^2}\right)\frac{\Delta\theta^2}{24}$ is, in every case, less than 0.1 per cent of the final result. The terms involving higher orders of derivatives have been omitted because their effect upon the result is less than 0.01 per cent.

Equation (11) is used in computing the values of the Joule-Thomson coefficient, μ. Since values of μC_p are required in equation (13), the products of the observed values of μ and interpolated values of C_p are given, in Table 6, and compared with computed values of μC_p. The differences between the observed and computed values of μC_p, although rather large in percentage, correspond to only 0.005° C. or less in the measurement of μ, which is comparable with the accuracy attained in the calibration of the thermometers.

The computed values of μC_p were obtained, by means of the general relation $\mu C_p=\theta\left(\frac{\partial v}{\partial\theta}\right)_p-v$, from the following empirical "equation of state" for ammonia,

$$v=\frac{R\theta}{p}-\frac{A}{\theta^3}-\frac{Bp+C}{\theta^{11}}-\frac{Dp^5}{\theta^{19}}-E+\theta.f(p)$$

in which v is expressed in cm^3/g, p in atmospheres, and θ in ° C. (abs), and

$$R=4.8187 \qquad C=3.6934\times10^{26}$$
$$A=3.40645\times10^{8} \qquad D=7.1166\times10^{40}$$
$$B=3.2820\times10^{26} \qquad E=2.6000$$
$$f(p)=(5955.66-528.45p+24.589p^2-0.3538p^3)\ 0.10^{-6}$$

This equation is not only in agreement with experimental results on p,v,θ within their estimated limit of accuracy, but is thermodynamically consistent with equations representing experimental results on other properties of the vapor, notably C_p, and H at saturation. It was developed for the purpose of computing tables of thermodynamic properties of ammonia, given in Bureau of Standards Circular No. 142, which contains the same equation in engineering units. The constants in the equation were derived, in part, from the empirical equation for C_p given in this paper, and, in part, from the saturation data and unpublished data on the specific

volume of the superheated vapor obtained at this bureau. The last two or three digits in most of the constants are insignificant in computations of v to an accuracy of 1 part in 1,000, but they become significant if the equation is used in computing other properties.

The derived equation for μC_p is

$$\mu C_p = \frac{1.816 \times 10^8}{\theta^3} + \frac{(5.91 + 5.25p)\ 10^{26}}{\theta^{11}} + \frac{1.90\ p^5 \times 10^{41}}{\theta^{19}} + 0.347$$

where μC_p is expressed in joules per gram per meter of mercury, p in atmospheres, and θ in degrees absolute (° C. + 273.1°). The curves shown in Figure 8 represent values computed from this equation and the circles represent observed values of μC_p. Since the equation is in fair agreement with the experimental results on μ, and since determinations of μ were not made at each of the states desired, all values of μC_p used in the computation of C_p were computed from the above equation or, in reality, obtained from the original drawing of Figure 8.

Values of the thermal leakage coefficient, x, were obtained from Figure 6. The upper line in Figure 6 was assumed for all the computations in Table 5.

VII. FORM OF EMPIRICAL EQUATION

An empirical equation of the form, $C_p = f\ (p,\ \theta)$, was chosen for two reasons, (1) because that form is most convenient for correlating the specific heat and specific volume measurements by means of the Clausius equation

$$\left(\frac{\partial C_p}{\partial p}\right)_\theta = -\theta\left(\frac{\partial^2 v}{\partial \theta^2}\right)_p$$

and (2) because the final results of the experiments yield values of C_p at definite pressures and temperatures. A form of the function, $f\ (p,\theta)$ was sought which would represent the experimental results closely and which could be handled easily as regards differentiation and integration.

For use over an extended range, the equation should satisfy the conditions that C_p become infinite at the critical point and that the heat added for any finite temperature change be finite.

An equation which satisfied these conditions and at the same time gave the proper form for v at the critical point would probably be very complex. Since the desired equation and others derivable in part from it, were to be used in computing a table of the properties of superheated ammonia vapor which covered only the range of the experiments, it seemed preferable to make the equation as simple as

possible and not attempt to satisfy the conditions at the critical point.

A first approximation for the function, $f(p,\theta)$, was obtained from a simple "equation of state," similar to the one used by Callendar [16] for steam, namely,

$$v=\frac{R\theta}{p}-\frac{A}{\theta^3}$$

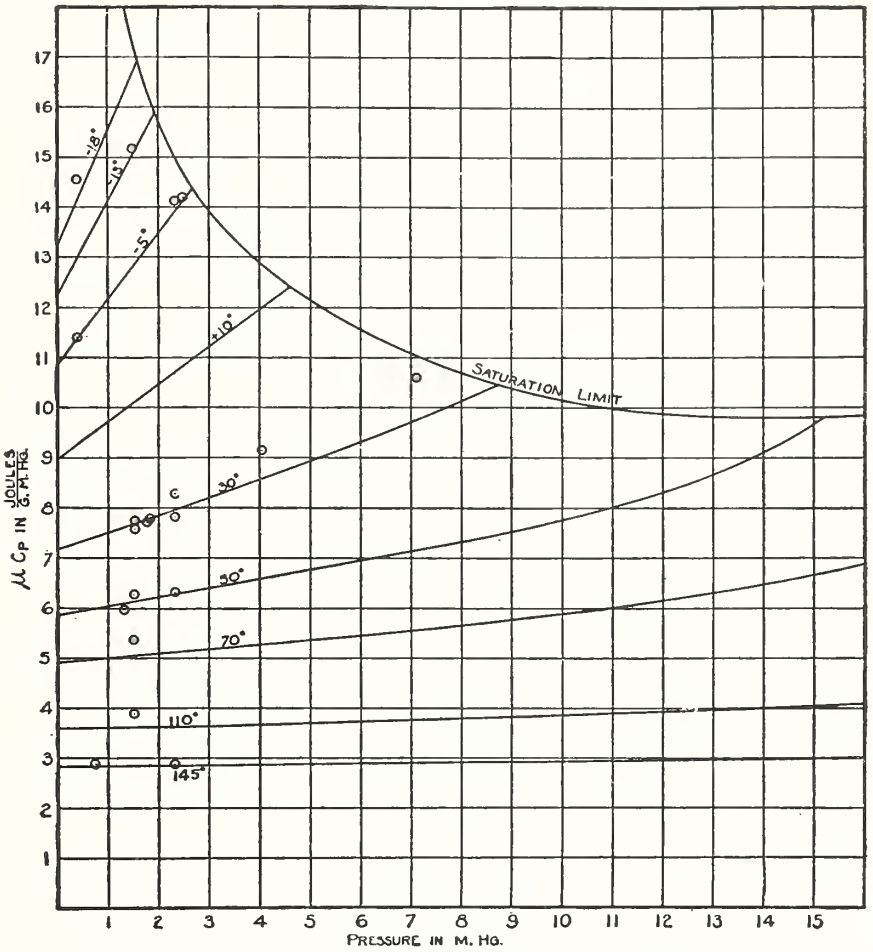

FIG. 8.—*Comparison of observed values of Joule-Thomson effect, μC_p, for ammonia vapor with curves calculated from empirical equation*

which was found to represent the experimental results on the specific volume within about 0.5 per cent. This equation when taken in conjunction with the Clausius equation, gave an equation of the form

$$C_p=C_{p0}+\frac{A'p}{\theta^4}$$

[16] "Thermodynamical Properties of Gases and Vapors," Proc. Royal Society (London), 67A, p. 266;, 1900. Also "Properties of Steam," Longmans, Green & Co., London; 1920.

where C_{p_0} represents the limiting values of the specific heat at zero pressure, and is a function of temperature only.

The extrapolation of the experimentally determined isothermals of Figure 10 to zero pressure, gives values of C_{p_0} which bear approximately a linear relation to the temperature, but are more closely represented by a function of the form

$$C_{p_0}=A+B\theta+\frac{C}{\theta}$$

Using then as an approximate equation

$$C_p=A+B\theta+\frac{C}{\theta}+\frac{Dp}{\theta^4}$$

and operating on the residuals, it was found necessary to use two additional terms in order to fit the results in the neighborhood of the saturation limit.

The form finally adopted to represent the results of the present investigation is

$$C_p=A+B\theta+\frac{C}{\theta}+\frac{Dp}{\theta^4}+\frac{p\,(E+Fp)}{\theta^{12}}+\frac{Gp^6}{\theta^{20}}$$

An equation, somewhat similar in form, has been found by Eichelberg [17] to represent well the experimental results on the specific heat of steam.

VIII. DISCUSSION OF RESULTS

The aggregate result of the entire series of determinations is represented by the following empirical equation:

$$C_p=1.1255+0.00238\theta+\frac{76.8}{\theta}+\frac{5.45p10^8}{\theta^4}+\frac{p(6.5+3.8p)10^{27}}{\theta^{12}}+\frac{2.37p^6 10^{42}}{\theta^{20}}$$

where C_p is expressed in joules per gram per degree centigrade, p in meters of mercury at 0°C. and standard gravity, and θ in degrees absolute (°C. + 273. 1°). The agreement between observed values of C_p and values computed from this equation is shown in Tables 4 and 5.

It may be noted that Table 4 contains the results of 108 complete experiments which give the value of the specific heat at 35 points in the pressure temperature range. These experiments were purposely made at chosen pressures and temperatures for convenience in the analysis and each point was established by two or more experiments. By interpolating over small intervals of temperature and pressure,

[17] "Zur Thermodynamik des Wasserdampfes," Zeitschrift des Vereines Deutsher Ingenieure, **61**, p. 750; 1917.

the results were corrected to seven temperatures (−15, 0, 35, 55, 75, 115, and 150° C.) and seven pressures (0.38, 1.5, 2.3, 4.05, 7.1, 10.4, and 15.1 m Hg). The average result at each point was used in

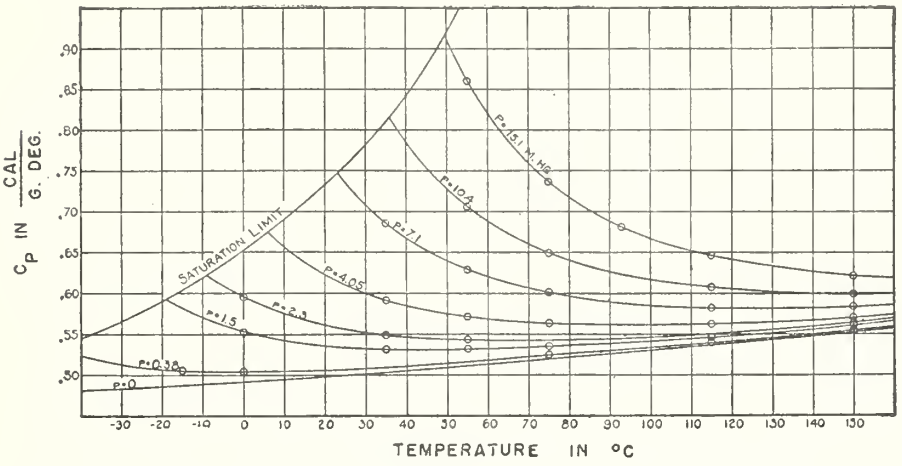

FIG. 9.—*Specific heat of ammonia vapor at constant pressure*

determining the constants in the empirical equation. The results at the 35 distinct points are shown graphically in Figures 9 and 10 with temperature and pressure, respectively, as the abscissas. The con-

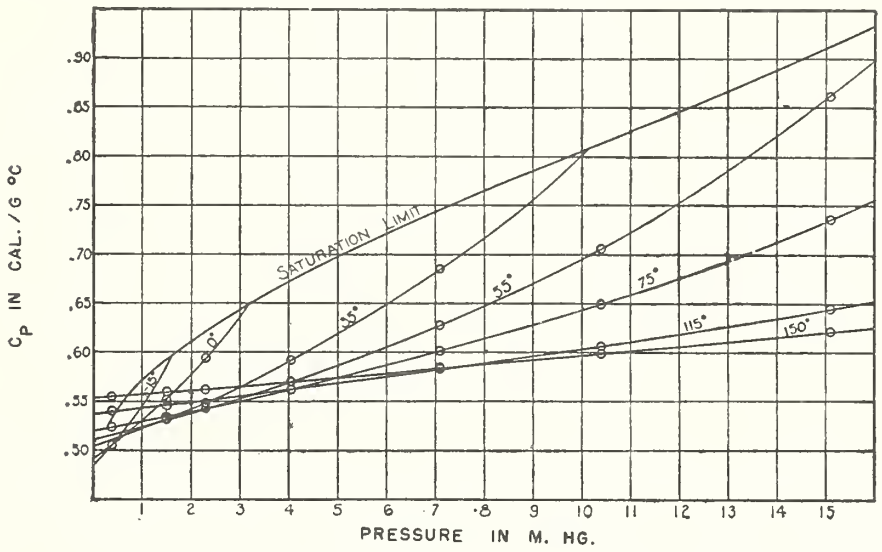

FIG. 10.—*Specific heat of ammonia vapor at constant pressure*

stant pressure and constant temperature lines represent values computed from the empirical equation and the circles, experimental determinations. The saturation limit of C_p is obtained by extrapola-

tion and is determined by the empirical equation taken simultaneously with the empirical equation for the vapor pressure.[18]

It may be noted in Table 3 that the experimental conditions were varied considerably in the various experiments. For example, experiments were made with temperature rises of approximately 5, 10, and 50°, and with rates of flow which varied by a factor of 4. These variations were introduced in order to note their effect upon the result and to detect sources of systematic errors. By examination of the deviations from the values given by the empirical equation it has not been possible to detect any systematic error.

An estimate of the accuracy of the measurements may be obtained by assigning average and maximum errors to each element which enters into the final result. Table 7 contains a tabulation of the magnitudes of these errors, which were estimated from the experience gained in making the measurements. They apply particularly to experiments with 10° temperature rise. The agreement between the observed and estimated average errors indicates that the empirical equation fits the results, to about the estimated precision attained in the measurements. It will be noted that the maximum deviation from the equation is less than the estimated maximum error, which means that all of the possible errors were probably not cumulative in any single experiment.

TABLE 7.—*Estimation of errors*

[All errors are expressed in per cent produced in the final result, C_p]

Source of error	Average error	Maximum error
Energy	±0.02	±0.05
Temperature rise	.05	.15
Rate of flow	.05	.15
Thermal leakage	.03	.10
Joule-Thomson correction	.02	.10
Total estimated	±.05	±.55
Observed deviations from empirical equation	±.07	±.26

IX. PREVIOUS DETERMINATIONS

Previous determinations of the specific heat of ammonia vapor are few in number and have been limited to determinations at one atmosphere pressure. A summary of these determinations is given in Table 8, which contains also a comparison with the present results within the temperature range of the latter.

[18] B. S. Sci. Papers, 16, p. 1; 1920 (Sci. Paper No. 369). Also in A. S. R. E. Jour., 6, p. 307; 1920, and in J. Am. Chem. Soc., 42, p. 206; 1919.

TABLE 8.—*Previous experimental determinations of C_p at one atmosphere pressure*

Date	Observer	Number of observations	Temperature range	Mean temperature	Mean observed C_p	Maximum deviation from mean	Deviation from present results
			° C.	° C.		Per cent	Per cent
1862	Regnault [1]	2	24–216	120	0.5084	0.2	−7.0
1876	Wiedemann [2]	12	25–100	62.5	.5202	2.3	−.6
1876	do	11	25–200	112.5	.5356	2.6	−.9
1910	Nernst [3]	4	365–569	467	.605	5.3	
1910	do	2	480–680	580	.658	1.8	
1915	Haber and Tamaru [4]	4	219–401	310	.605	.4	Arrangement B.
1915	do	6	337–508	422	.646	1.9	Arrangement A.
1915	do	3	337–508	423	.646	.4	Arrangement B.
1915	do	4	440–605	523	.693	.9	Arrangement B.

[1] Mémoires de L'Acadamie des Sciences, II, p. 161; 1862.
[2] Pogg. Ann. 157, p. 1; 1876.
[3] Zeit. für Elektrochemie, 16, p. 96; 1910.
[4] Zeit. für Elektrochemie, 21, p. 228; 1915.

Regnault and also Wiedemann used a method which consisted essentially of passing the heated vapor through a water calorimeter and observing the rate of flow of the vapor and the rise in temperature of the water. Their results on ammonia are in accord with their results on other gases and vapors in being systematically lower by a few per cent in general than those obtained by later experiments.

Nernst employed a comparative method in which various vapors passed through a preheater and then through a silver block which was inclosed in an electric furnace at a higher temperature. Adopting previously determined values of the specific heat of water vapor and carbon dioxide, he computed the specific heat of ammonia vapor from the observed rates of flow and the lowering of the temperature of the silver block. It may be remarked incidentally that the values of the specific heat adopted as standards are several per cent lower than those recently compiled by Holborn, Scheel, and Henning.[19] The variations in the experimental conditions were not sufficient to warrant an estimate of the accuracy of the results, although in the one case in which the rate of flow was doubled approximately an apparent increase of 10 per cent in the value of the specific heat was observed. Tests were made which indicated that no appreciable decomposition of the ammonia vapor took place at the temperatures used.

Haber and Tamaru used the continuous-flow electric method with a preheater partially inclosed in the furnace surrounding the calorimeter. The rate of flow of the ammonia vapor was varied by a factor of three. The main uncertainty in their results lies in the evaluation of the heat leakage. Two experimental arrangements were employed which differed only in the shielding of the electric heater. They state that the measurements with arrangement A constitute an absolute determination of C_p, while those with arrangement B constitute only

[19] Wärmetabellen, Friedr. Vieweg. & Sohn, Braunschweig: 1919.

relative determinations. The heat leakage with arrangement A, amounting from 10 to 25 per cent of the heat added electrically, was found to be independent of the rate of flow and was evaluated by the method of extrapolation to infinite flow. With arrangement B the heat leakage was found to be a function of the rate of flow and its magnitude was inferred from other experiments on air and carbon dioxide.

A comparison of the experimental determinations of C_p at one atmosphere pressure is shown graphically in Figure 11. It seems probable that the extrapolation of the present authors' empirical equation leads to high values of the specific heat at high temperatures. It is evident that the results of Nernst and of Haber and Tamaru are somewhat inconsistent with the present results and do not indicate

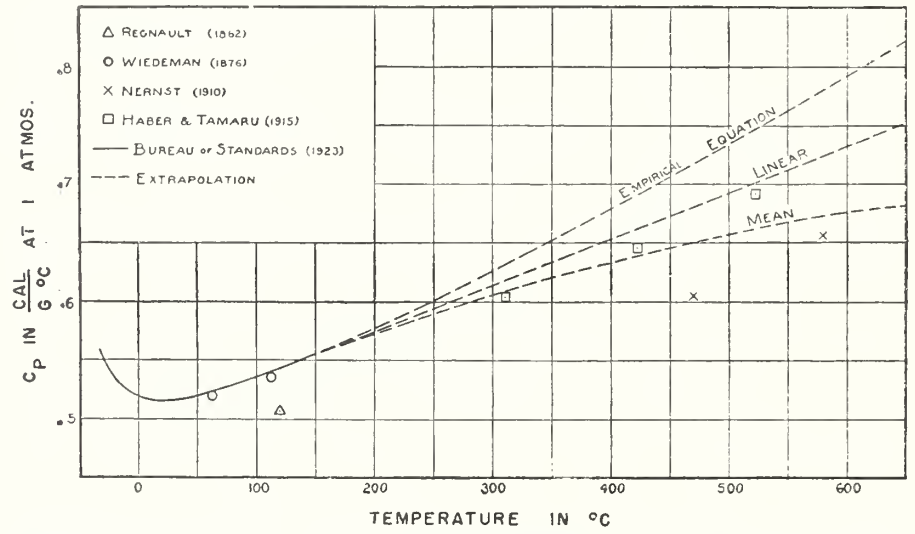

FIG. 11.—*Comparison of experimental determinations of specific heat of ammonia vapor at one atmosphere*

with certainty the trend of the curve at high temperatures. The assumption of a constant error of a few per cent in the results of Haber and Tamaru suggests the linear extrapolation shown in Figure 11. The lower curve represents the mean of the two sets of results.

With experimental determinations of C_p at one atmosphere pressure available, it is possible to derive values of C_p at higher pressures by means of an "equation of state." Goodenough and Mosher,[20] and Keyes and Brownlee,[21] have published, in their respective ammonia tables, the results of such a computation. Their equations, although widely different in form and based upon different data, give values of the specific volume of the superheated vapor which agree with the

[20] Univ. of Ill. Exp. Station, Bulletin No. 66; 1913.

[21] Thermodynamic Properties of Ammonia, John Wiley & Sons; 1916.

values given in the Bureau of Standards tables [22] to about 1 or 2 per cent, in general. It is interesting, therefore, to note the comparison of their computed values of C_p with the results of the present experiments as shown in Figure 12. For convenience in showing this comparison graphically, the values resulting from the present experiments are represented by the zero line and the curves show the percentage deviation of the computed values at various pressures.

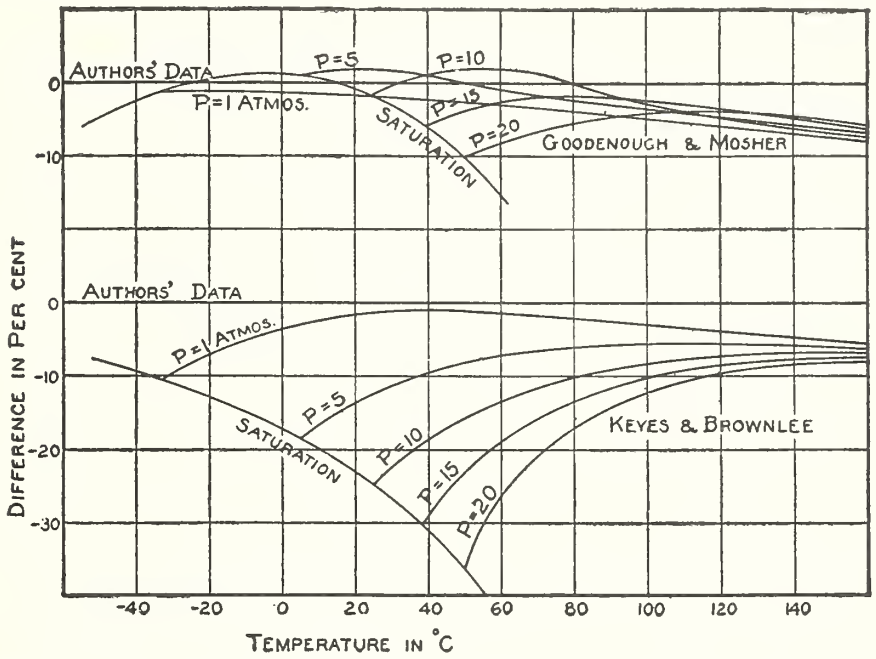

FIG. 12.—*Comparison of values of specific heat of ammonia vapor from earlier formulations with authors' experimental data*

X. SUMMARY

(1) A series of measurements of the specific heat of superheated ammonia vapor at constant pressure were made to supply data for tables of thermodynamic properties of ammonia suitable for use in refrigerating engineering.

(2) The continuous-flow electric method was employed, which consists of observing the rise in temperature produced by a measured electric power added as heat to a steady stream of vapor flowing at a measured rate. The advantages of this method for measurements of the specific heat of gases are pointed out. An abridged description is given of the flow calorimeter, which was especially designed and constructed for making these measurements on ammonia. The design is appropriate for similar measurements on other vapors and gases at

[22] Tables of Thermodynamic Properties of Ammonia, B. S. Circular No. 142, 1st edition; 1923.

temperatures below 150° C. and pressures below 100 atmospheres. Several features of this calorimeter are: Utility over a wide range of temperature and pressure; small thermal leakage; small size and heat capacity, requiring, therefore, only small samples of the purified material and a short time in coming to a steady state. A brief description is given of the thermoregulated baths, the temperature-control unit used for each bath, and the special devices used for regulating the rate of flow of the vapor. Many other details are described which have a bearing on the accuracy of the results obtained.

An expression is developed for the specific heat at constant pressure for a definite temperature and pressure which contains the three principal quantities observed—temperature rise, power input, and rate of flow—and, in addition, correction terms for thermal leakage, pressure drop, and the variation of the specific heat with temperature.

(4) The process of purification of the ammonia used in the measurements is described briefly. Tests made upon several samples, which were purified by this process, indicated the presence of less than 0.01 per cent by weight of water and less than 0.01 per cent by volume of noncondensing gases in the vapor phase.

(5) The procedures followed in the experiments and in the calibration of the instruments are described in detail. The correction for thermal leakage rarely exceeded 0.2 per cent of the heat supplied electrically in any experiment. The crucial test of the proper corrections for thermal leakage and pressure drop is the constancy of the final result with various rates of flow of the vapor.

(6) The results of 108 complete experiments serve to establish the value of the specific heat at 35 points in the temperature range -15 to $+150°$ C. and the pressure range 0.5 to 20 atmospheres. Several determinations of the Joule-Thomson coefficient were made in order to evaluate the correction for pressure drop in the specific heat experiments.

(7) An empirical equation of the form $C_p = f(p, \theta)$ was chosen to represent the experimental results within the range covered by the experiments.

(8) Values of C_p computed from the empirical equation agree with the experimental values within 0.3 per cent in all cases. The average agreement is 0.07 per cent.

(9) Previous measurements of the specific heat of ammonia vapor are briefly reviewed and tabulated.

(10) A table containing values of C_p at convenient intervals of pressure and temperature is appended.

XI. APPENDIX: TABLE OF C_p

TABLE 9.—*Specific heat of ammonia vapor at constant pressure*

[Calories per gram per degree centigrade]

Temperature °C.	Pressure in atmospheres. (Saturation temperature in italics.)										
	0	1 *−33.35°*	2 *−18.57°*	3 *−8.91°*	4 *−1.54°*	5 *+4.50°*	6 *9.67°*	7 *14.21°*	8 *18.27°*	9 *21.96°*	10 *25.34°*
Sat.	--------	0.5593	0.5935	0.6214	0.6457	0.6676	0.6877	0.7065	0.7242	0.7411	0.7575
−30	0.4829	.5513	--------	--------	--------	--------	--------	--------	--------	--------	--------
−20	.4856	.5344	--------	--------	--------	--------	--------	--------	--------	--------	--------
−10	.4885	.5247	.5704	--------	--------	--------	--------	--------	--------	--------	--------
0	.4917	.5194	.5532	.5931	.6392	--------	--------	--------	--------	--------	--------
10	.4950	.5168	.5426	.5724	.6062	.6440	.6860	--------	--------	--------	--------
20	.4985	.5161	.5364	.5593	.5848	.6130	.6438	.6775	.7142	--------	--------
30	.5021	.5167	.5330	.5510	.5708	.5924	.6158	.6410	.6682	.6974	.7289
40	.5058	.5181	.5315	.5461	.5619	.5788	.5970	.6164	.6371	.6592	.6826
50	.5097	.5201	.5313	.5434	.5562	.5699	.5843	.5997	.6158	.6329	.6510
60	.5137	.5227	.5322	.5423	.5529	.5641	.5759	.5883	.6012	.6148	.6290
70	.5178	.5256	.5338	.5423	.5513	.5607	.5704	.5806	.5912	.6022	.6136
80	.5220	.5288	.5359	.5432	.5510	.5589	.5671	.5756	.5844	.5935	.6029
90	.5262	.5323	.5385	.5449	.5515	.5583	.5654	.5726	.5800	.5877	.5955
100	.5306	.5359	.5414	.5470	.5528	.5587	.5648	.5710	.5774	.5839	.5905
110	.5350	.5397	.5446	.5496	.5547	.5598	.5651	.5705	.5760	.5817	.5874
120	.5394	.5437	.5481	.5525	.5570	.5616	.5662	.5710	.5758	.5807	.5856
130	.5440	.5478	.5517	.5557	.5597	.5637	.5679	.5721	.5763	.5806	.5850
140	.5486	.5520	.5555	.5591	.5627	.5663	.5700	.5737	.5775	.5813	.5852
150	.5532	.5563	.5595	.5627	.5660	.5692	.5725	.5759	.5792	.5826	.5860

Temperature °C.	10 *25.34°*	11 *28.47°*	12 *31.40°*	13 *34.15°*	14 *36.74°*	15 *39.19°*	16 *41.52°*	17 *43.75°*	18 *45.88°*	19 *47.92°*	20 *49.89°*
Sat.	0.7575	0.7734	0.7890	0.8044	0.8199	0.8355	0.8513	0.8674	0.8839	0.9009	0.9186
30	.7289	.7629	--------	--------	--------	--------	--------	--------	--------	--------	--------
40	.6826	.7077	.7346	.7634	.7946	.8286	--------	--------	--------	--------	--------
50	.6510	.6700	.6902	.7117	.7345	.7590	.7854	.8140	.8452	.8795	.9173
60	.6290	.6439	.6595	.6759	.6932	.7115	.7310	.7518	.7741	.7982	.8244
70	.6136	.6255	.6379	.6508	.6643	.6784	.6933	.7090	.7255	.7432	.7621
80	.6029	.6126	.6227	.6330	.6438	.6550	.6667	.6789	.6916	.7051	.7192
90	.5955	.6036	.6119	.6204	.6292	.6383	.6477	.6574	.6675	.6781	.6890
100	.5905	.5974	.6043	.6115	.6188	.6263	.6341	.6420	.6502	.6587	.6674
110	.5874	.5932	.5992	.6052	.6114	.6178	.6242	.6308	.6376	.6446	.6518
120	.5856	.5907	.5958	.6011	.6064	.6118	.6173	.6229	.6286	.6345	.6404
130	.5850	.5894	.5939	.5984	.6030	.6077	.6124	.6172	.6222	.6271	.6322
140	.5852	.5891	.5930	.5970	.6010	.6051	.6093	.6134	.6177	.6220	.6263
150	.5860	.5895	.5930	.5965	.6001	.6037	.6073	.6110	.6147	.6185	.6223

WASHINGTON, July 21, 1924.

Journal of Research of the National Bureau of Standards Vol. 59, No. 2, August 1957 Research Paper 2775

Thermal Conductivity of Beryllium Oxide From 40° to 750° C

David A. Ditmars and Defoe C. Ginnings

The thermal conductivity of beryllium oxide has been measured by an absolute method from 40° to 750° C. The apparatus employed steady-state longitudinal heat flow along a rod of high-fired beryllium oxide, surrounded by a tube with matching temperature gradient to minimize radial heat loss. The estimated accuracy of the measurements is about 3 percent. However, the values of thermal conductivity of the ideal beryllium oxide crystal are probably considerably higher than the values given because of the lower density (87 percent theoretical) of the sample used.

1. Introduction

Not only is beryllium oxide useful as a moderator in the utilization of atomic energy, but it has an unusually high thermal conductivity, much higher than other nonmetals and even higher than most metals over a limited temperature range. At room temperature, its thermal conductivity is about that of aluminum, whereas its electrical conductivity is extremely low. It was the purpose of this investigation to measure the thermal conductivity of beryllium oxide in the high-temperature range.

2. Sample

The beryllium oxide was originally fabricated by the Norton Co. by hot-pressing. A rough sample was taken from this material and machined, at the Oak Ridge National Laboratory, to a cylindrical rod about 0.5 in. in diameter and 6 in. long. From information obtained on this material, together with that obtained from a spectrographic analysis, it seems likely that its impurities (other than carbon) were less than 0.2 percent. It is possible that carbon was present in larger amounts in the sample, although it was white, with only occasional dark inclusions. The sample was fired in the NBS Mineral Products Division at about 1,700° C and machined to the form of a true cylinder having a diameter of 0.4524 in. at room temperature and an average density of 2.62 g/cm^3 (87 percent of single crystal). The method of original fabrication by hot-pressing may have caused a variation in density in the sample of several percent.

3. Method and Apparatus

The method and apparatus have been described briefly in technical reports [1, 2].[1] The method used was absolute in that the results were obtained without comparison with another material. A longitudinal heat flow was used to establish a temperature gradient in the sample. From the measured values of heat flow, temperature gradient, and the cross section of the sample, the thermal conductivity of the sample was calculated. Longitudinal rather than radial heat flow was used in order to obtain a reasonable temperature gradient in a conveniently shaped sample. The temperature gradient on the sample was determined by measuring the temperatures along the sample. The longitudinal heat-flow method, as applied to relatively long samples, has the inherent disadvantage that radial heat losses to the surroundings may reduce the accuracy of the results. However, in this case, the conductivity of the BeO was so high that radial heat losses did not seriously limit the accuracy of the results.

A scale diagram of the essential parts of the apparatus is shown in figure 1. Measured electrical heat, introduced in the "sample heater" at the top of the sample (BeO), flowed down the sample and its "adapter" to a heat sink. The sample heater consisted of six small helices of No. 38 Nichrome wire located in holes in the top of the sample. The adapter was used here to position the sample, as well as to fill in the needed length, because the apparatus was built to accommodate samples longer than 6 in. Anhydrous boric oxide was used to give good thermal contact between the sample and adapter, and between the adapter and the sink. This compound has a very low vapor pressure and has excellent wetting properties, maintaining good thermal contact at temperatures far below its melting point. The sink was cooled with either water or air, depending on the temperature range, and was equipped with a heater and thermocouple so that it could be automatically kept at a constant temperature.

The temperatures along the sample were measured with three thermocouples (No. 36 AWG platinum-platinum-rhodium) having reference junctions at 0° C and principal junctions on the sample at the three levels shown in figure 1. In addition to these three absolute thermocouples, a differential thermocouple was also used to ascertain directly the temperature difference between the upper and lower levels on the sample. All of the thermocouples on the samples were made with junctions peened into small holes (about 0.6 mm in diameter and depth) in the cylindrical surface of the sample. In order that the temperature gradient measured on the sample would correspond to the electric heat put into the top of the sample, precautions were taken to minimize radial heat loss along the sample. For this purpose, the sample was surrounded by a "guard tube"

[1] Figures in brackets indicate the literature references at the end of this paper.

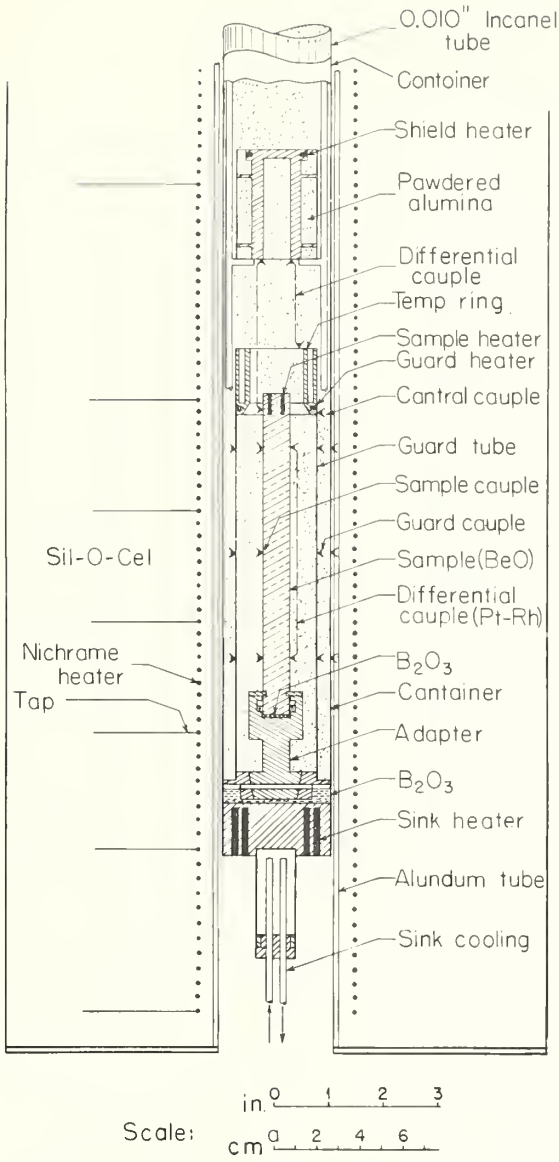

FIGURE 1. *Thermal-conductivity apparatus.*

(Inconel, 0.03-in. wall), with temperatures corresponding to those in the sample. Temperatures along the guard tube were measured with three platinum–platinum-rhodium thermocouples, with principal junctions attached to the guard tube at levels corresponding to those of the sample thermocouples. Three additional thermocouples, at the same levels on the guard tube but at different azimuths, were also provided. The top of the guard tube was heated by the "guard heater", and its temperature was controlled automatically, using the "control couple" close to the heater. Another heater with a control thermocouple (not shown in fig. 1) was provided at the bottom of the guard tube, but it was found unnecessary to use it when the furnace temperatures were suitably controlled. The top portion ("tempering ring") of the guard tube was made of thick nickel to which the electrical leads to the sample were thermally connected, so that it served as a tempering region for bringing the leads to the temperature of the top of the sample, and thus to reduce heat conduction along them. A "thermal shield" (nickel) and heater, placed above the sample and tempering ring, also served for this purpose and to prevent heat transfer upward through supports and insulation.

Although the apparatus shown in figure 1 has been used only for measuring the thermal conductivity of solids, it was designed so that it could be used also for high-conductivity liquids. For this application, the liquid would be contained in a thin-walled tube equipped with a suitable heater and a liquid expansion chamber extending up into the shield. To obtain the thermal conductivity of the liquid, it would be necessary to account for the thermal conduction in the container tube by making another experiment with the liquid replaced by a powder of very low and known thermal conductivity.

The whole assembly, supported by rods extending down to the bottom of the guard, was filled with fine aluminum oxide powder for insulation and enclosed in a 0.010-in. Inconel tube, which served to hold the powder. This tube, fitting closely in the "container" (0.035-in. Inconel tube) centered along the axis of the furnace, facilitated assembly. Thermocouple and heater leads were brought out from this container through an insulating seal at the top (not shown in fig. 1), so that the conductivity apparatus could either be evacuated or filled with argon. Because experiments with the apparatus had shown the electrical insulation to fail when it was evacuated at high temperatures, the apparatus was filled with argon after evacuation at moderately high temperatures to outgas the aluminum oxide. The thermal-conductivity apparatus was maintained at the chosen temperature by the surrounding furnace, which was equipped with numerous taps on the heater winding to give the desired vertical temperature gradients. Two automatic regulators, actuated by thermocouples in the furnace, were used to maintain constant temperatures.

4. Experimental Procedure

Two basic types of experiment were performed for each measurement of thermal conductivity. In the first type (called a *conductivity experiment*), the furnace temperature was controlled to the desired value, a known constant electric power was put into the sample heater, the temperatures of the guard and shield were adjusted to match those on the sample as closely as possible, and the sink temperature was adjusted to a constant value. After a steady state was obtained, several consecutive sets of observations of thermocouple emf and sample power were recorded. In the second type of experiment (called *calibration experiment*), no power was put into the sample heater, but in other ways, the experimental procedure was similar to the first. The purpose of this experiment was to correct for errors that did not depend on the power transmitted through the sample. Errors of this type are those due to differences, in thermocouples and those resulting from unknown heat leaks, which presumably were the same in both

types of experiments. Several other experiments were made to detect other errors and to determine their importance. Some of these experiments are described later.

Several hours were usually required to bring the various parts of the apparatus to the desired temperatures and to make sure that these temperatures were not changing significantly. The final data were usually obtained in a period of about 30 min, subsequent to an interval of about an hour during which the temperatures were observed to be constant. Automatic thermoregulators were used to control the temperatures of the furnace, guard, and sink.

5. Calculation of Results and Uncertainties

The conductivity values were calculated from the observed quantities by means of the equation

$$k=\frac{\dot{Q}\Delta X_0}{A_0(1+\alpha t_a)\Delta t},$$

where

k=thermal conductivity (watts cm^{-1} deg^{-1} C) at temperature t_a.
t_a=average temperature of sample between thermocouples.
$\dot{Q}$=heat-flow rate (watts).
ΔX_0=thermocouple spacing at 0° C (cm).
A_0=cross-sectional area at 0° C (cm^2).
α=coefficient of linear thermal expansion (deg^{-1} C).
Δt=temperature difference (deg C) between thermocouples.

This equation is valid for steady-state longitudinal heat flow over a small temperature interval. The determination of these factors in the conductivity equation, together with a consideration of their uncertainties, will now be discussed individually. The uncertainties referred to in this report are the authors' estimates (based on their judgment) on the basis that the observed quantity would have about an equal chance of being within that limit as being outside it, and that the sign of the uncertainty is just as likely to be positive.

5.1. Heat-Flow Rate ($\dot{Q}$)

a. Electric Power

Heat was generated by direct current in the sample heater, and power was measured in a conventional manner, using a potentiometer in conjunction with a high-resistance volt box to measure the potential drop across the heater, and a standard resistor in a current lead to measure the current. The errors in these electrical measurements were almost negligible. In measuring the potential drop across the heater, the potential terminals were located to evaluate properly the heat that went to the sample. Because the sample heater was made with very high resistance (relative to that of the heater leads), the uncertainty in the location of the potential terminals resulted in only about 0.1-percent uncertainty in the measured thermal conductivity.

b. Heat Flow From Sample to the Tempering Ring

In addition to the electric-power input to the top of the sample, it is necessary to consider the heat transfer between the sample and its surroundings. Because of the excess temperature of the sample heater, heat flowed along the heater leads to the tempering ring; the uncertainty in this heat flow (taken to be 50 percent of the correction) averaged about 0.24 percent of the total heat flow in the sample. In addition to this heat flow, there was the heat flow between the top part of the sample and the tempering ring. The evaluation of this was difficult because of the configuration and the temperature distribution on the top part of the sample where the sample heater was located. Using differential thermocouples, observations were made of the temperature difference between the isothermal tempering ring and a point on the top part of the sample. The location of this point was determined by calculation so that the net heat flow from the top of the sample to the tempering ring would be proportional to the emf of the differential thermocouple. The height of the top of the sample relative to the guard was made so that the bottom of the sample heater was at the same level as the bottom of the tempering ring. In the actual experiments, the tempering-ring temperature depended on the power in the guard heater and was indicated by the differential thermocouple to be 2 or 3 deg higher than the temperature of the sample, making necessary a correction for the resulting heat flow. It was found convenient to evaluate this correction experimentally by making two conductivity experiments in which only the tempering-ring temperature was changed and the furnace temperature adjusted to maintain the match between the guard and sample thermocouples. Using the resulting change in sample gradient, the data were corrected to correspond to no difference in temperature as indicated by the differential thermocouple. However, there still remained an uncertainty in heat flow due to some uncertainty in the proper location of the thermocouple junction on the sample head. It was estimated that the uncertainty in the heat flow between the sample and tempering ring, excluding heat flow along leads mentioned above, resulted in an uncertainty in measured conductivity averaging about 0.5 percent.

c. Heat Flow Down the Insulating Powder

Even when the guard temperatures matched sample temperatures, some of the heat input to the sample necessarily went to maintain some of the longitudinal heat flow in the insulating powder between the sample and guard. The conductivity of the aluminum oxide powder with argon gas was determined approximately by a few experiments as it was used in the apparatus. The temperature distribution in the insulation had been previously estimated with a resistance analog computer, setting up boundary conditions corresponding to the configuration and assumed temperatures of the sample and guard. It was estimated from these results

that when the thermocouple on the top part of the sample indicated the same temperature as the guard ring, the sample heater contributed only 16 percent of the total longitudinal heat flow in the powder, the remainder of the heat being furnished by the guard. Under this condition, about 0.2 percent of the heat of the sample heater flowed down through the insulating powder. The uncertainty of this correction was estimated to give less than 0.1-percent uncertainty in the measured thermal conductivity.

d. Heat Flow Between Sample and Guard

Because it was found impractical to match the sample and guard temperatures exactly during all conductivity experiments, experiments were made that permitted calculation of corrections for imperfect matching. For each guard thermocouple, two thermal-conductivity experiments were made, varying only the difference between that guard thermocouple and the corresponding thermocouple on the sample. From the resulting change in temperature gradient on the sample in these two experiments, it was possible to estimate a correction for small differences in matching guard and sample thermocouples. It was calculated that there was an uncertainty of about 50 percent in correcting for heat flow between the sample and the guard. This uncertainty resulted in an average uncertainty in measured conductivity of about 0.3 percent.

e. Heat Flow Into Heat Capacity of Sample

If the temperature of the sample were changing with time, some of the heat input would go to produce this change, and the temperature gradient on the sample would not correspond to the heat input at the top of the sample. In all experiments, the rate of temperature change was less than 0.8 deg C/hr, corresponding to an effect of 0.5 percent in the calculated value of conductivity. The average uncertainty in the correction for this was negligible.

5.2. Thermocouple Spacing (ΔX_0)

The distance between the principal junctions of the upper and middle sample thermocouples was 4.97 cm at 0° C, whereas the corresponding distance for the middle and lower thermocouples was 5.05 cm; this gives 10.02 cm for the distance between the extreme absolute thermocouples. The distance between junctions on the differential thermocouple was 10.01 cm. These distances, taken as the lengths between centers of the thermocouple holes, were measured to better than 0.01 cm with a traveling microscope, but because the thermocouples were peened into holes 0.06 cm in diameter, the possibility of nonuniform thermal contact makes a tolerance of 0.03 cm appear more realistic. This tolerance corresponds to 0.3-percent uncertainty in the 10-cm spacing between the sets of thermocouples used in the conductivity calculations. The effect of thermal expansion on both thermocouple spacing and cross-sectional area is lumped into the correction $(1+\alpha t_a)$, which is described later.

5.3. Cross-Sectional Area (A_0)

The sample was ground to have a uniform diameter of 0.4524 ± 0.0003 in., corresponding to a cross-sectional area of 1.038 cm^2. The uncertainty in this area was estimated to be less than 0.1 percent.

5.4. Thermal-Expansion Correction $(1+\alpha t_a)$

Thermal-expansion changes the thermocouple spacing by the factor $(1+\alpha t_a)$, and the cross-sectional area by the factor $(1+\alpha t_a)^2$, resulting in the $(1+\alpha t_a)$ term given in the conductivity equation. The coefficient of linear thermal expansion (α) has been determined by White and Schremp [3]. At the highest temperatures (747° C) of the conductivity experiments, the correction for expansion amounted to about 0.6 percent, with negligible uncertainty in the measured conductivity.

5.5. Temperature Difference (Δt)

The accurate measurement of the temperature difference on the sample was difficult, requiring a number of tests to eliminate or evaluate certain errors. As described in section 3, two different thermocouple systems were used to measure the temperature difference over the 10-cm length on the sample. The two independent thermocouple systems served to check on each other, usually agreeing on the measured temperature difference to better than 1 percent.

All temperatures were measured with platinum–platinum-rhodium thermocouples of No. 36 AWG wires. A sample thermocouple was calibrated at several points between 0° and 1,000° C in the Pyrometry Laboratory of the National Bureau of Standards. No significant difference was observed between the thermoelectric power of this sample and that given in the standard tables [4]. Even though the thermocouples were all made from wire off the same spools, it was possible that they had slightly different thermoelectric powers. Although these differences might not be serious for measurement of absolute temperatures, they could be significant for measurement of small temperature differences at high temperatures. These differences were automatically accounted for by the calibration experiments mentioned previously, in which no power was put into the sample heater. These calibration experiments gave differences in thermocouple readings, which increased regularly up to 470° C, and amounted to as much as 7 μv at this temperature. At temperatures approaching 750° C, the differences became both larger and more irregular, so that after each conductivity experiment, a calibration experiment was made to evaluate the differences.

In addition to the differences described above, the evaluation of Δt was uncertain because of the occasional effect of high humidity on the potentiometer used to measure the thermocouple emf. This effect was observed as a reading on the potentiometer, even when the potential across its terminals was

zero. When the value of Δt was observed, using the differential thermocouple, the value was subject to the full potentiometer uncertainty (about 2 μv) because only one reading was involved. When the value of Δt was determined by using the two absolute thermocouples, most of this potentiometer uncertainty was reduced (to about 0.5 μv) because the value of Δt was obtained from a difference of two readings. It is for this reason that the uncertainties in the value of Δt, using the differential thermocouple, were larger than the uncertainties when using the absolute thermocouples, averaging about 1.5 percent as compared to 0.4 percent. That the two thermocouple systems usually agreed to better than 1 percent is evidence that the error due to the humidity effect on the potentiometer was not excessive.

6. Results

The results of the individual thermal-conductivity measurements on beryllium oxide are given in table 1. Values of observed conductivity (k) are given as determined by using each of the thermocouple systems (absolute and differential) at the average temperature (t_a) of that portion of the sample measured by the thermocouples. At the lower temperatures, where the thermal conductivity of the beryllium oxide changes rapidly with temperature, small corrections to conductivity were made for the curvature of the conductivity-temperature function. In this table, the quantities given are corrected for all known errors. In the previous discussion, each uncertainty has been estimated by the authors on the basis that the observed quantity would have an equal chance of being within that limit as being outside that limit. These uncertainties have been combined (square root of the sum of the squares) and arbitrarily increased by over a factor of 2 to give more realistic values of estimated error listed in table 1.

Table 1 indicates that the results, using the absolute thermocouples, seem to be reliable to about 2 percent. The experiments under 60° C are not as accurate as the other experiments. This is due to the smaller temperature drop in the sample, first because the limitations of the heat sink made it necessary to use lower power, and second, because the thermal conductivity of the beryllium oxide was so high in this low-temperature range. The larger error estimated by using the differential thermocouple in this low-temperature region is due to the humidity trouble mentioned previously. No results are given for measurements with absolute thermocouples above 500° C because of failure of their electrical insulation.

A smooth function of thermal conductivity was obtained graphically from the observed values in table 1, giving greatest weight to those values having the smallest estimated errors. Table 2 gives smoothed values of the conductivity at even temperatures as obtained from the graph. Figure 2 gives the deviations of the results (obtained with the two different thermocouple systems) from the smooth

TABLE 1. *Experimental results*

Date (1954)	t_a	Power	Absolute thermocouples			Differential thermocouples		
			Δt	Observed k	Estimated error [a]	Δt	Observed k	Estimated error [a]
	°C	w	°C	w/cm-°C	%	°C	w/cm-°C	%
Aug. 25	38.2	0.8960	3.95	2.19	5.4	4.11	2.10	19.2
Aug. 26	46.2	1.4452	6.84	2.04	3.2	7.03	1.98	10.7
Aug. 25	52.6	1.8894	9.41	1.94	2.6	9.61	1.90	7.9
Aug. 27	59.7	2.3620	12.15	1.879	2.1	12.33	1.849	6.2
Aug. 24	85.8	3.3179	19.16	1.674	1.6	19.28	1.661	4.0
Oct. 8	86.2	3.8007	21.88	1.679	1.7	22.09	1.660	3.6
Sept. 29	86.9	3.6073	20.90	1.668	2.1	21.07	1.652	3.9
Sept. 23	87.3	3.6084	20.86	1.672	1.8	21.08	1.652	3.7
Sept. 30	87.3	3.6138	21.01	1.662	1.7	21.17	1.647	3.7
Aug. 31	91.4	2.5903	15.20	1.647	2.0	15.10	1.655	4.9
Sept. 1	123.8	2.4474	16.26	1.454	1.7	16.33	1.446	5.4
Sept. 15	153.0	2.4894	18.27	1.316	1.7	18.36	1.308	4.1
Sept. 2	153.4	2.4795	18.27	1.311	1.8	18.37	1.302	4.2
Oct. 11	202.0	3.9603	33.80	1.131	2.0	33.65	1.135	2.6
Aug. 23 [b]	202.1	3.8745	33.29	1.124	1.6	33.10	1.128	2.4
Aug. 18	241.5	3.7312	36.20	0.995	1.7	35.87	1.002	2.3
Aug. 19	241.4	3.7396	36.51	.989	2.2	36.19	0.996	2.7
Aug. 20 [b]	251.4	0.8739	8.95	.942	2.2	8.85	.952	6.5
Sept. 20	287.3	2.3441	25.93	.872	1.8	25.54	.884	2.8
Sept. 17	287.7	2.3378	25.87	.872	1.9	25.71	.876	2.9
Oct. 7	379.5	3.5169	48.12	.704	1.5	47.77	.709	2.0
Oct. 5	380.4	3.5378	48.64	.701	1.9	47.60	.715	2.3
Oct. 12	439.2	3.3054	51.83	.614	1.2	51.82	.614	1.7
Oct. 18	517.2	2.9239	------	------	------	53.63	.524	2.7
Oct. 19	578.7	2.5664	------	------	------	51.54	.478	3.5
Oct. 20	646.7	2.7048	------	------	------	59.94	.433	2.4
Nov. 2	747.9	2.6370	------	------	------	65.84	.384	4.3

[a] Estimated error is the authors' estimate, considering only the various uncertainties mentioned in the text.
[b] The results on August 20 and 23 represent averages of 2 experiments on each day.

function. At 50° C and below, the observed values deviate markedly from the smooth function, giving values at 40° C that are 4 percent different. These deviations are probably due to the very small temperature difference of 4° C in the sample, so that errors in the measurement of this temperature difference have greater influence on the result. Figure 2 also shows the results at 251° C to be about 3 percent lower than the other results. It seems probable that this departure is also due to the lower temperature difference on the sample resulting from the lower power; the power here was only one-fourth the power in the other experiments in this temperature range. If it is assumed that there existed an unknown constant absolute error in either heat flow or temperature difference, the deviations of about 3 percent in the low-power experiments would indicate that the experiments with the higher power might be in error by about 0.8 percent. Consequently, the authors believe that the over-all accuracy of the results is more likely to be about 3 percent instead of the 2 percent indicated by the estimated errors listed in table 1.

TABLE 2. *Thermal conductivity of* BeO *(density=2.62 g/cm³)*

(Smoothed values)

t	k	t	k
° C	*w/cm-° C*	° C	*w/cm-° C*
30	2.155	400	0.666
50	1.967	450	.598
100	1.581	500	.541
150	1.328	550	.498
200	1.131	600	.462
250	0.972	650	.433
300	.845	700	.406
350	.746	748	.384

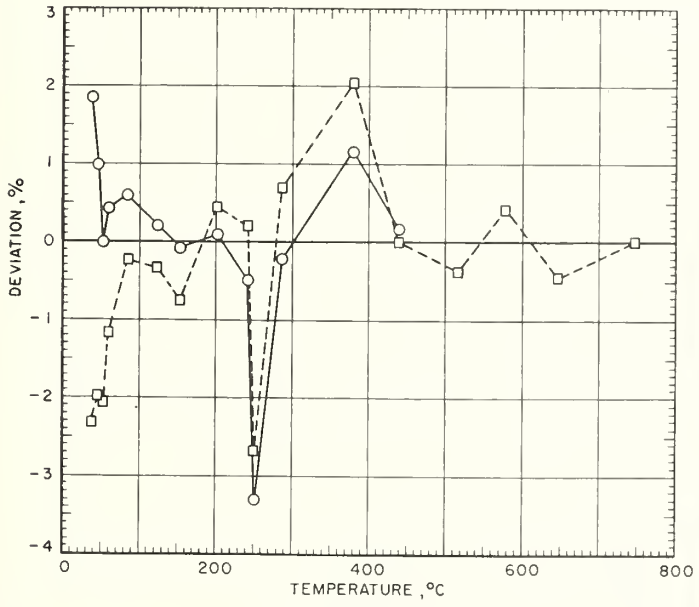

FIGURE 2. *Deviations of beryllium oxide thermal-conductivity data.*

Base line=NBS smoothed data.
○, NBS (absolute couples); □, NBS (differential couples).

No attempt has been made to correct the thermal-conductivity values for the NBS sample to correspond to zero porosity. Because the density of this sample was only 2.62 g/cm³ compared to about 3.0 for the ideal crystal, the thermal conductivity of the crystal should be significantly higher than the values given in table 2. From the investigation of Francl and Kingery [5], it would appear that the conductivity of the ideal crystal would be about 15 percent higher. However, the measurements of Powell [6] on beryllium oxide specimens (densities 1.85 to 2.82 g/cm³) would indicate a much larger correction. The authors feel that the correction for porosity is uncertain and that there are other factors beside porosity that also should be accounted for. One of these factors is the degree of bonding of the individual particles by the firing process.

7. Comparison With Other Results

Figure 3 gives a comparison of the results of the NBS measurements on BeO with the results of measurements at other laboratories on other samples. At the lower temperatures, the agreement with Scholes [7] is probably as good as the physical states of the two samples permit. Scholes used a sample having a density of about 2.97 g/cm³ as compared with the NBS sample having a density of 2.62. At higher temperatures, the results of Francl and Kingery [5] are consistently higher than the NBS results. They used a sample having a density of 2.86 g/cm³, but this would probably account for only a small part of the difference. The results of

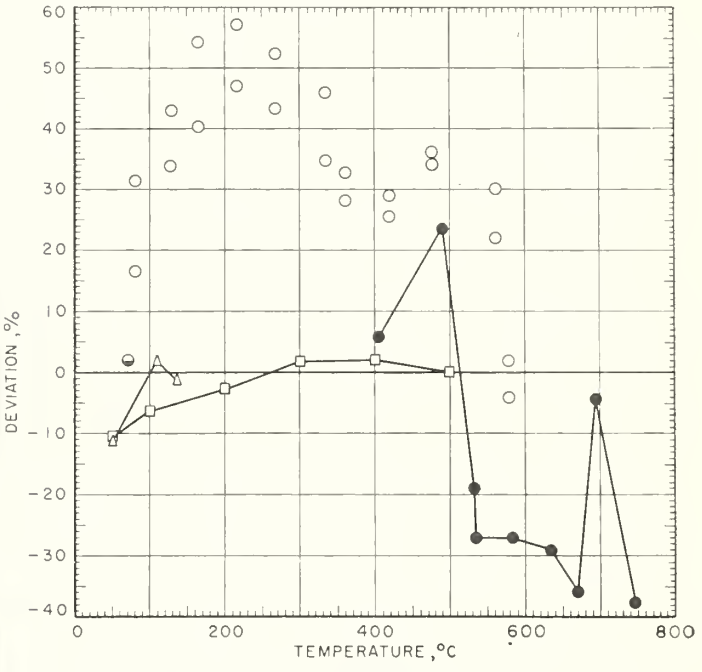

FIGURE 3. *Comparison of beryllium oxide thermal-conductivity data.*

Base line=NBS smoothed data.
△, Scholes (1950); ○, Francl and Kingery (1954); ●, Adams (1954); □, Powell (1954); ◒, Weeks and Seifert (1953).

Adams [8] are lower than the NBS results at higher temperatures, even though the samples had about the same densities (2.7 as compared to 2.62). Powell [6] measured the thermal conductivities of several samples of BeO having densities ranging from 1.85 to 2.82. His results, shown in figure 3, are interpolated for a density of 2.62 to compare with the NBS results; in general, the agreement is very good. Weeks and Seifert [9] determined the conductivity of a sample of BeO (density 3.0) at 70° C. Their agreement with the NBS value is probably better than the differences in the samples warrant.

The authors thank L. M. Doney, Oak Ridge National Laboratory, for furnishing the BeO sample used in this investigation, and S. M. Lang, National Bureau of Standards, for firing the sample at a high temperature.

The work described in this paper was sponsored by the Wright Air Development Center. The results that are given were taken from a report [2] submitted to that agency.

8. References

[1] E. D. West, D. A. Ditmars, and D. C. Ginnings, Technical Report 53–201, Part 5, to Wright Air Development Center (1954).
[2] D. A. Ditmars and D. C. Ginnings, Technical Report 53–201, Part 6 (1955).
[3] H. E. White and R. M. Schremp, J. Am. Ceram. Soc. **22,** 185 (1939).
[4] Reference tables for thermocouples, NBS Circular 506 (1951).
[5] J. Francl and W. D. Kingery, J. Am. Ceram. Soc. **37,** 80 (1954).
[6] R. W. Powell, Trans. Brit. Ceram. Soc. **53,** 389 (1954).
[7] W. A. Scholes, J. Am. Ceram. Soc. **33,** 111 (1950).
[8] Milton Adams, J. Am. Ceram. Soc. **37,** 74 (1954).
[9] J. L. Weeks and R. L. Seifert, Rev. Sci. Instr. **24,** 1054 (1953).

Washington, August 22, 1955.

Thermal Conductivity of Nitrogen from 50° to 500°C and 1 to 100 Atmospheres*

R. L. Nuttall[1] and D. C. Ginnings

A new apparatus has been constructed for measurements of the thermal conductivity of gases up to 500°C and 100-atmosphere pressure. The parallel-plate method was used with a spacing of about 0.5 millimeter between the hotplate and coldplate. A capacitance method was used to measure the effective spacing and area of the plates under the conditions of the experiment. No solid material was used between the plates. The effect of radiation was minimized by use of polished silver parts and was accounted for by experiments with the conductivity cell evacuated. Measurements on nitrogen were made at 1, 50, and 100 atmospheres, and from 50° to 500°C. It is believed that the accuracy of the results is about 0.5 percent, except at the highest gas densities.

1. Introduction

Accurate data on the thermal conductivity of gases are needed for two reasons. First, they are needed to check present theories of heat conduction in gases. Experimental measurements at very high temperatures and pressures are extremely difficult, so that theoretical means of predicting thermal conductivities in this range are needed. Second, accurate data are needed on at least one gas so that engineering data on other gases can be obtained with relatively simple apparatus by a comparison method. The present apparatus was constructed primarily to furnish very accurate data for use as standards by others making thermal-conductivity measurements on gases. Nitrogen was chosen as the first gas to be measured for several reasons. More measurements have been made on nitrogen than on any other pure gas. It is readily available in a state of high purity and is entirely suitable as a standard reference gas for use in calibrating apparatus for relative measurements.

2. Method

Measurements of thermal conductivity of gases in a steady state have been made by two general methods, radial heat flow and linear heat flow. Most measurements have been made with radial heat flow, either from a hot wire or between coaxial cylinders. In principle, these measurements are susceptible to convection errors. Elimination of these errors at the high pressures requires extremely small dimensions, which may be difficult to determine. The linear heat flow method is free from convection if the heat flow is downward. For this reason, the parallel-plate method was chosen for these measurements up to 100 atm. The spacing between the plates was made small to minimize the error caused by radial heat transfer. In addition, the small spacing reduces the possibility of convection in case the plates are not quite horizontal.

The correction for heat transfer by radiation between the hotplate and the coldplate was evaluated by an experiment with the conductivity cell evacuated. Of course, this assumes that no appreciable part of the radiation is absorbed by the gas in the conductivity experiment. In all the experiments, it was necessary to know the effective spacing between the plates. Frequently, solid spacers (of known dimensions) are used between the hotplate and coldplate. No such spacers were used in this apparatus because it was believed that the heat transfer through the contact area of the spacers and plates might be different with gas present than with the cell evacuated. The radiation correction experiment would thus be partially invalidated. The effective spacing was measured by a capacitance method under the actual conditions of the experiment. This method has several advantages over the usual method with measured spacers. First, the above-mentioned uncertainty in the effect of contact is eliminated. Second, the capacitance method automatically accounts for any change in dimensions. Third, because the direct capacitance between the hotplate and coldplate is measured, nonlinear heat flow at the circumference of the hotplate is accounted for.

The thermal conductivity, k (w cm^{-1} deg C^{-1}), for heat flow between parallel plates is given by the equation

$$k=\frac{\dot{Q}\Delta X}{\Delta t A}, \tag{1}$$

where Q is the rate of heat (watts) flowing only by conduction from the hotplate through the gas to the coldplate, Δt is the temperature difference (deg C) between the hotplate and coldplate, ΔX is the effective distance (cm) between the two plates, and A is the effective area (cm^2) of the hotplate. The factor $\Delta X/A$ may be considered as the constant of the "conductivity cell" determined by the capacitance method, so that

$$k=\frac{0.0885516\dot{Q}}{C\Delta t}, \tag{2}$$

*This work was supported in part by the National Advisory Committee for Aeronautics.

[1] Present address Argonne National Laboratory, Lemont, Ill.

where C is the direct capacitance (micromicrofarads) between the hotplate and the coldplate, assuming the material between the plates to have a dielectric constant of unity corresponding to a vacuum. With the gas between the plates, a small correction must be made for its dielectric constant. The conduction equation (2) would apply, of course, to any two surfaces, as well as to parallel plates, provided only that the temperature and electric fields are geometrically similar.

3. Experimental Procedure

3.1. Apparatus

The general assembly of the thermal-conductivity cell, the pressure vessel, and the surrounding furnace is shown in figure 1. The hotplate (H), coldplate (J), guard (F), and auxiliary guard (E) are shown schematically. The pressure vessel (G) is made of stainless steel and is sealed with a Monel gasket (D). This vessel is surrounded by a furnace (K) and furnace "neck" (C), which are made of aluminum and are equipped with electric heaters in numerous porcelain tubes in the aluminum. The furnace temperature was automatically controlled by means of a platinum resistance thermometer and bridge circuit. The furnace neck was controlled relative to the furnace by means of a thermocouple. The pressure vessel extends upward out of the furnace region so that the electric leads can be brought out of the pressure vessel in a cold region. The cooling coil (B) dissipates the heat from the furnace, so that the top is cool. The electric leads (all No. 32 gold wire) are brought up from the auxiliary guard through three Inconel tubes, which serve as electrostatic shields, as described later. There are 29 of these leads, which are brought out of the pressure vessel through a pressure seal, A. These leads go out radially between two "Kel-F" (polychlorotrifluoroethylene) disks, which are pressed together for the seal.

A number of difficulties were encountered before obtaining a successful seal at A. At first, the material Teflon (polytetrafluoroethylene) was used, but it was found to flow excessively at the high pressures necessary for the seal. The method finally used for this seal was to mold Kel-F around the gold wires at about 200° C.

The vital parts of the thermal-conductivity cell are shown in figure 2. The hotplate (M), coldplate (O), guard (E), and auxiliary guard (B) are all made of silver to minimize temperature gradients and heat transfer by radiation. The hotplate is made of three parts, silver-soldered together. The hotplate heater (L) is located between the lower parts and consists of about 55 ohms (at 25° C) of (0.05-mm diameter) platinum wire insulated with mica. Gold leads from this heater are brought out through the tempering region located at H between the upper two silver pieces of the hotplate and then to the thermal tie-down, F. The purpose of this thermal tie-down

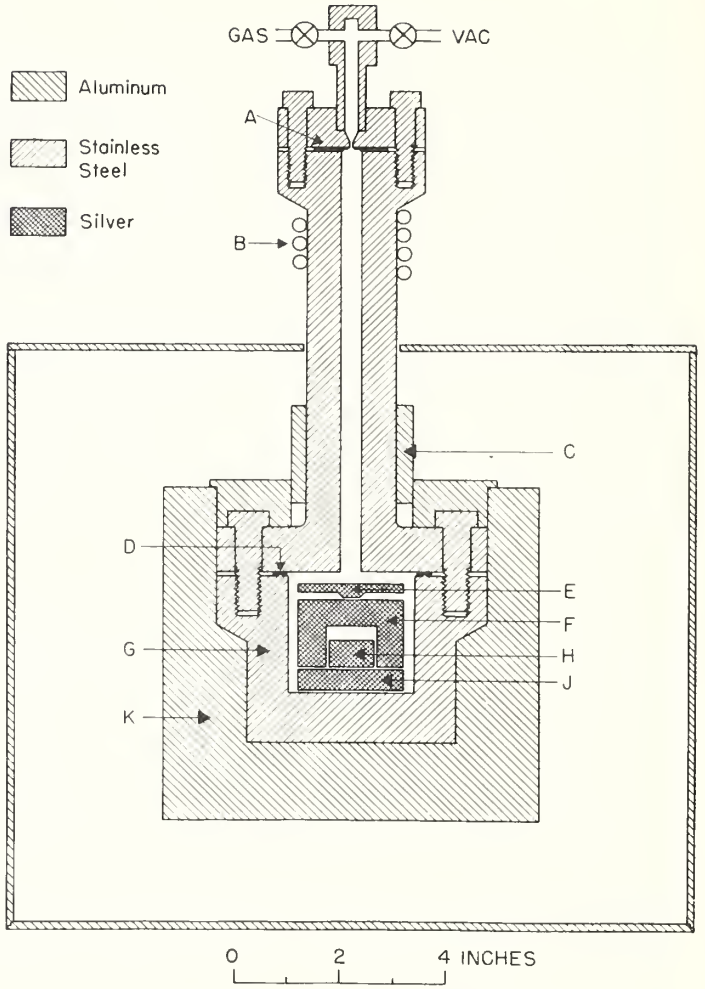

FIGURE 1. *Thermal-conductivity apparatus.*

A, Pressure seal for electric leads; B, cooling coil; C, furnace neck; D, Monel gasket; E, auxiliary guard; F, guard; G, pressure vessel; H, hotplate; J, coldplate; K, furnace.

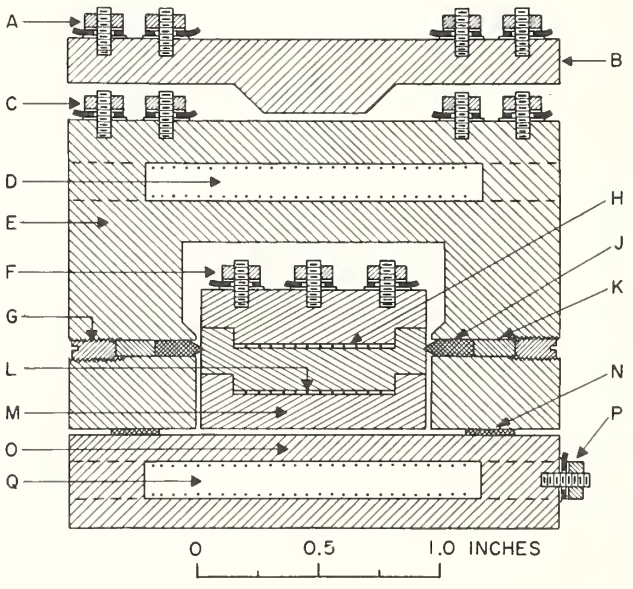

FIGURE 2. *Thermal-conductivity cell.*

A, C, F, H, P, Thermal tie-downs for electric leads; B, auxiliary guard; D, Q, platinum resistance thermometers; E, guard; G, silver screw; J, quartz supports for hotplate; K, aluminum insert; L, hotplate heater; M, hotplate; N, quartz spacers; O, coldplate.

is to bring the leads as close as possible to the temperature of the silver. This type of tie-down is used extensively throughout the apparatus and consists of a gold terminal insulated between thin mica disks and held down to the silver by a nut threaded on a machine screw. The gold terminal is spaced around the screw so that it is insulated from it.

The hotplate is supported by the guard ring at three points, using quartz supports (J), so that the bottom plane of the hotplate is in the same plane as the bottom of the guard ring. Because the coefficient of thermal expension of quartz is lower than that of silver, an aluminum insert (K) having a higher coefficient than quartz was used with the quartz for compensation. The quartz is held tightly against the hotplate by the silver screw (G) pressing against the aluminum insert. The guard (E) surrounds the hotplate, except where it is exposed to the coldplate. In the vital region near the coldplate, the guard is spaced about 0.5 mm from the hotplate. The assembly of the guard and hotplate is held about 0.5 mm from the coldplate by three quartz spacers (N) between the guard and coldplate. In this region, the silver was highly polished to reduce heat transfer by radiation. Heaters (not shown) are installed in both the guard and coldplate.

The temperatures of the guard and coldplate are measured by using the platinum resistance thermometers (D) and (Q), respectively, in conjunction with a Mueller bridge. These strain-free thermometers are not sealed. All leads (gold) from these two thermometers are thermally tied down at C and P, respectively, so that the temperatures of the platinum resistance thermometers are not affected by heat conduction along the leads. The temperature difference between the guard and hotplate is determined by means of a multiple-junction thermopile, using four No. 36 Chromel P-Alumel thermocouples in series. This thermopile has one set of electrically insulated junctions at F on the hotplate and the other set at C on the guard.

Experiments indicated the desirability of providing another thermal tie-down zone for all electric leads before they go out from C to the cold region. For this purpose, the silver auxiliary guard (B) was used with a heater built in to provide the bulk of the heat flow up along the electric leads. All three silver pieces, (B), (E), and (O), are held together by long machine screws fastened in the bottom of the surrounding pressure vessel. These four pieces are all electrically insulated from one another.

The effective operation of the thermal-conductivity apparatus depended upon the proper temperature control of the various components. For this purpose, five automatic thermoregulators were used to control the temperatures of the coldplate, guard, auxiliary guard, furnace, and the furnace neck. These thermoregulators were actuated by thermocouples or resistance thermometers (not the measuring resistance thermometers), and they consisted essentially of "chopper-amplifiers" operating saturable reactors in the heater circuits. The guard was maintained at the same temperature as that of the hotplate by means of the differential thermopile previously mentioned. This temperature control was the most important; it maintained constancy of temperature to about 0.001 deg C. The auxiliary guard was maintained at the same temperature as the guard by a single differential thermocouple. As a result of the effectiveness of the thermoregulation in the thermal-conductivity apparatus, all the observations on the thermal conductivity of nitrogen were made by one person. Both the electric power in the hotplate heater and the thermocouple readings were observed with a precision potentiometer.

A capacitance bridge was used to measure the capacitance between the hotplate and the coldplate. This bridge permitted the accurate measurement of small direct capacitances, even though relatively large capacitances exist between the "ground" and the plates. To eliminate, as far as possible, errors of measurement in capacitance, a calibrated capacitor having about the capacitance of the thermal-conductivity cell (about 10 $\mu\mu$f) was used as a reference and the measurements made by a substitution method. In this measurement, the same internal capacitance to ground was kept in the bridge circuit, so that the capacitance measurement approached very closely to the ideal comparative measurement, giving an accuracy comparable with the accuracy of the calibrated capacitor. Much care was taken to avoid significant capacitance between the leads from the hotplate and coldplate. They were effectively shielded from each other by bringing leads out through separate grounded Inconel tubes and by proper location of the leads that pass through the pressure seal.

For the measurement of the pressure of the gas in the conductivity cell, calibrated Bourdon gages were used. The requirement for accuracy on these gages was not great because the variation of thermal conductivity with pressure was much smaller than the change with temperature.

3.2. Purity of Nitrogen

The nitrogen used was extra-dry high-purity, obtained from the Linde Air Products Co., who stated that impurities did not exceed 100 ppm. Cryoscopic measurements made by G. F. Furukawa at the National Bureau of Standards with an adiabatic calorimeter showed liquid-soluble solid-insoluble impurities to be about 10 ppm. The conductivity cell was filled with this nitrogen, which had been passed through a silica-gel dryer and a filter made of glass wool.

3.3. Procedure

The general procedure was to set the furnace controls to the desired temperature, fill the conductivity cell with gas at the desired pressure, and put in a chosen electric power in the hotplate. With the coldplate automatically regulated to a constant temperature and the guard temperature automatically controlled to the temperature of the hotplate, the hot-

plate temperature became constant. After the capacitance between the two plates was measured, alternate measurements of electric power (W) and temperature difference (Δt) between the plates were made until the constancy of their values indicated that a steady state had been reached. The power in the hotplate was then changed so that similar measurements were made at three or more powers. The gas pressure was then changed and measurements were repeated for each of the pressures 0.7, 50, and 100 atm. All of these measurements were made at 50°, 100°, 200°, 300°, 400°, and 500°.

According to eq (2), the three quantities needed to determine the thermal-conductivity coefficient, k, are the rate of heat flow, $\dot{Q}$, the temperature difference, Δt, and the direct capacitance, C, between the hotplate and coldplate. Each of these quantities is discussed in detail below.

In order to obtain $\dot{Q}$ from W, the measured electric power in the hotplate, it is necessary to account for all heat flow from the hotplate other than by conduction through the gas. The possible paths of this heat flow are (1) to the surrounding guard by conduction and convection through gas, conduction through lead wires, and radiation, (2) to the coldplate by convection, and (3) to the coldplate by radiation.

Preliminary experiments were made to determine the heat-transfer coefficient between the guard and hotplate. Results of these experiments showed that an uncertainty in conductivity of less than 0.1 percent would be caused by a temperature difference between the guard and the hotplate of 0.001° C. It was found possible to control the temperature difference automatically to about this value.

The conductivity cell was designed to eliminate any convection currents. If convection does exist, it will cause an apparent change in the value of k with change in power input. At the lower gas densities, no such change was observed, and convection effects seemed absent. However, at the higher gas densities, k appeared to vary with power. The apparent k values were corrected by extrapolating to zero power input. This apparent change in k with power is believed to be due to a "chimney"-type convection resulting from gas flowing into the space between the guard and coldplate and out of the holes (not shown in fig. 2) provided for electric leads in the top of the guard. It is expected that blocking of these spaces would have eliminated this effect.

The heat transfer by radiation was accounted for by measurements with the cell evacuated. This power (W_r) transferred between two parallel plates can be expressed as

$$W_r = eA\sigma(T_2^4 - T_1^4), \tag{4}$$

where e is an effective emissivity of the surfaces, A is an effective area, σ is the Stefan-Boltzmann constant, and T_1 and T_2 are the absolute temperatures. If the temperature difference, Δt, is small compared to the average temperature, $T = 0.5\ (T_2 + T_1)$, then the transfer equation can be simplified to

$$W_r = 4\ eA\sigma T^3 \Delta t = BT^3 \Delta t. \tag{5}$$

The constant B was evaluated in preliminary experiments over the entire temperature range with the conductivity cell evacuated. The gas pressure in the cell in these experiments was estimated to be less than 10^{-5} mm of mercury. During the progress of the experiments with gas, the constant B was checked periodically at temperatures of 350° C and below to test for possible changes in emissivity with time. Higher temperatures were not rechecked for reasons to be discussed later with temperature measurement.

The direct capacitance (C) between the hotplate and coldplate was measured by a substitution method using a calibrated standard and a Sylvania type 125 capacitance bridge. The precision of the bridge reading was better than the certified accuracy of the standard capacitor.

The capacitance, C, in eq (2) is that measured in vacuum. For measurements with gas in the cell, correction must be made for the dielectric constant, ϵ, of the gas. ϵ was determined by using the Clausius-Mosotti equation

$$\frac{\epsilon - 1}{\epsilon + 2} = D\rho, \tag{6}$$

where D is a constant independent of temperature for nonpolar gases, and ρ is the gas density. The value used for D was 1953×10^{-7} [1] [2] when ρ is in Amagat units [2]. Although the correction for the dielectric constant of the nitrogen may amount to 1 or 2 percent at the highest densities, it is believed that the uncertainties in k due to this correction are less than 0.01 percent.

Temperature measurements were made with the resistance thermometers in the coldplate and the guard, together with the four-junction thermopile between the guard and the hotplate. These resistance thermometers were calibrated by the NBS Temperature Measurements Section before assembly of the cell. It was found, however, that when the system was kept under high vacuum at temperatures above 400° C, the thermometer characteristics changed slightly. This was probably due to contamination of the platinum by other metals in the system. Such a change took place during the determination of radiation corrections at 500° C. Rather than dismantle the apparatus to recalibrate the thermometers, it was thought that sufficient accuracy could be retained if the two thermometers were compared in place. In this way, the temperature difference would be known more accurately than the absolute temperature. This procedure is valid only because the evaluation of the temperature *difference*, Δt, is the important factor, whereas the change in thermal conductivity with temperature is small. It is estimated that after this procedure, the accuracy of the measurement of Δt was 0.002 deg C and of average temperature T was 0.01 deg C.

[2] Figures in brackets indicate the literature references at the end of this paper.

4. Results

The results of the measurements are given in table 1. The first column gives the temperature of the experiment, which is the mean of the hotplate and coldplate temperatures. The second column gives the power (W) put into the hotplate (as measured electrically) with nitrogen in the conductivity cell. Values of power W_r, given in the third column, are based on experiments with the conductivity cell evacuated and are calculated from eq (5). These values are subtracted from the corresponding values of W to give $\dot{Q}$, as used in eq (2). Over 40 experiments were made to determine the value of B in this equation. A value of $B=4.90\times10^{-12}$ w/deg^4 in this equation was found to fit the results best. The values of B calculated from the individual vacuum experiments deviated on the average about 4 percent from the above value, and seemed to be independent of temperature. Because the *maximum* values of W_r are only 3 percent of the corresponding values of W, an error of 4 percent in B would cause a maximum error of only about 0.1 percent in conductivity k.

The values of temperature difference Δt given in column 4 are based on measurements with the two resistance thermometers and the thermopile, which was used only as a "null" indicator. Column 5 gives the values of capacitance C (as used in eq (2)) between the hotplate and coldplate as determined at the same time and under the same conditions of the conductivity experiment. These values have been corrected for the dielectric constant of the nitrogen.

The values of "apparent" thermal conductivity, k^*, given in column 6, were calculated from eq (2). These values, when corrected to even temperatures, seem to be free from error due to convection in that they are usually independent of power, except at some of the highest pressures, as mentioned earlier. Because this effect is believed to be due to a chimney-type convection, it should diminish at lower power inputs. Therefore, the values of k^* were extrapolated to zero power to give "true" conductivities, k. In the worst case, at 100-atm pressure and 50° C, the extrapolation is over a large range of values of k^*. However, it is believed that this extrapolation should introduce only a relatively small error. The results from the three experiments at different powers were fitted by the method of least squares to a linear equation in power. The maximum deviation of the observed values of k^* in this linear equation was only 0.28 percent, so that it is believed that the linear extrapolation was adequate.

At low pressures the effect of temperature discontinuity near the walls may become significant. This has been taken into account for the 0.7-atm data by use of the equation

$$k=k^*\left(1+\frac{2g}{\Delta X}\right). \tag{7}$$

TABLE 1. *Experimental results on nitrogen*

Temperature, t	Power— With nitrogen, W	Power— With vacuum, W_r	Temperature difference, Δt	Capacitance, C	Apparent conductivity, k^*
Pressure, 0.7 atm					
°C	w	w	°C	μμf	10^{-4} w/cm deg
51.03	0.05107	0.00027	1.647	9.786	2.790
52.75	.1039	.00056	3.332	9.789	2.804
57.85	.2630	.0015	8.306	9.797	2.846
100.13	.05895	.00042	1.664	9.975	3.122
101.87	.1202	.0009	3.371	10.049	3.120
106.68	.2927	.0022	8.117	10.017	3.165
200.09	.07569	.00088	1.696	10.450	3.737
201.50	.1387	.0016	3.101	10.455	3.744
205.02	.2981	.0035	6.614	10.463	3.769
204.86	.2971	.0035	6.615	10.435	3.767
300.48	.09072	.0148	1.704	10.80	4.293
302.17	.1818	.0030	3.404	10.82	4.299
304.25	.2972	.0049	5.534	10.85	4.312
306.64	.4308	.0072	7.991	10.83	4.336
306.56	.3719	.0066	6.891	10.85	4.326
401.02	.1064	.0026	1.706	11.17	4.822
402.65	.2177	.0053	3.484	11.18	4.829
406.43	.4732	.0116	7.539	11.20	4.841
501.60	.1311	.0040	1.776	11.71	5.408
502.93	.2369	.0073	3.205	11.71	5.416
506.46	.5248	.0164	7.045	11.77	5.430
Pressure, 50 atm					
50.59	0.04416	0.00021	1.290	9.761	3.090
51.02	.05938	.00029	1.718	9.762	3.120
52.46	.1138	.0005	3.179	9.772	3.228
55.76	.2511	.0011	6.519	9.788	3.470
99.69	.04457	.00030	1.172	9.987	3.348
100.31	.06805	.00045	1.781	9.980	3.368
101.94	.1345	.0009	3.434	9.996	3.445
105.15	.2748	.0018	6.716	10.021	3.592
200.26	.09102	.00101	1.937	10.456	3.937
201.61	.1569	.0017	3.322	10.456	3.956
206.33	.3966	.0044	8.165	10.481	4.058
301.54	.1589	.0025	2.835	10.84	4.505
305.68	.4077	.0064	7.158	10.87	4.567
302.85	.2365	.0037	4.194	10.84	4.535
400.81	.1060	.0025	1.616	11.16	5.085
402.30	.2105	.0048	3.197	11.16	5.104
405.86	.4699	.0108	7.067	11.18	5.145
501.57	.1331	.0039	1.720	11.72	5.674
502.98	.2575	.0076	3.316	11.74	5.685
507.42	.6426	.0191	8.195	11.77	5.724
Pressure, 100 atm					
50.12	0.03336	0.00014	0.835	9.809	3.591
50.83	.06738	.00026	1.576	9.813	3.843
51.82	.1210	.0005	2.615	9.821	4.158
99.86	.0597	.0004	1.423	10.007	3.689
101.10	.1195	.0007	2.675	10.014	3.926
104.96	.3421	.0018	6.689	10.036	4.490
199.70	.07664	.00083	1.603	10.41	4.023
201.08	.1502	.0016	3.021	10.43	4.177
204.51	.3473	.0035	6.556	10.46	4.440
299.62	.04732	.00082	0.889	10.83	4.276
300.79	.1150	.0019	2.048	10.83	4.516
302.76	.2366	.0038	4.079	10.84	4.662
305.30	.4068	.0065	6.811	10.84	4.802
400.79	.1059	.0024	1.570	11.17	5.231
402.68	.2468	.0055	3.641	11.19	5.244
405.56	.4650	.0104	6.778	11.20	5.303
501.21	.1342	.0039	1.698	11.69	5.816
502.66	.2612	.0075	3.290	11.70	5.836
506.68	.6218	.0180	7.727	11.75	5.890

The "temperature-jump distance", g, is related to the "accommodation coefficient", a, by the relation [16]:

$$g=\frac{2-a}{a}(2\pi RT)^{0.5}\frac{k}{(\gamma+1)C_vP}, \quad (8)$$

in which R is the gas constant, T the absolute temperature, k the thermal conductivity, C_v the constant-volume specific heat, γ the specific-heat ratio, and P the pressure of the gas. Values of a for nitrogen on silver vary from about 0.8 at room temperature to 0.4 at 800° C [6]. The value of 0.5 was chosen as the most probable for the temperature range of these experiments.

Values of observed conductivity k, corrected to even temperatures, are listed in column 2 of table 2. In order to facilitate interpolation of the results between the observed points, empirical equations were derived to give conductivity as a function of temperature at each of the three pressures. These equations are as follows:

$$k=1.059\eta\left(C_v+\frac{9}{4}R\right) \quad \text{(pressure, 0.7 atm)}, \quad (9)$$

$$10^4k=2.714+0.005897t \quad \text{(pressure, 50 atm)}, \quad (10)$$

$$10^4k=3.161+2.9317\times10^{-3}t+9.0761\times10^{-6}t^2-8.8318\times10^{-9}t^3 \quad \text{(pressure, 100 atm)} \quad (11)$$

In these equations, k is in watts cm^{-1} deg^{-1}, t is in deg C, η is viscosity (poise), C_v is heat capacity (j g^{-1} deg^{-1}), at constant volume, and R is the gas constant (8.317/28.016 j g^{-1} deg^{-1}). The values of viscosity and heat capacity used in eq (9) were obtained from NBS Circular 564 (Nov. 1955), which tabulates heat-transport properties for a number of gases. The constants of these equations were obtained by the method of least squares. Values of k given in column 3 of table 2 are calculated from these equations. Column 4 gives the deviations of the observed results from these calculated values. The results are also given in figure 3, where the circles represent observed values and the solid lines the values from the above equations.

The empirical eq (10) and (11) fit the observed values at 50- and 100-atm pressure, respectively, almost as well as would be expected from the precision of the data. The average deviation of eq (10) (which is linear in t) from the observed conductivities is only 0.1 percent, with a maximum deviation of 0.3 percent. The deviations from eq (11) are also quite small except below 200°C, where there was increased difficulty, both experimentally and in fitting the observed points with an equation. The deviations of eq (9) from the observed values seem to be larger than can be attributed to experimental errors. Equation (9) is the same semi-empirical equation proposed by Eucken [3], except for the constant factor. A factor of 1.059 was found to fit the present data, as compared to a factor of 1 originally proposed by Eucken. More recent modifications of Eucken's equation by other investigators generally have predicted a value slightly greater than 1. An alternative equation for 0.7 atm, which fits well up to 400°C, and which may be easier for use in numerical interpolation in this region, is

$$k=2.495\times10^{-4}+6.366\times10^{-7}t-1.065\times10^{-10}t^2, \quad (12)$$

TABLE 2. *Thermal conductivity of nitrogen*

Temperature	Conductivity, k		Observed minus calculated
	Observed	Calculated	
Pressure, 0.7 atm			
° C	10^{-4} w/cm deg	10^{-4} w/cm deg	%
50	2.794	2.818	−0.9
100	3.129	3.131	−.1
200	3.750	3.727	+.6
300	4.308	4.308	.0
400	4.836	4.857	−.4
500	5.430	5.381	+.9
Pressure, 50 atm			
50	3.003	3.009	−0.2
100	3.303	3.304	.0
200	3.905	3.893	+.3
300	4.477	4.483	−.1
400	5.075	5.073	.0
500	5.660	5.662	.0
Pressure, 100 atm			
50	3.340	3.329	+0.3
100	3.513	3.536	−.6
200	4.060	4.040	+.5
300	4.612	4.619	−.1
400	5.218	5.221	.0
500	5.794	5.792	.0

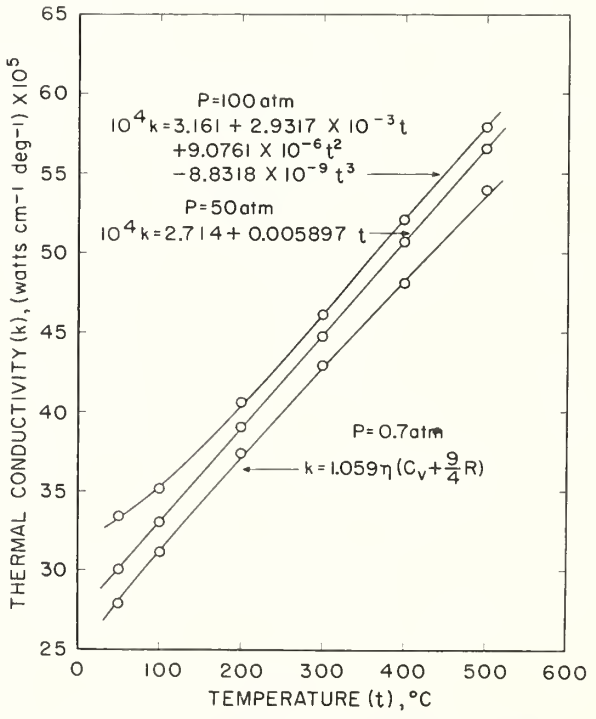

FIGURE 3. *Thermal conductivity of nitrogen.*

where k is in w cm^{-1} deg^{-1}, and t is in deg C. Although all of these equations are suitable for interpolation at their respective pressures, they may not be valid for extrapolation beyond the experimental range. Equation (9) is probably the most suitable for extrapolation to higher temperatures.

5. Discussion of Results

5.1. Accuracy

In order to estimate the accuracy of the final results, it is necessary to consider the effect of each of the terms in the conductivity equation

$$k=\frac{0.0885516\dot{Q}}{C\Delta t}.$$

The constant 0.0885516 is a conversion factor to allow for the system of units. It has negligible uncertainty in its use here. Some possible sources of error in the measured capacitance, C, are the capacitance between electric leads and the relatively large capacitance to ground (the guard is grounded) of the hotplate and coldplates. The electric leads were carefully shielded to avoid significant error from this source. The effect of the ground capacitance is largely eliminated by the design of the bridge used in its measurement. Use of a substitution method that compares the conductivity-cell capacitance with that of a standard capacitor minimizes a number of possible errors. By using this method, it is believed that this comparison is accurate to better than 0.1 percent. The absolute value of the standard capacitor is certified by the NBS (with a high probability) to only 0.3 percent.

In the experiments with nitrogen, the effect of the dielectric constant of the gas must be considered. It is estimated that uncertainty in the value of the dielectric constant of nitrogen is less than 0.01 percent, giving the same uncertainty in C and k. The total uncertainty in the capacitance measurement is believed to be about 0.3 percent. This is the largest uncertainty in most of the measurements, and it is based on 1 chance in 10 that the error will be larger than 0.3 percent.

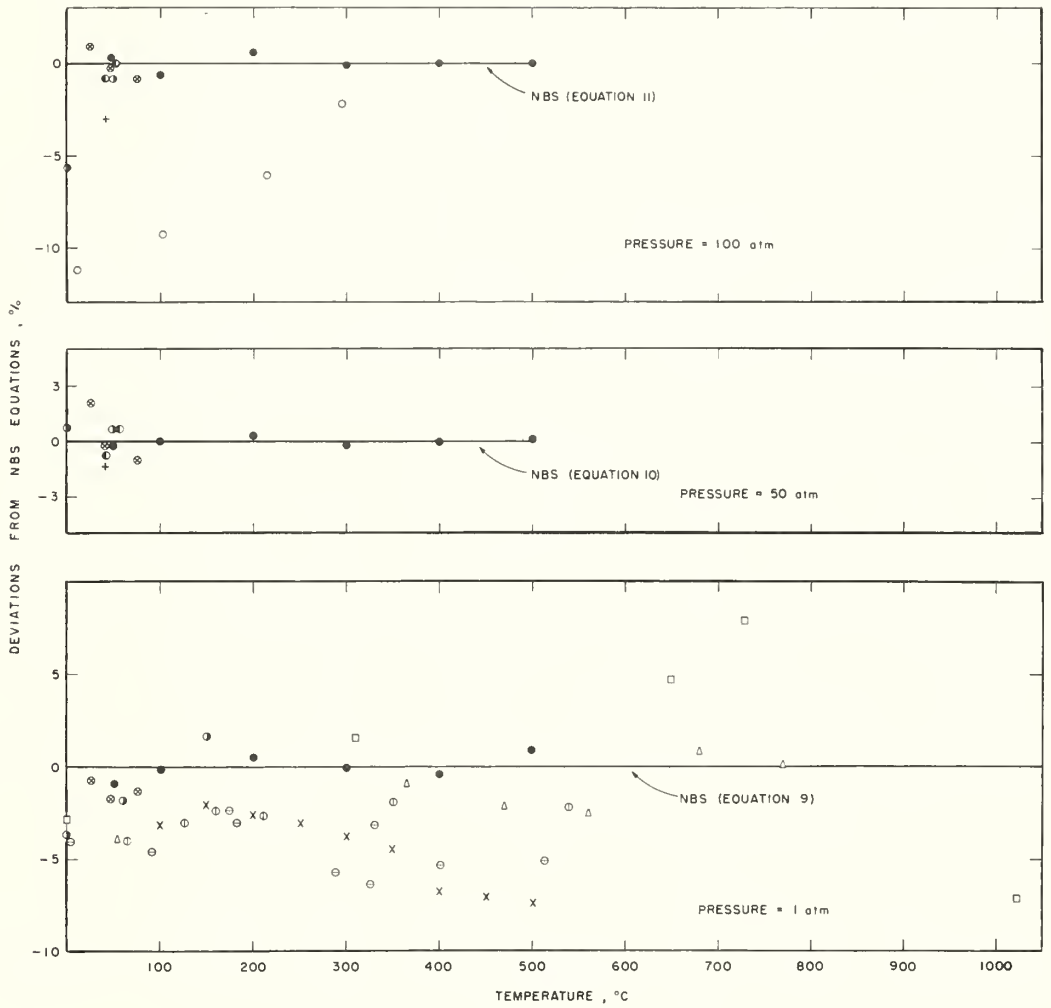

FIGURE 4. *Comparisons with others.*

●, NBS; ○, Stolyarov, Ipat'ev, and Teodorovich; ◑, Keyes; ◐, Vargaftik; ⊖, Frank; ⊕, Vargaftik and Oleschuk; ×, Schottky; △, Rothman and Bromley; ⊗, Michels and Botzen; □, Stops; +, Lenoir and Comings.

The factor $\dot{Q}$ in eq (2) is evaluated from the two powers W and W_r. The electrical measurement of W is believed to have negligible error. The uncertainty in the value of W_r determined from vacuum experiments is estimated to be less than 0.1 percent, except at the highest temperatures, where it may be as large as 0.1 to 0.2 percent. It is possible that the vacuum experiments do not account completely for all heat flow (other than $\dot{Q}$) from the hotplate during the gas experiments. This may be due to imperfect matching of the guard temperature to the hotplate temperature. It is estimated that the error from this source is less than 0.1 percent.

The measurement of Δt, which has been discussed earlier, has an estimated uncertainty of 0.002 deg C. This introduces uncertainties in the values of k of from 0.02 to 0.2 percent, depending on the magnitude of Δt. The uncertainty in the temperature scale, estimated to be about 0.01 deg C, is believed to introduce negligible error in k.

In estimating the over-all accuracy of the results, the authors believe that with most of the results, there is only 1 chance in 10 that the true conductivity values will deviate more than 0.5 percent from the observed values given in table 2. In the case of a few values at the highest pressures, it is believed that this tolerance might be increased by as much as 1 percent.

5.2. Comparison With Others

A comparison of the results of this investigation with the observed conductivity values from some other recent researches is given in figure 4. No attempt was made to include in the figure all the available data at low temperatures and low pressures, although all known high-pressure data are given. The data are plotted as deviations from eq (9), (10), and (11), which represent the NBS data for the three pressure ranges. At low pressures (approximately 1 atm), Frank [4] and Schottky [5] made measurements up to 500° C, Rothman and Bromley [6] up to 800° C, Stops [7] up to 1,020° C, Michels and Botzen [8] up to 75° C, and Vargaftik and Oleschuk [9] up to 541° C. Keyes and Sandell [10] have also made measurements up to 400° C at various pressures. Their results are not shown here because they believe their conductivity values to be too low over most of the temperature range. Later observed values of Keyes [11] up to 150° C are shown. Further measurements by Keyes [12] have been made up to about 350° C, but no observed values of conductivity have been published. At higher pressures, Michels and Botzen [8] made measurements up to 2,500 atm and 75° C, Stolyarov, Ipat'ev, and Teodorovich [13] up to 300 atm and 300° C, Vargaftik [4] up to 90 atm and 62° C, and Lenoir and Comings [15] up to 200 atm at 41° C. As in the low-pressure measurements, the results of Keyes and Sandell are not shown, although later results of Keyes are given up to 100 atm and 50° C.

6. References

[1] Handbook der Physik **12,** 517 (1927).
[2] NBS Circular 564 (November 1955).
[3] Physik Z. **2,** 1101 (1911).
[4] Z. Elektrochem. **55,** 636 (1951).
[5] Z. Elektrochem. **56,** 889 (1952).
[6] Ind. Eng. Chem. **47,** 899 (1955).
[7] Nature **164,** 966 (1949).
[8] Physica **18,** 605 (1952).
[9] Izvest. VTI **15,** #6, 7 (1946).
[10] Trans. ASME **72,** 767 (1950).
[11] Trans. ASME **73,** 597 (1951).
[12] Trans. ASME **74,** 1303 (1952).
[13] J. Phys. Chem. (U. S. S. R.) **24,** 166 (1950).
[14] Tech. Phys. U. S. S. R. **4,** 341 (1937).
[15] Chem. Eng. Progr. **47,** 228 (1951).
[16] E. H. Kennard, Kinetic theory of gases (McGraw-Hill Book Co., Inc., New York, N. Y., 1938).

Washington, December 27, 1956.

Journal of Research of the National Bureau of Standards Vol. 48, No. 1, January 1952 Research Paper 2279

Absolute Viscosity of Water at 20° C

J. F. Swindells, J. R. Coe, Jr., and T. B. Godfrey

An accurate knowledge of the viscosities of liquids in absolute units is of fundamental importance in many scientific fields. The measurement of these viscosities is almost universally based upon the absolute viscosity of water at 20° C as a primary standard. During the past 50 years there has been an increasing need for a more accurate determination of this standard. Consequently, with the cooperation of the Society of Rheology and some financial assistance from the Chemical Foundation, this project was undertaken by the National Bureau of Standards and has now been completed.

The determination was made by the method of capillary flow. By means of a calibrated injector, various known constant rates of flow were produced in capillaries of measured dimensions, and observations were made of the corresponding pressure drops through the capillaries. The effects of the ends of the capillaries were rendered negligible by the simultaneous treatment of data obtained with pairs of capillaries having essentially the same diameters but different lengths.

The value found for the viscosity of water is 0.010019 poise as compared with 0.01005 poise, which has generally been accepted for the past 30 years. The estimated accuracy of the new determination is ±0.000003 poise.

As a result of this work, beginning on July 1, 1952, the National Bureau of Standards is planning to use the value 0.01002 poise for the absolute viscosity of water at 20° C as the basis for the calibration of viscometers and standard-sample oils. It is recommended that other laboratories adopt this value as the primary reference standard for comparative measurements of viscosity.

1. Introduction

The viscosity of a liquid is its internal resistance to flow. The accurate measurement of viscosity in absolute units is a difficult undertaking, and the difficulty is magnified greatly as the accuracy desired is increased. However, if the viscosity of one liquid is known, viscosities of other liquids in terms of that of the known may be determined very accurately with relative ease. Because of its ready availability, water at 20° C has been generally adopted in the United States as the primary reference standard, its viscosity being taken to be 0.01005 poise [1].[1] Other values reported in the literature [2], however, are in disagreement with this value by as much as ±4 parts in 1,000.

In view of this uncertainty, in October 1931, chiefly at the instance of the late E. C. Bingham, the National Bureau of Standards began a redetermination of the viscosity of water at 20° C. This work had the cooperation of the Society of Rheology, through whom (during the first 2 years) considerable financial assistance was obtained from The Chemical Foundation. The problem was assigned to J. R. Coe, with the program subject to the review of N. E. Dorsey, who gave valuable advice and encouragement. It was agreed that, although other methods might also be explored, measurements should be made by the capillary flow method. An accuracy of at least 1 part in 1,000 was to be sought.

By the end of 1932, the apparatus and experimental procedures described below had been largely determined upon, much of the apparatus had been designed in detail, and some of it had been built or procured. In addition, rough experiments to establish the feasibility of the method had been concluded.

Initially, sufficiently uniform tubes were not easily available, and a machine to lap the bores of glass tubes was built as an alternative to attempting to find suitable tubes by the examination of many. This work was described in a progress report in December 1932 [3]. This part of the project was not completed, because it was found in 1933 that satisfactory capillaries were then being made by the Jena Glass Works in Germany. During the period 1933 to 1938, work on the project was subjected to frequent interruptions and necessary delays.

In the fall of 1938 conditions made it possible for T. B. Godfrey to join J. R. Coe in the work, which was continued without interruption until the fall of 1941, when it was again delayed by reason of the war. During the period 1938 to 1941 the apparatus was completed and assembled, the methods of calibration and flow measurement worked out in detail, and two series of flow measurements completed. Tentative values for the viscosity of water at 20° C [2] and at other temperatures based on these early measurements were reported in a letter to the Editor of the Journal of Applied Physics [4]. It was recognized, however, that with the completion of so small a part of the contemplated series of measurements, only the necessity of indefinitely suspending work justified any statement at that time.

Work on the determination was resumed in January 1947 by J. F. Swindells, who completed the experimental program and reduced all the data.

2. Theory of the Capillary Method

When accurate viscometric measurements are desired it is necessary to limit the conditions to laminar flow within the capillary tube. Turbulent flow is governed by factors that make conditions

[1] Figures in brackets indicate the literature references given on p. 23.

[2] The value of 0.010020 poise for the viscosity at 20° C, which was reported at that time, is in good agreement with the value 0.010019 ±0.000003, which is the final result of the completed determination.

unsuitable for evaluating the viscosity. According to the laws of similarity, it has been shown [5] that the type of flow in a capillary is characterized by a dimensionless ratio, the Reynolds number, $2vrD/\eta$, in which v is the mean velocity, r is the radius, and D and η are the density and viscosity, respectively, of the flowing liquid. Under ordinary conditions of capillary flow, sustained turbulence is not to be expected [5, chapter III] at Reynolds numbers less than 2,000. The present measurements were conducted in the range 100 to 650, and consequently the flow is assumed to be laminar, except possibly at the ends of the capillaries.

The system under consideration consists of a capillary having square-cut ends and located between two chambers that are large with respect to the bore of the capillary. The liquid in one chamber is accelerated from essential rest to the velocity in the capillary and then is brought to essential rest in the exit chamber. The measured quantities used in calculating the viscosity are P, the pressure drop between the two chambers; l, the length of the capillary; r, its radius; and Q, the volume rate of flow.

In the portion of a cylindrical tube remote from the ends the distribution of velocities across the tube is parabolic, and Poiseuille's laws are known to apply when the flow is laminar. These laws are expressed by the equation

$$\frac{dp}{dl}=\frac{8\eta Q}{\pi r^4}, \tag{1}$$

where dp/dl is the pressure gradient. Two kinds of corrections are necessary to modify eq 1 so that in its integrated form it will hold for a tube of finite length, in which account must be taken of the special conditions existing at the ends of the tube. First, the liquid entering the capillary is accelerated at the expense of the measured pressure drop. The amount of this conversion of static pressure to kinetic energy may be expressed as a part of the measured pressure drop by the addition of a term

$$\frac{mDQ^2}{\pi^2 r^4},$$

in which m is a coefficient whose magnitude depends in part upon the flow pattern at the entrance end of the tube. Within the range of Reynolds numbers covered here, it is probable that the kinetic energy of the flowing liquid is entirely dissipated as heat in the exit chamber [6]. However, if there should be some conversion of kinetic energy to static pressure in the process of deceleration, it would be accounted for in the magnitude of m.

The second correction that is required to account for the phenomena peculiar to the ends of the tube is the result of the work done against viscous forces in the rearrangement of the velocity distribution. The effect of this resistance in the converging and diverging streamlines at the ends of the tube is proportional to the radius and may be expressed as a hypothetical addition to the length. The effective length of the tube then becomes $l+nr$, in which n is a constant. A rather complete discussion of both of these corrections is given by Barr [7].

The complete equation for the flow through a capillary tube is usually expressed in one of the following equivalent forms:

$$\eta=\frac{\pi r^4 P}{8Q(l+nr)}-\frac{mDQ}{8\pi(l+nr)}, \tag{2}$$

$$P=\frac{8Q\eta}{\pi r^4}(l+nr)+\frac{mDQ^2}{\pi^2 r^4}, \tag{3}$$

$$\frac{P}{Q}=\frac{8\eta}{\pi r^4}(l+nr)+\frac{mD}{\pi^2 r^4}\cdot Q. \tag{4}$$

To calculate the viscosity from measurements made with a single capillary, numerical values must be assigned to m and n. If, for a given liquid, the values of the pressure drop corresponding to various rates of flow are measured, values of P/Q may be plotted against Q, and a straight line results as long as m and n remain constant. Such data may be used to demonstrate the constancy of m and n under given conditions and also to evaluate m for a particular capillary through use of eq 4.

When using capillaries of relatively large length-radius ratios, it is obvious that n is less significant. Conversely, this fact has prevented its evaluation with much certainty. Most of the published experimental values lie between zero and unity [7], but in many cases the experimental error is nearly as large as the quantity being measured. The most reliable work seems to have been performed by Bond [8], who concluded that $n=0.566\pm0.020$ for the tubes that he used. However, some of Bond's measurements were made with capillaries that were not sufficiently long for the parabolic distribution of velocities to become completely established, and consequently his results may not be strictly applicable to longer tubes.

It is desirable, therefore, to calculate the viscosity from flow measurements that render uncertainties in the value of n completely negligible. This may be accomplished through the simultaneous solution of data obtained in two capillaries having the same radius but different lengths. If we denote the measured quantities associated with the longer capillary by the subscript 1, and those pertaining to the shorter by the subscript 2, we obtain from eq 3 for the longer capillary

$$P_1=\frac{8Q\eta}{\pi r^4}(l_1+nr)+\frac{mDQ^2}{\pi^2 r^4}, \tag{5}$$

and for the same rate of flow in the shorter

$$P_2=\frac{8Q\eta}{\pi r^4}(l_2+nr)+\frac{mDQ^2}{\pi^2 r^4}. \tag{6}$$

Subtracting eq 6 from eq 5

$$P_1-P_2=\frac{8Q\eta}{\pi r^4}(l_1-l_2),$$

from which

$$\eta=\frac{\pi r^4(P_1-P_2)}{8Q(l_1-l_2)}. \tag{7}$$

However, it is not practicable to select two lengths of capillary having identical radii, even if they are cut from the same length of tubing. Also, while the flow data may show m and n to be constants for each tube, they may not be the same for both. Consequently, assigning the proper subscripts to r, m, and n in eq 5 and 6 and proceeding as before, the more general equation becomes

$$\eta=\frac{\frac{\pi}{8Q}(P_1r_1^4-P_2r_2^4)-\frac{DQ}{8\pi}(m_1-m_2)}{(l_1-l_2)+(n_1r_1-n_2r_2)}. \tag{8}$$

But if any reasonable values whatever are assigned to n_1 and n_2, and r_1 does not differ greatly from r_2, the quantity $(n_1r_1-n_2r_2)$ will be negligible with respect to (l_1-l_2) within the order of accuracy with which the lengths can be measured. Accordingly, the viscosity may be calculated by the equation

$$\eta=\frac{\frac{\pi}{8Q}(P_1r_1^4-P_2r_2^4)-\frac{DQ}{8\pi}(m_1-m_2)}{l_1-l_2}, \tag{9}$$

in which values for m_1 and m_2 are obtained from the flow data through use of eq 4, as mentioned above.

3. Apparatus

3.1. General Description

The experimental method involves flowing water through a capillary at various known constant rates and measuring the corresponding pressure drops through the capillary by means of a differential mercury manometer. The general arrangement of the apparatus used in making the flow measurements is shown diagrammatically in figure 1. The main elements are the viscometer, the injector for producing the flow of water through the capillary, and the differential mercury manometer. The

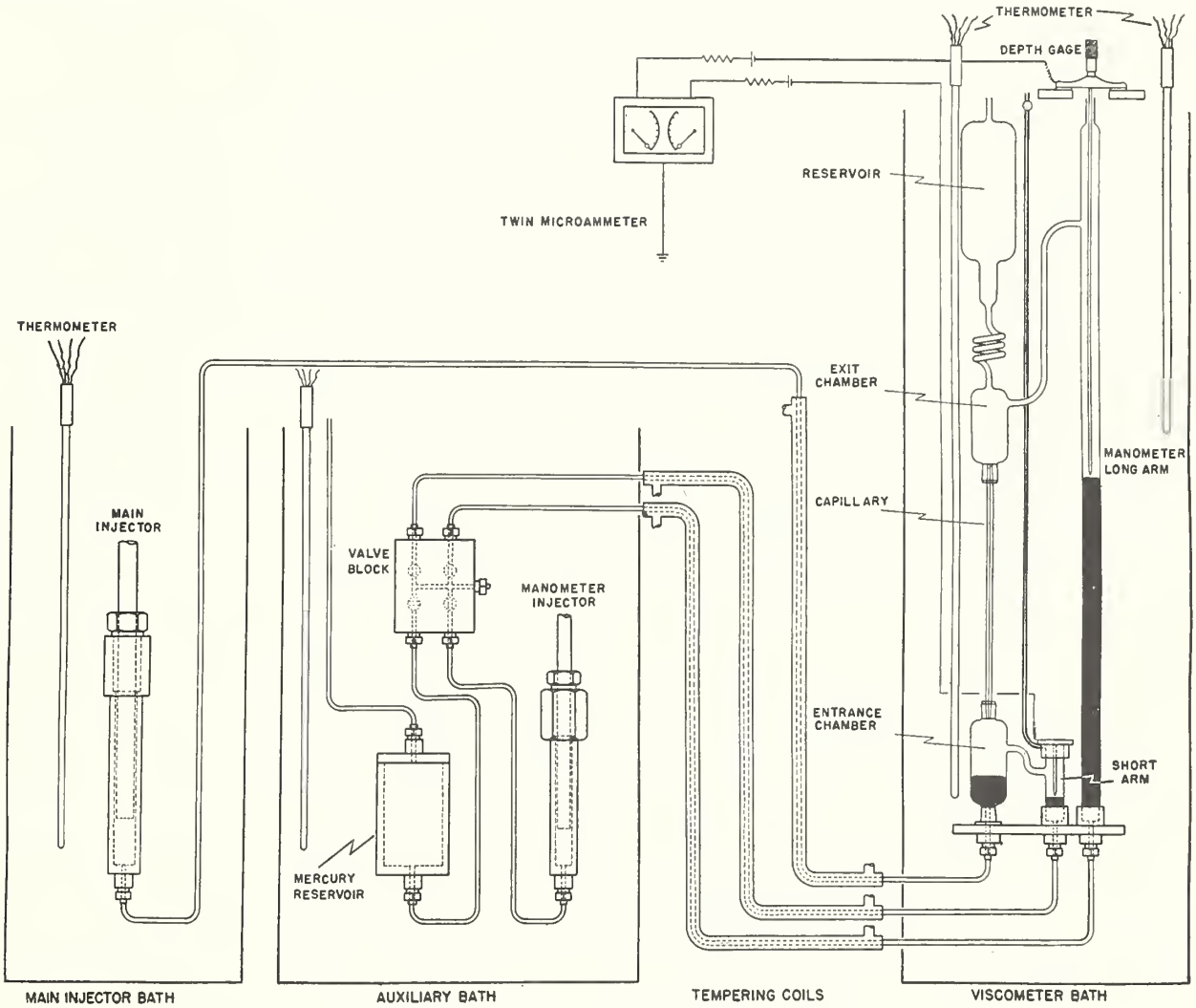

FIGURE 1. *Schematic diagram of apparatus.*

viscometer consists of a capillary mounted vertically between glass entrance and exit chambers. Glass tubes connect the entrance and exit chambers to the short and long arms of the manometer, respectively. A reservoir above the viscometer is connected to the exit chamber by a spiral of glass tubing as shown. Mercury in the entrance chamber and the two arms of the manometer is represented by the black areas. The parts of the viscometer and manometer above the mercury are filled with water to a level in the reservoir that is higher than the point where the side tube from the exit chamber connects with the manometer.

The various rates of flow are produced in the capillary by injecting mercury into the entrance chamber at various constant rates, thus displacing water upward through the capillary. The water flows from the exit chamber into both the long arm of the manometer and the reservoir, maintaining the same level in each. The mercury is injected by means of an accurately ground and lapped piston driven at a uniform rate. The piston is geared to a synchronous motor operating on a source of electric power of controlled frequency. Different rates of flow are obtained by changing the gear combinations.

The manometer consists of a mercury-filled U-tube, in which the short arm level is adjusted to a fixed height, and the level in the long arm is adjusted by addition or removal of mercury until the resulting mercury column balances the pressure drops through the capillary. The mercury in the manometer is manipulated by means of the manometer injector and mercury reservoir shown in the auxiliary bath. Constant-volume stopcocks are provided to shut off the two arms of the manometer from each other and for injecting mercury into either arm independently.

The viscometer and manometer are mounted together in a liquid bath maintained at the test temperature of 20° C. The temperatures of the main injector and the auxiliary apparatus for the manometer are held constant in separate baths, which are maintained somewhat above room temperature for ease in thermostatting. The connecting mercury lines between the injector and auxiliary baths and the viscometer bath are jacketed with liquid pumped from the viscometer bath to bring the mercury nearly to 20° C before it enters the manometer or viscometer.

3.2. Main Injector

The function of the injector mechanism is to provide a known constant flow of mercury into the entrance chamber of the viscometer, thus forcing water through the capillary at a rate that is constant when the manometer is at equilibrium.

Figure 2 shows the injector and its driving mechanism without the constant-temperature bath.

The injector consists of a vertically mounted, mercury-filled steel cylinder into which a steel piston is forced by a rigidly coupled screw. The screw, held from turning by outriders bearing on tracks parallel to its axis, is moved by a rotating nut held between thrust-type ball bearings. On the periphery of the nut is a worm gear driven by a worm on a horizontal drive shaft. This mechanism is driven through a change gear box by a synchronous motor.

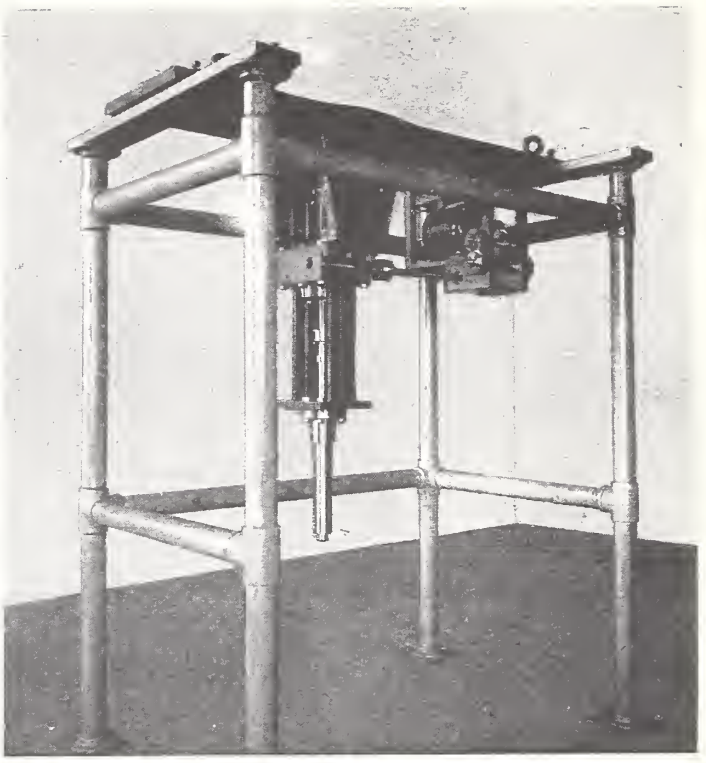

FIGURE 2. *Main injector with thermostat removed.*

The piston, nominally 1 in. in diameter, is made of hardened, ground, and lapped Ketos steel. Its diameter is uniform to ± 0.00004 in. The piston enters the steel cylinder through a vacuum-tight gland that contains cloth impregnated with ceresin wax. The cylinder has an inside diameter of 1⅛ in.; thus there is a 1/16-in. radial clearance between cylinder and piston. With a clearance of this magnitude, the formation of voids is unlikely except in the packing gland, and the volume of mercury expelled from the cylinder should be precisely the volume of the entering piston. The cylinder was thoroughly pumped out and filled with mercury under vacuum.

The screw is made of hardened steel. It has a maximum diameter of 1 in., and an 8-pitch Acme thread. The mating threads of the nut are made of Babbit metal. The worm gear that forms the periphery of the nut is of mild steel, and the mating worm is of hardened steel. These parts were specially machined so as to have no periodic error greater than 1 part in 10,000 of their lead. The worm and gear give a 40-to-1 reduction.

Speeds are changed by changing one or both pairs of meshed gears mounted outside the gear box. These are commercial grade, 32-pitch, ½-in. face, helical gears. The drive is a 3-phase, 110-volt, ¼-horsepower, synchronous motor.

Power for driving the injector mechanism is obtained from a constant-frequency generator driven by a special motor that takes its power from the commercial lines but has its speed automatically held in synchrony with a highly accurate 60-cycle

signal originating in a quartz-crystal oscillator maintained by the Radio Division of the Bureau. The piston and cylinder are immersed in a stirred oil bath whose temperature can be maintained at a chosen point within ±0.002° C. The worm-gear mechanism, gear box, and motor are in a cork-lined inclosure directly above the oil bath.

The rate of delivery of mercury from the injector is calculated from the measured delivery per turn of the worm drive shaft and the rotational speed of the shaft. The speed of the shaft is calculated from the motor speed and the ratio of the gears employed. Variations in speed caused by imperfections in the change gears can be neglected as they are of short period and tend to be integrated by the slow reaction of the manometer to changes in pressure. (The time constants for the system will be discussed later.) Variations in motor speed arising from frequency fluctuations in the power supply are guarded against. A permanent magnet, held in a collar, is installed on the drive-motor shaft in such a way that it induces pulses in a stationary coil with every revolution. The frequency of these pulses is compared with that of the 60-cycle control signal. If the power supply shifts more than 120° in phase with respect to the 60-cycle control signal, a buzzer sounds. An oscillograph is used to determine whether buzzer warnings indicate oscillations or actual gain or loss of cycles. With these safeguards in operation, the drive speed is taken to be 1,800 rpm without error.

The displacement of mercury by the piston per drive-shaft turn was determined by advancing the piston through its stroke in steps, catching and weighing the mercury displaced in each step. For this purpose a revolution counter and a divided drum were attached to the drive shaft, permitting reading of intervals to ±0.001 turn. The mercury is ejected through a delivery tube attached to the mercury line from the cylinder. This tube, similar to those used in ice calorimetry [9], was made by blowing a small spherical bulb at one end of a glass capillary tube. This bulb was then ground off in a plane perpendicular to the axis of the tube until the wall at the bottom was just broken through. With such a terminal configuration, the tube being mounted vertically, the mercury thread tends to break, leaving the bulb full, and variations in the delivery of mercury are minimized.

The smallest interval into which the total stroke of the piston can be divided is governed by the precision with which the mercury thread in the delivery tube can be broken, and the constancy of volume of the somewhat elastic cylinder and connecting tube. Repeated measurements of the mass delivered by the piston over a short part of its stroke showed a standard deviation of 3 mg from the mean.

The total delivery for a complete stroke of the piston is 109 cm^3 (1,470 g of mercury). The drive shaft makes 2,700 turns in driving the piston through this distance. For calibration, the total stroke was divided into 20 approximately equal intervals, each corresponding to about 135 turns of the drive shaft and a displacement of 73.5 g of mercury. In each interval the injector was driven under power for the required number of turns and allowed to coast to rest. The next interval was begun from this point of rest. In this way the slack in the drive was always kept in the same direction, minimizing variations arising from play in the driving gears and screw. The determination of the exact length of a particular interval in terms of number of turns of the drive shaft was obtained from the difference of two readings of the counter and divided drum on the shaft. As each reading was made to ±0.001 turn, the length of each interval could be determined to ±0.002 turn, or 1.5 parts in 100,000.

The increments of mercury were weighed with an accuracy of about 0.3 part in 100,000.

The mean rate of delivery for the entire stroke, expressed as mass displacement of mercury per turn of the drive shaft, was calculated by summing the masses of mercury delivered in all of the intervals and dividing by the total number of turns for the complete stroke. The uniformity of the rate of displacement throughout the stroke was obtained by a comparison of the rate calculated for each interval with the mean rate.

The first calibrations of the injector indicated that rate of displacement was not constant throughout the entire stroke of the piston, being more uniform during the second half of the stroke. As a consequence, only the second half of the piston stroke was employed in the earlier measurements.

Six calibrations were completed prior to 1941, five being made with the injector at 30° C and one at 35° C. The mean rates of delivery obtained in these calibrations for the portion of the stroke used in the flow measurements (intervals 12 through 19) are given in table 1. The rates at 35° C were computed from the calibrations made at 30° C, using 37.8×10^{-6}/°C as the cubical coefficient of thermal expansion for the Ketos steel piston [12] and 181.0×10^{-6}/°C for the coefficient for mercury. (See appendix A.)

TABLE 1. *Main injector calibrations, March 1939 through January 1940*

Calibration	Date	Measured rate of delivery at calibration temperature—		Rate of delivery at 35° C
		30° C	35° C	
		g/turn	*g/turn*	*g/turn*
1	3/17/39	0.54398	----	0.54359
2	3/21/39	.54397	----	.54358
3	3/27/39	.54398	----	.54359
4	3/29/39	.54396	----	.54357
5	1/2/40	----	0.54357	.54357
6	1/5/40	.54399	----	.54360
Mean	----	----	----	0.54358

Deviations from the mean rates of delivery for each calibration are shown in table 2. The computed standard deviation from the mean of a given calibration is given, and the standard deviation from the mean of each interval is given for the six calibrations. On the basis of the experiments with the delivery tube

which showed a standard deviation of 3 mg of mercury as previously stated, the deviation to be expected from this cause would be ±4 parts in 100,000 for intervals of this size. It is seen that the deviations in the first four calibrations are about twice this great and are over 10 times as large in the last two. It must be concluded then that variations in rate of delivery do exist along the piston. There are also real variations from calibration to calibration, especially in the last two. The relatively large changes between the fourth, fifth, and sixth may have been caused by slight shifts in the packing gland. These variations are not considered serious as the agreement between the mean rates, as shown in table 1, is very good for all six calibrations, and short-period variations along the stroke of the piston tend to be integrated by the manometer.

TABLE 2. *Deviations in parts per 100,000 from the mean rate of delivery for each calibration*

Interval	Calibration						Standard deviation each interval
	1	2	3	4	5	6	
12	−1	−3	+3	−5	−31	+13	±12
13	+21	+16	−1	+4	+78	−5	±27
14	−2	−5	+4	−1	−58	+60	±30
15	−5	−2	+5	+3	+7	+18	±8
16	+4	−2	−6	−16	+52	−66	±33
17	−17	−10	−7	+9	−10	+41	±22
18	−2	+1	−1	+5	−31	−51	±26
19	+2	+6	+3	+1	−8	−12	±8
Standard deviation	±9	±8	±5	±8	±46	±44	

It should be pointed out that the variations in the separation of the mercury at the end of the delivery tube enter only twice in the determinations of the mean rates given in table 1. A deficiency in delivery at the end of 1 interval results in a high delivery in the following interval, and only the start of the first and the end of the last interval have any effect. The expected deviation from this cause is thus reduced to ±0.5 part in 100,000 for the portion of the piston 8 intervals long.

The earlier flow measurements (series I and II, to be identified later) were made with this filling with the injector thermostatted at 35° C, and rates of flow in the viscometer were based on the value of 0.54358 g/turn, which is the mean of the values given in table 1.

Following these calibrations, work on the project was interrupted until January 1947. When the work was resumed in January 1947, the laboratory was air-conditioned. This made it possible to thermostat the injector at 30° C instead of 35° C. After the injector had been disassembled, cleaned, and refilled, three calibrations of the rate of delivery of the injector at 30° C were completed before making flow measurements. These data indicated that the useful part of the stroke of the piston could be extended to include intervals 5 through 19 without seriously affecting uniformity of delivery. Consequently this longer portion of the stroke was used for the later measurements.

Six calibrations were made in 1947 and 1948 on this filling of the injector before the injector was again refilled. The results of these six calibrations are given in table 3. In calibrations 10, 11, and 12, the stroke of the piston was not interrupted at the end of each interval, the total delivery of the injector for intervals 5 through 19 being collected and weighed in one bulk. The weighings of these relatively large quantities of mercury were made by the Mass Section of the Bureau with an accuracy of 1 part in 100,000. No significant difference was apparent in the mean rate of delivery as determined in bulk as compared with the calibrations by intervals.

TABLE 3. *Calibrations with second filling of injector*

Calibration	Date	Measured rate at 30° C
		g/turn
7	4/2/47	0.54391
8	7/7/47	.54393
9	7/22/47	.54393
10 [a]	8/4/47	.54392
11 [a]	1/3/48	.54391
12 [a]	1/3/48	.54390
Mean		0.54392

[a] Calibrations not made by increments.

The deviations for calibrations 7, 8, and 9 are given in table 4. They are seen to be somewhat larger than those for the first four calibrations with the initial filling but are much smaller than those for 5 and 6.

TABLE 4. *Second filling of injector*

Deviations in parts per 100,000 from mean rate of delivery for each calibration

Interval	Calibration			Standard deviation each interval
	7	8	9	
5	−8	−2	+2	±6
6	−1	−29	−15	±14
7	−25	−12	−17	±8
8	+7	+9	−8	±11
9	−18	−19	−13	±3
10	+13	+13	+15	±2
11	−12	−10	−14	±2
12	+1	+1	+10	±6
13	+24	+24	+27	±2
14	−9	+2	−3	±6
15	+6	+13	+14	±5
16	−8	+3	−9	±8
17	+6	−27	−19	±20
18	+18	+8	+10	±5
19	+3	+26	+19	±14
Standard deviation	±14	±17	±17	

Flow series III and IV were made with this second filling with the injector thermostated at 30° C, and rates of flow were calculated by using the mean value of 0.54392 g/turn shown in table 3.

Following the fourth series of flow tests, the injector was again cleaned and refilled. The results of the five calibrations made with this third filling are given in tables 5 and 6. The deviations shown in

table 6 are about the same as were found for the second filling. The data given in table 5 indicate an increase in the delivery rate of about 7 parts in 100,000 over the period of about a year and a half covered by these calibrations. This was not considered serious, and as with the previous fillings, the mean of the five calibrations was used in calculating the flow rates. The latest flow tests, series V through XII, were completed with this filling, 0.54396 g/turn being taken as the rate of delivery for the injector.

TABLE 5. *Calibrations with third filling of injector*

Calibration	Date	Measured rate at 30° C
		g/turn
13	5/24/48	0.54393
14	12/8/48	.54395
15	1/6/49	.54396
16	8/19/49	.54397
17	10/21/49	.54397
Mean		0.54396

TABLE 6. *Third filling of injector*

Deviations in parts per 100,000 from mean rate of delivery for each calibration

Interval	Calibration					Standard deviation each interval
	13	14	15	16	17	
5	−7	−4	+4	+5	+5	±7
6	−20	−10	−5	0	−6	±6
7	−9	−17	−8	−2	+6	±8
8	+19	+21	+22	+26	+24	±3
9	−20	−23	−7	−25	−13	±8
10	−2	+13	−6	+20	+10	±11
11	+12	+6	+11	+23	+22	±8
12	−17	−8	−22	−2	+2	±11
13	+30	+29	+25	+21	+30	±4
14	+2	−12	−5	−10	+4	±8
15	+4	+1	−4	−6	−9	±6
16	−6	−6	−9	−28	−32	±15
17	−31	−25	−31	−30	−58	±13
18	+17	+8	−7	−1	−7	±11
19	+31	+27	+43	+8	+23	±13
Standard deviation	±19	±18	±18	±18	±22	

The over-all performance of the injector was very satisfactory. No significant changes in the mean delivery rate were found even after the injector had been idle for the period of 6 years between the first and second fillings. The mean of the six calibrations with the first filling was recalculated to include the intervals 5 through 19 and found to be 0.54394 g/turn. This result compares very favorably with the values of 0.54392 and 0.54396, which were obtained with the second and third fillings, respectively, and it is felt that the mean rates of delivery used were known to somewhat better than 1 part in 10,000.

3.3. Manometer

The general operation of the manometer has been described above. Both arms of the manometer are constructed of glass tubing, the inside diameter of which is 0.97 in.

The lower ends are ground on a taper and cemented into matching stainless-steel seats, which connect to the mercury lines, as shown in figure 1. These connectors are mounted in a duralumin frame, which also supports the upper parts of the manometer and viscometer.

The short arm is about 3.5 in. high and is ground at the top to fit a stainless-steel cap which is cemented in place. The small tube that runs from the side of the cap to a gas-tight valve situated above the liquid level in the bath, serves to vent air from the top of the short arm when the apparatus is being filled with water. A weight, not shown in the figure, bears on the cap to prevent its being unseated under pressure.

The level of the mercury in the short arm is adjusted until it just makes contact with a fixed stainless-steel rod that projects downward from the cap as shown. This rod terminates in a point having an included angle of 60°. Contact between mercury and rod is determined electrically as described below.

The heights of mercury in the long arm are measured from a fixed surface plate above the mercury by means of calibrated stainless-steel depth gage rods, which fit in a micrometer head having a range of 1 in. These rods are $\frac{3}{16}$ in. in diameter and cover the range from 11 to 50 in. in 1-in. steps. They terminate in pointed tips similar to the tip of the fixed rod in the short arm. The surface plate is bolted to the duralumin frame, which supports the viscometer and manometer. The depth gage is clamped in a position directly over the long arm, as shown in the figure. Glass flats are used to insulate the gage electrically from the surface plate. The rods pass through a hole in the steel plate and enter the long arm, which extends above the liquid level in the viscometer bath.

The electric circuit in each arm, used to locate the mercury surface, consists of a 1.5-volt dry cell, a 30,000-ohm resistor, and a microammeter, all in series with the contact. With pointed tips on the rods and reasonably clean mercury-water interfaces, the mercury does not cling to the point, and contact is sharply indicated. It was found essential that the potential of the rods be negative with respect to the mercury. When the rod is made positive a nonconducting layer is immediately formed. Even with negative contacts, some electrolytic action takes place, and if the current is left on too long (several hours) a troublesome precipitate may form on the mercury surface. It is not necessary to insulate the rods from the water. For convenience in matching the contacts in the two arms, twin microammeters having 50-μa scales are mounted side-by-side.

The long arm is mounted as nearly vertical as possible, and the surface plate is carefully leveled. Nevertheless, the rods did not always make contact with the mercury in the center of the meniscus. In these cases the rods were rotated in the gage head until a minimum micrometer reading was obtained. This procedure was followed during the first three series of flow measurements. Thereafter the gage

rod in use was provided with a brass centering disk fastened near its tip. This disk has a diameter of ¾ in. Thus the tip was constrained within a ¼-in.-diameter circle at the center of the mercury meniscus. Calculation of the shape of the mercury meniscus [11] indicates that the error in locating the apex is not more than 0.0003 in. with the tip so restricted.

Loss of sensitivity in the long arm was encountered occasionally when the meniscus became contaminated with foreign matter. This surface was cleaned by applying vacuum to a long glass tube that was inserted in the long arm until its tip just touched the mercury surface.

It is estimated that the height of the column of mercury in the manometer may be measured with a precision of 0.0005 in. or better over the range of 0 to 40 in.

The auxiliary apparatus for manipulating the mercury in the manometer system has been mentioned previously. Coarse adjustment of the mercury in the long arm is attained by forcing mercury from the reservoir by gas pressure applied through a connection in the gas-tight cover, as shown in figure 1. Fine adjustments in either arm are made with the manometer injector. This injector is essentially similar in design to the main mercury injector. It has a ¾-in. piston fixed to a 12-pitch Acme screw. The piston is driven manually through a worm and gear having a 40-to-1 ratio. One turn of the hand crank on the drive shaft raises or lowers the mercury level in one arm by 0.0012 in.

The valves in the steel valve block are of the plug-and-barrel type. The rotating plugs are Ketos steel cylinders, hardened, ground, and lapped into hardened Ketos steel sleeves held in the mild steel body of the valve block. In the open position, ⅛-in. transverse holes through the plug and block are brought into alinement. In the closed position reliance is placed upon the very small clearance between plugs and sleeves to insure mercury tightness. The valve stems pass through vacuum-tight packing glands, which permit evacuation of the system for filling with mercury.

The first step in using the manometer is to obtain the manometer zero, which is a measure of the vertical distance between the contact point in the short arm and the surface plate on which the micrometer depth gage head rests. With no flow of mercury into the entrance reservoir of the viscometer, the manometer will come to equilibrium with the mercury at the same level in each arm. Mercury is added to the manometer system until this equilibrium is reached at the level of the contact in the short arm. The mercury level in the long arm is then measured from the surface plate, using the longest rod in the depth gage. The micrometer head reading for this condition is a measure of the desired vertical distance and is called the manometer zero. This reading is designated by M_0.

To obtain the height of mercury in the manometer for a given flow condition, mercury is forced into the long arm until it stands at its anticipated height. Then, with the main injector running and water flowing through the capillary at the desired rate, the two arms of the manometer are opened to each other. Mercury is added or withdrawn from the manometer system as necessary until equilibrium is reached with the mercury in the short arm at the level of the contact point. The mercury then stands as shown approximately in figure 1. The distance from the surface plate to the level of mercury in the long arm is measured by means of a gage rod of suitable length. The micrometer head reading for this condition is designated by M_Q. The differential height of mercury in the manometer is calculated from the difference between this reading and the manometer zero. The height of mercury is equal to M_0 minus M_Q plus the difference in length between the longest gage rod and the particular rod used in obtaining M_Q.

When the differential heights of mercury are measured in this manner, the actual lengths of the gage rods need not be known, and hence only differences between the longest, which is used in obtaining the manometer zero, and each of the other rods are determined. As it was not practical to cut the rods such that the differences in length were in steps of exactly 1 in., this was closely approximated, and the actual differences were measured, using Hoke gage blocks. These calibrations were repeated as often as was necessary to follow the changes in the lengths of the rods. It is felt that the corrections were known to within at least 0.0004 in. The results of these calibrations are given in detail in appendix B.

3.4. Viscometer

The viscometer is arranged as shown in figure 1. The capillary is mounted vertically between two terminal chambers. Terminal pieces are permanently cemented to the ends of the capillary with a phenolic elastomer (Permacel JX–5). The outer surfaces of the terminal pieces are conically ground to fit the tapered joints in the hemispherical ends of the chambers, as shown. The tapered joints are sealed with Apiezon, Hard Wax W to insure water tightness and permit the interchanging of the different capillaries used in the viscometer. The lower, or entrance, chamber is constructed of glass and is about 2.2 in. in diameter and 4.5 in. high. Its lower end terminates in a tapered joint that is cemented with the Hard Wax W, to the end of a fitting connecting to the mercury line from the main injector. The wax joints are coated with an automobile gasket shellac to protect the wax from the solvent action of the bath oil. The exit chamber, also of glass, is about 1.7 in. in diameter and 4 in. high. It is connected by glass tubing to both the reservoir and the long arm of the manometer, as shown. By this means the same water level is maintained in both the viscometer and manometer. The capacity of the reservoir is sufficient to accommodate the volume of water that is displaced through the capillary by a full stroke of the main injector.

In this system, an increase or decrease in the height of mercury in the short arm of the manometer

requires a corresponding flow of water out of, or into, the short arm through the side tube connecting it with the entrance chamber. Thus, until equilibrium is reached, the rate of flow of water through the capillary will not correspond to the rate of flow of mercury into the entrance chamber, but at any time will depend on the pressure indicated by the differential height of mercury, h, in the manometer. If q is the rate of flow through the capillary and Q is the rate of flow of mercury into the entrance chamber, it can be shown that q approaches Q as h approaches the limiting value corresponding to flow Q through the capillary.

As there is flow through the tube connecting the exit reservoir with the long arm, this tube offers some viscous resistance in series with the capillary. It can be shown that the pressure drop through the capillary plus this connecting tube is given by $h(D_{Hg}-D_W)g$, where D_{Hg} and D_W are the densities of mercury and water, respectively, and g is the acceleration of gravity. However, neglecting for the time being the small viscous resistance offered by the connecting tube, and using only the relatively large first term in eq 3, we can write

$$h=\frac{8\eta(l+nr)}{\pi r^4(D_{Hg}-D_W)g}\cdot q. \tag{10}$$

If

$$\frac{8\eta(l+nr)}{\pi r^4(D_{Hg}-D_W)g}=k,$$

eq 10 is rewritten

$$q=\frac{h}{k}. \tag{11}$$

For the condition where q is not equal to Q, the flow of water into or out of the short arm of the manometer is given by $A(1/2)dh/dt$, in which A is the cross-sectional area of the manometer tubing and dh/dt is the rate of change of pressure head. The total flow may then be expressed as

$$Q=\frac{h}{k}+\frac{A}{2}\frac{dh}{dt}. \tag{12}$$

Integrating with Q constant gives

$$h=kQ+C\cdot e^{-\frac{2t}{kA}}, \tag{13}$$

in which C is a constant. This equation shows that the height of mercury in the manometer approaches a value corresponding to flow Q through the capillary, being precisely kQ at infinite time.

In practice, the manometer is preset to approximately its final height and then allowed to approach its precise equilibrium value. The flow time until final readings may be taken depends on the accuracy attainable in measuring the height of mercury in the manometer.

Letting Δh_0 represent the amount by which h differs from kQ at the start of flow and Δh_t the difference after time t has elapsed, we can write

$$\frac{\Delta h_0}{\Delta h_t}=e^{\frac{2t}{kA}}, \tag{14}$$

from which

$$t=\frac{kA}{2}\,ln\left(\frac{\Delta h_0}{\Delta h_t}\right). \tag{15}$$

Thus, through use of eq 15 one can calculate the time required to reduce Δh_t to any desired fraction of Δh_0.

The results are given in table 7 for each of the capillaries used. These times are designated as time constants of the manometer and are shown for various values of the ratio $\Delta h_t/\Delta h_0$. The capillary designations given in the table will be identified later.

TABLE 7. *Manometer time constants in minutes*

$\frac{\Delta h_t}{\Delta h_0}$	Capillary			
	2.5	2.5a	1.4	1.4a
1/2	7	4	16	8
1/5	16	8	38	19
1/10	24	12	55	27

It is evident that with time constants of the magnitudes shown in table 7, periodic variations in Q resulting from imperfections in the change gears and injector delivery will not introduce appreciable error in the measured pressure.

As mentioned before, the measured pressure includes the pressure drop through the tube connecting the exit reservoir and the long arm. If P is the difference in pressure between the end reservoirs, l_T is the length of the connecting tube, r_T is the radius of the connecting tube, B is the cross-sectional area of the reservoir, and the other symbols are as before, it is seen that

$$h(D_{Hg}-D_W)g=P\left[1+\frac{l_T}{l}\cdot\frac{r^4}{r_T^4}\left(\frac{A}{A+B}\right)\right], \tag{16}$$

or

$$P=h(D_{Hg}-D_W)g\left[\frac{1}{1+\frac{l_T}{l}\cdot\frac{r^4}{r_T^4}\left(\frac{A}{A+B}\right)}\right]. \tag{17}$$

The calculated value of this factor by which $h(D_{Hg}-D_W)g$ must be multiplied to give the pressure drop across the capillary alone is as follows for each capillary used:

Capillary	Factor
2.5	0. 999995
2.5a	. 999980
1.4	. 999997
1.4a	. 999991

While these corrections are insignificant relative to the precision with which the manometric measurements were made, the corrections were applied.

3.5. Temperature Control

The oil baths by means of which the temperatures of the various parts of the apparatus are maintained constant consist of metal tanks insulated with a minimum thickness of 3 in. of ground cork. Inside each tank and close to the side is a vertical stirrer tube 6 in. in diameter extending from above the oil surface to a point a few inches above the bottom. A propeller on an axial shaft in the tube draws oil from the bath through a port just below the oil level and discharges it into the tank near the bottom with sufficient velocity to keep the main body of oil in fairly rapid motion. Electric heating coils and mercury-in-steel thermoregulators, annular in form, are mounted, one above the other, in the stirrer tubes in such fashion that oil flows down over both their inner and outer surfaces.

The viscometer bath is held at 20° C by artificial cooling. To effect this cooling a tank of light oil is maintained at 15°±0.1° C by a refrigerating system in conjunction with an automatically controlled electric heater. The oil from this tank is pumped at a steady rate through a coil in the stirrer tube in the viscometer bath, and the temperature is controlled by a thermostatically regulated heater. This system of temperature regulation was used during the first two series of flow measurements and provided control to ±0.004 deg C. Following these tests the apparatus was idle for 6 years. When work was resumed, it was found that this thermoregulator was insensitive. For the later flow measurements this bath was controlled by manual regulation of a variable transformer. Although tedious, the control was of the order of ±0.001 deg C. As the viscosity of water changes by only 1 part in 10,000 for a temperature change of 0.004 deg C in the neighborhood of 20° C, this control was more than adequate.

The main injector and auxiliary baths were held above room temperature, and therefore no artificial cooling was required. The injector bath was found to hold its temperature consistently to ±0.002 deg C. The thermoregulator in the auxiliary bath was not designed to be as sensitive as the other two, and the temperature control in this bath was ±0.01 deg C. Temperature variations of the magnitudes found in these baths cannot affect the measurements by as much as 1 part in 100,000.

Standard electric circuits were used with the thermoregulators. Steady currents through the heating coils, not quite sufficient to maintain temperature, were periodically augmented by intermittent currents controlled by the regulators. By means of motor-driven variable resistors, the steady currents were automatically adjusted to changing room temperature, temperature distribution in bath insulation, and line voltage.

Two thermometers were used in the viscometer bath, one at the level of the entrance chamber of the viscometer and the other at the level of the exit chamber. Temperature gradients were so small that readings on these two thermometers always agreed within 0.002 deg C.

When flow measurements are being made the mercury leaves the injector at a temperature 10 deg or more higher than that of the viscometer bath. In order to bring the temperature of the mercury close to 20 deg C before it enters the entrance chamber of the viscometer, oil is pumped from the viscometer bath through a copper jacket placed around the mercury line. The returning oil is discharged into the top of the viscometer bath stirrer tube, and hence its effect is to improve stirring rather than to increase temperature gradients throughout the bath. Experiments were performed to measure the effectiveness of the precooling of the mercury entering the viscometer. A thermometer was introduced into the entrance chamber through the ground joint normally holding the capillary. With the viscometer bath at 20° C and the main injector bath at 35°C, the temperature of the water in the chamber was measured at various rates of flow of mercury into the chamber. Even at the highest rates of flow used (0.25 cm^3/sec), no measurable temperature difference between the water and the bath liquid was observed.

Temperatures were measured with platinum resistance thermometers and a Mueller thermometer bridge. The thermometers were calibrated several times at the steam and sulfur points, and more frequent readings were taken at the ice point or triple point of water. Every 2 months, or oftener, the bridge was calibrated in terms of a 10-ohm secondary standard. Regular calibrations of the standard were made by the Resistance Measurements Section of the Bureau. It is believed that temperature measurements were made with an accuracy of ±0.001 deg C.

4. Capillaries and Their Measurement

4.1. Selection and Preparation

Flow measurements were made with four capillaries. One length of capiallary was selected in each of two diameters, and, after measuring their dimensions and making the necessary flow measurements, they were cut in half, and the measurements were repeated with one half-length of each tube. In this manner flow data were obtained on two pairs of capillaries, the tubes in each pair being close to the same diameter but having different lengths.

The capillaries were selected from FS Precision-Bore capillary tubing obtained from the Fish-Schurman Corp. The first selection was made in 1938 from three tubes of Jena Duran Glass 3891–III having external diameters of about 5 mm and internal diameters of about 0.5 mm. The capillary selected was numbered 2.5 and the half-length, which was later cut from this tube, was numbered 2.5a. Three more tubes were obtained from the same company in 1947. These were of Pyrex and had about the same external diameter but had a bore diameter of 0.4 mm. The capillary chosen from this stock

was designated as No. 1.4 and the half-length as 1.4a.

The tubes were chosen for uniformity and straightness of bore and freedom from blemishes. The character of the inner surfaces was examined under a microscope with the bores filled with water, while the examination for uniformity of bore was made with the tubes mercury-filled. The uniformity of the tubes was such that the selection could be made from the first few obtained.

An unused length from the stock of Jena glass was sectioned part way along its bore in such a way as to expose the surface of the bore for examination. A portion of the exposed surface was photographed at a magnification of ×200 and is shown in figure 3, A.

This section is typical of the surface of the bore of capillaries 2.5 and 2.5a. The surface shown in figure 3, B is typical of the Pyrex capillaries 1.4 and 1.4a. It is seen that both of these surfaces are characterized by many longitudinal grooves. These grooves vary in width between about 0.002 and 0.008 mm and are considerably less deep than wide. The Pyrex capillaries are singularly free from very many other markings. The Jena capillaries have regions of pits and elevations superimposed upon the grooved markings. All of these surface markings are so small in relation to the diameters of the capillaries, however, that it is believed their viscometric effects cannot be serious.

To examine for uniformity of bore the mercury-filled capillary was immersed in oil having the same index of refraction as the glass. Diameter measurements were made with a microscope having a filar micrometer eyepiece. Such measurements were made at points spaced 5 cm apart, except that the points nearest the two ends of a tube were taken 1 cm from the end. Measurements were made at each point in four radial directions spaced 45° apart. The results obtained with capillary 2.5 are given in table 8. The micrometer eyepiece was not accurately calibrated, and therefore the numbers in the table are in arbitrary units. The precision of the measurements was about 1 part in 500. The ends of this tube were designated as 1 and 2, and the distances to the points at which the diameter measurements were made were taken from end 1.

TABLE 8. *Optical measurements of the diameter of capillary 2.5, arbitrary units*

Distance from end 1	Radial direction—			
	0°	45°	90°	135°
cm				
1	1124	1123	1128	[a] 1120
5	1124	1121	1127	1121
10	1125	1127	1124	1123
15	1129	1123	1131	1126
20	1127	1122	1131	1123
25	1124	1124	1123	1129
30	1125	1121	1126	1128
35	1122	1121	1131	1123
40	1129	1127	1131	1124
45	1129	1123	[a] 1132	1124
49	[a] 1120	1124	1124	1126

[a] Highest and lowest values.

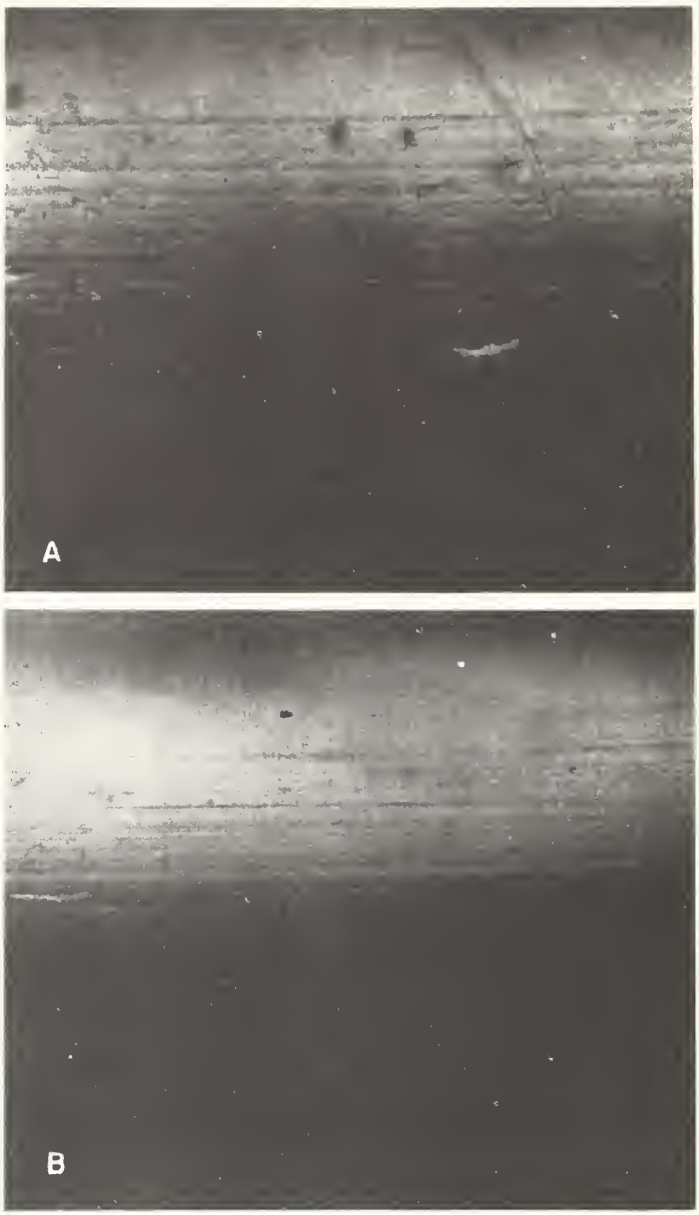

FIGURE 3. *Photomicrographs of surface of capillary bores.* Magnification ×200. A, typical of Jena glass; B, typical of Pyrex glass.

It is seen that the maximum variation shown by the measurements given in table 8 is only 1 percent. The effect of variations of this order will be discussed later under "Caliber corrections."

Similar measurements made on capillary 1.4 are given in table 9. The ends of this tube were numbered 4 and 5, and the distances are measured from end 4. The bore of this capillary is seen to be about as uniform as that of capillary 2.5, showing a maximum variation of 1.3 percent.

Following this selection, the ends of the capillaries were fitted with glass terminal pieces so that the bores terminate in circular planes 1 cm in diameter. The end planes of the terminals were ground normal to the axis of the bores and then polished until good sharp edges were obtained at the intersections of the cylindrical bores with the terminal planes.

When the longer capillaries 2.5 and 1.4 were cut in half, new terminal pieces were cemented at the cut

TABLE 9. *Optical measurements of the diameter of capillary 1.4, arbitrary units*

Distance from end 4	Radial direction—			
	0°	45°	90°	135°
cm				
1	895	892	887	892
5	896	892	889	892
10	893	895	888	891
15	895	894	888	893
20	889	893	892	892
25	893	895	893	895
30	892	891	891	892
35	891	895	888	[a] 897
40	890	892	889	896
44	889	890	[a] 885	892

[a] Highest and lowest values.

ends only. Thus, the shorter capillaries 2.5a and 1.4a each had one new end and one end from the original tube. Capillary 2.5a retained the original end number 1 from capillary 2.5, and its new end was numbered 3. Similarly, capillary 1.4a had the original end No. 4, and the new end was numbered 6. These numbers will be used later in identifying the direction of flow through the capillaries during the flow measurements.

The ends of the bores of the capillaries are shown in figure 4. The finished edges of the bores were not always perfect, as shown particularly by A and F. The badly chipped edges shown in D occurred after the flow measurements involving this end had been nearly completed. The three series of flow measurements had been completed with capillary 1.4, and the chipped places appeared on disassembling the apparatus after the first series with capillary 1.4a. The second series with 1.4a was made after the chips were discovered. It will be apparent from the data given later that these chipped places did not measurably affect the results.

4.2. Mean Radii of the Capillaries by the Gravimetric Method

Although optical measurements of diameter are useful in describing the variations in shape and area of cross section of the bore along a tube, such measurements cannot be made with sufficient accuracy to deduce a mean radius that may be used in calculating the resistance to viscous flow offered by the tube. Consequently, other methods were used to obtain the mean radii of the capillaries.

The first method used involves the weighing of the quantity of mercury required to fill the tube. The mean area of cross section is calculated by using the known density of mercury and the length of the tube.

For these determinations a clamp was made so that one end of the capillary could be closed off by means of a glass optical flat clamped against the polished face of the terminal piece. The optical flat extended sufficiently beyond the edge of the terminal piece to permit a nickel ring to be cemented to it to hold mercury as a vacuum seal when the capillary was supported vertically. By means of a ground glass joint, the terminal piece at the upper end of the capillary was cemented to a vacuum system. The tube was then filled under vacuum with double-distilled mercury and disconnected

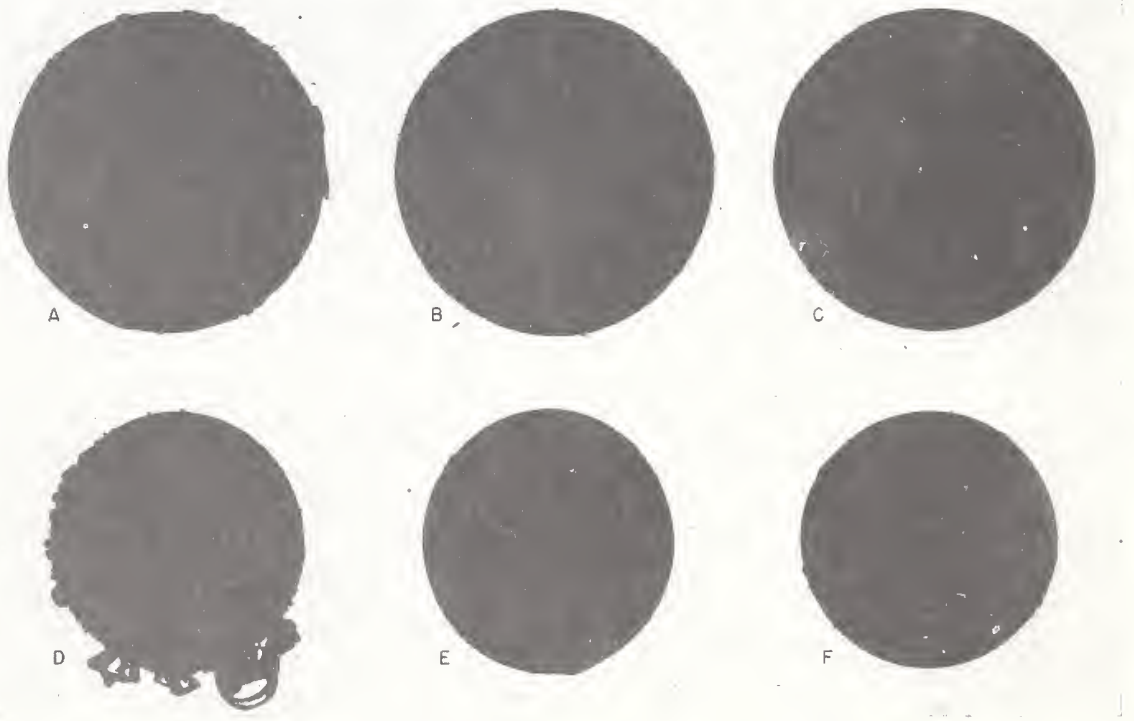

FIGURE 4. *Photomicrographs of the ends of the capillaries.*

Magnification ×75. A, Capillary 2.5, end 1; B, capillary 2.5, end 2; C, capillary 2.5, end 3; D, capillary 1.4, end 4; E, capillary 1.4, end 5; F, capillary 1.4, end 6.

from the vacuum system. The mercury-filled tube was mounted vertically in a well-stirred water bath with temperature control. A platinum resistance thermometer was used to determine the temperature of the water in the bath. The upper end of the capillary was allowed to extend about 4 mm above the water level, and on the flat horizontal surface of the end piece was placed a small glass optical flat through which the suitably illuminated end of the bore could be observed with the aid of a magnifying glass. Observations were then made to determine the exact temperature at which the bore was completely filled. As the temperature was increased the area of contact between the mercury and the optical flat increased until the area became equal to the cross-sectional area of the bore. The appearance of the interference fringes between the flat and the face of the end piece aided in determining when the flat was in close contact with the face and not pushed up by the mercury.

Having determined the temperature at which the bore was just full, the bath temperature was lowered until the mercury was no longer in contact with the flat. The flat was then removed and the capillary taken out of the bath and dried. The mercury in the bore was then ready to transfer to a small bottle for weighing. This was accomplished by first carefully removing the mercury from the seal at the clamped end. The capillary was mounted in a position about 30° from horizontal with the closed end high, and the clamp seal was opened slowly allowing the mercury to flow into the weighing bottle. Occasionally the mercury thread would break leaving a small filament of mercury in the end of the tube. This was removed by the gentle application of air pressure at the opposite end. The capillary was then examined with a magnifying glass to make certain that no mercury remained.

Measurements of the air temperature made in the region up to about 3 cm above the liquid level in the bath showed that, under the prevailing conditions, the temperatures were about 0.5 to 1 deg C above that of the bath. This was found to be the case for bath temperatures between 20° and 31° C for all room temperatures experienced. On this basis, the error in determining the mass of mercury required to fill the capillary, introduced by not correcting for the temperature of the 4 mm of capillary exposed above the bath liquid, was less than 3 parts per million for any of the capillaries used.

A further calculation showed that the dilation of the tube and the compression of the mercury caused by the pressure exerted by the column of mercury changed the mass required to fill the tube by not more than 3 parts per million for any of the capillaries. This correction was also neglected.

As the capillaries were to be used at 20° C, the dimensions at this temperature were required.

If M_θ is the mass of mercury that just fills the capillary at θ° C, D_{20} is the density of mercury at 20° C, α is the temperature coefficient of linear expansion of glass, β is the temperature coefficient of density of mercury, $\Delta\theta=(\theta-20)$, and r_{20} and l_{20} are the capillary radius and length at 20° C, we can write

$$M_\theta=\pi r_{20}^2\,(1+\alpha\Delta\theta)^2 l_{20}\,(1+\alpha\Delta\theta)\,D_{20}\,(1-\beta\Delta\theta). \quad (18)$$

Also

$$M_{20}=\pi r_{20}^2 l_{20}\,D_{20}, \quad (19)$$

in which M_{20} is the mass of mercury that would be required to fill the capillary at 20° C. Combining eq 18 and 19, we can say, with more than sufficient accuracy for the purpose,

$$M_{20}=\frac{M_\theta}{1+(3\alpha-\beta)\,\Delta\theta}. \quad (20)$$

Through use of eq 19 and 20, values of r_{20} are computed corresponding to the measured quantities θ and M_θ.

The capillaries were cleaned prior to each measurement of the radius. The cleaning procedures involved the discreet use of either nitric or chromic acids, followed by distilled water and drying air. When chromic acid was used, after the removal of the bulk of acid and preliminary rinsing, the bores were soaked with distilled water for at least 1 hour before the final rinsing with water. The cleaning agents and distilled water, as well as the drying air, were always passed through a sintered-glass filter before being introduced into the capillary. Radius measurements made at various times provide good evidence that the sizes of the bores were not changed by any of these cleaning procedures by any measurable amounts (see table 11).

The measurements of the lengths of the four capillaries were made by the Gage Section of the Bureau by comparison with Hoke end gages.

The results are as follows:

Capillary	l_{20}
2.5	48.736
2.5a	24.316
1.4	45.208
1.4a	22.525

It is believed that all the figures given are significant.

The weighings of the quantities of mercury were made by the Mass Section of the Bureau. The details of the weighings concerned with capillary 2.5 are not known. For the other capillaries each quantity of mercury was weighed twice. In connection with the weighings made on the fillings of capillaries 2.5a and 1.4a, a detailed study of the behavior of the glass weighing bottles used in the measurements was made in the Mass Section under the direction of L. B. Macurdy. The results of this study are given in appendix C.

It was concluded that the masses of the samples

from the fillings of capillaries 2.5a, 1.4, and 1.4a were known with an accuracy of ±0.01 mg or better. The samples from the fillings of capillary 2.5 were probably weighed with comparable accuracy.

In the calculation of M_{20} through the use of eq 20 the values used for α were those recommended by the manufacturers. These values are 3.6×10^{-6}/° C for the Jena Duran Glass 3891–III, of which capillaries 2.5 and 2.5a are made, and 3.2×10^{-6}/° C for Pyrex capillaries 1.4 and 1.4a. The density of mercury at 20° C was taken as 13.54589 g/cm^3 and β as 180.9×10^{-6}. These values were obtained from the work of Beattie [12] (see appendix A).

Five separate fillings of each capillary were made, the results of which are shown in table 10. The temperatures given are those at which the bores were judged to be exactly filled. The values of M_θ given for capillaries 2.5a, 1.4, and 1.4a are the means of the two weighings made on each quantity of mercury. The values of M_{20} are calculated by using eq 20.

TABLE 10. *Computations of mean radii by the gravimetric method*

Capillary	Date	θ	M_θ	M_{20}	r_{20}^2	r_{20}
		°C	g	g	cm^2	cm
2.5	5/10/41	19.91	1.313 12	1.313 10		
	5/14/41	20.18	1.313 19	1.313 23		
	5/15/41	19.22	1.313 36	1.313 19		
	5/16/41	19.82	1.313 15	1.313 11		
	5/17/41	20.94	1.312 84	1.313 05		
			Mean	1.313 14	6.3315×10^{-4}	2.5162×10^{-2}
2.5a	1/17/50	27.19	0.654 305	0.655 106		
	1/18/50	25.62	.654 488	.655 114		
	1/19/50	27.79	.654 187	[a].655 055		
	1/20/50	24.23	.654 641	.655 113		
	1/23/50	27.12	.654 326	.655 119		
			Mean	0.655 113	6.3309	2.5161
1.4	11/22/48	23.28	0.774 995	0.775 431		
	11/23/48	23.59	.774 943	.775 420		
	11/24/48	24.68	.774 733	[a].775 355		
	11/30/48	23.26	.774 983	.775 416		
	11/30/48	24.82	.774 774	.775 414		
			Mean	0.775 420	4.0305	2.0076
1.4a	1/24/50	27.52	0.386 255	0.386 753		
	1/25/50	31.39	.386 015	.386 770		
	1/26/50	29.87	.386 099	.386 753		
	1/27/50	28.14	.386 217	.386 756		
	1/27/50	30.68	.386 052	.386 759		
			Mean	0.386 758	4.0348	2.0087

[a] Determinations discarded.

With capillary 2.5a the result of the third filling shows a deviation from the mean of the order of 10 times as great as the other four. This is also the case with the third filling with capillary 1.4. As no discrepancies are found in the weighings, it seems evident that in these cases there was an undetected loss of mercury in the transfer from the capillary into the weighing bottle, and the results of these two fillings were discarded. The values of r_{20}^2 given in the table were calculated from the mean values of M_{20} for each capillary and represent the squares of the radii of right circular cylinders of the same volumes and lengths as the capillaries measured.

4.3. Mean Radii of the Capillaries by the Electric Resistance Method

The second method used for the precise determination of the mean radii of the boresof the capillaries is based upon the electric resistances of the bores when filled with mercury.

The electric resistance, R, of a cylindrical conductor of length l, radius r, and resistivity ρ is given by

$$R = \frac{\rho l}{\pi r^2}. \tag{21}$$

As the resistivity of mercury is accurately known, eq 21 affords a means of calculating the mean cross-sectional area of the bore of a capillary.

To adapt this method to the measurement of the mean radii of the capillaries, glass terminal bulbs were constructed with ground joints to fit the terminal pieces of the capillaries. A capillary with the terminal bulbs cemented in place is shown mounted in its supporting frame in figure 5. The bulbs are cylindrical with hemispherical ends and are 5 cm long with an internal diameter of 2.2 cm. Two tubes of 0.5-cm inside diameter are brought up from each terminal bulb, as shown in the figure. The distance from the face of the terminal piece of the capillary to the level of the side tube in the upper bulb is 2.4 cm. The corresponding distance in the lower bulb is 1.5 cm.

For making a measurement, the apparatus was evacuated and completely filled with double-distilled mercury up to a level within about 1 cm of the tops of the four tubes leading up from the terminal bulbs. Special electric connectors were placed on the tops of the four tubes, as shown in the figure. Each connector was made from a short piece of glass tubing sealed at the middle to separate the two end portions of the tube. A platinum wire was passed through the seal to make electric connection between the end portions of the tube. The connectors fitted loosely on the tubes leading from the terminal bulbs with the platinum wires making contact with the mercury in the tubes. The connectors were filled above the glass seals with mercury, into which the copper lead wires to the resistance bridge were dipped. The ends of the copper lead wires were amalgamated electrolytically, and the platinum wires were immersed in mercury for several months before use. With these connectors good electric contact is made without contaminating the mercury in the capillary with copper from the lead wires.

The resistance measurements were made with a Mueller resistance bridge. With the two leads connected to each terminal bulb, the procedure was similar to that used with a four-lead resistance thermometer. The mean of the two readings taken was the resistance of the mercury between the branch points in the two terminal bulbs. This resistance, corrected for the resistance in the terminal bulbs, yielded the resistance of the column of mercury in the capillary bore.

It has been shown (see, for example, Maxwell [13])

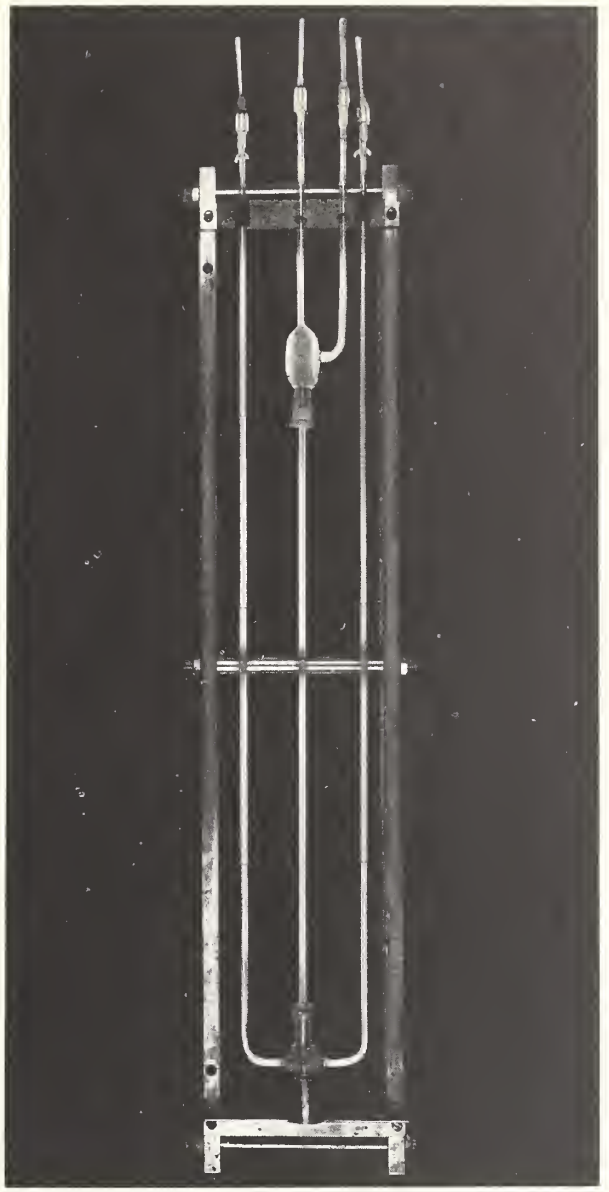

FIGURE 5. *Capillary mounted for the determination of its mean radius by the electric resistance method*

that the amount to be added to the measured resistance to account for the flow of electricity at the end of a tube may be expressed as an additional length equal to a constant times the radius of the bore at the end. A calculation by Rayleigh [14] yields a value of 0.82 for this constant. As the optical measurements of the diameters of the four capillaries showed that the mean radii at the ends of a capillary never differed from the mean for the whole tube by more than 0.3 percent, we can say that the sum of the corrections for the two ends is $2\times0.82\times r$, where r is the mean radius for the whole tube. Including the corrections for the ends, eq 21 then becomes

$$R=\frac{\rho\,(l+1.64r)}{\pi r^2}. \tag{22}$$

If subscripts refer to the temperature in ° C, we can introduce the coefficient of expansion of the glass into eq 22, which then becomes

$$R_\theta=\frac{\rho_\theta\,(l_{20}+1.64r_{20})\,(1+\alpha\Delta\theta)}{\pi r_{20}^2\,(1+\alpha\Delta\theta)^2}, \tag{23}$$

from which

$$r_{20}^2=\frac{\rho_\theta}{R_\theta}\left[\frac{l_{20}+1.64r_{20}}{\pi\,(1+\alpha\Delta\theta)}\right]. \tag{24}$$

For the solution of this equation, an approximate value of r_{20} is substituted in the second term on the right.

In all of this work the resistances are measured in absolute ohms. The following equation was used to calculate the resistivity of mercury in absolute ohm-centimeters at the temperature of the measurement:

$$\rho_\theta=94.1232\times 10^{-6}(1+889.15\times10^{-6}\cdot\theta+0.99360\times10^{-6}\cdot\theta^2), \tag{25}$$

in which θ is in ° C, and 94.1232×10^{-6} is the resistivity of mercury at 0° C. (See appendix A.)

The diameter of each capillary was measured at several different times by this method. For these measurements the capillary with the attached terminal bulbs was immersed either in a liquid bath, whose temperature was controlled within close limits, or in an ice-and-water bath. The results obtained with the four capillaries are given in table 11.

TABLE 11. *Computations of mean radii by the electric resistance method*

Capillary	Date	θ	R_θ	r_{20}^2	r_{20}
		° C	Ohms	cm^2	cm
2.5	3/25/41	+20.000	2.35007	6.3315×10^{-4}	
	3/25/41	+41.336	2.39665	6.3316	
	3/27/41	+31.971	2.37596	6.3315	
	3/29/41	+8.259	2.32532	6.3315	
	7/11/47	+20.000	2.35013	6.3313	
	4/20/48	−0.007	2.30827	6.3315	
	4/28/48	+23.912	2.35846	6.3315	
			Mean	6.3315	2.5162×10^{-2}
2.5a	2/18/49	−0.002	1.15287	6.3302	
	5/3/49	−.003	1.15282	6.3305	
	11/19/49	−.006	1.15287	6.3302	
			Mean	6.3303	2.5160
1.4	10/18/48	−0.003	3.36341	4.0302	
	11/17/48	−.004	3.36334	4.0303	
	1/10/49	−.001	3.36333	4.0303	
	2/16/49	−.001	3.36332	4.0303	
			Mean	4.0303	2.0076
1.4a	8/18/49	−0.005	1.67520	4.0347	
	10/7/49	−.004	1.67520	4.0347	
			Mean	4.0347	2.0087

The measurements on capillary 2.5 made over quite a range of temperatures are in good agreement, which tends to confirm the values of the constants in eq 25 in this temperature range. However, as it is believed that the resistivity of mercury is known best at 0° C, of the later measurements only those made close to 0° C were included in the calculations of the radii. The coefficient of expansion of the

glass need not be known accurately for use in eq 24, because an uncertainty in its value of as much as 1 part in 32 will result in an uncertainty of only 2 parts in a million in the value of r_{20}^2 as calculated from a measurement made at 0° C.

The radius measurements on a particular capillary were always made at times embracing the period during which the capillary was being used in the flow measurements. With each capillary, the agreement among the different determinations is good, and there is no evidence of any trend with time or use, even with capillary 2.5, on which measurements were made during 1941 and later in 1947 and 1948.

4.4. Caliber Corrections

The derivation of eq 2, expressing the resistance to the viscous flow of a liquid through a tube, is based upon the bore having the shape of a right circular cylinder. The optical measurements of the diameters of the capillaries used here have shown that they all depart somewhat from this ideal condition. Consequently, a correction must be applied to a measured radius to account for the difference between the viscous resistance in the actual capillary used and in an equally long one of uniform circular cross section. The determination of the mean radius by the gravimetric method has yielded the radius of a right circular cylinder of length and volume equal to those of the bore of the capillary. This radius may then be corrected appropriately for substitution in eq 2. However, the resistance to flow of electricity is also affected by the variable cross section of a tube. Therefore, the radii of the capillaries as measured by the electric resistance method must first be corrected to yield the radii of equally long capillaries of uniform cross-sectional areas and then be corrected again for substitution in the equation for the resistance to viscous flow.

In estimating the magnitudes of these corrections, the data given in tables 8 and 9 are used for describing the actual shapes of the capillaries. Various investigations of the effects of conicality and ellipticity of bore upon viscosity measurements have been made, but the above data on these tubes show that they cannot be considered conical. Their cross sections are irregular and resemble an ellipse in only a few places. The tubes are therefore treated as circular in section but with the area of section varying along the tubes. The mean of the diameters measured in the four radial directions at a particular point is taken as the diameter of the assumed circular section at that point. The mean diameters at the points measured along capillaries 2.5 and 1.4 are given in tables 12 and 13. The areas of section S calculated for each measured point are also given in these tables. Since only arbitrary units are used, S is taken equal to d^2 and, for the present purpose, can be assumed to be known exactly. Part of the data given in these two tables also apply to capillaries 2.5a and 1.4a, as they were cut from the longer capillaries 2.5 and 1.4.

Figure 6 shows values of S plotted against position along the tube for each of the four capillaries. These areas are represented by the plotted points, and the mean cross section for each capillary is shown by a horizontal dashed line.

TABLE 12. *Variations in cross-sectional area along capillary 2.5, arbitrary units*

Position along tube	Mean diameter	Area of cross section
cm		
1	1123.75	126 281
5	1123.25	126 169
10	1124.75	126 506
15	1127.25	127 069
20	1125.75	126 731
25	1125.00	126 563
30	1125.00	126 563
35	1124.25	126 394
40	1127.75	127 182
45	1127.00	127 013
49	1123.50	126 225

TABLE 13. *Variations in cross-sectional area along capillary 1.4, arbitrary units*

Position along tube	Mean diameter	Area of cross section
cm		
1	891.5	794 77
5	892.3	796 20
10	891.8	795 31
15	892.5	796 56
20	891.5	794 77
25	894.0	799 24
30	891.5	794 77
35	892.8	797 09
40	891.8	795 31
44	889.0	790 32

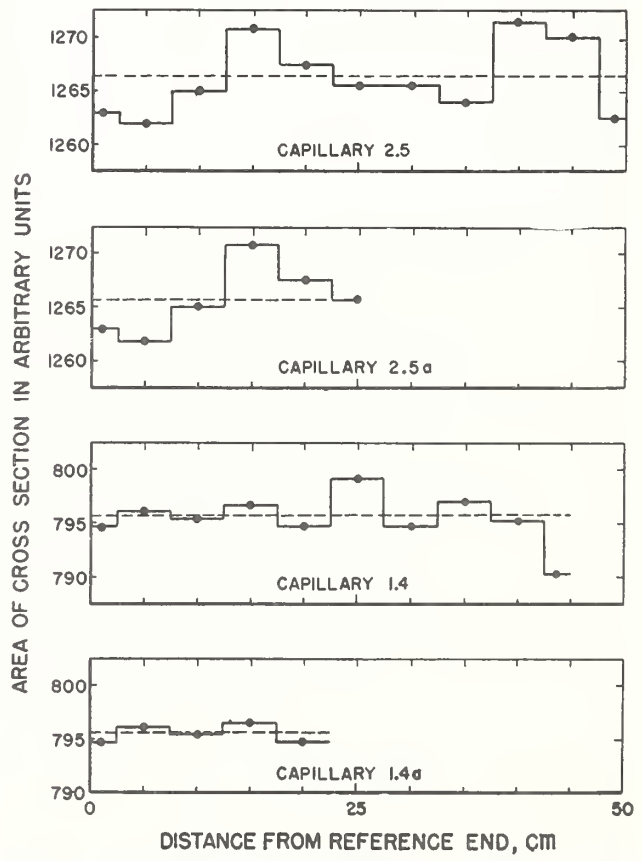

FIGURE 6. *Cross-sectional area of bore at regular positions along the capillaries.*

For one method of calculating the effects of such variations on the electric and viscous resistance offered by a capillary, the bore is assumed to be made up of a series of right circular cylinders, each having a cross-sectional area equal to the value of the corresponding plotted points and a length equal to the distance between the points. The area of section is then assumed to vary along the tube, as indicated by the stepped curve. Suppose the capillary of length l be divided into n such intervals of equal length l_i. Let S be the cross-sectional area in any interval and S_m be the mean cross-sectional area for the whole tube, as calculated by the relation $S_m=(1/n)\Sigma S$. Then the resistance to the flow of electricity through the variable cross section is proportional to $\Sigma(l_i/S)$, and the electric resistance offered by a tube of the same length but having a uniform cross-sectional area S_m is proportional to l/S_m. From these relations the percentage increase in the resistance to the flow of electricity of the nonuniform tube over the uniform one is given by

$$\frac{\Sigma(l_i/S)-l/S_m}{l/S_m}\times 100. \qquad (26)$$

For the laminar flow of liquids through the tubes, the viscous resistance is proportional to $\Sigma(l_i/S^2)$ for the nonuniform case and to l/S_m^2 for a uniform tube. In this case the percentage increase in the viscous resistance is given by

$$\frac{\sum(l_i/S^2)-l/S_m^2}{l/S_m^2}\times 100. \qquad (27)$$

As an example, this method is applied to the data on capillary 2.5 in the following way. The value of S calculated from the readings taken at the 5-cm position is assumed to be the mean for the 5-cm interval from 2.5 to 7.5 cm. As shown by the stepped curve in figure 6, this is repeated for each position, giving nine 5-cm intervals covering the length from 2.5 to 47.5 cm. The two 2.5-cm lengths at each end of the tube are combined to give a tenth 5-cm interval with a value of S equal to the mean of the areas at 1 cm and 49 cm. These data are then substituted in eq. 26 and 27 to give the desired corrections.

Similar procedures were followed with the other three capillaries, and the results obtained with all four are given in table 14. The signs are applied as follows: The signs are such as to correct the square of the radius as measured by the electric resistance method to yield the square of the radius of a uniform tube. The signs of the correction for viscous resistance are such as to correct the radius, calculated on the basis of a uniform bore, appropriately for substitution in the equations for viscous flow. It should be noted that the corrections given in the table are applied to the radius squared in the electric resistance measurements, whereas those for correcting the viscous resistance are applied to the fourth power of the radius.

TABLE 14. *Corrections to electric and viscous resistance measurements as a result of nonuniformity of bore*

Capillary	Corrections in parts per million	
	Electric resistance	Viscous resistance
2.5	+6	−21
2.5a	+6	−23
1.4	+5	−19
1.4a	+1	−3

It is seen in figure 6 that capillaries 2.5, 2.5a, and 1.4 show roughly harmonic variations in S. Assuming this type of variation, integration under these curves yields essentially the same corrections as those given in table 14.

As a third method of describing the variations in area of section, straight lines are drawn between the plotted points, and the integration is performed under these irregular curves. As would be expected, this method usually leads to somewhat smaller corrections than those obtained by the other two treatments.

The only case where these corrections are of any significance is the correction for viscous resistance in capillary 2.5. This correction was applied by using the value given in the table.

A summary of the measurements of the dimensions of the four capillaries is given in table 15. The values

TABLE 15. *Final dimensions of the capillaries*

Capillary	Length	Method	On the basis of a uniform bore		Effective for viscous flow	
			Radius [2]	Radius [4]	Radius [4]	Radius
	cm		*cm* [2]	*cm* [4]	*cm* [4]	*cm*
2.5	48.736	Gravimetric	6.3315×10^{-4}			
		Electric	6.3315			
		Mean	6.3315	4.0088×10^{-7}	4.0087×10^{-7}	2.5162×10^{-2}
2.5a	24.316	Gravimetric	6.3309			
		Electric	6.3303			
		Mean	6.3306	4.0076	4.0076	2.5161
1.4	45.208	Gravimetric	4.0305			
		Electric	4.0303			
		Mean	4.0304	1.6244	1.6244	2.0076
1.4a	22.525	Gravimetric	4.0348			
		Electric	4.0347			
		Mean	4.0347	1.6279	1.6279	2.0087

of the radius squared, as obtained by the two independent methods, were weighted equally, and the mean value was used for each capillary. It is seen that in each case the agreement between the two methods is very good. The maximum discrepancy occurred with capillary 2.5a and is only about 1 part in 10,000.

5. Viscosity Determinations

The viscometer was assembled and filled for the first series of tests at 20° C in the fall of 1940. The measurements made with this filling were designated as series I. In this series several independent observations of the pressure drop through the capillary were made at each of four rates of flow. Each measurement of the pressure drop corresponding to a particular rate of flow was assigned a run number in the order in which it was obtained within the series. In general, check runs at a given rate of flow were separated by measurements made at other rates of flow in order that the observations in a given run be as independent as possible of the influence of a preceding run. A similar procedure was followed each time the viscometer was filled, and a new roman series number was assigned to identify the particular filling. Between fillings the viscometer and manometer were disassembled and thoroughly cleaned.

The series I tests were used primarily for developing operating techniques and acquiring experience with the apparatus. The results of this series are therefore not considered as reliable as those of the succeeding 11 flow series and are not included in the final calculations. As a consequence of these preliminary flow tests, the experimental procedure that finally evolved is as follows:

After assembling the viscometer and manometer some mercury is injected into the entrance chamber of the viscometer and both arms of the manometer. Freshly distilled water from a laboratory still is introduced into the system through the open tube at the top of the overflow reservoir until the desired level is reached. Trapped air is removed by working the main injector back and forth through its stroke. The air trapped in the top of the short arm is forced out through the bleed tube (shown in fig. 1) by a forward stroke of the injector. After all of the air is removed and the tube is filled with water, the gas-tight valve at the top end of the tube is shut off.

All of the baths are adjusted to their proper temperatures, and mercury is introduced into the short arm of the manometer until the proper height is indicated by the fixed electric contactor. The longest of the gage rods, number 50, is then fixed in the depth-gage head, inserted in the long arm of the manometer, and the gage head is clamped in position. The gage head is set at its expected reading for the "manometer zero", and mercury is injected into the long arm until proper contact is made with the tip of the rod. The two arms of the manometer are now opened to each other. Any change in the height of mercury in the long arm with time is observed, and mercury is added or withdrawn in sufficient quantity so that when the final equilibrium position is established, the mercury in the short arm makes proper contact with the fixed contactor, and the level in the long arm is at the same height. In judging when this equilibrium position is reached, due consideration is given to the time constant for the particular capillary being used. These adjustments and readings of course are made when there is no flow of mercury from the main injector into the entrance chamber of the viscometer. The head reading of the micrometer for this final equilibrium condition is referred to as the "manometer zero" and is designated by M_0.

Manometer heights under flow conditions are measured in a similar manner. The change gears in the main injector drive are selected to give the desired rate of flow, and the mercury in the long arm of the manometer is preset at an expected height, using the gage rod of proper length. The injection of mercury into the entrance chamber of the viscometer is started, and the two arms of the manometer are then opened to each other. As in determining the manometer zero, mercury is added or withdrawn until the quantity of mercury in the manometer is such that the mercury level is at the contactor in the short arm when the equilibrium pressure corresponding to the particular rate of flow through the capillary is reached. It is often the case that this condition is not realized during a single stroke of the injector. In these cases the long arm of the manometer is shut off before stopping the main injector. With the manometer still closed the stroke of the injector is then reversed. After the forward stroke of the injector is started a second time, the manometer is again opened. In this manner the stroke of the injector is repeated as many times as are necessary to establish equilibrium. The reading of the micrometer head for this equilibrium condition is designated by M_Q. This process comprises a run, and a run number is assigned. Usually two or three such runs, together with a repeat observation of the manometer zero, can be completed in a working day. In this manner all of the flow data on a single filling of the viscometer may be obtained in about 2 weeks.

There is no known reason for measurable variations in readings of the manometer zero made with the same filling of the viscometer, and any observed differences in its value are attributed to experimental error. Consequently, at the completion of a series of flow tests all of the observations of M_0 are averaged and the mean value is used in calculating the pressure drop for each run. However, the value of M_0 will differ between different fillings of the viscometer as a result of the dismantling and reassembly of the short arm for cleaning purposes.

When measurements are being made a second operator keeps a continuous check on the temperature of the viscometer bath and records the thermometer readings every 5 minutes. Occasional readings of the temperatures of the other baths are taken, to be assured that they are operating properly. From these records the mean temperature in the viscometer bath is judged for each period during which a run is being made.

In general, this procedure was followed, beginning with series II, except for the following changes:

(a). In series II, readings of the manometer depth gage were recorded to 0.0001 in. In view of the general sensitivity encountered with the depth gage, together with other considerations, the readings in series III and the subsequent series were recorded only to the nearest 0.0005 in.

(b). As mentioned previously, beginning with series IV, a centering disk was used with the depth-gage rods for restricting the possible region of contact of the tips to a central area of the mercury meniscus.

(c). During all of the experiments intermittent electric contact was observed between the gage rods and surfaces in the manometer. This was caused by vibration of the stirring motor and pumps associated with the thermostating of the viscometer bath. During the first six series the manometer readings were taken matching the fluctuations in the readings of the microammeter in the long-arm circuit with those in the short arm. It was felt that in this manner the effects of these motions in the mercury surfaces would be minimized. However, beginning with series VII, after equilibrium had been reached, as shown by observations made in the above manner, both arms of the manometer were shut off, and the stirring motor and other sources of vibration were stopped. Readings were then taken with the mercury surfaces quiet. The two methods of taking the readings usually yielded essentially the same calculated height of the mercury column. Nevertheless, in a few instances differences as great as 0.006 in. were found. In the cases where any differences were shown, the readings taken with the quiet surfaces were used.

The results obtained in flow series II, III, and IV with capillary 2.5 are given in table 16. In the first column the arabic number accompanying the series number indicates the end of the capillary that was mounted as the lower, or entrance, end in the viscometer. The rates of flow Q were calculated from the calibrated delivery rate of the main injector, together with the gear ratios of the particular combinations of change gears used. The identical gear ratios were used in series III and IV as were used in II, the differences in the values of Q being a consequence of the different delivery rates of the injector. The injector was thermostated at 35° C for series II, and the mean delivery rate shown in table 1 was used. For series III and IV a longer stroke of the injector piston was used with the injector thermostated at 30° C, and the rates of flow were calculated from the mean rate of delivery given in table 3. In the third column of the table, values of the Reynolds number corresponding to each rate of flow are given to indicate the range covered in the experiments. The values given for P, the pressure drop through the capillary, are in each case the mean of several runs at the particular rate of flow. The detailed calculations of the values of P are given in appendix D.

Using the data in table 16, the values given for the viscosity were calculated by means of eq 4. This equation is equivalent to

$$\frac{P}{Q}=a+bQ, \tag{28}$$

in which

$$a=\frac{8}{\pi r^4}(l+nr)\eta$$

and

$$b=\frac{mD}{\pi^2 r^4}.$$

Introducing the measured dimensions of capillary 2.5 and the known density of water at 20° C, and taking the value of n as 0.57, the values of η were obtained from the relation

$$\eta=3.2292\times10^{-9}\times a.$$

Similarly, the values of m for the capillary were calculated by the equation

$$m=3.9635\times10^{-6}\times b.$$

The values of a and b were obtained from least-squares solutions of the straight lines represented by eq 28. In these solutions, Q was assumed to be without error, and the corresponding values of P/Q were weighted equally. These assumptions seem

TABLE 16. *Results of flow tests at 20° C with capillary 2.5*

Series number—entrance end	Q	Reynolds number	P	P/Q observed	a	b	η	m	P/Q, calculated	Deviation from line, observed—calculated
	cm^3/sec		$Dynes/cm^2$				Poise			
I–2	0.072232	182	0.225581×10⁶	3.12301×10⁶	3.10213×10⁶	0.2913×10⁶	0.010017	1.15	3.12317×10⁶	−160
	.128412	324	.403177	3.13971					3.13954	+170
	.192618	486	.608355	3.15835					3.15824	+110
	.256824	648	.815885	3.17683					3.17694	−110
III–2	.072277	182	.225762	3.12357	3.10245	.2923	.010018	1.16	3.12358	−10
	.128492	324	.403487	3.14017					3.14001	+160
	.192739	486	.608767	3.15850					3.15879	−290
	.256985	648	.816622	3.17770					3.17757	+130
IV–1	.072277	182	.225775	3.12375	3.10323	.2919	.010021	1.16	3.12433	−580
	.128492	324	.403718	3.14197					3.14074	+1230
	.192739	486	.608808	3.15872					3.15949	−770
	.256985	648	.816800	3.17840					3.17824	+160
				Mean values..	3.10260	0.2918	0.010019	1.16		

justified from the spread of the pressure data shown in tables 26 through 36 in appendix D, which indicate that the probable accuracy of P/Q is essentially independent of pressure. Furthermore, the results of the repeat calibrations of the injector suggest that Q was always known better than the corresponding equilibrium pressure, and hence Q was taken as without error.

The calculated values of P/Q given in table 16 were obtained by using eq 28 and substituting the values of a and b as given for each series. The deviations of the observed points from the calculated straight lines are also given and serve to indicate the constancy of m and n over the rates of flow covered.

With series II and III the observed values of P/Q are all within 0.01 percent of the calculated line. Differences of these magnitudes are attributable to experimental error, and m and n are demonstrated to be constant within the accuracy of the measurements. The relatively larger deviations shown for series IV are not explained, there being no known reason for questioning any of these data.

The spread in the values of a and b between the three series was taken to be experimental error, and therefore the values of η and m calculated from the mean values of a and b are believed best to represent the results of the flow measurements with this capillary alone.

Similar treatments of the flow data for the other three capillaries are given in tables 17, 18, and 19. With these capillaries also there is no evidence that m and n are not constant, the data being well represented by straight lines in agreement with eq 28. With these capillaries also the flow data are believed to be represented best by using the mean values of a and b as given in the tables.

The calculation of the viscosity by using the flow data with each capillary as an independent determination, as is done in tables 16 through 19, may be in error as a result of the uncertainty in the choice of a value for the constant n. However, as was outlined previously, the effect of an uncertainty in the value of n may be rendered negligible by simultaneous treatment of the flow measurements with each pair of capillaries. Taking capillaries 2.5 and 2.5a as one pair and 1.4 and 1.4a as another, the capillaries in each pair have very nearly the same radii but different lengths. The dimensions and flow data for each pair can then be substituted in eq 9 and the viscosity calculated without assuming a value for n. However, in making the actual calculations eq 9 was transformed somewhat.

If the least-squares line, based on the mean values of a and b, best represents the flow data for a particular capillary, that is equivalent to saying that the calculated value of P/Q at a particular value of

TABLE 17. *Results of flow tests at 20° C with capillary 2.5a*

Series number—entrance end	Q	Reynolds number	P	P/Q, observed	a	b	η	m	P/Q, calculated	Deviation from line, observed—calculated
	cm^3/sec		$Dynes/cm^2$				*Poise*			
VII-1	0.096376	243	0.151899×10^6	1.57611×10^6	1.54783×10^6	0.2957×10^6	0.010012	1.17	1.57633×10^6	−220
	.128502	324	.203807	1.58602					1.58583	+190
	.192753	486	.309368	1.60500					1.60483	+170
	.257004	648	.417293	1.62368					1.62382	−140
IX-3	.096376	243	.151927	1.57640	1.54822	.2938	.010015	1.16	1.57654	−140
	.128502	324	.203825	1.58616					1.58597	+190
	.192753	486	.309333	1.60482					1.60485	−30
	.257004	648	.417303	1.62372					1.52373	−10
X-1	.096376	243	.151915	1.57627	1.54749	.2970	.010010	1.18	1.57611	+160
	.128502	324	.203741	1.58551					1.58566	−150
	.192753	486	.309305	1.60467					1.60474	−70
	.257004	648	.417349	1.62390					1.62382	+80
				Mean values----	1.54785	.2955	.010012	1.17		

TABLE 18. *Results of flow tests at 20° C with capillary 1.4*

Series number—entrance end	Q	Reynolds number	P	P/Q, observed	a	b	η	m	P/Q, calculated	Deviation from line, observed—calculated
	cm^3/sec		$Dynes/cm^2$				*Poise*			
V-5	0.033674	106	0.239859×10^6	7.12297×10^6	7.09913×10^6	0.6911×10^6	0.010015	1.11	7.12240×10^6	+570
	.072282	228	.516662	7.14786					7.14908	−1220
	.096376	305	.690667	7.16636					7.16574	+620
	.128502	406	.923673	7.18800					7.18794	+60
VI-4	033674	106	.239831	7.12214	7.09874	.7009	.010014	1.13	7.12234	−200
	.072282	228	.516787	7.14959					7.14940	+190
	.096376	305	.690695	7.16665					7.16629	+360
	.128502	406	.923732	7.18846					7.18881	−340
VIII-4	.033674	106	.239866	7.12318	7.09965	.7023	.010015	1.13	7.12330	−120
	.072282	228	.516874	7.15080					7.15041	+390
	.096376	305	.690736	7.16708					7.16733	−250
	.128502	406	.923917	7.18990					7.18990	0
				Mean values----	7.09917	.6981	.010015	1.12		

TABLE 19. *Results of flow tests at 20° C with capillary 1.4a*

Series number—entrance end	Q	Reynolds number	P	P/Q, observed	a	b	η	m	P/Q, calculated	Deviation from line, observed—calculated
	cm^3/sec		$Dynes/cm^2$				*Poise*			
XI-4	0.033674	106	0.119681×10^6	3.55411×10^6	3.53065×10^6	0.7136×10^6	0.010015	1.15	3.55468×10^6	−570
	.072282	228	.258981	3.58292					3.58223	+690
	.096376	305	.346951	3.59996					3.59942	+540
	.128502	406	.465395	3.62169					3.62235	−660
XII-4	.033674	106	.119687	3.55429	3.53066	.7096	.010015	1.14	3.55456	−270
	.072282	228	.258938	3.58233					3.58195	+380
	.096376	305	.346882	3.59925					3.59905	+200
	.128502	406	.465379	3.62157					3.62185	−280
				Mean values	3.53066	.7116	.010015	1.15		

Q is better than an observed value. Hence, the best values of the pressure drops through the capillaries for substitution in eq 9 will be those obtained from the calculated values of P/Q. To illustrate this treatment, any particular value of Q may be chosen that is within the rates of flow common to the data on both capillaries in the pair. The values of a and b appropriate to the longer capillary are substituted in eq 28, and the value of P/Q is calculated for the particular rate of flow chosen. Multiplying this value of P/Q by Q gives the value of P_1, the pressure drop through the capillary. In a similar manner the value of P_2 is calculated for the shorter capillary at the same rate of flow. These values of the pressure drops corresponding to the rate of flow Q in each capillary are then substituted in eq 9, together with the capillary dimensions and the mean values of m as determined for the two capillaries. The identical results are obtained more simply, however, by a calculation using the intercepts for the two capillaries.

In a manner similar to that in which eq 8 and 9 were derived, it may be shown that

$$\eta=\frac{\pi}{8}\left[\frac{a_1r_1^4-a_2r_2^4}{(l_1-l_2)+(n_1r_1-n_2r_2)}\right], \qquad (29)$$

in which a_1 is the intercept in eq 28 for the longer capillary, and a_2 is the intercept for the shorter. As before, if r_1 and r_2 do not differ greatly, the quantity $(n_1r_1-n_2r_2)$ may be neglected.

The values of the measured quantities in eq 29 are given in table 20 for each of the four capillaries. The intercepts used are the mean values for each capillary, as given in tables 16 through 19. The values of the viscosity as calculated from the data for the pairs 2.5 and 2.5a, and 1.4 and 1.4a are given in table 21. These two calculations result in values that cover about the same range as the spread of values obtained in the previous calculations, using each capillary individually. For these two pairs it is evident that the quantity $(n_1r_1-n_2r_2)$ may be neglected.

In addition, calculations were made pairing capillary 2.5 with 1.4a and 1.4 with 2.5a. These results are also given in table 21. The value of 0.57 was used for both n_1 and n_2. The magnitude of the quantity $(n_1r_1-n_2r_2)$ is small in comparison with (l_1-l_2) in each case, and therefore the calculations are not seriously affected by uncertainties in n_1 and n_2. The agreement between the values of the viscosity as calculated through the use of these four pairs indicates an over-all consistency in the data.

TABLE 20. *Quantities used in the calculation of the viscosity, by means of equation 29*

Capillary	a	ar^4	l	$0.57r$
			cm	*cm*
2.5	3.10260×10^6	1.24374	48.736	0.014
2 5a	1.54785	0.62032	24.316	.014
1.4	7.09917	1.15319	45.208	.011
1.4a	3.53066	0.57476	22.525	.011

TABLE 21. *Values of the viscosity η, calculated from the data for pairs of capillaries*

Pair	η at 20° C	η at 20° C mean values	l_1-l_2	$n_1r_1-n_2r_2$
	Poise	*Poise*	*cm*	*cm*
2.5 and 2.5a	0.010022	0.010018	24.420	0.000
1.4 and 1.4a	.010014		22.683	.000
2.5 and 1.4a	.010022	.010020	26.211	+.003
1.4 and 2.5a	.010018		20.892	−.003

6. Discussion of Results

6.1. General

In work of this nature, where the result is dependent upon so many individual factors, it is difficult to evaluate the final result in terms of the estimated accuracy of each factor. It is believed that the error in each contributing measurement was reduced to 1 part in 10,000, or better, except perhaps in the measurement of the equilibrium pressures less than 10 in. of mercury. As the calculation of the viscosity involves the extrapolation of the observed data, however, the final result would not necessarily be this accurate.

The calculation of the viscosity by means of eq 29 probably represents the most reliable treatment of the data, because uncertainties in the magnitude of the constant n are minimized. The values given in table 21 for the results with the capillary pairs

2.5+2.5a and 1.4+1.4a are completely independent of the magnitude of n. The calculations for the pairs 2.5+1.4a and 1.4+2.5a, however, are given equal weight, because the introduction of any reasonable value for n will not affect the mean of these two by as much as 1 part in 10,000. The mean of the four values given in table 21 is

$$0.010019 \pm 0.000002,$$

where the deviation given is the standard deviation of the mean.

The values of the viscosity calculated by eq 28, obtained by treating the data for each capillary individually, and given in tables 16 through 19, show a spread from 0.010012 to 0.010019 poise, with a mean value of 0.010015. This would indicate that 0.57 is too high for the value of n. By taking these same data and assuming $n=0$ for all four capillaries, the following values result:

Capillary	η
2.5	0.010022
2.5a	.010018
1.4	.010017
1.4a	.010020

The mean of these values is 0.010019, which is the same as was obtained in the calculations with the capillaries in pairs. Although the assumption that $n=0$ results in better over-all agreement in the calculated values of the viscosity, the measurements are so insensitive for the evaluation of n, that no accurate conclusions may be reached as to its magnitude. It is pertinent, however, to note that the results of the calculations with eq 29 given in table 21 are not significantly changed by taking $n=0$. For $n=0$ the value of the viscosity calculated by using capillaries 2.5 and 1.4a is increased to 0.010023 poise, and the value derived from the pair 1.4+2.5a is reduced to 0.010017. Thus the mean value remains the same, but the standard deviation of the mean is increased to ± 0.000003. In consideration of this uncertainty in the value of n, the best result obtained from the data is

$$\eta_{20}=0.010019 \pm 0.000003.$$

No attempt is made to assign an accurate value to the constant m on the basis of this work, as the values of the slope b given in tables 16 to 19 may be appreciably in error as a result of heating effects in the capillaries. The incomplete dissipation of the heat generated by work done against viscous forces results in a temperature rise in the flowing liquid. The possible effects of such temperature rises in the capillaries were investigated through the use of equations developed by Hersey [15] and Hersey and Zimmer [16]. Their equations were expected to yield either too high or too low an effective temperature rise, depending upon what extreme conditions of temperature distribution in the capillary were assumed. Calculations based on these equations show that for any of the conditions covered by these equations, the values of the intercepts a, as given in tables 16 to 19, are unchanged. Hence, for the purpose of calculating the viscosity, it is not necessary to attempt to evaluate the effects of heating in the capillaries.

On the other hand, the heating effects may have a marked influence upon the calculated values of m. In fact, if certain assumptions are made with regard to the distribution of temperatures in the capillaries, it is possible to account for the differences in the calculated values of m for the four capillaries. As the real distribution of temperatures in the capillaries under the particular flow conditions is not known, no reliance is placed upon such calculations.

In attempting to compare the value obtained here for the absolute viscosity of water at 20° C with the results of other observers, it is found that all of the earlier determinations are subject to criticism, and therefore no good agreement is to be expected. The three most recent careful determinations were made by Thorpe and Rodger [17], Hosking [18], and Bingham and White [19]. Their results at 20° C are given in table 22. With regard to these results, it should be pointed out that none of these investigators attempted to make their measurements with the accuracy of the present work. Furthermore, with the capillaries that they were able to obtain, the deviations of the bores from right circular cylinders were large and in most cases not accurately known.

TABLE 22. *Viscosity of water at 20° C by other investigators*

Investigator	η_{20}	m	n
	Poise		
Thorpe and Rodger (1894)	0.010015	1.00	0
Hosking (1909)	.01003	1.158	1.64
Bingham and White (1912)	.01005	1.12	0

In all three of the determinations referred to in table 22 the viscosity was calculated from the observed pressures and rates of flow by means of eq 2. It is seen that Thorpe and Rodger's value is in best agreement with the value of 0.010019 obtained here. Seemingly, this is simply fortuitous, as there is no evidence that their determination was made with greater accuracy than the other two given in the table. They made no determination of m for their capillary, and the value of 1.00, which they used on theoretical grounds (probably not sound) is lower than most experimentally determined values. They were not convinced of the existence of the length correction involving the constant n, and hence assumed that $n=0$.

In Hosking's work neither the value of m nor n may be regarded as determined. He evaluated m for both directions of flow through each of four capillaries and obtained results varying from 1.128 to 1.216, with a mean of 1.158. He then recalculated some of his earlier results obtained with other capillaries, taking $m=1.158$ and $n=1.64$ and arrived

at $\eta_{20}=0.01006$ as the best result from his work. The value of $n=1.64$ was assumed, as with this correction, certain of his data were more self-consistent.

Bingham and White assumed that $m=1.12$ on the basis of calculations presented in a series of papers by Boussinesq [20]. They determined the value of n for several combinations of capillaries and concluded that its best value was zero. This value was then assumed for the capillary in which the determination of the viscosity of water was made.

In view of the uncertainties in all three of these determinations the lack of agreement with the present determination is not significant.

6.3. Application in Practical Viscometry

One aim in this investigation was to obtain a value for the absolute viscosity of water at 20° C that could be used as a standard in practical viscometry. Accordingly, beginning on July 1, 1952, the National Bureau of Standards is planning to use the value of 0.01002 poise for the absolute viscosity of water at 20° C as the basis for the calibration of viscometers and standard sample oils. It is recommended that other laboratories adopt this value as the primary reference standard for comparative measurements of viscosity.

In evaluating the work reported here, consideration is now given to any limitations in the general applicability of the results obtained under the particular conditions of these experiments. In this connection, various factors must be considered.

(a) *Purity of the water with respect to deuterium oxide.* At 20° C, D_2O is about 1.245 times as viscous as H_2O [21], and consequently the deuterium content in the water used must be considered. Fortunately, surveys (for example, [22] have shown that the variation in the isotopic concentration in water from a variety of world-wide sources is only a few parts per million. This variation is not great enough to affect the viscosity by as much as 0.01 percent [23].

(b) *Other impurities.* Unpublished results, obtained with water from various types of stills at the Bureau, have shown that a simple distillation, such as is accomplished by a commercial laboratory still, yields water of sufficiently uniform composition.

(c) *Change of viscosity with pressure.* Hardy and Cottington [21, p. 575], using a Master Fenske viscometer, found no measurable effect of pressure in the range, 1 to 3.4 atm.

(d) *Change of viscosity with rate of shear.* The fact that the data presented here are well represented by eq 28 may be considered as evidence that the viscosity does not vary with rate of shear in the range covered (5,000 to 20,000 reciprocal seconds). Furthermore, Griffiths and Vincent [24] could detect no difference between the viscosity of water measured at a rate of shear of 0.013 reciprocal second and that measured at 5,000 to 10,000 reciprocal seconds.

The authors acknowledge the following contributions to the project: N. E. Dorsey and C. S. Cragoe for their advice and encouragement; R. L. Cottington for his painstaking assistance in gathering many of the data.

7. References

[1] E. C. Bingham and R. F. Jackson, Standard substances for the calibration of viscometers, Bull. BS **14** (1918) S298.
[2] E. C. Bingham, Notes on the fluidity of water in the vicinity of 20° C, J. Rheology **2,** 403 (1931).
[3] J. R. Coe, Progress report on the determination of absolute viscosity, Physics **4,** 274 (1933).
[4] J. R. Coe and T. B. Godfrey, Viscosity of water, J. Applied Phys. **15,** 625 (1944).
[5] L. Prandtl and O. G. Tietjens, Applied hydro- and aeromechanics chap. II (McGraw-Hill Book Co., Inc., New York, N. Y., 1934).
[6] S. Erk, On the deviations of the pressure drop in a capillary from the Poiseuille law, J. Rheology **2,** 205 (1931).
[7] G. Barr, A monograph of viscometry, chap. II (Humphrey Milford, New York, N. Y., 1931).
[8] W. N. Bond, Viscosity determination by means of orifices and short tubes, Proc. Phys. Soc. (London) **34,** 139 (1922).
[9] Ostwald-Luther, Physico-Chemische Messungen, 5th ed., p. 467 (Leipzig, Germany, 1931).
[10] Informal communication of results obtained in the Thermal Expansion Section of the National Bureau of Standards.
[11] B. E. Blaisdell, The physical properties of fluid interfaces of large radius of curvature, Part I, J. Math. and Phys., MIT **19,** 186 (1940).
[12] J. A. Beattie, B. E. Blaisdell, J. Kaye, H. T. Gerry, and C. A. Johnson, The thermal expansion and compressibility of vitreous silica and the thermal dilation of mercury, Proc. Am. Acad. Arts Sci. **74,** 371 (1941).
[13] Maxwell, Treatise on electricity and magnetism, 3d ed., I, Art. 308, 309 (Oxford, Clarendon Press, 1873).
[14] Rayleigh, On the approximate solution of certain problems relating to the potential, Proc. Math. Soc. VII, 74 (1876).
[15] M. D. Hersey, Note on heat effects in capillary flow, Physics **7,** 403 (1936).
[16] M. D. Hersey and J. C. Zimmer, Heat effects in capillary flow at high rates of shear, J. Applied Phys. **8,** 359 (1937).
[17] T. E. Thorpe and J. W. Rodger, On the relations between the viscosity (internal friction) of liquids and their chemical nature, Roy. Soc. (London) Phil. Trans. **185A,** 397 (1894).
[18] R. Hosking, The viscosity of water, Phil. Mag. [6] **18,** 260 (1909).
[19] E. C. Bingham and G. E. White, Fluiditat und die Hydrattheorie, 1. Die Viskositat von Wasser, Z. Physik, Chem. **80,** 670 (1912).
[20] J. Boussinesq, Compt. rend. **110,** 1160, 1238, 1292 (1890); **113,** 9, 49 (1891).
[21] R. C. Hardy and R. L. Cottington, Viscosity of deuterium oxide and water in the range 5° to 125 C, J. Research NBS **42,** 573 (1949) RP1994.
[22] E. W. Washburn and E. R. Smith, An examination of water from various natural sources for variations in isotopic composition, BS J. Research **12,** 305 (1934) RP656.
[23] G. Jones and H. J. Fornwalt, The viscosity of deuterium oxide and its mixtures with water at 25° C, J. Chem. Phys. **4,** 30 (1936).
[24] A. Griffiths and P. C. Vincent, The viscosity of water at low rates of flow, Proc. Phys. Soc. (London) **38,** 291 (1926).
[25] W. Jaeger and H. von Steinwehr, Die Widerstandsanderung des Quecksilbers swischen 0° und 100°, Ann. Physik [4] **45,** 1089 (1914).
[26] N. E. Dorsey, Properties of ordinary water substance (Reinhold Pub. Co., Inc., New York, N. Y., 1940).

[27] K. L. Cook, Gravity measurements in the buildings of the U. S. Bureau of Standards, Washington, D. C., unpublished report of the U. S. Department of the Interior, Geological Survey (March 1948).
[28] Units of Weights and Measures, NBS Misc. Pub. 121 (1936).

8. Appendix A. Values of the Various Constants and Quantities Used in the Calculations

8.1. Density of Mercury

From the work of Beattie, et al. [12], and using the relation 1 ml = 1.000027 cm³,

$$D_{Hg,\ 0°C} = 13.59546 \text{ g/ml, or } 13.59509 \text{ g/cm}^3.$$

Also,

$$D_{Hg,\ 20°C} = 13.54589 \text{ g/cm}^3.$$

The values of β for use in eq 20 were calculated from Beattie's results and found to be as follows in the ranges in which they were used:

Temperature range	β
°C	
19 through 24	180.9×10^{-6}
25 through 32	181.0

8.2. Resistivity of Mercury

From the ICT value of 9.40766×10^{-4} international ohm-mm, and converting, using the relation 1 international ohm = 1.000495 absolute ohms,

$$\rho_0 = 9.41232 \times 10^{-4} \text{ absolute ohm-mm.}$$

The equation of Jaeger and von Steinwehr [25],

$$\rho_\theta = \rho_0 (1 + 889.15 \times 10^{-6}\theta + 0.99360 \times 10^{-6}\theta^2),$$

is used to calculate the resistivity at other temperatures.

8.3. Density of Water

The density of water at 20° C, used in the calculation of the pressure drop through a capillary from the height of mercury in the manometer, was calculated from the properties of water as given by Dorsey [26]. He gives the value of 0.9982336 g/ml, or 0.998207 g/cm³ (1 ml = 1.000027 cm³), for the density of air-free water at 20°C and a pressure of 1 atm. From Dorsey's table 92, the corresponding value for water saturated with air is 0.998206 g/cm³.

The pressure on the water, and therefore its density, varies throughout the viscometer and manometer system, and also varies with the height of mercury in the manometer. In appendix D the calculations of the pressure drops were made on the basis of a mean value for the density of water. This mean was calculated on the basis of a mean pressure of 1.25 atm on the water in the apparatus. The density at this pressure was calculated from the data given in table 105 of Dorsey's book and found to be 0.99822 g/cm³.

The use of this mean value of the density instead of the actual densities for each condition will in no case introduce an error greater than 2 parts per million in the calculation of the pressure drop through the capillary.

8.4. Acceleration of Gravity

The value used for the acceleration of gravity is 980.080 cm/sec², absolute gravity, Dryden reduction. This value is based upon accurate measurements [27] made on the same floor of the building in which the work was done.

9. Appendix B. Calibration of the Gage Rods Used With the Mercury Manometer

The calibration of a gage rod consists in the determination of the interval of length between that rod and the longest gage rod. The result is expressed as a correction to the nominal length of the interval.

The rods were calibrated with Hoke gage blocks in a room where the temperature was controlled close to 20° C. A shallow glass dish about 10 cm in diameter and containing mercury was placed on a leveled surface plate. A steel plate with a ¾-in.-diameter hole was supported above the dish on parallel bars which rested on the surface plate. Hoke gage blocks, wrung together in suitable combinations, were placed vertically on the ground surface of this plate, and the micrometer depth gage was seated on top of the gage blocks. The gage rods were clamped successively in the depth gage, passing through the holes in the gage blocks and steel plate to make contact with the surface of mercury in the dish. Contact was indicated by the same electric circuit as that employed in the manometer.

In this way the intervals between the longest rod and each of the others were determined on various occasions, with the results as given in table 23. After the first two calibrations, only the rods that covered the particular heights used in the tests were further calibrated.

TABLE 23. *Calibration of gage rods*

[The values given are corrections to the nominal lengths of the intervals in ten thousandths of an inch]

Rod	Nominal interval	Date of calibration							
		Jan. 1940	Mar. 1941	Dec. 1941	June 1947	Feb. 1948	Jan. 1949	Apr. 1949	Oct. 1949
	in.								
50	0	0	0	0	0	0	0	0	0
47	3	+183	+177						
46	4	+103	+98	+94				+59	+135
45	5	−34	−41	−44				−75	−78
44	6	+42	+35	+28			−4	+3	+3
43	7	+48	+41	+38	+30	+29	+11	+11	
42	8	+34	+26			+13	+29	+33	+25
41	9	+2	−6			−22	−34	−35	
40	10	+5	−3	+5		+6	−9	−9	−12
39	11	−33	−41	−41		−44	−48	−48	−53
38	12	+47	+39			+18	+6	+6	
37	13	−28	−32	−33	−43	−41	−44	−41	−47
36	14	0	−9	−12		−6	−8	−17	
35	15	−36	−45	−43		−48	−50	−57	−61
34	16	+21	+11			−2	−4	0	
33	17	+75	+68	+67		+48	+41	+42	
32	18	+51	+44			+16	+8	+12	
31	19	−44	−51	−53	−54	−61	−65	−66	
30	20	+38	+31			+12	+7	+10	
29	21	+43	+35			+25	+17	+19	
28	22	+27	+21			+4	+9	+11	
27	23	−62	−69	−70		−93	−99	−96	
26	24	−227	−235			−246	−256	−255	
25	25	−159	−167			−188	−196	−190	
24	26	−182	−191	−195	−195	−207	−219	−215	
23	27	−81	−93			−109	−121	−115	
22	28	+222	+212			+205	+191	+195	
21	29	−33	−43				−59	−46	

The rods were numbered according to their nominal lengths in inches. The second column gives the nominal difference in length between each rod and rod 50, which was the one used in obtaining the manometer zero. The corrections given for each rod are corrections to the nominal length of the corresponding interval in inches. In all of the calibrations, measurements with each rod were repeated at least once, and the corrections entered in the table are mean values. Repeated measurements on a given rod showed agreement within 0.0002 in. in almost all cases.

It was not possible to attribute the changes in the lengths to any one cause. In general, the changes were in the direction of the intervals shortening with time, but the magnitudes of the changes were not proportional to the interval

lengths and therefore were not explained by uniform shrinkage of the rods. It is probable that growth and shrinkage of the rods, together with possible electrolytic wear of the tips, were all involved in varying extents. However, these changes were followed closely, and it is felt that the corrections were known to within at least 0.0004 in. of their true values at all times when flow measurements were being made.

10. Appendix C. Radii by the Gravimetric Method. Details of the Weighings

For determining the mean radii of the capillaries by the gravimetric method, the quantities of mercury from the fillings of the capillaries were weighed in small glass-stoppered bottles.

In the weighings concerned with capillaries 2.5 and 1.4a, three bottles, 3, 6 and 25, were used. Bottles 3 and 6 were used in the weighing of the mercury, and bottle 25 was weighed each time as a blank. The weighing procedure was designed to determine the effects, if any, of possible variations in the surface condition of the glass upon the constancy of weight of the bottles. The three bottles were first weighed empty, and the mercury was transferred from the capillary to bottle 3 and weighed. It was then transferred to bottle 6 and weighed. After this, the mercury was discarded, and bottle 6 was weighed again empty. Before each weighing the bottles were held in steam momentarily to condense moisture of the surface so as to dissipate any electrostatic charges. The bottle caps were loosened and replaced. Then the bottles were placed in the balance and weighed after about 5 minutes.

The results of the weighings of the empty bottles are given in table 24. The weighings show small erratic changes, and

TABLE 24. *Mass of weighing bottles, empty*

Date	Relative humidity	Bottle—		
		3	6	25
	Percent	*mg*	*mg*	*mg*
1/17/50	18	2199.037 2199.038	2291.281 2291.278	2401.135 2401.134
1/17/50	17	2199.042 ----------	2291.283 2291.282	2401.135 ----------
1/18/50	31	---------- ----------	2291.290 2291.287	2401.147 ----------
1/19/50	18	2199.046 ----------	2291.289 2291.291	2401.146 ----------
1/20/50	15	2199.049 2199.040	2291.294 2291.294	2401.151 ----------
1/23/50	38	2199.059 ----------	2291.295 2291.302	2401.151 ----------
1/24/50	40	2199.062 ----------	2291.298 2291.302	2401.156 ----------
1/25/50	48	2199.053 ----------	2291.299 2291.301	2401.153 ----------
1/26/50	44	2199.051 ----------	2291.300 2291.300	2401.156 ----------
1/27/50	27	2199.053 ----------	2291.300 2291.299	2401.164 ----------
1/27/50	22	2199.058 ----------	2291.297 2291.306	2401.163 ----------

evidence a definite over-all gain in weight of all three bottles during the period of their use. The gain in weight of bottles 3 and 6 is probably not attributable to residues left by the mercury samples, as bottle 25 showed the same increase.

In the course of the weighings, the relative humidity in the room where the weighings were made was varied through the wide range given in the table. Apparently the weighings were not affected by these variations.

The results of the two weighings of each sample of mercury are given in table 25. Samples A to E were from repeat fillings of capillary 2.5a; F to J were from capillary 1.4a. The agreement between the two weighings of each sample is better than 0.01 mg in all cases. The mean values of these duplicate weighings are given in table 10 and were used in the calculations. Considering all sources of error, it is probable that these mean values are within 0.01 mg of the true masses of the samples.

TABLE 25. *Mass of samples of mercury from fillings of capillaries 2.5a and 1.4a*

Sample	Date	Weighed in bottle—	
		3	6
		mg	*mg*
A	1/17/50	654.303	654.307
B	1/18/50	654.490	654.485
C	1/19/50	654.185	654.190
D	1/20/50	654.638	654.643
E	1/23/50	654.329	654.324
F	1/24/50	386.252	386.258
G	1/25/50	386.016	386.013
H	1/26/50	386.099	386.099
I	1/27/50	386.214	386.221
J	1/27/50	386.056	386.047

11. Appendix D. Data and Calculation of the Pressure Drops Through the Capillaries

Tables 26 to 36 give the observations made in the 11 series of flow measurements and the detailed calculations of the pressure drops. The values of Q given in column 3 of these tables were calculated by the relation

$$Q = \text{speed of drive shaft} \times \frac{\text{grams mercury}}{\text{turn of drive shaft}} \times \frac{1}{D_{Hg,20^\circ C}}.$$

The speeds of the drive shaft in revolutions per second were calculated from the motor speed and the ratio of the gears used in each case. The rate of delivery of the injector in grams per turn of the drive shaft was taken appropriately from table 1, 3, or 5. The value used for the density of mercury at 20° C is 13.59546 g/cm³ (see appendix A).

The gage-rod corrections given in appendix B were plotted as a function of time, and the corrections entered in column 5 were taken from these curves.

Each observation of the manometer zero is entered in the lower part of the tables. The mean of the observations in a particular series was used in the computation of the pressures for that series.

Values of M_Q, the micrometer depth-gage head readings under the flow conditions, are given in column 6. In column 7, Δ = mean $M_0 - M_Q$.

The differential heights of mercury in the manometer are given in column 8. These are computed by the relation

$$h_\theta = \Delta + \text{interval} + \text{rod correction},$$

in which the interval is the nominal difference in length between the rod and rod 50.

The difference between the actual temperature of each run and 20° C is entered in column 9. On the basis of these temperature differences, the corrections to h_θ entered in column 11 were computed by using 0.0025%/0.001 deg C for the change in the viscosity of water with temperature at temperatures close to 20° C [4]. The sign of each correction is such that $h_{20} = h_\theta + \Delta h$, in which h_{20} is the height of mercury for a corresponding run at 20° C. Expansions or contractions in the duralumin frame, gage rods, mercury in the manometer, etc. were computed and found to be completely negligible for these small temperature differences.

The mean value of h_{20} for each rate of flow is given in column 12, and the standard deviation of the mean is given in column 13.

The pressure drops in dynes per square centimeter were calculated from the mean values of h_{20} and entered in column 14. The calculations were made using the relation

$$p_{20}=2.540005\times g\times(D_{Hg}-D_W)_{20^\circ\ C}\times h_{20},$$

in which 2.540005 is the factor for converting inches to centimeters [30]. Substituting for g and $(D_{Hg}-D_W)_{20^\circ\ C}$ their values from appendix A,

$$p_{20}=3.12363\times 10^4\times h_{20}.$$

As was mentioned in the description of the manometer, the values of p_{20} given in column 14 include the pressure drop through the side tube connecting the exit chamber with the long arm of the manometer. Values of this pressure drop, which is equal to the second term on the right hand side in eq 16, are given in column 15. This correction was applied to p_{20} yielding the pressure drops across the capillary alone, which are entered in column 16. Standard deviations in dynes per square centimeter are entered in column 17.

TABLE 26. *Series II, capillary 2.5*

[Calculation of the pressure drops]

1	2	3	4	5	6	7	8	9	10	11	12	13	14	15	16	17
Date	Run	Q	Gage rod	Gage-rod correction	M_Q	Δ	h_θ	$\Delta\theta$	Δh	h_{20}	h_{20}, means	Standard deviation of the mean	p_{20}	Correction for side tube	P	Standard deviation of the mean
		cm³/sec		*in.*	*in.*	*in.*	*in.*	*°C*	*in.*	*in.*	*in.*	*in.*	*Dynes/cm²*	*Dynes/cm²*	*Dynes/cm²*	*Dynes/cm²*
8/4/41	2	0.072232	43	+0.0040	0.6294	+0.2141	7.2181	0.000	0.0000	7.2181						
8/5/41	3	.072232	43	+.0040	.6275	+.2160	7.2200	+.009	+.0016	7.2216						
8/8/41	11	.072232	43	+.0040	.6276	+.2159	7.2199	+.007	+.0013	7.2212						
9/26/41	15	.072232	43	+.0040	.6195	+.2164	7.2204	+.004	+.0007	7.2211						
10/3/41	19	.072232	43	+.0040	.6180	+.2179	7.2219	−.005	−.0009	7.2210	7.2218	$\pm6\times10^{-4}$	0.225582×10^6	−0.000001	0.225581×10^6	±19
10/9/41	22	.072232	43	+.0040	.6155	+.2204	7.2244	−.006	−.0011	7.2233						
10/27/41	25	.172232	43	+.0040	.6165	+.2194	7.2234	+.002	+.0004	7.2238						
10/28/41	28	.072232	43	+.0040	.6166	+.2193	7.2233	−.002	−.0004	7.2229						
10/29/41	29	.072232	43	+.0040	.6166	+.2193	7.2233	.000	.0000	7.2233						
8/4/41	4	.128412	37	−.0032	.9375	−.0940	12.9028	+.013	+.0042	12.9070						
8/6/41	5	.128412	37	−.0032	.9366	−.0931	12.9037	+.001	+.0003	12.9040						
9/30/41	16	.128412	37	−.0032	.9246	−.0887	12.9081	+.004	+.0013	12.9094						
10/1/41	18	.128412	37	−.0032	.9248	−.0889	12.9079	.000	.0000	12.9079	12.9074	±9	.403179	−.000002	.403177	±28
10/8/41	21	.128412	37	−.0032	.9240	−.0881	12.9087	.000	.0000	12.9087						
10/28/41	26	.128412	37	−.0032	.9246	−.0887	12.9081	+.001	+.0003	12.9084						
10/29/41	30	.128412	37	−.0032	.9260	−.0901	12.9067	.000	.0000	12.9067						
8/4/41	1	.192618	31	−.0052	.3671	+.4764	19.4712	−.002	−.0010	19.4702						
8/6/41	6	.192618	31	−.0052	.3620	+.4815	19.4763	−.001	−.0005	19.4758						
8/6/41	8	.192618	31	−.0052	.3635	+.4800	19.4748	+.003	+.0015	19.4763						
8/7/41	9	.192618	31	−.0052	.3660	+.4775	19.4723	−.004	−.0019	19.4704						
8/8/41	13	.192618	31	−.0052	.3675	+.4760	19.4708	+.015	+.0073	19.4781	19.4760	±12	.608358	−.000003	.608355	±37
10/3/41	20	.192618	31	−.0052	.3502	+.4857	19.4805	−.005	−.0024	19.4781						
10/10/41	23	.192618	31	−.0052	.3518	+.4841	19.4789	+.001	+.0005	19.4794						
10/28/41	27	.192618	31	−.0052	.3544	+.4815	19.4763	.000	.0000	19.4763						
11/3/41	31	.192618	31	−.0052	.3510	+.4849	19.4797	.000	.0000	19.4797						
8/6/41	7	.256824	24	−.0193	.7110	+.1325	26.1132	.000	.0000	26.1132						
8/7/41	10	.256824	24	−.0193	.7102	+.1333	26.1140	+.001	+.0007	26.1147						
8/8/41	14	.256824	24	−.0193	.7060	+.1375	26.1182	+.006	+.0039	26.1221	26.1199	±30	.815889	−.000004	.815885	±94
9/30/41	17	.256824	24	−.0193	.6958	+.1401	26.1208	+.006	+.0039	26.1247						
10/10/41	24	.256824	24	−.0193	.6930	+.1429	26.1236	+.002	+.0013	26.1249						

Observations of M_0, August 1941 data

Date	8/4	8/4	8/5	8/5	8/6	8/7	8/7	8/8	8/8
Time	a. m.	p. m.	a. m.	p. m.	a. m.	a. m.	p. m.	a. m.	p. m.
M_0	0.8433	0.8433	0.8432	0.8432	0.8434	0.8437	0.8440	0.8438	0.8438

Mean value=0.8435. Standard deviation of the mean=±0.0001

Observations of M_0, September, October, and November 1941 data [a]

Date	9/26	9/26	9/29	9/29	9/30	9/30	10/1	10/3	10/3	10/8	10/8
Time	a. m.	p. m.	a. m.	p. m.	a. m.	p. m.	a. m.	a. m.	p. m.	a. m.	p. m.
M_0	0.8374	0.8349	0.8357	0.8364	0.8355	0.8323	0.8354	0.8369	0.8372	0.8362	0.8363
Date	10/9	10/9	10/10	10/10	10/27	10/27	10/28	10/28	10/29	10/29	11/3
Time	a. m.	p. m.	a. m.	p. m.	a. m.	p. m.	a. m.	p. m.	a. m.	p. m.	a. m.
M_0	0.8359	0.8361	0.8361	0.8359	0.8351	0.8364	0.8360	0.8360	0.8358	0.8359	0.8367

Mean value=0.8359. Standard deviation of the mean=±0.0002

[a] Following the August measurements certain shims were removed from under the surface plate on which the depth gage was mounted. Hence, these data are expected to be different from the August data.

TABLE 27. *Series III, capillary 2.5*

[Calculation of the pressure drops]

1	2	3	4	5	6	7	8	9	10	11	12	13	14	15	16	17
Date	Run	Q	Gage rod	Gage-rod correction	M_Q	Δ	h_θ	$\Delta\theta$	Δh	h_{20}	h_{20}, means	Standard deviation of the mean	p_{20}	Correction for side tube	P	Standard deviation of the mean
		cm^3/sec		*in.*	*in.*	*in.*	*in.*	°C	*in.*	*in.*	*in.*	*in.*	*Dynes/cm²*	*Dynes/cm²*	*Dynes/cm²*	*Dynes/cm²*
10/29/47	1	0.072277	43	+0.0029	0.4600	+0.2275	7.2304	−0.001	−0.0002	7.2302						
19/30/47	2	.072277	43	+.0029	.4600	+.2275	7.2304	.000	.0000	7.2304						
10/31/47	7	.072277	43	+.0029	.4615	+.2260	7.2289	−.003	−.0005	7.2284						
10/31/47	8	.072277	43	+.0029	.4605	+.2270	7.2299	−.001	−.0002	7.2297						
10/31/47	9	.072277	43	+.0029	.4630	+.2245	7.2274	+.009	+.0016	7.2290						
10/31/47	10	.072277	43	+.0029	.4620	+.2255	7.2284	+.003	+.0005	7.2289	7.2276	$\pm12\times10^{-4}$	0.225763×10^6	−0.000001	0.225762×10^6	±37
11/ 5/47	21	.072277	43	+.0029	.4705	+.2170	7.2199	−.006	−.0011	7.2188						
11/ 5/47	22	.072277	43	+.0029	.4670	+.2205	7.2234	−.006	−.0011	7.2223						
11/ 7/47	23	.072277	43	+.0029	.4620	+.2255	7.2284	+.005	+.0009	7.2293						
11/ 7/47	24	.072277	43	+.0029	.4615	+.2260	7.2289	.000	.0000	7.2289						
11/ 5/47	17	.128492	37	−.0042	.7670	−.0795	12.9163	−.002	−.0006	12.9157						
11/ 5/47	18	.128492	37	−.0042	.7640	−.0765	12.9193	−.002	−.0006	12.9187						
11/ 5/47	19	.128492	37	−.0042	.7655	−.0780	12.9178	−.004	−.0013	12.9165	12.9173	±6	.403489	−.000002	.403487	±19
11/ 5/47	20	.128492	37	−.0042	.7645	−.0770	12.9188	−.005	−.0016	12.9172						
11/ 7/47	25	.128492	37	−.0042	.7665	−.0790	12.9168	+.005	+.0016	12.9184						
11/ 3/47	13	.192739	31	−.0060	.1910	+.4965	19.4905	+.001	+.0005	19.4910						
11/ 4/47	14	.192739	31	−.0060	.1915	+.4960	19.4900	−.007	−.0034	19.4866	19.4892	±12	.608770	−.000003	.608767	±37
11/ 4/47	15	.192739	31	−.0060	.1895	+.4980	19.4920	−.007	−.0034	19.4886						
11/ 4/47	16	.192739	31	−.0060	.1875	+.5000	19.4940	−.007	−.0034	19.4906						
10/30/47	3	.256985	24	−.0205	.5270	+.1605	26.1400	.000	.0000	26.1400						
10/30/47	4	.256985	24	−.0205	.5260	+.1615	26.1410	−.001	−.0007	26.1403						
10/30/47	5	.256985	24	−.0205	.5220	+.1655	26.1450	.000	.0000	26.1450						
10/30/47	6	.256985	24	−.0205	.5225	+.1650	26.1445	.000	.0000	26.1445	26.1435	±12	.816626	−.000004	.816622	±37
11/ 3/47	11	.256985	24	−.0205	.5260	+.1615	26.1410	+.006	+.0039	26.1449						
11/ 3/47	12	.256985	24	−.0205	.5235	+.1640	26.1435	+.004	+.0026	26.1461						

Observations of M_θ

Date	10/29/47	10/29/47	10/30/47	10/30/47	10/31/47	10/31/47	11/ 3/47	11/ 3/47	11/ 4/47	11/ 5/47	11/ 5/47	11/ 7/47	11/ 7/47
Time	a. m.	p. m.	a. m.	p. m.	a. m.	p. m.	a. m.	p. m.	a. m.	a. m.	p. m.	a. m.	p. m.
M_θ	0.6890	0.6870	0.6885	0.6890	0.6880	0.6870	0.6870	0.6865	0.6870	0.6870	0.6870	0.6870	0.6875

Mean value=0.6875. Standard deviation of mean=±0.0003

TABLE 28. *Series IV, capillary 2.5*

[Calculation of the pressure drops]

1	2	3	4	5	6	7	8	9	10	11	12	13	14	15	16	17
Date	Run	Q	Gage rod	Gage-rod correction	Q	Δ	h_θ	$\Delta\theta$	Δh	h_{20}	h_{20}, means	Standard deviation of the mean	p_{20}	Correction for side tube	P	Standard deviation of the mean
		cm^3/sec		*in.*	*in.*	*in.*	*in.*	°C	*in.*	*in.*	*in.*	*in.*	*Dynes/cm²*	*Dynes/cm²*	*Dynes/cm²*	*Dynes/cm²*
12/18/47	1	0.072277	43	+0.0029	0.4655	+0.2230	7.2259	+0.006	+0.0011	7.2270						
12/18/47	2	.072277	43	.0029	.4645	+.2240	7.2269	+.004	+.0007	7.2276						
12/22/47	5	.072277	43	.0029	.4665	+.2220	7.2249	+.002	+.0004	7.2253						
12/22/47	6	.072277	43	.0029	.4655	+.2230	7.2259	+.003	+.0005	7.2264	7.2280	$\pm8\times10^{-4}$	0.225776×10^6	−0.000001	0.225775×10^6	±23
12/26/47	15	.072277	43	.0029	.4620	+.2265	7.2294	+.001	+.0002	7.2296						
12/26/47	16	.072277	43	.0029	.4620	+.2265	7.2294	+.002	+.0004	7.2298						
12/29/47	17	.072277	43	.0029	.4620	+.2265	7.2294	+.004	+.0007	7.2301						
12/26/47	13	.128492	37	−.0042	.7620	−.0735	12.9223	+.003	+.0010	12.9233						
12/26/47	14	.128492	37	−.0042	.7620	−.0735	12.9223	+.004	+.0013	12.9236	12.9247	±9	.403720	−.000002	.403718	±28
12/29/47	18	.128492	37	−.0042	.7590	−.0705	12.9253	+.002	+.0006	12.9259						
12/29/47	19	.128492	37	−.0042	.7590	−.0705	12.9253	+.002	+.0006	12.9259						
12/23/47	9	.192739	31	−.0060	.1955	+.4930	19.4870	+.004	+.0020	19.4890						
12/23/47	10	.192739	31	−.0060	.1990	+.4895	19.4835	+.005	+.0024	19.4859	19.4905	±22	.608811	−.000003	.608808	±69
12/24/47	11	.192739	31	−.0060	.1920	+.4965	19.4905	+.002	+.0010	19.4915						
12/24/47	12	.192739	31	−.0060	.1880	+.5005	19.4945	+.002	+.0010	19.4955						
12/19/47	3	.256985	24	−.0205	.5220	+.1665	26.1460	+.002	+.0013	26.1473						
12/19/47	4	.256985	24	−.0205	.5210	+.1675	26.1470	+.002	+.0013	26.1483						
12/23/47	7	.256985	24	−.0205	.5210	+.1675	26.1470	+.004	+.0026	26.1496	26.1492	±10	.816804	−.000004	.816800	±31
12/23/47	8	.256985	24	−.0205	.5190	+.1695	26.1490	+.004	+.0026	26.1516						

Observations of M_θ

Date	12/18/47	12/18/47	12/19/47	12/22/47	12/22/47	12/23/47	12/24/47	12/24/47	12/26/47	12/26/47	12/29/47	12/29/47
Time	a. m.	p. m.	a. m.	a. m.	p. m.	a. m.	a. m.	p. m.	a. m.	p. m.	a. m.	p.m.
M_θ	0.6870	0.6870	0.6870	0.6900	0.6895	0.6900	0.6890	0.6910	0.6880	0.6880	0.6870	0.6880

Mean value=0.6885. Standard deviation of mean=±0.0003

TABLE 29. *Series VII, capillary 2.5a*

[Calculation of the pressure drops]

1	2	3	4	5	6	7	8	9	10	11	12	13	14	15	16	17
Date	Run	Q	Gage rod	Gage-rod correction	M_Q	Δ	h_θ	$\Delta\theta$	Δh	h_{20}	h_{20}, means	Standard deviation of the mean	p_{20}	Correction for side tube	P	Standard deviation of the mean
		cm³/sec		*in.*	*in.*	*in.*	*in.*	*°C*	*in.*	*in.*	*in.*	*in.*	*Dynes/cm²*	*Dynes/cm²*	*Dynes/cm²*	*Dynes/cm²*
3/3/49	10	0.096376	45	−0.0075	0.8090	−0.1319	4.8606	0.000	0.0000	4.8606	4.8630	±14×10⁻⁴	0.151902×10⁶	−0.000003	0.151899×10⁶	±44
3/4/49	13	.096376	45	−.0075	.8060	−.1289	4.8636	.000	.0000	4.8636						
3/4/49	17	.096376	45	−.0075	.8050	−.1279	4.8646	+.001	+.0001	4.8647						
3/2/49	5	.128502	44	+.0003	.1525	+.5246	6.5249	+.001	+.0002	6.5251	6.5248	±3	.203811	−.000004	.203807	±9
3/2/49	8	.128502	44	+.0003	.1530	+.5241	6.5244	.000	.0000	6.5244						
3/3/49	9	.128502	44	+.0003	.1525	+.5246	6.5249	+.001	+.0002	6.5251						
3/4/49	14	.128502	44	+.0003	.1530	+.5241	6.5244	.000	.0000	6.5244						
3/2/49	6	.192753	40	−.0009	.7715	−.0944	9.9047	−.001	−.0002	9.9045	9.9043	±3	.309374	−.000006	.309368	±9
3/3/49	11	.192753	40	−.0009	.7725	−.0954	9.9037	.000	.0000	9.9037						
3/4/49	15	.192753	40	−.0009	.7715	−.0944	9.9047	.000	.0000	9.9047						
3/2/49	7	.257004	37	−.0042	.3135	+.3636	13.3594	.000	.0000	13.3594	13.3595	±14	.417301	−.000008	.417293	±44
3/3/49	12	.257004	37	−.0042	.3155	+.3616	13.3574	−.001	−.0003	13.3571						
3/4/49	16	.257004	37	−.0042	.3110	+.3661	13.3619	.000	.0000	13.3619						

Observations of M_θ

Date	3/2/49	3/2/49	3/3/49	3/3/49	3/4/49	3/4/49
Time	a. m.	p. m.	a. m.	p. m.	a. m.	p. m.
M_θ	0.6785	0.6780	0.6775	0.6765	0.6770	0.6750

Mean=0.6771. Standard deviation of the mean=±0.0005

TABLE 30. *Series IX, capillary 2.5a*

[Calculation of the pressure drops]

1	2	3	4	5	6	7	8	9	10	11	12	13	14	15	16	17
Date	Run	Q	Gage rod	Gage-rod correction	M_Q	Δ	h_θ	$\Delta\vartheta$	Δh	h_{20}	h_{20}, means	Standard deviation of the mean	p_{20}	Correction for side tube	P	Standard deviation of the mean
		cm³/sec		*in.*	*in.*	*in.*	*in.*	*°C*	*in.*	*in.*	*in.*	*in.*	*Dynes/cm²*	*Dynes/cm²*	*Dynes/cm²*	*Dynes/cm²*
3/28/49	6	0.096376	45	−0.0075	0.8570	−0.1300	4.8625	0.000	0.0000	4.8625	4.8639	±10×10⁻⁴	0.151930×10⁶	−0.000003	0.151927×10⁶	±31
3/30/49	8	.096376	45	−.0075	.8560	−.1290	4.8635	+.001	+.0001	4.8636						
3/31/49	14	.096376	45	−.0075	.8540	−.1270	4.8655	.000	.0000	4.8655						
3/28/49	7	.128502	44	+.0003	.2020	+.5250	6.5253	.000	.0000	6.5253	6.5254	±4	.203829	−.000004	.203825	±12
3/30/49	9	.128502	44	+.0003	.2025	+.5245	6.5248	.000	.0000	6.5248						
3/31/49	15	.128502	44	+.0003	.2015	+.5255	6.5258	+.001	+.0002	6.5260						
3/30/49	10	.192753	40	−.0009	.8250	−.0980	9.9011	.000	.0000	9.9011	9.9032	±12	.309339	−.000006	.309333	±38
3/30/49	12	.192753	40	−.0009	.8220	−.0950	9.9041	.000	.0000	9.9041						
3/31/49	16	.192753	40	−.0009	.8220	−.0950	9.9041	+.001	+.0002	9.9043						
3/30/49	11	.257004	37	−.0042	.3640	+.3630	13.3588	.000	.0000	13.3588	13.3598	±9	.417311	−.000008	.417303	±28
3/31/49	13	.257004	37	−.0042	.3635	+.3635	13.3593	.000	.0000	13.3593						
3/31/49	17	.257004	37	−.0042	.3615	+.3655	13.3613	.000	.0000	13.3613						

Observations of M_θ

Date	3/28/49	3/28/49	3/30/49	3/30/49	3/31/49	3/31/49
Time	a.m.	p.m.	a.m.	p.m.	a.m.	p.m.
M_θ	0.7290	0.7275	0.7260	0.7270	0.7255	0.7270

Mean value=0.7270. Standard deviation of mean=±0.0005

TABLE 31. *Series X, capillary 2.5a*

[Calculation of the pressure drops]

1	2	3	4	5	6	7	8	9	10	11	12	13	14	15	16	17
Date	Run	Q	Gage rod	Gage-rod correction	M_Q	Δ	h_θ	$\Delta\theta$	Δh	h_{20}	h_{20}, means	Standard deviation of the mean	p_{20}	Correction for side tube	P	Standard deviation of the mean
		cm³/sec		*in.*	*in.*	*in.*	*in.*	*°C*	*in.*	*in.*	*in.*	*in.*	*Dynes/cm²*	*Dynes/cm²*	*Dynes/cm²*	*Dynes/cm²*
8/12/49	1	0.096376	45	−0.0078	0.9635	−0.1280	4.8642	0.000	0.0000	4.8642						
8/12/49	5	096376	45	−.0078	.9650	−.1295	4.8627	+.006	+.0007	4.8634	4.8635	$\pm3\times10^{-4}$	0.151918×10^6	−0.000003	0.151915×10^6	±9
8/15/49	7	.096376	45	−.0078	.9650	−.1295	4.8627	.000	.0000	4.8627						
8/16/49	12	.096376	45	−.0078	.9640	−.1285	4.8637	.000	.0000	4.8637						
8/12/49	2	.128502	44	+.0003	.3125	+.5230	6.5233	.000	.0000	6.5233						
8/12/49	6	.128502	44	+.0003	.3130	+.5225	6.5228	.000	.0000	6.5228	6.5227	±9	.203745	−.000004	.203741	±27
8/15/49	8	.128502	44	+.0003	.3115	+.5240	6.5243	.000	.0000	6.5243						
8/16/49	13	.128502	44	+.0003	.3155	+.5200	6.5203	.000	.0000	6.5203						
8/12/49	3	.192753	40	−.0012	.9335	−.0980	9.9008	+.001	+.0002	9.9010						
8/15/49	9	.192752	40	−.0012	.9330	−.0975	9.9013	.000	.0000	9.9013	9.9023	±8	.309311	−.000006	.309305	±25
8/15/49	11	.192753	40	−.0012	.9310	−.0955	9.9033	.000	.0000	9.9033						
8/16/49	14	.192753	40	−.0012	.9310	−.0955	9.9033	+.001	+.0002	9.9035						
8/12/49	4	.257004	37	−.0047	.4700	+.3655	13.3608	.000	.0000	13.3608						
8/15/49	10	.257004	37	−.0047	.4700	+.3655	13.3608	.000	.0000	13.3608	13.3613	±8	.417357	−.000008	.417349	±24
8/16/49	15	.257004	37	−.0047	.4685	+.3670	13.3623	.000	.0000	13.3623						

Observations of M_0

Date	8/12/49	8/12/49	8/15/49	8/15/49	8/16/49	8/16/49	8/16/49
Time	a. m.	p. m.	a. m.	p. m.	a. m.	Noon	p. m.
M_0	0.8355	0.8345	0.8335	0.8360	0.8355	0.8360	0.8375

Mean=0.8355. Standard deviation of the mean=±0.0004.

TABLE 32. *Series V, capillary 1.4*

[Calculation of the pressure drops]

1	2	3	4	5	6	7	8	9	10	11	12	13	14	15	16	17
Date	Run	Q	Gage rod	Gage-rod correction	M_Q	Δ	h_θ	$\Delta\theta$	Δh	h_{20}	h_{20}, means	Standard deviation of the mean	p_{20}	Correction for side tube	P	Standard deviation of the mean
		cm³/sec		*in.*	*in.*	*in.*	*in.*	*°C*	*in.*	*in.*	*in.*	*in.*	*Dynes/cm²*	*Dynes/cm²*	*Dynes/cm²*	*Dynes/cm²*
12/20/48	5	0.033674	42	+0.0029	0.9090	−0.3225	7.6804	+0.002	+0.0004	7.6808						
12/20/48	6	.033674	42	.0029	.9105	−.3230	7.6799	+.003	+.0006	7.6805	7.6789	$\pm13\times10^{-4}$	0.239860×10^6	−0.000001	0.239859×10^6	±41
12/21/48	8	.033674	42	.0029	.9125	−.3250	7.6779	+.003	+.0006	7.6785						
12/22/48	13	.033674	42	.0029	.9150	−.3275	7.6754	+.002	+.0004	7.6758						
12/23/48	14	.072282	34	−.0002	.0460	+.5415	16.5413	+.004	+.0016	16.5429						
12/23/48	15	.072282	34	−.0002	.0480	+.5395	16.5393	+.002	+.0008	16.5401	16.5405	±14	.516664	−.000002	.516662	±44
12/28/48	17	.072282	34	−.0002	.0495	+.5380	16.5378	+.002	+.0008	16.5386						
12/20/48	7	.096376	28	+.0010	.4780	+.1095	22.1105	+.001	+.0006	22.1111						
12/21/48	9	.096376	28	.0010	.4755	+.1120	22.1130	+.002	+.0011	22.1141	22.1111	±11	.690669	−.000002	.690667	±34
12/28/48	18	.096376	28	.0010	.4800	+.1075	22.1085	+.002	+.0011	22.1096						
12/28/48	19	.096376	28	.0010	.4800	+.1075	22.1085	+.002	+.0011	22.1096						
12/21/48	10	.128502	21	−.0059	.0110	+.5765	29.5706	+.004	+.0030	29.5736						
12/21/48	11	.128502	21	−.0059	.0125	+.5750	29.5691	+.002	+.0015	29.5706	29.5706	±11	.923676	−.000003	.923673	±34
12/22/48	12	.128502	21	−.0059	.0130	+.5745	29.5686	+.002	+.0015	29.5701						
12/23/48	16	.128502	21	−.0059	.0150	+.5725	29.5666	+.002	+.0015	29.5681						

Observations of M_0

Date	12/20/48	12/21/48	12/21/48	12/22/48	12/22/48	12/23/48	12/23/48	12/28/48	12/28/48
Time	p. m.	a. m.	p. m.	a. m.	p. m.	a. m.	p. m.	a. m.	p. m.
M_0	0.5850	0.5865	0.5875	0.5845	0.5890	0.5865	0.5895	0.5875	0.5915

Mean value=0.5875. Standard deviation of mean=±0.0009

TABLE 33. *Series VI, capillary 1.4*

[Calculation of the pressure drops]

1	2	3	4	5	6	7	8	9	10	11	12	13	14	15	16	17
Date	Run	Q	Gage rod	Gage rod correction	M_Q	Δ	h_θ	$\Delta\theta$	Δh	h_{20}	h_{20}, means	Standard deviation of the mean	p_{20}	Correction for side tube	P	Standard deviation of the mean
		cm³/sec		*in.*	*in.*	*in.*	*in.*	*°C*	*in.*	*in.*	*in.*	*in.*	*Dynes/cm²*	*Dynes/cm²*	*Dynes/cm²*	*Dynes/cm²*
2/7/49	1	0.033674	43	+0.0011	0.0005	+0.6770	7.6781	0.000	0.0000	7.6781	7.6780	±2×10⁻⁴	0.239832×10⁶	−0.000001	0.239831×10⁶	±6
2/9/49	3	.033674	43	+.0011	.0005	+.6770	7.6781	+.001	+.0002	7.6783						
2/10/49	7	.033674	43	+.0011	.0010	+.6765	7.6776	.000	.0000	7.6776						
2/9/49	4	.072282	34	−.0002	.1350	+.5425	16.5423	.000	.0000	16.5423	16.5445	±13	.516789	−.000002	.516787	±41
2/10/49	8	.072282	34	−.0002	.1320	+.5455	16.5453	.000	.0000	16.5453						
2/11/49	10	.072282	34	−.0002	.1315	+.5460	16.5458	.000	.0000	16.5458						
2/9/49	5	.096376	28	+.0010	.5670	+.1105	22.1115	.000	.0000	22.1115	22.1120	±3	.690697	−.000002	.690695	±9
2/10/49	9	.096376	28	+.0010	.5665	+.1110	22.1120	.000	.0000	22.1120						
2/11/49	11	.096376	28	+.0010	.5660	+.1115	22.1125	.000	.0000	22.1125						
2/7/49	2	.128502	21	−.0059	.1015	+.5760	29.5701	.000	.0000	29.5701	29.5725	±14	.923735	−.000003	.923732	±45
2/9/49	6	.128502	21	−.0059	.0995	+.5780	29.5721	+.001	+.0007	29.5728						
2/11/49	12	.128502	21	−.0059	.0970	+.5805	29.5746	.000	.0000	29.5746						

Observations of M_0

Date	2/7/49	2/9/49	2/9/49	2/10/49	2/10/49	2/11/49	2/11/49
Time	a. m.	a. m.	p. m.	a. m.	p. m.	a. m.	p. m.
M_0	0.6760	0.6755	0.6780	0.6785	0.6785	0.6765	0.6795

Mean=0.6775. Standard deviation of the mean=±0.0006

TABLE 34. *Series VIII, capillary 1.4*

[Calculation of the pressure drops]

1	2	3	4	5	6	7	8	9	10	11	12	13	14	15	16	17
Date	Run	Q	Gage rod	Gage-rod correction	M_Q	Δ	h_θ	$\Delta\theta$	Δh	h_{20}	h_{20}, means	Standard deviation of the mean	p_{20}	Correction for side tube	P	Standard deviation of the mean
		cm³/sec		*in.*	*in.*	*in.*	*in.*	*°C*	*in.*	*in.*	*in.*	*in.*	*Dynes/cm²*	*Dynes/cm²*	*Dynes/cm²*	*Dynes/cm²*
3/10/49	1	0.033674	43	+0.0011	0.1005	+0.6754	7.6765	+0.001	+0.0002	7.6767	7.6791	±14×10⁻⁴	0.239867×10⁶	−0.000001	0.239866×10⁶	±45
3/11/49	4	.033674	43	.0011	.0970	+.6779	7.6790	+.001	+.0002	7.6792						
3/15/49	10	.033674	43	.0011	.0955	+.6804	7.6815	.000	.0000	7.6815						
3/10/49	2	.072282	34	−.0002	.2290	+.5469	16.5467	.000	.0000	16.5467	16.5473	±8	.516876	−.000002	.516874	±23
3/11/49	5	.072282	34	−.0002	.2275	+.5484	16.5482	+.001	+.0004	16.5486						
3/14/49	6	.072282	34	−.0002	.2290	+.5469	16.5467	.000	.0000	16.5467						
3/10/49	3	.096376	28	+.0010	.6650	+.1109	22.1119	+.001	+.0006	22.1125	22.1133	±8	.690738	−.000002	.690736	±24
3/14/49	7	.096376	28	.0010	.6630	+.1129	22.1139	+.001	+.0006	22.1145						
3/15/49	11	.096376	28	.0010	.6635	+.1124	22.1134	−.001	−.0006	22.1128						
3/14/49	8	.128502	21	−.0046	.1935	+.5824	29.5778	+.001	+.0007	29.5785	29.5784	±2	.923920	−.000003	.923917	±5
3/14/49	9	.128502	21	.0046	.1935	+.5824	29.5778	+.001	+.0007	29.5785						
3/15/49	12	.128502	21	.0046	.1925	+.5834	29.5788	−.001	−.0007	29.5781						

Observations of M_0

Date	3/10/49	3/11/49	3/11/49	3/14/49	3/14/49	3/15/49	3/15/49
Time	a. m.	a. m.	p. m.	a. m.	p. m.	a. m.	p. m.
M_0	0.7755	0.7780	0.7765	0.7745	0.7750	0.7745	0.7770

Mean value=0.7759. Standard deviation of mean=±0.0005

TABLE 35. *Series XI, capillary 1.4a*

[Calculation of the pressure drops]

1	2	3	4	5	6	7	8	9	10	11	12	13	14	15	16	17
Date	Run	Q	Gage rod	Gage-rod correction	M_Q	Δ	h_θ	$\Delta\theta$	Δh	h_{20}	h_{20}, means	Standard deviation of the mean	p_{20}	Correction for side tube	P	Standard deviation of the mean
		cm^3/sec		*in.*	*in.*	*in.*	*in.*	°*C*	*in.*	*in.*	*in.*	*in.*	*Dynes/cm²*	*Dynes/cm²*	*Dynes/cm²*	*Dynes/cm²*
9/14/49	1	0.033674	47	+0.0135	0.0830	+0.8176	3.8311	0.000	0.0000	3.8311	3.8315	$\pm10\times10^{-4}$	0.119682×10^6	−0.000001	0.119681×10^6	±31
9/15/49	5	.033674	47	+.0135	.0810	+.8196	3.8331	.000	.0000	3.8331						
9/15/49	9	.033674	47	+.0135	.0840	+.8166	3.8301	+.001	+.0001	3.8302						
9/14/49	2	.072282	42	+.0025	.6105	+.2901	8.2926	.000	.0000	8.2926	8.2911	±9	.258983	−.000002	.258981	±28
9/15/49	6	.072282	42	+.0025	.6125	+.2881	8.2906	.000	.0000	8.2906						
9/15/49	10	.072282	42	+.0025	.6130	+.2876	8.2901	.000	.0000	8.2901						
9/14/49	3	.096376	39	−.0053	.7855	+.1151	11.1098	−.002	−.0006	11.1092	11.1074	±13	.346954	−.000003	.346951	±41
9/15/49	7	.096376	39	−.0053	.7875	+.1131	11.1078	.000	.0000	11.1078						
9/15/49	11	.096376	39	−.0053	.7905	+.1101	11.1048	+.001	+.0003	11.1051						
9/14/49	4	.128502	35	−.0061	.9940	−.0934	14.9005	−.001	−.0004	14.9001	14.8993	±6	.465399	−.000004	.465395	±19
9/15/49	8	.128502	35	−.0061	.9950	−.0944	14.8995	.000	.0000	14.8995						
9/15/49	12	.128502	35	−.0061	.9965	−.0959	14.8980	+.001	+.0004	14.8984						

Observations of M_0

Date	9/14/49	9/14/49	9/15/49	9/15/49
Time	a. m.	p. m.	a. m.	p. m.
M_0	0.9000	0.9005	0.9005	0.9015

Mean=0.9006. Standard deviation of the mean=±0.0003.

TABLE 36. *Series XII, capillary 1.4a*

[Calculation of the pressure drops]

1	2	3	4	5	6	7	8	9	10	11	12	13	14	15	16	17
Date	Run	Q	Gage rod	Gage-rod correction	M_Q	Δ	h_θ	$\Delta\theta$	Δh	h_{20}	h_{20}, means	Standard deviation of the mean	p_{20}	Correction for side tube	P	Standard deviation of the mean
		cm^3/sec		*in.*	*in.*	*in.*	*in.*	°*C*	*in.*	*in.*	*in.*	*in.*	*Dynes/cm²*	*Dynes/cm²*	*Dynes/cm²*	*Dynes/cm²*
9/26/49	1	0.033674	47	+0.0135	0.0860	+0.8186	3.8321	0.000	0.0000	3.8321	3.8317	$\pm4\times10^{-4}$	0.119688×10^6	−0.000001	0.119687×10^6	±14
9/26/49	5	.033674	47	.0135	.0860	+.8186	3.8321	.000	.0000	3.8321						
9/27/49	9	.033674	47	.0135	.0870	+.8176	3.8311	−.001	−.0001	3.8310						
9/26/49	2	.072282	42	+.0025	.6180	+.2866	8.2891	.000	.0000	8.2891	8.2897	±3	.258940	−.000002	.258938	±8
9/27/49	6	.072282	42	.0025	.6175	+.2871	8.2896	.000	.0000	8.2896						
9/27/49	10	.072282	42	.0025	.6170	+.2876	8.2891	+.001	+.0002	8.2903						
9/26/49	3	.096376	39	−.0053	.7945	+.1101	11.1048	.000	.0000	11.1048	11.1052	±3	.346885	−.000003	.346882	±10
9/27/49	7	.096376	39	−.0053	.7945	+.1101	11.1048	.000	.0000	11.1048						
9/27/49	11	.096376	39	−.0053	.7935	+.1111	11.1058	+.001	+.0003	11.1061						
9/26/49	4	.128502	35	−.0061	1.0000	−.0954	14.8985	.000	.0000	14.8985	14.8988	±3	.465383	−.000004	.465379	±8
9/27/49	8	.128502	35	−.0061	.9990	−.0945	14.8995	.000	.0000	14.8995						
9/27/49	12	.128502	35	−.0061	1.0000	−.0954	14.8985	.000	.0000	14.8985						

Observations of M_0

Date	9/26/49	9/26/49	9/27/49	9/27/49
Time	a. m.	p. m.	a. m.	p. m.
M_0	0.9050	0.9035	0.9055	0.9045

Mean value=0.9046. Standard deviation of mean=±0.0005

WASHINGTON, February 16, 1951.

Precise Measurements With Bingham Viscometers and Cannon Master Viscometers

J. F. Swindells, R. C. Hardy, and R. L. Cottington

A critical study has been made of the techniques used at the National Bureau of Standards with Bingham viscometers and Cannon kinematic viscometers. All corrections applicable to measurements with these instruments were critically examined. Instruments of each type were calibrated using the viscosity of water at 20° C as the primary viscosity standard. The viscometers were used to determine the viscosities of four hydrocarbon liquids in the range 0.4 to 40 centipoises. With each liquid, the values obtained in the two types of viscometers were in agreement by 0.05 percent or better, indicating that no gross error was involved in the use of either instrument. It is considered, however, that the inherent relative simplicity of operation of the kinematic viscometer makes it a preferable instrument for this type of measurement.

1. Introduction

As the result of a recent determination [1] [1], the National Bureau of Standards on July 1, 1953, adopted the value of 1.002 centipoises (cp) for the absolute viscosity of water at 20° C as the primary standard for viscosity determinations. The American Society for Testing Materials, The National Physical Laboratory in England, and the Physikalisch Technischen Bundesanstalt in Germany have concurred in this action. Previous to this, the values of the secondary standards of viscosity issued by the Bureau were based upon 1.005 cp for the viscosity of water at 20° C. In connection with the reevaluation of the secondary standards on the basis of the new value for water, a comparative study has been made of the use of two types of viscometers for relating the viscosities of other liquids to that of water as a primary standard. Bingham viscometers and Cannon viscometers were used, and comparisons were made of the viscosities of four hydrocarbon liquids in the range 0.4 to 40 cp and of the viscosity of each liquid as determined in each type of instrument. This paper presents in some detail the techniques used in making these determinations to describe the methods employed in evaluating the National Bureau of Standards standard viscosity samples and to call attention to the magnitude of certain corrections often neglected in viscometry. The extension of these techniques to the calibration of viscometers with larger capillaries suitable for the measurement of the viscosities of more viscous liquids is relatively simple and involves the same methods as are covered here.

2. The Bingham Viscometer

2.1. General

A short treatment of the use of the Bingham viscometer, shown diagrammatically in figure 1, has been given previously [2], and it will be assumed that the reader has some familiarity with the instrument. With the usual procedure, pressure is applied to the right limb of the viscometer, and the rate of flow is determined by measuring the time required for the meniscus in the left limb to pass from the fiducial mark d to mark c. To avoid the necessity for drainage corrections, each determination is made with the bulb A initially dry. This is accomplished by introducing the sample into bulb B with a special pipet, sufficient liquid being added to fill the viscometer between the marks d and g at the test temperature. With the exception of certain calibration runs with water, the viscometer is cleaned and a fresh sample is introduced for each measurement. By this procedure the volume of flow is kept constant for each instrument regardless of the viscosity or rate of flow.

Pressure is applied to the liquid in the viscometer by air supplied from a tank having a capacity (about 60,000 cm^3) sufficiently large that the increase in volume (about 4 cm^3) in the pressure system during the flow of liquid from bulb B causes no significant reduction in pressure. The tank is thermally insulated to prevent rapid changes in its temperature

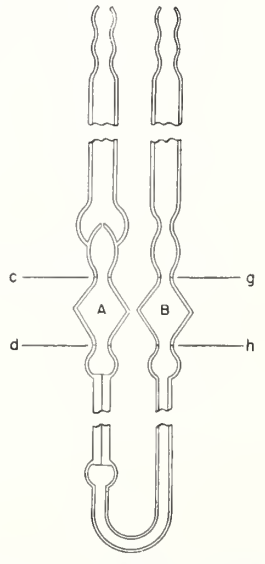

FIGURE 1. *Bingham viscometer.*

[1] Figures in brackets indicate the literature references at the end of this paper.

with fluctuations in the ambient temperature. In general, pressures above 150 mm Hg are read with a mercury manometer, a water manometer being used for lower pressures; differences in liquid levels in the manometer up to 600 mm are read with a cathetometer and greater differences are read by using a calibrated steel tape and reading telescopes. The heights were read to about 0.02 mm with the cathetometer and 0.1 mm with the steel tape.

Times of flow are measured using a stopclock operated from a constant-frequency source of power.

All of the flow measurements reported here were made with the viscometers immersed in a well-stirred, 30-gal oil bath whose temperature was controlled by supplying a heater from the output of a manually adjusted variable transformer. When operating below ambient temperature, heat was taken from the bath through cooling coils in which cold water was circulated at a constant rate. Temperatures were measured with a resistance thermometer, and their recorded values are believed to be accurate to $\pm 0.002°$ C.

2.2. Calibration

The usual form of the modified Poiseuille equation for the calculation of viscosity by the capillary method is

$$\eta=\frac{\pi r^4 Pt}{8V(l+nr)}-\frac{m\rho V}{8\pi(l+nr)t}, \tag{1}$$

where

r=radius of capillary
P=mean effective pressure drop through the capillary
V=volume between fiducial marks
t=time for volume V to flow
l=length of capillary
m, n=coefficients associated with the flow at the ends of the capillary
η, ρ=the absolute viscosity and density of the liquid whose viscosity is to be determined:

As over a considerable range of rates of flow, m and n can be taken as constant for capillaries having square-cut ends [3], certain of the quantities in eq (1) are usually grouped to give two constants for the instrument. Equation (1) then takes the form

$$\eta=CPt-C'\rho/t, \tag{2}$$

where

$$C=\frac{\pi r4}{8V(l+nr)} \text{ and } C'=\frac{mV}{8\pi(l+nr)}.$$

With viscometers having capillary bores small enough for calibration with water, these two constants are commonly evaluated by measuring the times of flow of water at 20° C for various applied pressures. The product Pt is plotted against $1/t$, and C and C' are evaluated from the resulting straight line by introducing known values for η and ρ. For the two water-calibrated viscometers used in the work reported here, however, it was found that such plots did not yield straight lines over the complete range of rates of flow in which the instruments were to be used, indicating that m and n were both varying, and consequently C and C' could not be treated as constants. For this reason and for simplicity, the purely empirical formula,

$$\eta=fPt, \tag{3}$$

was used with the viscometers. In this equation, f is a multiplying factor that varies with the conditions of flow. It is convenient to assume that the conditions peculiar to a given rate of flow are characterized by the corresponding value of the Reynolds number as calculated for the flow in the capillary ($R=2V\rho/\pi r\eta t$), and therefore f will have a definite value for each value of the Reynolds number. The calibration of these instruments, then, consists of determining the value of f as a function of the Reynolds number.

Although the Bingham viscometer is designed to minimize the effect of hydrostatic head in the instrument, actually small head corrections to an applied external pressure, p_0, are necessary to give an exact value of P. The first correction, which will be called the level head, arises from the fact that, despite careful construction, the two bulbs (A and B in fig. 1) will not be geometrically identical and at the same level. This condition results in a residual hydrostatic head that is of the same magnitude but opposite sign for flow right to left (R-L) and left to right (L-R) in the viscometer. The correction is largely independent of the magnitude of the applied external pressure but is proportional to the density of the liquid. The level head was evaluated in this work by making flow measurements in the L-R direction and then repeating in the R-L direction, using approximately the same applied pressure. The runs were made at the lowest applied pressure that could be accurately measured, and under conditions chosen to insure that the volume of flow was the same in each direction. Under these conditions, the difference in the time of flow for the two directions was attributed to a corresponding difference in pressure. Then, knowing the applied pressures, the magnitude of the correction was calculated.

A second head correction, which becomes very significant at low values of the applied pressure, is the commonly termed logarithmic head correction. If we neglect for the moment the level head discussed above, the initial pressure drop through the capillary is p_0+x, where x is the initial hydrostatic head of liquid, and the final pressure is p_0-x, but the mean effective pressure is not exactly p_0, the arithmetic mean of the two, since the higher pressures during the first part of the run cause more rapid flow and are therefore effective for a proportionately shorter

time. For bulbs of regular shape, however, the effective pressure is readily calculable. For this work, the calculations were made by using Barr's equation [4]. This equation is written $P(1+y^2/10+y^4/35+\ .\ .\ .)=p_0$, [approximately, where $y=x/p_0$. Barr states that this equation is derived "for a bulb that has the form of a pair of opposed cones, each of a height equal to the radius of the common base, discharging into air, or for such a bulb discharging symmetrically into a similar one, as in Bingham's viscometer". The correctness of this expression was verified in an independent derivation, but because the radius of the common base dropped out in the derivation, it is concluded that the expression holds for cones of any height-to-base ratio. It is of importance to note in connection with runs at low pressures, that the logarithmic head is a function of the ratio of the initial and final pressures, and therefore it increases in absolute magnitude as the applied pressure is reduced. The sign of the correction is always negative, no matter which direction of flow is being used in the viscometer, and therefore it does not affect the determination of the level head, as described above.

The design of the Bingham viscometer is such as to minimize the effect of surface tension upon P. Calculations of the net contribution of surface tension to the mean effective pressure indicate a maximum correction of about 0.001 mm Hg, which was neglected in this work.

A more complete discussion of the above corrections is given by Barr [3, chap. 3].

The three Bingham viscometers used are identified in table 1. Of these, viscometers 1 and 20 were calibrated with water, whereas number 5 was calibrated subsequently by using two hydrocarbon oils whose viscosities were determined in viscometers 1 and 20. In making the calibration runs with water an exception was made to the usual procedure of flowing into a dry bulb, most of the runs being made with the fiducial bulb wet. Following each R-L run, the liquid was drawn back at such a rate as to require about 80 sec with viscometer No. 1, and 120 sec with No. 20 for the fiducial bulb to empty. After allowing about 18 min for further drainage from the walls of the bulb, another R-L run was started. In this manner a reproducible volume of flow was obtained without the necessity of drying the instrument between runs. The difference between the volume of flow under this wet-bulb condition and the true volume of the fiducial bulb was obtained from the differences in the product Pt between wet and dry-bulb runs made with the same applied pressure. On this basis, all the wet-bulb runs were corrected to dry-bulb conditions.

TABLE 1. *Essential dimensions of Bingham viscometers*

Viscometer	Capillary		Volume of flow
	Radius	Length	
	cm	*cm*	*cm*³
1	0.012	10.2	3.96
20	.011	12.3	5.07
5	.017	10.0	4.00

The calibration data obtained with water at 20° C for viscometers 1 and 20 are given in appendices 7.1 and 7.2. All runs were made in the R-L direction, except for the few special runs made for the determination of the level head corrections. From these data the plots of Pt versus R given in figures 2 and 3 were constructed. Each plotted point represents the mean of at least two runs made at approximately the same pressure. For each viscometer, it is seen that the plot is not linear at certain values of R, as was mentioned previously. Since the data are not adequate to position accurately the curves at the lowest Reynolds numbers, the lines were drawn horizontal in this region on the basis of theoretical considerations [5]. From these curves values of Pt corresponding to selected values of R were obtained and, taking $\eta=0.01002$ poise, were substituted

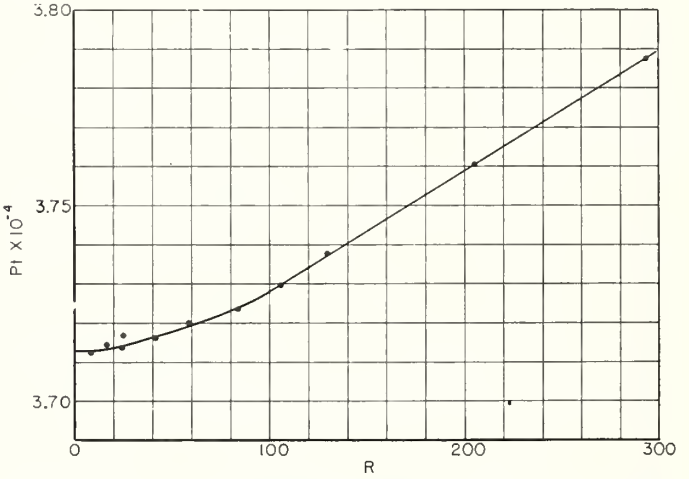

FIGURE 2. *Pt as a function of Reynolds number for Bingham viscometer number 1.*

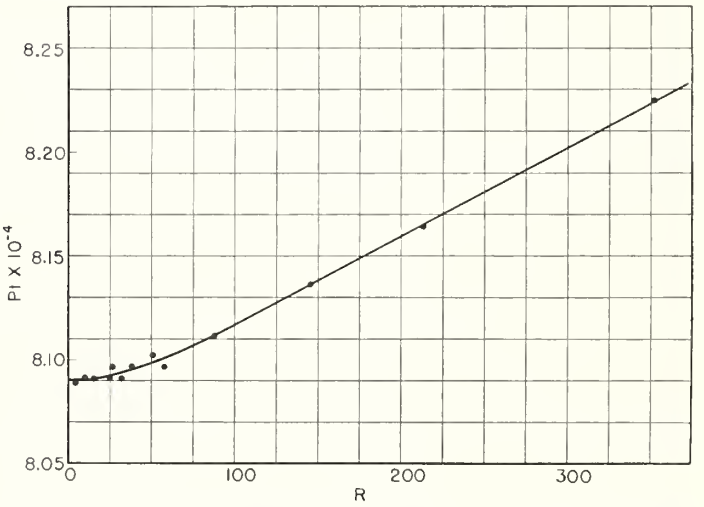

FIGURE 3. *Pt as a function of Reynolds number for Bingham viscometer number 20.*

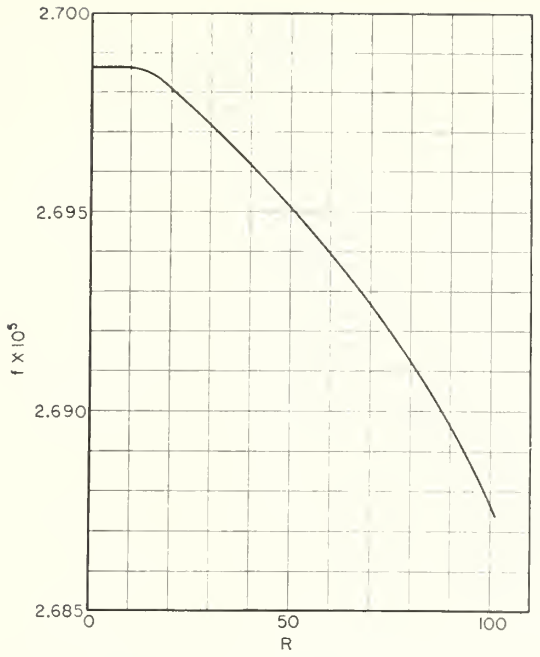

FIGURE 4. *Calibration curve for Bingham viscometer number 1.*

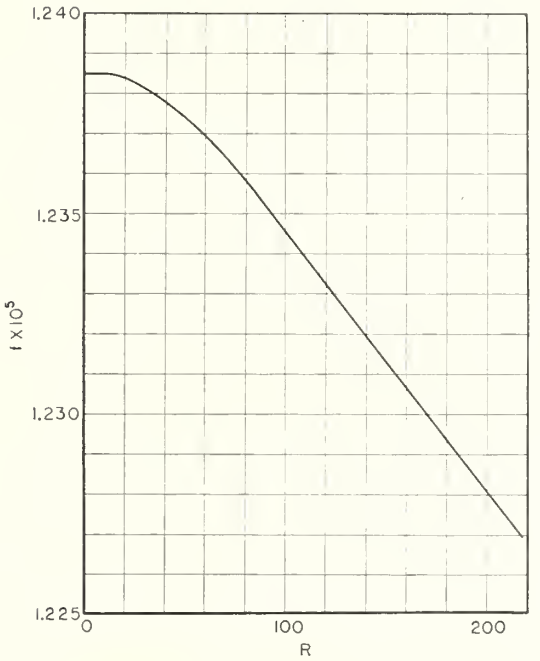

FIGURE 5. *Calibration curve for Bingham viscometer number 20.*

in eq (3) to calculate corresponding values of f. The values of f were then plotted as a function of R, yielding the calibration curves for viscometers 1 and 20 shown in figures 4 and 5, respectively.

To calculate the unknown viscosity of a liquid from flow data obtained in one of these viscometers, it is necessary to choose a value f from the calibration curve corresponding to a tentative value of the Reynolds number based on an estimate of the viscosity of the unknown. If the viscosity value calculated by substituting this value of f, together with the measured values of P and t, in eq (3) differs materially from the first estimate of the viscosity, a second calculation is required.

Viscometer No. 5 was calibrated with oils A and B (to be identified later), using values of their viscosities as determined in viscometers 1 and 20. These calibration data are given in appendix 7.3. As all calibrating runs and viscosity measurements made in viscometer 5 were at Reynolds numbers less than 10, it was assumed that f in eq (3) was constant for this viscometer under these conditions. The level head was measured and the logarithmic head calculated for this viscometer as outlined previously.

2.3. Results with Bingham Viscometers

The viscosities of normal heptane and three additive-free hydrocarbon oils were measured at 20° C. The mean results are given in table 2, and

TABLE 2. *Results at 20° C with Bingham viscometers*

Oil	Viscometer	R	η	η, mean
			cp	*cp*
n-Heptane	1	98.9	0.4112	0.4111
Do	20	154.3	.4110	
A	1	28.2 and 2.4	1.9250	1.9250
A	20	18.1	1.9251	
B	1	2.4	7.609	7.610
B	20	1.5	7.610	
C	5	0.2 and 0.5	42.82	42.82

data from individual runs in appendix 7.4. Normal heptane was included to furnish comparative results with a liquid whose viscosity is less than that of water. The heptane was not of highest purity, but was taken from a lot which met specifications for a primary reference fuel for the determination of octane number [6] and was at least 99.5 percent pure. The viscosities of *n*-heptane and oils A and B were determined in viscometers 1 and 20, employing the normal procedure of running in the R-L direction with the fiducial bulb initially dry. Oil A was run at as high and as low Reynolds numbers as was practical. Higher applied pressures were avoided because experience has shown that oils as light as A dissolve air rather rapidly under these conditions, with a consequent lowering of their viscosities. Conditions for the other runs were chosen to strike a balance between optimum conditions for accurate measurement of pressure and of time. In calculating the viscosities, small corrections were made to account for the change of viscosity of the oils with pressure. Observed viscosities were reduced to a pressure of 1 atm, as described elsewhere [2], by adding a second term to eq (3), which then becomes

$$\eta = fPt - \frac{F}{t}P\eta, \qquad (4)$$

where F is a factor representing the fractional change in η for unit change in pressure. Good agreement was found between results obtained in the two viscometers 1 and 20, the largest discrepancy being 0.05 percent with n-heptane. In addition, results obtained with oil A in viscometer 1 at R=28.2 and R=2.4 were in equally good agreement (see appendix 7.4), which tends to confirm the shape of the calibration curve at the lower range of Reynolds numbers (fig. 4).

Runs made with oil C in viscometer 5 at high and at low pressures were in good agreement (see appendix 7.4), indicating that the corrections applied for change of viscosity with pressure are not in serious error.

3. The Cannon Viscometer

3.1. General

In outline, the techniques used at the National Bureau of Standards with the Cannon viscometers, shown in figure 6, are substantially as described by Cannon [7], the principal differences consisting of a more rigorous treatment of the various corrections to be applied to the observed data. With instruments of the kinematic type the value of P applicable to eq (1), neglecting surface tension effects, is given by

$$P=hg(\rho-\rho_a), \tag{5}$$

in which h is the mean effective head, ρ is the liquid density, and ρ_a is the mean density of the air column in the left arm of the viscometer, as shown in figure 6. For application to the Master viscometers, eq (1) then becomes

$$\frac{\eta}{\rho}=\frac{\pi r^4 g}{8V(l+nr)}\,h\left(1-\frac{\rho_a}{\rho}\right)t-\frac{mV}{8\pi(l+nr)t}. \tag{6}$$

If we let

$$\frac{\pi r^4 g}{8V(l+nr)}\,h\left(1-\frac{\rho_a}{\rho}\right)=K$$

and

$$\frac{mV}{8\pi(l+nr)}=B,$$

eq (6) becomes

$$\frac{\eta}{\rho}=Kt-\frac{B}{t}. \tag{7}$$

It is apparent that K and B will not be constant for all test conditions, but their values will reflect any variations in m and n with Reynolds number. As is done with the Bingham viscometers, these changes in m and n are implicitly determined experimentally as a part of the viscometer calibration. In addition, the value of K changes with any change in h or $(1-\rho_a/\rho)$, and a small correction for variation in the value of g may be required if the instrument is used

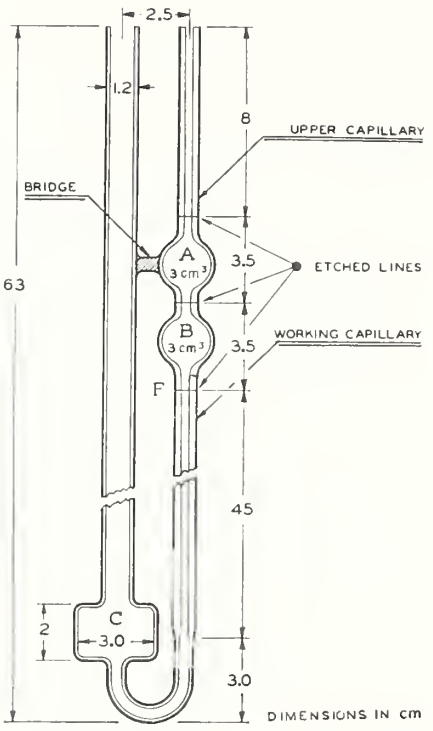

FIGURE 6. *Cannon Master viscometer.*

at a location other than where it is calibrated. If we let K_c be the determined value of K under the particular hydrostatic head at calibration, we can find from it the value of K under other test conditions by calculating changes in h and $(1-\rho_a/\rho)$. Since a change in $(1-\rho_a/\rho)$ is equivalent to a change in h, it is grouped with the other factors which affect h. For any test condition, eq (7) may then be written

$$\frac{\eta}{\rho}=K_c\left(1+\frac{\Delta h}{h}\right)t-\frac{B}{t}, \tag{8}$$

in which Δh is the difference in effective head between test and calibrating conditions, and is made up of the sum of Δh_1, Δh_2, etc., arising from the several factors involved. In practice it is convenient to treat K as a constant equal to K_c, and to apply the corrections to the time of flow t. The viscosity is calculated by means of the equation

$$\frac{\eta}{\rho}=K_c t_c-\frac{B}{t}, \tag{9}$$

in which $t_c=t(1+\Delta h/h)$.

Of the factors affecting h, the filling volume will be considered first. To introduce a reproducible volume of liquid into the viscometer, the viscometer and the liquid must both be at some standard temperature (20° C for this work) each time the viscometer is charged. To obviate the inconvenience of this procedure, fillings are made at ambient temperature, which is observed, and an appropriate correction, Δh_1, is then calculated to account for

any difference between the filling at the observed temperature and a standard filling at a temperature of 20° C. The calculation of this correction is similar to that of Δh_2, which follows.

A second factor affecting h, which gives rise to a correction Δh_2, is the change in effective head with differences between the calibration temperature and that of subsequent runs. The calculation of this correction is based on the cubical expansion of the viscometer and test liquid, together with the mean diameter of the working part of reservoir C, figure 6, [8]. For the most precise work an accurate knowledge of the internal diameter of C is necessary. This measurement was made by plugging the lower end of the capillary with wax and then filling the bottom part of the viscometer with mercury to a low level in C. Weighed increments of mercury were added, and the resulting increases in level in C were measured with a depth gage, from which data a mean internal diameter was calculated.

From differences in the factor $(1-\rho_a/\rho)$ between calibrating and operating conditions a Δh_3 is calculated. The density of the air in the viscometer is a function of the temperature and amount of water vapor present, neither of which is known accurately, but no serious errors are introduced by assuming the air to be 50-percent saturated and at the test temperature.

The factor most difficult to evaluate is the variation of the mean head with surface tension. In the work reported here, viscosity measurements of oils made in water-calibrated viscometers required the most careful estimates of the effects of surface tension. In the case of water, the contribution of surface effects to the effective head was determined experimentally and also calculated. The experimental determination was made with a glass bulb blown as nearly as possible to the size and shape of the fiducial bulb in the viscometer. The bulb was connected through a U-shaped tube to a cylindrical glass tube about 1 cm in diameter and held vertically close to the side of the bulb. The bulb and tube were then mounted in a small bath of oil having close to the same index of refraction as the bulb. Water was introduced into the tube until the level stood in the neck at the bottom of the bulb. The difference between the liquid levels in bulb and tube was then measured with a micrometer microscope mounted for vertical measurements. From this difference and a calculated value for the capillary rise in the cylindrical tube, the rise at this particular level in the bulb was obtained. The calculation of the rise in the cylindrical tube was made by using Sugden's table [9]. A known volume of water was then added and the measurements repeated. The portion of the added volume going into the bulb was the difference between the added volume and the volume increase in the tube as calculated from the change in level in the tube. This process was repeated, taking about 20 increments of volume to fill the bulb. From these data and a measured value of the head in the viscometer at a known level in the bulb, a value of the mean head in an interval, h_i, was estimated for each of the 20 intervals. Then, knowing the volume, ΔV, and the capillary rise, h_γ, for each interval, terms of the form $\Delta V h_\gamma/h_i$ were calculated for each interval. The quotient

$$\frac{\sum \frac{\Delta V}{h_i} h_\gamma}{\sum \frac{\Delta V}{h_i}}$$

then gave a time-weighted mean value for the capillary rise in the bulb as a whole. The rise in the cylindrical lower reservoir was calculated by using Sugden's table and subtracted from the mean value for the bulb to get a net effect for water in the viscometer. The same techniques were used to determine a net value of the surface tension for each of the oils tested. From the difference between water and oil, a correction, Δh_4, was calculated for application to data obtained with oil.

The net surface tension effect for water in the viscometer was also obtained by calculation alone. For this purpose, a vertical section through the fiducial bulb was plotted on a large scale as accurately as possible. The bulb was then divided into 13 sections, and a value of $\Delta V h_\gamma/h_i$ was calculated for each. With the aid of Bashforth and Adams' tables [10], each value of ΔV was calculated by using the geometry of the bulb as plotted and the calculated change in meniscus volume between the top and bottom of the section. The tables were also used in calculating h_γ for each section. This method has been given in more detail by Barr [11]. The mean value for the bulb was obtained weighting each section with respect to time, as was done in the experimental method. The calculations yielded a value within 0.01 percent of the experimental result, which lent confidence to both methods. Because of limited range of Bashforth and Adams' tables, the calculation could not be made for the oils.

Thus far in the treatment of the factors affecting K in eq (7), it has been assumed that the volume of flow, V, is constant under all conditions. For application to the work reported here, the validity of this assumption was carefully tested. Bulbs similar in size and shape to the fiducial bulbs in the Cannon viscometers were blown with capillary stems about 1 cm long above and below the bulb. To detect differences in the volume of flow of water and the several oils from a bulb, a capillary was attached below the bulb with neoprene tubing so that the bulb could be quickly disconnected. The capillary bore was selected to give about the same time of flow for a particular liquid as was found in the Cannon viscometer. By weighing the test bulb empty and again after a liquid had been run from it at the rate controlled by the resistance of the capillary, the volume of liquid remaining on the walls of the bulb was obtained. From the difference between results obtained with

a calibrating liquid and a test liquid, a correction to K_c could be calculated. Only one instance of a correction as large as 0.01 percent was found, and this so-called drainage correction was applied.

The viscometer is filled by holding it in an inverted position with the end of the upper capillary immersed in the liquid under test. Liquid is drawn into the viscometer by applying suction to the other arm until the level reaches a position slightly beyond the mark F (fig. 6). Applying just enough suction to hold the liquid level at approximately this position, the upper capillary is lifted from the liquid and the operator's finger is placed over its end. With the instrument still inverted, excess liquid is carefully bled out of the capillary past the finger tip until the liquid level reaches F. The viscometer is then returned to its normal upright position, and the finger is removed with a gentle wiping action. In this manner a reproducible filling volume is introduced. After filling the viscometer it is mounted in its bath, and sufficient time is allowed for the fiducial bulb B to empty and for the sample to come to the bath temperature before starting a test. To make a determination, the liquid is pushed up under 17-mm-Hg air pressure until the upper meniscus stands about 5 mm above the mark at the top of bulb B. The air pressure is then released, and the time for bulb B to empty is observed. With relatively low viscosity oils, raising the liquid with vacuum at the start of a run sometimes results in a time of flow slightly higher than when air pressure is used. Such differences are attributed to the removal of air from the sample under reduced pressure. It is therefore considered better technique to use air pressure as any change in the amount of air dissolved in the oil will start at the surface farthest removed from the liquid passing through the capillary.

When the liquid is pushed up at the start of a run, the meniscus level in reservoir C is lowered, leaving some liquid behind on the walls. The amount of liquid left on the walls influences the level in C and hence the value of h. By always using the same pressure in pushing the liquid up, the level in C is lowered at a rate inversely proportional to the liquid viscosity, which leaves about the same amount of liquid on the walls for each test. Calculations indicate that this procedure eliminates significant variations in h.

3.2. Calibration and Results

The calibration of the Cannon viscometers consists in evaluating K_c and B in eq (9). To illustrate the method, eq (9) is rewritten

$$\frac{\eta}{\rho t_c}=K_c-\frac{B}{t_c^2}, \tag{10}$$

in which t_c^2 is substituted for $t_c t$ without detectable error. Liquids having different kinematic viscosities (η/ρ) are run in the viscometer, and values of $\eta/(\rho t_c)$ are plotted against $1/t_c^2$. Values of K_c and B are then obtained from the resulting curve. As unpublished results in this and other laboratories have shown that B may not remain constant over the useful range of Reynolds numbers for this type of viscometer, the calibration must embrace the range in which the instrument is to be used. In practice, therefore, the calibration curve consists of a plot of $\eta/(\rho t_c)$ as a function of $1/t_c^2$ or R, and for a particular viscosity determination values of K_c and B are obtained from the curve at the appropriate value of $1/t_c^2$ or R.

The four Cannon viscometers used in this work are identified in table 3. Of these, M25–1 and M25–2 were calibrated with water, whereas M104 and M105 were calibrated subsequently with two hydrocarbon oils whose viscosities were determined in M25–1 and M25–2. The calibration data obtained with M25–1 and M25–2 are given in appendix 7.5, and from these data the calibration curves in figure 7 were plotted.

The curves were arbitrarily drawn through the values of $\eta/(\rho t_c)$ at Reynolds numbers of about 15, which were obtained with water at 20° C, because a value for the viscosity of water at 20° C was taken as the primary standard for calibration. The points at higher Reynolds numbers were obtained with water at 40°, 60°, and 80° C. The values used for the properties of water at these temperatures are given in appendix 7.6. As K_c refers to the conditions existent with water at 20° C, times of flow obtained at the higher temperatures were corrected by appropriate values of the factor $(1+\Delta h/h)$ in eq (8).

It is evident that the value of B is zero $(m=0)$ for these two viscometers up to a Reynolds number of at least 110. Because they were used at values of R never exceeding 50, the determinations made in these instruments were calculated by means of the equation

$$\frac{\eta}{\rho}=K_c t_c. \tag{11}$$

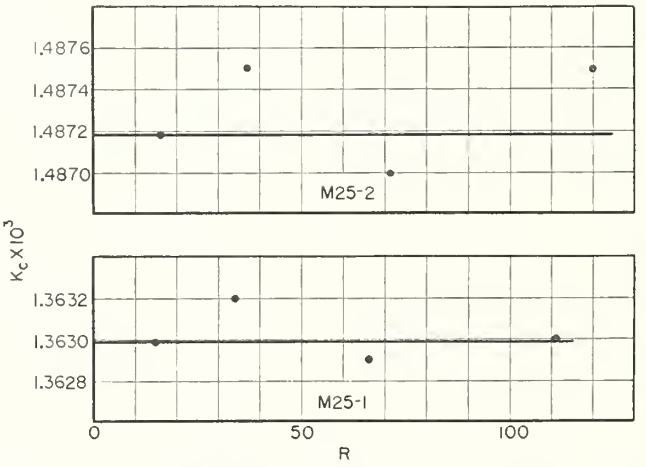

FIGURE 7. *Calibration curves for Cannon viscometers numbers M25–1 and M25–2.*

TABLE 3. *Essential dimensions of Cannon viscometers*

Viscometer	l	r	V	h	Filling volume	Radius of reservoir
	cm	*cm*	*cm*^{3}	*cm*	*cm*^{3}	*cm*
M25–1	44.5	0.0180	3.11	46.5	6.85	1.52
M25–2	44.5	.0185	3.13	46.3	6.77	1.50
M104	44.3	.0294	3.64	46.6	7.68	1.53
M105	44.5	.0293	3.54	46.6	7.53	1.55

Viscometers M104 and M105 were calibrated with oils A and B, using values of their viscosities as determined in M25–1 and M25–2. The calibration data are given in appendix 7.7. These viscometers were calibrated and used at $R<10$, and hence it was assumed that $B=0$ and eq (11) was applicable. For consistency, the values of K_c for these viscometers were also calculated for the conditions that would exist with water, even though water was never run in these viscometers. The values of the viscosites of *n*-heptane and the three mineral oils, as determined in the Cannon viscometers, are given in table 4. Detailed calculations are given in appendix 7.8. In table 4, kinematic viscosities are converted to absolute units for comparison with the measurements made in the Bingham viscometers. The results obtained independently in the two types of viscometers are in good agreement, the largest discrepancy being 1 part in 2,000 in the case of *n*-heptane. As the techniques employed and the nature of the corrections applied are quite different with the two types of instruments, it is not likely that similar errors are involved in both methods. Hence, there is indication that the treatments of the data obtained in both types of viscometers are free of gross error.

TABLE 4. *Results at 20° C with Cannon viscometers compared with Bingham results*

Oil	Viscometer	η/ρ	η/ρ mean	ρ	η	η, by Bingham
		cs	*cs*	*g/cm*^{3}	*cp*	*cp*
n-Heptane	M25–1	0.60070	0.60070	0.6841	0.4109	0.4111
Do	M25–2	.60069				
A	M25–1	2.4641	2.4643	.78110	1.9249	1.9250
A	M25–2	2.4645				
B	M25–1	9.1809	9.1812	.82907	7.612	7.610
B	M25–2	9.1815				
C	M104	49.583	49.584	.8637	42.83	42.82
C	M105	49.585				

4. Discussion of Results

4.1. Sources of Error in Using Bingham Viscometers

From a thorough examination of the various factors involved in the use of the Bingham viscometers, it appears that the greatest source of uncertainty arises from the unavoidable use of relatively low pressures in establishing the portion of the calibration curve corresponding to low Reynolds numbers. The lower pressures are more difficult to maintain relatively steady and measure with a given relative precision, and larger errors are introduced for given uncertainties in the values of the head corrections. This point is illustrated from the data for viscometer number 1 by a comparison of run 1–24, made at a Reynolds number of 8.5, with run 1–38 made at $R=41$ (see appendix 7.1). For run 1–38, with an applied pressure of 73 mm Hg (100 cm H_2O), the level head correction is 0.07 percent, and the logarithmic head correction is 0.01 percent, whereas for run 1–24 with an applied pressure of 15 mm Hg (21 cm H_2O), the level head correction is 0.31 percent, and the logarithmic head correction is 0.24 percent. Thus in the necessary extension of the calibration curve from $R=41$ down to $R=8.5$, the sum of the head corrections is increased from 0.08 percent to 0.55 percent of the applied pressure. For each of the three Bingham viscometers used in this work the value of the level head was determined experimentally, as described previously, the accuracy of the determinations being limited chiefly by the precision with which the pressures could be measured. The experimental evaluation of the logarithmic head corrections with sufficient accuracy, however, was not found feasible, and hence, the corrections were calculated, use being made of an equation given by Barr [4], by which the mean effective pressure for a run is calculated from the known initial and final pressures. This equation was developed on the assumption that each bulb of the viscometer had the shape of two cones placed base-to-base. Although this simple geometry is not exactly realized in any of these viscometers, the correction is not very sensitive to instrument dimensions. Further confidence is lent to the calculations by the fact that good agreement is always found between viscosity measurements made first under conditions where the correction is relatively large and again when the correction is small. This is shown to some extent by the viscosity determinations made on oil A in viscometer 1 (see appendix 7.4). This oil was run first at a pressure of 20 mm Hg, with a logarithmic head correction of 0.08 percent, and then at a pressure of 237 mm Hg, where the correction is negligible. The agreement between these runs is very good, which indicates that the shape of the calibration curve, and the values of the head corrections applied are essentially correct.

It has been shown [12] that the viscosity of water is not significantly affected either by change in the amount of air in solution or by change in pressure under the conditions of these tests. Although the viscosities of the hydrocarbon liquids are more sensitive to these variables, the experimental conditions were chosen such that the variations in the dissolved air under the different test conditions would not be expected to have measurable effects. Furthermore, unpublished experiments at the Bureau have shown that the corrections as applied for the change of viscosity of these hydrocarbon liquids with pressure [2] are probably not in error by more than 30 percent. In the tests recorded in Appendix 7.4, the largest correction occurs with runs 5–17 and

5–18 on oil C, with an applied pressure of 595 mm Hg. As the pressure correction for these runs is 0.08 percent, an error of 30 percent in the correction will amount to only 0.02 percent in the viscosity determination.

4.2. Sources of Error in Using Cannon Viscometers

The first considerations are concerned with the establishment of the calibration curves given in figure 7 for the two viscometers calibrated with water. In the work reported here these viscometers were used at Reynolds numbers in the range 0.03 to 42, and hence only factors affecting this portion of each curve will influence the results. As the determinations in the viscometers were to give results based on a value for the viscosity of water at 20° C, each calibration curve was arbitrarily put through the point at a Reynolds number of about 15, which represents the data obtained at this temperature. At this point, uncertainties in the value of K_c, which is equal to $\eta/\rho t_c$, will depend only on errors in t_c, as the value of η is taken without error and ρ is known with high accuracy. With reference to appendix 7.5, it is seen that for the data at 20° C, t_c is obtained from the observed time of flow t, by applying only a relatively small correction for filling temperature. This correction is readily calculable and is not considered as a source of error. Of the factors affecting t, the effects of errors in temperature measurement, or of temperature variations, are probably small. Both the platinum resistance thermometer and the Mueller G–2 bridge used for measuring temperature were calibrated shortly before or after tests were made, so that no error larger than 0.001 deg C is expected in the measured temperatures. Observed temperature variations during the tests were 0.002 deg C or less, with the mean temperature closer than is indicated by this spread. It is probable that the actual bath temperatures were within 0.002 deg of 20° C, which is equivalent to an uncertainty of only 0.005 percent in the viscosity of water. Calculations [2] of the precision of the mean values of t as recorded in appendix 7.5 indicate an uncertainty in the mean time of flow for viscometer M25–1 of ± 0.03 percent and for viscometer M25–2 an uncertainty of ± 0.007 percent. These limits reflect errors due to variations in filling the viscometers, bath temperature, timing, and unrecognized factors. From the above considerations, the values of K_c at $R=15$ for the two viscometers are probably within ± 0.03 percent of their true values.

Having established one point on each calibration curve, the other important factor is the shape of the curves in the range $R<50$. From theoretical considerations [3], with increasing values of R these curves should be horizontal lines until some value of R is exceeded and a gradually increasingly negative slope begins to develop. No known theory can account for a positive slope at these Reynolds numbers. The values of $\eta/\rho t_c$ for water at 40°, 60°, and 80° C were therefore obtained and plotted to indicate whether the curves could be assumed to have zero slope up to $R=50$. These values of $\eta/\rho t_c$ were computed by using the values of η/ρ given in appendix 7.5 and are believed to be accurate within 0.1 percent. It is seen that zero slope is indicated in the range of Reynolds numbers covered, and unreasonably large errors in the values of $\eta/\rho t_c$ for water at 40°, 60°, and 80° C would be required to change the positions of the calibration curves at $R<50$ by as much as 0.01 percent.

The calculations of the viscosities of n-heptane and oils A and B from the data obtained with these two water-calibrated viscometers are recorded in appendix 7.8. These data show that the times of flow for repeat fillings of a given viscometer with a given oil are in even better agreement than was the case with repeat fillings with water. It is estimated that the mean times of flow for the two fillings with each oil should be within ± 0.01 percent of their true values, based upon 99-percent confidence limits.

In appendix 7.8 the values of t_c are obtained by applying at least three corrections to the observed times of flow. Of these, $\Delta h_1/h$ is calculated without significant error. With reference to section 3.1 it is seen that $\Delta h_3/h$ is dependent upon differences in ρ air/ρ liquid between calibrating and test conditions. The values of $\Delta h_3/h$ were calculated by assuming the air in the viscometers to be 50-percent saturated under all conditions, which was not always the case. No significant error is introduced by this assumption, however, as the difference between the values of $\Delta h_3/h$, assuming dry air and again assuming saturation, affects t_c by only 2 parts in 100,000. The third correction, $\Delta h_4/h$, which is applied to account for the difference in head caused by the difference in surface tension between water and the oils, is perhaps the greatest source of uncertainty. As described previously, the calculated value of the effect of surface tension for water at 20° C was in good agreement with the experimental value, but both calculations and experiments were sufficiently complex as to make it difficult to estimate the accuracy of either. It is believed no error greater than ± 0.02 percent is introduced by this correction, but this can not be said with certainty.

The drainage factors recorded in appendix 7.8 based upon experiments described in section 3.1, are believed to be known to about 0.002 percent and are therefore not significantly in error. No satisfactory explanation has been found for the different behavior of oil A, as compared with n-heptane and the other two oils, in bulbs of similar shape and volume to the fiducial bulbs of viscometers M25–1 and M25–2 (see fig. 6). Oil A did not show this different behavior in a somewhat more elongated bulb similar to the fiducial bulbs of viscometers M104 and M105.

In the calibration of viscometers M104 and M105 with oils A and B and the subsequent determinations of the viscosity of oil C, the sources and magnitudes of error are essentially the same as described above for the oil runs in viscometers M25–1 and M25–2.

[2] The calculations were made by the American Society for Testing Materials' methods [13], assuming that the true value of the mean will lie within the limits given 99 times in 100.

4.3. Heating Effects in Capillaries

So far in the treatment of the data it has been assumed that, once the liquid under test has reached the temperature of the bath in which the viscometer is immersed, it remains at this temperature during the measurement. Because heat is generated in the liquid as it is sheared in the capillary, it is obvious that this assumption cannot be strictly true. As the temperature will vary from point-to-point within the capillary, the viscosity will vary accordingly, and what is measured is a mean value of the viscosity corresponding to some effective mean value of the temperature within the capillary. In attempting to calculate this mean effective temperature, one is unable to postulate what conditions of temperature distribution and heat transfer exist for a given flow condition. Hersey [14] and Hersey and Zimmer [15] have derived equations for calculating the mean effective temperature rise, first assuming conditions of adiabatic flow and then for conditions of thermal equilibrium in the liquid flowing in the capillary. Corrections based on these equations have been calculated for the data in both the Bingham and Cannon viscometers. Referring to appendices 7.4 and 7.8 it is seen that oil C was run in a Bingham viscometer at pressures of 595 mm Hg (runs 5–17 and 5–18) and 303 mm Hg (runs 5–15 and 5–16), and also in Cannon viscometers at 29 mm Hg. If we should assume the conditions defined by Hersey and Zimmer as incomplete adiabatic flow and calculate corrections, using their eq (5) [15], we get a viscosity correction of +0.70 percent for the tests in the Bingham viscometer at 595 mm Hg, and a correction of +0.02 percent for the tests in the Cannon viscometers. On this basis the tests at 595 mm Hg uncorrected, should be about 0.7 percent lower than the runs at 29 mm Hg. As the results recorded in table 4 and appendix 7.4 are in good agreement at all three pressures without these corrections, it must be concluded that conditions of incomplete adiabatic flow are not approximated in these tests. Calculations based on Hersey's eq (13) [13], which assumes flow under the conditions of thermal equilibrium, yield negligibly small corrections, in agreement with the evidence of the tests referred to above.

It should be noted that the effects of heating in the capillary are not only probably negligibly small under the conditions of the tests reported here, but in addition, through the course of calibration and use of a viscometer, the effects tend to be minimized. In the calibration of an instrument, heating effects result in a negative correction to the calibration constant, while in a subsequent determination made in the viscometer the effects result in a positive correction to the time of flow. Thus, even though no corrections are applied, the product of the instrument constant and the time of flow tends to yield a correct result in the viscosity determination. Of course this will only be strictly true when the pressure drop through the capillary is the same for both the calibration and the determination, and when the liquid whose viscosity is being determined and the calibrating liquid have the same heat capacity and temperature coefficient of viscosity. The pertinent physical properties of the liquids involved will usually be sufficiently alike, however, to minimize an accumulation of errors in the usual laboratory practice of calibrating a series of viscometers, graduated as to capillary diameter, by calibrating a larger capillary with an oil whose viscosity has been determined in a smaller one.

4.4. Variability of End Corrections With Reynolds Number

The possible existence of curvature in Pt versus R plots for viscometers of the Bingham type, such as shown in figures 2 and 3, has not been generally recognized. Most observers have confined their calibrations to the higher rates of flow in order to obtain more accurate pressure measurements, and in addition, there has often existed a disregard or inaccurate estimation of the level head and logarithmic head corrections, which may mask the true nature of the calibration curve at the lower Reynolds numbers. The curvature found in the plots for viscometers 1 and 20, however, is not inconsistent with the theory of end corrections and may be explained through a consideration of the nature of the coefficients m and n in eq (1).

The value of m is dependent upon the work done in accelerating the liquid from essential rest to the parabolic distribution of velocities existing after a sufficient entrance length has been traversed. This work is done not against viscous forces, but only imparts kinetic energy to the flowing liquid at the expense of the applied pressure. The value of n arises in part from the excess work done against viscous forces in the entrance length as compared with an equivalent length where the distribution of velocities is parabolic throughout. At sufficiently high Reynolds numbers the kinetic energy of the liquid streaming out of the exit end of the capillary is dissipated as heat [16] in the enlarged part of the viscometer past the capillary. For this condition, the phenomena at the exit end will make a negligible contribution to the values of m and n. At lower Reynolds numbers, however, part or all of the kinetic energy may be expended against viscous resistance close to the exit of the capillary. The value of m for a given Reynolds number will then depend upon the difference between the work done in acceleration at the entrance end and the amount of kinetic energy used in overcoming viscous resistance at the exit end. The magnitude of n will be the sum of the extra work done against viscous resistance at the two ends. It follows then that higher values of m correspond to lower values of n and conversely. Also, when m is constant over a range of Reynolds numbers, n should also be constant. Dorsey [5] has treated this subject at some length and concludes that, for capillaries with square-cut ends, m is zero, and n has a constant value of 1.14 up to a Reynolds number of 10, while at higher Reynolds numbers, $m=1$ and n has a constant value of 0.57. He

recognizes, however, that the values of m and n will be affected by the geometry of the entrance and exit ends of the bore. In the construction of the Bingham viscometers some glass blowing was done at the ends of the capillaries so that they are not precisely square-cut, but evidence slight fire polishing at the edge of the bore. With this geometry it is not surprising that these viscometers show an extended transition region (approximately $R=10$ to 60) between the range where $m=0$ and the range above $R=60$ where m becomes constant.

For Bingham viscometer 1 the constant value of m is 1.12, which is in agreement with values reported by others for capillaries with squarecut ends [3]. The lower value of $m=0.95$ found for Bingham No. 20, may be the result of some peculiarity in the shape of the ends of the capillary bore as a result of glass blowing. With the Cannon viscometers M25–1 and M25–2, it was found that $m=0$ up to at least a Reynolds number of 120, which is as high as the calibration was carried. This condition is undoubtedly associated with the gradual tapers through which the bores of these capillaries expand. It is probable that at sufficiently higher rates of flow these calibration curves would also pass through a transition region and then assume a constant slope corresponding to a value of m which is close to one.

5. Conclusion

In making the measurements reported here, every reasonable precaution was taken so that the results would reflect the accuracy of which each viscometric method was capable. The viscosity values of the four liquids as determined independently by the two methods were in better agreement than was anticipated, and hence it is believed that both methods are relatively free of error. Reviewing the techniques and sources of error critically, however, it is apparent that the necessary steps in calibrating the Bingham viscometers are more complicated and contain more possibilities of uncertainty than are present in calibrating the Cannon viscometers. The experimental difficulties in establishing the calibration curve with water at low Reynolds numbers and the uncertain effects of heating in the capillary are perhaps the weakest points in the method. On the other hand, the relative simplicity of the method with the Cannon viscometers makes this method singularly attractive and inherently more accurate. The greatest difficulty with this method seems to lie in adequately correcting the head for the difference in the surface tensions of water and oil. The procedures described here for evaluating this correction are cumbersome and time consuming to the extent that less accurate estimates of the correction are resorted to in most laboratories. It is possible that a redesign of the shape of the fiducial bulb of the viscometer would simplify the evaluation of this correction. For example, a cylindrical bulb with a conical top and bottom would present simple geometric shapes for which surface tension effects are readily calculable by Barr's method [11]. Any redesign of this nature, however, would have to be accompanied by considerations of the drainage characteristics of the bulb as well.

6. References

[1] J. F. Swindells, J. R. Coe, Jr., and T. B. Godfrey, J. Research NBS **48,** (1952) RP2279.
[2] J. F. Swindells, J. Colloid Sci. **2,** 177 (1947).
[3] G. Barr, A monograph of viscometry, chap. 2 (Humphrey Milford, New York, N. Y., 1931).
[4] G. Barr, J. Chem. Soc., London, 1793 (1935).
[5] N. E. Dorsey, Phys. Rev. **28,** 833 (1926).
[6] 1952 Am. Soc. Testing Materials, Manual of engine test methods for rating fuels, Supp. II, Sec. 217 (a).
[7] M. R. Cannon, Ind. Eng. Chem. **16,** 708 (1944).
[8] M. R. Cannon and M. R. Fenske, Ind. Eng. Chem., An. Ed. **10,** 297 (1938).
[9] S. Sugden, J. Chem. Soc., London, **119,** 1483 (1921).
[10] F. Bashforth and J. C. Adams, Capillary action (University Press, Cambridge, 1883).
[11] G. Barr, Proc. Phys. Soc., London, **58,** 575 (1946).
[12] R. C. Hardy and R. L. Cottington, J. Research NBS **42,** 573 (1949) RP1994 (see p. 575).
[13] Am. Soc. Testing Materials, Manual on presentation of data (1945 printing).
[14] M. D. Hersey, Physics **7,** 403 (1936).
[15] M. D. Hersey and J. C. Zimmer, J. Appl. Phys. **8,** 359 (1937).
[16] S. Erk, J. Rheol. **2,** 205 (1931).

7. Appendices

7.1. Calibration of Bingham Viscometer 1 with Water at 20° C

Run	Direction of flow	Condition of bulb	P_0	Level head	Log head	P	t	Pt Wet bulb	Correction wet to dry	Pt Dry bulb	Pt Dry bulb Mean	P Mean
1	2	3	4	5	6	7	8	9	10	11	12	13
			mm Hg	*mm* Hg	*mm* Hg	*mm* Hg	*sec*					
1–24	R-L	Wet	15.093	+0.047	−0.036	15.104	2456.00	37095.4	+24.0	37119.4	37124	8.5
1–25	R-L	Wet	14.835	+.047	−.036	14.846	2498.71	37095.8	+24.0	37119.8		
1–34	R-L	Wet	15.132	+.047	−.036	15.143	2450.62	37109.7	+24.0	37133.7		
1–31	L-R	Wet	15.225	−.047	−.036	15.142	2448.02	37067.9	+24.0	37091.9	37125	8.5
1–32	L-R	Wet	15.161	−.047	−.036	15.078	2460.65	37101.7	+24.0	37125.7		
1–33	L-R	Wet	15.005	−.047	−.036	14.922	2486.90	37109.5	+24.0	37133.5		
1–35	L-R	Wet	15.244	−.047	−.036	15.161	2448.81	37126.4	+24.0	37150.4		
1–26	R-L	Wet	29.335	+.047	−.018	29.364	1264.24	37123.1	+24.0	37147.1	37143	16.5
1–27	R-L	Wet	29.313	+.047	−.018	29.342	1264.81	37112.1	+24.0	37136.1		
1–42	R-L	Wet	29.142	+.047	−.018	29.171	1272.52	37120.7	+24.0	37144.7		
1–40	R-L	Wet	42.970	+.047	−.013	43.004	862.94	37109.9	+24.0	37133.9	37135	24.2
1–41	R-L	Wet	43.029	+.047	−.013	43.063	861.81	37112.1	+24.0	37136.1		
1–28	R-L	Wet	43.199	+.047	−.013	43.233	859.04	37138.9	+24.0	37162.9	37170	24.6
1–29	R-L	Wet	43.805	+.047	−.013	43.839	847.51	37154.0	+24.0	37178.0		
1–38	R-L	Wet	72.831	+.047	−.007	72.871	509.55	37131.4	+24.0	37155.4	37161	41.4
1–39	R-L	Wet	73.846	+.047	−.007	73.886	502.71	37143.2	+24.0	37167.2		
1–36	R-L	Dry	104.169	+.047	−.005	104.211	356.94			37197.1	37200	58.6
1–37	R-L	Wet	104.169	+.047	−.005	104.211	356.77	37179.4	+24.0	37203.4		
1–15	R-L	Wet	149.480	+.047	−.004	149.523	248.89	37214.8	+24.0	37238.8	37237	84.2
1–16	R-L	Wet	150.074	+.047	−.004	150.117	247.88	37211.0	+24.0	37235.0		
1–1	R-L	Dry	187.703	+.047	−.003	187.747	198.64			37294.1	37296	106.0
1–5	R-L	Dry	187.270	+.047	−.003	187.314	199.08			37290.5		
1–7	R-L	Dry	187.832	+.047	−.003	187.876	198.57			37306.5		
1–9	R-L	Dry	190.737	+.047	−.003	190.781	195.48			37293.9		
1–11	R-L	Dry	190.678	+.047	−.003	190.722	195.51			37288.1		
1–23	R-L	Dry	188.862	+.047	−.003	188.906	197.48			37305.2		
1–2	R-L	Wet	187.480	+.047	−.003	187.524	198.78	37276.0	+24.0	37300.0	37296	106.0
1–6	R-L	Wet	187.039	+.047	−.003	187.083	199.27	37280.0	+24.0	37304.0		
1–8	R-L	Wet	187.655	+.047	−.003	187.699	198.54	37265.8	+24.0	37289.8		
1–10	R-L	Wet	191.037	+.047	−.003	191.081	194.97	37255.1	+24.0	37279.1		
1–12	R-L	Wet	190.810	+.047	−.003	190.854	195.36	37285.2	+24.0	37309.2		
1–17	R-L	Wet	232.251	+.047	−.002	232.296	160.79	37350.9	+24.0	37374.9	37378	130.0
1–18	R-L	Wet	232.011	+.047	−.002	232.056	160.98	37356.4	+24 0	37380.4		
1–19	R-L	Wet	368.515	+.047	−.001	368.561	101.97	37582.2	+24.0	37606.2	37604	205.2
1–20	R-L	Wet	368.476	+.047	−.001	368.522	101.97	37578.2	+24.0	37602.2		
1–21	R-L	Wet	531.552	+.047	−.001	531.598	71.22	37860.4	+24.0	37884.4	37875	293.7
1–22	R-L	Wet	531.285	+.047	−.001	531.331	71.22	37841.4	+24.0	37865.4		

7.2. Calibration of Bingham Viscometer 20 with Water at 20° C

Run	Direction of flow	Condition of bulb	P_0	Level head	Log head	P	t	Pt Wet bulb	Correction wet to dry	Pt Dry bulb	Pt Dry bulb Mean	R Mean
1	2	3	4	5	6	7	8	9	10	11	12	13
			mm Hg	*mm* Hg	*mm* Hg	*mm* Hg	*sec*					
20–26	R-L	Wet	14.914	−0.097	−0.034	14.783	5470.29	80867	+33	80900	80893	5.2
20–27	R-L	Wet	14.229	−.097	−.035	14.097	5735.43	80852	+33	80885		
20–28	L-R	Wet	15.255	+.097	−.033	15.319	5276.28	80827	+33	80860	80893	5.5
20–29	L-R	Wet	15.207	+.097	−.033	15.271	5299.55	80927	+33	80960		
20–30	L-R	Wet	15.189	+.097	−.033	15.253	5299.06	80827	+33	80860		
20–31	R-L	Wet	28.974	−.097	−.017	28.860	2803.05	80896	+33	80929	80916	10.5
20–32	R-L	Wet	29.190	−.097	−.017	29.076	2782 02	80890	+33	80923		
20–51	R-L	Wet	28.910	−.097	−.017	28.796	2808.12	80863	+33	80896		
20–52	R-L	Wet	29.098	−.097	−.017	28.984	2790.56	80882	+33	80915		
20–33	R-L	Wet	43.374	−.097	−.012	43.265	1869.48	80883	+33	80916	80913	15.6
20–34	R-L	Wet	43.191	−.097	−.012	43.082	1877.25	80876	+33	80909		
20–43	R-L	Wet	74.965	−.097	−.007	74.861	1081.15	80936	+33	80969	80966	27.0
20–44	R-L	Wet	74.714	−.097	−.007	74.610	1084.69	80929	+33	80962		
20–37	R-L	Wet	69.628	−.097	−.007	69.524	1163.14	80866	+33	80899	80910	25.2
20–38	R-L	Wet	69.853	−.097	−.007	69.749	1159.70	80887	+33	80920		
20–35	R-L	Wet	87.942	−.097	−.006	87.839	920.63	80867	+33	80900	80910	31.7
20–36	R-L	Wet	87.731	−.097	−.006	87.628	923.06	80886	+33	80919		
20–39	R-L	Wet	105.450	−.097	−.005	105.348	768.21	80929	+33	80962	80963	38.0
20–40	R-L	Wet	105.919	−.097	−.005	105.817	764.80	80929	+33	80962		
20–41	R-L	Dry	105.452	−.097	−.005	105.350	768.40			80950		
20–42	R-L	Wet	105.196	−.097	−.005	105.094	770.22	80946	+33	80979		
20–45	R-L	Wet	140.328	−.097	−.004	140.227	577.66	81004	+33	81037	81027	50.5
20–46	R-L	Wet	140.074	−.097	−.004	139.973	578.56	80983	+33	81016		
20–15	R-L	Wet	159.491	−.097	−.003	159.391	507.81	80940	+33	80973	80961	57.4
20–16	R-L	Wet	158.835	−.097	−.003	158.735	509.75	80915	+33	80948		
20–17	R-L	Wet	244.479	−.097	−.002	244.380	331.89	81107	+33	81140	81115	88.0
20–18	R-L	Wet	244.589	−.097	−.002	244.490	331.68	81092	+33	81125		
20–25	R-L	Wet	244.963	−.097	−.002	244.864	331.05	81062	+33	81095		
20–47	R-L	Wet	244.297	−.097	−.002	244.198	332.05	81086	+33	81119		
20–48	R-L	Wet	243.924	−.097	−.002	243.825	332.53	81079	+33	81112		
20–24	R-L	Dry	245.341	−.097	−.002	245.242	330.68			81097		
20–2	R-L	Wet	400.796	−.097	−.001	400.698	202.94	81317	+34	81351	81363	144.9
20–4	R-L	Wet	410.912	−.097	−.001	410.814	198.05	81362	+34	81396		
20–6	R-L	Wet	406.918	−.097	−.001	406.820	199.97	81352	+34	81386		
20–8	R-L	Wet	404.893	−.097	−.001	404.795	200.89	81319	+34	81353		
20–10	R-L	Wet	404.433	−.097	−.001	404.335	201.12	81320	+34	81354		
20–12	R-L	Wet	403.796	−.097	−.001	403.698	201.36	81288	+34	81322		
20–49	R-L	Wet	403.883	−.097	−.001	403.785	201.43	81334	+34	81368		
20–50	R-L	Wet	403.961	−.097	−.001	403.863	201.40	81338	+34	81372		
20–1	R-L	Dry	400.860	−.097	−.001	400.762	202.97			81343	81362	145.4
20–3	R-L	Dry	410.850	−.097	−.001	410.752	198.18			81403		
20–5	R-L	Dry	407.486	−.097	−.001	407.388	199.76			81380		
20–7	R-L	Dry	404.853	−.097	−.001	404.755	200.94			81331		
20–9	R-L	Dry	404.632	−.097	−.001	404.534	201.13			81364		
20–11	R-L	Dry	404.078	−.097	−.001	403.980	201.38			81353		
20–19	R-L	Wet	595.256	−.097	−.001	595.158	137.12	81608	+34	81642	81642	212.9
20–20	R-L	Wet	595.038	−.097	−.001	594.940	137.17	81608	+34	81642		
20–21	R-L	Wet	994.445	−.097		994.348	82.67	82203	+34	82237	82250	353.2
20–22	R-L	Wet	995.422	−.097		995.325	82.64	82254	+34	82288		
20–23	R-L	Wet	994.676	−.097		994.579	82.64	82192	+34	82226		

7.3. Calibration of Bingham Viscometer 5 with Oils at 20° C

Run	Oil	Direction of flow	Condition of bulb	p_0	Level head	Log head	P	t	Pt	Pt Mean	R	η	$C_3P\eta$	f
1	2	3	4	5	6	7	8	9	10	11	12	13	14	15
				mm Hg	*mm* Hg	*mm* Hg	*mm* Hg	*sec*				*cp*		
5–3	A	R–L	Wet	20.069	−0.045	−0.017	20.007	884.28	17691.8	17690.6	----	------	------	----------
5–6	A	R–L	Wet	20.679	−.045	−.017	20.617	857.90	17687.3		----	------	------	----------
5–9	A	R–L	Wet	19.883	−.045	−.017	19.821	892.62	17692.6					
5–2	A	L–R	Wet	20.029	+.045	−.017	20.057	881.80	17686.3	17691.2	----	------	------	----------
5–5	A	L–R	Wet	20.589	+.045	−.017	20.617	858.30	17695.6					
5–8	A	L–R	Wet	19.973	+.045	−.017	20.001	884.54	17691.7					
5–1	A	R–L	Dry	19.946	−.045	−.017	19.884	889.86	17694.0	17692.1	6.8	1.9250	0.00003	1.0881×10^{-4}
5–4	A	R–L	Dry	20.285	−.045	−.017	20.223	874.32	17681.4					
5–7	A	R–L	Dry	19.996	−.045	−.017	19.904	889.03	17695.3					
5–14	A	R–L	Dry	19.940	−.045	−.017	19.878	890.32	17697.8					
5–10	B	R–L	Dry	296.132	−.048	−.001	296.083	236.36	69982	69946	6.9	7.6097	.00224	1.0883
5–11	B	R–L	Dry	296.112	−.048	−.001	296.063	236.22	69936					
5–12	B	R–L	Dry	296.924	−.048	−.001	296.875	235.63	69953					
5–13	B	R–L	Dry	296.722	−.048	−.001	296.673	235.66	69914					

7.4. Determinations in Bingham Viscometers

Oil	Viscometer	Run	p_0	Level head	Log head	P	t	Pt	Pt Mean	f	fPt	$C_3P\eta$	η	R
1	2	3	4	5	6	7	8	9	10	11	12	13	14	15
			mm Hg	*mm* Hg	*mm* Hg	*mm* Hg	*sec*						*cp*	
n-Heptane	1	1–52	43.133	+0.032	−0.006	43.159	354.51	15300.3	15299.1	2.6878×10^{-5}	0.41121	0.00001	0.41120	98.9
Do	1	1–53	42.992	+.032	−.006	43.018	355.65	15299.4						
Do	1	1–54	43.310	+.032	−.006	43.336	353.00	15297.6						
Do	1	1–55	43.321	+.032	−.006	43.347	352.95	15299.3						
Do	20	20–60	106.122	−.066	−.002	106.054	314.75	33380.5	33386.8	1.2310	.41099	.00002	.41097	154.3
Do	20	20–61	106.025	−.066	−.002	105.957	315.15	33392.3						
Do	20	20–62	106.172	−.066	−.002	106.104	314.67	33387.7						
A	1	1–49	20.002	+.037	−.016	20.023	3562.24	71326.7	71330.8	2.6986	1.9249	.00003	1.9249	2.4
A	1	1–50	20.010	+.037	−.016	20.031	3561.22	71334.8						
A	1	1–43	237.532	+.037	−.001	237.568	300.45	71377.3	71380.2	2.6973	1.9253	.0003	1.9250	28.2
A	1	1–44	237.133	+.037	−.001	237.169	300.97	71380.8						
A	1	1–45	237.415	+.037	−.001	237.451	300.62	71382.5						
A	20	20–53	237.405	−.076	−.001	237.328	655.16	155488	155478	1.2384	1.9254	.0003	1.9251	18.1
A	20	20–54	237.704	−.076	−.001	237.627	654.30	155479						
A	20	20–55	237.460	−.076	−.001	237.383	654.92	155467						
B	1	1–46	296.634	+.039	−.001	296.672	950.80	282076	282046	2.6986	7.6113	.0022	7.6091	2.4
B	1	1–47	296.674	+.039	−.001	296.712	950.45	282010						
B	1	1–48	296.394	+.039	−.001	296.432	951.49	282052						
B	20	20–56	296.751	−.081	−.001	296.669	2071.92	614674	614654	1.2385	7.6125	.0022	7.6103	1.5
B	20	20–57	296.679	−.081	−.001	296.597	2072.19	614605						
B	20	20–58	296.650	−.081	−.001	296.568	2072.65	614682						
C	5	5–15	302.259	−.050	−.001	302.208	1302.81	393720	393716	10.882	42.844	.017	42.827	0.2
C	5	5–16	303.062	−.050	−.001	303.011	1299.33	393711						
C	5	5–17	595.110	−.050	−.001	595.059	661.92	393881	393830	10.882	42.857	.034	42.823	.5
C	5	5–18	595.070	−.050	−.001	595.019	661.79	393778						

7.5. Calibration of Viscometers M25–1 and M25–2 with Water

Viscometer	Filling	Temperature	t	t, mean	t, adjusted for mean[a]	$\Delta h_1/h$	$\Delta h_2/h$	$\Delta h_3/h$	$\Delta h_4/h$	$(1+\Delta h/h)$	t_c	$\eta/(\rho t_c)$	R
		° C	sec	sec	sec						sec		
M25–1	1	20	736.33	736.46	736.46	+0.00002	0.00000	0.00000	0.00000	1.00002	736.47	1.36299×10^{-3}	15
M25–1	2	20	736.53										
M25–1	3	20	736.58										
M25–1	4	20	736.42										
M25–1	1	40	482.72	482.72	482.81	+.00002	−.00012	+.00008	+.0001	1.00008	482.85	1.3632	34
M25–1	2	60	348.17	348.17	348.14	+.00002	−.00031	+.00016	+.0002	1.00007	348.16	1.3629	66
M25–1	3	80	267.90	267.90	267.85	+.00002	−.00056	+.00026	+.0003	1.00002	267.86	1.3630	111
M25–2	1	20	674.95	674.96	674.96	+.00002	.00000	.00000	.00000	1.00002	674.97	1.48718	16
M25–2	2	20	674.95										
M25–2	3	20	674.97										
M25–2	1	40	442.43	442.43	442.44	+.00002	−.00012	+.00008	+.0001	1.00008	442.48	1.4875	37
M25–2	2	60	319.07	319.07	319.07	+.00002	−.00031	+.00016	+.0002	1.00007	319.09	1.4870	71
M25–2	3	80	245.44	245.44	245.44	+.00002	−.00056	+.00026	+.0003	1.00002	245.44	1.4875	120

[a] The observed differences in the times of flow at 20° C for the different fillings are assumed to be largely due to differences in the volume of liquid charged into the viscometers. Since the data at 40°, 60°, and 80° C were obtained with different single fillings, the observed times of flow at these temperatures were adjusted to correspond to a hypothetical filling represented by the mean of the observed times at 20° C.

7.6. Properties of Water

Temperature	γ[a]	η[b]	ρ[c]	η/ρ
° C	Dynes/cm	cp	g/cm³	cs
20	72.7	1.0020	0.99821	1.0038
40	69.6	0.6531	.99222	0.6582
60	66.2	.4665	.98321	.4745
80	62.6	.3548	.97180	.3651

[a] International Critical Tables.
[b] Hardy and Cottington [12], based on $\eta_{20}=1.005$ cp and converting to $\eta_{20}=1.002$ cp.
[c] N. E. Dorsey, Properties of ordinary water substance, table 93, in grams per milliliter and converting to grams per cubic centimeter, using 1 ml = 1.000027 cm³.

7.7. Calibration of Viscometers M104 and M105 with Oils

Viscometer	Oil	Filling	t	t, mean	$\Delta h_1/h$	$\Delta h_3/h$	$\Delta h_4/h$	$(1+\Delta h/h)$	t_c	η/ρ	K_c	Kc, mean
			sec	sec					sec	cs		
M104	A	1	298.08	298.08	+0.00009	−0.00034	+0.00144	1.00119	298.44	2.4642	8.2572×10^{-3}	8.2569×10^{-3}
M104	A	2	298.09									
M104	B	1	1110.54	1110.57	+.00009	−.00025	+.00142	1.00126	1111.97	9.1811	8.2566	
M104	B	2	1110.60									
M105	A	1	291.30	291.28	+.00009	−.00034	+.00144	1.00119	291.63	2.4642	8.4499	8.4496
M105	A	2	291.25									
M105	B	1	1085.11	1085.26	+.00009	−.00025	+.00142	1.00126	1086.63	9.1811	8.4492	
M105	B	2	1085.40									

7.8. Results Obtained with Cannon Viscometers

Oil	Viscometer	Filling	t	t, mean	$\Delta h_1/h$	$\Delta h_3/h$	$\Delta h_4/h$	$(1+\Delta h/h)$	Drainage factor	t_c	K_c	η/ρ	R
			sec	*sec*						*sec*		*cs*	
n-Heptane	M25–1	1	440.36	440.37	+0.00009	−0.00055	+0.00126	1.00080	1.00000	440.72	1.36299×10^{-3}	0.60070	42.0
Do	M25–1	2	440.38										
Do	M25–2	1	403.60	403.59	+.00009	−.00055	+.00126	1.00080	1.00000	403.91	1.48718	.60069	45.0
Do	M25–2	2	403.58										
A	M25–1	1	1806.05	1805.92	+.00008	−.00034	+.00144	1.00118	0.99990	1807.87	1.36299	2.4641	2.5
A	M25–1	2	1805.80										
A	M25–2	1	1655.44	1655.36	+.00008	−.00034	+.00144	1.00118	.99990	1657.15	1.48718	2.4645	2.6
A	M25–2	2	1655.28										
B	M25–1	1	6727.52	6727.41	+.00008	−.00025	+.00142	1.00125	1.00000	6735.82	1.36299	9.1809	0.2
B	M25–1	2	6727.30										
B	M25–2	1	6165.99	6166.06	+.00008	−.00025	+.00142	1.00125	1.00000	6173.77	1.48718	9.1815	.2
B	M25–2	2	6166.12										
C	M104	1	5997.22	5997.43	+.00007	−.00019	+.00139	1.00127	1.00000	6005.05	8.2569	49.583	.03
C	M104	2	5997.64										
C	M105	1	5860.62	5860.89	+.00007	−.00019	+.00139	1.00127	1.00000	5868.33	8.4496	49.585	.03
C	M105	2	5861.16										

WASHINGTON, September 16, 1953.

574278 O - 61 - 37

Selected Papers on

Mechanics

(Contents on page VI)

U. S. DEPARTMENT OF COMMERCE
HENRY A. WALLACE, Secretary
NATIONAL BUREAU OF STANDARDS
E. U. CONDON, Director

Circular of the National Bureau of Standards C454

PROVING RINGS FOR CALIBRATING TESTING MACHINES

By
BRUCE L. WILSON, DOUGLAS R. TATE,
and GEORGE BORKOWSKI

[Issued August 14, 1946]

UNITED STATES
GOVERNMENT PRINTING OFFICE
WASHINGTON : 1946

For sale by the Superintendent of Documents, U. S. Government Printing Office
Washington 25, D. C. - Price 15 cents

573/I

PREFACE

The trend in present-day engineering design is toward the use of efficient, lightweight structural elements and machine parts. Such elements have of necessity been utilized by aircraft and ordnance engineers, and their application is now being given increased attention by engineers in all fields. In the development of efficient designs it is necessary that materials be tested before being used as structural elements and machine parts to insure that they will have the required mechanical properties. Structures and subassemblies must also be tested to verify the soundness of design and point the way to still more efficient designs. This testing requires the use of accurate load-indicating testing machines. To insure the reliability of the test results obtained with load-indicating testing machines, frequent periodic calibration is recognized as being essential. A study of methods of calibrating testing machines, initiated at the Bureau some 25 years ago, showed the equipment then available to be inadequate and led to the development of the proving ring by H. L. Whittemore and S. N. Petrenko. The proving ring, because of its accuracy, constancy, and convenience, is now the most widely used device for the calibration of testing machines. Several hundred of these devices are now in service in commercial and government laboratories in this country and abroad. This Circular summarizes the Bureau's experience in the calibration and use of proving rings and makes recommendations for their proper use.

E. U. CONDON, *Director.*

PROVING RINGS FOR CALIBRATING TESTING MACHINES

By Bruce L. Wilson, Douglas R. Tate, and George Borkowski

ABSTRACT

A description is given of the proving ring, which was developed at the National Bureau of Standards to provide an accurate portable load-measuring device for calibrating testing machines. Methods are described for calibrating proving rings by dead weights for loads up to 111,000 lb and by means of other calibrated proving rings for higher loads. Rings which complied with the specification included in the paper were subjected to tests to determine the errors introduced by variations of the conditions of use. Provided reasonable care is exercised in using proving rings, the errors are shown to be small compared to ±1 percent, the generally recognized tolerance for testing machines.

CONTENTS

I. INTRODUCTION

Experience at the National Bureau of Standards and in other laboratories in using testing machines that apply forces to engineering materials and structures has indicated the advisability of frequent periodic calibration of such machines, if reliable test results are to be obtained. To insure the accuracy of the results obtained with a machine, it is necessary that the calibration include loads up to the capacity load of the machine. Some types of low-capacity machines may be calibrated to capacity by means of standard weights or by means of standard weights and proving

levers. Because these methods of calibration were not adequate for calibrating all types of small machines, and particularly, because they were inadequate for calibrating large testing machines, experiments were undertaken more than 20 years ago with portable elastic devices which could be calibrated under accurately known forces and then transported to the testing machine and used to measure the forces applied by the testing machine. These experiments led to the development of the proving ring [1, 2, 3][1] by H. L. Whittemore and S. N. Petrenko. The development and commercial production of the proving ring led to a greatly increased use of elastic calibration devices and made it necessary to provide facilities for the calibration of these devices. For calibrating devices up to 111,000 lb two dead-weight testing machines [4] have been installed at the Bureau. Methods of calibrating elastic devices for loads up to 300,000 lb by means of several 100,000-lb-capacity rings have been developed. The purpose of this paper is to describe the proving ring, its calibration, and performance under various conditions of use.

II. DESCRIPTION OF PROVING RINGS

1. DEFINITION

A proving ring is an elastic ring, suitable for calibrating a testing machine, in which the deflection of the ring when loaded along a diameter is measured by means of a micrometer screw and a vibrating reed mounted diametrically in the ring.

2. DESIGN

(a) SHAPE

A compression proving ring is shown in figure 1. Forces are applied to

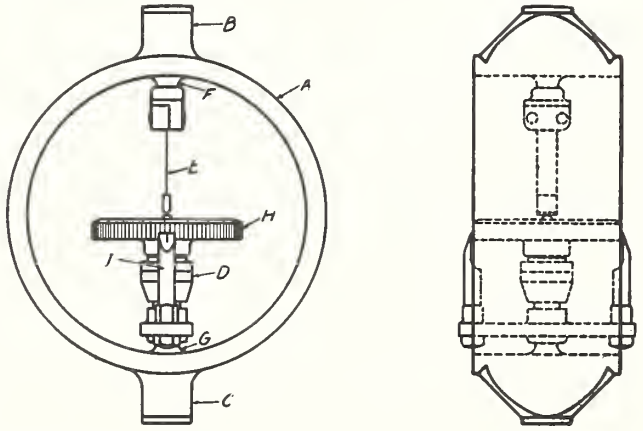

FIGURE 1.—*Proving ring for measuring compressive forces.*

the ring, *A*, through the integral external bosses, *B* and *C*. The resulting deflection of the ring is measured with a micrometer screw, *D*, and a vibrating reed, *E*, which are attached to integral internal bosses, *F* and *G*. By means of a graduated dial, *H*, and an index pointer, *I*, the deflection of the ring may be measured in divisions of the micrometer dial. A proving ring for measuring both tensile and compressive forces is shown in figure 2 with the tension fittings attached.

[1] Figures in brackets indicate the references given at the end of this paper.

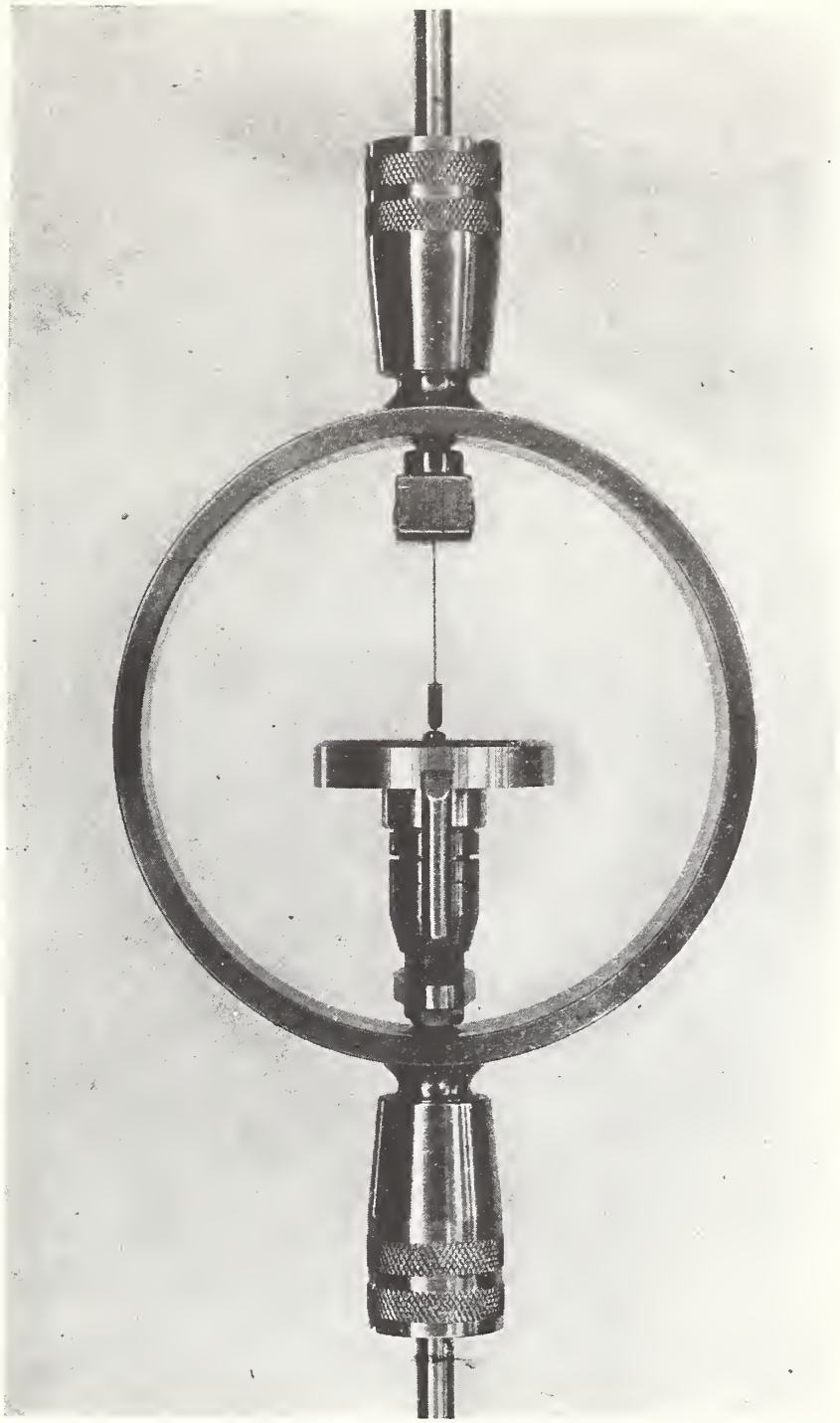

FIGURE 2.—*Proving ring for measuring both tensile and compressive forces, with tension fittings attached.*

The end of the lower external boss of a compression proving ring usually is plane and perpendicular to the axis of the bosses. The end of the upper external boss is usually convex. It is frequently made a portion of a sphere having as center the center of the end of the lower external boss and a radius equal to the over-all height of the ring. The external bosses of rings for measuring tensile forces are provided with tension fittings for applying forces to the ring. The fittings usually include spherical bearings to minimize eccentric loading of the ring.

(b) CAPACITIES

Compression rings having capacities from 300 lb to 300,000 lb, and tension rings having capacities as great as 100,000 lb have been submitted for calibration. The over-all heights of compression rings vary from about 6 in. for 2,000-lb rings to 19 in. for 300,000-lb rings. The weights of compression rings vary from about 2 lb for 2,000-lb rings to 150 lb for 300,000-lb rings.

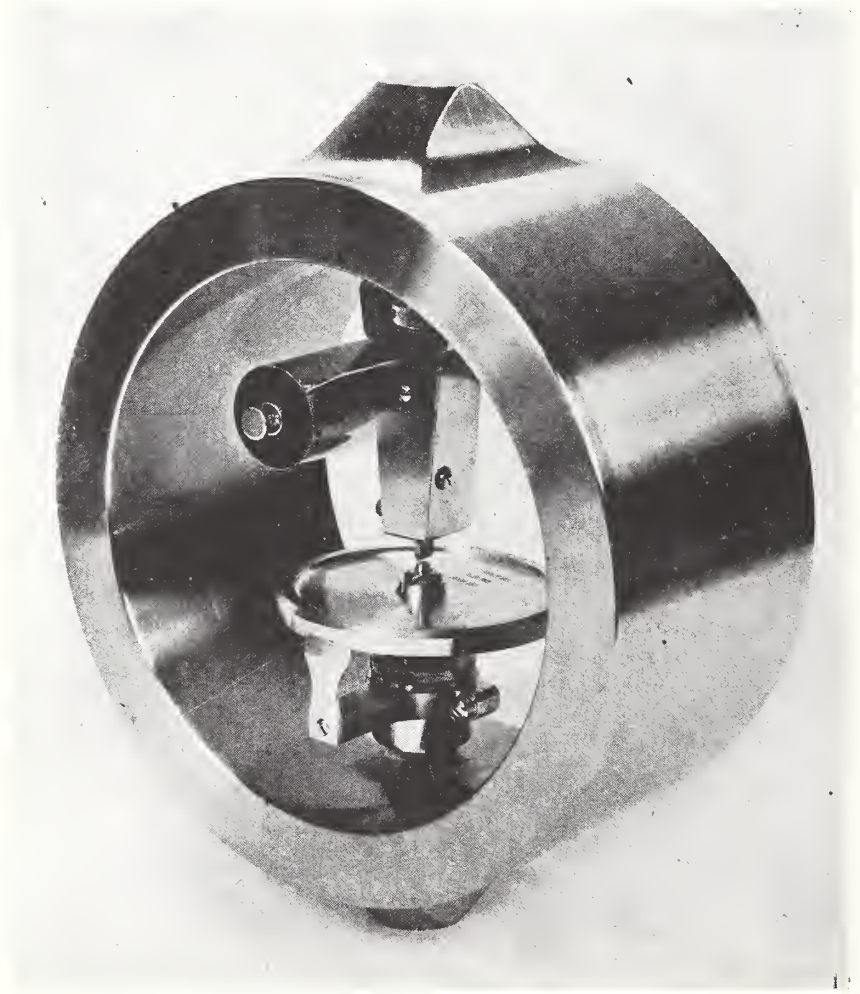

FIGURE 3.—*Proving ring equipped with electrically operated vibrating reed.*

The weights and heights of tension rings without tension fittings are a little greater than for compression rings of corresponding capacities.

(c) DEFLECTION-MEASURING APPARATUS

The vibrating reed and micrometer screw provide a sensitive and reliable means for measuring the change in diameter of the ring under load. When the reed is vibrating and the micrometer screw is adjusted so that the button on the spindle contacts the vibrating reed, a sensitive indication is produced, which varies rapidly as the button is advanced. Experience indicates that with micrometer screws having pitches varying from 40 to 64 threads per inch, as commonly supplied on most proving rings, readings may be made with a sensitivity of about one or two hundred thousandths of an inch.

Two types of vibrating reeds are used on proving rings; one type is operated manually and the other is driven electrically [5]. Figures 2 and 3 show proving rings having the two types of vibrating reeds. When reading a ring equipped with a manually operated vibrating reed, the lower end of the reed is pushed aside about ½ inch with the end of a pencil or other suitable object and released. Use of the finger is not recommended because changes in length of the reed with temperature change the reading of the ring. While the reed is vibrating, the dial is rotated, advancing the button into the path of the reed until a characteristic buzzing sound is produced, and the time required to reduce the amplitude from about ½ in. to zero amplitude is 2 or 3 seconds. Either or both of these effects may be used by the operator in setting the dial. With no contact between the reed and button, the vibration will continue from 10 to 15 seconds. An operator usually has no difficulty in obtaining reproducible readings to about ± 0.1 dial division at zero load. Different operators will obtain zero-load readings that differ by more than this amount, as will a single operator if he uses different sound intensities and different lengths of time for stopping the motion of the reed. As deflections of the ring are the differences between zero-load readings and load readings, it is important that the operator adjust the dial in the same way in making each reading. Different operators will obtain comparable deflections even though their methods of adjusting the dial differ.

With the electrically driven reed the best results are obtained by turning the dial to advance the button just far enough to interfere with the vibration of the reed. This condition can be detected better by watching the change in amplitude of the reed than by listening for the change in intensity or frequency of the sound. Readings taken by advancing the button until a large change in amplitude is produced or until the motion is nearly stopped have been found much less reliable than readings taken in the manner described above.

Experience indicates that the combination of a well-made micrometer screw and vibrating reed is about equal in sensitivity and superior in ruggedness and accuracy to dial micrometers for measuring the deflections of elastic devices. The best dial micrometers commercially available have errors several times the errors of well-made micrometer screws. For this reason, the American Society for Testing Materials [6] permits the use of devices having dial micrometers only at the test loads for which they have been calibrated.

(d) DEFLECTION

Proving rings are usually designed to have a deflection of 0.05 to 0.10 in. under capacity load. The dimensions of a ring that will have approximately a desired deflection may be computed by means of equations given in engineering textbooks. Equations for computing the deflection of plain rings loaded at opposite ends of a diameter have been published by Timoshenko, Bach and Baumann, and Larard [7, 8, 9, 10]. For a plain ring having a rectangular cross section, the equation given by Timoshenko reduces to the following:

$$d = \frac{Pr^2}{eElt}\left\{\frac{\pi}{4} - \frac{2}{\pi}\left(1 - \frac{e^2}{r^2}\right) + \frac{2e}{r}\left[\frac{2}{\pi}\left(1 - \frac{e}{r}\right) + 0.265\pi\right]\right\},$$

where

d = deflection of the ring in the direction of the loaded diameter, in.

P = applied load, lb

r = radius of the centerline of the ring, in.

E = Young's modulus of elasticity for the material of the ring, lb/in.^{2}

l = width of the cross section of the ring, in.

t = thickness of the cross section of the ring, in.

$$e = r - \frac{t}{\log_n \dfrac{1 + \frac{1}{2}\frac{t}{r}}{1 - \frac{1}{2}\frac{t}{r}}}.$$

Actually, the measured deflections of proving rings are about 25 percent less than the deflections computed by means of equations derived for plain rings because of the stiffening effect of the integral bosses. As the relationship between the deflection of a proving ring and the applied load is determined by applying accurately known forces to the ring, the derivation of an equation which would take into account the stiffening effect of the bosses is unnecessary.

(e) STRESS

To obtain satisfactory elastic behavior of a ring, the maximum stress must be less than the stress required to produce an appreciable permanent set in the material. Equations for computing the maximum bending moment in a plain ring loaded at opposite ends of a diameter are given by Timoshenko, Bach and Baumann, and Larard [7, 8, 9, 10]. The following equation derived from Timoshenko's results gives the maximum stress for a ring having a rectangular cross section:

$$\sigma_{max} = \frac{Pr}{elt\pi}\left(1 - \frac{e}{r}\right)\frac{\left(\frac{t}{2} - e\right)}{\left(r - \frac{t}{2}\right)},$$

where

σ_{max} = maximum fiber stress across the inner cylindrical elements passing through the load line, lb/in.^{2}

P = applied load, lb

r = radius of the centerline of the ring, in.

l = width of the cross section of the ring, in.
t = thickness of the cross section of the ring, in.

$$e = r - \frac{t}{\log_n \frac{1 + \frac{1}{2}\frac{t}{r}}{1 - \frac{1}{2}\frac{t}{r}}}.$$

This equation for plain rings does not apply accurately to proving rings having integral bosses (fig. 1) because the bosses influence the stress distribution in the plane containing the maximum bending moment. Experience has demonstrated that stress values calculated by the above equation are satisfactory for design purposes, provided there are adequate fillets where the bosses join the ring and no "stress raisers" are present. Breakage of some rings through holes and stamped numbers has indicated the desirability of avoiding holes, stamped numbers, tool marks, cracks, etc.

Except for rings having deflection-measuring apparatus attached by means of plugs or screws, computed working stresses as high as 150,000 to 165,000 lb/in.^{2} have been found satisfactory.

(f) MATERIAL AND FINISH

Proving rings are usually made of alloy steel, rough-machined from annealed forgings, heat treated, and then ground to size. Probably rings unpolished after heat treatment or finished by some other method would be satisfactory. One chromium-plated ring has given satisfactory service for several years at the Bureau.

Satisfactory proving rings designed along the lines indicated in the preceding sections have been made from a steel having the following chemical composition: Carbon, 0.50 percent; chromium, 1.00 percent; and nickel, 1.75 percent. This steel is heat treated to give about the following properties in tensile tests:

Yield strength (offset=0.05 percent)	210,000 lb/in.^{2}
Tensile strength	230,000 lb/in.^{2}
Elongation in 2 inches	8 percent.

III. CALIBRATION

1. GENERAL

All proving rings submitted for calibration at the National Bureau of Standards are calibrated for compliance with the performance specification given in the appendix, section VIII. This specification does not give detailed requirements for the design of proving rings, but it does include performance requirements that have been found necessary to insure that rings will maintain their calibrations satisfactorily with ordinary use and with the handling to which rings shipped by commercial carriers are subjected.

Proving rings are calibrated by determining the relationship between accurately known forces and the corresponding deflections.

2. LOADS NOT EXCEEDING 111,000 LB

Two dead-weight testing machines [4] have been installed at the National Bureau of Standards for calibrating elastic calibration devices.

With the larger machine, compressive and tensile loads from 2,000 lb to 111,000 lb by 1,000-lb increments may be applied. With the smaller machine, loads from 200 lb to 10,100 lb by 100-lb increments may be applied. The errors of the weights do not exceed about 0.01 percent.

3. LOADS EXCEEDING 111,000 LB

Calibration loads exceeding 111,000 lb are applied to large proving rings by means of three calibrated 100,000-lb-capacity proving rings as shown in figure 4. The three nearly identical calibrated rings are placed

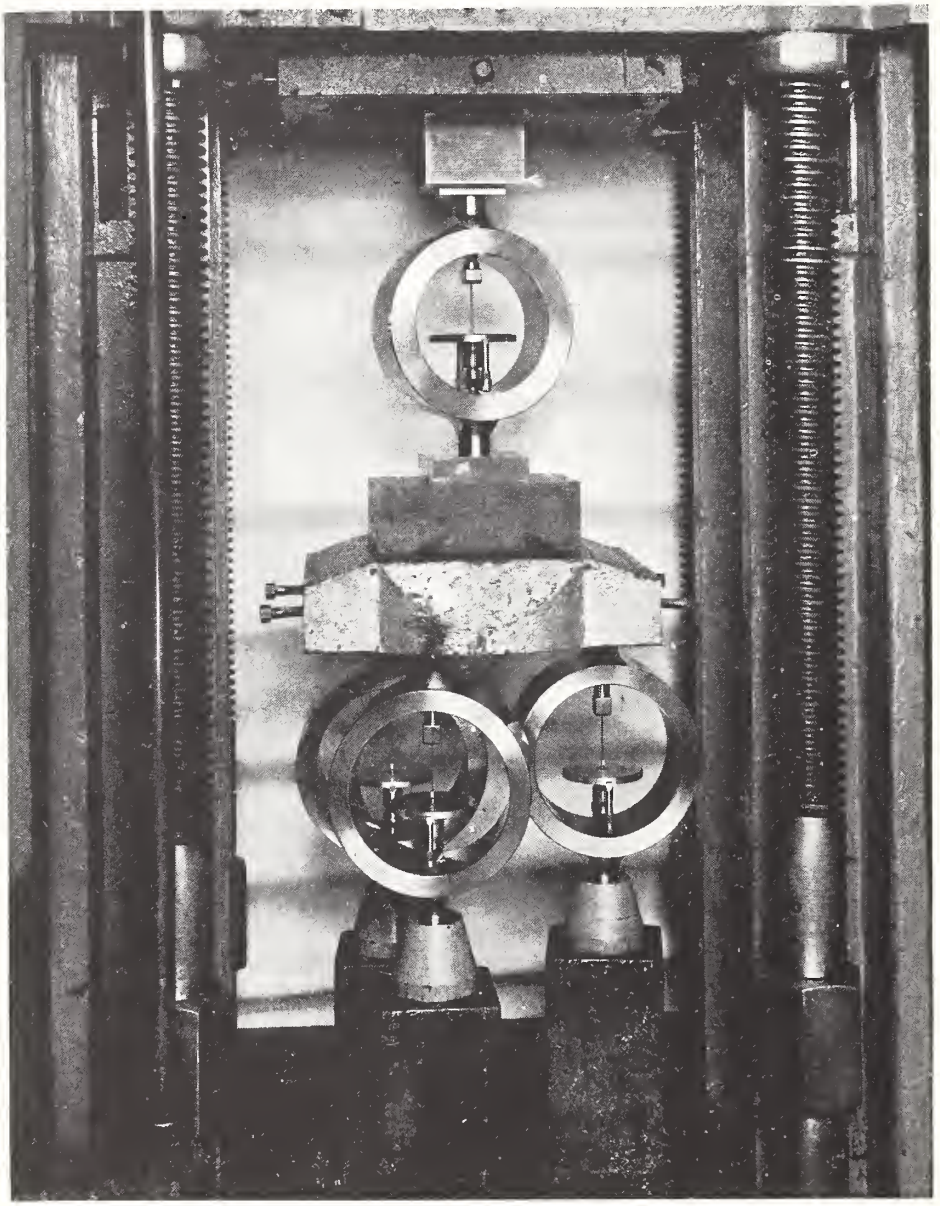

FIGURE 4.—*Calibration of a proving ring for loads exceeding 111,000 lb by means of three calibrated 100,000-lb-capacity proving rings.*

in a vertical testing machine at the corners of a triangle so oriented that the centroid of the triangle lies on the axis of the machine. A thick steel plate is placed over the upper bosses of the three rings. The ring to be calibrated is placed on a hardened block on the plate above the three rings and so located that when forces are applied to the rings by means of the testing machine, the deflections of the three lower rings are equalized to within about 1 percent.

During the calibration the load indicated by the testing machine is disregarded. The four proving rings are read simultaneously while the load is held constant or increased very slowly. The force applied to the ring being calibrated is the sum of the forces measured by the three previously calibrated rings.

This method of calibration has been used for loads up to 300,000 lb, the capacity load of the largest compression ring submitted for calibration. The errors of measuring the load applied to the ring being calibrated do not exceed 0.1 percent. Calibration factors (see below) computed from results obtained in the dead-weight machine and from results obtained on the same rings by the method described fit smooth curves about equally well. The relatively smaller observational error in determining the deflection of the ring for the higher loads compensates for the greater errors of the loads measured with the three rings so that the departure of individual calibration factors is little greater for a given ring for loads exceeding 111,000 lb than for loads applied by dead weights.

4. LOADING PROCEDURE

Proving rings are calibrated by increasing the loads to the test loads. Compressive loads, except those on concave and convex bearing blocks [appendix, paragraph II-5(d)], are applied to the lower boss of a ring through a plane, hardened steel bearing block and to the upper boss either through a ball or a soft-steel block. Tensile loads are applied to a ring through pulling rods provided with the ring. The tension fittings usually include two or more spherical bearings so that the ring will not be loaded eccentrically.

Proving rings are usually calibrated for 10 approximately equally spaced loads from 10-percent-capacity load to capacity load. A preliminary preload to capacity is desirable to stabilize the no-load reading of the ring. Before and after each load reading, a no-load reading of the ring is observed. The deflection of the ring is computed as the difference between the load reading and the average of the no-load readings observed immediately before and after the application of the load. For each deflection the calibration factor, which is the ratio of the load to the corresponding deflection, is computed.

5. CALIBRATION GRAPH

The calibration factors are plotted on the calibration graph as a function of the deflection, as shown in figure 5. Well-made rings in good condition exhibit a nearly linear relationship between the calibration factors and the deflection. The calibration factor for compression rings decreases with increasing ring deflection, as shown in figure 5. The calibration factor for tension rings increases with increasing ring deflection.

In using the ring the load is computed from the ring readings by multiplying the ring deflection by the calibration factor read from the calibration graph.

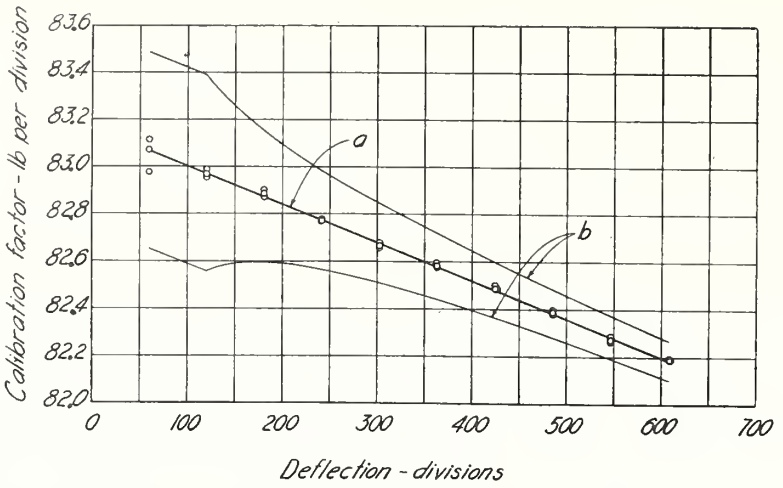

FIGURE 5.—*Calibration graph for 50,000-lb-capacity compression proving ring.*
Line "a" represents the calibration line for 70° F; line "b" represents the specification limits.

6. TEMPERATURE COEFFICIENT

Because the dimensions and the elastic properties of a ring change with temperature, the deflection of a ring for a given load varies with the temperature. The variation is not large for small temperature changes; usually it is less than 0.02 percent per degree Fahrenheit. Calibration results for proving rings are given for a temperature of 70° F. When the rings are used to calibrate testing machines and the ring temperature is different from 70° F, the results may be corrected for temperature by the formula

$$d_{70} = d_t \, [1 + K \, (t - 70)],$$

where

d_{70} = deflection of ring at a temperature of 70° F
d_t = deflection of ring at a temperature of t degrees Fahrenheit
K = temperature coefficient of the ring
t = temperature, degrees Fahrenheit, during test.

The temperature coefficient, K, depends primarily upon the temperature coefficient of Young's modulus for the material of the ring. The temperature coefficient of Young's modulus for steels depends upon the chemical composition of the steel and its heat treatment. For rings made of steels having a total alloying content not exceeding 5 percent, the value $K = -0.00015$ per degree Fahrenheit has been found sufficiently accurate. For some other steels, values of the temperature coefficient of Young's modulus of elasticity, that would result in values of K ranging from -0.00011 to -0.00024 have been observed. Most of the proving rings submitted for calibration are made of steel having a total alloying content not exceeding 5 percent.

Calibrations of proving rings in the dead-weight machines at the National Bureau of Standards are made at 70° F whereas calibrations at loads beyond the capacity of these machines are made at room temperature usually in the range 65° to 90° F, and then corrected to 70° F.

IV. USE

1. CALIBRATION OF TESTING MACHINES

Proving rings are used primarily for calibrating testing machines, the purpose for which they were developed. In figure 6, a 100,000-lb-capacity compression proving ring is shown in a vertical hydraulic testing ma-

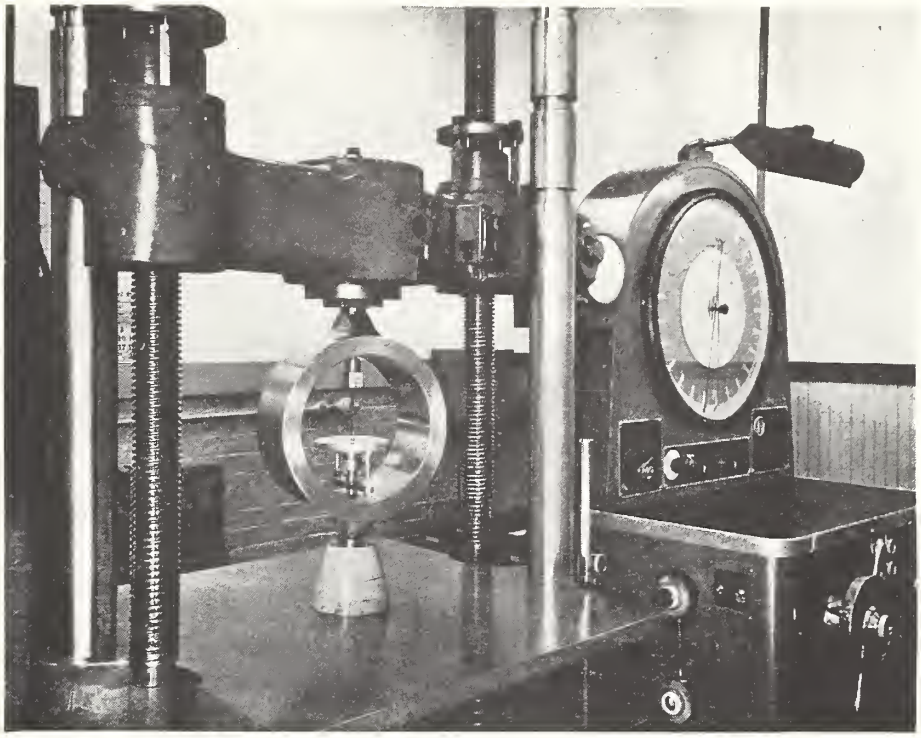

FIGURE 6.—*Proving ring in testing machine ready for the calibration of the testing machine in compression.*

chine. The ring, together with bearing blocks through which the loads are applied to the external bosses, takes the place of the specimen in the machine. When rings are used for calibrating horizontal testing machines, the no-load ring readings are taken with the rings supported by their external bosses.

In carrying out a calibration, two operators are required to read the indicated load of the testing machine and the ring simultaneously. The temperature of the air near the ring is recorded so that the proper temperature corrections may be applied.

A sample data sheet for the partial calibration of one scale range of a testing machine is given in table 1.

The results in the first three columns of table 1 were observed during the calibration. The results in the fourth column were obtained by subtracting from each load reading the average of the no-load readings taken before and after the load reading. The ring load was computed by multiplying the ring deflection for 70° F by the corresponding calibration factor. The error in pounds was computed by subtracting the ring load from the machine reading.

574278 O - 61 - 38

TABLE 1.—*Data sheet for the partial calibration of 200,000-lb scale range of hydraulic testing machine with a 100,000-lb-capacity proving ring*

Machine reading	Temperature	Ring reading	Ring deflection	Ring[a] deflection for 70° F	Calibration[b] factor	Ring load	Error of testing machine	Percentage error of testing machine
lb	° *F*	*div.*	*div.*	*div.*	*lb/div.*	*lb*	*lb*	
0	79	32.1						
60,000		442.7	410.6	410.05	145.85	59,806	+194	+0.32
0		32.1						
80,000		581.2	549.05	548.31	145.58	79,823	+177	+ .22
0		32.2						
100,000		719.6	687.4	686.47	145.31	99,751	+249	+ .25
0		32.2						
60,000		442.8	410.6	410.05	145.85	59,806	+194	+ .32
0		32.2						
80,000		580.8	548.6	547.86	145.58	79,757	+243	+ .30
0		32.2						
100,000		719.4	687.4	686.47	145.31	99,751	+249	+ .25
0	79	31.8						

[a] Ring deflection for 70° F = Ring deflection for 79° F $(1 - 9 \times 0.00015)$
[b] Read from the calibration curve or calculated from the equation:
Calibration factor = 146.66 − 0.00197 × deflection for 70° F.

To obtain information concerning the reproducibility of the readings of a testing machine the errors are frequently determined for two or more

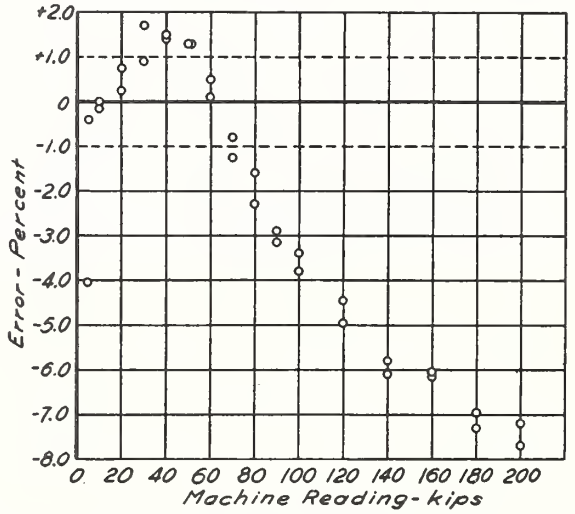

FIGURE 7.—*Calibration results obtained on a 200,000-lb-capacity testing machine in need of repairs.*

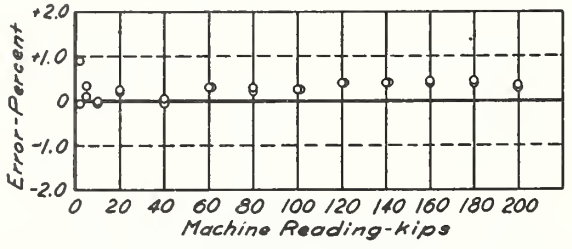

FIGURE 8.—*Calibration results obtained on a 200,000-lb-capacity testing machine in good condition.*

applications of the same indicated testing-machine loads. The results of complete calibrations of two testing machines are given in figures 7 and 8 to illustrate results for machines in unsatisfactory and satisfactory conditions. The American Society for Testing Materials [6] tolerance lines of ± 1 percent are shown by the dashed lines. The machine found to be unsatisfactory (fig. 7) had been in regular use prior to its calibration.

Several rings may be used together, as shown in figure 9, to calibrate machines having capacities exceeding the capacity of a single ring. The

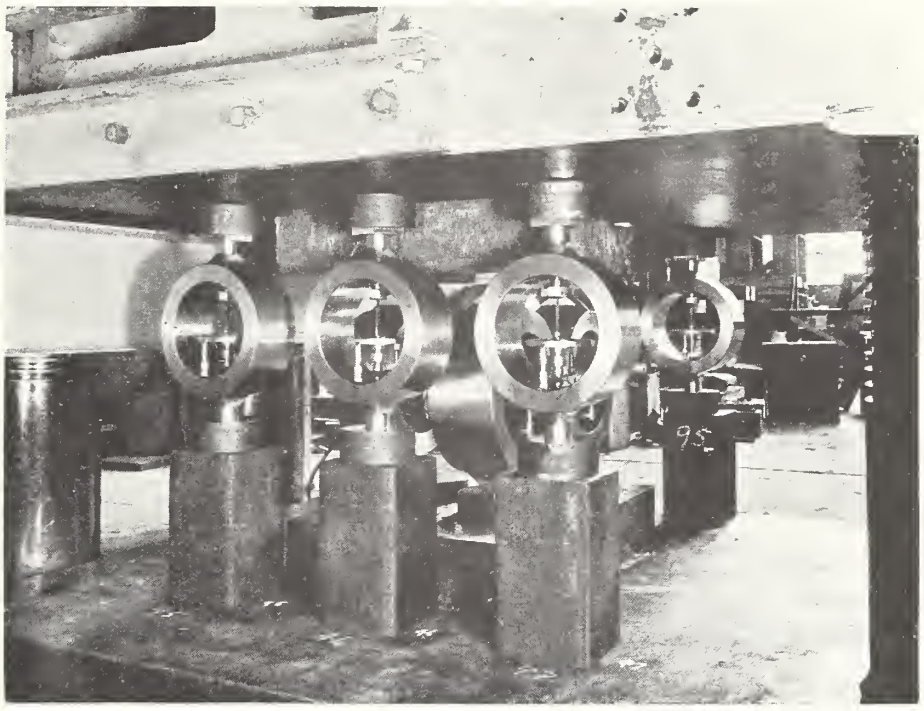

FIGURE 9.—*Eight compression proving rings arranged to be loaded in parallel to obtain test loads equal to the sum of the forces applied to the individual rings.*

indicated load of the testing machine and the rings are read simultaneously, and the ring load is computed as the sum of the loads carried by the individual rings. By this method, calibrations have been made with proving rings for loads up to about 2 million pounds.

2. OTHER USES

Proving rings have also been used as dynamometers, for weighing elevator cars, and for weighing bridge reactions [11].

V. ERRORS

1. ERRORS DUE TO VARIATIONS IN LOADING SCHEDULE

During calibration proving rings are read within a few seconds after the load is applied or removed and a no-load reading is observed before and after each load reading. It is not always possible to follow such a time schedule in using proving rings, and it is sometimes necessary to use them for measuring decreasing as well as increasing loads. To de-

termine the errors that might result from such variations in the conditions of use, dead-weight tests at 70° F were made on three rings having capacities of 3,000 kg, 20,000 lb, and 100,000 lb. Each of the rings had been calibrated and found to comply with the requirements of the specification given in the appendix.

After having been unloaded for more than 24 hours, each ring was loaded to capacity and kept under capacity load for 3 hours. Ring readings were observed as soon as possible after the load was fully applied and again after intervals from ½ minute to 3 hours after application. The maximum observed creep under capacity load for the 3-hour period was 0.05 division, or 0.01 percent of the capacity load.

After each ring had remained under capacity load for 3 hours, the load was completely removed. The no-load reading of the ring was observed as soon as possible and again after intervals from ½ minute to 3 hours after removal of the load. In every case the no-load reading changed during the first half-hour of the 3-hour period. The maximum observed zero shift was 0.4 division, or 0.06 percent of the capacity deflection. Within 32 minutes for the 3,000-kg and 20,000-lb rings and within 64 minutes for the 100,000-lb ring, the no-load readings equalled the no-load reading observed before the application of the capacity load.

The hysteresis at half-capacity load was determined for each ring by computing the difference between the ring readings at half-capacity load observed before and after the application of capacity load. The results indicated a hysteresis of 0.10 percent for the 3,000-kg and 100,000-lb rings and 0.15 percent for the 20,000-lb ring.

2. ERRORS DUE TO INSTANTANEOUS TEMPERATURE EFFECT

When a proving ring is loaded, both tensile and compressive stresses are set up in the material of the ring. An increase in temperature occurs in the material subjected to compressive stresses, and a decrease in temperature occurs in the material subjected to tensile stresses [12, 13]. Consequently, the reading of a suddenly loaded (or unloaded) proving ring changes as the temperature throughout the material of the ring becomes equalized. This equalization occurs so rapidly that it may be ignored without significant error in rings not exceeding 100,000-lb capacity. For larger rings, errors due to this cause become negligible if readings are taken no sooner than 30 seconds after removal of load. No delay in taking readings under load is necessary because with ordinary testing machines the time required to apply and adjust the test load and read the ring is great enough to permit nearly complete temperature equalization.

3. ERRORS DUE TO ANGLE OF LOAD LINE

If a proving ring is loaded through suitable bearing blocks or tension fittings in a testing machine whose platens are plane and parallel, the load line will be very nearly coincident with the axis of the bosses of the ring. For compression rings a lack of parallelism of the heads of the testing machine may result in an inclination of the load line with respect to the axis of the bosses of the ring.

To determine the magnitude of the error introduced by an inclination of the load line, a 100,000-lb-capacity compression proving ring was loaded in the 111,000-lb-capacity dead-weight machine through 2- and 4-degree wedges, as shown in figure 10. The errors resulting from these

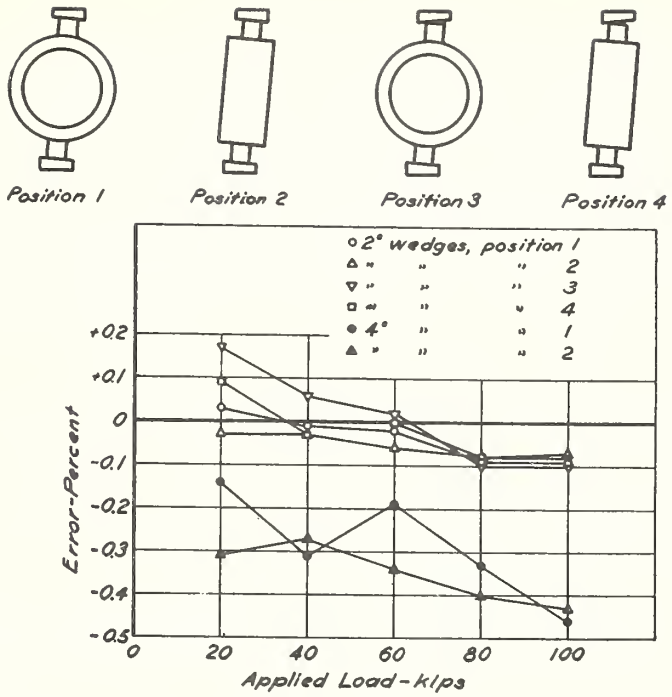

FIGURE 10.—*Effect of the angle of the load line on the calibration of a 100,000-lb-capacity proving ring.*

conditions of loading are plotted in percent as a function of the applied load. The maximum errors introduced by the 2-degree wedges were about 0.17 percent at 20-percent-capacity load and 0.1 percent at capacity load, values which do not exceed the tolerances of 0.5 percent and 0.1 percent, respectively, given in the Bureau specification for proving rings. The maximum error introduced by the 4-degree wedges was about 0.46 percent at capacity load.

As an angle of less than 2 degrees can easily be detected by inspection, there is no reason for the occurrence of appreciable errors due to inclination of the load line.

4. ERRORS DUE TO CHANGE OF CALIBRATION WITH TIME

The relationship between the deflection of a proving ring and the applied load depends not only upon the dimensions of the ring but also upon the elastic constants of the material of the ring. Provided the dimensions are not altered by removing material or by plating the surface, and provided a ring has not been overloaded or subjected to sufficient wear to introduce errors from these causes, a study of the constancy of the calibration with time may be expected to indicate the magnitude of any change in elastic constants with time.

Experience indicates that there is no appreciable aging effect for rings made of the steel described on page 7. The results of a study of the calibrations of three 300,000-lb-capacity rings for a 12-year period are given in figure 11. Each ring was calibrated seven times during this

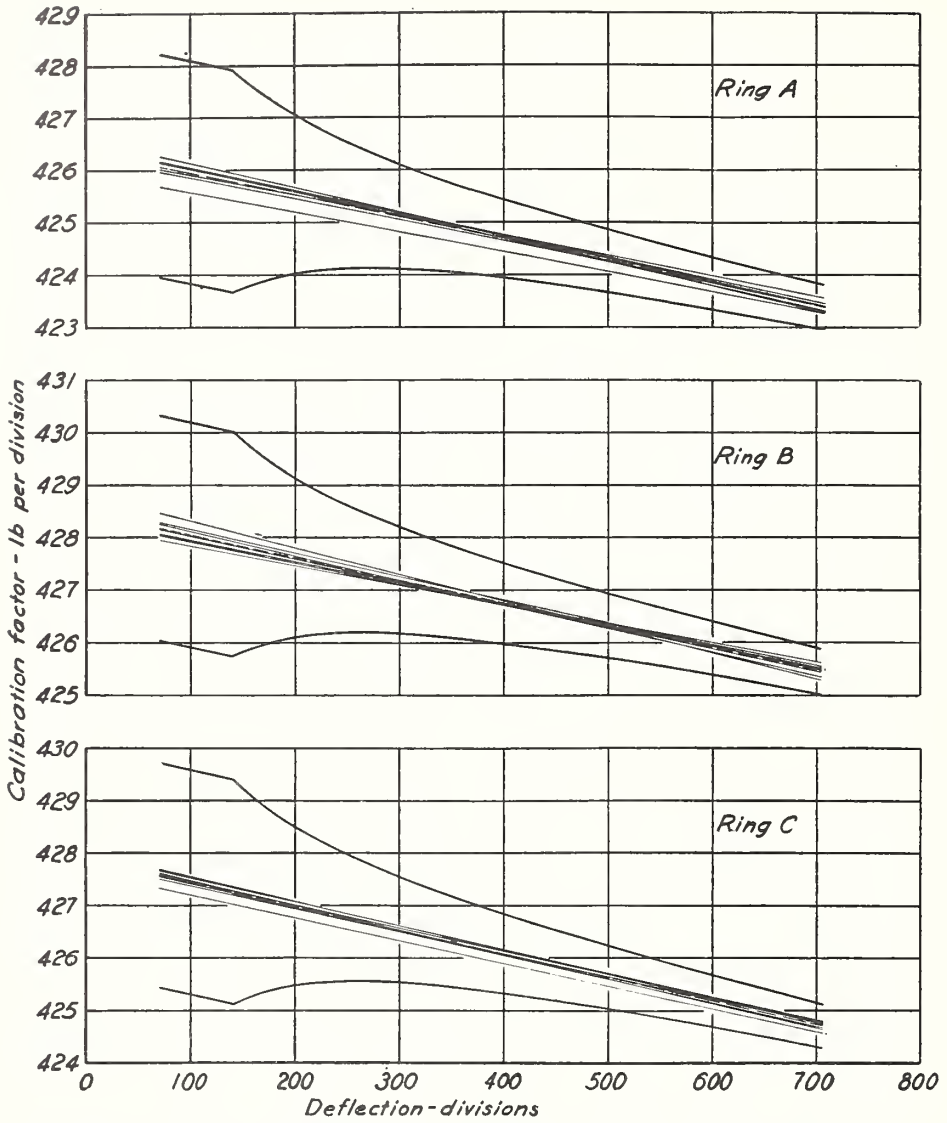

FIGURE 11.—*Effect of time and use on the calibrations of three proving rings for calibrations spaced over a period of years.*

The dashed line represents the average of the individual calibration lines indicated by the light lines which were drawn to represent experimental points not shown. The curved lines are the specification limits corresponding to the average calibration line.

period. The individual lines drawn to represent each calibration are shown as solid lines. An "average" calibration line for each ring is shown by a dashed line. Specification limits corresponding to the dashed line, computed as defined in the appendix, are shown for each ring. It is evident that the changes in calibration with time are small compared to the tolerances for constancy. Furthermore, the small changes observed indicated no progressive trend but were apparently random changes of a magnitude about equal to the experimental error of determining a given calibration line. Experience with other capacities of rings is in accord with the results given for the 300,000-lb rings.

5. ERRORS DUE TO WEAR

Each time the reading of a proving ring is observed, the end of the vibrating reed repeatedly strikes the button on the spindle of the micrometer screw, tending to wear the contacting surfaces. Although the rate at which metal is worn away varies with the operator and frequency of use, ultimately the alteration in the shapes of the surfaces leads to errors in the measured deflections of the ring.

Errors of this type generally may be observed as a cyclic departure of the calibration points from the straight line of the calibration curve,

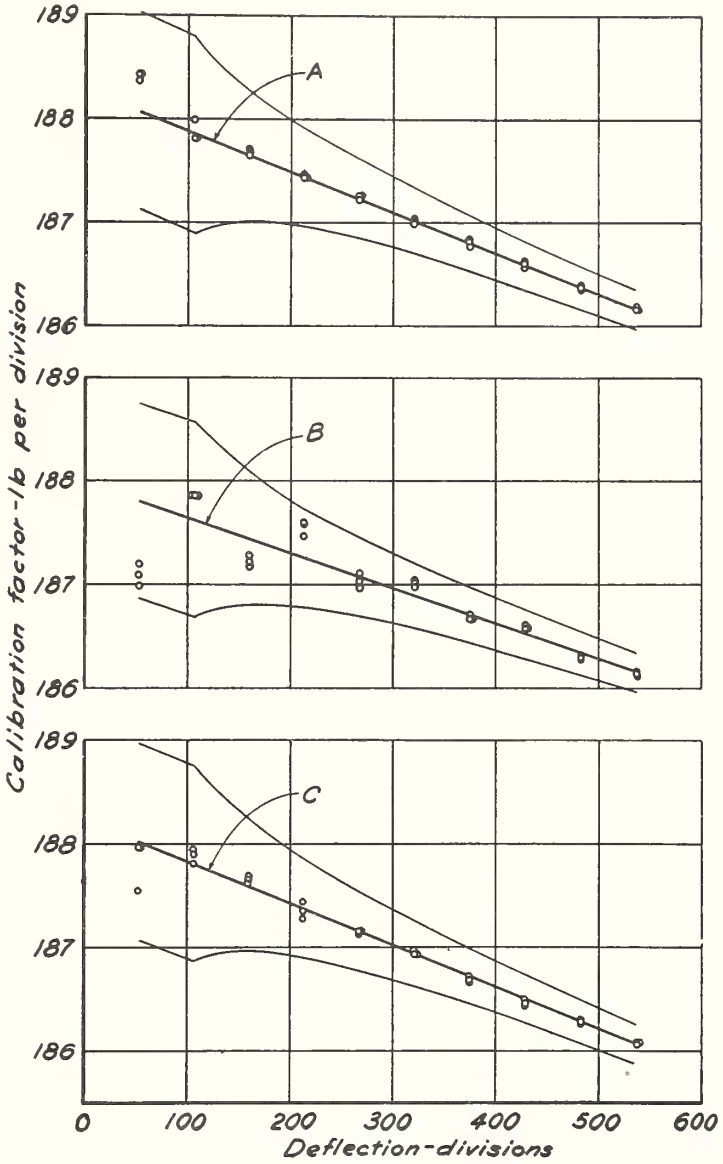

FIGURE 12.—*Effect of wear on the calibration results.*
A, Original calibration of a new ring; *B*, calibration of the same ring after considerable use; and *C*, calibration of the same ring after reconditioning of the worn surfaces of the deflection-measuring apparatus after the calibration marked *B*.

as shown in figure 12. In this figure, *A* shows the original calibration of a 100,000-lb-capacity ring, *B* shows the calibration made after considerable use, and *C* shows the calibration made after the worn surfaces of the deflection-measuring apparatus had been refinished. Experience indicates that for rings used frequently the worn surfaces should be refinished at intervals of 2 or 3 years.

The calibration of a ring that has been overloaded sufficiently to produce a set is permanently changed, and the ring should be recalibrated after any necessary repairs. A considerable number of rings have been recalibrated after having been overloaded and reconditioned and have shown satisfactory performance.

VI. CONCLUSIONS

Proving rings that comply with the specification included in the appendix are suitable for determining the errors of the indicated loads of testing machines. Such rings, provided they are not overloaded, subjected to excessive wear or otherwise damaged, maintain their calibrations without significant change over periods as long as 12 years. However, it is recommended that rings be recalibrated after intervals of from 1 to 2 years. Even under unusual conditions of use the errors of proving rings certified to comply with the specification given in the appendix are small compared to the generally recognized tolerance of ± 1 percent for testing machines.

VII. REFERENCES

[1] Proving ring. U.S. Patent 1,648,375 issued to H. L. Whittemore and S. N. Petrenko.

[2] Proving ring. U.S. Patent 1,927,478 issued to H. L. Whittemore and S. N. Petrenko.

[3] S. N. Petrenko, Elastic ring for verification of Brinell hardness testing machines, Trans. Am. Soc. Steel Treating C.22, 420 (1926).

[4] B. L. Wilson, D. R. Tate, and G. Borkowski, Dead-weight machines of 111,000- and 10,100-pound capacities, Circular of the NBS C446 (1943).

[5] Testing instrument. U.S. Patent 1,694,187 issued to R. B. Lewis.

[6] ASTM Standards, 1944, part I, Metals, p. 953–961.

[7] S. Timoshenko, Strength of materials, part II, second edition, ch. 2 (D. Van Nostrand Co. Inc., New York, N. Y., 1941).

[8] C. Bach and R. Baumann, Elastizitat und Festigkeit, 9th edition, p. 502 (Julius Springer, 1924).

[9] C. E. Larard, The elastic ring acted upon by equal radial forces, Phil. Mag. [7] C.22, 129–143 (1931).

[10] C. E. Larard, The elastic ring. A comparison of strains determined experimentally with the strains calculated from the elastic ring theory, Phil. Mag. [7] C.22, 1183–1188 (1931).

[11] C. M. Spofford and C. H. Gibbons, Weighing bridge reactions with proving rings, Eng. News Rec. C.22, 446–449 (1935).

[12] M. F. Sayre, Thermal effects in elastic and plastic deformation, Proc. ASTM, part II, C.22, 584 (1932).

[13] L. B. Tuckerman, discussion, Proc. ASTM, part II, C.22, 594 (1932).

VIII. APPENDIX

NATIONAL BUREAU OF STANDARDS SPECIFICATION FOR PROVING RINGS FOR CALIBRATING TESTING MACHINES

(Letter Circular LC 822, April 15, 1946)

INTRODUCTION

The National Bureau of Standards has had more than twenty-five years of experience in calibrating testing machines which apply forces to engineering materials. This experience has indicated the advisability of frequent periodic calibration of such machines, if reliable test results are to be obtained. It also indicated the need for a calibrating device which would be sufficiently accurate for the purpose and at the same time more readily portable and convenient in use than the devices previously available. Proving rings were developed at the National Bureau of Standards to meet this need.

This specification is the result of over 20 years' experience in the development of proving rings and in calibrating them periodically in dead-weight calibrating machines. It contains requirements which have been found necessary to insure that proving rings complying with them will be satisfactory, reliable instruments for calibrating testing machines.

These technical requirements are identical with those in Letter Circular 657, which this specification supersedes. The simplified procedure for the recalibration of rings previously certified is justified by the experience of the past 7 years.

I. DEFINITIONS

1. PROVING RING

A proving ring is an elastic ring, suitable for calibrating a testing machine, in which the deflection of the ring when loaded along a diameter is measured by means of a micrometer screw and a vibrating reed mounted diametrically in the ring.

2. READING

A reading is the value indicated by the micrometer dial when it has been adjusted to contact the vibrating reed.

3. DEFLECTION

The deflection of the ring for any load is the difference between the reading for that load and the reading for no load.

4. CALIBRATION FACTOR

The calibration factor for a given deflection is the ratio of the corresponding load to the deflection.

II. COMPLETE CALIBRATION

1. MARKING

The maker's name, the capacity load, and the serial number of the ring shall be legibly marked upon some part of the instrument.

2. MICROMETER DIAL

(a) The dial of the micrometer shall be of the uniformly graduated type. When successive graduation lines on the dial are set to one fixed index line, the positions of successive graduation lines nearly diametrically opposite referred to another fixed index shall differ from each other by not more than 1/20 of the smallest division of the dial.

(b) The smallest division of the dial shall be not less than 0.05 inch and not more than 0.10 inch.

(c) The width of any graduation line on the dial shall not exceed one-tenth of the average distance between adjacent graduation lines.

(d) The width of any index line shall be not less than 0.75 and not more than 1.25 times the average width of the graduation lines on the dial.

3. OVERLOAD

The ring shall be overloaded repeatedly to a load of not less than 9 percent nor more than 10 percent in excess of the capacity load. The difference between the

no-load reading after the first overload and the no-load reading after any subsequent overload shall not exceed one-tenth of one percent of the deflection of the ring under capacity load.

4. STIFFNESS

Under the capacity load the ring shall deflect not less than 0.040 inch.

5. CONSTANCY

(a) *Range 1/10 to 2/10-Capacity Load.*—The observed deflection of the ring, for an applied load of not less than one-tenth nor more than two-tenths of the capacity load, shall differ from the average of at least three successive observations for the same applied load by not more than one-half of one percent of the deflection for the applied load.

(b) *Range 2/10 to Capacity Load.*—The observed deflection of the ring, for any applied load not less than two-tenths nor more than the capacity load, shall differ from the average of at least three successive observations for the same applied load by not more than one-tenth of one percent of the deflection for the capacity load.

(c) *Disassembling.*—The difference between the deflections of the ring, observed before and after the deflection-measuring apparatus is removed and then replaced, shall be not greater than the maxima specified in paragraphs II-5(a) and II-5(b) of this specification, under the loads there specified.

(d) *Bearing Blocks.*—A compression proving ring shall be loaded through plane, concave, and convex bearing blocks. The deflections of the proving ring for the minimum load and for the maximum load applied by dead weights during the calibration shall be determined when the load is applied to the lower boss of the ring through concave and convex bearing blocks. The difference between the average deflections observed using the concave bearing block and the average deflections observed using a plane bearing block for the same loads shall not exceed the maxima specified in paragraphs II-5(a) and II-5(b) of this specification. The differences between the average deflections observed using the convex bearing block and the average deflections observed using a plane bearing block for the same loads shall not exceed the maxima specified in paragraphs II-5(a) and II-5(b) of this specification. The concave and convex bearing blocks shall comply with the following requirements:

(1) They shall be steel.
(2) The Brinell numbers shall be not less than 400 and not more than 600.
(3) The radii of curvature of the spherical surfaces shall be not less than 9 feet and not more than 10 feet.

III. RECALIBRATION

1. CONSTANCY

(a) *Range 1/10 to 2/10-Capacity Load.*—The observed deflection of the ring, for an applied load of not less than one-tenth nor more than two-tenths of the capacity load, shall differ from the average of at least three successive observations for the same applied load by not more than one-half of one percent of the deflection for the applied load.

(b) *Range 2/10 to Capacity Load.*—The observed deflection of the ring, for any applied load not less than two-tenths nor more than the capacity load, shall differ from the average of at least three successive observations for the same applied load by not more than one-tenth of one percent of the deflection for the capacity load.

(c) *Comparison with Last Calibration.*—The observed deflections of the ring during recalibration shall differ from the deflections observed at the time of the last calibration by not more than the maxima specified in paragraphs III-1(a) and III-1(b) of this specification, under the loads there specified.

(d) *Alternative Procedure.*—If the ring fails to comply with the requirements of paragraph III-1(c) of this specification, the deflection-measuring apparatus shall be removed and then replaced. The difference between the deflections observed before and after this is done shall be not greater than the maxima specified in paragraphs III-1(a) and III-1(b) of this specification, under the loads there specified.

IV. METHOD OF CALIBRATION

1. COMPLETE CALIBRATION

The proving ring shall be calibrated in accordance with the requirements given in section II, Complete Calibration:

(a) If the ring has not been calibrated by the National Bureau of Standards since the revision of this specification on April 4, 1934.

(b) If the ring was not certified when last calibrated by the National Bureau of Standards.
(c) If the ring has been repaired or modified since its last calibration by the National Bureau of Standards.

2. RECALIBRATION

Except as provided in paragraphs IV-1(a), IV-1(b), and IV-1(c), Complete Calibration, a ring shall be recalibrated in accordance with the requirements given in section III, Recalibration.

3. LOADS NOT EXCEEDING 110,000 LB

For loads not exceeding 110,000 lb the proving ring shall be calibrated by applying dead weights known to within 0.02 percent.

4. LOADS EXCEEDING 110,000 LB

For loads exceeding 110,000 lb the applied load shall be known to within 0.1 percent.

5. LOADING PROCEDURE

The proving ring shall be calibrated under increasing loads. Compressive loads, except as provided in paragraph II-5(d), shall be applied to the lower boss of the ring through a plane, hardened-steel bearing block and to the upper boss either through a ball or a soft-steel block. Tensile loads shall be applied to the ring through the pulling rods provided with the ring.

6. TEMPERATURE CORRECTION

To compensate for temperature changes which occur during calibration, the deflections of the proving ring shall be corrected for temperature using the formula

$$d_{70} = d_t [1 + K (t - 70)],$$

where

d_{70} = deflection of ring at a temperature of 70° Fahrenheit

d_t = deflection of ring at a temperature of t degrees Fahrenheit

K = temperature coefficient

t = temperature, degrees Fahrenheit, during test.

The coefficient K depends upon the chemical composition of the steel of which the ring is made and its heat treatment. For steels having a total alloying content not exceeding five percent, the value $K = -0.00015$ per degree Fahrenheit is sufficiently accurate. For some other steels, values of K have been found ranging from -0.00011 to -0.00024. When the proving ring is submitted for calibration, the value of K shall be furnished this Bureau by the person submitting the ring or by the manufacturer of the ring.

V. METHOD OF REPORTING RESULTS

1. CERTIFICATES OF CALIBRATION

For a ring which complies with the requirements of this specification, a certificate of calibration will be issued including a calibration graph showing the calibration factor as a function of the ring deflection.

2. REPORTS

For a ring which does not comply with the requirements of this specification, a report will be issued giving the results in the form of a table and stating wherein the ring fails to comply.

WASHINGTON, March 25, 1946.

U. S. DEPARTMENT OF COMMERCE
JESSE H. JONES, Secretary
NATIONAL BUREAU OF STANDARDS
LYMAN J. BRIGGS, Director

CIRCULAR OF THE NATIONAL BUREAU OF STANDARDS C446

DEAD-WEIGHT MACHINES OF 111,000- AND 10,100-POUND CAPACITIES

By
BRUCE L. WILSON, DOUGLAS R. TATE, GEORGE BORKOWSKI

[Issued June 1943]

UNITED STATES
GOVERNMENT PRINTING OFFICE
WASHINGTON : 1943

596/I

PREFACE

The calibration of testing machines, for applying forces to specimens of engineering materials and structures, has long been recognized as an important problem by both producers and users of engineering materials. Many methods of calibration have been devised for calibrating small testing machines, but only by means of elastic calibration devices can the larger testing machines be calibrated to capacity. The development at the National Bureau of Standards of the proving ring, one type of elastic calibration device, resulted in a greatly increased use of elastic calibration devices and made necessary the provision of facilities for the calibration of such devices. The two dead-weight machines described in this Circular were designed and installed to calibrate such devices. In these machines the accurately known tensile or compressive forces necessary for the calibration of elastic devices may be applied.

LYMAN J. BRIGGS, *Director.*

DEAD-WEIGHT MACHINES OF 111,000 AND 10,100-POUND CAPACITIES

By Bruce L. Wilson, Douglas R. Tate, and George Borkowski

A dead-weight testing machine of 102,000-lb capacity was installed at the National Bureau of Standards in 1927 to provide means for calibrating elastic calibration devices, which are used to calibrate force-indicating testing machines. To obtain a larger number of test loads the original machine was altered by the addition of nine 1,000-lb weights and an operating mechanism. To obtain the smaller test loads necessary for the calibration of elastic calibration devices having smaller capacities a new machine of 10,100-lb capacity was installed. The two machines are described and the errors of the weights of the machines are discussed.

CONTENTS

I. INTRODUCTION

To meet the increasing need for determining the errors in the force indications of testing machines used for determining the strength and other properties of structural materials, the Whittemore-Petrenko proving ring,[1] one type of elastic calibration device, was developed. Briefly, this device consists of a heat-treated steel ring having integral external bosses through which forces are applied to the ring and integral internal bosses to which a vibrating reed and micrometer screw deflection-measuring apparatus is attached. The deflection of such a ring bears a definite relationship to the applied load. After this relationship has been determined by applying accurately known forces to the ring in dead-weight machines,[2] the ring may be used to determine the errors of the indicated loads of testing machines. The development of the proving ring, which made available a convenient, accurate, portable calibrating device, led to a greatly increased use of elastic calibration devices, displacing some of the other methods of calibration which are outlined in the American Society for Testing Materials Standard Methods of Verification of Testing Machines.[3]

[1] Proving ring. U. S. Patents 1,648,375 and 1,927,478, issued to H. L. Whittemore and S. N. Petrenko.
[2] L. B. Tuckerman, H. L. Whittemore, and S. N. Petrenko, *A new dead-weight testing machine of 100,000-pounds capacity*, BS J. Research 4, 261 (1930) RP147.
[3] Am. Soc. Testing Materials Standards I, 889 (1942).

They are used for the original adjustment of the weighing systems of new machines and for the regular recalibration of machines. This has led to a greatly increased demand for the calibration of elastic calibration devices by the National Bureau of Standards.

Experience in using the 102,000-lb-capacity dead-weight machine installed at the Bureau in 1927 (see footnote 2) indicated the necessity of applying 8 or 10 different test loads to determine with sufficient accuracy the relationship between the load and the deflection of an elastic calibration device. With this original machine only 11 test loads from 2,000 lb to 102,000 lb by 10,000-lb increments could be applied. It was, therefore, not adequate for calibrating devices having capacities less than about 100,000 lb.

To provide adequate facilities for calibrating elastic devices having capacities less than 100,000 lb, the original machine was altered, and a new, smaller machine was installed. With the large machine, test loads from 2,000 lb to 111,000 lb by 1,000-lb increments may now be applied. With the small machine, test loads from 200 lb to 10,100 lb by 100-lb increments may be applied.

The machines are suitable for calibrating elastic calibration devices, but they are not suitable for determining the strengths of materials or structures.

II. DESCRIPTION OF THE 111,000-POUND-CAPACITY MACHINE

A diagrammatic sketch of the 111,000-lb-capacity dead-weight machine is shown in figure 1. Drawings of the weight linkages and bevel seats are shown in figure 2, and the machine is shown in figures 3, 4, 5, and 6.

The machine (fig. 1) consists essentially of a hydraulic jack, an upper and a lower frame, and flat cylindrical weights. The weights, not all of which are shown in the sketch, may be applied to the lower frame. The upper frame is supported by a ball that rests on the ram of the jack. The upper frame is connected to the lower frame only by the elastic calibration device.[4] Loads are applied to the calibration device by raising the upper frame with the jack. The calibration device, being connected between the upper and lower frames, lifts the lower frame and the weights supported by it as the upper frame is raised. The number of 10,000-lb weights applied to the lower frame depends on the height to which the frame is raised. The number of 1,000-lb weights applied to the lower frame is adjusted by means of motor-driven gearing attached to the upper frame.

The machine, which is located in the laboratory of the Bureau's Engineering Mechanics Section, is about 30 feet high by about 12 feet wide. The weights are on the first floor of the laboratory building, the forces are applied to calibration devices on the second floor, and the hydraulic jack for lifting the weights is on the third floor. The room on the second floor through which the frames of the machine pass is equipped with temperature-control apparatus by means of which the temperature may be maintained constant to within $\pm 0.5°$ F.

[4] The term "elastic calibration device" is defined by the American Society for Testing Materials (see footnote 3) as follows:

"An elastic calibration device for use in verifying the load readings of a testing machine consists of an elastic member to which loads may be applied combined with a mechanism for indicating the magnitude of deformation under load."

The term "elastic calibration device" includes proving rings, solid bars, hollow bars, elastic loops, and other members whose elastic deformation can be measured.

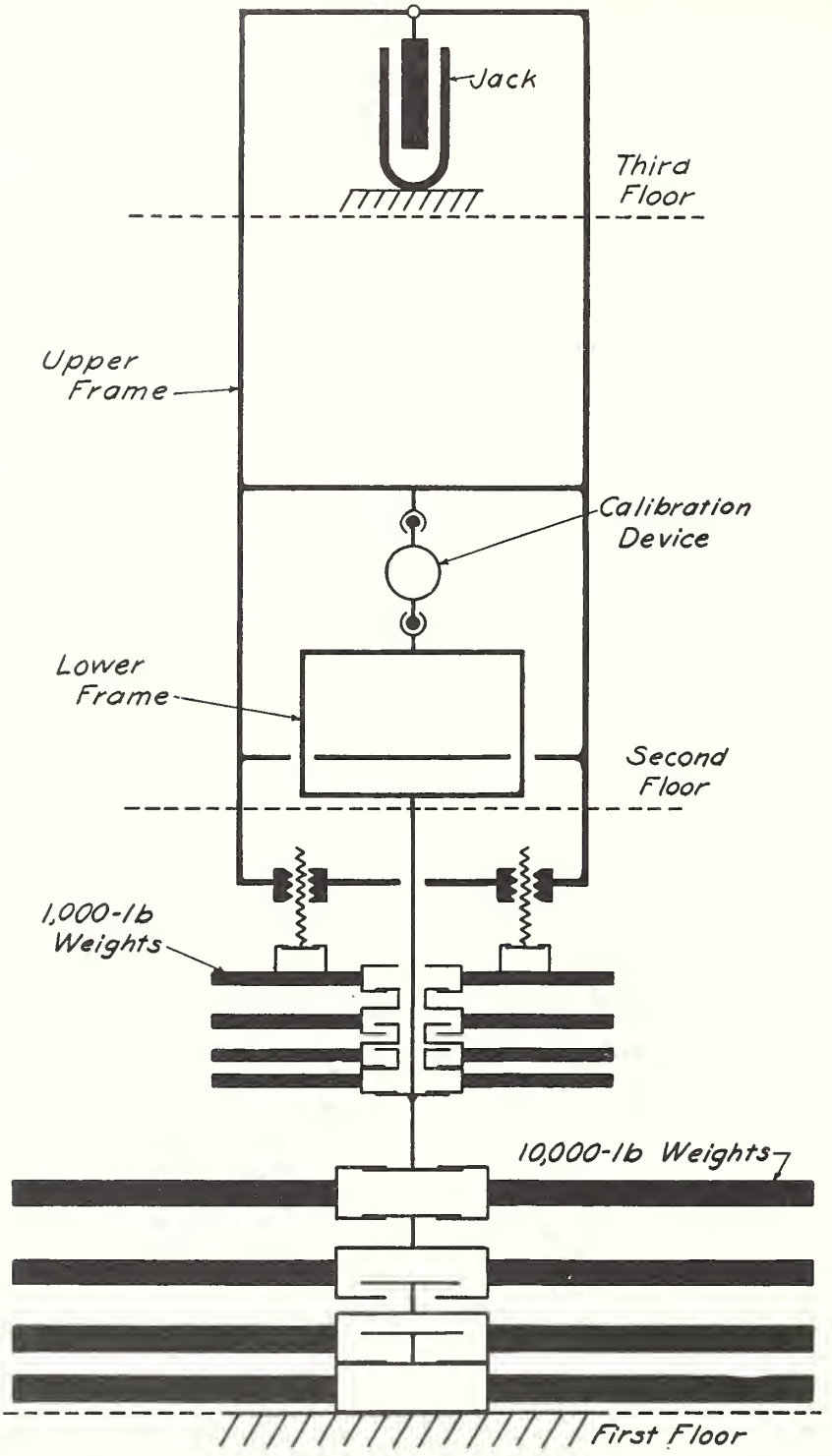

FIGURE 1.—*Diagrammatic sketch of the 111,000-lb-capacity dead-weight machine.*

The machine consists essentially of a hydraulic jack, an upper and a lower frame, and weights that may be applied to the lower frame. Forces are applied to the calibration device, which forms the only connection between the upper and lower frame, by raising the ram of the jack.

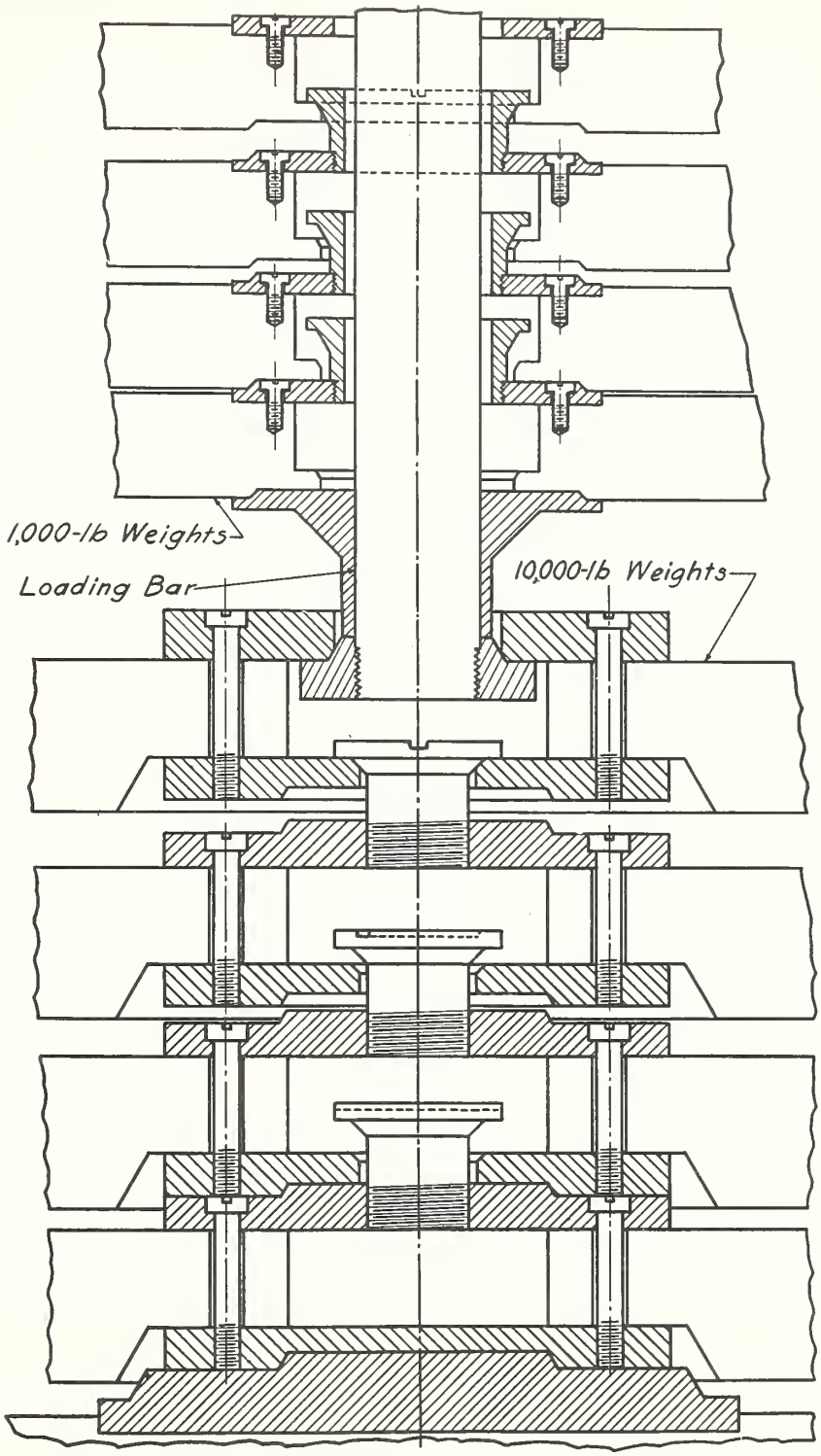

FIGURE 2.—*Bevel seats and weight linkages of the 111,000-lb-capacity dead-weight machine.*

574278 O - 61 - 39

It is normally kept at 70° F. The frame of the machine consists of two reinforced-concrete columns, *A–A* (figs. 3 and 4), which extend from the concrete foundation of the machine to the third floor where two steel I-beams, *B* (fig. 6), are placed across the tops of the columns. A bevel seat (fig. 2) for the bottom 10,000-lb weight is built into the

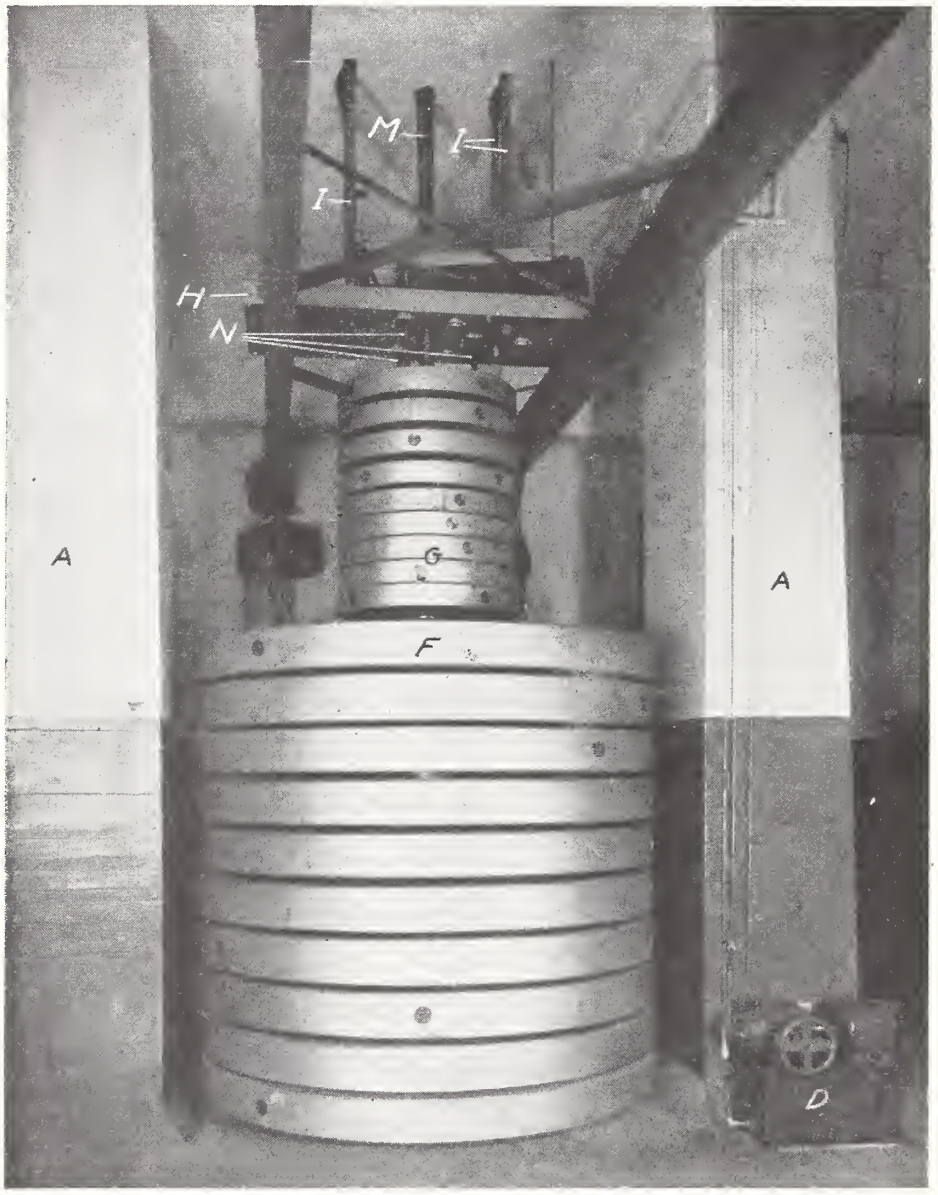

FIGURE 3.—*Part of the 111,000-lb-capacity dead-weight machine located between the first and second floors.*

Any number of the nine 1,000-lb weights, *G*, and the ten 10,000-lb weights, *F*, may be applied to the loading bar, *M*, which is suspended from the lower frame. The two I-beams and chain hoists suspended from the second floor are completely independent of the machine. They are used only to lift the weights during disassembly and assembly of the machine.

foundation. The hydraulic jack, *C* (fig. 6), which is operated by an electrically driven multiple cylinder pump, *D* (fig. 3), is supported by the I-beams. Control valves and electrical switches for operating the machine are located in the case, *E* (figs. 4 and 5), on the second floor.

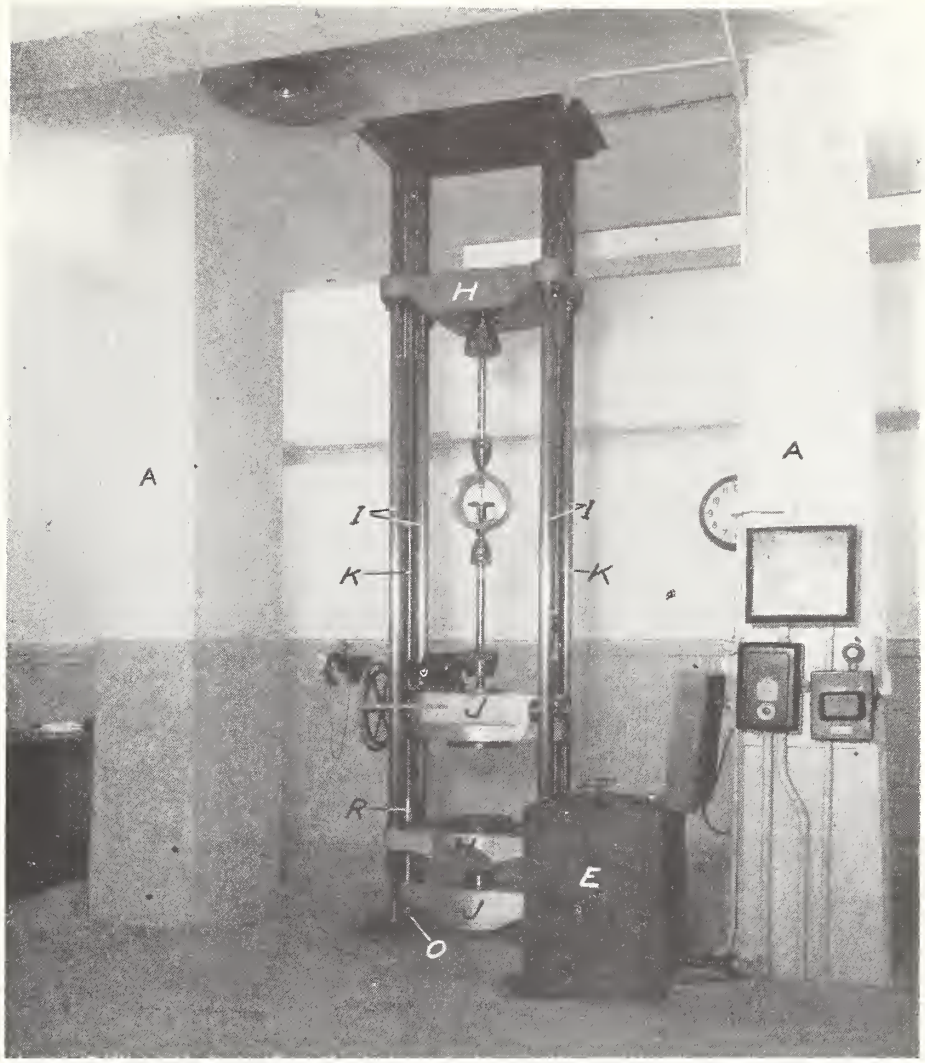

FIGURE 4.—*Part of the 111,000-lb-capacity dead-weight machine located between the second and third floors.*

The upper frame *H–H* and *I–I* is raised by the hydraulic jack on the floor above. The loading bar, to which the weights may be applied, is suspended from the lower frame, *J–J* and *K–K*. The 100,000-lb-capacity proving ring ready for calibration in tension connects the upper and lower frames.

The cast-iron 10,000-lb weights, *F* (fig. 3), are about 7½ in. thick by 84 in. in diameter. The steel 1,000-lb weights, *G* (fig. 3), are about 4 in. thick by 33½ in. in diameter. The adjusting cavities in the sidewalls of the weights are closed by threaded plugs.

The apparatus for applying forces to the device to be calibrated consists of two frames. The upper frame consists of four yokes, *H*, connected by four rods, *I* (figs. 3, 4, 5, and 6). To limit swinging of the upper frame, guides are provided for the rods where they pass through the second floor. The top yoke, *H* (fig. 6), rests on a steel ball on the ram of the jack. The bottom yoke, *H* (fig. 3), carries the operating mechanism for the 1,000-lb weights. The two intermediate

yokes, *H*, which are the lower compression and upper tension heads of the machine, are fixed in position on rods *I*.

The lower frame consists of two yokes, *J* (figs. 4 and 5), connected by two rods, *K* (figs. 4 and 5). The upper, unthreaded portions of these rods move vertically in guides, which can be rotated by hand to decrease the friction on rods *K* in the upper yoke *H* of the upper frame shown in figure 4. These guides are sufficient to keep the lower frame in proper alinement with respect to the upper frame, provided cali-

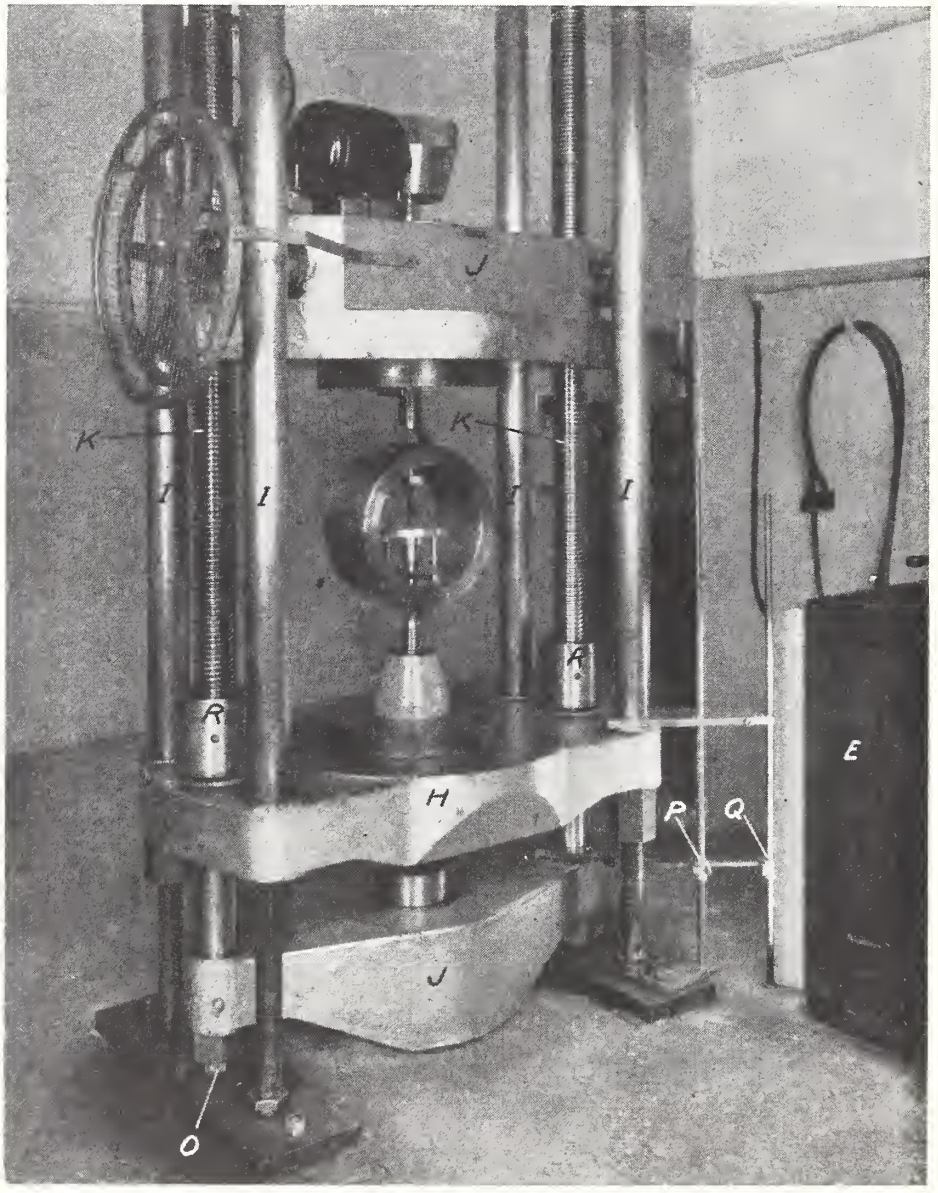

FIGURE 5.—*Lower part of the 111,000-lb-capacity dead-weight machine located between the second and third floors.*

The 100,000-lb-capacity proving ring ready for calibration in compression connects the upper and lower frames.

bration devices are properly centered in the machine. Tests have shown that the friction does not produce any detectable difference in the readings of the devices calibrated in this machine. The upper yoke of the lower frame, which is the upper compression and lower tension head of the machine, may be adjusted vertically on the

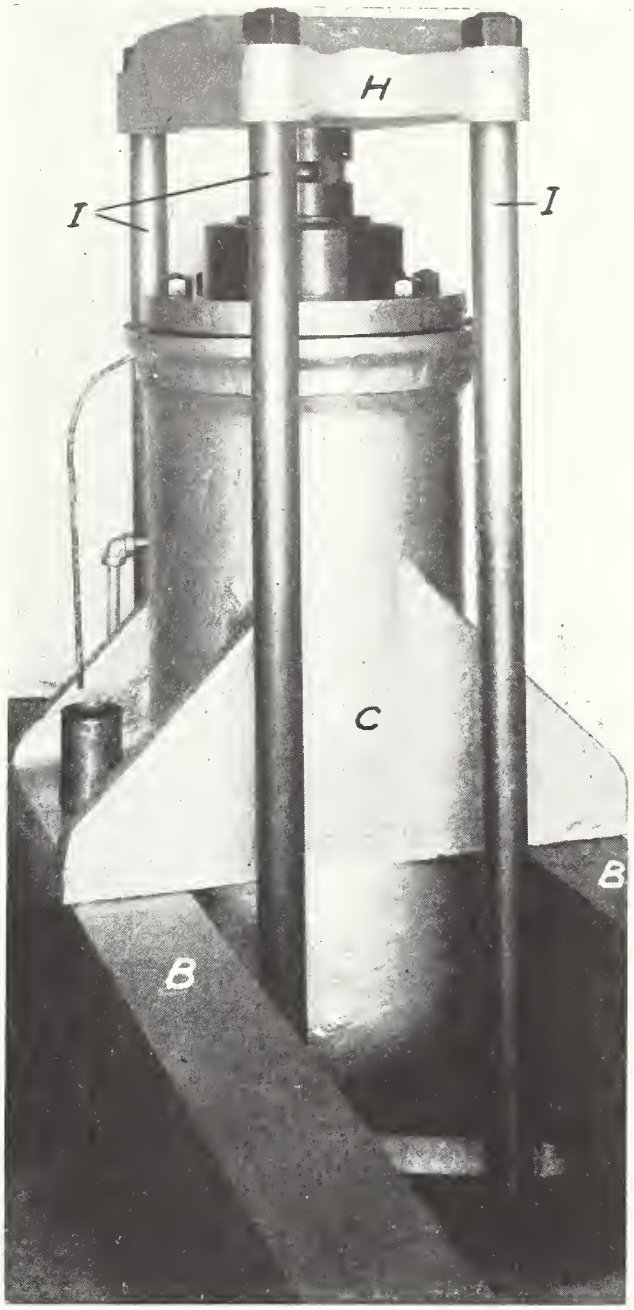

FIGURE 6.—*Part of the 111,000-lb-capacity dead-weight machine located above the third floor.*

The upper frame, *H* and *I–I*, is supported by a ball on the axis of the ram of the jack. Forces are applied to the device to be calibrated by raising the ram of the jack.

threaded rods, K, by rotating the nuts in the yoke by means of the electric motor and gearing shown in figures 4 and 5. Devices up to about 6 ft in length can be calibrated in either tension or compression.

The loading bar, M (fig. 3), is suspended from lower yoke J. This bar passes through the bottom yoke of the upper frame and the nine 1,000-lb weights. At its lower end it carries a bevel seat (fig. 2) for the bottom 1,000-lb weight and a head which projects below a plate (fig. 2) attached to the top 10,000-lb weight.

The 1,000-lb weights are supported by three threaded rods, N (fig. 3), which engage bevel seats in plates attached to the top 1,000-lb weight. These rods may be moved vertically by means of an electric motor and gearing attached to the bottom yoke of the upper frame. With the upper frame and the loading bar at any heights within their operating ranges, any number of the nine 1,000-lb weights may be supported from the rods N by means of the connecting pieces which link the weights together. The weights not supported from the rods N are supported on the bevel seat attached to the loading bar, each weight above the bottom weight being supported on a bevel seat on the weight below. A movement of about 11 in. of the rods N is required to transfer the support of all the weights from the loading bar to the rods N.

When the loading bar is not in contact with the top 10,000-lb weight, the bottom 10,000-lb weight is supported on the bevel seat (fig. 2) built into the foundation, and each of the other weights rests on a similar seat (fig. 2) on the weight below. The 10,000-lb weights are supported by the loading bar when the jack, through a calibration device, lifts the lower frame. When the loading bar has been raised about ¾ in. from its lowest position, the head on the end of the bar engages a bevel seat on the lower side of a plate attached to the top weight, thus applying the top weight to the loading bar. As the bar is raised farther, a connecting piece attached to the second weight engages a bevel seat in the top weight, and similarly the other weights are suspended in succession. All 10 weights are suspended when the loading bar has been raised about 10 in.

When the lower frame of the machine is not supported by a calibrating device, it is supported on two bevel seats, O (figs. 4 and 5), which are supported by the second floor of the building.

The position of the lower frame and the number of weights supported by the loading bar are shown by indicators P and Q (fig. 5). The total weight supported by a calibration device is the sum of the weight of the lower frame, 2,000 lb, and the weights shown on indicators P and Q.

If a calibrating device should fail under load, the weights it carried would fall. To prevent possible damage from this cause, the nuts, R (figs. 4 and 5), on the threaded rods, K, are adjusted so that there is a small clearance between their lower surfaces and the upper surface of one of the yokes of the upper frame. This limits to a safe distance the possible fall of the weights.

A proving ring of 100,000-lb capacity is shown in the dead-weight machine ready for calibration in tension in figure 4. The same ring is shown ready for calibration in compression in figure 5. To insure that forces applied to calibration devices will be axial, devices placed in the machine are carefully centered so that the axes of the devices coincide with the axis of the machine.

III. DESCRIPTION OF THE 10,100-POUND-CAPACITY MACHINE

The 10,100-lb-capacity dead-weight machine is shown in figures 7 and 8. Figure 7 shows the machine as it was originally installed on the first floor of the laboratory building. The machine as it is now installed is partially shown in figure 8.

The machine is about 14 ft high by about 5 ft wide. It rests on a concrete column, the top of which is about 10 ft above the first floor of the building. The machine projects through the second floor into the temperature-controlled room, which also surrounds the frames of the 111,000-lb-capacity machine. The column and the machine

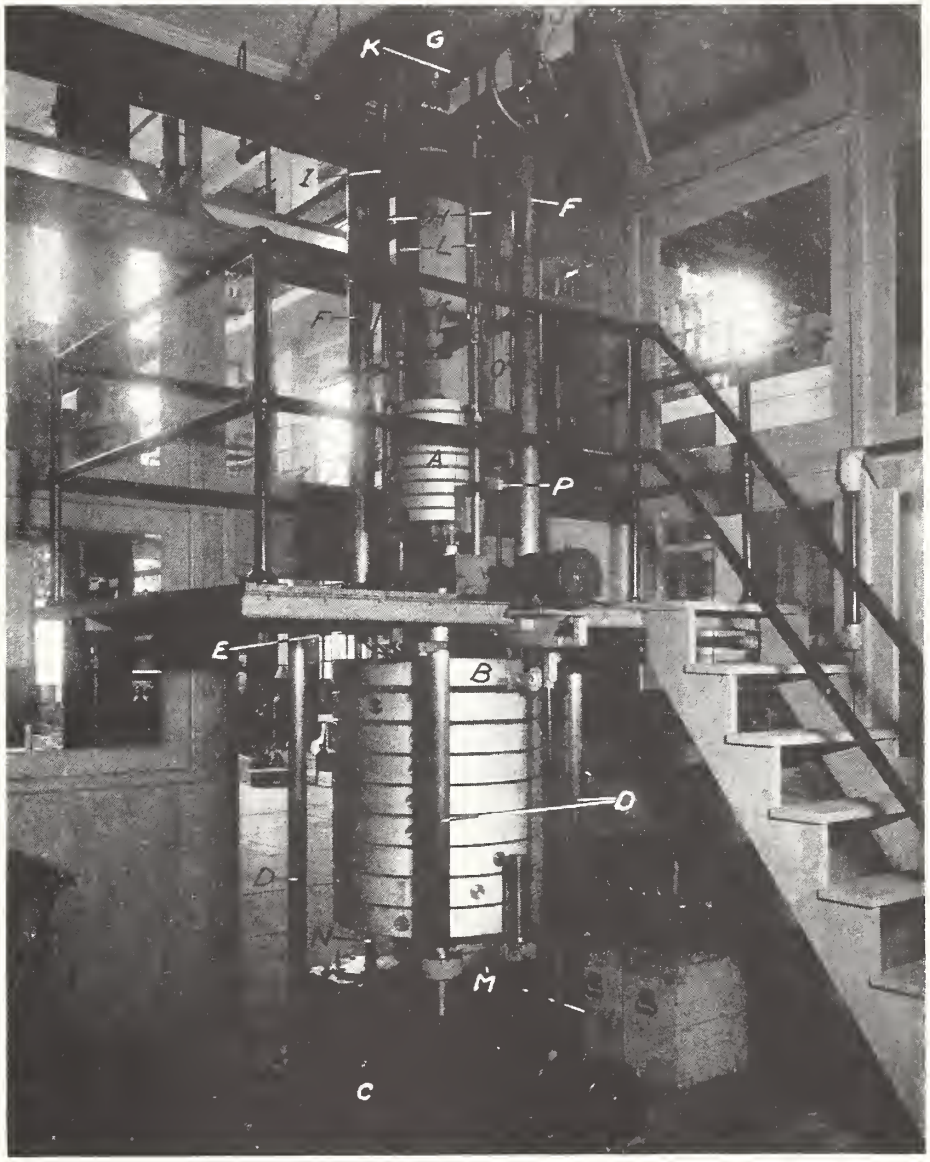

FIGURE 7.—*10,100-lb-capacity dead-weight machine as it was originally installed.*

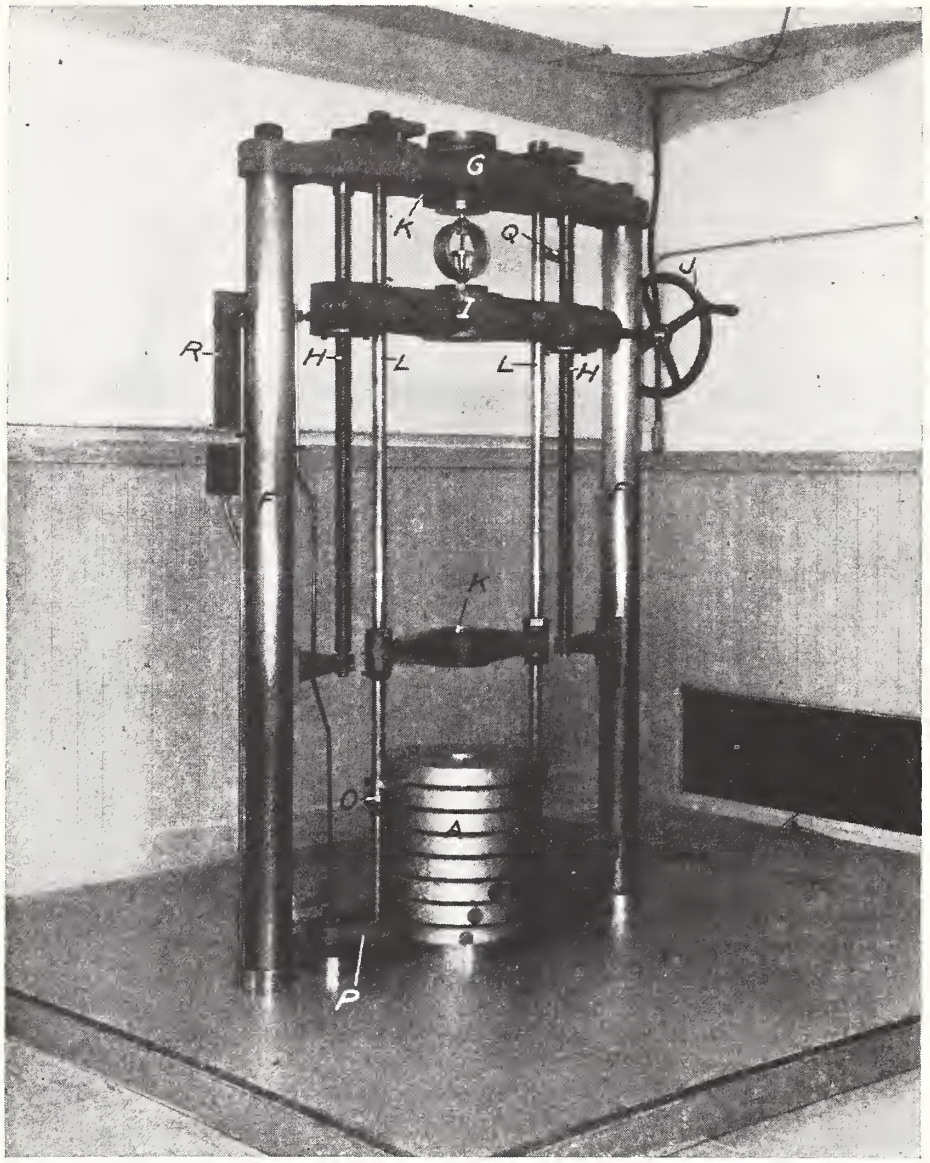

FIGURE 8.—*Loading frame and 100-lb weights of the 10,100-lb dead-weight machine.*

A 3,000-kg. capacity proving ring is shown ready for calibration in compression.

are not connected structurally to the floors of the building or the platform around the machine.

Both the 100-lb weights, *A* (figs. 7 and 8), and the 1,000-lb weights, *B* (fig. 7), are steel. The 100-lb weights are about 2 in. thick by 15½ in. in diameter, and the 1,000-lb weights are about 4 in. thick by 33 in. in diameter. The adjusting cavities in the sidewalls of the weights are closed by threaded plugs.

The frame of the machine consists of a base-plate, *C* (fig. 7), connected by four rods, *D* (fig. 7), to an upper plate, *E* (fig. 7), which supports two rods, *F* (figs. 7 and 8), the upper ends of which are connected by yoke *G* (figs. 7 and 8). Two screws, *H* (figs. 7 and 8),

are attached to yoke *G*, and by these, yoke *I* (figs. 7 and 8) is supported. Yoke *I* may be moved vertically by means of gears which are actuated by turning the handwheel, *J* (figs. 7 and 8). Devices up to 34½ in. in length may be calibrated in either tension or compression.

The loading frame consists of three yokes, *K* (figs. 7 and 8), connected by two rods, *L* (figs. 7 and 8). The bottom yoke *K*, which connects the lower ends of rods *L*, does not show in the photographs. In this smaller machine, friction due to the rubbing of the frame against other parts of the machine, which is negligible in the 111,000-lb machine, could produce appreciable error. For this reason an electronic device is used to indicate mechanical contact of the loading frame and the weights suspended from it with other parts of the machine. By taking readings only when there is no such contact, no frictional errors are introduced into the forces applied to calibration devices.

When the connecting piece attached to the top 1,000-lb weight is not in contact with the loading frame, the weights are supported on the crosspiece, *M* (fig. 7), which is moved vertically by means of the motor-driven screws, *N* (fig. 7). The bottom weight rests on a bevel seat in *M*, and each of the other weights rests on a similar seat on the weight below. As the crosspiece is lowered the connecting piece attached to the top weight engages a bevel seat in the bottom yoke of the loading frame, and the weight is supported by the loading frame. As the crosspiece is lowered farther, the weights are transferred one after another to the loading frame. A movement of about 6 in. is required to transfer all of the nine 1,000-lb weights from the crosspiece to the loading frame. The weights are removed by raising the crosspiece.

When the lugs attached to the top 100-lb weight are not in contact with the bevel seats, *O* (figs. 7 and 8), on the loading frame, the weights are supported on yoke *P* (figs. 7 and 8), which is moved vertically by means of motor-driven screws. The bottom weight rests on a bevel seat in yoke *P*, and each of the other weights rests on a similar seat on the weight below. As yoke *P* is lowered, the lugs attached to the top weight engage the bevel seats on the loading frame and the weight is transferred to the loading frame. As the yoke is lowered farther, the weights are transferred one after another to the loading frame. A movement of about 9 inches is required to transfer all of the nine 100-lb weights from yoke *P* to the loading frame. The weights are removed by raising yoke *P*.

The bevel seats and connectors for the individual weights in this machine are similar in principle to those for the 10,000-lb weights of the 111,000-lb machine shown in figure 2.

When the loading frame is not supported by a calibration device, it is supported on two bevel seats attached to the yoke *G*. The position of the loading frame is shown by the pointer, *Q* (fig. 8). The total weight supported by a calibration device, which consists of the loading frame, 200 lb, and the weights applied to the loading frame, is shown on the indicator, *R* (fig. 8). Auxiliary weights are added to the frame to obtain test loads which are not multiples of 100 lb.

A proving ring of 3,000-kg capacity is shown in the machine ready for calibration in compression in figures 7 and 8.

IV. ACCURACY OF THE MACHINES

1. THE 111,000-LB-CAPACITY MACHINE

The maximum error in the weight of the lower frame or any one of the 10,000-lb weights was determined to be about 0.1 lb when the machine was installed in 1927.

The maximum error of the 1,000-lb weights was determined to be about 0.0005 lb when they were installed in 1931.

The errors of the weights and the lower frame were redetermined in 1938. The nine 1,000-lb weights were calibrated by the method of substitution against standard weights on a special testing beam. The nine 1,000-lb weights and 1,000 lb of standard weights were combined to form the standard which was used to calibrate the 10,000-lb weights by the method of substitution on a 10,000-lb capacity platform scale. The smaller parts of the lower frame were calibrated on a balance, and the larger parts were calibrated by the method of substitution against standard weights on a platform scale. For each of the ten 10,000-lb weights no mean computed error exceeded 1 lb, or 0.01 percent. For each of the nine 1,000-lb weights no mean computed error exceeded 0.05 lb, or 0.005 percent. The 2,000-lb lower frame differed from the nominal value by less than 0.5 lb, and it was adjusted to weight 2,000.0 lb. No adjustment was made to the weights because the observed errors were of the same order of magnitude as the errors of the calibration equipment.

2. THE 10,100-LB-CAPACITY MACHINE

The maximum error of the 1,000-lb weights did not exceed 0.005 lb when the machine was installed in 1931. The maximum error of the 100-lb weights did not exceed 0.001 lb when the machine was installed in 1931. The error of the 200-lb frame did not exceed 0.01 lb.

The errors of the weights and the loading frame were redetermined in 1938. The nine 1,000-lb and the nine 100-lb weights were calibrated by the method of substitution against standard weights on a special testing beam. Part of the loading frame was weighed on the special testing beam and the remainder was weighed on a balance. For each of the nine 1,000-lb weights the maximum error did not exceed 0.05 lb, or 0.005 percent. For each of the nine 100-lb weights the maximum error did not exceed 0.005 lb, or 0.005 percent. The error of the 200-lb loading frame did not exceed 0.005 lb. No adjustments were made to the weights or frame because the observed errors were of the same order of magnitude as the errors of the calibration equipment.

V. USE OF THE MACHINES

The dead-weight machines are used to calibrate elastic calibration devices, which are used to calibrate testing machines. The American Society for Testing Materials Standard Methods of Verification of Testing Machines (see footnote 3) requires that an elastic calibration device be calibrated by dead weights known to be accurate within 0.02 percent for loads not exceeding 100,000 lb. Since no other machines which comply with this requirement are available in the United States, the machines described are used not only for calibrating

elastic calibration devices for government laboratories, but also for calibrating devices for the public.

The machines are not suitable for determining the strengths of materials or structures.

VI. CONCLUSIONS

The dead-weight machines described in this paper are suitable for calibrating proving rings and other elastic calibration devices under test loads from 200 lb to 111,000 lb. Test loads from 200 lb to 10,100 lb by 100-lb increments and from 2,000 lb to 111,000 lb by 1,000-lb increments may be applied. The errors of the test loads do not exceed 0.02 percent.

The maximum observed errors of any of the weights was less than 0.01 percent in 1938, which is less than one-tenth the maximum allowable percentage error for elastic calibration devices. The maximum allowable error specified by the American Society for Testing Materials for primary standards for calibrating elastic calibration devices is 0.02 percent. It is believed that the weights of the machines are now sufficiently stable so that the errors will not, under normal circumstances, exceed 0.02 percent for a period of 10 or 20 years.

The machines were designed by the Bureau's Engineering Mechanics Section, under the supervision of L. B. Tuckerman and H. L. Whittemore, in cooperation with The A. H. Emery Co., Stamford, Conn., and built by The A. H. Emery Co. They were installed with the assistance of A. H. Stang and L. R. Sweetman.

The weights of the machines were calibrated by the Bureau's Division of Weights and Measures, under the supervision of F. S. Holbrook and R. W. Smith.

Washington, January 25, 1943.

U. S. Department of Commerce
National Bureau of Standards

Research Paper **RP1726**
Volume 37, July 1946

Part of Journal of Research of the National Bureau of Standards

Temperature Coefficients for Proving Rings

By Bruce L. Wilson, Douglas R. Tate, and George Borkowski

Proving rings for calibrating testing machines are not compensated for change in elastic properties and dimensions with temperature. For this reason, temperature-correction factors must be used in computing ring loads from deflections obtained at temperatures that differ from the temperature of calibration. Temperature coefficients for 14 representative rings were computed from calibration results obtained at temperatures of 70° and 100° F. The temperature coefficient of one ring for the range +70° to −93° F was determined from measurements of the natural frequencies at these temperatures. The temperature coefficient of a proving ring is shown to be equal to the temperature coefficient of Young's modulus of elasticity plus twice the coefficient of thermal expansion of the material of the ring.

I. Introduction

The proving ring is the most widely used elastic calibration device [1][1] for calibrating testing machines that apply forces to engineering materials and structures. About four-fifths of such devices submitted to the National Bureau of Standards for calibration during the past year were proving rings. The rings are not compensated for the change in elastic properties and dimensions with temperature, therefore, a knowledge of the temperature coefficient is required for use in computing ring loads from deflections obtained at temperatures that differ from the temperature during the calibration of the ring.

The tests described were undertaken (a) to determine experimentally the temperature coefficients of a number of representative proving rings for the usual range of room temperatures, (b) to determine the coefficient of a representative

[1] Figures in brackets indicate the literature references given at the end of this paper.

Contents

ring at a temperature near −100° F, and (c) to determine whether the temperature coefficient may be calculated with sufficient accuracy from measured values of the temperature coefficient of Young's modulus of elasticity and the coefficient of thermal expansion for the material of a ring.

II. Description of Proving Ring

The proving ring has been described in a previous paper [2]. Briefly, it is an elastic ring in which the deflection of the ring, when loaded along a diameter, is measured by means of a micrometer screw and a vibrating reed mounted diametrically in the ring. One of the rings used in the tests reported is shown in figure 1. This ring, which was used for the tests at −93° F, was made of steel having the following chemical composition: C, 0.50 percent; Cr, 1.00 percent; and Ni, 1.75 percent. It was heat treated to show a Vickers number of about 475 (diamond indenter, load=120 kg). It is believed that each of the proving rings tested had a total alloying content not exceeding 5 percent.

Proving rings are usually calibrated in dead-weight machines [3], in which their deflections are determined for 10 uniformly spaced loads. The calibration factor, the ratio of the load to the deflection of the ring, is calculated, and the results are shown graphically as in figure 2. When a ring is used to measure loads, the observed deflection is multiplied by the product of the calibration factor read from the calibration graph and a temperature correction factor.

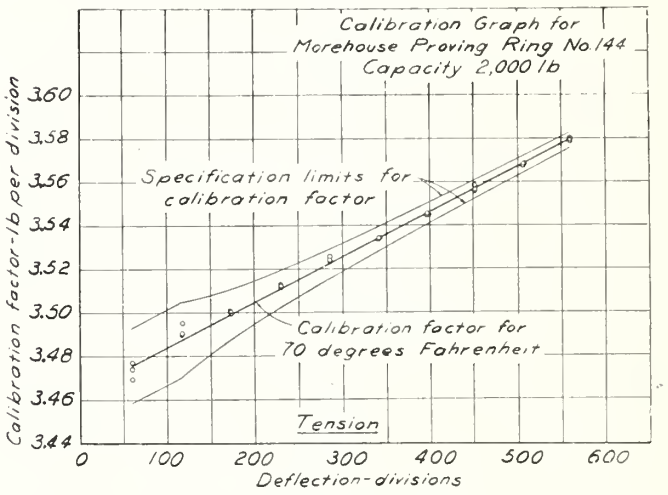

FIGURE 2.—*Calibration graph for Morehouse proving ring No. 144.*

III. Theory of Thermal Effects

1. Relationship Between Temperature Coefficient and Deflection for Proving Rings

The temperature coefficient, k, of a proving ring is defined by the equation

$$k=(1/F_c)(dF/dt), \tag{1}$$

in which F_c is the calibration factor for the ring at the standard temperature of calibration.

The calibration factor F_t for any temperature, t, becomes

$$F_t=F_c[1+k(t-t_c)], \tag{2}$$

where

F_t=calibration factor for a temperature of t degrees
t_c=standard temperature of calibration.

Equation 2 may be written in terms of deflections measured in dial divisions as

$$d_c=d_t[1+k(t-t_c)], \tag{3}$$

in which

d_c=deflection of the ring at a temperature of t_c degrees
d_t=deflection of the ring at a temperature of t degrees.

Solving equation 3 for the temperature coefficient

$$k=\frac{d_c-d_t}{d_t(t-t_c)}. \tag{4}$$

By means of equation 4 the temperature coefficient for a ring may be computed from deflections for the same load obtained at different temperatures.

2. Relationship Between Temperature Coefficient of Proving Ring and Temperature Coefficient of Young's Modulus of Elasticity and Coefficient of Thermal Expansion

The deflection in the direction of the load of a closed circular ring of rectangular cross section

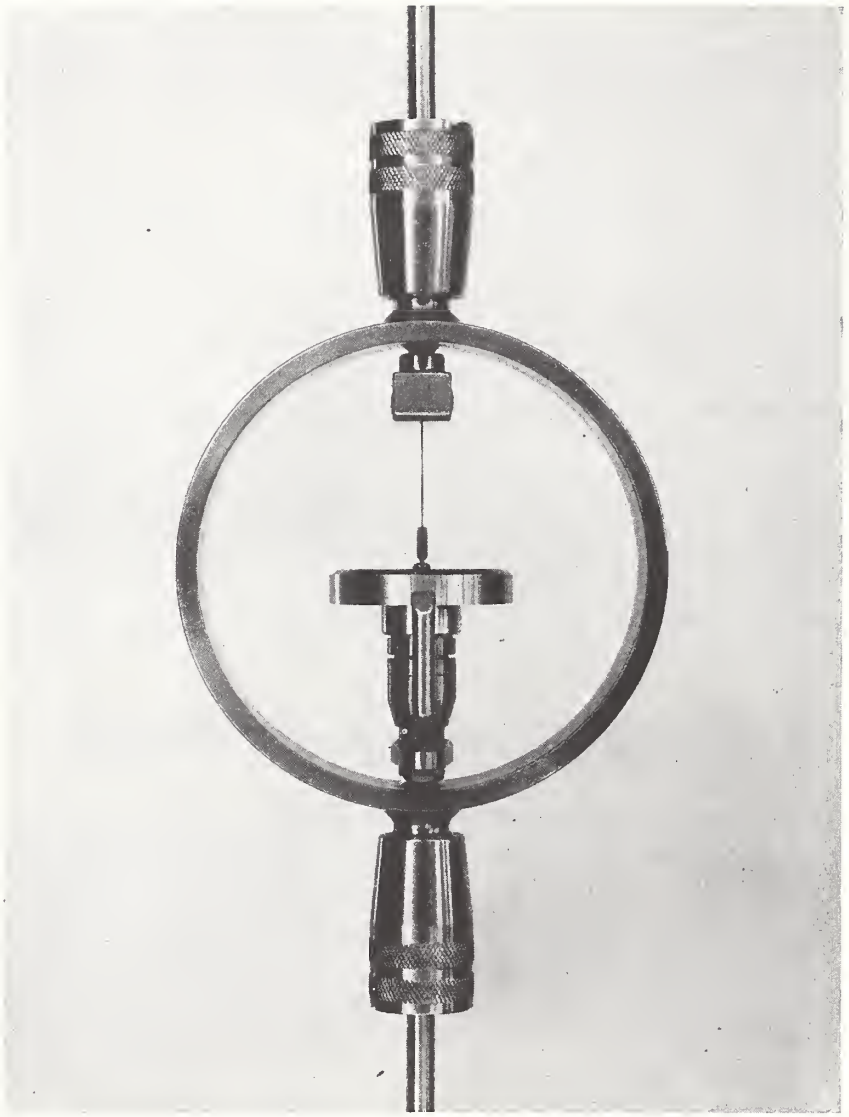

FIGURE 1.—*Morehouse proving ring No. 144, capacity 2,000 lb, with tension fittings attached to external bosses.*

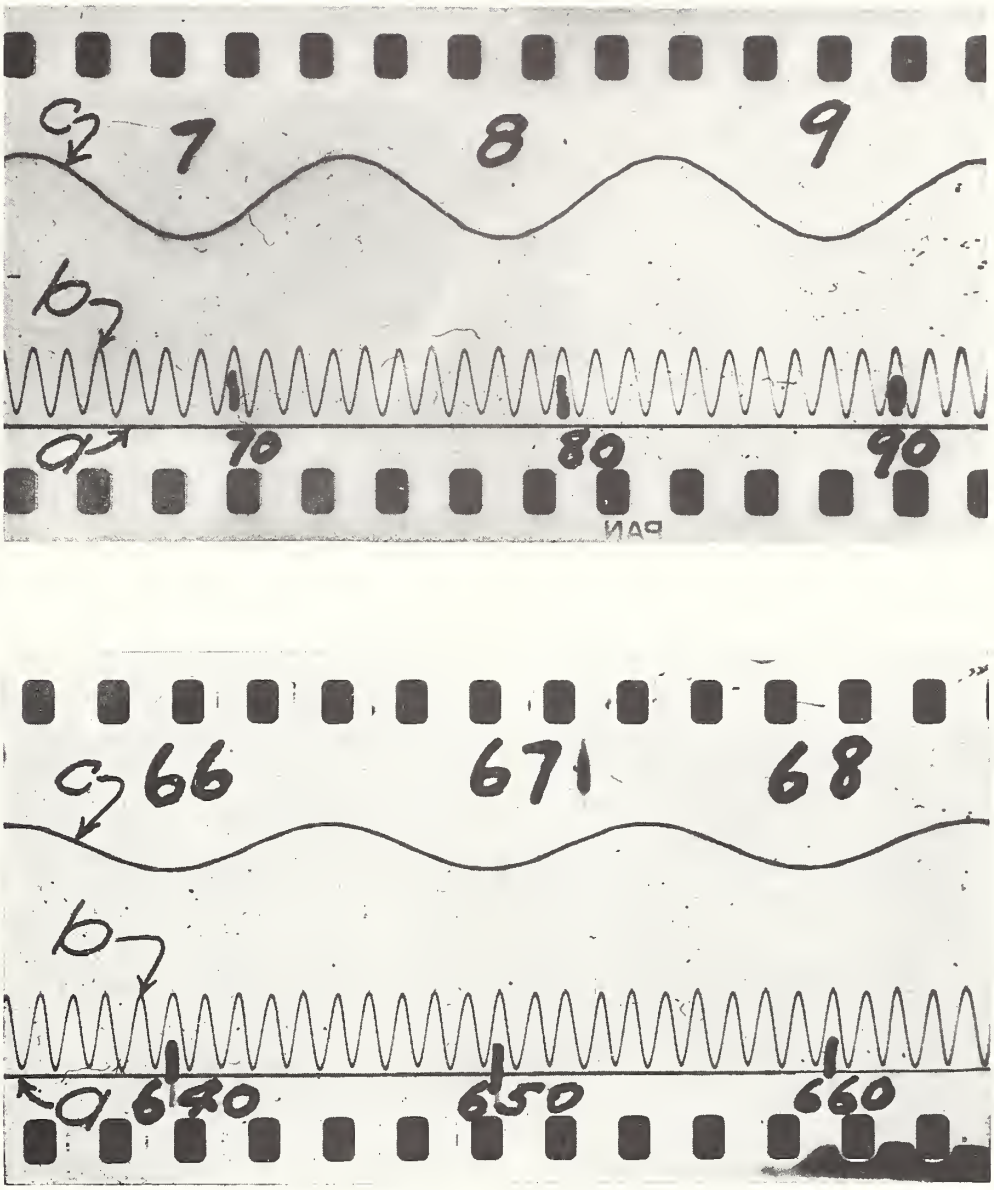

FIGURE 4.—*Reproductions from film exposed in the autographic autocollimator; (a) reference line, (b) time scale, (c) ring vibration as indicated by Tuckerman strain gage.*

loaded at opposite ends of a diameter is given approximately by the expression eq 4
where

$$d=APr^3/Elh^3, \tag{5}$$

d=deflection of the ring in the direction of the forces
A=a numerical constant
P=load on the ring
r=initial radius of curvature of the neutral surface
E=Youth's modulus of elasticity of the material of the ring
l=width of the cross section of the ring
h=thickness of the cross section of the ring.

The deflection of a proving ring is not exactly proportional to the load as indicated in equation 5. The calibration factor increases slightly with increasing tensile load as shown in figure 2. Usually the calibration factor for 10-percent capacity load differs from the calibration factor for capacity load by less than 3 percent.

As the calibration factor of a proving ring is, by definition, the ratio of the load to the deflection of the ring measured in dial divisions, the effect of changing temperature on the micrometer screw should be included in the expression for the calibration factor. Usually the micrometer screw is made of steel and has about the same coefficient of thermal expansion as the ring. If the axial travel of the micrometer screw per unit dial division is denoted by N, the calibration factor F may be written as

$$F=(PN/d). \tag{6}$$

After combining equations 5 and 6 the result may be expressed as

$$F=BEL^2, \tag{7}$$

in which

B=a numerical quantity, constant for a given ring
E=Young's modulus of elasticity, lb/in.^{2}
L=a quantity having the dimensions of length, in.

Differentiating equation 7 with respect to temperature and then dividing by equation 7,

$$\frac{1}{F}\frac{dF}{dt}=\frac{1}{E}\frac{dE}{dt}+\frac{2}{L}\frac{dL}{dt}. \tag{8}$$

Since the value of F changes by less than 1 percent over the temperature range in which proving rings are ordinarily used, it is permissible to write

$$\frac{1}{F}\frac{dF}{dt}=\frac{1}{F_c}\frac{dF}{dt}=k,$$

the temperature coefficient of the ring.
Since

$$\frac{1}{E}\frac{dE}{dt}=e.$$

the temperature coefficient of Young's modulus of elasticity

$$\frac{1dL}{Ldt}=\alpha,$$

the coefficient of linear thermal expansion.
Equation 8 may be written

$$k=e+2\alpha. \tag{9}$$

By means of equation 9 the temperature coefficient of a proving ring may be calculated from the temperature coefficient of Young's modulus of elasticity and the coefficient of thermal expansion.

3. Relationship Between Temperature Coefficient and Spring Constant for Proving Rings

The temperature coefficient of a proving ring may be computed from measurements at two temperatures of the natural frequency of the elastic system consisting of the ring and its load of dead

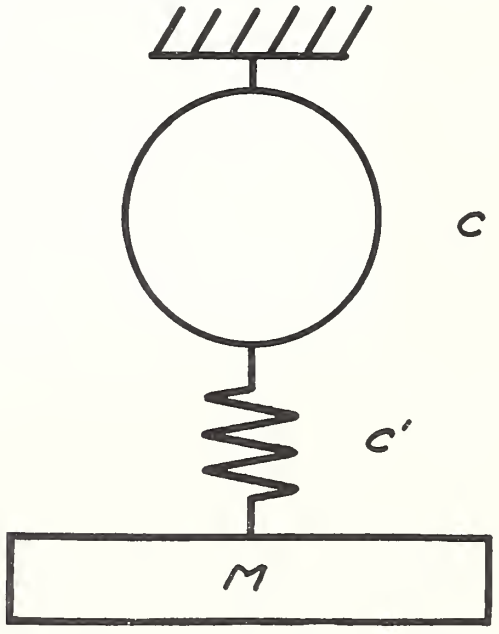

FIGURE 3.—*Elastic system used in the vibration tests.*

The load applied to the ring is represented by M, the spring constant of the ring by c, and the spring constant of the loading fixtures by c'.

weights shown in figure 3. The natural frequency of the system may be written [5]

$$f=\frac{1}{2\pi}\sqrt{\frac{cc'}{(c+c')m}}, \tag{10}$$

in which

f=natural frequency of the system
c=spring constant, load per unit deflection, for the proving ring
c'=spring constant for the loading fixtures
m=mass suspended from the ring.

From equation 10 the spring constant for the ring at any temperature, t, is

$$c_t=\frac{mc'(2\pi f)^2}{c'-m(2\pi f)^2}. \tag{11}$$

An expression for the temperature coefficient in terms of the spring constants of the ring may be derived from equation 4, which gives the relationship between the temperature coefficient and the deflections of the ring. It may be shown that

$$k=\frac{c_t-c_c}{c_c(t-t_c)}+\alpha, \tag{12}$$

in which

c_t=the spring constant of the ring for the temperature t degrees
c_c=the spring constant of the ring for the temperature t_c degrees
α=the coefficient of linear thermal expansion.

The last term in equation 12 is due to the change in pitch of the micrometer screw with temperature. By means of equation 12 the temperature coefficient of a proving ring may be calculated from the spring constants of the ring for two different temperatures and the thermal coefficient of linear expansion of the material of the ring.

IV. Experimental Procedure

1. Temperature Range 70° to 100° F

The tests were made in dead-weight testing machines [3], the loading frames of which are inclosed in a temperature controlled room. The air temperature of the room could be maintained near 70° or 100° F and held constant to within one-half degree Fahrenheit.

During the calibrations a steel block having a section approximately equal to the section of the ring being calibrated and long enough to reduce thermal end effects was placed near the ring. The bulb of a sensitive calibrated thermometer was sealed into a hole bored to the center of the block. The calibrations of the rings were made with both the block temperature and the air temperature maintained within one-half degree Fahrenheit of the desired temperature. The average temperature of the block during the interval of calibration was taken as the average temperature of the ring.

2. Temperature Range +70° to −93° F

For tests at −93° F the ring was inclosed in a wire-mesh cage, which in turn was inclosed in a box supported by the upper pulling rod. For the low-temperature tests the space between the wire-mesh cage and the box was packed with solid carbon dioxide. The box and cage were so designed that, although the ring was almost completely surrounded by solid carbon dioxide, sufficient clearance was provided for the ring to vibrate without damping effects produced by friction with the cage or the walls of the box. Vibration tests at 70° were made with the box in place.

The temperature of the ring was measured by means of five calibrated chromel P-alumel thermocouples in contact with the surface of the ring. It is believed that the errors of the temperature measurements did not exceed 1 degree Fahrenheit. During the low-temperature tests, the temperature of the ring differed from point to point due to conduction of heat along the pulling rods, but in no case did the temperature measured at any point differ from the average temperature by more than 5 percent of the total temperature range.

Vibration of the ring was produced by a single impact of a small hammer swung from a constant height about a fixed axis. The hammer swung freely, struck a rubber pad, and was caught on the first rebound. Therefore, the initial amplitude of the ring vibration was very nearly constant.

The natural frequency of the vibration of the 2,000-lb-capacity ring loaded to about 60-percent-capacity load was measured by means of a Tucker-

574278 O - 61 - 40

man strain gage attached to projections on the pulling rods of the ring. The images from the gage, a reference mirror, and a vibrating mirror controlled by the standard 60-cycle-frequency signal from the Bureau's Radio Section were photographed in an autographic autocollimator. The film was moved continuously by a synchronous motor at a speed of approximately 10 inches per second. The length of film exposed during each run was sufficient to photograph at least 60 complete wavelengths of the ring vibration. Typical records are shown in figure 4.

The frequency was determined from measurements of the number of time waves corresponding to a fixed number of wavelengths of the ring vibration. By projection, the number of time wavelengths was determined to within 0.1 time wavelength. In no case, it is believed, did the error in the measurement of the frequency exceed 0.02 percent.

The effect of damping on the frequency was calculated from measurements of the amplitudes on each film. In no case was the calculated error due to damping greater than 0.001 percent.

Under ordinary conditions of use sufficient time elapses after the application or removal of load to a proving ring to permit almost complete temperature equalization before readings are observed, and the action may, therefore, be considered isothermal [6]. During the vibration tests the frequency was about 12 cycles per second, and the action was nearly adiabatic. As the difference between temperature coefficients for steel rings determined under isothermal and adiabatic conditions can be shown to be less than 1 percent [7], no correction was considered necessary.

The spring constant of the loading fixtures (c', equation 10) was nearly independent of the temperature of the ring as the temperature of the air surrounding the rods and frame of the deadweight machine was constant. The constant c' was evaluated by substituting in equation 11 a value of c_t derived from the calibration graph of the ring for 70° F and the measured natural frequency of the system for a ring temperature of 70° F.

V. Results

1. Temperature Range 70° to 100°F

The temperature coefficients were determined for 14 proving rings for the range of temperatures from 70° to 100° F. In preliminary tests it was observed that the result obtained by computing the coefficient for the three highest of the 10, uniformly spaced test loads applied to the ring, e. g., 80, 90, and 100 percent of capacity, did not differ significantly from the result computed for 10 uniformly spaced test loads. Therefore, the temperature coefficients were determined for the three highest test loads. The temperature coefficient, k (equation 4) was computed for each ring by the method of least squares.

Typical average deflections for a 100,000-lb-capacity compression proving ring are as follows:

	Applied load—		
	80,000 lb	90,000 lb	100,000 lb
Deflection, for 101.6° F, divisions	484.21	545.33	606.67
Deflection, for 70.2° F, divisions	482.07	542.82	603.82
Difference, divisions	2.14	2.51	2.85

TABLE 1.—*Temperature coefficients for proving rings for the temperature range 70° to 100° F*

Capacity	Temperature coefficient, k	
	Compression per ° F	Tension per ° F
MOREHOUSE MACHINE CO. PROVING RINGS		
Pounds		
2,000	−0.000144	−0.000134
10,000	−.000148	----------
10,000	−.000143	----------
10,000	−.000152	----------
10,000	−.000146	----------
20,000	−.000155	−.000147
50,000	−.000155	----------
100,000	−.000160	−.000149
100,000	−.000146	----------
100,000	−.000150	----------
100,000	−.000158	----------
TINIUS OLSEN TESTING MACHINE CO. PROVING RINGS		
2,000	−0.000123	----------
20,000	−.000155	----------
100,000	−.000151	----------

Average value of the temperature coefficient for proving rings, $k = -0.000148$/° F

The temperature coefficient calculated from these data by the method of least squares is

$$k = -0.000146 \text{ per degree Fahrenheit}$$

Temperature coefficients for the 14 proving rings are given in table 1.

The temperature coefficients for proving rings varied from −0.000123 to −0.000160, the mean value being −0.000148 per degree Fahrenheit. This value corresponds to the value −0.000149 per degree Fahrenheit calculated by means of equation 9 from values for the coefficients of Young's modulus of elasticity and thermal expansion reported by Dadourian [8]. Keulegan and Houseman [9] reported results from which computed values were obtained ranging from −0.000132 to −0.000146 per degree Fahrenheit for steels of less than 5 percent total alloying content.

The temperature coefficient of one of the rings differed from the average value for all of the rings by 0.000025 per degree Fahrenheit. For this ring, correction by means of the average value for a temperature difference of 30° F, a considerably greater temperature difference than is ordinarily encountered, would result in an error of 0.075 percent. This is less than the tolerance (0.1 percent) for proving rings [2].

2. Temperature Range +70° to −93° F

Low-temperature measurements were made on the proving ring shown in figure 1. The calibration graph for this ring for a temperature of 70° F is shown in figure 2.

The temperature-correction coefficient was calculated from measurements of the natural frequency of vibration recorded on six films. The following results were obtained.

Temperature	Frequency	Spring constant of ring	Temperature coefficient per °F
°F	c/s	lb/in.	
69.4	12.391	23,050	−0.00023
−93.2	12.585	23,940	----------

The value −0.00023 obtained for the temperature range +70° to −93° F differs considerably from the average value of −0.00015 obtained for the temperature range 70° to 100° F. Benton [10] also reported a considerable increase in the temperature coefficient of Young's modulus at low temperatures. The greatest source of error in the low-temperature tests was the nonuniformity of the temperatures of different portions of the ring. Nevertheless, it is believed that the value reported is not in error by more than 1 part in 23.

As a check on the method used in the low-temperature tests, the temperature coefficient of a ring was measured by the same method over a temperature range of 70° to 178° F by means of heaters mounted in the box used for the low-temperature tests. A value $k = -0.000153$ per degree Fahrenheit was obtained, which agrees with values obtained in the dead-weight machines.

VI. Conclusions

The temperature coefficients of a group of 14 proving rings were measured for the temperature range 70° to 100° F and found to average −0.00015 per degree Fahrenheit. This value is in agreement with values calculated from the results of other observers for this temperature range.

The work of Keulegan and Houseman [9] has indicated that the temperature coefficient of Young's modulus changes very slowly in the range of temperatures ordinarily encountered in the operation of testing machines. It is believed, therefore, that for rings made of steel having a total alloying content not exceeding 5 percent, the temperature coefficient will not vary more than 10 percent from 30° to 120° F. An error of 10 percent in the temperature coefficient will introduce less than 0.05-percent error in the calculated ring load for a temperature difference of 30° F, a greater difference than is usually encountered.

The temperature coefficient of a proving ring was also measured for the temperature range +70° to −93° F and found to be −0.00023 per degree Fahrenheit.

The temperature coefficients of rings made of steels having a total alloying content exceeding 5 percent may be expected to differ significantly from the values reported.

VII. References

[1] Am. Soc. Testing Materials Standards 1944, part I, Metals, p. 954.

[2] B. L. Wilson, D. R. Tate, and G. Borkowski, Proving rings for calibrating testing machines, Circular NBS C454 (1946).

[3] B. L. Wilson, D. R. Tate, and G. Borkowski, Dead-weight machines of 111,000- and 10,100-pound capacities, Circular NBS C446 (1943).

[4] S. Timoshenko, Strength of materials, part II, ch. 2 (D. Van Nostrand Co., Inc., New York, N. Y. 1930).

[5] Den Hartog, Mechanical vibrations, second edition, p. 41–49 (McGraw-Hill Book Co., Inc., New York, N. Y., 1940).

[6] L. B. Tuckerman, discussion, Proc. Am. Soc. Testing Materials, part II, **32,** 594 (1932).

[7] J. H. Poynting and J. J. Thomson, A text-book of physics-heat, ninth edition, pp. 284–304 (Charles Griffin & Co. Ltd., London, 1928).

[8] H. M. Dadourian, Phys. Rev. [II], **XIII,** 337 (1919).

[9] G. H. Keulegan and M. R. Houseman, BS J. Research **10,** 289 (1933) RP531.

[10] J. R. Benton, Phys. Rev. **16,** 17 (1903).

Washington, April 16, 1946.

Journal of Research of the National Bureau of Standards Vol. 57, No. 4, October 1956 Research Paper 2714

Calibration of Vibration Pickups by the Reciprocity Method

Samuel Levy and Raymond R. Bouche

The reciprocity theory for the relationship between mechanical force and velocity and electric current and voltage is presented for a linear electrodynamic vibration-pickup calibrator having a driving coil, a velocity-sensing coil, and a mounting table. The theory takes account of flexibility in the calibrator structure and in the coils, electric coupling between different parts of the same coil and between parts of one coil and parts of the other, and flexibility in the magnet structure. The theory shows what measurements are required in using a linear electrodynamic calibrator for the absolute calibration of vibration pickups.

A description is given of the mechanical arrangement and electric circuitry used at the National Bureau of Standards in calibrating calibrators by the reciprocity method. A typical velocity-sensing-coil calibration curve is presented showing the effect of pickup mass on the calibration factor. Typical examples of measurement of calibration factor and mechanical impedance of pickups are also presented.

Practical limitations of the reciprocity method due to nonlinearity resulting from lack of tightness of mechanical joints, resonance effects, amplitude effects, etc., are discussed.

1. Introduction

An early application of the reciprocity method to the measurement of mechanical quantities was that by R. K. Cook [1] [1] in 1940. He applied the method to the absolute calibration of microphones. This was followed in 1948 with papers by H. M. Trent [2] and A. London [3], who showed how the reciprocity method could be used for the absolute calibration of vibration pickups. The reciprocity method was applied to the calibration of electrodynamic transducers in 1948 by S. P. Thompson [4] and to the calibration of piezoelectric accelerometers in 1952 by M. Harrison, A. O. Sykes, and P. G. Marcotte [5].

Commercially available calibrators for vibration pickups have a mounting table that is connected by a relatively rigid internal structure to a driving coil and to a velocity-sensing coil. This internal structure is supported from the frame by flexure springs or guide wires. John C. Camm, formerly of NBS, in 1953 showed how the reciprocity method could be applied to the calibration of the velocity-sensing coil of such a calibrator in connection with work for the Office of Naval Research. In 1955 the authors of the present report, in connection with work for the Diamond Ordnance Fuze Laboratories, extended Camm's theory to take account of pickup mass and flexibility in the internal structure for the frequently occurring case where the driving coil, sensing coil, and mounting table are mechanically joined at a point.

The present report gives a broader basis for the application of the reciprocity method to the calibration of the velocity-sensing coil of calibrators, by considering both the internal structure and the magnet to be flexible and by taking account of electric-coupling effects. It also shows how the calibrator, once its velocity-sensing coil has been calibrated by the reciprocity method, can be used to determine the calibration factor and to measure the mechanical impedance of vibration pickups.

2. Reciprocity Theory for Flexible Vibration-Pickup Calibrators

In the appendix the general reciprocity theory for a calibrator is presented. This theory is applicable to a calibrator operating in any frequency or amplitude range in which it can be considered to be a linear system. Neither the internal structure nor the magnet structure need be considered rigid. The theory is applicable, for example, not only at low frequencies and at frequencies near certain resonances, but also at frequencies above axial resonance where

[1] Figures in brackets indicate the literature references at the end of this paper.

the driving coil and mounting table move in opposite directions. The theory is also applicable where there is electric coupling between different parts of the same coil and between parts of one coil and parts of the other.

The positive terminals of the driving and sensing coils are designated as those having positive voltages when the mounting table is moving inward. Conversely, positive current in the coils produces outward velocity at the mounting table.

When the calibrator is energized with current in the driving coil at any particular frequency, the calibration factor, F, is defined as the ratio of the voltage in volts in the velocity-sensing coil to the velocity in inches per second at the surface of the mounting table. It is shown in the appendix that

$$F=a+bY_p \tag{1}$$

where Y_p is the pickup mechanical impedance (lb-sec/in.), and all the symbols represent complex numbers in the manner commonly used for alternating-current electrical theory. The calibrator constants, a and b, are determined by the following two experiments and computational procedure.

Experiment 1: The equipment is shown in figure 1 (a). Attach weights to the mounting table and measure for each weight the transfer admittance in amperes per volt, G, between the driving and sensing coils:

$$G=\frac{I_o^D}{E_o^S} \tag{2}$$

where

I_o^D=current in driving coil.

E_o^S=voltage generated in open-circuited sensing coil. (It is permissible to leave a voltmeter permanently connected to the sensing coil. If this is done, the open-circuit condition is obtained when no other connection is made to the sensing coil.)

Experiment 2: The equipment is shown in figure 1 (b). Couple a second vibration exciter to the calibrator being calibrated at the mounting table, and measure the ratio, R, of open-circuited voltages generated in the sensing and driving coils:

$$R=E_o^S/E_o^D. \tag{3}$$

Computational Procedure: Determine the ordinate intercept, J, and the slope, Q, of the function $W/(G-G_o)$ when plotted against the weight, W, attached to the mounting table in experiment 1, where G_o is the value of G when $W=0$. Constants a and b in eq (1) are then given by

$$a=0.01711\sqrt{j\omega JR}, \qquad b=6.601Q\sqrt{R/(j\omega J)}, \tag{4}$$

where ω is the frequency in radians per second, and j is the unit imaginary vector.

It is shown in the appendix that the vibration-pickup calibrator calibrated by the reciprocity method can be used to determine the mechanical impedance, Y_p, of a pickup by measuring the admittance, G_p, eq (2), with the pickup attached to the mounting table, and the admittance, G_o, when nothing is attached to the table, by use of the relationship

$$Y_p=j\left(\frac{\omega}{386}\right)\left(\frac{J(G_p-G_o)}{1-Q(G_p-G_o)}\right). \tag{5}$$

To carry out the calibration of a pickup the following procedure is used: The driving coil of the calibrator is energized at the desired frequency and the value of Y_p is determined. The

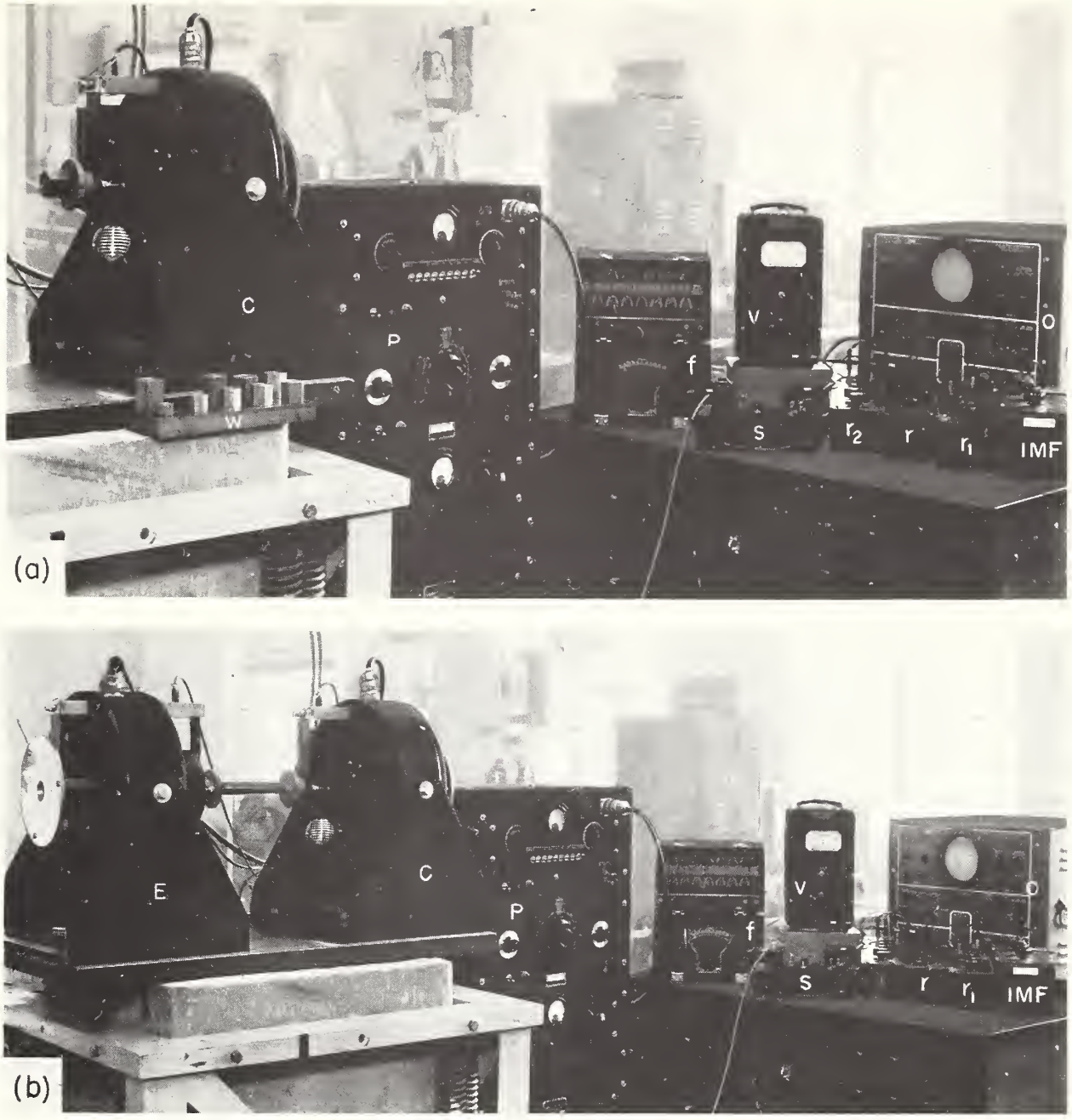

FIGURE 1. *Measurement of constants of vibration-pickup calibrator.*

(a) Weights, *W*, are attached to mounting table of calibrator, *C*, in experiment 1. (b) External vibration exciter, *E*, is required to provide sinusoidal motion to calibrator, *C*, in experiment 2.

calibrator is then driven at the desired amplitude as indicated by the voltage, E_o^s, in the sensing coil, and then the velocity is given by

$$v = E_o^s / F, \tag{6}$$

where F is obtained by substituting Y_p in eq (1). The output of the pickup corresponding to this excitation is then measured. Ordinarily the term bY_p in eq (1) for F is negligibly small, except at frequencies high enough to cause relative displacements between the mounting table and the sensing coil. Where it is known that bY_p is negligibly small, the determination of Y_p may be omitted from the calibration procedure.

3. Measurement of Constants

3.1. Accuracy of Weights

The weights attached to the table in carrying out experiment 1 at the Bureau are shown at W in figure 1 (a). The weights increase in 0.1-lb steps from 0 to 1 lb. They vary less than 0.1 percent from their rated values. Their attachment surface has a stud that engages the mounting table and a contacting ring, ⅛ in. wide, which provides a connection of high rigidity. A film of oil is wiped on this ring before engagement to eliminate air in the contact surface.

3.2. Accuracy of Frequency Measurements

The frequency was measured with a calibrated electronic frequency meter. The indicated audio oscillator frequency did not differ from the measured frequency by more than 0.2 percent.

3.3. Measurement of Transfer Admittance

The circuit shown in figure 2 (a) is used to measure the transfer admittance. With the switch in the "up" position, the values of r and r_1 are adjusted until the voltage drops $|E_{12}|$ across terminals 1 and 2, and $|E_{13}|$ across terminals 1 and 3, are equal as measured on a high-impedance voltmeter. The magnitude of G is then given by

$$|G|=\frac{r+r_1+r_2}{rr_2}. \tag{7}$$

The accuracy of $|G|$ determined in this manner depends only on the accuracy of the circuit elements and the repeatability of the voltmeter reading, but not on the accuracy of the voltmeter. Values of the resistances are chosen to load the amplifier suitably. Typical values for this calibrator are r_2, equal to 10 ohms, and $r+r_1$, approximately 1,000 times greater than r_2.

Voltage $|E_{23}|$ across terminals 2 and 3 is then read from the voltmeter. The switch is lowered to the "down" position. The value of r_1 is adjusted until $|E_{14}|$ equals $|E_{13}|$, and voltages $|E_{13}|$ and $|E_{43}|$ are read on the voltmeter. The phase angle, ϕ_G, of the transfer admittance, G, is the phase angle of I_o^D with respect to E_o^S. Because the currents in r, r_1, and r_2 are in phase with I_o^D, phase angle ϕ_G can be determined from a construction of a polygon of voltages as

$$\phi_G=\cos^{-1}\left(1-\frac{1}{2}\frac{|E_{23}^2|}{|E_{13}^2|}\right). \tag{8}$$

A suitable value of r_2 is used so that $r_1\omega 10^{-6}$ is greater than 100; then the approximate value of

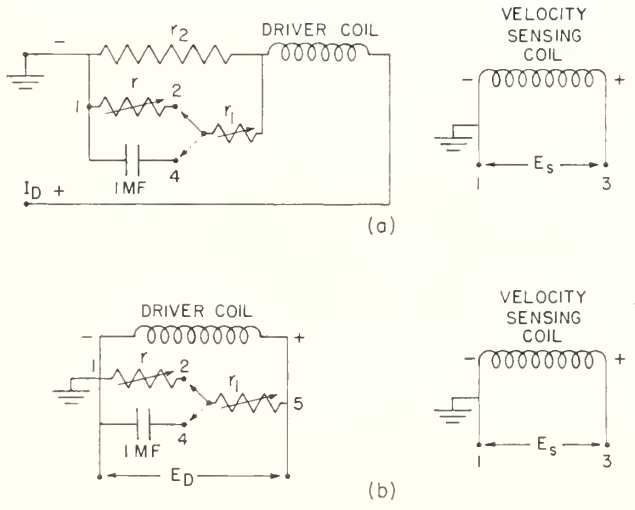

FIGURE 2. *Circuits used in the measurement of constants of vibration-pickup calibrator.*

(a) Measurement of transfer admittance. (b) Measurement of voltage ratio.

ϕ_G can be determined from

$$(\phi_G)\ \text{approx}=90°-\cos^{-1}\left(1-\frac{1}{2}\frac{|E_{34}^2|}{|E_{13}^2|}\right). \tag{9}$$

The use of both eq (8) and (9) determines the magnitude and quadrant for ϕ_G. It happens, though, except near certain resonances, that ϕ_G is near $\pm 90°$. Small errors in $|E_{43}|$ or $|E_{13}|$ result in large changes in the angle

$$\cos^{-1}\left(1-\frac{1}{2}\frac{|E_{43}^2|}{|E_{13}^2|}\right)$$

when ϕ_G is near $-90°$. Difficulty in measuring the small value of $|E_{43}|$ results in error when ϕ_G is near 90°. Therefore, eq (8) is used to determine the magnitude of ϕ_G and (9) its quadrant.

3.4. Measurement of Voltage Ratio

The circuit shown in figure 2(b) is used to measure the ratio of the open-circuit voltages of the driving and sensing coils when the calibrator being calibrated is driven by an external vibration exciter. With the switch in the "up" position and with r_1 set at 10,000 ohms, resistor r is adjusted until the voltages across terminals 1 and 2 and terminals 1 and 3 are equal. The magnitude of the voltage ratio, R, is then given by

$$|R|=\frac{r}{10{,}000+r}. \tag{10}$$

(In the case of a calibrator for which 10,000 ohms is not effectively an infinite impedance across the driving coil, r_1 in figure 2(b) should be increased to an adequate value and eq (10) correspondingly modified.)

To determine the phase angle of R, $|E_{13}|$ and $|E_{23}|$ are measured. The switch is then put in the "down" position, r_1 is adjusted until $|E_{14}|$ equals $|E_{13}|$, and $|E_{43}|$ is measured. Then from a construction of a polygon of voltages

$$\phi_R=\cos^{-1}\left(1-\frac{1}{2}\frac{|E_{23}^2|}{|E_{13}^2|}\right), \tag{11}$$

and

$$\phi_R=\cos^{-1}\left(1-\frac{1}{2}\frac{|E_{43}^2|}{|E_{13}^2|}\right)-\cos^{-1}(|R|). \tag{12}$$

It happens that ϕ_R is near either 0° or 180°. Equation (11) is insensitive for these angles, either because $|E_{23}|$ is very small for ϕ_R near 0° or because the cosine is insensitive to small changes in $|E_{23}|$ near 180°. Therefore, eq (12) is used to determine the magnitude of ϕ_R and eq (11) only its quadrant.

4. Typical Results

4.1. Calibration of Sensing Coil

Results obtained in the calibration of the sensing coil of a typical calibrator having a nominal 50-lb driving-force rating are now presented. All measurements were made after thermal equilibrium was approached. The positive terminals of the driving and sensing coils were determined as those having positive voltage when the mounting table had inward velocity. Positive velocity is then outward.

First, the transfer admittance, G, experiment 1, was measured for a sequence of weights, W, on the mounting table at each frequency for which a calibration was desired. Typical results at frequencies of 900 and 5,000 cps are presented in figure 3. In figure 4 are the corresponding plots of $W/(G-G_o)$ against W. The data were fitted by a weighted least-squares procedure for a straight line. The weighting as determined by a consideration of the expected error in $1/(G-G_o)$ was 1, 2, 3, . . ., 10 for W=0.1, 0.2, 0.3, . . ., 1.0 lb. Intercepts J and

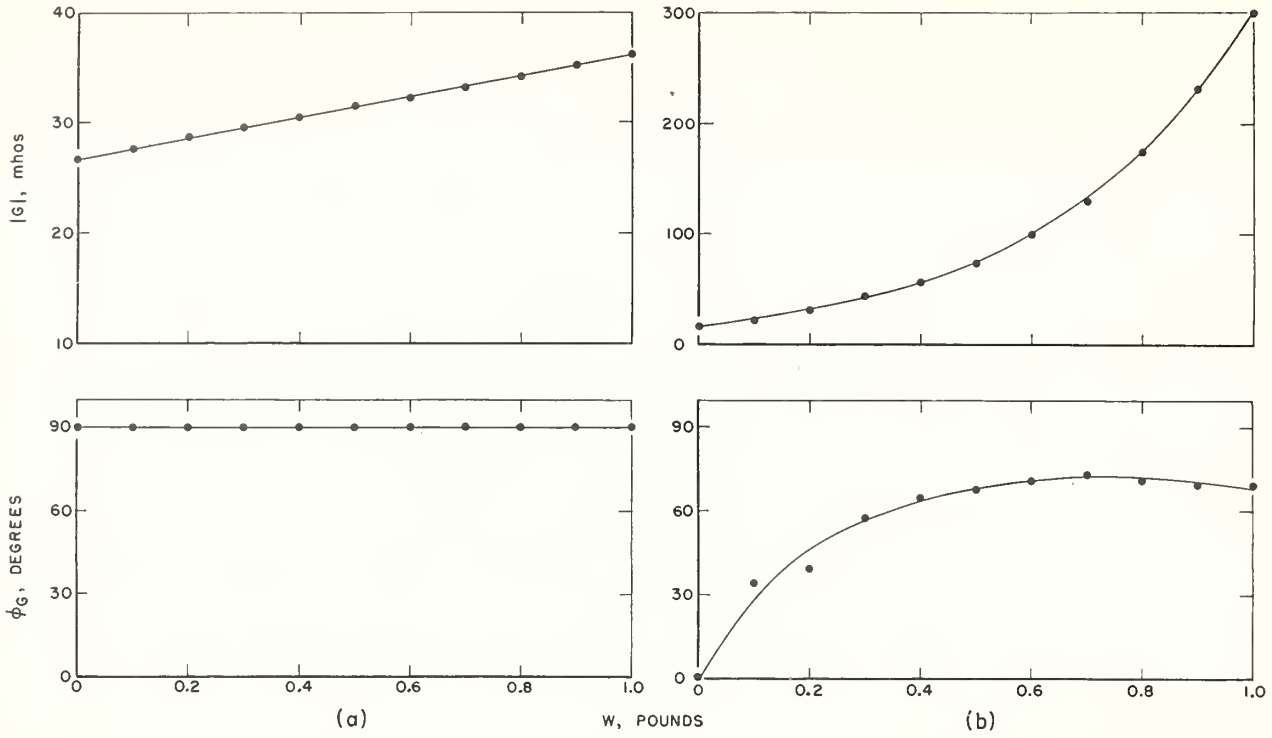

FIGURE 3. *Variation of transfer admittance, G, with weight, W, on the mounting table for a typical vibration pickup calibrator at frequencies of (a) 900 cps and (b) 5,000 cps.*

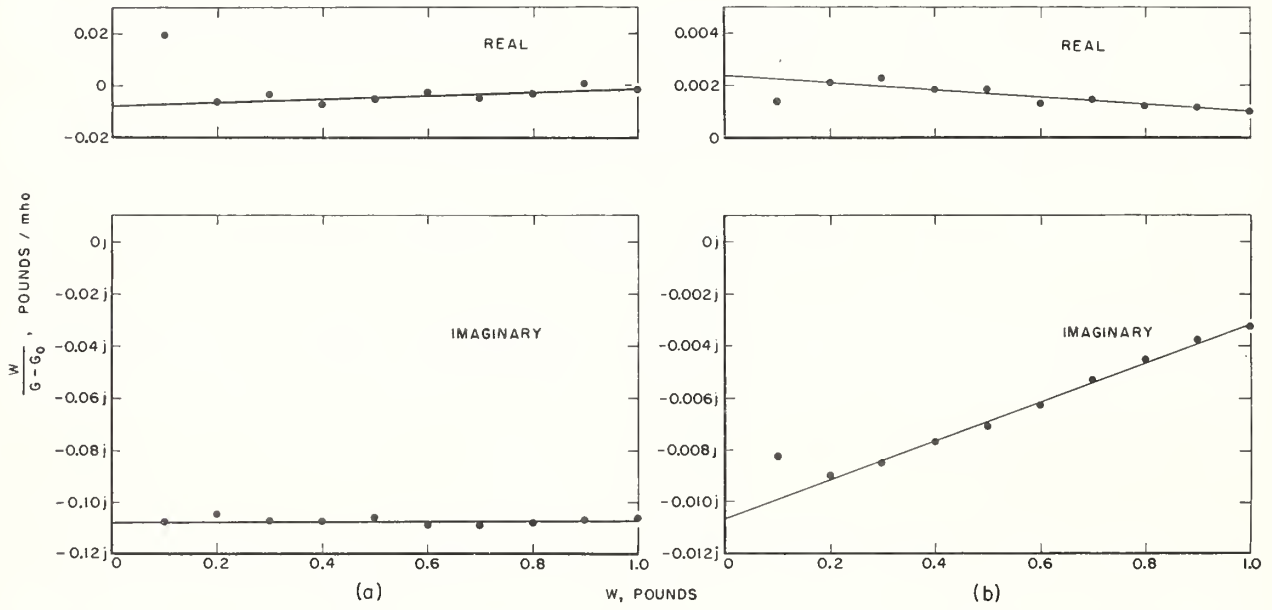

FIGURE 4. *Plot of $W/(G-G_o)$ as a function of W for a typical vibration pickup calibrator at frequencies of (a) 900 cps and (b) 5,000 cps.*

slopes' Q, determined by this procedure, are at 900 cps $J=0.1089/\underline{-94.2°}$ lb-ohm, and $Q=0.00767/\underline{11.8°}$ ohm, and at 5,000 cps, $J=0.01094/\underline{-77.4°}$ lb-ohm, and $Q=0.00765/\underline{100.4°}$ ohm.

The voltage ratio, R, when driven by an external vibration exciter, experiment 2, was then determined as $R=0.1090/\underline{-2.6°}$ at 900 cps and $R=0.2495/\underline{-2.0°}$ at 5,000 cps. Next the constants a and b in eq (4) were computed. Substituting their values in eq (1) gave calibration factors of the sensing coil with a pickup of mechanical impedance Y_p on the mounting table,

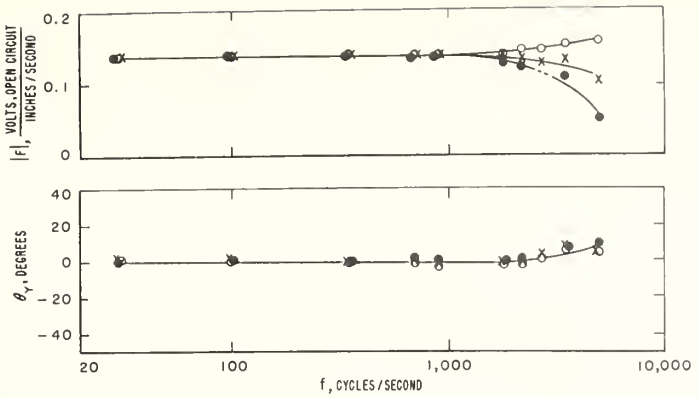

FIGURE 5. *Variation of calibration factor of velocity-sensing coil with frequency and pickup weight for a typical vibration pickup calibrator.*

○=0 lb, ×=½ lb, ●=1 lb.

at 900 cps, $F=0.1402/\underline{-3.4°}+0.000674/\underline{12.6°}\ Y_p$ v-sec/in., and at 5,000 cps, $F=0.1584/\underline{5.5°}+0.001360/\underline{93.1°}\ Y_p$ v-sec/in.

In figure 5 are shown the magnitude and phase angle of the calibration factor of the velocity-sensing coil of this typical vibration-pickup calibrator as a function of frequency for pickups having a mechanical impedance Y_p corresponding to weights W of 0, 0.5, and 1.0 lb ($Y_p=j\omega W/386$). It is evident that, for this particular vibration-pickup calibrator, the calibration factor of the velocity-sensing coil is nearly independent of frequency and pickup weight up to 900 cps. The curve for 1 lb is dotted in the vicinity of 2,700 cps because the plot similar to that shown in figure 4 was not linear beyond 0.5 lb. The source of this nonlinearity could not be localized. This nonlinearity has not been found in other calibrators of the same make and model number calibrated at the same frequency.

4.2. Calibration of a Variable-Resistance-Type Accelerometer and a Piezoelectric-Type Accelerometer

Results obtained in the calibration of a variable-resistance-type accelerometer and piezoelectric-type accelerometer are now presented. In these calibrations the circuit shown in figure 2 (a) was used with the pickup terminals designated 6 and 7, in place of velocity-sensing-coil terminals 1 and 3. The method given in section 3.3 was then used for the measurement of G_p, the value of G with the pickup attached to the mounting table.

For the piezoelectric pickup, the value of G_p obtained at 900 cps was $G_p=I_o^D/E_o^S=28.51/\underline{91.8°}$ mhos, and at 5,000 cps, $G_p=37.9/\underline{43.6°}$ mhos. With terminal 6 grounded and terminal 7 replacing terminal 3, the same procedure gave, at 900 cps, $I_o^D/E_p=16.35/\underline{2.5°}$ mhos, and at 5,000 cps, $I_o^D/E_p=3.201/\underline{-44.6°}$ mhos, where E_p is the output voltage of the pickup. From eq (5), the mechanical impedance, Y_p, of the pickup was computed by using, at 900 cps, $G_o=26.81/\underline{92.0°}$ mhos, and at 5,000 cps, $G_o=16.51/\underline{18.1°}$ mhos, and the values of J and Q obtained in section 4.1. This gave, at 900 cps, $Y_p=2.712/\underline{83.3°}$ lb-sec/in. and at 5,000 cps, $Y_p=18.23/\underline{70.5°}$ lb-sec/in. Using these values of Y_p in eq (1), the velocity sensing-coil calibration factors at 900 cps and 5,000 cps, respectively, are $F=0.1399/\underline{-2.7°}$ v-sec/in. and $F=0.1357/\underline{9.2°}$ v-sec/in. The pickup acceleration calibration factor, F_p, is

$$F_p=\frac{(I_o^D/E_o^S)}{(I_o^D/E_p)}\frac{Fg}{j\omega} \tag{13}$$

where $Fg/(j\omega)$ is the acceleration calibration factor of the sensing coil. Using this equation, at 900 cps, $F_p=0.0166/\underline{-3.4°}$ v/g, and at 5,000 cps, $F_p=0.0197/\underline{6.5°}$ v/g. Figure 6 shows the complete calibration of the piezoelectric-type accelerometer.

The calibration of the variable-resistance-type accelerometer, which was performed in a similar manner, is shown in figure 7. To compute the results on the variable-resistance

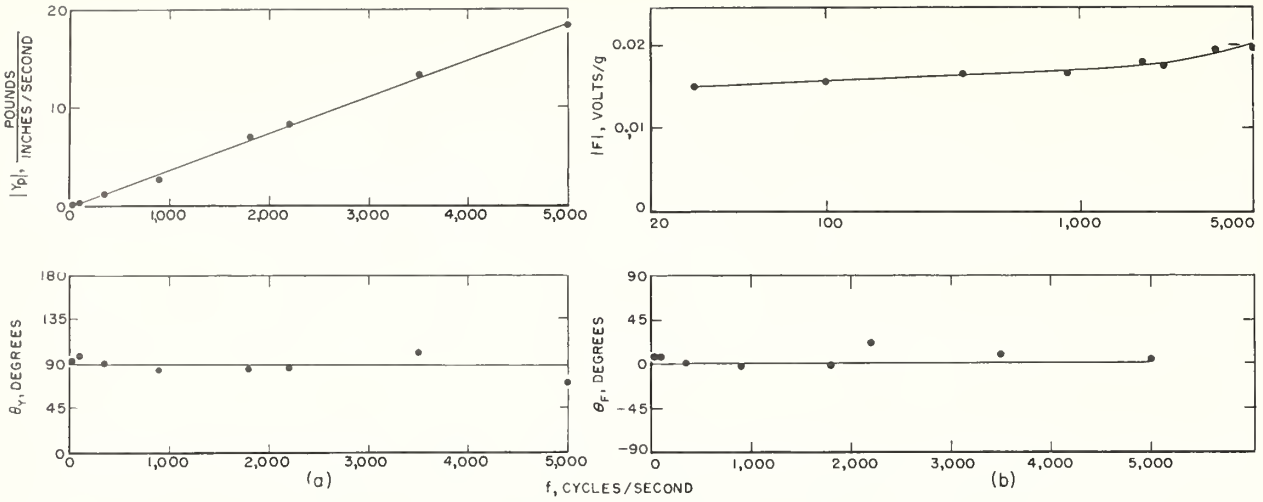

FIGURE 6. *Calibration of piezoelectric-type accelerometer at a nominal acceleration level of 2 g.*

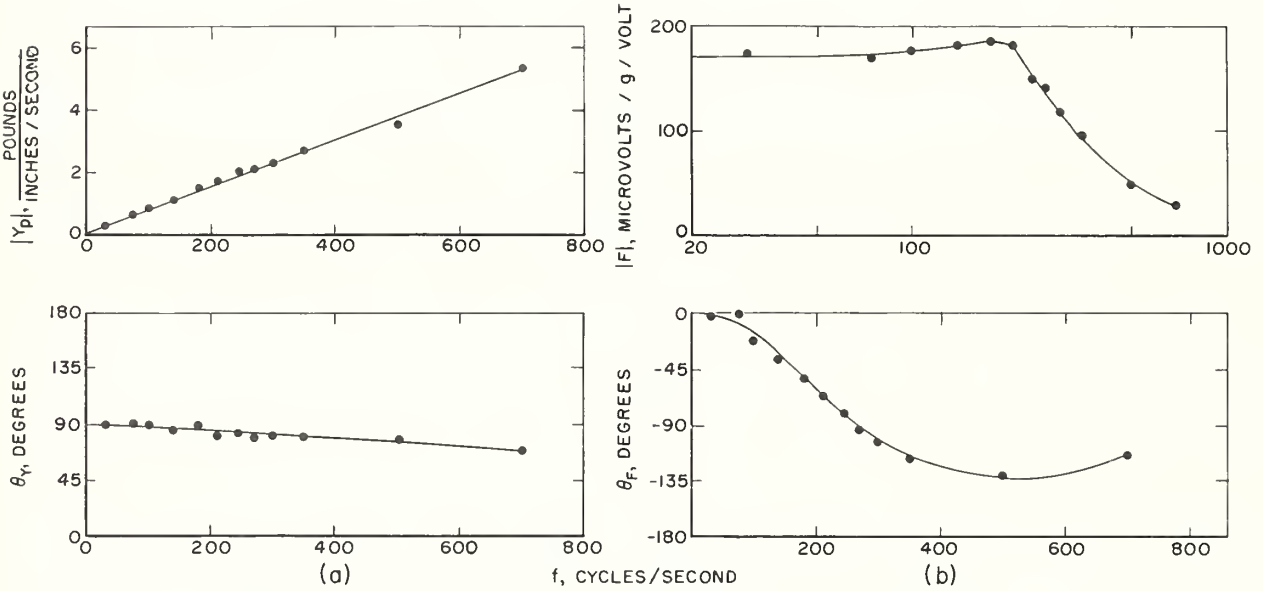

FIGURE 7. *Calibration of variable-resistance-type accelerometer at a nominal acceleration level of 2 g.*

pickup at frequencies other than those at which the vibration-pickup calibrator was calibrated, it was necessary to interpolate suitably for a, b, R, and Q, and compute J from eq 4. This interpolation was only used at frequencies below 900 cps. In this frequency range, such interpolation results in no appreciable error for this calibrator when the resonant frequencies of the flexures are avoided. The frequencies used for the pickup calibration were not those at which flexure resonance was present.

5. Effects of Calibrator Construction on Accuracy

Inaccuracy in the reciprocity method, exclusive of electrical measurements, arises primarily from deviations from true linearity in the calibrator performance. The more important forms of nonlinearity are discussed below.

5.1. Resonance Effects

Resonance accentuates inaccuracy due to nonlinearity because relatively small changes in the calibrator constants, which are caused by very small changes in the structure of the calibrator and small changes in the exciting frequency, can cause large changes in the amplitude of vibration. Even when such changes do not occur, the large amplitudes associated with resonance may exceed the linear range. The resonance of the driving coil relative to the velocity-sensing coil reduces the accuracy of the reciprocity calibration over a small frequency range because $|R|$ is very small and therefore difficult to measure, and because the large amplitude of the driver coil may exceed its linear range. Operation of the calibrator near resonance frequencies should therefore be avoided. Some common resonance conditions in their usual order of appearance with increasing frequency follow:

a. Resonance of mounting table and coils as a rigid body on the guiding flexures.
b. Local resonance in the flexures.
c. Transverse vibration of the shaft connecting mounting table and driving coil.
d. Longitudinal resonance of shaft connecting mounting table and driving coil.
e. Local resonance in table or coils.

5.2. Transverse Motion

Transverse motion from any source invalidates the reciprocity method, which requires the mounting table to have uniaxial motion. Transverse motion occurs at the resonance frequencies of the flexures and at the transverse resonance frequencies of the shaft on which the moving parts are mounted. At resonance, the amplitude will vary substantially for small changes in frequency and the resonance may occur at a frequency that is a harmonic of the driving frequency. Flexures can be detuned by attaching small weights to them.

5.3. Tightness of Mechanical Joints

The tightness of the mechanical joints in a calibrator will have little effect on its performance at low frequencies, where the moving assembly of mounting table and coils acts as a "rigid body." At frequencies approaching those for internal resonance in the assembly, looseness in the joints can affect behavior by, for example, changing the structural stiffness or by introducing coulomb friction. At very high frequencies, joints normally thought to be tight may be a source of erratic behavior, which is difficult to eliminate as tightness will ordinarily vary with temperature and time. Coating all joints with oil improves their rigidity.

5.4. Amplitude Effects

The nonuniformity of the magnetic fields surrounding the coils is a primary source of nonlinearity. This effect tends to be greatest at low frequencies, where the displacement amplitude is large for a given acceleration. At high frequencies, the displacement amplitude is relatively small, and this effect is negligible. The change in equilibrium position of the moving assembly of a calibrator, when its orientation is changed, may cause a change in calibration factor due to change in the effective field strength.

The structure of a calibrator will ordinarily experience small deformations in its linear range at permissible current intensities. At resonance, the deformations are larger. Little is known about the linearity of structural damping for a structure as complicated as a calibrator; however, so long as the damping is small, its possible lack of linearity would affect only the resonant response.

5.5. Temperature Effects

Changes in temperature cause moderate changes in elastic constants and in the tightness of joints, and in this way can affect the calibrator performance near resonance. Changes in temperature may also affect the field flux density, and thus the electrical characteristics of the driving coil, but should not ordinarily affect the calibration factor of the velocity-sensing coil.

5.6. Purity of Electric-Power Sources

If the magnets are excited by direct current containing an alternating-current ripple, this ripple may appear in the velocity output of the calibrator owing to currents included in the driving coil by transformer action from the field. Such a disturbance can readily be detected by exciting the field and observing the velocity of the mounting table with the driving coil short-circuited.

Any harmonic content in the power supply to the driving coil will excite the calibrator at the harmonic frequencies, as well as at the primary frequency. The techniques described in this paper are applicable only for excitation at a single frequency.

6. Conclusions

It is concluded that the reciprocity methods described can be used for the accurate calibration of vibration pickups and calibrators having linear response. The accuracy is limited primarily by the accuracy of electrical measurement, by deviations from true linearity in construction, and by impurities in power supplies to the field and driving coils. The frequency range is limited theoretically only to frequencies for which the mechanical impedance of the weights attached to the mounting table can be computed. Ordinarily this limits the range to that at which the weights act as though they were rigid bodies. Practically, the calibrator used as an example in this report is most suited for use at frequencies of 900 cps and below, where its calibration factor is not affected by the mechanical impedance of most vibration pickups that would be attached to its mounting table. The calibrator is suited for use above 900 cps, however, with some loss in precision primarily due to the electromechanical properties of the calibrator being less constant with respect to field-coil temperature than they are at lower frequencies. The upper acceleration range of most calibrators, when resonance is avoided, is below 50 g. This would be the limit for calibrating by the reciprocity method.

7. Appendix. General Reciprocity Theory

7.1. Reciprocity for Electric Circuit

If a complicated electric circuit is considered to be made up of a number of meshes, the almost trivial fact that the common impedance between meshes i and k, for example, is the same as that between k and i is the basis for the proof of the reciprocity theorem. This proof is elegantly presented by Guillemin on page 152 of reference [6]. Guillemin states on page 276 that the reciprocity theorem can be proved for both transient and steady-state performance. This means, for example, that if we impress a voltage in mesh 5 of a given network and measure the current, say in mesh 2, and then place the voltage in mesh 2 instead of in mesh 5 and measure the current in mesh 5, we will find the current exactly the same in the two cases, both in magnitude and phase.

7.2. Reciprocity for Mechanical System

If a complicated mechanical system can be replaced by an equivalent system having discrete mass-points joined by springs and dashpots, the fact that the spring and dashpot connecting points i and k is the same as that connecting points k and i makes possible a proof of the reciprocity theorem for mechanical systems completely analogous with that for electric circuits. (Reference [7] gives a proof of this theorem for conservative systems.) In other words, this reciprocity theorem states, for example, that if we impress a force on point 5 of a given system and measure the velocity, say at point 2, we will find the same velocity in magnitude and phase when we place the force at point 2 instead of at point 5 and measure the velocity at point 5. It should be mentioned that it is possible to have a mechanical system consisting of discrete elements that is not reciprocal, for example, if it contains gyroscopic elements.

7.3. Reciprocity for Combined System

In developing the reciprocity theorem for the combined electric-mechanical system of a calibrator, we will use matrix notation. This will permit us to consider the coils as flexible bodies and take account of electric coupling between coils, as well as deformation in the field and movable structure. The notation and theorems given by Frazer, Duncan, and Collar [8] will be used.

Currents and voltages in the velocity-sensing coil will be indicated by S and in the driving coil by D. We will consider the coils subdivided into a sufficient number of segments so each moves as a rigid body and number them consecutively in the two coils. The subscript o will indicate terminal values. Complex notation used in alternating-current electrical theory will be used throughout. All symbols represent vector quantities, unless otherwise noted. An English system of units (inches, pounds, and seconds) will be used.

Current I_o^S at the terminals of the sensing coil is given by

$$I_o^S=\frac{E_o^S}{z_{oo}^{SS}}+\frac{E_o^D}{z_{oo}^{SD}}+[z^S]\{E\}, \tag{A1}$$

where

E_o^S=voltage at terminals of coil S.

E_o^D=voltage at terminals of coil D.

z_{oo}^{SS}=impedance at terminals of coil S.

z_{oo}^{SD}=transfer impedance from terminals of coil S to terminals of coil D.

$[z^S]=\left[\frac{1}{z_{o1}^S}\ \frac{1}{z_{o2}^S}\cdots\frac{1}{z_{on}^S}\right]$, where z_{on}^S is the transfer impedance from segment n to the terminals of coil S.

$\{E\}=\begin{bmatrix}E_1\\E_2\\\cdot\\\cdot\\\cdot\\E_n\end{bmatrix}$, E_n is the voltage generated in segment n.

A similar expression can be written for I_o^D. Both of these expressions can be expressed as

$$\{I_o\}=[z_o]\{E_o\}+[z]\{E\}, \tag{A1a}$$

where

$$\{I_o\}=\begin{bmatrix}I_o^S\\I_o^D\end{bmatrix};\quad \{E_o\}=\begin{bmatrix}E_o^S\\E_o^D\end{bmatrix}.$$

$$[z_o]=\begin{bmatrix}\frac{1}{z_{oo}^{SS}} & \frac{1}{z_{oo}^{SD}}\\ \frac{1}{z_{oo}^{DS}} & \frac{1}{z_{oo}^{DD}}\end{bmatrix}$$

$$[z]=\begin{bmatrix}\frac{1}{z_{o1}^S} & \frac{1}{z_{o2}^S} & \cdots & \frac{1}{z_{on}^S}\\ \frac{1}{z_{o1}^D} & \frac{1}{z_{o2}^D} & \cdots & \frac{1}{z_{on}^D}\end{bmatrix}.$$

The current in any segment is given by

$$\{I\}=[z]'\{E_o\}+[Z]\{E\}, \tag{A2}$$

where

$\{I\}=\begin{bmatrix} I_1 \\ I_2 \\ . \\ . \\ . \\ I_n \end{bmatrix}$, I_n is the current in segment n,

$[Z]=\begin{bmatrix} \frac{1}{z_{11}} & \frac{1}{z_{12}} & \cdots & \frac{1}{z_{1n}} \\ \frac{1}{z_{21}} & \frac{1}{z_{22}} & \cdots & \frac{1}{z_{2n}} \\ . & . & & . \\ . & . & & . \\ . & . & & . \\ \frac{1}{z_{m1}} & \frac{1}{z_{m2}} & \cdots & \frac{1}{z_{mn}} \end{bmatrix}$, z_{mn} is the transfer impedance from segment m to segment n,

$[z]'$=transpose of $[z]$.

Velocity v_o at the mounting table, taken positive outward, is given by

$$v_o=\frac{F_o}{Y_{oo}}+L_1[y][k]\{I\}, \tag{A3}$$

where

F_o=the force at the mounting table.

Y_{oo}=the mechanical impedance at the mounting table.

$L_1=2.249\times10^{-7}$, a conversion factor.

$[y]=\begin{bmatrix} \frac{1}{y_{o1}} & \frac{1}{y_{o2}} & \cdots & \frac{1}{y_{on}} \end{bmatrix}$, where y_{on} is the transfer mechanical impedance from the mounting table to segment n.

$[k]=\begin{bmatrix} B_1l_1 & 0 & 0 & \cdots & 0 \\ 0 & B_2l_2 & 0 & \cdots & 0 \\ 0 & 0 & B_3l_3 & \cdots & 0 \\ . & . & . & & . \\ . & . & . & & . \\ . & . & . & & . \\ 0 & 0 & 0 & \cdots & B_nl_n \end{bmatrix}$, where B_n is the flux density, and l_n is the length for segment n.

In eq (A3), the product $L_1 B_n l_n I_n$ gives the force, in pounds, at segment n when I_n is the current, in amperes. The velocity of the various segments is given by

$$\{v\} = [y]' F_o + L_1 [Y][k]\{I\}, \tag{A4}$$

where

$\{v\} = \begin{bmatrix} v_1 \\ v_2 \\ . \\ . \\ . \\ v_n \end{bmatrix}$, v_n is the velocity of segment n.

$[y]'$ = transpose of $[y]$.

$[Y] = \begin{bmatrix} \frac{1}{y_{11}} & \frac{1}{y_{12}} & \cdots & \frac{1}{y_{1n}} \\ \frac{1}{y_{21}} & \frac{1}{y_{22}} & \cdots & \frac{1}{y_{2n}} \\ . & . & & . \\ . & . & & . \\ . & . & & . \\ \frac{1}{y_{m1}} & \frac{1}{y_{m2}} & \cdots & \frac{1}{y_{mn}} \end{bmatrix}$, y_{mn} is the transfer mechanical impedance from segment m to segment n.

The corresponding velocity in the magnetic field at the various segments is given by

$$\{v^M\} = L_1 [Y^M][k]\{I\} + [y^M]' F_o, \tag{A4a}$$

where

$\{v^M\} = \begin{bmatrix} v_1^M \\ v_2^M \\ . \\ . \\ . \\ v_n^M \end{bmatrix}$, v_n^M is the velocity of the magnetic field at segment n.

$[Y^M] = \begin{bmatrix} \frac{1}{y_{11}^M} & \frac{1}{y_{12}^M} & \cdots & \frac{1}{y_{1n}^M} \\ \frac{1}{y_{21}^M} & \frac{1}{y_{22}^M} & \cdots & \frac{1}{y_{2n}^M} \\ . & . & & . \\ . & . & & . \\ . & . & & . \\ \frac{1}{y_{m1}^M} & \frac{1}{y_{m2}^M} & \cdots & \frac{1}{y_{mn}^M} \end{bmatrix}$, y_{mn}^M is the transfer mechanical impedance from the location of segment m to that of segment n in the magnetic field.

$$[y^M]' = \begin{bmatrix} \frac{1}{y^M_{o1}} \\ \\ \frac{1}{y^M_{o2}} \\ \\ \vdots \\ \\ \frac{1}{y^M_{on}} \end{bmatrix}$$, y^M_{on} is the transfer mechanical impedance from the mounting table to the magnetic structure opposite segment n.

The voltage generated in each segment is

$$\{E\} = -L_2[k]\{v\} + L_2[k]\{v^M\}, \tag{A5}$$

where $L_2 = 2.540 \times 10^{-8}$, a conversion factor. In eq (A5), $-L_2 B_n l_n (v_n - v_n^M)$ is the electromotive force generated in segment n, in volts, when the relative velocity between segment n and the magnetic field, in inches per second, is $(v_n - v_n^M)$. Substituting (A2) into (A4) and (A4a), and substituting the results into (A5) gives

$$\{E\} = -F_o L_2[k][y - y^M]' - L_1 L_2[K][z]'\{E_o\} - L_1 L_2[K][Z]\{E\}, \tag{A6}$$

where

$$[K] = [k][Y][k] - [k][Y^M][k]. \tag{A7}$$

Letting

$$[V^{-1}] = [1] + L_1 L_2[K][Z], \tag{A8}$$

where

$$[1] = \begin{bmatrix} 1 & 0 & 0 & \cdots & 0 \\ 0 & 1 & 0 & \cdots & 0 \\ 0 & 0 & 1 & \cdots & 0 \\ \vdots & \vdots & \vdots & & \vdots \\ 0 & 0 & 0 & \cdots & 1 \end{bmatrix}$$, the unit matrix,

$[V^{-1}]$ = inverse of $[V]$.

$$\{E\} = -F_o L_2[V][k][y - y^M]' - L_1 L_2[V][K][z]'\{E_o\}. \tag{A9}$$

Substituting (A9) into (A1a),

$$\{I_o\} = [z_o]\{E_o\} - F_o L_2[z][V][k][y - y^M]' - L_1 L_2[z][V][K][z]'\{E_o\}. \tag{A10}$$

Substituting (A9) in (A2) and the result in (A3) gives

$$v_o = \frac{F_o}{Y_{oo}} - L_1 L_2 F_o[y - y^M][k][Z][V][k][y - y^M]' + L_1[y - y^M][k][V]'[z]'\{E_o\}, \tag{A11}$$

using

$$[V]' = [1] - L_1 L_2[Z][V][K]. \tag{A12}$$

The proof of eq (A12) is obtained as follows: By using (A8),

$$\begin{aligned}[1]-L_1L_2[Z][V][K]&=[K^{-1}]([K]-L_1L_2[K][Z][V][K])\\&=[K^{-1}]([K]+(1-[V^{-1}])[V][K])\\&=[K^{-1}][V][K].\end{aligned}\tag{A13}$$

Also, premultiplying both sides of (A8) by $[K^{-1}]$,

$$[K^{-1}][V^{-1}]=[K^{-1}]+L_1L_2[Z].\tag{A14}$$

As $[K]$ is symmetric, $[K^{-1}]$ is symmetric. As $[Z]$ is also symmetric, $[K^{-1}][V^{-1}]$ is symmetric. Its inverse $[V][K]$ is therefore also symmetric. The transpose of a symmetric matrix is itself or

$$[V][K]=[K]'[V]'=[K][V]'.\tag{A15}$$

Substituting (A15) in (A13) gives (A12).

The current in the velocity-sensing coil is always zero,

$$I_o^S=[1\ 0]\{I_o\}=0.\tag{A16}$$

Substituting (A10) into (A16) and solving for E_o^S gives

$$E_o^S=\frac{F_oL_2z_{oo}^{SS}[z^S][V][k][y-y^M]'-E_o^D\left(\frac{z_{oo}^{SS}}{z_{oo}^{SD}}-L_1L_2z_{oo}^{SS}[z^S][V][K][z^D]'\right)}{1-L_1L_2z_{oo}^{SS}[z^S][V][K][z^S]'}.\tag{A17}$$

The current in the driving coil is

$$I_o^D=[0\ 1]\{I_o\}.\tag{A18}$$

Substituting (A17) into (A10) and the result into (A18) gives

$$\begin{aligned}I_o^D=F_oL_2\frac{\left(\frac{z_{oo}^{SS}}{z_{oo}^{SD}}[z^S][V][k][y-y^M]'-[z^D][V][k][y-y^M]'\right.}{1-L_1L_2z_{oo}^{SS}[z^S][V][K][z^S]'}\\\frac{\left.+L_1L_2z_{oo}^{SS}[z^S][V][K][z^S]'[z^D][V][k][y-y^M]'-L_1L_2z_{oo}^{SS}[z^S][V][K][z^D]'[z^S][V][k][y-y^M]'\right)}{1-L_1L_2z_{oo}^{SS}[z^S][V][K][z^S]'}\\+E_o^D\frac{\left(\frac{1}{z_{oo}^{DD}}-\frac{z_{oo}^{SS}}{(z_{oo}^{SD})^2}-L_1L_2\frac{z_{oo}^{SS}}{z_{oo}^{DD}}[z^S][V][K][z^S]'+2L_1L_2\frac{z_{oo}^{SS}}{z_{oo}^{SD}}[z^S][V][K][z^D]'-L_1L_2[z^D][V][K][z^D]'\right.}{1-L_1L_2z_{oo}^{SS}[z^S][V][K][z^S]'}\\\left.+L_1^2L_2^2z_{oo}^{SS}[z^S][V][K]([z^S]'[z^D]-[z^D]'[z^S])[V][K][z^D]'\right)\end{aligned}.\tag{A19}$$

Substituting (A17) into (A11) gives

$$\begin{aligned}v_o=F_o\frac{\left(\frac{1}{Y_{oo}}-L_1L_2[y-y^M][k][Z][V][k][y-y^M]'-L_1L_2\frac{z_{oo}^{SS}}{Y_{oo}}[z^S][V][K][z^S]'\right.}{1-L_1L_2z_{oo}^{SS}[z^S][V][K][z^S]'}\\+L_1^2L_2^2z_{oo}^{SS}[z^S][V][K][z^S]'[y-y^M][k][Z][V][k][y-y^M]'\\\left.+L_1L_2z_{oo}^{SS}[z^S][V][k][y-y^M]'[z^S][V][k][y-y^M]'\right)\\-L_1E_o^D\frac{\left(\frac{z_{oo}^{SS}}{z_{oo}^{SD}}[z^S][V][k][y-y^M]'-[z^D][V][k][y-y^M]'\right.}{1-L_1L_2z_{oo}^{SS}[z^S][V][K][z^S]'}\\\left.+L_1L_2z_{oo}^{SS}[z^S][V][K][z^S]'[z^D][V][k][y-y^M]'-L_1L_2z_{oo}^{SS}[z^S][V][K][z^D]'[z^S][V][k][y-y^M]'\right)\end{aligned}.\tag{A20}$$

The coefficient of L_2F_o in equation (A19) equals the coefficient of $-L_1E_o^D$ in (A20). Equations (A19) and (A20) are subjected first to the condition $v_o=0$ and then to the condition $I_o^D=0$. Eliminating E_o^D in (A19), when $v_o=0$, and F_o in (A20), when $I_o^D=0$, we obtain

$$\left.\frac{F_o}{L_1I_o^D}\right|_{v_o=0}=-\left.\frac{E_o^D}{L_2v_o}\right|_{I_o^D=0}. \tag{A21}$$

This is the reciprocity relation that exists in the combined electromechanical system.

Equations (A20), (A19), and (A17) can be written for brevity as

$$v_o=CF_o+AL_1E_o^D \tag{A22}$$

$$I_o^D=-AL_2F_o+BL_1E_o^D \tag{A23}$$

$$E_o^S=HF_o+NL_1E_o^D, \tag{A24}$$

where the constants A, B, C, H, and N depend only on the calibrator construction.

In eq (1) a relationship is given for the calibration factor, defined as $F=E_o^S/v_o$, as a function of the mechanical impedance, Y_p, of the object on the mounting table. We will determine this equation in terms of the calibrator constants A, B, C, H, and N of eq (A22) to (A24). If the force, F_o, is only the reaction to driving a mechanical impedance Y at a velocity v_o,

$$v_o=-F_o/Y. \tag{A25}$$

Substituting (A25) in (A22) and solving for F_o,

$$F_o=-E_o^D\frac{AL_1}{C+1/Y}. \tag{A26}$$

Substituting (A26) into (A24) and (A25) and forming the ratio E_o^S/v_o,

$$F=\frac{E_o^S}{v_o}=\frac{N}{A}+\left(\frac{NC}{A}-H\right)Y. \tag{A27}$$

We see that N/A in eq (A27) is a in eq (1) and $(NC/A)-H$ in eq (A27) is b in eq (1) when Y is Y_p.

$$a=N/A, \qquad b=(NC/A)-H. \tag{A28}$$

In experiment 1, section 2, the transfer admittance $G=I_o^D/E_o^S$ is determined for a series of weights, W, attached to the mounting table. Substituting (A26) into (A23) and (A24) and forming the ratio G,

$$G=\frac{I_o^D}{E_o^S}=\frac{B+(BC+A^2L_2)Y}{N+(NC-AH)Y}. \tag{A29}$$

In experiment 1, Y is the mechanical impedance $j\omega W/g$, where W is the weight on the mounting table, ω the frequency in radians per second, and g the acceleration of gravity, 386 in./sec^2. Making this substitution in (A29) and forming $W/(G-G_o)$, where G_o is the value of G when $Y=0$, we find

$$\frac{W}{G-G_o}=\frac{386}{j\omega}\frac{N^2}{A^2NL_2+ABH}+\frac{N^2C-AHN}{A^2NL_2+ABH}W. \tag{A30}$$

We see that the intercept J and slope Q found in determining $W(G-G_o)$ experimentally are

$$J=\frac{386}{j\omega}\frac{N^2}{A^2NL_2+ABH} \tag{A31}$$

$$Q=\frac{N^2C-AHN}{A^2NL_2+ABH}. \tag{A32}$$

In experiment 2, section 2, the voltage ratio, $R=E_o^S/E_o^D$, is determined when I_o^D is zero. Eliminating F_o between (A23) and (A24) and setting $I_o^D=0$, we see that

$$R=E_o^S/E_o^D=\frac{HBL_1+ANL_1L_2}{AL_2}. \tag{A33}$$

Equation (4) is obtained when eq (A31) through (A33) are substituted into (A28) and L_1 and L_2 have the values given previously.

From eq (A29), $G_o=B/N$, when Y is zero, that is, G_o is the value of G when nothing is attached to the mounting table of the calibrator. If G_p is the value of eq (A29) when $Y=Y_p$, where Y_p is the mechanical impedance of a pickup to be determined, we find that

$$Y_p=\frac{N^2(G_p-G_o)}{(A^2L_2N+AHB)-(N^2C-AHN)(G_p-G_o)}. \tag{A34}$$

The substitution of eq (A31) and (A32) into (A34) gives eq (5) for determining the mechanical impedance of a pickup attached to the mounting table of the calibrator.

We are indebted to L. R. Sweetman for guidance in setting up the laboratory equipment, and to Richard Harwell, Jr., for the careful machining of the masses and the various fixtures used. Ruth Woolley performed the least-squares calculations and Carol Waldron prepared the figures.

8. References

[1] Richard K. Cook, Absolute pressure calibrations of microphones, J. Research NBS **25**, 489–505 (1940) RP1341.

[2] Horace M. Trent, The absolute calibration of electromechanical pickups, J. Appl. Mechanics **15**, 49–52 (1948).

[3] Albert London, The absolute calibration of vibration pickups, NBS Tech. News Bul. **32**, 8–10 (1948).

[4] Sanford P. Thompson, Reciprocity calibration of primary vibration standards, Naval Research Laboratory Rept. F–3337, 8 p. (August 16, 1948).

[5] M. Harrison, A. O. Sykes, and P. G. Marcotte, The reciprocity calibration of piezoelectric accelerometers, David Taylor Model Basin Rept. 811, 14 p. (March 1952).

[6] Ernst A. Guillemin, Communication networks (John Wiley & Sons, Inc., New York, N. Y., 1931).

[7] Horace Lamb, On reciprocal theorems in dynamics, Proc. London Math. Soc. **19**, 144–151 (1889).

[8] R. A. Frazer, W. J. Duncan, and A. R. Collar, Elementary matrices (MacMillan Co., New York, N. Y. 1947).

Washington, March 12, 1956.

Reprint from the
Symposium on Elevated Temperature Strain Gages
SPECIAL TECHNICAL PUBLICATION NO. 230
Published by the
American Society for Testing Materials
1958

A FACILITY FOR THE EVALUATION OF RESISTANCE STRAIN GAGES AT ELEVATED TEMPERATURES

By R. L. Bloss[1]

Synopsis

Because of the urgent need for making strain measurements under elevated temperature conditions, a number of "high-temperature" strain gages have recently become available. Although most of the companies producing these gages provide some performance information, potential users are in need of much more complete information in order to choose a gage suitable for their needs and to interpret test results obtained with it. Such information will also assist in the development of better gages. A facility which is being established at the National Bureau of Standards for the comprehensive evaluation of these gages is described and some typical results of the evaluation tests are shown.

As the need for obtaining strain measurements at elevated temperatures increased, the effort devoted to developing a gage for this purpose was expanded. This is reflected in the appearance in the past few years of a number of strain gages of different designs, mostly of the bonded resistance type. As these gages were used, however, it became obvious that they had shortcomings which had not been anticipated and were not necessarily predictable. Discussions at various meetings and conferences as to the need for these gages and of their shortcomings pointed to the desirability of establishing an evaluation facility. Such a facility could provide information to assist in the development of more satisfactory gages at the same time that it was providing data on the performance of the available gage types. In order to best use equipment and techniques that had been previously developed for the evaluation of room-temperature gages (1),[2] post-yield gages (2), and temperature-compensating gages (3), the Department of the Navy and Department of the Air Force have sponsored the establishment of such an evaluation facility at the National Bureau of Standards.

Scope of Evaluation

In the beginning there was little available information regarding expected gage performance at elevated temperatures. Frequently the manufacturer provided only a gage factor for room temperature which was sometimes a theoretical value based only

[1] Physicist, Engineering Mechanics Section, National Bureau of Standards, Washington, D. C.

[2] The boldface numbers in parentheses refer to the list of references appended to this paper, see p. 66.

upon gage geometry and wire characteristics. In some cases not even the gage factor was given. On the other hand, potential users recognized the need for much more complete information and compiled lists of gage requirements which, although perhaps somewhat idealistic, provided a guide for selecting tests to which the gages

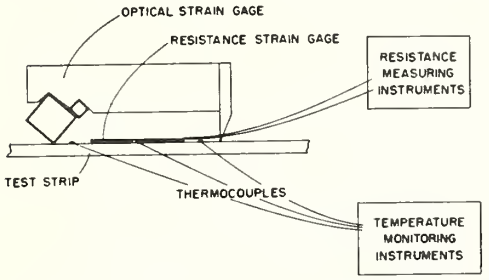

FIG. 1.—Method for Determining Gage Factor.

should be subjected. The selection of evaluation tests was also influenced by conferences and informal conversations with people involved in the development, manufacture, and use of these gages. The tests selected were designed to determine the following characteristics:

1. The variation of gage factor with temperature and strain history,
2. The linearity of the relative change of resistance with strain,
3. The relative change of resistance of the gage with time at nearly constant temperature and with no mechanically applied strain,
4. The relative change of resistance of the gage due to small temperature fluctuations and large changes in temperature,
5. The ability of the gages to withstand storage under various humidity conditions,
6. The effects of transient heating and cooling on the installed gages.

It is expected that other factors will be evaluated as the need arises and if the performance of a gage warrants such evaluation.

Considering the number of gages available for evaluation and the number of variables involved in test facilities where they might be used, it seemed that complete evaluation for all gages under all conditions would be impractical if not impossible. Therefore an attempt has been made to establish a facility which could provide sufficient information to permit a logical choice of gage type for a particular test condition and to minimize the evaluation work which would be required before the gages could be used for a particular test.

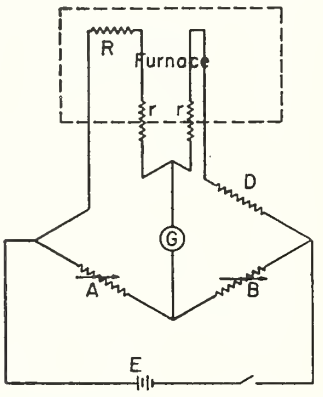

FIG. 2.—Wheatstone Bridge Circuit for Resistance Measurements.

EQUIPMENT AND PROCEDURE

The method adopted for obtaining gage factor values and determining linearity is similar to that described by Campbell (1) and is illustrated in Fig. 1. The resistance gage to be tested is attached to a test strip of uniform cross-section following the recommended installation procedure. An optical strain gage (4) spans the gage being tested and serves as a standard strain measuring device. Electrical leads to the gage and thermo-

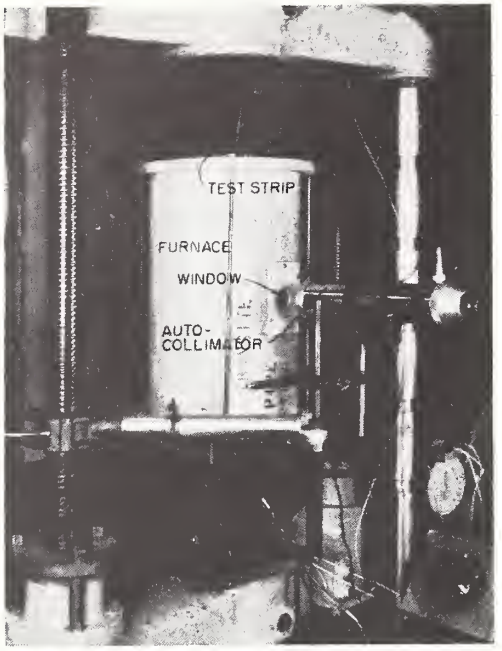

FIG. 3.—Test Equipment for Gage Factor Determination.

couples pass either through or around the knife edge of the optical gage to the electrical measuring equipment. The change of resistance of the gage as it is strained is measured by means of the Wheatstone bridge circuit shown in Fig. 2. Variable resistances A and B are contained in a Wenner ratio set, D is a fixed resistor of known value, R is the gage being tested, and r is the resistance of the leads to the gage. This lead resistance is made small and is also duplicated in an adjacent arm of the bridge circuit to provide compensation for lead resistance variations. Arm A is variable in steps of 1 ppm of its nominal resistance and arm B is variable in steps of 400 ppm. The galvanometer, G, has sufficient sensitivity to indicate clearly a change of resistance of 1 ppm, the smallest increment of arm A. The relative change of resistance of the gage, $\frac{\Delta R}{R}$, can be expressed in terms of the A and B arm dial settings (a_0, a_1, a_2, b_0, b_1, and b_2), the fixed resistance, D, the initial gage resistance, R, and the lead resistance, r, as

$$\frac{\Delta R}{R} = \frac{1}{100}\left[\frac{100+(a_2-a_0)}{1+0.04(b_2-b_0)} - \frac{100+(a_1-a_0)}{1+0.04(b_1-b_0)}\right]\frac{D+r}{R}$$

After the bridge circuit is initially balanced, tests are conducted by setting a predetermined change of resistance onto the Wenner ratio set and loading the test strip until the bridge is again balanced, at which time an optical gage reading is taken. This process is repeated to obtain a series of readings for increasing and decreasing loads. After corrections for temperature fluctuations, elapsed time, and instrument calibration are applied, the gage factor is determined as the slope of the curve of relative change of resistance *versus* strain, that is, $K = \frac{\Delta R}{R}/\epsilon$. This value

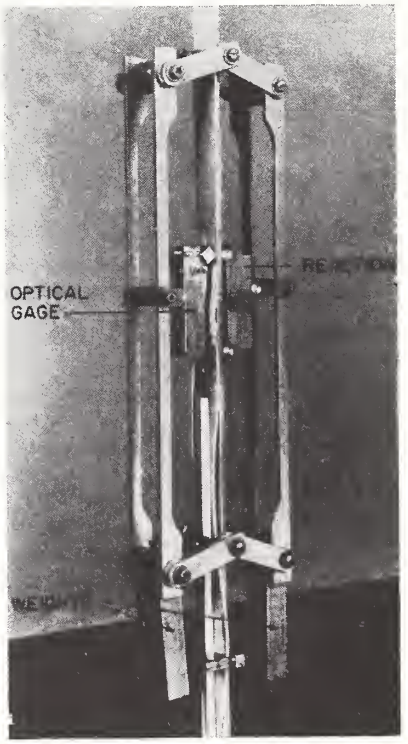

FIG. 4.—Optical Strain Gage Mounting.

is obtained from a line fitted to the data by least squares. The departure of the experimental points from the least squares curve shows the non-linearity of the gage response.

The equipment originally used for these tests is shown in Fig. 3. It consisted of the test strip extending through a furnace which was mounted in a universal testing machine. A window in the furnace permitted the optical gage readings to be obtained with the autocollimator. This arrangement had several disadvantages, the principal ones being,

1. Difficulty in maintaining a uniform temperature due to chimney effect,
2. The limiting of tests to tension loading, and
3. Difficulty in mounting the optical gage onto the test strip. (The method which was used to hold the optical gages is shown in Fig. 4.)

In order to overcome these disadvantages, equipment using a horizontal test strip which can be loaded in either tension or compression was designed. This machine is shown in Fig. 5. A test strip is held in wedge-type grips and also fits tightly against a compression bearing member at each end. The load is applied by a variable speed mechanical drive through a gear chain, linear motion being assured by a torque arm. The optical gage is held onto the specimen by means of a suitable weight. The furnace is mounted on a carriage to permit easy adjustment of its position as well as to facilitate inserting the test specimen into the machine. Evaluation tests are conducted in the same manner as was outlined above.

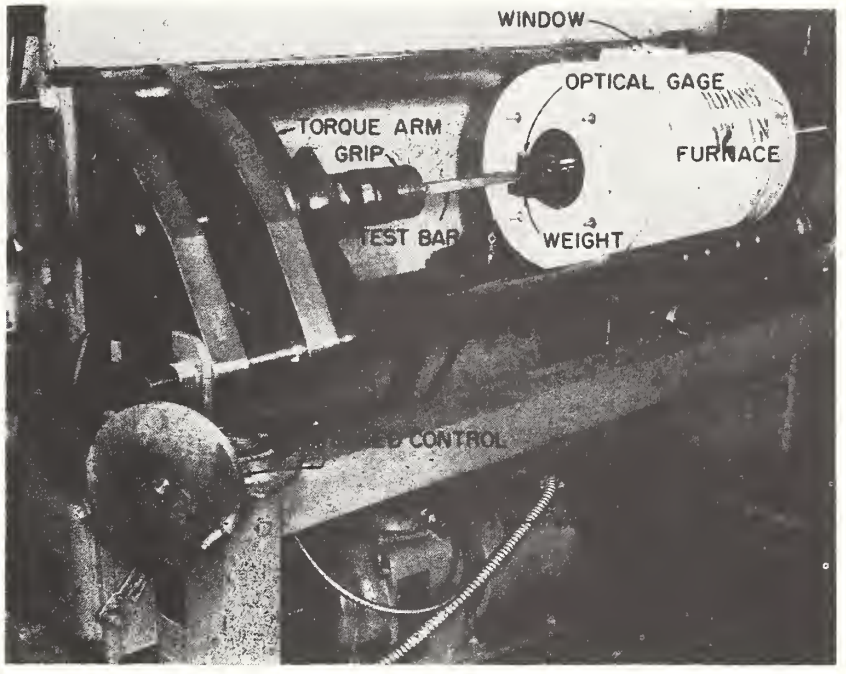

Fig. 5.—Horizontal Test Equipment for Gage Factor Determination.

It was soon found that the change of gage resistance with time at elevated temperature (drift) could be great enough to be a serious problem. In

order to measure this change of resistance satisfactorily, the equipment shown in Fig. 6 was assembled. It consists of a small furnace and a stand and holder for holding a small test strip in the furnace without applying a load or restraint upon it. Electrical leads and thermocouples are brought out to electrical measuring instruments. Since

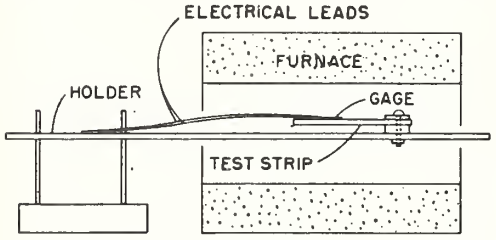

FIG. 6.—Equipment for Drift Determination.

the resistance changes are frequently too large and rapid to follow with the Wenner ratio set, a Baldwin SR-4 strain indicator which had been previously calibrated was used to measure the relative change of resistance. In practice, the furnace is preheated to the desired test temperature, the test strip is inserted into the furnace and allowed to come to temperature, and then the apparent strain indicated by the gage and the temperature of the test strip are noted at frequent intervals for at least one hour. Corrections are applied to the data for the temperature fluctuations which occur during this time.

In order to apply the proper corrections for temperature fluctuations during gage factor and drift tests, values of temperature coefficient of resistance are required. These "temperature coefficients" are obtained for each gage at each test temperature by causing the temperature to increase a few degrees and decrease a similar amount during which time the resistance change is noted. The temperature coefficient, α, is then determined by eliminating the drift rate, β, from the simultaneous equations

$$\alpha \Delta T_1 + \beta \Delta t_1 = A$$
$$\alpha \Delta T_2 + \beta \Delta t_2 = B$$

where:

ΔT_1 and ΔT_2 are the temperature changes,

Δt_1 and Δt_2 are the corresponding time intervals, and

A and B are the measured apparent strains, or resistance changes.

It should be noted that this method assumes that the temperature coefficients and drift rates are constants, independent of small temperature variations, of direction of temperature change, and of time. It should also be noted that this temperature coefficient is for a gage installed on a test strip and is therefore a function of the coefficient of resistance of the gage element, of the coefficient of linear expansion of the gage element and the test strip, and of the gage factor. It is also quite possible that the cement will be a contributing factor. It is assumed that all of these factors remain constant over the time and temperature intervals involved.

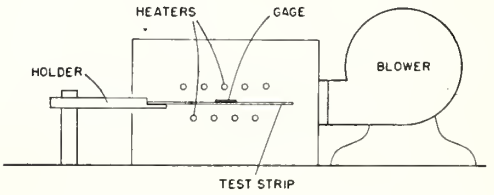

FIG. 7.—Equipment for Transient Heating.

In order to evaluate the ability of the gages to withstand storage at different humidity levels, test chambers consisting of desiccator jars with saturated salt solutions to provide relative humidity levels of about 12, 55, and 93 per cent (5) were assembled. These chambers are used to store gages in three conditions: (1) as received from the manufacturer, (2) in contact with

uncured cement, and (3) in contact with cement cured according to the gage manufacturer's recommendations. The resistance of each of the gages is measured at suitable intervals, usually once a week. A significant change of resistance would be evidence of deterioration of the resistance element, the bonding agent, or both.

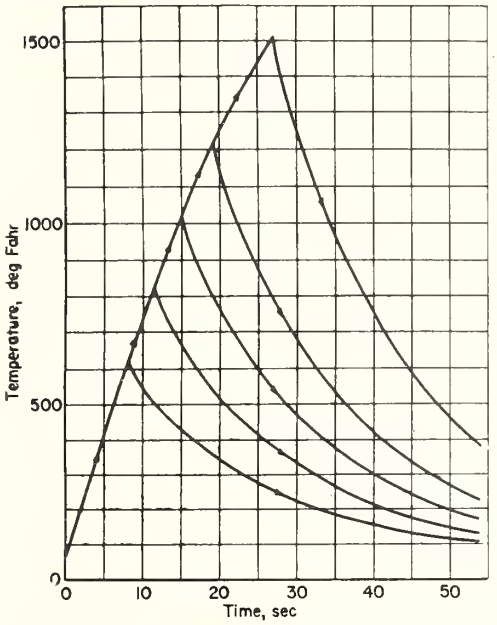

FIG. 8.—Transient Heating Temperature Cycles.

Since many of the tests for which high-temperature strain gages are needed involve transient heating, it seemed necessary to determine how rapid temperature changes would affect the gages, to evaluate their performance characteristics under such conditions, and to define some of the problems associated with the use of gages under these conditions. For this purpose the apparatus shown in Fig. 7 was assembled. It consists of an open-ended transite box through which are inserted nine quartz tube radiant heat lamps. This box is mounted at the output of a centrifugal blower. A holder for a test strip is mounted at the other end of the box. The heaters, normally rated 500w at 125v, are operated at 208v. When the heaters are turned on, an automatic system takes over to turn the lamps off and the blower on when the test strip reaches a preset temperature. The heating and cooling of a small stainless steel test strip (1 by 0.050 in.) obtained with this apparatus is shown in Fig. 8. The maximum heating rate is about 60 F per sec.

During such temperature cycles the relative change of resistance of the gage, indicated by the output voltage of a bridge circuit of which the gage is one arm, is recorded as a function of the test strip temperature which is measured by a thermocouple spot-welded to the strip. An Electro-Instrument Model 225 X-Y recorder is used to record these values.

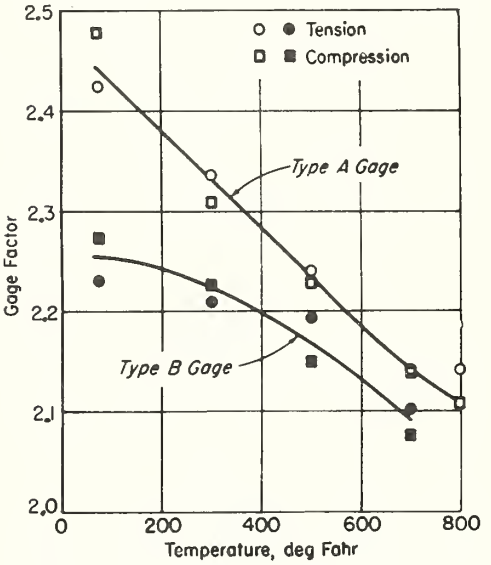

FIG. 9.—Gage Factor Values for Two Gages.

TEST RESULTS

Gage factor values obtained in tension and compression tests of two gage

types are shown in Fig. 9. It was not felt practical to carry out static gage factor determinations for these gages at temperatures higher than shown because of the high drift rates that would have been encountered. Even at these temperatures, the application of rather large corrections to the loading cycle data was required as shown in Fig. 10. Drift rate and temperature coefficient values for use in making these corrections were determined when the individual gages were being evaluated. Since the temperature fluctuations were small, perhaps 1 F, during these gage factor tests, the greater part of these corrections are for drift.

The departure of the gage response from the straight line relationship $\frac{\Delta R}{R} = K\epsilon$ is shown in Fig. 11. These values were obtained after the corrections of Fig. 10 had been applied.

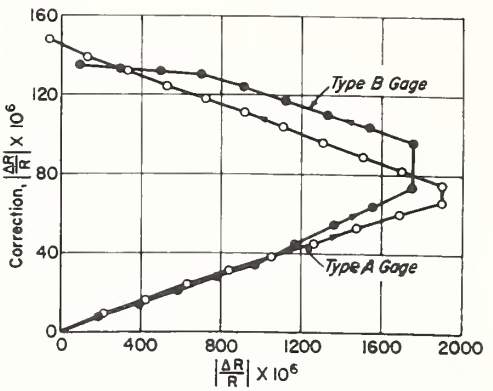

FIG. 10.—Corrections for Drift and Temperature Fluctuations.

The magnitude of the corrections shown in Fig. 10 indicate that drift can be a serious problem. In order to find at what temperatures this characteristic would preclude static gage factor determinations, drift was measured at temperatures as high as 1000 F. Typical values for one type of gage are shown in Fig. 12. It is interesting to note that the drift can be either positive

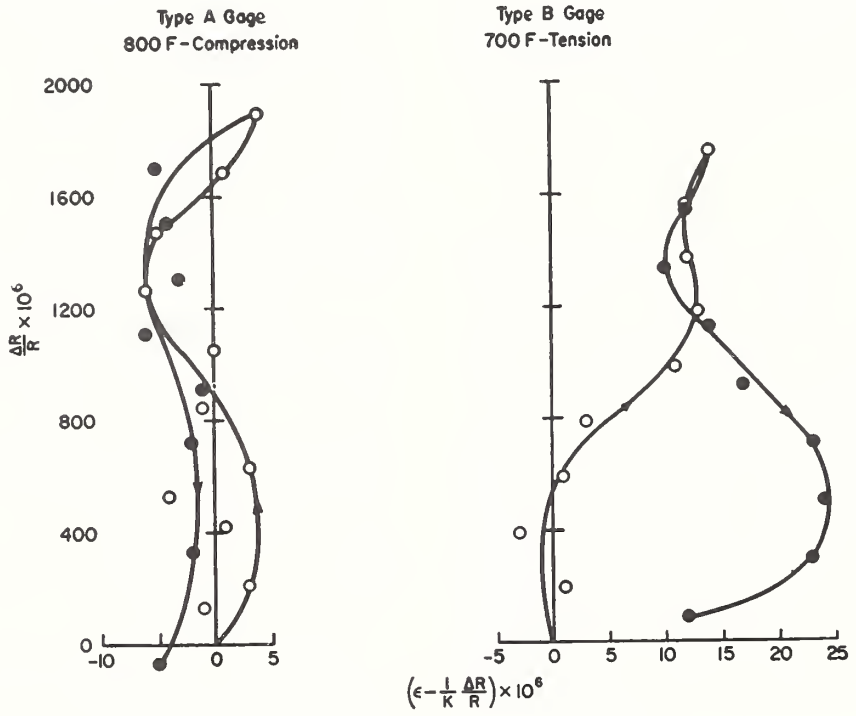

FIG. 11.—Strain Deviation of Two Gages.

or negative depending upon material and temperature. It has also been found that its magnitude and sometimes its direction can be changed by thermal history. This is shown in Fig. 13 which shows the drift behavior of four gages of one type at 800 F with different thermal histories.

The temperature coefficient of the gages varied considerably from gage to gage of one type. The curve of Fig. 14 is drawn through the average values obtained from four or more gages at each temperature; each gage had been subjected to a different thermal history. The vertical lines show the range of values obtained at each temperature. In this case some of the discrepancy, especially at the higher temperatures, may be due to an invalidity of the assumption that the temperature coefficient does not vary rapidly with temperature. In other instances there is some doubt about temperature coefficient and drift rate being nearly independent of time, temperature, and direction of temperature change even over the small time and temperature intervals involved.

An example of relative change of resistance of a gage while being subjected to temperature changes of about 60 F per sec is shown in Fig. 15. The curves shown are for two heating cycles of the same gage. The large difference in the slopes of the curves shows that the resistance - temperature characteristics of the gage were drastically changed by this treatment. The difference in the curves for heating and cooling may be due to a number of factors. The most probable of these are: (*a*) the resistance-temperature characteristics of the gage may depend upon the direction of temperature change, (*b*) there may be a permanent change in the gage wire characteristics due to thermal history, or (*c*) a temperature difference which may depend upon temperature and direction and rate of temperature change

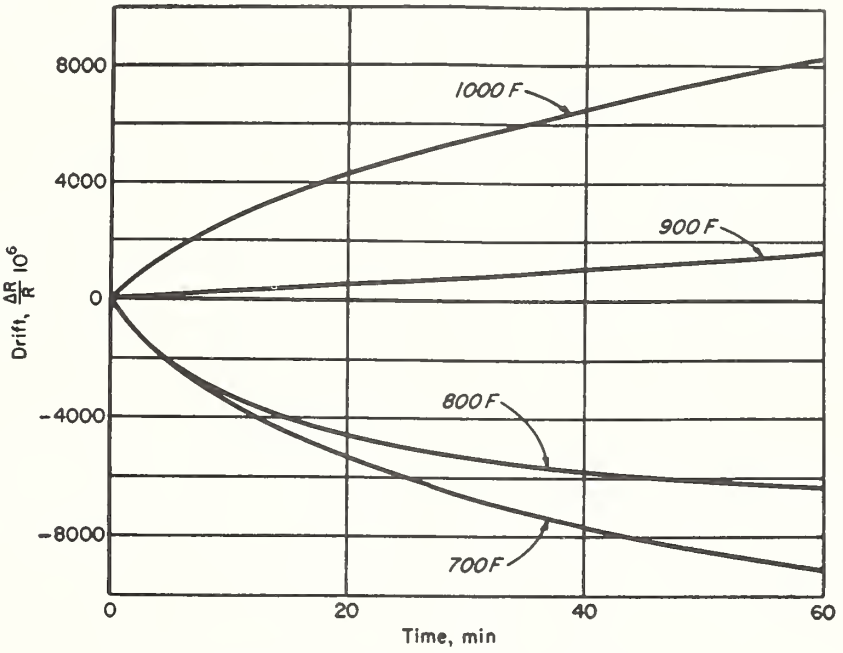

FIG. 12.—Drift Behavior at First Test Temperature.

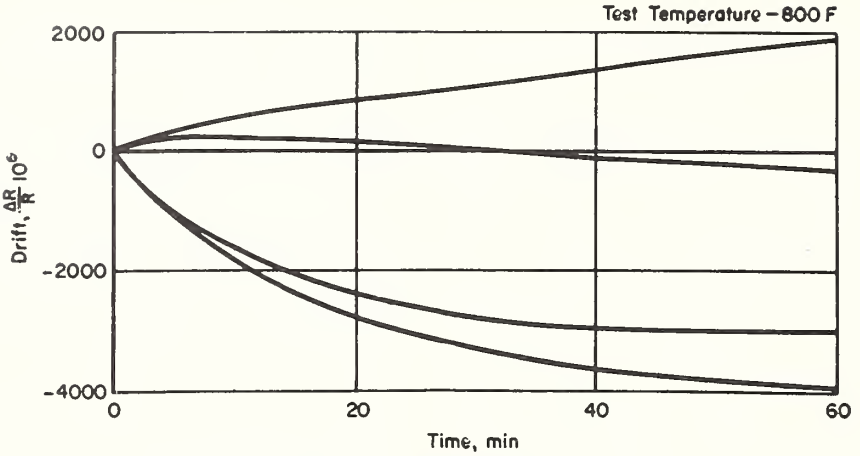

FIG. 13.—Effect of Thermal History on Drift.

may exist between the gage and the test strip. Until a better understanding of these factors can be obtained, these results can only serve to point out a potential source of serious error in using resistance strain gages for tests under transient heating conditions.

CONCLUSIONS

The number of variables encountered in the use of resistance strain gages at elevated temperatures is considerably greater than for room temperature use. It is therefore essential that a complete evaluation of the performance characteristics be made in order that the effect of these characteristics can be known for the gages under various test conditions. Since the number of test conditions is large, it is not practical for one facility to evaluate all gages for all test conditions. There should, however, be a central evaluation facility to provide sufficient information about the various gage types to guide users in their selection of a particular gage type and to minimize the additional evaluation that may be necessary prior to the use of these gages.

FUTURE PLANS

Although the current facility is suitable for obtaining considerable gage performance information at temperatures up to 1000 F (higher for some characteristics), it is inadequate for some needs. The most urgent need is for a more rapid method of evaluation to supplement the present facility by determining which gage types are suitable for a more complete evaluation and by providing performance data,

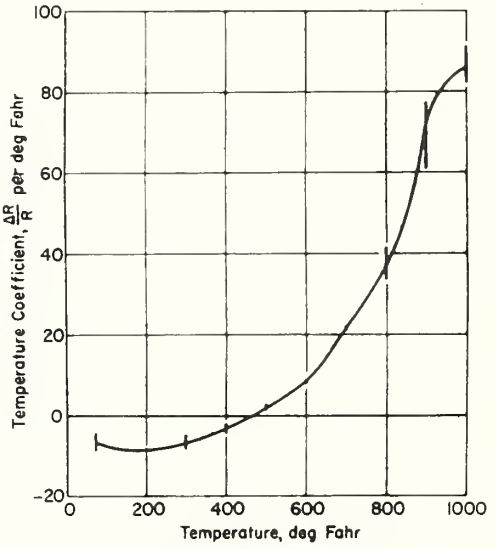

FIG. 14.—Average Temperature Coefficient of Several Gages.

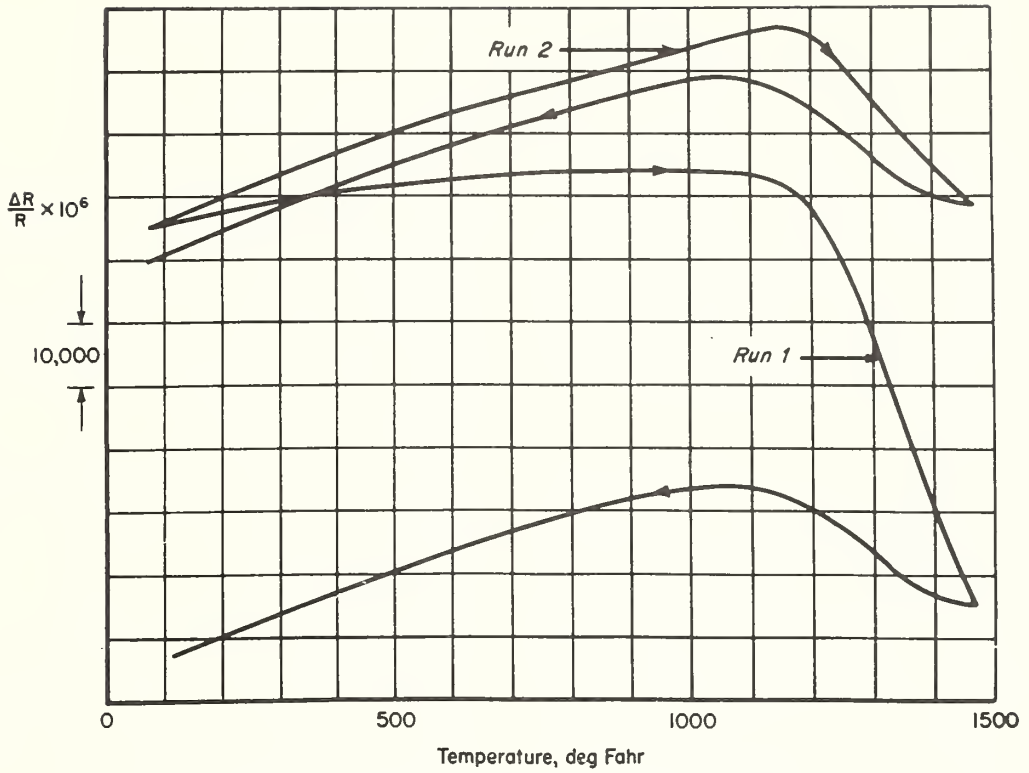

FIG. 15.—Response of Gage with Transient Heating.

although less complete, at an earlier date. More information is also needed on gage performance for test conditions which require transient heating conditions, including higher heating rates than those obtained with the present facility; dynamic, including transient, loading conditions; long time stability; slow temperature changes; and exposure to radioactive radiation and strong electric and magnetic fields. Plans currently are being made, and in some cases equipment is being assembled, to establish facilities for some of this work. Work on some of the phases, such as the effect of radiation exposure, which would require elaborate and specialized equipment has not yet been undertaken, but as these phases become increasingly important facilities for evaluation in these areas will need to be established.

REFERENCES

(1) W. R. Campbell, "Performance Tests of Wire Strain Gages I—Calibration Factors in Tension," *NACA TN 954,* Nat. Advisory Committee Aeronautics (1944).

(2) D. Namkoong, D. W. Hinze, and W. R. Campbell, "Characteristics of SR-4 and G-H Post Yield Resistance Strain Gages," *NBS Report 2537,* Nat. Bureau Standards (1953).

(3) D. W. Hinze, D. Namkoong, and W. R. Campbell, "Characteristics of Two Types of Temperature Compensating Resistance Strain Gages," *NBS Report 2552,* Nat. Bureau Standards (1953).

(4) P. R. Weaver, "An Optical Strain Gage for Use at Elevated Temperatures," *Proceedings,* Soc. Experimental Stress Analysis, Vol. IX, No. 1 (1951).

(5) A. Wexler and S. Hasegawa, "Relative Humidity-Temperature Relationships of Some Saturated Salt Solutions in the Temperature Range 0 to 50 C," *Journal of Research, RP 2512,* Nat. Bureau Standards, Vol. 53, No. 1, July 1954.

Reprinted from the Transactions of the ASME for October, 1958

Liquid-Flowmeter Calibration Techniques

By M. R. SHAFER[1] and F. W. RUEGG,[2] WASHINGTON, D. C.

Calibration techniques for liquid flowmeters are discussed with emphasis on problems which are known to influence the accuracy of calibration procedures. Also, reference methods which have been used to evaluate the comparative accuracy of different calibrators are described. The results of comparative accuracy tests on four calibrators of different designs are presented and it is shown that the agreement between these is within ±0.15 per cent in the test range of 10,000 to 100,000 lb per hr. The many precautions necessary to approach this precision from the traditionally accepted "plus and minus one per cent" are given in detail.

Introduction

In the course of a continuing program of research and development at the National Bureau of Standards on aircraft fuel-metering-accessory test equipment, conducted under the sponsorship of the Bureau of Aeronautics, the performance of various liquid flowmeters has been investigated as well as equipment and techniques for their calibration. Experience has demonstrated that absolute accuracies better than ±0.3 per cent are possible in the calibration of direct-indicating flow-rate meters. It is believed that the calibration techniques used to attain such accuracies are of sufficient general interest to warrant presentation here. Thus the objectives of this paper are to present a discussion on flowmeter-calibration techniques; to present data obtained at the National Bureau of Standards and elsewhere; to demonstrate the present state of the flowmeter-calibration art; and to describe some of the limitations of existing calibration equipment and procedures.

The techniques discussed herein are applicable to totalizing meters for which calibration procedures are established and defined (1).[3] However, our primary interest and experience have been restricted to direct-reading liquid flowmeters operating under steady-flow conditions in the range 5 to 100,000 lb per hr.

A meter calibration may be considered accurate only for the conditions existing at the time the calibration data were taken. Thus those quantities which can influence the performance of the meter must be known, measured, and controlled during precise calibration work. Factors influencing the performance of the different type meters have been investigated and reported in numerous papers, among which are (2 to 7). These factors are the density, viscosity, and temperature of the liquid; upstream, and to a lesser extent, downstream flow disturbances; the vapor pressure and absolute pressure level; and the orientation and scale sensitivity of the meter. Of course, the influence of these varies widely among the different type meters.

Summarizing the possible influences on meter performance, it may be noted that the influence of density usually can be predicted through analysis. The erratic effects of viscosity are most pronounced with the smaller sized meters and can be established only through calibration tests. Temperature exerts its influence through its effects upon the configuration of the meter and upon the physical properties of the test liquid. Vapor pressure and pressure level should have no appreciable influence provided compressibility of the liquid is not significant and the pressure level is sufficient to prohibit vapor formation. Finally, meters are sensitive to external flow disturbances, and this effect generally increases with meter size and flow rate. In fact, inadequate control of flow disturbances is one of the greatest sources of error in precise work.

Although meter characteristics may seem a separate problem from that of calibration, it must be stressed that precise calibration work cannot be performed unless these are given ample consideration in specifying and controlling the conditions of calibration.

Selection and Calibration of Instrumentation

Extreme accuracy is now possible in the measurement of mass, time, and those other quantities required for the flowmeter calibration. Perhaps some thoughts regarding the selection and calibration of the separate instrumentation items may be of value before discussing representative calibration systems. The calibrator will require a timer, scales for the measurement of mass or prover tanks for volumetric determinations, thermometers, density-measuring instruments, and perhaps a viscometer. Each of these must have sufficient sensitivity and accuracy to serve its intended purpose.

Electronic-counter timers are preferred for measuring the time interval. Many different makes are now available which operate on the principle of counting the pulses from a tuning fork or quartz-crystal oscillator. These usually indicate in units of 0.001 sec and have provisions for electronic actuation. They are considered to be better suited for this application as compared to synchronous clocks and stop watches which are dependent upon the frequency of the power supply, have minimum scale divisions of 0.1 sec, and utilize mechanical methods of actuation. Standards of time and frequency are broadcast by the National Bureau of Standards over station WWV in Maryland and WWVH in Hawaii (8). These precise signals, accurate 2 parts in 100 million, are adequate and convenient references for the calibration of timers.

Volumetric calibrating systems will require prover tanks. Specifications and calibration procedures for these are given in (1). Accuracies better than 0.1 per cent of the nominal tank volume can be attained with prover tanks provided adequate and proper temperature corrections are applied.

For the gravimetric-type calibrator a scale of conventional design, equipped with weighbeam and counterpoise is recommended. The addition of quick-weighing or automatic indication devices is not considered necessary and possibly might prove detrimental to over-all accuracy as compared to the free-swinging lever system. For smaller capacities, a straight lever system or even the equal-arm balance should be used. Balances of the torsion-tape and/or flexure-plate type also will prove suitable because of their inherent stability. Features influencing their selection and use will include capacity, smallest weighbeam graduations, and sensitivity which can be adjusted by the manufacturer as required.

Before placing the scale in service, two tests extending over the

---

[1] Research Engineer, National Bureau of Standards.

[2] Physicist, National Bureau of Standards.

[3] Numbers in parentheses refer to the Bibliography at the end of the paper.

Contributed by the Research Committee on Fluid Meters and presented at the Annual Meeting, New York, N. Y., December 1–6, 1957, of The American Society of Mechanical Engineers.

Note: Statements and opinions advanced in papers are to be understood as individual expressions of their authors and not those of the Society. Manuscript received at ASME Headquarters, July 24, 1957. Paper No. 57—A-70.

load range at which it will be used should be conducted. The first should be made before, the other after installation of the weigh tank and its connections. If the two are not in agreement, connections are likely interfering with proper functioning of the scale and the conditions should be corrected. This calibration should be done with test weights that meet C tolerances (9 and 10) and not by the comparison of one scale with another. Test weights may be secured from state or city Weights and Measures Departments, or if these are not available, the services of the scale manufacturer should be secured. The National Bureau of Standards will certify test weights in Washington, D. C., or at the National Bureau of Standards Master Scale Depot located in the Clearing Industrial District of Chicago, Ill. A self-contained or built-in type scale is desired to prevent damage to which portable type scales are subject during moving and handling. Also, the scale must be protected from wind and air currents while in use, since even light air currents produce weighing errors of appreciable magnitude.

Temperatures should be indicated preferably with mercury-in-glass thermometers usually of the range 0 to 120 F graduated in single degrees and accurate to one degree or better. Standards, specifications, and methods of testing liquid-in-glass thermometers are reported in (11) for the range −110 to +750 F. This reference lists the range, subdivisions, maximum permissible scale error, and installation instructions for the numerous types of thermometers used in test work.

In those calibration applications requiring a conversion between volumetric and gravimetric units, the measurement of liquid density is of extreme importance. Instruments for determination of liquid gravity or density include the hydrometer, pycnometer, and Westphal balance. The hydrometer is the simplest of these and it yields fairly accurate results. Specifications, tolerances, and methods of certification for hydrometers are described (12). If the test liquid is a petroleum product, any necessary conversion from specific-gravity units to density and corrections for temperature differentials can be made conveniently on the basis of Petroleum Measurement Tables (13) which contain conversion and thermal-expansion factors for all liquid-petroleum products within the specific gravity range 0.46 to 1.10.

A Static Weighing Calibration System

Calibration of a liquid flowmeter involves a determination of the time interval required for a measured mass or volume of fluid to pass through the meter, at a constant indicated rate, under the specified conditions of calibration. As extreme accuracy is possible in the measurement of mass and time, the limiting factors in the procedure are the technique, the sensitivity of the meter, the constancy of the indicated flow rate, the mechanics of collection of the fluid, and the method of timer actuation.

In presenting this discussion of a representative flowmeter-calibrating system, an apparatus which was designed and constructed at the National Bureau of Standards will be described. This was developed to obtain a precision of about 0.1 per cent with two basic features in mind: (*a*) A way was sought to collect the fluid with a minimum disturbance to the steady state of flow through the meter; and (*b*) a method was desired whereby the mass of the liquid collected could be measured under a "static" condition of no flow into the collection tank. In this way the problem of accurate measurement of mass and time could be reduced to a minimum as nearly all dynamic considerations were eliminated. A schematic diagram of the apparatus is presented in Fig. 1. This particular system was used for the evaluation of flow rates in the range 5000 to 100,000 lb/hr,

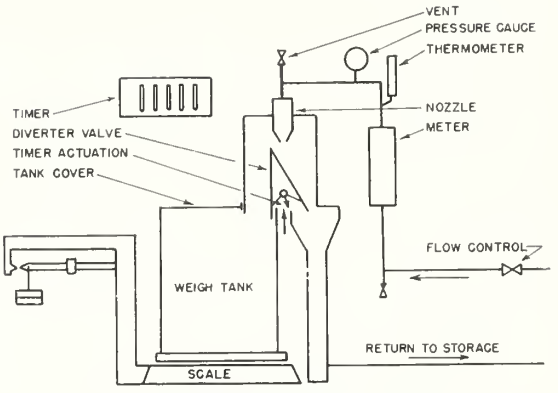

Fig. 1 NBS static weighing calibrator

which can be extended through the techniques described herein. Essential components are the flow-rate supply and control, the meter under calibration, a flow-diverter valve, an electronic timer, and a platform scale and tank.

The function of the flow-rate supply-and-control system is to deliver filtered liquid, of known physical properties, at a closely controlled temperature to the meter under test. Additional functions are to eliminate surges and pulsations within the fluid and to provide a convenient, sensitive method of control whereby all desired flow rates may be set and maintained to within 0.1 per cent of the desired value. Also, this system must contain provisions to assure positive elimination of all gas and vapor from the liquid before entering the meter with special consideration being given to the possibility of vapor formation during the throttling action of the flow-control valve.

Quantities influencing the performance of the meter under test have been discussed briefly. Of these, the upstream flow disturbances are the most difficult to detect and control when working to tolerances of a few tenths of one per cent. Such disturbances include flow distribution, pulsations, and rotational flow which originate within the pumps and fuel-supply components. They cannot be conveniently eliminated completely by placing a straight length of pipe upstream of the meter.

Some success has been obtained with a flow straightener consisting of bundles of small tubing and screens placed within a larger tube installed at or near the entrance of the meter under test. This helps in defining the calibration conditions. Also, the flow straightener in conjunction with master meters provides a more stable secondary reference for evaluating the comparative accuracy of different calibrators. As a final remark on this subject of upstream disturbances, the throttling valve should never be installed at the entrance to the meter as erratic disturbances may be introduced which will impair the precision of calibration. Rather, this valve should be located on the downstream side if possible.

The function of the diverter valve is to direct the flow as desired to storage or to the weigh tank without disturbing the rate of flow through the meter. Leak detectors should be provided to assure that none of the metered flow can bypass the weigh tank during the weigh-time interval. Also, in the static test method, the diverter valve should actuate the timer during its traverse and divert the flow quickly.

The particular diverter used in our apparatus was made of 0.035-in. cold-rolled steel in the form of an inverted V, each side being 15 in. long and 12 in. wide, with an included angle of 30 deg. The center of rotation was $2^1/_2$ in. above the base. Angular displacement was performed by a pneumatic-piston device having equal speeds in both directions with pneumatic cushions provided

574278 O - 61 - 42

at the end of the stroke. Time of positioning of the diverter was such that about 30 millisecond were required to cut through the liquid stream.

The counter-type timer should be actuated by electronic means, and in our apparatus actuation was accomplished by the diverter valve at the mid-point of its travel. This timer indicated in units of 0.001 sec and was calibrated against the standard reference time signal.

The platform scale used in this work was purchased on the open market. The scale is a self-contained, straight-lever type equipped with suspension main load-bearing assemblies and a single bar weighbeam graduated to 100 lb in $^1/_2$-lb divisions. A complement of counterpoise weights provided a total capacity of 5000 lb. Modifications performed at the National Bureau of Standards included the installation of a vernier scale on the main sliding poise to give readings to 0.05 lb. Also, concrete supports were provided for all main-lever-fulcrum bearings and for the weighbeam assembly to give a "built-in" scale. Thus the possibility of damage to which portable scales are subject during transit was eliminated.

The balance-ball elevation was adjusted to give a sensibility reciprocal of 0.1 lb at a load of 1000 lb. Sensibility reciprocal is defined as the amount of weight required to shift the weighbeam from an equilibrium position at the middle, to equilibrium at either extremity of the trig loop. Immediately prior to the flowmeter-calibration work, a scale calibration was made using 50-lb test weights known to be accurate within Class C maintenance tolerances of ± 40 grains. Both ascending and descending loads were used in the range of loads to be encountered and no hysteresis was observed. Considering the sensitivity, precision of calibration, and constancy of the scale as determined by the tests, it was practicable to determine minimum net weights of 400 lb to an absolute accuracy of better than 0.05 per cent.

The weigh tank had a capacity of 64 cu ft. No connection of any kind was attached to the tank when weigh determinations were being made, and the tank was emptied by inserting the inlet hose of a transfer pump. However, a drain valve would be adequate if the tank has sufficient elevation with reference to the liquid reservoir. In installations requiring permanent, flexible tank connections, tests must be conducted to assure that these are not interfering with the proper operation of the scale.

Calibration of a meter at a selected rate of flow was performed by first determining the tare weight while the diverter valve directed the flow to "return to storage." The diverter was then operated to direct the liquid into the weigh tank and this operation automatically started the timer. After collection of an appropriate amount of liquid, the diverter was repositioned to return to storage, automatically stopping the timer. The gross weight was then measured and the net determined for the indicated time interval. It should be noted that weight determinations were not made while liquid was entering the scale tank. Weights determined by this method require a correction for air buoyancy (1) magnitude 0.1 to 0.2 per cent, to obtain the true weight.

Another important consideration in precise calibration techniques is the piping between the meter and the weigh system. This must be such as to assure that all of the flow and only that flow indicated by the meter is collected in the weigh tank during the calibration run. Aside from the obvious requirement of no leakage or bypass from these connections, complete elimination of gas and vapor must be assured so gas compression or expansion cannot occur. Always remember, one of the greatest sources of measurement inaccuracy is improper gas elimination. Thus the meter-discharge lines should be as short and small as possible with vents provided at high points for gas elimination. As a general rule, the volume of the discharge piping should not exceed 5 or at most 10 per cent of the flow collected during a calibration run.

Discharge connections of small volume also reduce the effects of thermal expansion and contraction of the liquid if an appreciable change in temperature is encountered during a run. For instance, the coefficient of cubical expansion of petroleum products is about 0.06 per cent per deg F, and 10 deg F change in temperature during the test could introduce an error of 0.06 per cent if the volume of piping is only 10 per cent of the volume of fluid collected.

Volatility of the liquid is an important consideration because of loss by evaporation. Our weigh tanks and diverter valves were provided with covers to reduce loss of vapor and the test liquid was a naphtha having a Reid vapor pressure of less than 0.1 psi. No measurable evaporation loss was detected. However, for high vapor-pressure liquids, such as gasoline, considerable refinement to the techniques described herein is required to eliminate both loss by evaporation and vapor formation in the meter-discharge lines. The ideal solution appears to be a pressurized weigh system, but this will introduce many additional complications.

Examples of Dynamic Weighing Calibrators

The static weighing method of flowmeter calibration is time-consuming and thus not well suited for those applications in which convenience of operation is important. Thus dynamic weighing is utilized frequently. This determines the time interval required to collect a preselected weight of liquid, the weighing being performed while the liquid is entering the scale tank or other weight-determining collector. Although experience has demonstrated that the accuracy of dynamic calibrators can be just as good as the static method described, additional dynamic factors must be considered.

Three different dynamic calibrators will be considered briefly. Method 1, shown schematically in Fig. 2, utilizes a free-swinging lever scale. With this arrangement, the weight of the fuel in the tank increases until it overcomes the resistance of the counterpoise weights on the end of the weighbeam which then rises and actuates the timer. At this time an additional weight is added to the pan depressing the weighbeam. When it rises again the timer is stopped. This procedure requires acceleration of the scale just prior to both the start and stop actuation of the timer.

Three important dynamic phenomena take place during this weigh cycle. They are: The change in the impact force of the falling liquid between the initial and final weigh points; the collection of an extra amount of fluid from the falling column by the rising level in the tank; and the change in inertia of the scale and weigh tank with the resultant change in time required to accelerate the weighbeam past the timer trip point.

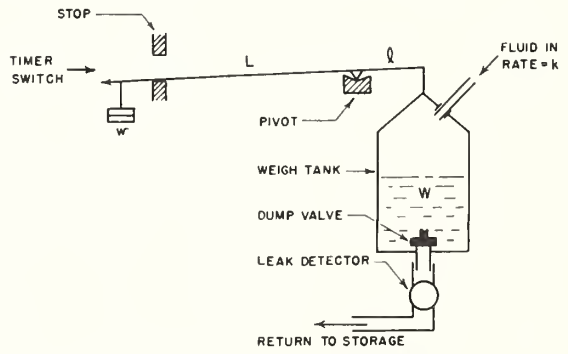

Fig. 2 Dynamic weighing calibrator 1

It can be demonstrated that the decrease in impact force is essentially equal and opposite to the additional weight collected from the falling column. Thus even though each of these may be appreciable, they cancel each other. The effect of change in inertia between the initial and final weigh points can become appreciable and should be considered whenever the weight of liquid collected contributes significantly to the inertia of a scale system requiring a relatively large travel of its weighbeam to the point of timer actuation. This method of weighing is used frequently in other situations, and an explanation of the inertia errors involved may be of interest.

Consider a scale consisting of a single, massless lever, as illustrated in Fig. 2, having arms of length l and L. When fluid is added to a tank at a mass rate k, the collected weight W eventually will balance the counterpoise weights w. A further collection of liquid will then deflect the lever past the point of timer actuation as a result of the unbalance kt and its corresponding torque $ktgl$, where t is time measured from the instant of balance and g is the acceleration of gravity.

As a first approximation, this torque is equal to the product of the moment of inertia of the fluid and counterpoise weight and the angular acceleration $d^2\theta/dt^2$. If the scale ratio L/l is large, the moment of inertia is essentially that of the counterpoise weights, and the equation of motion of the scale may be written

$$ktgl \simeq wL^2 \frac{d^2\theta}{dt^2} \quad \ldots\ldots [1]$$

which reduces to

$$ktg \simeq WL \frac{d^2\theta}{dt^2} \quad \ldots\ldots [2]$$

as w is approximately equal to Wl/L.

Integrating twice, using constants of integration equal to zero, and rearranging, gives the time required for deflection through an angular displacement θ

$$t \simeq \left(\frac{6L\theta W}{kg}\right)^{1/3} \quad \ldots\ldots [3]$$

Thus for a constant deflection and flow rate, the time required for deflection should be approximately proportional to $W^{1/3}$. This was tested on one dynamic weighing calibrator having a scale ratio of 50:1 and constant values of $\theta = 0.007$ radian and $k = 6.4$ lb per sec. The results, plotted in Fig. 3, give a least-squares curve of

$$t = 0.031 W^{0.43} \quad \ldots\ldots [4]$$

This value of 0.43 for the exponent of W is in reasonable agreement with the derived value of 1/3 considering the precision of the experimental work and the approximations used in deriving Equation [3].

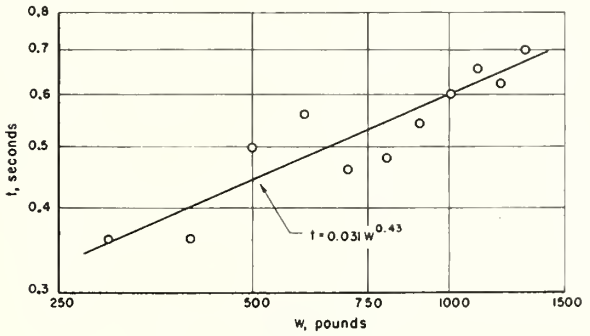

Fig. 3 Scale deflection time

The error of interest in dynamic weighing is the difference Δt between the time required for the deflection of the weighbeam at the final weight W_2 and at the tare weight W_1. Referring to Equation [3] this is derived as

$$\Delta t = t_2 - t_1 \simeq \left(\frac{6L\theta}{g}\right)^{1/3} \frac{(W_2^{1/3} - W_1^{1/3})}{k^{1/3}} \quad \ldots\ldots [5]$$

which is the inertia error in the measured time interval $T = (W_2 - W_1)/k$ required to collect the net weight of liquid. Dividing by T the percentage error is

$$\text{Per cent error} = \left(\frac{\Delta t}{T}\right) 100 \simeq 100 \left(\frac{6L\theta}{g}\right)^{1/3} k^{2/3} \left(\frac{W_2^{1/3} - W_1^{1/3}}{W_2 - W_1}\right) \quad \ldots\ldots [6]$$

The relation expressed in Equation [6] was checked by comparing dynamic calibrator 1 with the NBS static calibrator using a method to be described later. The results are plotted in Fig. 4, in which different symbols are used to designate the various flow rates. Values obtained from Equation [6], with $L = 2.2$ ft and $\theta = 0.007$ radian, are shown by the solid line. Equation [4], transposed to the co-ordinates of the figure, is shown as a dashed line.

The data of Fig. 4 are in reasonable agreement with Equations [6] and [4]. Thus it is believed that these are a measure of the inertia errors involved in this form of dynamic weighing. When the deflection of the weighbeam was reduced from 0.007 to about 0.0004 radian, the inertia effects became indistinguishable from the other small errors of the system.

At the time the tests were conducted to obtain the data of Figs. 3 and 4, we were not attempting an evaluation of the inertia error, but only demonstrating its presence. W_1 was not determined and it was necessary to estimate its value in these analyses. Thus the data should not be considered precise. However, it is believed these data are sufficient for the purpose of demonstrating that significant inertia errors may result from this method of dynamic weighing.

Dynamic calibration method 2, shown in Fig. 5, collects the liquid in a tube or cylinder of known cross-sectional area and uses the pressure existing at the bottom as a measure of the weight of liquid collected. The vertical rise in liquid between the initial or tare and the final weigh positions is usually in the range 2 to 20 ft. Thus it is necessary to measure and/or indi-

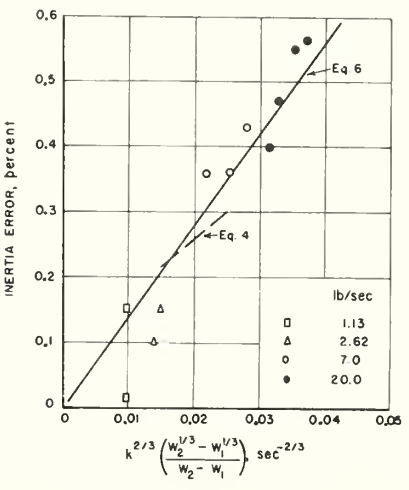

Fig. 4 Inertia error of dynamic method 1 for $(L\theta)^{1/3} = 0.249$

cate this pressure difference of 1.5 to 15 in. of mercury to a precision better than 0.1 per cent. The majority of installations use mercury manometers as the pressure-measuring device with electrodes, corresponding to different collected weights, spaced at accurately determined intervals. Contact between these and the mercury, in conjunction with electronic circuitry, provides the impulse for actuation of the timer. The contact spacing in these manometers must remain constant and any dirt or oil film which may effect the contact closure must be eliminated.

Important considerations for method 2 are: Effects of thermal expansion on the standpipe cross-sectional area and on the density of the manometer fluid; incomplete drainage of the cylinder walls before commencing the weigh-time determination, a significant factor in working with high-viscosity liquids; and changes in air pressure within either the cylinder or manometer column during the timing interval. The line between the cylinder and manometer well must never contain air or vapor. Also, the difference in elevation between its connections to the cylinder and manometer should be small so changes in the density of liquid within this line will have no influence on the height of the mercury. This is especially important when test-liquid temperatures differ from either that of the room or the mercury.

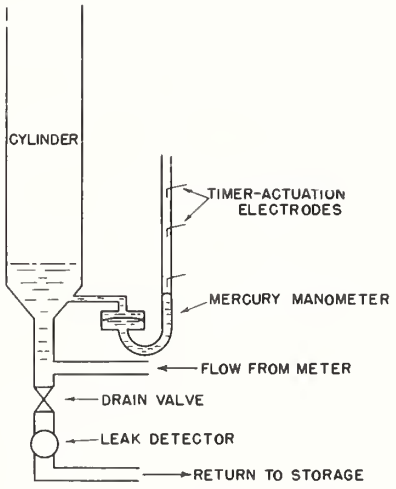

Fig. 5 Dynamic weighing calibrator 2

Dynamic considerations applicable to method 2 are first to ascertain that the pressure-measuring device has completed its acceleration and attained a constant velocity before the weigh-time interval is commenced. Also, oscillations resulting from the natural frequency of the pressure indicator must not exist. The other dynamic consideration is that of air compression in the collection vessel, especially at higher flow rates, resulting from restrictions such as flame arresters placed in the vent. It is readily seen that appreciable errors indicating higher than actual flows can result when such restrictions exist.

Dynamic calibration method 3, Fig. 6, employs bench dial scales for the measurement and indication of the weight of liquid. Nine light-beam intercepting paddles were added to the indicating dial, each corresponding to a predetermined weight. In operation, when sufficient liquid has entered the weigh tank to overcome the selected tare, the indicating mechanism of the scale commences to move around the dial. The first interruption of the light beam, occurring when the tare weight is balanced, starts the timer. An adjustable time-delay relay is provided whereby the phototrip circuit will not stop the weigh cycle until a selected time interval has been exceeded. Thereafter, when the next paddle intercepts the light beam the timer is stopped, the

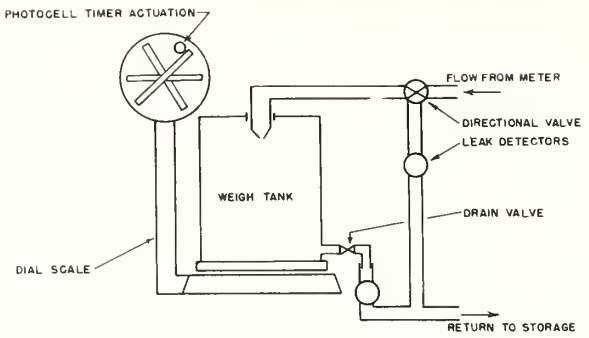

Fig. 6 Dynamic weighing calibrator 3

weight corresponding to that paddle is recorded, and the time is observed and recorded.

Dynamic considerations of method 3 are impact force and decrease in height of the falling liquid column as explained for method 1. Another consideration is the acceleration of the scale and its indicating mechanism to a constant velocity prior to the starting of the timer and maintenance of this velocity until the end of the weigh-time interval. Also, bench dial scales usually have constant sensitivity which, even when adequate at full scale, leads to larger percentage errors at the smaller weights. Thus good precision cannot be expected when the lower portion of the dial or range of the scale is used.

No attempt has been made to reveal all possible sources of dynamic errors in this discussion. These, of course, vary considerably with the different methods utilized. However, an attempt has been made to demonstrate that a static check and calibration of the instrumentation are not sufficient to prove the absolute accuracy of a dynamic-weighing method of calibration, as the response of the instrumentation used under transient conditions is a very important consideration.

Evaluation of Calibration Procedure and Equipment

The evaluation of calibration procedures and equipment includes a consideration of the ease and convenience of operation. Features which may be considered here are: The sensitivity and stability of the flow control; the temperature control; the time required to perform a weigh-time determination; and the time interval required to empty the weigh system between successive runs. All of these are of interest to the engineer in deciding whether a particular unit meets the general requirements of its intended purpose. These are not always the same for different applications, as more emphasis upon calibration time is necessary in a stand designed for production tests as compared to one used occasionally for high-accuracy tests of reference meters.

However, after these general performance characteristics are deemed satisfactory for the intended application, there still remains the all-important questions as to the precision of the measurement procedure and the absolute accuracy. The term precision as used in this paper refers to the variations or differences between repeat measurements. In the construction and operation of any calibrating unit, considerable attention will be directed towards refining the measurement procedure to reduce the variation so that it becomes insignificant. Unfortunately, this state is not always achieved and it may be necessary to evaluate the magnitude of the variations obtained.

The methods of statistics (14) define many units of variation by which the precision of a measurement procedure may be expressed. Among these are the "standard deviation," the "standard deviation of the average," the "confidence interval," and the "difference between duplicates." These are extremely useful to the engineer concerned with measurements and should

be used more extensively in flowmeter-calibration work. The ISO/TC-30 Committee of Fluid Measurements has recommended the use of twice the standard deviation as the tolerance limit in fluid-metering. An application of this tolerance is discussed by Jorissen (15).

It is beyond the scope of this paper to explain and demonstrate the application of statistics to precision of flow measured. However, the precision of the calibration procedure must be evaluated and the standard deviation provides a useful comparative unit for this purpose. A few representative statistical values will be presented to demonstrate the precision of flowmeter-calibration procedures attained in our laboratory. When data for ten successive runs are compared, using nominal timing intervals of 60 sec, the following representative values of precision result:

Standard deviation = 0.08 per cent
Standard deviation of the average = 0.03 per cent
Ninety-five per cent confidence interval = 0.06 per cent
Difference between duplicates does not exceed 0.12 per cent 80 per cent of the time

These data were obtained during calibration of sensitive float-type flowmeters. Naturally, they are dependent upon the sensitivity of the meter under calibration and meters with low-scale sensitivity will reduce this precision considerably.

Large differences between duplicate runs will be encountered occasionally. These are caused by insufficient time in bringing the meter and the liquid to operating temperature and incomplete purging of the system of gases. This happens frequently when small meters are calibrated on large-capacity stands. Other causes of large differences are insufficient tare time, with dynamic calibrators, and continuous readjustment of flow when such is necessary to provide a steady flow indication. In fact, experience generally demonstrates that minimum variability results when the flow-control valve can be left at a constant setting during the calibration time-interval.

After the calibration procedure and equipment have been adjusted to give satisfactory precision of measurement, a check of the absolute accuracy is desirable to detect the presence of constant errors. The best method for such a check is to use two or more different experimental procedures to measure the same quantity. Errors are then noted when averages disagree by an amount larger than is to be expected from the precision of the measurements. Perhaps our experience will be of help to others concerned with this problem.

In 1954 the National Bureau of Standards was requested to evaluate three dynamic weighing calibrators, one each of the designs of Figs. 2, 5, and 6, to determine whether their absolute accuracies were within the tolerance of ± 0.25 per cent. Two of these stands, A and B, were in our laboratory. It was decided that the best method of detecting constant errors in these would be through the use of a different experimental procedure to measure the same flow rate. A static weighing stand, NBS, similar to that of Fig. 1, was constructed for this purpose. The third calibrator, C, is installed at another facility and some other technique was required as moving the NBS stand was not convenient. Thus it was decided to use direct-reading flowmeters as secondary references.

The following procedure was used for the determination of the accuracy of calibrators A and B at our laboratory. The calibrating stand under evaluation provided storage of liquid, pumps, filter, and flow and temperature control. In operation, the unknown flow rate was maintained constant as indicated by a sensitive float-type flowmeter operating at a constant temperature with a liquid of constant physical properties. This constant flow rate was evaluated alternately by the calibration stand under test and by the NBS static weighing method, the flow being

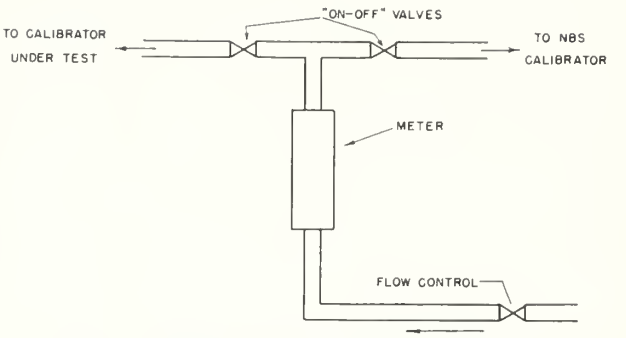

Fig. 7 Comparative accuracy-evaluation procedure

directed as desired by "on-off" valves placed downstream from the meter as shown in Fig. 7. The averages of four or five flow determinations made by each apparatus were then compared to obtain the difference between the calibrator under test and the NBS apparatus for the particular flow rate. This method has two important advantages: (*a*) The same quantity was being measured by two different procedures; and (*b*) upstream connections to the meter and downstream connections for a reasonable distance are never disturbed in directing the flow as desired to one of the two calibrating methods. Thus the conditions of calibration at the meter are identical.

For the evaluation of calibrator C, two secondary reference meters were selected. The first, range 7000 to 27,000 lb per hr, is of the float-type design having a logarithmic taper, a constant scale sensitivity of about 4 mm per per cent of indicated flow, and a stainless-steel float. All liquid passes through the metering tube. The larger meter is an experimental prototype design, range 35,000 to 100,000 lb per hr, and consists of the foregoing meter in parallel with a fixed orifice. As will be demonstrated later, this was not suitable as a secondary reference and a third meter was used. The third meter has a range 30,000 to 100,000 lb per hr, is a float-type having a 500-mm scale, and all of the flow passes through the glass metering tube. This served as an adequate secondary reference in the determination of the accuracy of calibrator C with a single exception.

Prior to the initial calibration of the three reference meters, the inlet and outlet connections were standardized. This included a 2-in. orifice upstream discharging into about 6 ft of 4-in. tubing connected to the meter inlet. The orifice was used in an attempt to obtain identical entrance flow conditions on the different calibrators. The meters were calibrated first at a few selected test points with the NBS apparatus and were then taken to calibrator C where the tests were repeated again by the same operator. Test fluids having a Reid vapor pressure of 0.1 psi and a kinematic viscosity of 1.10 centistokes were used at each location. Corrections were computed and applied for the different specific gravities of 0.783 and 0.779.

The final results of the tests are given in Fig. 8 which shows the per cent deviation of the individual calibrators from the average results for all four. Different symbols are used to designate the calibrators and each plotted point is the average of four to six separate determinations of rates of flow. Since some of these data may be considered proprietary information, we are not attempting to present the specific performance of any particular method other than the NBS static weighing apparatus represented by the open circles. Rather, the primary purpose is to show the extent of agreement obtained between four different methods of determination of flow rate. Where two identical symbols are plotted for the same flow rate, they represent the use of two different weights with corresponding timing intervals of about 30 and 60 sec. The average from which the deviations

were computed was obtained from the data within the ±0.15 per cent band with each calibrator assigned an equal weight.

As can be seen, the great majority of points are within ±0.15 per cent and the exceptions will now be discussed. Three deviations of about 1 per cent were obtained in the range 40,000 to 70,000 lb per hr with calibrator C. It must be understood that these are not an indication of the accuracy of this calibrator. Rather, they have been included to demonstrate difficulties encountered with the secondary reference meter of the orifice-bypass type. These deviations represent a change in the performance of this meter as a result of different upstream flow disturbances between the two calibrators, NBS and C. It has been concluded that a significant swirl or rotational flow difference existed between the two stands which was sufficient to affect the performance of the orifice-bypass meter by about 1 per cent.

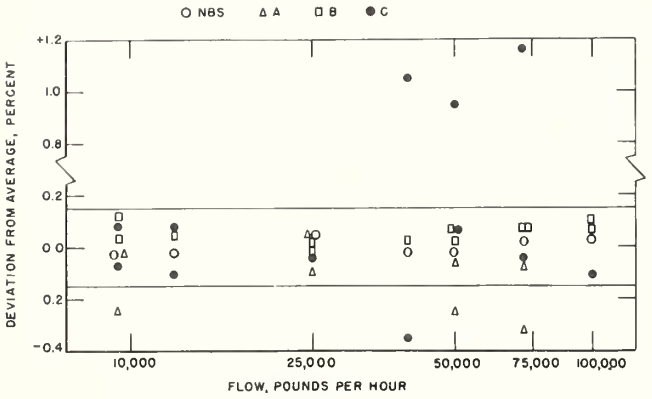

Fig. 8 Comparison of four calibrators

Still referring to Fig. 8, good results were obtained on calibrator C in the range 50,000 to 100,000 lb per hr with the third reference meter. A low reading of −0.35 per cent was obtained at 40,000 lb per hr, the lowest float position where sensitivity of this meter to upstream disturbances is a maximum. Thus it is demonstrated that two different calibrators can both be accurate and yet give different calibration results because of the influence of different upstream flow disturbances on the meter under test.

The other three low points of Fig. 8 were obtained using small test weights on a weighing mechanism of insufficient sensitivity. It is also possible that some unevaluated dynamic effects were present here.

Excluding the extreme points of Fig. 8, the resulting agreement between the four different methods of flow-rate determination may be considered quite good as it is within ±0.15 per cent. The program also enabled the detection of inertia errors of about 0.5 per cent and influences of disturbances upstream from the meter of about 1.0 per cent in one case and 0.4 per cent in another. Thus, through the procedures described herein, it has been possible to detect and correct errors in calibration equipment and procedures having magnitudes of less than 1 per cent.

Conclusions

Precise calibration of flow-rate meters requires a knowledge and control of each parameter which may influence the performance of the meter under test. Among these are the physical properties and temperature of the test liquid, at times the absolute pressure level, and the influence of upstream flow disturbances. The latter is perhaps the most difficult to specify and control when working to accuracies better than 1 per cent and is one of the primary reasons for apparent discrepancies in results between different calibrators.

Extreme accuracy is now possible and certified standards are available for the measurement of mass, time, temperature, and density which a calibrator is required to control or indicate. However, in designing a specific calibrator, an intelligent selection of the instrumentation for range and sensitivity is necessary if adequate precision and accuracy are to result. Also, provisions must be included to insure that all of the liquid and only that liquid which passes through the meter will be collected in the calibrator.

Examples of both static and dynamic weighing calibrators have been presented. For the particular calibrators and flow ranges investigated, there is not a significant difference in the absolute accuracies. However, dynamic weighing methods are subject to errors which are not exposed by a static calibration of the instrumentation. Thus it seems desirable that dynamic weighing calibrators of new designs should be evaluated for accuracy by comparisons with other calibration methods.

Acknowledgments

The suggestions and assistance of H. H. Russell of the Mass and Scale Section and H. S. Bean of the Fluid Meters Section, in advising on problems related to this work, are gratefully acknowledged. Also, we freely admit that many of the techniques and possible sources of errors described herein have been pointed out by others who have been more than liberal in advising us of their experiences. Among these are V. P. Head of Fischer and Porter Company, and A. W. Brueckner of G. L. Nankervis Company.

Bibliography

1 "ASME-API Code for Installation, Proving, and Operation of Positive Displacement Meters in Liquid Hydrocarbon Service," American Petroleum Institute Code No. 1101, Revised January, 1952, American Petroleum Institute, New York, N. Y.

2 "Discharge Coefficients of Square-Edged Orifices for Measuring the Flow of Air," by H. Bean, E. Buckingham, and P. Murphy, *National Bureau of Standards Journal of Research*, vol. 2, March, 1929, Research Paper No. 49.

3 "The Laws of Similarity for Orifice and Nozzle Flow," by J. L. Hodgson, TRANS. ASME, vol. 51, 1929, part 1, FSP-51-42, pp. 303–332.

4 "Fluid Meters, Their Theory and Application," fifth edition, 1957, in press, prepared by ASME Research Committee on Fluid Meters, ASME, New York, N. Y.

5 "Coefficients of Float-Type Variable-Area Flowmeters," by V. P. Head, TRANS. ASME, vol. 76, 1954, pp. 851–862.

6 "Correcting for Density and Viscosity of Incompressible Fluids in Float-Type Flowmeters," by M. R. Shafer, et al., *National Bureau of Standards Journal of Research*, vol. 47, no. 4, 1951, Research Paper No. 2247, pp. 227–238.

7 "Survey of Mass-Rate Flow-Measuring Principles," by Y. T. Li and S. Y. Lee, ASME Paper No. 55—SA-72, unpublished.

8 "Standard Frequencies and Time Signals WWV and WWVH," Letter Circular LC-1023, June, 1956, National Bureau of Standards Boulder Laboratories, Boulder, Colo.

9 "Precision Laboratory Standards of Mass and Laboratory Weights," National Bureau of Standards Circular 547, August, 1954, available from Superintendent of Documents, U. S. Government Printing Office, Washington, D. C.

10 "Specifications, Tolerances, and Regulations for Commercial Weighing and Measuring Devices," National Bureau of Standards Handbook H44, September, 1949, available from Superintendent of Documents, Washington, D. C.

11 "ASTM Standard on Thermometers," by T. W. Lashof and L. B. Macurdy, prepared by ASTM Committee E-1, American Society for Testing Materials, Philadelphia, Pa., December, 1953.

12 "Testing of Hydrometers," by J. C. Hughes, National Bureau of Standards Circular 555, October, 1954, available from Superintendent of Documents, Washington, D. C.

13 "ASTM-IP Petroleum Measurement Tables," ASTM Designation D1250, American edition, American Society for Testing Materials, Philadelphia, Pa

14 "Statistical Methods for Chemists," by W. J. Youden, John Wiley & Sons, Inc., New York, N. Y., second printing, 1955.

15 "On the Evaluation of the Accuracy of the Coefficient of Discharge in the Basic Flow-Measurement Equation," by A. L. Jorissen, TRANS. ASME, vol. 75, 1953, p. 1323.

Discussion

R. L. Galley.[4] A most interesting and thorough exposition of the pitfalls awaiting the novice in calibrating flowrate-measuring devices, this paper is one of the most practical treatments of a long-neglected subject that has come to the writer's attention. The authors are to be commended on their work and on this paper. It deserves wide circulation.

As one engineer who has devoted over a quarter of a century to the measurement of flow, the writer has seen the pitiful results of many amateur calibrators who did not know of all the precautions that should be observed, as the authors point out. The following comments are offered:

1 One assumes that the work deals only with volumetric and not with the so-called "mass" or gravimetric flowmeters. Of course, the same techniques would apply with either.

2 The problem of vapor pressure in testing hydrocarbon fuels is well explained, but the user is well advised that in calibrating certain turbine-type flow sensors in the same fuels, even a satisfactory line pressure does not always preclude the possibility of local cavitation in the region of the turbine blades. This can throw results way off, and one would never suspect the reason by the vapor-pressure criterion alone.

3 The authors do not mention Reynolds numbers, and the reader is left to assume that flow conditions at the test meter are sufficiently turbulent.

4 Gravity flow through the test rig is much safer than pumped flow, as this provides a better test condition.

S. R. Grotta.[5] A flow-correlation program similar to that described in the paper was carried out by the writer's company. A different approach was made, however, in the type of meter used as a reference.

It was felt that a reference meter should feature portability and ease of installation. Since the turbine meter fills this requirement in the higher flow ranges (above 250 lb per hr) better than the variable-orifice meter, an investigation was conducted to evaluate its suitability for this application. The program involved tests of flowmeter repeatability under various conditions which probably would affect all types of volumetric flowmeters.

Most of the tests were conducted with matched pairs (same make and size) of turbine meters installed in a recirculating flow system. The output signal of each flowmeter was fed into a separate electronic pulse counter. Since the output pulse is a measure of volumetric flow, permitting the counter to totalize these pulses for a sufficient period of time a direct indication of the total volume of fluid passed through the meter was produced. When the two turbine meters were placed in series and the counting sequence started and stopped simultaneously, the total counts from the two were nearly equal, with a slight difference being due to manufacturing tolerances. The ratio of the total counts (meter A divided by meter B) was found to remain constant over a wide range of flow. The standard deviation for 15 observations was 0.02 per cent. The maximum deviation from the mean was 0.03 per cent. By interchanging the meter positions in the pipeline and repeating tests we found that the effect of the initial plumbing configuration was less than 0.05 per cent.

The effect of flow-system-plumbing configuration on meter performance was investigated using this test procedure. Valves and elbows were placed in the pipe at the locations shown in Fig. 9. An elbow immediately upstream of a 1-in. meter produced an error as great as 0.9 per cent. The addition of a straight pipe 6 diameters in length ahead of the meter reduced this error to less than 0.2 per cent. The different makes of turbine meters tested were all affected by the flow pattern set up by the elbow. The degree of effect, however, varied from make to make.

After the selection of turbine meters suitable for reference use was made, a correlation program was carried on between the NBS calibrator and the Pratt & Whitney flow-calibrating standpipes. These standpipes, as company standards, are used to perform several hundred calibrations per year. Fig. 10 shows a portion of the correlation data. These data are plotted as pulses per gallon versus frequency (cps). As can be seen, the results of the correlation were very encouraging. A distinct advantage of the turbine flowmeter for correlation studies is that the accuracy of the data

[4] Consulting Engineer, Flowmeter Specialist, Woodland Hills, Calif.

[5] Experimental Engineer, Pratt & Whitney Aircraft, East Hartford, Conn.

PLUMBING CONFIGURATION FLOW DIRECTION →	1" DIAMETER TURBINE FLOWMETERS		
	MAKE I	MAKE II	MAKE III
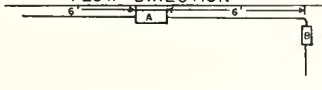	.91	.69	.84
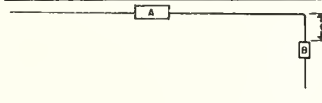	.21	.23	00
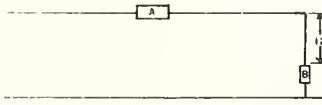	.15	.06	.00
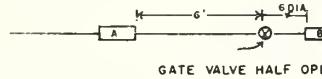 GATE VALVE HALF OPEN	.10	METER ERRATIC	.15
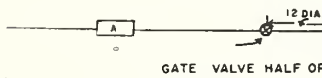 GATE VALVE HALF OPEN	.02	METER ERRATIC	.14

FIGURES ARE AVERAGE OF THREE OBSERVATIONS

Fig. 9 Per cent error in flow measurement caused by close proximity of elbow or valve to turbine flowmeter

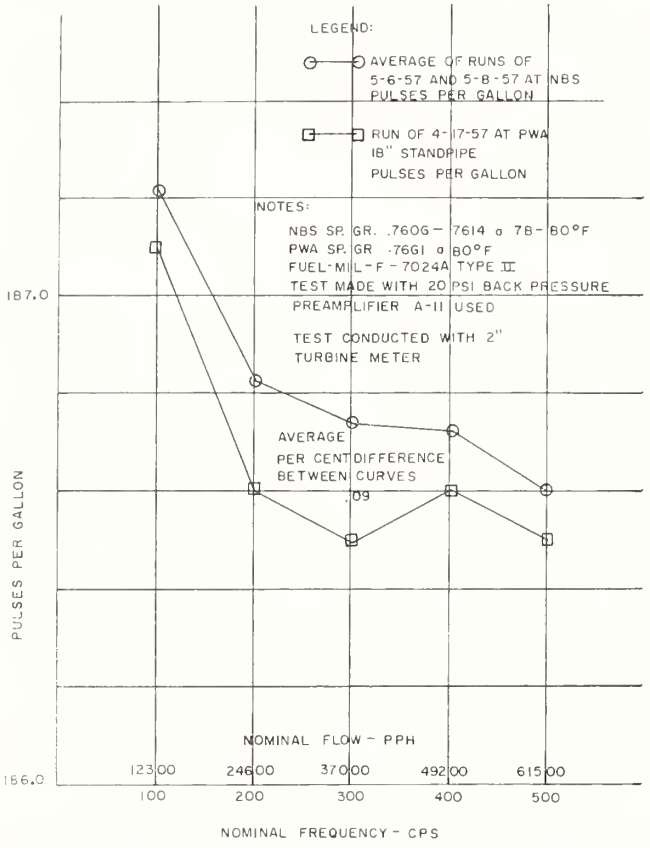

Fig. 10 National Bureau of Standards flowmeter correlation with Pratt & Whitney Aircraft

is not affected by small flowrate variations during the run. The flowrate is, in effect, averaged by the totalizing counter and timer the same as it is averaged by the weigh tank or standpipe used for calibration.

Turbine meters are not immune to all problems, however. Great care must be taken to keep the turbine rotor free of lint or other foreign material and protected from being nicked or scratched by hard objects. The observations made by the authors, emphasizing the importance of specific gravity and temperature measurements for the float-type meters, are even more important for turbine-meter applications. We also have found, as has been stated with regard to float-type meters, that air or vapor in the system causes serious error. Cavitation at the turbine-meter outlet also has been a source of trouble. This difficulty was eliminated by the application of back pressure.

It is apparent that many pitfalls have to be avoided both in calibrating turbine flowmeters and employing them for correlation studies. We feel that a document setting forth recommended procedures in the installation and use of turbine flowmeters would be very useful to those industries requiring a high degree of accuracy in flow measurements.

Finally, consideration should be given to means for conducting calibrations and correlations at elevated temperatures, up to 500 F and at pressures to 1000 psi.

V. P. Head.[6] Every fluid-mechanics laboratory should profit from the authors' treatment of inertia error. Beam travel from rest to timer operation is often $^1/_4$ or $^1/_2$ in. Note in Equation [6] that $L\theta$ is the displacement, y, of the counterweight end of the beam. Neglecting tare weight, and noting that W/k is the duration of the run T, and denoting per cent error by e, Equation [6] becomes

$$y = \frac{g}{6} T^2 \left(\frac{e}{100}\right)^3 \quad \ldots\ldots\ldots\ldots\ldots\ldots [7]$$

Using $g = 386$ in./sec^2, an average 60 sec time run requires y to be less than 0.00023 in. for 0.1 per cent, or 0.028 in. for 0.5 per cent, or $^1/_2$ in. for 1.3 per cent inertial error. Diverse beam scale dynamic rigs prevalent in university and aircraft test laboratories in past years are at best 1 per cent devices, and increasing use of the diverter, authors' Fig. 1, is to be encouraged, especially with water at low temperature where evaporation rates are negligible.

After a year of dynamic weighing experience at General Electric's A G T Division, we were using two scales and timers with pump and flowmeter between, and with 50 to 200 lb actual weights moved from receiver scale to supply scale after timers were started. Flexible hoses were hopeless. Small vertical pipes of outside diameter d extended almost to the bottom of both cylindrical liquid tanks of inside diameter D. Buoyancy of the volume of pipe plus its contained liquid was corrected by

$$W_{\text{actual}} = W_{\text{indicated}} \left(1 - \frac{d^2}{D^2}\right) \quad \ldots\ldots\ldots\ldots [8]$$

This system served only to detect gross errors in damaged meters and provide meter corrections, accurate within about 0.5 per cent, for the effects of large viscosity variations. Otherwise, meters were probably more accurate without the supposed corrections.

The writer then undertook the development of a new primary standard for liquid-mass measurement, and a number of other aircraft laboratories contributed to its perfection. Known as the standpipe liquid weigher, and illustrated in the authors' Fig. 5, this new primary standard is not proprietary, and educational as well as industrial laboratories are encouraged to construct their own. While dynamic weighing is almost always used, static weighing by means of a single micrometer-actuated contact also could be employed, with a synchronized diverter-timer switch as in the authors' Fig. 1. When regarded as primary, with the mass per inch of mercury W/H calculated from Equation [9] (which follows), performance has consistently been ± 0.15 per cent. Attempts to determine W/H by weighing withdrawn fluid on conventional scales has led to errors as large as 0.6 per cent and proved that conventional scales are secondary devices in need of constant restandardization.

Let ρ_{hg} = mercury density at 70 F, ρ_l and ρ_a = average liquid and atmospheric densities, grams per cc. Let A_l = standpipe area, A_W = manometer well area, and A_t = manometer tube area, all in square inches at 70 F. The constant including atmospheric-buoyancy correction is

$$W/H = 0.0361276 \frac{\rho_l A_l}{\rho_l - \rho_a} \left[\rho_{hg}\left(1 + \frac{A_t}{A_W}\right) - \rho_a\left(1 + \frac{A_t}{A_l}\right) - \rho_l\left(\frac{A_t}{A_W} - \frac{A_t}{A_l}\right)\right] \quad \ldots\ldots [9]$$

Small thermal corrections, Fig. 11, are used when necessary. Variations of ρ_l and ρ_a from assumed average values have trivial effects. In the writer's opinion, this primary liquid-weight standard is as reliable as any in the world, though, of course, the many factors affecting flowmeters as well as those producing difference between flow at the meter and flow into the standard, so capably emphasized by the authors, always must be kept in mind.

[6] Director of Hydraulic Research, Fischer & Porter Co., Hatboro, Pa. Mem. ASME.

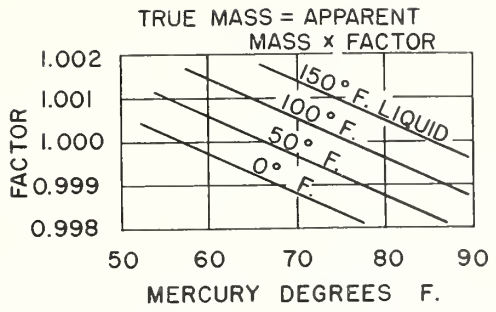

Fig. 11 Thermal-expansion corrections for standpipe liquid weigher

T. M. Morrow.[7] The authors are to be commended on the clear, concise presentation of the problems encountered in the calibration of flowmeters with dynamic weighing calibrators. They also are to be complimented on the conservative evaluation of the effect of these problems on the state-of-the-art of liquid-flow measurement.

Obviously, it is impossible to discuss in detail each source of measurement error noted in the paper. This discussion, therefore, will be limited to the presentation of an over-all picture of the effect which the results of this study can produce in the art of liquid-flow measurement.

The techniques used in the comparisons are obviously the result of careful study and planning to achieve more accurate flowmeter calibrations. Each problem is discussed with clarity noting the effects produced not only in the flow range tested, but also in the higher ranges of flow.

The careful planning and execution of the tests should be noted. Only through closely controlled and monitored test conditions could such significant results be obtained. Such tests are necessary to detect errors which many manufacturers of flowmeter-calibrating equipment consider insignificant.

To evaluate fully the extent of these errors it is necessary to have very accurate information concerning all the factors influencing the test. Only when each of these tests can be repeated a sufficient number of times to determine the existence and extent of the error, can a true evaluation be made of total error effect. By repeated tests and quantitative analysis the authors have determined that these errors are significant and their effects should be considered in precise flowmeter calibrations.

The Naval Bureau of Ordnance calibration program is confronted with accuracy requirements increasing from the nominal 1 or $1/2$ per cent at industrial level to a primary standard level of better than 0.1 per cent. This accuracy is not only required at the flowrates at which the National Bureau of Standards tests were conducted, but over the range of flows from 15 lb per hr to more than 2,500,000 lb per hr. This paper, therefore, represents a step toward the achievement of the required accuracy over this range. The limiting factor, until now, has been an inability to determine the rate of increase of these potential errors at higher flowrates in dynamic weighing calibration systems.

The tests and results presented in this paper are being studied carefully by the Naval Bureau of Ordnance to find a means of applying the equipment and techniques found therein to the area of high-flow, high-accuracy, liquid-flow measurement. Before further progress can be made in adapting present, or developing new, flow-measuring devices to newly developed fuels, hydraulic fluids, and liquid oxidizing agents, the characteristics peculiar to these liquids must be determined and evaluated.

These evaluations and the errors discussed in this paper should be considered for their effect on higher accuracy requirements.

[7] Measurement Standards Division, U. S. Naval Inspector of Ordnance, Pomona, Calif.

It is suggested, indeed urged, that the authors continue their program of research and evaluation of the errors of liquid-flowmeter calibrators and that it be expanded to meet existing and future requirements of increased accuracy and higher flow ranges.

E. A. Spencer.[8] It is interesting to compare the equipment developed by the authors with that used to test flowmeters at the Government's Mechanical Engineering Research Laboratory at East Kilbride, Glasgow.

This laboratory, which is one of the research stations of the Department of Scientific and Industrial Research, has a number of circuits, using water as the working fluid to cover a wide range of sizes and flowrates, the maximum capacity being 6,000,000 lb/per hr (30 cu ft per sec). A smaller version of the main rig is comparable with the NBS static calibrator and was designed for flowrates up to 180,000 lb per hr through 6-in. piping. Early experiments indicated that very high accuracies could be obtained more easily with a static weighing technique than with volumetric tanks[9] and in fact direct weighing has been adopted in all the flow-calibration systems of the laboratories. In the main rig a weighbridge capable of weighing 30 tons of water was installed while for the smaller version a 2000-lb platform machine having a sensitivity of $1/4$ oz has been found adequate, the minimum period for diversion into the measuring tanks being 30 sec. Like the NBS system the movement of the diverter past its mid-travel position actuates an electronic counter and the diversion time can be measured in milliseconds.

One of the major differences between the authors' system and MERL is in the siting of the flow-control valve. In the latter a spear valve similar to that used for a Pelton wheel is situated at the end of the calibration line and the round jet issuing from this is changed to a thin rectangular stream by a fishtail nozzle attached to the valve. High-speed cine films have shown that the diverter moves across this stream in about 40 millisec. Experience with this method of flow control which ensures a safe positive pressure at the meter position has been very satisfactory and is considered preferable to the upstream position selected by the authors. In view of their remarks on the dangers of upstream throttling the reason for not siting the valve between the meter and the tee-junction to the calibrators is not apparent.

Although as the authors point out a calibration is only absolutely true for the actual conditions at the time of the test, the value of such a test on a flowmeter is that it should provide data which can be applied to the subsequent use of the meter in its final installation. The introduction of flow straighteners at or near the upstream entry to the meter may produce artificial conditions which will differ substantially from those experienced in practice and give rise to significant errors. Are the authors recommending that in effect a flow straightener should become part of the meter? Even with this arrangement it is desirable that the laboratory installation should be free from rotational disturbances such as those indicated by the extreme test points in the comparison of the four calibrators. Were the authors able to measure the amount of the swirl upstream from the reference meters?

The authors are to be congratulated on the very high standards of precision achieved with the equipment in calibrating flowmeters. These figures which are dependent on the sensitivity of the meter could usefully be supplemented by results on the steadiness of the rate of flow by comparing the successive measurements of the actual flowrate determined by the NBS calibrator. At MERL it has been found that the standard deviation of such repeated determinations with the control valve at a set position is

[8] Principal Scientific Officer, Fluid Mechanics Division, Mechanical Engineering Research Laboratory, Glasgow, Scotland.

[9] "The Accurate Calibration of Flowmeters With Water," by E. A. Spencer and A. T. J. Haward, *Trans. Society of Instrument Technology*, vol. 9, 1957, p. 1.

0.1 per cent. It should, however, be noted that the supply to the calibration lines is from a constant-head tank and not direct through a pump.

Authors' Closure

The authors wish to express their appreciation for the encouraging comments of the discussers. Regarding the comments by Mr. Galley, it is correct to state that the techniques are equally applicable to either volumetric or gravimetric flowmeters. His observations on cavitation in turbine sensors are important as the high velocity at the turbine blades, with its corresponding reduction in static pressure, frequently is a cause of vapor formation especially with hydrocarbon liquids. The authors are also in agreement that the flow must be uniformly turbulent at the test meter, and that gravity flow provides a better test condition for precision work.

Mr. Grotta brings out an important characteristic to be considered in the selection of reference meters; namely, much greater precision can be obtained with reference meters of the totalizing type having a calibration constant essentially independent of flow rate. The newer electronic methods of digital readout can be employed with these and the absence of an exact flow setting will not influence the results significantly. This eliminates the human error associated with the observation and setting of flow rate and greatly increases the precision of the calibration procedure.

The treatment of inertia error by Mr. Head is correct for the assumption of zero tare weight and a massless scale and weigh tank. As they are never attained actually, his dynamic errors are the maximum to be expected. However, even if these are given due consideration, the possibility of a significant inertia influence should be considered when dynamic weighing is used.

Mr. Morrow has effectively presented the fact that the old industrial tolerances of one per cent are no longer adequate, at least in the field of national defense, and has discussed a requirement for standards approaching the accuracy level of 0.1 per cent. Although the various individual components and instruments required for this precision are available, Spencer[9] has demonstrated the considerable work involved in attempts to attain such accuracy. The problem becomes even more complicated when one realizes that new hazardous liquids at both high and low temperatures and throughout wide pressure ranges are involved.

With reference to Dr. Spencer's very constructive comments it should be mentioned that a fundamental difference in objectives exists. Dr. Spencer is attempting to establish a flow rate laboratory having the highest possible accuracy, whereas the apparatus described in this paper was constructed for the single purpose of evaluating the performance and accuracy of three dynamic type calibrators of commercial manufacture. These had been designed for installation in industrial facilities for the calibration of flowmeters used in the aircraft industry. Thus in this particular work it was necessary to use the pumps, heat exchangers, and flow control valves supplied with the calibrators as part of the evaluation procedure. This is the reason the flow control valve was located upstream from the meter. The authors are in complete agreement that throttling should be accomplished downstream from the meter whenever possible.

Regarding the subject of flow straighteners, every type of flow rate indicating meter is influenced by the upstream flow conditions. The authors still recommend that flow straighteners should be considered part of the meter in applications requiring accuracies of a fraction of one per cent. This is especially true in the aircraft field where meter installation conditions deviate considerably from the ideal. Sprenkle and Courtright[10] have recently discussed a few types of straighteners and have demonstrated their effect upon the precision of flow measurement with orifice-type metering elements.

No attempt was made to measure the swirl upstream from the reference meters, it being deemed sufficient for our purposes merely to demonstrate that its presence contributed a significant influence. The authors are in agreement that laboratory calibrators should be free from rotational disturbances and pulsations. Naturally, such is best accomplished by utilizing a gravity supply. However, this is not always feasible in industrial installations especially those using hazardous liquid-hydrocarbons as the working fluid.

---

[10] "Straightening Vanes for Flow Measurement," by R. E Sprenkle and N. S. Courtright, *Mechanical Engineering*, vol. 80, February, 1958, p. 71.

UNITED STATES DEPARTMENT OF COMMERCE • Charles Sawyer, *Secretary*
NATIONAL BUREAU OF STANDARDS • E. U. Condon, *Director*

Density of Solids and Liquids

by Peter Hidnert and Elmer L. Peffer

National Bureau of Standards Circular 487
Issued March 15, 1950

659/I

Preface

Density is one of the significant physical properties of materials that is important in science and industry.

This Circular is issued to supply a demand for information about various methods for determinations of the densities of solids and liquids. The Circular also indicates that density determinations may be used to identify materials, and to obtain relationships between density, chemical composition, thermal and mechanical treatments, etc.

This Bureau has published during the past four decades the results of investigations on the densities of various materials. A list of these publications will be sent upon request to anyone interested.

E. U. Condon, *Director.*

Contents

Density of Solids and Liquids

by Peter Hidnert and Elmer L. Peffer*

Density data may be used for obtaining relationships between density, chemical composition, thermal and mechanical treatments of materials, etc. This circular defines density and specific gravity, describes 11 methods (hydrostatic weighing, picnometer, flotation, hydrometer, falling drop, balanced column, Boyle's law, electromagnetic, elastic helix, ice calorimeter, and volumetric) for determinations of the densities of solids and liquids, and indicates the accuracy of various methods.

I. Introduction

1. Definitions and Terms

Density is a significant physical property of materials, and is important in science and industry. The extensive literature on density shows that determinations of the density of materials is a constant and recurrent problem. For example, density determinations may be used to identify materials, and to obtain relationships between density, chemical composition, thermal and mechanical treatments of materials, etc.

In any list of the physical properties of a substance, its density or specific gravity is usually included. If the values of the density of a substance are to be relied upon when obtained by different observers or by different methods, it is important that they be both accurate and comparable.

Density is the mass per unit volume and is usually expressed in grams per cubic centimeter (or per milliliter)[1] at some definite temperature.

Specific gravity is an abstract number expressing the ratio of the weight of a certain volume of the material in question to the weight of the same volume of some other substance taken as standard at a stated temperature. Water is usually used as the standard substance. Both the temperature of the material and the temperature of the standard substance should be indicated.

Density and specific gravity, while fundamentally different, are nevertheless determined in the same way and may have the same numerical values. The two terms are often used synonymously as expressing the "heaviness" of a substance. Care must be taken, however, to state the units employed and the temperatures involved, otherwise there is danger of confusion and misinterpretation of results.

Specific gravity may be determined at any convenient temperature and referred to water at any desired temperature. For example, specific gravity may be determined at 20° C and referred to water at 20°, 15°, 4° C, or any other temperature. It is then expressed as specific gravity at 20°/20° C, 20°/15° C, or 20°/4° C. If determined at 25° C, the specific gravity is expressed as 25°/20° C, 25°/15° C, or 25°/4° C.

Specific gravity is often expressed in terms of water at the same temperature as that at which the substance is weighed; for example, 15°/15° C, 20°/20° C, or 25°/25° C. It is preferable, however, especially in the case of liquids, to express all specific gravities in terms of water at 4° C. The values are then directly comparable, since they are measured in terms of the same unit, and if the change of specific gravity per degree change of temperature is known they may all be easily reduced to the same temperature. There is also the additional advantage that specific gravities when so expressed are numerically the same as densities in grams per milliliter. For example, specific gravity at 20°/4° C is numerically the same as density at 20° C expressed in grams per milliliter. This is obvious, since, by definition, 1 milliliter of water at 4° C weighs 1 gram.

In making specific gravity determinations on a series of samples of the same kind, it is likely that the temperatures of the various samples will differ somewhat unless a constant temperature bath is used. Suppose the temperatures range as follows: 23.5°, 24.4°, 25.0°, 25.6°, and 26.2° C. The specific gravities may then be calculated at 23.5°/4°, 24.4°/4°, 25.0°/4°, 25.6°/4°, and 26.2°/4° C, and, if the change of specific gravity per degree centi-

*Deceased.

[1] The cubic centimeter (that is, the volume of a cube 1 cm on a side) is not equal to the milliliter, but the difference is so slight as to be negligible in all ordinary determinations. The milliliter is equal to 1.000028 cubic centimeters. In volumetric measurements the unit of volume usually employed is the milliliter (ml), though it is sometimes erroneously referred to as the cubic centimeter (cc). When the cubic centimeter is actually intended it should be written "cm^3" and not as "cc". The cubic centimeter is usually employed to express volumes calculated from linear measurements.

grade is known, the values can at once be reduced to 25°/4° C by multiplying the change per degree centigrade by the difference between the temperature of observation and 25° C. For example, if the samples are linseed oil, of which the change in specific gravity is 0.00068 per degree centigrade, the specific gravities can be reduced to 25°/4° C by subtracting from the observed values of the successive samples 0.00068 times 1.5, 0.6, 0.0, −0.6, and −1.2.

If the above specific gravities had been expressed in terms of water at the temperature of observation, they would have been at 23.5°/23.5°, 24.4°/24.4°, 25.0°/25.0°, 25.6°/25.6°, and 26.2°/26.2° C, and would not then have been directly comparable or easily reducible to the same basis, since the correction to be applied in each case would then involve both the expansion of the sample itself and the change of the unit of measurement, that is, the density of water.

For purposes of comparison, specific gravities are sometimes shown in parallel columns at 15°/15° and at 25°/25° C. This method does not make possible a real comparison since the values given in the two columns are measured in different units. It shows only the difference between the expansion of the sample in question and that of water over the same temperature range. If it should happen that the sample in question had the same rate of expansion as water then the specific gravities of the sample at 15°/15° and at 25°/25° C would be identical, that is, it would appear that the specific gravity of the sample did not change with change of temperature.

In all determinations one should distinguish between apparent and true specific gravity. In case the true specific gravity is desired, this can be obtained either by correcting all weighings for air buoyancy before determining the ratio of the weights, or by applying a correction to the apparent specific gravity.

Table 1 [1][2] gives corrections to be applied to apparent specific gravities in order to obtain true specific gravities. These corrections are based on specific gravities at 25°/25° C, but they are sufficiently accurate for practical purposes at ordinary laboratory temperatures. For substances having specific gravities that do not differ much from unity, the difference between apparent and true specific gravity is small, but for substances with specific gravities far from unity, the difference between apparent and true specific gravity is correspondingly large.

In case it is desired to correct the apparent weight of a body for air buoyancy, this correction may be calculated by means of an appropriate table of air densities at various temperatures and pressures. The buoyancy correction to be added to any apparent weight, to reduce it to true weight

[2] Figures in brackets indicate the literature references at the end of this Circular.

TABLE 1. *Corrections to be applied to apparent specific gravities in order to obtain true specific gravities at 25°/25° C (U. S. Pharmacopoeia)*

Apparent specific gravity	Correction	Apparent specific gravity	Correction
0.6	0.00047	2.0	−.00118
.7	.00035	3.0	−.00236
.8	.00024	4.0	−.00353
.9	.00012	5.0	−.00471
1.0	.00000	6.0	−.00589
1.1	−.00012	7.0	−.00706
1.2	−.00024	8.0	−.00824
1.3	−.00035	9.0	−.00942
1.4	−.00047	10.0	−.01060
1.5	−.00059	11.0	−.01177
1.6	−.00071	12.0	−.01295
1.7	−.00082	13.0	−.01413
1.8	−.00094	14.0	−.01530
1.9	−.00106	15.0	−.01648

in vacuum, is calculated by multiplying the air density by the difference in volume between the body weighed and the weights required to balance it on an even arm balance, or

$$B=\rho(V-V_w), \tag{1}$$

where B is the air buoyancy, ρ the air density, V the volume of body weighed, and V_w the volume of weights.

The numerical values of V and V_w can be arrived at by an approximation which may be carried to any desired degree of accuracy. The value of V may be obtained from the relation

$$V=\frac{m}{d}, \tag{2}$$

where m is the mass, and d is the density of the body. For a first approximation m may be taken as the uncorrected weight, and d as the apparent density. In the same way V_w may be taken as the apparent weight divided by the assumed density of the weights (8.4 for brass weights). This gives an approximate value for B which may be applied to the apparent weights and by this means a more exact value for V and V_w can be determined and with these values of V and V_w a more exact value of B can be obtained. This process may be continued until the successive values of V, V_w, and B differ by negligible amounts. In most cases the second approximation will be found to be sufficiently exact, and in many cases, only the first approximation will be required.

The weight of a body in vacuum may also be computed from the equation

$$\begin{aligned} M&=W+\rho\left(\frac{M}{d_1}-\frac{W}{d_2}\right)=W\frac{d_1}{d_2}\left(\frac{d_2-\rho}{d_1-\rho}\right)\\ &=W\frac{d_1}{d_1-\rho}\left(1-\frac{\rho}{d_2}\right)=W\left[1+\frac{\rho}{d_2}\left(\frac{d_2-d_1}{d_1-\rho}\right)\right]\\ &=W+\frac{kW}{1000}, \end{aligned} \tag{3}$$

where M is the weight of body in vacuum, W the apparent weight of body in air, ρ the density of air, d_1 the density of body, d_2 the density of weights, and k the correction factor. Table 2 gives correction factors for $\rho=0.0012$ (dry air at 21° C and 760 mm pressure).

The weighings are reduced to vacuum by means of a special device originally designed for use in correcting weighings of water in tests of volumetric apparatus. This device consists of a glass bulb of such volume that, when suspended from one arm of a balance and counterpoised against a brass weight of equal mass, the number of milligrams that must be added to the pan from which the bulb is suspended to secure equilibrium is equal to the air buoyancy on a liter of water weighed against brass weights. This buoyancy constant when divided by 881.3 ml (the difference in volume between the glass bulb and the brass weights) gives the air density. The bulb is suspended in a glass case to protect it from disturbing air currents. Correction is made for the difference in temperature between this case and the balance where density determinations are made. The density of the brass weights for the purpose of correcting for displaced air is assumed to be 8.4 g/cm³.

If greater precision is required, the true value for ρ depending on temperature, humidity, and pressure, should be substituted in eq 3. Values for ρ for dry air containing 0.04 percent of CO_2 at various temperatures and pressures may be obtained from table 29 of a previous Bureau Circular [2].

TABLE 2. *Correction factors (buoyancy) for $\rho=0.0012$*

[BS Circular 19, 6th ed.]

Density of body weighed	Correction factor, k			Density of body weighed	Correction factor, k		
	Pt-Ir weights $d=21.5$ g/cm³	Brass weights 8.4	Quartz or Al weights 2.65		Pt-Ir weights $d=21.5$ g/cm³	Brass weights 8.4	Quartz or Al weights 2.65
g/cm³				g/cm³			
0.5	2.35	2.26	1.95	5.0	0.18	0.10	−0.21
.6	1.95	1.86	1.55	6.0	.15	.06	−.25
.7	1.66	1.57	1.26	7.0	.12	.03	−.28
.8	1.45	1.36	1.05	8.0	.10	.01	−.30
.9	1.28	1.19	0.88	9.0	.08	−.01	−.32
1.0	1.14	1.06	.75	10.0	.06	−.02	−.33
1.1	1.04	0.95	.64	11.0	.05	−.03	−.34
1.2	0.94	.86	.55	12.0	.04	−.04	−.35
1.3	.87	.78	.47	13.0	.04	−.05	−.36
1.4	.80	.72	.40	14.0	.03	−.06	−.37
1.5	.74	.66	.35	15.0	.02	−.06	−.37
1.6	.69	.61	.30	16.0	.02	−.07	−.38
1.7	.65	.56	.25	17.0	.01	−.07	−.38
1.8	.61	.52	.21	18.0	.01	−.08	−.39
1.9	.58	.49	.18	19.0	.01	−.08	−.39
2.0	.54	.46	.15	20.0	.00	−.08	−.39
2.5	.42	.34	.03	21.0	.00	−.09	−.40
3.0	.34	.26	−.05	22.0	.00	−.09	−.40
3.5	.29	.20	−.11	23.0	.00	−.09	−.40
4.0	.24	.16	−.15	24.0	−.01	−.09	−.40

II. Types of Apparatus for Density Determinations

Eleven methods for determinations of the densities [3] of solids and liquids will be described. Free use has been made of publications of many authors, particularly those of the National Bureau of Standards. In order to conserve space it is necessary to omit descriptions of some variations and modifications of the density methods described in this Circular. Some of the illustrations were redrawn with minor changes in order to conform with this Bureau's editorial policy.

1. Hydrostatic Weighing Method

The hydrostatic weighing method may be used for determining the density of solids and liquids.

(a) Solids

For the determination of the density of a solid it is first weighed in air, and then weighed while suspended in a liquid of known density. This is done by attaching one end of a silk thread or fine wire to one arm of an equal arm balance and the other end of the thread or wire to a small basket in which the solid sample is placed. It is necessary to have the thread or wire pass through the surface of the liquid with the basket attached in taking the balance reading before the solid sample is placed in the basket in order that errors due to the weight of this attachment and to the effect of surface tension of the liquid on the suspension thread or wire may be avoided. A fine wire is preferable to a silk thread since large errors may be introduced on small samples by the use of the latter.

The density of the solid sample is computed from the weight in air divided by its volume. This volume is equal to the loss of weight of the sample divided by the density of the liquid at the temperature of observation.

(b) Liquids

The density of a liquid may be determined by weighing in the liquid a sinker of known mass and volume. The arrangement of apparatus used at the National Bureau of Standards is shown in figures 1 to 4. The densimeter tube containing

[3] At the request of the American Society for Testing Materials, the National Bureau of Standards completed in 1941 an investigation of instruments available to industry for the determination, indication, or recording of the specific gravities of gases. Eleven different instruments were investigated with the use of 15 test gases of known specific gravities. Determinations were made of the accuracy and reproducibility, of the effects of changes of temperature, relative humidity and water content of the surrounding air, and of sources of error and applicable corrections. The test gases ranged in specific gravity from helium (0.15), in steps of approximately 0.15, to butane (2.06). The probable errors in the values of the specific gravities of the test gases and mixtures used as reference standards averaged ±0.00004, which made it possible to fix the errors of the instruments to 0.0001 specific gravity unit. The results of this investigation have been published by Smith, Eiseman, and Creitz [3].

the liquid and the immersed sinker E is shown in figure 1. A special cap is used for closing the densimeter tube when weighings are not being made. This cap consists of a brass cover, A, fitted to the tube by a soft rubber bushing, B. Through the center of the cover is a hole, which may be closed by a tightly fitting brass plug, C. To the upper and lower faces of this plug is attached the suspension wire. When weighings are in progress, the suspension is as shown in figure 1, b, access of the outer air being only through the hole in the cap. When weighings are not in progress, this hole is closed by the plug, as shown in figure 1, a, to avoid changes in concentration of the liquid, caused by evaporation or by absorption of water vapor from the air. In figures 2 and 3 the densimeter tube, H, is shown fixed in place in the inner water bath.

The water in the inner bath is kept in constant circulation by the propeller I. This bath is immersed in an outer bath kept in constant circulation by means of a motor-driven propeller,

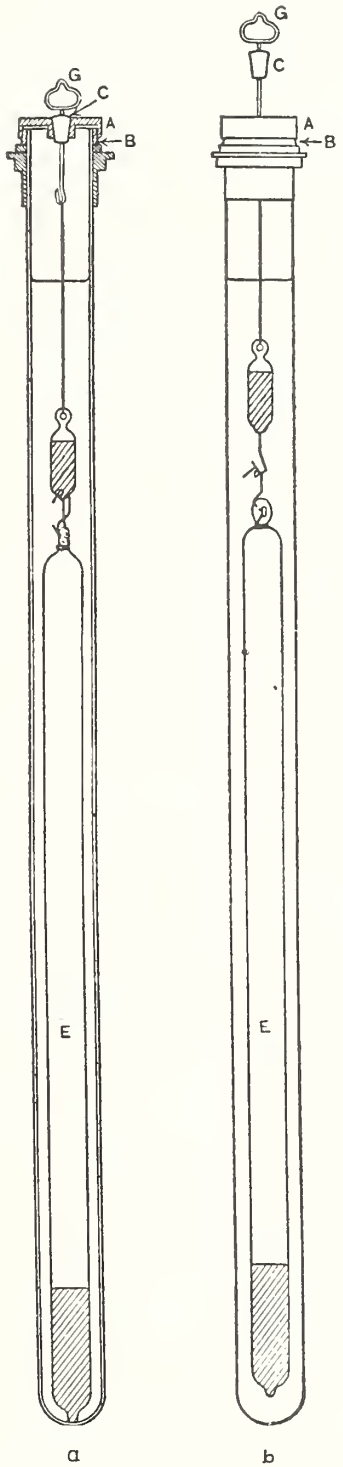

FIGURE 1. *Densimeter tube, one-third size (Osborne).*

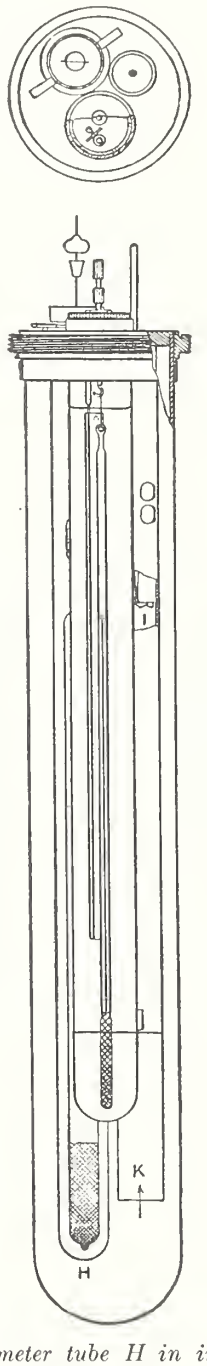

FIGURE 2. *Densimeter tube H in inner water bath, one-fourth size (Osborne).*

574278 O - 61 - 43

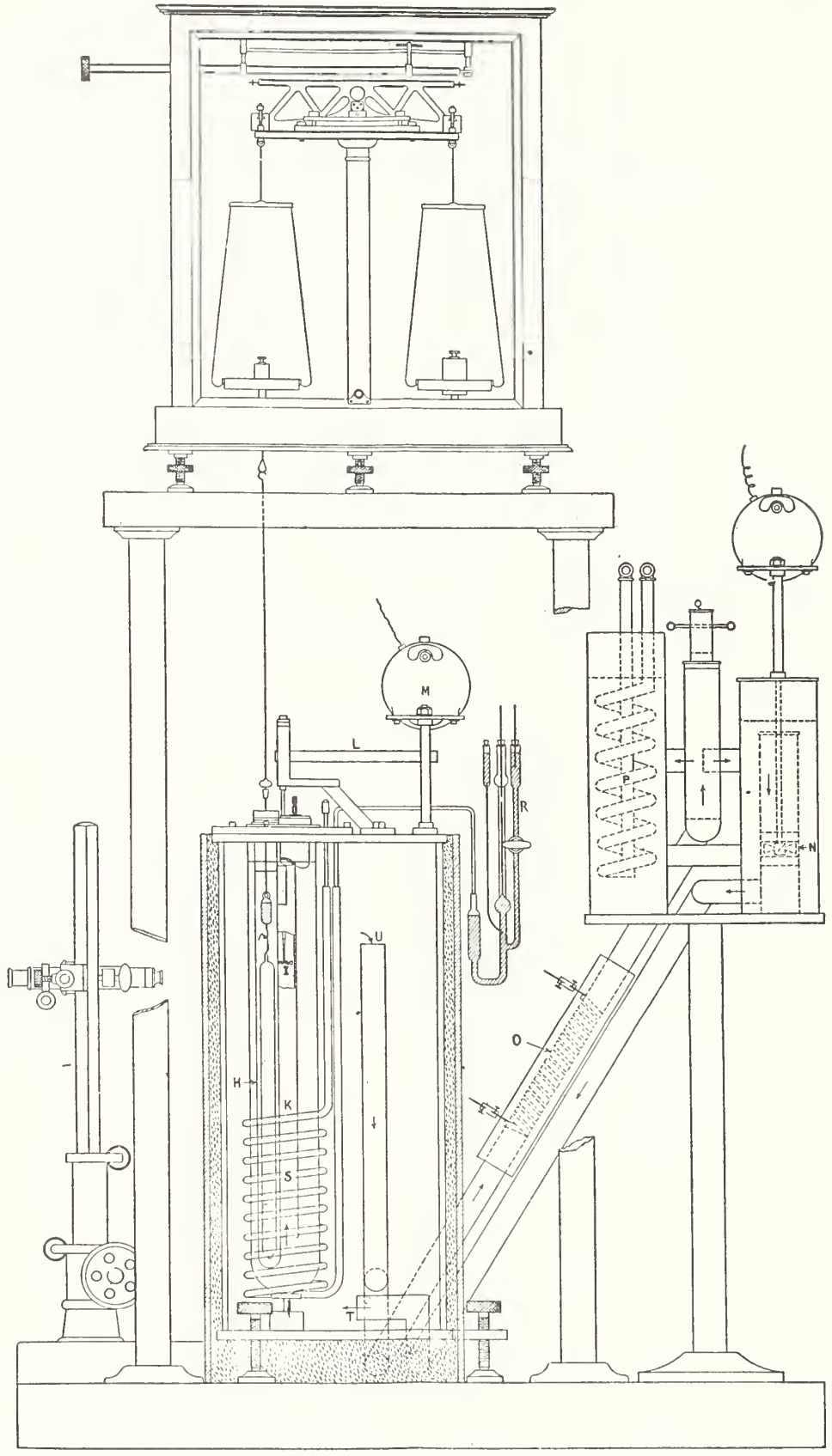

FIGURE 3. *Apparatus for determination of density by hydrostatic weighing method, one-ninth size (Osborne).*

N, placed outside the bath. The temperature of this outer bath is maintained constant or changed at will by means of the electric heating coil, O, surrounding the return pipe and by the tubular coil, P, connected with a refrigerating unit maintained at a temperature below 0° C. The flow of cooled liquid in this coil is adjusted by means of a valve. By means of special valve, Q, the flow of water in the circulating apparatus may be directed entirely through the cooling chamber, directly through the circulating propeller, or divided, part going either way at will, thus regulating the quantity of heat removed from the system by the refrigerating unit. The cooling is made slightly in excess of the heat acquired from the surrounding air and that produced by the circulation, the balance being maintained by means of the heating coil.

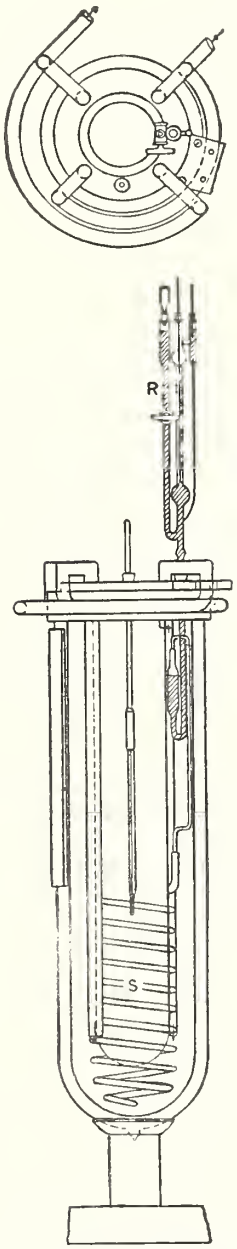

FIGURE 4. *Bath for use in determination of density by hydrostatic weighing method, one-eighth size (Osborne).*

This coil, which has a resistance of 10 ohms, is made of Chromel A or Nichrome V ribbon, wound over mica on the brass tube through which the return flow takes place. It is used both for regulation of temperature and for rapid heating when changing the temperature. For regulation it is connected in series with a variable resistance consisting of a sliding contact wire rheostat and a bank of parallel connected lamps. Another lamp bank is connected as a shunt on this variable resistance in the circuit of which is a relay operated by a thermoregulator, R. The bulb of this thermoregulator is the tubular copper coil S, containing about 20 ml of xylol.

A rise in temperature closes an electric circuit, the relay is thus energized, the shunt circuit broken, and the current in the heating coil diminished. When the temperature falls sufficiently, this action is reversed. The sensitivity of the regulation varies with conditions. Under the most adverse conditions the regulating energy used in the heating coil is from 100 to 140 watts and maintains the outer bath constant within 0.05 deg C. Under the best conditions the energy varies from 10 to 20 watts, keeping the temperature of the bath constant within 0.01 deg C. The periodic variation in temperature of the outer bath is in either case far too rapid to produce any perceptible change in the inner bath. For rapid heating, the small regulating current is replaced, using a double-throw switch, by a heavier current supplying about 1,500 watts in the heating coil.

The outer bath as first arranged is shown in figure 3. It was contained in a rectangular tank with plate-glass walls and brass bottom and top. The insulation consisted of cotton between two layers of heavy cardboard. The water entered at T and left at U, thus insuring complete circulation. Owing to the repeated difficulty on account of leakage of the joints, this tank was replaced by a double-walled glass cylindrical vacuum jacket as shown in figure 4. The top was closed by a brass cap cemented to the glass. The water enters by two tubes extending to the bottom and leaves by two tubes at the top. The greatest difficulty with this container for the outer bath was the distortion of the image of the thermometers, owing to the cylindrical surface of the container. This difficulty was remedied to a considerable extent by cementing a plane glass plate to the outside surface of the container, forming a cell which when filled with water corrected most of the aberration. The cylindrical container is covered with nickeled paper or aluminum foil in order to exclude or minimize radiation. Windows are cut in the paper or foil to permit observations to be made.

The temperatures are observed on two mercury

thermometers [4] suspended in a tube of water, the position of which is symmetrical in the inner bath to that of the densimeter tube. The thermometers are so mounted on a movable cap that by its rotation they may be successively brought into position for reading. They are read with the aid of a long-focus microscope so mounted as to be movable vertically. The object of placing the thermometers in a tube instead of directly in contact with the water of the inner circulating bath is to eliminate, as far as possible, errors due to temperature lag within the densimeter tube. Since the liquid sample is separated from the circulating bath by the densimeter tube, the thermometers should be separated from the circulating bath by a similar tube so that when a constant temperature is indicated by the thermometers the same constant temperature shall obtain within the densimeter tube.

The apparatus shown in figures 1 to 4 and described above has now been modified in several respects. The tubular copper coil, *S*, has been replaced with a sinuous glass tube having vertical segments. Thermocouples have been placed in the outer and inner baths and in the thermometer tube to detect small temperature changes.

A sinker made of annealed Jena 16^{III} glass, ballasted with mercury, is used. Its volumes are calculated from its weight in vacuum and its apparent weights in twice distilled water at various temperatures, using known values for the density of water [2, 5]. The sinker should have a volume of 50 to 100 ml.

The sinker is suspended by a hook from a small secondary sinker attached to a wire let down from one pan of a balance as shown in figure 3. The secondary sinker has a mass sufficient to keep the suspension wire straight and in its proper position, and is always immersed in the liquid, whether the larger sinker (of known mass and volume) is attached or not.

The platinum suspension wire passing through the surface of the liquid sample, has a diameter [5] of 0.2 mm and is covered with a fine layer of unpolished gold by electrodeposition. In the case of liquids which imperfectly wet the suspension wire, this roughening of the surface of the wire is essential, but with such liquids as linseed oil and turpentine it is probably unnecessary.

The weighings are made on a sensitive balance by the method of substitution, that is, a constant mass is kept on one pan of the balance and the weighings made on the other pan. Sufficient weights are placed on the latter pan to secure equilibrium, first with the sinker attached and then detached. The weights were calibrated in terms of known standards and were accurately adjusted, so that the maximum error of any possible combination of weights is so small in comparison with accidental errors as to be negligible.

In making density determinations of a liquid by the hydrostatic weighing method, the procedure is as follows:

The water in the outside circulating bath is brought to the desired temperature and, before observations are begun, sufficient time is allowed to elapse for the apparatus to reach the steady state. When the thermometers in the inner tube indicate a constant temperature it is assumed that the liquid in the densimeter tube is at the same constant temperature and observations are begun. First, a weighing is made with the sinker suspended in the liquid sample, then the temperature is observed on each of two thermometers; next, a weighing is made with the sinker off, then a second weighing with the sinker on, and after that a second observation of temperature. The temperature may then be changed to a different temperature and the same procedure followed.

The density of the liquid sample is calculated by means of the equation

$$D_t = \frac{W - \frac{(w - w_1) + (w - w_2)}{2}\left(1 - \frac{\rho}{d_w}\right)}{V_t}, \qquad (4)$$

where D_t is the density of liquid sample at temperature t, W is the weight of sinker in vacuum, w is the weighing with sinker off, w_1 and w_2 are the weighings with sinker in the liquid, ρ is the air density, d_w is the density of weights (8.4 is usually assumed for brass weights), and V_t is the volume of sinker at temperature t.

With this method it is possible to obtain densities of ordinary liquids that are accurate to within 2 units in the fifth decimal place. However, Redlich and Bigeleisen [7] and Prang [4] claimed an accuracy of approximately 4 units in the seventh place and 4 to 5 units in the eighth place, respectively.

Additional information about the hydrostatic weighing method used at the National Bureau of Standards is given in publications by Osborne [8], Bearce [9], and Bearce and Peffer [10]. Wirth [11], Prang [4], Schulz [6], and Redlich and Bigeleisen [7] also described the hydrostatic weighing method used by them for determinations of the densities of liquids.

The Westphal balance indicated in figure 5 is a direct-reading instrument for determinations of the density of liquids by hydrostatic weighing. The balance consists of a pivoted beam graduated on one arm from which is suspended a sinker by means of a fine platinum wire. The movable weights (riders), in terms of density, represent units, tenths, hundredths, thousandths, and ten-thousandths. The Westphal balance should be in equilibrium when the sinker is suspended in water at a given temperature and the unit weight is in

[4] Prang [4] used a copper-constantan differential thermoelement for determining the temperature of a large sinker to within 0.0005 deg C (corresponding to 0.03 mg in weight).

[5] Prang [4] and Schulz [6] used platinum suspension wires 0.05 and 0.02 mm in diameter, respectively.

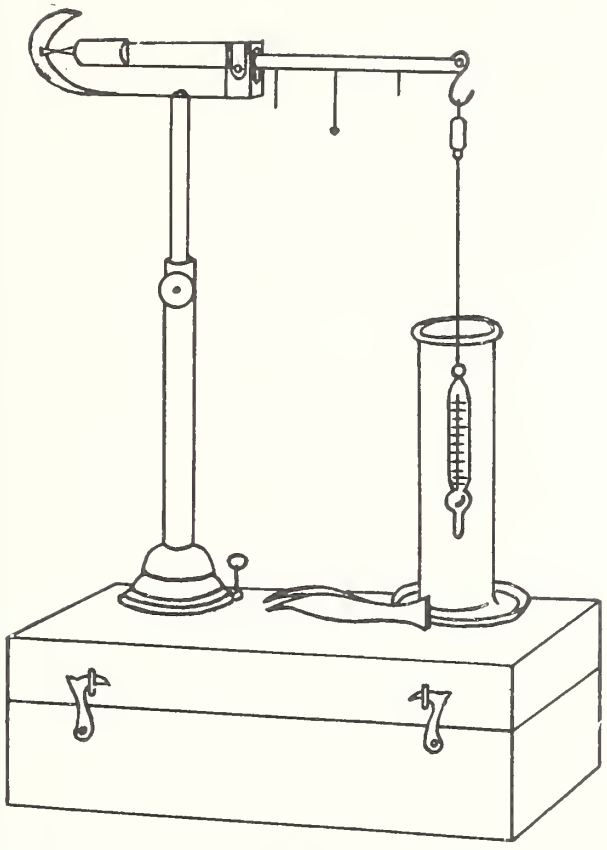

FIGURE 5. *Westphal balance for determinations of the density of liquids (Wright).*

proper position on the beam. When the sinker is suspended in another liquid at the same temperature, different weights may be required to bring the balance to equilibrium. The density is read directly from the values of the weights and their positions on the beam.

The Westphal balance is in general about as accurate as a hydrometer but not as convenient. Its principal advantage is that it can be used on small samples of liquids.

Forziati, Mair, and Rossini [12] described a density balance which is similar in principle to the Westphal balance. They used the balance shown in figure 6 for measurements of the density of purified liquid hydrocarbons and of mixtures of hydrocarbons, on samples as small as 9 ml in volume, with a precision of several parts per 100,000.

The scale on this particular balance ranges [6] from 0.65 to 0.95 g/ml, with the smallest division on the scale corresponding to 0.0001 g/ml and readings with the vernier being made to 0.00001 g/ml.

The balance was calibrated for measurements of density by making observations on a series of seven hydrocarbons for which values of density were determined by the picnometer method, for air-saturated material at 20°, 25°, and 30° C with an estimated over-all uncertainty of ±0.00002 g/ml.

[6] Other ranges of scale readings may be obtained as required.

In reducing the scale readings, corrections (from zero to 0.00003 g/ml) were made for slight inequalities in the spacing of the notches on the beam, which inequalities were determined by measurements with known masses hanging from the left arm of the beam as the rider on the beam was moved successively from one notch to another.

As the density of liquid hydrocarbons changes about 0.00001 g/ml for a change in temperature of 0.01 deg C, and as the sensitivity of the balance is 0.00001 g/ml, changes in temperature of the sample under observation in excess of 0.01 deg C will be indicated as changes in the scale readings at balance. For precise work, it is desirable to have thermometric control that produces a maximum variation in the temperature of the sample of not more than 0.01 deg C.

The effect of differences in surface tension of samples of various liquid hydrocarbons, with different forces on the fine platinum wire supporting the sinker, was calculated to be negligible. As the surface tension of hydrocarbons varies in a more or less regular manner with density, the main effect of differences in surface tension in going from hydrocarbons of low density to those of high density becomes incorporated as part of the calibration correction. The net effect of surface tension then reduces to the effect of the difference in surface tension for hydrocarbons of the same or nearly the same density. Examination of published data in the range of density 0.60 to 0.90 indicates that hydrocarbons of the same or nearly the same density have values of surface tension that differ by not more than about 1 dyne/cm. This corresponds to a maximum error of 0.000005 g/ml in density.

2. Picnometer Method

The picnometer method may be used for determining the density of liquids and solids.

(a) Liquids

The hydrostatic weighing method described in the preceding section is applicable only to such liquids as are of sufficient fluidity to allow the sinker to take up a position of static equilibrium when suspended in the liquid. With the more viscous liquids the sensitivity of the balance is greatly reduced and the weighings become more difficult, and of doubtful accuracy. For such liquids it is therefore necessary, or at least desirable, to use some other method. The method usually resorted to is that of the picnometer or specific gravity bottle.

In the construction of a picnometer the elements desired are as follows:

(a) A form adapted to the rapid attainment of the constant temperature of a surrounding bath.

(b) Means of filling with minimum contact of liquid sample with air.

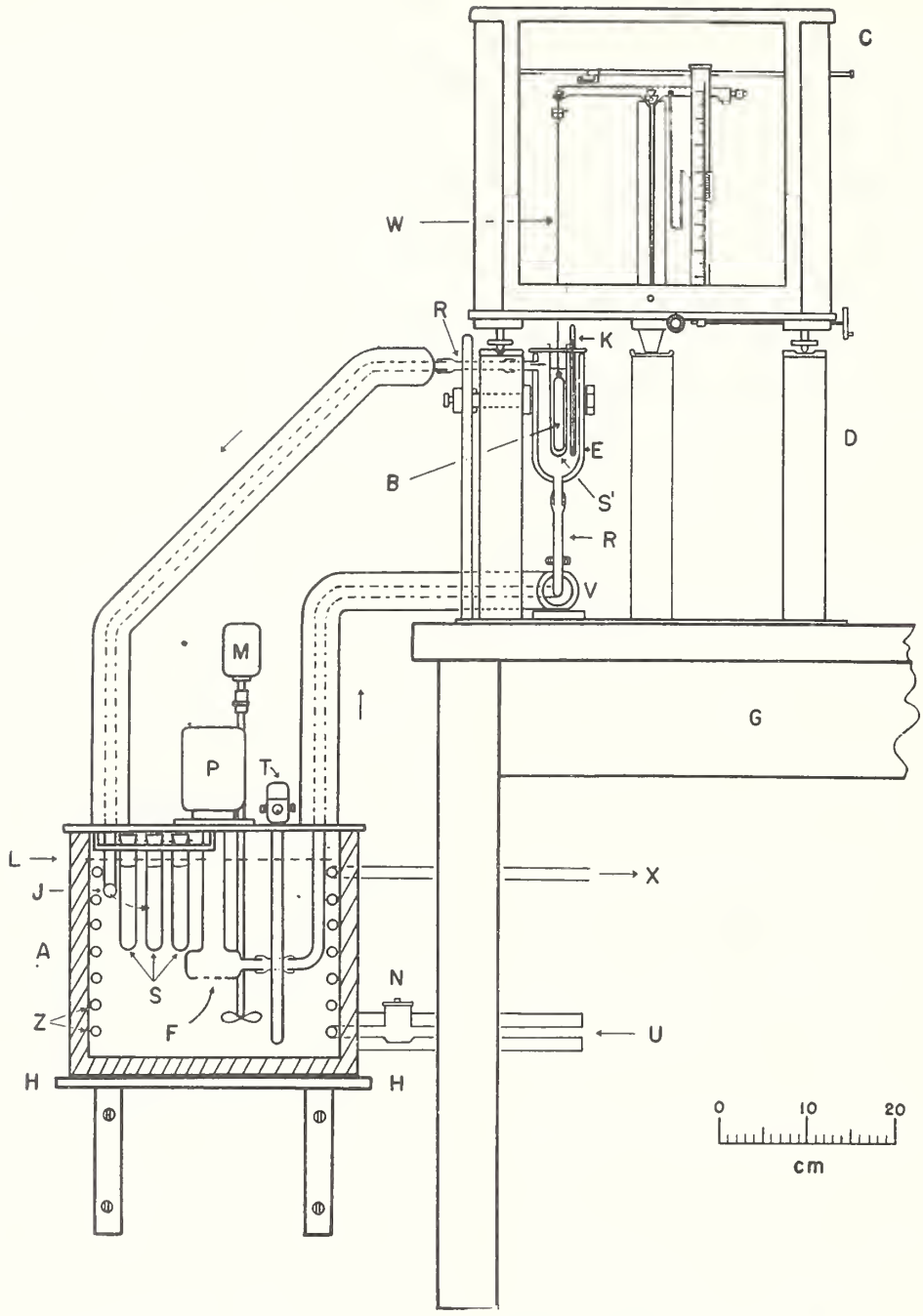

FIGURE 6. *Density balance for determinations of the density of liquids (Forziati, Mair, and Rossini.)*

A, Constant-temperature water reservoir; B, bob or sinker (volume 5 ml); C, chainomatic balance; D, metal supporting stand; E, vacuum-jacketed glass water bath; F, water inlet to pump; G, table; H, shelf (fastened to wall); J, water return from E; K, special mercury-in-glass thermometer (graduated from 19.90° to 20.10°, or from 24.90° to 25.10°, or from 29.90° to 30.10° C, with a sensitivity on the scale of 1 mm equal to 0.05° C); L, level of water; M, motor for stirrer; N, solenoid valve; P, water pump; R, connection of rubber tubing; S,S′, test tubes for containing samples of liquids; T, mercury-type thermoregulator; U, inlet for cooling water; V, valve for controlling flow of water through E; W, platinum wire, 0.003 in. in diameter; X, outlet for cooling water; Z, coil for cooling water.

(c) Protection after filling from change of weight by evaporation or absorption of moisture.

(d) Precision of filling.

Special picnometers on the principle of the Ostwald-Sprengel type have been designed and constructed for use at the National Bureau of Standards [13, 10]. The form of the picnometers is illustrated in figures 7 to 9. They were all made of Jena 16^{III} glass [7] and thoroughly annealed. They are adapted to immersion in the constant-temperature bath described in the preceding section. One of the picnometers (fig. 7) is the

[7] Pesce and Hölemann [14], Shedlovsky and Brown [15], and Washburn and Smith [16] used picnometers made of fused quartz. The volume of Pesce and Hölemann's picnometer was about 25 cm^3, which they claimed could be determined to within 0.0001 cm^3 at various temperatures between 25° and 85° C. Washburn and Smith stated that the volumes of their picnometers were determined with an accuracy of 0.1 percent.

Rudolphi [17] form, consisting of a hollow cylinder, which permits a rapid attainment of temperature but at the expense of total volume. Another picnometer (fig. 8) is of the plain cylindrical form. The cap with stopcock attached, as shown in figure 8, is used to control the internal pressure when filling the picnometer. The bulb containing the liquid to be investigated is joined to the picnometer by the ground joint *b*. By proper manipulation, such as inclining the picnometer at a suitable angle and properly varying the air pressure, liquid is introduced into the picnometer after filling, cap *a* is replaced. With the picnometer in position in the water bath, leaving only the upper portions of the capillaries emergent, the adjustment of the quantity of liquid is approximated as the temperature approaches constancy. Liquid may be introduced if necessary by means of a pipette placed with its tip to the aperture of the capillary with proper adjustment of pressure through tube *C*. Small quantities of liquid may be removed by means of a strip of filter paper applied at the tip of the capillary. Enough liquid is removed to bring the meniscus just to the line *e* on the capillary. The inside of the enlargement, *d*, of the tube is dried, either by means of filter paper or by a stream of dry air. The picnometer itself serves as a sensitive thermo-indicator, and until

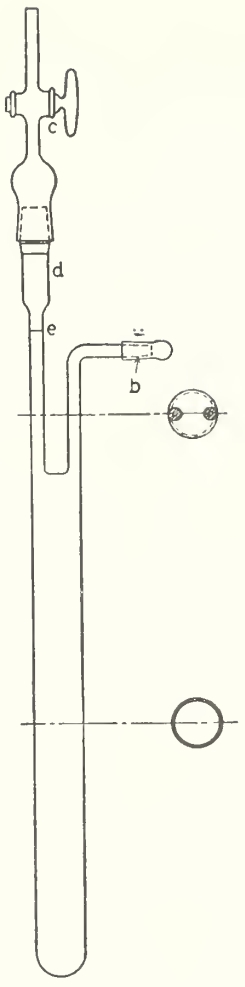

FIGURE 8. *Picnometer, one-fourth size (Osborne).*

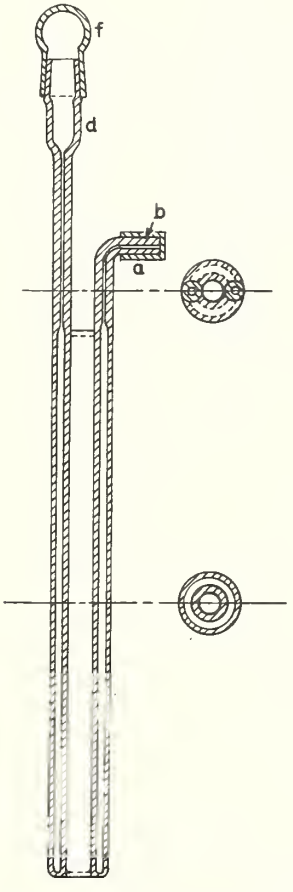

FIGURE 7. *Picnometer, three-tenths size (Osborne).*

the temperature becomes constant the final adjustment of the quantity of liquid should not be made. When the temperature appears steady, 5 or 10 minutes more are allowed as a margin of safety, and the filling is then completed. The picnometer is closed to prevent evaporation or absorption of moisture by means of cap *f*, shown in figure 7.

Figure 9 shows a third picnometer used at the National Bureau of Standards. The essential features are tube *E* extending nearly to the lower end of the picnometer, tube *D* extending up through the bottom of reservoir *I*, funnel *G*, and the attachment *F* provided with a stopcock. In filling the picnometer the liquid is placed in funnel *G* and drawn in through *E* by exhausting the air through *F*. By this procedure much time is saved in filling the picnometer, and the method is equally efficient in emptying and cleaning the picnometer when it is desired to introduce another liquid sample. When the filling is completed, *F* and *G* are replaced by caps *A* and *B*, all parts being provided with well-fitting ground joints. The picnometer is then placed in the temperature-control bath and brought to the desired temperature which is recorded. The quantity of liquid

in the picnometer is so adjusted that when temperature equilibrium has been established the liquid surface is just flush with the tips of the capillary tubes C and D. The excess liquid in reservoir I is removed and its interior carefully cleaned with the aid of a pipette and filter paper. The picnometer is removed from the bath, and the instrument and its contents are allowed to come to room temperature. The picnometer is dried and then weighed. From the previously determined mass, internal volume, and external volume of the picnometer, and the data obtained for a liquid sample at a given temperature, it is possible to calculate the density of the liquid from the equation

$$D_t = \frac{w\left(1-\frac{\rho}{d_w}\right)+\rho v - P}{V_t} = \frac{M}{V_t} \qquad (5)$$

where D_t is the density of liquid sample at temperature t, w is the apparent mass of picnometer filled with liquid sample at temperature t, ρ is the density of air, d_w is the density of weights (8.4 is usually assumed for brass weights), v is the external volume of picnometer, P is the mass of empty picnometer, V_t is the internal volume of picnometer at temperature t, and M is the mass of liquid sample contained in picnometer.

With the picnometers described it is possible to obtain densities of liquids that are accurate to within 1 unit in the fifth decimal place.

Shedlovsky and Brown [15], Robertson [18], and Wibaut, Hoog, Langedijk, Overhoff, and Smittenberg [19] described a picnometer with two graduated capillary tubes of uniform bore, as indicated in figure 10. With this graduated picnometer it is possible to make a density determination of a liquid comparatively quickly for once the picnometer is accurately calibrated the volume of the liquid sample need only be adjusted sufficiently closely to bring the liquid levels somewhere within the graduated regions of the capillary tubes at the temperature in question. After weighing, the picnometer is suspended in a constant-temperature bath provided with a side

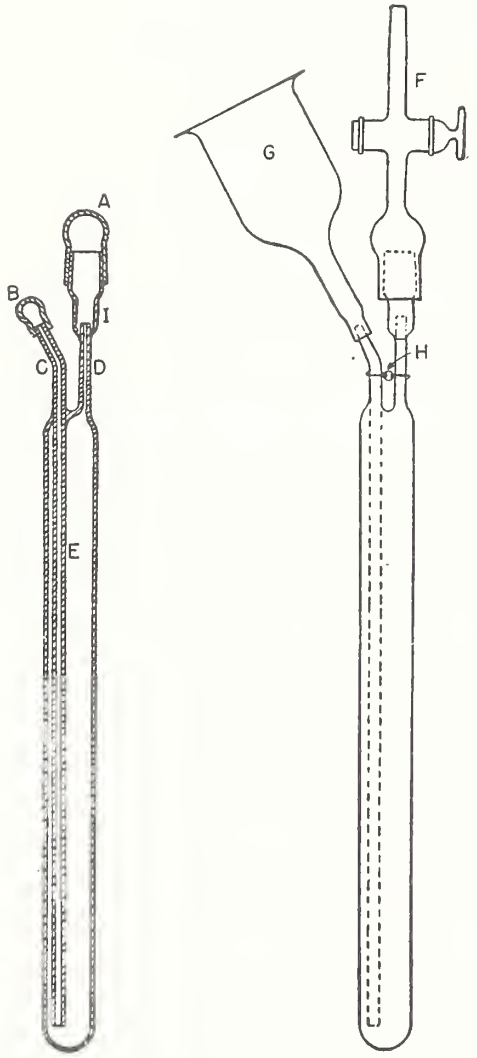

FIGURE 9. *Picnometer (Bearce and Peffer).*

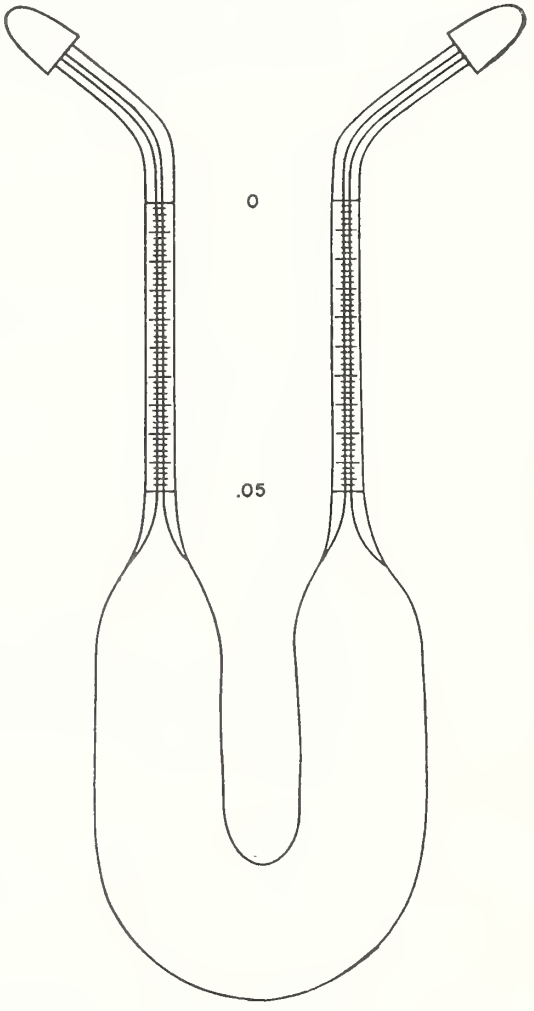

FIGURE 10. *Graduated picnometer (Robertson).*

window through which the meniscus levels can be read with the aid of a lens. The volume of the liquid corresponding to the known weight is thus determined. This picnometer has several obvious advantages over the Sprengel type of picnometer that is commonly used. Besides being more rapid and simpler to use, it avoids two likely sources of error in the Sprengel type, namely, possible variations in the liquid level at the tip and of the temperature in the process of withdrawing the liquid when bringing the meniscus to the reference mark.

Washburn and Smith [16] used a differential picnometer method for determining differences in density of water with a precision of 1 part in 1 million. Two fused-quartz picnometers very closely the same in size and weight, and of the shape shown in figure 11, were used. The capillary stem of each picnometer had a reference mark less than 0.01 cm in thickness, made with a diamond point, and the volume per unit length of the capillary was determined with an accuracy of 0.1 percent by calibration with mercury. The volume of each picnometer up to the reference mark was determined with an accuracy of 0.1 percent by weighing empty, filling with distilled water to any suitable height in the capillary, as read with a cathetometer while the picnometer was in a constant temperature bath, again weighing, and applying a correction for the volume of water in the capillary above the mark.

In making a measurement of the difference in density between a given sample of water and normal water, the first picnometer was filled with normal water and the second with the sample to any suitable heights in the capillaries. The filling was conveniently done with a fine silver capillary and the aid of a low vacuum line, as

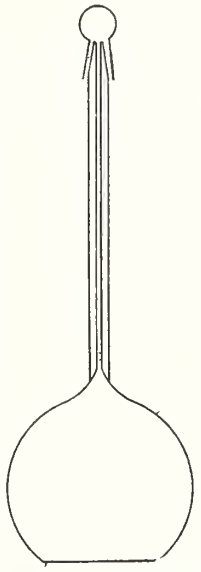

FIGURE 11. *Fused-quartz picnometer (Washburn and Smith).*

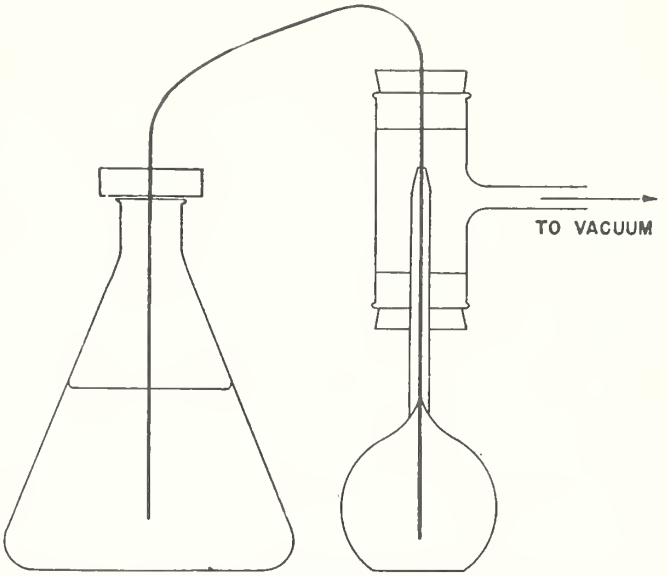

FIGURE 12. *Device for filling picnometer (Washburn and Smith).*

illustrated in figure 12. The picnometers were then placed side by side, with their ground stoppers loosely in place, in a constant temperature bath containing distilled water and having front and back of plate glass. After thermal equilibrium was attained, the height of the meniscus above the reference mark in each capillary was read with the cathetometer. The picnometers were next taken out of the bath, wiped dry, placed on opposite pans of a balance with their stoppers tightened in place, and the difference in their weights was determined. After the weighing, they were emptied and refilled so that the first picnometer then contained the sample water and the second contained normal water. Again they were placed in the bath in the same positions as before and the capillary heights recorded. They were again taken out, dried, placed on the same balance pans and the second difference in weight determined. The expression for the difference in density is obtained as follows:

Let

P_1=weight of picnometer 1
P_2=weight of picnometer 2
V_1=volume of picnometer 1 to the reference mark
V_2=volume of picnometer 2 to the reference mark
D =density of sample investigated
D_0=density of normal water.

$\Delta V_1'$, $\Delta V_1''$, $\Delta V_2'$, $\Delta V_2''$=volume of water above the reference mark in the capillary of picnometer 1 in the first and second fillings and picnometer 2 in the first and second fillings, respectively.

m_1=difference in masses after the first filling
m_2=difference in masses after the second filling.

If pichometer 1 is always placed on the right-hand pan of the balance,

$$P_2+V_2D+\Delta V'_2D=P_1+V_1D_0+\Delta V'_1D_0+m_1 \quad (6)$$

$$P_2+V_2D_0+\Delta V''_2D_0=P_1+V_1D+\Delta V''_1D+m_2. \quad (7)$$

Subtracting eq 7 from eq 6 and rearranging gives

$$(V_1+V_2)(D-D_0)=(m_1-m_2)+(\Delta V'_1D_0-\Delta V''_1D)-(\Delta V'_2D-\Delta V''_2D_0). \quad (8)$$

As this method is used only for the measurement of small differences in density, where $D-D_0<0.001$ g/ml, eq 8 may be written as

$$D-D_0=\frac{(m_1-m_2)+D_0[(\Delta V'_1-\Delta V''_1)-(\Delta V'_2-\Delta V''_2)]}{V_1+V_2}. \quad (9)$$

A bulb volume of about 50 ml and a capillary diameter of about 0.1 cm were found suitable. For a precision in $D-D_0$ of 1 part in 1 million with picnometers of this size, a convenient distribution of precision in the measurements is:

1. The temperature of the stirred water in the bath is held constant to within 0.01 deg C, because with extreme fluctuations of the bath temperature less than 0.01 deg, the lag in the picnometers is sufficient to maintain them constant to within 0.002 deg C.
2. The capillary heights are read to 0.001 cm.
3. The weighings are made to 0.03 mg.

It is advantageous to adjust the capillary heights to make the correction $(\Delta V'_1-\Delta V''_1)-(\Delta V'_2-\Delta V''_2)$ small and thus avoid the necessity for a very precise calibration of the capillaries. It is to be noted that:

1. The dry weights of the picnometers are not required.
2. The two picnometers should be so closely alike that effects of varying humidity are balanced.
3. The temperature of the water in the picnometers should be constant and uniform.
4. The effect of barometric and hydrostatic pressure on the capillary heights is balanced.
5. The (negligible) evaporation past the ground-glass stoppers is balanced.
6. The fused-quartz bulbs should show no measurable temperature hysteresis over the temperature range involved.
7. The small effect of dissolved air is balanced and it is not necessary to prepare air-free water.
8. The correction for air buoyancy affects only the difference of the differences, $(\Delta V'_1-\Delta V''_1)-(\Delta V'_2-\Delta V''_2)$, in the capillary volumes and with proper adjustment of the heights is negligible.

The earliest micromethods for determinations of densities of liquids are based on the use of small picnometers. Capillary tubes are used as containers for small amounts of liquid samples, but these tubes have the disadvantage of being fragile. Micropicnometers of the pipette type are the most practical.

Alber [20] described the two types of micropicnometers shown in figure 13. One type of micropicnometer (fig. 13, a) holds a definite volume, 0.1 ml, and is used in decigram procedures. The other type (fig. 13, b) serves for the measurement of varying volumes according to the amount of sample available and is recommended in two sizes—as a centigram pipette for volumes from 20 to 80 mm³, and as a milligram pipette for volumes from 6 to 16 mm³. The micropic-

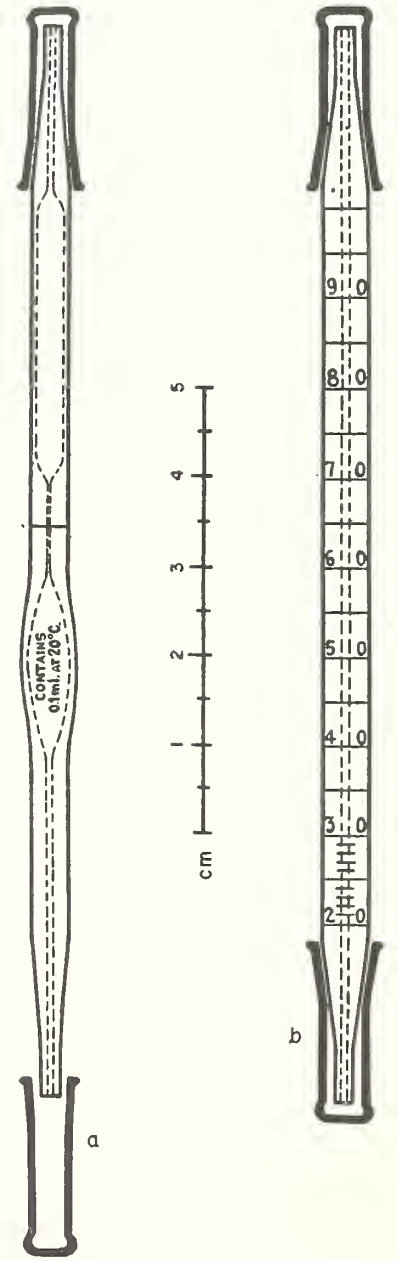

FIGURE 13. *Two types of micropicnometers (Alber).*

a, Decigram pipette, volume 100 mm³; b, centigram pipette if bore=1 mm, volume 20 to 80 mm³; milligram pipette if bore=0.5 mm, volume 6 to 16 mm³.

nometers are equipped with caps, rubber tubing, a mouthpiece filled with some drying agent, and a counterpoise of approximately the same shape and surface (glass rods). Furter [21] described a technique for using a graduated pipette micropicnometer for determinations of the densities of liquids at temperatures up to 300° C.

Other forms of picnometers or modifications of those indicated in this section have been described by Lipkin, Davison, Harvey and Kurtz [22], Newkirk [23], Hall [24], Parker and Parker [25], Scott and Frazier [26], Snyder and Hammond [27], Smith [28], Hennion [29], and Fontana and Calvin [30]. It has been claimed that the most accurate measurements by the picnometer method attain a precision of about 1 part in a million.

(b) Solids

The picnometer method described for liquids may be used in a similar manner for determinations of the densities of solid substances such as powders, crystals, or other solids. For some materials, appreciable errors may be introduced by the expulsion and solution of air and moisture by the picnometer liquid and the adsorption of the picnometer liquid on the surfaces of the materials. The choice of a picnometer liquid depends on the nature of the solid to be investigated. A satisfactory picnometer liquid should have a high degree of wetting power, that is, ability to expel air. The liquid should not combine with or be adsorbed on the surface of the solid and should not dissociate or polymerize during use.

The density of a solid may be computed from the equation

$$D=\frac{dS}{S+P+Vd-W}, \qquad (10)$$

where D is the density of solid, d is the density of picnometer liquid, S is the weight of solid, P is the weight of dry, empty picnometer, V is the internal volume of picnometer, and W is the total weight of picnometer, solid, and liquid necessary to fill the picnometer.

With a given picnometer and a liquid of known density, eq 10 becomes

$$D=\frac{dS}{S+k-W}, \qquad (11)$$

where k equals $P+Vd$. With this equation it is only necessary to determine the weight of the solid and the total weight of the picnometer, solid, and liquid required to fill the picnometer.

Figure 14 shows 2 small picnometers used by Russell [31] with a centrifuge. The stoppers, which can be made from thick-walled capillary of 0.5- to 1-mm bore, should be very carefully ground in, so that the picnometer volume will be very accurately and reproducibly defined. A fine line encircles the capillary stopper in order to aid in defining the picnometer volume. The picnometer is covered by a cap with a ground-glass joint to prevent any slight evaporation of the picnometer liquid. The volume of the picnometer is determined at the temperatures of use, which in any case should be above the highest balance room temperature that will be encountered. This precaution prevents the picnometer from overflowing and causing a loss of liquid.

Baxter and Wallace [32] used a 25-ml graduated flask, the neck of which was constricted to about 2.5 mm in diameter. For determinations of densities of halogen salts of sodium, potassium, rubidium and cesium, they used toluene for the picnometer liquid. They secured an accuracy in setting of about 0.3 mg of toluene. The neck of the flask was dried before the meniscus was set. Before weighing, the outside of the flask was washed with a dilute solution of ammonia, wiped with a clean, slightly damp, cotton cloth and was allowed to stand in the balance room for at least one hour.

Nutting [33] stated that tetrahydronaphthalene ("tetralin"), dichloroethyl ether ("chlorex"), tetrachloroethane, and the mono-, di- and trichlorobenzenes are quite satisfactory for picnometer liquids in determinations of densities of clays and soils. These liquids are but slightly adsorbed on soil grains, decompose or polymerize very little in use, disturb existing hydrates very slightly if at all, have low vapor pressures, moderate densities, and moderate coefficients of expansion.

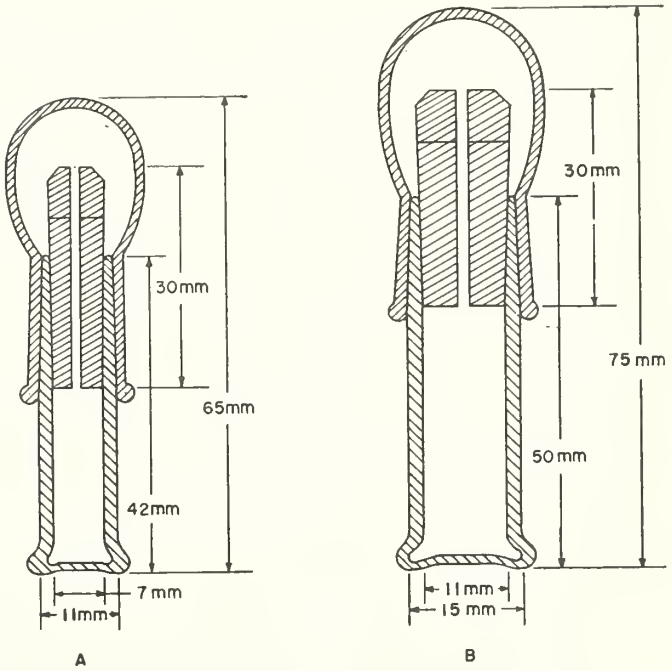

FIGURE 14. *Picnometers for solids (Russell).*

A, Small picnometer, volume about 1 ml; B, larger picnometer, volume about 3 ml.

With the apparatus shown in figure 15, Gooden [34] succeeded in removing air smoothly from fine powder immersed in the liquid of a picnometer, by controlled agitation while the sample is under vacuum. The source of agitation is a vibrator, V, of the type used for massaging the face and scalp. A special head, H, which holds the picnometer flask, F, is used instead of the original vibrator head. This special head consists of a one-hole rubber stopper in which three nails are inserted at a slight angle to grasp the body of the flask. The vibrator is mounted head upward on a heavy base, B, which rests on a thick rubber sheet, G, covering the top of a wooden block, W. The rubber sheet serves as a gasket between the block and a vacuum bell jar, J, which covers that part of the apparatus so far described. One or more air holes, A, cut in the gasket, prevent the central portion from being lifted when the jar is evacuated. A round-bodied electric lamp cord is run from the vibrator down through the gasket into the block and out at one side, the passage through the wood being bushed airtight with a rubber stopper, S. A coupling, C, between the vibrator and the gasket may be inserted for convenience in handling.

The following procedure is used by Gooden for adjustment of the vibration intensity and of the pressure reduction: The apparatus is plugged into a continuously variable transformer, T, with voltage range from 0 to about 115. The rubber tube from the bell jar to a vacuum line has a branch connected to a manometer, M, and another branch left open at the end, E. The operator controls vibration and vacuum with one hand on the adjusting knob of the transformer and the index finger of the other hand resting lightly over the tube end, E. If it is desired to maintain a particular adjustment for some time without attention, the transformer may be set for the necessary voltage and the vacuum kept fairly constant by leakage through a screw pinchcock, P. If the maximum vacuum is desired, the end of a cork stopper may be left resting against E.

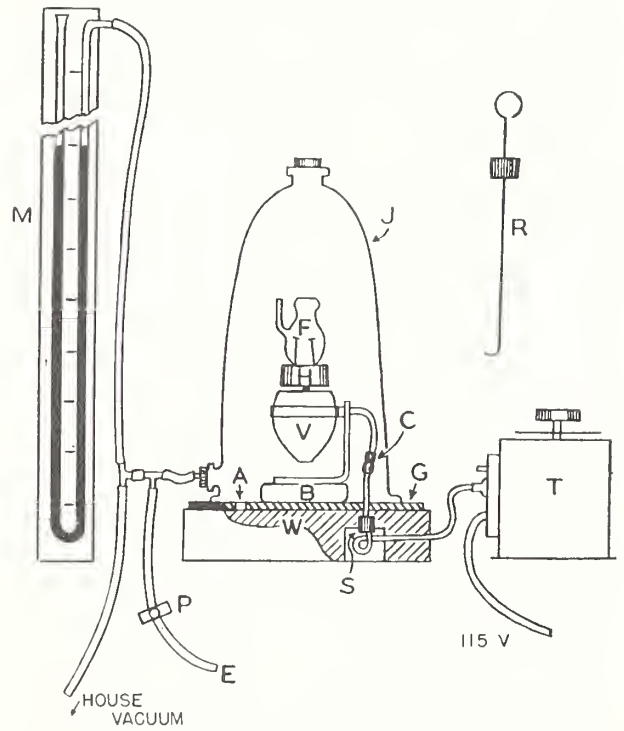

FIGURE 15. *Apparatus for removal of air from samples of powder in picnometer liquid (Gooden).*

Continuous but not violent bubbling until the amount of air remaining does not sensibly affect the volume of the sample, is recommended. A test for completeness of air removal is to observe whether the height of the liquid in the picnometer changes on application or removal of vacuum. If the last significant traces of air are persistent, two methods may be used for hastening their removal. One method is to stir the sample with a stiff wire rod, R, extending through a flexible rubber stopper in the top of the bell jar. Another method, which is more convenient, is to jerk the flask repeatedly by jiggling the electric plug that connects the transformer to the electric outlet.

3. Flotation Method

The flotation method of determining the densities of materials may be considered as a development or modification of the hydrostatic weighing method. In the flotation method the object floats in the liquid and no suspension thread or wire is required. Retgers [35] used this method by mixing two liquids until he obtained a mixture in which a submerged solid body floated. The density of the solid body is the same as the density of the mixture which could be determined later by another method.

Pisati and Reggiani [36] were among the earliest investigators to use the flotation method for determinations of the density of liquids.

Figure 16 shows the float used by Warrington [37] for determinations of the densities of liquids. By slipping small ring-shaped platinum weights over the submerged stem, the density of the float may be made to approximate that of the liquid sample. The temperature is then allowed to change very slowly until a temperature is reached at which the float neither sinks nor rises.

The float used by Warrington for determinations of the densities of solids, is indicated in figure 17. He made determinations with the float in water, first with the float loaded with mercury alone, and then with the float loaded with the solid and mercury. The mercury and the solid were in contact with the water. The density of the solid may be computed from the following equation:

$$d_S = \frac{d_M d_w W_S}{W_S d_M + (W_M - W_{M'})(d_w - d_M)}, \qquad (12)$$

where d_S is the density of the solid, d_M is the density of mercury, d_w is the density of water, W_S the weight of solid in vacuum, W_M the weight of mercury required to bring the float to floating equilibrium, and $W_S+W_{M'}$ is the sum of weights of solid and mercury required to bring float to floating equilibrium. Warrington claimed an accuracy of 1 part in 100,000 for densities of solids, and 1 part in a million for liquids.

Richards and Shipley [38, 39] and Richards and Harris [40] used small floats (not exceeding 5 ml volume) of fused quartz, Jena glass, and soft glass, shaped like a buoy or a fish, as illustrated in figure 18. Aging of the floats before calibration and use was found to be important. They found that such floats are easily changed from sinking to rising in aqueous solutions by a fall in temperature of 0.001 deg C near the temperature of floating equilibrium. Their method depends upon noting the precise temperature at which the liquid sample attains the same density as a given, previously calibrated float. This equality of density is indicated when floating equilibrium is attained, that is, when the entirely immersed float neither rises nor sinks in the liquid. Data of a single determination from Richards and Shipley [38] in table 3, indicate that the temperature of floating equilibrium can be determined within 0.001 deg C.

Richards and Shipley used a thermostat capable of maintaining a constant temperature within 0.001 deg C and of easily changing this temperature. The liquid sample is placed in a flask, immersed in a stirred constant temperature bath. The float within the flask is viewed by reflection in a small inclined mirror beneath the water of the bath. Care must be taken to prevent air bubbles from attaching themselves to the float.

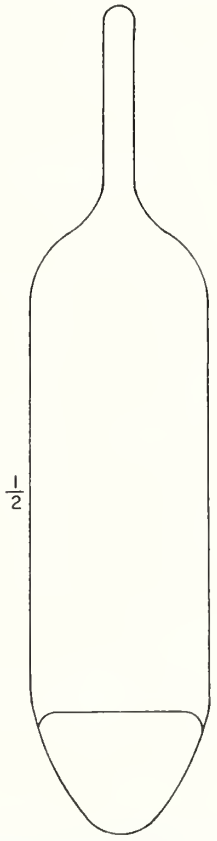

FIGURE 16. *Float for determination of density of liquids, one-half size (Warrington).*

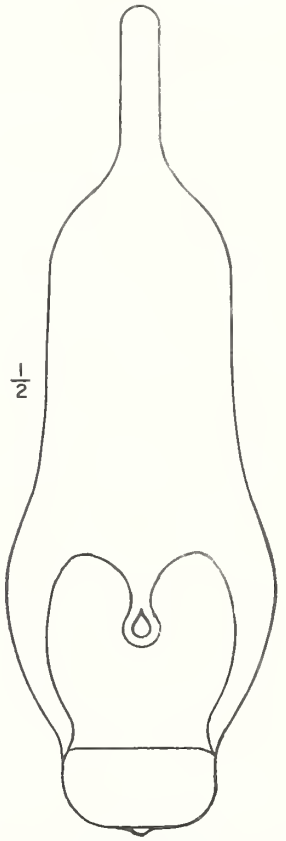

FIGURE 17. *Float for determination of density of solids, one-half size (Warrington).*

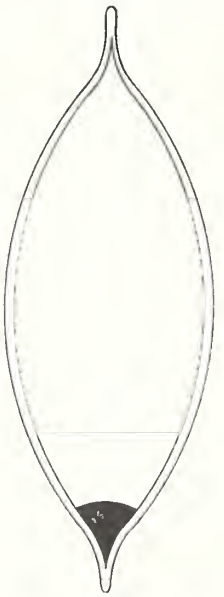

FIGURE 18. *Float for determination of density of liquids (Richards and Shipley).*

TABLE 3. *Movement of float near temperature of floating equilibrium (Richards and Shipley.)*

Temperature	Movement of float	Temperature	Movement of float
° C		° C	
15.394	Sinking.	15.390	Rising.
15.390	Rising.	15.391	Sinking.
15.392	Sinking.		

Figure 19 shows the float used by Lamb and Lee [41] for determinations of densities of aqueous solutions. A piece of soft iron is enclosed in the bulb of the float. By means of an electric current through an external circuit, an electromagnetic attraction is exerted upon the bulb in a vertical direction, in order to obviate the difficulty of varying the buoyancy of the float by small amounts. Lamb and Lee claimed an accuracy of several units in the seventh decimal place.

A fused-quartz float with a cobalt-steel permanent magnet sealed in the bottom of the float was used by Hall and Jones [42]. By slowly reducing the current through a coil the voltage was found which just prevented the float from rising in the liquid sample.

Richards and Shipley varied the temperature of the liquid sample and Lamb and Lee used a magnetic control in order to obtain floating equilibrium in their determinations of densities of liquids. Gilfillan [43] held the temperature of the liquid sample constant at 0° C and altered the buoyancy of the float by varying the hydrostatic pressure. Measurements are made in test tubes connected to a pump and manometer system by means of ground joints. The tubes are kept immersed in a thermostat at 0° C and the movement of the Pyrex-glass float weighted with mercury, is observed through a double-walled evacuated window by means of a telescope.

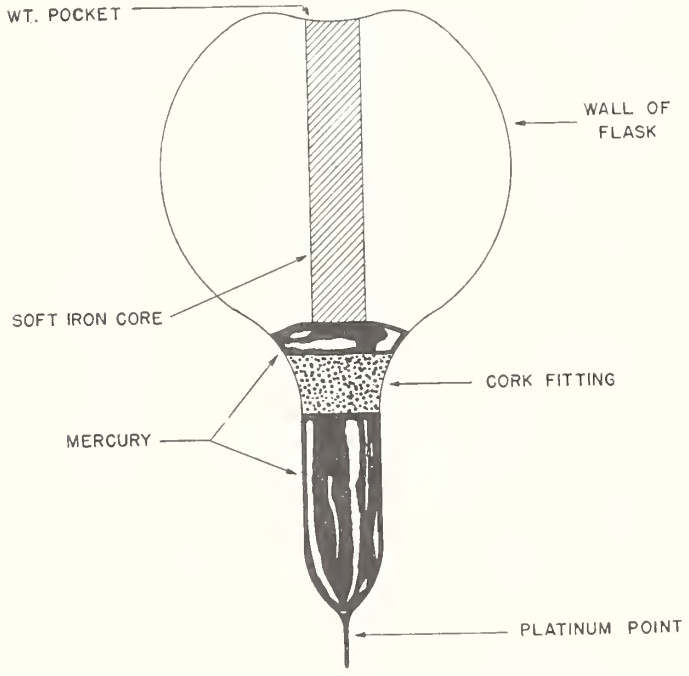

FIGURE 19. *Float for determination of density of liquids (Lamb and Lee).*

For determinations of the density of small crystals, Bernal and Crowfoot [44] applied the centrifuge in the flotation method. A small quantity of the substance (about 0.05 mg or less) is placed in a suitable liquid contained in a small test tube. Air bubbles are removed from the crystals and liquid by evacuation in a vacuum desiccator. The test tube is then placed in a centrifuge and spun for several minutes at a speed of 2,000 to 4,000 revolutions per minute. A heavier or lighter liquid is added to the tube, according to whether the crystals sink or rise. The process is repeated until the submerged crystals float in the liquid. The density of the crystals is then equal to the density of the liquid, which can be determined by any of the known methods.

Yagoda [45] published a list of organic liquids and solutions of inorganic salts that have been used in density determinations by the flotation method. This list is given in table 4. In adding one liquid to another, it is necessary to choose liquids that are miscible and in which the solid sample is not soluble or is only slightly soluble. The liquids should preferably be colorless or lightly colored, mobile, and not highly volatile.

TABLE 4. *Liquids used for determinations of density by flotation method (Yagoda)*

Liquid	Specific gravity [a]
ORGANIC LIQUIDS	
Toluene	0.866
Benzene	.879
Carbon bisulfide	1.26
Carbon tetrachloride	1.58
Ethyl iodide	1.94
Ethylene bromide	2.19
Methylene bromide	2.50
Bromoform	2.88
Acetylenetetrabromide	2.97
Methylene iodide	3.33
SATURATED AQUEOUS INORGANIC SALT SOLUTIONS	
Thoulet's solution [b]	3.2
Cadmium borotungstate	3.28
Cobalt borotungstate	3.34
Rohrbach's solution [c]	3.5
Thallium formate at 20°	3.40
Thallium formate at 50°	4.11
Thallium formate at 90 °	4.76

[a] Temperature not indicated.
[b] Contains potassium and mercuric iodides in the molecular ratio of 2:1 (1 part of KI and 1.3 parts of HgI_2 by weight); the salts combining in solution to form the complex K_2HgI_4. By boiling off the excess water until a fragment of fluorite is floated on the surface, a pale amber-colored solution results, with a specific gravity of about 3.2 at room temperature.
[c] Is an analogous complex of barium mercuric iodide (see footnote b).

A procedure for the preparation of a set of floats for use as indicators for determining the densities of liquid or solid samples of materials, has been described by Blank [46]. These floats prepared

from glass tubing (1½ cm in length and 1 cm in diameter) and lead foil, may be used for densities from about 1 to 11.

Emeléus and coworkers [47] considered fused quartz as the ideal material for floats because of its small thermal expansion, great elasticity, mechanical strength, permanence and insolubility. They found that a slim cylindrical float is better than a fish-like form, for the movement of the former responds more rapidly and certainly to small differences in the density of a liquid. Their floats were about 75 mm long and 4 mm in diameter and had a ring at the top so that they could be handled conveniently by means of a glass hook.

Additional information about the flotation method is given by Lewis and MacDonald [48], Randall and Longtin [49], Johnston and Hutchison [50], and Hutchison and Johnston [51]. Randall and Longtin described a microfloat of Pyrex glass for determinations of the density of very small samples of water, as small as 0.1 ml. They made floats about the size of a grain of wheat.

4. Hydrometer Method

The hydrometer consists of a graduated cylindrical stem and a bulb weighted with mercury or lead. For a determination of the density or specific gravity of a liquid by this method, it is necessary to use a suitable hydrometer that will sink in the liquid to such position that a part of the graduated stem extends above the surface of the liquid.

Some hydrometers (thermohydrometers) have a thermometer in the stem to indicate the temperature of the liquid. If the thermometer is not made as a part of the hydrometer, the thermometer should be so placed that the bulb can assume the temperature of the liquid, and as much of the mercury column as is feasible should be immersed. This is important, especially if the temperature of the liquid differs greatly from that of the surrounding air. In reading the thermometer accurately, care must be taken that the line of sight is perpendicular to the thermometer scale in order to avoid parallax. The temperature of a liquid should be read to a degree of accuracy that is comparable with the accuracy of the determination of the density of the liquid.

Hydrometers should be made of smooth, transparent glass without bubbles, striae, or other imperfections. The glass should be of a kind that adequately resists the action of chemical reagents and also possesses suitable thermal qualities, such as would adapt it to use for thermometers.

Each section of a hydrometer perpendicular to its axis should be circular. The stem should be uniform in cross section and no irregularities should be perceptible. The outer surface should be symmetrical about a vertical axis. There should be no unnecessary thickening of the glass walls and no abrupt constrictions which would hinder convenient cleaning. The capillary stem of a thermohydrometer should be parallel to the axis and should extend at least 10 mm above the scale. It should contain an enlargement that will permit heating to 120° C.

Before graduation and adjustment all hydrometers should be thoroughly annealed.

Material used for ballast should be confined to the bottom of the instrument, and no loose material of any sort should be inside a hydrometer. The disposition of the weight should be such that the hydrometer will always float with its axis vertical.

Only the best quality of paper should be used for scales and designating labels inside the hydrometer. The paper usually known as first-class ledger paper is suitable for this purpose. The scales and labels should be securely fastened in place by some material which does not soften at the highest temperature to which the hydrometer will be exposed in use and which does not deteriorate with time. The scale should be straight and without twist.

The hydrometer should be perfectly dry on the inside when sealed. Thermometer bulbs and capillary tubes should be free from air.

The hydrometer stem should extend above the top of the scale at least 1.5 cm and below the scale should continue cylindrical for at least 3 mm. The thermometer scale should not extend beyond the cylindrical portion of the containing tube nor beyond the straight portion of the capillary. It is desirable that the thermometer scale should include the ice point (0° C).

The total length of a hydrometer should not exceed 45 cm and should generally be much less than this for the sake of convenience. The top of the stem should be neatly rounded, but not unnecessarily thickened. The graduations and inscriptions should be in permanent black ink, such as india ink. They should be clear and distinct.

The length of the smallest subdivisions of the scales should, in general, be from 1 to 2 mm. The division lines must be perpendicular to the axis of the hydrometer; that is, horizontal when the instrument is floating.

The lengths of division and subdivision lines both on hydrometer and thermometer scales should be so chosen as to facilitate readings. Sufficient lines should be numbered to indicate clearly the reading at any point. The numbers at the ends of the scale intervals should be complete, but those intermediate may be abbreviated.

The division lines of the hydrometer scale should extend at least one-fourth around the circumference of the stem and be adjacent to or intersect a line parallel to the axis indicating the front of the scale. The division lines of the thermometer scale should extend behind and on both sides of the capillary. To facilitate readings

near the ends of the hydrometer scale the graduations should be continued a few divisions beyond the ends of the principal interval.

The hydrometer scale for density indications should be divided in 0.001, 0.0005, 0.0002, or 0.0001 unit of the density. For percent or degree indications the hydrometer scale should be divided into whole, half, fifth, or tenth percents or degrees. The thermometer scale should be divided into whole or half degrees.

The hydrometer scale or a suitable special label should bear an inscription that indicates unequivocally the purpose of the instrument. This inscription should denote the liquid for which the hydrometer is intended, the temperature at which it is to be used, and the character of the indication, including definition of any arbitrary scale employed.

Hydrometers are seldom used for the greatest accuracy, as the usual conditions under which they are used preclude such special manipulation and exact observation as are necessary to obtain high precision. It is, nevertheless, important that they be accurately graduated to avoid, as far as possible, the use of instrumental corrections, and to obtain this result it is necessary to employ certain precautions and methods in standardizing these instruments.

The methods of manipulation described below are, in general, employed at the National Bureau of Standards in testing hydrometers and should be followed by the manufacturer and user to a degree depending on the accuracy required.

The hydrometer should be clean, dry, and at the temperature of the liquid before immersing to make a reading. The liquid should be contained in a clear, smooth glass vessel of suitable size and shape. By means of a stirrer which reaches to the bottom of the vessel, the liquid should be thoroughly mixed. The hydrometer is slowly immersed in the liquid and pushed slightly below the point where it floats naturally and then allowed to float freely. The reading on the graduated stem should not be made until the liquid and the hydrometer are free from air bubbles and at rest.

The correct method of reading the hydrometer is illustrated in figure 20. The eye should be placed slightly below the plane of the surface of the liquid (fig. 20, A) and then raised slowly until this surface, seen as an ellipse, becomes a straight line (fig. 20, B). The point at which this line cuts the graduated stem of the hydrometer should be taken as the reading of the instrument (fig. 20, B). The reading gives the density or specific gravity directly or it may be reduced to density or specific gravity by means of an accompanying table.

In case the liquid is not sufficiently clear to allow the reading to be made as described, it is necessary to read from above the liquid surface (apparent reading) and to estimate as accurately as possible the point to which the liquid rises on the hydrometer stem. As the hydrometer is calibrated to give correct indications when read at the principal surface of the liquid, it is necessary to correct the apparent reading above the liquid surface by an amount equal to the height to which the liquid creeps up on the stem of the hydrometer. The amount of this correction may be determined with sufficient accuracy for most purposes by taking corresponding readings in a clear liquid and noting the difference.

In order that a hydrometer may correctly indicate the density of a liquid, it is essential that the liquid be uniform throughout and at the temperature at which the hydrometer was calibrated.

To insure uniformity in the liquid, stirring is required shortly before making the observation. This stirring should be complete and may be well accomplished by a perforated disk or spiral at the end of a rod long enough to reach the bottom of the vessel containing the liquid. Motion of this stirrer from top to bottom serves to disperse layers of the liquid of different density.

The liquid should be at nearly the temperature of the surrounding atmosphere, as otherwise its temperature will be changing during the observation, causing not only differences in density but also doubt as to the actual temperature. When

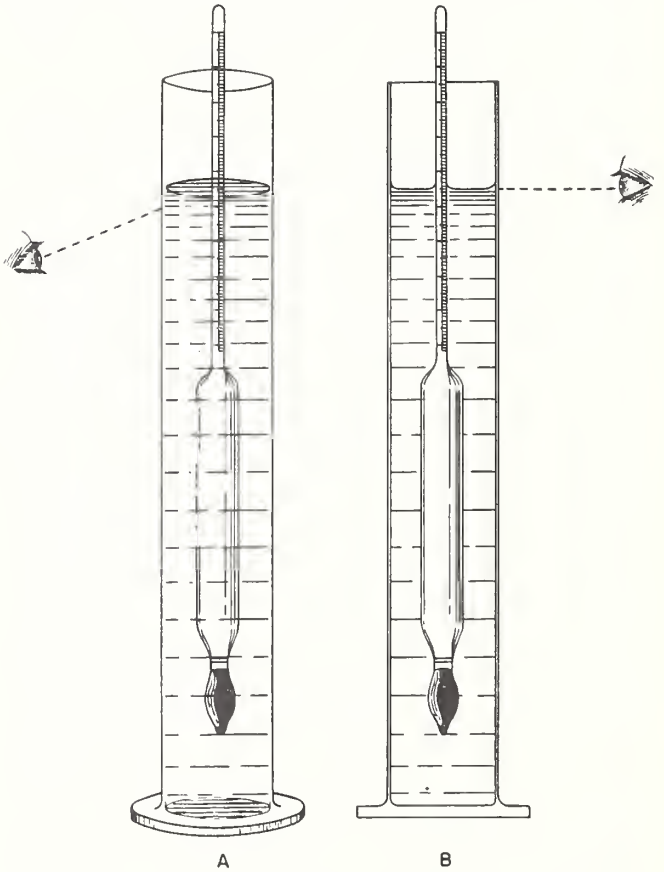

FIGURE 20. *Method of reading hydrometer (NBS Circular C410).*

the temperature at which the hydrometer is observed differs from the temperature at which the hydrometer was calibrated, the reading is not truly the density according to the basis of the hydrometer. The indicated reading differs from the normal reading by an amount depending on the difference in temperature and on the relative thermal expansion of the hydrometer and the liquid. Tables of corrections may be prepared for use with hydrometers at various temperatures. Such tables should be used with caution, and only for approximate results when the temperature differs much from the temperature at which the hydrometer was calibrated or from the temperature of the surrounding air.

Effects of surface tension on hydrometers are a consequence of the downward force exerted on the stem by the meniscus or curved surface, which rises about the stem, and affects the depth of immersion and consequent scale reading. Because a hydrometer will indicate differently in two liquids having the same density but different surface tensions, and since surface tension is a specific property of liquids, it is necessary to specify the liquid for which a hydrometer is intended. Although hydrometers of equivalent dimensions may be compared, without error, in a liquid differing in surface tension from the specified liquid, comparisons of dissimilar hydrometers in such a liquid must be corrected for the effect of the surface tension.

In many liquids spontaneous changes in surface tension occur due to the formation of surface films of impurities, which may come from the liquid, the vessel containing the liquid, or the air. Errors from this cause are avoided by the use of liquids not subject to such changes or by the purification of the surface by overflowing immediately before reading the hydrometer. The latter method is used at the National Bureau of Standards for testing hydrometers in sulfuric-acid solutions and alcohol solutions, and is accomplished by causing the liquid to overflow from the part of the apparatus in which the hydrometer is immersed by a small rotating propeller which serves also to stir the liquid. The apparatus is shown in figures 21 and 22.

A simpler but less precise apparatus designed to permit renewal of the surface of a liquid by overflowing, is shown in figure 23. The cylinder is filled nearly to the spout by the liquid, the density of which is desired or in which hydrometers are to be compared. The hydrometer is then immersed in the liquid and permitted to float freely until it has assumed the temperature of the liquid. The hydrometer is raised to permit thorough stirring of the liquid and the temperature is observed. From a beaker containing the liquid at the same temperature a sufficient amount is poured into the funnel to cause the liquid to overflow and run out the spout, where it is caught in a convenient vessel. The hydrometer is then read. The completeness of the cleansing of the surface of the liquid may be tested by repeating the operation. The readings of the hydrometer will approach a constant value as the surface becomes normal.

The necessity for such special manipulation is confined to the reading of hydrometers in liquids which are subject to surface contamination. Such, in general, are aqueous solutions or mixtures of acids, alkalies, salts, sugar, and weak alcoholic mixtures. Oils, alcoholic mixtures of strength above 40 percent by volume, and other liquids of relatively low surface tension are not, in general, liable to surface contamination sufficient to cause appreciable changes in hydrometer readings.

The accuracy of hydrometer readings depends, in many cases, upon the cleanness of the hydrometers and of the liquids in which the observations are made. In order that readings shall be uniform and reproducible, the surface of the hydrometers,

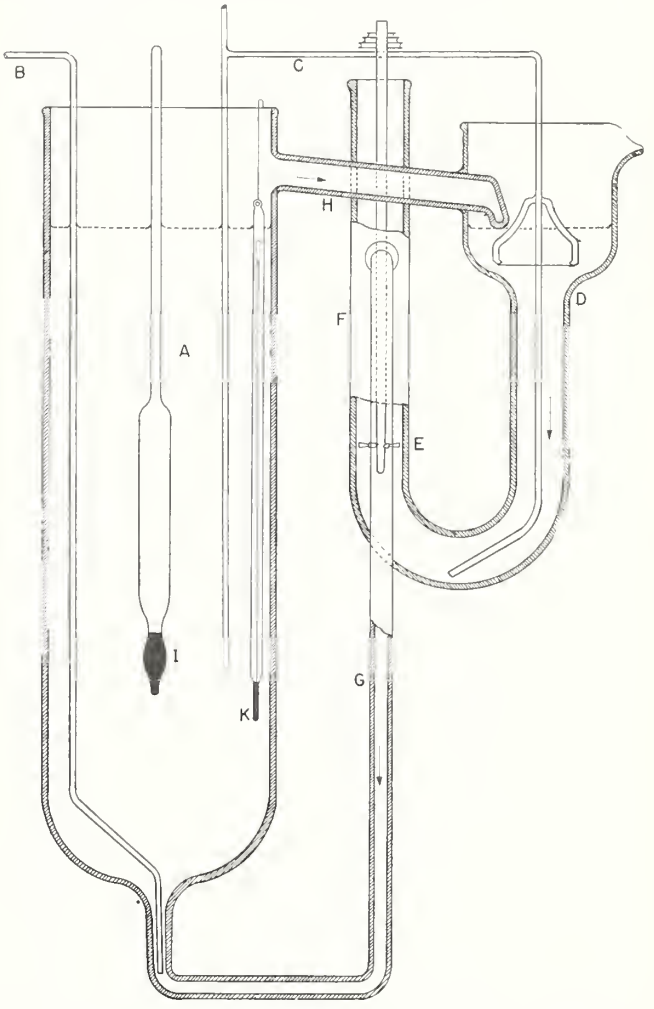

FIGURE 21. *Section of hydrometer comparator (Peffer and Blair, NBS Circular 477).*

A, Cylinder containing the test liquid; B, glass tube for filling and emptying A; C, siphon for removing the liquid from D into A; E, propeller that stirs the liquid and raises it in the tube F, making it flow through G into A and through the cross tube H, into D; I, hydrometer; K, thermometer.

574278 O - 61 - 44

and especially of the stem, must be clean, so that the liquid will rise uniformly and merge into an imperceptible film on the stem. The readiness with which this condition is fulfilled depends somewhat upon the character of the liquid. Certain liquids, such as mineral oils and strong alcoholic mixtures, adhere to the hydrometer stem very readily, while with weak aqueous solutions of sugar, salts, acids, and alcohol, scrupulous cleaning of the stem is required in order to secure the normal condition. Before use, the hydrometer should be thoroughly washed in soap and water, rinsed, and dried by wiping with a clean linen cloth. If the hydrometer is to be used in aqueous solutions which do not adhere readily, the stem should be dipped into strong alcohol and immediately wiped dry with a soft, clean, linen cloth.

A careful observer can, by using a hydrometer that has been accurately calibrated, obtain results that are correct to within one of the smallest subdivisions of the scale. For example, a "precision" hydrometer should yield densities that are accurate to one unit in the third decimal place, or, if graduated in percentages, to 0.1 percent. This degree of accuracy can be considerably improved by the exercise of special precautions as to temperature control, cleanliness, etc.

There are a number of arbitrary scales in use to represent the densities or specific gravities of liquids.

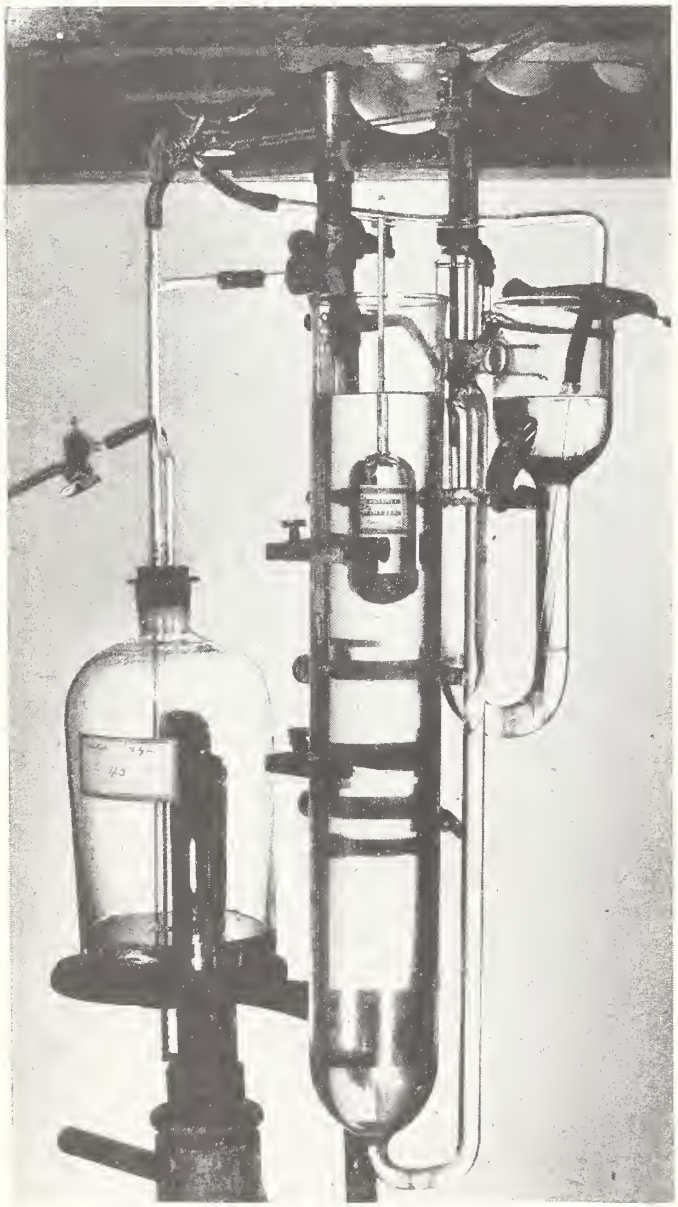

FIGURE 22. *Hydrometer comparator (Peffer and Blair, NBS Circular 477).*

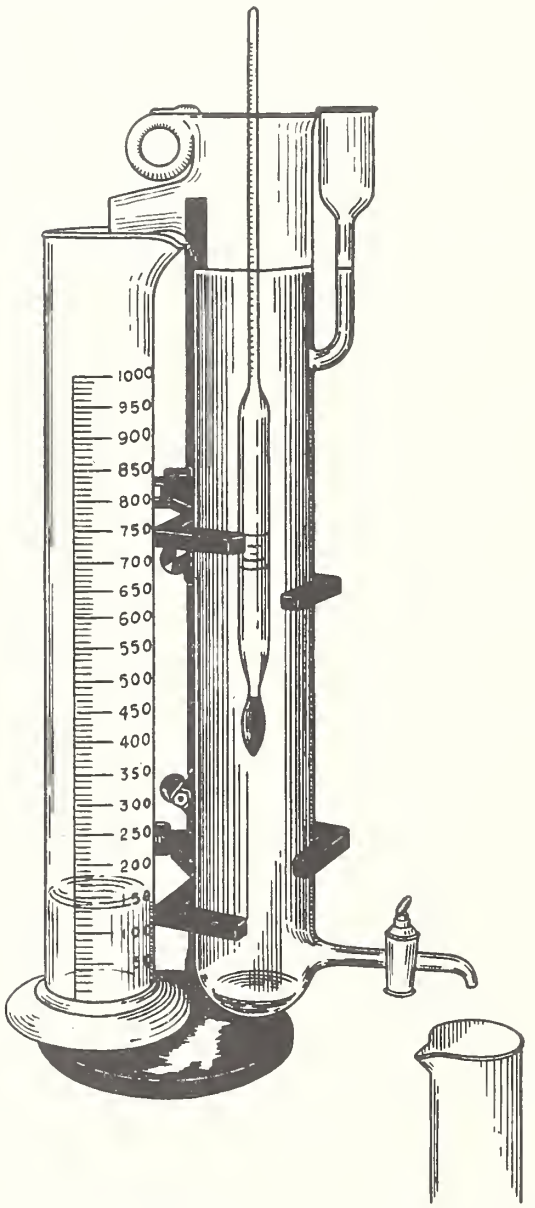

FIGURE 23. *Apparatus for renewal of surface by overflowing (NBS Circular 16).*

Two Baumé hydrometer scales are in general use in the United States. The following formula is used for liquids heavier than water:

$$\text{Degrees Baumé} = 145 - \frac{145}{\text{sp gr } 60°/60° \text{ F}}. \quad (13)$$

For liquids lighter than water, the formula is

$$\text{Degrees Baumé} = \frac{140}{\text{sp gr } 60°/60° \text{ F}} - 130 \quad (14)$$

The modulus 141.5 instead of 140 in eq 14 was also used in the petroleum-oil industry. In order to overcome the confusion that existed in this industry by reason of the use of two so-called Baumé scales for light liquids, the American Petroleum Institute, the U. S. Bureau of Mines, and the National Bureau of Standards in December 1921 agreed to recommend that in the future only the scale based on the modulus 141.5 be used in the petroleum-oil industry, and that it be known as the API scale. The relation of degrees API to specific gravity is expressed by the formula

$$\text{Degrees API} = \frac{141.5}{\text{sp gr } 60°/60° \text{ F}} - 131.5 \quad (15)$$

The Baumé scale based on the modulus 140 continues to be in general use for other liquids lighter than water. Tables of specific gravities corresponding to degrees Baumé for both heavy and light liquids and to degrees API for petroleum oils, have been published [2, 52].

Hydrometers or lactometers for determining the specific gravities of milk are usually read in Quevenne degrees. The relation of Quevenne degrees to specific gravity is expressed by the formula

$$\text{Quevenne degrees} = 1000 \text{ (sp gr} - 1). \quad (16)$$

On account of the opaqueness of milk, it is customary practice of manufacturers to calibrate lactometers to be read at the top of the meniscus at 60° F.

The Bureau of Dairy Industry, United States Department of Agriculture [53] recommends the following procedure in preparing a sample of milk prior to a determination of its specific gravity. If the milk is freshly drawn or has been unduly shaken in transit or handling so that considerable air has been incorporated, it should be held at a temperature not lower than 50° F for 3 or 4 hours to allow trapped air to escape. Cool the sample of milk rapidly to a temperature between 35° and 40° F and hold it at this temperature 4 to 6 hours. Then allow the milk to warm up slowly during at least a half-hour period to 55° F. Mix the cream layer into the milk by pouring carefully back and forth several times, each time allowing the milk to run down the inside wall of the receptacle to avoid incorporating air. Taking the same care, pour the mixed milk into a cylinder which, with the lactometer, has been previously cooled in a water bath to 58° F. Immerse the cylinder in the water bath and bring the water bath and milk rapidly to a temperature of 60° F, taking care not to exceed that temperature. Before reading the mark on the lactometer stem at the top of the meniscus be sure that the lactometer floats freely and that the stem above the milk is clean and dry.

Plato, Domke, and Harting [54] derived the following relation between the specific gravity and the percentage of sucrose in sugar solutions:

$$\text{Sp gr } 15°/15°\text{C} = 1 + (387.7655p + 1.33945p^2 + 0.0048303p^3 - 0.0000053546p^4 - 0.00000008400p^5)10^{-5}, \quad (17)$$

where p is the percentage of sucrose from 2.5 to 76. A table of specific gravities corresponding to various percentages of sucrose by weight (Brix) from 0 to 95 and to Baumé (modulus 145) degrees from 0 to about 49.5, was published by Snyder and Hammond [55].

The barkometer, Twaddle (also spelled Twaddell), and Baumé hydrometer scales are in common industrial use in the leather-tanning industry for determinations of the specific gravities of tanning extracts. The following formulas give the relations between specific gravity and barkometer and Twaddle degrees, respectively:

$$\text{Degrees barkometer} = \frac{\text{Sp gr } 60°/60° \text{ F} - 1}{0.001}, \quad (18)$$

$$\text{Degrees Twaddle} = \frac{\text{Sp gr } 60°/60° \text{ F} - 1}{0.005}. \quad (19)$$

The relation between degrees Baumé and specific gravity is given by eq 13. Tables giving corrections to observed degrees barkometer, Twaddle, and Baumé, at various temperatures between 50° and 100° F in order to obtain corresponding degrees at 60° F, have been published by Blair and Peffer [56].

5. Falling-Drop Method

The falling-drop method for determining the density of liquids was developed by Barbour and Hamilton [57, 58]. This method consists in measuring the falling time of a small drop of liquid of known size through a definite distance in an immiscible liquid of known density. The latter liquid (reference liquid) should have a slightly lower density than the liquid drop. Using bromobenzene-xylene mixtures for the reference liquids, Barbour and Hamilton [59] obtained the densities of 0.01 ml of aqueous solutions to an accuracy of 0.0001. Vogt and Hamilton [60] refined this

method by means of accurate temperature control and an improved pipette so that it is possible to determine the densities of 10-mm^3 (approx. 0.01 ml) samples to within 2.5 parts per million.

The density of a falling drop of liquid may be computed from eq 20 or 21 derived from Stokes' law.

$$D=D_0+\frac{18V\mu}{gd^2} \tag{20}$$

or

$$D=D_0+\frac{k}{t}, \tag{21}$$

where

D=density of drop of liquid
D_0=density of reference liquid
V=velocity of drop of liquid
μ=coefficient of viscosity of reference liquid
g=acceleration due to gravity
d=diameter of drop of liquid
k=a constant depending upon the viscosity of the reference liquid, the size of the falling drop of liquid, and the distance over which the drop is timed
t=time of fall of drop over a fixed distance.

Figure 24 shows the apparatus used by Hoiberg [61] for determining the specific gravity of petroleum oils by the falling-drop method. Three Pyrex-glass tubes with a 1.3-cm bore and 50 cm long, were marked with lines 30 cm apart, extending all the way around the tubes, one line being 5 cm from the end of the tube. Rubber stoppers were inserted to close the ends of the tubes nearest to the lines. The tubes were mounted in a 2-liter cylinder by means of a brass plate standing on three 1-cm legs and with a cap on the top. The three holes fitting the glass tube in the brass plate and cap were drilled with their centers on the apexes of an equilateral triangle and 3.5 cm apart. Holes were also drilled in the cap for a thermometer, a 250-watt knife-blade heater, and an expansion-type thermoswitch. Copper tubing 0.3 cm in diameter was run down the side of the cylinder to supply air for stirring the water bath. A leveling stand and leveling screws were provided. The thermometer was suspended so that it could also be used as a plumb bob to adjust the glass tubes in a vertical position.

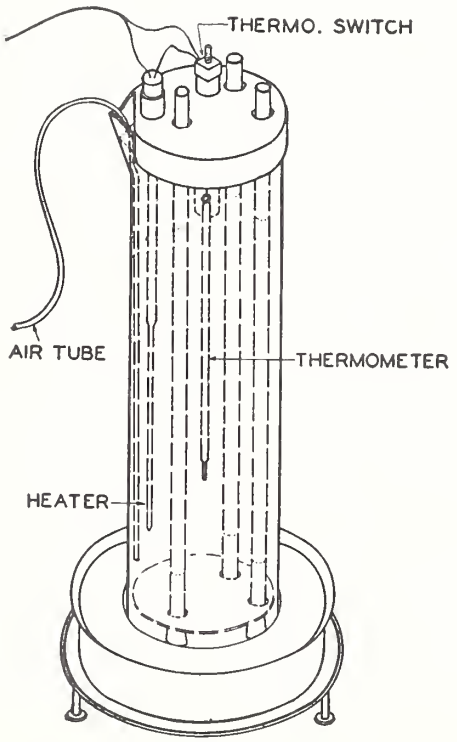

FIGURE 24. *Apparatus for determining the specific gravity of liquids by falling-drop method (Hoiberg).*

Solutions of ethyl alcohol and distilled water were mixed to cover the range in specific gravity of various petroleum oils. Before filling the glass tubes the solutions were heated to boiling under a reflex condenser to dispel air. The temperature of the solution in the glass tubes should be maintained constant.

A falling-drop pipette calibrated to deliver 2 drops of 0.01 ml volume each was used by Hoiberg to form the drop of petroleum oil, a pipette controller being used to regulate the delivery of the pipette. The time of fall of the drop was measured with an electric timer to within 0.1 second, and the specific gravity was obtained from a calibration curve.

Pipettes for obtaining drops of liquids of uniform size for determinations of density by the falling drop method have been described by Hochberg and LaMer [62] and Rosebury and van Heyningen [63].

Because bromobenzene and xylene mixtures are volatile, Frilette and Hanle [64] used solutions of phenanthrene in α-methylnaphthalene as reference liquids in measuring the specific gravity of water samples having D_2O contents ranging from 10 to 40 percent. Keston, Rittenberg, and Schoenheimer [65] used *o*-fluorotoluene as a reference liquid for determinations of density of water (with low contents of deuterium oxide). Frilette and Hanle state that *o*-fluorotoluene is not suitable for water that has a deuterium-oxide content much above 7 percent, for the precision of the falling-drop method falls off rapidly as the difference in density of the water and reference liquid increases.

Kagan [66] used a mixture of methyl salicylate and mineral oil as a reference liquid in determinations of the specific gravity of blood serum and plasma by the falling-drop method. Table 5 gives a comparison of the specific gravities of samples of serum and plasma by the falling-drop method and the picnometer method.

TABLE 5. *Comparison of specific gravities of samples of serum and plasma by the falling-drop method and the picnometer method (Kagan)*

Specific gravity		Difference
Falling-drop method	Picnometer (2 ml) method	
SERUM		
1.0285	1.0288	−0.0003
1.0256	1.0254	+.0002
1.0222	1.0222	.0000
1.0281	1.0283	−.0002
1.0283	1.0283	.0000
1.0306	1.0304	+.0002
1.0280	1.0280	.0000
1.0286	1.0290	−.0004
1.0280	1.0283	−.0003
1.0289	1.0292	−.0003
1.0303	1.0302	+.0001
1.0283	1.0279	+.0004
1.0209	1.0210	−.0001
1.0277	1.0279	−.0002
1.0285	1.0286	−.0001
1.0278	1.0274	+.0004
1.0297	1.0295	+.0002
1.0220	1.0220	.0000
1.0287	1.0284	+.0003
1.0261	1.0262	−.0001
OXALATED PLASMA		
1.0234	1.0233	+0.0001
1.0310	1.0312	−.0002
1.0268	1.0268	.0000
1.0330	1.0328	+.0002
1.0234	1.0232	+.0002
HEPARINIZED PLASMA		
1.0272	1.0274	−0.0002
1.0297	1.0298	−.0001
1.0221	1.0223	−.0002

Temperature changes in the reference liquid, variations in the size (diameter) of the falling drop, and errors in measurement of the time of fall of the drop, are important sources of error.

6. Balanced-Column Method

If one arm of a communicating U-tube contains a liquid having a density D_1 at any temperature and pressure, and the other arm contains an immiscible liquid having a density D_2 at the same temperature and pressure, then

$$\frac{D_1}{D_2}=\frac{h_2}{h_1}, \tag{22}$$

where h_1 is the height of the liquid in the first arm of the U-tube, and h_2 is the height of the liquid in the second arm (both heights are measured from the separating horizontal plane between the two liquids). If the density of one liquid is known, the density of the other liquid can be computed from eq 22.

Wiedbrauck [67] found that the densities of several liquids (ethyl alcohol, methyl alcohol, benzol, 10-percent solution of potassium hydroxide, and sulfuric acid) that he determined by the balanced-column method are accurate to 0.2 percent when compared with determinations by the hydrostatic weighing and picnometer methods. Frivold [68] claimed an accuracy of about 2×10^{-7} in his determinations of the differences of the density of water by this method.

An apparatus for simultaneous determinations of the densities of two or more liquids by the balanced-column method was described by Ciochina [69].

7. Method Based on Boyle's Law

Gallay and Tapp [70] applied Boyle's law to determine the density of leather by a simple method making use of the displacement of air. Their precision on a sample of about 2 g is approximately 0.3 percent. Thuau and Goldberger [71] and Edwards [72] also applied methods based on Boyle's law. The former gave no data. Edwards used a complicated procedure, which he admitted was in error by about 1.3 percent.

Kanagy and Wallace [73] determined the density of leather with an apparatus similar to that used by Gallay and Tapp. A diagram of the apparatus used by Kanagy and Wallace is shown in figure 25. A vessel, A, is connected at both ends with capillary tubing. The volume was calibrated between points X and Y on the capillaries and was found to be 10.734 ml. B is another vessel, which serves as the container for the sample and is connected to A with capillary tubing and the three-way stopcock, F. A and B have an

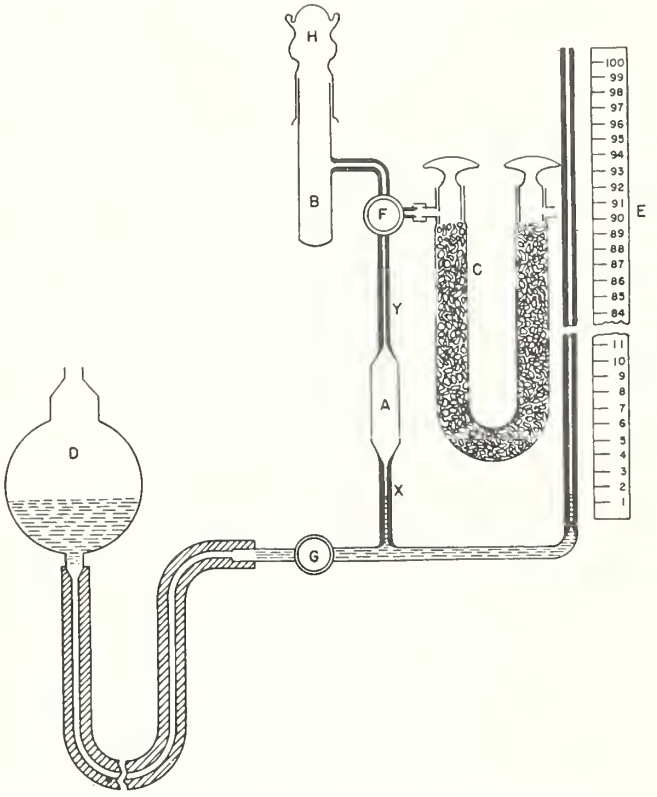

FIGURE 25. *Diagram of apparatus for density by method based on Boyle's law (Kanagy and Wallace).*

inlet through stopcock F and the U-tube, C, which contains anhydrous calcium sulfate to dry the air drawn into vessel A and to prevent the condensation of water vapor in B on compression. The volume of B, including the capillary arm to Y, is about 18 ml. Cap H fits over the outside of B, thereby eliminating the possibility of the leather coming into contact with the lubricating grease. The cap is fitted with glass lugs and held securely by means of wire springs. D, a cup containing mercury, is attached to the main apparatus with rubber tubing and is used to raise and lower the mercury level in A.

With stopcock F open to the U-tube C and the vessel A, the mercury level in A is raised to Y by lifting mercury cup D. Then dry air is drawn into A through C by lowering the mercury to X. F is closed to C and opened to A and B. The sum of the volumes of A, B, and the connecting capillaries may be represented by V_1, and the barometric pressure by P_1. The mercury level is then raised from X to Y, and stopcock G is closed. The volume of B and the capillary arm to Y may be represented by V_2, and the barometric pressure, P, plus the increase in pressure shown on manometer E caused by the compression (ΔP_1), by P_2. All values of pressure are read in centimeters of mercury. Then substituting in Boyle's law for a given mass of gas at a given temperature,

$$P_1V_1=P_2V_2 \tag{23}$$

$$P(A+B)=(P+\Delta P_1)B \tag{24}$$

or

$$B=\frac{PA}{\Delta P_1}. \tag{25}$$

The volume of B is calculated from eq 25. When a sample of leather having a volume L is placed in vessel B and the procedure repeated,

$$P(A+B-L)=(P+\Delta P_2)(B-L) \tag{26}$$

or

$$L=B-\frac{PA}{\Delta P_2}. \tag{27}$$

The density of the sample is then

$$D=\frac{M}{L}, \tag{28}$$

where D is the density, M is the mass of the sample, and L is the volume of the sample.

Kanagy and Wallace made density measurements on samples of leather weighing from 2 to 6 g. The samples were conditioned for at least 48 hours at 65 ± 2 percent relative humidity and $70°\pm2°$ F, and all determinations were made in a room controlled at these conditions.

The precision of the determinations is influenced largely by two factors—pressure measurements and the size of the sample. On repeat measurements, the manometer readings varied about 0.5 mm. This variation is equivalent to 0.016 ml for a 2-g sample having a volume of 1.5 ml, or an error of approximately 1 percent. To test the apparatus, the volume of a piece of copper wire 100 cm in length and of uniform diameter was determined from dimensional measurements. Its volume was then determined by the apparatus. The volume by dimensional measurement was 1.319 cm^3 and as determined by the apparatus 1.303 ml. These values illustrate the precision of the method for volumes less than 2 ml. For a 6-g sample having a volume of about 4 ml, the error is equivalent to about 0.007 ml or less than 0.2 percent. The apparatus was again tested with a piece of brass tubing that had a larger volume than the copper wire. The volume calculated by dimensional measurements was 4.014 cm^3, whereas that determined with the apparatus was 4.010 ml. The difference is smaller than that calculated from the reproducibility of the readings, and illustrates the precision possible for samples having volumes greater than 2 ml. Unfortunately no comparison was made of densities by this method and by another density method, such as hydrostatic weighing or the use of a picnometer.

A reported value of the density of a sample of leather should be accompanied by a statement of the temperature and relative humidity at which it was determined.

8. Electromagnetic Method

Richards [74] constructed an apparatus for rapid determinations (about two hundred 5-ml samples of liquids every 8 hours) of the densities of small samples of liquids. Ordinary hydrometers and picnometers were unsuitable for his purpose, since the former require at least 20-ml samples, whereas the latter are too slow.

The essential parts of the apparatus consist of a small glass float held under the surface of the sample of liquid by an adjustable stop and a small coil surrounding the lower portion of the sample tube. If current passing through the coil is gradually increased, the resulting magnetic field will eventually exceed a critical value, such that the force on an armature (made from a short piece of an iron nail) will become sufficient to draw the float away from a stop. The density of the sample of liquid may be determined by measurement of the critical current, from the equation

$$D=kI^2+D_F, \tag{29}$$

where D is the density of the sample of liquid, k is a constant, I is the critical current, and D_F the density of float.

Richards used alternating current from a step-transformer in the field coil to prevent permanent magnetization of the armature and to minimize

sticking of the float. The value of I in eq 29 is, in practice, the value obtained with an alternating-current milliammeter. The sensitivity of the apparatus is increased and the range decreased by increasing the size of the float, reducing the size of the armature, and reducing the number of turns in the field coil. Surface-tension effects are eliminated by the electromagnetic method because the float is submerged.

A diagram of the apparatus for determinations of the density of liquids by the electromagnetic method is shown in figure 26. The float, A, constructed of Pyrex glass, encloses the armature. The average density of the float is adjusted by adding or removing glass at the tip until it just floats in liquid, the density of which corresponds to the lowest value of the range required. The inside diameter of the float tube should be about 2 mm greater than that of the float to ensure a free passage. The float is centered on the bottom of the stop. The lower end of the float tube is sloped to allow drainage, and the drain tube allows 0.5-mm clearance around the tail of the float. A three-way stopcock is sealed on after the coil is mounted; the lower limb is used as a drain, and the side limb serves to admit air for drying the apparatus. The bearing for the adjustable stop is cemented in place after insertion of the float.

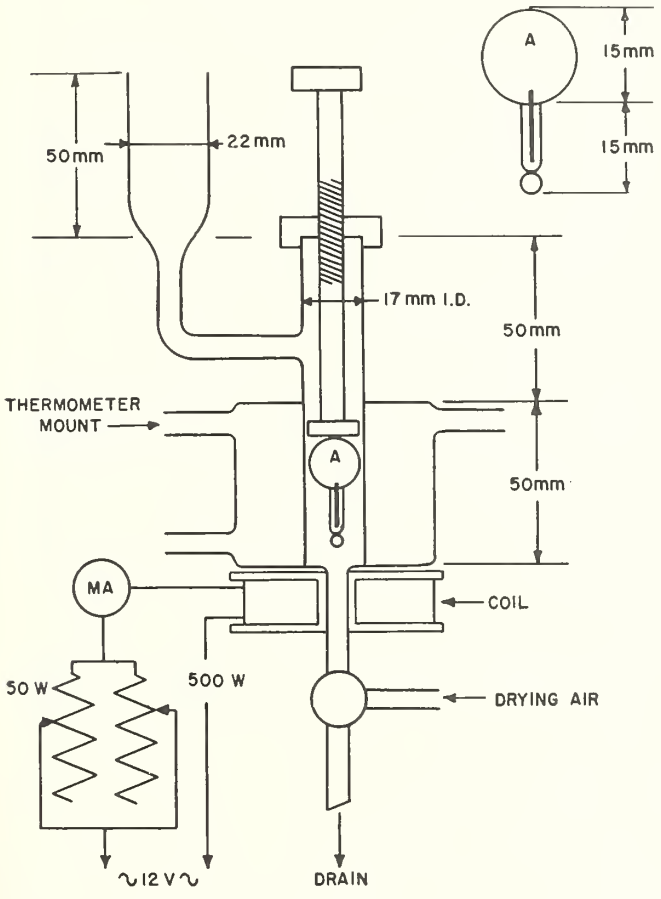

FIGURE 26. *Diagram of apparatus for determinations of the density of liquids by electromagnetic method (Richards).*

The coil is wound on an ebonite former with a thin core and consists of about 28 g of double cotton-covered copper wire No. 23 AWG. It is connected in series with a 20-volt alternating-current transformer and a variable-resistance assembly.

A water jacket surrounding the float chamber is used to maintain a constant temperature during determinations. Richards found it easy to maintain a temperature constant to within 0.2 deg C, which produces an error of less than 0.0002 g/ml in the densities of gasoline fractions.

A comparison of densities obtained by the electromagnetic and picnometer methods is given in table 6. The first column gives the critical currents used in the former method.

TABLE 6. *Comparison of densities obtained by electromagnetic and picnometer methods (Richards)*

Current	Density		Difference
	Electromagnetic method	Picnometer method	
amp			
0.085	0.626	0.6255	0.000
.152	.637	.6370	.000
.179	.643	.6429	.000
.223	.656	.6563	.000
.302	.684	.6842	.000
.383	.723	.7230	.000
.397	.732	.7309	+.001
.424	.746	.7445	+.002
.425	.747	.7458	+.001
.445	.759	.7598	−.001
.459	.768	.7673	+.001
.475	.778	.7795	−.002
.477	.780	.7811	−.001
.488	.788	.7874	+.001
.500	.797	.7962	+.001
.502	.798	.7974	+.001
.515	.807	.8082	−.001
.521	.813	.8146	−.002

9. Elastic Helix Method

In the elastic helix method by Wagner, Bailey, and Eversole [75], a fused-quartz helix and a fused-quartz bob suspended in a homogeneous medium (liquid or gas) were used to determine the density of this medium. The helix and the bob are buoyed up according to Archimedes' principle, causing a change in the length of the helix. The length of the helix can be related to density by calibration in a series of media of known density.

The relative density of a medium can be calculated from the equation

$$D=D_S+\frac{a(T_S-T)-(L_S-L)}{b}, \qquad (30)$$

where L is the length of the helix in a medium of density D at a temperature T, L_S is the length of the helix in the standard medium of density D_S at the standard temperature T_S, and a and b are constants.

The absolute density of a medium can be computed from eq 31.

$$D=\frac{a(T_S-T)-(L_S-L)}{-\left(\frac{\partial L}{\partial M}\right)_T (V_b+V_h)}, \tag{31}$$

where L is the length of the helix in a medium of density D at a temperature T, L_S is the length of the helix in the standard medium of density D_S at the standard temperature T_S, V_b is the volume corresponding to the apparent effective mass of the bob, V_h is the volume corresponding to the apparent effective mass of the elastic helix, and $(\partial L/\partial M)_T$ can be determined from the changes in length of the helix caused by the addition of small weights to a platinum bucket suspended from the helix in a medium of constant density and temperature.

The elastic-helix method should be useful for measurements of densities in systems that are not accessible to measurements by other methods. Liquid or vapor densities can be determined accurately to the fourth significant figure by this method.

10. Ice Calorimeter Method

An ice calorimeter was used by Ginnings and Corruccini [76] for determining the density of ice at 0° C. In this device, the heat to be measured is allowed to melt ice that is in equilibrium with water in a closed system, and the resulting volume decrease is determined by means of mercury drawn into the system. The calibration factor, K, of this ice calorimeter (ratio of heat input to mass of mercury intake) is related to the heat of fusion, L, of ice, the specific volumes of ice, v_i, and water, v_w, and the density of mercury, d_m, by the equation

$$K=\frac{L}{(v_i-v_w)d_m}. \tag{32}$$

By using eq 32, the density of ice at 0° C and 1-atmosphere pressure may be calculated from the calibration factor of the ice calorimeter, the heat of fusion of ice, and the densities of water and mercury. Using 270.37 int. j/g of mercury for the calibration factor, 0.999868 g/ml for the density of water, 13.5955 g/ml for the density of mercury, and 333.5 int. j/g for the heat of fusion of ice, Ginnings and Corruccini calculated the density of ice to be 0.91671 g/ml at 0° C and 1-atmosphere pressure. The largest uncertainty in this calculation is believed to be caused by the uncertainty of 0.06 percent in the heat of fusion of ice, which is equivalent to 0.00005 g/ml in the density of ice.

Numerous measurements of the density of ice have been reviewed by Dorsey [77]. The results of these measurements have been so scattered that some observers have believed the density of ice to be not strictly constant. The value given in the International Critical Tables [78] for the density of ice at 0° C and 1-atmosphere pressure is 0.9168 $\pm$0.0005 g/ml. Ginnings and Corruccini believe that the ice-calorimeter method provides the most accurate determination of the density of ice, since this method is free from many of the difficulties inherent in other methods. On account of the filaments and cracks that all samples of ice appear to have, any experimental method that measures the "bulk" density of ice will obviously give a different result from methods, such as the ice-calorimeter method, which determine the true density. No evidence has been obtained with the ice calorimeter that the true density of ice is anything but constant.

11. Volumetric Method

The approximate density of a solid having a definite geometrical form may be determined by a volumetric method. In this method the volume is computed from measurements of the dimensions of the solid. The weight of the solid is obtained in a convenient manner. The density of a solid determined by this method is probably accurate to about 1 percent.

Peffer [79] was unable to obtain accurate determinations of the density of artificial graphite by the hydrostatic weighing method, because this material absorbs liquids such as water, kerosine, toluol, etc. He therefore used the volumetric method for determinations of the densities of five samples of artificial graphite.

III. References

[1] U. S. Pharmacopoeia, revision of 1910.
[2] Standard density and volumetric tables, Circular BS C19, 6th ed. (1924).
[3] F. A. Smith, J. H. Eiseman, and E. C. Creitz, Tests of instruments for the determination, indication, or recording of the specific gravities of gases, NBS Miscellaneous Pub. M177 (1947).
[4] W. Prang, Über die Konzentrations-abhängigkeit von Dichte und Brechungsindex sehr verdünnter wässriger Lösungen starker Elektrolyte, Ann. Physik **31** (5), 681 (1938).
[5] L. W. Tilton and J. K. Taylor, Accurate representation of the refractivity and density of distilled water as a function of temperature, J. Research NBS **18,** 205 (1937) RP971.
[6] G. Schulz, Dichtemessungen an Lösungen organischer Säuren in Benzol, Dioxan und Cyclohexan, Z. physik. Chem. **40** (B), 151 (1938).
[7] O. Redlich and J. Bigeleisen, Molal volumes of solutes. VI. Potassium chlorate and hydrochloric acid, J. Am. Chem. Soc. **64,** 758 (1942).
[8] N. S. Osborne, Density and thermal expansion of ethyl alcohol and of its mixtures with water, part 2, Bul. BS **9,** 371 (1913) S197.
[9] H. W. Bearce, Density and thermal expansion of linseed oil and turpentine, Tech. Pap. BS 9 (1912).
[10] H. W. Bearce and E. L. Peffer, Density and thermal expansion of American petroleum oils, Tech. Pap. BS 77 (1916).
[11] H. E. Wirth, The partial molal volumes of potassium chloride, potassium bromide and potassium sulfate in sodium chloride solutions, J. Am. Chem. Soc. **59,** 2549 (1937).
[12] A. F. Forziati, B. J. Mair, and F. D. Rossini, Assembly and calibration of a density balance for liquid hydrocarbons, J. Research NBS **35,** 513 (1945) RP1685.
[13] N. S. Osborne, Density of ethyl alcohol and of its mixtures with water, part 3, Bul. BS **9,** 405 (1913) S197.
[14] G. Pesce and P. Hölemann, Zur Bestimmung von Dichten und Brechungsindices von Lösungen bei höheren Temperaturen, Z. Elektrochem. **40,** 1 (1934).
[15] T. Shedlovsky and A. S. Brown, The electrolytic conductivity of alkaline earth chlorides in water at 25°, J. Am. Chem. Soc. **56,** 1066 (1934).
[16] E. W. Washburn and E. R. Smith, An examination of water from various natural sources for variations in isotopic composition, BS J. Research **12,** 305 (1934) RP656.
[17] M. Rudolphi, Eine neue Pyknometer-form (Hohlcylinder-Pyknometer), Physik. Z. **2,** 447 (1901).
[18] G. R. Robertson, A graduated pycnometer, Ind. Eng. Chem., Anal. Ed. **11,** 464 (1939).
[19] J. P. Wibaut, H. Hoog, S. L. Langedijk, J. Overhoff and J. Smittenberg, A study on the preparation and the physical constants of a number of alkanes and cycloalkanes, Rec. Trav. Chim. Pays-Bas **58,** 329 (1939).
[20] H. K. Alber, Systematic qualitative organic microanalysis; Determination of specific gravity, Ind. Eng. Chem., Anal. Ed. **12,** 764 (1940).
[21] M. Furter, Beiträge zur Bestimmung und Kenntniss der Molekular-Refraktion. I, Helv. Chim. Acta **21,** 1666 (1938).
[22] M. R. Lipkin, J. A. Davison, W. T. Harvey, and S. S. Kurtz, Jr., Pycnometer for volatile liquids, Ind. Eng. Chem., Anal. Ed., **16,** 55 (1944).
[23] W. B. Newkirk, A picnometer for the determination of density of molasses, Tech. Pap. BS 161 (1920).
[24] R. E. Hall, The densities and specific volumes of sodium chloride solutions at 25°, J. Wash. Acad. Sci. **14,** 167 (1924).
[25] H. C. Parker and E. W. Parker, Densities of certain aqueous potassium chloride solutions as determined with a new picnometer, J. Phys. Chem. **29,** 130 (1925).
[26] A. F. Scott and W. R. Frazier, The solubilities and densities of saturated solutions of sodium and potassium halides at 25°, J. Phys. Chem. **31,** 459 (1927).
[27] C. F. Snyder and L. D. Hammond, Determination of weight per gallon of blackstrap molasses, Tech. Pap. BS **21,** 409 (1927) T345.
[28] G. F. Smith, The purification and some physical constants of formamide, J. Chem. Soc., p. 3257 (1931).
[29] G. F. Hennion, A self-filling pycnometer, Ind. Eng. Chem., Anal. Ed. **9,** 479 (1937).
[30] B. J. Fontana and M. Calvin, Semimicropycnometer for heavy water, Ind. Eng. Chem., Anal. Ed. **14,** 185 (1942).
[31] W. W. Russell, A new method in pycnometric analysis, Ind. Eng. Chem., Anal. Ed. **9,** 592 (1937).
[32] G. P. Baxter and C. C. Wallace, The densities and cubical coefficients of expansion of the halogen salts of sodium, potassium, rubidium and cesium, J. Am. Chem. Soc. **38,** 259 (1916).
[33] P. G. Nutting, Adsorption and pycnometry, J. Wash. Acad. Sci. **26,** 1 (1936).
[34] E. L. Gooden, Removal of air from powders in density determinations, Ind. Eng. Chem., Anal. Ed. **15,** 578 (1943).
[35] J. W. Retgers, Die Bestimmung des spezifischen Gewichts von in Wasser löslichen Salzen, Z. physik Chem. **3,** 289 (1889).
[36] S. Pisati and N. Reggiani, Gli areometri a totale immersione, Rend. R. Accad. dei Lincei [4] **6,** 99 (1890).
[37] A. W. Warrington, Hydrometers of total immersion, Phil. Mag. [5] **48,** 498 (1899).
[38] T. W. Richards and J. W. Shipley, A new method for the quantitative analysis of solutions by precise thermometry, J. Am. Chem. Soc. **34,** 599 (1912).
[39] T. W. Richards and J. W. Shipley, A convenient method for calibrating thermometers by means of floating equilibrium, J. Am. Chem. Soc. **36,** 1 (1914).
[40] T. W. Richards and G. W. Harris, Further study of floating equilibrium, J. Am. Chem. Soc. **38,** 1000 (1916).
[41] A. B. Lamb and R. E. Lee, The densities of certain dilute aqueous solutions by a new and precise method, J. Am. Chem. Soc. **35,** 1667 (1913).
[42] N. F. Hall and T. O. Jones, A redetermination of the protium-deuterium ratio in water, J. Am. Chem. Soc. **58,** 1915 (1936).
[43] E. S. Gilfillan, Jr., The isotopic composition of sea water, J. Am. Chem. Soc. **56,** 406 (1934).
[44] J. D. Bernal and D. Crowfoot, Use of the centrifuge in determining the density of small crystals, Nature **134,** 809 (1934).
[45] H. Yagoda, The measurement of density by the flotation method, Chemist-Analyst **21,** 4 (Nov. 1932).
[46] E. W. Blank, Construction of density standards, J. Chem. Ed. **10,** 618 (1933).
[47] H. J. Emeléus, F. W. James, A. King, T. G. Pearson, R. H. Purcell, and H. V. A. Briscoe, The isotopic ratio in hydrogen: A general survey by precise density comparisons upon water from various sources, J. Chem. Soc. (London), p. 1207 (1934).
[48] G. N. Lewis and R. T. MacDonald, Concentration of H^2 isotope, J. Chem. Phys. **1,** 341 (1933).
[49] M. Randall and B. Longtin, Determination of density differences by the flotation temperature method, Ind. Eng. Chem., Anal. Ed. **11,** 44 (1939).

[50] H. L. Johnston and C. A. Hutchison, Efficiency of the electrolytic separation of lithium isotopes, J. Chem. Phys. **8,** 869 (1940).
[51] C. A. Hutchison and H. L. Johnston, Determination of crystal densities by the temperature of flotation method. Density and lattice constant of lithium fluoride, J. Am. Chem. Soc. **62,** 3165 (1940).
[52] National standard petroleum oil tables, Circular NBS C410 (1936).
[53] P. A. Wright, Testing milk and cream, U. S. Department of Agriculture Miscellaneous Publication 161, (May 1940).
[54] F. Plato, J. Domke and H. Harting, Die Dichte, Ausdehnung und Kapillarität von Lösungen reinen Rohrzuckers in Wasser, Wiss. Abhandl. Kaiserlichen Normal-Aichungs-Komm., II. Heft (1900).
[55] C. F. Snyder and L. D. Hammond, Weights per United States gallon and weights per cubic foot of sugar solutions, Circular NBS C457 (1946).
[56] M. G. Blair and E. L. Peffer, Hydrometer correction tables and thermal-density coefficients for vegetable tanning extracts, Circular NBS C449 (1945).
[57] H. G. Barbour and W. F. Hamilton, Blood specific gravity; its significance and a new method for its determination, Am. J. Physiol. **69,** 654 (1924).
[58] H. G. Barbour and W. F. Hamilton, The falling drop method for determining specific gravity, J. Am. Med. Assn. **88,** 91 (1927).
[59] H. G. Barbour and W. E. Hamilton, The falling drop method for determining specific gravity, J. Biol. Chem. **69,** 625 (1926).
[60] E. Vogt and W F. Hamilton, Determination of the concentration of "heavy water" by means of the falling drop method, Am. J. Physiol. **113,** 135 (1935).
[61] A. J. Hoiberg, Specific gravity of petroleum oils by the falling drop method, Ind. Eng. Chem., Anal. Ed., **14,** 323 (1942).
[62] S. Hochberg and V. K. LaMer, Microdetermination of density by the falling-drop method, Ind. Eng. Chem., Anal. Ed. **9,** 291 (1937).
[63] F. Rosebury and W. E. van Heyningen, A modified micropipet for density determinations in heavy water analysis, Ind. Eng. Chem., Anal. Ed. **14,** 363 (1942).
[64] V. J. Frilette and J. Hanle, Gravitometry of heavy water. New reference liquids for the falling-drop method and precision attainable, Ind. Eng. Chem., Anal. Ed. **19,** 984 (1947).
[65] A. S. Keston, D. Rittenberg, and R. Schoenheimer, Determination of deuterium in organic compounds, J. Biol. Chem. **122,** 227 (1937).
[66] B. M. Kagan, A simple method for the estimation of total protein content of plasma and serum. I. A falling drop method for the determination of specific gravity, J. Clin. Investigation **17,** 369 (1938).
[67] E. Wiedbrauck, Apparat zur schnellen spezifischen Gewichtsbestimmung kleiner Flüssigkeitsmengen, Z. anorg. Chem. **122,** 167 (1922).
[68] O. E. Frivold, Dichtebestimmungen an Lösungen, nebst Bestimmung der Dichteunterschiede zwischen Wasser und Wasser mit Luft gesättigt, Physik. Z. **21,** 529 (1920).
[69] J. Ciochina, Apparat zur Bestimmung des spezifischen Gewichtes von Lösungen, Z. anal. Chem. **98,** 416 (1934).
[70] W. Gallay and J. S. Tapp, The determination of the real density of leather, J. Am. Leather Chem. Assoc. **37,** 140 (1942).
[71] U. J. Thuau and A. Goldberger, La densité du cuir, J. Int. Soc. Leather Trades Chem. **15,** 415 (1931).
[72] R. S. Edwards, A note on the determination of the real density of sole leather, J. Int. Soc. Leather Trades Chem. **17,** 358 (1933).
[73] J. R. Kanagy and E. L. Wallace, Density of leather and its significance, J. Research NBS **31,** 169 (1943) RP1556.
[74] A. R. Richards, An electromagnetic densitometer, Ind. Eng. Chem., Anal. Ed. **14,** 595 (1942).
[75] G. H. Wagner, G. C. Bailey and W. G. Eversole, Determining liquid and vapor densities in closed systems, Ind. Eng. Chem., Anal. Ed. **14,** 129 (1942).
[76] D. C. Ginnings and R. J. Corruccini, An improved ice calorimeter—the determination of its calibration factor and the density of ice at 0° C., J. Research NBS **38,** 583 (1947) RP1796.
[77] N. E. Dorsey, Properties of ordinary water substance, p. 466 (Reinhold Publishing Corp., New York, N. Y., 1940).
[78] International Critical Tables **3,** 43 (McGraw-Hill Book Co., Inc., New York, N. Y., 1928).
[79] E. L. Peffer's values were published in table 2 of paper by P. Hidnert and W. T. Sweeney, Thermal expansion of graphite, Tech. Pap. BS **21,** 223 (1927) T335.

Washington, June 15, 1949.

U. S. Department of Commerce National Bureau of Standards

RESEARCH PAPER RP1685

Part of Journal of Research of the National Bureau of Standards, Volume 35, December 1945

ASSEMBLY AND CALIBRATION OF A DENSITY BALANCE FOR LIQUID HYDROCARBONS[1]

By Alphonse F. Forziati,[2] Beveridge J. Mair, and Frederick D. Rossini

ABSTRACT

The assembly and calibration are described of a density balance for rapidly measuring the densities of liquid hydrocarbons on samples as small as 9 milliliters in volume. The reproducibility of the measurements is ±0.00002 to ±0.00003 gram per milliliter and the over-all uncertainty is estimated to be about ±0.00005 gram per milliliter.

CONTENTS

I. INTRODUCTION

In connection with the work of this laboratory on the analysis, purification, and properties of hydrocarbons, it has been necessary to make measurements of the density of purified liquid hydrocarbons, and of mixtures of hydrocarbons, on samples as small as 9 ml in volume, rapidly and with a precision of several parts per 100,000. This report describes the assembly and calibration of a density balance for such measurements.

II. APPARATUS

The assembly of the density balance is shown in figure 1, with the detailed parts described in the legends.

A diagram of the controls for the density balance is shown in figure 2, with details given in the legend.

The scale on this particular balance ranges[3] from 0.65 to 0.95 g/ml, with the smallest division on the chainomatic scale corresponding to 0.0001 g/ml and readings with the vernier being made to 0.00001 g/ml.

For containing the samples to be measured, test tubes having an inside diameter of 14 mm and an inside depth of 138 mm were se-

[1] This investigation was performed at the National Bureau of Standards as part of the work of the American Petroleum Institute Research Project 6 on the "Analysis, purification, and properties of hydrocarbons."

[2] Research Associate on the American Petroleum Institute Research Project 6 at the National Bureau of Standards.

[3] Other ranges of scale readings may be obtained as required.

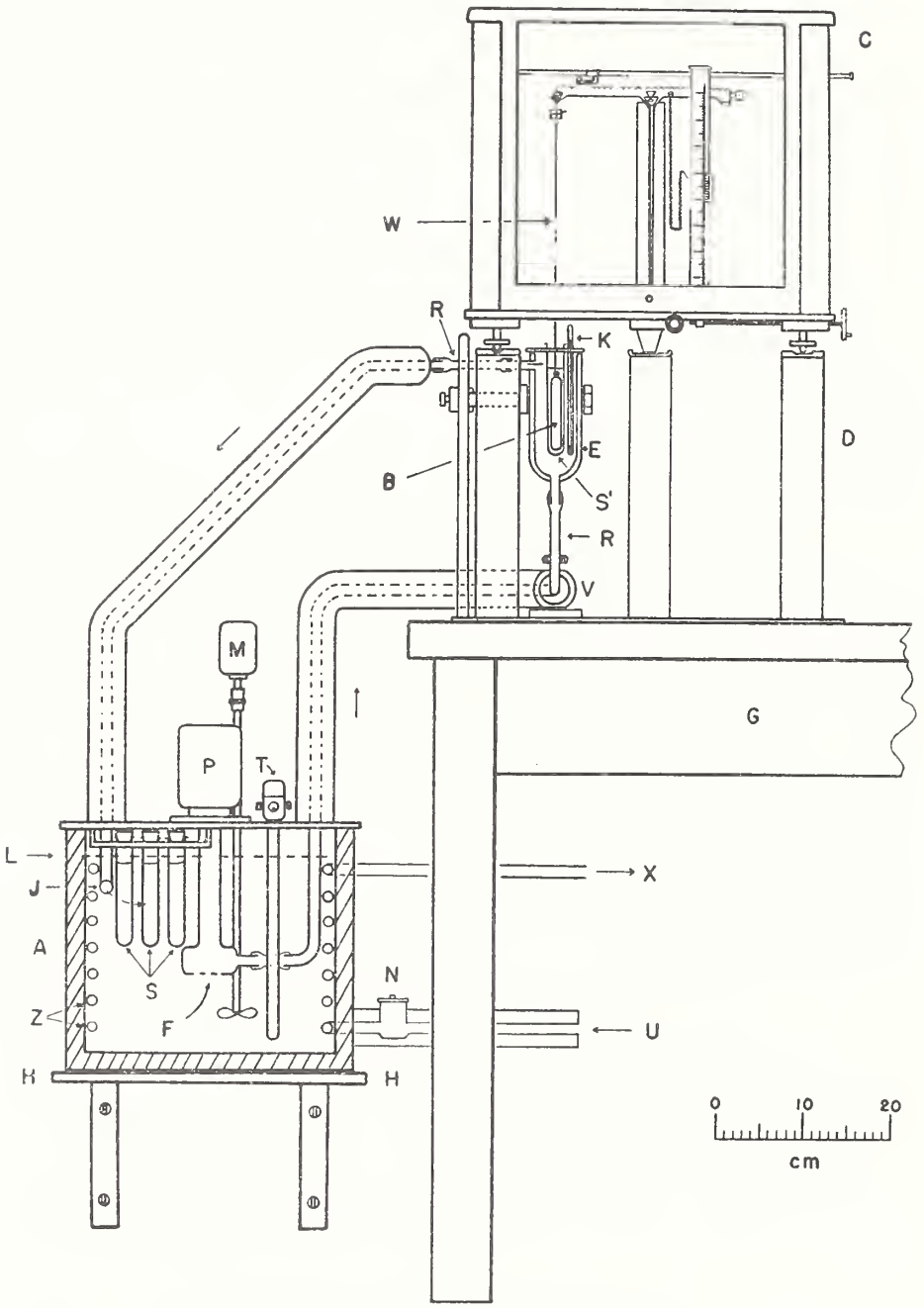

FIGURE 1.—*Assembly of density balance.*

A, Constant-temperature water reservoir; *B*, bob or plummet (volume 5 ml); *C*, chainomatic balance (see text); *D*, metal supporting stand; *E*, vacuum-jacketed glass water bath; *F*, water inlet to pump; *G*, table; *H*, shelf (fastened to wall); *J*, water return from *E*; *K*, special mercury-in-glass thermometer (graduated from 19.90 to 20.10, or from 24.90 to 25.10, or from 29.90 to 30.10, with a sensitivity on the scale of 1 mm equal to 0.05° C); *L*, level of water; *M*, motor for stirrer; *N*, solenoid valve; *P*, water pump; *R*, connection of rubber tubing; *S*, *S'*, test tubes for containing samples under observation; *T*, mercury-type thermoregulator; *U*, inlet for cooling water; *V*, valve for controlling flow of water through *E*; *W*, platinum wire, 0.003 inch in diameter; *X*, outlet for cooling water; *Z*, coil for cooling water.

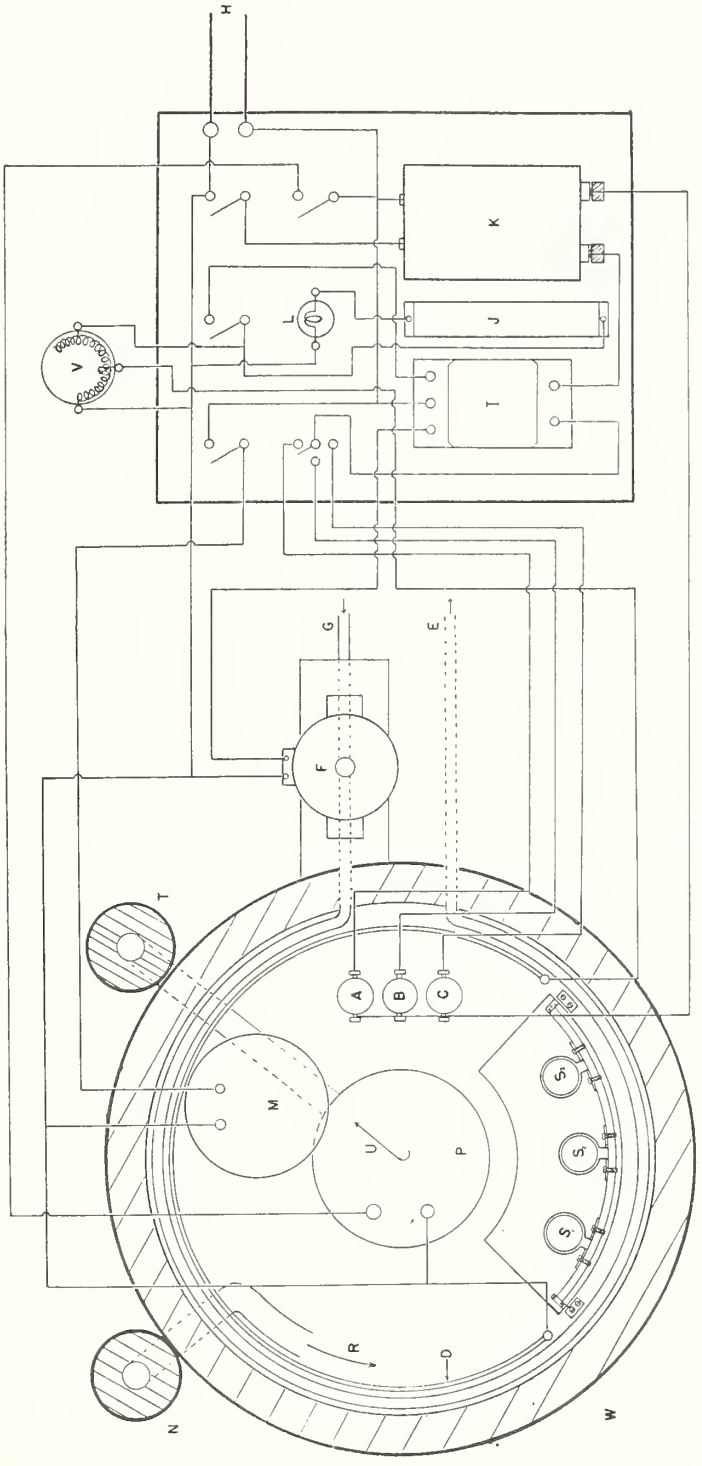

FIGURE 2.—*Diagram of controls of the density balance.*

A, *B*, *C*, Mercury-type thermoregulators, set to control at 20°, 25°, and 30° C, respectively, with a maximum amplitude in the control cycle of about 0.005° C; *D*, 100-watt heater in copper tube; *E*, discharge for water; *F*, solenoid valve (⅜-in. iron-pipe connections); *G*, inlet for cooling water; *H*, electric-power line, 110-volt alternating current; *I*, relay (midget); *J*, 1,000-ohm resistance (10 watts); *K*, rectifying transformer, 110-volt alternating current to 6 volts, direct current; *L*, miniature lamp, 14 volts; *M*, stirrer motor; *N*, return for water; *P*, circulating water pump; *R*, water from *N*; *S*, *S*, *S*, test tubes containing samples for observation; *T*, thermally insulated pipe connecting large water reservoir and the vacuum-jacketed glass water bath; *U*, path of water to *T*; *V*, variable transformer, 115 volts alternating current, 100 watts; *W*, constant-temperature water reservoir.

lected from standard Pyrex glass stock. On each tube was engraved a number (1, 2, 3, etc.) and also a horizontal line to mark a volume of 10 ml. The smallest volume that could be measured with the apparatus as assembled was 9 ml.

In more recent measurements on purified hydrocarbons,[4] special sample tubes with ground caps are being used in order to reduce loss by evaporation and contact with air. A cap with a hole in it, permitting free passage of the platinum wire supporting the plummet and being held in position by a special clamp, is used on the sample during the measurements. At other times, a closed cap (having the same standard ground joint) covers the sample tube.

III. PROCEDURE

The procedure in performing the measurements is as follows (the letters referring to fig. 1 legend):

Three of the samples to be measured (usual volume, 10 ml; minimum volume, 9 ml) are introduced by means of a small funnel into test tubes, care being taken to avoid wetting the lips of the test tubes. Stoppers of Neoprene rubber are then placed on the tubes to avoid loss of hydrocarbon by evaporation, and the tubes are then placed in the rack, S, in the large bath, A, with a time of 15 to 20 minutes allowed for a given sample to approach the temperature of measurement.

Tube 1 is then removed from the rack, S, unstoppered, and placed in position at S' in the small bath, E. The small bath, E, is then elevated into position so that the plummet, B, is completely immersed in the liquid with the top of the tying loop of platinum wire on the plummet being 1 mm below the surface of the liquid. (The depth of immersion of the platinum wire must be kept constant within ± 1 mm to reduce the error from this source to about ± 0.000005 g/ml.) The valve, V, is then opened and adjusted so that the flow of water is just less than the drainage capacity of the tube, J. (This maintains a substantially constant level of water in the bath, E.) The plummet, B, is then centered in the test tube, S', by sighting, at right angles, from the front and the left. (This operation is facilitated by having a mirror placed in appropriate position at the left side.) At this point, test tube 4, containing another sample, may be placed in the rack, S, in the position vacated by tube 1.

The beam of the balance is then partially released and the rider placed in position. After the beam is completely released, the chainomatic crank is turned rapidly to obtain a near balance. As the liquid dampens the motion of the plummet, a final reading is obtained by approaching the "balance" position very slowly, both from above and below, alternately three times in each direction. The final reading is taken as the average of these six readings, the maximum difference among which will seldom exceed 0.00002 g/ml.

The beam is then clamped, the valve, V, is closed, and the bath, E, is lowered and rotated about the supporting rod away from the suspended plummet, B. The latter is then rinsed by immersion in a test tube containing acetone, twice for the compounds of higher volatility (C_7 and lower) and three times for those of lower volatility (C_8 and higher).

[4] A. F. Forziati and F. D. Rossini, National Bureau of Standards. American Petroleum Institute Research Project 6. Unpublished data.

A period of 10 minutes is allowed for the plummet to become dry before immersing it in the next sample. During this interval, test tube 1 is removed from the small bath, *E*, the outside of the test tube is dried with a clean cloth, the sample is transferred to its original container, and the tube is cleaned by means of several rinsings with acetone and placed on the suction rack for drying.

At the beginning, middle, and end of each series of measurements, one of the standard reference liquids (2,2,4-trimethylpentane for paraffins, methylcyclohexane for naphthenes, and toluene for aromatics) is included among the samples measured in order to check the calibration of the balance (see following section).

The above procedure, which requires about 20 minutes per sample in steady operation, is that followed for the precise measurements on purified hydrocarbons. For routine analytical measurements (to ± 0.0001 g/ml) on a series of fractions of distillate, considerable time is saved by eliminating some of the above steps; reducing the time of waiting for temperature equilibrium, eliminating some of the calibrations, etc. The abbreviated procedure requires about 10 minutes per sample in steady operation.

IV. CALIBRATION

The balance was calibrated for measurements of density by making observations on a series of seven hydrocarbons (including the three NBS Standard Samples of hydrocarbons, which are certified with respect to values of density, namely, 2,2,4-trimethylpentane, No. 217; methylcyclohexane, No. 218; and toluene, No. 211 a), for which values of density were determined [5] under the supervision of E. L. Peffer in the Bureau's Capacity and Density Section, for air-saturated material, at 20°, 25°, and 30° C, with an estimated over-all uncertainty of ± 0.00002 g/ml. In reducing the scale readings, corrections (from zero to 0.00003 g/ml) were made for slight inequalities in the spacing of the notches on the beam, which inequalities were determined by measurements with known masses hanging from the left arm of the beam as the rider on the beam was moved successively from one notch to another.

The results of the observations on the calibrating samples are given in figure 3, which gives on the scale of abscissas the scale reading and on the scale of ordinates the scale reading less the certified value of density, in 10^{-5} g/ml. For the measurements, the balance was adjusted so that, for 2,2,4-trimethylpentane (NBS Standard Sample 217) at 25° C, the scale reading was identical with the certified value for this temperature. Linear calibrating lines were drawn for each of the three temperatures, as shown, with the line for 25° C being made to go through zero at the density for the Standard Sample of 2,2,4-trimethylpentane.

Table 1 summarizes departure of the observed points in figure 3 from the appropriate calibrating line. It is seen that the maximum departure is ± 0.00003 g/ml and that the average departures are ± 0.00002 g/ml.

[5] The method is described in Tech. Pap. BS T77(1916) and Bul. BS **9**, 405 (1913) S197.

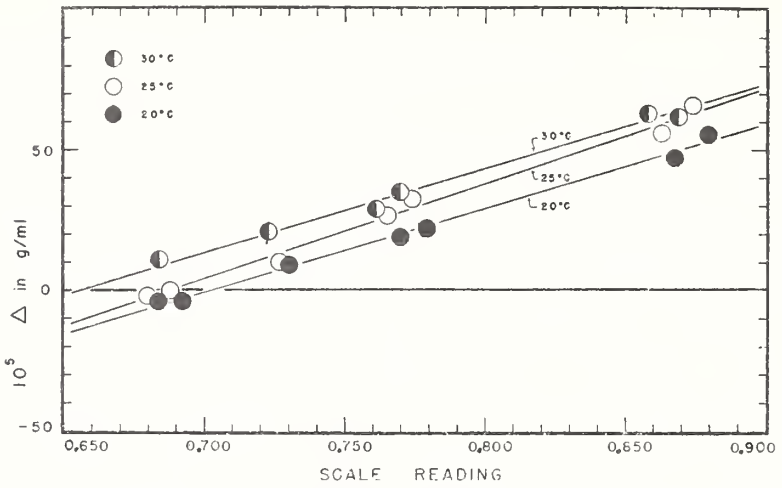

FIGURE 3.—*Calibrating data for the density balance.*

The scale of ordinate gives 10^5 times the value of the difference, scale reading less the value of density certified for the given hydrocarbon, at the given temperature. The scale of abscissas gives the scale reading. The three sets of measurements apply to 20°, 25°, and 30° C, as indicated.

TABLE 1.—*Departures of the observations on the certified samples from the respective calibrating lines*

Sample	Departure of the observed value from the value given by the calibrating line		
	20° C	25° C	30° C
	10^{-5} g/ml	*10^{-5} g/ml*	*10^{-5} g/ml*
n-Heptane	1½	½	
2,2,4-Trimethylpentane	−1	0	2½
n-Decane	1	−3	1
Methylcyclohexane	−1	½	−2½
Cyclohexane	−1	3	1
Toluene	−2½	−3	2½
Benzene	2½	3	−2
Average	±1½	±2	±2

V. DISCUSSION

As the density of liquid hydrocarbons changes about 0.00001 g/ml for a change in temperature of 0.01 deg C, and as the sensitivity of the balance is 0.00001 g/ml, changes in temperature of the sample under observation in excess of 0.01 deg will be reflected as changes in the scale readings at balance. For precise work, it is desirable to have a thermometric control that produces a maximum variation in the temperature of the sample of not more than 0.01 deg. In the apparatus assembled in this laboratory, the thermometric control produced temperatures having a maximum variation of about 0.005 deg. The absolute value of the temperature of the measurements made at the three controlled temperatures was determined at appropriate intervals by placing a platinum resistance thermometer (25 ohms) in place of the plummet and determining the resistance of the platinum thermometer with a Mueller bridge. The same observations yielded the magnitude of the variation of the temperature.

The effect, on this method of measuring density, of differences in surface tension of the samples under investigation, with resulting different forces on the thin platinum wire supporting the plummet, was calculated to be negligible. Because the surface tension of hydrocarbons varies in a more or less regular manner with density, the main effect of differences in surface tension in going from hydrocarbons of low density to those of high density becomes incorporated as part of the calibration correction. The net effect of surface tension then reduces to the effect of the difference in surface tension for hydrocarbons of the same or nearly the same density. Examination of the available data indicates that, in the range of density 0.60 to 0.90, hydrocarbons of the same or nearly the same density have values of surface tension that differ by not more than about one dyne/cm. This would correspond to a maximum error of 0.000005 gm/ml in density.

The effect, on the density, of absorption by the hydrocarbon of water vapor from the air was determined by measuring the difference between the density of a sample dried by filtration through silica gel and of this same sample subsequently saturated with water. The observed differences, density of sample saturated with water less the density of the dried sample, were 0.00001, −0.00001, and −0.00003 g/ml for 2,2,4-trimethylpentane, methylcyclohexane, and toluene, respectively. During the measurements on the material saturated with water, a globule of water was permitted to lie at the bottom of the tube containing the hydrocarbon. With normal precautions, it appears that errors from this source are well within the limits of uncertainty.

In order to ascertain whether the measurements as made are for hydrocarbon saturated with air, the difference was determined between the density of a freshly distilled sample and of this same sample subsequently saturated with air. The observed differences, density of freshly distilled sample less that of the air-saturated sample, were −0.00001, 0.00001, and 0.00001 g/ml for 2,2,4-trimethylpentane, methylcyclohexane, and toluene, respectively. It appears that measurements made by the present procedure may be ascribed, well within the limits of uncertainty, to hydrocarbon material saturated with air.

From the results of repeated observations on various samples, the reproducibility of the observations made with this density balance is estimated to be ±0.00002 to ±0.00003 g/ml. From the data given in table 1 and figure 3, the over-all uncertainty of the measurements of density of a given sample is estimated to be about ±0.00005 g/ml.

The authors are indebted to E. L. Peffer, chief of the Bureau's Capacity and Density Section, for providing the absolute values of the densities of the reference and Standard Samples used in the calibrations reported in this paper.

WASHINGTON, June 1, 1945.

574278 O - 61 - 45

UNITED STATES DEPARTMENT OF COMMERCE • Charles Sawyer, *Secretary*
NATIONAL BUREAU OF STANDARDS • E. U. Condon, *Director*

Methods of Measuring Humidity and Testing Hygrometers

Arnold Wexler and W. G. Brombacher

National Bureau of Standards Circular 512

Issued September 28, 1951

For sale by the Superintendent of Documents, U. S. Government Printing Office, Washington 25, D. C.

Price 20 cents

698/I

Contents

Methods of Measuring Humidity and Testing Hygrometers

A Review and Bibliography

Arnold Wexler and W. G. Brombacher

This paper is a review of methods for the measurement of the water-vapor content of air and other gases and for the production and control of atmospheres of known humidity for hygrometer testing and calibration and for general research. Among the hygrometric techniques discussed are psychrometry, mechanical hygrometry, dewpoint measurement, electric hygrometry, gravimetric hygrometry, thermal conductivity, index of refraction, pressure and volume measurements, and dielectric constant. Descriptions are given of suitable equipment for establishing desired humidities over a wide range of temperature. A list of 157 selected references pertaining to hygrometry is included.

1. Introduction

The conditions under which the relative or absolute humidity of gases are measured, recorded, or controlled vary greatly, and as a result, many methods of humidity measurement have been developed or proposed. However, for some applications there is at present no satisfactory method available for such measurements, and the available information on methods and instruments for measuring humidity is quite scattered. This Circular, with the appended references, is intended to answer inquiries on humidity measurement in a more comprehensive manner than may be done by correspondence.

Knowledge of the moisture content of solid materials, particularly paper, wood, and grain, is often required during some stage of processing or storage. The equipment, known as moisture meters, used for this purpose is not discussed in this Circular.

In many cases a substantial gaseous equilibrium exists between the solid and the surrounding atmosphere. A satisfactory determination of the moisture content of the solid can be made by the relatively easy measurement of the humidity of the atmosphere, once the relation between the two has been established. The same is true, of course, for liquids of definite composition, except that the water content may vary.

2. Definitions

Relative humidity is the ratio, usually expressed in percent, of the pressure of water vapor in the gas to saturation pressure of water vapor at the temperature of the gas. In engineering, relative humidity is sometimes defined as the ratio of the weights per unit volume of the water vapor in the gas mixture and the saturated vapor at the temperature of the gas mixture. The two definitions are equivalent for all practical purposes.

Absolute humidity of a gas mixture may be defined as the pressure of water vapor, or as the weight per unit volume of water vapor.

Specific humidity, a term of use in air conditioning, is the weight of water vapor in air per unit weight of the dry air.

Dewpoint is the temperature to which water vapor must be reduced in order to obtain a relative humidity of 100 percent that is, to obtain saturation vapor pressure.

Instruments from which the relative humidity is determined are called either psychrometers or hygrometers. Generally, the dry- and wet-bulb instrument (described later) is called a psychrometer, and direct indicators of relative humidity are called hygrometers.

Hygrographs are recorders of relative humidity.

3. Classification of Instruments

Humidity-measuring instruments and methods may be divided into the following classes for convenience. No exhaustive search of the literature was made to insure a complete listing of all proposed instruments, so that it is anticipated that some omissions exist.

Dry- and wet-bulb. Measurements depending on the change in temperature due to rate of evaporation from wet surfaces, an example of which is the dry- and wet-bulb or sling psychrometer.

Mechanical hygrometers. Measurement of a change in a dimension of an absorbing material, such as human hair or goldbeater's skin.

Dewpoint indicators and recorders. Instruments which indicate or record the temperature at which dew from the gas (air and water vapor) mixture under test will just form. A common type employs a mirror for observing the formation of the dew.

Electrical hygrometer. Measurement of the electrical resistance of a film of moisture absorbing material exposed to the gas under test.

Gravimetric hygrometer. Measurement of weight of moisture absorbed by a moisture absorbing material.

(a) Increase in weight of a drying agent as gas with a constant moisture content is passed through it.

(b) Change in weight of an absorbing material with change in moisture content of the gas under test.

Thermal conductivity method. Measurement of the variation in thermal conductivity of a gas sample with water vapor.

Spectroscopic method. Measurement of the change in intensity of selected absorbing spectral lines with change in humidity of the gas under test.

Index of refraction. Measurement of change in index of refraction of a moisture absorbing liquid with change in ambient humidity.

Pressure or volume. Measurement of the pressure or volume of the water vapor in a gas sample.

Thermal rise. Measurement of the temperature rise of a material exposed to water vapor.

Mobility of ions. Measurement of the change in mobility of ions due to the presence of water vapor.

Dielectric constant. Measurement of the dielectric constant of a gas with change in water-vapor content.

Critical flow. Measurement of the variation of pressure drop across two combinations of nozzles, operating at critical flow, with a desiccant between one pair of nozzles.

Diffusion hygrometer. Measurement of effects due to diffusion of gases with and without water vapor.

Chemical methods. Procedures involving chemical reactions or phenomena.

For sources of supply for the instruments indicated as commercially available, consult *Thomas Register of American Manufacturers* or *The Instruments Index.*

4. Description of Instruments

4.1. Dry- and Wet-Bulb Psychrometer

The psychrometric method of determining humidity is of importance in the fields of meteorology, air conditioning, refrigeration, and the drying of foods, lumber, etc. Its basic simplicity and fundamental calibration have made it the dominant means for measuring the moisture content of air. The elemental form of the psychrometer comprises two thermometers. The bulb of one thermometer is covered with a moistened cotton or linen wick and is called the wet-bulb, whereas the bulb of the other thermometer is left bare and is referred to as the dry-bulb. The evaporation of water from the moistened wick of the wet-bulb thermometer produces a lowering in temperature and from the readings of the two thermometers and the air or gas pressure, the humidity, absolute or relative, may be determined. It is current standard practice to ventilate the thermometers by slinging, whirling, or forced-air circulation.

To obtain the relative or absolute humidity, the relation between the wet- and dry-bulb readings and the actual pressure of the water vapor must be known. This correlation was obtained by Ferrel (26)[1] in 1886, based on the data of Marvin and Hazen, who made numerous observations of wet- and dry-bulb readings with sling and whirled psychrometers and simultaneous determinations of dewpoints with Regnault and Alluard dewpoint apparatus. Ferrel, after reducing these data, fitted them into the expression

$$e = e' - AP(t - t')$$

where, in metric units,

$A = 6.60 \times 10^{-4}\ (1 + 0.00115t')$

e = partial pressure of water vapor in mm Hg at the dry-bulb temperature t°C

e' = saturation pressure of water vapor in mm Hg at the wet-bulb temperature t'°C

P = total pressure (which, in the case of meteorological observations, is atmospheric pressure) in mm Hg

[1] Figures in parentheses indicate the literature references at the end of this paper.

and where, in English units,

$A = 3.67 \times 10^{-4} [1 + 0.00064 (t' - 32)]$

e = partial pressure of water vapor in. Hg at the dry-bulb temperature t°F.

e' = saturation pressure of water vapor in in. Hg at the wet-bulb temperature t'°F

P = total pressure in in. Hg.

Starting from fundamental concepts, several theories have been developed that attempt to explain the phenomena that occur at the wet-bulb and which, at the same time, yield expressions of the form used by Ferrel. The first equations for use in psychrometry were developed by Ivory (21) in 1822 and extended by August (22) in 1825 and Apjohn (23) in 1837. The so-called convection theory is the result of their work. In 1911, Carrier (28, 42) and in 1922, Lewis (40) reestablished the basis of this theory and renamed it the adiabatic saturation theory. This theory, which depends on a heat balance at the wet-bulb, found wide acceptance in the air-conditioning and refrigerating industries and has been used extensively in the construction of phychrometric charts. The agreement between theory and experimental data was investigated by Carrier (28) and Dropkin (87). Their results indicate that for most work of engineering accuracy, the adiabatic saturation theory is adequate for predicting the vapor pressure of water vapor from wet- and dry-bulb readings. Maxwell (11) in 1877 deduced an equation based on the diffusion of heat and vapor through a surface gas film on the wet-bulb. In recent years, further work has been done experimentally (71) and theoretically (73) on psychometric theory, and in reviewing the subject (93).

As the psychrometric formula gives the partial pressure of the water vapor of the gas under test, a computation is necessary to convert to humidity in other terms. The relative humidity, for example, is obtained from the equation

$$RH = \frac{e}{e_s} \times 100,$$

where

e = the partial pressure of water vapor as determined by the psychrometric formula

e_s = the saturation pressure of water vapor at the dry-bulb temperature

RH = the relative humidity, in percent.

In practice, calculations directly involving the use of the psychrometric formula are rarely made. The customary procedure is to employ tables (1, 4, 5, 7, 13, 14, 15, 16, 18, 44, 67, 81, and 96) or charts or curves (1, 9, 18, 77, 82, 100, 107, 115) that conveniently and rapidly yield the relative humidity, vapor pressure, or dewpoint from the dry- and wet-bulb thermometer readings and the air pressure.

The sling psychrometer (1, 8, 12, 15, 60), using two mercury thermometers, is the common form of this instrument. It is relied upon principally by meteorologists and is widely used by other scientists and by engineers for measuring relative humidity. Ventilation is obtained by swinging the thermometers to produce a minimum air velocity of 900 ft/min at sea level (higher at altitude). It is supplied by firms manufacturing meteorological instruments and by many laboratory apparatus supply houses. Stationary thermometers, with ventilation produced by a motor-driven fan or blower integral with the instrument, are known as Assmann or aspiration psychrometers (1, 8, 12, 60). These are also commercially available from a smaller number of firms. Unventilated psychrometers are unreliable and hence rarely used.

In addition to the mercury-in-glass thermometer, other temperature measuring devices may be adapted for psychrometric use. Resistance thermometers (47, 64, 70) thermocouples (68, 69, 72, 89, 90, 108), and bimetal thermometers (148) can be used for both indicating, recording, and control. Thermocouples are of special interest where low lag is important, where there is little or no ventilation (72, 89, 90) or where very low relative humidities (91) are to be measured.

Instead of direct temperature measurements, the temperature of the thermometers may be equalized (140). In this method the temperature of the wet-bulb is raised to that of the dry-bulb and the heat measured which is required to maintain equilibrium. This is accomplished by winding a manganin wire heater around the wet-bulb and under the wick and measuring the current when the wet- and dry-bulb thermometers read alike. A convenient arrangement utilizes a differential thermocouple psychrometer whose output is read on a galvanometer. The current to the wet-bulb heater is adjusted until the galvanometer no longer deflects.

The psychrometric method often may be applied in specialized or unconventional conditions. At temperatures below freezing, the psychrometer continues to function, but the magnitude of the depression is greatly reduced and proper precautions must be taken to obtain reliable data (121). At elevated temperatures or low relative humidities, special instruments (56), tables (67) and techniques (74) must be used. Most tables and charts are designed for use at atmospheric pressures. When low or high pressures are encountered, either special tables (15, 44) or charts (82) must be used or the relative humidity must be computed.

Where the moisture content of gases other than air is to be determined, the psychrometric constant A must be modified, to account for the physical properties of the particular gas. Values of A for several mono-, di- and triatomic gases are given by Brauckhoff (143).

Among the factors influencing the performance and accuracy of the psychrometric method are (a) the sensitivity, accuracy and agreement in reading of the thermometers, (b) the speed of air past the

wet-bulb thermometer, (c) radiation, (d), the size, shape, material and wetting of the wick, (e) the relative position of the dry- and wet-bulb thermometers, and (f) the temperature and purity of the water used to wet the wick. A discussion of these factors will be found in (1, 8, 12, 15, 35, 37, 46, 60, 74, 78, 90, 98, 121, 151).

The thermometers used in psychrometry should be high-grade matched instruments, else appreciable error may be introduced. While a calibration of the thermometers is desirable, an intercomparison at several temperatures to determine whether they read alike usually suffices. In addition, when high accuracy is desired and low relative humidities are measured, corrections for the emergent stem of the wet-bulb thermometer should be applied.

Thermometer errors may combine in several ways to influence the accuracy of the relative humidity. Thus either the dry-bulb thermometer or the wet-bulb thermometer or both may be in error. The magnitude of the error in relative humidity will depend not only on the magnitude of the thermometer errors, but also on their particular combination, since both the dry-bulb temperature and the wet-bulb depression are required for a determination. Occasionally, in psychrometric work, instead of measuring both the dry- and wet-bulb temperatures separately, the dry-bulb temperature and the wet-bulb depression are measured, from which the wet-bulb temperature can be computed for use in entering commonly available tables. The latter is obtained by measuring the temperature difference with, say, a differential thermocouple, one end of which is maintained dry and the other wet. Here the errors may occur either in the dry-bulb measurement or in the depression measurement or in both. Errors in the depression, however, may be considered as equivalent to errors in the wet-bulb reading, so that essentially the combinations of errors are the same as those first listed.

In order to obtain an estimate of the errors in relative humidity arising from thermometer errors, it will be assumed that psychrometric measurements are made at atmospheric pressure (29.92 in. Hg), at dry-bulb temperatures of 150°, 100°, 75°, 50°, and 32° F, and at wet-bulb depressions of 0.1, 1.0, and 10° F. For these given conditions, the errors in relative humidity, due to (a) a negative error of 1° F in wet-bulb temperature with the dry-bulb temperature correct, (b) a positive error of 1° F in dry-bulb temperature with the wet-bulb temperature correct, (c) an error of 1° F in dry-bulb temperature and an error of 1° F in wet-bulb temperature, both errors being negative, and (d) a positive error of 1° F in dry-bulb temperature and a negative error of 1° F in wet-bulb temperature, have been determined and are given, correspondingly, in table 1. It is seen in (c), table 1, that the errors are greatly reduced if the thermometers are matched.

TABLE 1. *Error in relative humidity due to uncorrected errors in the thermometers*

(a) Dry bulb thermometer reads correctly; wet bulb thermometer reads 1 deg F low

Dry bulb temperature	Error in relative humidity at a wet bulb depression of—		
	0.1 deg F	1.0 deg F	10 deg F
°F	%	%	%
150	2.6	2.6	2.1
100	3.6	3.5	2.9
75	4.6	4.5	3.7
50	6.7	6.6	5.6
32	10.5	10.3	----------

(b) Dry bulb thermometer reads 1 deg F high; wet bulb thermometer reads correctly

Dry bulo temperature	Error in relative humidity at a wet bulb depression of—		
	0.1 deg F	1.0 deg F	10 deg F
°F	%	%	%
150	2.6	2.5	2.0
100	3.5	3.4	2.6
75	4.5	4.4	3.1
50	6.6	6.4	4.3
32	9.8	9.4	----------

(c) Dry bulb thermometer reads 1 deg F low; wet bulb thermometer reads 1 deg F low

Dry bulb temperature	Error in relative humidity at a wet bulb depression of—		
	0.1 deg F	1.0 deg F	10 deg F
°F	%	%	%
150	0.00	0.02	0.11
100	.00	.03	.32
75	.00	.05	.51
50	.00	.11	1.24
32	.02	.26	----------

(d) Dry bulb thermometer reads 1 deg F high; wet bulb thermometer reads 1 deg F low

Dry bulb temperature	Error in relative humidity at a wet bulb depression of—		
	0.1 deg F	1.0 deg F	10 deg F
°F	%	%	%
150	5.1	5.0	4.1
100	7.0	6.8	5.4
75	8.9	8.7	6.7
50	13.0	12.7	9.8
32	19.8	19.3	----------

The psychrometric constant, A, in the Ferrel formula is not invariant but is a function of the velocity of ventilation across the wet-bulb thermometer, and reaches a minimum value as the velocity is increased. This is reflected as a maximum wet-bulb depression. Any further increase in velocity will have negligible effect. When the velocity is sufficiently high so that A, is constant, then the magnitude of the velocity need not be measured or estimated. For most mercury-in-glass thermometers with bulbs ¼-inch diameter or less, the acceptable minimum rate of ventilation is

900 ft/min. If this velocity is not achieved, then the measured wet-bulb depression will not be a maximum, and the use of the psychrometric formula, tables or charts will yield values of relative humidity that are too high.

The heat absorbed by the wet-bulb due principally to radiation tends to raise the wet-bulb temperature so that a true depression is not attained. To minimize this effect, radiation shielding is commonly employed. One method of such shielding, successfully used in some ventilated psychrometers, is to surround the wet-bulb with an external primary metal shield and to insert an auxiliary shield between the primary external shield and the wet-bulb, this auxiliary shield being covered with a wick so that, upon moistening, the auxiliary shield may be brought close to the wet-bulb temperature thereby practically eliminating the source of radiation and conduction due to the difference between the dry- and wet-bulb temperatures.

The function of the wick is to retain a thin film of water on the wet-bulb so that evaporation may continue until the true wet-bulb temperature is reached. Cotton or linen tubing of a soft mesh weave serves well for this purpose because of its excellent water-absorbent properties. Sizing in the wick material, encrustations forming after use and lack of a snug fit interfere with the maintenance of a continuous film of water. Substances in solution in the wick water, due either to impurities on the wick or in the water used for moistening will change the saturation vapor pressure of water and hence affect the results. Wicks should therefore be cleaned and replaced frequently, and distilled water should be used for moistening. The wick should extend beyond the bulb and onto the stem of the thermometer, for an inch or so, in order to reduce heat conduction along the stem to the bulb.

Although the temperature of the water used to moisten the wick is often at dry-bulb temperature, it should be preferably that of the wet-bulb or slightly higher. The use of water that has been brought to the wet-bulb temperature is especially important when the ambient temperature is high and when the relative humidity is low.

If the temperature of the water used to wet the bulb is too high, it may take a long time for the bulb to cool to wet-bulb temperature, and before this point is reached the water may have evaporated sufficiently so that the thermometer never reaches the wet-bulb temperature. If the moistening water temperature is appreciably lower than the wet-bulb temperature, the thermometer temperature will climb throughout the period of ventilation, remaining constant at the wet-bulb temperature only as long as there is sufficient water to keep the bulb surrounded with a film of water. If the temperature of the water used for moistening is at, or slightly above or below, the wet-bulb temperature, then the wet-bulb will remain or quickly attain the wet-bulb temperature and remain at this value for an appreciable length of time so that it can be read easily and accurately.

A separation of the dry- and wet-bulbs is necessary in order to prevent the air that passes the wet-bulb, and is thereby cooled by the evaporating water, from contacting the dry-bulb and giving rise to an erroneous dry-bulb reading. To avoid this, the thermometers may be arranged so that the air flows across the dry-bulb before it reaches the wet-bulb or the air sample may be divided so that one part flows across the wet-bulb and the other part across the dry-bulb.

4.2. Mechanical Hygrometer

In hygrometers of this type, human hair is commonly used as the sensing element. In indicators the midpoint of a bundle of hairs under tension is connected by the simplest possible lever system to a pointer. In recorders a pen arm, which is substituted for the pointer, traces an ink record on a clock-driven drum.

The hair hygrometer indicates relative humidity directly over a wide range of temperature, but its reliability rapidly decreases as the ambient temperature decreases below freezing (0° C).

At temperatures below freezing (0° C) the hair hygrometers indicate relative humidity in terms of the vapor pressure of supercooled water, not that of ice (117).

The chief defect is the lack of stability of the calibration under usual conditions of use. However, tests recently completed at this Bureau on two good quality recorders indicated little average shift in calibration over a period of almost 1 year; the hysteresis (difference in indication, humidity increasing and decreasing) was of the order of 3-percent relative humidity. See (1, 8, 12, 38, 45, 83, 88, 117) for performance data.

Reliable data on the lag of the hair hygrometer are lacking, particularly at low temperatures. Suddenly subjecting hygrometers at about 25° C to a change in relative humidity requires of the order of 5 minutes to indicate 90 percent of the change in relative humidity; this time interval increases with decrease in temperature of the hairs, and is of the order of 10 times greater at −10° C. The effect of temperature on the calibration of hygrometers commercially available is not well established for temperatures below 0° C.

At the best, indications of the hair hygrometer have a reliability of about 3 percent in relative humidity at room temperature when exposed to a constant relative humidity long enough to obtain equilibrium. The large time lag of the hair hygrometer is a serious barrier to accuracy if changing humidity is being measured.

The hair hygrometer is made by a large number of industrial instrument companies, including meteorological instrument firms; the hair hygro-

graph (recorder) is made by a smaller but still large number of these firms.

The hair element with suitable accessories is widely used as a humidity controller in air-conditioning and other applications. The zero shift so evident in instruments measuring ambient humidity is less troublesome when the relative humidity about the element is maintained nearly constant (50, 62, 129). Controllers are available from a sizable number of industrial instrument firms.

A recent development in this country has been the use of goldbeater's skin in disk form by Serdex (139). It is claimed, but not yet generally accepted, that the performance is essential better than that of the human-hair type. See (134) for performance data at low temperatures; as for the hair hygrometer, the indication at temperatures below freezing of instruments reading correctly above freezing, is in terms of relative humidity of the vapor pressure of supercooled water.

Many organic materials are hygroscopic. Thus wood fibers have been used as a sensing element. Also plastics (152) in a form similar to bimetal have some application and perhaps are the most open to exploration. A cotton filament as a torsion element (53) has been tried. None of these seem to give essentially better, if as good performance as human hair and thus far have had only limited application.

4.3. Dewpoint Indicators and Recorders

When water vapor is cooled, a temperature is reached at which the phase changes to liquid or solid. At this temperature, condensation continues until an equilibrium between the vapor and liquid or solid phase is established. The temperature at which the vapor and liquid or vapor and solid phases are in equilibrium uniquely fixes the pressure of the vapor phase (saturation vapor pressure) and therefore determines the absolute humidity.

If the temperature at which water vapor must be cooled for it to be in equilibrium with its liquid or ice state is measured, then the humidity is obtained directly from it. The dewpoint method provides a convenient technique for ascertaining this temperature. Basically, the procedure is to reduce the temperature of a mirror until dew or frost just condenses from the surrounding air or gas sample. The temperature at the surface of the mirror at the instant dew or frost appears is defined as the dewpoint. If the temperature of the air or gas sample is measured and the initial humidity of the sample surrounding the mirror is kept unaltered, the initial relative humidity can be computed from a knowledge of the saturation vapor pressures at the two temperatures.

It should be noted that the formation of frost is not always positive because of the lack of a crystal nucleus, so that supersaturation may occur. Supersaturation is less likely to occur with respect to the liquid phase than with the ice phase. At a given saturation pressure, if ice does not form on the mirror, dew will form as the mirror temperature is lowered, hence there is always a little uncertainty whether the first clouding of the mirror represents the dewpoint (with condensed water) or the frost point.

Values of the saturation vapor pressure of water, at temperature above and below freezing, are readily available in various handbooks and compilations (1, 2, 4, 6, 15, 16, 17, 18, 128). There is some discordance in the values given in the listed references. However, for most applications in the field of humidity measurement or control, there is little to be gained in the use of any one table in preference to the others. The values given in table 2 are reproduced from the Smithsonian Meteorological Tables (16). At temperatures below 0° C, the saturation vapor pressures refer to water vapor in equilibrium over ice. Saturation vapor pressures of water vapor below 0° C in equilibrium over supercooled water are given in table 3 and are reproduced from the International Critical Tables (17).

The dewpoint instrument serves as a useful research tool for the determination of humidity in meteorology as well as for the determination of water vapor content in flue gases, gasoline vapors, furnace gases, compressed gages, and closed chambers. While the dewpoint instrument has been under considerable development in the past decade, principally along the line of improving the temperature control, means of indication, and automatic recording, it has been used in elemental form as far back as the early part of the last century. Dalton and Daniells used simple dewpoint hygrometers. Regnault (24) developed an instrument that has been used as a prototype and standard for many years in the measurement of atmospheric humidity. Essentially, it consisted of a thin polished silver thimble containing ether. Air was aspirated through the ether to cause evaporation and hence cooling of the thimble. The temperature of the ether at the appearance and disappearance of dew was observed and the mean taken as the dewpoint. A thermometer in a second thimble, near the first, gave the ambient temperature and, by comparison, the second thimble helped in the recognition of the appearance and disappearance of dew on the first thimble. Improvements and variations of the Regnault design were made by Alluard (25), and others (32, 41, 45, 55, 57).

The early models used ether for cooling and mercury-in-glass thermometers for temperature and measurement. Recent models have employed such cooling schemes as compressed carbon dioxide, dry ice, liquid air (for very low dewpoints) and mechanical refrigeration. In addition, metal mirrors are now commonly used, the

TABLE 2. *Saturation vapor pressure of water vapor in millimeters of mercury with respect to water above 0°C and with respect to ice below 0°C*

(Reproduced from the Smithsonian Meteorological Tables)

Temp, °C	0	1	2	3	4	5	6	7	8	9
−70	0.0019									
−60	.0080	0.0070	0.0061	0.0053	0.0046	0.0040	0.0035	0.0030	0.0026	0.0022
−50	.0294	.0260	.0229	.0202	.0178	.0156	.0137	.0120	.0105	.0092
−40	.0964	.0859	.0765	.0680	.0605	.0537	.0476	.0421	.0373	.0329
−30	.2878	.2591	.2331	.2094	.1880	.1686	.1511	.1352	.1209	.1080
−20	.7834	.7115	.6456	.5854	.5303	.4800	.4341	.3923	.3541	.3194
−10	1.9643	1.7979	1.6444	1.5029	1.3726	1.2525	1.1421	1.0406	.9474	.8618
−0	4.5802	4.2199	3.8868	3.5775	3.2907	3.0248	2.7785	2.5505	2.3395	2.1445
0	4.5802	4.924	5.291	5.682	6.098	6.541	7.012	7.513	8.045	8.610
10	9.210	9.846	10.521	11.235	11.992	12.794	13.642	14.539	15.487	16.489
20	17.548	18.665	19.844	21.087	22.398	23.780	25.235	26.767	28.380	30.076
30	31.860	33.735	35.705	37.775	39.947	42.227	44.619	47.127	49.756	52.510
40	55.396	58.417	61.580	64.889	68.350	71.968	75.751	79.703	83.830	88.140
50	92.639	97.33	102.23	107.33	112.66	118.20	123.98	130.00	136.26	142.78
60	149.57	156.62	163.96	171.59	179.52	187.75	196.31	205.19	214.41	223.98
70	233.91	244.21	254.88	265.96	277.43	289.32	301.63	314.38	327.59	341.25
80	355.40	370.03	385.16	400.81	416.99	433.71	540.99	468.84	487.28	506.32
90	525.97	546.26	567.20	588.80	611.08	634.06	657.75	682.18	707.35	733.28
100	760.00									

TABLE 3. *Saturation vapor pressure of water vapor in mm mercury with respect to supercooled water*

(Reproduced from the International Critical Tables)

Temp, °C	0	1	2	3	4	5	6	7	8	9
−0	4.579	4.258	3.956	3.673	3.410	3.163	2.931	2.715	2.514	2.326
−10	2.149	1.987	1.834	1.691	1.560	1.436				

warming of which by heat from the ambient atmosphere has been augmented by electric resistance or induction heating. The temperature of the mirror surface is frequently measured by thermocouples affixed several hundredths of an inch below the surface or actually on the surface of the mirror. While mercury-in-glass thermometers are still used, their high lag introduces an uncertainty in the temperature reading. In one instrument, the temperature is measured by a carbon dioxide vapor pressure thermometer in which the mirror is integral with the bulb (19). Visual observation of dew or frost has often been replaced by photoelectric detection of reflected or scattered light from the mirror and is indicated on an electrical meter, or automatically recorded. The output of the photoelectric circuit has been used also to control the heat input to the mirror and thereby to maintain the mirror temperature at the dewpoint. Photoelectric observation below the frost point has several advantages. Electronic circuits may be employed that automatically maintain a constant film thickness on the mirror. There can then be little question of whether the liquid or solid phase is involved, for supercooled liquid will not long exist under such conditions without changing to ice. There will be no supersaturation for lack of a crystal nucleus.

For information on these later forms of dewpoint indicators and recorders operating at atmospheric pressure, see (79, 95, 97, 102, 104, 110, 127, 135, 142, 144, 145, 146). Dewpoint indicators requiring visual observation and manual operating of the cooling system are available from dealers in scientific laboratory equipment. Dewpoint indicators and recorders employing photoelectric detection are made by a limited number of manufacturers.

Several dewpoint indicators have been developed that are of novel form or of specialized use. An instrument for use at high pressures is described in (133). In another instrument the sample of gas under test is pumped into a closed chamber and is then cooled by adiabatic expansion to a lower pressure. By repeated trials a pressure ratio can be secured so that a cloud or fog is just formed when the pressure is suddenly released. The dewpoint is computed from the ratio of the initial to final pressure and the measurement of the initial temperature. One version of this instrument (45) employs a vacuum pump for exhausting a reservoir into which the gas sample eventually is expanded. A commercial version (130) uses a small hand pump for compressing the gas sample and then expands the gas into the atmosphere. No adequate data on performance limits are available.

A polished rod or tube of high thermal conductivity, heated at one end and cooled at the other end so that dew forms on part of the rod (43) has been used to obtain the dewpoint. The temperature of the rod measured at the dew boundary is the dewpoint. There has been no commercial development of this device. Unpublished data indicate that it is unreliable at dewpoints below the ice point (0° C) because no satisfactory ice—no ice boundary is obtainable.

Use has been made of the change in conductivity

between electrodes on a glass thimble for detecting the dewpoint (45, 59).

The dewpoint method may be considered a fundamental technique for determining vapor pressure or humidity. However, the certainty of the dewpoint measurement is influenced by several factors, some of which are of such indeterminate nature as to make an estimate of the accuracy difficult. It is not always possible to measure the temperature of the mirror at the surface or to assure that no gradients exist across the surface. The visual detection of the inception of condensation cannot be made with complete assurance nor is it probable that two different observers would detect the dew or frost at the same instant. It is usual practice for the dewpoint to be taken as the average of the temperature at which dew or frost is first detected, on cooling of the mirror, and the temperature at which the dew or frost vanishes, on warming of the mirror. This procedure does not assure a correct answer since care must be taken to locate the thermometer, so that no temperature gradient exists from the cold source to the mirror face or to the gas as a whole. The photoelectric detection of the dewpoint usually depends upon achieving an equilibrium condition on the mirror surface during which the amount of dew or frost remains constant. It has been reported (146) that the dewpoint so measured, down to $-35°$ C, agrees on the average to 0.1 deg C with the dewpoint measured visually with a Regnault instrument.

The uncertainty of measuring the dewpoint decreases with decrease in temperature. Below low 0° C uncertainty definitely exists if the eye is used for detecting the first sign of condensation, for it cannot distinguish or differentiate between the liquid and ice phase with the minute trace of water involved. With a photoelectric system in which the mirror alternately cools and then warms so that condensation forms and evaporates, the photocell is likewise incapable of determining whether the condensate is liquid or solid. With a photoelectric system in which a constant film thickness is automatically maintained on the mirror, ice will form on the mirror, for, as previously explained, supercooled water cannot long exist on a free and exposed surface.

Dewpoint instruments have been built with reported sensitivities of 0.1° C (27) and 0.01° C (97) and with reported accuracies of ± 1 percent of the vapor pressure (27) at temperatures above freezing and $\pm 1°$ C at $-70°$ C (127).

4.4. Electrical Hygrometers

Dunmore. These hygrometers commonly depend upon the change in electric resistance of a hygroscopic material with change in humidity. In one design, largely developed by Dunmore (94, 99, 103), two parallel wires of a noble metal are wound upon a polystyerene cylinder or strip. A hygroscopic coating of polyvinyl acetate or polyvinyl alcohol and dilute lithium chloride solution is placed between the wires. At constant temperature the logarithm of the electrical resistance between the parallel wires varies approximately linearly with the logarithm of the relative humidity and is measured by a suitable Wheatstone bridge, preferably using alternating current, or other suitable electric circuits. The electric resistance at constant relative humidity is highly dependent upon temperature, especially at temperatures below 0° C.

The hygrometer was primarily developed for use in radiosondes in which the output is fed to a radio transmitter and controls an audio frequency. It is widely used for this purpose and is manufactured by a number of firms. An indicator and a controller for industrial use is now available commercially.

An elementary theory of the electric hygrometer has been proposed by Schaffer (132).

Similarly, as for the hair hygrometer, the chief defect has been in stability of calibration, which seems to have been overcome in the model for industrial use. The continuous application of direct current causes polarization with a resultant shift in calibration and ultimate deterioration. At temperatures above freezing, the response to humidity changes is rapid, but at lower temperatures, time lags are appreciable. Some data on the performance at low temperatures are given in (134 and 150). One of the advantages of this design is that it is remote indicating an adaptable for control. See also (113 and 114).

Dewcel. Another form of the electric hygrometer is the "dewcel", which is remote indicating and can be used for control (136, 154). Essentially it indicates the dewpoint temperature. The sensing element, similarly as the Dunmore element, has a parallel wire winding with the material between the wires kept wet with a wick impregnated with a saturated solution of lithium chloride. The element is heated by an electric current passed between the parallel wires until its temperature is such that the element neither loses nor gains moisture from the surrounding atmosphere. The electric resistance of the element increases if the temperature is above the equilibrium temperature, since the solution concentration increases by evaporation, and vice versa, and thus the vapor pressure of the solution on the element is automatically brought to and maintained in equilibrium with the surrounding vapor pressure. The temperature of the element, which is measured either by a resistance or liquid filled thermometer, determines the vapor pressure of the lithium chloride solution which in turn equals the pressure of the water vapor in the surrounding atmosphere. The scale can be graduated in terms of dewpoint insofar as the vapor pressures for saturated lithium chloride are accurately known. It is approximately 15 percent of that of water

down to temperatures of about 0° C. With certain restrictions the dewpoint is measurable in the range −16 to +160° F. Stability of calibration under service conditions is claimed.

This instrument can be used for remote indicating, recording and control. It functions best in still air, and when the ventilation of the sensitive element becomes excessive (greater than 50 ft/min), suitable means must be used to reduce the ventilation, if accuracy is to be maintained.

Weaver. Weaver and Riley (147) have developed a type of electric hygrometer which has application in routine checking of water vapor content of gases, particularly those in high pressure cylinders.

The sensitive element is a film of electrolyte, usually phosphoric and sulfuric acid, with suitable electrodes for use in measuring the electric resistance of the film, all mounted in a small case, as an aviation engine spark plug, suitably modified. Since the electric resistance of the film is unstable, a comparison procedure is resorted to, in which the resistance of the film in equilibrium with the atmosphere to be measured is immediately matched by exposing to an atmosphere, the moisture content of which can be controlled in a known way.

In the primary use of the instrument, in measuring the dryness of aviator's oxygen, pressure control was found to be most convenient and is described here only in its most elemental form. Gas, usually nitrogen, is humidified 100 percent while at high pressure. A sample of this nitrogen, at atmospheric pressure, is passed through the cell and the resistance noted, usually as the reading of a galvanometer in an unbalanced alternating-current Wheatstone bridge. Then a sample from the compressed gas under test is passed through the cell, at a pressure which is reduced until the same reading is obtained. From the measured pressures and the known water content of the saturated sample, either the weight of water vapor per unit volume, vapor pressure, or relative humidity of the test sample can be computed.

The instrument is characterized by speed, the use of a small sample and greater sensitivity than is possessed by other instruments or methods comparable in these respects. It is available commercially.

Lichtgarn. The variation in electric resistance with relative humidity of selected underfired clays has been investigated by Lichtgarn. The performance data are incomplete as yet, and no elements appear to be commercially available (137).

Gregory humidiometer. Gregory (120) has utilized the electric resistance of cotton impregnated with LiCl or $CaCl_2$ solution to measure humidity. This method has been applied to the measurement of humidity on the skin and clothes of a human subject (131).

Burbidge and Alexander. The variation in electric resistance of cotton wool and human hair has been investigated by Burbidge and Alexander (51). The logarithm of the resistancy of these materials is proportional to relative humidity.

4.5. Gravimetric Hygrometry

a. Change in Weight of Drying Agent

The well-known gravimetric method is accepted as the most accurate for determining the amount of water vapor in a gas. The gas mixture of measured volume and known pressure and temperature is passed over a moisture absorbing chemical, usually phosphorous pentoxide for results of the highest accuracy, and its increase in weight determined. For the data, the weight of water vapor per unit volume and the relative humidity of the gas sample can be computed. Considerable care is required to obtain reliable data (3, 27, 66, 149). This method is employed only in fundamental calibration of instruments or exact determinations of water vapor content.

b. Change in Weight of Absorbing Material

In this type of hygrometer a moisture absorbing material such as human hair, or a chemical, or combinations of both to obtain a structure convenient to handle, is continuously weighed by a delicate balance with an indicator and calibrated humidity scale. The weight of the material must change only with change in the relative humidity of the ambient air (109, 118, 119). Instruments of this type are not known to be available commercially.

4.6. Thermal Conductivity

The difference in thermal conductivity between air (or other gases) and water vapor is utilized so that the temperature, and thus the electric resistance of a hot wire in a small cell varies with change in humidity of the air sample. Two hot wires, one in a reference cell exposed to dry air, are in a bridge circuit, the output of which is a function of the vapor pressure of water in the sample. The theory has been developed by Daynes (31) and Shakespear (34). A model was built by Leeds & Northrup (61, 76). This hygrometer is limited in sensitivity at low temperatures owing to the low vapor pressure of water vapor existing at these temperatures. It has considerable promise as a recorder of humidity in a closed space and in meteorology. It is limited by the fact that it is not specific for water vapor but indicates any change of composition of the gas entering the instrument.

Schwarz (138) has called attention to the possibility of subjecting the water-vapor sample to an inhomogeneous electric field in a thermal conductivity apparatus. Since the water molecule is a dipole, an additional circulation of the water

vapor, in contrast to that obtained with air, is secured. This effect can be expected to add to the effect of differences in the heat conduction of air and water vapor. No development work appears to have been done on this possibility.

4.7. Spectroscopic Method

Instruments have been developed in which infrared bands which are absorbed by water vapor are compared in intensity with another band not so absorbed. The sample of air under analysis may be in a tube (116, 125) with the spectral bands obtained from a lamp or may be the entire atmosphere with the sun furnishing the spectral bands (124). The effect of water vapor upon the energy of the received radiation may be measured by phototubes or thermocouples. The instrument is not made commercially.

4.8. Index of Refraction

Some experimental work has been done on the variation of the index of refraction of a thin film of glycerine with water vapor content of the ambient air (29 and 48). The method, even if successfully developed, appears to have only limited application.

4.9. Measurement of Pressure or Volume

The volume of water vapor in a gas sample can be measured if its change in volume is measured at constant pressure before and after the water vapor is absorbed. Conversely, if the volume is held constant, the change in pressure gives the pressure of the water vapor. These methods are useful only in laboratory investigations. The difficulty of obtaining accurate determinations increases rapidly with decrease in temperature of the gas sample. See (1 and 8) for descriptions of a number of instruments of this type.

In one form of constant pressure apparatus a manometer and also a graduated tube containing an absorbing liquid, such as sulfuric acid, are connected to a gas container. In operation sulfuric acid is slowly admitted to the container to absorb the water vapor in the sample and at the same time in sufficient volume to maintain constant the absolute pressure of the gas, as indicated by the manometer and a barometer. The volume of acid admitted is the volume of water vapor in the sample, subject to corrections for lack of constancy of temperature or of the reference pressure.

If the apparatus just described is modified so that the sulfuric acid forms part of the original volume, a constant volume apparatus results. In this case the change in pressure as the water vapor is absorbed is the water-vapor pressure.

The tilting form of absorption hygrometer described by Mayo and Tyndall (33) is essentially a constant volume instrument. Here the absorbing material is installed in a piston which moves from one end of the cylinder containing the gas sample to the other as the cylinder is oscillated, thus forcing the gas through the absorbing chemical. This piston action reduces the time required for complete absorption of the water vapor. The fall in gas pressure which is measured is the water vapor pressure. The device is proposed as a working standard in calibration of hygrometers. It is not available commercially.

One version of constant-volume hygrometer (105) completely dispenses with an absorbing chemical and, instead, uses low temperatures to condense part of the water vapor content of a gas sample, and from a measurement of the temperature and reduction in pressure, permits the determination of the initial vapor pressure. In this instrument, two identical vessels, one containing dry gas and the other the gas sample of unknown water vapor content, are sealed and connected through a differential manometer. The vessels are then immersed in a liquid bath and gradually cooled until the differential manometer registers a pressure difference, indicating that condensation of water vapor has taken place in the gas sample. At this point the temperature and pressure difference are read. From the saturation pressure at the observed temperature and from the pressure difference, the initial water vapor content is then computed.

By employing a liquid-air trap, the moisture in a large volume of gas can be condensed and then suitably measured. The known volume of gas is passed through the trap and, while the low temperature is maintained, the trap is evacuated. The apparatus is then allowed to warm up, preferably in a thermostatted bath, and the vapor pressure measured. Experience with this method at this Bureau indicates that for frost points below $-20°$ C, it is better than the direct determination of the frost point. When using this method with gases containing carbon dioxide, the temperature of the air trap is raised above $-78°$ C before evacuation. This permits any condensed carbon dioxide to be vaporized and removed from the trap.

For additional information on absorption hygrometers, see (30, 85, 86, 101, 111).

4.10. Thermal Rise

The rise in temperature accompanying the exposure of dry cotton wool to moist air has been employed as a means of indicating humidity (see (36 and 45) for details).

4.11. Mobility of Ions

The change in the mobility of ions, produced by α-rays and γ-rays, due to the presence of water

vapor has been investigated (45, 51). While a small effect has been observed, no practical hygrometer has been developed.

4.12. Dielectric Constant

Birnbaum has developed a recording microwave refractometer (153) of high sensitivity that can continuously sample and record the dielectric constant of a stream of air or gas. Since the dielectric constant of air varies with water-vapor content, this instrument may be employed as a recording hygrometer. The refractometer operates by comparing two identical cavity resonators. Into one of these cavities, the test sample is introduced. The resulting differences in resonance frequency between the two cavities is then a measure of the dielectric constant of the test sample. In addition to its high sensitivity, the refractometer has a time response, limited by the response of the recording milliammeter, of about one-half second to discrete changes in dielectric constant. A similar instrument has been reported by Crain (157).

4.13. Critical Flow

Wildhack (156) has proposed a means of measuring relative humidity which utilizes sonic, or critical, flow through small nozzles. Two sets of two nozzles in series are arranged in parallel, with critical flow maintained through all nozzles. At critical flow the mass flow through each nozzle is independent of the downstream pressure, and is directly proportional to the entrance pressure. An absorber of water vapor is placed between one series pair of nozzles, which reduces the mass flow and hence the gas pressure at the entrance to the downstream nozzle. Measurement of the difference in entrance pressures between the two downstream nozzles, of the absolute pressure of the gas at the entrance to the referenced downstream nozzle, and of the gas temperature, will serve to determine the relative humidity of the gas.

4.14. Diffusion Hygrometer

The difference in density of completely and partially saturated air, at the same temperature, has been employed to measure air humidity (49). Esentially, a column of atmospheric air is balanced against a column of saturated air. The difference in density of the two columns causes the lighter saturated air to diffuse upward into the atmosphere and the atmospheric air, because of its greater density to diffuse downward into a saturation chamber where it, in turn, becomes fully humidified. The rate of diffusion is then directly related to the vapor pressure of the atmospheric air and is detected and measured by means of the deflection produced in a suspended vane. It is claimed that this water vapor diffusion method can operate over a wide temperature range, is continuously indicating or recording, is easy to operate and is portable.

A different approach was used in the hygrometer described by Greinacher (122). His instrument is based on the difference in diffusion of water vapor and air through a semipermeable membrance. A porous clay plate cemented to an opening in the wall of an enclosed vessel containing a desiccant preferentially permits air diffusion and prevents water vapor diffusion. A differential manometer, communicating with the enclosed vessel and the ambient atmosphere (whose humidity is being measured), registers a pressure drop Δp_1 that is directly proportional to the partial pressure e of the water vapor in the ambient atmosphere. In order to avoid consideration of the constant of proportionality of the apparatus a similar vessel with an identical porours clay plate and manometer, but containing water instead of the dessicant, is employed. The pressure drop Δp_2 indicated by the latter arrangement is directly proportional to the difference between the saturation vapor pressure e_s and the ambient partial pressure e at the ambient temperature. The relative humidity is given by the relation.

$$RH = 100 \times \frac{e}{e_s} = 100 \times \frac{\Delta p_1}{\Delta p_1 + \Delta p_2}$$

Further theoretical consideration of this hygrometer are presented by Spencer-Gregory and Rourke (141). The instrument is reported to be extremely sensitive to rapid temperature changes which may give rise to erroneous readings.

4.15. Chemical Methods

Several methods are available for the determination of the moisture content in gases by chemical means. A very simple and qualitative indicator may be made based on the change in color, from blue to pink, of cloth or paper impregnated with cobaltous chloride, as the humidity increases. When a color comparison scale is employed with this indicator, a rough estimate of the relative humidity is obtained (75). Cobaltous bromide may similarly be used, with a threefold increase in sensitivity. The colors of these cobalt salts are affected by temperature as well as humidity. The quantitative measurement of water vapor has been successfully made by using cobaltous bromide as an indicator in a visual (112) and in a photoelectric (123) colorimetric method.

There is a series of compounds of ketones and Grignard reagents which can form internal ions accompanied by the development of intense color, induced by the presence of water. Some useful compounds are the complexes of Michler's ketone (tetramethyl-diaminobenzophenone) and Grignard reagent (ethyl magnesium bromide, methyl

magnesium iodide, or phenyl magnesium iodide). An apparatus, employing the color change of these compounds, has been developed, primarily for detecting moisture in compressed oxygen (19). The apparatus and method involves sealing a measured amount of compound with dry sand in a glass ampule. Then, under a controlled and uniform rate of gas flow, the ampule is broken and the time for the movement of the resultant color front along a specified distance is measured. This time, for a given batch of ampules identically made, is a function of the moisture content, the temperature and rate of flow.

A method for the analytical determination of the water content in a wide range of materials was proposed by Karl Fischer in 1935 (84). His reagent, a solution of iodine, sulfur dioxide and pyridine in methanol, is the basis of titrimetric procedures that have been applied to moisture determinations in gases (20).

5. Test Methods

The testing and calibration of hygrometers involve the production and control of atmospheres of known relative humidity over a wide range of temperatures. While the methods of humidity production are varied, they may be classified, conveniently, into several categories. The equipment for producing the known relative humidity must be designed so that hygrometers to be tested can be conveniently exposed to the controlled atmosphere.

The sections below are restricted largely to the description of methods of producing a constant humidity of known amount useful for calibration of hygrometers.

5.1. Basic Methods

Relative humidity is related, through the fundamental gas laws, to such parameters as temperature, pressure, and water-vapor content. Several convenient and practical methods are available of directly establishing atmospheres of known relative humidity with sufficient precision and accuracy by the measurement and control of these parameters, without requiring auxiliary humidity measuring and sensing instruments.

The principle of divided flow may be employed, when flow is permissible, to produce any desired humidity. Apparatus, based on this principle, has been described in (76) for use at temperatures above freezing and in (134 and 149), for use at temperatures below 0° C (32° F). A stream of dry air is divided accurately, usually by means of a proportioning valve, into two parts. One part is saturated, with respect to water or ice; the other part is maintained dry. The two parts are then recombined in a test chamber and exhausted into the air. The relative humidity is given by the ratio of the division. A simplified schematic diagram of this method is shown in figure 1.

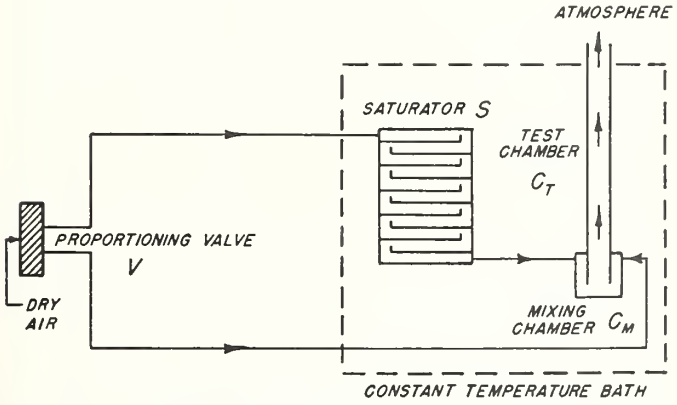

FIGURE 1. *Simplified schematic diagram of the principle of operation of the divided-flow humidity apparatus.*

In the recirculation or two-temperatures method, a stream of air is saturated at a controlled temperature and then the temperature of the mixture is elevated, without loss or gain in moisture. A measurement of the two temperatures serves to determine the relative humidity. To insure complete saturation at the lower temperature, the air stream is recirculated in a closed system from the saturator (at the lower temperature) to a test chamber (at the higher temperature) and back to the saturator. The temperatures must be accurately measured and controlled; for example, at 20° C (68° F) an error of 0.2° C (0.3° F) in either temperature measurement represents 1 percent error in relative humidity, which error increases at lower temperatures. Laboratory equipment of this type has been built (106, 155), but none is commercially available. The method is illustrated in figure 2.

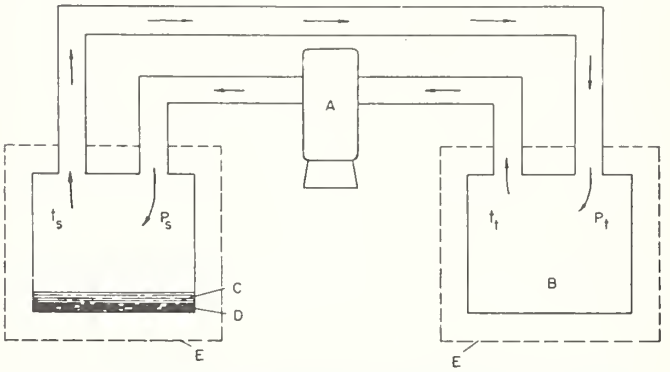

FIGURE 2. *Simplified schematic diagram of the two-temperature recirculating method of relative-humidity production.*

A, gas pump; B, test chamber; C, water; D, saturator; E, thermostatted bath.

In the two-pressure method (147) a stream of air (or some other gas) at an elevated pressure is saturated and the pressure of the saturated air is reduced as required to obtain any desired humidity. Since the desired relative humidity is required, usually, at atmospheric pressure, the elevated pressure is so adjusted that the air, upon expansion to atmospheric pressure, will be at the proper relative humidity. The pressure of the air and water vapor mixture is measured at both the elevated and reduced pressures, and so are the temperatures, if they differ. To insure that the saturator and test chamber temperatures remain the same, and also to provide a means of controlling and establishing any desired temperature, the saturator and test chamber are immersed in a thermostatted bath. To prevent condensation the saturated air temperature must not fall below the dewpoint, which may require heating the mixture at or before it flows through the pressure-reducing valve. Even at room temperature, control of the saturator temperature will be necessary if the air flow is appreciable. At constant temperature, the relative humidity is roughly the ratio of the two pressures, assuming ideal gas laws. More accurate computation of the relative humidity takes into account deviations from the ideal gas laws (147).

One type of saturator employed in this method consists of a cylinder filled with clean sand and water through which the air passes. Another type similarly consists of a cylinder into which water has been added, but the air in this type enters the cylinder tangentially to and above the water (or ice) surface and, after swirling around many times over the water, emerges through a central port at the top. A sketch of this method is shown in figure 3.

In the water or steam injection method for the precise control of relative humidity, moisture and dry air are mixed in desired proportions, using nozzles, orifices or other metering elements in conjunction with pressure reducers. See (67) for one application.

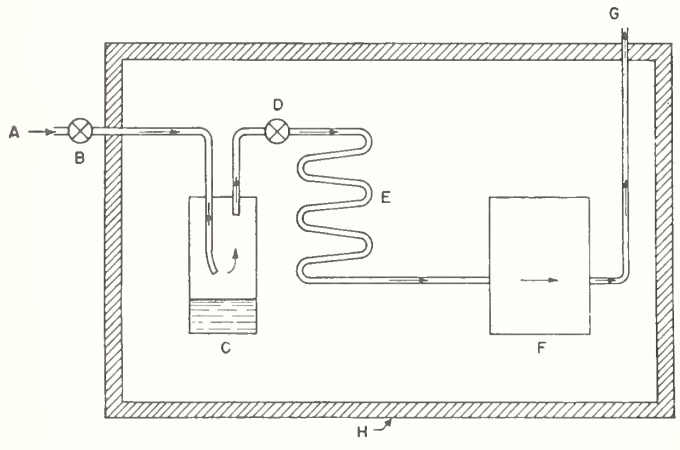

FIGURE 3. *Simplified schematic diagram of the two-pressure method of relative-humidity production.*

A, High-pressure source; B, pressure reducer; C, saturator (water or ice); D, valve; E, heat exchanger; F, test chamber; G, to atmosphere; H, thermostatted bath.

5.2. Secondary Methods

Very convenient methods exist for establishing atmospheres of known relative humidity which depend upon the equilibrium vapor pressure of water when a chemical is dissolved in it. These methods are ideally suited for controlling the relative humidity of a small closed space. Equilibrium conditions are more rapidly established when air circulation or stirring, as by means of a fan or blower, is employed. In all these methods, the test chamber should be kept free of hygroscopic materials, such as wood.

The saturated salt solution method is inexpensive and simple and produces constant relative humidities that are roughly independent of temperature. This method is used frequently for calibrating mechanical type hygrometers. A sealed chamber is required, for which a large glass jar or bell jar is often suitable. The salt solution is made up as a slushy mixture in a glass or enameled tray or in the glass jar, if used, with the solution spreading over as large an area as practicable. Distilled water and chemically pure salts must be used. The salts listed in table 4 have been found useful; for a list of others see (4). The data in table 4 are based partly on the vapor pressure data given in the International Critical Tables (17) and partly on dewpoint measurements made at this Bureau.

TABLE 4.—*Saturated salt solutions suitable for use in humidity control*

KNO_3 = potassium nitrate
NaCl = sodium chloride
$Mg(NO_3)_2.6H_2O$ = magnesium nitrate
$MgCl_2.6H_2O$ = magnesium chloride
LiCl = lithium chloride

Temperature		Relative humidity of saturated salt solution				
		KNO_3	NaCl	$Mg(NO_3)_2.6H_2O$	$MgCl_2.6H_2O$	LiCl
°C	°F	%	%	%	%	%
0	32	97	76	54	34	19
5	41	96	76	54	33	16
10	50	95	75	53	33	14
15	59	95	75	53	33	13
20	68	94	75	53	33	12
25	77	93	75	52	33	11
30	86	92	75	52	32	11
35	95	90	75	51	32	11
40	104	89	75	51	31	11

Water-sulfuric-acid mixtures (39, 52, 63) produce atmospheres of relative humidity that depend on composition and temperature. Two techniques may be employed. The liquid may be exposed in a suitable tray in a sealed chamber to give the equilibrium vapor pressure of the mixture, or air may be bubbled or otherwise brought into intimate contact with the liquid. Wilson's data (39) are reproduced in table 5.

TABLE 5. *Relative humidity obtained from water-sulfuric acid solutions*

Relative humidity	Percentage of H_2SO_4 (by weight) at—			
	0° C	25° C	50° C	75° C
%				
10	63.1	64.8	66.6	68.3
25	54.3	55.9	57.5	59.0
35	49.4	50.9	52.5	54.0
50	42.1	43.4	44.8	46.2
65	34.8	36.0	37.1	38.3
75	29.4	30.4	31.4	32.4
90	17.8	18.5	19.2	20.0

Water-glycerine mixtures (63) will similarly produce atmospheres of known relative humidity. The techniques employed with water-sulfuric acid mixtures work equally well with water-glycerine mixtures. The relative humidity obtainable at 25° C from various water-glycerine solutions are given in table 6.

TABLE 6. *Relative humidity obtained from water-glycerine mixtures at 25° C*

Relative humidity	Glycerine (by weight)	Specific gravity
%	%	
10	95	1.245
20	92	1.237
30	89	1.229
40	84	1.216
50	79	1.203
60	72	1.184
70	64	1.162
80	51	1.127
90	33	1.079

5.3. Control Methods

In response to a sensing element, such as a mechanical hygrometer, electrical hygrometer, or psychrometer, the humidity of a closed space may be raised by water, spray or steam injection, by exposure to a water surface or wet wicks, or by the introduction of saturated or high humidity air (or gas), or the humidity may be lowered by chemical absorption, or the introduction of dry air (or gas). The controls that are used may be manual or automatic.

One type of controlled-humidity chamber design (32, 45) consists, essentially, of a sealed chamber, such as a bell jar, in which air circulation is obtained by means of a fan. Two trays, each with a tight cover that can be raised and lowered externally, are placed in the chamber. One tray contains a chemical absorbent, such as sulphuric acid, silica gel or Drierite, while the other contains distilled water, preferably with exposed cotton or linen wicks. The cover of the appropriate tray is raised until a hygrometer indicates that the desired relative humidity has been attained. The cover is then dropped and, since the chamber is sealed, the humidity remains constant. This chamber may be made automatic by using the output of a sensing element, through an appropriate circuit, to raise or lower the required cover.

See (8, 10, 12, 50, 54, 58, 62, 65, 92, 114, and 129), for additional suggestions and details.

5.4. Comparisons with Standards

While it is preferable to use atmospheres of known relative humidity for testing or calibration, it is often desirable to make spot checks of mechanical hygrometers and hygrographs under prevailing atmospheric conditions or even, in some cases, to test or calibrate hygrometers in chambers where the humidity is not known or only known approximately. Under these conditions, the readings of the instrument under test may be compared with those of a standard instrument.

It is generally considered that the primary standard in hygrometry is the gravimetric method of water vapor measurement. However, except for work of the highest order of accuracy, this method is seldom used as a working standard. On the other hand, proved designs of dewpoint indicators and recorders are frequently employed as working standards where accuracy is desired. Many models are in the nature of laboratory instruments, especially those depending on visual observation and manual temperature control, requiring skilled personnel for successful operation so that they are not usually used in routine calibrations. The dry- and wet-bulb psychrometer is particularly suited for rapid routine work. It should be used with caution in small enclosures, for evaporation from the wet-bulb may increase the relative humidity of the space being measured. If adequate ventilation is secured and proper precautions are observed, the psychrometer is calibrated merely by having its thermometers calibrated.

6. Selected References

6.1. Books and Pamphlets

(1) Feuchtigskeitmessung. H. Bongards. R. Oldenburg, Berlin. 322 p (1926). (Excellent general treatise)

(2) Properties of ordinary water substance. N. Ernest Dorsey. Reinhold Publ. Co. (1940).

(3) Dictionary of applied physics. Section on humidity by Skinner (1923). Glazebrook.
(Describes psychrometric, dewpoint and gravimetric methods of humidity measurement.)

(4) Handbook of chemistry and physics. p. 1925, 30th ed. (1946). Chemical Publ. Co., 26 Court St., Brooklyn 2, N. Y. $6.00.

(5) Heating, ventilating and air conditioning guide. American Society Heating & Ventilating Engrs., New York (1944).

(6) Wärmetabellen der Phys. Tech. Reich. L. Holborn, K. Scheel, and F. Henning. Friedr. Vieweg & Sohn, Braunschweig (1919).

574278 O - 61 - 46

(7) Psychrometertafeln. Jelineks. VII Aufl., Leipzig (1929).
(8) Handbuch der Meteorologischen Instrumente. E. Kleinschmidt. Julius Springer, Berlin (1935). (Section on measurement of atmospheric humidity and evaporation.)
(9) Mechanical engineers handbook. Lionel S. Marks. McGraw-Hill (1941).
(10) Controlled humidity in industry. M. C. Marsh. Charles Griffin & Co., Ltd. (London) (1935).
(11) Diffusion. C. Maxwell. Encyl. Brit. 9th ed., 7, 218 (1877).
(12) Meteorological instruments. W. E. K. Middleton. University of Toronto Press (1941). (Chapter on measurement of atmospheric humidity.)
(13) Chemical engineers handbook. J. H. Perry. McGraw-Hill Book Co., New York, 2d ed. (1941).
(14) Aspirations-Psychrometertafeln des Preus. Met. Inst. III Aufl. Preuss. Met. Inst. Braunschweig (1927).
(15) Psychrometric tables. U. S. Weather Bureau WB No. 235 (1912). (Supt. of Documents, Washington 25, D. C.) 15¢.
(16) Smithsonian meteorological tables. Smithsonian Institution (1939).
(17) International critical tables, III, 211. E. W. Washburn. McGraw-Hill Book Co., New York.
(18) Psychrometric tables and charts. O. T. Zimmerman and I. Lavine. Industrial Research Service, Dover, N. H. (1945) $7.50.
(19) Oxygen research. Summary technical report of Division 11, NDRC, 1 (1946) chap. 14. Instruments for testing oxygen. S. S. Prentiss. p. 320.
(20) Aquametry. Applications of the Karl Fischer reagent to quantitative analysis involving water. John Mitchell, Jr. and Donald Milton Smith. p. 168 Interscience Publishers, Inc., New York (1948).

6.2. Articles

(21) On the hygrometer by evaporation. J. Ivory. The Philosophical Magazine and Journal 60, 81 (1822).
(22) Über die Verdunstungskalte under deren Anwendung auf Hygrometrie. E. F. August. Annalen der Physik und Chemie 335, 69 (1825).
(23) On the theory of the moist bulb hygrometer. Apjohn. Trans. Roy. Irish Acad. 17, 275 (1837).
(24) Etudes sur l'Hygrométrie. V. Regnault. Ann. Chim. Phys. (3) 15, 129 (1845).
(25) Kondensationhygrometer. Alluard. Symons Month. Met. Mag. 13, 55 (1877).
(26) Annual Report, Chief, U. S. Signal Officer. Ferrel. Appendix 24, pp 233–259 (1886).
(27) Report on hygrometric methods; first part, including the saturation method and the chemical method, and dewpoint instruments. W. N. Shaw. Phil. Trans. Royal Soc. 179, 73 (1888).
(28) Rational psychrometric formulae. W. H. Carrier. Trans. ASME 33, 1005 (1911).
(29) Determination of relative humidity of the air by refractometry. Giraud. J. Physique 3, 900 (1913). (Used change of index of refraction of glycerine with humidity.)
(30) Improved methods of hygrometry. A. N. Shaw. Trans. Roy. Soc. Can., Ser. 3, 10, 85 (1916). (Absorption hygrometers.)
(31) The theory of the katharometer. H. A. Daynes. Proc. Roy. Soc. London A97, 273 (1920). (Thermal conductivity method.)
(32) Some modified forms of hygrometers. E. Griffiths. Trans. Phys. Soc. London 35, VIII (1921–2). (Description of psychrometer, dewpoint apparatus and humidity chamber.)
(33) The tilting hygrometer; a new form of absorption hygrometer. H. G. Mayo and A. M. Tyndall. Proc. Phys. Soc. London 34, lxvii (1921–22). (Moisture abstracted from air sample by P_2O_5 and change of pressure measured.)
(34) The katharometer. G. A. Shakespear. Proc. Phys. Soc. London 33, 163 (1921). (Thermal conductivity method of humidity measurement.)
(35) The wet and dry bulb hygrometer. P. S. Skinner. Trans. Phys. Soc. London 34, lx (1921–22). (Some experimental work on psychrometric formula.)
(36) A thermal hygrometer. A. M. Tyndall and A. P. Chattock. Proc. Phys. Soc. London 34, lxxii (1921–22). (Method depends on exposing dry cotton wool to damp air and measuring temperature rise.)
(37) Note on psychrometry in a wind tunnel. R. A. Watson Watt, Proc. Phys. Soc. London 34, lxiv (1921–22). (Effect of ventilation on psychromethric constant.)
(38) The theory of the hair hygrometer. F. J. W. Whipple. Trans. Phys. Soc. London 34, 1 (1921–22). (Mathematical treatment.)
(39) Humidity control by means of sulphuric acid solutions with critical compilation of vapor pressure data. R. E. Wilson. J. Ind. & Eng. Chem. 13, 326 (1921). (Data percent sulfuric acid solution against relative humidity at 0°, 25°, 50° and 75° C.)
(40) The evaporation of a liquid into a gas. W. K. Lewis. Mech. Eng. 44, 325 (1922) and 55, 567 (1935).
(41) Direct determination of gasoline-air mixtures. W. A, Gruse. Ind. Eng. Chem. 15, 796 (1923).
(42) The temperatures of evaporation of water into air. W. H. Carrier and D. C. Lindsay. Trans. ASME 46, 36 (1924).
(43) A new method for determining the temperature of the dewpoint. M. Holtzmann. Phys. Zeitschrift 25, 443 (1924). In German. (Polished rod type dewpoint indicator.)
(44) Hygrometry in deep mines. R. S. Jones. Colliery Guardian (England) 128, 1437–38, 1499–1500 (1924).
(45) The measurement of humidity in closed spaces. Ewing and Glazebrook. Spec. Report No. 8, Food Investigation Board, Dept. of Scientific and Ind. Research (London) (1925). Revised ed., E. Griffiths (1933).
(46) Energy transformations in air currents and applications in the measurement of atmospheric humidity. Paine. Proc. Nat. Acad. Sci. 11, 555 (1925).
(47) A new relative humidity recorder. L. Behr. J. Opt. Soc. Am. 12, 623 (1926). (A circuit and recorder for automatically giving relative humidity by the phychrometric method using resistance thermometers.)
(48) A hygrometer employing glycerine. E. Griffiths and J. H. Awbery. Proc. Phys. Soc. London 39, 79 (1926). (Used change of index of refraction of glycerine with humidity.)
(49) Continuous indicating hygrometer. Romberg and Blau. J. Opt. Soc. Am. 13, 717 (1926).
(50) An automatic humidity control. W. H. Apthorpe and J. J. Hedges. J. Sci. Inst. 4, 480 (1927). (Hair element controls a circuit which controls supplies of moist and dry air to the chamber.)
(51) Electrical methods of hygrometry. P. W. Burbidge and N. S. Alexander. Trans. Phys. Soc. London 40, 149 (1927–28). (Used resistance of cotton wool and human hair; also measured change in mobility of ions due to water vapor.)
(52) The vapor pressure of water over sulfuric-acid-water mixtures at 25° C and its measurement by an improved dewpoint apparatus. J. R. I. Hepburn. Proc. Phys. Soc. London 40, 249 (1927). (Revision of Wilson's data, ref. 37.)
(53) Influence of humidity on the elastic properties of cotton. Mann. Shirley Inst. Memoirs 6, 53

(1927). Also J. Text. Inst. 18, T253 (1927). (Torsion hygrometer from cotton filament.)
(54) Notes on temperature and humidity control cabinets. Circ. No. 310 Paint & Varnish Manufacturers Assoc. (May 1927).
(55) Determination of volatility of gasoline. R. Stevenson and J. A. Babor. Ind. End. Chem. 19, 1361 (1927). (An apparatus for determining the dewpoints of air-gasoline mixtures. Visual observation of optical change of a platinum black mirror.)
(56) A hygrometer for use in timberseasoning kilns. E. Griffiths. Trans. Phys. Soc. London 41, 426 (1928).
(57) Dehumidification of air. C. S. Keevil and W. K. Lewis. Ind. & Eng. Chem. 20, 1058 (1928). Dewpoint apparatus.)
(58) Humidity test equipment. E. B. Wood. Instruments 1, 135 (1928). (Describe air-conditioned test room, controlled by sprays and radiators, chambers controlled by sulfuric acid-water mixtures, and chambers controlled by saturated salt solutions.)
(59) An electrical method for the determination of the dewpoint of flue gases. H. F. Johnstone. U. Ill. Eng. Exp. Station. Cir. 20. (1929). (Automatic method for recording dewpoint depending upon conductivity between platinum electrodes on glass thimble.)
(60) Industrial humidity instruments. M. F. Behar. Instruments 3, 549, 605, 659 (1930).
(61) A high-sensitivity absolute-humidity recorder. C. Z. Rosecrans. Ind. & Eng. Chem. Anal. Ed. 2, 129 (1930). (Thermal conductivity apparatus.)
(62) A simplified humidity control. W. H. Apthorpe and M. C. Marsh. J. Scientific Insts. 8, 152 (1931). (Hair element equipped with contacts.)
(63) Control of relative humidity in a small enclosed space. F. T. Carson. Paper Trade Journal (Oct. 1931). (Describes water-sulfuric acid and water-glycerine mixture method of humidity control.)
(64) Resistance thermometers for the measurement of relative humidity or small temperature differences. D. C. Rose, Can. J. Research 5, 156 (1931).
(65) An improved method of maintaining constant humidity in closed chambers. R. H. Stoughton. J. Sci. Inst. 8, 164 (1931). (Hygrotstat controls air circulation past a wet muslin surface.)
(66) The water content of saturated air at temperatures up to 100° C. J. H. Awbery. Proc. Phys. Soc. London 44, 143 (1932). (Determined by gravimetric method.)
(67) The basic law of the wet- and dry-bulb hygrometer at temperatures from 40 to 100° C. J. H. Awbery and E. Griffiths. Proc. Phys. Soc. London 44, 132 (1932). (Description of experimental determination of psychrometric chart at elevated temperatures based on gravimetric and dewpoint measurements. Data presented.)
(68) Über thermoelektrische Feuchtigkeitsmessung. L. Kettenacker. Z. für Instrumentenkunde 52, 319 (1932).
(69) Determination of relative humidities by means of thermocouples. J. H. Lanning. Ind. Eng. Chem. Anal. Ed. 4, 286 (1932).
(70) Apparatus for the measurement of relative humidity. J. H. Orchard. Trans. Phys. Soc. London 44, 224 (1932). (Description of a platinum resistance thermometer psychrometer).
(71) An experimental study of the wet-bulb hygrometer. T. K. Sherwood and E. W. Comings. Trans. Am. Insti. Chem. Eng. 28, 88 (1932).
(72) Ein Psychrometer ohne künstliche Belüftung. H. Wald, Z für d. ges Kalte-Ind. 39, 111 (1932).
(73) The theory of the psychrometer. J. H. Arnold. Physics 4, 255 (1933).
(74) Some improvements in psychrometry. D. B. Brooks and H. H. Allen. J. Wash. Acad. Sci. 23, 121 (1933).
(75) Color changes in hygroscopic salts and their use for humidity measurements. Alfred Swartz. Messtechnik 9, 87 (1933).
(76) Supplying atmospheres of known humidity. A. C. Walker. Bell. Lab. Record VII, 169 (1933). (Dry and saturated air mixed to produce desired relative humidities. Method used to test L&N thermal conductivity humidity recorder.)
(77) The Mollier Psychrometric Chart. F. Keppler Refrig. Eng. 27, 136 (1934).
(78) The present state of psychrometric data. Keyes and Smith. Refrig. Eng. 27, 127 (1934).
(79) An apparatus for the determination of the dewpoint. E. B. Moss. Proc. Phys. Soc. 46, 450 (1934).
(80) A formula and tables for the pressure of saturated water vapor in the range 0 to 374°C. N. S. Osborne and C. H. Meyers. J. Research NBS 13, 1 (1934) RP691.
(81) An investigation of the wet- and dry-bulb hygrometers at low temperature. J. H. Awbery and E. Griffiths. Proc. Phys. Soc. of London 47, 684 (1935).
(82) Psychrometric charts for high and low pressures. D. B. Brooks. NBS Pub. M146 (1935) (out of print).
(83) The transient condition of the human hair hygrometer element. A. F. Spilhaus. Mass. Inst. Tech. Meteoro. Course (Cambridge, Mass.). Professional Notes No. 8 (1935).
(84) A new method for the analytical determination of the water content of liquids and solids. Karl Fischer. Angew. Chem. 48, 394 (1935).
(85) A sulfuric acid hygrometer. A. Blackie. J. Sci. Inst. 13, 6 (1936). (Absorption hygrometer that gives vapor pressure of water directly.)
(86) A vapor pressure hygrometer. J. J. Dowling. J. Sci. Inst. 13, 214 (1936). (Moisture content of air determined by reduction in pressure of a fixed volume due to absorption by a chemical drying agent.)
(87) The deviation of the actual wet-bulb temperature from the temperature of adiabatic saturation. D. Dropkin. Cornell U. Eng. Exp. Stat. Bul. No. 23 (1936).
(88) The behavior of a single-hair hygrometer under varying conditions of temperature and humidity. W. G. Iles and K. Worsnop. Trans. Phys. Soc London 48, 358 (1936).
(89) Messung der Luftfeuchtigkeit mit Thermoelementen ohne künstliche Beluftung. Von We. Koch. Gesundheits-Ingenieur 59, 504 (1936).
(90) The use of thermocouples for psychrometric purposes. R. W. Powell. Trans. Phys. Soc. London 48, 406 (1936).
(91) The measurement of very low relative humidities. A. Simons. Proc. Phys. Soc. London 48, 135 (1936).
(92) A humidity control device for ovens. C. T. Webster. J. Sci. Inst. 13, 412 (1936). (Psychrometer controls steam injection and excess moisture condensation.)
(93) A review of existing psychrometric data in relation to practical engineering problems. W. H. Carrier and C. O. Mackey. ASME Trans. 59, 32 and 528 (1937).
(94) An electrical hygrometer and its application of radio meteorography. F. W. Dunmore. J. Research NBS 20, 723 (1938) RP1102.
(95) Determination of low humidity with dewpoint potentiometer. A. K. Frank. G. E. Rev. 41, 435 (1938).
(96) New tables of the psychrometric properties of air-vapor mixtures. W. Goodman. Heating, Piping

and Air Cond. **10**, 1, 119 (1938). (Based on Keenan and Keyes steam tables.)

(97) Accurate determination of dewpoint. A. W. Hixson and G. E. White. Ind. & Eng. Chem. Anal. Ed. **10**, 235 (1938).

(98) The effect of radiation on psychrometic reading. D. Dropken. Cornell U. Exp. Stat. Bul. 26 (Oct. 1939).

(99) An improved electrical hygrometer. F. D. Dunmore. J. Research NBS **23**, 701 (1939) RP1265.

(100) The psychrometric chart, its application and theory. W. Goodman. Heating, Piping and Air Cond. **11**, 357, 421, 485, 549, 613, 671, 749 (1939); **12**, 6, 107, 171, 239, 303, 367, 431, 486 (1940).

(101) Study of Rideal absorption hygrometer. H. W. Harkness. Rev. Sci. Inst. **10**, 237 (1939).

(102) Dewpoint hygrometer for use at low temperature. C. A. Winkler. Canadian J. of Research **17**, Sec. D, 35 (1939).

(103) An improved radiosonde and its performance. H. Diamond, W. S. Hinman, F. W. Dunmore, and E. G. Lapham. J. Research NBS **25**, 327 (1940) RP1329. (Electric hygrometer.)

(104) A dewpoint recorder for measuring atmospheric moisture. C. W. Thornthwaite and J. C. Owen. Monthly Weather Review **68**, 315 (1940).

(105) Studies with the condensation hygrometer. T. Okada and M. Tamura. Proc. Imp. Acad. (Tokyo) **16**, 141 and 208 (1940).

(106) Equipment for conditioning materials at constant humidities and at elevated temperature. J. G. Wiegerink. J. Research NBS **24**, 639 (1940) RP1303.

(107) A new psychrometric chart for low temperatures and humidities. C. W. Deverall. Heating and Ventilating **38**, 51 (June 1941). (Expanded scale at low temperature.)

(108) The construction and use of a thermoelectric psychrometer. C. Lorenzen, Jr. Temperature—Its measurement and control in science and industry. American Institute of Physics, p. 660 (1941).

(109) The optical hygrometer and its working. L. D. Mahajan. Indian J. Physics **15**, 425 (1941).

(110) Electric dewpoint recorder. R. H. Reed. In symposium on Temperature—Its measurement and control in science and industry. American Institute of Physics, p. 655 (1941).

(111) Chemical absorption hygrometer as meteorological instrument. C. W. Thornthwaite. Trans. Am. Geophys. Union, pt II, 417 (August 1941).

(112) On the measurement of water vapor in gases. F. C. Todd and A. W. Gauger. Proc. Amer. Soc. Test. Mat. **41**, 1134 (1941). (Colorimetric method described using cobaltous bromide in n-butyl alcohol as an indicator).

(113) Study of electric hygrometer. R. N. Evans and J. E. Davenport. Ind. & Eng. Chem. (Anal. ed.) **14**, 507 (1942).

(114) Bridge controlled relay circuit for Dunmore relative humidity elements. R. L. Andrews. Rev. Sci. Inst. **14**, 276 (1943).

(115) Two nomographs for low and high wet-bulb range solve psychrometric problems. E. Berl and G. A. Sterbutzel. Chem. & Met. Eng. **50**, 142 (Dec. 1943). (Alignment charts for obtaining relative humidity from dry- and wet-bulb readings.)

(116) A spectroscopic hygrometer. L. W. Foskett and N. B. Foster. Bul. Am. Meteoro. Soc. **24**, 146 (1943). Abstract, Aero. Eng. Rev. **2** (April 1943).

(117) Calculation of the relative humidity from hair hygrometer readings during balloon ascents. E. Glückauf. Qtr. J. Royal Meteoro. Soc. **70**, 293 (1944). (Theoretrical investigation of low temperature lag of hair hygrometers and method of correcting radiosonde data.)

(118) Humid hysteresis of Mahajan's optical hygrometer and others. L. D. Mahajan. Indian J. Physics **18**, 216 (1944).

(119) Time lag and humid fatigue of hygrometers. L. D. Mahajan. Indian J. Physics **18**, 293 (1944).

(120) Meteorological investigations at Rye, Part I. Instruments Branch (British) Air Ministry, JMRP No. 17 (May 1944). (Gregory humidiometer; relative humidity measured as a function electrical resistance of Egyptian cloth soaked in LiCl or $CaCl_2$ solution.)

(121) Psychrometry in the frost zone. D. D. Wile. Refrig. Eng **48**, 291 (1944).

(122) Ein neuer Feuchigkeitsmesser; das Diffusionshygrometer. H. Greinacher. Hel. Phys. Act. **17**, 437 (1944).

(123) A colorimetric method for determining the water vapor content in fuel gases utilizing the Evelyn colorimeter. R. J. Pfister and D. J. Kirley. Amer. Soc. Test. Mat. Bul. **127**, 17 (1944).

(124) Spectrophotometer for determination of water vapor in vertical column of atmosphere. N. B. Foster and L. W. Foskett. J. Optical Soc. Am. **35**, 601 (1945). (Use phototube to measure changes in absorption of sun's spectral band, 9340 angstroms, due to water in path.)

(125) A photoelectric hygrometer. B. Hamermesh, F. Reines, S. Korff. Nat. Adv. Com. Aero. Tech. Note 980 (1945). (Absorption of spectral band measured by photoelectric means.)

(126) Hitemp psychrometric chart. O. T. Zimmerman and I. Lavine. Industrial Research Service, Dover, N. H. (1945). $12.50.

(127) Meteorology of the lower stratosphere. G. M. B. Dobson. Proc. Roy. Soc. **A185**, 144 (1946).

(128) Low-pressure properties of water from —160 to +212°F. J. A. Goff and S. Gratch. Heating, Piping and Air Conditioning, (1946).

(129) Recorder and controller for temperature and humidity. V. D. Hauck, R. E. Strum and R. B. Colt. Electronics **19**, 96 (1946). (Human hair element periodically controls an electrical resistance.)

(130) Illinois Testing Laboratories dewpoint indicator. Instruments **19**, 278 (1946).

(131) A method of measuring temperature on the skin and clothing of a human subject. L. W. Ogden and W. H. Rees. Shirley Institute Memoirs **XX**, 163 (1946). (Description of electric hygrometer made by boiling cotton fabric in LiCl solution. Relative humidity is a function of resistance and temperature.)

(132) A simple theory of the electric hygrometer. W. Schaffer. Bul. Am. Meteoro. Soc. **27**, 147 (1946).

(133) Hygrometer for high pressure gases. W. W. Beuchner and L. R. McIntosh. Rev. Sci. Inst. **18**, 586 (1947).

(134) Investigation on absorption hygrometers at low temperatures. E. Glückauf. Proc. Phys. Soc. London **59**, 344 (1947). (Description of divided flow type of test apparatus, performance of goldbeater's skin elements, and the electric hygrometer as a function of temperature.)

(135) An improved continuous indicating dewpoint meter. F. A. Friswold, R. D. Lewis and R. C. Wheeler, Jr. NACA Tech. Note No. 1215. Washington, D. C. (Feb. 1947).

(136) Humidity measurement by a new ssytem: Dewcel. W. F. Hicks. Refrig. Eng. **54**, 351 (1947). Also Instruments **20**, 1128 (1947). (Foxboro electric hygrometer.)

(137) New method of measuring relative humidity. F. Lichtgarn. Instruments **20**, 336 (1947). (Preliminary results on the use of ceramic materials as electrical resistance elements.)

(138) Analysis of gas mixtures containing a para-electric component. N. Schwarz. Physica (Holland) **A1**, 47 (1947). (Thermal conductivity effect increased by an electric field imposed on gas sample.)

(139) Serdex hygrometer. Rev. Sci. Inst. **18**, 591 (1947). (Goldbeater's skin hygrometer.)

(140) The measurement of humidity. H. S. Gregory. Instrument Practice **1**, 367, 447 (1947).

(141) A theoretical basis for the diffusion hygrometer. H. Spencer Gregory and E. Rourke. Phil. Mag. **38**, 573 (1947).

(142) Surface Combustion Corp. furnace-atmosphere humidity recorder. Instruments **20**, 730 (1947).

(143) Psychrometric moisture determination in gases. H. Bruckhoff. Arch. Tech. Messen. *Issue No. 152*, T17 (1947).

(144) A method for the continuous measurement of dewpoint temperatures. D. N. Bussman. Report of Dept. of Meteorology, U. of Chicago.

(145) An automatic dewpoint meter for the determination of condensable vapors. T. T. Puck. Rev. Sci. Inst. **19**, 16 (1948).

(146) Moisture measurement with an electronic dewpoint indicator. V. E. Suomi. Instruments **21**, 178 (1948).

(147) Measurement of water in gases by electrical conduction in a film of hygroscopic material and the use of pressure changes in calibration. E. R. Weaver and R. Riley. J. Research NBS **40**, 169–214 (1948) RP1865. (For a description of of commercial model see Instruments **20**, 160 (1947). (Electric hygrometer). (Supt. of Documents, Washington 25, D. C.). 25¢.

(148) Weston all-metal humidity indicator. Rev. Sci. Inst. **19**, 123 (1948).

(149) Divided flow type, low temperature humidity test apparatus. Arnold Wexler. J. Research NBS **40**, 479 (1948) RP1894. (Supt. of Documents, Washington 25, D. C.). 10¢. (Describes method of combining dry and saturated air to produce desired relative humidities.)

(150) Low temperature performance of radiosonde electric hygrometer elements. Arnold Wexler. J. Research NBS **43**, 49 (1949) RP2003. (Supt. of Documents, Washington 25, D. C.). 10¢

(151) Some possible sources of error in operating the Assmann psychrometer. M. E. Woolcock. Instrument Practice **4**, no. 1, 13 (1949).

(152) Biplastic strip hygrometer. Mod. Plastics **26**, 73 (March 1949).

(153) A recording microwave refractometer. George Birnbaum. Rev. Sci. Inst. **21**, 169 (1950).

(154) Test and adaptation of the Foxboro dewpoint recorder for weather observatory use. J. H. Conover. Bul. Am. Meteoro. Soc. **31**, no. 1, 13 (Jan. 1950). (Tests on Dewcel for accuracy, lag and utility for meteorological use.)

(155) Recirculating apparatus for testing hygrometers. Arnold Wexler. J. Research NBS **45**, 357 (1950) RP2145.

(156) Versatile pneumatic instrument based on critical flow. W. A. Wildhack. Rev. Sci. Inst. **21**, 25 (1950).

(157) Apparatus for recording fluctuations in the refractive index of the atmosphere at 3.2 centimeters wavelength. C. M. Crain. Rev. Sci. Inst. **21**, 456 (1950).

UNITED STATES DEPARTMENT OF COMMERCE • Sinclair Weeks, *Secretary*
NATIONAL BUREAU OF STANDARDS • A. V. Astin, *Director*

Electric Hygrometers

Arnold Wexler

National Bureau of Standards Circular 586

Issued September 3, 1957

For sale by the Superintendent of Documents, U. S. Government Printing Office, Washington 25, D. C.
Price 20 cents

718/i

Contents

Electric Hygrometers

Arnold Wexler

This Circular is a review of the art of measuring the moisture content of air by the methods of electric hygrometry. The basis of these methods is the change in electrical resistance of a hygroscopic material with change in humidity.

1. General Introduction

Many, if not most, materials sorb and desorb water vapor as the ambient relative humidity increases or decreases. Associated with this sorption, there is usually a corresponding change in electrical resistance of the material. Materials which display a humidity-dependent change in resistance can be utilized as humidity sensors. However, for a sensor to be of practical use, it should have a reversible and reproducible humidity-resistance characteristic. Such sensors, or elements, when coupled with suitable measuring circuits constitute the electric hygrometer class of instruments. An electric hygrometer, therefore, may be defined as an instrument for determining the moisture content of air (or any gas) by the measurement of the electrical resistance of a hygroscopic material with change in humidity. In line with this definition, instruments that may use electrical meters or recorders or electronic devices in their circuitry, or that may require electric current for their operation, but that do not measure the resistivity or conductivity of a hygroscopic material are not discussed.

It is convenient to classify the sensors, in accordance with their basic principles of operation, into those that depend upon (a) the conductivity of aqueous electrolytic solutions, (b) the surface resistivity of impervious solids, (c) the volume resistivity of porous solids, (d) the resistivity of dimensionally-variable materials, and (e) the temperature of saturated salt solutions. These categories are not necessarily mutually exclusive nor do they include all possible ways in which resistance can be used for humidity sensing. They simply provide a basis for a description and discussion of many of the sensors that are in use or have been proposed.

2. Conductivity of Aqueous Electrolytic Solutions

2.1 General Theory

One type of electric hygrometer sensor is an aqueous solution of an ionizable substance. There are several variations of this type of sensor, but they all have the same theoretical basis of operation. Briefly, the electrical resistance of the sensor is a function of the concentration of the solution which, in turn, is a function of the ambient relative humidity and temperature. Some of the fundamental and theoretical considerations of sensor operation are discussed by Schaffer [1] [1] whereas Evans and Davenport [2] have studied, experimentally, the conduction mechanism.

If a nonvolatile solute is dissolved in water at a constant temperature, the equilibrium vapor pressure will be lowered below the saturation vapor pressure of pure water at that temperature. As the concentration of the solution is increased, the equilibrium vapor pressure is decreased. With many solutes, such as salts, a point is reached at which the further addition of solute to water will produce no further depression of the vapor pressure. The solution, at this point, will be saturated and the equilibrium vapor pressure will remain constant. Under certain conditions, a supersaturated solution can be produced, but, for the purposes of this discussion, it will be assumed the maximum solubility is reached at saturation.

For any given concentration and temperature of an aqueous solution, there is a corresponding equilibrium vapor pressure. If the solution is surrounded by an open space, there will be a continual flow of water vapor into and from the solution. If the vapor pressure of the space is greater than the equilibrium vapor pressure of the solution, there will be a net flow into the solution; conversely, if the vapor pressure of the space is less than the equilibrium vapor pressure of the solution, there will be a net flow of vapor from the solution into the space. This net vapor flow will continue until either the vapor pressure of the space and solution are equalized, or the water is evaporated completely from the solution. If a solution of finite volume is surrounded by an

[1] Figures in brackets indicate the literature references at the end of this Circular.

infinite space of constant vapor pressure, only the concentration of the solution will change until the equilibrium vapor pressure of the solution equals that of the ambient space. The concentration of the solution, at equilibrium, is a measure, therefore, of the ambient vapor pressure or relative humidity. One method of determining the concentration of the solution is by measuring its electrical conductivity. Thus, an aqueous solution of an ionizable material can be utilized as an electric hygrometer sensor.

Some of the factors that influence or control the use, in this fashion, of an aqueous electrolytic solution are as follows:

(a) *Minimum relative humidity.* If the solute has a finite solubility in water, then at saturation, the solution will have attained its minimum relative humidity. If the ambient relative humidity is less than this minimum equilibrium relative humidity of the solution, the water will evaporate leaving only the solute. The equilibrium relative humidity for the saturated solution is the lower operational limit of the solution. Sulfuric acid is miscible with water in all proportions and has no minimum of this kind; this is the reason for its use in some sensing elements. With lithium chloride, a salt that is commonly used in sensors of the electrolytic class, the minimum theoretical relative humidity that may be measured is 14.7 percent at 0° C, 12.0 percent at 25° C, and 11.4 percent at 50° C [3]. With sodium chloride, the minimum theoretical relative humidity, over the range of 0° to 50° C, is 74.7 percent to 75.8 percent [3]. The proper choice of a salt depends, in part, on the minimum relative humidity that the sensor will be expected to measure.

(b) *High relative humidity.* There is a practical upper relative humidity operational limit for the solution. As the relative humidity increases, the dilution of the solution increases, until at a relative humidity of 100 percent, water vapor will be sorbed continually as the solution tends to approach infinite dilution. (In most practical sensors, the solution should not be exposed to a relative humidity of 100 percent.)

(c) *Hydrates.* Many solutes possess the property of forming chemical compounds with their solvents. If the solvent is water, then these compounds are known as hydrates. The formation of a hydrate will occur at a specified temperature and concentration. Solutes which form hydrates will exhibit discontinuities in their equilibrium vapor pressure data at the hydration temperatures. In addition, the solution conductivity at the hydration temperature will change markedly, and during the change, there will be an uncertainty regarding the ambient relative humidity.

(d) *Cryohydric point.* The addition of a nonvolatile solute to water lowers the freezing point of the water. As the concentration of the solution is increased, and the temperature lowered, a point is reached at which the solute is in equilibrium with both ice and liquid water. The maximum depression of freezing point is attained under this condition. The lowest temperature of freezing, for a given solute and water is known as the cryohydric point. If the temperature is decreased below this point, the solution will separate into pure solute and ice. The cryohydric point is the lowest theoretical temperature at which an aqueous solution of a finitely soluble solute can be used as an electric hygrometer.

(e) *Volume.* In theory, there is no limit to the volume of solution that may be employed. In practice, the volume should be kept as small as feasible. A small volume permits the solution to reach concentration equilibrium with the ambient relative humidity much more rapidly than a large volume. A small volume will respond to temperature changes more rapidly, and will affect the atmosphere of a confined space less, which is often an important consideration.

(f) *Polarization.* Either alternating or direct current can be used in the circuit for measuring the conductivity of the solution. If direct current is used, then the solution undergoes electrolysis, and there is a migration of ions to the electrodes. Associated with this migration of ions is the phenomenon of polarization. Polarization may be due to a chemical or physical change on the surface of the electrode, or to the deposition of a film of gas or oxide or other material, or it may be due to a change in concentration of the electrolyte in the neighborhood of the electrode. Polarization manifests itself by a change in the conductivity of the solution with time. If alternating current is used, then electrolysis is eliminated and polarization reduced or eliminated. However, the electrical capacitance of the solution, as well as that of the measuring circuit introduces a complicating factor. The physical dimensions of the solution may be varied to reduce the electrical capacitance and a measuring circuit may be used which balances out this capacitance. Unless this is done, the solution, for low ambient relative humidities, may approach a minimum conductance (maximum impedance).

(g) *Electrodes.* The electrodes employed should be materials that do not corrode or react with the electrolyte. Noble metals are usually the most satisfactory materials for use as electrodes.

(h) *Solution carrier or retainer.* Some convenient means must be provided for physically containing or supporting the solution and the electrodes. Of course an actual volumetric vessel or container may be used for this purpose. The surface of the solution in contiguity with the ambient atmosphere, should be as large as feasible for a given volume. If a vessel or container is used it will be limited usually to a fixed position to avoid spillage. Because of this and other limitations, volumetric containers are seldom, if ever, used. One approach is to apply a thin layer of solution, by brushing, dipping or spraying, to an impervious insulator on which electrodes have

been affixed. Another approach is to disperse the solution in an inert binder of high viscosity or adhesiveness and then to apply a thin film of the resultant mixture to an impervious insulator. Natural or synthetic fibers or fabrics are more or less porous and will absorb and retain liquids. They can be impregnated therefore with a suitable electrolytic solution. In a similar fashion there are inorganic materials that are highly porous and these also can be impregnated with appropriate solutions.

2.2. Electrolytic Solution on Impervious Insulating Surfaces

a. Weaver Water Vapor Indicator

The use of an electrolytic solution on an impervious insulator as a moisture detector was studied as early as 1923 by Weaver and Ledig [4, 5]. They found that of the materials they investigated, sulfuric and phosphoric acids were the most useful, for with these acids, extremely low moisture contents could be detected. However, it was necessary to use alternating current in the measuring circuit to prevent polarization and to mix the electrolyte with gelatin or a similar binder to prevent "creeping" of the film of electrolyte after it has been coated on the surface of a detector. Even with these precautions, the calibration changed so rapidly that very frequent recalibrations were necessary. This method was little used until a need developed for measuring the moisture content of cylinders of compressed oxygen. Weaver and Riley [6] then devised a simple and rapid calibration technique whereby the resistance of the electrolytic film, soon after a measurement, could be translated into a measure of the moisture content.

The detector of the Weaver water vapor indicator comprises two closely spaced concentric platinum electrodes, separated by an insulating material, usually glass, and housed in a high pressure case such as an aviation engine spark plug. A small amount of electrolyte is applied to the detector and wiped across the surface, say, with a clean cloth, leaving a thin film. The detector is then exposed to an atmosphere of unknown humidity and the resistance of the film measured with an alternating current bridge or similar circuit. The detector is now exposed to a gas, such as air, oxygen, or nitrogen, the moisture content of which can be controlled in a known way. This is accomplished by saturating dry gas at a high pressure and expanding to a lower pressure. The pressures are adjusted so that the resistance of the detector in the atmosphere of known water vapor content is identical to that in the atmosphere of unknown humidity. In essence, this is a null method in which an electric hygrometer is used to balance an unknown humidity against a known humidity.

Figure 1 is a simplified flow diagram of the apparatus. A pressure regulator is used to set the pressure in the saturator at any desired value,

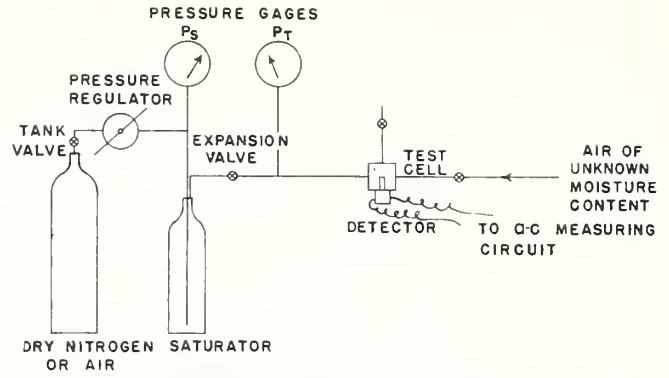

FIGURE 1. *Simplified flow diagram of Weaver water vapor indicator.*

P_S, and an expansion valve reduces the pressure of the saturated gas to P_T. The saturator may be one or more high pressure metal cylinders filled with moistened pumice or gravel. The detector is inserted into a test cell which can be filled either with the test gas of known moisture content or with the atmosphere of unknown humidity. Alternatively, the detector may be inserted directly into the atmosphere of unknown humidity, and after a reading has been made, it then may be inserted in the test cell for calibration.

Assume that the gas of unknown humidity, at an absolute pressure P_i, is expanded to an absolute pressure P_X at which pressure it produces a suitable reading on the detector. Assume also that the desired information is the moisture content of this gas at an absolute pressure P. If the pressure changes occur at constant temperature, and if the water vapor-gas mixture obeys the ideal gas laws, then the moisture content, W, at P is related to the moisture content W_X at P_X by

$$W = W_X \frac{P}{P_X}. \tag{1}$$

Let the gas, used in the calibration procedure, be saturated at an absolute pressure P_S and expanded to an absolute pressure P_C. If the saturation and expansion are isothermal, and if gas ideality is again assumed, then the moisture content W_C, at pressure P_C is related to the moisture content W_S, at P_S by

$$W_C = W_S \frac{P_C}{P_S}. \tag{2}$$

If the resistance of the electric hygrometer, that is, the water vapor detector, is the same at P_C with the gas of known moisture content as at P_X with the gas of unknown humidity, then the moisture contents of these two gases, at their respective pressures are equal, that is, $W_X = W_C$. Therefore, the moisture content of the gas of unknown humidity is obtained by substituting eq (2) into (1) to give

$$W = W_S \frac{P_C}{P_S} \frac{P}{P_X}. \tag{3}$$

The moisture content may be expressed in any of several ways: (a) water vapor density, in mass of water vapor per unit volume; (b) vapor pressure; or (c) relative humidity. The densities and vapor pressures of saturated water vapor are given in standard tables [7] so that for any given temperature, the appropriate value for W_S can be obtained. In terms of relative humidity W_S is always equal to 100 percent.

For many meteorological applications, where the moisture content of atmospheric air is to be measured, the detector will be exposed, usually, to the atmospheric air at atmospheric pressure and its moisture content will be desired at atmospheric pressure. Thus P is equal to P_X and eq (3) reduces to

$$W=W_S\frac{P_C}{P_S}. \tag{4}$$

The quantity of vapor that exists in equilibrium with the liquid or solid phase of water, in the absence of any other vapor or gas, is a function solely of the temperature. In the presence of an inert gas, the nature of the gas and the pressure of the gas influences the equilibrium quantity of vapor. Weaver [6, 8] has shown that for such gases as air, oxygen, and nitrogen, for pressures up to 6,000 psi, and for temperatures of −45° to +38° C, an empirical relation may be used to account for the pressure effect. Thus, eq (3) becomes

$$W=W_S\frac{P_CP(1-KP_C+K'P_C^2)(1-KP+K'P^2)}{P_SP_X(1-KP_S+K'P_S^2)(1-KP_X+K'P_X^2)} \tag{5}$$

and eq (4) becomes

$$W=W_S\frac{P_C(1-KP_C+K'P_C^2)}{P_S(1-KP_S+K'P_S^2)} \tag{6}$$

where

$$K=1.9\times10^{-4} \text{ and } K'=1.4\times10^{-8}.$$

With phosphoric acid as the electrolyte on the detector, moisture concentrations as low as 8 μg of water vapor per liter are adequately measured and moisture concentrations as low as 3 μg/liter can be detected. With sulfuric acid as the electrolyte, concentrations as low as a fraction of a microgram per liter can be detected. In terms of dewpoint with respect to ice, these concentrations are approximately equivalent to dewpoints of −62°, −69°, and −80° C. The thickness of the electrolytic film on the detector is not critical. However, a thick film is more sensitive, and slower in response, than a thin film.

The main use of the Weaver water vapor indicator is to measure low moisture contents, especially the moisture content of compressed gases. Because of the relative instability of calibration of the sensitive film on the detector, the preferred technique for procuring a reliable reading is to calibrate the film immediately after exposure to a gas of unknown humidity. A film may maintain its calibration without appreciable change for 15 min. The indicator can therefore be utilized to follow, for short intervals of time, changing humidity conditions. In general, it is not too well adapted for giving continuous readings of changing moisture concentrations for extended periods of time. The accuracy of this device depends, in large measure on (a) the accuracy of the water vapor content of the test gas at saturation, (b) the accuracy of the pressure measurements, (c) the accuracy of the pressure correction term, and (d) on the absence of moisture sources and sinks within the equipment. In the present state of development, the saturator, test cell, and detector are operated at room temperature. The temperature of these components varies, more or less, with ambient temperature. Errors in the temperature of these components, or differences in temperature, are reflected as errors in the indicated moisture content. For example, an error of 1° C in the temperature of the saturator, or a difference of 1° C between the saturator and test cell or detector that is not corrected for in the computation, will introduce an error of about 6 percent in the measured moisture content at an ambient temperature of about 25° C.

b. Dunmore Hygrometer

In exploring the possibilities of electric hygrometry for measuring the moisture content of the upper air during a radiosonde flight, Dunmore [9, 10] experimented with the use of various electrolytic solutions, such as calcium, zinc, and lithium chloride salts, sulfuric and phosphoric acid, and mixtures of these materials, coated on glass cylinders. As a result, he developed a hygrometer that consisted of a thin wall flint glass tube, 10 mm in diameter, 0.3 mm in thickness, and 12.7 cm long, roughened by sand blasting or etching, and having a bifilar coil of No. 38 AWG bare tinned copper wire, with a pitch of 20 turns per inch, wound on its outer surface. When coated with a dilute aqueous solution of lithium chloride, the resistance of the unit, between the two coil windings, was a function of the ambient relative humidity and temperature. Figure 2 is typical calibration. Although this hygrometer was subject to the same defects as that of Weaver and Ledig, Dunmore found that if he held it at a constant relative humidity prior to use, and calibrated it within a few days of use, it was capable of giving indications accurate to ±5 percent relative humidity. He also found that the long time aging or instability was due to either the oxidation or corrosion of the tinned copper electrodes and that the hysteresis was associated with the roughened surface of the glass. By using platinum or palladium electrodes and a smooth polystyrene base, he was able to improve the performance of the hygrometer so that it held its calibration to within ±3 percent for 6 months.

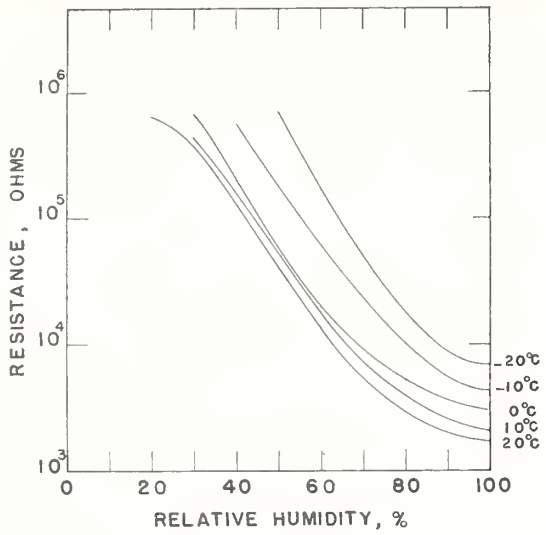

FIGURE 2. *Typical calibration of an electrolytic type of electric hygrometer.*

Roughened glass tube with bifilar coil electrodes coated with 5 percent (by volume of a saturated solution and water) lithium chloride solution. After Dunmore.

c. Larach Hygrometer

Although such electrolytes as lithium chloride, zinc chloride, phosphoric acid, and sulfuric acid have been favored for sensor use, there has been a continuing search for materials which have such improved characteristics as increased sensitivity, less temperature dependence, faster speed of response and less polarization. Solutions of the tetrachlorides of the metals tin, zirconium, hafnium, and lead, have been proposed by Larach [11] for use as sensors. A thin layer of such a solution is applied to an insulator, say a glass slide with fused silver electrodes, and heated at about 80° to 100° C until it partially dries and becomes tacky. A hygrometer element made in this way has a nonlinear relation between the logarithm of the resistance and the relative humidity, as shown in figure 3. The S-shape nature of this curve gives rise to the greatest sensitivity for the middle range of relative humidities and reduced sensitivities for both low and high humidities. The purported advantage of such a sensor is the reduction or elimination of polarization.

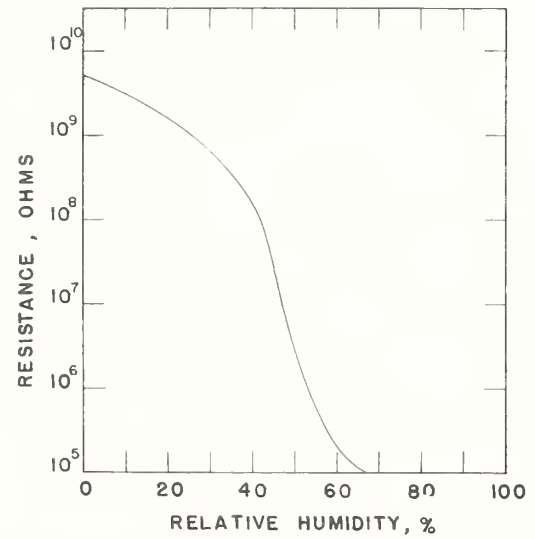

FIGURE 3. *Typical calibration curve of a Larach hygrometer.*

Insulator coated with a solution of the tetrachloride of either tin, zirconium, hafnium, or lead.

d. Gregory Hygrometer

An electric hygrometer has been developed by Gregory [12] in which glass wool yarn, impregnated with an electrolytic solution, is used as the sensitive element. One variant of this sensor is made by winding 9 feet of yarn around four platinum-clad nickel-iron core electrodes. The electrodes are connected in pairs. The yarn consists of 100 fibers, each about 25×10^{-5} cm in diameter; about 0.6 mg of calcium chloride in solution is spread over the yarn. Each fiber of the yarn acts as an impervious insulating surface, but the yarn, to some extent, is partially a porous medium so that solution is held and retained in the spaces between adjacent fibers. Such a sensor exhibits a near linear relationship between the logarithm of the resistance and the logarithm of the relative humidity, as shown in figure 4.

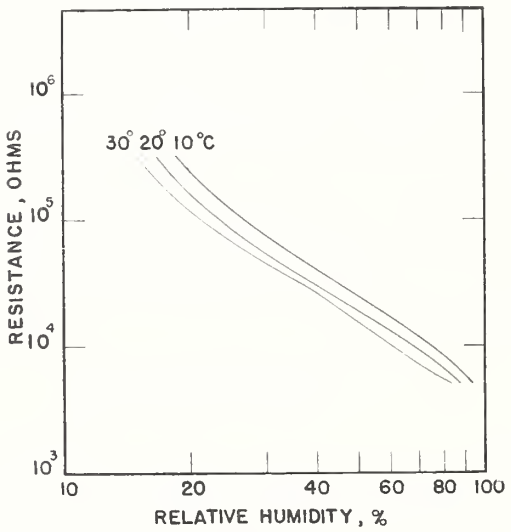

FIGURE 4. *Typical calibration curves of the Gregory hygrometer.*

Glass fibers coated with calcium chloride solution.

The range of this type of sensor has been extended to relative humidities of 1 percent or less by a modification in which the impregnated glass wool yarn is wound on a platinum electrode $\frac{1}{16}$ in. in diameter. A second electrode, comprising a platinum strip 0.001 in. in thickness and 0.01 in. in width is wound over the yarn. The conducting path is across the diameter of the yarn. Such an element can be made with a resistance that varies from 1.5 megohms at 1 percent relative humidity to 8,000 ohms at 10 percent relative humidity. Normal range elements, using the former construction, have been developed that have an over-all size of $10\times6\times6$ mm [13]. These miniature elements are probably accurate to ±2 percent relative humidity. After a discrete change in

relative humidity, at room temperature, the miniature element undergoes a 63 percent change in indication in 2 to 2½ min and a 90 percent change in indication in 3 to 5 min.

2.3. Electrolytic Solutions in Organic Binders

One difficulty with the direct application of aqueous electrolytic solutions to impervious insulating surfaces is the tendency for the solution to break up into globules of liquid, or to move or "creep", particularly when under the influence of such forces as gravity, and even to drip from the substrate surface. In order to keep the solution on the surface, the latter has sometimes been treated to make it rough, as, for example, the sandblasting or etching of glass when it is used as the insulator. If the surface treatment is too extensive, then the insulator may approach the category of a porous medium whereby the solution is retained in pores or capillaries of the insulator. An alternative method can be used to keep the solution on a smooth surface. The electrolytic solution is mixed with a binder, usually organic, that has excellent adhesive properties and the resultant mixture is applied to the insulating surface. What is particularly desired in such a binder is the ability to mix readily with the solution and to permit water vapor to diffuse rapidly through the mixture. A binder which forms a highly pervious structure on drying, and which has proved to be excellently suitable for electric hygrometer sensor use is partially hydrolyzed polyvinyl acetate [14,15]. Another good binder is polyvinyl alcohol [16]. Agar-agar, pectin, gelatin [17], alkyl aryl poly-ether alcohol [18], and methyl methacrylate [6] also have been used as binders. The addition of a binder increases the lag of the electric hygrometer because water vapor has to diffuse through the structure of the binder in order that equilibrium conditions may be attained. On the other hand, the binder may enhance the even distribution of solution on the substrate surface, leading to greater reproducibility between elements fabricated under uniform conditions. Then too, it has been established that a binder may act to reduce polarization, as in the case of partially hydrolyzed polyvinyl acetate and lithium chloride solution films [14]. Elements made with solutions in binders, when not exposed to severe temperature extremes, or to high relative humidities for extended intervals of time, will maintain their calibration and perform well for periods in excess of 1 year.

a. Dunmore Hygrometer

One of the most successful of the electric hygrometers of this type is that developed by Dunmore [14, 15]. In his early researches, Dunmore experimented with aqueous solutions on impervious insulators. It was not until he conceived the idea of combining a dilute aqueous solution of lithium chloride with an alcoholic solution of partially hydrolyzed polyvinyl acetate that he produced an excellent sensor that subsequently found wide application in meteorology and in industrial applications.

The early version of this sensor was made by coating a thin-walled aluminum tube with a polystyrene solution to form an insulating layer over the aluminum. In a later version, the aluminum tube was replaced with a polystyrene tube. A bifilar coil of No. 38 AWG bare palladium wire is wound on the tube; the two wires of the coil act as the electrodes. The unit is coated by dipping into a binder-electrolyte mixture of appropriate concentration and withdrawing at a constant rate. It is then aged under room conditions for 10 to 14 days, or inserted in an atmosphere of gently circulating air at 60 percent relative humidity at 26° C for 2 days. During the aging period, the resistance decreases and settles down to a final value.

By choosing the proper number of turns of wire, pitch, tube diameter, and concentration of lithium chloride, the resistance of the film can be made to vary over an appreciable range for a desired relative humidity range. Sensors have been designed that have the same resistance range, for increments of relative humidity of 16 percent; eight such sensors cover the range of relative humidities from 6 to 99 percent.

For radiosonde use, a single element has been developed that has a resistance range of 4,000 ohms to 6 megohms, as the relative humidity, at 20° C, goes from 100 to 15 percent. This element is a flat sheet of polystyrene, 3 x 1/16 x 1/32 in. with tin electrodes affixed to the long edges by sputtering. The element is coated, by dipping, in a binder and lithium chloride solution mixture. The calibration characteristics of such an element are shown in figure 5. At room temperature, with an air velocity of 768 ft/min parallel to the long edge of the element, the 63 percent speed of response is 3 to 6 sec and the 90 percent speed of

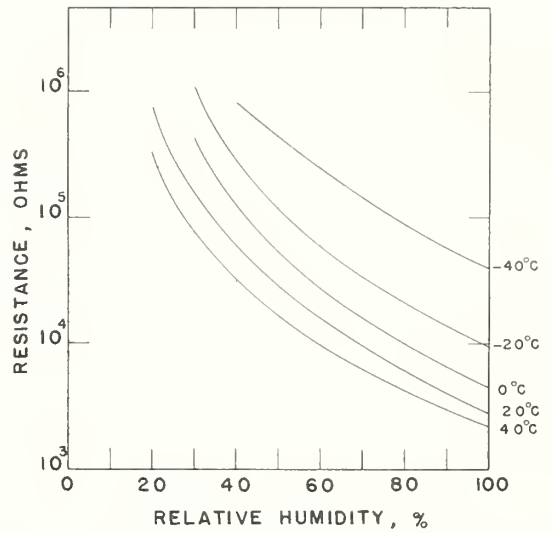

FIGURE 5. *Standard calibration curve of the narrow width, lithium chloride, electric hygrometer element used with the radiosonde.*

response is 25 to 35 sec. Temperature has a marked effect on the speed of response. At −20° C, the 63 percent speed of response, at air velocities of 525 ft/min is 50 to 150 sec [19]. Actually, the speed of response is an involved function of temperature, magnitude and direction of the relative humidity change, initial relative humidity, orientation of the element, and air velocity [19, 20].

The Dunmore hygrometer is manufactured commercially for industrial and scientific applications in both tubular and flat strip forms [21, 22, 23]. Units have been designed for special applications where small size is important [24, 25].

2.4. Electrolytic Solutions on Fibers and Fabrics

Most organic fibers are somewhat porous and have a capacity for absorbing liquids. When fibers are woven into fabrics, not only do the fibers absorb liquids, as they would singly, but the interstices between the fibers of the fabric can retain additional liquid. This ability of fibers and fabrics to absorb liquids lends itself readily to electric hygrometry, for an electrolytic solution can be used to impregnate these materials and so form humidity sensors. The fiber or fabric acts as a carrier for the solution. At the same time, it also inhibits the rapid equilibrium between ambient humidity and solution concentration, for as with the binder discussed above, water vapor has to diffuse through the capillaries within the fiber and the interstices between fibers.

It is possible to utilize such natural fibers as hair, cotton, silk, or such synthetic fibers as rayon, nylon, or saran [18]. Further, fabrics from these fibers or materials such as paper or asbestos cloth are suitable bases for treatment with electrolytic solutions [26, 27, 28, 30, 32, 33]. The electrolyte must be one that will not react with the base material. O'Sullivan [29] has been demonstrated that the conduction of cellulosic materials impregnated with salt is ionic.

a. Gregory Hygrometer

The Gregory hygrometer is an example of how an electric hygrometer of the salt-impregnated fabric type can be made and of how it may be expected to perform [30, 31, 32, 33]. In the version used by Ogden and Rees [33], a thin, grey, rectangular piece of cotton fabric, is boiled in a 1-percent solution of lithium chloride and allowed to air dry. This material is clamped, along each long edge by a thin piece of copper foil, leaving a narrow strip of exposed fabric $\frac{1}{8}\times 1$ in. Contact and adhesion between the copper foil and the cloth is increased by using colloidal graphite as a bonding agent. The copper foil strips serve as electrodes. The weft threads are removed from the fabric to increase the porosity and improve the speed of response of the element. Copper wires are attached to the electrodes to function as leads, and both the wires and electrodes are insulated by coating with polystyrene cement. Figure 6 is a sketch of the unit.

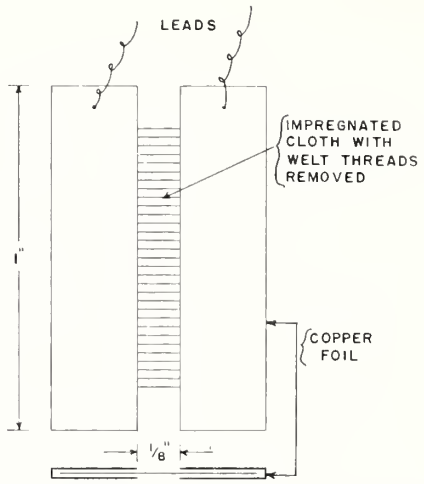

FIGURE 6. *Ogden and Rees version of the Gregory hygrometer.* Cotton fabric impregnated with one percent lithium chloride solution. Copper foil electrodes.

A typical calibration curve for the hygrometer is shown in figure 7. There is a hysteresis effect and a temperature effect on the calibration. It is claimed that an accuracy of ±2 percent can be obtained from this hygrometer.

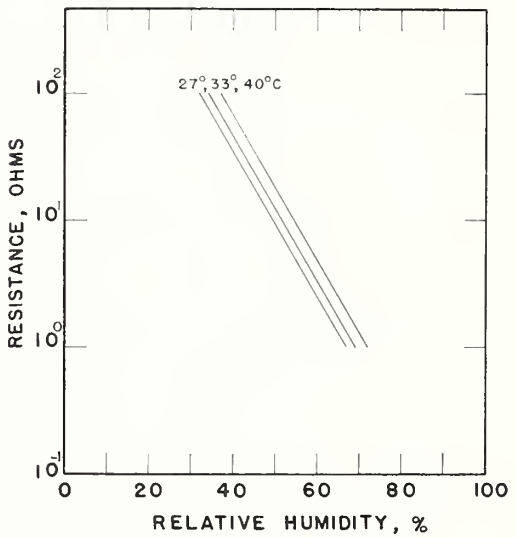

FIGURE 7. *Typical calibration of the Ogden and Rees version of the Gregory hygrometer.*

2.5. Electrolytic Solutions in Porous Ceramics

A porous ceramic can be impregnated with a salt solution to form a sensor in which the current flow is ionic. Such a sensor has been developed by White [34]. The core for this element is pure low-fired alumina. It is saturated with a solution of a salt such as lithium chloride or sodium dichromate. Two helical spiral coils of small diameter platinum wire are wound on the surface and so arranged that current can flow from coil

to coil, in proportion to the resistivity of the impregnated core, and a heating current can be passed through one coil to raise the temperature of the core. The circuit is shown in figure 8. In this way, the temperature of the core can be adjusted to any desired value above ambient;

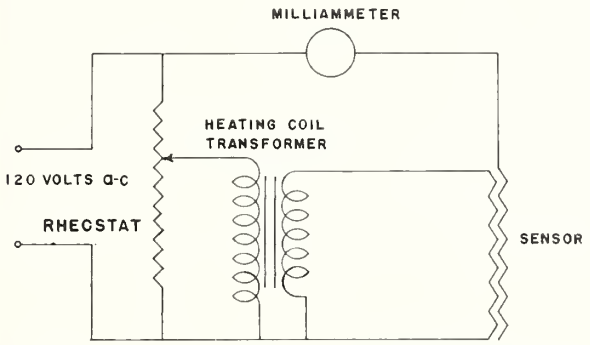

FIGURE 8. *Circuit diagram of the White hygrometer.*
Porous low-fired alumina core impregnated with salt solution.

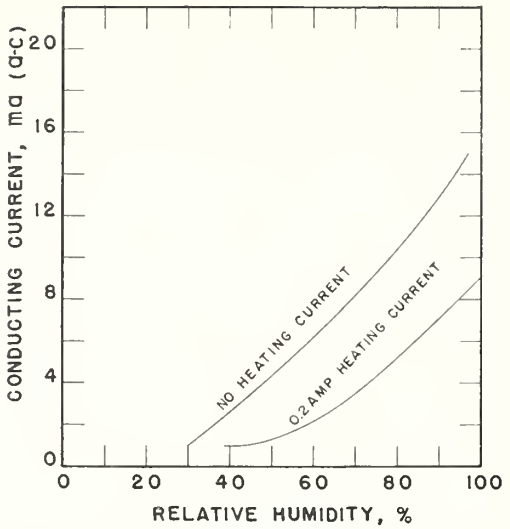

FIGURE 9. *Typical calibration curves for the White hygrometer.*

yet the sensor still functions in the usual fashion by a variation in resistance with relative humidity. Typical calibration curves, with and without heating current, are shown in figure 9. Within limits, variations in electrical characteristics from element to element, changes in ambient temperature, line voltage, and heater currents produce curves that are nearly parallel. This facilitates the use of slight changes in heater current to compensate for most of the variables encountered.

The speed of response of the sensor is a function of ambient temperature and relative humidity. For high humidities and high temperatures, it is several minutes; at temperatures around 0° C and relative humidities under 30 percent, it is 1 hour or even longer.

3. Surface Resistivity of Impervious Solids

3.1. General Theory

The surface resistivity of some impervious materials, in particular, electrical insulators such as glass, porcelain, and plastics, varies in a marked way with ambient relative humidity. Water vapor is adsorbed on the surface of these materials, and retained by physical bonding forces, forming a thin film whose thickness, and possibly continuity, is a function of the relative humidity. This film of moisture provides a leakage path for current flow. There probably are minute quantities of soluble salts or gases present on the surface of the insulator which contribute to the conductivity of the film. The net effect is that the surface resistivity may decrease six or more decades as the relative humidity of the surrounding air increases from 0 to 100 percent. Because the material has an impervious surface, little or no water vapor will penetrate or diffuse into the body. The water vapor that is sorbed remains on the surface. It is to be expected, therefore, that the attainment of equilibrium between adsorbed water vapor and ambient relative humidity will be relatively fast. Materials normally classified as impervious are seldom completely so; there is usually some diffusion of water vapor into or out of the interior. Diffusion is a relatively slow process. Thus, a material may exhibit an initial fast response to a change in relative humidity, but also the time for reaching final equilibrium may be prolonged by the slow diffusion of a small amount of vapor.

The magnitude of the surface resistivity of an insulator is very high. This requires the use of special measuring circuits and techniques. Provided one can measure the high resistances involved, impervious insulators form a class of electric hygrometer sensors that are especially useful where fast response is needed.

3.2. Nonporous Insulators

One of the first to propose the use of an impervious insulator as a moisture detector was Pionchon [35]. His device was a glass tube, with silvered electrodes. With a voltage impressed across the electrodes, a galvanometer was able to detect the flow of current when the detector was moved from a dry to a moist atmosphere. Curtis [36] and Field [37] investigated the surface sensitivity properties of a large variety of insulating materials and showed that the resistivity decreased through several orders of magnitude as the relative humidity increased from 0 to 100 percent. These studies indicated that some materials take hours or days to reach equilibrium, due to their porous structure. The laws of film

formation on glazed surfaces appear to be logarithmic [38].

Lubach [39] and Polin [40] proposed hygrometers that use glass, porcelain, glass wool, hard rubber, and ceramics as moisture sensors. Dunmore [10, 11] attempted to use glass tubing, roughened by sandblasting or etching, and wound with a bifilar bare copper wire coil for electrodes, as a sensor. Although he found that he obtained usable indications from such a sensor, he discarded it in favor of the electrolytic solution. Edlefsen [41] proposed the use of glass wool, in a cell with electrodes, for measuring relative humidity. A hygrometer employing a glass wool cell as a detector now appears to be commercially available [42]. This instrument has a relative humidity range of 42 to 100 percent, a temperature range of −40° to 80° C, and a corresponding resistance range of 100 megohms to 40,000 ohms.

3.3. Salt Film

Consider a thin film of salt deposited on an insulator and exposed to a constant relative humidity. If the ambient relative humidity does not exceed the equilibrium relative humidity of a saturated solution of the salt, then the film will sorb only enough water vapor that can be held by physical bonding forces. The quantity of adsorbed water vapor will be a function of the ambient relative humidity. The resistance of the film will be a measure of the ambient relative humidity.

A sensor of this type has an upper limit equal to the equilibrium relative humidity of the saturated solution of its salt. Thus, if the sensor is to be exposed to the full range of relative humidities, the salt should have an equilibrium relative humidity that is as close to 100 percent as possible. This implies that the salt should be practically insoluble in water. Even though the salt may be insoluble in water, or the sensor never exposed to relative humidities equal to or greater than that of the saturated solution of the salt, it is probable that some molecules of the salt ionize in the adsorbed water vapor and therefore contribute to the measured conductivity of the surface film.

Salt films, used in the manner described above, have been proposed or developed as electric hygrometer sensors by McCulloch [43], Auwarter [44], and Wexler et al. [45]. Anderson [46] had used a bead of calcium chloride, containing two copper wire leads separated by a 1 mm gap as a moisture detector. In a dry atmosphere, the resistance was 30,000 ohms; in the presence of water vapor the resistance dropped to 200 ohms. Fiene [47] designed detectors made with fused salt. He utilized the increased conductivity of the detector, when it formed a saturated solution, to designate the ambient relative humidity. Both Anderson and Fiene relied on the pronounced change in the resistance of a soluble salt, as it went into solution, and in this respect their sensors differ from those of McCulloch, Auwater, or Wexler et al.

a. McCulloch Hygrometer

The McCulloch sensor [43] consists of a coating of beryllium fluoride applied to a Pyrex tube on which there is a bifilar coil that functions as electrodes. The electrodes, 0.002-in. diameter nickel wire, are wound on a ¾-in. diameter Pyrex tube. Each electrode has 10 turns of wire and the two electrodes are spaced ¾-in. apart. The tube is dipped in a boiling 3 percent aqueous solution of beryllium fluoride, dried, and baked at about 300° C. The calibration of this sensor is shown in figure 10. The resistance at 97 percent

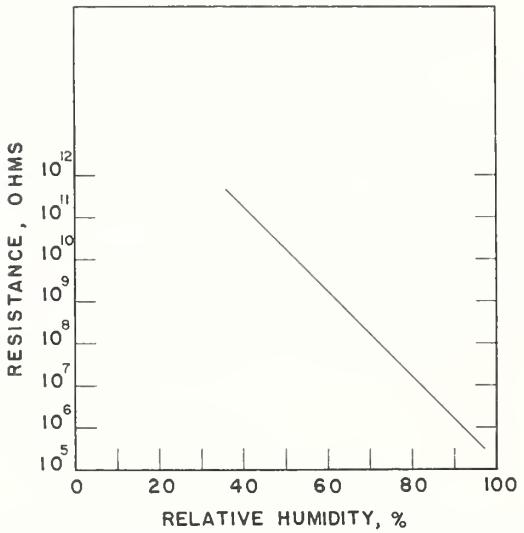

FIGURE 10. *Calibration curve of the McCulloch hygrometer.* Beryllium fluoride film on Pyrex.

relative humidity is about 3×10^{5} ohms and at 30 percent is about 10^{12} ohms.

b. Auwarter Hygrometer

In the Auwarter hygrometer [44], a thin film of a metallic fluoride, such as magnesium fluoride, aluminum fluoride or cryolite, is deposited, in vacuum, upon an impervious insulating material with spaced metallic electrodes. The film so formed has a thickness of the order of 4×10^{-4} to 10^{-5} in. The logarithm of the resistance, except at low relative humidities, is a linear function of the relative humidity. A speed of response, at room temperature, of less than 1 sec, is claimed.

c. Wexler et al. Hygrometer

In investigating the possibilities of improving the means for upper air humidity sensing with the radiosonde, Wexler and his associates [45] developed a fast responding hygrometer that uses, as the moisture sensitive material, a thin film of potassium metaphosphate deposited on an insulat-

ing base. In one form of the sensor, potassium metaphosphate is vacuum deposited on a glass slide, $3\times\frac{1}{2}\times\frac{1}{32}$ in., that contains parallel silver electrodes, $\frac{1}{8}$ in. wide, along the long edges. The thickness of the film is about 3 μin. Figure 11

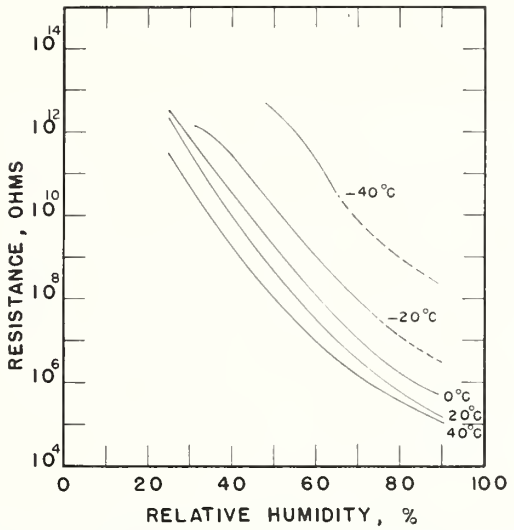

FIGURE 11. *Calibration of the fast responding potassium metaphosphate film hygrometer developed by Wexler et al.*

shows the calibration curves of this sensor for the temperature range of −40° to +40° C. The logarithm of the resistance is approximately linear with relative humidity at constant temperature. The resistances vary from 4×10^4 to 10^{13} ohms. The manufacturing process is sufficiently well controlled so that elements, made in the same or in different batches, closely conform to a mean calibration curve. The standard deviation of an individual element from the mean calibration, over the −40° to 40° C range, is 2.9 percent relative humidity. The average hysteresis is 2.7 percent relative humidity. The polarization effect for reversed current loading (1-min cycles) is of the order of 0.3 percent relative humidity at the end of 2 hours; it is of the order of 2 percent for intermittent direct current loading (15 sec on, 45 sec off). The speed of response at room temperature, with an air velocity of 768 ft/min parallel to the long edge of the sensor, is about 0.1 to 0.4 sec for a 63 percent change in indication; at −20° C, with an air velocity of 800 ft/min, it is about 2 to 3½ sec.

3.4. Oxide Film

a. Jason Hygrometer

Oxide layers can be formed on aluminum by anodization in acid electrolytes. These layers can be made porous in which state they offer a large surface area for the sorption of water vapor. As the water vapor is adsorbed or desorbed from the oxide film, there is a corresponding change both in its capacitance and resistance. This phenomenon has been utilized in the development of a capacitance-resistance hygrometer [48, 49, 50, 51, 52, 53].

Any method of anodizing which yields porous aluminum oxide films will produce sensitive elements; nonporous films show no great variation of capacitance or resistance with humidity change. After formation, aging occurs during which time the capacitance decreases and resistance increases until stabilization is attained. Elements formed in sulfuric acid still exhibit an appreciable sensitivity whereas those formed in other acids or by other processes appear to have lost their wide response to relative humidity.

Koller [53] was one of the first to propose the use of oxide films on metallic substances as humidity sensors. His element is made by electrolytically anodizing a plate of aluminum in sulfuric acid to form an oxide film 0.0004 in. thick. Gold leaf, 4 μin. thick, is placed over the oxide film and electrical leads are attached to both the leaf and the substrate.

A typical Jason sensor [49] is made by degreasing an aluminum rod, anodizing one end, and thoroughly washing off the electrolyte. The untreated surface is coated with an insulating layer which is made to overlay the oxide layer slightly. A thin porous conducting material is deposited over the oxide and extended over the insulation. This porous material may be a thin film of a colloidal suspension of carbon, or it may be a thin film of metal chemically or vacuum deposited. Wires are attached to the aluminum rod and porous conducting film, the rod and film being the electrodes of the element. The construction is shown in detail in figure 12.

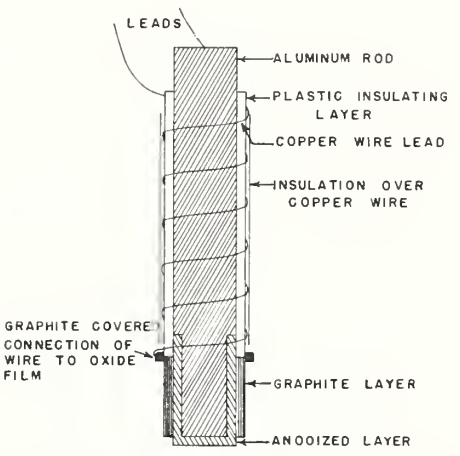

FIGURE 12. *Construction of the Jason hygrometer.*

The capacitance and resistance, as a function of relative humidity, are shown in the curves of figure 13. Cutting et al. [49] claim that the sensor is almost independent of temperature from 0° to 80° C. Underwood and Houslip [50] have

574278 O - 61 - 47

found a pronounced temperature effect. With care in the construction, elements anodized simultaneously have the same calibration curve. At relative humidities of 90 percent or more, the response is slow and there is a small irreversible drift. This gives rise to positive hysteresis on returning to lower relative humidities. Prolonged exposure to saturation destroys the sensitivity of the element. Applied voltages greater than 80 percent of the formation voltage cause temporary breakdown of the oxide. Surface contamination by oil or grease interferes with proper performance.

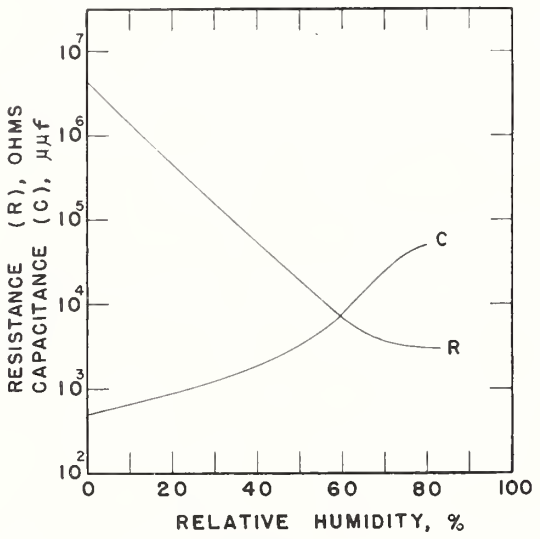

FIGURE 13. *Typical calibration of a Jason hygrometer.* Aluminum oxide film on aluminum rod.

3.5. Ion Exchange Resins

A conventional ion exchange resin [54] consists of a high polymeric, cross-linked structure containing as an integral part of its structure polar groups of positive or negative charge (anion and cation exchangers, respectively). Associated with these polar groups are ions of opposite charge which are held by electrostatic forces to the fixed polar groups. One feature of such a resin is that it is hydrophilic. In the presence of water or water vapor, the electrostatically held ions become mobile, and, when a voltage is impressed across the resin, the ions are capable of electrolytic conduction. Materials such as cross-linked phenol formaldehyde, resorcinol formaldehyde, phenol furfural, cresol formaldehyde, xylenolformaldehyde, divinylbenzene-polystyrene copolymer, and similar high polymeric cross-linked plastics are capable of being made into ion exchange resins by suitable treatment with a variety of reagents including concentrated sulfuric acid, fuming sulfuric acid, sulfur trioxide and chlorosulfonic acid. As an example, polystyrene can be treated with sulfonic acid whereby the sulfonic radical is made an integral part of the structure whereas the hydrogen ion (anion) is bound to the radical by electrostatic forces. Any cation which will satisfy the condition that the resin be electrostatically neutral can take the place of, or exchange with, the hydrogen ion. Hence the name ion exchange resin.

a. Pope Hygrometer

An ion exchange resin can be adapted to humidity sensing, as demonstrated by Pope [55], for it sorbs water vapor from the ambient atmosphere and eventually reaches an equilibrium state with the surrounding relative humidity. Because such a resin is a highly porous material, water vapor will move through it by diffusion. Thus, if used in bulk form, an ion exchange resin would respond relatively slowly to changes in ambient humidity. However, rather than using it in bulk form, a thin layer is formed on the surface of, and integral with, the parent polymer. A base is chosen that is thermally stable and is a nonconductor. The surface is hygroscopic, insoluble in water, and electrically conductive. The principal difference between the base and the surface layer is that the latter contains polar constituents with electrostatically attached ions that have ion exchange properties. Electrodes can be attached to the surface of the resin to form the humidity sensor.

A typical hygrometer element is made from a rod of polystyrene which is submerged in concentrated sulfuric acid, at 100° C, using 0.5 percent, by weight, silver sulfate as a catalyst. The time of sulfonation may be varied from 1 to 60 min. depending on the conductivity desired at a given relative humidity. The greater the sulfonation time, the thicker the layer formed, and the slower the speed of response. After sulfonation, the rod is rinsed with water, boiled in sulfuric acid for 1 hour, rinsed again with distilled water, and air dried. Electrodes are added by painting with conductive metallic paint. Typical calibration curves, for elements made in this fashion, for different sulfonation times, are shown in figure 14. Figure 15 indicates the effect of temperature on the calibration.

Among the interesting characteristics of this type of hygrometer are the following: (a) the relative permanence of the sensitive surface layer when compared against films of electrolytic solution; (b) the ability of the element to operate at temperatures as high as 100° C; (c) the possibility of washing the surface with water or, perhaps, steam, if contamination interferes with the performance; and (d) the control of resistance range and speed of response by control of the sulfonation time, i. e., by control of the thickness of the porous layer of ion exchange resin.

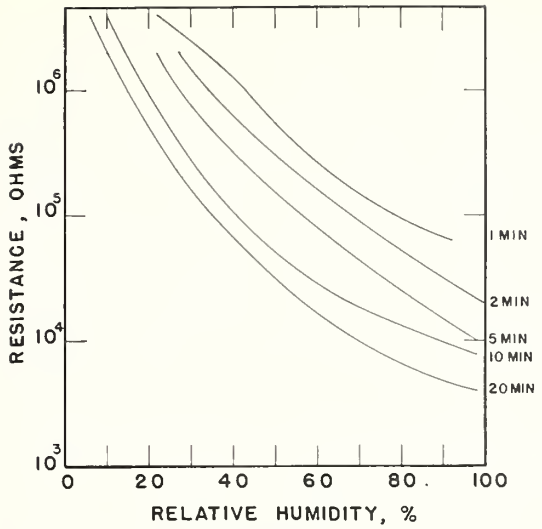

FIGURE 14. *Typical calibration, at 25° C, for the Pope hygrometer.*
Polystyrene base sulfonated for various times.

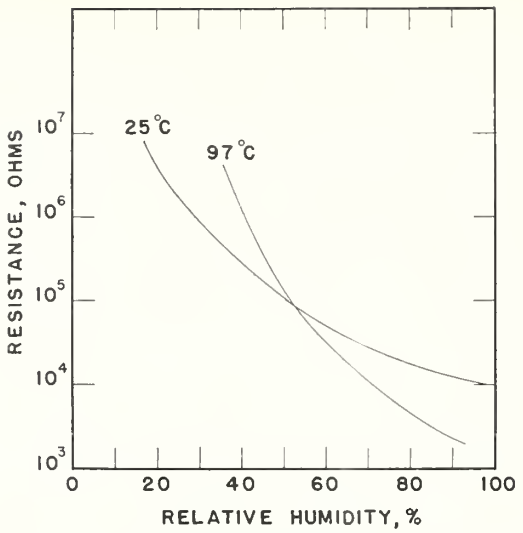

FIGURE 15. *Effect of temperature on the calibration of the Pope hygrometer.*
Polystyrene base sulfonated one hour.

4. Volume Resistivity of Porous Solids

4.1. General Theory

In a manner analogous to the use of the variation of the surface resistivity of impervious solid insulators with ambient relative humidity, the variations of the volume resistivity of some porous materials with ambient relative humidity can be utilized for humidity sensing. There are many substances that absorb water vapor, but relatively few that do so with sufficient reversibility and reproducibility [56, 57, 58]. Highly porous substances, as, for example, underfired clays, natural fibers, and textiles, have a high capacity for moisture absorption. Water vapor diffuses and permeates into the capillaries and pores of these substances, greatly affecting their volume resistivities. Unfortunately, the porous nature of these materials, which makes them so highly hygroscopic, often contributes undesirable characteristics that seriously detract from their usefulness as sensors. For one, the time involved for a porous material to reach equilibrium with any change in relative humidity is often excessively long. Then too, a porous material too often possesses hysteresis and drift. In spite of their shortcomings porous solids find some application as electric hygrometer elements.

4.2. Porous Insulating Materials

The variations in resistance of porous materials with relative humidity were first investigated because of their bearing on the insulating properties of dielectrics. Evershed [59], Curtis [36], and Kujirai [60] studied a large number of substances and determined that, in general, such materials decreased in resistivity by many orders of magnitude as the relative humidity increased from 0 to 100 percent. Further studies were made, not only on bulk insulating materials but also on textile materials and individual fibers [61, 62, 63, 64, 65, 66, 67]. The application of such materials to electric hygrometry was attempted in 1921 by Barr [68]. He made a sensor by gilding a glass tube, wrapping cotton around the tube, then winding gilt wire over the cotton. One model of this sensor has a resistance of 850 ohms at 90 percent relative humidity and 780,000 ohms at 33 percent relative humidity. The logarithm of the resistance is nearly linear with relative humidity. The lag is considerable. Parsons and Laws [69] used a piece of leatheroid wound around a metal cylinder; a bare metal wire is wound over the leatheroid and the resistance between it and the metal cylinder is used as an indication of ambient relative humidity. Burbridge and Alexander [70] devised hygrometers from both cotton and human hair. A layer of pure cotton wool, thin enough to be semitransparent, is placed between two electrodes in the form of a grid, as shown in figure 16. At constant temperature, the logarithm of the resistance is

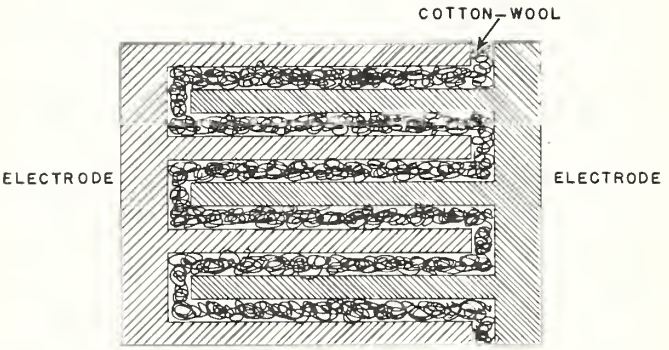

FIGURE 16. *Burbridge and Alexander cotton-wool hygrometer.*

linear with relative humidity. The resistance varies one decade for each 20 percent change in relative humidity. The lag is a function of the thickness of the layer; for one design of sensor, this is of the order of 5 to 6 min in air stirred by a fan. The hysteresis is about 2 percent. The hair hygrometer uses hair degreased by repeated extraction with alcohol. The logarithm of the resistance is nonlinear with relative humidity; the change in resistance is small in the 0 to 50 percent relative humidity range and greater at higher relative humidities. An alternate form of cotton sensor was proposed by Starkins [71]. Two separate lengths of cotton-covered copper bell wire are wound on a porcelain tube to form a bifilar coil. The copper wires act as electrodes and the cotton insulation changes its resistance with ambient relative humidity.

Both Cleveland [17] and Kersten [72] use hydrophilic gels as the humidity responsive material. Typical gels are gelatin, pectin and agar-agar. Films of gels are deposited on a rigid insulator or on clear photographic film containing electrodes.

Lichtgarn [73, 74] and others [75, 76, 77] have used underfired clays, sintered ceramics, and plaster of Paris. These are highly porous materials that are able to absorb relatively large amounts of water vapor. They can be fabricated in a diversity of shapes and forms. An attempt is usually made to devise an element that has as large a surface area, for a given volume, as practical. A sintered ceramic block $4\times3\times2$ mm, is able to change in resistance from 1,000 megohms to 1 megohm for a relative humidity change of 10 to 95 percent [77].

5. Resistivity of Dimensionally-Variable Materials

5.1. General Theory

There is a class of electric hygrometer sensors that depends on dimensional changes to produce changes in resistance. Many materials change in length or volume or both as they absorb or desorb water vapor. The classic examples are hair, vegetable fibers, and wood. These materials are used in hygrometry to actuate mechanical systems that move pointers over dials for indicating relative humidity, or operate switches in humidity control systems. Materials, dimensionally-variable with relative humidity, may be coated or impregnated with conductive substances. The latter will expand or contract as the humidity sensitive materials expand or contract. By the proper choice of the conductive substance, a measurable change in resistance is achieved. Consider a film whose conductivity depends on the presence of discrete particles of carbon, metal dust, or other electronic (as opposed to ionic) conducting medium. As the film expands, the particles separate and the resistance increases; as the film contracts the reverse occurs. Dimensionally-variable humidity sensitive materials expand with increasing relative humidity and contract with decreasing relative humidity. A particle type of conducting film or conducting impregnation on such a material will therefore increase in resistance with increasing relative humidity and decrease in resistance with decreasing relative humidity. This behavior is the inverse of that observed with electrolytic-film sensors, surface-resistivity sensors, or volume-resistivity sensors. Now, in addition to the change in resistance due to the dimensional changes in the conducting film or impregnation, there is the resistance change in the humidity sensitive base material. Thus the resistance of this humidity sensor is made up of two parallel resistances. As one increases, the other decreases. Depending on the relative magnitudes of these two resistances, the measured resistance may be monotonic with relative humidity, or it may go through a maximum so that a single value of resistance may correspond to either of two relative humidities.

5.2. Carbon Element

Dimensionally-dependent resistance sensors were made by Welco [78] using, for hygroscopic materials, hair, cellophane, and paper and coating them with India ink. The cellophane and paper elements were 20 cm$\times$1.25 cm whereas the hair element consisted of 27 segments in parallel, each 2.5 cm in length, degreased by boiling in ethyl ether. These sensors had limited humidity and resistance ranges.

Smith and Hoeflich [79] have described the development of a carbon film hygrometer element that uses a plastic binder as the material that is dimensionally variable with relative humidity. A polystyrene strip, 100 mm long, 18 mm wide, and 1.2 mm thick, serves as the blank on which the sensitive film is deposited. There are two metal (tin) electrodes along the long edges. The clear space between the electrodes is 11 mm. A mixture composed of 45 percent carbon, 32 percent hydroxyethyl cellulose, 16 percent polyoxy ethylene sorbitol, and 7 percent alkyl aryl polyether alcohol is sprayed on both sides of the blank. The hydroxyethyl cellulose functions as a binder. It changes its volume with relative humidity and in doing so, alters the relative positions of the conducting carbon particles. The polyoxy ethylene sorbitol is a humectant type plasticizer that modifies and controls the sensitivity of the element. The alkyl aryl polyether alcohol is a non-ionic dispersing agent which is needed to insure a uniform distribution of carbon in the film.

The calibration for a typical carbon film hygrometer element is shown in figure 17. The element has low sensitivity at low relative humidities. As the relative humidity increases the sensitivity increases. At relative humidities of 80 percent or

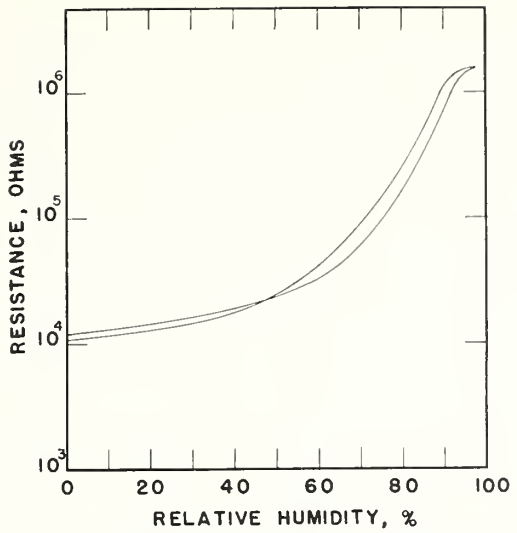

FIGURE 17. *Calibration curve for a typical carbon film sensor at temperatures between 0° and 40° C.*

above, there is a decided tendency for the calibration curve to have a "hump," that is, to undergo a reversal so that for a range of resistances, there are two values of relative humidity for each value of resistance. To avoid this "hump" requires the careful elimination of even small traces of ionic substances. Thus, in making elements of this type, deionized or freshly distilled water is used, the dispersing agent is cleaned by dialysis, and the binder is specifically prepared to be free of ionic content.

With this element, there is an average hysteresis of about 5 percent relative humidity, the hysteresis being more pronounced at lower relative humidities. There is relatively little polarization. This is due, possibly, to the fact that the mechanism of conduction is primarily electronic rather than electrolytic. The speed of response, at $-20°$ to $-30°$ C, for a 90 percent change in indication, is about 30 to 60 sec.

When the element is exposed to atmospheric air over a period of time, it tends to acquire impurities and to shift in calibration. For such long time exposures, a protective moisture-permeable envelope should be used. There is, of course, an accompanying large increase in lag, for now the moisture has to diffuse through the envelope.

6. Temperature-Controlled Saturated Salt Solutions

6.1. General Theory

Consider a saturated salt solution in a closed space. If equilibrium conditions prevail, the partial pressure of the water vapor in the space will be uniquely determined by the temperature, as the temperature of the solution is increased from its freezing point to its boiling point. At any given temperature, this partial pressure will be less than the saturation vapor pressure of pure water. Now let the saturated salt solution, at some given temperature, be exposed to an ambient atmosphere having a higher vapor pressure than the equilibrium vapor pressure of the saturated salt solution. Normally, there will be a net flow of vapor from the ambient atmosphere to the saturated salt solution, with a dilution of the latter until the vapor pressures are equal. On the other hand, if the temperature of the saturated salt solution be increased, a point will be reached where two vapor pressures will be equal whereas the solution will remain at the same concentration. A measurement of this temperature determines the ambient vapor pressure. Similarly, if the saturated solution, at some given temperature, is exposed to an ambient atmosphere with lower vapor pressure than the equilibrium value of the saturated salt solution, the temperature of the latter can be reduced until the two vapor pressures are equal, and a measurement of the solution temperature determines the vapor pressure. If there were some means for determining when the vapor pressures equalize it would be possible to use the temperature of the saturated salt solution as a hygrometric indicator.

The conductivity or resistance of a salt solution is a good indicator of its concentration. As the concentration increases or decreases, the resistance increases or decreases. Now, consider a saturated solution in which suitable electrodes are arranged so that its resistance may be measured. If the vapor pressure of this solution is in equilibrium with the ambient atmosphere, then the resistance remains constant; if the vapor pressure of the solution is greater than that of the ambient atmosphere, water vapor will evaporate and the resistance will increase; and conversely, if the vapor pressure of the solution is less than that of the ambient atmosphere, water vapor will be sorbed by the solution with a corresponding decrease in resistance. By adjusting the temperature of the saturated solution, a point will be reached at which the resistance remains constant. The temperature of the solution is now a measure of the ambient vapor pressure.

6.2. Dewcel

The temperature-controlled saturated solution principle has been successfully utilized in a form of hygrometer known as the "dewcel" [80]. A thermometer bulb (usually of the resistance or vapor pressure type) is surrounded by a glass wool wick impregnated with a saturated solution of lithium chloride. Two silver wire electrodes are wound on the outside of the wick to form a bifilar coil. Alternating current is impressed across the electrodes, through a ballast tube, as shown in the circuit diagram of figure 18. The flow of current through the solution generates enough heat to raise the temperature of the device. As the temperature increases, water evaporates

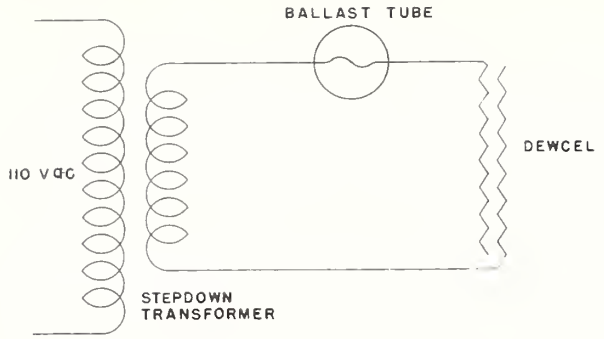

FIGURE 18. *Circuit diagram of the "dewcel" hygrometer.*

from the solution, the resistance increases, the current decreases, and the heat generated by the current flow decreases. The device then tends to cool because of the decrease in heat input. Thus, the application of current to the saturated solution provides automatic temperature control. The solution attains a temperature that corresponds to a constant resistance, which, of course, means that the solution and ambient vapor pressures are equal. The temperature, as measured by the thermometer, can be indicated or recorded.

Figure 19 is a plot of the vapor pressure, as a function of temperature, of pure water and of a saturated solution of lithium chloride. These curves show the relation between the measured dewcel temperature, the ambient vapor pressure and the ambient dewpoint. For example, if the equilibrium temperature of the dewcel is 51° C, then the ambient vapor pressure is 10 mm of Hg, as obtained from the lithium chloride curve. The dewpoint is read from the ordinate, by intersecting the water curve at the same vapor pressure. For the above case, the dewpoint is 11° C.

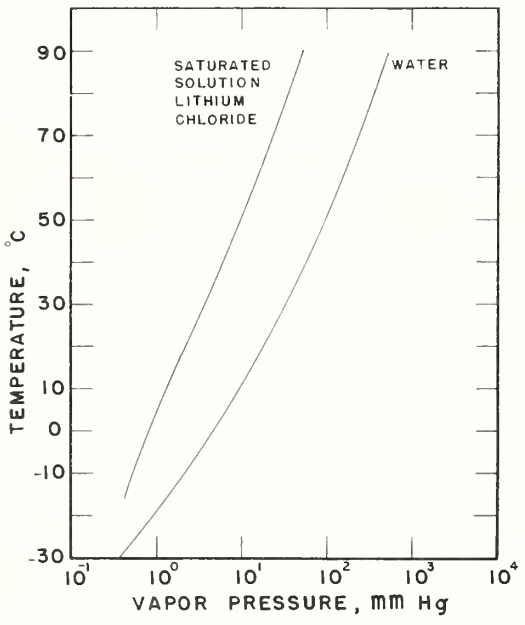

FIGURE 19. *Vapor pressure as a function of temperature, for water and a saturated solution of lithium chloride.*

There are several important considerations regarding the design and use of the dewcel. The speed of response of the unit depends primarily on the rate at which it can be heated or cooled. Hence, the thermal mass must be small if high lags are to be avoided. When the dewcel is exposed to high ambient vapor pressures, with no power across the electrodes or after a power failure, all the salt may dissolve to form a dilute solution. The wick must be of sufficient absorbency to retain the salt and to prevent any loss from dripping. However, if there is a loss of salt, it can be easily replenished without disturbing the fundamental calibration. After a period of inoperation, and particularly after applying fresh solution or exposure to high humidity, the resistance of the solution may be relatively low. On applying current to the electrodes, there may be a high enough flow of current to damage the structure. To avoid this, a ballast resistor is used in the input circuit as a current limiting device. The dewcel functions best in still, or near still air. High air speeds, say above 50 ft/min conducts too much heat away from the device, lowering the equilibrium temperature and shifting the calibration.

There is a limited range of humidities that the dewcel can measure at any ambient temperature. This range in terms of relative humidity, extends from 100 percent to the equilibrium value of the saturated salt. At room temperature, the range is 100 to 11 percent; at lower temperatures, the range narrows as indicated in the curve of figure 20. The lowest ambient temperature, at which the dewcel will operate is, theoretically the freezing point of a saturated solution of the salt, that is −80° C. Actually, the practical minimum temperature is about −29° C (−20° F).

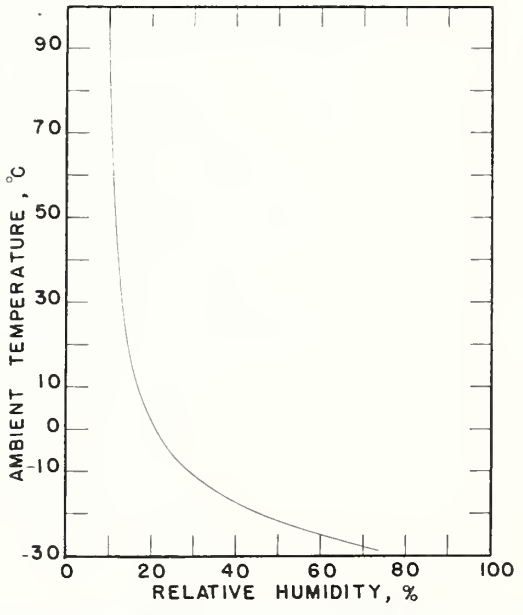

FIGURE 20. *Minimum relative humidity that can be measured with the "dewcel" at various ambient temperatures.*

The dewcel has been investigated for its applicability to meteorology [81]. The accuracy of the instrument is about ±3° F in dewpoint. The speed of response is 0.8 to 3.5 min for a 98 percent change in indication.

6.3. Wylie Hygrometer

A form of hygrometer has been proposed by Wylie [82] which differs from the dewcel in that a single crystal or a transparent group of crystals is used on which a thin film of saturated solution forms rather than a wick impregnated with a saturated salt solution. Further, whereas in the dewcel the solution can be temperature controlled only above ambient, in the Wylie hygrometer there is provision for both heating above and cooling below ambient.

One construction of the hygrometer consists of a small isothermal metal enclosure, about 1 in. long and 1 in. in diameter, in which a suitable ionic crystal is mounted between two chemically inert electrodes. The gas under test is forced through the enclosure after it has been brought to the enclosure temperature by passing through channels cut in the enclosure or by passing through an attached coil of metal tubing. The enclosure is cooled by passing a refrigerant through appropriate channels. Compressed carbon dioxide gas, expanding through a small needle valve, serves as a satisfactory refrigerant. An insulated coil of resistance wire, wound directly on the metal enclosure, is used to provide heat electrically. The temperature of the enclosure is measured with a resistance thermometer wound directly on it or with a directly attached thermocouple.

The conductivity of the crystal is measured on a deflecting type of instrument, or, by electronic means, is made to control the heating and cooling of the enclosure. Crystals of such salts as potassium sulfate or lithium chloride can be used. With potassium sulfate, the equilibrium relative humidity at room temperature is 97 percent; with lithium chloride it is 12 percent. With the former salt, cooling is generally necessary whereas with the latter, heating is usually required.

7. Electrolysis of Water

7.1. General Theory

Water is electrolyzed into gaseous oxygen and hydrogen by the application of a voltage in excess of the thermodynamic decomposition voltage (2 v). The mass of water electrolyzed is directly related to the electrolysis current by Faraday's law.

$$M_{H_2O}=\frac{It}{96500}\times\frac{W_{H_2O}}{Z} \tag{7}$$

where

M_{H_2O}=mass of water, grams

I=electrolysis current, amperes

W_{H_2O}=gram—molecular weight of water

Z=valance

t=time, seconds.

Consider, now, a mixture of air and water vapor and let the water vapor be electrolyzed completely. From the perfect gas laws and Amagat's law of partial volumes, it follows that

$$\frac{V_{H_2O}}{V_{air}}=\frac{M_{H_2O}}{M_{air}}\times\frac{W_{air}}{W_{H_2O}} \tag{8}$$

or

$$M_{H_2O}=\frac{V_{H_2O}}{V_{air}}\times\frac{W_{H_2O}}{W_{air}}\times M_{air} \tag{9}$$

where

M_{air}=mass of air, grams

V_{H_2O}=partial volume of water vapor, cm³

V_{air}=partial volume of air, cm³

W_{air}=gram—molecular weight of air.

The current flow, during electrolysis is

$$I=\frac{96500}{18.016}\times 2\times\frac{V_{H_2O}}{V_{air}}\times\frac{W_{H_2O}}{W_{air}}\times\frac{M_{air}}{t} \tag{10}$$

or

$$I=6660\,\frac{V_{H_2O}}{V_{air}}\times\frac{M_{air}}{t}. \tag{11}$$

Thus, the current flow is directly proportional to the volume ratio of water vapor to air and to the mass flow of air. If the mass flow of air is kept constant, then the current flow is directly proportional to the volume ratio. If the volume ratio is expressed in parts of water vapor per million parts of air, equation (11) becomes

$$I=0.00666\text{ ppm}\times\frac{M_{air}}{t}. \tag{12}$$

7.2. Keidel Hygrometer

Keidel [86] has described a hygrometer that operates by electrolyzing, continuously and quantitatively, the water vapor content of a water vapor-gas mixture. Figure 21 is a flow diagram of the instrument. A sample of water vapor and air enters the instrument, under pressure, and is divided into two parts. A constant mass flow of dry air is maintained in the electrolytic cell while the remainder of the sample is by-passed,

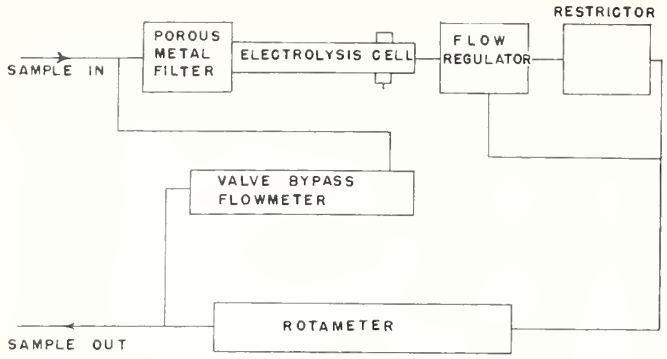

FIGURE 21. *Flow diagram of the electrolysis hygrometer.*

through a flowmeter, and exhausted at the outlet. The part of the sample that passes through the cell, then flows, in turn, through a pressure regulator, an adjustable restrictor, a flowmeter and finally exhausts at the outlet. The flow through the sample flowmeter is adjusted to 100 cm^3/min at a pressure of 760 mm of Hg and a temperature of 25° C. Under these conditions, the electrolysis current is 13.2 μa/ppm.

The electrolysis cell is a Teflon tube, the inside of which is coated with a thin, viscous film of partially hydrated phosphorous pentoxide. Two platinum wire electrodes are spirally wound on the inside of the Teflon tube in contact with the film. The film absorbs the water vapor from the sample gas. The application of a d-c potential across the electrodes electrolyzes the water and the resultant current is measured on a microammeter, or, if desired, recorded.

This instrument has full scale ranges of 10 to 1,000 ppm. It is claimed that the accuracy is 5 percent of the indication from 1 to 1,000 ppm. If the efficiency of electrolysis is 100 percent, then the accuracy is limited by the constancy of the mass flow of the air and performance of the electrical components. The speed of response, for a 63 percent change in indication, is about 1 min. in the increasing humidity direction and about 2 min in the decreasing direction. The response time varies with water vapor concentration, applied cell voltage, and film thickness.

Because the sample flow through the cell is controlled on a volumetric rather than a mass basis, and measured on a rotameter, there is a temperature effect. If the instrument is used at other than its design temperature, the correction is 0.3 percent per ° C.

8. Measuring Circuits

There are several simple circuits that are commonly used to measure the resistance of the sensor, or, a related parameter, such as current. The output of the circuit is displayed on a meter or a recorder, sometimes in the measured variable, but more often in units of relative humidity.

The d-c ohmmeter and the d-c Wheatstone bridge are two standard circuits for measuring resistance. They are not, however, well suited to electric hygrometry, for a preponderance of the better sensors are wholly or partly ionic conductors and so are subject to polarization. With d-c circuitry, even with small impressed voltages on the sensor, there is a significant error due to polarization. Except in specialized applications, d-c circuitry is to be avoided. The outstanding exception is the radiosonde where pulsating d-c is applied to the sensor. Because a radiosonde flight normally is of no more than 2 hours duration, the amount of polarization that occurs in this time can be tolerated.

Figure 22 is a diagram of a typical a-c circuit [14]. The transformer reduces the 110 input voltage to a desired lower value, sometimes to 100 v although it may be much lower. The limiting resistor prevents the current through the sensor from exceeding a maximum value. With Dunmore sensors, the current is limited, preferably, to 100 μa. The lower the maximum current, the greater the life of the sensor. A rectifier converts the alternating current to direct current so that it can be measured on a d-c microammeter. Alternatively, or in addition, a dropping resistor can be used in the d-c part of the circuit and the voltage drop

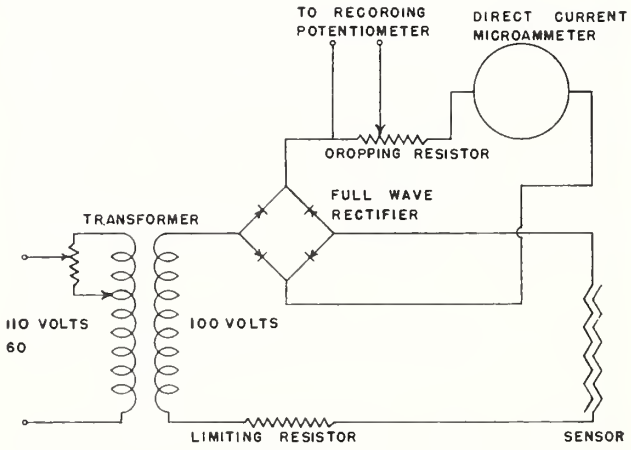

FIGURE 22. *Alternating current measuring circuit.*

across it recorded on a strip chart potentiometer. With this circuit, there is a loss in sensitivity at both low and high resistances. A typical sensor calibration curve, in terms of indicated current, is shown in figure 23. Dunmore elements are often used in sets of eight, each covering a relative humidity span of about 16 percent, the set covering about 7 to 98 percent. The salt solution concentration of each element is so chosen that the same resistance range is encompassed by each element for its limited relative humidity span. Thus, the calibrations, with the same circuit, will appear as parallel displaced curves of the same shape as in figure 23.

It is occasionally advantageous to make the entire relative humidity range correspond to the

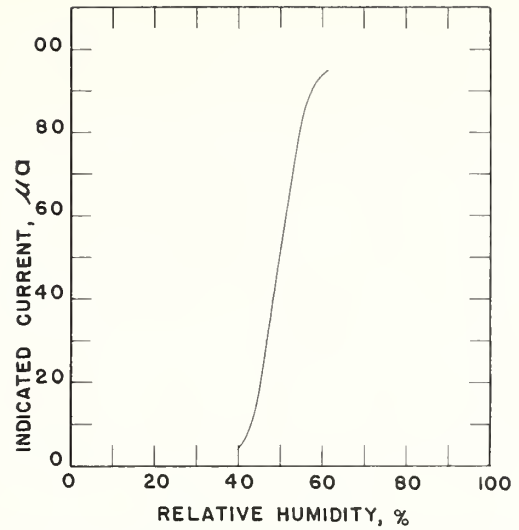

FIGURE 23. *Typical calibration of a limited range Dunmore sensor when used with the a-c measuring circuit of figure 22.*

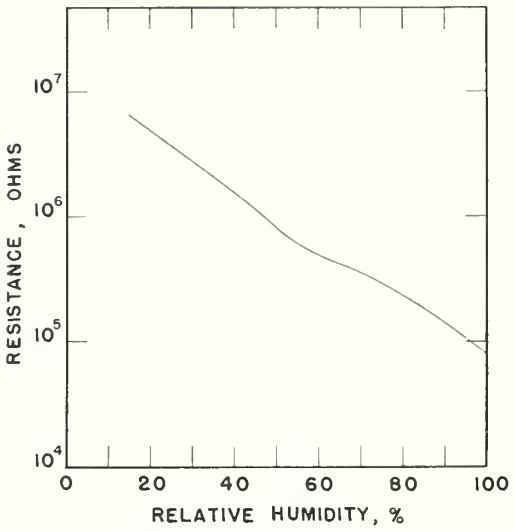

FIGURE 25. *Typical calibration curve at 24° C of five limited range Dunmore elements arranged as shown in figure 24.*

range of the indicating and recording instrument. Dunmore [14] has described an arrangement of sensors and resistors, as shown in figure 24, which accomplishes this. A set of five sensors, with appropriate resistors, will produce a calibration

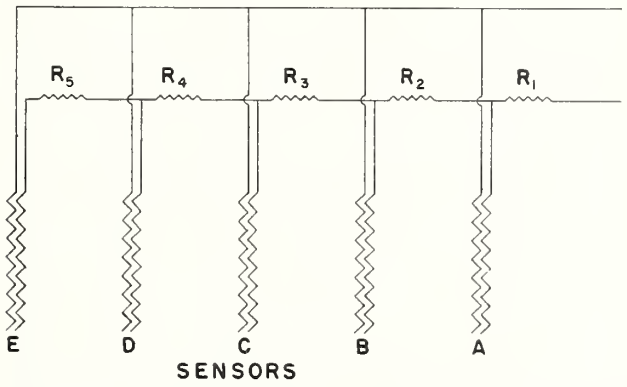

FIGURE 24. *Arrangement of limited range sensors and resistors to cover full relative humidity range.*

curve, in terms of resistance versus relative humidity, of the type shown in figure 25. At high relative humidities the resistance of sensors B, C, D, and E are very low, but resistors R_2, R_3, R_4, and R_5 prevent any significant current flow; sensor A and resistor R_1 control. At low relative humidities the resistances of sensors A, B, C, and D are sufficiently high so that sensor E, in combination with resistors R_1, R_2, R_3, R_4, and R_5 control. At intermediate relative humidities, sensors B, C, and D control in a like manner.

A standard a-c Wheatstone bridge circuit can be employed for the measurement of sensor resistance. Weaver [6] has used several different variants of the a-c bridge with his sensor. For extremely high resistances, say 10^6 ohms and greater, simple a-c circuits, such as that of figure 22, are unsuitable because the sensor capacitance becomes the controlling factor, limiting the upper value of the resistance that can be measured. The standard d-c circuits are often unsuitable too because the high voltage required to give a measurable current flow results in polarization. In addition, to cover the many decades of resistance of some sensors a range switch is necessary. Garfinkel [83] has devised an interesting electrometer circuit, figure 26, which impresses about 1.25

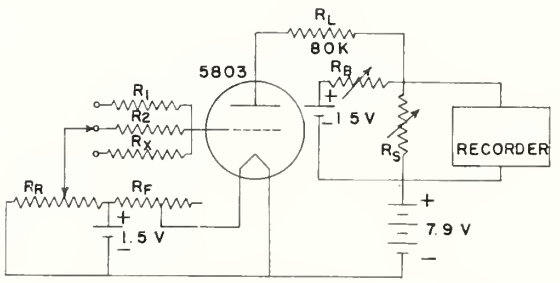

FIGURE 26. *Garfinkel electrometer circuit.*

R_1 and R_2 are precision resistors used for calibration. R_F and/or R_R are used to adjust or compensate for changes or drifts in calibration. R_X is the unknown (electric hygrometer sensor). R_S and R_B are adjusted so that the full range of the recorder corresponds to the full range of R_X,

v on the sensor, limits the current flow to about 100 μa, and yields an output that is proportional to the logarithm of the sensor resistance. Thus, eight decades of resistance can be indicated on the scale of an output meter or recorder without range switching. There is also a provision for adjusting the zero and range.

There are other circuits and schemes that may be used with electric hygrometer sensors, but the above ones indicate some of the main types. Because sensors usually have a temperature coefficient, circuits have been designed to automatically correct or compensate for this [84, 85].

9. Discussion

There are certain advantageous features in the use of electric hygrometry in meteorology. The sensor is small and relatively inexpensive, although the cost of the measuring circuit may not necessarily be low. The indications are in terms of electrical quantities so that remote indicating or recording is feasible. On the other hand, except for the temperature-controlled saturated solution and water electrolysis types, the electric hygrometer is an empirical device that requires a calibration. Furthermore, it usually has an appreciable temperature coefficient so that the calibration must cover a range of temperatures and, with each measurement with the hygrometer, there must be a temperature measurement. To a limited extent, the hygrometer circuit can be designed to compensate for temperature, obviating the necessity of a direct temperature measurement.

Several other factors influence the performance of the electric hygrometer. Polarization introduces an error, but this can be avoided by the use of a-c circuitry. Exposure to saturated air, fog or clouds, or wetting as by rain, is usually deleterious to a sensor. Contamination of the sensitive surface, especially by ionizable materials, will shift the calibration if not ruin the sensor.

These are some of the gross characteristics of the electric hygrometer that must be assessed for a given application. Within its limitations, the electric hygrometer is an extremely useful instrument.

Among the various sensors, there are relative advantages and disadvantages. The Weaver water vapor indicator, for example, is an excellent instrument for measuring very low humidities, but is not too well suited to continuous recording. It is best used in situations where discrete measurements are to be made. It requires an operator. Those sensors that use an aqueous solution, without binder, on an impervious surface are inherently faster in response than the binder type or the impregnated fiber, fabric, or ceramic. When high speed of response is required, the former sensors are the logical choice of the electrolytic solution class. However, the stability and life of the former may be expected to be less than the latter.

Of all the sensors, those that depend on surface adsorption will probably have the fastest response. The dry salt films appear to be best in this regard. They have one major limitation. It is their high resistance. To measure the high resistances requires special circuitry and handling. The oxide film sensor, as in the Jason hygrometer, has a more reasonable resistance range, but it has such drawbacks as an upper relative humidity limit, hysteresis, and loss of sensitivity after extended exposure to high humidity.

Sensors whose function is based on volume resistivity tend to be very sluggish in response, to exhibit hysteresis and drift. They can usually be made to have any desired resistance range.

The carbon element is difficult to make without a high relative humidity "hump". Because it conducts electronically, rather than ionically, it is free of polarization. It appears to be faster in response than the lithium chloride hygrometer and to have less of a temperature coefficient.

With all these sensors, the performance at low temperatures is related to the lag. With decreasing temperature, the lag increases exponentially. Sensors which will adequately respond at normal temperatures may become so sluggish at low temperatures that their indications have little value. Elements through which water vapor diffuses, must be made very thin in cross section to reduce their inherently high lag; even then, the speed of response may be too slow for these elements to be of practical value in meteorology. Surface resistivity sensors have an obvious advantage here, for they depend on surface adsorption rather than volume adsorption and diffusion. They, too, slow down at low temperatures, probably because there is some volume adsorption accompanying the surface adsorption.

The hygrometers using a temperature controlled saturated salt solution or a water electrolysis cell are based on quantitative laws. The latter is capable of measuring very low moisture contents and so may be adaptable to upper air or arctic meteorology.

10. References

[1] W. Schaffer, A simple theory of the electric hygrometer, Bull. Am. Meteorol. Soc. **27,** 147 (1946).

[2] R. N. Evans and J. E. Davenport, A study of the electric hygrometer, Ind. Eng. Chem. (Analytical Ed.) **14,** 507 (1942).

[3] A. Wexler and S. Hasegawa, Relative humidity-temperature relationships of some saturated salt solutions in the temperature range 0° to 50° C, J. Research NBS **53,** 19 (1954) RP2512.

[4] E. R. Weaver and P. G. Ledig, Detector for water vapor in closed pipes, Ind. Eng. Chem. **15,** 931 (1923).

[5] E. R. Weaver and P. G. Ledig, Detection of water in closed pipes, Tech. Pap. BS **17,** 637 (1923) T242.

[6] E. R. Weaver, and R. Riley, Measurement of water in gases by electrical conduction in a film of hygroscopic material and the use of pressure changes in calibration, J. Research NBS **40,** 169 (1948) RP1865; Instr. **20,** 160 (1947); Anal. Chem. **20,** 216 (1948).

[7] R. J. List (Editor), Smithsonian Meteorological tables, 6th rev. ed. (1951).

[8] E. R. Weaver, Electrical measurement of water vapor with a hygroscope film, Anal. Chem. **23,** 1076 (1951).

[9] F. W. Dunmore, An electrical hygrometer and its application to radio meteorography, J. Research NBS **20,** 723 (1938) RP1102.
[10] F. W. Dunmore, Humidity measuring, U. S. Patent 2,295,570, Sept. 15, 1942.
[11] S. Larach, Humidity sensitive device, U. S. Patent 2,609,688, Sept. 9, 1952.
[12] H. S. Gregory and E. Rouke, Modern aspects of hygrometry, Trans. Soc. Instr. Tech. **4** (3), 125 (1952).
[13] E. B. Edney, Construction and calibration of an electrical hygrometer suitable for microclimatic measurements. Bull. Entomol. Research **44,** 333 (1953).
[14] F. W. Dunmore, An improved electric hygrometer. J. Research NBS **23,** 701 (1939) RP1265.
[15] F. W. Dunmore, Humidity variable resistance, U. S. Patent 2,285,421, June 9, 1942.
[16] W. R. Steiger, A new development in the measurement of high relative humidity, Science **114,** 152 (1951).
[17] H. W. Cleveland, Electric resistance film hygrometer, U. S. Patent 2,458,348, Jan. 4, 1949.
[18] C. Harmantas and D. A. Mathews, Sensing element for the electric hygrometer, U. S. Patent 2,710,324, June 7, 1955.
[19] Arnold Wexler, Low temperature performance of radiosonde electric hygrometer elements, J. Research NBS **43,** 49 (1949) RP2003.
[20] E. Gluckauf, Investigation on absorption hygrometers at low temperatures, Proc. Phys. Soc. (London) **59,** 344 (1947).
[21] Anon., Electric hygrometer, Chem. Eng. News **24,** 1434 (1946).
[22] R. H. Munch, Instrumentation, Ind. Eng. Chem. **39,** 83A (Jan. 1947).
[23] J. R. Green, New developments in systems for measurement and control of humidity and temperature in ceramic driers, Bull. Am. Ceram. Soc. **32** (1), 18 (Jan. 1953).
[24] J. A. Van den Akker, Application of the electric hygrometer to the determination of water-vapor permeability at low temperature. Paper Trade J. **124** (No. 24), 51 (1947); **126** (No. 1), 32 (1948).
[25] W. A. Brastad and L. F. Borchardt, Electric hygrometer of small dimensions, Rev. Sci. Inst. **24,** 1143 (1953).
[26] Richard Brown and Edwin H. Perry, Moisture Indicator, U. S. Patent 2,009,760, July 30, 1935.
[27] E. Moen, Electronic humidity meter, Electronics **14,** 76 (June 1941).
[28] Kenneth C. Brown and Frederic J. Weyher, Apparatus for controlling the humidity of spaces, U. S. Patent 2,234,858, Mar. 11, 1941.
[29] J. B. O'Sullivan, The conduction of electricity through cellulose. Parts I, II, III, IV. Shirley Institute Memoirs **XX,** 109–143 (1946).
[30] Meteorological investigations at Rye, Part I, Instruments Branch (British) Air Ministry, JMRP No. 17 (May 1944).
[31] O. M. Ashford, Accuracy of Gregory humidiometer, Air Ministry, Met. Res. Comm. MRP 227 (Mar. 26, 1945).
[32] A. M. Firesah, An electrolytic hygrometer, Proc. Math. Soc. Egypt **2,** 3 (May 1942).
[33] L. W. Ogden and W. H. Rees, A method of measuring temperature on the skin and clothing of a human subject, Shirley Inst. Memoirs **XX**, 163 (1944).
[34] W. C. White, A new electrical hygrometer, Elec. Eng. **73,** (No. 12), 1084 (Dec. 1954).
[35] J. Pionchon, Electric hygroscope of great sensitiveness, Compt. rend. **146,** 809 (1908).
[36] H. L. Curtis, Insulating properties of solid dielectrics, Bul. BS **11,** 359 (1915) S 234.
[37] R. F. Field, The formation of ionized water films on dielectrics under conditions of high humidity, J. Appl. Phys. **17,** 318 (1946).
[38] Smail, Brooksbank, and Thornton, The electrical resistance of moisture films on glazed surfaces, J. Inst. Elec. Eng. **69,** 427 (1931).
[39] Walter Lubach, Electric hygrometer, U. S. Patent 1,749,826, Mar. 11, 1930.
[40] H. S. Polin, Hygrometer, U. S. Patent 2,015,125, Sept. 24, 1935.
[41] N. E. Edlefsen, A glass wool cell for measuring aqueous vapor pressure, Rev. Sci. Instr. **4,** 345 (1933).
[42] Anon., Humidity measurement and control, Electronic Eng. **25,** (304), 267 (June 1953).
[43] L. McCulloch, Hygrometer, U. S. Patent 2,381,299, Aug. 7, 1945.
[44] M. Auwarter, Electric hygrometer, U. S. Patent 2,715,667, Aug. 16, 1955.
[45] Arnold Wexler, et al., A fast responding electric hygrometer, J. Research NBS **55,** 71 (1955) RP2606.
[46] P. Anderson, Some properties of hydrogen desorbed from platinum and palladium, J. Chem. Soc. (London) **121,** 1153 (1922).
[47] Marcus E. Fiene, Device for indicating the humidity of the air, U. S. Patent 2,064,651, Dec. 15, 1936.
[48] F. Ansbacher and A. C. Jason, Effect of water vapor on the electrical properties of anodized aluminum. Nature **171,** 177 (1953).
[49] C. L. Cutting, A. C. Jason, and J. L. Wood, A capacitance-resistance hygrometer, J. Sci. Inst. **32,** 425 (1955).
[50] C. R. Underwood and R. C. Houslip, The behavior of humidity-sensitive capacitors at room temperatures, J. Sci. Inst. **32,** 432 (1955).
[51] A. C. Jason and J. L. Wood, Some electrical effects of the adsorption of water vapor by anodized aluminum, Proc. Phys. Soc. (London) **B68,** 1105 (1955).
[52] MacDowall and Cutting, Jason and Wood, A capacitance-resistance hygrometer, J. Sci. Instr. **33,** 284 (1956).
[53] L. R. Koller, Electric hygrometer, U. S. Patent 2,237,006. April 1, 1941.
[54] R. Kunin and R. J. Myers, Ion exchange resins. (John Wiley & Sons, Inc., New York, N. Y., 1950).
[55] M. Pope, Electric hygrometer, U. S. Patent 2,728,831, Dec. 27, 1955.
[56] R. E. Wilson and T. Fuwa, Humidity equilibria of various common substances, J. Ind. Eng. Chem. **14,** 913 (1922).
[57] T. Kujirai, Y. Kobayaski, and Y. Toriyama, Absorption of moisture by fibrous insulating materials, Sci. Papers Inst. Phys. Chem. Research (Tokyo) **I**(6), 79 (1923).
[58] M. Harris, Handbook of textile fibers (Harris Research Laboratories, Inc., 1246 Taylor St., N. W., Washington 11, D. C., 1954).
[59] S. Evershed, The characteristics of insulation resistance. J. I. E. E. **52,** 51 (1914).
[60] T. Kujirai and T. Akahari, Effect of humidity on the electrical resistance of fibrous insulating materials, Sci. Papers Inst. Phys. Chem. Res. (Tokyo) **I** (7), 94 (1923).
[61] F. P. Slater, A sensitive method for observing changes of electrical conductivity in single hygroscopic fibers, Proc. Roy. Soc. (London) **B 96,** 181 (1924).
[62] E. J. Murphy and A. C. Walker, Electrical conduction in textiles. I, J. Phys. Chem. **32,** 1761 (1928).
[63] E. J. Murphy, Electrical conduction in textiles. II, J. Phys. Chem. **33,** 200 (1929).
[64] E. J. Murphy, Electrical conduction in textiles. III, J. Phys. Chem. **33,** 509 (1929).
[65] A. C. Walker, Effect of atmospheric humidity and temperature on the relation between moisture content and electrical conductivity of cotton, J. Textile Inst. **24,** T145 (1933).
[66] M. C. Marsh, and K. Earp, The electrical resistance of wool fibres, Trans. Faraday Soc. **29,** 173 (1933).
[67] S. P. Hersh and D. J. Montgomery, Electrical resistance measurements on fibers and fiber assemblies, Text. Research J. **22,** 805 (1952).

[68] G. Barr, Part of "Discussion on hygrometry," Proc. Phys. Soc. (London) **34,** LXXXVII (1921).
[69] C. A. Parsons and A. H. Law, Means for detecting or measuring moisture, U. S. Patent 1,383,233, June 28, 1921.
[70] P. W. Burbridge and N. S. Alexander, Electrical methods of hygrometry, Trans. Phys. Soc. (London) **40,** 149 (1927–28).
[71] W. R. Starkins, System for detecting and controlling humidity variations, U. S. Patent 1,694,107, Dec. 4, 1928.
[72] H. J. Kersten, Humidity responsive device, U. S. Patent 2,377,426, June 5, 1945.
[73] Fred Lichtgarn, Electrical device, U. S. Patent 2,358,406, Sept. 19, 1944.
[74] Fred Lichtgarn, New method of measuring relative humidity, Instruments **20,** 336 (1947).
[75] G. Bouyoucos, Electric hygrometer, U. S. Patent 2,367,561, Jan. 16, 1945.
[76] Herman Kott, Humidity measuring device, U. S. Patent 2,047,638, July 14, 1934.
[77] A. G. Thomson, Measuring relative humidity, Elec. R. (London) **147,** 640 (1950).
[78] L. A. Welco, Humidity-resistance relations in carbon-coated hygroscopic materials, Nature **134,** 936 (1934).
[79] Walter K. Smith and Nancy J. Hoeflich, The carbon film electric hygrometer element, Bull. Am. Met. Soc. **35,** (2), 60 (1954).
[80] W. F. Hicks, Humidity measurement by a new system, Refrig. Eng. **54,** 351 (1947).
[81] J. H. Conover, Test and adaptation of the Foxboro dew-point recorder for weather observatory use, Bull, Am. Meterol. Soc. **31,** (1), 13 (1950).
[82] R. G. Wylie, A new absolute hygrometer of high accuracy, Nature **175,** 118 (1955).
[83] S. B. Garfinkel, An eight decade logarithmic ohmmeter, ISA Journal **3,** 54 (1956).
[84] R. E. Hadady, Automatic temperature-compensated humidity indicator, U. S. Patent 2,684,592, July 27, 1954.
[85] R. S. Feigal, Humidity measuring apparatus, U. S. Patent 2,689,479, Sept. 21, 1954.
[86] F. A. Keidel, A novel, inexpensive instrument for accurate analysis for traces of water (Presented at the Pittsburgh Conference on Analytical Chemistry and Applied Spectroscopy, February 27, 1956).

WASHINGTON, March 18, 1957.

Humidity Standards*

Arnold Wexler

This paper describes and discusses instruments which may serve as primary and secondary humidity standards, including a gravimetric hygrometer, now under development at the National Bureau of Standards, to serve as its basic reference for humidity measurements. The use of precision humidity generators for producing atmospheres of known humidity is outlined. Methods and techniques of obtaining fixed humidity points are given.

1. Introduction

A variety of instruments are used in the measurement of the moisture content of gas. Many of these are purely empirical and require testing and calibration. Some instruments have a theoretical basis. Even these sometimes require calibration for the highest accuracy. Then, too, instruments operating on different principles, and, occasionally, instruments operating on the same principle, will yield divergent results. A method of test or calibration, or a standard against which other instruments may be compared, is necessary if consistent and accurate measurements of humidity are to be made.

The testing and calibration of hygrometers may be approached in either of two ways. An instrument or method that has a firm theoretical basis and is capable of giving highly accurate and reproducible absolute measures of the moisture content of gas may be chosen as a standard.. Hygrometers may then be calibrated by direct comparison with the standard when simultaneously exposed to various humidities. Alternately, atmospheres of known humidity may be produced and controlled. Hygrometers may then be exposed to the known atmospheres, or, the gas of known humidity may be fed to the instruments under test.

2. Hygrometer Standards

2.1 Primary Standard

The gravimetric method of water vapor measurement is gener-

*Scheduled for publication in Tappi, Spring 1961.

ally considered the most precise and accurate in hygrometry. In this method, the mass of water vapor admixed with a volume of gas is absorbed by a desiccant and then the volume of the dry gas is measured directly. Since these quantities are fundamental, this method yields an absolute measure of the humidity. Because of this, and its relatively great inherent accuracy, the gravimetric method is often used as a primary standard against which other methods and instruments are compared. However, to achieve the inherent accuracy of the gravimetric method there must be careful attention to details. Measurements are time consuming, especially those involving low moisture contents. The results are average values. Hence it is usually necessary, when calibrating other instruments against the gravimetric method to employ a humidity generator that produces air of constant humidity. This method is principally used for research work of the highest accuracy or for making fundamental calibrations.

The gravimetric method has a long and well established history of use. In 1845, Regnault [1] employed it to determine the density and vapor pressure of saturated water vapor in air. Subsequently, in 1888, Shaw [2] repeated some of Regnault's work as part of an extensive investigation on the hygrometric methods in use at that time. Awberry [3] utilized it to measure the water content of saturated air at elevated temperatures while Awberry and Griffiths [4] used it as a standard for low temperature calibrations. Bartlett [5] and Saddington and Krase [6] measured the water content of gases saturated at high pressures with the gravimetric method while Goff et al. [7, 8] utilized it to determine the interaction constant of moist air. Walker and Ernst [9] and Wexler [10] have utilized this method for calibrating and checking the accuracy of precision humidity generators. It has also been used extensively in investigations of the vapor pressures of liquids and solutions, particularly salt solutions [11-24].

An experimental set-up for making a moisture determination with the gravimetric method is shown in figure 1. Gas of constant water vapor content is issued from a humidity generator and a sample withdrawn through an absorption train, saturator and laboratory wet gas meter, etc. The moisture is absorbed by the train of U-tubes. The first U-tube removes all, or nearly all, of the water. If the absorbent in the first U-tube is near exhaustion or if the gas flow is too rapid some moisture may remain in the effluent gas. The second tube will remove the amount that is still left. The third U-tube serves as a guard to prevent water vapor from diffusing back from the saturator or gas meter. The first two tubes are weighed before and after a run to give the mass

[1] Figures in brackets indicate the literature references in this paper.

of water vapor removed from the air. The volume of dry gas emerging from the absorption train is measured by a laboratory wet gas meter. The gas meter, however, saturates the gas that flows through, so that the indicated volume is that of moist air.[28] To insure that the gas is completely saturated before entering the gas meter so that no changes in water level will occur due to evaporation, a saturator is inserted immediately upstream of the gas meter. This saturator may be a container or, preferably a series of containers, filled with water-washed gravel or pumice that is moistened with water. Since the gas meter measures the volume of saturated gas the indicated volume must be corrected to give the volume of dry gas associated with the absorbed water vapor. The mass of dry gas is obtained by multiplying the volume by the density.

The absolute humidity, r, in terms of mass of water vapor/unit mass of dry gas, is given by

$$r = \frac{M_w}{V \times c \times \left(\frac{\rho}{1+.00367t}\right)\left(\frac{P-e_s}{760}\right)}, \qquad (1)$$

where

M_w = mass of water vapor absorbed in the first two U-tubes, g
V = indicated gas meter volume, cm^3
c = calibration factor for gas meter (a function of rate of flow)
ρ = density of dry gas at standard pressure and temperature (760 mm Hg and $0^\circ C$)
t = temperature of the gas in the gas meter, $^\circ C$
P = absolute pressure of the gas in the gas meter, mm Hg
e_s = saturation vapor pressure at temperature t, mm Hg

The procedure in making a run is as follows: The test gas is drawn through the absorption train, saturator, gas meter and flowmeter. The rate of flow is adjusted and controlled at a constant value by the vacuum control valve. After a predetermined volume of test gas has been sampled, the control valve is closed, the absorption tubes sealed and the change in weight of U-tubes Nos. 1 and 2 is determined.

Although this procedure appears to be simple, certain precautions should be observed to reduce and eliminate sources of error. A constant rate of flow should be maintained through the system. The wet gas meter is flow-dependent so that the calibration constant (c in eq (1)) will depend on the flow. The rate of flow should be kept low,

preferably below one lpm, if complete absorption of the water vapor from the sample gas is to be assured. U-tube No. 1 is filled with anhydrous magnesium perchlorate, $Mg(ClO_4)2$, while No. 2 and No. 3 are filled with phosphorous pentoxide, P_2O_5. Anhydrous magnesium perchlorate is a granular material with an excellent drying efficiency[25, 26], and is easy to handle, while phosphorous pentoxide, which has the greatest known drying efficiency[27], is a powder that readily deliquesces and must be handled with care. In filling the absorption tubes, the desiccant should be packed loosely so that no appreciable pressure drop is introduced. Furthermore, it is desirable to insert glass wool plugs at intervals between the desiccant to avoid channeling of the gas on passage through the tubes. It is well to remember that the maximum permissible pressure drop across a wet gas meter is about 0.3-in. water. A greater pressure differential may blow the water seal in the meter, causing gas to by-pass the measuring compartments. Furthermore, the typical gas meter is a low pressure device, built for operation at a differential of a few inches of water pressure with respect to ambient pressure. Excessive pressures may distort the case, cause the shaft stuffing box to leak, and produce a bind on the drum thereby affecting the meter accuracy. The gas meter must be carefully leveled, the water level properly adjusted, and only integral revolutions used as a measure of the volume[29-30].

In making precision weighings of the absorption tubes such factors as buoyancy, change in weight of the internal gas volume, change in external surface conditions, static charge, and thermal gradient within the balance case contribute errors that may be easily overlooked. The use of an identical dummy absorption tube as a tare will tend to compensate for buoyancy. If this tare is treated and handled in a similar fashion as the tubes in the absorption train, then some of the other errors may be reduced. The internal pressure within the tare is adjusted to that within the test absorption tube by momentarily opening it at the same time that the latter is being sealed for weighing. The tare and main tube should never be handled with bare hands, for moisture and oil from the hands will affect the weight. Both may be wiped with a damp cloth to remove static charge prior to insertion into the balance case. One technique for insuring that the balance pans do not accumulate static charge is to keep an ionizing source (e.g., a radioactive salt) within the case. Furthermore, the balance should be in a room that is maintained at a fairly constant temperature and where there are no sources of heat radiation that could induce temperature gradients, and hence convection currents, within the case. The relative humidity within the balance case should be constant, for changes in

humidity may shift the balance rest point.

It is important that no hygroscopic materials be used in the experimental set-up other than the drying agents in the absorption train. Rubber and some plastics, for example, are sufficiently hygroscopic as to act as moisture sources and sinks. For this reason, tubing and stoppers fabricated from such materials must not be used. The set-up should be made from glass or glass and metal. Seals, such as on the absorption tubes, are achieved with ground glass stopcocks. Pneumatic connections between components may be made through mercury seals or "0" ring seals. Every effort must be made to eliminate the possibility of error from moisture sources or sinks.

A typical absorption tube weighs about 70 g. The duration of a gravimetric determination can be adjusted so that at least 0.2 g of water is absorbed. An analytical balance, with a capacity of 200 g and a sensitivity of 0.1 mg will weigh the absorbed water vapor with sensitivity of 1/2000. Assuming that all precautions with regard to buoyancy, etc. have been taken, an accuracy in weighing of 1/1000 may be expected. If more water is absorbed greater accuracy may be obtained.

The accuracy of measurement of volume with the gas meter is limited at best to 1/500[29, 30]. The pressure measurement can be made with an accuracy of at least 1 mm Hg and the temperature measurement can be made to better than 0.1°C. Thus these two measurements will be better than about 1/760.

It is apparent that the overall accuracy is limited by the volume measurement. If greater overall accuracy is required a water aspirator can be substituted for the gas meter. A further refinement would be to use an oil aspirator. If an oil with negligible vapor pressure is chosen (say, butyl phthalate) then the saturator may be eliminated too. In that case, eq (1) becomes

$$r = \frac{M_w}{V\left(\frac{\rho}{1+.00367t}\right)\frac{P}{760}} \qquad (2)$$

The National Bureau of Standards has developed a gravimetric hygrometer to serve as its primary standard for humidity measurement. Figure 2 is a block diagram and figure 3 is a flow diagram of this hygrometer. It consists of a solid desiccant absorption train (main drying train), a gas volume measuring system, a vacuum pump, temperature and pressure measuring instruments, and suitable valves

574278 O - 61 - 48

and control. The test gas is continuously withdrawn at a nominally constant flow rate from a humidity generator, passes through the main drying train and gas volume measuring system and discharges added to the vacuum pump. The gas volume measuring system comprises two calibrated stainless steel cylinders, each with a nominal internal capacity of 30 l, immersed in a thermostatted oil bath. Through the proper sequencing of the on-off position of valves attached to the inlet and exit ports of the cylinders, by means of a pressure switch and valve sequencing and control circuit, each cylinder is alternately evacuated and filled with the test gas to a predetermined pressure. The internal capacity of each cylinder, together with the pressure and temperature of the gas therein, provide a highly accurate measure of the gas volume. The total gas volume is the sum of the individual fillings of each cylinder.

The gravimetric method yields a measure of the humidity in terms of mixing ratio. Two fundamental quantities are determined directly: The mass of water vapor and the volume of dry gas. The latter, through the known density of the test gas, is converted into mass of gas. Thus, the value of the moisture content of the gas has been obtained in terms of an absolute definition by direct measurement. By recourse to the laws of gaseous behavior it is possible to convert from mixing ratio to such terms as vapor pressure, specific humidity, relative humidity or saturation deficit. However, the accuracy with which the humidity can be expressed in units or terms derived from the mixing ratio is limited by the degree of validity of the laws of gaseous behavior and vapor pressure. The accuracy with which the mixing ratio can be determined directly is limited only by the accuracy of the measurement of fundamental quantities.

With the Bureau's gravimetric hygrometer, an attempt is being made to measure the various parameters that determine the mixing ratio with an accuracy of 1/10,000 with the expectation that the mixing ratio itself will thus be known to 1/1000.

2.2 Secondary Standards

The time, work, painstaking care, and skilled personnel required for setting up and using the gravimetric method preclude its general use except for fundamental calibration work. There is a need, therefore, for one or more types of instruments that could serve as secondary or working standards. The secondary standard is one which can be calibrated against the primary standard and then, in turn, used

for routine calibrations. It would appear that to be acceptable as a secondary standard an instrument should directly measure the humidity of the air in terms of fundamental quantities, or should have a firm theoretical basis for its operation so that its indication can be related to the humidity through known physical laws. It is intended, at the National Bureau of Standards, to investigate for possible use as secondary standards such instruments as the dewpoint hygrometer, the microwave hygrometer, and the psychrometer.

3. Precision Humidity Generators

Several convenient and practical methods are available for producing atmospheres of known humidity with sufficient precision and accuracy that the use of auxiliary hygrometers for direct measurement is not required. Equipment incorporating these methods may be called precision humidity generators.

3.1 Pressure Humidity Apparatus

In this type of apparatus, a stream of air at an elevated pressure is saturated and the pressure of the saturated air is reduced as required to give any desired humidity. If the temperature is held constant during saturation and after expansion, and the perfect gas laws are obeyed, then the percentage relative humidity, RH, at the lower pressure, P_t, is the ratio of the absolute values of the lower pressure, P_t, to the higher pressure, P_s, that is,

$$RH = \frac{P_t}{P_s} \times 100. \qquad (3)$$

Water vapor-air mixtures depart from ideal gas behavior. Furthermore, air, when saturated with water vapor at high pressure, does not hold the same amount of moisture as at atmospheric pressure [5, 31]. Equation (3), therefore, does not strictly define the relative humidity, particularly at high values of P_s. Weaver[32, 33] has shown that an empirical equation of the form

$$RH = 100 \times \frac{P_t}{P_s} \frac{(1 - KP_t + K'P_t^2)}{(1 - KP_s + K'P_s^2)}$$

more closely yields the true relative humidity where the constant K has a value of 1.9×10^{-4} and K' is equal to 1.4×10^{-8} when the pressure is expressed in pounds per square inch. The magnitude of the ratio

$(1 - KP_t + K'P_t^2) / (1 - KP_s + K'P_s^2)$ does not differ from unity by more than 1/4 of 1 percent when P_t is at atmospheric pressure and P_s is no greater than 150 psig. For these pressures, the relative humidity will be in the range of 10 to 100 percent.

The pressure method was used by Weaver and Riley[32] for the calibration of electrically conducting hygroscopic films employed in the measurement of water vapor in gases. Their equipment was designed for low rates of gas flow and was used under room-temperature conditions. Wexler and Daniels [34] used the two-pressure principle in the design of a precision humidity generator that produced atmospheres of known relative humidity from 10 to 98 percent over a temperature range from -40 to +40°C with an accuracy to within 1/2 of 1 percent RH, or better.

Figure 4 is a simplified schematic drawing illustrating the principle of operation of the apparatus, while figure 5 is a block diagram and figure 6 a schematic of a practical version of the apparatus. The apparatus is a continuous-flow device. Air from a high-pressure source is dried and cleaned by a low-temperature drying and filtering system. It is then heated in a warm-up unit prior to entering the humidifying system. Two pressure regulators in series reduce and control the pressure in the saturators at any desired value. After emerging from the humidifying system, the air passes through an expansion valve into a test chamber, where its pressure is maintained constant, usually at atmospheric pressure, and then allowed to exhaust into the room or a vacuum source. The drying and filtering systems are immersed in a bath of dry ice and Stoddard's solvent. The humidifying system, expansion valve and test chamber are immersed in a thermostatted bath whose temperature can be controlled at any desired value.

Instruments undergoing test or calibrations can be inserted into the test chamber or, alternatively, air from the test chamber can be fed to the test hygrometer. Provided one can assure complete saturation, the accuracy with which the pressure humidity apparatus can generate air of known relative humidity is limited by a) the accuracy with which the pressure is measured, b) the uniformity or constancy of the temperature from the final saturator through to the test chamber, and c) the degree of validity of the correction term of eq (4). By using suitable pressure measuring instruments, the accuracy of the pressure measurements can be made to 1 part in 500. The temperature can be held constant to at least 0.05°C. The correction term can be determined, by the gravimetric method, with corresponding accuracy. It is estimated that the pressure humidity apparatus will

produce a relative humidity that is known to within 1/2 of 1 percent RH, or better.

The question may arise as to whether complete saturation is obtained. This can be ascertained by a simple experiment. The apparatus has an external saturator which can be charged with water and operated at any desired temperature, or it can be maintained dry. If this external saturator is maintained dry, then the humidifying system within the thermostatted bath must provide all the moisture necessary to saturate the air at the bath temperature. The apparatus is operated, therefore, with the external saturator dry and the moisture content is measured by inserting a precision hygrometer in the test chamber, or by sampling the air and making a gravimetric determination. Water is added, now, to the external saturator and its temperature is adjusted to some value above that of the thermostatted bath. Without changing any other operating conditions, air is passed through the apparatus. Since the external saturator supersaturates the air with respect to bath temperature, the humidifying system within the thermostatted bath precipitates and condenses out the excess water. The moisture content is measured again and compared to the previous measurement. If the two are identical, they give sufficient assurance that complete saturation is obtained.

Basically, this equipment generates a known relative humidity. From a measurement of the temperature and pressure within the test chamber and with the application of the gas laws and the saturation vapor pressure of water the relative humidity can be converted to other units of humidity measurement.

3.2 Two-Temperature Humidity Apparatus

The method employed in this apparatus for producing atmospheres of known relative humidity is to saturate a stream of air with water vapor at a given temperature and then to raise the temperature of the air to a specified higher value. If t_s is the temperature of saturation, e_s the saturation pressure of water vapor at temperature t_s, t_t the elevated temperature, and e_t the saturation pressure of water vapor at temperature t_t, then the relative humidity, RH, at temperature t_t is

$$RH = \frac{e_s}{e_t} \times 100. \qquad (5)$$

In eq (5), the assumption is made that the absolute pressure of

the air at the elevated temperature, t_t, is the same as the absolute pressure of the air at the saturation temperature, t_s. If these two pressures are not identical, then a pressure correction must be introduced. If P_s is the absolute pressure of the air at t_s, and P_t is the absolute pressure of the air at t_t, then the relative humidity is

$$RH = \frac{e_s}{e_t} \times \frac{P_t}{P_s} \times 100. \qquad (6)$$

The inherent accuracy of this method depends not only on the accuracy with which the temperatures and pressures are measured, but also on the completeness of saturation and on the degree of accuracy or validity of the temperature-vapor pressure relationship for water. The latter may be considered to have been established with sufficient exactness for most purposes in hygrometry [35, 36]. Both the temperature and pressure can be measured to an accuracy of at least 1/1000. The completeness of saturation can be assured by employing a recirculating scheme. Thus this method has considerable inherent accuracy. Its main limitation is the time required for changing from one relative humidity to another, for this involves a temperature change.

The two-temperature principle has been used successfully in research laboratory equipment. Shaw [2] used it in a laboratory set-up for investigating the performance of hygrometers. Wiegerink [37] constructed equipment, based on this principle, for conditioning materials at constant humidities and elevated temperatures. Wexler [38] developed an apparatus capable of producing any desired relative humidity over a wide range of temperatures. Burcham [39] described a humidity oven, operating over the temperature range of 30 to 100°C, in which he achieved relative humidities of 30 to 95 percent.

A simplified schematic diagram illustrating how the two-temperature method may be employed on an apparatus is shown in figure 7. By means of a gas pump, air is circulated from a saturator into a test chamber and then back into the saturator. The temperature, t_s, of the saturator and the temperature, t_t, of the test chamber are maintained at the respective desired values by thermostatted baths. Complete saturation is achieved simply and efficiently by recirculation of air over water (or ice) in the saturator, in a closed system. Once equilibrium has been established the saturator does not have to change the absolute moisture content of the recirculated air but only to maintain it.

The design of a practical system, based on this method, is

shown in figure 8. It differs from the elementary design of figure 7 in that the test chamber temperature is controlled by means of a heater inserted in the air stream rather than by immersing the test chamber in a thermostatted bath. The elimination of a thermostatted bath for the test chamber, with the resultant simplification in design and construction, is made possible by the fact that the saturator must necessarily be maintained at a lower temperature than the test chamber, and hence the only requirement for achieving any desired test chamber temperature is the introduction of the requisite amount of heat into the air stream.

It is sometimes desirable to be able to make a rapid change of relative humidity from one discrete value to another. This can be achieved in this equipment by utilizing a number of identical but independent systems that are arranged in such a fashion that their test chambers may be interchanged easily and quickly. Thus if a different saturator temperature, t_s, is maintained in each of, say, four saturators, and if the same temperature, t_t, is maintained in each of four test chambers, then the relative humidity in each test chamber is different. By interchanging the saturators used with a test chamber, several different relative humidities at the same temperature can be provided in it in rapid succession.

The arrangement is shown schematically in figure 9 for two systems. The interchange of saturators is effected by a special pneumatic switch. It consists of two ground and lapped plates, with suitable ports, to which the test chambers are attached and through which air may pass. A turn of the top plate with respect to the bottom plate advances each test chamber to a new position and connects each test chamber with a different saturator. Two such switches can be used instead of one, for greater convenience and versatility in changing saturators.

3.3 Divided Flow Humidity Apparatus

The principle of divided flow is employed in this apparatus to produce any desired humidity. Equipment based on this principle has been described by Walker and Ernst[9] for use at temperatures above freezing and by Gluckauf[40] and Wexler [41] for use at temperatures below 0°C. A stream of dry air is divided accurately, usually by means of a proportioning valve, into two parts. One part is saturated with respect to water or ice; the other part is maintained dry. The two parts are then recombined in a test chamber and then exhausted into the room. The relative humidity is given by the ratio of the division.

Figure 10 is a simplified schematic diagram illustrating the principle of operation. By means of a proportioning valve, V, a flow of dry air is divided into two parts in a known ratio. One part is passed through a saturator, S, until it is completely saturated. The saturator shown in figure 10 is designed solely for ice. It consists of a series of trays into which water can be poured and then frozen. Other types of saturators can be used equally well; the design is not limited to ice saturators. The air after emerging from the saturator is then mixed in a mixing chamber, C_M, with the other stream that has been maintained dry, and then allowed to exhaust through a test chamber, C_T, into the atmosphere. The saturator, mixing chamber, and test chamber are kept immersed in a constant temperature bath.

By direct measurement, the total pressure, P_s, in the saturator and the total pressure, P_c, in the test chamber are known. The fraction, X, of air flow that is directed through the saturator is given by the setting of the proportioning valve. Since everything is at a known constant temperature, the pressure e_s of the saturated water vapor within the saturator, is also known (by recourse to standard tables of vapor pressure). The relative humidity in the test chamber is determined by these known parameters.

Consider a unit mass of air entering the proportioning valve and dividing into two parts; one part passes through the saturator and is saturated with water vapor while the other by-passes the saturator and remains dry. The portion, X, of air emerging from the saturator, will contain Xr_s mass of water vapor, where r_s is the saturation mixing ratio, that is, mass of saturated water vapor per unit mass of dry air at the saturator temperature. After the two streams recombine, the air will contain r mass of water vapor per unit mass of dry air. The total mass of water vapor of the two separate streams is equal to the mass of water vapor of the recombined stream, i.e.,

$$Xr_s = r$$

or

$$X = \frac{r}{r_s} \quad . \qquad (7)$$

The relative humidity in the test chamber is defined by

$$RH = \frac{e}{e_s} \times 100, \qquad (8)$$

where e is the partial pressure of the water vapor in the test chamber.

From Dalton's law of partial pressures, and assuming the perfect gas laws to apply, it follows that the mixing ratio of the air-water vapor mixture in the test chamber is

$$r = \frac{M_w}{M_a} \frac{e}{P_c - e} \qquad (9a)$$

and that the saturation mixing ratio in the saturator is

$$r_s = \frac{M_w}{M_a} \frac{e_s}{P_s - e_s}, \qquad (9b)$$

where

M_a = molecular weight of air,

or

M_w = molecular weight of water.

Therefore

$$\frac{r}{r_s} = \frac{e}{e_s} \frac{(P_s - e_s)}{(P_c - e)}. \qquad (10)$$

By substituting eqs (7) and (8) into eq (10), the relative humidity is obtained in terms of known quantities

$$RH = \frac{X P_c}{P_s - (1-X)e_s} \times 100. \qquad (11)$$

If the pressure drop from the saturator to the test chamber is made sufficiently small, then P_s may be considered equal to P_c. Furthermore, at low temperature, say below $0^\circ C$, e_s is negligible compared to P_s.

Equation (11) therefore reduces to

$$RH = 100\ X. \qquad (12)$$

At higher temperatures, where the saturation pressure of water is no longer negligible, the relative humidity in the test chamber should be computed by eq (11).

Only under the stated conditions of small pressure drops and low temperatures is the relative humidity given by the proportioning ratio, X. On the other hand, the proportioning ratio X is a precise value of the percent mixing ratio and so is a direct measure of the absolute humidity produced by the divided-flow apparatus.

A divided-flow apparatus designed specifically for use at temperatures below freezing is shown schematically in figure 11. It comprises the following functional units: (a) The drying system, (b) the proportioning system, (c) the humidifying system, (d) the mixing chamber, (e) the test chamber, (f) the cooling system, and (g) the thermostatting system for temperature control.

Air from a high pressure source is dried by freezing in a dry ice and Stoddard's solvent bath. The dry air is then brought to room temperature, its pressure reduced and controlled by a regulator, and passed through the proportioning system.

One type of proportioning system which is used consists of a valve which divides the air in a definite ratio by means of orifices. In one design of valve six orifices of equal cross-sectional area are so arranged that by a turn of the knob of the valve, the incoming air can be divided to produce any of seven ratios: 0, 1/6, 1/3, 1/2, 2/3, 5/6, and 1. These ratios are the fractions of air entering the valve that emerge through one of the exit channels. Since this exit channel is made to communicate with the saturating system, these ratios may be used as the values for X in eqs (7), (9), (11), and (12). To assure that the air will divide in accordance with one of these given fixed ratios, the pressures downstream of the proportioning valve must be equalized. This is achieved by use of two variable resistances (pressure equalization valves) and a differential mercury manometer.

The two air streams, on leaving the proportioning system, flow through the humidifying system in parallel channels, into the mixing chamber where they are combined and centrifugally mixed, then into the test chamber and are finally discharged into the atmosphere. The saturators, mixing chamber and test chamber are immersed in a liquid bath that can be controlled at any desired temperature. For this particular apparatus, the temperature range is 0 to -40°C.

The divided-flow apparatus is a continuous-flow device in which the air speed through the test chamber can be adjusted and controlled. The rotation of the proportioning valve and the adjustment of the equalization valves are the only operations required for changing the relative humidity. The time involved is usually a matter of 1 or 2 sec. This permits any hygrometer under test in the test chamber to be subjected to a discrete change in relative humidity, a desirable advantage in the study of lag characteristics.

3.4 Apparatus Employing Combined Principles

Each of the generators so far described is based on a single principle of operation. It is, of course, possible to combine several of the principles for humidity generation into one apparatus. For example, the pressure humidity apparatus can be made more versatile by separately controlling the saturator and test chamber temperatures. The advantage of this is that low relative humidities can be reached without the need of extremely high saturator pressures. The relative humidity is then given by

$$RH = 100 \frac{P_t}{P_s} \times \frac{e_s}{e_t} \frac{(1 - K P_t + K' P_t)}{(1 - K P_s + K' P_s)}, \quad (13)$$

where

P_t = test chamber pressure
P_s = saturator pressure
e_s = saturation vapor pressure at the saturator temp.
e_t = saturation vapor pressure at the test chamber temp.

In a similar fashion, the divided-flow apparatus can be designed so that the saturator system and test chamber are in separate temperature baths.

4. Fixed Humidity Points

Very convenient methods exist for establishing atmospheres of known relative humidity which depend upon the equilibrium vapor pressure of water when a chemical is dissolved in it. The solution of a material in water lowers the vapor pressure of the water. The magnitude of the lowering depends on the concentration and temperature of the solution. These methods essentially provide fixed humidity points. They are ideally suited for controlling the relative humidity of a small space. Usually, little more is required than an enclosed space and an appropriate amount of chemical and water. Equilibrium conditions are more rapidly established, however, when air circulation or stirring, as by means of a fan or blower, is employed. When air circulation is used, the motor for driving the fan or blower is mounted externally to the test chamber to reduce any tendency for the chamber to warm up due to motor heat. The air circulation should be moderate, to reduce heating effects. In all these methods, the attainment of equilibrium depends on maintaining the chamber free of humidity sources or sinks. For this reason, the chamber should be fabricated from non-hygroscopic materials, preferably metal or glass. Materials which are highly hygroscopic, like wood, should not be used.

4. 1 Saturated Salt Solutions

The saturated salt solution method is inexpensive, simple and produces relative humidities that are roughly independent of temperature. The decided advantage of a saturated solution is that it can be made without measuring either the amount of salt or water. Since the concentration is fixed, for a given temperature, the ambient relative humidity is fixed. A saturated solution therefore provides an easily attained fixed humidity point. It is only useful at temperatures above the freezing point of the solution. A sealed chamber is required for which a large glass jar or bell jar is often suitable. The salt solution is made up as a slushy mixture in a glass or enameled tray or in the glass jar, if used, with the solution spreading over as large an area as practicable. Distilled water and chemically pure salts must be used. Stirring the solution may accelerate the attainment of equilibrium.

Data for a number of saturated salt solutions have been compiled by various authors and in various handbooks[42, 43, 44] . The salts listed in table 1 have been particularly useful for hygrometer calibration work. The data in this table are based on dewpoint measurements[45] . In general use, saturated salt solutions should not be expected to control the relative humidity to closer than about one percent relative humidity.

Table 1. Saturated salt solutions values of relative humidity versus temperature

Temperature	Relative humidity over saturated salt solution							
	$LiCl \cdot H_2O$	$MgCl_2 \cdot 6H_2O$	$Na_2Cr_2O_7 \cdot 2H_2O$	$Mg(NO_3)_2 \cdot 6H_2O$	NaCl	$(NH_4)_2SO_4$	KNO_3	K_2SO_4
°C	%	%	%	%	%	%	%	%
0	14.7	35.0	60.6	60.6	74.9	83.7	97.6	99.1
5	14.0	34.6	59.3	59.2	75.1	82.6	96.6	98.4
10	13.3	34.2	57.9	57.8	75.2	81.7	95.5	97.9
15	12.8	33.9	56.6	56.3	75.3	81.1	94.4	97.5
20	12.4	33.6	55.2	54.9	75.5	80.6	93.2	97.2
25	12.0	33.2	53.8	53.4	75.8	80.3	92.0	96.9
30	11.8	32.8	52.5	52.0	75.6	80.0	90.7	96.6
35	11.7	32.5	51.2	50.6	75.5	79.8	89.3	96.4
40	11.6	32.1	49.8	49.2	75.4	79.6	87.9	96.2
45	11.5	31.8	48.5	47.7	75.1	79.3	86.5	96.0
50	11.4	31.4	47.1	46.3	74.7	79.1	85.0	95.8

4.2 Water-Sulfuric Acid Solutions

Water-sulfuric acid mixtures produce atmospheres of relative humidity that depend on composition and temperature[46, 47, 48, 49, 50, 51]. The concentration of the mixture, at a given temperature, determines the ambient relative humidity. The temperature effect is small. The liquid may be exposed in a suitable tray in a sealed chamber to give the equilibrium vapor pressure of the mixture, or air may be otherwise brought into intimate contact with the liquid. Values of relative humidity, as a function of temperature and concentration, are given in table 2. Collins' data[48] are used for temperatures of 20 through 70°C while Wilson's compilation[46] is used for 0°C.

To obtain a desired relative humidity, it is necessary to prepare a solution of proper concentration. In use, the concentration of the solution may change and some technique is needed to periodically check or measure the concentration. One scheme is to titrate a sample with a standard base of known concentration; another is to measure the density or specific gravity. Values of specific gravity, as a function of concentration, at 20°C assuming the density of water at 4°C as unity, are listed in table 2 and are abridged from the Handbook of Chemistry and Physics[44]. The concentration of the sulfuric acid solution can then be adjusted, if necessary, by the addition of a suitable amount of water or acid.

Table 2. Relative humidity obtained from water-sulfuric acid solutions

Percent sulfuric acid by weight	Specific gravity at $\frac{20}{4}$ °C	Temperature, °C					
		0	20	25	30	50	75
		Relative humidity					
		%	%	%	%	%	%
10	1.0661	95.9	95.6	95.6	95.6	95.6	95.6
20	1.1394	87.8	88.0	88.0	88.0	88.2	88.5
25	1.1783	81.8	82.4	82.5	82.6	83.1	83.6
30	1.2185	73.8	75.0	75.2	75.4	76.2	77.2
35	1.2599	64.6	66.0	66.3	66.6	67.9	69.5
40	1.3028	54.2	56.1	56.5	56.9	58.5	60.5
45	1.3476	44.0	45.6	46.1	46.6	48.5	50.8
50	1.3951	33.6	35.2	35.7	36.2	38.3	41.0
55	1.4453	23.5	25.3	25.8	26.3	28.5	31.1
60	1.4983	14.6	16.1	16.6	17.1	19.0	21.4
65	1.5533	7.8	9.2	9.7	10.1	11.8	14.0
70	1.6105	----	3.4	3.7	4.1	5.4	7.2

4.3 Water-Glycerin Solutions

Water-glycerin mixtures will similarly produce atmospheres of known relative humidity[52, 53]. The techniques employed with water-sulfuric acid mixtures work equally well with water-glycerin mixtures. An important advantage of water-glycerin mixtures over water-sulfuric acid is that they are non-corrosive. The relative humidities obtained from various water-glycerin solutions are given in table 3. The values are based on the work of Grover and Nicol[53], who measured the vapor pressure at 20°C and applied Duhring's rule to compute the vapor pressures at other temperatures. Table 3 also contains values of specific gravity, at 20°C assuming the density of water at 4°C as unity, abridged from the Handbook of Chemistry and Physics[44]. A measurement of the specific gravity of a glycerin-water mixture provides a check on the concentration.

Table 3. Relative humidity obtained from water-glycerin mixtures

Percent glycerin by weight	Specific gravity at $\frac{20\ °C}{4}$	Temperature, °C			
		0	20	40	70
		Relative humidity,			
		%	%	%	%
20	1.0470	90.0	94.2	93.9	93.1
40	1.0995	82.2	86.5	86.6	86.2
60	1.1533	70.0	73.8	73.8	74.4
80	1.2079	49.6	51.7	50.9	50.5
90	1.2347	32.4	32.0	30.9	30.3

5. Humidity Chambers

In response to a sensing element, such as a mechanical hygrometer, electrical hygrometer, or psychrometer, the humidity of a closed space may be raised by water, spray or steam injection, by exposure to a water surface or wet wicks, or by the introduction

of saturated or high humidity air or the humidity may be lowered by chemical adsorption or the introduction of dry air. Either manual or automatic controls may be used to achieve the desired humidity. The basic feature about humidity chambers of this kind is that they require or depend upon auxiliary humidity measuring devices for an indication of the moisture content of the air. There are many chambers of this sort described in the literature [54-64] . Most of them are meant to be used at room temperature, or, perhaps, elevated temperatures, for testing materials and electrical instruments for the deleterious effects of high humidity. Some chambers have been designed for vapor absorption or permeability studies.

Figure 12 is a sketch of the humidity chamber. Two trays, each with a tight cover that can be raised and lowered by external manipulation, are placed in the chamber. One tray contains a chemical absorbent, such as sulfuric acid, silica-gel, or Drierite, while the other contains distilled water, preferably with exposed cotton or linen wicks. The cover of the appropriate tray is raised until a hydrometer indicates that the desired relative humidity has been attained. The cover is then dropped and since the chamber is sealed, the humidity remains constant. The chamber may be made automatic by using the output of a sensing element, through an appropriate circuit [62, 63] , to raise or lower the required cover.

6. References

[1] Regnault, M. V., Études sur l'hygrometrie, Ann. Chim. Phys. Serie 3, 15, 129 (1845).

[2] Shaw, W. N., Report on hygrometric methods, Trans. Roy. Soc. London [A] 179, 73 (1888).

[3] Awberry, J. H., The water content of saturated air at temperatures up to 100°C, Proc. Roy. Soc. London 44, 143 (1932).

[4] Awberry, J. H., and E. Griffiths, An investigation of the wet-and-dry bulb hygrometer at low temperatures, Proc. Phys. Soc. London 47, 684 (1935).

[5] Bartlett, E. P., The concentration of water vapor in compressed hydrogen, nitrogen and a mixture of these gases in the presence of condensed water, J. Am. Chem. Soc. 49, 65 (1927).

[6] Saddington, A. W., and N. W. Krase, Vapor-liquid equilibria in the system nitrogen-water, J. Am. Chem. Soc. 56, 353 (1934).

574278 O - 61 - 49

[7] Goff, J. A., and A. C. Bates, The interaction constant for moist air, Trans. ASHVE 47, 1 (1941).

[8] Goff, J. A., J. R. Andersen and S. Gratch, Final values of the interaction constant for moist air, Trans. ASHVE 49, 269 (1943).

[9] Walker, A. C., and E. J. Ernst, Jr., Preparation of air of known relative humidity and its application to the calibration of an absolute-humidity recorder, Ind. and Eng. Chem. Anal. Ed. 2, 134 (1930).

[10] Wexler, A., Divided flow, low-temperature humidity test apparatus, J. Research NBS 40, 479 (1948).

[11] Tamman, G., Über eine dynamische Methode zur Bestimmung der Dampfspannungen, Annalen der Physik (Wied) 33, 322 (1888).

[12] Walker, J., Über eine Methode zur Bestimmung der Dampfspannungen bei niederen Temperaturen, Z. physik Chem. 2, 602 (1888).

[13] Linebarger, C. E., On the vapor-tensions of mixtures of volatile liquids, J. Am. Chem. Soc. 17, 615 (1895).

[14] Orndorff, W. R., and H. G. Carrell, The vapor pressure method of determining molecular weights, J. Phys. Chem. 1, 753 (1897).

[15] Perman, E. P., The evaporation of water in a current of air, Proc. Roy Soc. London 72, 72 (1903).

[16] Carveth, H. R., and R. E. Fowler, Saturation by the method of air-bubbling, J. Phys. Chem. 8, 313 (1904).

[17] Earl of Berkley and E. G. J. Hartley, The determination of the osmotic pressures of solutions by the measurement of their vapor pressure, Proc. Roy. Soc. London 77, 156 (1906).

[18] Lincoln, A. T., and D. Klein, The vapor pressure of aqueous nitrate solutions, J. Phys. Chem. 11, 318 (1907).

[19] Krauskopf, F., The vapor pressure of water and aqueous solutions of sodium chloride, potassium chloride and sugar, J. Phys. Chem. 14, 489 (1910).

[20] Derby, I. H., F. Daniels, and F. C. Gutsche, An apparatus for the measurement of vapor pressures by the dynamic method and determinations of the vapor pressure of water at 24.97°, J. Am. Chem. Soc. 36, 793 (1914).

[21] Washburn, E. W., and E. O. Heuse, The measurement of vapor pressure lowering by the air saturation method, J. Am. Chem. Soc. 37, 309 (1915).

[22] Goff, J. A., and J. B. Hunter, Measurement of latent heat by the gas-current method, J. Appl. Mech. 9, 21 (1942).

[23] Hunter, J. B., and H. Bliss, Thermodynamic properties of aqueous salt solutions, Ind. Eng. Chem. 36, 945 (1944).

[24] Johnson, E. F., Jr., and M. C. Molstad, Thermodynamic properties of aqueous lithium chloride solutions, J. Phys. Colloid. Chem. 55, 257 (1951).

[25] Bower, J. H., Comparative efficiencies of various dehydrating agents used for drying gases (a survey of commercial drying agents), J. Research NBS 12, 241 (1934).

[26] Bower, J. H., Revised results obtained with certain dehydrating agents used for drying gases, J. Research NBS 33, 199 (1944).

[27] Morley, E. W., Amount of moisture in a gas, Am. J. Sci. 30, 140 (1884); 34, 199 (1887).

[28] Smith, F. A., and J. H. Eiseman, Saturation of gases by laboratory wet test meters, J. Research NBS 23, 345 (1939).

[29] Waidner, C. W., and E. F. Mueller, Industrial gas calorimetry, B.S. Tech. Paper No. 36 (1914).

[30] Bean, H. S., Gas measuring instruments, NBS Circ. 309 (December 8, 1926).

[31] Pollitzer, F., and E. Strebel, Über den Einfluss indifferente Gase auf die Sattigungs - Dampfkonzentration von Flüssigkeiten, Z. Phys. Chem. 110, 768 (1924).

[32] Weaver, E. R., and R. Riley, Measurement of water in gases by electrical conduction in a film of hygroscopic material and the uses of pressure changes in calibration, J. Research NBS 40, 169 (1948).

[33] Weaver, E. R., Electrical measurement of water vapor with a hygroscopic film, Annal. Chem. 23, 1076 (1951).

[34] Wexler, A., and R. D. Daniels, Jr., Pressure humidity apparatus, J. Research NBS 48, 269 (1952).

[35] Goff, J. A., and S. Gratch, Low pressure properties of water from -160 to 212 F, Trans. ASHVE 52, 95 (1946).

[36] Smithsonian Meteorological Tables, 6th revised ed. (The Smithsonian Institution (1951).

[37] Wiegerink, J. G. Equipment for conditioning materials at constant humidities and at elevated temperatures, NBS J. Research 24, 639 (1940).

[38] Wexler, A., Recirculating apparatus for testing hygrometers, J. Research NBS 45, 357 (1950).

[39] Burcham, J. N., Variable temperature and humidity oven, J. Sci. Instr. 30, 335 (1953).

[40] Glueckhauf, E., Investigation on absorption hygrometers at low temperatures, Proc. Phys. Soc. London 59, 344 (1947).

[41] Wexler, A., Divided flow type, low temperature humidity test apparatus, J. Research NBS 40, 479 (1948).

[42] O'Brien, F.E.M., The control of humidity by saturated salt solutions - a compilation of data, J. Sci. Instr. 25, 73 (1948).

[43] Washburn, E. W., International critical tables, Vol. III, 211 (McGraw-Hill Book Co., New York, N.Y.).

[44] Hodgeman, C. D., Handbook of Chemistry and Physics (Chemical Rubber Pub. Co., Cleveland, Ohio).

[45] Wexler, A. and S. Hasegawa, Relative humidity-temperature relationships of some saturated salt solutions in the temperature range 0° to 50°C, J. Research NBS 53, 19 (1954).

[46] Wilson, R. E., Humidity control by means of sulfuric acid solutions with a critical compilation of vapor pressure data, Ind. Eng. Chem. 13, 326 (1921).

[47] Hepburn, J.R.I., The vapor pressure of water over sulfuric acid-water mixtures at 25°C, and its measurement by an improved dewpoint apparatus, Proc. Phys. Soc. London, 40, 249 (1928).

[48] Collins, E. M., The partial pressures of water in equilibrium with aqueous solutions of sulfuric acid, J. Phys. Chem. 37, 1191 (1933).

[49] Shankman, S. and A. R. Gordon, The vapor pressure of aqueous solutions of sulfuric acid, J. Am. Chem. Soc. 61, 2370 (1939).

[50] Stokes, R. H., The measurement of vapor pressure of aqueous solutions by bi-thermal equilibrations through the vapor phase, J. Am. Chem. Soc. 69, 1291 (1947).

[51] Stokes, R. H. and R. A. Robinson, Standard solutions for humidity control at 25°, Ind. Eng. Chem. 41, 2013 (1949).

[52] Washburn, E. W., Int. Crit. Tables III, 291 and 293 (McGraw-Hill Book Co., New York, N.Y.).

[53] Grover, D. W., and J. M. Nicol, The vapor pressure of glycerin solutions at 20°, J. Soc. Chem. Ind. 59, 175 (1940).

[54] Griffiths, E., Some modified forms of hygrometers, Trans. Phys. Soc. London, 35, viii (1921-22).

[55] Matthews, I. C., and A. M. Burgess, Laboratory humidity cabinet, Ind. Eng. Chem. 20, 1239 (1928).

[56] Ewing and Glazebrook, The measurement of humidity in closed spaces, Spec. Report No. 8, Food Investigation Board, Dept. of Scientific and Ind. Research (London, 1925). Revised ed. by E. Griffiths (1933).

[57] Kleinschmidt, E., Handbuch der meteorologischen Instrumente (Julius Springer, Berline, 1935).

[58] Lonsdale, T., Small constant humidity chamber, Engineering 139, 321 (1935).

[59] Webster, C. T., A humidity control for ovens, J. Sci. Inst. 13, 412 (1936).

[60] Humphries, F. E., Some notes on the control of humidity and the construction of a constant-temperature and -humidity cabinet for lab. use, J. Intern. Soc. Leather Trades Chem. 22, 224 (1938).

[61] Middleton, W.E.K., Meteorological instruments (University of Toronto Press, 1941).

[62] Andrews, R. L., Bridge controlled relay circuit for Dunmore relative humidity elements, Rev. Sci. Inst. 14, 276 (1943).

[63] Hauck, V. D., R. E. Strum, and R. B. Colt, Recorder and controller for temperature and humidity, Electronics 19, 36 (1946).

[64] Cram, L. A., An apparatus for producing air of controlled relative humidity for hygrometer calibration and testing, J. Sci. Instr. 33, 273 (1956).

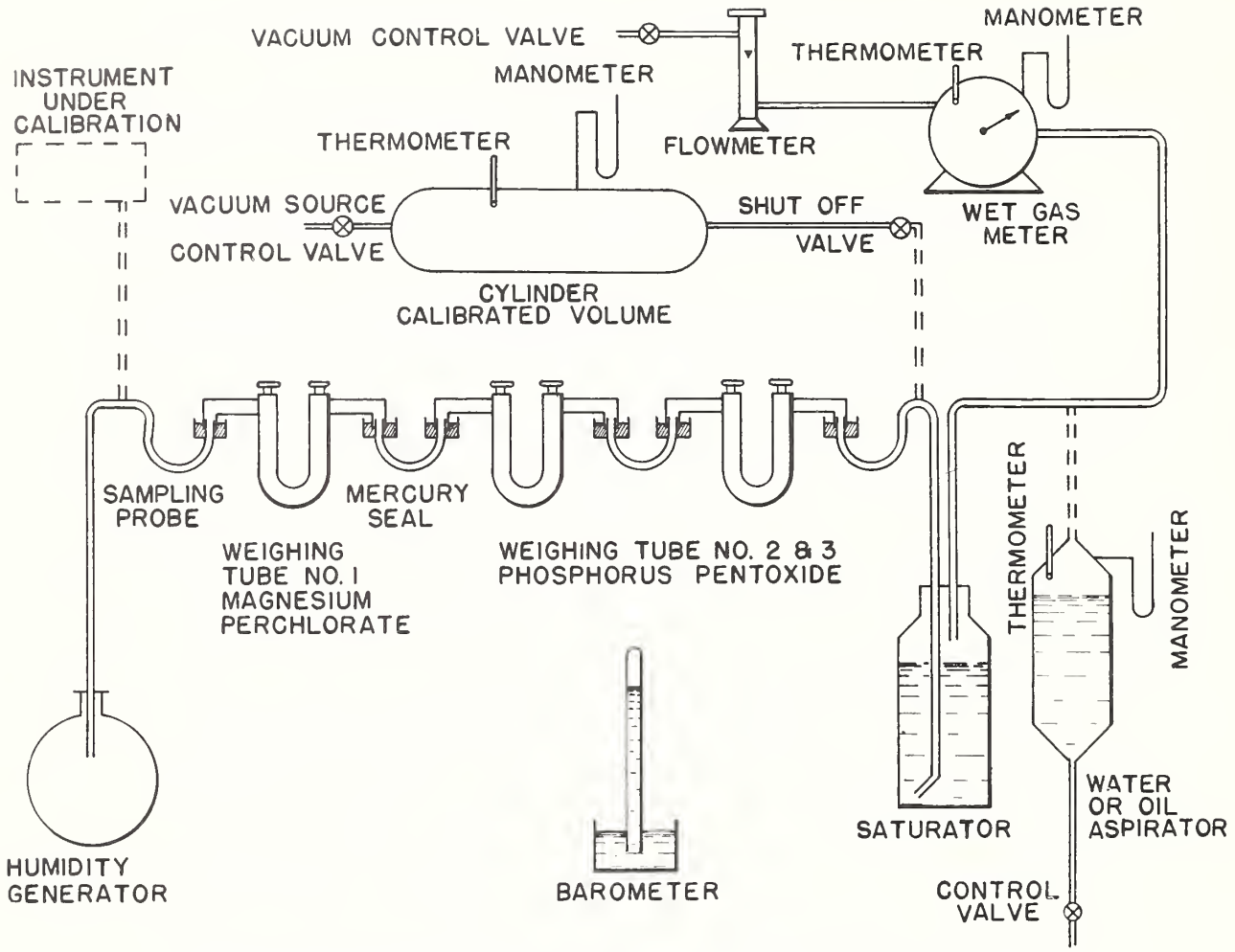

Figure 1. Gravimetric method of moisture measurement.

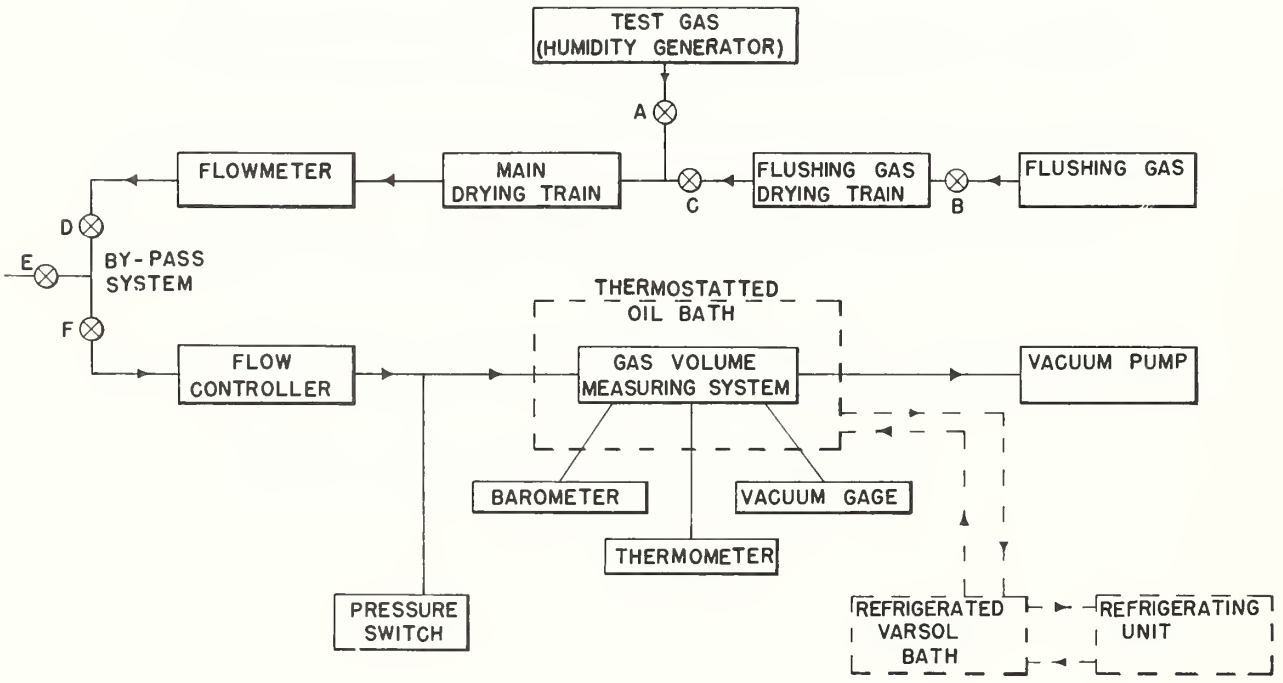

Figure 2. Block diagram of NBS gravimetric hygrometer.

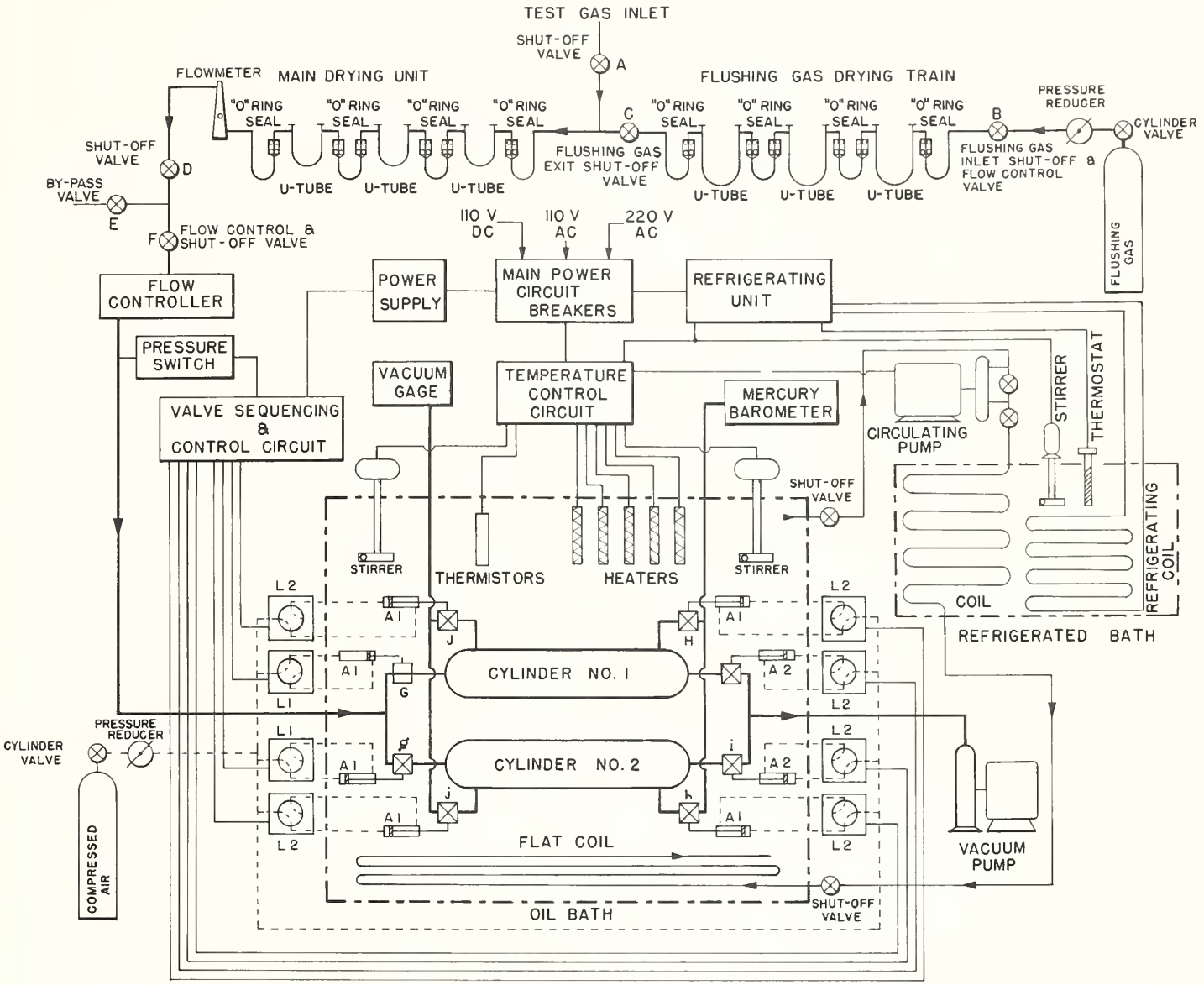

Figure 3. Flow diagram of NBS gravimetric hygrometer.

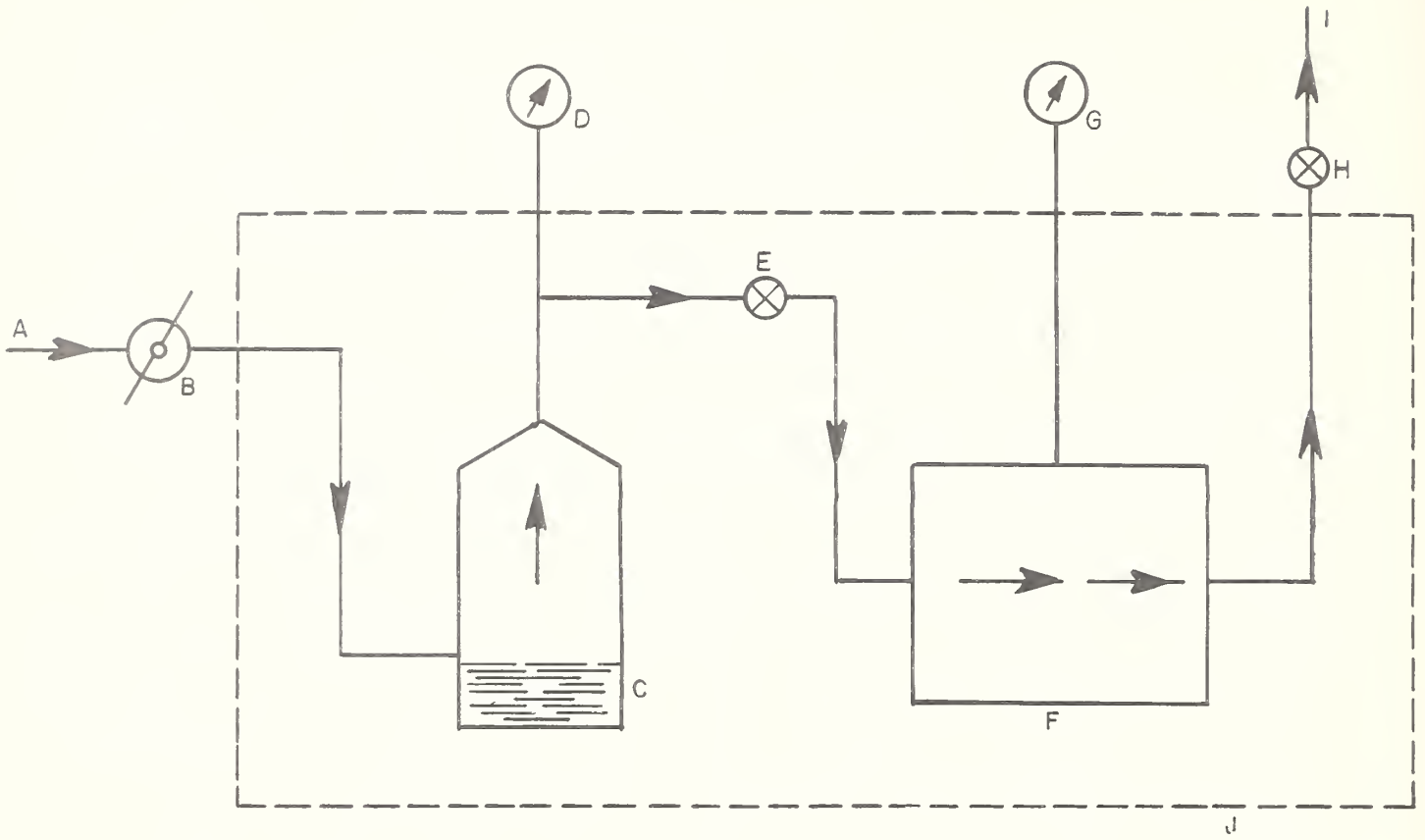

Figure 4. Simplified schematic drawing of pressure humidity generator.

A - Source of high pressure air
B - Pressure regulator
C - Saturator
D - Precision pressure gage
E - Expansion valve
F - Test Chamber
G - Precision pressure gage
H - Control valve
I - Atmosphere or vacuum source

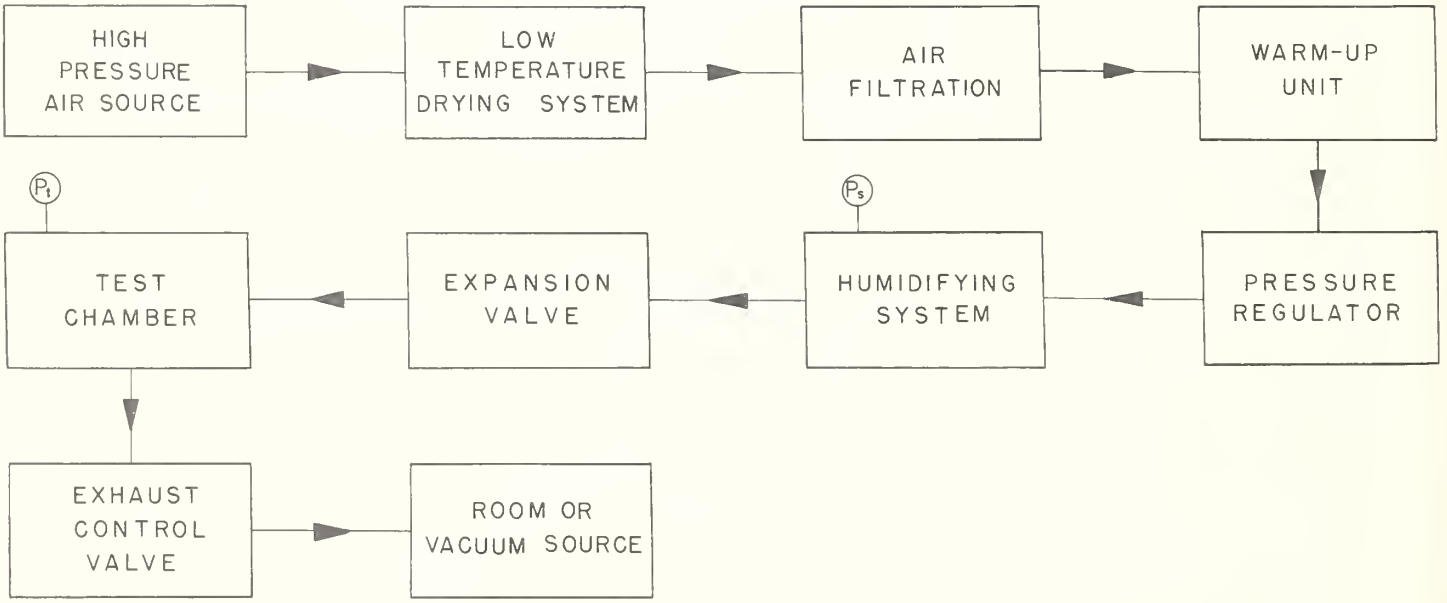

Figure 5. Block diagram of NBS pressure humidity generator.

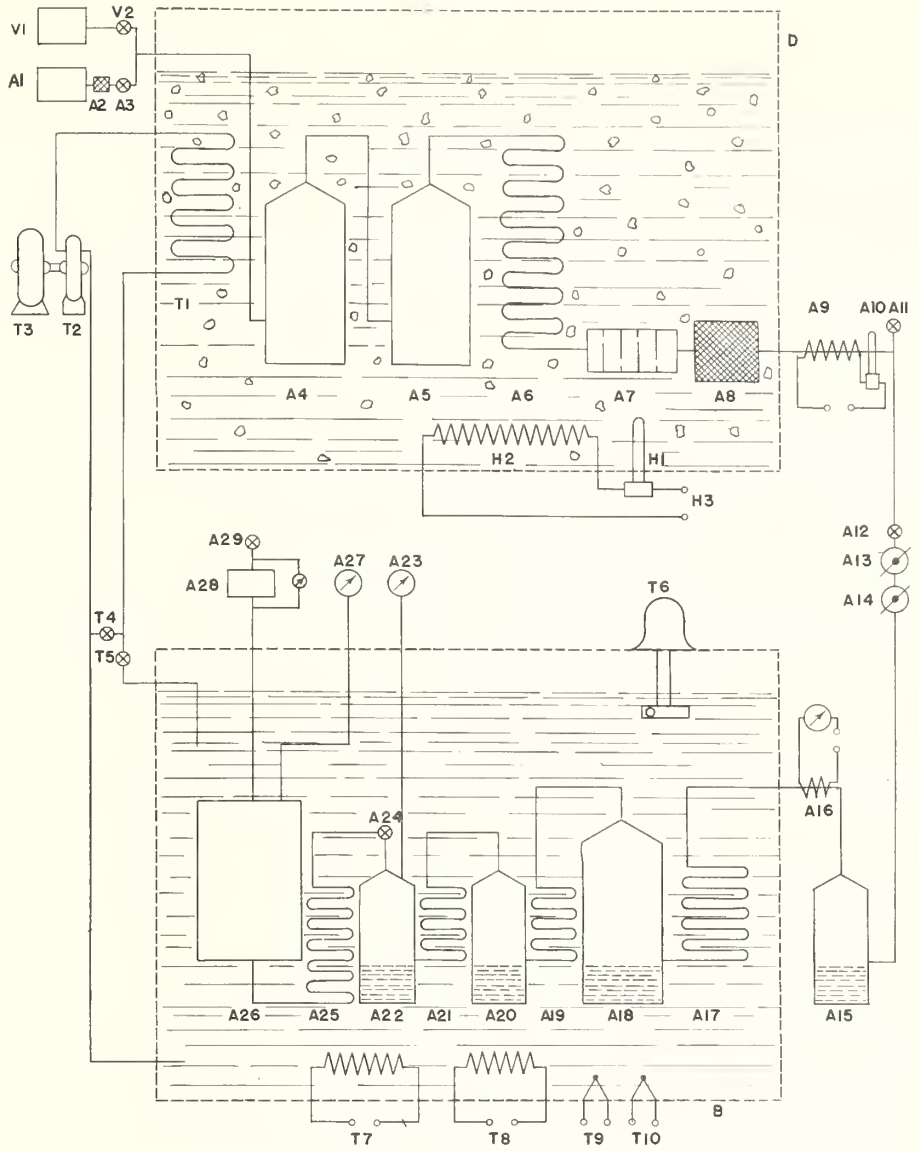

Figure 6. Schematic drawing of NBS pressure humidity generator.

A 1 - High pressure source
A 2 - Filter
A 3 - Valve
A 4, 5 - Centrifugal water separator
A 6 - Copper cooling coil
A 7 - Fin air dryer
A 8 - Low temperature filter
A 9 - Electric heater
A 10 - Bimetal thermregulator
A 11 - Air reversal valve
A 12 - Shut-off valve
A 13, 14 - Pressure regulator
A 15 - External gross saturator
A 16 - Resistance thermometer and indicator
A 17, 19, 21, 25 - Copper coil heat exchangers
A 18, 20, 22 - Centrifugal saturators
A 23, 27 - Pressure gages
A 24 - Expansion valve
A 26 - Test chamber
A 28 - Linear flowmeter
A 29 - Exhaust control valve
B - Insulated liquid (varsol) constant temperature bath
D - Insulated dry ice bath
H 1 - Bimetal thermoregulator
H 2 - Electric heater
H 3 - Input voltage
T 1 - Varsol cooling coil
T 2 - Positive rotary displacement pump
T 3 - Motor
T 4 - Varsol by-pass valve
T 5 - Varsol control valve
T 6 - Centrifugal stirrer
T 7 - Constant electric heater
T 8 - Intermittent electric heater
T 9, 10 - Thermistors
V 1 - Vacuum source
V 2 - Vacuum shut-off valve

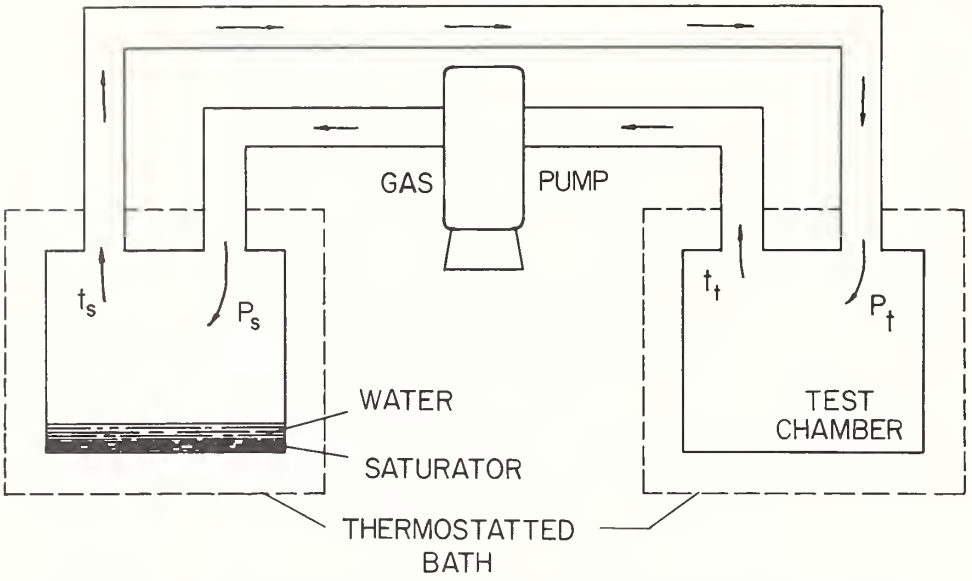

Figure 7. Simplified schematic drawing of two-temperature humidity generator.

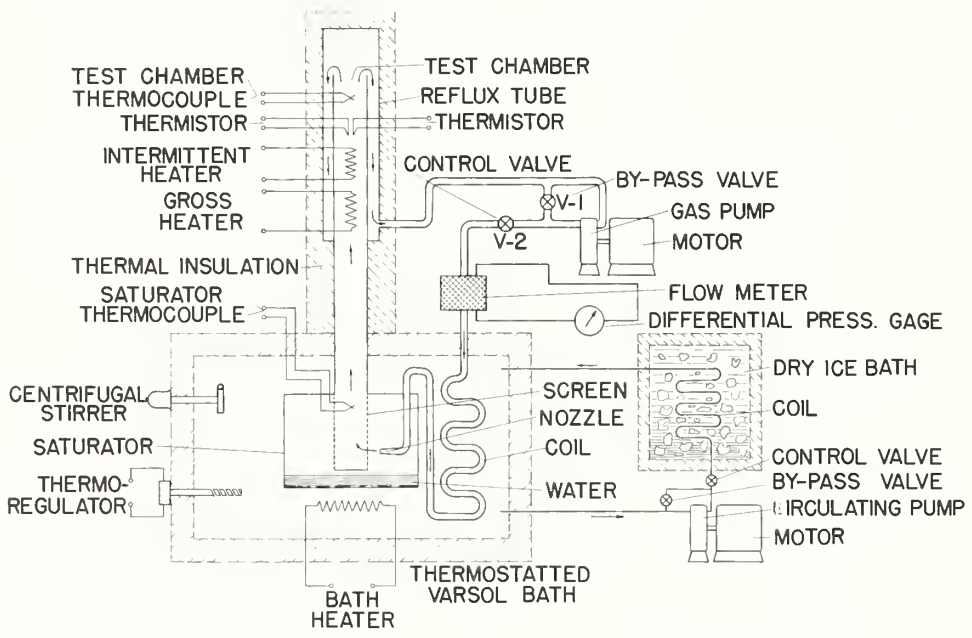

Figure 8. Schematic drawing of NBS two-temperature humidity generator.

Single recirculating system shown.

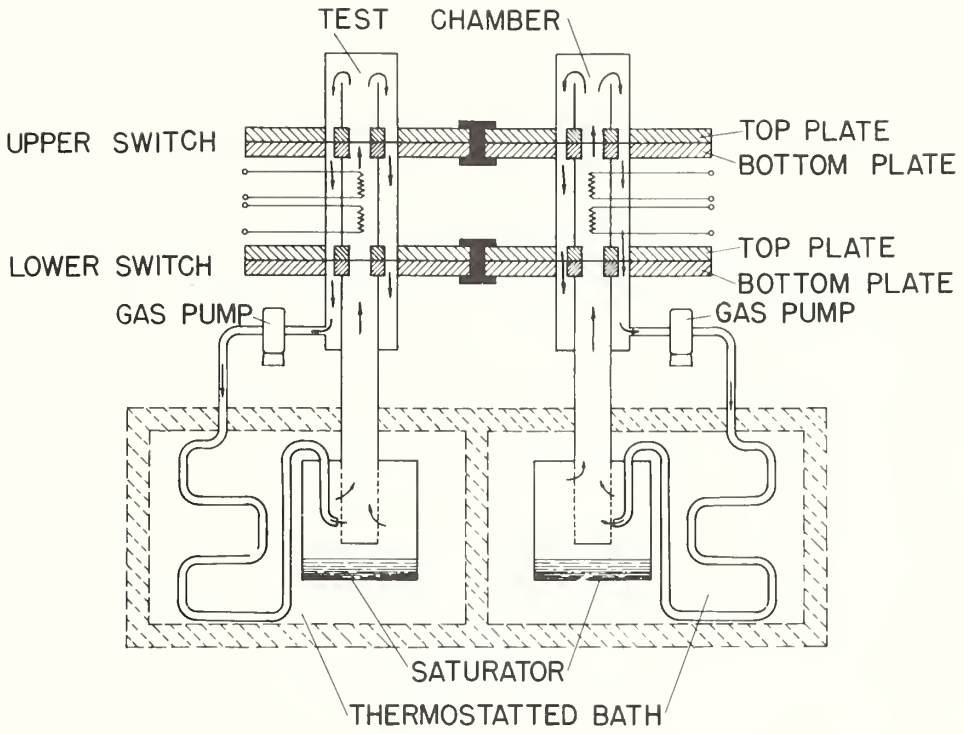

Figure 9. Schematic diagram of pneumatic switches for interchanging test saturators of NBS two-temperature humidity generator.

Only two of four recirculating systems shown.

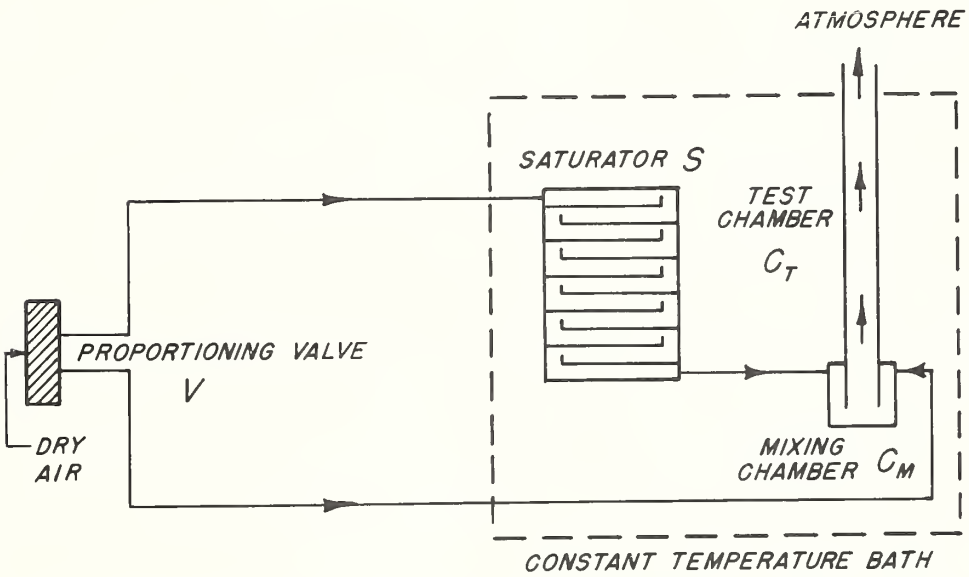

Figure 10. Simplified schematic drawing of divided-flow humidity generator.

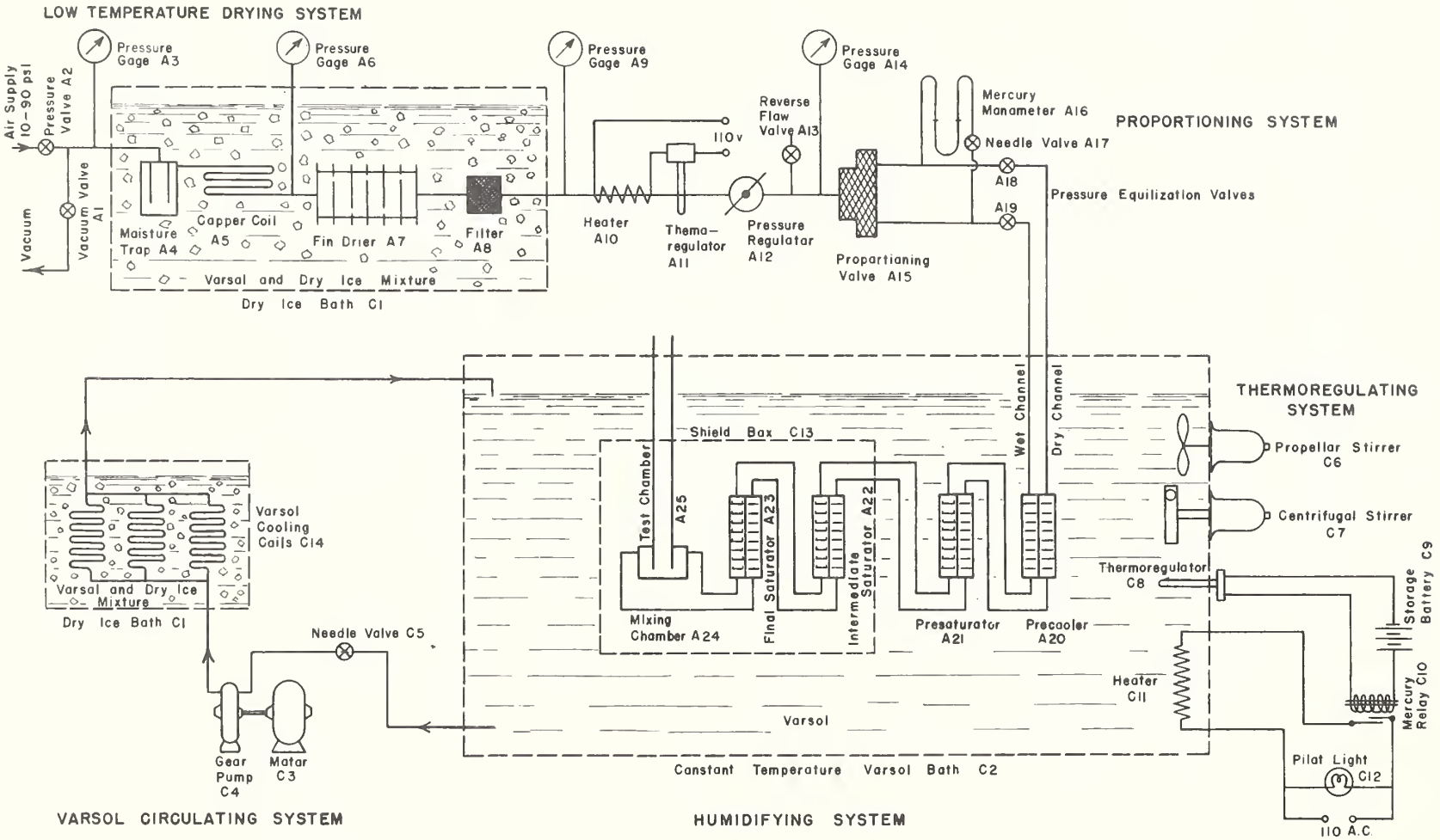

Figure 11. Schematic drawing of NBS divided-flow humidity generator.

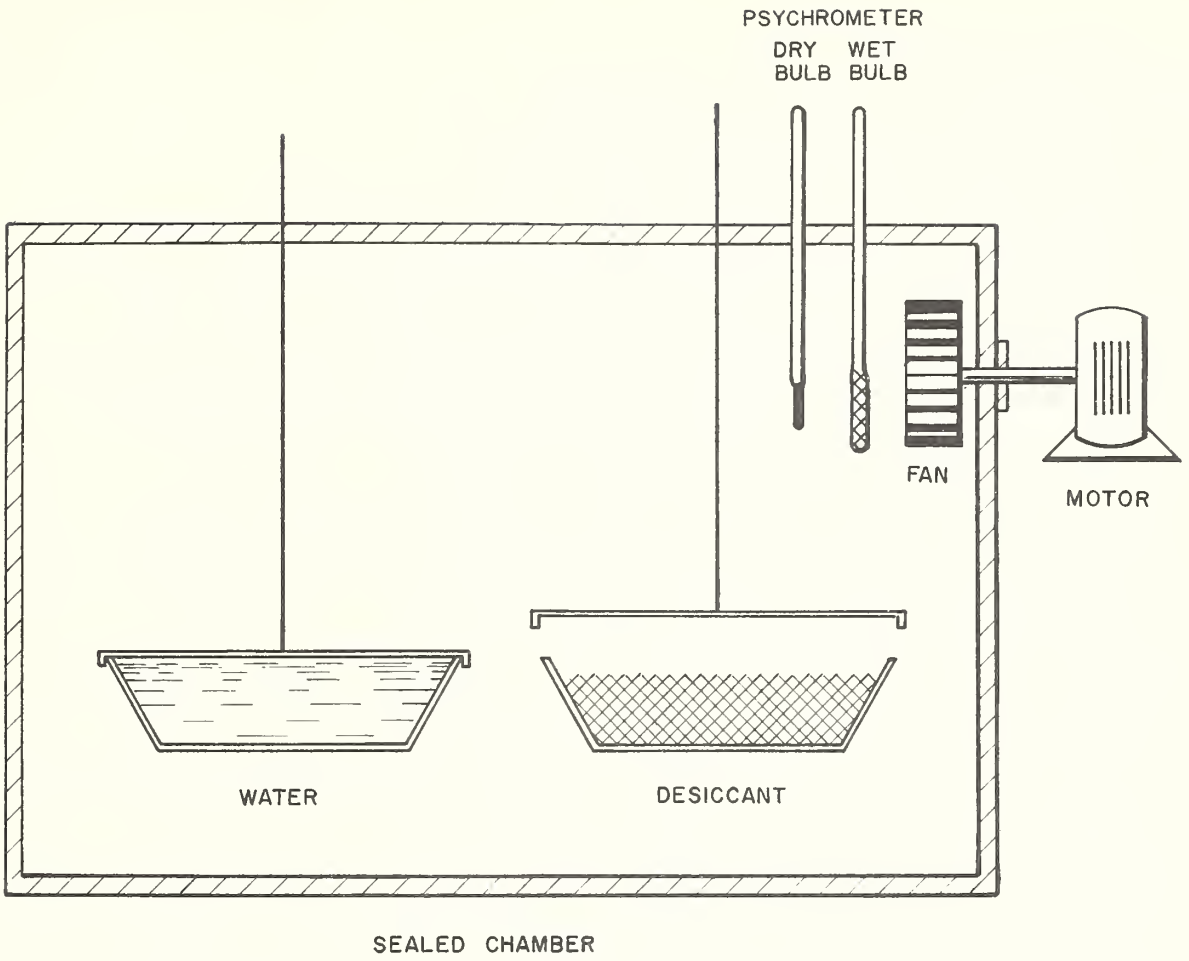

Figure 12. Simple humidity chamber.

Recirculating Apparatus for Testing Hygrometers [1]

By Arnold Wexler

An apparatus that was developed for producing atmospheres of known relative humidity is described. It was designed, principally, for research on and calibration of radiosonde hygrometer elements at temperatures above freezing, but is equally useful at temperatures down to −40° C. It operates by saturating air at one temperature and then raising the air temperature sufficiently to give any desired relative humidity. The air is recirculated continuously in a closed system. Four identical, but independent, recirculating systems are employed. Discrete changes in humidity and temperature are obtained by means of a novel pneumatic valve that permits the hygrometers under test to be switched, easily, from system to system. Checks on the performance of the apparatus by means of the gravimetric method of moisture determination and the psychrometric method show an average difference in relative humidity of ±1.2 percent.

I. Introduction

In the meteorological sounding of the upper atmosphere by means of the radiosonde, the device commonly employed for sensing the water vapor content of the air is the electric hygrometer.[2] [3] During a flight, the hygrometer may be subjected to a wide range of temperatures and humidities, as well as to air flows, corresponding to rates of ascent of the balloon, of 1,000 ft/min or more. These conditions of use have created a need for some convenient means of producing and maintaining atmospheres of known relative humidity, at any of the temperatures encountered in a radiosonde flight, for calibration and research purposes.

An apparatus has been developed to fulfill this need. It was designed for operation, principally, at temperatures above 0° C but is equally useful at temperatures down to −40° C. Provision was made for obtaining discrete changes in humidity and temperature and for maintaining given air speeds. It supplements an apparatus of the divided-flow type previously built for use at temperatures below freezing.[4]

II. Theory

A fundamental method for producing an atmosphere of known relative humidity is to saturate a stream of air with water vapor at a given temperature and then to raise the temperature of the air to a specified higher value. If t_s is the temperature of saturation, e_s the saturation pressure of water vapor at temperature t_s, t_t the elevated temperature, and e_t the saturation pressure of water vapor at temperature t_t, then the relative humidity, H, at temperature t_t is

$$H=100\,\frac{e_s}{e_t}. \tag{1}$$

In eq 1 the assumption is made that the absolute pressure of the air at the elevated temperature, t_t, is the same as the absolute pressure of the air at the saturation temperature, t_s. If these two pressures are not identical, then a pressure correction must be introduced. If P_s is the absolute pressure of the air at t_s, and P_t is the absolute pressure of the air at t_t, then the relative humidity is

$$H=100\,\frac{e_s}{e_t}\,\frac{P_t}{P_s}. \tag{2}$$

A simplified schematic diagram illustrating how the two-temperature method may be employed in an apparatus is shown in figure 1. By means of a gas pump, air is circulated from a saturator into a test chamber and then back into the saturator. The temperature, t_s, of the saturator and the temperature, t_t, of the test chamber are maintained at their respective desired values by thermostatted baths. Complete saturation is achieved simply, and efficiently by recirculation of air over water in the saturator, in a closed system. The relative humidity, H, in the test chamber is given by eq 2, where the saturation vapor pressures, e_s and e_t, corresponding to temperatures t_s and t_t, are obtained from standard tables, and the absolute pressures, P_s and P_t, are measured values.

The design of a practical system, based on this method, is shown in figure 2. It differs from the elementary design of figure 1 in that the test-chamber temperature is controlled by means of a heater inserted in the air stream rather than by

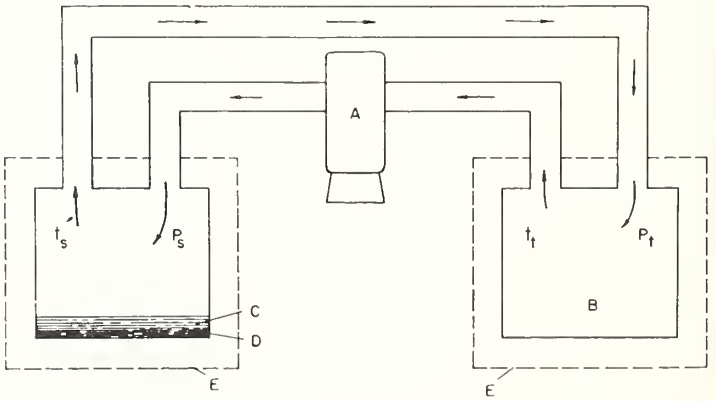

FIGURE 1. *Simplified schematic diagram illustrating the two-temperature recirculating method of relative humidity production.*

A, Gas pump; B, test chamber; C, water; D, saturator; E, thermostatted bath.

[1] This apparatus was developed for the Bureau of Ships, Department of the Navy.
[2] F. W. Dunmore, J. Research NBS **20**, 723 (1938) RP1102.
[3] F. W. Dunmore, J. Research NBS **23**, 701 (1939) RP1265.
[4] A. Wexler, J. Research **40**, 479 (1948) RP1894.

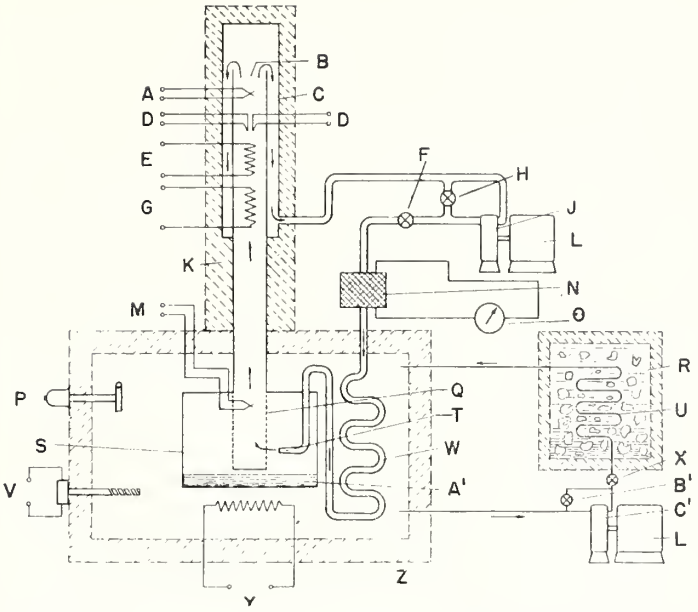

FIGURE 2. *Schematic diagram of a practical two-temperature recirculating humidity apparatus.*

A, Test-chamber thermocouple; B, test chamber; C, reflux tube; D, thermistor; E, intermittent heater; F, control valve (air); G, gross heater; H, bypass valve (air); J, gas pump; K, thermal insulation; L, motor; M, saturator thermocouple; N, flow meter; O, differential pressure gage; P, centrifugal stirrer; Q, screen; R, dry-ice bath; S, saturator; T, nozzle, U, coil (liquid); V, thermoregulator; W, coil (air); X, control valve (liquid); Y, bath beater; Z, thermostatted Varsol bath; A′, water; B′, bypass valve (liquid); C′, circulating pump.

immersing the test chamber in a thermostatted liquid bath. The elimination of a thermostatted bath for the test chamber, with the resultant simplification in design and construction, is made possible by the fact that the saturator must necessarily be maintained at a lower temperature than the test chamber, and hence the only requirement for achieving any desired test-chamber temperature is the introduction of the requisite amount of heat into the air stream. A novel feature of the test-chamber design is the concentric tube arrangement. The air from the saturator flows upward through the inner tube, then reverses its direction and returns downward in the annular space between the inner and outer tubes. The outer tube is thermally insulated. This reflux action contributes to temperature control and a reduction in thermal losses, for it surrounds the test space, which is at the upper end of the inner tube, with air at or near the test-chamber temperature.

The important features of the saturator are its simplicity of design, its adaptability for temperatures below as well as above the freezing point of water, and its effective saturation of air at both high and low flows. These features are achieved in large measure by imparting a centrifugal action to the entrant air stream. The saturator is a cylindrical chamber to which water is added to a convenient depth. Air is discharged through a nozzle into the chamber above the water surface and tangential to the vertical walls and is exhausted through a central port in the top. The centrifugal action creates a whirlpool and thoroughly mixes water vapor with the air. Spray and liquid droplets are forced to the walls by centrifugal force, with the result that there is little tendency for liquid water to emerge through the exit port, except at very low air flows. A multilayer fine wire screen baffle is used at the exit to trap and prevent water from passing out of the saturator at the low flows. As the air does not bubble through the water but only passes over its exposed surface, the water may be frozen without impairing the functioning of the saturator. The saturation pressure of the water vapor in the saturator (for use in eq 2) is taken, then, with respect to ice.

A desirable requirement in a humidity apparatus is a scheme or mechanism whereby the relative humidity may be changed quickly and in discrete steps. Such a scheme is necessary for lag studies on hygrometers. It is achieved in this equipment by utilizing four identical but independent systems that are arranged in such a fashion that their test chambers may be interchanged easily and rapidly. Thus, if a different temperature, t_s, is maintained in each of the four saturators, and if the same temperature, t_t, is maintained in each of the four test chambers, then the relative humidity in each test chamber is different. By interchanging the test chambers, the relative humidities therein undergo discrete changes, as each test chamber now communicates with a different saturator.

The arrangement is shown schematically in figure 3 for two of the four systems. The interchange of test chambers is effected by a special pneumatic switch. It consists of two ground and lapped plates to which the inner and outer tubes are attached and which contain ports through which the air may pass. A quarter turn of the top plate with respect to bottom plate advances each test chamber to a new position and connects each test chamber with a different

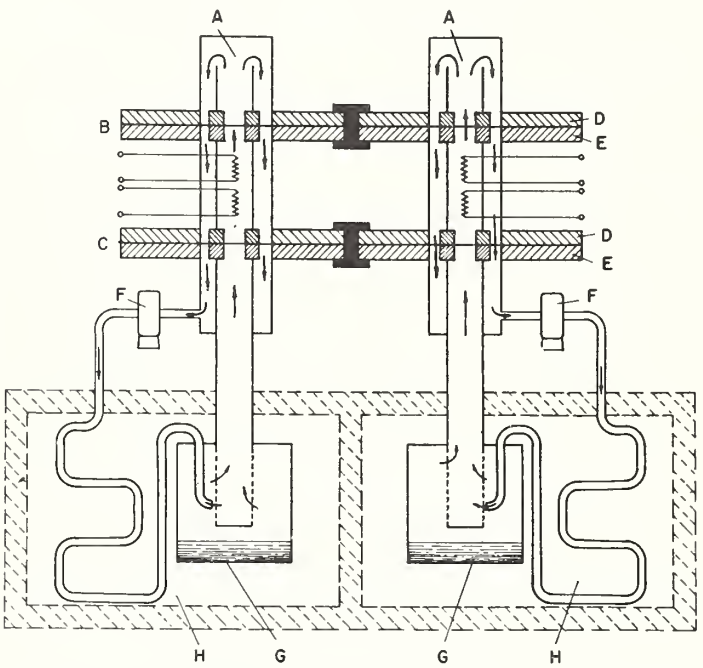

FIGURE 3. *Schematic diagram of pneumatic switches for interchanging test chambers; only two of the four systems are shown.*

A, Test chamber; B, upper switch; C, lower switch; D, top plate; E, bottom plate; F, gas pump; G, saturator; H, thermostatted bath.

saturator. Two such switches are used instead of one for greater convenience and versatility. For lag studies only, the upper switch is used. The speed with which the relative humidity can be changed is of the order of 1 to 2 seconds and depends primarily on the speed with which the switch can be rotated.

III. Design Details

An oil-free impeller-type gas pump is used to circulate air continuously through each system. The flow is controlled by means of a bypass valve, as shown in figure 2, and is measured by a glass-wool linear flowmeter that is calibrated in terms of air speed through the test chamber. The air flows through a copper tube coil, immersed in the same thermostatted liquid bath as the saturator and reaches bath temperature before it passes into the saturator. The cooling coil is essential for satisfactory operation, for unless the air enters the saturator at the bath temperature, an uncertainty in saturation temperature ensues. The saturator is a brass cylinder, 5 in. in diameter and 4 in. deep. The inner tube of the reflux portion of the system is polystyrene with 1¼-in. outside diameter and ⅛-in. wall thickness, while the outer is brass tubing with 2-in. outside diameter and 1/32-in. wall thickness.

The copper tube coil and saturator are immersed in a varsol bath, whose temperature is closely regulated. Varsol is used so that low temperatures may be attained. A bimetal thermoregulator controls a heater through a power relay. The circuit is shown in figure 4. A positive rotary displacement pump

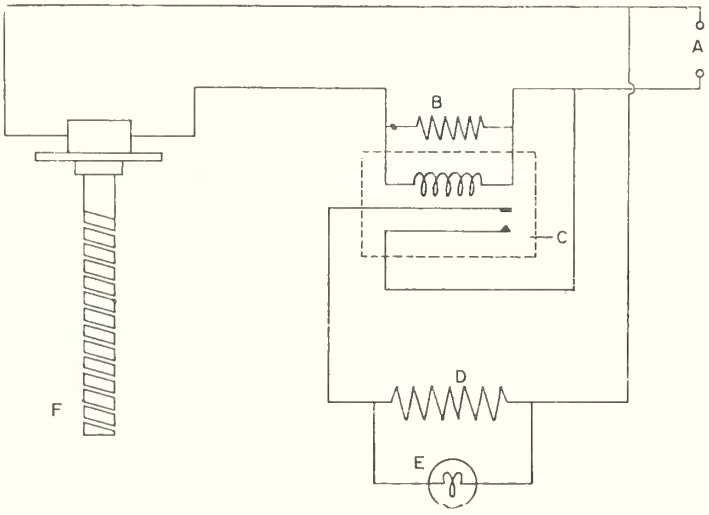

FIGURE 4. *Varsol bath temperature control circuit.*

A, 110-v alternating current; B, shunt resistor; C, power relay; D, bath heater; E, pilot lamp; F, bimetallic thermostat.

withdraws varsol from the bath, circulates it through another cooling coil and discharges it back into the bath. This second cooling coil is maintained at −78° C by crushed dry ice. The cold varsol flow is adjusted, by means of valves, so that the bath temperature will tend to drop very slightly. The heater is arranged to go on when the bath temperature drops below the control point and will go off when the bath temperature is at or above the control point. On-off regulation is thereby achieved. The bath is actively agitated by a centrifugal stirrer.

The temperature of the moving air stream in the test chamber is controlled by two heaters; a gross heater supplies constant heat, the amount manually adjusted, by means of a rheostat, as shown in figure 5; an intermittent heater supplies heat on demand, the amount also manually adjusted by a rheostat and the demand determined by two thermistors acting as the temperature sensitive elements. The gross heater supplies most of the heat, whereas the intermittent heater supplies heat, as required, to raise the temperature to the control point. Figure 6

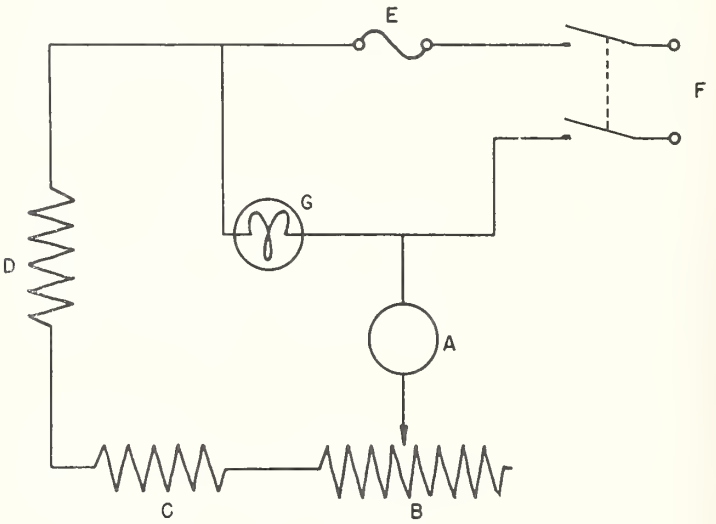

FIGURE 5. *Test-chamber gross-heater circuit.*

A, Ammeter; B, rheostat; C, limiting resistor; D, gross heater; E, fuse; F, 110-v alternating-current regulated supply; G, pilot lamp

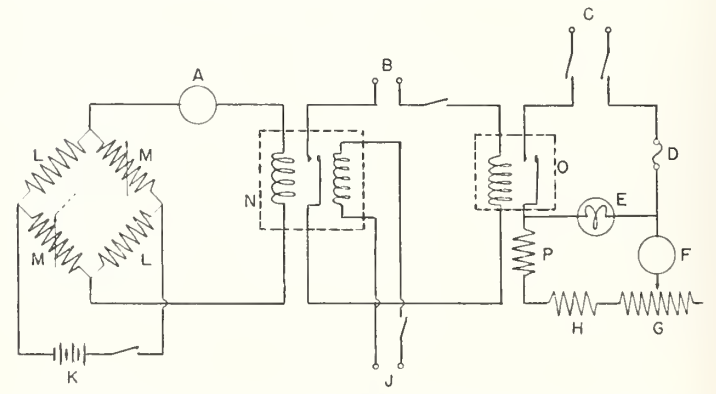

FIGURE 6. *Test-chamber intermittent-heater control circuit.*

A, Microammeter; B, 6-v direct current; C, regulated 110-v alternating current; D, fuse; E, light; F, milliammeter; G, rheostat; H, limiting resistor; J, 28-v pulsing circuit; K, 22½ v; L, thermistor; M, decade resistance box; N, galvanometer relay; O, power relay; P, intermittent heater.

is a circuit diagram of the intermittent heater control circuit. The desired control temperature is established by resistances, *M* (coupled decade resistance boxes) in a Wheatstone bridge circuit containing thermistors, *L*. The bridge balance is sensed by a galvanometer relay. A current of ½ microampere deflects the pointer against a magnetic contact, actuating a power relay and, in turn, the intermittent heater. The operation of an electromagnetic

plunger returns the pointer to a sensing position. If the bridge is balanced, the pointer does not move; if the bridge is unbalanced, the pointer deflects. An electronic pulsing circuit periodically triggers the plunger at a frequency that is adjustable from 2 times a minute to 60 times a minute, so that the galvanometer may sense the balance of the bridge.

The completed apparatus is shown in figure 7. Figure 8 shows the apparatus with the cover raised showing the four thermostatted baths.

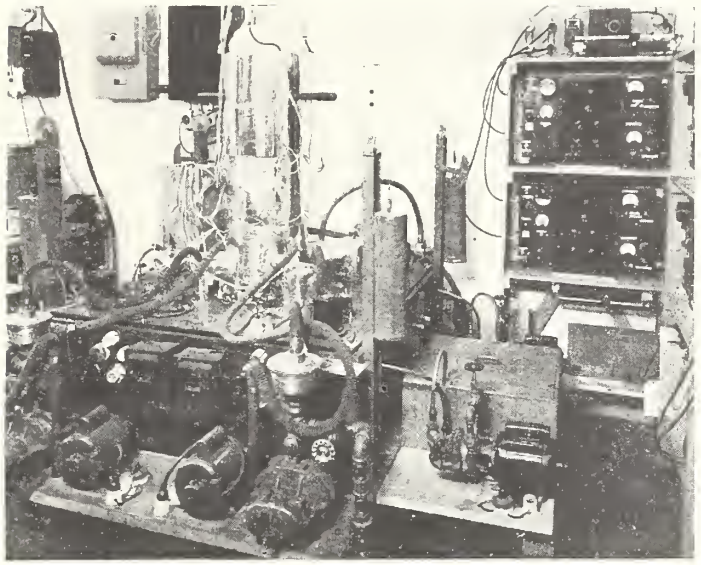

FIGURE 7. *Humidity apparatus.*

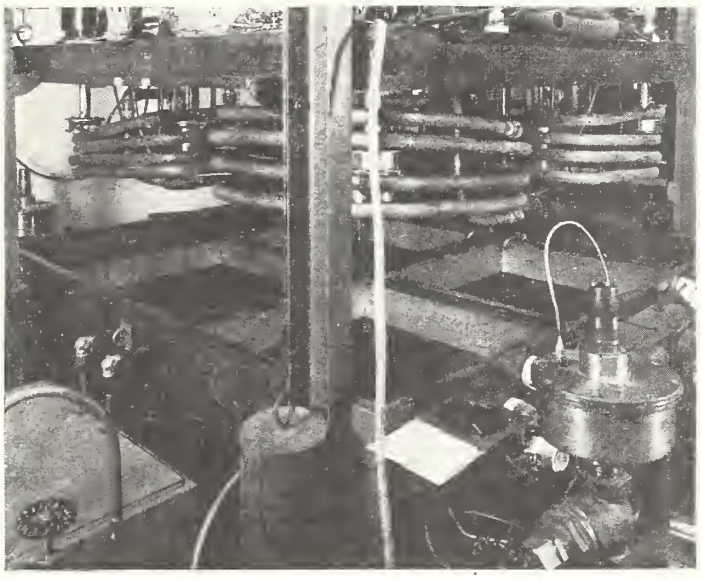

FIGURE 8. *View of apparatus with cover raised showing the four independent thermostatted baths.*

IV. Performance Characteristics

The performance of the apparatus has been investigated to determine the accuracy and the usable temperature and humidity ranges. The gravimetric method of moisture determination (see footnote 4) was used to give an independent check on the relative humidity produced by the apparatus for various saturator and test-chamber temperatures and various speeds of air flow. The results are given in table 1. As an additional check on the accuracy, a thermocouple psychrometer was employed to measure the actual relative humidity in the test chamber. The results are given in table 2. These tests show an average difference in percentage of relative humidity of ± 1.2 percent between the gravimetrically measured relative humidity and the apparatus relative humidity given by eq 2; and an average difference in percentage of relative humidity of ± 0.9 percent between the psychrometric measurements and the apparatus values given by eq 2.

TABLE 1. *Gravimetric calibration*

Run	Date, 1949	Air velocity	Test-chamber temperature	Relative humidity		
				Apparatus	Gravimetric	Difference
		ft/min	*°C*	*Percent*	*Percent*	*Percent*
14	10/28	50	24.52	39.2	39.6	−0.4
15	10/28	250	25.45	37.0	37.8	−.8
16	10/28	500	26.41	34.7	35.8	−1.1
17	10/28	1,000	27.61	32.3	32.6	−0.3
18	11/1	500	−3.85	46.0	47.0	−1.0
19	11/1	500	−3.54	22.8	23.4	−0.6
20	11/4	50	20.53	95.0	95.0	.0
21	11/4	1,000	21.41	87.6	84.7	+2.9
22	11/4	50	17.37	83.9	84.0	−0.1
23	11/4	1,000	17.83	81.1	81.6	−.5
24	11/9	1,000	4.75	88.9	85.1	+3.8
25	11/9	1,000	14.98	44.6	44.5	+0.1
26	11/9	1,000	9.68	97.5	94.6	+2.9
27	11/9	1,000	9.68	97.2	96.3	+0.9
28	11/14	1,000	15.71	89.3	88.7	+.6
29	11/14	1,000	15.71	89.2	86.6	+2.6
30	11/14	1,000	15.68	89.5	88.2	+1.3
Average						±1.3

TABLE 2. *Psychrometric calibration*

(Air velocity=1,000 ft/min)

Test-chamber temperature (°C)	Relative humidity		
	Apparatus	Psyehrometer	Difference
	Percent	*Percent*	*Percent*
15.88	88.6	88.8	−0.2
15.90	88.6	88.2	+.4
15.01	65.1	63.8	+1.3
15.05	64.9	65.5	−0.6
5.93	72.1	71.6	+.5
5.83	72.1	72.3	−.2
10.92	51.1	50.1	+1.0
10.71	51.9	51.2	+0.7
10.72	52.1	51.3	+.8
17.22	34.1	33.3	+.8
17.05	34.7	33.7	+1.0
17.12	34.2	32.9	+1.3
21.10	37.2	38.5	−1.3
21.17	37.0	38.5	−1.5
21.08	36.9	38.4	−1.5
21.10	36.9	38.2	−1.3
Average			±0.9

As the precision and accuracy of the apparatus is to a large extent a function of the precision and accuracy of the temperature regulation and measurement of the test chambers and saturators, these temperatures must be adequately controlled and suitably measured. Temperatures are measured

574278 O - 61 - 50

with calibrated copper-constantan thermocouples and a precision potentiometer to a precision of 0.01 deg C. Because of the fair size of the liquid bath, bimetallic regulation is adequate for maintaining saturation temperatures constant to ±0.02 deg C over time intervals of 1 hour and constant to ±0.1 deg C over long time intervals. The thermistor-Wheatstone bridge circuit maintains test chamber temperatures constant to ±0.04 deg C over time intervals of 1 hour and constant to ±0.1 deg C for long time intervals.

The distribution of temperature within the saturator was explored by means of thermocouples located at the inlet, in the water, and at the outlet. The temperature of the air emerging from the saturator is within ±0.04 deg C of the temperature of the air entering the saturator; the temperature of the air entering the saturator is within ±0.06 deg C of the temperature of the water in the saturator; and the temperature of the air emerging from the saturator is within ±0.08 deg C of the temperature of the water. These temperature differentials may account for errors of ±½-percent relative humidity.

The difference in temperature between the saturator and bath was also investigated. The air entering the saturator is within ±0.07 deg C of the bath temperature; the water temperature is within ±0.04 deg C of the bath temperature; and the air emerging from the saturator is within ±0.09 deg C of the bath temperature.

Although the gas pump is capable of producing very high rates of flow, the coupling between motor and pump is set to allow a maximum air speed of 1,500 ft/min in the test chamber. By proper adjustment of the bypass valve, any lesser air speed is obtainable.

The upper relative humidity limit is determined by the saturation temperature, the air velocity and the efficiency of the thermal insulation and refluxing action surrounding the test chamber. The thermal leakage through the insulation is 2.2 cal/min for each degree centigrade temperature difference between the test chamber and room. The maximum relative humidities that may be obtained with air speeds of 50 and 1,000 ft/min for various saturator temperatures and with the apparatus in a room at 30° C are given in table 3. It is apparent that at high air velocities, the thermal leakage does not seriously limit the relative humidity range. At very low air flows, the maximum relative humidity obtainable is seriously limited, especially at the low saturator temperatures. Fortunately, in electric hygrometer calibration and research, high air speeds are used in order to simulate radiosonde flights, hence relative humidities sufficiently high for all practical purposes can be obtained.

TABLE 3. *Computed maximum attainable relative humidities*

Saturator temperature (°C)	Maximum relative humidity at test-chamber air velocity of—	
	50 ft/min.	1,000 ft/min
	Percent	*Percent*
25	95	99
15	86	99
5	77	98
−5	64	97
−20	49	96

For any test chamber temperature, the lowest attainable relative humidity is limited by the lowest attainable saturator temperature, which is about −55°C. It is possible to reduce the relative humidity to about 16 percent at a test-chamber temperature of −40°C, and to lower values at higher test-chamber temperatures.

The saturator temperature must not be permitted to exceed room temperature, for then there is a possibility for the system above the saturator to assume a temperature less than that of the saturator with resultant condensation of water vapor. Equation 2 then would no longer give the relative humidity in the apparatus.

The internal diameter of the test chamber is 1 in. Two standard radiosonde electric hygrometers (4 in.×5/16 in.×1/32 in.) can be inserted into the test chamber. If all four channels or systems of the apparatus are operated simultaneously, then eight elements can be tested at one time.

The ratio of the absolute pressures in the test chamber and saturator, P_t/P_s, used in eq 2, varies somewhat with air velocity and negligibly with temperature. Its variation with velocity may be once determined and then applied as a pressure correction. This correction is very small, and except for the high air velocities may be neglected for most work. Even for an air velocity of 1,000 ft/min, the correction is only of the order of 0.6 percent. The pressure ratio corrections are shown in table 4.

TABLE 4. *Pressure ratio corrections*

Air speed	Pressure ratio corrections, P_t/P_s
ft/min	
0	1.0000
100	1.0000
200	0.9997
400	.9989
600	.9978
800	.9962
1,000	.9938

V. Discussion and Summary

An apparatus particularly suited for research and calibration of electric hygrometers of the Dunmore type has been designed, developed, and constructed. It operates by saturating air at one temperature and then raising the air temperature sufficiently to give any desired relative humidity. The important feature in this method is the continuous recirculation of air in a closed system and the use of a simple and efficient centrifugal saturator that can be used below 0° C, as well as above. Air speeds up to 1,500 ft/min are obtainable. A novel switching mechanism is utilized for giving rapid and discrete changes

in relative humidity. This switching mechanism also is adaptable for giving rapid and discrete changes in temperature.

It is designed to operate at test-chamber temperatures above 0° C, but may readily be used at temperatures as low as −40° C. The low temperatures are achieved, however, at some sacrifice of the maximum attainable relative humidity. For most of the test-chamber temperature range, practically any desired relative humidity may be produced by the apparatus.

Independent checks on the performance of the apparatus by means of the gravimetric method of moisture determination and the psychrometric method show an average agreement in relative humidity of 1.2 percent as measured and as given by the apparatus, eq 2.

The author gratefully acknowledges the assistance of R. A. Baun of the Shop Division in the construction of the apparatus and of E. T. Woolard in the experimental work.

WASHINGTON, August 14, 1950.

U. S. Department of Commerce
National Bureau of Standards

Research Paper RP1894
Volume 40, June 1948

Part of the Journal of Research of the National Bureau of Standards

Divided Flow, Low-Temperature Humidity Test Apparatus[1]

By Arnold Wexler

An apparatus is described, based on the principle of divided flow, for producing air of known relative humidity at temperatures below 0° C with an average error of 3 percent. It was designed primarily for testing and calibrating at low temperature the electric-hygrometer elements used in radiosondes, although any device with a diameter less than 1⅛ in. may be inserted into the test chamber of the apparatus. It is capable of producing rapid and discrete changes in relative humidity at constant temperature, a desirable feature for studying lag characteristics. It is provided with a control for obtaining any air velocity up to 1,500 ft/min.

I. Introduction

An apparatus has been developed for producing air of known relative humidity at temperatures from 0° to −40° C. The primary purpose for building this apparatus was to provide a means for investigating the behavior of radiosonde hygrometers at low temperatures, especially electric-hygrometer elements of the Dunmore type. In their use, on radiosondes, the elements are subjected to rapidly changing humidity conditions and to air velocities of about 700 ft/min. It was felt desirable in studying and calibrating these elements to be able to do so under simulated conditions of use. Therefore, in the design of the apparatus, provision was made to permit rapid change from one discrete value of relative humidity to another, and a device was incorporated for controlling the velocity of the air.

II. Theory

The method utilized for producing an atmosphere of known relative humidity was to divide accurately a current of dry air into two streams, one of which was maintained dry and the other saturated with respect to ice, and then to recombine the two. It was employed by Gluckauf [2] in an investigation on absorption hygrometers and by Walker and Ernst, Jr.[3] in a laboratory setup for preparing constant mixtures of air and water vapor. Figure 1 is a simplified schematic diagram of the basic components of the apparatus illustrating the principle of operation. By means of the proportioning valve, V, a flow of moisture-free air is divided into two parts in a known ratio. One part is passed through the saturator, S, over a series of trays containing ice until it is completely saturated. It is then mixed in the mixing chamber, C_M, with the other part that has been maintained dry, and allowed to exhaust through the

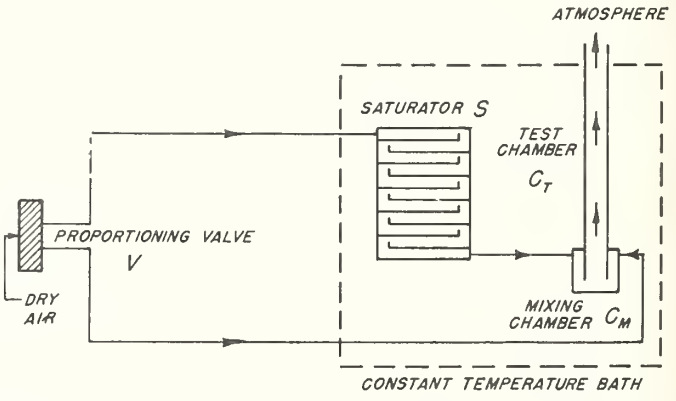

FIGURE 1. *Simplified schematic diagram illustrating the principle of operation of the humidity apparatus.*

[1] This development was financially supported by the Bureau of Ships, Department of the Navy.

[2] E. Gluckauf, Proc. Phys. Soc. 59, 344 (1947).

[3] A. C. Walker and E. J. Ernst, Jr., Ind. & Eng. Chem. Anal. Ed. 2, 134 (1930).

test chamber, C_T, into the atmosphere. The saturator, mixing chamber, and test chamber are kept immersed in a constant temperature bath. In order to subject a hygrometer or other device to air of known and constant relative humidity, it is inserted into the test chamber, C_T.

The relative humidity in the test chamber is a function of (a) the fraction of air that passes through the saturator, (b) the total pressure in the saturator, (c) the total pressure in the test chamber, (d) the saturation pressure, and (e) the partial pressure of the water vapor in the test chamber. Under ideal conditions, which the apparatus approaches with sufficient closeness, all variables except one drop out, and the relative humidity becomes equal to the fraction of air that passes through the saturator. If X is the fraction of air that passes through the saturator, W_S is the ratio by weight of the water vapor to the dry air of the mixture leaving the saturator, and W_C is the ratio by weight of the water vapor to the dry air of the mixture passing through the test chamber, then

$$W_C=XW_S. \tag{1}$$

From Dalton's law of partial pressures, and assuming the perfect gas laws apply, it follows that for an air-water vapor mixture the ratio by weight W of the water vapor to the weight of dry air is

$$W=\frac{M_w}{M_a}\frac{p}{P-p}, \tag{2}$$

where M_a and M_w are the molecular weights respectively of air and water vapor, p the partial pressure of the water vapor in the mixture and P the total pressure of the mixture. Substituting the value of W in eq 2 into eq 1 yields

$$X=\frac{(P_S-p_S)p_C}{(P_C-p_C)p_S}. \tag{3}$$

Relative humidity is defined as the ratio of the actual vapor pressure to the saturation pressure of water. The relative humidity, H, in the test chamber, C_T, is therefore

$$H=\frac{p_C}{p_S}. \tag{4}$$

Combining eq 3 and 4 leads to

$$H=\frac{X}{\left(\frac{P_S}{P_C}-\frac{p_S}{P_C}\right)\frac{P_C}{P_C-p_C}}. \tag{5}$$

If the pressure drops from the saturator to the test chamber and from there to the atmosphere are made small, then $P_S=P_C=P_A$, the atmospheric pressure. At 0° C, $p_S/P_C=p_S/P_A=0.006$, at −10° C it equals 0.0025, and at −20° C it equals 0.001. Also $P_C/P_C-p_C=P_A/P_A-p_C$, where p_C equals or is less than p_S. Therefore, for the applicable conditions eq 5 reduces without significant error to

$$H=X. \tag{6}$$

III. Description of Apparatus

The essential functional units of the apparatus are (a) the drying system, (b) the proportioning system, (c) the humidifying system, (d) the mixing chamber, (e) the test chamber, (f) the cooling system, and (g) the thermo-regulating system for temperature control. Figure 2 schematically shows these functional units and their component parts.

Air is supplied to the drying system at pressures from 70 to 90 psi. Water from the air at the supply pressure is removed by freezing in the dry ice-varsol bath, *C1*, in which the temperature is well below −70° C. The vapor pressure of the water in the air emerging from the drying system, upon expansion to 1 atmosphere, is probably less than 0.0003 mm Hg. Particles of dirt, ice, or oil are caught by the filter, *A8*.

The dry air is brought to room temperature by means of the electric heater, *A10*, is reduced and controlled in pressure by regulator, *A12*, and then passes through the proportioning system. The pressure regulator also serves to control the speed of air in the test chamber, *A25*, permitting adjustments up to 1,500 ft/min.

The proportioning valve, *A15*, figure 2, which divides the air in a definite ratio consists of six orifices of equal cross-sectional area so arranged that by a turn of the knob of the valve, the incoming air can be divided to produce any of seven ratios, 0, 1/6, 1/3, 1/2, 2/3, 5/6, and 1. These ratios are the fractions of air entering the valve that emerge through one of the exit channels of

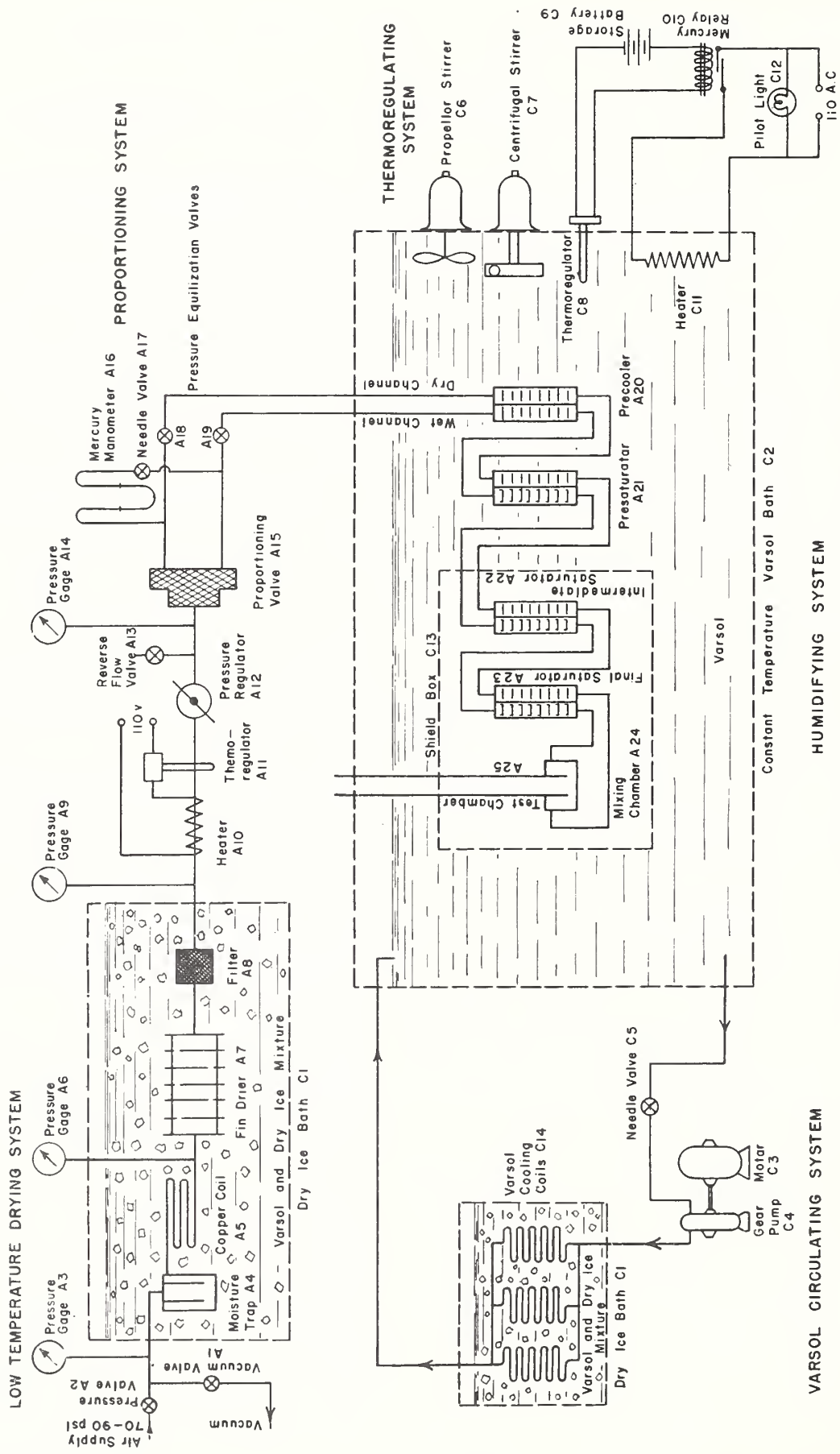

FIGURE 2. *Schematic drawing of the functional units and component parts of the humidity apparatus.*

the valve. If they are considered to apply only to that part of the air that subsequently becomes saturated, then they may be used as the values of X in eq 5 and 6. To assure that the air will divide in accordance with one of these given fixed ratios, the downstream pressures must be equalized. To achieve this, the differential mercury manometer, *A16*, and the two variable resistances (pressure equalization valves), *A18* and *A19*, are installed.

The construction of, and the flow of air through, the proportioning valve are shown in figures 3 and 4. Essentially the valve, *A15*, consists of a brass base, *B*, a brass top, *T*, a steel orifice plate, *P*, and a Bakelite knob, *K*. The incoming air enters the valve through a central hole in the base, *B*, continues through two 3/16-in. diameter holes in the midsection of the orifice plate, *P*, strikes the top, *T*, reverses its flow and again passes through the steel orifice plate, *P*, this time through six 1-mm diameter orifices, and exits in two streams from the base, *B*. The base, *B*, has two circular grooves on a 1½ in. diameter, 3/16-in. wide, ¼ in. deep and separated ¼ in. at the ends. Each groove is connected to an outlet, *O*. The orifice plate, *P*, rests on the base, *B*, in such a fashion that the orifices communicate with either or both grooves, depending upon the angular position of the plate, *P*, with respect to the base, *B*. The surfaces of contact between the plate, *P*, and base, *B*, are ground and lapped and coated with a thin film of stopcock grease to provide a leaktight but rotatable joint. By means of a steel shaft, *S*, that connects the orifice plate, *P*, to the Bakelite knob, *K*, through the valve top, *T*, and a steel packing nut, *N*, that seals the shaft, *S*, in the top, *T*, the orifice plate, *P*, can be rotated to any one of the seven possible settings. Upon turning the knob, *K*, two spring actuated snap pins, *Q*, in the knob, *K*, click and seat in a series of holes on the outer surface of the valve top, *T*, corresponding to the seven desired positions of the orifice plate, *P*, with respect to the valve base, *B*.

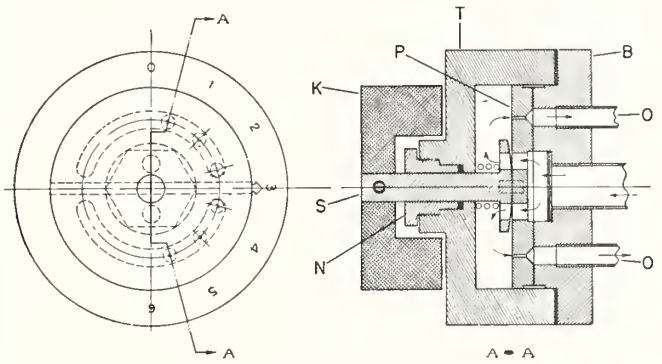

FIGURE 3. *Cross-sectional view of the proportioning valve showing the flow of air.*

B, Brass base; *T*, brass top; *P*, steel orifice plate; *K*, Bakelite knob; *O*, air outlet; *S*, steel sbaft; *N*, steel packing nut.

The two air streams, upon leaving the proportioning system, flow through the humidifying system in parallel channels, thermally in contact with one another to allow heat interchange and temperature equilibrium between the two streams to be achieved and maintained. Saturation is ac-

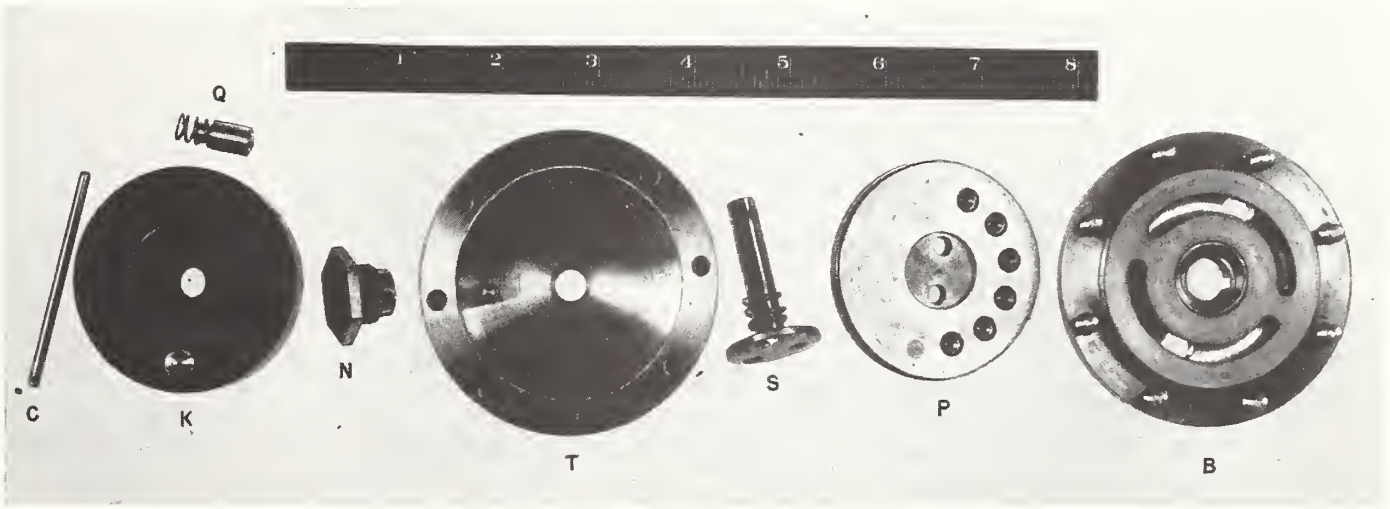

FIGURE 4. *Essential parts of the proportioning valve.*

B, Brass base; *P*, steel orifice plate; *S*, steel shaft; *T*, brass top; *N*, steel packing nut; *K*, Bakelite knob; *Q*, spring-actuated snap pin; *C*, steel pin for fastening *K* to *S*.

complished in four stages. The air to be humidified is first brought to ambient temperature in a precooler, *A20*, figure 2. It then passes through three saturators, *A21*, *A22*, and *A23*. The precooler, *A20*, consists of staggered shelves, one series for each of the two currents of air. Each series is pneumatically isolated from, but in thermal contact with, the other. The saturators are similarly built, except that trays replace one series of shelves. The trays can be filled with water and the water frozen. Thus, in the saturator, in one channel air passes over trays of ice and in the parallel adjoining channel, air passes over shelves. From the final saturator, *A23*, the saturated air and the dry air are centrifugally mixed in the mixing chamber, *A24*, and discharged into the atmosphere through the test chamber, *A25*.

The humidifying system, the mixing chamber, *A24*, and the test chamber, *A25*, are immersed in a varsol bath, *C2*, whose temperature is closely regulated. This is done by circulating the varsol of the bath through cooling coils, *C14*, immersed in dry ice. The bimetal thermoregulator, *C8*, through the relay, *C10*, controls the heater, *C11*, to keep the bath termperature at any desired value. The bath, *C2*, is actively agitated. As an aid in averaging and stabilizing the variations of the bath temperature, the intermediate and final saturators, *A22* and *A23*, the mixing chamber, *A24*, and the test chamber, *A25*, are encased in the copper shield box, *C13*, to provide a unit of high heat content that assumes the mean temperature of the bath. The shield box, *C13*, keeps varsol away from direct contact with the enclosed components.

The thermoregulating system is capable of controlling the temperature of the humidifying system to $\pm 0.05°$ down to $-15°$ C, to $\pm 0.1°$ down to $-30°$ C and to $\pm 0.2°$ down to $-40°$ C for runs up to 10-hr duration. For short periods of time of ½ to 1 hr, the temperature can be maintained to $\pm 0.02°$ C. Calibrated copper-constantan thermocouples and a precision potentiometer are used for measuring the temperature in the apparatus with an accuracy of $\pm 0.02°$ C.

Measurements of the temperatures at the inlets and outlets in the final saturator, *A23*, under various conditions, indicate that at the inlets the two air streams are on the average within 0.07° C of one another, and at the outlets they are on the average within 0.02° C of one another. In the humidifying side of the final saturator, *A23*, the inlet and exit temperatures are on the average within 0.03° C of each other. The temperature in the test chamber is on the average 0.08° C warmer than the air emerging from the final saturator, *A23*.

Since no further saturation can occur subsequent to the exit of the air from the final saturator, *A23*, the pressure at the exit may therefore be considered as the P_S of eq 5. The difference between P_S and atmospheric pressure, P_A, for various test chamber air velocities, is shown in the curve of figure 5. At an air velocity

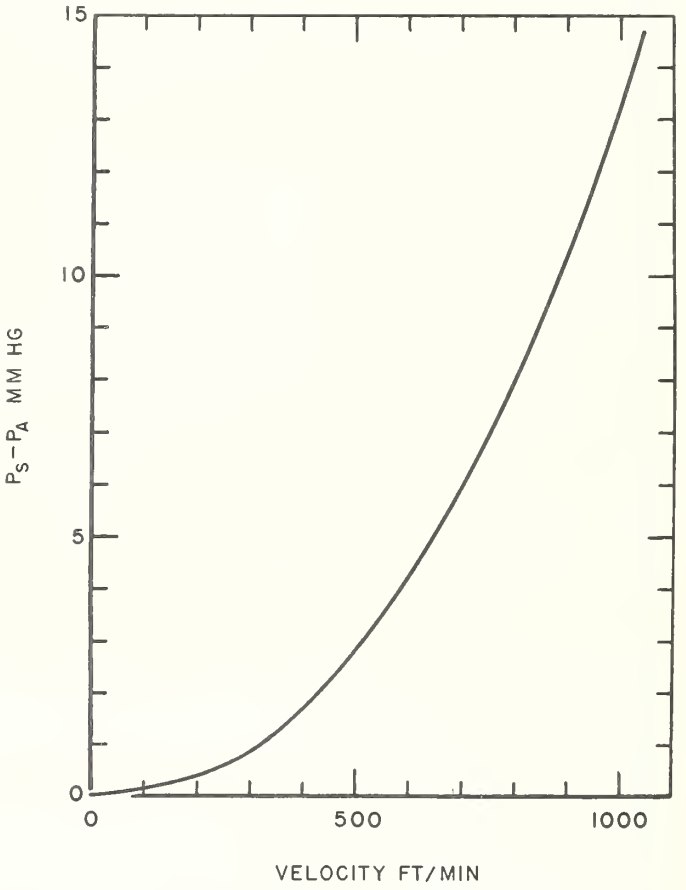

FIGURE 5. *Difference in pressure between the exit of the final saturator, P_s, and atmospheric pressure, P_A, for various test chamber air velocities.*

of 525 ft/min, the assumption that $P_S = P_A$ introduces an error in H of 0.4 percent, at 850 ft/min, the error is 1.2 percent, and at 1,140 ft/min, the error becomes 2.5 percent. If eq 5 instead of eq 6 is used for calculating the relative humidity produced by the apparatus, these errors are avoided.

IV. Calibration

1. Theory

In order to check the over-all performance of the apparatus, a series of tests was made to compare the actual humidity it produces with the humidity given by eq 6. The gravimetric method of moisture determination was selected as the means for measuring the water vapor content of the air in the test chamber under operating conditions. By definition, the relative humidity in the test chamber is

$$H=\frac{p_w}{p_{sw}}, \tag{7}$$

where p_w is the partial pressure of the water vapor in the air, and p_{sw} is the saturation pressure of the water vapor. Assuming that air and water vapor from room temperature to $-60°$ C and at a pressure of 1 atmosphere obey Dalton's law of partial pressures and the perfect gas law, then

$$p_a+p_w=P_C, \tag{8}$$

$$p_wV=\frac{m_w}{M_w}RT_C, \tag{9}$$

and

$$p_aV=\frac{m_a}{M_a}RT_C, \tag{10}$$

where p_a is the partial pressure and P_C is the total pressure of the air in the test chamber, V is the volume, m_w and m_a are the weights of water and air respectively in volume V, M_w and M_a are the molecular weights of water and air, R is the universal gas constant, and T_C is the absolute temperature in the test chamber.

Since the air in the air–water-vapor mixture from the test-chamber exhausts with negligible pressure drop into the atmosphere, then $P_C=P_A$, where P_A is atmospheric pressure. Dividing eq 9 by eq 10 and substituting into eq 8 yields

$$p_w=\frac{P_A}{1+\frac{m_aM_w}{m_wM_a}}. \tag{11}$$

If, from a sample of air taken from the test chamber, the weight of water vapor and air be determined and the pressure measured, the partial pressure of the water vapor could easily be calculated using eq 11, and the relative humidity would follow from eq 7. Figure 6 is a schematic diagram of the setup used for obtaining m_a, m_w, and P_A. A glass probe was inserted into the test chamber and a sample of air withdrawn. The water vapor was removed from the sample by passing it through an absorption tube containing phosphorous pentoxide and accurately weighed. The volume, pressure, and temperature of the same sample of air were measured, and from these data m_a was obtained.

Now

$$m_a=V_ad_a, \tag{12}$$

where d_a is the density of dry air at the pressure and temperature of V_a, the volume of dry air. In this particular setup, V_a was measured by a laboratory wet gas meter at a temperature t_g.

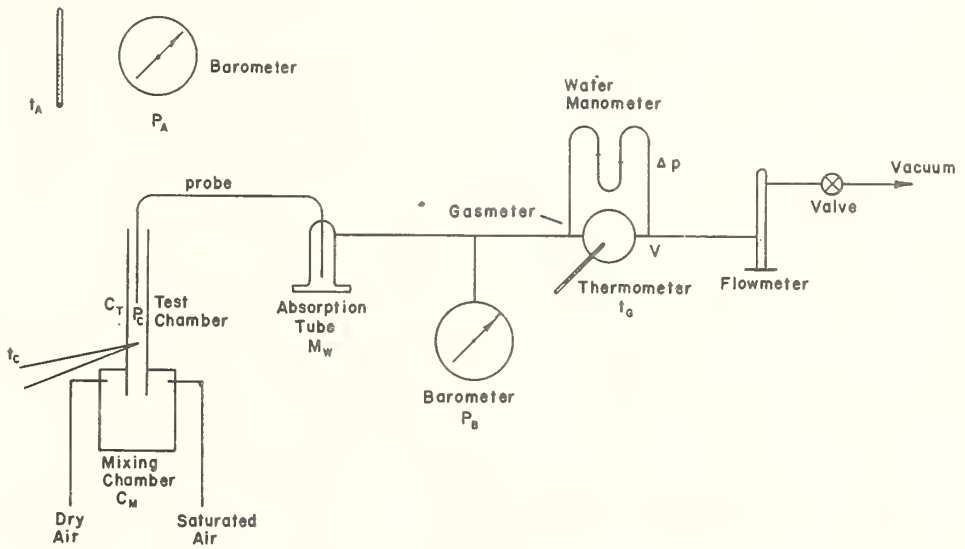

FIGURE 6. *Diagram of gravimetric calibration setup.*

This gasmeter completely saturates the air passing through it so that the partial pressure of the dry air in the gasmeter is given by $P_B - p_g - 1/2\Delta p$, where P_B is the pressure at the inlet to the gas meter, p_g is the saturation pressure of water vapor at the temperature, t_g, of the air in the gas meter, and Δp is the pressure drop across the gas meter. The weight of the dry air in the sample, in terms of observable data and the density of dry air under standard conditions, becomes

$$m_a = \frac{V_a(P_B - p_g - 1/2\Delta p)(0.001293)(273.1)}{760(273.1 + t_g)}. \quad (13)$$

Substituting from eq 13 and 11 into eq 7 yields the desired expression for the relative humidity in the test chamber in terms of known and measurable quantities

$$H = \frac{P_A/p_{sw}}{1 + \frac{V_a(P_B - p_g - 1/2\Delta p)(0.00028898)}{m_w(273.1 + t_g)}}. \quad (14)$$

With the proportioning valve set to produce a relative humidity of 100 percent, and the pressure regulator adjusted to give an air velocity in the test chamber of 525 ft/min, a number of gravimetric determinations was made in the temperature range of −10° to −40° C. Then with the air velocity maintained at 525 ft/min, and at an ambient temperature of −10°C, a run was made at each setting of the proportioning valve. Finally, at an ambient temperature of −10° C and with the proportioning valve set at 100 percent, two runs were made, one at an air velocity of 850 ft/min and the other at 1,140 ft/min.

2. Procedure and Results

In making a gravimetric determination, the humidity apparatus was set into operation and brought to equilibrium conditions. The sample of air was withdrawn by the glass probe at the rate of 1 liter per minute. An attempt was made to collect 50 mg of water vapor in the absorption tube. This required withdrawing air for periods varying from ½ to 10 hr. The weight of the water was determined with an accuracy of ½ to 1 percent.

For the duration of the run, frequent readings were made at equal time intervals of the temperatures and pressures. The pressure, P_B, at the inlet of the gas meter was determined with an accuracy of ±0.2 mm Hg and the atmospheric pressure, P_A, was determined with an accuracy of ±0.1 mm Hg, both by means of precision aneroid barometers. A mercury-in-glass thermometer, accurate to 0.1 deg, gave the temperature, t_g, of the air in the gas meter. A water manometer that could easily be read to ½ mm or better was used to obtain the pressure drop, Δp, across the gas meter.

The results of these determinations are given in table 1, based upon the saturation pressures with respect to ice presented in the Smithsonian Tables,[4] in Wärmetabellen,[5] and in Goff's table.[6] It is estimated that the vapor pressures have been gravimetrically determined with an accuracy of 1 to 2 percent. The difference, D, without regard to sign, between each test result and the setting of the proportioning valve is also given. The differences depend upon the vapor pressure tables used in the computation. The best agreement between the gravimetric determinations and the valve settings of the humidity apparatus is obtained by utilizing the Wärmetabellen values of vapor pres-

Table 1. *Gravimetric calibration*

Run number	Saturation temperature	Air velocity	Proportioning valve setting	Relative humidity					
				Smithsonian		Wärmetabellen		Goff	
				Result	D	Result	D	Result	D
	°C	ft/min	%	%	%	%	%	%	%
1	−10.30	525	100	100.6	0.6	101.6	1.6	101.5	1.5
8	−11.09	525	100	97.3	2.7	98.2	1.8	98.1	1.9
9	−11.01	525	100	94.9	5.1	95.8	4.2	95.7	4.3
10	−11.30	525	100	94.1	5.9	95.0	5.0	94.9	5.1
1a	−14.57	525	100	98.9	1.1	100.0	0.0	100.0	0.0
5	−28.65	525	100	96.6	3.4	99.1	.9	97.6	2.4
6	−28.61	525	100	98.0	2.0	100.3	.3	99.1	0.9
7	−40.94	525	100	94.4	5.6	99.6	.4	94.4	5.6
11	−39.77	525	100	96.0	4.0	99.1	.9	96 3	3.7
2	−10.30	525	83.3	81.3	2.0	82.2	1.1	82.0	1.3
3	−10.10	525	66.7	63 3	3.4	63.9	2.8	63.8	2.9
4	−10.02	525	50.0	49.7	0.3	50.2	0.2	50.2	0.2
12	−10.50	525	33 3	32.9	.4	33 2	.1	33.2	.1
13	−10.48	525	16.7	15.4	1.3	15.5	1.2	15.5	1.2
14	−10.01	525	0	0.4	0.4	0.4	0.4	0.4	0.4
15	−10.36	850	100	94.2	5.8	95.6	4.4	95.5	4.5
16	−10.75	1,140	100	102.3	2.3	103.3	3.3	104.6	4.6
1b	−14.42	525	66.7	64.2	2 5	64.9	1.8	64.9	1.8
Avg..	-------	-----	-----	-----	2.7	-----	1.7	-----	2 4

[4] Smithsonian Meteorological Tables, 5th ed. (1939).

[5] L. Holborn, K. Scheel, and F. Henning, Wärmetabellen der Physikalisch-Technischen Reichsanstalt (1919).

[6] John A. Goff, ASHVE Journal Section; Heating, piping, and air conditioning, 355 (June 1945).

sure. The average difference between the valve settings and the test results for the temperature range of −10° to −40° C and for air velocities up to 1,140 ft/min, based on the Warmetabellen is 1.7 percent, on Goff's table is 2.4 percent, and on the Smithsonian tables is 2.6 percent. These results show that the humidity apparatus, over the temperature and velocity ranges tested, produced air having a relative humidity that averaged within 3 percent of the orifice ratio setting of the proportioning valve.

V. Discussion

This apparatus is particularly suited for the investigation and calibration of hygrometers, psychrometers, and dewpoint apparatus at temperatures below 0° C. The rotation of the proportioning valve and the adjustment of the pressure equalization valves are the only operations necessary for changing the relative humidity. The time involved is usually a matter of 1 or 2 seconds. This readily permits any device under test to be subjected to a sudden discontinuous change in relative humidity, a desirable advantage in the study of lag characteristics. The air velocity in the test chamber can easily be adjusted to any value up to 1,500 ft/min within several seconds by adjusting the pressure regulator. The size of an object that can be tested is limited by the inside diameter of the test chamber, which is 1⅛ in. For applications where high air velocities are not necessary, the diameter of the test chamber may be increased to allow larger devices to be inserted.

There is no provision in the apparatus for introducing discrete and rapid changes in ambient temperature. To change the ambient temperature may require up to an hour to reach equilibrium conditions.

There are two ways in which this apparatus may be used to produce known dewpoints. If the proportioning valve is set to 100, then the emerging air will have a dewpoint equal to the test chamber temperature, or, more closely, to the temperature of the air in the final saturator. A change in dewpoint is made by altering the bath temperature. On the other hand, if recourse to standard vapor-pressure tables and eq 4 is made, then for any given bath temperature, several vapor pressures, equivalent to dewpoints at temperatures below that of the bath, are obtainable by rotation of the proportioning valve. The dewpoints thus obtained may have an average error of 0.3 deg C based on an average error in the humidity of 3 percent.

The author thanks R. B. Kennard, for designing the proportioning valve and preliminary models, and E. G. Clarke for constructing some of the units, especially the saturators.

Washington, March 3, 1948.

Pressure-Humidity Apparatus[1]

Arnold Wexler and Raymond D. Daniels, Jr.

An apparatus for producing atmospheres of known relative humidity, based on the "two-pressure principle", is described. It has a working space (test chamber) of 1 cubic foot, in which the relative humidity may be varied and controlled from 10 to 98 percent, the temperature from −40° to +40° C, the air flow up to 150 liters per minute, and the test-chamber pressure from ½ to 2 atmospheres. The humidity in the test chamber may be set and maintained to an accuracy of at least ½ of 1-percent relative humidity.

1. Introduction

The pressure-humidity equipment is a laboratory apparatus for producing atmospheres of known relative humidity by control of the pressure in the test chamber of air saturated at a higher pressure. As this apparatus was developed primarily for hygrometer research and calibration, especially on electric hygrometer elements, which, during use, are subjected to a wide temperature range, it was essential that the temperature of the working space should be adequately controlled and maintained at any desired value from −40° to +40° C. Futhermore, it was desirable that any relative humidity, from 10 to 98 percent, should be conveniently produced and that a change could be made rapidly from any one value of relative humidity to any other value. Finally, it was also desirable to have a means of varying the rate of air flow through the working space, selected to have a volume of about 1 ft^3.

An apparatus has been developed that successfully meets the above requirements. It operates on what may be called the "two-pressure principle." Basically, the method, shown in elemental schematic form in figure 1, involves saturating air, or any gas, with water vapor at a high pressure and then expanding the gas to a lower pressure. If the temperature is held constant during saturation and upon expansion, and the perfect gas laws are assumed to be obeyed, then the relative humidity, RH, at the lower pressure, P_t, will be the ratio of the absolute values of the lower pressure, P_t, to the higher pressure, P_s, that is, $RH=100\times P_t/P_s$.

Water vapor-air mixtures depart from ideal gas behavior, so that the simple pressure ratio does not strickly define the relative humidity. Weaver [2] [3] has shown that an empirical equation of the form

$$RH=100\times\frac{P_t}{P_s}\frac{(1-KP_t)}{(1-KP_s)},$$

where the constant K has a value of 0.00017 when the pressure is expressed in pounds per square inch, more closely yields the true relative humidity. The magnitude of the correction introduced by the term $(1-KP_t)/(1-KP_s)$ is shown in table 1 for the applicable range of test-chamber pressures (½ to 2 atm) and relative humidities (10 to 100%). With atmospheric pressure in the test chamber the maximum error does not exceed ¼ of 1-percent relative humidity and hence, for most work, may be neglected. Even at a test-chamber pressure of 2 atm, the maximum error is less than 0.5-percent relative humidity. For very precise work, it is preferable to use the empirical equation.

TABLE 1. *Error due to nonideal behavior of water-vapor–air mixtures*

Test-chamber pressure	Relative humidity, percent					
	100	80	60	40	20	10
	Error in relative humidity, percent					
abs atm						
½	0	0.02	0.05	0.08	0.10	0.11
1	0	.05	.10	.15	.20	.23
2	0	.10	.20	.30	.41	.47

The pressure method was developed by Weaver and Riley (see footnote 2) for the calibration of electrically conducting hygroscopic films used in the measurement of water vapor in gases. Their equipment was designed for low rates of gas flow and was used under ambient room-temperature conditions.

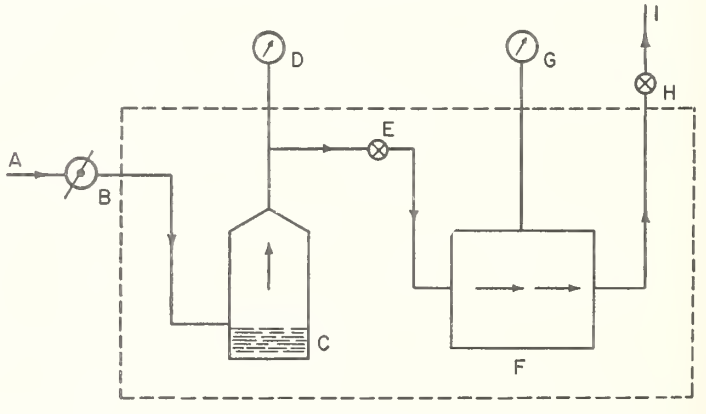

FIGURE 1. *Simplified schematic drawing of the principle of operation of the pressure-humidity apparatus.*

A, high-pressure air source; B, pressure regulator; C, saturator; D, pressure gage; E, expansion valve; F, test chamber; G, pressure gage; H, exhaust valve; I, atmosphere or vacuum source; J, constant-temperature bath.

[1] The development of this apparatus was sponsored by the Aerology Branch of the Bureau of Aeronautics.
[2] E. R. Weaver, and R. Riley, J. Research NBS **40**, 169 (1948) RP1865.
[3] E. R. Weaver, Anal. Chem. **23**, 1076 (1951).

Their saturator was a small cylinder, containing water and filled with fragments of pumice or stream-washed gravel through which the gas could be bubbled under pressure.

2. Description of Apparatus

The apparatus is shown in block diagram in figure 2 and schematically in figure 3. It consists, essentially, of the following functional components, through which air flows continuously: A high-pressure air source, a low-temperature drying system, a filtering system, a warm-up unit, a pressure regulator, a humidifying system, an expansion valve, a test chamber, and an exhaust control system.

Air is supplied from a 250-psig reciprocating compressor, *A1*, figure 3, capable of delivering 5 ft^3/min of free air at room temperature. This air is filtered (*A2*) to remove pipe scale, dirt, dust, or other solid material, and is then introduced into the drying system (fig. 4).

Water from the air at the supply pressure is removed by freezing in a train of four drying units immersed in a bath, *D*, containing a mixture of dry ice and Stoddard solvent. The first two units, *A4* and *A5*, are large-capacity centrifugal water separators. These are followed by a copper coil, *A6*, and a baffle dryer, *A7*. Particles of snow or ice and droplets of oil (from the compressor) are caught by a filter, *A8*, which is maintained immersed in the same low-temperature bath, *D*.

The air emerges from the dryer at about −78° C. It is then heated in the warm-up unit to a temperature somewhat greater than that being maintained in the thermostatted liquid bath, *B*. The warm-up unit consists of an electric heater, *A9*, that is controlled by a thermoregulator, *A10*. Two pressure regulators, *A13*, and *A14*, in series reduce the pressure and maintain it constant in the hymidifying system.

Saturation is accomplished in four stages. The air is first passed through the external gross saturator, *A15*, which is kept at a higher temperature than the bath, *B*, and then through the three bath saturators, *A18*, *A20*, and *A22*. The gross saturator, because of its higher temperature, introduces water vapor in excess of that required for complete saturation at bath temperature. The combination of heat exchangers *A17*, *A19*, and *A21* and centrigfugal saturators *A18*, *A20*, and *A22* precipitates this excess water vapor so that just complete saturation is obtained in the final saturator, *A22*. The bath saturators and heat exchangers are shown in figure 5.

The saturators are simple in design and function equally well below as well as above the freezing point of water. They are similar to a type previously used [4] with considerable success. Each saturator consists of a cylinder to which water is added to a convenient depth. Air is discharged through a nozzle into the chamber above the water surface and tangential to the vertical walls and is exhausted through a central port in the top. The centrifugal force creates a whirlpool action that thoroughly mixes the water vapor with air. Spray and liquid water are forced to the walls by centrifugal force, so there is little tendency for liquid water

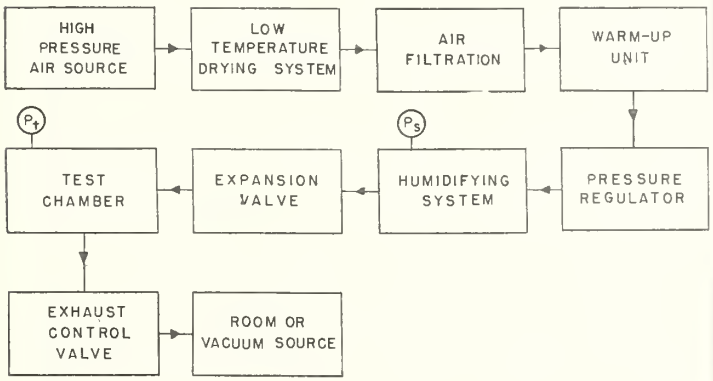

FIGURE 2. *Block diagram of the pressure-humidity apparatus.*

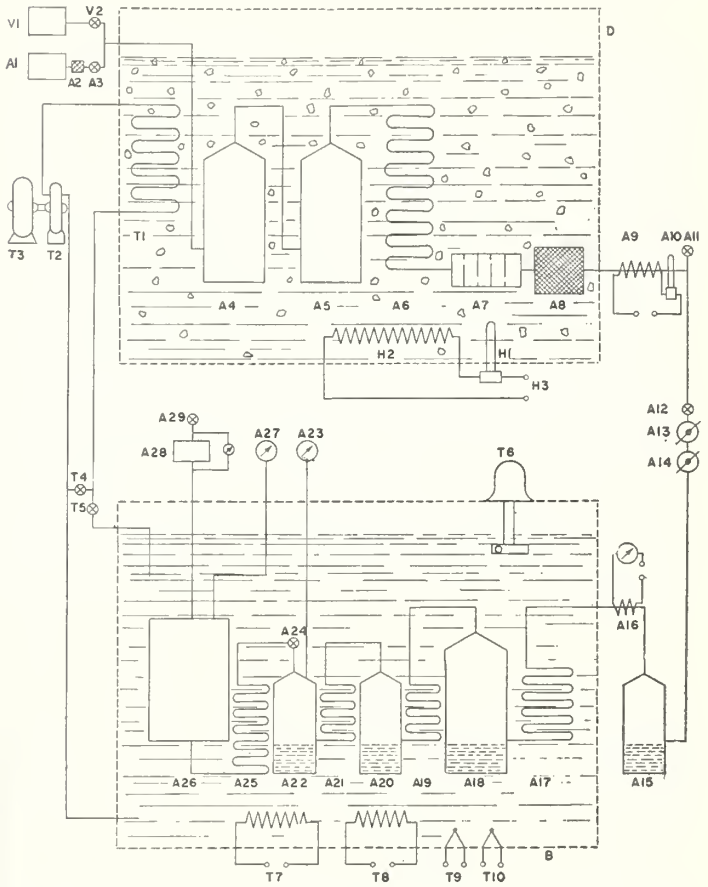

FIGURE 3. *Schematic flow diagram of the pressure-humidity apparatus.*

A1, high-pressure source; A2, filter; A3, valve; A4, centrifugal water separator; A5, centrifugal water separator; A6, copper cooling coil; A7, fin air dryer; A8, low-temperature filter; A9, electric heater; A10, bimetal thermoregulator; A11, air reversal valve; A12, shut-off valve; A13, pressure regulator; A14, pressure regulator; A15, external gross saturator; A16, resistance thermometer and indicator; A17, 19, 21, 25, copper coil heat exchangers; A18, 20, 22, centrifugal saturators; A23, 27, pressure gages; A24, expansion valve; A26, test chamber; A28, linear flowmeter; A29, exhaust control valve; B, insulated liquid (Stoddard solvent, constant-temperature bath; D, insulated dry-ice bath; H1, bimetal thermoregulator; H2, electric heater; H3, input voltage; T1, Stoddard solvent cooling coil; T2, positive rotary displacement pump; T3, motor; T4, Stoddard solvent bypass valve; T5, Stoddard solvent control valve; T6, centrifugal stirrer; T7, constant electric heater; T8, intermittent electric heater; T9, 10, thermistors; V1, vacuum source; V2, vacuum shut-off valve.

[4] Arnold Wexler, J. Research NBS **45**, 357 (1950) RP2145.

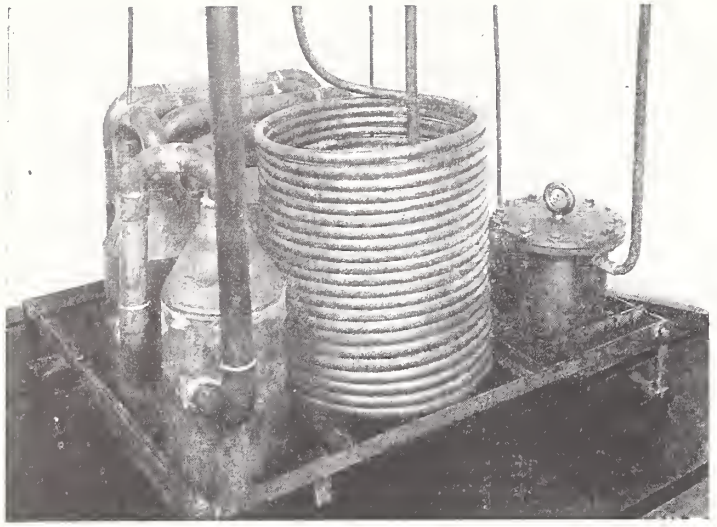

FIGURE 4. *Drying system and Stoddard solvent cooling coil.*

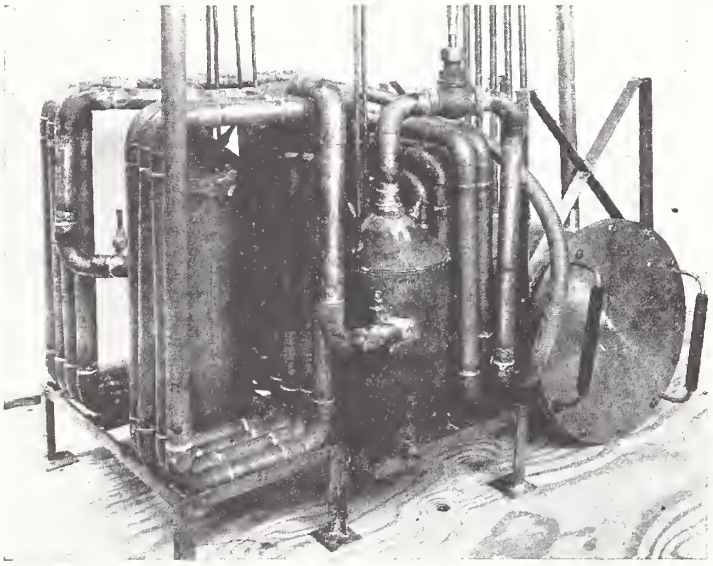

FIGURE 5. *Bath saturators, heat exchangers, and test chamber.*

to emerge through the exit port. A multilayer fine-wire screen baffle is used at the exit as a further guard against the escape of liquid water. As air does not bubble through the water but only passes over its exposed surface, the water may be frozen without impairing the functioning of the saturator.

Upon emerging from the final saturator, *A22*, the pressure of the air is reduced by expansion valve *A24*. Because a temperature drop may occur in the air at the expansion valve, a final heat exchanger, *A25*, is provided for bringing the air to bath temperature before it enters the test chamber, *A26*.

The working space, *A26*, is a cylindrical chamber having a nominal volume of 1 ft^3. It is shown with the cover removed in figure 6. Tubular outlets extend from the chamber to allow electric leads to be brought in and out of the working space. The air discharges from the chamber into a linear flowmeter, *A28*, and then through an exhaust control valve, *A29*, into a vacuum source or simply into

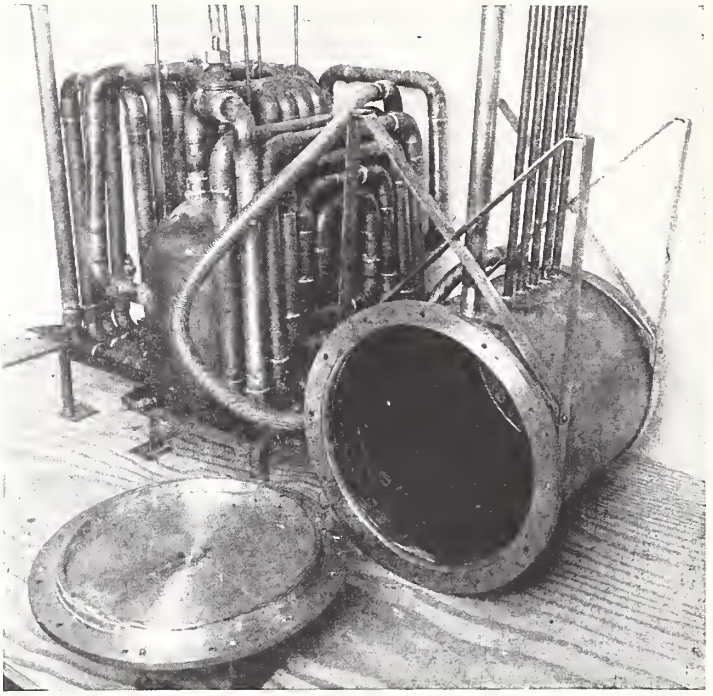

FIGURE 6. *Test chamber with cover removed.*

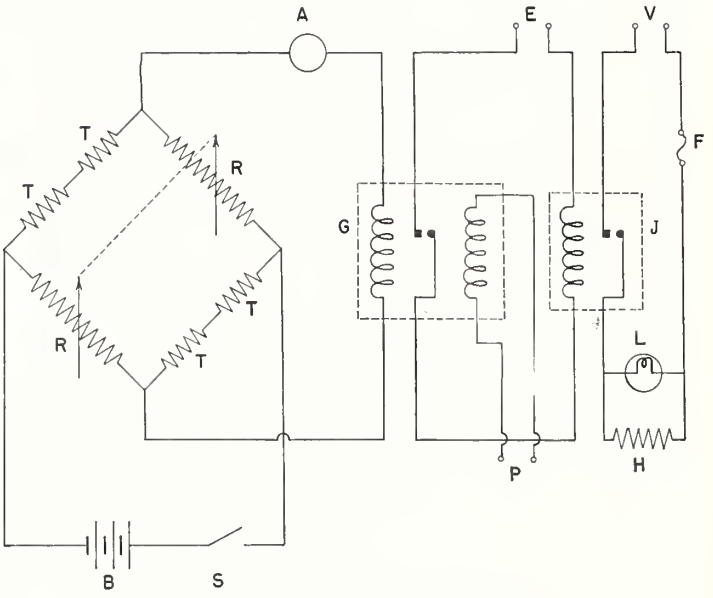

FIGURE 7. *Temperature control circuit.*

T, Thermistor; R, precision helical rheostat; B, 22½-v battery; S, battery switch; A, microammeter; G, ½ a galvanometer relay; P, input from pulsing circuit; F, fuse; J, power relay; E, input voltage for power relay coil; H, intermittent bath heater; V, input voltage for intermittent heater; L, pilot lamp.

the room air. The chamber is suspended from a counterweight system so that it can be easily raised above or immersed into the liquid bath, *B*. A length of flexible metal hose, between the test chamber, *A26*, and the final heat exchanger, *A25*, permits the test chamber to have the required motion.

The saturation pressure, P_s, is measured in the final saturator, *A22*, by gage *A23*, and the test pressure is measured in the test chamber by gage *A27*. These measurements are made with high-precision

laboratory test gages that have been calibrated against the National Bureau of Standards pressure standards. For atmospheric or reduced pressures, a high-quality calibrated aneroid barometer is used. From atmospheric pressure up to 2 atm, a mercurial manometer is employed. The higher pressures are determined with either a 0- to 50-psig or a 0- to 200-psig Bourdon tube gage.

The temperature of the liquid bath, *B*, can be adjusted to and closely regulated at any temperature from −40° to +40° C by a simple on-off thermostatting system. Stoddard solvent, which is used as the bath liquid so that low temperatures may be attained, is actively agitated by a centrifugal stirrer, *T6*, and is circulated from the bath, *B*, by a positive rotary displacement pump, *T2*, through a copper coil, *T1*, immersed in a mixture of dry ice and Stoddard solvent in bath *D* and back into bath *B*. By proper manual setting of a bypass valve, *T4*, and a control valve, *T5*, the rate of Stoddard solvent flow is adjusted so that the bath *B* tends to cool slightly. The desired bath temperature is established by resistances (coupled helical precision rheostats), *R*, in a Wheatstone bridge circuit, figure 7. Thermistors, *T*, with temperature coefficients of 4 percent/deg C, are employed as the temperature-sensitive elements. Any cooling disturbs the bridge balance, which is sensed by a galvanometer relay, *G*. A current of ½μa deflects the galvanometer pointer against a magnetic contact, actuating a power relay, *P*, and, in turn, intermittent bath heater, *H*. The operation of an electromagnetic plunger returns the pointer to a sensing position. If the bridge is unbalanced, the pointer will deflect and again throw on the heater; if the bridge is in balance, the pointer will remain in a null position. An electronic pulsing circuit, *P*, periodically triggers the plunger so that the pointer may sense the bridge balance.

3. Operation of Apparatus

The method of operation of this equipment is simple. The instrument, material, or device under investigation is inserted into the test chamber, the latter closed and immersed into the liquid bath. Distilled water is added to each saturator to an appropriate depth. Solid carbon dioxide is then added to the dry-ice bath, *D*. The temperature of the liquid bath is brought to and maintained at the desired value. Air from the high-pressure source is allowed to pass through the apparatus and the pressures in the saturators and test chamber adjusted to give any preselected relative humidity. The thermoregulator controlling the temperature of the air passing through the warm-up unit is set to maintain a temperature in the external saturator several degrees higher than in the liquid bath. When thermal equilibrium had been established in the components in the liquid bath, the pressure ratio indicates the correct relative humidity in the test chamber. Changing the relative humidity primarily involves adjusting the pressure regulators so that they will maintain a new pressure in the saturators. To maintain a constant air flow, a minor adjustment of the expansion valve is also made.

When atmospheric pressure is desired in the test chamber, the air emerging from the chamber is allowed to exhaust directly into the room. Elevated pressures in the chamber are obtained by throttling the flow from the chamber by means of the exhaust control valve, *A29*, figure 3. Reduced pressures in the chamber are achieved by attaching a vacuum source to the exhaust control valve and adjusting the valve to give the required reduced pressure.

In operating below freezing, one precaution must be observed. The level of the water in each saturator must be kept below the inlet nozzle, otherwise, on freezing, the opening will be sealed by ice.

The equipment may be operated continuously for 8 to 16 hr, after which the accumulated water in the dryer should be removed. Failure to do so may result in clogging of the dryer by ice and the reduction, or even complete stoppage, of air flow.

The removal of water from the dryer is accomplished in two steps. First the dry ice bath is raised to room temperature by a thermostat, *H1*, and heater, *H2*. Then suction is applied by vacuum source *VI* and room air drawn through the reversal valve, *A11*, and dryer until all the water has been evaporated. Overnight operation usually suffices to remove most of the water.

4. Performance and Accuracy

The psychrometric and dew-point methods of humidity measurement were used independently to evaluate the accuracy of the humidity produced by the equipment. A thermocouple wet-and-dry-bulb hygrometer was employed over a wide range of relative humidities and at temperatures from 0° to 30° C. A dew-point instrument having a thermocouple embedded just below the surface of a small (¼ in. in diameter) mirror for temperature measurement, manually controlled heating and cooling of the mirror, and visual observation through a telescope for dew and frost detection, was constructed and used to measure dew points from room temperature down to −27° C. A series of experiments was made in which the relative humidity measured by the above two methods was compared with the relative humidity given by the ratio of the test-chamber pressure to the saturator pressure. The results are shown in table 2. The average difference in percentage of relative humidity between the psychrometrically determined values and the apparatus values given by the pressure ratio is ±0.4 percent, and the average difference in percentage of relative humidity between the value determined by dew-point measurement, and the apparatus value given by the pressure ratio is ±0.6 percent. Similarly, the algebraic average differences are −0.2 and 0.0 respectively. It may be assumed that as there is no marked tendency for the differences to be either positive or negative, the air passing through the saturators emerges neither supersaturated or undersaturated.

TABLE 2. *Summary of calibration*

Date of run	Nominal ambient bath temperature	Relative humidity produced by pressure-humidity apparatus	Relative humidity measured by—		Difference in relative humidity between pressure-humidity apparatus and—	
			Dew-point hygrometer	Psychrometer	Dew-point measurement	Psychrometric measurement
	°C	%	%	%	%	%
3-28-51	23.5	96.1	----	96.2	-----	−0.1
		90.1	----	91.1	-----	−1.0
		81.6	----	82.3	-----	−0.7
		74.4	----	75.2	-----	−.8
		59.6	----	59.7	-----	−.1
		50.1	----	50.5	-----	−.4
		38.0	----	38.4	-----	−.4
		25.1	----	25.4	-----	−.3
3-28-51	9.7	92.9	----	92.4	-----	+.5
		79.8	----	79.8	-----	.0
		61.0	----	61.0	-----	.0
		49.5	----	49.3	-----	+.2
		37.2	----	37.0	-----	+.2
		24.6	----	24.2	-----	+.4
3-28-51	30.4	92.6	----	92.9	-----	−.3
		78.3	----	78.6	-----	−.3
		59.6	----	59.7	-----	−.1
		49.2	----	49.4	-----	−.2
		37.0	----	37.2	-----	−.2
		24.9	---	24.8	-----	+.1
4-6-51	24.7	97.9	96.7	----------	+1.2	-----
		88.8	88.7	----------	+0.1	-----
		77.6	75.9	----------	+1.7	-----
		77.4	77.9	----------	−0.5	-----
		54.8	55.4	----------	−.6	-----
		36.9	37 3	----------	−.4	-----
		23.0	23.9	----------	−.9	-----
4-16-51	6 0	96.9	97.0	96.9	−.1	0.0
		90.6	92.1	91.4	−1.5	−.8
		77.9	78.6	78.5	−0.7	−.6
		57.7	58.5	58.2	−.8	−.5
		42.7	42.9	42.6	−.2	+.1
4-18-51	6.0	96.2	96.3	94.7	−.1	+1.5
		53.9	54.7	53.8	−.8	+0.1
		36.6	36.6	36.7	.0	−.1
		28.3	28.4	28.8	−.1	−.5
		23.2	23.1	23.5	+.1	−.3
4-19-51	−4.8	96.8	97.1	----------	−.3	-----
		86.0	86.7	----------	−.7	-----
		74.7	74.7	----------	.0	-----
4-24-51	−9.6	76.4	75.9	----------	+.5	-----
		68.3	68.2	----------	+.1	-----
		54.1	53.5	----------	+.6	-----
4-25-51	−19.8	96.3	95.6	----------	+.7	-----
		88.0	89.1	----------	−1.1	-----
		78.7	78.2	----------	+0.5	-----
		66.4	65 0	----------	+1.4	-----
		56.7	55.6	----------	+1.1	-----
				Arithmetic avg	±0.6	±0.4
				Algebraic avg	.0	−.2

The relative-humidity range obtainable is limited by the range of ratios of test-chamber pressure to saturator pressure. The maximum saturator pressure that can be employed with this apparatus is about 150 psi. When the test chamber is maintained at its maximum pressure (about 2 atm), the minimum relative humidity is about 20 percent. At atmospheric pressure, a relative humidity as low as 10 percent is readily produced, and at a reduced pressure of ½ atm, the minimum relative humidity decreases to 5 percent.

The temperature range of the equipment extends from −40° to +40° C. The upper end is limited by the flash point of the bath liquid (Stoddard solvent). However, by substituting water for Stoddard solvent as the bath liquid, the upper end of the temperature range may be extended to about 90° C.

The accuracy with which any desired relative humidity may be established is a function of the uniformity of temperature in the apparatus, particularly in the final saturator and the test chamber. The relative humidity in the test chamber will be equal to the pressure ratio of the test chamber to final saturator only if these two units are at the same temperature. The distribution of temperature within the saturators, test chamber, and surrounding liquid bath was explored by means of thermocouples, located at the inlet, outlet, and in the water of each saturator, near the front and rear of the test chamber, and at four separate points within the liquid of the bath. As an indication of the variations in temperature that may exist in the apparatus, data are presented in table 3 of the average temperatures at various locations for three 2-hour runs at different ambient temperatures. It may be seen that the differentials are of minor magnitude, especially between the final bath saturator and the test chamber.

TABLE 3. *Temperature distribution*

Location	Temperature		
Initial bath saturator:	°C	°C	°C
Air inlet	9.55	23.33	30.24
Air outlet	9.57	23.30	30.25
Water	9.66	23.29	30.30
Intermediate bath saturator:			
Air inlet	9.63	23.35	30.45
Air outlet	9.65	23.36	30.44
Water	9.63	23.29	30.39
Final bath saturator:			
Air inlet	9.64	23.39	30.48
Air outlet	9.65	23.40	30.44
Water	9.66	23.36	30.43
Test chamber:			
Front	9.64	23.35	30.40
Rear	9.61	23.35	30.37
Bath:			
Side of test chamber	9.64	23.38	30.40
Expansion valve	9.64	23.39	30.40
Rear of test chamber	9.61	23.39	30.39
Bottom	9.58	23.38	30.39

The constancy of bath temperature is of importance, for quite often materials or hygrometers under investigation are temperature dependent. The control system has effectively regulated the bath at temperatures from −40° to +40° C. For periods of time of 2 to 5 hours, average fluctuations of 0.02 to 0.05 deg. have been observed.

5. Discussion

This equipment has been used successfully for calibration testing and research. The working space of 1 ft^3 is ample for most instruments, materials, and devices that have to be completely immersed in an atmosphere of known relative humidity. There is no theoretical limitation on the size of the test chamber that may be employed with this type of

equipment; a larger sized chamber would simply require a larger surrounding liquid bath. Neither is there any limitation on the geometry of the test chamber. A cylinder was chosen in this case for ease of construction, but any other space configuration can be substituted. Even in the present design, the cylindrical test chamber can be uncoupled from the setup, and, within the limitation of the available bath space, any other size, shape, or design of chamber can be attached.

Occasionally air of known or preestablished dew point is required at a place or instrument remote from the test chamber. The desired dew point can be readily produced by the apparatus, and all or part of the air from the test chamber can be piped wherever needed. The only limiting factor involves the temperature of the ambient air, which must not drop below the dew point of the air flowing through the transmission tubing, because condensation may occur in the lines.

The range of relative humidities obtainable with this type of equipment may be extended to much lower values by using a higher pressure source. A 250-psig compressor, operating between 150 to 200 psig, is used in the present design and provides relative humidities that are sufficiently low for most purposes. Much higher pressures would necessitate components capable of withstanding those high pressures. Similarly, for flows in excess of 5 ft^3/min, a compressor having a larger volume capacity would be required.

The rapidity with which the relative humidity may be changed depends primarily on the time involved in adjusting the pressure regulator, which controls the saturation pressure. Minor adjustments of the expansion valve and the exhaust control valve may be required after the major pressure adjustment has been made. These operations can easily be executed within 30 sec. At low rates of flow, the limiting factor ceases to be the time required for performing the above mechanical operations and becomes, instead, the time involved in purging air of one relative humidity, with air of another relative humidity. The component with the maximum air volume is the test chamber. It has a space of about 1 ft^3, so that the purging time depends upon the rate of air flow through this 1-ft^3 volume.

6. Summary

An apparatus of versatility and convenience for producing atmospheres of known relative humidity has been developed and constructed at the Bureau. It operates on the "two-pressure principle," whereby air is saturated at a high pressure and expanded to a lower pressure, the relative humidity at the lower pressure being the ratio of the lower to higher pressure, provided the operation is performed at constant temperature.

Important parameters can be varied and controlled over wide ranges: relative humidity from 10 to 98 percent; temperature from −40° to +40° C; flow up to 150 liters/min; test-chamber pressure from ½ to 2 atm. The relative humidity can easily be changed from one value to another within 30 sec.

Independent checks on the accuracy of the relative-humidity production with the psychrometric and dew-point methods have yielded average agreements of ±0.4 to ±0.6 percent. As the latter methods of measurement are probably no more accurate than about ±0.5 percent, it is reasonable to assume that the apparatus produces relative humidities that are known to at least ±0.5-percent relative humidity.

Washington, December 12, 1951

574278 O - 61 - 51

Relative Humidity-Temperature Relationships of Some Saturated Salt Solutions in the Temperature Range 0° to 50° C[1]

Arnold Wexler and Saburo Hasegawa

The relative humidity-temperature relationships have been determined in air in equilibrium with saturated salt solutions of lithium chloride, $LiCl \cdot H_2O$; magnesium chloride, $MgCl_2 \cdot 6H_2O$; sodium dichromate, $Na_2Cr_2O_7 \cdot 2H_2O$; magnesium nitrate, $Mg(NO_3)_2 \cdot 6H_2O$; sodium chloride, NaCl; ammonium sulfate, $(NH_4)_2SO_4$; potassium nitrate, KNO_3; and potassium sulfate, K_2SO_4, over a temperature range of 0° to 50° C, using the dewpoint method. The relative humidity is a continuous function of temperature, and, except for sodium chloride, is monotonic. The curve for sodium chloride increases from 74.9-percent relative humidity at 0° C to a maximum of 75.6 percent at 30° C and then gradually decreases to 74.7 percent. The maximum change in relative humidity with temperature, about 15-percent relative humidity as the temperature increases from 0° to 50° C, occurs with saturated salt solutions of sodium dichromate and magnesium nitrate.

1. Introduction

Saturated salt solutions are very useful in producing known relative humidities, principally for testing and calibrating selected hygrometers and hygrographs at temperatures above 0° C. The saturated salt solution is made up as a slushy mixture with distilled water and chemically pure salt in a glass or enameled tray and is enclosed in a sealed metal or glass chamber. When equilibrium conditions, usually hastened by forced air circulation or stirring, are attained, the chamber space is at a constant relative humidity. Some saturated salt solutions produce relative humidities that are roughly independent of temperature.

The equilibrium values of relative humidity of the saturated solutions of several salts used in calibration and testing are listed in NBS Circular 512 [1][2] and are based partly on vapor-pressure data given in the International Critical Tables [2] and partly on dewpoint measurements made at NBS. The relative humidity-temperature relationships of these, as well as several other, saturated salt solutions have been redetermined and are the subject of this paper.

The measurement of vapor pressure or vapor pressure lowering of a salt solution may be made in several ways. The differential methods are based on the determination of the difference in vapor pressure between the solution and solvent, using a sensitive differential manometer. In the dynamic method, the boiling point of the solution is determined under reduced pressure. The transpiration, or gas-saturation, method involves the gravemetric measurement of the water-vapor content of an inert gas saturated by passage over or through the salt solution. The dewpoint method consists in reducing the temperature of a mirror surface until condensation occurs.

The dewpoint method was utilized in this investigation. With this method, measurements could readily be made in the presence of an air atmosphere under conditions similar to those occurring in the use of saturated salt solutions for humidity-control purposes. Furthermore, other than using chemically pure salts of reagent grade and distilled water, no special precautions were taken. Thus the salts contained trace impurities, and the water was air saturated.

2. Description of Apparatus

The experimental setup shown in figure 1 was used to determine the equilibrium vapor pressure of a saturated salt solution. The bottom of a 2-liter Wolff flask, A, was filled to a depth of 2 inches with a saturated solution of a salt, B, made up as a slushy mixture with a pure reagent grade chemical and distilled water. A dewpoint apparatus, C, was inserted through one side neck of the flask; an air stirrer, D, was inserted through the central neck of the flask; and two copper-constantan thermocouples, E and F, were inserted through the other side neck of the flask. The Wolff flask was immersed in a liquid bath, O. Automatic temperature control of the bath was achieved by a system in which thermistors, in a bridge circuit, detected the temperature unbalance and a heater, H, supplied heat in proportion to the unbalance. Below room temperature, a cooling system, I, was used to reduce the bath temperature.

The shaft of the air stirrer, D, was supported in a close-fitted bearing and driven, through a belt and pulley, by an external remotely positioned motor.

Thermocouple, E, measured the air temperature within the Wolff flask, thermocouple, F, measured the temperature of the saturated salt solution, and thermocouple, H, measured the temperature of the liquid bath. These thermocouples were made with cotton-covered Bakelite-insulated wire. To insure that no spurious electromotive force would be

[1] This investigation was financially supported by the Aerology Branch, Bureau of Aeronautics, Department of the Navy.

[2] Figures in brackets indicate the literature references at the end of this paper.

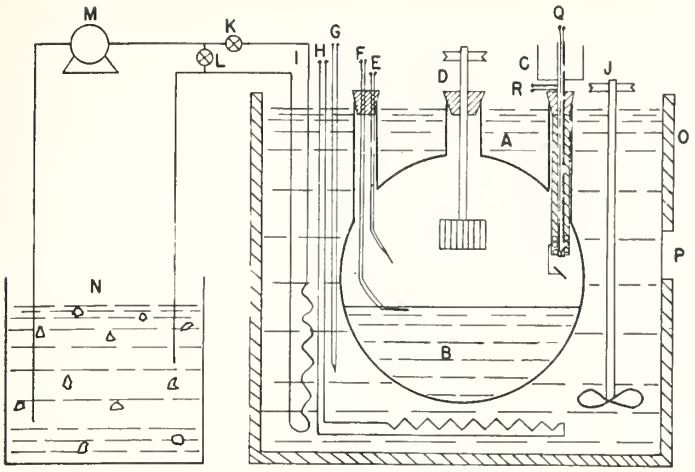

FIGURE 1. *Experimental setup.*

A, 2-liter Wolff flask; B, saturated salt solution; C, dewpoint apparatus; D, air stirrer; E, thermocouple for measuring air temperature; F, thermocouple for measuring temperature of saturated salt solution; G, thermocouple for measuring bath temperature; H, bath heater; I, cooling system; J, liquid bath stirrer; K, cooling system control valve; L, cooling system by-pass valve; M, cooling system pump; N, Stoddard's solvent mixed with dry ice; O, liquid thermostated bath; P, position external to bath from which a light is projected on the dewpoint mirror and from which the dewpoint mirror is observed with a telescope.

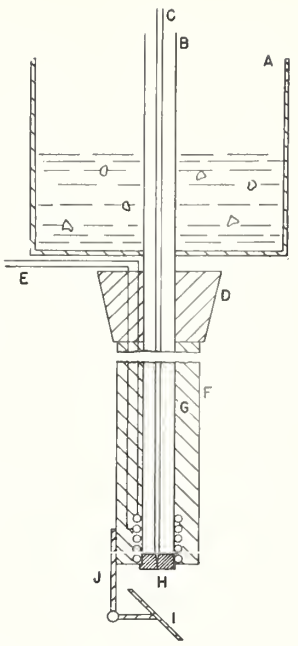

FIGURE 2. *Dewpoint apparatus.*

A, Brass cup; B, copper cooling tube; C, thermocouple; D, rubber stopper; E, heater; F, Bakelite tube; G, glass wool insulation; H, dewpoint mirror; I, viewing mirror; J, support braeket.

introduced because of electrolytic action, each junction was coated and protected with polystyrene cement. The thermocouple leads were covered with grounded equipotential shields. A precision potentiometer was used to measure the thermocouple electromotive force with a precision of better than 1 microvolt.

A light was projected on the dewpoint mirror and the mirror was viewed, through a telescope, from position, P, external to the liquid bath.

Details of the dewpoint apparatus are shown in figure 2. A brass cup, A, 3 inches in diameter and 3 inches deep, was attached to one end of a ¼-inch-outside-diameter copper tube, B, $\frac{1}{32}$-inch in wall thickness. A dewpoint mirror, H, was soldered to the other end of the copper tube. This mirror, ¼-inch-outside-diameter and ⅛ inch thick, was machined from copper, with a recess equal to the wall thickness of the copper tube so that it would fit snuggly in the end of the tube. The reflective surface of the mirror was first ground and polished, then plated with chromium, and finally lapped to within one-half fringe of optical flatness. A 1-mm-diameter hole was drilled in the center of the mirror, from the rear, to within about $\frac{1}{64}$ inch of the front reflective surface. A copper-constantan thermocouple, C, B&S gage No. 30, was inserted into the hole and soldered to the mirror.

An insulated-wire heater, E, was wound around the copper tube close to the mirror end. This heater was controlled by a variable transformer from a 60-cycle a-c power source. Glass-wool insulation, G, was wrapped around the copper tube and retained in position by a Bakelite tube, F, ¾-inch outside diameter. A galvanometer mirror, I, attached to the Bakelite tube by a metal bracket, J, allowed convenient viewing of the dewpoint mirror.

The addition of dry ice and alcohol to the brass cup, A, figure 2, served as a cold source for cooling the dewpoint mirror, H, through conduction along the copper tube, B. By decreasing the voltage applied to heater, E, the temperature of the dewpoint mirror could be lowered gradually until dew or frost was detected. By increasing the voltage applied to heater, E, the temperature of the mirror could be raised slowly until all dew or frost disappeared. The dewpoint mirror temperature corresponding to the instant of appearance and disappearance was measured by thermocouple, C.

3. Experimental Procedure

The procedure employed in making observations was to adjust the liquid-bath temperature to some desired value and then permit the Wolff flask, with its contents to come to temperature equilibrium. After equilibruim had been established, an observer would manipulate the dewpoint heater control and simultaneously view the dewpoint mirror until he had obtained five successive appearances and disappearances of dew or frost on the dewpoint mirror. A second observer would then repeat the process under the same operating conditions. Occasionally, the two observers would take repeat sets of observations. In this fashion, for any one salt, data were obtained at 10-deg. intervals from 0° to 50° C.

4. Results

For purposes of this investigation, it was assumed that the dewpoint corresponded to the mean of the observed temperature at which dew first appeared and then disappeared. For a given observer, each dewpoint therefore corresponded, usually, to the average of a minimum of 10 temperature observa-

TABLE 1. *Observed temperature-relative humidity data*

Lithium chloride $LiCl \cdot H_2O$						
Temperature °C	0.23	9.56	19.22	29.64	39.64	46.76
Relative humidity %	14.7	13.4	12.4	11.8	11.8	11.4
Magnesium chloride $MgCl_2 \cdot 6H_2O$						
Temperature °C	0.42	9.82	19.53	30.18	39.96	48.09
Relative humidity %	35.2	34.1	33.4	33.2	32.7	31.4
Sodium dichromate $Na_2Cr_2O_7 \cdot 2H_2O$						
Temperature °C	0.60	10.14	19.82	30.04	37.36	47.31
Relative humidity %	60.4	57.8	55.5	52.4	50.4	48.0
Magnesium nitrate $Mg(NO_3)_2 \cdot 6H_2O$						
Temperature °C	0.39	9.85	19.57	30.47	40.15	48.10
Relative humidity %	60.7	57.5	55.8	51.6	49.7	46.2
Sodium chloride NaCl						
Temperature °C	0.92	10.23	20.25	30.25	39.18	48.30
Relative humidity %	75.0	75.3	75.5	75.6	74.6	74.9
Ammonium sulfate $(NH_4)_2SO_4$						
Temperature °C	0.39	10.05	20.04	30.86	39.97	47.96
Relative humidity %	83.7	81.8	80.6	80.0	80.1	79.2
Potassium nitrate KNO_3						
Temperature °C	0.62	10.17	20.01	30.70	40.35	48.12
Relative humidity %	97.0	95.8	93.1	90.6	88.0	85.6
Potassium sulfate K_2SO_4						
Temperature °C	0.54	10.08	19.81	30.44	39.94	48.06
Relative humidity %	99.0	98.0	97.1	96.8	96.1	96.0

tions. The dewpoint, for a salt at a test temperature, was taken as the mean of the dewpoints obtained by each observer.

The ambient temperature was assumed to be the mean of the air temperature and the salt temperature within the Wolff flask. As these temperatures were relatively stable for appreciable periods of time, only one such set of temperature readings was obtained by each observer for his corresponding set of dewpoint observations.

The relative humidity in equilibrium with the saturated salt solution is given by

$$RH = \frac{e_d}{e_a} \times 100,$$

where e_d is the vapor pressure of pure water at the dewpoint temperature, and e_a is the vapor pressure of pure water at the ambient temperature. The vapor pressures given in the Smithsonian Tables [3] were used in this computation.

The mean relative humidity at each observed test temperature is presented in table 1 for eight different saturated salt solutions ranging in relative humidity from about 11 percent to 99 percent. The data for each salt were plotted, and the best smooth curve obtainable by eye was drawn through the plotted points. The faired values from this smooth curve are given in table 2. They represent the best estimates of the relative humidities obtained with these salts at the selected temperatures.

TABLE 2. *Faired values of relative humidity versus temperature*

Temperature	Relative humidity of saturated salt solution							
	$LiCl \cdot H_2O$	$MgCl_2 \cdot 6H_2O$	$Na_2Cr_2O_7 \cdot 2H_2O$	$Mg(NO_3)_2 \cdot 6H_2O$	NaCl	$(NH_4)_2SO_4$	KNO_3	K_2SO_4
°C	%	%	%	%	%	%	%	%
0	14.7	35.0	60.6	60.6	74.9	83.7	97.6	99.1
5	14.0	34.6	59.3	59.2	75.1	82.6	96.6	98.4
10	13.3	34.2	57.9	57.8	75.2	81.7	95.5	97.9
15	12.8	33.9	56.6	56.3	75.3	81.1	94.4	97.5
20	12.4	33.6	55.2	54.9	75.5	80.6	93.2	97.2
25	12.0	33.2	53.8	53.4	75.8	80.3	92.0	96.9
30	11.8	32.8	52.5	52.0	75.6	80.0	90.7	96.6
35	11.7	32.5	51.2	50.6	75.5	79.8	89.3	96.4
40	11.6	32.1	49.8	49.2	75.4	79.6	87.9	96.2
45	11.5	31.8	48.5	47.7	75.1	79.3	86.5	96.0
50	11.4	31.4	47.1	46.3	74.7	79.1	85.0	95.8

TABLE 3. *Scatter of data about smooth curves*

Nominal temperature	Relative-humidity deviation of data from curve of saturated salt solution							
	$LiCl \cdot H_2O$	$MgCl_2 \cdot 6H_2O$	$Na_2Cr_2O_7 \cdot 2H_2O$	$Mg(NO_3)_2 \cdot 6H_2O$	NaCl	$(NH_4)_2SO_4$	KNO_3	K_2SO_4
°C	%	%	%	%	%	%	%	%
0	0	+0.3	0	+0.2	+0.1	0	−0.5	0
10	0	−.3	0	−.3	−.1	0	+.4	+.1
20	0	−.2	+.2	+.8	0	0	−.2	−.1
30	0	+.3	−.1	−.3	0	0	+.1	+.2
40	+.2	+.5	−.1	+.5	−1.0	+.4	+.1	−.1
50	−.1	−.2	+.2	−.6	0	0	0	+.1
Average	0	±0.3	±0.1	±0.6	±0.2	±0.1	±0.2	±0.1

The plots of relative humidity versus temperature yield curves that are continuous and, generally, vary little with temperature over the temperature range of 0° to 50° C. These plots are shown as solid-line curves in figures 3 to 10. The maximum variation of relative humidity with temperature occurs with saturated solutions of sodium dichromate and magnesium nitrate. For these salts there is an absolute decrease in relative humidity of about 15 percent as the temperature increases from 0° to 50° C. The scatter of the mean experimental values above the smooth curves is given in table 3. The greatest scatter of the data occurs with sodium chloride and is ±0.6 percent relative humidity. For the other salts, the scatter is equal to or less than ±0.3 percent relative humidity.

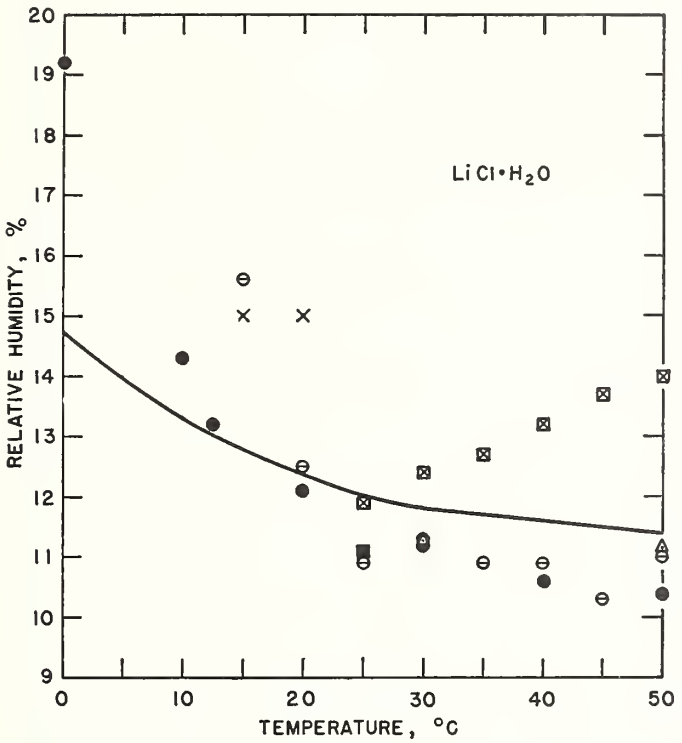

FIGURE 3. *Comparison of the faired NBS results with results of other experimenters.*

Figures 3 to 10, inclusive, show a comparison of the faired NBS results, as solid-line curves, with the results of other experimenters. The following symbol notation is used throughout these figures:

- ● ICT [2]
- ○ Foote, Saxton, and Dixon [4]
- + Leopold and Johnston [5]
- △ Sakai [6]
- □ Adams and Merz [7]
- ◇ Burns [8]
- × O'Brien [9]
- ▲ Speranskii [10, 15]
- ▽ Prideaux [11]
- ♦ Edgar and Swan [12]
- ■ Stokes and Robinson [13]
- ✳ van't Hoff [14]
- ▼ Carr and Harris [16]
- ◑ Lescoeur [17]
- ▭ Derby and Yngve [18]
- ⊕ Konduirev and Berezovskii [19]
- ◒ Ewing, Klinger, and Brandner [20
- ◬ Johnson and Molstad [21]
- ⊖ Huttig and Reuscher [22]
- ⊠ Gokcen [23]

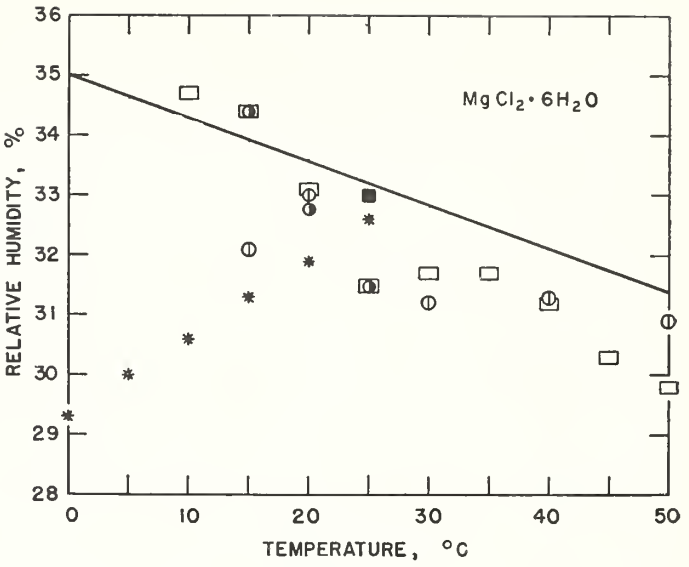

FIGURE 4.
(See fig. 3)

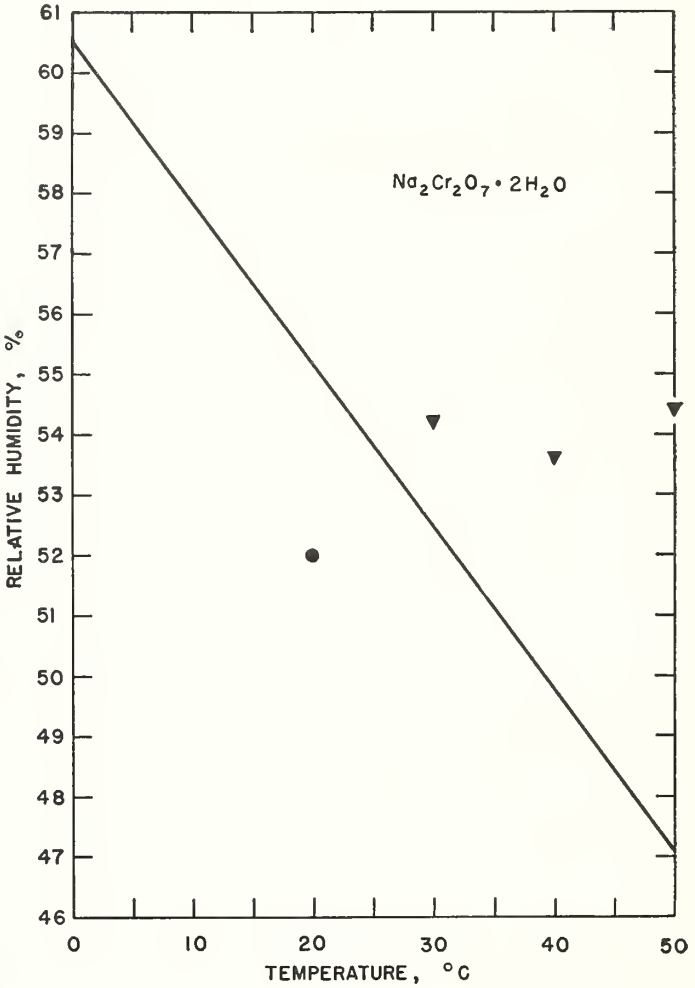

FIGURE 5.
(See fig. 3)

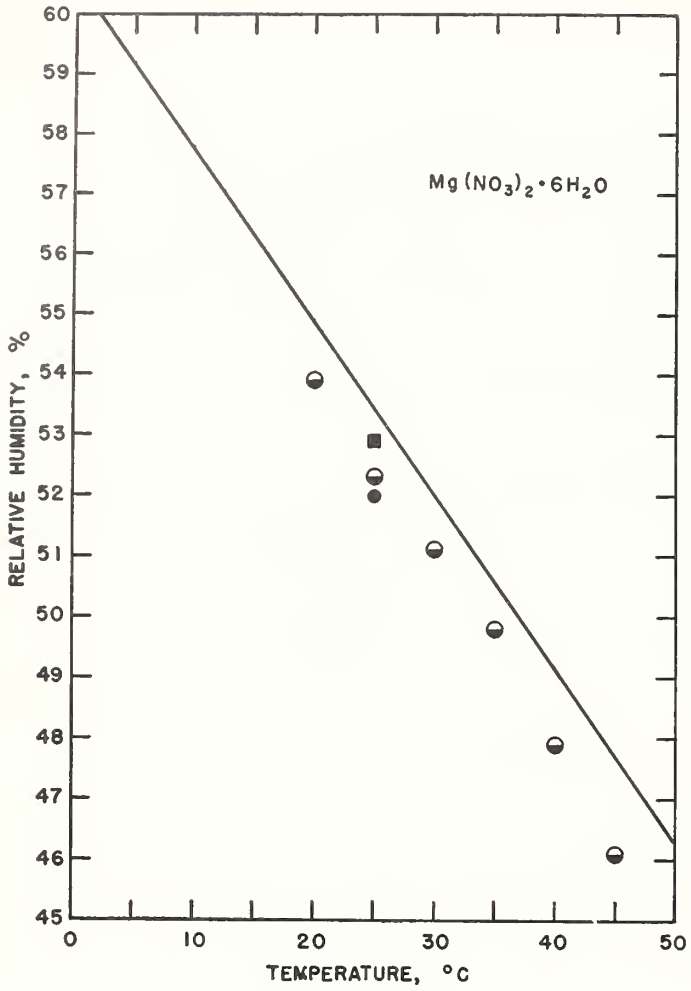

FIGURE 6.
(See fig. 3)

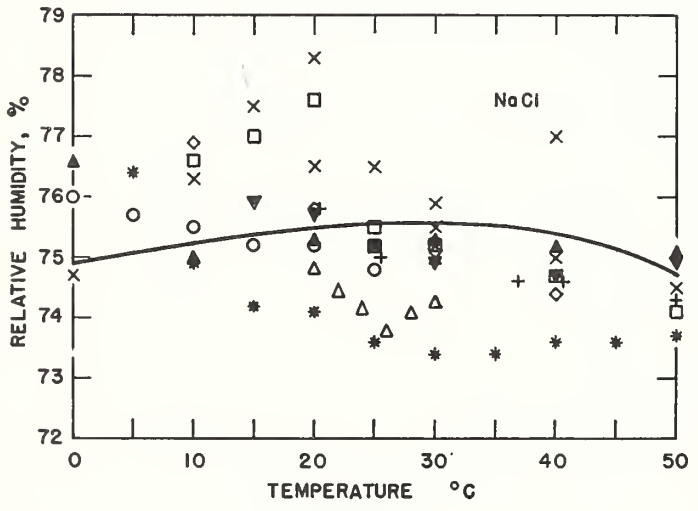

FIGURE 7.
(See fig. 3)

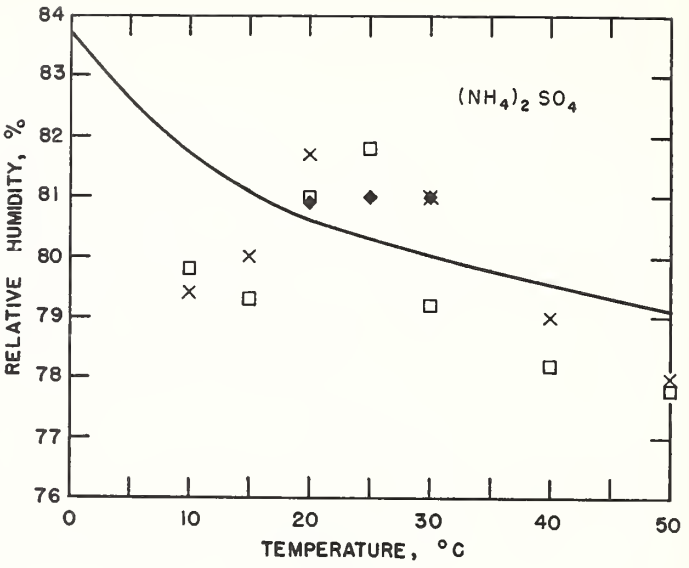

FIGURE 8.
(See fig. 3)

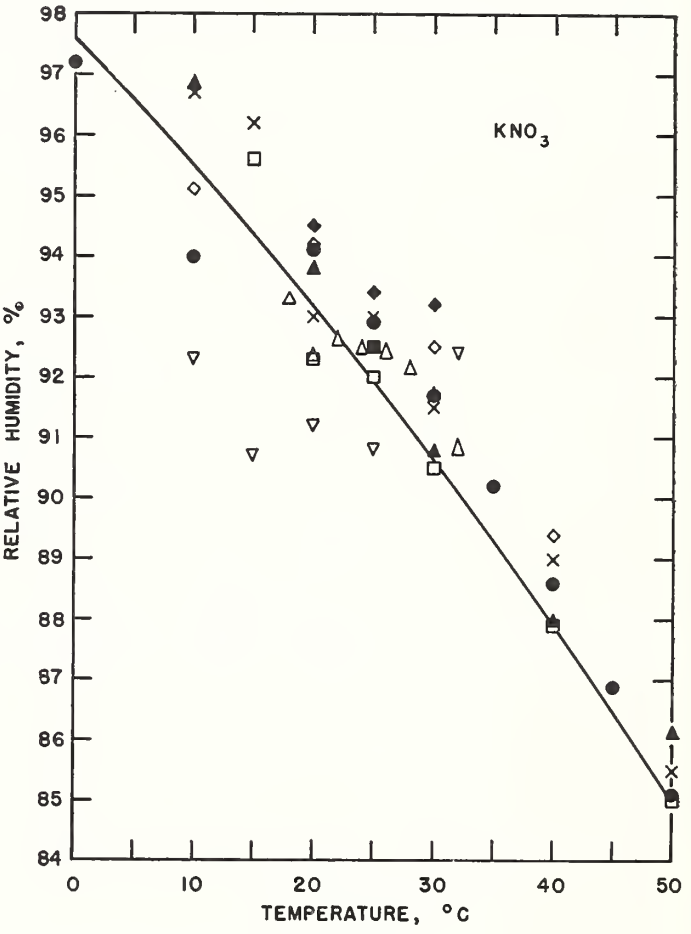

FIGURE 9.
(See fig. 3)

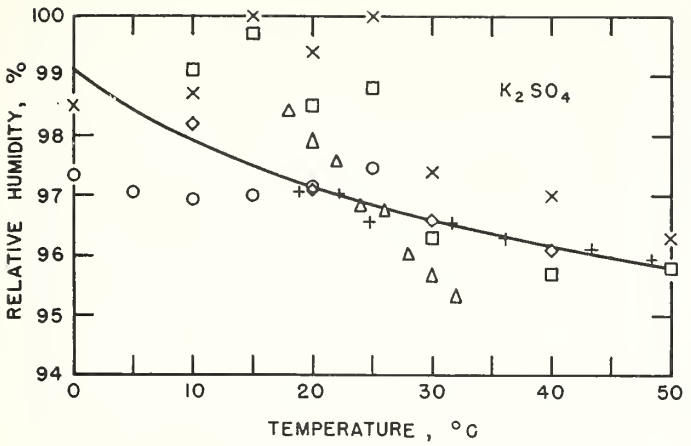

FIGURE 10.
(See fig. 3)

5. Discussion

5.1. General

There are several advantages to the use of the dewpoint method in determining the equilibrium relative humidity over a saturated salt solution. The experimental setup can be relatively simple, requiring only a temperature-controlled liquid bath for maintaining the salt solution and its containing vessel at some fixed temperature and a dewpoint detector. The dewpoint can be measured in the presence of an air (or other noncondensible) atmosphere. Methods that depend on the direct measurement of vapor pressure, either absolute or differential, require careful elimination of all gases and vapors except the water vapor from above the salt solution as well as the elimination of any dissolved gases in the solution because these would produce a serious error in the vapor pressure. The absolute accuracy of the vapor-pressure measurement increases with decreasing dewpoint for a given accuracy in the dewpoint measurement. For example, if the dewpoint is measured with an accuracy of 0.1 deg C, the corresponding accuracy in vapor pressure is 0.008 mm Hg at −20° C, 0.034 mm Hg at 0° C, 0.109 mm Hg at 20° C, and 0.296 mm Hg at 40 °C. The accuracy, in terms of percentage of vapor pressure, is 0.8 percent at −20° C, 0.7 percent at 0° C, 0.6 percent at 20° C, and 0.5 percent at 40° C. Thus, the percentage accuracy in vapor-pressure determination by the dewpoint method, for a given dewpoint accuracy, is roughly independent of dewpoint or vapor pressure. The dewpoint method is an indirect method; it yields a temperature from which the vapor pressure is obtained by recourse to tables. One of the inherent limitations of the method lies in the basic accuracy of the tables. For most work, and particularly for this investigation, the standard tables are considered to have adequate accuracy.

5.2. Errors

In determining relative humidity by the dewpoint method, the principal errors arise in the measurement of the dewpoint temperature and the ambient temperature. The precision of the temperature measurement, using calibrated single-junction copper-constantan thermocouples and a calibrated precision potentiometer, was 0.01 deg C, but the accuracy was probably no better than 0.05 deg C. As (1) the thermocouple for measuring the dewpoint was imbedded only several hundredths of an inch below the surface of the dewpoint mirror, (2) the body of the mirror was copper, and (3) the rates of heating and cooling were uniform and slow, it seems reasonable to assume that any temperature differentials within or across the mirror were negligible, say, no more than 0.01 to 0.02 deg C. Because of the relatively low thermal conductivity of liquid water, the temperature differential across the thickness of a dew film was possibly of greater magnitude. In cooling, the mirror was colder than the exposed dew surface and in heating, it was warmer. Two factors tend to reduce the importance of this. First, by averaging the temperatures at which dew is first observed to appear and then disappear, the errors due to the differentials across the dew, because they are of opposite sign, tend to cancel. Second, by keeping the thickness and quantity of dew small, the differentials can be reduced to a minimum.

The manually operated and visually observed dewpoint hygrometer required a certain degree of skill for successful use. After some experience in its use, it was possible to control the rate of heating and cooling so that the mirror temperature could be followed easily with a potentiometer, the appearance and disappearance of dew could be detected readily, and the thickness of the dew deposit kept as small as desirable. An observer could repeat a series of, say, five dewpoint determinations, at any one time, with an average deviation of a single determination from the mean of 0.04 deg C, with an average deviation of the mean of 0.01 C, and with an average range of 0.13 deg C. The average difference in temperature between the appearance and disappearance of dew was 0.5 deg C, whereas the maximum difference ever observed was 2 deg C. The dewpoint appeared to be independent of the various observed differences in temperature between the appearance and disappearance of dew.

The dewpoint (the average, usually, of five repeat determinations) obtained by any one observer had an average deviation from the mean of two or more observers of 0.07 deg C. The average deviation of the mean dewpoint of all observers for a salt solution at any temperature was 0.04 deg C. The mean range in dewpoint for all of the test conditions for two or more observers was 0.16 deg C.

Because the dew was visually detected, it is likely that different observers used different criteria for defining the appearance or disappearance of dew.

This may account to some extent for the spread in dewpoint from one observer to another.

Below 0° C, either frost or dew (supercooled water) may be deposited on the surface of the dewpoint mirror. In all cases (which included dewpoints as low as −23° C) the deposit first detected was dew. If the mirror temperature was not permitted to fall too far below the dewpoint, then dew remained on the mirror throughout the determination. If the mirror temperature dropped appreciably below the dewpoint, the dew changed to frost.

The ambient temperature was taken as the mean temperature of the salt solution and air. These latter two temperatures differed from each other because of the heat sources and sinks associated with the setup. The fan used for stirring the air within the chamber introduced heat through agitation; conduction along the shaft added or abstracted heat, depending on whether the room temperature was above or below that of the test chamber. The dewpoint hygrometer served as a serious heat sink, for, by the very nature of its operation, it has to be maintained below test-chamber temperature. Although the insulation surrounding the conduction rod aided appreciably in reducing the magnitude of the heat loss, there was still enough loss to produce a temperature differential between the salt solution and air. The test-chamber temperature may therefore have an average uncertainty, because of this differential, of 0.09 deg C.

The root-mean-square uncertainty in the dewpoint determination is 0.07 deg C and in the ambient (test chamber) temperature is 0.10 deg C. The corresponding uncertainty in relative humidity varies from a maximum of 1.2 percent for the high-humidity saturated salt solutions to 0.2 percent for the low-humidity saturated salt solutions.

5.3. Comparison of Results With Those of Other Investigators

The NBS results are compared with those of other investigators in figures 3 to 10, in which the NBS results are shown as solid-line curves. The results of some workers were reported for a limited temperature range or, occasionally, for only one temperature. Wherever necessary, results that were presented in terms of vapor pressure were converted into relative humidity.

It is apparent from these figures that there is a certain degree of scatter among the values reported by other researchers as well as some disagreement between the NBS results and those values. In general, these other results fall within a band of values that is, on an average, roughly within ±1½-percent relative humidity of the NBS results.

5.4. Use of Saturated Salt Solutions

When saturated salt solutions are employed for humidity control, experience has shown that certain precautions must be observed in order that the theoretical values may be used without the need of measurement. It is necessary to enclose the saturated salt solution in a sealed chamber. The chamber and the fixtures therein must be made of nonhygroscopic materials, preferably metal or glass, else the time required for humidity equilibrium to be achieved may be very great, sometimes of the order of days or weeks. The chamber, salt solution, and ambient air should be brought to temperature equilibrium. It is desirable for the salt solution to occupy as large a surface area as possible and for some means of air ventilation or circulation to be provided. In the latter regard, if at all possible, the motor that drives the fan or blower should be external to the chamber. Otherwise, the heat dissipated by the motor will gradually raise the internal chamber temperature and introduce some uncertainty in the equilibrium relative humidity. The time required for humidity equilibrium to be reached with saturated salt solutions depends on several factors: (1) the ratio of free surface area of the solution to chamber volume, (2) the amount of air stirring, and (3) the presence of hygroscopic materials. It is conjectured that agitating the saturated salt solution may increase the rate at which equilibrium is achieved.

As ideal conditions are rarely obtained in practice, it is probable that the theoretical values of relative humidity are seldom reached. In general use, saturated salt solutions should not be expected to control the relative humidity to closer than about 1-percent relative humidity of the theoretical values.

6. References

[1] Arnold Wexler and W. G. Brombacher, Methods of measuring humidity and testing hygrometers, NBS Circular 512 (1951).

[2] International Critical Tables **1,** 68 (McGraw-Hill Book Co., New York, N. Y., 1927).

[3] Smithsonian Meteorological Tables, 6th Revised Edition (1951).

[4] H. W. Foote, Blair Saxton, and J. D. Dixon, The vapor pressures of saturated aqueous solutions of certain salts, J. Am. Chem. Soc. **54,** 563 (1932).

[5] H. Geneva Leopold and John Johnston, The vapor pressure of the saturated aqueous solutions of certain salts, J. Am. Chem. Soc. **49,** 1974 (1927).

[6] W. Sakai, The study of urea, 1. The hygroscopic properties of (the) double substance. The vapor pressure of saturated solution(s) of salts, J. Soc. Chem. Ind. Japan, **43,** Suppl. binding 104 (1940).

[7] J. R. Adams and A. R. Merz, Hygroscopicity of fertilizer materials and mixtures, J. Ind. Eng. Chem. **21,** 305 (1929).

[8] Robert Burns, Conditioning of insulating materials for test, Bell Telephone System Monograph B–986 (1937). Source of material not given.

[9] F. E. M. O'Brien, J. Sci. Instr., **25,** 73 (1948).

[10] A. Speranskii, The vapor pressure and integral heat of solution of saturated solutions, Z. physik. Chem. **78,** 86 (1912).

[11] E. B. R. Prideaux, The deliquescence and drying of ammonium and alkali nitrates and a theory of the absorption of water vapor by mixed salts, J. Soc. Chem. Ind. **39,** 182–5T (1920).

[12] G. Edgar and W. O. Swan, Factors determining the hygroscopic properties of soluble substances, I. Vapor pressure of saturated solutions, J. Am. Chem. Soc. **44,** 570 (1922).

[13] R. H. Stokes and R. A. Robinson, Ind. Eng. Chem. **41,** 2013 (Sept. 1949).
[14] J. H. van't Hoff, E. F. Armstrong, W. Hinrichsen, F. Weigert, and G. Just, Gips und Anhydrit, Z. physik. Chem. **45,** 257 (1903).
[15] A. Speranskii, Vapor pressure of saturated solutions, Z. physik. Chem. **70,** 519 (1910).
[16] D. S. Carr and B. L. Harris, Ind. Eng. Chem. **41,** 2014 (Sept. 1949).
[17] M. H. Lescoeur, Researches sur la dissociation des hydrates salines et des composés analogues, Ann. Chem. Phys. (7) **2,** 85 (1894).
[18] I. H. Derby and Victor Yngve, Dissociation tensions of certain hydrated chlorides and the vapor pressures of their saturated solutions, J. Am. Chem. Soc. **38,** 1439 (1916).
[19] N. V. Konduirev and G. V. Berezovskii, Vapor pressure of saturated solutions and hydrates of magnesium chloride, J. Gen. Chem. (USSR) **5,** 1246 (1935).
[20] Warren W. Ewing, Ernest Klinger, and John D. Brandner, Vapor pressure-temperature relations and the heats of hydration, solution and dilution of the binary system magnesium nitrate-water, J. Am. Chem. Soc. **56,** 1053 (1934).
[21] Ernest F. Johnson, Jr., and Melvin C. Molstad, Thermodynamic properties of aqueous lithium chloride solutions. An evaluation of the gas-current method for determination of thermodynamic properties of aqueous salt solutions, J. Phys. & Colloid Chem. **55,** 257 (1951).
[22] F. H. Huttig and F. Reuscher, Studien zur Chemie des Lithiums. I. Über die Hydrate des Lithiumchlorids und Lithiumbromids, Z. anorg. Chem. **137,** 155 (1924).
[23] Nevzat A. Gokcen, Vapor pressure of water above saturated lithium chloride solution, J. Am. Chem. Soc. **73,** 3789 (1951).

WASHINGTON, February 19, 1954.

Reprinted from The Journal of the Acoustical Society of America, Vol. 26, No. 3, 428–433, May, 1954

An Acoustic Method for the Measurement of Vibration Amplitudes*

Walter Koidan
National Bureau of Standards, Washington, D. C.
(Received December 11, 1953)

By means of a modification of the pistonphone, a technique has been developed to obtain the response of a capacitance type vibration pickup probe using the reciprocity calibration of a condenser microphone as a reference. The raised, center portion of a circular piston, driven by a barium titanate cylinder, projects into one end of a cavity, the shelf of the piston being located outside of the enclosure. A calibrated condenser microphone coupled to the other end of the cavity responds to the sound pressure developed by the piston. The output of an annular capacitance type vibration pickup, which detects the motion of the piston shelf, is compared with the generated microphone voltage. With the microphone removed from the cavity, the output of a capacitance probe located adjacent to the top surface of the piston is compared with that of the annular pickup. The probe response is computed from these measurements and the microphone response.

From considerations of checks by independent methods, an accuracy of about 0.5 db is indicated from 100 to 10 000 cps. Using a sensitive probe, vibration amplitudes as small as 10^{-9} cm have been measured with a comparable degree of accuracy.

INTRODUCTION

THE first reference to the pistonphone is in a paper by Wente,[1] who describes it as a device for calibrating condenser microphones from 20 to 200 cps. A piston and a condenser microphone are coupled to the same cavity, a known sinusoidal motion imparted to the piston by means of a motor-crank arrangement, and the pressure in the cavity calculated from the piston displacement. The expression for the pressure can be derived from a consideration of the approximately adiabatic process involved. Differentiating the expression pV^γ = a constant, there results, for small displacements,

$$p = -Ap_0\gamma\Delta d/V, \tag{1}$$

where p = sound pressure, Δd = piston displacement, A = cross-sectional area of piston, V = cavity volume, p_0 = ambient pressure, and γ = ratio of specific heats for the gas. Equation (1) is valid under the conditions that (a) the walls of the cavity are perfectly rigid, (b) the cooling effect of the walls is negligible, and (c) standing wave patterns do not exist in the gas.

The nature of these assumptions has been discussed by Ballantine[2] and Cook.[3] In a paper by DiMattia and Wiener,[4] a comparison is made of the determinations of the reciprocity response of a condenser microphone by three laboratories. The data indicate that with modern experimental techniques, reciprocity calibrations are performed with an over-all estimated accuracy of 0.2 db or better from 50 to 10 000 cps. In view of the availability of the condenser microphone as an accurate pressure measuring device, it was suggested by London[5] that the original use of the pistonphone be reversed to determine the amplitude of motion of the piston from the measured sound pressure over an extended frequency range. The known motion could then be used to calibrate a vibration pickup. In proceeding with this work, a capacitance probe was developed as the vibration pickup which would electrically reproduce the motion of the surface under observation with negligible mechanical loading.

CAPACITANCE TYPE VIBRATION DETECTOR

A schematic diagram of the capacitance vibration detector is shown in Fig. 1. The design is an adaptation of a circuit described by Van Zelst,[6] and modified for use as a vibration detector. At the mechanical input, C represents a capacitance formed by placing a conducting surface in proximity to a vibrating piston, which is maintained at ground potential. L and C, shown as a probe in Fig. 1, constitute one branch of a bridge circuit, the other three branches being made up of a variable resistance (R) and two capacitors of equal

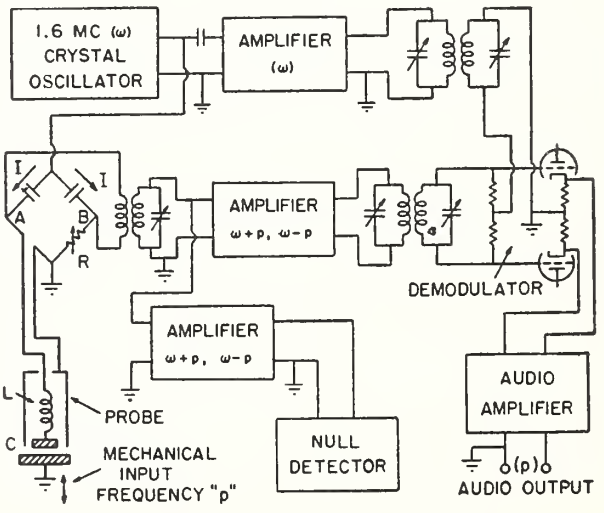

Fig. 1. Schematic diagram of the capacitance vibration detector using a probe.

* This work was supported by the Office of Basic Instrumentation of the National Bureau of Standards.

[1] E. C. Wente, Phys. Rev. **10**, 48 (1917).
[2] S. Ballantine, J. Acoust. Soc. Am. **3**, 319 (1932).
[3] R. K. Cook, J. Research Natl. Bur. Standards **25**, 498 (1940).
[4] A. L. DiMattia and F. M. Wiener, J. Acoust. Soc. Am. **18**, 341 (1946).
[5] A. London, J. Appl. Mech. **15**, 391 (1948).
[6] J. J. Z. Van Zelst, Philips Tech. Rev. **9**, 357 (1947–1948).

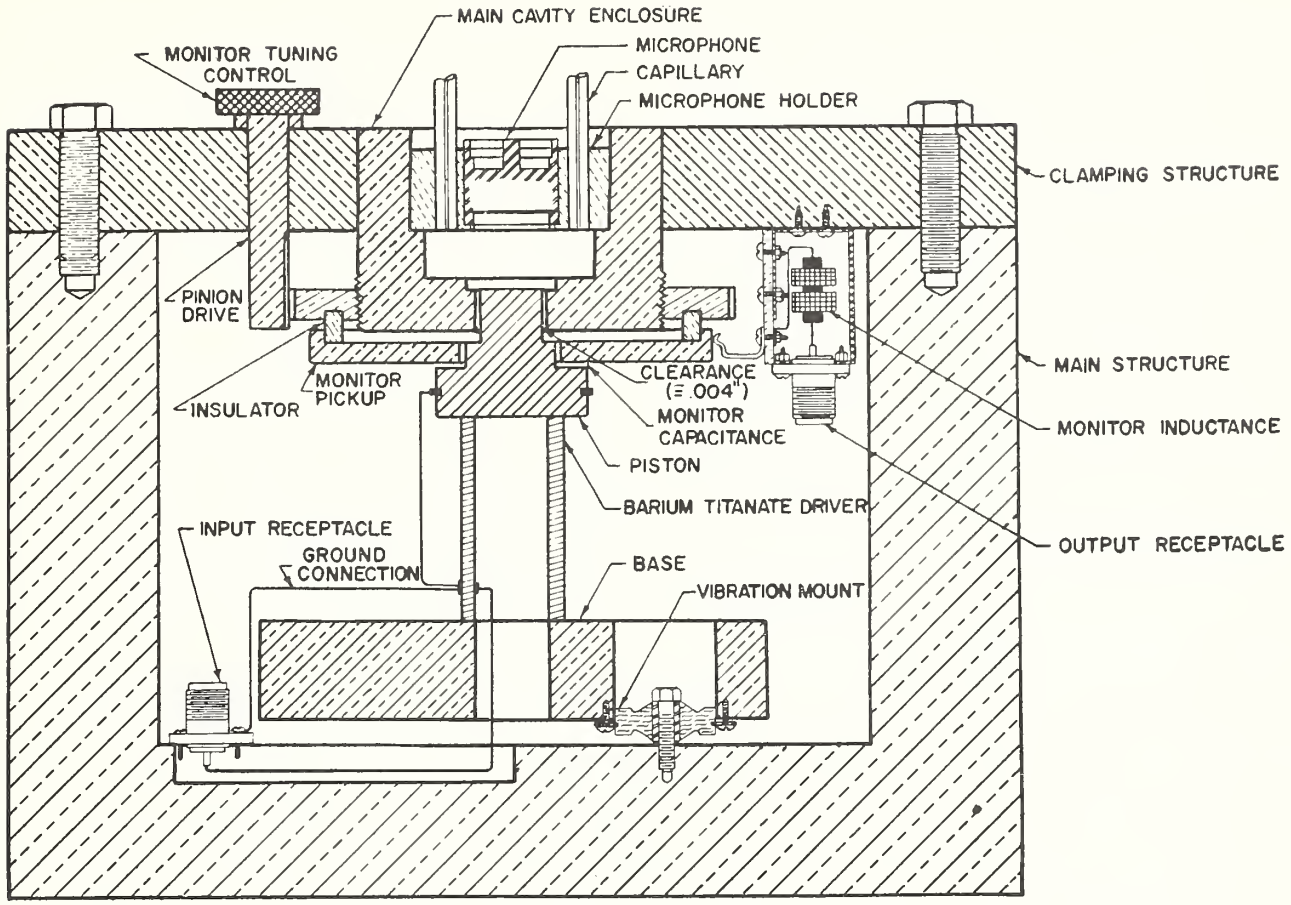

FIG. 2. Cross section of the pistonphone, showing the arrangement of the driver, monitor, and microphone.

value. A 1.6 mc signal from a crystal controlled oscillator is injected into the bridge and a balance is obtained by alternately varying C and R until the null detector reads a minimum. This occurs when L and C are tuned to series resonance at 1.6 mc and R is adjusted to equal the effective resistance of the L-C branch. The two capacitors in the upper branches of the bridge are chosen to present a high impedance to the oscillator source, while the output of the bridge, taken between points A and B, has a relatively low impedance. Because of the low impedance of the L-C combination, the capacitance to ground of the cable which connects the probe inductance to point A does not adversely affect the operation of the bridge and can be balanced by a capacitance between point B and ground, the adjustment being not at all critical.

When the piston is set into motion at an angular frequency, p, the bridge output is given by[7]

$$v_0 = j\frac{I}{\omega C^2}\Delta C\frac{1}{2}\left[\cos(\omega-p)t-\cos(\omega+p)t\right], \qquad (2)$$

where v_0 = instantaneous output voltage, I = peak carrier current in bridge, ω = angular frequency of carrier, C = total capacitance of pickup element, and ΔC = peak variation in capacitance.

[7] See appendix for derivation.

Voltage v_0 is a suppressed carrier, containing both the upper and lower side bands, $(\omega+p)$ and $(\omega-p)$, but not the carrier, ω. In order to extract the audio-frequency, the suppressed carrier and the original carrier are combined to produce an amplitude modulated wave, which is demodulated in a push-pull infinite impedance detector. The balanced audio output corresponds to the mechanical input to C. Reversion to single-ended operation is added for convenience in instrumentation.

PISTONPHONE-MONITOR COMBINATION

Figure 2 shows the pistonphone arranged for an acoustic calibration. The driver is a hollow barium titanate cylinder, polarized to produce a longitudinal elongation for a voltage applied between the inside and outside surfaces. A step-shaped piston is cemented to the upper end of the driver; the lower end is cemented to a circular brass base supported by four vibration mounts, the need for which will be discussed below. The main structure of the instrument supports a clamping structure, which in turn supports the cavity and its accessories. The walls of the cavity are made up of the main cavity enclosure, the piston surface, the diaphragm of a Western Electric type 640AA condenser microphone, a Lucite microphone holder, and the ends of two glass capillary tubes.

The motion to be correlated with the sound pressure in Eq. (1) is that of the top surface of the piston, since it is this surface which develops the pressure in the cavity. Although it would be desirable, it is not feasible to operate a capacitance vibration detector in proximity to the piston surface at the same time that the microphone is coupled to the cavity. A "monitor" vibration detector is therefore included to obtain calibrations independent of the driver characteristics. The monitor detects the change in capacitance between the shelf of the piston, maintained at ground potential, and an annular pickup element. The pickup is electrically insulated from the main structure and arranged to rotate on a screw thread for adjustment, by pinion and gear, of its capacitance to ground. The associated series inductance is mounted adjacent to the capacitance and is connected to the electronic circuit of the vibration detector through an output receptacle and a cable.

The six-pound mass of the driver base and the four vibration mounts comprise a mechanical system resonant at about 15 cps, the purpose of which is to reduce mechanical coupling between the driver and the main structure. If the driver base is rigidly clamped to the body of the instrument, standing waves set up in the structure result in relative motion of the capacitance pickup and give rise to spurious effects. As will be seen in the experimental results, the use of vibration mounts is decidedly effective in reducing mechanical coupling, but due to building vibration, the mass-stiffness system introduces an ambient low-frequency noise output. This effect can be minimized by connecting a high or band pass filter to the audio output.

Another mechanical coupling factor which must be eliminated is the rubbing that can occur between the piston and the cavity enclosure. A clearance of approximately 0.004 in., sealed with Vaseline to prevent leakage of gas, is therefore provided.

The glass capillary tubes assure that atmospheric pressure exists inside the cavity and also provide an inlet for hydrogen, which is used in the cavity at frequencies above 3000 cps to prevent the onset of standing wave patterns in the gas within the frequency range in which the calibrations are made. The pistonphone cavity has a volume of 19.9 cc, a diameter of 1.688 in.; and a diameter-to-length ratio of 3.4. The section of the piston which projects into the cavity is $\frac{5}{8}$ in. in diameter.

ACOUSTIC CALIBRATION OF THE PISTONPHONE MONITOR

The response of the monitor is obtained by comparing its output with the microphone open circuit voltage. A switching arrangement is used to substitute the monitor capacitance and its associated inductance into the bridge circuit in place of the probe shown in Fig. 1, so that when the piston is driven, the variation in capacitance between the piston shelf and the monitor pickup element produces an output from the vibration detector circuit. At the same time, the motion of the piston develops a sound pressure in the cavity given by

$$p = e_{oc}/\rho, \tag{3}$$

where p = sound pressure, e_{oc} = open circuit microphone voltage, and ρ = microphone response.

In order to determine the monitor response, it is not necessary to know either the pressure or the piston displacement. An explicit expression for the monitor response is obtained by combining Eq. (1) and (3):

$$\frac{e_m}{\Delta d} = -\frac{\rho A p_0 \gamma}{V}\frac{e_m}{e_{oc}}, \tag{4}$$

where e_m = audio output of the detecting circuit using the monitor pickup.

Using a variation of the usual substitution method, the ratio e_m/e_{oc} is measured by introducing the voltage e_m, through an attenuator, across the insert resistance of the microphone preamplifier.

CAPACITANCE PROBE AND ITS CALIBRATION

To provide a practical method for transferring the acoustic calibration, the capacitance probe shown in Fig. 3 was developed. The probe consists of a pickup element, an inductance, a Lucite insulating tube, a brass shield, and a threaded holder. Adjustment of the distance between the pickup element and the vibrating surface is by a knob, which through a double reduction gear, turns the screw to raise or lower the probe.

The probe response is obtained by comparing its output with that of the monitor. The microphone and its holder are removed from the cavity, the probe support rigidly bolted to the top clamping structure of the pistonphone, and the probe brought into position directly over the top surface of the piston by tuning the bridge circuit for a null indication. Two bridge circuits are now brought into use: one incorporating the monitor capacitance, inductance, and resistance, and the other containing the probe capacitance, inductance, and resistance. Making use of the switching arrangement to read both monitor and probe output

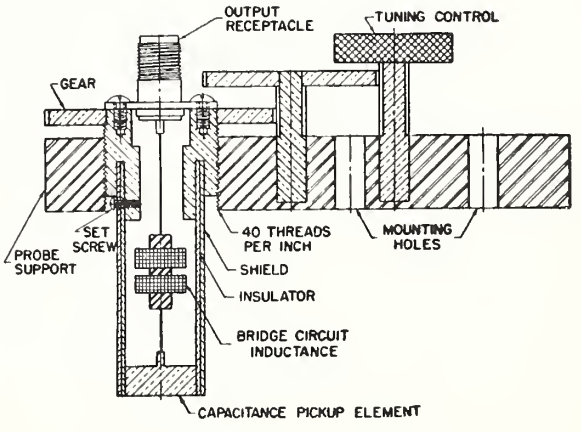

FIG. 3. Cross section of a capacitance probe.

voltages from the detecting circuit, the probe to monitor output ratio is obtained for each frequency.

The complete expression for the response of the capacitance vibration detector using a probe is

$$\frac{e_p}{\Delta d} = -\frac{\rho A p_0 \gamma}{V} \frac{e_m}{e_{oc}} \frac{e_p}{e_m'}, \tag{4a}$$

where e_p = audio output of the detecting circuit using a capacitance probe.

The design of a probe involves the choice of an inductance, which, with the stray capacitance of the probe, plus the desired parallel plate capacitance between the pickup element and the piston surface, establishes series resonance at the crystal oscillator frequency. Since C in Eq. (2) is the total capacitance of the pickup element, including stray capacitance, the stray capacitance obviously affects the response; hence the need for a shield to eliminate possible changes in the response in transferring the probe from the calibrating instrument to other shakers. Two probes were built, one designed primarily for high sensitivity and the other for practical applications. The former, designated as probe No. 1, operates at a spacing of approximately 0.06 mm, and has a mid-frequency range response of 1.40×10^6 volts/cm, while the latter, probe No. 2, operates at a spacing of about 0.5 mm, with a response of 8.92×10^4 volts/cm.

Referring to Eq. (2), it is seen that the response of the capacitance vibration detector is proportional to $\Delta C/C^2$. If no stray capacitance were present in the probe, this expression could be rewritten as $-\Delta d/A$, where A is the area of the parallel plate capacitor, with air dielectric, formed by the pickup element and the vibrating surface. This indicates that for a given area, changing C by means of varying the spacing, and revising the inductance to obtain series resonance, will not affect the response. However, if C includes stray capacitance, a closer spacing in conjunction with a smaller value of inductance will yield a greater response. The response can thus be increased by decreasing the spacing until the stray capacitance becomes negligible compared to the parallel plate capacitance. Beyond this point, it appears that the response may be increased by decreasing the area of the probe to require a closer spacing for a given value of probe inductance.

EXPERIMENTAL RESULTS

Two acoustically determined response curves of the capacitance vibration detector, using probe No. 2, are shown in Fig. 4. The absolute value of the response at low frequencies was verified by microscope measurement of the amplitude of vibration of a separate shaker, illuminated by a stroboscopic light source. With the light source adjusted to a slightly different frequency from that of the shaker, the vibration was observed in slow motion and measurements made with a microscope eyepiece. The results of the microscope measurements are plotted in Fig. 4 for comparison with the pistonphone calibrations. The relative response of the detecting circuit as a function of frequency, shown in Fig. 4, was measured electronically by disconnecting the bridge circuit and oscillator section of the vibration detector, and substituting an amplitude modulated wave input. The decrease in response with frequency thus measured is seen to approximate that of the response determined acoustically.

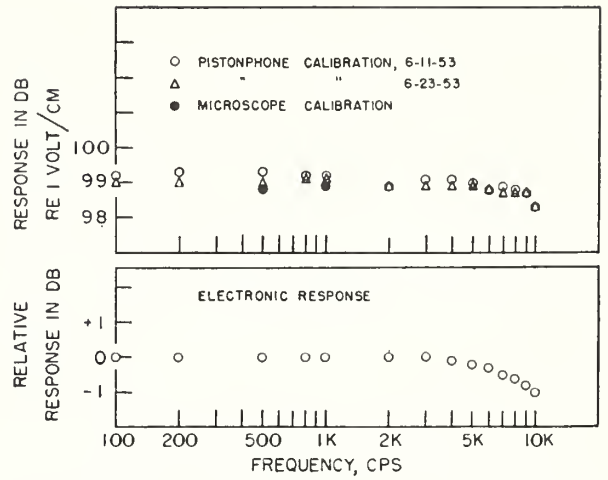

FIG. 4. Response of the capacitance vibration detector. The upper set of curves shows the response, measured acoustically with the pistonphone, using probe No. 2, two calibrations being plotted to indicate the precision of the measurements. At 500 and 1000 cps, the response was verified by microscope measurement using a stroboscopic light source. The lower curve shows the relative response of the vibration detector as a function of frequency measured electronically by substituting an amplitude modulated wave input in place of the bridge.

Above 200 cps, the output noise level of the detecting circuit is less than 50 microvolts rms in a band width of 20 cps. When referred to the response of probe No. 1, the more sensitive probe, this noise corresponds to a peak vibration amplitude of 5.05×10^{-11} cm, permitting accurate measurements of less than 10^{-9} cm.

The upper amplitude limit is determined either by distortion in the electronic amplifiers, or when the amplitude of vibration is large enough to cause Eq. (2) to become invalid. If the peak vibration amplitude is permitted to vary up to 2 percent of the spacing, considerations of measured noise level and response indicate a useful dynamic range of about 100 db.

The ratio of probe to monitor output, measured as a function of frequency, increases by about 0.3 db in the range from 100 to 10 000 cps. There are at least three possible explanations for the slight increase in this ratio: (a) the output impedance of the bridge circuit is different for the probe than for the monitor, permitting optimum adjustment of the radio-frequency transformers for only one input condition at a time, (b) residual mechanical coupling may exist between the driver and pickup devices, and (c) flexural modes of vibration may occur in the piston at higher frequencies.

Several pistonphone calibrations were performed before clearance between the piston and cavity enclosure was provided, and before the driving system was placed on vibration mounts. Consistent results were obtained from 100 to 1000 cps, but above 1000 cps the data were somewhat erratic. The acoustic calibration range was extended to 2000 cps by providing the small clearance between the piston and cavity enclosure to prevent mechanical coupling due to rubbing of the surfaces; however, above 2000 cps erratic results were again encountered. By the addition of the vibration mounted driver system with maintenance of the clearance, the range was extended to 10 000 cps.

To observe the effects of mechanical coupling, the probe was tuned over the top clamping plate of the pistonphone. With this arrangement, an output from the probe would indicate vertical motion of the clamping plate. When the vibration mounts were removed and the driver base rigidly clamped to the main structure, strong outputs were observed at several frequencies between 2000 and 10 000 cps. Using vibration mounts, but with the moving structure unbalanced so that rubbing occurred between the piston and the cavity enclosure, the same effect was noticed. With vibration mounts and correct balancing, so that rubbing did not occur, no output was detected.

In estimating the accuracy of the pistonphone calibration of the capacitance vibration detector using a probe, the microphone reciprocity calibration and the pistonphone measurements must both be considered. As pointed out in the Introduction, the microphone response is known to have an accuracy of 0.2 db or better. The error introduced in the pistonphone calibration as a result of volume effects, cooling losses, and contributions from standing waves in the gas, is estimated at approximately 0.1 db. An attenuator, accurate to within 0.1 db, was used to measure the two voltage ratios which appear in Eq. (4a), introducing an estimated error of 0.1 db in each of these two measurements. No attempt was made to evaluate the error introduced by residual mechanical coupling or acoustical coupling between the driver and the capacitance pickup devices; however, the experimental data mentioned above on the ratio of probe to monitor output as a function of frequency are a strong indication that the coupling effects on the pickup devices are small. Furthermore, it is seen from Eqs. (4) and (4a) that acoustic reaction on the driver does not affect the value of the response obtained for either the monitor or the probe since the driver motion affects the numerator and denominator of these expressions equally. From these considerations and from the experimental results shown in Fig. 4, the accuracy of the probe response is estimated at about 0.5 db up to 1000 cps. Although no direct microscope measurements were feasible above this frequency, agreement of the relative response between the upper and lower curves indicates a comparable degree of accuracy from 1000 to 10 000 cps.

ABSOLUTE ELECTRONIC CALIBRATION

An independent method was developed for calibrating the capacitance vibration detector at low frequencies. The method is of interest because it is based upon the measurement of a direct displacement instead of upon the sound pressure calibration of a microphone. Although the method was not fully exploited experimentally, agreement with the acoustic calibration was found to be within about 1 db, and it should be possible to reduce the difference by further refinement.

The output of the null detector is connected through an amplifier and a thermocouple to a dc microammeter. When the capacitance probe is at the correct spacing, d, the null detector output is small, and the microammeter reading is close to zero. From this position, the probe is detuned by a known distance, Δd_d, changing the capacitance by ΔC_d. The unbalanced bridge produces a carrier output sufficient to heat the thermocouple and obtain a reading on the microammeter. From Eq. (16) of the Appendix, the instantaneous null detector output is

$$v_{od} = K\Delta C_d \sin\omega t, \tag{5}$$

where $K \propto jI/\omega C^2$. The rms value of this voltage is

$$V_{odrms} = K\Delta C_d/\sqrt{2}. \tag{6}$$

The probe is then retuned to a null and the piston given an unknown sinusoidal motion of peak value Δd_a. The output from the null detector now represents an increase in the null reading. From Eq. (15), the null detector output for this condition is

$$v_{oa} = K\Delta C_a \tfrac{1}{2}[\cos(\omega - p)t - \cos(\omega + p)t], \tag{7}$$

where ΔC_a = peak variation in capacitance. The rms value of v_{oa} is,

$$V_{oarms} = K\Delta C_a/2. \tag{8}$$

For small displacements, direct or alternating,

$$\Delta C/C_e = -\Delta d/d, \tag{9}$$

where C_e = capacitance of pickup element, not including stray capacitance. Relating Eqs. (6), (8) and (9),

$$\Delta d_a = -\sqrt{2}\Delta d_d V_{oarms}/V_{odrms}. \tag{10}$$

The ratio of the voltages in Eq. (10) is found by taking the square root of the ratio of the microammeter readings for the two conditions, since these readings, obtained by means of the thermocouple, are proportional to the square of the rms value of the null detector output. The response of the probe is computed from Eq. (10) and the audio output voltage of the detecting circuit, measured for the sinusoidal motion of the piston. In employing this method, the requirement that the displacement be small compared to the spacing applies to the direct displacement of the probe as well as to the motion of the piston.

APPLICATIONS

In order not to affect the response of the probe in its application to the absolute measurement of vibration amplitudes, it should be used adjacent to a plane surface no smaller than the outer diameter of the probe shield. The vibrating surface is placed at ground potential in the electronic circuit of the capacitance vibration detector, and the probe is tuned to a null directly over the surface for adjustment of the spacing at which it is designed to operate. A piezoelectric accelerometer, having an exposed plane surface perpendicular to the direction of vibration, can be calibrated by tuning the probe in proximity to this surface.

In establishing a frame of reference for the support of the probe, mechanical coupling between the driver and the probe must be avoided. It is usually advantageous to clamp the probe to a structure separate from that of the driver. However, this introduces a low-frequency ambient vibration noise level into the output of the capacitance vibration detector, which, as in the case of the vibration mounted pistonphone driver, must be eliminated by a high or band pass filter.

APPENDIX

Derivation of Expression for v_0

Referring to Fig. 1, the current through the L-C branch is equal to that through R under conditions of balance. Calling the peak value of this current I, the instantaneous voltage at point A is

$$v_A = I \sin\omega t\left[r + j\left(\omega L - \frac{1}{\omega(C+\Delta C \sin pt)}\right)\right], \quad (11)$$

where r = effective resistance of the L-C branch. At point B,

$$v_B = IR \sin\omega t. \quad (12)$$

When the bridge is correctly adjusted, $R=r$, and the output voltage is

$$v_0 = v_A - v_B = jI \sin\omega t\left(\frac{\omega^2 LC + \omega^2 L\Delta C \sin pt - 1}{\omega(C+\Delta C \sin pt)}\right). \quad (13)$$

Since $\omega^2 LC = 1$, and $\Delta C \sin pt \ll C$,

$$v_0 = j\frac{I}{\omega C^2}\Delta C \sin\omega t \sin pt. \quad (14)$$

By a trigonometric substitution,

$$v_0 = j\frac{I}{\omega C^2}\Delta C\frac{1}{2}\left[\cos(\omega - p)t - \cos(\omega + p)t\right]. \quad (15)$$

If ΔC is introduced under static conditions by simply detuning the bridge, Eq. (14) becomes

$$v_0 = j\frac{I}{\omega C^2}\Delta C \sin\omega t. \quad (16)$$

ACKNOWLEDGMENT

The author is indebted to the late Dr. Albert London for the guidance and encouragement which made this work possible. Acknowledgment is also due Mr. Irving Levine for his work on the capacitance vibration detector which preceded that of the author's.

Reprinted from The Journal of the Acoustical Society of America, Vol. 30, No. 9, 867–870, September, 1958

Stroboscopic Interferometer for Vibration Measurement*

E. R. Smith, S. Edelman, E. Jones, and V. A. Schmidt
National Bureau of Standards, Washington, D. C.
(Received May 15, 1958)

This paper describes measurement of vibration amplitude with a Fizeau type interferometer using pulses of monochromatic light of adjustable phase. The interferometer is used to calibrate vibration pickups over the frequency range from 100 to 20 000 cps.

I. INTRODUCTION

THE stroboscopic interferometer is a development of work described previously.[1] The objective of the work is the development of methods and equipment for accurate calibration of vibration measuring instruments over the audio-frequency range. Preliminary experiments led to the statement (see reference 1, p. 734) that there was promise of improvement of the earlier work by combination of the interferometric with the stroboscopic technique. This improvement has been developed sufficiently now to be usable in calibration.

A pattern of straight-line fringes is formed by interference of light reflected from two nearly parallel plane surfaces, one stationary and one vibrating.

The position of a fringe in relation to a fiducial mark in the field of view at any instant is determined by the distance between the stationary surface and the vibrating surface at that instant, and varies with the motion. The stroboscopic effect is obtained by driving the lamp with voltage pulses which are synchronized with the vibration. One short flash of light occurs in each cycle of vibration. If the phase of the flash is constant relative to the phase of the motion, the interference pattern appears to be motionless. If the phase of the flash is varied slowly, the pattern appears to move in a direction perpendicular to the fringes. The amplitude of the motion of the fringes is proportional to the amplitude of the vibration. Since the distance between fringes corresponds to a displacement of $\frac{1}{2}$ the wavelength of the light,[2] the amplitude of vibration is determined by measuring the excursion of a fringe and the distance between fringes on the same scale. The vibration amplitude is then expressed in fractions of a wavelength of light and converted to meters by using the known value of the wavelength of the monochromatic light used. The voltage from the pickup being calibrated and the frequency of vibration are measured at the same time. These three quantities furnish the information necessary for calibration.

Measurement of small displacements by the use of interferometric fringes illuminated by stroboscopic light pulses of adjustable phase is not new.[3–9] However, our need for equipment capable of handling a variety of vibration measuring instruments over a wide frequency range introduced problems which were somewhat different from these faced by previous workers.

II. OPTICAL EQUIPMENT

The Fizeau type interferometer is shown schematically in Fig. 1. The lower reflecting surface is the top of a fused quartz optical flat cemented to the shake table. The upper reflecting surface is the bottom of a similar flat supported on leveling screws about 1 mm above the lower flat. The spacing is made as large as possible without spoiling the sharpness of the fringes to reduce the effect of the sound pressure generated by the vibrating flat on the upper flat.

The flats are coated with multilayer dielectric films which give reflectivities of about 90% for light of 5876 A with little absorption.[10,11] The multiple beam interference pattern resulting from the use of such coated flats consists of fine dark lines on a bright background.

A point source of light of 5876 A is formed by a Cenco helium spectrum tube, a combination of interference and gelatin filters, and a pinhole. The source is placed slightly more than 1° off the axis in the focal plane of the collimating lens. The light reflected from the flats after passing through the collimating lens is deflected by a front surface mirror into the viewing system. This consists of an iris diaphragm in the focal plane of the collimating lens, a lens for shortening the image distance to a convenient size, and a filar micrometer eyepiece modified so that both the cross hair and the scale are movable.

* The work reported here was carried out as part of a program of Basic Instrumentation Research cooperatively supported at the National Bureau of Standards by the Office of Naval Research, the Air Force Office of Scientific Research, the U. S. Atomic Energy Commission, and the National Bureau of Standards.

[1] Edelman, Jones, and Smith, J. Acoust. Soc. Am. 27, 728 (1955).

[2] C. F. Bruce, "Some applications of interferometry to precision measurement," National Standards Laboratory Technical Paper No. 4, Commonwealth Scientific and Industrial Research Organization, Melbourne, Australia, 1954.

[3] Paul Paasche, Z. tech. Phys. 9, 411 (1928).

[4] W. D. Dye, Proc. Roy Soc. (London) A138, 1 (1932).

[5] G. F. Hull, Rev. Sci. Instr. 15, 340 (1944).

[6] Bruce, Macinante, and Kelly, Nature 167, 520 (March 31, 1950).

[7] S. Tolansky and W. Bardsley, Proc. Phys. Soc. (London) B64, 224 (1951).

[8] Bruce, Macinante, and Kelly, Australian J. Appl. Sci. 4, 28 (1953).

[9] E. A. G. Shaw, J. Acoust. Soc. Am. 28, 38 (1956).

[10] D. Jacquinot and C. Dufour, J. phys. radium 11, 427 (1950).

[11] Belk, Tolansky, and Turnbull, J. Opt. Soc. Am. 44, 5 (1954).

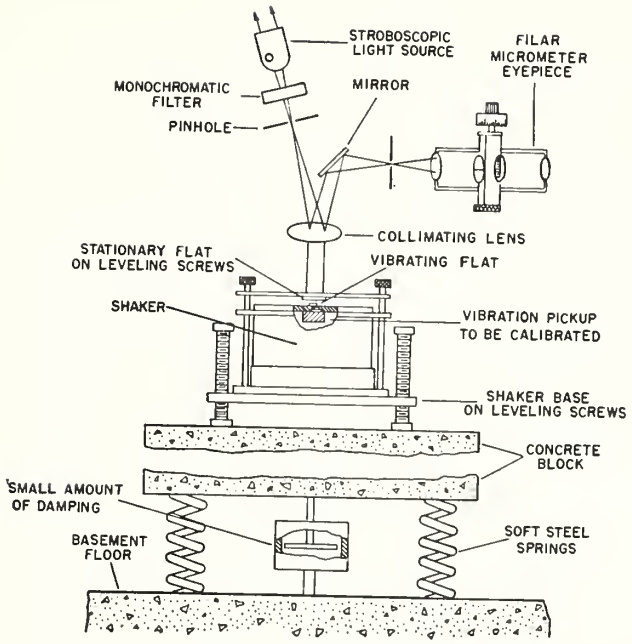

FIG. 1. Fizeau type interferometer.

III. MECHANICAL EQUIPMENT

The light source, collimating lens, and viewing system are mounted on a drill press spindle. The shaker and flats are mounted on a vibration isolator consisting of a 2-ft cube of concrete which is suspended on soft helical steel springs. The natural frequency of the isolator is about 1 cps. Sponge rubber damping causes any vibrations which may arise to be damped out in a short time.

The shaker used for the measurements reported here is a stack of barium titanate annular disks 6 in. in outer diameter and 2 in. in inner diameter. The bottom of the stack is on a steel base supported by leveling screws and the top of the stack is cemented to an aluminum shake table.

The vibration pickup being calibrated is attached as rigidly as practicable to the underside of the shake table, and the lower optical flat is cemented to the upper side of the shake table directly above the pickup. This insures that the sensitivity determined by the calibration is the voltage from the pickup for a measured vibration of the surface to which the pickup is attached. If the pickup is attached to the top of the shake table in the usual way, the optical flat must be placed at another point on the shake table or on top of the pickup. In either case, at high frequencies, incorrect calibration may result from relative motion between the surface to which the pickup is attached and the surface of the flat where motion is measured.

The upper flat is held in an aluminum clamping ring supported on leveling screws which also provide a means for adjusting the spacing between flats. At the suggestion of Dr. T. M. Perls, a small, light, vibration pickup is cemented to the clamping ring close to the flat to detect any motion of the top plate, e.g., motion caused by sound pressure or due to transmission through the base of the shaker and the leveling screws. No such motion has been present during any of the measurements made so far.

IV. ELECTRONIC EQUIPMENT

The electronic circuit is shown schematically in Fig. 2. The light flashes are synchronized with the motion by using the same oscillator to drive the lamp and the shaker. The frequency of the oscillator signal is determined by using an electronic counter to measure the ratio of the oscillator frequency to the frequency of one of the National Bureau of Standards standard frequencies.

The shaker drive circuit following the oscillator consists of a McIntosh power amplifier followed by an inductance chosen to resonate with the capacitance of the shaker at the frequency in use. The signal at the input of the shaker is measured by a vacuum tube voltmeter and monitored by a cathode-ray oscilloscope.

The lamp drive circuit following the oscillator is the same as that described in our earlier paper[1] except that a Model 2120A Electro-Pulse, Inc., pulse generator was used.

The signal from the instrument being calibrated is monitored with a Hewlett-Packard distortion meter at intervals and especially whenever there is reason to suspect anything other than clean sinusoidal excitation. Even slight distortion is indicated by nonuniform or nonrectilinear motion of the interference fringes.

V. ALIGNMENT

The structural isolation of the flats from each other, necessary to prevent transmission of vibration, causes some difficulty in orienting them so that fringes are visible. With the viewing system and the upper flat removed, the shaker with the lower flat attached is placed so that an image of the point source of light is seen centered in the plane of the iris diaphragm. The upper flat is then placed on its supports and lowered by means of the leveling screws until the reflecting surfaces

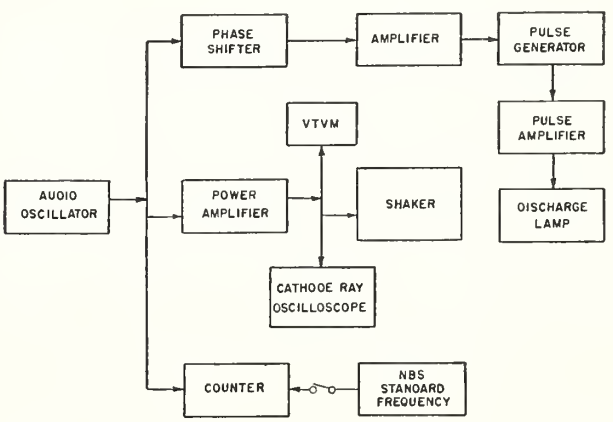

FIG. 2. Block diagram of stroboscopic interferometer.

574278 O - 61 - 52

are approximately parallel and about a millimeter apart. As the reflecting surfaces approach the parallel condition, a number of images of the light source become visible in the mirror. The fainter images are moved closer to the brightest image and finally into coincidence by further manipulation of the leveling screws. The fringe pattern can then be seen. The viewing system is attached to the interferometer and the leveling screws are again used to orient the fringes for convenient measurement and to separate them. We found it convenient to have four of the dark fringes in the field of view.

VI. CALIBRATION PROCEDURE

As described briefly in Sec. I, the basis of the method is the use of the same scale to measure the excursion of a fringe and the distance between fringes so that the excursion is expressed as a fraction of the wavelength of light. The scale is the graduated wheel of the micrometer screw which moves the cross hair in the eyepiece of the viewing system. The screw graduations are supplemented by a scale at one side of the field of view of the eyepiece which can be moved parallel to its length by an ungraduated micrometer screw in the eyepiece. The eyepiece is constructed so that one hundred graduations of the graduated micrometer screw wheel constitute a revolution and move the cross hair one unit on the scale.

Distance between fringes is measured in terms of micrometer screw graduations by using the ungraduated micrometer screw to set one of the lines of the scale on one of the fringes, using the graduated micrometer screw to set the cross hair on the next fringe, and then noting the number of graduations of the micrometer screw required to bring the cross hair into coincidence with the line of the scale which was first set on the fringe.

Similarly, the excursion of a fringe is measured in terms of micrometer screw graduations by using the ungraduated micrometer screw to set one of the lines of the scale on one of the extremes of the excursion, using the graduated micrometer screw to set the cross hair on the other extreme of the excursion, and then noting the number of graduations of the micrometer screw required to bring the cross hair into coincidence with the line of the scale which had been set.

In each case, the procedure starts by marking the extremes of the distance to be measured by setting a mark on each extreme separately. Then, when the two marks are set correctly, simultaneously, the distance is measured without further reference to the fringe pattern. This reduces errors which might otherwise arise because of drift of the fringe pattern during the time required to move a mark from one extreme of the distance to the other. It has not been possible to prevent drift of the fringe pattern.

VII. PRECISION OF MEASUREMENT

Results of a typical set of measurements are presented in Table I. These measurements were made to determine the response of the shaker rather than to calibrate a pickup, but the measurements are of the same kind and the results are representative.

TABLE I. Response of stack shaker determined by stroboscopic interferometer.

Freq. cps	Signal driving shaker rms volts	Measured excursion A	rms amplitude A	Shaker response A/volt
108	56	306	108.2	1.93
	56	304	107.5	1.92
	56	284	100.4	1.81
	56	303	107.1	1.91
	56	306	108.2	1.93
	56	297	105.0	1.87
	56	306	108.2	1.93
	56	300	106.1	1.89
2292	52	275	97.2	1.87
	52	265	93.7	1.80
	52	274	96.9	1.86
	52	272	96.2	1.85
	52	263	93.0	1.79
	52	265	93.7	1.82
	52	247	87.3	1.70
5000	96	645	228	2.36
	98	622	220	2.26
	98	604	214	2.18
	98	627	222	2.26
	98	629	222	2.28
	98	590	209	2.13
10 000	47	808	286	6.1
	48	780	278	5.8
	50	781	276	5.5
	49	800	283	5.8
	50	842	298	6.0
20 000	20	651	230	11.2
	20	588	208	10.4
	20	567	200	10.0
	20	631	223	11.2
	20	616	218	10.9
	20	618	218	10.9
	20	638	226	11.0
	20	596	211	10.3

It can be seen that the repeated measurements of excursion at each frequency fall within a range of $\pm 6\%$. If a fringe pattern is made stationary by shutting off the vibration and connecting the reflecting surfaces with a rigid mechanical bond, the hairline can be set repeatedly on the center of one of the narrow dark lines with a variation of about 5 A. The much larger variation in the measured excursions is ascribed to drift of the fringe pattern, irregularities in the pulse triggering voltage, lack of precision in the measurement of voltage, and lack of flatness in the reflecting surfaces. The last of these appears to be most serious. The presence of local irregularities in the flats was shown by bends and kinks in the dark fringes, which changed shape as the fringe pattern moved across the field of view. The measured displacement of the fringes thus contained a component due to the change of shape of the fringe as it

moved from one extreme of the motion to the other. A new set of flats with all departures from flatness smaller than those in the present set by at least a factor of 10 has been ordered. It is hoped that their use will result in a corresponding improvement in precision.

In spite of thermal shielding of the interferometer, it was not found possible to prevent drifting of the fringe pattern. The effects of drift were minimized by the technique of setting marks at both extremes of the motion simultaneously, as described above, but it added considerably to the time and effort required to make a measurement and had some part in the spread of the measurements.

Irregularities in the pulse triggering voltage were caused by noise in the driving signal and combined with noise in the discharge lamp to broaden the fringes slightly over their width with steady light. This effect was only rarely present and it is not considered a serious trouble. It can be reduced to insignificance by proper amplification and filtering if the other sources of variation are reduced sufficiently to make this worth the trouble.

The voltage driving the shaker was measured to two significant figures on a vacuum tube voltmeter which had been compared with a calibrated thermal voltmeter. It is likely that the spread would have been reduced somewhat if the voltage had been read to three significant figures, but such precision was not needed for the purpose of the measurements.

Attempts were made to improve the precision by averaging over different parts of the field of view and also by driving the phase shifter with a slow electric motor so that the fringe pattern appeared to be in constant slow motion. Neither practice resulted in any appreciable improvement.

VIII. CONCLUSIONS

The use of an optical interferometer illuminated by stroboscopic monochromatic light makes it possible to measure excursions of the order of 300 A corresponding to rms amplitudes of vibration as small as 100 A over the audio-frequency range, with an uncertainty no greater than 6%.

The frequency had no apparent effect on the ease of measurement. A few measurements made at considerably greater amplitude, which were not part of the results reported here, seemed to indicate that the variations in repeated measurements of excursion were about the same for large amplitudes as for small, so that the percentage of variation decreased with amplitude.

The measuring technique reported here is time consuming and leads to serious eye fatigue. It is planned to improve the sensitivity of the method and to reduce the fatigue by using steady light and achieving the stroboscopic effect by the use of an image converter with pulsed focusing voltage.

If the total excursion of the fringe pattern is more than a few half wavelengths, the technique reported here becomes unreasonably tedious. Calibrations can then be performed by the use of a photocell and electronic counter to count the fringes passing a slot. This method of measurement, which uses averaging provided by an imposed linear drift in addition to the vibration, was reported at the October, 1957, Meeting of the Acoustical Society and will be the subject of a subsequent paper.

IX. ACKNOWLEDGMENTS

The work reported here was started by a suggestion made by Dr. Charles P. Saylor. Mr. Theodore R. Young designed the interferometer and provided considerable constructive criticism. Mr. Thomas F. Scrivener and Mr. Robert R. Brooks made most of the measurements.

NATIONAL BUREAU OF STANDARDS
Washington, D. C.

December 1959

Impedance Tube Method of Measuring Sound Absorption Coefficient

The method was first described by H. O. Taylor in 1913. (Phys. Rev. 2, 1913, p 270). More recent developments are discussed in a book "Acoustic Measurements" by L. L. Beranek, p 308.

The measurements are made in accordance with the Tentative Method of Test C-384-56T of the American Society for Testing Materials. Standing sound waves are set up in a tube which is closed at one end by the material to be tested. The ratio of the maximum and minimum pressures of the standing waves is measured, and from it the sound absorption coefficient for normal incidence is calculated. If desired, a semi-empirical formula can then be used to obtain an approximation to the random-incidence coefficient. This latter coefficient is the one usually measured in a reverberation room. The formula used is discussed in a paper "Determination of Reverberant Sound Absorption Coefficients from Acoustic Impedance Measurements", A. London, Journal of the Acoustical Society of America, Vo. 22, March 1950.

Measurements are made on three samples of each material, all three coefficients and their average being reported.

It should be borne in mind that in most impedance tube methods the sample is inserted in the tube, whereas here the sample overlaps the end of the tube. This latter arrangement is more convenient experimentally. The inaccuracy in the measured coefficient due to the sound energy which escapes through the open edge of the sample we estimate to be very slight, since the diameter of the tube is large relative to the thickness of the acoustic materials tested.

The tube is made of 3/16" aluminum; it is 8" in diameter and 24" long. The sound source is a 6" speaker mounted at one end of the tube. The sound is picked up on a crystal microphone, the response of which is amplified, filtered and measured on a vacuum tube voltmeter.

The disadvantages of the method are 1., that the normal incidence coefficient is measured and not the more useful random incidence coefficient and 2., that mounting conditions used in actual installations cannot be duplicated very well on the small samples used. Thus, normal incidence coefficients as measured by this method are not generally of direct use to the architect, but they are useful in the development and manufacturing control of acoustic materials.

Frequencies at which coefficients are measured.

500 cps only.

Accuracy of Tests.

Coefficients measured by the long tube method are repeatable within ±0.03 on the same piece of material.

Amount of material required for a test.

Three pieces of material are needed, each having no lateral dimension less than 10-1/2" and preferably with no dimension greater than 15".

Types of mounting available.

Acoustical tiles are backed by a rigid steel plate, 1/2" thick.

Some materials are flexible enough to absorb sound by diaphragmatic action, that is, by flexural vibration of the piece of material. However most acoustic materials absorb sound in a different manner by remaining stationary and allowing the air vibrations to be damped out in the pores. In cases where diaphragmatic absorption is considerable a particular support or backing should be specified; or such absorption can be eliminated by bonding the material to a rigid base.

If a plaster or sprayed-on material is to be tested, the standard types of application are used.

Procedure for painting samples.

Materials may be painted as for the reverberation room test.

Cost of test.

The fee is $83.00 for each material.

Time required for test.

Results are usually reported within 3 weeks of receiving samples.

Procedure for requesting a test.

Before a test can be started, a purchase order or letter formally requesting the test must be received. Letters should be addressed to: Dr. A. V. Astin, Director, National Bureau of Standards, Washington 25, D. C., and marked for the attention of Dr. R. K. Cook, Chief, Sound Section.

Returning of test material.

Test materials are not returned unless this is requested.

Reprinted from The Journal of the Acoustical Society of America, Vol. 22, No. 2, 263–269, March, 1950

The Determination of Reverberant Sound Absorption Coefficients from Acoustic Impedance Measurements

Albert London
National Bureau of Standards, Washington, D. C.
(Received November 1, 1949)

A method is described for utilizing normal absorption coefficient or acoustic impedance measurements to predict reverberant sound absorption coefficients. The average of coefficients for the six standard frequencies determined from acoustic impedance measurements agrees closely with the average reverberant coefficient, for cases where the material may be said to obey the normal impedance assumption. The normal absorption coefficients of some 26 different acoustic materials were measured at 512 c.p.s. Using the method given in the paper, the predicted reverberant coefficient deviated from the measured reverberant coefficient by 0.05 or less for 18 materials, while in only 3 cases were the deviations greater than 0.10. The method should be particularly applicable to the problem of acceptance testing of installed acoustic materials.

In the theoretical development, best agreement with experiment was obtained by introducing a new kind of reverberant statistics which associates with each wave packet in a random field a scalar quantity equal to the square of the absolute value of the sound pressure in each packet, instead of the customary energy flow treatment. Also, it was found necessary to carry out the analysis using a concept of equivalent real impedance to replace the usual complex impedance.

I. INTRODUCTION

IT would be of considerable technological importance if it were possible to determine from laboratory measurements on small samples the sound absorption coefficient one might expect to measure on large samples placed in a reverberant test chamber. A similar problem is that of the field measurement of an acoustic material already applied to the walls of a room. In particular, difficulty is often experienced with acoustic plasters whose acoustic properties may be ruined by improper application. In this case it is of prime importance to be able to measure the coefficient in the field in order to check compliance with purchase specifications which are based on reverberation room coefficients.

In large rooms or auditoriums it may be possible to obtain an approximate idea of the field absorption coefficient by measuring the reverberation time. However, in small rooms, corridors, or other open spaces, it is not possible to use the reverberation time technique. Measurement of the acoustical impedance of the material using tube methods, or short tube methods as developed by Cook[1] and Mawardi[2] seems to be a practical procedure readily applicable to use in the field on those materials for which the absorption is due to the surface and not to mounting effects.

In any acoustic impedance tube measurement, what is in reality measured is the absorption coefficient for normal incidence. Accordingly, the problem reduces to one of relating the reverberant, or random incidence absorption coefficient to the normal incidence coefficient. In the following, we deduce such a relationship which apparently agrees on the average with data obtained for a considerable number of materials. There are certain difficulties associated with the treatment which will be discussed in detail.

[1] R. K. Cook, J. Acous. Soc. Am. **19**, 922 (1947).
[2] O. K. Mawardi, J. Acous. Soc. Am. **21**, 84 (1949).

II. RELATION BETWEEN ACOUSTIC IMPEDANCE AND NORMAL AND RANDOM INCIDENCE COEFFICIENTS

Paris[3] first derived an expression (Eq. (1)) for the sound absorption coefficient, α_θ, for a wave incident at angle θ on an acoustic material which has an acoustic impedance Z:

$$\alpha_\theta = 1 - \left| \frac{(Z/\rho c)\cos\theta - 1}{(Z/\rho c)\cos\theta + 1} \right|^2, \tag{1}$$

where ρc is the acoustic impedance of air.

Let

$$Z/\rho c = z = r + jx. \tag{2}$$

Then Eq. (1) may be written

$$\alpha_\theta = \frac{4r\cos\theta}{(r\cos\theta+1)^2 + x^2\cos^2\theta}. \tag{3}$$

From (3) the normal incidence coefficient α_0, is

$$\alpha_0 = \frac{4r}{(r+1)^2 + x^2}. \tag{4}$$

Using the customary reverberant sound field statistics, the random incidence coefficient $\bar{\alpha}$, is defined by

$$\bar{\alpha} = 2\int_0^{\pi/2} \alpha_\theta \cos\theta \sin\theta d\theta \tag{5}$$

and substituting (3) into (5) results in

$$\bar{\alpha}_P = \frac{8r}{x^2+r^2}\left\{1 + \frac{r^2-x^2}{x(x^2+r^2)}\tan^{-1}\left(\frac{x}{1+r}\right) - \frac{r}{x^2+r^2}\ln[(1+r)^2+x^2]\right\}. \tag{6}$$

[3] E. T. Paris, Proc. Roy. Soc. **115**, 407 (1927).

Equation (6) was first derived by Paris[4] in terms of the acoustic admittance while similar formulations are given by Morse, Bolt, and Brown[5] and by Morse.[6]

In the paper by Morse, Bolt, and Brown,[5] $\bar{\alpha}_P$ was compared with the reverberant sound absorption coefficient $\alpha_{A.M.A.}$ given by the Acoustic Materials Association for four different commercial acoustic materials. The acoustic impedance measurements were those of Beranek.[7] Their conclusions were:

(1) Above 2000 c.p.s., $\alpha_{A.M.A.}$ corresponds to $\bar{\alpha}_P$, indicating adequate diffusion in the sound chamber such that the conditions of random incidence and uniform energy distribution are satisfied.

(2) Below about 500 c.p.s., $\alpha_{A.M.A.}$ usually approximates what Morse, Bolt, and Brown call α_n, the normal absorption coefficient, which is the coefficient for normal incidence for a large number of normal modes and which has the approximate value of

$$\alpha_n \simeq 8r/(r^2+x^2). \tag{7}$$

In the cases where $\alpha_{A.M.A.}$ is larger than α_n at low frequencies, they attribute this discrepancy to mounting conditions and sample size. At low frequencies, then, there is presumed to be incomplete diffusion in the reverberant chamber.

(3) The region between 500 to 2000 c.p.s. is intermediate in the diffusion between that corresponding to α_n and that corresponding to the completely random coefficient $\bar{\alpha}_P$.

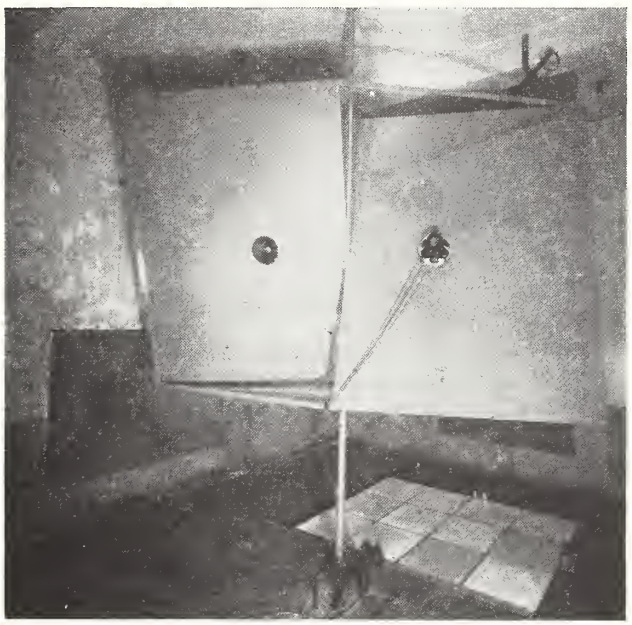

FIG. 1. View showing vanes in the reverberation room of the National Bureau of Standards.

(4) For low frequencies the decay curve will be a broken line, the slope of the initial straight portion, covering approximately the first 30 db of decay, corresponding to α_n.

In discussing the above conclusions relative to the experimental technique utilized in the reverberant test chamber of the National Bureau of Standards, one must raise the following points:

(1) It is difficult to see how a very close approximation to complete diffusion cannot help but be assured by the use of two vanes some 8 feet by 8 feet in size (Fig. 1).

(2) Even at low frequencies linear decay curves are obtained over a range of at least 50 db at 128 c.p.s. and up to 70 db at 256 c.p.s.

(3) Linear decay curves can be obtained by restricting the amount of material introduced into the chamber to 72 sq. ft. in accordance with the results obtained by Chrisler.[8] This material is placed on the floor which has a total area of 750 sq. ft.

In what follows, we shall consider a somewhat different method of deriving a reverberant sound absorption coefficient, one which on the average is in better agreement with experiment than $\bar{\alpha}_P$. In addition a somewhat simplified and hence semi-empirical method will be described which enables one to predict the reverberant coefficient from a measurement of r and x, to within an accuracy of 0.05 in the average absorption coefficient for the range of 128 to 4096 c.p.s.

It will be convenient to discuss the latter method first.

Davis[9] in his book *Modern Acoustics* discusses the relationship between the reverberant coefficient and the coefficient obtained from a tube measurement which he calls the stationary-wave coefficient but which in reality corresponds to the coefficient α_0. Figure 2 is a reproduction of Fig. 80 in his book in which is shown a graph of the relationship between the ratio of reverberant to stationary-wave coefficient as a function of stationary-wave coefficient at a frequency of about 500 c.p.s. The best smooth curve was drawn through 11 experimental values. It should be noted that the experimental points were deduced from published values of reverberation coefficients obtained at different times and in different countries while α_0 was measured by Davis and Evans.[10]

The curve of Fig. 2 can be almost fitted exactly by the following procedure:

(1) It is assumed that for a given value of α_0, determined from r and x by Eq. (4), one can define an equivalent impedance z_e, which is real, and which

[4] E. T. Paris, Phil. Mag. 5, 489 (1928).
[5] Morse, Bolt, and Brown, J. Acous. Soc. Am. 12, 217 (1940).
[6] P. M. Morse, *Vibration and Sound* (McGraw-Hill Book Company, Inc., New York, 1948), 2nd edition, p. 388.
[7] L. L. Beranek, J. Acous. Soc. Am. 12, 14 (1940).
[8] V. L. Chrisler, J. Research Nat. Bur. of Stand. 13, 169 (1934), RP 700.
[9] A. H. Davis, *Modern Acoustics* (G. Bell and Sons, London, 1934), p. 216.
[10] A. H. Davis and E. J. Evans, Proc. Roy. Soc. 117, 89 (1930).

therefore may be obtained from Eq. (1) by writing

$$\alpha_0=1-\left(\frac{z_e-1}{z_e+1}\right)^2=\frac{4z_e}{(z_e+1)^2}. \tag{8}$$

Equation (8) thus results in two solutions for z_e. However only the solution,

$$z_e=\frac{1+(1-\alpha_0)^{\frac{1}{2}}}{1-(1-\alpha_0)^{\frac{1}{2}}} \tag{9}$$

is compatible with experimental results.

(2) The random incidence coefficient, α_e^*, corresponding to α_0 is then defined by

$$\alpha_e^*=\frac{\int_0^{\pi/2}\{1-[(z_e\cos\theta-1)/(z_e\cos\theta+1)]^2\}\sin\theta d\theta}{\int_0^{\pi/2}\sin\theta d\theta}. \tag{10}$$

Here we note two departures from the definition of random incidence coefficient $\bar{\alpha}$ as given in Eq. (5). First, we make use of a different type of reverberant statistics, or averaging with respect to θ, as evidenced by the fact that the $\cos\theta$-factor does not appear in the integral. A discussion of this type of statistics appears below. The * superscript will be used to refer to this type of averaging. Second, in α_θ, Eq. (1), we have introduced the equivalent impedance z_e and use the resulting expression in Eq. (10). The subscript e will be used to indicate the introduction of z_e.

Carrying out the integration (10) results in the following equation:

$$\alpha_e^*=\frac{4}{z_e}\left[\ln(1+z_e)-\frac{z_e}{1+z_e}\right] \tag{11}$$

or substituting (9) into (11), we have

$$\alpha_e^*=4\left[\frac{1-(1-\alpha_0)^{\frac{1}{2}}}{1+(1-\alpha_0)^{\frac{1}{2}}}\right]\times\left\{\ln 2-\tfrac{1}{2}-\ln[1-(1-\alpha_0)^{\frac{1}{2}}]-\frac{(1-\alpha_0)^{\frac{1}{2}}}{2}\right\}. \tag{12}$$

It will also be of interest to evaluate

$$\bar{\alpha}_e=\frac{\int_0^{\pi/2}\left\{1-\left[\frac{(z_e\cos\theta-1)}{(z_e\cos\theta+1)}\right]^2\right\}\cos\theta\sin\theta d\theta}{\int_0^{\pi/2}\cos\theta\sin\theta d\theta}, \tag{13}$$

which turns out to be

$$\bar{\alpha}_e=\frac{8}{z_e^2}\left[1+z_e-\frac{1}{1+z_e}-2\ln(1+z_e)\right] \tag{14}$$

or substituting (9) into (14), we have

$$\bar{\alpha}_e=8\left[\frac{1-(1-\alpha_0)^{\frac{1}{2}}}{1+(1-\alpha_0)^{\frac{1}{2}}}\right]^2\left\{\frac{2}{1-(1-\alpha_0)^{\frac{1}{2}}}-\frac{1-(1-\alpha_0)^{\frac{1}{2}}}{2}-2\ln\left[\frac{1-(1-\alpha_0)^{\frac{1}{2}}}{2}\right]\right\}. \tag{15}$$

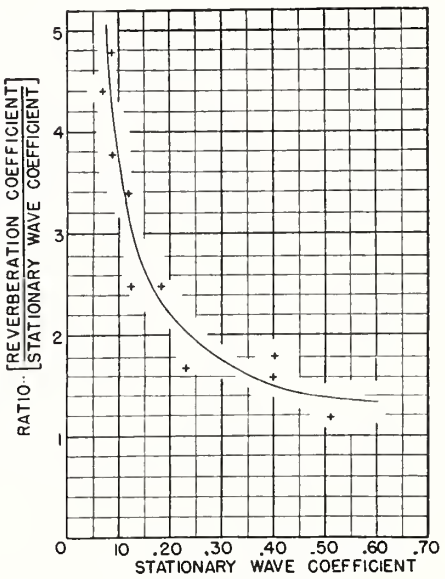

FIG. 2. Plot showing the relationship between the ratio of reverberant to stationary-wave coefficient as a function of stationary wave coefficient at a frequency of about 500 c.p.s. as given by Davis and Evans.

Figure 3 is a comparison between α_e^*/α_0 *vs.* α_0 as computed from Eq. (12), $\bar{\alpha}_e/\alpha_0$ *vs.* α_0 as computed from Eq. (15) and α_{rev}/α_0 *vs.* α_0 as given by Davis where α_{rev} is the absorption coefficient measured in a reverberant test chamber. It will be seen, that for α_0 below 0.40, the α_e^*/α_0 curve is in much better agreement with the experimental values than the $\bar{\alpha}_e/\alpha_0$ curve. For $\alpha_0>0.40$, both α_e^*/α_0 and $\bar{\alpha}_e/\alpha_0$ are in close agreement. Experimental values of α_0, however, do not exceed 0.60 so that it is not possible to check the extent to which α_e^* or $\bar{\alpha}_e$ agrees with experiment for the larger values of α_0.

Figure 4 is a plot which gives directly α_e^* and $\bar{\alpha}_e$ as a function of α_0.

We are thus led to the tentative conclusion that the star-type statistics as defined by Eq. (10) appears to be in better agreement with experiment than the bar-type statistics, as defined by Eq. (14). Further corroboration of this tentative conclusion will be given below in connection with the four commercial materials previously mentioned, for which we will compare α_{rev}, α_e^*, $\bar{\alpha}_e$, α^*, and $\bar{\alpha}_P$, where in the latter two coefficients we drop the equivalent treatment and work directly with the real and imaginary component of the impedance. That is, α^* is defined by analogy with

Eq. (10) as

$$\alpha^*=\frac{\int_0^{\pi/2}\{1-|(z\cos\theta-1)/(z\cos\theta+1)|^2\}\sin\theta d\theta}{\int_0^{\pi/2}\sin\theta d\theta} \quad (16)$$

or

$$\alpha^*=\frac{4r}{x^2+r^2}\left\{\frac{1}{2}\ln[x^2+(r+1)^2]-\frac{r}{x}\tan^{-1}\left(\frac{x}{1+r}\right)\right\}. \quad (17)$$

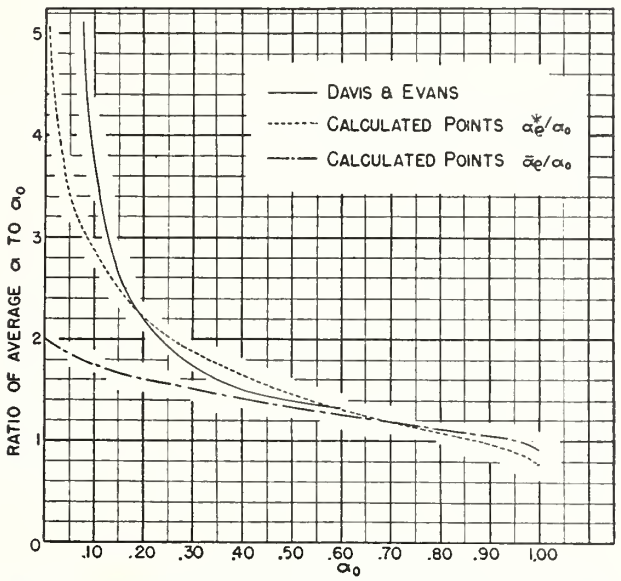

FIG. 3. Comparison between the Davis and Evans curve (Fig. 2), α_e^*/α_0 *vs.* α_0, and $\bar{\alpha}_e/\alpha_0$. See text.

It is advantageous at this point to discuss the assumptions inherent in the star-type statistics. We consider (Fig. 5) a point 0 of the elementary area dS located at the origin of a spherical coordinate system. We assume that wave packets strike point 0 uniformly from all directions. The number of packets striking 0 from a solid angle $d\Omega$ will thus be proportional to $d\Omega$. We assume that each wave packet carries with it a scalar quantity $|p_i|^2$ which does not vary with angle of incidence and which is the square of the acoustic pressure in the wave. Thus, if P_i^2 is the sum of the individual $|p_i|^2$ wave packets incident at 0, then

$$P_i^2=B|p_i(\theta)|^2\int_0^{2\pi}d\phi\int_0^{\pi/2}\sin\theta d\theta, \quad (18)$$

where B is a constant of proportionality, while the total amount which is absorbed is given by

$$P_{abs}^2=B\int_0^{2\pi}d\phi\int_0^{\pi/2}\alpha_\theta|p_i(\theta)|^2\sin\theta d\theta \quad (19)$$

since α_θ is in reality given by[11]

$$\alpha_\theta=1-\left|\frac{p_r(\theta)}{p_i(\theta)}\right|^2 \quad (20)$$

where $p_r(\theta)$ is the reflected pressure amplitude of a wave incident at angle θ while $p_i(\theta)$ is similarly the incident pressure amplitude. Thus

$$\alpha^*=\frac{P_{abs}^2}{P_i^2}=\frac{\int_0^{\pi/2}\alpha_\theta\sin\theta d\theta}{\int_0^{\pi/2}\sin\theta d\theta}, \quad (21)$$

since $|p_i(\theta)|^2=|p_i|^2$, independent of angle of incidence.

It is to be noted that had we used energy as the scalar quantity associated with each wave packet, it would have been necessary to define the intensity as the amount of energy transmitted through unit area per unit time. This would immediately have required the amount of energy striking dS to be proportional to $dS\cos\theta$ and to the solid angle $d\Omega$, thus giving rise to the usual bar-type statistics. It seems more reasonable to associate the quantity $|p|^2$ with each wave packet for two reasons:

(1) The absorption coefficient as a function of angle of incidence, α_θ, is given by Eq. (20) directly in terms of the ratio of squares of the absolute values of pressures.

(2) In any reverberant test chamber setup, it is customary to use pressure microphones, so that the quantity $|p|^2$ is what is actually measured.

While it is still necessary that the sound field be completely random in phase in order to sum the $|p|^2$ of the individual packets, it is not necessary to assume that $|p|^2$ is proportional to total energy. In many cases, especially at the lower frequencies, this may not be true at all.

The extent to which the star-type statistics is superior to the bar-type statistics is indicated in Table I. Here we list the four commercial materials discussed by

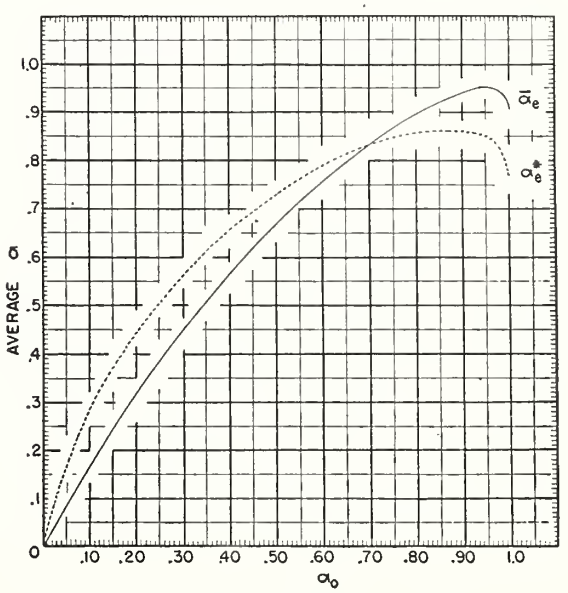

FIG. 4. Plot of $\bar{\alpha}_e$ and α_e^* *vs.* α_0. See text.

[11] See reference 6, p. 367.

Morse, Bolt, and Brown.[5] The impedance terms r and x were read directly from the curves given by Beranek.[7] The coefficients α_{rev} are the A.M.A. coefficients as read from the graphs,[5] while $\bar{\alpha}_P$, the reverberant coefficient of Paris, Eq. (6), were also read from the graphs. The coefficients α_e^*, $\bar{\alpha}_e$, α^* have been previously defined.

In Table II, the difference in average coefficient (average for all frequencies) relative to the experimental α_{rev} is listed.

In practically every case the star-type coefficient is equal to or better than the corresponding bar-type coefficient. Whereas, $\bar{\alpha}_e$ is usually a close approximation to $\bar{\alpha}_P$, α_e^* is usually much closer to α_{rev} than α^*. The coefficient α_e^* in each case gives the closest approximation to α_{rev}, and with the exception of Acoustex is within 0.05 of α_{rev}. In the case of Acoustex, there is some indication that the reverberant coefficient is too high at the three lowest frequencies relative to other results obtained on the same material. The results on α_{rev} given in Table I were apparently obtained from Bulletin VII of the Acoustic Material Association published in April, 1940. Bulletin No. VIII published June, 1941 lists Acoustex mounted on 1×2 furring strips, which customarily gives higher results at the lowest frequencies than the rigid mounting coefficients reported in Table I, with coefficients of 0.09 and 0.25 at 128 and 256 c.p.s. respectively, while some data obtained and published in Letter Circular LC-506, October, 1937, at the National Bureau of Standards, lists coefficients of 0.19 and 0.41 at 256, and 512 c.p.s., which are in close agreement with α_e^*. It is not known to what extent the acoustic impedance samples were selected from the same batch or samples which were used in the reverberation tests. In fact, it would appear that this was not done, the reverberant coefficients apparently being taken from published data of the A.M.A. The only reliable procedure would be to carry out the acoustic impedance measurements and reverberation measurements on the same batch. In any event, it still appears that, technologically speaking, α_e^* is a close approximation on the average to α_{rev} and hence may be a useful tool in field measurements.

It will be of interest to apply this type of analysis to an absorbent material which, on the basis of previous experiments, apparently does not have a normal acoustic impedance; that is, the ratio of pressure to normal component of velocity is not independent of angle of incidence. In this event, α_θ is not given by Eq. (1) and the variation of α with θ must be determined if an integration of α over θ is to be carried out. Cook and Chrzanowski,[12] in an investigation at the National Bureau of Standards of the absorption of sound by spheres having a hair-felt surface, concluded that the normal impedance assumption apparently was not valid for hair-felt. Inasmuch as they give both acoustic impedance measurements and reverberation room coefficients made on the same bath of hair-felt, uncertainty on this score will be eliminated.

[12] R. K. Cook and P. Chrzanowski, J. Acous. Soc. Am. **21**, 167 (1949).

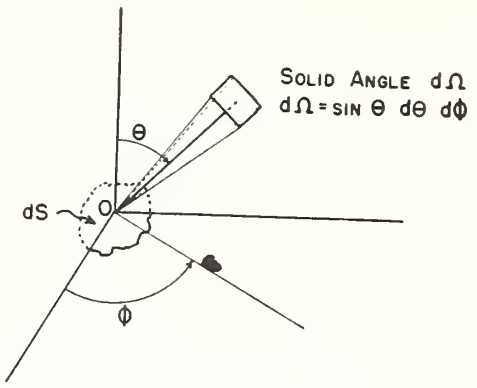

FIG. 5. Representation of solid angle used in star-type statistics.

In Figs. 6 and 7 we compare α_{rev}, α_e^*, and $\bar{\alpha}_P$ for

TABLE I.

f(c.p.s.)	r	x	α_0	α_{rev}	α_e^*	$\bar{\alpha}_e$	α^*	$\bar{\alpha}_P$
			Acoustex, $\frac{7}{8}$″					
128	2.6	−21.0	0.023	0.24	0.09	0.04	0.07	0.09
256	1.9	−11.2	0.057	0.29	0.19	0.10	0.13	0.12
512	1.5	− 5.2	0.180	0.60	0.42	0.30	0.28	0.27
1024	1.5	− 1.6	0.681	0.95	0.83	0.82	0.69	0.74
2048	2.2	+ 1.3	0.738	0.83	0.85	0.86	0.79	0.85
4096	4.3	− 0.6	0.605	0.75	0.79	0.76	0.79	0.77
Av. (128–4096)				0.61	0.53	0.48	0.46	0.47
			Celotex C-4, $1\frac{1}{4}$″					
128	2.6	−12.0	0.066	0.27	0.22	0.12	0.16	0.13
256	2.5	− 6.2	0.197	0.46	0.44	0.32	0.34	0.32
512	2.6	− 1.8	0.642	0.98	0.81	0.79	0.75	0.86
1024	2.8	+ 2.0	0.607	0.79	0.79	0.76	0.74	0.72
2048	5.4	+ 5.0	0.327	0.55	0.59	0.48	0.55	0.48
4096	10.0	+ 0.5	0.330	0.51	0.60	0.49	0.60	0.48
Av. (128–4096)				0.60	0.58	0.49	0.52	0.50
			Permacoustic, 1″					
128	3.2	−13.7	0.062	0.21	0.20	0.10	0.15	0.14
256	3.6	− 6.6	0.222	0.48	0.48	0.36	0.40	0.36
512	4.0	− 3.3	0.446	0.76	0.69	0.62	0.64	0.58
1024	5.0	− 1.8	0.510	0.72	0.74	0.68	0.73	0.68
2048	4.0	− 1.6	0.580	0.75	0.78	0.74	0.76	0.73
4096	3.0	− 1.6	0.646	0.74	0.81	0.80	0.78	0.78
Av. (128–4096)				0.61	0.62	0.55	0.58	0.55
			Temcoustic, $\frac{1}{2}$″					
128	13.5	−30.4	0.048	0.16	0.16	0.08	0.15	0.11
256	14.5	−17.0	0.110	0.28	0.31	0.18	0.28	0.16
512	13.5	−11.0	0.163	0.43	0.39	0.27	0.37	0.28
1024	12.0	− 6.5	0.227	0.49	0.48	0.36	0.47	0.38
2048	12.2	0	0.280	0.44	0.54	0.43	0.54	0.44
4096	9.8	+ 2.5	0.318		0.58			
Av. (128–2048)				0.36	0.37	0.30	0.36	0.27

TABLE II. Difference in average coefficient relative to α_{rev}.

	α_e^*	$\bar{\alpha}_e$	α^*	$\bar{\alpha}_P$
Acoustex $\frac{7}{8}$″	−0.08	−0.13	−0.15	−0.14
Celotex C-4, $1\frac{1}{4}$″	−0.02	−0.11	−0.08	−0.10
Permacoustic, 1″	+0.01	−0.06	−0.03	−0.06
Temcoustic, $\frac{1}{2}$″	+0.01	−0.06	+0.00	−0.09

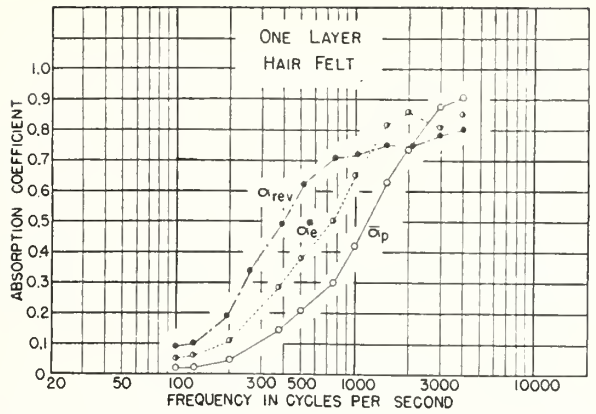

FIG. 6. Comparison between measured reverberant coefficient and predicted reverberant coefficient α_e^* for a single layer of hair-felt. $\bar{\alpha}_P$ is the reverberant coefficient first derived by Paris. Hair-felt is presumed to violate the normal impedance assumption.

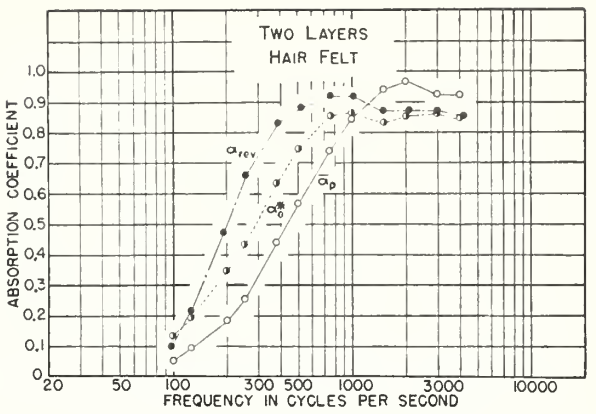

FIG. 7. Comparison between measured reverberant coefficient and predicted reverberant-coefficient α_e^* for two layers of hair-felt. $\bar{\alpha}_P$ is the reverberant coefficient first derived by Paris Hair-felt is presumed to violate the normal impedance assumption.

TABLE III. Hair felt coefficients.

Frequency c.p.s.	Single layer α_{rev}	Single layer α_e^*	Single layer $\bar{\alpha}_P$	Double layer α_{rev}	Double layer α_e^*	Double layer $\bar{\alpha}_P$
128	0.10	0.06	0.02	0.20	0.19	0.10
256	0.34	0.17	0.08	0.66	0.44	0.26
512	0.62	0.38	0.21	0.88	0.75	0.57
1024	0.72	0.66	0.43	0.92	0.86	0.86
2048	0.75	0.86	0.75	0.87	0.85	0.96
4096	0.80	0.86	0.91	0.85	0.85	0.92
Av. (128–4096)	0.55	0.50	0.40	0.73	0.66	0.61

a single and double layer of hair-felt. It will be seen that in each case α_e^* is a much closer approximation to α_{rev} than $\bar{\alpha}_P$. In Table III we consider the average values of the various coefficients for the six standard frequencies.

The lack of very close agreement between α_e^* and α_{rev} may in part be attributed to the failure of the normal impedance assumption.

A further test of the extent of agreement between α_e^* and α_{rev} was made in our laboratory at 512 c.p.s. by measuring[13] the α_0 of samples which had been measured in the reverberation room. A tube having a $9\frac{3}{4}$ inch diameter was used and α_0 was obtained directly by measuring the ratio, ρ, of a pressure maximum to the adjacent pressure minimum. The absorption coefficient, α_0, is given by[9]

$$\alpha_0 = 4\rho/(1+\rho)^2. \qquad (22)$$

Table IV lists the results obtained on twenty-six different materials. Measurements were made on several different pieces of tile (usually 3) of the 72 sq. ft. used in the reverberation room test. In most cases, α_e^* as measured had a maximum deviation of about 0.04 for different pieces of the same material. The coefficient listed in the table is the average for the several pieces used in the measurements. In cases where α_e^* varied excessively between different tiles, the individual measurements are listed.

Of the 26 materials listed in Table IV, 18 values of α_e^* deviate from α_{rev} by 0.05 or less, 5 deviations fall in the range of 0.06 to 0.10, while only three have deviations greater than 0.10. It is interesting to observe that entries 1, 2, and 5, which are Acousti-Celotex tiles, all deviate by 0.10 or more, indicating that possibly the mechanism of sound absorption is such as to violate the normal impedance assumption. Inasmuch as it is impossible to get an α_e^* greater than 0.86, one would expect 1 and 2 to deviate. In the case of 1, the α_0 which

TABLE IV. Tabulation of $\alpha_e^* - \alpha_{rev}$ *vs.* α_{rev} at 512 c.p.s.

Material	α_{rev}		$\alpha_e^* - \alpha_{rev}$
1. $1\frac{1}{4}$″ C-4 Celotex R.I. finish	0.97		−0.11
2. $1\frac{1}{4}$″ C-4 Celotex slow burning	0.94		−0.10
3. 1″ Certile	0.83		−0.07
4. 1″ Fiberglas tile perforated	0.79		−0.05
5. $\frac{3}{4}$″ C-9 Celotex	0.78		−0.10
6. $\frac{13}{16}$″ Travacoustic fissured	0.78		−0.05
7. $\frac{3}{4}$″ Certile	0.75		−0.03
8. $\frac{3}{4}$″ Travacoustic fissured	0.72		−0.04
9. $\frac{3}{4}$″ Fiberglas tile perforated	0.71		+0.04
10. $\frac{3}{4}$″ Firtex, perforated	0.71		−0.01
11. $\frac{13}{16}$″ Kelly Island tile, perforated	0.69		−0.02
12. $\frac{3}{4}$″ Fiberglas tile fissured	0.68		+0.03
13. 1″ Quietone, perforated	0.68		+0.04
14. 1″ Firtex, perforated	0.68		−0.04
15. $\frac{11}{16}$″ Insulite acoustilite	0.66	−0.16[a] −0.06 −0.15	−0.12
16. $\frac{13}{16}$″ Dantore fissured	0.66		−0.02
17. $\frac{3}{4}$″ Fiberglas tile plain	0.65		+0.07
18. $\frac{13}{16}$″ Dantore fissured	0.65		−0.03
19. $\frac{1}{2}$″ Hansonite perforated	0.62		−0.05
20. $\frac{5}{8}$″ Travacoustic fissured	0.62		−0.01
21. $\frac{1}{2}$″ Firtex perforated	0.55		−0.02
22. 1″ Softone	0.53	−0.04[b] −0.15	−0.10
23. Sabinite No. 1 Plaster	0.48		+0.03
24. Sabinite No. 2 Plaster	0.48		+0.04
25. $\frac{3}{4}$″ Softone	0.41		−0.05
26. $\frac{3}{4}$″ Acoustex, type 40 R	0.37		+0.19

[a] Individual differences for 3 pieces of tile.
[b] Individual differences for 2 pieces of tile.

[13] These measurements were made by Seymour Edelman and Earle Jones.

TABLE V. $\alpha_e^* - \alpha_{rev}$ *vs.* α_{rev}.

Material	α_{rev}	$\alpha_e^* - \alpha_{rev}$ 12″×12″ tile flush	$\alpha_e^* - \alpha_{rev}$ 9¾″ diameter sample in tube
5. ¾″ C-9 Celotex	0.78	−0.12	−0.14
9. ¾″ Fiberglas perforated	0.71	+0.01	−0.24
14. 1″ Firtex, perforated	0.68	−0.07	−0.09
26. ¾″ Acoustex, type 40 R	0.37	+0.19	−0.01

was observed gave exactly the maximum value of α_e^*, i.e., 0.86.

One other feature of these tube measurements should be clarified. All of the measurements listed in Table IV were made using a 12 in.×12 in. tile which was placed in flush contact with a rubber gasket mounted on the end of the tube. In the case of acoustic plasters, a sample having the approximate dimensions of 30 in.×30 in. was used. The reasons for not cutting the samples to fit inside the tube were twofold. First, in any field measurement using the tube, it would not be possible to deface the surface of the installed material, and second, the materials were not expendable, since only at most three pieces had been saved from the reverberation room tests, for identification purposes.

However, some of the materials were cut to fit inside of the tube. The results are listed in Table V for an individual tile before and after cutting to fit inside of the tube.

The results in the table show that Celotex and Firtex have no appreciable absorption due to propagation of the sound wave in the material outside of the geometrical area intercepted by the tube, whereas, both the Fiberglas and Acoustex materials do.

In summary, then, it would appear that the proper procedure for utilizing α_e^* to check field coefficients for agreement with laboratory coefficients is as follows:

(1) Determine α_0 or the acoustic impedance and α_{rev} in the laboratory.

(2) Compute α_e^* from α_0 or from the acoustic impedance measurements.

(3) If the average α_e^* agrees closely with the average α_{rev}, then a field measurement of α_0 or of the acoustic impedance should be sufficient to determine the extent of compliance with the reverberation coefficient.

(4) If the average α_e^* as determined in the laboratory does not agree with the average α_{rev}, it would still be possible, however, to find an average α_e^* in the field from the α_0 or acoustic impedance measurements and the extent of compliance of the field α_e^* with the laboratory α_e^* could then be used as a criterion for acceptability.

III. CONCLUSIONS

A procedure has been outlined whereby normal absorption coefficient or acoustic impedance measurements may be utilized to predict reverberant sound absorption coefficients. The average of coefficients for the six standard frequencies determined from acoustic impedance measurements agrees closely with the average reverberant coefficient, for cases where the material may be said to obey the normal impedance assumption. In the case of normal absorption coefficient measurements, for a large number of materials, good agreement was obtained between the predicted and measured reverberant coefficient. A method of utilizing field measurements of the normal absorption coefficient or of the acoustic impedance for acceptance testing has been indicated which should be applicable even in cases where the normal impedance assumption is violated.

On the theoretical side, we have found best agreement with experiment by utilizing a new kind of statistics which associates with each wave packet in a random field a scalar quantity equal to the square of the absolute value of the sound pressure in each packet, instead of the customary energy flow treatment. On the other hand, it has been necessary to utilize a semi-empirical concept of equivalent impedance as distinguished from the usual complex impedance treatment. The best which can be said for the introduction of this bit of empiricism is that it works, although no reasons for its success are deduced here.

Reprinted from The Journal of the Acoustical Society of America, Vol. 29, No. 7, 813–816, July, 1957

The Condenser Microphone as a Displacement Detector Calibrator

Walter Koidan
National Bureau of Standards, Washington, D. C.
(Received March 28, 1957)

The absolute calibration of a variable capacitance type displacement detector was performed by using the diaphragm of a condenser microphone as a reference moving surface. The detector was calibrated by coupling its associated probe to the front end of the microphone to detect the variation in capacitance between the diaphragm and the probe, when the diaphragm was driven by applying an electrical signal to the microphone terminals. Computation of the displacement detector response was made in two ways: one based upon the reciprocity relationship in a set of two linear equations describing the microphone as a reversible transducer; the other, upon the acoustical impedance of a cavity with rigid walls. Measured values of the displacement detector response are plotted from 10 cps to 40 000 cps.

INTRODUCTION

THE lightweight diaphragm and high coupling coefficient of the condenser microphone make it suitable as a displacement generator over a wide frequency range, including infrasonic and low ultrasonic frequencies. For example, if the diaphragm of a Western Electric Company type 640AA microphone is driven below its resonance frequency by applying an excess potential of 14 volts to the electrical terminals, the equivalent linear displacement averaged over the diaphragm is about 10^{-5} cm. The displacement is approximately proportional to the open-circuit microphone response, and at 40 000 cps is about 7×10^{-7} cm.

Motion in this amplitude range can be measured conveniently by a displacement detector of the variable capacitance type described in an earlier paper.[1] Briefly, the detector makes use of a probe consisting of an inductance connected to a pickup element which forms one plate of a capacitance, the other plate being any external conducting surface placed in proximity to the pickup element. The inductance-capacitance combination, located in a bridge circuit, is tuned to series resonance at an auxiliary carrier frequency by adjusting the distance between the probe and the external conductor. This resonance is indicated by a null. The output of the detecting circuit is proportional to the linear displacement of the external surface relative to the probe, when this motion is small compared to the separation of the capacitor plates at resonance.

PROBE CONSTRUCTION

If the motion is not uniform over the surface, the detector will respond to the displacement averaged over that part of the surface to which it is in proximity. A basis is thus provided for the design of a probe to measure the average motion of a microphone diaphragm when it is driven electrically at the microphone terminals.

Figure 1 shows such a probe adjusted for calibration at the front end of a Western Electric Company type 640AA condenser microphone. It will be noted that the microphone diaphragm consists of an essentially clamped annular section enclosing a central circular section free to move.

The capacitive pickup element of the probe is a circular metal disk, perforated with uniformly spaced holes, and with an outside diameter equal to that of the central section of the microphone diaphragm. A ring-shaped shield for the disk is provided, electrically insulated from it by thin spacers. The disk and shield were machined from gridded caps furnished with 640AA microphones. The outside of the shield is threaded, so that the probe can be screwed into the front end of the microphone; the proper spacing for series resonance is precisely indicated by a zero reading on the null indicator.

The motion of the diaphragm due to a change in the applied electrical field between the diaphragm and the backplate produces a proportional change in capacitance between the diaphragm and the perforated disk. The holes in the disk, which reduce the acoustic impedance seen by the diaphragm, must be distributed in such a

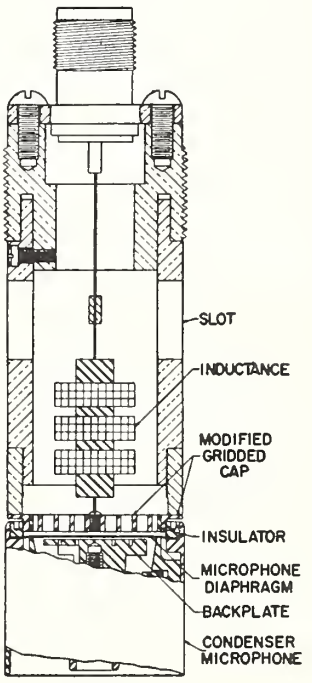

Fig. 1. Displacement detector probe arranged for calibration at the diaphragm end of a Western Electric Company type 640AA condenser microphone. In this arrangement, the displacement detector responds to the volume displacement of the microphone diaphragm. The ratio of the voltage driving the microphone at its electrical terminals to the voltage obtained from the output of the displacement detector circuit is used to compute the detector response.

[1] W. Koidan, J. Acoust. Soc. Am. **26**, 428 (1954).

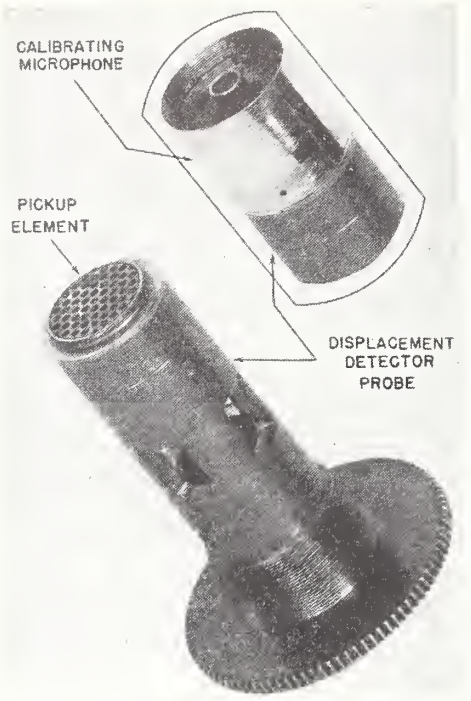

FIG. 2. Photograph of the probe. The upper inset shows how a microphone is coupled to the probe to calibrate the displacement detector.

way as to permit the pickup to respond to the average motion.

Figure 2 is a photograph of the probe, showing its perforated disk pickup element. The upper inset indicates how the microphone is coupled to the probe for the purpose of calibrating the displacement detector. Figure 3 shows the probe mounted vertically to measure the motion of a vibrating conducting surface located just below the displacement pickup element, and separated from it by about 0.5 mm. The detector probe, as mounted, responds only to a net displacement of the moving surface along a vertical axis. Thus, lateral motion and certain kinds of rotational motion would not be detected in the arrangement shown.

The procedure for calibrating the displacement detector is essentially an extension of the reciprocity technique for calibrating a microphone; additional measurements only of voltage ratio are required. Two methods for computing the detector response will be described.

DIAPHRAGM VELOCITY METHOD

Two equations describing the condenser microphone as a linear reversible transducer are

$$e=Z_{11}i+Z_{12}u,$$
$$p=Z_{21}i+Z_{22}u,$$

where e is the voltage at the electrical terminals, i is the current into the electrical terminals, u is the volume velocity of the diaphragm, p is the excess pressure at the diaphragm, and the Z coefficients are functions of frequency and of the equivalent four terminal network parameters.

We define the open circuit pressure response, ρ, of the microphone as $-(e/p)_{i=0}$. From the above equations and the assumption that $Z_{12}=Z_{21}$, the following relationships hold:

$$\rho=-(e/p)_{i=0}=-Z_{12}/Z_{22}=-Z_{21}/Z_{22}=(u/i)_{p=0}.$$

Denoting the electrical admittance of the microphone for zero acoustic load as $(i/e)_{p=0}=(g+j\omega C)_{p=0}$, where g and C are the microphone conductance and capacitance, respectively, $j=\sqrt{-1}$, and ω is the frequency in radians per second, we can perform the following operations:

$$(u/i)_{p=0}(i/e)_{p=0}=(u/e)_{p=0}=\rho(g+j\omega C)_{p=0}$$
$$=j\omega S(\xi/e)_{p=0}, \quad (1)$$

where S is the active area of the microphone diaphragm and ξ is the equivalent linear diaphragm displacement averaged over its surface.

With the probe properly adjusted in front of the microphone diaphragm, a voltage e is applied to the electrical terminals of the microphone, and the voltage ratio e/e_c measured by means of an attenuator, where e_c is the output voltage of the detecting circuit. Defining the response of the displacement detector, M, as e_c/ξ (see Appendix), and combining with Eq. (1), we obtain:

$$M=\frac{j\omega S}{\rho(g+j\omega C)_{p=0}}\left(\frac{e_c}{e}\right)_{p=0}.$$

Since $g^2\ll\omega^2C^2$ at all frequencies, the expression for the magnitude of the detector response reduces to

$$|M|=\frac{S}{\rho}\left(\frac{e_c}{e}\frac{1}{C}\right)_{p=0}. \quad (2)$$

The capacitance of the microphone for zero acoustic load at the diaphragm is obtained by measurements in a quarter wave length tube. The directly measured

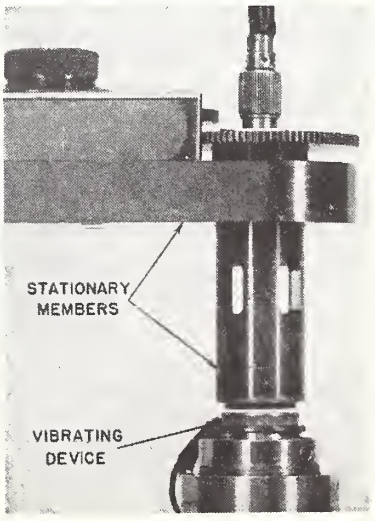

FIG. 3. The manner in which the calibrated probe can be used to measure the vibration of a device. The probe is mounted in a fixed frame of reference and placed in proximity to an exposed plane surface of the vibrating device.

voltage ratio, e_c/e, requires a correction for the reaction on the microphone diaphragm, since the acoustic load will in general not be zero when the probe is coupled to the microphone.

The procedure for making this correction is illustrated schematically in Fig. 4. The probe is disconnected from the detecting circuit bridge, and the microphone, with an associated inductance, is substituted. The condenser microphone and inductance are tuned to series resonance at the auxiliary carrier frequency, whose source is in the detecting circuit. The diaphragm is driven at the desired frequency of vibration by applying an electrical signal, e_{in}, to the microphone terminals, through the inductance. The output, e_{out}, is proportional to the change in capacitance between the diaphragm and the backplate; the electrical signal driving the microphone is rejected by the detecting circuit. Measurements of e_{in}/e_{out} are made with the probe in front of the diaphragm and also with a quarter wave length tube as the acoustic load to obtain the difference in diaphragm motion for the two conditions. The measured correction factor in decibels is essentially zero up to 500 cps. Figure 4 shows its magnitude at discrete frequencies from 1000 to 40 000 cps.

In the notation of Simmons and Biagi[2] for the microphone parameters, $Z_{11}=1/j\omega C_0$ and $Z_{12}=-\phi/j\omega C_0$, where C_0 is the blocked capacitance and ϕ the electromechanical coupling constant of the microphone, the following relation can also be derived from the two transducer equations:

$$\left(\frac{e}{u}\right)_{p=0}=\frac{1}{j\omega C_0}\left(\frac{1}{\rho}-\phi\right).$$

This equation leads to another expression for the displacement detector response:

$$M=\frac{S}{C_0}\left(\frac{1}{\rho}-\phi\right)\left(\frac{e_c}{e}\right)_{p=0}. \tag{3}$$

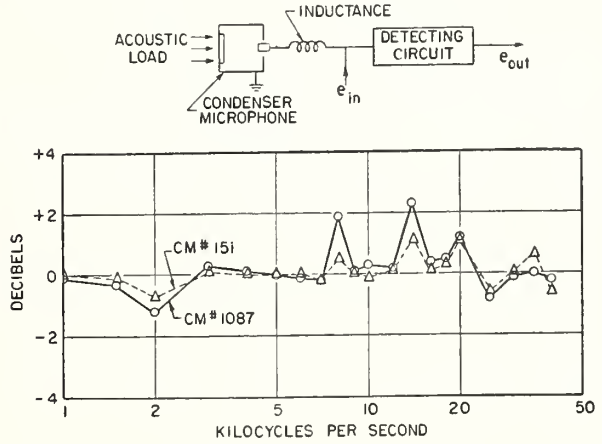

FIG. 4. Corrections for the effect of acoustic load on the diaphragms of two microphones when coupled to the detector probe. The ordinate denotes the diaphragm motion for zero acoustic load minus that for probe load.

As shown in reference 2, ϕ can be evaluated from $\phi=(C_L-C_0)/\rho_L C_L$, where C_L and ρ_L are the low frequency microphone capacitance and response, respectively. Although ϕ is small compared to $1/\rho$, its inclusion is necessary at many frequencies. The terms $1/\rho$ and ϕ are complex, and evaluation of Eq. (3) requires a knowledge of the phase angle between them.

ACOUSTICAL CAVITY METHOD

A second method of obtaining the detector response requires the same voltage ratio measurement of e/e_c and a similar correction for the reaction on the diaphragm. However, the computation is made from the response of an auxiliary microphone whose capacitance need not be known.

This method uses an additional voltage ratio measurement made as part of the procedure in an acoustical reciprocity calibration of the microphones. Two condenser microphones are coupled to a cavity, one for use as a sound source, and the other as a receiver. The source is driven by a voltage, e', and the receiver generates a voltage, e_R, proportional to the sound pressure produced in the cavity. The ratio, $e'/e_R=R_1$, is measured under these conditions.

For an adiabatic process within the cavity, $PV^\gamma=$a constant, where P is the pressure, V the cavity volume, and γ the ratio of specific heats. Upon differentiation, $p=-\gamma SP_0\bar{\xi}'/V$, where S is the active area of the driver microphone diaphragm, P_0 the static pressure, and $\bar{\xi}'$ the equivalent linear displacement of the driver microphone diaphragm averaged over its surface.

The response of the receiver microphone, ρ_R, is defined as $-(e_R/p)$, so that

$$p=-\frac{\gamma SP_0}{V}\bar{\xi}'=-\frac{e_R}{\rho_R}=-\frac{e'}{R_1\rho_R}. \tag{4}$$

With the probe coupled to the driver microphone as in the diaphragm velocity method, the voltage ratio, $e/e_c=R_2$ is measured. The detector response can then be written as

$$M=e_c/\bar{\xi}=e/\bar{\xi}R_2.$$

When the correction is made for the reaction on the diaphragm, $e/\bar{\xi}R_2$ becomes $e'/\bar{\xi}'R_2'$, where R_2' is R_2 corrected for the acoustic load of the probe relative to that of the acoustic coupler. Substituting $e'/\bar{\xi}'$ from Eq. (4), we get

$$M=\rho_R\frac{\gamma SP_0}{V}\frac{R_1}{R_2'}. \tag{5}$$

[2] B. D. Simmons and F. Biagi, J. Acoust. Soc. Am. 26, 693 (1954).

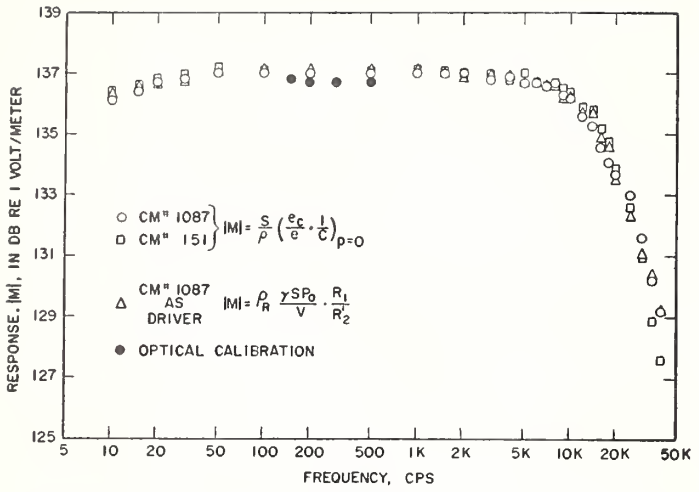

FIG. 5. Measured response of the displacement detector from 10 cps to 40 000 cps. The optical calibration points are shown to indicate the degree of accuracy obtained.

Equation (5) does not depend on the method of determining the pressure response, ρ_R; however, it can be combined with the expression for the response of the receiver microphone derived by the acoustical reciprocity method[3] to obtain $M=(S/R_2')(R_1Q\gamma P_0/VC)^{\frac{1}{2}}$, where Q is the ratio of the response of the receiver microphone to that of the driver, and C is the capacitance of the driver for a zero acoustic load.

Theoretical corrections can be applied to R_1 for standing wave patterns in the acoustic coupler at very high frequencies,[2] and for the cooling effect of the coupler walls at very low frequencies.[4]

RESULTS

Figure 5 shows the measured response of the displacement detector, using the probe, from 10 cps to 40 000 cps. Two response curves computed from Eq. (2) are shown, using different microphones; one curve computed from Eq. (5) is plotted for comparison. The response obtained from Eq. (3) is not shown, since the results are essentially identical with (2).

As an independent check, optical calibration of the displacement detector was performed at four frequencies by measuring the motion of an electrodynamic vibration exciter with the probe, and also with a microscope using a stroboscopic light source. These points, shown as the filled in circles in Fig. 5, fall within about 0.3 decibel of the responses determined by the diaphragm velocity and acoustical cavity methods.

[3] R. K. Cook, J. Acoust. Soc. Am. **12**, 415 (1941).
[4] F. Biagi and R. K. Cook, J. Acoust. Soc. Am. **26**, 506 (1954).

ACKNOWLEDGMENTS

The author wishes to thank Dr. R. K. Cook for suggesting this work, and Mr. Earle Jones for performing the optical calibration.

APPENDIX

The following proof is included to show that for small diaphragm displacements and curvatures, the detector responds to an equivalent linear diaphragm motion, $\bar{\xi}$, defined by Eq. (1).

The capacitance in mks units for an elemental diaphragm area S_i can be written as $C_i=\epsilon_0 S_i/x_i$, where x_i is the distance between the diaphragm element and the displacement probe, and ϵ_0 is the permittivity of free space. Differentiating with respect to x_i,

$$dC_i=-\epsilon_0(S_i/x_i^2)dx_i.$$

The distance x_i is made up of the sum $x_0+\Delta x_i$, where x_0 is the uniform spacing before application of the polarizing voltage and Δx_i is the nonuniform change in spacing due to the polarizing voltage. Expanding,

$$dC_i=-\frac{\epsilon_0}{x_0^2}S_i dx_i+\frac{2\epsilon_0}{x_0^3}\Delta x_i S_i dx_i-\cdots.$$

If second and higher order terms are neglected, the total change in capacitance is

$$dC_T\approx-\frac{\epsilon_0}{x_0^2}\sum_i S_i dx_i=-\frac{\epsilon_0}{x_0^2}dv,$$

where dv is the volume displacement.

Thus, the detector responds essentially to small volume displacements of the microphone diaphragm. For an equivalent uniform linear displacement, $\bar{\xi}$, the detector responds to a volume displacement $\bar{\xi}S$.

Reprinted from The Journal of the Acoustical Society of America, Vol. 30, No. 2, 114–121, February, 1958

Reverberation Chamber Study of the Sound Power Output of Subsonic Air Jets

Richard V. Waterhouse and Raymond D. Berendt
National Bureau of Standards, Washington 25, D. C.

(Received April 15, 1957)

The reverberation chamber technique was used to determine the sound spectra and acoustic power radiated by air jets over a range of subsonic velocities. Different air jets were used with round and square velocity profiles; nozzles of circular cross section, and nozzles with saw-tooth and corrugated ends were also used. Of these nozzles only the latter type gave a significant (9 db) reduction in sound power output for a given exit-pressure ratio. A study was made of the limitations of the reverberation chamber technique caused by the absorption in the chamber. When this absorption became considerable, the measurement of sound pressure level in a circle around the sound source revealed a directional pattern, and the assumption of uniform energy distribution in the chamber became invalid. This situation was noticeable at frequencies above 5 kc in the National Bureau of Standards chamber, owing to air absorption.

INTRODUCTION

THE object of the work reported here was to measure the sound power output and spectra of model air jets. Several papers have appeared[1,2] in which the sound pressure levels were measured at a few fixed points in a jet sound field, but only a few papers have presented figures for the total sound power output of jets. At the time the work reported here was initiated (1952), two sets of the latter type of data[3,4] had appeared and they were not in good agreement.

There are certainly several difficulties in the way of obtaining reasonably accurate figures (for example within ± 5 db) for the sound power output of jet sources. Two methods of measurement can be used; the reverberation chamber method is convenient for a directional sound source like an air jet as the multiple reflection of the sound at the walls of the chamber gives a sound field of approximately uniform energy density throughout the chamber. Then the sound power output of the source in each frequency band can be computed from one sound pressure level measurement. The other method available is the free-field method.

Both methods however have their difficulties. In the former method the diffusion of the sound field becomes inadequate at high and low frequencies, while in the latter difficulties are presented by the vagaries of the weather and the reflecting action of the ground, which extends the near sound field. If a large anechoic chamber is used to avoid the latter difficulties, it is still necessary to make measurements at many points to delineate the directional pattern of the source.

The reverberation chamber method is probably somewhat less accurate than the free-field method, for reasons discussed in more detail later, but it seemed appropriate for these measurements as it combined reasonable accuracy with convenience.

A semireverberant enclosure has been used in some investigations[3] in place of a reverberation chamber. However, such an enclosure has the disadvantages (a) that the effective absorption of the enclosure varies with the directional pattern of the sound source and (b) that the absorption of the enclosure for any kind of source cannot be measured accurately; for example, the measured absorption would depend on where the microphones and source were placed. These factors

[1] L. W. Lassiter and H. H. Hubbard, Natl. Advisory Comm. Aeronaut. Tech. Mem. 2757 (1952).
[2] A. Powell, Aeronaut. Quart. 4, 341 (1954).
[3] H. M. Fitzpatrick and R. Lee "Measurements of noise radiated by subsonic air jets," U. S. Navy Department, TMB Report 835, 1952.
[4] R. Lee, "Free field measurements of sound radiated by subsonic air jets," U. S. Navy Department, TMB Report 868 (1953).

574278 O - 61 - 53

tend to reduce the accuracy of power output measurements in semireverberant enclosures.

It appeared that the following factors may have contributed to the discrepancies between the results of references 3 and 4. (1) The amount of turbulence present in the air used was unknown. (2) The nozzles used were of different shapes and unspecified flow characteristics. For these nozzles the assumption of isentropic flow used in calculating the flow velocity from pressure measurements [see Eq. (3)] may have been invalid. (3) Neglect of the variation of the directional pattern of the jet source with frequency may have introduced errors. (4) The estimates of the absorption of the semireverberant enclosure may have been in error.

In the measurements described here efforts were made to avoid errors from these sources by using (1) a pressure regulated air supply and a calming tank, which gave stable operating conditions, and an air jet with negligible initial turbulence; (2) nozzles known to give isentropic flow[5]; and (3) and (4) a reverberation chamber of known absorption and diffuse sound field characteristics. Also the sound-pressure measurements were made sufficiently far from the source to ensure that far-field conditions obtained.

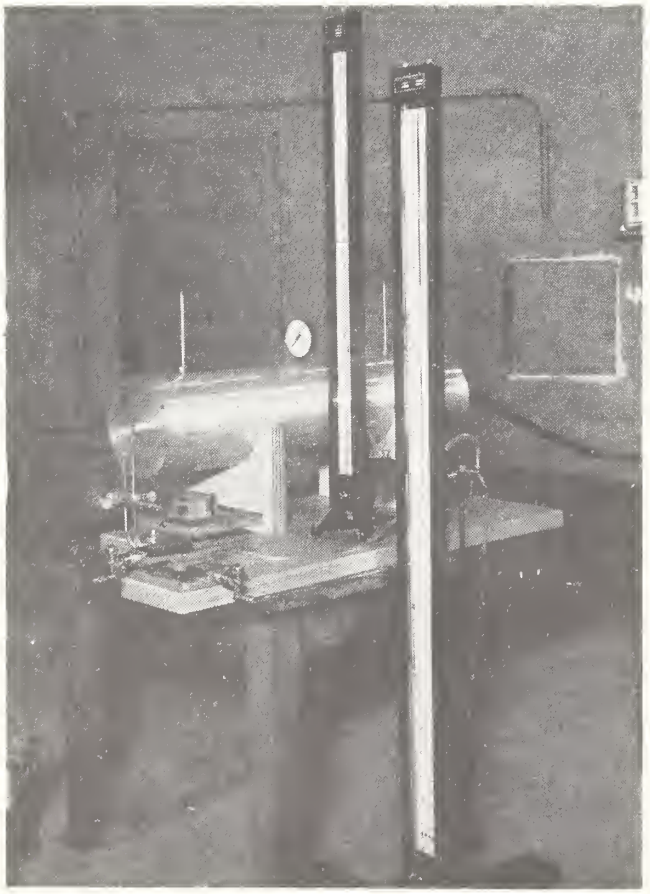

FIG. 1. Experimental setup in the National Bureau of Standards reverberation chamber showing calming tank and Pitot tubes.

[5] Bean, Buckingham, and Murphy, J. Research Natl. Bur. Standards 49, 561 (1929).

It is emphasized that the measurements reported here were of total sound-power output. The spatial distribution of the sound radiated by the air jet was ignored, although this factor is, of course, important in practice. It is quite possible that a silencing device could reduce the peak sound levels without reducing the total sound-power output of a jet, by altering the directional pattern. Such a situation could not be investigated in a reverberation chamber, however; it would require a free-field technique.

The first measurements were made with nozzles having circular orifices. Later measurements were made on nozzles having saw-tooth and corrugated ends, as such nozzles had been claimed to reduce the sound power output for a given thrust.[6] Isentropic flow was assumed in computing the mean jet velocities for all of the nozzles.

APPARATUS

The measurements were carried out in the reverberation chamber of the National Bureau of Standards. The chamber was 25 ft×30 ft in plan and 20 ft in height and contained two large vanes which were rotated to give a more uniform distribution of the sound energy. The experimental setup is shown in Figs. 1 and 2.

A 100-lb/in.^{2} compressed air line was connected to two pressure regulators in cascade and delivered an outlet pressure constant within ± 0.05 lb/in^2. A high pressure hose, $\frac{3}{4}$ in. i.d., connected the regulators to a calming tank. The tank, made of Duralumin, was 3 ft long, 8 in. in o.d. and $\frac{3}{8}$ in. in wall thickness, and contained acoustic treatment to reduce noise generated within the system as shown in Fig. 2. In all cases, the noise produced within the system was negligible compared to that of the emergent air jet.

The tank was terminated with a $\frac{1}{2}$ in. i.d. long-radius nozzle, i.e., a nozzle with a high contraction ratio, whose longitudinal section was a segment of an ellipse as shown in Fig. 3. The emergent air jet had a square velocity profile and negligible initial turbulence, as shown in Fig. 4. The circles represent the experimental points and the solid and broken curves represent the

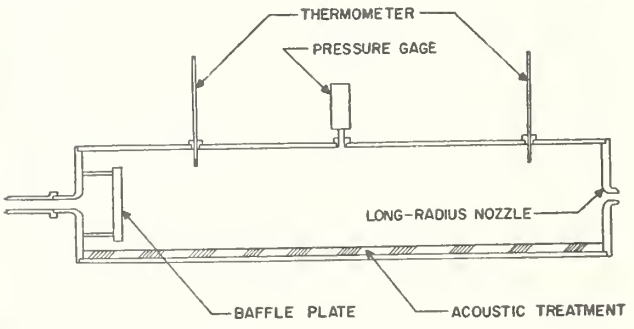

FIG. 2. Schematic of calming tank, showing long-radius nozzle in end plate.

[6] F. B. Greatrex, Engineer 200, Nos. 5188, 5189, 5190, pp. 23–25, 45–47, and 92–93 (1955).

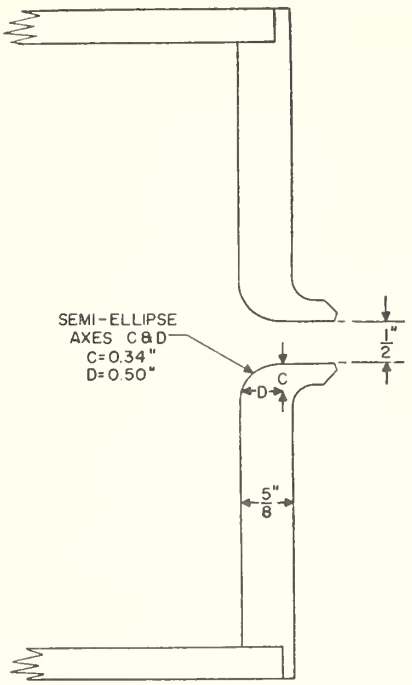

FIG. 3. Detail of long-radius nozzle.

velocity distributions obtained by Deissler[7] for flow through a tube at distances of 100 diameters and 1.5 diameters from entrance, respectively.

A cylindrical brass pipe of $\frac{1}{2}$ in. i.d., 2 ft length, and with $\frac{1}{16}$ in. wall thickness replaced the calming tank and nozzle for tne measurements on the fully developed, or round velocity profile, air jet. The exit end of the pipe was faced off square.

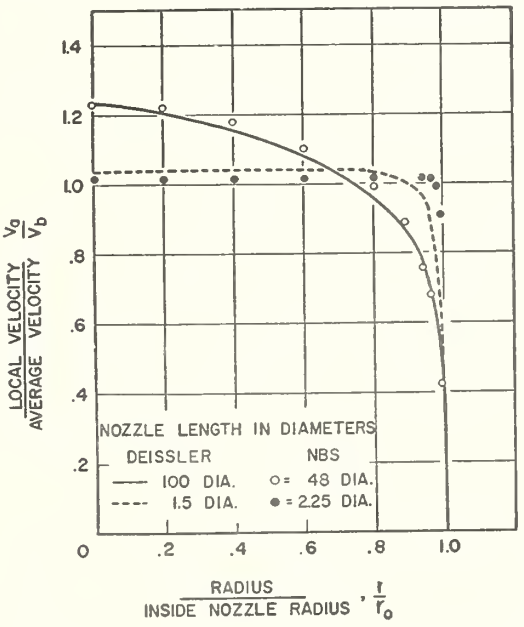

FIG. 4. Velocity profiles of air jets from long-radius and cylindrical nozzles as compared with velocity profiles of pipe flow with turbulence at different stages of development.

[7] R. G. Deissler, Natl. Advisory Comm. for Aeronaut. Tech. Notes 2138 (1950).

The saw-tooth nozzle used in some of the measurements was made of $\frac{1}{2}$ in i.d. brass pipe, 14 in. in length, and $\frac{1}{16}$ in. in wall thickness. The nozzle, shown in Fig. 5, had 4 teeth which were 1 in. long and parallel to the axial line.

Measurements were made also on two nozzles, one with shallow and one with deep corrugations.[6] The first consisted of 1 in. length of $\frac{1}{2}$ in. i.d. brass pipe which flared into a conical section of 6 corrugations approximately $\frac{1}{2}$ in. in length, as shown in Fig. 6. The second was similar to the first except that the corrugations were extended to a length of $\frac{15}{16}$ in. with the inner walls of the corrugations converging onto a circular cross section approximately $\frac{3}{64}$ in. in diameter. The outer walls diverged onto a circular cross section $\frac{7}{8}$ in. in diameter thus forming 6 deep corrugations. The cross-sectional area of the exhaust passage was constant throughout the length of each corrugated nozzle. The corrugated parts of the nozzles were made of copper electroplated on an interior form which was later removed. For the sound measurements, the corrugated nozzles were connected to the long-radius nozzle at the exit end of the calming tank.

TABLE I. Reverberation chamber absorption at relative humidity 60%. Volume of chamber = 15 000 cu ft.

Frequency cps	m,[a] attentuation coefficient per ft	Computed air absorption in sabins	Total measured chamber absorption in sabins
2000	0.0007	40	100
4000	0.002	120	180
6000	0.004	240	310
8000	0.006	360	450
10 000	0.008	480	600

[a] Figures taken from Knudsen and Harris, *Acoustical Designing in Architecture* (John Wiley and Sons, Inc., New York, 1950), p. 160.

To obtain figures for the mean velocity of the air jets from the cylindrical and long-radius nozzles, impact and static pressure traverses were made across the exit planes of the nozzles by means of pitot static probes which were supported in a coordinate vise. With this device the probes could be positioned within 0.001 in.

The pitot and static probes were made from steel hypodermic tubing 0.037 in. o.d. The static pressure holes were 0.009 in. in diameter and were situated 10-tube diameters downstream from the hemispherical probe tip. The probes were reinforced with $\frac{1}{8}$ in. o.d. brass tubing about 1 in. above the pressure holes to prevent vibration of the measuring heads.

The sound-pressure level measurements were made with a dynamic microphone, a calibrated sound level meter, and band-pass filters.

MEASURING PROCEDURE

Since the reverberation chamber effectively integrated the directional pattern of the air jet source, only

one measurement at each frequency band was needed to obtain the sound power output. For all the sound measurements the microphone was placed 9 ft from the jet source and at an angle of 90° to the jet axis. Both the jet source and microphone were approximately 40 in. above and parallel to the floor. These positions were not critical.

All the sound pressure level and Pitot static pressure measurements were made under steady state conditions. Impact pressure traverses for various jet velocities were made at 0.05 in. intervals across the horizontal diameter of the nozzle, approximately 0.1 in. upstream from its exit edge. The static pressure measurements were made in the same manner. Air temperature measurements were made in the calming tank or in the jet stream and from these data the free stream temperatures were computed. The measured temperatures were within 3°C of room temperature, which was kept at about 20°C. From these data, the velocity profiles and absolute jet stream velocities were computed.

The Pitot static probes were removed from the jet stream after use, to eliminate noise, before the sound pressure levels for the corresponding jet velocities were measured.

The sound power of the source was calculated from the measured sound pressure levels as follows.

The sound power output W of a source in the central region of a reverberation chamber for a certain frequency band is given by[8]

$$W=\frac{A\langle p^2\rangle}{4\rho c}, \tag{1}$$

where A = absorption of the reverberation chamber for the frequency band considered, $\langle p^2\rangle$ = mean squared sound pressure measured in the diffuse part of the sound field, and ρc = acoustic impedance of air. If W_{16} is the power level expressed in db above 10^{-16} watt and A is in sabins (ft²), in air at ordinary temperature and barometric pressure, Eq. (1) becomes

$$W_{16}=\text{SPL}+10\log_{10}A+23.5\text{ db}, \tag{2}$$

where SPL is the sound pressure level (with the customary reference pressure of 0.0002 microbar) measured in the diffuse part of the sound field; i.e., sufficiently far away from the source and reflecting surfaces.

The local or absolute jet velocities V_a were computed from the following equations.[9]

$$p_0/p=[1+(\gamma-1)M^2/2]^{\gamma/(\gamma-1)}, \tag{3}$$

$$T=T_0/[1+(\gamma-1)M^2/2], \tag{4}$$

$$c=49.02T^{\frac{1}{2}}, \tag{5}$$

[8] P. M. Morse, *Vibration and Sound* (McGraw-Hill Book Company, Inc., New York, 1948), pp. 384, 414.

[9] H. W. Liepmann and A. E. Puckett, *Introduction to Aerodynamics of a Compressible Fluid* (John Wiley and Sons, Inc., New York, 1947), pp. 21–27, 75.

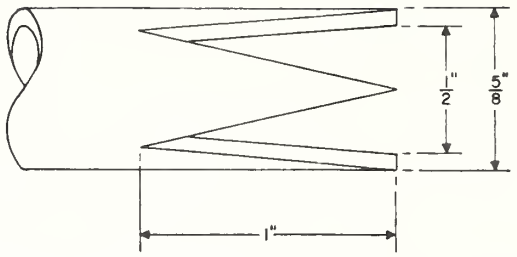

FIG. 5. Detail of saw-tooth nozzle with 4 teeth parallel to axis.

and

$$V_a=cM, \tag{6}$$

where p = pressure outside reservoir, p_0 = reservoir pressure, $\gamma=1.40$, the ratio of specific heats for air, M = local Mach number, T = free stream temperature in degrees Rankine (°R), and T_0 = stagnation temperature in °R, c = local speed of sound. The quantities p, p_0, and T_0 were measured directly.

The thrusts for the cylindrical pipe and the long-radius nozzle were computed from the measured velocity profiles by numerical integration. The other nozzles were compared not on the basis of equal thrust but on the basis of equal centerline velocity or equal exit-pressure ratio.

LIMITATIONS OF REVERBERATION CHAMBER TECHNIQUE

In a large reverberation chamber, the assumption of uniform sound energy distribution is invalid at high frequencies, since at these frequencies the absorption in the chamber is appreciable. The measured variation of absorption with frequency for the National Bureau of Standards reverberation chamber is given in the final column of Table I. A large part of the absorption is caused by the air, as can be seen upon comparison with the computed air absorption also given in the table.

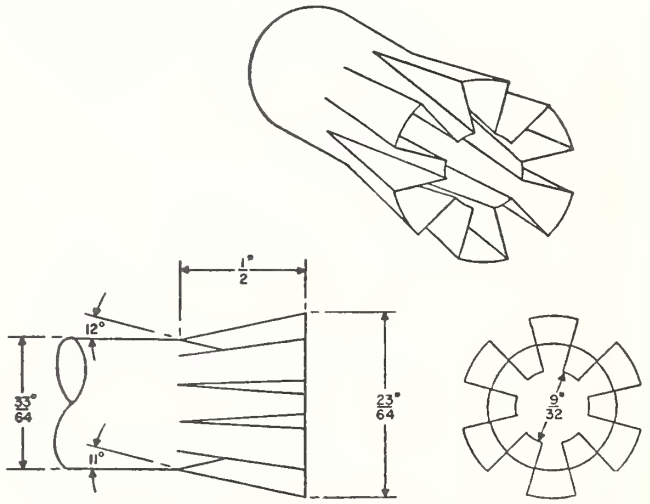

FIG. 6. Detail of shallow corrugated nozzle. (Note: The fraction $\frac{23}{64}$ should read $\frac{23}{32}$.)

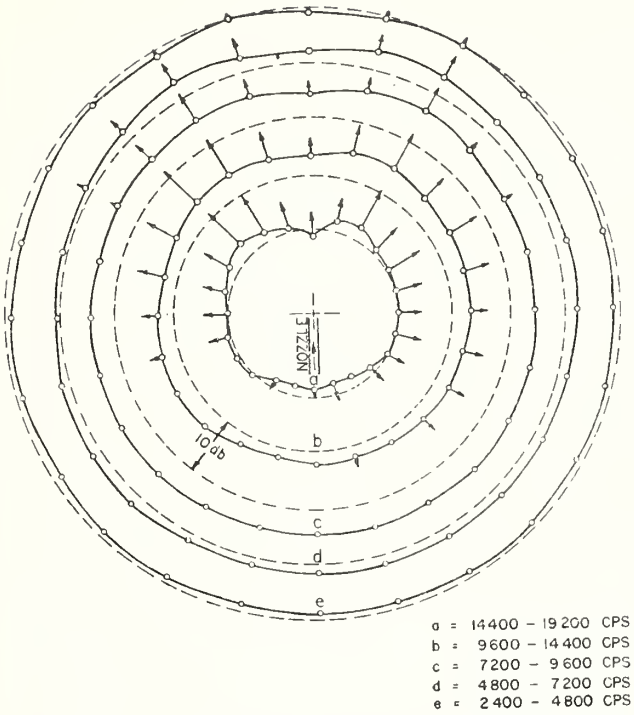

FIG. 7. Polar distribution in various frequency bands of relative sound pressure level caused by an air jet from a long-radius nozzle of $\frac{1}{2}$ in. diameter in the National Bureau of Standards reverberation chamber. $M=0.9$. All microphone positions were 9 ft from the estimated center of the noise source; see text. The relative levels for the several frequency bands are arbitrary.

In connection with the measurements of sound power output, the energy distribution in the chamber was examined over a frequency range 1000 to approximately 19 000 cps. Relative sound pressure levels were measured under steady state conditions at 15° intervals around the jet source. The relative humidity was controlled at about 60%.

At frequencies above 5000 cps, the directional pattern of the jet source became apparent, as shown in Fig. 7. However, quite accurate computations (see later section on accuracy of results) of sound energy could be made at frequencies up to about 7000 cps, since the sound field in the chamber was still reasonably diffuse at this frequency as the figure shows. The microphone was cylindrical in shape, with the diaphragm at one end. The closed curves connect the sound pressure levels measured with the microphone directed at right angles to a radius vector from the estimated center of the noise source. The effective center of the jet noise source was taken to be a point on the axis and 14 diameters downstream from the exit of the nozzle.

The arrowheads indicate the pressure levels measured with the microphone pointing inward along this radius vector. The length of the arrow is governed by the directional characteristics of the microphone and the nonuniform distribution of sound energy in the chamber.

The directional characteristics of the W.E. 633A dynamic microphone are given in the literature.[10] Using these figures with the data of Fig. 7, one can arrive at an approximation of the angular distribution of sound pressure at the microphone positions.

The arrows in Fig. 7 give a rough idea of the directional pattern of the air jet source, and evidently at the higher frequencies the assumption of equal energy density throughout the chamber is not valid. To obtain accurate measurements of the power output of a source emitting considerable energy at frequencies above 7000 cps either a small reverberation chamber or a free-field method would have to be used.

Nevertheless, for the sources used in the above work it was considered that reasonable accuracy was obtained by the use of the large reverberation chamber.

It is generally considered that the frequency of the peak of the sound spectrum of a jet source is related to

TABLE II. Sound spectra of air jets with rounded and square velocity profiles.[a]

Profile:	Round	Square	Round	Square	Round	Square
M on center line	0.90	0.90	0.69	0.69	0.50	0.50
V_a, ft/sec, on center line	940	948	748	751	550	553
V_b mean, ft/sec	782	932	614	740	445	545
Frequency range cycles per second	Sound power level in db *re* 10^{-16} watt					
75–150	99.6	103.2	90.7	96.6		
150–300	106.9	110.4	100.9	104.4	93.4	96.9
300–600	115.4	119.0	108.8	111.7	100.8	103.7
600–1200	123.2	127.3	115.5	119.3	106.8	110.3
1200–2400	129.9	133.9	121.6	125.1	111.2	114.9
2400–4800	131.9	136.1	122.1	126.3	111.9	115.6
4800–9600	128.2	132.3	118.4	122.2	107.2	110.9
Total sound power level	135.4	139.5	126.3	130.1	116.0	119.7

[a] M is the local Mach number. V_a and V_b are absolute air jet velocities. Both nozzles were $\frac{1}{2}$ in. i.d.

TABLE III. Sound spectra of air jets with rounded and square velocity profiles.[a]

Profile:	Round	Square	Round	Square	Round	Square
V_b mean, ft/sec	782	776	614	612	445	446
V_a, ft/sec, on center line	940	788	748	621	550	450
M on center line	0.90	0.73	0.69	0.57	0.50	0.40
Frequency range cycles per second	Sound power level in db *re* 10^{-16} watt					
75–150	99.6	98.2	90.7			
150–300	106.9	105.4	100.9	98.9	93.4	92.4
300–600	115.4	113.2	108.8	106.3	100.8	98.7
600–1200	123.2	120.5	115.5	113.0	106.8	104.5
1200–2400	129.9	126.9	121.6	118.1	111.2	108.4
2400–4800	131.9	128.6	122.1	118.8	111.9	108.4
4800–9600	128.2	123.9	118.4	114.4	107.2	103.4
Total sound power level	135.4	132.1	126.3	122.9	116.0	113.0

[a] V_a and V_b are absolute air jet velocities. M is the local Mach number. Both nozzles were $\frac{1}{2}$ in. i.d.

[10] L. L. Beranek, *Acoustic Measurements* (John Wiley and Sons, Inc., New York, 1950), p. 226.

the diameter of the source. For a large source of 20 in. diameter the sound output may peak at a low frequency, around 500 cps, while for a small source of $\frac{1}{2}$ in. diameter the corresponding figure may be around 5000 cps.

Thus to improve the accuracy of reverberation chamber measurements of sound power output, the possibility existed of using a nozzle larger than $\frac{1}{2}$ in. diameter, so that less of its sound output would lie in the high-frequency region where measurements were less accurate. This was not done since the noise levels of a larger nozzle at the Mach numbers used would have been unpleasantly high for the observer in the chamber; to handle all the measurements by remote control would have been very cumbersome.

RESULTS

Spectra and sound power output figures for various nozzles are given in Tables II, III, IV, and V. The differences between the sound power outputs of the various nozzles can be summarized as follows.

1. For a given jet diameter and mean velocity (thrust) the sound power level of the round profile jet was about 3 db greater than that of the square profile jet. This increase in sound power probably resulted from the greater (about 21%) centerline velocity of the round profile jet.

2. For a given jet diameter and centerline velocity, the sound power level of the square profile jet was about 4 db greater than that of the round profile jet. However, the thrust was about 45% greater in the former case.

3. The total sound power output of the air jet with round velocity profile varied as the 7.7 power of the mean velocity, the standard deviation being 0.3. For the square velocity profile jet, the value was 8.2 with a standard deviation of 0.2. See Fig. 8.

4. For a given jet diameter and centerline velocity, the sound power level of the saw-tooth-end nozzle was about $1\frac{1}{2}$ db greater than that of the cylindrical nozzle.

TABLE IV. Sound spectra of air jets emerging from cylindrical pipes (circular cross section) with square and saw-tooth ends.[a]

	Square end	Saw-tooth end
M on center line	0.79	0.79
V_a, ft/sec, on center line	835	836
Frequency range cycles per second	Sound power level in db re 10^{-16} watt	
75–150	97.2	97.2
150–300	103.4	103.9
300–600	111.9	112.4
600–1200	119.5	120.0
1200–2400	125.9	126.6
2400–4800	128.1	129.8
4800–9600	124.2	127.2
Total sound power level	131.5	133.1

[a] The pipes were 14 in. long with $\frac{1}{2}$ in. i.d. M is the local Mach number. V_a is the absolute air jet velocity.

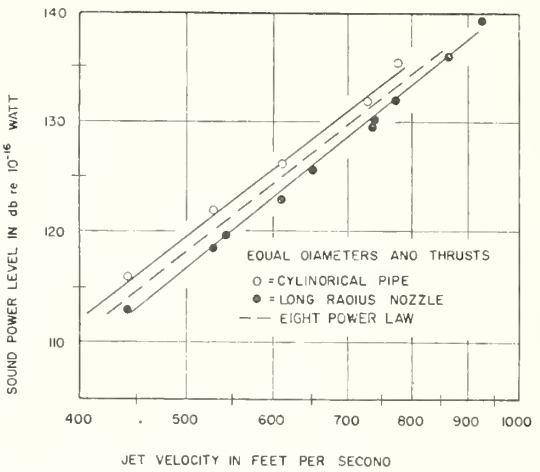

FIG. 8. Total sound power radiated by two air jets as a function of mean jet velocity.

5. For a given exhaust passage area and exit pressure ratio [corresponding to $M \simeq 0.9$, using Eq. (3) above], the sound power levels of both types of corrugated nozzle were approximately 9 db less than that of the long-radius nozzle.

TABLE V. Sound spectra of air jets emerging from long-radius and corrugated nozzles of equal exhaust passage areas.[a]

	Sound power level in db re 10^{-16} watt $M = 0.90$		
Frequency range c/s	Long radius nozzle	Shallow corrugated nozzle	Deep corrugated nozzle
75–150	102.5	98.8	100.1
150–300	109.1	106.1	106.6
300–600	118.1	112.4	111.9
600–1200	126.0	117.5	116.5
1200–2400	132.2	121.7	121.2
2400–4800	134.2	123.7	123.5
4800–9600	130.2	123.2	123.2
Total sound power level	137.7	128.2	128.0
	M = 0.70		
75–150	96.5	88.6	99.5
150–300	103.8	99.1	105.1
300–600	111.2	104.9	109.4
600–1200	119.0	110.2	114.0
1200–2400	123.9	114.2	117.2
2400–4800	125.5	115.7	120.0
4800–9600	121.4	115.2	118.9
Total sound power level	129.2	120.5	124.3
	M = 0.50		
75–150			94.7
150–300	96.1	91.6	98.1
300–600	103.1	96.6	100.9
600–1200	109.5	101.2	106.5
1200–2400	113.9	105.7	110.7
2400–4800	114.7	108.5	113.0
4800–9600	109.9	106.9	110.4
Total sound power level	118.8	112.5	116.9

[a] The Mach number M was calculated from the ratios of pressures inside and outside the calming tank, assuming isentropic flow, by use of Eq. (3) above.

ACCURACY OF RESULTS

The total sound power levels given above are probably slightly below the true levels, since the sound energy at frequencies above 9600 cps was not measured. Extrapolating the figures to account for this would give increases in the total power levels of less than $\frac{1}{2}$ db for Tables II, III, and IV, and up to 1 db for Table V.

Taking this and other possible sources of error into account, it is probably safe to say that the total power levels of Tables II, III, and IV are within ± 2 db of the true values, and that they are correct within ± 1 db for comparative values; for Table V the figures are ± 3 db and ± 2 db. Thus when the sound power output of the corrugated nozzle is given as 9 db less than that of the long-radius circular nozzle for a given thrust, we judge the figure 9 db to be correct within ± 2 db.

We estimate the individual velocity figures and Mach numbers to be within $\pm 1\%$ of the true values.

The variation of sound power level with $\log_{10}$ (mean jet velocity) was found to follow a straight line as shown in Fig. 8. The slope of this straight line was computed by the method of least squares, using a weighting for each point to account for its margin of error. Five points were used in the calculation for the round profile jet, and 10 points for the square profile jet.

The standard deviation of individual points (i.e., values of sound power level at a given jet velocity) was 0.6 db. That is, given the original estimates of possible error (± 2 db) for the power levels, and assuming a straight line dependence of power level on $\log_{10}$ (mean jet velocity), the chances were 68 out of 100 that the measured power levels lay within 0.6 db of the true values.

DISCUSSION

The figures given above for sound power output are generally lower than those of Fitzpatrick[3] and Lee.[4] Depending on the jet velocity, the present sound power levels were from 8 to 11 db less than those given in reference 3 and from 3 to 6 db less than those in reference 4. Most of the difference is probably due to the causes discussed in the introduction.

The differences were not significant between the sound powers radiated by the nozzles of circular cross section giving rounded and square velocity profiles, for the same thrust. Lassiter and Hubbard,[11] and Powell,[2] have also discussed this matter, and reached this conclusion.

Concerning the variation of the sound power with mean flow velocity, the values of 7.7 and 8.2 obtained for the exponent of the latter are in quite good agreement with the earlier[12] prediction of Lighthill. This agreement may be fortuitous, since that theory was restricted to homogeneous isotropic turbulence and low Mach numbers. A later paper[13] by that author discusses reasons why the exponent might exceed 8. The value for the exponent found by Lee[2] was 6.4, while Tyler and Perry[14] obtained the value 8 in later experiments. Of course, the sound intensity at a point in the sound field of a jet is a different matter, and the dependence of this intensity on the mean jet velocity varies considerably with the position of the measuring point.[15]

As regards the frequency distribution of the sound power radiated by various nozzles, the spectra shown in Fig. 9 were obtained with air jets of round and square velocity profiles, under the same thrust conditions. Although the velocity profiles of the two types of air jets are very different, their spectra and sound power outputs are extremely similar.

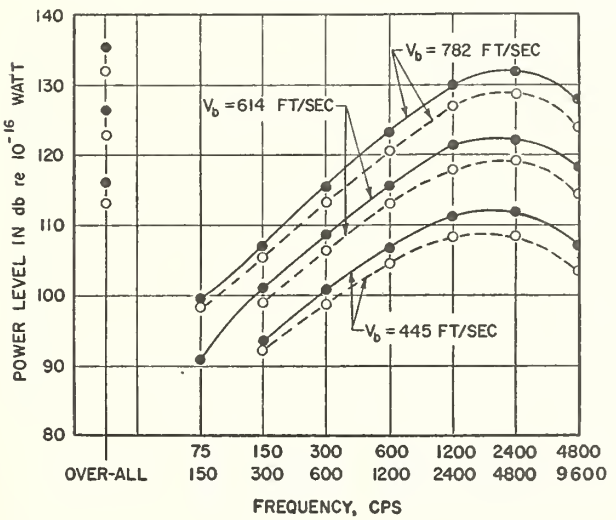

FIG. 9. Sound spectra of two air jets at various mean velocities: solid circles ●, cylindrical nozzle (round profile); open circles ○, long-radius nozzle (square profile). See Table III.

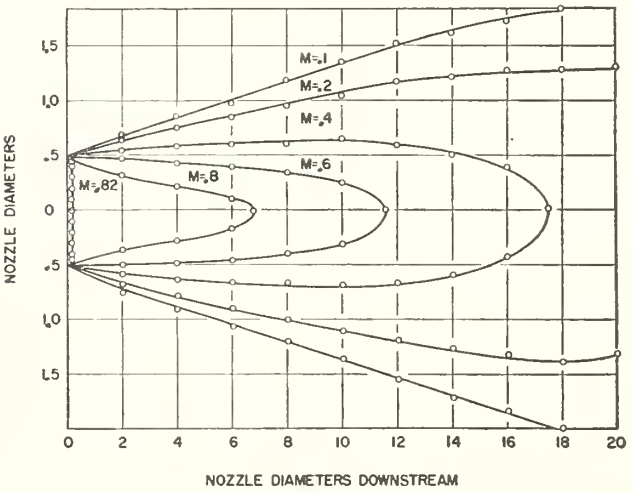

FIG. 10. Mach number contours of an air jet in the vicinity of $\frac{1}{2}$-in. diameter long-radius nozzle. Mean flow velocity $V_b = 862$ ft/sec at exit edge of nozzle. Mach numbers were computed from pitot measurements without correction for turbulence.

[11] L. W. Lassiter and H. H. Hubbard, J. Acoust. Soc. Am. **27**, 431–437 (1955).

[12] M. J. Lighthill, Proc. Roy. Soc. (London) **A211**, 564–587 (1952).

[13] M. J. Lighthill, Proc. Roy. Soc. (London) **A222**, 1–32 (1954).

[14] J. M. Tyler and E. C. Perry, S. A. E. Trans. **63**, 308–320 (1955).

[15] A. Powell, Aircraft Eng. **26**, 2–9 (1954).

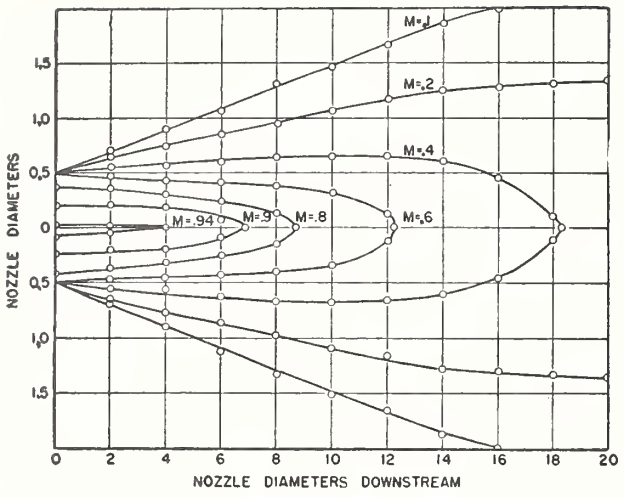

FIG. 11. Mach number contours of an air jet in the vicinity of a $\frac{1}{2}$-in. diameter cylindrical pipe. Mean flow velocity $V_b = 810$ ft/sec at exit edge of nozzle. Mach numbers were computed from pitot measurements without correction for turbulence.

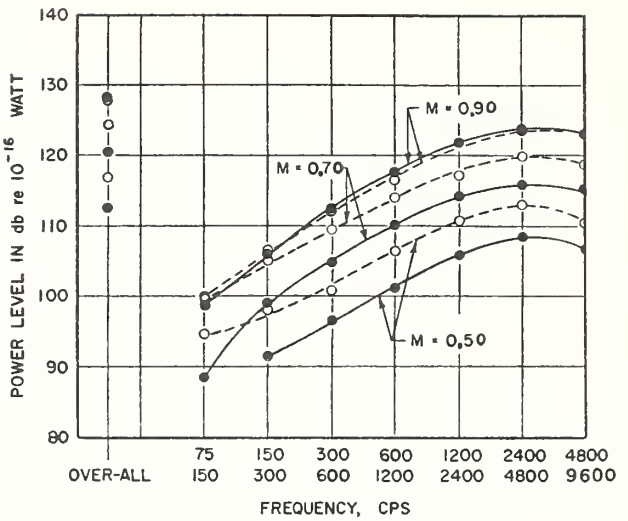

FIG. 12. Sound spectra of air jets from two types of corrugated nozzle; see Table V. Solid circles ●; shallow corrugated nozzle; open circles ○; deep corrugated nozzle.

A possible explanation for this is that a large fraction of the jet noise is generated some distance downstream from the exit edge of the nozzle. Figures 10 and 11, which show contours of Mach number* in the vicinity of the nozzles, tend to support this explanation insofar as the two sets of contours are extremely similar downstream from the nozzles and differ only near their exit edges. The angle of divergence of the air jet was about the same in both cases.

The spectra of the sound radiated by the corrugated nozzles are shown in Fig. 12. At the higher jet velocities, the two types of corrugated nozzles performed equally as noise reducers; but at the lower jet velocities the nozzle with shallow corrugations was considerably better than the one with deep corrugations.

Of the various nozzles used, only the corrugated type gave a significant reduction (9 db) in sound power level. This figure is in fair agreement with the reduction of 7 db obtained by Greatrex[6] for a full-scale corrugated nozzle mounted on a jet engine, using a free-field technique. The reason for this reduction in sound power is not known, although it has been suggested[6] that it is primarily due to the increased divergence of the air jet.

The saw-tooth nozzle also increased the divergence of the air jet, compared to the nozzles having a circular orifice. However, the sound power output was not reduced in this case, possibly owing to additional noise being generated by the air flowing over the teeth.

We are of the opinion that the reduction in sound output of an air jet given by both the corrugated nozzle and the metal screen[16] is closely related to the changes these devices produce in the development of turbulence in the escaping air jet. It is hoped to study this relation further in the future.

* The Mach numbers plotted in Figs. 10 and 11 were derived from pitot tube readings, using Eq. (3) above. No correction was made for the effect of turbulence.

[16] E. E. Callaghan, and W. D. Coles, Natl. Advisory Comm. Aeronaut., Tech. Notes 3452 (1952).

Reprinted from The Journal of the Acoustical Society of America, Vol. 30, No. 1, 4–13, January, 1958

Output of a Sound Source in a Reverberation Chamber and Other Reflecting Environments*

Richard V. Waterhouse
National Bureau of Standards, Washington, D. C.
(Received October 21, 1957)

It is important to know the output of a source as a function of position in a reverberation chamber. Expressions are given for the sound power output of simple monopole and dipole sources as functions of source position in various reflecting environments. They are obtained by the use of the method of images and a general formula due to Rayleigh for the output of a number of simple sources. The cases of a dipole source near a reflecting plane and a simple source near a reflecting edge and corner are treated, and the effect of the band width of the source is considered. The results apply when the reflectors enclose the source, as in a reverberation chamber, unless the distance in wavelengths between parallel walls is small and the absorption in the enclosure is low. Some experimental data are given, and the reverberation chamber method of measuring the power output of sources is discussed. In the general case of an extended source emitting nonspherical waves near reflecting surfaces, it may be more convenient to find the variation of power output with position by experiment than by calculation.

INTRODUCTION

An important property of sound sources is that their sound power output and directional patterns in general vary when they are placed in different positions near reflecting surfaces.

The effect is caused by the sound reflected from the reflectors reacting back on the source. This reaction can be considered as an impedance reflected onto the source. The reflected impedance varies with the environment, and thus in general the sound power output of the source varies with the environment.

The effect is discussed in the literature,[1–3] and Fischer[4] has given expressions for the dependence on source-reflector separation for a simple source near a plane. In this paper expressions are given for various source-reflector systems that are of interest in architectural acoustics, including the case of a dipole source near a reflecting plane, and a simple source near a reflecting edge and corner.

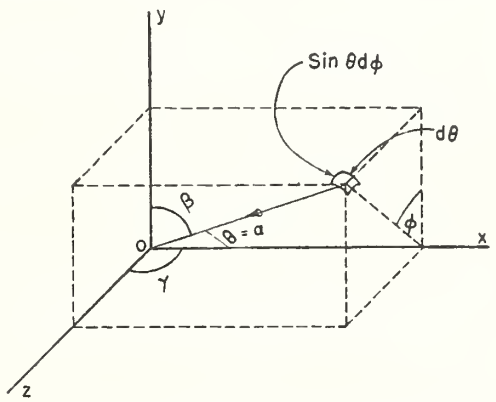

Fig. 1. Coordinate axes used in derivations in text. $\cos\alpha=\cos\theta$, $\cos\beta=\sin\theta\cos\phi$, and $\cos\gamma=\sin\theta\sin\phi$. Element of area on a sphere of radius d with center 0 is $d^2\sin\theta d\theta d\phi$.

These expressions follow from the use of the method of images and a formula due to Rayleigh for the output of a number of simple sources. It is shown that, in general, the power output of the source differs significantly from the free-field value if the distance of the source from the reflector is less than the wavelength of the sound emitted.

These results are of practical importance in several ways. For example, they show where a source must be located in a reverberation chamber if the free-field value of the power output of the source is to be measured. They also enable one to estimate to what extent noise can be reduced or increased by manipulating reflectors near a source. Such manipulation of reflectors could also be used to match a source into a medium.

We first obtain expressions for the power output variations of some simple types of source and reflector, and then consider their application to the more complicated source-reflector systems met in practice.

OUTPUT OF SOURCE NEAR PLANE REFLECTOR

Rayleigh's formula[5–8] for the directional pattern DP of a number of simple sound sources of uniform strength and frequency, placed at arbitrary positions in space, can be written

$$DP \propto \sum_m \sum_n \cos(kd_{mn}+\epsilon_{mn}), \qquad (1)$$

where $k=\omega/c_0$, $\omega=2\pi f$, c_0 is the sound velocity, and f is the frequency of the sound sources.

* A lecture on this topic was given at a meeting of the Acoustical Society of America on December 15, 1955.

[1] Lord Rayleigh, *Theory of Sound* (Dover Publications, New York, 1945), Vol. 2, pp. 108–112.

[2] H. Lamb, *Dynamical Theory of Sound* (Edward Arnold and Company, London, 1931), second edition, pp. 229 and 233.

[3] L. L. Beranek, *Acoustics* (McGraw-Hill Book Company, Inc., 1954), pp. 319–320.

[4] F. A. Fischer, Elek. Nachr.-Tech. **10**, 19 (1933).

[5] Rayligh, *Collected Papers* (Cambridge University Press, London, 1912), Vol. 5, p. 137.

[6] H. Stenzel, Elek. Nachr.-Tech. **6**, 165 (1929).

[7] H. Stenzel, *Leitfaden zur Berechnung von Schallvorgaengen* (Berlin, 1939) (English translation by A. R. Stickley, published by Naval Research Laboratory, Washington, D. C.).

[8] E. Rhian, J. Acoust. Soc. Am. **26**, 704 (1954).

The path difference of rays from sources m and n in the direction with direction cosines $\cos\alpha$, $\cos\beta$, $\cos\gamma$ (see Fig. 1) is d_{mn}, i.e.,

$$d_{mn}=(x_m-x_n)\cos\alpha+(y_m-y_n)\cos\beta+(z_m-z_n)\cos\gamma, \quad (2)$$

where (x_m,y_m,z_m) are the position coordinates of the mth source. ϵ_{mn} is the phase difference between sources m and n. The term "directional pattern" is defined here as the part varying with direction in the expression for the mean squared pressure in the far field of a source.

The sound output W of all the N sources is obtainable by integrating (1) over a sphere, and can be written

$$W/W_f=N+2\sum(\cos\epsilon_{mn})j_0(r_{mn}'), \quad (3)$$

where the sum is taken over every pair of sources. If only one source is real, the rhs of (3) is divided by N. $W_f=2\pi k^2\rho_0 c_0$ is the free-field power output of one source. The spherical Bessel function is $j_0(r_{mn}')=(\sin r_{mn}')/r_{mn}'$, and $r_{mn}'=4\pi r_{mn}/\lambda$, i.e., 4π times the distance in wavelengths between sources m and n.

$$r_{mn}=[(x_m-x_n)^2+(y_m-y_n)^2+(z_m-z_n)^2]^{\frac{1}{2}}. \quad (4)$$

From these formulas we can obtain comparable expressions for the output of a single source near certain reflecting surfaces, by the use of the method of images.[2,9] In this method, sound reflected by the reflector is considered to emanate from one or more image sources. These image sources are placed so that their radiation combines with that of the object source to satisfy the boundary conditions of the problem.

We consider that the reflectors are rigid and 100% reflecting, so the boundary condition is that on the reflecting plane the normal component of particle velocity is zero. The strength, i.e., peak volume velocity, of the source is fixed, and independent of the environment of the source.

For the case of a simple source near a plane reflecting surface, as shown in Fig. 2(a), one image source is enough to satisfy this boundary condition, the image source being equal in strength and phase to the object source.

The directional pattern of the source plus reflector is then, from (1)

$$DP\propto\cos^2 a, \quad (5)$$

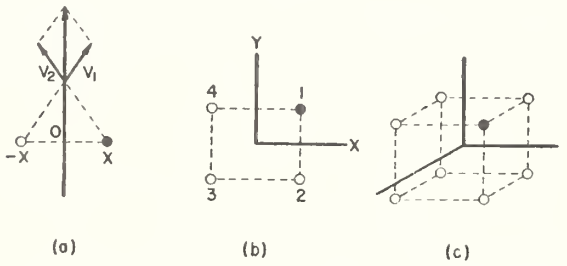

FIG. 2. ● Point source. ○ Image source. Acoustic images at one-wall, two-wall, and three-wall reflectors when one point source is present. The black lines represent the profiles of the reflectors.

[9] H. Lamb, *Hydrodynamics* (Dover Publications, New York, 1945), p. 129.

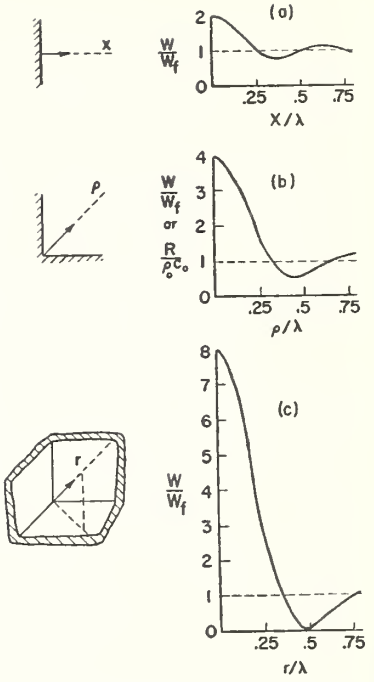

FIG. 3. Theoretical curves for the relative power output W/W_f of a simple source as a function of position near one-, two- and three-plane reflectors at right angles. ρ and r are the distances of the source from the origin along the lines of symmetry, and $k=\omega/c_0$ is the wave number. When the source is many wavelengths away from the reflectors, its power output W approaches the free field value W_f asymptotically. The dashed lines are the asymptotes. See Table II for the expressions plotted here.

where $a=kx\cos\alpha$; the reflecting plane is the yz plane of Fig. 1, and the source is a distance x from it.

The power output W of the source plus reflector[4] is found from (3) to be

$$W/W_f=1+j_0(x'). \quad (6)$$

W_f is the output of the source in a free field, for example, suspended on a string in an anechoic chamber. The spherical Bessel function $j_0(x')=(\sin x')/(x')$, and $x'=4\pi x/\lambda$, i.e., 4π times the distance in wavelengths from source to reflector.

The power output of the source-reflector combination can also be obtained by calculating the impedance seen by the source, as shown in Appendix II.

Expression (6) is plotted in Fig. 3(a). It can be written in terms of the other variables f, the frequency, or k, the wave number, as

$$W/W_f=1+j_0(2kx) \quad (7)$$

$$=1+j_0(4\pi fx/c_0). \quad (8)$$

The form (6) is used here since it is compact and helps to underline the fact that the position in space of the source, measured in wavelengths, is the important variable here.

SOURCE OF ARBITRARY DIRECTIONAL PATTERN

For a sound source of arbitrary directional pattern $A_1=A(\theta,\phi)$, the method of images can still be used, but the image sources must now have particular directional patterns. If the source is distant x from an infinite rigid reflecting plane, an image source with directional pattern $A_2=A(\pi-\theta,\phi)$ is needed to satisfy the boundary condition.

From (1) we then obtain for the directional pattern DP of source and reflector

$$DP \propto A_1^2+A_2^2+2A_1A_2\cos 2a. \tag{9}$$

The power output of the combination is then proportional to

$$\int_0^{\pi/2}\int_0^{\pi}(A_1^2+A_2^2+2A_1A_2\cos 2a)\sin\theta d\theta d\phi, \tag{10}$$

using the coordinate system of Fig. 1. The constant of proportionality is determined by normalization. This expression can be calculated if the functions $A_1=A(\theta,\phi)$ and $A_2=A(\pi-\theta,\phi)$ are given.

As an example, we take $A_1=\cos\theta$, using the coordinate system of Fig. 1, yz being the reflecting plane. This gives the source a figure-of-eight directional pattern like that of a dipole source in a free field with the dipole axis parallel to the x axis. When the source is distant x from the plane reflector, the directional pattern of the combination is found from (9) to be

$$DP \propto \cos^2\alpha \sin^2 a, \tag{11}$$

and the power output from (10) is given by

$$W/W_f=1-j_0(x')+2j_2(x'), \tag{12}$$

where W_f is the free-field value of the power output of the source, $x'=4\pi x/\lambda$, $j_0(x')=(\sin x')/x'$, $j_1(x')=[j_0(x')-\cos x']/x'$, and $j_2(x')=(3/x')j_1(x')-j_0(x')$.

Equation (12), which is the same as Eq. (21) given later in this paper, is plotted in Fig. 4.

EFFECT OF BAND WIDTH

The foregoing results apply to sources emitting sound at one frequency only. For sources emitting sound at a few discrete frequencies, i.e., a line spectrum, the resultant effects are obtained by summing arithmetically the effects at the various single frequencies. For sources emitting continuous bands of noise, analogous results can be found by an integration, as follows.

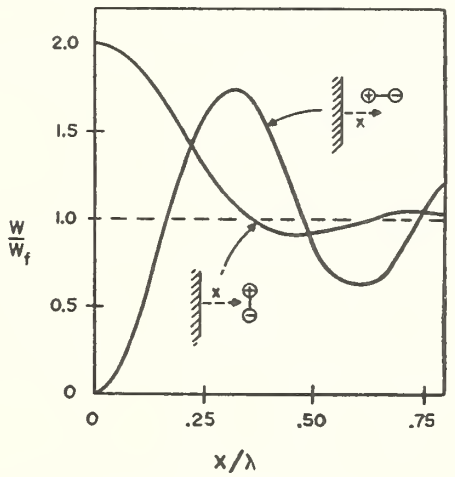

FIG. 4. Theoretical curves for the relative power output W/W_f of a dipole source *versus* distance x/λ in wavelengths from a plane reflector. Two cases are shown, with the dipole axis normal and parallel to the reflector. See Eqs. (21) and (19). The dashed line is the asymptote.

For a point source emitting noise with a continuous band width f_1 to f_2, (5) becomes

$$DP \propto [1/(f_2-f_1)]\int_{f_1}^{f_2}\cos^2 a\, df, \tag{13}$$

$$\propto 1+[(\sin Bf_2-\sin Bf_1)/B(f_2-f_1)], \tag{14}$$

where $B=(4\pi x\cos\theta)/c_0$.

The relative power output of the source, from (6) and (8) is

$$W/W_f=1+[1/(f_2-f_1)]\int_{f_2}^{f_1} j_0(4\pi fx/c_0)df. \tag{15}$$

The integral is the sine integral, which is tabulated. Graphs of (15) for band widths of $\pm 10\%$, one octave, and 5 octaves are given in Fig. 5. It is apparent that even with the wide band of 5 octaves the main feature of the curve remains.

Dipole Source

Expressions for the directional pattern and power output of a dipole source as functions of distance from a plane rigid reflector are obtainable from the general formulas (1) and (3).

When the dipole is in the xy plane of Fig. 1, and its axis makes an angle η with the reflector (yz plane), its directional pattern is

$$DP \propto \sin^2\eta\cos^2\alpha\sin^2 a+\cos^2\eta\cos^2\beta\cos^2 a, \tag{16}$$

and its power output W in terms of W_f, the free-field output of the dipole, is

$$(W/W_f)=1+(3/x')j_1(x') +3\sin^2\eta[(1/x')j_1(x')-j_0(x')], \tag{17}$$

where $j_1(x')=[j_0(x')-\cos x']/x'$.

When the dipole axis is parallel to the plane, $\eta=0$ and

$$DP \propto \cos^2\beta\cos^2 a \tag{18}$$

$$(W/W_f)=1+j_0(x')+j_2(x'), \tag{19}$$

where $j_2(x')=(3/x')j_1(x')-j_0(x')$.

When the dipole axis is normal to the plane reflector, $\eta=90°$ and

$$DP \propto \cos^2\alpha\sin^2 a \tag{20}$$

$$(W/W_f)=1-j_0(x')+2j_2(x'). \tag{21}$$

The foregoing expressions† are tabulated in Table I, and graphs of (19) and (21) are given in Fig. 4.

These results are of some practical interest. For

† Results (18) to (21) were given in a lecture on this topic to the Acoustical Society of America on December 15, 1955. More recently, they were given by U. Ingard and G. L. Lamb, Jr., J. Acoust. Soc. Am. **29**, 743 (1957).

TABLE I. Expressions for the directional pattern and relative power output of a dipole source as functions of distance x from a plane reflecting wall.[a]

	Dipole makes angle η with wall	Dipole axis parallel to wall	Dipole axis normal to wall
Directional pattern, DP	$\sin^2\eta\cos^2\alpha\sin^2 a+\cos^2\eta\cos^2\beta\cos^2 a$	$\cos^2\beta\cos^2 a$	$\cos^2\alpha\sin^2 a$
Relative power output W/W_f	$1+(3/x')j_1(x')+3\sin^2\eta[(1/x')j_1(x')-j_0(x')]$	$1+j_0(x')+j_2(x')$	$1-j_0(x')+2j_2(x')$

[a] $a=kx\cos\alpha$; $x'=4\pi x/\lambda$; $j_0(x')=(\sin x')/x'$; $j_1(x')=[j_0(x')-\cos x']/x'$; $j_2(x')=(3/x')j_1(x')-j_0(x')$. In Fig. 1, the yz plane is reflecting, and the dipole is in the xy plane. See Fig. 4 for graphs of some of the expressions here for the relative power output.

example, at low frequencies a loudspeaker with no cabinet radiates like a dipole, as experimental results given later show.

OUTPUT OF SOURCE NEAR REFLECTING EDGE AND CORNER

When a point source is near 2 reflectors at right angles, 3 image sources are needed to satisfy the boundary conditions, as shown in Fig. 2(b).

The normal velocity components of the sound from sources 1 and 2, 3 and 4, cancel on the xz plane, and similarly for sources 1 and 4, 2 and 3, on the yz plane. Analogous arguments hold for the case of 3 reflectors at right angles, Fig. 2(c), where 7 image sources are needed.

Thus when the source is at (x,y,z) the images in the three reflector case lie at the points $(-x, y, z)$, $(x, -y, z)$, $(x, y, -z)$, $(-x, -y, z)$, $(x, -y, -z)$, $(-x, y, -z)$, $(-x, -y, -z)$, and analogously for the two-plane case.

Inserting these image positions in (1) and (3) we obtain the directional pattern and power output of a simple source near two-, and three-plane reflectors.

The directional pattern for a simple source at position xy near a reflecting edge [xz and yz planes reflecting, see Figs. 1 and 2(b)] is

$$DP\propto(\cos a\cos b)^2, \tag{22}$$

where $a=kx\cos\alpha$, $b=ky\cos\beta$, and the coordinate system and symbols of Fig. 1 are used.

The relative power output is

$$W/W_f=1+j_0(x')+j_0(y')+j_0(\rho'), \tag{23}$$

where $x'=4\pi x/\lambda$, $y'=4\pi y/\lambda$, and $\rho'=4\pi(x^2+y^2)^{\frac{1}{2}}/\lambda$.

If the source is confined to the line of symmetry from the origin, bisecting the angle xoy, its relative power output is

$$W/W_f=1+2j_0(\rho'/\sqrt{2})+j_0(\rho') \tag{24}$$

[see Figs. 3(b) and 9].

When the source is at position (x,y,z) near a reflecting corner the directional pattern is

$$DP\propto(\cos a\cos b\cos c)^2, \tag{25}$$

where a and b are as in (22) and $c=kz\cos\gamma$, (see Fig. 1).

The relative power output of the source is

$$W/W_f=1+j_0(x')+j_0(y')+j_0(z')+j_0(\rho_1')+j_0(\rho_2')+j_0(\rho_3')+j_0(r'), \tag{26}$$

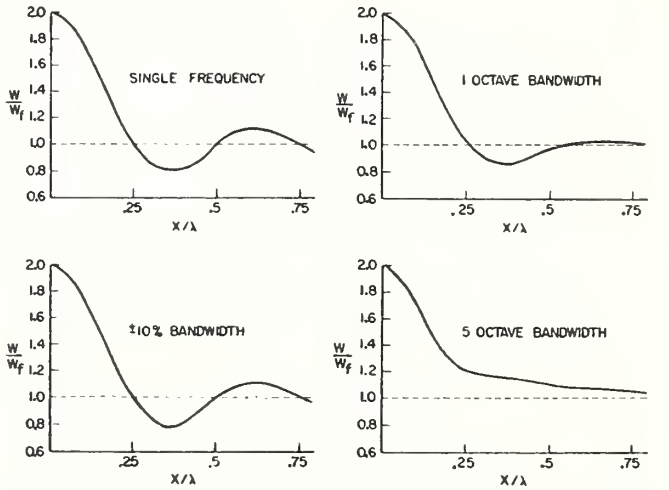

FIG. 5. Theoretical curves for the relative power output W/W_f of a simple source as a function of distance x/λ in wavelengths from a plane reflector, when the source vibrates with various band widths. In the abcissae $\lambda=(\lambda_1+\lambda_2)/2$ where λ_1 and λ_2 are the wavelengths at the extremes of the bands. The dashed lines are asymptotes.

where $\rho_1'=2k(x^2+y^2)^{\frac{1}{2}}$, etc., and $r'=2k(x^2+y^2+z^2)^{\frac{1}{2}}$.

When the source is confined to the line of symmetry from the corner, its relative power output is

$$W/W_f=1+3j_0(r'/\sqrt{3})+3j_0(r'\sqrt{\tfrac{2}{3}})+j_0(r'), \tag{27}$$

[see Fig. 3(c)].

The above results are tabulated in Table II, and some graphs are given in Figs. 3 and 6. The results were obtained by a different technique in a previous paper.[10] Contour maps of Eqs. (17) and (20) are being prepared with the aid of an electronic computer, and it is hoped to publish them in a later paper.

The curves in Fig. 3 are caused by interference, and depend only on the distance in wavelengths between source and reflector.

The power output variation can be considered to result from the source seeing a different radiation resistance R at different positions near the reflector, while the strength or volume velocity of the source remains the same. The ordinates in Fig. 3 can all be labeled $R/\rho_0 c_0$, as in Fig. 3(b).

The curves can also be considered from the standpoint of the method of images. For example in Fig. 2(a), when the source touches the reflector, it concides with its image: its strength is thus doubled, and its power

[10] R. V. Waterhouse, J. Acoust. Soc. Am. **27**, 247, 256 (1950).

TABLE II. Expressions for the directional pattern and relative power output of a simple source as functions of position (x,y,z) near 1-plane, 2-plane, and 3-plane reflectors at right angles.[a]

	1-plane reflector (yz plane)	2-plane reflector (xz, yz planes)	3-plane reflector (xy, xz, yz planes)
Directional pattern, DP	$\cos^2 a$	$(\cos a \cos b)^2$	$(\cos a \cos b \cos c)^2$
Relative power output, W/W_f	$1+j_0(x')$	$1+j_0(x')+j_0(y')+j_0(\rho')$	$1+j_0(x')+j_0(y')+j_0(z')+j_0(\rho_1')+j_0(\rho_2')+j_0(\rho_3')+j_0(r')$
	Along line of symmetry	$1+2j_0(\rho'/\sqrt{2})+j_0(\rho')$	$1+3j_0(r'/\sqrt{3})+3j_0(r'\sqrt{\tfrac{2}{3}})+j_0(r')$

[a] $a=kx\cos\alpha$, $b=ky\cos\beta$, $c=kz\cos\gamma$, $\cos\alpha=\cos\theta$, $\cos\beta=\sin\theta\cos\phi$, and $\cos\gamma=\sin\theta\sin\phi$. $\rho_1'=2k(x^2+y^2)^{\frac{1}{2}}$ etc. $r'=2k(x^2+y^2+z^2)^{\frac{1}{2}}$. $j_0(x')=(\sin x')/x'$. See Fig. 1 and Fig. 3 for graphs of the relative power-output functions above.

output integrated over a whole sphere would be quadrupled. However, only the radiation over $\frac{1}{2}$ a sphere can exist, i.e., in front of the plane wall, and the power output is thus double, not quadruple, the free-field value.‡

For similar reasons, the power output of a simple source goes up to 4 times the free-field value when the source is near a reflecting edge and up to 8 times near a reflecting corner.[11]

Figure 7 shows the interference of the sound-pressure waves from two point sources. The lower part of the figure shows the mean pressure distribution for each source along the line joining the two sources.

When the distance between the sources is less than one wavelength, the high intensity parts of the fields interact, and the total energy present is strongly dependent on the source separation. When the distance between the sources is a few wavelengths, the high-intensity central part of the field of each source is little affected by the interference of the weak outer field of the other source. As the separation of the sources increases, the effect of interference becomes negligible, and the power output of each source approaches the free-field value, as shown in Fig. 3(a).

One feature of the curves in Fig. 3 is that for certain source positions the power output is less than the free-field value. This occurs in all the regions of the graphs in Fig. 3 where the curve is below the dashed lines. In such regions the interference is predominantly destructive, and the power output of the simple source is not increased but diminished.

For example, in Fig. 2(c) the output is less than the free-field output when the source distance r from the corner is in the region $0.36\lambda<r<0.78\lambda$. If the source is fixed at a distance $r=1$ ft from the corner, the corresponding frequency range over which the output is diminished is approximately the octave 400–800 cps.

Figure 3(c) shows the interesting fact that the destructive interference of spherical waves near a reflecting corner can be almost complete. This is perhaps surprising at first sight, in view of the different geometry of the systems formed by the spherical waves and the rectangular reflectors.

When the simple source is moved out from the apex of the corner along the line of symmetry with respect to the three walls forming the corner, the power output reaches a minimum of about 7% of the free-field value at $r=0.49\lambda$. Thus the destructive interference is about 93% complete.

As this source is moved out from the corner, its output starts at 9 db above the free-field value, and then falls to 11.5 db below it in a distance of about $\lambda/2$. Thus at this point the drop in sound power output is 20 db from the initial value, a considerable reduction.

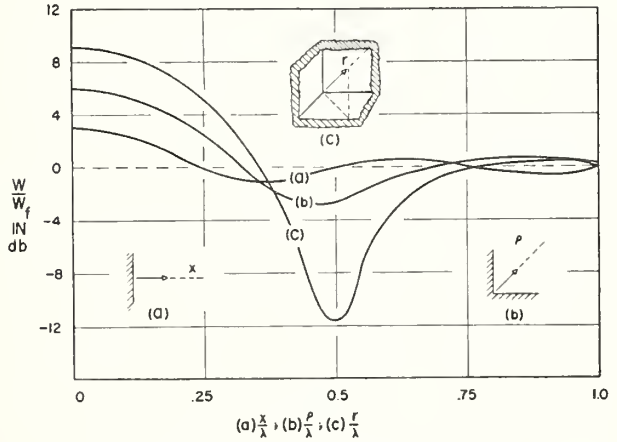

FIG. 6. Decibel plot of curves in Fig. 3.

APPLICATION TO ENCLOSURES

The above results for the power output of a source as a function of position near reflectors were derived under the assumption that the reflecting surfaces were of infinite extent, and the question arises as to whether the results are valid when the surfaces form part of an enclosure, such as a reverberation chamber or an ordinary room. When a source radiates in an enclosure, the sound can be reflected back and forth repeatedly, and evidently the impedance reflected back onto the source may differ substantially from the amounts computed above for nonenclosing reflectors.

In the next section of this paper, experimental evidence is given which shows that the results are valid in a large reverberation chamber. Here we will mention physical considerations which indicate that the results

‡ See reference 2. Lamb's *Hydrodynamics* contains an error on this point (see reference 9, p. 498, lines 5 and 6).

[11] H. F. Olson, *Elements of Acoustical Engineering* (D. Van Nostrand Company, Inc., Princeton, 1947), p. 28.

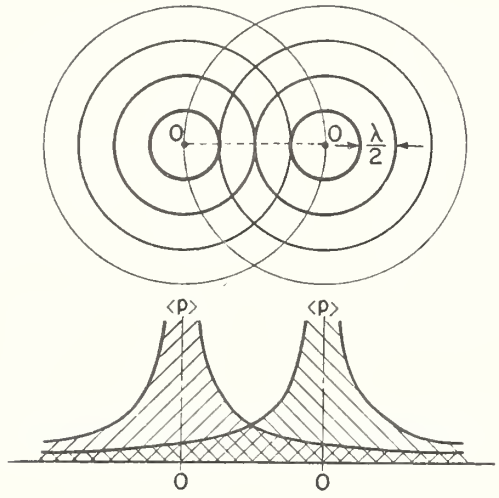

FIG. 7. Interference between the wave systems of two point sources. In the lower part of the figure the rms pressure $\langle p \rangle$ for each source is plotted along the line joining the two sources. Along this line $\langle p \rangle$ falls off according to an inverse first power law. λ is the wavelength.

are approximately true for any enclosure under two restrictions.

These restrictions are (a) that the surfaces of the enclosure other than those being considered as the reflectors must be distant at least a wavelength from the source, and (b) that the absorption in the enclosure must not be too small. Of course, the original limitations imposed on the reflecting surfaces associated with the source still hold, i.e., that these surfaces (c) must be rigid, and perfect or nearly perfect reflectors, and (d) must be large compared to the wavelength.

Under conditions (a) and (b), the reflected energy from the far walls of the enclosure (i.e., those walls not already considered to be associated with the source) will contribute little reflected impedance to the source.

As an example of the effect of a partial enclosure, we can consider the case of a simple point source equidistant from two plane parallel walls. The walls have a pressure reflection coefficient $R \leq 1$ which is independent of the angle of incidence of plane waves.

An analysis of this case is given in Appendix I. The power output of the source depends on the absorption of the walls, and the distance in wavelength separating the walls, as shown in Fig. 8. When the distance between the source and each wall exceeds the wavelength, the power output of the source differs from the free-field value by less than 1 db even when the wall absorption is low.

The image theory of the action of a reflecting environment on a source can be applied to a rectangular reverberation chamber, where the impedance reflected onto the source by the environment will vary with the distance of the source from the reflecting surfaces and the dissipation present. From physical considerations one would expect this to be the case whether the dissipation occurs at the walls or in the medium, and to be independent of room shape.

The next question to consider is whether quantitative criteria can be given for conditions (a) and (b) above. If the absorption of the enclosure is given, how many wavelengths away must reflecting surfaces be for the impedance they reflect on the source to be within given bounds?

Unfortunately, simple answers are possible only in simple cases, e.g., for a simple source near a corner, etc. It should be noticed that the directional pattern of the source is important here. The impedance reflected from a reflector onto a source with a pencil-shaped directional pattern is generally different from that reflected onto a source emitting spherical waves. For in the former case nearly all the sound radiated can be reflected back onto the source by a plane reflector several wavelengths away, while in the latter case only a small fraction can be so reflected.

The curves in Figs. 3, 5, and 8, and the experimental evidence in the next section indicate that for constant velocity sources of spherical waves, reflectors at distances greater than λ from the source will have small (less than 1 db or 25%) effect on the power output, even though the enclosure is very reverberant (e.g., average surface absorption coefficient about 3%).

For directional sources, the corresponding distance will depend on the orientation of the source, and may exceed λ. In such cases, and where the configuration of the reflecting surfaces is not simple, it may be easier to measure the variation of power output with position than to compute it.

EXPERIMENTAL RESULTS

Figure 9 gives some experimental evidence for these effects. The solid curve is a plot of Eq. (24), and gives the theoretical variation of the power output of a simple point source as it is moved away from two reflectors at right angles.

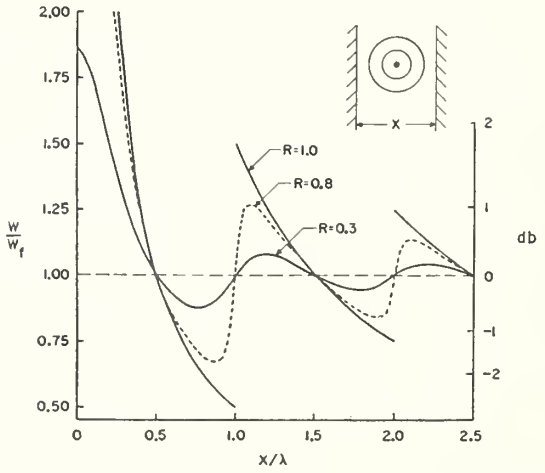

FIG. 8. Theoretical curve for the relative power output W/W_f of a simple point source equidistant from two plane parallel walls. x/λ is the distance in wavelengths between the walls. The walls have a pressure reflection coefficient $R \leq 1$ which is independent of angle of incidence for plane waves. The curve is a plot of Eq. (31).

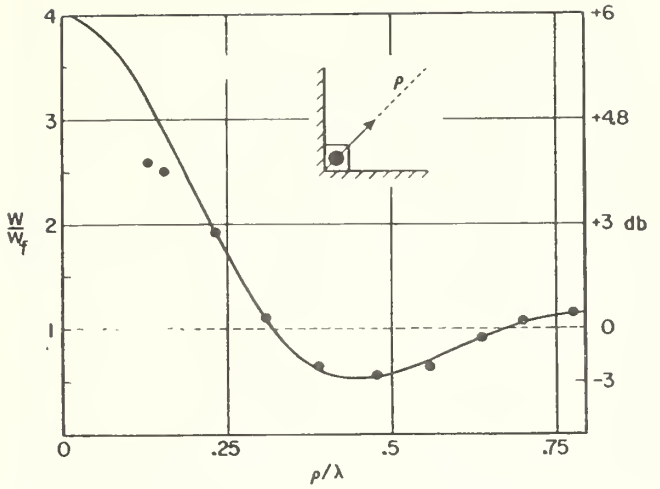

FIG. 9. Relative power output W/W_f of a simple source as a function of distance ρ along the line of symmetry from the origin at the vertex of a two-plane reflector. The solid line is the theoretical curve for a single frequency given by Eq. (24). The curve for a warbled frequency would be little different, see Fig. 5. The points are experimental data for a warbled signal 350±50 cps. The dashed line is the asymptote.

The black dots are experimental points, measured in the National Bureau of Standards reverberation chamber, two walls being used as the two reflectors.

Loudspeakers 4 in. in diam, mounted in small boxes filled with mineral wool, were used to simulate simple sources. They were driven with a warbled signal of frequency 350±50 cps, which gave a wavelength of about 3 ft, i.e., about 6 times the box diameter.

The voltage across each loudspeaker voice coil was kept constant throughout the experiment, in an attempt to make the loudspeaker cones vibrate with constant amplitude, as the theory required. The reasonable agreement obtained between theory and experiment (see the following, and Fig. 9) indicated that the loudspeakers used this way did resemble simple sources of constant strength, except for the near-field region.

One loudspeaker was put in each of the 4 lower corners of the reverberation chamber. The sound level in the chamber was measured by fixed microphones as the sources were moved along the floor away from the corners of the chamber. The measured sound levels gave the sound power output of the sources as functions of position; a uniform reverberant sound field in the central part of the chamber was assumed. Four sources were used instead of one to make the sound field more uniform. The walls of the reverberation chamber were brick, plastered and painted, giving a sound absorption coefficient of about 2% at this frequency.

Experimental points could not be obtained very near the corner owing to the physical dimensions of the loudspeaker box. The two experimental points shown nearest the corner are appreciably off the theoretical curve; this was probably caused by the departure of the loudspeaker field from the spherically symmetric field required by the theory. However, the rest of the data agree quite well with the theoretical curve.

In another experiment, one 4 in. diam loudspeaker was taken out of its box and used to simulate a dipole source. It turned out to be unnecessary to use 4 loudspeakers. A warbled frequency of 300±50 cps was used.

Figure 10 shows the results when the axis of the "dipole" was normal to a reflecting wall. The experimental curve is of the same type as that given by the theory for a dipole, and although there are significant differences between the 2 curves these can reasonably be attributed to the loudspeaker source differing from the ideal dipole source.

Similar experiments were made using 8 in. and 12 in. diam loudspeakers, and in all cases the main features of the theoretical curve were confirmed, but the details varied. It is quite entertaining to perform this experiment in a qualitative way, by moving a loudspeaker away from the wall of a reverberant room, the loudspeaker axis being normal to the wall. The increase in level from the minimum, obtained with the loudspeaker touching the wall, to the first maximum at a distance of about 0.3λ is quite striking.

Experiments with the axis of the loudspeaker dipole parallel to the wall were also performed, and give results which agreed with the theory in a similar way.

Additional confirmation that the theoretical results apply in a reverberation chamber is given by the experimental results already published[10] for the interference patterns that exist at the boundaries of a reverberant sound field.

In that case the source was fixed, and the microphone signal was measured as the microphone was moved along a certain path near the reflecting wall. If the chamber is kept constant, it follows from the theory of reciprocity that if the source and microphone are interchanged, and the source is now moved along the same path near the reflector, the microphone must record the same variation as it did before. This means the output of the source must vary with its position.

Thus the foregoing results for the source follow by reciprocity theory from the existence of the interference patterns in the reverberation chamber, subject to the restrictions that usually apply in reciprocity theory, for example that the source, microphone, and any absorbers present are linear.

An interesting example of reciprocity is that the variation in signal picked up by a velocity microphone when moved normal to a reflecting wall is the same as the variation in output of a dipole source moved along the same path, excluding the very-near-field region. This can be seen by comparing Fig. 4 and Eq. (21) of this paper with Fig. 9 and Eq. (6) on p. 253 of reference 10. Both the velocity microphone and the dipole source have the same figure-of-eight directional pattern, the first as a receiver and the second as an emitter. The orientation of this directional pattern with respect to the wall was the same in both cases, of course.

MEASUREMENT OF THE POWER OUTPUT OF A SOUND SOURCE

In considering some practical consequences of these effects, we first inquire how far one assumption used in deriving the above results will hold in practice. The assumption was that the volume velocity or vibration of the source was independent of changes in the impedance it worked into.

Apparently this is true for most sound sources met in practice, such as transformers, jet engines, appliances, and loudspeakers, although it is hard to find published evidence on this point. Such sources are not matched into the medium, and are little affected by impedance changes within the limits we are considering here.

The internal impedance of such sources is much higher than the radiation impedance of the air they work into. Thus they act analogously to constant current sources in electricity and deliver power proportional to the load resistance.

A related fact is that such sources are inefficient sound generators. A transformer whose whole mass is vibrating, dissipates much more energy in internal friction than in sound radiation, and its motion is evidently largely independent of the latter.

At the present time there is some interest in the measurement of the sound power output of sources; an American Standards Association standard on this topic is in preparation. In this paper we have shown that such measurements may be affected by the presence of a reflector in four ways. A reflector can change the power output, the directional pattern, the extent of the near field, and the radiation impedance of a sound source.

It is clear then that the position of the source relative to reflectors must be carefully considered in measuring its sound power output. One can measure the free-field value, or some other value near a reflector, or perhaps both. As an example, if a transformer is always used mounted on a concrete slab it is probably most useful to measure its power output in that position, and not bother with its free-field output.

In measuring the power output of a simple source by the reverberation chamber method, the source can in principle be placed anywhere in the reverberation chamber, and the results corrected to the free-field value (or the value corresponding to any other position near plane reflectors at right angles) by using the equations in Table II. However, the correction varies with frequency, and the composite correction for the power output of a broad-band source might be laborious to compute. Also the results would be restricted to simple sources.

Thus in practice if the free-field output of a source is required, it is probably most convenient to place the source and microphone(s) far enough away from all reflecting surfaces (walls, floors, ceilings, vanes, etc.) in the chamber for these interference effects to be negligible. For simple sources, the errors from these effects will in general be less than 1 db, if the source and microphones are placed at least $\lambda/2$ from the nearest boundaries, and at least 2λ, say, from the other boundaries of the chamber. See reference 10, p. 254.

For a source with a nonspherical-directional pattern of sound radiation, the corresponding distances will depend on the orientation of the source, and may exceed these. In such cases it may be more convenient to find the variation of power output with position by experiment than by calculation.

ACKNOWLEDGMENT

The author wishes to thank the members of the National Bureau of Standards, particularly Dr. R. K. Cook, for helpful discussions of various points in this paper.

APPENDIX I. OUTPUT OF A SIMPLE SOURCE BETWEEN TWO PARALLEL WALLS

A simple source is equidistant from two-plane parallel walls whose separation is x, and whose pressure reflection coefficient $R \leq 1$ is independent of the angle of incidence of plane sound waves.

At a point a small distance r from the source, on a line making an angle θ with the normal from the source to the reflectors, $r \ll x$ and $r \ll \lambda$, the potential caused by the direct and reflected waves is

$$\psi = (1/r)\cos(\omega t - kr) + (R/x)[\cos(\omega t - kx + kr\cos\theta) + \cos(\omega t - kx - kr\cos\theta)] + (R^2/2x)[\cos(\omega t - 2kx + kr\cos\theta) + \cos(\omega t - 2kx - kr\cos\theta)] + \cdots \quad (28)$$

$$= (1/r)\cos(\omega t - kr) + 2(A\cos\omega t + B\sin\omega t)\cos(kr\cos\theta) \quad (29)$$

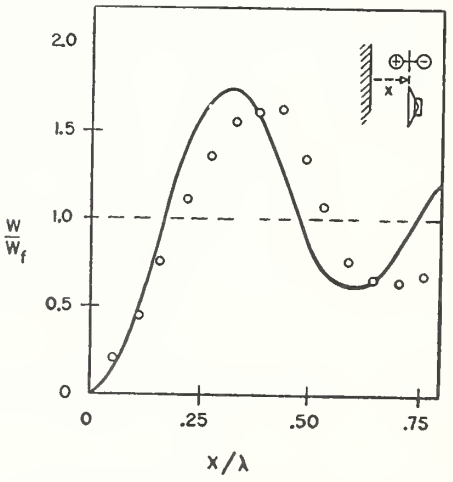

FIG. 10. The curve is taken from Fig. 4. The circles are experimental points measured in a reverberation chamber, for the relative power output W/W_f of a dipole source (axis normal to reflector) *vs* distance x/λ in wavelengths from a plane reflector. See text.

where

$$A=\sum_{n=1}^{\infty}(R^n/nx)\cos nkx$$

and

$$B=\sum_{n=1}^{\infty}(R^n/nx)\sin nkx. \tag{30}$$

From (29) we obtain the pressure $p=-\rho_0(\partial\psi/\partial t)$ and the radial particle velocity $v=\partial\psi/\partial r$. Next the mean value of pv, i.e. $\langle pv\rangle$, is taken, and this expression is integrated over the surface of the sphere of radius r. Then the power output of the source is

$$W=\lim_{r\to 0}4\pi r^2\int_0^{\pi/2}\langle pv\rangle\sin\theta d\theta$$

$$=2\pi\rho_0\omega k(1+2B/k)$$

i.e.,

$$W/W_f=1+(2/kx)\tan^{-1}[(R\sin kx)/(1-R\cos kx)],\qquad R<1, \tag{31}$$

where W_f is the output of the source in a free field.

For $R=1$,

$$W/W_f=1+(\pi/kx),\qquad 0<kx<2\pi$$
$$=1+(3\pi/kx),\quad 2\pi<kx<4\pi,\quad \text{etc.}$$

The solution is finite for all nonzero values of kx; the energy escapes between the walls. For $R=1$, the value of W/W_f jumps discontinuously from $\frac{1}{2}$ to $\frac{3}{2}$ at $kx=2\pi$, and jumps from $\frac{3}{4}$ to 5/4 at $kx=4\pi$, etc.

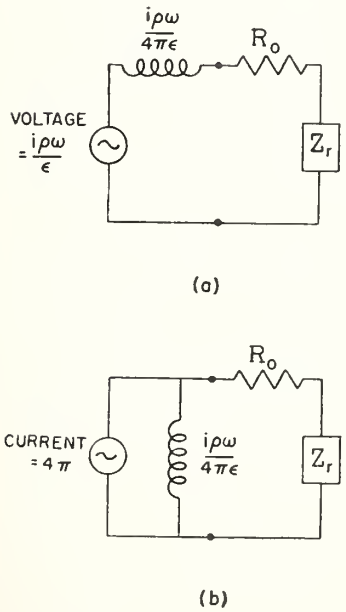

FIG. 11. Equivalent circuits for a sound source consisting of a small pulsating sphere of radius $\epsilon\ll\lambda$. Z_r is the reflected impedance caused by a plane reflector. In the $\lim_{\epsilon\to 0}$ the source becomes a simple point source.

Equation (31) is plotted in Fig. 8. Stenzel[12] gives expressions in the form of infinite series for the velocity potential in some more general cases of this type.

APPENDIX II. IMPEDANCE REFLECTED ONTO SIMPLE SOURCE BY PLANE REFLECTOR

The output of two point sources was calculated by Rayleigh[5] by finding the mean-squared pressure at a point in the far field, and integrating this over a spherical surface. A different method, based on the fact that the reaction of a source (or a reflector) on another source can be considered as a reflected impedance, is as follows.

We consider first a source similar to a simple point source, but with a small finite radius ϵ; the source is thus a pulsating sphere, with volume velocity independent of ϵ. The center of this sphere is distant x from a plane rigid reflector, $\epsilon\ll x$, $\epsilon\ll\lambda$.

The potential ψ at a distance r from the source center, $\epsilon<r\ll x$, λ, can then be written

$$\psi=(1/r)\exp i(\omega t-kr)$$
$$+(1/2x)\exp i(\omega t-2kx+kr\cos\theta). \tag{32}$$

The corresponding pressure and velocity are given by $p=-\rho(\partial\psi/\partial t)$, $v=(\partial\psi/\partial r)$, and the impedance seen by the source is

$$Z=p/4\pi r^2 v\quad\text{at}\quad r=\epsilon \tag{33}$$

$$=(\rho\omega k/4\pi)[1+(\sin 2kx/2kx)$$
$$+i(1/k\epsilon+\cos 2kx/2kx)], \tag{34}$$

dropping second-order terms. Thus $Z=Z_0+Z_r$, where Z_0 is the free-field value of the impedance, and Z_r is the reflected impedance. We then have

$$Z_0=\lim_{x\to\infty}Z \tag{35}$$

$$=(\rho\omega k/4\pi)(1+i/k\epsilon) \tag{36}$$

$$=R_0+iX_0. \tag{37}$$

Equation (34) is equivalent to the electrical circuit shown in Fig. 11(a) which can be transformed to that shown in Fig. 11(b). In the latter, the mass reactance proportional to $1/k\epsilon$ is shunted across the source and becomes infinite as the source approaches a point source of the same volume velocity, i.e., as $\epsilon\to 0$; the source then works into the free-field radiation resistance R_0, due to the medium, in series with the reflected impedance Z_r.

From (36), $R_0=\rho\omega k/4\pi$, and the free-field power output of the source is $\langle I^2\rangle R_0$, where $\langle I^2\rangle$ is the mean-

[12] H. Stenzel, Ann. Physik 43, 1–31 (1943).

574278 O - 61 - 54

squared volume velocity. The reflected impedance, due to the presence of the reflector, is

$$Z_r = R_r + iX_r \tag{38}$$

$$= (\rho ck^2/4\pi)[j_0(x') + in_0(x')] \tag{39}$$

$$= (\rho ck^2/4\pi)h_0(x'), \tag{40}$$

where $j_0(x')$ and $n_0(x')$ are spherical Bessel function of the first and second kind, and $x' = 2kx$; $h_0(x')$ is the spherical Hankel function. A plot of R_r *vs* X_r gives the usual impedance spiral, see Fig. 12. If the reflecting wall is not rigid, but gives a "pressure release" boundary condition ($p = 0$), the corresponding reflected impedance is the same as (40) but negative.

It is emphasized that these impedances[13] apply only to a simple point source. The same reflector will in general reflect a different impedance onto a different type of source, for example, a line source.

The power output of the point source in the presence of the reflector can be calculated in three different ways. (1) By integrating $\langle p^2 \rangle$, the mean-squared pressure, over a surface in the far field which encloses the source. (2) By integrating $\langle pv_{\text{normal}} \rangle$ over any convenient surface enclosing the source, as was done in Appendix I.

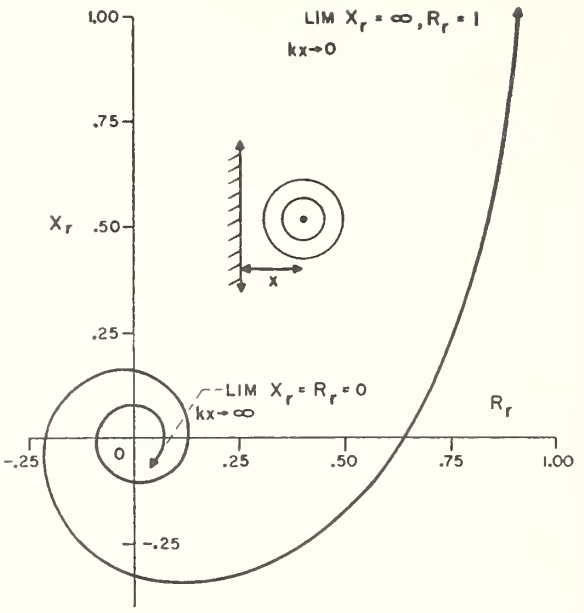

FIG. 12. Impedance diagram showing how the impedance $Z_r = R_r + iX_r$, reflected from a plane reflector onto a simple source, varies with kx.

(3) By taking the product $\langle I^2 \rangle \mathrm{Re}[\lim_{r\to 0}(p/4\pi r^2 v)]$ as above. From (34) this gives

$$\langle I^2 \rangle (\rho\omega k/4\pi)[1 + (\sin 2kx/2kx)] = W_f[1 + j_0(x')]$$

the same as (6).

[13] G. Laville and T. Vogel, Acustica 7, 101 (1957).

REVERBERATION CHAMBER METHOD OF MEASURING SOUND ABSORPTION COEFFICIENT

Raymond D. Berendt
National Bureau of Standards
September 1959

Description of Method:

In this method, the sound absorption coefficient is measured on a large sample of the material, about 72 square feet in area, mounted exactly as it would be in an actual installation. Owing to the size of the sample, variations of absorption due to non-uniformity of the product are largely averaged-out. Moreover, the material is measured in a sound field which approaches that existing in an actual large room. For these reasons, reverberation chamber coefficients are used universally for architectural purposes, and this test is accepted as the standard test by the acoustic materials industry.

The reverberation chamber at the National Bureau of Standards is a double wall rectangular enclosure with dimensions 25' x 30' x 20'. The walls are of brick, 8" thick and separated by a 4" airspace. The interior surfaces of the chamber are plastered and painted.

Measures are taken to produce the uniform distribution of sound energy required by theory. A pair of rotating vanes are mounted on a vertical shaft in the center of the chamber. Each vane measures approximately 10½' in height and 8' in width; the rate of rotation is 5 rpm.

The sound is produced by four 12" dia. loudspeakers fed with frequency modulated ("warbled") test signals, with approximately 10% band width and a modulation rate of 8 times per second. The speakers are enclosed in individual wooden boxes which are positioned on the floor in the four corners of the chamber. The faces of the speakers are tilted upward 45° with respect to the floor and directed toward the midpoint of the chamber.

The sound is picked up by four dynamic microphones positioned approximately 6' above the floor and about 4½' from the walls, at the four corners of the chamber.

After amplification and filtering, the microphone output is fed into a logarithmic recorder which automatically records the level of the decaying sound. Essentially linear decays covering a range of 50 db are obtained at the discrete frequencies. From this record the reverberation times are determined. First, the reverberation time of the chamber is measured when it is empty, and again when the sample is placed in the chamber. From the known constants of the chamber and the difference between the two reverberation times the absorption of the sample is computed, using the Sabine formula. The measurements are made with the chamber held at a minimum of 60% relative humidity and a temperature in the neighborhood of 70°F.

Area Effects:

The absorption of an acoustic material depends to a large degree on the size and shape of the sample tested. Because of diffraction effects, measurements on small samples indicate much greater absorption per unit area of material than do measurements on larger samples of the same material. It is not unusual, even on a sample as large as 72 square feet, to obtain apparent absorption coefficients greater than unity.

From a large number of measurements on areas of various sizes and different materials, it has been shown that the apparent absorption coefficient approaches a limiting value as the area of the test sample is increased indefinitely. Consequently, the sound absorption coefficients for surface materials obtained at the National Bureau of Standards are always reported after they have been corrected to what their calculated values would be for samples of infinite area. Such corrections cannot be applied to acoustic structures like space absorbers and irregularly shaped baffles, and the results in these cases are reported in terms of the number of units of sound absorbing power actually measured for the particular number and arrangement of the baffles used in the sound absorption tests.

Frequencies at which Absorption Coefficients are Measured:

Sound absorption coefficients are measured at 125, 250, 500, 1000, 2000, and 4000 cycles per second and are reported to the nearest 0.01. The noise reduction coefficient is the average to the nearest multiple of 0.05 of the coefficients for 250, 500, 1000, and 2000 cps.

Test Sample:

(a) Types of material: All types of material can be tested by this method, including acoustic structures such as space absorbers, suspended panels and irregularly shaped baffles.

(b) Size and Placement: In general, the test sample measures 72 square feet in area and 8' x 9' in plan. The sample is usually positioned centrally on the floor in one half of the reverberation chamber, with no part of the sample closer than 4 feet from reflecting surfaces, other than the floor.

(c) Mounting: The test sample is mounted in a manner closely simulating an actual installation. Some of the conventional types of mounting are listed on the last page of this pamphlet.

Accuracy of Test:

A statistical analysis of the accuracy of the sound absorption coefficient measurements, based on 10 different samples, indicated that the standard deviation is approximately 0.03 at 125 and 4000 cps, and 0.02 at the other frequencies.

Types of Mounting:

1. Cemented to gypsum wall-board. This is considered equivalent to cementing to plaster or masonry.

2. Nailed on 13/16" x 2" furring, 12" o.c., unless otherwise indicated.

3. Metal supports attached to 13/16" x 2" wood furring.

4. Laid directly on laboratory floor.

5. Nailed on 2 x 4's, 12" o.c., unless otherwise indicated.

6. Attached to metal suspension system, 3½" airspace (nominal 4") back of tile, unless otherwise indicated.

7. Acoustic tile nailed to 13/16" x 2" furring, 18" o.c., space between furring filled with mineral wool.

8. Nailed on 2 x 8's, 12" o.c., unless otherwise indicated.

9. Laid on 24 gauge sheet iron, nailed to 13/16" x 2" furring, 24" o.c.

10. Laid on 2 x 6's, 24" o.c., unless otherwise indicated.

Reprinted from The Journal of the Acoustical Society of America, Vol. 27, No. 6, 1072–1077, November, 1955

Measurement of Correlation Coefficients in Reverberant Sound Fields

Richard K. Cook, R. V. Waterhouse, R. D. Berendt, Seymour Edelman, and M. C. Thompson, Jr.
National Bureau of Standards, Washington, D. C.

(Received July 21, 1955)

Reverberation chambers used for acoustical measurements should have completely random sound fields. We denote by R the cross-correlation coefficient for the sound pressures at two points a distance r apart. $R=\langle p_1 p_2\rangle_{Av}/(\langle p_1^2\rangle_{Av}\langle p_2^2\rangle_{Av})^{\frac{1}{2}}$, where p_1 is the sound pressure at one point, p_2 that at the other, and the angular brackets denote long time averages. In a random sound field, $R=(\sin kr)/kr$, where $k=2\pi/$(the wavelength of the sound). An instrument for measuring and recording R as a function of time is described. A feature of this instrument is the use of a recorder's servomechanism to measure the ratio of two dc voltages. The results of correlation measurements in reverberant sound fields are given.

I. INTRODUCTION

REVERBERATION rooms, in which random sound fields can be established, are important tools in applied acoustics. Such rooms have long been used for measurement of the sound absorption coefficients of acoustical materials, and are useful also for determining the total output of sound radiators, the directivity index of microphones, and the sound transmission loss of building structures.

Two outstanding problems in applied acoustics are the production of random sound fields in reverberation rooms and the determination of whether or not a given sound field, once established, is random. We define a completely random sound field to be such that at every point within the field, plane waves near a particular frequency, having the same average intensity for all directions and phases, will have passed by after a sufficiently long time.

In this paper we shall consider a cross-correlation coefficient, R, for the sound pressures at two different points in a sound field, and we shall give a simple theoretical demonstration of how R varies with wave number $k(=2\pi/$the wavelength) and the distance r between the points in a random sound field. Conversely, the measured variation of R as a function of k and r in a reverberation room is a useful criterion for helping to determine whether or not a random sound field is present. On this account an instrument was developed for measuring and recording correlation coefficients as a function of time. A novel feature of this instrument is the use of a recorder's servomechanism to measure the ratio of two dc voltages.

Hershman[1] suggests that the cross-correlation coefficient defines the acoustic quality of a closed room more completely than the reverberation time does. Instruments have been devised for measuring correlation coefficients for various other physical phenomena.

[1] S. G. Hershman, Zhur. Tekh. Fiz. **21**, 1492 (1951).

Dryden[2] and his collaborators describe a system for measuring cross-correlation coefficients between velocity fluctuations at two points in a turbulent air stream. Brooks and Smith[3] constructed a recording correlation meter, for studying the propagation of radio waves, which utilizes data recorded on magnetic tapes. Seiwell[4] has devised a mechanical correlator which makes use of data recorded on paper tapes.

II. CORRELATION COEFFICIENTS FOR REVERBERANT SOUND FIELDS

We define the correlation coefficient between the sound pressures at two points A and B in a sound field as

$$R=\langle p_1 p_2\rangle_{Av}/(\langle p_1^2\rangle_{Av}\langle p_2^2\rangle_{Av})^{\frac{1}{2}}, \quad (1)$$

where $p_1(t)$ and $p_2(t)$ are the respective instantaneous sound pressures at time t at the two points, and the angular brackets denote long time average. Thus

$$\langle p_1 p_2\rangle_{Av}=(1/T)\int_0^T p_1(t)p_2(t)dt,$$

and

$$R=\int_0^T p_1(t)p_2(t)dt\Big/\left[\int_0^T p_1^2(t)dt\int_0^T p_2^2(t)dt\right]^{\frac{1}{2}}.$$

It will be interesting to point out a few simple properties of R. Schwarz's inequality shows that $-1\leqq R\leqq 1$. If $p_1(t)$ and $p_2(t)$ are both sinusoidal of the same frequency, but differ in phase by ϕ, so that $p_1=A\cos\omega t$, $p_2=B\cos(\omega t-\phi)$, then $R=\cos\phi$. Suppose a plane wave of wavelength λ passes over the points A and B and let ϑ be the angle between the normal to the wave fronts and the line AB (see Fig. 1). If $k=2\pi/\lambda$ and $r=$distance between A and B, then

$$R=\cos(kr\cos\vartheta). \quad (2)$$

The value of R for a random sound field can now be easily obtained from Eq. (2). Our definition of such a field assigns equal weights to all directions of the incident sound, and so the correlation coefficient is the average of Eq. (2) for all directions. This average is

$$\bar{R}=\int_0^{\pi}\int_0^{2\pi}\cos(kr\cos\vartheta)\sin\vartheta d\phi d\vartheta/4\pi$$
$$=(\sin kr)/kr, \quad (3)$$

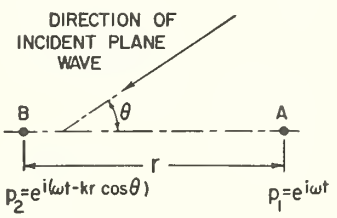

FIG. 1. Correlation in a plane wave.

[2] Dryden, Schubauer, Mock, and Skramstad, National Advisory Committee for Aeronautics Report No. 581 (1937).

[3] F. E. Brooks and H. W. Smith, Electrical Engineering Research Laboratory, University of Texas, Report No. 50 (May 1, 1951).

[4] H. R. Seiwell, Rev. Sci. Instr. 21, 481 (1950).

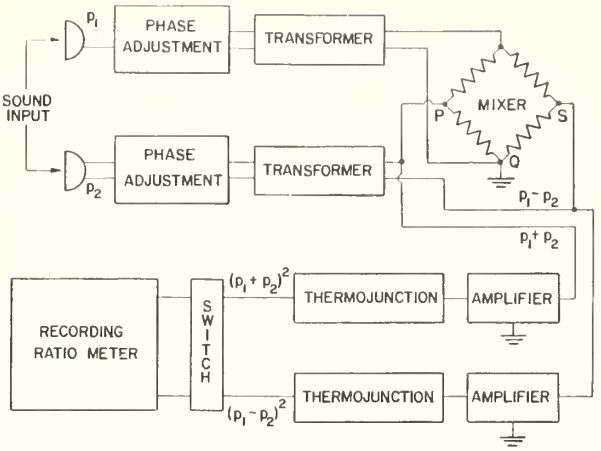

FIG. 2. Block diagram of recording correlation meter.

which is the cross-correlation coefficient for the sound pressure at two points, distance r apart, in a random sound field of wave number k.

If the sound field has a band of frequencies, all of equal weights, extending from k_1 to k_2, then the correlation coefficient for the two points is

$$\bar{R}=\int_{k_1 r}^{k_2 r}\sin u du/u(k_2 r-k_1 r)$$
$$=(\sin kr)/kr+\text{terms of the order of }[(k_2-k_1)/k]^2, \quad (4)$$

where $k=(k_1+k_2)/2$.

We can imagine a sound field to be random in two dimensions, so that the normals to the wave fronts all lie in the same plane, and all directions in the plane have equal weights. For such a field

$$\bar{R}=\int_0^{2\pi}\cos(kr\cos\vartheta)d\vartheta/2\pi$$
$$=J_0(kr), \quad (5)$$

where J_0 is the Bessel function of zero order.

The departure of any particular sound field from the three-dimensional random condition, as we have defined it, is shown by the departure of the measured variation of R as a function of k and r from the variation expressed in Eq. (3) and shown as the solid curves in Figs. 7, 8, and 9. The effect of such a departure from randomness in two particular cases can be seen by comparing Eq. (3) with Eq. (2) for plane waves and with Eq. (5) for a sound field random in only two dimensions. Equation (5) is plotted as the dotted curve in Fig. 9.

III. DESCRIPTION OF APPARATUS

One method of finding R, as defined in Eq. (1), is to measure separately $\langle(p_1+p_2)^2\rangle_{Av}$, $\langle p_1^2\rangle_{Av}$, and $\langle p_2^2\rangle_{Av}$. Then,

$$R=[\langle(p_1+p_2)^2\rangle_{Av}-\langle p_1^2\rangle_{Av}-\langle p_2^2\rangle_{Av}]/$$
$$2(\langle p_1^2\rangle_{Av}\langle p_2^2\rangle_{Av})^{\frac{1}{2}}. \quad (6)$$

This method was applied in some preliminary experiments with a single-channel amplifier system con-

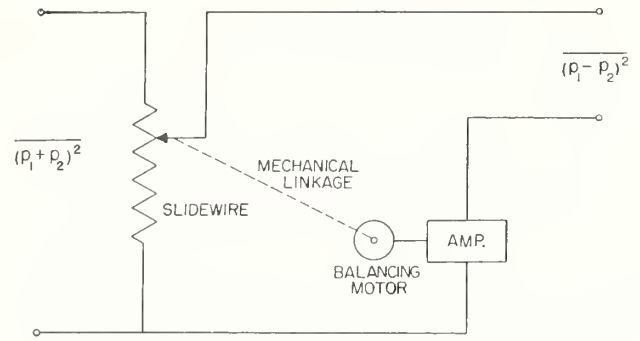

FIG. 3. Use of self-balancing recorder as a ratio meter.

sisting of a linear amplifier, a square-law (thermojunction) rectifier, and a galvanometer. Two moving-coil microphones, having approximately the same responses, were placed in the random sound field of the 15 000 cu ft reverberation room of the National Bureau of Standards. The galvanometer reading for $\langle(p_1+p_2)^2\rangle_{Av}$ at the desired frequency was got by connecting the two microphones in series with the amplifier system, and observing the galvanometer reading, $g\langle(p_1+p_2)^2\rangle_{Av}$, for a few minutes. The gain g is the constant ratio between the galvanometer reading and the time-averaged square of the sound pressure. Likewise observed for a few minutes were $g\langle p_1^2\rangle_{Av}$ and $g\langle p_2^2\rangle_{Av}$. The values of R were then computed by means of Eq. (6).

The observations on $\langle p_1^2\rangle_{Av}$ etc., had to be made consecutively since only one channel was available. This required (*a*) that g remain constant with time, and (b) that the acoustic output of the loudspeaker sources remain fixed. It was not difficult to keep constant the gain g of the microphone and amplifier system, but variations in the output of the loudspeaker system occasionally caused substantial errors in R. What was needed was a microphone-amplifier-computer system which would yield R immediately and record it as a function of time.

Such a system can be constructed from two channels, one yielding $S=\langle(p_1+p_2)^2\rangle_{Av}$ and the other yielding $D=\langle(p_1-p_2)^2\rangle_{Av}$. Consider

$$R=(1-D/S)/(1+D/S)=(S-D)/(S+D)$$
$$=2\langle p_1p_2\rangle_{Av}/(\langle p_1^2\rangle_{Av}+\langle p_2^2\rangle_{Av}). \quad (7)$$

If $\langle p_1^2\rangle=\langle p_2^2\rangle_{Av}$, then Eq. (7) is the same as Eq. (1). Even if $\langle p_1^2\rangle_{Av}$ and $\langle p_2^2\rangle_{Av}$ differ by as much as 40% (1.5 db) so that $\langle p_2^2\rangle_{Av}=1.4\langle p_1^2\rangle_{Av}$, the difference between values of the correlation coefficient deduced from Eqs. (1) and (7) will not exceed about one percent of R. A meter which indicates directly the ratio of two electric currents applied to it, can be used to indicate the ratio D/S which appears in Eq. (7). The scale of the ratio meter can be regraduated so as to read directly the values of R corresponding to various ratios. The possibility of using a commercially available electrical ratio meter was considered first, but it was finally decided to use the scheme described by Nier *et al.*,[5] in which a recording potentiometer is modified so as to indicate the ratio of two voltages. A block diagram of the apparatus (Fig. 2) shows how this was accomplished.

Pressure microphones (Western Electric type No. 633A) were used to pick up the sound signals at the two points A and B in the reverberation room, and two microphones were chosen whose outputs differed as little as possible in phase and amplitude. Even so, the microphone outputs differed in phase up to 20° at the higher frequencies and an adjustable RC circuit was used to balance out this difference.

The signals p_1 and p_2 were then passed through a step-up transformer into a bridge circuit which gave outputs (p_1-p_2) and (p_1+p_2). The principle of this bridge is shown in Fig. 2. The arms of the bridge were of equal impedance, and the output signals appeared across the resistors PQ and SQ, which were the grid resistors of amplifiers. The amplifiers were of conventional audio-frequency design, having variable gain up to 60 db. The output stages were transformer coupled to thermojunctions which performed a squaring operation.

The thermojunctions were capable of giving an output voltage of 50 mv, but outputs of less than 5 mv were used in order to obtain an accurate square-law characteristic. The time constant of each thermojunction was approximately 0.75 second, and this gave an averaging effect by minimizing fluctuations of a shorter time constant.

Having thus obtained signals $\langle(p_1-p_2)^2\rangle_{Av}$ and $\langle(p_1+p_2)^2\rangle_{Av}$, their ratio was recorded by a modified Honeywell-Brown potentiometer. Such instruments usually measure the ratio of the unknown voltage to a known voltage obtained from a standard cell. For the purpose of these measurements the standard cell was disconnected (see the article by Nier *et al.*[5]) and the signal $\langle(p_1+p_2)^2\rangle_{Av}$ substituted in its place, so that on leading in the $\langle(p_1-p_2)^2\rangle_{Av}$ signal as the unknown volt-

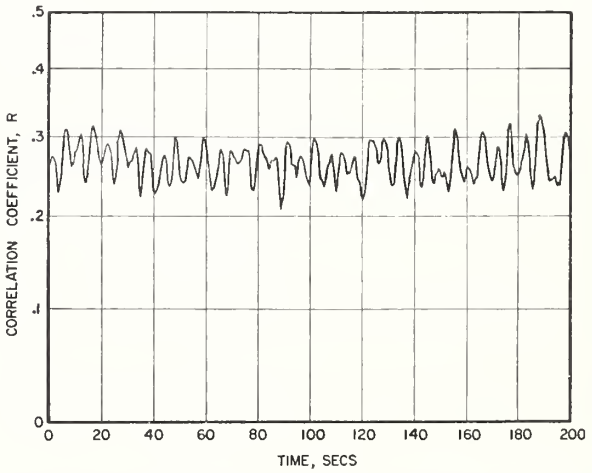

FIG. 4. Recordings of variations in correlation coefficient R with time. Microphones a fixed distance apart in a 15 000 cu ft reverberation chamber. Sound frequency 2000 cps, with ±10% warble 7 times/sec. Vanes rotating, with a 12 second period of rotation.

[5] Nier, Ney, and Inghram, Rev. Sci. Instr. 18, 294 (1947).

age the required ratio ρ was recorded (see Fig. 3). A scale was made for the instrument so that the correlation coefficient $R=(1-\rho)/(1+\rho)$ would be read directly from the recorder chart. In the case of negative correlation coefficients, where $\langle(p_1-p_2)^2\rangle_{Av}>\langle(p_1+p_2)^2\rangle_{Av}$, a switch was used to interchange the signals entering the potentiometer.

IV. RESULTS OF MEASUREMENTS

The apparatus described in Sec. III was used to measure correlation coefficients in the 15 000 cu ft reverberation chamber at the National Bureau of Standards, in order to compare them with the coefficients predicted theoretically in Eqs. (3) and (4) for a random sound field. The room, and the measures taken to diffuse sound in it, have been described elsewhere.[6] In brief, diffusion is achieved by frequency modulation of the audio signal and by use of large rotating vanes on which two loudspeakers are mounted.

Sound was produced in the room by two loudspeakers

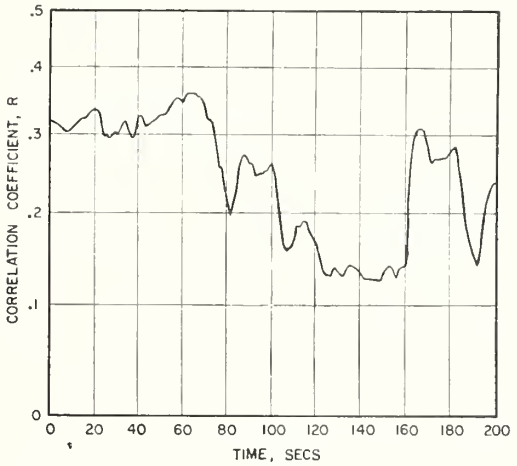

FIG. 5. Same as Fig. 4, except vanes stationary.

which were fed by a power amplifier preceded by a beat-frequency oscillator with a warbling device. The loudspeakers were driven with approximately 25 watts electrical power, which gave a convenient pressure level in the room. Theory indicated that the sound-pressure level should not affect the randomness of the sound field and the values of the correlation coefficients, and this was confirmed experimentally.

The microphones were suspended from a wire in the room, one being kept immobile in one position while the other was displaced from it a measured horizontal distance r along the wire. The two microphones were located about five feet above the floor, and the line joining them was in the north-south direction (parallel to the 25-ft wall). The correlation coefficient R was recorded for various values of r at each of three frequencies and R was plotted against kr, k being the wave number corresponding to the center frequency of the warbled band.

[6] L. L. Beranek, *Acoustic Measurements* (John Wiley and Sons, Inc., New York 1949), p. 864.

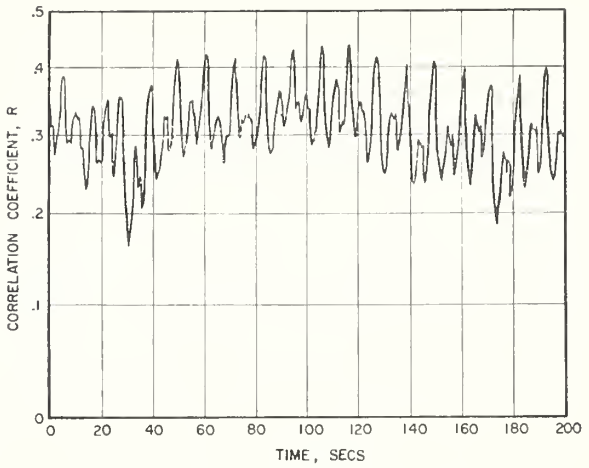

FIG. 6. Same as Fig. 4, except no warble.

At all settings of the microphones the records of R showed considerable fluctuations with time, a typical example being shown in Fig. 4. The most noticeable part of the fluctuation is periodic, the period of 12 seconds coinciding with the period of rotation of the vanes. This period corresponds to alternate peaks in the curve. The two sheet metal leaves of the vanes are symmetrically located relative to the axis of rotation, which suggests that the period of the recording in R should be six seconds. However, the two loudspeakers, one on each leaf of the vanes, might produce sound fields sufficiently different in amplitude and/or phase to account for the 12-second period. The details of the way in which the vane rotation causes periodicity in R is not known.

Figure 5 shows the lack of periodicity in the fluctuations of R when the vanes were not rotating, and Fig. 6 shows the increased variation in R when the warble was not used. These two records demonstrate the value of the warble and the rotating vanes in improving the randomness of the sound field in the reverberation chamber.

The fluctuations made it necessary to take records of sufficient length to ensure a reliable mean value for R.

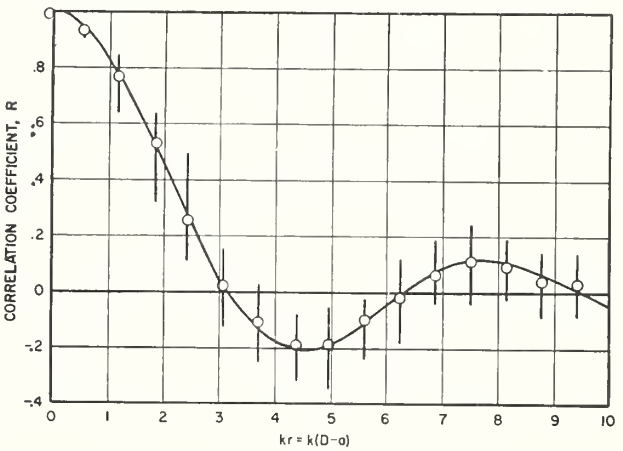

FIG. 7. Correlation coefficient R *vs* distance. Random sound field at 250 cps±10% warble, vanes rotating. ○ = measured R. Solid curve = $(\sin kr)/kr$.

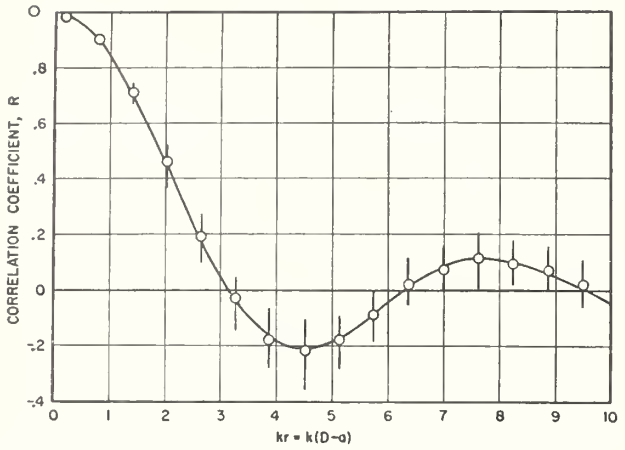

FIG. 8. Correlation coefficient R *vs* distance. Same as FIG. 7, except frequency = 1000 cps.

This mean value was estimated from the record as the value given by the straight line having equal areas of the R curve on either side of it. In the graphs (see Figs. 7–9) each value of R is plotted as a line whose length shows the amplitude of the fluctuation, with a circle on the line showing the mean value.

The fluctuations of R with time are of considerable interest in connection with the use of the reverberation chamber for measurement of sound power and sound absorption. They indicate that the sound pressures should be averaged over a time period of the order of at least 12 seconds in any measurements which depend on having a random sound field.

Correlation Coefficient Curves

Figures 7, 8, and 9 show the curves obtained in the National Bureau of Standards reverberation chamber at 250 cps, 1000 cps, and 2000 cps. The curves at 250 cps and 1000 cps are in good agreement with the theoretical curves for a random sound field, and the small divergencies that exist are within the limits of experimental error. This indicates that at these frequencies the sound field in the reverberation room approaches perfect randomness.

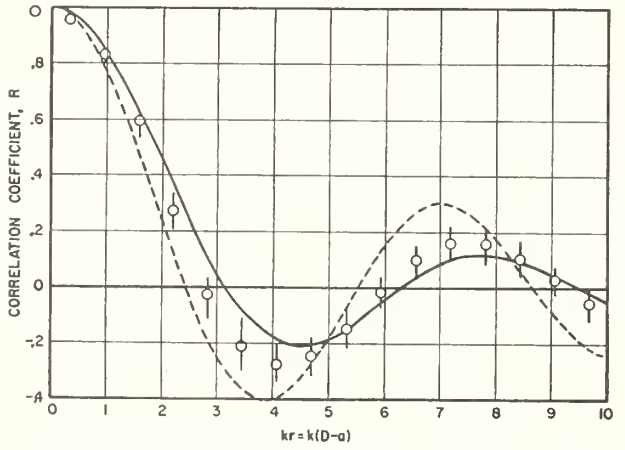

FIG. 9. Correlation coefficient R *vs* distance. Same as Fig. 7, except frequency = 2000 cps. Dotted curve = $J_0(kr)$.

At 2000 cps, the experimental points lie on a curve located between the curves derived for a random field and for a field in which only vibrations in a horizontal plane take place. This may mean that at this higher frequency, horizontal vibrations in the room predominate over vibrations in other planes giving a sound field that is not perfectly random. A partial explanation may lie in the approximate nature of the diffraction correction (see following).

The similarity of the two theoretical curves for a random field and a field in which only vibrations in a horizontal plane occur shows that large departures from randomness may cause relatively small changes in correlation coefficients and thus that measurements over a carefully chosen network of lines are necessary in assessing the randomness of sound fields from correlation coefficients.

The aforementioned measurements were made by moving the microphones along a horizontal line in the room. Similar results were obtained when the microphones were moved in other directions.

Diffraction Correction

In the graphs of the correlation coefficients shown in Figs. 7–9, a correction was made to D, the distance

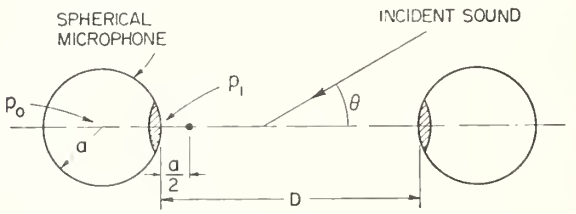

FIG. 10. Allowance for sound-wave scattering by microphones during correlation measurements.

between the front faces of the microphones, to allow for diffraction. This correction was derived as follows.

Figure 10 shows sound incident at an angle ϑ on a microphone, assumed to be spherical. In the absence of the sphere, in air, if the wave at p_0 is $e^{i\omega t}$, the wave at p_1 is $\exp[i(\omega t - ka\cos\vartheta)] \approx (1 - ika\cos\vartheta)e^{i\omega t}$, since $ka \ll 1$. With the sphere in place, the wave at p_1 becomes approximately $[1 - (3/2)ika\cos\vartheta]e^{i\omega t}$. Thus, the sphere retards the phase of the wave at its perimeter by $(1/2)ka\cos\vartheta$, owing to its diffracting effect. To correct this, we measure distances from a point $a/2$ in front of each sphere, instead of at the surface of each sphere.

Since $R = (\sin kD)/kD$ for air, then $R = \sin k(D-a)/k(D-a)$ for solid spheres of radius a in air.

Western Electric type 633A microphones were used in these measurements. These are roughly cylindrical in shape, three and one-half inches long, and of circular cross section, the radius being one inch. The aforementioned diffraction correction was used as being the best available, taking for a the radius of the microphone's circular cross section.

V. CONCLUSIONS

Correlation coefficients measured in a reverberation room agreed closely with the results predicted theoretically for a random sound field. It was demonstrated that this agreement was not obtained if either the warble tone or the rotation of the vanes was absent. Also, the agreement relied on averaging the sound field conditions over a sufficiently long time, which was found to be at least 12 seconds, the time of one complete rotation of the vanes.

The requirement that $R=(\sin kr)/kr$ in a random sound field is a necessary condition for such a field, but sufficient conditions are not yet available. We surmise that if the $(\sin kr)/kr$ condition is fulfilled when measurements are made along three mutually perpendicular directions, then the sound field will be random.

A practical question is, how can a sound field be made random if the $(\sin kr)/kr$ condition is not satisfied? For our 15 000 cu ft reverberation chamber, the experiments suggest that our rotating vanes ensure a random field, at least for frequencies between 250 and 2000 cps. Theoretical justification for the use of rotating vanes is not yet available.

Reprinted from The Journal of the Acoustical Society of America, Vol. 22, No. 6, 837–842, November, 1950

Calibration of Audiometers

E. L. R. Corliss and W. F. Snyder*
National Bureau of Standards Washington, D. C.
(Received May 19, 1950)

A general description is given of the procedure developed at the National Bureau of Standards for calibrating audiometers. The sources of calibration standards are presented, and there is a discussion of the physics underlying the present technique. Limitations on the validity of the threshold data are pointed out. A method for determining the calibration of audiometer earphones is described. Data on earphone response can be used to gain some insight into the malfunctioning of an audiometer, and the way in which this can be done is indicated.

INTRODUCTION

An audiometer is used to measure auditory threshold. The most widely used type of audiometer is an electronic instrument which generates pure tones of controllable intensity and frequency in an earphone (receiver). The setting of the intensity control when the tone is just audible to the person being tested is a measure of that person's hearing threshold. Whether the threshold is normal or not, however, can be decided only if the audiometer is calibrated in terms of the sound pressure at auditory threshold for people with normal, unimpaired hearing. The hearing loss of a person's ear is the ratio (expressed in decibels) of the sound pressure

* Formerly of the Sound Section, now with the Microwave Standards Section of the National Bureau of Standards.

at the threshold of audibility for that ear to the normal threshold pressure.

The following account is intended to describe a technique for calibrating audiometers, developed in large part at the National Bureau of Standards for the use of persons who manufacture or test these instruments. The procedure is embodied in the provisions of a proposed American Standard Specification,[1] developed by the American Standards Association and the National Bureau of Standards in a joint program.

THRESHOLD STANDARDS

Calibration of an audiometer is fundamentally the determination of the sound pressure produced by the earphone of the audiometer when it is placed on a standard coupler. The coupler consists of a heavy brass shell, enclosing a specified volume of air in an enclosure of simple geometric design. The earphone is placed over an opening in the coupler, and the sound pressures which it produces in the air volume are measured by means of a pressure-sensitive microphone. A diagram of Coupler No. 9A, designed at the National Bureau of Standards, is shown in Fig. 1. The volume of air within the coupler is about 5.7 cc, or approximately the volume within an average ear canal when an earphone is placed over the ear. The sound pressure in the coupler is measured with a calibrated condenser microphone. As shown, the coupler accommodates a Western Electric Type 640A or 640AA microphone; other condenser microphones may be used if they are of the same or smaller size and the coupler is modified so that it still encloses the same air volume.

The threshold voltage of an earphone at any frequency is the voltage which must be applied across its terminals to produce a sound pressure that is the threshold value for normal hearing at that particular frequency. The values in most common use in this country were determined by loudness-balancing from the data obtained during the National Health Survey of 1935–36.[2] From these data, the threshold voltages were determined for certain earphones (Western Electric Type 705A) kept at the Bureau. Because aging of the earphones might change the threshold voltages, the pressures produced in Coupler No. 9A by the audiometer earphones when threshold voltages were applied at their terminals were determined soon after completion of the survey. These pressures became the threshold standard for that particular type of receiver. They are independent of changes in response of the receivers.

The standard coupler pressures are not equal to the threshold pressures in the ear canal because the coupler does not present to the earphone an acoustic load

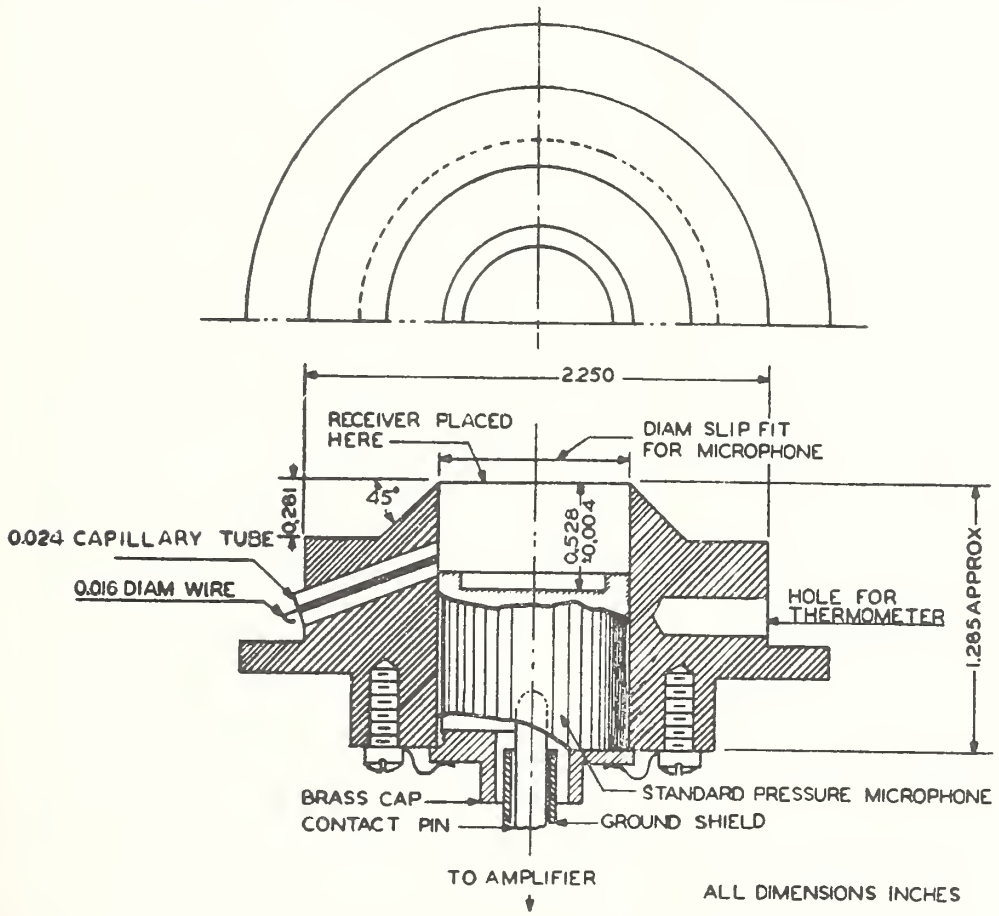

FIG. 1. N. B. S. Coupler No. 9A for calibration of audiometer receivers by means of Western Electric Types 640A or 640AA condenser microphones. The face of the receiver being calibrated rests on the upper edge with a coupling force equal to the weight of the receiver plus 400 g. The diaphragm of the microphone is located 0.528 in. (1.34 cm) below the upper edge of the cavity. The entire assembly is designed for use with a condenser microphone amplifier. (Volume = 5.7 cc.)

[1] American Standard Specification for Audiometers for General Diagnostic Purposes. Copies may be obtained from the American Standards Association, 70 East 45th Street, New York 17, New York.

[2] Reports of the National Health Survey, Hearing Study Series, Bulletin No. 5 (1935–36).

identical with that of the ear canal. Consequently, although the threshold pressures in the ear canal are presumably the same for all earphones, there is no reason to expect the standard coupler pressures to be identical for all types of earphones. A comparison is shown in Fig. 2. It was, of course, known from the beginning that the coupler did not duplicate the acoustic impedance of the ear. The ear presents additional loading due to compliance of flesh, and leakage of sound between the ear and the cap of the earphone, which are not provided by the coupler. It is this fact that makes it necessary to undertake the task of loudness-balancing to establish threshold coupler pressures for each new type of receiver. Until a coupler can be developed which presents a better replica of the ear's impedance over a wide frequency range, the alternative to loudness balancing is to make a complete threshold determination for each new type. If the acoustic load with which a human ear terminates the earphone were duplicated by the coupler, the standard threshold pressures would be identical with those in the average ear canal at threshold, and would be the same for all earphones designed to cover the ear.

Loudness balancing to establish standard threshold rests upon the premise that coupler standard threshold pressures are the same for all earphones of the same type. To determine standard coupler pressures for earphones of a new type, at least six subjects (12 ears) having approximately normal hearing make measurements of the voltages applied at the terminals of the new earphone and the standard earphone which will produce equally loud sounds at sound levels about 20 db above threshold. By combining these data with the measurement of the responses of the earphones when placed on Coupler No. 9A, the standard coupler threshold pressures at various frequencies for the new earphone may be found.

Standard threshold coupler pressures have now been determined for a number of different commercially available audiometer earphones. These values may be obtained from the Bureau by written request if they are needed by a testing laboratory. The threshold figures were originally determined for the octaves of 128 c/sec. Recently a change has been suggested in frequency standards for audiometer tests, from octaves of 128 c/sec. to octaves of 125 c/sec. This change is incorporated in the new American Medical Association and American Standards Association specifications. However, the National Health Survey measurements were made at octaves of 128 c/sec. The threshold pressures for 128 c/sec. octaves have been extrapolated to the new 125 c/sec. base by use of the minimum audible sound pressure curve determined by L. J. Sivian and S. D. White of Bell Laboratories.[3] At the present time, a project is under way at one of the sound laboratories in this country which will result in a direct determination

[3] L. J. Sivian and S. D. White, J. Acous. Soc. Am. 4, 288–321 (1933).

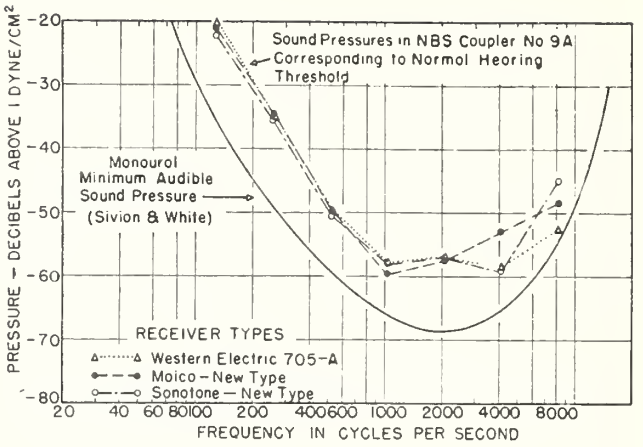

FIG. 2. Comparison of coupler pressures, corresponding to normal threshold for several types of commercial earphones, and the minimum audible pressure determination by Sivian and White. The form of the coupler pressure curve, derived from National Health Survey data, is in general agreement with the minimum audible pressure curve. Even if the coupler were to be a better replica of the ear, a difference of at least 5 db from the Sivian and White data is to be expected. The Sivian and White measurements were made with trained observers, and represent minimum rather than normal threshold.

of the auditory threshold pressures for 125 c/sec. octaves. Pending completion of that work, the extrapolated data are being used.

In Table I, standard threshold pressures in Coupler No. 9A are given for the Western Electric Type 705A earphone. Data for other types of earphones may be obtained by loudness-balancing against a Type 705A earphone or against other types for which standard threshold data are available. However, it might be well to consider that standard threshold data for receiver types other than the WE Type 705A were determined by a loudness-balance technique, and their use as comparison standards for loudness-balance implies an increase in the experimental uncertainty.

SOUND PRESSURE MEASUREMENT

To check the sound pressure output of the audiometer against standard threshold pressures, the sound pressure produced in Coupler No. 9A by the audiometer is measured at one hearing loss dial setting—usually 60 db—for each frequency. The audiometer is operated at the rated voltage stated by the manufacturer. Voltage regulation in the audiometer may be checked by making output pressure measurements at the extremes of line voltage likely to be encountered. The earphone is coupled to the condenser microphone through Coupler 9A. The microphone is connected to a preamplifier of the cathode follower type. An amplifier of fairly high gain is needed to bring the output of the cathode follower up to a level sufficient to actuate an output meter. If the same amplifier is to be used throughout the calibration procedure, gains of 80 to 120 db should be available.

A substituted voltage is used to determine the voltage output of the microphone. The arrangement for inser-

TABLE I. Standard threshold pressures in Coupler No. 9A. Western Electric Type 705A Receiver for octaves of 125 c/sec. and 128 c/sec. (Corresponding to the application of threshold voltages at the earphone terminals.)

Frequency (c/sec.)	Pressure (db above 1 dyne/cm²)	Frequency (c/sec.)	Pressure (db above 1 dyne/cm²)
125	−19.5	128	−20.1
250	−34.4	256	−34.9
500	−49.2	512	−49.5
1000	−57.3	1024	−57.5
2000	−57.0	2048	−57.0
4000	−58.9	4096	−58.5
8000	−53.1	8192	−52.3

tion of the voltage is shown in Fig. 3. With the hearing loss dial set at 60 db, the output meter is read. The hearing loss dial is then turned back to attenuate to a maximum the signal from the audiometer, and a calibrating voltage of the same frequency as that of the audiometer signal is inserted in series with the condenser microphone. The voltage is adjusted by means of a calibrated attenuator until the output meter reads the same as it did when the audiometer tone was being applied. From the amplitude of the calibrating voltage and the voltage response of the condenser microphone the sound pressure in the coupler can be computed. An attenuator of high quality should be used; the resistor across which the voltage is applied should terminate the attenuator with its characteristic impedance. A thermal voltmeter makes a good instrument for measuring the voltage at the input of the attenuator because it gives true R.M.S. readings.

ATTENUATOR DIAL

The pressure produced in the coupler at hearing loss dial settings other than 60 db can be derived from a calibration of the audiometer attenuator (hearing loss dial). For this measurement, the earphone is connected to the audiometer and placed on the coupler, so that the audiometer is loaded with the proper output impedance. A 500-ohm calibrated attenuator is placed in parallel with the earphone. (This impedance is suitable for many audiometer earphones, most of which have impedances of about 10 ohms.) The attenuator is connected to an amplifier and thence to a wave analyzer, which serves as a tuned amplifier and output meter. It is necessary to use a tuned amplifier in order to filter out electrical noise introduced by the high amplification required in the frequency range corresponding to maximum hearing acuity, since at those frequencies the signal voltages will be very low.

The hearing loss dial is checked against the calibrated attenuator by starting at the lowest hearing loss dial setting, with the parallel attenuator at a minimum setting. The difference between the dial steps and the attenuator steps is determined by adjusting the external calibrated attenuator to maintain the output meter readings at about the same point as the hearing loss dial is turned toward higher output settings.

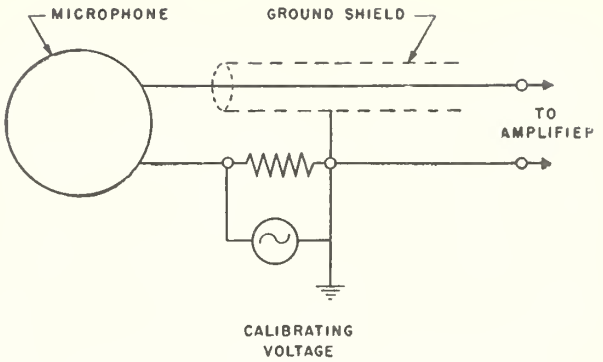

FIG. 3. Technique of introduction of calibrating voltage.

HARMONIC ANALYSIS AND FREQUENCY MEASUREMENT

It is usual for specifications to require that the fundamental of the pure tone signal from the audiometer be at least 25 db above the sound pressure of any harmonic. A harmonic analysis of the audiometer signal is performed with a modification of the assembly described above. The earphone is placed on the coupler, and its acoustic output is picked up by the condenser microphone, which is connected to an amplifier and a wave analyzer. The amplitudes of the various harmonics are measured by means of the wave analyzer.

The frequencies of the audiometer tones can be checked in various ways. They may be checked by audible beats against calibrated tuning forks, or against a calibrated beat frequency oscillator, using audible beats or Lissajous' figures on an oscilloscope. They may be compared with a standard timing frequency by means of electronic counters. The oscillator calibration can be determined by making use of the frequency broadcast from the National Bureau of Standards radio station WWV at Beltsville, Maryland. The standard frequency broadcast can also be used to provide the timing signal for the counters. Audio frequencies of 440 c/sec. and 600 c/sec. are broadcast on several radio carrier frequencies, including 2.5, 5, 10 and 15 Mc. Information on the broadcast schedule and means of making use of the standard frequencies may be secured by writing to the Central Radio Propagation Laboratory, National Bureau of Standards, Washington 25, D. C.

BACKGROUND NOISE LEVEL

The background noise level in the receiver output is evaluated by a weighted measurement of the sound level produced by the audiometer receiver in Coupler No. 9A when the audiometer is on, but the signal tone is interrupted. The relative weighting is that of the zero loudness level curve of intensity level *vs.* frequency This curve is shown in Fig. 4. The measurement is made for all settings of the hearing loss dial and at all settings of the frequency control, since it has been found that the general noise level varies somewhat with these settings. The characteristics of the power supply influence the

background noise in the audiometer. The noise background introduced by the power supply depends upon the voltage characteristics of the power line, which are described in terms of *TIF* (telephone influence factor).

The *TIF* of a power line is a numerical rating which describes the loudness of noise which it is likely to induce in telephone circuits. Methods for measuring *TIF* are described by Barstow, Blye and Kent.[4] The characteristics of a frequency weighting network for *TIF* measurements are shown in Fig. 5. An average for the *TIF* of power lines throughout the country has been found to be about 15 to 25 for a.c. lines and 80 to 120 for d.c. lines. Of course, if the *TIF* for the particular power lines on which the instrument is to be operated is known, the noise level should be measured when the instrument is operating on a line with that *TIF*, even though the *TIF* values may fall outside the limits of the average values given above.

EARPHONE RESPONSE

If an audiometer in service is suspected of giving incorrect readings, the source of trouble may often be located by making a measurement of the earphone's response. Audiometers are adjusted as a unit, for a particular earphone. If difficulty develops, and spurious threshold measurements are being made, it may be that the earphone has shifted in response, or that the output voltage of the audiometer has changed.

By combining the measured response of the earphone with the standard threshold pressures specified for that type of earphone, the voltages which should be applied to the terminals of the earphone to produce a given sound level may be found, and compared with the actual output voltages which the audiometer supplies across the earphone terminals. A level of 60 db above threshold might be chosen with advantage, so that the voltage to be measured is in a convenient range for accurate measurement. If the voltages put out by the audiometer depart systematically from the requisite values at all frequencies, or are low or high at only one particular frequency, the difficulty is probably in the audiometer circuit. Deviations due to drift in the earphone response usually show a dependence upon frequency.

The earphone response may be measured without a direct measurement of voltage, and this may prove to be a convenience when only part of a calibration is to be carried out on an audiometer. The method depends upon the use of a substitution voltage in the microphone circuit. The voltage is introduced across a resistor which is in series between the microphone shell and ground. Usually this is the terminal impedance of a low impedance attenuator (500 ohms or less), since stray pickup may give trouble if higher impedances are used. The reading of the output meter when the microphone is used as a sound detector is matched by applying a voltage across the terminal resistor which will give the same reading, and noting the attenuation which must be applied to the initial voltage. Since both the signal from

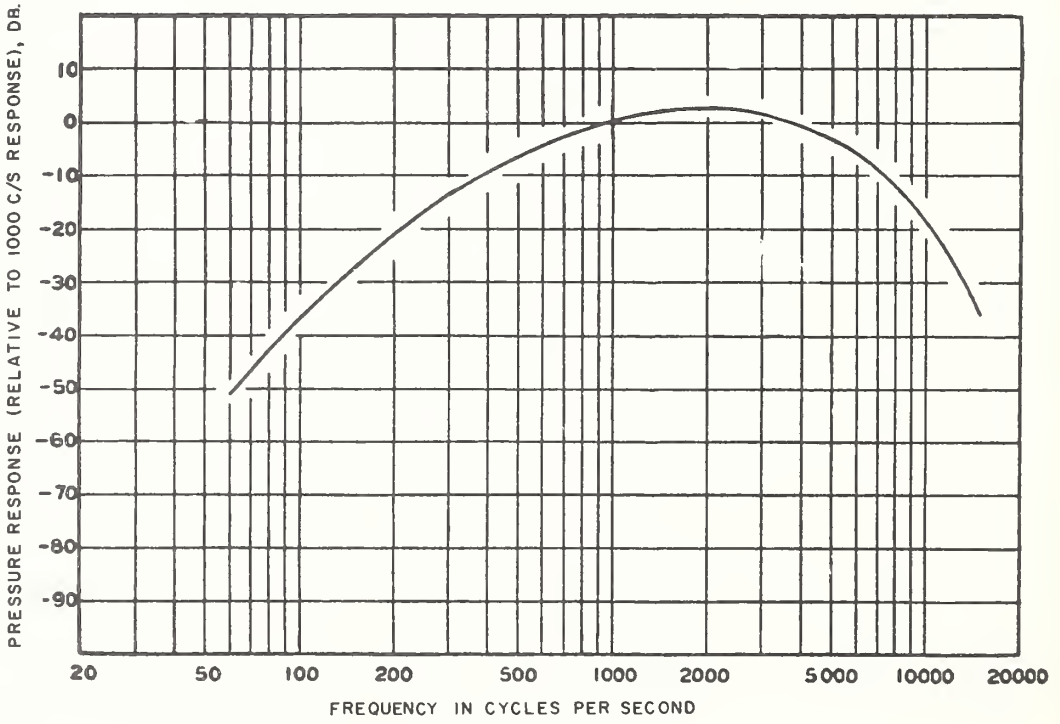

FIG. 4. Pressure response-frequency characteristic of equipment for measurement of noise in air-conduction receiver. (This curve is taken from that published in the article by L. J. Sivian and S. D. White), J. Acous. Soc. Am. 4, 313 (1933), and on page 124 of *Hearing* by S. S. Stevens and H. Davis (John Wiley and Sons, Inc. New York, 1938).

[4] Barstow, Blye, and Kent, Trans. A. I. E. E. 54, 1307 (1935).

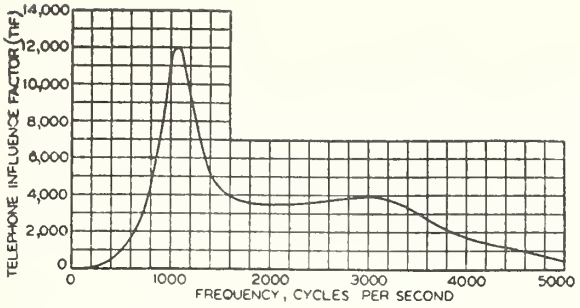

FIG. 5. Frequency weighting network for *TIF* measurements.

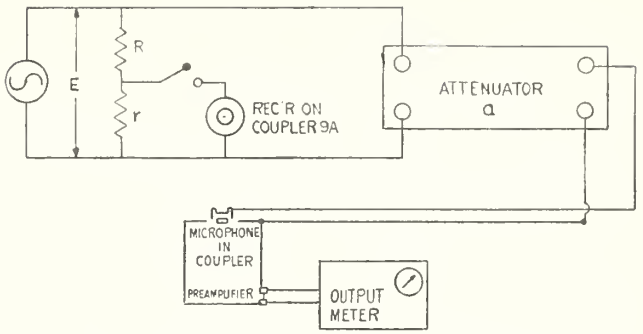

FIG. 6. Arrangement for earphone calibration.

the microphone and the signal from the attenuator are amplified via the same channel, the voltage output of the attenuator will be equal to the output voltage of the microphone. The network for this arrangement is shown in Fig. 4.

The value of resistor "r" (Fig. 4) should be made small so that the voltage across it is not changed appreciably when the earphone is shunted across it. A correction may be made if the impedance of the earphone is known. The value of "R" is chosen so that the attenuator readings are of convenient size. For low impedance earphones a convenient set of values is $R=10$ ohms and $r=0.1$ ohm.

The attenuator is set at a high value so that it contributes no signal when the earphone is serving as a source of sound, and the reading of the output meter is observed. The earphone circuit is then opened, and the attenuator is adjusted to give the same output meter reading.

Let the voltage applied to the input of the attenuator be "E." If the impedance of the earphone can be neglected, the voltage across the earphone is $(E\times r/R+r)$. Expressed in decibels, the voltage level across the earphone is then

$$20\log_{10}E+20\log_{10}r/(R+r).$$

Calling the observed attenuator reading "A," the substitute voltage is $20\log_{10}E-A$, which is the e.m.f. output of the microphone. The sound pressure level in the coupler is $20\log_{10}E-A-p$, where p is the response of the microphone in decibels relative to 1 volt-cm^2/dyne.

The response of the earphone in decibels relative to 1 dyne/cm^2-volt is the difference between the pressure level in the coupler and the voltage level across the earphone, when the levels are expressed in decibels. The response of the earphone represented by "P" is thus given by

$$P=20\log_{10}E-A-p-20\log_{10}E-20\log_{10}r/(R+r)$$

or,

$$P=-20\log_{10}r/(R+r)-A-p.$$

The computation of the threshold voltages from the standard threshold pressures in Coupler No. 9A and the earphone response is a simple subtraction. P, the earphone response, is given in decibels above 1 dyne/cm^2-volt. S, the standard threshold pressure, is given in decibels above 1 dyne/cm^2. The threshold voltage level, T, of the earphone is then given, in decibels above 1 volt, by the relation:

$$T=S-P.$$

The threshold voltage in volts can then be looked up as the antilogarithm of $T/20$ in a table of logarithms.

ACKNOWLEDGMENT

The procedure described in this paper has been evolved by the work of a large number of individuals. Auditory thresholds were determined on about 10,000 normal ears in the National Health Survey of 1935–36, under the supervision of Dr. Willis C. Beasley of the U. S. Public Health Service. An objective method for maintaining the threshold standards, and an earphone coupler for use in calibrating audiometer earphones were developed in the Sound Section of the National Bureau of Standards. Various improvements in technique have been contributed by several staff members during the course of their work on audiometry.

574278 O - 61 - 55

Reprinted from The Journal of the Acoustical Society of America, Vol. 26, No. 4, 506–509, July, 1954

Acoustic Impedance of a Right Circular Cylindrical Enclosure

Fernando Biagi and Richard K. Cook
National Bureau of Standards, Washington, D. C.
(Received April 12, 1954)

At low frequencies, the acoustic impedance of a right circular cylindrical enclosure (containing air, or other gases) is affected by the cooling effects of the walls. Analytical expressions for the temperature distribution have been obtained, and computations of the effect on the impedance are given in the form of plotted correction factors. These corrections are used in making absolute pressure calibrations of condenser microphones at low frequencies.

The solution presented for the average temperature distribution applies also to the heat-conductivity problem of a uniform volume distribution of sinusoidal heat sources, which are considered to be in phase, inside a cylindrical enclosure having isothermal walls.

In the past decade the reciprocity technique has been widely used for measuring the pressure response of condenser microphones to be used as sound pressure standards in air. The technique, which has been fully described in various places, makes use of a small enclosure, usually a right circular cylinder. The enclosure (called a coupler) contains air, or other gases, in which sound pressure is produced. The volume V of the enclosure (usually of the order of 10 cc) is chosen so that the pressure fluctuations occur adiabatically at audio frequencies. The acoustic impedance of the enclosure is made use of in the calculations. If B is the ambient barometric pressure, γ the ratio of specific heats of the enclosed gas, and ω the pulsatance of the sinusoidal adiabatic pressure fluctuations, then the impedance is $j\gamma B/\omega V$ ($j^2=-1$).

At infrasonic frequencies the acoustic impedance of the coupler is affected by the cooling effects of the walls. At sufficiently low frequencies, the sound pressure fluctuations occur isothermally, and the impedance is $jB/\omega V$. When the frequency is varied from the adiabatic to the isothermal region, the acoustic impedance can be regarded as a complex number which varies continuously from its adiabatic value to its isothermal value. The problem is to determine quantitatively what happens to the impedance at intermediate frequencies. As has been shown by F. B. Daniels[1] and others, the problem reduces to a determination of the space average of the temperature distribution within the coupler.

Expressions for the acoustic impedance of two parallel plates, a spherical enclosure, and an infinite cylinder have been obtained by Daniels.[1] Nomograms for them have been obtained by M. J. E. Golay.[2] Two infinite series solutions to the problem of the temperature distribution in a right circular cylindrical enclosure will be described in what follows.

SINGLY-INFINITE SERIES SOLUTION

If we apply the first law of thermodynamics and assume that the time-variations of the quantities involved are like $\exp(j\omega t)$, then it is possible to reduce the equation for the temperature distribution[3] to

$$\nabla^2 T=\beta^2(T-\alpha) \tag{1}$$

[1] F. B. Daniels, J. Acoust. Soc. Am. **19**, 569 (1947).
[2] M. J. E. Golay, Rev. Sci. Instr. **18**, 347 (1947).
[3] E. C. Wente, Phys. Rev. **19**, 333 (1922).

where

$$\beta^2 = j\omega\rho C_p/K, \quad \alpha = p/\rho C_p,$$

if the radiation term is neglected. In the above equations: C_p = specific heat at constant pressure; ρ = density of the medium; K = coefficient of thermal conductivity; p = amplitude of the sinusoidal sound pressure in the gas, constant throughout the coupler; T = variational temperature of the gas, which is a function of position in the coupler, and whose time-averaged value is zero; α = variational temperature (associated with the sound pressure) which would prevail throughout the gas if the walls had no cooling effect.

The boundary condition at the walls of an enclosure containing air is that the temperature is practically constant. Mathematically, if a = radius of the cylinder and l = its length (see Fig. 1), then

$$T=0 \text{ at } r=a, \text{ and } T=0 \text{ at } z=\pm l/2.$$

Substituting $\tau=(T-\alpha)/\alpha$, we have from Eq. (1)

$$\nabla^2\tau=\beta^2\tau.$$

Consider a cylindrical enclosure having isothermal walls, and containing a gas which is heated periodically by the absorption of thermal radiation, for example. The heat energy added is a sinusoidal function of time, and all parts of the gas receive heat at the same rate and in phase. Then the above differential equations apply, and the solution which we shall present for the temperature distribution in the acoustical problem, will be valid also for the heat conductivity problem.

Since the enclosure is axially symmetric the temperature will not depend on the angular parameter. We seek to construct a solution $\tau(r,z)$ by superposing solutions of the form $R(r)Z(z)$. We find that R and Z must satisfy

$$\frac{d}{dr}\left(r\frac{dR}{dr}\right)+\mu^2 rR=0,$$

$$\frac{d^2Z}{dz^2}+k^2Z=0, \quad k^2+\mu^2=-\beta^2.$$

Solutions to these equations are

$$R=CJ_0(\mu r)+DY_0(\mu r),$$
$$Z=A\cos(kz)+B\sin(kz).$$

The solution must be finite at $r=0$, therefore $D=0$. From the symmetry it is obvious that $B=0$. Thus choosing $C=1$, a general solution can be written as

$$\tau=\sum A\cos(kz)J_0(\mu r). \tag{2}$$

At the walls of the enclosure where $T=0$, $\tau=-1$ which can be substituted into Eq. (2). When $r=a$, τ becomes a function of z, which is equated to -1. When $z=\pm l/2$, τ is a function of r and this also must equal -1. In order to meet both conditions, we can use two series, each of which is zero when one variable

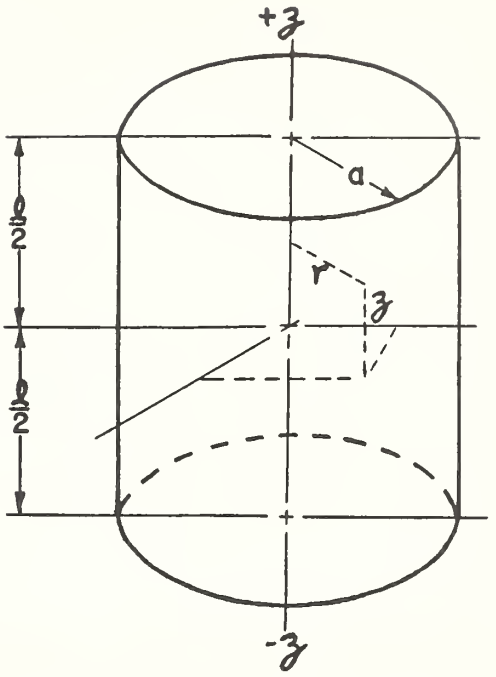

FIG. 1. Coordinates for a right circular cylindrical enclosure.

has the boundary value, and each of which has the value -1 when the other is zero. We will therefore divide the sum (2) into two sums over the indices n and ν. Thus

$$\tau=\sum_n A_n\cos(k_nz)J_0(\mu_nr)+\sum_\nu A_\nu\cos(k_\nu z)J_0(\mu_\nu r). \tag{3}$$

For $r=a$,

$$-1=\sum_n A_n\cos(k_nz)J_0(\mu_na)+\sum_\nu A_\nu\cos(k_\nu z)J_0(\mu_\nu a). \tag{4}$$

If we take $J_0(\mu_na)=0$, we shall be left with a sum over the index ν. We select A_ν and k_ν so that the sum is a Fourier series of cosine terms equal to the constant -1, each term being zero at $z=\pm l/2$. This gives us

$$A_\nu=4(-1)^{\nu+1}/lk_\nu J_0(\mu_\nu a), \quad k_\nu=(2\nu+1)\pi/l,$$
$$\mu_\nu^2=-(k_\nu^2+\beta^2), \quad \nu=0,\ 1,\ 2,\ 3,\cdots\infty.$$

We repeat this procedure at $z=\pm l/2$, where $r\neq a$. The sum over the index ν is zero, and we are left with the sum, over the index n, of Bessel's functions equal to -1. The μ_n and A_n are chosen so that the sum is a Fourier-Bessel series equal to -1. Hence

$$A_n=-2/\mu_naJ_1(\mu_na)\cos(k_nl/2), \quad J_0(\mu_na)=0,$$
$$k_n^2=-(\mu_n^2+\beta^2), \quad n=1,\ 2,\ 3,\cdots\infty.$$

Our solution for the spatial distribution of temperature in the coupler is

$$T/\alpha=1-\sum_{n=1}^{\infty}2\cos(k_nz)J_0(\mu_nr)/\mu_naJ_1(\mu_na)\cos(k_nl/2)$$

$$+\sum_{\nu=0}^{\infty}4(-1)^{\nu+1}\times\cos(k_\nu z)J_0(\mu_\nu r)/k_\nu lJ_0(\mu_\nu a). \tag{5}$$

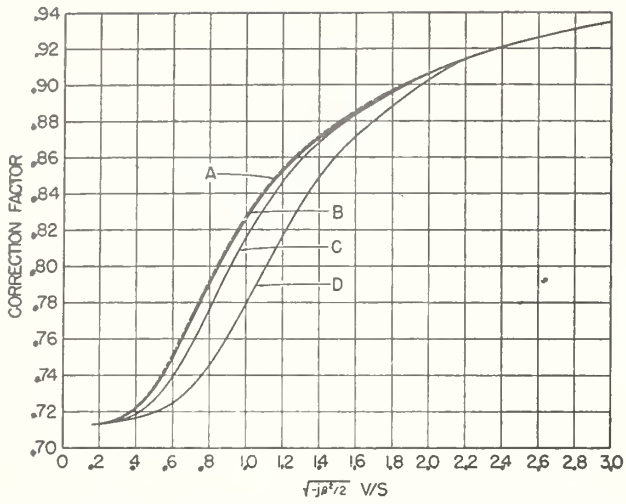

FIG. 2. Correction factors, for the cooling effects of the walls, to the acoustic impedance of various enclosures. V = enclosure volume, and S = surface area. A is for a right circular cylinder having $a/l = 1.185$. B is for a sphere. C is for an infinitely long circular cylinder. D is for two infinite parallel planes.

The average temperature within the enclosure is

$$\bar{T} = (2/a^2 l) \int_{-l/2}^{l/2} \int_0^a T r dr dz. \tag{6}$$

It can be shown that the integration of the infinite series (5) for T can be carried out term by term. The result is

$$\bar{T}/\alpha = 1 - 8 \sum_{n=1}^{\infty} \tan(k_n l/2)/k_n l(\mu_n a)^2 - 16 \sum_{\nu=0}^{\infty} J_1(\mu_\nu a)/\mu_\nu a k_\nu^2 l^2 J_0(\mu_\nu a). \tag{7}$$

DOUBLY INFINITE SERIES SOLUTION

The sum of a doubly infinite series of Fourier-Bessel functions can also be obtained as a solution for the temperature distribution. Consider the functions $\cos(\pi\mu z/l) \times J_0(\lambda r/a)$, where $\mu = 1, 2, 3, \cdots$, and λ = the positive roots of $J_0(\lambda) = 0$, arranged in ascending order of magnitude. These functions form a complete orthogonal set within the right circular cylindrical enclosure for functions $T(r,z)$ which are even in z. We write

$$T/\alpha = \sum_{\mu}^{\infty} \sum_{\lambda}^{\infty} A(\mu,\lambda) \cos(\pi\mu z/l) J_0(\lambda r/a). \tag{8}$$

On substitution of this expression into the differential equation (1), and making use of the expansion for unity, which is

$$1 = -\frac{8}{\pi} \sum_{\mu=1,3,\ldots}^{\infty} \sum_{\lambda=1}^{\infty} \frac{(-)^{(\mu-1)/2} \cos(\pi\mu z/l) J_0(\lambda r/a)}{\mu\lambda J_1(\lambda)}, \tag{9}$$

we find that μ takes on odd values only. The solution is

$$T/\alpha = -\frac{8}{\pi} \sum_{\mu=1,3,\ldots}^{\infty} \sum_{\lambda=1}^{\infty} \frac{(-)^{(\mu-1)/2} \beta^2 \cos(\pi\mu z/l) J_0(\lambda r/a)}{\mu\lambda J_1(\lambda)(\pi^2\mu^2/l^2 + \lambda^2/a^2 + \beta^2)}. \tag{10}$$

The average temperature $\bar{T}$ in the enclosure is

$$\bar{T}/\alpha = (32/\pi^2) \sum_{\mu=1,3,\ldots}^{\infty} \sum_{\lambda=1}^{\infty} \beta^2/\mu^2\lambda^2 \times (\pi^2\mu^2/l^2 + \lambda^2/a^2 + \beta^2). \tag{11}$$

The doubly infinite series (10) for $T(r,z)$ is uniformly convergent in the cylinder, $0 \leqq r \leqq a$, $-l/2 \leqq z \leqq l/2$. Its derivatives through the second order are all uniformly convergent within any closed region interior to the cylinder. Therefore they can be substituted into the differential equation (1). When this is done, it is found that the series (10) satisfies (1). It is evident that (10) satisfies the boundary conditions, and so it is a solution to the problem at hand.

If $l \to \infty$, so that the enclosure becomes an infinitely long cylinder, we find that both (5) and (10) reduce to the solution given by Daniels for such a cylinder. If $a \to \infty$, they also reduce to the solution for an enclosure formed of two infinite parallel plates.

CALCULATIONS

Expressions (5) and (10) are superficially different, but (5) can be readily transformed into (10) and vice versa. A similar remark applies to the two expressions for $\bar{T}$. Formula (7) can be directly transformed into (11) and vice versa. However it appears that Eq. (11) is more convenient for computation with SEAC (the National Bureau of Standards Eastern Automatic Computer). Equation (11) has the additional advantage over (7) that it does not require the use of transcendental functions with complex arguments.

Computations of the average temperature, for $a = 2.15$ cm and $l = 1.814$ cm, were made as a function of $-j\beta^2$. Pressure calibrations of condenser microphones are made at the Bureau of Standards in a coupler having these dimensions. The average temperatures were used to compute a correction factor to the acoustic impedance (see Daniels[1]). In Fig. 2 are plotted values

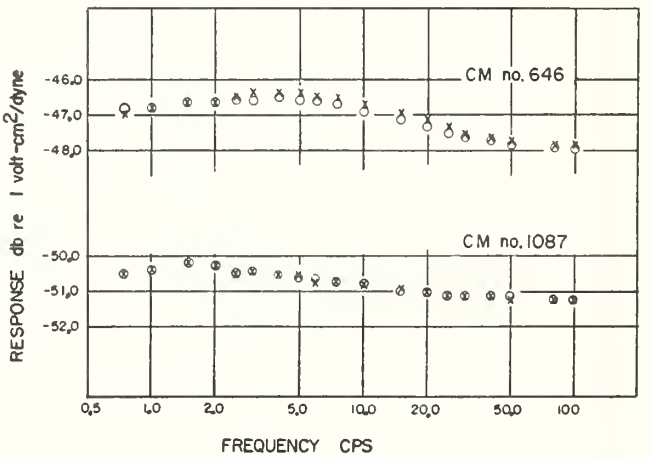

FIG. 3. Responses of Western Electric type 640AA condenser microphones Nos. 646 and 1087 at very low frequencies. ○ = calibration with a 3.18 cc coupler. × = calibration with a 20.1 cc coupler.

of the magnitude of the correction factor (for $\gamma=1.403$) *vs* the nondimensional parameter $(-j\beta^2/2)^{\frac{1}{2}}V/S$, where V is the volume and S the surface area of the enclosure, as curve A. All cylinders having the same ratio $a/l=1.185$ will have the same curve A. Curves B, C, and D are, respectively, those for a sphere, infinite cylinder, and parallel plates as obtained by Daniels. Curve A shows that the correction factor for this finite cylindrical enclosure approximates more closely that of a sphere rather than that of an infinite cylinder or that of parallel plates. Curve A is substantially different from the approximate curve given in Fig. 2 of the American Standard Method for the Pressure Calibration of Laboratory Standard Pressure Microphones, Z24.4-1949.

Curves for $a/l=0.2500$, 0.4138, and 0.7754 were also computed. In each of these cases, the curves were very close to curve A and curve B (for the sphere). The coding of Eq. (10) for numerical evaluation by SEAC will be kept available for some time to come.

APPLICATION TO CALIBRATION OF MICROPHONES

The pressure responses of two condenser microphones were measured utilizing the correction factor of Fig. 2 to the acoustical impedance. Two enclosures having different volumes were used, and the responses obtained are plotted in Fig. 3. The crosses represent calibration in the 20.1 cc coupler, and the open circles the calibration using the 3.18 cc coupler. A correction for the finite diaphragm impedance (0.1 cc equivalent added volume) was used for the calculations made with the 3.18 cc coupler. The results of these measurements and computations indicate that the correction for the temperature effect is small at these frequencies, but useful in that it permits calibration with either coupler with agreement within 2 percent.

Reprinted from The Journal of the Acoustical Society of America, Vol. 26, No. 5, 693-695, September, 1954

Pressure Calibration of Condenser Microphones above 10 000 cps

Bernard D. Simmons and Fernando Biagi
National Bureau of Standards, Washington, D. C.
(Received April 24, 1954)

A "plane wave" acoustic coupler and an electrical admittance method are described for the pressure calibration of condenser microphones in the ultrasonic frequency range. Calibration results are given for frequencies to 40 kc.

INTRODUCTION

THE standard method[1] for the pressure calibration of microphones utilizes an acoustic coupling cavity through which pressure is applied to the diaphragm of the microphone. Figure 1 is a diagram of the NBS 20-cc cavity, designed for use with the Western Electric 640AA condenser microphone, a "type L" standard.[2] Reciprocity calibrations using this cavity are made, with a precision of 1.0 percent and without correction for wave motion or diaphragm impedance, to a frequency of 3000 cps when the cavity is air filled and to 12 000 cps using hydrogen.

The frequency range is limited by the assumption that the ratio of the volume current produced by the driving transducer to the pressure over the microphone diaphragm, the "reciprocity parameter," is the lumped admittance $(\omega V/\rho c^2)$ of the volume V of gas enclosed. At low frequencies the pressure in the cavity is uniform and this assumption is valid provided the impedances of the transducer diaphragms are large compared to the cavity impedance. At higher frequencies, for which the wavelength is comparable to the cavity dimensions, wave motion complicates the pressure distribution. The result of departure from the lumped impedance assumption due to wave motion is shown by curve A of Fig. 2.

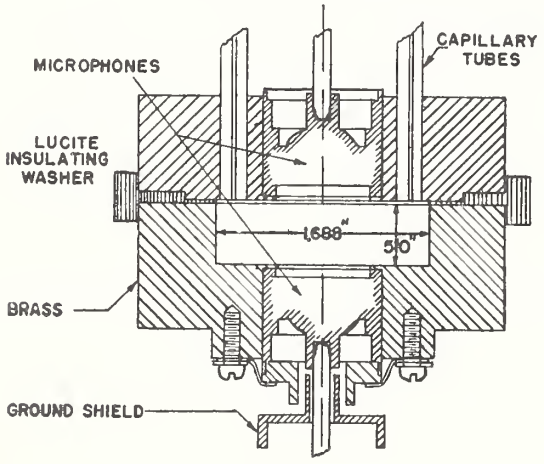

FIG. 1.

The "pattern factor" A is the experimentally determined response in the air-filled cavity relative to the response obtained in the hydrogen-filled cavity.

Considerations in the design of cavities for optimum performance without correction for wave motion are discussed in detail by Beranek,[3] with reference to the experimental work of DiMattia and Wiener. Cook[4] has discussed theoretically the relative influence of the length and radial modes, indicating an optimum ratio of diameter to length, which, for the 20-cc cavity, was experimentally determined to be 3.4/1. Reducing the size of the cavity with the same ratio of diameter to length leads to a slight improvement in frequency range. By a further reduction in size DiMattia and Wiener produced a design which, with a correction for diaphragm impedance, is intended for work in air to 6000 cps. This is probably the limit of what can be

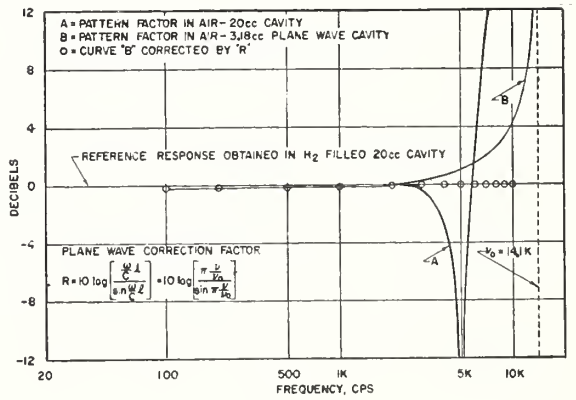

FIG. 2.

achieved with these microphones in the direction of maintaining uniform pressure in a cavity.

Plane Wave Cavity

A correction for wave motion in a cylindrical tube which takes into account both radial and longitudinal variation in pressure is complicated by interaction between the pressure and the modes of vibration of the diaphragms, and involves a knowledge of the diaphragm structures. A considerable simplification is obtained if the frequency of the first radial mode of the cavity is

[1] American Standard Z24.4-1949, American Standard Method for the Pressure Calibration of Laboratory Standard Pressure Microphones, American Standards Association, 70 East 45th Street, New York 17, New York.

[2] American Standard Z24.8-1949, American Standard Specification for Laboratory Standard Pressure Microphones.

[3] L. L. Beranek, *Acoustic Measurements* (John Wiley and Sons, Inc, New York), p. 140 ff.

[4] R. K. Cook, J. Acoust. Soc. Am. **16**, 102 (1944).

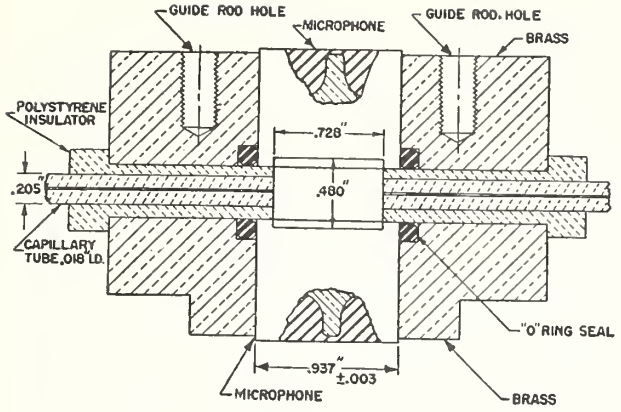

FIG. 3.

substantially above that of the first longitudinal mode. Then, if the impedance of the microphone diaphragm is sufficiently high, the pressure is uniform over the diaphragm surface, and, as is true at low frequencies, is still proportional to the volume velocity of the source.

The wave correction is the increase in pressure at the microphone diaphragm. The pressure and particle velocity in a plane wave are[5]

$$p(x)=Ae^{ikx}+Be^{-ikx}$$

$$u(x)=\frac{1}{\rho c}(Ae^{ikx}-Be^{-ikx}).$$

ρ is the density of the undisturbed medium. $k=2\pi\nu/c$ where ν is the frequency and c the sound velocity. Using the boundary conditions $u(l)=0$, corresponding to an effectively rigid diaphragm, and $u(0)=u$, the pressure at the microphone diaphragm ($x=l$) is

$$p(l)=2\rho cu/(e^{ikl}+e^{-ikl})=\rho cu/\sin kl.$$

At low frequencies as k approaches zero, $\sin kl$ approaches kl and the increase in pressure at higher frequencies is $kl/\sin kl$. In decibels, the correction to the response is

$$R=10\log_{10}\left[\frac{2\pi\nu l}{c}\Big/\sin\frac{(2\pi\nu)l}{c}\right].$$

With these considerations in mind the cavity shown in Fig. 3 was constructed for use with the W. E. 640AA microphone. The two cylindrical sections of the cavity are separated by a polystyrene insulator through which capillary tubes, shown in the cross section, lead into the cavity. The capillaries serve to introduce hydrogen into the cavity. The length l includes the microphone recesses, which vary slightly in depth from one microphone to another. The effective length can be accurately determined from the frequency ν_0 of the first (longitudinal) resonance ($l=\lambda/2$). For this purpose the foregoing expression may be put in the form

$$R=10\log_{10}\left[\frac{\pi\nu/\nu_0}{\sin(\pi\nu/\nu_0)}\right].$$

Using air ν_0 is about 14 kc and the frequency of the first radial mode is 22.7 kc. The volume of the cavity is 3.21 cc.

Response data up to 10 kc using the plane wave cavity are shown on Fig. 2. The zero reference level is the response obtained from the 20-cc hydrogen-filled cavity. Curve B is the uncorrected response obtained from the plane wave cavity when air filled. The circles are corrected values of B using the wave correction factor R. The agreement above 500 cps is close to 1.0 percent. Below 500 cps values diverge slightly (0.3 db) because of the finite impedance of the diaphragm.

The excellent results obtained to 10 kc/sec with the plane wave cavity using air, as compared with the usual results obtained with the 20-cc hydrogen-filled cavity, create a strong presumption that satisfactory calibration data can be obtained using hydrogen in the plane wave cavity at frequencies beyond 10 kc, where difficulties are encountered with the 20-cc cavity.

In order to check the cavity data above 10 kc, an alternate procedure was developed using electrical impedance data. This method will now be described.

Electrical Impedance Method

The performance of the condenser microphone is assumed to be described by the following pair of linear relations between the voltage e and current i on the electrical side and the pressure p and volume current u on the mechanical side.

$$e=\frac{1}{j\omega C_0}i+\frac{-\varphi}{j\omega C_0}u,$$

$$p=\frac{-\varphi}{j\omega C_0}i+Z_m u.$$

The parameter C_0 is the electrical capacitance with the diaphragm restrained from motion, and Z_m is the

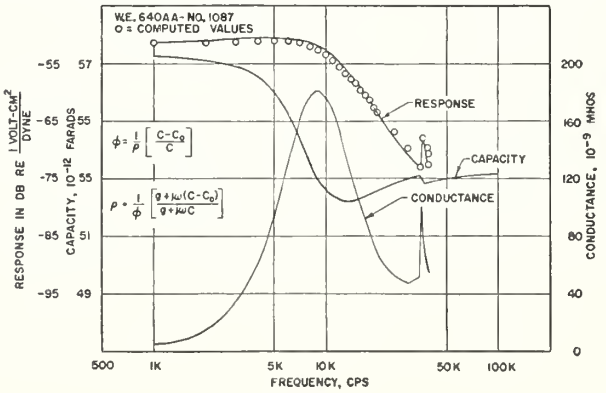

FIG. 4.

[5] P. M. Morse, *Vibration and Sound* (McGraw-Hill Book Company, Inc., New York, 1948), p. 238.

impedance on the mechanical side with the electrical side open circuited.

The parameter φ, which depends on the polarizing voltage and the geometry of the condenser plates, is considered in the following treatment to be independent of frequency.

The microphone response ρ, defined as the ratio of open-circuit voltage to pressure, is

$$\rho = -(e/p)_{i=0} = +\varphi/j\omega C_0 Z_m.$$

If the mechanical load impedance is small compared to Z_m, so that $p=0$, which experimentally was assured by using a quarter-wavelength coupling tube, the electrical admittance is

$$Y = (j\omega C_0) + \varphi^2 \Big/ \left(Z_m - \frac{\phi^2}{j\omega C_0} \right).$$

Solving for Z_m and substituting in the above expression for the response, we obtain

$$\rho = (Y - j\omega C_0) \Big/ \varphi Y = \frac{1}{\varphi} \left[\frac{g + j\omega(C - C_0)}{g + j\omega C} \right],$$

where $Y = g + j\omega C$.

The parameters C_0 and φ are determined experimentally in the following manner. At high frequencies, where the mass reactance of the diaphragm becomes large, the electrical capacitance approaches the blocked value C_0. The value of C_0 was measured at 100 kc. At low frequencies the conductance becomes small and the response is

$$\rho = C - C_0/\varphi\omega C.$$

φ can thus be determined from a value of response at low frequencies. Both φ and C_0 can be determined from values of response at low frequencies.

Figure 4 shows measured values of capacitance, conductance, and response and calculated values of response using the above method.

Figure 5 shows on an expanded scale data from three microphones. The zero reference value is the value of

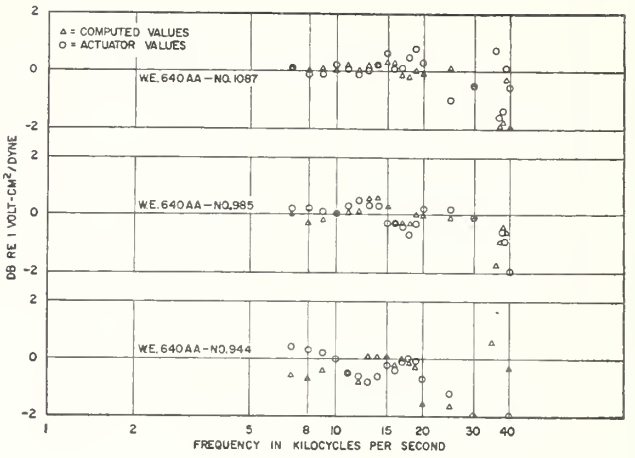

FIG. 5.

the response as measured by reciprocity using the plane wave cavity. The triangular points are the calculated values using the measured capacitance and conductance. The circular points are points which were determined by using an electrostatic actuator.[6] These results indicate a fair agreement between calculated and measured values of response up to about 40 kc.

CONCLUSION

With microphones having the diameter of the W. E. 640AA, a cylindrical enclosure permits calibration, within the usual accuracy (2 percent), up to about 10 kc in air using a correction based on plane wave transmission. With hydrogen in the cavity, results of about the same accuracy can be obtained up to 25 kc and with less accuracy up to 40 kc. Above 40 kc the radial mode of the coupler causes difficulties. However, values of response above 40 kc can still be calculated using impedance data with the assumption the microphone follows the simple four-terminal network theory on which the electrical impedance method is based.

The authors wish to express their appreciation to Dr. R. K. Cook for his interest and helpful suggestion in this work.

[6] Reference 3, p. 173.

Reprinted from The Journal of the Acoustical Society of America, Vol. 25, No. 5, 990–993, September, 1953

A Probe Tube Method for the Transfer of Threshold Standards between Audiometer Earphones*

Edith L. R. Corliss and Mahlon D. Burkhard
National Bureau of Standards, Washington, D. C.
(Received June 3, 1953)

To establish threshold standards for various types of earphones, from a set of threshold standards that has been determined for one particular type of earphone by a hearing survey, an empirical relationship must be found giving the sound pressures in the calibrating coupler corresponding to equal sound pressures in the ear. This has previously been accomplished by means of loudness balancing between earphones. The method described in this paper makes use of a direct probe measurement of the sound pressure developed by an earphone at the entrance to the ear canal. The experimental process is described and the results of tests to establish the equivalence of the probe method and loudness-balancing are given. In addition, several of the conditions under which loudness-balancing is carried out were investigated by the probe method. Equal loudness sensation was found to correspond to equal sound pressures at the ear, within the limits of experimental error.

INTRODUCTION

THE observed response of an earphone as a sound source is a function of the acoustic load with which it is terminated. Thus, if they differ in internal impedance, earphones that produce the same sound pressure in a human ear usually will not produce equal sound pressure in an ordinary calibrating coupler.† Our present difficulties with the standards for auditory threshold stem from the fact that we do not yet have earphone calibrating equipment that duplicates the physical conditions of measurements on the human ear.

The threshold voltage of an earphone at any frequency is the voltage which must be applied across its terminals to produce a sound pressure that is the threshold value for normal hearing at that particular frequency. Because earphones are calibrated on an "artificial ear" coupler, threshold standards for audiometric purposes are maintained in terms of the sound pressures produced by certain types of audiometer earphones in N.B.S. Coupler No. 9A.

The sound pressure produced by an earphone on the calibrating coupler is not in general the same as that which it would produce on an average human ear, because the coupler does not reproduce the acoustic load presented to the earphone by the ear. Since earphones of various types differ in their internal impedances, each type of earphone will have a different set of coupler pressures corresponding to the development of normal auditory threshold sound pressures in the ear. Therefore, once an auditory threshold survey has been made with a particular type of earphone, the results of this measurement cannot be applied directly to establish standards of normal threshold for earphones of any other type.

To obtain a set of threshold standards for a new type of audiometer earphone, either a complete new auditory threshold determination must be undertaken, or the threshold standards must be derived from existing threshold determinations on a standard type of earphone. This is achieved by determining what relationship of sound pressures in the calibrating coupler corresponds to the generation of equal sound pressures in the ear by both the new and the standard earphone. With present methods, it is not practical to establish for all types of earphones a relationship other than empirical between the response data obtained with a calibrating coupler and the actual response on the ear. As newer designs of earphones are developed, we have the problem of establishing normal threshold standards for them, so that they may be used in audiometry.

The method at present most generally used for the transfer of auditory threshold standards between earphones is a subjective technique, called "loudness balancing." In this process, the subject performing the "loudness-balancing" measurement is located in a sound-isolated room. He has at hand a signal generator, serving two calibrated voltage-dividing networks, each terminating in an earphone. The two earphones are attached to a single handset. One earphone is the standard earphone, for which threshold standards are known. The other earphone is the earphone for which threshold standards are to be determined by transfer from the known values for the standard earphone. The subject adjusts the signal applied to the standard earphone to a voltage level ascertained (from the known threshold standards and the calibration of the earphone) to produce a sound pressure corresponding to 20 db

* This work supported in part by the Office of the Surgeon General of the United States Army.

† A calibrating coupler, or "artificial ear," is a heavy-walled chamber of appropriate dimensions such that when an earphone is placed on it, the total enclosed volume is approximately the same as would be enclosed by the earphone on a human ear. The sound pressure in the coupler is measured with a pressure-sensitive microphone which forms part of the enclosure. See American Standard Z24.9–1949, American Standard Method for the Coupler Calibration of Earphones and American Standard Z24.5–1951, American Standard Specifications for Pure-Tone Audiometers for Hearing Diagnostic Purposes, available from the American Standards Association, 70 East 45 Street, New York, New York. An abridged version of Z24.9–1949 appeared in J. Acoust. Soc. Am. **22**, 609 (1950).

See also E. L. R. Corliss and W. F. Snyder, J. Acoust. Soc. Am. **22**, 837–842 (1950).

above normal auditory threshold. He then listens, in rapid alternation, to each of the earphones in turn, moving the handset rapidly back and forth so that first one earphone and then the other is presented to the same ear. While doing this, the subject adjusts the electrical signal applied to the second earphone until the sound it generates is equal in loudness to the sound he hears from the standard earphone. He then records the reading of the voltage divider on the second earphone. From this information, and from the calibration of this earphone on the calibrating coupler (NBS No. 9A or equivalent) the sound pressure in the coupler corresponding to normal auditory threshold for the secondary earphone can be computed. This determination usually is performed for at least six subjects having normal auditory acuity. It has been customary to make measurements for both ears of each subject.

It is possible, however, to use a probe inserted through the earphone cap to measure the actual sound pressures generated at the entrance to the ear canal,[1] and thus to determine the relative terminal voltages which must be applied to two earphones to produce equal sound pressures at the entrance to the canal. This objective method has the advantage of being simpler to carry out than loudness balancing, and it is much more rapid. By experiment, we have been able to show that this method gives substantially the same results as luodness-balancing. The probe method also makes it possible to investigate several of the assumptions upon which the entire idea of transferring threshold standards from one type of earphone to another is based.

ORIGIN OF PRESENT STANDARDS

The sound pressure standards for normal auditory threshold maintained by the National Bureau of Standards are derived from the National Health Survey of 1935–1936. The original measurements were determinations of voltages applied at the terminals of the audiometer earphones used in the survey. These voltages were averaged from the values that corresponded to threshold sensation for the 5000 persons whose auditory thresholds were being measured. The primary determination was thus given in terms of mean voltages applied to a specific group of earphones of particular design.

After completion of the survey, the threshold data were transferred to a group of standard earphones designed especially for stability in calibration. "Loudness balancing," as described above, was used to effect the transfer. The fixed voltages applied to the survey earphones were chosen to produce levels of 0 db, 20 db, and 40 db above average normal threshold. Although all three comparison levels yielded essentially the same results for the relative voltages to be applied to the new standard earphones, the data obtained by comparison at the 20-db level showed the least scatter. Hence the transfer process usually has been carried out at the 20 db level.

The loudness-balance measurement gave normal threshold values in the form of voltages applied at the terminals of standard earphones. Immediately after a loudness balance, the earphones were placed on a calibrating coupler and their response was measured. From the loudness-balance data and the earphone response, the sound pressures in the coupler that corresponded to normal auditory threshold were computed for the audiometric frequencies (octaves of 128 cps up to 8196 cps). These sound pressures constitute the normal threshold standard. They are independent of any subsequent aging of the earphone.

PHYSICAL FACTORS IN THE THRESHOLD STANDARDS

The usual calibrating coupler is a hard-walled cylindrical cavity closed at one end by a condenser microphone. When it is closed off by an audiometer earphone, the enclosed volume is approximately the same as the volume enclosed by an earphone held against a human ear. Comparison of the response of earphones on the ear and on the calibrating coupler shows that the coupler does not duplicate the acoustic load presented to the earphone by the ear.[2] For a given voltage applied to the earphone the sound pressures generated in the ear at low frequencies are significantly lower than the sound pressures generated in the coupler. Without phase measurements, it is not possible to decide whether this is due to leakage or to additional compliance.

At high frequencies there are sound patterns in both the ear and the coupler. At any single frequency, however, there is a fixed relationship between the sound pressure measured at the microphone in the coupler and the sound pressure present at the eardrum for each individual ear. The standard coupler 9A was designed so as to minimize pattern effects at particular fixed audiometric frequencies.

A set of threshold standards in terms of sound pressures in a coupler is valid for all earphones of a standard type provided that the high-frequency patterns in both ear and coupler remain constant for all earphones of the type. To maintain the pattern, all earphones of a given type must produce like geometric enclosures, although of course the enclosure on the coupler will differ from that on the ear. Constancy of pattern requires that all earphone cushions for a particular type of earphone be of controlled profile, thickness, and compliance; and that the distance from the front face of the moving diaphragm to the plane of the cushion be held constant.

If, in addition to maintaining the geometry of the

[1] F. M. Wiener and D. A. Ross, J. Acoust. Soc. Am. 18, 401–408 (1946).

[2] See, for example, M. D. Burkhard and E.L.R. Corliss, "The sound pressures developed by earphones in ears and couplers," National Bureau of Standards Report No. 1470 (Februrary 29, 1952).

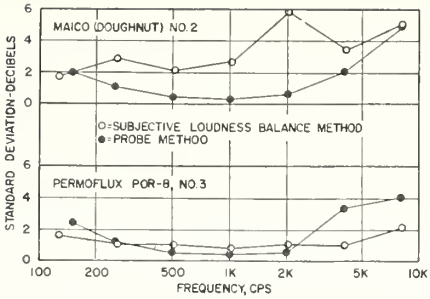

FIG. 1. Comparison of the standard deviations of the measurements on individual persons, arising from physical differences among individuals taking part in the measurements by each method. Six persons performed the loudness balance. Fourteen subjects were used in the probe method.

enclosure, the earphone is held against the ear with a constant coupling force, the acoustic leak at low frequencies for any individual ear will be approximately the same for all earphones of a particular type. However, it is in general not easy to meet this condition when subjective loudness balancing is being carried out, because the comparison and standard earphones must be interchanged rapidly. When threshold standards are transferred by means of the probe technique to be described here, the coupling force can be maintained constant.

So far as we know now, it can be assumed that auditory sensation for any normal individual is a function of the sound pressure presented at the eardrum. As we shall see later, our experimental measurements confirm this assumption. On this basis, the process of loudness balance is justified as a method for establishing a threshold standard for a new type of earphone. When a number of subjects, having hearing adequate for the task, determine what voltages applied to the earphone terminals give the same loudness sensation for both earphones, the sound pressures produced at the eardrum by the earphones are presumed to be equal.

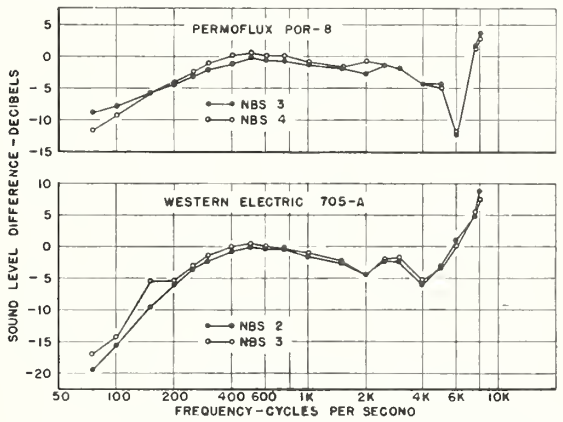

FIG. 2. A check on the basic assumption for transfer of coupler pressure standards for threshold. Difference between average sound level produced in ears and sound level produced in N.B.S. Coupler 9A, with the voltage applied to the earphone held constant. Each pair of curves was obtained with two earphones of the same type.

The loudness-balancing process is slow and unpleasant. It is practical only if it is done at relatively few frequencies and if the number of subjects in a jury is small, although the jury must be kept large enough to insure representative conditions. Because the determination is made at a rather low sound level, each subject must concentrate his attention on the sound, and can work only in especially quiet surroundings.

OBJECTIVE PRESSURE MEASUREMENT

Sound pressures developed by an earphone at the entrance to the ear canal can be observed by means of a probe microphone inserted through the earphone cap. These observations can be used to determine when two earphones, the comparison standard and the earphone for which threshold standards are to be determined, produce the same sound pressure at the entrance to the ear canal.

The transfer of threshold is carried out as follows: The response of each earphone is measured on the calibrating coupler. By probe techniques, the response is measured for each earphone when mounted on the ears of a number of human subjects.

TABLE I. Threshold transfer data. Sound pressures in N.B.S. Coupler No. 9A corresponding to normal auditory threshold.

	(Db re 1 dyne/cm²)			
	Permoflux type PDR-1 Maico "doughnut" cushion		Permoflux type PDR-8 MX41/AR cushion	
Frequency cps	Subjective	Probe	Subjective	Probe
125	−20.4 db	−25.2 db	−21.6 db	−25.4 db
250	−34.2	−34.5	−35.2	−34.7
500	−49.5	−48.7	−49.5	−49.0
1000	−59.4	−58.0	−57.5	−57.4
2000	−57.3	−56.4	−56.9	−58.8
4000	−53.0	−57.7	−59.5	−60.5
8000	−49.2	−52.4	−45.7	−48.1

Let us denote the response, expressed in decibels, of the standard earphone as measured on the coupler by C_s. Let the mean response of the standard earphone as measured on the group of human subjects be H_s. Designate the corresponding quantities for the new earphone by C_x and H_x, respectively. The coupler sound pressures in decibels corresponding to the standards of normal threshold for the new earphone are simply obtained by adding the quantity D to the standard pressures for the standard earphone corresponding to normal threshold, where

$$D=(C_x-H_x)-(C_s-H_s).$$

D is the ratio of the sound pressures developed by each of the earphones in the calibrating coupler for voltages at which they produce equal sound pressures in the ear.

EQUIVALENCE OF RESULTS

If the probe method is equivalent to loudness balancing, the results of the transfer of threshold by both methods should be substantially the same. For

two types of earphones on which the process of threshold transfer had been carried out by loudness balancing, the transfer of threshold was repeated by the probe technique. The responses of the test earphones were measured on both ears of 14 human subjects. The differences between these responses and those measured on the calibrating coupler (Coupler No. 9A) were computed. The same measurements were made for the comparison standard earphone (W. E. Type 705-A). Table I shows the threshold values for the two earphones as determined by both the loudness-balancing and probe techniques.

The group of persons used for the probe method was essentially different from the group used for loudness balancing. Only one person was common to both groups. The threshold values obtained by loudness-balancing are those determined originally when the transfer of threshold standards to these particular types of earphones was performed in our laboratory. From a study of the statistical variations involved, we conclude that the physical differences among individuals cause a major part of the differences shown here between the threshold transfer data determined by each of the methods.

The standard deviations for the two methods are plotted in Fig. 1. The deviation is that arising primarily from physical differences among individuals. The standard deviation for the loudness-balancing method also inevitably includes variations in judgment. That part of the deviation caused by variations among repeated measurements, on a single individual was found to be very small.

A measure for judging the difference between the results of threshold transfer by the two methods is is given by the factor $1/\sqrt{n}$ times the standard deviation, where n is the number of persons involved in the transfer measurements. This corresponds to a confidence level of 0.68. The differences appearing in Table I are significant in comparison to the uncertainties of the measurement only at 125 cps. This difference can be traced to the fact that the earphone is applied to the ear with controlled force when the probe method is used for transfer of threshold. In loudness balancing, the coupling force is not controlled. The force coupling the earphone to the ear has a strong influence upon the effective response of the earphone at low frequencies.[3]

The rather close agreement between the results of threshold transfer by the two methods indicates that the sensation of equal loudness corresponds directly to equal sound pressures at the entrance to the ear canal. This is a fundamental assumption upon which threshold transfer by loudness balancing is based.

Although the uncertainties of measurements are comparable for the two techniques, the probe method makes less demands on the subjects. In the probe technique, the subject is passive, and merely provides a suitable acoustic enclosure. Because no subjective judgment is involved, measurements can be made at convenient sound pressure levels. While the earphone is in place, there is a fairly good seal to the ear, and external noise is excluded to some extent. Measurements by the probe technique can be made quickly, and can be made at a much larger number of fixed frequencies than is feasible when subjective comparison must be relied upon. (Until further threshold determinations are made, however, threshold transfers are limited to the particular fixed frequencies at which the present standards were determined.) A large number of subjects can be used. Since immediate interchange of earphones to determine instantaneous equality is not required, the coupling force holding the earphone to the ear can be controlled.

[3] See reference 2, p. 14.

EXPERIMENTAL BASIS FOR TRANSFER OF THRESHOLD STANDARDS

The idea that threshold standards are applicable to all earphones of a given type implies that all earphones of the given type will show the same consistent difference between their performance on the calibrating coupler and their actual performance on the ear. This assumption can be checked easily by the probe technique. Several pairs of audiometer earphones were compared for this purpose. The results of the check are shown in Fig. 2.

Within the limits of experimental uncertainty, earphones of like type show the same ratio in response between their performance on the coupler and on the ear. This shows that the principle of establishing threshold standards in terms of sound pressure developed in a calibrating coupler is experimentally valid.

The same group of fourteen individuals was used throughout. It should be noted that the uncertainty of measurement sets a lower limit to the tolerance on sound-pressure outputs specified in audiometer adjustment. If the tolerance limits are set substantially closer than the experimental uncertainty in relating ear measurements to coupler measurements, the result does not contribute to the validity of audiometer readings.

Although the probe method for transfer of threshold standards is easier to carry out than loudness balancing, it is necessary with either method to make a transfer for each new type of earphone. Thus each time the design of earphones is changed, a number of human subjects must be assembled and a transfer of standards must be made. If a coupler that terminates earphones with the appropriate acoustic load can be made, it will be possible to make direct comparisons of earphones.

Reprinted from The Journal of the Acoustical Society of America, Vol. 26, No. 5, 679–685, September, 1954

The Response of Earphones in Ears and Couplers*

Mahlon D. Burkhard and Edith L. R. Corliss
National Bureau of Standards, Washington 25, D. C.

Applied voltage responses of seven earphones on both ears of fourteen people were obtained with the aid of a probe tube microphone inserted into the volume enclosed by the earphone. Treatment of the response data by the method of analysis of variance allowed separation of variance effects due to error in repeated measurement, dissimilarity between a given person's ears, and differences among individuals. The latter are found to be the most important effects to contend with in audiometric practice. Effects of application force on sound pressure output of an earphone are examined. Comparisons between the average response on ears and on three superficially different couplers are presented. Responses on ears were substantially different from responses on couplers over parts of the frequency range. Recommendations are given for improving the reliability of audiometric measurements by instrumental refinements.

I. INTRODUCTION

THE work reported in this paper results from a program being carried out at the National Bureau of Standards to improve the methods by which standards of auditory threshold are maintained. For audiometric purposes the threshold of hearing is defined as the minimum sound pressure at the entrance to the ear canal which produces a pitch sensation. A person's threshold of hearing by air conduction is usually measured with a pure-tone audiometer which introduces sounds at specific frequencies and controlled levels into the patient's ear by means of an earphone held over his ear.

The response of an earphone, i.e., its acoustic output as a function of electrical signal, depends upon the acoustic load with which it is terminated. The electrical signal required to produce arbitrary sound pressure levels is usually determined by means of an "artificial ear" coupler. The coupler connects the earphone acoustically to a microphone through a volume approximately the same as that enclosed by the earphone on an average human ear.

Artificial-ear calibrating couplers used in this country for calibration of audiometer earphones are of the hard-walled cylindrical volume type. It is well known that these couplers load an earphone with only volume reactance. As far as can be judged from response measurements, they simulate the ear's impedance over only a small portion of the audio-frequency range. The most satisfactory type of calibrating coupler for audiometry would be one which duplicates closely the termination presented by the average ear at all audiometric frequencies. This would obviate the procedures of making transfers of standard threshold pressure,[1] now needed when new earphone types are developed for audiometric use.

Other investigators have found much variation in the sound pressure under an earphone on an ear, both in regard to the uncertainty of repeated measurement on a person's ear and on the extreme range of pressures occurring in measurements on a number of individuals.[2,3] Thus it had seemed that development of calibrating couplers simulating the ear would not appreciably improve the precision of clinical audiometry. In the work described here the possible sources of the large variations were investigated by observing earphone responses under various conditions of application. One particularly useful result of this study was the finding that by controlling the force of application of the earphone to the ear, the uncertainty of repeated measurements on an ear could be materially reduced. Control of this factor also facilitated study of the other sources of variation.

Applied voltage[4] responses of earphones were studied on ears by means of a capillary probe tube microphone. These measurements and their significance are discussed in part II. In part III comparisons of earphone responses on three superficially different couplers are made.

In the following discussion we shall frequently refer to the sound pressure developed by an earphone in various circumstances. The applied voltage response of an earphone depends primarily on the conditions of earphone use or measurement. Thus, when observed responses differ, it is the result of production of different sound pressures for the same voltage at the earphone terminals.

* Supported in part by the Office of the Surgeon General, U. S. Army.

[1] For background see E. L. R. Corliss and M. D. Burkhard, J. Acoust. Soc. Am. 25, 990 (1953), and E. L. R. Corliss and W. Snyder, J. Acoust. Soc. Am. 22, 837 (1950); also, L. L. Beranek, *Acoustic Measurements* (John Wiley and Sons, Inc., New York, 1949), p. 367.

[2] OSRD Report No. 3105, Response characteristics of interphone equipment (Electro Acoustic Laboratory, Harvard University, Cambridge) (1944).

[3] F. M. Wiener and D. A. Ross, J. Acoust. Soc. Am. 18, 401 (1946).

[4] The applied voltage response of an earphone is defined as 20 times the logarithm to the base 10 of the absolute value of the ratio of the rms sound pressure generated to the rms voltage applied at the terminals of the earphone. This calibration procedure is outlined in the *American Standard Method for the Coupler Calibration of Earphones Z24.9–1949* (American Standards Association Inc., 70 East Forty-fifth St., New York 17, New York). Published in part in J. Acoust. Soc. Am. 22, 602 (1950).

II. EFFECT OF LOAD IMPEDANCE ON AN EARPHONE

Basically the system for which the response of an earphone is defined and the system by which the response is measured are similar in the measurements under discussion. Let us represent the earphone as a lossless generator of volume velocity shunted by an internal impedance Z_i. The ear or coupler is then treated as a load impedance Z_e in parallel with Z_i. In audiometric determinations it is desirable to produce the same ratio of sound pressure to applied voltage with a given earphone on all ears and in an appropriate calibrating coupler. To maintain the generator pressure output essentially independent of changes in its load Z_e, the internal impedance Z_i must be small relative to Z_e. The types of earphones we have tested do not appear to have internal impedances small enough over all the frequency range to keep the pressure response of the earphone the same for all ears.

III. EARPHONE RESPONSE ON EARS

(A) Experimental Procedure

For measurements on ears, a special head mounting was built to support an earphone and a probe microphone with its preamplifier. This mounting incorporated a calibrated sylphon bellows so that the force of the earphone against the ear could be controlled. It is shown in Fig. 1.

The probe microphone consisted of a capillary steel tube connected to a face-plate that screwed onto the front of a Western Electric 640AA condenser microphone. A small air volume was enclosed between the face-plate and the microphone diaphragm. Sound pressures at the far end of the probe were transmitted to the air volume and picked up by the microphone. The probe was calibrated both in free field and in a cavity against a standard condenser microphone. By inserting the probe into the space between the earphone cap and the ear, sound pressures there could be measured on each of a number of individuals over the frequency range from 75 to 8000 cycles per second.

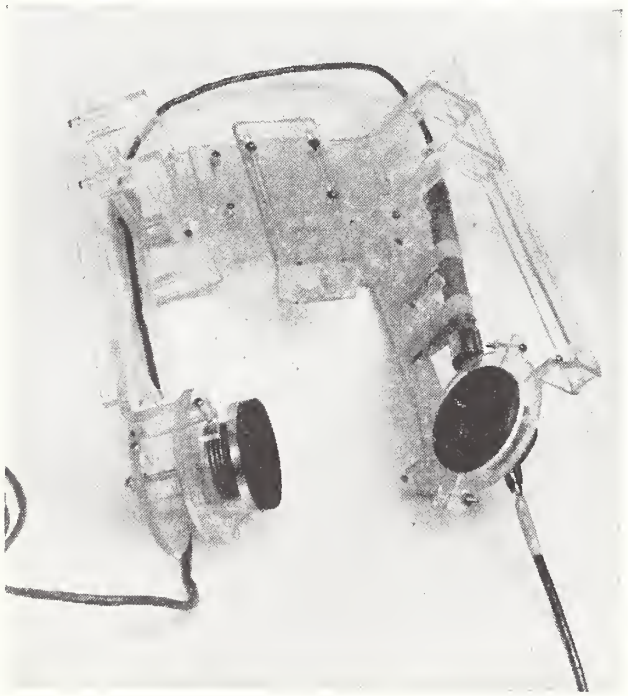

FIG. 1. Equipment for applying earphone to ear. Force is controlled by compression of sylphon bellows a known amount. The 640AA microphone and probe that detect the sound pressure are kept rigidly fixed relative to the earphone.

(B) Average Response of Earphones

Let us now discuss in detail the results of earphone response determinations on couplers and ears. Applied voltage responses were measured for seven standard earphones of four different types on the National Bureau of Standards calibrating coupler No. 9A and on both ears of fourteen individuals. The measurement for all seven earphones was performed twice on three of these subjects to evaluate the error of repeated meas-

TABLE I. Example of applied voltage response of earphones on ears. Data at three frequencies are given for a Permoflux Type PDR-8 earphone. Sequence of presentation has been arranged so that responses observed at 100 cps descend in magnitude. Application force on earphone is 1.5 kg.

Person	Ear	Earphone response, db re 1 dyne/cm²/volt Frequency—100 cps	1000 cps	5000 cps
EJ	L	39.2	40.7	32.8
BS	L	38.7	40.7	41.2
FB	R	38.5	40.7	32.8
AO	L	37.3	40.3	37.5
SE	L	37.0	40.5	35.6
RFB	L	36.9	39.0	28.1
FB	L	36.7	40.5	36.3
EC	L	36.6	39.3	31.9
JW	R	36.4	40.2	36.0
AO	R	36.1	39.6	40.3
RFB	R	35.7	37.4	24.6
EJ	R	35.4	38.9	36.2
EC	R	34.6	39.8	35.7
HL	L	34.2	37.0	39.1
SE	R	33.8	39.6	33.2
JW	L	33.7	40.3	35.3
BS	R	33.0	39.4	38.4
PB	R	32.6	40.7	37.4
MB	L	31.1	39.8	36.4
RDB	R	24.9	40.2	33.1
PB	L	24.5	40.4	38.0
HL	R	24.4	37.9	34.5
MB	R	23.6	40.6	36.3
WK	R	21.2	40.7	32.8
CR	L	20.1	39.9	40.2
RDB	L	19.7	41.7	35.8
WK	L	12.9	39.5	40.6
CR	R	11.7	42.7	29.1
Average response		30.7	39.9	35.4
Minimum response		11.7	37.0	24.6
Maximum response		39.2	42.7	41.2
Spread of observations		27.5	5.7	16.6

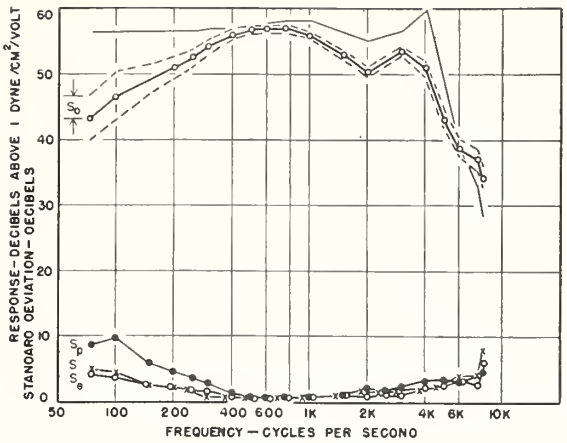

(a) Permoflux Type PDR-1 (MX41/AR cushion)

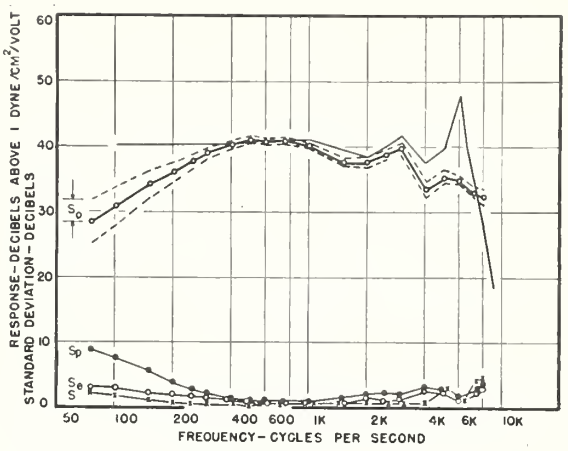

(b) Permoflux Type PDR-8 (MX41/AR cushion)

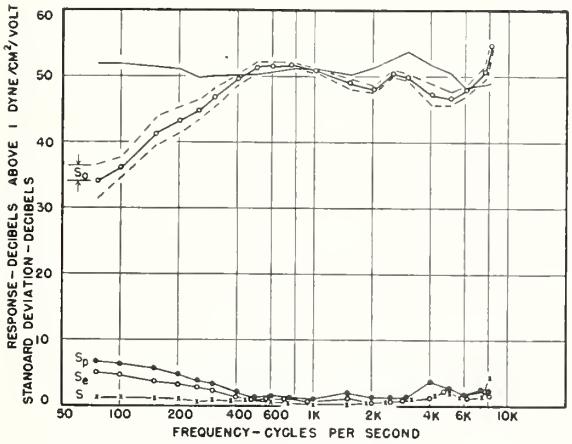

(c) Permoflux Type PDR-10 (MX41/AR cushion)

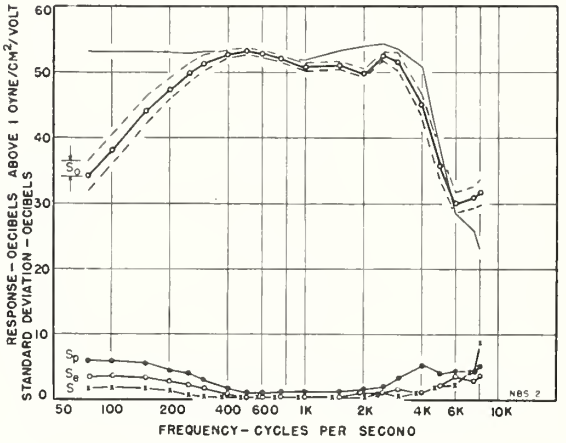

(d) Western Electric Type 705-A. Applied voltage response and precision indices. Heavy line is average of response on both ears of 14 individuals. Light line is response of earphone on coupler No. 9-A, included for reference. s_p, s_e, s, and s_o are statistical indices indicating the variation among responses due to individual physical differences among people, difference between a person's two ears, variation in repeated response determinations, and estimated standard deviation of the mean, respectively.

FIG. 2.

urement. No effort was made to establish clinical control of the people used but their ears were examined by Dr. Glorig of Walter Reed Hospital with an otoscope to note the absence of physical irregularities such as perforated drum membranes, and ear volumes were measured.

To illustrate the range of variation of sound pressures encountered when applying a constant voltage to an earphone on an ear, Table I presents typical applied voltage response determinations. Data at three frequencies are given for a Permoflux Type PDR–8 earphone for both ears of the fourteen individuals used. Noting that the sound pressures developed vary from person to person, we consider that each individual possesses his own particular value which can be found as the average of the earphone response for left and right ears. Also, there will be an average value of the sound pressure response of a particular earphone for a group of people. If an individual is chosen from the group and a measurement made on one ear, the values obtained, excluding measurement errors, differ in general from the population average because: (1) identical results may not be obtained on both ears of the same individual, and (2) the individual's average differs from the population average.

The variability of individual values about the average for our fourteen subjects, and of the discrepancy between the two ears and the individuals' average may be estimated. These estimates have been designated s_p^2, the variance due to the variability of individual averages including measurement errors, and s_e^2, the variance representing the variation between the ears of the same person, also including measurement errors. The positive square roots of these parameters have been plotted for a number of frequencies in Fig. 2 along with that of the estimate of the measurement error variance s^2.

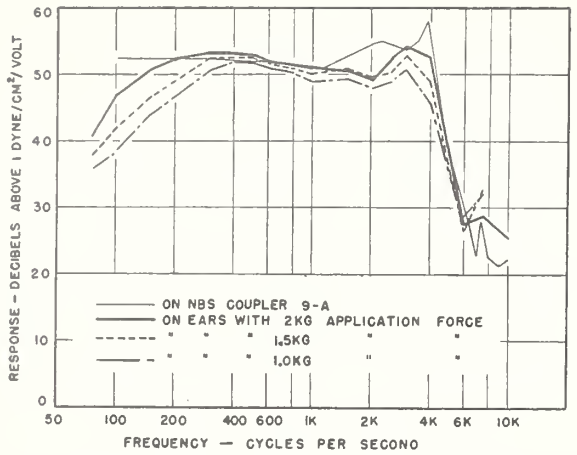

FIG. 3. Applied voltage response of a Western Electric Type 705-A earphone. Force used to hold the earphone on the ear is the parameter yielding the separate curves. Response on National Bureau of Standards Coupler No. 9-A is given for comparison.

Application of the F test[5] to the parameter s_e indicates that it is not significantly different from s, and hence shows that ears tend to occur in "matched pairs" with respect to the sound pressures produced in them by earphones. Using the same criteron, s_p has been found to be significant with few exceptions. The points which show no significance have not been considered important to the overall effect. Thus the dissimilarity noted between both ears of an individual probably results from the random measurement error of this type of measurement, but the variations among subjects result from individual differences which affect the acoustic load of the earphone. The high degree of repeatability of any observation, indicated by low values of the index s, is attributable to the fact that the earphone application force is closely controlled in all cases.

The estimated standard deviation of the average responses of these earphones is given by s_o computed from analysis of variance results. On the basis of the Student distribution[6] and a significance level of one in twenty, it is estimated that the true average response of the earphone for the whole population has a value within $\pm 0.6\ s_o$ of the average shown.

Over the small mid-frequency range of 500 to 1000 cps, the responses of the earphones we used are nearly the same on ears as they are when measured in Coupler No. 9A. Precision of measurement is best in this region, thus precluding the occurrence of this agreement by chance. At lower frequencies uncertainties of measurement become much greater while the average response on ears falls off. At higher frequencies the dissimilar geometries of the ear and coupler undoubtedly contribute much to the differences between the coupler and the ear. The same applies to the increase in uncertainty, because the length of the ear canal and the general shape and size of the external ear are peculiar to each individual. This personal characteristic determines the impedance encountered by an earphone when it is applied to the ear.

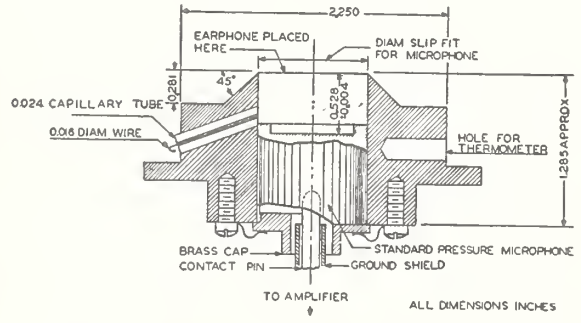

FIG. 4. National Bureau of Standards Calibrating Coupler No. 9-A. Standard threshold pressures for audiometer calibration are maintained in terms of sound pressures generated in this coupler. Volume = 5.7 cc.

[5] See any text on statistics, e.g., D. C. Villars, *Statistical Design and Analysis of Experiments for Development Research* (William C. Brown Company, Dubuque, Iowa, 1951).

[6] See e.g., D. C. Villars (reference 5).

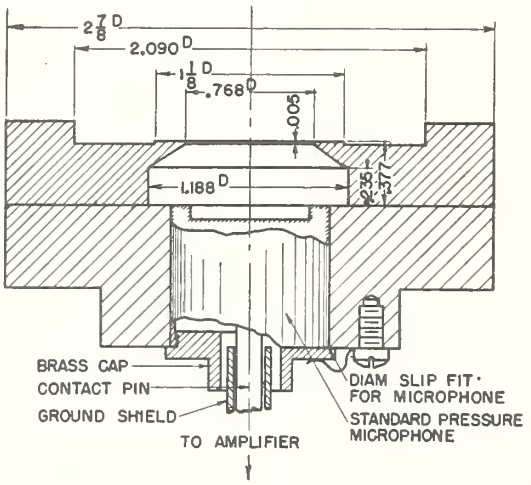

FIG. 5. Joint Radio Board (JRB) calibrating coupler. Earphone was calibrated with cushion removed. Volume = 6.0 cc. This differs only slightly in dimensions from the ASA Type I coupler.

We have obtained similar applied voltage response and uncertainty index characteristics for all of the earphones tested on ears by this method.

(C) Earphone Application Force Effect on Earphone Response

It is reasonable to expect that the force with which the earphone is applied to the ear affects the sound pressure developed by it in the ear. Because of the yielding properties of both the flesh and the rubber earphone cap, an increase of application force tends to reduce the volume enclosed under the earphone and at the same time probably tends to close off any acoustic leaks. Effects of earphone application force on earphone response are indicated in Fig. 3 where we show the average of some applied voltage earphone response measurements made on ears at forces of 1.0, 1.5, and 2.0 kg, and on the National Bureau of Standards 9–A calibrating coupler. Although the averages shown result

from comparatively few observations (3 persons with two repeats for 1.0 kg, 14 persons for 1.5 kg, 4 persons for 2.0 kg), differences to be noted in the average response curves shown are large enough to be statistically significant by the Student t test in most cases.

Apparently the acoustic termination to the earphone tends toward a volume reactance approximating a hard-walled calibrating coupler as the application force is increased. It still would not be practical to extrapolate to the conclusion that the difficulty of relating coupler pressures to ear pressures in calibration procedures can be avoided in this way. We have found that forces in excess of 2.0 kg become unbearably painful and that even a 2.0-kg force can be tolerated only for short periods.

IV. EARPHONE RESPONSE ON COUPLERS

Figures 4, 5, and 6 give cross-sectional drawings of the three artificial ear calibrating couplers investigated. National Bureau of Standards Coupler No. 9–A,[7,8] Fig. 4, is the one for which auditory threshold standards maintained by the Bureau of Standards are specified. It has a volume of 5.7 cc and presents nearly pure volume reactive acoustic load. The original Joint Radio Board 6 cc coupler,[2] Fig. 5, is essentially the same as the Type I coupler specified for Coupler Calibration of Earphones.[4] It, too, presents a load which is nearly pure volume reactance. The design of this coupler is such that the front cushion of the earphone must be removed while it is being calibrated. These couplers are intended to have an air volume approximating that enclosed by an earphone on an ear.

The third coupler is a copy of one used at the National Physical Laboratory, Teddington, England.[9] This coupler, designated B–1, is shown in Fig. 6 as modified to accommodate the type 640AA microphone. It is made up of a cylinder with volume of 5.17 cc having two tubes $14\frac{1}{2}$ feet long let into its side walls. Graduated lengths of wool yarn were drawn into the tubes in an attempt to make the tubes appear infinite in length. The design in theory is intended to produce impedance in accord with data reported by West,[10] and by Inglis, Gray, and Jenkins[11] for the acoustic impedance of ears.

Although the couplers differ somewhat in physical structure, an earphone's applied voltage response measured on each is substantially the same. The response of a 705–A type earphone, given in Fig. 7, showed greater dependence on the coupler structure than both the Type PDR–1 and Type PDR–8 earphones. Morrical *et al.*[12] found much similarity between the responses of an earphone measured on the 9–A and JRB couplers. It is interesting to note that addition of the acoustic leak in the B–1 coupler has not made it significantly different from the 9–A and JRB couplers.

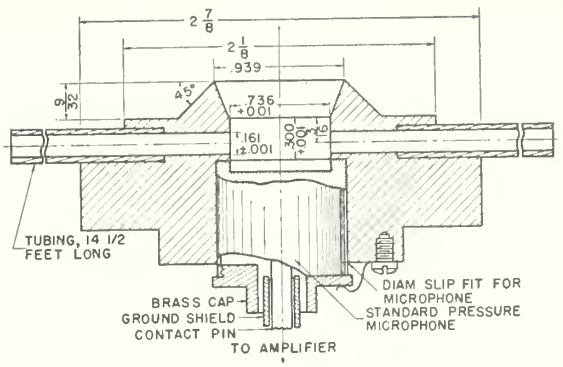

FIG. 6. B-1 Coupler. An adaptation of a coupler employed at the National Physical Laboratory, Teddington, England by R. S. Dadson. It has been modified for use with Type 640AA condenser microphone. Tubes at sides are partially filled with graduated lengths of wool yarn. Volume of cylinder = 5.17 cc.

Comparing responses for the same earphone applied to ears and these couplers, e.g., the data of Figs. 3 and 7, it is evident that the sound pressures produced in ears differ significantly from those in the coupler below 500 cps and above 1000 cps. At higher frequencies differences arise through wave motion effects. This comes about in part because on the ear the pressure was measured directly in front of the earphone but the coupler pressure is measured with a microphone at the coupler bottom. Differences between responses on ears

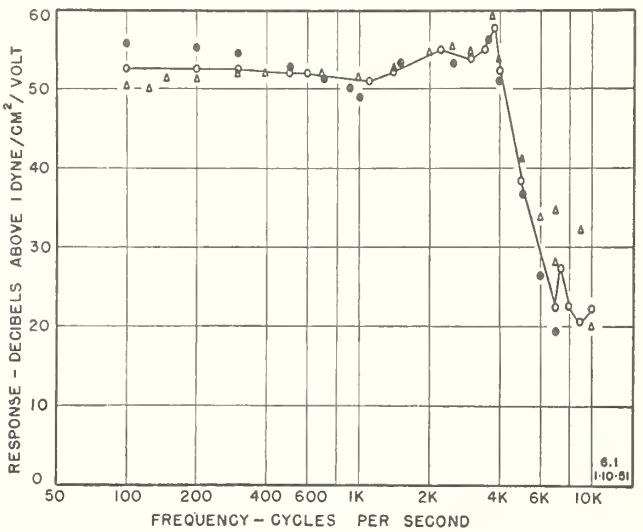

FIG. 7. Applied voltage response of a Western Electric Type 705-A earphone on three superficially different calibrating couplers: o—o on NBS coupler No. 9-A; △ on B-1 coupler; ● on JRB coupler.

[7] American Standard Specification for Audiometers for General Diagnostic Purposes, Specification Z24.5—1951. Available from American Standards Association, Inc., 70 East 45th St., New York 17, New York. Price $.50.

[8] American Standard Specification for Pure-tone Audiometers for Screening Purposes, Specification Z24.12—1952. Available from American Standards Association, Inc., 70 East 45th St., New York 17, New York. Price $.50.

[9] Hearing Aids and Audiometers, Special Report 261, Medical Research Council, His Majesty's Stationery Office, London, England (1947).

[10] W. West, British P. O. Elect. Engrs. J. **21**, 293 (1929).

[11] Inglis, Gray, and Jenkins, Bell System Tech. J. **11**, 293 (1932).

[12] Morrical, Glaser, and Benson, J. Acoust. Soc. Am. **21**, 183 (1949).

574278 O - 61 - 56

and couplers at lower frequencies cannot arise from wave effects. The average of the volumes enclosed under an earphone cap with contour typical of audiometer earphones on ears of 12 of our 14 subjects is 5.3 cc. Reducing coupler volumes to this amount would serve to make the sound pressure in the coupler even higher at low frequencies than it is on the ears.

One obvious source of difference is the mounting of the earphone on the ears and couplers. The coupler terminates in a circular aperture which forms a uniform seal either with the earphone cap or with the front face of the earphone mechanism. Irregularities in the contour of the side of the face prevent a uniform seal by the earphone on the ear. Simple computations show that there is at least one additional component in the acoustic load presented by the ear that is not provided in hard wall volume couplers. Although the acoustic leak in the *B*–1 coupler is designed to introduce a resistive element in the load, the output of the earphones at low frequencies is considerably lower on the ear than on this coupler. The agreement in the range 500 to 1000 cps suggests either that both ear and coupler impedance magnitudes are sufficiently larger than the mechanical impedance of the earphone so that they render the measured response independent of the load used, or that the effective impedances are alike. The former mechanism seems more likely since it would allow for the deviations between responses on the ear and on the coupler observed at frequencies outside this range.

The results indicate that the mechanical impedance of audiometer earphones may be too high relative to the load impedances which are encountered in practice. Because audiometric measurements require that the sound pressure at any frequency be maintained constant for all ears, it is evidently preferable to avoid impedance matching. Instead, earphones chosen for audiometry should exhibit low internal impedance.

VI. CONCLUSIONS

Normal threshold of audibility at a given frequency is the minimum sound pressure at the entrance to the external auditory canal which at that frequency produces an auditory sensation in ears. It is necessary therefore that an audiometer earphone produce the same sound pressure in all of the ears to which it may be applied, otherwise considerable inaccuracy in the threshold measurement may result.

Earphone calibration under prescribed and representative conditions is basic to the maintenance of the standards of auditory threshold. The calibrating coupler now specified for earphone calibrations does not duplicate the acoustic load of the human ear as closely as desired for audiometric work. As a result, the standards of auditory threshold apply only for the earphone with which the threshold determination was made. If a different earphone type is to be used for audiometry, either new threshold determinations must be made for this type of earphone or transfer of the threshold must be made from one earphone to the other. This may be accomplished either by loudness balancing between the earphones or by measuring the pressure under each earphone when it is held on an ear. If, however, the couplers were more representative of the average ear, all of the necessary information about any earphone which was proposed for audiometric measurements could immediately be obtained from the coupler calibration of the earphone. Therefore, a new artificial ear calibrating coupler that will more nearly duplicate the measured impedance of ears is needed. It is evident from sound pressure observations that there are resistive and reactive components in the impedance of an average human ear. At present the standard calibrating couplers in this country are of the hard-wall type, presenting chiefly volume reactive impedances.

Considerable reduction in the variability in sound pressure generated by an earphone on a particular ear has been made by controlling the application force of the earphone. The precision of all audiometric practices could be improved by control of the headband force so that it is the same for all subjects. A force of 1.5 kg has been found advantageous in this investigation. Most headbands now in use give a smaller variable force that depends on head size.

Variations in earphone response on the ears of a group of people will not be eliminated by specifying the application force, however, since the differences are due almost wholly to the physical characteristic of the particular ear on which the measurements were made. Because of this, for a given acuity of the ears of several individuals, observed thresholds will appear to be different to the extent that the responses of the earphone on these ears differ. Thus hearing losses apparently observed audiometrically may not actually exist. It follows directly from the measurements described here, that some cases of hearing loss of the order of 20 db to 30 db may only be due to a decrease in sound pressure at the entrance to the ear because of the acoustical termination which that particular ear presents to the earphone.

Earphones are usually designed empirically for maximum sound energy transfer, thus probably the magnitude of the impedance of the earphone matches the impedance of the ear. For audiometry, however, an earphone should be chosen or designed that has an acoustic pressure output substantially unaffected by acoustic load over the range of impedances encountered on ears. This requires an impedance mismatch, i.e., an earphone with a low driving impedance acting effectively as a constant pressure source.

VII. ACKNOWLEDGMENT

The statistical evaluation of the large quantity of data was carried out at the suggestion and with the

help of Mr. Joseph Cameron of the Statistical Engineering Section, National Bureau of Standards. Dr. Aram Glorig, otologist, of Walter Reed Hospital, Forest Glen Annex, made examinations of the ears of our subjects and was consulted on problems of medical and clinical interest in this work. Mr. R. F. Brown, Jr., and Mr. K. T. Lemmon performed some of the measurements reported here, and Mr. R. P. Thompson carried out some of the statistical computations. The authors greatly appreciate the cooperation of a number of their associates in the Sound Section who furnished their ears for observation.

U. S. Department of Commerce National Bureau of Standards

RESEARCH PAPER RP1341

Part of Journal of Research of the National Bureau of Standards, Volume 25, November 1940

ABSOLUTE PRESSURE CALIBRATIONS OF MICROPHONES

By Richard K. Cook

ABSTRACT

A tourmaline-crystal disk was used both as a microphone (direct piezoelectric effect) and as a sound source (converse piezoelectric effect). Application of a principle of reciprocity to the acoustic measurements gave an absolute determination of the piezoelectric modulus $d_{33}+2d_{31}$ of tourmaline under hydrostatic pressure. A condenser microphone was calibrated by the tourmaline disk. The same principle was applied to data obtained by using a condenser microphone as both source and microphone to secure an absolute calibration of another condenser microphone. It was proved experimentally that the tourmaline disk and the condenser microphones satisfied the principle of reciprocity. The absolute acoustic determination of the piezoelectric modulus gave $d_{33}+2d_{31}=2.22\times10^{-17}$ coul/dyne. The "reciprocity" calibrations agreed with the results of electrostatic actuator, pistonphone, and "smoke particle" calibrations, but disagreed with thermophone calibrations of the condenser microphones.

CONTENTS

I. INTRODUCTION

Absolute measurements of sound intensity are of basic importance in acoustics. Such measurements are most conveniently made by means of calibrated microphones, and it is important to have accurate methods of making both absolute pressure and absolute free-field calibrations of microphones. Absolute pressure calibrations are needed at low frequencies to supplement free-field Rayleigh-disk measurements at higher frequencies, and are needed to check Rayleigh-disk measurements in the frequency region in which both pressure and free-field calibrations should be the same. Absolute pressure calibrations are also needed in audiometric work.

First calibrations of a condenser microphone made with an electrostatic actuator and with a thermophone, both of conventional design, showed a difference much greater than the probable error of the determination. The difference between the thermophone and the free-field Rayleigh-disk calibrations of a condenser microphone, in the

frequency region in which both calibrations should be the same, was also greater than the probable error. It was decided to use piezoelectric crystals to throw some light on the discrepancies between the results obtained with the thermophone, the electrostatic actuator, and the Rayleigh disk.

II. PRINCIPLE OF RECIPROCITY

1. GENERAL

Shortly after the discovery of the direct piezoelectric effect by the brothers P. and J. Curie, M. G. Lippmann predicted the existence of a converse piezoelectric effect, and showed quantitatively how large it should be.

Lippmann's proof, generalized by W. Voigt [1][1], is in reality a special case of a principle of reciprocity. Other special cases of the principle are well known in applied mechanics, electrical engineering, and acoustics. This principle was discussed by Lord Rayleigh [2] for mechanical systems and electrical systems, and was discussed by S. Ballantine [3] for certain mixed mechanical and electrical systems. The same principle of reciprocity can be applied not only to piezoelectric crystals but also to condenser microphones, moving-coil microphones, and to the thermophone. By means of this principle, the output of a transducer (i. e., a device which is used as both sound source and microphone) as a sound source can be computed from its response as a microphone, and vice versa.

Suppose that a pressure sinusoidal in time

$$p=p_0e^{i\omega t}$$

is applied to the diaphragm of a transducer (e. g., a condenser microphone); suppose electric charge

$$q=q_0e^{i\omega t}$$

is released from the transducer. The release of this charge, q, by the pressure, p, is called the direct effect (see fig. 1). It is assumed that the charge released is directly proportional to the pressure. This assumption of linearity is sufficient for the application of the reciprocity principle.

If the proportionality between p and q is given by

$$q=\tau p, \tag{1}$$

the principle of reciprocity asserts that

$$v=\tau u, \tag{2}$$

where τ is numerically the same in both eq 1 and 2, if q, p, v, and u are all in the same system of units, and where

$$v=v_0e^{i\omega t}$$

[1] Figures in brackets indicate the literature references at the end of this paper.

is the change of volume caused by the motion of the diaphragm due to an applied voltage

$$u=u_0e^{i\omega t}.$$

The volume change, v, due to the voltage, u, is called the converse effect (see fig. 2). There might be differences in phase among the quantities q, p, v, and u. To account for phase differences, the

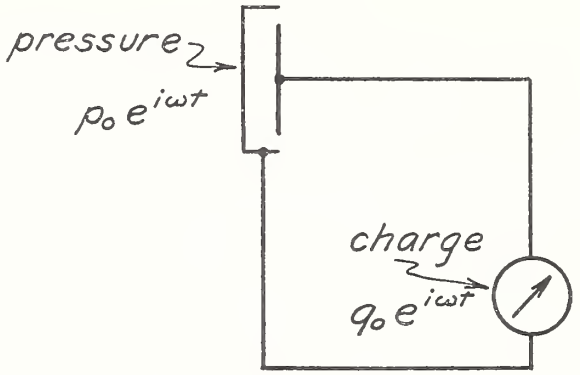

FIGURE 1.—*Direct effect.*
Transducer used as microphone.

coefficients q_0, p_0, v_0, and u_0, and the transduction coefficient, τ, are in general complex numbers, and τ might also be a function of frequency.

The principle of reciprocity applies without regard to the mechanism of operation of the transducer, provided only it is linear. The principle applies even if there are frictional forces or thermal actions in the

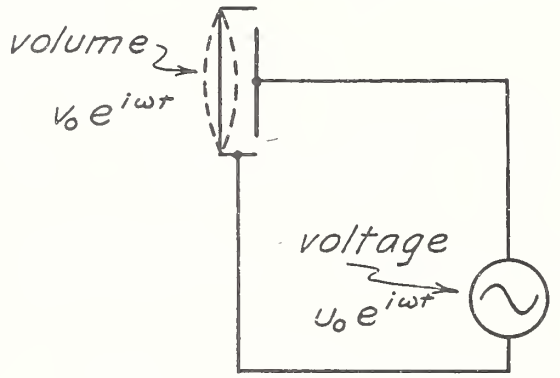

FIGURE 2.—*Converse effect.*
Transducer used as sound source.

transducer, provided these are linear (i. e., $\tau=q/p$ is independent of p). Thus a thermophone without a polarizing current is not linear when used as a sound source and the principle does not apply. Indeed, the thermophone used as a microphone under such circumstances has no response. But with a polarizing current the thermophone becomes a linear sound source (within certain limits), and the reciprocity theorem can be applied within these limits to compute the response as

a microphone from the output of the thermophone as a source of sound. Similarly, the principle can be applied to a condenser microphone having a polarizing voltage, but the principle is not applicable to an unpolarized condenser microphone.

Besides the assumption of linearity, it is also assumed that the only force applied in the direct effect is the pressure on the diaphragm (i. e., the electric terminals of the transducer are shorted, so that no electric forces are applied), and that the only force applied in the converse effect is the voltage on the electric terminals (i. e., the diaphragm volume change takes place with no reaction from the gas in front of the diaphragm). It presently will be shown how closely these conditions are realized in the laboratory, and how to take into account departures from the specified conditions.

If p and v are, respectively, in dynes per square centimeter and cubic centimeter and Q and E in coulombs and volts, then eq 1 and 2 become, in this mixed system of units,

$$\left.\begin{aligned} Q&=\tau p \\ v&=10^7\tau E \end{aligned}\right\} \tag{3}$$

and τ is in square centimeters coulomb per dyne. These units will be used throughout the remainder of this article. The quantities representing voltage, charge, pressure, and volume changes will henceforth have root-mean-square (rms) values.

2. APPLICATION TO PIEZOELECTRIC CRYSTALS

Tourmaline, a polar crystal of the trigonal system, acquires a uniform electric moment per unit volume under hydrostatic pressure. The magnitude of the moment per cubic centimeter is

$$M=(d_{33}+2d_{31})p \text{ coul/cm}^2,$$

and its direction is parallel to the principal (optic and piezoelectric) crystal axis. The quantities d_{33} and d_{31} (Voigt's [1] notation) are, respectively, the piezoelectric modulus for normal pressures on faces perpendicular to the principal axis, and a piezoelectric modulus for normal pressures on any two faces which are parallel to the principal axis and to each other. The quantity $d_{33}+2d_{31}$ is the piezoelectric modulus of the crystal under hydrostatic pressure.

Voigt's measurements on Brazilian tourmaline gave

$$d_{33}+2d_{31}=2.42\times10^{-17} \text{ coul/dyne.}$$

For a crystal cut in the shape of a circular disk of area A and having its parallel flat faces perpendicular to the principal axis, the electric moment per unit volume, M, will appear as a uniform electric charge per unit area, M, on the flat faces, or the total charge on each flat face will be

$$Q=AM=A(d_{33}+2d_{31})p \text{ coul.}$$

Then, by the principle of reciprocity, a potential difference of e'_s (volts) applied between the flat faces will cause a volume change of the crystal of amount

$$v=10^7A(d_{33}+2d_{31})e'_s \text{ cm}^3. \tag{4}$$

A tourmaline crystal is then used in the following way as both sound source and microphone to secure an absolute pressure calibra-

tion of (for example) a condenser microphone, and to secure also the hydrostatic piezoelectric modulus of the crystal.

Let the response of the condenser microphone be

$$\rho=\frac{e_m}{p}\text{cm}^2 \text{ volts/dyne},$$

where e_m is the voltage output of the microphone due to the sound pressure, p. The response of the crystal used as a microphone (direct effect) is

$$\frac{A(d_{33}+2d_{31})}{C}=\frac{Q}{Cp}\text{ cm}^2 \text{ volts/dyne},$$

where C (farads) is the capacity of the crystal microphone. The crystal response is expressed in this way because Q/C (the voltage output of the crystal microphone) can be readily measured, whereas it is not feasible to measure Q directly.

The first step is to measure the ratio of the condenser-microphone response to the crystal-microphone response. The ratio is

$$\frac{\rho C}{A(d_{33}+2d_{31})}=\frac{e_m}{e_s}, \tag{5}$$

and is got experimentally by applying the same pressure (or pressures in a known ratio) to both microphones and by measuring the ratio of the output voltages, e_m/e_s, by means of an attenuation box or known resistances. The voltage output of the condenser microphone is e_m, and that of the crystal for the same sound pressure is e_s.

The second step is to use the crystal as a source, acting on the condenser microphone as a microphone through a gas-filled cavity of volume, V (cm^3). If B (dynes/cm^2) is the barometric pressure in the gas and γ is the ratio of specific heats of the gas, then the piezoelectric volume change of the crystal given by eq 4 will give rise to a pressure

$$p=\left(\frac{10^7\gamma B}{V}\right)A(d_{33}+2d_{31})e'_s \text{ dynes/cm}^2,$$

provided v is small in comparison with V. The condenser microphone voltage output due to this pressure will be

$$e'_m=\left(\frac{10^7\gamma B}{V}\right)A(d_{33}+2d_{31})\rho e'_s \text{ volts}. \tag{6}$$

Simultaneous solution of eq 5 and 6 yields

$$\left.\begin{aligned}\rho&=\sqrt{\frac{10^{-7}V}{\gamma BC}\left(\frac{e_m}{e_s}\right)\left(\frac{e'_m}{e'_s}\right)}\text{ cm}^2 \text{ volts/dyne}\\ A(d_{33}+2d_{31})&=\sqrt{\frac{10^{-7}CV}{\gamma B}\left(\frac{e_s}{e_m}\right)\left(\frac{e'_m}{e'_s}\right)}\text{ cm}^2 \text{ coul/dyne}\end{aligned}\right\}. \tag{7}$$

Thus an absolute pressure calibration of a condenser microphone is obtained by absolute measurements of a volume, the barometric pressure, and a capacitance, and by measurements of two voltage ratios. An absolute determination of the adiabatic piezoelectric modulus of the tourmaline crystal under hydrostatic pressure is obtained by measurement of the crystal area in addition to the quanti-

ties enumerated above. The only quantity which is not measured directly is γ, whose values for air, hydrogen, and helium are accurately known.

Superimposed on the piezoelectric action in the direct effect will be the pyroelectric effect (since temperature changes in the gas which accompany pressure changes will penetrate into the crystal), and superimposed on the piezoelectric action in the converse effect will be the electrocaloric effect (since temperature changes in the crystal which accompany voltage changes will penetrate into the gas). But the principle of reciprocity will hold nevertheless, and eq 7 will give a quantity which represents a mixed piezoelectric and thermoelectric modulus at low frequencies, and which will approach asymptotically the adiabatic piezoelectric modulus at high frequencies.

In cavities of small volume, the elastic volume changes of the crystal (used as a microphone) due to an applied pressure, will in themselves give rise to a pressure superimposed on the applied pressure calculated on the assumption of no yielding of the crystal. The crystal suffers a volume change also if the faces are not at the same potential, because the potential difference, Q/C, acquired by the crystal causes a piezoelectric volume change by virtue of the converse effect, and likewise will give rise to a pressure superimposed on the calculated applied pressure. In effect, the piezoelectric modulus will appear to be a function of cavity volume, if the crystal volume changes are appreciable and due allowance is not made for them. This will be called the volume effect. For tourmaline the adiabatic compressibility is about 10^{-12} cm^2/dyne. Therefore, the ratio of the pressure caused by elastic volume change to the applied pressure is less than 10^{-6} for cavity volumes greater than 10 cm^3 and crystal volumes less than 4 cm^3. For tourmaline the adiabatic piezoelectric modulus is about 2.4×10^{-10} cm/volt. Therefore, the ratio of the pressure caused by piezoelectric volume change to the applied pressure is less than 10^{-8} for cavity volumes greater than 10 cm^3, crystal areas less than 15 cm^2, and crystal-microphone capacitance greater than 30×10^{-12} farad. With these restrictions, the volume effect for a tourmaline crystal used as a microphone is completely negligible, and by the principle of reciprocity the volume effect for a tourmaline crystal used as a source is also negligible, with the same restrictions. The volume effect for condenser microphones will be discussed in section 3.

Quartz and Rochelle salt have no electric moment under hydrostatic pressure. This conclusion is reached from considerations of the crystal symmetry of these materials. Consequently, such crystals cannot be used in the same way as tourmaline is used to obtain an absolute calibration of a microphone.

3. APPLICATION TO CONDENSER MICROPHONES

Let ρ_1(cm^2 volts/dyne) be the response and C_1 (farads) the capacitance of a condenser microphone, *I*, which is to be used as both source and microphone to calibrate a second condenser microphone, *II*, whose response is ρ_2(cm^2 volts/dyne). The equations of the direct and converse effects for the condenser microphone are

$$\left.\begin{aligned} Q&=\rho_1 C_1 p \\ v&=10^7\rho_1 C_1 E \end{aligned}\right\} \tag{8}$$

These correspond to eq 3. Microphone *I* is then used in exactly the same way as was the tourmaline crystal to secure an absolute pressure calibration of microphone *II*. That is to say, the first step is to obtain the ratio of the responses, ρ_1/ρ_2, by applying the same pressure to both microphones, and the second step is to couple microphone *I* (used as a sound source) to microphone *II* by means of a gas-filled cavity of known volume, from which is obtained the product of the responses, $\rho_1\ \rho_2$. The final equations for the responses, ρ_1 and ρ_2, are

$$\left.\begin{aligned}\rho_1&=\sqrt{\frac{10^{-7}V}{\gamma BC_1}\left(\frac{e_1}{e_2}\right)\left(\frac{e'_2}{e'_1}\right)}\ \text{cm}^2\ \text{volts/dyne}\\ \rho_2&=\sqrt{\frac{10^{-7}V}{\gamma BC_1}\left(\frac{e_2}{e_1}\right)\left(\frac{e'_2}{e'_1}\right)}\ \text{cm}^2\ \text{volts/dyne}\end{aligned}\right\}\qquad(9)$$

These correspond to eq 7. In these equations V (cm^3) is the volume of the cavity in which microphone *I* is used as a sound source, B (dynes/cm^2) is the barometric pressure in the cavity, γ is the ratio of the specific heats of the gas in the cavity, e_1 and e_2 are, respectively, the voltage outputs of microphones *I* and *II* for the same applied pressure, and e'_2 is the voltage output of microphone *II* for a voltage e'_1 applied to microphone *I* when used as a sound source (the two microphones being coupled by the cavity of volume V).

The condenser microphone diaphragm suffers a volume change if the potential difference between the diaphragm and back plate is not steady, because the alternating potential difference, Q/C, causes a volume change by virtue of the converse effect, and will therefore give rise to a pressure superimposed on the applied pressure calculated on the assumption of no volume change of the microphone. The ratio of the pressure caused by this volume change to the applied pressure is less than 5×10^{-3} for a condenser microphone having a response less than 3×10^{-3} cm^2 volt/dyne and a capacitance less than 3.5×10^{-10} farad, and for cavity volumes greater than 10 cm^3. This part of the volume effect was therefore neglected.

The compressibility (admittance) of the diaphragm gives rise to a volume effect which is not negligible. An absolute calculation of the amount would require an exact knowledge of the construction of the microphone. In the absence of such knowledge, the amount of the volume effect must be determined experimentally by making response measurements at several different cavity volumes. Unfortunately, at high-frequencies volume effects due to cavity resonances swamp those due to diaphragm compressibility, and there is no way of separating the two effects. This means that a precise determination of the volume effect can be made only at low frequencies. Let the compressibility of the diaphragm *II* be $c_2(\text{cm}^5/\text{dyne})$; that is, a pressure of $p(\text{dynes/cm}^2)$ on the diaphragm causes a volume change of $c_2p(\text{cm}^3)$. Then at frequencies less than the lowest natural frequency of diaphragm *II* the compressibility will have the effect of increasing the cavity volume which appears in eq 9 from V to $V+\gamma Bc_2$. It is clear from the principle of reciprocity that the same volume effect will be present when the microphone is used as a sound source. If c_1 is the compressibility of diaphragm *I*, then the total effect will be to increase

the volume which appears in eq (9) from V to $V+\gamma Bc_1+\gamma Bc_2$. The quantity $\gamma Bc(\text{cm}^3)$ will hereafter be denoted by $\kappa(\text{cm}^3)$, and will be called the volume constant of the microphone.

III. EXPERIMENTAL RESULTS

1. REVERSIBILITY OF TRANSDUCERS

A "reversible" transducer is one which satisfies the principle of reciprocity. A simple experimental way of ascertaining whether or not two transducers are reversible is the following. The transducers are coupled by a cavity of fixed volume. A voltage e_1 is applied to transducer *I* (source), and the corresponding voltage output e'_2 of transducer *II* (microphone) is measured. Then a voltage e_2 is applied to transducer *II* (source), and the corresponding voltage output e'_1, of transducer *I* (microphone) is measured. Then the over-all coupled system is reversible, if the equation

$$\frac{C_2}{C_1}=\left(\frac{e_1}{e'_2}\right)\left(\frac{e'_1}{e_2}\right) \tag{10}$$

is satisfied, where C_2 and C_1 are the capacitances of transducers *II* and *I*, respectively. Thus eq10 is a necessary condition for the reversibility of each transducer. If a third transducer is used and eq10 holds for each pair of transducers, this will be a sufficient condition for the reversibility of each of the three. Actually, it will be entirely safe to assume each of two transducers is reversible if eq10 holds when the two transducers are coupled. Thus the reversibility of a transducer is determined experimentally by purely electrical measurements of two voltage ratios and a capacitance ratio.

Such measurements were made on the following: A Western Electric condenser microphone type 394, No. 4829 (denoted hereafter as microphone 2); a Western Electric condenser microphone type D96436, No. 70 (denoted hereafter as microphone 70); a tourmaline crystal transducer (denoted hereafter as transducer *CD*). Transducer *CD* was made of black California tourmaline, 3.8 cm in diameter and 0.3 cm in thickness. The front face was coated with tin foil affixed with wax, and the tourmaline was wrung on to a brass block. The block was insulated from the outside brass block (at ground potential) which was connected to the tin foil.

The voltage ratios appearing in eq10 were measured at various frequencies by means of an attenuation box to the nearest decibel and by means of an output meter to the nearest one-tenth decibel. The capacitances were separately measured at 1,000 c/s (by means of a strict substitution method) with a variable capacitance calibrated in the capacitance section of this Bureau. The results are shown in figure 3. The gases which were used with each pair of transducers are indicated in the legend. The sound pressure was about 2×10^{-2} dyne/cm^2 with the tourmaline transducer *CD* as source, and about 10 dynes/cm^2 with transducer *CD* as microphone. In the other two cases plotted in figure 3, the pressure was about 1 dyne/cm^2.

The estimated probable error in 20 $\log_{10}$ (C_2/C_1) is 0.1 db, and in 20 $\log_{10}$ (e_1/e'_2) (e'_1/e_2) is less than 0.2 db. The conclusion from the results plotted in figure 3 is, that within the experimental uncertainty

eq10 is satisfied. Consequently, condenser microphones 2 and 70 and tourmaline transducer *CD* are reversible. This is a direct experimental proof of the equality of the direct and converse piezoelectric moduli in tourmaline under hydrostatic pressure.

After Lippmann's theoretical proof of the equality of the direct and converse piezoelectric moduli, J. and P. Curie made an attempt to verify the equality for the modulus, d_{11} in quartz, but experimental difficulties enabled them to obtain only a very rough agreement between the two moduli. Since then, H. Osterberg and J. W. Cookson [4] have concluded that measurements of d_{11} by some observers who used the direct effect only have agreed on the whole with measurements of d_{11} by other observers who used the converse effect only.

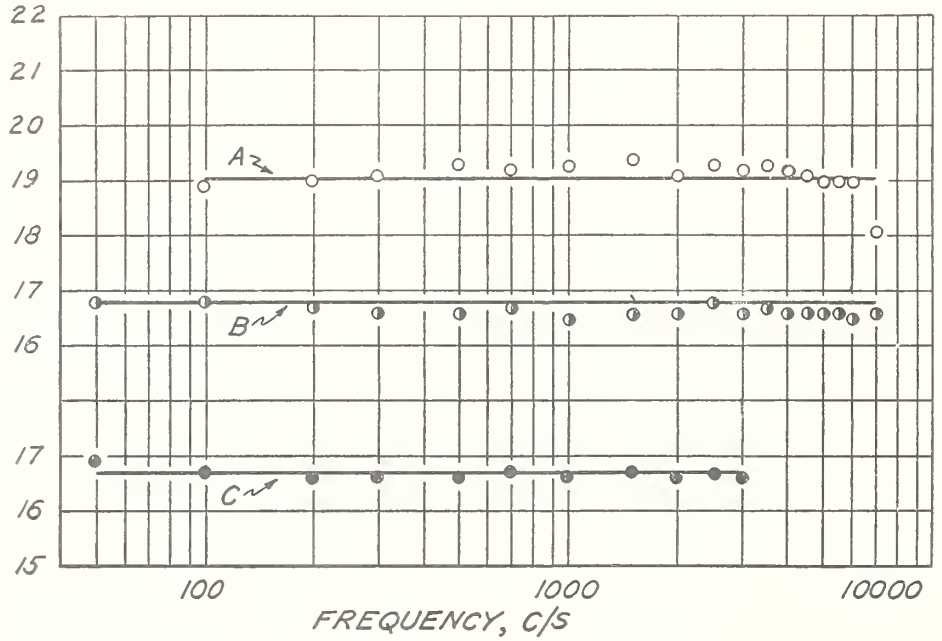

FIGURE 3.—*Graph showing reversibility of tourmaline transducer and condenser microphones.*

○=20 $\log_{10}$ (e_1/e'_2) (e'_1/e_3), and curve A=20 $\log_{10}$ (C_2/C_1) at 1,000 c/s, for condenser microphone 2 and tourmaline transducer *CD*, in helium.

◑=20 $\log_{10}$ (e_1/e'_2) (e'_1/e_2), and curve B=20 $\log_{10}$ (C_2/C_1) at 1,000 c/s, for condenser microphones 2 and 70, in helium.

●=20 $\log_{10}$ (e_1/e'_2) (e'_1/e_2), and curve C=20 $\log_{10}$ (C_2/C_1) at 1,000 c/s, for condenser microphones 2 and 102, in air.

Because of variations in the composition of tourmaline from different sources, it is not possible, in order to decide the equality of the two moduli for tourmaline, to compare the results of some observers who used the direct effect only with the results of other observers who used the converse effect only.

2. MICROPHONE CALIBRATIONS

The reversibility of condenser microphones 2 and 70 and of transducer CD having been established, the principle of reciprocity was applied to data obtained with these transducers to secure absolute pressure calibrations of microphones 2 and 70.

The results are shown in figures 4 and 5. The reciprocity calibrations are those obtained with condenser microphone 2 used as both source and microphone. The cavity volumes and gases which were used are indicated in the legends. The estimated probable error of measurement is 0.2 db. The volume effects of the microphone diaphragms and the cooling effect of the walls of the cavity have not been included in the responses, which were computed directly from eq 9 (the geometrical volume of the cavity being used for V). These omissions introduce systematic errors not much greater than the probable error stated above. The amounts of these are deduced in the following paragraph.

Measurements of the volume constant, κ, gave $\kappa_2=1.3 \pm 0.2$ cm^3, and $\kappa_{70}=0.3 \pm 0.2$ cm^3. These values are experimentally the same in air, hydrogen, and helium, and are experimentally independent of whether the sound source used in the measurements is a thermophone, a tourmaline crystal, or a condenser microphone. Measurements from which the above values of κ are obtained were made usually at cavity volumes of 15, 30, and 40 cm^3. The fact that the thermophone yields the same value for κ as does the other sound sources is surprising, since Ballantine [5] has shown that the diaphragm motion of a condenser microphone should react on the thermophone foil strips in such a way as to result in a net effect different for different gases and in any case much smaller than the experimental value found above for condenser microphone 2. The value of κ_2 found above is also somewhat greater than the value computed by L. J. Sivian [6] for microphones of the same type. Direct measurements of cos ϕ (where ϕ is the phase angle between the pressure applied to the microphone diaphragm and the voltage output of the microphone) showed that the values of κ_2 and κ_{70} are practically independent of frequency below 3,000 c/s. Because of the difficulty of measuring κ above about 3,000 c/s (although the results of the measurements of cos ϕ show that κ_2 and κ_{70} become zero at about 6,000 c/s and become negative at higher frequencies), it was decided to make the reciprocity measurements at cavity volumes of 40 cm^3 so as to keep the volume effects small. Omission of the volume effects means that the computed response of microphone 2 is low by 0.3 db and of microphone 70 is low by 0.1 db below 3,000 c/s. The cooling effect of the walls of the cavity must also be considered. It is usually incorrectly assumed that the temperature variation of the gas at the walls of the cavity is zero, on the grounds that the thermal conductivity of the metal walls is much greater than that of the gas. However, in a quasi-stationary temperature distribution (all temperatures sinusoidal functions of the time) the quantity of importance is the thermal diffusivity, which is the thermal conductivity divided by the product of density and specific heat. The thermal diffusivities of brass, air, hydrogen, and helium are, respectively, at room temperature and barometric pressure 0.34, 0.28, 1.67, and 1.78 cm^2 sec. From these values it can be deduced that a better boundary condition at the walls of the cavity is that the rms temperature at the walls is one-half the rms temperature in the gas at a distance from the walls. The inclusion of this boundary condition in the reciprocity calibrations raises the computed responses of microphones 2 and 70 by less than 0.1 db, for frequencies greater than 50 c/s and a cavity volume of 40 cm^3, and for any of the three gases mentioned above. The upshot of all the fore-

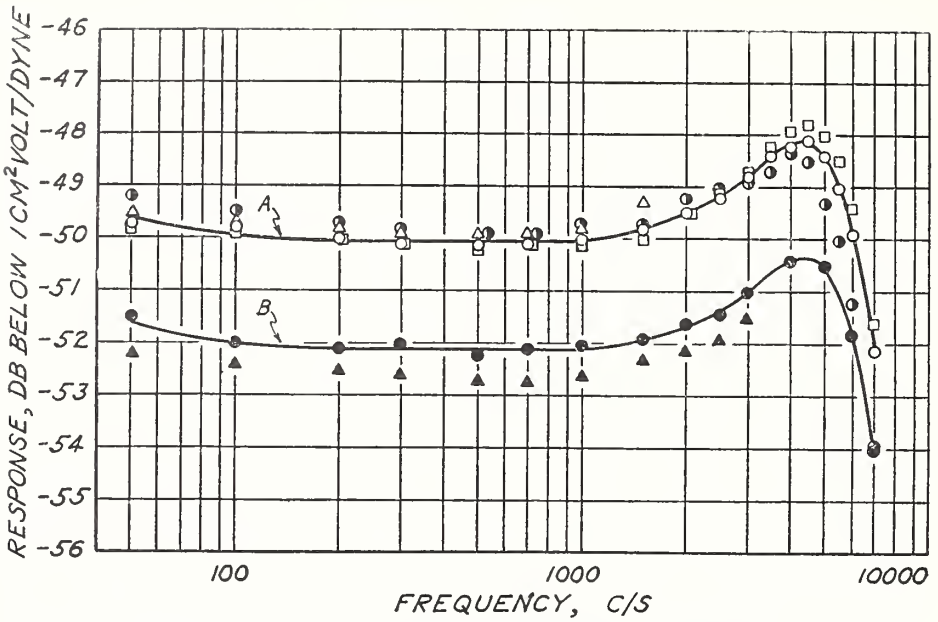

FIGURE 4.—*Calibration graph of condenser microphone 2.*

○ and curve *A* = reciprocity in hydrogen, cavity volume 40 cm³.
△ = reciprocity in air, cavity volume 40 cm³.
□ = reciprocity in helium, cavity volume 40 cm³.
◑ = electrostatic actuator.
● and curve *B* = thermophone in hydrogen, cavity volume 8.5 cm³.
▲ = thermophone in air, cavity volume 8.5 cm³.

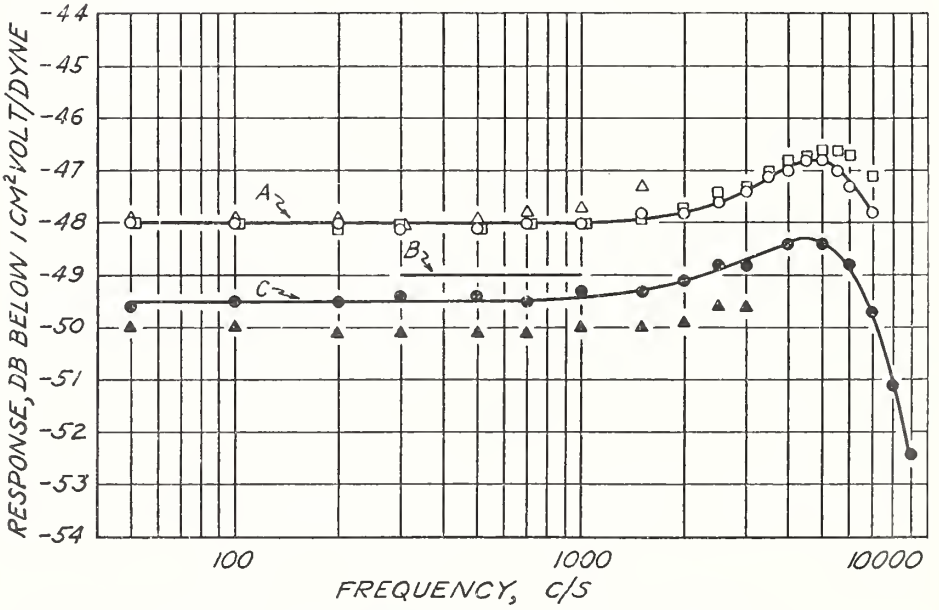

FIGURE 5.—*Calibration graph of condenser microphone 70.*

○ and curve *A* = reciprocity in hydrogen, cavity volume 40 cm³.
△ = reciprocity in air, cavity volume 40 cm³.
□ = reciprocity in helium, cavity volume 40 cm³.
Curve B = Rayleigh disk.
● and curve *C* = thermophone in hydrogen, cavity volume 10.8 cm³.
▲ = thermophone in air, cavity volume 10.8 cm³.

going is that the systematic errors introduced into the reciprocity calibrations by omission of the volume effects and cooling effects amount to a lowering of the response of microphone 2 by 0.3 db and of microphone 70 by 0.1 db.

The reciprocity calibrations of condenser microphones 2 and 70 obtained with the tourmaline transducer *CD* used as both sound source and microphone agree (within the estimated probable error) with the reciprocity calibrations obtained with the condenser microphone 2 used as both sound source and microphone.

Figure 4 shows also the results of electrostatic actuator calibrations of microphone 2. The actuator measurements were made with a "solid" grille having 25 holes each 0.7 mm in diameter and 3 mm long, and with a slotted grille having grille bars each 1.53 mm wide and 3 mm deep and grille slots each 0.88 mm wide. The pressure produced by the slotted grille was computed by means of nomographs made for such grilles by S. Ballantine [5]. The results with the slotted grille at frequencies higher than 1,000 c/s are plotted, in spite of the presence of numerous small "resonances" which appeared in the output of microphone 2 and which vitiate the results at such frequencies. Below 1,000 c/s the electrostatic actuator calibrations and the reciprocity calibrations in air, hydrogen, and helium of condenser microphone 2 all agree within the estimated probable error.

Figures 4 and 5 also show the results of gold foil thermophone calibrations of condenser microphones 2 and 70. The thermophone results were computed with the formula given by S. Ballantine [5], except for minor corrections which will be presently discussed. The thermophone cavity volumes are about the sizes used by several other observers. The estimated probable error of the individual thermophone determinations below 1,000 c/s is 0.2 db, but the estimated probable error of the difference between the air and hydrogen calibrations of a particular microphone is less than 0.2 db. The response obtained by the thermophone of a microphone of the same type as No. 2 had a value 0.3 db lower in helium than in air. It is plain that the thermophone calibrations in air, hydrogen, and helium disagree among themselves and disagree with the reciprocity calibrations in the regions of safe comparison below 1,000 c/s by amounts much greater than the probable errors of the differences. The inclusion of the volume effects will increase the responses of both microphones 2 and 70 below 3,000 c/s, so that the thermophone calibrations in air (which are more reliable than those in hydrogen and helium because of smaller systematic errors) will be below the reciprocity calibrations by 1.5 db for each microphone. This difference is still much greater than the estimated probable error. The disagreement between the thermophone calibrations in air, hydrogen, and helium is unchanged by inclusion of the volume effects.

The thermophone formula and calculations given by S. Ballantine [5] require correction because they are based on the assumption of no temperature variation in the gas at the walls of the cavity (this assumption was discussed above) and on the assumption that commercial gold foil has the same specific heat as pure gold. The specific heat of the gold foil, calculated from the results of a chemical assay, was 0.0328 cal/g° C, whereas that of pure gold is 0.0313 cal/g° C. The two corrections are in opposite directions and almost nullify one

another, thus leaving calculations made from Ballantine's thermophone formula practically unchanged.

Pistonphone measurements were made by Guy Cook and the author on a condenser microphone of the same type as microphone 2. The measurements were made between 50 and 200 c/s in a cavity of 15 cm^3 at a sound pressure of about 5 dynes/cm^2. Air, hydrogen, and helium were used. The piston was driven by a loudspeaker coil, and its amplitude of motion was measured by means of an optical lever and autocollimator. The amplitude measurements were checked by a microscope having a calibrated graticule. The computed probable error of the pistonphone results was 0.3 db, and the results agreed with an electrostatic actuator calibration of the same microphone within the probable error.

Resonant-tube measurements were made by Guy Cook and the author on the same condenser microphone. The microphone was placed at one end of the resonant tube. The amplitude of motion of illuminated tobacco-smoke particles was observed (with a microscope having a calibrated graticule) at the central displacement loop in the gas in the resonant tube. Observations were made at 95 and 285 c/s at a sound pressure of about 75 dynes/cm^2. The estimated probable error of the resonant tube results was 0.5 db, and the results agreed with the electrostatic actuator calibration of the same microphone within the estimated probable error.

The disk curve *B* in figure 5 is placed 0.5 db above the thermophone calibration in hydrogen, and is the result of Rayleigh-disk and thermophone comparisons between 300 and 1,000 c/s on several other microphones of the same type as microphone 70. The Rayleigh-disk measurements were made in the free field by Guy Cook.

The conclusion is, that in the usually accepted thermophone formula there are systematic errors which are different for different gases, and which are much greater than the error of measurement. The trouble probably lies in the assumed modus operandi of the thermophone. It has been suggested that the gold foil possibly adsorbs and emits gas during each thermal cycle. Another suggestion is, that viscosity forces have an effect on the pressure produced by the thermophone. The computed responses in air, hydrogen, and helium are in the same order as the viscosity coefficients of these gases.

3. PIEZOELECTRIC MODULI

The results of acoustic measurements, based on the principle of reciprocity, of the adiabatic piezoelectric modulus $d_{33}+2d_{31}$ of California tourmaline are shown in figure 6. The tourmaline was crystal *CD*, which was used as both source and microphone.

The results of static testing-machine measurements (by use of the direct effect) of the modulus d_{33} and Voigt's [1] static measurements (also by use of the direct effect) on Brazilian tourmaline are also given in figure 6. The frequency scale of the abscissas does not apply to the horizontal lines representing the static tests; these lines were drawn merely to facilitate comparisons with the acoustic measurements. Static measurements yield isothermal moduli, whereas the acoustic measurements yield adiabatic moduli. However, D. A. Keys [7] has shown from thermodynamic considerations that the difference between the isothermal and adiabatic moduli is less than

0.3 percent. Below 500 c/s the acoustic measurements do not yield the adiabatic modulus, since the droop in the measured modulus $d_{33}+2d_{31}$ at low frequencies is due to the superposition of thermoelectric effects on the piezoelectric action. The droop above 3,000 c/s is caused by cavity resonances.

The testing-machine measurements of the modulus d_{33} were made at loads between 1,000 and 3,000 lb in a hydraulic testing machine. A preassigned load was applied to a crystal disk 3.8 cm in diameter and 0.15 cm thick, and the electric charge released from the crystal on sudden release of the testing-machine load was measured by a calibrated ballistic galvanometer. A check of the experimental setup

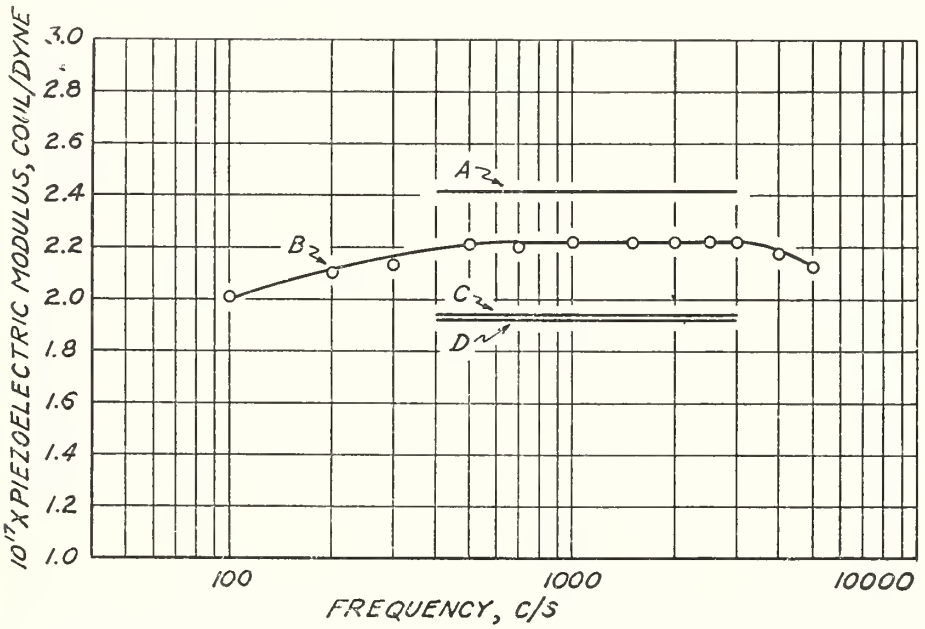

FIGURE 6.—*Graph of piezoelectric moduli of tourmaline.*

○ and curve B=acoustic measurements of $d_{33}+2d_{31}$ for California tourmaline.
Curve A=static measurements by Voigt of $d_{33}+2d_{31}$ for Brazilian tourmaline.
Curve C=static testing-machine measurements of d_{33} for California tourmaline.
Curve D=static measurements by Voigt of d_{33} for Brazilian tourmaline.

was made by measuring the piezoelectric modulus d_{11} of quartz, which is well known. The estimated probable error in the measured value of the modulus d_{33} for black California tourmaline is 2 percent.

The curious discovery was made that it is absolutely essential to load the crystal through rigid (e. g., steel) bearing blocks. Erroneous results were obtained when the tourmaline and quartz were loaded through Plexiglass (a methacrylate resin of low modulus of elasticity) bearing disks. It was established that these anomalies were not due to friction. Evidently the crystal is subjected to thermal actions and to large shearing stresses (in addition to the compressive stresses) when loaded through Plexiglass disks in contact with the crystal, and these thermal actions and shearing-stresses cause the anomalous piezoelectric effects.

The following measurements were made on California tourmaline, used as a sound source, in addition to the measurements of $d_{33}+2d_{31}$ given in figure 6. Three crystals (each 3.8 cm in diameter and 0.15

574278 O - 61 - 57

cm thick) cut from the same batch of tourmaline had identical piezoelectric moduli. When two of these disks were wrung together with vaseline so that the analogous ends of their crystal axes pointed in the same direction, the piezoelectric modulus was the same as that of a single disk, which shows that the acoustically measured modulus is independent of the crystal thickness. When the same two disks were wrung together so that the analogous ends of their axes pointed in opposite directions, the piezoelectric modulus was zero. Each disk suffered a volume change under the applied voltage, but the net volume change was zero, since the individual volume changes differed in phase by π. The piezoelectric modulus was independent of applied voltage in the range from 130 to 1,300 volts. The foregoing measurements were made in air, between 200 and 1,000 c/s, in a cavity of about 20-cm^3 volume. It is understood that the conclusions are valid only within the experimental uncertainty, which is about 2 percent of the modulus $d_{33}+2d_{31}$. In addition, a determination of the volume constant, κ, for a crystal yielded $\kappa=0$, within the experimental uncertainty of about 0.3 cm^3, which confirms the theoretical conclusion that a crystal used as a transducer should have no detectable volume effect.

A quartz-crystal disk, 3.6 cm in diameter and 0.46 cm thick, having its flat faces perpendicular to one of the three diagonal axes of the quartz, was used as a sound source in a cavity of about 20 cm^3. The measured piezoelectric modulus was about 1 percent of that of tourmaline at 500 c/s. At lower frequencies the disk had a small sound output, evidently due to electrocaloric effects superimposed on the piezoelectric. The conclusion is, that within the experimental uncertainty, the piezoelectric modulus of quartz under hydrostatic pressure is zero. This confirms experimentally the theoretical conclusion reached from considerations of crystal symmetry.

IV. INSTRUMENTS AND TECHNIQUE

The cavities were made of simple geometrical shapes (e. g., right circular cylinders), and the volumes were computed from measurements of the linear dimensions. The scale and micrometer calipers used in these measurements were compared with secondary standards kept in this Bureau. The estimated probable error in the measurement of volume is 0.4 percent.

The barometric pressure was measured by an aneroid barometer which from time to time was compared with a mercury barometer. The estimated probable error in the measurement of pressure by the aneroid barometer is 0.1 percent.

Microphone capacitances were measured by a strict substitution method. A variable air condenser, calibrated in the capacitance section of this Bureau, was used as a secondary standard. As a check on the technique, a particular condenser was measured in both the sound chamber and in the capacitance section. The estimated probable error in capacitance measurement is about 1 percent.

Voltage ratios were measured by means of an attenuation box to the nearest decibel, and by a copper oxide rectifier output meter to the nearest 0.1 db. The attenuation box was calibrated by comparison with a calibrated potentiometer, and had errors less than 0.1 db. The estimated probable error in the measurement of voltage ratio is

0.1 db. The output meter was used over a range not exceeding 0.5 db.

Nearly all the experimental measurements were made at room temperatures between 20° and 25° C, and at barometric pressures between 742 and 758 mm Hg. Within these limits there was no dependence of the responses of the condenser microphones on temperature or barometric pressure. Small variations in the responses (about 0.5 db in range) seemed to be entirely random in character.

Various tricks of technique were used to detect and eliminate spurious voltages in the microphone circuit. Such voltages are the commonest cause of trouble. For example, electrostatic coupling between the gold foil of the thermophone and the high-potential side of the tourmaline microphone causes a spurious voltage in the tourmaline-microphone voltage output. This will easily occur because the voltage applied to the thermophone is about 10^4 times greater than the voltage output of the tourmaline microphone. In another case, resistance coupling between the tourmaline-crystal sound-source circuit and the low-potential (ground) side of the condenser microphone causes a spurious voltage in the condenser-microphone voltage output. This might happen because the voltage applied to the crystal source is about 10^6 times greater than the voltage output of the condenser microphone. Reversal of the polarizing voltage on the condenser microphone (or, in the case of the thermophone, reversal of the polarizing current) will change the phase of the spurious voltage with respect to the voltage generated in the microphone by π, and the voltage output of the microphone will not be independent of polarity (as it should be), if the spurious voltage is appreciable. In crystal measurements, substitution of a dummy glass (or any nonpiezoelectric material) transducer for the crystal transducer will readily reveal spurious voltages.

V. SUMMARY

Application of a general principle of reciprocity to the action of a piezoelectric crystal or to a microphone yields absolute pressure calibrations of another microphone, and also yields absolute values of the adiabatic piezoelectric modulus under hydrostatic pressure. Absolute measurements of a volume, the barometric pressure and a capacitance are needed in addition to measurements of two voltage ratios; also, the ratio of specific heats of the gas used in the cavity is required.

Calibrations secured in this way are in good agreement with electrostatic actuator, pistonphone, and "smoke particle" calibrations of a condenser microphone. Thermophone calibrations in air, hydrogen, and helium disagreed among themselves and with the reciprocity calibrations of the same microphones by amounts much greater than the experimental uncertainty.

Absolute acoustic measurements of the adiabatic piezoelectric modulus of black California tourmaline under hydrostatic pressure gave $d_{33}+2d_{31}=(2.22\pm0.06)\times10^{-17}$ coul/dyne. It was experimentally proved that the direct and converse piezoelectric moduli $d_{33}+2d_{31}$ are equal, within the experimental uncertainty.

The following is a tentative set-up for securing absolute pressure calibrations of condenser microphones. A tourmaline-crystal source, calibrated by application of the principle of reciprocity, will be the

primary standard. A condenser microphone will serve as a secondary-standard source, which will be calibrated from time to time by the primary tourmaline standard.

There are common crystalline household substances which are piezoelectric under hydrostatic pressure, and which might be used as sound sources. Such are sucrose (cane sugar) and tartaric acid (sour salt). The latter at room temperatures has a piezoelectric modulus about double that of tourmaline.

The theoretical conclusions and experimental results contained in this article were reported at the meeting of the Acoustical Society of America in Washington, D. C., in April 1940. Similar theoretical conclusions were reached by W. R. MacLean [8] and published in the July 1940 issue of the Journal of the Acoustical Society of America.

I thank Elias Klein, of the Naval Research Laboratory, for securing loans of tourmaline and equipment, and for his kind help and encouraging suggestions.

VI. REFERENCES

[1] W. Voigt, *Lehrbuch der Kristallphysik* (B. G. Teubner, Leipzig, 1910).
[2] Rayleigh, *The Theory of Sound* (Macmillan & Co., London, 1896).
[3] S. Ballantine, Proc. Inst. Radio Engrs. **17,** 929 (1929).
[4] H. Osterberg and J. W. Cookson, Rev. Sci. Instr. **6,** 347 (1935).
[5] S. Ballantine, J. Acous. Soc. Am. **3,** 319 (1932).
[6] L. J. Sivian, Bell System Tech. J. **10,** 96 (1931).
[7] D. A. Keys, Phil. Mag. [6] **46,** 999 (1923).
[8] W. R. MacLean, J. Acous. Soc. Am. **12,** 140 (1940).

Washington, August 14, 1940.

Reprinted from THE JOURNAL OF THE ACOUSTICAL SOCIETY OF AMERICA, Vol. 32, No. 5, 611, May, 1960

Method for Measurement of $|E'/I'|$ in the Reciprocity Calibration of Condenser Microphones

WALTER KOIDAN
National Bureau of Standards, Washington 25, D. C.
(Received February 19, 1960)

A simple method is described for accurately measuring the ratio of the driving current through a capacitor-type sound source to the open-circuit voltage of a microphone used as the sound receptor. Determination of this ratio in a reciprocity calibration procedure eliminates the need for measurement of the capacitance of the reversible microphone.

A SIMPLE technique has been developed for accurately measuring the ratio $|E'/I'|$ in the reciprocity calibration of condenser microphones,[1] where I' is the driving current through the reversible microphone used as a sound source, and E' is the open-circuit voltage of the receptor microphone.

Nielsen's method[2] for performing this measurement makes use of an auxiliary calibrated capacitor through which the microphone driving current flows. The voltage across this capacitor is then observed with the aid of a cathode-follower preamplifier.

The method described below and illustrated schematically in Fig. 1 uses a resistance standard. No preamplifier, other than one for the receptor, is required.

The shell of the reversible microphone is not connected to ground, but rather to one side of a calibrated decade resistance box, R. An insulating ring and shielded calibrating line[3] is used to make this connection. The microphone is driven from a signal generator through a single-conductor shielded cable; stray capacitance across the microphone terminals is controlled by means of a ground shield.[3]

Switches 1 and 2 can be ganged for convenience, connections being made to points A and A' in one position and points B and B' in the other position. At each frequency two adjustments are required:

(1) First, the attenuator is adjusted so that voltmeter V_1 reads the same in both positions of switch 1. The position of switch 2 does not affect this measurement. The voltage which appears across the output of the attenuator is then equal in magnitude to the open-circuit voltage E' of the receptor microphone.

(2) Secondly, resistance R is adjusted so that voltmeter V_2 reads the same in both positions of both switches. The voltage across R is then equal to $|E'|$. The ground shields ensure that the current through R is the same as that through the sound source.

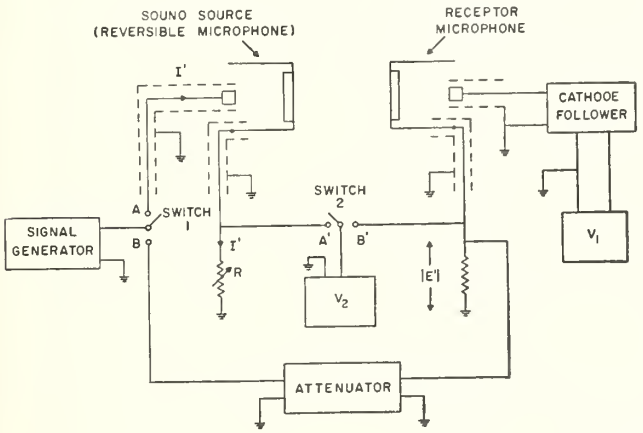

FIG. 1. Schematic diagram of the method for measuring the ratio $|E'/I'|$. Polarizing-voltage supplies and blocking capacitors were omitted from the diagram for clarity.

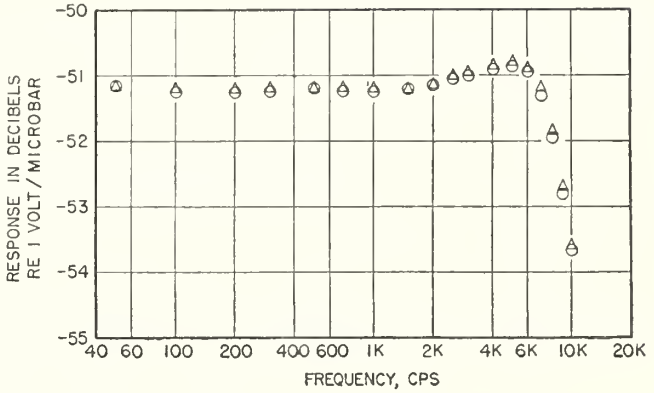

FIG. 2. Pressure response of a Western Electric Company type 640 AA condenser microphone measured by two variations of the reciprocity technique. The circles represent the response calculated from measurements of $|E'/I'|$; the triangles were obtained from measurements of capacitance and voltage-to-voltage ratios.

The desired voltage-to-current ratio is therefore

$$|E'/I'| = R. \tag{1}$$

This result is independent of the attenuator reading; in fact, the signal generator output can be a function of switch positions without affecting the value of R.

The method is adaptable to both pressure (coupler) and free-field calibrations. In a typical pressure calibration of a Western Electric Company type 640 AA condenser microphone, the resistance R varied from 24 350 ohms at 50 cps to 57.5 ohms at 10 kc. The variation of resistance with frequency is in the proper direction to minimize the effect of stray capacitance across R, which can be as large as about 1000 $\mu\mu$farad.

When attenuator readings are also taken, byproducts are the voltage-to-voltage ratio appearing in Cook's formula[4] and the magnitude of the electrical driving-point impedance of the reversible microphone. If the ratio $|E'/E| = A$, where E is the driving voltage, then from Eq. (1), the electrical impedance is $|R/A|$.

A pressure response curve for a type 640 AA microphone obtained by measuring the voltage-to-current ratio is shown in Fig. 2. For comparison, the response curve obtained by capacitance measurements with a Schering bridge and the voltage-to-voltage ratio is also plotted.

Miss June O. Magruder assisted in the laboratory measurements.

[1] W. R. MacLean, J. Acoust. Soc. Am. **12**, 140 (1940).
[2] A. K. Nielsen, Acustica **2**, 112 (1952).
[3] American Standards Association Standard Z24.4-1949, Fig. 6.
[4] R. K. Cook, J. Acoust. Soc. Am. **12**, 415 (1941).

ASA
Reg. U. S. Pat. Off.
Z24.4-1949
UDC 621.395.61:
621.3.089.6

American Standard Method for the

Pressure Calibration of Laboratory Standard Pressure Microphones

SPONSOR

Acoustical Society of America

Approved December 27, 1949

American Standards Association

Incorporated

894/1

An American Standard implies a consensus of those substantially concerned with its scope and provisions. The consensus principle extends to the initiation of work under the procedure of the Association, to the method of work to be followed, and to the final approval of the standard.

An American Standard is intended as a guide to aid the manufacturer, the consumer, and the general public. The existence of an American Standard does not in any respect preclude any party who has approved of the standard from manufacturing, selling, or using products, processes, or procedures not conforming to the standard.

An American Standard defines a product, process, or procedure with reference to one or more of the following: nomenclature, composition, construction, dimensions, tolerances, safety, operating characteristics, performance, quality, rating, certification, testing, and the service for which designed.

Producers of goods made in conformity with an American Standard are encouraged to state on their own responsibility, in advertising, promotion material, or on tags or labels, that the goods are produced in conformity with particular American Standards. The inclusion in such advertising and promotion media or on tags or labels of information concerning the characteristics covered by the standard to define its scope is also encouraged.

American Standard

Registered United States Patent Office

First Edition: Z24.4-1938
Revised Edition: Z24.4-1949

Published by
AMERICAN STANDARDS ASSOCIATION
INCORPORATED
70 East Forty-fifth Street
New York 17, N. Y.

Price, Seventy-five Cents

Copyright 1950 by American Standards Association, Incorporated

Universal Decimal Classification 621.395.61:621.3.089.6

895/2

Foreword

(This Foreword is not a part of the American Standard Method for the Pressure Calibration of Laboratory Standard Pressure Microphones, Z24.4-1949)

This American Standard comprises a part of a group of definitions, standards, and specifications for use in acoustical work. It is a revision of the American Recommended Practice for the Calibration of Microphones, Z24.4-1938, which was approved by the American Standards Association in March, 1938. Information concerning the reasons for publishing this revision is included in the introduction to this document.

In May, 1932, following a proposal of the Acoustical Society of America, the American Standards Association initiated a standardization project on Acoustical Measurement and Terminology under the sponsorship of the Acoustical Society of America, and with the following scope:

> Preparation of standards of terminology, units, scales, and methods of measurement in the fields of acoustics and mechanical vibration.

A committee in charge of the work was organized, and its organization meeting was held in May, 1932. Numerous changes in both the personnel and the organizations represented on this committee have been made since 1932. Also, in May, 1942, the scope of the work was extended to include vibration. Various subcommittees have been organized to take care of the committee's program. They are:

Acoustical Terminology
Fundamental Sound Measurements
Noise Measurement and Sound Level Meters
Sound Insulation and Sound Absorption Measurement
Audiometry and Hearing Aids
Vibration and Shock Measurement

A subcommittee on Underwater Sound Measurement also existed, but upon completion of its work was discharged in September, 1949.

Suggestions for improvement gained in the use of this standard will always be welcome. They should be sent to the American Standards Association, Incorporated, 70 East 45th Street, New York 17, N. Y.

The organizations which participated in this work and the names of their representatives are as follows:

VERN O. KNUDSEN, *Chairman* — C. F. WIEBUSCH, *Vice-Chairman*

J. W. MCNAIR, *Secretary*

Organization Represented	*Name of Representative*
Acoustical Society of America (*Sponsor*)	L. L. BERANEK
	V. O. KNUDSEN
	K. C. MORRICAL
	C. F. WIEBUSCH
Acoustical Materials Association	JOHN S. PARKINSON
	LYLE F. YERGES
Air Conditioning and Refrigerating Machinery Association	LEONARD C. BASTIAN
	WILLIAM B. HENDERSON (*Alt*)
American Gas Association	F. E. HODGDON
American Hearing Aid Association	FRED W. KRANZ
American Institute of Electrical Engineers	P. W. BLYE
	C. R. HANNA
	P. L. ALGER
	B. F. BAILEY (*Alt*)
	ELLSWORTH D. COOK (*Alt*)
	H. M. TURNER (*Alt*)
American Institute of Physics	L. L. BERANEK
American Medical Association	HOWARD A. CARTER
	HALLOWELL DAVIS (MD)
American Otological Society, Inc	EDMUND P. FOWLER (MD)
American Physical Society	EDWARD C. WENTE
American Society for Testing Materials (*Liaison*)	R. E. HESS
American Society of Heating and Ventilating Engineers	T. A. WALTERS
	PAUL D. CLOSE (*Alt*)

Organization Represented	*Name of Representative*
American Society of Mechanical Engineers	Raymond V. Parsons (*Alt*)
Canadian Standards Association (*Liaison*)	T. D. Northwood
Department of the Air Force	Harry Schecter
	J. Edwin Wilson
Department of the Army, Medical Corps	Colonel Merritt G. Ringer
	Colonel Austin Lowrey, Jr (*Alt*)
Department of the Army, Signal Corps	Raoul A. Faralla
Department of the Navy, Bureau of Ships, Code 665	P. J. Weber
	P. M. Barzilaski (*Alt*)
	V. L. Chrisler (*Alt*)
	C. K. Smith (*Alt*)
Electric Light and Power Group	W. T. Smith (*Alt*)
General Radio Company	Arnold P. G. Peterson
Institute of Radio Engineers	E. Dietze
	Harry F. Olson
International City Managers Association	Edward S. Clark
Motion Picture Research Council, Inc	Gordon Edwards
	Gordon Sawyer
National Association of Fan Manufacturers	R. D. Madison
	J. L. Lennon (*Alt*)
National Bureau of Standards, U. S. Department of Commerce	Richard K. Cook
National Electrical Manufacturers Association	W. E. Pakala
	E. J. Erdelsky
	J. J. Smith
	A. H. Fiske, Jr (*Alt*)
	Ira Reindel (*Alt*)
	H. C. Werner (*Alt*)
Radio Manufacturers Association	Hugh S. Knowles
Hermon Hosmer Scott, Inc	H. H. Scott
Society of Automotive Engineers	L. M. Ball
	Paul Huber
Society of Motion Picture Engineers	Frederick C. Schmid
ASA Telephone Group	B. C. Burden
	G. W. Gilman
	A. H. Inglis
	C. H. G. Gray (*Alt*)
	Benjamin Olney (*Alt*)
	J. A. Parrott (*Alt*)
U. S. Public Health Service	George D. Clayton
	Dohrman H. Byers (*Alt*)
Members-at-Large	L. Batchelder
	Floyd A. Firestone
	R. B. Lindsay
	H. A. Leedy
	F. V. Hunt
	A. M. Small
	Wallace Waterfall

Subcommittee B on Fundamental Sound Measurement, which was responsible for the development of this standard, has the following personnel:

Leo L. Beranek, *Chairman*

L. J. Anderson
B. B. Bauer
R. K. Cook
G. S. Field
F. A. Firestone
M. G. Kolmes
Frank Massa
Keron Morrical
Harry F. Olson
Arnold P. G. Peterson
F. F. Romanow
Harry Schecter
H. H. Scott
A. Stephan
W. Wathen-Dunn
P. J. Weber
P. M. Barzilaski (*Alt*)
C. K. Smith (*Alt*)
J. Edwin Wilson

The Writing Group directly responsible for the drafting of this standard is as follows:

B. B. Bauer
L. L. Beranek
R. K. Cook
F. F. Romanow
F. M. Wiener

Contents

Introduction

The technique for the primary calibration of standard microphones described herein is based on the results of experience gained over the past few years at the National Bureau of Standards, the Bell Telephone Laboratories, and Harvard University. The technique for secondary calibration of general laboratory microphones by comparison with standard microphones will be developed in another specification. The original calibration techniques described in American Recommended Practice for the Calibration of Microphones, Z24.4-1938, have been superseded by the reciprocity technique, and while it is not the intent to reject the older methods of calibration (use of thermophone, pistonphone, Rayleigh disc, etc), it is believed that the methods described herein represent the best practice consistent with the present state of the art. This relatively new technique will yield more accurate results over a wider frequency range than any of the older methods, and in addition is more convenient to use in the laboratory. Although numerous problems still exist, particularly at high audio frequencies in the free field, it is believed that sufficient progress has been made to warrant this revision and it is hoped it will assist industry and research laboratories working on acoustical measurements.

American Standard Method for the

Pressure Calibration of Laboratory Standard Pressure Microphones

1. Scope and Purpose

1.1 This standard describes a method for securing absolute primary calibrations of laboratory standard pressure microphones as described in American Standard Specification for Laboratory Standard Pressure Microphones, Z24.8-1949, by the reciprocity technique. Also described is the procedure for making secondary calibrations of standard microphones.

2. Definitions

2.1 Open-Circuit Voltage. The root-mean-square (rms) open-circuit voltage of a microphone at a given single frequency is the voltage appearing at its terminals when the microphone is working into an effectively infinite electrical impedance.

Unit: Volt

NOTE: *Substitution Method.* The open-circuit voltage of a microphone for which Thevenin's theorem applies is determined by the following method: The two accessible electrical terminals of a microphone, on which sound pressure is acting, can be regarded as the terminals of a generator having an internal electrical impedance connected in series with an open-circuit voltage. The open-circuit voltage is measured by connecting a source of known and adjustable voltage, in series with the microphone and an amplifier-indicator system. The microphone diaphragm is terminated acoustically with the same impedance when the calibrating voltage is applied as when the sound field is applied. The calibrating voltage is adjusted until the same indicator reading is produced as is produced by the electromotive force generated by a given sound pressure acting on the microphone diaphragm in the absence of the calibrating voltage. The open-circuit voltage is then equal in magnitude to the calibrating voltage. The connection of the known calibrating-voltage source to the microphone adds an accessible electrical terminal to the microphone and calibrating-voltage system. The new terminal is at ground potential (Fig. 1, p 10) and serves as a shield to fix the impedance between the terminals of the microphone. The rms value of the open-circuit voltage shall be expressed in absolute volts.* In actual practice a guard ring such as that shown in Fig. 6 must be used.

2.2 Pressure Response. The pressure response of a microphone at a given single frequency is 20 times the logarithm to the base 10 of the ratio of the rms, open-circuit voltage, to the rms sound pressure when the sound pressure is uniformly applied over the surface of the pressure-sensitive element (diaphragm).

*Prior to January 1, 1948, the practical volt accepted in this country equalled one international volt. Since that date, however, the absolute volt has been adopted. One international volt = 1.00033 absolute volts.

The ratio of the open-circuit voltage to the sound pressure causing it is generally a complex number. The pressure response is 20 times the logarithm to the base 10 of the absolute value of this complex ratio.

Cgs unit: db relative to 1.00 volt $dyne^{-1}$ cm^2 (volt $microbar^{-1}$)

Mks unit: db relative to 1.00 volt $newton^{-1}$ m^2

2.3 Pressure-Response Phase Angle. The pressure-response phase angle of a microphone at a given single frequency is the phase angle between the open-circuit voltage and the sound pressure uniformly applied over the surface of the pressure-sensitive element (diaphragm).

Unit: Degrees

2.4 Free Field. A free field is a field (wave or potential) in a homogeneous, isotropic medium free from boundaries. In practice it is a field in which the effects of the boundaries are negligible over the region of interest.

NOTE: The actual pressure impinging on an object (*e.g.*, electroacoustic transducer) placed in an otherwise free sound field will differ from the pressure which would exist at that point with the object removed, unless the acoustical impedance of the object matches the acoustical impedance of the medium.

2.5 Free-Field Voltage Response (Receiving Voltage Sensitivity). The free-field voltage response of an electroacoustical transducer used for sound reception is the ratio of the voltage appearing at the output terminals of the transducer when the output terminals are open-circuited to the free-field sound pressure existing at the transducer location prior to the introduction of the transducer in the sound field.

The free-field voltage response is usually expressed in decibels, *viz*, 20 times the logarithm to the base 10 of the quotient of the observed ratio divided by the reference ratio, usually 1 volt per microbar. The free-field response is defined for a plane progressive sound wave whose direction of propagation has a specified orientation with respect to the principal axis of the transducer.

Cgs unit: db relative to 1.00 volt $dyne^{-1}$ cm^2 (volt $microbar^{-1}$)

Mks unit: db relative to 1.00 volt $newton^{-1}$ m^2

2.6 Microphone Location. Microphone location is a point in space fixed with respect to the sound source which coincides with the arbitrary microphone center during calibration. For pressure microphones, this point is chosen to be in the plane of the pressure-sensitive element (diaphragm).

2.7 Electrical-Output Impedance. For pressure or free-field calibrations, the electrical-output impedance of a microphone at a given single frequency is defined as the complex ratio of the voltage applied across its electric terminals to the resulting current.

This impedance is a function of the acoustical impedance loading the microphone.
Unit: Absolute ohm

2.8 Acoustical Impedance of a Microphone. The acoustical impedance of a microphone at a given single frequency is the complex ratio of the sound pressure uniformly applied over the surface of the pressure-sensitive element (diaphragm) to the volume velocity.
Units: Acoustical ohm (dyne sec cm^{-5})

NOTE: The value of this quantity depends upon the electrical termination.

2.9 Equivalent Volume of a Microphone. In dealing with closed cavity measurements (coupler measurements), it is convenient to express the acoustical input impedance of a microphone of the type described in terms of the acoustical impedance of an equivalent volume V_e of a gas enclosed in a rigid cavity by use of the following relation

$$V_e = \frac{\gamma P_a}{j\omega Z_a}$$

where

	Cgs System	Mks System
V_e = equivalent volume	cm^3	m^3
γ = ratio of specific heats	number	number
P_a = ambient pressure	dyne cm^{-2}	newton m^{-2}
$\omega = 2\pi f$	rad sec^{-1}	rad sec^{-1}
f = frequency	cps	cps
Z_a = acoustical impedance of the microphone	dyne sec cm^{-5}	newton sec m^{-5}

NOTE: The equivalent volume of a microphone should be specified by the designer or the manufacturer.

2.10 Reversible Microphone. Consider a linear, passive, electroacoustical transducer. Let p = pressure applied to the diaphragm and E = voltage applied to the electric terminals. Both p and E are sinusoidal and of the same frequency. Let u = diaphragm volume velocity, and i = current through the electric terminals. The equations of the transducer are

$$\begin{aligned} z_{11}i + z_{12}u &= E \\ z_{21}i + z_{22}u &= p \end{aligned} \qquad \text{(Eq 1)}$$

where z_{22} is the acoustical impedance looking into the transducer when the electric terminals are open, and z_{11} is the electrical impedance looking into the transducer when the mechanical motion is stopped (diaphragm blocked). The transducer is said to be reversible if the transduction coefficients z_{12} and z_{21}, when expressed in a consistent system of units, are such that $|z_{12}| = |z_{21}|$.

3. Primary Calibration

3.1 General. The primary calibration technique is based on an application of the reciprocity principle to a microphone which is reversible.

3.2 Pressure Calibration. Let e_b and e_c' be the open-circuit voltages of microphones B and C, respectively, when the same sound pressure p in dynes cm^{-2} is applied to the microphones. Let ρ_b be the complex ratio of e_b/p, and Z_b the electrical-output impedance in ohms of the reversible microphone B which is used both as a sound source and as a microphone to calibrate microphone C. Similarly, let ρ_c be the complex ratio e_c'/p of microphone C.

Since microphone B is reversible, its transduction coefficients B_{12} and B_{21} for the mixed system of units comprised of absolute electrical and cgs acoustical units are related by

$$B_{12} = 10^{-7} B_{21} e^{j\beta}$$

where
ϵ = the base of natural logarithm
$j = \sqrt{-1}$
β = a real number

First obtain the ratio ρ_b/ρ_c by applying the same sound pressure p to both microphones and measuring the ratio of the output voltages e_b/e_c'. Then

$$\frac{\rho_b}{\rho_c} = \frac{e_b}{e_c'} \qquad \text{(Eq 2)}$$

This ratio is obtained by placing microphones B and C in succession in the lower wall of a coupler, a typical one of which is shown in Fig. 4 (p 12). A third microphone, placed in the upper wall of the cavity, serves as a source of sound of adjustable frequency.

Second, use microphone B as a source of sound, and microphone C as a microphone. By application of the

reciprocity principle to microphone B, the volume velocity u_b in cm³ per second of the diaphragm of microphone B due to a voltage E_b'' applied to the microphone is

$$u_b = 10^7 \epsilon^{-j\beta} \rho_b E_b''/Z_b$$

The sound pressure due to the volume velocity u_b of microphone B is

$$p'' = \frac{\gamma P_a u_b}{j\omega V} \qquad \text{(Eq 3)}$$

where

p'' = sound pressure in dynes per cm² due to volume velocity of microphone B
γ = ratio of the specific heats of the gas in the cavity (at 25 C and 1 atmosphere for air $\gamma = 1.402$; for hydrogen $\gamma = 1.408$)
P_a = ambient static pressure in the cavity in dynes per cm²
$\omega = 2\pi f$, f = frequency in cycles per second
V = volume of coupler cavity in cm³

Let e_c'' be the open-circuit voltage of microphone C due to the sound pressure p'' produced by microphone B when voltage E_b'' is applied to it. Combination of the equations above yields

$$\rho_b \rho_c = \frac{10^{-7} j\omega Z_b V}{\gamma P_a} \cdot \frac{e_c''}{E_b''} \epsilon^{j\beta} \qquad \text{(Eq 4)}$$

Simultaneous solution of Equations (2) and (4) results in the following values of ρ_b and ρ_c.

$$\rho_b = \pm \sqrt{\frac{10^{-7} j\omega Z_b V}{\gamma P_a} \cdot \frac{e_b}{e_c'} \cdot \frac{e_c''}{E_b''} \epsilon^{j\beta}} \ \frac{\text{cm}^2 \text{ volts}}{\text{dynes}}$$

$$\rho_c = \pm \sqrt{\frac{10^{-7} j\omega Z_b V}{\gamma P_a} \cdot \frac{e_c'}{e_b} \cdot \frac{e_c''}{E_b''} \epsilon^{j\beta}} \ \frac{\text{cm}^2 \text{ volts}}{\text{dynes}} \qquad \text{(Eq 5)}$$

The pressure responses are $20 \log_{10} | \rho_b |$ and $20 \log_{10} | \rho_c |$ in db relative to 1 volt dyne^{-1} cm². The pressure-response phase angle for the microphone is the phase angle of ρ_b or ρ_c expressed in degrees.

3.3 Correction Factors. In the derivation of Equation (3) above, it is assumed that the acoustical impedance of the volume V is negligibly small with respect to the acoustical impedances of the transducer diaphragms and can be calculated from the simple relationship, $\gamma P_a/(j\omega V)$. Such a simple relationship only exists if (*a*) there is no appreciable change in the impedance because of the presence of the capillary tubes used for admitting the hydrogen, if (*b*) the ratio of the volume of the cavity to the product of its surface area times the square root of the wavelength is a sufficiently large quantity so that heat conduction at the sidewalls can be neglected, and if (*c*) the maximum dimensions of the cavity are small relative to the wavelength of sound. If conditions (*a*), (*b*), or (*c*) are violated singly or together the value of the acoustical impedance is not equal exactly to $\gamma P_a/j\omega V$.

3.3.1 *Capillary Correction.* The acoustical impedance Z_c of two capillary tubes of equal length in parallel is given by the relation

$$Z_c = \frac{4\pi\eta d}{(\pi r^2)^2} + j \frac{2\omega\rho d}{3\pi r^2} \text{ acoustical ohms} \qquad \text{(Eq 6)}$$

where

η = coefficient of viscosity in poise (at 25 C and 1 atmosphere for air $\eta = 187 \times 10^{-6}$; for hydrogen $\eta = 88.6 \times 10^{-6}$)
d = length of each of the capillary tubes in cm
r = radius of each of the capillary tubes in cm
ρ = density in gms per cm³ (at 25 C and 1 atmosphere for air $\rho = 1.185 \times 10^{-3}$; for hydrogen $\rho = 0.082 \times 10^{-3}$)

The impedance of the capillaries shunts the impedance due to the cavity volume resulting in an effective cavity impedance denoted by Z_T given by

$$Z_T = \frac{\gamma P_a}{j\omega V} \frac{Z_c}{Z_c + \gamma P_a/j\omega V} \qquad \text{(Eq 7)}$$

To allow for the impedance of the capillaries, $\gamma P_a/j\omega V$ in Equation (5) should be replaced by Z_T. This would add to the pressure response $20 \log_{10}(\rho)$ the term

$$10 \log_{10} | 1 + \gamma P_a/j\omega V Z_c | \text{ db} \qquad \text{(Eq 8)}$$

The phase angles of Equation (5) should be corrected by subtracting from them one-half of the phase angle of the quantity inside the brackets of Equation (7).

3.3.2 *Heat Conduction Correction.* The correction term "A" in decibels and the phase angle in degrees necessary to include the effects of heat conduction at the walls of the cavity are plotted graphically in Fig. 2 (p 11). The meanings of the symbols are indicated on the graphs.

3.3.3 *Equivalent Microphone Volume Correction.* If the equivalent volume of the microphone exceeds approximately ½ percent of the volume V of the coupler cavity, twice the equivalent volume of the microphone should be added to the value of V in Equation (5).

3.3.4 *Wave-Motion Correction.* The correction due to wave motion to be added to $20 \log_{10} | \rho |$ obtained from Equation (5) is given by $10 \log_{10} r_w/r_{fw}$ where r_w is the ratio of the voltage applied to the sound source to the open-circuit voltage generated by the

microphone and r_{fw} is what this ratio would be were the cavity free from wave motion. The correction can be determined by measuring the above voltage ratio with the coupling cavity filled with air in one case and with hydrogen in another. The correction for air in the chamber is then obtained by letting the voltage ratio for air equal r_w and the voltage ratio for hydrogen (with the effects of differences in thermal conductivities, capillary impedances, and ratios of specific heats between air and hydrogen discounted), equal to r_{fw}. The correction for the cavity filled with hydrogen is the same as that for air with the frequency scale shifted by the ratio of the velocity of sound in hydrogen to that in air. At the higher frequencies, the difference in the voltage ratios thus obtained may not give the complete correction, since some wave motion may exist for the chamber filled with hydrogen.

The wave motion correction is a function of the chamber dimensions. The ratio of the diameter to the length of the chamber of Fig. 4 (p 12) is near the optimum for best chamber performance. When filled with hydrogen at 25 C and one atmosphere, the wave-motion correction for this chamber is less than ± 0.1 db up to 15 kc.

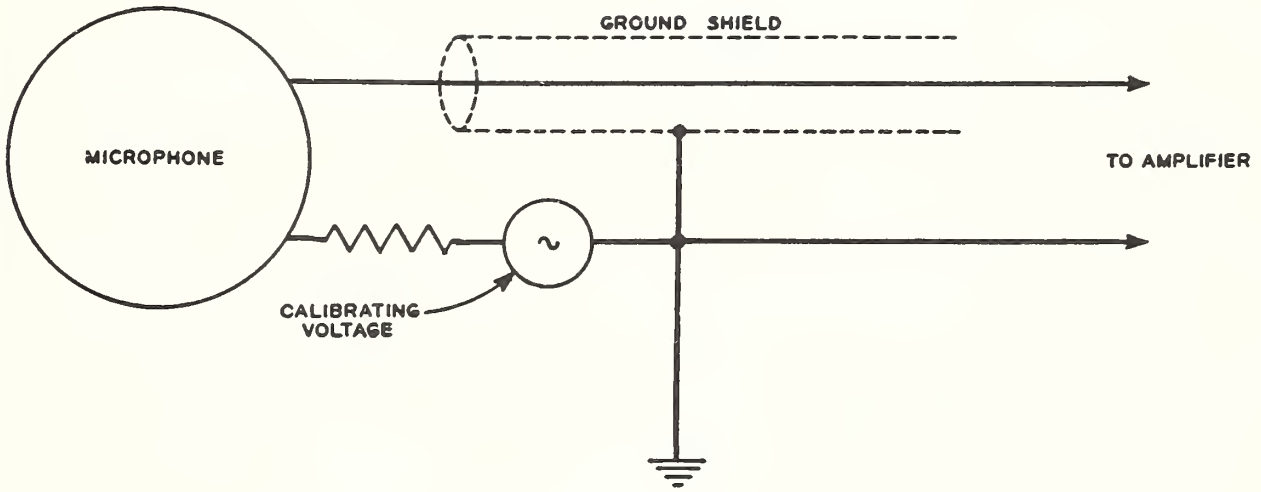

FIG. 1
Technique of Introducing Calibrating Voltage

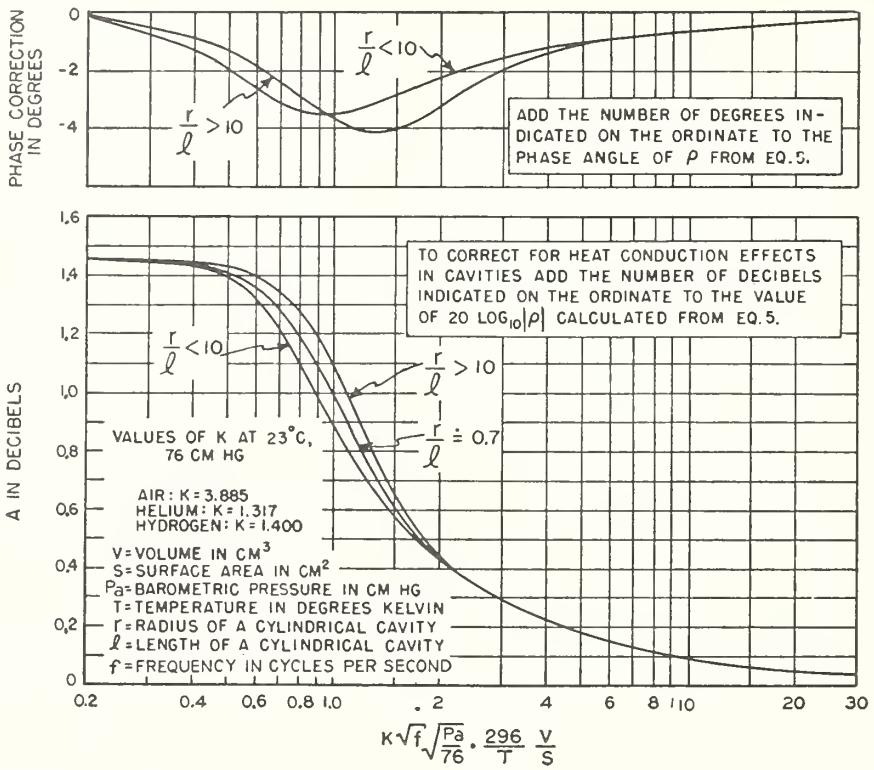

FIG. 2
Chart for Determining Heat Conduction Correction for Couplers

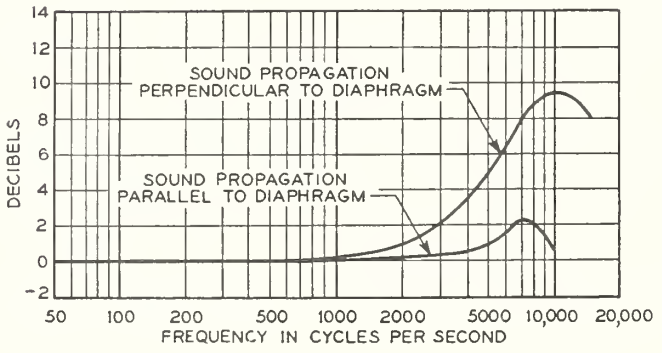

FIG. 3
Free-Field Responses Minus Pressure Response for a Type-L Laboratory Standard Pressure Microphone when Attached to a Mounting as Shown in Fig. 5

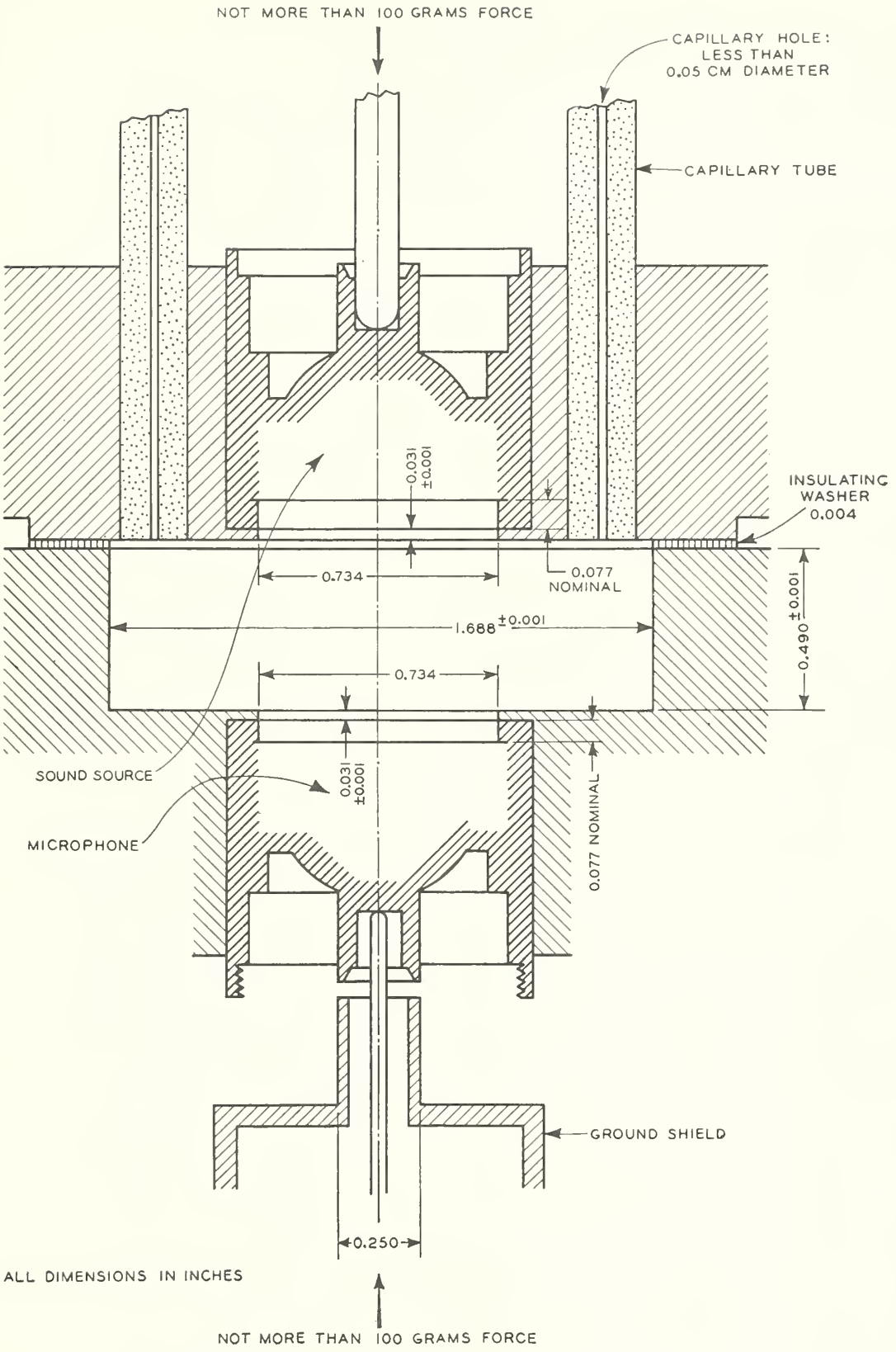

FIG. 4
Typical Cavity for Reciprocity Calibration of Type-L Laboratory Standard Microphones

574278 O - 61 - 58

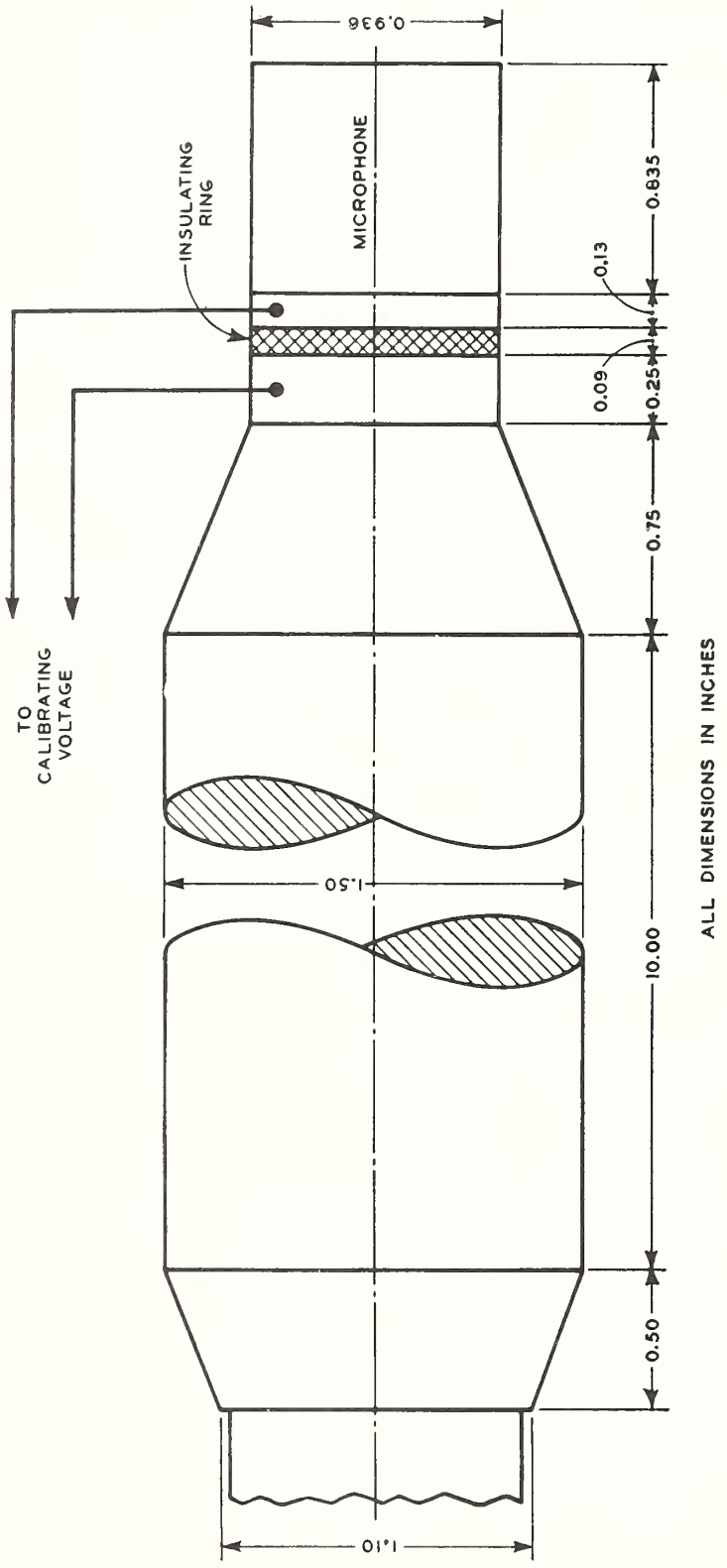

FIG. 5
Outline Drawing of Type-L Laboratory Standard Microphone and Preamplifier
Used in Obtaining Data of Table 1 and Fig. 3

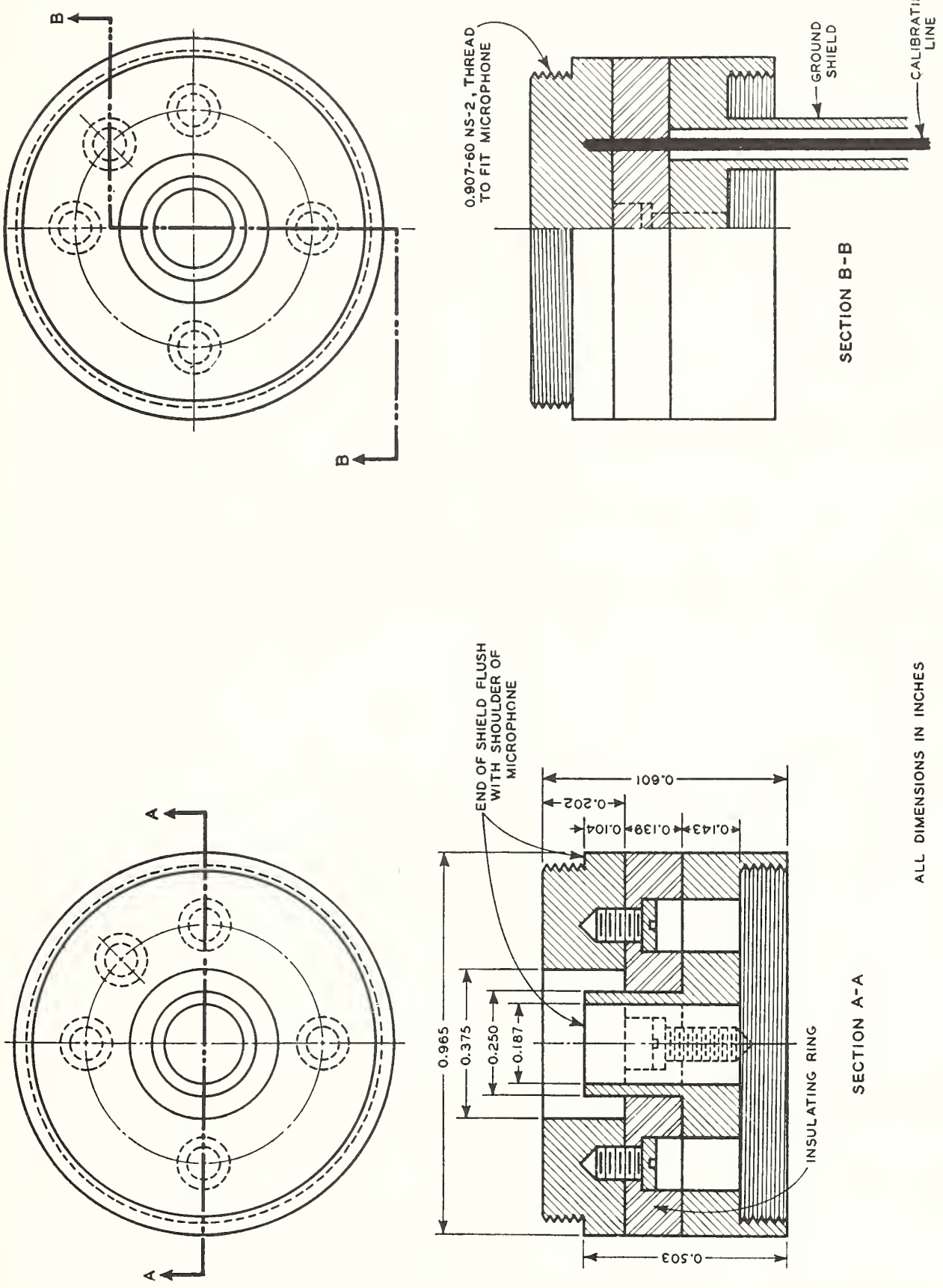

FIG. 6
Insulating Ring and Ground Shield Used at National Bureau of Standards when Calibrating Type-L Standard Microphone

Appendix

This Appendix is not a part of the American Standard Method for the Pressure Calibration of Laboratory Standard Pressure Microphones, Z24.4-1949, but is included to aid users of the standard.

A1 Secondary Pressure Calibration. A standard microphone whose pressure response is not known is calibrated by comparison with another standard microphone which has a known primary pressure calibration. The comparison is made by placing the microphones in succession in the lower wall of a coupler such as that shown in Fig. 4 (p 12). A third microphone, placed in the upper wall of the cavity, serves as a source of sound of adjustable frequency. The differences of the pressure responses are obtained from ρ_2/ρ_1, which is computed as in 3.2, Equation (2).

A2 Plane-Wave Free-Field Calibration. The method of making free-field calibration is beyond the scope of this standard. However, for the convenience of the users of this standard, information is given in Table 1 and Fig. 3 (p 11) which permits the determination of the plane-wave free-field calibration of a Type-L laboratory standard pressure microphone when attached to the mounting shown in Fig. 5 (p 13). The differences obtained by subtracting the pressure response from the free-field response for both the case in which the approximate plane wave is propagated in the same direction as the inward normal to the diaphragm and the case in which the propagation is parallel to the diaphragm are given in Table 1. In Fig. 3 are given curves plotted from these values. Free-field responses may be obtained by adding these values to the pressure response.

A3 Reciprocity Pressure Calibration Formula which Includes the Acoustical Impedances of the Transducer Diaphragm. The analysis of 3.2, Pressure Calibration, is simplified by assuming that the acoustical impedance of the coupling chamber is negligibly small compared to that of the transducer diaphragms and that the impedance of the chamber is given by $\gamma P_a/j\omega V$. In the analysis below neither of these assumptions is made but it is assumed that the wavelength of sound is so large that uniform pressure exists throughout the chamber. The formulas derived here, therefore, require no corrections due to (*a*) the finite values of the diaphragm impedances, (*b*) capillary leaks, and (*c*) heat conduction to chamber walls. However, if wave motion exists, a corresponding correction must be applied.

The measurements on which this analysis is based are the same as those of 3.2, Pressure Calibration. Three transducers A, B, and C are used. Two transducers at a time are coupled to the chamber and at each

TABLE 1
Differences of Free-Field Response Minus Pressure Response for a Type-L Laboratory Standard Pressure Microphone Having the Dimensions and Mounting of Fig. 5 (p 13)

Frequency cps	Free-Field Response Minus Pressure Response in db	
	Sound propagated perpendicular to diaphragm	Sound propagated parallel to diaphragm
300	0.0	—
500	0.1	0.0
700	0.2	—
1000	0.3	0.0
1500	0.5	—
2000	0.9	0.2
2500	1.5	—
3000	2.2	0.3
4000	3.5	0.5
5000	4.9	1.1
6000	6.5	1.5
6500	7.3	—
7000	7.9	2.2
7500	8.4	—
8000	8.8	1.9
9000	9.2	1.5
10000	9.4	0.7
11000	9.4	—
12000	9.2	—
13000	8.9	—
14000	8.4	—
15000	7.9	—

frequency of measurement the ratio of the open-circuit voltage generated by one to the voltage applied to the other is measured. Three such measurements are made as follows:

Measurement	Sound Source Transducer	Microphone Transducer	Ratio Measured
1	A	B	e_b/E_a
2	A	C	e_c'/E_a'
3	B	C	e_c''/E_b''

The small e's represent the open-circuit voltages and the large E's represent applied voltages.

The electrical impedance loading the transducers, when used as microphones, is represented by Z_l. The acoustical impedance of the chamber, with both transducer diaphragms blocked, is represented by Z_v. Z_v includes such effects as the shunt impedance of the capillary tubes and the reduction in impedance due to heat conduction to the chamber walls. The impedance elements of transducer A are defined below. Corresponding symbols with b and c replacing a apply respectively to transducers B and C.

a_{11} = the electrical impedance with the diaphragm blocked

a_{12} = a transduction coefficient and equals the negative of the ratio of the generated open-circuit voltage to the volume velocity applied to the diaphragm

a_{21} = the other transduction coefficient and equals the negative of the ratio of the effective generated blocked pressure to the current applied

a_{22} = the acoustical impedance of the diaphragm with the electrical terminals open circuited

u_a = the volume velocity of the diaphragm

The equations of motion for Measurement 1 are

$$\begin{aligned} I_a a_{11} + u_a a_{12} &= E_a \\ I_a a_{21} + u_a(a_{22}+Z_v) - u_b Z_v &= 0 \\ -u_a Z_v + u_b(Z_v+b_{22}) + i_b b_{21} &= 0 \\ +u_b b_{12} + i_b(b_{11}+Z_l) &= 0 \end{aligned} \qquad \text{(Eq 1)}$$

It is assumed that the system of units being used is consistent and that transducer B is reversible, therefore, we have

$$b_{12} = b_{21}\epsilon^{j\beta} \qquad \text{(Eq 2)}$$

where

β = a real number

ϵ = the base of natural logarithm

The open-circuit voltage generated by transducer B is given by

$$e_b = \lim_{Z_l \to \infty} i_b Z_l \qquad \text{(Eq 3)}$$

Solving Equation (1) for i_b and taking the limit gives

$$e_b = E_a\left(\frac{a_{21}b_{12}}{a_{22}b_{22}}\right)\left(\frac{a_{22}b_{22}Z_v}{a_{22}b_{22}+a_{22}Z_v+b_{22}Z_v}\right)\left(\frac{1}{a_{11}-a_{12}a_{21}/[a_{22}+b_{22}Z_v/(b_{22}+Z_v)]}\right) \qquad \text{(Eq 4)}$$

The second term in brackets is the acoustical impedance of the chamber in parallel with the open-circuit acoustical impedances of transducers A and B. Let this impedance be denoted by Z_{vab}. The denominator of the third term in brackets is the electrical impedance of transducer A with transducer B open-circuited. Denote this impedance by Z_{avb}. Using these symbols Equation (4) becomes

$$e_b/E_a = (a_{21}b_{12}/a_{22}b_{22})\ (Z_{vab}/Z_{avb}) \qquad \text{(Eq 5)}$$

Similar equations for measurements 2 and 3 are

$$e_c'/E_a' = (a_{21}c_{12}/a_{22}c_{22})\ (Z_{vac}/Z_{avc}) \qquad \text{(Eq 6)}$$

$$e_c''/E_b'' = (b_{21}c_{12}/b_{22}c_{22})\ (Z_{vbc}/Z_{bvc}) \qquad \text{(Eq 7)}$$

A simultaneous solution of Equations (5), (6), and (7) gives

$$\frac{b_{12}b_{21}}{b_{22}^2} = \frac{(e_b)}{(E_a)}\frac{(E_a')}{(e_c')}\frac{(e_c'')}{(E_b'')}\frac{(Z_{vac})}{(Z_{vab}Z_{vbc})}\frac{(Z_{avb}Z_{bvc})}{(Z_{avc})} \qquad \text{(Eq 8)}$$

The ratio of the open-circuit voltage generated by B to the open-circuit pressure applied to its diaphragm may be obtained from the definitions of b_{12} and b_{22} and is given by

$$\rho_b = -b_{12}/b_{22} \qquad \text{(Eq 9)}$$

Similarly

$$\rho_c = -c_{12}/c_{22} \qquad \text{(Eq 10)}$$

From Equations (2), (8), and (9) we have

$$\rho_b = \pm\left(\frac{(e_b)}{(E_a)}\frac{(E_a')}{(e_c')}\frac{(e_c'')}{(E_b'')}\frac{(Z_{vac})}{(Z_{vab}Z_{vbc})}\frac{(Z_{avb}Z_{bvc})}{(Z_{avc})}\epsilon^{j\beta}\right)^{1/2} \qquad \text{(Eq 11)}$$

In a similar manner we may obtain from Equations (2), (5), (6), (7), and (10)

$$\rho_c = \pm\left(\frac{(E_a)}{(e_b)}\frac{(e_c')}{(E_a')}\frac{(e_c'')}{(E_b'')}\frac{(Z_{vab})}{(Z_{vac}Z_{vbc})}\frac{(Z_{avc}Z_{bvc})}{(Z_{avb})}\epsilon^{j\beta}\right)^{1/2} \qquad \text{(Eq 12)}$$

Equations (11) and (12) reduce to the expression of Equation (5) of 3.2, for the following conditions in combination; (a) if the impedances of the diaphragms are high relative to the chamber impedance; (b) if the chamber impedance can be expressed by $\gamma P_a/j\omega V$; (c) when the acoustical terms are in cgs units and the electrical terms are in absolute units and (d) if E_a' equals E_a''.

A4 Miscellaneous Remarks. The coupler used for calibration consists basically of a cavity having a right, circular, cylindrical shape. The ratio of the diameter of

the cavity to its height should be approximately 3.5 if freedom from wave-motion corrections is desired over a wide range. (See typical coupler shown in Fig. 4, p 12.) The volume of the cavity is large enough so that the absolute value of its acoustical impedance is at most 2 percent of the absolute value of the acoustical impedance of the microphone diaphragm of a Type-L laboratory standard pressure microphone (see American Standard Specification for Laboratory Standard Pressure Microphones, Z24.8-1949, Table 1).

In making measurements at frequencies between 50 and 3000 cps, the cavity of the coupler shown in Fig. 4 (p 12) is filled with air. For frequencies higher than 3000 cps, the cavity should be filled with pure hydrogen at barometric pressure.

The electrical-output impedance Z_1 of a microphone can be measured by means of a suitable bridge. A Wagner grounded Schering bridge has been found suitable for this purpose when the impedance is mainly capacitative. The ground shield of the microphone (see Figs. 1, 4, and 6) is connected to ground when the microphone is measured in such a bridge.

Bibliography

Reciprocity Calibrations:

(1) Schottky, W.: Tiefempfangsgesetz. *Zeitschrift fur Physik*, **36,** 689 (1926)

(2) Ballantine, S.: Reciprocity in electromagnetic, mechanical, acoustical, and interconnected systems. *Proceedings of the Institute of Radio Engineers*, **17,** 929 (1929)

(3) Dubois, R.: Methodes electrotechniques permettant d'etudier completement les microphones reversible dans l'air et dans l'eau. *Revue d'Acoustique*, *Part I*, **2,** 253-287 (1933) *Part II*, **3,** 27-46 (1934)

(4) Mac Lean, W. R.: Absolute measurement of sound without a primary standard. *Journal of the Acoustical Society of America*, **12,** 140 (1940)

(5) Cook, R. K.: Absolute pressure calibration of microphones. *National Bureau of Standards Journal of Research*, **25,** 489-505 (1940) (Also published in abbreviated form in *Journal of the Acoustical Society of America*, **12,** 415 (1941)

(6) Olson, H. F.: Calibration of microphones by the principles of similarity and reciprocity. *RCA Review*, **6,** 36-42 (1941)

(7) Wiener, F. M.: Reciprocity calibration of a miniature condenser microphone in free space. *Journal of the Acoustical Society of America*, **13,** 119 (1941)

(8) Foldy, L. L. and Primakoff, H.: General theory of passive linear electroacoustic transducers and the electroacoustic reciprocity theorem I. *Journal of the Acoustical Society of America*, **17,** No. 2, 109-120 (1945)

(9) Primakoff, H. and Foldy, L. L.: A general theory of passive linear electroacoustic transducers and the electroacoustic reciprocity theorem II. *Journal of the Acoustical Society of America*, **19,** No. 1, 50 (1947)

(10) Miles, J. W.: Coordinates and the reciprocity theorem in electromechanical systems. *Journal of the Acoustical Society of America*, **19,** No. 5, 910 (1947)

(11) McMillan, E. M.: Further remarks on reciprocity. *Journal of the Acoustical Society of America*, **19,** 922 (1947)

(12) Harvard University: *Report of Psycho-Acoustic Laboratory, PNR-4.* On the technique of absolute pressure calibration of condenser microphones by the reciprocity method.

General Calibration Procedures:

(13) Arnold, H. O. and Crandall, I. B.: The thermophone as a precision source of sound. *Physical Review*, **10,** 22-38 (1917)

(14) Wente, E. C.: A condenser transmitter as a uniformly sensitive instrument for the absolute measurement of sound intensity. *Physical Review*, **10,** 39-63 (1917)

(15) Webster, A. G.: The absolute measurement of sound. *Engineering*, **111,** 763-765 (1921)

(16) Wente, E. C.: The thermophone. *Physical Review*, **19,** 333-345 (1922)

(17) Wente, E. C.: Sensitivity of the electrostatic transmitter for measuring sound intensities. *Physical Review*, **19,** 498-503 (1922)

(18) Paris, E. T.: Doubly resonated hot-wire microphones. *Royal Society Proceedings*, **101,** 391-410 (1922)

(19) Tucker, W. S.: The hot-wire microphone and its applications. *Royal Society Articles*, Journal **171,** 121-134, 134-137 (1923)

(20) Gerlach, E.: Messungen von schalldruckamplituden. *Wissenschaftliche Veroffnungen, a.d. Siemens Konzern*, **3,** 139-143 (1923)

(21) Von Hippel, A.: Experimentelle untersuchung des thermomikrophones. *Annallen der Physik*, **76,** series 4, 590-618 (1925)

(22) Aldridge, A. J., Cohen, B. S., West, W.: The frequency characteristics of telephone systems and audio frequency apparatus, and their measurement. *Journal of the Institute of Electrical Engineers*, **64,** 1023-1064 (1926)

(23) Skinner, C. H.: Anomalous action of the Rayleigh disk. *Physical Review*, **27,** 346-350 (1926)

(24) Hartmann, C. A.: Messungen an mikrophonen und telephonen. *Electrische Nachrichten-technik*, **3,** 458 (1926)

(25) Meyer, E.: Uber die messung der geschwindigkeitsamplitude un der druckamplitude in schallfeldern. *Elektrische Nachrichten-technik*, **4,** 86 (1927)

(26) Barnes, E. J. and West, W.: The calibration and performance of the Rayleigh disk. *Journal of the Institute of Electrical Engineers*, **65,** 871-880 (1927)

(27) Ballantine, S.: Note on the effect of reflection by the microphone in sound measurements. *Proceedings of the Institute of Radio Engineers*, **16,** 1639-1644 (1928)

(28) Ballantine, S.: Note on the effect of reflection by the microphone in sound measurements. *Physical Review*, **32,** 988-992 (1928)

(29) Sivian, L. J.: A modification of the Rayleigh disk method for measuring sound intensities. *Philadelphia Magazine*, **5,** 615-620 (1928)

(30) West, W.: Pressure on the diaphragm of a condenser transmitter. *Proceedings of the Institute of Electrical Engineers*, **5,** 145 (1930)

(31) Ballantine, S.: Effect of cavity resonances on the frequency responses characteristic of the condenser microphone. *Proceedings of the Institute of Radio Engineers*, **18,** 1206 (1930)

(32) Oliver, D. A.: An improved condenser microphone for sound pressure measurements. *Journal Scientific Instruments*, **7,** 113 (1930)

(33) Sivian, L. J.: Absolute calibration of condenser microphones. *Bell System Technical Journal, X*, No. **1,** 108 (Jan. 1931)

(34) Paris, E. T.: Singly resonant hot-wire microphones. *Proceedings of the Physical Society of London*, **43,** 72 (1931)

(35) Drysdale, C. V.: Acoustic measuring instruments. *Physical Society, Discussion on Audition*, 62-78 (June 19, 1931); discussed 135-151

(36) Andrade, E. N. da C.: The absolute measurement of sound amplitudes. *Physical Society, Discussion on Audition*, 79-81 (June 19, 1931); discussed 135-151

(37) Olson, H. F.: Mass controlled electrodynamic microphones: the ribbon microphone. *Journal of the Acoustical Society of America*, **3,** 56 (1931)

(38) Andrade, E. N. da C.: Absolute measurements of sound amplitudes and intensities. *Royal Society Proceedings*, **134,** 445 (1931)

(39) Carriere, Z.: Measures absolues des grandeurs fondamentales en acoustique, Part 2, measurements of amplitudes. *Revue d'Acoustique*, **1,** 110-125 (1932)

(40) Chavasse, P.: Quelques considerations sur l'evolution et l'etat actuel de la technique microphonique. *Revue d'Acoustique*, **1,** 176-221 (1932)

(41) Kotowski, P.: Measurements with Rayleigh disks. *Electrische Nachrichtentechnik*, **9,** 404-406 (1932)

(42) Ballantine, S.: Technique of microphone calibration. *Journal of the Acoustical Society of America*, **3,** 319 (1932)

(43) Abbott, E. J.: Calibration of condenser microphones for sound meters. *Journal of the Acoustical Society of America*, **4,** 235 (1933)

(44) Gorsser, W.: Sensitive Rayleigh disks for sound measurement. *Archivs fur Electrotechnik*, **27,** 329-334 (1933)

(45) Geffcken, W. and Keibs, L.: Investigation of acoustic threshold values: the thermophone and its use for acoustic measurements. *Annallender Physik*. **16,** series 4, 404-430 (1933)
(46) Marshall, R. N. and Romanow, F. F.: A non-directional microphone. *Bell Systems Technical Journal,* **15,** 405 (1936)
(47) Kaye, G. W. C.: Microphone calibration with the Rayleigh disk. *Journal of the Acoustical Society of America*, **7,** 174 (1936)
(48) Andrade, E. N. da C. and Parker, R. C.: A standard source of sound and the measurement of minimum audibility. *Royal Society Proceedings*, **15,** 507 (1937)
(49) Castelliz, H. and Schiller, P. E.: Research on new sound-measuring probes. *Akustisches Zeitschrift*, **2,** 11-17 (1937)
(50) Lehmann, K. O.: Ein neuer akustischer gleichrechter. *Zeitschrift fur Technische Physik*, **18,** 309 (1937)
(51) West, W.: Free field calibration of microphones. *Nature*, **39,** 142 (1938)
(52) Woelke, B.: Electroacoustic measurements with the Rayleigh disk. *Funktech Monashefte*, 281-286 (Sept, 1938)
(53) Hayashi, T. and Kobayashi, M.: A Rayleigh disk of resonance type. *Electrotechnical Journal, Institute of Electrical Engineers of Japan. The Denki-Gakkwai,* **2,** 277-280 (Tokyo) (1938)
(54) Ernsthausen, W.: Absolute calibration of microphones. *Akustische Zeitschrift*, **4,** 13 (1939)
(55) Baumzeiger, B. and Glover, R. P.: Moving coil pistonphone for measurement of sound field pressure. *Journal of the Acoustical Society of America*, **10,** 200. (1939)
(56) Merrington, A. C. and Oatley, C. W.: Accuracy of Konig's formula for the Rayleigh disk. *Royal Society Proceedings*, **171A,** 505-524 (1939)
(57) Hayashi, T.: Calibration of microphone and loudspeaker response by interrupted sound wave. *Nippon Electrical Communication Engineering,* **19,** 165-168 (1940)
(58) Wood, A.: Intensity of sound. *Acoustics*, Chapter XI, 287-313 Interscience Publishers, Inc (New York) (1941)
(59) Boner, C. P. and Kennedy, W. J.: Absolute pressure generator and its application to the free-field calibration of a microphone. *Journal of the Acoustical Society of America*, **14,** 19 (1942)
(60) Rosenberry, H. H. and Smith, W. C.: The Rayleigh disk as a laboratory instrument. *Journal of the Acoustical Society of America*, **16,** 123 (1944)
(61) Scott, R. A.: An investigation of the performance of the Rayleigh disk. *Royal Society Proceedings*, **183A,** 296-316
(62) Daniels, F. B.: Acoustical impedance of enclosure. *Journal of the Acoustical Society of America*, **19,** 569 (1947)
(63) Beranek, L. L.: *Acoustic Measurements*, **IV,** 111-176 John Wiley & Sons, Inc (New York) (1949)
(64) Osrd Report No. 1817: Design, operation, and calibration of the sound pressure meter. (September 25, 1943)
(65) Massa, Frank: Working standard for sound pressure measurements. *Journal of the Acoustical Society of America*, **17,** 29-34 (1945)
(66) Cook, Richard K.: Measurement of the electromotive force of a microphone. *Journal of the Acoustical Society of America*, **19,** 503 (1947)

Revised
October
1960

U. S. DEPARTMENT OF COMMERCE

NATIONAL BUREAU OF STANDARDS
Washington 25, D. C.

List of
Publications
LP36

ENGINEERING MECHANICS

Publications by Members of the Staff of the

National Bureau of Standards

Notes on aerodynamic forces on airship hulls, L. B. Tuckerman. NACA Tech. Note 129 (1923).

An analysis of the deformation of the mooring spindle of the "Shenandoah", L. B. Tuckerman and C. S. Aitchison. Tech. Pap. BS 18, 609 (1925).

Inertia factors of ellipsoids for use in airship design, L. B. Tuckerman. NACA Tech. Report 210, 11th annual report (1925).

Technical aspects of the loss of the U. S. S. Shenandoah, J. Am. Soc. Naval Engrs. 38, No. 3 (1926).

Strength of tubing under combined axial and transverse loading, L. B. Tuckerman, S. N. Petrenko, and C. D. Johnson. NACA Tech. Note 307 (1929).

Strength of welded joints in tubular members for aircraft, H. L. Whittemore and W. C. Brueggeman. NACA Tech. Reports 16, No. 348 (1930). J. Am. Welding Soc. 9, 107 (1930).

Strength of rectangular flat plates under edge compression, L. Schuman and G. Back. NACA Tech. Reports 16, No. 356 (1930).

Contribution to the design of compression members in aircraft, W. R. Osgood. J. Research NBS 13, 157 (1934) RP698.

Aircraft: Materials and testing, Edgar Marburg Lecture, L. B. Tuckerman. Proc. Am. Soc. Testing Materials 35, Pt. II, 3 (1935).

An interesting case of sub-multiple resonance, L. B. Tuckerman and W. Ramberg. Phys. Rev. 49, No. 11, 862, 2d series (1936).

Strength of welded aircraft joints, W. C. Brueggeman. NACA Tech. Reports 23, No. 584 (1937).

Torsion tests of tubes, A. H. Stang, W. Ramberg and G. Back. NACA Tech. Reports 23, No. 601 (1937).

Column strength of tubes elastically restrained against rotation at the ends, W. R. Osgood. NACA Tech. Reports 24, No. 615 (1938).

Fatigue testing of wing beams by the resonance method, W. M. Bleakney. NACA Tech. Note 660 (1938).

Experimental study of deformation and effective width in axially loaded sheet-stringer panels, W. Ramberg, A. E. McPherson and S. Levy. NACA Tech. Note 684 (1939).

Calculation of stresses and natural frequencies for a rotating propeller blade vibrating flexurally, W. Ramberg and S. Levy. J. Research NBS 21, 639 (1938) RP1148.

The column strength of two extruded aluminum alloy H-sections, W. R. Osgood and Marshall Holt. NACA Tech. Reports 25, No. 656 (1939).

Compressive test of a monocoque box, W. Ramberg, A. E. McPherson, and S. Levy. NACA Tech. Note 721 (1939).

Principles of moment distribution applied to stability of structural members, W. R. Osgood. Discussion. Proc. 5th Intern. Congress for Appl. Mechanics 149 (1939).

Dimensionless coefficients applied to the solution of column problems, W. R. Osgood. Discussion. J. Aeronaut. Sci. 8, No. 1, 23 (1940).

Mechanical properties of flush-riveted joints, W. C. Brueggemen and F. C. Roop. NACA Tech. Report 701 (1940).

Mechanical properties of flush-riveted joints submitted by five airplane manufacturers, W. C. Brueggeman. NACA Wartime report W-79 (1942).

Rectangular plate loaded along two adjacent edges by couples in its own plane, W. R. Osgood. J. Research NBS 28, 159 (1942) RP1450.

Bending of rectangular plates with large deflections, S. Levy. NACA Tech. Report 737 (1942).

Square plate with clamped edges under normal pressure producing large deflections, S. Levy. NACA Tech. Report 740 (1942).

Normal-pressure tests of circular plates with clamped edges, A. E. McPherson, W. Ramberg, and S. Levy. NACA Tech. Report 744 (1942).

Torsion test of a monocoque box, S. Levy, A. E. McPherson, and W. Ramberg. NACA Tech. Note 872 (1942).

Normal-pressure tests of rectangular plates, W. Ramberg, A. E. McPherson, and S. Levy. NACA Tech. Report 748 (1942).

Bending with large deflection of a clamped rectangular plate with length-width ratio of 1.5 under normal pressure, S. Levy and S. Greenman. NACA Tech. Note 853 (1942).

Effect of rivet and spot-welded spacing on the strength of axially loaded sheet-stringer panels of 24S-T aluminum alloy, S. Levy, A. E. McPherson, and W. Ramberg. NACA Tech. Note 856 (1942).

Bending tests of a monocoque box, A. E. McPherson, W. Ramberg, and S. Levy. NACA Tech. Note 873 (1942).

Buckling of rectangular plates with built-in edges, S. Levy. J. Appl. Mech. 9, No. 4, A-171 (1942).

Large-deflection theory for end compression of long rectangular plates rigidly clamped along two edges, S. Levy and P. Krupen. NACA Tech. Note 884 (1943).

Large-deflection theory of curved sheet, S. Levy. NACA Tech. Note 895 (1943).

The center of shear again, W. R. Osgood. J. Appl. Mech. 10, No. 2, A-62 (1943).

Effect of curvature on strength of axially loaded sheet-stringer panels, W. Ramberg, S. Levy and K. L. Fienup. NACA Tech. Note 944 (1944).

Torsion test to failure of a monocoque box, A. E. McPherson, D. Goldenberg, and G. Zibritosky. NACA Tech. Note 953 (1944).

Effect of developed width on strength of axially loaded curved sheet stringer panels, A. E. McPherson, K. L. Fienup, and G. Zibritosky. NACA Wartime Report W-51 (1944).

Simply supported long rectangular plate under combined axial load and normal pressure, S. Levy, D. Goldenberg, and G. Zibritosky. NACA Tech. Note 949 (1944).

Axial fatigue test of 10 airplane wing-beam specimens by the resonance method, W. C. Brueggeman, P. Krupen, and F. C. Roop. NACA Tech. Note 959 (1944).

Notes on columns, W. R. Osgood. Discussion. J. Aeronaut. Sci. 11, No. 3, 196 (1944).

Corrections for lengths of columns tested between knife edges, W. R. Osgood. J. Aeronaut. Sci. 11, No. 4, 378 (1944).

Column formulas, W. R. Osgood. Proc. Am. Soc. Civil Engineers 70, No. 1 (1944).

Axial fatigue tests at zero mean stress of 24S-T aluminum alloy sheet with and without a circular hole, W. C. Brueggeman, M. Mayer, Jr., and W. H. Smith. NACA Tech. Note 955 (1944).

Analysis of square shear web above buckling load, S. Levy, K. L. Fienup, and R. M. Woolley. NACA Tech. Note 962 (1945).

Axial fatigue tests at two stress amplitudes of 0.032-inch 24S-T sheet specimens with a circular hole, W. C. Brueggeman, M. Mayer, Jr., and W. H. Smith. NACA Tech. Note 983 (1945).

Strength of wing beams under axial and transverse loads, W. Ramberg, A. E. McPherson, and S. Levy. NACA Tech. Note 988 (1945).

Instability of extrusions under compressive loads, W. Ramberg and S. Levy. J. Aeronaut. Sci. 12, No. 4, 485 (1945).

Plastic bending - approximate solution, W. R. Osgood. J. Aeronaut. Sci. 12, No. 4, 408 (1945).

Analysis of deep rectangular shear web above buckling load, S. Levy, R. M. Woolley, and J. N. Corrick. NACA Tech. Note 1009 (1946).

Clamped long rectangular plate under combined axial load and normal pressure, R. M. Woolley, J. N. Corrick, and S. Levy. NACA Tech. Note 1047 (1946).

Effect of normal pressure on strength of axially loaded sheet-stringer panels, A. E. McPherson, S. Levy, and G. Zibritosky. NACA Tech. Note 1041 (1946).

Instability of outstanding flanges simply supported at one edge and reinforced by bulbs at other edge, S. Goodman and E. Boyd. NACA Tech. Note 1433 (1947).

Instability of simply supported square plate with reinforced circular hole in edge compression, S. Levy, R. M. Woolley, and W. D. Kroll. J. Research NBS 39, 571 (1947) RP1849.

Computation of influence coefficients for aircraft structures with discontinuities and sweep-back, S. Levy. J. Aeronaut. Sci. 14, No. 10, 547 (1947).

Reinforcement of a small circular hole in a plane sheet under tension, S. Levy, A. E. McPherson, and F. C. Smith. J. Appl. Mech. 15, No. 2, 160 (1948).

Experimental verification of theory of landing impact, W. Ramberg and A. E. McPherson. J. Research NBS 41, 509 (1948) RP1936; NBS Tech. News Bul. 32, 42 (1948).

Axial fatigue tests at zero mean stress of 24S-T and 75S-T aluminum-alloy strips with a central circular hole, W. C. Brueggeman and M. Mayer, Jr. NACA Tech. Note 1611 (1948).

Primary instability of open section stringers attached to sheet, S. Levy and W. D. Kroll. J. Aeronaut. Sci. 15, No. 10, 581 (1948).

The dynamic response of a simple elastic system to antisymmetric forcing functions characteristic of airplanes in unsymmetric landing impact, J. B. Woodson. J. Appl. Mech. 16, No. 3, 310-316 (1949).

Compression tests of curved panels with circular hole reinforced with circular doubler plates, W. D. Kroll and A. E. McPherson. J. Aeronaut. Sci. 16, No. 6, 354 (1949).

Stress distribution near reinforced circular hole loaded by pin, S. Levy and F. C. Smith. J. Research NBS 42, 397 (1949) RP1979.

Transient vibration in an airplane wing obtained by several methods, W. Ramberg. J. Research NBS 42, 437 (1949) RP1984.

Elastic buckling of outstanding flanges clamped at one edge and reinforced by bulbs at other edge, S. Goodman. NACA Tech. Note 1985 (1949).

Instability in shear of simply supported square plates with reinforced hole, W. D. Kroll. J. Research NBS 43, 465 (1949) RP2037.

Influence of wing flexibility on force-time relation in shock strut following vertical landing impact, A. E. McPherson, J. Evans, Jr., and S. Levy. NACA Tech. Note 1995 (1949).

Comparison of fatigue strengths of bare and alclad 24S-TS aluminum-alloy sheet specimens tested at 12 and 1000 cycles per minute, F. C. Smith, W. C. Brueggeman, and R. H. Harwell, Jr. NACA Tech. Note 2231 (1950).

Lateral elastic instability of hat-section stringers under compressive load, S. Goodman. NACA Tech. Note 2272 (1951).

Fatigue and static tests of flush-riveted joints, D. M. Howard and F. C. Smith. NACA Tech. Note 2709 (1952); Product Engineering - 1955 Annual Handbook, p. G-2.

Influence coefficients of tapered cantilever beams computed on SEAC, S. Levy. J. Appl. Mech. 30, No. 1 (1953).

Calculation and measurement of normal modes of vibration of an aluminum-alloy box beam with and without large discontinuities, F. C. Smith and D. M. Howard. NACA Tech. Note 2884 (1953).

Investigation of sandwich construction under lateral and axial loads, W. D. Kroll, L. Mordfin, and W. A. Garland. NACA Tech. Note 3090 (1953).

Structural analysis and influence coefficients for delta wings, S. Levy. J. Aeronaut. Sci. 20, No. 7, 449 (1953).

Tests of bonded and riveted sheet-stringer panels, L. Mordfin and I. E. Wilks. NACA Tech. Note 3215 (1954).

NBS Research and Development in Aeronautics. NBS Tech. News Bul. 38, 100 (1954).

Adhesive bonded aircraft structures. NBS Tech. News Bul. 39, 11 (1955).

Cumulative fatigue damage of axially loaded alclad 75S-T6 and alclad 24S-T3 aluminum-alloy sheet, I. Smith, D. M. Howard, and F. C. Smith. NACA Tech. Note 3293 (1955).

Creep and creep rupture characteristics of some riveted and spotwelded lap joints of aircraft materials, L. Mordfin. NACA Tech. Note 3412 (1955).

Computation of vibration modes and frequencies on SEAC, W. F. Cahill and S. Levy. J. Aeronaut. Sci. 22, No. 12, 837 (1955).

Thermal stresses and deformations in beams, S. Levy. Aeronaut. Eng. Rev., Inst. Aeronaut. Sci. 15, No. 10 (1956).

Creep behavior of structural joints of aircraft materials under constant loads and temperatures, L. Mordfin and A. C. Legate. NACA Tech. Note 3842 (1957).

Effect of rib flexibility on the vibration modes of a delta-wing aircraft, W. D. Kroll. J. Research NBS 60, 335 (1958) RP2852.

The reports on structural properties of house constructions, designated as Building Materials and Structures Reports (BMS), are listed in List of Publications LP11. This List of Publications can be obtained free on request to the National Bureau of Standards.

Tests of large bridge columns, J. H. Griffith and J. G. Bragg. Tech. Pap. BS (1918) T101.

The compressive strength of large brick piers, J. G. Bragg. Tech. Pap. BS (1918) T111.

Tests of hollow building tiles, Bernard D. Hathcock and E. Skillman. Tech. Pap. BS (1919) T120.

Load strain-gage tests of 150-ton floating crane for the Bureau of Yards and Docks, U. S. Navy Department, L. J. Larson and R. L. Templin. Tech. Pap. BS13 (1920) T151.

Results of some compressive tests of structural steel angles, A. H. Stang and L. R. Strickenberg. Tech. Pap. BS 16, 651 (1922) T218.

Welded pressure vessels. Bul. No. 5 Am. Bureau Welding; J. Am. Welding Soc. 2, 11 (1923).

Loading tests of a hollow tile and reinforced concrete floor of Arlington Building, Washington, D. C., L. J. Larson and S. N. Petrenko. Tech. Pap. BS 17, 405 (1923) T236.

Some compressive tests of hollow tile walls, H. L. Whittemore and B. D. Hathcock. Tech. Pap. BS17, 513 (1923) T238.

Stresses in a few welded and riveted tanks tested under hydrostatic pressure, A. H. Stang and T. W. Greene. Tech. Pap. BS17, 645 (1923) T243.

Strength of ideal walls, Brick and Clay Record 62, No. 4, 313 (1923).

Spot-welded girders and columns tested for strength, L. B. Tuckerman. Eng. News-Record 92, 982 (1924).

Strength of steel tubing under combined column and transverse loading including tests of columns and beams, T. W. Greene. Tech. Pap. BS18, 243 (1924), T258.

Bibliography on riveted joints. Am. Soc. Mech. Engineers (1924).

Proper construction of welds for pressure vessels, H. L. Whittemore. Eng. News-Record 92, 462 (1924).

Tests of some girder hooks, H. L. Whittemore and A. H. Stang. Tech. Pap. BS18, 305 (1924) T260.

Tangent modulus and the strength of steel columns in tests, O. H. Basquin. Tech. Pap. BS18, 381 (1924) T263.

Tests of I-beams in torsion, L. B. Tuckerman. Discussion. Eng. News-Record 93, 882 (1924).

Compressive strength of sand-lime brick walls, H. L. Whittemore and A. H. Stang. Tech. Pap. BS19, 57 (1925) T276.

Tests of hollow tile and concrete slabs reinforced in one direction, D. E. Parsons and A. H. Stang. Tech. Pap. BS 19, 465 (1925) T291.

Compressive and transverse strength of hollow-tile walls, A. H. Stang, D. E. Parsons, and H. D. Foster. Tech. Pap. BS 20, 317 (1926) T311.

Strain lines, structural members. Delaware Bridge. NBS Misc. Publ. 72 (1926).

Steel trusses carry 22 stories in Chicago Hotel. Eng. News-Record 96, No. 16, 641 (1926).

Investigation of the behavior and of the ultimate strength of riveted joints under load, E. L. Gayhart, Comdr., U.S.N. Trans. Soc. Naval Architects and Marine Engineers (New York, N. Y.) 34, 55 (1926).

Compressive strength of column web plates and wide web columns, R. S. Johnston. Tech. Pap. BS 20, 733 (1926) T327.

Tests of large columns with H-shaped section, L. B. Tuckerman and A. H. Stang. Tech. Pap. BS21, 1 (1926). T328.

Stresses in a rail due to a falling weight, A. H. Stang. J. Am. Welding Soc. 6, No. 3, 64 (1927).

The strength of solid and hollow walls of brick, A. H. Stang. Ceramic Age 10, No. 6, 198 (1927); Architect, Builder and Industrial News, 4, No. 7, 141 (1928); Building Economy, 4, No. 1, 20 (1928).

Strength of interlocking-rib tile walls, A. H. Stang, D. E. Parsons, and A. B. McDaniel. Tech. Pap. BS22, 389 (1928) T366.

574278 O - 61 - 59

The effect of strength of brick on compressive strength of brick masonry, J. W. McBurney. Proc. Am. Soc. Testing Materials 28, Pt. II, 605 (1928).

Compressive strength of clay brick walls, A. H. Stang, D. E. Parsons, and J. W. McBurney. BS J. Research 3, 507 (1929) RP108.

Transverse tests of H-section column splices, J. H. Edwards, H. L. Whittemore, and A. H. Stang. BS J. Research 4, 395 (1930) RP157; J. Am. Welding Soc. 9, 7 (1930).

Test of composite beams and slabs of hollow tile and concrete, D. E. Parsons and A. H. Stang. BS J. Research 4, 815 (1930) RP181.

Compressive tests of bases for subway columns, J. H. Edwards, H. L. Whittemore, and A. H. Stang. BS J. Research 5, 619 (1930) RP218; J. Am. Welding Soc. 10, 20 (1931).

Strength of welded shelf angle connections, J. H. Edwards, H. L. Whittemore, and A. H. Stang. BS J. Research 5, 781 (1930) RP230; J. Am. Welding Soc. 10, 29 (1931).

Report of structural steel welding committee. Am. Bureau Welding (1931).

Inspection service for welded structures seen as need, H. L. Whittemore. Steel 88 (1931); Welding Engineer 16, 49 (1931).

Stress distribution welded steel pedestals, J. H. Edwards, H. L. Whittemore, and A. H. Stang. BS J. REsearch 5, 803 (1930) RP232; J. Am. Welding Soc. 10, 46 (1931).

Strain measurement in the reinforcement for the dome of the Natural History Building, W. C. Lyons, H. L. Whittemore, A. H. Stang, and L. R. Sweetman. BS J. Research 6, 183 (1931) RP268.

Compressive tests of jointed H-section steel columns, J. H. Edwards, H. L. Whittemore, and A. H, Stang. BS J. Research 6, 305 (1931) RP277.

Tests of cellular sheet-steel flooring, H. L. Whittemore and J. M. Frankland. BS J. Research 9, 131 (1932) RP463; J. Am. Welding Soc. 12, 4 (1933).

Final report committee on welded rail joints. Am. Bureau Welding (1932).

The areas and tensile properties of deformed concrete reinforcement bars, A. H. Stang, L. R. Sweetman, and C. Gough. BS J. Research 9, 509 (1932) RP486.

Column curves and stress-strain diagrams, W. R. Osgood. BS J. Research 9, 571 (1932) RP492.

Shear tests of reinforced brick masonry beams, D. E. Parsons, A. H. Stang and J. W. McBurney. BS J. Research 9, 749 (1932) RP504.

Wind bracing connection efficiency, W. R. Osgood. Discussion. Proc. Am. Soc. Civil Engineers (New York 18, N. Y.) 58, 675 (1932).

Compressive strength of steel columns incased in brick walls, A. L. Harris, A. H. Stang, and J. W. McBurney. BS J. Research 10, 123 (1933) RP520.

Test of a flat steel plate floor under load, L. B. Tuckerman, A. H. Stang, and W. R. Osgood. BS J. Research 12, 362 (1934) RP662.

Neutral axis in a reinforced concrete member subjected to combined stress, W. R. Osgood. Civil Eng. 4, No. 10, 546 (1934).

Stresses in space structures, W. R. Osgood. Discussion. Proc. Am. Soc. Civil Engineers 60, 1085 (1934).

Tests of Mesnager hinges, D. E. Parsons and A. H. Stang. J. Am. Concrete Inst. 6, 304 (1935).

The double-modulus theory of column action, W. R. Osgood. Civ. Eng. 5, No. 3, 173 (1935).

Rational design of steel columns, W. R. Osgood Discussion. Proc. Am. Soc. Civil Engineers 61, No. 3, 391 (1935).

Test of steel tower columns for the George Washington Bridge, A. H. Stang and H. L. Whittemore. J. Research NBS 15, 317 (1935) RP831.

Accelerated service test of pintle bearings, A. H. Stang and L. R. Sweetman. J. Research NBS 15, 591 (1935) RP854.

Some tests of steel columns incased in concrete, A. H. Stang, H. L. Whittemore, and D. E. Parsons. J. Research NBS 16, 265 (1936) RP873.

Tests of eight large H-shaped columns fabricated from carbon manganese steel, A. H. Stang, H. L. Whittemore, and L. R. Sweetman. J. Research NBS 16, 595 (1936) RP896.

Tests of steel chord members for the Bayonne Bridge, A. H. Stang, H. L. Whittemore, and L. R. Sweetman. J. Research NBS 16, 627 (1936) RP897.

Strength of a riveted steel rigid frame having straight flanges, A. H. Stang, M. Greenspan, and W. R. Osgood. J. Research NBS 21, 269 (1938) RP1130.

Strength of a riveted steel rigid frame having a curved inner flange, A. H. Stang, M. Greenspan, and W. R. Osgood. J. Research NBS 21, 853 (1938) RP1161.

Heterostatic loading and critical astatic loads, L. B. Tuckerman. J. Research NBS 22, 1 (1939) RP1163.

A theory of flexure for beams with non-parallel extreme fibers, W. R. Osgood. Trans. Am. Soc. Mech. Engrs. 61, A-122 (1939).

Strength of a welded steel rigid frame, A. H. Stang and M. Greenspan. J. Research NBS 23, 145 (1939) RP1224.

Steel rigid frames, W. R. Osgood. Discussion. Proc. Am. Soc. Civil Engineers 67, 472 (1941).

Stresses in a rectangular knee of a rigid frame, W. R. Osgood. J. Research NBS 27, 443 (1941) RP1431.

Refinement in design to conserve materials, W. R. Osgood. Eng. News-Record 128, No. 17, 58 (1942).

Perforated cover plates for steel columns: Program and test methods, A. H. Stang and M. Greenspan. J. Research NBS 28, 669 (1942) RP1473.

Perforated cover plates for steel columns: compressive properties of plates having ovaloid perforations and a width-to-thickness ratio of 40, A. H. Stang and M. Greenspan. J. Research NBS 28, 687 (1942) RP1474.

Perforated cover plates for steel columns: compressive properties of plates having ovaloid perforations and a width-to-thickness ratio of 68, A. H. Stang and M. Greenspan. J. Research NBS 29, 279 (1942) RP1501.

Perforated cover plates for steel columns: compressive properties of plates having ovaloid perforations and a width-to-thickness ratio of 53, A. H. Stang and M. Greenspan. J. Research NBS 30, 15 (1943) RP1514.

Perforated cover plates for steel columns: compressive properties of plates having circular perforations and a width-to-thickness ratio of 53, A. H. Stang and M. Greenspan. J. Research NBS 30, 177 (1943) RP1527.

Perforated cover plates for steel columns: compressive properties of plates having a net-to-gross cross-sectional-area ratio of 0.33, A. H. Stang and M. Greenspan. J. Research NBS 30, 411 (1943) RP 1540.

Axial rigidity of perforated structural members, M. Greenspan. J. Research NBS 31, 305 (1943) RP1568.

Perforated cover plates for steel columns: compressive properties of plates having ovaloid, elliptical, and "square" perforations, A. H. Stang and B. S. Jaffe. J. Research NBS 40, 121 (1948) RP1861.

Perforated cover plates for steel columns: Summary of compressive properties, A. H. Stang and M. Greenspan. J. Research NBS 40, 347 (1948) RP1880.

Bending tests of large welded-steel box girders at different temperatures, A. H. Stang and B. S. Jaffee. J. Research NBS 41, 483 (1948) RP1934; J. Am. Welding Soc. 28, No. 3, 89-S(1949).

Stress studies of welded ship structure specimens, W. R. Campbell. J. Am. Welding Soc. 30, No. 2, 68-S (1951).

Stress studies of bulkhead intersections for welded tankers, W. R. Campbell, L. K. Irwin, and R. C. Duncan. J. Am. Welding Soc. 31, No. 2, 68-S (1952).

Failures in welded ships, an investigation of the causes of structural failures. NBS Tech. News Bul. 37, 24 (1953).

Tensile tests of large specimens representing the intersection of a bottom longitudinal with a transverse bulkhead in welded tankers, L. K. Irwin and W. R. Campbell. Ship Structure Committee Report SSC-68 (1953).

Creep and static strengths of large bolted joints of forged aluminum alloys under various temperature conditions, L. Mordfin, G. E. Greene, N. Halsey, R. H. Harwell, Jr., and R. L. Bloss. Presented at 26th Annual Mtg. of Inst. Aeronaut. Sci. (New York) Preprint No. 779 (1958).

MACHINE ELEMENTS

The friction and carrying capacity of ball and roller bearings, H. L. Whittemore and S. N. Petrenko. Tech. Pap. BS14 (1921) T201.

Experimental use of liquid air and explosives for tightening body-bound bolts, H. L. Whittemore. Am. Machinist 56, 524 (1922).

The strength of bolt threads as affected by inaccurate machining. G. M. Deming. Mech. Engineering 45, 583 (1923).

Tests of ball bearings for rotating beam fatigue machines, L. B. Tuckerman and C. S. Aitchison. Am. Machinist 61, 369 (1924).

Failures of aircraft engine parts and causes thereof, L. B. Tuckerman. Discussion. Proc. Am. Soc. Testing Materials 30, Pt. II, 195 (1930).

Note on the electrical resistance of contacts between nuts and bolts, F. Wenner, G. W. Nusbaum, and B. C. Cruickshanks. BS J. Research 5, 757 (1930) RP227.

The relation of torque to tension for thread-locking devices, H. L. Whittemore, G. W. Nusbaum, and E. O. Seaquist. BS J. Research 7, 945 (1931) RP386.

Impact and static tensile properties of bolts, H. L. Whittemore, E. O. Seaquist, and G. W. Nusbaum. J. Research NBS 14, 139 (1935) RP763.

The tensile forces in tightened bolts, A. H. Stang. Prod. Eng. 22, No. 2, 118 (1951).

A pretied tie for communication line wires, C. R. Ballard and R. R. Bouche. REA Conf. Paper No. CP 58-266 (1958).

Handmade bolts support the Capitol dome, L. K. Irwin. Fasteners 13, No. 3 (1958).

MISCELLANEOUS

Strength and other properties of wire rope, J. H. Griffith and J. G. Bragg. Tech. Pap. BS (1919) T121.

Physical tests of motor truck wheels, C. P. Hoffman. Tech. Pap. BS13 (1920) T150.

Results of some tests of manila rope, A. H. Stang and L. R. Strickenberg. Tech. Pap. BS15 (1921) T198.

Tests of rotary drill pipes, A. H. Stang. Iron Age 108, 804 (1921); 109, 359 (1922).

Size standardization by preferred numbers, L. B. Tuckerman. Am. Soc. Mech. Eng. (1922).

Investigation of oxyacetylene welding and cutting blowpipes, with special reference to their design, safety and economy in operation, R. S. Johnston. Tech. Pap. BS15 (1922) T200.

Some tests of steel wire rope on sheaves, E. Skillman. Tech. Pap. BS17, 227 (1923) T229.

Laboratory strength tests of motor truck wheels, T. W. Greene. J. Soc. Automotive Engineers XV, 150 (1924).

Testing gas welds, H. L. Whittemore. Welding Engineer 12, 38 (1927); Am. Machinist 66, 40 (1927); Power 65, 211 (1927); Acetylene J. 28, 330 (1927); Welding J. XXIV, 46 and 156 (1927).

Comparative tests of six-inch cast iron pipe of American and French manufacture, S. N. Petrenko. Tech. Pap. BS21, 231 (1927) T336.

Control for welding, H. L. Whittemore. J. Am. Welding Soc. 7, 52 (1928).

Efficiency of machinists' vises, H. L. Whittemore and L. R. Sweetman. BS J. Research 3, 191 (1929) RP91.

Corrosion of open valley flashings, K. H. Beij. BS J. Research 3, 987 (1929) RP123.

Procedure control for aircraft welding, H. L. Whittemore, J. J. Crowe, and H. H. Moss. Proc. Am. Soc. Testing Materials 30, Pt. II, 140 (1930); Welding 1, 589 (1930).

Seams for copper roofing, K. H. Beij. BS J. Research 5, 585 (1930) RP216.

A welded dredge pipe, H. L. Whittemore. Industry and Welding 2, 12 (1931).

Welding research, H. L. Whittemore. Industry and Welding 2, 7 (1931).

A welded steam pipe, H. L. Whittemore. Industry and Welding 2, 2 (1931).

Thermal effects in elastic and plastic deformation, L. B. Tuckerman. Discussion. Proc. Am. Soc. Testing Materials, 32, Pt. II, 594 (1932).

These consulting engineers, H. L. Whittemore. Industry and Welding 4, 17 (1932).

Safe welding practice, H. L. Whittemore. Eng. News-Record 112, 237 (1934).

Flow in roof gutters, K. Hilding Beij. BS J. Research 12, 193 (1934) RP644.

Report of the joint board of review appointed to investigate the causes of the accident to the balloon "Explorer", L. B. Tuckerman. Member of the Board. Natl. Geographic Soc. contributed tech. papers stratosphere series, No. 1, 71 (1935).

Ballast requirements and performance of the stratosphere balloon "Explorer II", L. B. Tuckerman, W. Ramberg, and F. D. Swan. Natl. Geographic Soc. contributed tech. papers stratosphere series, No. 2, 250 (1936).

Load distribution and strength of elevator cable equalizers, A. H. Stang and L. R. Sweetman. J. Research NBS 17, 291 (1936) RP912.

Inspection and tensile tests of some worn wire ropes, W. H. Fulweiler, A. H. Stang, and L. R. Sweetman. J. Research NBS 17, 401 (1936) RP920.

Approximation to a function of one variable from a set of its mean values, M. Greenspan. J. Research NBS 23, 309 (1939) RP1235.

The sliding of metals, W. R. Osgood. Engineer 168, 426 (1939).

Effect of a small hole on the stresses in a uniformly loaded plate, M. Greenspan. Quart. Appl. Math. II, No. 1, 60 (1944).

The Hankinson Formula, W. R. Osgood. Comment and discussion. Eng. News-Record 135, 646 (1945).

Impact strength of nylon and of sisal ropes, S. B. Newman and H. G. Wheeler. J. Research NBS 35, 417 (1945) RP1679.

Dynamic tensile tests of parachute webbing. A. H. Stang, M. Greenspan, and S. B. Newman. J. Research NBS 36, 411 (1946) RP1710.

Theory for axial rigidity of structural members having ovaloid or square perforations, M. Greenspan. J. Research NBS 37, 157 (1946) RP1737.

On the intensity of light reflected from or transmitted through a pile of plates, L. B. Tuckerman. J. Opt. Soc. Am. 37, No. 10, 818 (1947).

PHYSICS - Contributions of electricity to mechanics, W. Ramberg. J. Wash. Acad. Sci. 39, No. 9, (September, 1949).

Response of accelerometers to transient accelerations, S. Levy and W. D. Kroll. J. Research NBS 45, 303 (1950) RP2138.

Errors introduced by finite space and time increments in dynamic response computations, S. Levy and W. D. Kroll. Proc. 1st U. S. Natl. Congress of Appl. Mech., June 11-16, 1951 (1952); J. Research NBS 51, 57 (1953) RP2431.

Damping of elastically supported element in a vacuum tube, S. Levy, E. V. Hobbs, W. D. Kroll, and L. Mordfin. J. Research NBS 50, 71 (1953) RP2391.

Determination of loads in the presence of thermal stresses, S. Levy. J. Aeronaut. Sci. 21, No. 10, 659 (1954).

Radiant-heat transfer between nongray parallel plates, S. Goodman. J. Research NBS 58, 37 (1957) RP2732.

Wind-induced vibration of telephone and distribution conductors, R. R. Bouche, A. A. Lee, C. R. Ballard, and F. J. On. REA Conf. Paper. AIEE Middle East. Dist. Meeting (Washington, D. C., 1958).

Aerodynamic heating and fatigue, W. D. Kroll. NASA Memo 6-4-59W (1959).

Elastic deformations in strips with holes loaded through pins, M. Chi and L. K. Irwin. J. Research NBS 62, 147 (1959).

Effect of internal radiant heat transfer on temperature distribution, thermal stress and deflection in box beams, S. Goodman, S. B. Russell, and C. E. Noble. J. Research NBS 62, 175 (1959).

PROPERTIES OF MATERIALS

Impact tests for woods, NACA Tech. Note 78 (1922).

Fatigue or progressive failure of metals under repeated stress, L. B. Tuckerman. Discussion. Proc. Am. Soc. Testing Materials 22, Pt. II, 266 (1922).

Mechanical meaning of hardness numbers, S. N. Petrenko. Mech. Engineering 46, 926 (1924).

Hardness and hardness testing, L. B. Tuckerman. Mech. Engineering 47, 53 (1925).

Report of conference on fatigue phenomena of metals, H. L. Whittemore. Natl. Research Council, Div. of Eng. and Ind. Research 21 (1927).

The strength of brick in tension, J. W. McBurney, J. Am. Ceram. Soc. 2, No. 2, 114 (1928).

Fatigue resistance of some aluminum alloys, L. B. Tuckerman. Discussion. Proc. Am. Soc. Testing Materials 29, Pt. II, 344 (1929).

Fatigue studies of non-ferrous sheet metals, L. B. Tuckerman. Discussion. Proc. Am. Soc. Testing Materials 29, Pt. II, 365 (1929).

Aircraft materials, L. B. Tuckerman. Discussion. Proc. Am. Soc. Testing Materials 30, Pt. II, 175 (1930).

Failures of aircraft engine parts and causes thereof, L. B. Tuckerman. Discussion. Proc. Am. Soc. Testing Materials 30, Pt. II, 195 (1930).

Physical properties of electrically welded steel tubing, H. L. Whittemore, J. S. Adelson and E. O. Seaquist. BS J. Research 4, 475 (1930) RP161; J. Am. Welding Soc. 9, 17 (1930).

Mechanical properties of aluminum alloy rivets, W. C. Brueggeman. NACA Tech. Note 585 (1936).

The crinkling strength and the bending strength of round aircraft tubing, W. R. Osgood. NACA Tech. Reports 24 (1938).

A rational definition of yield strength, W. R. Osgood. J. Appl. Mech. 7, No. 2, A-61 (1940).

Effect of aging on mechanical properties of aluminum-alloy rivets, F. C. Roop. NACA Tech. Report 724 (1941).

Material shortages - redesign and substitution, H. L. Whittemore. Eng. News-Record 128, 114 (1942).

Tensile and pack compressive tests of some sheets of aluminum alloy, 1025 carbon steel, and chromium-nickel steel, C. S. Aitchison and J. A. Miller. NACA Tech. Note 840 (1942).

Tensile and compressive properties of some stainless steel sheets, C. S. Aitchison, W. Ramberg, L. B. Tuckerman, and H. L. Whittemore. J. Research NBS 28, 499 (1942) RP1467.

Round heat-treated chromium-molybdenum-steel tubing under combined loads, W. R. Osgood. NACA Tech. Note 896 (1943).

Description of stress-strain curves by three parameters, W. Ramberg and W. R. Osgood. NACA Tech. Note 902 (1943).

Tensile and compressive tests of magnesium alloy J-1 sheet, C. S. Aitchison and J. A. Miller. NACA Tech. Note 913 (1943).

Mechanical properties of metals and alloys, John L. Everhart, W. Earl Lindlief, J. Kanegis, P. G. Weissler, and Frieda Siegel. NBS Circ. 447, 481 (1943)$3.50.

Symposium on the significance of the hardness test of metals in relation to design, L. B. Tuckerman. Discussion. Proc. Am. Soc. Testing Materials 43, 847 (1943).

Significance of the secant and tangent moduli of elasticity in structural design, W. R. Osgood. Discussion. J. Aeronaut. Sci. 11, No. 1, 91 (1944).

Plastic bending, W. R. Osgood. J. Aeronaut. Sci. 11, No. 3, 213 (1944).

Micro-deformation under tension and compression loads of thin aluminum alloy sheets for aircraft construction, J. A. Miller. Discussion. Proc. Am. Soc. Testing Materials 44, 683 (1944).

Plastic bending - further considerations, W. R. Osgood. J. Aeronaut. Sci. 12, No. 3, 253 (1945).

Stress-strain formulas, W. R. Osgood, J. Aeronaut. Sci. 13, No. 1, 45 (1946).

Stress-strain and elongation graphs for aluminum alloy R301 sheet, J. A. Miller. NACA Tech. Note 1010 (1946).

Determination and presentation of compressive stress strain data for thin sheet metal, W. Ramberg and J. A. Miller. J. Aeronaut. Sci. 13, No. 11, 569 (1946).

Poisson's ratio of some structural alloys for large strains, A. H. Stang, M. Greenspan, and S. B. Newman. J. Research NBS 37, 211 (1946) RP1742.

Stress-strain and elongation graphs for alclad aluminum-alloy 75S-T sheet, J. A. Miller. NACA Tech. Note 1385 (1947).

A statistical analysis of some mechanical properties of manila rope, S. B. Newman and J. H. Curtiss. J. Research NBS 39, 551 (1947) RP1847.

Stress-strain and elongation graphs for alclad aluminum-alloy 24S-T sheet, J. A. Miller. NACA Tech. Note 1512 (1948).

Stress-strain and elongation graphs for alclad aluminum-alloy 24S-T81 sheet. NACA Tech. Note 1513 (1948).

Mechanical properties of human bones. NBS Tech. News Bul. 32, 118 (1948).

The elasticity and strength of some long bones of the human body, C. O. Carothers, F. C. Smith, and P. Calabrisi. Naval Medical Research Inst. Proj. NM 001 056 02 13 (October, 1949).

Stress-strain and elongation graphs for aluminum-alloy 75S-T6 sheet. J. A. Miller. NACA Tech. Note 2085 (1950).

Stress-strain and elongation graphs for alclad aluminum-alloy 24S-T86 sheet, J. A. Miller. NACA Tech. Note 2094 (1950).

Effective modulus in plastic buckling of high-strength aluminum-alloy sheet, J. A. Miller and P. V. Jacobs. NACA RM51G11 (September, 1951).

Dynamic stress-strain curves for mild steel using the tangent modulus procedure, W. R. Campbell. J. Wash. Acad. Sci. 43, No. 4, 102 (1953).

Poisson's ratio of aircraft sheet materials for large strains, S. Goodman and S. B. Russell. Proc. 1st Mid-western Conf. on Solid Mechanics, (April, 1953).

Mechanical tests on specimens from large aluminum-alloy forgings, J. A. Miller and A. L. Albert. NACA Tech. Note 3729 (1956).

Investigation of bearing creep of two forged aluminum alloys, L. Mordfin, N. Halsey, and P. J. Granum. NBS Tech. Note 55 (PB161556) (1960) $1.00.

TESTING METHODS

Comparison of five methods used to measure hardness, R. P. Devries. Tech. Pap. BS (1912) T11.

Airplane tensiometer, L. J. Larson. NACA Report 32, 4th Annual Report (1918).

The hardness testing of metals. Report of Committee of Eng. Div. of Nat. Research Council. Mech. Engineering 43, 445 (1921).

Optical strain gages and extensometers, L. B. Tuckerman. Proc. Am. Soc. Testing Materials 23, Pt. II, 602 (1923).

New developments in electrical telemeters, O. S. Peters and R. S. Johnston. Proc. Am. Soc. Testing Materials 23, Pt. II, 592 (1923).

Equalizer apparatus for transverse tests of brick, H. L. Whittemore. Tech. Papers. BS18, 107 (1924) T251.

A simple fixture for testing belting. Am. Machinist 60, 722 (1924).

Cable reel of simple design, H. L. Whittemore. Machinery 30, 925 (1924).

Design of specimens for short-time fatigue tests, L. B. Tuckerman and C. S. Aitchison. Tech. Pap. BS19, 47 (1924) T275.

Table of Brinell hardness numbers. NBS Misc. Publ. 62 (1924).

Tests of thin gage metals, H. L. Whittemore. Discussion. Proc. Am. Soc. Testing Materials 24, Pt. II, 1006-1011 (1924).

Comparative slow bend and impact notched bar tests of some metals, S. N. Petrenko. Tech. Pap. BS19, 315 (1925) T289.

Strain detection in mild steel by wash coating, R. S. Johnston. British Iron and Steel Inst. CXII, 342 (1925).

Elastic ring for verification of Brinell hardness testing machines, S. N. Petrenko. Trans. Am. Soc. Steel Treating IX, 420 (1926).

A fabric tension meter for use on aircraft, L. B. Tuckerman, G. H. Keulegan, and H. N. Eaton. Tech. Pap. BS 20, 581 (1926) T320.

Methods of socketing fiber rope and tensile strength tests, H. L. Whittemore and C. T. Ervin. Cord Age 9, No. 6, 12 (1926).

Impact testing of insulating material, H. L. Whittemore. Discussion. Proc. Am. Soc. Testing Materials 26, Pt. II, 653 (1926).

Standardizing the Brinell test, H. L. Whittemore, L. B. Tuckerman, and S. N. Petrenko. Discussion. Am. Soc. Steel Treating XI, 67 (1927).

A portable apparatus for transverse tests of brick, A. H. Stang. Tech. Pap. BS21, 347 (1927) T341.

The Whittemore strain gage, H. L. Whittemore. Instruments I, 299 (1928).

Rings for checking accuracy of testing machines, W. S. Morehouse. Iron Age 123, 945 (1929).

The determination and significance of the proportional limit in testing metals, L. B. Tuckerman. Discussion. Proc. Am. Soc. Testing Materials 29, Pt. II, 538 (1929).

Report of Committee E-1 on methods of bend testing, L. B. Tuckerman. Discussion. Proc. Am. Soc. Testing Materials 29, Pt. I, 503 (1929).

A new dead weight testing machine of 100,000 lb. capacity, L. B. Tuckerman, H. L. Whittemore, and S. N. Petrenko. BS J. Research 4, 261 (1930) RP147; Metals and Alloys 1, 661 (1930).

Relationships between rockwell and Brinell numbers, S. N. Petrenko. BS J. Research 5, 19 (1930) RP185.

Specimens for torsion tests of metals, L. B. Tuckerman. Discussion. Proc. Am. Soc. Testing Materials 30, Pt. II, 545 (1930).

A method of exciting resonant vibrations in mechanical systems, L. B. Tuckerman, H. L. Dryden, and H. B. Brooks. BS J. Research 10, 659 (1933) RP556.

Determination of stresses from strains on three intersecting gage lines and its application to actual tests, W. R. Osgood and R. G. Sturm. BS J. Research 10, 685 (1933) RP559.

A propeller-vibration indicator, H. L. Dryden and L. B. Tuckerman. BS J. Research 12, 537 (1934), RP678.

A method for determining stresses in a non-rotating propeller blade vibrating with a natural frequency, W. Ramberg, P. S. Ballif, and M. J. West. J. Research NBS 14, 189 (1935) RP764.

An extensometer comparator, A. H. Stang and L. R. Sweetman. J. Research NBS 15, 199 (1935) RP822; Mechanical World and Engineering Record XCVIII, 473 (1935).

Determination of principal stresses from strains on four intersecting gage lines 45° apart, W. R. Osgood. J. Research NBS 15, 579 (1935) RP851.

Determination of the Brinell number of metals, S. N. Petrenko, W. Ramberg, and B. L. Wilson. J. Research NBS 17, 59 (1936) RP903.

Speed control for screw-power testing machines driven by direct-current motors, A. H. Stang and L. R. Sweetman. ASTM Bull. No. 87 (August, 1937).

Compensation of strain gages for vibration and impact, W. Bleakney. J. Research NBS 18, 723 (1937) RP1005.

Calibration of testing machines under dynamic loading, B. L. Wilson and C. Johnson. J. Research NBS 19, 41 (1937) RP1009.

Graphical computations of stresses from strain data, A. H. Stang and M. Greenspan. J. Research NBS 19, 437 (1937) RP1034.

The "pack" method for compressive tests of thin specimens of materials used in thin-wall structures, C. S. Aitchison and L. B. Tuckerman. NACA Tech. Reports 25 (1939).

The significance of tests, W. E. Emley and L. B. Tuckerman. ASTM Bull. No. 99 (1939).

Extension of pack method for compressive tests, C. S. Aitchison. NACA Tech. Note 789 (1940).

Symposium on the significance of the tension test, W. R. Osgood. Discussion. Proc. Am. Soc. Testing Materials 40, 583 (1940).

Note on plane strain, W. R. Osgood. J. Appl. Mech. 9, A-26 (1942).

Proposed method of verification and classification of strainometers, B. L. Wilson. ASTM Bull. No. 117, 83 (1942).

A portable calibrator for dynamic strain gages, A. E. McPherson. NACA Tech. Note 887 (1943).

Adaptor for measuring principal strains with Tuckerman strain gage, A. E. McPherson. NACA Tech. Note 898 (1943).

Dead-weight machines of 111,000-and 10,100-pound capacities, B. L. Wilson, D. R. Tate, and G. Borkowski. NBS Circ. 446 (1943).

A subpress for compressive tests, C. S. Aitchison and J. A. Miller. NACA Tech. Note 912 (1943).

Guides for preventing buckling in axial fatigue tests of thin sheet-metal specimens, W. C. Brueggeman and M. Mayer, Jr. NACA Tech. Note 931 (1944).

Characteristics of the Tuckerman strain gage, B. L. Wilson. Proc. Am. Soc. Testing Materials 44, 1017 (1944).

Performance tests of wire strain gages I - calibration factors in tension, W. R. Campbell. NACA Tech. Note 954 (1944).

A comparison of microhardness indentation tests, D. R. Tate. Trans. Am. Soc. for Metals 35, 374 (1945).

A transfer strain gage for large strains, M. Greenspan and L. R. Sweetman. J. Research NBS 34, 595 (1945) RP1658.

Performance tests of wire strain gages II - calibration factors in compression, W. R. Campbell. NACA Tech. Note 978 (1945).

Performance tests of wire strain gages III - calibrations at high tensile strains, W. R. Campbell. NACA Tech. Note 997 (1945).

Errors in indicated strain for a typical wire strain gage caused by prestraining, temperature changes, and weathering, W. R. Campbell. NACA Tech. Note 1011 (1946).

A fixture for compressive tests of thin sheet metal between lubricated steel guides, J. A. Miller. NACA Tech. Note 1022 (1946).

Performance tests of wire strain gages IV - axial and transverse sensitivities, W. R. Campbell. NACA Tech. Note 1042 (1946).

Proving rings for calibrating testing machines, B. L. Wilson, D. R. Tate, and G. Borkowski. NBS Circ. 454 (1946) 15 cents.

Temperature coefficients for proving rings, B. L. Wilson, D. R. Tate, and G. Borkowski. J. Research NBS 37, 1 (1946) RP1726.

Vacuum-tube acceleration pickup, W. Ramberg. J. Research NBS 37, 391 (1946) RP1754.

Device for measuring principal curvatures and principal strains on a nearly plane surface, A. E. McPherson. NACA Tech. Note 1137 (1947).

Performance test of wire strain gages V - Error in indicated bending strains in thin sheet metal due to thickness and rigidity of gage, W. R. Campbell and A. F. Medbery. NACA Tech. Note 1318 (1947).

A vacuum tube for acceleration measurement, W. Ramberg. Electrical Engineering 66, No. 6, 555 (1947).

The measurement of acceleration with a vacuum tube, W. Ramberg. Proc. Am. Inst. Elec. Eng. Paper 47-108 T Section,66 (1947).

Performance tests of wire strain gages VI - Effect of temperature on calibration factor and gage resistance, W. R. Campbell. NACA Tech. Note 1456 (1948).

Tests of six types of bakelite-bonded wire strain gages, W. R. Campbell. NACA Tech. Note 1656 (1948).

Calibration of accelerometers, S. Levy, A. E. McPherson, and E. V. Hobbs. J. Research NBS 41, 359 (1948) RP1930.

Resistance wire strain gages and their application, W. Ramberg. InterAvia 4, No. 1, 27 (January, 1949); InterAvia 4, No. 2, 87 (February, 1949).

The improved Ramberg vacuum-tube accelerometer, W. Ramberg. NBS Tech. News Bul. 34, 180 (1950).

Fatigue testing machine for applying a sequence of loads of two amplitudes, F. C. Smith, D. M. Howard, I. Smith, and R. H. Harwell, Jr. NACA Tech. Note 2327 (1951).

Recent developments in the Ramberg vacuum tube accelerometer, S. Levy. Proc. of the Soc. for Exp. Stress Anal. 9, No. 1, 151 (1951).

An optical strain gage for use at elevated temperatures, P. R. Weaver. Proc. of the Soc. for Exp. Stress Anal. 9, No. 1, 159 (1951).

Determination of stress-strain curve in shear by twisting square plate, W. Ramberg and J. A. Miller. Proc. 1st U. S. Natl. Congress of Appl. Mech., June 11-16, 1951 (1952).

Mechanical testing of solid materials, W. Ramberg. Appl. Mech. Rev. 5, 241 (1952).

Calibration of load measuring devices, B. L. Wilson. Recent Developments and Techniques in the Maintenance of Standards, National Physical Laboratory (1952).

The measurement of forces acting on a pilot during crash landing, A. E. McPherson. Proc. of the Soc. for Exp. Stress Anal. 9, No. 2, 159 (1952).

Improved photogrid techniques for determination of strain over short gage lengths, J. A. Miller. Proc. of the Soc. for Exp. Stress Anal. 10, No. 1, 29 (1952).

Determination of dynamic stress-strain curves from strain waves in long bars, W. R. Campbell. Proc. of the Soc. for Exp. Stress Anal. 10, No. 1, 113 (1952).

NBS Limit-load gage, P. R. Weaver. NBS Tech. News Bul. 36, 131 (1952).

Twisted square plate method and other methods for determining the shear stress-strain relation of flat sheet, W. Ramberg and J. A. Miller. J. Research NBS 50, 111 (1953) RP2397.

574278 O - 61 - 60

Stress-strain relation in shear from twisting test of annulus, W. Ramberg and J. A. Miller. J. Research NBS 50, 125 (1953) RP2398.

High capacity load calibrating devices. NBS Tech. News Bul. 37, 137 (1953).

A dual-amplitude axial-load fatigue machine, A. E. McPherson. Proc. of the Soc. for Exp. Stress Anal. 10, No. 2, 143 (1953).

Application of resistance-wire strain gages to high-capacity load-calibrating devices, D. R. Tate. NBS Circ. 528, 121 (1954) $1.50.

Preliminary investigation of the strain sensitivity of conducting films, W. R. Campbell. NBS Circ. 528, 131 (1954) $1.50.

Longitudinal impact tests of long bars with a slingshot machine, W. Ramberg and L. K. Irwin. Am. Soc. Testing Materials Spec. Tech. Publ. No. 176, 111 (1955).

A large vibration machine, NBS Tech. News Bul. 39, 24 (1955).

Calibration of vibration pickups by the reciprocity method, S. Levy and R. R. Bouche. J. Research NBS 57, 227 (1956) RP2714.

Electrodynamic Standards for vibration pickups, NBS Tech. News Bul. 41, No. 1 (1957).

Calibration of shock and vibration pickups, W. Ramberg. Noise Control, 3, No. 5, 23-33 (September, 1957).

A facility for the evaluation of resistance strain gages at elevated temperatures, R. L. Bloss. Am. Soc. Testing Materials Spec. Tech. Publ. No. 230 (1958).

Autographic stress-strain recorders, R. R. Bouche and D. R. Tate. Am. Soc. Testing Materials Tech. Paper 39 (1958).

Vibration pickup calibration, NBS Tech. News Bul. 43, 161 (1959).

Improved standard for the calibration of vibration pickups, R. R. Bouche. Soc. Experimental Stress Anal. Paper No. 570 (1959).

The evaluation of resistance strain gages at elevated temperatures, R. L. Bloss. Am. Soc. Testing Materials Preprint No. 74a (1960).

Revised
1960

U. S. DEPARTMENT OF COMMERCE
NATIONAL BUREAU OF STANDARDS

List of
Publications
LP33

PRESSURE MEASUREMENTS

Books and Periodical References

Compiled by

W. G. Brombacher

Pressure & Vacuum Section

1. MISCELLANEOUS REFERENCES

1.1 W. A. Wildhack, Pressure drop in tubing in aircraft instrument installations, NACA Tech. Note 953 (Feb. 1937).

1.2 W. G. Brombacher, Instrumentation for flight testing airplanes, Instruments 20, 700 (1947). (Classification of devices for measuring pressures in aircraft.)

1.3 Manometer tables, Inst. Soc. Am. RP2.1, 32 pages (1948).

1.4 W. G. Brombacher, Some problems in the measurement of pressure, Instruments 22, 355 (April 1949).

1.5 K. J. DeJuhasz, The engine indicator, its design, theory and special applications (Instrument Publishing Co., New York, N. Y., 1934).

1.6 H. C. Roberts, Mechanical measurements by electrical methods, 357 pages (Instrument Publishing Co., Pittsburgh, Pa., 1946).

1.7 W. P. Mason, Electromechanical transducers and wave filter, 419 pages (D. Van Nostrand Co., Inc., New York, N. Y., 1948).

1.8 D. R. Church and D. K. Hart, Balanced pressure engine indicators, Mech. Eng. 72, 389 (1950).

1.9 Anon, Internal ballistics, 311 pages (Great Britain Ministry of Supply, London, H. M. Stationery Office, 1951). (340 references.)

1.10 DuMont Laboratories, Transducers, 151 pages (Allen B. DuMont Laboratory, Inc., 1953).

2. MERCURIAL BAROMETERS

2.1 F. A. Gould, Barometers and manometers, Dict. Applied Physics 3, 140 (1923). (Edited by R. Glazebrook.)

2.2 K.C.D. Hickman, The mercury meniscus, Rev. Sci. Instr. 19, 190 (1929).

2.3 J. E. Sears and J. S. Clark, New primary standard barometer, Proc. Roy. Soc. (London) 139, 130 (1933).

2.4 F. A. Gould and J. C. Evans, A new form of barostat, J. Sci. Instr. 10, 215 (1933).

2.5 A. Klemeno and O. Bankowski, The capillary depression of mercury in large bore tubes, Naturwissenschaften 22, 10 (1934).

2.6 E. Kleinschmidt, Handbuch der Meteorologischen Instrumente, 733 pages (Julius Springer, Berlin, 1935). (Chapter on measurement of air pressure.)

2.7 W.E.K. Middleton and A. F. Spilhaus, Meteorological instruments, 3d ed., 286 pages (Univ. of Toronto Press, 1953).

2.8 H. F. Stimson, The measurement of some thermal properties of water, J. Wash. Acad. Sci. 35, 201 (1945).

2.9 Smithsonian Meteorological Tables, 6th ed. (1951).

2.10 C. F. Marvin, Barometers and the measurement of atmospheric pressure, Circulr F, Instrument Division, U. S. Weather Bureau (1912).

2.11 S. Haynes, Automatic calibration of radiosonde baroswitches, Electronics 24, 126 (May 1951).

2.12 H. J. Svec and D. S. Gibbs, Recording mercurial manometer for pressure range 0-760 mm Hg, Rev. Sci. Instr., 24, 202 (1953).

3. MANOMETERS, LIQUID TYPE

3.1 B. Tockepeiser, New types of sensitive silica manometers, J. Sci. Instr. (May 1930).

3.2 Malmberg and Nicholas, A simple manometer utilizing a non-volatile liquid of low density, Rev. Sci. Instr. 3, 440 (1932).

3.3 E. Ower, Measurement of airflow, 2d ed. (Chapman & Hall, London, England, 1933). (See chapter on Manometers.)

3.4 R. Warden, An improved multitube tilting manometer, Aero Research Committee, Rept. & Mem. 1572 (London, 1939).

3.5 H. Reichardt, Pressure gage for very small pressure differences, (Micromanometer) Z. Ver. deut. Ing. 79, 50 (1935).

3.6 F.V.A.E. Engel and R. J. Wey, Mechanical flowmeters, Engineer 160, 555, 584, 612 (1935). (Describes special forms of liquid manometers, including float and ring types.)

3.7 Micromanometers, (Aerodynamische Versuchsanstalt, Göttingen, Oct. 1936).

3.8 Roger Gelmont, Theory and operation of a Cartesian Diver type manostat, Ind. Eng. Chem., Anal. Ed. 18, 633 (1946). (Made by Emil Greiner.)

3.9 J. L. Wilson, H. N. Eaton, and H. B. Henrickson, Use and testing of sphygmomanometers, Techn. Pap. BS 21 (1927) T352. OP. (Contains an elementary treatment of manometers.)

3.10 I. E. Puddington, Sensitive mercury manometer, Rev. Sci. Instr. 19, 577 (1948).

3.11 J. Reilly and W. N. Rae, Physico-chemical methods 1, 822 (D. Van Nostrand Co., Inc., New York, N. Y., 1939).

4. ABSOLUTE-PRESSURE GAGES

4.1 R. H. Field and G. C. Cowper, The aneroid barometer and altimeter, Topographical Survey, Bull. 63 (Dept. Interior, Canada, 1931).

4.2 P. Werkmeister, Metallbarometer System Paulin, Z. Instrumentenk 51, 435 (1931).

4.3 W. G. Brombacher, Measurement of altitude in blind flying, NACA Tech. Note 503 (1934).

4.4 Pioneer sensitive altimeter, Aviation, 39 (Dec. 1936); Aero Digest, 54 (Dec. 1936); U. S. Air Services, 34 (Dec. 1936).

4.5 Kollsman improves the altimeter, Western Flying, 38 (July 1938); Aero Digest, 104 (Aug. 1938); Aviation, 41 (Aug. 1938).

4.6 H. J. Van der Maas and J. H. Greidanus, The accuracy of altitude measurements with the aneroid-type altimeter, Report V1162, National Luchtvaart Laboratorium (1939). (In Dutch.)

4.7 L. F. Curtiss, A. V. Astin, L. L. Stockman, and B. W. Brown, An improved radio meteorograph on the Olland principle, J. Research NBS 22, 97 (1939) RP1169. OP. (Time between contacts controlled by aneroid pressure element.)

4.8 W. S. Hinman, F. W. Dunmore, and E. G. Lapham, An improved radiosonde and its performance, J. Research NBS 25, 327 (1940) RP1324. OP. (Switch type aneroid pressure element described.)

4.9 Philip Kissam, Precision altimetry, Photogrammetric Engineering, 25 (Jan., Feb., Mar. 1944).

4.10 Frederick Koppel, Recent progress in the measurement of atmospheric pressure, Rev. Sci. Instr. 18, 850 (Nov. 1947). (Quartz barograph and hypsometer.)

4.11 Daniel P. Johnson, Calibration of altimeters under pressure conditions simulating dives and climbs, NACA Tech. Note 1562 (1948).

4.12 Daniel P. Johnson, D. I. Steel and M. de Novens, Measurement of drift and recovery in aircraft altimeters, NBS Report 1953.

5. PRESSURE GAGES, DIFFERENTIAL AND GAGE

5.1 H. T. Owens, Research and development of high pressure oxygen gauges, Acetylene J. (Jan. 1924).

5.2 A. Graham, Note on the structure of turbulence in a natural wind, containing also a description of sensititive pressure gage, Aero Research Committee, Rept. & Mem. 1704 (London, 1936). (Diaphragm-type gage.)

5.3 David S. Evans and K. Mendelssohn, The physics of blood pressure measurement, Proc. Phys. Soc. (London) 54, pt. 3, 211 (1942).

5.4 P. S. White, Seasoning Bourdon tube systems, Instruments 16, 356 (June 1943).

5.5 Harry Matheson and Murray Eden, Highly sensitive differential manometer, Rev. Sci. Instr. 19, 502 (1948).

5.6 A. G. Keenan and R. L. McIntosh, A strain-sensitive resistance wire manometer, Rev. Sci. Instr. 19, 338 (1948).

5.7 M. P. White, Application of Bourdon tubes to pressure indicating devices, Instruments 23, 1068 (1950).

5.8 J. E. Witherspoon, Electronic-recorder pickups, Instruments 26, 429 (1953).

5.9 L. Ollivier and D. J. Tricebock, Precise pressure measurement, Elec. Mfg. 52, 114 (Aug. 1953).

6. HIGH-PRESSURE MEASUREMENT

6.1 James H. Boyd, Jr., A manometer for the measurement of small pressure differentials at high pressures, J. Am. Chem. Soc. 52, 5102 (1930).

6.2 P. W. Bridgman, The physics of high pressure, 398 pages (Macmillan Co., New York, N. Y., 1931); with supplement (G. Bell, London, 1949).

6.3 C. H. Meyers and R. S. Jessup, A multiple manometer and piston gages for precision measurements, BS J. Research 6, 1061 (1931) RP324. OP.

6.4 J. A. Beattie and Walter L. Edel, Über Messungen mit der Kolbendruckwaage, I Der Einfluss des Druckes auf die Waagenkonstante, Ann. Physik 7, 633 (1931).

6.5 J. A. Beattie and O. C. Bridgman, Über Messungen mit der Kilbendruckwaage. II Einfluss von Alterung and Olviskositat auf die Waagenkonstante; Beziehung zwischen dem Wirksamen und dem Wirklichen Durchmesser des Kolbens, Ann. Physik 12, 827 (1932).

6.6 A. Michels, The calibration of a pressure balance in absolute units, Proc. Roy. Acad. Amsterdam 35, 994 (1932).

6.7 A. Michels and M. Lenssen, Electric manometer for pressures up to 3000 atmospheres, J. Sci. Instr. 11, 345 (1934).

6.8 E. Schmidt, Measurement of small pressure differences at high pressures, VDI 80, 635 (1936).

6.9 J. R. Roebuck and W. Cram, Mercury manometer for 200 atmospheres, Rev. Sci. Instr. 8, 215 (1937).

6.10 L. H. Adams, R. W. Goranson, and R. E. Gibson, Manganin resistance pressure gage, Rev. Sci. Instr. 8, 230 (1937).

6.11 N. H. Sage and W. N. Lacey, Apparatus for study of pressure-volume-temperature relations of liquids and gases, Am. Inst. Mining Met. Engrs. Tech. Pub. 1127 (1939).

6.12 H. Ebert, Establishment of a pressure scale and experimental realization up to 20,000 atm., Z. Angew. Phys. 1, 331 (1949).

6.13 H. E. Darling and D. H. Newhall, A high-pressure wire gage using goldchrome wire, Trans. ASME 75, 311 (1953).

6.14 P. W. Pridgman, Measurement of hydrostatic pressure to 30,000 kg/cm^2, Proc. Am. Acad. Arts Sci. 74, 1 (1940).

6.15 P. W. Bridgman, Recent work in the field of high pressures, Revs. Modern Phys. 18, 1 (1946). (674 references.)

6.16 D. P. Johnson and D. H. Newhall, The piston gage as a precise measuring instrument, Symposium on high pressure, ASME Trans. 75, 301 (1953).

7. VACUUM MEASUREMENT

7.1 M. Pirani and R. Neuman, High vacuum gages, Electronic Eng. 17, 277, 322, 367 (1944-45).

7.2 Saul Dushman, Manometers for low pressures, Instruments 20, 234 (1947). (A review of existing vacuum gages.)

7.3 G. W. Monk, The vacuum divider; a low pressure multiplier, Rev. Sci. Instr. 19, 396 (1948).

7.4 V. H. Dibeler and F. Cordero, Diaphragm-type micromanometer for use on a mass spectrometer, J. Research NBS 46, 1 (1951) RP2167. OP.

7.5 J. M. Los and J. A. Morrison, A sensitive differential manometer, Rev. Sci. Instr. 22, 805 (1951).

7.6 R. J. Havens, R. T. Koll and H. E. LaGow, The pressure, density and temperature of the earth's atmosphere to 160 km, J. Geophys. Res. 57, 59 (1952).

7.7 D. B. Cook and C. J. Danby, A simple diaphragm micromanometer, J. Sci. Instr. 30, 238 (1953).

8. DYNAMIC-PRESSURE MEASUREMENT

8.1 Kalman J. De Juhasz, The engine indicator, 235 pages (Instrument Publishing Co., Pittsburg, Pa., 1934). (Covers all types of dynamic pressure measurement available up to 1934.)

8.2 C. M. Bouton, H. K. Griffith, and P. L. Golden, Accuracy of manometry of explosions, comparative performance of some diaphragm-type explosion manometers when using hydrogen-air mixtures, U. S. Bur. Mines Tech. Paper 496 (1931).

8.3 Bernard Lewis and G. von Elbe, Combustion, flames and explosion of gases, 415 pages (Academic Press, 1941). (Section on pressure measurement.)

8.4 Robert E. Tozier, The NACA optical engine indicator, NACA Tech. Note 634 (Jan. 1938).

8.5 F. R. Caldwell and E. F. Fiock, Some factors influencing the performance of diaphragm indicators of explosion pressures, J. Research NBS 26, 175 (1941). RP1368. OP.

8.6 J. C. Karcher, A piezoelectric method for the instantaneous measurement of high pressures, BS Sci. Pap. 18 (1922) S445. OP.

8.7 R. H. Kent and A. H. Hodge, The use of the piezoelectric gage in the measurement of powder pressures, Trans. ASME 61, 197 (1939).

8.8 N. J. Thompson and E. W. Cousins, Measuring pressures of industrial explosions, Electronics, 90 (Nov. 1947). (Capacitance pickup, 2 to 3000 psi.)

8.9 A. G. Keenan and R. L. McIntosh, Strain-sensitive resistance wire manometer, Rev. Sci. Instr. 19, 336 (May 1948).

8.10 C. S. Draper, E. S. Taylor, J. H. Lancor, and R. T. Coffey, Development of a detonation detector suitable for use in flight, NACA Tech. Note 977 (1944).

8.11 R. D. Meyer, Applications of unbonded-type resistance gages, Instruments 19, 136 (Mar. 1946).

8.12 H. Schaevitz, The linear variable differential transformer, Proc. Soc. Exper. Stress Analysis 4, 79 (1947).

8.13 P. B. Smith, A recording optical manometer for transient pressures, J. Sci. Instr. 24, 134 (1947).

8.14 L. H. Montgomery and J. W. Ward, Measurement of transient hydraulic pressures, Rev. Sci. Instr. 18, 289 (1947).

8.15 R. H. Cole, Underwater explosions, 437 pages (Princeton Univ. Press 1948).

8.16 C. S. Draper and Y. T. Li, A new high-performance engine indicator of the strain-gage type, J. Aer. Sci. 16, 593 (1949).

8.17 M.O.W. Wolfe, Measurement of fluctuating fluid pressures, Aircraft Eng. 21, 368 (1949).

8.18 D. R. Church and D. K. Hart, Balanced pressure engine indicators, Mech. Eng. 72, 389 (1950).

8.19 J. H. Hett and R. W. King, Jr., A frequency modulation pressure recording system, Rev. Sci. Instr. 21, 150 (1950).

8.20 W. D. MacGeorge, The differential transformer as applied to the measurement of substantially straight line motions, Proc. Inst. Soc. Am. 4, 28 (1950); Instr. 23, 610 (1950).

8.21 Characteristics and applications of resistance strain gages, NBS Circular 528, 140 pages (1954). $1.50.

8.22 H. R. Bierman and R. Jenkins, A hypodermic pressure manometer utilizing the bonded wire resistance strain gauge, Rev. Sci. Instr. 22, 268 (1951).

8.23 C. D. McKinney, Jr. and M. Kilpatrick, An apparatus for measuring the rates of some rapid reactions, Rev. Sci. Instr. 22, 590 (1951).

8.24 A. G. Boggis, Design of differential transformer displacement gauges, Proc. Soc. Exper. Stress Analysis 9, 171 (1952).

8.25 W. J. Levedahl, Instrumentation for detonation research, Instr. Soc. Am. Proc. 7, 343 (1952).

8.26 J. L. Patterson, A miniature electrical pressure gage utilizing a flat diaphragm, NACA Tech. Note 2659, 47 pages (1952).

8.27 E. M. Sharp, B. A. Coss, and L. Jaffe, A digital automatic multiple-point pressure-recording system, Instr. Soc. Am. Proc. 7, 236 (1952).

8.28 I. Glass, W. Martin, and G. N. Patterson, A theoretical and experimental study of the shock tube, Inst. Aero Physics, Univ. Toronto Report 2, 281 pages (1953). (73 references.)

8.29 B. Lewis, H. C. Hottel, and A. J. Nerad, Fourth symposium (international) on combustion (combustion and detonation waves), 926 pages (Williams and Wilkins Co., 1953).

8.30 J. Alman, Pressure recorder for rocket motor studies, Electronics 26, 146 (May 1953).

8.31 I. G. Baxter, Differential capacitance manometer, J. Sci. Instr. 30, 358 (1953).

8.32 J. F. Kinkel and R. R. Mawson, Automatic calibration of transducers, Instruments 26, 1526 (1953).

8.33 D. W. St. Clair, L. W. Erath, and S. L. Gillespie, Sine-wave generators; Frequency-response symposium, ASME Paper 53-A12, 7 pages (1953).

8.34 C. B. Vogel, Piezoelectric well hydrophones, J. Accoust. Soc. Am. 25, 711 (1953).

8.35 Y. T. Li, High-frequency pressure indicators for aerodynamic problems, NACA Tech. Note 3042, 52 pages (1953).

8.36 R. T. Eckenrode and H. A. Kirshner, Measurement of pressure transients, Rev. Sci. Instr. 25, 33 (1954). (112 references.)

8.37 C. G. Hylkema and R. B. Bowersox, Experimental and mathematical technique for determining dynamic response of pressure gages, Inst. Soc. Am. J. 1, 27 (Feb. 1954); Proc. ISA 8, 115 (1953).

8.38 H. F. Rondeau, An introduction to the resistance wire strain gage, Inst. Soc. Amer. J. 1, 17 (Feb. 1954). (176 references.)

8.39 J. Grey, Pressure transducers, Product Eng. 25, 174 (Jan. 1954).

8.40 H. C. Roberts, Mechanical measurements by electrical methods, 357 pages (Instrument Publishing Co., Pittsburgh, Pa., 1946).

8.41 W. G. Brombacher and T. W. Lashof, Bibliography and index on dynamic pressure measurements, NBS Circular 558 (Feb. 1955). $.75.

9. FLAT AND CORRUGATED CIRCULAR DIAPHRAGMS

9.1 Stanley Smith, On the depression of the center of a thin circular disc of steel under normal pressure, Trans. Roy. Soc. Can. 16, Ser. 3, Sec. 3, 217 (1922).

9.2 M. D. Hersey, Diaphragms for aeronautic instruments, p. 157, NACA Tech. Rept. 165 (1923).

9.3 H. N. Eaton and C. T. Buckingham, Non-metallic diaphragms for instruments, NACA Tech. Rept. 206, 149 (1924).

9.4 A. A. Griffith, The theory of pressure capsules (Air Ministry T. 2541 and A.) Aero Research Committee, Rept. & Mem. 1136, 1-14 (London 1928).

9.5 K. Stange, Der Spannungszustand einer Kreisringscale, Ingenieur-Archiv. 11, pt. 1, 47 (1931).

9.6 Theodore Theodorsen, Investigation of the diaphragm-type pressure cell, NACA Tech. Rept. 388, 507 (1931).

9.7 E. Meissner, Uber das Knicken Kreisringformiger Scheiben, Schweiz Bauzt. 101, No. 8, 87.

9.8 Stewart Way, Bending of circular plates with large deflection, Paper No. APM-56-12, Trans. ASME 56, No. 8, 627 (Aug. 1934).

9.9 W. A. Wildhack and V. H. Goerke, Corrugated metal diaphragms for aircraft pressure-measuring instruments, NACA Tech. Note 738, 41 pages (Nov. 1939).

9.10 Fernand Charron, Étude des capsules anéroides, Pubs. sci. et techn. ministère air (France) 160 (Feb. 1940).

9.11 W. G. Brombacher, V. H. Goerke, and F. Cordero, Sensitive aneroid diaphragm capsule with no deflection above a selected pressure, J. Research, NBS 24, 31 (1940) RP 1270. OP.

9.12 W. A. Wildhack and V. H. Goerke, The limiting useful deflections of corrugated metal diaphragms, NACA Tech. Note 867 (Dec. 1942).

9.13 L. B. Hunt, Beryllium copper in instrument design, J. Sci. Instruments 21, 97 (June 1944).

9.14 H. G. Williams, Test methods for predicting diaphragm performance, The Instrument Maker 14 (March - April 1946).

9. FLAT AND CORRUGATED CIRCULAR DIAPHRAGMS (CONTINUED)

9.15 Properties and applications of Wilco Ni-Span "C" constant modulus alloy, Eng. Data Bulletin (H. A. Wilson Co., Mar. 1946).

9.16 Alfred Pfeiffer, A note on the theory of corrugated diaphragms for pressure-measuring instruments, Rev. Sci. Instruments 18, 660 (1947).

9.17 E. W. Pike and N. E. Gibbs, A study on aneroid capsules, J. Applied Phys. 19, 106 (Jan. 1948).

9.18 P. G. Exline, Pressure responsive elements, Trans. ASME 60, 625 (1938).

10. BOURDON TUBES

10.1 H. Lorenz, Theory of the flexible tube manometer, Physik. 18, 117 (Mar. 1917), abstracted in Science Abstracts, Section A-Physics No. 573 (July 1917).

10.2 L. Mauerer, On the deformation of Bourdon aneroid spirals, Arch. Math. Leipzig 1, 260 (3 Reiche 6, 1903).

10.3 G. Klein, Unterscuchung and Kritik von Hochdruckmessen, Dissertation Köng. Tech. Hochschule, Berlin (Sept. 1908).

10.4 C. Susa, Determining range of helical Bourdon springs, Instruments 5, 85, 88 (April 1932).

10.5 C. B. Biezeno and J. J. Koch, On the elastic behavior of the Bourdon tube, Proc. Acad. Amsterdam 44 (1951).

10.6 Walter Wuest, Die Bewegungslehre von Röhrenfedern, Z. Instrumentenk. 63, 416 (Dec. 1943).

10.7 Irwin Vigness, Elastic properties of curved tubes, Trans. ASME 65, 105 (Feb. 1943).

10.8 Alfred Wold, Elementary theory of the Bourdon gauge, J. Applied Mechanics 68, A207; Discussion, Journal (June 1947) p. A165, by Eastman Smith.

10.9 L. M. Vander Pyl, Bibliography on Bourdon tubes and Bourdon tube gages, ASME Preprint 53-IRD-1 (Sept. 1953).

ACOUSTICS

"Long-Tube Method for Field Determination of Sound-Absorption Coefficients", Earle Jones, Seymour Edelman, and Albert London, J. Res. NBS 49, 1 (July 1952).

"The Determination of Reverberant Sound Absorption Coefficients from Acoustic Impedance Measurements", Albert London, J. Acous. Soc. of Am., 22, 263 (1950).

"Effect of Paint on the Sound Absorption of Acoustic Materials", V. L. Chrisler, J. Res. NBS 24, 547 (1940).

"Dependence of Sound Absorption upon Area and Distribution of Absorbent Material", V. L. Chrisler, J. Res. NBS 13, 169 (1934).

"Transmission of Reverberant Sound through Walls", Richard V. Waterhouse, Acustica, 4, 290 (1954) (Proceedings of First ICA Congress, 1953).

"Methods for Determining Sound Transmission Loss in the Field", A. London, J. Res. NBS 26, 419 (1941).

"Recent Sound Transmission Measurements at the National Bureau of Standards", V. L. Chrisler and W. F. Snyder, J. Res. NBS 14, 749 (1935).

"Theory and Interpretation of Experiments on the Transmission of Sound through Partition Walls", Edgar Buckingham, Sci. Pap. BS, 20, 193 (1925).

"Interference Patterns in Reverberant Sound Fields", R. V. Waterhouse, J. Acous. Soc. Am., 27, 247 (March 1955).

"Sound Insulation of Wall and Floor Construction", Sound Section Staff (February 25, 1955).

"Some Developments in Vibration Measurement", Seymour Edelman, Earle Jones, and Ernest R. Smith, J. Acous. Soc. Am., 27, 4 (July 1955).

"A Basic Method of Determining the Dynamic Characteristics of Accelerometers by Rotation", W. A. Wildhack and R. O. Smith, J. Instr. Soc. Am., 1, 12, Paper No. 54-40-3 (December 1954).

"Pressure Calibration of Condenser Microphones above 10,000 cps", B. Simmons and F. Biagi, J. Acous. Soc. Am., 26, 693 (September 1954).

"High Speed Stroboscope for Accelerometer Calibration", P. G. Sulzer, E. R. Smith and S. Edelman, Rev. Sci. Inst., 25, 837 (August 1954).

"Acoustic Impedance of a Right Circular Cylindrical Enclosure", F. Biagi and Richard K. Cook, J. Acous. Soc. Am., 26, 506 (July 1954).

"An Acoustic Method for the Measurement of Vibration Amplitudes", W. Koidan, J. Acous. Soc. Am., 26, 428 (May 1954).

"Laboratory Standard Microphones", R. K. Cook, Acustica 4, 101 (1954).

"Subharmonic Crystal Oscillators", M. Thompson, Jr., C. Tschiegg, and M. Greenspan, Rev. Sci. Inst., 25, 8 (1954).

Wide-Range Calibrator for Vibration Pickups", W. A. Yates and Martin Davidson, Electronics, 26, 183 (September 1953).

An Accurate Time-Modulated Pulse Circuit", Carroll Tschiegg and Martin Greenspan, Rev. Sci. Instr., 24, 183 (February 1953).

"An Eleven Megacycle Interferometer for Low Pressure Gases", Martin Greenspan and Moody C. Thompson, Jr., J. Acous. Soc. Am., 25, 92 (January 1953).

"A Logarithmic Slidewire for a Self-Balancing Potentiometer", M. Greenspan and M. Thompson, Jr. Rev. Sci. Inst., 22, 799 (1951).

"Absolute Calibration of Vibration Pickups", A. London, Tech. News Bul., 32, 8 (January 1948).

"Remarks on Measurement of Electromotive Force of a Microphone", Richard K. Cook, J. Acous. Soc. Am., 20, 874 (1948).

"Measurement of Electromotive Force of a Microphone", R. K. Cook, J. Acous. Soc. Am., 19, 503 (1947).

"A Short-Tube Method for Measurement of Impedance", R. K. Cook, J. Acous. Soc. Am., 19, 922 (1947).

"Absolute Pressure Calibration of Microphones", R. K. Cook, J. Res. NBS, 25, 489 (1940); also published in abbreviated form in J. Acous. Soc. Am., 12, 415 (1941).

"Principles, Practice and Progress of Noise Reduction in Airplanes", A. London, Tech. Notes National Advisory Committee for Aeronautics No. 748 (1940).

"The Response of Earphones in Ears and Couplers", Mahlon D. Burkhard and Edith L. R. Corliss, J. Acous. Soc. Am., 26, 679 (September 1954).

"Probe Tube Method for the Transfer of Threshold Standards between Audiometer Earphones", E. L. R. Corliss and M. D. Burkhard, J. Acous. Soc. Am., 25, 990 (September 1953).

"Calibration of Audiometers", E. L. R. Corliss and W. F. Snyder, J. Acous. Soc. Am., 22, 837 (1950).

574278 O - 61 - 61

"Anelasticity of Quartz", R. K. Cook and R. C. Breckenridge, Phys. Rev., 92, 1419 (December 1953).

"Piezoelectric Constants of Alpha- and Beta-Quartz at Various Temperatures", R. K. Cook and Pearl G. Weissler, Phys. Rev., 80, 712 (1950).

"Thermal Voltages of a Quartz Crystal", R. K. Cook, M. Greenspan and P. G. Weissler, Phys. Rev., 74, 1714 (1948).

"Decay Constant in Vibrating Systems", R. D. Laughlin, Radio-Electronic Eng. Section, Radio and Television News, 49, 11 (April 1953).

"Measurement of Dynamic Properties of Rubber", R. S. Marvin, Ind. and Eng. Chem., 44, 696 (April 1952).

"Federal Specification SS-A-118b for Acoustical Units", Prefabricated Acoustical Materials Subcommittee to the Committee on Heat Insulating Materials, Federal Specification Board.

"The Electrometer at High Frequencies", Martin Greenspan, J. Wash. Acad. Sci., 45, 229, July 1955.

"Effect of Dissolved Air on the Speed of Sound in Water", M. Greenspan and C. E. Tschiegg, J. Acous. Soc. Am., 28, 501 (1956).

"Temperature Coefficient of Speed of Sound in Water near the Turning Point", Martin Greenspan, Carroll E. Tschiegg, and Franklin Breckenridge, J. Acous. Soc. Am., 28, 500 (1956).

"Speed of Sound in Water by a Direct Method", Martin Greenspan, J. Res. NBS 59, 249 (1957), RP 2795.

"A Sing-around Ultrasonic Velocimeter for Liquids", Martin Greenspan and Carroll E. Tschiegg, Rev. Sci. Inst. 28 (November 1957).

"Mechanical Impedance of the Forehead and Mastoid", E. L. R. Corliss and W. Koidan, J. Acous. Soc. Am., 27, 1164, November 1955.

"The Condenser Microphone as a Displacement Detector Calibrator", Walter Koidan, J. Acous. Soc. Am., 29, 813, July 1957.

"Microphone Diaphragm Null Method for Sound Pressure Measurement", Walter Koidan, J. Acous. Soc. Am., 32, 505, April 1960.

"Calibration for Carrier Operated Microphones and other Reversible Transducers", M. D. Burkhard, E. L. R. Corliss, W. Koidan, and F. Biagi, J. Acous. Soc. Am., 32, 501, April 1960.

"Method for Measurement of |E'/I'| in the Reciprocity Calibration of Condenser Microphones", Walter Koidan, J. Acous. Soc. Am., 32, 611, May 1960.

"Method of Measuring Airborne and Impact Sound Transmission Loss of Building Constructions", R. V. Waterhouse and R. D. Berendt, November 28, 1958.

"Sound Transmission Loss of Some Building Constructions", R. V. Waterhouse, R. D. Berendt, and R. K. Cook, Noise Control, 5, 40, July 1959.

"New Method of Recording the Sound Transmission Loss of Walls as a Continuous Function of Frequency", R. V. Waterhouse and R. K. Cook, J. Acous. Soc. Am., 27, 967, September 1955.

"On Standard Methods of Measurement in Architectural Acoustics", R. V. Waterhouse, J. Acous. Soc. Am., 29, 544, May 1957.

"Measurements on Sound Absorbers for Jet-Engine Test Cells", R. V. Waterhouse, R. K. Cook, and R. D. Berendt, J. Acous. Soc. Am., 28, 688, July 1956.

"Interference Patterns in Reverberant Sound Fields", R. V. Waterhouse, J. Acous. Soc. Am., 27, 247, March 1955.

"Precision of Reverberation Chamber Measurements of Sound Absorption Coefficients", R. V. Waterhouse, Proceedings of Third International Acoustics Congress, Stuttgart (1959).

"Stroboscopic Interferometer for Vibration Measurement", E. R. Smith, S. Edelman, E. Jones, and V. Schmidt, J. Acous. Soc. Am., 30, 867, September 1958.

"Measurement of Correlation Coefficients in Reverberant Sound Fields", R. K. Cook, R. V. Waterhouse, R. D. Berendt, S. Edelman, and M. C. Thompson, Jr., J. Acous. Soc. Am., 27, 1072, (November 1955).

"Variation of Elastic Constants and Static Strains with Hydrostatic Pressure: A Method for Calculation from Ultrasonic Measurements", R. K. Cook, J. Acous. Soc. Am., 29, 445, April 1957.

"Experimental and Theoretical Investigation of the Magnetic Properties of Iron Oxide Recording Tape", Eric D. Daniel and Irving Levine, J. Acous. Soc. Am., 32, 1, January 1960.

"Determination of the Recording Performance of a Tape from its Magnetic Properties", Eric D. Daniel and Irving Levine, J. Acous. Soc. Am., 32, 258, February 1960.

"Apparatus for the Direct Determination of the Dynamic Bulk Modulus", John S. McKinney, Seymour Edelman, and Robert S. Marvin, J. Applied Physics, 27, 425, May 1956.

"American Standard Method for the Pressure Calibration of Laboratory Standard Pressure Microphones", Z24.4-1949.

"American Standard Method for the Free-Field Secondary Calibration of Microphones", Z24.11-1954.

"American Standard Specification for Laboratory Standard Pressure Microphones", Z24.8-1949.

"American Standard Method for the Coupler Calibration of Earphones", Z24.9-1949

"American Standard Specification for Audiometers for General Diagnostic Purposes", Z24.5-1951.

"American Standard Specification for Pure-Tone Audiometers for Screening Purposes", Z24.12-1952.

"American Standard Method for Measurement of Characteristics of Hearing Aids", Z24.14-1953.

"American Standard Recommended Practice for Laboratory Measurement of Air-Borne Sound Transmission Loss of Building Floors and Walls", Z24.19-1957.

Subject Index

Combined subject index for the three volumes of NBS Handbook 77

Author Index

Combined author index for the three volumes of NBS Handbook 77

PUBLICATIONS PROGRAM OF THE NATIONAL BUREAU OF STANDARDS

Results of fundamental and applied research at the National Bureau of Standards in physics, chemistry, engineering, and mathematics are published in the Bureau's own series of publications. Papers are also published in the journals of professional and scientific societies and in technical and trade publications.

JOURNAL OF RESEARCH

reports National Bureau of Standards research and development in physics, mathematics, chemistry, and engineering. Comprehensive scientific papers give complete details of the work, including laboratory data, experimental procedures, and theoretical and mathematical analyses. Illustrated with photographs, drawings, and charts.

The Journal presents review articles by recognized authorities and compilations of information on subjects closely related to the Bureau's technical program.

Selected NBS nonperiodical publications and articles by the Bureau staff in professional journals are abstracted in the appropriate section of the Journal. In addition, each section carries a complete listing of all Bureau publications that are not abstracted in that section.

Four Sections ---------- Separately Available

A. PHYSICS AND CHEMISTRY

Papers of interest primarily to scientists working in these fields. This section covers a broad range of physical and chemical research, with major emphasis on standards of physical measurement, fundamental constants, and properties of matter. Issued six times a year. Annual subscription: Domestic, $4.00; foreign, $4.75.*

B. MATHEMATICS AND MATHEMATICAL PHYSICS

Studies and compilations designed mainly for the mathematician and theoretical physicist. Topics in mathematical statistics, theory of experiment design, numerical analysis, theoretical physics and chemistry, logical design and programing of computers and computer systems. Short numerical tables. Issued quarterly. Annual subscription: Domestic, $2.25; foreign, $2.75.*

C. ENGINEERING AND INSTRUMENTATION

Reporting results of interest chiefly to the engineer and the applied scientist. This section includes many of the new developments in instrumentation resulting from the Bureau's work in physical measurement, data processing, and development of test methods. It also covers some of the work in acoustics, applied mechanics, building research, and cryogenic engineering. Issued quarterly. Annual subscription: Domestic, $2.25; foreign, $2.75.*

D. RADIO PROPAGATION

Reporting research in radio propagation, communications, and upper atmospheric physics. Topics covered include propagation in ionized media, scattering by turbulence, effect of irregular terrain on propagation, diffraction and scattering by solid obstacles, propagation through time-varying media, surface waves, and antennas. Issued six times a year. Annual subscription: Domestic, $4.00; foreign, $4.75.*

*Difference in price is due to extra cost of foreign mailing.

OTHER PERIODICALS

The following periodicals may be obtained on a 1-, 2-, or 3-year subscription basis (although no reduction in rates can be made) from the Superintendent of Documents, U.S. Government Printing Office, Washington 25, D.C.:

Technical News Bulletin. Summaries of current research at the National Bureau of Standards are published in the Bulletin. The articles are brief, with emphasis on the results of research, chosen on the basis of their scientific or technologic importance. All publications by Bureau staff are announced in the Bulletin. Annual subscription: Domestic, $1.50; foreign, $2.25.

Basic Radio Propagation Predictions. The Predictions provide the information necessary for calculating the best frequencies for communication between any two points in the world at any time during the given month. The data are important to users of long-range radio communication and navigation, including broadcasting, airline, steamship, and wireless services, and to investigators of radio propagation and ionosphere. Each issue, covering a period of 1 month, is released 3 months in advance. Annual subscription: Domestic, $1.50; foreign, $2.00.

NONPERIODICALS

Applied Mathematics Series. Mathematical tables, manuals, and studies.

Monographs. Major contributions to the technical literature on various subjects related to the Bureau's scientific and technical activities. These comprise much of the type of material previously published in the larger National Bureau of Standards Circulars.

Handbooks. Recommended codes of engineering and industrial practice (including safety codes) developed in cooperation with interested industries, professional organizations, and regulatory bodies.

Miscellaneous Publications. Charts, administrative pamphlets, annual reports of the Bureau, conference reports, etc.

Technical Notes. This series consists of communications and reports (covering both other agency and NBS-sponsored work) of limited or transitory interest. NBS Technical Notes are designed to supplement the Bureau's regular publications program. They are for sale by the Office of Technical Services, U.S. Department of Commerce, Washington 25, D.C.

Catalog of NBS Publications

A complete listing of National Bureau of Standards publications is given in NBS Circular 460, Publications of the National Bureau of Standards, issued from 1901 to June 30, 1947, and its Supplement issued from July 1, 1947, to June 30, 1957. Technical abstracts are given for the publications issued since January 1, 1942. The price of the Circular is $1.25 and the Supplement is $1.50. These documents may be purchased from the Superintendent of Documents, Government Printing Office, Washington 25, D.C. (see "Purchase Procedure" below).

Announcements of New Publications

The Bureau's *Technical News Bulletin* and the *Journal of Research* contain monthly announcements of new NBS publications. Besides listing the Bureau's own publications, the Bulletin and the Journal announce papers by Bureau staff members published in non-Bureau periodicals.

Other Government Sources of Information on NBS Publications

Business Service Checklist. Weekly announcement of publications of the Department of Commerce. Lists titles and prices of National Bureau of Standards publications, and those of other parts of the Department of Commerce. Available from the Superintendent of Documents. $1.50 a year (foreign $3.50).

Monthly Catalog of United States Government Publications. Issued by the Superintendent of Documents. $3.00 a year (foreign $4.50).

Government Printing Office Price Lists. Lists of Government publications on particular subjects. Free from the Superintendent of Documents.

In addition, many of the technical journals carry notices of new Bureau publications of interest in their respective fields.

Purchase Procedure

Most NBS publications are for sale ONLY by the Superintendent of Documents, Government Printing Office, Washington 25, D.C. (PLEASE DO NOT SEND ORDERS TO THE NATIONAL BUREAU OF STANDARDS.) Payment in advance is required, and may be made by coupons sold in sets of 20 for $1.00 and good until used, postal money order, express order, check, or by currency (at sender's risk). A discount of 25 percent is allowed to purchasers of 100 or more copies of a single publication to be mailed to one address. Postage is not required for orders mailed to the United States and possessions. Remittances from foreign countries should be made by international money order or draft on an American bank, and should include an additional one-fourth of the purchase price for postage.

Some purchasers of Government publications prefer to use the "deposit account" service provided by the Superintendent of Documents. Deposits of $10 or more are accepted, against which orders may be placed without making individual remittances or first obtaining quotations. Order blanks are provided by the Superintendent of Documents for the convenience of users of the deposit account arrangement. Orders on these blanks are returned with notations showing the publications supplied, explanations regarding those not sent, the amount charged, and the balance on deposit.

Out of print NBS publications are available for reference use in many scientific, technical, and public libraries. The Bureau's Catalog of Publications, NBS Circular 460, contains a list of Government Depository Libraries that receive selected Bureau publications. Some libraries are equipped to provide photostat or microfilm copies of out of print documents.

U.S. GOVERNMENT PRINTING OFFICE: 1961 O—574278